

REPORT DOCUMENTATION PAGE

Form Approved
OMB No. 0704-0188

Burden for this collection of information is estimated to average 1 hour per response, including the time for reviewing instructions, searching existing data sources, gathering and maintaining the data needed, and completing and reviewing the collection of information. Send comments regarding this burden estimate or any other aspect of this collection of information, including suggestions for reducing this burden, to Washington Headquarters Services, Directorate for Information Operations and Reports, 1215 Jefferson Davis Highway, Suite 1204, Arlington, VA 22202-4302, and to the Office of Management and Budget, Paperwork Reduction Project (0704-0188), Washington, DC 20503.

1. AGENCY USE ONLY (Leave blank)

2. REPORT DATE
15 June 2001

3. REPORT TYPE AND DATES COVERED
Final Report, 1 October 00 - 30 September 2001

4. TITLE AND SUBTITLE
D/F 01: FINAL REPORT OF THE AIAA STUDENT AIRCRAFT DESIGN, BUILD & FLY COMPETITION

5. FUNDING NUMBERS
G: N00014-98-1-0493
PR: 97PR04749-00

6. AUTHORS
By Gregory Page, Chris Bovias, Michael Selig and the student participants of D/B/F 2001.
Compiled by Stephen Brock, AIAA Student Programs

7. PERFORMING ORGANIZATION NAME(S) AND ADDRESS(ES)

American Institute of Aeronautics and Astronautics
ATTN: AIAA Foundation
1801 Alexander Bell Dr., Ste 500
Reston, VA 20191-4344

8. PERFORMING ORGANIZATION
REPORT NUMBER

2001DBF7630

9. SPONSORING/MONITORING AGENCY NAME(S) AND ADDRESS(ES)

Office of Naval Research
800 North Quincy St (ONR 351)
Arlington, VA 22217-5660

10. SPONSORING/MONITORING AGENCY
REPORT NUMBER

11. SUPPLEMENTARY NOTES

12. DISTRIBUTION/AVAILABILITY STATEMENT

APPROVED FOR PUBLIC RELEASE

12b. DISTRIBUTION CODE

13. ABSTRACT (Maximum 200 words)

This report is made up of the combined reports of 28 separate teams of students who entered the 2001 Design, Build & Fly Competition. The objectives of the Design, Build & Fly Competition were to have students teams design, build and fly unmanned remote control electric aircraft designed for two specific missions: a short-field cargo sortie and a cruise/ferry sortie. A "fly-off" took place on the Webster Field near St. Inigoes, MD, in April 2001. Winners of the contest: 1st place, Oklahoma State University; 2nd, California Polytechnic Institute; 3rd, Oklahoma State University. The Design, Build & Fly Competition was supported by Cessna, the Office of Naval Research and the AIAA Foundation.

14. SUBJECT TERMS

Unmanned / Remote / Control / RC / Aircraft / Student / Design / Build / Fly / AIAA

15. NUMBER OF PAGES

1809

16. PRICE CODE

17. SECURITY CLASSIFICATION OF
REPORT

18. SECURITY CLASSIFICATION OF
THIS PAGE

19. SECURITY CLASSIFICATION OF
ABSTRACT

20. LIMITATION OF ABSTRACT
SAR

540-01-280-5500

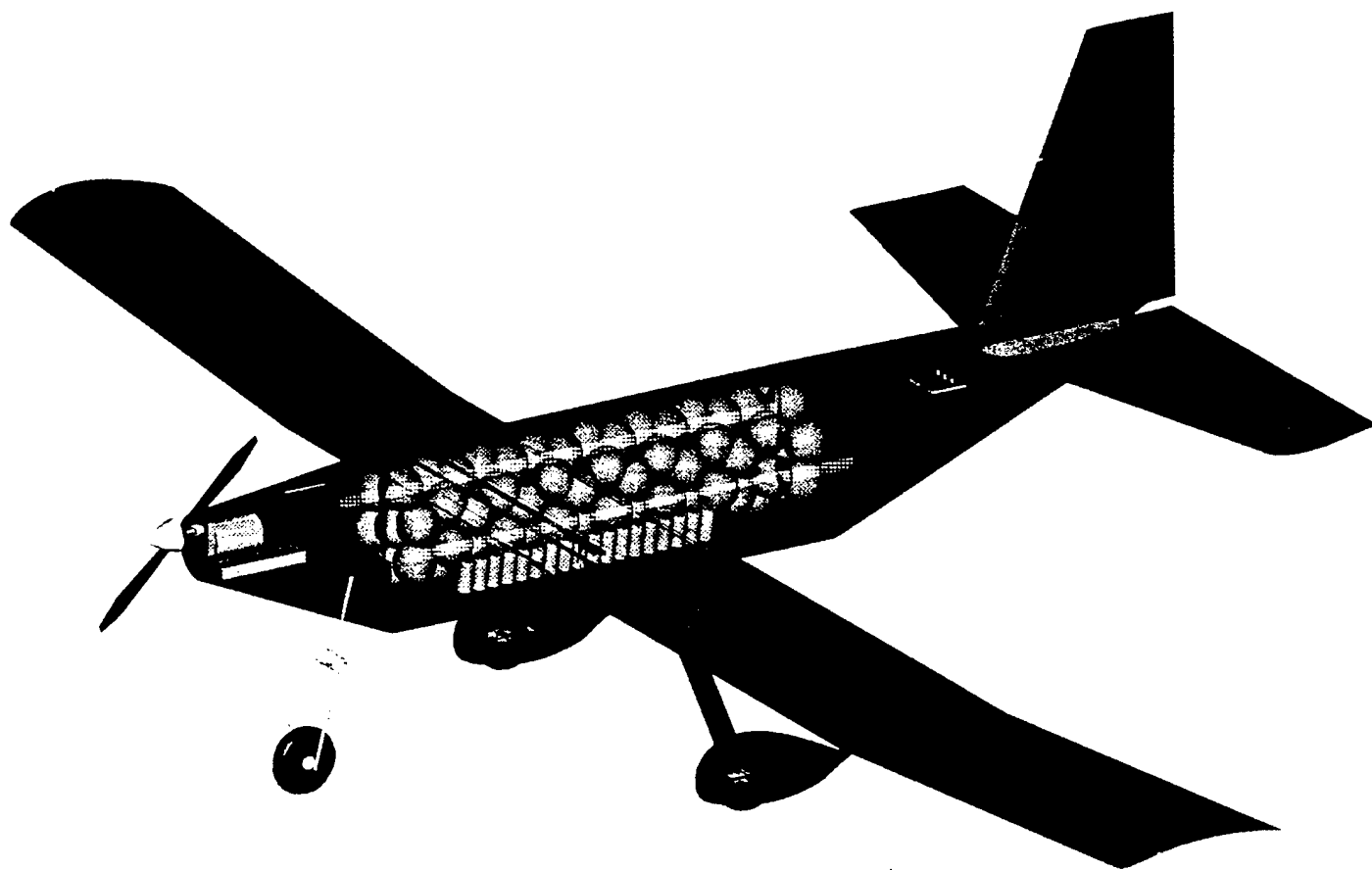
Computer Generated

STANDARD FORM 298 (Rev 2-89)
Prescribed by ANSI Std Z39-18
298-102

20010621 010

2000/01 AIAA Foundation
Cessna/ONR
Student Design/Build/Fly Competition

Proposal Phase Design Report



Oklahoma State University
orange team

March 13, 2001

1	EXECUTIVE SUMMARY	3
1.1	SUMMARY OF DESIGN DEVELOPMENT	3
1.2	MAJOR DEVELOPMENT PROCESS AREAS FOR FINAL CONFIGURATION	3
1.3	RANGE OF DESIGN ALTERNATIVES INVESTIGATED	3
1.4	DESIGN TOOLS USED IN EACH PHASE	4
2	MANAGEMENT SUMMARY	5
2.1	TEAM ARCHITECTURE	5
2.2	ASSIGNMENT AREAS	5
2.3	MANAGEMENT STRUCTURES	6
3	CONCEPTUAL DESIGN	8
3.1	MISSION ANALYSIS AND STRATEGY DEVELOPMENT	8
3.2	ALTERNATIVE CONCEPTS INVESTIGATED	9
3.3	IMPORTANT DESIGN PARAMETERS	10
3.4	FIGURES OF MERIT	10
3.5	RATED AIRCRAFT COST FOR CONCEPTS	12
3.6	FEATURES THAT PRODUCED THE FINAL CONFIGURATION	13
4	PRELIMINARY DESIGN	14
4.1	DESIGN PARAMETERS INVESTIGATED AND FIGURES OF MERIT	14
4.1.1	<i>Aerodynamics Group</i>	14
4.1.2	<i>Structures Group</i>	18
4.1.3	<i>Propulsion Group</i>	21
4.2	ANALYTICAL METHODS	22
4.2.1	<i>Aerodynamics Group</i>	22
4.2.2	<i>Structures Group</i>	23
4.2.3	<i>Propulsion Group</i>	23
4.3	CONFIGURATION AND SIZING DATA	24
4.3.1	<i>Aerodynamics Group</i>	24
4.3.2	<i>Structures Group</i>	28
4.3.3	<i>Propulsion Group</i>	29
4.4	FEATURES THAT PRODUCED THE FINAL CONFIGURATION	34
4.4.1	<i>Aerodynamics Group Summary</i>	34
4.4.2	<i>Structures Group Summary</i>	34
4.4.3	<i>Propulsion Group Summary</i>	34
5	DETAIL DESIGN	35

5.1	PERFORMANCE DATA.....	35
5.2	COMPONENT SELECTION AND SYSTEMS ARCHITECTURE.....	39
5.2.1	<i>Propulsion</i>	39
5.2.2	<i>Structures</i>	40
5.3	INNOVATIVE SOLUTIONS	41
5.3.1	<i>Fuselage</i>	41
5.3.2	<i>Wing</i>	41
5.3.3	<i>Tail</i>	41
5.3.4	<i>Landing Gear</i>	42
5.3.5	<i>Hinges</i>	42
6	MANUFACTURING PLAN.....	42
6.1	MANUFACTURING PROCESSES INVESTIGATED	42
6.2	PROCESS FOR MANUFACTURE OF MAJOR COMPONENTS	43
6.2.1	<i>Fuselage</i>	43
6.2.2	<i>Wing</i>	43
6.2.3	<i>Tail</i>	43
6.2.4	<i>Landing Gear</i>	44
6.3	ANALYTICAL METHODS.....	44
6.3.1	<i>Cost</i>	44
ITEM.....		44
ESTIMATED COST		44
6.3.2	<i>Skills</i>	44
6.3.3	<i>Scheduling</i>	45
6.4	INNOVATIVE SOLUTIONS	45
7	DRAWING PACKAGE	45

1 Executive Summary

The Oklahoma State University Orange Team began searching for an optimum design for this year's Design/Build/Fly competition by evaluating the mission requirements and determining the critical constraints on the design. The objective of this year's contest is to carry alternating payloads of as much steel as possible and as many tennis balls as possible for each sortie. The aircraft design must meet the following criteria as established by the rules of the contest.

- Wingspan of a maximum of 10 ft.
- Aircraft must be propeller driven and electric powered with a commercially available motor from the AstroFlight or Graupner brushed motor families
- Aircraft must use shrink wrapped, commercially available NiCad batteries
- Battery pack must weigh no more than 5.0 lb
- Aircraft must weigh a maximum of 55 lb at takeoff
- Aircraft must be able to withstand a 2.5g load case

1.1 Summary of Design Development

The initial approach in solving this particular design problem involves a systematic mission analysis. This analysis integrates the contest rules with other physical limitations to find the performance needed to score well in the competition. This mission analysis program was then expanded to include propulsion, aerodynamic, and structural information. The program was then used to evaluate and define flight performance and mission strategy.

1.2 Major Development Process Areas for Final Configuration

The first major step in the design process for the Orange team was the development of the mission analysis program. This mission analysis lead to the preliminary configuration selection that allowed the team to move into the next design phase. The program was then refined to include experimental data obtained by the propulsion group through wind tunnel testing. While the refinement of the mission analysis was being done, the structures group began work on the major sub-assemblies of the aircraft. When the mission analysis refinement was completed and the design of the subassemblies finished, then the team moved on to construction of a prototype aircraft. This prototype allows the team to do flight testing to refine the design for the final aircraft.

1.3 Range of Design Alternatives Investigated

The team investigated configurations running from the more experimental to the common and well tested. Configurations considered included flying wing, canard, conventional, multi-engine, and twin fuselage. Different manufacturing processes were also investigated including conventional balsa and monokote and carbon fiber.

1.4 *Design Tools used in each Phase*

During the conceptual and preliminary design phases there were two major design tools utilized. The aerodynamics group centered on developing an involved and expandable mission analysis program. The propulsion team utilized wind tunnel testing of previous propulsion systems. Once this data was gathered, it could be integrated into the mission analysis program and used to develop an optimal propulsion system for the desired flight profile.

Once the data was gathered, the equipment desired and purchased or built and put through more wind tunnel testing. This allowed for further analysis and refinement of systems and techniques that can be implemented in the detailed design of the structure and systems.

The culmination of the detailed design phase is the building and flight testing of a prototype aircraft. Here any unexpected issues in systems integration and performance can be explored and addressed for use in the building of the final aircraft.

2 Management Summary

2.1 Team Architecture

The Orange team is divided into three technical groups, aerodynamics, propulsion, and structures. This technical group division helps the efficiency of the team as a whole. The team personnel were divided up into the technical groups based on their personal interests, their technical background, and the need in each area. Each group has an appointed leader who reports to the chief engineer. The chief engineer is responsible for facilitating communication between the groups and delegating responsibilities to each of the groups. Although not official members of the team, our advisors have provided very valuable information and guidance. Below is a chart illustrating the architecture of team management.

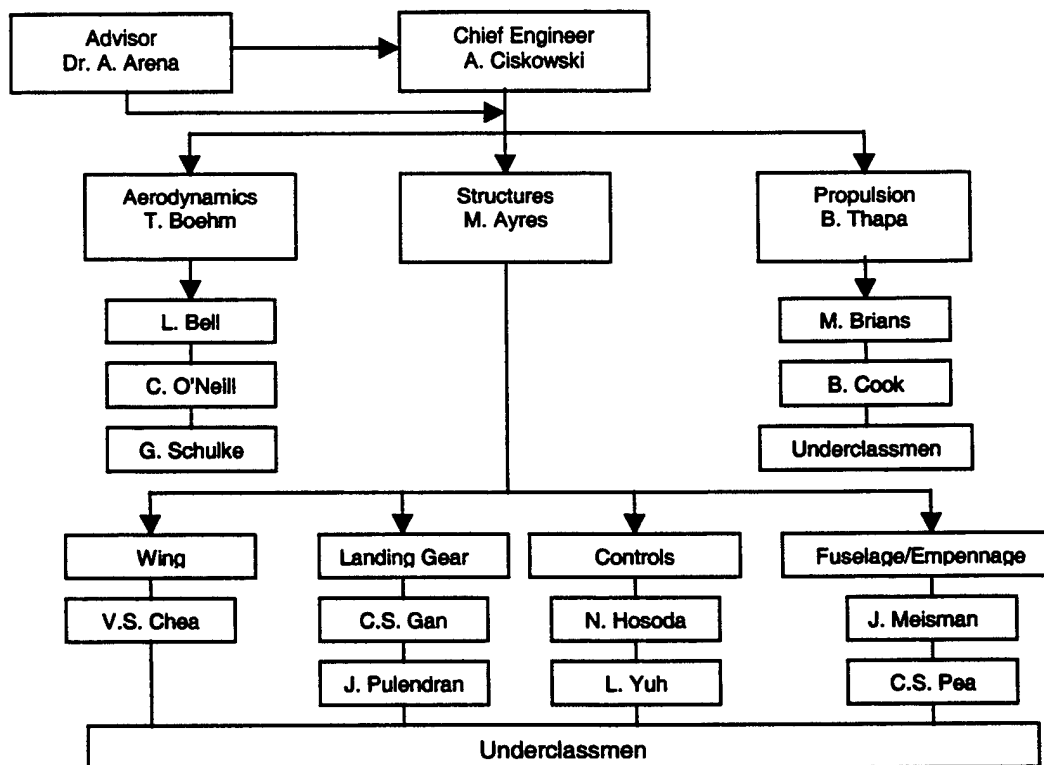


Figure 2.1-1: Team Architecture

2.2 Assignment Areas

The aerodynamics team is the primary configuration group. This team develops and refines a mission analysis program based upon the objectives and guidelines of the competition. The aerodynamics team is responsible for the external configuration and layout including airfoil design. This group is also responsible for the evaluation of aircraft performance in all phases of flight.

The propulsion team is responsible for testing and evaluating possible components of the propulsion system to supply data to the Aerodynamics group. They are responsible for motor, battery and propeller selection. This group is also responsible for working with the aerodynamics group to integrate the propulsion systems into the airframe. They are also responsible for the maintenance of the propulsion system.

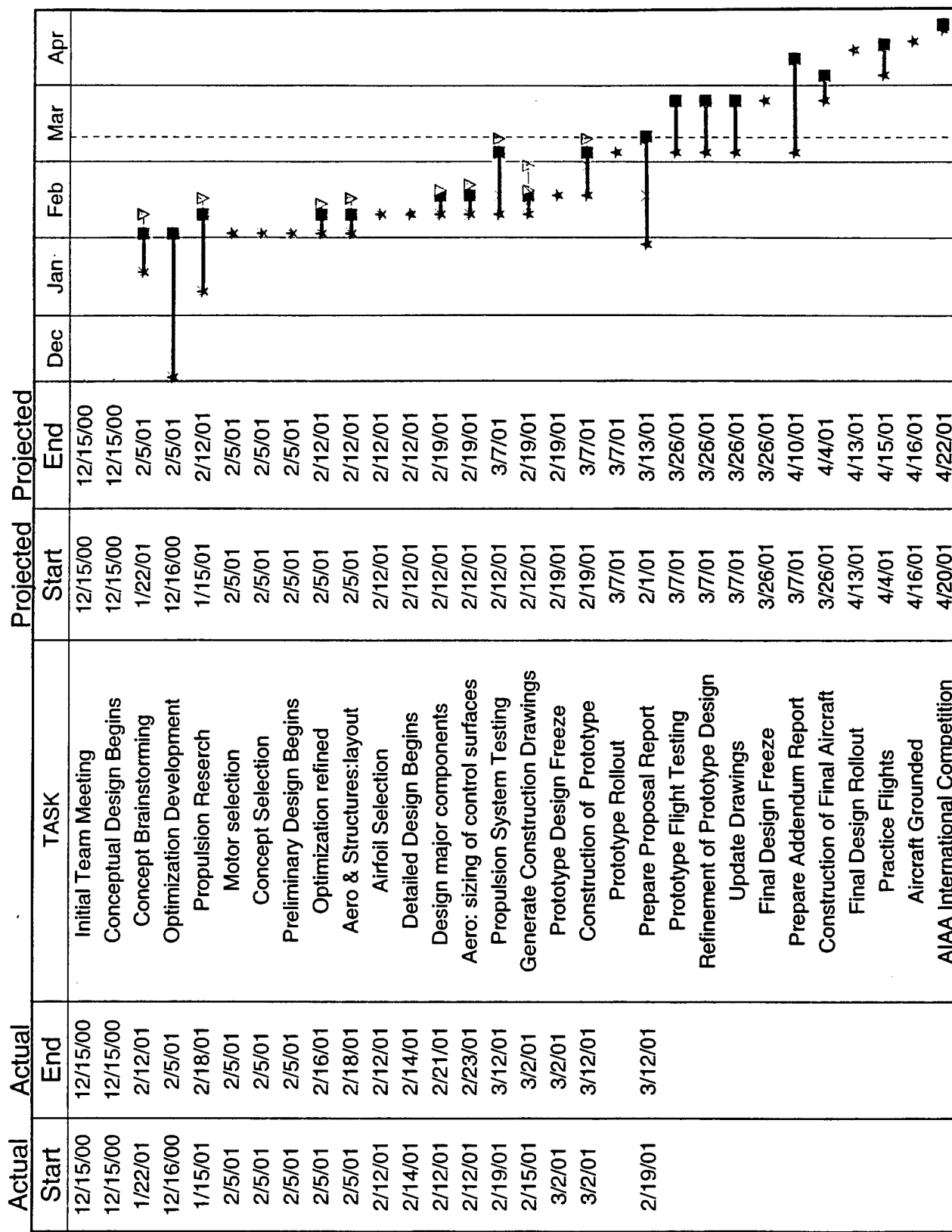
The structures team is primarily responsible for the construction of the aircraft. This team conducts the stress analysis of the structural design. They are responsible for internal layout and component placement in the aircraft. In addition to the testing and analysis of all structural components, this group is responsible for preparing the construction drawings, and the selection of the construction method and materials.

2.3 Management Structures

The design team meets formally twice a week as an entire group. During these team meetings, the chief engineer and the advisor bring to light any issues that require the attention of the entire team. These team meetings are also when the majority of the team brainstorming is conducted.

Aside from the team meetings, each technical group meets separately during the week. At these technical group meetings, the group leads address the issues pertinent only to their particular group. The technical groups also meet at other times each week to do the necessary group work such as wind tunnel testing. During construction the team will function more as a whole. The aerodynamics and propulsion groups will shift to help the structures team with construction of the aircraft. This is to minimize miscommunications between those responsible for the design and those responsible for the construction.

At the beginning of each week the chief engineer and the technical group leads meet to discuss the progress made during the previous week, the important issues for the upcoming week and make sure every group is aware of their schedule and upcoming deadlines.



★ Projected Time

★ Actual Time

Figure 2.3-1: Orange Milestone Chart

3 Conceptual Design

The objective of the conceptual design phase is to identify and develop possible solutions. Governing physics and the competition rules are used to initiate and guide the design search. Design parameters are created to predict performance from each of the conceptual designs. Figures of Merit and Rated Aircraft Cost (RAC) are introduced to evaluate each conceptual design's effectiveness. Finally, a configuration is produced from the results of the conceptual design phase.

3.1 Mission Analysis and Strategy Development

In trying to get a feel for the breadth and depth of the design problem, a computer program was created to assist with aircraft selection and flight performance estimation. The ultimate goal was to allow the program to optimize the specified aircraft geometry with respect to score. The requirements of this optimization are twofold. The contest rules and governing physics must be satisfied. Second, selection of aircraft geometry with a high score is desired. The multi-dimensional design space defined by combination of contest rules and physics prevents an aircraft based on a heuristic or intuition from being an optimum.

The payload related score consists of the summation of total carried payload weight determined by the number of sorties and the individual payload weight carried for each. The 10-minute mission window and the available propulsion energy limit the total number of sorties possible during a mission. Overall aircraft weight is constrained by the contest rules at 55 pounds maximum with specific limitations on the minimum payload weights to be carried. The number of sorties and the overall payload weights are clearly coupled. It is expected that the overall best score will not result from either carrying a massive payload for one sortie or carrying a small payload multiple times. With the heavy lifting endpoint, the aircraft encounters the overall 55 pound gross weight limit. With multiple sorties, the payload reloading time overruns the total mission time.

In order to reduce pilot workload, the profile was broken into three constant power settings: full power, cruise power, and idle. Additionally, these velocities should be low enough for controllability while high enough to prevent overpowering wind effects. A cruise height of above 20 feet is needed for error recovery and spotting, while under 200 feet is needed to prevent excessively long climbs

Several parameters were set up as being key to competition performance. These parameters were all integrated into a system of equations using the constraints of the competition and aerodynamic principles to relate the parameters. This system was evaluated to the maximum score potential of a particular configuration.

A non-linear conjugate-gradient method was selected with the understanding that multiple guess values were required to avoid local maximums. A computer program was created which combined the conjugate-gradient method, relevant aerodynamics, propulsion performance, structural estimates and the contest rules. Six parameters were evaluated; steel payload weight, tennis ball payload weight, maximum battery power, wing area and the cruise powers for both steel and tennis ball sorties. All other variables

were calculated involving the six evaluated parameters. Passing the variables to the relevant aerodynamic, propulsion or structural subroutine integrated performance estimates.

Limits on wingspan, total time, payload and takeoff distance were required to keep the aircraft within the DBF mission constraints. The RAC design criteria established in the DBF rules meant that the aircraft geometry heavily influenced the final score. Estimates of aircraft weight as a function of geometry were derived. The propulsion system was modeled through calculations of power, time and energy throughout the flight. Experimental values for the total energy available and efficiency obtainable were used.

Aerodynamic subroutines calculated takeoff, climb, cruise, approach and landing characteristics of the aircraft. Time, velocity and power for the segments were calculated. See the profile Figure 3.1-1.

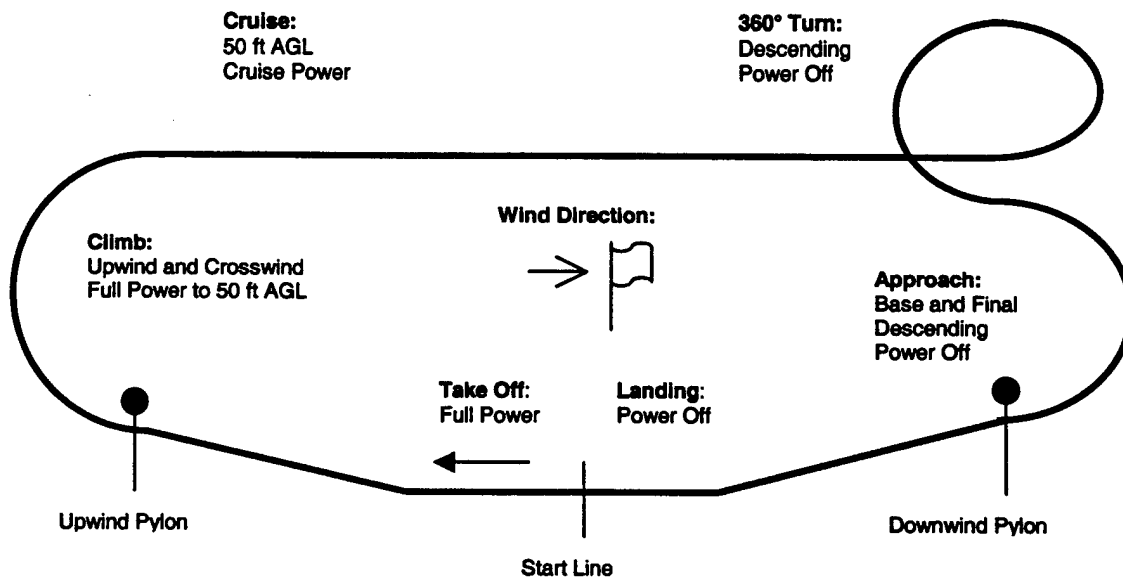


Figure 3.1-1: Flight Profile

3.2 Alternative Concepts Investigated

During the brainstorming activities of the team, no concept was judged or eliminated. This phase involved solely gathering every possible idea to give a foundation for developing the final aircraft. The next stage was then to begin selecting the most promising designs for further investigation. In this initial elimination, several parameters were used to aid in the selection of the most promising designs. Among them were our ability to build the concept with limited time and resources, the performance possibility of the aircraft, and the ability to compete in the mission assigned by the contest. A total of five possible configurations were selected for further evaluation. These five configurations are shown in Figure 3.2-1.

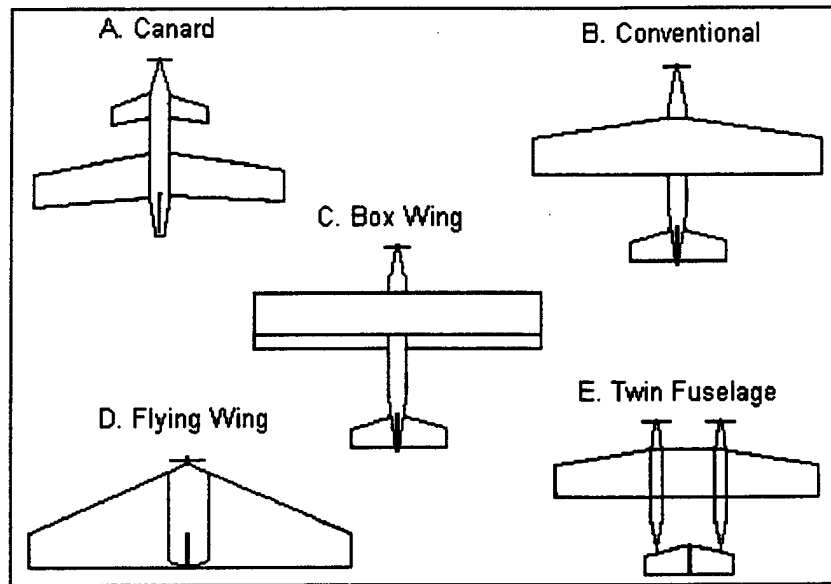


Figure 3.2-1: Preliminary Configurations

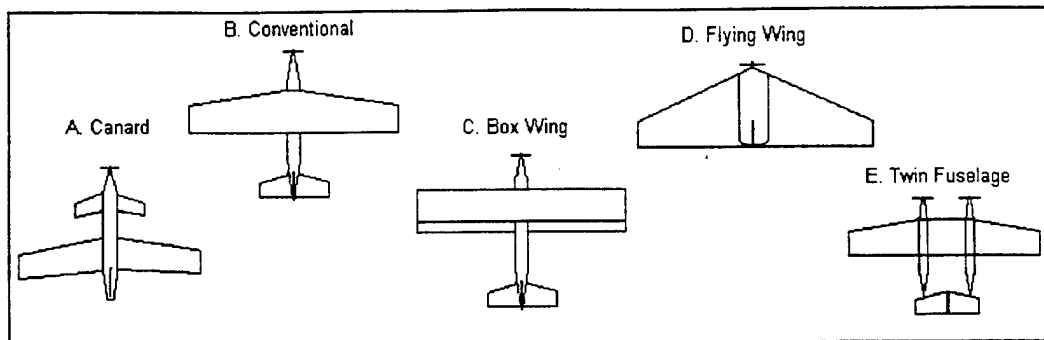
3.3 Important Design Parameters

Primary design parameters are needed to efficiently set the aircraft geometry and performance. The chosen parameters must be capable of entirely describing the dominant aerodynamic characteristics of an aircraft while still allowing for uncertainties. These design parameters are:

- Maximum Available Power
- Cruise Powers
- Payload Weights
- Number of Sorties
- Wing Area
- Take-off lift coefficient

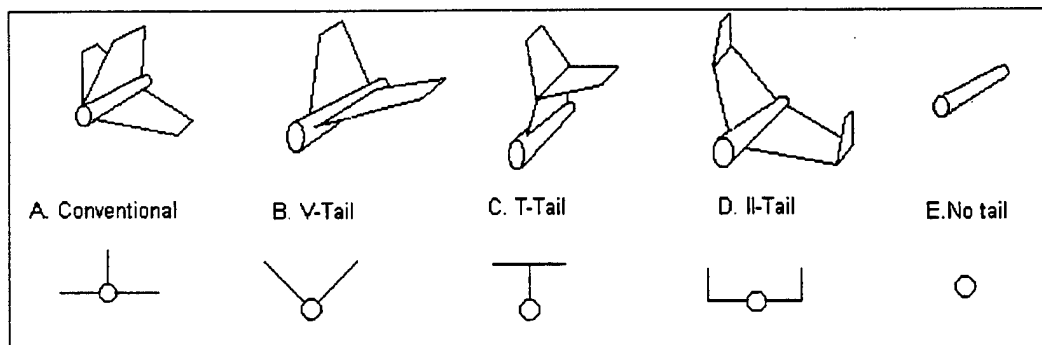
3.4 Figures of Merit

The main configuration was selected with the assistance of Figure 3.4-1. Once the main configuration was selected, several other decisions had to be made regarding the empennage type, shown in Figure 3.4-2, and wing placement. Table 3.4-1 below shows the FOM for the wing placement evaluation. Explanations of FOM usage are found in section 3.6.



Figures Of Merit	Weight Factor	A	B	C	D	E
SCORE / RAC	0.3	1	1	0	-1	0
Stability and Control	0.2	1	1	1	-1	0
Payload Capability	0.2	0	1	1	-1	1
Propulsion	0.1	0	0	0	0	1
Ease of Construction	0.1	0	1	-1	-1	-1
Production Costs	0.1	1	1	0	-1	-1
Total Score	1	0.6	0.9	0.3	-0.9	0.1

Figure 3.4-1: Configuration Figures of Merit Chart



Figures Of Merit	Weight Factor	A	B	C	D	E
RAC Impact	0.3	0	0	0	-1	1
Stability and Control	0.3	0	-1	0	-1	-1
Reliability	0.1	1	0	1	0	-1
Ease of Construction	0.1	1	-1	0	0	1
Servo Location	0.1	1	1	0	0	1
Production Costs	0.1	1	1	1	0	2
Total Score	1	0.4	-0.2	0.2	-0.6	0.3

Figure 3.4-2: Tail Figures of Merit Chart

Figures Of Merit	Weight Factor	High Wing	Mid Wing	Low Wing
Stability and Control	0.2	1	0	0
Payload Access	0.3	0	0	1
Ease of Construction	0.1	1	1	1
Fuselage Volume Affected	0.2	0	-1	0
Landing Gear Interface	0.1	0	0	1
Total Score	1	0.3	-0.1	0.5

Table 3.4-1: Wing Placement Figures of Merit Chart

3.5 Rated Aircraft Cost for Concepts

An important step in exploring the performance possibility of a concept in this contest is to evaluate the rated aircraft cost of the different configurations. The main breakdown of the equation for rated aircraft cost is shown in the table below.

Using the rated aircraft cost equation breakdown and information from the mission analysis program, the total rated aircraft cost for each of the five final designs considered can be evaluated. The results are as shown in Table 3.5-1.

Canard				RAC	5.076
MEW	13	13	100	1500	
REP	1*30*1.2*36	1296	1	1296	
MFRH	Wing	45	20	900	
	Body	29	20	580	
	Tail	20	20	400	
	Systems	10	20	200	
	Propulsion	10	20	200	
Conventional				RAC	5.076
MEW	13	13	100	1500	
REP	1*30*1.2*36	1296	1	1296	
MFRH	Wing	45	20	900	
	Body	29	20	580	
	Tail	20	20	400	
	Systems	10	20	200	
	Propulsion	10	20	200	
Box Wing				RAC	6.792
MEW	14	14	100	1500	
REP	2*30*1.2*36	2592	1	2592	
MFRH	Wing	66	20	1320	
	Body	29	20	580	
	Tail	20	20	400	
	Systems	10	20	200	
	Propulsion	10	20	200	
Flying Wing				RAC	4.016
MEW	11	11	100	1100	
REP	1*30*1.2*36	1296	1	1296	
MFRH	Wing	45	20	900	
	Body	7	20	140	
	Tail	10	20	200	
	Systems	9	20	180	
	Propulsion	10	20	200	
Twin Fuselage				RAC	5.696
MEW	15	15	100	1500	
REP	1*30*1.2*36	1296	1	1296	
MFRH	Wing	45	20	900	
	Body	50	20	1000	
	Tail	20	20	400	
	Systems	10	20	200	
	Propulsion	20	20	400	

Table 3.5-1: Rated Aircraft Cost for Configurations Considered

3.6 Features that produced the Final Configuration

Once the mission analysis program had developed the performance needed to score well, there were a great many decisions to be made regarding the numerous possibilities for aircraft design. Although the program had answered many questions, it couldn't give all the information for more intangible things. In order to systematically make those comparisons, several categories were established under which to compare the designs. These categories were rated according to their estimated importance in getting the mission accomplished. In systematically making the decisions necessary to create this aircraft, several figures of merit were used. The main categories for comparison are given below.

Score / Rated Aircraft Cost: The first category for comparison was the configurations rated aircraft cost. Since the main goal is to perform as well as possible in the contest, obviously the higher score possibility for the configuration, the better. The lowest value for rated aircraft cost was desired in order to have a lower divisor of the points earned by amount of payload carried. The mission analysis program developed by the team was used in order to evaluate the score potential of each configuration.

Stability and Control: Stability and control issues were considered to be a very important category for evaluation as well. In order to perform well at the competition, the aircraft must be stable and easily controlled by the pilot. Although an unstable aircraft could have been used, it was shown in the mission analysis program that the aircraft was going to have to fly numerous sorties per mission and therefore an aircraft that could be controlled well was a must. After all, if the aircraft is difficult to fly and is not controllable then it won't be able to give the performance desired by the program.

Reliability: In order to compete with this aircraft in a situation that requires as many as eighteen flights to be competitive, the aircraft design must be reliable. While the aircraft's manufacturing processes and materials heavily affect this, there are also some designs where the performance is more reliable in a varying number of wind conditions and other situations. This concept is tied somewhat to the stability and control of the aircraft.

Payload Capability: Since the purpose of this aircraft is to carry payload, the ability of the basic design to do so was an important parameter for evaluation. The differences in the types of payload to be carried add another level of complexity. The tennis ball payload requires a volumetric consideration more than a shear lifting capability. The steel payload, however, would be limited only by what the aircraft can lift.

Propulsion: Before selecting propulsion system components several possible configurations were developed. These included single and multi-motor configurations. These configurations differ significantly in weight and RAC impact, so it was important to choose the configuration that would best

serve the design goals. The single motor configuration gave the best score in the mission analysis program. The DBF battery specifications, 5 lbs of NiCad batteries, left the task of finding the battery type and brand that would give the performance developed by the mission analysis program. The selection process for the batteries was conducted through research into different products that were offered by several manufacturers. The propeller selection was aided by performance parameters that were dictated by the aerodynamics team later in the design process. The gearbox for the motor depends on the propeller size and was initially assumed to be between 2.4:1 and 3:1.

Ease of Construction: Even the greatest concepts are meaningless to us if they cannot be built. Because of this fact, as well as the relative inexperience of our team members in aircraft construction, manufacturing simplicity was deemed an important consideration. Given more time and resources, more complexity could have been allowed, but that was not the case in our current situational constraints.

Material Selection: As with any aerospace application, weight is a critical factor. With the recent innovations of carbon fiber used in building this type of aircraft, this was one of the first materials explored. The other major material considered seriously was balsa-monokote construction. Because of its strength to weight ratio, durability and ease of repair, carbon fiber stood out in the conceptual design phase.

4 Preliminary Design

Once the main configuration decisions were made in the conceptual design phase, further evaluations and refinements were made in the preliminary design phase. Information was generated in the form of selection of fuselage shape and sizing of components. The mission analysis program was further developed to aid in the refinement of the design.

4.1 Design Parameters Investigated and Figures of Merit

4.1.1 Aerodynamics Group

The aerodynamics group's goal was to predict and then increase the competition score. Performance characteristics such as C_D , C_L , and S from the conceptual design phase were further investigated. Among the most important of these needed for design refinements were aircraft drag and airfoil performance.

Drag Calculation Overview

Drag affects aircraft during all operational phases. Drag analysis was performed for the fuselage, lifting surfaces and miscellaneous components with preliminary sizing information. Figure 4.1-1 shows the contributions of the various components to the overall drag coefficient

Fuselage: In order to consider many fuselage configurations, circular as well as elliptical formulas were found to compute effective diameters for the form factor equations available in Raymer's Aircraft Design: A Conceptual Approach. The analysis then calculated Reynolds Numbers and subsequent flat-plate skin-friction coefficients. These were multiplied by the fuselage form factor and wetted surface area to obtain the overall fuselage component.

This analysis was then developed to specify a diameter for the payload region and a separate one for the remainder of the fuselage. This ability helped to approximate the total fuselage drag in a single calculation versus multiple single diameter ones. This allowed a length for the payload area to be calculated using test data for an average volume displacement presented by the tennis balls.

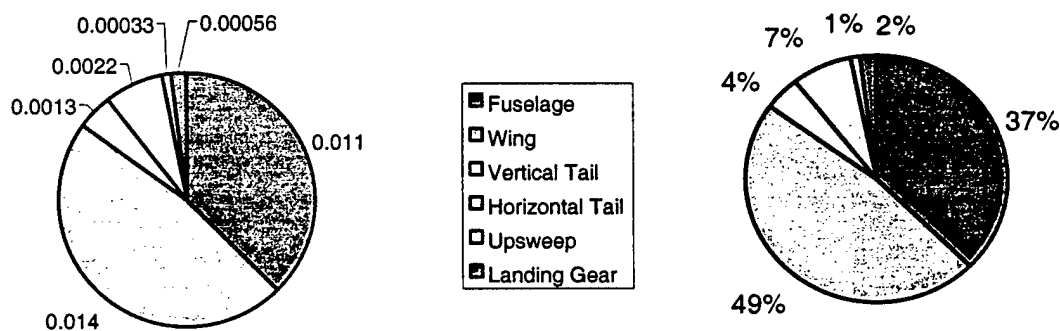


Figure 4.1-1: Aircraft Drag Breakdown

Lifting Surfaces: The wing calculation assumed a flat-plate skin-friction coefficient utilizing parameters such as the location of the maximum thickness, sweep angle, and thickness to chord ratio. Using the polar plot for the specific airfoil used refined the drag calculation for the wing. The analysis of the horizontal and vertical tail was similar to the wing computation.

Other Components: Landing gear and upsweep of the aft fuselage to the tail were also addressed. For the landing gear, total frontal areas of the tires and struts were assumed using historical data. Both of these areas produced a significant percentage of the overall drag and steps could be taken to reduce the effect. For example, by adding a fairing to a strut and wheel the gear coefficient was reduced by 48%. In the case of fuselage upsweep, there was almost sixteen times the amount of drag generated by increasing the upsweep angle from five degrees to fifteen.

Interference factors on the individual aircraft components were estimated using historical data. Our assumptions included a moderately filleted low wing configuration that corresponded to approximately twenty percent interference, a horizontal and vertical tail of four percent, and fuselage interference to be negligible. Drag associated with gaps and voids between mating surfaces was not calculated for each individual component. Rather, a 7.5% additional drag is added to the component total to compensate.

Airfoil Selection

Through the use of the mission analysis program, the total aircraft weight, wing platform area, and design airspeeds were determined. From that program, it was discovered that the high take-off lift and cruise velocity were critical parameters. To achieve an airfoil of with these performance characteristics, special detail was given to the maximum coefficient of lift and low drag over a wide range of lift values.

Airfoil Analysis: For the scale of the aircraft and low velocities, the only airfoils analyzed were those tested for Reynolds numbers below 300,000. To achieve the highest accuracy, low-speed wind tunnel data was used. Majority of the information was taken from the websites of the University of Illinois at Urbana-Champaign's Low-Speed Airfoil Tests and the Nihon University Aerospace Student Group's Airfoil Database. Of the 1100 airfoils listed on the UIUC Airfoil Test Site, the selection was reduced to the following families due to their high lift capabilities: Eppler, Wortmann, Liebeck, Selig, and Selig-Donovan. By comparing the plots of coefficient of lift (C_L) versus coefficient of drag (C_D) and coefficient of lift versus angle of attack (α) provided by the Nihon University website, it was possible to conveniently analyze the airfoil data.

Airfoil Comparisons: The primary constraint on the airfoil selection was the high lift needed for take-off within 200 ft. Exploration of the mission analysis program showed that the coefficient of lift desired was greater than 1.5 and that the final score increased directly with the higher lift coefficients. Consideration was given to the addition of high lift devices (i.e., flaperons), but was nullified due to increased mechanics and construction complications. Preliminary comparisons of unaltered airfoils produced five choices that

provided the greatest lift: the Eppler 423, Wortmann FX74-CL5-140, Wortmann 63-137, Selig 1210, and Selig 1223.

The second constraint of selection was the drag. Since the aircraft will operate for the majority of the time in cruise, airfoils were then examined to minimize drag and, hence, increase performance. Preliminary calculations given by the mission analysis program indicated that the aircraft would require a cruise velocity of 65 mph. Based on a 55-pound design weight, the aircraft required an airfoil with lift coefficients in the range of 0.6-0.8. Therefore, from the previous selected airfoils, the highest consideration was given to those airfoils that had the lowest drag coefficients in lift coefficient range of 0.8-1.0. Assuming lift coefficients within this range of values would account for the drag losses incurred by the actual aircraft. The polar plots for the three final airfoils considered are shown in Figure 4.1-2.

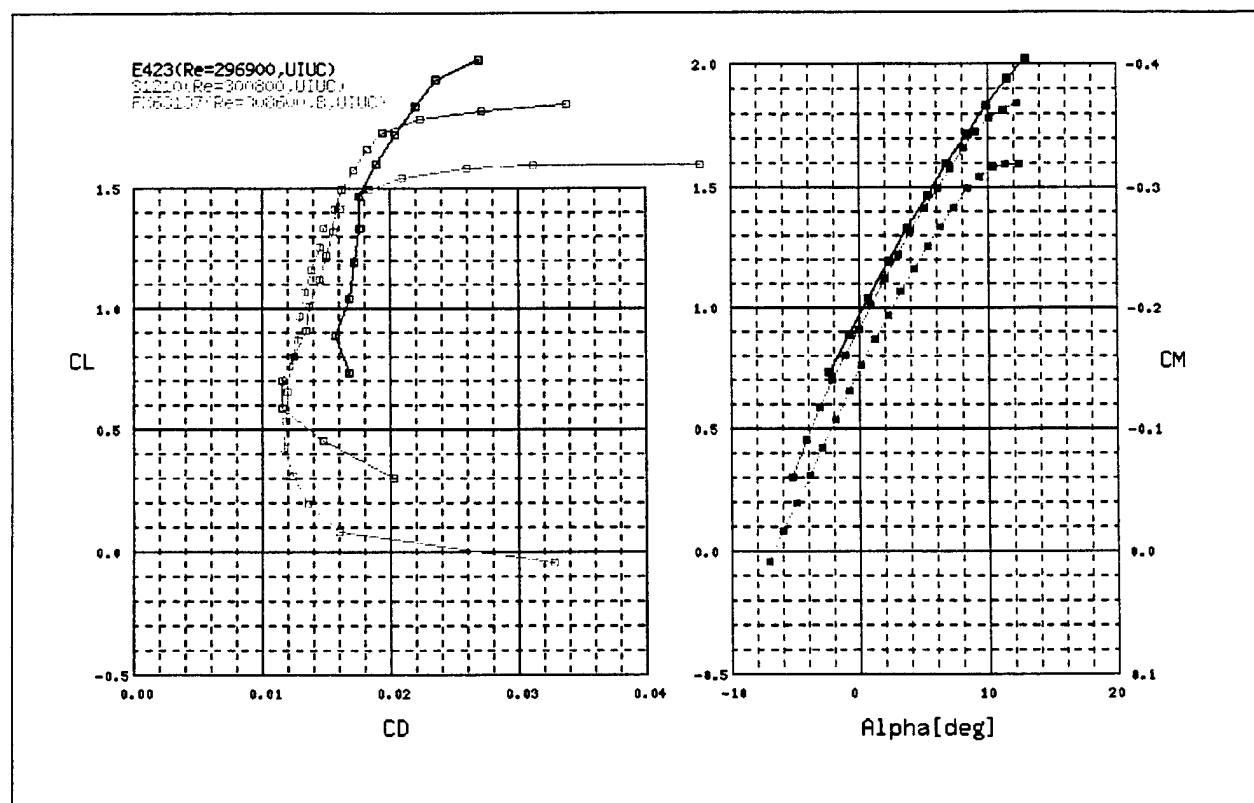


Figure 4.1-2: Polar curves for selected airfoils

It was evident from the polar curves that the drag increase due to increased angle of attack varied significantly for each airfoil. From the performance standpoint, the desired airfoil would possess a C_L vs. C_D curve that was very steep. With this qualification, both the Selig 1223 and Wortmann FX74-CL5-140 were eliminated from consideration. At this point, the Eppler 423 was the front-runner based upon maximum lift characteristics. However, further sensitivity analysis of the mission analysis

program yielded a large correlation between increased drag and lower score. Although consideration of the high lift characteristics of the Eppler 423 airfoil was considered, the score reduction due to drag was too critical. The Eppler 423 airfoil was chosen for the main wing. Compared to the Selig 1210, the Eppler 423 is worth 2.5 points even with the 30% extra cross sectional area that increases weight. The Selig 1223 has an unfavorable drag curve forcing the cruise lift coefficient into the drag bucket. Since the scores are similar between the E423 and the Selig 1223, the added flexibility of the Eppler 423 is a benefit.

4.1.2 Structures Group

In order to investigate the important features of each component based on its function, the aircraft was broken down into sections. The wing, fuselage, tail section, landing gear, and speed loader all have figures of merit specific to their function in the airplane.

Fuselage: Preliminary design of the fuselage included examining designs for load carrying structures through the length of the fuselage. Several structural members were investigated for their ability to carry bending load through the fuselage. Figures of merit for these structural members include:

- Ability to carry bending moment
- Strength to weight ratio
- Ability to withstand torsion

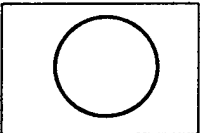
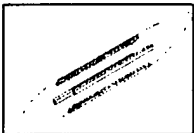

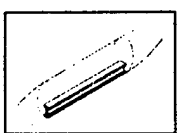
Figures of Merit	Weight Factor	 Reinforced Skin	 Longerons	 Stringers	 Keelson
Weight	0.4	-1	1	0	0
Bending Strength	0.35	-1	1	0	1
Connection Interface	0.15	1	-1	0	-1
Construction complexity	0.1	1	-1	0	-1
Rating		-.5	.5	0	.1

Figure 4.1-3 Fuselage Structure Type Figures of Merit Chart

Wing: With the chosen material for construction of the wing, the most important design consideration was the bending moment that would be carried. With an estimated aircraft weight of 38 to 55 pounds, the bending moment at the root chord could be up to 1650 in lb. The method of mounting the wing to the fuselage is also very critical. The section of wing mounted within the fuselage is only six inches wide over the ten-foot span. The following figures of merit are critical for the wing design and its connection to the fuselage:

- Strength of center section/attachment points
- Weight
- Manufacturability
- Ability to carry Bending Moment

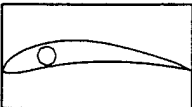
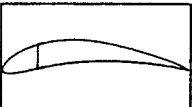

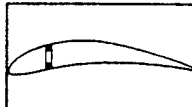
Figures of Merit	Weight Factor	 Tube Spar	 C-Channel Spar	 End Grain Balsa Spar	 Hybrid Spar
Weight	0.4	-1	1	1	0
Bending Strength	0.35	-1	0	1	1
Connection Interface	0.15	1	-1	0	1
Construction complexity	0.1	1	-1	1	0
Rating		-.25	.5	.85	.5

Figure 4.1-4: Spar Type Figures of Merit Chart

Tail: The tail must be mounted in a fashion that will allow incidence angles to be finely tuned before permanently mounting the tail into place. An ideal tail design would also allow the control linkages to be placed entirely within the fuselage to reduce drag. This would be accomplished by reducing the amount of carry-through structure through the fuselage. These things considered, the following are figures of merit for narrowing down a final tail design:

- Able to carry bending moment
- Ease of mounting stabilizers
- Small carry-through structure
- Transmission of torsion to fuselage

Speed Loader: The speed loader is an extremely mission sensitive component of the airplane. Not only does the speed loader design directly affect the sizing and design of the fuselage and carry through structure, but it also affects the Rated Aircraft Cost. If the speed loader is part of the fuselage, the weight

of the speed loader is counted in the empty weight of the aircraft, increasing the rated aircraft cost. The design of the speed loader is also critical to minimize reloading time between sorties.

Landing Gear: The anticipated gross weight of the aircraft initially ranged from 38 to 55 lbs. Taking this into consideration, special attention had to be paid to the landing gear. The goal was to design the gear to be as light as possible while providing sufficient strength to withstand the anticipated loads and retaining flexibility to reduce the force transferred to the aircraft structure. Due to the extent of taking off, landing and taxiing that will be necessary to complete multiple laps, ground handling characteristics of the aircraft should also be exceptional.

Two gear configurations were initially considered: conventional landing gear, and tricycle landing gear. Without a nose wheel, the plane can pitch over if too much brake is applied. Conventional landing gear aircraft are naturally unstable on the ground. So, a conventional landing gear aircraft can be difficult to control when landing or taking off. The tricycle landing gear has the main wheels located at each side of the centerline behind the center of gravity, with a nose wheel on the forward centerline. The tricycle landing gear configuration is noted for ease of ground handling and is difficult to ground loop unless steered into a skid. Taking all of this into account, the tricycle landing gear was selected.

Four different designs were analyzed for feasibility. Figures of merit were used to aid the analysis process Figure 4.1-5. The main characteristics taken into account in the construction of the decision matrix was weight of the gear, drag contributions of the gear, ground handling, dependability and construction complexity. In conjunction with the design parameters investigated, weight and drag contributions were sized as the main priority. Relative importance was placed on ground handling and dependability of the gear while little importance was paid to construction complexities.

Since the ratings of the respective designs were extremely close, a decision had to be made by considering another factor is the ease of replacement. This was to be based solely on whether the design would be easily replaceable if the unforeseen happens. Since, three of the designs were struts, this meant that the main gears would have to be placed at the wing. If this were the case, it would be difficult to replace the gear if it were to fail. Replacement could only be made if a hatch were incorporated into the wing section. This could be avoided by using the bow type gear. The bow type gear will be attached to the wing but at a location where it will be located directly below the fuselage. Taking this consideration, the gear would be bolted directly from the fuselage. This configuration allows one to change the gear easily as there would already be a hatch incorporated into the design to accommodate the speed loader.

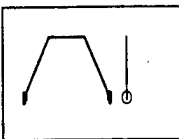
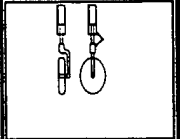
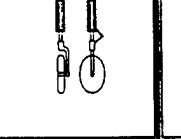
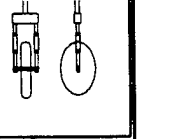
Design Criterion	Weight Factor	 Conventional Bow	 Non-expandable	 Expandable	 Two-Stroke
Weight	0.4	1	0	0	0
Drag	0.2	-1	0	0	-1
Ground Steering ability	0.15	-1	1	1	1
Dependability	0.15	0	0	0	1
Manufacturability	0.1	1	-1	-1	-1
Rating		.15	.05	-.05	0

Figure 4.1-5: FOM Decision Matrix used for Landing Gear Selection

4.1.3 Propulsion Group

The parameters that we considered to be important in the design of our propulsion system were power output, thrust produced, overall efficiency, and weight. The power produced by our system is very important because it is the determining factor in how many laps we will be able to complete. Therefore, we selected our batteries based on how much power we could get out of a 5lb pack. The thrust was also an important consideration because we are lifting up to 50 lbs over a length of 200 feet. Efficiency and weight also affect the performance of the plane, so we designed for maximum efficiency and relatively low weight.

The FOMs that we constructed aided in our propulsion system component selection. In each FOM the areas of consideration are weighted according to their importance. The alternatives are then rated on their level agreement with each area of consideration. The final score for each alternative is a result of the weights and ratings and gives us a good idea of which component best satisfies our needs. For the propulsion system selection we have constructed FOMs for the batteries and the motor. These figures, used in conjunction with analytical data and test results help us to choose the best possible propulsion system according to our needs.

4.2 Analytical Methods

4.2.1 Aerodynamics Group

Performance

The mission analysis program discussed in section 3.1 evolved throughout the design development. As shown in Figure 4.2-1, the process was iterative with further expansion for detailed design. The mission analysis program was modified to include experimental airfoil lift and drag as well as propulsion data. Sensitivity analysis was performed to verify the validity of initial assumptions and to select better flight routines. Inclusion of these functions allowed a more robust and versatile mission analysis program. Experimental low speed airfoil data was found in the UIUC low speed airfoil tests (<http://amber.aae.uiuc.edu/~m-selig/>). This allows the mission analysis program to use a piecewise best-fit line of the airfoil's polar plot. The modification of the mission analysis also allowed propulsion data such as batteries, speed controller, motor and propeller to be included.

Sensitivity analysis was performed to verify the validity of initial assumptions and to select the best flight routine and aircraft geometry. Important score increasing tactics were found from performing sensitivity analysis on the sortie laps, tennis ball packing, wing airfoil, wind velocity, weight, landing distance and cruise height.

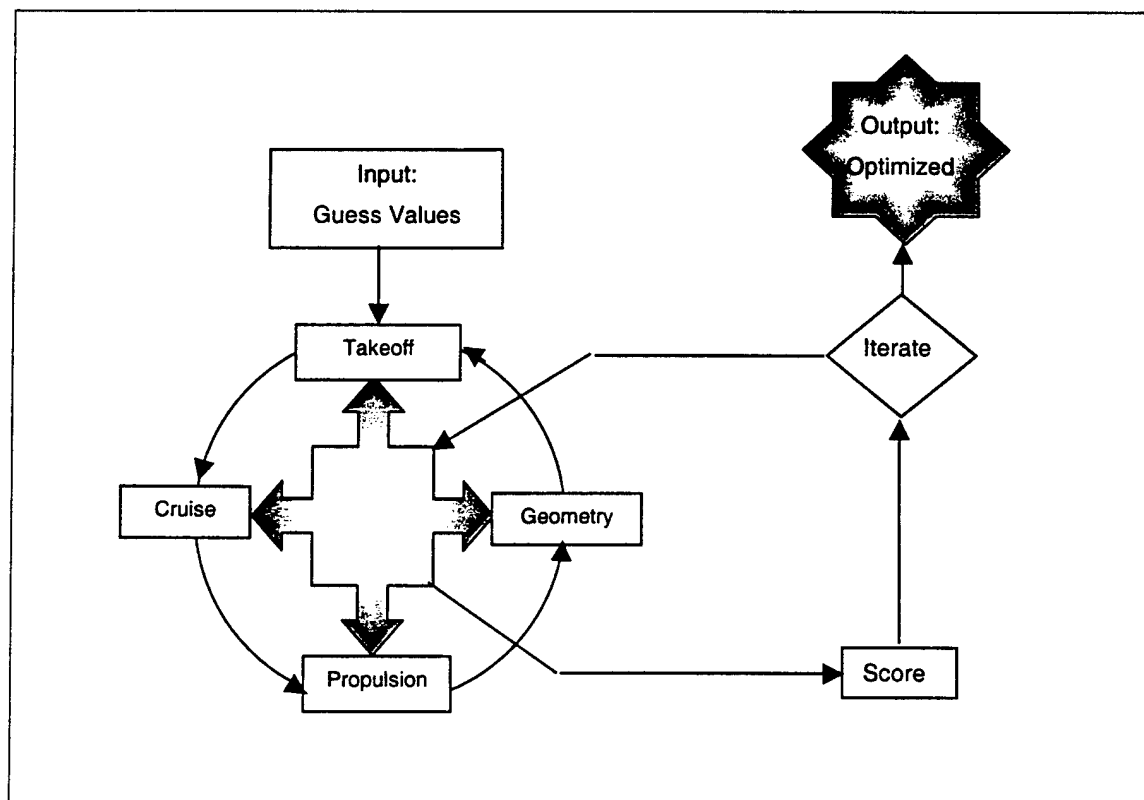


Figure 4.2-1: Mission Analysis Program Flowchart

Drag

The method used to estimate parasite drag was the component buildup method. This method sums the individual drag components of the aircraft by calculating a flat-plate skin-friction coefficient and a form factor that estimates the pressure drag due to viscous separation across the surface. Additionally, an interference factor is used to approximate the interference component between surfaces. Each component is comprised of the product of the drag factor, interference factor, wetted area, and form factor. The major components considered in this buildup method include fuselage, wing, horizontal tail, vertical tail, landing gear, and fuselage upsweep. Other drag components include induced drag from lift and trim drag.

4.2.2 Structures Group

Landing Gear

First and foremost, the location of the main and nose gear had to be calculated. Overturn angle and tip over angle had to be taken into consideration on deciding upon the location. It is noted that the minimum static load has to be greater than 6% of the aircraft weight. Calculations have shown that the CG could vary from 0 to 1 inch of the present center of gravity (25.4 inches from the nose of the aircraft). Taking these into consideration, calculations were performed by taking the sum of moments about the center of gravity. The following was obtained:

Distance between nose gear and main gear = 19 inches

Distance between nose of airplane and nose gear = 6.12 inches

The height of the landing gear is approximately 6 inches from the bottom of the wing to the ground. This distance was the minimum length needed in order for the propeller to have an appropriate clearance.

The main landing gear was based on 4g load for structural integrity where we assumed we assumed the worst case for the plane when it landed without flaring on one wheel. Calculations were also made to determine the dependability of the gear. A bolt-member analysis was conducted using Rotsher's pressure cone method for stiffness calculation to obtain the type and number of bolts that would be needed to secure the gear to the aircraft. Calculations show that two- $\frac{1}{4}$ inch SAE Grade 1 steel bolts would give a factor of safety of 2.4 against fracture. Shear stress analysis showed that by placing the bolts at 5 inches apart, a factor of safety of 3.12 is obtained against shear.

4.2.3 Propulsion Group

In order to achieve the maximum performance possible from our system we incorporated an mission analysis spreadsheet created using MathCAD software. This analysis allowed us to get theoretical thrust, velocity, efficiency, and power results for any combination of batteries, motors, and propellers, before we ordered and tested any of our components. This was invaluable in the preliminary

design phase because it gave us a good overall picture of what was happening with different combinations of components.

In addition to using theoretical analysis tools, both static and dynamic tests were performed. The static tests were bench tests performed using a dynamometer. The static tests included: battery endurance tests (at various fixed power settings and at variable power), motor parameter tests, installed performance tests (20%, 50%, and 80% blockage, as well as streamlined cowling effects), charge rate effects test, motor and battery cooling effects, and fuse effects. The dynamic tests were performed in the wind tunnel using the dynamometer. Wind tunnel tests included experiments on propeller efficiency, variations on takeoff, and predicted flight profile. The use of wind tunnel tests were highly beneficial because the combination of components of the propulsion system create highly coupled behavior that is complicated and difficult to predict using analytical methods.

4.3 Configuration and Sizing Data

4.3.1 Aerodynamics Group

Stability and Control

Stability and control issues include several aspects, such as tail size, fuselage size, wing parameters, and control surface size and deflection angles. There are two main categories and characteristics under which stability and control operates, longitudinal and lateral control which each contain static and dynamic considerations. Static stability is present if the forces resulting from a disturbance return the aircraft to the original state; dynamic stability is evident if the dynamic characteristics of the aircraft return it to an initial condition. The process by which it returns is dependent upon the aircraft center of gravity and forces resulting from the control surface deflections. All equations, approximations, and historical design values came from Raymer's Aircraft Design: A Conceptual Approach.

Longitudinal Stability

Initial Horizontal Tail Sizing: The first step in the stability and control analysis included sizing the horizontal stabilizer. This calculation came from approximating the distance from the wing quarter chord to the horizontal quarter chord to be sixty percent of the fuselage length. The provided aspect and taper ratios related wing reference area and tail volume coefficients.

Aircraft Pitching Moment: The next process comprises the governing moment equation for the entire plane. Moments for the fuselage and wing as well as the wing and horizontal tail lift moments were added to the moment resulting from the thrust.

The magnitude of the pitching moment derivative changes with the aircraft center of gravity. Power off neutral point is calculated by setting the derivative to zero. This defines the most aft aircraft center of gravity, also known as the aircraft neutral point, location to be determined for stable flight. The static margin is computed from the neutral point location. If the center of gravity is ahead of the aircraft

neutral point, the static margin is positive and the total pitching moment negative. This results in a stable configuration as shown in Figure 4.3-1.

A static margin of 15% is assumed to be adequate in maintaining stability. Upon calculation and comparison, the sensitivity to the static margin is large. The difference between the center of gravity location and the wing aerodynamic center is approximately an inch, which is better defined as the difference between a stable and an unstable aircraft.

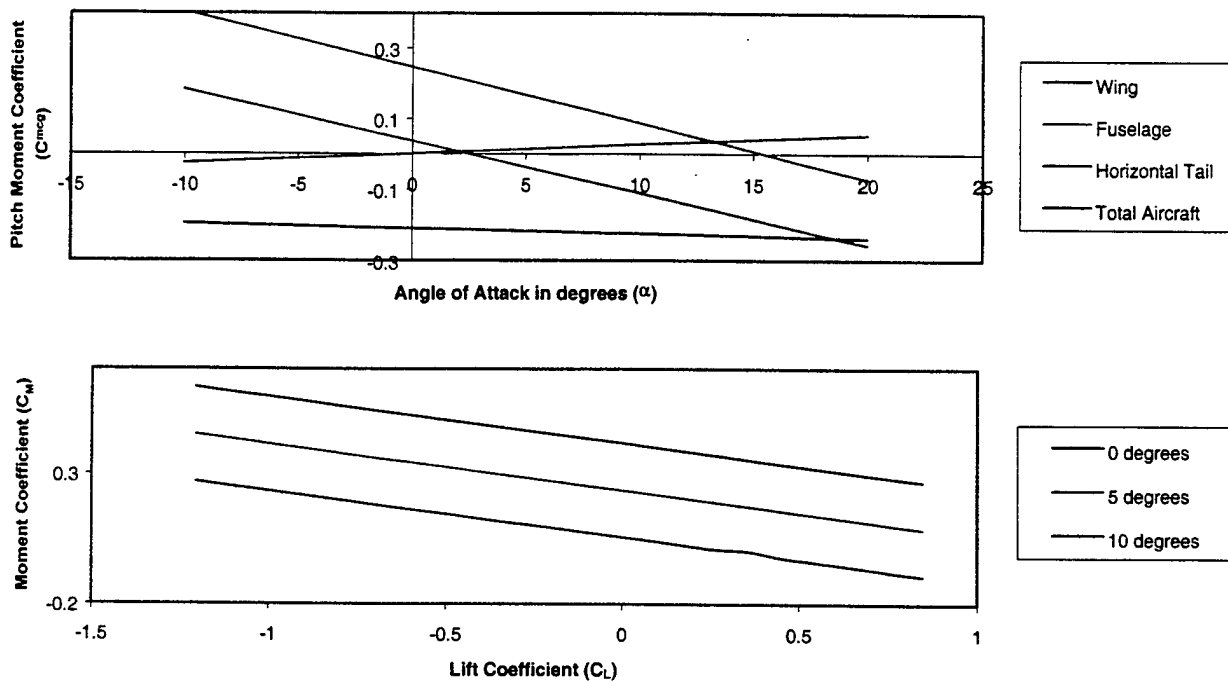


Figure 4.3-1: Pitching Moment and C_M vs. C_L at Changing Elevator Angle

Trim Analysis and Tail Resizing: The next step involved the trim characteristics at various angles of attack and elevator deflection. This is accomplished by calculating the total aircraft moment (C_M) and the lift coefficients (C_L). Since the weight of the aircraft and the wing platform area are previously defined, the total aircraft lift coefficient needed in cruise flight is a simple relation of aircraft weight, wing area, and dynamic pressure. The trim elevator deflection angle for a specific C_L is found graphically where the aircraft C_M is zero.

The initial C_M versus C_L graph does not provide a reasonable elevator deflection during cruise for the range of necessary aircraft lift coefficients. To adjust the trim graph, the horizontal tail area, elevator percentage of the horizontal chord, and horizontal tail incidence angle are adjusted until the elevator deflection is near neutral for the range of aircraft lift coefficients.

Takeoff considerations were also considered. Additional moments were added to the total aircraft pitching moment for the drag forces resulting from rolling wheel friction and the weight on the rear landing

gear as the aircraft changes angles of attack. This takeoff check assumes that the aircraft has eighty percent of the takeoff thrust and can produce a positive aircraft C_M with elevator deflection.

After completing these two flight scenarios, the horizontal tail area and aspect ratio were set to allow the aircraft to fly with little or no elevator deflection. Although the horizontal tail platform area is significantly larger than the initial estimates, the short coupling of the fuselage, to reduce RAC, combined with a large wing lift force dictates that the horizontal surface will have to be significantly enlarged to provide a stabilizing moment.

Horizontal Tail Airfoil Selection: Once the horizontal tail specifications were determined, an airfoil had to be selected. Two types of airfoils that were considered: symmetrical and cambered. Symmetric airfoils provided the best drag solution and ease of construction. However, in the trim analysis the incidence angle was set at -5° to achieve the necessary tail lift; this does not provide for low drag in cruise because the horizontal tail is not aligned with the flow. Cambered airfoils provide the next option.

In selecting the airfoil, several parameters had to be known and considered. Mean aerodynamic chord, lift coefficient in cruise, and required lift coefficient during takeoff dictate the airfoil operating parameters. The first consideration includes the mean aerodynamic chord of the horizontal surface. The Reynolds number over the airfoil decreases with the chord; in a low Reynolds number range the airfoil becomes less effective and efficient in providing lift. The surface is operating in a low Reynolds range but is not approaching the lower limit ineffectiveness. Thus, low Reynolds number airfoils are the major limitation in the horizontal selection.

Additional parameters include the lift coefficients needed in cruise and takeoff. These are found from the trim analysis by solving for the horizontal tail lift coefficient component. Many low Reynolds number airfoils were plotted on polar graphs using the data from the University of Illinois at Urbana-Champaign website. The airfoils that operated in the required C_L range were compared with the final having a combination of low drag coefficient and steep C_L versus C_D slope. The Eppler 387 airfoil was selected.

Aerodynamic Balance: From the drag, propulsion, and score mission analysis, the aircraft is optimized for low drag and high speed. Concern arises in the event of a steep negative aircraft angle of attack coupled with high velocity. In this situation, the elevator servo can become overpowered by the dynamic pressure and thus be ineffective at restoring pitch control of the aircraft. This can be catastrophic in the end results for both the aircraft and spectators. Therefore, an aerodynamic balance analysis was performed on the horizontal surface.

For this analysis the maximum speed of the aircraft was assumed to be twenty percent above the full throttle cruise speed with the elevator at maximum deflection. The servo torque is set equal to the difference between the moment from the elevator and aerodynamic balance surface resulting from dynamic pressure. From this relation, the span of the aerodynamic balance is solved in terms of horizontal tip chord, horizontal span, and elevator chord.

Lateral Stability

Aircraft Roll and Yaw Moments: Initial vertical tail sizing was conducted in the same manner as the horizontal with wing to tail relations. Historical aspect and taper ratios and distance between the center of gravity and mean aerodynamic chord of the vertical tail were used. The main driver in lateral stability calculations is the roll and yaw moments with the change in side slip angle (β). Moments from the wing, fuselage, ailerons, and vertical tail are summed to complete the aircraft roll and yaw moments.

While the longitudinal moments can determine the aircraft center of gravity, these equations do not refine this estimate. These moments are less influential over center of gravity location compared to the aircraft pitch moment considerations.

The roll stability ensures the aircraft will restore a wings level position when disturbed. If roll stability is not present, the resulting roll moment will be in the same direction as the perturbation and thus reinforce the roll rate. When roll stable, the roll moment created by the sideslip will counteract the disturbance and return the aircraft to a wings level attitude. Roll moment is composed of several components; the most important being the dihedral effect from the wings, fuselage effect, and the vertical tail.

The greatest contributor to roll stability is the dihedral effect from the dihedral angle of the wings. For this low wing design, the fuselage is destabilizing while the vertical tail adds slightly to the stability. Stability is achieved through a negative slope, which can be seen in Figure 4.3-2.

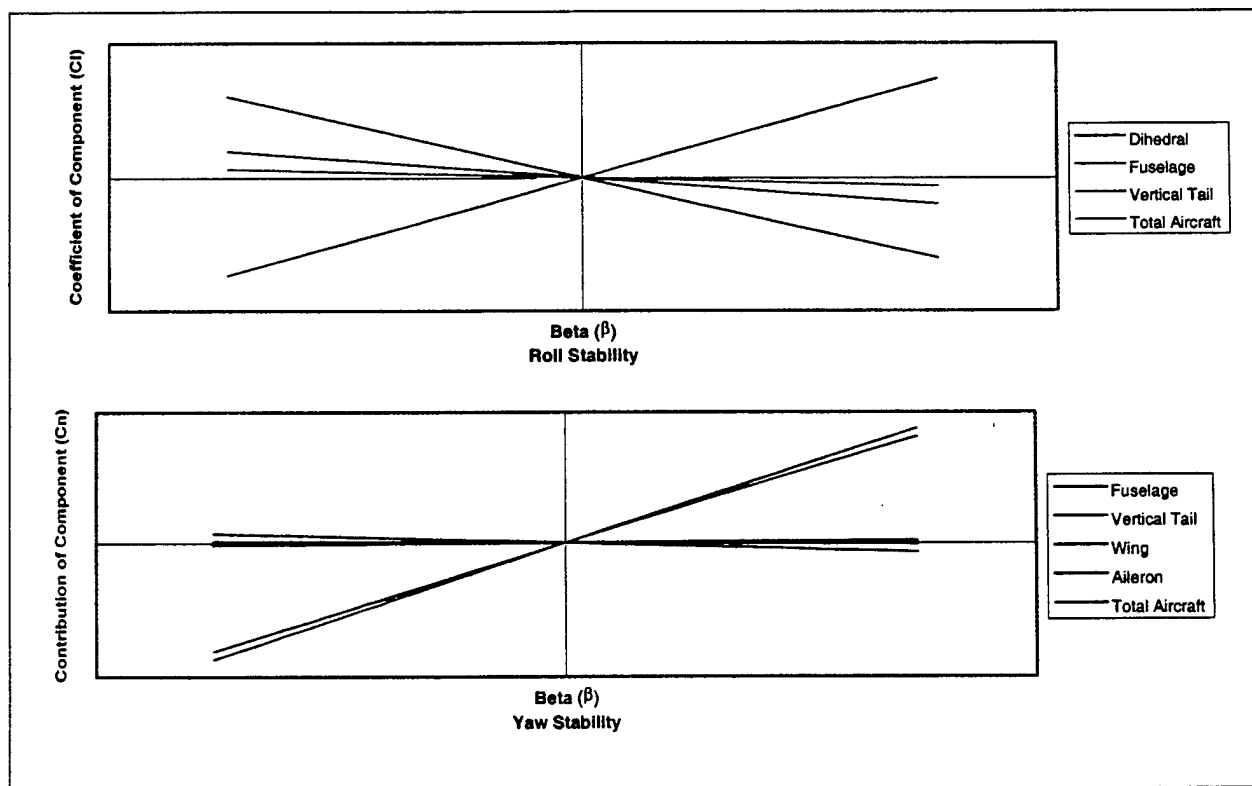


Figure 4.3-2: Static Stability Contributions

The yawing moment is comprised of components from the vertical tail, fuselage, wing, and aileron deflection. The major component is the lateral lift from the vertical tail. Rudder deflection increases this effect, which counteracts the destabilizing fuselage component. Yaw stability is characterized by positive slope, as can be seen in Figure 4.3-2, elevon deflection is arbitrary.

Rudder Sizing: Completing the lateral stability is the sizing of the rudder and elevon effectiveness. This is done simultaneously with the roll and yaw moment graphs. Since the size of the elevator has been set in the longitudinal analysis, only the effectiveness of elevon control can be computed rather than sizing considerations. Initial parameters were obtained from Raymer and these measurements were further refined for our specific aircraft through simultaneous solving.

4.3.2 Structures Group

Fuselage: The choices for fuselage structural members were a combination of bulkheads, longerons, keelson, stringers, and reinforced skins. A combination of longerons and bulkheads mounted to reinforce skin was chosen to fulfill all of the figures of merit for the fuselage. This combination provides bending moment and torsional strength, which will allow the aircraft to remain rigid.

The bending moment strength of a longeron is eight times greater than that of a stringer with a factor of two increase in weight. Torsion will be resisted by the bulkhead and reinforced skin interaction. The keelson was eliminated due to its method of reinforcement. A keelson would run the length of the plane through the floor of the aircraft, which in our design is interrupted by the recessed wing. This structure would have to be bent around the wing and would therefore be less effective than a longeron and much more difficult to construct. These factors, previously weighed out in section 4.1.2, justify the selection of longerons for structural reinforcement.

Wing: To carry the large bending moment in the center of the wing, a spruce spar separated by a foam block and covered with carbon fiber twill will be utilized. Balsa wood in the center section of the wing along the leading edge will strengthen the connection of the wing to the fuselage. This design choice allows a strong spar to carry the bending moment with the carbon fiber skin acting as a safety factor. The balsa wood center section allows a good surface to connect the wing to the fuselage with pins and bolts.

Other methods of carrying loads from the wing to the fuselage and well as carrying the bending loads in the wing were also considered. A center section composed of honeycomb was an alternative to the balsa wood, but did not provide a good surface for mounting pins to for a secure connection of the fuselage. Additionally, a spar comprised of concentric carbon fiber tubes was considered. The spruce spar was chosen over this design in order to provide a greater moment of inertia with less weight and

utilize the weight added to the wing to the fullest. These factors were weighted in Section 4.1.2 to show the final selection of a hybrid spar composed of spruce and carbon fiber twill.

Tail: The chosen tail design is a strategically ribbed tail allowing carbon arrow shaft to be firmly mounted and then inserted through the fuselage for transmission of bending and torsion forces. The relatively small diameter shafts would allow the control linkages to pass through the rear of the fuselage. In order to firmly attach the stabilizers to the tail, the inboard sections will be made of balsa wood that will be shaped and glued to the fuselage surface.

The chosen design fulfills all of the figures of merit outlined for tail design. The carbon fiber arrow shafts provide a spar for the large tail as well as acting as carry through and attachment structure to the fuselage. Although a carbon fiber tube is not the optimum shape for carrying bending forces, it is an excellent compromise to perform all of the functions the tail components must satisfy as indicated by the figures of merit for the tail in Section 4.1.2.

4.3.3 Propulsion Group

Battery Sizing: The battery type that will be used was predetermined by the competition rules, which stated that the power supply must consist of Nickel-Cadmium batteries, and must weigh 5 lbs or less. The battery selection was a very high priority for the propulsion team. Batteries designed for high voltage, with high capacity, and able to withstand the harsh conditions of high performance applications were needed. It was found that the Sanyo Fast Charge Batteries (R-Series) best suited the performance needs. Data for the different sizes of the Sanyo batteries is shown in Table 4.3-4.3-1.

Part Number	Size	Capacity (mAh)	Mass (g)	Price (US Dollars)	Capacity per Mass (mAh/g)
N-800AR	A	800	34	3.00	23.53
N-1300SCR	Sub-C	1500	52	2.25	25
N-4000DRL	D	4000	160	5.50	25
N-1250SCRL	4/5 Sub-C	1250	43	3.50	29.06
N-3000CR	C	3000	84	4.50	34.71
N-1900SCR	Sub-C	1900	54	3.50	35.19
RC-2400	Sub-C	2400	54	5.50	44.44

Table 4.3-4.3-1 Sanyo Fast Charge Battery Statistics – Provided by TNR Technical

After considering the performance curves for several types of batteries and looking at the manufacturers performance data RC-2400 battery were selected for the propulsion system. The RC-2400 had the highest capacity per gram and was relatively lightweight. At 1.9 ounces per cell the RC-2400 would allow us to have more cells in our battery pack than the higher capacity batteries and still provide us with 24.3 % more overall capacity.

Decision Factor	Weight	N-1900SCR	RC-2400	N-3000CR
Weight	.4	0	1	-1
Efficiency	.2	0	1	1
Capacity/Mass	.3	0	1	1
Cost	.1	0	-1	-1
	Total	0	.8	0

Table 4.3-2: FOM Decision Matrix for Battery Selection

Figure 4.1-3 demonstrates the maximum velocity attainable for different throttle settings limited by battery power and physical constraints of the aircraft. The chart verifies the power plant chosen will produce enough power to achieve the desired cruise velocity and then some. The intersections illustrate the maximum velocity at a given throttle setting for different loading conditions based on the propeller discussed in the next section.

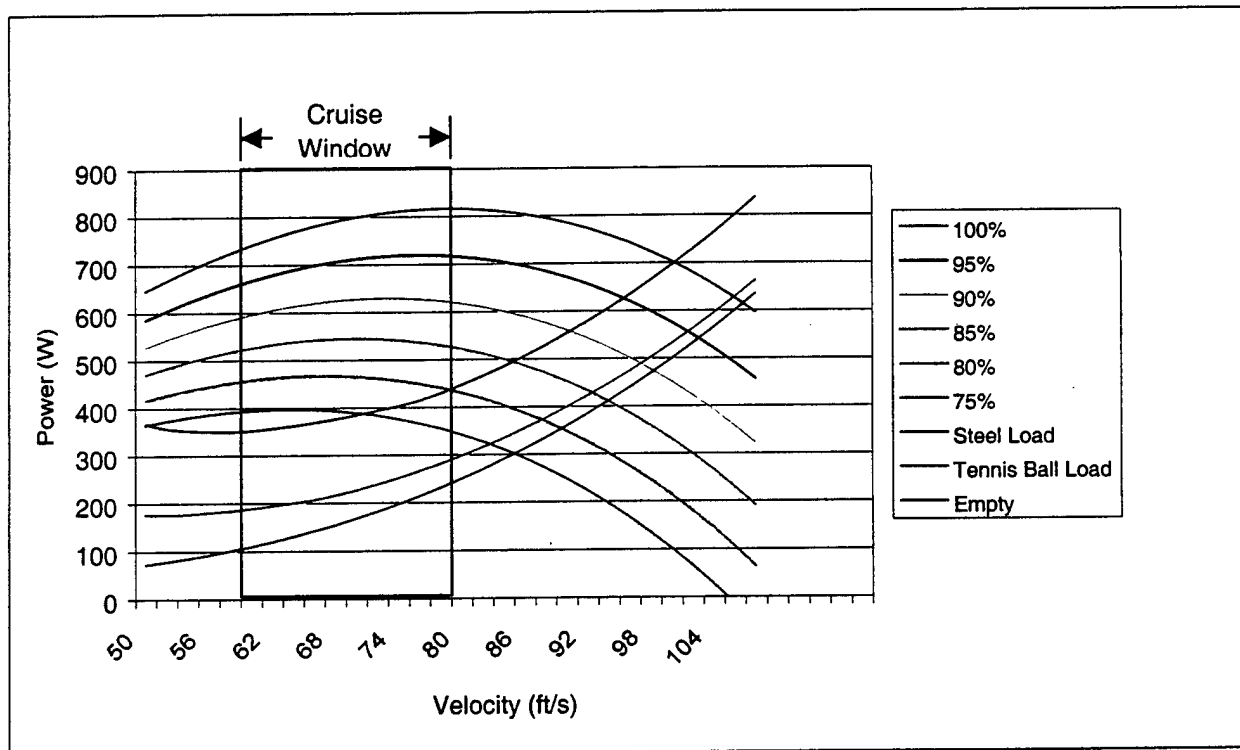


Figure 4.3-3: Power Available vs. Power Required for Various Throttle Settings

Motor Sizing: The AstroFlight Cobalt 60 (#661), 90 (#691), and 40 (#640) motors with Super Box gearing were examined. In determining which motor would best suit the performance needs, parameters including current, weight, power produced by the assembled propulsion system, and efficiency were considered. The initial design concept called for a propulsion system that could handle 1500 Watts of power, produce a minimum of 9 lb of static thrust, and have high efficiency. Analysis was begun with a conservative estimate of an overall efficiency of 40% based on historical data.

Basic motor performance analysis was performed using data supplied by the manufacturer. Theoretical analysis showed that the 40-size motor would not provide enough thrust for takeoff. High current (30 Amps) damage was also a concern. However, the efficiency of the 640 was slightly higher than for the other two motors. The 661's efficiency was quite close to the 640's efficiency and it produced much more thrust. It also had the ability to handle larger current and voltage inputs. There was a concern over the weight gained from using the larger motor, however this was determined to be acceptable for the thrust and efficiency combination of the motor. The 690 produced more thrust than the 661, however the efficiency dropped off. The 690 would require a larger propeller and the combined weight and length issues would impact the RAC and other flight systems such as landing gear. Figure 4.3-4 shows the torque and efficiency curves for each of the three motors that we considered. Table 3.4-1 shows the other motor parameters that we considered. By making direct comparisons between the motors we were able to select the motor that would best serve our needs. It appeared to us that the 661 would be a good compromise between the 640 and 690 motors.

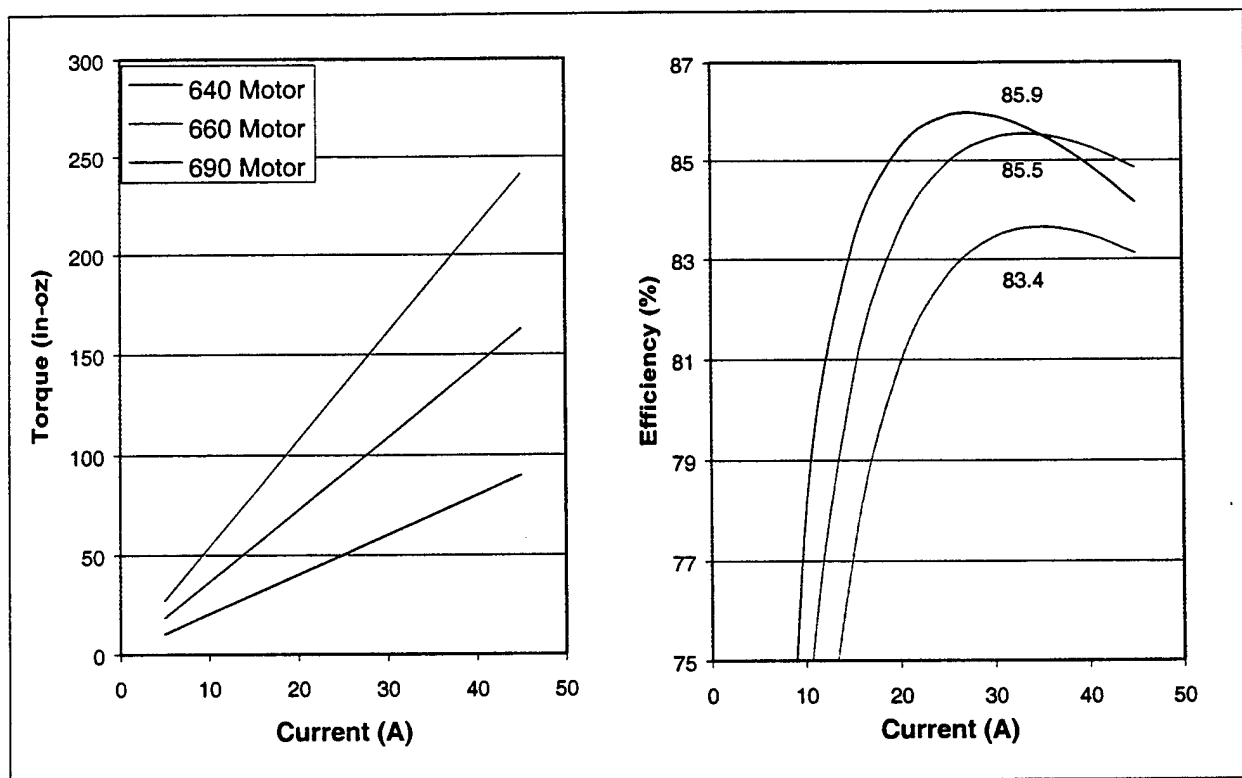


Figure 4.3-4: Performance for selected AstroFlight motors

Using the decision matrix shown in Table 4.3-2 and collaboration with the Aerodynamics team, we concluded that to get the best performance we should use the AstroFlight 60 size motor. The Aerodynamics team required about 1200 Watts of power for takeoff and climb and about 680 Watts for cruise, with approximately 9 lbs of static thrust for takeoff. They also wanted the efficiency of the

propulsion system to be at least 40% based on historical data. Using MathCAD as our primary analysis tool we found that the AstroFlight 60 motor could meet all our criteria for the propulsion system to power our airplane.

Decision Factor	Weight	Astro 40	Astro 60	Astro 90
Power Output	.2	-1	0	1
Efficiency	.3	0	0	-1
Ability to Handle Current Load	.1	-1	0	0
Cost	.1	0	0	1
Weight	.2	1	0	-1
Availability	.1	0	0	0
Score		-1	0	-2

Table 4.3-3: FOM Decision Matrix for Motor Selection

Propeller Sizing

The final component of the propulsion system to be selected was the propeller. The primary analysis of the propellers came from performance curves generated from experimental analysis. Using MathCAD to compute parameters for different P/D ratios, gear ratios, and propeller diameters we were able to determine thrust produced during different portions of the flight, overall efficiency of the system, current drawn, power available, and speed of the airplane. All of these parameters could be determined for both steel and tennis ball sorties. The graphs in Figure 4.3-5 show how the available power changes with P/D at different C_T , C_P , and η values. These graphs were used to determine what size and pitch needed for the propeller.

The values in Figure 4.3-6 gave us a baseline for further propeller testing and selection. Utilizing this information, we were able to obtain a reasonable range of propellers to then test dynamically. We performed flight profile tests and propeller efficiency tests on several types and sizes of propellers including wooden, APC, and carbon fiber as well as two- and three-bladed propellers.

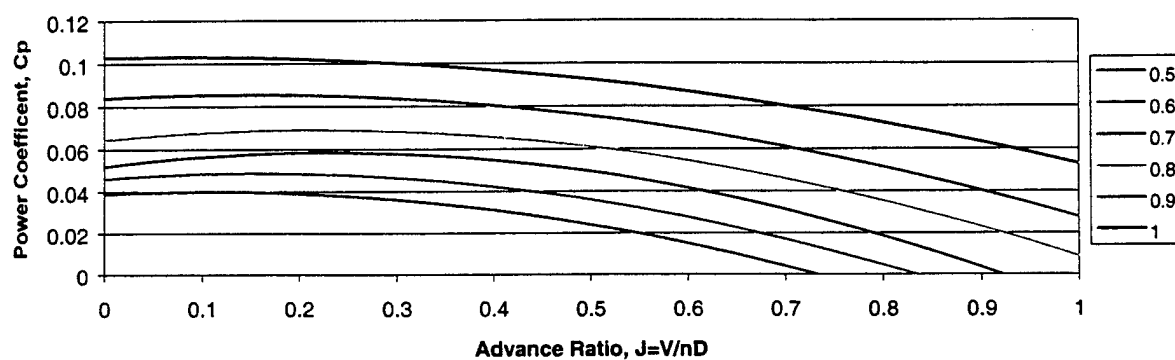
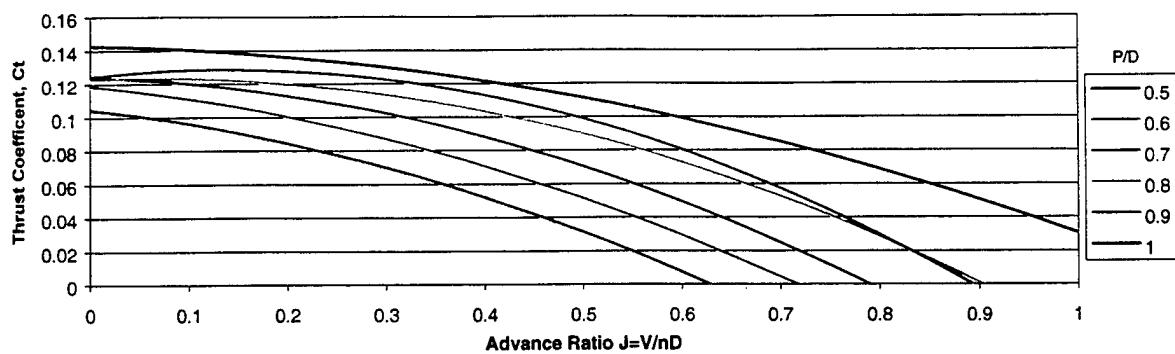


Figure 4.3-5: Advance Ratio vs. Thrust and Power

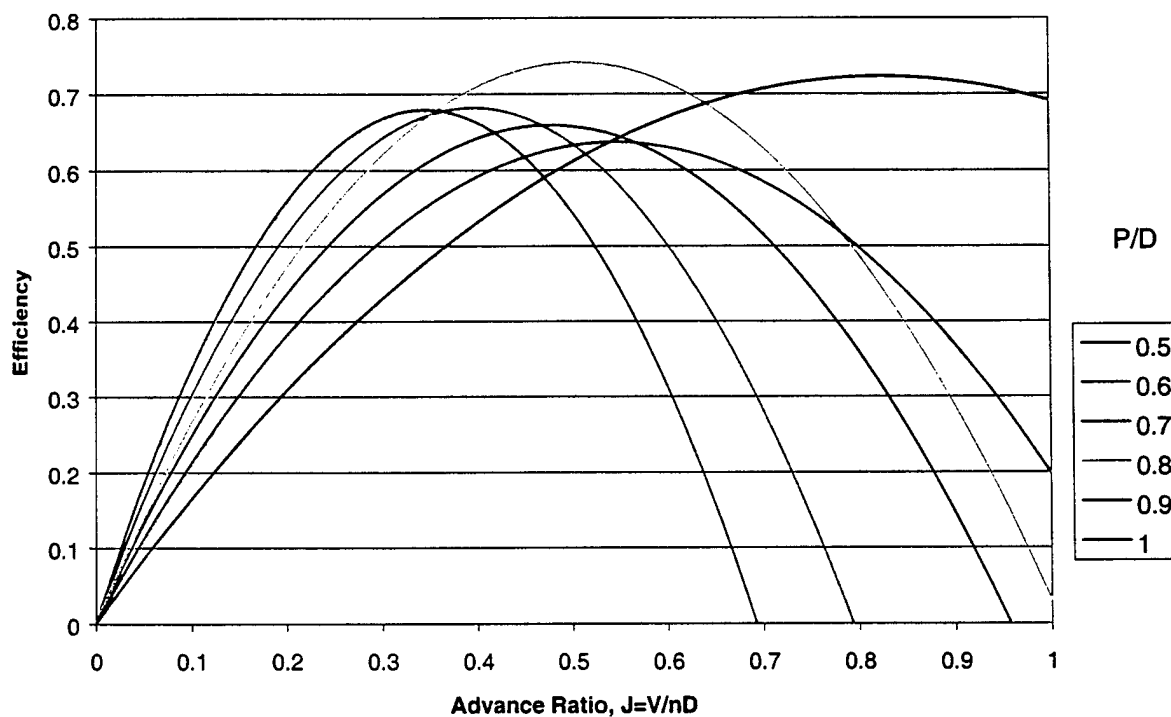


Figure 4.3-6: Advance Ratio vs. Efficiency

4.4 Features that produced the Final Configuration

4.4.1 Aerodynamics Group Summary

During the preliminary design phase the aerodynamics team analyzed the drag generated by the aircraft and explored methods for reducing the overall drag. Among those methods were wheel pants, careful selection of wing airfoil, and tail airfoil and incidence angle. The performance needed by the aircraft demanded a high-lift airfoil and the Eppler 423 was selected for the main wing as well as adding polyhedral for added stability. The short-coupled fuselage called for a moderate-lift, inverted airfoil for the horizontal stabilizer. For this the Eppler 387 was selected, with a negative incidence angle of 1° . A NACA 0009 airfoil was chosen for the vertical stabilizer. Aerodynamic balances were added to the horizontal stabilizer to aid in the servo's ability to overpower flight forces.

4.4.2 Structures Group Summary

Preliminary design yielded the following parameters for the final aircraft, which is to be built entirely from carbon fiber and foam. The fuselage skin will consist of a foam sandwich structure reinforced with longerons and bulkheads constructed from either foam or end grain balsa sandwich structures. The wing will consist of an airfoil cut from foam, covered in carbon fiber skin, and reinforced to carry bending moment with a hybrid spar constructed from a spruce and carbon fiber twill sandwich. The tail section will be structurally reinforced to carry bending moment, made simple to mount to the fuselage at the correct incidence angle, and transfer torsion to the fuselage through the use of carbon fiber tubes mounted in plywood ribs. The speed loader will consist of a cylinder mounted inside the center section of the fuselage to which a foam hatch will attach for fast removal. This hatch will be removable from the speed loader for placement in the fuselage without the speed loader itself. Finally, the landing gear will consist of a bow gear fabricated from multiple layers of carbon fiber and attached to the aircraft with two steel bolts.

4.4.3 Propulsion Group Summary

The propulsion system will consist of the 661 motor, 37 RC-2400 batteries, a gear ratio of 2.7, which was selected through analytical analysis and performance optimization, and a 22-inch propeller with a 12-inch pitch. This system provides 14 lbs of takeoff thrust with a cruise thrust of 3.59 lbs, a cruise velocity of 73.87 ft/s, and 800 Watts of cruise power for the steel payload. For the tennis ball payload the cruise thrust is 2.89 lbs at 72.45 ft/s and 600 Watts of power. The maximum power from the batteries is 1076 Watts and the usable power will last for 585.6 seconds. With our planned sortie runs we will use 89.7% of our energy. The power margin will allow us the option of making an extra lap if the conditions are favorable.

5.1 Performance Data

A conventional configuration monoplane with the parameters shown in Table 5.1.1 below was found to be the optimum combination. This particular configuration is a maximum score while still providing for uncertainties in the flight profile. In particular, the mission profile is well under 600 seconds with battery power still available.

The number of steel and tennis ball laps ultimately determines the final score. Because the number of laps is influenced by the energy available, allowable time and individual sortie payload, flying the optimum profile is critical. The time requirement of ten minutes essentially prevents more than 8 total sorties. The maximum score without wind for each legal combination of steel and tennis ball laps is given in Figure 5.1-1. The optimal payload profile is 3 steel and 3 tennis ball laps.

Geometry	
Wing Span	10 ft
Wing Area	8.85 ft ²
Aspect Ratio	11.3
Fuselage Length	5 ft
Empty Weight	14.8 lb
Gross Weight	52 lb
Payload Fraction	72%
RAC	4.56

Performance	
Max Velocity	70 mph
Steel Cruise	50 mph
Tennis Ball Cruise	51 mph
Stall Speed (Gross Weight)	39 mph
Stall Speed (Empty)	23 mph
Glide Ratio (Gross Weight)	17.8:1
Steel Takeoff Distance	180 ft
Tennis Ball Takeoff Distance	60 ft
Landing Distance (Gross Weight)	240 ft

Payload	
Steel Wind 0 mph	26 lbs
Steel Wind 5 mph	32 lbs
Steel Wind 10 mph	35 lbs
Steel Wind 15 mph	35 lbs
Tennis Balls	100

Endurance	600 s.
Range	24000 ft.

Handling Qualities	
Stable in all axis	
Nose wheel steering	
5 Control Surfaces	
Brakes	

Table 5.1-1: Aircraft Specifications

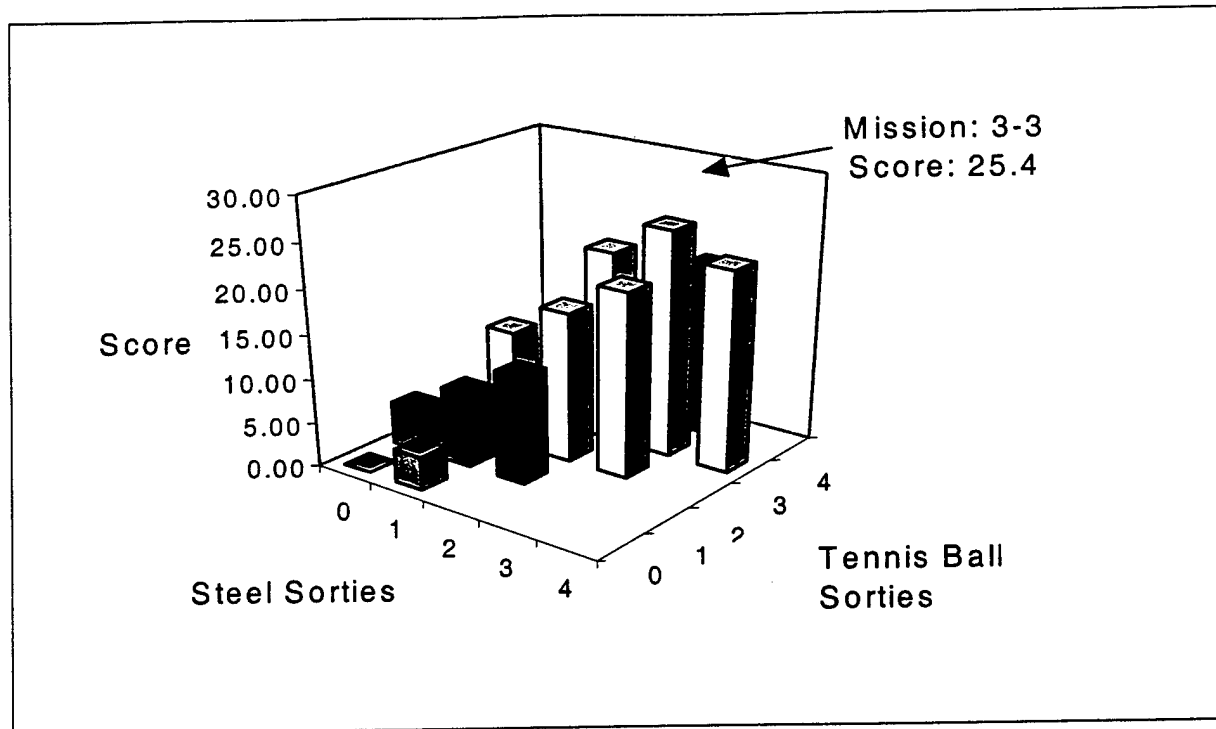


Figure 5.1-1: Sortie Mission analysis

The tennis ball packing influences drag and RAC. Because efficiently packing tennis balls requires certain fuselage cross section sizes, only the first four reasonable tennis ball cross section configurations were analyzed. The configurations were a 4, 7, 10 and 14 ball cross sections. Small configurations required a long fuselage while larger configurations had excessive drag. Figure 5.1-2, the highest score was achieved with using a 10 ball cross section. From this analysis, the relationship between possible geometries and ultimate score has been constrained by the ultimate score.

There was strong sensitivity of the score to the empty weight. From Figure 5.1-2, a 1-pound change in empty weight yields a 1.3-point change. The increase in score is due to both the Rated Aircraft Cost and the ability to carry more payload. While decreasing the weight always increases the optimization's score, reality requires a structurally sound and durable aircraft. As expected, low structural weights must be balanced with a structural integrity.

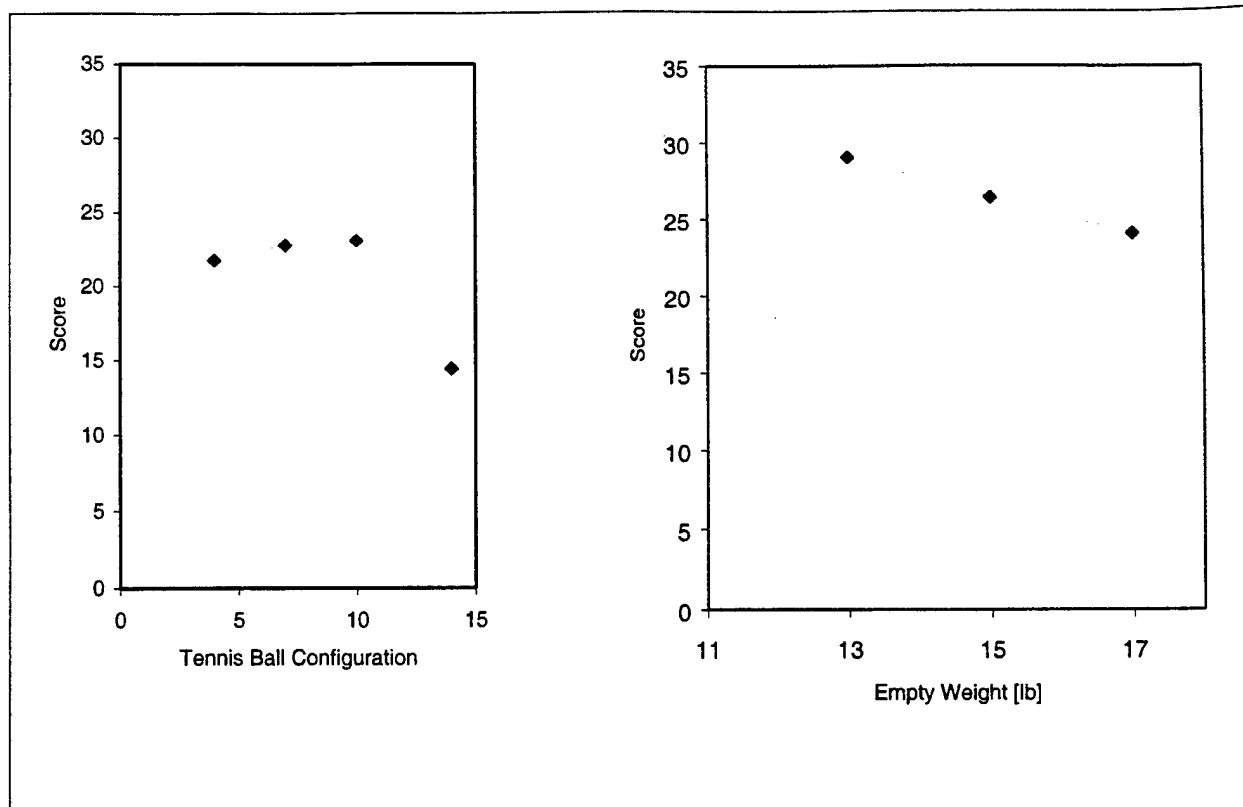


Figure 5.1-2: Configuration Trends

As expected, wind affects the score. An upwind takeoff increases the maximum steel weight due to the 200-foot takeoff distance constraint. Below the optimized wind velocity, the aircraft is unable to takeoff without exceeding the maximum takeoff distance. From Figure 5.1-3, the wind increase causes a near linear increase in score. Researching the historical wind speeds at Patuxent River, Maryland during the April competition time period yielded valuable results. A six year record of average wind speed yielded an 8.8 mph daily average wind speed. Partial data for the average low wind yielded a wind of over 5 mph. Wind strongly affects the score due to the takeoff distance limitation. For each 5 mph increment in wind velocity, the score increases by approximately 3 points. At a wind speed of 15 mph, the aircraft is at the 55-pound weight limitation with a score of 36. From the wind analysis, it was decided to optimize for a 5 mph wind.

Cruise height sensitivity analysis indicated that score was a weak function of cruise height. From Figure 5.1-4, the maximum score was nearly constant for heights below 100 feet. Although unexpected, having the score uncoupled from the cruise height will be beneficial to the pilot. The pilot will be able to choose a comfortable altitude and not be concerned with flying low.

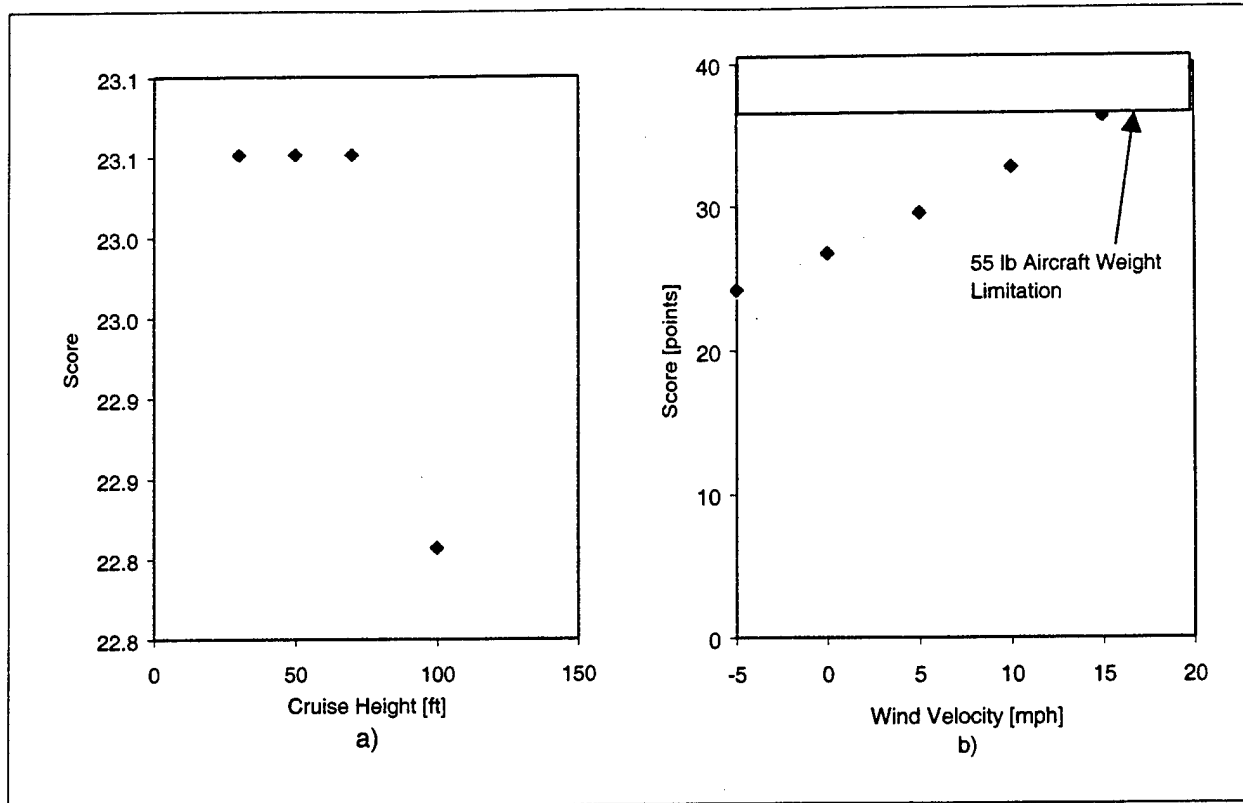
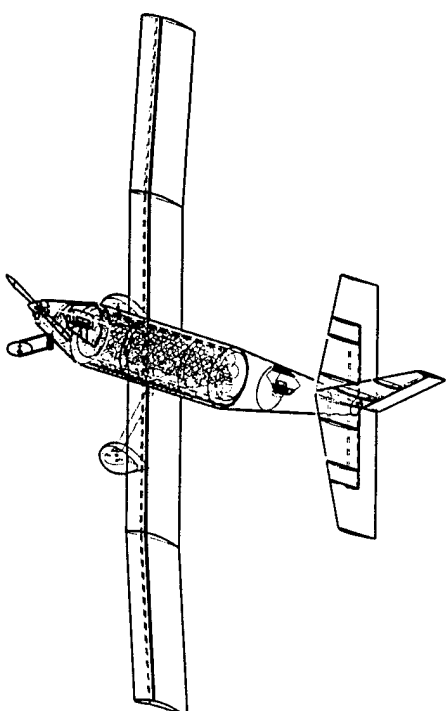
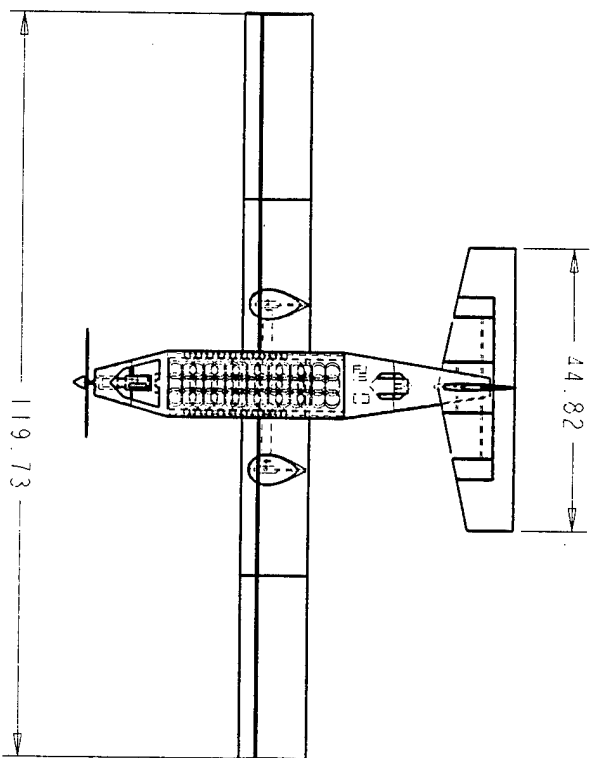
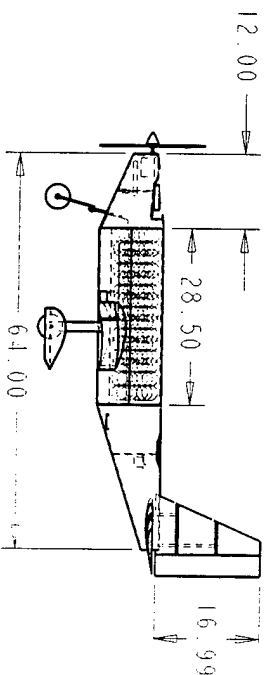
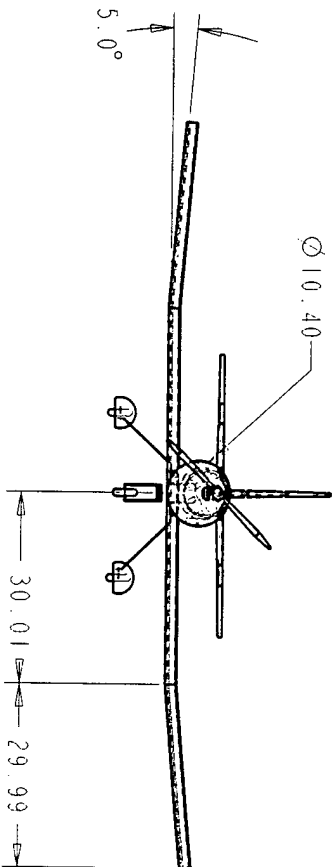


Figure 5.1-3 Score Sensitivity to (a) Cruise Height (b) Wind Velocity

With the higher speeds predicted and required by the aircraft, landing and roll out distances need to be considered. An analysis of landing ground roll distance is disturbing. For this ground roll sensitivity analysis, the aircraft was loaded to give the highest score for the given wind. As discussed in the wind sensitivity analysis, an increase in wind also increases the carried payload weight. From Figure 5.1-4, a no-wind 20 lb steel payload sortie is estimated to take 650 feet to stop. A 10 mph wind with a 30 pound steel payload decreases the distance to 430 feet. Thus, an effective stopping method needs to be considered. To resolve this problem, an investigation into the effectiveness of brakes on ground roll distance was performed. The mission analysis program was modified to include braking during the ground roll. To test the brake sensitivity, a worst-case scenario of a zero-wind with the corresponding optimized steel payload weight was considered. Test results are given in Figure 5.1-4. With no brakes, the estimated roll out distance was 720 feet. With a braking force equal to only 10% of the aircraft weight, the ground roll distance was slashed to just over 270 feet. It appears that even small braking forces are effective in reducing ground roll distances. A brake system is beneficial.



SCALE 0.050



Cessna/ONR
Student
Design/Built to Fly
Competition

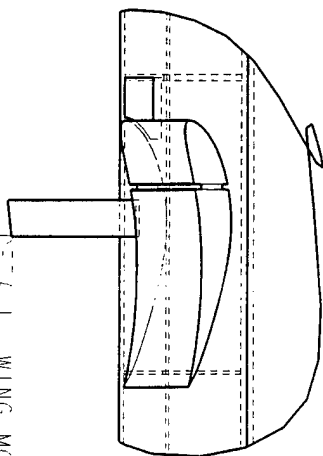
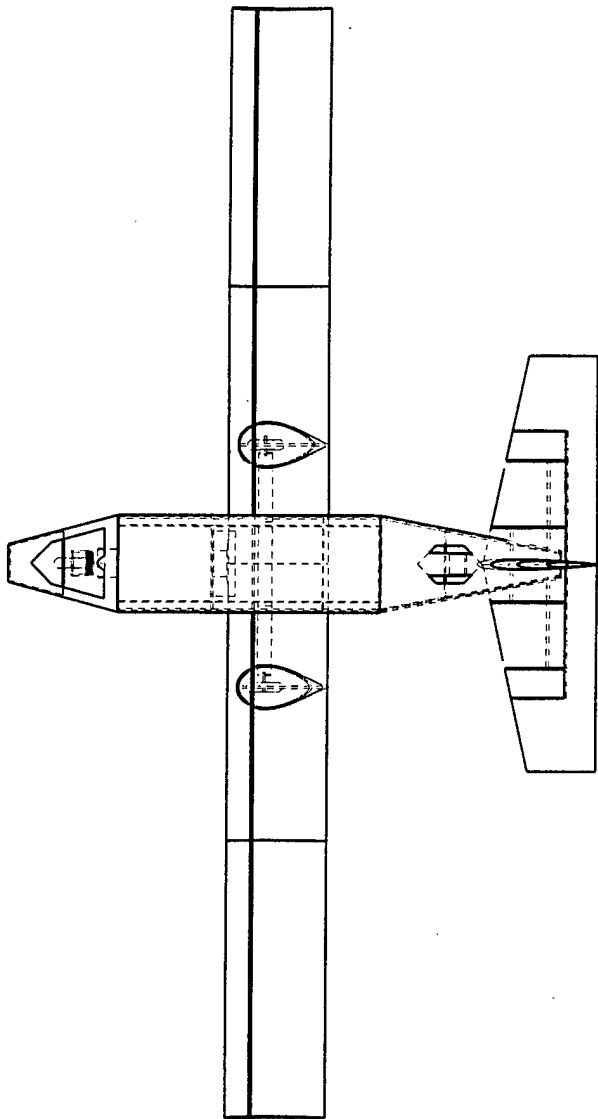
2000/2001

Refined Design

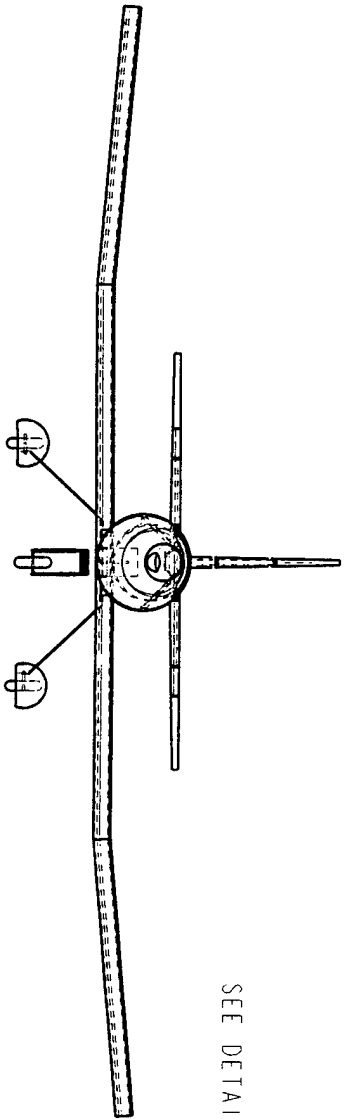
OKLAHOMA STATE UNIVERSITY

13 May 2001

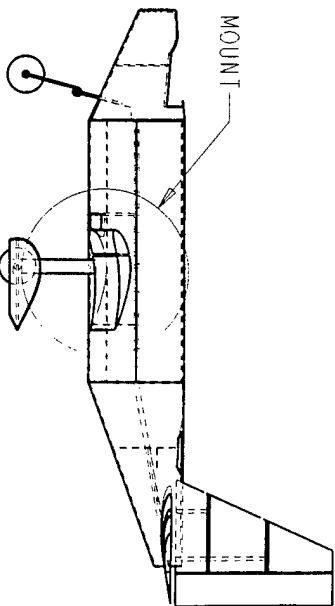
OKLAHOMA STATE UNIVERSITY



DETAIL WING MOUNT
SCALE 0.200



SEE DETAIL WING MOUNT



Cessna/ONR
Student
Design/Build/Fly
Competition

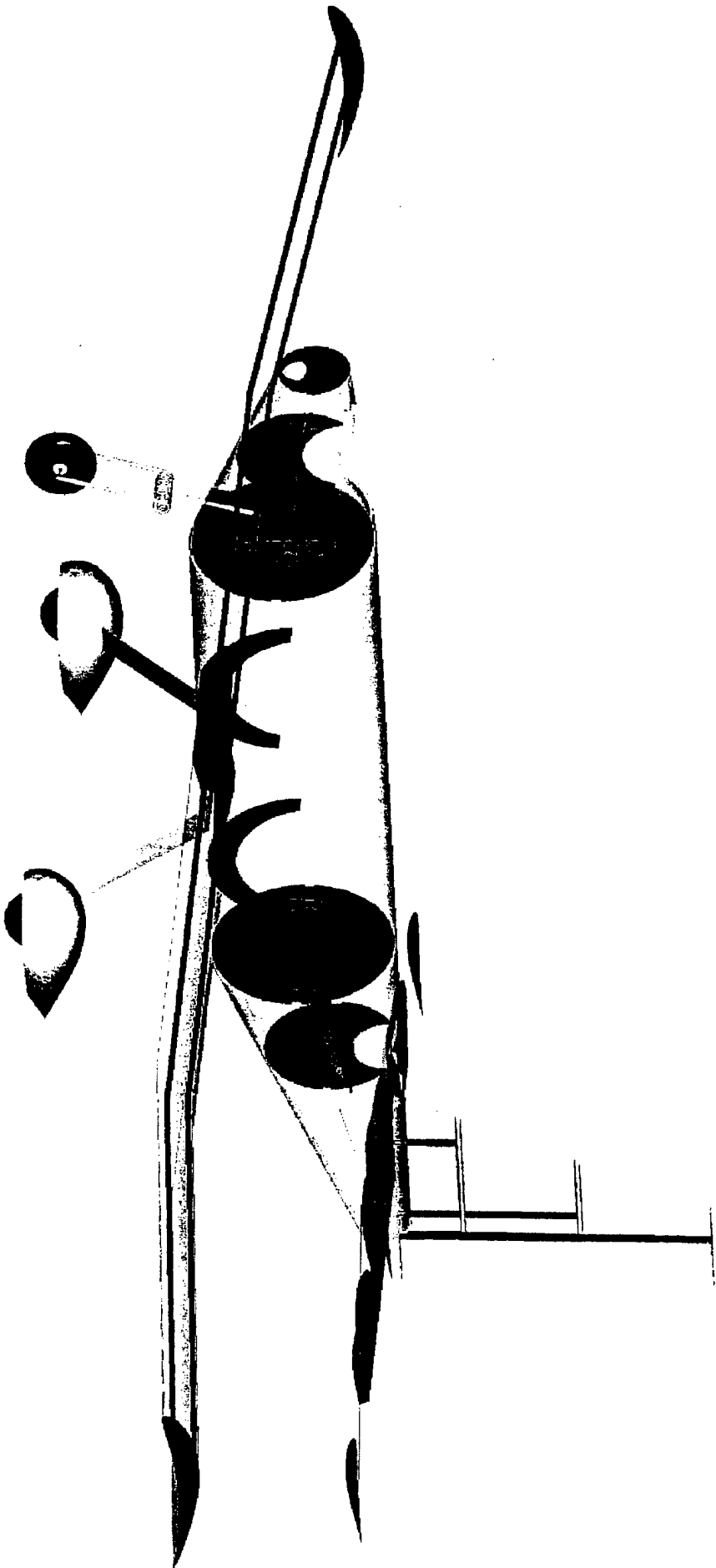
2000/2001

Structure & Assembly

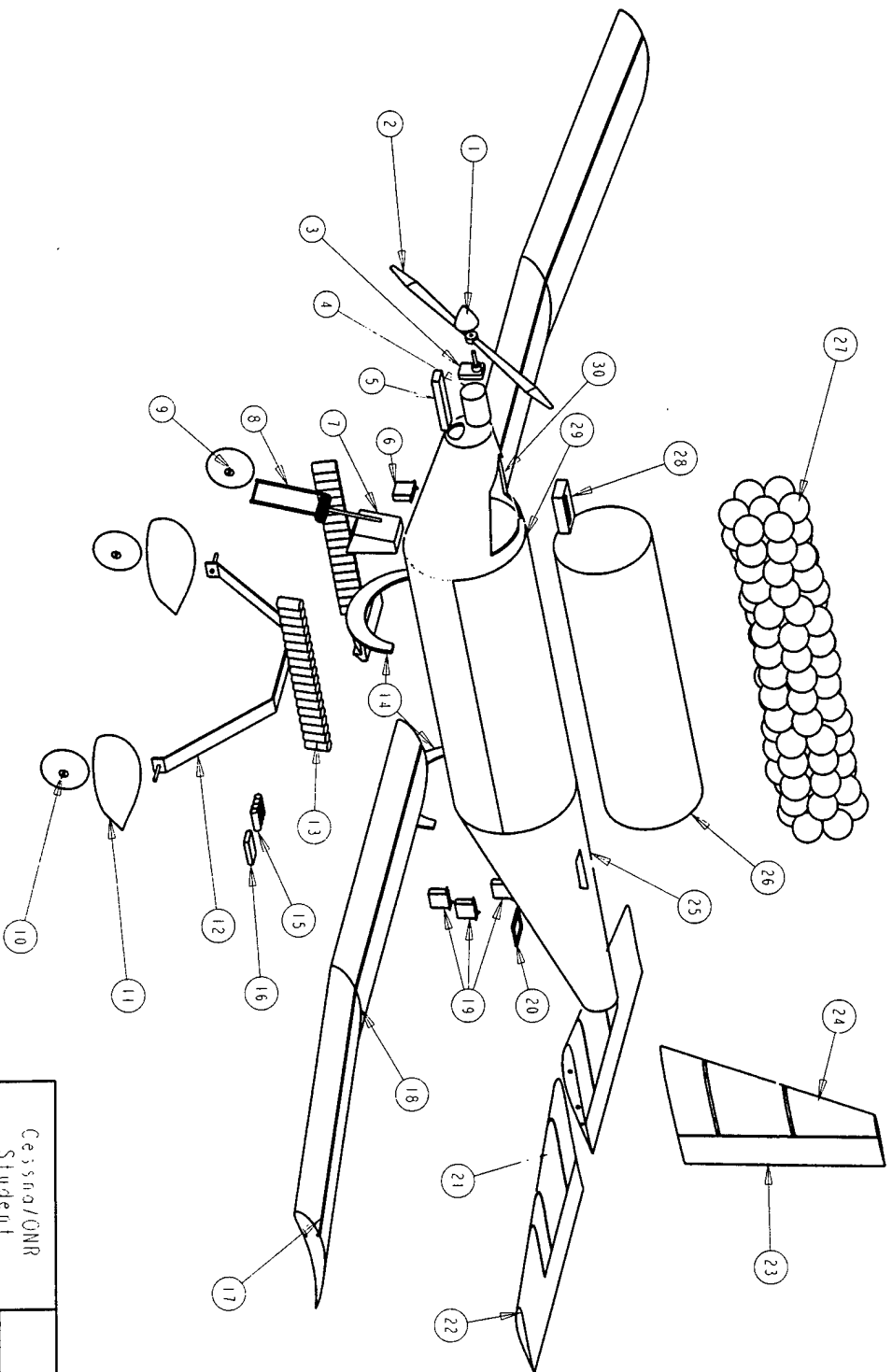
OKLAHOMA STATE UNIVERSITY

13 Mar 2001

Final Design Project



Cessna/OMB Student Design/Build/ity Competition		Structural Isometric Rendering	
2000/2001		OKLAHOMA STATE UNIVERSITY	
		13 Mar 2001	1:50 Scale per Page



No.	Item	Qty
1	Spinner	1
2	Propeller	1
3	Gearbox	1
4	Electric motor	1
5	Speed control	1
6	Nose gear servo	1
7	Nose gear mount	1
8	Nose gear	1
9	Nose wheel	1
10	Main wheel	2
11	Wheel post	2
12	Main gear	1
13	Battery pack	2
14	Wing mount	1
15	Receiver pack	1
16	Receiver	1
17	Wing spar	2
18	Polyhedral wing	2
19	Tail servos	3
20	Servo mount	1
21	Horiz. stabilizer	2
22	Elevator	2
23	Rudder	1
24	Vert. stabilizer	1
25	Rear hatch	1
26	Speed loader	1
27	Tennis balls	100
28	Wallmeter	1
29	Speedloader, hatch	1
30	Forward hatch	1

Exploded View

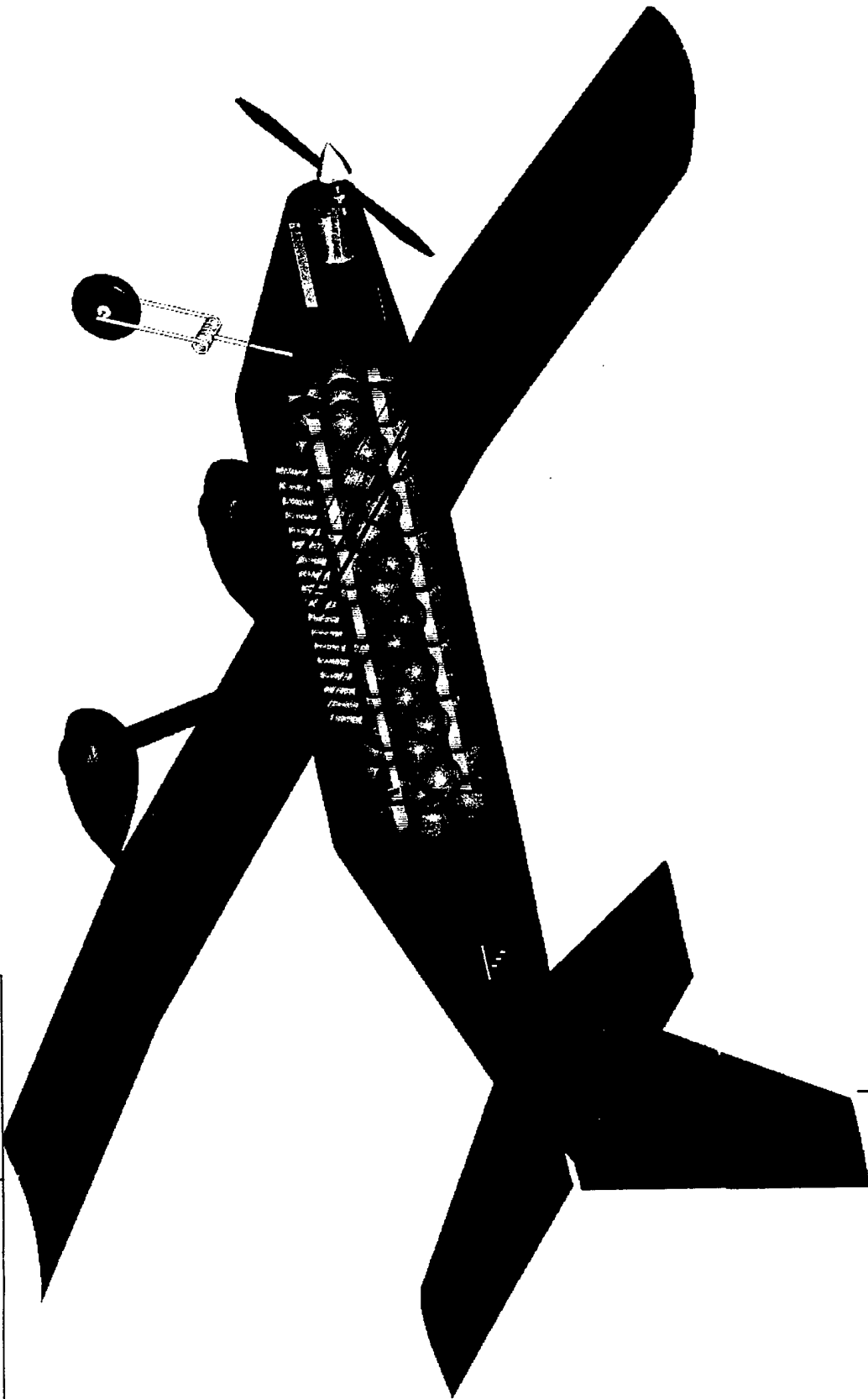
Cessna/ONR
Student
Design/Build/Fly
Competition

OKLAHOMA STATE UNIVERSITY

2000/2001

13 Mar 2001

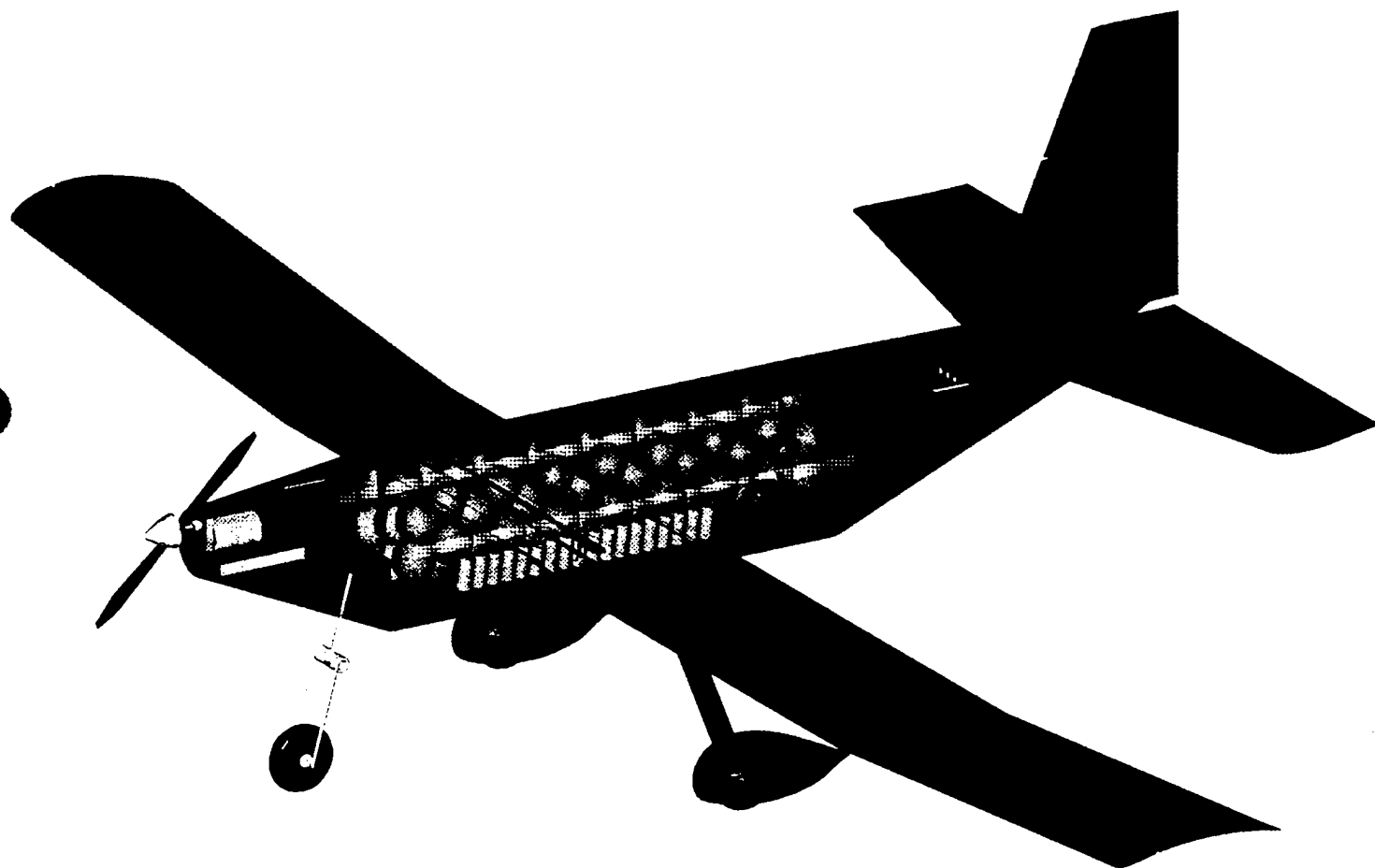
OTU Charge Team



Cessna/ONR Student Design/Build/Fly Competition		Isometric Rendering	
2000/2001		OKLAHOMA STATE UNIVERSITY	
		13 Mar 2001	07:00:00 to 16:20

2000/01 AIAA Foundation
Cessna/ONR
Student Design/Build/Fly Competition

Addendum Phase Design Report



Oklahoma State University
orange team

April 10, 2001

1	EXECUTIVE SUMMARY	3
1.1	SUMMARY OF DESIGN DEVELOPMENT.....	3
1.2	MAJOR DEVELOPMENT PROCESS AREAS FOR FINAL CONFIGURATION.....	3
1.3	RANGE OF DESIGN ALTERNATIVES INVESTIGATED.....	3
1.4	DESIGN TOOLS USED IN EACH PHASE.....	4
2	MANAGEMENT SUMMARY.....	5
2.1	TEAM ARCHITECTURE.....	5
2.2	ASSIGNMENT AREAS	5
2.3	MANAGEMENT STRUCTURES	6
3	CONCEPTUAL DESIGN.....	8
3.1	MISSION ANALYSIS AND STRATEGY DEVELOPMENT	8
3.2	ALTERNATIVE CONCEPTS INVESTIGATED.....	9
3.3	IMPORTANT DESIGN PARAMETERS	10
3.4	FIGURES OF MERIT	10
3.5	RATED AIRCRAFT COST FOR CONCEPTS	12
3.6	FEATURES THAT PRODUCED THE FINAL CONFIGURATION.....	13
4	PRELIMINARY DESIGN.....	14
4.1	DESIGN PARAMETERS INVESTIGATED AND FIGURES OF MERIT	14
4.1.1	<i>Aerodynamics Group</i>	14
4.1.2	<i>Structures Group</i>	18
4.1.3	<i>Propulsion Group</i>	21
4.2	ANALYTICAL METHODS	22
4.2.1	<i>Aerodynamics Group</i>	22
4.2.2	<i>Structures Group</i>	23
4.2.3	<i>Propulsion Group</i>	23
4.3	CONFIGURATION AND SIZING DATA	24
4.3.1	<i>Aerodynamics Group</i>	24
4.3.2	<i>Structures Group</i>	28
4.3.3	<i>Propulsion Group</i>	29
4.4	FEATURES THAT PRODUCED THE FINAL CONFIGURATION.....	34
4.4.1	<i>Aerodynamics Group Summary</i>	34
4.4.2	<i>Structures Group Summary</i>	34
4.4.3	<i>Propulsion Group Summary</i>	34
5	DETAIL DESIGN.....	35

5.1	PERFORMANCE DATA	35
5.2	COMPONENT SELECTION AND SYSTEMS ARCHITECTURE.....	39
5.2.1	<i>Propulsion</i>	39
5.2.2	<i>Structures</i>	40
5.3	INNOVATIVE SOLUTIONS	41
5.3.1	<i>Fuselage</i>	41
5.3.2	<i>Wing</i>	41
5.3.3	<i>Tail</i>	41
5.3.4	<i>Landing Gear</i>	42
5.3.5	<i>Hinges</i>	42
6	MANUFACTURING PLAN.....	42
6.1	MANUFACTURING PROCESSES INVESTIGATED.....	42
6.2	PROCESS FOR MANUFACTURE OF MAJOR COMPONENTS	43
6.2.1	<i>Fuselage</i>	43
6.2.2	<i>Wing</i>	43
6.2.3	<i>Tail</i>	43
6.2.4	<i>Landing Gear</i>	44
6.3	ANALYTICAL METHODS	44
6.3.1	<i>Cost</i>	44
6.3.2	<i>Skills</i>	44
6.3.3	<i>Scheduling</i>	45
6.4	INNOVATIVE SOLUTIONS	45
7	DRAWING PACKAGE	45
ADDENDUM		
8	LESSONS LEARNED	53
8.1	PROTOTYPE FLIGHT TESTING RESULTS	53
8.2	AIRCRAFT DIFFERENCES FROM THE PROPOSAL DESIGN AND JUSTIFICATION	55
8.2.1	<i>Aerodynamics Group</i>	55
8.2.2	<i>Structures Group</i>	55
8.2.3	<i>Propulsion Group</i>	56
8.3	TIME AND COST REQUIRED TO IMPLEMENT CHANGE/IMPROVEMENT REALIZED.....	56
8.4	AREAS FOR IMPROVEMENT IN NEXT DESIGN AND MANUFACTURING PROCESS	57
9	AIRCRAFT COST	58

8 Lessons Learned

8.1 Prototype Flight Testing Results

Once the prototype aircraft was assembled and deemed flight worthy, the flight-testing phase began. Pictures from the flight-testing phase are shown in Figure 8-1. The flight-testing phase compared the predicted and actual aircraft performance. Data obtained during flight-testing was analyzed to determine the aircraft's flight performance. The parameters assessed include stability and control, handling qualities, speed, lift capability, energy used per lap, endurance and were ultimately used to determine the final strategies.



Figure 8-1: Pictures of prototype flight-testing

Stability and control and handling qualities were verified by pilot opinion. As a result of the pilot's input, ailerons were incorporated into the final design in lieu of a rolling tail, which was included in the original design to reduce RAC of the wing. This change resulted in a reduction in the overall tail size.

After verification of the handling qualities as well as the stability and control of the aircraft, a speed run was conducted. The speed run was conducted at full power over a set course. The average up wind and down wind speed was then obtained. The resulting average speed was 70 feet per second. Since this was considerably lower than the predicted max speed of 102 feet per second, the calculations were reviewed and the aircraft inspected. Upon completion of this assessment, a difference in motor constants was discovered. Due to a delay in delivery of the contest motor, an old motor of the same size was used

in the prototype. This motor, however, has different motor constants than that of the final motor ordered. These differences were overlooked prior to flight-testing. After discovering the discrepancies, adjustments were made to the calculations to verify the max speed for the test motor. Those calculations revealed a max speed of 71 feet per second.

Lift capability was the next parameter to be investigated. This evaluation was conducted by stepping up the steel weights from empty to maximum weight. Maximum weight successfully lifted was determined by two factors, take-off distance and climb rate. It was determined that climb rate was the limiting factor as to the amount of weight the aircraft can lift. As a result, the maximum gross take-off weight was determined to be 40 lbs instead of the 55 lbs originally predicted.

The energy used per lap was greater than predicted. For each tennis ball lap the actual energy used was 0.6 – 0.65 Ah compared to the predicted value of 0.44 Ah. There was less of a difference in the energy used per steel. This changed from 0.39 Ah predicted to 0.4 – 0.45 Ah actually used. These differences were a result of higher than predicted parasite drag on the aircraft.

Finally, with all the previously mentioned tests completed, multiple contest missions were executed. The results of these missions lead to the conclusion that a 3-3 mission was not possible due to the change in capacity limitation of the battery pack to be discussed in section 8.2.3. However, the information obtained lead to the development of two alternative strategies. The first strategy, 3 steel – 2 tennis ball laps, involves light payload weight and low wind conditions. The second strategy, 2 steel – 2 tennis ball laps, evolved from the discovery of a sensitivity of the aircraft's performance to wind conditions. This strategy is utilized for wind speeds greater than 10 mph and was governed mainly by the aircraft's total time in flight.

The following chart summarizes the predicted versus actual flight-test data used for refinements on the competition aircraft.

	Predicted	Actual
Max Speed	71 ft/s *	70 ft/s
Endurance	2400 mAh	2100 mAh
Energy used per tennis ball lap	0.44 Ah	0.6 – 0.65 Ah
Energy used per steel lap	0.39 Ah	0.4 – 0.45 Ah
Flight profile (low wind speed)	3 steel – 3 tennis ball laps	3 steel – 2 tennis ball laps
Flight profile (high wind speed)	3 steel – 3 tennis ball laps	2 steel – 2 tennis ball laps
Gross take-off weight	55 lbs	40 lbs

* Value for adjusted motor constants

8.2 Aircraft differences from the proposal design and justification

8.2.1 Aerodynamics Group

The sizing of the horizontal tail changed for several reasons. The major factor in this revision came from the necessity of ailerons to adequately control the aircraft under various loading and environmental conditions. Since ailerons are used for roll control, this requirement for the rolling tail sizing became unnecessary. The second factor in the resizing came from pilot response. The pilot determined the pitch stability and control to be overly adequate. Overall aircraft weight reduction comprised the final consideration.

Through analyzing the lateral stability and control equations, reducing the horizontal tail area by 6.5% did not significantly change the horizontal lift coefficient to require a new horizontal airfoil selection. This change brings the aircraft stability closer to 15% static margin and reduces the overall aircraft weight and drag coefficient. Parameters such as aspect ratio, taper ratio, percentage of the chord as elevator, and aerodynamic balance assumptions remained constant from the prototype.

8.2.2 Structures Group

There are several structural modifications to the design of the aircraft that have been integrated into the final airplane to be flown at the contest. These differences were introduced to improve the weight of the aircraft, the ability of the aircraft to perform the contest mission, and the crashworthiness of the aircraft.

The original design of the fuselage called for longerons that were eliminated due to the extremely strong fuselage skin that was obtained by the foam/carbon fiber sandwich. The extra bending moment that would be withstood by longerons was not required and would only have added weight to the aircraft. The fuselage was not over designed in all areas, however. The bulkheads in the prototype comprising the wing carry through structure delaminated after a few flights and were doubled before catastrophic failure occurred.

The wing was also modified from the original design. The spar, which was to be made of $\frac{1}{4}$ " X $\frac{1}{4}$ " spruce material, was increased to $\frac{3}{8}$ " material to yield an acceptable deflection under the maximum gross weight the aircraft will weigh in with at the contest.

The wing attachment to the fuselage was also modified from a combination of bolting and pinning to bolting only with nylon shear bolts. This modification was integrated to provide greater crashworthiness. The shearing bolts will not damage the leading edge of the wing or carry through structure in the fuselage in the event of abnormal loading conditions. In an effort to reduce interference drag, fillets were added at the fuselage to wing interface as well as the fuselage to tail surfaces interface.

The landing gear design was also modified. An aluminum two stroke nose gear called out in the design would have been difficult to manufacture and was therefore replaced with a commercially produced steel spring type gear that was tested on the prototype. This gear performed well and weighed very close to previous teams manufactured nose gear.

Finally, the speed loader configuration has also been modified. The original design of the speed loader specified that the fuselage hatch be mounted to the speed loader, allowing only one movement be required to replace the speed loader between sorties. This design did not take into consideration the weight and awkward nature of a payload carrying tube and the hatch will now be a separately removed from the aircraft allowing better handles be design to manipulate the speed loader into and out of the fuselage.

8.2.3 Propulsion Group

The propulsion system for the final design stage did not undergo any major changes other than the propeller sizing. After running several dynamic tests on the proposed system it was determined that a different size of propeller better served the needs of the design. The proposed propeller was a 22/12 and the final propeller was a 22/20, however there is still the option of changing out propellers to get the optimum performance at different wind speeds. The propellers that are useful for the projected wind and plane speeds are the 22/12, 22/20, 24/14, and 24/24 propellers. Having these propellers on hand will provide a wide range of options at the contest so that maximum performance of the airplane will be achieved. The only other change in the propulsion system was a minor adjustment of the gearing. Rather than using a linear gear system, which sometimes backs into the motor housing, a helical gear system is implemented. The rest of the components remain unchanged in the final design. However, the manufacturer's specifications on the battery packs stated an available capacity of 2400 mAh. After extensive testing both in the field and in the wind tunnel, it was determined that the battery packs would only safely supply 2100 mAh of capacity. This new capacity has since been used as the maximum capacity. This change in capacity means that a 3 steel – 3 tennis ball flight profile is no longer possible due to battery limitations. So, a change of the strategy originally developed, as discussed earlier in the prototype flight-testing results, was necessary.

8.3 Time and cost required to implement change/improvement realized

The intention of the team from the beginning was to build two planes, a prototype and a competition aircraft. In this way, the learning was done on the prototype and the changes, which would have been costly in both monetary means and time, were applied to the final aircraft from the learned lessons of the prototype. This allowed for all changes to be planned for in advance of the final construction and therefore not increase the cost of the project to realize the improvements.

The improvements realized from these changes between the prototype and final aircraft include a lighter structure, a stronger structure, and a structure that will perform the mission task better as indicated by each of the justifications listed for the improvements that were made. The most significant change between the prototype and the final aircraft is the tail sizing.

The time and cost of the change to the horizontal tail is minimal for several reasons, but very beneficial in the RAC calculations due to the resulting reduction in empty weight for the aircraft. For the prototype, a MathCAD program set up the lateral stability and control equations and coupled the

appropriate graphs for the prototype sizing. Initial sizing came from a dependency upon a known platform area; resizing included modifying the platform area until the output and graphs produced an appropriate solution. The MathCAD program calculated all dimensions for the stabilizer, elevator, and aerodynamic balance.

Little production time was required to revise the construction drawings; the use of Professional Engineer allowed these dimension changes to be made easily. Foam templates were the only prototype hardware that could not be reused for the final. Structure ribs, spars, and foam cores had to be produced for the final aircraft regardless of design changes; the altered dimensions of these items did not add production time. Assembly of the tail and subcomponents occurred in the same manner as the prototype. The same materials were used in the final assembly of the tail and its subcomponents resulting in no monetary cost difference from the original design.

8.4 Areas for improvement in next design and manufacturing process

Although many improvements were integrated into the aircraft that will be flown at the contest, other refinements to the design and manufacturing process would be integrated into a future aircraft. Many items in the prototype were replaced with items made of lighter materials. This improved the rated aircraft cost by reducing the empty weight of the aircraft. There are still several components, however, that could be replaced in the final aircraft to further reduce the weight. These changes were not made in the final aircraft because of the time and cost of implementing them.

The first item is the blue foam used extensively in the structure of the aircraft. This material is excellent for forming aircraft components such as wing cores, but it is heavy. For a future aircraft, other foam types would be investigated to find one that is formable, light, and will stand up to the vacuum pressure needed to cure the carbon fiber/foam composite structures. Another item that is perhaps not ideal is the carbon fiber arrows that were used as spars in the tail section. Although these items allowed for easy tail section mounting to the fuselage, the circular shape is not ideal for a structural member designed to withstand bending forces. A future aircraft would integrate a lighter spar, possibly a lightweight carbon fiber beam, to replace these arrows.

The manufacturing process utilized in the final aircraft was not modified greatly from the prototype. This process was refined before manufacturing of the prototype by discussion with previous members of the team. There are, however, some improvements that will be passed on to next year's team. One improvement in the foam cutting technique that would be integrated into a future aircraft is to cut the airfoil cores over a shorter length of foam. This year's airfoils have a slight sag in the leading edge due to the wire lagging as it passes through the center of the foam. Another improvement is to use honeycomb in the fuselage skin as opposed to foam. The thin cross section of foam was difficult to cut over the conical sections of the fuselage due to the slower section of the hot wire melting additional material.

Flight-testing would remain a very high priority in the next design and manufacturing process. Actual results from the flights would be compared to the dynamic test results and the analytical data to how the plane performs in the air. This would require faster design and manufacturing processes, but

cost will not be increased. Another area for improvement for the next design involves the battery charging methods. By changing the way that the batteries are initially charged the overall power output will be greater.

9 Aircraft Cost

The following pages are documentation of the rated aircraft cost for the OSU Orange team plane. First, Table 9-1 shows a complete account of the rated aircraft cost. Then, in Figure 9-1 there is a visual breakdown of the percentage contribution of each category to the total rated aircraft cost and another breakdown of each structure's contribution to the total number of manufacturing man hours.

Engine Power Empty Weight			
Actual Weight (lbs)	MEW Multiplier (\$/lb)		RAC
14 13.6	\$100.00		\$1,400.00
Rated Engine Power			
Number of engines	Fuse Rating	Number of cells	Voltage per cell
1	20	37	1.2
Rated Engine Power (watts)			888
Rated Engine Power Multiplier (\$/watt)			1
Total Rated Engine Power RAC Contribution			\$888.00
Manufacturing Cost			
Wing			
Unit	Quantity	Multiplier (hr/unit)	WBS Contribution
Wing	1	15	15
Projected Area	8	4	32
Strut or brace	0	2	0
Control Surface	2	3	6
Total Wing WBS Contribution (hrs)			53
Fuselage			
Unit	Quantity	Multiplier (hr/unit)	WBS Contribution
Body	1	5	5
Length (ft)	5.333	4	21.332
Total Fuselage WBS Contribution (hrs)			26.332
Empennage			
Unit	Quantity	Multiplier (hr/unit)	WBS Contribution
Basic	1	5	5
Vertical Surface	1	5	5
Horizontal Surface	1	10	10
Total Empennage WBS Contribution (hrs)			20
Flight Systems			
Unit	Quantity	Multiplier (hr/unit)	WBS Contribution
Basic	1	5	5
Servo or controller	5	2	10
Total Flight Systems WBS Contribution (hrs)			15
Propulsion Systems			
Unit	Quantity	Multiplier (hr/unit)	WBS Contribution
Engine	1	5	5
Propeller or fan	1	5	5
Total Propulsion Systems WBS Contribution (hrs)			10
Total Manufacturing Man Hours			124.332
Manufacturing Cost Multiplier (\$/hr)			20
Total Manufacturing Cost RAC Contribution			\$2,486.64

Table 9-1: Detailed breakdown of RAC

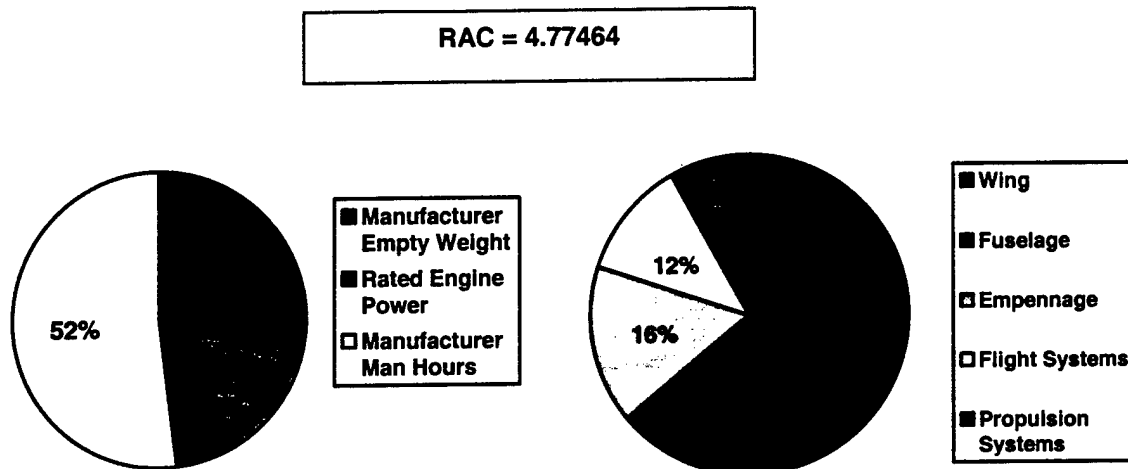


Figure 9-1: Visual Breakdown of Rated Aircraft Cost and Manufacturing Man Hours

Stealin' Balls
Design Report – Proposal Phase

2000/2001 Cessna/ONR/AIAA Student Design/Build/Fly Competition

Aeronautical Engineering Department

California Polytechnic State University, San Luis Obispo

Authors: John Asplund, James Bach, Jeremy Rocha, Francesco Gianinni

March 13, 2001

Table Of Contents

1.0 Executive Summary.....	3
2.0 Management Summary	5
3.0 Conceptual Design	7
3.1 Introduction.....	7
3.2 Design Parameters	7
3.3 Figures of Merit	8
3.4 Conclusions.....	9
4.0 Preliminary Design.....	11
4.0 Preliminary Design.....	12
4.1 Figures of Merit	12
4.2 Design Parameters Investigated.....	12
4.2.1 Mission Sizing	12
4.2.2 Battery Selection.....	13
4.2.3 Propulsion System	14
4.2.4 Wing Design	15
4.3 Analytical Methods.....	16
4.4 Features that produced the final configuration selection	17
5.0 Detailed Design	22
5.1 Takeoff Performance	22
5.2 Payload Fraction	22
5.3 Payload Configuration	22
5.4 Performance.....	23
5.5 Propulsion System	23
5.6 Landing Gear	23
5.7 Mass Properties.....	23
5.8 Stability and Control.....	24
5.8.1 Methods of Control.....	24
6.0 Manufacturing Plan.....	30
6.1 Design Drivers.....	30
6.1.1 Ease Of Construction	30
6.1.2 Cost.....	30
6.1.3 Weight.....	30
6.1.4 Tooling.....	31
6.1.5 Time.....	31
6.2 Manufacturing Processes	31
6.2.1 Wing	31
6.2.2 Fuselage	32
6.2.3 Tail Surfaces	32
6.2.4 Landing Gear	32
6.3 Analytical Methods.....	33
6.4 Manufacturing Timeline	33
References	36

1.0 Executive Summary

A team of students at Cal Poly San Luis Obispo has undertaken the task to design and build an airplane to participate in the Cessna/ONR Student Design/Build/Fly competition. The competition involves designing and building an electric powered, radio controlled airplane capable of flying tennis balls and steel around a designated course as many times as possible in a ten-minute time period. The payloads must be alternated between laps where a "Heavy Payload" lap is done with the steel and a "Light Payload" lap is done with the tennis balls. The maximum number of tennis balls that can be carried at once is 100. The score per lap for carrying tennis balls is 20 points where each tennis ball yields $1/5$ of a point. The steel laps are scored one point per pound of steel carried. A sortie is defined as one complete ten-minute time period. The final score is a result of the average of three sorties. The final score is calculated by multiplying the average from the best three laps times the report score, divided by the Rated Aircraft Cost (RAC) of the configuration. The RAC is calculated based on the geometry of the aircraft, the empty weight, and the motor power required to fly the aircraft.

A variety of constraints were placed on the design team by the contest officiators. Each of the design constraints received consideration during the entire design process. The major design constraints are the time limitation of 10 minutes, takeoff distance of 200 feet, max wingspan of 10 feet, 5-pounds of batteries, and internally housed payload. At the beginning of the conceptual design, the design team investigated several possible airplane configurations. The team rated each airplane configuration based on a number of criteria referred to as the figures of merit (FOM). The initial FOMs for the conceptual design phase were used to screen competing concepts based on the contest design constraints and limitations within the design team. After possible concepts had been narrowed down to four airplane configurations, a detailed score analysis for each configuration was done using a Visual Basic program. These designs were a conventional low wing monoplane, a biplane, a tandem wing, and a flying wing. The program started with a takeoff model to size the wing and propulsion system for a given payload and gross takeoff weight. The best cruise speed, time required to complete the course, and RAC were calculated to find the scoring potential of each design. The sizing program evolved and grew more refined throughout each phase of the design process. The competing designs were also quantitatively evaluated to determine the most viable concept. The design that maintained a high scoring potential with inherently good handling qualities was the low wing monoplane. The low wing offers the accessibility to the payload while providing direct load paths to the primary structure for both in-flight and landing loads. The design is predictable and simple, with opportunity for innovation with the aircraft structure and landing gear. This configuration was selected for the final design.

During the preliminary design phase, the configuration was optimized to achieve the highest score using more detailed analysis. Because aircraft design is highly assumption driven, it relies heavily on the

experience of the senior team members. The background of the team, and the enthusiasm for the project has contributed to the design and fabrication of a winning design. California Polytechnic State University, San Luis Obispo is proud to present Stealin' Balls, their 2000/2001 entry for the Cessna/ONR Student Design/Build/Fly Competition.

2.0 Management Summary

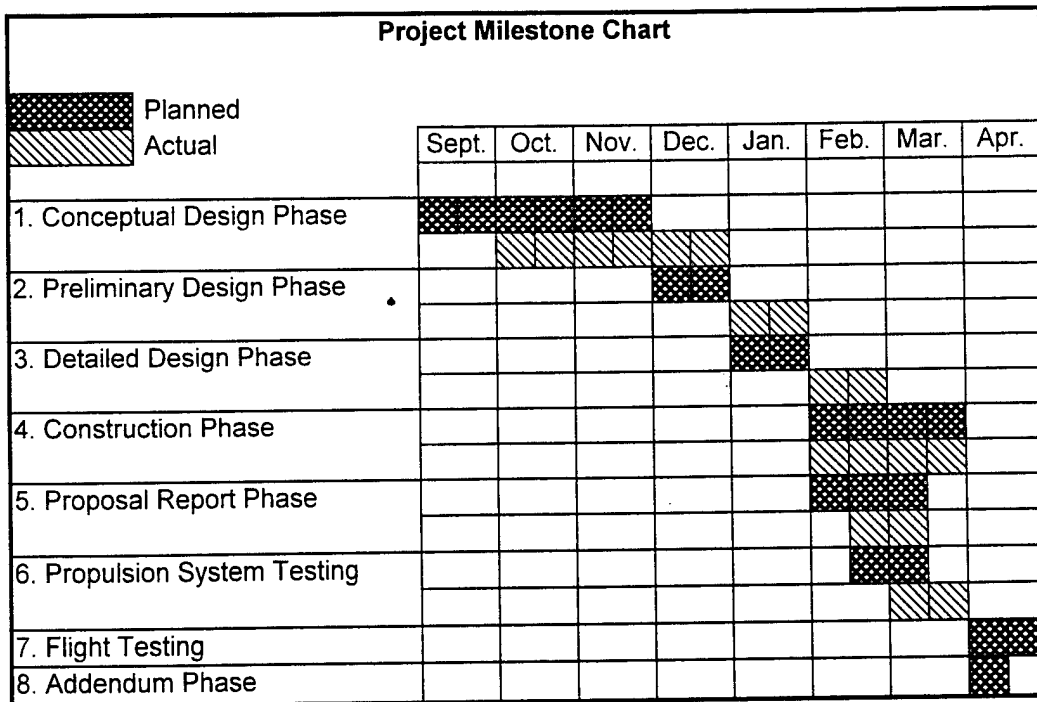
This years Cessna/ONR Student Design/Build/Fly (DBF) team at California Polytechnic State University (Cal Poly) is comprised of 20 students. The break down of the team is as follows:

- 2 graduate students
- 5 seniors
- 3 juniors
- 4 sophomores
- 4 freshmen

All but one of the students are Aeronautical engineering students. The other student is a mechanical engineering student. Initially, during the preliminary design phase, the group of students was divided up into several different design tasks. Younger students were paired with senior students to help teach them the design process. One group worked on the drag prediction and integrated it with the sizing routine in Excel. A second group worked on the performance including takeoff, landing and time prediction. The third group was responsible for propulsion and stability and control.

The two graduate students on the team, James Bach and John Asplund, have been involved in the DBF competition before. These two students orchestrated the design and construction of this year's airplane. The group leader, Jeremy Rocha, kept the team on schedule and motivated throughout the duration of the project. Jay Garcia, one of the junior team members, was responsible for fund raising and soliciting companies for materials. The less experienced members of the group participated in the design process while contributing to the report. The fabrication experience of the graduate students was used to train the underclassmen how to build using modern composite fabrication techniques. Passing the skills and knowledge down to the rest of the group is essential for the success of the future Cal Poly Design/Build/Fly teams. The milestones for the project are illustrated in Figure 2.1.

Figure 2.1 Project Milestones



3.0 Conceptual Design

3.1 Introduction

To determine the most viable configuration concept for the mission, several parameters were considered for comparison. Although there are many concepts that could complete the mission, the following four were chosen for comparison:

- Flying wing
- Monoplane
- Biplane
- Tandem wing

These concepts were evaluated based on the specific requirements of the mission to establish the best design.

3.2 Design Parameters

The design parameters used to screen competing designs include: payload capability, cost effectiveness, scoring potential, handling qualities, time, and take-off distance. The most useful analytical tool used throughout the conceptual design was a program written in Visual Basic simulating the entire flight.

To better understand the nature of the mission, a simple model that predicted the flight time required to complete the mission was written. With the ten-minute time limit, a first cut analysis showed that flying faster did not necessarily increase the total number of laps completed. Figure 3.1 illustrates the trend of cruise speed versus total time. Using conservative values for landing and reload, it was found that completing six laps was a reasonable goal considering the ten minute time limit. In addition, the total energy required to complete the mission increases as cruise speed is increased. Therefore it does not make sense to fly faster unless the aircraft is clearly capable of completing another lap. With six total laps as the performance goal, sizing of the competing configurations was performed to evaluate each design quantitatively.

The relaxed takeoff distance requirement does not drive the design as much as the other parameters. With the increased span limitation and a fixed amount of batteries, the takeoff requirement is not a parameter the design is exclusively optimized for like the previous years of competition.

The payload capability of each design directly drives the size and weight of the airplane. The rules state that payload must be carried internally and not within the wing. For this reason, a flying wing must be equipped with a large pod to enclose the payload. When considering the pod required to carry the payload, the benefits of the low RAC of the flying wing are overshadowed. To carry both the steel and

the tennis balls, the aircraft must have a large cargo bay that is easily accessible. The tandem wing, monoplane and biplane all have similar internal volumes to contain the payload.

The cost of each competing design is an important factor when the total score is considered. Since the score is divided by the cost, the most cost effective solution could provide the highest scoring aircraft. A tandem wing concept is a very inexpensive aircraft because essentially half of the wing area is considered a tail and charged accordingly. A concept with a shorter fuselage or a lower empty weight could also provide an inexpensive aircraft. These factors were all taken into consideration when comparing the concepts.

The scoring potential of each design was carefully investigated using fundamental design parameters specific for the mission. These include payload quantity, climb rate, and takeoff performance. The scoring potential for each concept was evaluated by keeping these parameters constant and running each concept through a mission simulation. The results are illustrated in Figure 3.2. The tandem wing is capable of scoring slightly higher, with the conventional configuration scoring just half of one point less. The flying wing was close as well, and the biplane had the lowest scoring potential. Just considering the scoring potential alone and building the highest scoring airplane is not the best method for winning the competition. Handling qualities and configuration risk are important considering a competition of this nature. Based on past experience, good handling configurations can increase the chances for success immensely. Therefore, concepts that have potential handling issues maintain less merit than the conventional configurations. The tandem wing is a high-risk concept because the flying characteristics are not as well known as conventional designs.

Initially, the optimal payload weight carried by the design was not well understood. However, after comparing the 50, 75, and 100 tennis ball configurations, the score was clearly maximized by the 100 ball design. In addition, because the aircrafts size was optimized to carry a specific payload weight, the optimal steel payload weight was equal to the tennis ball weight. All configurations were sized accordingly.

3.3 Figures of Merit

To find the optimal design it is important to take into consideration all of the elements the competition presents. The factors considered when determining the best concept for the mission are listed below:

- Empty weight
- Score
- Handling

- Risk
- Energy consumption

These parameters are known as Figures of Merit (FOM). The competing concepts are put into a matrix to weigh the advantages and disadvantages of each. The rating for each FOM goes from A through F with A representing the highest rating and F representing the lowest rating. The FOMs are listed with the most important at the top descending to the least important. Refer to Table 3.1 for the concept evaluation.

3.4 Conclusions

There are many different configurations that can adequately perform the mission. However, the four concepts evaluated showed that the low wing monoplane was the best compromise when considering the entire mission. The monoplane is very predictable to build and fly, and can achieve a very high score. The energy consumption of a monoplane is higher than the flying wing but overall the design is optimal for the entire mission. In addition, the performance prediction for the aircraft is greatly simplified by using a standard configuration. The flying characteristics are very predictable for the monoplane so the risk involved is very low.

Figure 3.1 Lap Potential

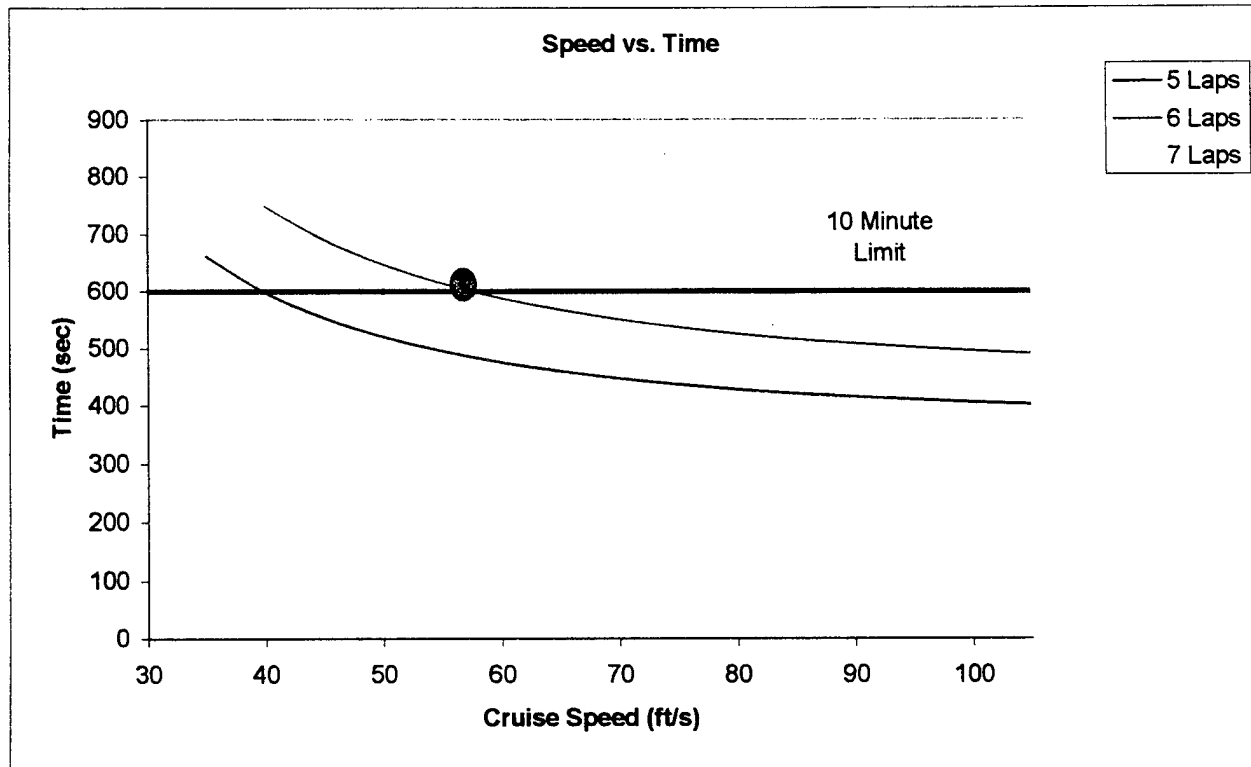


Figure 3.2 Concept Trade Study

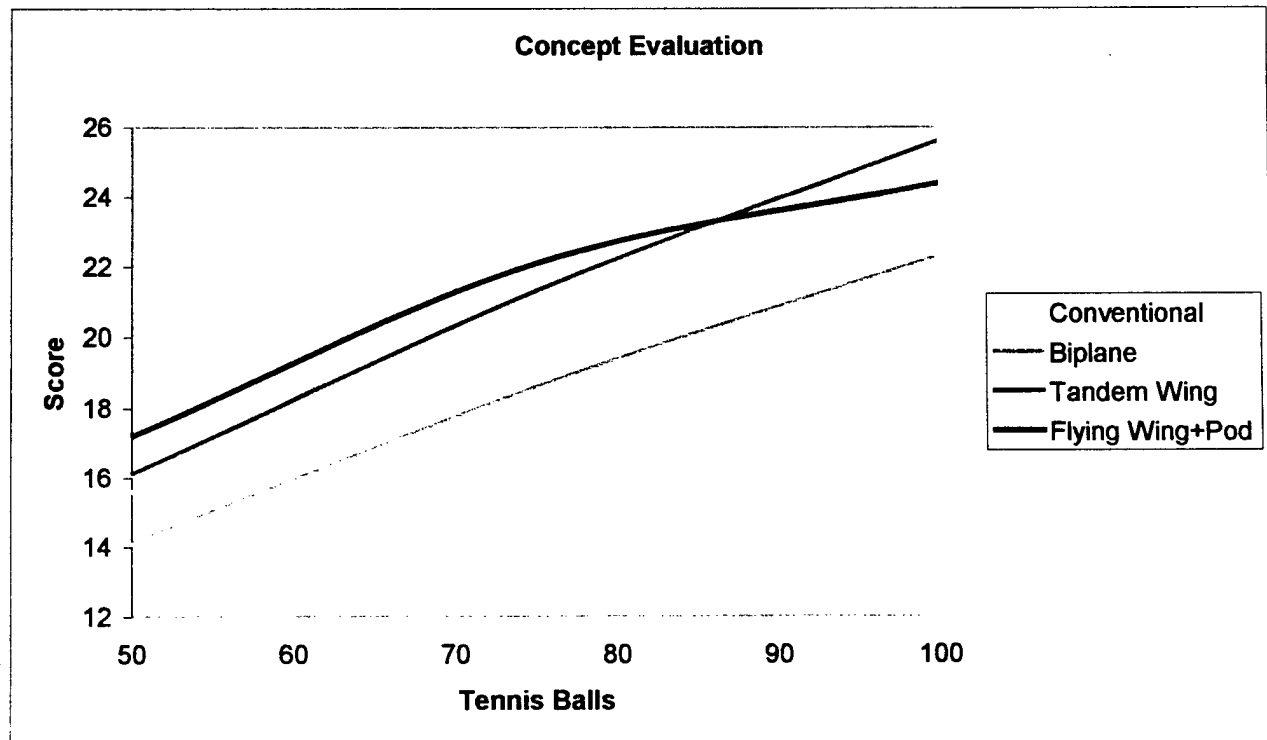


Table 3.1 Figures Of Merit

FOM/Concept	Tandem Wing	Biplane	Monoplane	Flying Wing
Empty Weight	C	D	B	A
Score	A	D	B	C
Handling	C	A	A	B
Risk	D	B	A	D
Energy	C	C	B	A

4.0 Preliminary Design

4.1 Figures of Merit

All preliminary design work was evaluated based on the following figures of merit:

- Impact on Maximum Score
- Handling / Easy to Fly
- Availability of Components/ Materials

Continually referring to these figures allowed each team member to make decisions that were best for the entire system. By understanding the sensitivity of each design parameter to the figures of merit, the team could focus their efforts optimizing the parameters that directly drove the design.

4.2 Design Parameters Investigated

The following areas of the design were investigated in detail because they had great impact on both the rated aircraft cost and the aircraft's ability to meet performance requirements:

- Mission Sizing
- Battery Selection
- Propulsion System Selection
- Wing Design

4.2.1 Mission Sizing

During preliminary design, it was determined that an aircraft sized for carrying the maximum 100 tennis balls with equal weight of steel would score the highest. This aircraft would be capable of completing six sorties within the ten minute mission time. It was also found that a conventional mono-wing configuration would be very cost competitive while minimizing the risk associated with exotic configurations. After this was determined, it was necessary to study the effect of wing aspect ratio, wing loading, and maximum lift coefficient on various aspects of performance including final score. This analysis was accomplished by tying together all the various tools for analyzing the design including models for propulsion system, aerodynamics, weight estimation, takeoff performance, cost, and tail sizing into a mission simulation program. The simulation flew the candidate aircraft through the mission to determine energy usage, time required and also checked key performance requirements. Different design parameters could be varied allowing their impact on the design to be understood.

Figure 4.1 shows the results of varying wing loading and aspect ratio on energy usage and final score for a 100 tennis ball, six sortie, monoplane configuration. Each configuration was sized with enough batteries to complete six sorties. A 10ft/sec minimum climb rate was imposed at gross weight on all the designs based on input from the pilot. If a design could not meet this requirement, a larger motor and or larger battery pack was substituted and the design was re-sized. Depending on the design, propulsion

makes up 15-40% of the aircraft cost. Because propulsion system cost was directly rated to maximum power, designs that had more the 15ft/sec climb rate at gross weight generally were not very competitive due to high cost. These designs were reconfigured to allow acceptable climb rate with a more competitive cost. At high wing loadings, sizing for a fixed climb rate caused the aircraft to be incapable of meeting the 200ft takeoff requirement.

The results indicate that below aspect ratios of 8, the aircraft required more than the maximum battery weight of five pounds to complete 6 laps. Even though the empty weight of these aircraft was comparatively low, the poor cruise and turn efficiency make the designs incapable of completing the mission. Higher aspect ratio wings enable the aircraft to complete the mission with less than five pounds of Nickel Cadmium batteries (NiCds) at the expense of higher empty weight due to higher structural weight. Up to the span limit of ten feet, the trade between aspect ratio and final score was very soft. Additionally, input from the pilot suggested that he would prefer to fly a lower aspect ratio aircraft because of handling and it's lower sensitivity to gusts.

The design showed fairly high sensitivity to wing loading. For fixed climb rate, lowering wing loading caused the design to move further away from the zero wind takeoff constraint but also reduced maximum score. Wing loading did not heavily drive the mission energy usage for the aircraft. The final tradeoff for wing loading was between pushing the takeoff distance and pilot familiarity with "hot" airplanes versus achieving the highest possible score.

The final design configuration was chosen after carefully considering these factors with a wing aspect ratio of ten, and a maximum wing loading of 57oz/ft².

4.2.2 Battery Selection

The propulsion system must be powered by a NiCd battery pack no more than 80 oz in weight as described in the contest rules. Many different types and sizes of NiCd batteries were available. Essentially, by limiting the weight of the battery, the total energy available for propulsion is limited. Depending on the characteristics and type of NiCd cell used, it also limits the maximum power. Research on the characteristics of NiCd cells was conducted to choose the best battery to fulfill both the aircraft's energy and maximum power requirements. The voltage and maximum current capabilities of the available motors were also considered during the search.

Two styles of NiCd cells were investigated in detail, the high capacity Sanyo KR series, and the NiCd cells typically used for electric powered R/C models, the fast charge Sanyo R series. Table 4.1 shows the characteristics of each cell type.

The fast charge cells are designed to handle high maximum currents and therefore are well suited for typical electric aircraft motors. The specific power density of these cells is on the order of 25 Watts/oz. These cells have a specific energy density of approximately 1.2 Watt-Hours/oz. The Sanyo RC-2400 sub-C cell has the highest energy density and excellent power density compared to all of the fast charge cells.

The high capacity KR cells were considered because of their higher energy density (1.6 Watt-hours/oz). The compromises in the cell design which gave it high capacity also hurts the cell's internal resistance and their maximum discharge rate. Because of this, the power density is only half that of the fast charge cells, approximately 11 Watts/oz. Unfortunately, most of the design concepts required over 1000 Watts peak power to meet the minimum climb requirement, rendering the high capacity cells unsuitable. Additionally, NiCd cells delivering power at their maximum rate are not operating efficiently which significantly reduces their delivered energy. Most electric motors available for powering a 25 lb aircraft require 20-50 Volts input instead of the near 100 Volts that a series pack of high capacity cells would be. A combination parallel-series pack was considered to reduce the voltage and increase the current capabilities, but the difficulties in charging and maintaining balance between the cells eliminated this idea.

The final NiCd cells chosen for the design were the Sanyo RC-2400 cells because of their availability, performance, and the team member's familiarity with the cell.

4.2.3 Propulsion System

After initial sizing, it was determined that the aircraft needed a propulsion system able to run on approximately 28-34 NiCd cells, and be capable of handling 900-1200 Watts for takeoff and climb performance. Both single motor and twin motor configurations were considered. It was determined universally that for a given power requirement, the single motor solutions outperformed the twins in final score. This was caused by the additional cost of having more than one motor and speed controller, because for a given power level, two smaller motors, gearboxes and propellers weigh more than a single large motor. In addition, larger motors generally have higher efficiency.

To evaluate the performance of the motors available for the aircraft, a Visual Basic subroutine modeling electric motors was written. This model uses motor parameters including Kv (RPM/V), idle current, armature resistance, RPM and thermal limits to calculate output power and efficiency for DC motors. This program was used in conjunction with a propeller model and the mission simulation to compare the various motors offered by Astro Flight and Graupner.

Performance, reliability and availability were considered in selecting the motor. In the United States, the larger Graupner Ultra motors are not very popular nor are they regularly stocked by hobby vendors. The

team members were also very familiar with the Astro product line and felt confident in their reliability. Although the Ultra motors significantly outperformed the equivalent Astro Flight motors, the lack of availability and absence of suitable gearboxes for the Graupner's caused the team to consider only Astro Flight products.

The power requirements for the design fell between two motors in the Astro product line, the Cobalt 40 and the Cobalt 60. Table 4.2 shows the four Astro Flight motors seriously considered for the aircraft. The performance model showed that the electrical efficiency of both these motors were comparable. Although the 60 is capable of running reliably at 1600 Watts input power, the motor is over half a pound heavier than the 40. The 40 is normally rated at 700 Watts input power, but after careful bench testing, it was found to be capable of running at higher voltages allowing it to be run at 1200 Watts for short periods. The mission profile calls for short periods at full power for takeoff and climb followed by extended cruise periods well within the normal power limits for the 40. The disadvantage of running the motor at such high power levels is premature erosion of the brushes and commutator. For a limited use contest aircraft, this was deemed an acceptable compromise. The team decided to use the Astro 40 8T with 3.1:1 gear reduction over the Astro 60 because of the significant reduction in empty weight and improved scoring potential.

The propeller performance model indicated propellers 14 to 15 inches in diameter with 12 to 14 inches of pitch would load the selected motor to the required 1175 Watts. The relatively high pitch of the propeller was chosen because of the aircraft's high cruise speed (60ft/sec). This pitch was a compromise between the advance ratio required for efficient cruise, and thrust required for takeoff and climb performance. Because of variation in efficiency and power absorption between different propeller manufacturers, the propeller model was calibrated using data gathered from the motor manufacturer and with testing performed with an Astro 40. Final propeller selection will occur during flight testing.

Early motor bench testing conducted with fuses indicated that all fuses failed at significantly higher current levels than their rated value. This was especially noted when the fuse was mounted within the propeller slip stream. Because the propulsion system cost is directly related to the current rating of the fuse, it will be possible to safely increase final score by choosing a slightly lower current fuse for use in the airplane.

4.2.4 Wing Design

Early in the design phase, it was recognized that the cost of the wing represented 20-40% of the total cost of the airplane. Wing cost was largely dependent on wing area, so in order to reduce cost as much as possible, the wing was designed to operate efficiently at high lift coefficients. This was a function mainly of the airfoil selected for the design. The wing plan form was also considered in the

design because of its impact on handling, aerodynamic efficiency, and the maximum lift achievable given a constant wing area.

Several airfoils were compared using X-foil, an airfoil design tool. The design Reynolds number for takeoff was 200,000 while the cruise condition was $Re(CL)^{0.5} = 250,000$. Figures 4.2 and 4.3 show the four airfoils considered for the design. Each of the airfoils shared similar physical characteristics, thickness ratios above 10% and camber above 3.6%. Maximum lift coefficient, drag at cruise (CL 0.8-1.2), usable CL range, and behavior near stall were considered. Of these requirements, the wing section drag impacted the maximum score the least. This was because the viscous drag was dominated by the contributions of the large fuselage and landing gear. The JA13 airfoil showed the best compromise between these factors and was chosen for the design. Figure 4.4 shows the airfoil with its characteristics.

The impact on score from wing plan form was also investigated in attempt to understand sensitivity. Constant chord, single taper, and multi-taper wings were evaluated. It was found that a constant chord, zero twist wing of aspect ratio 10 was only capable of achieving 88% of the lift of an elliptically distributed chord wing's maximum lift, before the root stalled. However, this ensures safe stall characteristics compared to the elliptical chord distribution. A compromise plan form was chosen which was capable of 95% the maximum lift to ensure reasonable handling. The expected lift distribution is shown in Figure 4.5.

4.3 Analytical Methods

Many of the tools used in the design process were created by the team members using Visual Basic or in Microsoft Excel. Nearly all the programs were written some time before work on the 00/01 Design/Build/Fly aircraft began and have been already well tested and validated. These programs include an electric motor/ propeller model, an aerodynamic model, a weight estimation spreadsheet, a longitudinal static stability model, takeoff and climb simulation, and a lift distribution spreadsheet. These tools were incorporated into a 00/01 DBF mission simulation model which included a cost model. To check validity, aircraft with known performance from the 99/00 competition were also run through the simulation successfully.

The only tool not developed by the team members was X-foil, written by Mark Drela. After learning to use X-foil, results from low Reynolds number wind tunnel testing performed at University Illinois Urbana Champaign were compared with data produced by X-foil. At the relatively high Reynolds numbers that this aircraft will fly at, the correlation between test data and predicted performance was excellent.

4.4 Features that produced the final configuration selection

During the design process, care was taken to identify the important aspects of the mission. By understanding the sensitivity of each design parameter, the team could focus their design efforts on the areas which would produce the highest scoring aircraft. Guided with experience and careful modeling of the system, the following features of the aircraft were found to be critical for attaining the highest score and were incorporated in the team's design. They are listed in order of importance.

- Low Empty Weight
- 100 Tennis Balls/ Equivalent Weight Steel Payload
- Conventional Design/ Conventional Handling
- Six Laps
- Aircraft Appropriately Sized for Mission
- Minimize Wing Area
- High Lift Airfoil

Because of these features, the Cal Poly 00/01 Design Build Fly should perform very well at the competition in April.

Figure 4.1 Mission Sizing

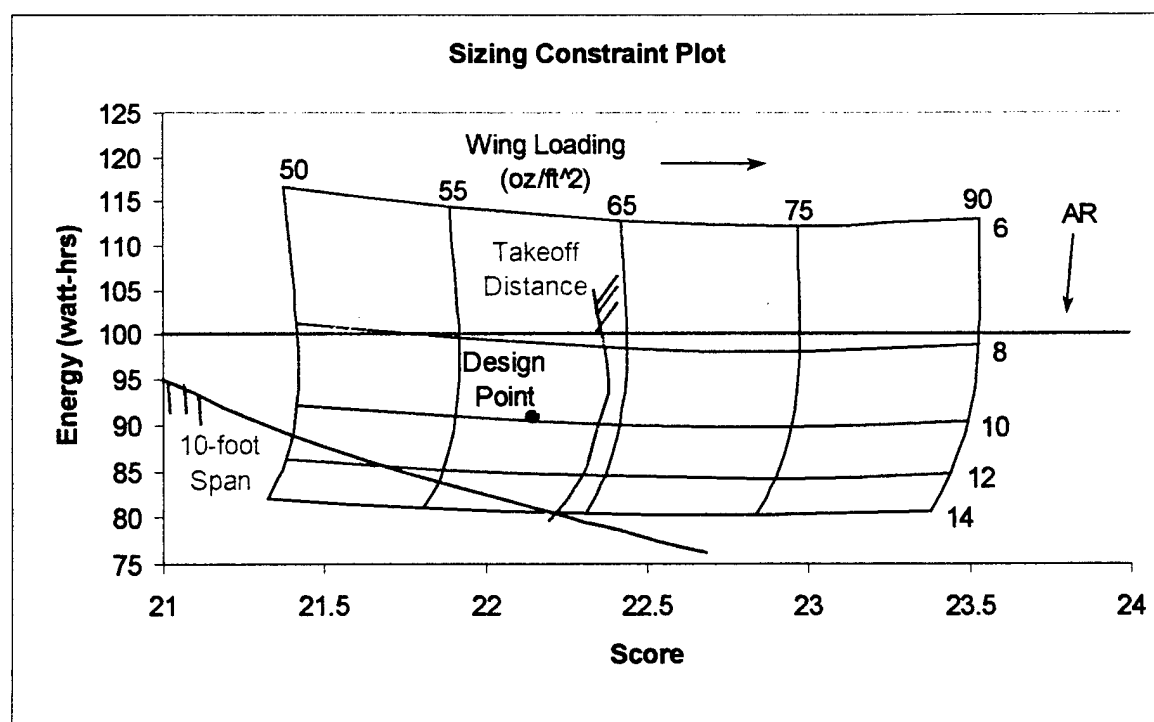


Table 4.1 Battery Pack Trade

NiCd Cell	mAh	Weight (oz)	Package	Cells in 80oz Pack	mOhm /cell	Pack Voltage	Amps @ 1.0V/cell	Pack Max Watts	Pack Watt-hr
KR-1100AAU	1100	0.85	AA	94	20	113	10	941	124
KR-1500AUL	1500	1.09	4/5A	73	16	88	13	917	132
KR-1700AU	1700	1.25	A	64	14	77	14	914	131
N-1250SCR	1250	1.50	4/5sub C	53	4.5	64	44	2370	80
RC-2000	2000	2.00	sub C	40	3.8	48	53	2105	96
RC-2400	2400	2.15	sub C	37	3.6	44	56	2067	107
N-3000CR	3000	3.00	C	27	3.3	31	61	1616	96

Table 4.2 – Motor Selection

Motor	Weight (oz)	Gear Ratio	Propeller	Cells (RC2400)	Power In (Watts)	Max Efficiency	Cruise Efficiency
Astro 40 8T	14	3.1	15x12	30	1175	81%	77%
Astro 40 10T	14	2.75	18x18	32	1225	80%	78%
Astro 60 11T	22.5	2.75	20x18	32	1300	82%	76%
Astro 60 7T	22.5	2.75	14x10	30	1300	84%	69%

Figure 4.2 Airfoil Comparison

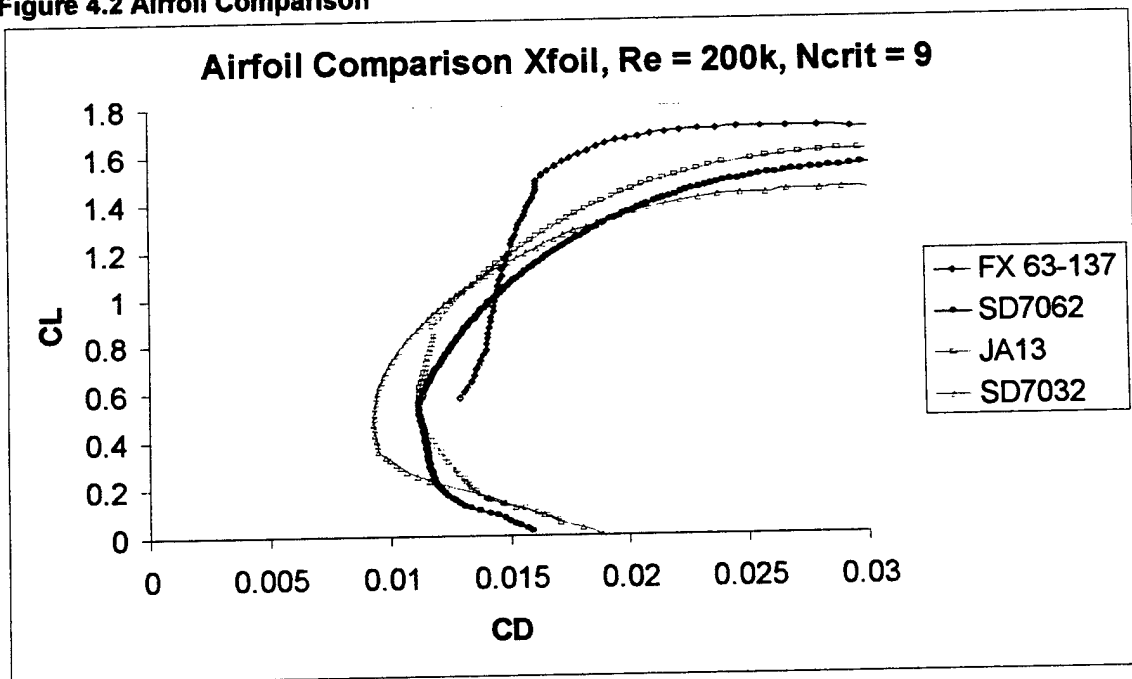


Figure 4.3 Airfoil Comparison

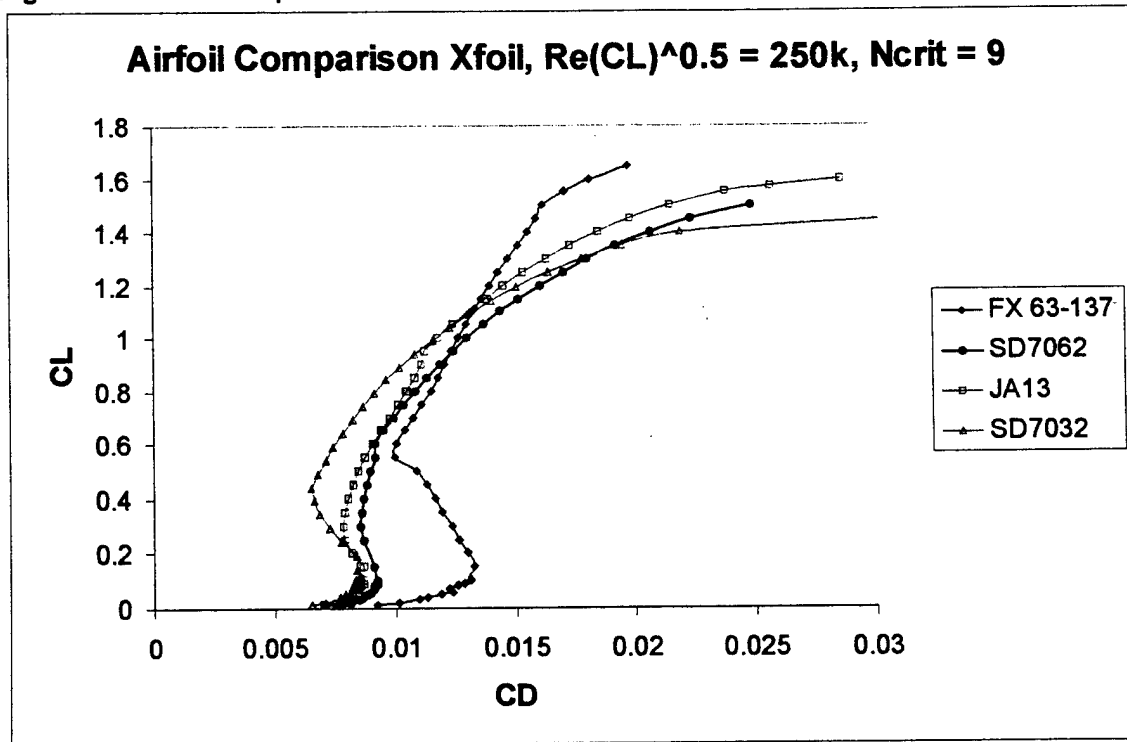


Figure 4.4 JA13 Airfoil

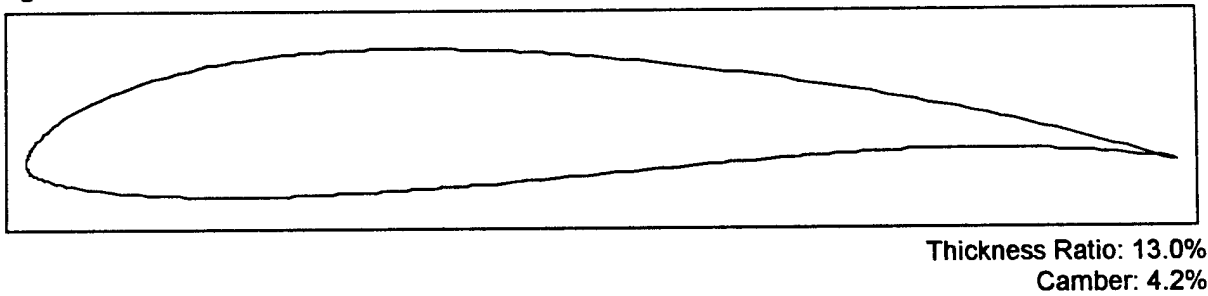
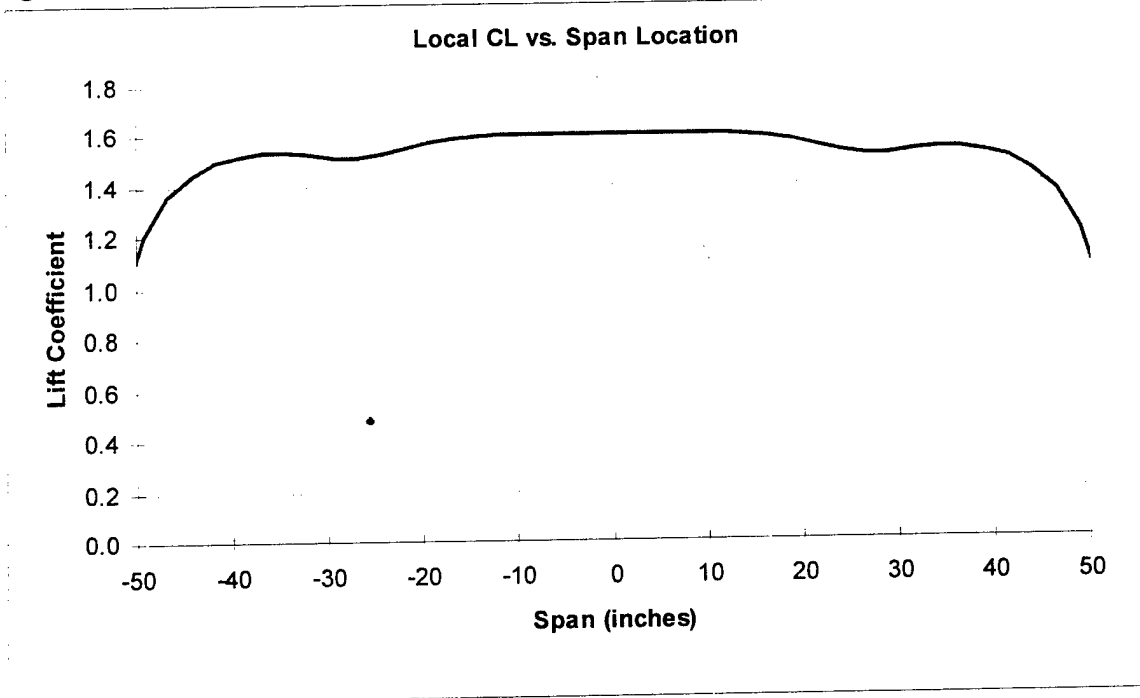


Figure 4.5 Wing Lift Distribution



5.0 Detailed Design

The three-view layout is illustrated at the end of the detailed design section. The payload carrier is sectioned with the fuselage in the side view to display loading and structural detail.

5.1 Takeoff Performance

The final configuration's takeoff performance is listed in Table 5.1. These distances were calculated with a time based simulation using the equations of motion. The program incorporates a simple propulsion, aerodynamics and rolling resistance model to calculate the forces on the aircraft. This model was developed two years ago for the 98/99 DBF contest and has been validated over the past two years of competition.

Based on past team experience, it was decided to size the aircraft for comfortable takeoff margin with zero head wind. Too many teams in the past have wasted competitive scoring sorties because of missing the takeoff distance during the competition.

5.2 Payload Fraction

The final configuration's mass properties are listing in Table 5.2. The payload fraction for the design is nearly 50%. Careful structural design, the use of composites, and experienced builders allow the airplane to be very lightweight. •The final scoring potential is heavily driven by manufacturers empty weight. Not only does it drive the aircraft sizing for performance, it makes up nearly one-third of the cost. Based on the type of construction seen on competing schools aircraft over the past few years of the contest, this aircraft should have a significant advantage because of it's lightweight and innovative structural design.

5.3 Payload Configuration

Several different packing configurations for 100 tennis balls were considered. The final configuration needed to cleanly fit within the fuselage of a conventional, low wing airplane. The stacking orientation that suited the design the best was consecutive rows of six balls arranged in a "six shooter" shape. The seventh ball of each row would be offset in between rows in the center of the "six shooter". This packing arrangement fits all 100 tennis balls with a 8.3 inch diameter cylinder, 40 inches in length.

For quick loading and unloading during a sortie, the tennis balls are carried within a "speed loader". The speed loader is constructed using thin transparent mylar wrapped into a cylindrical shape. The alternate payload, steel bars, which is a much higher density payload, easily fits within the cargo area designed for the tennis balls.

5.4 Performance

The drag model used for the design work calculates the viscous drag of each airframe component based on Reynolds number, shape, and area. For the wing and tail, airfoil drag polars generated in X-foil were used with a table lookup arrangement to estimate viscous drag. Induced drag was calculated using conventional methods. Because the team had no way to verify the drag estimates during the design phase, very conservative numbers were used. This decision was made to ensure that the airplane would have at least the expected performance, if not better than anticipated. Figure 5.1 shows the expected aerodynamic performance of the final configuration. Figure 5.2 shows the climb performance for the final configuration. The aircraft has an acceptable climb rate at gross weight of 15ft/sec.

During sizing, the available energy stored within the NiCd pack was estimated conservatively to allow some margin of error in performance estimation and for safety while flying the mission. It was assumed that the batteries would only deliver 85% of their rated capacity. This gave the 32 cell pack of RC2400 NiCds an energy storage of 80 Watt-hours. Table 5.3 shows the expected energy usage while flying the mission.

5.5 Propulsion System

The propulsion configuration for the design is a single nose mounted brushed DC electric motor. The motor chosen for the design is the Astro 40 8Turn Geared Cobalt motor with 3.1:1 spur gear reduction. Electrical power for the system is provided by 32 Sanyo RC-2400 Nickel Cadmium batteries assembled in series. The motor is throttled with an Astro Flight 204D electronic speed controller. The motor turns a 15-inch diameter by 12-inch pitch two bladed propeller at 7000 RPM. As part of the aircraft cost rules, a fuse must be placed within the motor system to determine the current capabilities of the motor. The expected full throttle input voltage for the motor is 35 Volts with a corresponding current of 35 Amps.

5.6 Landing Gear

The landing gear configuration is a tricycle design. The team manufactured a carbon fiber pre-preg main gear that attaches to the bottom of the wing. The steerable nose gear is a Robart RoboStrut 500 lightweight strut. The gear will use standard heavy duty R/C airplane rubber tires. Provisions are being made to fabricate a main wheel braking system if during flight testing, brakes are deemed necessary.

5.7 Mass Properties

A firm understanding of the location of the center of gravity (cg) is crucial for a good-handling airplane. The design allows for flexibility of component locations if initial weight estimates are not as

predicted. Refer to Table 5.4 for a weight and balance table. The moments are all calculated from a datum plane one inch in front of the nose. The location of the cg corresponds to 35 percent of the mean aerodynamic chord (MAC).

5.8 Stability and Control

A good-handling airplane can greatly increase the chances for success in a competition of this nature. The emphasis on handling qualities is evident throughout the entire design process. One key performance trade off is obvious in the plan form of the wing. An elliptical lift distribution is optimal for generating lift efficiently. However, the trade-off is a decrease in overall stall characteristics. The plan form is tailored to get near elliptical lift distribution without sacrificing the handling qualities during stall.

The only penalty for a slightly oversized tail was an increase in structural weight and a minor increase in drag. For this reason, the vertical and horizontal tails were sized with generous tail volumes. The tail volumes are 1.25 and .075 for the horizontal and vertical respectively. The large horizontal tail allowed for a wide range of flyable CG locations while providing excellent pitch damping characteristics. The vertical tail provides control power in a strong crosswind. The large vertical also assists stall characteristics during gusty conditions by minimizing yaw excursions. Good ground handling qualities are key in minimizing time on the ground from touchdown to take-off. The conditions at Webster field are often unpredictable, so the chances of landing in a crosswind are high. Tail draggers classically have difficulty tracking straight without a lot of pilot skill. For this reason, the tricycle gear configuration is the best choice for a good-handling airplane.

The payload and batteries drive the location of the cg heavily. For this reason, the payload and the batteries are located on the cg. The size of the tail allows the cg to move while maintaining adequate control power and stability. The cg is located at 35 percent of the MAC to provide a design static margin of 10 percent. The lower than normal design static margin is a result of pilot preference.

5.8.1 Methods of Control

The aircraft is controlled in roll by deflecting the ailerons differentially to avoid adverse yaw. Dihedral provides spiral mode stability at the cost of poor crosswind performance. For this reason, the aircraft has no dihedral. The roll however is coupled to yaw by mixing the two controls electronically with the radio. The rudder provides yaw control and pitch is controlled by the elevator. Each control surface has one servo, refer to Figure 5.5 for the layout. The nose wheel is controlled by one servo that is electronically mixed to the rudder stick.

Three view and Payload Layout

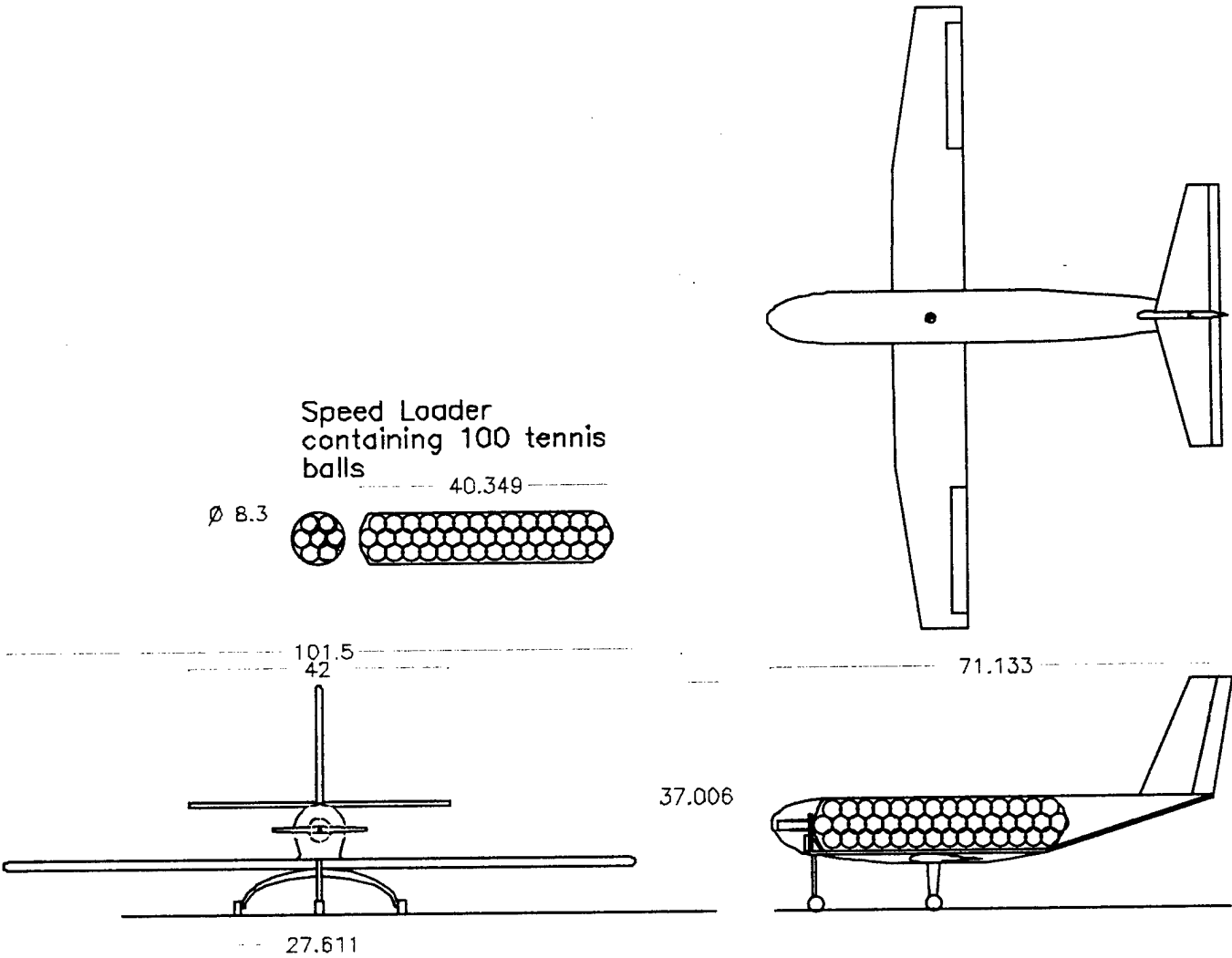


Table 5.1 Takeoff Distance

<i>Head Wind (mph)</i>	<i>Ground Roll (ft)</i>
0	160
5	130
10	90
15	40

Table 5.2 Weight Breakdown

<i>Component</i>	<i>Weight (lb)</i>	<i>Mass Fraction</i>
Wing	2.09	8.0%
Tails	1.17	4.5%
Fuselage	2.15	8.3%
Landing Gear	0.96	3.7%
Motor Sys	1.36	5.2%
Batteries	4.32	16.6%
Radio gear	0.98	3.8%
Empty Weight	13.03	50.1%
Payload	13.00	49.9%
Gross Weight	26.03	

Table 5.3 Flight endurance

<i>Steel Lap</i>	<i>Time (seconds)</i>	<i>Energy (Watt-Hr)</i>
Takeoff	7	2.7
Climb	9	3.5
Turns	17	4.3
Downwind	11	1.5
Landing	12	0.3
Lap Total	56	12.4
<i>Tennis Ball Laps</i>		
Takeoff	7	
Climb	9	3.6
Turns	17	4.3
Straight Legs	25	3.3
Landing	12	0.3
Lap Total	69	14.2
<i>Six Lap Total</i>	375	80.0

Figure 5.1 Aerodynamic Performance

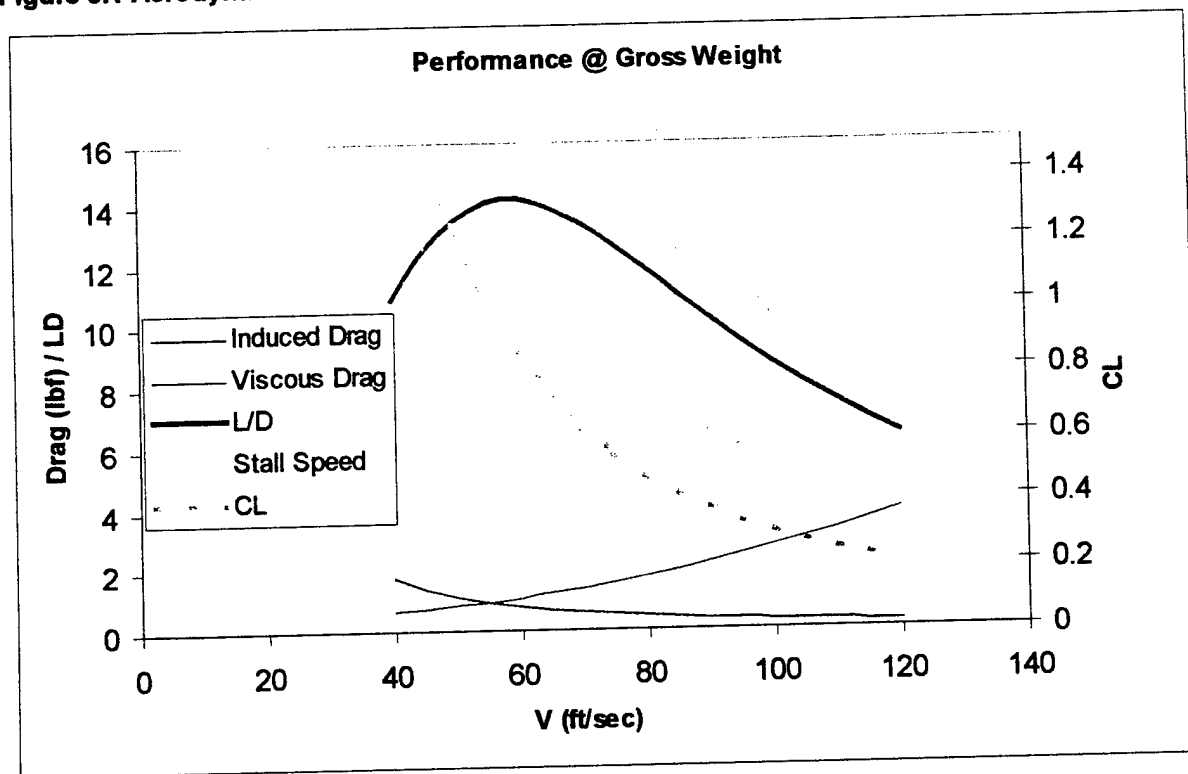


Figure 5.2 Climb Performance

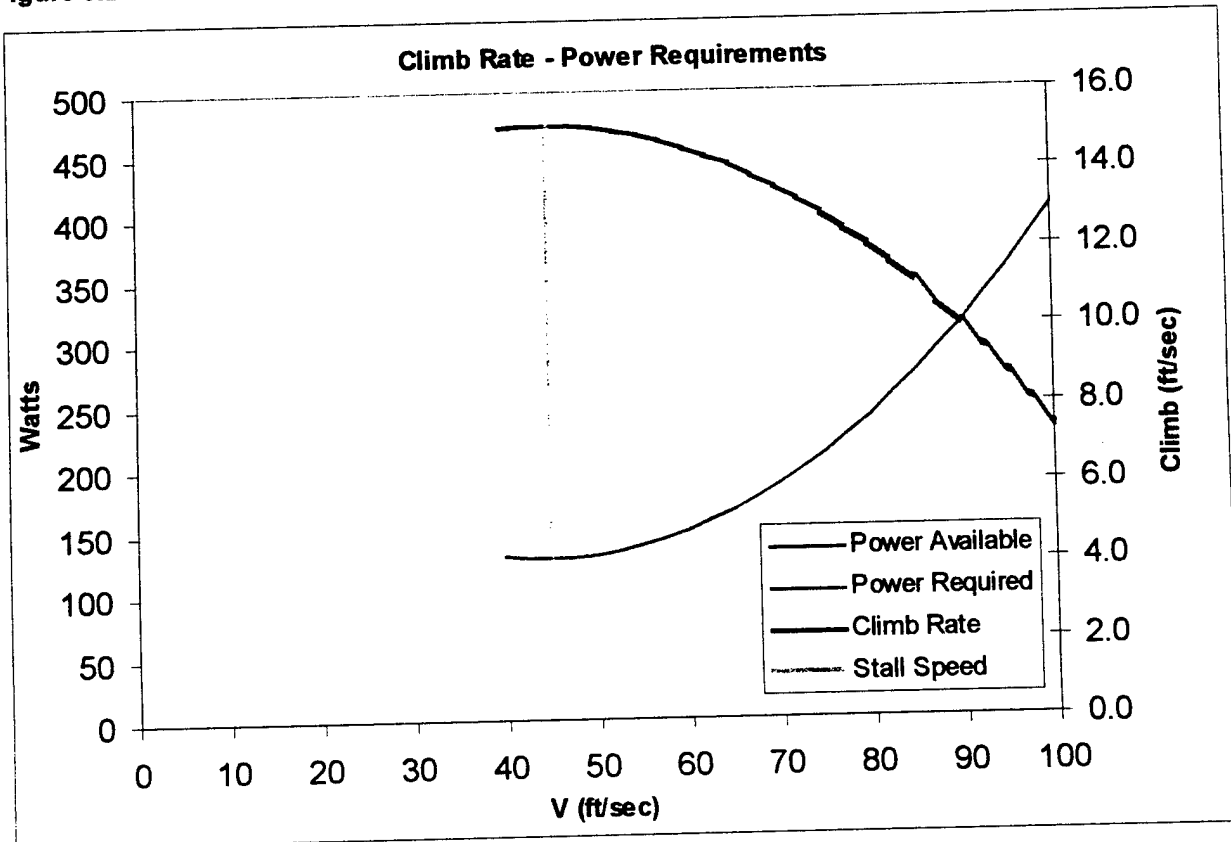


Figure 5.3 Systems Layout

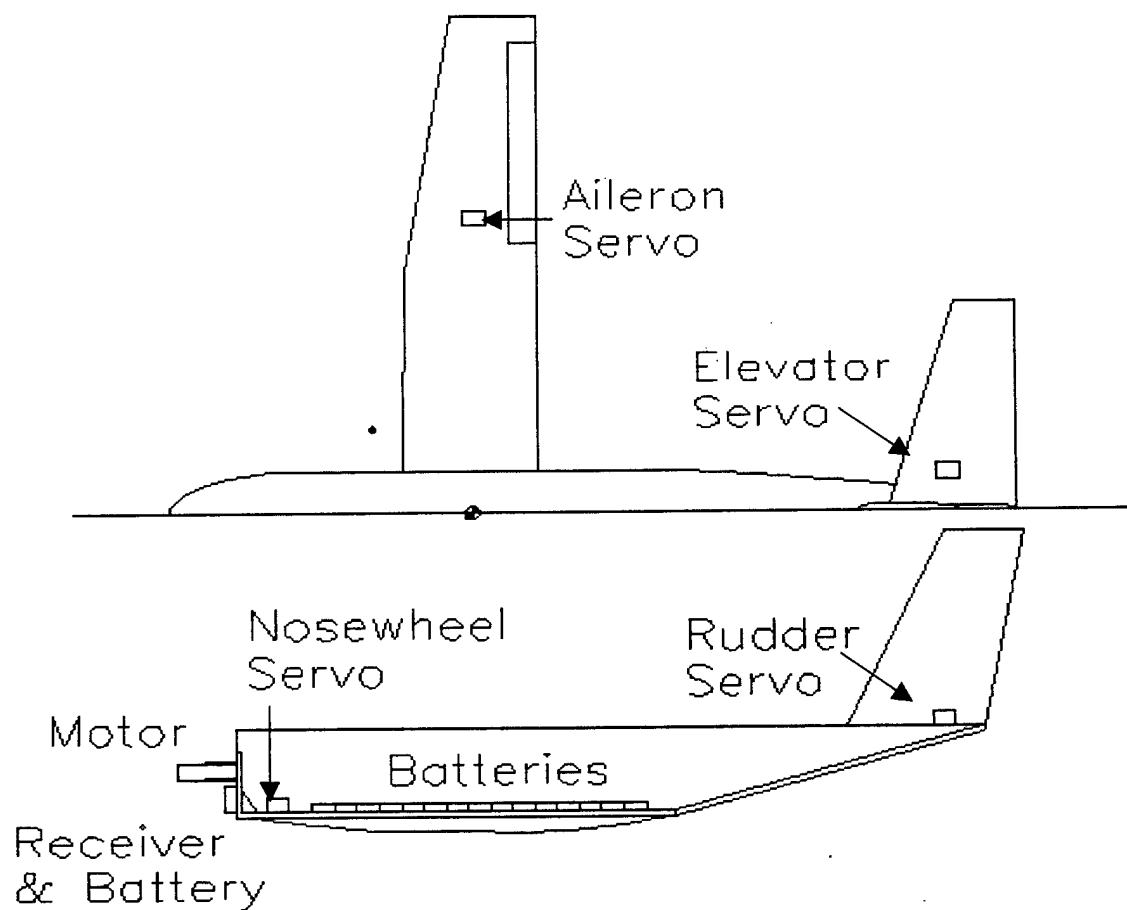


Table 5.4 Weight and Balance

Component	weight (oz)	arm (in)	Moment (in-oz)
Main Gear	10	28	280
Nose Gear	5	8.7	43.5
Horizontal Tail	13	68	884
Vertical Tail	7	68	476
Wing	33.5	28	938
Batteries	69	27	1863
Fuse	34	30	1020
Motor+Controller+Propeller	22	5.2	114.4
Radio Gear	15.5	9	139.5
Payload	208	28.2	5865.6
Totals	417		11624
CG Location	27.9		

6.0 Manufacturing Plan

6.1 Design Drivers

The figures of merit (FOM) driving the manufacturing of the aircraft include: ease of construction, durability, weight of materials, tooling, time, and availability of materials. The value of each FOM is illustrated in Table 6.1. The main goal of the manufacturing was to make the lightest possible structure to decrease the empty weight cost of the aircraft.

6.1.1 Ease Of Construction

The ease of construction was a driving FOM throughout the design. With experienced model builders on the team, there were many designs that could easily be discarded due to obvious construction complications. Experience in this area was what made the final design a feasible aircraft to manufacture. The entire aircraft took advantage of the simple manufacturing processes it was designed for. The fuselage is a simple foam core with a carbon keel and a Kevlar skin. The wing was hot-wired from Dow blue foam (density 1.8 lb/ft³) and vacuum bagged using a carbon spar cap and a Kevlar skin as the primary structure for bending and torsion loads. Similarly, the horizontal and vertical tails are made from Dow foam with a carbon spar cap and Kevlar skin. The aircraft easily lends itself to post-design modifications due to the simplicity of the entire manufacturing process. In addition with a foam core structure, the aircraft is very durable.

6.1.2 Cost

There were two aspects of cost considered throughout the design and manufacturing of the aircraft: monetary value of the materials used and the Rated Aircraft Cost (RAC) stated in the rules. The cost of materials was a concern due to the minimal budget the team had to work with. The high-end materials such as carbon, Kevlar, and Rohacell were the most expensive part of the empty weight of the airplane. The systems including batteries, motor, controller and receiver were all very expensive items that were essential to the success of the aircraft as well. Overall very few compromises had to be made to stay within budget due to generous donations from Northrop Grumman and Lockheed Martin Skunk Works.

The RAC drove the design and manufacturing trades throughout all phases of the design process. The most effective way to build an inexpensive aircraft was to make it very light. All of the main structure was optimized for minimal weight to keep the RAC of the aircraft low.

6.1.3 Weight

Careful consideration for weight was taken while choosing the materials and methods for construction. The design takes advantage of hybrid materials that provide astounding strength to weight ratios. Carbon fiber is very strong, light and workable. The total empty weight of the aircraft needed to

be kept to a minimum in order to maximize the payload fraction and keep the RAC down. Experience was definitely a factor in efficiently strengthening the heavily loaded areas of the aircraft.

6.1.4 Tooling

Various molding methods for manufacturing the aircraft were briefly considered, however, the time spent designing and constructing a mold for the wing and fuselage was better spent building the airplane. However, the landing gear was constructed using a male mold and pulling a female part due to the simple geometry. The entire landing gear construction process only represents a small fraction of the total work done on the aircraft.

6.1.5 Time

Manufacturing time was a driving factor throughout the entire design process. Cal Poly's participation in the Design/Build/Fly competition is extracurricular, so all the work had to be done during the team's spare time. The time allotted provided for very little experimentation with different construction techniques. The team decided to use the construction methods they were familiar with. The decision was made early to also simplify the construction of the aircraft. In so doing, many potential problems were completely avoided.

6.2 Manufacturing Processes

6.2.1 Wing

A molded wing was immediately rejected due to the lengthy process of fabricating the molds. Obechi was considered, however, the material introduced an increase in weight to achieve the same ultimate strength. Refer to Table 6.2 for the qualitative evaluation of the wing construction

The team had experience with wet lay-up, so it was decided to cut the airfoil from DOW foam with a Kevlar skin and a carbon spar cap. Using the lift curve slope generated from the plan form data of the wing, the lift force was known at any location along the span. The wing was divided up into one-inch increments so the lay-up schedule could be optimized. Since carbon gets very expensive as the thickness is decreased, 2.9-oz/yd² unidirectional (uni) cloth was used as the primary bending load member. With a fixed thickness, the width of the carbon was tapered to match the local moment of inertia required to prevent the wing from failing. With a thick airfoil, three layers of carbon at the root provided the strength to withstand 15 g's. Refer to Figure 2 for the lay-up schedule.

The foam was purchased from the local hardware store. The carbon and Kevlar were wetted out on two pieces of Mylar. The Mylar sandwiched the core, and was put into a vacuum bag. The panel was cooked at 100 degrees for 24 hours. The other wing panel and the tail are constructed using the same methods.

6.2.2 Fuselage

The fuselage is the area where the most innovation is evident. There are two parts to the fuselage: the skin and the keel. The keel absorbs all the flight and landing loads and provides hard points for the wing, tail, landing gear, payload, batteries, and motor. The keel is designed for both stiffness and ultimate stress. The keel is constructed using Rohacell foam (4.7 lb/ft^3) and carbon to create a sandwich. The Rohacell provides nearly ten times the compression strength of the Dow foam, and only weighs twice as much. The trade off is essential in making a strong, durable fuselage structure. The designed ultimate stress of carbon vacuum bagged over Rohacell is $100,000 \text{ lb/in}^2$. A trade study was done to determine the best combination of Rohacell and carbon to meet the load requirements. The moment of inertia increases with the square of the thickness of the Rohacell. However, the Rohacell is very heavy compared to a few layers of carbon. The best combination of foam and carbon is at the bottom of the bucket in Figure 6.3. However, Rohacell conveniently comes in 0.5-inch thick sheets. To save time and maintain accuracy, the 0.5-inch thick foam was used as illustrated by the red dot in Figure 6.3.

6.2.3 Tail Surfaces

The methods explored to build the tail include a wood build-up, balsa over foam, and balsa with fiberglass over foam. A foam core tail covered with balsa wood alone tends to be heavy due to the amount of resin required to adequately bond the wood to the foam. A wood built-up tail is very fragile and time consuming. Using the same construction method for the wing, the tail construction was simple and fast. The ranking of the processes is displayed in figure 6.4.

6.2.4 Landing Gear

The landing gear presented another area for innovation and optimization. Historically landing gear are about 10 percent of the total weight of the airplane. For a 30-pound airplane that is three pounds. With prior experience using carbon and foam, the landing gear was optimized for both ultimate stress and bending stiffness. The gear was sized for a pilot error on landing resulting in a 6-ft/sec impact with the runway. Assuming two inches of travel on the main gear, this sink rate is equivalent to a 10-g landing. The difficulty when sizing the gear was achieving the ultimate strength with two inches of deflection without failing. There are a few ways to meet both of these criteria. The gear could be designed for a constant stress by decreasing the moment of inertia from the root to the wheel. A tapered width landing gear is an easy way to decrease the inertia. Another way is to taper the thickness, or number of layers of carbon along the length of the gear. Both of these methods were employed to meet the design criteria. In addition, selecting the best combination of core and skin thickness could minimize the weight of the gear. Figure 6.2 illustrates the results of this optimization with the red dot representing the thickness with a factor of safety added for integrity. The nose gear was purchased from Robart due to its robustness and low cost.

6.3 Analytical Methods

The analysis method for screening the manufacturing processes was evaluation based on experience, instead of using elaborate models. A simple spreadsheet was created to compare the impact on wing weight using various densities of materials. The team has a good feel for what it takes to design and build a good aircraft. Simplicity proved to be the best analytical method available. By keeping the design basic, the skill-level required was significantly reduced. Time for construction and testing was always a factor throughout the project. Each construction technique was highly scrutinized to ensure ample flight test time to reduce the chance for pilot error.

6.4 Manufacturing Timeline

To complete the project on time, a tight schedule was adhered to throughout the design and fabrication processes. Milestone chart illustrated in Figure 6.3 was constructed to avoid the last minute crunch.

Table 6.1 Qualitative Ranking of The Figures Of Merit

Figure of Merit	Ranking		
	5	3	1
Ease of Construction	easy	medium	hard
Durability	High	medium	low
Weight	light	medium	heavy
Tooling	none	some	required
Time	short	average	long
Materials Avail.	easily acquired	average	difficult to find

Table 6.2 Ranking of The Figures Of Merit For The Wing

Figure of Merit	Ranking		
	<i>molded</i>	<i>obechi over foam</i>	<i>wet lay-up</i>
<i>Ease of Construction</i>	1	5	5
<i>Durability</i>	1	3	5
<i>Weight</i>	5	1	5
<i>Tooling</i>	1	5	5
<i>Time</i>	1	3	5
<i>Materials Avail.</i>	3	3	5
Total	12	20	30

Table 6.3 Ranking of The Figures Of Merit For The Tail Surfaces

Figure of Merit	Ranking		
	<i>built-up</i>	<i>balsa/foam</i>	<i>Kevlar/Carbon/Foam</i>
<i>Ease of Construction</i>	3	5	5
<i>Cost</i>	5	5	3
<i>Weight</i>	3	3	5
<i>Tooling</i>	5	5	5
<i>Time</i>	3	3	5
<i>Materials Avail.</i>	5	5	5
<i>Total</i>	24	26	28

Figure 6.1 Wing Lay-up Optimization

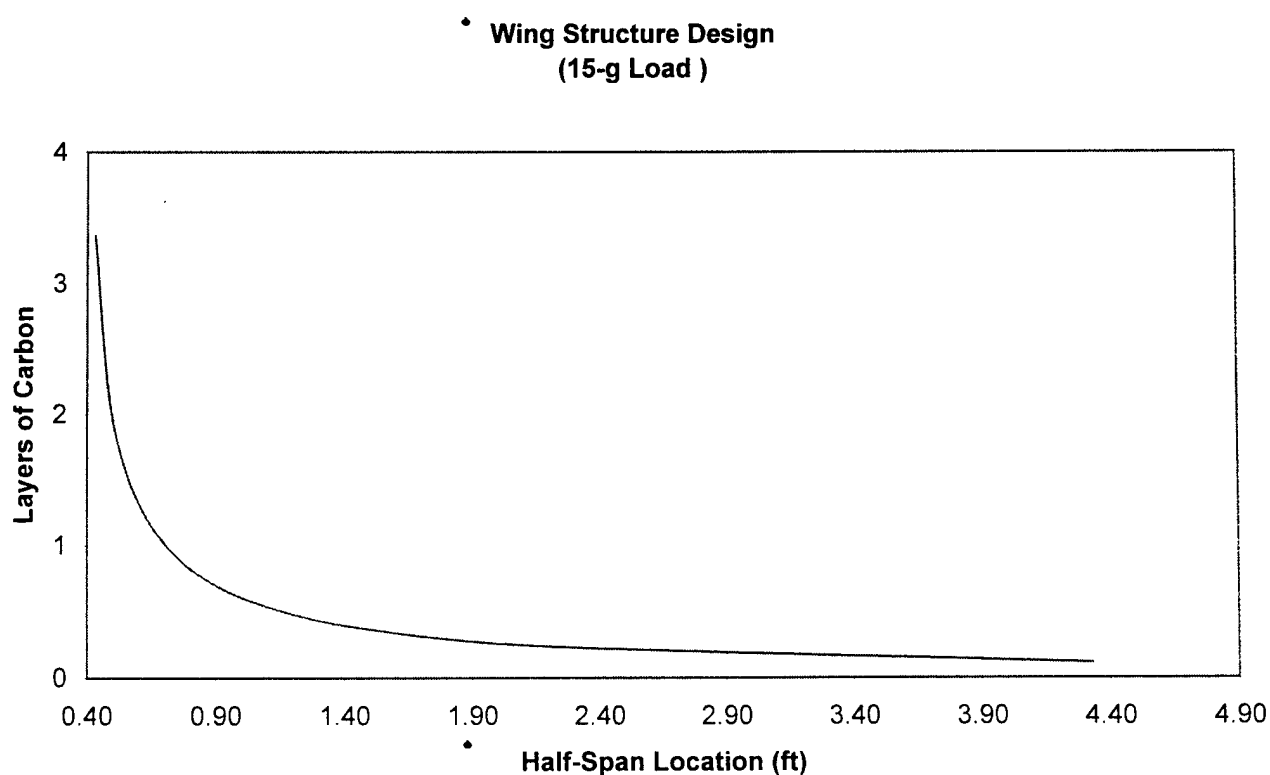


Figure 6.2 Keel Optimization

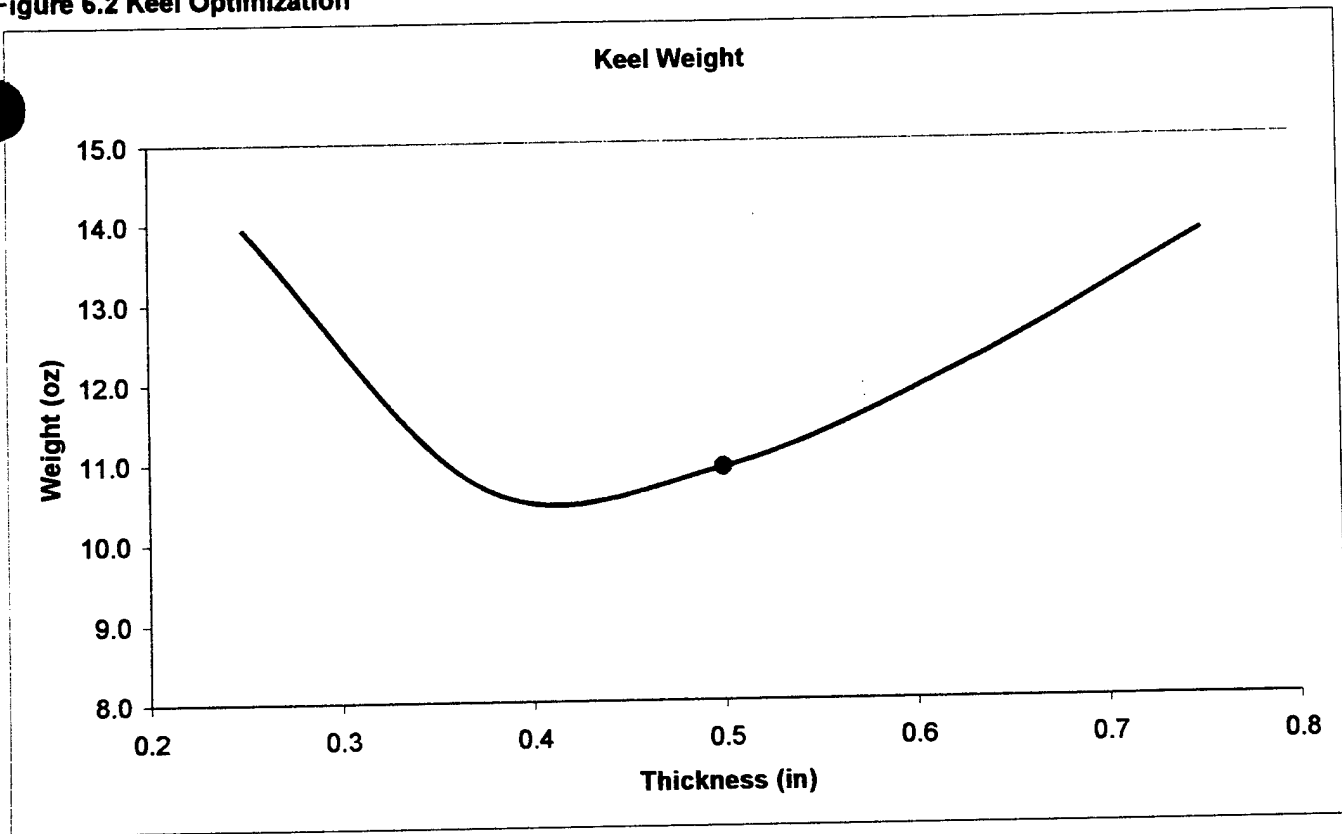
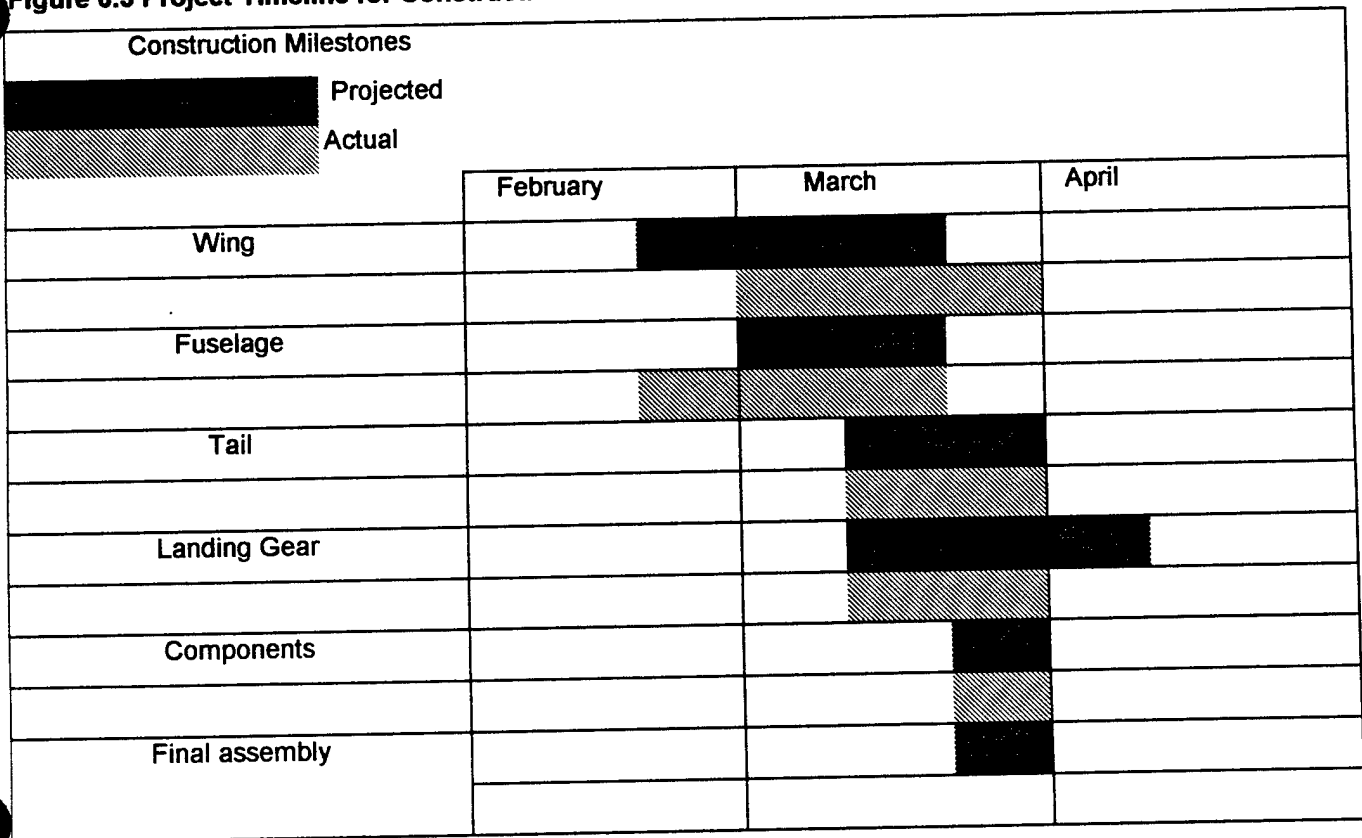


Figure 6.3 Project Timeline for Construction



References

1. Deyoung, J., "Induced Drag Ideal Efficiency Factor of Arbitrary Lateral-Vertical Wing Forms", NASA CR-3357, Dec. 1980
2. Raymer, D.P., *Aircraft Design: A Conceptual Approach*, 2nd ed., AIAA Education Series, Washington, D.C., 1994
3. Roskam, J., *Airplane Flight Dynamics and Automatic Flight Controls*, Roskam Aviation and Engineering Corporation, Ottawa, KS, 66067, 1979
4. Selig, M.S., Donovan, J.F., and Fraser, D.B., *Airfoils at Low Speeds*, SoarTech 8, SoarTech Publications, Virginia Beach, VA, 1989
5. Selig, M.S., Lyon, C.A., Gigure, P., Ninham, C., and Guglielmo, J.J., *Summary of Low Speed Airfoil Data-Vol. 2*, SoarTech Publications, Virginia Beach, VA, 1996
6. Shevell, R. S., *Fundamentals of Flight*, 2nd ed., Prentice Hall, New Jersey, 1989, pp. 290-303

Stealin' Balls
Design Report – Addendum Phase

2000/2001 Cessna/ONR/AIAA Student Design/Build/Fly Competition

Aeronautical Engineering Department
California Polytechnic State University, San Luis Obispo

Authors: John Asplund, James Bach, Jeremy Rocha, Francesco Gianinni

April 9, 2001

Table Of Contents

1.0 Executive Summary.....	3
2.0 Management Summary.....	3
2.1 Group Dynamics.....	4
2.2 Timeline.....	6
3 Conceptual Design.....	6
3.0 Introduction.....	6
3.1 Design Parameters.....	7
3.2 Figures of Merit.....	8
3.3 Conclusions.....	10
4.0 Preliminary Design.....	11
4.0 Preliminary Design.....	11
4.7 Landing Gear.....	13
5.0 Detailed Design.....	14
5.0 Detailed Design.....	15
6.0 Manufacturing Plan.....	15
6.1 Design Drivers.....	15
6.1.1 Ease Of Construction.....	15
6.1.2 Cost.....	15
6.1.3 Weight.....	16
6.1.4 Tooling.....	16
6.1.5 Time.....	16
6.2 Manufacturing Processes.....	16
6.2.1 Wing.....	17
6.2.2 Fuselage.....	17
6.2.3 Tail Surfaces.....	17
6.2.4 Landing Gear.....	18
6.3 Analytical Methods Used To Screen Manufacturing Processes.....	18
6.4 Manufacturing Timeline.....	19
7.0 Addendum.....	19
7.1 Weight Estimation.....	19
7.1.0 Structure.....	19
7.1.1 Landing Gear.....	20
7.2 Aircraft Performance.....	21
7.3 Propulsion.....	22
7.4 Lessons Learned.....	22
7.5 Cost.....	22

7.0 Addendum

Throughout the design process, there were several elements of the design that differed from the actual aircraft constructed. The main differences are a result of optimistic weight estimation for several main components of the aircraft. The weight increase had a large impact on other aspects of the design including the propulsion system, performance and cost.

7.1 Weight Estimation

Accurate weight prediction is essential when optimizing an aircraft for a competition of this nature. The performance of any aircraft hinges on the weight of the vehicle. For this reason, the weight prediction tools were tuned using existing model aircraft constructed using similar techniques. The result is a method that can predict the aircraft weight throughout the design process. However, as the scale of the aircraft increases the prediction methods deviate from the constructed aircraft because of several factors. These factors include higher than normal g loading, methods of construction and structural efficiency.

7.1.0 Structure

The airframe weight estimate without the motor was originally eight pounds. The actual weight of the aircraft was not as predicted for several reasons. There was a large deviation from the predicted weight estimation of the tail and fuselage. When building with carbon and Kevlar, it is often difficult to predict how much extra material must be added in highly loaded areas to avoid failure. There were also weight increases due to integration of the components of the aircraft. The hardware to mount the tail, landing gear, wing and the motor all contributed to increase in empty weight of the airplane.

The estimated weight of the tail was 10 ounces. The tail received extra material for integration to the fuselage that was not taken into consideration in the original weight estimate. There was also a small strip of Kevlar that provided enough torsional stiffness to prevent the elevator from flexing. The final weight of the tail is 16 ounces for these reasons.

The fuselage construction entailed hand-laid up Kevlar over white foam with a carbon and Rohacell main structure. The foam was hot-wire cut and sanded to shape. Kevlar was carefully laid over the foam and epoxy was applied. The foam provides great durability and is very easy to repair. However, the density of the foam and the total volume introduce a significant portion of the total weight of the fuselage. The weight reduction method was to remove all of the foam leaving a thin skin. Once completed, the team realized the foam provided added durability and strength for the fuselage. The weight prediction method did not account for added weight of the foam, causing a difference between the actual and predicted weight of the fuselage. As a result, the fuselage weight increased by nearly one pound.

7.1.1 Landing Gear

The other main component that contributed to the increase in weight is the nose gear. The mounting brackets and the down tube were both undersized in the original design, making the gear not adequate for the aircraft. In addition, the original tires that the airplane was sized with were several ounces lighter than the tires that are going to be used in the competition. After the modifications, the total weight of the nose gear increased by 0.5 pounds.

7.2 Aircraft Performance

During flight testing, key aspects of the final aircraft's performance were compared with the predicted performance. The areas tested and compared include climb rate, takeoff distance, power settings for cruise flight and endurance. These performance figures were critical for the aircraft to complete its mission.

At a gross weight of 30lb, the expected ground roll for the aircraft with half charged batteries and zero wind was predicted to be 170ft. Flight test data showed that when flown carefully, the aircraft easily left the ground before 200ft under those conditions. Climb rate at gross weight was also validated to be acceptable at approximately 10ft/sec half way through the battery pack.

An area where analysis did not match actual flight performance was cruise power and maximum endurance. During gross weight practice sorties, the aircraft would run out of batteries during the sixth payload lap. After careful consideration and testing, several parts of the design spreadsheet were identified to be slightly over optimistic. It was determined that the aircraft needed to use approximately 12% less energy, (11 Watt-Hrs) in order to complete the mission as intended. In an attempt to get back the sixth lap and improve performance, each contributor to system efficiency was ranked according to its impact. This list was then compared with the design teams ability to make changes to the aircraft in the short time remaining before the contest. The following changes were considered for improvement:

- Add NiCd cells
- Pilot smoothness
- Reduce payload capacity
- Reduce empty weight
- Propeller efficiency
- Speed controller efficiency
- Parasite drag clean-up

The easiest solution was to add more batteries to the aircraft. The maximum power could then be achieved by using a slightly smaller propeller at the higher voltage with less current. The difficulty with this solution was the Astro 40's ability to be run on high cell counts. The Astro 40 8T was designed to run on 26 cells but the team was planning on pushing the motor for the contest by running on 32 cells. In order to run on even higher voltage without destroying the motor, a higher turn armature would be

required to keep the motor RPM down. These custom armatures are available, but not in time frame before the contest.

Energy can also be conserved during the flight by careful flying technique. By flying the course tightly and by making sure that the airplane is flown at best L/D speed, more flight time could be achieved. Practicing the course during the next few weeks before the contest will help minimize energy consumption.

Another possibility would be to reduce the payload capacity of the airplane down to 90 tennis balls and 11 pounds of steel. This certainly will allow the flight to be completed while posting a reasonable score with some performance margin.

Most of the unexpected losses in the propulsion system were found to come from speed controller partial throttle inefficiency. In the performance model, speed controller efficiency was estimated at 95%. All of the sizing trades were conducted with this efficiency. The team found that during cruise flight, the power setting required was noticeably higher than anticipated. A static test was conducted to measure the actual efficiency to better understand the problem. To test controller efficiency, the motor and propeller combination were run on a bench power supply at the voltage and current expected for cruise. The propeller RPM was measured indicating a certain power level output from the motor. The motor was then run through the speed controller with the input voltage set at the full 36 volts of the battery pack. Then using the same propeller, throttle setting was then set to achieve the same propeller RPM. The input power was carefully noted and compared to the previous D.C. test. The team found that the input power increase by 17% when running with the speed control. This test indicated that the efficiency of the controller was only 85%. Unfortunately, no higher efficiency controller technology seems to be available for electric R/C aircraft. The team will investigate higher efficiency controllers for next years contest.

Both drag cleanup and propeller efficiency were considered to improve performance. However, the impact of improvements in these two areas was fairly small compared to other changes in the aircraft. In order to accurately measure propeller efficiency, careful testing would be required in the wind tunnel. This testing would be very useful, but compared to the relatively little time required to make other significant improvements to the aircraft, the team's time would be better spent in other areas. Reducing parasite drag by building wing root fairings, landing gear fairings, and an engine cowl could improve performance, but again is fairly time consuming for little gain.

7.3 Propulsion

During preliminary design, optimistic estimates of empty weight were used for sizing the aircraft. The power requirements for the design lied between two Astroflight motors, the Astro 40 and 60. Because empty weight drove the design strongly, the original design utilized the Astro 40, a smaller,

lighter motor. The final aircraft empty weight was 35% higher than anticipated, the original motor no longer fit the power requirements for the design and the decision was made to switch the larger Astro 60. This decision was also made for reliability issues because the Astro 40 was not designed for kilowatt power levels. Another advantage of using the larger motor is its capability of running reliably on higher cell number packs, a solution to the endurance problem. Testing of the Astro 60 will be conducted in the following weeks to optimize the number of cells required to complete the mission.

7.4 Lessons Learned

The aircraft design process provides a platform for learning for every vehicle designed. Likewise, there were many valuable lessons learned throughout the design of this aircraft as well. Foremost is the optimism that can lead to underestimating weights. This seems universal in all aircraft design; the airplane comes out overweight and more power is needed to get the desired performance. The aircraft needed the larger motor, more cells and a bigger propeller because of the increase in weight. We also learned that taking chances with various aspects of the design could take valuable time away from completing the aircraft on time. If we had just chosen the larger motor from the beginning, the time spent trying to make the smaller motor work could have been used to optimize other components of the aircraft.

The competition is driving a design that is easily repairable and very predictable. Since three 10-minute flying periods must be completed, a well-handling airplane is essential for success. Flight test data has shown the overall handling qualities of the airplane are very predictable.

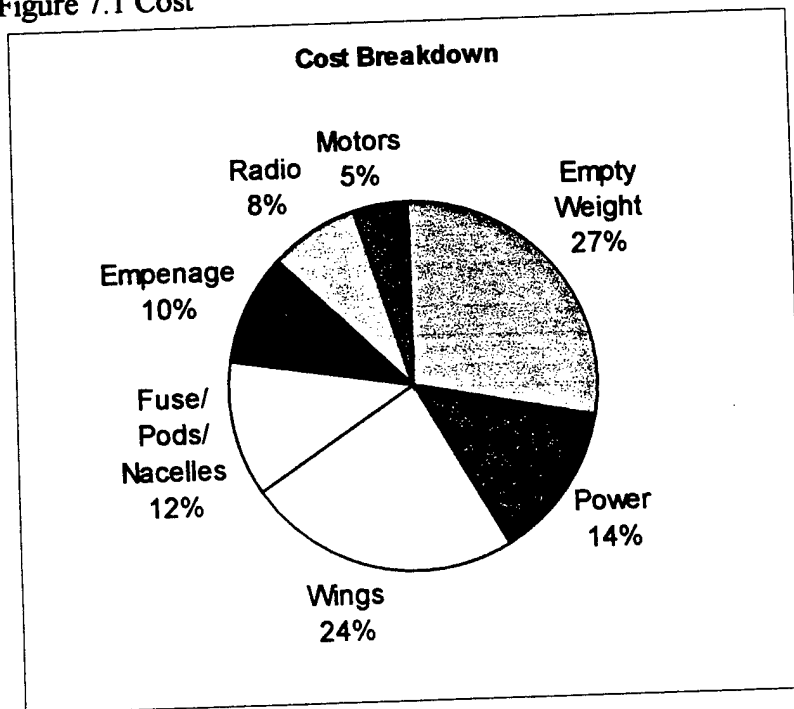
7.5 Cost

The rated aircraft cost (RAC) was a large design driver throughout the design process. The RAC was calculated using the supplied cost model in the rules for the competition. The RAC was carefully taken into consideration throughout the design process. The work breakdown structure (WBS) is provided in Table 7.1. According to the WBS, the majority of the man-hours are from the manufacturing of the wing. The percent breakdown of each portion of the cost is illustrated in Figure 7.1. The pie chart shows that the majority of the cost comes from the empty weight and wing area of the aircraft. The weight could have been shaved down to make a cheaper aircraft but the durability and survivability would have been compromised. The wing area was minimized for both efficiency and cost. The aircraft represents a highly optimized design for each aspect of the contest.

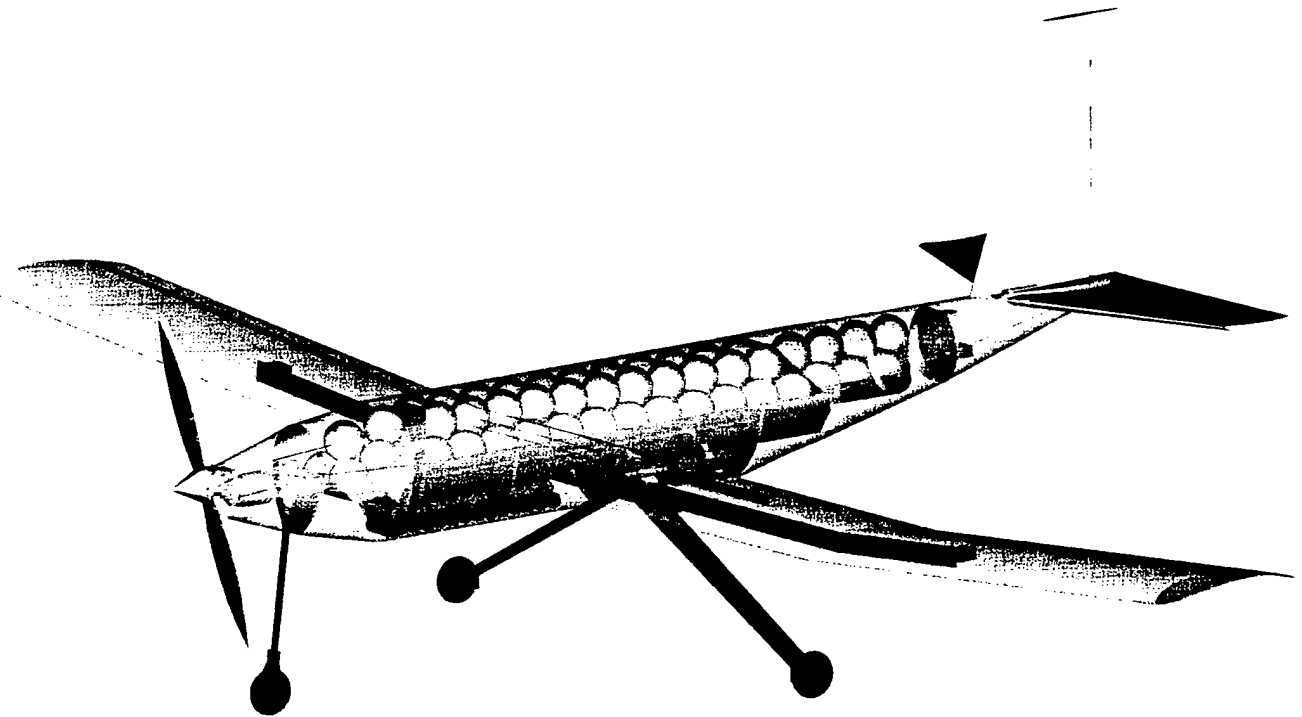
Table 7.1 Cost Breakdown

Empty Weight	11.7	lb	1170
Power	32	cells	576
Current	15	amps	
Wings	1	#	1004.8
Total Area	7.31	ft2	
Surfaces	2	#	
Fuse/ Pods/ Nacelles	1	#	500
Total Length	5	ft	
Empennage	1	#	400
Vertical	1	#	
Horizontal	1	#	
Radio	1	#	340
Servos	5	#	
ESCs	1	#	
Propulsion			
Motors	1	#	200
Props	1	#	
Total			4.1908

Figure 7.1 Cost



**AIAA/CESSNA/ONR
Design/Build/Fly Competition**



Design Report - PROPOSAL PHASE

**OSU Black
Oklahoma State University
March 13, 2001**

Table of Contents

1.0 Executive Summary.....	3
2.0 Management Summary	4
2.1 Architecture of the Design Team.....	4
2.2 Design Personnel and Assignment Areas.....	5
2.3 Personnel Assignments, Schedule Control, and Configuration Control.....	6
2.4 Milestone Chart	7
3.0 Conceptual Design	8
3.1 Mission Analysis and Strategy Development	8
3.1.1 Pre-Conceptual Design	9
3.1.2 Phases of Mission Operation	9
3.1.3 Primary Design Parameters	10
3.1.4 Operational Constraints.....	11
3.1.5 Sensitivity Analysis.....	11
3.1.6 Strategy Development.....	12
3.1.7 Contest Strategy.....	12
3.2 Alternative Concepts Investigated	13
3.2.1 Conceptual Planform Layout Alternative	14
3.2.2 Wing Placements Alternatives.....	14
3.2.3 Alternative Fuselage Concepts	15
3.2.4 Alternative Tail Concepts	15
3.2.5 Alternative Landing Gear Concepts	16
3.2.6 Alternative Propulsion Concepts	16
3.2.7 Material Selection Alternatives	18
3.3 Figures of Merit and Their Mission Features	18
3.4 Final Ranking Chart	20
3.5 Features of the Final Conceptual Configuration	20
4.0 Preliminary Design.....	21
4.1 Design Parameters Investigated.....	21
4.1.1 Operational Constraints.....	22
4.2 Figures of Merit	22
4.3 Analytical Methods, Expected Accuracy, and Reasoning	23
4.3.1 Analytical Methods	23
4.3.2 Experimental Methods.....	24
4.4 Configuration Sizing Data	24
4.4.1 Airfoil Selection.....	24
4.4.2 Pitch Stability	25
4.4.3 Yaw Stability.....	26
4.4.4 Roll Stability.....	27
4.4.5 Horizontal Tail Planform Layout Selection	27
4.4.6 Horizontal Tail Airfoil Selection.....	28
4.4.7 Flight Stability Derivatives	29
4.4.8 Fuselage Shape Consideration	39
4.4.9 Wing Structure Design	31
4.4.10 Landing Gear Design	33
4.4.11 Motor and Battery Selection	33
4.4.12 Propeller Selection	35
4.4.13 Overall Configuration Sizing Data Summary.....	36
4.5 Features that Produced the Final Configuration Selection	37
5.0 Detail Design.....	38
5.1 Performance Data.....	38
5.1.1 Takeoff Calculations	38
5.1.2 Handling Qualities	38
5.1.3 Range	39
5.1.4 Endurance	39

5.1.5	Payload.....	39
5.2	Component Selection and Systems Architecture	39
5.2.1	Propulsion Component Selection and System Architecture	39
5.2.2	Structures Component Selection and System Architecture	40
5.3	Drawing Package.....	40
5.4	Innovative Configuration Solutions, Manufacturing Process, Cost Reduction	40
6.0	Manufacturing Plan	42
6.1	Manufacturing Processes Investigated, Cost and Skill Required	42
6.2	Process Selected for Major Component Manufacture.....	43
6.3	Individual Processes Investigated and Figures of Merit Used.....	43
6.3.1	Fuselage Process.....	43
6.3.2	Wing and Tail Process	44
6.3.3	Landing Gear Process.....	44
6.4	Analytical Methods Including Cost, Skill Matrix, and Scheduling	44
6.4.1	Manufacturing Schedule.....	45
6.5	Innovative Configuration Solutions, Manufacturing Process, Cost Reduction	45

1.0 Executive Summary

This report summarizes the approach of taken by the OSU Black Team to design an aircraft that would perform well in the 2000/2001 Design/Build/Fly (D/B/F) contest. The goal of this year's competition was to design and build a propeller-driven, electric, unmanned airplane that would be capable of carrying both cargo volume and heavy payloads around a specified course. These payload laps, or sorties, must be completed within a ten-minute time period. The challenge of the competition is to design an aircraft that will achieve a superior score within the requirements set by the contest officials. The contest score specified by the contest rules is a function of the written report score, the total flight score, and the rated aircraft cost.

The first step the OSU Black Team took in the design process was to divide the team into technical groups, to review the AIAA DBF mission requirements and then define technical, operational and support requirements. The three groups – aerodynamics, propulsion, and structures-- then each conducted research into design, power, and construction techniques. During this "pre-conceptual phase," one of the biggest achievements of the aerodynamics group was the development of an optimization code. This code used iterative and nonlinear mathematical solving techniques to locate the best score within the contest constraints. The optimization program allowed the contest parameters to be analyzed in a way that decided the major components of the competition such as wing sizing, sortie configuration, payload sizes, power needed, etc.

After gathering research material, optimization analysis was performed. The teams collaborated to begin the conceptual phase where both non-conventional and conventional designs, capable of performing to the requirements of the optimization, were analyzed and compared. This analysis focused mainly on the aerodynamic properties and the manufacturing feasibility of each design. The Rated Aircraft Cost (RAC) was developed using the six primary design parameters. The team reviewed six alternative planforms, six wing placement options, three fuselage shapes, five tail configurations, five landing gear concepts, four propulsion layouts and four material/construction techniques.

At the start of the preliminary phase a monoplane with a polyhedral, low-wing, circular fuselage with a conventional tail was chosen as the optimum design. The propulsion group selected the battery and motor combination of the SR2400 and the Astroflight 661 motor. The aerodynamics group found the static stability and the control surface sizes. The structures group completed the stress and load calculations. The structures group started the technical drawings.

During the detail design phase, the major components were set, and the manufacturing processes were determined. The aerodynamics group completed the dynamic stability calculations and finalized detailed

optimization. The propulsion group selected a propeller to take full advantage of the battery-motor combination within the design performance envelope.

The final design includes an Astroflight 661 motor with a 22-inch propeller and a power source made up of 37 cells of SR2400 NiCad batteries. The wings of the plane will be of polyhedral form using a Selig S1210 airfoil. The ailerons will be powered by 50 oz-in servos. The horizontal stabilizer of the plane will be made with an Archer 18 airfoil and an NACA 0009 airfoil on the vertical stabilizer. Both the elevator and rudder will use horns to reduce the hinge moments on the control surfaces. The fuselage will be built primarily out of foam-supported carbon fiber. The main landing gear will be bow type and built using carbon fiber. The nose gear will be a steerable aluminum Oleo strut design.

The projected mission performance for the steel payload is a take off roll of 160 feet, with a climb rate of 13 feet per second at full power and a cruise speed of 91 feet per second. The 100 tennis ball payload will have a take off roll of 95 feet, a climb rate of 17.5 feet per second and cruise speed of 92 feet per second.

2.0 Management Summary

2.1 Architecture of the Design Team

The design team, led by a chief engineer, is composed of three groups: aerodynamics, propulsion, and structures. Each group is composed of a lead engineer and component specialists; this arrangement can be seen in Figure 2.1. The structure of the team is designed with the chief engineer overseeing the progress of the overall project and the lead engineers' progress, and then the lead engineers oversee the progress of assigned specialists' tasks. Together, the chief and lead engineers assure that all aspects of design and construction are completed on schedule.

At the beginning of the project, the chief and lead engineers assigned certain tasks to each group. The aerodynamics group's first responsibility was optimizing the plane's design and performance within the contest parameters. As the conceptual design was finalized, the aerodynamics group worked with the structures and propulsion group to develop a design that meet the requirements of the contest and was acceptable from the standpoint of the other two teams. After the initial optimization is completed, the aerodynamics members break into integrated product teams with propulsion and structures. Here they conduct trade studies, size control surfaces, and suggest drag reduction methods.

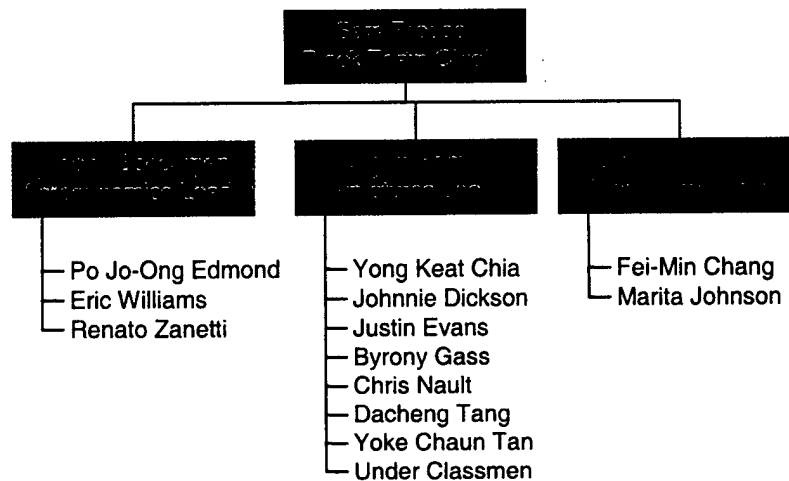


Figure 2.1: Architecture Chart for OSU Black Team

The propulsion group is responsible for the design of the motor, propeller, and battery configuration. After testing, researching, and experimenting, they work with the other two groups to check that the chosen power configurations are sufficient to propel the final design. The structures group is responsible for the structural integrity of the aircraft, lofting and manufacturing work. The integrated products teams are built around structural components of the aircraft such as landing gear, tail structure, and power sources.

2.2 Design personnel and Assignment Areas

The aerodynamics group is primarily responsible for the optimization code, and checking the relevant design constraints. They determine the aerodynamic loads and set design requirements, such as power from the propulsion system, maximum empty weight and component location. They are responsible for predicting and modifying the behavior of the aircraft.

The propulsion group's priority is supplying the plane with power. They have developed an efficient combination of batteries, motors, and propellers that best suites the aircraft. To do this requires knowledge of numerous testing, research, and experimental techniques.

The structures group is responsible for aircraft construction. In order to insure that a suitable and feasible plane is designed, they worked closely with the other two teams during the design phases. This is the

group that must make sure that the plane is strong and durable enough to withstand the loads the plane will encounter. They performed structural analysis on the major components of the plane, decided on the appropriate construction methods, and produced the construction drawings.

Team Member	Title	Assignment Areas
Sam Preece	Chief Engineer	
Anthony Boeckman Po Jo-Ong Edmond Eric Williams Renato Zanetti	Aerodynamics Lead	Optimization/Stability Calcs CG Calcs/Tail Sizing Control Surfaces Airfoil Selection/Wing Sizing
Chad Stoecker Fei-Min Chang Marita Johnson	Propulsion Lead	Motors/Prop Fuses/Prop Batteries
Dustin Hamill Young Keat Chia Johnny Dickson Justin Evans Byrony Gass Chris Nault Dacheng Tang Yoke Chuan Tan	Structures Lead	Fuselage/Materials Construction/Jigs Landing Gear Design Tail Design/Servo Design Construction/Fuselage Tech Drawing/Landing gear Wing Structure Construction/Jigs

Table 2.1: Design Personnel and Assignment Areas

2.3 Personnel Assignments, Schedule Control, and Configuration Control

The team, since it was split into three independently function groups, had to be careful to stay on schedule and make the necessary progress. To do this effectively, a few methods were used. The chief engineer developed a milestone chart seen in Table 2.2 to plan out the project. At least once a week, the chief engineer and group leads would to discuss progress and developments. The group leads then each communicated with their groups to remain on schedule. This also controlled the configuration of the plane. With the leads in constant communication no overlapping of design occurred. Any configuration changes were always discussed during these meetings and then worked out between the involved groups, so each group was always aware of the developments of the others.

2.4 Milestone Chart

Table 2.2 documents the actual and predicted timing of the major events in the aircraft design. This table was used as a time management tool to coordinate the actions of the team. The three groups worked together to stay in the expected schedule seen in Table 2.2 to control configuration decisions in a timely manner.

OSU Black Team Milestone Chart

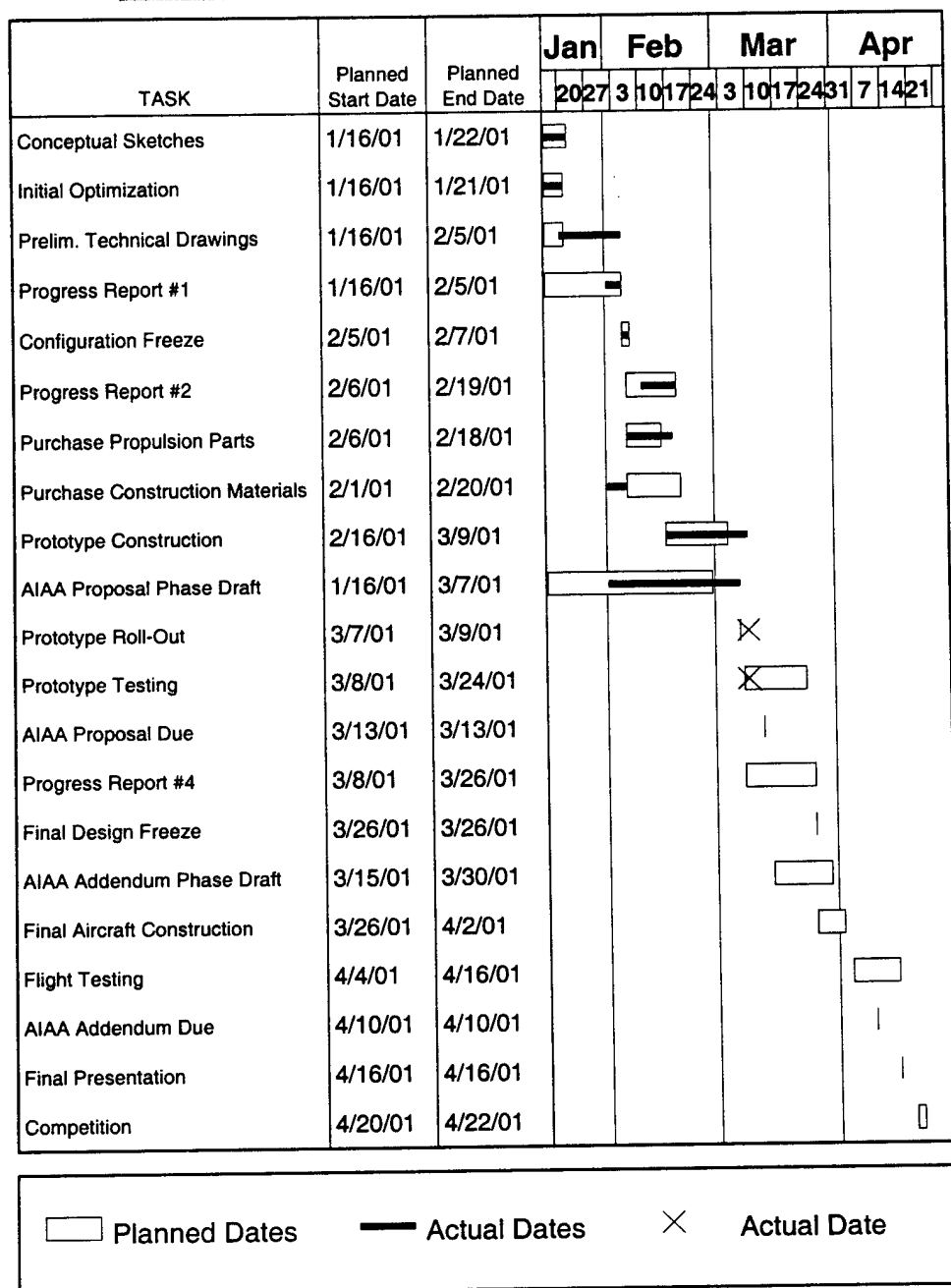


Table 2.2: Milestone Chart for OSU Black Team

3.0 Conceptual Design

3.1 Mission Analysis and Strategy Development

The mission profile this year for the AIAA Design/Build/Fly contest was to design a plane that can carry two different payloads on two different sortie courses. For the steel payload, or the heavy payload, the sortie is once around the course with a 360° turn in the middle of the sortie. The plane must carry no less than five pounds of steel. For the tennis ball payload, or the volume payload, the plane must fly the course twice without the turn in the middle. The plane could carry no less than ten tennis balls and no more than one hundred. The rules require that the plane be powered by an electric motor and have no more than five pounds of batteries. The plane must also take off within 200 feet and complete all scoring laps within a ten-minute time limit. The wingspan is also limited to ten feet. The current that the motor could draw was limited to 40 amperes. The weight of the loaded plane was set at a maximum of 55 pounds. The flight score for a contest round is the sum of the number of tennis balls carried divided by five plus the weight of steel carried. The round's score is then divided by the Rated Aircraft Cost, RAC. The RAC is a penalty that relates the wing area, the length of the fuselage, the power available to the motor, the empty weight of the plane and the difficulty of construction. These rules and scoring functions set up the initial conditions that the team would use to optimize the plane design.

3.1.1 Pre-conceptual Design

Before any design work began, the aerodynamics group set to work analyzing the mission the contest created. In order to reduce the number of parameters compared and simplify the models for various elements in the RAC and the Score, the optimization model was expressed in terms of eight primary design parameters. Each phase of operation that the plane will see in the contest mission was then modeled. Next, the constraints of operation and contest rules were developed. This mission inspection was improved for each design phase. The model's accuracy and estimates improved as more design details were decided upon. The optimization codes allowed the aerodynamics group to perform sensitivity studies on operational and design constraints. The optimization drove the design through the engineering process and well past the detailed design phase.

3.1.2 Phases of Mission Operation

The aerodynamics group began by defining each phase of operation for the contest mission. A total of three phases were found to be important: takeoff, climb and cruise. These phases of operation are depicted in Figure 3.1. Although the plane only operates in three different phases, the model must account for the two different payloads and sorties requirements. Next, equations for power, velocity, and time were found for each of the flight conditions. All of these equations were functions of the optimization parameters.

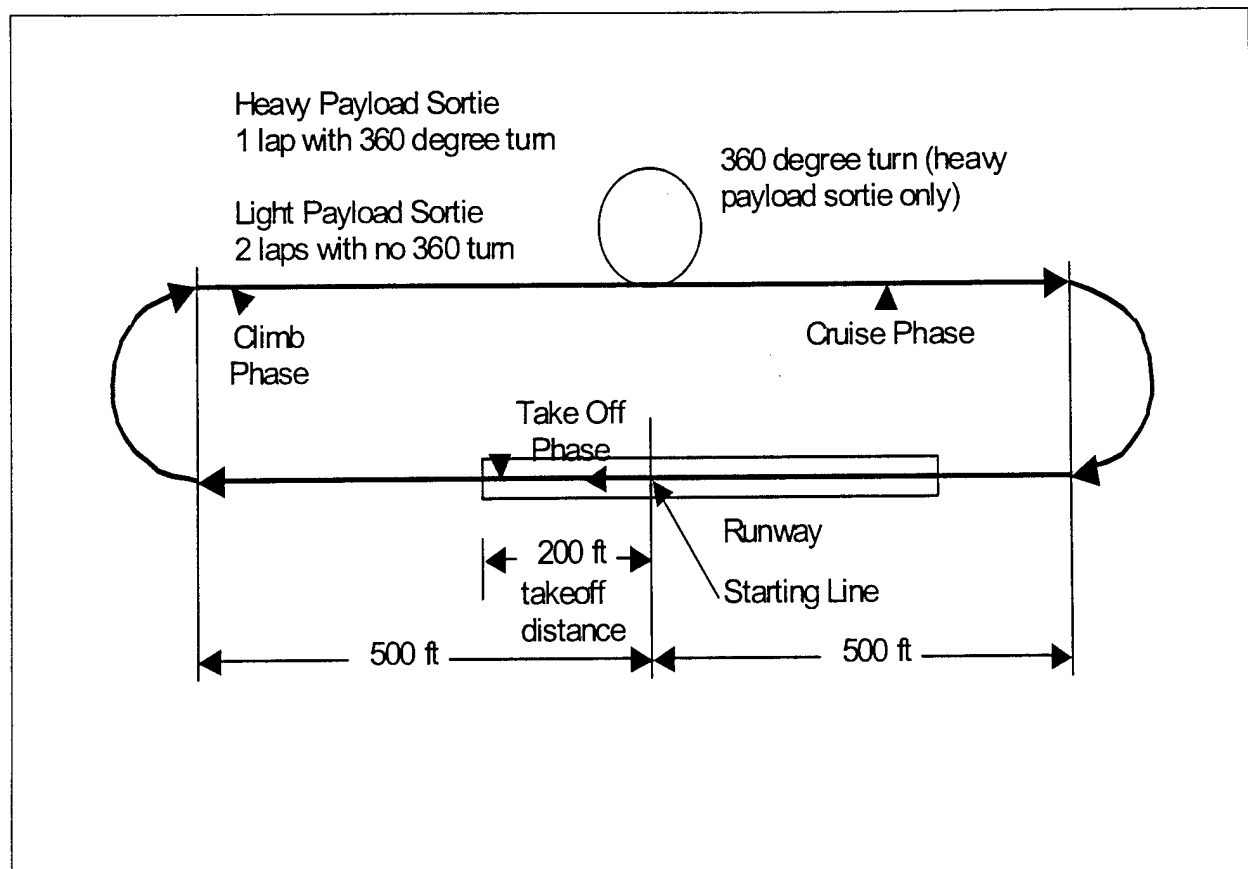


Figure 3.1: Graphic representation of the mission sorties

The first condition of flight was takeoff. The power used in takeoff was assumed to be the same for both the steel and tennis balls. This reduced the workload on the pilot and was found to be reasonable in the final optimal point for the conceptual design. The takeoff was modeled using the equation for takeoff from stand still to takeoff velocity. The model provided a check to make sure the plane could get off the ground within the distance limit and then found the time and energy used to do so.

The next phase of flight was the climb to altitude. Cruise altitude was an operational parameter set by the pilot and designers. This phase model assumed that the plane would continue at the takeoff power and lift coefficient until the cruise altitude was reached. The model of climb assumed that the plane could generate the power to climb, which should be the same as the power needed to take off. The end result of the model was the time required to climb and the forward velocity during the climb.

The last phase of flight was the cruise phase. This is the phase where the plane should spend most of its time during the contest round. The cruise velocity and power were found from the relationship between drag, lift needed to remain aloft, and the power needed to produce that lift. The model found the power used in the cruise phase and the time spent cruising.

To model the time spent on the ground changing payloads and the time spent taxiing from landing stop to the start line, a constant time per sortie flown was assumed.

3.1.3 Primary Design Parameters

To write the optimization code, eight primary parameters of the design were found. These limitations were found to be the core elements of the optimization during the early stages of design. These were not the only parameters, but were judged to be the parameters that mostly heavily influenced the design.

- Planform Wing Area, S : This parameter affects several areas. It and the coefficient of lift determine the amount of lift generated by the wing at a given air speed. The wing area sets the weight of the wing. Wing area is also penalized in the RAC formula.
- Payload Weight of Steel, W_{ST} : The weight of the steel directly impacts the overall score of the plane. The weight of steel carried is summed and used as part of the score. In the code, it is used to check that the plane can generate enough power to get off the ground and have enough power to cruise around the course of the contest.
- Payload Weight of Tennis Ball, W_{TB} : The weight of the tennis balls affects much more than the score. The number of tennis balls is used to find the overall score, but the volume of the tennis balls has a greater influence. The tennis ball capacity determines the length of the fuselage, which in turn affects the weight of the plane. The weight of the tennis balls also affects the power drain in the tennis cruise laps of the contest run.
- Power to Take Off, P_{TO} : For the initial optimization, the power needed to take off was assumed to be the same for both the steel and the tennis ball runs. It was also assumed that the take off power would be the maximum power the plane ever saw. This value was set to the Rated Engine Power in the Rated Aircraft Cost formula. A limit, defined by the maximum allowable power in the contest rules, was set to constrain the optimization.
- Power to Cruise in the Steel Lap, P_{ST} : The power generated on a steel lap was used to find the energy used for the steel flights and check that the plane was capable of flight for the steel lap cruise.
- Power to Cruise in the Tennis Ball Lap, P_{TB} : The power generated on a tennis ball lap was used to find the energy used for the tennis ball flights and check that the plane was capable of flight for the tennis ball lap cruise.
- Number of Steel Laps, N_{ST} : The number of steel laps was used in the score to find the overall score for the steel payload runs. This number should be as high as possible, but is constrained by the energy stored in the batteries and the time allowed.
- Number of Tennis Ball Laps, N_{TB} : The number of tennis ball laps was used in the score to find the overall score for the tennis ball payload runs. The number should also be as high as possible, but again, is constrained by the energy stored in the batteries and the time allowed.

3.1.4 Operational Constraints

The operational constraints this year were a combination of both the rules of the contest, and the realistic challenges of flying an airplane. The limits imposed by the contest rules include the time allowed, the endurance limits due to battery weight (energy storage capacity), and the take off distance limit. The realistic limits include the allowable range of C_L , the time on the ground needed for payload transfer, and the cruise altitude.

3.1.5 Sensitivity Analysis

Once the optimization code was written and tested, the aerodynamics group determined the sensitivity of the overall score, flight score and RAC, to several factors. The factors with the most importance were the number of laps of the two payloads. This can best be viewing in Figures 3.2 and 3.3. This analysis also found the importance of power available, the lift coefficient, the wind speed, and the drag. Although the drag has less drastic impact than the lift, it does affect the score. The importance of achieving a high lift on take off is offset by the ability to travel the course faster, fitting in more laps. The plane was also designed with a wind of five miles per hour. The wind speed has a drastic effect in the that it can gain three points of overall score for only five more miles per hour of wind speed. This sensitivity lead the designs to favor concepts that pushed the factors in direction with positive score effects.

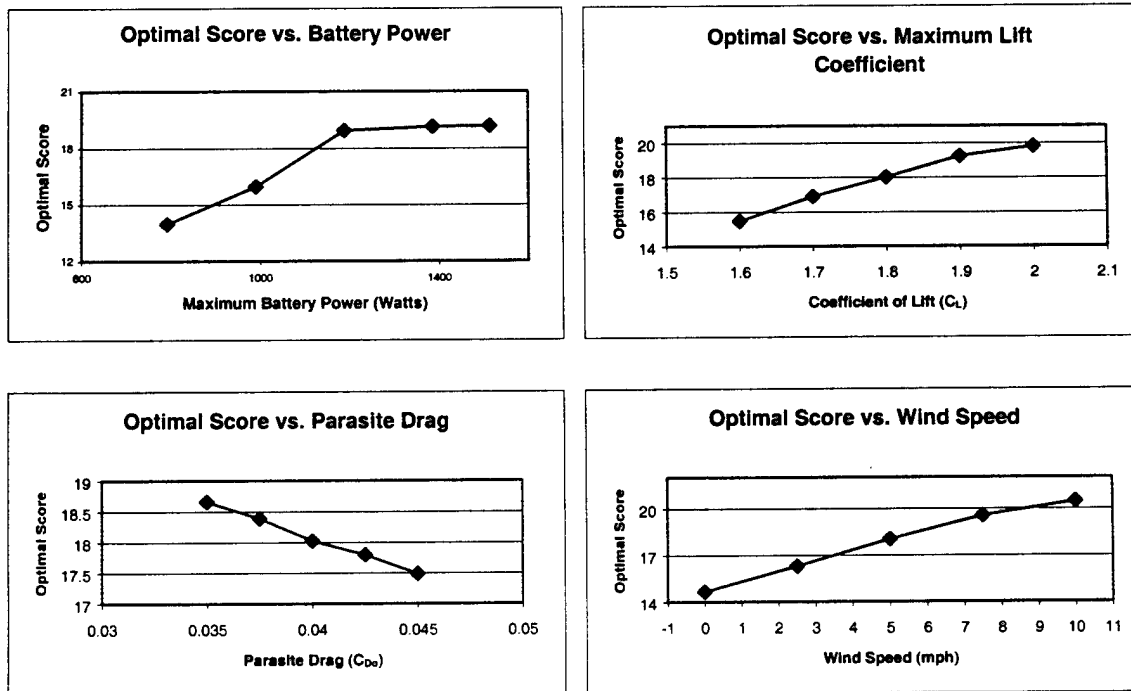


Figure 3.2: The sensitivity of the overall flight score to the Maximum Power out of the batteries, the coefficient of lift, the coefficient of drag and the wind speed.

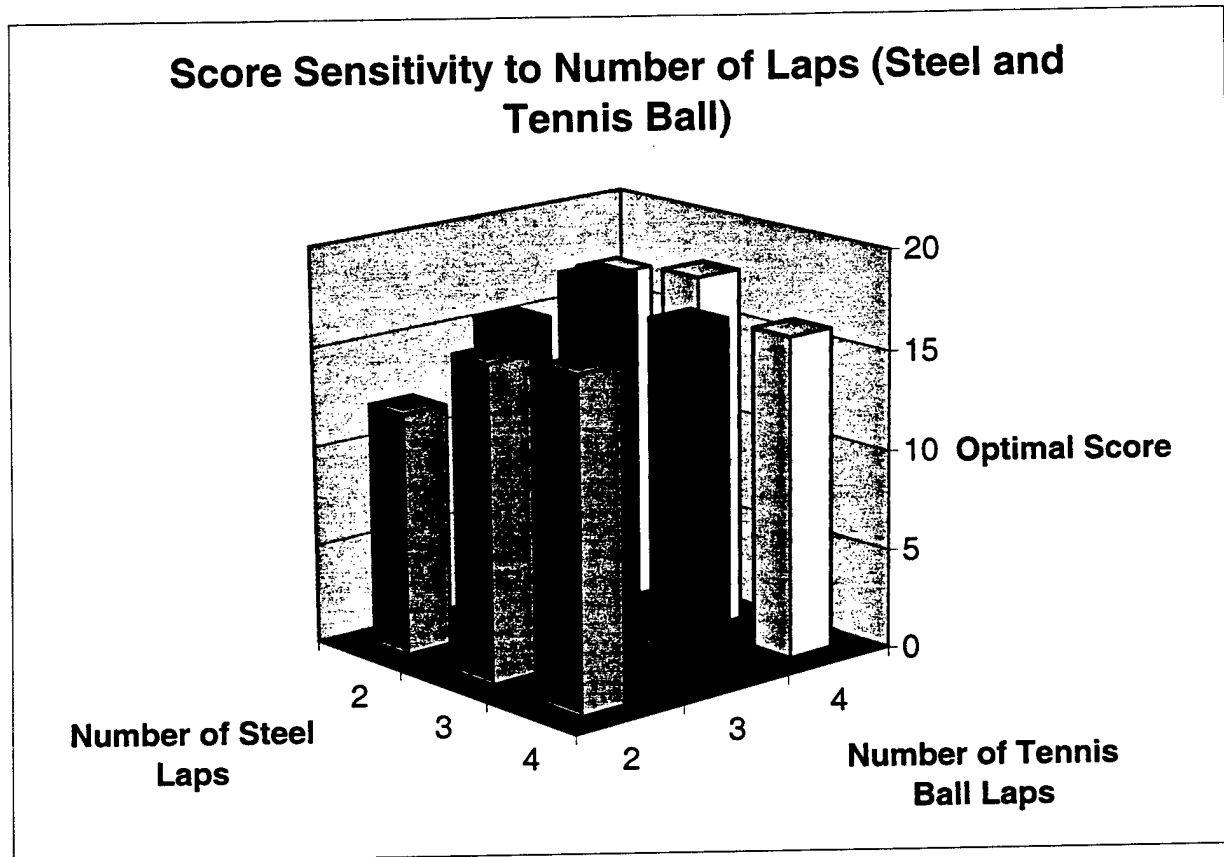


Figure 3.3: The sensitivity of the overall flight score to the number of laps or steel and the number of laps of tennis balls.

3.1.6 Strategy Development

The goal of developing the models of operation and performance for the aircraft was to optimize the overall score function. The code used a conjugant-gradient solving technique to local the maximum of the score design space. To insure that the global maximum was located, the optimization was run repeatedly with randomized initial guesses. The optimization used score as a function not only of the weight of steel and the number of tennis balls, but also of the maximum power used and the surface area of the wing, which are also factors in the Rated Aircraft Cost. The code searches for the optimal point within the design space set by the operational constraints. Once the optimal point was found for the operational and secondary design parameters, the optimization was analyzed for sensitivity to changes in these parameters.

3.1.7 Contest Strategy

The optimization produced a strategy and airplane to be designed by the team. The sensitivity showed some factors to be very important and others not. The code illustrated that a low drag, high lift plane would be required to reach the highest possible score. This data is summarized in Table 3.1

S	9.4 Square Feet	P_{TO}	1188 Watts
P_{ST}	669 Watts	P_{TB}	670 Watts
W_{ST}	13 Pounds	W_{TB}	13 Pounds
C_{LMAX}	1.8	C_D	0.04
N_{ST}	3 Laps	N_{TB}	3 Laps
Rated Aircraft Cost	5.143	SCORE	18.8

Table 3.1: Design Parameters Determined by Strategy Development

3.2 Alternative Concepts Investigated

As the real start of the conceptual design was the development of conceptual sketches by all members of

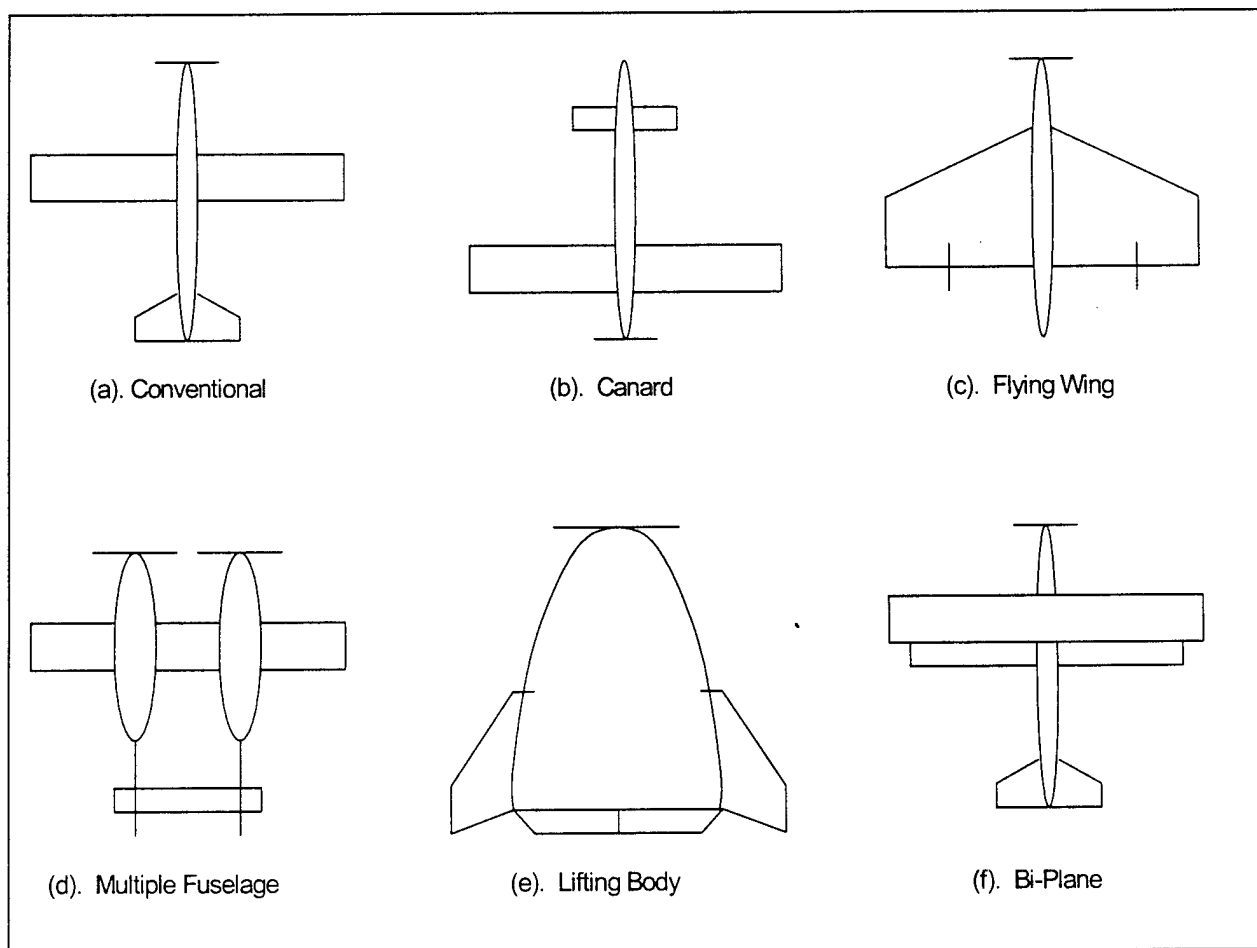


Figure 3.4: Sketches of the planform layout of the plane

the team. After all members submitted ideas for the final plane, the team began debating the merits of each concept and the producing new ideas by synthesis of several concepts and proposal of entirely new ideas. The result was a set of viable concepts from which the final design would emerge.

3.2.1 Conceptual Planform Layout Alternatives

The following list of alternatives was considered for the general planform of the aircraft. The selection of planform concept affected all the following conceptual decisions. The sensitivity of conceptual design to the overall score was performed as the figures of merit were analyzed in section 3.3. Graphical representations of the concepts can be found in Figure 3.4.

- a. Conventional Design: This is the standard configuration of most aircrafts. The wing can achieve maximum lift. The design is easily controlled, and combines low cost, quick construction and intuitive piloting. It has an average Rated Aircraft Cost (RAC). The conventional design is the standard to which the other concepts are compared.
- b. Pusher prop with canard: The canard has good aerodynamics, but the wing can never achieve the maximum lift coefficient out of the airfoil for good stall characteristics. The increased weight in the rear due to motor placement also reduces the attractiveness of this design. The RAC is slightly higher than average because the wing area must be large enough to accommodate the lower C_{Lmax} of the canard-wing combination.
- c. Flying wing: The RAC of this design warranted further investigation, but the difficulty in construction and control make the concept unattractive.
- d. Multiple Fuselage: This design is simple to build, but has a high RAC, with two engines, two vertical tails and three fuselages.
- e. Lifting body: This is a great design with very low RAC. Unfortunately, lifting body usually only works at high speeds and has extreme difficulty of control. This design would have a low RAC, the reason it was considered, but the gain in score was of no value since the problems implementation would overcome the advantages.
- f. Biplane: This configuration provides a lot of lift, but has high drag and a high cost. The RAC is higher than that of most designs due to wing struts and the added cost of having two wings, even if the area is the same.

3.2.2 Wing Placement Alternatives

The wing placement was next set of alternatives to be considered. The planform concept decision is a major factor in the feasibility of all the following options. The selection of the wing placement option was made after the planform decision.

- a. Straight Low Wing: The straight wing is the easiest wing to construct. The low placement allows easy access to a speed loader hatch. The low wing does not exhibit stable tendencies about the roll axis, making it unfeasible as a selection.
- b. Straight Mid-Wing: This design would also be easy to produce, but the obvious loss of cargo space where the wing carries through is a negative aspect.
- c. Low Wing Polyhedral: This wing is more complicated to build than a straight wing, but has the advantage of roll stability and leaving the upper surface of the fuselage open for speed loader access. The multiple joints do make the concept less desirable because of construction reasons and added weight.
- d. Low Wing Dihedral: The low wing dihedral is also more complicated than a straight wing. It also has the advantages of roll stability and the open upper fuselage surface. Joining the wings to the base of the fuselage could be a problem, and the angles have to be precise.
- e. Straight High Wing: design allows for roll stability and easy construction. The high wing limits the amount of hatch surface available to the speed loader.
- f. High Wing Anhedral: design has the same concerns and advantages as the high straight wing. The anhedral high wing does reduce the roll stability of the aircraft.

3.2.3 Alternative fuselage Concepts

The following three options existed for the fuselage shape: rectangular, hexagonal, and circular/oval. These three possibilities all have their own advantages and obstacles.

- a. Rectangular: This design offers the easiest construction and payload configuration. It makes wing attachment easier but weighs more. Aerodynamically the rectangular shape is the worst out of the three because it has the most drag.
- b. Hexagonal: A compromise between the rectangular and circular/oval configurations. Weighing less, this shape offers better drag performance than the rectangular shape while still having flat surfaces for easier construction and wing attachment.
- c. Circular/oval: This shape has the lowest drag of the three candidates and has the lowest weight. Wing attachment with the circular/oval fuselage will be slightly more difficult.

The most important decision factors are drag and weight, based on the above information the circular/oval shape fuselage was chosen. The length of the fuselage was determined by the optimization and therefore was not addressed in conceptual design.

3.2.4 Alternative Tail Concepts

The aerodynamics and structures group worked together to determine the best tail configuration. The concepts listed here are those that were considered for the conceptual design. It is important to note that the tail decision was dependent on the planform selected.

- a. Conventional Tail: This tail is the tail to which all other designs will be compared. Its advantages include simple construction, ease of servo placement, good overall performance.
- b. T-tail: The T-tail puts the horizontal stabilizer further out of the prop wash and gives the opportunity to reduce drag due to surface area. The surface area of the tail remains the same as the Conventional tail. But with the relocation of the horizontal stabilizer, the root of the vertical tail has to be reinforced and the installation of the servo for the elevator becomes more complex.
- c. Cruciform: The Cruciform tail adds complexity to both manufacturing and servo location. It adds complexity to both control surface implementation and construction concerns. The benefits are minimal considering it does not fully move the horizontal stabilizers out of the propeller wash. Overall this is not an attractive configuration.
- d. Twin tail: The twin tail would offer slightly greater control and redundancy, but the increased RAC offsets this advantage. The increase in controls is also unnecessary. A single large vertical tail will likely produce less drag than the twins, since they have twice the number of sharp corners to interfere with the flow and are more area within the prop wash.
- e. V-tail: A V-tail would require the same amount of surface area as a conventional tail, while adding complexity in construction and the need to mix the control channels.

3.2.5 Alternative Landing Gear Concepts

The only way that landing gear effect RAC is through the M.E.W. so gear weight was a concern. The major area of concern for landing gear is the load path incorporated with landing.

- a. Bow type: A simple design that could be easily attached to the bottom of the fuselage. The load path associated with a bow type gear transmits directly to the fuselage. This is a definite advantage over the other types.
- b. Oleo Shock-Strut: A design with one connecting point to the wing. A down side of the oleo is that the single strut must withstand longitudinal and lateral bending moments when landing, thus translating these loads to the wing.
- c. Trailing Link: An effective design that eliminates bending moments in the wing. Some of the negative wing loading would still exist with this design. This design is also more complicated to build and design.

3.2.6 Alternative Propulsion Concepts

The conceptual Design of the propulsion system was driven by the rules of the competition, the rated aircraft cost, and the requirements realized from the score optimization. The rules of the competition restrict the design of the propulsion system to three main areas, motor selection, prop selection, and battery selection. Four different propulsion configurations were considered.

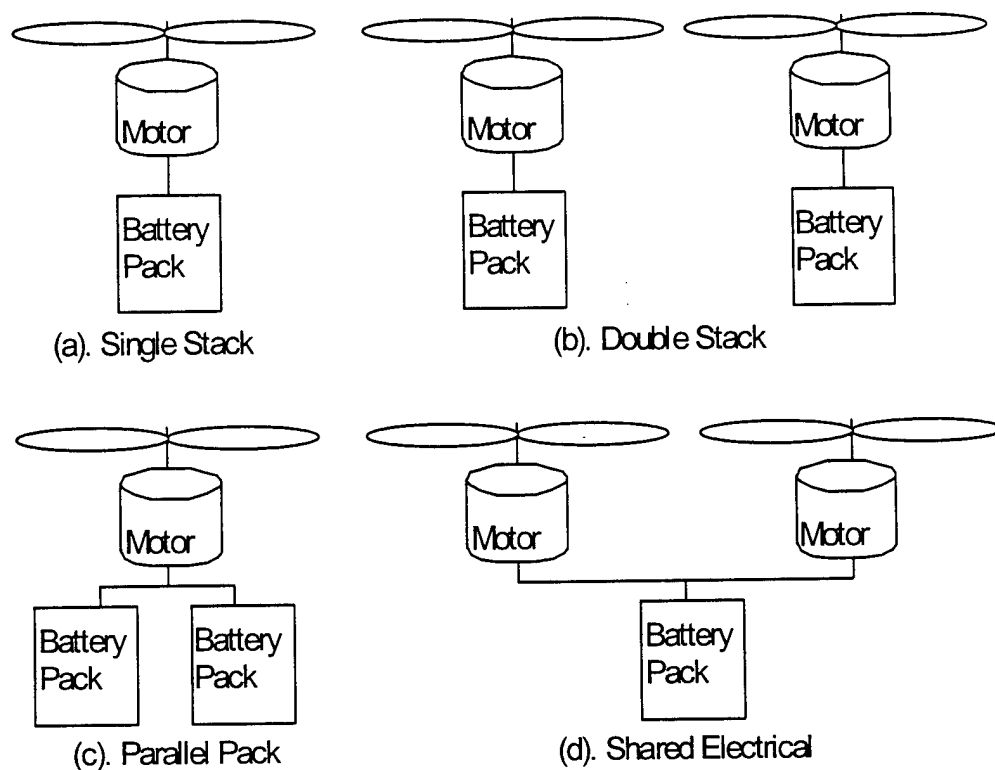


Figure 3.5: Motor-Battery-Propeller concepts investigated

- a. **Single Stack**: A single motor, single battery, single propeller makes up the single stack. This configuration was the most basic choice for a propulsion system. It has the advantages of simplicity and low rated aircraft cost.
- b. **Double Stack**: The double stack consists of two separate battery-motor-propeller systems. This configuration was found to be a poor performer. The two engines doubled the rated aircraft cost. In addition, separate electrical systems meant two fuses, which again doubled the rated aircraft cost, resulting in a four-fold increase in the rated aircraft cost as compared to the single stack.
- c. **Parallel Pack**: The parallel pack consists of two battery packs wired in parallel to a single motor. The primary advantage of the parallel pack is that a lot more batteries can be placed in the battery pack without resulting in a voltage that will damage the motor. Unfortunately, if the individual packs discharge at different rates causing the polarity of one of the packs could be reversed and ruining the entire battery pack. The advantages of wiring battery packs in parallel do not outweigh the disadvantages. There is no difference in the rated aircraft cost between the parallel pack and the single stack.

- d. Shared Pack: The shared electrical system consists of two motor connected to a single battery pack. The shared electrical system is much better, in terms of rated aircraft cost, than the double stack but still results in twice the rated aircraft cost of the single stack because of the two motors. Two motors will produce more thrust and power. However, it was thought that enough power and thrust could be obtained from a single stack.

It was determined that all propulsion configurations could produce the power required to take off. Therefore the propulsion configuration was chosen on rated aircraft cost and simplicity. The simplest and the lowest in terms of RAC was the single stack. Therefore, the single stack was chosen as the propulsion configuration.

3.2.7 Material Selection Alternatives

The types of materials to use in the construction were considered. The 2 alternatives discussed here were the 2 that were best suited to size of the plane and the production capacity of the structures group.

- a. Balsa and Monocoat: Balsa and monocoat are the conventional construction techniques for small scale aerial vehicles. The construction is straight forward, within the skill range of the structures group and low cost. Plane weight would be higher than other methods increasing the RAC.
- b. Carbon Fiber: This method of construction is more expansive and more complicated. The skills to build with this technique were available to the structures group. The final plane will have a lower weight than the conventional construction, with lower RAC, and more durability.

3.3 Figures of Merit and Their Mission Features

Many figures of merit went into the design decisions. The following list of figures of merit were all ranked in Table 3.3:

- Rated Aircraft Cost: The plane was designed with the intent of winning the contest. For this reason, the best combination of RAC and total points was desired. The lower the RAC, the better the score was of the figure of merit.
- Cost: The budget was the limiting factor of the design. All the money used, was received in the form of sponsorship. Designs that can be constructed inexpensively were scored higher.
- Ease of Construction: The structures group must design a method of construction for all parts. Carbon fiber fabric reduces the complexity of most parts, but it requires more lead-time and greater skill. Concepts that are inherently difficult to produce in the workshop received low scores.
- Ease of Design: This figure refers to the knowledge base needed to successfully complete the design. The design is limited to the current understanding of the aerodynamic, propulsion and structures groups. Designs that required intense study of obscure areas of these fields were abandoned as too time consuming for a one semester project. Complicated designs that required knowledge of advanced subjects or operations were scored low.

- Aerodynamic Effects: This FOM accounts for the aerodynamics portion of the design. The design receives a high rating with low drag and high lift. Designs that would have had inherent problems generating lift or generating high drag receive low marks. Those design that are difficult to stabilize or balance also scored low.
- Durability: At the contest the plane will most likely land and take-off well over thirty times. The plane must withstand cyclic loading and stresses for extended periods of time. Designs with areas that are prone to destruction because of fatigue were scored low.
- Weight: The maximum total weight of the plane is 55 pounds. Every pound of empty plane weight was one less pound of payload the plane could carry. In addition, the empty plane weight was penalized in the RAC. Low weight planes received high scores.
- Ease of Repair: Although it is desired for the plane to never crash, planes with good repair characteristics were valued over a craft that is difficult to modify or fix. Aircraft with easy repair and modification earned high scores.
- Ease of Operation (Stability and Control): The plane must be flown by a pilot, placing too much load on the operator will result in impaired performance. A mediocre design that allows the pilot to focus on piloting can work better than a high performance configuration that relies highly on pilot performance. Easily flown crafts received high scores.

Figures Of Merit	Flying Wing, no fuselage	Flying Wing, with short fuselage	Monoplane	Biplane	Multi- fuselage, boom Tail	Lifting Body
Ease of Construction	-1	0	1	1	0	-1
Construction Time	0	1	1	1	1	-1
RAC	1	1	0	-1	-1	1
Durability	1	1	1	1	1	1
Ease of Operation	-1	-1	1	1	1	-1
Cost	0	1	1	1	1	0
Payload Capacity	1	1	0	0	-1	0
Aero Effects (Lift/Drag)	0	1	0	0	0	-1
Repair/Modify	-1	-1	1	1	1	-1
Access to Speed Loader	1	1	1	1	0	1
Total	1	5	7	6	3	-2

Table 3.2: Initial decision matrix for the overall configuration

The initial decision matrix, Table 3.2, was used to remove designs that the team found by simple comparisons to be least feasible, or desirable. The matrix used a simple comparison (-1,0, or 1) to find overall planform concepts that meet best suited the strategy requirements. The results were summed up and the best three of the six compared were analyzed in more depth for the final ranking chart.

3.4 Final Ranking Chart

The initial decision matrix for the planform layout of the aircraft was in Table 3.2. The final decision matrix, Table 3.3, uses a weighted score of each concept for each figure of merit that was found to vary substantially. After the planform layout was determined, the combinations of wing structure and fuselage cross-section were explored.

Figure Of Merit	Maximum Value	Monoplane	Biplane	Flying Wing, Short Fuselage
Maximum Value found by the optimization Routines	There is no "Maximum" Flight Score	18.92	15.9	19.7
Stability and Control Complexity of Design	5	5	5	2
Stability and Control Pilot Comfort	5	5	5	3
Difficulty of Construction, Construction Time	10	10	8	4
Total	20 + 19.7	38.92	33.9	28.7

Table 3.3: The final decision matrix for the plane configuration

The best configuration was found to be the conventional monoplane. The monoplane was easy to build and easy to control. The flying wing with a short fuselage design was found to be difficult to design and a high load on the pilot, who must also manage the power during flight. The Biplane design had potential due to increased lift, but the higher RAC, second wing penalty, reduced the scoring ability too much.

3.5 Features of The Final Conceptual Configuration

The final configuration of the aircraft was chosen based on the decision matrix in Table 3.3. The best description for the plane is a low polyhedral wing, circular cross-sectional fuselage with a conventional tail. The plane will use tricycle landing gear of either oleo or bow type. This configuration meets the requirements of the optimization, has a low weight estimate, and meets the demands of construction and time. The two-piece wing design has two semi-spans that will be built, permanently bonded together, and connected to the bottom of the fuselage by shear pins. Both of the semi-spans will have the polyhedral angle built into them, eliminating the need for secondary connections at these points. Also the connection to the fuselage would be simplified because the wings would not connect to the fuselage at an angle as with pure dihedral. This perpendicular joining design offers the simplest method of connection. As a result, it leaves the largest room for error in construction. The circular fuselage cross-section was chosen based on information from past experience and newly available tools. The standard configuration tail was chosen to reduce weight, keep low RAC and avoid control surface actuators placement problems.

4.0 Preliminary Design

As the preliminary design began, the focus of the optimization shifted from finding the best combination to improving the estimates and data for the optimization code. The propulsion group began to develop more accurate methods for finding power and the true energy storage of the batteries. The structures team developed better plane weight models and requirements for payload weights. As well as laying out the internal structure of the plane, and the volume needed to contain the tennis ball payload were refined. The aerodynamics group refined estimates of the drag coefficient and began a search to find airfoils that could meet or exceed the lift requirements found from the optimization. The aerodynamics group also began control surface sizing, found flight derivatives, and made initial center of gravity calculations.

4.1 Design Parameters Investigated

Moving from conceptual to preliminary design the parameters investigated changed slightly. The conceptual design decisions gave guidance to a refined set of parameters. The weight of tennis balls carried added a cargo volume, and the demands of the propulsion system helped define the battery, motor and propeller. The weights of the payload helped the structures group develop stress analyses for the fuselage and landing gear.

- Payload Weight, W_{st} , W_{tb} : Normally, the maximum payload weight would be considered a figure of merit. The optimization, however, used the payload weights to determine the best strategy. The weight of payload that can be handled was then a parameter for which the plane was designed rather than a positive feature of a potential design.
- Cargo Volume: Again, this parameter could be a figure of merit. The optimization found that the best score could be achieved with a plane carrying the maximum number of tennis balls; therefore, plane was designed to carry 100 tennis balls.
- Power – Take off and Cruise, P_{to} , P_{st} , P_{tb} : These factors were found to be important in reaching the optimal score. It was found from the optimization that power management is critical for a high score. The plane must be designed with the ability to hit the optimal power use at both the take off and cruise conditions.
- Surface Area of the Wing, S : This parameter was used to find the lift of the wing and minimize the Rated Aircraft Cost score. The optimization program determined the smallest wing that can generate the needed lift a takeoff within the limits of the lift coefficient. The lift coefficient was varied to find the sensitivity to the total score and the wing area.
- Lift Coefficient: For the optimization to produce results, a C_L must be supplied. Using experimental results for known sources and previous experience, a reasonable estimate to the maximum lift coefficient was determined. A sensitivity analysis to this factor was performed, and the C_L was found to be an important score factor.

- Drag Coefficient: This factor became important, as the speed of plane is critical to reaching the planned strategy. The right combination of coefficient of lift and drag is a goal of the preliminary design.
- Number of Laps, Endurance: The strategy developed from the returns of the optimization dictated the number of laps of both the heavy and light payload laps. Achieving both goals is necessary to reach the optimum score.

4.1.1 Operational Constraints

Due to the contest rules, the strategy and aerodynamics the following constraints were enforced.

- Cruise Altitude: This value was set by consolation between the designers and the pilot. The altitude of 70 feet was found to be acceptable to both.
- Time on Ground: This is an estimate of the time the plane is on the ground, including landing rollout, cargo exchange, and time needed to taxi to the starting line. This time was estimated from previous competition experience.
- Distance of Cruise: The contest officials set this value. The length was padded to allow for error.
- Runway Limit: A value of 200 ft was set by the competition rules, for the optimization a value of 180 ft was used to leave room for error.
- Battery Weight and Endurance: The weight of the batteries is another operational constraints set of the contest. The endurance of the batteries must be enough to hit the optimal score.
- Completion of planned strategy within time limit: Another design consideration is that the plan is able to complete the contest course with the intended number of laps of each payload with the allotted time.

4.2 Figures of Merit

Several figures of merit were used for the preliminary design. The following list describes each figure of merit and their respective missions features.

- Score Effects: This FOM is also a design parameter, but falls under the figure of merit as well. Every aspect of the plane takes into consideration the effect it will have on the overall score.
- Durability: In order to win with the current contest strategy, the plane will have to land at least 18 times before its finished. The plane will also be designed for transportation to the contest as well. As such it must be able to survive being disassembled and reassembled repeatedly.
- Ease of Modification of Design: The prototype airplane will be tested to reveal design defects and inadequacies. Design that allows the modification will be preferred over other designs.
- Weight: Each part will be considered for its individual weight penalty. The overall weight of the plane should be the optimal value or less.
- Ease of Construction: The difficulty in construction of complex fuselages, wings or tails was weighed. Designs that require skills or tools unavailable to the structure team were disregarded.

- Aerodynamic Effects: Designs with high lift and low drag were considered. For this contest, it was of great interest to reduce drag.
- Stability and Control: Designs with inherent control problems were valued less when compared to designs with well-known stability characteristics.
- Access Points for a Speed Loader: The different designs were compared for areas of access to the speed loader. Designs with ease and quick access to the cargo compartment were preferred.
- Cost: This is the one figure of merit that can place an absolute cap on a design. The cost of the projected design was considered in the materials selection and in the inherent cost of a design.
- Efficiency: The maximum motor-battery efficiency is obtained by multiplying the motor efficiency by the battery efficiency. The battery efficiency is found by taking into account the losses due to the internal resistance of the batteries. The motor efficiency is found by taking into account the copper and iron losses in the motor. A higher battery-motor efficiency results in a higher score.
- Total Energy: The total energy of the batteries is a measure of the total energy stored in the batteries. Sensitivity analysis shows that that an increase in total energy storage results in a higher flight score. The total energy does not have a direct effect on the rated engine power score.

4.3 Analytical Methods, Expected Accuracy, and Reasoning

During the design phases the team used both analytical and experimental methods to find results. The aerodynamics group used several analytical techniques to define the characteristics of the aircraft. The propulsion group used wind tunnel and static dynamometer test to characterize the propulsion system.

4.3.1 Analytical Methods

For the initial optimization, the aerodynamics group used simple models for take off thrust, take off distance, and climb rate. The steady and level flight of the cruise phase was model by solving the equilibrium equation between drag and thrust. As the optimization was refined with better data from the structures and propulsion groups, the equations were improved. The take off function more accurately modeled the thrust from the propeller. The drag estimate was refined from first order estimates (guesses from experience) to calculations from charts available in Raymer's *Aircraft Design, A Conceptual Approach*. The accuracy of drag predictions is difficult to quantify, as drag is difficult to model.

When the stability calculations were started the aerodynamics team chose to use the stability estimates in Nelson's *Flight Stability and Automatic Control*. The linearized flight equations of motion assumption were found to hold true for the team's design. The assumption of only small disturbances was valid, as the plane was designed as a cargo transport. The control surface estimates held under the same assumption. The approximations of the modes of flight vary due to how well the small disturbance theory holds. The estimates for the Short Period, Roll and Dutch Roll are known to vary no more than five percent with in

the assumption envelope. The Phugoid motion can be inaccurate to about 30 percent, however the period of the Phugoid is large enough that the sortie will finish before the Phugoid can diverge. The Spiral estimate can be inaccurate as well. The Spiral mode is one that the pilot will damp out naturally by his control of the plane. If the prototype proves to be susceptible to any divergence, the aerodynamics group will reanalyze the aircraft and redesign to damp out the mode of motion.

4.3.2 Experimental Methods

Extensive experimental tests were conducted to determine the best propulsion system. The primary tool for testing was a dynamometer built for testing scaled propellers. This dynamometer could measure the thrust of the propeller, the torque of the propeller, and the rotational speed of the propeller. The second most important tool was an experimental quality wind tunnel. The wind tunnel has a 9 square foot cross sectional testing area and is capable of producing wind speeds of up to 120 ft/s depending upon ambient conditions.

Tests were conducted under static conditions, with the dynamometer outside the wind tunnel, and dynamic conditions, with the dynamometer in the wind tunnel. This data was then non-dimensionalized to obtain the coefficient of thrust, the coefficient of power, and the efficiency versus advance ratio curves. In addition to this, extensive testing was done on last year's motor and battery pack. Thermocouples were used to measure the temperature of the batteries and the motor. The power, amperage, and watt-hour reading of the batteries were also recorded. The performance of the batteries and motors was tested under static and dynamic conditions at various discharge amperages. A test was also conducted to determine the effect of a blockage placed behind the propeller. This testing resulted in a marked improvement in this year's propulsion system.

4.4 Configuration Sizing Data

4.4.1 Airfoil Selection

The optimization assumed a maximum coefficient of lift, which was used during take off and climb. The optimization determined the lift coefficient at cruise for both payloads for velocity and power requirements. These considerations drove the airfoil selection. The first step in the airfoil search was to find candidates with sufficient maximum lift coefficient. It was assumed that the lift coefficient during take off is slightly less than 1.5, which is eighty percent of the maximum lift coefficient of 1.8. During cruise the lift coefficient varies from 0.7 to 0.9. The wing chord and airspeed yield a Reynolds number of 300,000. This search produced several possibilities. The candidates were screened to further reduce the number of possible airfoil.

In the optimization a total parasite drag coefficient of 0.04 was assumed. Because of other contributions such as fuselage, landing gear, tail, etc., the portion of the drag allocated to the wing/airfoil is less than

0.02. Many drag polar curves were compared while looking for reliable experimental data. When possible, airfoils with maximum lift coefficients, even those greater than 1.8, were analyzed. Airfoils that were unable to exhibit reliably predictable relationships between lift, drag, and stall point were removed as too great a risk. Furthermore, this extra lift will be useful especially in the prototype, which is error-prone, and might need more lift during take off. The airfoil that satisfied these requirements was the Selig S1210. Its characteristic drag polar is in Figure 4.1.

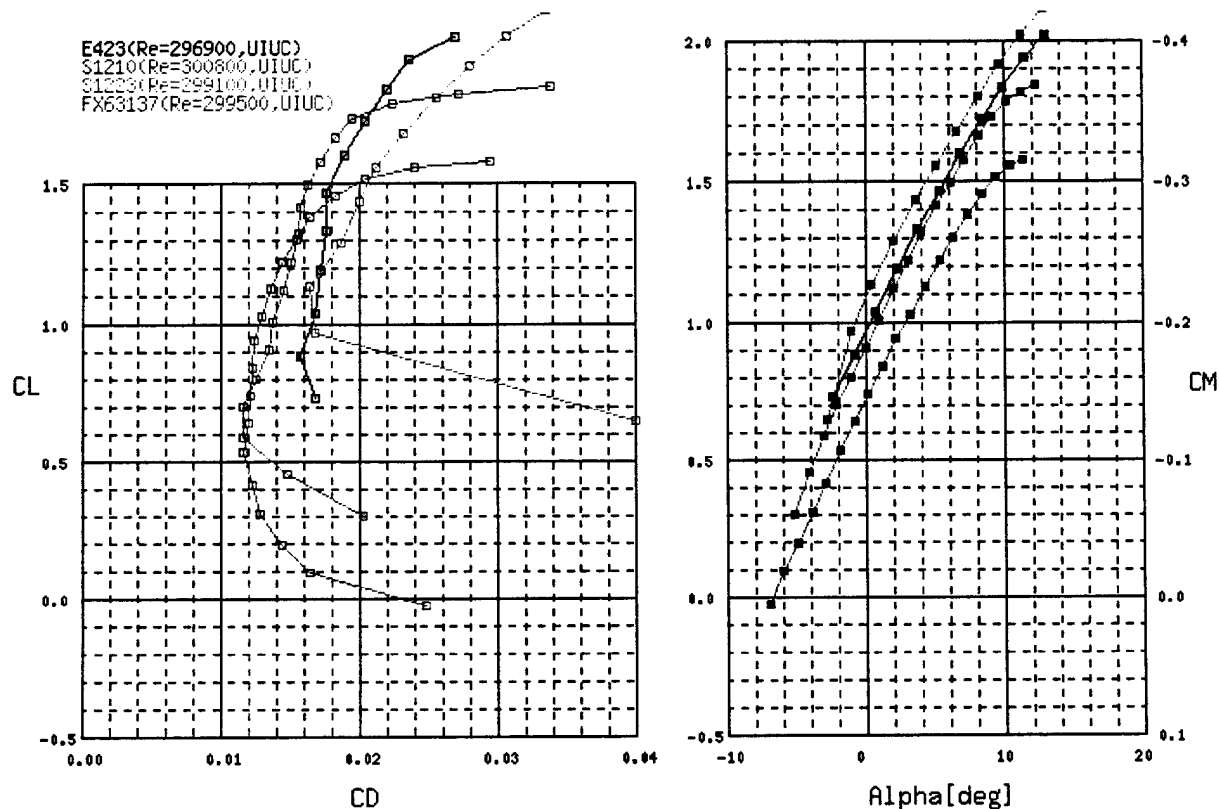


Figure 4.1: Drag polar Comparing four candidates for wing airfoil; the S1210 was selected due to its range of operation and low drag characteristics.

4.4.2 Pitch Stability

The calculations of the pitch stability determined the size of the vertical tail and its incidence angle. Aspect ratios of 4 and a taper ratio of 0.5 for the tail were chosen. These values correspond to the desired tail shape and rules of thumb from literature sources. This reduced the tail sizing variables to two unknowns, the root chord of the horizontal stabilizer and the coefficient of lift of the tail, C_{L_t} . The first calculation performed was the fuselage contribution to the pitch stability using an equation summing the contribution of each section of the fuselage to the overall stability.

Next, the non-dimensional location of the neutral point was found. The center of gravity was known from initial estimates and the position of the payload center of gravity. The stick-fixed static margin was used to find the tail chord and coefficient of lift necessary to achieve the desired pitch stability.

In order to find the tail chord and C_{L_t} , the stick-fixed static margin was set at 15% of static stability. This was a large value, as it was preferred to have a strong stability for the prototype. Literature on the subject stated a value of 0.05 to be adequate. The value would be reduced if the flight-tests showed it to be acceptable.

The next step was to find the necessary contribution of the tail to pitch moment coefficient at zero angle of attack, C_{M_0} , such that the plane is stable at the cruise angle of attack, α_{cruise} . To find the need downward force from the tail the moment must be found from all other sections of the airplane. Adding together the pitch moment from the wing, fuselage and thrust yields the total moment that the tail must counter. The airplane pitch coefficient at zero pitch angle was found to be a function of the tail's lifting force, even though it is directed down. With the force from the tail known, the pitch stability contribution of the other parts was found and added together to find the airplane's pitch moment coefficient versus pitch angle derivative, C_{M_α} . This value must be negative in order to achieve stability. With the values of C_{M_0} and C_{M_α} known the pitch moment can be expressed as a function of the angle of attack and the force generated by the tail.

Our wing cruise angle of attack was -0.85 degrees, so C_M was set to be zero at that angle, in order to have the desired trim during cruise flight. The tail characteristics for a tail at an effective angle of attack of zero were found. The coefficient of lift for a tail with an aspect ratio of 4 was found to be 0.35. The size of the tail root chord was set to 9.5 inches. The selection of the horizontal stabilizer's airfoil is discussed in section 4.4.6.

The tail chord was oversized to 10.5 inches for two reasons. The first was to have a bigger security margin in the pitch stability. The second was to allow the elevators to be oversized as well. This increased the static margin to 0.206.

4.4.3 Yaw Stability

The size of the vertical tail was dependant upon acceptable yaw stability. With the shape of the fuselage and the wing already known their contributions to directional stability were calculated. Since the vertical stabilizer must be symmetric, the NACA 0009 airfoil was selected, as there is abundant information about the airfoil available. The vertical tail contribution was found to be a function of the vertical tail surface.

It was known that to have stability it was necessary to have a positive $C_{N\beta}$. The Literature suggested a $C_{N\beta}$ of 0.05 for the cruise velocity Reynolds number. A vertical surface of 1.13 square feet was found to be adequate to meet stability requirements. To account for any errors a 1.25 feet square vertical tail surface would be used.

4.4.4 Roll Stability

A similar approach as that used for yaw stability was used to find the polyhedral angle of the wing. The contribution of the low wing (without the polyhedral effects) and the fuselage was calculated. This value was found to be destabilizing as the low wing and fuselage work to promote instability. Then the contribution of the polyhedral angle of the wing (Γ) was calculated as a function of this angle. The wing had a polyhedral angle only toward the tip, from 2 to 5 feet on each semi-span.

Adding the coefficient of roll moment from the wing and body together resulted in the roll moment coefficient versus yaw angle derivative for the total airplane as a function of Γ , so setting this coefficient to a $C_{l\beta}$ of -0.05 multiplied by the maximum lift coefficient, easily found the polyhedral angle. An angle of 4.735 degrees was found and rounded up to a 5 degrees polyhedral angle.

4.4.5 Horizontal Tail Plan-form Layout Selection

When choosing the tail, various options for the plan-form layout were considered. The options included the straight tail, the straight tapered, swept tapered, and the straight swept. It was decided that the swept tapered style best fit the rest of the design requirements. This decision was based on the following criteria: weight, drag, ease of construction, and rated aircraft cost. When determining the best selection for the weight criterion, the weights of various options were computed. These weights were based on similar surface areas. The options ranked in as follows:

1. Straight Tail .374 lbf
2. Swept Un-tapered .374 lbf
3. Swept Tapered .44 lbf
4. Straight Tapered .44 lbf

The difference in weight is from the fact that, for a longer chord, more foam is required for the thickness needed.

When determining the best alternative in terms of drag it is necessary to look at the causes of drag on the tail surface. When trying to reduce drag, eliminating any portion of the tail that would cause flow separation was important. Gapless hinges were required to minimize the drag. The straight tapered tail would force the use of gapped hinges. This would be a high drag configuration. The swept un-tapered configuration required multiple control surfaces and would therefore raise rated aircraft cost. In the other two design configurations it was possible to use gapless hinges for the control surfaces. Overall, these

two styles were preferred. The swept tapered was preferred over the straight tail because of the "Oswald Efficiency Comparison." The swept tapered had an Oswald Efficiency of .95 where as the Oswald Efficiency of the straight tail was .75. For the given performance characteristics, the swept tapered configuration was chosen. We decided to implement horns into the tail control surfaces in order to reduce the strain on the servos used to drive them. By creating a force balance between the horn and the control surface, the surfaces could be moved with less effort, making them more efficient.

4.4.6 Horizontal Tail Airfoil Selection

After strenuous consideration using a decision matrix, it was decided that adapting the A18SM (Archer) airfoil for the airplane was the most suitable. The selection of airfoil was based mainly on the aerodynamic considerations. The figures of merit (FOM) for the airfoil selection were the following: Cruise lift coefficient at zero angle of attack, cruise drag coefficient at zero angle of attack, thickness/weight, lift coefficient range.

First, based on the stability calculations, the tail required a lift coefficient of 0.35 at zero angle of attack. Only a few airfoils met the requirements. The airfoils were then compared to for drag characteristics. Airfoils were compared for lowest drag at zero angle of attack and for the range of low drag. As speed was critical to the optimal strategy, reduced drag had a high priority.

Weight of the tail was one of the critical aspects of design. The weight of the tail had two effects. The first was an increase in empty weight of the plane, which drove down the overall score. The second was center of gravity effects, because larger tails shift the center of gravity toward the rear of the plane. Weight was influenced by the maximum thickness of the airfoil. The cross-sectional area and volume of foam would be higher as the maximum thickness increases, therefore, the lower the maximum thickness of the airfoil, the more favorable it was to the overall plane design. Two candidates met these requirements, the A18SM and the BE50SM.

FOM	A18SM	BE50SM
Thickness/Weight	1	1
Cruise CL @ $\alpha=0$ deg	1	0
Cruise CDo @ $\alpha=0$ deg	1	1
CL Range at min CD	1	1
Total Score	4	3

Table 4.1: Decision matrix for the horizontal tail airfoil

The final condition was the operational lift coefficient range of the airfoil. Looking only at the difference between the minimum and maximum value was not enough. As mentioned earlier the airfoil would be operating at a lower lift coefficient region so A18SM was chosen for the horizontal tail. A comparison matrix between the two best options for the horizontal stabilizer airfoil is included in Table 4.1.

4.4.7 Flight Stability Derivatives

The following values are the flight derivatives of the preliminary plane design. Table 4.2 shows the longitudinal flight stability derivatives, and Table 4.3 the lateral. Table 4.5 shows flight control derivatives in both longitude and latitude. A static margin of 0.204 was used, due to an upsized tail.

Wing		$C_{L_{\omega}}$	0.731
$C_{M_{\omega}}$	-0.246	$C_{M_{\alpha}}$	-0.227
$C_{L_{\omega}}$	4.639	$C_{M_{\omega}}$	-0.123
Fuselage			
$C_{M_{\omega}}$	-0.041	$C_{M_{\alpha}}$	0.589
Tail			
$C_{M_{\omega}}$	0.09	$C_{M_{\alpha}}$	-0.952

Table 4.2: Flight Stability Derivatives: Longitudinal, Static Margin: 0.206

$C_{N_{\beta fw}}$	-0.031	$C_{N_{\beta v}}$	0.097
$C_{N_{\beta}}$	0.066	$C_{l_{\beta wf}}$	0.011
$C_{l_{\beta d}}$	-0.085	$C_{l_{\beta}}$	-0.075

Table 4.3: Flight Stability Derivatives: Lateral

Longitudinal			
$C_{M_{\delta e}} = -0.785 \text{ 1/rad}$			
Lateral			
$C_{N_{\delta r}} = -0.035 \text{ 1/rad}$	$C_{l_{\delta r}} = 0.021 \text{ 1/rad}$	$C_{l_{\delta a}} = 0.097 \text{ 1/rad}$	$C_{N_{\delta a}} = -0.014 \text{ 1/rad}$

Table 4.4: Flight Stability Control Derivatives, Static Margin: 0.206

4.4.8 Fuselage Shape Consideration

The payload of tennis balls is the driving parameter in determining the volumetric size of the fuselage, a study was conducted to see how ball configurations and the number of tennis balls for a given design affected two parameters, weight and fuselage drag. Figure 4.2 shows the different ball configurations considered including the configuration that the team chose, the Black Pack. It is shown only as the 100 ball configuration.

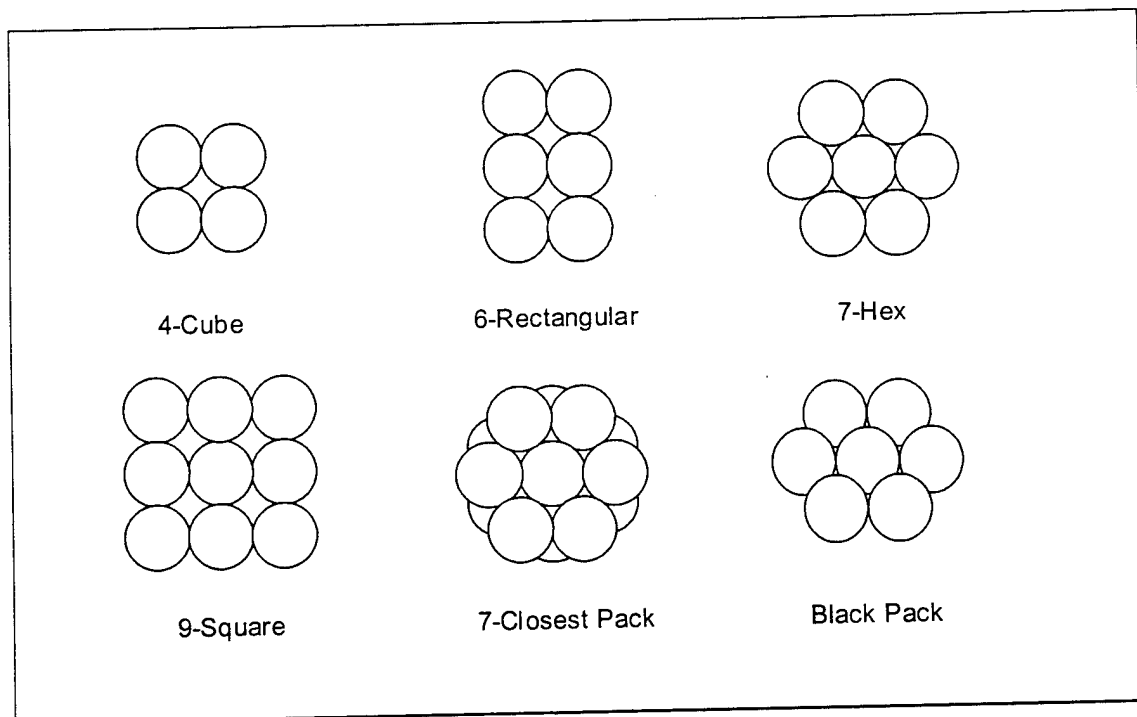


Figure 4.2: Fuselage tennis ball cross-section configurations considered in the trade study

From the team's aircraft optimization, the optimal tennis ball cargo stayed between 70 and 100 tennis balls for a payload. The trade study examines only this range for each configuration. The results of the skin weight portion of the fuselage configuration trade study are shown in Figure 4.3. The fuselage weight chart shows that as payload size increases, so do the fuselage size and the fuselage skin weight. The fuselage skin weight is based on the fuselage being constructed out of a carbon fiber/Styrofoam core sandwich. This construction technique weighs half as much as conventional construction. One result from the data is that the square and rectangular fuselages are not as light as rounded fuselages.

The fuselage drag coefficient, which was calculated using methods from Raymer (1999, p. 342-346), is nondimensionalized in terms of the wing area. An assumption made by the equations is that the entire fuselage experiences fully developed turbulent flow as a result of propwash. The results of this part of the trade study are shown in Figure 4.3. The results show the rectangular fuselages at real disadvantage with respect to the more rounded fuselages, also, the shorter length gained by the 7-Closest Pack configuration is better than the standard 7-Hex configuration.

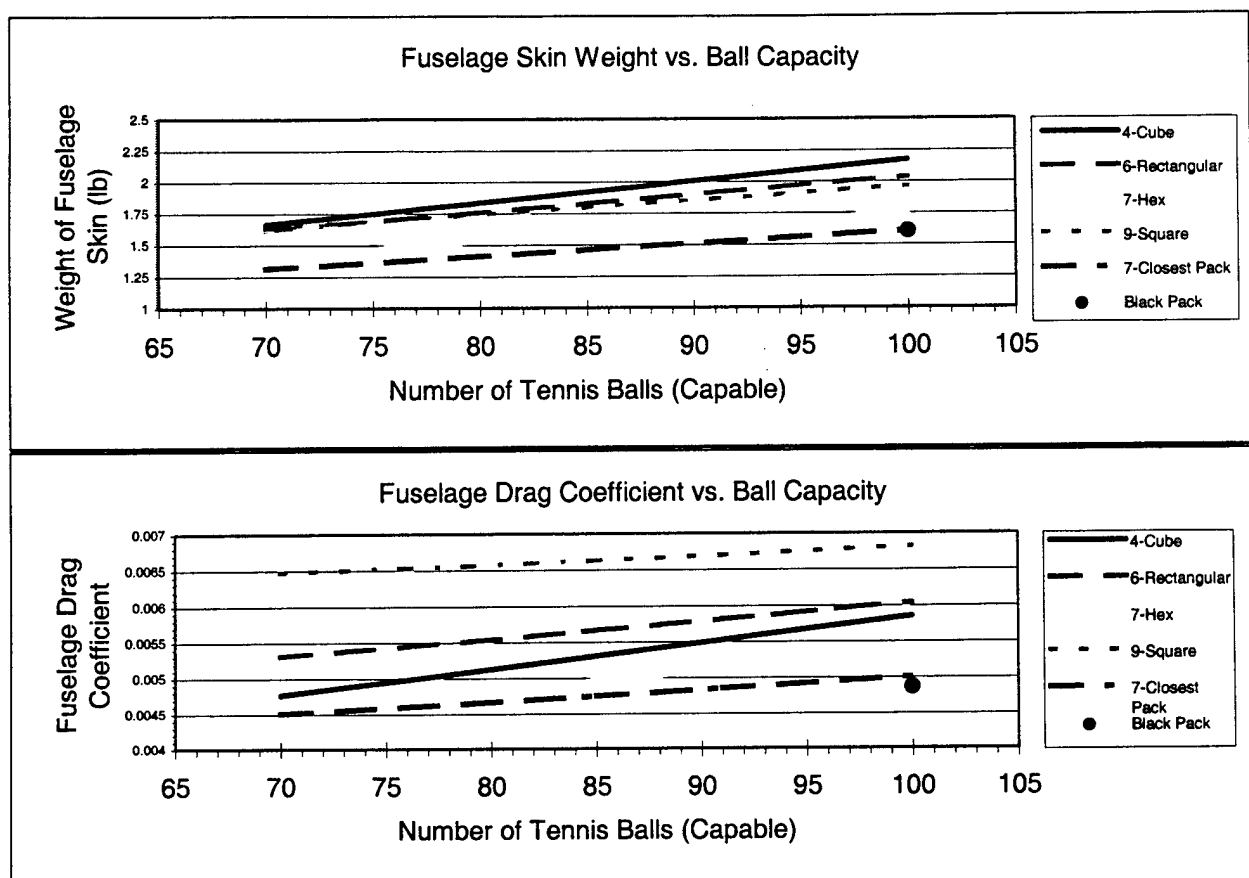


Figure 4.3: The effect of tennis ball payload capacity on weight and drag coefficient

From this study, the team chose another variation in the 7-Hex configuration, the Black Pack configuration, which is a slanted back 7-Hex cross section. Like the 7-Closest Pack configuration, the Black Pack is a two-dimensional closest pack arrangement. This configuration was chosen over the 7-Closest Pack configuration because it eased the placement of batteries. Thus, it is no surprise that the 7-Closest Pack and the 2-dimensional closest pack Black Pack have nearly the same fuselage skin weight. Whenever the drag data from the two bodies were looked at, the similarities disappeared. The team's preliminary fuselage design has a slight advantage in drag coefficient due to its more economical use of fuselage volume for payload with respect to the 7-Closest Pack configuration because it incorporates a more efficient use of nose and tail space than the standard configurations.

4.4.9 Wing Structure Design

Two trade studies also resulted for the wing. The first was the wing construction study, which looked at the weight from the two leading candidates for construction. The first was a foam core construction with carbon fiber skin. Second, was a carbon fiber, foam, carbon fiber sandwich construction. Figure 4.4 shows the varying of wing weight with respect to the wing area for a wing span held at a constant 10ft. For the optimized wing area value of 9.4 ft², the foam core wing came in 0.3 lb lighter than the sandwich.

For the Selig 1210 airfoil, the sandwich only begins to be viable at a wing area greater than 12 ft², and that is assuming that the sandwich skin is stiff enough carry the aircraft without an internal wing structure. From this trade study the team decided on using the foam core wing construction.

A second wing trade study performed looked at the effect of wing taper on wing weight, assuming that the tapered wing and rectangular wing generate the same amount of lift. Figure 4.4 shows the wing dimensioning definitions used in the trade study. The foam core Selig 1210 airfoil was used to find the weights. The graph clearly shows that the rectangular wing maintains the lowest wing weight. This is a result that the wing foam weight increases as a result of the square of the chord. The weight saved at the tips is overshadowed by the weight increase at the root of the wing.

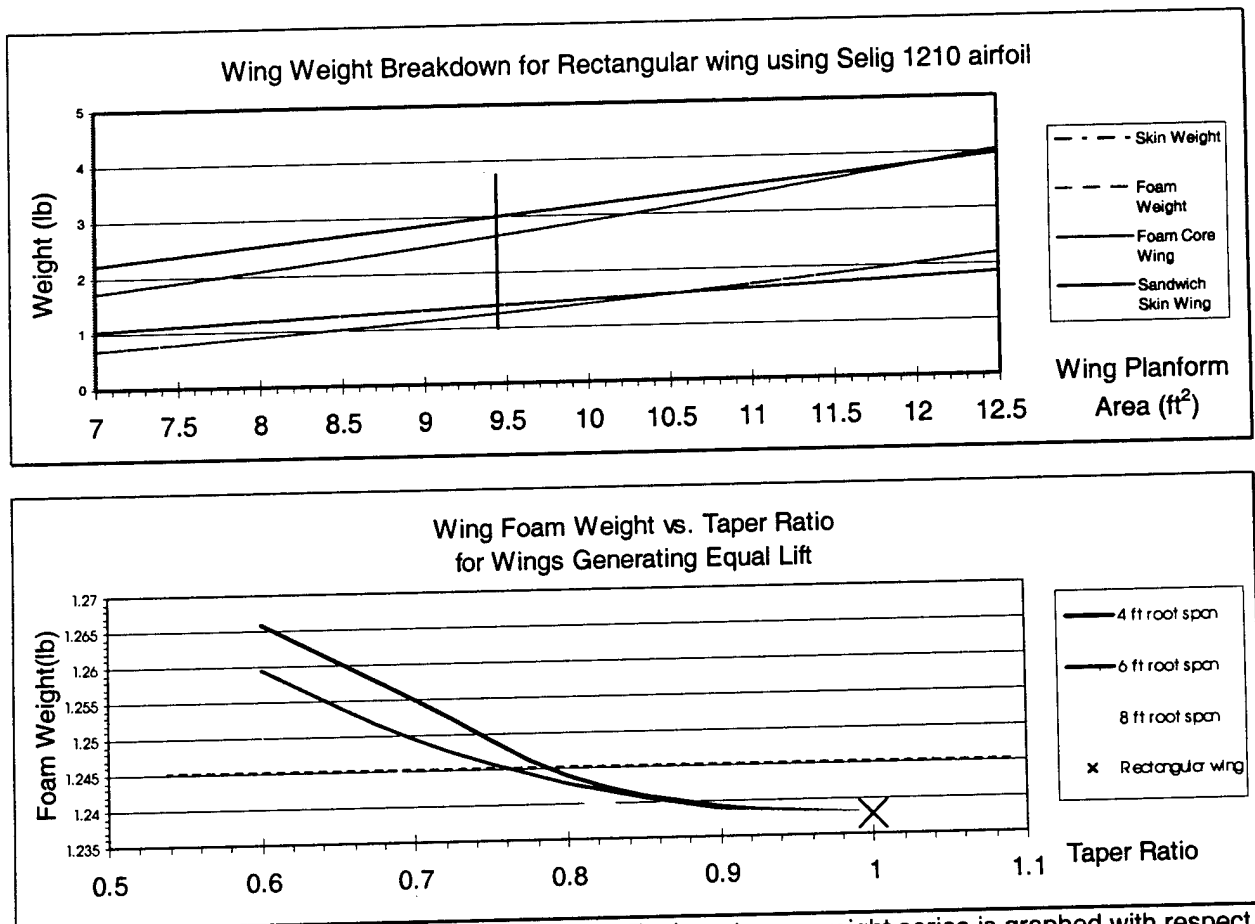


Figure 4.4: Results of the wing taper weight study. Each root span weight series is graphed with respect to the varying taper ratio.

With the method of wing construction decided a stress analysis was performed. The maximum wing loading will occur during the tip test when the plane is placed on a test stand supported only at the tips of its wings. The highest stress levels occur at the wing roots. With an 150% load of 85 pounds, the stress on the top of a 1/8 in. thick main spar is 481.6 ksi. For reinforcement a second spar was added in the wing. To account for the high stress, the spar will be strengthened with a 3-ply C-channel reinforcement

about the root of the wing with 0.4 in flanges. The maximum stress at the root of the wing with just the C-channel reinforcement would then be 87.3 ksi, less than one-fifth of the previous value. The most common carbon fiber failure mode is delamination from a second surface and buckling. Since the C-channel is one piece, that cannot happen.

4.4.10 Landing Gear Design

Several designs were considered to try to effectively transmit the loads induced while landing to the main structure of the plane. Options for a landing gear type that connected to the wing included connecting the gear to the main wing spar or building a load distribution system into the wing. While providing an effective path for the loads these designs could not alleviate some of the local problems such as crushing of the foam and delamination of the wing skin. For a bow gear these problems do not exist. A bow gear design was originally thought to be heavier and to produce more drag than a wing-mounted design.

After further research and investigating new construction techniques a solution was reached. A carbon fiber bow gear would be used. Properly designed this type of landing gear could solve all of the design challenges. The advantage to this designed lied in the fact that the carbon fiber arms of the bow could be made to any shape desired. This meant an aerodynamic, low weight design could be implemented. Realizing this technique allowed the team to create efficient main landing gear.

The nose gear presented a different challenge. Ground handling requirements dictated that the plane have steerable front landing gear. Another design requirement was to use front brakes on the plane, to make more efficient use of the time on the ground. With these requirements in mind an oleo type gear was chosen. To lighten the weight of the nose gear a carbon fiber tube was used for the main strut.

4.4.11 Motor and Battery Selection

The first task of propulsion preliminary design was to conduct an exhaustive search for different types of batteries. Information was compiled on approximately 135 batteries. Previous OSU planes used the Sanyo KR-2300SCE battery. These batteries were built to have an extended life and be used for very low amperage discharge rates. Experimental results showed that they had a very poor performance at a high amperage discharge rate. This degradation in performance can be avoided by using a high discharge type battery. It was also felt that a quick charge battery is needed to effectively compete in the contest. The type of application for which each battery was designed was also investigated. The high performance, "racing" batteries were all designed for applications that drained the voltage at a high current. For these reasons, a choice was made to consider only the quick charge, high performance, high discharge, racing batteries. This choice left 15 high charge/discharge, "racing" batteries for consideration. The four batteries that gave the highest total energy were selected as the top performers. The decision matrix in Table 4.5 was used to pick the best battery out of the top four performers.

The batteries were chosen on the basis of the total energy provided by all the batteries allowed by the 5 lb limit and the overall battery efficiency. These figures of merit are listed at the left of the matrix. The value for the total energy for the SR-2400 was significantly higher than any other battery. In addition it had the second highest battery efficiency. The SR-2400 was the top choice heading into the motor selection phase.

Figures of Merit	Batteries			
	SR-2400	SR-2000	SR-3000	N-RC2400
Total Energy (Kwatts-sec.)	435	372	415	373
Battery Efficiency (%)	90	90	92	86

Table 4.5: Battery selection decision matrix

The next step was to choose the motor. According to the rules, the motor must be a brush type motor. Oklahoma State University has a long relationship with Astroflight. Based on past experience, they have the best motors on the market, and worked well with teams from OSU. Astroflight is located in California, while Graupner is a German company. Choosing a motor from Graupner would add logistical concerns. In addition, Astroflight has always given OSU a substantial discount off the retail price of their motors. Astroflight was chosen as the manufacturer to purchase from.

Astroflight produces two series of motors, the "60's" and the "90's", which can operate at the planned voltages and currents. When comparing motors, the two important parameters are the mechanical power out of the motor and the motor efficiency. The mechanical power and motor efficiency for the different motors with the SR-2400 battery were compared in Figure 4.5. The 661 motor was a clear winner for both mechanical power out of the motor and the overall motor-battery efficiency. Figure 7 also shows that with the 661 motor, the highest mechanical power out of the motor is achieved with the SR-2400 battery. Thus the Astroflight 661 motor and the SR-2400 battery were chosen for our propulsion system. Having chosen a battery and motor, propeller and gearbox selection were next studied.

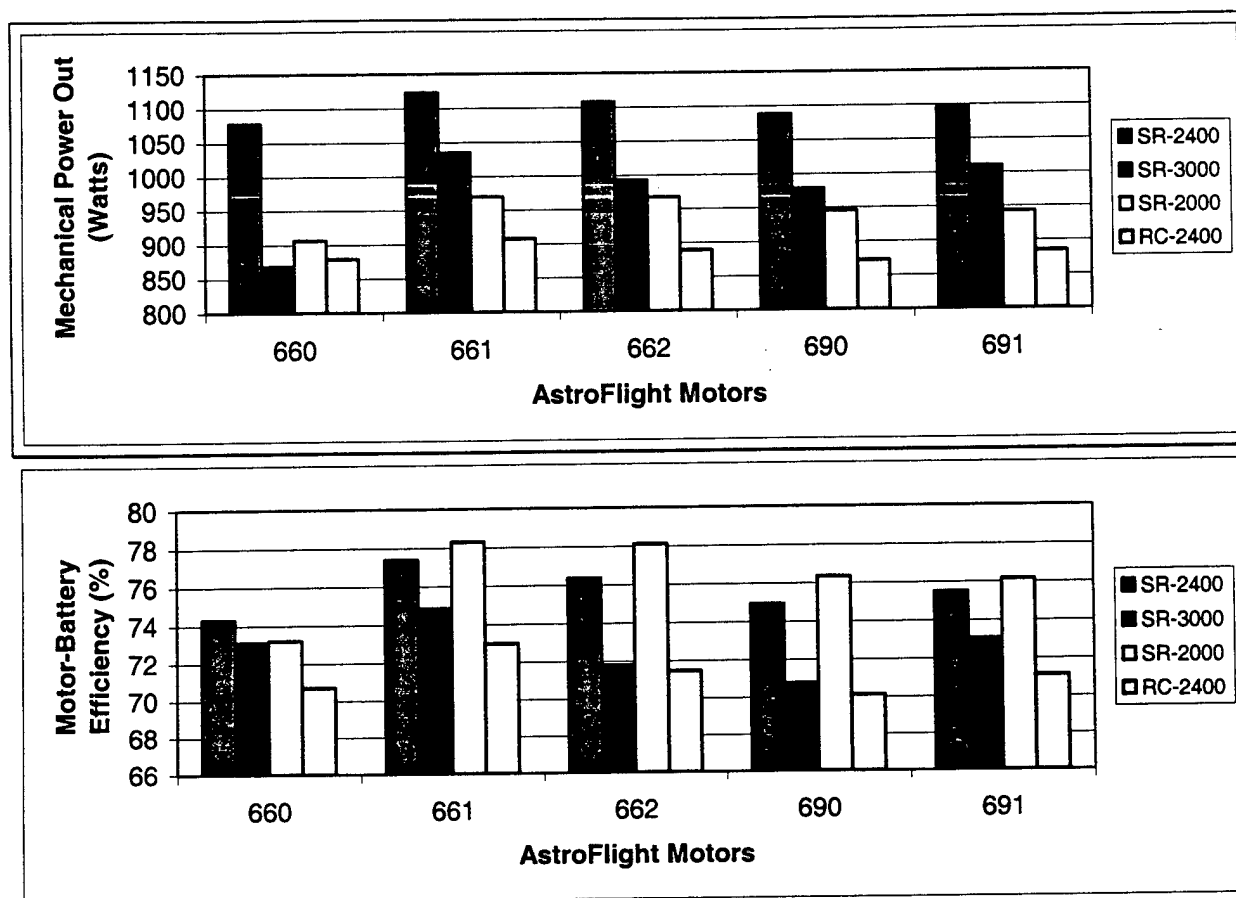


Figure 4.5: Mechanical Power Out of the Motor for Different Motor Battery Combinations (Top) and Motor-Battery Efficiency for Different Motor Battery Combinations (Bottom).

4.4.12 Propeller Selection

There were six main parameters for propeller selection--propeller size, propeller pitch over diameter (P/D) ratio, thrust from the propeller, torque from the propeller, power drawn by the propeller, and motor current used by the propeller. Extensive tests were conducted by performing experiments on twelve different propellers using a dynamometer and a wind tunnel to determine these six parameters. Data gathered from experimental tests was non-dimensionalized as four parameters--the coefficient of thrust (C_T), the coefficient of power (C_P), the overall propulsive efficiency (η), and the advance ratio (J). Graphing C_T , C_P , and η versus J gives definitive performance data of each propeller as shown in Figure 4.6. In addition, second-degree polynomials were fit to the C_T and C_P graphs. These polynomials were added to the computer models of the propulsion system. This allowed an accurate simulation of our propulsion system.

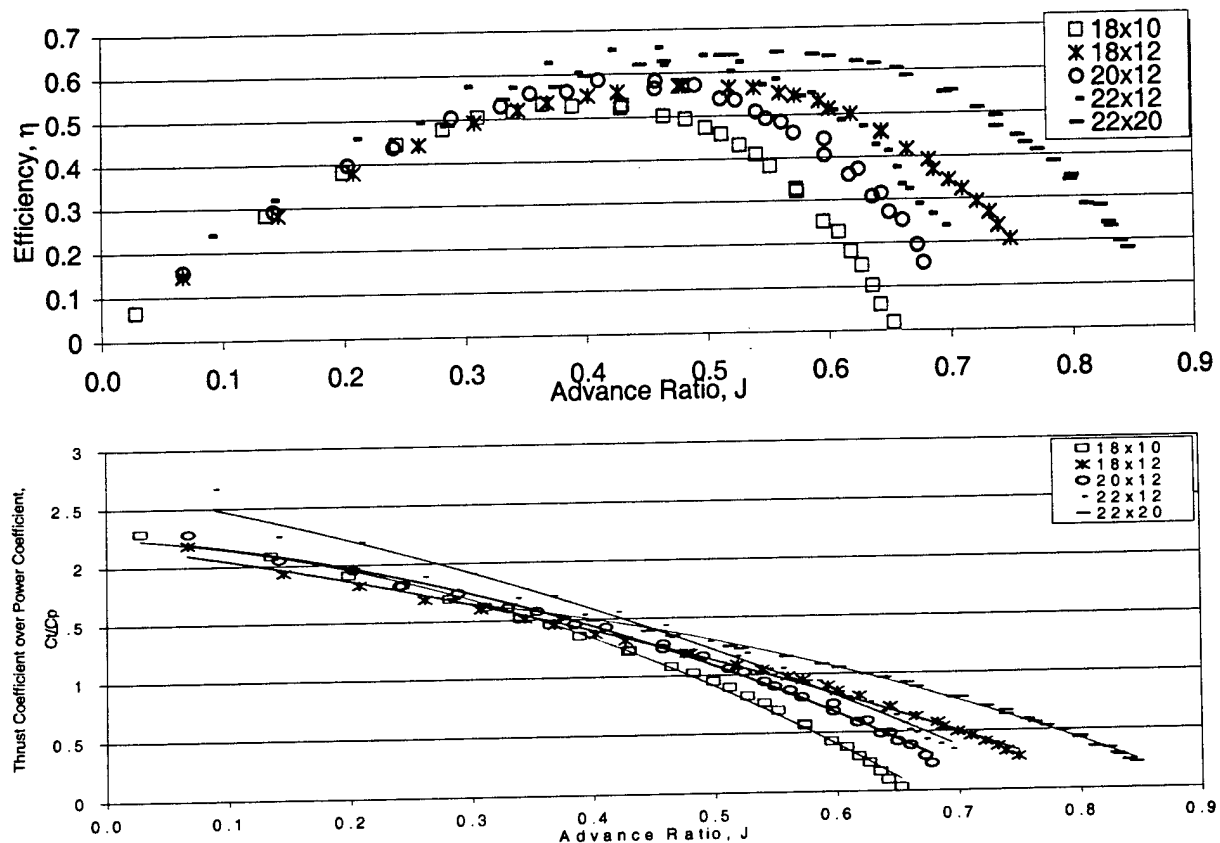


Figure 4.6: The overall efficiency of the propulsion system versus the advance ratio (Top) and the ratio of the thrust produced by the propeller to the power drawn by the propeller versus the advance ratio (Bottom)

Using the characteristic data from each propeller, the propeller size and the pitch over diameter ratio (P/D) were then iterated, to find the best propeller for the flight characteristics desired. Based on the optimization of the overall score, a 22-inch propeller was chosen.

Computer models, based on the experimental data, were then developed to give the performance of the propeller and the current drawn by the motor. The current drawn by the motor was used to estimate battery endurance. Using these models, iteration was begun to find the best gear ratio for the 22-inch propeller. That gear ratio was found to be 2.7:1.

4.4.13 Overall Configuration Sizing Data Summary

The preliminary design produced a plane that will reach the contest strategy requirements. The preliminary design is summarized in Table 4.6.

Wing Airfoil	Selig S1210
Wing Area	9.4 ft ²
Wing Span	10 ft
Wing Chord	11.28 in
Wing Angle of Incidence	0°
Aspect Ratio of the Wing	10.68
Aileron Area	0.705 ft ²
Polyhedral Angle	5°
Horizontal Tail Airfoil	Archer 18 (A18SM)
Horizontal Tail Area	1.75 ft ²
Horizontal Tail Root Chord	10.5 in
Horizontal Tail Span	31.5 in
Horizontal Tail Taper Ratio	0.5
Horizontal Tail Angle of Incidence	0°
Elevator Area	0.45 ft ²
Vertical Tail Airfoil	NACA 0009
Vertical Tail Area	1.25 ft ²
Vertical Tail Root Chord	12 in
Vertical Tail Span	17 in
Vertical Tail Taper Ratio	0.5
Rudder Area	0.32 ft ²
Fuselage Length	71.6 inches (6 feet)
Battery	SR-2400
Number of Batteries (in 5 lbs)	37
Motor	AstroFlight 661
Propeller Diameter	22 inches
Gross Take Off Weight, no cargo	18.25 lb.
Gross Take Off Weight, Volume cargo	31.25 lb.
Gross Take Off Weight, Heavy Payload	39.25 lb.

Table 4.6: Configuration Sizing Data

4.5 Features that Produced the Final Configuration Selection

During the preliminary phase many of the details of the plane's configuration were finalized. An Astroflight 661 motor will power the plane, with a power source made up of 37 cells of SR2400 NiCad batteries. To propel the plane, a 22-inch propeller will be used. The wings of the plane will be of polyhedral form using a Selig S1210 airfoil. The ailerons will be powered by 50 oz-in servos, in order to control the plane. The tail of the plane will be made with an Archer 18 (A18SM) airfoil in the horizontal direction, and an NACA 0009 airfoil in the vertical direction. The plane body will be built primarily out of foam-supported carbon fiber. The main landing gear will be bow type and built using carbon fiber. The nose gear will be a steerable aluminum/carbon fiber Oleo strut design.

5.0 Detail Design

5.1 Performance Data

With the tail and control surfaces sized, the aerodynamics team began to investigate the modes of motion and general dynamic stability of the airplane. Other values that had been included in the optimization, but never explicitly stated are include here as well.

5.1.1 Take Off Calculations

During the optimization, the distance and time required to take off was calculated. The calculations took into account the ground effects and estimated friction forces on the wheels. After the design was finalized the take off calculations were checked for the performance unloaded. The values are summarized in Table 5.1.

Take Off Condition	Distance (feet)	Time (seconds)
Heavy Payload (21 lbs)	161.0	6.6
Volume Payload (13 lbs)	92.7	4.3
No Payload	24.0	1.5

Table 5.1: Take Off Values

5.1.2 Handling Qualities

Once the static stability was set, the team began the dynamic stability and modes of motion calculations. The Eigenvalues of the modes can be seen in Table 19, and the modes of motion are summarized in Table 20. The Short Period motion was found to have a period of 0.832 seconds with a damping ratio of 0.536. The Phugoid motion was found to have a period of 9.037 seconds with a damping ratio of 0.041. The Dutch Roll motion was found to have a period of 1.589 seconds with a damping ratio of 0.39. The rules of thumb from literature predicted that these values would be acceptable in flight

	Eigenvalue
Short Period	$-4.0 \pm 6.3i$
Phugoid	$-0.03 \pm 0.69i$
Roll	-17.7
Spiral	-0.01
Dutch Roll	$1.544 \pm 3.64i$

Table 5.2: Eigenvalues

Mode of Motion	Frequency (Hz)	Damping Ratio	Period (seconds)
Short Period	7.55	0.53	0.83
Phugoid	0.69	0.04	9.03
Dutch Roll	3.95	0.39	1.58

Table 5.3: Motion Modes

5.1.3 Range

Since the plane was design to fulfill a specific mission profile, the range of the plane is best expressed in the number of laps of each type that can be completed. The plane is designed to handle 3 laps of the heavy payload, steel, and 3 laps of the light payload, tennis balls. The total distance flown should be approximately 24000 feet or 4.5 miles.

5.1.4 Endurance

Similar to the Range the endurance of the craft is best expressed in terms of the scoring laps that can be completed. Since the optimal score point is found by using all the energy in the batteries in the exact limit of the contest run time, the plane is designed for 10 minutes of flight.

5.1.5 Payload

The payload configuration of the plane was one of the primary design parameters during conceptual and preliminary design. For the volume payload, the plane was structured around a tennis ball configuration that contained the 100 tennis balls of the optimal score value. For the heavy payload, the structures teams designed to the maximum weight allowed under the contest rules, 55 pounds. This will allow the team to vary the amount of steel carried based on the conditions at the contest site. The tennis ball configurations can be varied as well, allowing the team to pursue any strategy within the limits of the plane's performance characteristics. The estimated Gross Take Off Weight, GTOW, for the tennis ball lap is 31.25 lb. The GTOW for the steel is estimated at 39.25 lb.

5.2 Component Selection and Systems Architecture

The configuration of the plane can be divided into two main sections: propulsion and structures

5.2.1 Propulsion Component Selection and System Architecture

As mentioned previously, the SR-2400 battery was chosen as the best battery for the flight conditions. After talking to SR, it was decided to buy pre-manufactured matched packs. Each packs consists of 37 cells and is separated into a front pack, consisting of 27 cells, and a rear pack, consisting of 10 cells. This pack configuration fits around the wing carry through structure under the payload area. The 37-cell pack gives a nominal operating voltage of 44.4 volts. The optimization called for take off current of 30 amps and cruise current of approximately 20 amps. Based on experimental results of last year's battery

packs, it is felt that seven or eight take offs can be achieved. The motor chosen was the AstroFlight 661 motor. The factory-supplied gearbox of 2.7:1 will be used. The plane will have a cruise speed of 80 ft/sec so a high P/D ratio propeller was chosen. A higher P/D ratio results in peak efficiency at higher speeds. A 22-inch propeller was chosen.

5.2.2 Structures Component Selection and System Architecture

The Structural system of the plane consisted of the fuselage, wings, tail and landing gear.

The fuselage is designed to carry the required payload while weighing as little as possible. To do this it made the most efficient use of space to maintain a short length and small volume. The fuselage must also support the aerodynamics and propulsions systems. The shape of the fuselage was also designed to reduce frontal surface area and therefore drag.

The wings will be made of Selig 1210 airfoils; they are equipped with ailerons to control the plane while turning. Each wing also contains one main spar that was designed to withstand the tip test imposed at the beginning of the competition.

The tail horizontal the Archer 18 (A18SM) airfoil, and the vertical tail the NACA 0009 airfoil. The Archer airfoil was used to reduce the size of the tail required for the plane, this aided in both weight and drag reduction.

The final structural component is the landing gear. The demands of the landing gear are high. It was designed to withstand the rigors of landing the plane while being as light as possible. The final landing gear design has considered all the possible loads that could be induced upon landing and how to properly transmit these loads to the structure of the plane.

For a visual of the systems architecture please see the drawing package.

5.3 Drawing Package

To view the drawing package, please turn to the last five pages of the report.

5.4 Innovative Configuration Solutions, Manufacturing Process, Cost Reduction

Many of the design decisions were made to reduce cost, and are discussed in their respective sections. The rules of the contest actually aid in reducing cost since the plane is penalized for size and smaller planes are cheaper. Also, the more efficiently the plane was built, the cheaper it should be. Most of the innovative design decisions had to do with the manufacturing process and can be seen in the following list.

- Ball Configurations: The seven ball hexagonal form was slanted to further reduce frontal area of the plane.
- Fuselage construction: The bottom of the fuselage was laid up as one piece for structural purposes. The wing carry through was also included in the fuselage mold so that it could be simultaneously laid up to reduce stress concentrations at the connection.
- Female molds were used to get a smooth surface on the outside surfaces of the aircraft.
- The polyhedral was laid up as one piece and baked at the correct angle into the wing. The ability to use the same mold for both sides guarantees the angles for both the right and left sides of the wing should be identical.
- The structural bulkheads and longerons were designed and built around the batteries to make efficient use of the space.
- Moving some of the tennis ball payload into the nose and tail of the plane reduced fuselage length.
- Carbon fiber bow main landing gear with a nonrectangular cross-section was implemented to reduce weight. Similarly a carbon fiber strut was used on the nose gear also to reduce weight.

All of these innovative configurations helped to make the manufacturing process more efficient or the plane less expensive.

6.0 Manufacturing Plan

6.1 Manufacturing Processes Investigated, Cost and Skill Required

Several methods of fuselage mold preparation were researched. For any of these methods, a master mold had to be made to either the dimension of the inner mold line (IML) or outer mold line (OML) of the aircraft. There were three processes investigated for making a master mold: Computer Numeric Controlled (CNC) machining a block of tooling dough/foam, wire cutting sections of foam, or carving tooling dough by hand.

By CNC machining a master mold, excellent tolerances and smooth surfaces could be achieved. This method would be very expensive because a CNC was not available to the team. This then would require subcontracting to make the molds. This makes the availability of this process very low.

The method of foam wire cutting had advantages in that the foam was inexpensive, and the skill level matched that of the team. The foam must be cut in sections using parallel templates. The parallel templates made it difficult to align all the sections and produce a blended shape. The cost of the foam was much less than that of the tooling dough, and CNC machining. This method also required less time to manufacture since foam sheets were readily available from local suppliers.

The carving of tooling dough by hand had advantages in that it is cheaper than CNC machining. Also, it can be made in one piece making the master more rigid than foam. Tooling dough was more expensive than foam, and the geometric tolerances would be difficult to maintain. Also, the team had no experience with tooling dough. After comparing the candidates with the decision matrix seen in Table 6.1, the decision was made to make the molds out of foam.

Figure of Merit	CNC	Tooling Dough	Foam
Cost	3	3	4
Skill Required	1	1	2
Availability	1	2	2
Total	5	6	8

Table 6.1: Manufacturing Decision Matrix

The next manufacturing decision involved two competing carbon fiber lay-up ideas. The team could either make a thin female mold out of fiberglass off an OML master, cut the OML master down to an IML master and lay-up the carbon fiber fuselage on an IML master plug with the flexible OML mold bagged to the outside for surface finish, or make a rigid female mold off an OML master and lay-up carbon fiber on the that OML female.

The OML female is the industry standard for many parts. For this purpose, the female mold should make the outside smooth to reduce drag. An OML female mold required additional backup structure in order for the mold to hold its dimension under vacuum.

During the detailed design phase, it was decided to use a foam core for much of the fuselage skin. This core was a thin cut off the OML foam master. For the structure the most critical dimension was the IML because speed loaders and batteries must fit precisely. Thus, an IML plug allowed the pieces to be laid-up from the inner dimension out. The designed 1/8-inch foam core between the outer and inner fuselage skins would be difficult to maintain precisely. Using an OML female mold, any core dimension errors would affect crucial internal areas. In the end, it was decided to lay-up carbon fiber on the male IML foam plug to save cost and time.

6.2 Process Selected for Major Component Manufacture

After the detail design was complete, final manufacturing plans were laid out. The team decided to use carbon fiber 2X2 3K twill as a sandwich with primarily foam core for the entire airplane. In order to use either pre-impregnated carbon fiber or a wet-lay-up fabric, a mold must be used to acquire the correct shape. The blended fuselage design required proper mold planning in order to achieve a light and durable structure and a smooth outer surface finish. The fuselage design involved four separate parts--bottom fuselage, motor cover, speed loader hatch, and upper aft section.

In mold design it is crucial to be able to remove the mold after curing it. Proper mold design and release techniques were planned as methods for this reason. For each of the fuselage parts, a separate mold was required. In order to secondary bond surfaces, a peel-ply material was purchased for use in the lay-up. Proper release films, breather, bagging films and sealants were all acquired for carbon fiber lay-up.

6.3 Individual Processes Investigated and Figures of Merit Used

For the manufacturing process, the figures of merit used were the main components of the plane. Each component, along with an investigated manufacturing process is discussed in the sections below.

6.3.1 Fuselage Process

The foam for the fuselage masters was to be first cut into accurate blocks of foam by gluing pieces together and wire cutting the blocks to dimension. By using templates cut to dimension and a rotating wire cut, rounded foam sections were used. These rounded sections were aligned on a tooling board. OML flexible fiberglass females were laid and cured on the OML plugs. An IML plug was aligned on a tooling board using the reduced sections. The fuselage parts were made by laying up carbon fiber, foam core, carbon fiber, and the flexible female molds on the IML plugs, and then vacuum bagging the entire lay-up.

6.3.2 Wing and Tail Process

The wing molds were easier to design since foam core was chosen for the airfoils. When cutting out the wing with templates, female cradles were formed simultaneously. To obtain a smooth finish on the wing, proper treatment of the foam cradles was important. It was decided to coat the cradles with a thin epoxy resin and wet-sand the surface until smooth. To increase efficiency, one female cradle was designed with the capacity to cook both wings using the same mold. In order to get the polyhedral bend in the wings, a five-degree foam angle block was cut and glued to the cradles. The wing spars were made in three parts. A "C" spar was laid up on a precision-machined piece of oak mold. Two additional rectangular spars were also added. Servo wire slots were cut into the wings with a hot wire.

Like the wing, the horizontal and vertical tails were made by cutting a foam core and female cradles. They were also composed of a single layer of carbon fiber on the foam core.

6.3.3 Landing Gear Process

The bow gear mold was made again with foam. The surface finish was acquired by applying epoxy and sanding both top and bottom mold surfaces. Several sets of bow gear were planned for spares in case of failure. The nose gear was machined out of aluminum and bonded with a carbon fiber tube.

6.4 Analytic Methods Including Cost, Skill Matrix, and Scheduling

As discussed previously, each of the different manufacturing methods had different costs, time to order and receive, and skill required. To CNC the molds would require a lot of time just to make the molds. This was time that would be better spent actually making the carbon fiber parts. Making the molds with tooling dough would require a higher skill than the team had available and would cost more. Foam cutting would require a lot of time and the necessary tools, but fortunately OSU owns the tools needed.

6.4.1 Manufacturing Schedule

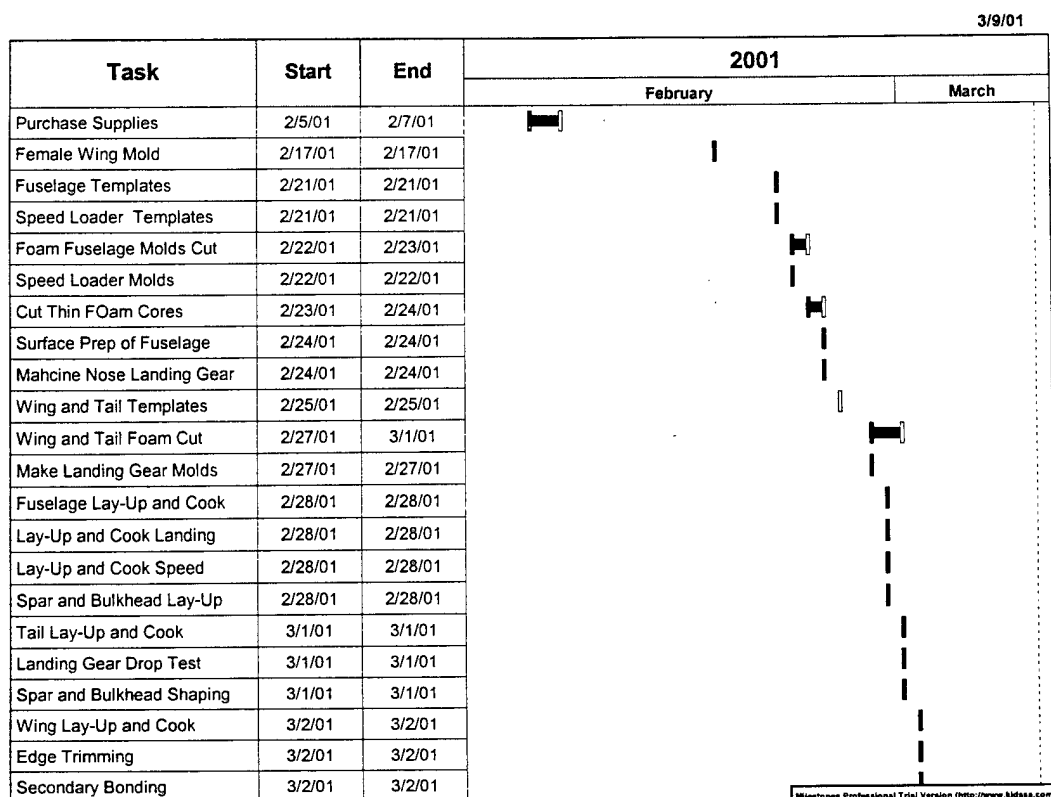
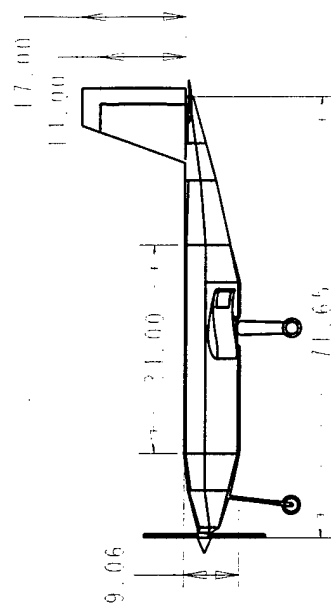
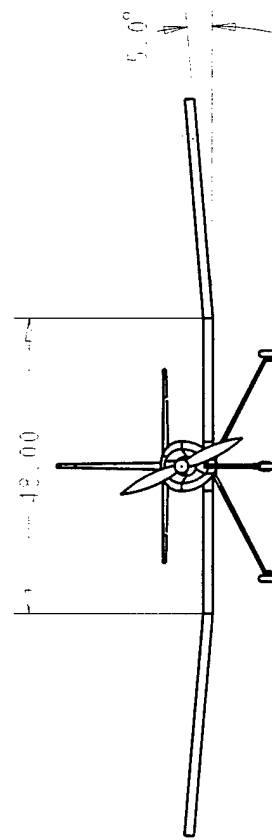
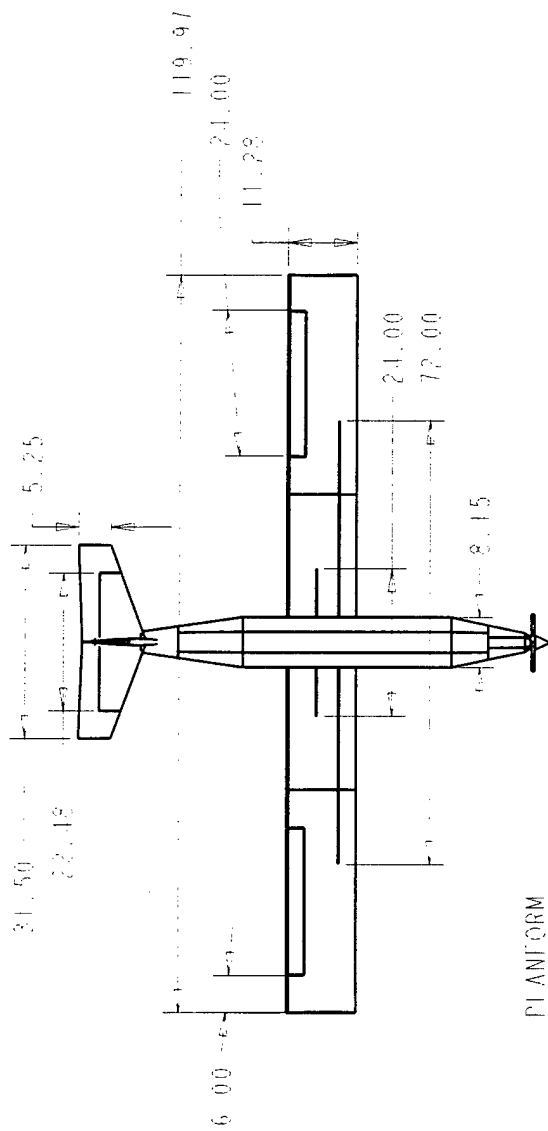


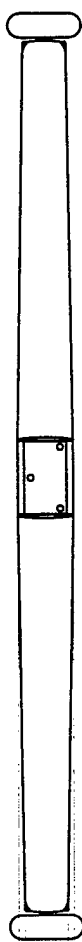
Figure 6.1: manufacturing schedule for the prototype

6.5 Innovative Configuration Solutions, Manufacturing Process, and Cost Reduction

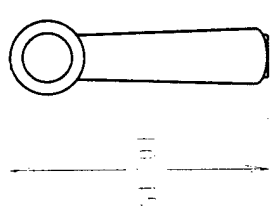
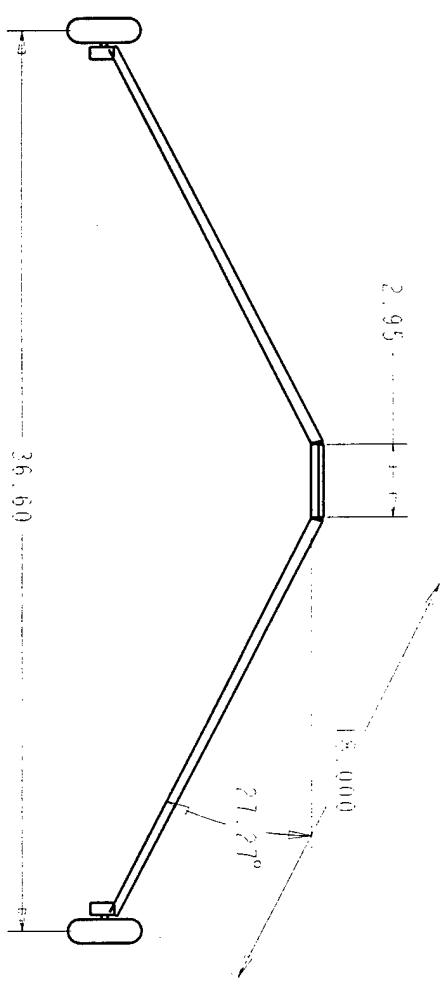
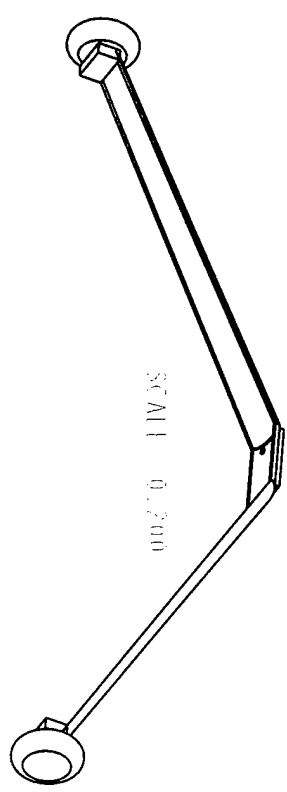
To reduce cost of manufacturing, the team made a few innovative decisions. In the past, OSU teams have a history of using carbon fiber, but usually their molds were not re-useable. This year, the molds were treated in a way that they would be reusable. Since the team will be building both a prototype and the final plane, this process will reduce both cost and time. The wing lay-up procedure is also time and cost reducing procedure (see Wing Process 6.2.3). Most of the cost-reducing, innovative details of the configuration have been discussed in the previous sections 5.4, 6.2 and 6.3.



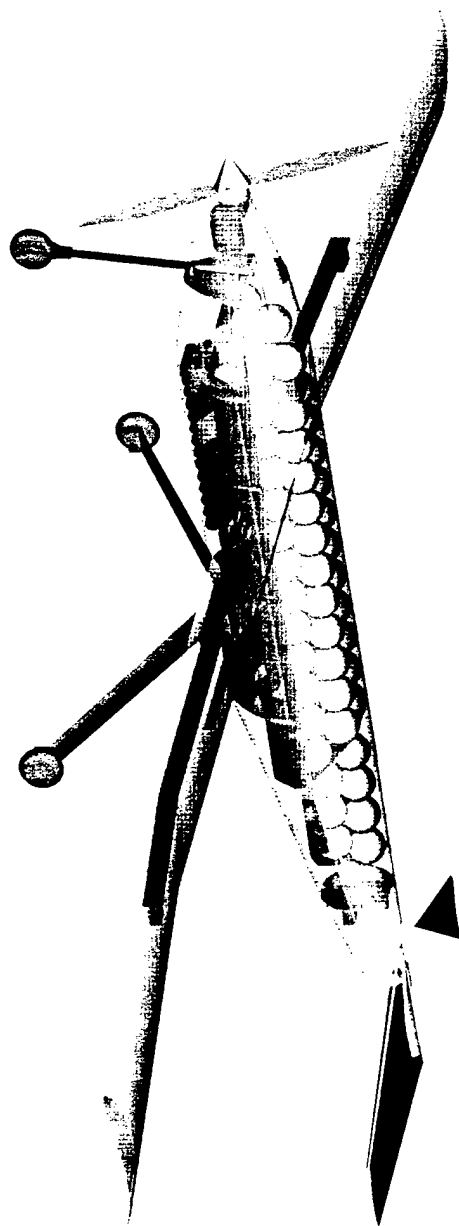
PORT VIEW	
COSY H BLACK HAM	
CAUSE 9.95	



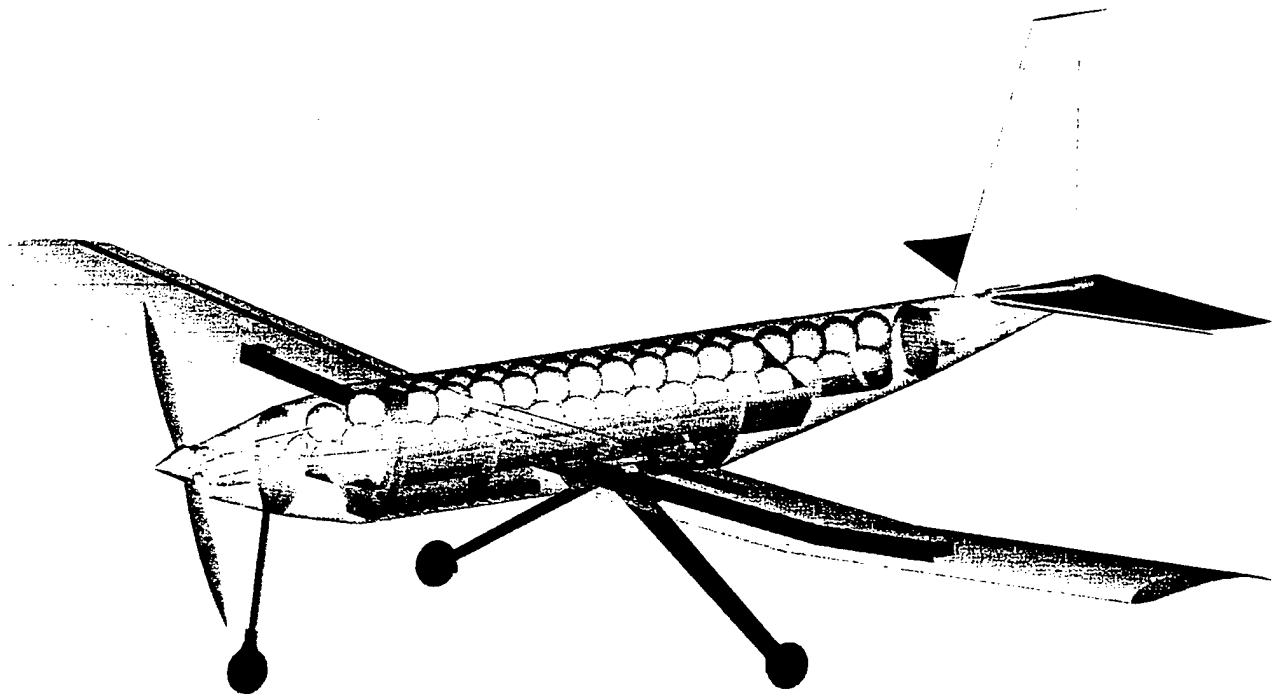
1.75
2.25



MAIN LABELING OF AIR	
OUTER AIR IN AIR	
10.15	



**AIAA/CESSNA/ONR
Design/Build/Fly Competition**



Design Report - ADDENDUM PHASE

**OSU Black
Oklahoma State University
April 10, 2001**

Table of Contents

PROPOSAL PHASE

1.0 Executive Summary.....	3
2.0 Management Summary.....	4
2.1 Architecture of the Design Team.....	4
2.2 Design Personnel and Assignment Areas.....	5
2.3 Personnel Assignments, Schedule Control, and Configuration Control.....	6
2.4 Milestone Chart.....	7
3.0 Conceptual Design.....	8
3.1 Mission Analysis and Strategy Development.....	8
3.1.1 Pre-Conceptual Design.....	9
3.1.2 Phases of Mission Operation.....	9
3.1.3 Primary Design Parameters.....	10
3.1.4 Operational Constraints.....	11
3.1.5 Sensitivity Analysis.....	11
3.1.6 Strategy Development.....	12
3.1.7 Contest Strategy.....	12
3.2 Alternative Concepts Investigated.....	13
3.2.1 Conceptual Planform Layout Alternative.....	14
3.2.2 Wing Placements Alternatives.....	14
3.2.3 Alternative Fuselage Concepts.....	15
3.2.4 Alternative Tail Concepts.....	15
3.2.5 Alternative Landing Gear Concepts.....	16
3.2.6 Alternative Propulsion Concepts.....	16
3.2.7 Material Selection Alternatives.....	18
3.3 Figures of Merit and Their Mission Features.....	18
3.4 Final Ranking Chart.....	20
3.5 Features of the Final Conceptual Configuration.....	20
4.0 Preliminary Design.....	21
4.1 Design Parameters Investigated.....	21
4.1.1 Operational Constraints.....	22
4.2 Figures of Merit.....	22
4.3 Analytical Methods, Expected Accuracy, and Reasoning.....	23
4.3.1 Analytical Methods.....	23
4.3.2 Experimental Methods.....	24
4.4 Configuration Sizing Data.....	24
4.4.1 Airfoil Selection.....	24
4.4.2 Pitch Stability.....	25
4.4.3 Yaw Stability.....	26
4.4.4 Roll Stability.....	27
4.4.5 Horizontal Tail Planform Layout Selection.....	27
4.4.6 Horizontal Tail Airfoil Selection.....	28
4.4.7 Flight Stability Derivatives.....	29
4.4.8 Fuselage Shape Consideration.....	39
4.4.9 Wing Structure Design.....	31
4.4.10 Landing Gear Design.....	33
4.4.11 Motor and Battery Selection.....	33
4.4.12 Propeller Selection.....	35
4.4.13 Overall Configuration Sizing Data Summary.....	36
4.5 Features that Produced the Final Configuration Selection.....	37
5.0 Detail Design.....	38
5.1 Performance Data.....	38
5.1.1 Takeoff Calculations.....	38
5.1.2 Handling Qualities.....	38

5.1.3	Range	39
5.1.4	Endurance	39
5.1.5	Payload.....	39
5.2	Component Selection and Systems Architecture	39
5.2.1	Propulsion Component Selection and System Architecture	39
5.2.2	Structures Component Selection and System Architecture	40
5.3	Drawing Package.....	40
5.4	Innovative Configuration Solutions, Manufacturing Process, Cost Reduction	40
6.0	Manufacturing Plan	42
6.1	Manufacturing Processes Investigated, Cost and Skill Required	42
6.2	Process Selected for Major Component Manufacture.....	43
6.3	Individual Processes Investigated and Figures of Merit Used	43
6.3.1	Fuselage Process.....	43
6.3.2	Wing and Tail Process	44
6.3.3	Landing Gear Process.....	44
6.4	Analytical Methods Including Cost, Skill Matrix, and Scheduling	44
6.4.1	Manufacturing Schedule.....	45
6.5	Innovative Configuration Solutions, Manufacturing Process, Cost Reduction	45

ADDENDUM PHASE

7.0	Lessons Learned	53
7.1	Prototype Testing	53
7.1.1	Speed Trials	54
7.1.2	Endurance (Energy Usage) Trials	54
7.1.3	Contest Lap Trials	55
7.2	Areas for improvement in the Final Design and Manufacturing Process	55
7.2.1	Aerodynamic and Propulsion Improvements	55
7.2.2	Structural and Manufacturing Improvements	56
7.3	Aircraft Differences Between Proposal and Final Design	56
7.3.1	Landing Gear	56
7.3.2	Fuselage and Tail	57
7.3.3	Contest Strategy	58
7.4	Time and Cost to Implement Design Changes	58
8.0	Aircraft Cost	59
8.1	Documentation of Rated Aircraft Cost	59

7.0 Lessons Learned

7.1 Prototype Testing

As the OSU Black Team finished the prototype, the name *RAVEN* was attached to it due to its resemblance to the bird of the same name. Once the prototype plane was completed, the team began testing. The Ditch Witch airport facility in Perry, Oklahoma was used. The paved runway simulates the contest site rather well. As testing was conducted, it was found that a set of checklists were necessary to prepare the plane and avoid mistakes. The tests focused on determining how closely the strategy requirements were met. The strategy development techniques used by the design team would be proven or disproven by the performance of the *RAVEN*. Images of the flights are in Figures 7.1.

The prototype testing had one main goal, to determine how well the plane would perform at the contest. To reach that goal a series of tests were devised to test the *RAVEN's* performance at the contest. The tests to learn how the plane would score were the lap time trials and the energy usage trials. Other aspects of the flight tests were to measure its durability, landing performance, lifting capacity, taxiing, braking and ground speed tests. The plane was taxi tested in a parking lot for steering control and nose gear tracking. The brakes on the nose gear were tested at this time for braking power. The nose gear brake was satisfactory. The plane was flown first without payload to allow the pilot to trim the plane

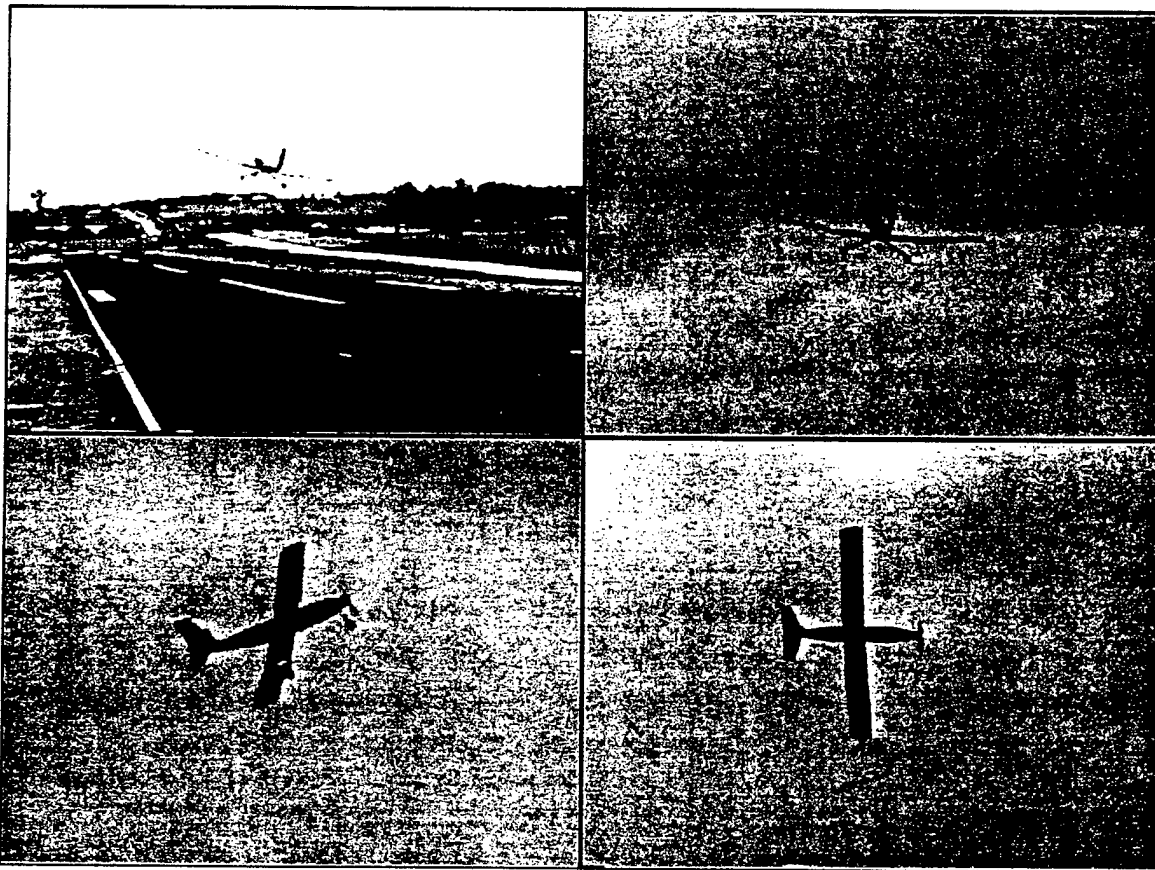


Figure 7.1: *RAVEN* in flight

and become familiar with the handling qualities. After the pilot felt comfortable with the *RAVEN*, the team moved into lift testing. The *RAVEN* was tested with payload up to 13.4 lb. (35 lb. gross weight). The plane could take off with more weight, but this payload would be used for the speed trials, landing tests and energy usage tests. The landing tests were, of course, performed each time the *RAVEN* flew. The last area of interest was how well the plane aged as it went through the flights and crashes. The wing and fuselage impacted and slid on the paved runway more than once. The *RAVEN* was still performing well on the last prototype flight. The prototype had only taken minor damage over the course of the ten flights and landings. The tests for the speed trials, the energy usage and lap times are explained in detail as these tests are most important to the performance at the contest.

7.1.1 Speed Trials

Once it was confirmed that the plane could lift a 13.4 lb. payload (gross weight of 35 lbs.), the speed tests were run. The tests were run for both full throttle and minimum power to remain aloft. In order to remove the effect of the wind, the test was done both up and down wind. The two were then averaged. The tests involved measuring the time for the *RAVEN* to travel the distance of 580 feet. Table 7.1 lists the results for the speed trials.

Full Power	Ground Speed (ft/sec)	Predicted Speed (ft/sec)
Upwind	64.44	-
Downwind	72.5	-
Average Speed (ft/sec):	68.47	79
Minimum Power	Ground Speed (ft/sec)	Predicted Speed (ft/sec)
Upwind	38.67	-
Downwind	52.73	-
Average Speed (ft/sec):	45.70	44.7

Table 7.1: Results for the Speed Trials, 13.4 lb. payload, 35 lb. gross weight

It is important to note that gearbox, 3.1 to 1, used on this trial was that of the design, 2.7 to 1. The design gearbox should produce less thrust, but more speed. The loss of thrust would not be a problem as the correct gearbox was used in later experiments and the *RAVEN* did not develop any thrust related problems. The results matched well for a prototype. The speeds were found to be acceptable to the design strategy.

7.1.2 Endurance (Energy Usage) Trials

With speed runs complete, the team moved into the endurance test phase. The goal of these tests was to determine the amount of energy used for each of the two contest sorties, steel and tennis ball. By this point a gearbox with the correct ratio was available. The results of these tests are in Table 7.2. The energy usage estimates were accurate. However, a new problem was found during these tests. The

actual useful energy stored in the batteries was not 2.4 amp-hours as specified by the manufacturers. The batteries actually held only about 2.1 amp-hours of useful power at the discharge rates used. The last lap of the contest run could not be run as the batteries were drained of energy. This required a redesign of the contest strategy.

Tennis Ball Lap	
Energy Used (Ahr)	Prediction (Ahr)
0.444	0.475
Steel Lap	
Energy Used (Ahr)	Prediction (Ahr)
0.339	0.343

Table 7.2: Energy used on each of the two contest sorties for a 13.4 lb. payload

7.1.3 Contest Lap Trials

With the endurance and airspeed trials finished the team started timing the contest laps as the plane made a circuit around the course. The *RAVEN* proved to be close to predictions for the steel payload, off by 7 seconds. The tennis ball lap was not as good, a difference of 24 seconds. For the power levels that are needed to conserve batteries, the speed around the course is too slow. The comparisons are in Table 7.3.

Tennis Ball Lap	
Actual Time (sec)	Prediction (sec)
105	81
Steel Lap	
Actual Time (sec)	Prediction (sec)
60	53

Table 7.3: Time for each of the two contest sorties and prediction, 13.4 lb. payload

7.2 Areas for improvement in the Final Design and Manufacturing Process

The prototype performed well. The improvements will be discussed in two sections. The first is Aerodynamic and Propulsion Performance. The second section is Structural and Manufacturing Processes.

7.2.1 Aerodynamic and Propulsion Performance Improvements

These improvements centered on reducing the drag of the plane and reconfiguring the contest strategy to handle the true capacity of the batteries. The high drag was a result of poor surface finish on the wings and tail. The interface between the tail and the fuselage added to the drag. This area had tight corners

with rough surfaces. The main landing gear connection point contained several exposed bolt heads and sharp corners.

The weakness in the propulsion system was battery endurance. The power plant stopped producing useful power after the 2.1 amp-hour point. After researching battery performance, it was found to be unlikely that any battery would store more total energy. This new information would be used to update the optimization routines.

7.2.2 Structural and Manufacturing Improvements

The construction of the *RAVEN* demonstrated some of the flaws with the proposal design. The prototype tests, and crashes, found others. During one of the first test flights, the nose gear snapped off. The problem was found to be due to change in material at the point of failure. The main landing gear failed as well after bouncing twice on touch down. A reworking of the landing gear was required.

The fuselage and tail became an area of continued difficulty. When the fuselage was removed from the male plug mold, it was discovered that the fuselage had not kept the shape of the outer mold well. While mounting the tail section onto the fuselage, the tail was found to be structurally weak and in need of reinforcement. The upper and lower fuselage sections mated imperfectly.

7.3 Aircraft Differences Between Proposal and Final Design

During the prototype testing each major component of the *RAVEN* was considered for improvement. The prototype wing was found to work well and the final wing would be made using the same methods as the original. There were several other areas where minor improvements were needed. Some of the areas that received minor changes were: servo wiring, control surface servos and control rods connection and placement, and the mounting of the nose gear to the firewall. The areas where major changes in design or manufacturing process took place were the landing gear, fuselage and tail, and contest strategy.

7.3.1 Landing Gear

During the first flights of the *RAVEN*, the nose gear broke off when the prototype rolled off the runway into the grass. After inspection, it was found that the gear broke at the interface of aluminum with graphite shaft. The gear was replaced with an all aluminum piece. The new gear performed better for only a small increase in weight. To make up for the weight of the nose gear, the mounting material was changed from aluminum to delron, a lightweight structural plastic.

The main landing gear appeared to function well until the last of the prototype tests when on landing the *RAVEN* bounced twice and then broke the main gear. After inspection, the gear was redesigned for lighter weight and more strength. The shape of the cross-section of the gear was modified so that a

greater number of composite layers could be used with more strength at an equivalent weight. The wheelbase was shortened to reduce weight and drag. The height was reduced for similar reasons. The new landing gear centered on using honeycomb along the entire length of the gear from the wheel attachment to the connection with the fuselage. The honeycomb use meant that the complex curves of the original design were abandoned, as the honeycomb cannot form the shapes of the original design.

7.3.2 Fuselage and Tail

As the fuselage was made, several errors were found. The first of which was that the horizontal tail was placed on top of the circular fuselage. The interface between the flat tail and the round fuselage became complicated, and the weight of the tail as a whole increased due to the need for structural reinforcement. To fix this flaw, the horizontal stabilizer was moved down until it joined the fuselage at the widest point of the aft section's circumference. This also allowed the control rods connecting the control surfaces and the servos to remain within the fuselage with only a small exit port close to the surfaces.

The final aircraft will benefit from the lessons learned during the prototype construction. The fuselage will be constructed using a female mold to insure that the proper outside dimensions are reached (See Fig 7.2). The prototype was built using a male plug that could only maintain the inside shape of the fuselage

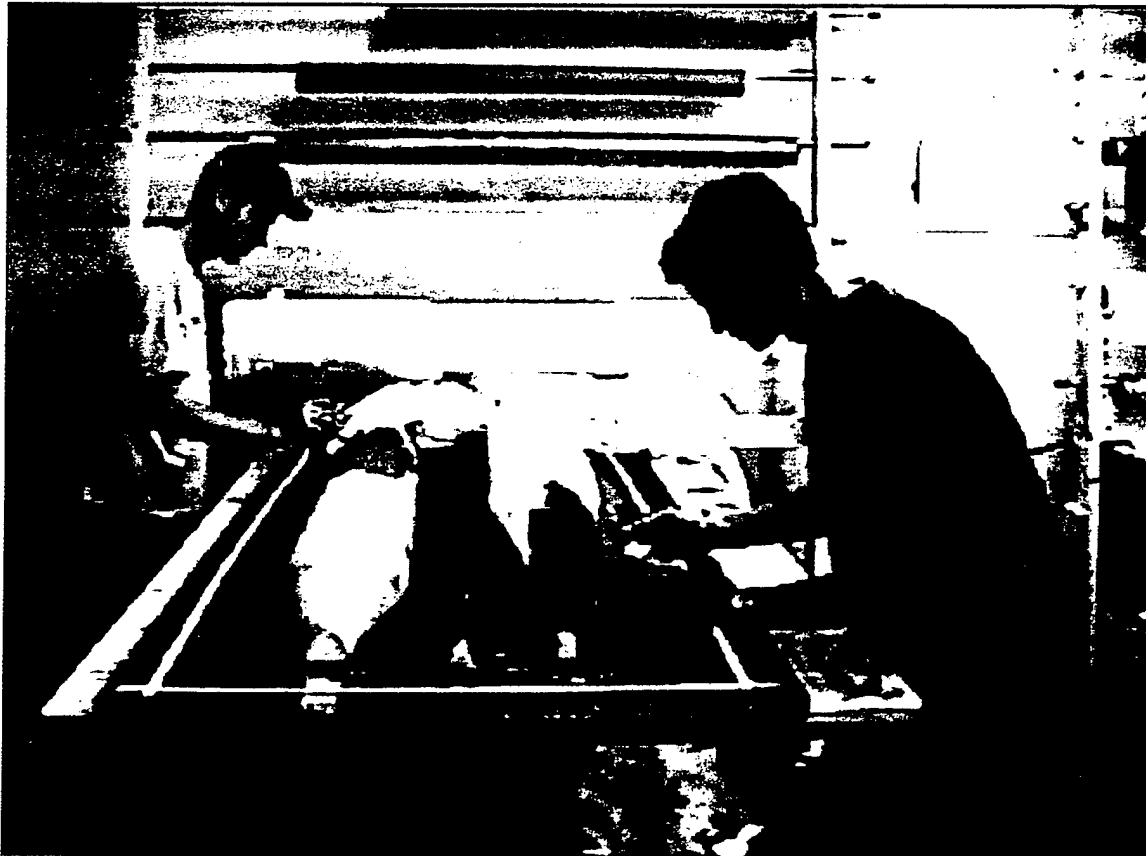


Figure 7.2: The male master plugs being prepared to make the female molds

properly. The fuselage was left long on the sides in the final so that the meeting of the upper and lower section could be more easily made to mate. To correct a problem with the motor mount, a torque tube was added into the design of the final. The tube should handle the stresses on the mount from the motor. The hinge and securing mechanisms for the speed loader hatch were designed with this new manufacturing process in mind.

7.3.3 Contest Strategy

As the data on the performance of the *RAVEN* was collected, the optimization routines used to determine the strategy for the contest were updated. The proposal phase contest strategy was found to be too optimistic. The strategy of three laps each of steel and tennis balls was not possible due to the limits of the battery storage. The optimization was refined and the new combination of two steel laps and three tennis ball laps was selected as the best possible strategy for the competition. The computer optimization routines zeroed in on a full payload of tennis balls (100) and a payload of 15.3 pounds of steel. The new strategy has more flexibility than the proposal phase strategy and can let the team take advantage of wind conditions at the contest site, whatever the conditions are. The plane was design with the idea of flexibility strategy foremost in mind.

7.4 Time and Cost Required to Implement Design Changes

The final plane will have the benefit of the refinements made for the prototype. Most of the changes made in the redesign of the *RAVEN* were easy to implement with known manufacturing techniques. The material requirements for the two planes, prototype and final, were the same therefore the cost did not change appreciably. The time to complete the tail, wing and landing gear all dropped significantly. The team had experience fabricating these parts, so the process took less time. The time for fuselage construction went up drastically as the female molds were new to the structures group and they take inherently more time. In addition, the motor mount and torque tube were laid up with the lower fuselage as one piece. This was a new process that needed to be tested. The changes made in the final plane reduced the Rated Aircraft Cost. The two pounds of Manufactures Empty Weight that the final lost reduced the RAC by 0.2.

8.0 Aircraft Cost

8.1 Documentation of Rated Aircraft Cost

The aircraft parameters that apply to the Rated Aircraft Cost and the calculation of the RAC are in Table 8.1. A breakdown of the RAC by percentages is included in Figure 8.1.

Description	Supplied Cost Model	Aircraft Parameter	Man Hour Score	Coefficient Cost Multiplier	RAC Contribution (\$ thousands)
MEW Manufacturers Empty Weight	Actual airframe weight, lb., without payload or batteries	18 ^{12.7} lb.	-	\$100/lb.	1.3
REP Rated Engine Power	# engines Fuse Rating # cells	1 motor 20 Amps 37 cells			
	REP = (# engines * Fuse Rating * 1.2 V/cell * # cells)	888 watts	-	\$1/watt	0.888
MFHR Manufacturing Man Hours	WBS 1.0 Wing(s)				
	15 hr/wing	1 wing	15		
	+4 hr/sq ft Projected Area	8.8 sq. ft.	35.2		
	+2 hr/strut or brace	0 struts or braces	0		
	+3 hr/control surface	2 control surfaces	6		
	Subtotal of ManHours for 1.0 Wing(s):		56.2	\$20/ManHr	1.124
	WBS 2.0 Fuselage and/or pods				
	5 hr/body	1 fuselage	5		
	+4 hr/ft of length	5.9 ft. of length	23.6		
	Subtotal of ManHours for 2.0 Fuselage and/or pods:		28.6	\$20/ManHr	0.572
	WBS 3.0 Empenage				
	5 hr. (basic)	1 empenage	5		
	+5 hr./vertical surface	1 vertical surface	5		
	+10 hr./horizontal surface	1 horizontal surface	10		
	Subtotal of ManHours for 3.0 Empenage:		20	\$20/ManHr	0.4
	WBS 4.0 Flight Systems				
	5 hr. (basic)	1 Flight System	5		
	+2 hr./servo or controller	5 servos	10		
	Subtotal of ManHours for 4.0 Flight Systems:		15	\$20/ManHr	0.3
	WBS 5.0 Propulsion Systems				
	5 hr./engine	1 motor	5		
	+5 hr./propeller or fan	1 propeller	5		
	Subtotal of ManHours for 5.0 Propulsion Systems:		10	\$20/ManHr	0.2
MFHR = Sum of WBS hours		Total of ManHours:	129.8		
				RAC:	4.784

Table 8.1: Calculation of the RAC

4.754

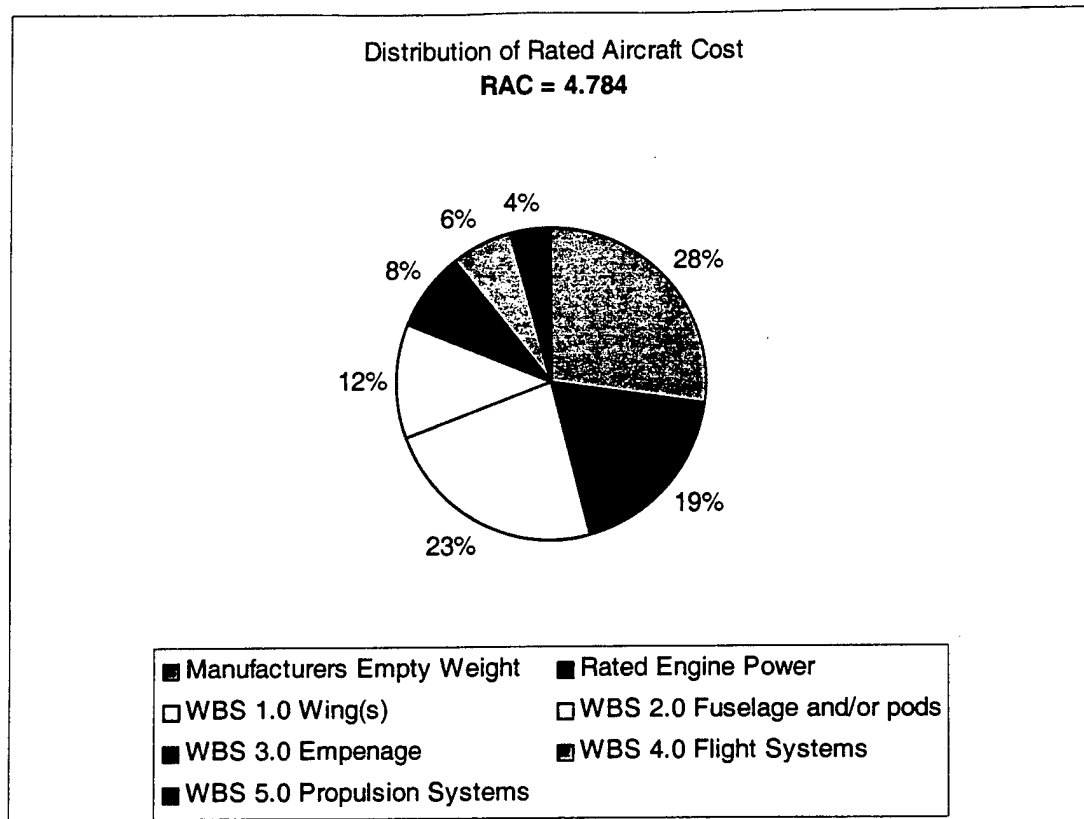
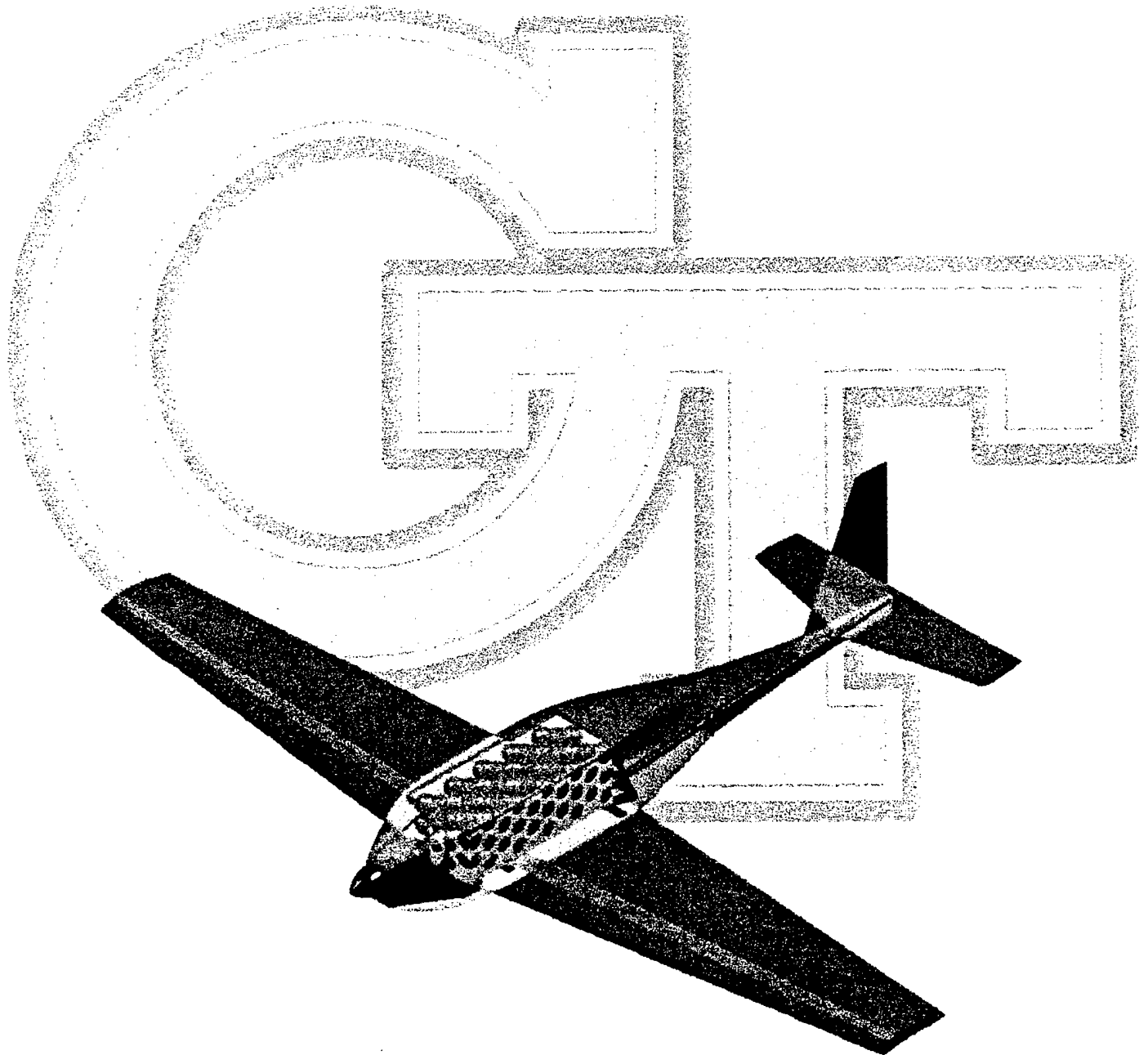


Figure 8.1: Breakdown of the RAC into its component values

AIAA Design, Build, Fly Competition Proposal



The Georgia Institute of Technology
Presents

Mananmu

2000-2001
AIAA Design/Build/Fly Competition

School of Aerospace Engineering
Georgia Institute of Technology
Atlanta, GA 30332

Advisor: Dr. Dimitri Mavris
Team Leader: Adam Broughton

Mark Birney
Jared Wikler
Ben Hopwood
Karen Feigh
Randy Reese
Harlan McCullough
Jordan Drewitt
Drew Smallwood
Tiago Perez
Phillip Frye
Alisa Hawkins
Kristen Wilhelm
Michael Matthews

Special Thanks to Dr. Dimitri Mavris for his support.

1. Executive Summary	2
2. Management Summary	6
3. Conceptual Design Phase	10
3.1 Problem Definition	10
3.2 General Solution Characteristics	11
3.3 Solution Concepts	12
3.4 Initial Screening	13
4. Preliminary Design Phase	17
4.1 Figures of Merit.....	17
4.2 Initial Assumptions.....	18
4.3 Preliminary Wing and Tail Configuration	20
4.4 Preliminary Propulsion Design	20
4.5 Preliminary Structural Design	24
5. Detailed Design Phase.....	33
5.1 Wing Arrangement.....	33
5.2 Empennage	36
5.3 Wingtip Design	38
5.4 Handling and Control Characteristics	39
5.5 Radio Telemetry	39
5.6 Performance and Flight Testing.....	40
6. Manufacturing Plan.....	41
6.1 Fuselage Shell.....	44
6.2 Empennage	46
7. References.....	48

The American Institute of Aeronautics and Astronautics (AIAA) in coordination with Cessna Aircraft and the Office of Naval Research sponsor the annual Student Design, Build, Fly Competition to "...encourage innovation and maintain a fresh design challenge." The Academy of Model Aeronautics (AMA) sanctioned event involves the drafting and building of an unmanned remotely operated aircraft to fly a designated flight course while carrying a heavy payload and within a specified time limit. The total score for a school's entry is based on three components; the design report score, the manufacturing cost model score, and the total flight score. For this 2000-2001 contest season, some of the major restrictions in the contest rules are:

- 10 ft. limit on the wingspan
- 5 lbs. limit on propulsion battery
- propeller driven, non-rotary wing aircraft
- 10 minute flight period
- 200 ft. takeoff ground roll limit
- 55 lb. total aircraft weight limit
- electrically powered motor
- 50 page limit on design report

The Design, Build, Fly (DBF) project at Georgia Tech is not just an opportunity for students to participate in an aircraft design competition. It is also a highly educational opportunity for engineering students to apply classroom theory in developing an engineering task from its initial conception through all design phases to its end product. The competitive environment pushes team members to set high standards in an engineering environment. Poor engineering in ANY component of the aircraft may result in failure to meet contest goals.

The recent movement over the past several years within Georgia Tech Aerospace Engineering has been toward broad range concepts and development of new aircraft engineering methods. These methods include developing the project as a whole, not just the aircraft itself. Similarly, the project development for the Georgia Tech DBF team has traditionally been research and application of new concepts to gain a competitive advantage over more traditional designs (discussed further in the Conceptual Design Section). However, a more detailed look at project development reveals that much time can be wasted trying to research highly innovative designs. Full understanding of a new design takes literally thousands of man-hours of research, not to mention expensive equipment and costly experiments. This realization is true for the design of any new component of an aircraft, and there are literally hundreds of components working together in a complete aircraft. In the past, confidence in a design may have come from ignorance about its faults.

The first paragraph of the first page of the AIAA DBF web site says that the competition "...will provide a real-world aircraft design experience for engineering students by giving them the opportunity to validate their analytic studies." It was not the place of the team to explore new concepts and revolutionary designs, but rather to apply known concepts. The team realized that conceptual knowledge is much more valuable

when it has been validated by experience, and exploring new concepts would only fragment the understanding of aerospace engineering as a whole.

Georgia Tech's DBF team for the 2000-2001 contest season was entirely undergraduates, which meant that knowledge and experience resources were limited. Careful management of the team's limited resources was therefore key to developing a successful platform. The recognition of broad range concepts engineering and the limitations on experience of the team members were probably the most valuable assets of all. The team leaders took every step to continually review what concepts were most important to goal accomplishment, and were conscious of not wasting time on developments that were highly complex.

The students working on the DBF project were divided into three teams for better organization. These teams were the Aerodynamics and Configuration Team, the Structures Team, and the Propulsion Team. The Aerodynamics and Configuration Team was responsible for aircraft configuration, flight performance, airfoil selection, and controllability analysis. The Structures team was responsible for the airframe, wing construction (including spar design), and materials selection. The Propulsion Team optimized the battery/motor/propeller combination that would maximize duration and thrust.

Each team had a team leader, and there was one group leader to manage the activities of the three teams. The activities of the teams follow the Conceptual, Preliminary, and Detailed Design phases as outlined by AIAA's contest rules. All Georgia Tech DBF members were full-time students and voluntarily worked on the project in addition to regular class work.

Student activity on the 2000-2001 Design, Build, Fly competition began early in the contest season. As soon as the new contest rules were posted on the Cessna/ONR web site, the team began reviewing the rules and discussing the nature of the competition. The members of the team who participated in the previous season contributed learned skills to the new project. New team members brought in fresh ideas.

Because many students were off campus during the summer term, the project did not seriously develop until the beginning of the fall semester at Georgia Tech. At that time, the Conceptual Design Phase was officially begun and the team carried over summer progress to begin full commitment on the project. Most of the Conceptual and Preliminary Design was done during this term. Beginning with the winter/spring semester at Georgia Tech, the team finished the construction of prototype aircraft and began flight testing and refining the contest plane. This phase of research was considered the Detailed Design phase. Over all three terms, the development of the project was fully documented and summarized in this design report.

After the first review of the competition rules the team estimated the aircraft flying weight, takeoff airspeed, and cruise airspeed. The most desirable wingspan was determined to be 10ft. From these rough numbers, the team began to explore the aircraft configurations that would maximize payload capability, airspeed, and duration. Flying wing, box wing, biplane, monoplane and others were all investigated. Consideration was given to accessing the cargo bay area, removing and replacing the propulsion battery

pack, flight controllability, reliability of flight performance analysis, and configuration strength issues. References included textbooks, graduate students, and professors.

Only the monoplane and biplane were investigated beyond the first analysis of aircraft configurations. The primary argument against other alternative designs was the reliability of flight performance calculations. Monoplane configuration was preferred over the biplane for structural simplicity and lower cost model score. It took the Aerodynamics and Configuration Team several weeks to finally conclude that not only was a monoplane a strong candidate, but it was a better choice than a biplane. A low-wing monoplane (as opposed to high-wing or mid-wing configurations) was decided upon for cargo accessibility issues.

The Propulsion Team conducted fundamental research into the basics of electric propulsion systems. It was determined that one, large motor and propeller would be more efficient than several smaller motors and propellers. Having one motor and propeller would also lower the cost model score. This analysis and the analysis on aircraft configuration is summarized in the Conceptual Design Phase section of this report.

The Preliminary Design then began with the airfoil selection and wing planform design. Some of the issues discussed during this phase of the design were control surface size, wing loading, induced drag, profile drag, dihedral, washout, ground effect, interference effects, and tail blanketing at high angles of attack. The airfoil analysis program SNACK was used for most airfoil performance analysis. The University of Illinois Airfoil Data web site was also referenced for airfoil research.

The Structures Team estimated dynamic flight loads and researched spar designs. The Structures Team was also involved in designing in speed-loader for the cargo bay during this phase.

The Propulsion Team developed a thorough understanding of electric propulsion systems and created several EXCEL spreadsheets to analyze design alternatives. Varying the diameter, pitch, RPM and airspeed were analyzed to see the response on thrust and power. The Propulsion Team also used combined blade element theory (CBEMT) to estimate thrust.

The Aerodynamics and Configuration team noted that much of the traditional theory about airflow around a surface assumes relatively large surfaces and high airspeeds. The combination of small wings and low airspeeds results in extremely low Reynolds numbers, and the characteristics of wing stalls at low Reynold's numbers were found to be unlike the stalls found on larger aircraft. Tip effects were also found to be considerably different. Most full size aircraft have stall speeds above the estimated cruise airspeed of model aircraft. This prompted detailed research into stall characteristics specific to model aircraft and redirected the thinking of the design team.

One of the most important realizations about airflow around a surface was that the boundary layer is essentially scaled to the Reynold's number. Laminar flow separation therefore occurs much earlier on the surfaces of scale aircraft. The design team then decided that smoothly contoured surfaces were much more important than originally thought and began to plan the wing, tail and fuselage accordingly. Some of the most significant changes were new plans to construct a fiberglass fuselage and wing, and to research

wingtip design more thoroughly. Wing faring was determined more important than previously thought, as was control surface joints. Planning for these details was important in the performance estimates of the Preliminary Design Phase. The complete discourse is summarized in the Preliminary Design Phase section of this report.

At the beginning of the Detailed Design Phase, the wing design was known, the internal and external configuration was known, and the size and placement of the tail were calculated. All that remained were to finalize the details of the components that would make up the constructed airplane. The Detailed Design Phase was approached with two functions in mind: (1) Develop the construction of the aircraft as needed, and (2) validate the design through experimentation. Construction began with the drafting the internal frame and attaching components. Then the frame was built and evaluated for functionality. The construction of the wing and tail surfaces followed, as did the outer shell of the fuselage. During this time, the propulsion system was wind tunnel tested to validate research done in the Preliminary Design Phase.

The two Georgia Tech teams previous to this season's entry have placed fourth place overall in DBF competition. After the disappointing finish in April of 2000, professors and students met in several sessions to discuss improvements to the DBF program. Team management was a serious problem in the previous seasons, and students wanted more participation in the project developments. Dr. Dimitri Mavris recognized that the complexity of the program opens opportunities for students of all majors to participate in a multidisciplinary application of classroom knowledge. These educational benefits were the motivation to refine the architecture of the program. Faculty and staff also recognized that proficiency in the DBF competition would promote Georgia Tech as a leader in aerospace engineering design education. It was for these reasons that regular meeting times, revised class schedules, better lab access, and new lab meeting times were implemented. Local funds supported the renovation of the DBF laboratory (formerly Georgia Tech Aerial Robotics) and the purchase of new laboratory equipment.

Those students who had participated in DBF in previous years, or had model airplane flying/building experience were very valuable to the DBF effort at Georgia Tech. In previous years much of the time the students spent developing the project was spent researching the complexities of model aircraft. Very little time was ever spent actually optimizing the features of the aircraft. With the improved management program, the experience of these team members allowed faster progress through peer-learning.

The broad scope of the project requires more than just experienced students and broad plans. As with any project team, some kind of hierarchical structure must exist to delegate tasks and enforce progress. During project planning in the very early stages of the project, it was recognized that there were essentially three schools of thought that divided the project. The aerodynamics of the aircraft are the primary interest of most team members, but the aircraft propulsion system also requires much attention. The need to lighten the airframe as much as possible was also recognized. Having the lightest airframe possible means a higher weight fraction that can be dedicated to cargo, thus increasing flight score.

These three areas of study were given the names the Aerodynamics and Configuration Team, the Propulsion Team, and the Structures Team respectively. Each team was designated a team leader, and all three teams were headed by one group leader. The group leader was Adam Broughton, an industrial and systems engineering undergraduate with nine years of flying and building experience with UAVs. Mr. Broughton was a key contributor to Georgia Tech's 1999-2000 DBF entry, and is currently conducting research on UAVs for the Aerospace Systems Design Laboratory. Mark Birney, an aerospace engineering senior, was designated as the team leader for the Aerodynamics and Configuration Team. Mr. Birney is active in graduate studies and does part-time work for General Electric Aircraft Engines. Ben Hopwood, a mechanical engineering junior, was chosen to lead the Structures Team. Mr. Hopwood is highly proficient in static mechanics and composite materials. The Propulsion Team was lead by Jared Wikler. Mr. Wikler is an aerospace engineering senior, and although involved in a cooperative education program with Lockheed Martin, he was an instrumental leader in the development of the project. All other

team members assigned to research teams based on personal interest, and were allowed to belong to multiple teams. The list of design personnel and their assignment areas is shown in Figure 2.1.

Team Member	Design Group	Major Contributions
Adam Broughton, IE/SR	***Group Leader***	team organization, process control, scheduling, budgeting, project development
Mark Birney, AE/SR	AeroConfig Team Leader	flight performance optimization, design report leader, airfoil selection, aircraft synthesis
Ben Hopwood, ME/JR	Structures Team Leader	airframe design, spar design, stress analysis, wing design
Jared Wikler, AE/SR	Propulsion Team Leader	CATIA/CAD specialist, performance estimation, configuration design, airfoil selection
Phillip Frye, AE/JR	Propulsion Team	propeller thrust performance, energy accounting
Kristen Wilhelm, AE/JR	Structures Team	manufacturing, major construction design, speed loader development
Jordan Drewitt, AE/JR	AeroConfig Team	Empennage design and performance calculation, empennage manufacture.
Kenny Gow, MGT/FR	--independent	sponsorship relations, financial control
Michael Matthews, AE/ JR	AeroConfig Team	airfoil selection, score optimization
Randy Reese, AE/SO	Structures Team	flaps performance, wing manufacture
Harlan McCullough, ME/SR	Structures & Propulsion Team	aircraft construction design, wing manufacture, flight duration, thrust estimation
Karen Feigh, AE/SR	AeroConfig & Structures	flight performance, stress analysis of dynamic flight loads
Alisa Hawkins, AE/SR	AeroConfig Team	empennage performance calculation, aircraft configuration, score optimization
Vien Ngo, AE/JR	AeroConfig Team	wingtip design
Tiago Perez, AE/SO	Propulsion Team	thrust estimation, flight duration calculations
Drew Smallwood, AE/JR	Structures Team	cargo load analysis, speed loader design and manufacture

Table 2.1: Team Composition

The group leader and team leaders coordinated together to plan out the schedule of major developments. In the previous season, the complete synthesis of the aircraft did not occur until a few

weeks before the competition. The first flights with full payload did not occur until the day of the competition. This season's DBF team recognized that much more time is needed to optimize the flight performance of the aircraft before the competition, and scheduled the first flights of the prototype for December 2000. The schedule of major developments (such as the configuration, airfoil selection, propulsion system design) was planned to accommodate this deadline. However as unanticipated complications arose, and students became busy with academics, this schedule was adjusted several times in order to accommodate unforeseen delays. Every two weeks, the team generated a report to faculty and staff on the accomplishments and schedule maintenance.

The original schedule has been adapted to the Milestone Chart in Figure 2.1. This chart reflects what the DBF team originally intended to follow, and what actually occurred. For flight-testing and insurance against a possible crash, the team decided to get a prototype aircraft flying as soon as possible (December on the first schedule). A second and possibly third aircraft were planned for the winter/spring term.

The delays in the Conceptual and Preliminary Design of the project were mostly due to unreliable information. The team was not willing to dedicate time to building a prototype aircraft if it wasn't absolutely sure of the design. Maintaining the schedule purely for the sake of keeping schedule would mean neglecting further research into the basics of the design; which are difficult to change once the aircraft is constructed. Details of full functionality were essential to the construction of the prototype for accuracy of results, and security against an unexpected crash.

The construction began only when the team was absolutely confident with the design. From that point, difficulties with cutting foam wing cores was the major delay. The fuselage was constructed in just a few days, but it took the team nearly 6 weeks to produce a satisfactory wing. The remainder of the aircraft synthesis followed in a few days. Flight-testing however was delayed until more progress on the design report and fuselage could be made.

The team is generally satisfied with the progress speed of the new management structure. Thorough design of a new aircraft is alone a difficult task. When that difficult task is conducted by inexperienced engineering students, under a closed time frame, while studying full time at a major institution, the difficulties begin to compound. However the assets of the team are not only the contest entry, but the vast amount of practical experience the team will carry into their aerospace careers.

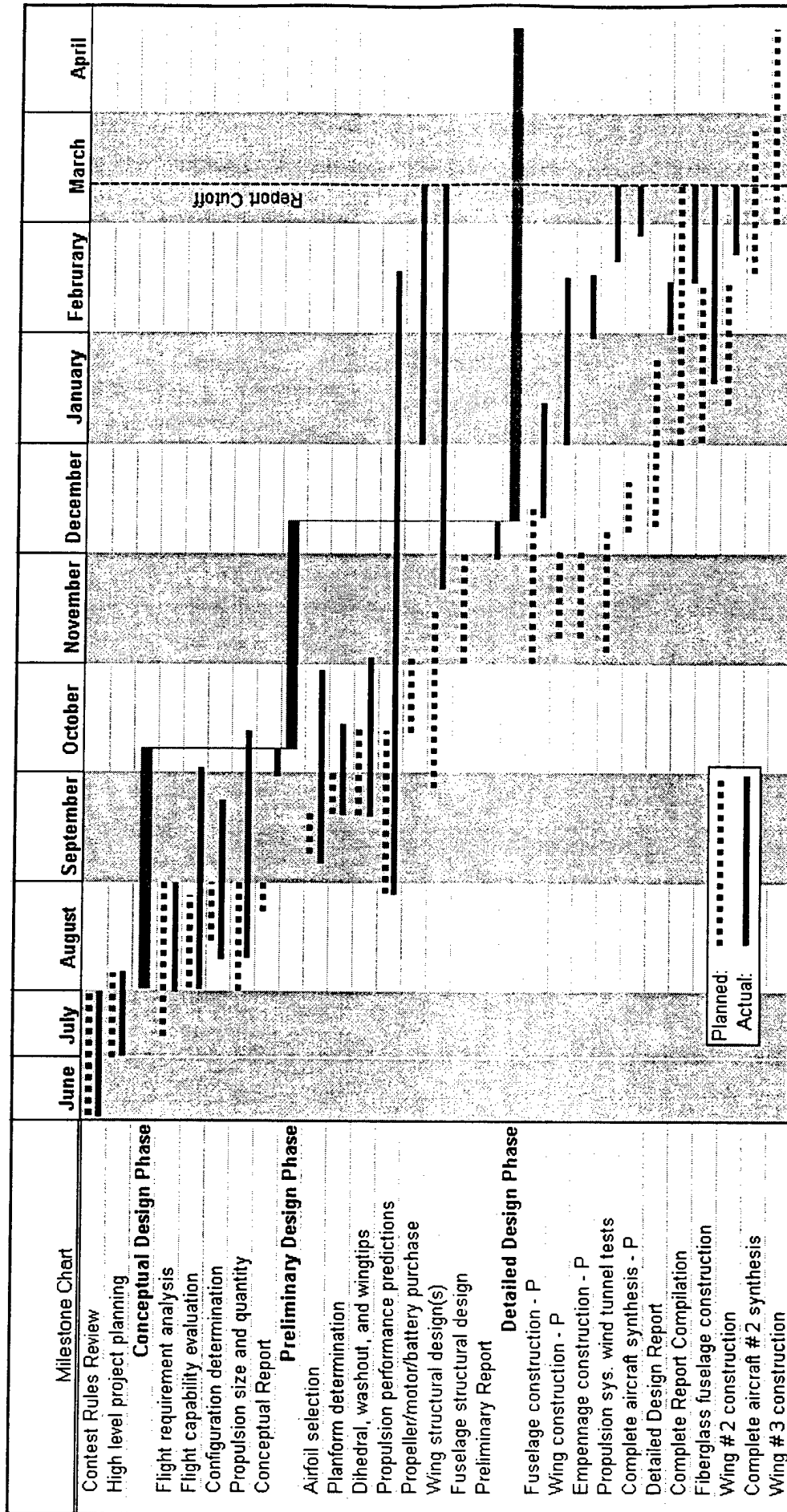


Figure 2.1: Milestone Chart

3.0

Conceptual Design

The conceptual design phase was begun by examining the rules for this year's Design, Build, Fly competition. From these rules, a mission profile and mission requirements were developed to guide the selection of possible aircraft configurations. Potential aircraft configurations were then screened using Figures of Merit derived from the mission requirements and from several underlying principles decided upon by the team leaders. These Figures of Merit helped to define which requirements were most important and should therefore take the greatest consideration in the selection of a configuration. The screening process narrowed possible configurations to a conventional type monoplane or biplane, to be assessed later in preliminary design at a more detailed and quantitative level.

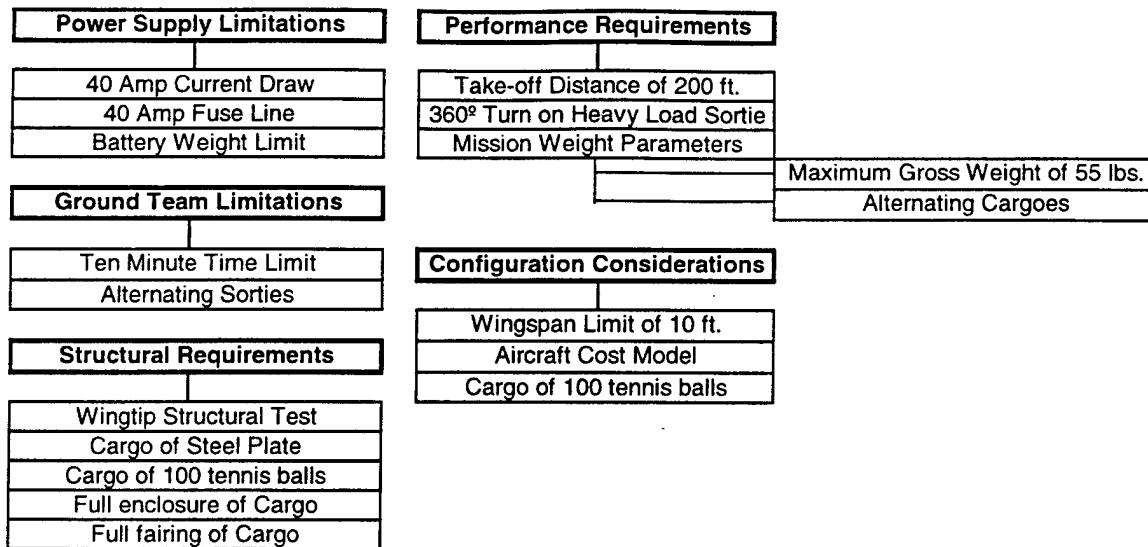
At the beginning of the initial, conceptual design process, several tools were selected, and several ground-rules established to guide this phase of the design. The tools selected for use came from Georgia Tech's Integrated Product and Process Design Methodology, and included Affinity Diagrams for concept categorization, and a Pugh Matrix for solution screening. Further, the team decided to pursue a historically based design approach which would eliminate the need to do extensive research when such work has already been done. Lastly, the need to keep concepts, future analysis, and manufacturing at an undergraduate level was recognized and incorporated into the conceptual design process.

3.1 Problem Definition:

The mission requirements for this year's competition involve carrying up to one-hundred tennis balls and as much steel as possible on alternating sorties around a specified course. As many sorties as possible must be completed within ten minutes. These requirements make the primary challenge of the design being to have an aircraft that can carry both a heavy cargo and a light cargo with a large volume. The aircraft will also be required to make a 360° turn on the heavy cargo legs which it will not be required to make on the light cargo legs.

Important constraints to consider include limits upon the wingspan and maximum gross weight, limits upon the current draw and fuse line for the battery, a battery weight limit, and a required take-off distance limit. Further, a structural test to be conducted on the aircraft requires that the wings be able to support the aircraft at maximum payload capacity when lifted at the wingtips. The requirement that the payload be fully enclosed and fully faired appeared to be self-evident, but worthy of note for any designs considered.

These requirements coming directly from the rules were listed and then categorized in the Affinity Diagram depicted in Figure 3.1. This diagram illustrates how some of the requirements affected the similar aspects of the design. Some of the requirements were repeated because they could fit into more than one category. These categories fit the major design considerations for most aircraft, and were helpful in showing what needed to be considered for any candidate configuration.



**Figure 3.1: Mission Requirements
Affinity Diagram**

3.2 General Solution Characteristics:

Since this design is being formulated by undergraduate students with neither extensive design experience, sophisticated test facilities, nor a very large time frame, the overall approach will be to use general historical data and trends to develop the design. Specifically, relevant data on radio controlled aircraft and aircraft in the category of low-speed general aviation and homebuilts will be used to form a design which will satisfy the unique requirements of this competition. The strength of this approach is that the straightforward task of lifting a required payload with configuration limitations has been accomplished many times, with various trends and approaches proven successful since human flight began. Rather than attempting to use student innovation to solve the challenges of this competition, this design will rather focus on formulating a strong historically based design with sufficient time to test the design in a prototype to validate the various investigations performed.

Because of performance deterioration for small Reynolds numbers, it was argued that a large wing of a given airfoil would be more efficient in generating lift than a proportionally smaller wing. Further, it was observed from historical data that aircraft become more efficient in terms of payload capacity relative to empty weight as the aircraft reaches larger sizes. This argument was sufficient to pursue the largest wing possible that would give low drag for the chosen weight. This argument implies that more overall energy is needed to pull the airplane through the air, such that battery capacity should be maximized for maximal duration. The energy density of battery cells is higher for larger cells, thus reinforcing the argument that larger airplanes are favorable to smaller ones.

A more concrete analysis revealed that for additional cargo weight the aircraft had increasingly large costs in induced drag. From a strategic standpoint, this means that the aircraft should carry as much weight as possible up to its ability to complete an additional lap around the course as long as there is sufficient battery capacity. For example, if an airplane can carry 40 lbs. around the course 5 times and score 200 points with some capacity left over, it may be able to carry 35 lbs. around the course 6 times and score 210 points. For conceptual design, the first conclusion was to create an aircraft of 10ft wingspan, maximize capacity as per the voltage needed for the motor(s), and of efficient aerodynamic design.

This last statement raises another important conceptual design point. How many motors should the aircraft have? The question can be answered regardless of aircraft design, ignoring drag or other flight requirements. The argument was made that electric motors will draw a certain amount of base current regardless of throttle (voltage) setting, thus making multiple motors less efficient. If one motor was found to have reasonable thrust and current draw, then multiple motors would not be necessary. Since motors are limited to the Graupner or AstroFlight brushed motors, the choice of appropriate power plants was very limited. Because of the size of our aircraft, only two motors, the AstroFlight Cobalt 60 and 90, were found to produce reasonable thrust and current draw to produce the thrust to accelerate even a 45 lb. airplane to lifting speeds within 200 ft. Since these motors are available for use in our design, we concluded that it was most appropriate to have only one motor to power the aircraft.

Up to this point the design team had concluded that the aircraft would be 10 ft. span, 5 lbs. of battery, and of only one electric motor. The next step was to decide the aircraft configuration. The approach to the deciding the aircraft configuration involved a rather lengthy discussion about "non-traditional" aircraft designs. The central leading arguments in favor or against an alternative design were a historical knowledge of the design and the complexity of analysis of that design. The team did not feel as though it would be productive to pursue a design that deviated greatly from more traditional designs. This feeling was based on the fact that there has been a tremendous amount of research done on alternative aircraft configurations outside of Georgia Tech, and these designs have not shown such dramatic improvements in lifting efficiency that they have replaced more traditional designs. Such a conservative approach to the design of the competition aircraft eliminates the risky probability of entering an aircraft that is incapable of efficiently accomplishing the team's mission. It is faulty logic to think that an extremely competitive aircraft has to be one that has an extremely innovative design. In previous year's competitions some other teams with highly radical aircraft configurations have not performed well, and may have assumed that a radical design was most suited for the competition requirements. However, an exotic design brings the issue of a lack of understanding in the characteristics or behavior of the aircraft.

3.3 Solution Concepts:

In response to this mission and its requirements, several different configuration options were proposed which could meet the requirements. Only general configuration concepts were considered,

leaving some mission requirements for analysis under preliminary and detail design, or for inclusion in the Figures of Merit. The general design issues considered in terms of selecting a starting configuration included:

- High Weight Cargo
- High Volume Cargo
- Limited Wingspan
- Aircraft Cost Model

Based upon these issues, the aircraft needed was characterized as a cargo or transport type aircraft. From this characterization, four major design configurations were suggested.

1. **Box-Wing Aircraft:** A monoplane with a wing arrangement connected to a smaller wing located above the main wing and near the back of the aircraft fuselage. This concept is a blend of the monoplane and biplane.
2. **Monoplane:** Conventional aircraft with a single wing, fuselage and tail for stability and control.
3. **Biplane:** Aircraft with two wings stacked vertically around the fuselage, and having a tail for control.
4. **Flying Wing:** An aircraft constructed of a single wing, with no separate fuselage or tail. All cargo and controls contained within the wing.

These concepts were proposed based upon historical cargo-type aircraft, and continued to avoid difficult revolutionary concepts, or extremely unusual designs.

3.4 Initial Screening:

The next step was to define figures of merit based upon these mission requirements and upon the general design approaches desirable for this type of competition. These figures of merit could then be used to help select between the several possible design configurations. These merits were also weighted from 1-9, using odd numbers to make differentiation easier. Higher numbers indicate a combination of both great importance as well as close correlation to the configuration selection, while lower numbers indicate some lesser importance or lesser correlation.

1. **Turn-around Time (3):** Since the aircraft must make several circuits around the course involving the change of cargo with each sortie, quick removal and loading of cargo are important so that time is not wasted on the ground.

2. **Fuselage Capacity (5):** One of the main challenges associated with this design is the carriage of a large number of tennis balls, meaning that the fuselage must accommodate a large volume.
3. **Ease of Analysis (7):** Since this design team is made up primarily of students at the undergraduate level, consideration must be taken for simplicity of analysis. Complicated or revolutionary designs may show conceptual promise, but become impossible to analyze at the appropriate level to make quantitative decisions.
4. **Cost Model Score (9):** The configuration and capabilities of the aircraft should minimize total rated cost model score. The cost model is 1/3 of the score components of the competition and so was analyzed very carefully at this stage. A computational spreadsheet to estimate the cost model for each concept was generated as shown in Figure. From this comparative study, quantitative data could be drawn from the anticipated configurations and used in comparing the different configurations during the screening test.
5. **Drag (9):** Flight duration (number of laps around the course) should be maximized by minimizing drag. For conceptual design, drag consideration was used to settle the choice between two similar competing designs when one design favored lower drag.
6. **Strength/Weight (7):** The construction of the aircraft should feature a configuration that minimizes necessary structure for normal flight operations. Weight savings were not discussed in terms of extra pods, wings, booms or other components, but rather in the necessary internal structure needed to make the airplane robust. Every ounce and even half-ounce of unnecessary weight removed from the plane was seen as highly advantageous.
7. **Maintainability (5):** Aircraft design and construction should be chosen with consideration to operation and maintenance of the aircraft. As with any aircraft, full-scale or model, some routine service and maintenance is necessary in order to keep the craft flying. The previous year's entry was very difficult to transport, assemble, and maintain, and the design team felt that simplicity in design would better facilitate overall operations.
8. **Construction Feasibility (7):** Construction of the aircraft should be within the limits of skill and materials resources of the students. Although composite materials are very strong for their weight, they are very difficult to construct, and require a substantial knowledge of composite construction in order to proficiently build. Experienced team members have seen competition aircraft projects that have been built much stronger than necessary, thus sacrificing flight performance.

The cost model for These merits and their values were then entered into the Pugh Assessment Matrix shown in Table 3.1. The different designs were then compared in terms of these figures of merit to the biplane, which was chosen as a baseline. These positive or negative comparisons were then weighted according to the merit weights, and a final score tallied. Based upon the overwhelming strength of the

monoplane in terms of qualitative score from the Pugh Matrix, the configuration was selected as the preferred one for continued design. However, the major design requirement which could not be shown qualitatively by this process was the wing span limit, and so the biplane had to remain a candidate until it was shown that a monoplane could give the needed lift for the competition. This analysis and the final selection of the monoplane configuration was done in the preliminary design phase.

For the selection of a monoplane over a biplane, the primary issue of discussion was the increased lift of a biplane compared to its potential drag penalties. According to Raymer (65) a biplane will give an induced drag of $\frac{1}{2}$ that of a monoplane when the biplane has two wings of equal size to the monoplane. However, due to interference effects, this will be decreased by about 30%, and will not be as substantial as shown by the ideal calculations. Since the addition of a wing and so much wing area would have significant effects upon the cost model, if the monoplane could meet the needed lift and drag requirements established by the payload and the engine, then decision was made to proceed with the simpler monoplane.

Table 3.1: Pugh Selection Matrix

Figure of Merit	Weight	1. Biplane (Baseline)	2. Mono- plane	2. Box-Wing	3. Flying Wing
Turn-Around Time	3	0	+	0	+
Fuselage Capacity	5	0	0	0	-
Ease of Analysis	7	0	+	-	-
Cost Model Score	9	0	+	0	+
Drag	9	0	+	-	+
Strength/Weight	7	0	0	-	0
Maintainability	5	0	+	-	-
Construction Feasibility	7	0	0	0	-
(Baseline)					
<i>Positives</i>		0	5	0	3
<i>Negatives</i>		0	0	4	4
<i>Sum</i>		0	5	-4	0
<i>Weighted Score</i>		0	33	-28	-3

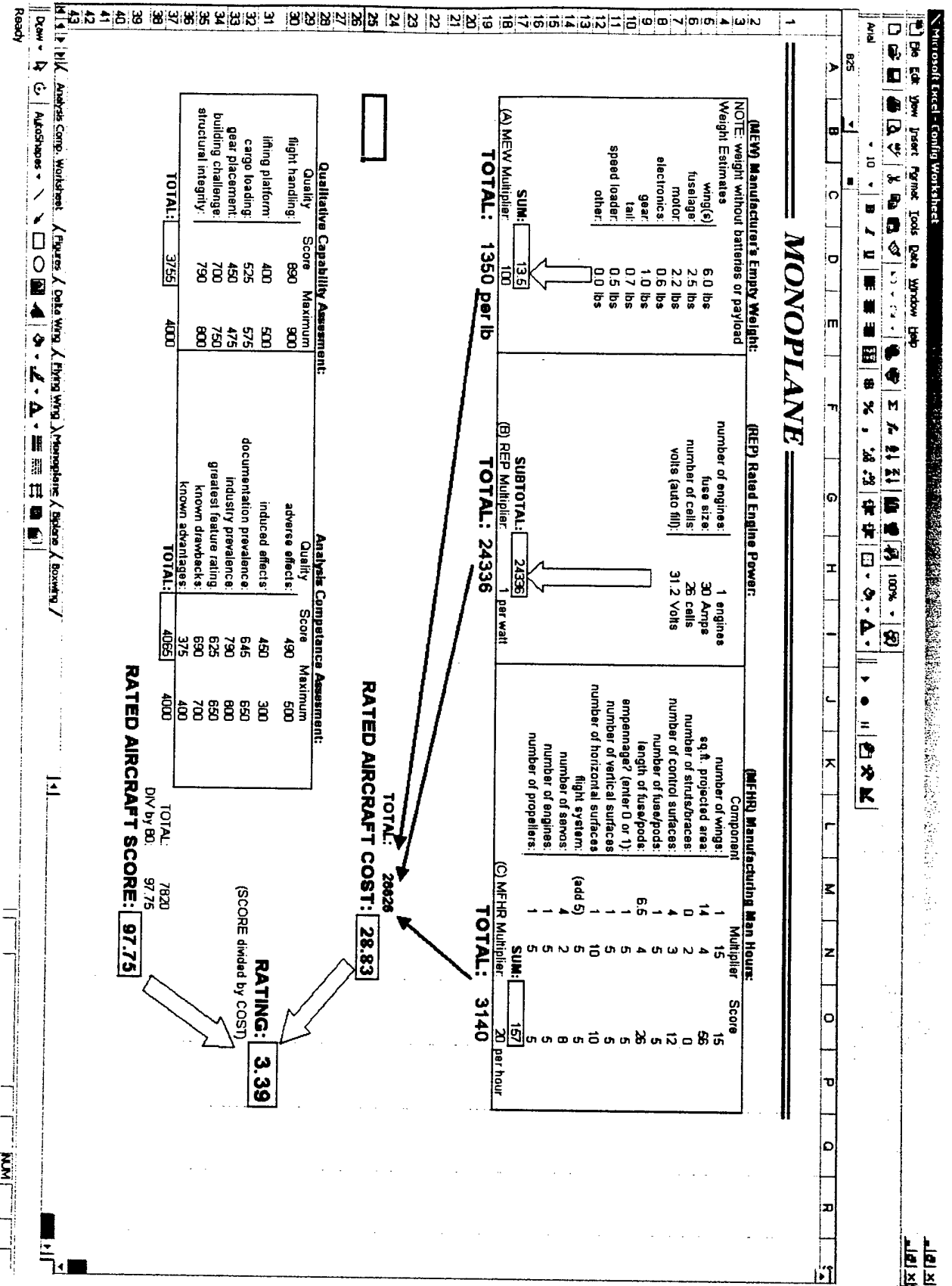


Figure 3.1: Aircraft Cost Impact Spreadsheet

4.0

Preliminary Design

The purpose of the preliminary design phase was to provide initial values for the design, and to make a final determination of whether a biplane would be needed, or if a monoplane would suffice. Qualitatively, a monoplane would be preferred, however, the required wingspan limit means that additional wing area may be needed to get the aircraft into the air. The initial calculations performed at this point served as initial aircraft sizing values from which the details of the aircraft could later be derived. The tools at this stage included historical data and trends, and a performance spreadsheet created in Excel.

Only the last 4 months of the project were spent on the construction of the aircraft. Much more attention was dedicated to reinforcing arguments for the design rather than developing manufacturing methods. The design team could afford to do this because several of the team members have experience building and flying UAVs and did not have to spend time learning how to construct model aircraft.

It was noted that the aircraft in these competitions are generally under-powered and overweight. The aircraft are also new, untested designs that are pushed to their limits of flight capability. The very nature of the competition yields aircraft that are highly likely to fail either structurally or aerodynamically. The design team therefore chose to build *at least* one prototype and one competition aircraft for the DBF competition. The first prototype was intended to validate performance estimations and serve as a backup aircraft in the event that the competition aircraft was damaged and could not be repaired by the competition date. The final competition aircraft would be the same configuration. The only differences would be the construction of the two airplanes.

4.1 Figures of Merit

For this stage of the design, several figures of merit had to be established to guide the design decisions. These remained similar to those figures used in the conceptual design phase and were used to help make the decisions in arriving at the initial numbers for the aircraft.

The ideal aircraft in response to this competition would be the smallest, lightest plane possible, carrying the most weight for the longest period of time. This approaches an optimum condition as the weight limit is carried around the competition course by an infinitely small aircraft for the maximum allowable time of ten minutes. However, not all of these conditions can be met at the same time, and so several figures of merit were chosen to help gage the trade-offs involved in various decisions. The figures of merit were stated in the form of questions to be asked as each decision at this stage was made. Figures of merit selected included:

1. **Effect on Cost Model (High Importance):** How does the decision impact the cost model for the aircraft? An example of a configuration argument that reduced cost model score was the

idea to incorporate deep dihedral and eliminate wing control surfaces, thereby dropping two servos and relying on yaw-to-roll coupling to control the aircraft.

2. **Strength to Weight Ratio (High Importance):** Does the decision provide the needed strength in the aircraft while keeping the structural weight as low as possible?
3. **Handling Characteristics (Moderate Importance):** Does the decision maintain adequate conceptual stability for the aircraft? This is a little less important for this aircraft since complicated maneuvering will not be required.
4. **Effect On Overall Drag (High Importance):** Will this decision help to minimize the drag of the aircraft? Since it has already been anticipated that the aircraft will be underpowered, it is highly desirable to keep the drag
5. **Constructability (Moderate Importance):** Can this design option be adequately constructed using model aircraft techniques and with the resources available? Some options may be too difficult to build in terms of technique, may require excessive time commitment, or may be too expensive to construct.
6. **Ease of Analysis (Moderate Importance):** Can this option be satisfactorily analyzed using available methods and/or software?

4.2 Initial Assumptions:

Based upon the model aircraft flying experience of some of the team members, take-off and cruising speeds were estimated. A take-off gross weight of 45 lbs. was selected to insure that the aircraft would be capable of carrying a maximum or near maximum allowable payload in the event that the propulsion system caused a high cargo weight to maximize the flight score. Forty-five pounds was selected to allow for pushing the design to its limits during the competition in terms of cargo capacity and weight carrying ability while remaining under the maximum allowable aircraft weight. However, when calculating the wing parameters, a weight of 55 lbs. was used to ensure that the aircraft would be capable of lifting any range of cargo weights.

At this stage, an Oswald efficiency factor and the aspect ratio of the wing could also be set. A relatively low value of .80 was selected to account for the anticipated "dirty" manufacturing for a scratch built radio control aircraft. This factor may range from values as low as .45 to values about .90, but is normally set in the range of .80-.90. The low value in that standard range was selected as a conservative estimate.

From historical data, it appeared that the most desired aspect ratio for the wing would be somewhere from 7-9. However, the wing span limit of ten means that the only value which may be varied in determining the aspect ratio is the wing area. A wing area of 11 ft.² gave an aspect ratio of just above nine, however, initial calculations showed that a coefficient of lift of 2.66 would be required on take-off. This value is outside of those which may be achieved with conventional wings and without advanced

high-lift devices. Further, since the potential cost saving achieved by using flaperons on the wing may limit the effectiveness of the increase on C_L during take-off, a more conservative value for $C_{L_{required}}$ was desired. A final wing area of 14 was decided upon, which gave a $C_{L_{takeoff}}$ required of 2.09 and could be more easily achieved using a conventional wing and flapperons. This set the aspect ratio to 7.14, within the desired range. The initial assumptions are summarized in Table 4.1.

Velocity Parameters		
	mph	ft./s
Vto	27	39.6
Vcruise	38	55.73
Selected Max Take-off weight		
Wto	45 lbs.	
Selected Wing Parameters		
e	0.8	
b	10	ft.
S	14	ft.^2
AR	7.14	

Table 4.1: Initial Design Parameters

At this stage, it appeared that a monoplane was a feasible configuration, and that the design values fell within those desired by the design team and within competition rules. Based upon Raymer, the only benefit that a biplane might have provided—lower induced drag—will exist only if the “total span is limited for some reason to a value less than that desired for a monoplane” (66). Since a monoplane does meet the desired values, it was assumed that a biplane would not provide any appreciable benefit.

From these specific initial assumptions, other values of importance (See Table 4.2) could be calculated, including wing-loading, lift-to-drag ratio, $C_{L_{required}}$ for take-off and cruise, and drag for these conditions. These initial performance parameters are summarized in Table 4.2. The drag is especially important for continued analysis of the propulsion system. At this point the take-off thrust required to take off in 200 ft. was calculated according to Hale, pp. 67-68. Neglecting drag, the required thrust was determined to be 5.53 lbs. Added to the take-off drag of 5.47 lbs., the total average thrust required for take-off in 200 ft. is 11 lbs., with uncertainty due to ground effect and ground friction. This thrust is within the estimated range of the engine output, and so indicates that this design will be able to get off the ground within the required distance for the 45 lb. case. Returning again to the philosophy of optimistic design prior to flight testing, the engine will largely limit the aircraft's performance, and so this may be regarded as the limiting case for the payload and will require specific attention during flight testing and during detail design.

Take-off			Cruise		
Clmax	1.708098	(required from wing)	Clmax	0.862329	(required from wing)
Cdi	0.162523		Cdi	0.041422	
Cdo	0.0472		Cdo	0.0472	
Cdtot	0.209723		Cdtot	0.088622	
L/D	8.144558		L/D	9.730385	
W/S	3.214286	lbs./ft. ²	W/S	3.214286	lbs./ft. ²
Drag	5.525162	lbs.	Drag	4.624689	lbs.

Table 4.2: Take-off and Cruise Characteristics**4.3 Preliminary Wing and Tail Configuration:**

A low-wing configuration was selected for this design. A high wing would provide greater stability, however, the benefit of a low wing is that there will be greater accessibility to the cargo area. This is important to reduce turn-around time at the competition itself. The stability issue may be dealt with in terms of adding dihedral to the wing, which will be more difficult to build. However, it was decided that the extra construction effort would be worth it in order to improve the turn-around time between sorties.

Several tail designs are available to aircraft designers. We analyzed the feasibility of these options in order to decide which would be most beneficial to our specific airplane. We discussed options such as conventional, T-tail, V-tail, inverted V-tail, H-tail, and Y-tail, among others.

The T-tail reduces the height of the vertical stabilizer, but may result in pitch-up problems; it is also more complicated to construct and heavier than other configurations. The V-tail and inverted V-tail provide a creative incorporation of yaw-roll coupling, as well as a theoretical reduction in wetted area. The main disadvantage to these configurations is the complicated control method needed to steer the aircraft with such a system. The simplicity of the conventional tail was chosen as the most appropriate configuration for our flight characteristics. We are also most familiar with this design and are more able to accurately assess its performance.

4.4 Preliminary Propulsion Design:

The design of the propulsion system was so important to the team, that a small group of students was dedicated to researching it for the duration of the project. The batter/motor/propeller selection was greatly simplified in this year's competition with the restriction on motor manufacturers. The team quickly identified that the AstroFlight Cobalt 90 was the motor that was to be used on the aircraft. This left only the other two components undetermined.

Thorough understanding of the motor was required before the dynamics of the electric propulsion could be explored. Much of the information on electric motor performance was taken from the Electric

Motor Handbook by Robert J. Boucher. The book outlines the basics of electric motor performance for electric motors and is catered to the AstroFlight family of electric motors. Sufficient formulas are given in the book for the Propulsion Team to account for all power and efficiency calculations. Table 4.3 shows the table that was constructed to compare electric motors and their outputs given a set of inputs.

Motor research showed that the output performance of the electric propulsion system is highly dependent on the load placed on the motor for a given set of input factors. This load comes from the required torque needed to spin a propeller at a given RPM and airspeed. At constant RPM, this required torque comes from aerodynamic drag factors from the propeller and internal resistance factors within the motor. Faster RPMs, larger propellers, or low airspeeds all increase the load on the system. Higher loads draw more current from the battery, and these high discharge rates shorten effective capacity and output performance suffers.

The Propulsion Team investigated these relationships and found that as airspeed increases, the required torque per RPM decreases up to an "advance ratio" of one. The *advance ratio* is a term used to describe the amount of theoretical slip of a propeller and is equal to the forward velocity divided by RPMs*Diameter (some text use actual velocity divided by pitch speed). Beyond the airspeed for which the pitch speed equals one, the aircraft is flying faster than the propeller's output and the required torque is negative. For any given propeller design, this relationship between thrust and airspeed (for a given RPM) is unique and dependent on pitch, diameter, airfoil, planform, air density, tip effects, and other factors. This relationship, called the *unloading characteristic curve*, may also be affected by the design of helical twist, the surface texture of the propeller, and the rigidity of the material used to construct the propeller.

Variable	Magnitude	Units			
Voltage Constant, K_v :	230	RPM / Volt			
Torque Constant, K_t :	5.891304348	in-oz / Amp			
Terminal Resistance, R_m :	0.155	Ohms			
Input Voltage, V_{in} :	30	Volts			
Net Effective Voltage, V_m :	29.85483871	Volts			
No Load Current, I_o :	2.5	Amperes			
Stalled Current, I_{stall} :	193.5483871	Amperes	Shaft Output:		
Input Current, I_{in} :	25	Amperes	Gear Ratio:	2.75	:1
Net Effective Current, I_m :	22.5	Amperes	Ideal Speed:	6900	RPM
Power Input, P_{in} :	750	Watts	Speed at I_{in} :	6008.75	RPM
Power Output, P_{out} :	587.8125	Watts	Geared Shaft Speed:	2185.00	RPM
Heat Loss:	162.1875	Watts	RPM Drop:	1.29	%
Torque:	132.5543478	in-oz	→ Torque: 364.5244565 in-oz		
Efficiency	78.38%				
Max Efficiency Current:	21.99706725	Amperes			
Max Efficiency Percentage:	88.63%				

Table 4.3: Comparative Motor Outputs

Model aircraft propellers are commonly defined by only the pitch and diameter, from which the pitch-to-diameter ratio can be calculated. The Propulsion Team used this pitch-to-diameter ratio to roughly indicate the slope of the unloading characteristic curve, and the diameter was used indicate the magnitude of the load placed on the motor. Further defining factors would later better fit calculations of the theoretical unloading characteristic curve to the actual unloading characteristic curve.

The team identified other variables that may affect thrust performance. Because Reynold's numbers are very small, laminar flow separation characteristics are quite different from larger, full size counterparts. These characteristics have yet to be thoroughly explored, and are difficult to predict in performance calculations. Its is known that the boundary layer is much smaller for low Reynold's numbers, and small imperfections in the surface of the blade may have significant effects on thrust performance. Manufacturing irregularities in the camber of the airfoil (such as runs in the paint) may cause early flow separation and seriously degrade the performance of the propeller blade.

The theoretical slope of the unloading characteristic curve is a smooth, continuous curve from an advance ratio of zero (at which point the thrust is infinite) up through all positive values. However, the first experimental tests of propellers in a wind tunnel suggested that in reality, high pitch propellers at low airspeeds often experience stalling until the advance ratio increases to the point where the angle of attack of the propeller blade decreases to below stalling. This characteristic is seen as a slight dip from the theoretical unloading characteristic curve at low airspeeds. For higher airspeeds (and thus advance ratios) the realized thrust closely follows the theoretical thrust.

Several methods were used to estimate the actual unloading characteristic curve. The best of which was taken from methods used by helicopter design engineers at Georgia Tech. The method of Combined Blade Element Theory (CBEMT) as explained to the DBF team was as follows: The blade is sectioned into evenly spaced increments from the root to the tip. The sections near the root that do not produce lift (such as those forming the hub or covered by the spinner) and those near the tip that are adversely affected by tip effects are ignored. The remaining sections are used to calculate lift just as one would when figuring the lift from a wing section. The angle of attack at each section is figured from a parabolic curve fitting the root and tip angles of attack. The airspeed varies linearly from root to tip and is figured from the climb ratio (forward velocity) and RPM. The coefficients of lift and drag are calculated from airfoil data at each section. The differential increment of coefficients of thrust and power are summed along the blade from root to tip to give total thrust and power for the propeller. The results of the CBEMT spreadsheet that the Propulsion Team developed were accurate within 9% of actual thrust results for the Master Airscrew series of propellers that were tested.

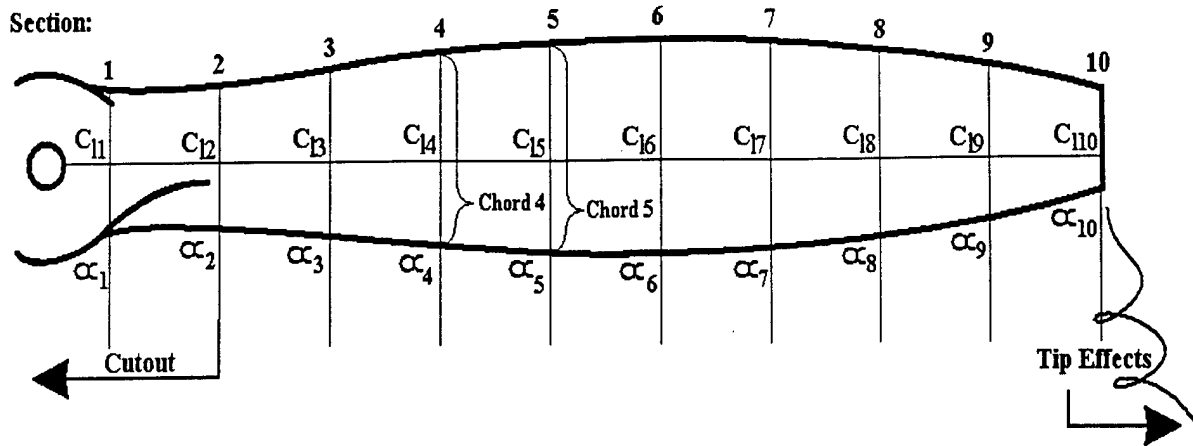


Figure 4.1: Analysis Division of Propellor Blade

The thrust predictions from the CBEMT spreadsheet were used to identify the range of propellers that gave acceptable thrust for takeoff within 200ft. The power absorbed by these propellers was used with an efficiency coefficient (power absorbed to thrust produced) to determine the drain on the battery and estimate duration. Motor efficiency was also taken into account with the ratio of electrical power into the motor to physical power (torque per time) out of the motor.

The optimal propeller for the application has been tentatively decided as a Mejzlik 26x12, but the group of best candidates is still being considered. These propellers are those that provide just enough thrust to reach liftoff speeds around 190ft from beginning ground roll and still provide adequate thrust at cruise. Test flights will better indicate the flight capabilities of the aircraft, and if necessary, cargo weight will be decreased to increase duration.

The propulsion battery pack was the last component to be determined in the propulsion system. Based on the propeller energy requirements, the battery was chosen by using the highest capacity cell that would provide the necessary voltage to turn the propeller the minimum takeoff RPM. Currently, the Propulsion Team has tentatively decided on 26 Sanyo 3000mAh cells.

4.5 Preliminary Structural Design:

The Structures Team coordinated with the Aerodynamics and Configuration team to develop the lightest aircraft that could carry the most weight. The team members did not know how much payload the aircraft was capable of carrying at the time the internal structure of the aircraft needed to be decided upon. The team also did not know the empty weight of the aircraft. However it was known that adding payload up to the 55lb weight limit would maximize the total score. By carefully estimating the weight of each known component of the aircraft, the empty weight of the aircraft was estimated to be 13lbs. Subtracting the weight of the 5lb battery left 37lbs available for cargo weight. This weight was set as the required minimum test weight for the wing.

The design of the internal frame of the aircraft followed a few simple principles. The first principle was that heavy weight should be set as low in the airplane as possible for stability, and as close to the wing as possible for maneuverability. The second principle was that the structural members should be as simple as possible. Structural failures often occur at glue joints because of either failure of the glue or concentration of stress. Therefore, the design of the internal structure should minimize the number of combined members. A third principle is that the design team also wanted to keep the entire structure as lightweight as possible, with the idea that the structure should only be as strong enough to withstand dynamic loads, and no stronger. Any additional strength meant excess material and therefore excess weight. The major exception to this principle is the wingtip test for the safety inspection of the competition. The three-point wingtip test does not approximate any spanwise load distribution the aircraft will experience while in flight.

Dynamic loads were the main concern with the design of nose and tail support. These components have long moment arms to the CG. On hard landings or heavy wind shear, these ends of the aircraft will put a tremendous bending strain on the airframe. A 4-g dynamic load for wings and a 24-inch drop for landing gear were used at the tests for the most extreme loads the aircraft must endure.

Materials selection for the construction of any aircraft should be taken seriously. Aircraft need the strength to withstand rigorous flight loads, but simultaneously need to be lightweight in order to perform well. Maximizing the strength-to-weight ratio for an aircraft involves creative arrangement of components that will make the most use of their internal strength. Following the principle stated earlier, the aircraft was designed to use materials only dense enough to provide the necessary strength, and no more. Aside from weight, the materials that have the highest bulk modulus, shear modulus, modulus of elasticity, or tensile strength may not always be the best material for a certain application because of limiting factors such as ease of manipulation, cost, or availability.

Fastening these components together is another consideration in the design of the airframe and the choice of materials. Components can be glued, welded, soldered, bolted, screwed, or some other alternative fastening method (such as Velcro). Components that may be taken apart or adjusted later will be bolted or screwed, but permanent bonds would use an adhesive or weld. Epoxy is generally not appropriate for joining two pieces of balsa because balsa has such low density as compared to epoxy.

Such a joint would be heavier and stronger than necessary. White glue has very low bonding characteristic as compared to epoxy, but can be thinned with water and spread more easily than epoxy for large surface bonds that do not require high local strength. Permanent bonds in which a glue joint may not be trusted may incorporate screws, bolts, or pins for additional security. Each fastening method has an optimal application given the material and strength requirement, and all of the listed above have been qualitatively investigated.

Of the glues, there are the white glues (e.g., Elmer's® brand), several types of epoxy, cements, cyanoacrylates, and polyurethane glues. The epoxies are one of the most commonly used methods used to join two surfaces. There are basically two types of epoxies. There are the "gluing" type epoxies and "laminating" type epoxies. Laminating epoxy is usually much less viscous than gluing epoxies so that the epoxy can wick its way into the fibers of the laminating material. Much of the reason epoxies bond so tightly is that they cure from a chemical reaction (and thus always mixed from two parts) rather than "air drying" from exposure to the atmosphere. This allows the bonding medium to be fluid enough to soak into the texture of the surface, and then cure to a very rigid form. This is why two-part epoxy bonds very well to wood and foam, but not to metals. Although it gives an excellent bond between wooden components, epoxy can add a significant amount of weight to an aircraft if not used sparingly. Some types of epoxy have such low viscosity to be used on woven fabrics, such as fiberglass and carbon fiber, to make very strong, lightweight components. This laminating application is discussed in more detail later.

Cyanoacrylate (CA) type glues are lighter weight and has a viscosity similar to water. CA type glues are best suited for bonding balsa wood because the CA wicks into the highly porous wood to give a bond beyond the contacting surfaces. These types of glues do not work well on plywood because the glue used by the manufacturer to bond the laminates has a neutralizing effect on the CA. CA does adhere fairly well to some unpolished metals (such as the 1000 and 2000 series Aluminums) but is not suited for the styrene-type plastics. CA-type adhesives will dissolve any polystyrene material, and precautions must be taken to keep CA and CA accelerators away from polystyrenes.

The polyurethane glues were the third type of glue used to construct the aircraft. Polyurethane glues are fairly non-reactive and readily available at most hardware stores. There are two types of polyurethane glues, and both expand while curing, resulting in a lightweight bond. Water-activated polyurethane glue has a minimal expanding characteristic that works well to laminate balsa wood sheeting to a polystyrene foam core. Using a vacuum bag retains the airfoil fairly well while the glue expands. The Elmer's® brand of water-activated polyurethane was used by the Georgia Tech DBF team. Air curing polyurethane is not generally used as adhesive, but was found in 1999 to be an excellent lightweight adhesive for gap filling applications. The Great Stuff® brand of air curing polyurethane was used by the Georgia Tech DBF team.

Another type of adhesive is plastic cement. These types of adhesives are not generally considered "glues" because they do not join surfaces by mating to the surface texture of the two components. Cements are used exclusively on ABS plastics and chemically "melt" the plastic, then air

cure to give a very strong, weld-like bond. Cements were only used in experimentation and not used by the Georgia Tech DBF team on the final production aircraft.

The Structures Team decided to explore only those materials commonly used on UAVs and light aircraft for the historical knowledge available on those materials in that specific application. This greatly simplified the choice of materials. However some of these materials require a high degree of skill in order to exploit to full potential, and many DBF members have little or no experience with these materials. Some materials are more readily available than others, and some materials cost much more money than others that may be able to do the same job.

Noticing these dynamics, the team began to evaluate all the costs associated with a certain material. These costs included team member experience with the material, analytical certainty/uncertainty, monetary costs, man-hours to manipulate, strength reliability, end-result strength-to-weight ratio, etc... The sum of all these costs was a total attractiveness level associated with that material, reflected as "Relative Cost" in the qualitative matrix below. Low relative cost represents a high attractiveness level. Also shown are the

	Density	Strength to Weight	Shear Failure	Bulk Modulus	Availability	Manipulation Skills	Spanning Surface	Relative Cost
Carbon Fiber Plates	very high	very high	brittle	extreme	low	very difficult	excellent	very high
Fiberglass Plates	very high	very high	brittle	very high	low	difficult	excellent	high
Balsa wood	low	very high	flexible	fair	high	very easy	fair	low
Basswood	high	high	brittle	very high	low	easy	very poor	low
Spruce	medium	very high	brittle	very high	low	easy	poor	medium
Basswood Plywood	high	high	brittle	very high	high	easy	poor	medium
Poplar Light Plywood	medium	medium	brittle	high	high	easy	poor	medium
Polyvinyl	high	high	flexible	poor	high	easy	excellent	medium
ABS Plastic	high	medium	flexible	fair	medium	difficult	good	low
Aluminum	very high	high	flexible	good	high	fair	good	low
Styrene	high	medium	flexible	fair	medium	fair	good	low
Polystyrene (expanded)	low	low	brittle	good	high	fair	poor	medium
Polystyrene (extruded)	low	medium	brittle	good	medium	fair	poor	medium
Lexan	high	medium	brittle	fair	medium	fair	good	low
Paper	medium	low	flexible	poor	high	easy	poor	low

Table 4.4: Construction Material Characteristics

Wings:

Aside from the propulsion system, the primary performance unit of the aircraft is, of course, the wing. With the airfoil and planform known, the construction of the wing was the next major task. The Structures Team had the lead on this project and developed the construction design arguments for several of the most favorable options. The team determined that the highest bending loads would come from lifting the fully loaded airplane by the wing tips (three-point stress test). During flight, the load is distributed fairly elliptically across the span. The construction designs that the Structures Team developed were based on the need to retain the exact airfoil, the need for a glossy-smooth lifting surface, the need for low weight, and the strength to support the three-point stress test. As with the conceptual design, the team found it more productive to explore conventional design rather than develop revolutionary new designs.

The combinations of construction designs are seemingly infinite. One could use a fabric with epoxy to form the outer shell, but there are fiberglass, carbon fiber, Kevlar, Aramid, silk, and other fabrics from which to choose. Within each type of fabric, there are also many different weights and weave patterns. There are many different types of epoxy to choose from. One could also use such composites to construct the spar. However, with a strong enough outer shell, a spar may not be needed. Once a fabric, weave, and epoxy are chosen, one can also vary the number of layers, and the placement/orientation of the fabric in order to maximize strength. Aside from composites, there are many types and densities of foam, wood, and other materials that are all good candidates for constructing a wing.

It is this complexity that makes strength analysis virtually impossible. The team could choose a set of materials in a specific design and calculate a static analysis or a CAD finite element analysis, but the results could not be reliable because the high error that results from the extremely high number of input factors affecting the response. Accuracy of inputs, human error, and analysis competence are other sources of error.

The question then arises of how to obtain the lightest, strongest wing that will outperform all other designs. This implies that there is one optimal design with all others being subordinate. However, one, single, optimal design may not exist. There could be several good candidates, each offering different features. After addressing such arguments, the team decided to identify a small set of best candidates, and construct the most robust design first. Flight testing and three point testing will then verify how well the wing suits the performance needs of the design.

Two of the wing requirements were to hold the airfoil shape accurately and provide a glossy-smooth lifting surface. The team decided to use a foam core with a composite shell to meet these two requirements. For foam wings, it was not clear whether or not a spar should be used. Composites technology in making hollow core (no spar at all) composite wings popular in the homebuilt aircraft industry, and from this movement it was noted by the design team that lighter spars could be used with heavier wing skins. Heavier spars would carry more load and thus require less strength from the shell. The tradeoff between the weight of the spar and the additional weight of a thicker shell is not clear. It

would require extensive strength testing of foam, spars and laminate skins in order to accurately predict the performance of such a composite wing.

After extensive discussion about load distribution and strength requirements, the design team developed four wing designs that offer significantly different designs. The four designs were ordered from the most reliable to the most suspect. Shown in Figure 4.2, the four designs cover most of the discussion about wing construction. The team's plan was to build each wing, and use the wing proven to offer sufficient strength at the lowest weight.

The wing designs as shown in the figure are in the order that the team wanted to build the wings. Time restriction was always a concern, and the team knew that it was possible that time would run out and the team would have to use whatever had been built up to that point. Therefore, the team chose to build the strongest wing with the best flying surface first.

At the time the wing construction began in January, the team was far behind schedule. As a precaution the team decided to add a spar to the wing design. The spar would ensure the strength of the wing and allow for some experimentation with spar design.

High-density (2lbs per cubic foot) blue extruded polystyrene was chosen for the wing core. Extruded polystyrene has a homogenous consistency that makes it stronger than white expanded polystyrene of the same density. Extruded polystyrene is also available in pink (1.3lbs per cubic foot) and gray (approximately 0.78lbs per cubic foot). However, these densities are not readily available in blocks large enough to cut a single wing panel of our design.

The choice for the first constructed wing was the blue foam core wing covered in fiberglass, as shown in the figure.

Spar Design:

For security, the DBF team thought that it would be wise to design the construction of the first wing to be stronger than absolutely necessary. It was safer for the team to err on the side of too strong rather than too weak. It was suspected that a foam core wing covered in fiberglass would be strong enough to withstand the wingtip test, but without a reliable means of estimating strength from these types of constructions, the team could not be sure. There was also the possibility that a lighter foam, inside of a thinner shell, along with the use of a well designed spar may have a higher overall strength-to-weight ratio than the other. At the time, it was suspected that a spar could be designed to support the load without the surrounding wing. This would mean that the wing would not have excess material designed to support the other part of the load. The general idea for designs supporting a spar was that the wing would feature a strong "spine" from which the body of the wing was attached.

The two strength systems in these designs that the team identified were the composite outer shell, and the internal spar. The Structures Team wanted to determine the relative strengths and weight of each system and how to optimally integrate them.

One of the main concerns of the Aero-Configuration team about wing structure was that uneven loading of the wing may result in twisting while in flight. The Structures Team began research into these dynamics began with Semobeam, a Unix shell program designed to calculate loading patterns on thin shelled models. The team first analyzed the reinforced spar and reinforced spar with outer fiberglass modeling. This modeling process was entirely script based and required a substantial training period. Both models were completed with spar positions at 15, 20, 25, 30, and 35 percent chord.

The outputs of the program showed irregular load distribution along the cross section of the systems, and it was suspected that data entry errors were the cause. Two weeks of investigation did not reveal what was causing the problem with the output, and the program was abandoned.

Now two months into the project without any reliable outputs for wing design, the Structures team began looking for alternatives. One of the Structures Team members found an article on model aircraft spar designs in the October 1990 issue of Remote Control Modeler magazine. This article described a series of tests that were done on carbon fiber reinforced spars. In the tests, 6-ft. spars 2.5-in tall underwent 3 point flexure tests. Some of the key points that were learned in this testing were:

- Buckling was the primary cause of failure
- Carbon fiber in compression needed to be three times as thick as in tension
- Thus, compression caps *must* be thicker than tension caps
- 1/16" Carbon fiber did not buckle
- Carbon fiber was roughly 4.5 times as strong as spruce
- Vertical grain webs were 25% stronger than horizontal grain webs
- Gap-filling CA was found to be best suited for construction
- The shear web is a vital element of the spar

Because each of the test spars were 6-ft in this test, each of the force-to-break results were multiplied by 6/10 to normalize the results to the 10' DBF spar. This comes to 92 lb of force-to-break resultant for the 6' spars. The two spars of interest in the test were:

Top Cap	-	.203" wide / 0.062" thick Carbon Fiber
Bottom Cap	-	.203" wide / 0.021" thick Carbon Fiber
Shear Web	-	.125" wide / 2.500" thick Spruce
Weight	-	.328 oz/ft
Force-to-break (6')	-	69 lb
Force to break (10')	-	41.8 lb

Top Cap	-	.250" wide / 0.080" thick Carbon Fiber
Bottom Cap	-	.250" wide / 0.031" thick Carbon Fiber
Shear Web	-	.250" wide / 2.500" thick Balsa

Weight	—	.328 oz/ft
Force to break (6')	—	80 lb
Force to break (10')	—	48 lb

The results of these tests were encouraging because these spars were rated up to the equivalent of 41.8 lb and 48 lb. respectively for a 10' spar. Additionally, at .328 oz/ft, a 10' spar would weigh roughly 3.28 oz. These strength-to-weight results effectively nullified the need for the fiberglass skin to add support for the wingtip test. From these figures, 4.75-oz/sq.ft fiberglass covering at 14-sq.ft surface was suspected a poor candidate for reinforcement when the spar can relatively easily be reinforced at a low weight to the desired strengths. However, later results would show that considerable strength could be obtained from such an outer shell.

For a more refined analysis, the Structures Team began to draw several wing designs in CATIA, with the intention of running a finite element (FE) analysis for three point loads. As the students gathered more knowledge about FE models, it was decided that such analysis is beyond the capabilities of an undergraduate research team. Strength in the outer shell depends on the type of cloth (fiberglass, carbon fiber, Aramid, Kevlar, silk, etc...), the weight of that cloth, the number of layers, the orientation of layers, and the type of epoxy used. Reliability of such an analysis also assumes flawless human construction, something not likely with inexperienced students. FE analysis for spars suffered the same scenario, but with even more materials from which to choose. There are literally millions of combinations which could be analyzed.

At this point in the Structures Team's progress, the aircraft was already behind schedule for production. The team had to decide on how to structure a wing and estimate its strength. The team reassessed what was known about wing structural design and necessary strength. It was known that a foam core would hold an airfoil shape well, but that foam could not be configured to carry shear loads. However when a hard outer shell is supported by from to resist compression, the foam can be used to greatly increase the strength of a wing. For spar design, it was known that the vertical component of the I-beam shape served the same purpose as the foam did for the outer shell. That is, to resist compression and hold the "caps" in place.

The team knew that a strong wing was needed to ensure that at least one successful wing would be produced before the competition. Therefore blue foam, which is more homogeneous and more dense than Acrospan, 1-lb/cu. ft white foam, was chosen to make the foam core. With the proper fiberglass covering, this wing would probably be strong enough to withstand the fully loaded wingtip test. However, a very strong yet lightweight spar was constructed for installation in the wing for additional strength. This spar was made from yellow poplar plywood (similar to spruce in the analysis above). The 0.080: think

Fuselage:

Model helicopter aircraft construction inspired the construction decided upon for the prototype. The structure is essentially two side frames fairly close together and braced to each other through cross members. The parallel side frames are spaced 3" apart, but the aircraft is 10" wide; leaving a little more than three inches on either side for the battery packs. The proximity of the two side frames gives a rigid center section with a light outer shell. The empennage is attached to the frame by a 1" aluminum tube, and the tube is clamped to the frame by hardwood blocks. The 2lb electric motor on the nose end of the plane is mounted between the two frames on a plywood plate that is pinned between the side frames. The nose gear is mounted on a similar plywood plate just aft of the motor.

The two frames carry all major loads that are required of the fuselage. The remainder of the internal material serves primarily to cradle the speed loader box. Two spruce runners joining fore and aft top airframes were added to work in tension and resist the downward moments caused by the motor and tail sections.

The outer shell of the aircraft was not intended to support any of the loads required of the fuselage. The design is therefore neither monocoque nor semi-monocoque, but rather a small flying frame inside of a lightweight, non-load bearing shell. The first shell was constructed with basswood and spruce runners that form a truss-like frame; then covered in polyvinyl heat-shrink film. This shell was intended only to approximate the smooth contour of the final product. The final product shell was designed to be made from a fiberglass mold of the lofted CAD drawing.

Construction	Spar	Features	Cost
Blue foam (2lb/cu ft) solid core, Fiberglass shell	Carbon composite	Very strong, excellent lifting surface	Expensive materials, low man-hours
White foam (1lb/cu ft) solid core, Balsa sheeted, Fiberglass Shell	No spar or short landing gear spar	Moderately strong, lightweight, excellent lifting surface	Expensive materials, medium man-hours
Wooden internal construction	Spruce caps with balsa shear webs	Light weight, fairly strong wing	Inexpensive materials, highly labor intensive
Blue foam ribs, balsa sheeted, covered	Carbon composite	Very light, very strong, excellent lifting surface	Expensive materials, highly labor intensive

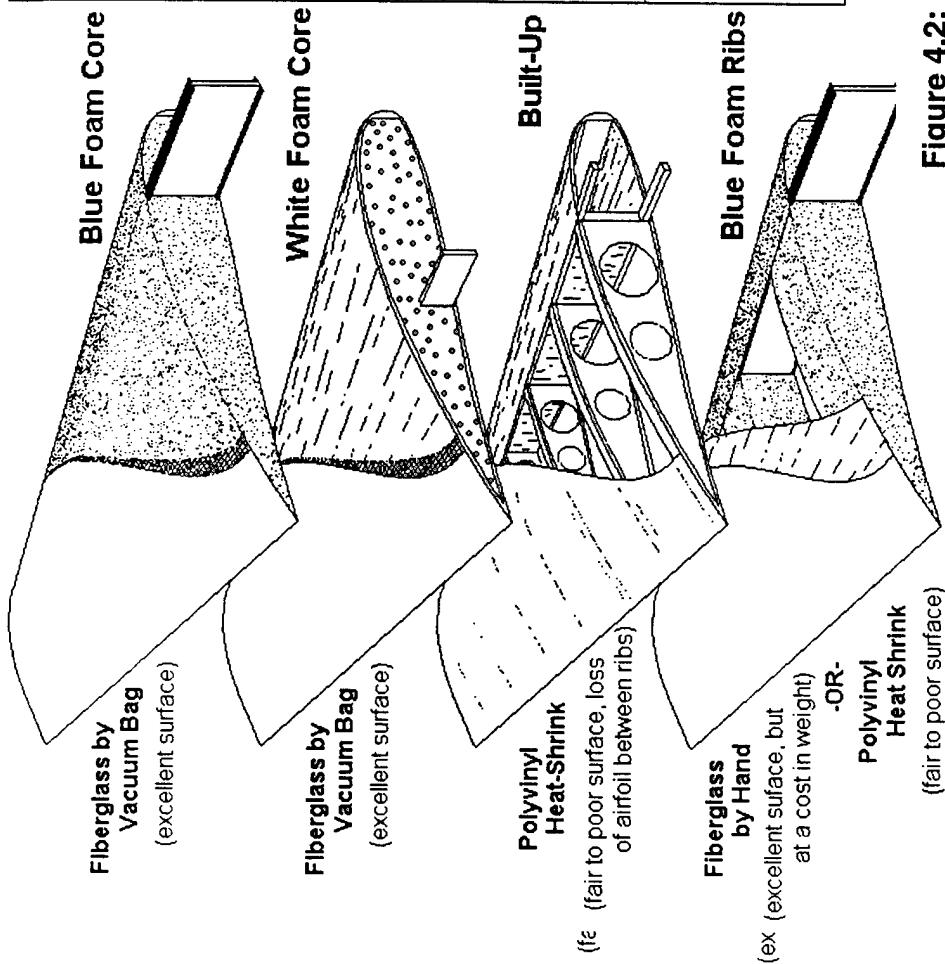


Figure 4.2: Wing Construction Concepts

(Illustration by DBF member Adam Broughton)

5.0

Detailed Design

Throughout the design process, the team carefully thought out the design of each component so that it would perform as well as possible for the competition. However, the team knows that what works in theory may not always work in reality. As components were fabricated and evaluated, the team could see first hand how well their concepts fit practical applications. It is this kind of education that makes such a project so valuable to team members.

With the basic dimensions of the aircraft such as wingspan, gross weight, required $C_{L_{cruise}}$ and $C_{L_{takeoff}}$ known, the details of the aircraft could now be addressed and clearly defined. These sections of the aircraft include the wing, the fuselage, the empennage, aircraft handling and control, and the structural arrangement of the aircraft.

5.1 Wing Arrangement:

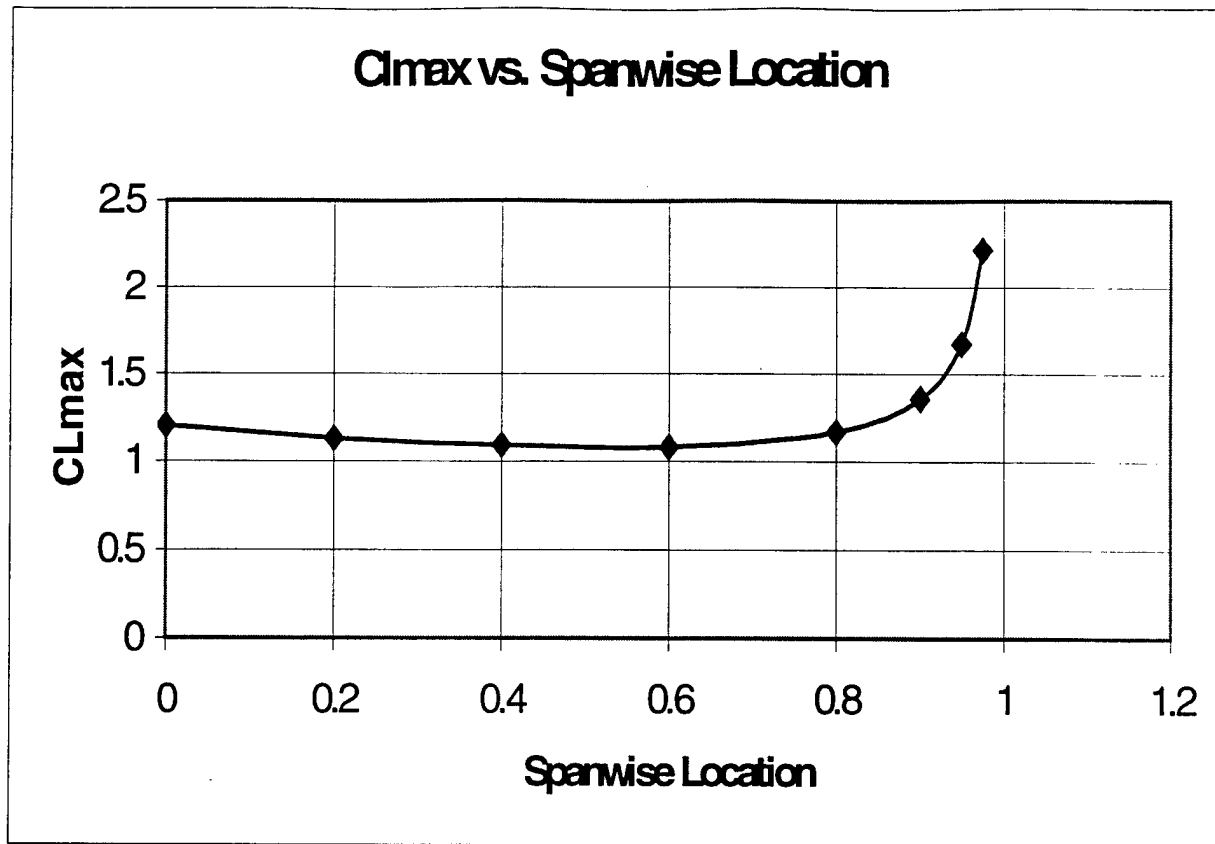
The general wing characteristics were selected from historical trends. A leading-edge sweep of 1.2° was selected because most aircraft at similar low speeds have a leading edge-sweep of zero, but a sweep of 1.2° would allow the main wing spar to be perpendicular to the fuselage. A taper ratio of .45 was selected as this ratio most closely approximates elliptical loading for a trapezoidal shaped wing according to Raymer. The wing geometry is summarized in Table 5.1.

	ft.	in.
Co	1.931034483	23.17241
Ct	0.868965517	10.42759
L.E. sweep	0 degrees	
Taper	0.45	

Table 5.1: Wing Planform Characteristics

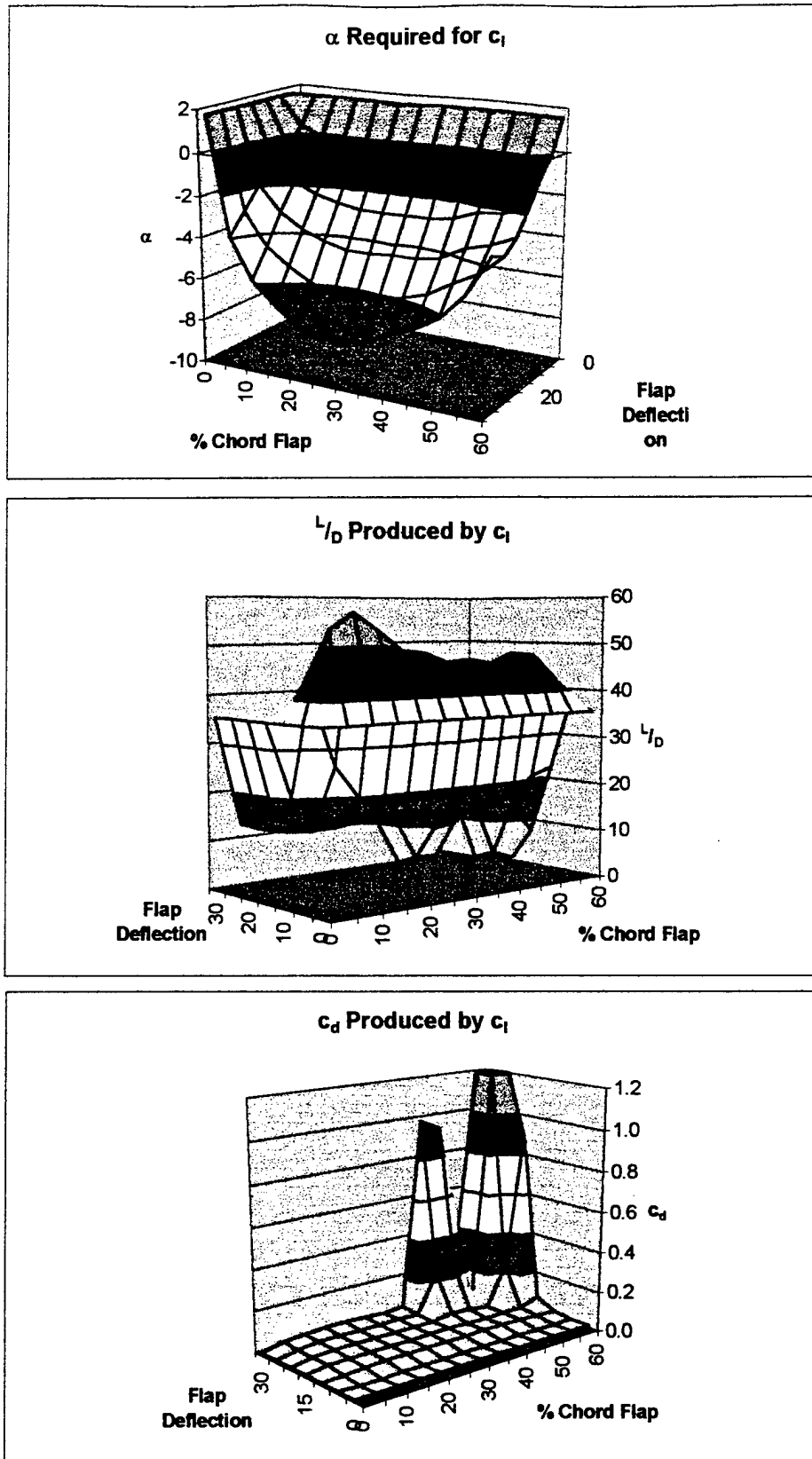
The airfoil for this aircraft was chosen by taking the $C_{L_{max}}$ for cruise at the heaviest flight condition, and modifying it for three-dimensional effects using a method in Abbott and Doenhoff's Theory of Wing Sections. The results of this study are summarized in Figure 5.1. The lowest spanwise C_l is the C_L which the wing must be able to generate, and in this case was a C_l of 1.082. The goal was to find an airfoil which would meet this cruise requirement, and then use flaps or flapperons to achieve the required C_L which is required.

Figure 5.1: Coefficient of Lift Distribution



The two candidate airfoils selected were the LNV109A and the NACA 58012-93, two relatively high lift, cambered airfoils. These were chosen because of their appropriate thickness to the speeds involved. Historically, airfoils at such low speeds range from 12-15% thickness, with a lower thickness helping to decrease the overall drag. These two airfoils were analyzed using a spreadsheet optimization for varied flap deflections with varied flap widths relative to the span, showing the required angle of attack, the resulting induced drag, and the lift to drag ratio produced by the airfoil. These optimizations took into account the different required C_L s for the four primary parts of the mission, including cruise and take-off for the light and heavy conditions. The summary analysis charts for the LNV109A are shown in Figure 5.1. From the results of both analyses revealed that both were very similar in performance and very close to the desired C_{Lmax} . However, the NACA 58012-93 appeared to have a slightly lower coefficient of drag for the heavy take-off and light cruise situations and so was chosen for this aircraft.

Flapperons were chosen for this aircraft because they permit a lower drag for identical lift produced by an aircraft with only partial wing-length flaps. Further, the use of flapperons reduces the overall cost model score of the aircraft by decreasing the number of servos required. The use of flapperons may make handling more difficult since the roll authority is generally reduced by their use. However, for this mission, no complicated maneuvering other than a turn on the heavy loading leg will be required, and so flight testing will be used to see if this provides sufficient control.



**Figure 5.2: Flap Effects on LNV109A
Performance Characteristics**

5.2 Empennage:

The choice of tail location (horizontally with respect to the wing quarter chord) was made based primarily on historical data. An idea that occurred to the team leader was to have a variable-arm horizontal tail arrangement for the prototype. Therefore we chose a shorter distance (meaning larger area) in order to obtain a conservative value that could be used with several arm lengths. This way, we could experimentally test which location provided maximum benefits at the time of flight. The chosen length was determined to be 4.5ft (from the quarter chord of the wing to the quarter chord of the horizontal tail), with the testing range between 4 and 5.5ft.

The vertical location with respect to the wing was also chosen based on a downsizing of typical home-built aircraft. An important factor to consider was to ensure that the wing wake would not blanket the action of the control surfaces (namely elevator) during takeoff, flight, and maneuvering. Thus, a height of 4 inches above the wing mean chord line was chosen.

Several methods were used to determine the horizontal and vertical tail areas including NACA reports and historical data. The best method for the calculation of tail area was the Tail Volume Coefficient method, which uses the following equations:

$$S_{VT} = \frac{c_{VT} b_w S_w}{L_{VT}}$$

$$S_{HT} = \frac{c_{HT} \bar{C}_w S_w}{L_{HT}}$$

where S_{VT} and S_{HT} are the areas of the horizontal and vertical tails, c_{VT} and c_{HT} are the horizontal and vertical tail volume coefficients, b_w is the wing span, S_w is the wing area, \bar{C}_w is the average mean chord of the wing, and L_{VT} and L_{HT} are tail moment arms.

Using Raymer's home built model typical values the vertical tail volume coefficient was chosen to be 0.04 and the horizontal tail volume coefficient as 0.4.

The NACA Report 293 described a method for arriving at a value of c_{VT} and c_{HT} that required assumptions which we believed were not conducive to accurate results. During the conceptual design phase, precise values of properties such as aspect ratios, moment considerations, and efficiency factors were not known. Therefore our best approximation was not very reliable, and we chose to abandon this method in preference for the simpler Raymer's equations used previously.

Last year's DBF design produced an Excel spreadsheet to calculate the tail areas. After finding our values, we used the spreadsheet to verify our results. A comparison to last year's configuration was also made. The final sizing values can be seen in Table 5.2.

The horizontal tail has two important aspects to consider: first, the aspect ratio needs to have a high enough value for effective pitch control, but lower than the wing's aspect ratio in order not to stall before the wing. Second, the taper ratio is chosen such that it approximates most closely an elliptical lift distribution, which minimizes induced drag. This ratio is 0.45. The pitch control surface takes the form of a single elevator that spans the width of the tail. It comprises the two last inches of the horizontal tail chord.

The vertical tail area of 1.25 square feet (determined from the volume coefficient method) is distributed between height and width. We originally equated the root chord of the horizontal tail to that of the vertical tail. However, a simple Hershey bar application with that chord dimension made the vertical tail too tall. Any tapering performed on the vertical tail was essentially useless aerodynamically speaking, although it added an aesthetic quality. In addition, tapering resulted in an even taller tail, unless the root chord was made longer than the horizontal tail root chord. As of now, a final decision has not been made as to the tapering of the vertical tail. However, this is not a major decision because the total aerodynamic performance is not significantly altered one way or another. Regardless of the decision, the vertical tail is placed forward of the horizontal tail to avoid blanketing of the rudder by the horizontal surfaces.

	Variable	Value	Unit
Airfoil		NACA 0012	
Area	S_{HT}	2.1	ft ²
Span	b_{HT}	39	in
Mean Chord	C_{HT}	7.75	in
Tip Chord	C_{HTtip}	4.8	in
Root Chord	C_{HTroot}	10.7	in
Moment Arm	L_{HT}	4.5	ft
Taper Ratio		.45	
Elevator Chord		2	in

Table 5.2: Horizontal Tail Sizing

	Variable	Value	Unit
Airfoil		NACA 0012	
Area	S_{VT}	1.25	ft ²
Moment Arm	L_{VT}	4.5	ft

Table 5.3: Vertical Tail Sizing

	Variable	Value	Unit
Area	S_w	14	ft ²
Span	b_w	10	ft
Mean Chord	C_w	16.7	in

Table 5.4: Required Wing Characteristics**5.3 Wingtip Design:**

Induced drag from tip effects is a commonly known source of drag. The team suspected that incorporating wingtips could reduce overall drag. Wingtips were found to increase the effective wing span and decrease induced drag with negligible increases in weight or area. The team searched for discussions on wingtip design in airplane design books, including Raymer's and Roskam, and aerospace related websites on the Internet. Originally the team chose the Hoerner wing tip design, which is a low-drag wingtip design commonly used for full-scale aircraft. The end of the wing is cut at a 45-degree angle with the top surface longer than the bottom surface. The theory behind this design is that the airflow on the underside of the wing flows outward to the tips, pushing the vortices away from the wing. Raymer argued that this tip design provides the most effective span increase for the least amount of weight addition. This would also not increase our effective wing area in the cost model.

After further analysis, the Hoerner wingtip was found to not be a better choice for low Reynolds number airplanes. It was discovered that a downward pointing wingtip would actually be a better design. The main advantage to this design would be protection of the control surfaces. This protection becomes important during landing and takeoff. If gusts or unstable flight occur near the ground, the wingtips (and therefore the ailerons) are the first to hit the ground, especially in a low-wing configured airplane.

Another solution to reduce the induced drag and increase the effective aspect ratio of the wing is to use the upward sloping winglet. The advantage this wing tip solution is to effectively add span to the wing (aspect ratio up, induced drag down) as well as move the wingtip vortices outward and upward.

Unfortunately, the construction is rather complex and the team did not feel confident about the accuracy of modeling the flow-field (to place the vortices correctly). There was also concern that, at low speeds, the winglet efficiency would not outweigh its costs in weight, skin friction, and form drag. Thus, it was decided that a downward sloping wingtip was the best choice for the team's application. The addition of the wingtips will take place as flight testing progresses, as no apparent way to theoretically analyze the full effect of the tips was found.

5.4 Handling and Control Characteristics

The first main decision was to use a low-wing configuration. A high-wing would provide greater stability, however, this would have required a T-tail, which has apparent weight penalties (Raymer). A low wing, while requiring more stability consideration would allow for fast loading in the field, and would permit a conventional tail structure. Further, stability could be induced through the use of dihedral in the wing

The control of the aircraft is sufficient, as it used an approximate method which usually overestimates the size needed for control surfaces.

5.5 Radio Telemetry:

The team knew that flight-testing would be essential to perfecting the design. The entire prototype was based on estimates and theory. Until the complete synthesis of all components working together could be tested, it would not be known how well the design met the desired performance. Early in the project development, it was recognized that "testing" would entail more than just flying the airplane with specified cargo, propeller, battery, etc... Otherwise, the only conclusion that can be drawn is "Yes, it flies."

The team knew that it would have to gather some data from the test flights to see what kind of performance was actually occurring. On-board flight data gathering equipment for model aircraft are virtually nonexistent or extraordinarily expensive, and so the team decided to build their own equipment. A local graduate student specializing in aircraft controls, Aaron Kahn, was willing to advise the team on how to build the equipment. Mr. Kahn gave explicit instructions on what equipment to purchase, and how to arrange the equipment to feed back the necessary data.

The data that the team wanted to gather was airspeed, motor RPM, voltage, current, and motor temperature. The airspeed indicator was constructed with a small pressure transducer at the end of a long ¼-inch aluminum tube. The motor RPM gauge was constructed with a photo gate at the edge of a 4-inch wheel mounted behind the propeller. The wheel had a small hole in it that allowed the beam of light to pass through the gate and count each revolution. The voltmeter and ammeter signals were taken from an AstroFlight wattmeter. The motor temperature was taken on the outside of the motor can with a small thermocouple.

The five signals were recorded together in real time and transmitted through a radio transmitter on board the aircraft to a receiver on the ground, which was linked to a laptop computer, which recorded the data strings. The team used a cheap hand-held RC hobby transmitter, similar to the one controlling

the aircraft, to send the signals to the computer. The voltage from each sensor was scaled to fit the input signals to the transmitter, then sent to the receiver. The data is later interpreted in the laboratory. Currently, the team is re-scaling the instruments to fit the bandwidth of the transmitter, and hopes to have the unit fully operational again within days.

5.6 Performance and Flight Testing:

The first flight of the prototype was on Monday, February 26th, 2001. Sky conditions were overcast, there were light winds from the southeast, and density altitude was reported at 1860 ft. at a local airport. The aircraft was fixed with a 24x12-inch propeller on two 26 cell battery packs linked in parallel. Total aircraft weight was near 24 lbs., and takeoff ground roll was estimated at 60 feet with full (30 degrees) flaps. Problems with the wire landing gear limited the flight testing that afternoon, and the team has not had an opportunity to continue flight-testing since then. Further testing will be documented in the Addendum Phase of this report.

Of the two flights that have been made on the aircraft, the team is proud to report that handling qualities were beyond expectations. With a minor adjustment to the center of gravity, stall characteristics were very predictable and at very low airspeeds. Climb rates were as expected for the propulsion system, and power off glide with 9 lbs. of battery was outstanding. Unfortunately, few conclusions can be drawn from these flights, but the team looks forward to further flight testing with the radio telemetry and full payload.

The construction of the aircraft coincided with the Detailed Design Phase. The materials selection was based upon the strength requirements, weight, ease of manipulation, and cost. The structural configuration of these materials was based upon thorough investigation of static and dynamic loads of known components. As discussed earlier, the team decided to build at least two aircraft. The first would be a fully operational prototype and the second would be a lighter, more streamlined version of the prototype.

The first aircraft would feature a strong, but heavy wing, and a boxy wood-frame fuselage. The second aircraft would feature a lighter wing, and a more streamlined fiberglass fuselage.

Once the configuration of the design was known, the team began to draft the assemblies that would compose the aircraft. The internal frames were dimensioned, components were sized, and the layout of electrical equipment was organized. Drafting by hand and with the use of the CAD package CATIA greatly facilitated this task. Once the students could actually see the components together on the design before it was built, refinement of the structural concept could be very easy. Using drafting aids reduced build time, wasted materials, and valuable man-hours.

The experience and skills of the team members was a known limitation. Some team members had experience with traditional wood-frame model aircraft, but composite materials were known to be great materials for building lightweight, strong aircraft. It was suspected that a lighter, stronger aircraft of more streamlined design could be created by using composite materials. These materials were therefore evaluated early in the project to determine if using composites was appropriate for the team's applications. Advice from local experts, composite dealers, and composites oriented websites led the team to conclude that they could produce satisfactory composite wing and fuselage at a reasonable cost.

As discussed in the Preliminary Design report, there were four wings of different designs. The first wing that the team wanted to construct was the blue foam core covered in fiberglass. Fiberglass was also planned for the construction of the fuselage and would require a great deal of man-hours to construct. Because none of the team members had any experience with fiberglass, it was decided to begin the wing before the fiberglass fuselage. This procedure would ensure that the lifting platform of the aircraft would be ready for flight on a wood-frame fuselage if unexpected delays did not allow ample time to build the fiberglass fuselage. At the time, these "unexpected delays" were suspicions that the wing may not realize the predicted strength estimates, and an alternative design would have to be constructed.

The team began to build the wing and internal frame simultaneously once it was decided that structural design was satisfactory. Both components were constructed with the idea that this newly designed aircraft would be a predecessor to the aircraft actually used in the competition. Unfamiliar composite techniques and inexperience proved to degrade the desired quality of a competitive platform. Learned skills would later produce a much better aircraft.

Carbon fiber or fiberglass plates were originally planned to be used for the internal frames. However, these materials are difficult to cut and shape, not to mention expensive. Monetary and human costs were too high for an unproven design, and the team decided to make the frames from 1/8" yellow poplar plywood. At \$12 for a 1/8x12x48 inch sheet, the team cut frame costs by nearly 80% for G-10 fiberglass, and over 90% for multidirectional carbon fiber laminates. Not planned, but yellow poplar light plywood was later found to be easier to fasten together than bolting composite plates. Completion of the internal frames arrived sooner than planned, allowing students to focus efforts on building the first wing.

Recall that the first wing was blue foam core covered in a light fiberglass shell. The setup for cutting foam cores involved a six-foot hotwire bow, two endplate templates, 200 lbs. of steel plates, a voltage power source, and two operators.

End plate templates were made from plywood rather than a metal that would absorb heat from the wire (causing an irregular cut). The end plate templates were cut from full size printouts of the airfoil. The printout was set 1/64th of an inch below the desired airfoil shape to accommodate the thickness of the fiberglass to be applied later. A thin strip of unidirectional carbon fiber tape was glued to the templates to prevent the wire from burning into the wood and then checked to ensure the template fit the airfoil. After some adjusting, the template fit the airfoil to within 1/100th of an inch. The templates were then marked with evenly spaced numbers and scaled to each other. The hotwire operators would use these numbers to ensure that the wire was at the same place on the templates as it made the cut through the foam. The planform was cut first, then the templates were secured to the ends of the foam block. The templates were aligned along a datum that had been printed with the airfoils, and the tip template was rotated three degrees at 25% cord to provide the correct washout. The steel was used to hold the foam down to a flat surface (checked with a laser) and prevent bowing in the core as the foam cooled to room temperature.

Using a hotwire bow to obtain smooth cuts through blue polystyrene proved to be a very difficult task. A considerable amount of time was spent developing the method for cutting foam cores, but once a satisfactory method was found, the team spent little time actually constructing the wing.

The foam cores are cut from 4x24x96 inch blue foam with 0.020 inch diameter nickel-chromium wire under high tension. When cutting blue foam, the best results were found when the wire was under high tension, high temperature, and using the smallest diameter wire. Poor cuts resulted from oscillations in the wire as the hot wire liquefied the foam. These oscillations were reduced by the combination of high temperature, high tension, and low forward pressure (causing the wire to lag behind in the middle). The first attempts with 28-gauge (0.0126 inch diameter) nickel-chromium showed that thermal expansion caused a dramatic drop in wire tension. Several attempts were made to stretch the wire while hot, but because the wire was very thin, the team had problems with the wire breaking at the tips. The breaks would occur on the wire that extended beyond the edges of the foam. There, the wire was not being cooled by dissipating heat to the foam, and therefore hotter. This excess heat caused the electrical resistance to go up, and therefore become even hotter from the high current passing through it. The extreme heat weakened the wire and caused it to fail.

Larger 22 gauge (0.0253 inch diameter) nickel chromium wire was then used to protect against failing at high tension and high temperature. However, when this wire was heated enough to resist oscillations, the large diameter carried so much heat that it would melt the foam unevenly as it made the cut. Smooth cuts could never be made without arranging a mechanical device to provide a perfectly consistent pull through the foam. One alternative was to use a smaller diameter wire that carried less heat, but the smaller diameters are more prone to breaking and cannot be strung as tightly (resulting in oscillations). The solution the team developed was to use a wire size between the two gauges already tried, and of a slightly different composition. A satisfactory cut was finally made with 24 gauge (0.0201 inch diameter) Inconel® nickel-chromium iron. The iron in the wire minimizes thermal expansion and aids in tensile strength. Using this wire produced good results on both white (1lb. per cubic foot density) and blue foam.

After two months of difficulties with cutting foam, the team finally obtained an acceptable wing core. This core was cut vertically at 25% cord for the spar. The spar used on the first wing was constructed by splicing three pieces of poplar light plywood together, then gluing the unidirectional carbon fiber strips on the top and bottom to form the I-beam shape. The carbon fiber on the top of the spar was thicker than the carbon fiber on the bottom. The argument here was that the top of the spar need to resist bulk compression, and the bottom would resist tension when loaded from above. The team used 0.060x0.250 inch unidirectional carbon fiber on top, and 0.022 x 0.250 inch unidirectional carbon fiber on bottom. The spar was built with a ten-degree bend in the center section to give the wing panels five-degrees of dihedral. The spar was set 1/8 below the surface of the foam core to preserve the shape of the airfoil. It was noted that the spar would no longer be glued to the fiberglass shell as originally planned, transferring strength directly to the shell. However the rigidity of the carbon fiber made accurate shaping of the surface very difficult.

The foam cores are cut to fit the spar, and the spar and foam pieces are put inside the blue foam shells (negatives) and then all are placed in a vacuum bag at 25"Hg until the polyurethane glue has cured. Two large sheets of Mylar are then cut to fit the top and bottom of the wing. The sheets are waxed with mold release wax, then polished. Six coats of wax were applied and polished on both sides of both sheets. Then 0.73oz and 3 oz. fiberglass cloth were cut to fit the two sheets. E-Z Lam® epoxy was mixed and spread onto the fiberglass and Mylar until all wrinkles were gone. Then the two sheets were placed on the reassembled wing and put back into the vacuum bag. After three days in the vacuum bag, the wing was taken out of the bag.

The control surfaces were formed by cutting a 3/4 inch groove through the underside of the wing up to the fiberglass on top. Instead of completely cutting the control surface off, it is left to hinge on the top layer of fiberglass. There are several advantages to making the control surface this way. First of all, the shape of the control surface is ensured to fit the shape of the wing because it was once part of the wing. Secondly, there is no gap between control surface and wing to allow air to slip from high pressure to low pressure, thus the surface is more effective. Third, there is no hinge to disrupt the flow of air over the

hinge line. Because there are no hinges, there is less work to assemble the complete wing. The team was very satisfied with the results of the completed wing.

6.1 Fuselage Shell:

As was discussed in the Preliminary Design report, the fuselage the fuselage was designed as neither monocoque nor semimonocoque. There are two components: the internal frame and the outer shell. The internal frame carries the loads of the aircraft, and the outer shell streamlines the airframe for low drag. The shell itself is what allows the fuselage to be very lightweight and very strong. By concentrating the weight near the wing, less structure is needed to support normal flight loads, thus allowing the outer shell to be light enough to support only its own weight and no more. Since the outer shell does not carry any loads, the shell walls can be made very thin. The thickness of paper is a good comparison. Since the shell is so thin as to not be able to support its own weight, structural supports position the shell around the frame and keep it in place.

The outer shell was the central design feature of the fuselage. Using one layer of 2-oz/sq yd fiberglass cloth, the entire seven-foot long outer shell would weigh slightly more than half of one pound. Although this design gives high strength at extremely low weight, it does require a great deal of man-hours and skill in order to construct.

It was not known if the team would have enough time to construct this shell before the date of the competition. Construction of a working prototype had priority, as there were many other tasks that would occupy the team's time. A working fuselage made from poplar light plywood and a polyvinyl heat-shrink shell over a light wooden frame. A second set of wings and the fiberglass outer shell began construction while this fuselage was being tested for functionality.

The fiberglass shell is made from a two-part mold, which was formed from a two-part plug of the desired shape. The procedure for generating this plug is as follows: The CAD drawing of the aircraft's shell is divided in to cross sections beginning and the nose of the airplane and separated every four inches all the way to the tail. The wing and tail surfaces are removed as they will not become part of the shell. Each of these cross sections shows the shape of the fuselage at that point along the longitudinal axis. A datum is drawn from the nose to the tail to give the cross sections orientation to each other. Then the cross sections are printed to scale and cut out from the white paper. Also printed with the cross sections is the full-scale profile view of the aircraft, with the datum drawn in place.

Then two profiles are cut from a large 3/16" plywood sheet. These are sanded together to exactly fit the printout and each other. Holes are drilled though both sheets and wooden dowels are placed in the holes and glued to only one of the profiles. The dowels will hold the two profiles together in a press-fit.

The cross section printouts are cut from the centerline inward 3/16-inch to account for the thickness of the plywood profile. Then the two mirror image cross sections are glued to scrap pieces of blue foam (four inches thick). Once the glue cures, the cross sections are cut from the blue foam with a generous margin. Each of these cutouts are then glued to the profiles in the appropriate order to form a

rough shape of the fuselage. The blue foam is then sanded to smooth contours until the paper can be seen in the joints between foam sections. At that point, it is known that the outer limits of the shell have been reached.

After final sanding of the foam, the plug is layered with several layers of light (2-oz) fiberglass. Each layer is left to cure, then sanded smooth. Three layers of light fiberglass have been shown to be adequate. Then a final layer of very fine fiberglass cloth is applied to give a fine texture to the outside of the plug. A thick coat of epoxy over this final layer gives some boundary for sanding.

Once cured, the plug is sanded smooth and filled where necessary until the entire outside of the shell has a regular contour. Then the plug is painted and gloss coated. At this point, the two halves of the plug have a perfectly shaped outer surface with a glossy-smooth texture. These halves are cut along the center where the two plywood profiles are mated. Then the two halves are pried apart, and one is set aside.

The other is placed with the flat side (profile side) down on a large panel of glass. Where the outside of the plug meets the glass, there is a gap from the thickness of the blade which separated the two halves. This gap is filled with putty and then shaped to match the outside of the plug. The plug is then waxed and polished on the glass panel.

At this point, there is no gap between the plug half and the glass panel. Then the process of layering fiberglass on top of the plug begins. Fiberglass is laid over the plug half and onto the glass. The first layers are of lightweight cloth (.5 to .75-oz cloth). As additional layers are added, the cloth used is heavier. The last layers are of fiberglass matting (not a weave) which gives strength to the mold.

Having prepared the other plug half in the same manner as the first, the plug and its mold are lifted from the glass. The second plug half is pressed in place to the first plug half, and the procedure of layering fiberglass is repeated on the first plug and its mold (instead of on the glass panel). Before separating the two molds holes are drilled through both molds in the overlay of fiberglass outside the plug. These holes will align the two molds later on. The plug is no longer needed, and the two mold halves can be separated and the plug can be removed.

The next step is to cut out the wing hole, motor hole, and holes for the tail surfaces. These holes are cut through the fiberglass mold anywhere there will be no shell on the final product. The inside surface of the mold is then waxed and polished. This completes the negatives of the plug.

To form the final shell, one layer of fiberglass (with epoxy) is laid on the inside of the mold. The mold halves need to sit with the open side upward, so that gravity will keep the fiberglass in the mold. After the epoxy has set (usually about 12 hours) the excess fiberglass is trimmed precisely at the seam. The two mold halves are then bolted together. Reaching through the holes in the molds, epoxy is then spread across the joint to bond the two halves. The whole shell is set aside to cure for 24 hours, then the halves can be unbolted and the shell can be removed. The hatch on top is cut from the shell after the shell has cured.

At the time this report was generated, the team was midway through this process.

6.2 Empennage:

The tail surfaces would never be required to withstand "unusual" loading, such as the wing tip test for wings. The only loads they experience are the aerodynamic loads placed on them when the control surface is deflected. These loads are small in comparison to the wing loads under full cargo. Therefore the construction of tail surfaces can afford to be somewhat less robust.

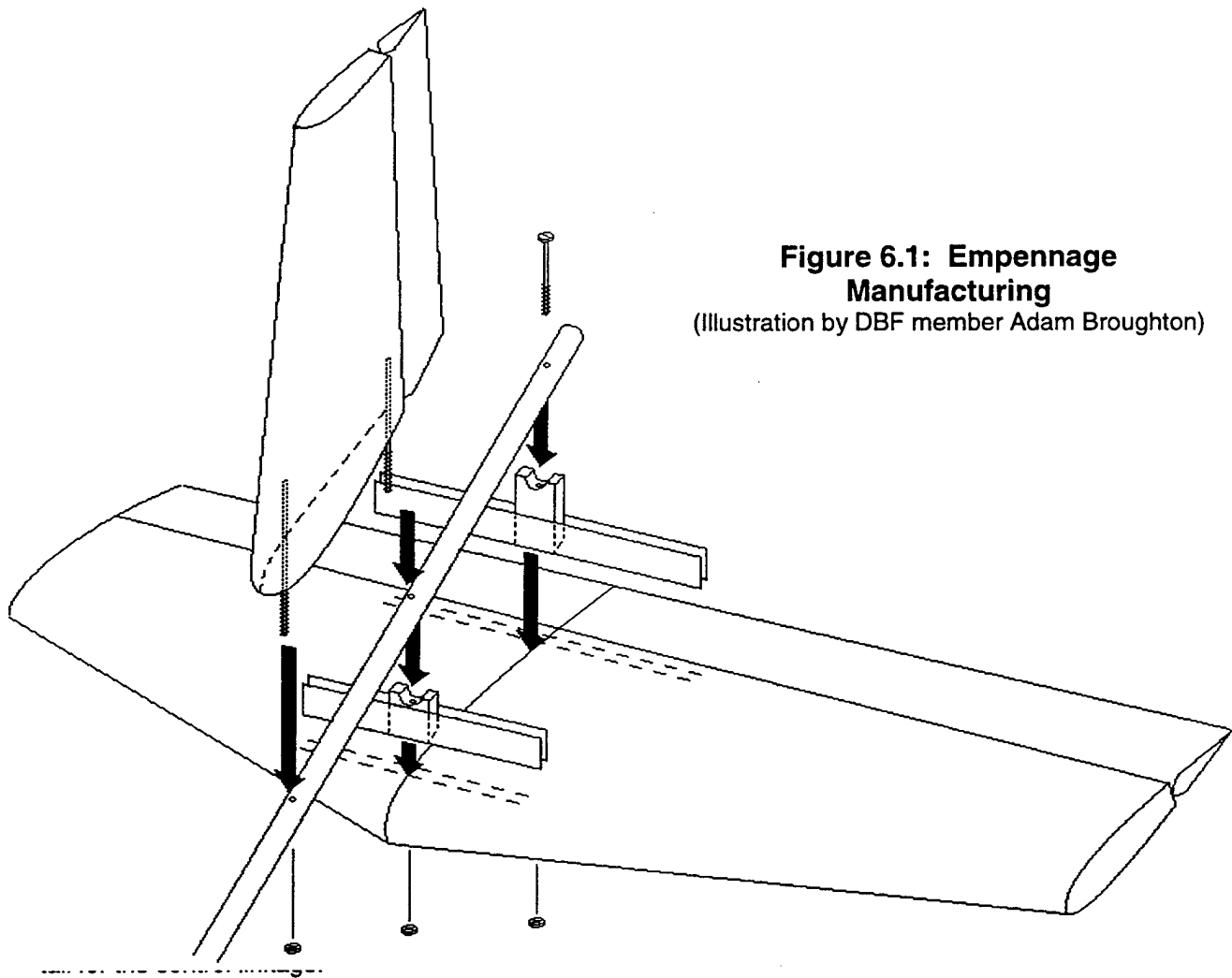
The first tail section that was constructed was one of the simplest components that were manufactured. Printouts of the root and tip airfoils were cut out of poplar light plywood, and then attached to blue foam blocks cut in the shape of the planform. The horizontal stabilizer and elevator halves were cut in one panel and the roots were glued with polyurethane glue. The fin and rudder were cut out in the same manner. The elevator and rudder were cut away and divided into 1/2-inch ribs. These ribs were sheeted in 1/16-inch balsa sheeting and used as the control surface. All surfaces were covered in polyvinyl heat-shrink covering.

The biggest concern of the Structures Team was how to rigidly attach the tail surfaces to the round tail boom. Dynamic flight loads may cause uneven loading of the tail surfaces, causing them to twist on the boom. Although maximum flight speeds would be fairly low, the stabilizer and rudder needed to be fastened securely enough to resist flutter while in flight.

The previous year's entry also used a 1-inch Aluminum tail boom to support the tail section, and the method of attachment worked well enough to be duplicated again on the horizontal stabilizer. The method of attachment was to use a 1/4-inch basswood block laminated between two larger strips of 1/32-inch birch plywood. The plywood strips were sunk into the blue foam, and glued in place. The block had a semicircle cut out of one end to fit the aluminum pipe. A hole was drilled through the pipe and block, and the stabilizer was attached with a 6-32 steel bolt.

The fin was attached in a somewhat different manner. The root of the fin was cut out to fit tightly against the pipe. Then, two 10-inch sections of 6-32 threaded rod were partially imbedded vertically into the foam and secured with polyurethane glue. One was imbedded near the leading edge, and the other near the rudder. The part of the rod not imbedded into foam was run through the aluminum pipe and secured with a nut on the other side.

Although these tail surfaces were simple to construct, they did not satisfy the Aerodynamics and Configuration team. The heat-shrink covering was constantly wrinkling and creating a poor surface. The problem was that the appropriate heat could not be applied because it would melt the foam underneath. However, these tail surfaces were adequate for the prototype, and allowed flight-testing to begin while stronger, lighter tail constructions were investigated. Later, the team would construct white foam tail surfaces covered in fiberglass in the same manner as the first wing.



**Figure 6.1: Empennage
Manufacturing**
(Illustration by DBF member Adam Broughton)

The fin/rudder attachment was also modified. The sides of the box were always perpendicular to the plane of the horizontal tail, and so these sides were extended to partially cover about an inch of the root of the fin. The foam shells left over from cutting tail cores were trimmed to fit the gap between the box sides and the fin. Then a bolt was run through the box sides and the root of the fin in three places to secure it to the aluminum pipe. The end result was a tail section that was lighter, smoother, and much more rigid than before.

Boucher, Robert J. (1995) Electric Motor Handbook. Los Angeles, California: AstroFlight, Inc.

Hale, Francis J. (1984) Introduction to Aircraft Performance, Selection and Design. New York, New York: John Wiley & Sons, Inc.

Georgia Institute of Technology: AE 6370 Design for Affordability through Integrated Product and Process Design. Fall 2000. Dr. D. Mavris, Instructor.

Raymer, Daniel P. (1992) Aircraft Design: A Conceptual Approach. Washington D.C.: American Institute of Aeronautics and Astronautics, Inc.

Roskam, Jan. (1997) Airplane Design (Part I). Lawrence, Kansas: DARcorporation.

Roskam, Jan. (1997) Airplane Design (Part II). Lawrence, Kansas: DARcorporation.

Selig, Michael. University of Indiana Airfoil Data. Department of Aeronautical and Astronautical Engineering. <http://www-aero.aae.uiuc.edu/~m-selig/ads.html>. September 15, 2000. University of Illinois at Urbana-Champaign, Urbana, Illinois 61801

Simmons, Martin. (1978) Model Aircraft Aerodynamics. Great Britain: A. Wheaton & Co Ltd.

AIAA Design, Build, Fly Competition Addendum

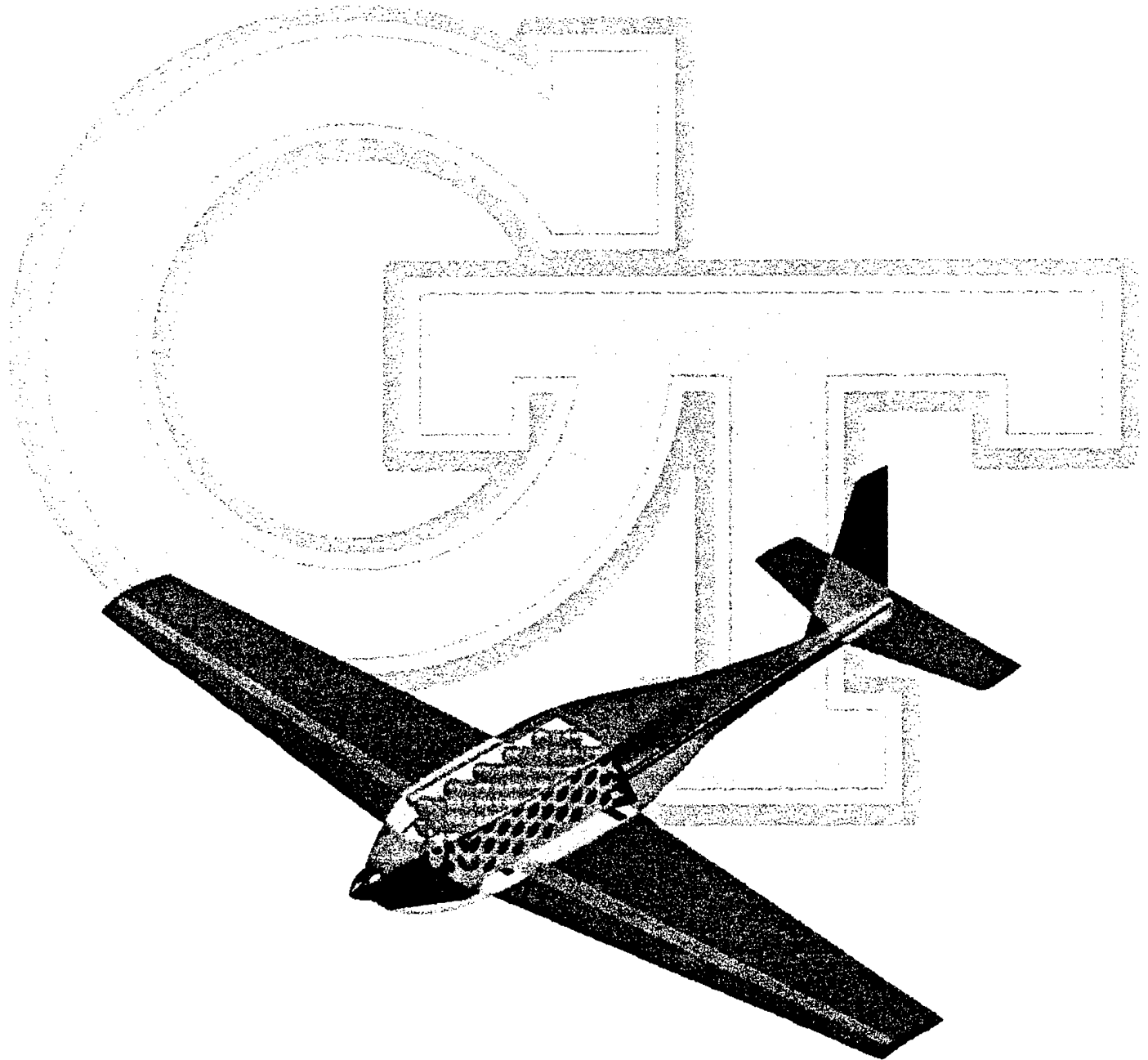


Table of Contents

1. Executive Summary	2
2. Management Summary	6
3. Conceptual Design Phase	10
3.1 Problem Definition.....	10
3.2 General Solution Characteristics.....	11
3.3 Solution Concepts	12
3.4 Initial Screening	13
4. Preliminary Design Phase.....	17
4.1 Figures of Merit	17
4.2 Initial Assumptions	18
4.3 Preliminary Wing and Tail Configuration	20
4.4 Preliminary Propulsion Design	20
4.5 Preliminary Structural Design.....	24
5. Detailed Design Phase	33
5.1 Wing Arrangement	33
5.2 Empennage.....	36
5.3 Wingtip Design	38
5.4 Handling and Control Characteristics.....	39
5.5 Radio Telemetry.....	39
5.6 Performance and Flight Testing	40
6. Manufacturing Plan	41
6.1 Fuselage Shell	44
6.2 Empennage.....	46
7. References	48
8. Addendum.....	51

Continued Propulsion Work

The initial performance calculations assumed a 55lb aircraft with a propulsion system capable of 11lb of static thrust. These assumptions were used to figure thrust requirements at takeoff and cruise, which were 10.8lbs of static thrust for takeoff, and roughly 4lbs of thrust for cruise. However, flight-testing showed that the aircraft was not lifting as early as predicted for takeoff. The team speculated possible sources of error, such as too much drag and too little thrust. Without working telemetry equipment (discussed later) it was difficult to pinpoint exactly what the problems were.

Without ways to significantly reduce drag, the team had no option but to try to increase thrust. The Mejzlik 26x10 propeller was used for the first series of flight-testing. Lower pitch propellers were found to produce higher static thrust, but lower cruise speeds. Higher pitch propellers have a flatter unloading characteristic, resulting in lower static thrust, but are capable of producing more thrust at cruise than lower-pitched propellers. The initial performance calculations assumed that the motor would turn a 26x10 around 3800 RPM, but test measurements showed around 3000 RPM for static conditions. The team was not able to locate the reason for the large error in estimation, but knew that if RPM drops were consistent across a range of propellers, then a larger propeller could be used to generate more thrust at a similar RPM.

The team simultaneously increased pitch and diameter for experimentation with larger propellers. Using a Bolly 28x14 significantly improved the overall thrust for the aircraft, allowing it to take off in as little as 40 ft. at empty weight. Several flights were made with this propeller, and although flight performance was improved, the aircraft was still flying much slower than was satisfactory. Because of the heavy weight of the Bolly carbon fiber propeller, the motor was not able to reach full RPM as quickly as with a wooden propeller or a hollow carbon fiber Mejzlik. It is for these reasons that the team is still investigating better options for propellers.

The team would like to have a more scientific approach than just trial and error, but without accurate data gathering equipment, there are few alternatives. Several months were spent arranging a wind tunnel test stand for battery-motor-propeller combinations, but early in the experimental testing the test stand was destroyed in an accident. The team was not able to obtain the necessary resources to continue experimental testing before the competition.

Radio telemetry equipment was also planned for data gathering during flight testing, but this project was also plagued with problems. Delays in the assembly of the equipment and calibration of the instruments have kept the team from having these tools for data gathering. Although the telemetry equipment is not planned on being used in this year's entry, the completion of the equipment will facilitate DBF and other UAV design efforts in the future.

Landing Gear Changes

The landing gear was originally ¼ inch diameter steel wire with small control rods used as struts. The nose leg was a commercially produced dual strut purchased at a local hobby store. Because of the problems with propulsion and the tendency to stall, the aircraft made several hard landings during flight-testing and destroyed the wire landing gear. An 1/8 inch plate of T-6 aluminum was used to make a replacement gear. This new gear is what is currently used on the aircraft.

Wing Reconstruction

In the Proposal Phase of this report, the wing was described as blue foam core covered in fiberglass. This wing was used for flight testing, but another wing is currently in the completion stages and may be used at the competition. This second wing is white foam core sheeted in 1/16 inch balsa. There are two short spars of 1/8 inch poplar light plywood extending 24 inches from the centerline. The two short spars are 4.5 inches apart, and the landing gear blocks are mounted between them under the balsa sheeting. All other design points are identical to the blue foam core wing used for flight-testing. Estimated weight savings are 1.2 lbs. The cost model spreadsheet indicates the heavier 6.9 lb. blue foam core wing.

Project Difficulties

It has been noted in the past that AIAA's Design, Build, Fly competition requires a great deal of resources just to meet contest requirements and be competitive. Most of these resources are information resources, and without experienced members leading the design team, much of the time spent on the project is managing people (the inexperienced members) and not making project developments. In order for inexperienced undergraduate students to make valuable contributions to the DBF effort, they need very extensive guidance in all the many complexities that go into developing a winning platform. The leader members noted that such efforts become programs in UAV education, and not design competitions.

Georgia Tech has had a history of struggling with this issue, and it has not yet become clear how DBF "should be" conducted. Each of the other schools who participate in the competition seem to have their own interpretation AIAA's intent, and students in previous years have been frustrated with the equality of design programs.

If DBF means a multidisciplinary education program in which students of all majors can participate in a fun and interesting project while strengthening engineering education, then Georgia Tech is a true winner. The Georgia Tech design team began the project with eighteen members, of which only three had participated in the competition previously. There were only two members with UAV experience outside of the DBF effort, and only one member had extensive experience with building UAVs. By the end of the project however, every member had participated in broad range engineering program. Few students at any engineering education institution ever get the

opportunity to participate in a complete design process; from conceptual design to product testing.

The design process used this year by Georgia Tech can be improved upon greatly. The team used what knowledge it had to begin the process, but did not have a clear methodology and so overlooked such needed details as certain performance calculations to fully understand the flight envelope apart from take-off and cruise. The use of historical data and concepts worked very well in terms of the conceptual design, but the details of the design require a proactive and detailed engineering approach. Determining these details are the real challenge of the project development, and an understanding of the overall process of aircraft design is essential to proficient engineering. The Georgia Tech DBF team recognized the difference in component design and systems design. Where an individual component may have been designed extraordinarily well, its performance may not be appropriate for the system as a whole.

Aircraft Cost Model

The following page shows the table for the rated aircraft cost as per the AIAA's DBF rules

(MEW) Manufacturer's Empty Weight:		(REP) Rated Engine Power:		(MFHR) Manufacturing Man Hours:		
NOTE: weight without batteries or payload						
Weight Estimates		number of engines:	1 engines	number of wings:	1	Score
wing(s)	6.9 lbs	fuse size:	30 Amps	sq. ft. projected area:	14	15
fuselage:	2.5 lbs	number of cells:	26 cells	number of struts/braces:	0	56
motor:	2.2 lbs	volts:	31.2 Volts	number of control surfaces:	4	0
electronics:	0.6 lbs			number of fuse/pods:	1	12
gear:	1.0 lbs			length of fuse/pods:	6.5	5
tail:	0.7 lbs			empennage? (enter 0 or 1):	1	26
speed loader:	0.5 lbs			number of vertical surfaces:	1	5
other:	0.0 lbs			number of horizontal surfaces:	1	5
				flight system: (add 5)	5	10
				number of servos:	4	5
				number of engines:	1	8
				number of propellers:	1	5
SUM:	14.4	SUBTOTAL:	936	SUM:	157	5
(A) MEW Multiplier:	100 per lb	(B) REP Multiplier:	1 per watt	(C) MFHR Multiplier:	20 per hour	
TOTAL:	1440	TOTAL:	936	TOTAL:	3140	

TOTAL RATED AIRCRAFT COST: 2379

5.566



PROPOSAL FOR THE DESIGN OF AN UNMANNED AIR VEHICLE

Syracuse University

Reid Thomas, Project Leader

Victoria Garnier

Jessica Lux

Jeffery Robinson

Scott Todd

Eliza Honey

Renea LaRock

Michael Nagy

Michael Czabaj

Benjamin Nesmith

Brian Foo

Dr. V.R. Murthy, Faculty Advisor

Acknowledgments

The Syracuse University 2000/2001 Design/Build/Fly team would like to extend special thanks to:

Dr. Vadrevu R. Murthy
Professor, Syracuse University

Dr. Barry D. Davidson
Associate Professor, Syracuse University

Dr. Eric F. Spina
Associate Dean, L.C. Smith College of Engineering and Computer Science, Syracuse University

Syracuse University
L.C. Smith College of Engineering and Computer Science
Department of Mechanical, Aerospace, and Manufacturing Engineering

Syracuse University Composite Materials Laboratory

Any others who have helped us this year

Without the help, support and encouragement of those mentioned above, this year's plane would not have been possible. Thank you all for your support.

Table of Contents

Acknowledgments	i
Table of Contents	ii
1. Executive Summary	1
1.1 Overview	1
1.2 Design Development	1
1.3 Design Tools Utilized	2
2. Management Summary	3
2.1 Design Team Architecture	3
2.2 Design Deadlines	4
3. Conceptual Design	6
3.1 Initial Concepts	6
3.1.1 Figures of Merit	6
3.1.2 Alternative Concepts	8
3.2 Twin Boom Conceptual Design	8
3.2.1 Wing Trade Studies	8
3.2.2 Fuselage Trade Studies	9
3.2.3 Empennage Trade Studies	9
3.3 Subsystem Trade Studies	10
3.3.1 Landing Gear	10
3.4 Propulsion	10
4. Preliminary Design	11
4.1 Initial Sizing	11
4.1.1 Figures of Merit	11
4.1.2 Weight Estimation	12
4.1.3 Fuselage Sizing	13
4.1.4 Wing Sizing	14
4.1.5 Empennage Sizing	14
4.2 Motor Sizing	15
4.2.1 Motor Estimations	15
4.3 Airfoil Selection	16
4.3.1 Figures of Merit	16
4.3.2 Airfoil Comparison	16
4.4 Aircraft Information	21
5. Detailed Design	22
5.1 Handling Qualities	22
5.1.1 Stability Derivatives	22
5.1.2 Control Surface Sizing	23
5.2 Performance Analysis	23
5.2.1 Maximum Load Factor	23
5.2.2 Instantaneous Turn Rate	24
5.2.3 Sustained Turn Rate	24
5.2.4 Stall Speed	24
5.2.5 Take-Off Performance	24
5.2.6 Drag Polar	24
5.2.7 Cruise Performance	26
5.3 Final Sizing	26
5.3.1 Wing	26
5.3.2 Fuselage	27
5.3.3 Cooling	27
5.3.4 Empennage	27

5.3.5 Final Weight Estimation and CG Location	27
5.4 Structural Analysis	28
5.4.1 Wing	28
5.4.2 Fuselage	28
5.5 Subsystems	29
5.5.1 Landing Gear	29
5.5.2 Radio Control Devices	29
5.4 Aircraft Information	30
6. Manufacturing Plan	36
6.1 Figures of Merit	36
6.2 Wing Manufacture	36
6.3 Speed Loaders	37
6.4 Fuselage	39
6.5 Tail	39
6.6 Systems Integration	40
References	41

1. EXECUTIVE SUMMARY

1.1. OVERVIEW

This document presents the design, analysis, and manufacturing details for Syracuse University's 2000-2001 entry in the AIAA/Cessna/ONR student Design/Build/Fly competition. The conceptual, preliminary, and detailed design phases of Team Syracuse's entry, termed Der Gabelschwanz Teufel, are presented below. A manufacturing plan and summation of team organization are included.

1.2. DESIGN DEVELOPMENT

Initially, the design team considered seven configurations for the DGT – a conventional design, conventional with twin boom, a biplane, a canard configuration, a joined wing configuration, a flying wing configuration, and a blended wing fuselage. Along with figures of merit, other inherent advantages and disadvantages were discussed for each of these designs. One of the most important figures of merit is payload volume. In order to allow for the larger ranges of tennis balls, configurations with greater internal cargo space were rated higher. With this in mind a twin boom configuration was selected for further development. This design has several advantages over the baseline conventional configuration and the other options considered. It's major advantage being a superior payload capacity; a second important consideration is the availability of empirical data on similar aircraft. The design does incur a Rated Aircraft Cost (RAC) increase over the baseline configuration, but the advantage of additional payload space outweighed the increase of RAC.

Due to the twin boom design, with initial consideration for a center fuselage, the DGT is named after a well-known military twin boom aircraft—the P-38, or "The Forked Tailed Devil," as the German Luftwaffe titled it.

With a design configuration, important parameters such as wing loading, wing aspect ratio, payload capacity, and thrust loading were used to find initial sizes. Propeller propulsion was selected, as past experience with ducted fans has been unsatisfactory. The conceptual design stage also included wing seating, empennage type and location, and payload estimations.

Motor selection was more limited this year, so the team settled upon the Astro Flight 640(G) motors after eliminating other options due to their thrust output or amp requirements. During preliminary design more details were finalized, including airfoil selection and empennage geometry.

For detailed design, aircraft performance was calculated. All necessary parameters, including take-off performance, G-load capabilities, range and endurance, and payload fraction were found. Handling qualities were estimated through stability derivatives and a more detailed flight regime that included maximum speed, stall speed and turning rates.

With the design of the DGT finalized, the development of a manufacturing plan was initiated. After comparing both composite materials and wood materials for the construction of the fuselage, an ultra-lightweight balsa frame wrapped in a composite skin was selected. This provides high strength, low weight and no significant increase in manufacturability. The wing is manufactured from a foam core wrapped in fiberglass. The use of a foam core enables the team to manufacture the composite skin without the use of a mold, resulting in a more time- and cost-effective design.

1.3. DESIGN TOOLS UTILIZED

Tools employed in the design of the DGT include AutoCAD, Calcfoil, Microsoft Excel, MotoCalc, Profili, the UIUC airfoil database, PV-WAVE, and the internet.

The internet proved to be an excellent research tool during the conceptual and preliminary design phases. The team utilized searching capabilities to find empirical data on similar designs, research motor, battery, landing gear, and propeller manufacturers, explore the possibility of having foam core wings commercially cut, and locate other component retailers. Two of the above listed design tools—the UIUC airfoil database and Calcfoil—are only available over the Internet.

Calcfoil [<http://beadec1.ea.bs.dlr.de/Airfoils/calcfoil.htm>] utilizes a conformal mapping method to determine the aerodynamic coefficients of various airfoils. The team used Calcfoil to evaluate the lift, drag, and pitching moments of various airfoils considered.

The UIUC airfoil database [http://www.uiuc.edu/ph/www/m-selig/ads/coord_database.html] was utilized in airfoil selection. It provides coordinates and descriptions of over eleven hundred airfoils.

The Italian airfoil plotting program Profili was used to print scale diagrams of the airfoils selected for the wing, tail, and fin. Profili provides a scale drawing of any airfoil in its database based on a user-specified chord length. These printed drawings were then used in the manufacturing of the wing, tail, and fin.

Microsoft Excel proved especially useful during preliminary and detailed design. A number of spreadsheets were created to analyze several of the key aspects of the DGT's final design, including sizing, stability, and performance data.

PV-WAVE was used primarily in the airfoil selection process. A small program was written to compare the values found using Calcfoil. This comparison helped reduce the number of airfoils before a final selection was made.

AutoCAD R14 was used to make all drawings contained in this report.

2. MANAGEMENT SUMMARY

2.1. DESIGN TEAM ARCHITECTURE

Team Syracuse consists of students with varying experience levels and backgrounds. Leading the group is junior aerospace engineering major Reid Thomas; other juniors include aerospace engineering majors Victoria Garnier, Jessica Lux, Matt Tundermann, and Jeff Robinson, along with mechanical engineering major Scott Todd. Sophomore members are aerospace engineering majors Eliza Honey and Renea LaRock, and freshmen team members include Mike Czabaj, Mike Nagy, Ben Nesmith, and Brian Foo.

Thomas and Lux both are entering their third year of Design/Build/Fly competition while Garnier, Honey, and LaRock are second-year members. This year, many team members are participating for the first time—juniors Robinson, Todd, and Tundermann, and freshmen Czabaj, Nagy, Nesmith, and Foo.

The team met once a week starting in September to design the DGT. The first task everyone worked on was conceptual design; seven aircraft configurations were ranked based on selected Figures of Merit (FOM). After the team selected a twin boom design, individual work become much more specialized. During weekly meetings members updated the team on their progress and received group input. Once building began, all team members worked on the construction of the aircraft.

Thomas is a veteran Design/Build/Fly team member; using his experiences from past competitions and personal model aircraft he has built, he was able to coordinate and direct the design and construction of the aircraft. Besides leading the team, Thomas contributed a great deal to the project: he was widely involved in all design stages and his responsibilities included performance calculations, initial drawings of the aircraft, composites research, and structural analysis of the wing and booms.

Garnier, Honey, Lux, and LaRock are the rest of the team members with previous Design Build Fly experience. In the early stages of design, LaRock performed airfoil research, Garnier researched propulsion, and Honey investigated batteries and battery configurations. Lux designed a thrust test stand and researched methods of charging the plane's batteries. Thomas and Honey also performed CG calculations for the aircraft. All of these members worked on cost analysis and materials purchasing, and Lux and Garnier also finalized the logistics for the trip.

First year upperclassmen on the team are Todd, Tunderman, and Robinson. Scott Todd designed the speed loaders and created the final CAD drawings for the aircraft, and Tunderman and Robinson assisted with the building of the aircraft.

Freshmen Czabaj and Nagy have previous experience with hobby aircraft and were able to offer practical construction tips. Nesmith and Foo helped with initial research for the aircraft and contributed

many hours to aircraft construction. The new freshmen will be a valuable asset to the team in future years, due to the skills that they learned on the team this year.

2.2. DESIGN DEADLINES

A milestone chart was developed to keep the design team on target and aware of upcoming deadlines; these deadlines included those both self-imposed and contest-mandated. This milestone chart, with team goals and actual completion dates, is reproduced in Table 2.1.

The dates listed in this milestone chart represent continued improvement in meeting target goals. Team Syracuse began the conceptual design phase in early September, rather than late October as in past years, and moved the manufacturing start date up to late January. The team was able to adhere to this schedule by posting it in team workspace and updating progress continually.

Thomas also met with faculty members throughout the process in order to get advice as well as update them on the design and manufacturing process. At the end of the first semester, a brief meeting was held with the department chair to update him on Team Syracuse's progress. In early March, the team presented a progress update and final budget analysis to the engineering faculty at Syracuse University. This presentation kept the design team to a fixed deadline for finishing detailed design and starting construction on the DGT. Lux and Thomas prepared the presentation, and all members of the team assisted in presentation of the material.

Table 2.1 Milestone Chart

FALL SEMESTER		
Task	Projected Completion Date	Actual Completion Date
Empirical Database	9/15/00	9/29/00
Conceptual Design	10/1/00	10/4/00
Configuration Selection	10/4/00	10/4/00
Weight Estimation	10/11/00	10/11/00
Wing Sizing	10/18/00	10/18/00
Initial Design	10/18/00	10/20/00
Component Placing	10/18/00	11/1/00
Preliminary Sizing	10/25/00	10/25/00
Landing Gear Selection	10/25/00	10/25/00
Entry Form Due	10/31/00	10/30/00
Airfoil Selection	11/1/00	11/1/00
Preliminary Design	11/1/00	11/1/00
Power Configuration	11/1/00	11/8/00
CG Location	11/1/00	11/8/00
Control Surface Sizing	11/15/00	12/1/00
Optimization	12/1/00	12/18/00
Detailed Design	12/8/00	1/25/01
SPRING SEMESTER		
Begin drafting report	1/25/01	2/7/01
Begin manufacturing	1/28/01	1/28/01
Fuselages Framed up	2/7/01	2/14/01
Speed loaders assembled	2/14/01	2/7/01
Rough Draft of Report Done	2/16/01	2/16/01
Wing Fiber-glassed	2/28/01	
Tail framed up	2/21/01	2/22/01
Presentation to Faculty	3/2/01	3/2/01
Hand report to faculty	3/2/01	3/5/01
Fuselages Fiber-glassed	3/6/01	
Components placed	3/7/01	2/28/01
Report Due	3/13/01	3/13/01
Aircraft Complete	4/1/01	
Flight testing	4/2/01	
Addendum completed	4/5/01	
Addendum Due	4/10/01	
Final Modifications	4/12/01	
Competition	4/20/01 – 4/22/01	4/20/01 – 4/22/01

3. CONCEPTUAL DESIGN

3.1 INITIAL CONCEPTS

The initial stage of the conceptual design phase consisted of proposing as many potential airplane configurations as possible. The team defined seven possible configurations—a conventional design, conventional with twin boom, biplane, canard configuration, joined wing configuration, flying wing configuration, and a blended wing fuselage. Those proposed configurations were ranked quantitatively by Figures of Merit (FOM) in order to make a final configuration decision. The FOM covered four basic categories: design/mission specification issues, manufacturing concerns, flight performance, and Rated Aircraft Cost (RAC). Each candidate configuration was ranked on a point scale regarding more specific criteria within every major category. A final configuration decision was based on these rankings. The FOM for each element involved weight, cost, manufacturing complexity, strength, power and durability.

3.1.1 Figures of Merit

The figures of merit used to evaluate the seven different configurations constitute four basic categories:

- Design/mission specification issues
- Manufacturing concerns
- Flight performance
- Rated Aircraft Cost (RAC)

The FOM, seven configurations, and quantitative rankings are provided in Table 3.1. The highlighted column illustrates the optimal design, and the highlighted rows illustrate the two most heavily ranked FOM.

Table 2.1. Conceptual Design Ranking

	Standard Configuration	Biplane	Flying Wing	BWF	Tail Boom	Joined Wing	Canard
Light Payload (volume)	0	0	1	1		0	0
Heavy Payload (volume)	0	0	1	1		0	0
Manufacturing Complex.	0	0	-2	-2		-1	-1
Manufac. Cost: Manpower	0	-1	-2	-2		-1	-1
Manufac. Cost: Materials	0	-1	0	0		-1	0
RAC	0	-3	1	0		-1	0
Design: Control	0	1	-2	-1		-1	-2
Design Database	0	0	-2	-3		-1	-2
Weight	0	-1	1	0		0	0
Durability	0	0	-2	-2		0	0
Flightworthiness	0	1	-3	-2		0	-2
Stability	0	0	-3	-2	0	-1	-1
Design Difficulty	0	-1	-3	-3	0	-2	-3
Total	0	-6	-15	-15		-9	-12

The design/mission specification category of FOM include light/heavy payload carrying ability, design difficulty, amount of design information available, and control over the design factors of a particular configuration. Since the mission specifies that the airplane alternately carry tennis balls and steel blocks for light and heavy payload cycles, respectively, the ideal configuration must have enough room to carry both the relatively large, low-density tennis balls as well as high-density steel blocks. The best configuration, from a design point of view, does not entail a great degree of design difficulty, has a large amount of information available concerning the design, and has widely available data on similar configuration; allowing the team maximum control over design factors.

A design can look great on paper, but it must be practical from a manufacturing and flight standpoint. For this reason, the team considered manufacturing concerns such as overall complexity, man-hours required, and cost of materials when evaluating configurations.

Flightworthiness is another important consideration, so the FOM related to in-flight performance were considered for each configuration. These included durability, stability, and ease of control from the pilot's standpoint.

In the interest of overall team score, Rated Aircraft Cost (RAC) was also evaluated qualitatively during configuration selection. Since RAC is the divisor for the team's final score, the lowest possible RAC is the most desirable. Rated Aircraft Cost is related to the airplane's weight, number of engines, and manufacturing man-hours as outlined in the competition rules.

3.1.2 Alternative Concepts

There were seven basic configurations considered: conventional, biplane, flying wing, blended wing fuselage, twin boom, joined wing, and canard.

A conventional configuration allows the team to make the best use of previous experience and involves fewer unknowns in both the design and manufacturing stages. A biplane adds to manufacturing cost and, due to competition rule changes for this year, greatly increases RAC, but may be easier to fly than a conventional airplane. The flying wing configuration allows more room for payload than a conventional airplane but adds considerable manufacturing complexity and does not allow the team the desired control over design factors. A blended wing fuselage is similar to a flying wing in most respects, but the team has considerably less data on the design. This makes a blended wing fuselage significantly more difficult to design. A twin boom allows the team considerably more room for light payload but it has a slightly higher RAC. A joined wing is much more difficult to design than a conventional airplane, and there is very limited data available on similar aircraft. The canard configuration is even more difficult to design than a joined wing airplane, does not provide enough empirical data, and is less stable in flight than a conventional airplane.

After considering all seven proposed configurations in light of the given FOM's, a twin boom configuration was selected. This configuration effectively balances maximized design ability, minimized manufacturing difficulties, best flight performance, and lowest RAC.

3.2 TWIN BOOM CONCEPTUAL DESIGN

Once a configuration was chosen, the design of major components of the aircraft began. Material selection occurred alongside of design work; the team's goal was to minimize weight, cost, and manufacturing complexity while maximizing strength, power and durability. Overall, weight was the most important factor considered, followed by cost and complexity.

3.2.1 Wing Trade Studies

The team evaluated two types of wings: a balsa wing, and a foam/fiberglass wing. The team has equal amounts of experience with each type.

A more traditional balsa wing is less expensive than a foam wing and presents fewer manufacturing difficulties. A foam wing is difficult to cut correctly and, until it is fiberglassed, easily to damage. Fiberglassing the wing also poses a separate set of problems. Foam cannot be vacuum-bagged because it is highly susceptible to crushing and twisting, a condition that must be taken into account before fiberglassing. The conclusion reached is that foam core wings are stronger than balsa wings but incur a manufacturing penalty, while balsa wings are heavier and weaker.

With previous knowledge of how vacuum bagging and twisting can destroy a foam core wing, the team carefully weighed the consequences before making a decision: since it is too difficult to cut, the foam core would need to be purchased from an outside manufacturer, and the wing would need to be fiber glassed by the team. Though these steps add significant cost and manufacturing complexity to wing construction, the finished product is lighter and much stronger than a balsa wing.

After weighing these possibilities, the team made a decision to use a foam-core/fiberglass wing, considering weight to be the highest priority in this case. The team also felt that they has learned from past experiences and would be able to fiberglass the wing effectively and efficiently.

3.2.2 Fuselage Trade Studies

Fuselage material is of utmost importance in a twin boom configuration, since the surface area of the fuselages is greater than that of a single fuselage. The materials considered were plywood, fiber glassed balsa wood, and carbon fiber composite.

Manufacturing the fuselage out of plywood is relatively simple: once designed, pieces would simply have to be cut out and put together. The cost of a plywood fuselage is also relatively low in comparison to that of the other possibilities. The largest drawback to this selection, however, is the structural weight of wood thick enough to support the required loads.

The second material considered for fuselage manufacture was thin balsa sheeting covered with fiberglass. This option weighs considerably less than the plywood option for the same or greater strength, but costs more and adds an additional step (fiberglassing the balsa) to the manufacturing process.

The third, and final, fuselage material considered was a carbon fiber composite. This material allows the team maximum strength with minimum weight, but is considerably more expensive. Manufacturing follows the same procedure for the fiberglass, adding complexity above the wood fuselage.

After careful consideration of these options, including creating a test section of fiberglassed balsa sheeting to test the unconventional combination, fiberglassed balsa was selected for its lower weight, affordability, and sufficiently high strength.

3.2.3 Empennage Trade Studies

Two horizontal tail configurations were considered: a low tail mounted to the fuselages and a high tail mounted between the vertical tails. A low tail was discarded in order to accommodate the removal of payload; placing the tail between the booms would limit the options available for payload exchange. A high tail was chosen because it is attached between the vertical tails and therefore wouldn't have to be directly attached to the fuselage. This had the added benefit of increasing the efficiency of the vertical tails, by reducing tip effect inherent in finite wing sections. However, at high angles of attack, the wing

interferes with the flow over high tails; this was resolved by placing the horizontal tail high enough to avoid this at the expected angles of attack.

3.3 SUBSYSTEM TRADE STUDIES

3.3.1 Landing Gear

Two types of landing gear were taken into consideration by the team: fixed landing gear and retractable landing gear. Fixed landing gear is simpler to manufacture and less expensive than the retractable alternative, but creates more drag in flight. The reduction in drag with retractable landing gear is not sufficient, however, to warrant the doubled cost, higher degree of manufacturing complexity, and significantly higher weight that this option entails. Thus, in the interests of reducing weight and overall cost of the airplane, fixed landing gear were selected.

3.4 PROPULSION

The team contemplated two types of battery-powered propulsion for the airplane: ducted fans and propellers. Experience with both types allowed for an in depth analytical comparison.

Ducted fans are more expensive than propellers, more complex, draw more current than the 40-amp limit imposed by contest rules, and do not work as well as propellers for a short takeoff distance. Since ducted fans are not easily available in the correct size and have not been widely used on planes of this size, the team selected propellers.

4. PRELIMINARY DESIGN

The selection of an optimal configuration in the conceptual design phase led to the further design of a twin boom aircraft. Having selected a configuration, the next step was initial sizing. Physical sizes, as well as design parameters were estimated based upon previous team's entries and team-selected figures of merit. A first step towards this sizing was the creation of a historical aircraft database. This included all available data on past entries from the previous four years of competition; this data was collected from information posted on the competition website. Throughout the preliminary design phase the team relied upon this database, weekly meetings with the team's advisor, and general meetings with faculty members to verify design data.

4.1 INITIAL SIZING

4.1.1 Figures of Merit

In order to begin initial sizing of the aircraft, four figures of merit (FOM) were defined. These FOM were used for justification of sizing selections:

- Rated Aircraft Cost
- Wing Loading
- Power Loading
- Aspect Ratio
- Payload Capacity

The Rated Aircraft cost (RAC) is directly tied to a team's overall score. The cost matrix, defined in the competition rules, assigns cost values based upon the physical attributes of the aircraft design. The goal was to minimize this FOM, as RAC is the direct divisor of the final score.

Wing loading affects handling qualities, take-off weight, take-off field length, and is tied to structural weight. Of these factors, take-off weight is the most critical, this is due to the thrust limitations imposed in the rules with battery restrictions. The take-off, wheels off, distance was specified in the contest rules; this is important since lower wing loadings correspond to shorter take-off distances. However, all of the other characteristics improve with higher wing loadings. A compromise of these factors was the goal of this FOM analysis.

Power loading affects the performance of an aircraft. Acceleration, climb, maximum speed, and sustained turn rate all improve with lower power loadings. Lower power loads (unlike thrust-to-weight) increase all of the above performance criteria. This figure of merit was used to facilitate engine sizing.

Aspect ratio affects the induced drag: higher aspect ratio equates to lower induced drag. This does not come without a price, however, as higher aspect ratios lead to higher structural weights. The goal of this FOM was a high aspect ratio.

The final FOM, payload capacity, refers to the ability of the aircraft to carry payload. Steel, with a greater density than tennis balls, was not the primary factor of this FOM. Instead, the payload capacity of the aircraft was tied to the number of tennis balls the design could carry. The goal of this FOM was to carry as much payload as possible.

4.1.2 Weight Estimation

With a conceptual design chosen and figures of merit determined, a preliminary weight estimation was possible. Weights for all required components were found, and those for structural members were estimated from previous team experience. The resulting weight estimation is shown in Figure 4.1.

Weight Of Aircraft		
Group	Item	Weight(lbs)
Radio:	Receiver	0.09375
	Bat.	0.21875
	Switch	0.03125
	Servo-HT	0.9
Propulsion:	Motor	1.8125
	Spd Cnt	0.0272727
	Bat.	5
	Prop/cone	0.25
	Fuse/misc	0.3125
Structure:	Wing	1.5
	Boom	2
	Vert tail	0.25
	stab	0.25
	Gear	0.75
	misc	0.5
		13.896023

Figure 4.1 Initial weight estimation

With this weight estimation, the team made initial calculations of wing loading, payload weight, payload volume, and total weight. Total weight estimates, wing loading, and wing area (discussed in depth below) allowed thrust estimations to begin; this in turn allowed for the preliminary selection of motors to begin.

4.1.3 Fuselage Sizing

Fuselage sizing is dependent primarily upon payload capacity. As described in Section 4.1.1, payload capacity was driven by the number of tennis balls the design could carry. For this, three configuration types were considered: payload cross sections containing one, two or three tennis balls. This is an important factor because tennis balls are a direct multiplier from the flight score. In order to maximize the number of tennis balls carried, the cross section with three tennis balls was chosen. With the number per cross section chosen, it was found that a forty-two inch payload section would provide the room required for the tennis balls; this allows for fifty tennis balls to be carried in each boom for a total of one hundred tennis balls, the maximum number allowed.

From this, an initial cross sectional layout of the payload section was developed to include a circular cutout of approximately six inches to allow for the tennis balls. For the fuselage cross sectional shape through the payload section, two shapes, a circular cross section and a square cross section, were considered. A circular shape has less surface area and creates less skin friction drag, but is more difficult to produce, has a more complex wing joint, and has less internal room for components such as batteries and servos. For these reasons a square cross section was chosen.

Both the nose and tail section were approximated at this point. The nose section needed to be large enough to contain the motor, speed controller, air intake (for cooling), and the nose gear. A section twelve inches in length was chosen as long enough to encompass these components. This defined an initial placement of components, subject to further analysis and refinement for CG location. The nose section was approximated to converge to the centerline of the aircraft in that twelve inch section. This was an approximation until the motors were chosen and the geometry for the mounting screws was known. The aft section was also approximated at twelve inches. The aft section's sole purpose was a connection point for the empennage, and as such would be further refined with the final empennage sizing. The aft section was assumed to continue straight back at the upper surface of the fuselage, and taper from the bottom to the top through the twelve inch section. Independent of wing seating, low, mid, or high wing, the wing was assumed to join the fuselage at the center of the payload section; this was due to the varying weights that would be flown during the competition. This placed the estimated center of gravity of the payload at the quarter chord of the wing.

The spacing between the fuselages was also an important factor. For single engine out performance, the fuselage spacing needed to be minimized. The landing gear, a quad gear setup for the two booms, required the opposite condition: the landing gear needed to be spaced as far apart as possible to improve ground-handling qualities of the aircraft. As a compromise, the distance was approximated to twenty-four inches, centerline to centerline, as an allowance for the projected minimum spacing for the landing gear.

4.1.4 Wing Sizing

Wing sizing began with consideration of two of the figures of merit, aspect ratio and wing loading. Aspect ratio was the first considered: increasing the aspect ratio of a wing lowers induced drag, but increases structural weight. However, for this application, a small scale unmanned air vehicle (UAV), the increase in structural weight is negligible due to two factors. First, structural support in the fuselages is taken to be independent of the wing aspect ratio. This assumption is made due to the fact that the method of securing the wing to the fuselages does not change with wing size. It is recognized that a larger root chord produces a larger wing saddle; however, the main attachments at the forward and rear sections of the wing do not change. The second assumption is that the weight added to the wing itself would be at most one (excluding extremely large aspect ratios which are not the case here) extra ply layer, or a minimal number of extra balsa ribs. Extra weight comes from any added pieces to the two wing types considered, that is foam core – fiberglass skin and traditional balsa airfoil and spar approaches. After that consideration the maximum allowable span, ten feet, was chosen, as it would result in the highest possible aspect ratio.

With that done, consideration turned to the next figure of merit, wing loading. As described in Section 4.1.1, wing loading is very important for several aspects of the aircraft. For this stage, the most important role of wing loading considered was the take-off length requirement. The rules of the competition state that all aircraft must have wheels off by two hundred feet. With this as a starting point, historical values were used to determine an acceptable range for wing loading. With an initial weight estimation and take-off distance established, the range of acceptable wing loadings was estimated to be 1.8 – 3.2 lbs/ft². This allowed for an initial estimate of wing area.

Additionally, the geometry of the wing was estimated for the particulars of the mission: low subsonic transport. With the low speeds involved, compressibility effects were neglected. Because of this the wing was not swept in either direction, although this was reserved as a possible parameter for final CG location. A taper ratio of 0.45 was also assumed for the wing to best approximate an elliptical lifting surface. With these values as starting points the rest of the aircraft could begin to take more substantial form.

4.1.5 Empennage Sizing

With the initial sizing of the fuselage and wing complete, initial estimates for the horizontal and vertical tail began. The horizontal tail volume coefficient was estimated to be approximately 0.7 from reference (2). This led to a resizing of the aft end of the fuselage. In order to obtain a reasonable tail volume coefficient, the tail area and arm length were varied. In order to reduce drag, it is desirable to minimize the tail area; satisfying this pushes the horizontal tail farther back. Counter to this, the structural weight of the aircraft increases as the tail moves further back in respect to the wing. An initial balance

was formed with a horizontal tail chord length of sixteen inches. This increased the aft end of the fuselage by four inches. The balance of the horizontal tail was found to steady the pitching moment created by the wing. The pitching moment is dependent upon airfoil selection, which is discussed below in Section 4.3.2.

The horizontal tail was also shifted back slightly farther to obtain the desired tail volume coefficient. This shift necessitated that the vertical tails be swept back; this sweep angle was found to be just less than sixty degrees. The geometry of the vertical tails was then set by the requirements to join with the horizontal tail section. The chord length of the vertical tails is sixteen inches, and they are untapered. This results in a vertical tail coefficient larger than needed to maintain stability; however, the need to support the vertical tail outweighed the desire for a smaller volume.

Symmetrical airfoils were considered for both the horizontal and vertical tail sections. The driving factor of the airfoil selection was the minimization of drag. Also considered was the thickness of the airfoil, as a thicker airfoil would lead to more structural weight at the aft end of the fuselage. With these factors in mind, several symmetrical airfoils were compared, and the NACA 64-008A was selected for the horizontal and vertical tail sections.

4.2 MOTOR SIZING

The rules for this year's competition stipulate that the motors must be brushed and from the Graupner or Astro Flight catalogues. From the figures of merit it was desirable to find motors providing an adequate power loading. The limitations of the rules, however, did not allow sufficient motor selection to match thrust loading to an optimal size.

4.2.1 Motor Estimations

With the limitations imposed by the rules, the team began investigating both companies. Information on the Graupner line proved elusive, however, so propulsion studies were focused upon the Astro Flight families of motors. Past experience and preliminary battery estimations were for sixteen to twenty cells per motor. This limited options in the Astro Flight Cobalt catalogue to 'Ten to Twenty Cell Sport Motors', and 'Ten to Twenty Cell FAI Motors.' The FAI motors, however, were eliminated due to a current draw above the forty amp limit also imposed by the competition rules. This left the motor selection somewhat limited. All of the motors in the remaining category fit into the amp range allowed, leaving four motors to select from. Preliminary weight estimations pointed towards the selection of the larger motors in the 640 series. The remaining choices differed only in that one was a direct drive, and the other was a geared motor. Geared motors provide larger torque output, allowing the motor to swing a larger prop. For this reason, the Astro Flight 640G was chosen as the motor for the aircraft.

4.3 AIRFOIL SELECTION

Airfoil selection is a critical step in aircraft design. Many different factors go into the design of an airfoil, and a "good" airfoil can only be determined with a specific flight regime in mind.

4.3.1 Figures of Merit

As with aircraft sizing, several figures of merit were established as the initial criteria for airfoil selection. These were used along with the specifications of the flight regime to create a list of airfoils for further inspection:

- C_{lmax}
- Stall Angle
- C_d
- L/D

The maximum lift coefficient, C_{lmax} , is an important airfoil characteristic; it is used in take-off performance as related to the stall speed of the aircraft. Shorter take-off field lengths are obtained with higher values of C_{lmax} due to the lower stall speeds attainable.

Stall angle is an important characteristic for handling qualities. A higher stall angle allows for larger tolerances in flight. Aircraft with higher stall angles are also more maneuverable than those with lower stall angles. Maneuverability proves important in this application since pilots for small UAV's have fewer stall indications than pilots situated in full-size aircraft.

Drag is another important airfoil characteristic. Lower C_d values mean that the airfoil creates less drag in flight. This is directly tied into the next figure of merit: L/D

The L/D FOM is the ratio of lift to drag. This provides a good indication of the efficiency of an airfoil. This was weighted slightly more in overall considerations than the other figures of merit.

4.3.2 Airfoil Comparison

The flight characteristics of the competition allowed for several assumptions. The flight envelope of the plane would be at most 300 feet above sea level at very low subsonic speeds, thus making an assumption of incompressible flow very accurate. Airfoils from the UIUC Airfoil Coordinates Database (Reference (4)) were compared with the figures of merit defined above, and those that best fit the figures of merit were compared further. Comparisons were made using an online airfoil analysis program titled Calcfoil (Reference (8)). Calcfoil utilized conformal mapping with the Reynold's Number and airfoil coordinates as inputs. Comparisons of Calcfoil outputs and data published in Reference (9) were made, and the difference was negligible.

Upon review, the following nine airfoils were considered further:

- LS-413 Modified
- LS-417 Modified
- CLARK Y
- DAE51
- DEFCND2
- Eppler 1230
- Wortman FX 62-k-131
- Wortman FX 62-k-153/20
- Wortman FX 63-100

These were compared at Reynold's numbers of 200,000, 600,000, and 1,200,000. A comparison of the figures of merit is show in figures 4.2, 4.3, and 4.4 below for a Reynold's number of 200,000; Reynold's numbers of 600,000 and 1,200,000 produce the same rankings among the airfoils.

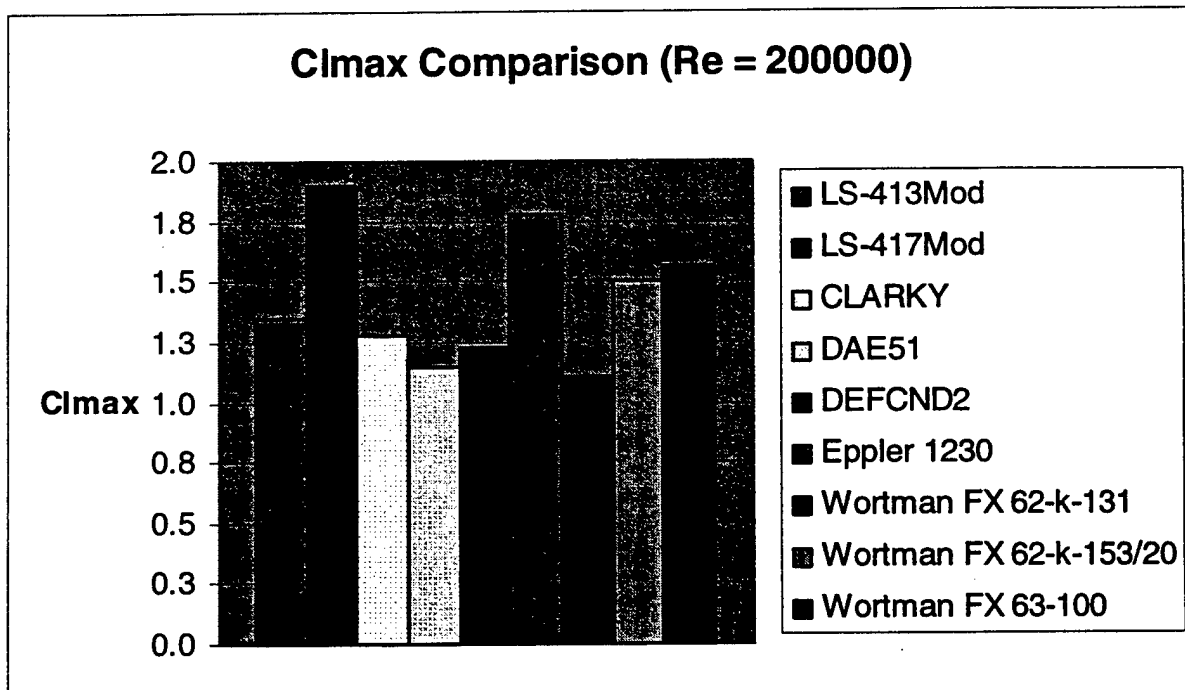


Figure 4.2 C_{lmax} Comparison

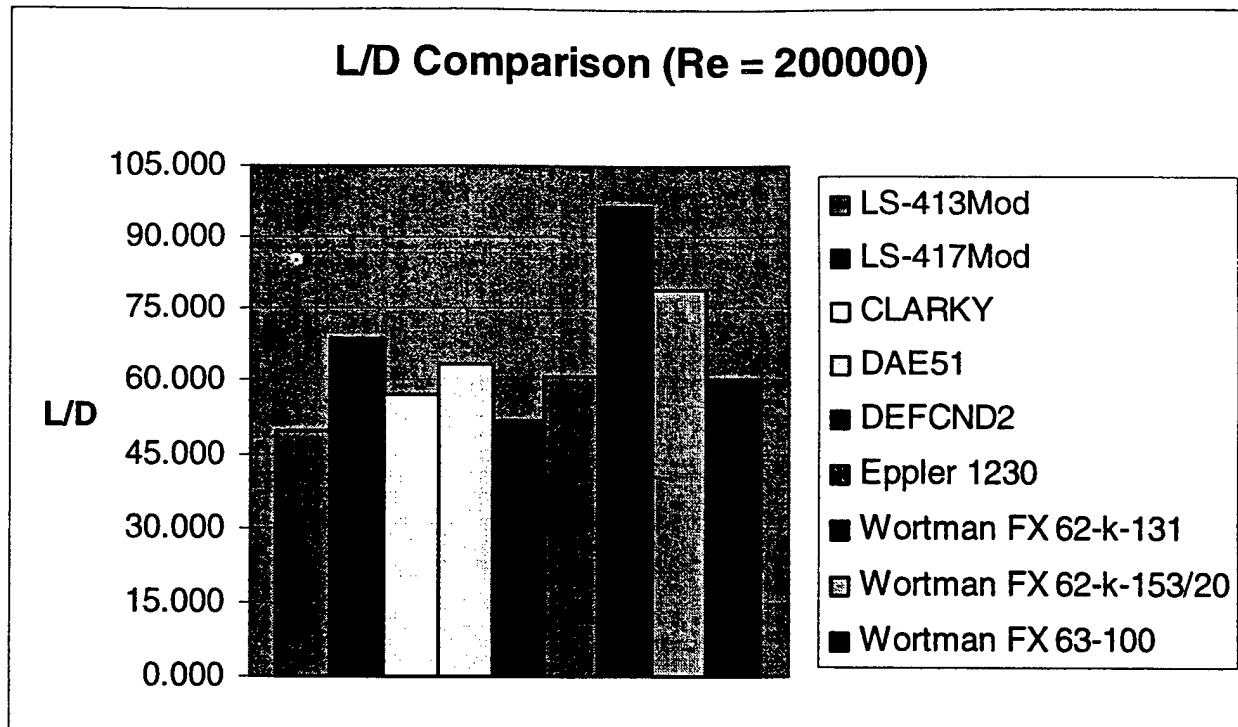


Figure 4.3 L/D Comparison

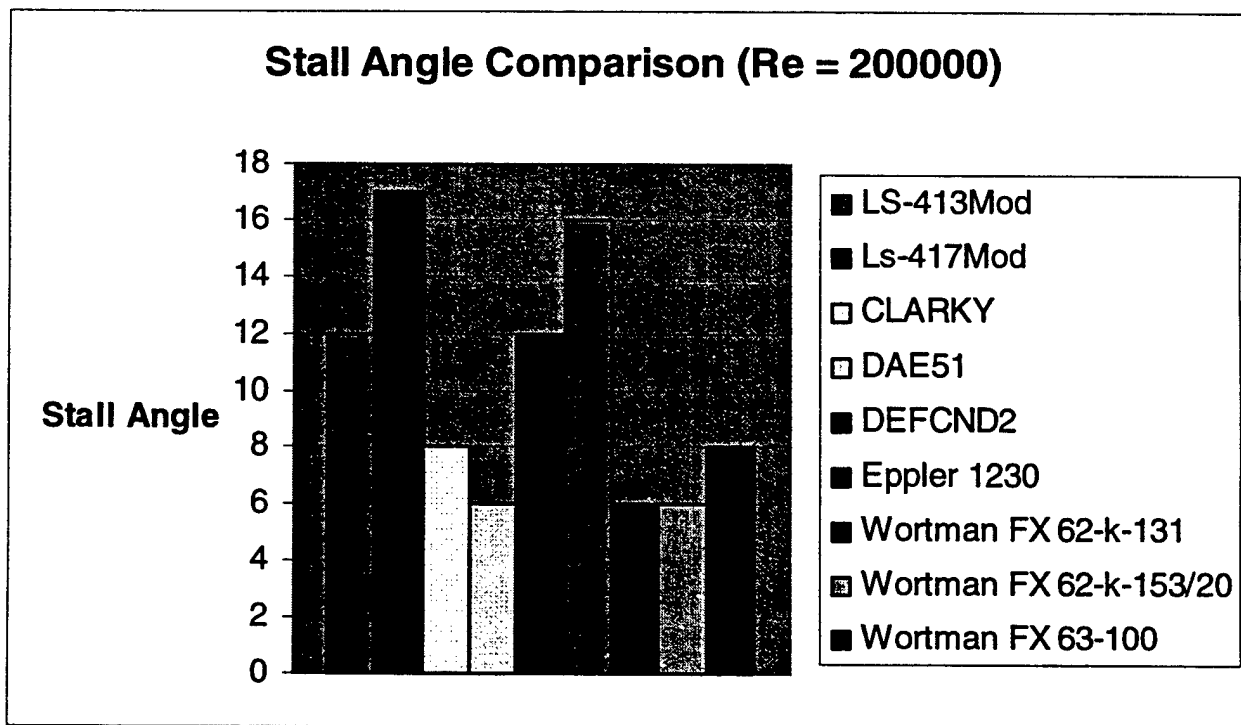


Figure 4.4 Stall Angle Comparison

Based on figures 4.2-4.4, the LS-417 Modified airfoil was selected. This is due to the high $C_{l_{max}}$, high stall angle and above average L/D ratio. The characteristics of the LS-417 Modified airfoil were further compared at an estimated aircraft Reynold's number of 2,300,000 for the aircraft. This data is presented below in figures 4.5, 4.6, and 4.7. This data is utilized for empennage sizing as well stability calculations in Section 4.

Flow separation over the airfoil was also considered. At very low Reynold's numbers laminar separation can occur, reattaching as a turbulent boundary layer, assuming the airfoil does not stall or C_l is less than $C_{l_{max}}$. The size of this laminar bubble will not be a problem in the Reynold's number range of the wing at the operating C_l values.

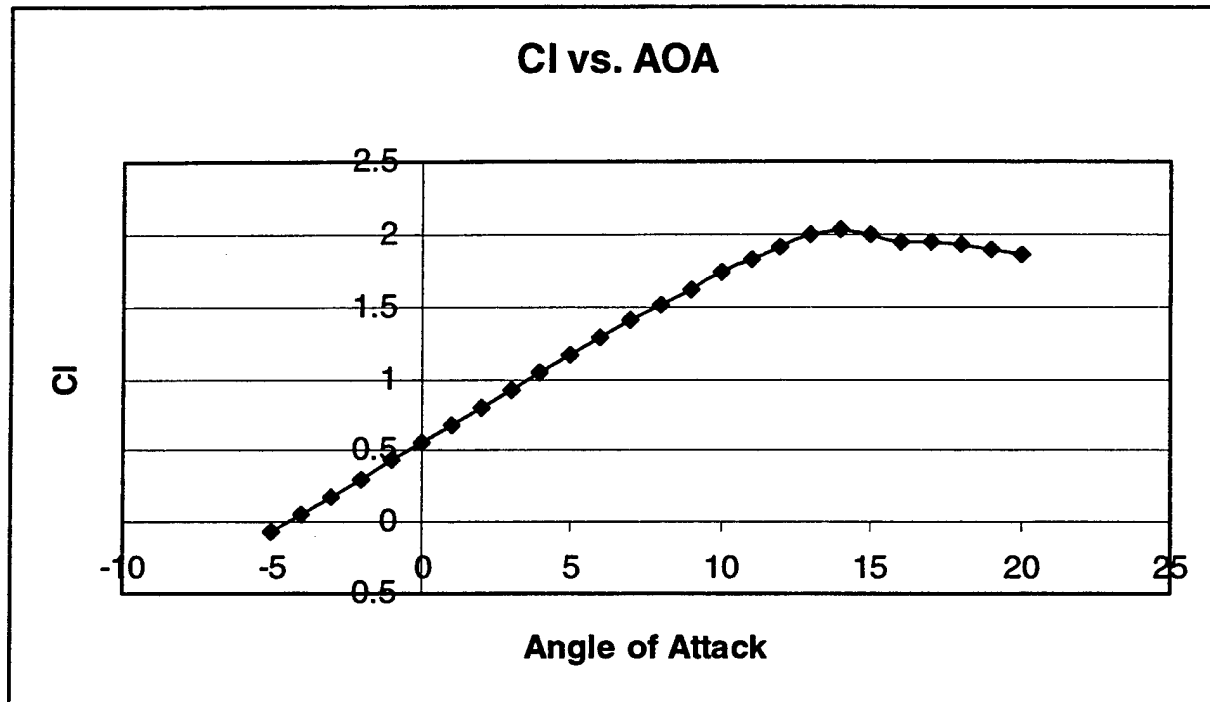


Figure 4.5 C_l versus Angle of Attack

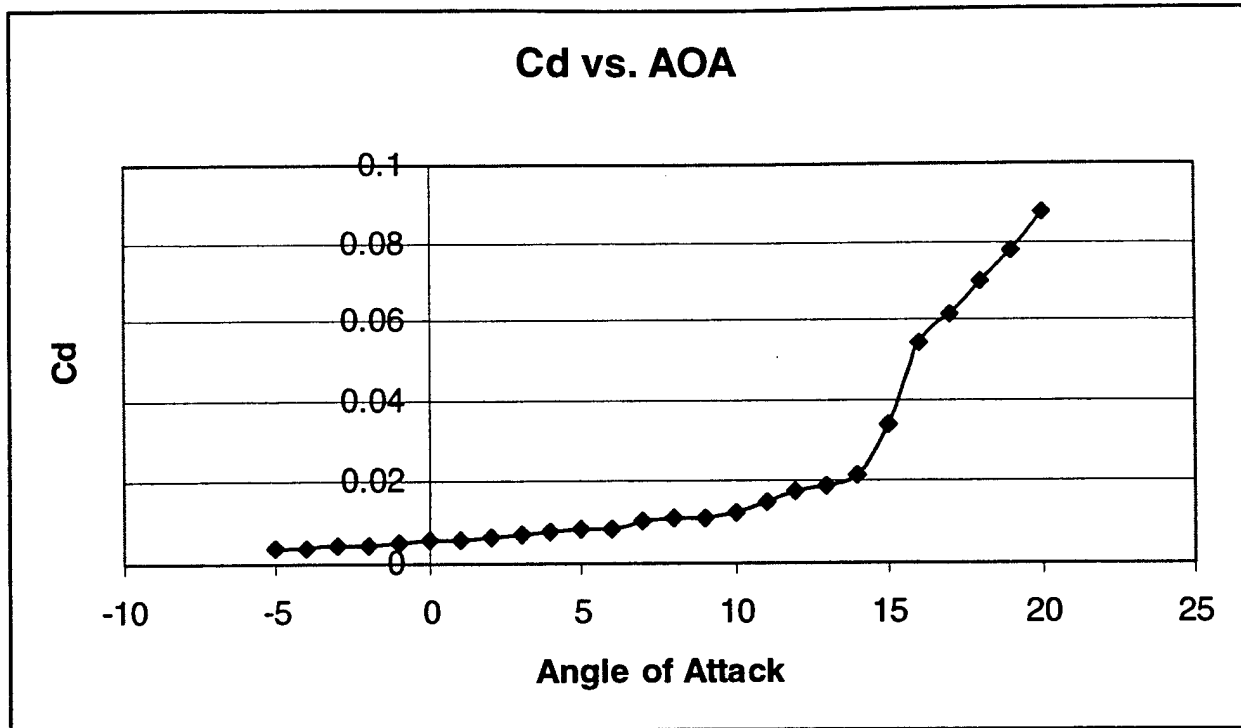


Figure 4.6 C_d versus Angle of Attack

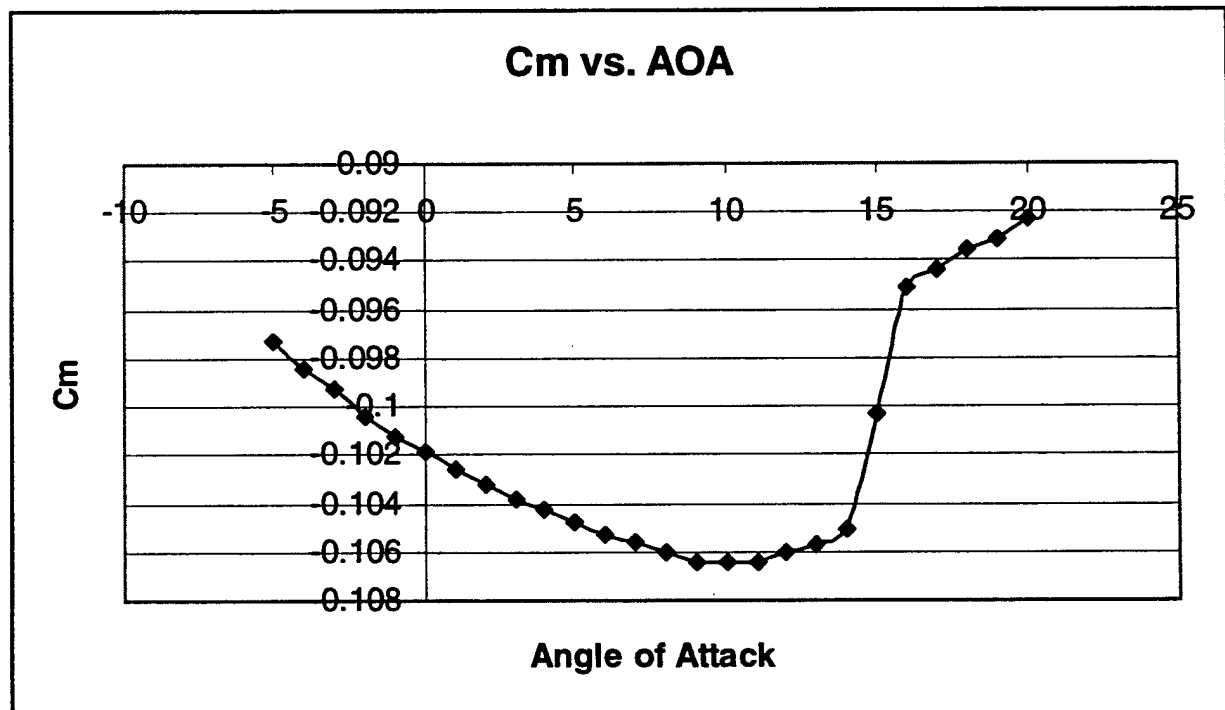


Figure 4.7 C_m versus Angle of Attack

4.4 AIRCRAFT INFORMATION

Name: DGT

Mission: UAV Cargo Transport

Fuselage:

42 inch payload section.

12 inch nose section.

16 inch aft section.

Wing:

10 ft. span.

10 ft² area.

Taper ratio: 0.45

High wing.

Horizontal tail:

16 inch chord.

2.67 ft² area.

High T-tail section.

Vertical tail:

16 inch chord.

60° sweep.

1.78 ft² area.

Batteries:

Sanyo 2000mah.

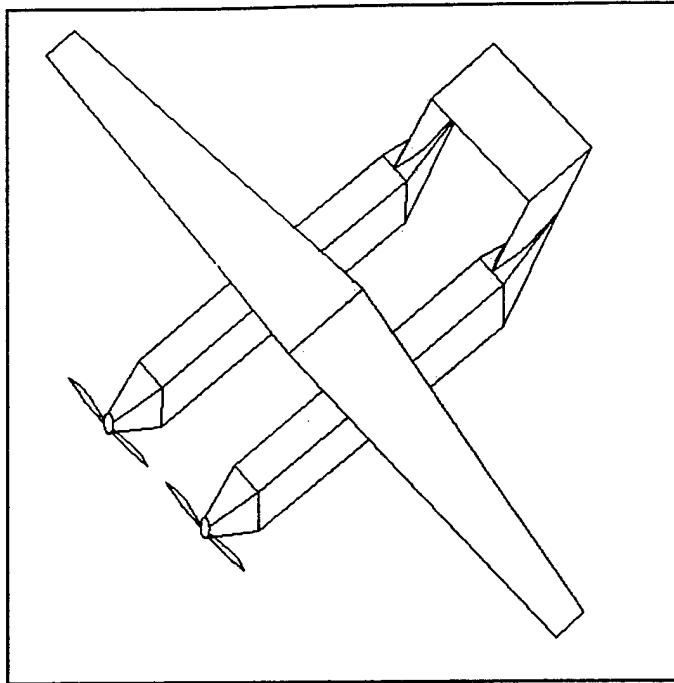
Total cells: 36; eighteen cells per motor

Motor: Astro Flight 640G (2)

Speed Controller: Astro Flight 204D

Rated Aircraft Cost: 7.5

Projected Single Flight Score: 60



5. DETAILED DESIGN

Design finalization involved several factors. The handling qualities needed to be balanced with sizing optimization, as well as performance data. The structural integrity of the aircraft also needed to undergo an analysis in order to determine the strength necessary for flight.

5.1 HANDLING QUALITIES

The airplane must be controllable and maneuverable in take-off, climb, cruise, descent and landing stages. The tasks involved in the handling qualities analysis are:

- Longitudinal Control
- Lateral and Directional Stability
- Minimum Control Speed
- Trim (longitudinal, lateral and directional trim)
- Static Stability (longitudinal, and directional)
- Dynamic Stability
- Stall Characteristics

Stability derivatives enter into the calculation of the handling qualities. The important ones are computed in the next section.

5.1.1 Stability Derivatives

With initial sizing estimates completed with the preliminary design, an analysis of stability derivatives was completed. The aircraft design was compared with the requirements for those derivatives to ensure that the aircraft would prove statically stable. As found in reference (3), the important stability derivatives are:

- $C_{l\alpha} > 0$ – aircraft lift curve slope
- $C_{m\alpha} < 0$ – pitching moment curve slope
- $C_{mq} < 0$ – variation of pitching moment coefficient with pitch rate
- $C_{Du} > 0$ – variation of drag coefficient with speed
- $C_{mu} > 0$ – variation of moment coefficient with speed
- $C_{y\beta} < 0$ – variation of moment coefficient with sideslip angle

The derivatives were found per the methods in reference (3). Two assumptions were made for the calculation of these derivatives; first, that compressibility effects could be ignored at the low speeds, and second, that the aircraft was flying at small angles of attack. For the aircraft design, they were found to meet the criteria necessary for static stability. The results of this analysis are displayed in table 5.1.

Table 5.1 Stability derivatives

$C_{l\alpha}$	1.126 rad^{-1}
$C_{m\alpha}$	-0.1126 rad^{-1}
C_{mq}	-1.032 rad^{-1}
C_{Du}	0.00
C_{mu}	0.00
$C_{y\beta}$	-0.2513 rad^{-1}

5.1.2 Control Surface Sizing

In addition to stability, all aircraft must have control mechanisms. These must be adequate to guide the aircraft through all anticipated flight regimes, as well as encompass a factor of safety. Values were found in percentages from reference (2). With the wing and tail geometries known, the control surface sizes could be found exactly. The elevator was set at 40% of the horizontal tail area. This area was fixed from balancing the pitching moment of the wing in the preliminary design phase. The rudder was taken as 35% of the total vertical tail area, which was then set at 18% per vertical tail section. Ailerons were taken as 25%C for 45% of the semi-span. High and low rate settings were selected for surface deflections. Aircraft functions known as dual rates were employed for the multiple rate settings. This is discussed further in Section 5.5.2.

5.2 PERFORMANCE ANALYSIS

Performance data on the aircraft was another vital statistic of the design. Performance data both validated the design selection and predicted competition flight scoring. Because the difference in weight between the two payload sorties was small, the calculations were done for a single weight, and the other payload sortie was approximated as identical. The weight of the steel payload was selected, as it provided a more precise measurement. A summation of performance data is included in table 5.2 at the end of section 5.2.

5.2.1 Maximum Load factor

The maximum load factor of the plane is an important characteristic. It is used in determining instantaneous turn rates, for performance, as well as the ultimate loads that the structure must be designed to handle. Maximum load factor, as described in reference (1) was found to be nearly four. With a standard aircraft factor of safety of 1.5, this fixed the load factor at six, or six – g's.

5.2.2 Instantaneous Turn Rate

With a maximum load factor, the instantaneous turn rate of the plane was calculated. This, along with the sustained turn rate, was needed in order to estimate range and endurance. This was found at the stall speed (detailed below), at the maximum lift coefficient. Using the maximum load factor found above, the instantaneous turn rate was found to be 123.94 Deg/s.

5.2.3 Sustained Turn Rate

Similar to instantaneous turn rate, the sustained turn rate is important for range and endurance calculations. The sustained turn rate was also found at the stall speed with the maximum lift coefficient. The sustained turn rate was found to be 81.732 Deg/s.

5.2.4 Stall Speed

The stall speed for the aircraft was found with the airfoil maximum lift coefficient, $C_{l_{max}}$. The basis for finding the stall speed was the realization that at level flight, $L = W$. With that, the stall speed was calculated at 31.22 mph.

5.2.5 Take-Off Performance

Take-off performance was one of the most important performance figures calculated, as a maximum take-off distance is stipulated within the competition rules. Take-off performance was calculated with several variables: C_l was taken at a zero incidence level, at 0.55. Thrust loading was taken at 70% of the total as estimated from reference (2). Take off velocity was estimated at 10% above stall speed. With these factors, the worst-case take-off distance was found to be 141 ft, well within the take-off distance allowed.

5.2.6 Drag Polar

In order to determine the range and endurance of the aircraft, an accurate measure of the drag is needed. A level one estimation was used for drag calculations; this was expected to provide an accurate drag prediction, with a slight tendency for over-prediction. Drag is comprised of three main components: induced, compressibility, and skin friction drag. Because of the low Mach numbers of the flight, drag due to compressibility effects was neglected. At this stage the drag polar could be evaluated by:

$$C_D = C_{D0} + KC_L^2 \quad (5-1)$$

Here C_D is the total drag, C_{D0} is the zero-lift drag, K is the induced drag constant, and C_L is the aircraft lift coefficient. Part of C_{D0} is the skin friction drag. This can be found after computing the skin friction coefficient for each body. Assuming a turbulent boundary layer, the skin friction coefficient is found with:

$$C_f = \frac{0.455}{[\log(Re)]^{2.58}} \quad (5-2)$$

C_f is the skin friction coefficient, and Re is the Reynold's number, based upon body length. Reynold's numbers were found at the stall speed of the aircraft. C_f values were found for both booms, the wing, both vertical stabilizers, and the horizontal stabilizer. This was found with:

$$C_{D0} = \frac{1.2(\sum C_{fbody} S_{wetbody})}{S} \quad (5-3)$$

In 5-3 the C_{fbody} is the skin friction coefficient of the specific body, and $S_{wetbody}$ is the wetted area of that body. Here S is the reference wing area.

This left the calculation of induced drag to finalize the aircraft drag polar. The induced drag coefficient was found as:

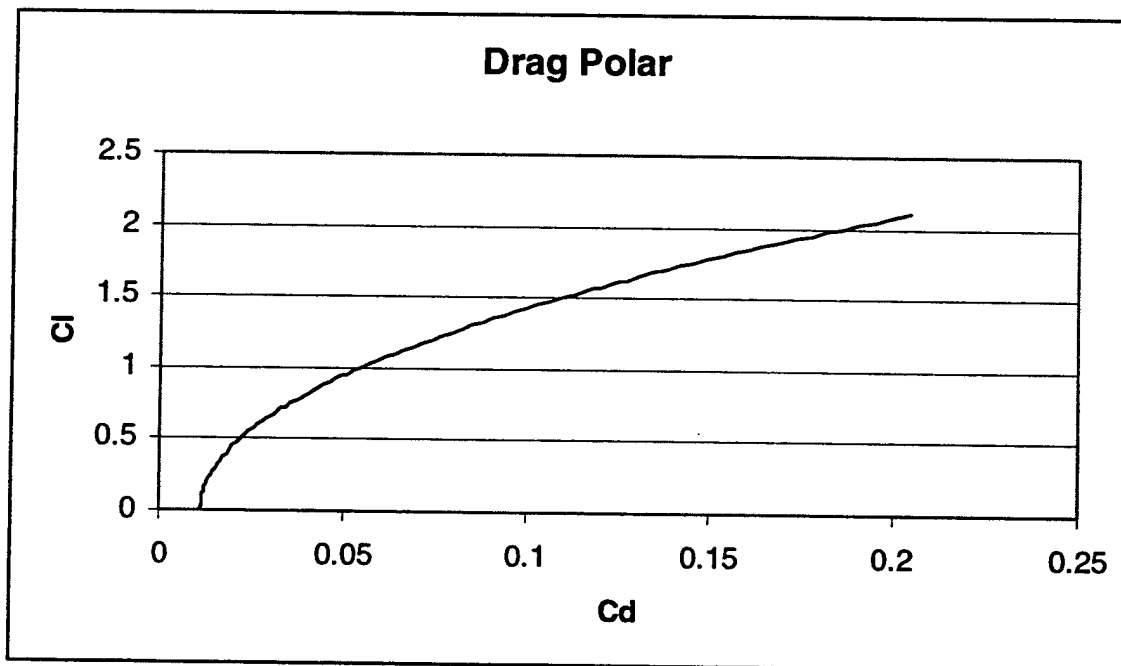
$$K = 1/\pi Ae \quad (5-4)$$

A is the aspect ratio of the wing and e is Oswald's span efficiency factor. With unswept wings this value is estimated with:

$$e = 1.78(1 - 0.045A^{0.68}) - 0.64 \quad (5-5)$$

The resulting drag polar is shown in Figure 5.1.

Figure 5.1 Drag Polar for Aircraft



5.2.7 Cruise Performance

At cruise conditions lift is equal to weight and thrust is equal to drag. With no time limit, these would be the optimization factors for the design. However, because of the time limit imposed, the maximum number of payload sorties will be flown by flying at the maximum cruise speed. Maximum cruise speed, for level flight, was found to be 60.13 mph. This was found from the balance of force equations in level flight presented in reference (1). With the course layout, maximum cruise speed, and sustained turning rate, the heavy steel payload sortie time was computed. This was found to be 37.5 seconds. For the tennis ball sortie, a flight time of 68.1 seconds was found. This allowed for two of each sortie to be flown for a total mission time of 3 minutes and 34 seconds. This was within thirty seconds of the projected run time calculated using Motocalc, an electric engine thrust and run time calculator. This allowed ample time for the exchanging of payloads between sorties.

Table 5.2 Summation of Performance Data

Maximum Load Factor	6 G's
Instantaneous Turn Rate	123.94 Deg/s
Sustained Turn Rate	81.732 Deg/s
Stall Speed	31.22 MPH
Take-Off distance	141 ft.
Maximum Cruise Velocity	60.13 MPH
Steel Payload Flight Time	37.5 s
Tennis Ball Payload Flight Time	68.1 s
Number of Sorties Flown	4

5.3 FINAL SIZING

With the performance estimations and stability derivatives satisfied, final sizing of the aircraft could be completed. With satisfactory performance estimations, no major changes were incorporated into the design. Because of this only minor sizing changes were made to facilitate the construction phase.

5.3.1 Wing

The wing construction method decided upon was a foam core wrapped in fiberglass. Previous experience had imparted the lessons needed in order to manufacture a high quality part. For ease of construction, the wing root and tip chord lengths were increased slightly. This led to a total wing area of 10.61 ft². Other wing parameters remained unchanged. A span of ten feet was still planned, with the Quarter chord left unswept, and the taper ratio of 0.45 unchanged.

5.3.2 Fuselage

The fuselages were left unchanged. A forty-two inch payload section still remained the main section. The nose was left at twelve inches, with the only changes being that the front bulkhead for motor attachment was moved slightly above centerline to accommodate the gearbox of the motor. The aft section remained the same, with doors splitting open to allow for easy removal of the payload. Bulkheads were placed with respect to component locations. These locations were finalized with the CG calculation in Section 5.3.4.

5.3.3 Cooling

Due to the large currents seen by the speed controllers, cooling must be provided to those units. It is also advisable to provide cooling to the main battery packs, as they also attain relatively hot temperatures compared with the aircraft. Cooling for both of these systems was provided through the use of NACA flush inlets. One is in the forward nose section to cool the speed controller, while two are in the aft end of the payload compartment to cool the batteries.

5.3.4 Empennage

The empennage was also left nearly unchanged. The vertical tail sections were left with a height of eight inches, swept back 60° . The only change was in the horizontal stabilizer. It was determined that for stability the horizontal tail would need two degrees of negative incidence to counter the pitching moment of the wing.

5.3.5 Final Weight Estimation and CG Location

With final sizing complete, a more detailed weight estimation was completed. The aircraft empty weight was found to be 14.15 lbs. The gross weight of the plane with the steel bars was found to be 25.5 lbs, for a payload fraction of 0.445. For the Tennis balls, the gross weight was found to be 25.05 lbs, for a payload fraction of 0.427.

With a final structural weight known, components could be placed. The CG was taken at the quarter chord of the wing, and the components balanced around that. Placement of the components allowed for final bulkhead placement in the booms.

5.4 STRUCTURAL ANALYSIS

Before construction begins, it is important to make sure the structure can support the loads it will encounter.

5.4.1 Wing

The construction method chosen for the wing was a foam core wrapped in fiberglass, producing a wing both lighter and stronger than one manufactured with conventional balsa. In order to determine the number of ply layers and the resulting strength of the wing, a simple structural analysis was done.

The wing was assumed to be a cantilever beam, fixed at the root. A limit load of three times the aircraft's weight was approximated at the tip. This load is the maximum load factor found above, divided on the two wing tips. The resulting force produces a bending moment at the root. For the analysis the foam cores were neglected, so the fiberglass skin was required to safely bear the moment produced. The moment was resolved into axial stresses, under the assumption that the upper skin would be in compression, and the lower skin in tension. The axial loads, compared with the tensile and compressive stresses of fiberglass, found in reference (5), were used to compute factors of safety and G-loads. The wing was found to have a factor of safety of 2.11 above the maximum load factor, allowing for the wing to sustain 12.7 G's. This is a relatively high G-loading, however past competitions have illustrated the wisdom of over designing for strength.

Additionally, the ply orientations were investigated. Layers of $[0/90]$ orientation were needed to support the bending load in the wing. However, it has been shown that ply layers of $[\pm 45]$ have a higher resistivity to impact damage, and as such, the outer ply layer is to be oriented in this manner.

5.4.2 Fuselage

The fuselage was also modeled as a beam. The fuselage was assumed to be a cantilevered beam secured at the CG. Because the CG represents a balance of moments, an analysis of only one side of the fuselage was necessary. For this analysis the bulkheads in the fuselage were neglected and all loads were assumed imparted to the fiberglass skin. A load of one half the aircraft weight was assumed with a moment arm of three quarters the length of the section. The moment at the CG was assumed to act upon the skin as axial loads, with the upper skin in tension and the lower skin in compression. From this it was found that the fuselage could sustain an 8.1 G-load, with a factor of safety of 1.35 above the maximum load factor.

5.5 SUBSYSTEMS

With all major design work completed, the remaining task was for a more detailed analysis of the components.

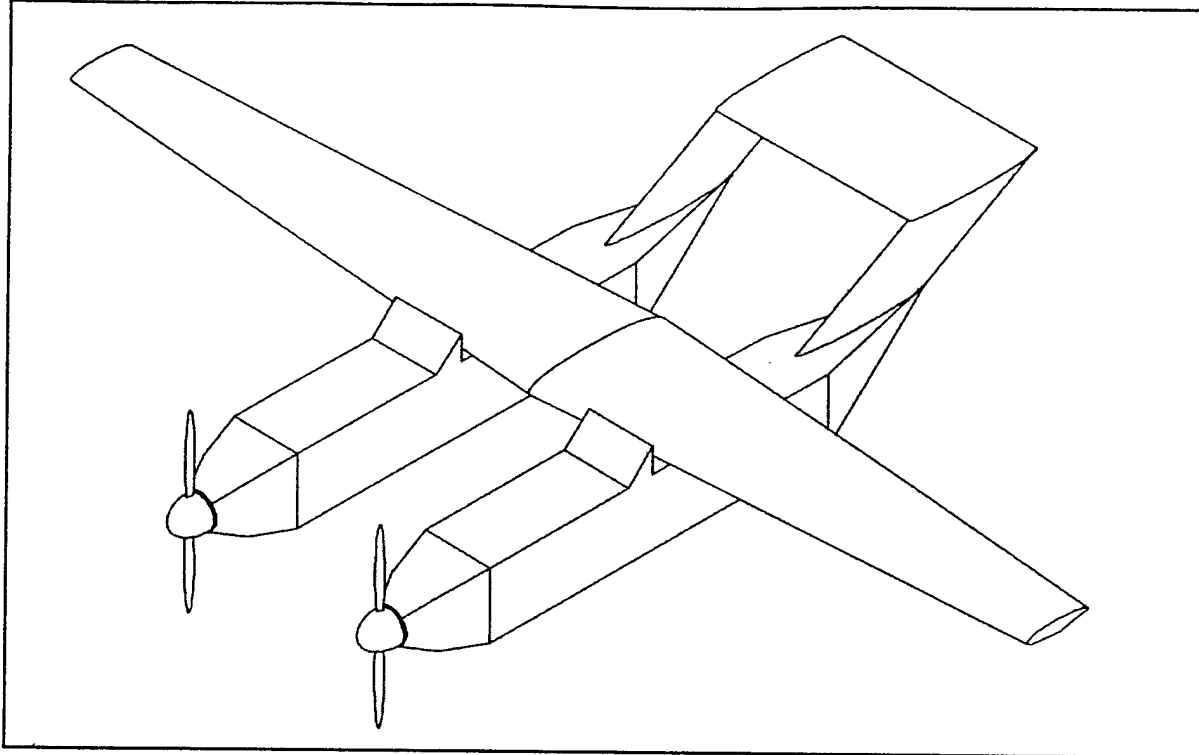
5.5.1 Landing Gear

The twin boom design of this year's aircraft necessitated a quad gear arrangement. Robart Robo-Struts will again be chosen for the landing gear. Robart is a well-known name in the model aircraft world with a reputation for quality and customer satisfaction. These gear feature fully functional oleo struts and are made from high-grade aluminum. Because of this Robart Gear was selected this year.

5.5.2 Radio Control Devices

Aircraft control will be provided with a Futaba 6XA computer radio. This transmitter is capable, along with the PCM receiver of providing the failsafe requirements stated in the rules. Rudder, Elevator, and Nose Gear servos will be Futaba quarter scale, S3202 servos. These are capable of handling higher torques necessitated by the scale of the aircraft. Aileron servos will be standard Futaba S3003's. These will be mounted in the foam core wing for direct connection with the ailerons. The radio has several built in functions, including flaperons. This is important should the decision be made after flight-testing to decrease take-off and landing distances. This radio also features dual rates, multiple settings for control throws of the servos. This allows for high and low movement settings to be selected for various parts of the flight regime, adding to the comfort of the pilot.

5.4 AIRCRAFT INFORMATION



Name: DGT

Mission: UAV Cargo Transport

Fuselage:

42 inch payload section.

12 inch nose section.

16 inch aft section.

Wing:

10 ft. span.

10.61 ft² area.

Taper ratio: 0.45

High wing.

Horizontal tail:

16 inch chord.

2.67 ft² area.

High T-tail section.

Vertical tail:

16 inch chord.

60° sweep.

1.78 ft² area.

Batteries:

Sanyo 2000mah.

Total cells: 36; eighteen cells per motor

Motor: Astro Flight 640G (2)

Speed Controller: Astro Flight 204D

Rated Aircraft Cost: 7.376

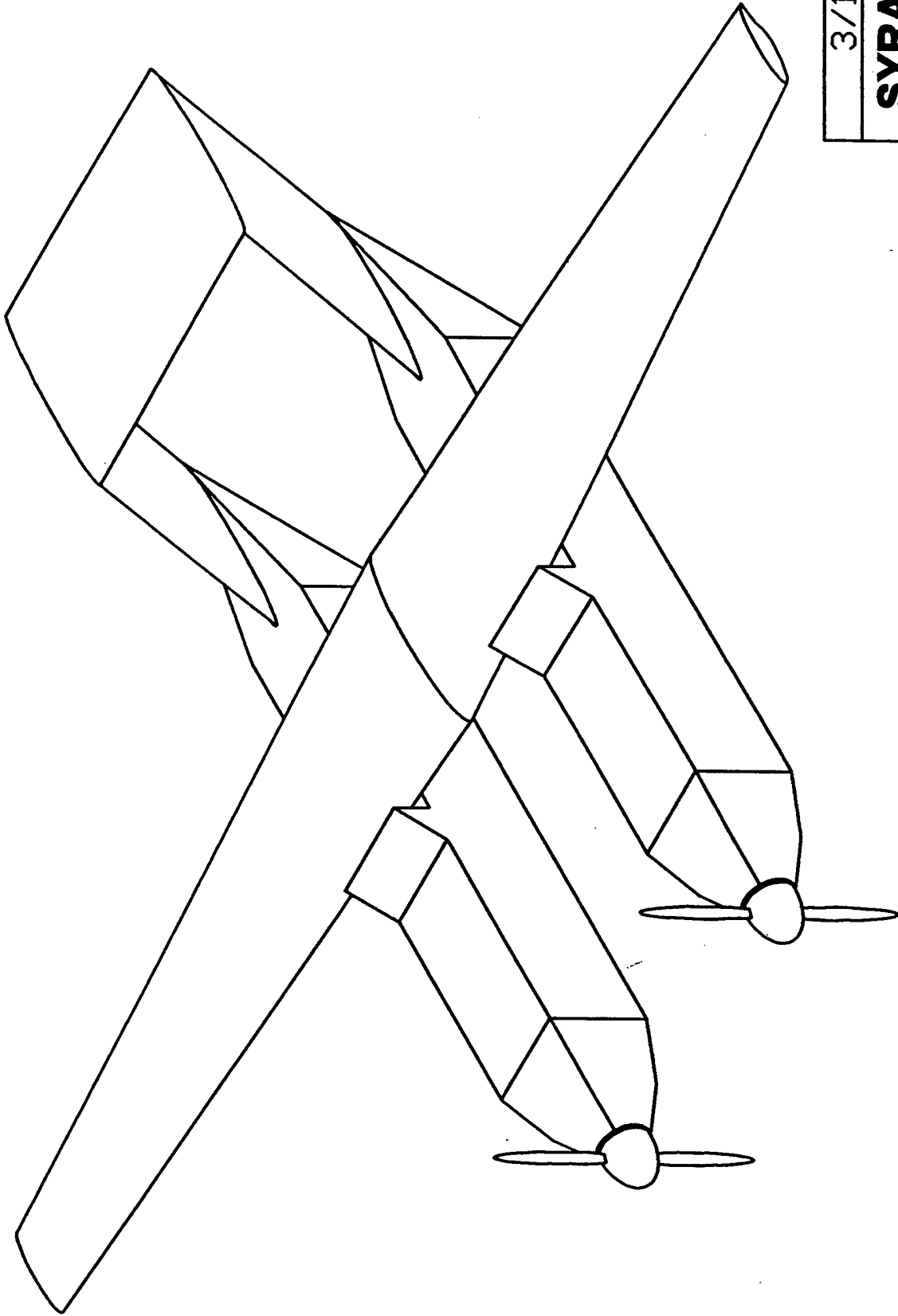
Projected Single Flight Score: 63

Max Speed: 60.1 MPH

Sorties: 4, 2 of each.

DRAWING PACKAGE

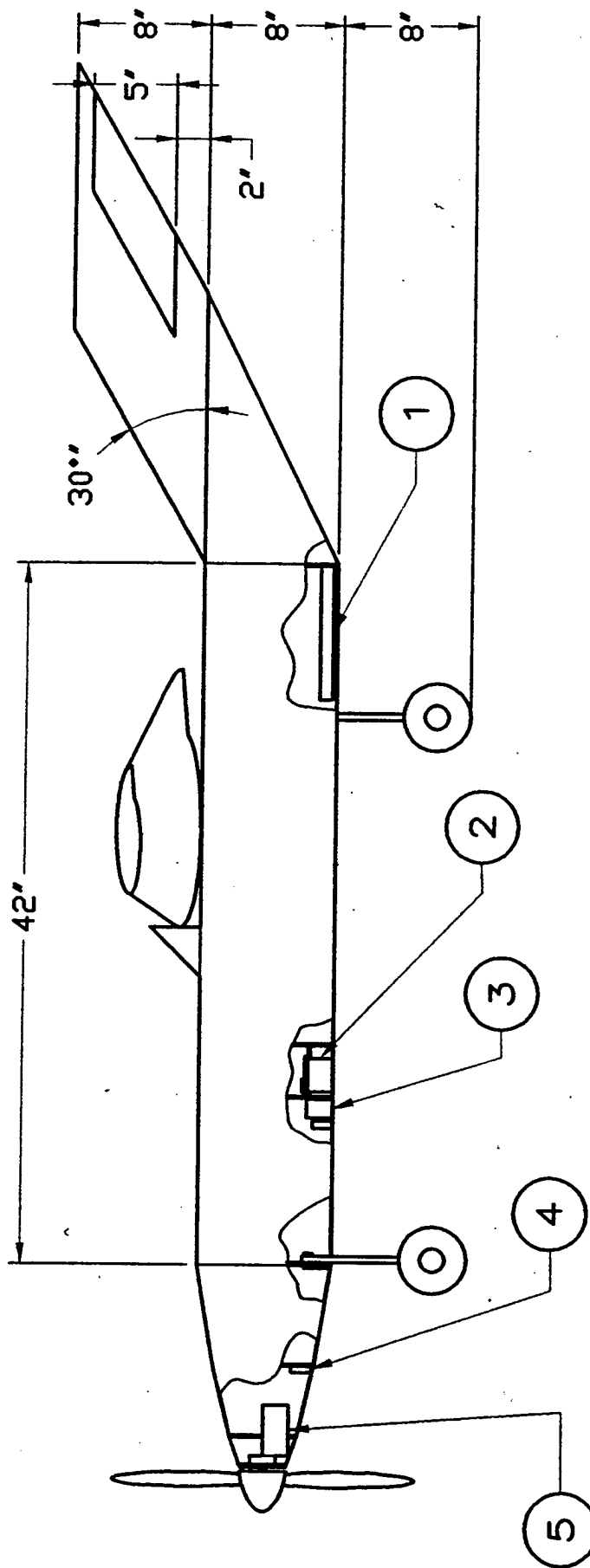
The drawings illustrate the configuration selected as well as sizing of the aircraft. Drawing four provides a cut-away view to illustrate component placement. All drawings were made with AutoCad R14.



3/13/01

**SYRACUSE
UNIVERSITY**

DGT-
ISOMETRIC



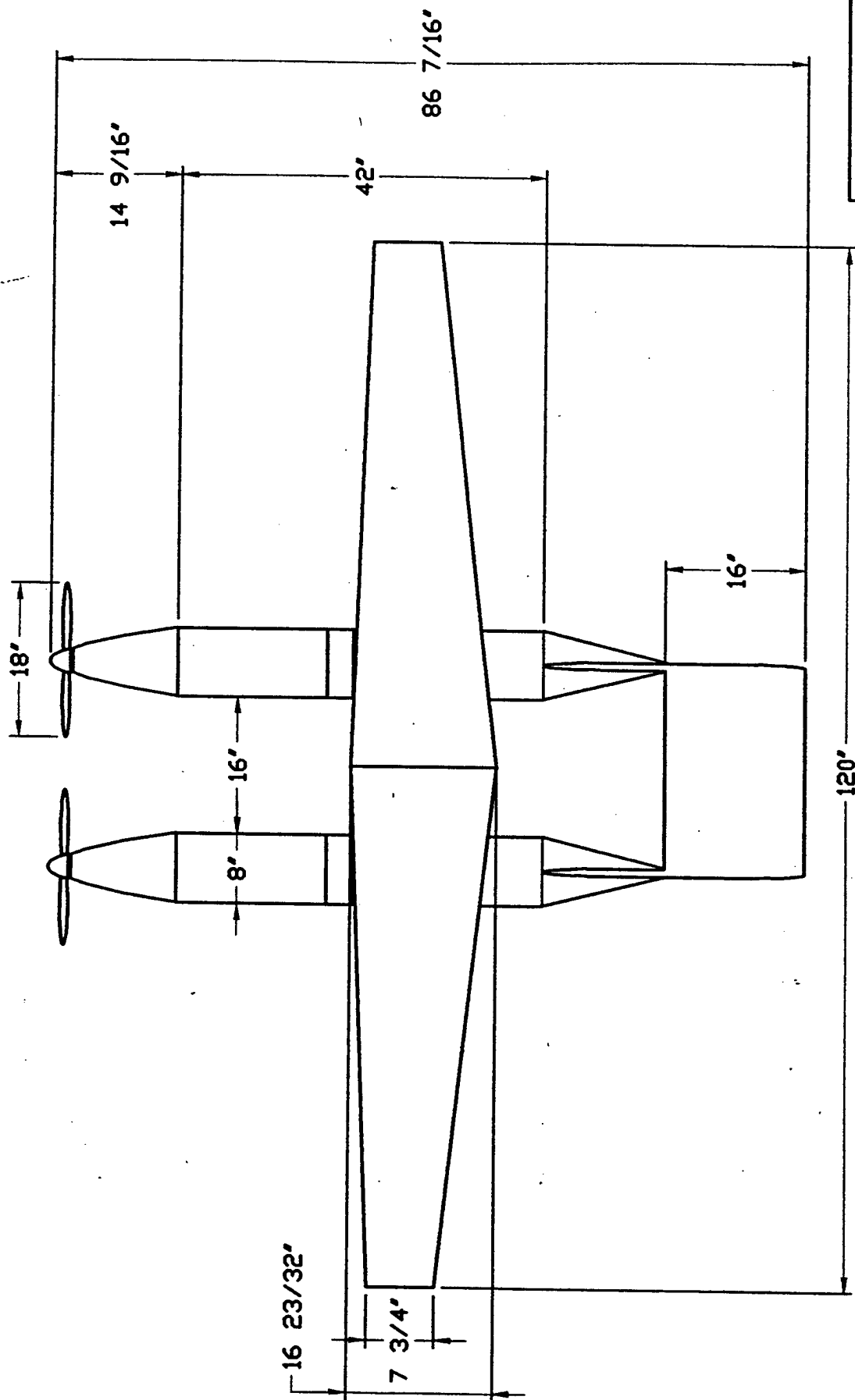
NO.	DESCRIPTION
1	BATTERY
2	SERVO
3	RECEIVER + BATTERY
4	SPEED CONTROLLER
5	ELECTRIC BRUSH MOTOR

3/13/01

**SYRACUSE
UNIVERSITY**

DGT-

RIGHT VIEW

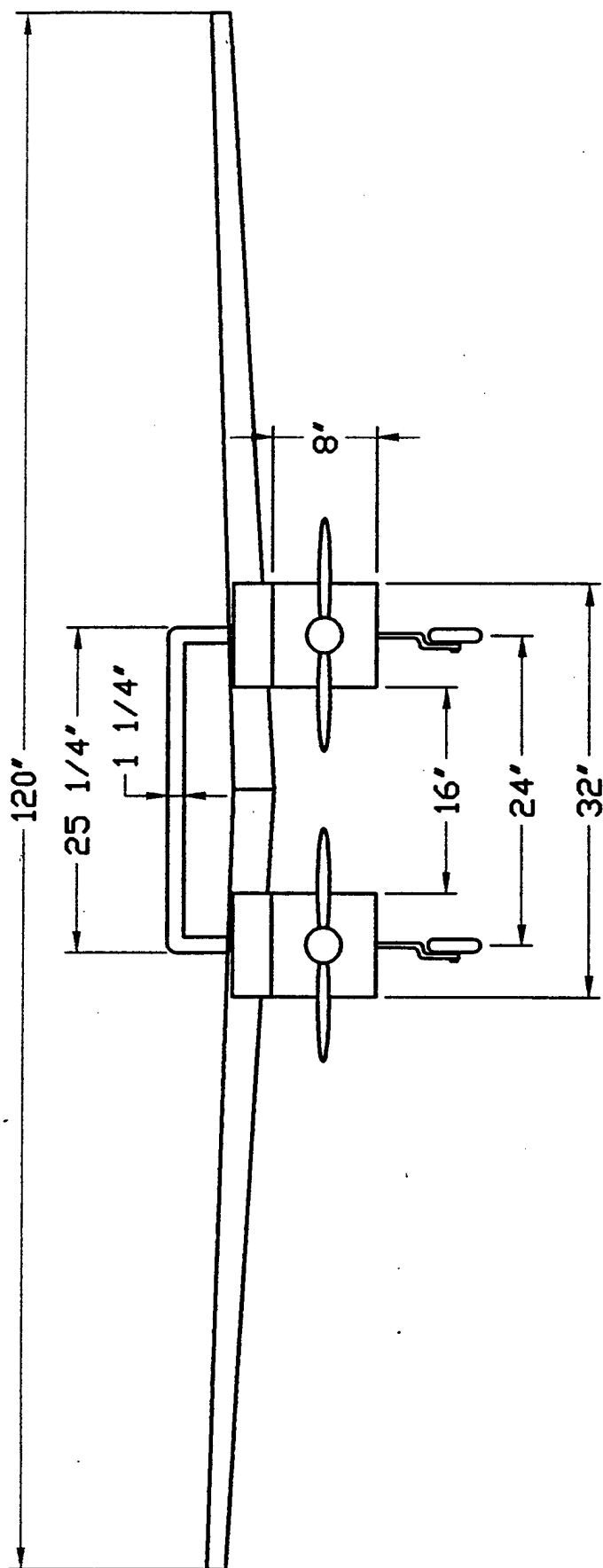


3/13/01

**SYRACUSE
UNIVERSITY**

DGT-

TOP VIEW



3/13/01

**SYRACUSE
UNIVERSITY**

DGT-

FRONT VIEW

6. MANUFACTURING PLAN

The manufacturing plan is designed to minimize cost and man hours while still providing a competitive aircraft. All materials and plan selections are made in accordance with chosen figures of merit while taking into account the team's modeling skills and past experiences. A manufacturing time table is presented at the end of this section, table 6.3.

6.1 FIGURES OF MERIT

The team used seven figures of merit (FOM) when considering manufacturing materials and plans:

- Availability
- Reparability
- Strength/Weight Ratio
- Skills Needed
- Past Experience
- Monetary Cost
- Man Hour Cost

The team is placing heaviest consideration on the Strength/Weight Ratio and Past Experience categories. Strength/Weight Ratio is an important consideration due to the twin boom configuration chosen for the plane; the team needs high-strength materials to carry the payload, but the addition of another boom adds significant weight to the aircraft. Past experience is also an important consideration because it allows the team to make decisions based on what has and has not worked instead of relying purely on theory.

6.2 WING MANUFACTURE

From an experience standpoint, wood is the best material for wing construction. It is easy to work with, inexpensive, and common in radio-controlled aircraft. However, balsa has a low strength/weight ratio and the team decided that a wood wing, when built to withstand design loads, is too heavy. Instead, it was determined that a foam core wing covered in a composite material is preferable: it has a higher strength/weight ratio and the team has past experience with it. The team looked at covering the wing in carbon fiber and fiberglass. Fiberglass was chosen because it is significantly less expensive than carbon fiber. A summation of the wing material comparison is presented in table 6.1.

Table 6.1. Figures of Merit

Material	Availability	Reparability	Strength/ Weight	Skills Needed	Past Experience	Time	Cost
Wood	5	5	2	1	5	2	2
Fiberglass	4	2	4	4	4	4	3
Carbon Fiber	2	2	5	4	2	4	5
Foam Core	2	3	2	5	4	2	3

The team decided that cutting the foam cores was too difficult and time consuming so the foam cores were ordered from a company that produces custom foam cores: RPV Industries. Past experience with RPV Industries taught the team that they are accurate and reliable in their production of foam cores.

RPVI's method of foam core manufacturing utilizes a hot-wire approach. For manufacturing, two thin metal templates of wing cross-sections are constructed: one of the tip and one of the root. The templates are then placed at the end of blocks of expanded polypropylene foam and a stainless steel wire is stretched the length of the blocks. A current is run through the wire, which then follows the templates and cuts the foam to the correct shape.

The wing cores were manufactured in two semi-span segments. Final sanding of these eliminated the imperfections left from the foam cutting. The two wing halves will be epoxied together at the root before further construction. Ailerons will be cut from the wing and set aside; servo compartments and wire runs will also be cut from the foam prior to fiberglassing. With all necessary sections cut out, the wing will be fiberglassed. Three plies of fiberglass will be used for the skin. These will be applied from the upper surface-trailing edge, and worked around the leading edge to the lower surface-trailing edge. This will be done to minimize the imperfections at the leading edge. Instead of vacuum bagging the wing, it will be placed back in the foam cradles it was cut from. This will allow the team to control the amount of twist in the wing. This also allows for the application of release cloth to improve the surface finish of the fiberglass. The wing will be primed and sanded several times to decrease surface irregularities. The final paint will be applied sparingly to minimize weight. The ailerons, previously cut from the wing, will be fiberglassed and finished in a similar fashion.

6.3 SPEED LOADERS

In the initial design stages for the plane, the team determined that the use of speed loaders would be desirable for competition. In selection of a material to construct the speed loaders, figures of merit, shown in table 6.2, were considered. An emphasis was placed upon strength/weight ratio, cost and skill matrix.

Table 6.2 Figures of Merit for Speed Loader Construction

<i>Material</i>	<i>Availability</i>	<i>Reparability</i>	<i>Strength/ Weight</i>	<i>Skill Matrix¹</i>	<i>Time¹</i>	<i>Cost</i>
Wood	5	5	2	5	5	5
Fiberglass	5	2	4	4	4	4
Carbon Fiber	4	2	5	2	2	2
Kevlar	3	2	5	2	2	1

It was decided that constructing speed loaders from fiberglass/epoxy composite would give the desired strength with a low weight. Because of the team's experience with the material in past years, the speed loaders would be easy to construct.

The next step in the design of the speed loaders was determining a configuration that was both easy to manufacture and had the least weight for the intended purpose. Since the loaders had to be identical in shape, the critical size was determined from the number of tennis balls. By using a tennis ball manufacturer's specifications for the weight of a typical tennis ball, the optimum number of balls for construction was determined as 48 with an arrangement of 16 rows of 3 balls. The team also decided that using a cylindrical tube was favorable for carrying the balls; a diameter of six inches was selected. This selection was based upon a minimum diameter for the three-ball configuration, as well as manufacturing needs and available sizes for molds. The optimal length of the speed loader was determined by finding the distance for 16 tennis balls to be placed in a line, which was determined to be approximately 40". PVC pipe with an ID of 6" was selected for the mold based on price and availability.

The PVC pipe mold was cut to a length of 48" to allow for extra material to be trimmed afterwards to the desired length or 42". The pipe was then cut longitudinally into three pieces. The number of lengthwise sections was selected from experience with composite materials and vacuum bagging. The mold was then put back together using duct tape on the inside seams to hold the shape. The outside of the mold was then covered in a liquid release film and wrapped in polyester release cloth. Based on experience with fiberglass composite, the number of plies was selected to be three to give the desired strength at the least weight. Three plies of fiberglass were wrapped around the mold and epoxied, with the excess removed, then covered by another polyester release cloth and finally breather/bleeder material. The entire mold and speed loader was then vacuum bagged using sealant putty to prevent leaks for a period of 24 hours.

After the speed loader was removed from the mold, a permanent cap of one fiberglass ply was fixed to one end of the speed loader. The other end was fitted with a removable end cap that attaches using three 4-40 cap head screws that are threaded into blind nuts fixed permanently into small wooden blocks. The three wooden blocks were glued to the side of the speed loader using 5-minute quick epoxy and the entire speed loader was sanded to give smooth surfaces for sliding into and out of the fuselage.

The team needed to manufacture 4 speed loaders: 2 for tennis balls and 2 for steel bars. In the two for steel, two small fiberglass pieces were added to slide the steel bars under and fix them into place to eliminate movement of the steel within the speed loader.

6.4 FUSELAGE

The design of the fuselage sections had to take into account design limitations based on the speed loader design. Because of the need for almost every bulkhead section to be cut for the insertion of the speed loaders, the team decided a composite material was necessary to give the fuselage the needed strength. Using skill matrix and cost as the major figures of merit, fiberglass/ epoxy was selected. The bulkheads were constructed from 3/32" balsa with a three plies of fiberglass laminated to each side. All the bulkheads, except for those where the front landing gear is mounted, were then cut for the speed loaders. Bulkhead placement was necessary to strengthen areas of high stress, specifically wing attachments, changes in shape, and landing gear attachments.

The frame was then constructed out of 3/16" balsa beams and covered using 1/32" balsa sheeting. Since the sheathing sections only provide a surface to mold the fiberglass/epoxy to and provide no structural strength, the smallest possible thickness of balsa was selected to lower the weight of the plane. The location of all servos and electronic equipment was carefully mapped out in order to ensure access hatches could be cut without compromising the strength of the fiberglass in the fuselage sections.

The fuselage will be fiberglassed and epoxied using three plies and oriented each in a specific manner. The first ply will be in a 0-90 grain direction with regards to the lengthwise direction of the fuselage, the second will be 45-45 and the third will be 0-90 again. The change in orientation of the grains of the second ply will give added strength in the diagonal direction since the composite is weakest diagonally to the grain, by orienting the plies in different directions, the entire composite will be stronger than if all the plies were oriented the same way. The fuselage will then be finished like the wing: primed and sanded smooth to minimize imperfections before finally being painted.

The rear of the fuselage was constructed separately in two pieces and each is attached using hinges and latched together. The two pieces swing open opposite each other and allow access to the speed loader compartment in the fuselage. Also, the speed loader compartment was lined with fiberglass/epoxy rails to slide the speed loader for easy insertion and removal. Rails were desired over sheathing the compartment because of weight and concerns with access to electrical components and servos.

6.5 TAIL

Like the fuselage, the horizontal and vertical tails were manufactured out of balsa, fiberglass, and epoxy resin. The tailpieces are assembled as a traditional wood wing and then covered in fiberglass and

the vertical tails are joined to the fuselage. Ribs will be cut out of 1/16" balsa and joined by an upper and lower spar at the quarter chord. The tails will then be sheeted with 1/32" balsa. A half inch gap will be cut at the hinge line and 1/4" balsa stock will be added to each section. The tail will then be fiberglassed w/ three plies of alternating 0-90, 45-45, and 0-90 oriented fiberglass and resin. The rudder will be joined to the tail w/ CA hinges and a control horn. The vertical tail will be attached to the rear of the fuselage with 30 minute epoxy resin. The horizontal tail is fitted between the two vertical tails and all pieces are painted.

6.6 SYSTEMS INTEGRATION

All servos are mounted on hardwood rails and located in the forward compartments and nose except for those controlling the ailerons, which are located in the wing. Pushrods are used to connect rudder and tail gear to the appropriate servo. The battery and receiver are wrapped in foam to reduce vibrations and are placed in a forward compartment.

Table 6.3 Manufacturing Time Schedule

Task	Target Date	Completed Date
Manufacturing Start Date	1/25/01	1/28/01
Fuselages Framed Up	2/7/01	2/7/01
Wing Ordered	2/7/01	2/15/01
Speed Loaders (initial)	2/14/01	2/16/01
Vertical Tail Assembled	2/16/01	2/16/01
Component Placement	2/21/01	2/16/01
Fuselage Interior Work	2/21/01	3/2/01
Speed Loaders (Final)	2/21/01	-
Wing Fiberglassed	3/9/01	-
Fuselages Fiberglassed	3/23/01	-
Horizontal Tail Assembled	3/28/01	-
Paint and Finishing	3/31/01	-
First Flight	4/1/01	-
Flight Test Modifications	4/1/01 – 4/18/01	-
Competition	4/20/01 – 4/22/01	-

References

1. Roskam, J. and Lan, C.; Airplane Aerodynamics and Performance; DARcorporation; Lawrence, 1997
2. Raymer, D.P.; Aircraft Design: A Conceptual Approach; American Institute of Aeronautics and Astronautics; Reston, 1999
3. Roskam, J.; Airplane Flight Dynamics and Automatic Flight Controls; Ottawa, 1979
4. Selig, M.; UIUC Airfoil Coordinates Database; http://amber.aae.uiuc.edu/~m-selig/ads/coord_database.html; University of Illinois; Urbana, 1995
5. Hibbeler, R.C.; Mechanics of Materials; Prentice Hall, Inc.; Upper Saddle River, 2000
6. Anderson, J.D.; Fundamentals of Aerodynamics; McGraw-Hill, Inc.; New York, 2001
7. Bruhn, E.F.; Analysis and Design of Flight Vehicle Structures; Tri-State Offset; USA, 1973
8. Calcfoil; <http://beadec1.ea.bs.dlr.de/Airfoils/calcfoil.htm>
9. Abbot, I.H. and Von Doenhoff, A.E.; Theory of Wing Sections; Dover Publications; New York, 1959



PROPOSAL FOR THE DESIGN OF AN UNMANNED AIR VEHICLE

Syracuse University

Reid Thomas, Project Leader

Victoria Garnier

Jessica Lux

Jeffery Robinson

Scott Todd

Eliza Honey

Renea LaRock

Michael Nagy

Michael Czabaj

Benjamin Nesmith

Brian Foo

Dr. V.R. Murthy, Faculty Advisor

Acknowledgments

The Syracuse University 2000/2001 Design/Build/Fly team would like to extend special thanks to:

Dr. Vadrevu R. Murthy
Professor, Syracuse University

Dr. Barry D. Davidson
Associate Professor, Syracuse University

Dr. Eric F. Spina
Associate Dean, L.C. Smith College of Engineering and Computer Science, Syracuse University

Syracuse University
L.C. Smith College of Engineering and Computer Science
Department of Mechanical, Aerospace, and Manufacturing Engineering

Syracuse University Composite Materials Laboratory

Any others who have helped us this year

Without the help, support and encouragement of those mentioned above, this year's plane would not have been possible. Thank you all for your support.

Table of Contents

Acknowledgments	i
Table of Contents	ii
7. Lessons Learned	1
7.1 Design Lessons Learned	1
7.2 Construction Lessons Learned	1
8. Rated Aircraft Cost	3
8.1 Rated Aircraft Cost	3

7. Lessons Learned

7.1 Design Lessons Learned

With the team architecture consisting entirely of underclassmen (no seniors), every step in the design process provided a new learning experience. The past two entries from Syracuse University have encompassed forward thinking designs, employing a Blended Wing Fuselage and a Control Canard with ducted fans. While these ideas were novel, and warrant future consideration, this year the team wanted to stay with a more classical approach. This allowed the team to compare sizes and parameters with previous work, thus providing a check that the team's sizing and performance calculations were within normal parameters. Continuing improvement was made in setting and reaching earlier goals in all sections of the design and construction phases. This helped, and continues to help ensure that errors relating to poor time management are reduced.

Past competition entries have encountered difficulties calculating accurate thrust and run time. The team attempted to reduce these errors this year. While MotoCalc was still utilized for the basic thrust and run time values, numbers produced were taken as initial values. A test bed was constructed in order to attain final thrust values, and to verify the MotoCalc data. The test bed proved to be very effective and showed the MotoCalc data to be within five percent of the actual thrust and run time numbers attained.

7.2 Construction Lessons Learned

The aircraft built is nearly identical to the one detailed in the report. No major elements of the design were changed; the only actual changes were made in rounding, in order to assume more convenient dimensions for construction.

The largest problem encountered with construction of this year's entry was with the structural weight. The initial weight estimation done for this year's design was done with past entries as reference. The hope was that by using composite materials the team would be able to meet, or perhaps lower, these values, leaving more weight available for payload. Unfortunately the aircraft's weight has turned out to be significantly higher than predicted.

During the fall semester the team constructed a payload test section. The goal of the test section was to validate the proposed manufacturing procedures and predict the weight of a composite section. The test section showed that the manufacturing process selected would indeed work, and was within the abilities of the team. However, this test section also helped lead to the predictions of low structural weight. In retrospect, this test section did not contain adequate information to provide weight data. Future designs would be better served with more accurate weight estimations. A very important part of next years design will be to work toward accurate weight estimation equations that are tailored towards Unmanned Air Vehicles (UAV's).

This year the team decided to again use a foam core, composite wrapped wing. Experience with these materials last year proved less than satisfactory, so improvements to the manufacturing process were made this year. Last year, the team discovered that vacuum bagging the wing had crushed the foam core. To avoid crushing the foam again, this year's wing was not vacuum bagged for curing. Last year's wing also had a large amount of twist due to the absence of structural support while curing. Therefore, more support was given to the foam structure while the composite material was being applied and cured. This produced an improved result. The final product maintained the wing dimension and airfoil cross sections specified. Also produced, however, were several wrinkles and bubbles in the fabric. These were highly undesirable, and as such were removed, and patched with further fabric. The overall effect of this was to reduce the strength of the composite. If this construction technique is used in future competitions, more refinement of the manufacturing process must be done. A possibility is to apply the composite to one side, top and bottom, at a time. Before this is done, however, a more detailed analysis of the structural effects would need to be done.

The work with composites on this aircraft has also been a relatively new experience for the team. Current team members only experience with composites had been with last years failed wing. The wing and booms for this year's aircraft have proved very challenging. Despite creating a test section for the booms, and working on the wing last year, many small adjustments needed to be made during fabrication to allow the fabric to follow the contours of the wing and booms. The improvisation needed to complete these tasks allowed the team to gain a much greater understanding of the possibilities composites offered, as well as the limitations of working with them.

Because various team members posses different degrees of manufacturing skills, areas that required more precision were left to those with previous building experience. However, this still led to some difficulties during construction. With multiple hands constructing delicate parts such as the tail surfaces; maintaining construction continuity became very difficult. Future years can benefit from more comprehensive manufacturing plan, detailing which team members are responsible for constructing specific parts of the aircraft.

Another goal that the team attempted to reach this year was finishing all aspects of the design, and most importantly the construction, sooner than in past years. This year the team was very successful in meeting this goal. However, this can still be improved upon. The sooner the process is completed and the aircraft is flight worthy, the sooner performance tests can begin. These tests help to establish how closely the aircraft behaves as compared with the predictions. This also allows time for any modifications needed to achieve optimal performance. The project timeline will always be a critical goal to maintain.

8. Rated Aircraft Cost

8.1 Rate Aircraft Cost

The basis for the Rated Aircraft Cost (RAC) is a guideline for developing a more efficient aircraft. The formula for calculating the RAC is specified in the competition rules. The Rated Aircraft Cost the DGT is **7.944**. Table 8.1 details the multipliers called for in the RAC formula.

Table 1.1 Rated Aircraft cost breakdown

Variable	Definition	Value
A	Manufacturers Empty Weight Multiplier	\$100/Lb
B	Rated Engine Power Multiplier	\$1/Watt
C	Manufacturing Cost Multiplier	\$20/Hr
MEW	Manufacturers Empty Weight	10.4
REP	Rated Engine Power	3648
MFHR	Manufacturing Man Hours	162.8
TOTAL		\$7,944

The Manufacturing man hours, Work Breakdown Structure (WBS), is further broken down in table

8.2

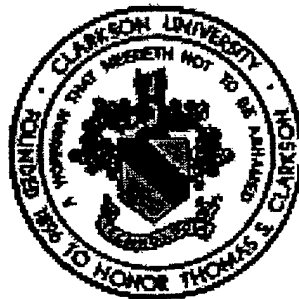
Table 8.2 Work Breakdown Structure

WBS	Subsection	Man Hours
Wing	Basic	15
	Area	42.44
	Strut/Brace	0
	Control Surface	6
Fuselage	Basic	10
	length	23.36
Empenage	Basic	5
	Vertical Surface	10
	Horizontal Surface	10
Flight Systems	Basic	5
	Servo	16
Propulsion	Motor	10
	Props	10
Total		162.8

AIAA Design Build Fly Competition

CLARKSON UNIVERSITY

Knight Hawk



Proposal Phase

Table of Contents

1. Executive Summary.....	4
1.1 Summary of Development	4
1.2 Alternative Designs	4
1.3 Design Tools	5
2. Management Summary	7
2.1 Architecture of the Knight Hawk Design Team	7
2.2 Assignment Areas.....	8
2.3 Milestone Chart	8
3. Conceptual Design	11
3.1 Alternative Designs.....	11
3.2 Design Parameters Investigated	13
3.3 Rated Aircraft Cost	14
4. Preliminary Design	15
4.1 Design Parameters	15
4.2 Airfoil Selection	15
4.3 Center of Gravity	17
4.4 Thrust and Weight	17
4.5 Overall Aircraft Layout	17
5 Detail Design	19
5.1 Data Analysis and Flight Performance Predictions	19
5.2 Predetermined Economical Flight Pattern	21
5.3 Stability and Control.....	22
5.3.1 Direction Stability and Control.....	26
5.3.2 Roll Stability and Control.....	28
5.3.3 Dynamic Stability Derivatives.....	30
5.3.4 Stability of Longitudinal Motion	30
5.3.5 Stability of Lateral Motion.....	32
5.4 Structural Analysis	34
5.5 Component Selection	41
5.6 Final Aircraft Configuration	42
6. Manufacturing Plan	43
6.1 Alternative Building Materials.....	43
7. Drawing Package.....	45

1. Executive Summary

1.1 Summary of Development

The Knight Hawk project for the Design, Build, Fly Team of 2000-2001 started with the fall 2000 semester at Clarkson University. The project is an extracurricular activity at Clarkson University, comprised of undergraduate students at all levels of education. The team's development of the aircraft was divided into two stages, which include the design and analysis phase, and the manufacturing stage. The conceptual design phase determined the aircraft configuration by weighing benefits versus costs for several proposed configurations. The team reduced the configuration possibilities to an improvement of the previous year's twin-fuselage canard design or a single fuselage canard configuration. While a conventional design provided a rather easily constructed and stable design, the team wished to challenge itself with a less common configuration as a means to learn more about aircraft design.. After a cost/benefit review of the two configurations, the single fuselage canard configuration was chosen. After selection of the aircraft type, the team moved into the preliminary design phase. The majority of the fall semester was used to perform analysis on the potential design and obtain the optimum configuration for the mission specifications.

With the completion of the detailed design phase late in the fall semester, construction began before the end of the semester. Upon the initial construction a plywood fuselage two team members discovered a new fuselage type which decreased the empty weight while making attachment points and the fuselage more resistant to forces and moments encountered in flight. With the start of the spring 2001 semester construction resumed. The team continued to make modifications to the aircraft and solve problems encountered when moving from the design phase to the manufacturing phase. The semester was also used to prepare the necessary reports for the competition and test the aircraft's actual performance and stability characteristics in flight.

1.2 Alternative Designs

The production of adequate lift to minimize takeoff distance and maximize payload capacity was the major driving design parameter. To produce an aircraft that has a limited wingspan and limited amount of power available, lifting surface configurations took the highest priority in the design research. Larger wing area would reduce the wing loading, thereby decreasing the stall speed. Since a lower stall speed decreases the takeoff speed, less power is required during the takeoff run. Takeoff is the active constraint when sizing motor power so a smaller motor can be used. The decrease in weight results in less required lift.

Several configurations were chosen for evaluation based on historical cases, namely the canard, conventional high wing, conventional low wing, biplane, wing body, and tandem wing. Primary concerns were lifting area, flight stability, airframe strength, ease of construction and propulsion integration. Other lesser concerns included maneuverability and drag. The team selected the canard configuration during the conceptual design. The possibility was left open for a three-surface configuration. It was believed that a stable, controllable aircraft could be made with the canard or three-surface aircraft. Historical examples of these types of aircraft were cited, such as Burt Rutan's designs. Both model and full size aircraft in these configurations have been flown successfully.

During the preliminary design phase, the airfoil was chosen for both wings, the fuselage layout was constructed and motor research was conducted. During the latter part of the preliminary design phase, a new fuselage concept was suggested. After a short time of weighing the advantages and disadvantages of the new configuration it was decided that an aluminum backbone fuselage was a more light weight design and it was adopted.

Detailed design included structural layout of the aircraft, final motor and battery selection and final sizing of control surfaces. It was decided that a hot-wire foam cutting technique would be the easiest manufacturing method and would produce accurate wings. A hot-wire cutter was constructed and tests were carried out to confirm its validity as a construction technique. The hot-wire method produced wings that were within design tolerances in planform and cross-section. The wings were constructed of Styrofoam with an aluminum spar. The fuselage was also made of aluminum. One AstroFight 90 engine was selected for propulsion. Forty sub-C NiCad cells were to be connected in series with the motor. The final aircraft had a payload capacity of 88 tennis balls, a canard configuration with an expanding fuselage between the wing and canard.

1.3 Design Tools

Several computer-based design tools were employed to aid in the different stages of the aircraft development. Among them were:

- Microsoft Excel
- Computervision DesignView
- Autocad 2000
- X-Foil by Mark Drela
- Laminar Research X-Plane
- ANSYS

Microsoft Excel was used to compute lift and drag data, set up center of gravity calculations, and size the tail fins and control surfaces.

DesignView is a parametric 2-dimensional drawing program that was used for wing and fuselage layout. Its programming features allowed for the resizing of the airframe by a simple change of one dimension. It was also used to calculate the neutral point for the aircraft.

Autocad was used to provide a 3-dimensional view of parts to be constructed. It aided in the construction process by providing a real-life simulation of part fitting.

X-Foil is a unix/X-windows based 2-dimensional airfoil analysis software. It provided a numerical estimation for various proposed airfoils. It was used to compute lift, drag and pitching moment in both viscous and non-viscous flow modes.

Laminar Research X-Plane is a software package that provides a design environment to create an aircraft and a flight simulator to test the aircraft. The software allows for the entry of drag data; airfoils; wing, fuselage and empennage geometry; center of gravity and propulsion placement and size. Using blade element theory the code breaks the aircraft down, performing aerodynamic calculations 15 times per second. The code also includes data output that allows the designer to see the motion of the aircraft. Several variables can be output to determine the stability and performance of the design. Also, many different aircraft views are available to allow the pilot to fly the aircraft from the exterior. The program was used to train students in the operation of model aircraft.

ANSYS is a finite element software package that allows users to generate parts or an entire model and apply forces, moments and other components in order to test bending, rigidity and strength. The software was useful in determining strength and rigidity in the aircraft.

2. Management Summary

2.1 Architecture of the Knight Hawk Design Team

The team was comprised of several members with varying commitment and knowledge. Past years had seen the team split into various groups such as configuration, performance, aerodynamics and propulsion but this created scheduling conflicts. This year a consensus from the general membership wished to organize the team as whole. During the preliminary and conceptual design phases the team the team leader acted as chief engineer and assigned research areas to fellow team engineers. The research results were presented to the entire team at meetings where designs decisions were made. The team leader's responsibility was to facilitate the integration of design decisions into a final design and to allow all team members to contribute ideas, thoughts and experiences.

J. Wayne Braun, a senior Aeronautical Engineer was chosen as team leader because of his past experiences with both the DBF competition, leadership on campus and senior experience. Wayne organized all meeting, was involved heavily in the design and sizing process, purchase and obtained components and headed construction.

Annie McLaughlin, a junior Aeronautical engineer acted as the team's financial manager. She ensured the group was staying within budget as well as obtaining funds for the team to operate from.

Tara Fornaro, a senior Aeronautical engineer documented the design process of the aircraft. This was vital as it was used to create the proposal. She also helped to obtain material for the aircraft.

Aroosh Naqvi, a freshman Aeronautical engineer was vital in research and development. Aroosh gathered information on the possible power plants and power supply for the aircraft. After selection of these components Aroosh coordinated the purchase of them.

Chuck Trail, Elizabeth Kenney, Mark Harrison, Jason Kuntz, Russ Zea, Daniel Van Ness, and Jason Camps contributed in the analysis and construction of the aircraft. These members were greatly involved in the project, spending many hour to ensure the completion of the aircraft.

Dr. Ken Visser, a professor in the Mechanical and Aeronautical Engineering Department at Clarkson University and graduate student Matt Duquette served as advisors for the Knight Hawk team.

2.2 Assignment Areas

The team produced six assignment areas for the design and analysis of the aircraft. These areas included stability and control, performance, configuration, aerodynamics, propulsion and power supply, and structures.

The stability and control area was assigned to J. Wayne Braun and Jason Camps. Wayne utilized Excel to model the aircraft with a simplistic method for the preliminary design while Jason used the X-plane software to generate a more complex model for the detailed design. The X-plane software allowed Jason to actually fly the plane and provided several modes of analysis and output for the aircraft.

The area of performance fell under the analysis and modeling of Jason Camps in the X-plane software. Using the X-plane software he insured that the performance specifications met the mission specifications.

The configuration area was assigned to J. Wayne Braun as chief engineer he oversaw the integration of the different component of the aircraft. Wayne also facilitated communication between groups to incorporate different designs.

The aerodynamic assignment area was given to Mark Harrison who investigated potential airfoils and the different aerodynamic advantage of each potential design. He also oversaw and managed the possible aerodynamic interference of the pusher prop, canard and wing along with the vertical tail and control surfaces.

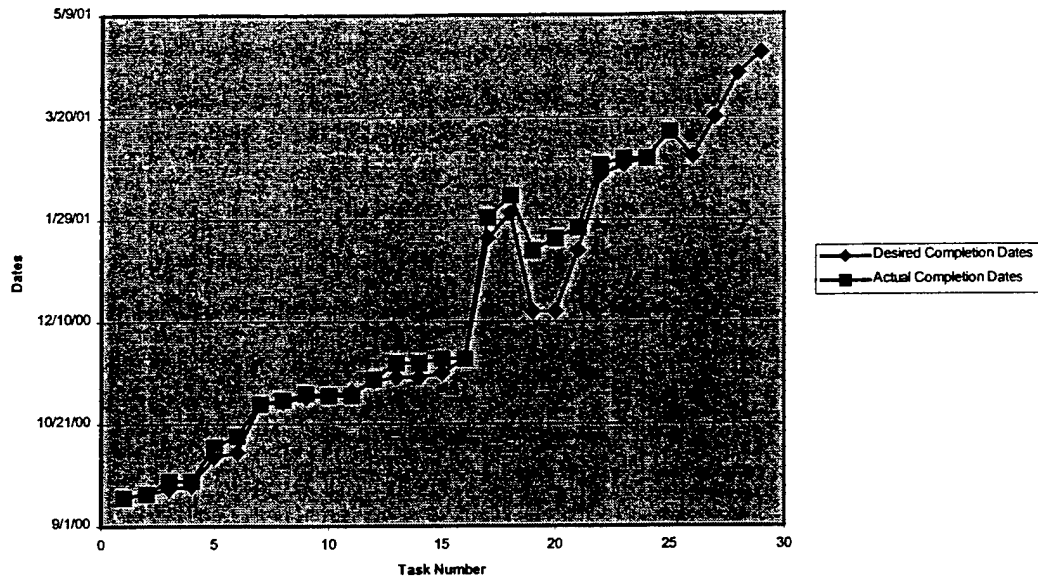
The propulsion and power supply area was assigned to Aroosh Naqvi and Charles Triall. These two members coordinated the research and gather of both the propulsion and power supply for the aircraft. These members also were vital in the integration of both the engine and battery packs into the desired design.

The structure area was given to Mark Harrison and Elizabeth Kenney who performed structural analysis on the aircraft utilizing ANSYS software. These reports gave insight into forces and moment experienced by the aircraft and provided information to prevent aero elasticity in the design.

Though these areas were assigned to certain team personnel, the team as a whole actively communicated with each other providing and included every member in each area of assignment.

2.3 Milestone Chart

The Milestone Milestone Schedule and Completion Chart in Figure 2.1 plots the progress of the Knight Hawk Program.



	Event	Desired Date	Actual Date
1	Begin Conceptual Design	9/15/00	9/15/00
2	Wing Concept	9/17/00	9/17/00
3	Fuselage Concept	9/19/00	9/23/00
4	Empennage Concept	9/21/00	9/23/00
5	Conceptual Design Complete	10/5/00	10/10/00
6	Begin Preliminary Design	10/7/00	10/15/00
7	Submit Electronic Entry Form	10/31/00	10/31/00
8	Preliminary Design Complete	11/1/00	11/2/00
9	Begin Detailed Design	11/3/00	11/5/00
10	Hot Wire Test	11/4/00	11/4/00
11	Construction Tests	11/6/00	11/4/00
12	Detailed Design Complete	11/11/00	11/12/00
13	Start Construction	11/13/00	11/20/00
14	Wing Construction Started	11/13/00	11/20/00
15	Canard Construction Started	11/15/00	11/22/00
16	Fuselage Construction Started	11/22/00	11/22/00

17	Vertical Tail Construction Started	1/20/01	1/30/01
18	Landing Gear Construction Started	2/1/01	2/10/01
19	Wing Construction Completed	12/15/00	1/14/01
20	Canard Construction Completed	12/15/00	1/20/01
21	Fuselage Construction Completed	1/14/01	1/25/01
22	Vertical Tail Construction Completed	2/20/01	2/25/01
23	Landing Gear Construction Completed	2/25/01	2/28/01
24	Final Assembly Completed	2/28/01	2/28/01
25	Proposal Phase Due	3/13/01	3/13/01
26	Rollout	3/1/01	
27	Testing Complete	3/20/01	
28	Addendum Phase Due	4/10/01	
29	Competition	4/20/01	

Figure 2.1: Milestone Schedule and Completion Chart

3. Conceptual Design

3.1 Alternative Designs

The conceptual design is inherently an iterative process. The team assessed the requirements and restrictions to brainstorm different designs that may be best suited for the competition.

The following configurations were considered:

- Canard
- Conventional High Wing
- Conventional Low Wing
- Biplane
- Wing Body
- Tandem Wing

The team felt that these configurations represented a sufficiently diverse pool of aircraft to evaluate and that they had potential to meet the objectives at hand. Table 3.1 shows the Figures of Merit.

Table 3.1 – Figures of Merit

Figures of Merit		1	2	3	4	5	6
3	Produced Lift	2.60	1.80	1.75	2.75	2.50	2.75
2	Stability	1.60	1.75	1.50	1.45	0.55	0.50
2	Ease of Manufacturing	1.50	1.30	1.60	0.25	1.00	0.75
2	Cost	1.00	1.25	1.10	0.50	0.75	0.45
1	Design Simplicity	0.60	0.50	0.50	0.55	0.50	0.25
10	Total	7.30	6.60	6.45	5.50	5.30	4.70

1. Canard
2. Conventional High Wing
3. Conventional Low Wing
4. Biplane
5. Wing Body
6. Tandem Wing

The canard configuration was chosen because it received the highest score based on the merit system. The major attraction of this design is that it is a double lifting surface where on conventional aircraft the tail acts as a down lifting surface. The selection on a non-conventional design was chosen to differentiate the Knight Hawk team and continue the team's history of unique designs along with a design that would challenge the Clarkson design team. Note that design 6 is the previous design of the Clarkson DBF team. Improvements on last years design was also considered because the methods and analysis were already performed however it scored lowest in the merit system and was determined to be inadequate.

3.2 Design Parameters Investigated

The following parameters were investigated:

- Fuselage Size and Configuration
- Propulsion Type and Integration
- Tail Configuration
- Wing Placement and Configuration
- Payload Access

The fuselage size and configuration was a major concern for the team. There were fears of not able to hold enough payload or be able to load the payload quickly. The underlying problem was in order to make the time during the flight; components need to be out of the way for the payload to be put in easily and quickly. It was also taken into consideration that the fuselage might also be able to generate extra lift and help carry more payload. The configuration was also a major concern for the team. There was discussion about whether to use a box configuration or a backbone for the fuselage. A box configuration would be easier for carrying the payload and components. But it would also add weight, thus affecting the amount of lift needed to get the plane in the air. A backbone configuration would be much lighter but would also make it harder to carry the payload and components.

Another consideration was the propulsion. The type and configurations were discussed because they both would affect the overall weight of the plane and the center of gravity. One discussion was over the number of motors to use, one or two. A cost/benefit study was performed to weigh the weight versus thrust gain in a two motor configuration. Furthermore, the team discussed propeller configuration. The merits of pusher and tractor propellers were discussed and the pusher configuration was chosen. The team decided to plan for the possibility of two motors, one in pusher and another in puller configuration centerline with the fuselage.

The team also considered the tail configuration. Both a conventional and canard configurations were investigated. Tail configuration is important because it affects the stability of the plane. The canard configuration would be less stable longitudinally. The conventional would be more stable longitudinally. But the canard adds more lift to the entire airplane whereas with the conventional configuration the horizontal tail subtracts to from the lift.

The team also spent a lot of time considering the wing placement and configuration. A canard, tandem, conventional high wing, conventional low wing, flying wing and biplane configuration was considered. Each of these configurations is stable though some are more stable then others. The amount of lift is also affected by the configuration. Once the team had decided on a configuration wing placement was

discussed. The placement of the wing causes the lift, stability and center of gravity to change. It would also vary the space we had to carry the payload and components.

The last parameter that was investigated was the accessibility of the payload. The payload needed to be easily accessible and quickly removable. This is because of the time constraint on the flight at the competition. The team brainstormed on how to place the payload so that we could remove and switch it easily. The fuselage would also need to be designed so that the payload was easily accessible.

3.3 Rated Aircraft Cost

The aircraft cost was not a determining factor in the team's choice of a configuration since the costs were determined to be relatively similar. A flying wing had the lowest cost, but it would not be worthwhile to reduce the cost and sacrifice the ability to meet the contest objectives.

<u>Configuration</u>	<u>Cost (Thousands of \$)</u>
Canard Configuration	8.60
Conventional High Wing	8.40
Conventional Low Wing	8.40
Biplane	8.50
Flying wing	8.30
Tandem Wing	8.50

4. Preliminary Design

4.1 Design Parameters

Several design parameters were considered in the preliminary design of the aircraft. These included:

- Airfoil Characteristics
- Stall characteristics
- Lift to Drag Ratio
- Wing Loading
- Location of Center of Gravity
- Payload
- Thrust to Weight Ratio
- Overall Aircraft Layout

4.2 Airfoil Selection

With lift being the major consideration for the competition, much effort needed to be invested in wing design. Airfoils on the University of Illinois online airfoil database were evaluated using an online airfoil analysis code written by Martin Hepperle. Design requirements called for an airfoil that had good lift characteristics (a C_{lmax} of about 1.8) at low speed (approximately 25 mph). Also the low drag high thickness to chord ratio and gentle stall characteristics were desired. Several airfoils were investigated as candidates for the wing. Some included the DAE-11, the Selig 4180, and the NACA 6412. The one that met most of the design requirements was the NACA 6412. It had the highest C_l -AoA curve and the better drag polar at high values of C_l . The lift-to-drag ratio also was the best among the possible choices. This is important because the less drag there is, the less power that will be needed to take off. Also with the low increase of drag with lift, it will provide a smoother transition into a stall, thus allowing the pilot to regain control easier. Aspect and taper ratio combinations were examined in an effort to create an elliptical lift distribution and thus make the plane more stable in low cruise speeds.

Characteristics of NACA 6412 Airf
(Re = 300,000)

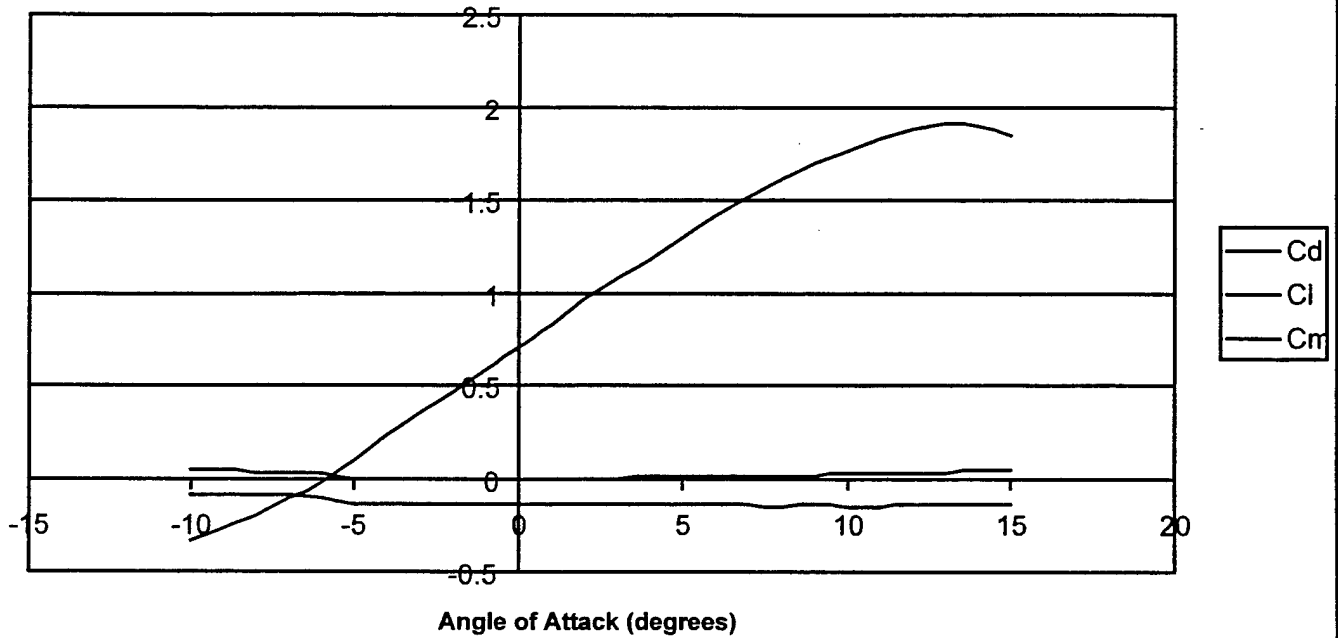


Figure 4.21: Characteristics of a NACA 6412 Airfoil

4.3 Center of Gravity

Wing loading and the location of the center of gravity were considered most from a point of view concerning stability and control. It was determined that placing the wing load closest to the mid span and as close to the main wing spar as possible would ensure small amounts of center of gravity travel for different loading configurations. However, this would affect the location of the center of gravity, which would most affect the stall characteristics. It was decided that center of gravity was most important in determining the placement of the payload and the battery locations, the heaviest pieces of gear to be carried. The five pound limit of batteries meant that a motor needed to be chosen that would produce enough output for the design the design points for the competition.

4.4 Thrust and Weight

The thrust of the plane is an essential factor in airplane design. During straight and level flight, the thrust and the weight are equal at a constant speed. This fact helped in the choosing of the correct motor. Because of the restrictions in the competition the only electric motors could be used. They also had to be commercially available. The two companies that could be used, set forth by the competition, were either Astroflight or Graupner. After several meetings it was decided to go with the Astroflight Cobalt 90 with 714 Superbox. Software was used to help evaluate the 2 motors. Points of interest for the motor were the torque, max thrust, amount of batteries to power the unit, gearboxes, and the efficiency factor. Battery configurations and propellers were also considered during the motor selection. The Cobalt 90 engine was chosen because it gave optimal thrust while minimizing battery drain for the ten-minute flight.

4.5 Overall Aircraft Layout

Main alternatives for the final layout of the aircraft were scrutinized. It was decided to go with the canard frame with the motor located in the tail. The size of the canard used was to be much smaller than the main wing. This is to decrease the drag from the canard and to keep the downwash from it small enough were as not to affect the flow over the main wing. The location of the payload was going to be attached to the underbelly of the aircraft. It acts like an external drop tank where during the dry flight. When the payload needs to be added, this method of carrying is quick and simple to attach. It allows for the tennis balls to be preloaded in to the payload box, taking only seconds to secure to the aircraft. This method reduces the size of the fuselage; amount just needed to carry radio gear and batteries. This reduction in the fuselage reduces the overall cost of the plane. It also reduces the Drag due to the fuselage components. Another way to reduce this would to use the Area Rule combining the fuselage more with the wing, slimming the overall size of the fuselage down more towards the tail providing more wing area.

The disadvantage of this configuration was if the canard were located too close to the main wing the flow across the main wing would be disturbed. This disturbance would produce increased drag. It might also cause the flow to separate earlier and therefore produce stall. The disadvantage for the drop payload was that it contributes more surface area which to produce drag. If the payload was housed inside the fuselage, the drag might be slightly reduced.

5 Detail Design

5.1 Data Analysis and Flight Performance Predictions

A detailed drag analysis was performed in order to predict longitudinal dynamic stability, power requirements in all phases of flight, and takeoff distance. The drag analysis can be seen in its tabulated form in Table 5.1.

Table 5.1 – Drag Analysis

Drag Analysis			
	C _d	Area (ft ²)	Drag Area
Fuselage	0.3000	0.50	0.15000
Canard	0.0294	4.0	0.11760
Wing	0.0294	20.0	0.58800
Tail	0.0100	0.03878	0.00039
Gear	2.0000	0.04167	0.08333
Sub Total		24.58045	0.93932
Interference		10%	
Total		Drag Area -> 1.03325	

Wing drag was based on 2-dimensional wing theory as determined by Calcfail, corrected for 3-dimensional effects. An interference drag addition of 10% was added to the overall drag estimation. The estimated drag in cruise flight at a zero angle of attack is approximately 2.9 lbs at 35 mph. The drag was cross-checked using Motocalc's built-in drag estimation feature. Motocalc's model is limited, not allowing for the analysis of a canard. A model was configured as a monoplane with an equivalent wing area of the canard and the wing of our aircraft. Despite the difference, Motocalc results showed drag within 10% of the analytic values at stall speed. Fuselage drag data is based off a report published by Hewitt Phillips and Bill Tyler, "Cutting Down the Drag." A series of tests in an MIT wind tunnel provided data for several model aircraft shapes. An interpolation between the different shapes was used to estimate the drag coefficient for the fuselages of the aircraft. Landing gear was assumed to be a flat plate. The vertical tail was considered a NACA 0004 airfoil due the leading and trailing edge taper.

Due to a peculiarly reward placing of the wing, Center of gravity positioning and stall speed was a major concern throughout the design of the aircraft each having drastic affects on its degree of controllability, motor selection, takeoff distance and turning radius. The stall speed was determined using a stall speed equation as provided in Anderson's text. With the full payload a stall speed of 18 mph was calculated.

A takeoff analysis, based on McCormick's method, shows a zero-flap liftoff occurring at approximately 123.5 feet. This is assuming a rotation initiation at a distance of 60 feet and a constant rotation throughout the remainder of the takeoff run. This results in an angle of attack between 9.5 and 10 degrees for the zero flap case. The analysis was performed using drag data obtained from the report mentioned above; drag and lift data from Calcfoil, and the takeoff equation and rolling resistance values as presented by McCormick. As calculated, the takeoff roll takes 6.75 seconds to complete. Takeoff analysis shows that runway departure speed is approximately double the calculated stall speed. The analysis does not take into affect the drag reduction and the lift enhancement from ground effect. The ground roll may be reduced by 5 to 10 percent in reality due to ground effect.

Using turn analysis from Anderson, the turn radius at a load factor of 1.2 it is 64 feet. For a load factor of 1.5 is 47 feet. Since stall speed increases by the square root of load factor the stall speed in a fully loaded configuration increases to 25 mph at a load factor of 1.2 and to 28 mph at a load factor of 1.5. The bank angle of a 1.2 g turn is 34 degrees. That increases to 48 degrees at a load factor of 1.5. This analysis was used in the flight pattern analysis described below. A summary of the turning Analysis can be seen in Table 5.2.

Table 5.2 – Turning Analysis

Turning Analysis			
n	ϕ (Rad)	ϕ (Deg)	Vel. Increase (%)
1	0.000	0	0.0
1.1	0.430	25	4.9
1.2	0.586	34	9.5
1.3	0.693	40	14.0
1.4	0.775	44	18.3
1.5	0.841	48	22.5
1.6	0.896	51	26.5
1.7	0.942	54	30.4
1.8	0.982	56	34.2
1.9	1.017	58	37.8
2	1.047	60	41.4

5.2 Predetermined Economical Flight Pattern

A power schedule was defined so as to maximize flight endurance with installed battery pack. The analysis was based on the published flight course, the turning analysis performed above and values that are obtained from the program Motocalc. Amperage ratings were used to determine total battery draw to maintain both level flight speed and turning radius. The course has an initial full throttle period of 20 seconds to allow for take-off roll and climb-out, which completes the upwind leg of the flight. Once at a safe altitude, a turn to downwind is performed at 75% power and 1.2 g. Power is kept at 75% to build airspeed for the 360-degree turn scheduled half down this leg of the flight. The downwind 360 degree turn is performed at 85% power and 1.5 g. The final downwind section of the flight will be flown at a maximum of 75% power, with reduced power depending on wind conditions. The final turn or base leg is performed at 25% power for 15 seconds and 1.2 g. The remainder of the flight is completed at minimum required gliding power. The total power use during a single sortie is 26 Amp-minutes. The full capacity of the 1900 mAh batteries is 108 Amp-minutes. The analysis is performed for a fully loaded aircraft (87 tennis balls). Twenty-four percent of the battery pack capacity is used in a single fully loaded water-carrying sortie. The total time aloft is estimated to be 1 minutes, 15 seconds. The estimated distance is 2700 feet. The course is flown at 30 mph except the takeoff run and the gliding phase to landing. An empty sortie would lack the downwind 360-degree turns. This results in a flight path that is 2400 feet.

Since two laps are needed for the ferry sortie, the total distance traveled is 4800 feet. Two minutes, ten seconds are needed to complete the full sortie. The energy used is 43 Amp-minutes. This is 40 % of the battery pack capacity. Hence, A full-load sortie and a ferry sortie consume 64 % of the battery pack. By this analysis, the flight periods can be performed in a cargo-ferry-cargo pattern or a ferry-cargo pattern on a single charge. Endurance calculations are included in Table 5-3.

5.3 Stability and Control

The lift-curve slope of the wing and horizontal tail were determined in 2-D then corrected for the 3-D values. Using C_l/C which is .25 for the Knight Hawk. The values of $(C_{l\delta})_{theory}$ from the figure was found to be 3.7 per rad for the 3-D corrected case. The value for the 3-D elevator effectiveness was then computed to be .058 per rad.

Because this aircraft not conventional the downwash parameter was computed as if the aircraft had a conventional tail. The downwash was also computed for the aircraft using the same equation as a conventional tail. The value obtained assuming this was a conventional aircraft is a downwash of .0097 per rad-ft and in the canard configuration it is .012 per rad-ft.

The aerodynamic centers for both the wing and the canard were calculated using the equation below. Enter a span of 10 and 4 for the wing and canard respectively yields an aerodynamic center of 1.67 ft for the wing and .67 ft for the canard. These values seem to aft under the assumption that the on most surfaces the MAC is located at 25% of the chord.

The aircrafts neutral point and longitudinal stability was computed by ignoring body effects. The calculated neutral point for this aircraft is .88 ft from the leading edge. The longitudinal stability $C_{m\alpha}$ was calculated using the following equation. The Knight Hawk has a longitudinal stability ($C_{m\alpha}$) of -0.029 .

The coefficient of lift as a function of the angle of attack was plotted using the following correlation equation. The plot generated was for a range of angles of attack from -5 deg to 15 deg for an elevator deflection of -10 deg, 0 deg, and 10 deg. The plot is displayed in Figure 5.31 below.

The pitching moment coefficient was computed as a function of angle of attack for three different elevator deflections -10 deg, 0 deg, and 10 deg respectively. Figure 5.32 displays the result of the function with the three different elevator deflections.

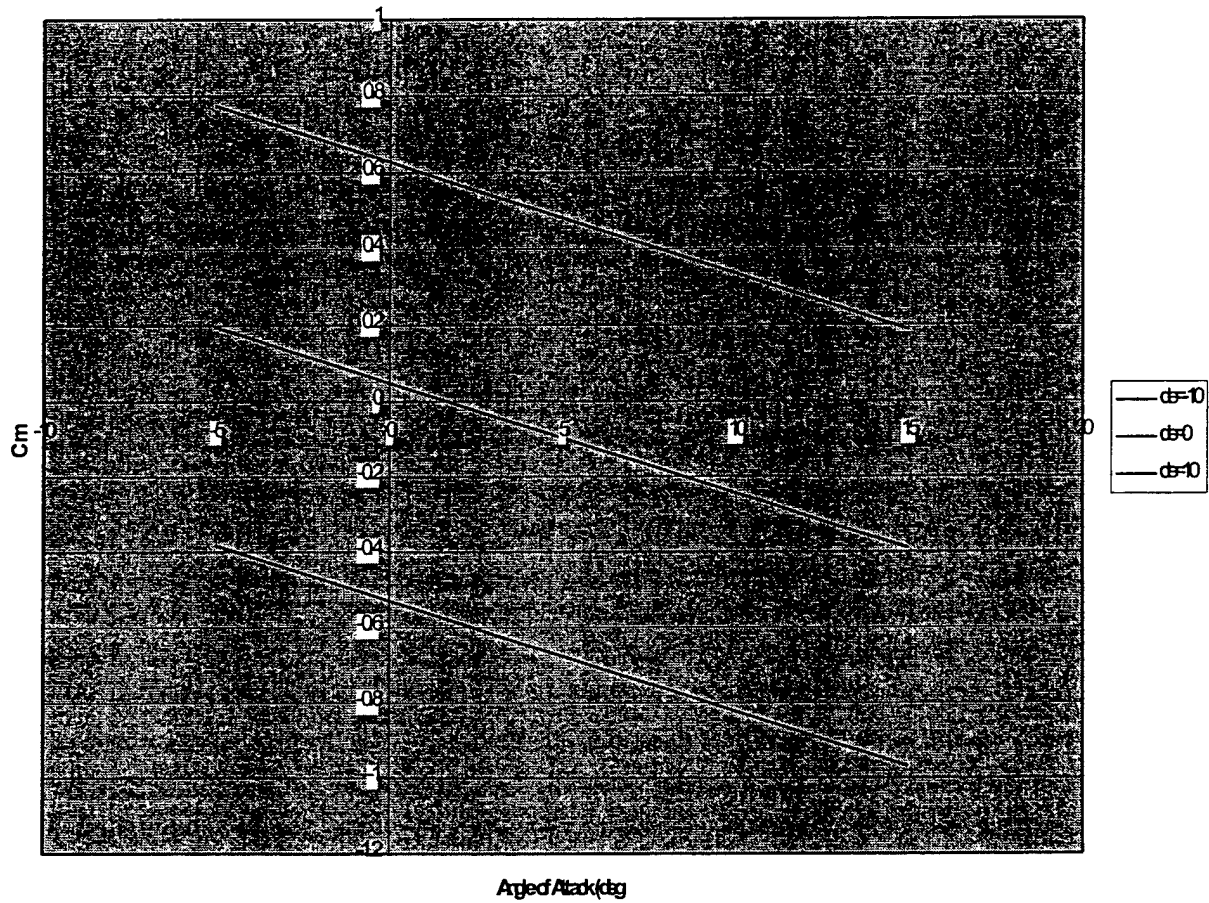


Figure 5.32: C_m vs. AOA

The coefficient of pitching moment decreases with an increase in angle of angle of attack. The coefficient of pitching moment shifts upwards with a positive deflection of the elevator. This trend is conducive to a stable aircraft.

The deflection trim was calculated as a function of angle of attack. This trimmed deflection is when the pitching moment is equal to zero.

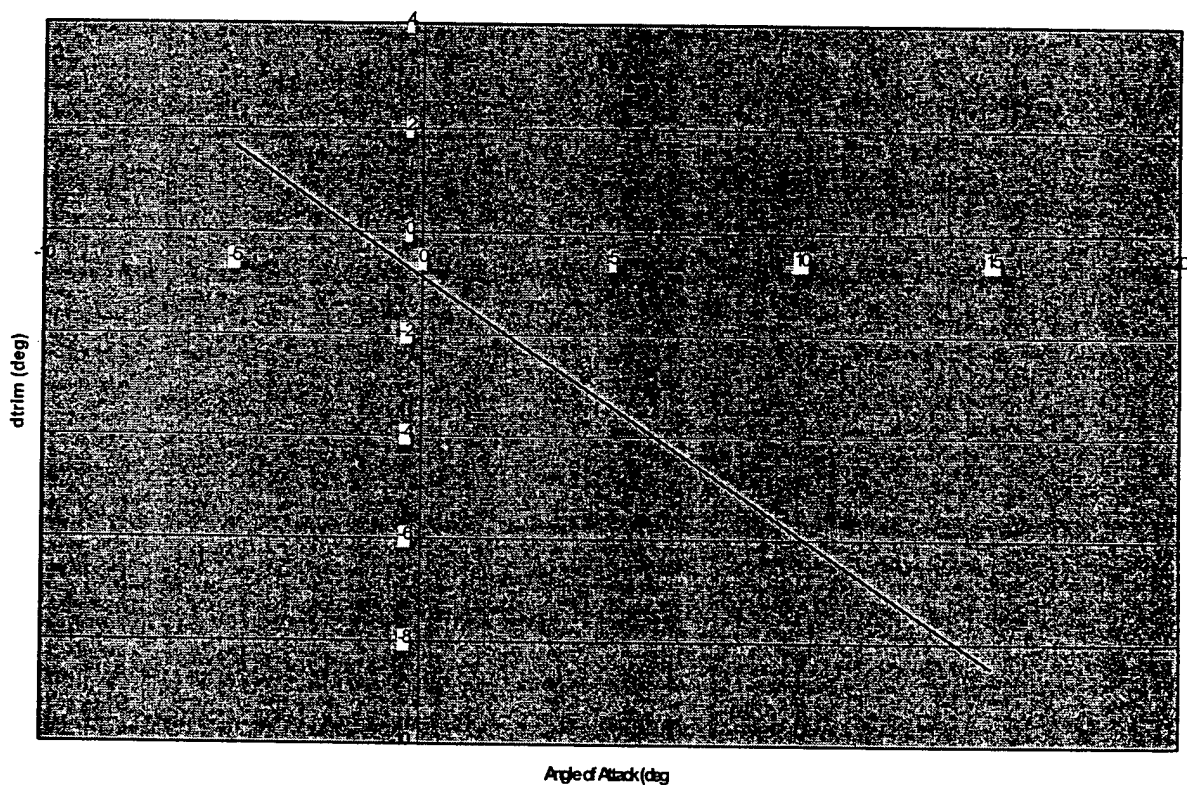


Figure 5.33: d_{trim} vs. Angle of Attack

The trimmed deflection is negatively increasing as the angle of attack increases. These calculations are based on a traditional aircraft. If this graph were to display a canard configuration the trimmed deflection would increase as the angle of attack increased because the canard is mounted in the front of the aircraft

and acts as a lifting surface. The horizontal tail on traditional aircraft actually experience a down force and canard experience an upward force due to their placement,

The coefficient of lift with respects to the trimmed condition was computed as a function of the angle of attack from 0 to 12 deg. Where the trimmed deflection for each angle of attack was found in the previous calculation and plotted in Figure 5.33. Figure 5.34 plots the relationship above for $0 < \text{angle of attack} < 12$.

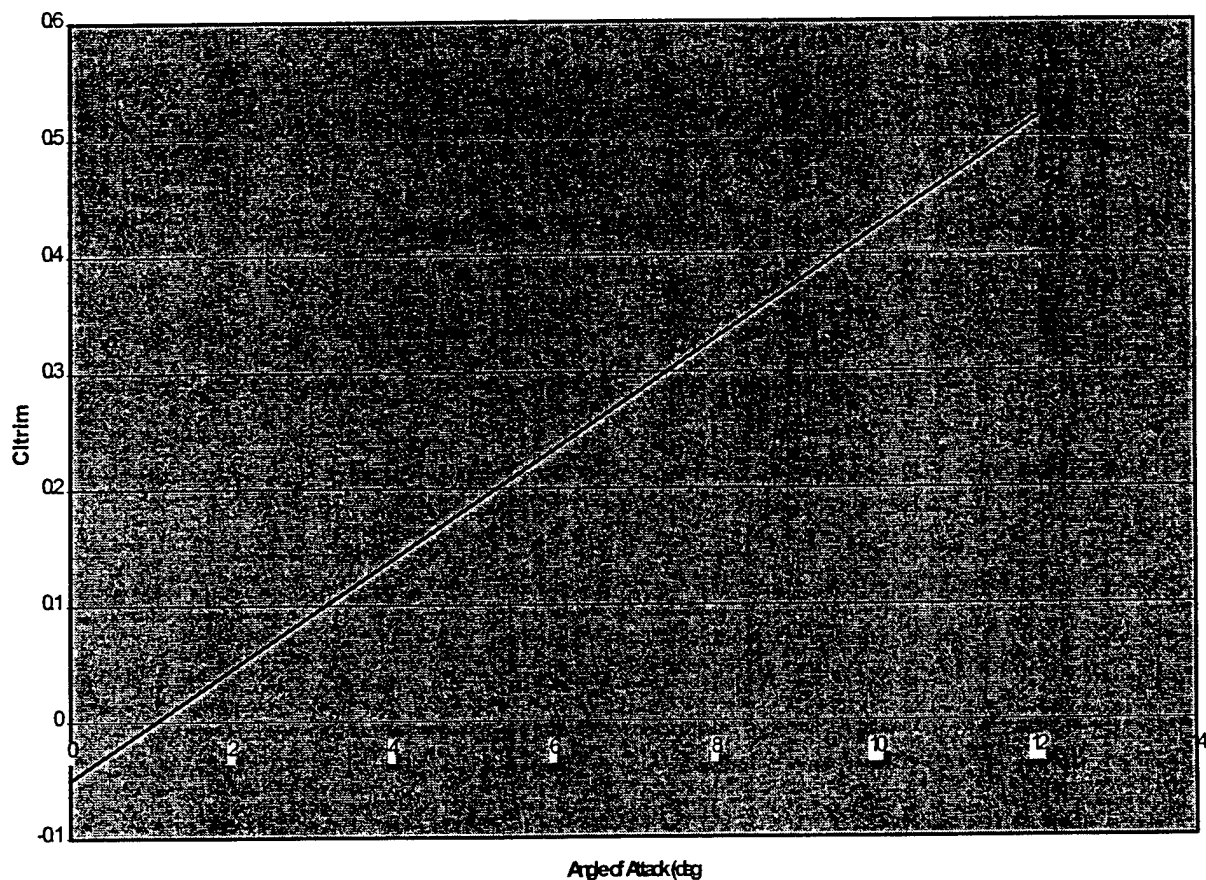


Figure 5.34: C_{ltrim} vs. Angle of Attack

The coefficient of lift for the trimmed condition increased with an increase in angle of attack. This graph displays the coefficients of lift for the aircraft when there is no pitching moment on the airplane.

5.3.1 Direction Stability and Control

The fuselage-wing contribution to directional stability was computed with the following equation. The value obtained for C_{nbf} is -.0003 for the fuselage-wing contribution.

The vertical tail contribution was obtained through historical data assumptions obtained from Datacom. However these approximations were compiled from historical data of swept wing aircraft with a horizontal tail. $A_{c/4}$ is the quarter chord sweep, which is equal to zero for the Knight Hawk because the wing is rectangular. The vertical tail contribution for the Knight Hawk is .0046. In addition the rudder effectiveness, C_{ndr} was calculated to be -0.018.

The coefficient of the yawing moment was plotted as a function of the sideslip angle β and separately as a

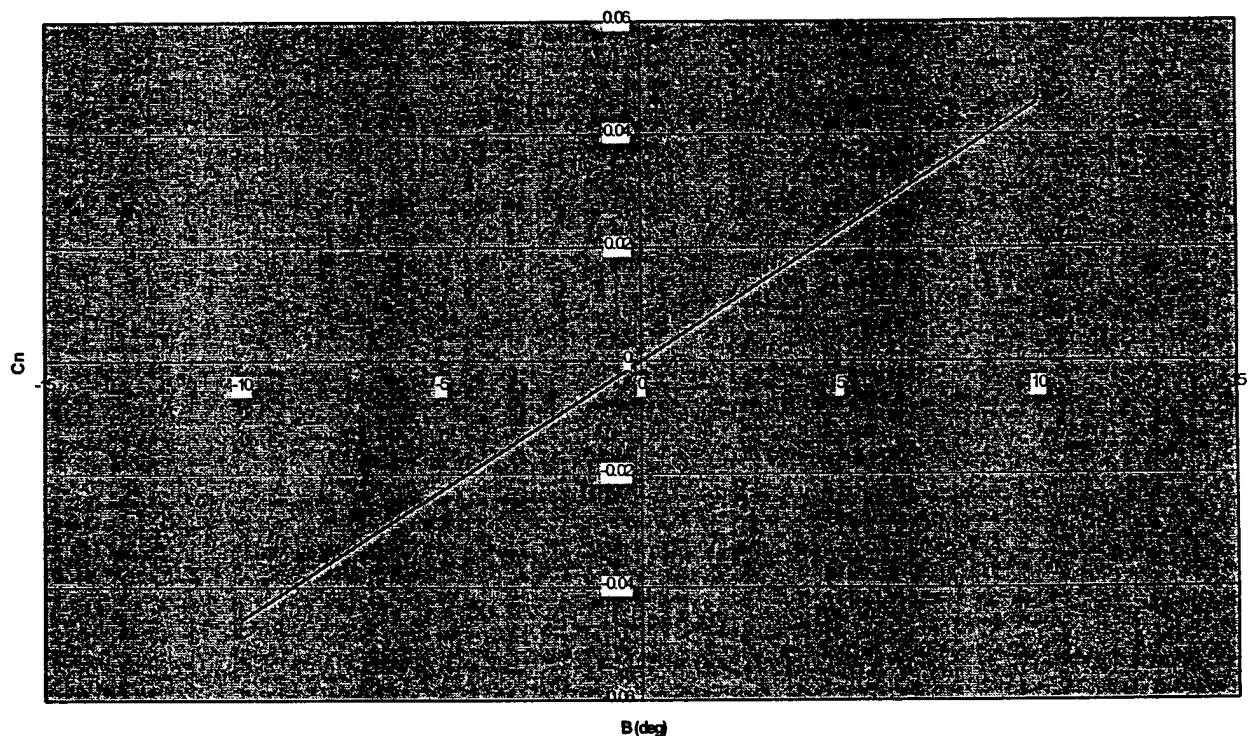


Figure 5.35: C_n vs. B

function of the rudder deflection. These were plotted in Figure 5.35 and 5.36. The range of sideslip angles ranges from -10 deg to 10 deg and the rudder deflections range from -20 deg to 20 deg.

With the increase in the sideslip angle the yawing moment coefficient increases both in the positive and negative regions.

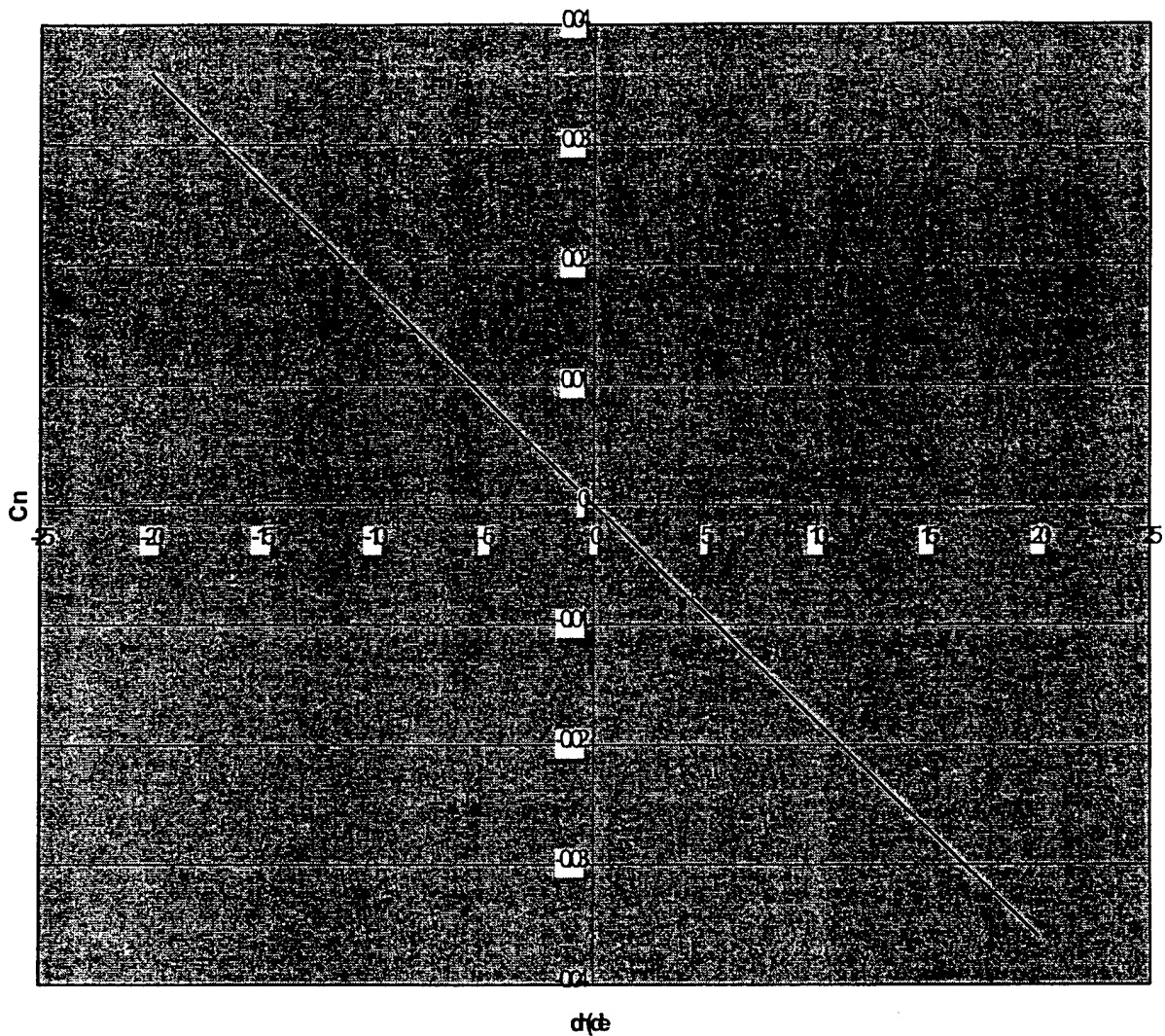


Figure 5.36: C_n vs. dr

The coefficient of the yawing moment increases with a negative rudder deflection and decreases with a positive rudder deflection. Note that a positive rudder deflection is to the right the right side when looking at the rudder from the behind the aircraft.

The maximum sideslip angle was determined for a steady sideslip with a maximum rudder deflection of 20 deg. The maximum sideslip angle for the condition stated above was 7.87 rad.

5.3.2 Roll Stability and Control

Wing dihedral and sweep contributions to an aircraft are significant in the roll stability of an aircraft however this aircraft does not have wing dihedral or sweep due to other manufacturing and structural constraints. Therefore the wing was made with no dihedral and no sweep. Thus calculations for these effects were not calculated.

The vertical tail contribution to the roll stability and control was calculated using the equation below. C_{l_b} for the vertical tail obtained from the equation above is -0.0046 . The aileron effectiveness was computed using strip theory however the equation simplifies because the aircraft has a rectangular wing. The equation yields a value of -0.018 for the aileron effectiveness.

The coefficient of the rolling moment was plotted as a function of the sideslip angle and the aileron deflection.

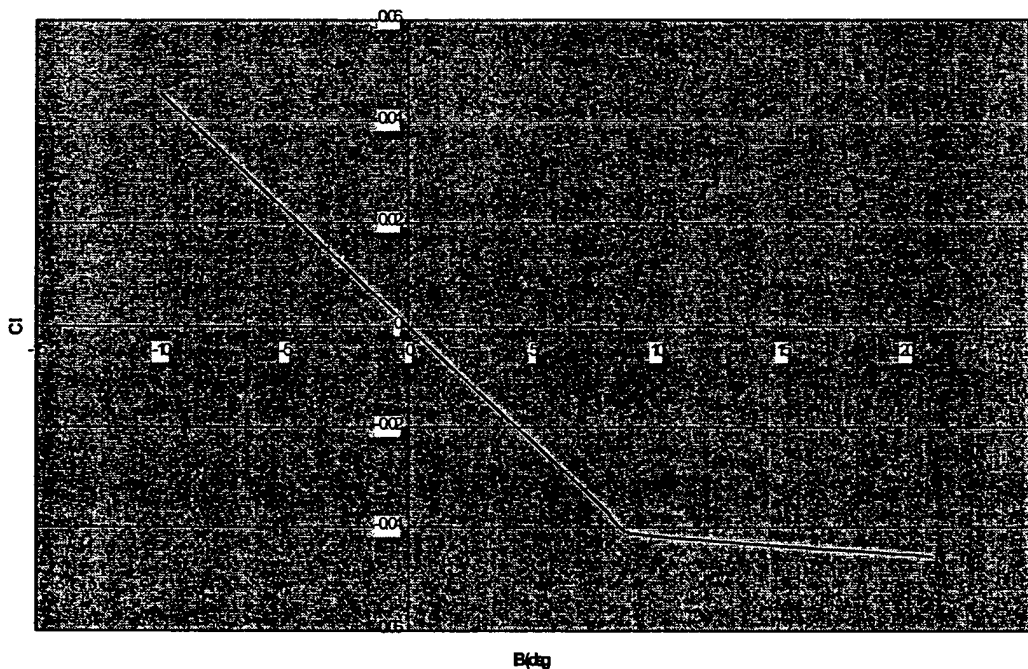


Figure 5.37: C_l vs. B

The rolling moment coefficient was calculated for a range of sideslip angles from -10 deg to 10 deg. Figure 5.37 is the plot of the rolling moment coefficient as a function of the sideslip angle. From the plot the rolling moment coefficient decreases at the sideslip angle increase however after 9 deg the rolling moment coefficient decrease at a lesser rate. Figure 5.38 plots the rolling moment coefficient as a

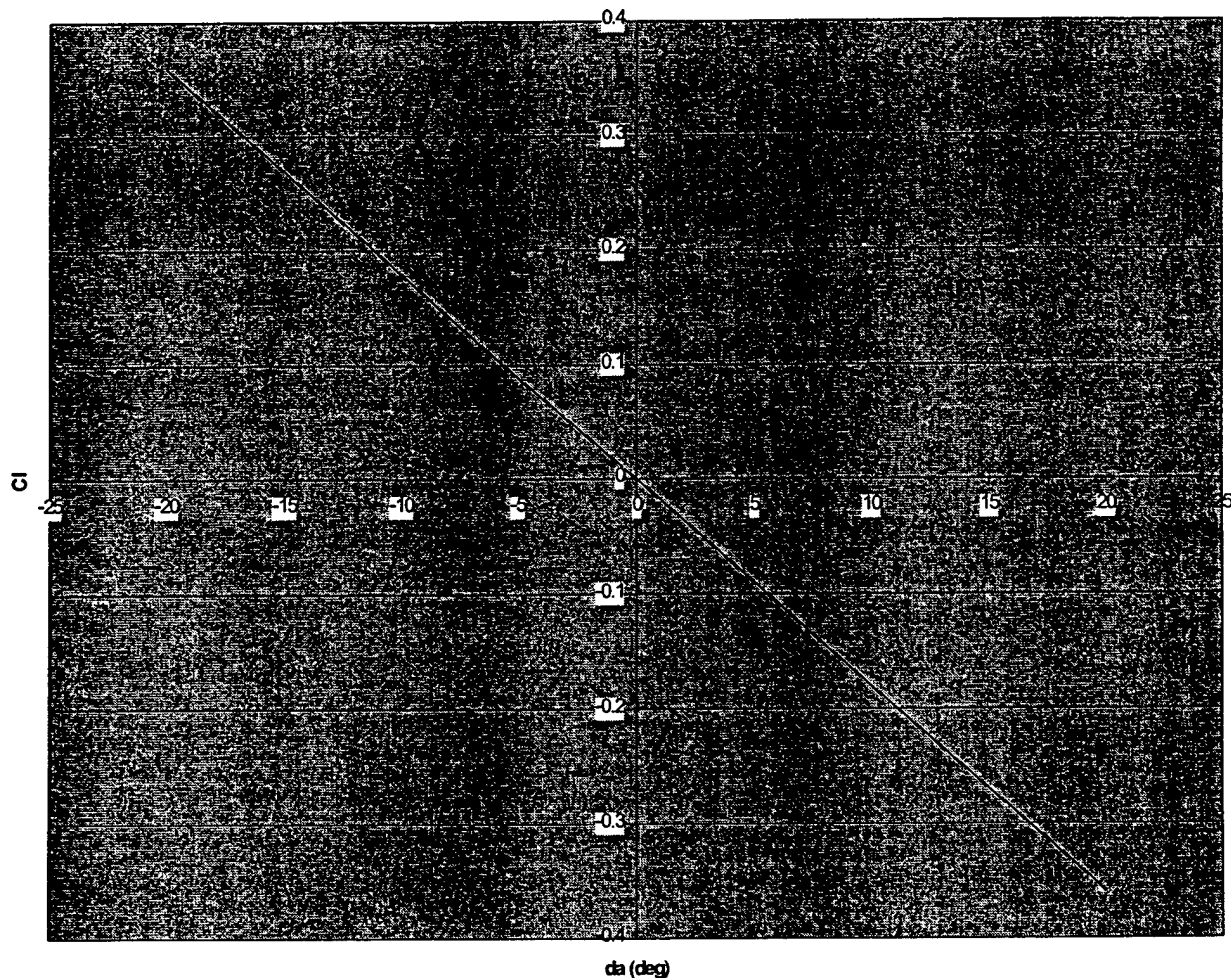


Figure 5.38: C_l vs. da

function of the aileron deflection from a -20 deg deflection to a 20 deg deflection. As the aileron deflection is increased the rolling moment decreases. C_l is positive for negative aileron deflection and negative for positive aileron deflection.

5.3.3 Dynamic Stability Derivatives

The speed derivatives X_u , and Z_u are calculated for the aircraft but M_u is assumed to be zero. Note that U_0 , C_{d0} and C_{l0} are values at a certain reference condition as they can be confused with other values with similar notation. The value of the speed derivative X_u was -0.0024 lb and the value of Z_u was -0.237 lb.

The pitch rate derivative M_q and the rate of change of angle of attack derivative M_α were calculated while Z_q and Z_α were assumed to be zero in this case. The coefficients were calculated first then converted to the derivatives by multiplying by the appropriate parameters. It should be noted that this is the C_{mq} for the tail and not the whole aircraft therefore a historical value of 1.1 is multiplied by the C_{mq} of the tail to obtain the value for the whole aircraft. The value of M_q for the aircraft is -0.005 lb-ft. This value is known as pitch damping because it is negative and opposes the pitching motion.

The rate of change of the angle of attack is computed in the same manner. It should be noted that downwash is included in this equation however this aircraft is unconventional so this value is a crude estimation of the actual value for a lack of a better estimation method. Using the same format in Equation 3.4 the coefficient was converted into the pitching moment with respects to the rate of change of angle of attack yielding a value of $-1.9E-05$ lb-ft.

The rolling moment with respects to the roll rate were calculated in the same manner as the moments above. The equation for the rolling moment is simplified by the fact that the aircraft has a rectangular wing planform. The value for the rolling moment with respects to the roll rate L_p was -0.75 lb-ft. This value is important because it is the roll damping moment, notice its negative value opposes a rolling moment.

The roll derivative N_p was also calculated. It should be noted that the roll derivative Y_p is assumed to be zero. Where C_L is the coefficient of lift at a reference condition. In this case the reference condition is at cruise in steady level flight. The roll derivative N_p was -0.556 lb-ft. The yaw rate derivatives including Y_r , N_r , and L_r were calculated. The result side force was calculated to be -0.135 lb. The yawing moment with respects to the pitch rate was calculated as -0.113 lb-ft. The rolling moment with respects to the yawing moment was found to be 1.12 lb-ft. This value is significantly higher than other moments on the aircraft, which could be a flaw with the design.

5.3.4 Stability of Longitudinal Motion

The variables for the equations of longitudinal motion were computed in the pervious sections. The equations were compiled in the state-space format and solved. The roots of these equations defined

parameters that dictate the longitudinal flying qualities of the aircraft. The state-space format of the longitudinal equations of motion is listed below in the following matrix format. Note that only the aircrafts natural stability is examined therefore the control matrix and control input is not included.

$$\begin{bmatrix} \Delta \dot{u} \\ \Delta \dot{w} \\ \Delta \dot{q} \\ \Delta \dot{\theta} \end{bmatrix} = \begin{bmatrix} -0.0237 & 0 & 0 & 32.2 \\ -2.37 & 0 & 50 & 0 \\ 15.38 & -6.49 & -324.57 & 0 \\ 0 & 0 & 1 & 0 \end{bmatrix} \begin{bmatrix} \Delta u \\ \Delta w \\ \Delta q \\ \Delta \theta \end{bmatrix}$$

Note that X_w and Z_w are assumed to be zero for lack of a better value. The determinate of this matrix was solved for in Maple. The root calculate by Maple was $-0.0103 \pm 1.236i$. The root was then used to determine the flying qualities of the aircraft in terms of the motions time period, the time for this motion to half, the number of cycles for the motion to half, the natural frequency and the damping ratio defined below.

Note these equations, as they will be used several times in both the longitudinal and lateral-directional motions. Below in Figure 4.1 are the values calculated for the aircrafts longitudinal flying qualities.

$$\begin{aligned} T &= 5.08s \\ T_{half} &= 67.28s \\ N_{half} &= 13.2cycles \\ w_n &= 1.24Hz \\ \zeta &= .008 \end{aligned}$$

Figure 5.39: Longitudinal Flying Qualities

Note that the time to half is greater than the total time period. This is abnormality in probably due to assumption of X_w and Z_w however this could be a potential stability and control problem with the aircraft, as it is an experimental aircraft. The other values seem reasonable but limited information is available on control and stability calculations of a RC canard aircraft.

The short period approximation calculations were performed using the fourth-order equations.

$$\begin{bmatrix} \Delta \dot{w} \\ \Delta \dot{q} \end{bmatrix} = \begin{bmatrix} 0 & 50 \\ -6.49 & -324.57 \end{bmatrix} \begin{bmatrix} \Delta w \\ \Delta q \end{bmatrix}$$

The determinate of the matrix was solved using Maple and returned a root of -1.003 and t_{half} of 0.693 sec for general reference. This root should have an imaginary number, which is probably effected by the assumed value of zero for Z_w .

The phugoid period approximation was calculated using the fourth-order. The phugoid period approximation determinate produced a root of $-0.0119 \pm 1.234i$ which was used to calculate the flying qualities in Figure 4.2.

$$\begin{aligned}T &= 5.08s \\T_{half} &= 58.23s \\N_{half} &= 11.4cycles \\w_n &= 1.24Hz \\\zeta &= .0096\end{aligned}$$

Figure 5.40: Phugoid Period Flying Qualities

The values compare closely with the original values for the longitudinal motion making this a remarkably fair approximation.

5.3.5 Stability of Lateral Motion

The lateral motion of the Knight Hawk was computed in the same way as the longitudinal motion but using a different matrix. Again the control matrix was not examined in this case.

$$\begin{bmatrix} \Delta \dot{v} \\ \Delta \dot{p} \\ \Delta \dot{r} \\ \Delta \dot{\phi} \end{bmatrix} = \begin{bmatrix} -0.0202 & 0 & -0.135 & 32.2 \\ 0.005 & -0.7548 & 1.12 & 0 \\ 0.005 & -0.5661 & -0.1132 & 0 \\ 0 & 1 & 0 & 0 \end{bmatrix} \begin{bmatrix} \Delta v \\ \Delta p \\ \Delta r \\ \Delta \phi \end{bmatrix}$$

The determinate of the matrix was solved for in Maple and produced the following roots.

Spiral Mode Root

0.445

Rolling Mode Root

-0.4851

Dutch Roll Mode Root

-0.4241 ± 0.8601

Figure 5.41: Longitudinal Motion

For reference purposes T_{half} was calculated for the spiral and rolling modes which are stated in Figure 5.2 below.

Spiral Mode Root

$$T_{half} = 1.56s$$

Rolling Mode Root

$$T_{half} = 1.43s$$

Figure 5.42: Spiral and Rolling Modes

For the dutch roll mode the time period, time to half, number of cycles to half, the natural frequency and the damping ratio were computed from the complex root found above. The values obtained (in order) are listed below.

$$T = 7.30s$$

$$T_{half} = 1.63s$$

$$N_{half} = .22cycles$$

$$\omega_n = 0.959 Hz$$

$$\zeta = .4422$$

Figure 5.43: Spiral and Rolling Mode Flying Qualities

Note that the cycles to half is much lower than previous calculation along with the natural frequency. However the damping ratio is relatively high showing that the aircraft flying qualities damp the dutch rolling motion, which is a favorable design characteristic.

The spiral mode approximation was computed in Excel as it includes a simple calculation rather than a matrix. The approximation root was found to be -1.235 with a reference T_{half} of 0.56 sec which is a poor approximation compared to the value of 1.56 s for T_{half} computed earlier. The approximation has a 64% difference from the original value calculated.

The root of the rolling moment was calculated as -0.75 with a T_{half} of 0.92 sec compared to an original T_{half} of 1.42 sec. Again this is a poor approximation with a 35% difference between the two values.

The dutch roll approximation is more involve than the pervious two approximations, which is defined by the 2×2 matrix below.

$$\begin{bmatrix} \Delta \dot{\beta} \\ \Delta \dot{r} \end{bmatrix} = \begin{bmatrix} -0.002 & -1.0027 \\ 0.2526 & -0.1132 \end{bmatrix} \begin{bmatrix} \Delta \beta \\ \Delta r \end{bmatrix}$$

Maple was used to solve the determinant of the matrix above producing the following root,

$-0.0576 \pm 0.5002i$. This root was then used to solve for the time period, time to half, number of cycles to half, the natural frequency, and the damping ratio which are stated in order below.

$$T = 12.55 s$$

$$T_{half} = 1.63 s$$

$$N_{half} = .96 cycles$$

$$\omega_n = 0.5035 Hz$$

$$\zeta = .1144$$

Figure 5.44: Dutch Roll Approximation Flying Qualities

The dutch roll approximation is a poor approximation for this mode. The time period, number of cycles, natural frequency and damping ratio are not similar to the values presented in Figure 5.44. The only value that is comparable is the time to half values, which is exactly as the original case.

These calculations can be considered a crude estimate for the control and stability of the Knight Hawk. The calculations can only be considered an estimate because of two reasons. The equations used are historically based on horizontal tail aircraft and the Knight Hawk has a canard configuration. The other reason is because the actual aircraft has not undergone any testing to determine some of the values that were merely assumed or roughly estimated. However the values calculated seem reasonable considering all the assumptions made. Considering that this aircraft was designed by students and is an experimental aircraft the stability and control parameters are reasonable enough to warrant the construction of the aircraft. A control and stability analysis of this magnitude for a radio controlled aircraft is unique therefore historical values are not available. Values can only be compared to full size aircraft of the same category and even those types of aircraft are limited in number. The control and stability parameters calculated prove that the aircraft is stable and will have desired control characteristics which validate the aircraft's production.

5.4 Structural Analysis

One of the challenges in designing the airplane for the Design, Build, and Fly competition is determining what material to use for the spar of the airplane. Typically, the spar is a 1" by 1" hollow box, with 1/8th thick walls. The material the spar is made out of must be able to withstand the loads placed upon it with minimal deflection, while having the lowest possible weight. If the deflection of the spar is too much, the

wing could lose its ability to effectively provide lift for the aircraft, or cause its control surfaces to stop functioning properly. Either of these will result in a crash for the airplane. On the other hand though, if the spar is made out a material that is too heavy, the airplane will never be able to leave the ground. A good spar material will provide a compromise between these two extremes.

Three different materials were analyzed for possible use in the spar. They were balsa wood, carbon steel, and aluminum. Each material was analyzed for deflection in two ways, once by hand calculations, and once by MARC. In addition, the maximum stress experienced by the spar was calculated to see if it exceeded the yield points of the materials. Since high wind shear is common while flying, after a material was selected for spar use, it was subjected to a gust loading of twice its normal load to see if it had the ability withstand the additional stress placed upon it.

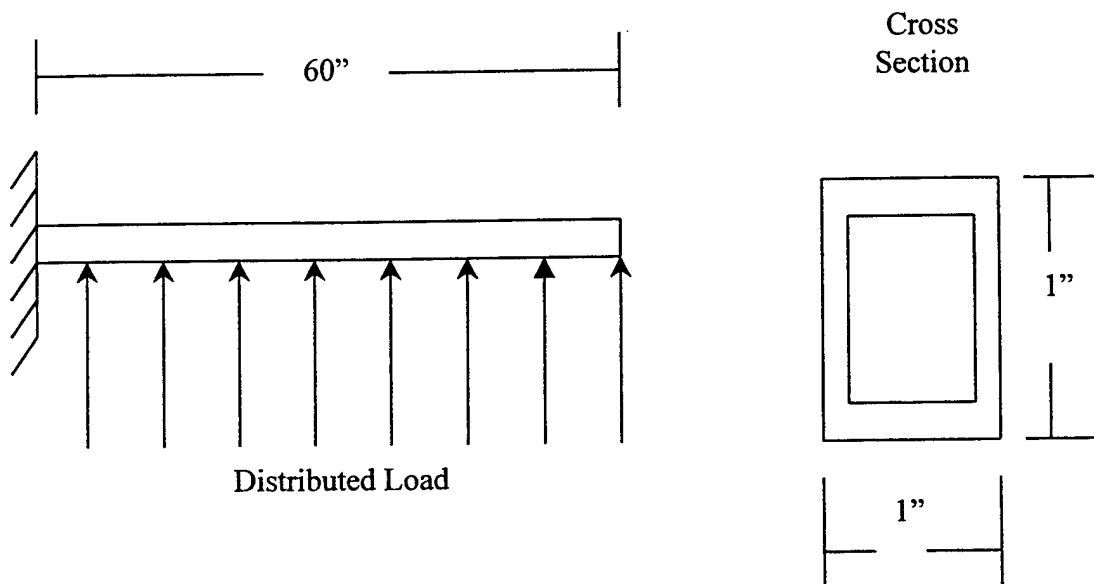


Figure 5.41: Spar Diagram

Since the spar is bolted to the body of the aircraft, it can be treated as a cantilever beam holding a distributed load. For hand calculations, this allows for the use of the equations:

$$\delta = \frac{PL^4}{8EI} \quad (5.41)$$

Where P is the distributed load, L is the length of the spar, E is the modulus of Elasticity, and I is the moment of Inertia.

$$\sigma = \frac{MC}{I} \quad (5.42)$$

Where M is the maximum moment applied, C is the distance from the neutral axis, and I is the moment of Inertia.

A FEM model of the wing spar was prepared using MSC MARC. The following geometric and material properties were entered into the model:

Table 5.5 - Material and Geometric Properties entered

	Balsa Wood	Aluminum	Carbon Steel
Young's Modulus (Psi)	1.75*10 ⁶	1.04*10 ⁷	30*10 ⁷
Poissons Ratio	0.45	0.334	0.292
I _{xx} (in ⁴)	4.88*10 ⁻⁴	4.88*10 ⁻⁴	4.88*10 ⁻⁴
I _{yy} (in ⁴)	0.28125	0.28125	0.288125
Cross Sectional Area (in ²)	0.4375	0.4375	0.4375
Density (lb/in ³)	0.010	0.1	0.284
Yield Stress (Ksi)	5	50	54

At this point the model was run using a 15 lbs distributed load (half the early weight estimates of the aircraft) as a static problem. This determined the stress and maximum deflection of each spar.

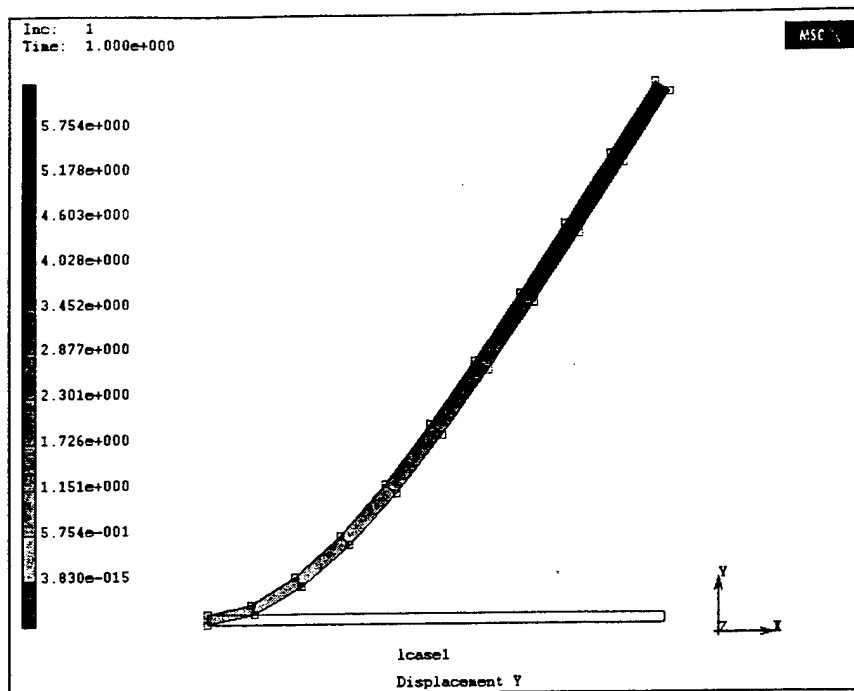


Figure 5.42: Balsa Wood Spar

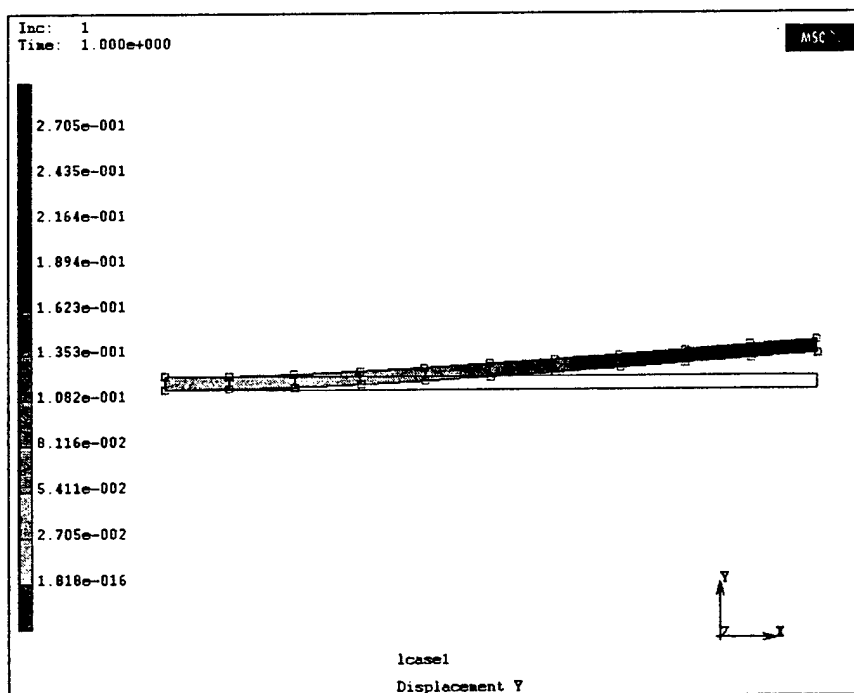


Figure 5.43: Aluminum Spar

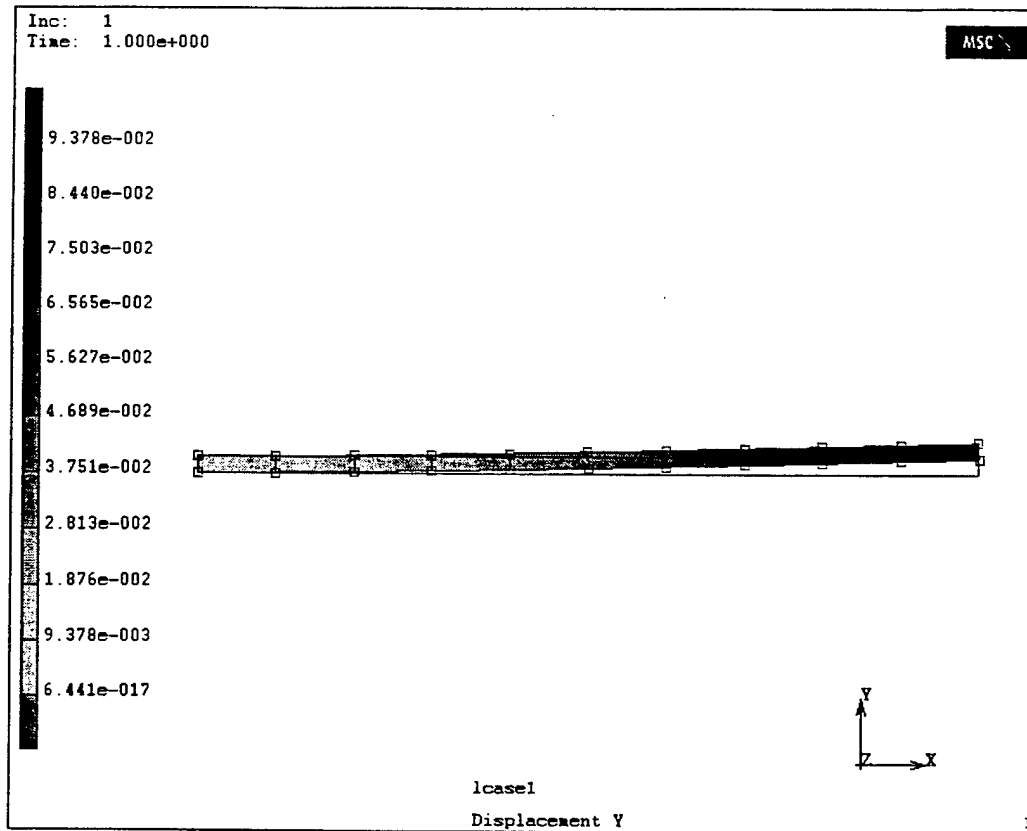


Figure 5.44: Carbon Steel Spar

All of these results correlated with the hand calculations performed.

Table 5.6 - Hand Calculated Deflections vs. MARC results

	Balsa Wood	Aluminum	Carbon Steel
Hand Estimates (in)	72.85	3.43	1.19
MARC Results (in)	69.05	3.25	1.13
% Difference	5.2	5.4	5.3

In addition, the maximum stress experienced by the spar was calculated both by hand, and with MARC. They were 19.8 Ksi and 20.3 Ksi respectively, which is a 2.7% difference. Using the above information it is possible to determine which material is best suited for making the spar. Balsa wood would not be a good choice due to the high deflection and the fact that the stress experienced at the root is higher than the 5 Ksi yield stress for Balsa Wood. On the other hand, both Aluminum and Carbon Steel have much

lower deflections than Balsa Wood, and neither of their yield stresses is exceeded at the root. Here, however, Aluminum has the advantage over Carbon Steel due to the fact that it is much lower in density, and thus will produce a much lighter spar than Aluminum. Thus it was decided that the spar would be made from Aluminum.

The problem was then re-run as a dynamic-transient model to incorporate gust loading. To simulate a strong gust, the load on the wing was doubled within a tenth of a second, and then relaxed it back to its original load of 15 lbs. The maximum stress experienced by the spar was then calculated to check that it did not exceed the yield point of the aluminum.

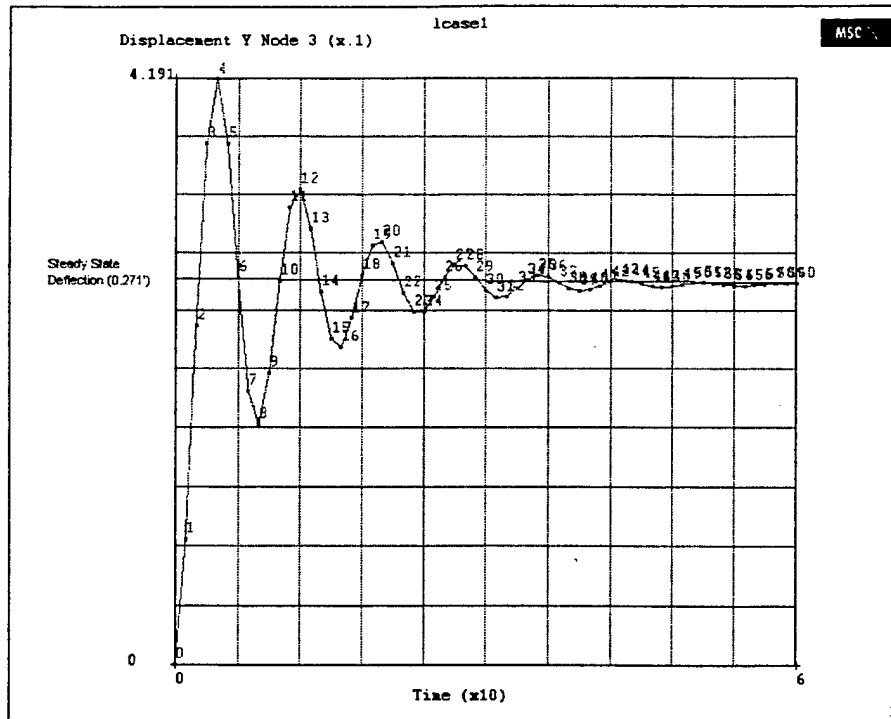


Figure 5.45: Displacement vs. Time for Gust-Loading

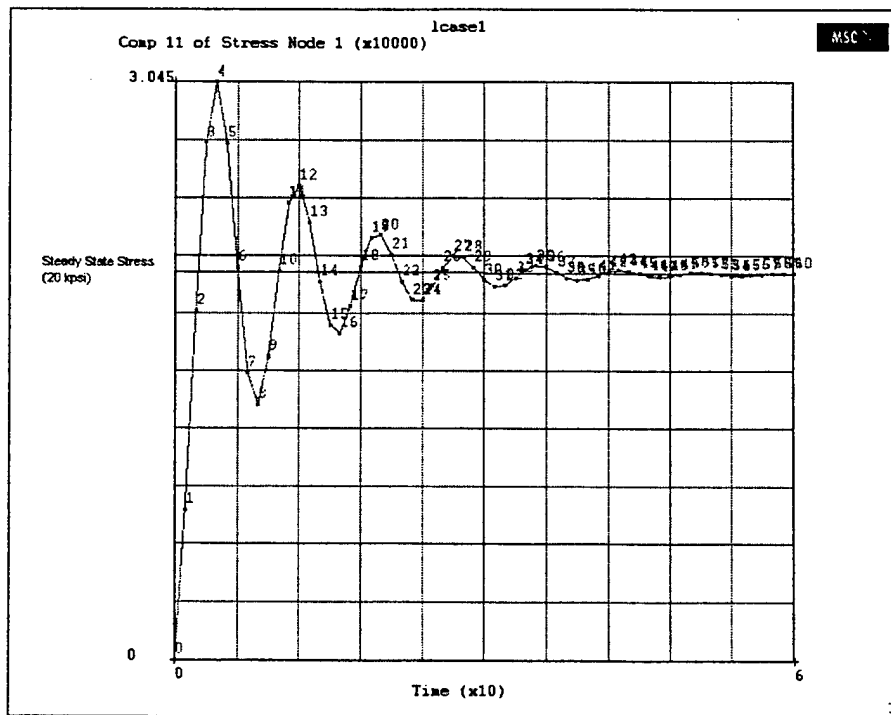


Figure 5.46: Stress vs. Time for Gust-Loading

The above Figures confirm that Aluminum is a good choice for the spar, as the deflection never exceeds five inches, and the stress never exceeds 30 Ksi, both of which are acceptable (the yield stress for aluminum is 50Ksi).

A solid spring landing gear was chosen for the aircraft due to its simplicity of design. This landing gear was also analyzed using MARC to ensure that it could withstand the weight of the aircraft sitting on the ground and also during landing. A preliminary analysis showed that the height of the main gear needed to be 13 inches in order to allow adequate clearance for the propeller on rotation. The gear was then designed to extend 12 inches down from the fuselage (assuming 2" diameter tires) and 9" out. As with the spar, both steel and aluminum were analyzed.

Using MARC, it was found that the maximum displacement occurred at the bottom of the landing gear, with the gear being pushed out and up. The deflections are as follows (positive x is away from the aircraft centerline, positive y is up)

Table 5.7 - Deflections

Material	Aluminum	Carbon Steel
x-deflection	0.59"	0.21"
y-deflection	0.55"	0.19"

Since during rotation, the weight will be transferred from the gear to the wings, it was determined that the aluminum would provide enough strength while saving weight over using steel.

5.5 Component Selection

One Astroflight 90 geared DC model aircraft motors provides propulsion for the aircraft. The motor has an Astroflight speed controller rated at a maximum current draw of 60amps. The motors are connected in series to a series-string of 40 Sanyo 1900 mAh RC type cells. Each cell is a Sub-C size. Total measured battery pack weight is 4.95 lbs. The batteries are in the cargo area at the bottom of the fuselage. This allows us to move the batteries around so as to obtain a precise predetermined Center of Gravity. Possible propellers range from 20 X 8 to a 26 X 9. Final propeller selection will be determined from static thrust testing. Analysis shows a 20 X 8 propeller is optimal.

A Futaba 6XAS 6-channel radio controls the airplane. Heavy duty servos are used for all control surfaces. Each servo produces 44 ounce-inches of torque. Flight-testing will determine if stronger servos are necessary for some or all control surfaces. An R148DP PCM receiver that provides failsafe features

on all channels is used. Four channels of the six available are used. Ailerons, elevators, and rudders provide control. The rudder and elevator and ailerons are controlled by single servos. Nose-wheel steering is Controlled by the same servo driving the rudder.

5.6 Final Aircraft Configuration

The final aircraft configuration and systems layout are shown in the attached drawing package. The final aircraft configuration is a canard design with a straight wing mounted towards the rear of the fuselage, and a motor in the tail to complete the pusher-canard configuration. The fuselage consists of a 1 inch aluminum square bar, with an extended cargo area between the wing and the nose. The landing gear consists of a main gear mounted at the center of gravity a standard nose wheel underneath the canard, and a propeller protector protruding from the rear fuselage of the tail, preventing the propeller from striking the ground on rotation. The aircraft has a wingspan of 10 feet, and an overall length of 6 feet. Estimated aircraft empty weight is 17.54 lbs. Estimated take-off weight is 35.25 lbs. (fully loaded)

6. Manufacturing Plan

6.1 Alternative Building Materials

Once the detailed design had been completed, the manufacturing processes for each individual component of the aircraft were investigated. The aircraft was divided into six major components: the main wing, the canard, the fuselage, a speed loader for the payload, the vertical tail, and the landing gear. Various building materials for each component were explored. Desired characteristics of materials would include both strength and lightweight.

The first and most important component of the aircraft is the wing. A lightweight material is desired to reduce the overall weight of the aircraft while still being strong enough to combat the effects of aeroelasticity. Two manufacturing processes were evaluated. The first was a wing design constructed of ribs and spars made from aircraft ply. A template would be made and copied for the ribs, which would be joined via wing spars. It would then be covered with a light skin such as monocoque. The second method would consist of forming the wing from insulation foam. Two templates would be fabricated from plywood and then attached to the end of a sheet of insulation foam. A hot-wire cutter would then be used to trace along the templates which would form the wing. The wood construction would provide an extremely strong wing however would cost the design in weight. The foam wing would be slightly weaker however adding a second spar would more than compensate while still being lighter than the wood construction. Because it was easier to construct, lighter in weight and also faster to construct, the foam wing was chosen.

Similar processes were considered for the canard. Because the canard was smaller the wood vs. foam weight would not be as critical as it was with the wing. The foam manufacturing process was selected because it was faster and there was still a slight reduction in weight. It should also be noted that in the event of a crash of the aircraft, the foam would be more likely to absorb the impact where the wood counterpart would most likely destruct. The foam would be easier to replace and repair if an incident occurred.

The man hours committed to the project were arranged in Figure 6.1.

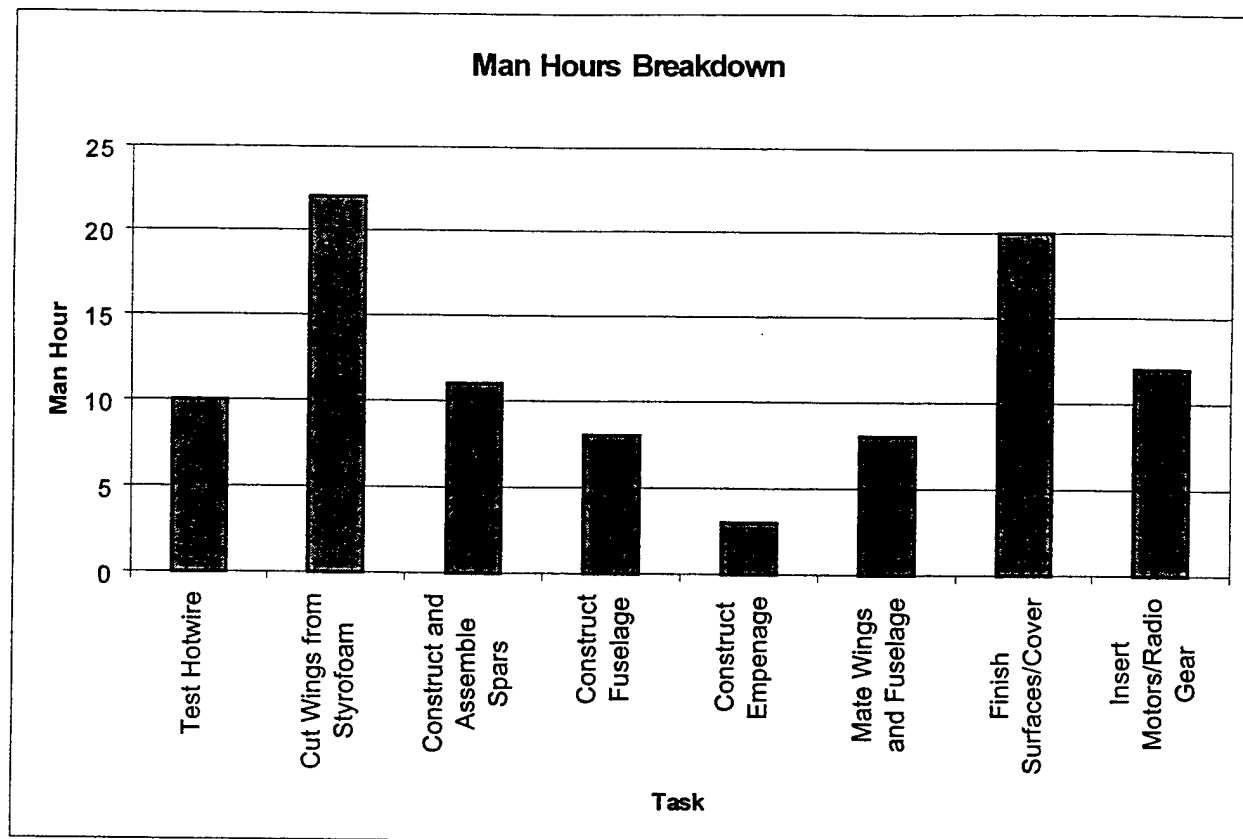


Figure 6.1: Manufacturing Man Hours Breakdown

References

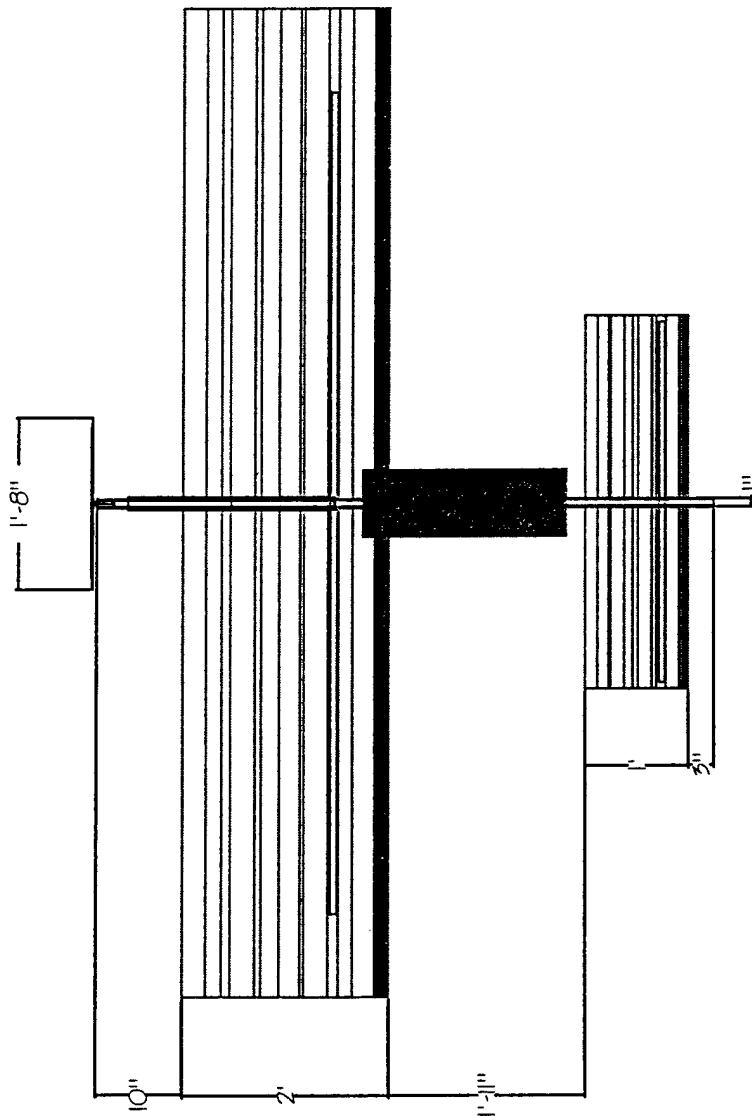
- Anderson, John D, Aircraft Performance and Design, McGraw-Hill, Boston, 1999.
- Etkin, Reid, Dynamics of Flight: Stability and Control, John Wiley & Sons, Inc., 3rd Edition, New York, 1996.
- Lennon, Andy, R/C Model Aircraft Design, Air Age, Ridgefield, CT, 1996.
- McCormick, Barnes W, Aerodynamics, Aeronautics, and Flight Mechanics, John Wiley, New York, 1979.
- Nelson, Robert C, Flight Stability and Automatic Control, McGraw-Hill, Boston, 1998.
- Avallone, Eugene A and Theodore Baumeister III, Marks' Standard Handbook for Mechanical Engineers, McGraw-Hill, Boston, 1996.
- Phillips, Hewitt and Bill Tyler, Cutting Down the Drag, Model Airplane News. Referenced from Lennon.

Drawing Package



REVISIONS

ZONE	REV	DESCRIPTION	DATE	APPROVED
------	-----	-------------	------	----------



Clarkson DBF

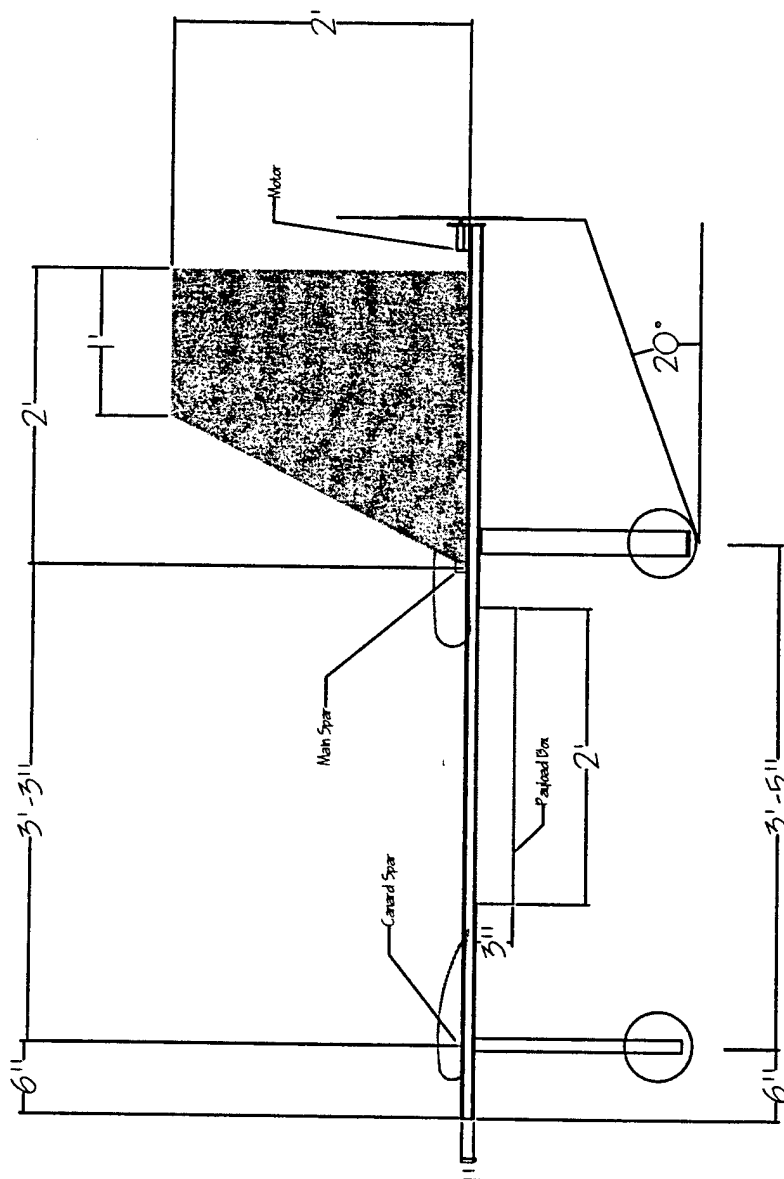
Top view

SIZE	FSCM NO.	DWG NO.	REV
SCALE			SHEET



REVISIONS

ZONE	REV	DESCRIPTION	DATE	APPROVED
------	-----	-------------	------	----------

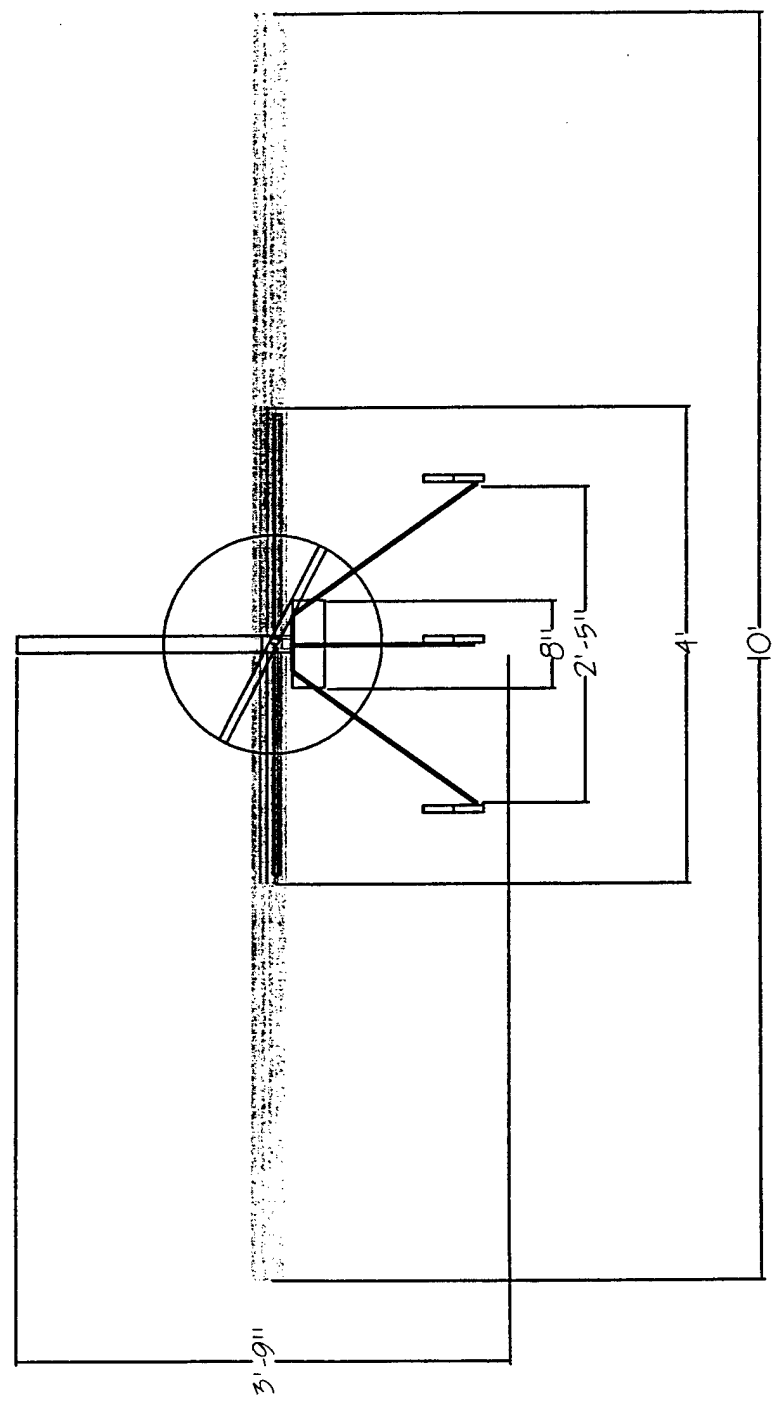


Clarkson DBF

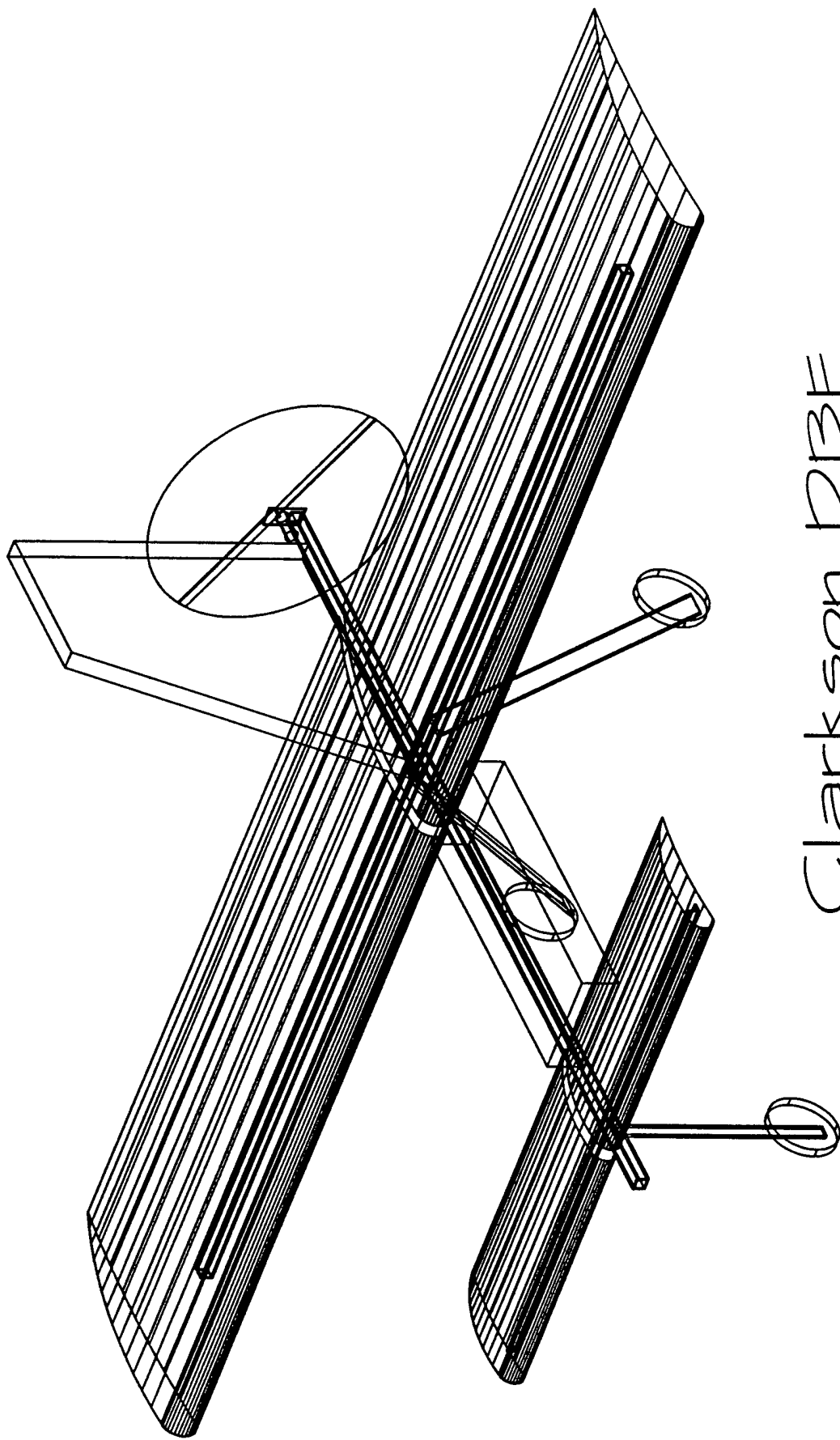
Side View

SIZE	FSCM NO.	DWG NO.	REV
SCALE		SHEET	

REVISIONS			
ZONE	REV	DESCRIPTION	DATE
			APPROVED



Clarkson DBF			
Front View			
SIZE	FSCM NO.	DWG NO.	REV
		3	
SCALE		SHEET	

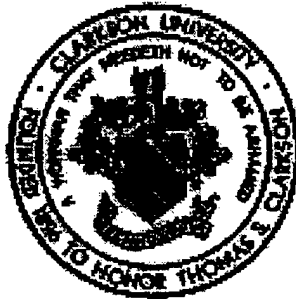


Clarkson DBF
3-D Isometric View

AIAA Design Build Fly Competition

CLARKSON **UNIVERSITY**

Knight Hawk



Addendum Phase

Table of Contents

List of Figures and Tables.....	4
1.0 Lessons Learned.....	5
1.1 Future Design Improvements.....	5
1.2 Manufacturing Process Improvements.....	5
2.0 Rated Aircraft Cost.....	7

List of Figures and Tables

Figure 1.1 – Final Aircraft Configuration Showing Twin Vertical Tails.....	6
Table 2.1 – Cost Breakdown by Component.....	8
Table 2.2 – Multiplier Values.....	8
Table 2.3 – Work Breakdown Structure.....	8

1.0 Lessons Learned

The final aircraft varied from the Proposal Phase due to the integration of the drawing board design and the manufacturing process. One of the most significant modifications was the decision to use two vertical tails 2 ft outboard of the main wing instead of a single center mounted vertical tail. Each vertical tail was made at 3/4th the size of the original tail. The design change was initiated because the original configuration would not have enough spin stability or sufficient yaw control. The new configuration increases the yawing moment, which will improve the directional stability and control of the aircraft. The new design was derived from aircraft that have two smaller vertical tails in order to be stored on aircraft carriers. Since the vertical tails are permanently mounted, the size of the smaller vertical tails allow for easier transport of the aircraft. The transport requirements were overlooked in the initial design phases. In addition the change in design saved time because the original configuration posed a more difficult integration near the engine. The cost function for each vertical tail was only 5 hours therefore the aircraft did not take a large hit by switching to the new design. Figure 1.1 shows the new twin-vertical tail configuration.

To reduce weight and create break-away points for major flying surfaces, steel hardware was replaced with nylon hardware at major joints. The nylon is not only lighter but will fracture under a smaller load in the event of a crash. This has the potential to reduce damage to major components in the event of accident. This change required 2 man-hours to re-drill holes for the larger nylon hardware.

1.1 Future Design Improvements

Improvements in the design process will include the addition of a preliminary design review and a critical design review with the team advisor and other selected faculty. The purpose of these reviews is to create tentative design completion dates and documentation of the design to date. The documentation and explanation of the engineering will not only create a better proposal phase report but also allow younger team members to become accustom to the design process.

1.2 Manufacturing Process Improvements

Due to the weight of standard aircraft materials in a aircraft this size, next year's aircraft will likely employ composite construction to decrease airframe weight. Many aluminum components can be replaced by properly designed composite components yielding a higher strength-to-weight ratio. While the process would take a greater amount of time the finished product would be stronger and lighter than the foam. The foam wing was light and easy to construct however the material was hard to finish correctly. In

addition a full conversion to nylon hardware will be use to reduce weight and allow for stress induced fractures in the case of a crash.

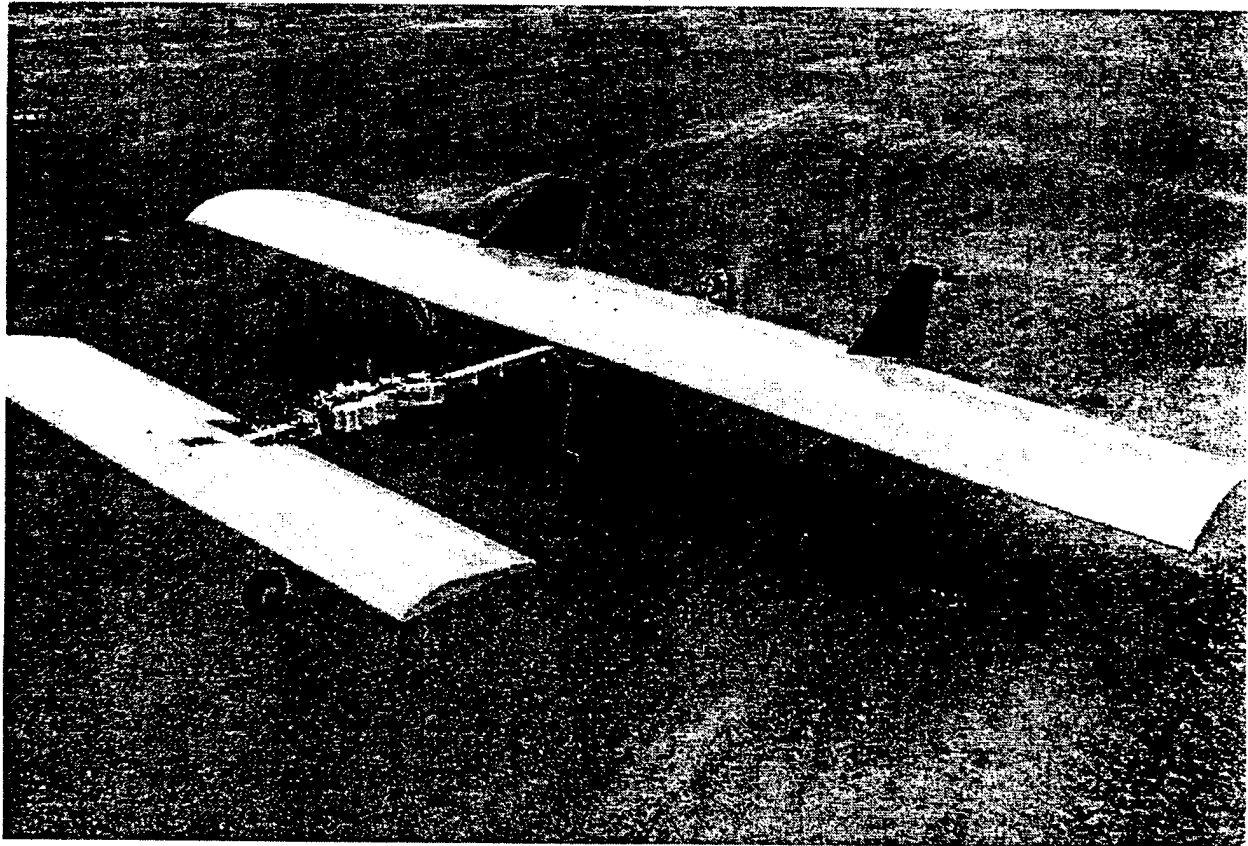


Figure 1.1 – Final Aircraft Configuration Showing Twin Vertical Tails

2.0 Rated Aircraft Cost

The total rated cost is \$7.70. Equation 2.1, as supplied by the competition coordinators was used to determine the rated cost. The aircraft consists of 1 pod totaling 8.2 feet long; a single wing of 20 ft²; a single horizontal stabilizer; two vertical stabilizers, one motor; a total of 38 Nicad cells; 4 servos; 1 controller; and two propellers. Its empty weight is 23 lbs. Table 2.1 shows the cost breakdown by each component. Table 2.2 shows the coefficients used in equation 2.1 to develop values for manufacturer's empty weight, rated engine power, and manufacturing man-hours.

$$\text{Rated Cost} = (A * \text{MEW} + B * \text{REP} + C * \text{MFHR}) / 1000 \quad (2.1)$$

The work breakdown structure (WBS) shows that the most rated man-hours were spent on the fuselage. The wings take up the second most time. The total number of rated man-hours was 178.8. Table 2.3 shows the WBS, organized into the separate construction categories as specified by the contest administrators.

To ensure the aircraft is within the contest rules, the battery pack was measured as 4.95 lbs., the wingspan is 10 feet, and the gross takeoff weight is less than 55 lbs.

Table 2.1 – Cost Breakdown by Component

			MFHR
	Number of Motors	1	5
	Number of Cells	38	
REP	Motor Rated Power (W)	1824	
	Number of Propellers	1	5
	Fuse Rating	40	
MEW	Empty Weight (lbs)	23	
	Wing Area (sqft)	20	80
	No. of Wings	1	15
	No. of Struts	0	0
	No. Control Surfaces	2	6
	Number of Fuselage + Pods	1	5
	Length Fuse + Pods (ft)	8.2	32.8
	No. of Vertical Surfaces	2	10
	No. of Horizontal Surfaces	1	10
	Number of Servos	5	10
		Total MFHR	178.8 <i>hours</i>
		Total Cost	\$7.70

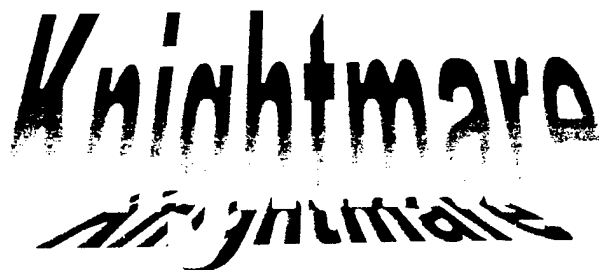
Table 2.2 – Multiplier Values

Empty Weight Multiplier	100	\$/lb
Engine Power Multiplier	1	\$/Watt
Manufacturing Cost Multiplier	20	\$/hour

Table 2.3 – Work Breakdown Structure

	Hours	Rated Labor Cost
1.0 Wings	101	\$2,020
2.0 Fuselage/Pods	37.8	\$756
3.0 Empenage	20	\$400
4.0 Flight Systems	10	\$200
5.0 Propulsion	10	\$200
Total	178.8	\$3,576

AIAA Electric Airplane



Team Members

Gary Ballmann
Adam Bojanowski
Kevin Chibar
Mirelis Cotto

Jennifer Creelman
Sebastian Echenique
Joshua Lobaugh
Kristina Morace

Arthur Morse
Jorge Pagán
Bernie Sam
la Whiteley

Mentors

Dr. Conway
Tconway@mail.ucf.edu

Dr. McBrayer
mcbayer@mail.ucf.edu

March 13, 2001

Table of Contents

1.0	Executive Summary	3
1.1	Major Development Areas	3
1.2	Design Alternatives Investigated	3
1.3	Design Tools Used	4
2.0	Management Summary	6
3.0	Conceptual Design	10
3.1	Introduction	10
3.2	Wing and Airfoil	10
3.3	Tail Boom	12
3.4	Fuselage	12
3.5	Landing Gear	14
3.6	Batteries	15
3.7	Motor and Propeller	15
3.8	Results	16
4.0	Preliminary Design	18
4.1	Wing	18
4.2	Fuselage	20
4.3	Prop/Engine	21
4.4	Batteries	23
4.5	RAC Comparison	24
4.6	Tail	26
4.7	Landing Gear	27
4.8	Results	27
5.0	Detailed Design	28
5.1	Hinge Design	28
5.2	Wing Design	28
5.3	Motor/Firewall Analysis	30
5.4	Landing Gear Analysis	32
5.5	Center of Gravity/Mass Properties	34
5.6	Tail Design	35
5.7	Flight Performance	37
5.8	Drawing Package	39
6.0	Manufacturing Plan	43
6.1	Introduction	43
6.2	Fuselage	45
6.3	Wing	45
6.4	Tail	46
6.5	Landing Gear	46
6.6	Engine	46
6.7	Safety	47
6.8	Figures of Merit	47
6.8.1	Cost	47
6.8.2	Availability	47
6.8.3	Required Skill Level	47
6.8.4	Timed Required	48
7.0	Concluding Remarks	49

1.0 Executive Summary

Knightmare is this year's University of Central Florida Design/Build/Fly (DBF) team #1 entry. The ideas used to design this aircraft were developed from the knowledge of those who attended the competition last year, as well as those who have never built an RC airplane before. The team aimed to optimize their design as best as possible by using innovative ideas as well as reusing old, proven ideas.

1.1 Major Development Areas

This report will show what progress there has been on the design of the aircraft including the wing design, airfoil, batteries, motor, fuselage design, cooling, and financial support. This will be shown by first performing an analysis of the problem by documenting the problem inputs, general limitations, design outputs, and stating the goals that are to be achieved by the design. After the analysis of the problem is complete, the group began to enounce possible solutions to the given problem. The group then began to go through the comparison analysis and summarize the solutions with what the group believes is the best course of action for winning this event.

The methods used to evaluate the problems were very systematic and revolve around the central idea of the Rated Aircraft Cost (RAC). The main purpose of this cost is to provide a numerical value for the physical size and complexity of the aircraft designed. In the final score the payload weight lifted by the aircraft is multiplied by the report score and then divided by the RAC for the final score. For this reason, if the RAC is kept to a minimal value the total score is maximized for the payload weight lifted by the aircraft. With this in mind, the group started to perform trade-off analyses to find the best solutions.

Four of the major design selections that make *Knightmare* unique are the hinged tail, the use of an air scoop, the rectangular/tapered wing, and the fiberglass cowling. Since easy access to the payload was required while out on the flight line, the hinged tail configuration simplified the ground crews job of exchanging the payload between sorties. The air scoop was designed after last year's team experienced over heating of the speed controller and batteries. The "quick fix" then was cutting holes in the skin to allow cooling over the speed controller and batteries. This year that problem was taken into consideration when initially designing the airplane. Since the team wanted to maximize the lift the full ten feet allotted by the competition rules was used in the design. The wing was designed to be a rectangular/tapered configuration to create a lift distribution similar to the elliptical wing. Finally, a fiberglass cowling was designed to help with the aerodynamics allowing a smooth flow over the nose of the plane. Another benefit of the cowling was the material selection because it decreased the weight the cowling would be in comparison to balsa or plywood.

1.2 Design Alternatives Investigated

Structural characteristics were chosen based on how they would affect the RAC. The choice between single or double boom tail designs is an excellent example of this thought process. The RAC of

the aircraft increases as the number of vertical stabilizers used increases. The double vertical stabilizer idea is sufficient for a high wind situation because of the decrease in cross-sectional area seen by the wind during flight, however, it increases the RAC because two vertical stabilizers are used. On the other hand, the single boom design has less sufficient handling characteristics in high wind, but the use of only one vertical stabilizer decreases our rated cost. Therefore, it becomes a trade-off of stability versus Rated Aircraft Cost.

The wing is very important when designing any aircraft. The airfoil and dimensions of the wing determine the lift, and consequently how much cargo can be carried. Along with the aerodynamic criteria, such as how much lift and drag would be produced by the proposed design, the airfoil and wing characteristics were also analyzed based on how much area the wing would consist of. The reasoning for this was that as the surface area of wing increased, the RAC increased also. Using this the team was able to find estimated values for the RAC, and then using the lifting capability of the wing determine a final score based on the preliminary values.

The physical dimensions of the fuselage also greatly affect the RAC, so these dimensions and the effect they had on the RAC were taken into account when analyzing the fuselage. The nature of the competition makes the interior size of the plane large due to the volume requirement of 10 tennis balls. Therefore, the fuselage had to be spacious enough to carry at the least ten tennis balls, but yet minimize the effects a stiff cross wind would have on the aircraft itself. The aircraft will be flying in St Inigos Maryland, at Webster Field, which is a part of the Patuxent River Naval Base. Webster field, from descriptions given, is on a peninsula very near the Chesapeake Bay, so strong winds off the bay are definitely a possibility.

The batteries were compared by the use of a power to weight ratio. This ratio is based on the milliAmp hour (mAh) rating of the battery and dividing it by the weight of the battery. This gave an idea of the batteries performance per unit weight so that the total weight of the aircraft could be kept low by maximizing the efficiency of the batteries. Another characteristic used was a "charge density". This is based on the physical volume of the battery as compared to the mAh rating of the battery. All of these ratios were important to maximize battery efficiency.

1.3 Design Tools Used

The computer was the main tool utilized during the trade off analysis. Use of the CAD program Pro/Engineer (Pro/E) provided a virtual model of the aircraft that was used to get an accurate model of the aircraft, as well as provide mass properties. Using this program greatly increased the ability to perform close approximations to the aircraft's actual RAC and a working model to visualize the layout of the components. The Microsoft spreadsheet program Excel was used to perform the number crunching of the RAC providing the ability to easily make variations in aircraft characteristics and see the effect of the score.

To further perform and complete analysis of the aircraft several design characteristic methods were used. The Pugh matrix method was utilized to help with the final selection of several design issues of the aircraft. In addition, using the Dominic method and House of Quality Matrix several designs could be discounted. All of these methods lend itself to comparative analysis. They are all based upon sighting designs and how they rate against the multitude of characteristics that are important to the overall success of the project.

Through this extensive trade off analysis, a final design was starting to develop into this year's AIAA Electric Airplane, *Knightmare*. By using all of the tools previously mentioned, the final design will meet the team's goals that include a highly efficient aircraft and will in turn meet the requirements set out by the competition.

2.0 Management Summary

As stated in the competition guidelines there were two main subdivisions of the team; the upperclassmen (undergraduate seniors) and the underclassmen (freshmen, sophomores, and juniors). The upperclassmen are the driving force, mainly because the aircraft is their senior project. As such the upperclassmen were subdivided into groups according to various aircraft components and the underclassmen were then assigned onto the various groups.

With that in mind, there are six seniors and six underclassmen on the team, all of them aerospace engineering students. The teams were separated into three groups of four members, each representing different aircraft sections. Two seniors and two underclassmen were assigned to the fuselage. Similarly four were assigned to the aircraft power, and another four to the wing and tail. Each group was subsequently responsible for researching, analyzing, and developing their sector and then reporting their findings/results to the entire team. The task breakdown for each individual and each group is shown in Figure 2.1.

As the project got underway, the team set up a meeting schedule with the advisors, Dr. James D. McBrayer and Dr. Ted Conway. In the early part of the project the team had a weekly meeting with the both advisors to discuss current findings and to ask any relevant questions. Then as time went, the team moved on to a biweekly meeting format because they felt it better to gather more information and accomplish more work between meeting times with the advisors. However, the groups and team continued with more frequent meetings. The team as a whole met at least twice per week, immediately following senior project class and various times as needed. The groups met at various times during the week, often after the team meetings. The important thing was that the groups accomplished what was needed so that the team could stay on schedule. The team proved itself worthy; it worked well as unit and accomplished the goals set forth. The timeline of events and milestones can be seen in Figure 2.2.

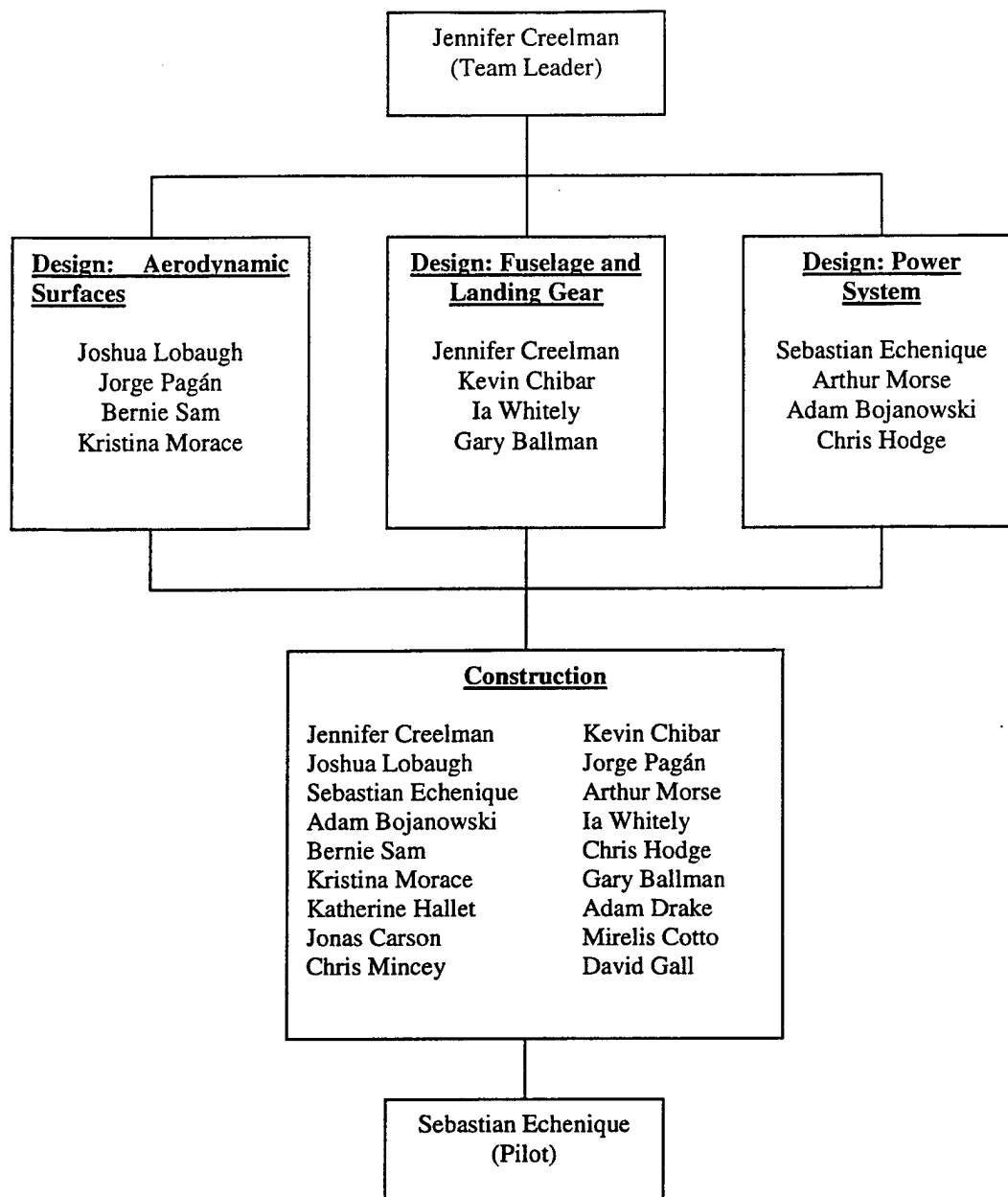


Figure 2.1. Task Breakdown.

ID	Task Name	Start Date	End Date	Duration	2000		
					September	October	November
1	Select team members	9/10/00	9/12/00	3d	■		
2	Explore team member experience	9/15/00	9/15/00	1d	■		
3	Recruit underclassmen	9/20/00	9/30/00	11d	■	■	
4	First design meeting	9/20/00	9/20/00	1d	■		
5	Separate team into 3 groups	9/20/00	9/20/00	1d	■		
6	Meeting with all gathered information	9/30/00	10/5/00	6d		■	
7	Use programs to calculate aircraft parameters	10/10/00	10/15/00	6d		■	
8	Choose motor	10/10/00	10/15/00	6d		■	
9	Select batteries	10/10/00	10/15/00	6d		■	
10	Select airfoil	10/10/00	10/15/00	6d		■	
11	Brainstorm body shape	10/10/00	10/15/00	6d		■	
12	Choose desirable RAC	10/10/00	10/15/00	6d		■	
13	Test motor	10/12/00	10/15/00	4d		■	
14	Select propeller	10/12/00	10/15/00	4d		■	
15	Use Excel to calculate RAC	10/12/00	10/20/00	9d		■	
16	Calculate wing area	10/12/00	10/20/00	9d		■	
17	Figure airplane length	10/12/00	10/20/00	9d		■	
18	Calculate total lifting weight	10/12/00	10/20/00	9d		■	
19	Give conceptual design presentation	10/26/00	10/26/00	1d			■
20	Send in entry form	10/30/00	10/30/00	1d			■
21	Perform stability calculations	10/30/00	10/31/00	2d		■	
22	Configure payload	11/1/00	11/1/00	1d			■
23	Configure batteries	11/1/00	11/10/00	10d		■	
24	Brainstorm wing construction and attachment	11/10/00	11/18/00	9d		■	
25	Design motor mount	11/10/00	11/24/00	15d		■	
26	Design hinge configuration	11/10/00	11/23/00	14d		■	
27	Do landing gear modeling and testing (FEM)	11/10/00	11/20/00	11d		■	
28	Do calculations for control surface sizing	11/15/00	11/20/00	6d		■	
29	Calculate flight performance	11/15/00	11/20/00	6d		■	
30	Put components into Pro/E and test for cg	11/15/00	11/20/00	6d		■	
31	Detailed design presentation	11/28/00	11/28/00	1d			■
32	Place all purchase orders	11/29/00	11/29/00	1d			■
33	Obtain sponsors	12/1/00	12/31/00	31d			■

Figure 2.2. Timeline

ID	Task Name	Start Date	End Date	Duration	2001			
					January	February	March	April
1	Redesigned fuselage for stability purposes	1/5/01	1/5/01	1d				
2	Redesign motor mount to be light plywood	1/6/01	1/6/01	1d				
3	Cut foam wing	1/8/01	1/8/01	1d				
4	Build spar	1/10/01	1/10/01	1d				
5	Build fuselage	1/15/01	1/20/01	6d				
6	Build horizontal and vertical stabilizers	1/20/01	1/20/01	1d				
7	Build tail boom	1/24/01	1/25/01	2d				
8	Shape mold for cowl	1/25/01	2/1/01	8d				
9	Build cowl	2/3/01	2/3/01	1d				
10	Build motor mount	2/2/01	2/2/01	1d				
11	Prepare wing for construction	2/10/01	2/15/01	6d				
12	Insert spar into wing	2/15/01	2/15/01	1d				
13	Design presentation	2/23/01	2/23/01	1d				
14	Calculate steel sizing	2/24/01	2/24/01	1d				
15	Assemble airplane components	2/27/01	2/27/01	1d				
16	Begin construction on second airplane	3/1/01	3/7/01	7d				
17	Carbon fiber/Vacuum bag the wing	3/4/01	3/4/01	1d				
18	Monokote all surfaces	3/4/01	3/12/01	9d				
19	Install electrical components	3/12/01	3/12/01	1d				
20	Check CG	3/12/01	3/12/01	1d				
21	Reposition batteries/receiver for CG adjustment	3/13/01	3/13/01	1d				
22	Test fly	3/30/01	3/30/01	1d				
23	Adjust airplane after test flight	4/3/01	4/3/01	1d				
24	Final design presentation	4/5/01	4/5/01	1d				
25	Airplane ready for competition	4/10/01	4/10/01	1d				

Figure 2.2. Timeline Continued.

3.0 Conceptual Design

3.1 Introduction

Many solutions exist for the electric airplane that range in plausibility. Any good airplane design, no matter what its mission objective, will consist of a series of compromises for each aspect of the vehicle. Every part may not have the best configuration possible because each one affects the other. A synthesis of all ideas must be found. This case is no different, and much deliberation has been put forth into this conceptual design.

3.2 Wing and Airfoil

An airplane is not an airplane unless it has a wing for the generation of lift, and ideas for the wing vary greatly. There is a virtual sea of airfoils that could have been used. Obviously, a thin airfoil that is made for supersonic speeds will not be of any use because of its lack of lift. A thicker airfoil with a reasonable amount of camber would provide the best lift. The NACA family had many choices, but the best one was found to lie in the small Selig family. Of those, the Selig 1223 airfoil (Figure 3.2.1), designed for high lift at low speeds, was chosen. In fact, this airfoil was designed for competitions like these. Although the NACA family had many choices, experience with the Selig airfoil has proven effective time and time again.

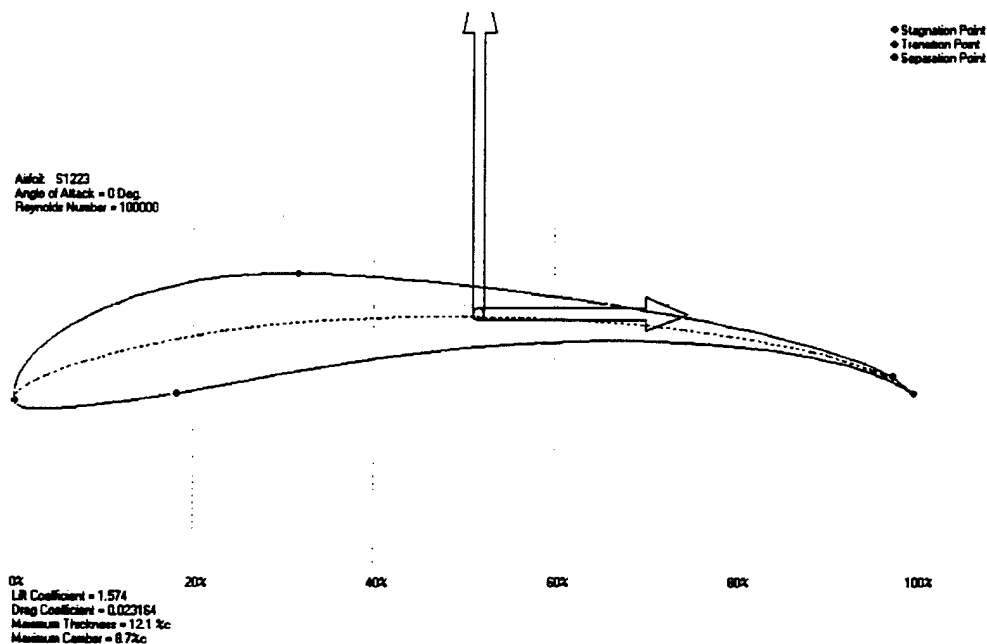


Figure 3.2.1. Selig 1223 Airfoil

The wing itself could have a small span and large chord (small aspect ratio), very long span and small chord (large aspect ratio), or be somewhere in the middle. The higher the aspect ratio, the higher the lift produced and the lower the induced drag, but the weight becomes greater. The maximum allowable wingspan for the competition is ten feet, and a ten-foot wingspan was chosen in order to obtain a higher aspect ratio. In order to counteract some of the adverse weight and lift effects, it was decided that the wing should be tapered. An additional advantage to tapering the wing is a decrease in area, resulting in a higher aspect ratio.

For lift enhancement and control, the concept of flaperons was considered. These devices would be used to increase lift at takeoff and landing (flap function), and to control roll (aileron function). Flaperons were chosen instead of separate flaps and ailerons in order to reduce cost without sacrificing performance significantly. A chart demonstrating the advantages of lift on an example airplane from the implementation of flaps can be seen in Figure 3.2.2.

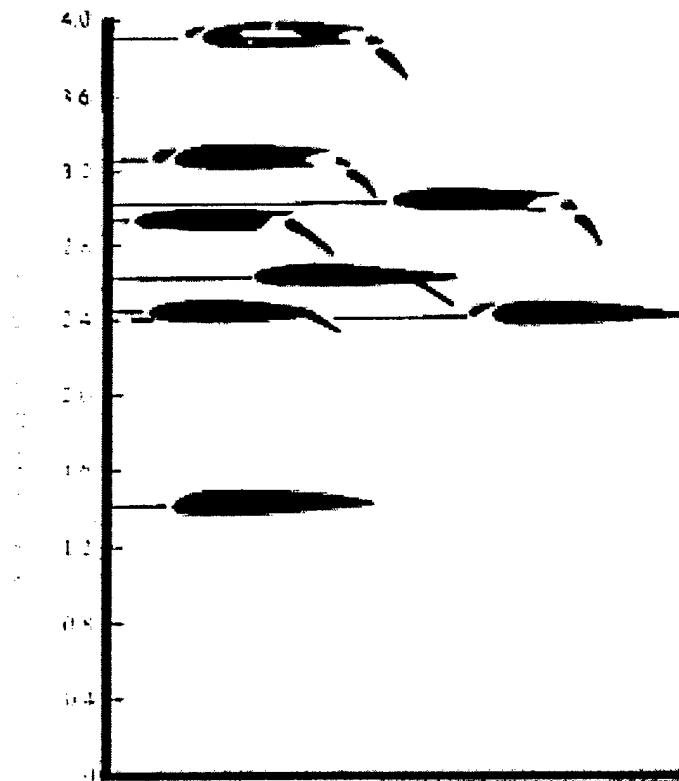


Figure 3.2.2. Flap Effects on Lift

Other important factors in the wing design included features such as single or double wings, the type of taper, and the actual structural makeup of the wing. These and other figures of merit for the wing can be seen in Table 3.1.

3.3 Tail Boom

The tail in an airplane works to balance adverse moments in pitch caused by the wing and to provide directional control and stability. Here the question was whether to choose a single vertical stabilizer and single tail boom or a double vertical stabilizer with twin tail booms. Then the decision had to be made as to whether to have that configuration in a high tail or low tail format.

A double vertical, single boom provides better control and stability but at a greater rate of cost. Another advantage of the double boom is that it provides easy access to the payload; the payload can be inserted and extracted between the booms. A single vertical, single boom lowers the cost, but is not as efficient in control and stability. By increasing the size of the tail surfaces, a single vertical and single boom can be used with a slight increase in control and stability, provided that the increase in total area is not too large. This seemed to be a reasonable compromise.

Another tail possible arrangement is the "T" tail. This configuration allows the horizontal tail to be lifted up away from the propeller wash and wing wake, making it more efficient. Inherent problems with the "T" tail are its heavier weight, difficult construction, and it does not help in stall recovery as well as other configurations.

A low tail configuration shapes the total airplane more aerodynamically than a high tail. On the other hand, a low tail places the empennage too close to the ground, which runs the risk of it hitting the ground upon takeoff and landing. The high tail configuration solves this problem by placing the boom higher off the ground.

The tail features discussed above were ranked and the results can be seen in the figure of merit chart (Table 3.1).

3.4 Fuselage

The fuselage of the airplane is of the utmost importance. Not only does it bind all the parts together, but it also distributes stresses, and carries the cargo. A large fuselage with a large amount of room for all the components would be ideal except for the fact that the larger the airplane, the heavier its weight and price in the Rated Aircraft Cost (RAC) equation. A lean fuselage that adequately carries all the components and cargo was the best choice overall. A circular cross-section would provide an adequate degree of streamlining as well. For strength and lightweight, the fuselage was to be made from a combination of balsa and light plywood.

Since the competing team can shape the steel cargo, it was decided to use the light payload (tennis balls) to shape the cargo area of the fuselage. Several options for this were available. The tennis

balls could be placed in one row, but that would make the fuselage unnecessarily thin and long. Stacked tennis balls are not very stable and dramatically increase the cross sectional area of the fuselage, so it was decided to use two rows of seven tennis balls (Figure 3.3.1). This provided for a fuselage that was not too wide, yet streamlined enough so as not to drive the RAC up. The steel cargo could be shaped to fit this area easily as well.

In order to efficiently and quickly load and unload both payload types, it was decided to use a speed loader. The competition rules state that the speed loader for both the heavy and light payloads must have the same external geometry, but more than one loader may be used with different internal geometry. This implies that different means to secure the payload internal to the container may be employed. This makes the selection of a design very important since both payloads must fit the same type of speed loader. Selection of the geometry was intuitive. The speed loader was designed to fit inside the fuselage ribs and was to be made from poster board material, lined inside with transparency sheets. The tennis balls fit into the loader without any internal modification. The steel, on the other hand, required a layer of foam around it that will secure it while in flight.

Other important factors considered included the manufacturing of the fuselage and its overall shape. All the figures of merit for the fuselage can be seen in Table 3.1.

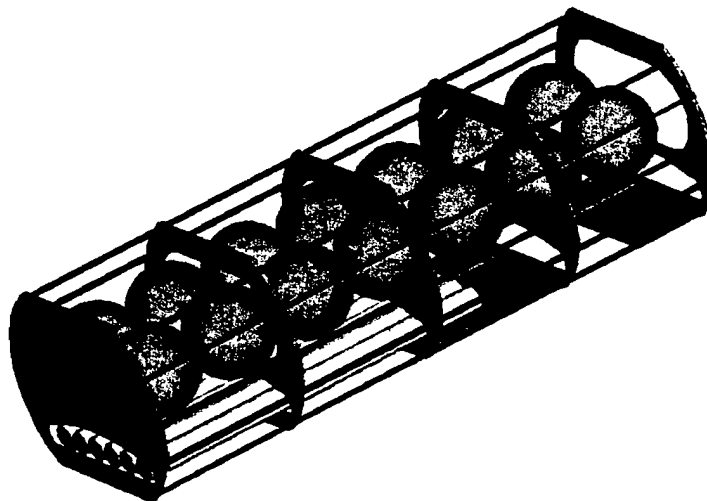


Figure 3.3.1. Fuselage Configuration with Light Payload.

3.5 Landing Gear

Aside from the aerial characteristics of the aircraft, the ground performance was another key consideration. This meant that a suitable landing gear had to be chosen. With that in mind, six different configurations for the landing gear were considered and can be seen in Figure 3.5.1. These were the single main, tail dragger, quadricycle, bicycle, tricycle, and multi-bogey as seen in the figure. Through a preliminary process of elimination the multi-bogey, single main, bicycle, and quadricycle types were immediately discarded. The multi-bogey configuration is used for extremely large aircraft and is just too much of an overbuilt design. Next, the single main and bicycle configurations were removed. The single main landing gear uses one wheel in the front of the aircraft, one wheel under each side of the wing, and one wheel on the tail. This configuration was decided against on the basis that it involves the wheels under the wing. The team has decided to keep a simple wing configuration that does not involve extra supports needed to hold up the forces of the landing gear on the ground. The bicycle configuration uses a single wheel in the front of the plane, a single wheel in the back and one wheel on each side of the wing. Again, the wheels under the wing kept us away from this design. Last, there is the quadricycle gear. This formation uses four wheels, two on each side of the fuselage. This gear was eliminated for the same reasons that the multi-bogey gear was eliminated; it was an overbuilt design for this type of aircraft.

The above features along with the physical makeup of the landing gear were important factors that were considered and ranked in Table 3.1.

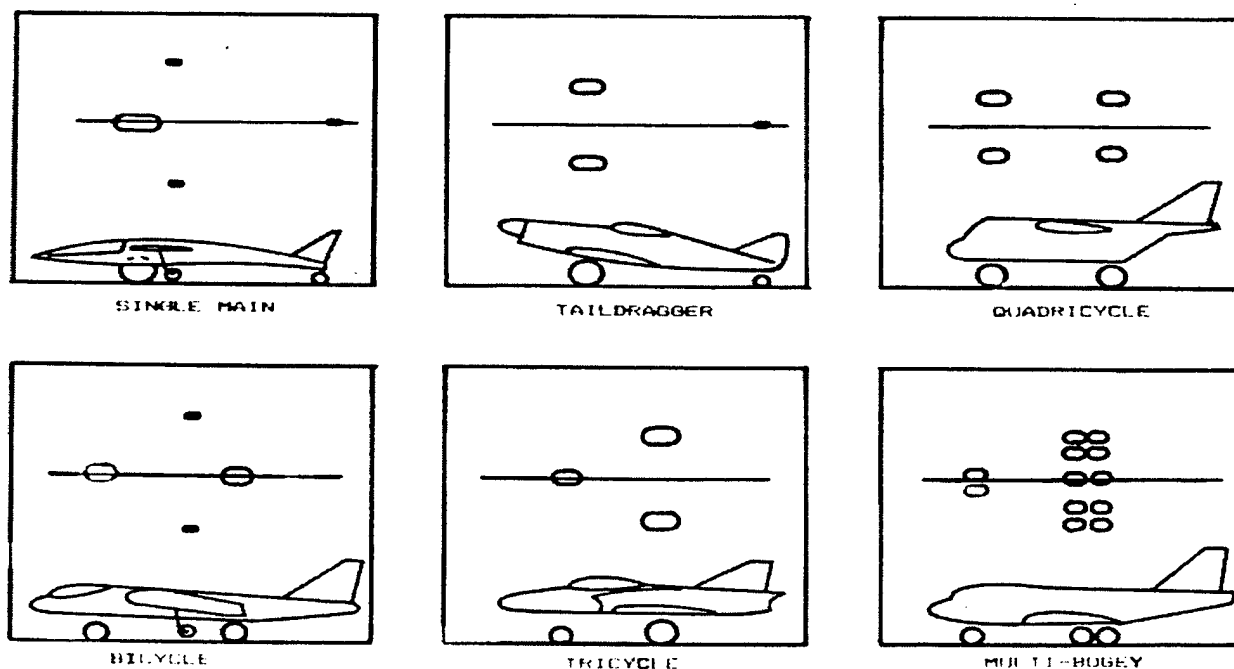


Figure 3.5.1. Landing Gear Configuration.

3.6 Batteries

Battery placement in the fuselage is critical. The batteries needed to be placed in a way that did not interfere with loading or unloading the cargo and in a way that kept them cool. Putting them in the cargo bay was out of the question because of interference with the speed loader and because of the lack of ventilation. Separating the batteries into different compartments may of kept them from heating each other up, but that would have made the wiring very difficult and tedious since they all needed to be connected to each other. They also had to be easily removable for recharging. It was decided that a separate compartment for all the batteries should be made in the fuselage. In this fashion they would all be together and out of the cargo bay. In order to counteract the heating effects, the compartment would be partly open to the outside air. This way while the airplane is in motion, cool air from the outside can flow over the batteries and keep them cooler than if they were all completely enclosed. The flow would then cool the cells and escape through an exit in the aft section of the aircraft. In order to prevent debris into the airplane, the scoop would be covered with some sort of screening or chicken wire. This solution came with a drawback of increased drag.

Other considerations for the batteries included the type of battery used. This is discussed in the next section because the batteries were intimately intertwined with the motor. These factors of merit can also be seen in Table 3.1.

3.7 Motor and Propeller

The coordinators of the competition have placed the constraint of Graupner or Astro Flight motors on all competitors. From previous experience with the two companies, Astro Flight motors are of better quality and durability. Astro flight offers the 40, 60, and 90 size motors. Choosing a motor is not as easy as going with the largest motor on the market. The weight and cost of the motor had to be taken into account, as well as, how those factors balance with the increase in torque. These and other figures of merit were ranked in Table 3.1.

The propeller is basically an airfoil that provides lift in the horizontal direction. Theoretically, the larger the prop the more thrust it generates, but there is a decrease in rpm (revolutions per minute) that reduces this benefit. Five props were tested to see what configuration provided the best results. Based on preliminary testing the 14X8 APC prop and the 13X8 APC PATTERN were kept for further testing.

The electric airplane's "fuel" is rechargeable Ni-Cad batteries, which come in all shapes and sizes. Because of their size, A-size batteries were deemed the only acceptable solution. Anything bigger would increase the overall aircraft weight because of the number of batteries needed. Selection was based on a power to weight ratio, and based on experience from previous years. Nothing less than 1700 milliAmps was considered, which narrowed the selection to two batteries:

Sanyo KR-1700 AU:	1700 mAh	36 g/battery	936g (24 batteries)	power/weight = 47.22
Gold Peak GP200AFK:	2000 mAh	43g/battery	1032g (24 batteries)	power/weight = 46.5

Because of the closeness of the power/weight ratios, either battery was a viable solution. Since they are so similar, the mAh was the deciding factor (the weight difference was negligible). Because of this, the Gold Peak battery was considered as the final selection.

3.8 Results

Looking at the chosen components, a conceptual visual representation of the electric airplane was made. The exploded view is shown below in Figure 3.8.1, and all detailed drawings are shown in the Detailed Design section of the paper. After all the aspects and parameters were taken into account, a chart documenting the possible solutions and their rated effects were created. This chart is seen in Table 3.1.

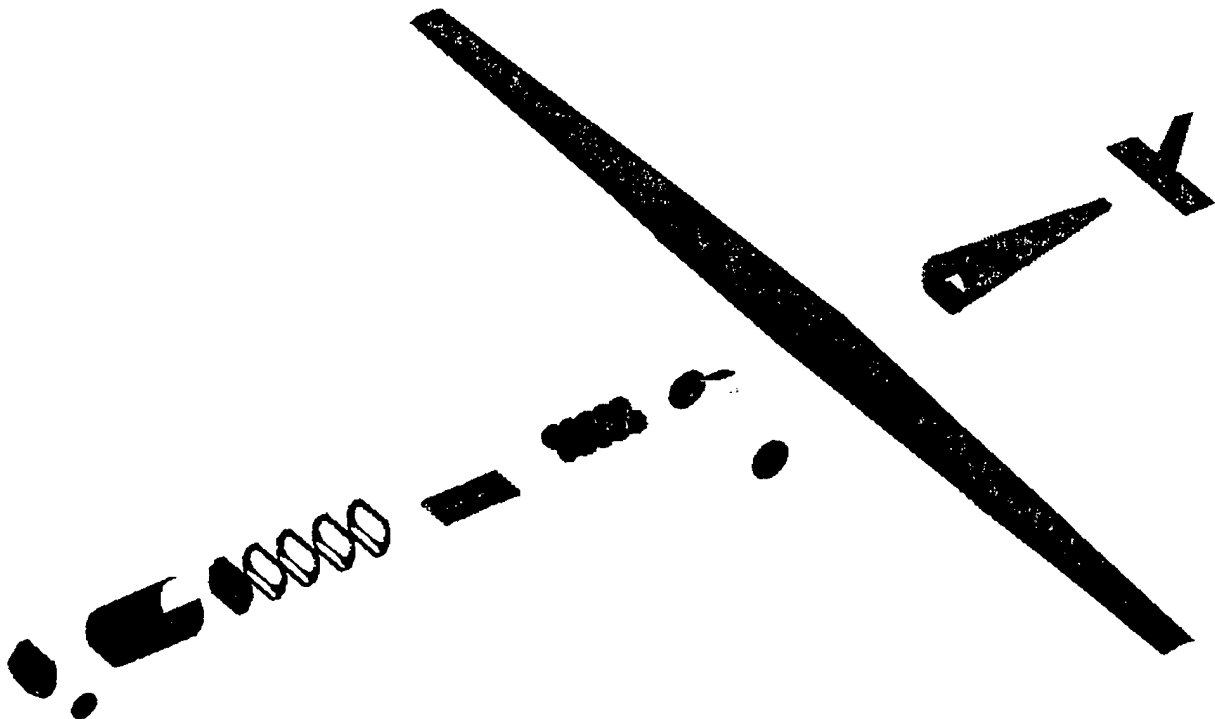


Figure 3.8.1. Exploded view of components.

Table 3.1. Figure of Merit Chart.

		Ease of Manufacture	Power Consumption	Handling Characteristics	Cost	RAC	Result
Wing	Tapered	0	1	1	0	1	3
	Rectangular	1	0	0	-1	-1	-1
	Elliptical	-1	1	1	0	0	1
	Rectangular/tapered	1	1	1	0	0	3
Number of wings	Mono-plane	1	0	0	1	1	3
	Bi-plane	-1	1	0	-1	-1	-2
Wing Structure	Foam, light ply spar, wooden sheeting	1	0	-1	1	0	1
	Carbon fiber spar, carbon fiber skin	-1	0	0	-1	0	-2
	Light ply spar, wooden sheeting (top), carbon fiber sheeting (bottom)	0	0	1	0	0	1
Tail boom Orientation	High tail	0	0	0	0	0	0
	Low tail	0	0	-1	0	0	-1
Tail boom	Single	1	0	0	0	1	2
	Double	0	0	1	0	-1	0
Tail configuration	T-tail	-1	0	1	0	0	0
	V-tail	-1	0	-1	-1	-1	-4
	Standard	1	0	0	1	0	2
Fuselage	Lifting body	-1	1	-1	-1	-1	-3
	Circular cross section	0	0	0	0	0	0
	Rectangular cross section	1	-1	0	0	0	0
Fuselage and Tail construction	Balsa, light ply	0	0	0	1	0	1
	Carbon fiber	-1	1	0	-1	1	0
Landing gear	Single main	-1	1	-1	-1	0	-2
	Bicycle	-1	1	0	-1	0	-1
	Quadracycle	-1	-1	-1	-1	-1	-5
	Tricycle	1	0	1	1	0	3
	Multibogey	-1	-1	-1	-1	-1	-5
	Tail dragger	0	0	0	0	0	0
Landing gear construction	Carbon fiber	-1	1	1	-1	0	0
	Aluminum	0	0	0	0	0	0
	Torsion bar	-1	1	1	-1	0	0
Motor	Astroflight 40	0	1	0	1	0	2
	Astroflight 60	0	0	0	0	0	0
	Astroflight 90	0	-1	0	-1	-1	-3
Propellers	APC	0	1	0	0	0	1
	Wood	0	0	0	0	0	0
	Nylon	0	0	0	0	0	0
Batteries	GP 2000	0	0	1	0	0	1
	KR 1700	0	0	0	0	0	0

1-Desirable, 0-Neutral, -1-Undesirable

4.0 Preliminary Design

4.1 Wing

The wing is one of the most important aspects of an airplane. The wing is what generates lift allowing the airplane to maximize the weight it can carry. Several variables determine how effective the wing will be on an airplane. Some of these variables include the lift generation, stability, weight, ease of manufacturing, rate of cost, and drag. For this year's UCF Electric Airplane, several wing options were looked at. These wing styles include a tapered wing, a rectangular wing, a swept wing, an elliptical wing, a wing with dihedral, and a rectangular and taper combination wing.

The Pugh and Dominic methods (as described in the Executive Summary) were used to determine the most effective wing for our purposes. The rectangular wing was used as the datum to compare all of the other wing designs that were being considered. The swept and dihedral wings were clearly not the choices for *Knightmare*. A swept wing is more effective at high speeds than at low speeds. At low speeds, a low Reynolds number is generated increasing the amount of drag on a swept wing. In addition, this type of wing would be difficult to manufacture, thus greatly increasing the time required to complete the wing. During flight, the loading on the wing will produce the effects of a dihedral wing. This is because the wing will be made from light materials such as foam, balsa, and carbon fiber, which can be easily deflected by the loading placed on the wing. Therefore, building a dihedral wing would be unreasonable because it would double the deflection the wing would create. Examples of the Pugh and Dominic methods for the wing are shown in Table 4.1.1.

A tapered wing when compared to a rectangular wing has a better lift distribution. According to Fundamentals of Aerodynamics, by John D. Anderson, a taper ratio between 0.4 and 0.5 would provide the best lift distribution. A taper ratio of 0.45 was chosen as a desirable number because it reduces the induced drag to a point that is only 1% greater than that for an elliptical wing. In addition, this wing weighs less, which would give it a lower RAC. Constructively, the drag would also be reduced by this design. The only disadvantage is that a tapered wing is slightly more difficult to make when compared with a rectangular wing. The next type of wing considered was a rectangular and tapered combination. This type of wing offers the same advantages of a tapered wing. Because this wing is more like an elliptical wing, it would generate a more uniform lift distribution than an untapered wing, which would in turn make it more stable. The final type of wing considered was the elliptical wing. This was determined to be the most effective type of wing because it gives the best uniform lift distribution. The only disadvantage to this wing is the difficulty of manufacture. This can even be seen in real aircraft. Most real aircraft do not use this type of wing due to the time and money that it takes to make this type of wing. Ease of manufacture was the only reason the team decided not to use this type of wing. For this purpose, *Knightmare* has a combination of a rectangular and tapered wing. This type of wing will generate the best possible lift distribution, the best stability, a lower weight and hence better RAC, and a lower coefficient of drag for the wing.

Pugh Method for Wing						
Alternatives						
Evaluation Criteria	Rectangular	Tapered Wing	Swept	Elliptical	Dihedral	Rectangular/Tapered
Lift Generation	S	+	S	+	S	+
Stability	S	S	-	+	+	+
Weight	S	+	S	+	S	+
Manufacturability	S	-	-	-	-	-
Rate of Cost	S	+	S	+	-	+
Drag	S	+	-	+	S	+
	+	-	4	2	5	1
Results	S	S	1	1	0	3
	-	-	1	3	1	2

Dominic Method for Wing						
A-Rectangular						
B-Tapered Wing						
C-Swept				High Priority-Weight, Rate of Cost		
D-Elliptical				Medium-Lift Generation, Manufacturability		
E-Dihedral				Low-Drag, Stability		
F-Rectangular/Tapered						
Alternative	High	Medium	Low			
A	G, P	G, E	F, G		E=Excellent	
B	E, G	G, G	G, G		G=Good	
C	G, G	G, P	P, G		F=Fair	
D	E, G	G, U	G, G		P=Poor	
E	G, G	G, P	G, G		U=Unacceptable	
F	E, G	G, G	G, G			
	H	M	L			
E	B D F	A				
G	A B C C D E E F	A B B C D E F F	A B B C D D E E F F			
F			A			
P	A	C E	C			
U		D				
————	Above is Excellent					
-----	Above is Good					
.....	Above is Fair					

Best rated is tied between tapered and a rectangular/taper combination.

Table 4.1.1 Pugh and Dominic Method.

The location of the wing was also a very important decision. A high wing would sit on top of the fuselage and would be one-piece. A mid wing or a low wing could either be a one-piece wing or two-piece wing joining through the fuselage. The problem with the low wing is that it would be mounted in the same location as the landing gear and experience heavy loading upon landings. This would cause unnecessary stress and fatigue on the wing and limit its lifetime. A two piece wing joining through the fuselage has been used numerous times on previous UCF aircraft. The problem with this configuration is that the two piece wing experiences a torsional effect, making the wing unstable. Attaching a mid wing cuts down on the payload area since the wing would be going through the middle of the fuselage. For these reasons a one-piece high wing was chosen for the optimal wing configuration.

4.2 Fuselage

The design of the fuselage is a very thorough and precise process. All elements of this airplane, including the fuselage, must be kept as light as possible. By keeping everything light, this will enable the aircraft to lift more weight. The fuselage needs to be designed to ensure that everything (receiver, speed controller, payload, and batteries) fits inside without allowing undesired excess space. Extra space in the fuselage means extra material, which means more weight. Using more material in certain sections will show that a high structural integrity is needed at that point. To help with the fuselage design Pro/E was used. With this program the team designed and configured the fuselage in different ways to make it as efficient as possible while keeping the rated aircraft cost as low as possible.

The fuselage design is based on the configuration of the tennis balls and batteries. The reasoning behind this is that the tennis balls and batteries will take up more room than the steel bars and batteries. To begin this design, a convenient arrangement of tennis balls must be found. The convenience will be how easily the tennis balls could be loaded and unloaded with the use of a speed loader. The team came up with five configurations that seemed to be the best, all creating a desired center of gravity directly in the middle of the payload stack. The optimum configuration was chosen based on the volume that the tennis balls occupied along with how easily they could be placed in and removed from the fuselage. Pro/E was used to determine the volume that each configuration would occupy in the fuselage and to also model the most aerodynamic body possible, while keeping the center of gravity in a reasonable place.

The fuselage utilizes the use of an "air scoop" as a method to have airflow through the bottom of the fuselage in an effort to cool the batteries. This air scoop was implemented with the design of the tennis ball configuration. The fuselage was also designed to incorporate the wing onto the top. This allows smooth flow of air over the top of the fuselage, as previously discussed.

The complete fuselage design is based upon how easily the payload can be accessed. The Figures of Merit for the fuselage are as follows:

- The volume needed for the payload
- The RAC of the fuselage
- An optimal center of gravity,

- Having an "air scoop" compatible design,
- The arrangement of batteries,
- The number of tennis balls that can be carried as payload

The most important of these aspects are the volume of the payload and batteries, and the RAC of the fuselage. The next most important aspects are having a center of gravity close to the lifting force and incorporating an "air scoop" into the fuselage. The final aspects considered were payload accessibility and the number of tennis balls the fuselage could carry.

The Pugh Method and the Dominic Method were used to determine which configuration would be optimal (Table 4.2.1). The previously mentioned criteria were used in these methods to determine the best fuselage design for our purposes. As explained for the wing, a datum or standard was used to compare the other design options against for the Pugh Method. The datum in this case was the two rows of seven tennis balls. This seemed to be the simplest configuration for loading/unloading and designing for the fuselage. Other arrangements of the light payload were considered, however none of the other arrangements had a smaller volume or more aerodynamic effect on the fuselage than the two rows of seven. The Dominic Method also showed similar results with the two rows of seven reflecting acceptable results. From the analysis of these two methods, it appeared that for the team's design purposes, the two rows of seven tennis balls was the most optimum and would be able to meet all the criteria in the above paragraph.

4.3 Prop/Engine

The choice for motors this year was limited by the competition rules. In previous years, a team could buy any off-the-shelf motor, but this year the team was restricted to two companies, Graupner and Astro Flight. A Graupner motor was used three years ago by a previous UCF team without very good results; on the other hand the electric airplane last year used an Astro Flight motor, getting exceptional results. As a team, the decision to go with the Astro Flight motor was based on good recommendations by numerous R/C modelers, and the fact that the team already had easy access to this brand of motor.

A comparison was done on three Astro Flight motors, sizes 40, 60, and 90. The 90-size motor was eliminated as an option, because the cost of the motor was 1/4 of the total airplane budget. The 40 and 60-size motors were closely compared using the Pugh and Dominic method and also by a comparative analysis done with the RAC. The RAC using the 40-size motor was lower, and as a result the total score was higher. The result of this comparison was definitely one of the major deciding factors. Additional factors also had an effect on the final decision for choosing the best motor, such as price and availability. A 40-size motor was readily available to the team. If the 60-size motor was chosen, it would have to be purchased at the price of \$325, and then delivery would take six weeks.

For testing on the motors, the team built a test stand composed of a sliding rail. There were two parts to the rail, a stationary part and a mobile part. The stationary part was clamped to a table and a fish scale was used to attach the stationary part to the mobile part via hook from the fish scale. With this

mechanism the team was able to do static thrust testing. Comparison between the thrust values from testing done with the 40-size motor and those given by the manufacturer gave similar results. From this testing, the team felt confident that the thrust values given by the manufacturer for the 60-size motor could be used for further analysis.

Using the manufacturer's information, calculations were done to see if using the 60-size motor would be more beneficial in regards to take off distance. The 60-size motor gave a shorter take off distance based on a total aircraft/payload weight of twenty pounds. With the 40-size motor, the plane was calculated to take off in 102 ft based on the same aircraft/payload weight. The rules of the competition stated that there was 200 ft. available, so there was not a big benefit with using the 60-size motor. Overall, the 40-size motor was the best choice for this competition, based on its power, size, price and availability.

After deciding on the motor, testing with different propellers began. The propeller selection could definitely make the difference between winning and losing. Propellers were found to come in many different shapes and sizes. There were two, three and even four-bladed propellers made out of plastic, composites, and wood. Different propeller lengths, pitch configurations, as well as different tips for the blades were all considered before selecting the final propeller for *Knightmare*. All of these characteristics impact the propeller efficiency and hence the output power of the motor.

The first step was to look at the number of blades on a propeller. Three and four bladed propellers are hard to find and can be costly. The two bladed propeller was the more practical choice since it was readily available, light (compared to the three and four bladed prop), and very inexpensive.

Propeller construction was a very important aspect. Plastic propellers are usually thrown out because they lose their shape very fast. As it spins the tips go forward and the propeller loses its efficiency. From testing, a wooden propeller was found to be light and kept its shape. These propellers have two types of tips; one is a square tip and the other is a round tip. The round tip gives more of an elliptical distribution increasing its efficiency. This prop was cheap but it shattered easily upon minimal impact to the ground. Since the airplane would have to land several times during the ten-minute period, it would not be possible to attach a new propeller on the flight line if one breaks. Propellers made from composite materials gave the best results in the team's testing, and the company confirmed that they were the most efficient propellers on the market. According to the test data and performance data, the tips of these propellers had an elliptical shape and the propeller maintained its shape during static thrust test; this did indeed support the company's theory.

Several size props were tested and considered. The 14x8 prop pulled 40 amps and the 13x8 props pulled 38 amps, as expected. These amp values are fairly close, so the deciding factor was the thrust developed. The developed thrust for the 14x8 prop was 7 lb. and the 13x8 props developed 6 lb. By this criterion the 14x8 prop was chosen.

4.4 Batteries

The choice of the batteries for the airplane was extremely important. The plane had to be light and powerful to maximize flight performance. It was very difficult to find someone knowledgeable of soldering cells together for this purpose. After many hours on the Internet and on the telephone, the team was able to talk to a representative at TNR Technical in California, and gain invaluable information.

The most important properties in choosing a cell are size, weight, shape, and Amps. The team decided to go with a round slender cell because of the numerous different configurations that could be achieved for the battery pack. With that criterion, two cells were extensively researched. The Sanyo KR-1700AU, and the Gold Peak 2000AFK. The representative of TNR confirmed that those were the best batteries for the job, that they would be more than happy to weld a pack together for a minimal fee, and that the battery pack would be guaranteed for one year.

To reach a final decision between these two cells, an Amps-to-weight ratio was obtained. The KR-1700AU had a power to weight ratio of 47.22 and the Gold Peak had a power to weight ratio of 46.5. Obviously, the Sanyo had a better power to weight ratio than the Gold Peak. The 1700mAh was determined to be adequate to make the plane fly with two steel sorties and two tennis ball sorties for the entire ten minute period. The team wanted to be on the safe side and make sure there would be extra time left in the batteries. The weight penalization for having the bigger battery was only 0.3 lbs. In comparison, testing with last year's batteries (1400mAh) showed that there was only enough power to fly for two steel sorties and one tennis ball sortie.

For arranging cells, there are two basic ways to form battery packs: one in series and the other in parallel. In series (see Figure 4.4.1.a) the voltage is added and the milli-Amp hours stay the same; the other configuration is parallel (see Figure 4.4.1.b) where the milli-Amp hours are added but the volts stay the same. Either method or both methods could be used. The higher the milli-Amp hours, the longer the flight time; the higher the voltage, the more thrust developed.

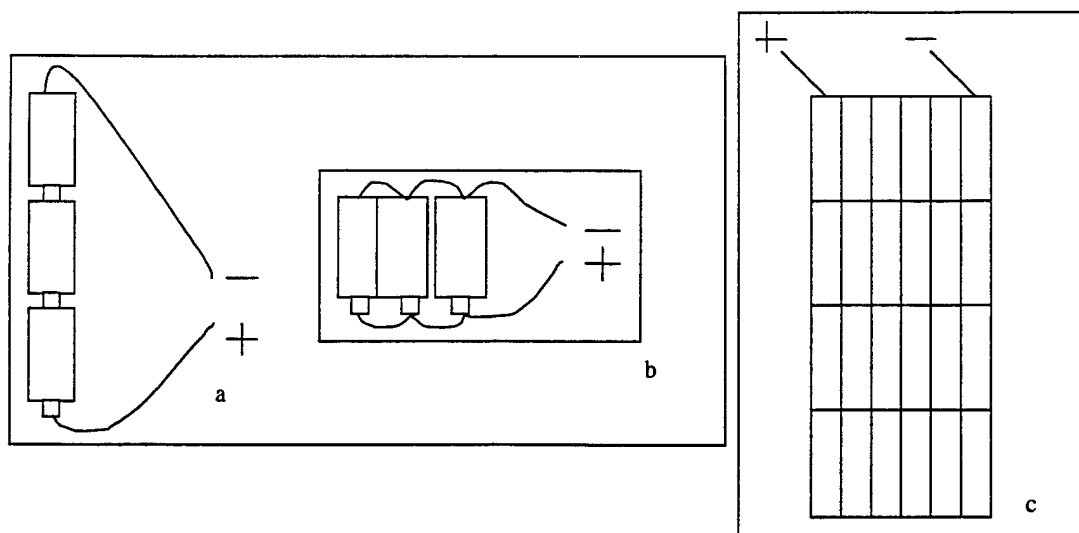


Figure 4.4.1. (a) Series (b) Parallel (c) Proposed Battery Pack

From all of this testing and research, the Gold Peak battery was chosen for use in this competition with a pack of 24 cells all in series. (Figure 4.4.1.c). The maximum number of cells that the motor can take is 24, and the manufacturer of the motor had recommended this number of batteries to the team. The configuration of the batteries actually decided the minimal dimensions of the fuselage, as mentioned in the conceptual design section. The battery configuration chosen also produced the most aerodynamic fuselage. Consequently, the battery pack is a configuration of six cells across and four back. From experience, the best idea is to have one connector coming out of the pack. This would eliminate the chances of short circuiting the batteries and shorting out the entire pack.

4.5 RAC Comparison

After the motor and number of batteries were decided upon, a comparison was done between the RAC for UCF's airplane and that of last year's winner, Utah State. As hoped, UCF came out with a greater score (200 points higher) than Utah State, showing a sufficient preliminary design thus far. This comparison can be seen in Table 4.5.1. Using Microsoft Excel, a spreadsheet was created to aid in comparing different fuselage and payload configurations to optimize the RAC. The optimum RAC computed was around a value of 3.3. Utilizing this value of the RAC, a total optimum score of approximately 2200 was calculated. This final value was computed with an accuracy range of ± 50 points.

UCF			
40 Sized Motor			
wing area=	7.42	Cells=	24
control surfaces=	2	Fuse(A)=	30
Body=	1		
Fuse Length(ft)=	4	Empty weight=	6
Verticals=	1		
Horizontal=	1	STEEL (lb)	75
Servos=	5	Tennis balls	42
Motors=	1		
Props=	1		
Strut=	0		

A	100/lb	100
B	1/W	1
C	20/hr	20
MEW		5.5
REP	#motors*Amp*1.2*#cell	864

MFHR	WING	#	
	15(hr) basic		15
	wing area (4/ft^2)	7.42	29.7
	surfaces (3/surface)	2	6
	Struts	0	0
	FUSE		
	body(5/body)	1	5
	Fuse length (4/ft)	4	16
	EMPENAGE		
	5(hr) basic		5
	Verticals (5/vertical)	1	5
	Horizontal (10/horiz)	1	10
	SERVOS		
	5(hr) basic		5
	servos (2/servo)	5	10
	PROPULSION		
	Engine (5/ engine)	1	5
	Prop(5/prop)	1	5
	Total		117

Paper	90
Rated Aircraft cost	3.75
Steel	75
Tennis balls /5	8.4
Score	2003.0

Utah state University			
wing area=	12	Cells=	36
control surfaces=	2	Fuse (A)=	40
Body=	1		
Fuse Length(ft)=	6	Empty weight=	18
Verticals=	1		
Horizontal=	1	STEEL (lb)=	110
Servos=	9	Tennis balls=	90
Motors=	1		
Props=	1		
Struts=	2		

A	100/lb	100
B	1/W	1
C	20/hr	20
MEW		18
REP	#motors*Amp*1.2*#cell	1728

MFHR	WING	#	
	15(hr) basic		15
	wing area (4/ft^2)	12	48
	surfaces (3/surface)	2	6
	Struts (2/strut)	2	4
	FUSE		
	body(5/body)	1	5
	Fuse length (4/ft)	6	24
	EMPENAGE		
	5(hr) basic		5
	Verticals (5/vertical)	1	5
	Horizontal (10/horiz)	1	5
	SERVOS		
	5(hr) basic		5
	servos (2/servo)	9	18
	PROPULSION		
	Engine (5/ engine)	1	5
	Prop(5/prop)	1	5
	Total		150

Paper	93
Rated Aircraft cost	6.528
Steel	110
Tennis balls /5	18
Score	1823.5

Table 4.5.1. Rated Aircraft Cost Comparison

4.6 Tail

The tail provides the stability for the aircraft. In addition to stability, the airplane will need to have a tail that allows easy access to the payload. The team has chosen to unload the payload out the back of the airplane instead of removing the wing to take it out of the top. This was because removing the wing would require too much time on the flight line since the wing was mounted on with four screws. Several options were looked at for both tail stability and payload access.

The difference between using a single or double boom, and one or two vertical stabilizers, is the amount of stability retained in the case of cross winds. Twin booms will allow the horizontal stabilizer to be connected at two "hard points" helping to prevent the tail from oscillating back and forth. A single boom gives an advantage of less weight if constructed using the minimum amount of material needed for structural stability. A double boom design had the capability of unloading the payload between the booms. A single boom design had the tail completely flip up on hinges to allow easier access to unloading the payload.

A single vertical stabilizer was thought of to keep the tail weight down and avoid the extra points that would be added to the RAC. A double vertical stabilizer would add weight to the tail and add more points to the RAC. However, an advantage to a double vertical stabilizer is that it would allow the tail to have a smaller profile area. A smaller area would give the tail better control in case of a crosswind, a crosswind that would tend to produce a greater yaw effect on a large vertical.

Several design configurations were thought of for the tail. Every combination of high tail, single or double boom, and single or double vertical stabilizers were looked at. In addition, a high tail with a single boom and a T-tail was looked at. A low tail was looked at to have a total airplane shape similar to that of an airfoil. However, as mentioned in the previous section a low tail would increase the possibility of hitting the ground upon takeoff and landing. The only options looked at for a low tail were single booms with one or two vertical stabilizers.

Again, the Pugh and Dominic methods were used to analyze the alternative designs. The criteria that the designs were evaluated under included stability, weight, payload access, complexity to build, clearance for landing/takeoff, and rated cost. With the Pugh method no alternative appeared better than using a high tail with a single boom and single vertical stabilizer. The high tail with a single boom and a T-tail configuration did rank quite similar to this configuration with the differences being in stability and complexity to build. The Dominic method gave similar results with the high tail with two vertical stabilizers and either one or two booms also acceptable.

Overall, a high tail was the definite choice. The decision had to be made between one or two booms and one or two vertical stabilizers. Having one vertical provided better results using both the Pugh and Dominic methods. The weight could be kept down and the tail would be better in the RAC. The only question for a single boom and single vertical stabilizer would be how structurally stable the tail could be made. One issue the team contemplated was how everything would be mounted. This will be looked at further in the detailed design section.

4.7 Landing Gear

The landing gear requires no analysis by Pugh or Dominic methods. The choice for this airplane was quite simple. As mentioned in the conceptual design section, six different types of landing gear were looked at for the design of this aircraft. Four were quickly eliminated and two were kept for further investigation; the tail dragger and the tricycle. The tail dragger would provide more propeller clearance, offer less drag and weight, and allow the wing to generate more lift for rough field operation than the tricycle gear. On the other hand, a tail dragger could also be unstable. The tail wheel is behind the center of gravity and causes a tighter turn, which could result in a wingtip hitting the ground. The aircraft must typically be aligned perfectly with the runway at touchdown to keep stability in landing. The next formation considered is the tricycle gear. This is the most commonly arrangement used today. Tricycle gear allows the center of gravity to be ahead of the main gear so the aircraft is stable on the ground and could even be landed with the nose unaligned to the runway. Upon looking at these arrangements of landing gear, the team decided to use the tricycle style of landing gear. For this design's purpose it appeared to be the configuration that would perform best under the given flight and runway conditions.

4.8 Results

Through the use of the Pugh and Dominic methods, a preliminary design was established. This design consisted of a high mono wing and single boom design. The power of the aircraft consisted of an Astro Flight 40-size motor with 24 cells in series used in conjunction with APC 14X8 propeller. With this preliminary design, the detailed design process was used to finalize and optimize particular aspects of the aircraft adequately.

5.0 Detailed Design

5.1 Hinge Design

The hinge is what provides access to the payload. As previously mentioned in the Executive and Preliminary sections, a hinged tail will give sufficient access to the payload in the fuselage while allowing the tail to be out of the way of the crew removing the payload. The hinge will be a simple hinge such as that found on a door only of a much smaller scale. One side of the hinge will be fixed to the fuselage while the other side is fixed to the tail. Washers and lock nuts will hold on the hinge. It will be placed on the outside of the airplane so the tail can flip upward.

The latch is affixed to the bottom of the airplane. The latch is of a simple kind used to hold the tail closed during flight, yet it is easily unlocked to allow access to the payload. Calculations were performed on the latch pin. The resulting conclusion is that the pin can absorb up to 50 lbf. before failure.

Any gaps between the fuselage and the tail is sealed with a gasket so that air will not be allowed to enter the fuselage. Any air entering into the plane could cause abnormal forces that could result in the failure of the mounting configuration. In addition, an abnormal airflow would increase the drag on the airplane that, in turn, would hinder its performance.

5.2 Wing Design

Again, the wing is, obviously, one of the more important parts of an airplane because it is what generates the lift to carry the airplane and its cargo. The design of a wing is a very detailed process. First, an airfoil must be selected that will produce the lift that is wanted for the airplane. Second, the wing size must be determined. The span and chord are very important in wing design. Then, a wing type should be decided upon. To review, a few examples of wing types are rectangular, elliptical, and tapered. Finally, the control surfaces on the wing must be chosen. Since the airfoil had been previously selected, the next aspect of the design was to determine the wing size. For this year's competition, the teams are limited to a 10-foot wingspan. To get the most lift out of our wing, the team decided to use the full 10-feet.

Now that the wing length was known, the type of wing geometry to use had to be decided. The most efficient wing has a uniform lift distribution. As discussed in the Preliminary Design section the wing that achieves this is an elliptical wing but due to construction difficulties, an elliptical wing was ruled out. A rectangular wing is very easy to build, but does not offer a uniform lift distribution. A rectangular wing creates excess lift at the tips, which increases induced drag. In addition to being inefficient at the tips, the additional area at the tips creates more weight for a heavier wing. From the previous examples, a tapered wing design was considered. This type of wing would have less area, which would also have a better effect on the rated aircraft cost. From research, a taper ratio of 0.45 was found to be the optimum for a tapered wing. A small tip chord would be very difficult to cut for such a cambered airfoil. For this reason, a tip chord of 4.5-inches was chosen, thus giving the wing a root chord of 10-inches. Experience in wing building told the team that this small taper ratio would be very difficult to build within a length of five feet from root to tip. Due to this fact, it was decided that a combination of a rectangular and tapered

wing would be used. As a comparison, an ellipse is fairly straight with most of the taper occurring towards the tips. So, the team's wing is straight and rectangular for approximately 60% of the wing with 20% on each tip for the tapered portion. A rectangular and tapered wing will still offer a uniform, semi-elliptical lift distribution while being much easier to manufacture. In addition, a rectangular and tapered wing does not have a significant effect on the rated aircraft cost.

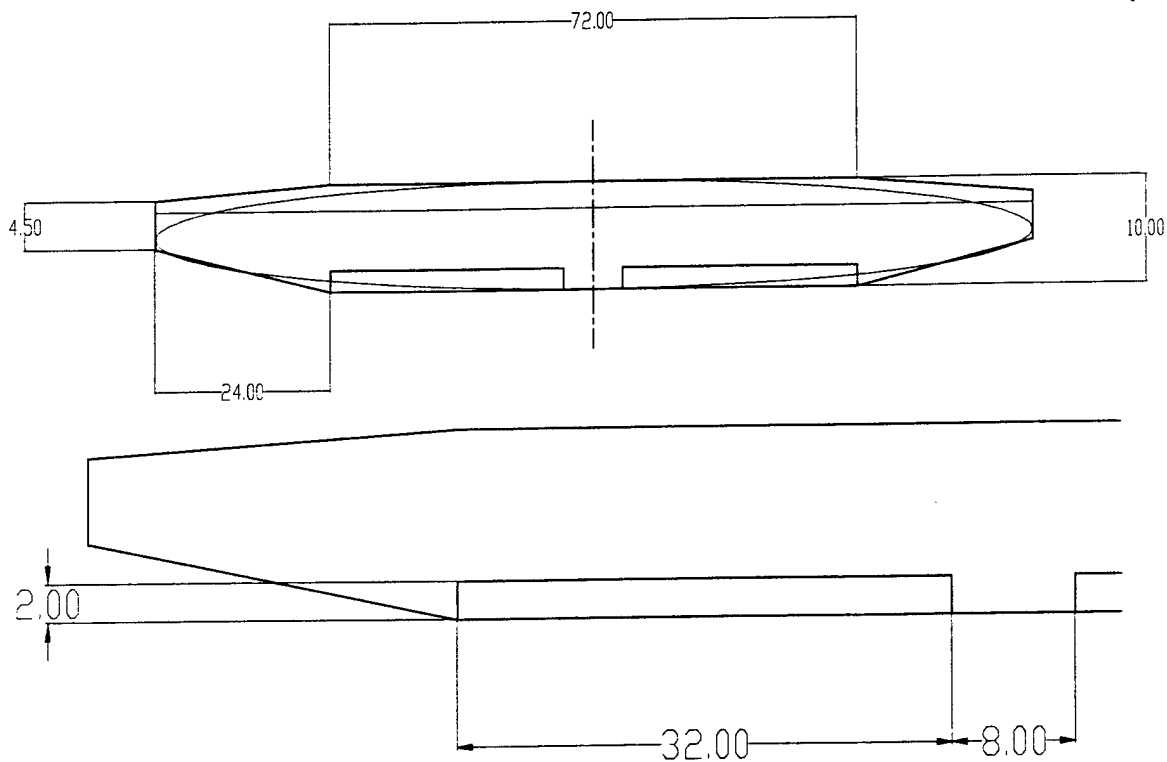


Figure 5.2.1. Wing Dimensions

The final component of the wing to consider is the control surfaces. On a wing, a flap is used to provide additional lift at takeoff while providing additional drag to slow down the airplane upon landing. While in flight, an aileron is used to provide roll for the airplane. Having both flaps and ailerons would require the wing to have four servos. This would weigh heavily on the rated aircraft equation given by the competition. It is the intent of this team to keep the rated aircraft cost as low as possible. For this purpose, the team decided to use flaperons on the wing, acting as both a flap and an aileron. Therefore, the flaperon will provide the lift and drag needed on takeoff and landing and providing the roll needed when in flight, while requiring only two servos. Research shows that the flaperon should extend 50-90% of the wingspan. For ease of control and construction, the flaperon was built on the rectangular section of the wing. With the rectangular portion being 72 inches, both flaperons will be 32 inches. This makes the flaperons 53% of the wingspan, which falls within the given range from research.

To ensure structural certainty, analysis was performed on the light ply wing spar. It was determined that spar itself can hold the weight of the aircraft, but the balsa and carbon fiber sheeting will be able to handle the additional dynamic loading.

Figure 5.2.1 gives a detailed picture of the wing.

5.3 Motor / Firewall Analysis

After the Cobalt 40 motor, Sanyo 2000 mAh batteries, and the 14x8 APC propeller were selected for *Knightmare*, an analysis of the force provided by the motor on the plane was done. *Knightmare* uses a "Firewall" as a means of protection for the motor in the event of a crash so that the steel payload does not rip out the motor and damage it. This firewall was made from a layer of fiberglass-coated balsa and a layer of light plywood. The purpose of this analysis was to see how much strain and deflection would be seen on the firewall and motor support with the seven pounds of thrust from the motor constantly acting on it. The first support was made from aluminum 2024-T3 with two reinforcing strips holding the support to the firewall. As shown in Figure 5.3.1(a), this configuration was considerably below the yield tensile strength of the aluminum and so it was decided that this support was too strong and added unnecessary weight to the aircraft.

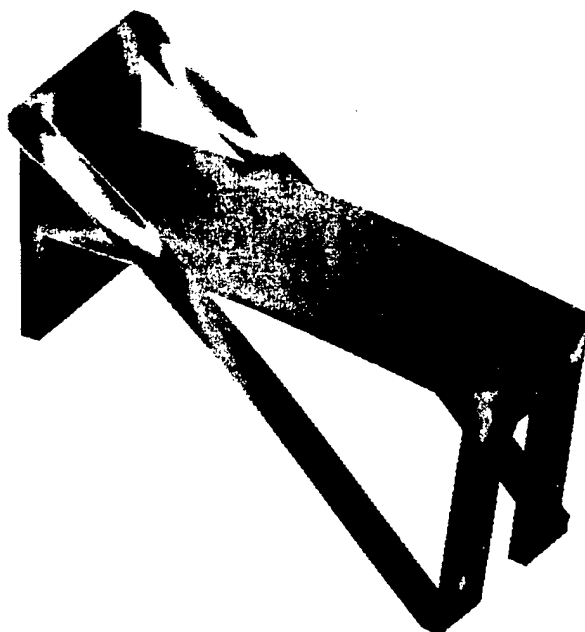
From the analysis of the first motor support, the design of the second motor support came about. This support was still below the maximum tensile strength of aluminum 2024-T3; however, it produced less weight, as well as, minimal deflection. The proposed design for the motor support can be seen below in Figure 5.3.1(b).

The proposed design above for the motor mount called for the frame to be made completely from aluminum. Looking at this design further it seemed costly and time consuming to construct, so alternatives had to be found. The alternative design used plywood and epoxy in the same design as above, but used side walls to give added strength and support (Figure 5.3.2). This alternative demonstrated adequate strength, from destructive testing, to withstand extreme landings. This new design proved easier to construct and lighter than the previous designs. By using the criteria of lightweight, strong, inexpensive and ease of construction, the plywood alternative was found to be the superior design. Analysis on this alternative, wooden motor support reveal that it would support a 10g landing and still be well below the yield strength of plywood.

RESULTS: 5- B.C. 1,STRESS_5,MOTOR
 STRESS - VON MISES MIN: 1.91E+01 MAX: 6.36E+03
 DEFORMATION: 1- B.C. 1,DISPLACEMENT_1,MOTOR
 DISPLACEMENT - MAG MIN: 0.00E+00 MAX: 7.78E-03
 FRAME OF REF: PART

paper

VALUE OPTION:ACTUAL



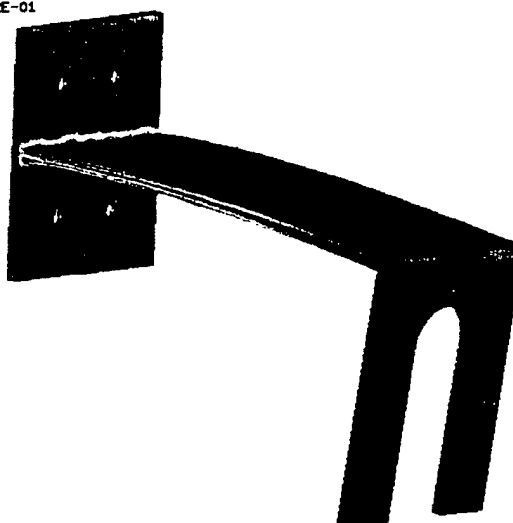
6.36D+03
 5.72D+03
 5.09D+03
 4.46D+03
 3.82D+03
 3.19D+03
 2.55D+03
 1.92D+03
 1.29D+03
 6.53D+02
 1.91D+01

(a)

RESULTS: 2- B.C. 2,STRESS_2,LOAD SET 1
 STRESS - VON MISES MIN: 7.47E-02 MAX: 2.64E+04
 DEFORMATION: 1- B.C. 2,DISPLACEMENT_1,LOAD SET 1
 DISPLACEMENT - MAG MIN: 0.00E+00 MAX: 3.72E-01
 FRAME OF REF: PART

/home/ugrad/alm/plexyglass.mfl

VALUE OPTION:ACTUAL



2.64D+04
 2.37D+04
 2.11D+04
 1.85D+04
 1.58D+04
 1.32D+04
 1.06D+04
 7.92D+03
 5.28D+03
 2.64D+03
 7.47D-02

(b)

Figure 5.3.1: (a) Configuration 1 for motor support
 (b) Configuration 2 for motor support

To house the motor, a cowl was made for the front of the aircraft. This cowl reduces the drag on the front of the aircraft and is constructed from fiberglass to attain minimal weight addition. A mold for the cowl was made from foam and was then layered with fiberglass cloth. Upon curing, the foam was removed leaving a strong and lightweight cowl. An air scoop was then cut out of the cowl to allow airflow into the fuselage. As mentioned before, this airflow is used to cool the batteries and the speed controller (which will heat up due to the extreme power output that will be generated during flight). The airflow then exits out of the tail of the aircraft just as the payload section of the fuselage ends.

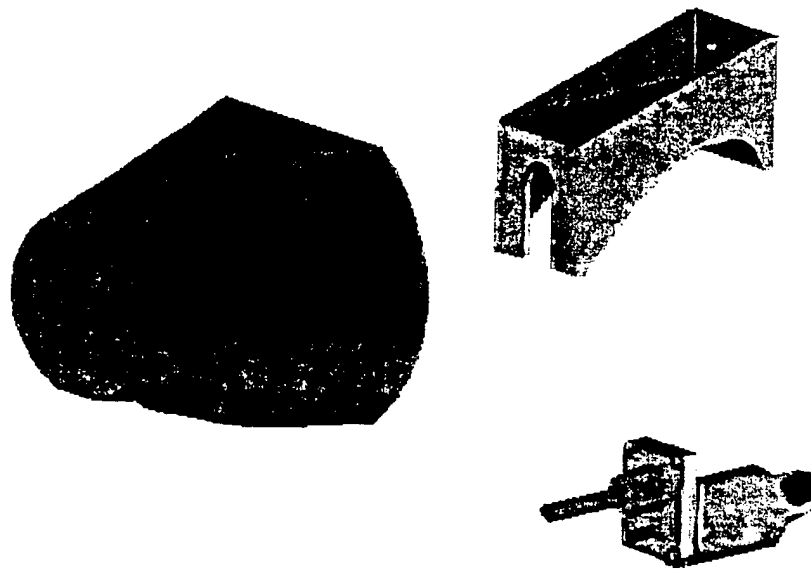
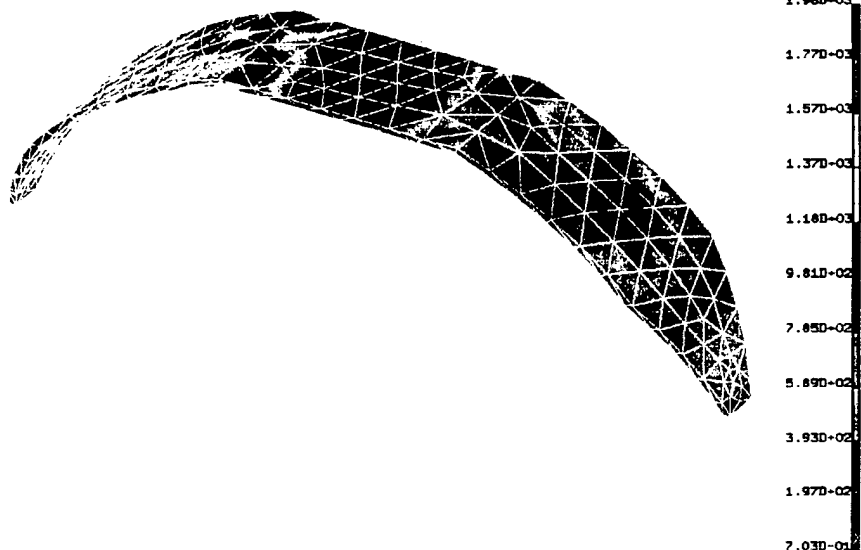


Figure 5.3.2. Fiberglass cowl and plywood motor mount.

5.4 Landing Gear Analysis

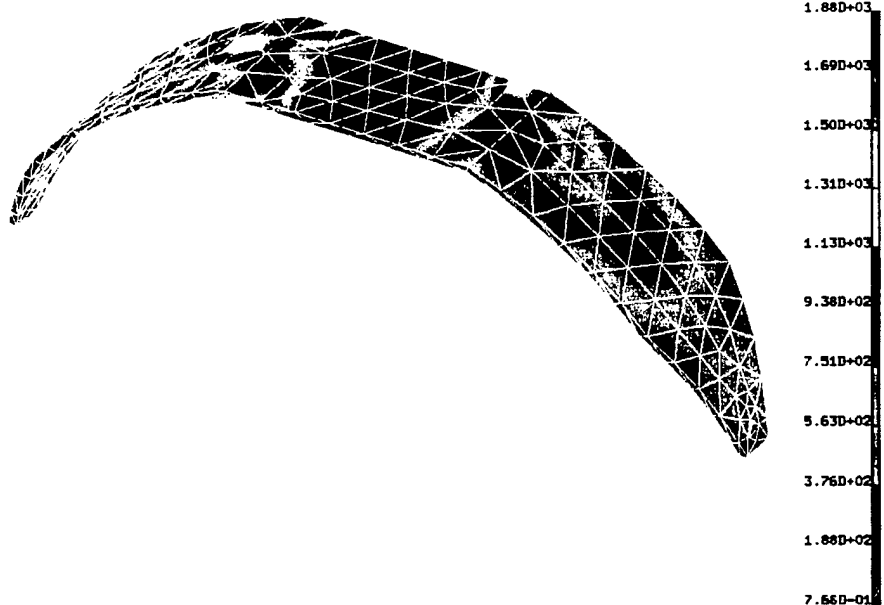
This year, UCF's electric airplane team had a different idea in mind for landing gear. Instead of designing a new main landing gear (since many existing designs already existed in the lab), the concept of "design reuse" surfaced. Why should manpower be wasted on a new design when an existing design could accomplish the task? With this in mind the team set out analyzing the pros and cons of each existing landing gear. The best main landing gear the team found, was one that was made from kevlar and carbon fiber. This design provided a combination of rigidity

/home/classes/fa00/en14535/kac/ARC/hate_ideas.mf1.2
 RESULTS: 3- B.C. 1,STRESS_3,LOAD SET 1
 STRESS - VON MISES MIN: 7.03E-01 MAX: 1.96E+03
 DEFORMATION: 1- B.C. 1,DISPLACEMENT_1,LOAD SET 1
 DISPLACEMENT - MAG MIN: 0.00E+00 MAX: 5.85E-03
 FRAME OF REF: PART



(a)

/home/classes/fa00/en14535/kac/ARC/hate_ideas.mf1.2
 RESULTS: 3- B.C. 1,STRESS_3,LOAD SET 1
 STRESS - VON MISES MIN: 7.68E-01 MAX: 1.88E+03
 DEFORMATION: 1- B.C. 1,DISPLACEMENT_1,LOAD SET 1
 DISPLACEMENT - MAG MIN: 0.00E+00 MAX: 1.05E-02
 FRAME OF REF: PART



(b)

Figure 5.4.1: (a) Carbon fiber model (b) Kevlar model

and flexibility that would be needed upon landing and would be sure to hold the weight of the plane during landing (its original use was for a heavy lift competition). It also provided the height that was needed to take off at various angles of attack without dragging the tail. The only change that was done to this landing gear was to change the wheel size. Since the team had no idea of the conditions of the runway the plane would be landing on, a larger wheel size was deemed necessary. Even though the team was confident this main landing gear would work, a simple analysis was done to ensure that this landing gear would not break. Using I-DEAS for the analysis, the landing gear was modeled first of carbon fiber/epoxy and then of kevlar/epoxy. This was because the team did not have the knowledge or resources to analyze the mesh of both materials. Knowing that the carbon fiber was more rigid, it was known that this would be the critical factor in determining the failure criteria for the main landing gear.

Figure 5.4.1 shows the stress and deformation of the main landing gear using an 8g force upon landing as a safety factor. As can be seen, the forces the landing gear sees is below the maximum tensile yield strength for both the kevlar and carbon fiber. The maximum deflection the main landing gear will see is .01 inches, with the stress concentration in the corners as is expected. This analysis proved to the team that the main landing gear would sustain the impact loads upon landing.

In performing the analysis on the landing gear mounting plate (fiberglass-coated balsa block), a very simplified approach was taken. The idea behind it is that the three-dimensional section of the plate that the landing gear contacted is isolated. Zero degree of freedom constraints were applied along the four edges perpendicular to the plate/gear-mounting surface. Then a distributed load was applied to the mounting surface to simulate the force of the landing gear on the plate. Using the best available property values for wood, the distributed force was varied and the appropriate data was taken. The stress values obtained were compared to the maximum tensile strength of the fiberglass balsa (50 MPa) because the assumption is that the plate would primarily see tensile loading. In the end, it was determined that the plate could take a maximum of a 4-g load, equivalent to 82 lbs.

5.5 Center of Gravity / Mass Properties

Now that all of the components had been selected, the final weight and center of gravity of the airplane could be determined. Using Pro/Engineer, the components and geometry were modeled and a total weight of 5.5 pounds was assessed to the plane. This weight was a good number since the team had set a limit of 5.5 pounds for the plane; however, it did not leave much room for changes upon manufacturing this design. The team tried numerous ways to cut the weight from the plane and was not able to cut it substantially, which lead to a critical assembly of *Nightmare*, being careful not go over the total weight.

Next, using Pro/Engineer, the center of gravity was found. As seen below, in Figure 5.5.1, the center of gravity (cg) lies right under the quarter chord. The red coordinate system on the figure below denotes the cg. This meets the criteria set out by the competition, which states that the cg should lie within the tip chord of the plane.

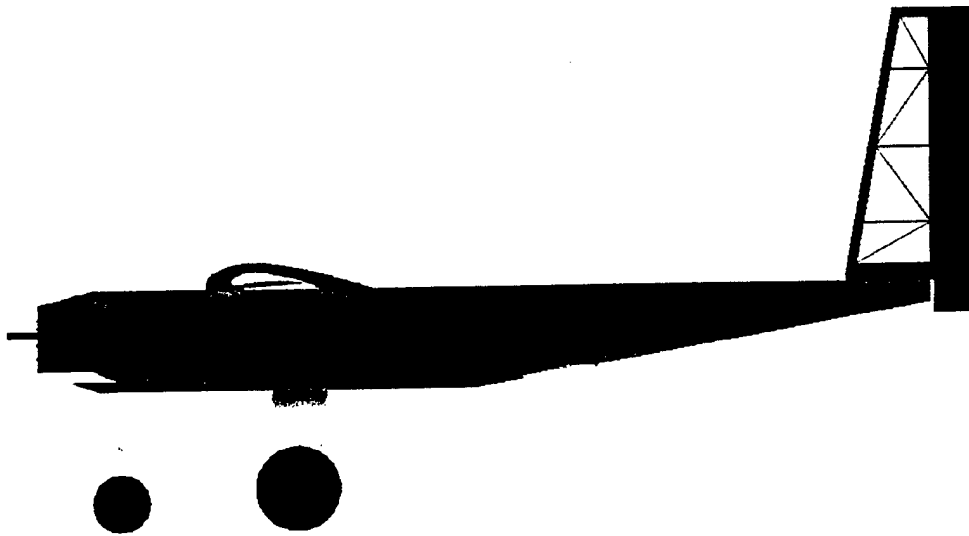


Figure 5.5.1. Center of Gravity of *Knightmare*.

5.6 Tail Design

As previously stated, it was decided that the payload should be removed from the fuselage out of the back so that the wing will not need to be removed. With this design, the tail design comes into play with regard to ease of payload removal. The tail had to be designed to extend the proper length from the fuselage, so as to provide the optimum moment for control and stability. Horizontal and vertical stabilizers also had to be designed to counteract this moment.

The design chosen for the tail, as mentioned before, is to use a single boom that would be hinged at the top of the fuselage and latched at the bottom. A tail that flips up on a hinge provides sufficient room to remove the payload from the fuselage. This tail was designed using ribs that would taper up from the fuselage to the rear of the tail. These ribs have stringers running down the sides for structural support. The entire tail was then sheeted in a thin balsa sheet. This tail design was chosen as the best for both ease of construction and payload access. The length of the tail was found using standard equilibrium equations with the lift from the wing, the weight acting at the center of gravity, the lift from the tail, and the distances between each. The length of the tail was then found to be two feet.

The horizontal and vertical stabilizers are sized both by modeler rules of thumb and equations. A person who builds model aircraft will say that a horizontal stabilizer should be 15-20% of the wing area or an aspect ratio of 3-4. The vertical stabilizer, on the other hand, should be 8-10% of the wing area or an

aspect ratio of 2-3. From AIAA Education Series Aircraft Design: A Conceptual Approach, by Daniel P. Raymer, using sizing equations for a tail and modeling this airplane off of a sailplane (small plane with long tail and large wingspan) a horizontal area of 160.2 in² and vertical area of 80.1 in² are found. These numbers fall within the range given by models for the area percentages. The team chose to have high aspect ratio stabilizers with lower areas. This makes the surfaces tall and thin. With all of these considerations, a final size of 26.7 inches long with a taper of 6.75 inches at the root to 3.6 inches at the tips is found for the horizontal stabilizer. The vertical stabilizer was found to be 15.5 inches high with a root chord of 6 inches and a tip chord of 4.4 inches. The surfaces were built using balsa rods with a truss system of balsa strips on the inside for structural stability. Single horizontal and vertical stabilizers are chosen to keep the rated aircraft cost down. The surfaces are tapered both to reduce weight and to lower the cross sectional area. Dimensions for the tail surfaces are shown in Figure 5.6.1.

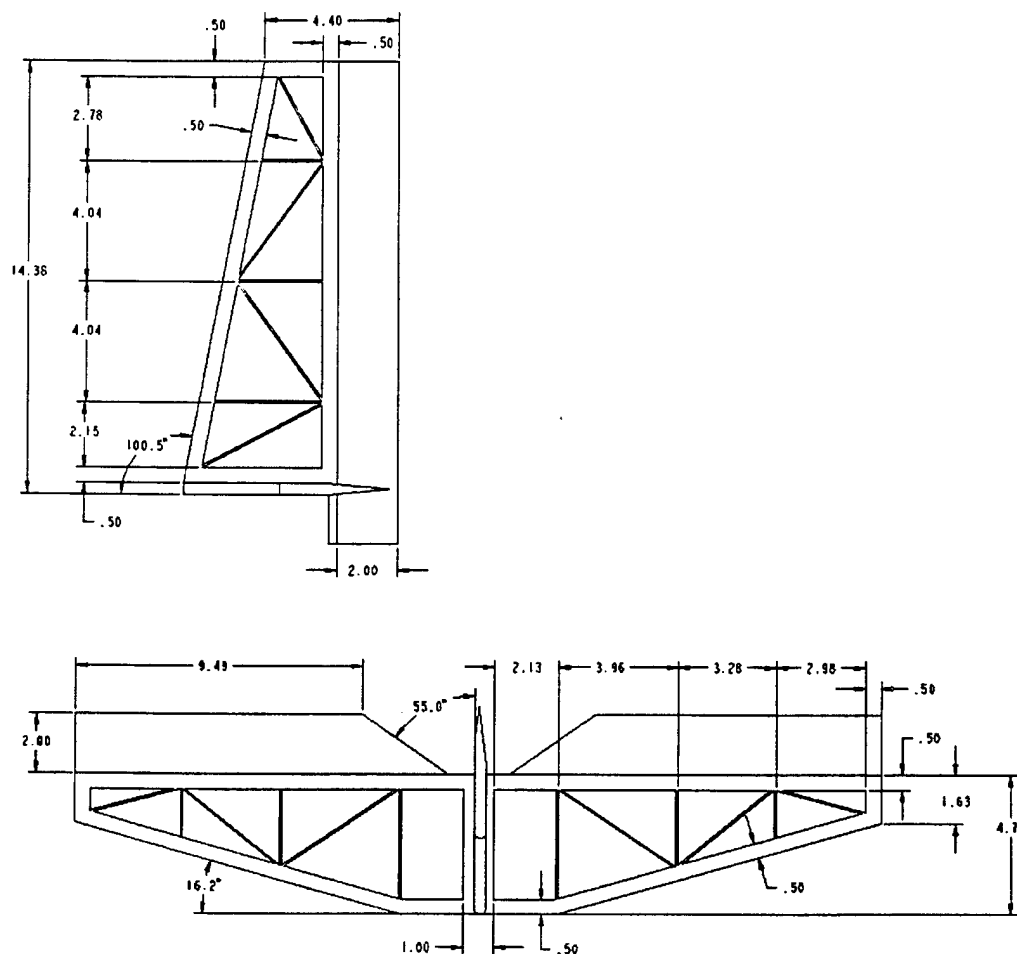


Figure 5.6.1. Tail Surface Dimensions.

5.7. Flight Performance

The notable difference in this particular UAV from a conventional aircraft is the fact that an electric engine powers it. This implies that the take off weight will be equal to the weight upon landing, thus range and endurance calculations cannot be performed in the traditional manner since the equations only deal with the use of fuel not electrical power.

Figure 5.7.1 below is the plot of thrust required versus thrust available curves. As shown by the intersection of the curves, a maximum velocity of 145 ft/sec (98.8mph) can be obtained. This velocity is for a plane flying at full throttle, however, *Knightmare* will be flying at a cruise velocity of approximately 35 mph, generating 23 pounds of lift.

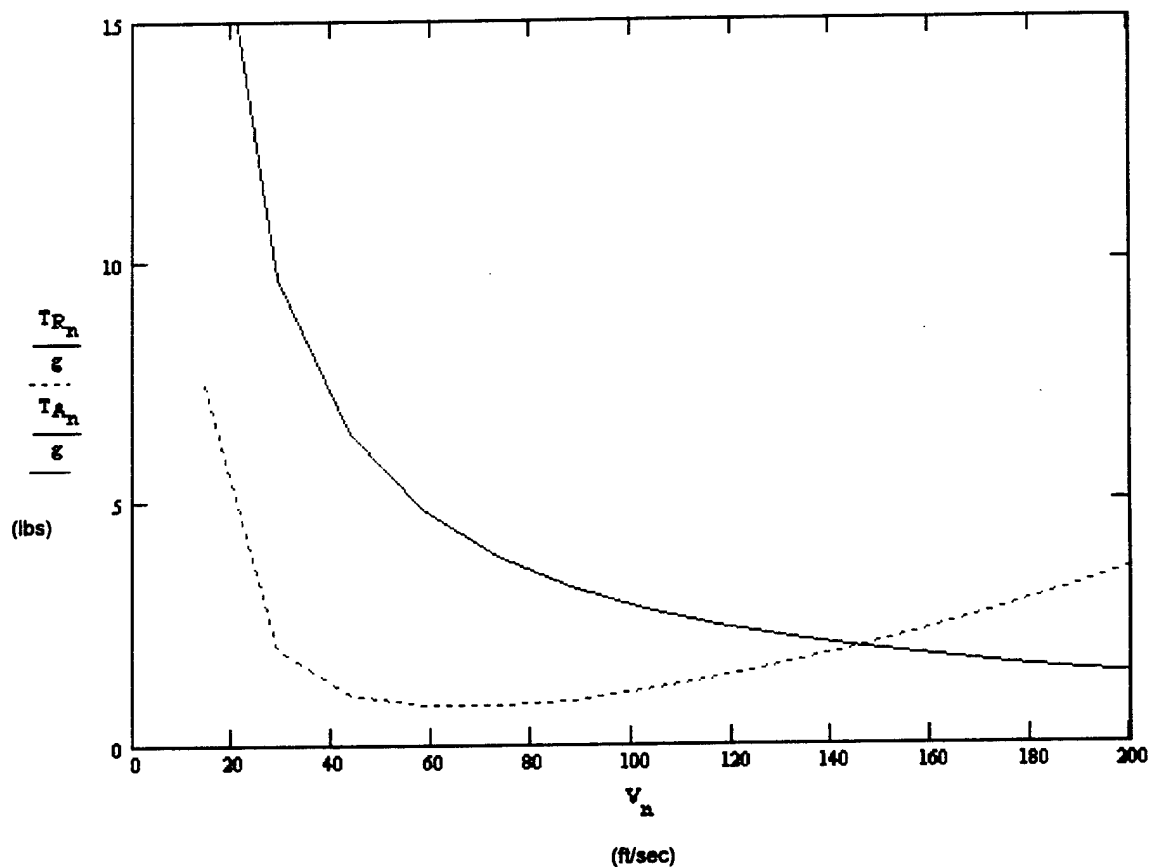


Figure 5.7.1. Thrust Available vs. Thrust Required.

Next the rate of climb curve was obtained as a function of velocity, and the maximum rate of climb was found to be 12 ft/sec, as shown below in Figure 5.7.2.

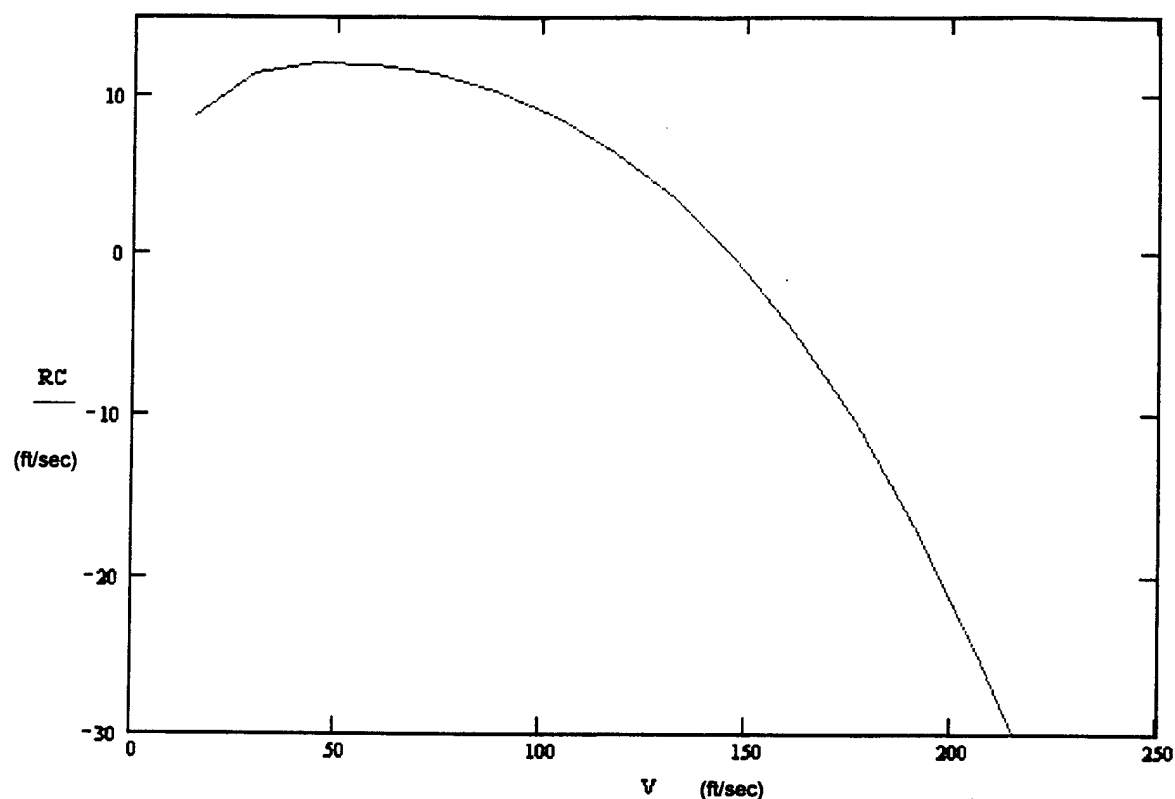


Figure 5.7.2. Rate of Climb.

One of the important requirements that the aircraft had to meet was the maximum takeoff distance of 200 feet. The takeoff distance was calculated using the heavy payload sortie by the equation where the 71bf is the thrust provided and s_{LO} is the takeoff distance. This yields a takeoff distance of 102

$$s_{LO} := \frac{1.44 \cdot W_{HeavySortie}^2}{g \cdot \rho \cdot S \cdot C_{Lmax} \left[71bf - \left[D + 0.02 \cdot (W_{HeavySortie} - L) \right] \right]}$$

feet, well below the limit. Similarly, the takeoff velocity is calculated by

$$V_{TO} := \sqrt{\frac{2 \cdot W_{HeavySortie}}{\rho \cdot S \cdot C_{Lmax}}}$$

yielding a takeoff velocity of 38 mph. Next, the stall velocity is calculated:

$$V_{Stall} := .7 \cdot 1.2 \sqrt{\frac{2 \cdot W_{HeavySortie}}{\rho \cdot S \cdot C_{Lmax}}}$$

providing a stall velocity of 21.6 mph. The ground roll distance on landing is provided by

$$S_L := \frac{1.69 \cdot W_{HeavySortie}^2}{g \cdot \rho \cdot S \cdot C_{Lmax} [D_L + 0.4 \cdot (W_{HeavySortie} - L_L)]}$$

with a landing distance of 360 feet. This of course means that some method of slowing the aircraft must be employed such as "wiggling" the aircraft on the runway upon landing.

The turn radius at cruise velocity is given by

$$R := \frac{2}{\rho \cdot C_L \cdot g} \frac{W_{HeavySortie}}{S}$$

yielding a value of 13.61 feet at cruise velocity with a coefficient of lift of 1.17. The induced drag was also of importance to us for obvious reasons. The following equation calculates the induced drag at cruise velocity

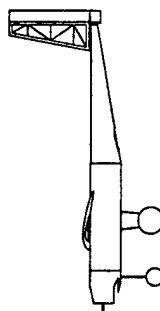
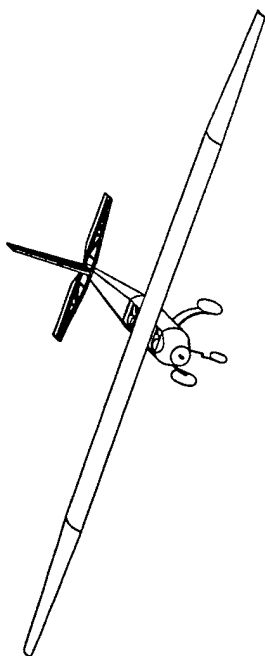
$$C_{di} := \frac{C_{Lcruise}^2}{\pi e \cdot AR}$$

giving a value of 0.048.

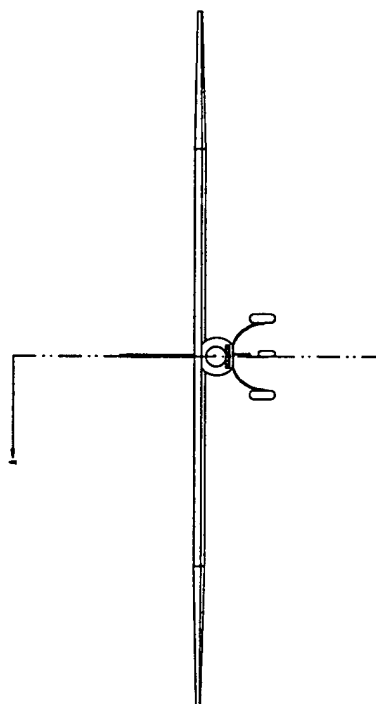
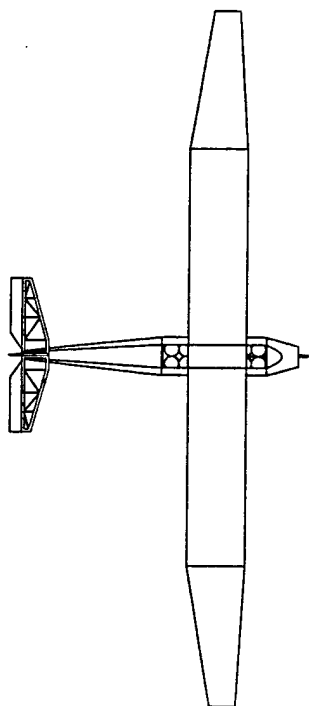
Another parameter of interest to the team as far as performance goes is the payload fraction. With a payload weight of 14.5 pounds and a total take-off weight of 20 pounds the payload fraction is calculated as 0.725.

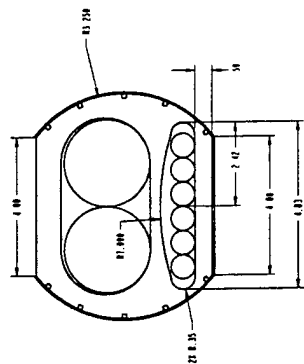
5.8 Drawing Package

Assembly drawings of *Knightmare* can be seen in the drawing package on the following three pages.

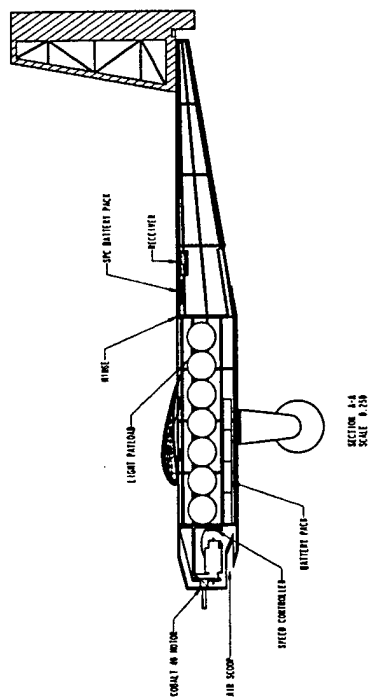


KNIGHTMARE

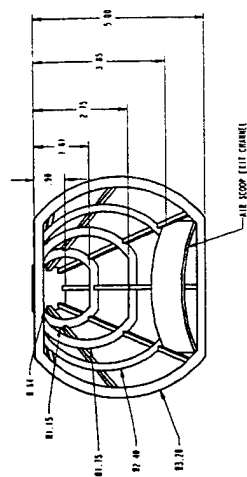
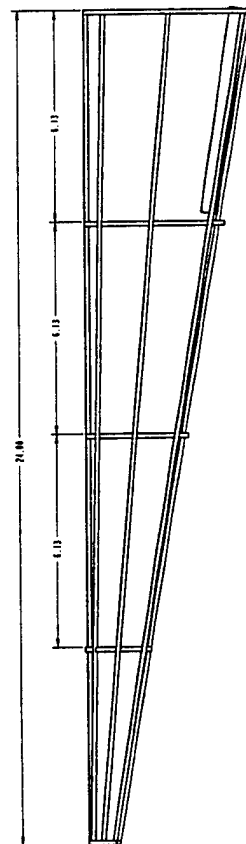




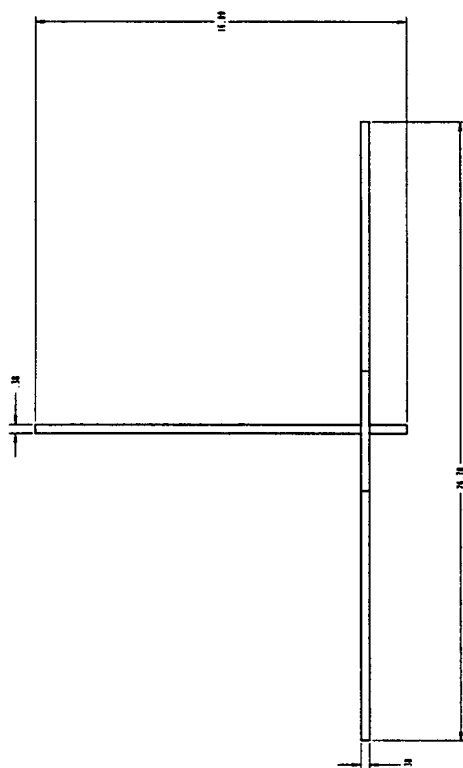
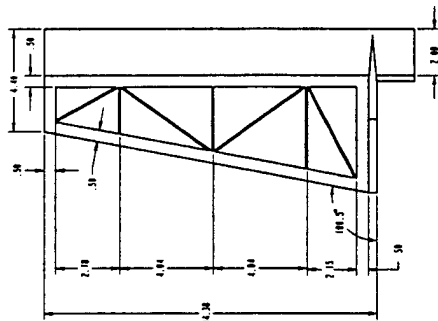
1. FUSELAGE TO BE SHEETED WITH 1/16 BALSA.
2. STRINGERS TO BE MADE FROM BALSA 3/8 X 3/8 X 18.13.



SECTION 1-1
SCALE 0.250

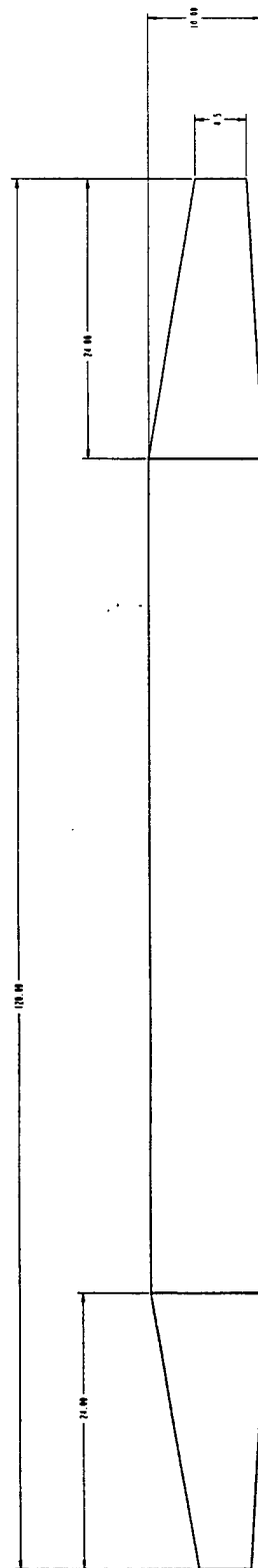


1. TAIL BOOM TO BE SHEETED WITH 1/16 Balsa.
2. STRINGERS TO BE MADE FROM Balsa 3/8 X 3/8 X APPLICABLE LENGTH.



TAIL STRUCTURE:

1. TAIL TO BE MADE OF BALSA TO DIMENSIONS SHOWN.
2. TRUSS SYSTEM IS SHOWN AND WILL BE MADE OF 1/16 BALSA STRIPS.



6.0 Manufacturing Plan

6.1 Introduction

With the design process completed, the implementation and manufacture of the design had to be undertaken. A design is conceived on paper but is delivered into the real world by the manufacturing process. The transition from one to the other is a delicate one that must be performed with great care and patience if the final product is to stay true to the design. It is important, therefore, to plan the manufacture of this airplane in a manner that is efficient, inexpensive, accurate, and feasible. In order to accomplish this, the manufacturing process must be narrowed down from all the available options. This section not only explains the chosen method of construction described in Figure 6.2 but also shows the reasons for selecting it based on an analysis of pertinent figures of merit. The budget breakdown of construction can be seen in Table 6.1.1.

Astro Flight

Product#	Description	Unit price	Quantity	Total
112D	Digital Peak Charger for 2 to 40 cell packs	\$150.00	1	\$150.00
204D	Airplane Speed Control 60 A@ 60V opto	\$100.00	2	\$200.00
529	13 Gage Silicone Wire 10 ft red, 10 ft black	\$12.00	1	\$12.00
Total				\$362.00

TNR Technical

Product #	Description	Unit Price	Quantity	Total
AF GP2000AFK	Gold Peak 2000mAh (17.5 mm*67.5 mm)	\$4.75	48	\$228
	Labor (configuration of packs with attached form)	\$11	2	\$22
Total				\$250

Tower Hobbies

Product #	Description	Unit Price	Quantity	Total
LXH274**	Futaba R148DP 8 Channel PCM Receiver	\$ 169.99	1	\$ 169.99
LXH446	Futaba AEC3 aileron extension	\$ 4.99	2	\$ 9.98
LXH447	Futaba AEC11 aileron extension 16"	\$ 5.99	2	\$ 11.98
LXK320	sand paper 80	\$ 4.99	1	\$ 4.99
LXK321	sand paper 150	\$ 4.99	1	\$ 4.99
LXK323	sand paper 220	\$ 4.99	1	\$ 4.99
LXH274**	Futaba S3002 Mini Ball Bearing w/metal gears	\$ 64.99	4	\$ 259.96
Total				\$ 466.88

Balsa USA

Product #	Description	Unit Price	Quantity	Total
Adhesives				
708	2 oz. Quik-Shot w/sprayer	\$ 3.25	1	\$ 3.25
710	2 oz. Un-Stik-It Debonder	\$ 3.95	2	\$ 7.90
712	Replacement Bottle Tips - Pkg of (2)	\$ 1.19	4	\$ 4.76
A702	(2) 2 oz. Thin	\$ 10.95	3	\$ 32.85
A705	(2) 2 oz. Thick	\$ 10.95	5	\$ 54.75
Epoxy				
544	5 Minute	\$ 5.49	2	\$ 10.98
545	12 Minute	\$ 5.49	2	\$ 10.98
546	30 Minute	\$ 5.49	1	\$ 5.49
42" Balsa sheets				
81	1/16*3	\$ 0.54	5	\$ 2.70
82	3/32*3	\$ 0.65	5	\$ 3.25
Total				\$ 136.91

Aerospace composites

Product #	Description	Unit Price	Quantity	Total
WF - 19	5.6 oz. Woven carbon plain weave 50" wide (\$/yard)	\$ 32.00	1	\$ 32.00
WF-16	3.7 oz S-Glass 27"	\$ 7.50	3	\$ 22.50
WF-15a	1.4 oz. S-Glass 50"	\$ 12.00	2	\$ 24.00
V-11	Mylar Bagging Film 60" wide per yard	\$ 1.50	3	\$ 4.50
V12E	Vac bagging Sealant tape 250 temp 25 ft	\$ 6.50	1	\$ 6.50
V-16	0.014 Du Pond Mylar 6ft	\$ 11.75	5	\$ 58.75
V-22	Breather Cloth 60" wide (per yd)	\$ 3.00	1	\$ 3.00
V-25A	China Bristle Epoxy brush 1" wide	\$ 1.00	1	\$ 1.00
V-26	Epoxy spreader 5" wide	\$ 1.00	1	\$ 1.00
V-28	3" Epoxy Roller Kit(Roller frame and two covers)	\$ 10.00	1	\$ 10.00
E80-R	Red Epoxy pigment past 2OZ	\$ 6.00	1	\$ 6.00
E60-03	EZ-Lam Epoxy 1-1/2 Qt Kit 60 48 oz.	\$ 38.00	1	\$ 38.00
Total				\$ 207.25
Total				\$ 1,423.04

Table 6.1.1 Total aircraft budget.

6.2 Fuselage

The fuselage is the part of the airplane that brings all of the components together and endures most of the rigors that are a result of normal operation. This implies that the fuselage be manufactured using extreme care in order to maintain the correct tolerances for the synthesis of the components as well as to maintain structural integrity.

As stated earlier the main fuselage was designed to mold around the light cargo and was to be made using a series of circular plywood ribs and balsa flanges that are lightweight, provide the necessary load carrying structure, and maintain aerodynamic efficiency.

Two processes were considered in the construction of these. The ribs would either be cut by hand using basic shop tools or they would be laser cut. The choice for this was intuitive. The ribs would be lasers cut because it provided more precision for all the cuts and almost perfect similarity between each rib.

After all the cutting had been finished the fuselage was covered by a balsa skin and then wrapped in monokote to provide a smooth outside surface. A groove was then cut in the upper portion of the cargo area to embed the main wing. Next the wing was connected to the fuselage by four nylon screws and locking helical inserts supported in a piece of light plywood.

6.3 Wing

The wing of the airplane had to be constructed in such a way that it provided the desired lift and was able to withstand the aerodynamic forces incurred during operation. Three main construction techniques were considered for construction. Since this airplane was designed to be small and light, a blue foam wing core and a light ply spar was taken into consideration. Second, a white foam wing with a carbon sheeting exoskeleton was considered. Finally, the team looked at a white foam wing, with a light ply spar reinforced with balsa on the top and carbon fiber sheeting on the bottom.

The first option was the easiest to build but was not strong enough. When tested in bending it deflected a total of 1.5625 inches. The carbon fiber exoskeleton wing deflected the least (.375 in.) but was the most expensive and difficult to construct. The team decided to manufacture the white foam wing with a light ply spar reinforced with balsa and carbon fiber sheeting because it only deflected .9375 in. and required only intermediate cost and building skills. Carbon fiber sheeting was used on the bottom while balsa sheeting was used on the top because carbon fiber performs better under tension than under compression. Even though this choice was not the easiest to manufacture, it was chosen for its strength characteristics.

Construction of this wing was performed using a hot wire that is guided by airfoil templates to cut the foam. It was made in four pieces: two inner rectangular sections and two outer, tapered sections due to large lengths of these (as shown in the Detailed Design section of the report). After this, the wing

pieces were individually cut at the quarter chord to make the compartment for the spar. The spar was then inserted and the pieces epoxied into one wing. Next, the balsa and carbon fiber sheeting was added, covered with Mylar and vacuum-sealed to obtain a tight bond.

6.4 Tail

The tail boom of the airplane was made in a similar fashion as the fuselage was. That is, lasers cut ribs were utilized to provide the geometry. It was attached to the fuselage using a hinge and locking mechanism obtained from a vendor and assembled by the team.

Since the horizontal and vertical stabilizers were basically flat plates, they were made of balsa and covered in monokote. The rudder and elevators are each controlled by their own servos for a total of two in the tail. Construction of the stabilizers was performed by manual cutting and adhered with epoxy.

6.5 Landing Gear

As stated in the detail design, the tricycle landing gear was chosen. There were two options available for the construction of the main landing gear. The first was to use a thin sheet of metal like aluminum for the struts, but this would weigh too much for the team's lightweight aircraft considerations. The other option was to use a composite. The team chose a strut made of layered carbon fiber and kevlar because it was both lightweight and provided the necessary strength to withstand the dynamic landing loads.

The landing gear struts were used from previous competitions. They were made using a molding procedure where the carbon fiber and kevlar were layered and bonded together with an epoxy resin.

The nose landing gear was an off the shelf component already designed to withstand more than the weight of the aircraft. One servo was used for the nose landing gear to provide for easier ground maneuverability.

6.6 Engine

A motor mount was connected to the firewall to provide support of the airplane's single engine. Two manufacturing options were considered for this, and, as stated in the detailed design, the one with the lightest weight was chosen. The motor mount was constructed of light plywood and used epoxy as the bonding agent.

With the engine properly mounted and housed in the cowling, the batteries needed to be placed. It was decided to evenly distribute all twenty-four batteries in a separate compartment in the cargo area of the fuselage that can be seen in Figure 3.3.1. To prevent overheating of the batteries while the airplane is in operation, an air scoop was cut in the leading edge of the cowling that allows the flow to cool the batteries and exit out of another small opening the aft section of the aircraft. This is one of the most innovative aspects of the vehicle, as it has not been incorporated in previous electric airplane designs at the University of Central Florida.

6.7 Safety

Safety was of paramount importance, both for the aircraft, and the ones who built it. It is a factor that had to be taken into account in all the phases of engineering. The aircraft had to be made to include a "kill" switch for the electrical system. This is required by the competition to ensure the safety of the flight crew during loading/unloading of the payload. Another safety factor that had to be built into the plane was the failsafe mode whereby the aircraft, upon engine failure during flight, automatically adjusts itself in the following manner:

Throttle closed

Full up elevator

Full right rudder

Full right (or left) flaperon

6.8 Figures of Merit

In the construction of the airplane, several figures of merit were taken into consideration in order to determine the best way to build. These included cost, availability, skill level, and time required. The matrix with the results can be seen in Figure 6.8.1.

6.8.1 Cost

Since the team was working under a budget, it was important not to choose components or manufacturing processes that required a considerable amount of money. Fortunately local sponsors that donated parts and use of facilities were readily available to support the team's design endeavors. Manufacturing processes that were costly are ranked with a minus sign, those that are expensive with a plus sign.

6.8.2 Availability

Availability of materials and components was of paramount importance. The materials needed to be found within the allotted time period to fit the team's manufacturing schedule. If the components were readily available they were given a plus, if they were difficult to find they were given a minus sign.

6.8.3 Required Skill Level

The team was made up of very diversified, talented people from different backgrounds who brought many skills with them. Despite this asset there were still many aspects of manufacturing with which the team was not familiar. By choosing a manufacturing process that the team was familiar with or could learn with relative ease the airplane could be constructed more efficiently. Processes that required easier skills were given a plus, while more difficult techniques were given a minus.

6.8.4 Time Required

The team desired to be completely finished with construction by mid March 2001 in order to have sufficient test and redesign time before the competition in April. Some manufacturing processes take more time than others do. In Table 6.8.1 if a process requires too much time it was given a minus, if it required a reasonable or little amount of time it was given a plus sign.

		Figures of Merit				
		Cost	Availabilit	Skill Level	Time Required	Total
Component	Process					
Wing	Foam / Spar	+	+	+	+	4
	Foam / Carbon Fiber	-	0	-	-	-3
	Foam / Carbon, Balsa Sheeting	+	+	0	0	2
Vertical / Horizontal Stabilizers	Airfoil & Foam	+	+	+	-	3
	Balsa Ribs & Flat Plate	+	+	+	+	4
Tail Boom	Ribs & Flanges	+	+	+	+	4
	Truss	-	+	-	-	-2
Fuselage	Ribs & Flanges	+	+	+	+	4
	Box Beam	+	+	+	-	3
Landing Gear	Composite Strut	-	+	0	+	1
	Metal Sheet	+	-	-	-	-2
Engine	Support Block	-	+	-	-	-2
	Simple Block	+	+	+	+	4

Table 6.8.1 Figure of Merits Breakdown

7.0 Concluding Remarks

With the design process now complete, all that remains is the actual manufacture of *Knightmare*. Assuming that the design will remain unchanged would be a rash assumption indeed. The design process is an iterative one that changes as the engineer proceeds. It is important to be open to options that present themselves while at the same time staying true to the overall spirit of the original, overall concept.

AIAA Electric Airplane

Nightmare

Team Members

Gary Ballmann
Adam Bojanowski
Kevin Chibar
Mirelis Cotto

Jennifer Creelman
Sebastian Echenique
Joshua Lobaugh
Kristina Morace

Arthur Morse
Jorge Pagán
Bernie Sam
la Whiteley

Mentors

Dr. Conway
Tconway@mail.ucf.edu

Dr. McBrayer
mcbrayer@mail.ucf.edu

April 10, 2001

Table of Contents

1.0 Introduction	3
2.0 Wing	3
3.0 Tail	4
4.0 Fuselage	4
5.0 Batteries	5
6.0 Test Flight	6
7.0 Sponsorship	7
8.0 Rated Aircraft Cost	7
8.1 Manufacturers Empty Weight	8
8.2 Rated Engine Power	9
8.3 Manufacturing Man Hours	9
8.4 Total Rated Aircraft Cost	9

1.0 Introduction

The manufacturing process brought about several problems that could not be foreseen during the design phase. The resourcefulness of each teammate could be seen by how each one overcame various obstacles in manufacturing. Often times, simple modifications could be made to the design to help overcome any obstacles.

The manufacturing of this aircraft brought about a few problems that were not seen in the design phase. Experience in this competition allowed the team to make simple modifications that would not affect the overall design of the aircraft.

A prototype aircraft proved to be quite beneficial to the final design. In building the prototype, several problems were encountered. These problems were fixed on the prototype, which allowed the final airplane to be built quickly and efficiently. In addition, things that were found time consuming or difficult on the prototype were manufactured differently on the final airplane. This section will discuss the problems encountered on the prototype and the measures taken to improve the design to make a better and more efficient final airplane for competition.

2.0 Wing

The post design phase of *Knightmare* revealed several features in the wing that needed to be reconsidered and learned from as well. Although the first design of the wing was adequate, the team contemplated if the first wing could be made lighter and stronger by manufacturing it differently. Upon consideration of this, it was decided to build a second wing. The first wing included a light plywood spar and had carbon fiber sheeting on the bottom surface with balsa sheeting on the upper surface. It also had a white foam core. For the second wing, the team considered removing the spar and using carbon fiber sheeting all around. The white foam would be changed to blue foam for additional strength. This idea was refined because blue foam would increase the weight of the wing since it had a greater density. The outcome was a second wing that included a light plywood spar with carbon fiber all around and a white foam core. This modification allowed for a stronger wing that provided an adequate amount of dihedral when loaded in flight.

The next feature that was reconsidered was the flaperons. In inspecting and moving the flaperons, the pilot expressed a concern about their size. It was feared that with a width of two inches there might not be enough surface area for the control surfaces to work properly. The team considered remedying this by increasing the width of the flaperons to three inches in the second wing. Upon actual flight testing of the airplane, it was determined that the original two-inch width was more than sufficient. Thus, no change was made to the control surfaces of the second wing.

3.0 Tail

Through every phase of design the flip-up tail was proven to be the best idea for unloading of the payload. Along with the fuselage, the tail was built using laser cut ribs. This made the assembly much easier than having to cut the ribs by hand.

An initial problem arose before building. The ribs for the tail were cut without notches for the stringers to be placed due to errors in the CAD drawing. For this reason, notches were cut by hand. This method brought about any human error that could be made in measuring for the notches. If another design is done with such a manufacturing technique, close attention needs to be done to ensure that every CAD model is perfect before the laser cutting process.

Upon building, another problem arose. The stringers on the top and bottom of the ribs noticeably turned out crooked. Each stringer was placed in the corner of each rib as the tail tapers down from front to back. It was noticed that, although the angle is calculated for the side stringers to taper down, the top and bottom stringer taper was not calculated properly. For this reason three new ribs were cut by hand with a slight length extension on the top and bottom of the ribs. The height of the ribs was kept the same dimension as before. This manufacturing of the new ribs put a delay on the tail building by about a day. This delay did not put a damper on the building process; instead it was simply an inconvenience.

The horizontal and vertical stabilizers were built by hand and kept the same dimensions as calculated from the area equations used in the preliminary design.

Overall, the tail did not change in design from each of the design phases. This can be attributed to the detailed comparison analysis done in early brainstorming sessions.

In the next design, a recommendation would be to accurately analyze every detail of the design before any manufacturing process, including laser cutting, is initiated. This helps both in speeding the manufacturing process and creating a problem free manufacturing process.

4.0 Fuselage

Second to the wing, the fuselage is probably the next most important part of the aircraft. It is the part that brings all the components together. The fuselage has to be structurally sound, while being as light as possible.

The key components of the fuselage are the ribs. As mentioned in the proposal phase, the ribs were professionally laser cut. The uniformity between ribs helped in the construction process because it reduced the chance of problems such as misalignment. This is contrary to the manufacturing of the tail ribs, because the fuselage ribs were laser cut with notches for attaching the stringers. The use of balsa stringers along the ribs was also deemed positive. They provided sufficient structural strength while still being lightweight. For the case of the wing, the original plan was to cut a groove in the top of fuselage for the wing to sit. But upon further inspection, it was determined that cutting the groove would compromise

structural integrity. With that idea discarded, the team decided to make a saddle from dense foam to place the wing onto.

After the proposal phase was complete, issues involving the battery and payload compartments were addressed that had not been dealt with in the proposal phase itself. The team decided to "sheet" the inside of both compartments. Sheeting the battery compartment was desired to create a sealed channel for air to flow over the batteries and out through the tail. Styrofoam stoppers were placed in front of and behind the battery pack to keep the battery pack stationary. The stoppers were made in the same basic shape as the battery pack so air could still flow over the top of the batteries. However, upon testing these battery stoppers it was found that they were actually blocking the flow through the air channel. To fix this, the team replaced the battery stoppers with balsa dowel rods that ran the length of the battery channel, preventing the batteries from moving inside of the aircraft. On the other hand, the reason behind sheeting the payload compartment was to allow the speed loader to be inserted and removed quickly and easily during competition. The material chosen to sheet both compartments was acetate because of its light weight and smooth surface.

As mentioned above a speed loader was constructed to enable the easy insertion and removal of the payload. Since the mission of the competition was to carry as much steel and as many tennis balls as possible within a ten minute time limit, it was necessary to have a quick and efficient method of exchanging the different payloads. To do this the team created a speed loader to house the light payload tightly and conform to its shape. The material used in fabricating this design was a thin, yet sturdy poster board sheeting. This same design was then used for the heavy payload; however, foam inserts were made to hold the steel in place since it would not take up as much volume as the light payload.

5.0 Batteries

The batteries were obtained from *TNR Technical*, where the team had them build the 24-cell pack. Having them build the pack was a significant advantage, cutting down on manufacturing time and complexity of the battery pack. On last year's competition aircraft, the team did all the soldering themselves. It was very time consuming and many cells were short-circuited. This year the team received the pack as one solid block with very clean solders, just what was desired. The biggest lesson that was learned from last year was that clean electrical connections are very important. Having one battery pack made everything much easier, which led to only one wire going from the pack to the motor.

The team ordered two speed controllers from Astro Flight and found a problem with one of them. The speed controllers came electronically blocked from the manufacturer and there was a sequence that the pilot had to go through with the radio to unlock it. After a brief period, that issue was subsequently resolved.

6.0 Test Flight

An early version of the team's design was flown for initial testing and feedback (Figure 6.1). The airplane was flown on a local radio controlled aircraft field on a windy day to simulate unfavorable flight conditions. It lifted off into a headwind in approximately 20 feet of runway. The only difference between the flown aircraft and final configuration was that a wooden propeller was used instead of a composite propeller.

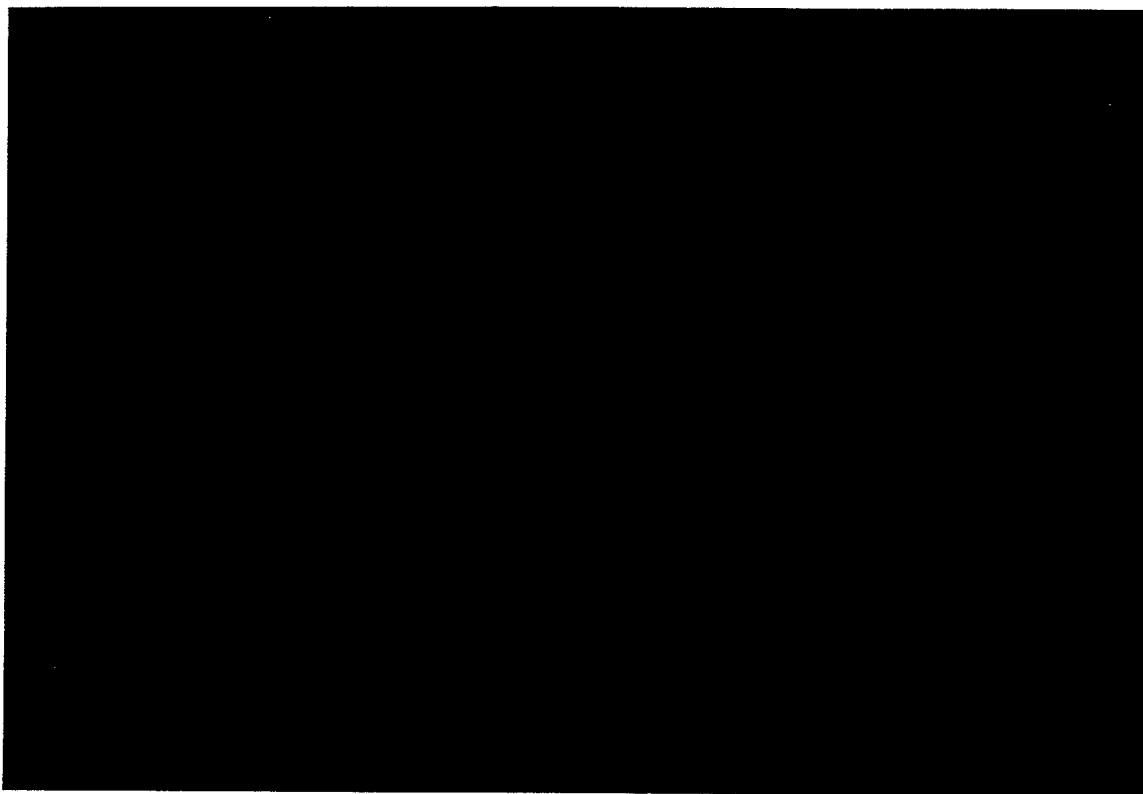


Figure 6.1. Initial Test Flight

Initially, the airplane flew well, though slowly because of the wind. There came a point, however, when the aircraft slowed down until it stopped and hung in midair. At this point the airplane banked to the right and hit the ground from an altitude of approximately 20 feet. The airplane broke in the places where sections were assembled and was able to be repaired in two hours.

It is believed that the use of a wooden propeller combined with a strong cross wind caused the airplane to stop in midair. Through testing, the team found that a wooden propeller was significantly less efficient than a composite one. The propeller wasn't the only reason for the disaster, prior to the heavy cross winds the aircraft flew and handled well, which led the team to believe that the wind played a considerable role in bringing the plane down to the ground forcefully. Presently, a second flight test is scheduled before the date of the competition.

7.0 Sponsorship

Building an electric aircraft has always been a costly project. Seeking sponsors has proven to be a necessity in past years along with this year. This is one aspect of this project that always seems to be put to the side and dealt with at a later date. Every year the money issue comes back to haunt the team near the competition time.

This year, the UCF Student Government supplied the team with an adequate amount of money to help build the plane. Even so, other sponsorship was still necessary. Letters were sent to companies in Orlando asking for any help that could be offered. This was done just before manufacturing begun. It was found that this was possibly a little too late to ask for sponsorship. In the future, sponsorship assistance should begin at the beginning and continue during the design process.

Two sponsors that proved extremely beneficial to the success of building *Knightmare* was the laser cutter *Full Spectrum* and the steel donator *Metal Supermarkets*. Having the ribs for the fuselage and tail laser cut proved to be extremely time saving and gave the airplane a smoother, more uniform look. The steel that was donated to the team was cut (by the sponsor) exactly to the team's specifications to ensure that it would fit inside the fuselage for the heavy payload. Good relations with *Full Spectrum* and *Metal Supermarkets* were kept to ensure future sponsorship.

8.0 Rated Aircraft Cost

The final score that is given to each team for the competition is dependent upon the written report, the flight score, and the rated aircraft cost. The equation used to calculate the final score is:

$$\text{Score} = \frac{\text{Written Report Score} * \text{Total Flight Score}}{\text{Rated Aircraft Cost}}$$

Throughout the entire design process, it was the team's goal to keep the Rated Aircraft Cost (RAC) as low as possible. The idea of minimizing the RAC would maximize the final score that *Knightmare* would accrue as indicated by the score breakdown above. More attention was paid to the report to attempt to achieve as high of a report score as possible. With a scoring format such as that for this competition, it would be very easy for a team to win the competition without lifting the most weight. It was the theory of this team that a larger overall score could be accomplished if the denominator of the score equation was kept minimal. A large airplane could lift a lot of weight, but encounter a large penalty from its large RAC. Dividing a large numerator by a large RAC could prove to give a smaller number than dividing a smaller numerator by a very small RAC. This year's team is out to prove that a small airplane can win this competition.

An Excel spreadsheet was generated to help aid in the analysis of the RAC. Thorough investigation of the RAC led to the conclusion that the most significant factor of the design was the amount of power that was generated. This is because the power contributed the most to the RAC as

compared with the other parameters (such as wing area, fuselage length, aircraft weight, etc.) included in the RAC calculation.

Table 8.1 shows the complete breakdown of *Knightmare's* Rated Aircraft Cost.

Table 8.1. Rated Aircraft Cost

Rated Aircraft Cost, \$(Thousands) = (A*MEW + B*REP + C*MFHR)/1000				
Coef.	Description	Value		
A	Manufacturers Empty Weight Multiplier	100/lb		
B	Rated Engine Power Multiplier	1/Watts		
C	Manufacturing Cost Multiplier	20/hr		
MEW	Manufacturers Empty Weight	lbs.		7.3
REP	Rated Engine Power	#motors*Amp*(1.2V/cell)*#cell		576
			Unit of Meas.	
MFHR	Manufacturing Man Hours	WING		
		15 (hr/wing)	1	15
		4 hr/sq. ft. projected area	7.417	29.668
		2 hr/strut or brace	0	0
		3 hr/control surface	2	6
		FUSELAGE		
		5 hr/body	1	5
		4 hr/ft. of length	4.4	17.6
		EMPENAGE		
		5 hr (basic)		5
		5 hr/vertical surface	1	5
		10 hr/horizontal surface	1	10
		FLIGHT SYSTEMS		
		5 hr (basic)		5
		2 hr/servo or controller	6	12
		PROPULSION SYSTEMS		
		5 hr/engine	1	5
		5 hr/propeller or fan	1	5
		Total		120.27
		<u>Rated Aircraft Cost=</u>		3.71

8.1 Manufacturers Empty Weight (MEW)

In designing an aircraft with a low rated aircraft cost in mind, the empty weight was an important factor. The multiplier for the MEW was \$100/lb. For this reason, the team wanted to keep the empty weight as low as possible. Upon completion of building, the total aircraft empty weight came out to be 7.3lb.

8.2 Rated Engine Power (REP)

A small aircraft does not require excessive power to lift it off of the ground. This allowed the team to only use 2.5 lbs. or 24 cells out of the allotted 5 lbs. The engine used will only draw 20 Amps, which also helped in the overall rated aircraft cost. The equation for REP is:

$$\text{REP} = \# \text{ engines} * \text{Amp} * 1.2\text{V/cell} * \# \text{ cells}$$

The multiplier for the REP is \$1/watt. Having such a small airplane only required one engine giving the REP a value of:

$$\text{REP} = 1 * 20 \text{ Amps} * 1.2 \text{ V/cell} * 24 \text{ cells}$$

This gives a REP value of 576 watts.

8.3 Manufacturing Man Hours (MFHR)

The MFHR includes the variables of the aircraft that can be adjusted during the design phase and is comprised of an estimated number of hours for each variable. For this airplane, the minimum number of each variable was used where applicable. For something such as the wing, the area was kept as low as possible while still giving the lift desired. The fuselage length was also designed to house just over the minimum number of tennis balls, as this is what determined the inside volume, not the steel blocks. Nothing extra was put into this aircraft that was not necessary. The breakdown of the MFHR can be seen in Table 8.1.

8.4 Total Rated Aircraft Cost

From Table 8.1 the values of each variable with its multiplier can be seen. The total rated aircraft cost is found from the equation:

$$\text{Rated Aircraft Cost, } \$(\text{Thousands}) = \frac{\$100/\text{lb} * 7.3 + \$1/\text{watt} * 576 \text{ Watts} + \$20/\text{hour} * 120.27 \text{ Hours}}{1000}$$

This gives a rated aircraft cost of 3.71 for this year's airplane.

East Stroudsburg University
of Pennsylvania

2001 AIAA/Cessna/ONR
Student Design/Build/Fly
Competition

Design Report



Proposal Phase

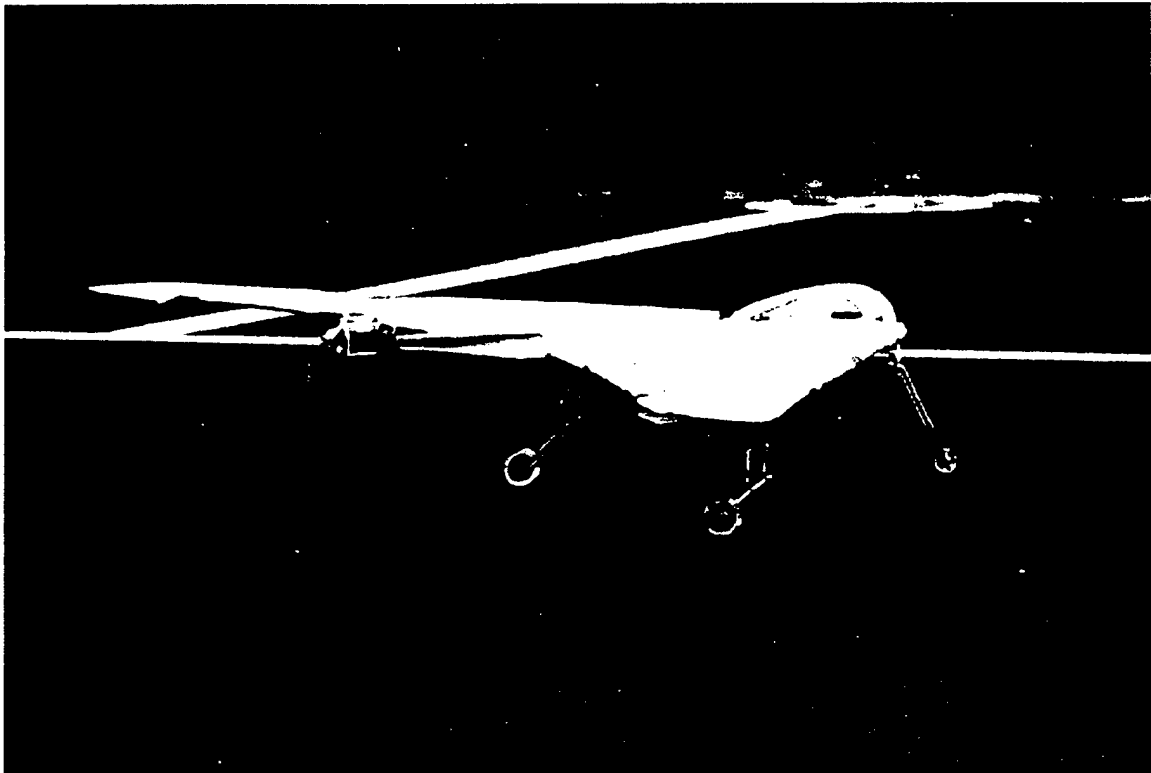
Contest Date: April 21-22

Contest Site: Patuxent River, MD

Electric Airplane Project
c/o Physics Department
East Stroudsburg University
East Stroudsburg Pa, 18301

Phone: 570-422-3341
Fax: 570-422-3505
Email: dlarrabee@po-box.esu.edu

Executive Summary



Executive Summary

With intent to compete in the Cessna/ONR 2001 Student Design/Build/Fly Competition, the team from East Stroudsburg University has prepared an original entry that satisfies the specified contest criteria. The entry has already demonstrated capable mission performance and efficient operation in accordance with its minimal rated aircraft cost. It is believed that the design shall serve to be far more competitive than the aircraft that was fielded by the team during the previous event.

The final design, christened the **ANSSIR BAT**, was chosen as a result of the factors arising from team debriefing after the 2000 contest and the new mission/contest requirements. The team placed 13th in a large field of competitors under difficult conditions in Kansas, and was one of the few teams returning with an undamaged aircraft. To build on this record of success, the team set the goal of placing within the top 5 teams for the next competition and began the design process to realize this. This year's team had the benefit of data acquisition and valuable experience gained from the ESU Impulse II, but decided to deviate from it and other conventional configurations in favor of the more competitive "all-wing" designs. Although the new aircraft is of flying-wing configuration and bares no resemblance to its predecessor, it was possible to keep a small number of aircraft components that were "contest proven" and required no alteration. This promoted rapid prototyping as the primary means by which, the final design would be ultimately frozen. Prototype flights were logged at least four months ahead of the contest and the final variant was flying at least one month before the scheduled event.

A broad range of alternatives was investigated during the conceptual stage of design. The team used a figure of merit exercise to select an unconventional planform that reflected the group's desire to effectively improve upon last year's entry while still retaining any successful equipment. Since battery-weight, span, takeoff distance, and rated aircraft cost posed considerable constraints, the primary emphasis was directed toward reduction in empty airframe weight through careful selection of materials. Composite materials were employed extensively. A higher skill matrix was necessitated with the incorporation of carbon-fiber construction, but was deemed acceptable in order to avoid the high weight penalty of other materials and to obtain the superb degree of stiffness required by a flying-wing.

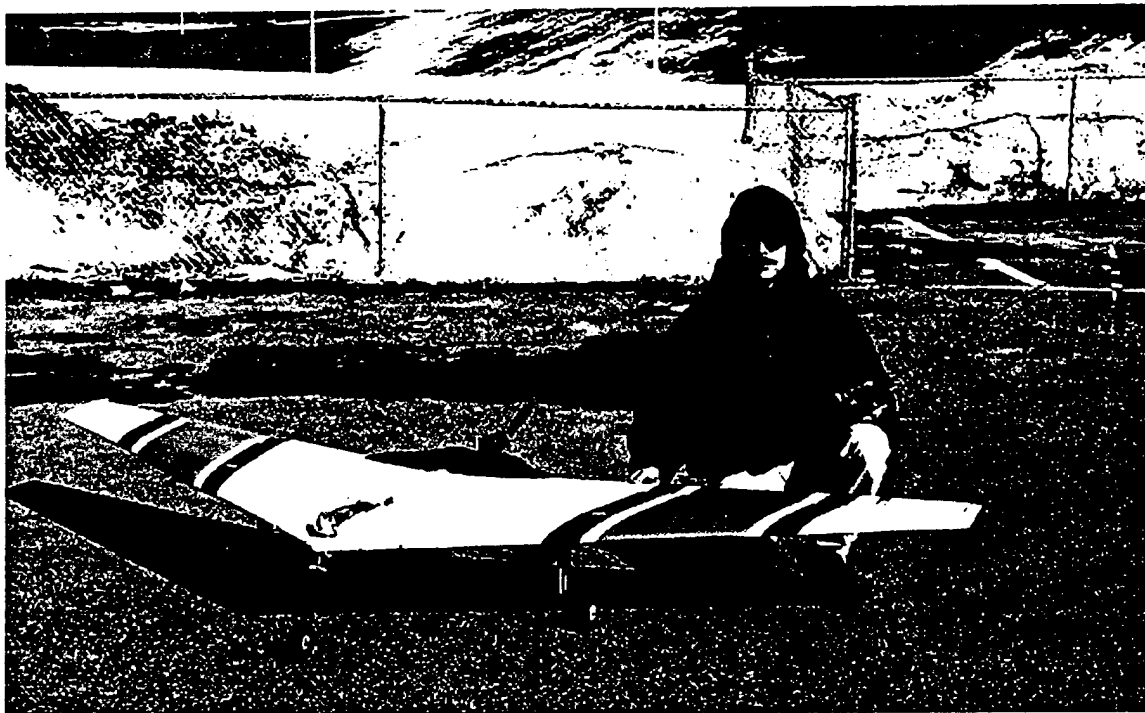
With respect towards sizing, no attempt was made to study an aircraft capable of carrying only the minimum payload since contest experience precludes the competitiveness of this approach. Instead only designs which could be made to carry the 100 tennis balls were considered viable. The ANSSIR BAT is an entry that operates at minimal cost, yet maintains maximum payload fraction. It is a 16lb aircraft (including 4.5lb. of batteries) that possesses a 10" span and is powered by one Astro Cobalt 60 motor on 32 SR Max cells. Depending on contest weather conditions, it can carry up to 13 lb. of cargo.

In the preliminary and detailed stage of design, MS-Works spreadsheets were used to calculate performance predictions and sizing optimization techniques. Math Soft's Mathcad 8 was used for longitudinal stability analysis and 2-D lifting line load distribution studies. Drafix Quick CAD and CAD Key

were employed for engineering drawing-based project applications. A multitude of research was done on the historical data concerning flying-wings, and several empirical relationships were discovered and utilized in the project.

The ESU ANSSIR BAT represents design, fabrication, and operation an "order of magnitude" greater than was possible with the ESU Impulse II. It is the most advanced entry ever fielded by the ESU team. We are confident that the team has produced the best pragmatic design under the imposed system of constraints and we are anxious to demonstrate its advertised capabilities at the 2001 contest in Maryland.

Managment Summary



Management Summary.

The East Stroudsburg University 2001 Cessna/ONR student design/build/fly competition airplane team is composed of nine members, each of whom was responsible for different aspects of the construction of the airplane.

The team met weekly to go over new concepts and any construction work or problems that needed to be addressed. During any other time of the week, the team members worked on the aircraft according to their schedules. Flight-testing was determined by the weather.

Our team leader is a General Science Graduate Student named Herbert Ziegler, III. Herb is a veteran member whose primary duties include the basic design of the aircraft, piloting the aircraft both in practice and at the contest, and delegating assignments to other members of the team. He was also responsible for the theories behind the characteristics of the aircraft. Herb wrote the Executive Summary, the Conceptual Design, and the Detailed Design sections of the Proposal Phase of the Tech Report and provided all of the CAD Drawings for the report. Herb also edited the technical content of the Proposal Phase of the Tech Report.

David Borofski, a senior and third year member of the team is majoring in secondary education with a concentration in Earth & Space Science. Dave was responsible for the installation of ancillary hardware in the aircraft.

Garrick Alt, a junior majoring in Physics, is a second year team member and team captain. He has been assigned detail work such as: making the foam forms for the leading edge, construction of the balsa wood ribs, machining an engine mount and a custom left-hand threaded propeller hub, milling the aircraft's wheels, and manufacturing the aircraft's landing gear. Garrick contributed to the conceptual design of the airframe as well. He is in charge of a new construction technique for a proposed second aircraft. Garrick wrote the Preliminary Design section of the Proposal Phase of the Tech Report and has been training to assume team leadership in the next competition.

Mark Harpel, also a second year team member, is a sophomore and computer science major. Mark was assigned to the construction of the landing gear and the balsa wood framework for the wing. Mark contributed to the Management Summary section of the Proposal Phase of the Tech Report.

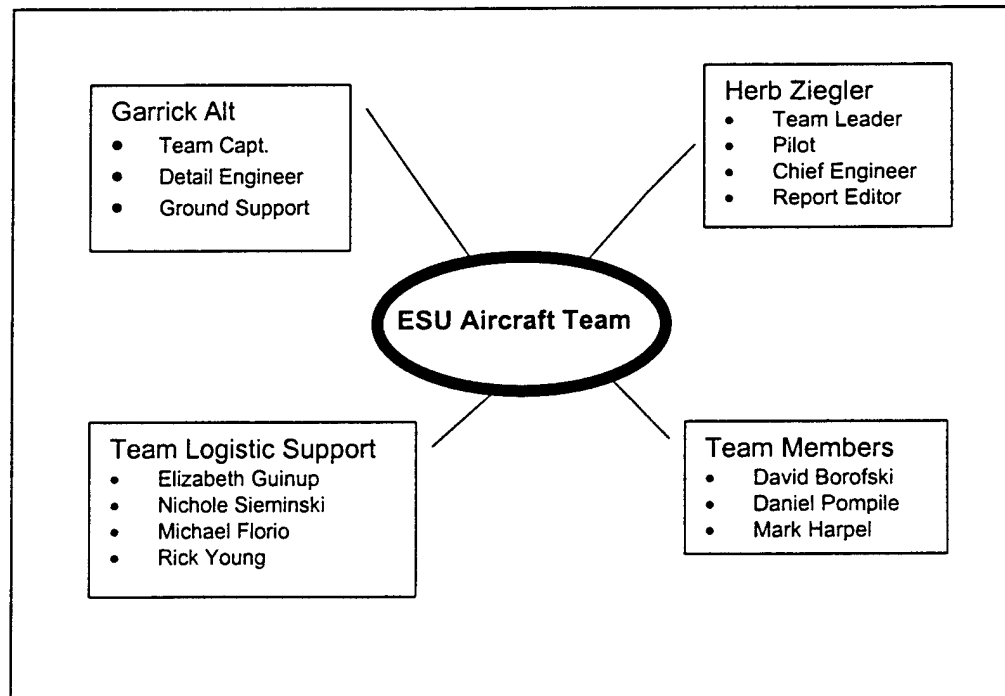
Daniel Pompile is a junior Earth & Space Science major. Dan worked on cargo pod construction and all components related to carbon fiber use. Daniel wrote the Manufacturing Plan section of the Proposal Phase of the Tech Report.

Michael Florio and Rick Young are freshmen who assisted other team members.

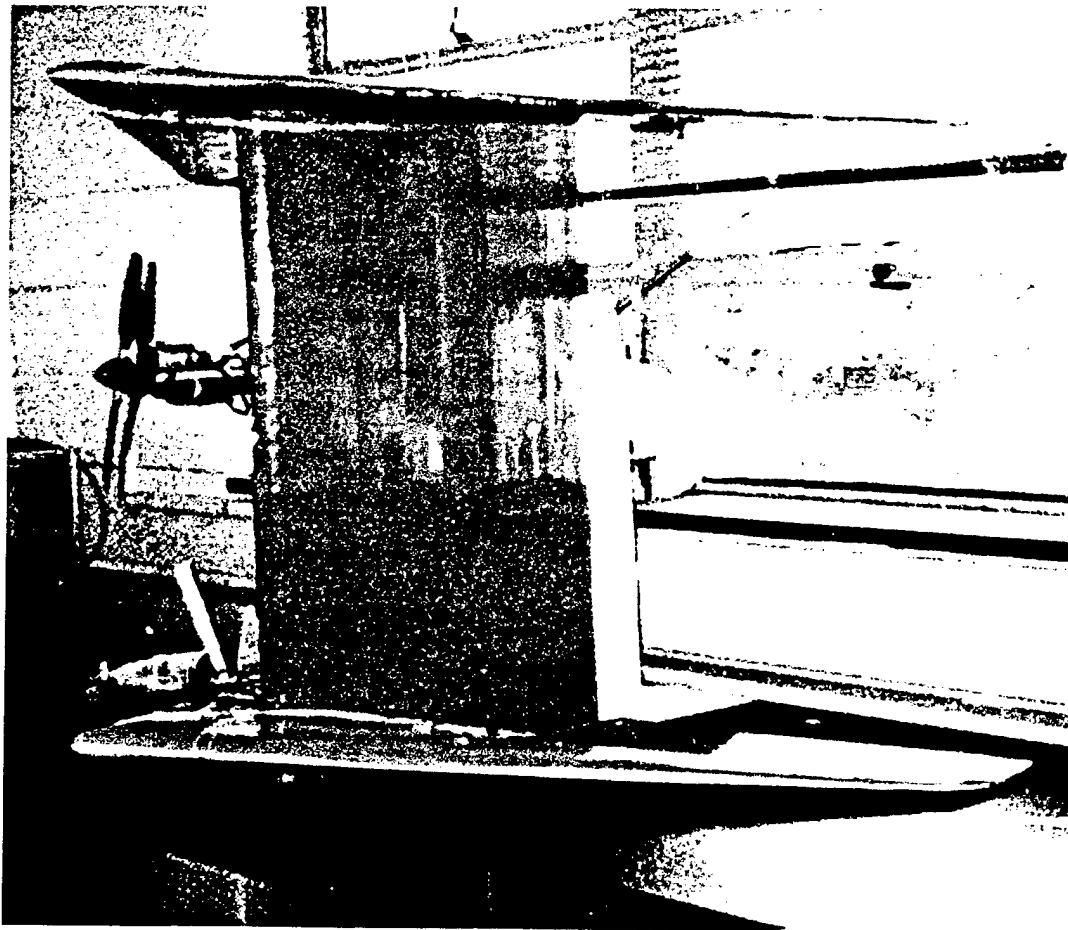
Elizabeth Guinup, a senior majoring in History with a minor in Political Science is serving as the Editor of the Tech Report.

Nichole Sieminski is a sophomore Elementary Education major and is the audio/visual technician.

Dates	Proposed	Actual
Sept. 25 - Oct. 20	Design airframe and propulsion system. Member assignments	Biplane flying wing model design, construction, testing
Oct. 23 - Nov. 17	New airframe design. New Member Assignments. New airframe construction	Flying wing design & construction begun. Cargo pod constructed.
Nov. 20 - Dec. 22	Landing gear construction. Determine weight & balance data. First test	Foam leading edge made & covered with carbon fiber. Balsa ribs installed.
Jan. 2 - Feb. 2	Airframe completed & Monokoted	Airframe completed & Monokoted
Feb. 5 - Feb. 16	Aircraft ground testing: taxiing, turning.	Weather prevented testing.
Feb. 17 - Mar. 20	Flight testing.	Flight testing.



Conceptual Design



Conceptual Design

Choosing the best design for a span-limited aircraft that must satisfy heavy payload mission requirements was very challenging. Many proposals had to be considered and tested in order to arrive at the optimum configuration. As a result of studying the multi-wing entries of the competitors that carried the maximum payload, the first design that was considered by the E.S.U. team was a tri-plane. Based on the notion of operating a slow-flying airplane with minimal power requirements and wing loading, the design consisted of three large lifting surfaces. Total wing area was greater than would be possible with a monoplane due to the contest-imposed span limitations. It was hoped that large wing area could be substituted for the minimal available power so that 100 tennis balls could still be carried around the contest course. A ½ scale prototype was constructed in the early summer, which bore a sport-scale appearance of the classic Fokker DR-1. However, it was found that the available propulsion system was inadequate to operate the aircraft. The aircraft with full cargo could not take off within the contest-defined runway limit. Once aloft the aircraft could not maintain a safe operating altitude, nor perform the required maneuvers unless operated at full throttle. This drained the battery pack at an unacceptable rate. The problems of operating multiple wings in close proximity clearly proved to be a disadvantage in accordance with classical predictions. The design was ultimately rejected because of these performance factors.

When the fall semester began the team decided to pursue a less conventional design. The second planform considered was a flying wing biplane. A central column that would also serve to contain the 100-ball cargo would separate two flying wings. The design called for placement of the wings approximately half a wingspan apart. Lifting surface theory suggests that this placement of the wings minimizes the interference between them, resulting in the lowest possible induced drag. The center column would additionally act as a rudder and would be placed aft of the center point of the wings. A horizontal tail was not included in the design because it was believed that the flying wings would provide sufficient pitch/roll stability for the entire aircraft.

By late September an approximately half scale foam-based model of this design was constructed and testing began. This model had a five-foot wingspan and a three-foot high center column. For the initial testing of the airframe, no motor was installed and the aircraft was launched via a hi-start system. Under conditions of low wind, the aircraft performed well. After several flight attempts under windy conditions, it was determined that the large rudder area furnished by the center column caused the aircraft to immediately weathervane. Due to the lack of a propulsion system, the aircraft was only capable of semi-controlled landings and as a result one wing was broken. Although this aircraft represented a highly original and workable design it had several problems, which seemed to scale unfavorably with increasing size. This made it unsuitable for the contest even with major revisions. The physical size of the full-scale aircraft

was simply too unwieldy to be manageable within the allotted construction space. The design also generated more drag than predicted and again the available propulsion system could not provide acceptable flight performance. The team engineered a custom configuration for this aircraft's propulsion system in an attempt to minimize the power-to-thrust ratio. The rotor assembly and gearbox from an RC helicopter was to be mated with an AstroFlight, Inc. Cobalt 60 electric motor and mounted on the center column in a pusher configuration. The collective function was to be used for variable pitch in flight so that proper blade loading would be maintained throughout all airspeeds. The cyclic function was to be used to aid in pitch and yaw stability. This would also have minimized the number of control surfaces needed on the airframe. Upon seeking the opinion of the judges as to the legality of this system, the team was told that this design constituted a custom prop and was therefore illegal under contest rules. This was the decision that ultimately precluded this aircraft from further consideration.

Because this ruling was made late in the semester, an attempt was made to utilize some of the work resulting from the biplane prototype. Consequently, 2/3 of the airplane was omitted and the decision was made to proceed with a conventional flying wing. The figure of merit exercise was completed; the results of which indicate our decision to compete with a pure flying wing. The following is a description of the FOM's that were utilized in the overall preliminary design process along with their general design implications. Ranking is accomplished by color. Red arrows signify maximum necessitated design attention followed by yellow and green arrows.

General Aircraft Requirements

- Can the design comply with all AIAA & AMA requirements regarding safety and competitive performance?



Design Implications of FOM

Limits on span, weight, propulsion, structural quality, crew and spectator safety must be implemented.

- Can the design be completed in accordance with the time constraints of the manufacturing and management milestone charts?



Charts reflect realistic goals toward design completion.

- Can the design be flown well in advance of the competition?



Team experience is paramount.

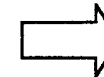
- Can the design be disassembled easily for transport to the specified contest site?



Considerations for travel must be carefully devised.

Mission Suitability

- How well can the design cope with unforeseen variables caused by weather?



Wind is expected to pose a problem in Maryland.

- Can a pilot of average skill operate the design?



The design should offer predictable flight qualities.

- Can the design possess a relatively low RAC?



The design should have low RAC, but flight performance comes first.

- Can the design adapt to different sortie strategies at the contest?



The design may carry different payload depending on weather.

Manufacturing Suitability

- How difficult will it be to fabricate the design?



Construction ease, though higher MFHR's than last year are acceptable.

- Can several copies of the design be built to serve as replacements?



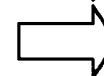
The team would like redundancy with its entry, though it is not essential.

- Can the design be built using the current team skill matrix?



The team has been able to expand its skills significantly since last year.

- Can the design be built with readily obtainable resources?



Carbon fiber has been added to our inventory

Figure of Merit Exercise (number (1-10) directly proportional to desirable effect)

<u>F.O.M.</u>	<u>Tri-plane</u>	<u>Biplane</u>	<u>Flying Wing</u>
Overall Complexity	4	5	7
Takeoff Distance	10	8	7
Max Gross Weight	7	6	4
Payload Fraction	6	7	8
Payload Variation	5	5	4
Rated Cost	3	5	10
Actual Cost	8	8	9
Power Required	3	5	8
Endurance	5	7	8
Turnover Angle	2	4	10
Ground Operation	3	4	10
Landing Distance	9	8	2
Transport Ease	3	5	10
Repair Ease	3	3	8
Manufacturing Time	4	5	6
Manufacturing Skill	3	5	8
Weather Capability	2	3	7
Piloting Skill	5	5	5
Visibility	10	10	4
Safe Operation	8	8	7
Total F.O.M. Points	103	116	142

Preliminary Design



Preliminary Design

In order to maximize an aircraft's overall contest score strictly by its design, the aircraft would have to possess the lowest possible rated aircraft cost, while maximizing the total flight score. It was apparent that this method, of overall contest score maximization, converged all possible designs to that of the flying wing design. This design would yield a significantly lower rated aircraft cost while maintaining a respectable performance. The flying wing design would require a fewer amount of control surfaces for flight. Due to enhanced ground effect characteristics the flying wing would require a take off distance that is one third of the distance for a conventional design. The flying wing design also possesses the lowest possible wetted aspect ratio, thus in theory possesses the lowest possible power requirement. These results would all be favorable for this competition, therefore making the flying wing design the best suited for the competition.

Initial sizing was accomplished by use of an analytical optimization exercise. The results of which were formatted into the traditional sizing matrix carpet plot. The crucial parameters of takeoff distance, gross weight, rated aircraft cost, and specific excess power were provided as functions of wing loading with respect to thrust-to-weight. According to standard format points above a given line imply excess performance beyond that required. Likewise points below a given line suggest that level of performance is unattainable. Therefore the logical, hence optimum, sizing is shown by the lowest intersection of performance characteristics still above the primary requirements. At this point the optimum thrust to weight and wing loading was discovered and provided the proper target values for the aircraft.

Historical research of Jack Northrop's wings showed that vertical stabilizers promoted wingtip stalling. Also vertical stabilizers would add to the rated aircraft cost. Thus the addition of vertical stabilizers should yield undesirable consequences. It was deduced that the optimal forms of yaw stabilization would be to install both the motor in the rear, making it a "pusher", and clam brakes. During yaw, with the prop in the rear, a component of the thrust vector would be designated to regain stable flight. In theory this would prevent the possibility of any diverging oscillations. Clam brakes could be used to enhance the control of yaw stability with a controlled input much like that of a rudder. Clam brakes could also be used to stop any Dutch roll oscillations. A configuration with both brakes open would serve as a recovery mode.

To maximize pendulum stability the pod will be placed on the bottom of the wing. Historically it is better to leave the top of the wing undisturbed. This allows the preservation of conventional aerodynamics. The pod's general shape would be dictated by the configuration of the tennis balls. In order to optimize the pod's shape, its wetted area would need to be as small as possible while still allowing room for 100 tennis balls. The pod would also be limited in length so that it does not exceed our predicted fuselage length and thus increasing the rated aircraft cost.

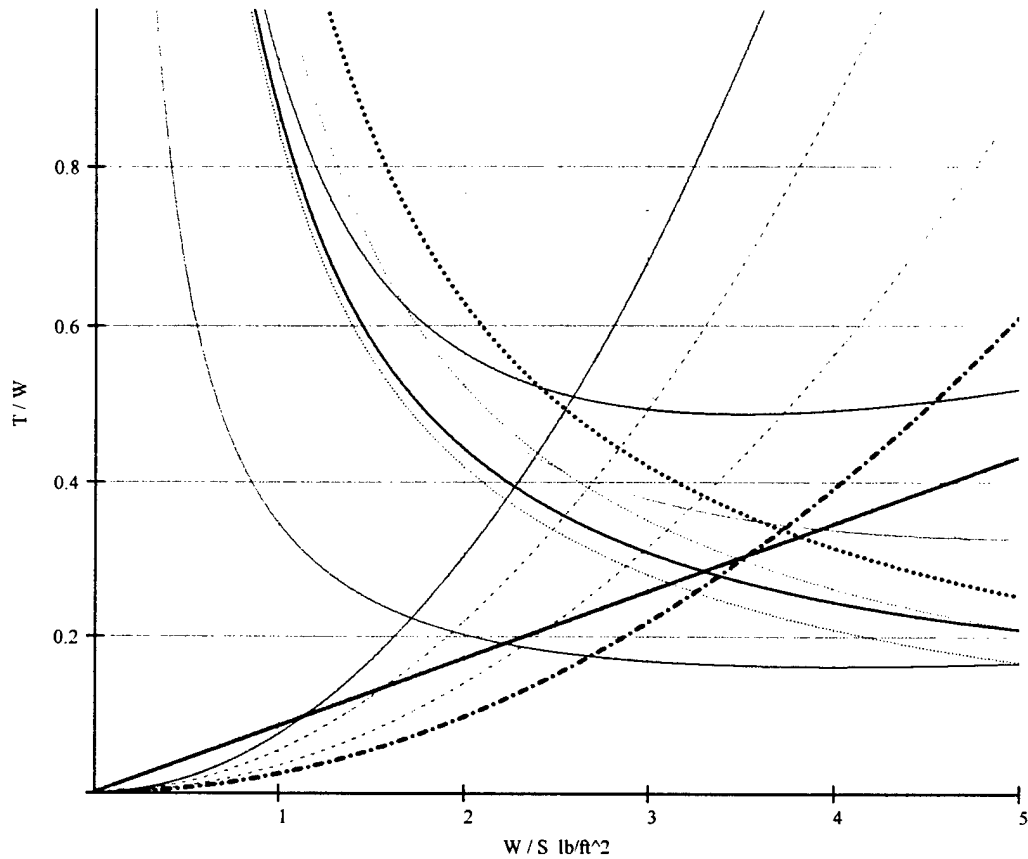
Due to the classical flying wing design methodology, the aircraft would require a symmetrical airfoil. The NACA 0009 airfoil would be chosen due to its well-known low pitching moment characteristics. The symmetrical airfoil would be chosen over a reflexed airfoil for this reason. This airfoil also possesses a moderate lift coefficient. For reasons of longitudinal stability the wing tips would need to be aft of the neutral point. This would be done by sweeping the leading edge of the wing thirty degrees. In order to maximize the wing area while keeping the center of mass close to the neutral point the trailing edge of the wing would be swept ten degrees. The wings required a washout angle of 6 degrees from center of wing to wing tip and was calculated using the empirical Pankin twist formula.

The performance of the landing gear on last year's *Impulse II* worked exceptionally well. Last year's gear design provided superb ground maneuverability and could handle a substantial landing gear load factor. This gear would also provide outstanding rough field capability. It was decided to keep the same gear design but add some slight modifications. The previous springs were temporarily replaced by stiffer springs that would compensate for the larger aircraft and provide better ground stability. After further experimentation it was determined that the gear would perform better if the springs were replaced with a gas shock. The gas shock provided the gear with a longer stroke and a spring constant that was more ideal for the desired performance. The previous year's nose gear frequently had a problem with bending due to hard landings. To remedy this problem, the original front gear set was replaced with a Fulgs-dual strut spring-loaded front gear set to prevent bending. This new nose gear allowed for its ground steering will be actuated by a dedicated servo.

For the third consecutive year the motor of choice will be the ASTRO 60 Cobalt Pattern Motor. It will be chosen due to its already known performance and limitations as well as its reliability. The ASTRO 60 produces performance that is suitable for the new flying wing design. This motor is also one of the remaining motors allowed for the competition after the new motor regulations. The high flight speeds necessitated by the flying wing seemed to preclude use of a gearbox and large diameter prop. Such an arrangement causes the propeller to unload too early in the performance envelope. Because of this it was decided to use a direct drive configuration consisting of 32 cells and a 14 x 10 prop. Experience has shown this to be the largest propeller that can be used with this battery compliment without exceeding the maximum motor wattage.

Discovery of a new battery manufacturer will allow a higher quantity of batteries. This should be a significant improvement because the new battery pack will produce the maximum voltage for the motor within the 5-lb weight limit. Compromising battery capacity in favor of higher pack voltage will no longer be a concern. In fact the new 2400 SR High Rate Max cells will not only maximize the motor voltage but will actually increase the capacity by twenty percent.

Sizing Matrix Plot



- $W_o=17$ ANSSIR BAT-T/W & W/S characteristics
- - - $W_o=20$
- - - $W_o=25$
- · - · $W_o=30$ lb
- 200ft Takeoff Parameter TOP=6
- 1 g at 25mph (must reside above curve for flight)
- 1g@40mph, $P_s=0$
- 2g@40mph, $P_s=0$
- 3g@40mph, $P_s=0$
- Min desirable T/W (assuming worst case 7lb thrust & $W_o=30$ lb)
- 5.00 RAC
- 5.25 RAC
- 5.50 RAC

Detail Design



Detail Design

The desire to have the absolute minimum cost formula has strongly influenced the decision to operate a flying wing. The cost formula revisions reward any attempt to minimize number of wings, control surfaces, servos, empty weight, motor current, tail surfaces, and fuselage length. If the traditional challenges tail-less aircraft handling can be overcome, a flying wing with minimal wetted area is the logical choice. The ESU ANSSIR BAT represents the contest variant of the prototype that can be fielded before April. It has already demonstrated capable flight performance and the ability to fly successfully with a payload fraction of .60. Any revisions in the actual contest aircraft will be slight, essentially encompassing further weight reduction in the manufacturing process to drive the payload fraction upwards.

The takeoff requirement of past events mandated a large amount of wing area previously obtained only with biplanes. However, the 2001 contest rules have made possible the use of a monoplane that can possess the correct wing area with greater aspect ratio that makes the use of a biplane questionable. The wing area was selected to minimize wing loading and maximize the aspect ratio based on the 10' span limitation. Sweep was chosen in accordance with the target aspect ratio the desired degree of effective dihedral, and the desired degree of longitudinal stability. No geometric wing dihedral was needed because of the swept wing configuration and its inherent equivalent dihedral effects. It was also realized that roll inertial would be greatly increased with payload carried below the roll axis and that geometric dihedral would further degrade roll responsiveness.

Since no advanced software dealing with computational fluid mechanics was available to the team, no precise modeling of the bell-shaped lift distribution was possible. Empirical relationships based on other flying wing designs were used to determine the appropriate degree of washout. The NACA 0009 was chosen as the wing section because of its known lift and pitching moment characteristics at expected vehicle Re. Based on the designs of Northrop, who did not favor the use of vertical fins, the control devices selected are conventional and effective when employed on flying wing aircraft. Large elevons are used in conjunction with wing tip clam brakes. The control deflection was determined by the practical limit of servo torque. Primary emphasis was toward maximizing movement but avoiding servo stall and high current drain. The elevons control pitch and roll and may incorporate any degree of differential throw necessary to discourage adverse yaw through radio mixing. Likewise the clam brakes have been electronically mixed to provide yaw control individually, or an emergency yaw-damp braking function when simultaneously applied. Use of these devices and careful piloting are the primary means by which, long oscillatory periods in the Dutch-roll mode are to be controlled. Inclusion of an on-board piezo-electric gyro was considered but rejected due to its inherent temperature drift error

and uncertainty of its response rate, which may actually aggravate adverse yaw recovery. Concerns still remain about the non-linear response rate of clam type drag brakes and testing will continue to determine the precise amount of required movement.

The primary contest constraint was viewed as the 200 ft take off distance. The plane was designed to takeoff fully loaded within this distance even with no head wind. Typically flying wing aircraft will require 1/3 the takeoff distance when compared to their conventional counterparts and this ground effect benefit was another reason for the chosen planform. In the event that higher winds are expected we will use the increase in takeoff performance as a safety margin rather than an opportunity to carry more cargo. This is not due to structural inadequacy of the spar, but rather the inability to significantly shift mass within the length of the pod without upsetting balance. It is believed that the virtual lack of lateral area will reduce drifting tendencies on takeoff in the gusty, crosswind environment that normally prevails during the contest.

The carbon fiber spars easily passed the contest-type structural verification test and it is unlikely that any flight maneuvers can exceed its limits in bending, shear, or torsion. Specific excess power curves show that it is not possible to attain high-g pulls from level flight and predicted top speed seems to limit ultimate loading to approximately 5 g (in a very non-contest-like dive!) The spar system incorporates two carbon fiber spars constructed of a carbon fiber/Fomular® sandwich. The leading edge coated back to the wing $\frac{1}{4}$ chord point and formed a rigid D-tube of varying cross section down the span. The secondary spar was of rectangular cross section and placed between the swept leading edges at the predicted center of pressure points of the wing. This also provided a logical location for the main gear mounts and a precise location for C.G. testing. Because the C.G. is significantly forward of the wing tips, the static contest safety inspection requires the team to utilize a *reward balance beam and subtract the appropriate amount of cargo from the pod such that the total cargo weight of 13 lb. is carried in the middle* while the wing is level and supported at the tips.

The battery-span loading concept has been instituted in this wing design, which has slightly decreased the structural requirements of the spar in flight. For reasons of longitudinal stability, it has also permitted the placement of battery mass as far forward as possible. In so doing however, the battery inertia loads associated with landing have been isolated primarily to the wing (along with cargo inertia loads), which may expose the wing to damage from rough landing. A tricycle undercarriage was selected with a steerable nose wheel. The main gear were placed in the wing to reduce turnover angle in ground operations and possess a significantly wide wheel track. Unfortunately, the characteristic short wheelbase of all flying wings is still apparent. The main gear are comprised of a levered trailing arm arrangement and have generous stroke to absorb landing loads. At full squat, the gear trail behind the C.G. is such that rotation for takeoff is still easily accomplished. Spring strut tension is adjustable to control trail for any vehicle weight. As installed in the wing, the main gear have shown the ability to tolerate a static drop

from 1.5ft corresponding to a gear load factor of 1.2 and a rate of sink equal to 3 ft/s. Failure of the system is predicted at a gear load factor of approximately 2.5, essentially a static drop from 3 ft with a vertical descent of 5 ft/s, whereby the gear will most likely separate from the rectangular secondary spar.

Cargo is housed in a conformal pod slung beneath the center of the wing. It was constructed from carbon fiber/Kevlar® yardage vacuum bagged around a mold. The volume was determined by the desire to carry the full 100-tennis ball maximum. Initially the concept of homogeneity was used for pod loading because the tennis balls would pack in uniformly without any special manipulation. However due to last minute ruling revision, the tennis balls will be arranged in a bag with a pod lid so that they are no longer capable of free distribution. Likewise the rectangular steel block may also be housed in the same pod with equivalent restraints. For purposes of speed loading, a separate but identical pod will be manufactured and pre-loaded in accordance with the new ruling. In no instance will the cargo be free to upset the C.G. of the aircraft. The pod is affixed to the aircraft with several types of fasteners, including snap fasteners, Dzus fasteners, and nylon bolts. Flight remains possible when the pod is removed from the aircraft, as was necessitated for initial flight -testing.

The propulsion unit was chosen based entirely upon its successful use demonstrated in the previous year, and the ruling that brushless motors have been banned. The AstroFlight Cobalt 60 pattern #661 can provide close to 1 hp within the battery limitations specified in this contest. On 32 SR 2400mah cells swinging a standard Zinger 14x10 prop it can deliver over 10lb. of static thrust while drawing 39 A. Because of the pusher orientation of the ANSSIR BAT and the fact that Zinger does not produce a 14x10 pusher prop, the motor was disassembled and timed for reverse rotation. Additionally, the armature shaft that mounts the prop was fashioned from a left-handed bolt so that the reverse rotation would not loosen the propeller nut. These modifications were pursued so that standard, tractor propellers can be utilized. This permits a greater selection in the choice of propellers, as the pusher type variety is limited. No abnormal motor or battery heating has been observed under operating conditions. The closest pusher prop manufactured is the 14x8 and it may be used in an emergency provided the motor direction is returned to normal, but the 14x10 is still the optimal selection.

Endurance of the primary pack is 6-7min at medium to full throttle settings. Depending on contest weather it may be possible to incorporate some gliding into the flights to help extend this. It is expected that propeller unloading at cruise will also increase run time. Rough range estimates predict that at cruise with full load, a flight segment of 3.5 miles is possible.

The team employed a new simulation program for pilot training and prediction of design performance in variable weather conditions. Great Planes' *Real Flight@ Generation 2* which, is the latest upgrade to the *Real Flight Standard Edition* software provided a valuable simulation capability never before possible. With the aircraft input parameters adjusted to those of the

ANSSIR BAT, virtually any foreseeable contest scenario could be flown. The plane underwent "virtual" testing in countless conditions ranging from 0 to 30mph winds with heavy gusting. Sortie strategies for flying in these conditions were explored and potential problems were identified. The program was also used to verify general handling predictions and takeoff performance within the specified distance. We were able to test our addition of spoilers and flaps not found on the ANSSIR BAT during its preliminary flights. The software used to allow only the use of glow-powered engines, excluding electric motor propulsion. This has been corrected with the new upgrade and it is now possible to simulate our aircraft quite accurately. We highly recommend this software and know that it has significantly aided our contest design development.

Table of Graphical Contents

Graphs

- General Specifications
- Drag Polar
- Critical Velocities vs. Weight
- Battery Pack Endurance vs. Current
- Power Required vs. Velocity
- Takeoff Distance vs. Payload Fraction
- Shear & Moment Variation in Semi-span
- Specific Excess Power vs. Velocity

CAD Package

- Exterior 3-View
- Payload Allocation
- Internal Systems
- Primary Structure

ANSSIR BAT General Specifications

Class

Type-	Radio-controlled electric UAV
Max. gross weight-	30.00lb
Empty airframe weight-	12.00lb
Empty weight plus batteries-	16.45lb
Max. # of tennis balls-	100
Total wetted area-	35ft ²
Frontal area-	2.0ft ²
Construction type-	40% Carbon Fiber/epoxy ,5% aluminum 35% balsa/plywood, 10% foam,10% other

Aircraft Cost Model

MEW	12
REP	1536
MFHR	126
Rated aircraft cost-	5.256

Fuselage

Length-	1.25ft
Height (no gear)-	1.25ft
Width-	1.75ft

Wing

Planform type-	swept, tapered, flying wing
Airfoil type-	NACA 0009
Span-	9.94ft
Root chord	2.42ft
Mean chord-	1.4ft
Max thickness-	0.22ft
Area-	15.8ft ²
Aspect ratio-	6.6:1
Thickness/chord ratio-	0.09
Taper ratio-	0.275
Washout	6°
Lift curve slope-	6.03
Max. L/D-	25.3:1
Cdi-	0.07
Cdo-	.005
Max. Cl-	1.0
Max. Alpha-	13°
Static margin	1"
C.G. % of root chord	38%

Powerplant

Configuration-	Single electric direct drive, pusher
Motor type-	Astro Cobalt 60 Pattern #661
Speed controller type-	AstroFlight 204D
Propeller type-	Zinger 14x10
Max. power-	1.0Hp
Static thrust-	10.5lb
Mean dynamic thrust-	5.5lb
Max current draw-	39.0A

Battery pack

Battery type- SR Max 2400 x 32
Pack weight- 4.45lb.
Pack voltage- 38.4V
Endurance- 5-10min

Undercarriage

Type- Tricycle, levered mains, dual-tire nose
Track- 3.52ft
Wheelbase- 2.08ft
Nose strut geometry- +30° caster
Main strut geometry- 0.0° camber, 3.0° toe-in, 2"-4" trail
Stroke- .25ft
Maximum descent velocity- 3.0ft/s
Load factor- 3.5
Longitudinal turnover angle- 30°
Later turnover angle- 40°
Brakes- none
Main tires- 2.8" diameter, roller blade
Nose gear tires- 5" diameter, foam

Radio Equipment

Radio type- Futaba T6XA PCM; Ch 48
Channels used- 6 total 1&2-elevon mix
3-throttle
4&5-rudder/clam brake mix
6-nose wheel steering

Servo type-

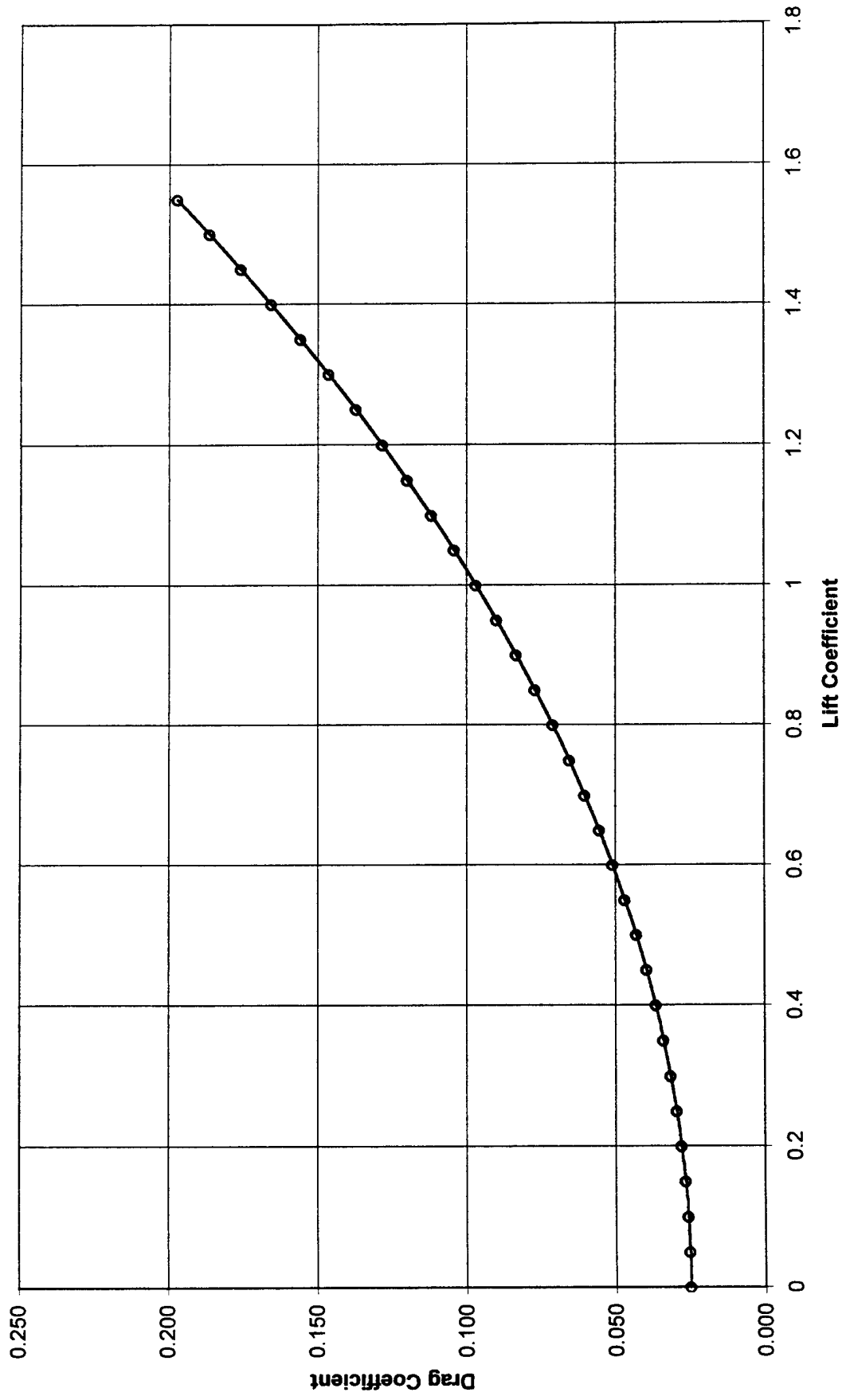
2 Tower 1/4 scale: elevons
1 Futaba S3003; nose gear
2 Tower micro, clam brakes

Elevon roll deflection- ± 20°
Elevon pitch deflection ± 35°
Clam yaw deflection- ± 30°
Clam brake deflection ± 30°
Nose gear deflection- ± 35°

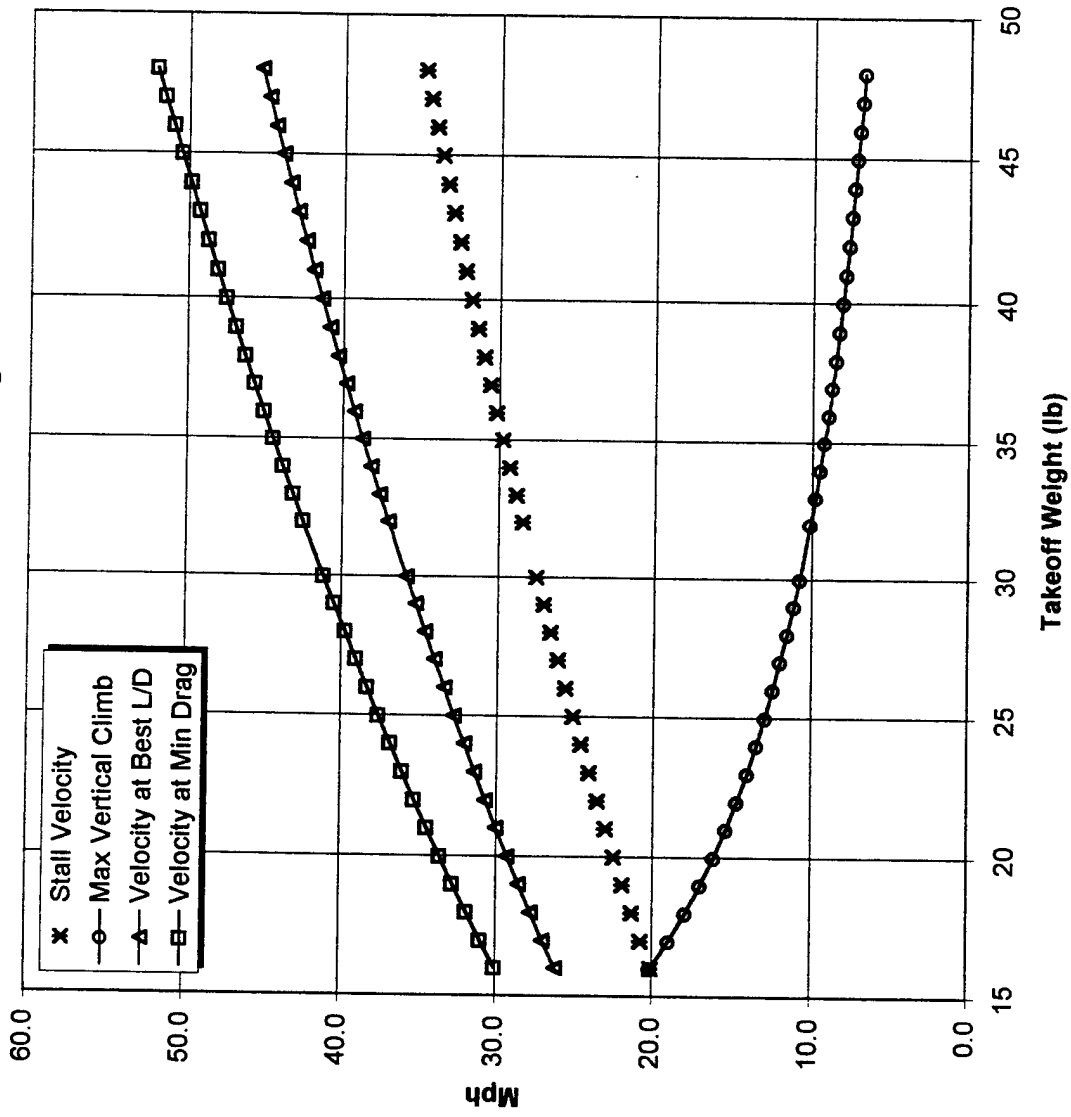
Performance

Max range at cruise (empty;full) 6.2mi;4.8
Empty takeoff distance 50ft
Max load takeoff distance 200ft at 1.31 payload fraction
Landing distance 350ft
Max speed 85mph
Max rate of climb (empty;full) 600fpm;28fpm
Stall speed (empty;full) 20mph;35mph
Cruise speed (empty;full) 31mph;48mph
Max loiter time (empty;full) 12min;6min
Max g loading 4.0
Max payload fraction 1.8, 1.3 for 200ft takeoff req.

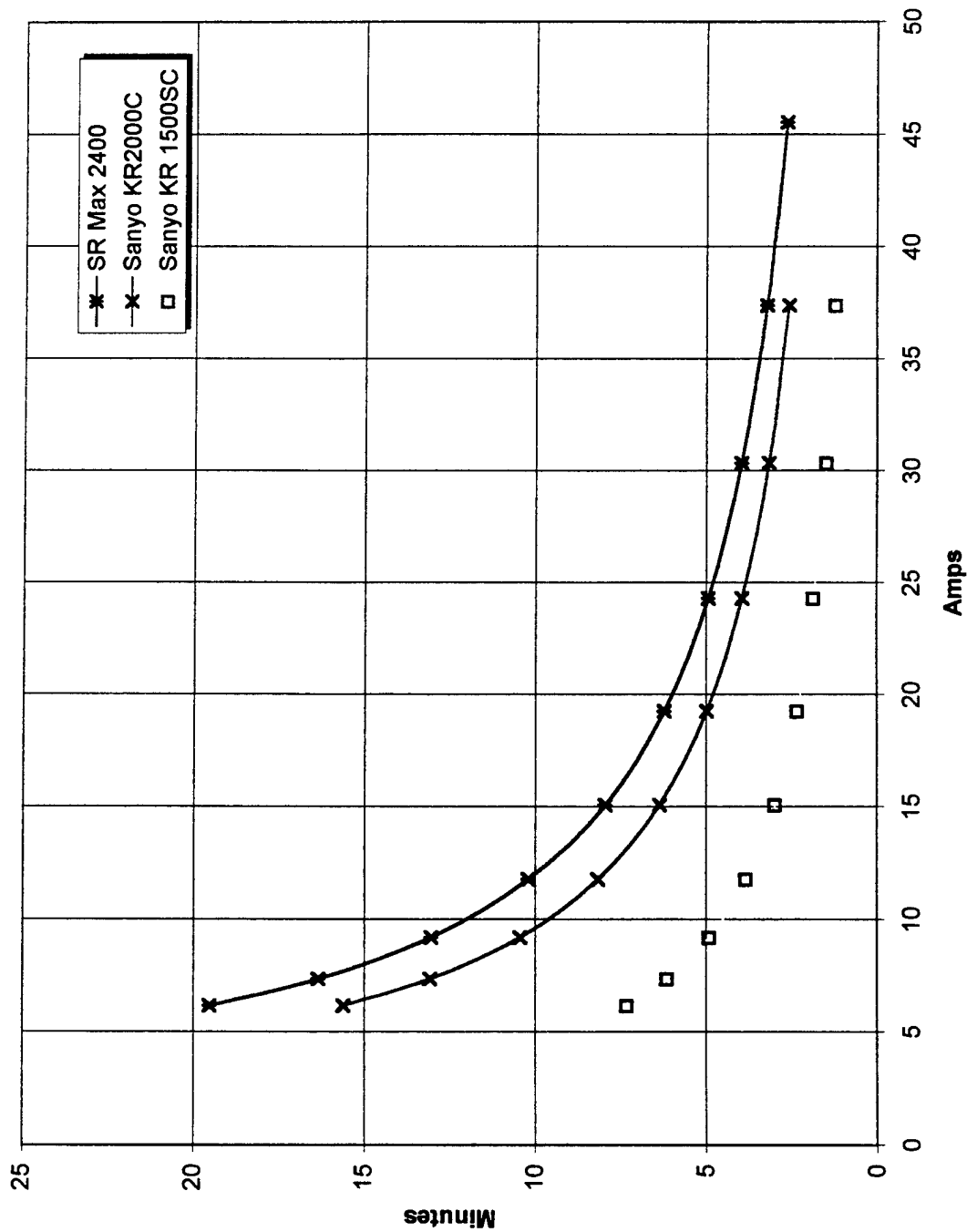
Drag Polar



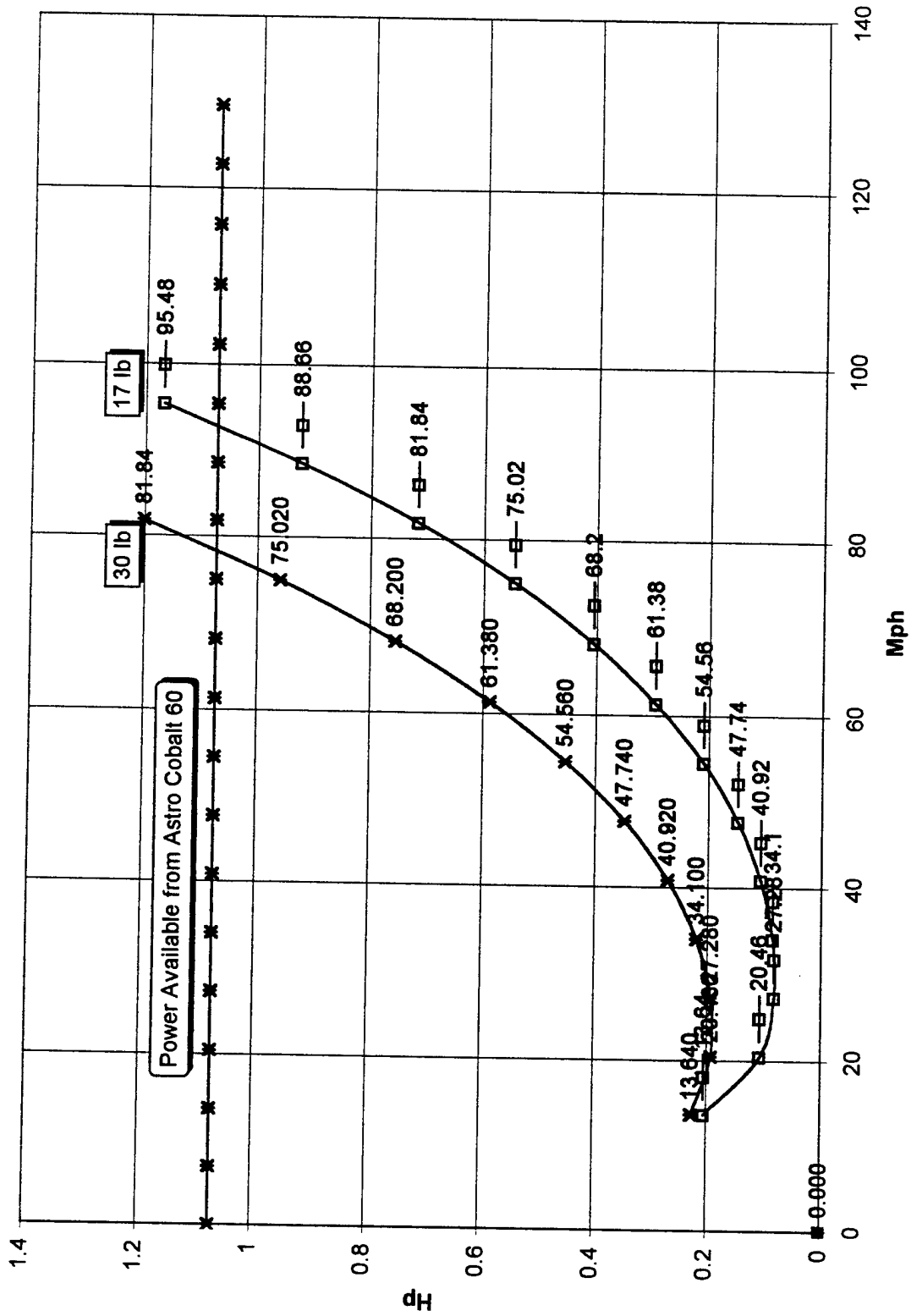
Critical Velocities vs Weight



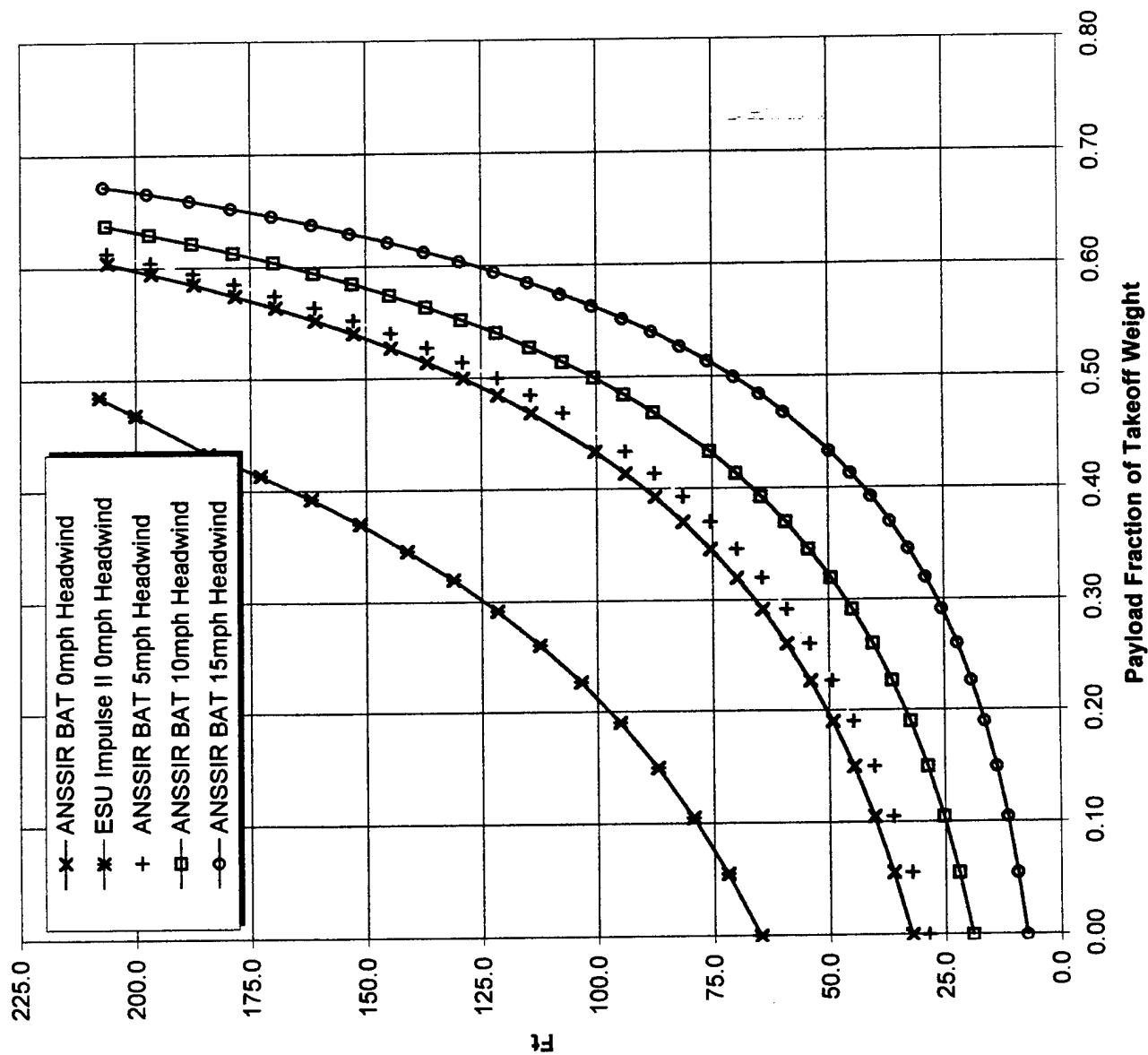
Battery Pack Endurance vs. Current

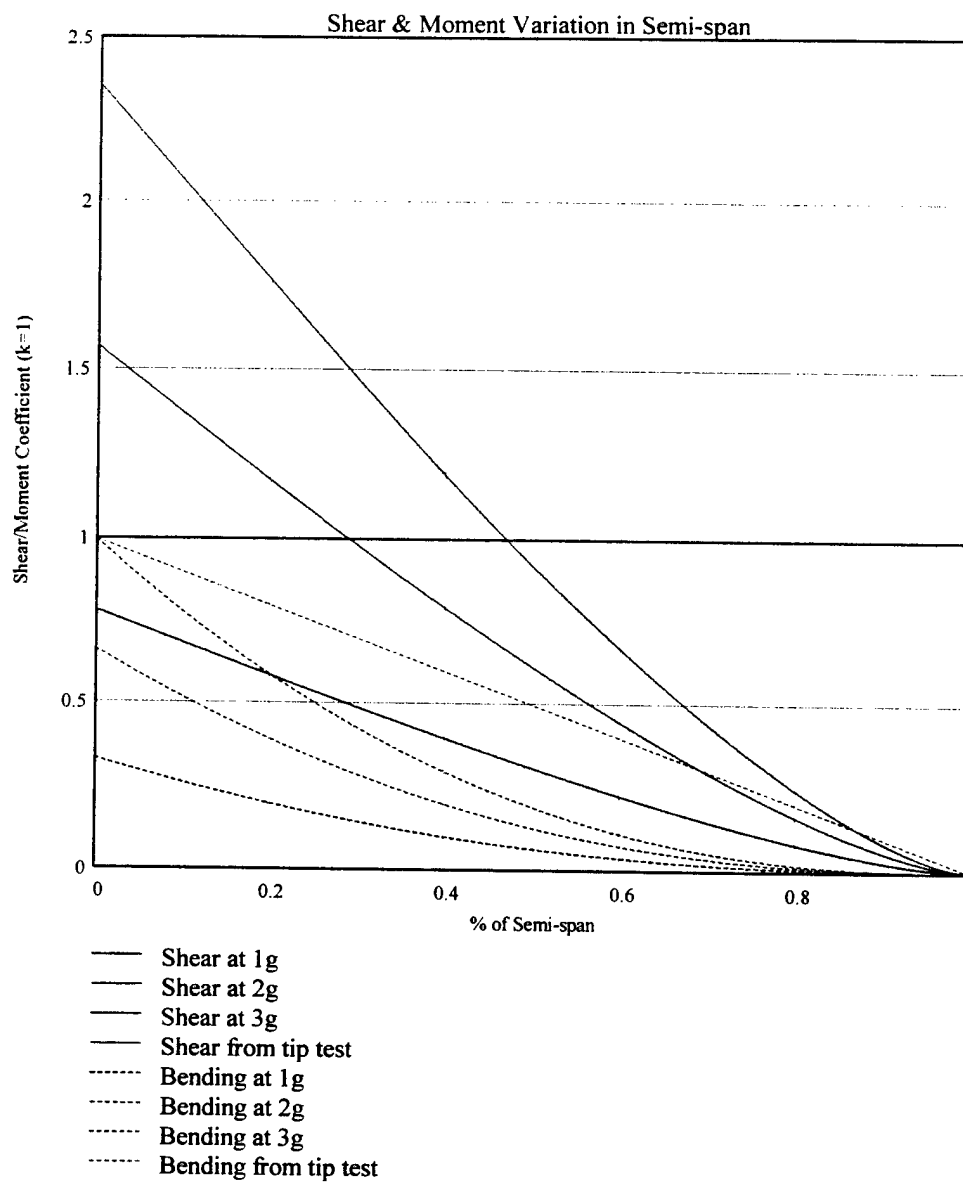


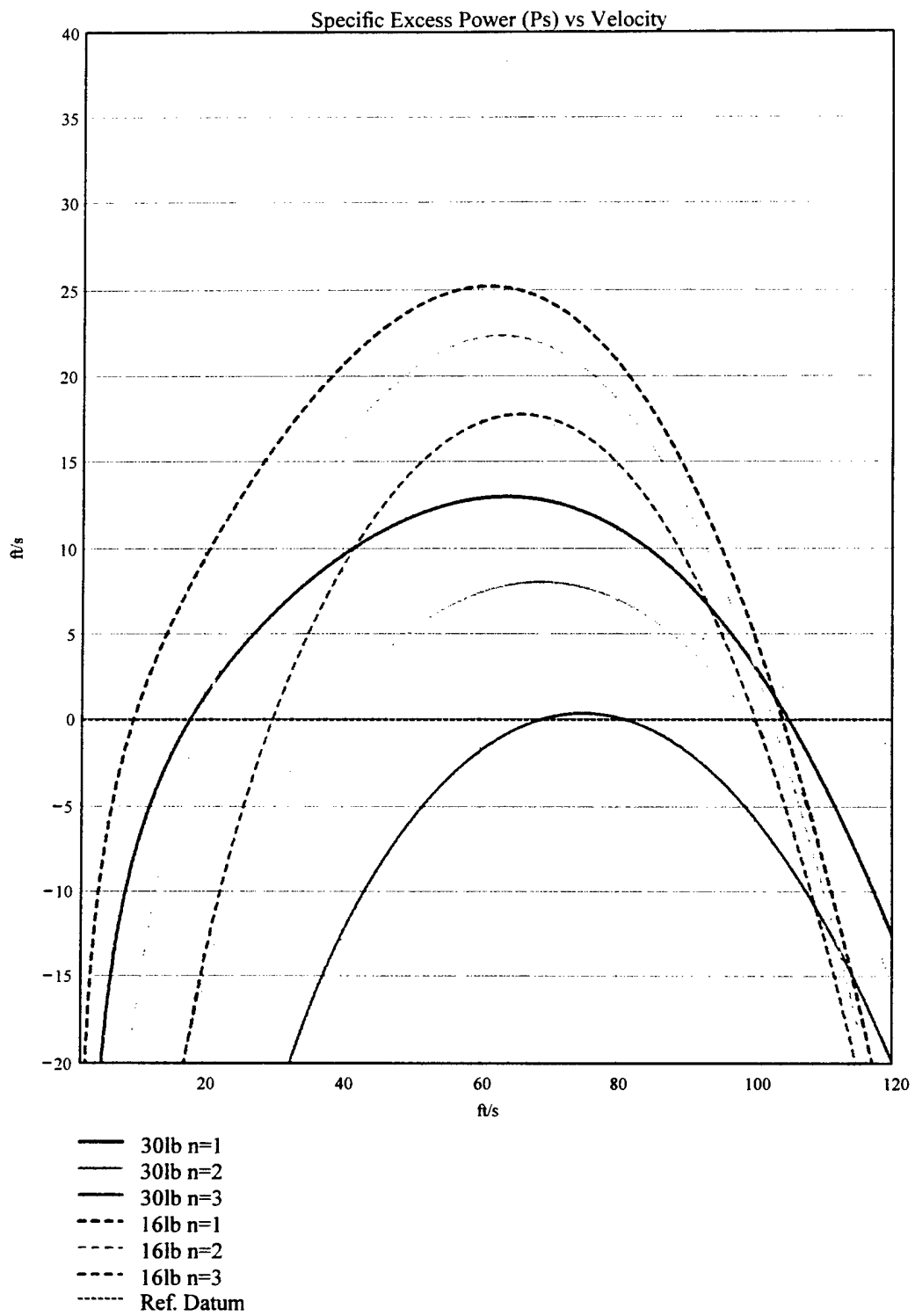
Power Required vs Velocity



Takeoff Distance vs Payload Fraction

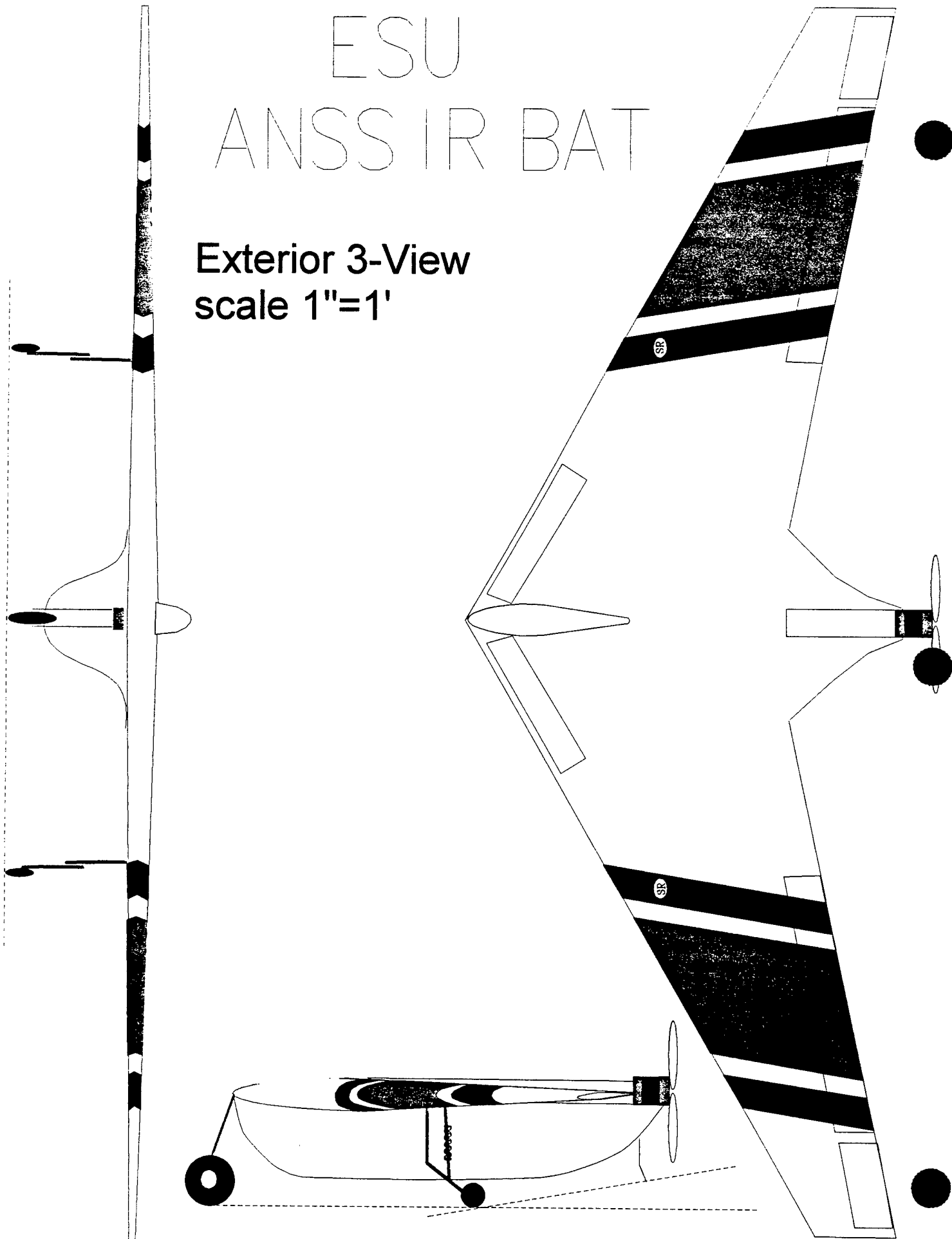






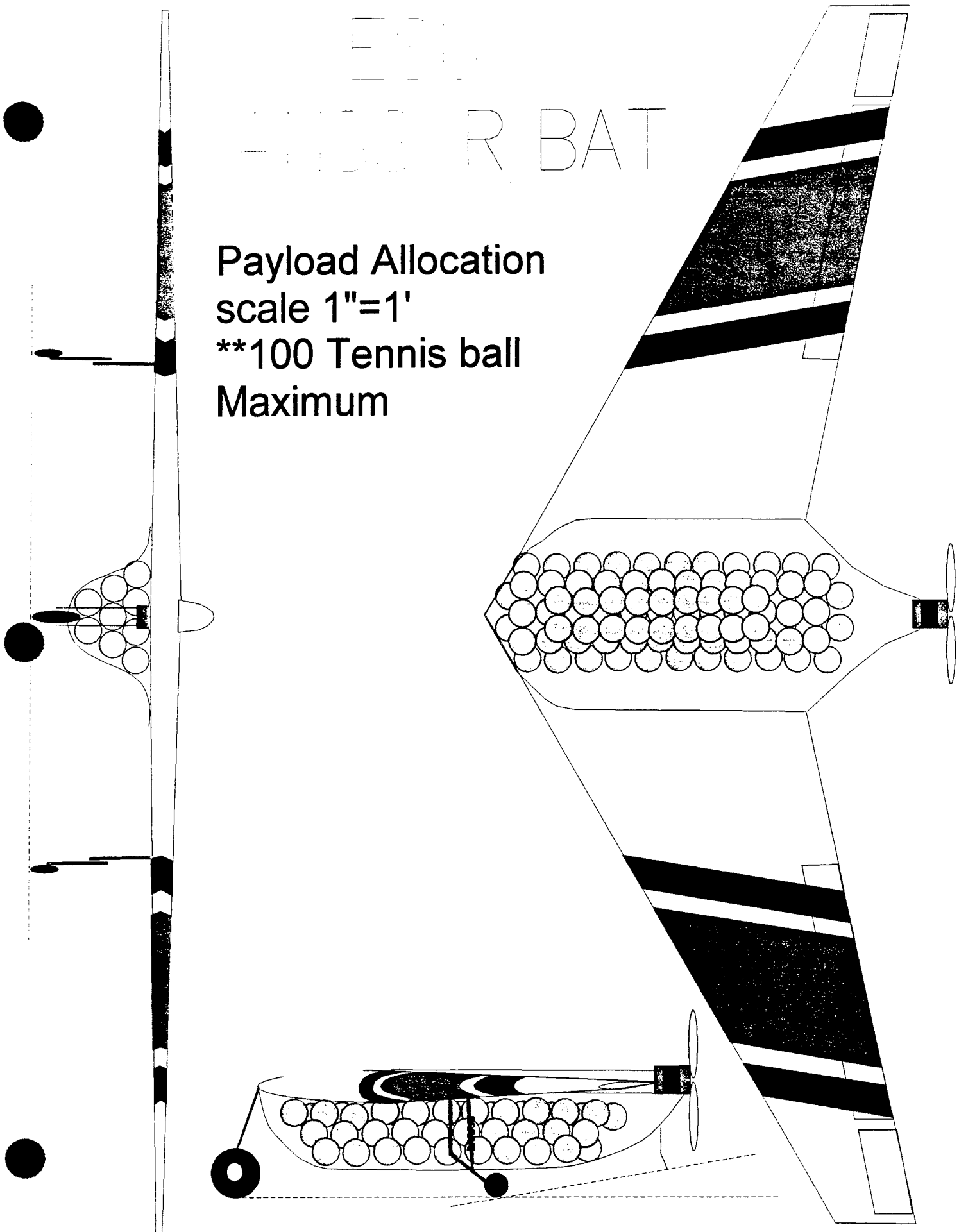
ESU ANSS IR BAT

Exterior 3-View
scale 1"=1'



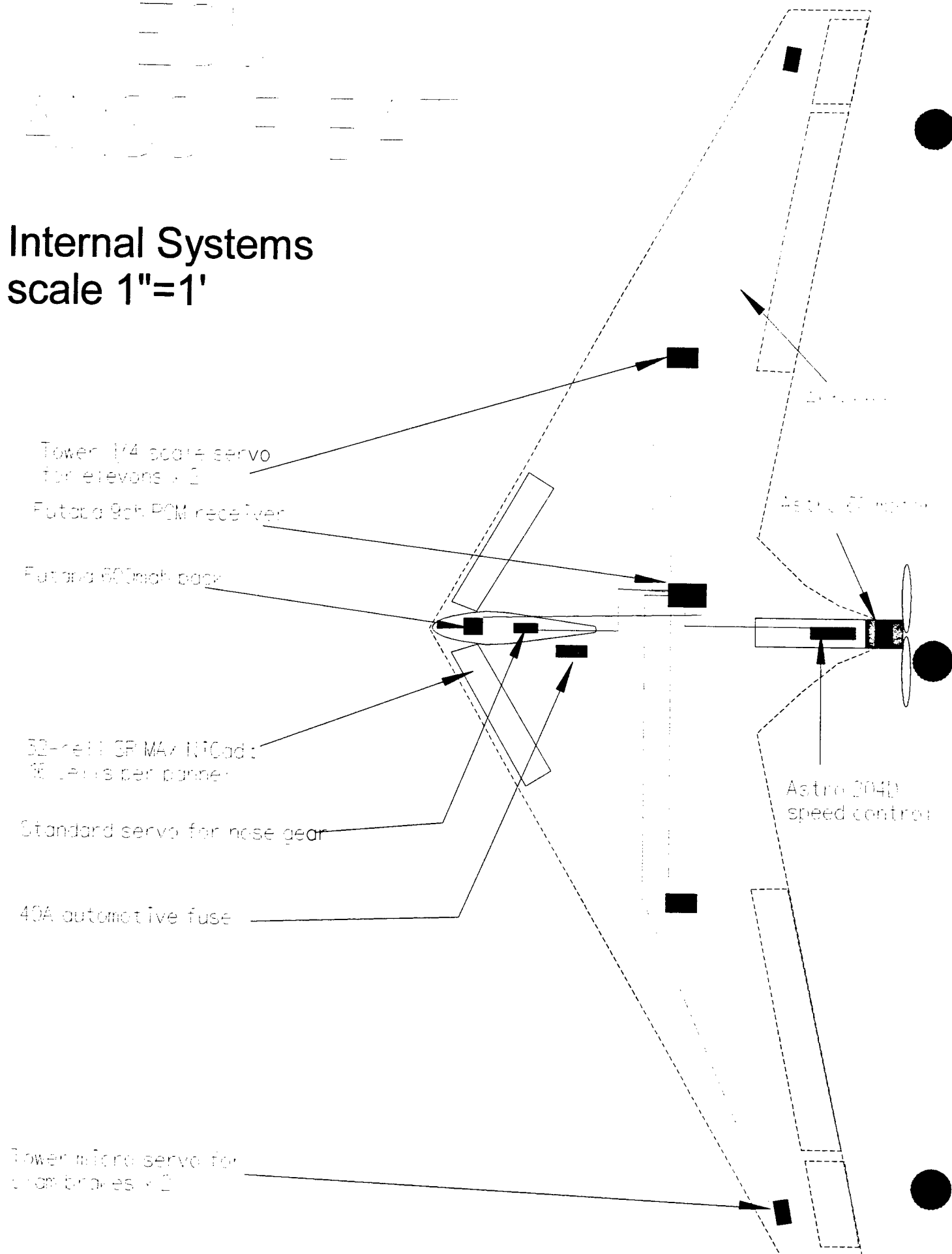
ERL 4000 R BAT

Payload Allocation
scale 1"=1'
**100 Tennis ball
Maximum

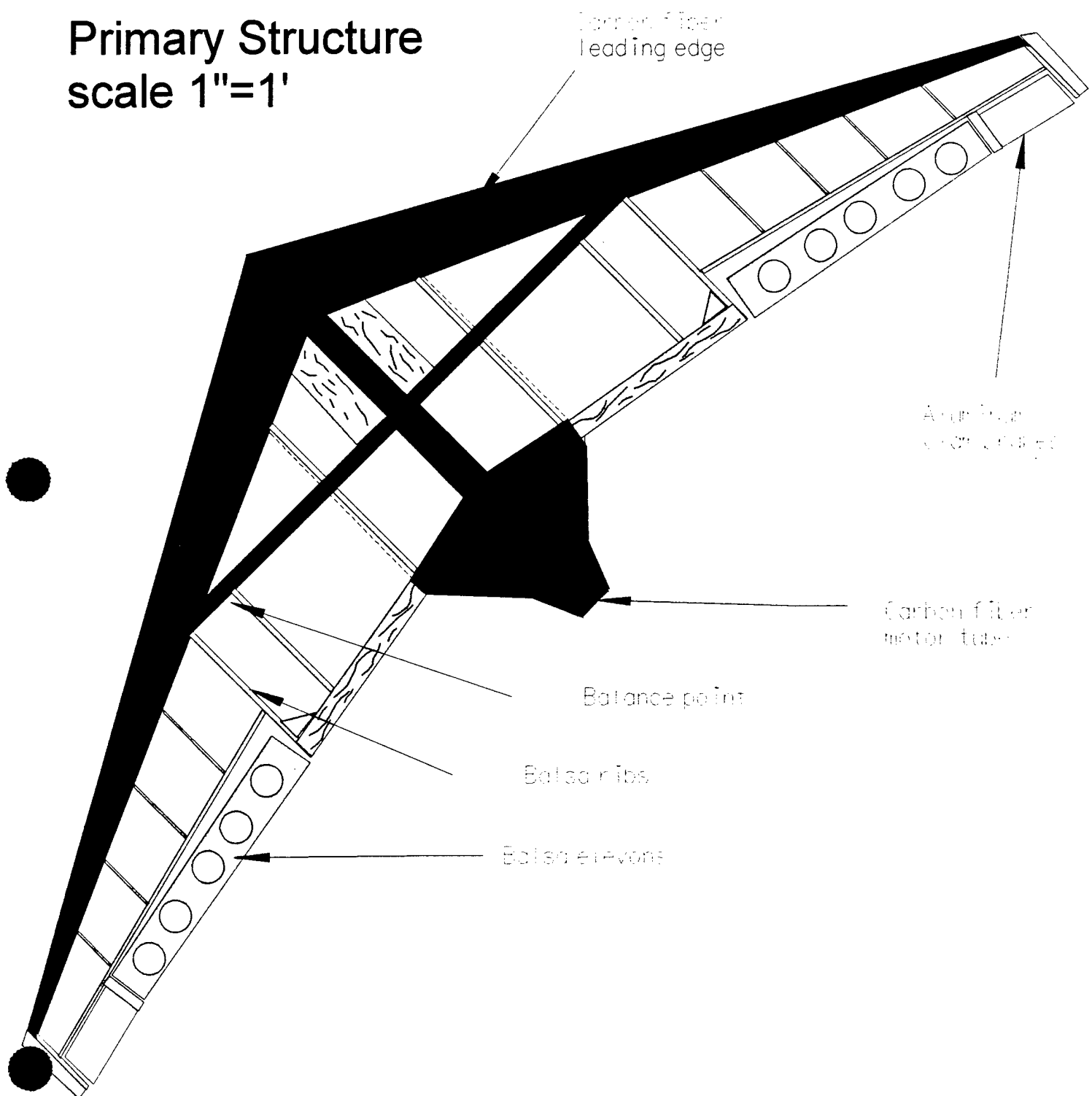


Internal Systems

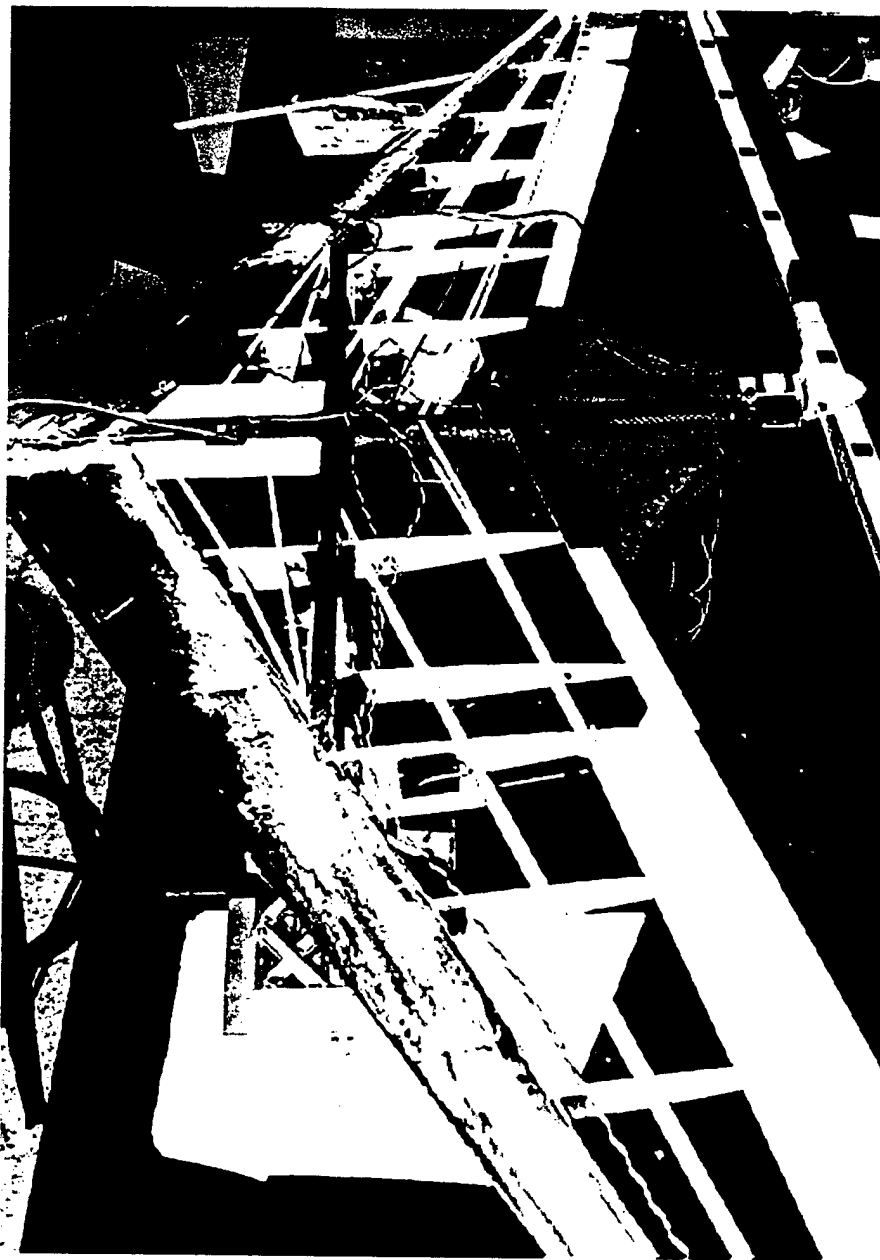
scale 1"=1'



Primary Structure scale 1"=1'



Manufacturing Plan



Manufacturing Plan

In designing the airplane this year a few key aspects were kept in mind toward kind of design that was going to be built. After much discussion, the team decided on a flying wing design. It was thought that this would be the best possible aircraft for the rules, stipulations, and tasks of this year's contest. Also the materials and skills available were a deciding factor in the production of the RC flying wing.

When the design was started it was obvious that the most important element of the plane was the wing. The team decided on a polystyrene foam core for the leading edge of the wing. The leading edge was broken up into two parts, each five feet long and joining at the center. The foam was placed in layers and glued together to obtain the proper size we needed for optimum lift. The foam was then cut using a taut electrically heated wire for a clean cut.

After both parts of the wings were cut and sanded to the desired shape we coated it with carbon fiber material to add strength and at the same time keep the weight low. The Carbon fiber was attached to the foam using a hardening epoxy. The wing was then again sanded down and a second coat of 10-minute epoxy was applied for additional strength. The spar was installed inline with the CG of the front edge only. It was also constructed of foam and carbon fiber material. We decided to go with a rectangular shape for ease of construction and strength.

The back portion of the wing uses ribs made of balsa wood. The balsa wood was attached to the front edge of the wing using cyanoacrylate (Zap-A-Gap). When the design was complete the entire wing was covered in Monokote. Bright florescent orange was strategically applied in bold geometric patterns to provide the best possible visual reference for the pilot in all aircraft attitudes. Historically, most military prototype aircraft have enjoyed success with similar paint schemes.

One addition to our wing was the use of clam brakes. On the tips of the back of the wing we installed two clam brakes in accordance with the elevons. They were made of thin sheet metal and were spring and servo actuated. It was thought that the incorporation of these brakes would help with yaw stability and speed control, but after testing the clam brakes it might be found that their effectiveness is insufficient.

To keep the rated aircraft cost formula down it was decided to use a pod instead of a standard fuselage. The pod was designed to be able to carry the maximum number of tennis balls and the least amount of steel allowed in competition flight. The pod was built by using a mold that was made from foam. The mold was covered in Monokote and release wax before placing a Kevlar-Carbon fiber material over it. Epoxy was used to laminate the form. The Kevlar®-carbon fiber was used for its abrasion resistance and low weight. The amount of structure inside the pod was minimized to a single bulkhead. After the pod cured it was tested to see if the tennis balls fit accordingly, and snap fasteners were employed to attach it to the front edge of the wing. The rest of the pod would be fastened with joiners drilled right into part of the

balsa wood frame of the wing. The pod was designed so that the tennis balls would fit in only one way possible; thus the balls would not be able to move about during flight. In accordance with the rules, a lid will be incorporated to the pod.

The batteries were stored along the front edge of the wing for ease of loading/unloading during charges, and more importantly for reasons of positive static longitudinal stability.

The design of the plane called for a pusher configuration. This was a problem due to the unavailability of pusher propeller selection in the retail market. The team had to modify the motor for reverse rotation. To stop the propeller from unfastening itself during flight we had to machine a left handed screw for the attachment of the propeller to the motor.

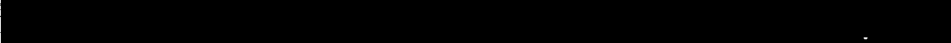
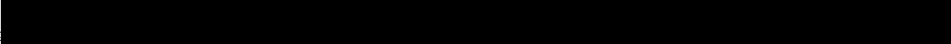
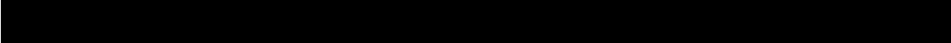
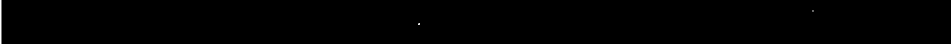
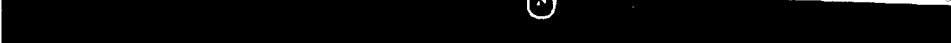
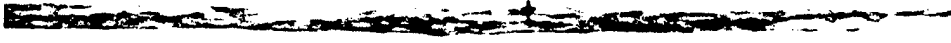
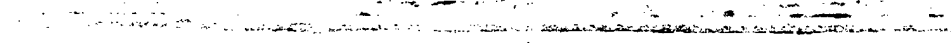
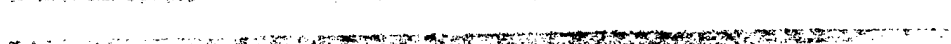
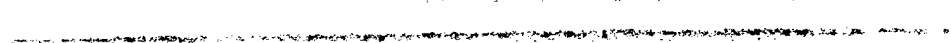
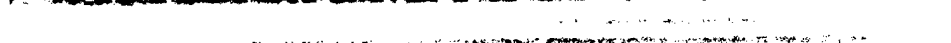
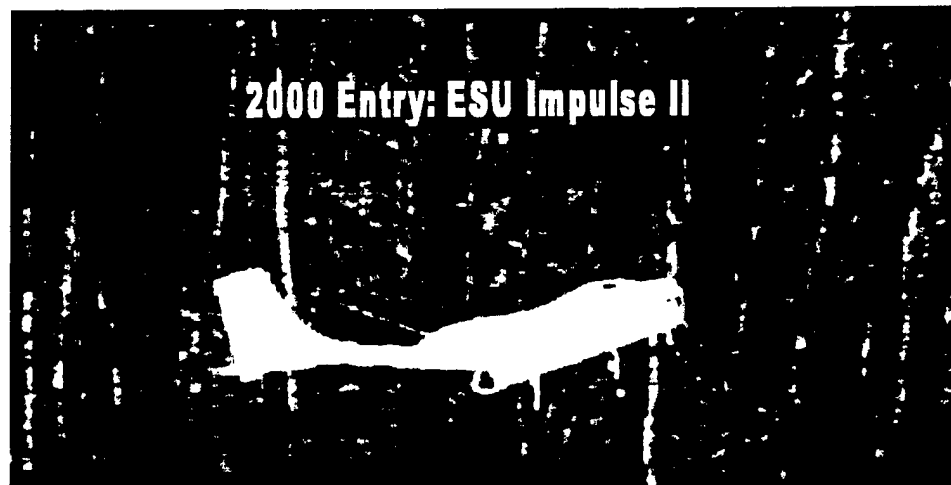
The motor pipe was a key aspect in the placement of the motor in the rear of the plane. The motor had to be placed down the centerline of the plane for pitch/yaw stability. The pipe was constructed of four layers of Carbon fiber for maximum strength. The motor pipe was then attached to the spar of the plane and attached to the ribs of the wing. A bump-stop wire was affixed to the end of the pipe to prevent prop strikes on rotation.

The landing gear is set up in a classic tricycle setup. The front wheel was arranged in such a fashion for steering the plane quite easily on the ground. It was unlike the two-rear landing gear in that there was no suspension on it. This was done so that it would not give under the weight and over rotate or nose-dive on landing. The main landing gear was originally made up of three pieces of hollow aluminum attached together and a spring on the support strut. This seemed adequate after trying different springs, yet a better idea was devised. The final decision was on constant force gas springs at fifteen pounds. The gear was fastened to the plane by using music wire and fastening it right to the spar of the plane. The wheels used on the plane were essential in the design. The front wheel is a soft foam wheel that makes turning very easy and makes for stable landings. The rear wheels used roller blade types with minimal rolling resistance and axle friction. They were milled to further reduce their weight.

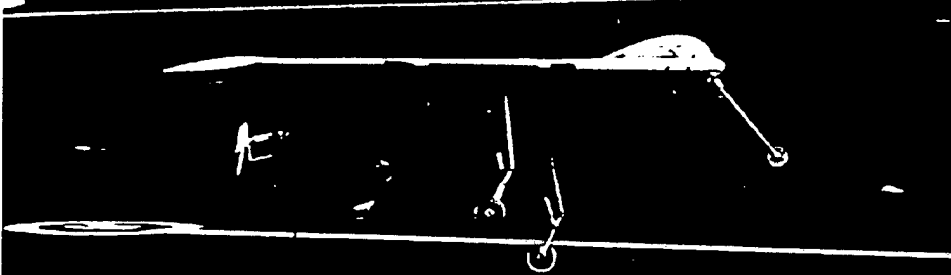
The design of the aircraft did not include a tail, a rudder or a fuselage to keep the rated aircraft cost minimized. The designers chose to use the maximum allowed wingspan. To keep the aircraft's weight as small as possible, carbon fiber was used in the construction of the leading edge spar and motor support. Balsa wood ribs were employed for the internal structure of the wing instead of making it completely out of the polystyrene foam.

After completion of the first plane the designers realized that some aspects of the plane could be altered so that it would be lighter, and have a lower rated cost. The leading edge of the wing could be done with polystyrene foam again, but prior to the Carbon fiber application holes or slots could be cut out of the foam. This would yield a lighter wing with more than sufficient strength. The cargo pod design could be more aerodynamic for less profile drag. The pod could be designed to make it easier and quicker to change between sorties.

2000 Entry: ESU Impulse II



2001 Entry: ESU ANSSIR BAT





**East Stroudsburg University
of Pennsylvania**

**2001 AIAA Cessna/ONR
Student Design/Build/Fly
Competition**

Design Report



Addendum Phase

Contest Date: April 21-22

Contest Site: Patuxent River, MD

Electric Airplane Project
c/o Physics Department
East Stroudsburg University
East Stroudsburg Pa, 18301

Phone: 570-422-3341

Fax: 570-422-3505

Email: dlarrabee@po-box.esu.edu

Lessons Learned

The ESU ANSSIR BAT has flown several times since the submission of the proposal phase of our design report. The team is pleased with its demonstrated handling qualities and has seen significant improvement in its ability to field a contest-worthy vehicle. Slight difficulties have been encountered and they have received additional design attention. It is expected that testing and optimization of the aircraft will continue until the contest date.

The most significant alterations to the aircraft involved both the deletion of the cargo pod and the addition of vertical fins. As initial flights were made, it became clear that the inherent yaw dampening provisions of the tail-less flying wing proved to be inadequate. Likewise the clam-brakes were ineffective in control. The decision was made to delete the clam brakes and large vertical fins with rudders were added to the wing tips. The fin area though large, was selected to provide additional yaw stability even in the presence of the huge destabilizing center, conformal pod. Additionally, it was hoped that the fins would provide a winglet effect at their span-wise location but they were primarily placed to take advantage of the longest possible tail-arm on the vehicle. Pod-less flights revealed exceptional and conventional control with the fins. They were a valuable addition to the airframe even with the ensuing cost formula increase.

As a flight was attempted with the pod after the fins had been installed, vehicle performance suffered tremendously. The ANSSIR BAT with 50 tennis balls was barely able to takeoff in 180ft and could not maintain altitude. The pod was the cause of this difficulty. The pod had been designed with the primary emphasis of fitting 100 tennis balls in the minimum possible volume. The aerodynamic effects of the under-wing conformal pod were unknown prior to the flight-test, but they were expected to be undesirable. Affecting the known characteristics of the NACA 0009 over the largest portion (center section) of the wing was very detrimental in the lift, and perhaps pitching moment characteristics of the wing. It was expected that the curvature of the pod would aggravate the Dutch-roll mode of stability were it not for the fins. The pod effectively blocked the propeller, which inevitably decreased available thrust. From a pragmatic point of view, attempts to load the pod hurriedly under contest like conditions were completely unacceptable. The possibility of adversely changing the C.G. was ever present and there was no good way to restrain the steel or tennis balls.

With the deletion of the pod, the only other alternative available to the team was the addition of external hard-points below the wing. Using the same attachment points as the pod, the two pylons will each mount 27 tennis balls in joined sections of commercial tennis-ball tubes. The use of pylons will effectively solve all of the problems incurred by the conformal pod. For testing, it may be possible to jettison the payload from the pylons if the aircraft experiences trouble. The cargo may be precisely loaded at the C.G. and will not shift. It will be easier to alter the amount of cargo during the contest to cope with weather variations. The weight of the new

system is slightly less than with the conformal pod. The stores will be several inches away from the wing, thus the section properties will be less effected and the propeller will no longer experience blockage. The only negative quality of the external pylon approach is that it will limit the total tennis ball load to approximately 54, instead of 100 as was possible with the pod. However since the pod hindered flight with only 50 tennis balls on board, the extra volume is essentially useless.

Motor and battery performance under contest-like conditions has forced the team to reconsider its competition strategy. Flight tests with no cargo system have shown that full throttle may continuously be used for no more than 4 minutes. Careful piloting and cargo reduction are mandated if use of the full competition period is expected. Thus reduction to approximately 7 lb. of cargo has been realized. It is not likely that 2 *Light Payload Tasks* will be accomplished and so, more than the minimum steel will be carried during the *Heavy Payload Task*.

The main gear has unexpectedly surpassed the performance and failure predictions found in our proposal phase. The traditional coil springs were replaced with 15lb constant-force gas struts commonly used on Xerox® machines. They have demonstrated the ability to handle landing in rough field conditions that would destroy other undercarriages. In one instance during flight tests with the loaded cargo pod, the pilot affected a takeoff within the 200ft takeoff run but found the plane was too heavily loaded. A fast landing and high vertical descent rate occurred in the unfinished field beyond the paved runway. There was no damage to the gear and the aircraft otherwise sustained minor damage. As mentioned before, an excessive turnover angle was deliberately built into the airplane, which enhances ground operation. This permits wonderful maneuverability and will facilitate taxiing back to the starting line if it is missed on landing. A nose wheel brake was never added to the aircraft because we did not want to add another servo, however the large foam wheel employed on the nose gear inherently offers mild braking when desired. The team tried 72mm roller-blade wheels on the ESU ANSSIR BAT and found that they significantly reduce the takeoff distance, though they are over twice the weight of conventional foam wheels. To eliminate the excessive stock wheel weight the roller-blade wheels were milled along their circumference, which resulted in a final weight very close to that of the foam wheels.

Weight reduction methodology is an ongoing process. The configuration of the ESU ANSSIR BAT will remain unchanged except for slight variations in external components. It is impossible to alter the airframe, which was designed to withstand the wingtip test at 13lb of cargo. Because our cargo will now be roughly 7lb, the airframe is too heavy. The fins, rudders, and elevons were manufactured out of light-density balsa reduce weight, and the airframe weight was virtually unchanged after the deletion of the clam brakes.

Regarding the next design and manufacturing process implementation for the ESU ANSSIR BAT, the use of carbon fiber over balsa framework is recommended. This would allow the true structural optimization of the vehicle albeit at the fiscal expense of material. The hand-

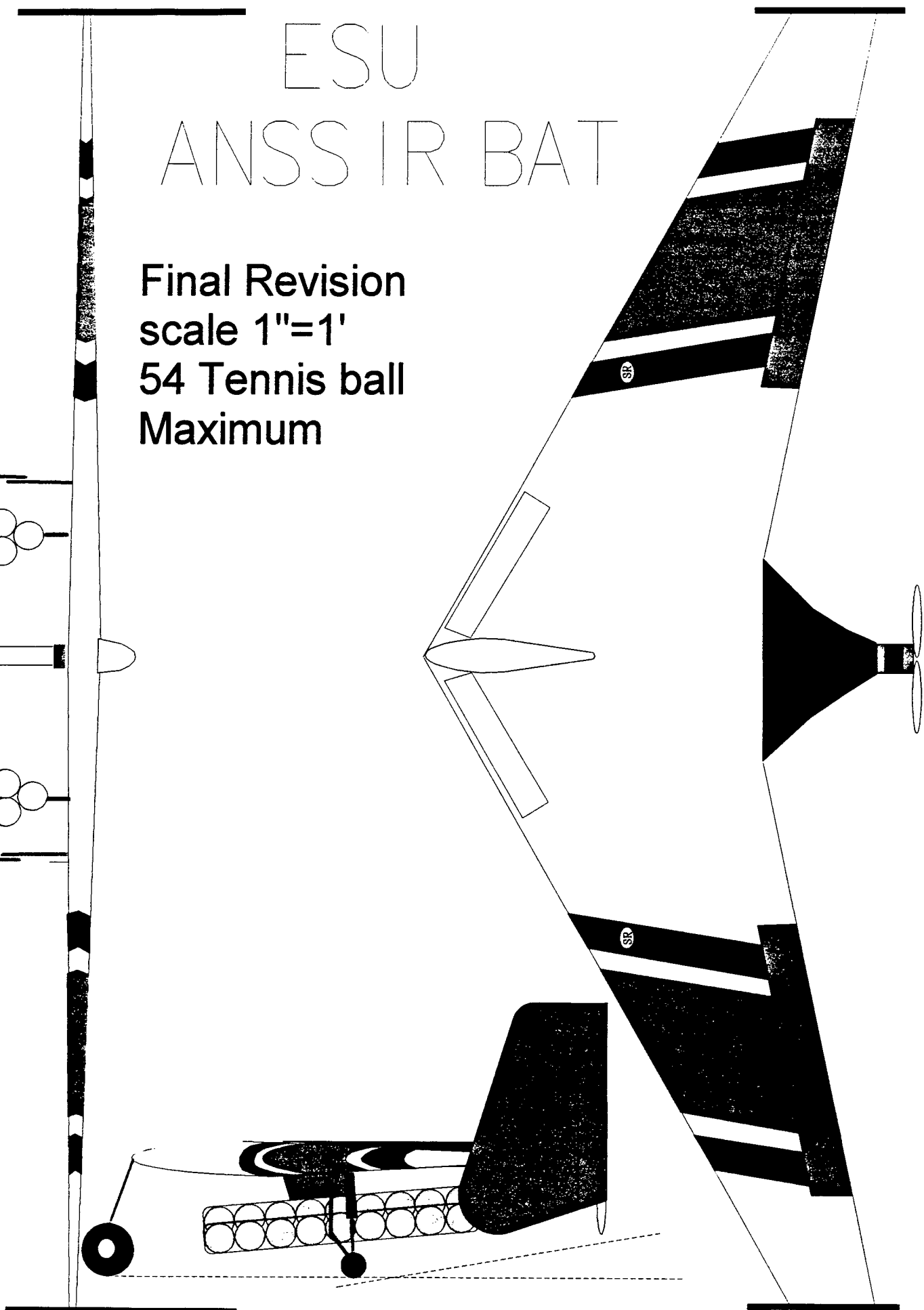
laid epoxy lamination technique works well with carbon fiber and foam but the results are dependent upon the precision of foam shaping and the weight of the foam core. It is believed that greater accuracy could have been obtained along with lighter weight, if the entire structure could have been fabricated beforehand with conventional balsa instead of foam. The precision of manufacture with respect to washout, sweep, taper, etc., items essential to a flying wing, would have been much better with this technique.

Additionally, we realize the need for additional flight-testing. We have been fortunate to have actual prototype flights 4 months prior to the competition and final variant flights 1 month beforehand. However we have not been able to test every conceivable contest scenario (other than on the simulator) because of weather, scheduling, obtaining a flying site etc.... This is the area of development that requires more effort, though it is much improved from last year's contest preparation period (the ESU Javelin flew just 4 days before the 1998-1999 contest).

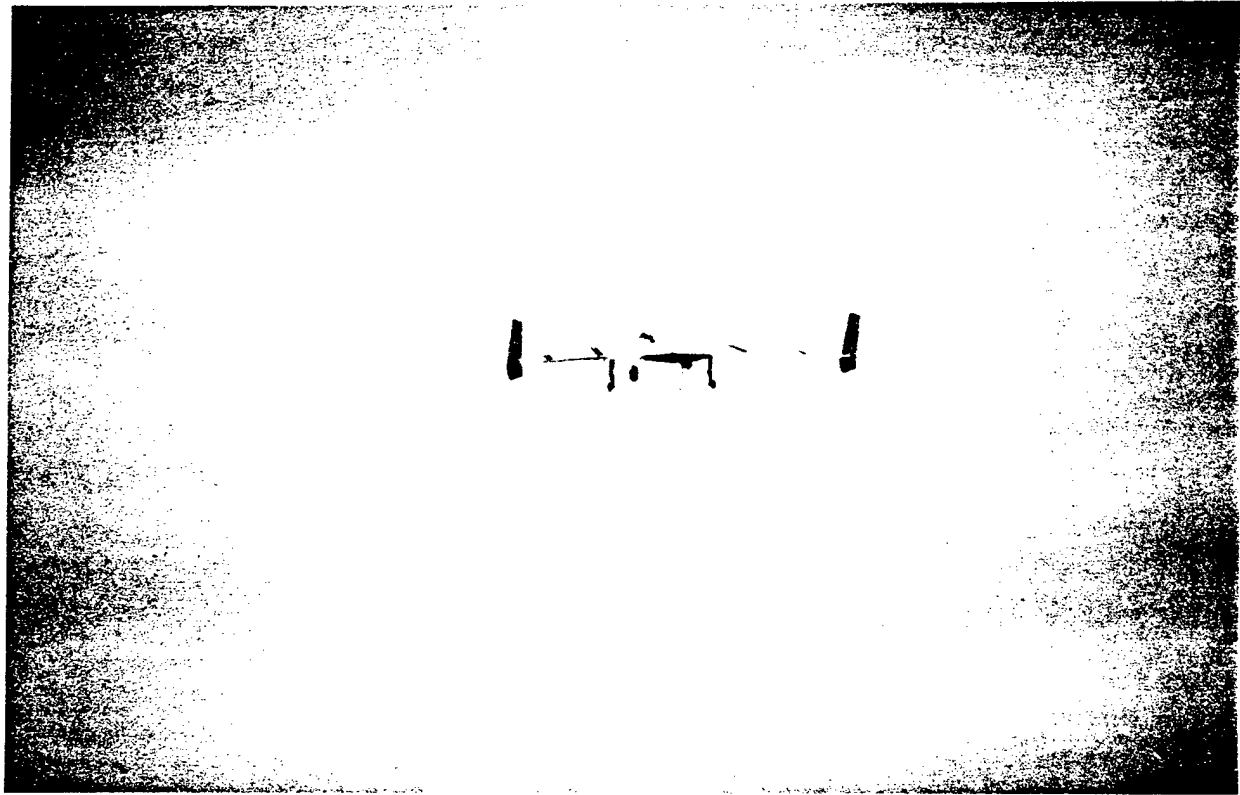
Finally, we recognize the need for more congruency between our analytical modeling and the fruition of our work in applied aerodynamics. The selection of a tail-less aircraft has reiterated this concern. Since our aircraft has been extremely successful, it would be beneficial to compile an extensive list of data from static and dynamic tests. It is conceivable that telemetry research should be conducted to verify all performance limitations on the aircraft for correlation with design equations and future reference. This is one area that must be addressed if we are to further advance our entry in the next Cessna/ONR student DBF contest.

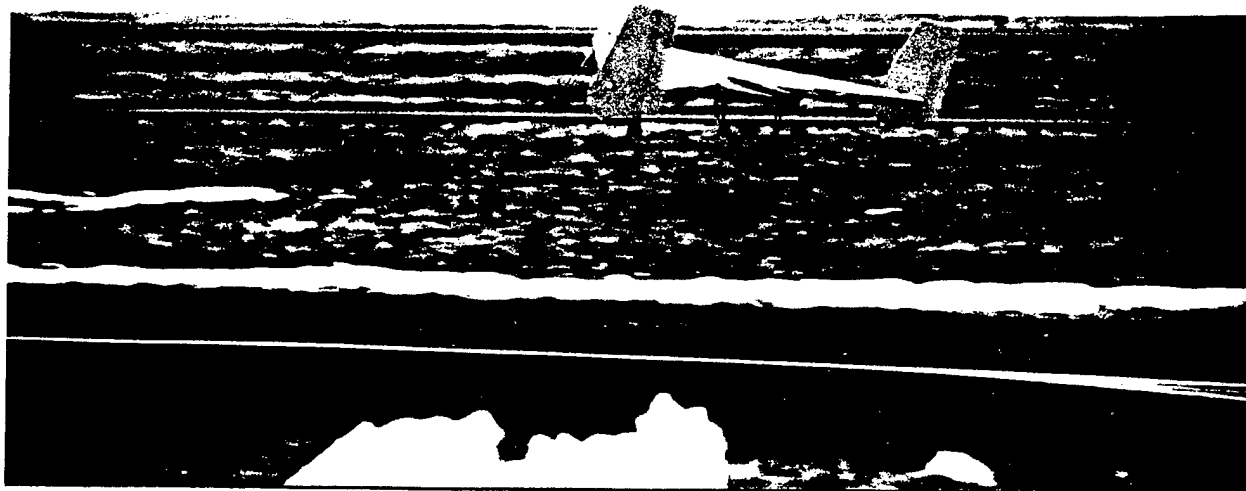
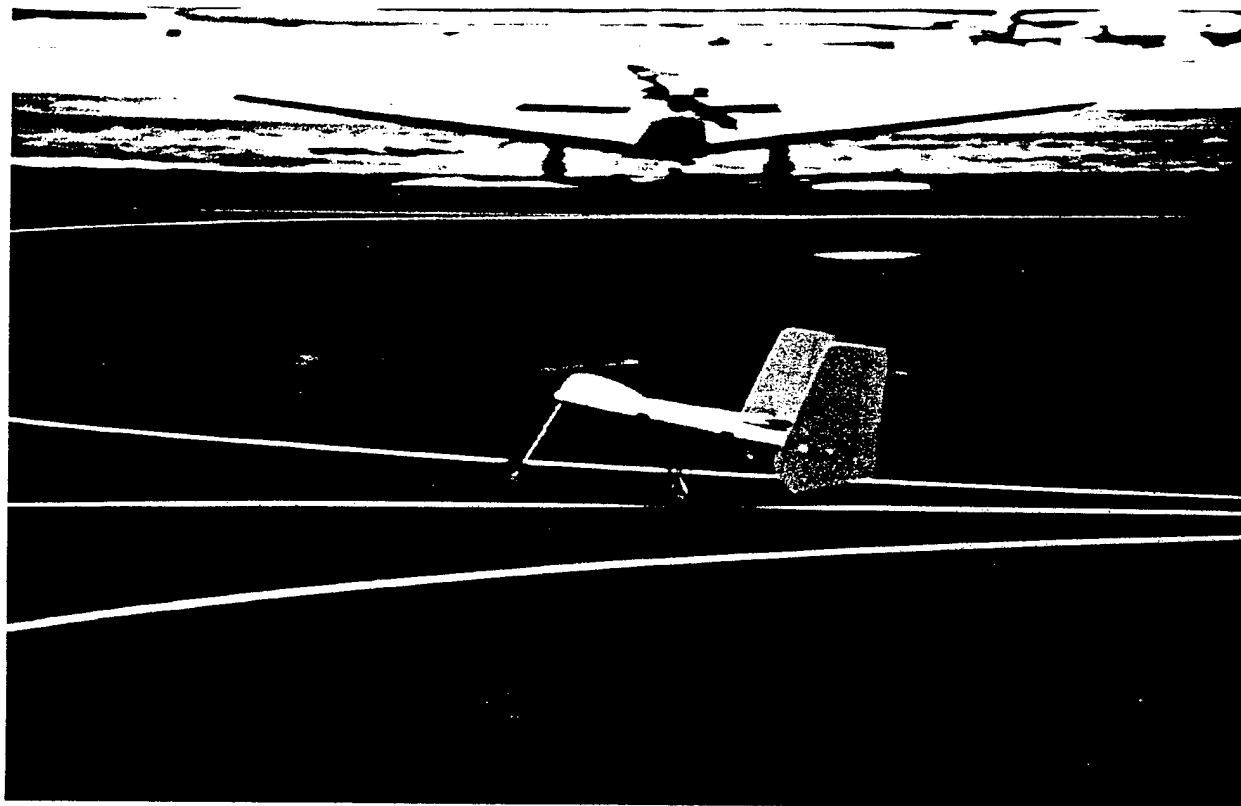
ESU ANSS IR BAT

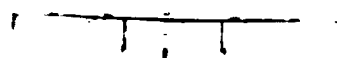
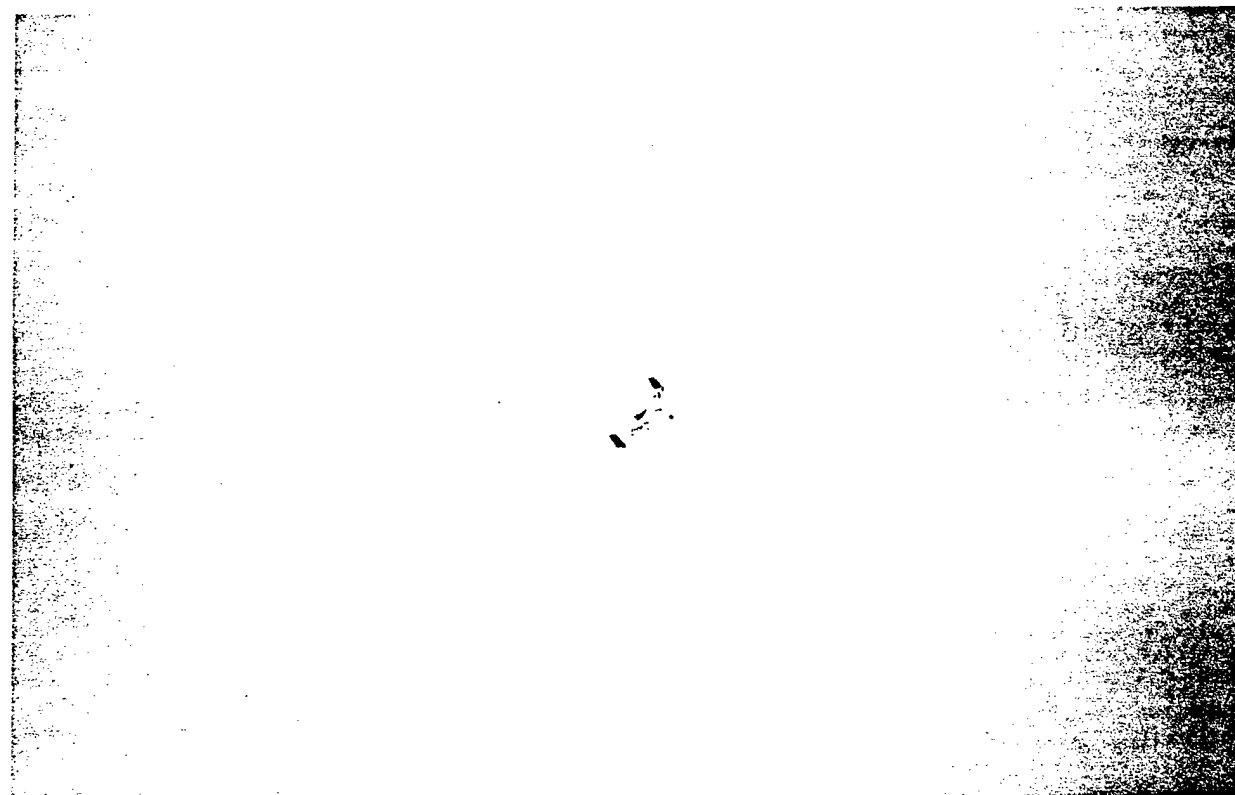
Final Revision
scale 1"=1'
54 Tennis ball
Maximum



<u>Rated Aircraft Cost Formula</u>					
<u>Manufacturer's Empty Weight</u>					14
<u>Rated Engine Power</u>					1536
[1x40x1.2x32=1536]					
# Motors	# Cells	Fuse A			
1	32	40			
<u>Manufacturing Man Hours</u>					156.92
[15x1+4x(15.8+2.93)+3x2+5x1+4x2.25+5x1+5x2+5x1+2x6+5x1+5x1=147.92]					
# Wings	Wing Area	# Struts/Braces	Total Fin Area		
1	15.8	0	2.93		
#Control Surfaces	# Bodies/Pods	Body/Pod length			
2	1	2.25			
# Empenage	#Vertical Surface	#Horizontal Surface			
1	2	0			
#Flight System	#Servos	#Propellers			
1	6	1			
<u>Rated Aircraft Cost</u>					6.0744
[100x14+1x1536+20x147.92=5.8944]					







UNITED STATES MILITARY ACADEMY

TEAM BLACK KNIGHT

CESSNA MONR STUDENT DESIGN BUILD
COMPETITION DESIGN REPORT



"GREY Balsa Fire"

WEST POINT, NEW YORK
MARCH 13, 2001

TABLE OF CONTENTS

1. Executive Summary	2
2. Management Summary	4
3. Conceptual Design Phase	7
3.1 Introduction	7
3.2 Identify Needs	7
3.3 Design Parameters	8
3.4 Figures of Merit	10
3.5 Morphological Analysis	11
3.6 Concept Determination	12
3.7 Concept Specifications	13
3.8 Results	15
4. Preliminary Design Phase	21
4.1 Introduction	21
4.2 Design Parameters	21
4.3 Numerical Methods Optimization	23
4.4 Materials Selection	27
4.5 Results	29
5. Final Design Phase	34
5.1 Introduction	34
5.2 Aircraft Performance	34
5.3 Aircraft Stability and Control	34
5.4 Stress Analysis	36
5.5 Component Selection	36
5.6 Systems Architecture	37
5.7 Innovative Configuration Solutions	37
5.8 Results	38
6. Manufacturing Plan	46
6.1 Introduction	46
6.2 Manufacturing Acquisition	46
6.3 Skill Assessment	47
References	50

In order to gain real-world aircraft design experience, a team of cadets from the United States Military Academy at West Point entered the Cessna/ONR Student Design/Build/Fly Competition. Under the guidance of the Civil and Mechanical Engineering Department, the team designed and built a remote-controlled aircraft to participate in the AIAA-sponsored event. The competition will take place on April 20-21 at Pax River Naval Air Station, Maryland.

The objective of the competition is to design, fabricate, and demonstrate the flight capabilities of an electrically powered R/C aircraft. The goal of the design team is to take first place at the competition by earning the highest score among all participants. The total score is the product of the report score and the flight competition score. The written report consists of both a Proposal Phase and an Addendum Phase which will be scored by AIAA officials.

The team incorporated two different design process models in order to ensure design quality. The first is the *Mechanical Design Process* written by David G. Ullman (Oregon State University). This book helped the team to establish the groundwork for the overall design process. The second is the *Philosophy of Airplane Design* written by John D. Anderson, Jr. This book was useful in providing information specific to the various components of aircraft design.

The design process includes several phases: specification, development, planning, conceptual design, preliminary design, detailed design, and manufacturing. Careful design and coordination between each of these areas is essential to designing a successful product.

In the specification, development, and planning phase; the team relied heavily on the design philosophy of Mr. David Ullman. Throughout this phase, Mr. Ullman focuses on forming the design team, understanding the problem, and planning the design. In forming the design team we created concurrent design teams as well as engineering design teams. This is covered in Section 2, Management Summary. Next, the team focused on understanding the problem. By using the tools outlined by Mr. Ullman, the team was able to effectively understand the problem at hand. The tools we used included the How/Why Analysis, Functional Decomposition, the Quality Function Deployment (QFD), and Mind Mapping.

The conceptual design phase absorbed a large amount of the team's focus in the early stages of the process. Using several reliable sources, the team was able to generate several design configurations that would be feasible for the mission. Ideas were also developed by browsing various sources including the world-wide web, patents, journals and aircraft from past competitions. By brainstorming, creating morphological charts, and mind mapping, we were able to come up with six general design concepts outlined in Section 3, Conceptual Design. The result of our Conceptual Design phase is a dual motor, low-wing configuration that utilizes a tail dragger landing gear and a standard empennage. We developed a maximum payload capacity by analyzing the engineering requirements. Using the seven intellectual pivot points for conceptual design, we were able to narrow some conceptual design phase requirements. These points can be viewed in Figure 3.1, located in the Conceptual Design section. By

using these model, we were able develop the conceptual design of our chosen aircraft. Some of the other configurations that we considered were the biplane, single motor, dual motors, tail-draggers, tricycle landing gears, high wing, mid wing, dual tail, standard tail, etc. The specifics of these designs are found in Section 3 of this report. In general, the aircraft took its form through the integrated design process in the conceptual design phase.

The aircraft began to take shape during the next phase—preliminary design. This phase determines the overall shape and sizing of the plane developed. Specifically, the team focused on the parameter and sizing tradeoffs of the aircraft. We used tools that incorporate several other modeling and finite element analysis software packages to develop the most appropriate values for each of the major components. For example, the preliminary design of the aircraft's wing used analysis from MathCAD and MatLab to select the wing sizing, airfoil shape, and chord length.

In the detail design phase, the team focused on the specifics of what the plane would look and perform like. This phase included a detailed analysis using our various computer programs to aid in the overall "paper trial" of the aircraft. We were able to effectively develop tools to predict the aircraft's performance before it was constructed. Computer programs such as PTC Pro-Desktop 2000 helped create the exact configuration to aid in the manufacturing process. Pro-D was incorporated with COSMOS Design STAR 2.1, which allowed us to run analytical studies on the structure and overall reliability of the aircraft using designated materials. Using these programs, the team was able to accurately predict where failure was most likely to occur. This analysis, along with the specifics of the design, is incorporated in Section 5 of this report (Detail Design).

The final phase is the actual manufacturing of the product. By using materials such as balsa wood, spruce, and limited composites, our aircraft was quickly built and was compatible with our limited building skills. Building to the specifications of the detailed design proved difficult, but became easier with experience.

From the above process we were able to develop a great design that will prove itself in the competition in Maryland. The airplane has a ten-foot wingspan, SD7003 airfoil, and a 15-inch chord length. The fuselage will be 74-in in length and is shaped using the familiar NACA 0024 classification. The tail empennage is a standard design that uses a NACA 0012 symmetric airfoil. The dual motors are Astroflight-40s and will enable our aircraft to take off and land with a gross weight of 36 pounds. The aluminum landing gear is configured as a tail dragger to minimize drag and weight.

In conclusion, the integration of two design process models has enabled team Black Knight to create the best aircraft design required to win the competition. The following report outlines our design configuration and the steps we took to create our aircraft.

2.0 MANAGEMENT SUMMARY

2.1 INTRODUCTION

In order to properly plan for the design and manufacture of the aircraft, the needs and mission profile were reviewed in excruciating detail. A detailed plan for design was established to facilitate a solid design methodology. In order to ensure design success the design schedule was established with extreme scrutiny and prioritized over all conflicting personal and academic requirements.

2.2 PLAN FOR DESIGN

Planning is another extremely important step in design. Consequently, we initially focused most of our attention on this step. "Traditionally, planning is the process used to develop a scheme for scheduling and committing the resources of time, money and people . . . Also, planning results in a map showing how product design process activities are scheduled" (Ullman, 77). With that in mind our first step was to determine the type of project we are participating in. After research, we decided that we are participating in the development of a new product for a single run. By designing for a single run instead of mass production, we did not have to take into serious account the careful manufacture and assembly timing involved. Then we assigned specific roles for each of the team members. Since our team only has ten members, each person had to assume additional duties.

2.2.1 Management Structure - The central hub for the operation is the team leader. Underneath the team leader, sub-team leaders include the building team leader and the report team leader. It is the responsibility of the team leader to ensure that during the design process the entire team is contributing to the design. In this capacity, all members were involved in all phases of the design process. With that in mind, a detailed plan was critical to design success. The list of design personnel and assignment areas enclosed in Table 2.1 shows the hierarchy within the design team.

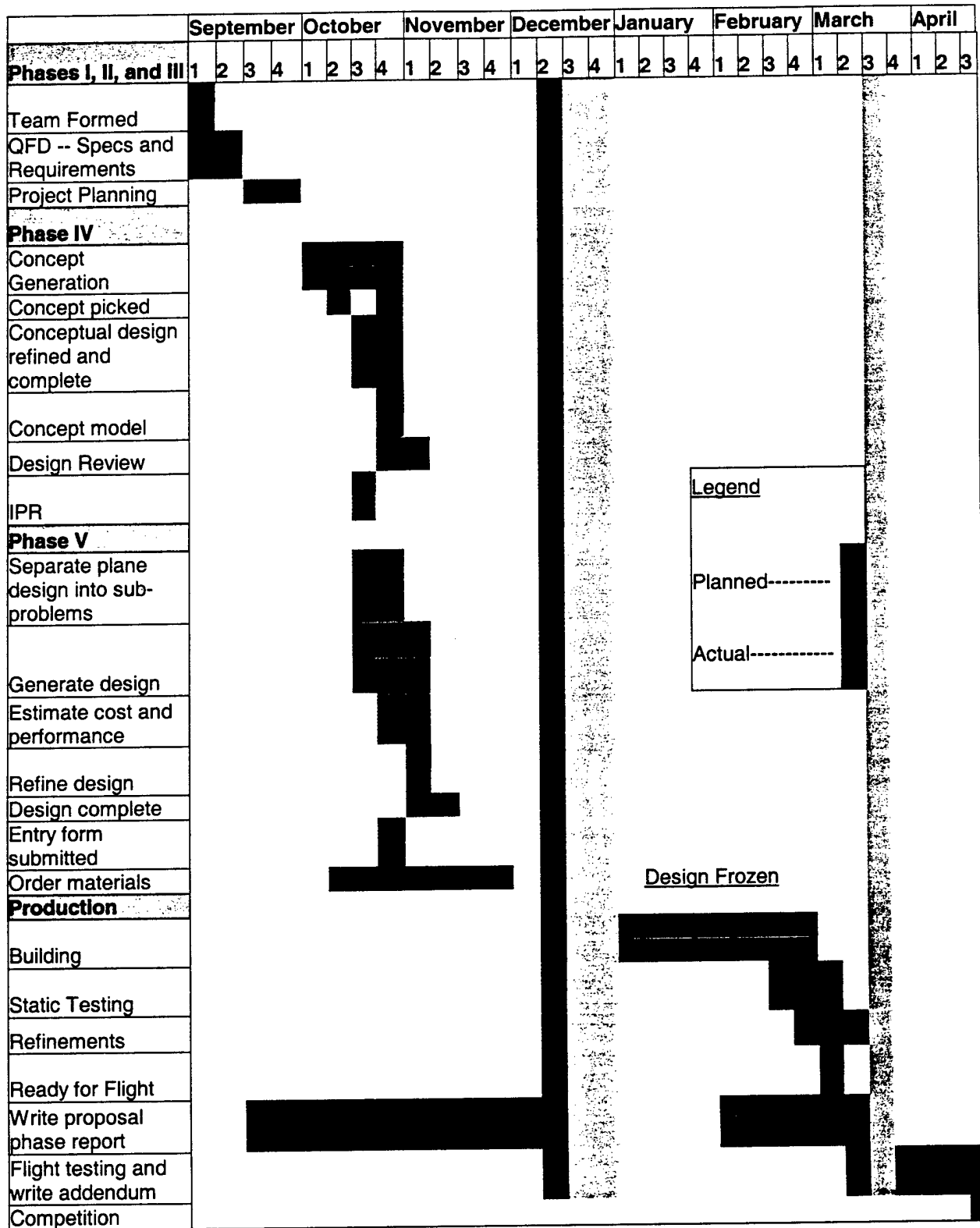
Index	Name	Primary Role	Area	Year
1	Schwark, Fred	Team Leader	Aero	2001
2	Lynch, Clayton	Building Leader	Aero	2001
3	Kolb, Kacie	Report Leader	Aero	2001
4	Holtz, Ryan	Budget Leader	Aero	2001
5	Lusk, Joe	Executive Officer	Aero	2001
6	Evangelista, John	Landing Gear	Mech	2001
7	Andreson, Kevin	Construction Team	Aero	2002
8	McArthur, John	Construction Team	Aero	2003
9	Thompson, Nathan	Construction Team	Aero	2002
10	Johannes, Andrew	Construction Team	Aero	2003

TABLE 2.1 Team Member Roles

The primary roles for each team member are shown above. In addition to each of these, every member carried additional duties.

2.2.2 Gannt Chart - Once roles were assigned, we performed the five steps in planning as defined by Ullman, which are: identify the tasks, state the objective for each task, estimate the personnel, time and other resources needed to meet the objectives, develop a sequence for the tasks, and estimate the product development costs. The compilation all the steps was then condensed into a Gannt Chart, Figure 2.1. This chart became a reference for task completion, personnel and time requirements. The actual progress of the design process is incorporated into Figure 2.1 to compare the effectiveness of our design plan.

FIGURE 2.1 Gannt Chart.- The planned schedule is compared to the actual design progress.



3.1 INTRODUCTION

The major drivers during the conceptual design process are aerodynamics, propulsion, and flight performance. Here, the general shape, size, weight and performance of the design are determined. The conceptual design phase determines such fundamental aspects as the shape of the wings (swept back, swept forward, or straight), the location of the wings relative to the fuselage, the shape and location of the horizontal and vertical tail, the use of a canard surface or not, engine size and placement, etc. (Anderson, 383). Such design parameters are derived from a list of concrete goals toward which the designers are aiming. In order to generate the optimal conceptual design the team used The Seven Intellectual Pivot Points for Conceptual Design (Anderson, 387). These seven points are listed in the block array shown in Figure 3.1.

3.2 IDENTIFY NEEDS

In the first step toward understanding the problem we conducted a How-Why Analysis, reference Figure 3.2. This tool helped us determine the problem needed to be solved and afforded a better understanding of the problem eventually leading to a problem statement. Therefore, our output was an initial problem statement that we used to guide our design process: ***To design an aircraft that optimizes both speed and carrying capacity.***

The next step we performed was the construction of a Mind Map. This design tool aided in our understanding of the depth and scope of the problem. By performing several iterations of the Mind Mapping technique we were able to recognize all aspects of the problem that needed to be considered throughout the design process, to include interrelationships, possible functions, and possible customer requirements.

The culmination of our efforts to identify the needs and functions of our future design is the Functional Decomposition, Figure 3.3. Keeping in mind that this is one of the most critical steps in design, we used the Functional Decomposition to identify the functions that our design must perform to successfully complete its mission. In this case, our design must deliver steel weights and tennis balls via air. Given this overall function we applied the "black box" method (Ullman, 124). Determining all the inputs such as energy, material and information flow, as well as the corresponding outputs, we grasped the conservation of energy, conservation of material, and required interfacing objects that we must consider when determining the sub-functions of our aircraft. A decomposition of these sub-functions follows in Figure 3.3. In order to develop these sub-functions we brainstormed what we wanted our design to do as opposed to how it is going to do it. From this list the main functions of our designed were developed to categorize the smaller sub-functions. These were: interact with the user, interact with the goods, and interact with the environment. All of this was refined into the functional decomposition. At this point we had identified the problem as well as the needs and functionality of the design.

3.3 DESIGN PARAMETERS

With a clear understanding of the problem and the establishment of design needs, the design team proceeded to evaluate specific design parameters relevant to the mission statement. These included such aspects of aircraft development applicable to the general shape and configuration of the design layout.

3.3.1 Propeller Configuration - The two main types of propeller configurations are tractor or pusher type. In a tractor configuration the propeller(s) are placed at the front of the aircraft, either at the nose of the fuselage or on the wings. This allows for a forward CG shift requiring smaller tail surfaces for stability. Additionally, the efficiency of the prop increases because it works in a clean air stream. However, this configuration has its disadvantages. The propeller slipstream disturbs the quality of airflow over the wing and fuselage decreasing lift and contributing to the skin friction. In a pusher configuration the fuselage and wing see undisturbed air. However, the prop itself does not experience clean air, thus decreasing its efficiency. Placing the motors in the rear shifts the center of gravity rearward, which, in turn, reduces longitudinal stability.

3.3.2 Wing Configuration - For the wing configuration there were two considerations: the geometric shape of the wing and its location relative to the fuselage. The wing can be elliptical, tapered, or rectangular in shape and be located on the fuselage in three different places (high, mid, or low). In addition a geometric twist and/or dihedral could be incorporated into the wing design. The wings can be swept forward or backward and have a leading edge sweep or a trailing edge sweep. Considering the magnitude of possible design variations, a relative comparison was performed to eliminate several of the options.

Wing Location. A high wing configuration, that is the wing is mounted on top of the fuselage, is the most stable in terms of lateral, rolling motion. However, the interference drag between the fuselage and the wing root is rather high. The mid-wing configuration provides the lowest drag of any of the three locations because the wing-fuselage interference is minimized. However, structurally speaking, the wing spar must pass through the fuselage. This means that the cargo area would be drastically reduced or inconvenienced. The major advantage to a low wing configuration is that the landing gear can be retracted into the wing box itself. Retractable landing gear can reduce drag, but is complicated and carries a rather significant weight penalty in this size of aircraft. The low wing configuration is also the least stable laterally. Another aspect of wing location is bi-wing vs. mono-wing configuration. The bi-wing configuration maximizes lift and load carrying capacity, but at the same time creates more drag, weight, and difficulty in design. The mono-wing is the more easily built and analyzed.

Wing Geometry. The wing geometry consists of either an elliptical, tapered, or rectangular shape. Elliptical wings offer the most favorable lift distribution, which in turn reduces induced drag. However, manufacturing an accurate elliptical wing is extremely difficult. A tapered wing offers somewhat

of a balance between manufacturing and obtaining a favorable lift distribution. However, manufacturing the required number of airfoils to produce a wing taper is still not an easy task. The rectangular wing is by far the easiest to manufacture, but causes the highest amount of induced drag.

Wing Sweep. Swept wings are relevant only at high-speed subsonic or supersonic airplanes. Therefore, this design parameter was not considered.

Wing Dihedral / Anhedral. A dihedral adds stability in roll to an airplane. When an airplane rolls, the lift vector tilts away from the vertical, and the airplane sideslips in the direction of the lowered wing. If there is dihedral, the extra component of flow velocity due to the side slipping motion creates an increased lift on the lowered wing, hence tending to restore the wings to the level equilibrium (Anderson, 429). The dihedral can start at the root of the wing or begin somewhere along the span of the wing. Anhedral is used in some high-wing aircraft in order to reduce their stability and allow them to roll more easily.

3.3.3 Tail Configuration - The tail consists of the horizontal tail, which provides pitch stability, and the vertical tail, which provides yaw stability. Each consists of a control surface, the elevator and the rudder, respectively. The size of each must be sufficient enough to provide stability and control of the aircraft. There were four different types of tail configurations considered.

A conventional tail provides reasonable stability and control. It is located aft of the center of gravity and is connected to the fuselage by means of a tail boom. This configuration is easily manufactured and analyzed. Perhaps its greatest credential is that it is found on nearly 70% of all aircraft.

A T-tail is similar to a conventional tail in that it is placed aft of the center of gravity and consists of both a horizontal and vertical stabilizer. The difference is in the location of the horizontal stabilizer—at the top of the vertical tail. In this configuration the horizontal tail acts as an endplate on the vertical tail decreasing the induced drag. Additionally, should the aircraft stall, the horizontal stabilizer does not inhibit the rudder. In order to ensure structural stability the strength of the vertical tail must be increased significantly. This adds drastically to the weight of the aircraft and shifts the center of gravity rearward.

A cruciform tail is a compromise between a T-tail and a conventional one. The horizontal stabilizer rests mid-height on the vertical tail. Some added strength is required to support the load and weight of the horizontal tail. Manufacturing this type of tail would be rather difficult due to the passing of the horizontal tail spar through the vertical tail.

A V-tail consists of two tails oriented in a V-configuration. Essentially, two tails at a certain angle act both as vertical and horizontal stabilizers. Aerodynamic analysis of such a configuration is often difficult.

3.3.4 Fuselage Configuration - The fuselage is perhaps the second most important component of the airplane. Not only does it carry the cargo, but it must also interface with every other piece of the airplane.

It must support the wings, the tail, the landing gear, the cargo, the battery, and the electrical equipment required to operate the airplane. Any failure in the fuselage would result in catastrophic failure of our design. There exist a limited number of fuselage configurations—conventional, lifting body, and flying wing. A flying wing avoids the added weight due to necessary tail surfaces incorporated in conventional designs. However, it is extremely difficult to analyze and design. A lifting body would help contribute to the overall lift of our airplane. However, the difficulty in joining all the components mentioned above and integrating a simple cargo box can be a very complex operation. A conventional design offers proven historical success. Additionally, analysis and design have been well documented. However, such a design increases weight and drag.

3.3.5 Landing Gear - A significant amount of attention was given to the design of the landing gear. A failure of the landing gear would cause incredible damage to the aircraft. Therefore, it had to be strong enough to support a worst-case scenario landing, but it couldn't be designed so strong that excess weight would limit the load carrying capacity of the aircraft. There are three configurations for landing gear to be considered: tricycle, bicycle, and tail-dragger. The benefits to a tricycle landing gear include easier maneuverability and less risk of a nose-over upon landing. The benefits of a bicycle landing gear include decreased weight and drag, but creates a more difficult takeoff and landing. The tail-dragger configuration is lighter than the tricycle but has an increased risk of a nose over during landing.

3.4 FIGURES OF MERIT

The most important aspect in creating a design is satisfying the customer requirements. There are many tools available that aid engineers in turning customer requirements into Figures of Merit or Engineering Requirements. The design tool used was Quality Function Deployment (QFD), also known as the "House of Quality" shown in Figure 3.4. The QFD guided the establishment of the design priorities and targets. The methodology for the QFD was to first identify the customers, determine the customer requirements, and then determine their relative importance. Then we benchmarked the competition, identified the engineering design requirements, assessed the competition and set engineering targets.

3.4.1 Identify Customers - Determining the customers means identifying every individual or agency impacting the success of our design. The design is being built for the purpose of winning a competition. The judges and sponsors of the competition act as primary customers for the design. They determine the requirements for the aircraft.

3.4.2 Determine Customer Requirements - In determining the customer requirements we extracted all the spatial constraints and performance parameters from the contest rules. Then we defined some of our own customer requirements through the goals that we have as a design team for the competition. Our customer requirements include objectives for performance, cost, assembly, regulatory requirements,

normal conventions, appearance, and safety. The completed list of customer requirements can be viewed in the QFD.

3.4.3 Relative Importance - It is nearly impossible to create a design that is able to meet every customer requirement. Therefore, a priority must be established among the requirements so that the design meets the most important aspects of the design. This was done by locating the requirements on a scale.

3.4.4 Benchmarking - In this step we conducted research on current models or assemblies that were applicable to our mission. We surveyed proficient R/C aircraft pilots and conducted patent searches on items such as remote controlled airplanes, unmanned-aerial vehicles, etc. The principle benchmark came from last year's aircraft submitted by USMA. All these products served as benchmarks for the competition analysis discussed later.

3.4.5 Figures of Merit - With the customer's requirements developed and the benchmarking complete, the engineering requirements were established. These represented qualitative or measurable interpretations of the customer's requirements. Then each of the customer requirements was correlated to the specific engineering requirement.

3.4.6 Assess Competition - By reviewing the competition we gain an understanding about the performance our design must achieve. After all, there's no point in designing an aircraft unless it will be better than the competition. We reviewed the competition performance of the USMA design the previous year. We felt we needed to improve the weight and load-carrying capacity for our design. We also assessed Utah State University's entry from the previous year. Other planes sold commercially were also considered.

3.4.7 Establish Engineering Targets - Keeping in mind the requirements of our customers, translated through engineering requirements, we were able to establish targets for our design. The absolute and relative importance of each of the requirements is determined through the correlation established earlier in the QFD process. Once the importance was established, each of the competitors was assessed for each engineering requirement. Once the assessment was made, the target values were established.

3.5 MORPHOLOGICAL ANALYSIS

The morphological analysis deals with the generation of design concepts. The Morphological Chart shown in Figure 3.5 incorporates the design functions from the Functional Decomposition in Figure 3.3 and the design parameters discussed previously. Each function was paired with appropriate design parameters in order to develop various concepts for evaluation. The specific components that we examined for each design are as follows: wing, fuselage, motor, propeller, power plant, tail and landing

gear. The morphological chart below outlines these six designs and addresses their specific features. Using the morphological chart as a guide we were able to determine each component's contribution to the engineering requirements and targets. The outputs of the morphological analysis were six concepts, labeled Alpha through Foxtrot, as shown in Figure 3.6. In addition to the configuration of each concept, a relative cost analysis was performed.

3.6 CONCEPT DETERMINATION

Using the concepts generated in the morphological analysis section, we underwent the process of determining which is best for the specified mission. A feasibility analysis first performed to ensure no concepts required technology or manufacturing processes not available to us. Next, a relative comparison using the engineering requirements and aircraft rated cost was performed to determine the best overall concept.

3.6.1 Feasibility Analysis – The feasibility of each of the design parameters is enclosed in Figure 3.4 along with the Morphological Analysis. Each possible configuration determined to be worth considering (WC), conditional (C), or not feasible (NF). There were five design parameters that were determined to be not feasible: elliptical and swept wings, lifting body and flying wing fuselage configurations, and a V-tail. We found that each of these would be either impossible to analyze aerodynamically or difficult to accurately manufacture given our limited expertise. The rest of the design possibilities were either conditional or worth considering.

3.6.2 Relative Comparison / Pugh's Method – Figure 3.7 shows the relative comparison conducted to evaluate the six previously generated concepts. The criterion for development of the Pugh's Method matrix stems from customer and engineering requirements. The requirements given by the customer and refined by the engineers focused the concept determination on quantitative variables. In order to accomplish this task, we used Pugh's Method to weigh the costs and benefits of each design. In this method, the criteria for the aircraft were weighted against each other and then applied to the different design concepts. Comparing the different concepts shows how each concept may be better than the other in certain areas and weaker in others. In general, this comparison relates each concept to the competitor and displays the best design for the mission. These issues are largely quantifiable and center on the ability for the engineer to accurately compare and contrast the varying concepts.

In the design of our aircraft, we described several criteria for concept determination. Specifically the following criteria the propulsion efficiency, landing gear strength, wing efficiency, payload capacity, range, take off distance, and cost of each concept was evaluated in the relative comparison. In the case of this competition the two with the highest weight for criterion were the payload capacity and the cost of the aircraft. The relative importance of this idea rest with the design and manufacture of the previous concepts.

We were able to choose our design based on the following matrix and the specific concept generations' techniques outlined in the previous section. From the analysis in Figure 3.7 it is clearly shown that concept Alpha best fits the criteria for a successful design.

3.7 CONCEPTUAL DEVELOPMENT

The overall conceptual development phase in aircraft design is based around seven aspects (Anderson, 387). These seven intellectual points can be viewed in the schematic in Figure 3.1. These "pivot points" were used as a guide for the conceptual design phase.

3.7.1 Requirements - The requirements for the aircraft were established previously in the QFD.

3.7.2 Weight Estimate - The factors affecting the weight of the aircraft include the fuel, the payload and the actual plane itself. In order to accurately estimate the weight of the airplane a significant amount of empirical data was analyzed. Much of this data included the empty weight of several equivalently sized RC airplanes sold commercially. Additionally, the load carrying capacity of several previous Cessna/ONR Design/Build/Fly competitors was reviewed. Based on the increase in wing span limit, it was determined that an increased load-carrying capacity was attainable. Thus, the initial cargo weight was chosen to be 18 pounds. The officials constrained the maximum weight of the batteries to 5 lb. Therefore, the weight of fuel carried will be such. The gross weight is a function of the payload weight and the ratio of fuel weight and empty weight to gross weight. Empirical data yielded the assumption that the ratio of empty weight to gross weight is .62 (Anderson, 394). Additionally, the ratio of fuel weight to gross weight is .159. Through algebraic manipulation, the gross weight was solved for, yielding 36 lbs. Therefore, the empty weight of the aircraft was estimated to be 18 lbs.

3.7.3 Critical Performance Parameters - There were four critical performance parameters to be determined prior to configuring our design. As shown in the QFD these include the maximum lift coefficient, the lift-to-drag ratio, the wing loading, and the thrust-to-weight ratio.

Lift-to-drag Ratio. The University of Illinois, Urbana-Champaign had the most comprehensive low Reynolds Number airfoil data. After downloading the data, the drag polar of several airfoils was plotted. The airfoil demonstrating the most favorable lift-to-drag ratio was chosen. Additionally, the thickness of the airfoil was considered since the wing had to contain the structural support to span 10 ft. An airfoil that was not thick enough might not be able to support the 2g test considering the limited amount of space for structural support. For this reason, several thin airfoils were neglected despite their rather high lift-to-drag ratios. Therefore, we selected ten airfoils that were valid candidates and took an average of their performance characteristics for calculations. This resulted in an average lift-to-drag ratio of 26.

Maximum Lift Coefficient. The average maximum lift coefficient at an estimated Reynolds Number of 500,000 was 1.2. In addition, the employment of flaps at 45 degrees increases the airfoil maximum lift coefficient by .9. Therefore, the average airfoil maximum lift coefficient is then 2.1. Finally, to account for three-dimensional effect, Raymer suggests that for finite wings with aspect ratio greater than 5 the 3-D maximum lift coefficient decreases by 10%. Assuming the aspect ratio is greater than five, the aircraft's estimated maximum lift coefficient becomes 1.9. The lift contributions of the fuselage, tail and other parts were neglected for the time.

Wing Loading. The wing loading is constrained by both the stalling speed and the takeoff distance. In the first case, the wing loading was based on the assumption that the stalling speed of the aircraft is 50 ft/s. Again, this was based on empirical analysis of various RC aircraft. Accordingly, the average estimated wing loading of the aircraft was 1.44 lb/ft². The maximum take off distance is 200 ft. Analysis of the takeoff distance constrained the wing loading to 1.6 lb/ft². As long as the wing loading is less than 1.6 lb/ft² the take off distance will be less than 200 ft. Therefore, the wing loading was determined from the specified stall velocity—1.44 lb/ft².

Thrust-to-weight Ratio. The thrust-to-weight ratio determines in part the takeoff distance, rate of climb, and maximum velocity. To obtain the design value of T/W, each of these three constraints was examined. Again, the takeoff distance is specified at 200 ft. The resulting estimated thrust-to-weight ratio was 0.4.

3.7.4 Configuration Layout - The configuration layout consists of a basic drawing of the aircraft up to this point in the design process. The major factor in configuration layout is the center of gravity of the aircraft. In order for aircraft stability, the center of gravity should be located on the quarter-chord of the wing. Therefore, the layout sizing of each of the components was based around this concept. With the basic configuration already chosen at this point in the process, the task at hand is the initial sizing of the aircraft and its components.

Wing. In order to obtain the correct critical performance parameters outlined previously, an iterative process was performed through program Black Knight to develop the ideal wing dimensions. The initial calculations put the wingspan at 10 feet and the chord length at 15 inches. From Basics of R/C Model Aircraft Design (Lennon, 125), the basic location for the wing should have the quarter-chord placed approximately twice the chord length from the nose of the aircraft. Therefore, our initial placement put the quarter-chord 30 inches from the nose of the aircraft.

Tail. In developing the accurate size of the tail, the team used design criteria as expressed in *Dynamics of Flight: Stability and Control* by Bernard Etkin. His method of determining the appropriate tail size was used to initially dimension tail.

Fuselage. The fuselage is the biggest factor when considering the center of gravity of the aircraft. Once the basic configuration was laid out, we made a basic weight estimate of each of the components of the aircraft and determined the location of the CG. There are many determining factors that go into the

design of the fuselage. The main considerations for the design were placement of the payload, placement of the batteries, attachment of the wing, tail, and landing gear, and basic dimensions. The basic proportions for an R/C aircraft according to Lennon outline the length of the fuselage as approximately 4-5 times the chord length (Lennon, 125). Therefore, the total length of the fuselage would be 74 inches. In order to allow potential error in our weight estimates, we decided to have a tray below the wing that would hold the battery pack and allow it to slide forward and back to make small adjustments in the CG. Our initial calculations put the CG at 28.3 inches from the nose, which is very near the quarter chord at 30 inches.

3.7.5 Better Weight Estimate- With the configuration layout in hand, a better weight estimate was developed. The amount of material was estimated and specific parts were researched to determine their weight. These values gave us a weight that was approximately 16 pounds. This weight was under our first estimate but allowed for potential error in the calculations.

3.7.6 Performance Analysis – Based on the preliminary aircraft's configuration, a rough performance analysis was conducted to ensure favorable performance characteristics. Such calculations included the stalling velocity, power loading, wing loading, etc. Table 3.1 summarizes the results of the performance analysis.

PERFORMANCE VARIABLE	VALUE
Wing Loading	2.88 lb/ft ²
Power Loading	21.429 lb/hp
Thrust-to-Weight Ratio	.4
$C_{D,0}$.011
K	.018
$(C_L)_{max}$	1.026
$(L/D)_{max}$	18.4
Stall Speed	48.5 ft/s
Takeoff Distance	114 ft

TABLE 3.1 Initial Performance Characteristics

3.8 RESULTS

After several different configurations were developed and numerically analyzed an optimum configuration emerged. Figure 3.7 shows the relative comparison of the six concepts. It can be seen that the best design—concept alpha—consists of a conventional fuselage and tail with a rectangular wing.

The initial dimensions and weights of the aircraft components is summarized in Table 3.2. Additionally, the estimated performance characteristics are included to show potential design success.

DESIGN PARAMETER	RESULT
Payload Capacity	18 lb
Gross Weight	36 lb
Rated Aircraft Cost	10.6
Wing Configuration	Rectangular
Wing Span / Chord Length	10 ft / 15 in
Fuselage Configuration	Conventional
Fuselage Length	74 in
Center of Gravity	28.3 in from nose
Tail Configuration	Conventional
Tail Location	44 in

TABLE 3.2 Conceptual Design Summary

FIGURE 3.1 The Seven Intellectual Pivot Points for Conceptual Design - Taken from *Aircraft Performance and Design* by Dr. John Anderson, this process was used to guide the initial configuration and sizing of the aircraft.

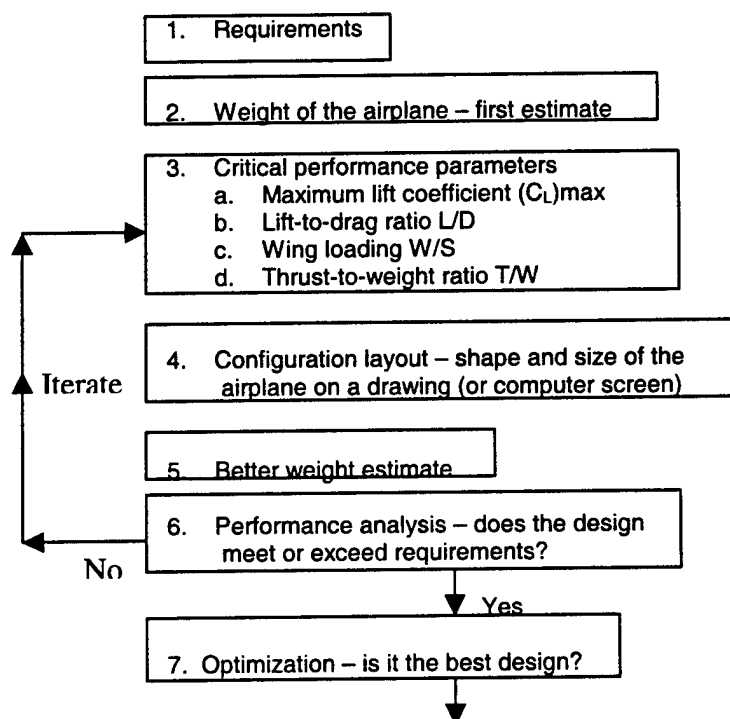


FIGURE 3.2 How-Why Analysis- This design tool was used to gain a clear understanding of the problem. The relations between each block helped develop a mission statement for the design team

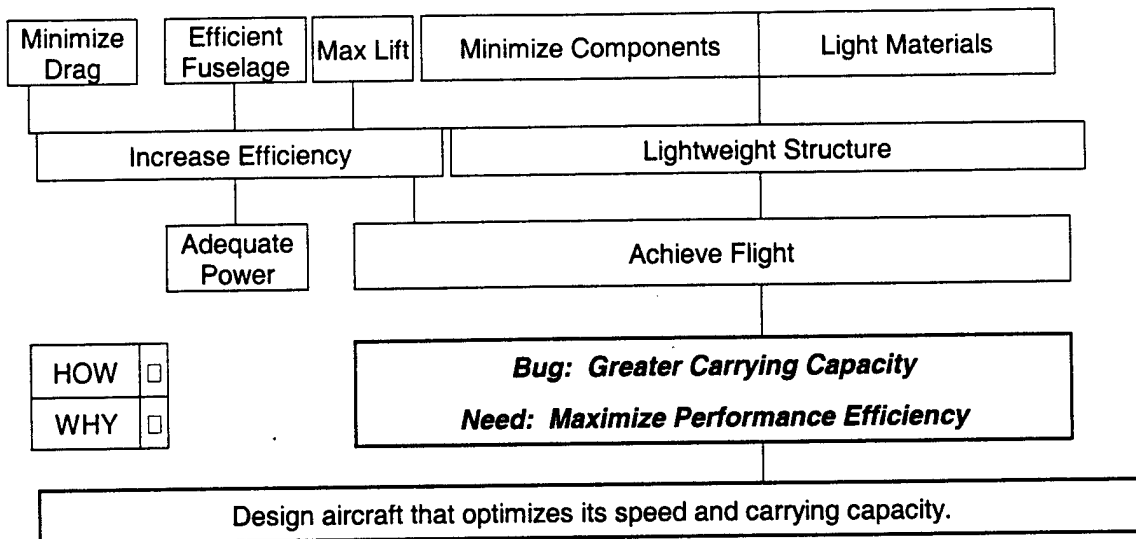


FIGURE 3.3 Functional Decomposition - This design tool helped the design team grasp the interrelations and functionality of the design. These sub-functions drive the concept generation in the morphological analysis.

1.0 Interact with user	1.1 Interface with user	1.1.1 Guide	1.1.1.1 Receive
			1.1.1.2 Send
2.0 Interact with Environment	2.1 Fly	2.1.1 Produce Lift	2.1.1.1 Produce thrust
		2.1.2 Maintain Forward Movement	2.1.2.1 Produce thrust
	2.2 Land	2.2.1 Ensure safety	
		2.2.2 Absorb shock	2.2.2.3 Absorb energy
		2.2.3 Stop movement	
3.0 Interact with payload	3.1 Load goods	3.1.1 Load easily	3.1.1.1 Access space
	3.2 Secure goods	3.2.1 Fasten	
		3.2.2 Compress	
	3.3 Carry goods	3.3.1 Provide space	
	3.4 Fasten door		
	3.5 Release goods		

FIGURE 3.4 Quality Functional Deployment

Symbols Key:

- △ Weak Correlation
- Medium Correlation
- Strong Correlation

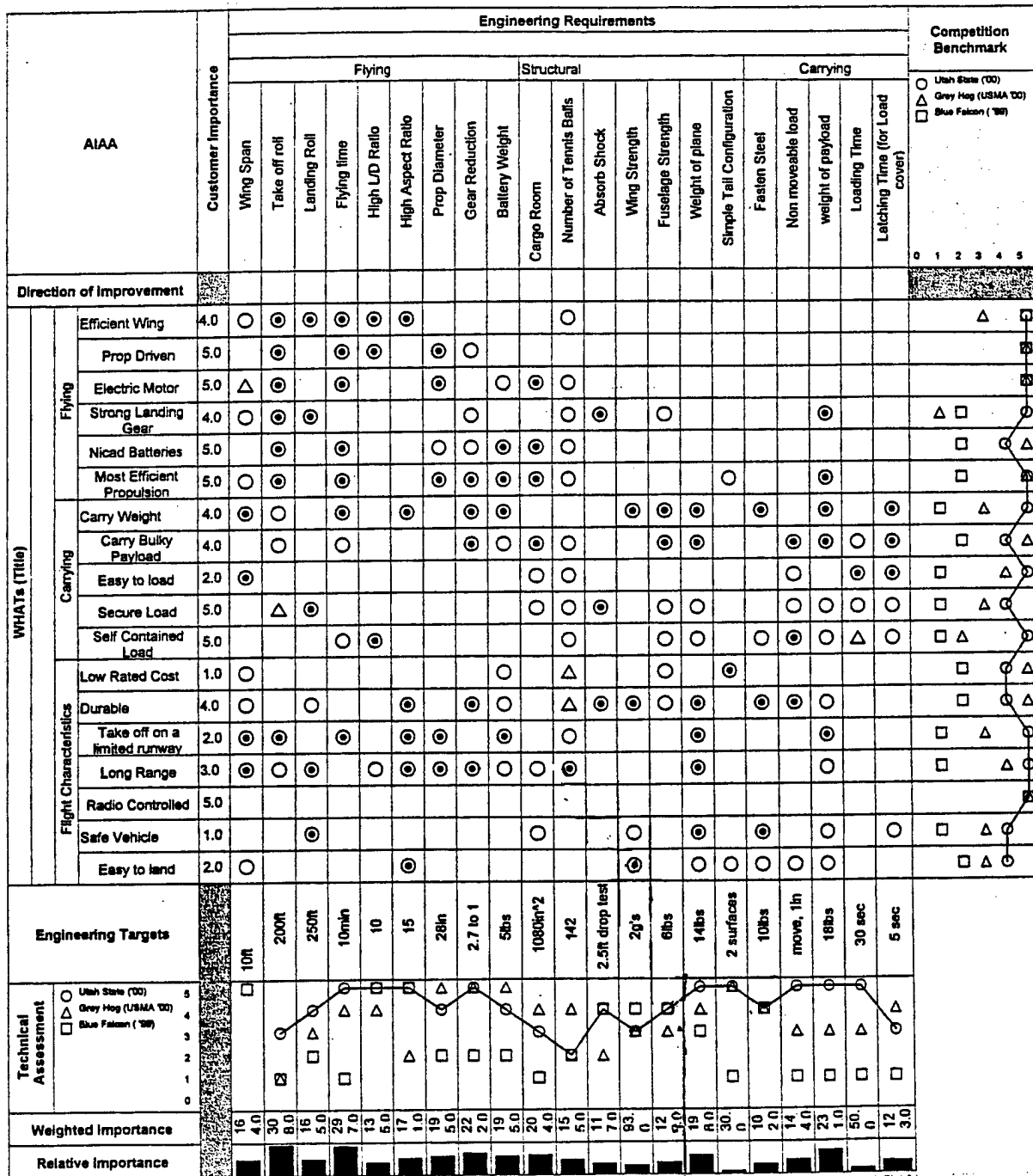


FIGURE 3.5 Morphological Analysis - WC- Worth Considering C- Conditional NF- Not Feasible

		Feasibility	Flight Performance	Structural	Transport	Cost	Manufacturability	Total
Wing Configuration	Wings		3	1.5	2.5	1	2	
Fuselage	high	WC	0.5	0	-0.5	0	0	0.25
	mid	WC	1	0	-1	0	0	0.5
	low	WC	0.5	0	1	0	0	4
	swept	NF						
	elliptical	NF						
	tapered	WC	0.5	0	0	-0.5	-0.5	0
	rectangular	WC	0	1	0	1	1	4.5
	dihedral	C	1	0	0	0	-1	1
	anhedral	C	1	0	0	0	-1	1
	mono-wing	WC	0.5	0	0	1	1	4.5
	Bi-wing	WC	1	-1	-0.5	-1	-1	-2.75
	standard	WC	0	1	1	1	1	7
	lifting body	NF						
	flying wing	NF						
Motor	Astro 90	WC	1	0	0	-1	0	2
	Astro 40	WC	1	0	0	1	0	4
Propeller Type	wood	WC	1	0	0	1	0	4
	nylon	WC	1	1	0	-1	0	3.5
	2 blade	WC	0.5	0	0	1	0	2.5
	3 blade	WC	1	0	0	-1	0	2
Power plant configuration	pusher	WC	1	0	0	0	-1	1
	tractor	WC	0.5	0.5	0	0	1	4.25
	twin prop	WC	1	0.5	1	0	-0.5	5.25
	single prop	WC	0.5	1	-1	0.5	1	3
Tail Configuration	conventional	WC	0	1	0	1	1	4.5
	T-tail	WC	1	-1	0	-1	-1	-1.5
	cruciform	WC	0.5	0	0	-1	-1	-1.5
	V-tail	NF						
Landing Gear	tricycle	WC	0	0	0	0	-0.5	-1
	bicycle	WC	0.5	0.5	0	0	0	2.25
	tail-dragger	WC	1	0.5	0	0	0.5	4.75

FIGURE 3.6 Generated Concepts – The general configuration of major components for the six concepts presented.

	Alpha	Bravo	Charlie	Delta	Echo	Fox-trot
Motors	Dual	Dual	Single	Single	Dual	Dual
	Astro 40s	Astro 40s	Astro-90	Astro-90	Astro 40s	Astro 40s
Wings	Rectangular	Rectangular	Rectangular	Tapered	Tapered	Tapered
	10ft span, c=15"	10ft span, c=15"	10ft span, c=15"	10ft span, c(ave)=15"	10ft span, c(ave)=15"	10ft span, c(ave)=15"
Fuselage	Streamline design	Streamline design	Streamline design	Streamline design	Dual Body Design	Rectangular Box
	max volume	max volume	max volume	max volume	Two compartments	max volume
Tail	Standard	Standard	Standard	Standard	Dual Vert Stabilizers	Standard
Landing Gear	Tail dragger	Tricycle	Tricycle	Tail Dragger	Tricycle	Tail Dragger
Rated Cost	8.8	8.9	6.6	6.4	10.5	8.7

FIGURE 3.7 Concept Comparison – Using Pugh's method, the six concepts were rated against each other under certain criteria. This shows Concept Alpha as the best design.

Components	Weighting	Alpha	Bravo	Charlie	Delta	Echo	Fox-trot
Motor Design Criteria	5	1	1	DATUM	0	1	1
Wing Design Criteria	7	0	0		-2	-2	-2
Fuselage Design Criteria	10	0	0		0	-1	0
Tail Design Criteria	1	0	0		0	-1	0
Landing Gear	4	2	0		2	0	2
Cost	8	-1	-1		0	0	0
Total		5	-3	0	-6	-20	-1

4.0 PRELIMINARY DESIGN

4.1 INTRODUCTION

In the preliminary design phase only minor changes are made to the configuration layout. In this phase serious structural and control system analyses took place. In this phase computational analysis was conducted to ensure no undesirable flight characteristics existed. At the end of this phase, the aircraft configuration was frozen and precisely defined.

4.2 DESIGN PARAMETERS

The design parameters driving the preliminary design change slightly from those developed in the conceptual design stage. In conceptual design the parameters helped determine the general shape and initial sizing of the aircraft. Now the design parameters focus on optimizing the size, shape, and location of the aircraft components. In order to optimize these components it was determined that aircraft performance was paramount. Drag, weight, and lift were considered as the three major components affecting the aircraft performance. Therefore, the chord, aspect ratio, wing span, fuselage length and several others design features were laboriously reviewed and optimized to maximize the performance of our aircraft. Next, a thorough materials analysis was conducted to ensure the proper structural support for major components is available.

4.2.1 Aspect ratio - The aspect ratio of the wing was the first design parameter reviewed. Typically, a high aspect ratio is most efficient because it reduces the induced drag due to wing tip vortices. In order to increase the aspect ratio a broad wing span and small chord are most favorable. However, there reaches a point of diminishing returns where the lift produced by a wing with a given chord begins to decrease. Additionally, structural considerations play an important role in determining the wingspan. With the optimum aspect ratio, the wingspan and chord length can easily be derived to produce a maximum amount of lift.

4.2.2 Airfoil - The conceptual design incorporated an average of several airfoils to estimate its performance. The selection of the airfoil plays a very important role in the efficiency and lift of the aircraft. Thin airfoils, while advantageous for higher maximum lift coefficients, demonstrate sharp stalling conditions. The effects of a sharp stall are rather obvious and could lead to a catastrophic failure of the design. However, with thicker airfoils, it is difficult to attain high maximum lift coefficients, but the stall occurs rather slowly.

The camber of the airfoil also drastically affects the performance of the aircraft. Highly cambered wings produce an extremely high coefficient of lift. However, drag is the penalty paid for producing the increased lift. The alternative, a symmetrical airfoil, lacks the ability to produce higher lift coefficients.

4.2.3 Ailerons - The ailerons control the angle of bank of an airplane. Therefore, ensuring the proper aileron sizing allows the pilot effectively turn the aircraft. The competition rules state that the aircraft must complete a 360-degree turn, in flight, during each cycle. Larger ailerons would allow the aircraft to turn easier in flight. Limiting the turning radius of the plane would shorten the flight time per cycle. On a negative note, the aileron acts to disrupt the airflow over the wing. This would break up any laminar flow across the wing and trip the air into a turbulent Reynolds number, resulting in unnecessary drag.

4.2.4 Tail Boom - The tail boom provides structural stability while connecting the tail to the fuselage. Two configurations of the tail boom were considered. First, the tail boom can consist of a rod extending from the fuselage to the tail. The advantage of this design is that it can provide structural stability at a relatively low weight. However, considering the volume required of the fuselage to carry the determined cargo, a significant amount of flow separation off the back of the fuselage will result. This would cause an increase in the form drag. Also, the flow separation would increase the amount of "dirty" air that the tail surfaces receive. This would reduce the effectiveness of the tail surfaces resulting in a reduction in control. The second design is an extension of the fuselage that tapers down as it approaches the tail. Certainly this design option is heavier, but the form drag would be drastically reduced.

4.2.5 Payload - Scoring most greatly affects the size and type of the payload to be carried. Should the aircraft be designed for heavy lifting (carrying steel weights) or volume (carrying tennis balls)? The answer to this question lies in what combination of the two maximizes the possible score. During conceptual design the payload-engineering target was determined to be 100 balls. The volume and configuration of this payload will directly influence the design of the fuselage.

4.2.6 Landing Gear - The previous year's USMA design experienced several problems with their landing gear. This caused severe damage to their motors, propellers, and fuselage. Therefore, analysis was conducted with a rather large factor of safety. Another problem confronting the fuselage design team was the ability to model impulses. The CAD programs available to the design team only allowed for constant loads. Therefore, the preliminary design of the landing gear assumed a 2-g constant load.

4.2.7 Tail Size - In order to provide the necessary stability, the horizontal and vertical stabilizers must be large enough. The tail should not be designed so large that an unnecessary amount of skin drag is produced. Similar to the wing, the aspect ratio becomes the design parameter. The proper span and chord length must be optimized to offer the required stability while minimizing the resulting skin drag. The control surfaces for the pitch and yaw conditions are the elevator and rudder, respectively. Again, similar to the ailerons on the wing, these control surfaces must be properly sized to ensure the proper amount of control.

4.3 NUMERICAL METHODS OPTIMIZATION FOR AIRCRAFT COMPONENTS

4.3.1 Wing Optimization - During the conceptual design process it was determined that the shape of the wing planform area would be rectangular. In preliminary design, the first design parameter evaluated with respect to the wing was the aspect ratio. Initially too many variables existed to optimize the aspect ratio. Therefore, the wingspan was fixed at 10 feet. This would surely produce the greatest lift possible increasing the load carrying capacity of the design. Given a wingspan, we iteratively stepped through planform areas from 10 ft² to 20 ft² while accounting for an increase in drag with an increase in planform area. The planform area that produced the greatest amount of lift given a 10 ft. wingspan was 12.5 ft². Thus, the wing chord length was determined to be 15 in. and the optimum aspect ratio was 8.

Once the precise dimensions of the wing were determined, the airfoil was selected. The source of airfoil data used was taken from volumes I-III of the University of Illinois at Urbana-Champaign's Low-Speed Airfoil Tests. The first constraint place on the airfoils dealt with the spar structure of the wing. The airfoil had to be thick enough to allow the spar to pass through it. For this reason, if the airfoil was not at least 1-in thick for a 15-in chord, it was not considered.

Another criterion for airfoil selection was efficiency. This was determined by the drag polar. Increases in the performance of the airplane calls for a reduction in drag and an increase in lift. For each of the airfoils considered a line was drawn from the origin tangent to the drag polar plot. The tangential point represented the maximum lift-to-drag ratio for the airfoil. The most efficient airfoil was the one with the highest maximum lift-to-drag ratio. Figures 4.3 and 4.4 show the comparison between airfoils. However, this was not the only selection criterion. The airfoil also had to reveal a good "drag bucket." That is, the percent deviation in the lift-to-drag ratio for a small change in angle of attack should be minimal. If it were too large, then the aircraft would pay severe drag penalties for variations in the wings angle of attack. Therefore, a limit was set at 10%. Any airfoil with a deviation in max L/D greater than 10% per degree about the optimum L/D was neglected. SD7003 emerged as the best airfoil with an L/D of 43 and the most prominent drag bucket of all airfoils considered.

With the airfoil selected and the wing shape and sizing determined, the last design parameter dealing with the wing was the aileron. Initial calculations called for an aileron size approximately 15% of the wing planform area. However, preliminary stability calculations revealed that 10% of wing planform area would suffice.

4.3.2 Payload - One of the engineering targets established through the QFD was to carry 100 tennis balls and 18-lb. of steel during a single sortie. To accomplish this, we had to design a cargo box that would carry all the balls without allowing them to shift during flight. We obtained the detailed dimensions and weight of a single tennis ball from the International Tennis Federation (ITF). Then, numerical analysis, we optimized the dimensions of a box, compatible with our fuselage design, that could contain all 100 balls. Accordingly, the box dimensions are 6-in x 9-in x 34-in. The weight of all the balls would be

approximately 13 pounds. This box needed to be easily accessible so that the payloads can be switched quickly. We determined that the box would be loaded into the fuselage through a hatch in the nose cone of the aircraft. The box would slide on rails for speed.

4.3.3 Fuselage – Initially we sought to reduce the overall drag created by the conventional fuselage configuration. In order to do this, it was decided that an airfoil-shaped fuselage would be most advantageous. The NACA 0024 airfoil was chosen in a method similar to the wing airfoil selection. In a further effort to reduce parasite drag, the fuselage was rounded like a bullet while still maintaining the shape of the NACA 0024 airfoil. Finally, we took the 40-in section of airfoil, and at its thickest point, added in a 10-in x 13-in x 34-in rectangular section to house the payload.

4.3.4 Tail - Similar to the wing, the tail had to be optimized for aspect ratio. The design of the tail set up is the least accurate part of the design process because it must rely on empirical data. Historical data was analyzed to determine the required tail surface area that would ensure effective control of the aircraft. The goal is to have the smallest horizontal and vertical stabilizer possible that will still give us positive control of the aircraft in order minimize both weight and drag. It should be noted that a longer tail boom will also reduce the size of the surfaces necessary since effectiveness of the control surfaces increases with the moment arm. This length is constrained by weight considerations and the amount of structure that would have to be added into the fuselage to handle an exceptionally long tail boom. Numerical methods proved that a fuselage length of 74-in was indeed long enough to ensure stability while minimizing both fuselage weight and tail surface area. With the chord, the fuselage length, area of the wing, and the empirical values for the other aircraft we have calculated a necessary horizontal area of 280-in². The vertical stabilizer is constrained by the same values, however we have added twenty percent to the required effectiveness for the vertical stabilizer since a twin-engine configuration introduced the potential for loss of yaw control should one engine fail. This increase in area would provide the pilot with enough control to safely land the aircraft without catastrophic failure. Thus, the amount of vertical stabilizer required is 210-in² with 50% of this surface being used as the rudder.

4.3.5 Landing Gear - In this portion of the design we achieved two main objectives with respect to the landing gear. First, to derive a rough mathematical model that simulates the response in the landing gear during an average landing. Second, to determine a suitable drop test height to simulate this. This would later serve as our primary evaluation of the landing gear.

Mathematical Model. In order to determine a rough idea of the mechanical response in the landing gear, a spring/damper-mass model was developed. The main assumptions in this model include:

- There is one degree of freedom in the response
- Each leg of the landing gear can be modeled with a spring and damper

- A vertical force F is placed on the mass from acceleration during landing and is calculated from the impulse on the landing gear

The mathematical model is shown in Figure 4.1 along with the resulting transient response, Figure 4.2. The differential equation of motion and the solution of the model above are as follows:

$$x'' + x'(c/m) + x(k/m) = F/m$$

$$x(t) = e^{-\zeta \omega_d t} * (b_1 \cos(\omega_d * t) + b_2 \sin(\omega_d * t)) + F/k$$

This model gave us an idea of what the response should look like in the landing gear. Additionally, it allowed us to choose reasonable spring and damping constants for the material. We used this primarily as a guideline to determine "rough guesses" at what the spring and damper constants should be for a desired response.

Drop Test Height. Determining a suitable drop test height was critical in our design because it would be our primary means to test the effectiveness of our final product before flying. In order to determine this height, we assumed that during an average landing we would have an average rate of descent of 35 mph at an angle of attack of 10 degrees. We then applied kinematics equations to solve for the height that would simulate such a landing when dropped freely. Friction was neglected. It was determined that a suitable drop test height would be 1.2 ft or 4.9 ft with a factor of safety equal to 2.

4.3.4 Motor - The next optimization of the major airplane components was made in determining the number of motors the aircraft will use. Two decisions had to be made concerning the motor selection; the types of motors and the numbers of motors to be used.

There are two types of motors allowed in the competition. These are Graupner and Astroflight. The selection of these motors was based on output from Ecalc software. This software is the industry standard for electric powered R/C aircraft. This program gives valuable information for the thrust, run time, estimated speed, amp draw, and watts created. Through the use of Ecalc, it was determined that in order to meet the thrust to weight requirement, the greatest amount of energy possible from the five pounds of batteries must be converted to mechanical power. The size of the motor needed was determined using the Quality Functional Deployment goal of 6 minutes of actual flight time (the rest of the time was assumed to be consumed by loading and unloading). Knowing the amount of energy, five pounds of batteries, the magnitude of amps that could be drawn for six minutes was determined. This was determined to be 19-22 volts. Therefore, the most efficient motor was one that produced the greatest mechanical output while operating under a 20-amp draw. Deciding which motor to use was a challenge made easier through the Ecalc software. By using the database this software offers, the motors with similar maximum amperage inputs could be used to compare the motor efficiency at various levels. Table 4.1 below shows comparison between the two motors.

PARAMETERS	Astro 40	Graupner S700bb
Thrust	173 oz.	158 oz.
Run Time (max throttle)	3.7 min	3.6 min
Max Speed	54 mph	52 mph
Pack Weight	70.2 oz.	70.2 oz
Watts Created	1364 W	1409 W
Watts Lost	142 W	206 W

TABLE 4.1 Motor Comparison - Ecalc outputs for two separate motors @ 20 amps.

This clearly shows that the Astro 40 is more efficient at that current. In addition, from Figure 4.5 we can see that there is a decreased loss of power with Astro. In order to achieve the maximum score the aircraft must fly as many circuits as possible during the competition. Previous exposure to electrical RC aircraft revealed the fact that the motors did not draw a continuous current from the power supply. Instead, the voltage potential declined with time. Therefore, the motors must be selected to maximize performance based on a weakening voltage source. The mechanical output of one versus two motors was numerically evaluated for comparison. Theoretically, the outputs should be the same, however, real-world variables created deviation from the theoretical analysis. For example, the increased wire resistance and decreased weight for a two motor configuration along with the increased prop size for a single motor configuration act to alter our initial predictions.

The required power to run the motors depended on the electrical load required. The load on the batteries was broken up into three categories: takeoff/climb, cruise and descent/landing. Take off and climb consume the most amount of power while it was assumed that no power was required for descent and landing. The required power to cruise was somewhere in between. The motor program accounted for different weights and required loads based on constant prop sizes and pitches. The prop analysis was conducted separate because it was felt that while directly related, the electrical load variation was proportionate to the change in prop size and pitch and could therefore be conducted in separate analyses. All aerodynamic data was taken from the optimization of major components above. Figure 4.6 shows that both one Astro 90 and two Astro 40 motors can produce the power necessary to fly for six minutes. However, this figure shows that with two motors our design can achieve a higher velocity with less drag. In addition, one engine comes with a slight weight penalty caused by the cobalt magnets and the sturdy housing. It was determined that two Astro 40 motors weigh four ounces less than one Astro 90. The motor efficiency of a single motor configuration is slightly better, however this is overcome by placing the two motors outboard on the wing. This allows for a reduction in the prop-wash effect along the fuselage. The propellers will both be in clean air in an outboard configuration. The major negative component of having two engines is the chance of one engine failing, but was neglected due to the reliability of electric power. The final important factor that pushed the design team toward two motors

was the desire to gear the motors down at a ratio of 3:1. This increases the mass flow rate of air through the propulsion unit producing more thrust at a lower electrical load per motor. To do this with a single motor would result in a propeller diameter too large for consideration.

4.3.5 Propellers - Available data for the purchased propellers was not available. Therefore, a series of static tests were developed to help determine the optimum propeller size and pitch. The tests were performed with an Astro 40 motor on the test stand depicted in Figure 4.7. For each propeller, the throttle was pushed until it drew 23 amps. The resulting thrust was measured using a calibrated spring scale. The results are enclosed in Table 4.2. The tests showed that the Top Flight 18 x 6 prop was most efficient.

Propeller	Diameter (in)	Pitch (°)	Current Draw (amps)	Thrust Force (lb)
Top Flight 15x8	15	8	23.5	6.5
Zinger 25x12	25	12	23.9	7.5
Top Flight 20x8	20	8	21.8	8.5
Classic 20x6	20	6	21.7	6
Graupner 3-Blade	18	6	23.5	5.9
Classic 18x10	18	10	23.5	6.5
Zinger 24X14	24	14	23	4.9

TABLE 4.2 Propeller Static Thrust Results

4.4 MATERIALS SELECTION

4.4.1 Wing Materials Analysis - The main consideration for construction of the wing was the 2-g test the aircraft must pass in order to be air worthy. Based on this requirement several materials were considered. The material selected should have characteristics that most favorably incorporate weight, strength, toughness and durability. First off, a few assumptions were made before materials analysis was performed. For the purpose of experimentation the size of the test specimen was assumed to be relative in finding the properties for the usage of the material. It was also understood that during the 2-g test, the spar would undergo pure bending, fixed at both ends with a load applied in the middle. Thus, it was assumed that pure bending analysis of various specimens would accurately predict their performance during the test.

The specific materials considered incorporated three classes of materials—polymers, composites, and metals. These materials were woods (balsa, ply, spruce, aspen, and brass-wood), Styrofoam, steel, blown foam, carbon fiber, and cardboard. It was impossible to construct each specimen in the exact shape. Whenever possible, the specimens were constructed 6 in. long, 1 in. wide and ¼ in. thick. Since the types of materials tested varied greatly in properties, stress-strain plots were developed to provide accurate data about each material. Once stress-strain plots were developed, the pure-bending

tests were conducted. The thirteen different materials proved to have varying degrees of strength and weight. In this case, the top three materials selected were balsa wood, plywood, and then Styrofoam. Material analysis determined that the ribs of the wing would be constructed out of balsa wood and the spar would be constructed out of plywood. A monocoque application will be placed over the balsa ribs to create the form of the airfoil.

4.4.2 Fuselage Materials Analysis - Materials chosen for the fuselage were those commonly used by RC airplane builders. The six most important materials considered were carbon fiber, fiberglass, magnesium, balsa wood, foam and aluminum. All these materials are composites that have a variety of good properties making them all good applications for fuselage construction. However, their properties were reviewed in detail to determine which is best.

A worst loading condition was assumed to be the design criterion. In this case, the airplane is in such a position that the fuselage would have 2g's of forces acting on it. The analysis conducted was based on the forces and stresses on the fuselage that occur at the 2g loading condition. The maximum static load distributed on the fuselage was estimated to be 36 lbs. However, under a 2g load this became 72 lbs. A free-body diagram of the fuselage under such a load revealed a normal force and bending moment act at various locations about the fuselage. The analysis of the fuselage shape was quite difficult. Therefore, the deciding factors were based strictly on material properties. These were ultimate tensile strength, yield strength, specific strength, specific modulus, density, hardness, toughness, and price.

For the fuselage plywood was chosen to be the best material. It offers the best combination of strength and weight. Its properties were determined to be the most efficient for the construction of the aircraft.

4.4.3 Tail Materials Analysis - Materials for the tail were chosen in a similar fashion to the wing materials selection. However, the loading felt by the tail surfaces was determined to be significantly less than that of the wing. Therefore, material testing and analysis revealed a balsa spar to be best.

4.4.4 Landing Gear Materials Analysis - The landing gear material design process was divided up into two steps. First, eight materials were evaluated to ensure they satisfied engineering requirements. Then the cost, ease of manufacture, availability and weight of each material were considered. The materials reviewed for design were Aluminum alloy 1100, Aluminum Alloy 2024, Titanium Alloy Ti-5 Al-2.5 Sn, Titanium Alloy Ti-6 Al-4V, Magnesium Alloy AZ31B, Magnesium Alloy AZ91D, Aramid fibers-epoxy matrix, and E-glass Fibers-epoxy matrix. All of these materials are relatively light and were therefore considered to be good candidates for landing gear application.

Several assumptions were made before analysis was conducted. First, it was assumed that each leg of the landing gear must be at least 10 inches apart to ensure taxiing stability. Also, in order to ensure

that the comparison of the materials is accurate, the shape and size of the landing gear for all materials remained the same throughout the analysis.

A program was created in Matlab to evaluate the behavior of the landing gear. The inputs to the program were the damping and stiffness coefficients for varying materials. It should be noted that each of these coefficients was the series sum of both the landing gear and wheel contributions. It was noticed that the landing gear contributes the most to the stiffness, whereas the tires contribute the most to the damping coefficient. This program delivered the material deflection by solving the derived differential equation of motion. The respective stresses for each material were calculated based on this deflection. Based on program outputs and the material decision matrix the material demonstrating the most favorable characteristics is Aluminum 6061.

4.5 PRELIMINARY DESIGN RESULTS

In general, the results generated from the preliminary design phase give the aircraft's overall dimensions. Table 4.3 outlines these results.

Component	Parameter	Value
Airfoil	Chord	15"
	Shape	SD7003
	Max thickness at chord	1"
Planform	Span	10'
	Dihedral	4 deg
	Aileron Area	15% wing
Fuselage	Length	74"
	Width	10"
	Height	10"
	Shape	Bullet
Motors	Type	Astroflight 40s (2)
	Amperage output (ave)	40 amps
	Propellers	20"
Tail	Shape	Standard
	Elevators Control %	10
	Vertical Stabilizer %	20
Landing Gear	Design	Tail dragger

TABLE 4.3 Preliminary Design Results

FIGURE 4.1 Landing Gear System Model – The spring / mass diagram of the landing gear was reduced to one degree of freedom. Appropriate differential equations of motion were derived from this model to describe the behavior of the landing gear.

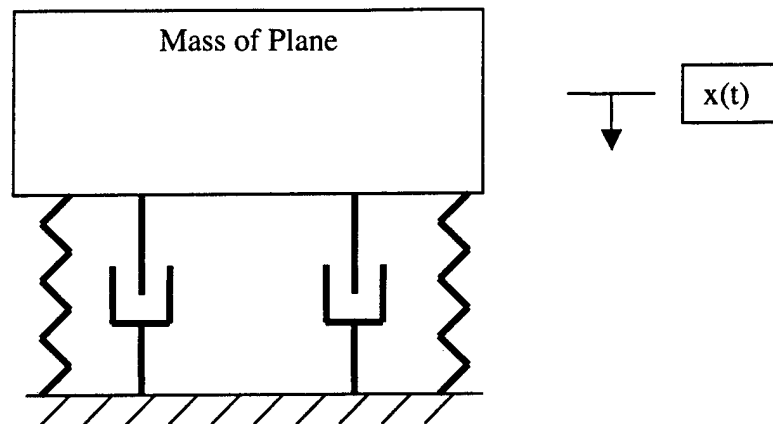


FIGURE 4.2 Landing Gear Transient Response – The landing gear will achieve steady state after 0.2 sec. This response is quite favorable.

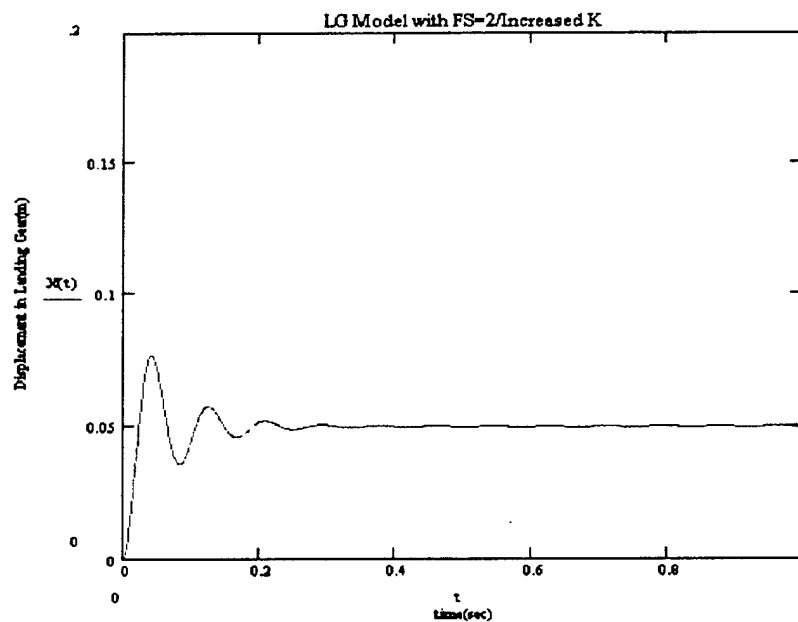


FIGURE 4.3 The Drag Polar for Selected Low Speed Airfoils – Reynolds numbers for the airfoils analyzed ranged from 480,000 to 504,000. This discrepancy was assumed to be negligible for airfoil selection. It can be seen that SD7003 has the greatest L/D ratio.

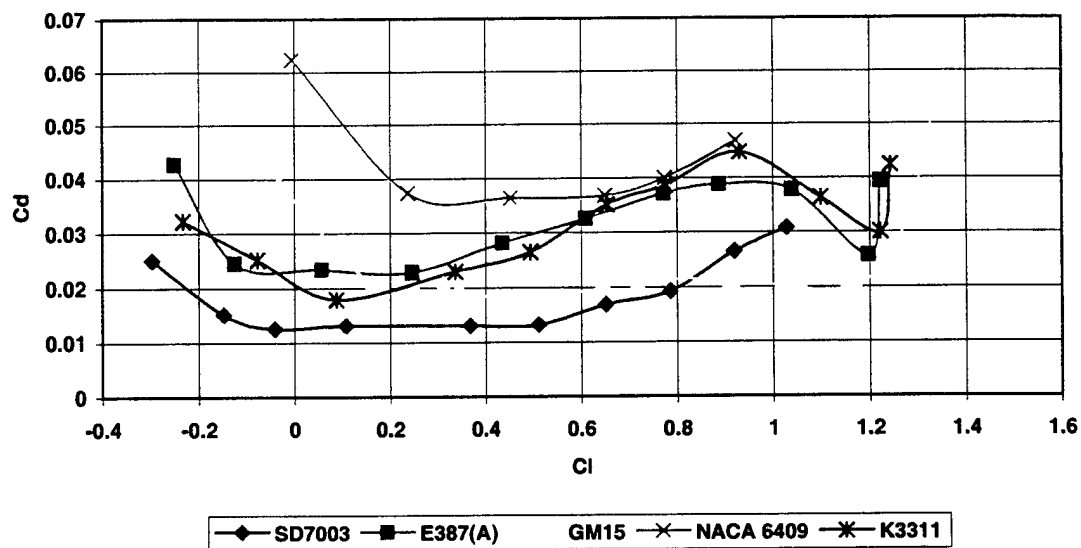


FIGURE 4.4 Coefficient of Lift v. Angle of Attack for Selected Low Speed Airfoils – SD7003 demonstrates the most favorable stall characteristics.

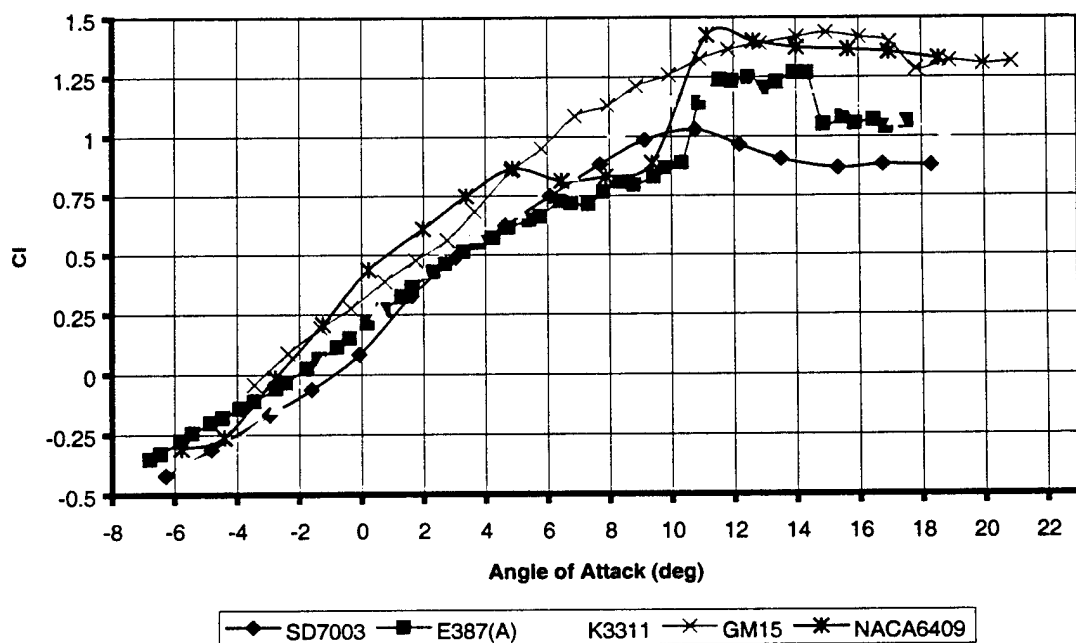


FIGURE 4.5 Power Loss Distribution: Astro40 vs Graupner 700bb – The pie charts below show that the Astro-brand motors are more efficient at a 20 amp draw. Less power lost in mechanical output for the Astro motors.

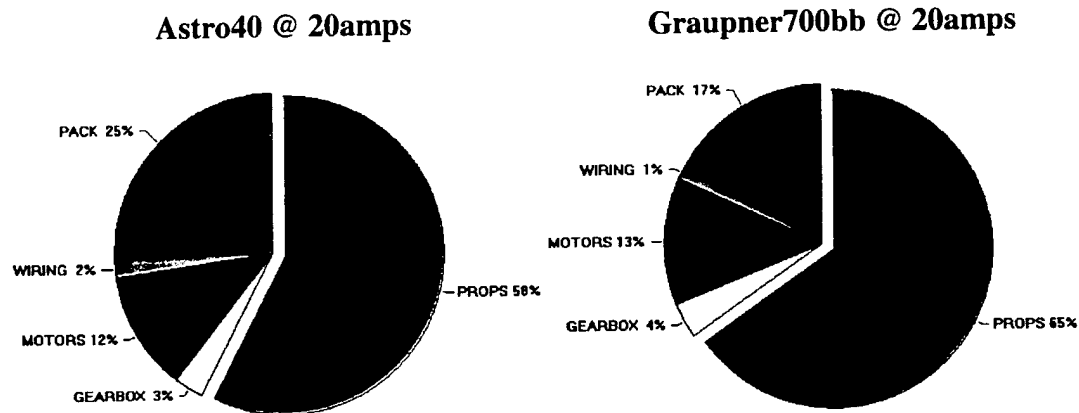


FIGURE 4.6 Flight Efficiency: One vs. Two Motors – Reviewing the two plots below shows that a two motor configuration is capable of producing a greater velocity at a lower drag than a single motor configuration.

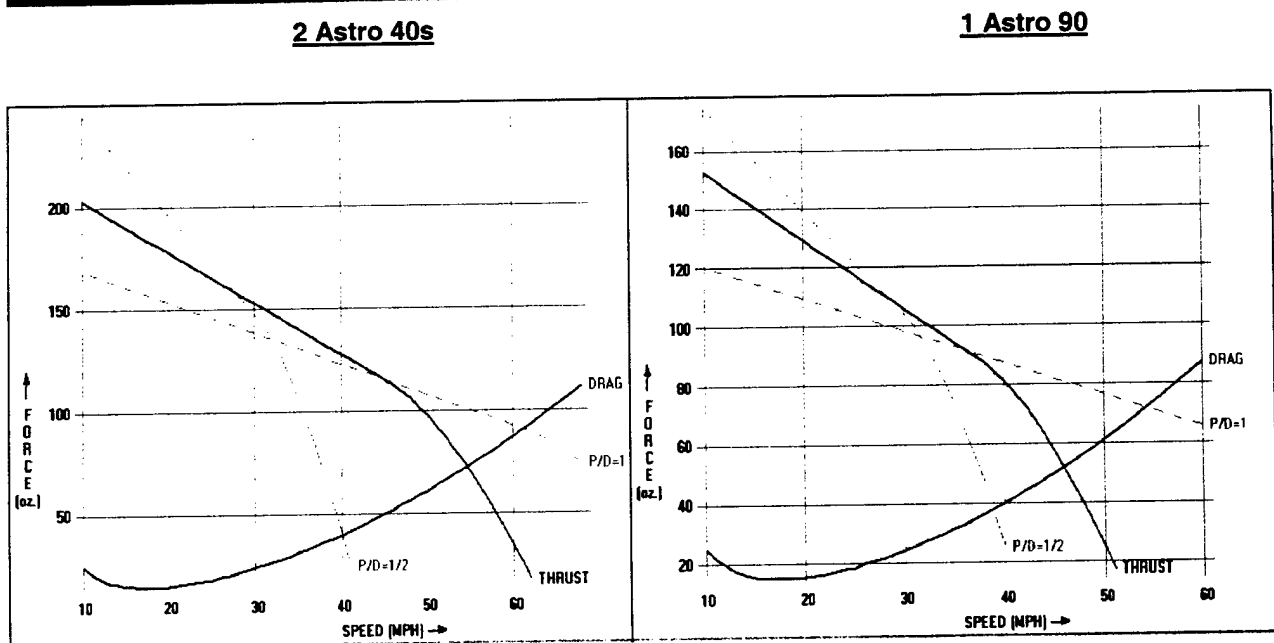


FIGURE 4.7 Motor Test Stand – This stand was developed to experimentally determine the static thrust produced by several props.

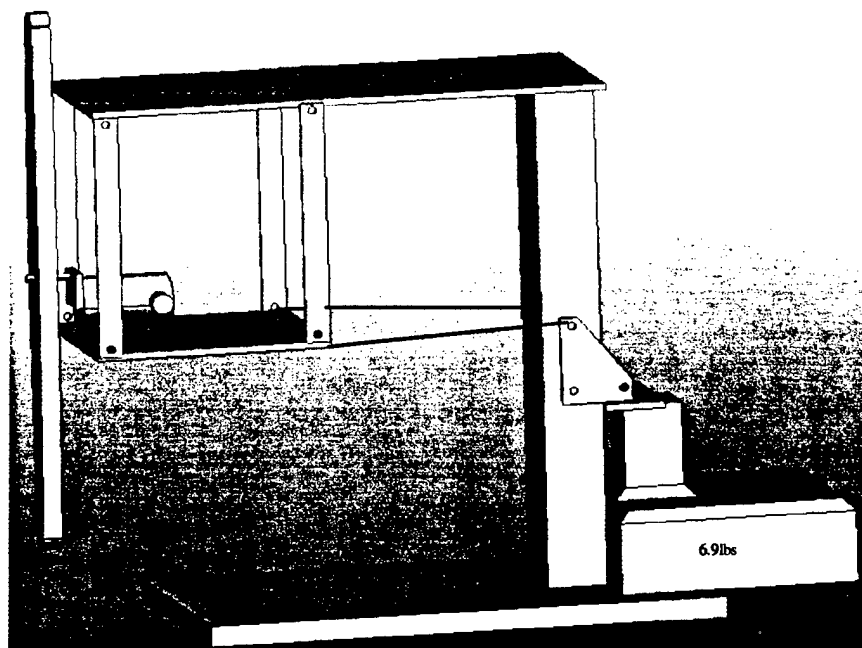


FIGURE 4.8 Rated Aircraft Cost – The cost was determined for the current configuration in accordance with the AIAA guidelines.

Aircraft Configuration			Cost (\$ Thousands)	
# Engines		2		
# Cells		37		
MEW	lbf	18		
# Wings		1		
Wing Projected Area	sqr ft	12.5		
# Fuselage		1		
Fuselage Length	ft	6		
# Vertical Surfaces		1		
# Horizontal Surfaces		1		
# Servos		4		
# Propellers		2		
Cost Terms				
A	100	-		
B	1			
C	20			
MEW	18			
REP	4440			
MFHR	128			
Rated Aircraft Cost			\$ (Thousands)	8.8
			WBS Wing	55
			WBS Fuselage	29
			WBS Empenage	20
			WBS Flight Systems	9
			WBS Propulsion System	15

5.1 INTRODUCTION

At this point stability and control of the designed aircraft is reviewed to ensure optimal flight performance. The aircrafts systems architecture was refined and components were selected. Then, 3-D drawings were created to check functional interference and component placement. Finally, stress analyses were performed on major components.

5.2 AIRCRAFT PERFORMANCE

5.2.1 TAKEOFF DISTANCE

Using the wing loading and thrust to weight ratio obtained from the previous design phases, the takeoff distance was calculated using the following equation:

$$S_g = \frac{1.21(W/S)}{g\rho_{\infty}(C_L)_{\max}(T/W)}$$

This equation delivered a takeoff distance of 114 ft (fully loaded).

5.2.2 Range and Endurance - For electric powered flight, the industry standard in calculating motor performance is the program Ecalc. This program gives valuable information for the thrust, run time, estimated speed, amp draw, and watts created. From this information, we were able to determine our range and endurance for the aircraft. The endurance of the aircraft was determined to be 8.8 minutes of flight at a cruise. At cruise, the range of the aircraft would be 7081 meters.

5.2.3 Power - Propeller-driven aircraft are rated in terms of power as opposed to thrust. The power available, or useful power, is a function of the propeller efficiency and the shaft power produced by the motors. The power required for straight level flight is a function of the thrust required and the velocity of the aircraft. A graphical analysis of the power required curve allowed the design team to determine the desired flight velocities of the aircraft. This graph can be viewed in Figure 5.1. For a propeller-driven aircraft the power available is essentially constant with velocity. The intersection of the maximum power available curve and the power required curve defines the maximum velocity for straight and level flight. Under the fully-loaded configuration it was determined that the maximum flight velocity for straight and level flight is 50.5 mph.

5.3 AIRCRAFT STABILITY AND CONTROL

5.3.1 Estimation of Aerodynamic Derivatives - In order to predict the performance and stability and control of the designed aircraft, certain aerodynamic derivatives had to be determined. Data for estimating aerodynamic derivatives came from the USAF Datcom (USAF, 1978).

5.3.2 Longitudinal Stability – The criterion for longitudinal stability is given by pitch stiffness or $C_{m,\alpha}$. The criterion to be satisfied is $C_{m,\alpha} < 0$, that is, positive pitch stiffness. USAF Datcom methods revealed $C_{m,\alpha}$ to be -2.769 , corresponding to positive pitch stiffness. This means that the aircraft will act to correct itself when it experiences a disturbance in pitch. The static margin, K_n also helped the team grasp the magnitude of longitudinal stability. The static margin is given by the difference between the neutral point and the center of gravity. For positive pitch stiffness, the static margin must be positive. That is, the design must have a neutral point, h_n , located aft of the center of gravity, h . The neutral point for an aircraft is similar to the mean aerodynamic center of the wing. It is the point where all aerodynamic forces act on the aircraft body. Consequently, the neutral point plays a vital role in the stability of the aircraft. Determination of the neutral point was given by:

$$h_n = h_{nwb} + \frac{a_l}{a} V_H \left(1 - \frac{\partial \varepsilon}{\partial \alpha} \right) - \frac{1}{a} \frac{\partial C_{m_p}}{\partial \alpha}$$

Since the motors were designed to be placed on same plane as the center of gravity, it was assumed that the change in moment produced by the propulsion units with respect to a change in the angle of attack was zero. The resulting neutral point was located at .916 percent of mean aerodynamic chord. In other words it is located 13.74 in. from the leading edge of the wing. The location of the center of gravity is at the quarter-chord point of the wing, or 3.75 in. from the leading edge. Therefore, the neutral point is located a sufficient distance aft of the center of gravity ensuring longitudinal stability of the aircraft in flight.

5.3.3 Weathercock Stability – Yaw stiffness describes the aircrafts weathercock stability. When the airplane is at an angle of sideslip β relative to its flight path, the yawing moment produced would be such as to tend to restore it to symmetric flight. For yaw stiffness the change in moment in the x-y plane with respect to a change in the sideslip angle β should be positive. That is, $C_{n,\beta}$ must be greater than zero. The governing equation for weathercock stability was:

$$\frac{C_{n,\beta}}{C_L^2} = \frac{1}{57.3} \left[\frac{1}{4\pi A} - \frac{\tan \Lambda_{c/4}}{\pi A (A + 4 \cos \Lambda_{c/4})} \left(\cos \Lambda_{c/4} - \frac{A}{2} - \frac{A^2}{8 \cos \Lambda_{c/4}} + 6(h_{n_w} - h) \frac{\sin \Lambda_{c/4}}{A} \right) \right]$$

In determining $C_{n,\beta}$ it was assumed that the aircraft was at a maximum lift coefficient. The resulting $C_{n,\beta}$ was .0001827. Therefore, the aircraft is stable in yaw. Further analysis was performed to determine the actual contribution of the vertical fin to weathercock stability. This would help gauge whether or not the sizing and optimization of the vertical stabilizer performed in previous design steps was sufficient.

5.3.4 Roll Stiffness – When the x-axis of the aircraft does not coincide with the relative wind a second order roll stiffness results through the medium of the derivative $C_{l,\beta}$. Rolling through an angle ϕ has affects in both the y and z planes. The angle of attack of the x-axis is defined as α_x . This variable is the criterion for roll stiffness. If α_x is greater than zero then there is a roll stiffness that resists rolling and acts to

keep the wings level. If $\alpha_x < 0$, then the stiffness is negative and the aircraft would rotate 180 degrees, the effects of which are easily understood. The roll stiffness was given by the following equation:

$$\frac{\partial C_l}{\partial \phi} = C_{l_\beta} \alpha_x$$

Numerical analysis revealed $\alpha_x = .00234$. Therefore, the aircraft will keep its wings level.

5.4 STRESS ANALYSIS

Another major portion of the detail design involved conducting stress analyses on critical components of the aircraft. The first of these involved the interface between the cargo bay, landing gear, wing and fuselage. This interface will experience the greatest load in flight and during landing/takeoff. Using Cosmos/M, we conducted a stress analysis on this joint. Figure 5.2 shows both the constraints, loads and respective stresses. This software does not have the capacity to model impulse loads. Therefore, we assumed a constant 2g load distributed across the interface. Under such a load it can be seen that we are within the allowable stress range. One concern raised was the stress concentrations around the bolts. From Figure 5.2 it can be seen that these areas experience higher loads. Therefore, we increased the number of bolts across the interface and included plywood washers to help increase the distribution area.

The second component requiring a stress analysis was the landing gear itself. In the preliminary design, the landing gear was designed using differential equations of motion and material properties. However, a stress analysis was required to highlight stress concentration areas so that questionable areas could be reinforced. Figure 5.3 shows the landing gear stress analysis. Again, a constant 2g load was assumed to act at the wheel attachments. The diagram revealed stress concentrations around the bolt areas. Therefore, we decided to reinforce these areas in a similar manner to the fuselage. The deflection of the landing gear was also checked to ensure the props would not contact the ground during a hard landing. The deflection animation was captured in three separate figures. Here we see the stress increase across the legs of the landing gear. However, it remains within a tolerable range. The deflection of the legs corresponded to a 2.5-in within the vertical plane. This allows ample room for propeller ground clearance.

5.5 COMPONENT SELECTION

5.5.1 Servos - The servos used in this airplane are off the shelf components since there is no need to design anything in this area, the only consideration was brand and servo size. When selecting the brand of servo to use we decided on Futaba since they manufacture the most Radio Control components and we have had excellent experience with them in the past. Futaba also manufactured our radio control transmitter and receiver unit thus keeping all of the control system compatible. For the tail dragger

configuration four servos will be used. These servos are the electrical to mechanical interface for the rudder, tail wheel, elevator, and both ailerons.

For the Elevator servo we used Futaba criteria for selecting a sufficient size. The result was a servo that is commonly used in 1/4 scale models. This servo is very large, but the weight is justified since any failure in the elevator control system would be catastrophic.

For the Rudder we used the same large servo. This servo needs to be able to handle a large load because it is providing control for both the rudder and the tail wheel. When taxiing, especially with a full load, this movement will take approximately 4lbs of force. This is just under the max force that the 1/4 scale servo can provide.

The aileron servos are important for precise handling especially in gusty conditions. We decided that two servos in the wing would provide a direct linkage giving better control for our aircraft. This also allows our pilot to easily add flaperons on the heaviest take offs and landings through the computer settings on our T6XA Futaba Radio.

5.5.2 Batteries - The batteries selected were the 2000 model batteries from Panasonic They are the top of the line and meet the Nicad requirements. The batter pack incorporates 37 cells under the 5lb limit. This will be possible by using very short lead wires to reduce pack weight. This will increase the voltage delivered to the motors and slightly increase our run time. For charging, we discovered that colder batteries can hold more amperage. Knowing this we will have a supply of plastic bags and a cooler of ice. This way we will gain a slight power advantage on the day of the competition.

5.6 SYSTEMS ARCHITECTURE

Upon completion of our detail design, we had several major components selected and drawn on Pro-Design. At this point, the way that all the systems fit together must be analyzed for the product to succeed. This was accomplished before any construction was started using the computer-aided drawing software Pro-Design. We found that each part can be assembled in to large conglomeration that allowed us to see the entire aircraft completely assembled. We were able to spot some problem areas where components did not have the necessary clearance and then iterate through the process again until all the components meshed into a functioning aircraft. This proved to be a major time saving step during this design process since we found problems before we built.

5.7 INNOVATIVE CONFIGURATION SOLUTIONS

In order to win the contest, our design has several design characteristics that will improve its performance. In order to do as many sorties as possible during the contest, it was important that we minimize the amount of loading and unloading time. Therefore, we designed the payload container to be easily taken in and out of the compartment within the fuselage. To do this, we decided to place the door for the payload in the nose cone of the aircraft. The nose cone is attached to the fuselage with a hinge

and can be swung open for easy access to the payload. The payload container is a lightweight balsa construction and slides on rails for easy loading and unloading. The center of gravity (cg) of the container sits directly on the cg of the aircraft so that there no change in cg position when any amount of payload is added. The container holds all 100 balls tightly, so that they will not shift during flight. In addition, the steel payload consists of steel sheets that will distribute their weight across the entire container, keeping stress concentrations to a minimum. Reference figure 5.4 to see how the seed loader interfaces.

Another aspect of our design is its reparability. Every feature on the aircraft is designed for easy repair so that we can be flying quickly during the unfortunate event of a crash. The aircraft is completely modular so that the broken components can be switched out immediately. In order to prevent problems with damaging the motors and propellers, the nose was designed so that in the event of a nose-over upon landing, the nose of the aircraft will hit first, not allowing the props to hit the ground. We knew the importance of this due to our tail-dragger configuration and problems that previous design teams have had with nose-overs.

5.8 FINAL DESIGN RESULTS

Empty Weight	18 lbs	Wing Construction	Rib and Spar
Loaded Weight	36 lbs	Horizontal Tail Area	280 sq in
Takeoff Distance(Loaded)	114 ft	Rudder	50%
CG Location (From Nose)	26.83 in	Vertical Tail Area	210 sq in
Airspeed (Cruise)	66 ft/s	Elevator	33%
Flight Time	8.8 min	Tail Airfoil	NACA 0012
Range	7081 m	Tail Construction	Balsa
Rated Cost (1000's)	8.8	Fuselage Length	74 in
Wing Shape	Rectangular	Fuselage Shape	NACA 0024
Wingspan	10 ft	Fuselage Height	13 in
Wing Location	Low	Fuselage Width	10 in
Chord Length	15 in	Fuselage Construction	Balsa and Foam
Airfoil Shape	SD7003	Maximum Payload	18 lbs Steel, 100
Wing Area	12.5 sq ft	Motors	2 Astro 40's
Alleron Area	10%	Propellers	Topflite 18x6
Dihedral	4 deg	Landing Gear Configuration	Tail Dragger

TABLE 5.1 Our Final Design!!!

Figure 5.1 Power Available vs Power Required Curve – The intersection of the required power curve and the available power curve give us with the optimum flight speed. This analysis was performed on both a loaded (red) and an unloaded (green) aircraft. Less power is required to fly unloaded, thus we can maintain a greater velocity.

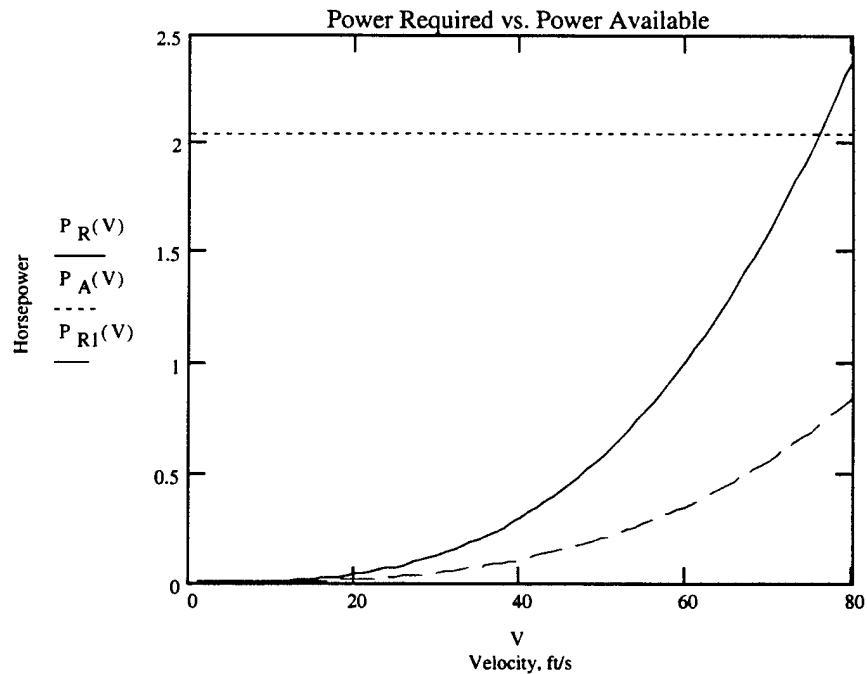


FIGURE 5.2 Fuselage Stress Analysis – The stress analysis showed us that the only areas for concern exist around the boltholes.

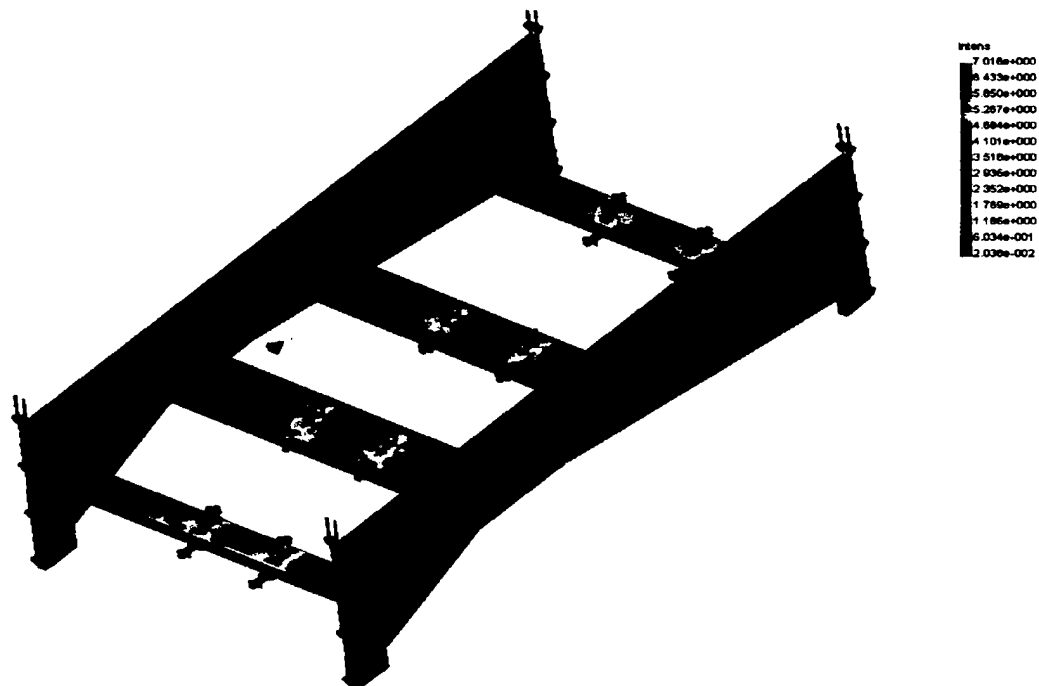


Figure 5.3 Landing Gear Stress Analysis – The deflection animation was captured in three separate figures showing the increase in stress with an increase in deflection. Additionally, the maximum deflection was small enough to ensure propeller ground clearance.

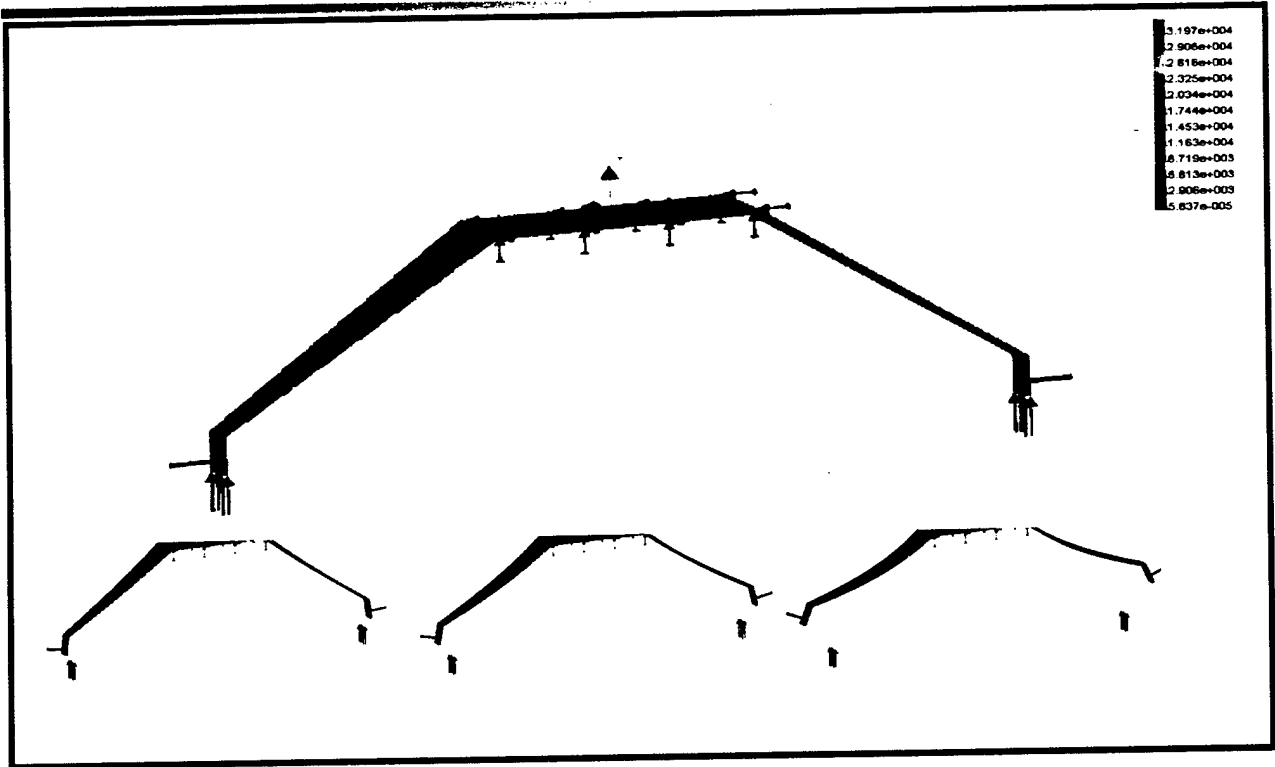


FIGURE 5.4 Speed-Loading Device

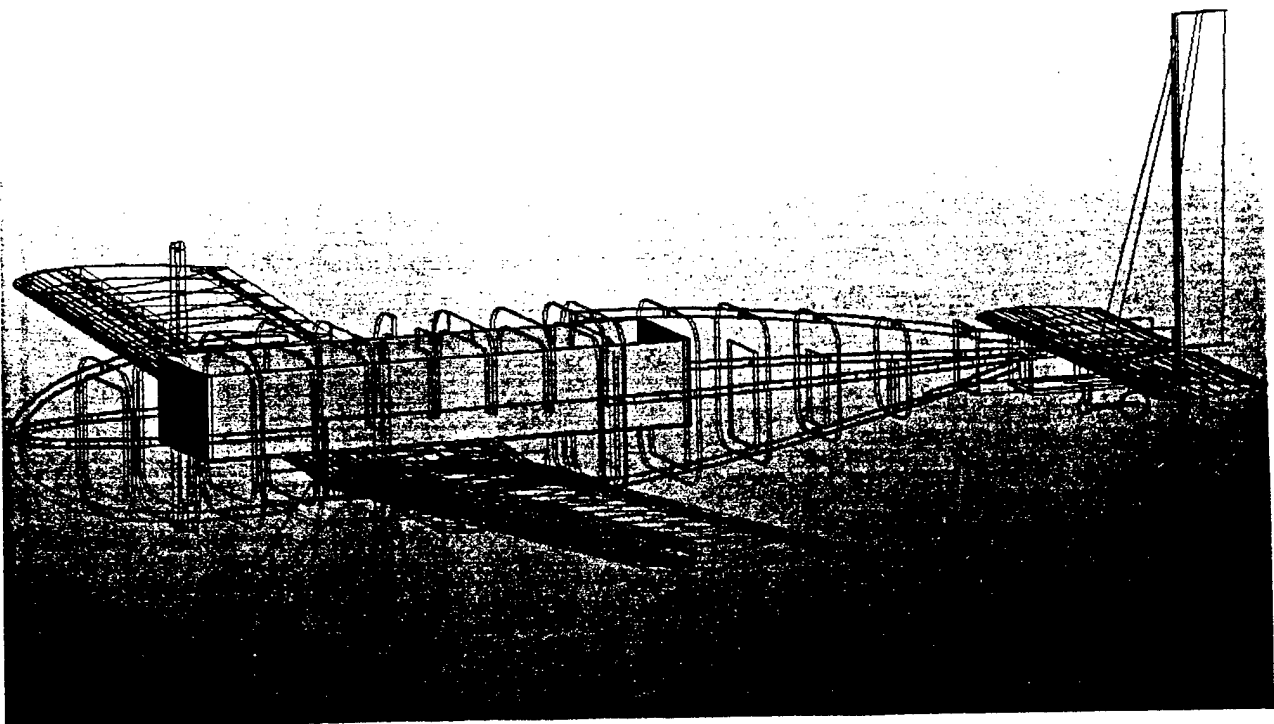


FIGURE 5.5 Exploded Aircraft Views

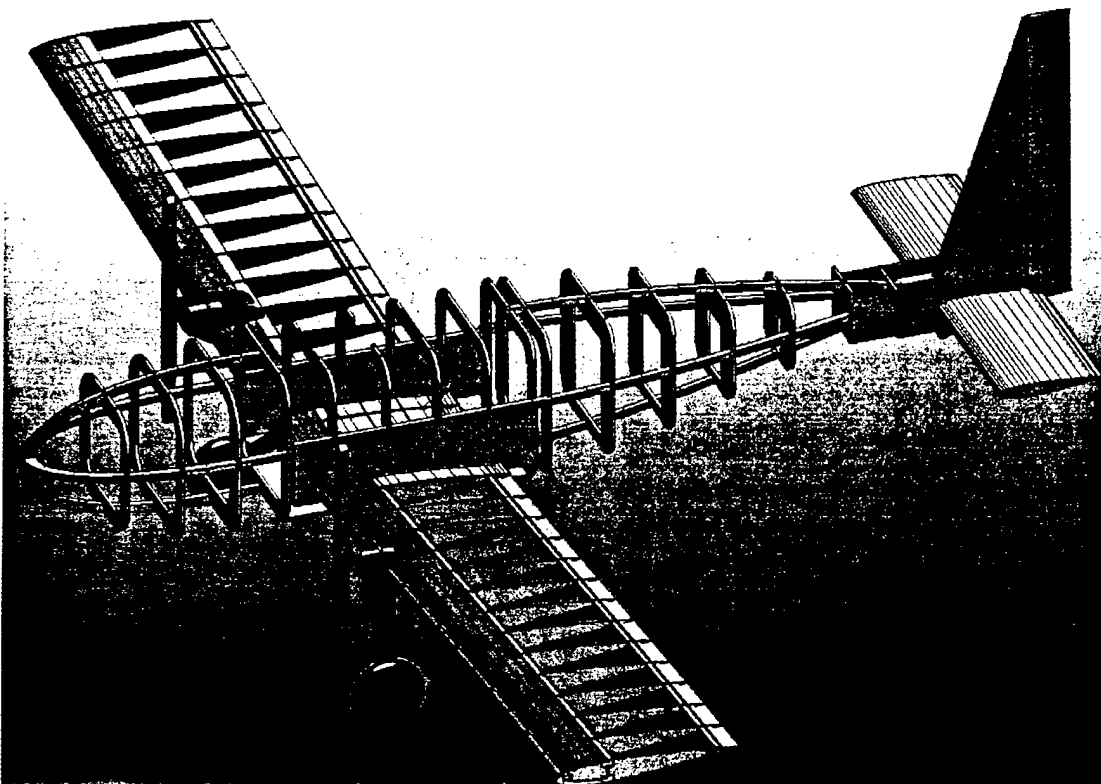
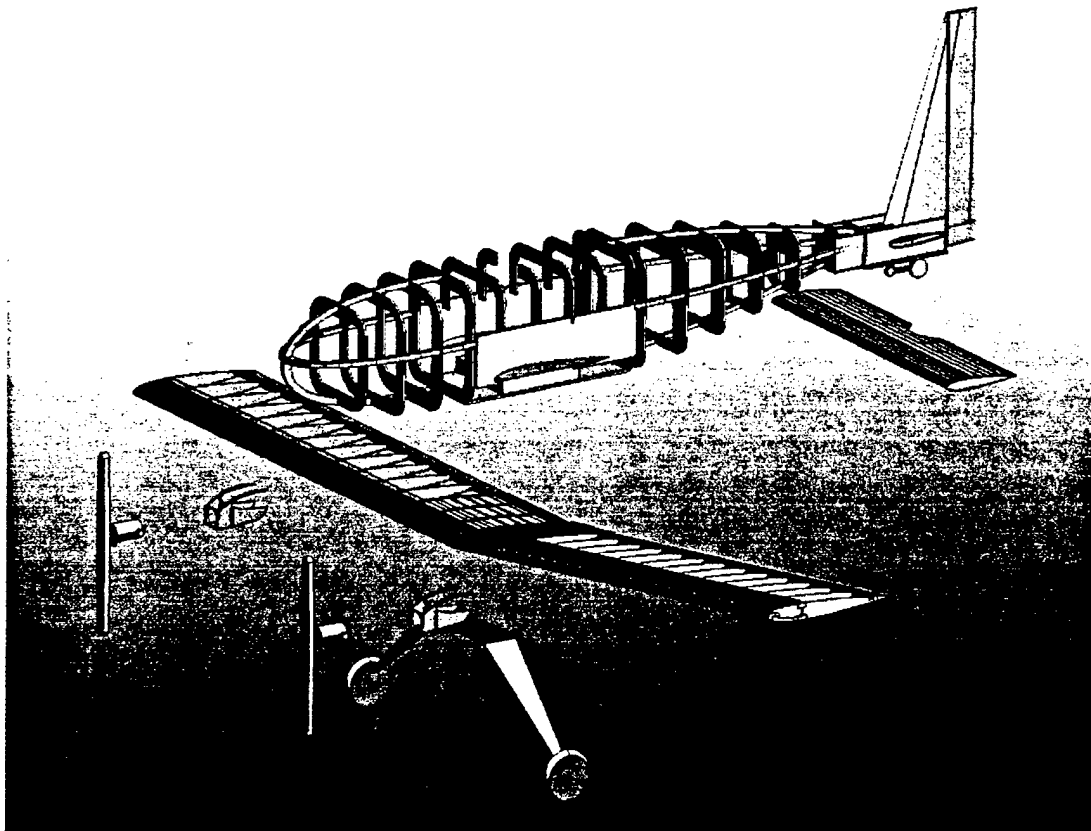


FIGURE 5.6 Wing Drawings

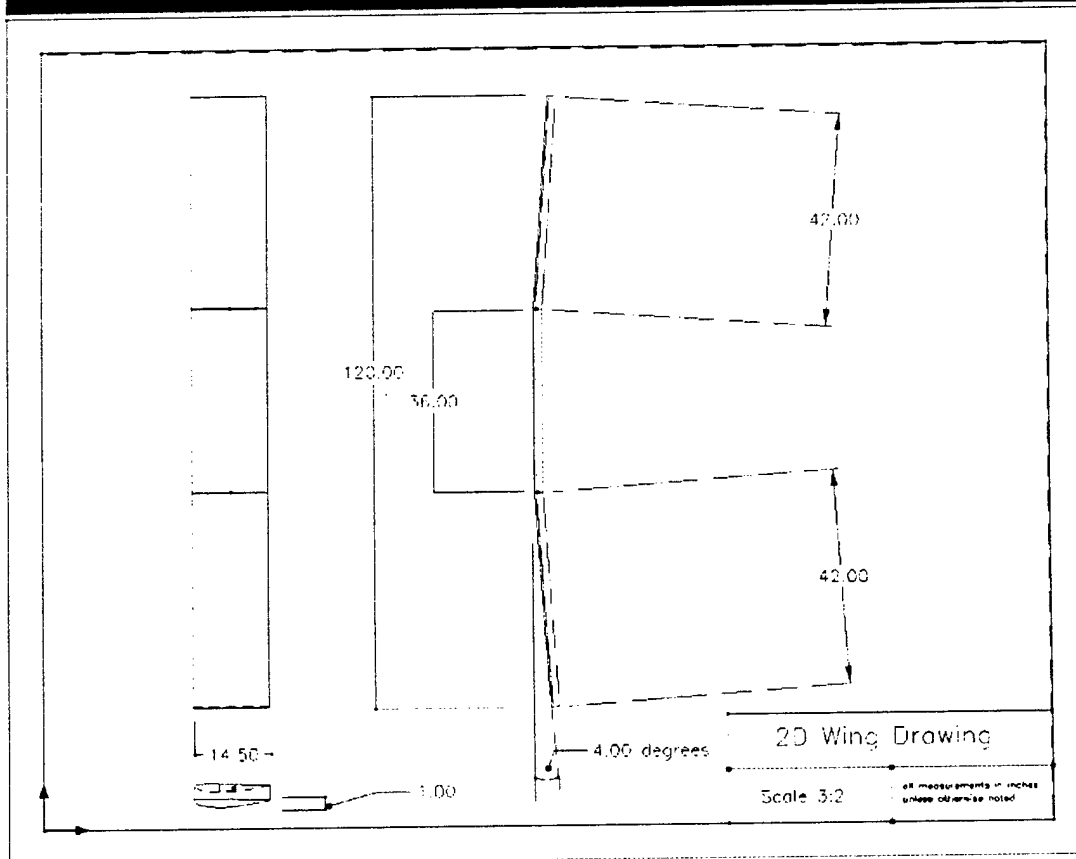


FIGURE 5.7 Fuselage Drawings

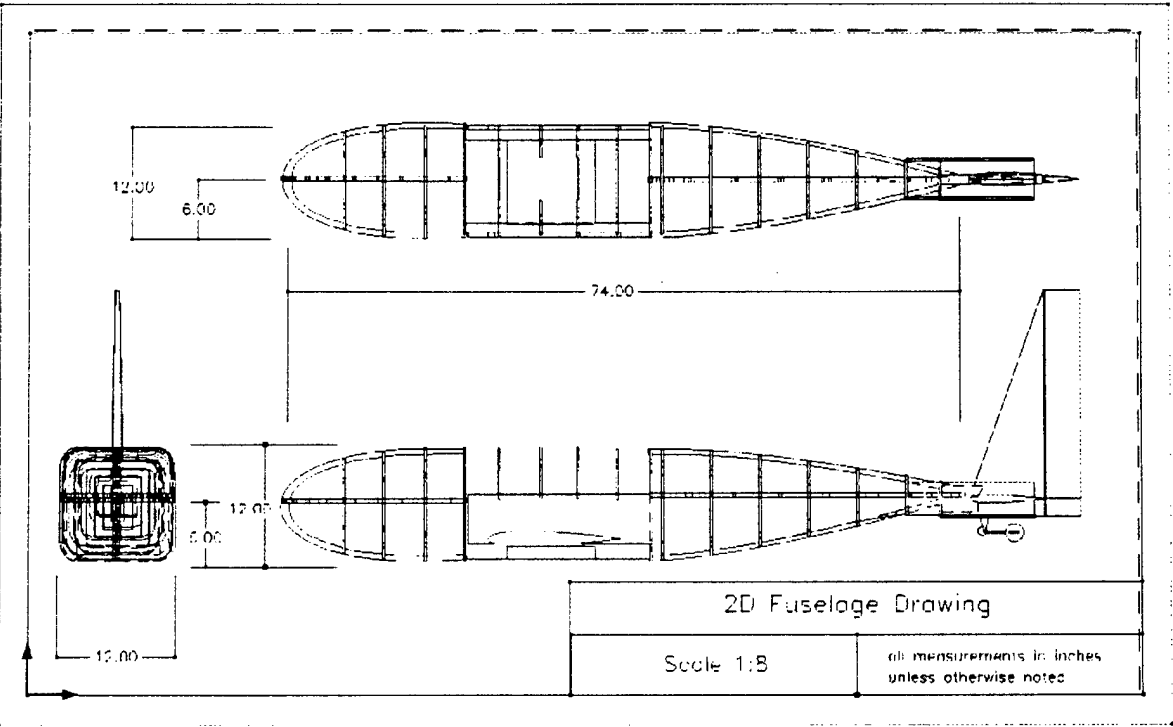
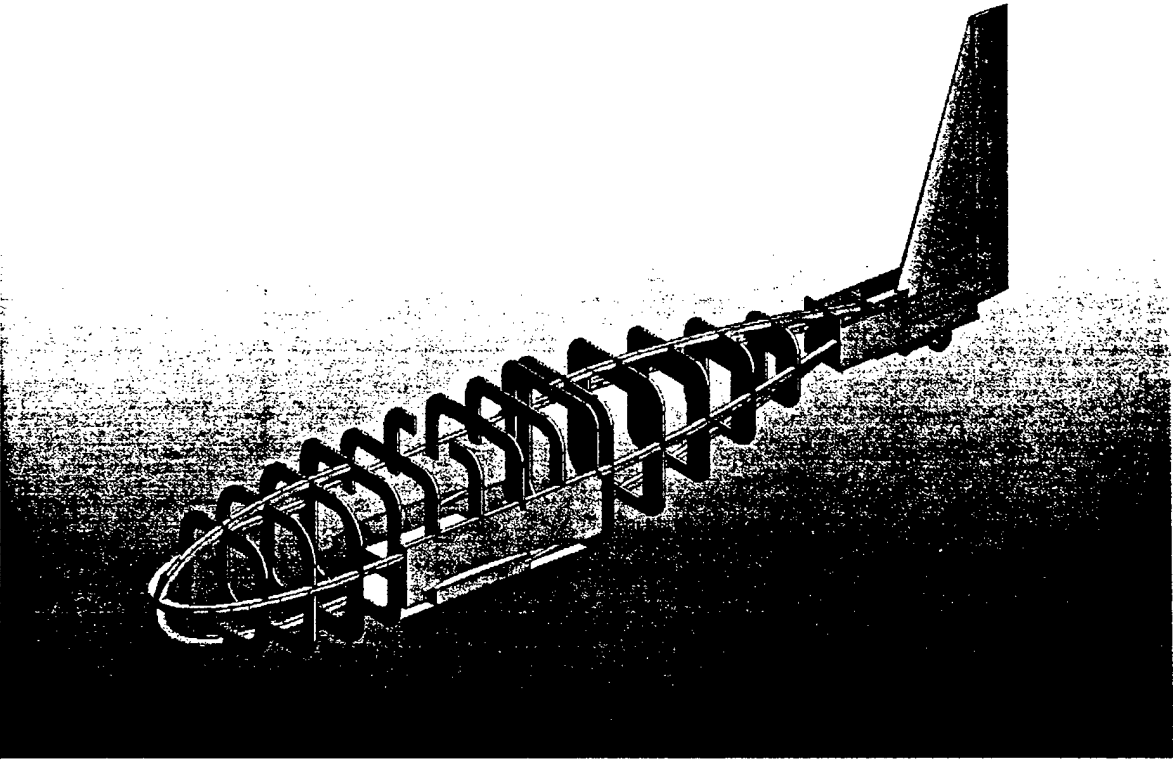


FIGURE 5.7 Tail Drawings

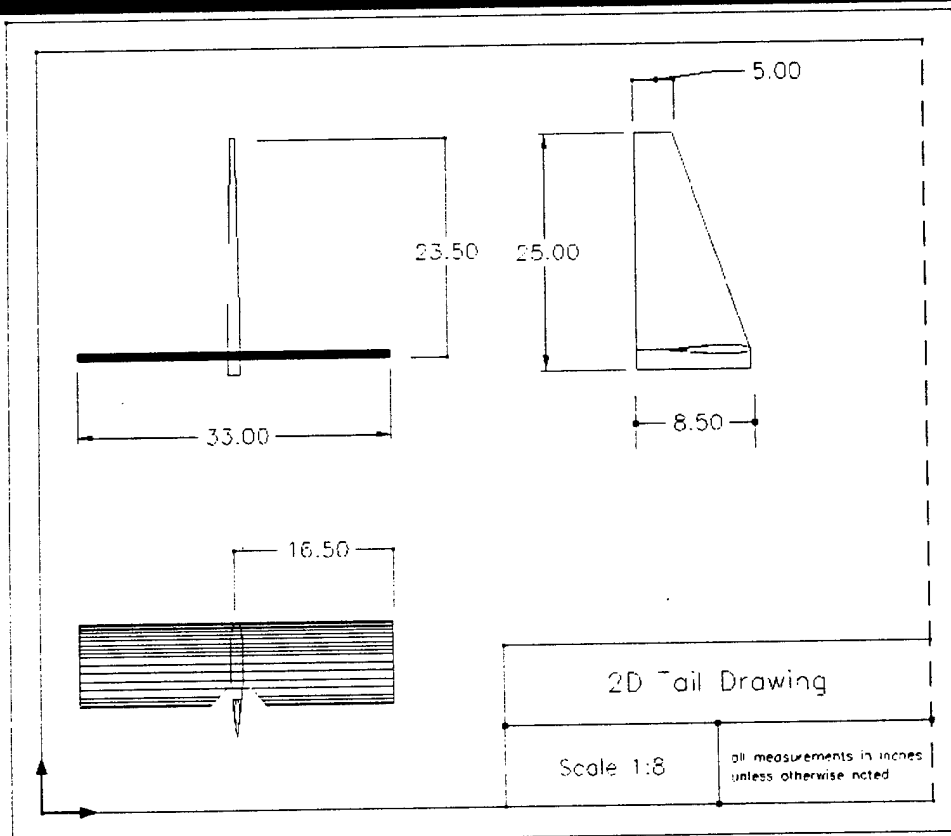
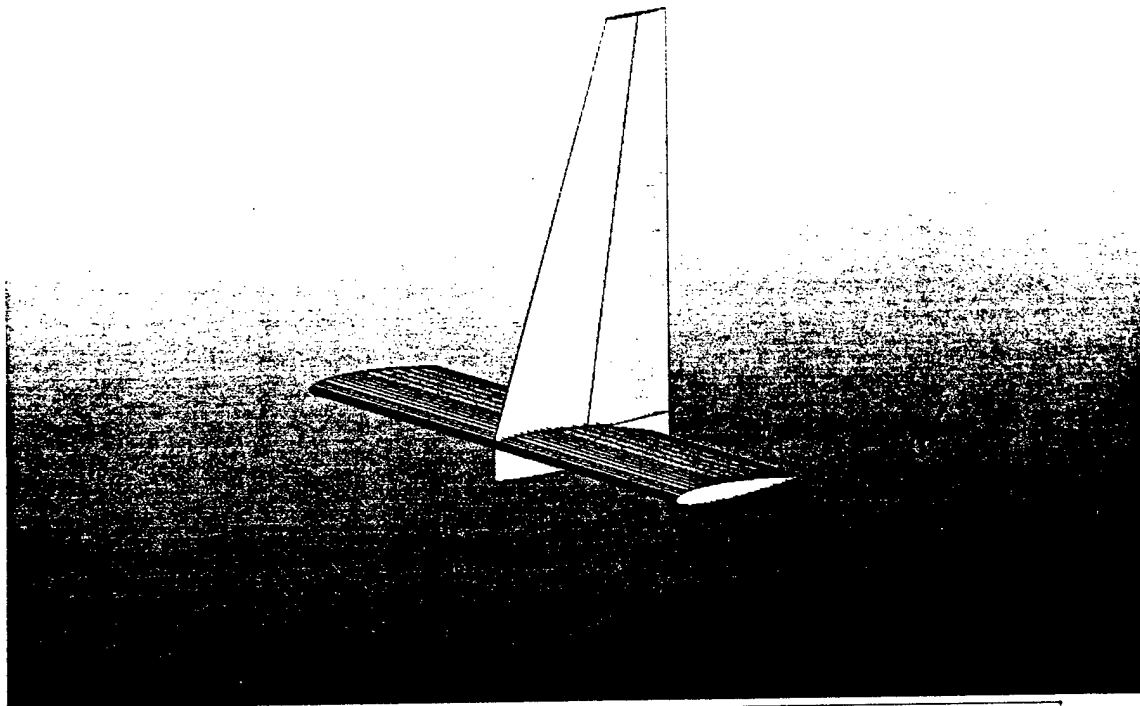
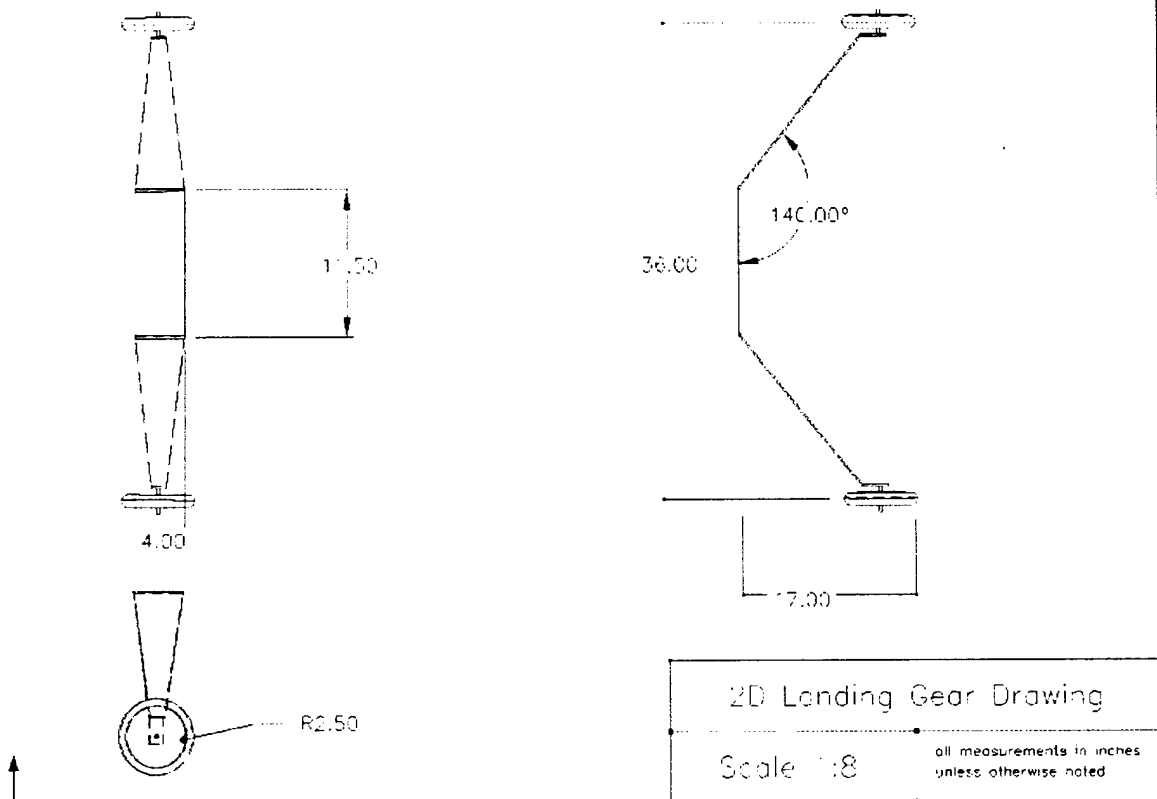
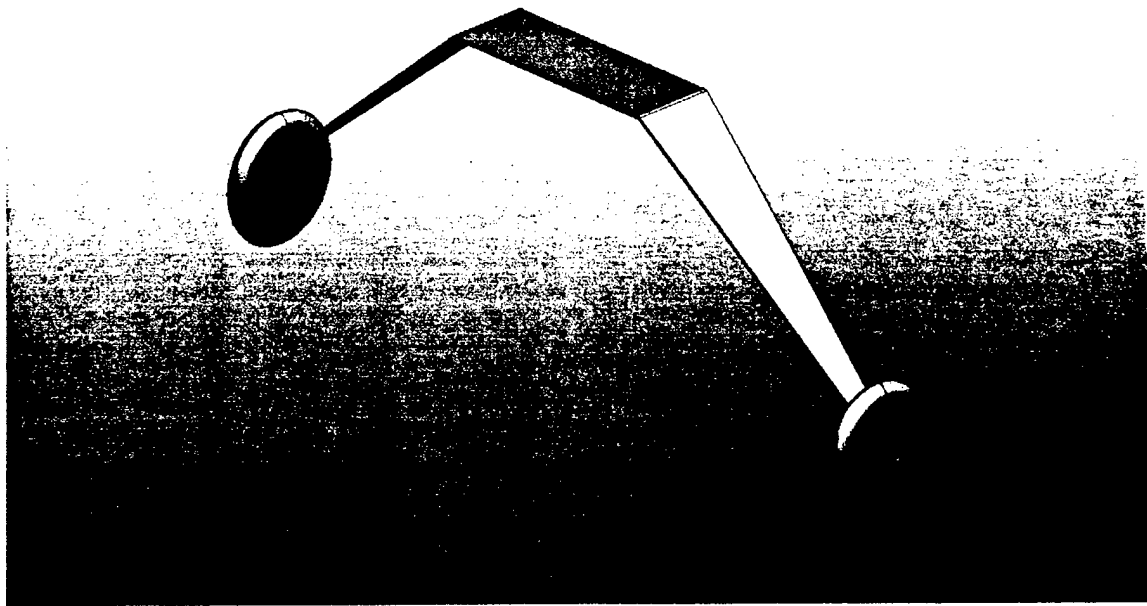


FIGURE 5.7 Landing Gear Drawings



6.1 INTRODUCTION

The Military engineering production process fundamentally parallels that which civilian counterparts incorporate into design manufacturing. The design phase outline shown in Figure 6.1 illustrates a guideline for design acquisition and production. In accordance with the manufacturing plan we entered this process in phase 2.

6.2 MANUFACTURING ACQUISITIONS AND PHASES

With concept exploration and program definition completed, we enter phase 2, manufacturing and development. The first run will be a Low rate initial production (LRIP) which allows us to work all the problems out of the manufacturing process. This will also allow us to use the initial aircraft to test our design and practice the competition before we actually compete. A major help in manufacturing this aircraft was the drawings from Pro-Design. Using a large scale plotter the full sized plans were printed and available for the construction teams. This helped with the sizing of parts and ensured accuracy. The manufacturing plan was broken down into four sections: fuselage, wing, tail and landing gear.

6.2.1 Fuselage - The plan for manufacturing the fuselage was based on simplicity and weight reduction. The standard stringer and bulkhead construction was determined to be the lightest construction method that could handle the load of a hard landing. Building on the conventional model building methods, we plan on using composite stringers to help make the complex shapes of the NACA 0024 airfoil that the fuselage was based on. Each stringer will be 1/8-in thick and consist of a 1/16-in layer of balsa and a 1/16-in layer of spruce. When these two are joined, the result will be a strong stringer with no inherent tension built into it. This will give us the strongest fuselage possible while still meeting our weight requirements. The bulkheads will be manufactured from common foam board. This material will give us enough strength to hold the stringers in place while also keeping the weight down. After testing several methods of fastening the bulkheads to the stringers the results showed that Elmers general purpose glue gave us the strongest joints.

6.2.2 Tail Components - The construction plan for the tail assembly is a framed construction with a balsa spar. The major consideration in building the tail was weight reduction. Research showed that built up surfaces made of balsa were much lighter than the foam or foam board alternatives. Cross bracing provided additional strength. Since a triangle is fundamentally stronger than a square, we incorporated that into the tail structures. This added some considerable time for building but was well worth the extra strength.

6.2.3 WING - For the wing we also plan to use classic built up construction with balsa ribs, leading edge stock, and trailing edge stock. The spar will be made out of plywood, spruce, and a balsa cap. We will

use a full-scale print out of the plan and a wing jig to ensure accuracy. The final product will be covered with Ultra-coat to give us a smooth tight covering while not adding excessive weight.

6.2.4 Landing Gear - A prefabricated landing gear was our primary choice. This ensured a professionally made design which would exceed the quality that we could fabricate.

The last portion of the landing gear that we left to the manufacturing design phase was the choice of wheels. The competition requirements state that the aircraft must take off within 200 ft. We will use washers and bushings to reduce the friction on the axle so that the level of friction is suitable for both take-off and landing. Standard RC aircraft rubber wheels will be used for the front portion of the landing gear and a standard tail wheel/spring mechanism for the rear wheel. We spent little time designing wheels for the plane since it seemed unreasonable to "reinvent the wheel."

6.3 SKILL ASSESSMENT

The skill level required for the construction phase of our manufacturing plan varied. To approach this in the most efficient manner, we constructed a skill level table that laid out the required parts to build. This can be viewed in Figure 6.3. We then examined the skill level necessary for each part. We also incorporated a rating system into this chart that would easily identify any parts that we expected to have trouble building. This allowed us ample time to research these problem areas.

We see that the wing is going to require the most amount of skill and so we have planned ahead for that. We also identified any of the tasks/parts that have a skill level of 3 and made special considerations for the research time involved for those parts.

FIGURE 6.1 Acquisition Milestones - This guide was used to develop milestones for the manufacturing plan.

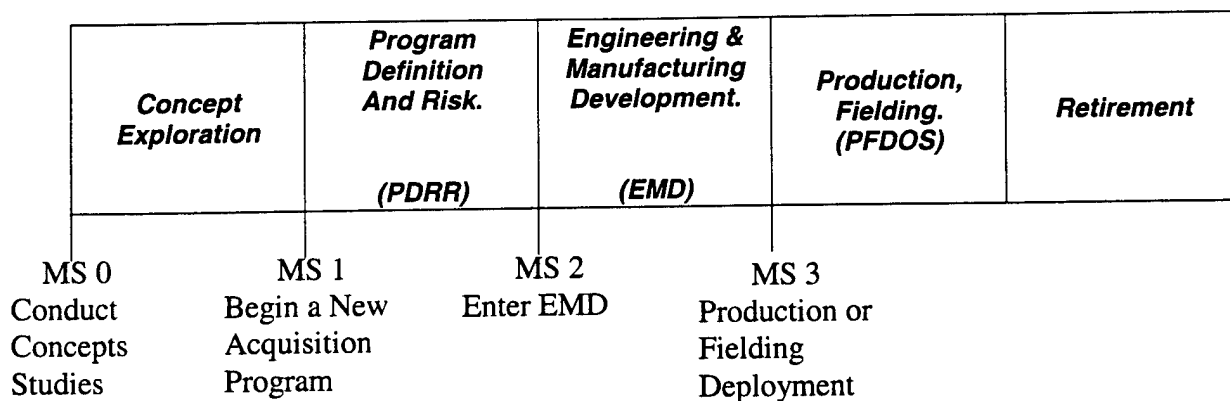


Figure 6.2 Manufacture Difficulty – The manufacture of each component was evaluated for difficulty using the following scale: skill level 1 requires common knowledge of manufacture. Skill level 2 calls for some research or consulting with experienced builders. Skill level 3 requires intense research and consulting.

Focus Area/Part	Fuselage	Wing	Tail Assembly	Landing Gear
Cutting Wood	1	1	1	0
Ribs	1	2	2	0
Spars	0	3	2	0
Stringers	3	1	1	0
Removable Parts	2	2	2	2
Linkages	2	2	2	0
Reinforcing	1	3	1	2
Covering	2	2	2	2
Control Surfaces	0	2	3	0
Motor Mounting	0	3	0	0
Battery Container	3	0	0	0
Duplicate Parts	1	1	1	1
Hinges/ Latches	2	0	0	0
SUMMARY	18	22	17	5

FIGURE 6.3 Manufacturing Milestones - Hthis calendar was created to fascilitate efficient production of our aircraft. We often remained ahead of schedule.

Manufacturing Milestone	December				January				February				March			
	1	10	20	30	1	10	20	30	1	10	20	28	1	10	20	30
First Cut	x															
Fuselage Formed				x												
Wing Built					x											
Tail Built				x												
Fuselage Covered												x				
Wing Covered													x			
Tail Covered													x			
Landing Gear on order					x											
Electronics installed													x			
Landing Gear Installed													x			
Back up landing gear started																
Final assembly													x			
First Taxi													x			
First Flight/testing																
Planned Deadline (o)																
Actual Deadline (x)																

EXTRA! EXTRA! EXTRA! Our aircraft broke contact with the ground on February 20, 2001—nearly one month early. This would not have been possible without a hardworking team, a strict adherence to the design schedule, and passion for aerodynamics. Go Black Nights!

REFERENCES

- [1] Anderson, J.D., *Fundamentals of Aerodynamics*, McGraw-Hill, Boston, MA, 1981.
- [2] Etkin, B.E., Reid, L.D., *Dynamics of Flight: Stability and Control*, 3rd Edition, Wile, New York, NY, 1996.
- [4] Lennon, Andy, *Basics of R/C Model Aircraft Design: Practical Techniques for Building Better Models*, Motorbooks International, New York, NY, 1996.
- [3] Raymer, Daniel, *Aircraft Design: A Conceptual Approach*, 2nd Edition, AIAA Education Series, American Institute of Aeronautics and Astronautics, Washington, 1992.

UNITED STATES MILITARY ACADEMY

TEAM BLACK KNIGHT

CESSNA/ONR STUDENT DESIGN BUILDING

COMPETITION DESIGN REPORT

ADDENDUM PHASE

"GREY Balsa Fire"

WEST POINT, NEW YORK
MARCH 30, 2001

TABLE OF CONTENTS

7. Lessons Learned	1
7.0 Introduction.....	1
7.1 Changes to Design after Proposal Phase.....	1
7.2 Areas for Improvement.....	2
8. Aircraft Cost	5

7.0 INTRODUCTION

Several changes were made to the "Grey Balsa Fire" following the Proposal Phase Report submission. Since the aircraft had already been constructed and test flown prior to the initial submission, most of the major "bugs" were worked out. Consequently, the design changes during the addendum phase are rather minor. An After Action Review involving every contributor to the project took place to identify potential areas for improvement and lesson learned. Finally, the completed aircraft's rated cost was determined for submission.

7.1 CHANGES TO DESIGN AFTER PROPOSAL PHASE

Many of the alterations made on the aircraft were driven by the comments of our pilot, COL David Allbee. One of his major complaints was that the aircraft had a nose-up tendency when he tried to trim the aircraft. The obvious solution was to shift the CG slightly forward. With this forward shift of the CG, we no longer needed the entire length of the battery box on the underside of the aircraft. The original design called for a long box so that the battery pack could be shifted to manipulate the CG. However, it was determined that a much smaller length was needed to gain the required CG shift. Therefore, to lighten the aircraft, we removed a significant portion of the battery box.

The pilot also desired more control in pitch. Therefore, we adjusted the elevator control horns to provide a greater range of deflection. This deflection was much greater than the required deflection range calculated in the proposal phase. We felt this was due to inconsistencies in manufacture and environmental factors such as wind and varying temperatures. The aircraft also had a slight tendency to roll right. We concluded that this was caused by a slight geometric twist across our wingspan. To correct this, we placed the wing in a homemade jig that straightened it out.

The most significant contribution of the flight test was the crash landing it took on its second flight. The crash revealed weaknesses in our structural design. In a thorough inspection of the aircraft, we discovered several locations that experienced minor fracturing and deformation. The fuselage interface with the wing and landing gear was the only location that required significant strengthening. Carbon fiber was placed across the joint and several balsa spars were added to bolster the interface. Larger washers were used to help distribute the load during landing. The empennage permanently deformed a slight amount during the crash. This caused the tail surfaces to become misaligned with the rest of the aircraft's control surfaces. Balsa struts were added to stiffen the empennage and return it to its original shape.

As a final modification to the original design, several holes were drilled to lessen the weight. A significant amount of material was removed from the fuselage bulkheads. These in no way added to the strength of the wing/fuselage/landing gear interface, nor did they add to the stiffening of the fuselage. Therefore, we felt completely justified in removing the material. We also removed material from the

plywood runners along the side of the fuselage. These were intended to distribute the load during a crash landing up and around the fuselage. However, as the crash revealed, the weaknesses were concentrated around the interface between the fuselage, wing and landing gear and not around the fuselage itself. Therefore, it seemed appropriate to lighten the structure there.

7.2 AREAS FOR IMPROVEMENT

The two sections we will focus on are the improvement in the overall design as well as in the manufacturing process for the aircraft.

7.2.1 Design - There were two areas that needed improvement in our design of the aircraft. The selection of the material and the sizing of the aircraft are two areas that need to be examined for correction.

Material Selection. We chose several different materials that need to be reexamined for next years aircraft. The first was the foam board used in the bulkheads for the fuselage. The fuselage design needs to be sturdy enough to carry the weight of the aircraft and support it through tough landings. In our design the force of the landing is transferred through the landing gear to the point of connection on the fuselage. The need for a stronger material is necessary to decrease the potential for failure. However, foam board is a good material to use because of its low weight.

The use of aluminum in the landing gear increased the weight of the aircraft. The landing gear was essentially over-designed. The angles used for the legs were based on a generally accepted rule of thumb equation for tail-draggers used by RC aircraft enthusiasts, yet the weight of the landing gear could have been reduced if the overall volume was decreased and perhaps a different material was used. Taking out additional sections to lower the weight, or decreasing the thickness would have been beneficial. Possible solutions to the materials problem might have included integrating carbon fiber, further examining the use of wood, or possibly choosing a completely different material such as titanium or a different type of aluminum.

Sizing. In designing the aircraft, we used various design techniques to determine the size of the components. In doing so, we over-designed the aircraft to counter the problems experienced by previous teams. In reflecting back, the size of the fuselage exceeded its design need. In limiting the size of this component, extra weight would have been removed. However, the fuselage does support the weight and volume of 100 tennis balls. This also is reflected in the design for the landing gear. The landing gear was over-sized because of the problems faced by previous teams in this competition. The area to improve would be to decrease the size of the aircraft's landing gear. This may also decrease the amount of clearance for the propellers.

7.2.2 Manufacturing Process - The manufacturing process needed improvement in four different areas: ordering of parts, duplicate parts manufacturing, the alignment of the motor mounts, and the use of balsa wood in consuming time.

Ordering Parts. We misappropriated a great deal of time waiting for parts to arrive. This hurt the overall scheduling by a small amount. The manufacturing of the plane went right on schedule, but the ordering of materials to make duplicate parts is time consuming. This slowed production down and limited our ability to create these duplicate parts necessary for competition day accidents.

Duplicate Part Manufacturing. We designed for a modular aircraft with which we could replace major end items immediately upon failure. These major end items included the nose section, main wing, fuselage, and tail section. To make this modular design successful, we planned on creating a duplicate of each of these major components to use during the competition. If a major part was damaged during a test or competition run, the goal was to be able to remove the damaged part and quickly replace it with a duplicate. The removal and subsequent reattachment would be facilitated by simple, lightweight, and sturdy plastic bolts that connect the major components together.

As we have found, the interfaces between the parts do not always match up as well as we would like. This is because smaller sub-components of the duplicate parts did not perfectly match the corresponding sub-components in the original parts. The reason for this is that we had completed the manufacturing of all the originals before beginning on the duplicates.

However, the duplicate parts would have been more similar to the original parts if we had constructed all of the sub-components at the same time. This was difficult for us, however, because we wanted to ensure that we had enough time and materials to construct one complete original plane before beginning work on the duplicate parts. Because of these time and material constraints, we were unable to manufacture a duplicate fuselage. However, we were able to finish construction on the parts that we deemed more likely to need replacement after a crash: the nosecone, main wing, and tail section.

Motor Mounts. During test flights, the pilot noted that the angle of the motors created stalling effects during low speeds. The aircraft's motor mounts were manufactured parallel to the wings. However, the pilot noted that the location of the CG versus the location of the thrust vector caused a torque in the way the aircraft flies. The effect is that in steady level flight the thrust vector is pointed upwards and not parallel to the flight of the aircraft. Also, the angle of attack the pilot is required to maintain in steady level flight is positive such that the motors are pointed upwards. This produced a thrust vector pointed upwards and created stalling effects at slow motor RPMs. After discovering the problem, we remounted the motors. Thus, next year's manufacturing should be more controlled and quality control should be implemented.

Time Consumption. In manufacturing the aircraft, a lot of time revolved around the manipulation of balsa wood. Balsa wood is used heavily throughout the plane and is very forgiving. However, working with the material is very difficult because of its unique material properties. Strength, ductility, and shearing are some of the weaknesses in using balsa in our design. These three factors coupled with the

exhausting nature of working with the various glues and fixing materials impeded work. In general, the area to improve would be the ability to become more familiar with the material and try to work with it more effectively in manufacturing. The material itself is the correct one for our design. It was the experience of the team to work with it that became frustrating. In the future, more emphasis needs to be put on working with balsa to improve craftsmanship.

8.0 INTRODUCTION

The aircraft cost model is used to determine the overall cost of the airplane. The model uses the different components of the aircraft to estimate a manufacturing cost. The wing, fuselage, tail, and control surfaces are some of the components that are used to determine the total aircraft cost. Table 8.1 below shows the total aircraft cost of our current design.

8.1 COST IN DESIGN PROCESS

Throughout the design process we examined the cost it would take to introduce several different components of the aircraft. For instance, the additional motor on the aircraft increases the overall cost tremendously. By making the aircraft a dual engine, the cost increased from around \$6,400 to \$8,400. However, the advantages to building a dual powered aircraft exceeded the design consideration of cost.

Another design consideration we looked at that dealt with cost was the area of the wing. The wing area plays a crucial role in designing an aircraft. As discussed in the Design Report, the aspect ratio of an aircraft's wing platform is very important to creating an efficient wing. However, this also increased our cost. By having a large platform area we increased the efficiency of the aircraft but also increased the cost. In determining our overall design we decided to run a higher efficiency aircraft instead of a cost efficient aircraft.

8.2 FINAL COST

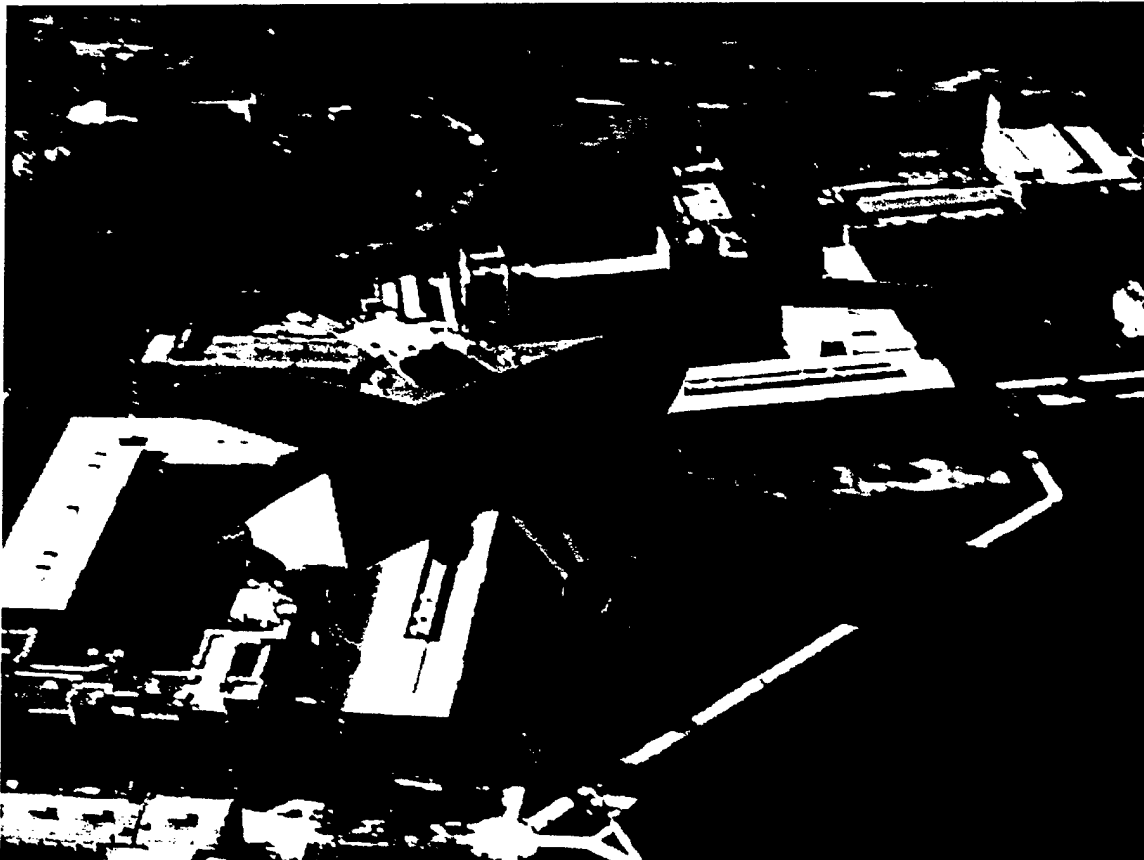
The aircraft's final cost was determined to be \$8,679. This cost is what is to be expected from the design of a dual motor R/C powered aircraft.

TABLE 8.1: Aircraft Cost Model

Constants			Key	
A =	100	Dollars per lb		Constants
B =	1	Dollars per watt		Inputs
C =	20	Dollars per hour		Intermediate Outputs
Manufacturers Empty Weight				Final Output
MEW	18	Pounds		
Rated Engine Power				
# Engines	2	Engines		
Amps	40	Amps		
Volts	1.2	Volts per cell		
# of cells	37	Cells		
REP				
Manufacturing Man Hours				
# Wings	1	Wings		
# Contol Surface	2	Control Surfaces		
Chord Length	1.21	Feet		
Span	10	Feet		
Proj. Area	4	Hour per sq.ft		
Hour per Wing	15	Hour per wing		
Hour per C.S.	3	Hr per control surface		
Wing WBS	69.3			
Fuselage	5	Hour per body		
# Body	1	Fuselage		
Length	6	Feet		
Hour per ft.	4	Hour per ft of length		
Fuselage WBS	29			
Empenage	5	Hours		
# Verticle Surface	1	Vertical Surface		
Hr per Vert Surf	5	Hour per Vert Surf		
# Horz Surf	1	Horizontal Surface		
Hr per Horz Surf	10	Hour per Horz Surf		
Empenage WBS	20			
Flight Systems	5	Hours		
# Servos	4	Servos or Controller		
Hr per Serv/Contr	2	Hour per Serv/Contr		
Flight Systems WBS	13			
Propulsion Systems	5	Hours per engine		
# Engines	2	Engines		
# Propellors	2	Props		
Hr per Prop	5	Hour per Prop		
Prop Systems WBS	20			
Total MFHR				
Rated Aircraft Cost			\$ (Thousands)	

**UNITED STATES MILITARY ACADEMY
WEST POINT, NY**

2001 DESIGN / BUILD / FLY COMPETITION



“Have A Nice Day”

Table of Contents

	<u>Page #</u>
1. Executive Summary	3
2. Management Summary	7
2.1 Design Team Assignment	7
2.2 Design Plan	7
3. Conceptual Design	10
3.0 Introduction	10
3.1 Design Goals and Philosophy	10
3.2 Design Parameters	11
3.3 Figures of Merit	15
3.4 Design Parameter Results	17
3.6 Conceptual Design Results	17
4. Preliminary Design	20
4.0 Introduction	20
4.1 Wing & Tail	20
4.2 Power Plant	21
4.3 Fuselage	23
4.4 Landing Gear	26
4.5 Preliminary Design Configuration	27
5. Detailed Design	30
5.0 Introduction	30
5.1 Component Selection & Architecture	30
5.2 Design Performance Data	37
5.3 Design Assessment	38
5.4 Detailed Drawing Package	39
6. Manufacturing Plan	43
6.0 Introduction	43
6.1 Wing & Tail	43
6.2 Power Plant	44
6.3 Fuselage	45
6.4 Landing Gear	46
7. References	48

1. Executive Summary

TTF Technologies, a team consisting of ten United States Military Academy cadets, entered the AIAA Cessna/ONR Student Design / Build / Fly Competition to compete and win with an originally designed remote control aircraft. The competition will be held on April 21-22, 2001, at Pax River, Maryland.

The task is to design, fabricate, and demonstrate the flight capabilities of an unmanned, electric powered, radio controlled aircraft that can best meet the specified mission profile. The goal of the contest is to create a balanced design that possesses good flight handling qualities while maintaining practical and affordable manufacturing requirements.

This year's mission profile includes two different tasks. The aircraft will fly as many sorties as possible within the given flight period. A single sortie is comprised of a take off and landing with a cargo load of steel followed by a take off and landing with a cargo load of tennis balls. The best three sorties will be summed to comprise the total flight score. The second portion of the contest involves the written report, which will be scored by the AIAA officials. The total team score for the competition equals the product of the written report score and total score, which is then divided by the rated aircraft cost.

The rules and constraints for the contest were used to formulate our team's figures of merit, customer requirements, engineering requirements, and engineering targets. The major constraints were payload configuration, take off length, wingspan, and motor type. The payload may not be carried internal to the wing, the take off length is extended from 100 feet to 200 feet, the wingspan has been expanded to 10 feet, and the motor must be from specified manufacturers.

The conceptual design began with the team considering all possible configurations for aircraft based on brainstorming techniques such as a how / why diagram, mind map, and functional decomposition. The team was then divided into four sub-design teams: team wing, team motor / prop, team fuselage, and team landing gear. Each group was tasked with researching their portion of the aircraft in depth and producing a conceptual design that coincided with the mission requirements and our figures of merit. At this point in the design process all component options and configurations were considered desirable and realistic. This fostered a more creative engineering process.

The first task for each sub-team was to develop their design parameters for the main aircraft components. These main aircraft components included the wing, tail, fuselage, power plant, propeller, and the landing gear. This phase allowed all sub-teams to better organize and research their component designs. Next, the team established figures of merit to better focus our design and manufacturing processes. Through a quality functional deployment we were able to link our figures of merit to weighted customer requirements. These customer requirements were cross-examined with our engineering requirements allowing our team to develop quantifiable engineering targets. Therefore, our figures of merit were directly linked to specific measurable quantities that could be used to check progress and aide in the design of the aircraft. The figures of merit included: modular design, low cost, manufacturability, thrust to weight ratio, strength to weight ratio, and handling characteristics. The results of our conceptual

design began the development of the Have A Nice Day (H.A.N.D.) aircraft. The specific conceptual configuration results are listed below.

Airplane Details for Conceptual Design	
Payload Capacity:	80 tennis balls 10 pounds steel
Wing Configuration:	2 piece Mid-Wing Mono Wing
Wing Material / Structure:	Carbon Fiber / Foam
Wing Planform Area:	12.5 square feet
Tail Configuration:	Conventional
Fuselage Configuration:	Single Body Fuselage
Speed Loader:	One Removable Cargo Box
# of Motors:	1
Propeller:	22 in – 28 in Tractor Mount
Landing Gear Configuration:	Tricycle

The preliminary design stage involved each sub-team refining design concepts by identifying governing parameters, choosing one design concept, and conducting preliminary calculations that will determine the form and function of each aircraft component. The configuration results for the preliminary phase are shown below.

Airplane Details for Preliminary Design	
Payload Capacity:	100 tennis balls 30 pounds steel
Wing Configuration:	2 piece Mid-Wing Mono Wing
Wing Material / Structure:	Carbon Fiber / Foam
Wing Shape	Rectangular
Aspect Ratio	7.14
Wing Planform Area:	14 square feet
Chord Length	1.4 feet
Dihedral	0 degrees
Airfoil Selection	Eppler 387
Tail Configuration:	Conventional
Fuselage Configuration:	Single Body Fuselage
Main Structural Bar:	Aluminum 3/4 inch hollow
Fuselage Length	44.5 inches
Tail Boom Length	23 inches
Wing Mount:	"U" Design
Speed Loader:	One Removable Cargo Box
Tennis Ball Configuration:	3 X 3 X 11
# of Motors:	1
Motor Type:	Astro 90
Gear box:	Astro Super Box 714
Battery Type:	SR Battery
# of Cells:	37
Propeller:	22 in – 28 in Tractor Mount
Landing Gear Configuration:	Tricycle
Landing Gear Clearance:	11 inches
Spring Shock System:	Front Landing Gear Spring

After determining the optimum design based on figures of merit and overall aircraft cost we established a more detailed design. Each component was now set for manufacturing and the design aspects were fine tuned by ensuring complete compatibility of the aircraft. The configuration results for the detail phase are shown below.

Airplane Parameters for Detail Design	
Payload Capacity:	100 tennis balls & 30 lb steel
Aspect Ratio	7.14
Wing Planform Area:	14 square feet
Chord Length	17 in
Airfoil Selection	Eppler 387
Main Structural Bar:	Aluminum $\frac{3}{4}$ inch hollow
Fuselage Length	44.5 inches
Aircraft Center of Gravity	26 in
Tail Boom Length	23 inches
Motor Type:	Astro 90
Gear box:	Astro Super Box 714
Battery Type:	SR Battery
# of Cells:	37
Total Projected Laps	29
Propeller:	26 in – 28 in Tractor Mount
Projected Thrust	13 lbf
Landing Gear Configuration:	Tricycle
Landing Gear Clearance:	11 inches
Spring Shock System:	Front Landing Gear Spring
Horizontal Tail Surface Area	545 in ²
Horizontal Tail Span	34.7 in
Horizontal Tail Chord	9.9 in
Vertical Tail Surface Area	201 in ²
Vertical Tail Span	20 in
Vertical Tail Chord	10 in
Take-off Distance	147 ft
Stall Velocity	20 mph
Coefficient of Profile Drag, $C_{D,0}$	0.024
Coefficient of Induced Drag, K	0.072
Optimal Velocity	41 mph

2.1 Design Team Assignment

TTF Technologies consists of six senior and four junior aerospace engineering majors from the Department of Civil and Mechanical Engineering at the United States Military Academy. Our mission is to design and build the winning aircraft for the 2001 AIAA Design/Build/Fly competition. The design and manufacture of the H.A.N.D. (Have A Nice Day) aircraft also serves as the final capstone design requirement for our undergraduate engineering education.

The TTF team is divided into four sub-design teams: team wing, team landing gear, team motor/prop, and team fuselage. Each sub-team worked collectively in the first phases of the design to ensure the compatibility of all aircraft components. Following the conceptual design the sub-teams worked independently to build the aircraft to the standard set by the predetermined figures of merit. The tail section of the aircraft became a collective effort due to an unexpected slow down in the building process. The wing team was designated responsibility for the research and development of the tail. Specialization assignments allowed each member to focus their work and ultimately become the subject matter expert on their specific aircraft component. As the aircraft progressed and started to take shape, the sub-design teams broke off to help with other components of the airplane that had not yet been completed. Figure 2.1 depicts the team member assignments used to focus the research, design, and manufacture of the aircraft.

2.2 Design Plan

The TTF design team initially met every other day to discuss goals, rules, and performance parameters. The conceptual design process was completed during these meetings, and our figures of merit were established. Through these initial steps we developed a how-why diagram, mind map, functional decomposition for each sub-design team, Gantt chart, quality functional deployment, engineering targets, and a morphological analysis for each sub-component. It was very important that our entire team be present during the preliminary design phase so that everyone could be focused on the same figures of merit. Figure 2.2 shows a modified Gantt chart, which expresses our team's timeline and suspense dates.

Our faculty advisor was present during these meetings to focus our thoughts and ideas towards our established engineering targets and figures of merit. He also organized guest speakers familiar with R/C aircraft to hold question and answer sessions during the conceptual phase. The TTF team also visited an R/C airfield where we talked to a few seasoned pilots about building a "user-friendly" aircraft.

During the preliminary design process the TTF sub-design teams focused all efforts on their particular part of the aircraft. Component interfacing problems were addressed, supplies were purchased, and prototype testing was done during this time. To ensure forward progress, the team met once every two weeks. This was a chance for everyone to ask questions, provide insight on any aircraft component, and address interface problems that one sub-component may have with another.

The detailed design stage involved all of the sub-design teams working together in the workshop to build the complete prototype aircraft. During this stage we kept close track of all past and proposed expenditures to ensure we stayed within our budget constraints. We also took pictures to keep a documented account of the building of our aircraft. The final phase will include flight testing to verify the airworthiness of the design, make any necessary design modifications and optimize our competition flight plan to achieve the highest possible score. The TTF Technologies team worked well to meet all of the figures of merit and produce an aircraft capable of winning the competition at the Pax River Airfield.

<i>Sub-Design Team Assignment</i>	<i>Team Members</i>
Wing	Scott Dunkle Bradley Townsend
Landing Gear	Will Fulton Jason Sienko
Motor & Prop	Bryan Lake John Njock David Meier
Fuselage	Eric Stoutenburg Joe Minor Kevin Kahre

Figure 2.1 Sub-Design Teams

This figure shows team member assignments used to focus individual research, design and manufacture of the aircraft.

1. <i>Phase 1 & 2</i> How-Why Analysis, Mind Map, Functional Decomposition, Gantt Chart	August 1 st – August 31 st
2. <i>Phase 3</i> QFD, Engineering Requirements & Targets	September 1 st – September 9 th
3. <i>Phase 4</i> Morphological Charts, Concept Design, Preliminary Drawings	September 10 th – October 20 th
4. <i>Engine and Battery Selection</i>	Completed by September 31 st
5. <i>Manufacturing Drawings & Design Refinement</i>	Completed by November 1 st
6. <i>Building Aircraft</i>	November 1 st – March 16 th
7. <i>Proposal Phase Report Due</i>	March 13 th
8. <i>Flight Testing</i>	March 26 th – April 13 th
9. <i>Addendum Phase Report Due</i>	April 10 th
10. <i>Competition</i>	April 20 th – April 22 nd

Figure 2.2 Detailed Timeline

This figure shows a modified Gantt Chart with suspense dates for each phase of the aircraft design.

3.0 Introduction

In the conceptual design phase, we developed the initial aircraft configuration to match the mission-oriented tasks. To do this we investigated the payload requirements and flight pattern for the aircraft to identify our engineering requirements. Given our engineering requirements we then meshed them with some of our constraints and engineering restrictions to produce figures of merit. With these figures of merit in mind the team embarked on the creative process of producing concepts for the general aircraft configuration. This initial process of developing alternative concepts is discussed in Section 3.2 Design Parameters. In order to determine an overall general aircraft concept, the team ranked and quantified the necessary design parameters based on a figure of merit system. The figure of merit system is discussed in Section 3.3 Figures of Merit. Figure 3.1, a quality functional deployment, shows the parameters our team decided to base the overall aircraft design with respect to the predetermined figures of merit.

At this point each major aircraft component was subdivided for further concept development, refinement, and evaluation. Some tools used during this phase include a functional decomposition and morphological chart to generate concepts for each component. The end product of this phase was a thorough understanding of the aircraft's performance requirements, our engineering requirements and constraints, and an initial aircraft configuration. These tools are discussed in Section 3.4 Design Parameter Results.

Each sub-team's iteration of component design was based on the lowest possible rated aircraft cost. Our functional decomposition and morphological charts helped to optimize the rated aircraft cost. These tools allowed for an iterative process of ideas to occur for each aircraft component. Upon completion of these charts the TTF design team was able to compare each concept to the aircraft cost model. The concept with a combination of the lowest rated cost and the highest figure of merit ranking became the optimized solution for each sub-team. These component optimizations are found in Section 3.5 Optimization Results.

3.1 Design Goals and Philosophy

Our ultimate goal is to win the competition with a competitive aircraft performance and written report. This immediately led us to set high engineering and performance targets. We also established that given our limited experience with RC aircraft we would make our design simple and modular. A simple design would allow us to produce a quality aircraft given our limited manufacturing skills and apply our aeronautical engineering knowledge that was grounded in simple conventional aircraft. A modular design would give us the opportunity to produce the aircraft and then continually modify components without having to reengineer the entire design. We believed that some of our best design innovations would come while we were constructing the aircraft and through iterations of the components design.

3.2 Design Parameters

The first portion of the conceptual design process involved determining the best properties on which to base our aircraft design. Each of these parameters were considered and evaluated with respect to our quality functional deployment. This tool helped us to better optimize our configurations around the predetermined figures of merit for our aircraft. These figures of merit were based on our research of previous years' competitions, production model R/C aircraft, modern cargo aircraft, information from the World Wide Web, and R/C aircraft books.

3.2.1 Wing Configuration

The design team immediately decided that we would design and build a rectangular wing, because of the simplicity of manufacturing. Most of the team members have had experience making smaller wings out of foam and the problems incurred by tapering the wing or attempting to make an elliptical wing outweighed the aerodynamic benefits. The ease of using an airfoil of constant chord for the entire planform area gives the team more manufacturing options and the ability to produce wings at a faster pace.

Three different configurations were initially considered for the wing. In past contests the bi-wing had a lot of success. However, the take off distance was increased to 200 feet this year, and the airplane's rated cost increases with additional wings. The second consideration was a high mono-wing configuration. A high wing yields the most roll stability to an aircraft and is prevalent in many privately owned aircraft such as the Cessna 152, 172 and 182. The third consideration was a mid mono-wing configuration. This wing would still lend a good deal of stability and would also be able to attach to the main structure of the fuselage without adding extra exterior bracing. The high mono-wing would likely have to be braced from the fuselage to the underside of the wing because of the ten foot wing span allowed for this years competition. Therefore, we decided on the mid-fuselage mono-wing configuration, because it is easier to fasten directly to the main interior supports of the fuselage and allows our team to plan on creating one big speed loader instead of two separate speed loaders for the front and back of the aircraft.

3.2.2 Wing Structure and Materials

We found many different methods and materials to build the wing structure. The ease of using a constant chord allowed our group to research the advantages and disadvantages of many different materials. The structure concepts include: balsa wood, carbon fiber/foam, Spyder Foam, foam with leading and trailing edges of balsa, fiberglass wrapped around a foam core, and foam covered with balsa sheeting. The traditional balsa wood wing is very light and can be made sturdy, but the manufacturing is tedious especially in the case of a 10 foot wing span. The team decided on using foam or foam core wing because of the ease of construction and the experience we already had with cutting smaller glider wings for previous design competitions. The carbon fiber / foam wing concept and foam / balsa sheeting wing concept were both carried over to the preliminary design phase. The foam is easy to mold using airfoil

templates and it will also give us a chance to produce a variety of different wing sections to test under certain loading conditions.

3.2.3 Spar Structure and Materials

The spar structure and material for a foam wing had to be carefully considered. We needed a lightweight and rigid material that could be inserted into the wing easily. Aluminum rods, wooden dowels, carbon tape, and carbon rods were all considered as possible spar structures. Unlike a traditional balsa wing, our spar would be a long cylinder instead of an I-beam structure. It would have to be able to bear the weight of the plane in the 2G test to enter the competition. This strength must be coupled with a material that is lightweight; therefore the wooden dowels and aluminum rods were eliminated from the possibilities.

The carbon tape and carbon fiber rods were both light weight and lent a high degree of strength to the wing. These two materials were carried into the preliminary design portion to either be used separately or in combination with each other. Our budget allowed for the team to order many different types of carbon fiber rods. These rods are made of either unidirectional or multi-directional fibers.

Carbon fiber rods are difficult to find in ten-foot sections. Therefore, our team initially planned on building a two-piece wing. If the two wing sections encountered interfacing problems then the two pieces could be connected using a carbon fiber sleeve to create a one piece wing. For a two-piece wing we could insert the pieces into a hollow cantilever beam, insert the extended spars into a slot and lock in place with a latch. Another option is to insert the wing into the spar, which would already be permanently attached to the fuselage. All of these methods for fixing the wing to the remainder of the aircraft were based on the ultimate goal of compatibility and modularity.

3.2.4 Tail

The tail of the aircraft would possess a conventional commercial aircraft, T-tail, or cruciform design. The conventional commercial aircraft configuration centers the horizontal and vertical portions on the tail end of the fuselage. This type of configuration has low structural weight compared to the other configurations while providing reasonable stability and control. For a T-tail, the structure is heavier, and the vertical tail must be strengthened to support the aerodynamic load and weight of the horizontal tail. However, this configuration does not blanket the rudder so interference is nonexistent in a commercial aircraft, but we would encounter problems running an efficient push rod system up to the elevator on the horizontal tail. The cruciform tail is basically a compromise between the conventional and T-tail configurations.

We choose the conventional tail design primarily for its more lightweight structure. The horizontal tail, vertical tail, and control surfaces are based on the wing planform area and the overall aircraft dimensions.

3.2.5 Fuselage

Since we wanted a simple and modular design, we decided early on that central to our aircraft configuration would be a simple bar to act as the main structural component. The bar, acting as a backbone would then support and connect all the other individual components. This is a design feature used in fighter aircraft, the new Commanche helicopter, and some RC aircraft.

The fuselage must contain the cargo in a stable position throughout the flight envelope. We decided to go with a single body fuselage. Six factors entered our decision to choose this concept. First was the securing of two payloads of different characteristics. One is volume payload that places a dimensional constraint and the other is a weight payload that places a structural constraint on the fuselage. Second, the rated cost considerations of various fuselage configurations lead us to select a single body. In the rated cost model, each fuselage or pod costs 5.0 manufacturing man-hours plus 4.0 hours per foot of length. The optimal configuration then is a single short body fuselage. This optimal cost configuration conflicts with our third fuselage consideration – low aerodynamic drag. A short fuselage would demand a large cross sectional area profile hitting the free stream air, which is undesirable. The fourth factor was a lightweight but durable structure. The fifth factor stemmed from the competition's execution of the mission tasks. Interchanging the cargo on successive missions within a 10 minute flight time meant that the ground crew would have to quickly switch the cargo loads. A speedloader was deemed the only feasible solution because any dumping of 100 tennis balls onto the runway just didn't sound like a good idea. Our concept also satisfied an additional requirement of being easy to manufacture. We selected a single body fuselage with a removable cargo box. This design maximized the factors listed above and met our engineering targets of carrying 100 tennis balls (approx. 13 lbs) and a minimum of 20 lbs of steel with a capacity up to 30 lbs.

For the speedloader, we had the options of either making the entire fuselage a removable structure or to have cargo contained within a box and placed internal to the fuselage body. The location of the wing at mid level meant that an entirely removable fuselage body was not feasible. We concluded that an access door or panel on top of the fuselage was the best option for putting the cargo in and out while the aircraft was on the ground. Whether the access panel would be a hinged door on the fuselage or a separate panel, we left for the preliminary design phase after some testing. By making the fuselage body thin skinned and light, we could cut down on the weight. For the cargo box, we designed it so it was light where it held only tennis balls and stronger only where the steel would sit. In order to simplify the design and construction of the fuselage we divided it into six sub-components: main bar, nose cone, tail cone, wing mount, fuselage body, and speed loader.

3.2.6 Power Plant & Propeller

Our first concern was to determine the number of motors we would use on our aircraft. We limited ourselves in this area to the choice of a single or dual motor configuration. We believed that the single motor configuration was better than the dual motor configuration for a few different reasons. First, in terms of the work breakdown structure, a single motor configuration would weigh in less on the

manufacturing man hours. This would help us keep the rated cost of our aircraft down. Second, in terms of simplicity we realized that designing, mounting, wiring, and controlling multiple motors simply might be beyond our capability. We did not have a great deal of model airplane building experience under our belts and felt that keeping our design simple would pay off for us when we were ready to build. Finally, we considered reliability as a factor. Although dual motors may seem more reliable because one motor may serve to power the aircraft in the case of the other going out, we focused more on the reliability of manufacturing a good dual motor aircraft. With this came knowledge of wiring multiple motors, placing them in order to provide thrust as desired with minimal control inputs, and the actual cost of the motors themselves. We did not have a lot of electrical wiring experience, we were skeptical as to how to time multiple motors to provide equal thrust and we believed that mounting the motors in the precise place in order to provide completely axial thrust would prove to be quite difficult. Therefore, we came to the conclusion that our design would be a single motor concept.

Once the number of motors was determined, we had to decide how exactly we would mount our single motor. We evaluated three separate concepts based on the following things: simplicity, manufacturability, propeller clearance potential, and modularity. Our actual concepts for mounting the motor were a motor "pod," a tractor configuration, and a pusher configuration. The motor "pod" was a wilder idea we had at first. We thought of it primarily for one reason: to prevent the propeller from striking the ground. This happened to the AIAA team last year and created setbacks for them. We wanted to avoid any potential reoccurrence of a prop strike. The major setbacks for the pod idea were that it would be difficult to manufacture and it was not a very simple design. The pusher prop had some potential, but eventually fell through because we believed it would be harder to mount and design the rest of the plane around it. Additionally, pusher props are much more difficult to find than tractor props. Finally, we found that a conventional tractor configuration would suit our needs.

Prop ranges for our single engine plane were expected to be between 22 and 28 inches. Further motor tests would yield the best results. We will test the amount of thrust produced by each motor / prop configuration with a wide variety of props of different lengths and pitches. Generally, the larger the propeller diameter, the larger the mass flow of air processed by the propeller. For the same thrust the larger propeller requires a smaller flow velocity increase across the propeller disk. This increases the propulsive efficiency. However the weight of the propeller usually increases with diameter and therefore drains more energy from the battery to turn the shaft of the motor.

3.2.7 Landing Gear

The landing gear must support the weight of the entire aircraft during taxiing, takeoffs, and landings. Our team decided on a tricycle landing gear configuration because it provides the most stability to our aircraft during landings by preventing the nose over effects, which are common for a tail dragger system. The landing is our team's primary focus of the sortie because of the terminating effect it had on last year's aircraft during the competition. Five factors entered our decision to choose our final concept. The first factor was maintaining a safe propeller clearance upon impact of numerous landings. This driving factor

in the design linked the necessary dimensions with the durability of the front and rear landing gear. We still needed to maintain an initial nose down attitude upon takeoff and ensure proper propeller clearance upon landing. Second, the ability of the landing gear to bear the gross weight of the plane with a full payload allowed the team to consider the amount of deflection desired in the shock absorption system, spacing between the front and rear landing gear, and the height ratio between the front and rear landing gear. Balance of the aircraft, the third factor, ties into the first and second engineering criteria. The balance of the aircraft with a full payload is crucial to the completion of as many sorties as possible. The height of the landing gear will directly determine the spacing between the wheels of the rear landing gear. The fourth factor was a system that allowed for a majority of the shock absorption to occur in the landing gear components. This factor led to the difficult task of designing a durable but lightweight system upon which most energy displacement would occur between the aircraft and the airstrip. The fifth factor imposed another engineering challenge of designing a simple and modular system. Upon failure of any part of the landing gear a quick and immediate change could be made while minimizing the impact upon the remainder of the aircraft. Our team decided to design a unique set of aluminum landing gear components in a tricycle configuration. Commercial and traditional landing gear components for remote control aircraft were researched and benchmarked to design a new system that would meet all of our engineering criteria.

3.3 Figures of Merit

Figures of merit were selected during the conceptual design stage in order to develop useful design parameters that would act as the driving mechanism towards our preliminary and detailed aircraft designs. Our figures of merit include: 1) Modular Design, 2) Thrust to Weight ratio, 3) Strength to Weight ratio, 4) Low Cost, 5) Manufacturability, and 6) Aircraft Handling. Each one of these figures of merit was broken down into weighted customer requirements for the development of the aircraft. Figure 3.1 shows the figures of merit on the left hand side of our quality functional deployment chart. This chart was used to link our figures of merit to engineering requirements and produce quantifiable engineering targets. These results are discussed in Section 3.4 Design Parameter Results.

3.3.1 Modular Design

The components of our aircraft should be able to be fixed or modified without affecting the performance of any other components. In order for this to occur we based our design around a modular framework. Every main piece of the aircraft would be able to be replaced without the need for major reconstruction. Designing a modular vehicle involves a much more critical and in-depth engineering process. Our goal was to possess an aircraft that could have at least one spare part for each component, and those spare parts could actually be used to put together another aircraft. The modularity of the aircraft is based on a piece-meal design, focused on maintainability and reliability, and will foster a quick loading plan for each sortie. These customer requirements were each weighted under the modular design figure of merit in the quality functional development.

3.3.2 Low Cost

The rated cost of our aircraft served an important role in the optimization process of our initial concepts. The team also managed a budget set by the Department of Civil and Mechanical Engineering. We had to track expenditures and predict future requirements for both the airplane and the trip to ensure we remained within our total budget allocation.

3.3.3 Manufacturability

In order to create a sound product we needed to have the ability to manufacture our designs. Taking an idea from paper to actual form is only viable if the team possesses the ability or experience to either build it on their own or have higher skilled machinists build their component based off of detailed drawings. TTF Technologies had access to the department tools and wood shop while also employing the skills of the West Point machinists on campus for more intricate parts of the aircraft.

3.3.4 Thrust to Weight Ratio

The thrust to weight ratio is one of the fundamental parameters that dictate airplane performance. It determines in part the takeoff distance, rate of climb, and maximum velocity. The team needs to create the most thrust to push our aircraft through the air while minimizing the aircraft's weight. The weighted requirements with respect to this figure of merit include: 55 pound aircraft weight limit, takeoff distance of less than 200 feet, low weight, electric motor, and wing span of equal to or less than 10 feet.

3.3.5 Strength to Weight Ratio

Structural integrity is very important aspect of our aircraft, however we do not want to sacrifice extra weight for the unnecessary over strengthening of individual components. We need to have enough structural integrity to withstand 2 Gs while using materials that are not very dense. The weighted requirements with respect to this figure of merit are ball and steel payload capacities, over-all low weight, and the fixed wing design.

3.3.6 Handling Characteristics

The H.A.N.D. must be able to function well on the airstrip and in the air. If the plane is unstable on the ground then landing the aircraft will be a very arduous task. The weighted requirements with respect to this figure of merit are flight agility, standard pilot controls, and functional fail-safe switches.

3.4 Design Parameter Results

The results for our design parameters are displayed in Figure 3.1, which shows the quality functional deployment with respect to the engineering requirements and figures of merit. This chart allowed us to focus on a quantifiable goal or engineering target throughout the design and manufacturing phase of our aircraft. Our figures of merit were linked to customer requirements and these requirements were then weighted in accordance to their importance from 1.0 to 16.0. The engineering requirements were then compared with each of these figures of merit to determine any type of relationship. If the relationship was highly involved then a dotted circle was put in the corresponding box. If it was involved then just a circle was given, and if it was only slightly involved a triangle was given. The program then took all of these

inputs and created a weighted and relative importance for each engineering requirement. From these results the team set the engineering targets in the bottom row of the quality functional deployment. These quantifiable results are directly linked to our figures of merit.

3.5 Conceptual Design Results

Upon completion of the quality functional deployment the alternative concepts were grouped to form the conceptual H.A.N.D. Aircraft. This was our first complete aircraft configuration section. Figure 3.2 lists all of the initial aircraft details for the conceptual design phase. This configuration was carried into the preliminary phase for further optimization.

Airplane Details for Conceptual Design

Payload Capacity:	80 tennis balls 10 pounds steel
Wing Configuration:	2 piece Mid-Wing Mono Wing
Wing Material / Structure:	Carbon Fiber / Foam
Wing Planform Area:	12.5 square feet
Tail Configuration:	Conventional
Fuselage Configuration:	Single Body Fuselage
Speed Loader:	One Removable Cargo Box
# of Motors:	1
Propeller:	22 in – 28 in Tractor Mount
Landing Gear Configuration:	Tricycle

Figure 3.2 Conceptual Design Airplane Details

This figure shows the main airplane details determined from the conceptual design portion of our engineering process.

4.0 Introduction

In the Preliminary Design phase, we continue to refine the concepts we developed in the Conceptual Phase. The first task is to identify what parameters will govern each component's design and why they are important. Second, we will use our figures of merit to evaluate engineering tradeoffs. Third, we conduct our analysis of all the components and assess the accuracy of our analysis. Fourth, we configure the components, their interfaces, and dimensions. Finally, we develop the final features of the design. The outcome of this phase is to produce a design of the aircraft that meets the engineering targets with analysis proof.

4.1 Wing

This section discusses the parameters for the wing. The first parameter that constrains our design is the wingspan; the rules state that the wing must not exceed ten feet. We must determine the wing shape, wing loading, chord length, dihedral, and airfoil selection.

4.1.1 Wing Shape

First, we determined that we would use a rectangular wing. We know that an elliptical and a tapered wing are more efficient because they have a more uniform downwash. However, our foam cutting machines allowed us to get a more exact airfoil shape by using a rectangular wing. We weighed the importance of good airfoil and an elliptical/tapered wing and determined that the airfoil shape was more important. The figure of merit of manufacturability is the dominant consideration here and a rectangular wing is the easiest to make.

4.1.2 Surface Area, Wing Loading, and Chord Length

We know that we want an aspect ratio (AR) of around 7.14. This is a common aspect ratio for cargo aircraft. The higher the aspect ratio the less induced drag the aircraft will have. This will increase the lift to drag ratio and allow us to lift more weight with our power plant. The design parameters support our figures of merit by reducing the induced drag as stated above. We can calculate all the parameters with the following formulas.

$$AR = 7.14 = \frac{b^2}{S}$$

$$S = 14 \text{ ft}^2$$

$$W / S = 35 \text{ lbs} / 14 \text{ ft}^2 = 2.5 \text{ lb} / \text{ft}^2$$

$$c = 1.4 \text{ ft}$$

4.1.3 Dihedral

From research, we found that 3-5 degrees is common for typical remote control airplanes. Dihedral insures lateral stability, which is a figure of merit for aircraft handling characteristics. The higher the wing sits in regard to the fuselage the less the dihedral you need because of the pendulum effect of the cargo weight. However, a dihedral conflicts with our figure of merit of manufacturability. To resolve these conflicting figures of merit, we made the judgment that putting in a dihedral vastly complicated the structural design of the aircraft, more so than the complications of no dihedral for aircraft flight stability. Our mid-wing design also facilitated our decision to go with a no dihedral wing. Additionally, the flex pattern of the wings will produce a natural dihedral that will assist lateral stability.

4.1.4 Airfoil Selection

We selected an airfoil based off data provided by UIUC Applied Aerodynamics (<http://www.uiuc.edu>). The data allows you to input the central parameter, the Reynolds number, to airfoil selection. Each airfoil operates at an optimum Reynolds number. The two airfoils that had excellent lift to drag ratios for a Reynolds number of about 100,000 were the Eppler 387 and the SD 7030 airfoils. What discriminated between the two was the Eppler 387 had better characteristics in very turbulent air. This is important for RC aircraft, which are adversely effected by even medium gusts of wind. Aircraft handling is an important figure of merit therefore using the Eppler 387 will help increase aircraft performance. Figure 4.1 shows the Eppler 387's performance with two different air conditions. Figure 4.2 shows the airfoil shape. Identifying airfoils given a Reynolds number with high lift to drag ratios and/or the highest coefficient of lift is a common approach to airfoil selection. It is of course only accurate for the flight condition for which it was selected. We chose the Reynolds number that would characterize the aircraft's primary flight condition. This condition changes drastically during take-off and landing sequences. Our airfoil selection is therefore an approximation that will put us within an acceptable performance range across all flight conditions even though the airfoil could perform less than optimal during some flight conditions.

4.2 Power Plant

In the conceptual design phase, we determined a single motor with a tractor configuration would be used for our airplane. The next step in dealing with the motor was to find a motor that would be suitable for our aircraft. It was determined that our airplane would be quite large with a wingspan of 10 feet and a fairly heavy gross weight of nearly 30 pounds.

4.2.1 Motor Selection

With those parameters, we set out to choose a motor to propel our airplane. We were limited in this first by a competition rule that our motor had to be a brushed motor from Astroflight or Graupner. We had another important factor play into our decision: we already had two Astro 90 cobalt motors left from last year's competition. Using these again would reduce the cost of our aircraft, which is an important figure of merit. After searching the Internet and hobby shops that knew anything about electric motors we came to the conclusion that an Astro 90 was the largest motor we had most readily available to us. We

also chose to use the commercially available Astro Superbox 714 with a gear ratio of 2.75 to 1. A gearbox will allow us to use a larger prop, which will result in more thrust. This will enable us to draw less on the battery while at the same time providing enough thrust to propel the airplane on take off and in a steady, level flight configuration. We decided on the Superbox 714 because it was readily available and recommended by the manufacturer. For the motor selection, the two most important figures of merit are the thrust to weight ratio and the manufacturability of the design. As outlined above, we selected what we identified as the largest commercial electric motor that would give us a significant amount of thrust. Our decision to stick with the Astro 90s of last year and to use the Astro gearbox simplified the design and reduced costs. The motor / prop team was then able to work with the Astroflight Company to put together a simple motor design.

4.2.2 Battery Selection

Another concern for the motor team was also to find a battery to serve as a power source for the motor. Again, due to lessons learned and equipment available to us, we used the same battery cell as last year's team. SR Batteries was able to build us a new battery pack, which had 37 cells and still stayed within the five pound limit. The additional cell over last year's pack will provide us with 1.2 more volts, which directly relates to the amount of power our motor can supply.

4.2.3 Propeller Selection

A third decision we had to make was what size and pitch propeller to use on our airplane. We used the Ecalc computer program to make a preliminary decision on the propeller. Using parameter estimates available at that time, we entered in values given to us by our teammates to try to simulate our conceptualized aircraft. We estimated a gross weight of twenty-five pounds and a planform area of 1440 in². Given the parameters chosen upon above, we found that a propeller with a 20.5 inch diameter and a pitch of 11.5 would allow us to fly for seven minutes. We felt this was reasonable at the time because we estimated a 30 second load/unload time between sorties. Competition flight limits the flying time to ten minutes. Based on this information we went in search of commercially available propellers. We found that propellers do not necessarily come with the specifications set forth above. The closest prop we could find was a 21 inch diameter by 12 inch pitch propeller by Metz. This initial estimate of the propeller diameter was important for finding our ground clearance. Additionally, we found that the AIAA team from last year chose to spin a 24 inch propeller. We realized that our airplane was a bit larger than theirs and it may be necessary to conduct motor tests with varying propellers on our own. The decision was made to order propellers ranging in size from 20 inches to 28 inches and test their thrust, power, and current draw characteristics to determine the optimum propeller. If our propeller is too small, it will not provide the thrust needed to rotate on take off. If our propeller is too large then there is the chance that it will cause the motor to draw too much current. This would be a bad situation because it could overload the speed controller and possibly damage the motor itself. We want to ensure that we have a high thrust to weight ratio, a dominant figure of merit. An analysis of this is discussed later in the detailed design section.

With respect to accuracy of the preliminary design stage for the motor team, we believe that we obtained good rough estimates to focus our final design. We know some limited information with respect to our motor, the Astro 90, because the manufacture supplied thrust and power characteristics data. We also believe our Ecalc simulations helped to decide upon a range of propellers to use, but certainly not a steadfast solution to our propeller question. To find a suitable motor combination we decided to run tests and use this information in conjunction with an analysis of electric flight to find a suitable motor/propeller combination. This analysis will be discussed in the detailed design portion below.

4.3 Fuselage

The primary figure of merit for the fuselage is low weight and cost. In the conceptual design, we selected a fuselage shape that would have a low rated cost, and in the preliminary design phase, low weight is the first consideration.

4.3.1 Main Bar Design

Preliminary design for the main bar involved determining it's dimensions, geometry, and material. The ideal geometry is a straight rod running from the engine mount in the front to the tail in the back. However, because of aerodynamics and a structural analysis the bent configuration diagrammed in figure 5.4.4 was the optimal solution. With the bar on the bottom of the fuselage, the weight of the cargo rested on top, the size of the landing gear could be reduced because the bar is lower to the ground, and it facilitated a top loading cargo area. In order to raise the tail and give it a cleaner airflow the tail boom portion is elevated above the main spar structure. The geometry of the bar was dictated by the required length for the fuselage body to contain the tennis balls, wing mount, and motor mount. This length was 45 inches – 8" for the wing mount, 6" for the motor mount, and 31" for the fuselage with tennis balls. The length of the tail boom was determined by the wing and tail design team as a requirement for the aerodynamic forces of the tail to produce a moment arm about the $\frac{1}{4}$ chord. This came out to be 23" for the straight part of the beam. The geometry of the bend was set at 45 degrees so we could make a tail cone that would provide a conical cargo space for servos and radio control receivers. The vertical height difference between the fuselage part of the bar and the tail boom part was designed so that the top of the fuselage body would be even with the tail boom. This height is 12 inches. We decided on aluminum for the material of the bar because it is lightweight, strong, and cheaper than alternatives like titanium or carbon fiber rods. The aluminum rod is square and hollow to decrease the weight while having flat surfaces to secure the components to. After testing different sizes, we determined that a $\frac{3}{4}$ inch square aluminum hollow rod had sufficient strength and stiffness for our design. Concerning our figure of merit, low weight, the main structural bar is perhaps heavier than alternative aircraft structures could be. However, an aluminum bar with lightening holes will have a high strength to weight ratio and will still offer us the modular design we desire.

4.3.2 Wing Mount Design

The design of the wing mount was a very challenging portion of our aircraft. With our single bar design the connection between the wings and the bar is critical since any kind of failure would be

catastrophic. Because of the variety of stresses that this connection would encounter during flight, we determined that an aluminum structure would ensure that there was no danger of failure because of the small bending moments felt by these beams. Aluminum was also a good choice because we wanted to keep the area around the mount relatively open in order to place our battery and steel payload near the $\frac{1}{4}$ chord of the wing (to minimize changes in CG location). Since our design has only one connection between the fuselage and the wing, we were concerned that the wing may bend without moving the fuselage. This would not only create stability and control problems, but would also place a great deal of stress on those connections. In an attempt to minimize this danger we decided on a "U" Design that would be as wide as the fuselage. This ensures that the aircraft banks with the wings as opposed to just the wing mount. Additionally, the "U" design provides two distanced contact points on the wing spars thus distributing the stress. Another advantage was the space between the wing connections in the "U" design provided a place to put the battery and steel payload that was under the $\frac{1}{4}$ chord. In order to reduce flexing we placed spacers connecting either side of "U" approximately 3 inches up either side to increase their rigidity. Although placing these spacers higher up the "U" may have been more effective, we did not want to interfere with the structure that would connect the wing to the "U." The wing mount is made of aluminum and braced with even lighter carbon fiber rods to lower the weight. This design provides sufficient strength to act as the torque box securing the wing and fuselage together and still satisfies our low weight figure of merit.

4.3.3 Fuselage Body

By the nature of our design the fuselage body must only cover the speedloader with an aerodynamic surface and have an access panel on the top. Since it serves no structural purpose, we selected a simple balsa wood frame and Ultracote covering to wrap up from the bar to the top of the speedloader cargo space. For the access panel on top, we decided that it would be a removable panel that connects to the bottom portion of the fuselage with pins. A hinged access panel, though convenient, would demand increased structural components, and hence weight, at the hinge points so we decided against it. Again a simple balsa wood frame and Ultracote covering was the best choice for the access panel as well. The fuselage body need only be big enough to house the speedloader and should be as thin as possible so that we reduce the frontal cross sectional area. The final dimensioning of it was done after the speedloader was manufactured. With no serious structural requirements, this design is as light as possible.

4.3.4 Speedloader Design

The speedloader (payload cargo box) has to hold the steel blocks and the tennis balls. The rules of the competition mandate that the speedloader must be the same in size and design for both payloads. Additionally, the containers must be reusable and the payload must be removable independently of the container. From our initial concept we wanted the tennis balls distributed on either side of the wing mount in the fuselage and the steel blocks secured above or below the wing mount. This would ensure a stable center of gravity location in either payload flight condition. It would have been ideal to place the steel

independently under the wing mount and have separate speedloaders for the tennis balls in front and behind the wing mount. The rules mentioned above were the primary constraints. We therefore decided to utilize the space above the wing mount to locate the steel blocks and secure the steel inside a "bridge" part of the speedloader. A 3 X 3 tennis ball configuration is a square 7 ¾ inches on a side. We put five 3 X 3 rows (45 tennis balls) on one side with a length of 13 inches and six 3 X 3 rows (54 tennis balls) on the other side with a length of 15 ½ inches. To meet our engineering target we wanted to carry up to 30 lb. For the portion of the speedloader that carries the steel, we were constrained by the wing mount over which the steel would sit. It was 7" X 8" so that meant a steel block of 7" X 8" X 2" would weigh 31 lb. The weight of the tennis balls (13 lb.) would rest on the main bar, but the weight of the steel would have to be transmitted down from above the wing mount to the bar. We decided to reduce this structural requirement we would incorporate the wing mount as part of the speedloader to secure the steel. After some testing we determined that a balsa wood skeleton structure was strong and light enough to be our speedloader. To remove the speed loader we needed a handle on top. We decided a carbon fiber rod running down the middle connecting the two ends and the steel container part would provide a good handle because it added to the strength of the speedloader, is lightweight, and allows us to pick up the loader from anywhere. The cargo box is light because it is constructed of balsa wood, one of our lightest engineering materials with sufficient strength.

4.3.5 Nose Cone Design

We wanted the nose cone to perform three functions: provide an aerodynamic shape, be lightweight, and act as a "hood" that we could remove and replace easily to gain access to the motor. This led us to a traditional balsa design covered by Ultracote. This is the lightest design. In order to gain access to the motor we decided on a design that could slide off the top even with the motor in place. A solid non-deflecting balsa tip on the front of the nose cone was necessary because of the prop wash experienced by the nose of the plane. We were also skeptical about placing Ultracote too close to the motor because it may melt. The solid balsa tip moved the first exposed Ultracote far enough away from the motor to alleviate all possibility of the motor melting the Ultracote under normal operating conditions. To make the cone removable we left the bottom of the cone open so that it could slide over the motor and onto the main bar. For the rear section of the cone, we elected to transition into the shape that best accommodated the 3x3 tennis ball arrangement we determined was optimal for holding our cargo.

4.3.6 Tail Cone Design

The tail cone was designed in much the same manner as the nose cone. We wanted it to be removable for ease of transport and replacement as well as light since it has no real load bearing requirements. We chose a simple cone that could be removed from the top and fit snugly onto the bar. The front of the cone was the same shape as the rear for the nose cone (optimal shape for 3x3 balls) and then tapers to a square size slightly larger than the tail boom to which it secures. With a balsa wood and Ultracote construction, it will be lightweight.

4.4 Landing Gear

The preliminary portions of the design involved selecting a landing gear configuration, load calculations of the front and rear landing gear, and spacing between the front and rear landing gear. The first task was to design the front landing gear. The rear landing gear would be designed second and compliment the functionality of the front configuration. The landing gear had to interact directly with the fuselage, the environment of the airstrip, and itself. The initial ideas focused on these interactions while meeting the engineering factors discussed earlier. Four concepts were produced based on the previous year's performance and research on commercially available landing gear. The landing gear is often a neglected design component of the aircraft. Last year's team had a landing gear fail that ruined the propeller and gearbox. For RC aircraft especially because of their hard landings, landing and taxiing is a critical flight envelope that is considered as a figure of merit under aircraft handling. Although the landing gear is only adding weight and drag during flight, the aircraft handling figure of merit takes precedence over the lightweight figure of merit. The landing gear is designed first to function properly and second to be lightweight.

4.4.1 Landing Gear Selection

The first front landing gear concept was an H-braced single wheel configuration. The shock resistance of the system was very low and consisted of a solid rubber wheel with a high compression strength spring on the exterior shaft of the main structure. In all concepts, the main structure of the landing gear that connects to the body of the aircraft is composed of a solid aluminum tube inside a slightly larger hollow aluminum tube. This structure allows for the design of a spring shock absorption system in the front landing gear. The spring shock absorption system provides only a small amount of deflection in the front landing gear. This dissipates landing shock while preventing propeller – runway surface contact. The second configuration consisted of two air filled rubber wheels, a single main structure, and an exterior spring. This system absorbs more energy from landings because of the air in the wheels, but still maintains a high compression strength spring. The third and forth concepts are the same as the second except the third uses two hollow tubes for the main structure and the fourth concept uses a high density foam inside the tubes to provide a shock absorption system.

The second concept was chosen through a relative and absolute comparison of the four concepts against our figures of merit. Upon this decision, concepts for the rear landing gear evolved into a single bent piece of aluminum that closely resembles those designed for traditional remote control aircraft. The main adjustments would be to the sizing and wheel spacing based on the height of the front landing gear. After design feasibility discussions with the team, our faculty advisor, and department professors the spring shock absorption system was changed to an interior spring configuration. The rear landing gear configuration was to be designed and based off the previous year's model while meeting our engineering targets.

4.4.2 Load Estimates on Landing Gear

A free body diagram can determine the forces the landing gear will experience. Some worst case scenarios we considered include a hard slap down on the front landing gear or the aircraft landing on one

of the rear wheels. Assuming we fly at the competition's maximum allowable weight of 55 lb. with a tricycle landing gear we could expect to see 41.25 lb. evenly distributed on the two rear wheels and 13.75 lb. on the front landing gear. The worst case scenarios would include one rear wheel making contact first with an estimated load of 25 lb. For a nose down slap we should consider the landing gear capable of taking a 20 lb. load. The spacing between the landing gear is important. The front landing gear will be placed rear of the motor mount portion of the main bar for structural reasons. The rear landing gear will be placed at a 15 degree angle to the rear of the $\frac{1}{4}$ chord. This location allows for a stable configuration during taxiing and is not so far to the rear as to create too large of a moment arm for the aircraft to nose up on take up. These load estimates are overestimates and therefore an analysis with these values will insure a factor of safety.

4.4.3 Landing Gear Sizing

The height of the landing gear is determined by the required propeller clearance plus a factor of safety that includes the deflection of the landing gear under a load. Maximum propeller diameter will be 28 inches so based on the vertical position of the motor, 11 inches is needed for ground clearance. The dimensions of the rear landing gear were based on a 1 to 2 degree nose down attitude that we needed to maintain when the aircraft remained at rest. This nose down attitude helps to suck the airplane down to the runway upon landing as soon as the front landing gear touches down. This allows the spring shock absorption system to work but the nose down attitude provides a damper system that keeps the spring from bouncing the nose of the aircraft off of the runway. The damper is created because our wing angle of incidence rests at zero degrees with respect to the spar. Therefore, when the nose of the plane comes down upon landing the negative angle of attack on our wing will help to hold the aircraft onto the runway. This slight nose down attitude will not hinder the aircraft on takeoffs. The rear landing gear will sit at 11.025 inches from the ground to provide the nose down attitude.

4.5 Preliminary Design Configuration

Figure 4.3 contains a summary of all the design parameters calculated in the preliminary design phase.

Airfoils at reduced Reynolds number 98863

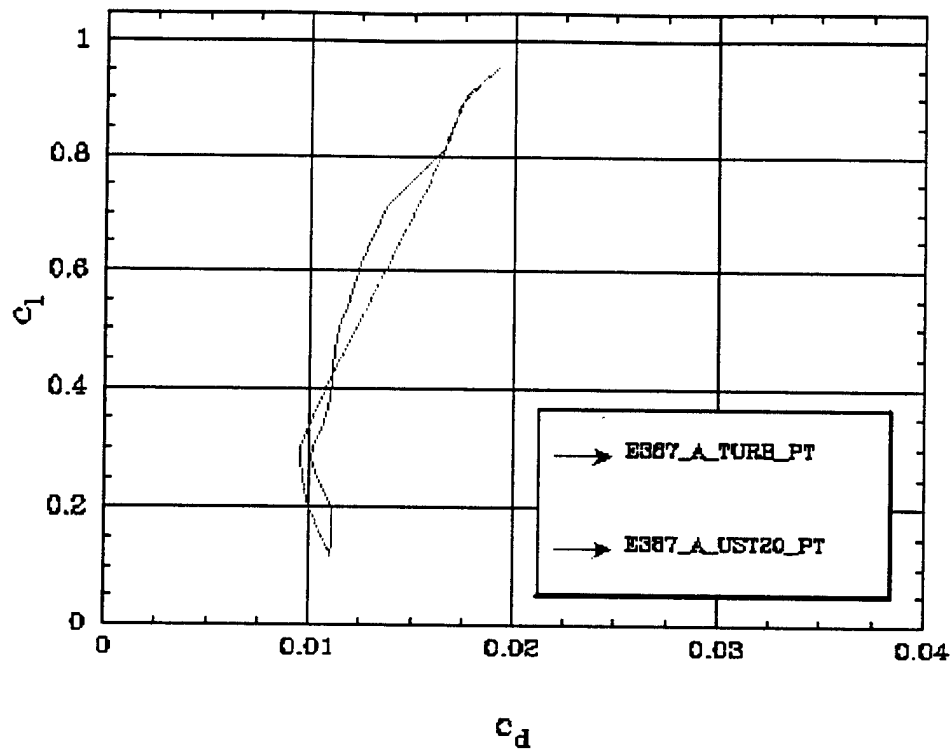


Figure 4.1 Eppler 387 Airfoil Lift to Drag ratio performance at 2 air conditions

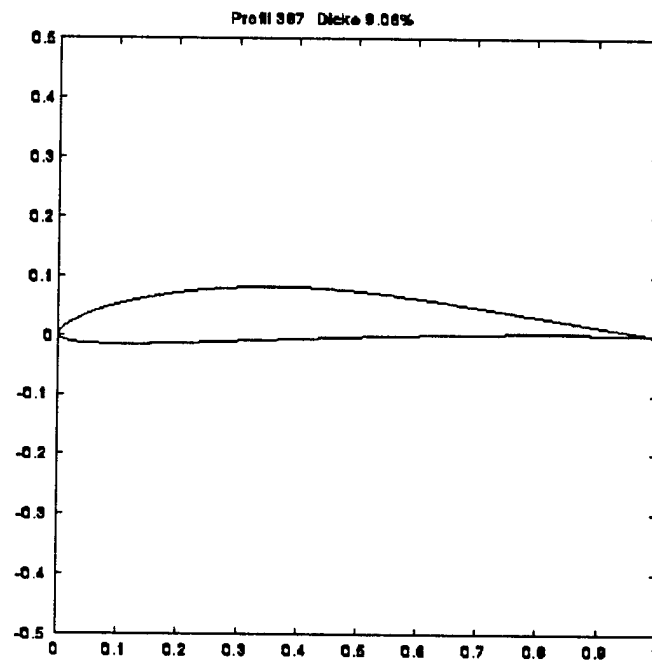


Figure 4.2 Airfoil Shape of the Eppler 387

Airplane Details for Preliminary Design

Payload Capacity:	100 tennis balls 30 pounds steel
Wing Configuration:	2 piece Mid-Wing Mono Wing
Wing Material / Structure:	Carbon Fiber / Foam
Wing Shape	Rectangular
Aspect Ratio	7.14
Wing Planform Area:	14 square feet
Chord Length	1.4 feet
Dihedral	0 degrees
Airfoil Selection	Eppler 387
Tail Configuration:	Conventional
Fuselage Configuration:	Single Body Fuselage
Main Structural Bar:	Aluminum 3/4 inch hollow
Fuselage Length	44.5 inches
Tail Boom Length	23 inches
Wing Mount:	"U" Design
Speed Loader:	One Removable Cargo Box
Tennis Ball Configuration:	3 X 3 X 11
# of Motors:	1
Motor Type:	Astro 90
Gear box:	Astro Super Box 714
Battery Type:	SR Battery
# of Cells:	37
Propeller:	22 in – 28 in Tractor Mount
Landing Gear Configuration:	Tricycle
Landing Gear Clearance:	11 inches
Spring Shock System:	Front Landing Gear Spring

Figure 4.3 Preliminary Design Airplane Details

5.0 Introduction

In the Detail Design section, we make materials selections and dimensioning finalized. Here we present each component's design in explicit detail to include a detailed drawing package. Additionally, we show any design performance data and begin to assess our design with the attempt to identify improvements. The result of this phase is a presentation of the finished product and an assessment of its actual or projected performance.

5.1 Component Selection and Architecture

In this section we refine the design and select the materials for the final aircraft. A great deal of our component selection and architecture was done in the lab as we were building. This hands on approach was tremendously helpful in completing the design.

5.1.1 Wing and Tail

We decided in the preliminary design to have two spars placed in the foam of the wing. Each spar extends to the tips of the wing for maximum support. We originally designed the wing to join in the middle of the fuselage for two reasons. First, was the ease of transportation of two five foot sections versus one ten foot section. The two spars would be placed at 4.25 and 10.5 inches from the leading edge. This would minimize the amount of twisting of the wing. From the previous calculations, we determined that two 0.315 inch hollow carbon fiber rods would support the load. After finding the rods at <http://www.cstsales.com/catalog.htm>, we could project the weight of the wing. The foam would weigh approximately 28.75 oz, the rods would weigh 7.34 oz, and the servos would weigh 3 oz. This would give a total weight of 39.09 oz for the wing. The aileron and tail design was done during this phase. For the ailerons, we researched and compared real airplane numbers to R/C airplane numbers. We determined from readings that 10% of the wing should be aileron. We knew that the area of the wing was 2016 in². Therefore, each aileron should be 100.8 in². We decided to use 2 inches as the chord, which meant that the aileron would be 54 inches long.

$$S_H = 0.55(c_w S_w) / D_H$$

$$S_H = 344.96 \text{ in}^2$$

For the tail, we used a relationship between the main wing and the tail surfaces. The distance (D_H) of the horizontal tail to the center of gravity of the main wing was 54 inches. With the horizontal tail area, we can determine the chord and span, knowing that we want an aspect ratio between 3 and 4.

$$b_H = \sqrt{AR \cdot S_H}$$

$$b_H = 34.7 \text{ in}$$

$$c_H = S_H / b_H$$

$$c_H = 9.9 \text{ in}$$

We did the same calculations for the vertical tail except that we wanted an aspect ratio between 2 and 4, and we also knew that the percentage of the main wing versus the vertical tail was .32 compared to the .55 for the horizontal tail.

These equations gave us the tail surface calculations:

$$S_v = 0.32(c_w \cdot S_w) / D_H$$

$$S_v = 200.7 \text{ in}^2$$

$$b_v = \sqrt{AR \cdot S_v}$$

$$b_v = 20 \text{ in}$$

$$c_v = S_v / b_v$$

$$c_v = 10 \text{ in}$$

5.1.2 Motor Mount

The first issue we resolved with respect to the motor was the method of attachment. We determined that a welded motor mount specifically detailed in the preliminary design met our needs. It is rigidly attached to the fuselage and allows for ample propeller clearance from the ground when utilized in conjunction with the front landing gear. Furthermore, the motor is completely detachable without having to breakdown the gearbox detachment. This goes well with our desire for the plane to be modular.

5.1.3 Motor Performance

When accessing the performance of the motor and the suitability of the motor/prop combination we had to analyze certain parameters for electric flight. In order to set up a suitable analysis we went to one of the leaders in electric flight, Bob Boucher of Astroflight. We used an electric flight analysis he outlined on his website at <http://www.astroflight.com/Contest.HTML>. Here he describes a way of analyzing resourcefulness of the power supply in terms of physics, specifically potential energy. The following is our own analysis:

We've decided upon a 37 cell SR Battery with approximately 1.25 volts/cell. The capacity of each cell is approximated at 1.75 amp hours. Therefore, our battery set up has the following potential power:

$$37 \text{ cells} (1.25 \text{ volts / cell} \cdot 1.75 \text{ amphours}) = 81 \text{ watt} \cdot \text{hours}$$

$$\text{converted : } 214,694 \text{ ft} \cdot \text{lb}$$

Potential Altitude Analysis:

We now assume that under ideal circumstances all of the potential energy in our batteries is converted to altitude. Given that our estimated, total aircraft weight is 30lbs.

$$\text{Altitude} = \left(\frac{214,694 \text{ ft} \cdot \text{lb}}{30 \text{ lbs}} \right)$$

$$\text{Altitude} = 7,157 \text{ ft}$$

Potential Range Analysis:

Assuming a glide ratio for our airplane of 10:1 we found the following:

$$\text{Range} = \text{Altitude} \cdot \text{Glide Ratio}$$

$$\text{Range} = 7,157 \text{ ft} \cdot (10/1)$$

$$\text{Range} = 71,570 \text{ ft}$$

We then convert the range to number of laps. We estimated the total distance of one lap is 2,500 feet. That gives an estimated 29 laps of battery power.

All of the calculations thus far are assuming completely ideal conditions. This is definitely not the case for our airplane. We took into account the Ecalc simulations and found that we should be running at an efficiency of approximately 65% for our motor and propeller combination. This means that we can expect at best to run 19 laps given the energy in our battery and assuming it is all converted to potential altitude.

Achieving Level Flight:

Based on the profile of our fuselage and the efficiency of our motor/prop combination we determined that it would take approximately 6.33 watts/lb in order to attain steady level flight given our 10 foot wingspan.¹

This translates into a total of 190 watts needed to sustain steady-level flight for our airplane.

Take Off Performance:

We must take off in 200 feet or less. Based on recommendations from the motor manufacturer, 19 watt/lb extra will be needed to take off. This will give us a climb out rate of 400 feet/minute which is suitable for reaching a safe altitude for the given course dimensions. This means that for take off we will need a minimum of 760 watts of power. These numbers allowed us to investigate which propeller to use with our Astro 90 motor.

Test Data

We performed some motor tests on a homemade motor stand to find solid numbers to compare with our required numbers from above. The test stand consisted of a fully charged battery pack, speed controller, an Astroflight wattmeter, radio receiver and controller, a spring scale, and a motor clamp. The stand was set up in such a way that we could take measurements for pounds of thrust, power of motor, current in motor, and potential of the system. The table below outlines our findings:

Propeller	Thrust (lbf)	Power (watts)	Current (amps)	Potential (volts)
21x10	9	780	18.3	42.6
24x14	11	1012	26.8	38.0
26x12	13	1050	28.8	36.5
28x8	13	937	27.8	33.7

There was one discrepancy in the tests. It seemed as if the battery was losing power when we got to the 28x8 propeller. However, it seems as if the 28x8 will not be needed because the 21x10, 24x14, and 26x12 props meet our needs. We plan on performing a few more tests on a 22 inch propeller to see the performance of it as well. Currently we are in the midst of preparing for flight tests with these three propellers to find the suitability for the pilot of the aircraft in terms of take off performance. We will also be conducting a cross check to see if the battery will last as long as expected.

Possible Errors:

In our assessment above, there are many places where some percent error could affect our results. First, we could not determine exactly the efficiency of our motor/prop combination in order to best determine

potential range based on our battery. Additionally, we had to assume that all of the potential energy in the battery would be converted to altitude. This means that our pilot must fly just the right profile for take off and steady flight. Additionally, we did not make an analysis on multiple take offs and the affect they may have on the battery. We are further investigating these affects in flight tests in order to resolve issues that may reduce the life of the battery. Finally, our motor tests were not perfect. The thrust readings were taken on a spring scale and the motor was not mounted completely parallel to the scale. There was also some additional friction in the system. Therefore, we concluded that our minimum thrust was determined. However, we believe that our readings on motor power, current, and potential were accurate. We used a digital wattmeter, which utilizes the latest in technology to obtain readings.

5.1.4 Wing Mount Refinement

The actual connection of the two carbon fiber wing spars to the wing mount "U" described in the preliminary design phase presented a design challenge. In our original design we had planned on a two piece wing that would slide through two holes in either side and connect in the middle. However, after we determined through testing that the two piece wing idea was impractical because of the difficulty of connecting the spars, we had to re-examine this connection. After the wing team decided on a one-piece wing with two carbon fiber spars approximately 7.5 inches apart, it was necessary to design a "top load" connector for the wing. After considering several different connection options, we chose a sandwich approach. This design has two rigidly connected boards connecting the front and back "U" with vertical slots. These two boards connect on the inside of the aluminum L-beams that form the "U." Two similar pieces fit on the outside of the aluminum beams. The top pieces are bolted to the aluminum frame and secure the graphite rods in place. The top boards are placed on the outside of the frame as opposed to on the inside, or directly on top of the bottom board so that the connection would tighten itself when the wings flexed upwards. If we had switched the location of the top and bottom boards the connection may have become loose when the spars flexed under a flight load. In addition to the small metal bolts on either side of the wooden collar, there are also two ¼ inch nylon bolts that connect the bottom slotted board to the top one. The nylon bolts help to relieve the stress from the two steel bolts at the end of the board. We considered using aluminum for these collars but we were concerned that the metal on graphite would damage the spar rods. The wood will be strong enough to hold the load of the wing under normal flight circumstances; in case of a crash we would rather have the connecting boards break than the wing spars. The wooden collars are much easier to manufacture/replace than the entire wing.

5.1.5 Center of Gravity Calculations

During the detailed design, one of the principal tasks for the fuselage team was to bring together all the components and calculate a projected center of gravity calculation for the aircraft. This would dictate where we would secure the wing mount. Conventional aircraft need a positive static margin where the center of gravity is ahead of the aerodynamic neutral point. This ensures longitudinal stability during flight. To make our preliminary center of gravity calculation we used the method in figure 5.1 with the moment arm referenced from the nose of the aircraft. The location of the rear landing gear must be 15

degrees back from the center of gravity. This ensures that the aircraft is stable while taxiing and is far enough forward to ensure that the nose can rotate up for take off. This meant that in the center of gravity calculations the rear landing gear moment arm is a function of center of gravity location plus the 15 degree rearward difference of 1.85". Our aircraft has three flight configurations – empty, tennis ball payload, and steel payload. The center of gravity calculations are done with the tennis ball payload 6 3x3 rows behind and 5 3x3 rows in front of the wing mount. For the empty flight configuration, the center of gravity is going to shift forward making the aircraft more stable but requiring more control surfaces. This is an acceptable condition. The same is true for the steel payload configuration. The center of gravity will shift forward only slightly because the steel is placed directly over the wing mount. This preliminary center of gravity calculation is a good estimate and allows us to proceed with the design. However, there is some error that we have taken into account with the design. We can vary the center of gravity by shifting a number of components. First, for slight shifts in the center of gravity we can move the battery pack. The battery pack weighing 5lbs sits under the wing mount and can move 2 inches back and forth. For larger shifts in the center of gravity we can reverse the tennis ball configuration so there is 5 3x3 rows in the back and 6 3x3 rows in the front. This design feature allows us to correct any errors of our preliminary center of gravity calculation.

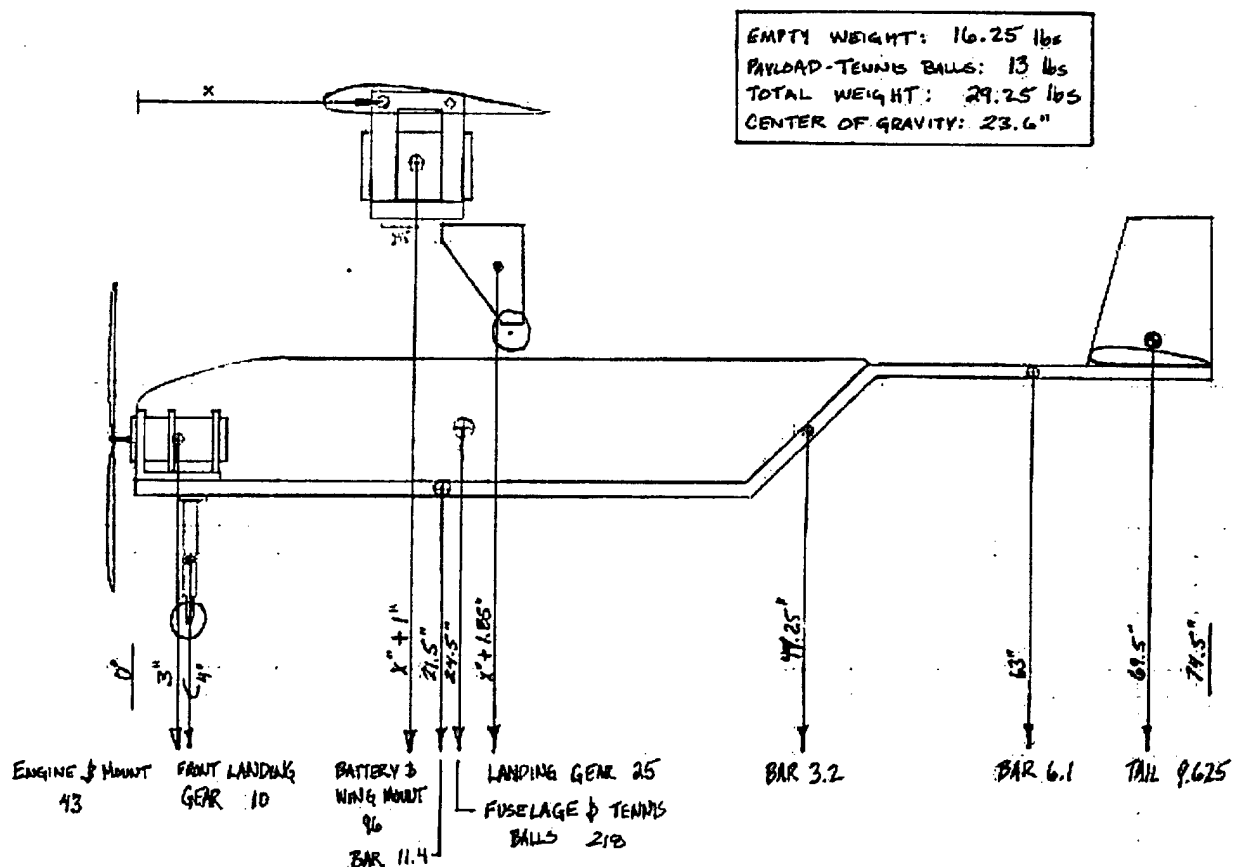


Figure 5.1 Preliminary Center of Gravity Calculation

5.1.6 Landing Gear

The preliminary portions of the design involved load calculations of the front and rear landing gear, spacing between rear and front landing gear, and initial detailed drawings. Figure 5.4.6 shows the final front landing gear configuration. The load calculations focused on the spring shock assembly. Research from the previous year's competitions illustrated that a single metal shaft can survive the competition landings. Calculations were made to determine the working length of the spring, the clash height of the spring, and maximum deflection of the spring induced by the force of the landing. The spacing of the landing gear was determined by the position of the quarter chord of the wing. All initial detailed drawings show the morphological procession towards the detailed phase of the design and ideas for critical connection interfaces between the landing gear and fuselage.

The front landing gear lends itself to the critical performance of absorbing shock while not allowing the plane to bounce around or the front prop to contact the runway surface upon landing. Therefore, the most critical portion of front landing gear assembly is the shock absorption system. First, the interior spring type must be determined. The interior spring is initially constrained by interior sizing of the outer aluminum tube. The interior diameter of the tubing is equal to 0.390 inches. Since we want there to be some room for compression the spring will be constrained to 3/8 inches (0.375 inches). Any more space than this would allow the spring to bend in the x direction when we want to constrain all spring movement to the y or vertical direction. This simplifying constraint allows us to concern ourselves with spring clash failure and ignore bending failure. For the initial calculations, we chose a spring from the Machinist's Handbook that fit the size constraints set by the tube. In our conceptual design engineering targets our team decided on maximum shock absorption of 55 pounds force. We are going to assume that the front landing gear will see one quarter of this force (13.75 lbf) since the tricycle landing causes the rear landing gear to take most of the force of the landing. We also assumed that 55 lbf in the y direction represents the worst case scenario since the aircraft will also be translating along the x-axis upon landing.

The following equation represents the multiple components of spring deflection that add to create the free or total spring length.

$$L_f = L_s + y_{clash} + y_{working} + y_{initial}$$

$$L_f = \text{Free Spring Length} = 2 \text{ in.}$$

$$L_s = \text{Shut Spring Length} = \text{Spring Gauge} \times \text{Number of Active Coils} = 0.054 \text{ in.} \times 18 = 0.972 \text{ in.}$$

$$y_{initial} = \text{Initial Pre-Load Deflection} = \text{Initial Force} / \text{Spring Rate} = 5 \text{ lbf} / (14.146 \text{ lbf/in}) = 0.353 \text{ in.}$$

$$y_{clash} = \text{Difference Between Minimum Working Length and Shut Length} = 0.15 \times L_f = 0.3 \text{ in.}$$

$$\text{Solving for } y_{working} = \text{Working Deflection} = 0.375 \text{ in.}$$

$$L_m = \text{Minimum Working Length} = L_s + y_{clash} = 1.272 \text{ in}$$

These preliminary calculations aided in choosing the proper spring and slot length drilled into the side of the outer aluminum tubing. The preliminary slot length was 1.4 inches, which allowed for 0.8 inches of

working space for the spring. The spring is held in place by a roll pin press fitted through the hollow aluminum tubing. The working space provided allows the spring to depress to a length of 0.8 inches. The shut length for the spring is 0.972 inches. So this means that the roll pin could not possibly collide with the aluminum. The force of the landing and the shear pin material (steel) would rip through the aluminum. The landing spring deflection must be solved for in order to determine if the spring will deflect past the minimum working length and proceed towards the shut spring length. The following equation calculates the spring deflection and gives an explanation of all the included variables.

$$y = \frac{8 \cdot F \cdot D^3 \cdot N_a}{d^4 \cdot G}$$

F = Force Exerted on Spring in the y-direction = $0.25 \times 55 \text{ lbf.} = 13.75 \text{ lbf.}$

d = Spring Gauge = 0.054 in.

D = Outer Spring Diameter – Spring Gauge = $0.375 \text{ in.} - 0.054 \text{ in.} = 0.321 \text{ in.}$

N_a = Number of Active Spring Coils = 18

G = Modulus of Rigidity for Spring Material = $11.2 \times 10^6 \text{ psi}$

Solve for $y = 0.688 \text{ in}$

The spring deflection felt upon the landing impact is 0.688 inches, which means that the spring will deflect to a length of 1.312 inches, which is well within the minimal working spring length of 1.272 inches and the length of the spring with respect to the slot (1.2 inches). In order to reach the minimal working spring length (1.272 in) a force of 14.556 lbf or 26.5% of the total landing impact (55 lbf) would have to be absorbed by the front landing gear. In order for the front landing gear shock absorption system to reach the spring shut length (0.972 in) a force of 20.555 lbf or 37.4% of the total landing impact would have to be placed on the front landing gear.

The interface between the fuselage and front landing gear is connected with a swivel bushing made out of bronze, which allows the front landing gear to securely fix to the main spar while maintaining the ability to steer the aircraft on the ground. The connection between the swivel bushing and the hollow aluminum tube will be secured with a 0.1 inch roll pin. All of the roll pins are pressure fitted and possess a higher shear modulus than the aluminum, so there is not a possibility of the pins failing upon landing impacts. The collar will be connected to the outside of the upper portion of the hollow tube and will provide a flange connection for the servo steering rod. The air-filled rubber wheels will be on a stainless steel axle that is press fit through the sold aluminum rod. The bearing for the wheels will be the plastic hub provided by the manufacturer. All of the parts will possess a high degree of modularity, so they can be changed out upon fatigue or wear.

The rear landing gear will composed of 1/8 in. thick aluminum. The mounting plate will be 6 inches by 6 inches. The legs of the rear landing gear will be at 45 degree angles with respect to the top of the mounting surface and 135 degrees with respect to the bottom of the mounting surface. The spacing between the wheels is 26.05 inches. The interior will be cut out with 1.5 inch thick walls to maintain enough rigidity but still provide a shock resistance upon landing. The most critical portion of the rear landing gear is the shear force applied between the rear landing gear structure and manufactured

axles. The axles will be store bought and made from stainless steel so that the shear force created upon impact will not shear the axle off. A balanced landing would evenly distribute 55 lbf between the two wheels. In the worst case the bent shape between the mounting plate and leg would see 25 lbf which does not come close to the force necessary for annealed or strain hardened aluminum to yield. Most of the force will be absorbed in the legs and the joint will not see the same force as the stainless steel axle.

5.2 Design Performance Data

Given some initial parameters we can make an estimate of our aircraft's flight performance before we fly it. Contained below is this estimate using a methodology for the design of propeller driven aircraft as outlined in *Aircraft Performance and Design*, by John Anderson.

5.2.1 Ground Roll

This is considered the take-off distance for the aircraft.

$$s_g = jN \sqrt{\frac{2W}{\rho S C_{L_{\max}}}} + \frac{j^2 (W/S)}{g \rho C_{L_{\max}} \mu_r}$$

$$W/S = 2.5; \rho = 0.002378; N = 3; j = 1.15; C_{L_{\max}} = 2.4; \mu_r = 0.4$$

$$s = 147 \text{ feet}$$

A take-off distance of 147 feet is well within the 200 feet constraint. This estimate shows we have met one engineering requirement.

5.2.2 Stall Velocity

This is the minimum velocity our aircraft can fly at steady level flight.

$$V_{\text{stall}} = \sqrt{\frac{2W}{\rho S C_{L_{\max}}}}$$

$$V_{\text{stall}} = 30 \text{ ft/s} = 20 \text{ mph}$$

Our aircraft's stall velocity is 20 mph.

5.2.3 Zero Lift Drag Coefficient

We use representative values from similar aircraft and flight conditions for this estimate.

$$C_{D,0} = (S_{\text{wet}}/S) * C_{fe}$$

$$C_{fe} = 0.0060; S_{\text{wet}}/S = 4$$

$$C_{D,0} = 0.024$$

Our zero-lift drag coefficient is estimated at 0.024.

5.2.4 Induced Drag Coefficient

This coefficient takes into account drag due to lift.

$$K = \frac{1}{4C_{D,0}(L/D)_{\max}^2} = \frac{1}{4(0.024)(12)} = 0.072$$

The induced drag coefficient is 0.072.

5.2.5 Optimal Velocity

This is the velocity at which the aircraft has the best $L^{3/2}/D$ ratio, also known as the best velocity for endurance of a propeller driven aircraft.

$$V_{optimal} = \left(\frac{2}{\rho} \sqrt{\frac{K}{C_{D,0}}} \frac{W}{S} \right)^{1/2} = 60 \text{ ft/s} = 41 \text{ mph}$$

At 41 mph the aircraft will be consuming the least amount of power. This is the flight speed we want to obtain at the competition.

5.3 Design Assessment

Overall, we are very pleased with our final product. One particular achievement was our constant consideration of the figures of merit throughout the design and building of aircraft. With nearly every component of the aircraft, a simple and modular design is apparent. This simple design philosophy allowed refinement of the various components as we went along. The modular design facilitates repair in the unfortunate, but likely, event the aircraft crashes. Additionally, the aircraft contains common features, which allowed for simple analysis of its projected performance.

Some initial improvements we would like to make prior to the competition or if we had the time and resources would be to begin lightening the aircraft's weight. The rear landing gear is a heavy design that has a substantial drag profile while in flight. Though a retractable landing gear is probably unfeasible, at least a lighter landing gear made of carbon fiber spars would greatly reduce the total aircraft weight. The main structural rod is also a major component that could use improvement. Here again, a different material would perhaps provide the solution. One of the reasons using a more expensive carbon fiber rod in the first place was eliminated was its cost and challenging manufacturing technique. Another alternative would have been to reduce the size of the bar consisting of the tail boom. The tail boom does not experience as great of forces as the main bar yet it is the same size. This was done primarily out of manufacturing convenience, but is certainly an over-engineered and weight penalizing component.

Some important things we learned concerning aircraft development include the iterative process of determining parameters. Critical values governed the design of the airplane and these values had to be determined early on in the preliminary phase. Additionally, we learned that dividing up the design of the aircraft into its four major components was useful, but that design team arrangement required good cross talk between the component teams. Otherwise the designs would not interface properly with each other. This was especially true of the fuselage team that was responsible for putting the components together with the main bar. Finally, with our aircraft complete over a month prior to the competition we have sufficient time to modify the design based on actual flight performance. We feel our flight testing will significantly improve our competition performance because we can optimize our loading configuration.

5.4 Drawing Package

Drawings of our components and the assembled plane are contained in figures 5.4.1 to 5.4.6. We did the drawings with the computer aided design software ProDesktop. The drawings are to scale; however, most fasteners and joiners have been left out for ease of viewing and component assembly with ProDesktop.

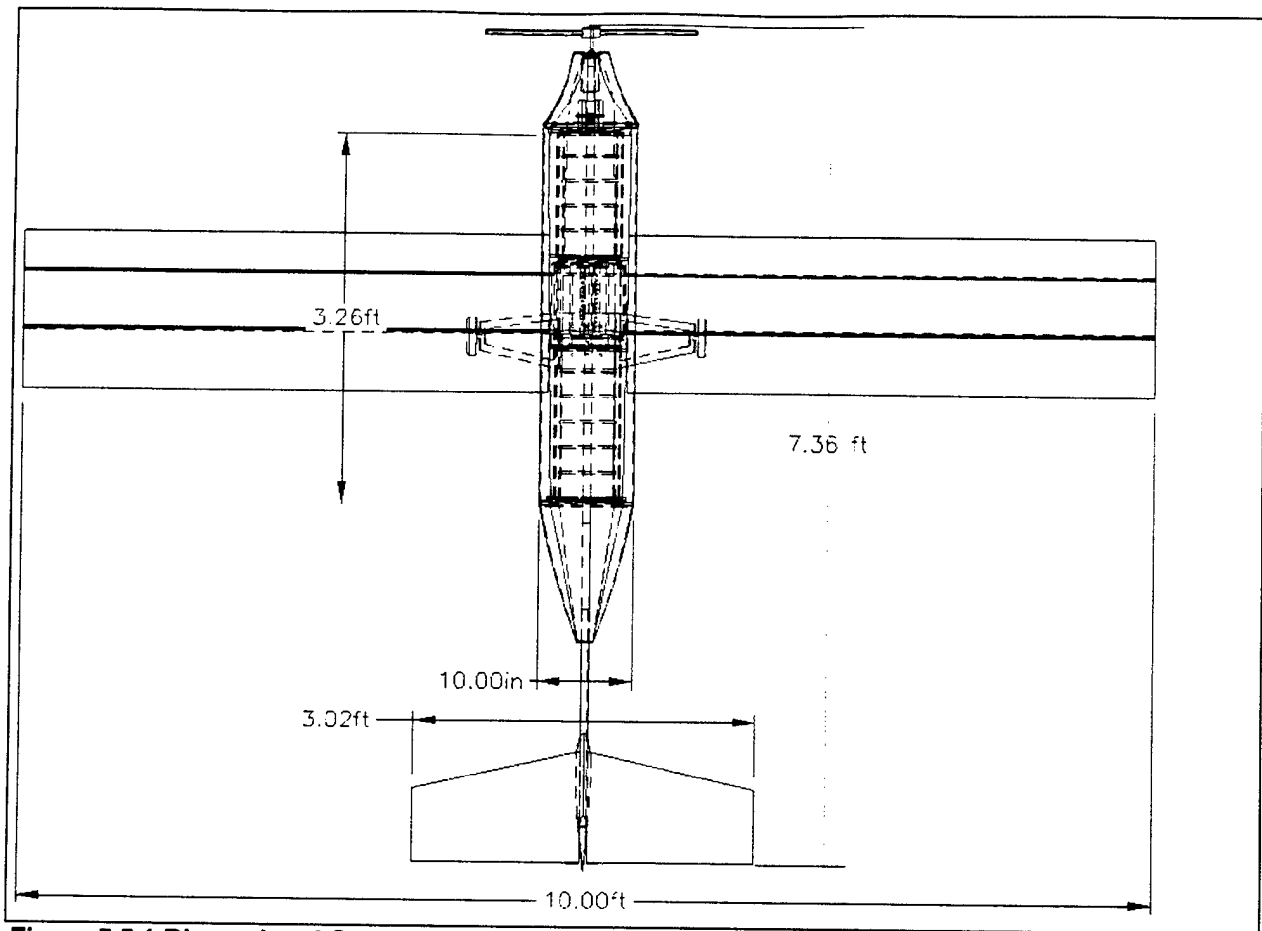


Figure 5.5.1 Dimensional Overview – Top View

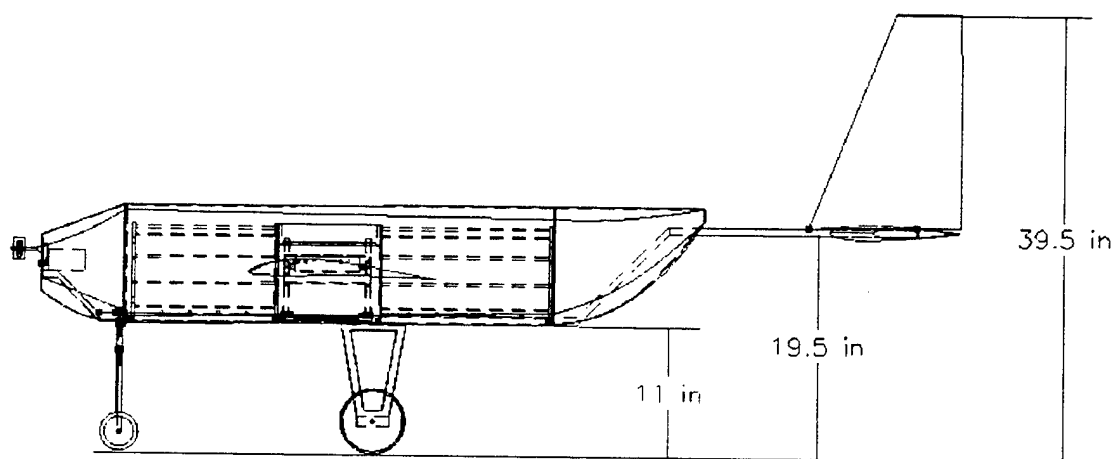


Figure 5.5.2 Dimensional Overview – Side View

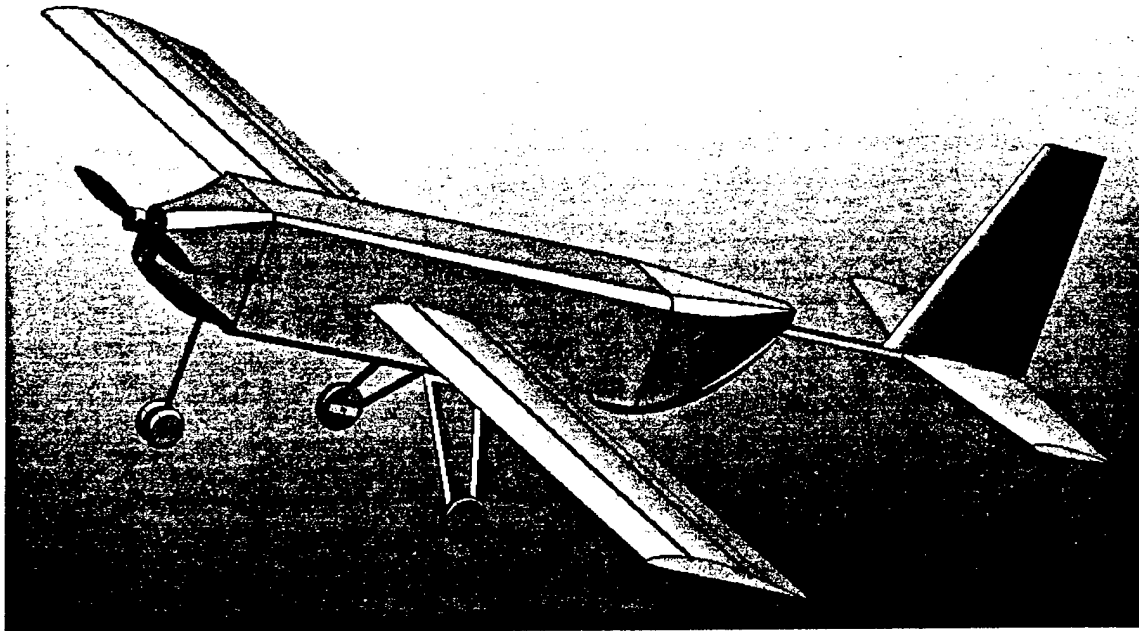


Figure 5.5.3 3-D View

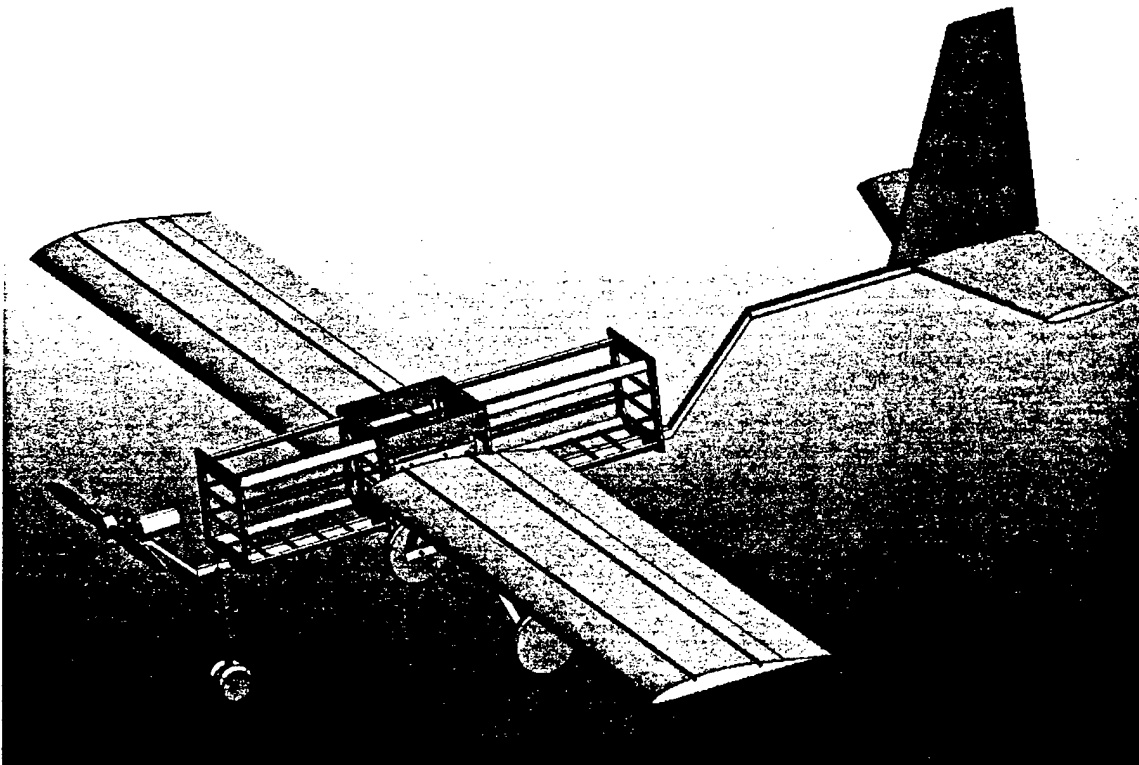


Figure 5.5.4 Structural View

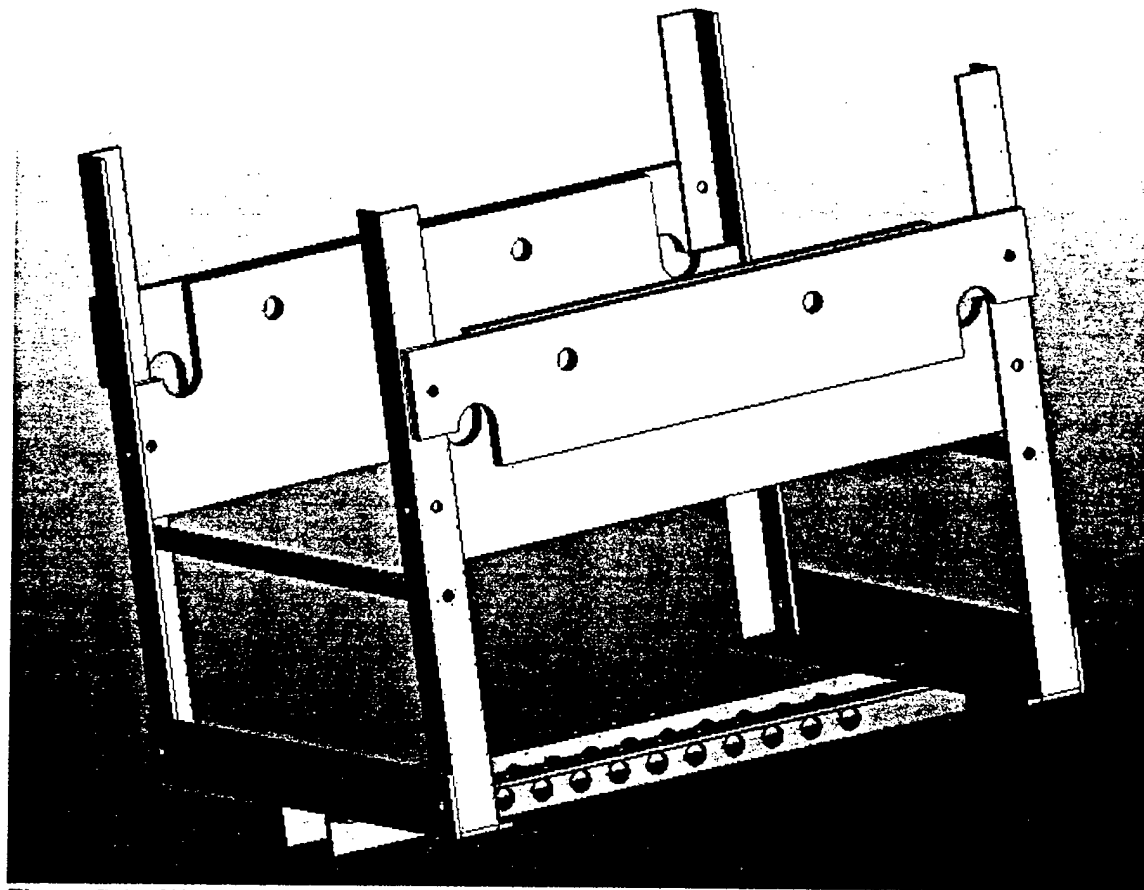


Figure 5.4.5 Wing Mount

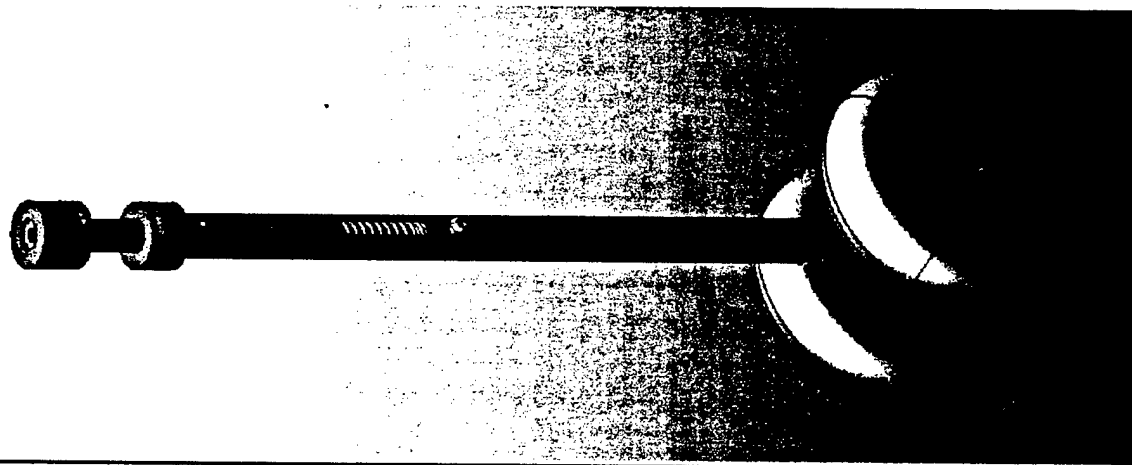


Figure 5.4.6 Front Landing Gear

6.0 Introduction

The basis of manufacturing our aircraft was simplicity. Our group was comprised of a team unfamiliar with the construction of model aircraft and remote control planes. Keeping all components modular and compatible throughout the design phases aided each group in the development of their portion of the aircraft. We combined two major avenues of approach in our manufacturing process. The first process involved the "do-it-yourself" Home Depot technique, which involved our team learning how to use all of the materials and machinery necessary to build a complete and functional aircraft component. The second process involved a more traditional business / engineering approach, which involved the early completion of detailed engineering drawings for our campus machinists. They used these drawings to create the component. This process involved numerous meetings between the engineers and machinists. The meetings and interaction helped to foster better component manufacturing and new design ideas. While building the aircraft our largest concerns were focused on the following figures of merit: strength to weight ratio, modularity, low cost, and of course manufacturability. The one advantage our team did have in the manufacturing process was our knowledge of shaping foam with hot wires and the effects of Ultracote on a foam surface.

6.1 Wing & Tail

The manufacturing of the wing posed many challenges to our team. The first challenge we faced was that the predicted 0.315 inch carbon fiber rods would not be strong enough. After a few point load tests we found that some type of reinforcement would be necessary or new rods would have to be purchased. Therefore, we went to a 0.5 inch carbon fiber rod. The carbon fiber rods came in four foot sections, so we used a wrapped mandrel to connect the rods together. We used six carbon fiber rods connected at four different points.

The foam we used was basic insulation foam found at any local Home Depot. This foam was used because we were not depending on the foam to provide any structural support and it was lighter than the traditional white or blue spyder foam. The airfoil shapes were cut using a foam wire cutter and sandpaper to sand the leading edge to the desired airfoil shape. Next, the grooves for the carbon fiber rods were put in the foam using a table saw. The rods were then placed into the foam and glued using Elmer's Polyurethane Glue. Multiple people at Home Depot and hobby shops recommended this glue. Once the glue dried (24 hours) the grooves were filled with foam filler and sanded to the original airfoil shape. We also drilled two inch diameter circles throughout the wing to reduce the weight. To ensure the wing could withstand the load, we used four strips of .003 inch fiberglass tape on the bottom of the wing for reinforcement. By doing this, we were able to eliminate 6 oz of foam. The next step was to cut the ailerons out of the airfoil. We used balsa wood for the aileron to ensure the necessary stiffness for proper airflow deflection across the aileron. The servos and extensions were then placed in the bottom side of the airfoil. We minimized the drag by turning the servos on their side and only allowing the control arm to

protrude from the airfoil. The next step was using Ultracote on the foam. We used Ultracote rather than Monocote because it is lighter and adheres to the foam surface better.

We used NACA 0012 for the airfoil shape of the tail. We needed a symmetrical airfoil and the Eppler 186 was too thin. We used the foam wire cutter to cut the tapered airfoil shapes. The taper was from 10 inches to 8.5 inches. We used .315 inch carbon fiber rods to connect the surfaces allowing them to be placed into the aluminum tube.

The vertical tail surface had a taper from 12 to 8 inches. This taper was also done by using the foam wire cutter. The vertical tail also had two .315 inch rods secured with epoxy. In the carbon rods we inserted steel bolts to secure the tail surfaces. This design allowed the vertical tail to secure the horizontal tail with only two bolts. The tail surfaces were also covered with Ultracote.

6.2 Power Plant

The manufacturing process for the motor portion of the airplane was limited in terms of actual work the team could perform. The motor itself, an Astro90 with gearbox, is an off-the-shelf, electric aircraft motor. The propellers we are using are also designed and manufactured by model aircraft companies, specifically Zinger and Metz. Therefore, all of the manufacturing for the motor portion of the airplane involved the development of a sturdy motor mount.

The motor mount was initially designed to be a completely modular piece of the aircraft. We designed it so that it could be detached with the motor if need be. After noting that this would interfere with one of our other figures of merit, manufacturability, we had to reconsider the design. The motor mount was adjusted to be a plate, which would be welded to the aluminum, main bar. We decided that no modularity would be lost because the motor itself is modular since it could easily be screwed and unscrewed to the plate. At this point we were able to create a few detailed hand drawings. The primary concerns for dimensions were that the plate had to be large enough to contain the front profile of the motor in addition to having the proper access and mounting holes. From these drawings we built a simple mock-up using wood and we attached it to the bar. We did this in order to see how well the potential design would mesh with the rest of the aircraft. At this point we realized that the front most portion of the fuselage butted directly up against the motor mount. This would have created a non-streamlined fuselage, which would have resulted in a lot of unnecessary drag. We then adjusted the motor mount to include a raised portion of the main bar in order to create a better profile for the front of the aircraft. This then forced us to redesign the actual mounting plate to which the motor assembly would be attached. This was a simple fix that resulted in reducing the height of the plate. We then built another mock up, only this time we made it out of aluminum.

The manner in which our aluminum, prototype plate was made was extremely simple. We used a hacksaw and a belt sander to shape it to the proper dimensions. Luckily after finding that our new design would work we were able to take more detailed drawings, containing exact placement of proper access and mounting holes. These drawings were then taken to machinists in order to reproduce exact

copies of our desired design. The final product aligned with our figures of merit because it was fairly easy to manufacture. It did not actually contribute to the rated aircraft cost or actual cost since we could have it manufactured for free, and it met our specifications for modularity.

6.3 Fuselage

To make our main bar we supplied the aluminum bar to our lab technicians with the dimensions we needed. They were able to weld good clean joints at the two bends in the bar. We were concerned that the bar would be weak at the joints but after some testing and assurances from the lab technicians that the weld was sufficient for our purposes, we found the bar strong enough.

Because of the modular/not typical nature of our design we used a number of different materials, this made for some interesting manufacturing. The nose cone was constructed by first making the balsa tip fit over the motor mount. Once it fit snugly excess wood was removed to give the tip the shape that we needed in order to transition to the square size of the fuselage. We also smoothed out the inside of the cone to give the motor more space for air circulation. Next we fabricated a piece of plywood that was the shape of the fuselage and ball holder. This piece was notched at the bottom to allow it to fit snugly against the bar. Once the two end pieces were constructed it was just a matter of connecting them with balsa strips and ultra coating over the outside. There was one modification to the original design when we discovered that the bottom of the bar stuck outside of a straight line connecting the front tip and rear support. To accommodate for this we added a piece of foam cut around the bar that would let us use straight strips along the bottom of the cone. This piece also provided a more precise fit around the bar.

The tail cone was built in the exact same manner. It was also necessary to place a foam "extension" on the fuselage side of the cone to allow straight strips along the bottom. After building the cone, we made a plate that would hold the servos to the bar inside of the tail cone. These servos control the rudder, elevator and front landing gear. By placing them in the tail cone area we avoided leaving this large space unused for any type of aircraft functionality. It was also the ideal location because of the straight and uninhibited path the push rods were able to take out the tail boom. There was also space in this area for our receiver, which was placed directly on top of the foam "extension" at the base of the fuselage side of the cone using industrial strength Velcro.

Construction of the wing mount was far more difficult because of the loads that it would see during flight. For this reason, the majority of the mount is made with ½ inch aluminum "L" bars. These bars are rigid enough to avoid any major disconnects in wing body movements. It would also fail by bending instead of snapping like a wood support may. The actual "collar" that supports the wings was made out of a ¼ inch aspen boards. The bottom pieces were rigidly attached to the body part of the wing mount the holes were drilled in to allow the wing to sit securely inside of the mount slots. The top pieces, also made from aspen are slightly thinner (1.5 inches tall in order to allow them to brake in the event of a crash. Besides the metal screws holding up the entire weight of the plane we choose to place two nylon

bolts connecting the top and bottom pieces of the "collar". This makes all four screws on each side bearing the positive loading resulting from flight.

The speedloader was constructed from various sizes of balsa wood. We took the original design structure and based our material choice off of spot strength tests. In our first assembly, we joined all the wood with epoxy and resin, but this added unnecessary weight to the structure. So in the second version of the speedloader, we joined all the wood with "CA+ glue," which is also easier to use because it requires no mixing and dries in seconds. For the carbon fiber rod handle on top of the box, we used an extra ¼ inch diameter piece not being used for the construction of the wing.

We constructed the fuselage body after the speedloader. This ensured that the speedloader fit onto the cargo region of the main bar and the fuselage body did not interfere with the placement of the speedloader. We simply constructed 4 balsa wood ribs joined by balsa wood spars and put Ultracote on the sides and connected to the nose and tail cones. We constructed the access panel last to ensure that it interfaced with the fuselage body and did not interfere with the top of the speedloader. We made it with the least amount of balsa wood possible and a Ultracote covering.

6.4 Landing Gear

A completely different approach to manufacturing was taken with respect to the landing gear. The process involved the only prototype being made at the machinist shop by our lab technicians. The front and rear landing gear of the aircraft were to be completely designed in CAD applications and a meeting was scheduled with the technicians to introduce our concept to them, ask for insight, and determine the feasibility of creating both fully functional prototypes in four weeks of turn around time.

The team reviewed the initial drawings before the landing gear sub-team met with the technicians. Going into the briefing we determined it would be best to buy as many materials as possible. We bought our initial aluminum materials at Home depot to include the hollow and solid aluminum tubing. All wheels and conceptual steering mechanisms were bought from Du-Bro remote control aircraft products. Later the team also used McNarra's Parts handbook to purchase stainless steel solid tubes for the axle, springs for the shock absorption system, and thrust bearings for the steering components.

The initial meeting was a complete success and the machinists were very informative on manufacturing methodology. For 4 weeks the landing gear team provided guidance at the shop every other day and supervised all progress on the tricycle landing gear. Upon completion of the tricycle system tests were performed to determine the deflection of the selected materials under different dynamic loads. After completing these tests the landing gear was modified slightly and put into production for three more copies. The drawings were modified to fit the final design.

Using this type of manufacturing process really helped our team to realize the capabilities of the very skilled machinists and technicians. Using this method exceeded our expectations based on the figures of merit. The modularity and compatibility of the landing gear system possesses a much higher level than we initially expected. The budget cost of manufacturing was minimal and only incurred by the

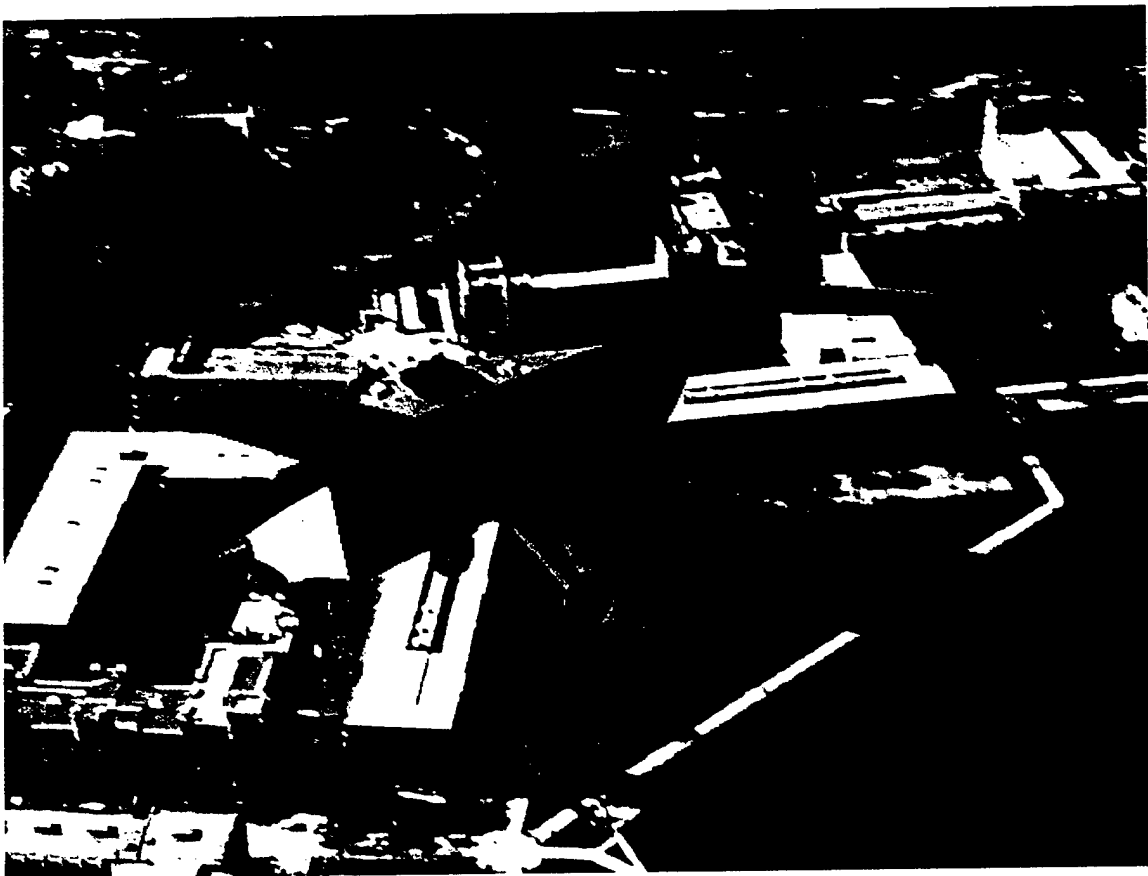
purchase of commercial products. The overall rated cost of the aircraft was not affected, and the manufacturability is now extremely easy. The prototype stage took four weeks and now the manufacturing turn around time for both components of the landing gear system takes only one week.

7. References

- [1] Anderson, J.D., *Aircraft Performance and Design*, McGraw-Hill, Boston, MA, 1999.
- [2] Anderson, J.D., *Fundamental of Aerodynamics*, McGraw-Hill, Boston, MA, 1991.
- [3] Boucher, Bob, "Winning the AIAA Student Design/Build/Fly Competition," from Astro Flight Inc. Website, [on-line], available from: <http://www.astroflight.com/Contest.HTML> , 1997.
- [4] Fan Wing, Website, [on-line], available from: <http://www.fanwing.com/>, 1999.
- [5] The Composite Store, Website, [on-line], available from: <http://www.cstsales.com/catalog.htm>, 2000.
- [6] NACA Airfoils, Website, [on-line], available from: <http://www.icemcfd.com/cfd/naca.html>, 2001.
- [7] UIUC Airfoil Coordinates Database, Website, [on-line], available from: http://amber.aae.uiuc.edu/~m-selig/ads/coord_database.html, 2000.
- [8] Aerospace Composite Products, Website, [on-line], available from: <http://www.acp-composites.com/>, 2001.

**UNITED STATES MILITARY ACADEMY
WEST POINT, NY**

2001 DESIGN / BUILD / FLY COMPETITION



“Have A Nice Day”

Design Report – Addendum Phase

Table of Contents

	Page #
1. Executive Summary	3
2. Management Summary	7
2.1 Design Team Assignment	7
2.2 Design Plan	7
3. Conceptual Design	10
3.0 Introduction	10
3.1 Design Goals and Philosophy	10
3.2 Design Parameters	11
3.3 Figures of Merit	15
3.4 Design Parameter Results	17
3.6 Conceptual Design Results	17
4. Preliminary Design	20
4.0 Introduction	20
4.1 Wing & Tail	20
4.2 Power Plant	21
4.3 Fuselage	23
4.4 Landing Gear	26
4.5 Preliminary Design Configuration	27
5. Detailed Design	30
5.0 Introduction	30
5.1 Component Selection & Architecture	30
5.2 Design Performance Data	37
5.3 Design Assessment	38
5.4 Detailed Drawing Package	39
6. Manufacturing Plan	43
6.0 Introduction	43
6.1 Wing & Tail	43
6.2 Power Plant	44
6.3 Fuselage	45
6.4 Landing Gear	46
7. References	48
8. Lessons Learned	4a
8.0 Introduction	4a
8.1 Tail Construction	4a
8.2 Wing Construction	4a
8.3 Wing Dihedral	5a
8.4 Control Surfaces	5a
8.5 Power Plant	5a
8.6 Fuselage	6a

8.7 Landing Gear.....	7a
8.8 Estimated vs. Actual Weight	8a
9. Aircraft Cost Model	10a
9.0 Introduction.....	10a
9.1 Aircraft Cost Model.....	10a

8.0 Introduction

Our team made many adjustments as the building and testing phases of our aircraft progressed towards completion. We faced many unexpected challenges not discovered in the earlier design phases. Most of these challenges involved connection methods between the different aircraft sub-components. In some cases these components were slightly altered to simplify manufacturing techniques or better interface with one another.

8.1 Tail Construction

The tail was easy to construct, but connecting it to the aluminum bar proved to be more of a challenge. We used the hot wire to cut the airfoil shapes, and carbon fiber rods were used as spars in the horizontal and vertical surfaces. The horizontal surface had two spars connecting the two surfaces with $\frac{3}{4}$ inch space between them. We cut two grooves in the aluminum bar and placed the horizontal surface snugly in place. Next, we placed two carbon fiber rods in the vertical surface and drilled two holes in the aluminum bar. The vertical surface was placed on top of the horizontal (securing it in place) and then tightened down with bolts. On our first attempt to remove the tail we found that the epoxy was not strong enough interface between the carbon rods and the insulation foam. The rods were spinning in the foam and we could not get the vertical surface off of the aluminum rod. This was fixed by placing a small piece of aluminum on the bottom of the vertical surface and securing the rod to the foam. Now, we could remove the vertical surface with ease. The time spent making the change was minimal.

8.2 Wing Construction

The original spars selected were 0.315 inches in diameter. Our original calculations were based on the data provided by the CST Composites Internet site. The 0.315 inch spar was tested in half of a wing and found that the wing deflected approximately 35 degrees under an increasing point load on the outer edge of the wing. This was too much deflection; therefore, we reworked our calculations and found the mistake. The new spar selected was the .5 inch carbon fiber rod. Two spars were placed full length in the wing and again tested for deflection. The deflection of the wing for the 2-G test was approximately 9.5 degrees, and the actual flight dihedral was approximately 5.5 degrees. We decided that we needed to reduce the actual flight dihedral to about 4 degrees for a mid wing configuration. We added a four foot spar located at the quarter chord to reduce the deflection. This reduced dihedral to the previously mentioned calculations of 6.5 and 3.7 degrees for the in flight and 2-G test dihedral respectively. Adding the spar was a timely task because the wing was already covered with Monocote. We cut the Monocote and had to form the groove by using a Dremel tool versus the table saw. The addition spar added very

little cost and weight to the over all wing. Now that we know the other spar must be added, we will be able to decrease the manufacturing time for a second wing.

8.3 Wing Dihedral

Originally, we wanted 3-5 degrees of dihedral. After a few load tests, we found that the wing was going to naturally deflect; therefore, we decided to eliminate the permanent dihedral. After building the wing, we tested it with a full load (approximately 50 lbs.) and found that the 2g test resulted in a dihedral of 6.5 degrees. This is a little more than we desired, but this was only for the 2g test. The 2g test is the worst case the wing will experience during flight and is a safety measure used to determine if the airplane is safe to fly. When flying, it will be experiencing a 3.7 degree dihedral, which is within our target dihedral of 3-5 degrees.

8.4 Control Surfaces

The control surfaces were designed around extensive research of passenger and R/C aircraft. After talking with our pilot, we learned that we wanted a larger rudder surface than we originally planned for. The pilot discussed the importance to slip through a turn versus using ailerons to turn. The slip allows the plane to use less power and causes the plane to be more stable. Therefore, we increased our rudder surface from 33% to 45% of the vertical tail planform surface.

8.5 Power Plant

Overall, the most difficult aspect when dealing with the power plant was the lack of knowledge about electric motors. Although every team member has taken a basic, electrical engineering course, our knowledge specifically about motors used for electric airplane flight was very small. Therefore we did as much research as possible before selecting a motor that would best meet the competition and aircraft requirements. Another problem emerged when we found it difficult to find information on Graupner Motors. We dealt with one hobby shop owner who claimed to have a large scale Graupner Motor that would out perform the Astro 90. When it came down to it, he had no documentation to prove his motor was actually built by Graupner. Since we decided on a single-motor configuration our best choice was to use the largest Astro motor we could buy. Therefore, a solution to this lesson is to leave a continuity file to future teams on where they can find information, and actual contacts that they could speak to when trying to learn about electric flight. Additionally, we also believe it would be beneficial to make this project more inter-disciplinary. Our entire team was made up of aerospace engineering majors. Since a major portion of the project is efficiency of the motor and battery we believe it would be useful to bring in an electrical engineering major. Finally, since the distributors and makers of the motors are pretty

limited, it is important to have a good rapport with them. It is important not to burn any bridges because it could seriously affect a team's ability to complete their airplane on time.

8.5.1 Props

Prop selection was also an area that could be improved upon. Our initial impression was that the E-calc program should be used as the guideline. We did this and bought props which were around the E-calc prop solution, both larger and smaller, to test. After speaking with a more knowledgeable, electric R/C pilot he said that E-calc was very accurate and it really wasn't necessary to test props on our own. We recommend that next year, the team spend a lot of time optimizing the prop selection based solely on E-calc. Actual testing only wasted time gathering data that was already available on the computer program.

8.6 Fuselage

The most significant lesson we learned from designing and manufacturing the fuselage is engineering for interfacing with all the other components. The fuselage must interface with nearly every component on the aircraft to include the motor, wing, tail, landing gear, and flight control systems. Additionally, it is internally constrained by the desired payload volume. As we designed the fuselage, we had to continually modify and adjust the configuration to accommodate the other components, particularly the wing. We found it is a tradeoff between either designing "in" from the components to the fuselage or "out" from the fuselage structure to the components. Since we gave primary consideration to the aerodynamic components we designed the fuselage with a generalized design that could accommodate slight changes in the configurations of the components. Along these same lines, communication among the design team cannot be stressed enough. We even found that designing a component should be done with the designers of an interfacing component present and not just with previously communicated input parameters.

An additional lesson we learned is to account for vibrations in mechanical structures. Our main beam is a thin aluminum square rod that transmits loads from the motor, wing, tail, and landing gear. The entire structure vibrates slightly if excited by an external force. Fortunately, the vibrations down the central beam do not effect the performance of the aircraft or jeopardize the structural integrity of the aircraft.

Because our design is based around a single aluminum bar to provide strength we did not design a very robust fuselage. However, we neglected to take into account the difficulties associated with placing the speed loader into the fuselage. Initially the top of the payload part of the fuselage was a single 5/16 square piece of balsa. However when the speed loader was placed in slightly crooked it would snap the balsa strip. Because of this problem we added a small carbon fiber rod below the 5/16 balsa to keep it from breaking during loading.

In building the top section for our fuselage we ran into problems connecting the lid to the bottom piece. Any kind of a hinge connection was impossible because of the foam pieces that

extend down to the top of the wing. Finding a place for securing pins was also difficult since the space between our fuselage wall and the speed loader was so small. As a solution we placed two pins in the middle section that would slide through the wing mount as well as the speed loader. This would secure both the lid and the speed loader to the main fuselage. We were concerned that these pins would rip through the foam so we glued some carbon tubes inside the foam to reduce the chances of the pins ripping out.

8.6.1 Speed Loader

In the proposal phase we had two options for the speed loader. The first one was to have the cargo box be part of a removable structure of the fuselage. The second option was to design a cargo box that would be contained inside the fuselage as an independent part. To be in conformity with the competition rules, but also to maintain a mid-wing configuration, we chose the second option. This option allows the fuselage to be independent from the speed loader, while facilitating an easier design that does not interfere with the wing at mid-span.

Two types of material were considered for the design of the speed loader. The first option was to build the speed loader out of thick sheets of foam where the tennis balls and steel blocks would sit tightly in holes drilled to match their respective geometries. However, for weight considerations, we made our final design out of balsa wood. The speed loader was built such that the tennis balls would be kept in a close and compact arrangement. The speed loader built in this fashion had three parts: two identical external containers and a small box in the middle.

The external containers were built to carry 54 and 45 tennis balls. They were made out of $\frac{1}{4}$ inch balsa bulkheads along the width and thin straight-edged pieces along the length. To strengthen the entire structure, squared rods were put in between the pieces along the width and the length. This way, all the open space in the container was filled with balls, and the balsa structure was on the outside constraining their movement.

The middle part of the speed loader was an open box made out of thicker balsa sheets with thin carbon fiber rods running along the bottom plane, on which the steel blocks would sit. For a load of tennis balls one ball would sit between two of the carbon fiber rods at the bottom of this middle section.

To connect the three parts of the speed loader, we ran carbon fiber rods along the length of whole structure and used epoxy to adhere the pieces to one another. Manufacturing is relatively time intensive for a removable device, but the modularity of this device will help us to unload and load the aircraft on each sortie.

8.7 Landing Gear

The main and nose landing gear required very few adjustments to the initial manufactured prototype. Only small adjustments were necessary to account for steering and wheel attitude. We were able to conduct bending and friction testing on the front landing gear.

This led to a few minor designing, dimensioning and manufacturing changes. These changes only cost a couple of days of turn around time with respect to the manufacturing process.

Initially the main landing gear wheels rested at a 20 degree angle canted outward from the bottom of the rear landing gear. This problem was due to the amount of weight transferred to the landing gear while it was fully loaded with our tennis ball payload. To correct for this problem the bottom flanges of the main landing gear were slightly bent inward about 8 degrees so the wheels would rest completely perpendicular to the runway surface.

A bending test was conducted on the front landing gear. This test was set up to resemble the worst case scenario of the aircraft landing off-centered on the front landing gear without the main landing gear touching first. The aircraft was fully loaded and canted off the table. The entire weight of the aircraft was held by the front landing gear as the aircraft was tipped to greater angles. The result was that the front landing gear did successfully hold the plane, but it suffered high bending stresses were the slot had been cut for the spring absorption system. This was expected and accounted for by redesigning the second generation landing gear with a slot width half that of the prototype model. This was a quick fix and affected manufacturing time very little since second generation landing gear manufacture had already been factored into our timetable.

The friction testing occurred between the two aluminum tubes that compose the main shaft of the front landing gear. Without lubrication aluminum on aluminum components usually gaul easily. Gaulling causes the shafts to stick to one another thus negating the effects of the spring absorption system. We tested two types of lubricants for the interior shaft; 1) an all purpose grease and 2) a Silicon based dry lubricant. We found that the grease corrodes the aluminum and causes the aluminum components to adhere to one another while the silicon based dry lubricant helps for the inner shaft to ride smoothly inside the hollow outer shaft. The latter provides more shock absorption and less chance for the nose gear to fail at the exterior slot.

Improvements in the rear landing gear can be made in the future by creating arrow shaft struts for the main landing gear rather than the 6061 Aluminum struts that are part of the current version. The arrow shafts are made from T6 aerospace quality aluminum, which will still provide shock absorption in the rear while being able to bear a greater load. The cost to this method is the time intensive work it takes to create the proper connection to hold the arrow shafts.

8.8 Estimated Weight vs. Actual Weight

Our team found that weight estimates were crucial to the design phase of the aircraft, however most of these estimates were based on last years competition. We found that our aircraft weight estimates based on last years model were relatively accurate. The figure below shows our weight estimates versus our actual weights for the different portions of the aircraft.

Component(s)	Estimated Weight (lbs)	Actual Weight (lbs)
Wings	2.4	3.95
Tail	1	0.75
Bar, Fuselage, Receiver, Wires, Servos	6.1	4.76
Nose Gear	1	1.25
Main Gear	3	3.5
Motor and Propeller	2.75	2.65
Total Aircraft Weight	16.25	16.86

Figure 8.1 Estimated vs. Actual Aircraft Weight

9.0 Introduction

The aircraft is assigned a rated aircraft cost based on a model the judges have created. The model calculates a rated cost of the aircraft by multiplying three parameters by a \$ cost. The three parameters are the manufacturers empty weight, the rated engine power, and the manufacturing man hours. The weight is in pounds as measured without the battery or payload. The engine power accounts for the battery used, number of engines, and the fuse from the battery to the controller. The manufacturing work hours are assigned according to the components of the aircraft. This total rated cost is divided into our overall score. Therefore, it is critical we have a low cost aircraft. In our initial design decisions, this rated cost model was examined so we could minimize the cost of our aircraft.

9.1 Aircraft Cost Model

See figure 9.1 for a diagram of the critical cost parameters listed below.

Manufacturers Empty Weight (MEW) = 16.86 lbs

Rated Engine Power (REP) = # engines * Amp * 1.2 V/cell * # cells
 = 1 engine * 40 Amps * 1.2 V/cell * 37 cells = 1776 W

Manufacturing Work Hours (MFHR)

1. Wing: 71 Work Hours

15 hr/wing * 1 wing + 4 hr/sq. ft of projected area * 14 ft² + 3 hr/control surface * 2 ailerons

2. Fuselage: 24.6 Work Hours

5 hr/body * 1 body + 4 hr/ft of length * 4.9 ft

3. Empenage: 20 Work Hours

5 hr basic + 5 hr/vertical surface * 1 vertical tail + 10 hr/horizontal surface * 1 horizontal tail

4. Flight Systems: 13 Work Hours

5 hr basic + 2 hr/servo * 4 servos

5. Propulsion Systems: 10 Work Hours

5 hr/engine * 1 engine + 5 hr/propeller * 1 propeller

Total Manufacturing Work Hours: 138.6 Work Hours

Costs	
A = Manufacturers Empty Weight Multiplier	\$100/lb
B = Rated Engine Power Multiplier	\$1/Watt
C = Manufacturing Cost Multiplier	\$20/hour

$\text{Rated Aircraft Cost, \$ (thousands)} = (A \cdot \text{MEW} + B \cdot \text{REP} + C \cdot \text{MFHR}) / 1000$

$\text{Rated Aircraft Cost} = (\$100/\text{lb} \cdot 16.86\text{lb} + \$1/\text{Watt} \cdot 1776\text{Watts} + \$20/\text{hour} \cdot 138.6\text{hrs}) / 1000$

Rated Aircraft Cost = \$6.234 (thousands)

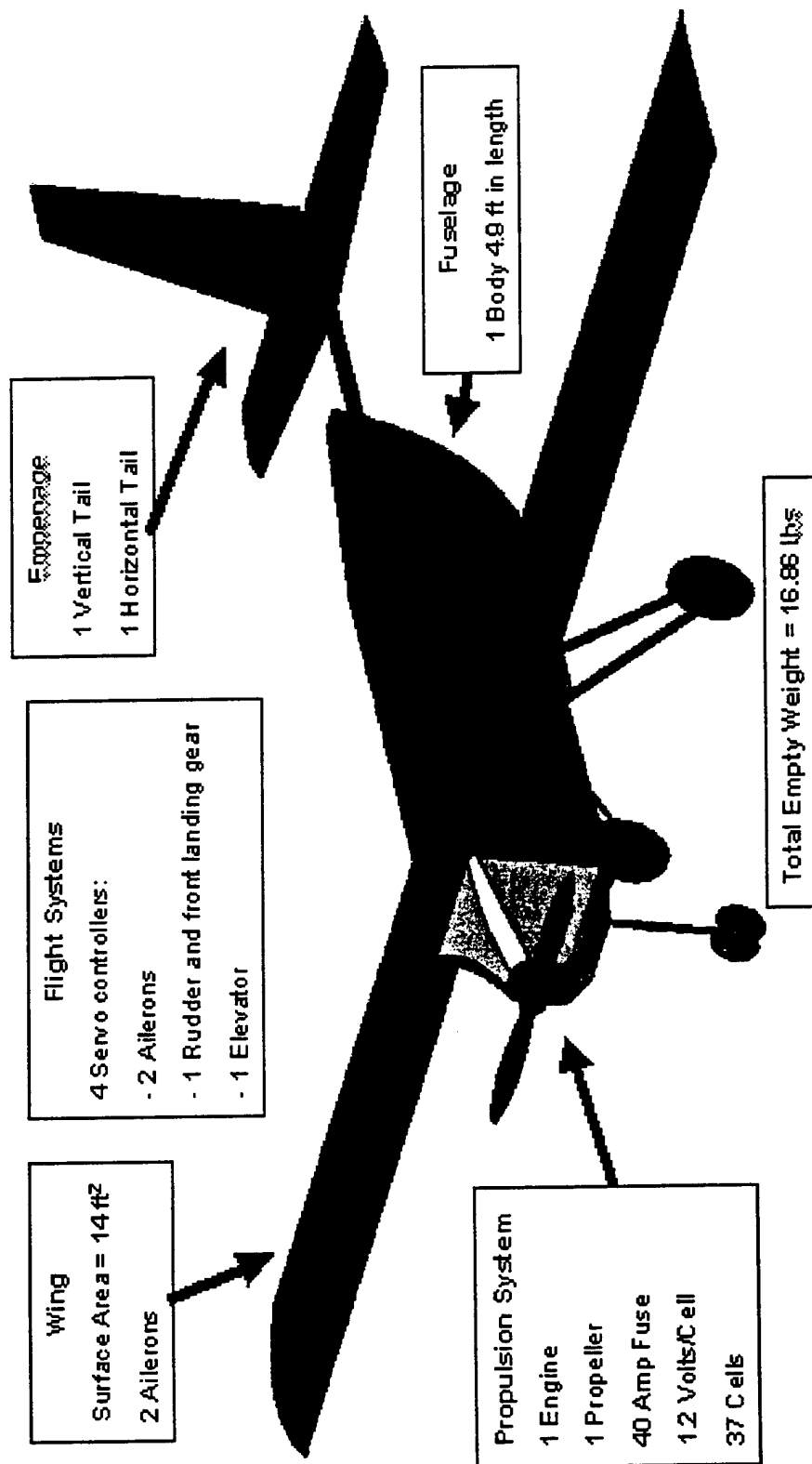


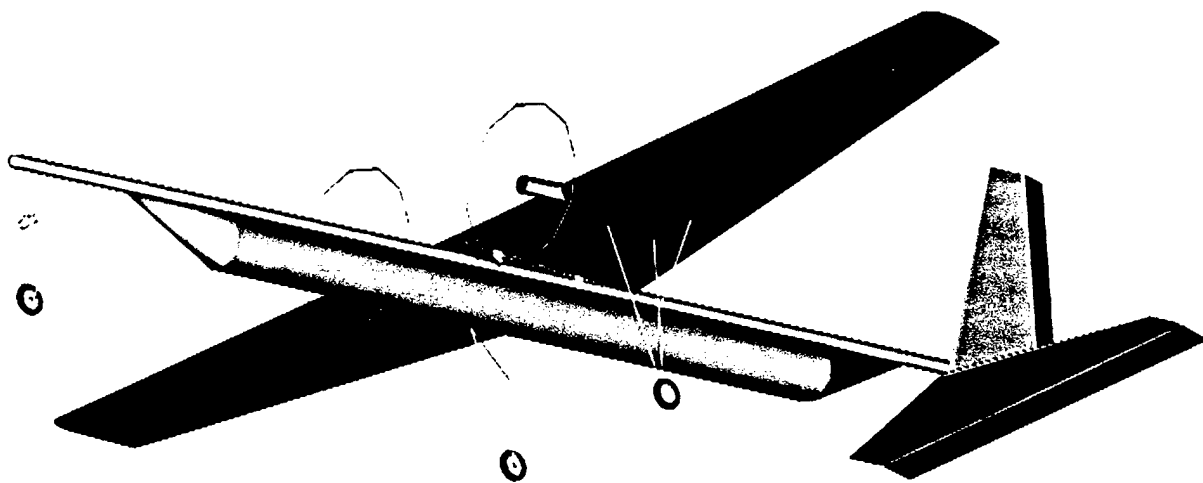
Figure 9.1 Rated Aircraft Cost Parameters

LOTHWORKS
WEST VIRGINIA UNIVERSITY

Proposal Phase

April 19th – 21st, 2001

Cessna ONR – Student Design/Build/Fly Competition



DEPARTMENT OF MECHANICAL AND AEROSPACE ENGINEERING

WEST VIRGINIA UNIVERSITY

MORGANTOWN, WV 26506

i. Table of Contents

i. Table of Contents	1
1. Executive Summary	3
2. Management Summary	4
Design Team	5
Design Configuration	5
Calculated Flight Score	5
3. Conceptual Design	6
3.0 Introduction	6
3.1 Material Selection and Construction Techniques	6
Balsa Wood.....	7
Foam Build-up.....	7
Composite Materials	8
Other Materials	8
3.2 Aircraft Parameters.....	8
Alternative Designs	8
Number of Motors	9
Number of Wings	9
Number of Fuselages.....	10
3.3 Conclusions	10
3.4 Conceptual Design Results	10
4. Preliminary Design	11
4.0 Introduction.....	11
4.1 Investigation of Design Parameters	11
Number of Tennis Balls.....	11
Steel Weight.....	11
Wing.....	12
4.2 Preliminary design rating system	12
4.3 Analytical Methods	12
4.4 Optimization Scheme Results	16
4.5 Structural Design	16
4.6 Wing Structure Analysis	16
4.7 Fuselage Structural Analysis	17
4.8 Preliminary Design Results	17
5. Detailed Design	26
5.0 Introduction.....	26
5.1 Detailed Design Parameters	26

Airfoil Selection	26
Wing Incidence	26
Wing Twist	27
Wing Dihedral	27
Wing Geometry	27
Wing Control Surface Sizing	27
Horizontal Tail Geometry and Sizing	28
Vertical Tail Geometry and Sizing	28
Propeller Selection and Motor Placement	28
Empennage Location	29
Landing Gear Configuration	29
Longitudinal Static Stability	29
5.2 Material Assessment	30
5.3 Composite Fiber Laminate Comparison	30
5.4 Truss-Core Sandwich Composite Stringers	31
5.5 Truss-Core Sandwich Composite Stringer Analysis	31
5.6 Fuselage Structural Analysis	32
5.7 Landing Gear Structural Analysis	33
5.8 Payload Configuration	33
5.9 Turn Rate	34
5.10 Conclusions	34
6. Manufacturing Plan	42
6.0 Introduction	42
6.1 Wing	42
6.2 Fuselage	43
6.3 Speed-Loader	43
6.4 Tail	44
6.5 Landing Gear	44
6.6 Motor Assembly	44
6.7 Final Assembly	44
7. References	46
8. Lessons Learned	47
9. Rated Aircraft Cost	47

1. Executive Summary

Back in September a group of engineering students from West Virginia University was assembled to begin work on this years airplane for the 2000-2001 Design Build and Fly Competition. Consisting of students from such fields as Mechanical/Aerospace, Electrical, Computer, and Civil Engineering, the team was made up of eight seniors, five juniors, two sophomores, a grad student, and remains under the direction of Dr. John Loth as it has for the past several years.

The competition which will be held April 21-22, 2001, is in its fifth year of succession, and once again sponsored by the AIAA in conjunction with Cessna Aircraft and the Office of Naval Research. The objective of the teams competing, is to design a propeller driven, electric powered, unmanned, RC type aircraft capable of carrying payloads of both tennis balls and steel in separate sorties of 10 minutes in duration.

The *LothWorks* entry utilizes a mono-wing planform accompanied with a taper and twist angle that makes for a near elliptical lift distribution. Powered by two AstroFlight Cobalt 640G electric motors, the airplane is driven by two 18-cell battery packs consisting of 2,400 mA-hr Sanyo high capacity racing cells. The above accessories allow the current load per motor to remain under the 40 amp limit, as well as fulfilling the requirement for five pounds of battery weight or less. Additional features of our aircraft include a conventional tail made from balsa wood, an aluminum fuselage, and a carbon-fiber speed-loader. A chart with the final configuration data for the *LothWorks* entry can be seen below.

Parameter	Value	Units
Horizontal Tail Area	3.00	ft ²
Vertical Tail Area	1.68	ft ²
Wing Aspect Area	8.33	
Wing Span	10.00	ft
Wing Taper Ratio	0.50	
Wing Root Chord	19.20	in
Wing Tip Chord	9.60	in
Wing Area	12.00	ft ²
Fuselage Length	8.34	ft
Fuselage Diameter	0.12	ft
Speed Loader Length	6.00	ft
Speed Loader Diameter	0.46	ft
Battery Rating	2400.00	mA-hr
# cells	38.00	
# motors	2.00	
# steel sorties	3.00	
# ball sorties	2.00	
Take-off Distance	200.00	ft
Flight Velocity	70.00	ft/s

2. Management Summary

A wide variety of students participated in West Virginia University's entry into the fifth annual Cessna/ONR Student Design, Build, Fly competition. The entire WVU team consisted of one aerospace engineering grad student, seven senior aerospace and mechanical engineering students, one senior electrical engineering student, five junior aerospace and mechanical engineering students, and two sophomore aerospace and mechanical engineering students. A total of sixteen team members with seven having experience from previous years. Preliminary work began during the summer of 2000 with several of the aforementioned students. Microsoft Excel spreadsheets were constructed for future design use, and some building materials were obtained.

With a large number of students enrolled on the team, it was decided that two WVU airplanes would be entered in the competition. Reasons for two entries centered mainly around the lack of workspace for sixteen people at one time, and the availability of materials and manpower. The team was split into two teams of eight. It was decided that seniors Timothy Leuliette, Elrond Driscoll, Sonny Hammaker, Robert Wolfe, and Garth Mathe; juniors Thomas Grindo and Matthew Lechlitter; and sophomore David Howell would comprise team *Lothworks*. Working in conjunction with the *Almost Heaven* team from WVU, the assessment of available materials and the public relations work associated with the donation of materials was accomplished.

The entire aircraft design was carried out by both WVU teams working in conjunction with each other, so as to compare the largest number of airplane designs and pick the best. Three design teams were established. These teams all designed around different speed loader configurations. One team designed for one large speed loader with a three tennis ball cross-section, another team designed for two shorter, side by side large speed loaders with three ball cross-sections, and the third designed for two small speed loaders with one ball cross-sections arranged side by side. The three design groups conducted sensitivity analyses on parameters affecting the total flight score. The computer programs written during the summer were used for this portion of the design. The sensitivity analyses took into account many variables, among them were: the number of tennis balls carried, the weight of steel carried, the wing and tail dimensions, the number and cross sectional size of speed loaders, flight velocity, available battery power, aerodynamic forces applied to the airplane, propeller effectiveness, and takeoff distance. These parameters and others were manipulated to provide the highest possible flight score. It should be noted that these initial designs did not include more detailed aspects such as structural soundness and material selection. **Table 2.1** shows the speed loader configurations designed with their tabulated theoretical flight scores. The configuration that produced the highest flight score was chosen to be built.

Table 2.1. Design pairs and calculated total flight scores.

Design Team	Design Configuration	Calculated Flight Score (report score assumed = 1)
Team 1	One speed loader, 3 ball cross-section, max 100 balls	9.025
Team 2	Two speed loaders, 3 ball cross-section, max 100 balls	6.007
Team 3	Two speed loaders, 1 ball cross-section, max 40 balls	8.864

After the preliminary design was complete, a detailed design was necessary. It was at this point that the entire WVU team was split into the two teams of eight. The *Lothworks* team was then split into two sub-groups: aerodynamics and stability & control, and structures. The aerodynamics and stability & control group was comprised of Timothy Leuliette, Elrond Driscoll, Matthew Lechlitter, and Thomas Grindo. The structures group was comprised of Sonny Hammaker, David Howell, Garth Mathe, and Robert Wolfe. As well as further detailed design in their respective areas, the aerodynamics and stability & control group was in charge of the construction of the wing, empennage, and electrical wiring, while the structures group was in charge of construction of the speed loaders, landing gear, fuselage, and the motor mounting gear. The report writing was conducted mainly by Sonny Hammaker and Garth Mathe, with input from all team members. **Table 2.2** shows a timeline of the planned and actual start and completion times of the design and report phases.

Table 2.2. Design and report timeline.

	Jul '00	Aug '00	Sep '00	Oct '00	Nov '00	Dec '00	Jan '01	Feb '01	Mar '01	Apr '01
Conceptual Design										
Preliminary Design										
Detailed Design										
Report Writing										
First draft										
Final draft										
planned completion										
actual completion										

3. Conceptual Design

3.0 Introduction

The conceptual design phase for any project serves as the foundation for what the final design will ultimately represent. For our particular design, the conceptual phase was split up into two additional phases. An Aircraft Parameters phase, and a Material Selection and Construction Techniques phase. Headed by the APG (aircraft parameter group), the responsibility of the first phase was to evaluate several different aircraft, and how they might fit in well with our common goal. The Material Selection and Construction Techniques phase was basically set up to consider the use of various materials made accessible to our team, and the various techniques used in implementing these materials. Also evaluated in this phase, was the skill level and craftsmanship present in each of the team members. Both phases were worked on by students not only knowledgeable in that particular field of study, but at the same time interested in learning a little bit more.

3.1 Material Selection and Construction Techniques

The main goal in constructing any UAV (unmanned aerial vehicle), is to make it as light as possible without any sacrifice in overall strength. However, in order to start the manufacturing of an aircraft, such things as skill level, cost of materials, funds available to the team, and time

allotted to finish the final product must be carefully evaluated. For team *LothWorks*, a few problems arose as a result of this evaluative process. Because the team consisted of students from various levels of academic standing (second semester freshmen---second semester grad students), the ability levels were all over the map. It was decided from this, that afternoon help sessions would be held in order to get the "rookies" caught up and on the same page as the experienced veterans. These sessions although few and brief, proved to be a great tool in creating team unity and understanding. As soon as everyone was caught up, discussions centered around the typical UAV construction techniques needed to be performed in order to manufacture the various components. The uses of balsa wood, foam build-up, and composites were the main topics discussed along with the limited uses of steel and aluminum.

Balsa Wood

One of the most common yet cheaper forms of building UAV's is with the use of balsa wood. Typically used in construction of light remote controlled aircraft, this material can prove to be very efficient in multiple applications. For our particular airplane, balsa wood was instrumental in adding strength while conserving weight internal to the wing as ribs, as well as in the total construction of the horizontal and vertical tails. In these applications, the wood was weight effective, and relatively easy to work with. On the other hand, in areas where strength is essential (ie. fuselage, external structure of the wing), balsa wood is generally ruled out as the main constructing material. This was no different in our case, for the concept of carrying as much payload as possible constituted a big portion of this years competition. The team members who had past experience in working with balsa were for the most part put in charge of the above tasks.

Foam Build-up

Perhaps the cheapest method in manufacturing parts for any type of UAV, is the method of foam build-up. Typically worked from a stock block of foam, materials can be easily formed into a desired airfoil shape by the use of a hot-wire. In order to increase its physical properties, a layer of composite and or thin layer of balsa wood can be applied where needed. This foam has a couple of drawbacks however. There is no room internal to a component made out of foam because it is just too weak to store anything. Also, many times a low density foam is accompanied with some sort of strengthening agent which ultimately adds to the weight of the component. This defeats the original purpose of using the foam (cut down on the weight) and should be stayed clear of whenever at all possible. For this year's airplane, foam was used to fabricate a plug to build our wing, used inside the speed loader carrying the steel, and for the construction of the airfoils encompassing the landing gear. Previous WVU entries designed mainly for speed have applied this method in constructing their wing, but with this years rules calling for the transportation of steel payloads, alternative methods were turned to.

Composite Materials

Composite materials are prevalent in nearly all forms of aircraft being manufactured in today's society. Defined as the combination of two or more materials used in creating a new material with enhanced mechanical and physical properties, a composite is generally found in one of two forms; fiberglass-epoxy or carbon-epoxy.

The advantages to using composite materials in aircraft are endless, but for applications specific to our entry, the main advantage is its strength to weight ratio. Fortunately for our team, a few members from last year's squad gained experience in working with the material, and over time learned how to construct lightweight yet very strong components. Another important factor, and key concept in working with composite materials, is the ability to manufacture multiple components in a portion of the time it would take with another material. Although time is needed to lay up a wing or a speed loader, once the mold is made, several parts can be manufactured in just a short time period. For this years airplane, the use of carbon fiber was instrumental in the overall design of our aircraft.

The only drawback in using the carbon-fiber composite is the obvious cost to buy it. The dry carbon fabric used for our design can cost in excess of \$100 per square yard, and can get real expensive if its usage isn't monitored. Thanks to the College of Engineering at West Virginia University, we can afford to purchase enough to fulfill the needs of our aircraft.

Other Materials

In addition to the above mentioned materials, steel as well as aluminum was used in the construction of this years entry *LothWorks*. Used primarily in the manufacturing of the landing gear, it was the decision of this year's team to use steel where previous year's teams used carbon fiber. The thought of preventing our behemoth of a plane from careening off the ground with carbon fiber landing gear seemed impractical. Bought in rod form, the quarter-inch mild steel was welded together and machined to make up the rear portion of the tricycle landing gear. For the frontal gear, an assembled piece was purchased for purposes of connecting to the aluminum fuselage. The sole other application where aluminum was used was in the manufacturing of the nacelle houses for the electric motors.

3.2 Aircraft Parameters

Alternative Designs

The purpose of the conceptual design phase of any project is to brainstorm for all the possible designs suitable to your aircraft. Because of the wide variety of academic standing present on this team, the ideas and concepts investigated were all carefully thought through before further development was commenced. Six different combinations were analyzed for our particular aircraft, and values were given to each component in terms of how it affected the overall performance of the plane. The three components evaluated included the motor(s), wing(s) and the fuselage. If multiple parts of the same component proved favorable to the

particular design entity, a value of +1 was assigned. On the other hand, if for example two wings proved to be too much of a hindrance to the overall performance of the airplane, a value of -1 was assigned. Likewise, a 0 value was assigned if it was deemed negligent on the performance of the airplane. These values were then totaled up and by process of elimination, the proper number of components needed to maximize our flight capabilities, and furthermore our total flight score was determined. This approach properly termed the "Figures of Merit" is represented in the table marked 3.1 below, and served as the basis of our initial design.

Table 3.1 Figures of Merit used to evaluate the baseline aircraft.

Figures of Merit	Number of Components	Energy Available	Empty Weight	Rac	Payload Weight	Drag Coefficient	TO Performance	Manufacturing Time	Cost	Strength	Overall Weight
Motor	1	1	0	0	-1	0	-1	0	0	0	-1
	*2	-1	0	-1	1	0	1	1	-1	0	0
Wing	*1	1	0	0	-1	0	-1	0	1	0	0
	2	-1	-1	-1	1	-1	1	0	-1	1	-2
Fuselage	*1	1	1	0	1	0	0	1	0	1	5
	2	-1	-1	-1	-1	-1	0	-1	-1	-1	-8
* Denotes the number of components used on <i>LothWorks</i>											

Number of Motors

The decision on how many electric motors to use brought about many questions. In using just one motor, take-off performance would be hurt significantly, but weight as well as funds would be salvaged. In using two motors, the rated aircraft cost would be driven up which entails driving our overall score down, but at the same time, the payload capabilities would be enhanced. As a team, we decided that without the use of two electric motors, we would be unable to accomplish some of the goals we set out for ourselves. These motors provide plenty of power at the expense of the batteries to power us for take-off, and to power us during our regular flight.

Number of Wings

When our team decided to go with the mono-wing configuration, aspects such as wing loading, take-off performance, payload weight and manufacturing time had to be carefully considered. An increase in the number of wings used would add significantly to the overall weight of the aircraft as well as to the overall carrying capacity. However, wanting to keep the weight at a minimum while still maintaining strength, we decided to go with the single wing structure with internal rib supports. This allowed for us to carry significant payload while limiting the overall weight of the wing at the same time. It also reduced the drag acting on the aircraft.

Time of manufacturing for the bi-wing configuration was another main deterrent. We knew that in manufacturing two wings for each aircraft, the quality of both would be sacrificed. Even though the molds were made up to mass-produce the wing, the time to do this takes away significantly from your schedule. Last but not least, the inclusion of a bi-wing configuration has a significant effect on the rated aircraft cost.

Number of Fuselages

Although we entertained the idea of more than one fuselage for some time, it was a unanimous decision to stray away from it. The addition of another fuselage meant many things in terms of overall performance and weight of the aircraft. Not only would a second fuse increase the empty weight of the plane, it would also require more battery power and increase the overall drag. We viewed both of these components as major players in the overall score of our aircraft and decided that the negatives outweighed the positives. In addition, the time needed to manufacture multiple fuselages was at a premium; as was the funds needed to purchase more carbon fiber. The increase in rated aircraft cost was also a major factor in choosing to fly with just a single fuselage.

3.3 Conclusions

Upon conclusion of the help sessions for the inexperienced team members, the conceptual design phase for *LothWorks*, went as planned. As a result of all the hard work and dedication put forth during this initial stage, a good basis for an aircraft was established. Perhaps the most difficult task during these first few weeks was assessing the overall skill and craftsmanship of the team members and analyzing the materials available as well as needed in order to complete our design in a timely manner.

3.4 Conceptual Design Results

As a result of past performances and the ability levels of the various team members, several options needed to be explored before an actual design was able to get underway. The hope of this initial stage was to carefully analyze all materials from both a cost effective and reliability point of view. In doing this, the team chose the carbon fiber composite material as the major component for constructing the airplane. Major parts including the wing and the speed-loader were deemed as being necessary components to be constructed out of this material if a competitive aircraft was to be built. In addition to using the carbon fiber, the balsa wood found itself being used as supporting ribs internal to the wing as well as the major component in constructing both the horizontal and vertical tails. The foam was instrumental in producing a plug to manufacture the wing and was also used along the inside of the speed-loader to help secure the steel. Not to be forgotten, the steel and aluminum played key roles in producing the landing gear and fuselage respectively.

4. Preliminary Design

4.0 Introduction

The preliminary design phase for our aircraft was set-up in a similar manner to that of the conceptual design. The main difference is that it provided a more in depth look at the materials, techniques, and configurations used while analyzing our airplane for the competition. This phase can only be as good as the prior phase (conceptual design), for it uses our original ideas and puts them into a more finalized structure.

4.1 Investigation of Design Parameters

There were three primary parameters investigated for further development during the preliminary design phase of our aircraft. The wing selection, number of tennis balls used, and amount of steel weight present were all further analyzed during this stage in order to improve the original baseline aircraft mentioned in the conceptual design. Once again, the structures group consisting of Sonny Hammaker, David Howell, Garth Mathe, and Robert Wolfe was put to the test in order to maximize the total flight score obtainable by the *LothWorks* aircraft. The three design parameters are discussed in detail, in the following few sections.

Number of Tennis Balls

The number of tennis balls carried per sortie had a major impact on our fuselage design as well as our total flight score and many other aerodynamic parameters. Since our team determined that we would try to maximize the number of tennis balls carried in order to yield an optimum score, the fuselage configuration played a key role in the drag acting on our aircraft. A large frontal area meant more drag, but a smaller fuselage meant less tennis balls carried and thus a lower total flight score. The battery power being used to fly the plane also needed to be determined, because as it increased, the number of possible sorties flown, decreased. The optimization model put into effect took all of the above factors and ran them through a Microsoft Excel program. This program allowed us to determine which fuselage diameter to use, how many tennis balls to be loaded, and how much battery energy would be spent while still achieving the highest possible score.

Steel Weight

The requirement to transport steel as a payload during one of the sorties allowed us to form a worst case scenario for most of our flight tests. Knowing that the increase in weight (compared to the tennis ball sorties) would increase our wing loading, and our battery usage during the take-off segment, we were able to determine how strong a wing we would need in order to get the plane off the ground. It was a relief to find out upon completion of our wing, that a tip test performed with nearly 30 lbs of steel resulted in less than a half an inch deflection at the center of the wing. We knew we had built a wing that would fulfill all the requirements at the competition.

Wing

Perhaps the parameter with the most influence on the rated aircraft cost, as well as the overall flight score is the wing area. Everything from the stall characteristics to the empty weight of the aircraft is effected by the total wing area. Similarly, the payload capabilities, battery energy used at take-off and landing, and appearance are affected. The overall influence the wing has on the performance was the main reason why it was selected as an independent variable for the optimization study.

Ideally, the loading of a wing should be elliptical. The best way to obtain elliptical wing loading is with an elliptical wing. In practice an elliptical wing is difficult to construct, so a trapezoidal half-span wing planform is substituted. For an unswept wing at subsonic speeds, a taper ratio of 0.45 allows for close to ideal wing loading. The reason for the taper is because a rectangular planform creates higher wingtip loading, which in turn creates approximately seven percent more drag due to lift than an elliptical wing of the same aspect ratio. For swept wings the taper ratio would be increased slightly to obtain more lift from the wing tips in an attempt to keep the ideal loading. These geometrical relations were kept in mind during the design, so as to obtain a final wing planform similar to that of a wing with ideal loading.

4.2 Preliminary design rating system

During the preliminary design phase, the team decided to replace the F.O.M method introduced in section three (3) (conceptual design), with a more reliable optimization model. We felt that this improved model would give us a better analysis of competing configurations.

4.3 Analytical Methods

The structures group performed optimum analysis on the number of tennis balls per sortie, amount of steel weight carried per sortie, maximum wing area, and optimum fuselage configuration all the while remaining within the amount of battery energy available. Once selected, the values used were compared in ratio form to the rated aircraft cost and analyzed against the alternative configurations. This method proved to be an easy way of comparing separate configurations as long as the design teams did a fairly good job in manufacturing.

The development of the final configuration stemmed from the analysis of the baseline aircraft from the conceptual design phase. As stated earlier, the preliminary design can only be as good as the conceptual design. An optimization program was developed by all members of the *LothWorks* team in an effort to equate the overall score, battery energy used, and steel payload weights as functions of the wing area, fuselage configuration, and number of tennis balls carried.

Initially, the total wing area, number of electric motors, and the various component weights were entered into the Excel spreadsheet. A rough estimate of the wing weight was used on the basis of last years wing, for similar construction techniques and materials were used, and

the remaining several parameters were defined in **Table 4.2**. Once the parameters were all accounted for, they were used to determine the available battery energy from equation 4.1 below.

$$E_{battery} = (\# cells) * (Volts/Cell) * (mA - hours) * (3.6) \quad (4.1)$$

The next parameter to be determined was the stall velocity of the airplane using the predicted wing loading. The number of tennis balls being used was varied from ten (10) to one-hundred (100), in increments of ten (10), and through the use of the computer program, the dimensions of the fuselage's diameter was able to be determined. The empty weight of the fuse was calculated by knowing the density of the material being used to build it, and the estimate of the fuselages dimensions given by the program. Weighing the tennis balls and then adding the total weight of the fuselage to the weight of the balls was how the loaded weight of the fuselage was found. Since it will be impossible to predict the weather conditions the day of the competition this far ahead of time, certain aspects were considered when determining the aircraft performance. Typically very windy at the site, a 30-fps (feet/second) headwind/tailwind was implemented in order to determine the effective distance the plane will travel in less than optimum conditions. This correction factor resulted in an increased "effective" distance flown by the aircraft. The equations used in determining the effective distance flown by our aircraft can be seen below labeled 4.2 and 4.3.

$$S_{effective,steel} = S_{steel} + 2000 \left(\frac{1}{1 - \left(\frac{V_{wind}}{V_{flight}} \right)^2} - 1 \right) \quad (4.2)$$

$$S_{effective,steel} = S_{steel} + 4000 \left(\frac{1}{1 - \left(\frac{V_{wind}}{V_{flight}} \right)^2} - 1 \right) \quad (4.3)$$

These effective distance correction equations allowed the team to be able to account for both an increase in time for a tailwind, and a decrease in flight time for a headwind.

The ball and steel sortie flight times were then estimated using the following two equations.

$$T_{balls} = \#sorties_{balls} * \left(\frac{S_{effective,balls}}{V_{flight}} \right) \quad (4.4)$$

In order to obtain the amount of time the team would need to make pit stops to change payload, the above value for time was subtracted from the ten-minute flight allowance given by the rules

$$T_{steel} = \# \text{ sorties}_{steel} * \left(\frac{S_{effective, steel}}{V_{flight}} \right) \quad (4.5)$$

committee.

Using the flight velocity (Ref. Table 4.1) and basing the fuselage Reynolds number on length, the turbulent friction coefficient of the fuselage was able to be determined from the following equation.

$$C_f = \frac{0.074}{Re_L^{0.2}} \quad (4.6)$$

Equation 4.6 was then used to find the fuselage parasitic drag coefficient from equation 4.7 below.

$$C_{D_o} = 0.47 + C_f * \frac{S_{wet, fuse}}{S_{frontal, fuse}} \quad (4.7)$$

The value 0.47 is a given number for the drag acting on a sphere simulating our nose cone. It was from this equation that we were able to calculate the parasite drag coefficient for the entire aircraft. It reads as follows:

$$C_{D_o, plane} = C_{D_o, wing} + C_{D_o, landing gear} * \frac{S_{LG}}{S_w} + C_{D_o, tail} * \frac{S_{tail}}{S_w} + C_{D_o, fuse} * \frac{S_{fuse}}{S_w} \quad (4.8)$$

The next step in this process was to determine the optimum lift coefficient by using the definition of the induced drag coefficient as a reference. The following equation was instrumental in this calculation.

$$C_{L, opt} = \sqrt{C_{Di} * \Pi * e * AR_{wing}} \quad (4.9)$$

From here, we were able to calculate the maximum lift to drag ratio by dividing the optimum lift coefficient (eq. 4.9) by the aircraft drag coefficient ($C_{D, plane}$). It is shown as equation 4.10 below.

$$\left(\frac{L}{D} \right)_{MAX} = \frac{C_{L, opt}}{C_{D, plane}} \quad (4.10)$$

Finding the weight of one tennis ball and then multiplying it by the number of balls used determined the weight of the payload during the tennis ball sorties. This value was then added to the weight of the fuselage as well as to the empty weight of the plane to calculate the total aircraft weight. Similar means were used for the steel sorties. With the above values already

determined, the lift coefficient, lift to drag ratio, and power required for the tennis ball sorties could be calculated. The latter is found from equation 4.11 shown below.

$$PR_{balls} = V_{flight} * \frac{W_{balls}}{(L/D)_{balls}} \quad (4.11)$$

The thrust required for flight during the tennis ball portion of the competition, and the power required for flight for the steel portion were found from the equations marked 4.12 and 4.13 respectively.

$$T_{R,balls} = \frac{W_{balls}}{(L/D)_{balls}} \quad (4.12)$$

$$PR_{steel} = \frac{(\#motors) * (\max power / motor) * (\%Power_{steel})}{100} * \eta_{total} \quad (4.13)$$

In finding the take-off thrust, a very important parameter in evaluating the take-off performance was determined. It was found by dividing the available power by the take-off velocity, and it can be seen in equation 4.14 below.

$$T_{take-off,avail.} = \frac{(\#motors) * (\max power / motor) * (\%P_{take-off} / 100)}{V_{take-off}} * \eta_{total} \quad (4.14)$$

Also needed in order to evaluate the take-off performance was the drag at take-off. It relates the drag of the plane with the velocity at take-off as well as the overall wing area. This equation can be used as follows.

$$D_{take-off} = C_{D,plane} * .5\rho V^2 * S_{wing} \quad (4.15)$$

Finally, with the above equations (4-14, and 4-15) solved for, the maximum weight of the aircraft was able to be determined for a set take-off distance of 200 feet. It was found from the following.

$$W_{max} = \frac{(64.4) * (X_{take-off}) * (T_{take-off} - D_{take-off})}{V_{take-off}^2} \quad (4.16)$$

The above equation (4.16) allowed us to calculate the maximum amount of steel we could carry without any problems to our airplane surfacing. Simply by subtracting the estimated empty weight value (W_{empty}) from the maximum weight value (W_{max}), the amount of steel able to be used could be found. In solving for the heavier of the two payloads, we knew the tennis ball payload would cause no problem. Throughout the course of plugging in values for the separate parameters discussed above, the steel payload weight was cross-referenced with the tennis ball payload to ensure that their weight didn't exceed that of the steel. Since the performance of our airplane was based on the weight of the steel, this was a crucial aspect to keep an eye on. As soon as the weight of both payload sorties was determined, a calculation for our total flight score

as well as the Rated Aircraft Cost was found. This allowed us to ultimately calculate an overall score for our aircraft. Simply put, the overall score is a combination of the values found from the Rated Aircraft cost, written report, and total flight score. The representation below forms a clear view on how to calculate this score.

$$SCORE = \frac{Total\ Flight\ Score * Written\ Report\ Score ***}{Rated\ Aircraft\ Cost} \quad (4.17)$$

*** Since we do not know the score on our written report, a value of 1 was used to simplify the calculations.

The configuration resulting in the highest overall score was the one chosen to represent West Virginia University. It was appropriately named *LothWorks*.

4.4 Optimization Scheme Results

Making an educated guess based on the experience of the team, and past years results, the value of the wing area was selected to fall somewhere in the 8 ft² to 13 ft² range. The optimization program we used allowed us to vary the wing area in increments of 1 sq.ft. in order to determine exactly what value would yield the highest overall score. For each wing configuration analyzed, the number of tennis balls used for the payload varied from ten (10), to one hundred (100) in increments of ten. At each increment, and at each wing design, an overall score was determined. The program yielded its highest overall score at exactly 100 tennis balls, and at a wing area equal to 12 sq. ft. Any area above the chosen 12-ft² mark resulted in a battery power usage higher than the 90 % mark, and a possibility for disaster. Thus, it was at the discretion of the team to choose the 100 ball, 12-ft² design for *LothWorks*.

4.5 Structural Design

The load factors that act on any aircraft while in flight express the maneuverability of an aircraft as a multiple of the acceleration due to gravity (32.2 ft/s²=g). For normal general aviation aircraft, $n_{pos} = 3.0$ and $n_{neg} = -1.0$. The V-n diagram shown on the accompanying page depicts the limit load factors as a function of airspeed. Both the maximum (positive) and minimum (negative) lift limit curves were calculated from equation 4.18.

$$n = \frac{0.5 * \rho_{alt} * V^2 * S_w * CL_{max}}{W_{TO}} \quad (4.18)$$

4.6 Wing Structure Analysis

Once the weights of each component were calculated (Ref. Table 4.2), the load, shear, and moment diagrams were generated. Similarly, in order to calculate, the forces acting on the wing, in both the y-z and x-z planes, the lift distributions, along with load and drag distributions were needed.

To graph the shear and moment diagrams in excel the trapezoidal approximation was implemented. This rule allows the engineer to divide the area under the curve into n-sections and

sum up the areas of each adjacent trapezoid. Equation 4.19 below shows how this rule is carried out, and **figures 4.6** and **4.7** graphically demonstrate this principle.

$$A = 0.5 * [f(x_{i-1}) + f(x_i)] * \Delta x \quad (4.19)$$

To find the lift along the span of the wing, three-inch sections were used in approximating an elliptical lift. From here, distributed loads along the wing accompanied with the concentrated loads of both the landing gear and electrical systems allowed for quick determination of the overall load distribution (Ref. **Figure 4.11**). Finally, the drag along the span of the wing, and the concentrated force due to the thrust of the motors was plotted in figures **4.9** and **4.10**.

4.7 Fuselage Structural Analysis

The load diagram of the fuselage was determined from the component weights listed in **Table 4.1**(also see **Figure 4.11**). Each entity was treated as a distributed load acting on the fuselage, and the power plant, avionics, and wing weights were lumped together. As a team, we chose to analyze multiple materials for use as a fuselage. We narrowed it down to aluminum and carbon fiber, for their properties (strength, and weight) were far superior to anything else we had access to. Although a carbon fiber fuselage would cut down significantly on the total weight of the aircraft, it was agreed upon to go with an aluminum fuselage for this year's design. For reasons of machineability and for the simple fact that the carbon could only be purchased in lengths of six feet to the 12 feet for aluminum, the final decision was relatively easy to make. It was also decided that the aluminum would be much more practical in areas where we wanted to thread various components to the fuselage (ie. nose gear, tail, and wing).

4.8 Preliminary Design Results

Upon conclusion of this phase, it was immediately realized that we had a strong foundation to start on the final design of our aircraft. At this time, all team members had become veterans, and all had played key roles in the development of the plane. The analysis performed on the various components was very thorough, and as a team we feel that our choice in selection of materials was the proper one.

In the preliminary phase, an optimization scheme was used to determine the maximum number of tennis balls we could carry along with the maximum steel payload capable of being transported. Our highest overall score turned out to be with payloads of 100 tennis balls, and 13.4 pounds of steel. This was made possible by our 12 ft² of wing area, and a battery usage just below the 90 % mark.

Table 4.1 Aircraft Parameters

Parameter	Value	Units
Landing Gear Frontal Area	0.18	ft ²
Horizontal Tail Area	3.00	ft ²
Vertical Tail Area	1.68	ft ²
Wing Aspect Ratio	8.33	
Wing Span	10.00	ft
Wing Taper Ratio	0.50	
Wing Root Chord	1.60	ft
Wing Tip Chord	0.80	ft
Wing Area	12.00	ft ²
Horizontal Tail Volume Coefficient	0.80	
Vertical Tail Volume Coefficient	0.07	
Tail Boom Length	5.00	ft
Fuselage Length	8.34	ft
Fuselage Diameter	0.12	ft
Speed Loader Length	6.00	ft
Speed Loader Diameter	0.46	ft
Overall Propulsive Efficiency	0.42	
Battery rating	2400.00	mA-hr
#cells	36.00	
Battery Energy	217940.70	ft-lb
%Power - Cruise	65.00	
%Power - Takeoff	95.00	
# motors	2.00	
CDo, gear	0.01	
CDo, wing	0.01	
CDo, h	0.01	
CDo, v	0.01	
Oswald Efficiency	0.80	
Max Current Draw	35.00	Amps
Max power per motor	700.00	W
Steel Sortie Distance	4000.00	ft
Ball Sortie Distance	6000.00	ft
# steel sorties	3.00	
# ball sorties	2.00	
Wing Maximum Lift Coefficient	1.20	
Takeoff Distance	200.00	ft
Flight Velocity	70.00	ft/s
Wing Reynold's Number	534257.35	
Typical Wind Speed	30.00	ft/s
Actual Stall Velocity	49.54	ft/s

Table 4.2 Weight fractions for steel and tennis ball sorties

"Lothworks"	Weight per part	Fraction of total weight	Weight per part	Fraction of total weight
Part	(lb)	(%)	(lb)	(%)
<i>Flap Pushrod L</i>	0.011	0.034	0.011	0.033
<i>Flap Pushrod R</i>	0.011	0.034	0.011	0.033
<i>Flap Servo L</i>	0.097	0.302	0.097	0.294
<i>Flap Servo R</i>	0.097	0.302	0.097	0.294
<i>Fuselage</i>	1.723	5.376	1.723	5.223
<i>H pushrod</i>	0.011	0.034	0.011	0.033
<i>H Servo</i>	0.097	0.302	0.097	0.294
<i>Main Battery L</i>	2.495	7.786	2.495	7.564
<i>Main Battery R</i>	2.495	7.786	2.495	7.564
<i>Main Gear L</i>	1.010	3.152	1.010	3.062
<i>Main Gear R</i>	1.010	3.152	1.010	3.062
<i>Main Wheel L</i>	0.163	0.508	0.163	0.494
<i>Main Wheel R</i>	0.163	0.508	0.163	0.494
<i>Motor L</i>	0.934	2.915	0.934	2.832
<i>Motor R</i>	0.934	2.915	0.934	2.832
<i>NG pushrod</i>	0.010	0.031	0.010	0.030
<i>Nose Brake</i>	0.033	0.103	0.033	0.100
<i>Nose Gear</i>	0.500	1.561	0.500	1.516
<i>Nose Pant</i>	0.067	0.209	0.067	0.203
<i>Nose Wheel</i>	0.163	0.508	0.163	0.494
<i>Prop L</i>	0.053	0.165	0.053	0.160
<i>Prop R</i>	0.053	0.165	0.053	0.160
<i>Rx</i>	0.070	0.220	0.070	0.213
<i>Rx Batt</i>	0.208	0.650	0.208	0.631
<i>Speed Control L</i>	0.122	0.380	0.122	0.369
<i>Speed Control R</i>	0.122	0.380	0.122	0.369
<i>Steel Payload</i>	0.000	0.000	13.440	40.760
<i>Tail</i>	0.649	2.026	0.649	1.970
<i>Tennis Ball Payload</i>	12.500	39.013	0.000	0.000
<i>V pushrod</i>	0.011	0.034	0.011	0.033
<i>V Servo</i>	0.097	0.302	0.097	0.294
<i>Wheel Pant L</i>	0.067	0.209	0.067	0.200
<i>Wheel Pant R</i>	0.067	0.209	0.067	0.200
<i>Wing</i>	6.000	18.730	6.000	18.190
<i>Totals</i>	<i>Total weight</i>	32.041	<i>Total weight</i>	32.981

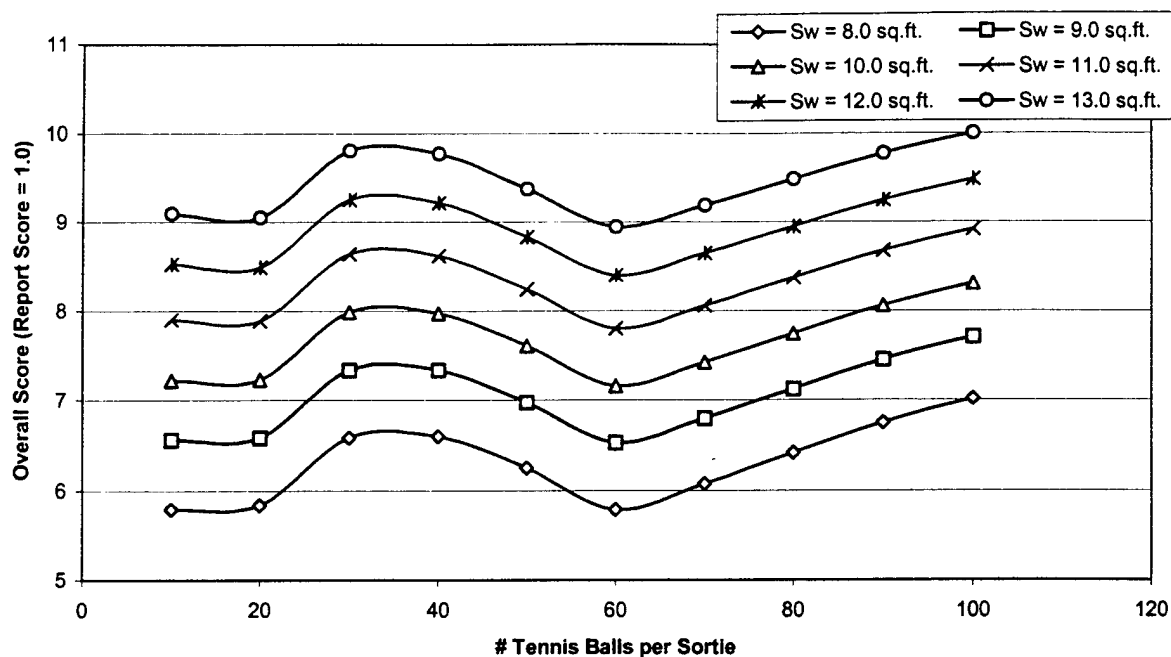


Figure 4.1 Overall Score Dependency on Number of Tennis Balls

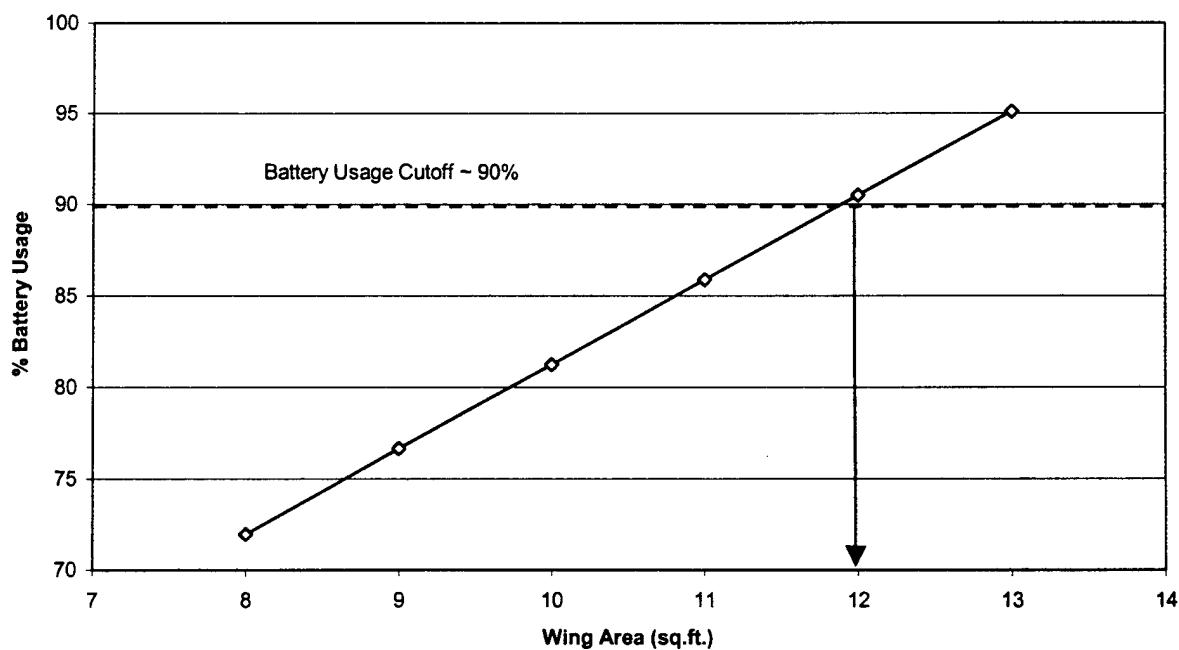


Figure 4.2 Battery Usage Dependence on Wing Area for 100 Tennis Balls

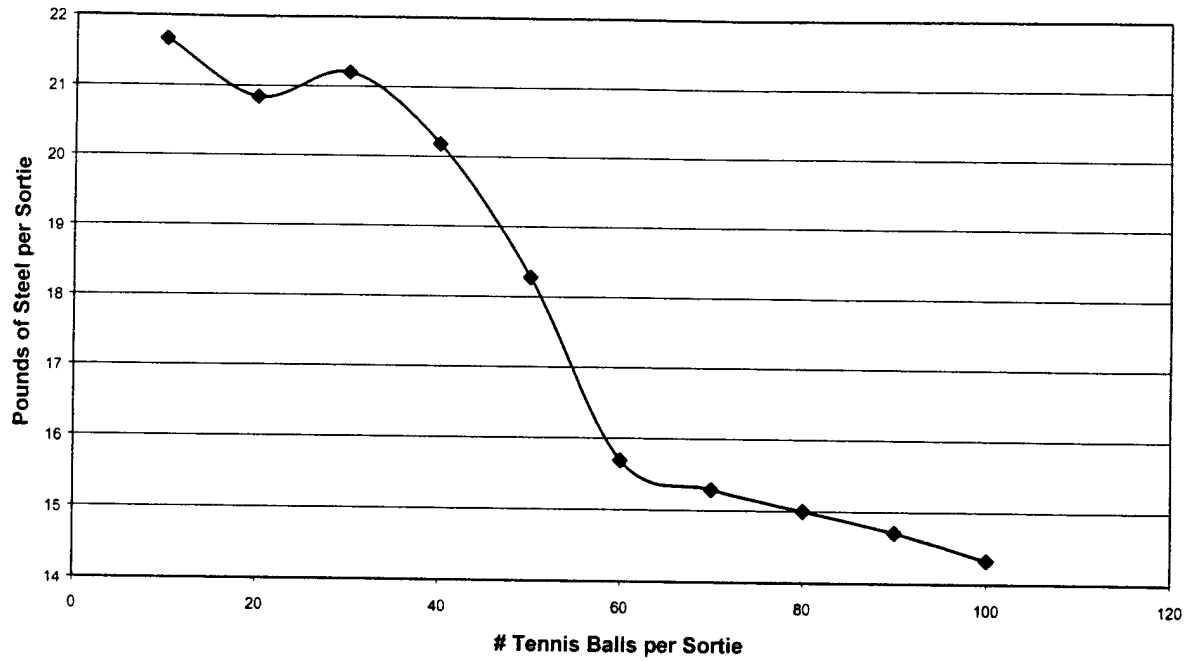


Figure 4.3 Comparison between pounds of steel and # of tennis balls per sortie

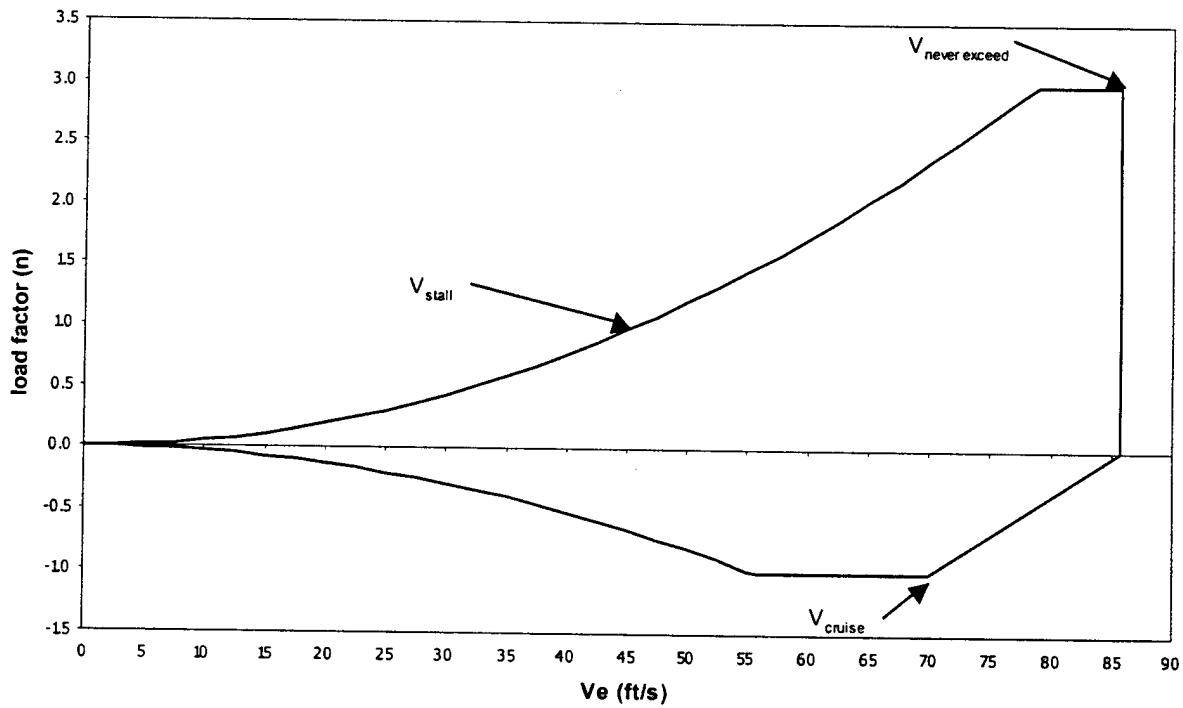


Figure 4.4 V-n Diagram for "LothWorks"

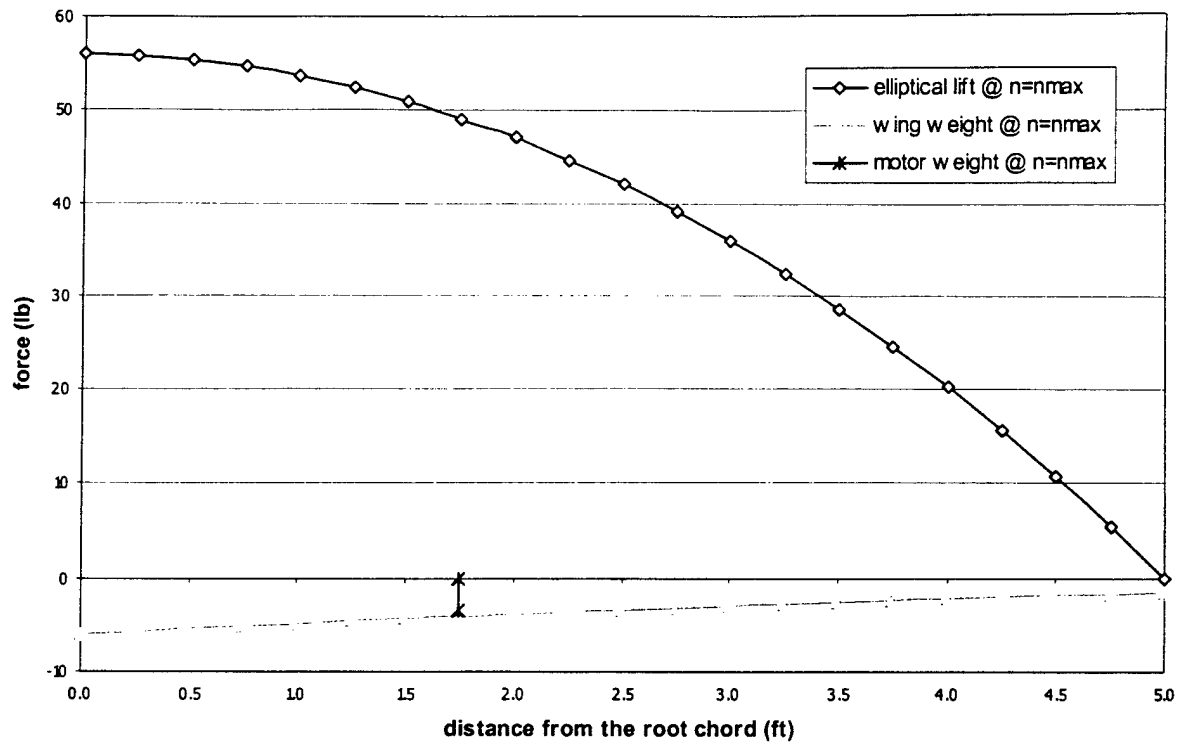


Figure 4.5 Load Diagram due to the lift and weight at $n=n_{max}$

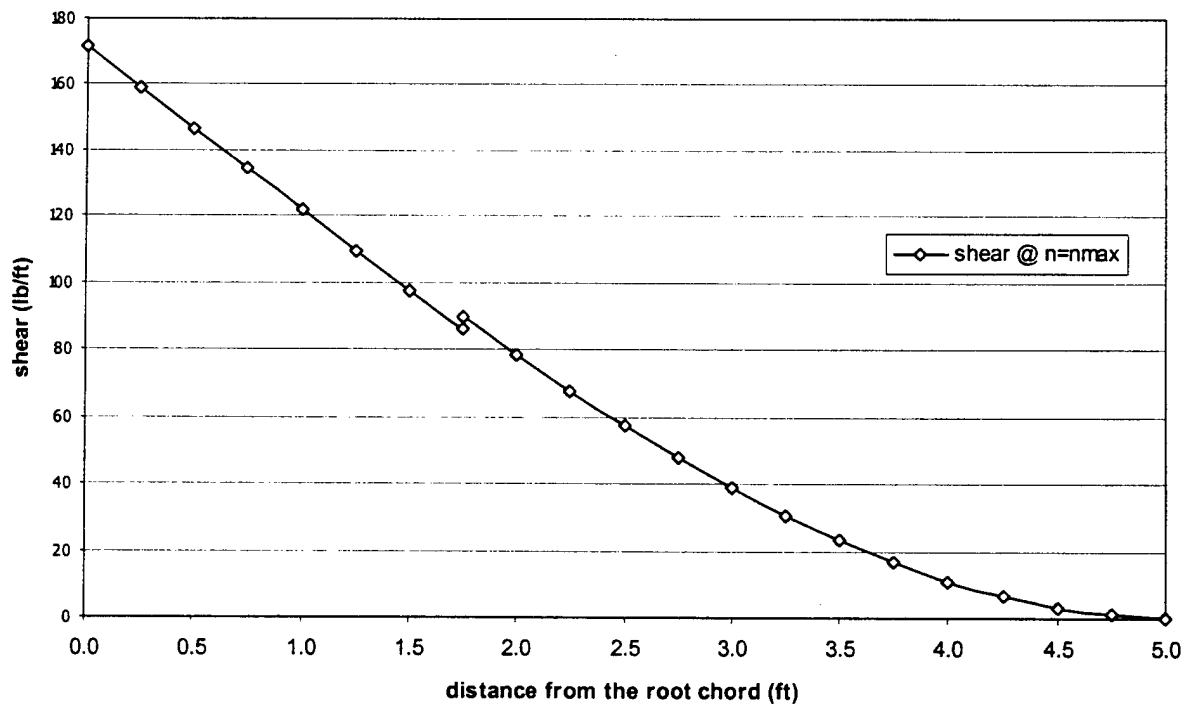


Figure 4.6 Shear Diagram due to the lift and weight at $n=n_{max}$

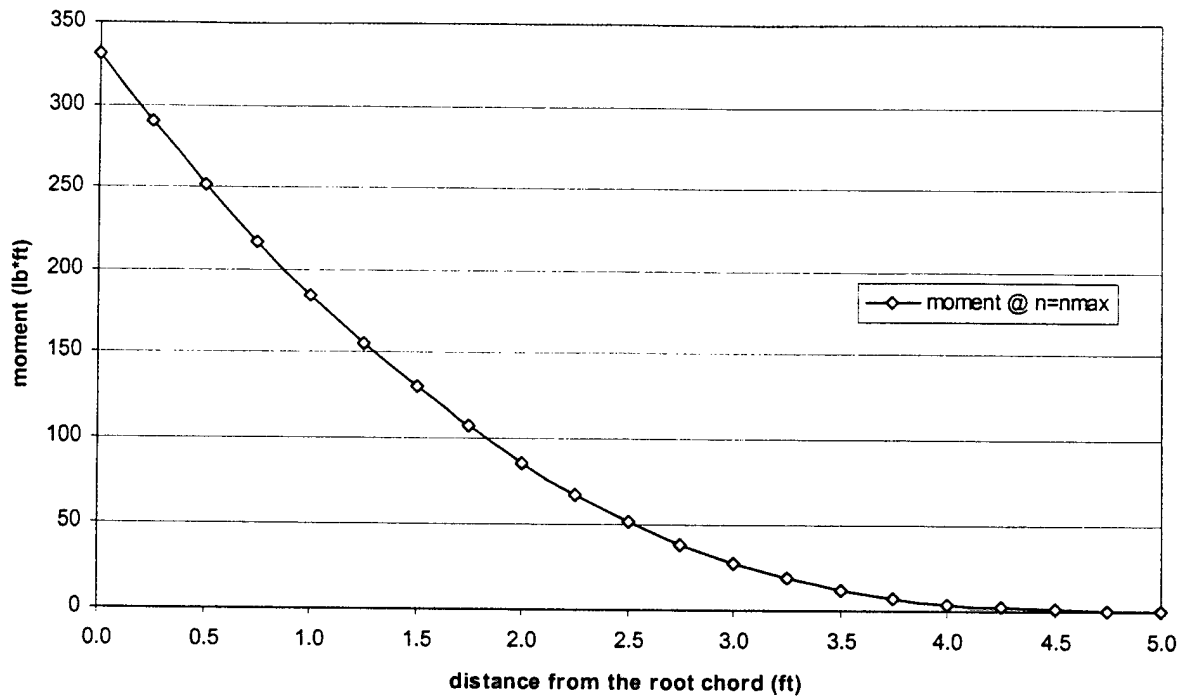


Figure 4.7 Flight bending moment due to the lift and weight at $n=n_{max}$

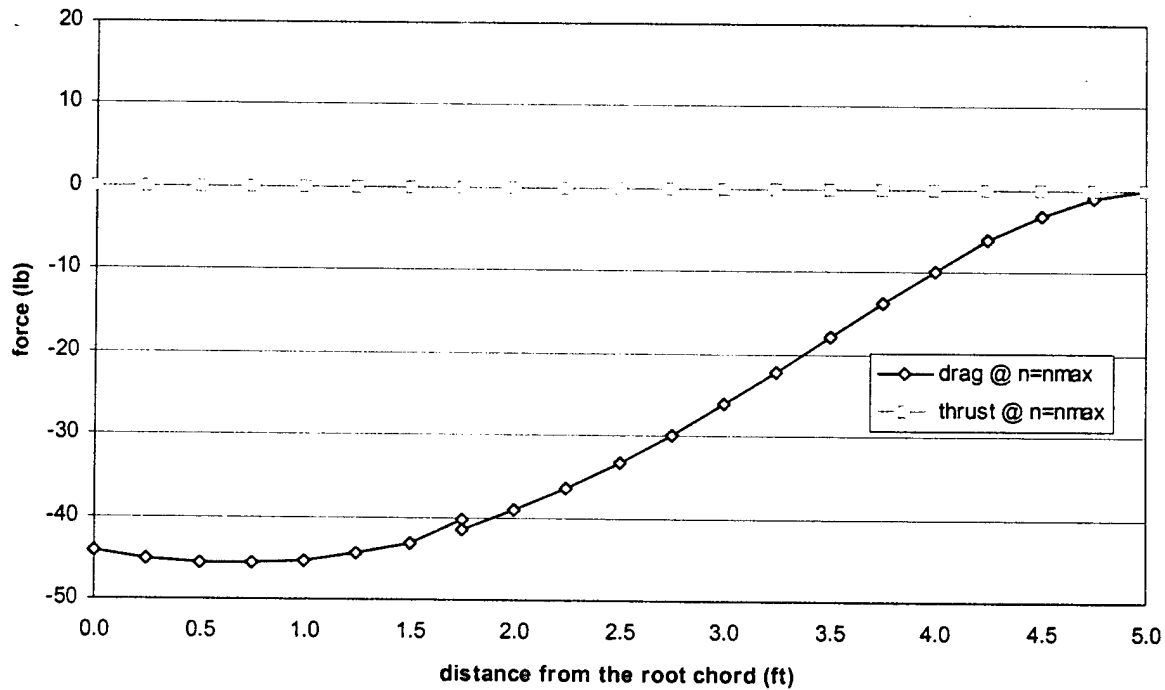


Figure 4.8 Flight load diagram due to the drag and thrust at $n=n_{max}$

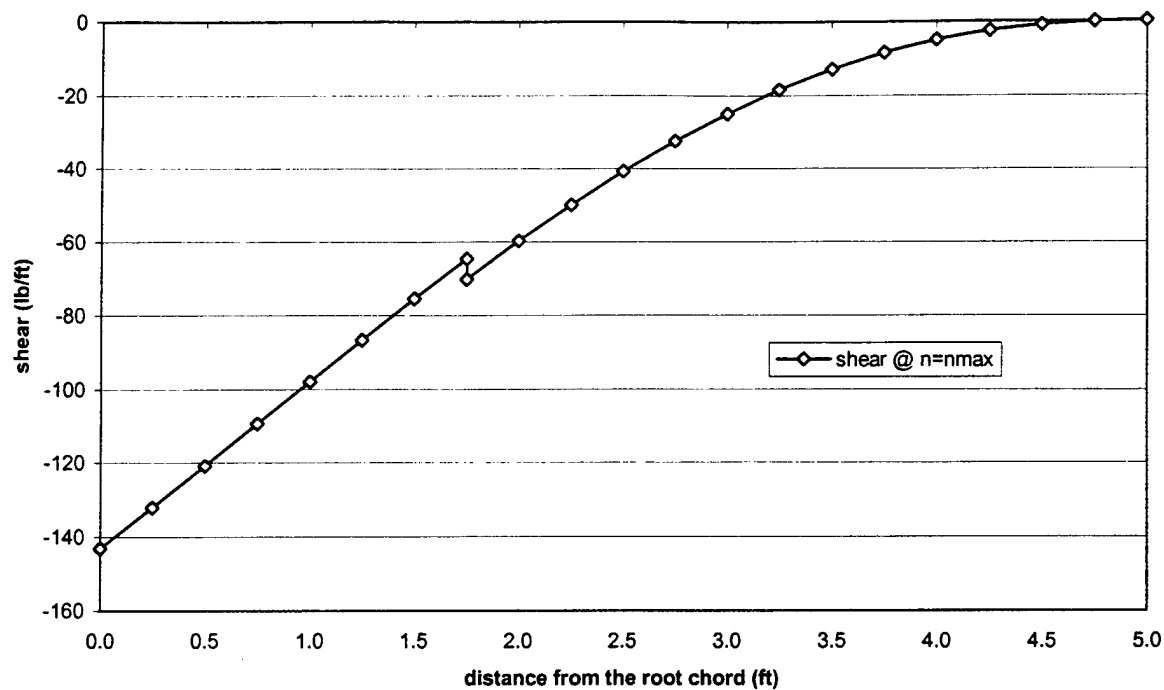


Figure 4.9 Flight shear diagram due to drag and thrust at $n=n_{max}$

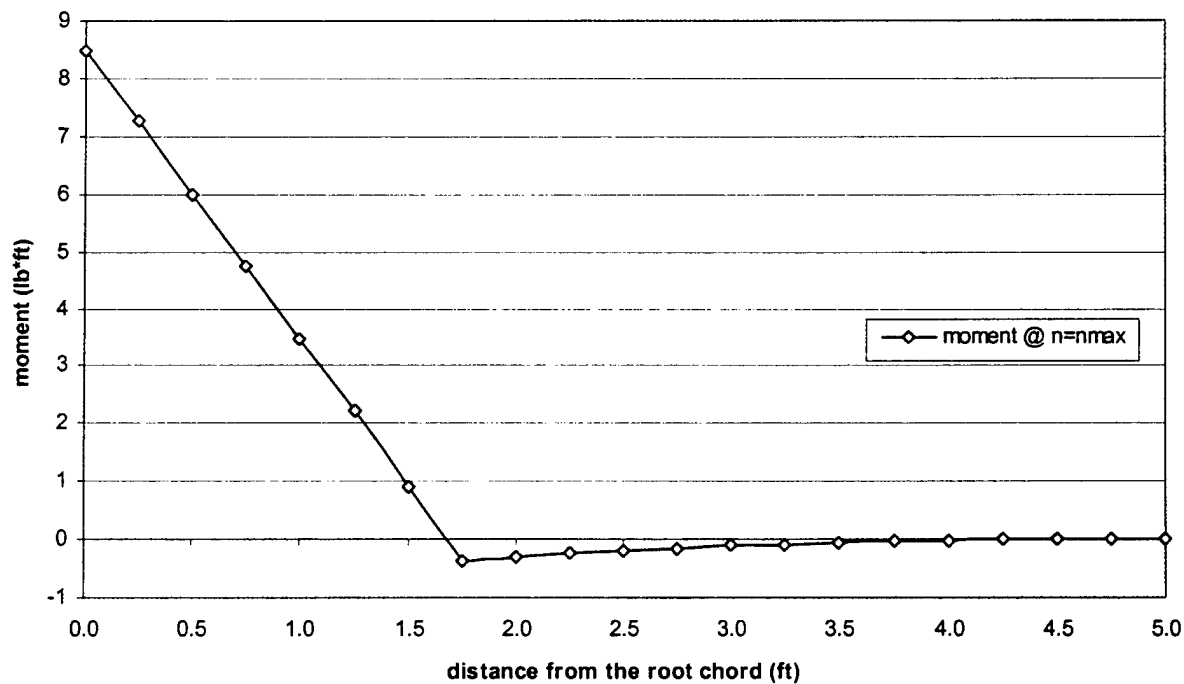


Figure 4.10 Flight moment diagram due to the drag and thrust at $n=n_{max}$

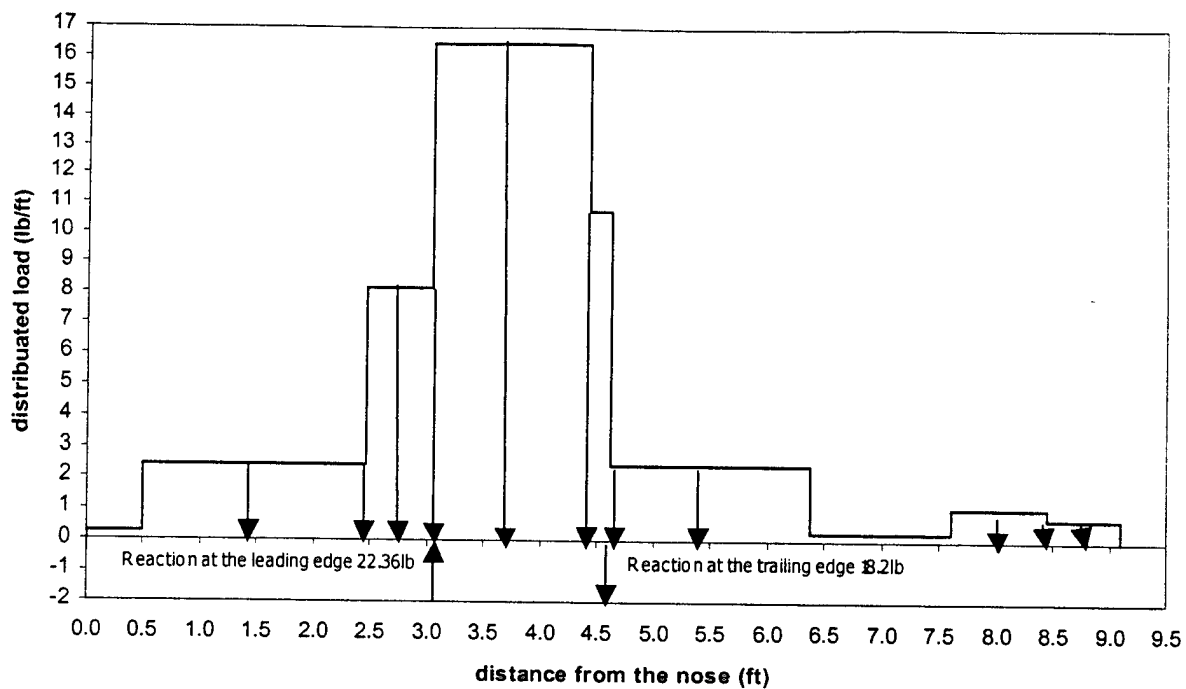


Figure 4.11 Diagram depicting loads acting on the fuselage

5. Detailed Design

5.0 Introduction

The purpose of the detailed design was determine the appropriate: airfoil, wing incidence, wing twist, wing dihedral, wing geometry, wing control surface sizing, tail geometry and control surface sizing, position of the tail, propeller, motor location, landing gear configuration, and longitudinal static stability. These parameters were designed around the aircraft weights and wing area determined in the preliminary design. Structural analyses of the main load bearing members of the aircraft were also carried out to ensure that critical parts would not fail during flight, takeoff, or landing.

5.1 Detailed Design Parameters

Airfoil Selection

The selection of an airfoil is one of the most important parts of an aircraft design. The airfoil will directly affect the airplane's lift, takeoff and landing distances, stall characteristics, and the overall aerodynamic efficiency.

Poor stall characteristics have sidelined several of WVU's entries in previous years. For this reason the stall performance of the chosen airfoil was to be the most important parameter taken into account. The team did not want all its hard work to be in vain because of a crash that could be avoided with proper design.

When plots of airfoil section lift coefficient versus the section angle of attack were compared, there were certain trends that were deemed desirable for good stall characteristics. First, the stall should occur at a fairly high sectional lift coefficient, and second, the loss in sectional lift coefficient should be gradual after the stall. If a rapid loss in sectional lift coefficient after the stall occurred for a given airfoil, that airfoil was eliminated from consideration for design. The thickness of the airfoil also has a large affect on its stall performance. A thin airfoil tends to promote flow separation at lower angles of attack than a thicker airfoil (around 15% chord length) with a larger leading edge radius.

With these ideals in mind, the NACA 4415 airfoil was chosen. **Figure 5.1** depicts the sectional lift coefficient versus the angle of attack for the 4415 airfoil. The gradual drop-off in sectional lift coefficient after the peak, or stall, of the graph should be noted.

Wing Incidence

The wing incidence at the root was determined from **eq. 5.1** to be 7.8 degrees.

$$i_{root} = \frac{C_{L_{root}}}{C_{L_{\alpha_{wing}}}} + \alpha_0 \quad (5.1)$$

The wing incidence at the tip was determined from **eq 5.2** to be 4.8 degrees.

$$i_{tip} = \frac{C_{L_{tip}}}{C_{L_{wing}}} + \alpha_0 \quad (5.2)$$

Wing Twist

It was decided that a twist (root is at a higher incidence angle than tip) would be applied to the wing in an effort to promote better stall characteristics. If a wing is not twisted, the wing will have a tendency to stall at the tips before the roots. This is not desirable as aileron control will be lost. A twist is applied so that the root is at a higher angle of incidence than the tip. A standard value of 3 degrees change from root to tip was implemented for the *Lothworks* entry. The root angle of incidence was raised 1.5 degrees and the tip angle of incidence was lowered 1.5 degrees.

Wing Dihedral

There are no set equations or rules for obtaining the proper amount of dihedral to use on an airplane, so historical values were used to determine this parameter. The dihedral was set to 2 degrees. 2 degrees of dihedral is actually rather small in comparison to many other airplanes, this value was justifiable due to the difficulty of constructing a wing with a higher amount of dihedral.

Wing Geometry

It was decided that the wingspan was to be as large as possible. The maximum allowable span of 10 feet was chosen to allow for a large aspect ratio. A large aspect ratio allows for slower transition from root stall to tip stall (total wing stall), and hence easier piloting. In order to prevent wing tip stall, which typically occurs for taper ratios below 0.45 for small model airplanes, a taper ratio of 0.5 was chosen for safety. From the previously determined wing area of 12 square feet, the aspect ratio was determined to be 8.33. The wing was also to be slightly swept so that the wing quarter chord angle could be normal to the aircraft centerline. When the quarter chord centerline is at 90 degrees, the maximum possible lift can be obtained from the wing. The sweep angle of the wing was determined to be 2.3 degrees from eq. 5.3.

$$\Lambda_{LE} = \arctan \left[\tan(\Lambda_n) + \frac{4n(1-\lambda)}{AR(1+\lambda)} \right] \quad (5.3)$$

Wing Control Surface Sizing

In order to use as few control surfaces as possible, for weight reasons associated with servos, etc., and to minimize deductions in total flight score, it was decided that flaperons would be the sole control surfaces on the wings. These control surfaces were sized as ailerons, but will serve as both flaps and ailerons. The flaperon sizing was based on historical data (Raymer, see references). An aileron chord to wing chord ratio of 0.28, and an aileron span to wing span ratio

of 0.35 were implemented to provide an adequate steady state rolling rate as well as increased lift for takeoff and increased drag for landing.

Horizontal Tail Geometry and Sizing

The sizing of the horizontal tail was based on the volume coefficient method. This can be seen in 5.4.

$$S_H = \frac{c_H MAC_W S_W}{L_H} \quad (5.4)$$

The horizontal tail volume coefficient, c_H , was determined from Raymer. The horizontal tail span and sweep angle were taken from historical data. These parameters were taken as 41-9/16 inches and 18.4 degrees respectively. The taper ratio was taken as 0.5. The elevator sizing was based on historical data and was taken as 30% of the horizontal tail mean aerodynamic chord.

Vertical Tail Geometry and Sizing

Like the horizontal tail sizing, the vertical tail sizing was based on the volume coefficient method. The area of the vertical tail was determined from 5.5.

$$S_V = \frac{c_V b_W S_W}{L_V} \quad (5.5)$$

The vertical tail volume coefficient, c_V , was determined from Raymer. The rudder sizing was taken from historical data to be 30% of the vertical tail mean aerodynamic chord. The vertical tail/rudder areas were also determined so as to provide adequate correcting force with one motor out conditions. The span of the vertical tail was taken as 20-25/32 inches and the leading edge sweep angle was taken as 18.4 degrees. The taper ratio was taken as 0.5.

Propeller Selection and Motor Placement

For propeller selection it was desirable to have a low drop-off in thrust with increasing flight velocity. It was also necessary that the moment of inertia of the propeller not be too large so as to force the motor to use more than 40 amps of electrical current. The software 'ElectriCalc' was used to compare propellers of different diameters, blade numbers, and blade pitches. The final propellers selected were TopFlight 15 X 8. The motors were placed on the leading edge of the wing in order to keep the heavy portions of the airplane near the center of gravity. This increased the steady state pitch rate, resulting in a more maneuverable aircraft. The increased pitch rate can also aid in a slightly faster climb as there is less gravity resistance holding the nose of the airplane down (as in a nose mounted motor). The motors were also situated as close as possible to the fuselage, without letting the airflow through the propellers be disturbed by boundary layer flow from the fuselage and speed loader, to reduce the yaw effect associated with a motor out condition.

Empennage Location

The horizontal and vertical tail leading edges were situated even with each other due to ease of construction and structural soundness. The tail structure was placed a distance of 60 inches from the quarter root chord of the wing to the quarter mean aerodynamic chord of the horizontal tail. This would allow flight with vertical tail (yaw) control to occur with a motor out situation.

Landing Gear Configuration

For the shortest takeoff distance attainable, it was determined that a tricycle landing gear configuration would be implemented. The idea of retractable landing gear was also considered, but eventually the idea was rejected due to construction complications and additions to rated aircraft cost. The retractable gear would also have used precious battery power, which would have affected the number of possible sorties. Fixed landing gear were chosen for their simple effectiveness and time tested reliability.

The tipback angle is defined as the maximum nose-up attitude with the most aft portion of the airplane touching the ground. In order for the airplane to be able to rotate correctly for takeoff and landing, the tipback angle needed to be between 15 and 25 degrees. The overturn angle, which is defined as the angle measured from the center of gravity to the main gear wheel, as seen from the rear at a location where the main wheel is aligned with the nose wheel. For land based aircraft the overturn angle should not exceed 63 degrees. The landing gear were designed and oriented such that the values of aforementioned angles were within their respective ranges.

Longitudinal Static Stability

Good longitudinal static stability is essential for the flight of any aircraft. The longitudinal stability calculations consisted of finding the aerodynamic center and center of gravity of the airplane. The aerodynamic center, the point at which the roll, pitch, and yaw motions revolve, was determined from 5.6.

$$\bar{X}_{ac} = \frac{C_{L_\alpha} \bar{X}_{ac_w} - C_{m_\alpha} + \eta_H \frac{S_H}{S_W} C_{L_{\alpha,H}} \frac{\partial \alpha_H}{\partial \alpha} \bar{X}_{ac_H} + \frac{F_{P_\alpha}}{qS_W} \frac{\partial \alpha_P}{\partial \alpha} \bar{X}_P}{C_{L_\alpha} + \eta_H \frac{S_H}{S_W} C_{L_{\alpha,H}} \frac{\partial \alpha_H}{\partial \alpha} + \frac{F_{P_\alpha}}{qS_W}} \quad (5.6)$$

In the above equation, the propeller force term, $\frac{F_{P_\alpha}}{qS_W}$ has been neglected and accounted for by

adding 0.05 to the static margin. The downwash term, $\frac{\partial \alpha_H}{\partial \alpha} = 1 - \frac{\partial \epsilon}{\partial \alpha}$ was determined through empirical methods. The pitching moment coefficient was found from 5.7.

$$Cm_{\alpha} = \frac{K_f W_f^2 L_f}{c S_w} \quad (5.7)$$

In the above equation, $K_f = 1 \cdot 10^{-7} x^3 + 6 \cdot 10^{-6} x^2 - 2 \cdot 10^{-4} x + 6.6 \cdot 10^{-3}$, where x is the location of the wing root quarter chord with respect to the total fuselage length. **Table 5.1** lists the above equation terms and their respective values. After the aerodynamic center was found, the aircraft components were rearranged so that an adequate static margin could be had. **Table 5.2** lists the various components of the aircraft, their weights, their distances from the quarter mean aerodynamic chord of the wing, and their moments about the quarter mean aerodynamic chord of the wing. In order to keep the aircraft stable with and without payload, the speed loader was designed to be carried with its center of gravity aligned with the aircraft's center of gravity.

5.2 Material Assessment

The first step in the construction phase was to determine what materials were already available to the team, and what materials would be needed for the complete construction of two airplanes. Some remnant materials from previous years were available to the team. These materials included some fibrous materials for use in composites as well as various wood products. Donations such as 1.7 oz. Kevlar 49, 3k carbon fiber, and Styrofoams of various densities were obtained from team sponsors. Purchases of epoxy resins, balsa, servos, push rods, and various tools were made to meet the team's needs.

5.3 Composite Fiber Laminate Comparison

The 1.7 oz. plain weave Kevlar and 3k carbon fiber materials had different properties, which suited them to certain applications. The Kevlar weave was much finer than the carbon fiber, which leant the Kevlar to applications where surface smoothness was very important. Unfortunately, not enough Kevlar was available to construct the entire aircraft, so specific surfaces were to be composed of Kevlar, while others were to be carbon fiber. The outer portion of the wing was chosen to be surfaces with the Kevlar due to its inherent smoothness.

Before any one portion of the aircraft was constructed, tests needed to be run on the composite materials to determine how many layers of a material, or a combination of materials, would be necessary for that particular component. Three laminate combinations were tested for rigidity, strength, and weight. **Table 5.3** compares three different laminates: three layers of [0,90] 1.7 oz. Kevlar 49, one layer of [0,90] 1.7 oz. Kevlar 49 and one layer of [0,90] 3k carbon fiber, and one layer of [0,90] 3k carbon fiber sandwiched between single layers of [0,90] 1.7 oz. Kevlar 49. **Table 5.3** shows that the laminate consisting of one layer of carbon fiber sandwiched between the single layers of Kevlar has higher first ply failure and higher fiber failure values than the other two laminates. An extra advantage of this laminate is that the Kevlar's tight weave is easier to work with than the loosely woven carbon fiber. When manually spreading the epoxy resin over

the carbon fiber, the loose fibers were easily moved out of place, whereas the Kevlar's tight weave was more receptive to working contact and held together better.

5.4 Truss-Core Sandwich Composite Stringers

Truss-core sandwich composite stringers were implemented at the quarter chord of the wing as the main load bearing structure of the wing. The composite stringers were designed to be very light, and due to their great strength the need for spars in the wing does not exist. The construction of the truss-core sandwich composite stringers also proved to be very simple and fast. The stringers, being made of Styrofoam and carbon fiber, were bonded directly to the wing so the fitting associated with spar construction was avoided altogether.

The stringers consisted of five Styrofoam strips, triangular in cross-section, with bases of 1.25 inches, and sides at 45 degree angles to the bases. Three of the strips were glued side by side to the inner wing. A strip of carbon fiber was then laid on top of the three triangular strips and the two remaining strips were laid on top of the carbon fiber in the gaps formed by the first three strips. A cross-section of the truss-core sandwich composite stringers can be seen in the **Drawing Package**.

5.5 Truss-Core Sandwich Composite Stringer Analysis

Composite materials are orthotropic, meaning their properties are not constant in the three dimensions. The material properties of the carbon fiber/epoxy composite between the Styrofoam strips of the truss-core are at +45 degrees and -45 degrees. The calculation of the material properties in these directions required a coordinate transformation matrix. The transformation matrix can be seen in 5.8.

$$[C] = [T]^T [C'] [T] \quad (5.8)$$

The components of the coordinate transformation matrix consist of the stiffness matrix, $[C]$, $[C] = [S]^{-1}$ in the global axis, and $[T]$ is the transformation matrix and can be seen in 5.9.

$$[T] = \begin{bmatrix} \pm \cos\theta & \pm \sin\theta & 0 \\ \pm \sin\theta & \cos\theta & 0 \\ 0 & 0 & 1 \end{bmatrix} \quad (5.9)$$

The sign of the terms depend on which web the properties are calculated for. The compliance matrix, $[S]$ can be seen in 5.10.

$$[S] = \begin{bmatrix} 1/E_1 & -v_{12}/E_1 & -v_{13}/E_1 & 0 & 0 & 0 \\ -v_{12}/E_1 & 1/E_2 & -v_{23}/E_2 & 0 & 0 & 0 \\ -v_{13}/E_1 & -v_{23}/E_2 & 1/E_3 & 0 & 0 & 0 \\ 0 & 0 & 0 & 1/G_{23} & 0 & 0 \\ 0 & 0 & 0 & 0 & 1/G_{13} & 0 \\ 0 & 0 & 0 & 0 & 0 & 1/G_{12} \end{bmatrix} \quad (5.10)$$

Laminates consisting of [0,90] Kevlar 49 - carbon fiber - Kevlar 49, [0,90] Kevlar 49 - carbon fiber, and [0,90] carbon fiber were modeled in CADEC-Macromechanics based on the material properties in eq.???. For a more accurate analysis of the wing, five stations were designated at equal increments of the semi span of the wing. These sections were then modeled in CADEC-Thin-Walled-Beams in order to analyze the stringer and airfoil geometries. First, each type of cell in the **Drawing Package** was analyzed separately, so that they could be added to the airfoil as concentrated stiffnesses. The axial stiffness, EA, and torsional stiffness, GJ, values were found for each concentrated stiffness and were then added to the airfoil model. Each of the concentrated stiffnesses created were then placed at the appropriate locations according to the drawing of the airfoil (Ref. **Drawing Package**). The test section was then evaluated and values for EA and GJ were calculated for the airfoil at each station. The results from CADEC showed that the Kevlar 49 - carbon fiber - Kevlar 49 laminate would provide adequate strength to support the aircraft at a load factor of $n_{pos}=3.0$.

5.6 Fuselage Structural Analysis

A 1-3/8 inch outside diameter aluminum pipe with a wall thickness of 0.058 inches was used as the fuselage of the airplane. The modulus of elasticity for the material, E, was equal to $10.1 \cdot 10^6$ pounds per square inch, the modulus of rigidity, G, was equal to $3.7 \cdot 10^6$ pounds per square inch, and Poisson's ratio, ν , was equal to 0.36. Using the loads from the fuselage load diagram (**Figure 5.2**), IDEAS Master Series 8 was used to model the loads on the fuselage. The fuselage is connected to the wing at three locations: 1 inch from the leading edge, 7 inches from the leading edge, and 13 inches from the leading edge. These points were taken as rigid and immovable and the appropriate loads were applied to the fuselage. The von Mises stress can be seen in **Figure 5.3**, where the maximum stress is $1.47 \cdot 10^3$ pounds per square inch where the pipe is fastened to the wing. It can be seen that the maximum displacement, $8.72 \cdot 10^{-2}$ inches, occurs at the tail of the airplane.

5.7 Landing Gear Structural Analysis

The landing gear are one of the most important parts of the aircraft. If the airplane cannot get off the ground or land safely it is, for most purposes, useless. Each of the main landing gear were designed to withstand the full impact of the airplane landing with a 10 feet per second vertical velocity towards the earth. The maximum static load the landing gear will see was found from eq. 5.11 to be 37 pounds.

$$(Max\ Static\ Load) = W \frac{N_a}{B} \quad (5.11)$$

In the above equation W is the weight of the airplane, N_a is the distance from the nose gear to the aft center of gravity, and B is the distance from the nose gear to the main gear.

With the strength of the gear as the main concern of the design, ¼ inch hot rolled, mild steel was chosen for the landing gear to be constructed of. Mild steel was chosen over a harder steel because a mild steel will bend under stress, while a harder, more brittle steel may shatter under heavy impact. To determine the buckling load of a single bar of ¼ inch mild steel 5.12 was used.

$$P_c = \frac{\pi^2 EI}{2L^2} \quad (5.12)$$

The buckling load of a single bar of the steel one foot long, with fixed ends was determined to be 105 lbs.

5.8 Payload Configuration

In order to minimize the area occupied by the tennis balls, for reasons of drag reduction, a speed loader frontal area of three tennis balls was implemented. The tennis balls were situated in a hexagonal close packed arrangement inside the loader. Hexagonal close packed is a reference to the molecular packing of the same name, and it is the closest possible amount of packing for spherical objects. The packing configuration can be easily explained as a triangle of three balls with another triangle of three balls, rotated 180 degrees, placed on top of the first triangle of balls. This pattern was repeated 33 times until a total of 99 tennis balls were fit into the speed loader. This produced a speed loader length of 72 inches. This configuration can be seen in Figure 5.4.

For steel transportation the same size speed loader was implemented. The only notable difference was that the steel was encased in a cylinder of low density Styrofoam. The Styrofoam prevents the steel from sliding in the speed loader while the aircraft is in motion, and can slip in and out of the speed loader for loading and unloading purposes.

The fore and aft faces of the speed loaders were also fitted with conical noses. The noses reduce induced drag at the fore portion of the loader, and base drag at the aft portion. The

noses, permanently bonded to the fuselage, also double as holders for the speed loaders, keeping them from shifting during flight.

5.9 Turn Rate

During a turn, the maximum total lift of the airplane is the load factor multiplied by the aircraft's weight. This value was found to be about 99 pounds. The turn rate was found from 5.13 and is equal to the radial acceleration divided by the velocity.

$$\dot{\Psi} = \frac{g\sqrt{n^2-1}}{V} \times 57.3 \text{ deg/rad} \quad (5.13)$$

The turn rate at the sortie flight speed of 70 feet per second and a load factor of 3 was found to be equal to 75 degrees per second.

5.10 Conclusions

The detailed design took all the critical factors of the entire aircraft and made them work with each other. As the last step before construction, the detailed design had to be completely correct so as not to ruin building materials with incorrect construction procedures. The detailed design process was looked over and agreed upon by all team members before construction began. This process was used as precautionary procedures to make sure no errors were abound.

Table 5.1 Stability parameters

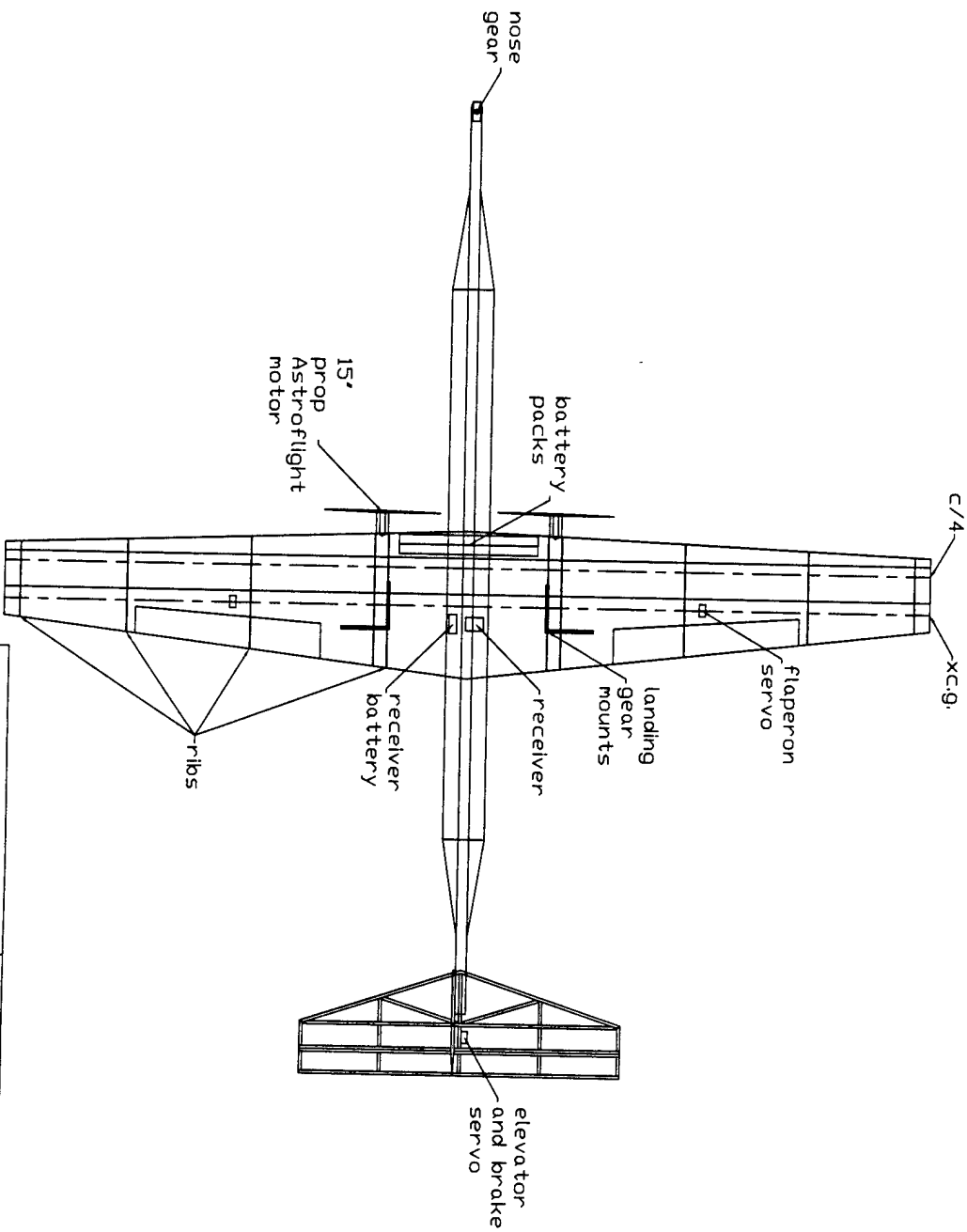
Parameter	Value	Description of Parameter
$C_{L\alpha}$	0.079/deg	Wing Lift Curve Slope
X_{acw}/MAC	0.294	Non-Dimensional Wing Aerodynamic Center Location
C_{Mofuse}	0.0017	Fuselage Pitching Moment Coefficient
η_H	0.96	Dynamic Pressure Ratio for Horizontal Tail
$C_{L\alpha H}$	0.06/deg	Horizontal Tail Lift Curve Slope
$\Delta\epsilon_H/\Delta\alpha$	0.495	Downwash Parameter
$\Delta\alpha_H/\Delta\alpha$	0.505	Horizontal Tail Effectiveness Parameter
X_{ach}/MAC	3.97	Non-Dimensional Horizontal Tail Aerodynamic Center Location
K_f	0.024	Empirical Fuselage Pitching Moment Factor

Table 5.3 Material properties of Kevlar 49/Epoxy and Carbon/Epoxy and comparison of laminates using available materials

Property	Kevlar 49/Epoxy	Carbon/Epoxy	Property	Kevlar 49 (3 ply)	Kevlar 49/Carbon	Kevlar 49/Carbon/Kevlar 49
E_1 (psi)	1.10E+07	2.06E+07	E_x (psi)	5.56E+06	7.62E+06	7.40E+06
E_2 (psi)	7.98E+05	1.49E+06	E_y (psi)	5.56E+06	6.18E+06	7.40E+06
G_{12} (psi)	3.00E+05	1.04E+06	G_{xy} (psi)	3.00E+05	8.00E+05	7.63E+05
ν_{12}	0.34	0.27	ν_{xy}	0.046	0.041	0.038
F_{1t} (psi)	2.00E+05	2.65E+05	*FPF	3.66E+03	4.82E+03	4.99E+03
F_{2t} (psi)	5.00E+03	8.27E+03	*FF	1.17E+04	1.87E+04	1.57E+04
F_6 (psi)	6.40E+03	1.03E+04	*Tsai-Wu Failure Criterion			
F_{1c} (psi)	8.50E+04	1.59E+05				
F_{2c} (psi)	2.00E+04	3.31E+04				
F_4 or F_5 (psi)	7.06E+03	-				

Table 5.2 Component weight in relation to moments and distance from mac/4.

Component	Weight (lb)	Distance From mac/4 (in)	Moment (lb-in)
Nose Gear	0.44	58.9	25.9
Nose Wheel	0.1628	58.9	9.59
Nose Brake	0.033	58.9	1.94
Nose Pant	0.0671	58.9	3.95
Pole	1.715428	-7.48	-12.8
Motor	0.93412	5.75	5.37
Motor	0.93412	5.75	5.37
Prop	0.0528	7.625	0.403
Prop	0.0528	7.625	0.403
Speed Control	0.12166	2.69	0.327
Speed Control	0.12166	2.69	0.327
Rx	0.0704	-7.32	-0.515
Rx Batt	0.20812	-7.3	-1.52
Main Batt	2.4948	2.62	6.54
Main Batt	2.4948	2.62	6.54
Nose Servo	0	39.89	0.0
H Servo	0.0968	-61.06	-5.91
V Servo	0.0968	-61.06	-5.91
Flap Servo	0.0968	-7.14	-0.691
Flap Servo	0.0968	-7.14	-0.691
Wing	4.9896	-4.99	-24.9
Tail	0.649	-58.1	-37.7
Main Gear L	0.001408	-8	-0.0113
Main Gear R	0.001408	-8	-0.0113
Main Wheel L	0.1628	-8	-1.30
Main Wheel R	0.1628	-8	-1.30
Wheel Pant L	0.0671	-8	-0.537
Wheel Pant R	0.0671	-8	-0.537
H pushrod	0.011	-61.06	-0.672
V pushrod	0.011	-61.06	-0.672
NG pushrod	0.011	58.9	0.648
Flap Pushrod L	0.011	-7.14	-0.0785
Flap Pushrod R	0.011	-7.14	-0.0785
Xcg (in) =	-1.74	from wing quarter chord	

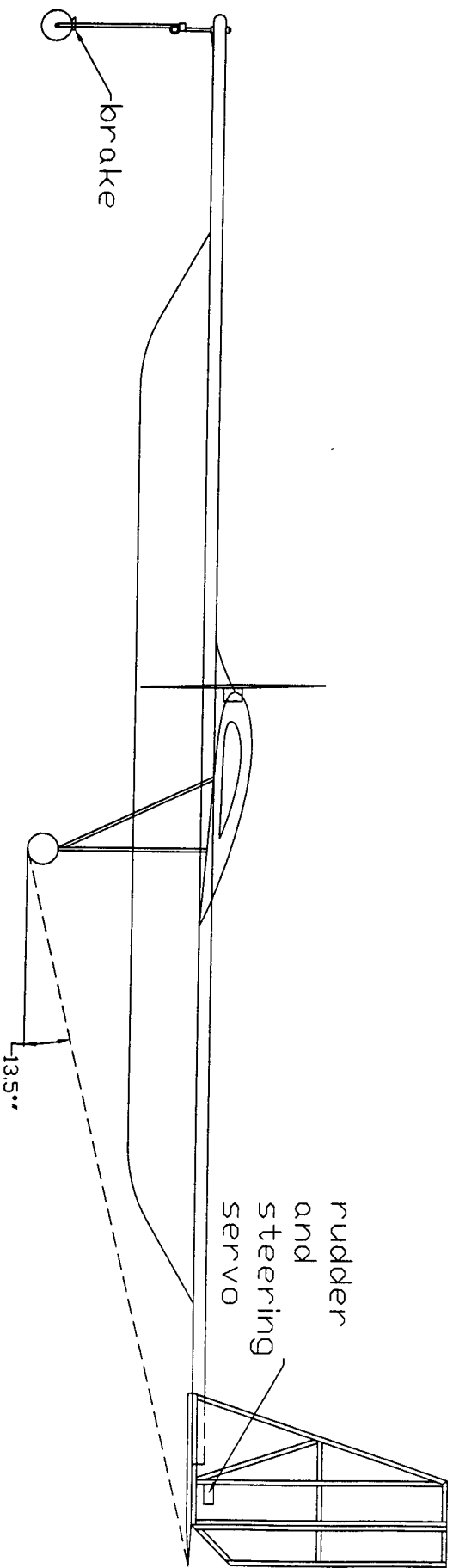


Wing Parameters	
Span	10'
Root Chord	19.2'
Tip Chord	9.6'
Angle of Twist	2.98°
Dihedral	2°
Angle of Attack	7.81°
Area	12ft ²
Aspect Ratio	8.33
Taper Ratio	0.5
Tail Parameters	
Span	41.5'
Root Chord	13.75'
Tip Chord	7'

West Virginia University
Morgantown, WV 26506

Lothworks Top View
Scale 0.8"=1'

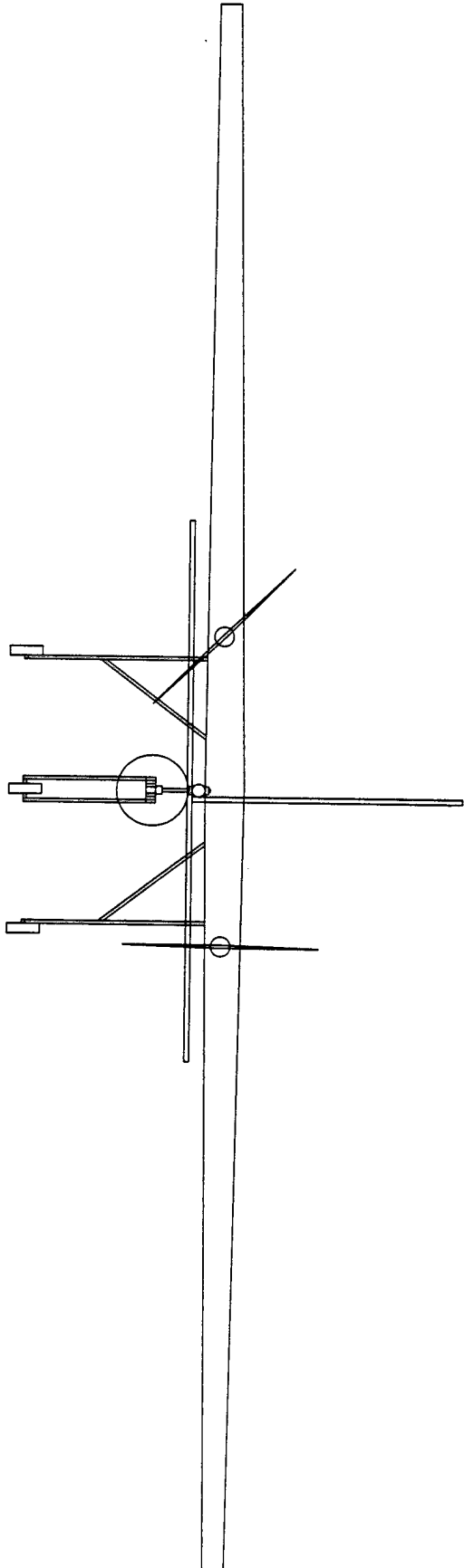
Drawn by: K. Ford
and T. Scarborough



West Virginia University
Morgantown, WV 26506

Lothworks Side View
Scale 1/4"=1'

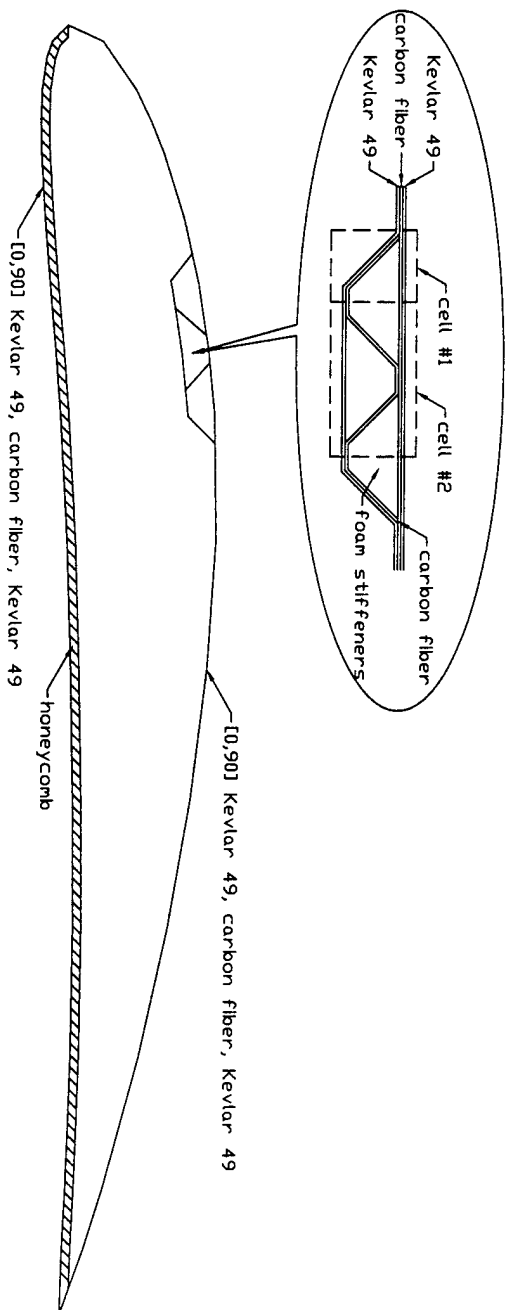
Drawn by: K. Ford
and T. Scarberry



West Virginia University
Morgantown, WV 26506

Lothworks Front View
Scale 1/4"=1'

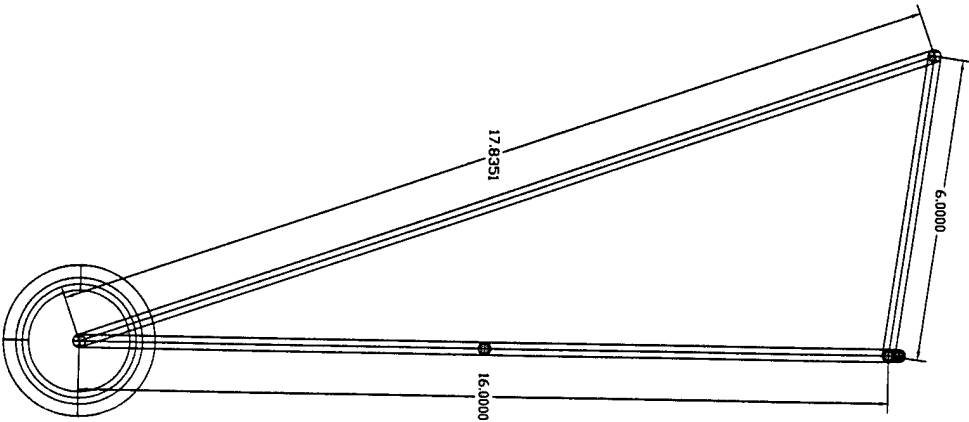
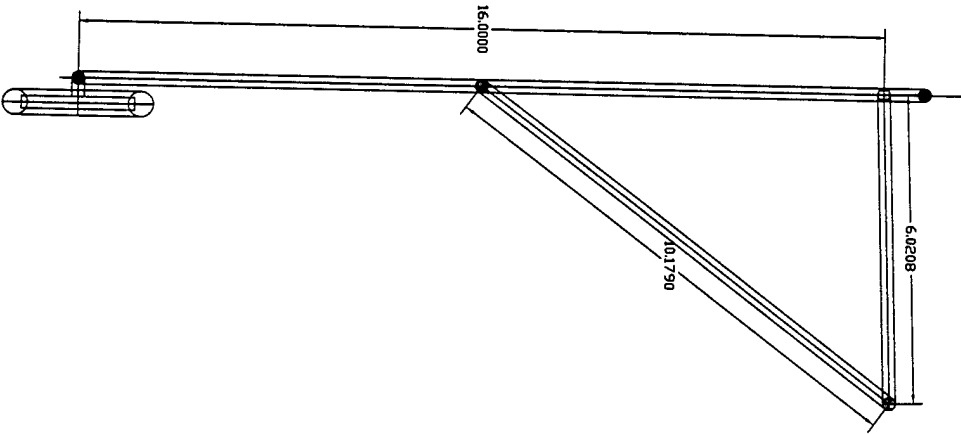
Drawn by: K. Ford
and T. Scarberry



West Virginia University
Morgantown, WV 26506

Lothworks
Wing Structure

Drawn by: K. Ford



West Virginia University
Morgantown, WV 26506

Lothworks
Landing Gear

Drawn by: K. Ford

6. Manufacturing Plan

6.0 Introduction

The construction of the aircraft needed to be done quickly and efficiently. It was necessary to complete construction and conduct flight tests of the aircraft to iron out any bugs before the competition time. Complete organization was necessary for the construction phase. To keep the building progressing in a timely fashion, tasks were handed out to certain individuals, and deadlines were set. The main difficulty of the construction phase was finding the time to put towards working. Many phases of the construction required several hours of constant work, which was difficult for the team to deal with. The divisions in the management summary were applied in order to help the construction phase flow as smoothly as possible.

6.1 Wing

The success of last year's entry into the design, build, fly competition led the team to implement the same type of fabrication techniques on this year's entry. The composite materials were laid-up by hand and vacuum bagged (to remove excess resin from the composite). This construction method was chosen due to the teams familiarity with the process and the availability of the necessary tools from previous years.

The first step in the creation of a composite wing was to build a plug that would be used, in turn, to build a wing mold. Full scale cross-sections of airfoils at various positions along the wing were cut from plywood. Using two of these differently sized airfoil templates, a section of Styrofoam wing was made. This was accomplished by placing one template on either side of a block of Styrofoam, with proper adjustments made for wing twist, etc., and running a hot wire through the Styrofoam along the borders of the templates. This produced a section wing that would be bonded to other such sections until a complete, full size, Styrofoam wing was completed. The Styrofoam wing was then sanded to get rid of imperfections. Even after sanding, small bumps remained on the wing plug, so balsa veneer sheets were used to coat the plug. In an attempt to attain the absolute smoothest plug, monocoat was used to cover the balsa veneer. The wing plug was then complete.

The construction of the wing mold was next. The plug was coated with several layers of mold release wax followed by several layers of polyvinyl acetate (PVA) and allowed to dry. These agents would ensure that composite materials would not stick to the plug when applied to it. A layer of surface coat resin, followed by several layers of fiberglass/epoxy, was applied to the plug and allowed to set up for 24 hours. This process was done for both the top and bottom of the plug so as to create two separate molds. When dry, the fiberglass composite molds were stiffened with plywood. Some imperfections in the mold were discovered when the plug was removed, as the heat released by the hardening of the epoxy melted some sections of the

monocoat and produced several air bubbles. These imperfections in the mold were filled with Bondo™ auto body filler putty and sanded to smoothness.

The next step was to actually construct a wing. Just as with the plug in the mold formation, the mold was coated with release wax and PVA. Pieces of Kevlar 49 and carbon fiber were hand coated with epoxy and scraped to remove excess. These pieces were then laid into the mold in their respective layers. The top layer of the still uncured composite was covered with a layer of perforated "perf-ply" polyethylene. Due to the molecular structure of the perf-ply material, the epoxy did not permanently bond to it. A layer of plastic filament batting was then laid over the perf-ply. This material was used to absorb the excess epoxy as it was sucked from the composite layers. A layer of high density polyethylene was then used to cover the batting and was made airtight through the use duct tape. A vacuum pump was then used to evacuate the air from the mold, and hence squeeze the excess epoxy from the composite. The vacuum was set to 13 inches of mercury, but not any higher due to the structural integrity of the mold being compromised. The resin was allowed 24 hours to set up, afterwards the wing half could be removed.

6.2 Fuselage

The fuselage was required to house the push rods used in steering and braking as well as support the various loads placed upon it during operation. An aluminum pipe was to be used, as they are strong, lightweight, and perfectly suited to the containment of the push rods. The wing mounting brackets were connected to the fuselage by epoxy and bolts. For ease of transportation the wing was designed to disconnect from the fuselage at the three mounting brackets. A new fuselage or wing could be paired with the parts of an already existing airplane for security in the event of an unfortunate mishap.

In an effort to minimize the weight and rated cost of the aircraft, the elevator and rudder servos doubled as brake and steering servos respectively. With less servos, the aircraft is further simplified, making repairs easier.

6.3 Speed-Loader

It was decided that for the maximum efficiency in changing payloads between sorties, a speed-loader would be implemented. The speed-loader was constructed of one layer of 3k carbon fiber. A 6 inch outside diameter PVC pipe was used as a mold for the speed-loader. The same processes outlined in the wing construction were followed in the speed-loader lay up. When cured, the loader was removed from the PVC pipe and sliced along its length. The diameter of the loader was then reduced to 5.5 inches in order to snugly accommodate the tennis balls. The rectangular steel pieces needed to be placed in the speed loader somehow. The simplest and best way to accomplish this was to cut cylinders out of low density Styrofoam that would slide into the speed loader. The steel would be cradled inside the Styrofoam cylinders, so that it would not move during flight.

A method of attaching and detaching the loader to the fuselage was then needed. Many different ideas were tossed around, but low drag, low weight, and simple to use zip ties were chosen above any other ideas.

6.4 Tail

The tail construction was rather straightforward. A balsa frame was glued together and draped with monocoat. Full size AutoCAD drawings were first made of the framework, so the builder could simply lay the tail surfaces on the drawing to check for correct construction.

6.5 Landing Gear

After the correct tipback and overturn angles were determined, the landing gear were designed. The main gear implement simple triangular framework to absorb the landing loads. Quarter inch mild steel was used on the main gear due to its high elasticity and resistance to brittle failure compared to some harder steels. A jig was first pieced together to keep the various legs of the main gear together and in the correct position during the welding procedure. The pieces were welded with a MIG welder and the excess weld ground off to reduce weight as much as possible. Wheels were placed on the gear through the use of simple axles.

6.6 Motor Assembly

The motor mounts were cut from 1.75 inch outside diameter, 0.058 inch wall thickness aluminum pipe. An 'L' shape was cut into the mounts so the motor would fit correctly into them. The cylindrical end of the pipe was situated in the leading edge of the wing, bonded to wing ribs for stability. The connection was reinforced with a fiberglass/epoxy composite to assure the mounts would not pull out of the wing during takeoff or flight. Hose clamps were used to hold the motors to the pipe. As well as providing sufficient squeeze on the motors to hold them in place, the hose clamps offered quick access to the motors for repairs.

6.7 Final Assembly

The overwhelming theme of the building process was that the aircraft had to be easily assembled and disassembled. For transportation and repair purposes this was a necessity. The main sections of the aircraft are the wing/landing gear/motor section, the fuselage/tail section, and the speed-loader. These sections are assembled with standard socket tool sets.

Figure 6.1 shows a breakdown of the manufacturing times of the various components of the aircraft. Both the scheduled and actual times of completion are shown.

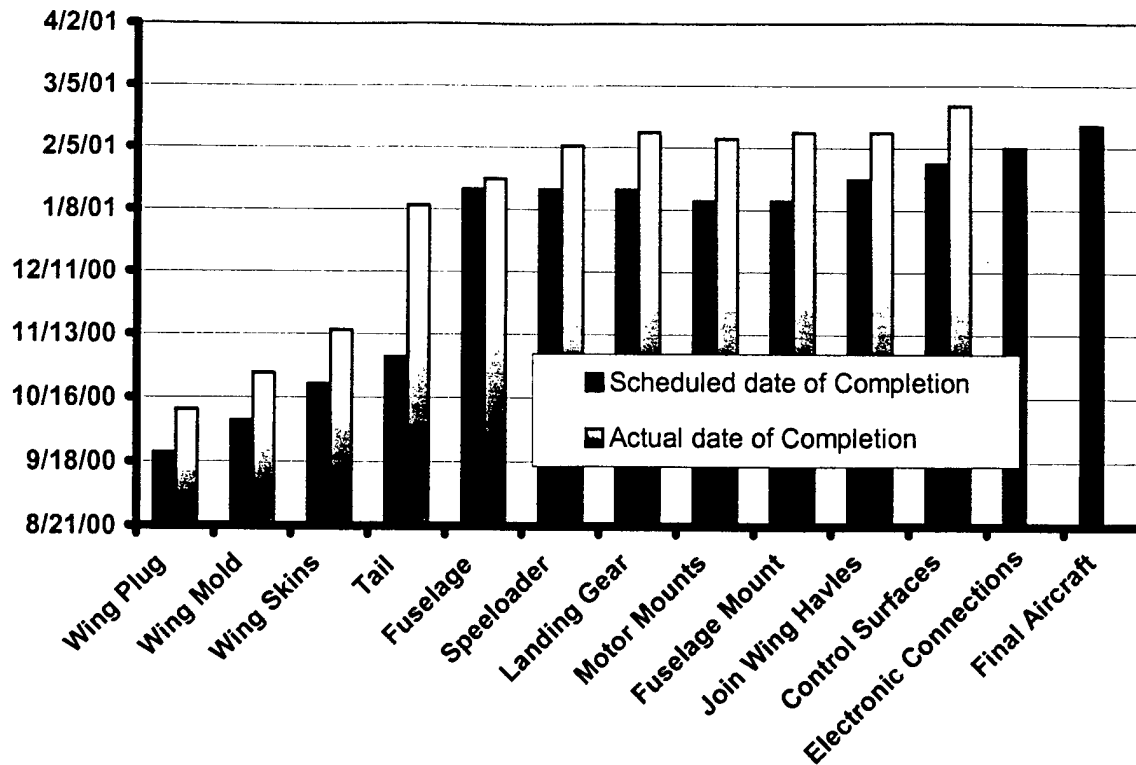


Figure 6.1 Manufacturing Milestone Chart

7. References

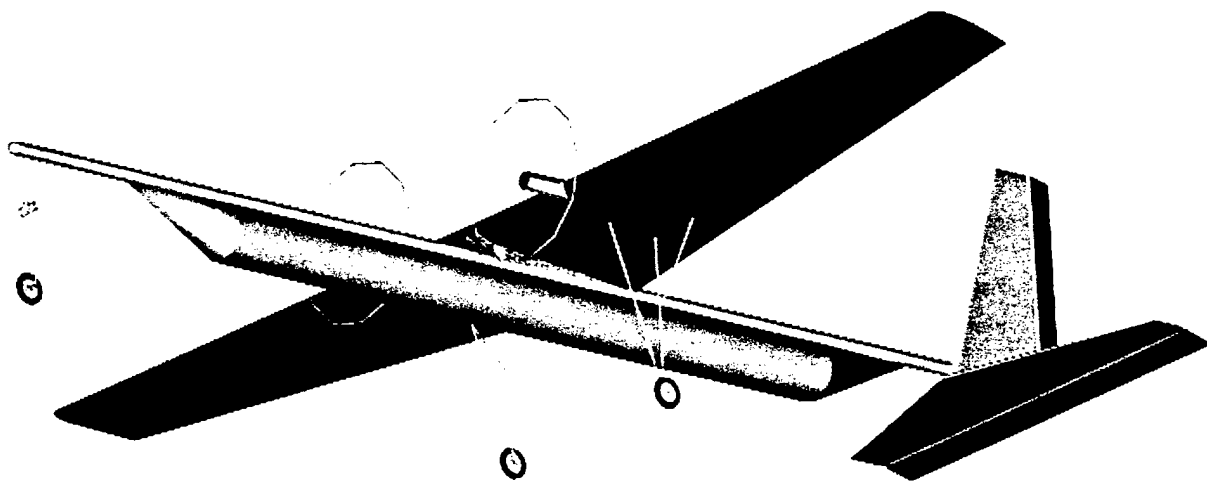
- [1] Raymer, Daniel P., "Aircraft Design: A Conceptual Approach Third Edition," American Institute of Aeronautics and Astronautics, Inc., Reston, VA 20191
- [2] Barbero, Ever J., "Introduction to Composite Materials Design," Taylor and Francis, Inc., Philadelphia, PA 19106
- [3] Tomblin, John; Chaffin, Michael; Rexrode, Timothy; Ringler, Todd, "Detailed Structural Design of the F-120 Fuselage MAE 162," Presented to Dr. Nithiam Sivaneri August 11, 1989, Morgantown, WV 26505
- [4] Sivaneri, N. "MAE 160 Design Project," West Virginia University, Morgantown, WV, 1999
- [5] Anderson, John D. Jr., "Fundamentals of Aerodynamics," McGraw-Hill, Inc.
- [6] Sun, C. T., "Mechanics of Aircraft Structures," John Wiley and Sons, Inc.
- [7] Ford, Kevin J., "UAV Truss-Core Sandwich Composite Wing," Mechanical and Aerospace Engineering Department, West Virginia University, Morgantown, WV 26505
- [8] Scarberry, Thomas T., "Electric Model Aircraft Propeller Analysis," Mechanical and Aerospace Engineering Department, West Virginia University, Morgantown, WV 26505
- [9] <http://cms.access.wvu.edu:8900/>, accessed online February 2001, Loth, John L.
- [10] Anderson, John D., "Introduction to Flight, 3rd Edition," McGraw Hill, 1989.
- [11] Roskam, Jan, "Airplane Flight Dynamics and Automatic Flight Controls, Part 1" Design, Analysis, and Research Corporation, 1995, Lawrence, Kansas

LOTHWORKS
WEST VIRGINIA UNIVERSITY

Addendum Phase

April 19th – 21st, 2001

Cessna ONR – Student Design/Build/Fly Competition



DEPARTMENT OF MECHANICAL AND AEROSPACE ENGINEERING

WEST VIRGINIA UNIVERSITY

MORGANTOWN, WV 26506

i. Table of Contents

i. Table of Contents	1
1. Executive Summary	4
2. Management Summary	5
Design Team	6
Design Configuration	6
Calculated Flight Score	6
3. Conceptual Design	7
3.0 Introduction	7
3.1 Material Selection and Construction Techniques	7
<i>Balsa Wood</i>	8
<i>Foam Build-up</i>	8
<i>Composite Materials</i>	9
<i>Other Materials</i>	9
3.2 Aircraft Parameters	9
<i>Alternative Designs</i>	9
<i>Number of Motors</i>	10
<i>Number of Wings</i>	10
<i>Number of Fuselages</i>	11
3.3 Conclusions	11
3.4 Conceptual Design Results	11
4. Preliminary Design	12
4.0 Introduction	12
4.1 Investigation of Design Parameters	12
<i>Number of Tennis Balls</i>	12
<i>Steel Weight</i>	12
<i>Wing</i>	13
4.2 Preliminary design rating system	13
4.3 Analytical Methods	13
4.4 Optimization Scheme Results	17
4.5 Structural Design	17
4.6 Wing Structure Analysis	17
4.7 Fuselage Structural Analysis	18
4.8 Preliminary Design Results	18
5. Detailed Design	27
5.0 Introduction	27
5.1 Detailed Design Parameters	27

9.1 Breakdown of the Rated Aircraft Cost	49
9.2 Manufacturer's Empty Weight Multiplier	50
9.3 Rated Engine Power	50
9.4 Manufacturing Man Hours	50
9.4.1 WBS 1.0 Wing	50
9.4.2 WBS 2.0 Fuselage/Pods	50
9.4.3 WBS 3.0 Empenage	51
9.4.4 WBS 4.0 Flight System	51
9.4.5 WBS 5.0 Propulsion System	51
9.5 Overall Score	51

8. Lessons Learned

During the construction of the aircraft, several modifications were made. These modifications stemmed from construction flaws and from factors that were overlooked in the design phase of the aircraft. Flaws in the plug used to make the wing proved to cause most of the headaches during construction. The tail servo locations and the landing gear were modified as well.

8.1 Wing

Overall, the construction techniques used to fabricate the aircraft worked well. Nonetheless, flaws in construction were present. This was due to a wide range of experience and skill in construction across the members of the team.

Of all the components of the aircraft, the wing had the most flaws. As stated earlier the wing was constructed out of composite materials using hand lay-up and vacuum bagging techniques. First, a male plug was produced, then a mold, and lastly the wing itself. This meant that any flaws in the plug would be visible in the mold and thus visible in the wing. As a result of the flaws in the plug and mold the wing endured several mistakes, some were cosmetic while some were aerodynamic. Using balsa wood and monocoat to sheet the plug was the first mistake. The balsa wood did not adhere well to the foam core and the monocoat wrinkled causing imperfections in the mold. These imperfections in the mold were fixed by filling them with surface filler. The balsa wood not adhering properly caused other problems. The dimensions of the wing and the shape of the airfoil were slightly altered. It was felt that these alterations would not cause enough problems to justify rebuilding another plug and mold. The team felt that if they had to do over again they would construct the plug from foam core and cover it with light weight fiberglass and bondo. The other aircraft components were not as complicated to construct as the wing was. Therefore, these components did not have the flaws present as did the wing.

8.2 Avionics

The servos located on the tail, rudder-steering and elevator-brake, were moved to make connections easier. Each servo was mounted directly behind the fuselage. The first advantage of this configuration was that it made it easier to run the pull-pull steering system and brake line to the nose gear. The steel cables run above the fuselage and through the wing-fuselage assembly. The second advantage was that this made it easier to run the servo wire to the receiver. The wire runs through the fuselage and into the wing, which houses the receiver.

8.3 Weight comparison

The empty weight of the aircraft is 26.0lbs. This is 6 pounds overweight. Most of the extra weight is in the wing. The weight of the wing is 8.5 pounds compared to the estimated 6 pounds. Several factors were overlooked on the estimate of the empty weight of the wing. First, the added weight of the control surfaces was not taken into account. The control surfaces were cut out of the wing and then trimmed with balsa wood and covered in fiberglass. The locations

were the hinges mounted to the wing and control surfaces were strengthened with the addition of balsa wood. Another area where additional weight was added was the motor mounts. Fiberglass was wrapped around the aluminum pipe and bolts were ran through the pipe to attach it to the adjacent ribs. The tail and wing-fuselage assembly also weighed more than what was estimated. Due to the additional weight of these components the cg of the aircraft was off. To compensate for this 1lb of lead was melted and fit inside the fuselage in front of the nose gear.

8.4 Improvements for Next Year

Organization, communication, and work ethic are perhaps the biggest improvements that need to be made for next year's team. The team leaders found it difficult to bring the team members together to work on the aircraft. Several team members were counted on to perform certain tasks and ended up doing nothing. Because of this most of the work fell on the shoulders of the team leaders.

For next year, several flights of this year's aircraft need to be video taped and analyzed. The takeoff distances and battery life need to be measured. Using these values the design program can be corrected.

9. Rated Aircraft Cost

The overall score of each team is a function of three parameters: the report score, flight score, and the rated aircraft cost (RAC). Each of these components is then further broken up into subsections. The report score is a summation of the proposal and addendum phases. The flight score is a summation of one-fifth the number of tennis balls transported and the weight of steel transported of each flight. The RAC is a more complicated score to tabulate. It is based on the "simplicity" of the aircraft and is calculated from a formula set forth by the competition officials. The following equation is used to calculate the overall score of the aircraft.

$$\text{Total Score} = \frac{\text{Written Report Score} + \text{Total Flight Score}}{\text{Rated Aircraft Cost}}$$

(9.1)

As one can observe to obtain the highest total score and win the competition, one must maximize the written report score and the total flight score while minimizing the RAC. Upon further examination of the RAC one will notice that minimizing the RAC and maximizing the total flight score are a closely related process.

9.1 Breakdown of the Rated Aircraft Cost

The overall rated aircraft cost (RAC) is calculated by the equation:

$$RAC, (\$ \text{thousands}) = \frac{A gMEW + B gREP + C gMFHR}{1000}$$

(9.2)

In the above equation, A, B, and C represent values of multipliers used to convert aircraft characteristics into manufacturing hours. The Manufacturer's Empty Weight Multiplier (MEW),

Rated Engine Power (REP), and the Manufacturing Man Hours (MFHR) are a breakdown of the different aircraft components to be converted to man-hours. A more detailed explanation of these parameters is described below.

9.2 Manufacturer's Empty Weight Multiplier

The manufacturer's empty weight multiplier, MEW, is comprised of the weight of the aircraft without the batteries or the payload. Of all the parameters that constitute the RAC the MEW affects the total flight score more than any other. Every additional pound the aircraft weighs increases the RAC by 0.1 point. Each pound saved on the construction of the aircraft can be replaced with an increased payload weight. This is crucial to the total score. Each additional pound of steel is multiplied by a factor five. Using these observations one sees that not only does the MEW affect the RAC it also affects the amount of payload carried which can make a significant change in the total score. In equation 9.2 A represents the manufacturer's empty weight multiplier and was given a value of \$100/lb. The MEW of 'Almost Heaven' is 2.60.

9.3 Rated Engine Power

The rated engine power, REP, was calculated using the following equation:

$$REP = \#engines gAmp_{fuse} \cdot .2V / \#cells$$

(9.3)

In equation 9.2 B represents the rated engine power multiplier and was given a value of \$1/Watt. The aircraft uses two engines, 36 battery cells, and a 40Amp fuse. The REP of Lothworks is 3.46.

9.4 Manufacturing Man Hours

The manufacturing man hours, MFHR, further breaks down the components of the aircraft into the work breakdown structure, (WBS), and takes into account the number of wings and their size, the number of fuselages/pods, and their size, the number of horizontal and vertical surfaces, the number of servos used, and the number of motors and propellers used. In equation 9.2 C represents the manufacturing cost multiplier and was assigned a value of \$20/hr. Table 9.1 is summary of the total number of manufacturing hours assigned to each component of the WBS. A value of 174.36 was used for the MFHR.

9.4.1 WBS 1.0 Wing

To achieve the highest total score possible the optimization program gave the results that the aircraft should have one wing with an area of 12ft² and two control surfaces. The rules state that 15hrs per wing, 4hrs per square foot of projected area, 2hrs per strut or brace, and 3hrs per control surface were to be used in the calculation of WBS 1.0. The total number of hours for WBS 1.0 is 69hrs (refer to Table 9.1).

9.4.2 WBS 2.0 Fuselage/Pods

WBS 2.0 consists of the number of fuselages and or pods and their respective lengths. 5hrs per body and 4hs per foot of length were assigned to the components of the

aircraft. Three components of the aircraft fall under this category, the fuselage and motor mounts. The length of the fuselage is 8.34' and the length of each motor mount that extends past the leading edge of the wing is 0.5'. The total number of hours for WBS 2.0 is 52.36hrs (refer to Table 9.1).

9.4.3 WBS 3.0 Empenage

WBS 3.0 is the number of vertical and horizontal surfaces on the aircraft. 5hrs were assigned for the construction of these components with an additional 5hrs per vertical surface and 10hrs per horizontal surface. The aircraft is comprised of 1 vertical surface and 1 horizontal surface. The total number of hours for WBS 3.0 is 20hrs (refer to Table 9.1).

9.4.4 WBS 4.0 Flight System

WBS 4.0 is the number of servos and controllers used on the aircraft. 5hrs were assigned for the basic flight control system. An additional 2hrs were assigned for each servo and controller used. The aircraft has 4 servos adding 8hrs to the MFHR (refer to Table 9.1)

9.4.5 WBS 5.0 Propulsion System

WBS 5.0 is the number of motors and propellers or fans used on the aircraft. 5hrs per motor, propeller, and fan were assigned. The aircraft has 2 motors and 2 propellers adding 20hrs to the MFHR (refer to Table 9.1)

9.5 Overall Score

Even though the overall score cannot be determined until the actual competition, the RAC component was calculated using the following equation:

$$RAC, (\$thousands) = \frac{100g26 + 1g3456 + 20g74.36}{1000} = 9.54 (\$thousands) \quad (9.4)$$

Table 9.2 is a comparison of the values for each airframe dependent parameter in the cost model. Figure 9.1 is a comparison of the different components of the RAC and the percentage that each adds to the overall RAC. As can be seen the REP is the largest contribution to the RAC. This occurs because the design uses the maximum allotted weight for the batteries and 2 motors. The MEW is the second largest contributor to the RAC. Better construction skills and time construct another aircraft would lower the empty weight. The value of the RAC may change by the time of the competition. Some additional weight may be added to the aircraft due to repairs or other unforeseen occurrences.

Table 9.1 Work Breakdown Structure for the aircraft

	component	characteristic	hours per characteristic	total number of hours per component
WBS 1.0 Wings	<i>number of wings</i>	1	15	15
	<i>wing area (ft²)</i>	12	4	48
	<i>struts and braces</i>	0	2	0
	<i>control surfaces</i>	2	3	6
WBS 2.0 Fuselage/Pods	<i>number of bodies</i>	3	5	15
	<i>total length of bodies (ft)</i>	9.34	4	37.36
WBS 3.0 Empenage	<i>basic cost</i>	-	5	5
	<i>number of vetical surfaces</i>	1	5	5
	<i>number of horizontal surfaces</i>	1	10	10
WBS 4.0 Flight System	<i>basic cost</i>	-	5	5
	<i>number of servos or controllers</i>	4	2	8
WBS 5.0 Propulsion System	<i>number of engines</i>	2	5	10
	<i>number of propellers or fans</i>	2	5	10
total number of hours				174.36

TABLE 9.2 COMPARISON OF THE AIRFRAME DEPENDENT PARAMETERS IN THE COST MODEL

Airframe Parameter	RAC (\$ thousands)
Manufacturer's Empty Weight, MEW	2.60
Rated Engine Power, REP	3.46
WBS 1.0 Wing	1.38
WBS 2.0 Fuselage and Motor Mounts	1.05
WBS 3.0 Empenage	0.40
WBS 4.0 Flight System	0.26
WBS 5.0 Propulsion System	0.40
Total RAC	9.54

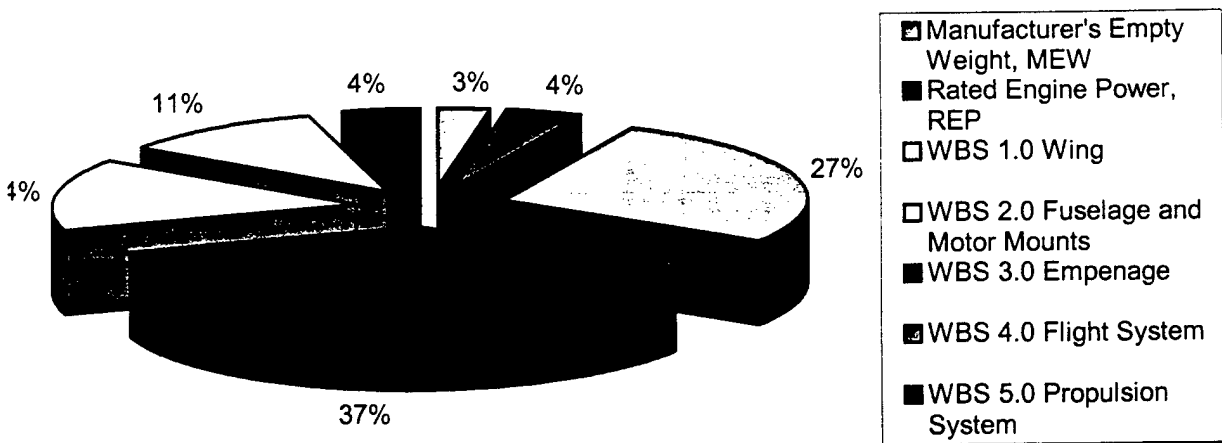


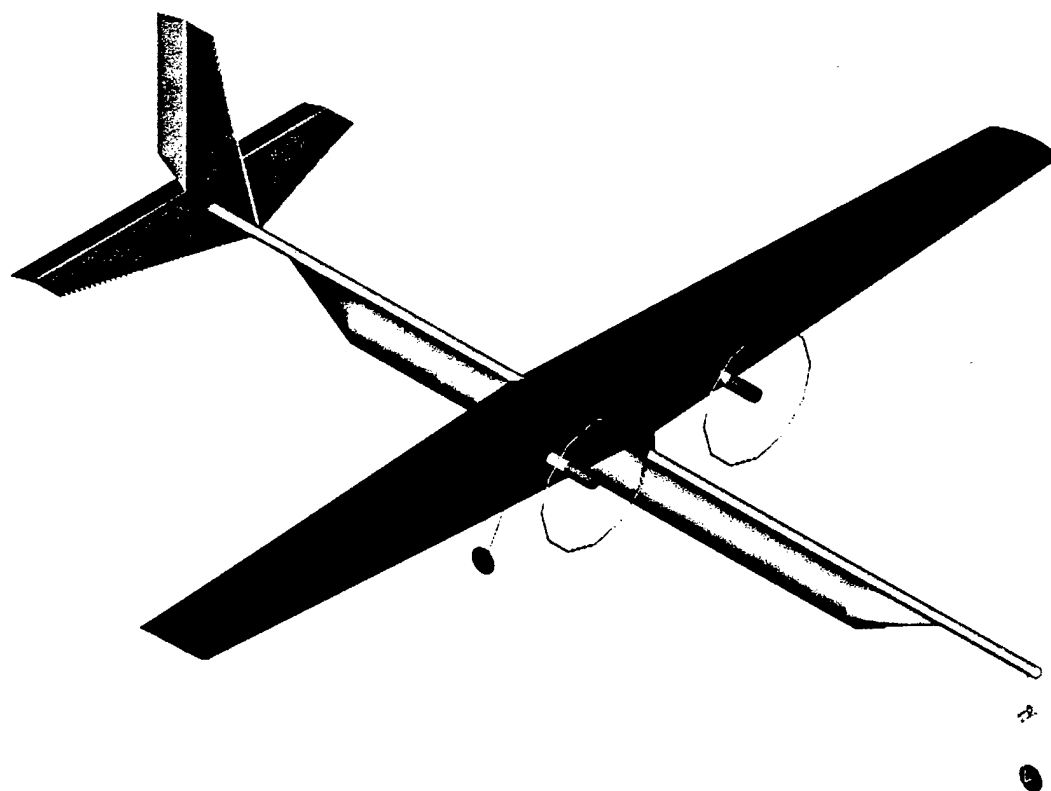
Figure 9.1 Comparison of the component's contribution to the rated aircraft cost

ALMOST HEAVEN
WEST VIRGINIA UNIVERSITY

Proposal Phase

April 19th – 21st, 2001

Cessna ONR – Student Design/Build/Fly Competition



DEPARTMENT OF MECHANICAL AND AEROSPACE ENGINEERING

WEST VIRGINIA UNIVERSITY

MORGANTOWN, WV 26506

i. Table of Contents

i. Table of Contents.....	1
1. Executive Summary.....	3
2. Management Summary	4
3. Conceptual Design	5
3.1 Aircraft Parameters	6
3.1.1 Alternative Concepts Investigated	6
3.1.2 Number of Motors	6
3.1.3 Number of Wings	6
3.1.4 Number of Speed Loaders.....	6
3.2 Material Selection and Construction Techniques.....	7
3.2.1 Balsa Wood.....	7
3.2.2 Foam Build-up.....	7
3.2.3 Composite Materials	7
3.2.4 Other Materials	8
3.3 Conceptual Design Results.....	8
4. Preliminary Design.....	10
4.1 Design Parameters Investigated	10
4.1.1 Wing Area	10
4.1.2 Number of Tennis Balls.....	10
4.1.3 Steel Payload Weight.....	11
4.2 Preliminary Design Rating System.....	11
4.3 Analytical Methods Used.....	11
4.4 Optimization Scheme Results	14
4.5 Structural design	14
4.6 Wing Structure Analysis	15
4.7 Fuselage Structure Analysis	15
4.8 Preliminary Design Results	15
5. Detail Design	25
5.1 Detailed Design – Aircraft Parameters Group.....	25
5.1.1 Airfoil Selection	25
5.1.2 Propeller Selection.....	26
5.1.3 Aileron Sizing	26
5.1.4 Horizontal Tail Sizing and Location	26
5.1.5 Vertical Tail Sizing	26
5.1.6 Wing Incidence, Twist, Taper, and Dihedral	27
5.1.7 Landing Gear Selection	27

5.1.8 Longitudinal Static Stability Analysis	27
5.1.9 Turning, Landing, and Climb Analysis	28
5.2 Assessment of available materials	28
5.3 Comparison of different laminates	29
5.4 Truss-Core Sandwich Composite Stringers	29
5.5 Truss-Core Sandwich Composite Stringer Analysis	30
5.6 Fuselage Structural Analysis	31
5.7 Landing Gear Structural Analysis	31
5.8 Payload Configuration	31
6. Manufacturing Plan	41
6.1 Wing	41
6.2 Fuselage	42
6.3 Speed Loader	42
6.4 Tail	43
6.5 Landing Gear	43
6.6 Power Plant	43
6.7 Final Assembly	43
7. References	44
8. Lessons Learned	46
9. Aircraft Cost	46

1. Executive Summary

This aircraft design presented is in response to the request for proposal submitted by the AIAA along with Cessna and the Office of Naval Research, for a radio-controlled, unmanned aerial vehicle. The aircraft must be capable of displacing a maximum number of tennis balls and a maximum number of pounds of steel during a 10 minute flight period, while minimizing the Rated Aircraft Cost. The proposed aircraft is the result of a "one-shot" optimization scheme in which all design parameters were taken into account and used to determine the proper payloads and wing area for the final configuration. This method provided a quick way to evaluate several competing concepts. The aircraft configuration was optimized to maximize the overall score.

The "Almost Heaven" entry utilizes a mono-wing planform, tapered and twisted to produce a nearly elliptical lift distribution. The aircraft is powered by twin AstroFlight Cobalt 640G electric brushed motors, which are driven by two 18-cell (5 pounds total) NiCd battery packs consisting of RC2400 Sanyo high capacity racing cells. A conventional tail was designed for ease of construction, as was the aluminum tube fuselage. A speed-loader has been used to facilitate a rapid payload exchange. Advanced composites such as Kevlar 49 and carbon fiber have been used to fabricate the aircraft, thereby reducing the empty weight, and increasing the payload capability. The final configuration for West Virginia University's entry, "Almost Heaven" is presented below:

Design Variable	Value	Units
<i>Wing Area</i>	12.00	ft ²
<i>Wing Span</i>	10.00	ft
<i>Wing Root Chord</i>	1.60	ft
<i>Wing Tip Chord</i>	0.80	ft
<i>Wing Aspect Ratio</i>	8.33	
<i>Wing Taper Ratio</i>	0.50	
<i>Horizontal Tail Area</i>	3.00	ft ²
<i>Vertical Tail Area</i>	1.68	ft ²
<i>Fuselage Length</i>	8.34	ft
<i>Fuselage Diameter</i>	0.115	ft
<i>Speed Loader Length</i>	6.00	ft
<i>Speed Loader Diameter</i>	0.46	ft
<i>Battery rating</i>	2,400.00	mA-hr
<i># cells</i>	36	
<i># motors</i>	2	
<i># steel sorties</i>	3	
<i># ball sorties</i>	2	
<i>Maximum Takeoff Distance</i>	200	ft
<i>Average Flight Velocity</i>	70.00	ft/s

2. Management Summary

Students at West Virginia University's Department of Mechanical and Aerospace Engineering embarked on a mission to win the fifth annual Cessna/ONR Student Design Build Fly competition. This year's team consisted of fourteen students; one graduate aerospace engineering student, six senior aerospace and mechanical engineering students, one senior electrical engineering student, five junior aerospace and mechanical engineering students, and one sophomore aerospace engineering student. Seven of the team members had experience working on past entries.

Several members of the team were at the university during the summer. These students laid the groundwork for the design and construction of the aircraft. During the summer the shop was organized and supplies were purchased. Once the fall semester began the team met and discussed the rules of the competition and began the conceptual design.

There were three branches to the total design team. The first branch was the Aircraft Parameters Group (APG). This group was responsible for the aerodynamics and performance as well as the stability and control of the aircraft. The aerodynamics and performance engineers were Tom Scarberry and Michael Plyler. The stability and control engineers were Benjamin Reid and Andy Mason. Mr. Scarberry was the leader for the aerodynamics and performance team while Mr. Reid was in charge of the stability and control. The second branch was the Structures and Materials Group (SMG). This group was responsible for the acquisition of materials as well as the structural design of the entire aircraft. The structural engineers were Kevin Ford and Joseph Quintana. Mr. Ford was the Structures and Materials Group leader. The third branch of the design team was the Manufacturing and Integration Group (MIG). This team was responsible for fabricating the aircraft and integrating the various components into the aircraft. The MIG was constantly in contact with each of the leaders from the other groups in order to ensure that all design changes were feasible. The manufacturing engineers were Jonathan Breckenridge and Peter Cooke. Mr. Breckenridge was the leader from the Manufacturing and Integration Group. Mr. Cooke was the team pilot and provided valuable experience in the fabrication of model aircraft. Although the MIG had the final say in the aircraft construction, every member of the design team was involved in building the WVU entry.

Communication between each design group was critical for maintaining deadlines as well as the overall success of the entire team. The team leaders from each group were responsible for overseeing the development of their particular aspect of the aircraft. This responsibility included making sure that all design changes were made known to the other team leaders and resolving the conflicts resulting from these changes. Each group leader was given total authority over their particular design variables. The entire team met once per week to discuss design changes, progress, and to clarify what needed to be done during the next week.

Mr. Scarberry and Mr. Ford were given total control over the entire design team since they had the most experience working on this competition. Mr. Scarberry oversaw the aerodynamics/performance/stability and control groups while Mr. Ford oversaw the structures/materials

and the MIG groups. They were responsible for setting and enforcing the deadlines. This approach to team leadership allowed conflicts to be resolved almost immediately. A set of easily modified drawings was created to allow feasibility studies of all design modifications. Perhaps the greatest advantage of pairing the team members was that new members of the team could quickly learn the overall process of designing a radio-controlled aircraft, which will be beneficial to next year's team. Each member developed the crucial skills required to work together as a team to accomplish a goal. Everyone on the team not only worked hard throughout the year, but each member contributed to the overall success of the team. Table 2.1 is a milestone chart of the planned and actual timing of the conceptual, preliminary, and detailed design stages, as well as the report preparation period.

Table 2.1 Design milestones

	Jul-00	Aug-00	Sep-00	Oct-00	Nov-00	Dec-00	Jan-01	Feb-01	Mar-01	Apr-01
Conceptual Design										
Preliminary Design										
Detailed Design										
Report Preparation										
Rough Draft										
Reviewed by Faculty										
Final Copy										
planned completion										
actual completion										

3. Conceptual Design

The conceptual design phase was divided into two sub phases: Aircraft Parameters phase and the Material Selection and Construction Techniques phase. During the Aircraft Parameters phase, the APG considered the advantages and disadvantages of previous UAV's, and evaluated the different types of aircraft and considered the advantages and disadvantages of each, according to how each type of aircraft would perform in this competition. During the Material Selection and Construction Techniques phase, the Structures and Materials group, along with the Manufacturing and Integration group, evaluated the availability and use of several different types of UAV materials and construction methods. In this phase the MIG and SMG took into account the materials available to the team from previous years, the cost of new materials, and the fabrication skills of the team members.

3.1 Aircraft Parameters

3.1.1 Alternative Concepts Investigated

In the conceptual design stage, several generic baseline aircraft configurations were considered for further development. These configurations consisted of six different combinations of different numbers of wings, motors, and speed loaders. The number of each particular component was then evaluated based upon a set of Figures of Merit determined by the Aircraft Parameters Group, according to how the different numbers of each component would affect various aspects of the aircraft performance. If the number of components was favorable to a particular design variable, a value of +1 was assigned to that number of components. If the number of components was unfavorable, a value of -1 was assigned. If the number of components had a negligible effect on the design parameter, a 0 was assigned. The number of motors, wings and speed loaders with the highest FOM sum was selected. The resulting configuration was then a baseline aircraft consisting of the number of wings, speed loaders, and motors determined by this process. Table 3.1 is a ranking chart used to evaluate the various configurations.

3.1.2 Number of Motors

The number of motors used on the baseline aircraft was extremely important. First, the number of motors was limited by the number of cells used in the battery pack, due to the five pound battery weight limit; however, takeoff performance would be enhanced by more than one motor. An increase in the number of motors used also translated into increased cost as well as an increased rated aircraft cost. An increased number of motors would enhance the payload weight capability, at the expense of battery life. The effect on the manufacturing time was negligible.

3.1.3 Number of Wings

The number of wings used on the baseline aircraft had a strong effect on the aircraft drag coefficient. This translated into an increase in the percent of battery energy used throughout the flight time. An increase in the number of wings used on the baseline configuration would mean a significant increase in the empty weight of the aircraft. The takeoff performance was limited by the number of wings used on the baseline aircraft. The increased wing area would effectively reduce the wing loading for a given payload weight, thus reducing the stall velocity and decreasing the takeoff distance. The possible number of wings was limited by the manufacturing time associated with making more than one wing (although mold construction techniques were used, time was still required to "build" the wing.) Also, the number of wings had a significant effect on the rated aircraft cost.

3.1.4 Number of Speed Loaders

The effect of using more than one speed loader had six detrimental effects on the baseline aircraft performance. First, more than one speed loader meant an increase in the aircraft drag coefficient and thus an increase in the battery energy used. This was significant due to the motor battery weight restriction. More than one speed loader meant a direct increase in the aircraft empty weight. In addition, the ability to produce more than one speed loader was limited by the manufacturing time and the cost of the materials. More than one speed loader meant an increase in the rated aircraft cost as well.

3.2 Material Selection and Construction Techniques

The main goal in constructing any aircraft is to make each component as strong and light as possible. Additionally, the team members had to take into account the required skill, cost, and time to construct the aircraft using different construction techniques. This posed several problems. The team member's experience was varied. Because of this limitation, special "classes" were set up by the senior team members to increase everyone's competence in different construction techniques. Time was also a limitation. Each member was taking a full course load, so construction time was limited. The team discussed typical UAV construction techniques in an attempt to determine the appropriate method needed to construct each component. Balsa wood, foam build-up, and composite material construction were investigated for each component.

3.2.1 Balsa Wood

One of the cheaper methods investigated, balsa wood construction is typically used to fabricate kit radio-controlled aircraft. This method consists of cutting ribs, spars, and stringers individually, and then assembling them to construct the wing, tail, or fuselage. However, as was learned with previous entries, this method is tedious and time consuming. Weight quickly increases with the use of adhesives, lowering the strength to weight ratio of balsa wood. However this method was not completely ruled out since some components require minimal strength. Several members had worked on a previous entry that used a balsa wing and ruled out the use of that type of wing due to the difficulties mentioned above. Analysis showed that the construction of the tail with balsa wood was very weight effective. This method was successfully used last year and is not labor intensive. Due to the strength to weight ratio of balsa wood and the cargo plane concept of this year's competition, balsa wood was ruled out for the construction of the fuselage.

3.2.2 Foam Build-up

The cheapest and easiest construction method is foam build-up method. This method has typically been used to construct UAV aircraft wings and consists of making templates of the desired airfoil shape and then using a hot-wire to cut the component out of a block of foam. A surface such as a thin layer of balsa wood or fiberglass is then applied. There are two drawbacks to this method. First, there is no space inside the component to house payload or avionics. Second, low-density foam must be used to ensure a lightweight component. The lighter foam is also weaker, requiring additional supports to be fabricated, increasing the component weight. Previous WVU entries used this method to build the wings; however, these entries were lighter planes designed for speed rather than moving heavy cargo. Due to the difficulties of adding additional strength and storing avionics in this type of wing, it was decided that this was an undesirable wing construction method. Like balsa wood, this technique was also more applicable to fabricate the tail.

3.2.3 Composite Materials

A composite material is formed by the combination of two or more distinct materials to form a new material with enhanced properties [1]. Fiberglass-epoxy and carbon-epoxy are the two primary

composite materials used in the aircraft industry. These materials are lightweight, yet strong enough to construct an unmanned aerial vehicle.

The main advantage to using composite materials is that last year's team learned the procedures for constructing strong, lightweight components. Several members of last year's team have returned and have experience working with composites. Weight and construction time were minimized using a new spar-less wing concept, the Ford-Guiler super beam, which is being developed at West Virginia University. Repeatability is another advantage of composites. Once the required mold has been constructed, it can be used several times to produce identical parts. Since composite materials can be easily molded into a hollow cylinder or a box, it was decided to use them for the speed loader. Previous WVU entries have utilized a composite landing gear. It was believed that this method would provide adequate strength but, at an increased weight, due to the length of the gear. Cost was the main disadvantage of using composite materials. Dry carbon fabric was priced at \$100 dollars a yard. Fortunately, the College of Engineering and Mineral Resources at West Virginia University is very active in the Society for the Advancement of Material and Process Engineering and has several contacts in industry. Therefore, most of the needed materials were donated.

3.2.4 Other Materials

Other materials considered by the team were steel and aluminum. Last year's landing gear was fabricated using steel rods. This method required a minimal amount of construction time. Because of the simple cylindrical shape of the speed loader, aluminum could have been used. The drawback with using aluminum sheet, is that it permanently deforms under impact. The fuselage tube was made of aluminum pipe.

3.3 Conceptual Design Results

According to Table 3.1 the final configuration consisted of one wing, one speed loader and two motors. This combination provided the most efficient means of achieving the maximum overall score.

After an initial assessment of the available materials and construction techniques, composite materials appeared to offer the most advantages considering the skill of our team members. Therefore, it was the preferred material for the construction of several major components of the aircraft: the wing, speed loader, and the landing gear attachment points. Balsa wood and foam build-up construction were also used. It was decided to use them where construction allowed simple building methods, such as the tail and where making molds and using composite materials would take too much time.

These decisions are shown in the Figures of Merit (FOM) listed in Table 3.2. This table is a compilation of the different structural components of the aircraft. The following scale was used to evaluate each component and the corresponding construction material/technique. A rating of 0 was used if the category was neutral to the material or technique. The ratings of 1 and 2 were used for medium and high scales respectively. If the rating was beneficial to the category then a positive value was used, if the rating was a hindrance to the category then a negative value was used. A brief explanation of the use of balsa wood for the construction of the wing is: Availability (0) – none is currently owned by the team and

is easy to purchase, Cost (-1) – the cost of balsa is small compared with other materials but would still need to be purchased, Team's manufacturing capabilities (1) – the team members could fabricate the wing using balsa wood but have no previous experience doing so, Time to build (-1) each method is tedious to construct thus each is given an equal rating, Strength to weight ratio (0) – the weight of the wing would be more than composite materials but adequate strength could be obtained. Using this method each material or technique was evaluated and the methods with the highest score were further investigated.

Table 3.1 Figures of Merit used to evaluate the baseline aircraft

	Number of Components	Energy Available	Empty Weight	RAC	Payload Weight	Drag Coefficient	TO Performance	Manufacturing Time	Cost	Strength	Overall Weight
Motor	1	0	0	0	-1	0	-1	0	0	0	-2
	2*	-1	0	-1	1	0	1	0	-1	0	-1
Wing	1*	1	0	0	-1	0	-1	0	1	0	0
	2	-1	-1	-1	1	-1	1	0	-1	1	-2
Speed Loader	1*	1	1	0	1	0	0	1	0	1	5
	2	-1	-1	-1	-1	-1	0	-1	-1	-1	-8
<i>*number of components used</i>											

Table 3.2 Figures of Merit for the structural components of the aircraft

		Availability	Cost	Team's manufacturing capability	Time to build	Strength to weight ratio	Overall weight
Wing structure	<i>composite materials</i>	2	0	2	-1	2	5
	<i>balsa wood</i>	0	-1	1	-1	1	0
	<i>foam build-up</i>	1	0	1	-1	-1	0
Fuselage structure	<i>aluminum pipe</i>	1	-1	2	1	1	4
	<i>carbon fiber tube</i>	1	-2	2	1	2	4
Tail structure	<i>composite materials</i>	2	0	2	-1	-1	2
	<i>balsa wood</i>	0	-1	2	1	1	3
	<i>foam build-up</i>	1	0	1	1	-1	2
Speed loader	<i>composite materials</i>	2	0	2	-1	2	5
	<i>PVC pipe</i>	0	-1	2	2	-2	1
	<i>aluminum flashing</i>	0	-1	2	1	-2	0
Landing gear structure	<i>composite materials</i>	2	0	2	-1	-1	2
	<i>metal</i>	1	0	2	1	1	5

4. Preliminary Design

The preliminary design phase was divided into sections similar to the conceptual design stage. Aircraft parameters were further analyzed to determine the optimum configuration. The construction materials and techniques were further analyzed to determine how the aircraft would be built.

4.1 Design Parameters Investigated

During the preliminary design phase, the APG continued to improve the baseline aircraft selected during the conceptual design phase. There were three primary design parameters investigated: wing area, number of tennis balls, and steel weight. These design variables were optimized using a program written by the APG in order to maximize the overall score. The program output is listed in Table 4.1.

4.1.1 Wing Area

The wing area was selected as an independent variable in the optimization model. The importance of the model being based on the wing area was due to the fact that the wing area directly affected the empty weight of the aircraft, the payload weight capability of the aircraft, the stall characteristics (and thereby the takeoff and landing performance), the battery energy used during each sortie as well as the rated aircraft cost.

4.1.2 Number of Tennis Balls

The number of tennis balls to be carried per sortie determined the speed loader configuration, since no payload was to be carried internal to the wing. This had a major impact on the drag coefficient of the aircraft. A small increase in the frontal area of the speed loader caused a large increase in the

parasitic drag coefficient of the aircraft; whereas an increase in length only had about half the increase in drag as an increase in frontal area. As a result, this caused the battery energy usage to increase, along with the takeoff and cruise power required. Therefore, a longer speed loader is better than one with a greater cross sectional area. As the battery energy usage increased, the number of possible sorties decreased. One goal of the optimization model was to determine the cutoff point at which the amount of payload was optimized for a preset number of possible sorties resulting in a maximum score. Another important consideration for the number of tennis balls was the speed loader, since its contribution to the rated aircraft cost was determined by the number of tennis balls carried.

4.1.3 Steel Payload Weight

The steel payload was assumed to be the heavier of the two sortie payloads, and as a result, determined the "worst case" takeoff performance. The heavier the payload, the higher the wing loading and the higher the stall velocity and takeoff power required.

4.2 Preliminary Design Rating System

During the preliminary design stage, the APG decided that the FOM method of evaluating competing configuration parameters should be replaced with an optimization model used to determine the overall score ratio (total flight score divided by RAC with report score equal to 1.0) for each possible configuration. The overall score for each configuration was found and checked against the percent battery usage, to ensure that there was enough power remaining to complete all the sorties. The mission feature supported by this method was a maximum overall score, safely utilizing all available battery energy.

4.3 Analytical Methods Used

The APG used an optimization model to select the optimum number of tennis balls per sortie, the optimum steel weight per sortie, the optimum wing area, and the optimum speed loader configuration, while remaining within the available battery limits. The calculated values for each of these parameters maximized the total flight score to rated aircraft cost ratio and were expected to be within the teams' construction accuracy. This method was selected because it provided an easy way to quickly compare several competing configurations. This optimization scheme was used to analyze the baseline aircraft arrived at in the conceptual design phase. The optimization process allowed the overall score, battery energy used and steel payload weights to be calculated as a function of wing area and number of tennis balls, and hence, speed loader configuration.

First, the wing area, number of motors and the various component weights were entered into the software. The wing weight was estimated from last year's aircraft since similar construction was used. Several parameters were then defined as shown in Table 4.2. Once these parameters were known, they were used to calculate the available battery energy using the following equation:

$$E_{battery} = (\# cells) \left(\frac{Volts}{cell} \right) (mA - hours) \left(\frac{3.6 A - sec}{mA - hours} \right) \quad (4.1)$$

The stall velocity was then estimated using the predicted wing loading. The number of tennis balls was then varied from 10 to 100 in increments of 10 balls. For each increment of tennis balls, the fuselage

dimensions required to hold that number of balls was calculated. Using trends from previous years, the fuselage weight was then estimated to arrive at a total empty weight estimate. Since the conditions at the contest site are typically very windy, provisions were made to account for this when determining the aircraft performance. To do this, an effective distance that the aircraft travels was found by superimposing a +/-30 fps headwind/tailwind on the aircraft, depending on whether the aircraft was flying into the wind or with the wind. This resulted in an increased "effective" distance flown by the aircraft as shown by equations 4.2 and 4.3:

$$S_{effective, steel} = S_{steel - nowind} + 2000 \left(\frac{1}{1 - \left(\frac{V_{wind}}{V_{flight}} \right)^2} - 1 \right) \quad (4.2)$$

$$S_{effective, balls} = S_{balls - nowind} + 4000 \left(\frac{1}{1 - \left(\frac{V_{wind}}{V_{flight}} \right)^2} - 1 \right) \quad (4.3)$$

In these equations, the 2000 and 4000 coefficients were the straight-away distances covered by the aircraft. This effective distance allowed the APG to account for the increased time and energy required to fly against a headwind. The ball and steel sortie times were then estimated using equations 4.4 and 4.5:

$$t_{balls} = \#sorties_{balls} \left(\frac{S_{effective, balls}}{V_{flight}} \right) \quad (4.4)$$

$$t_{steel} = \#sorties_{steel} \left(\frac{S_{effective, steel}}{V_{flight}} \right) \quad (4.5)$$

These sortie times were then subtracted from the total 10-minute flight time to obtain the allowable pit stop time.

Using the flight velocity the fuselage Reynolds number based on length was found. This was then used to estimate the fuselage turbulent friction coefficient [10],

$$C_f = \frac{0.074}{R_{e_l}^{0.2}} \quad (4.6)$$

which was then used to find the fuselage parasitic drag coefficient,

$$C_{Do_{fus}} = 0.47 + C_f \frac{S_{wet, fuse}}{S_{frontal, fuse}} \quad (4.7)$$

where 0.47 is the parasite drag coefficient for a sphere, to simulate the nose cone. Once this was known, the parasite drag coefficient for the entire aircraft was found using the following equation:

$$C_{Do_{plane}} = C_{Do_{wing}} + C_{Do_{LandingGear}} \frac{S_{LG}}{S_w} + C_{Do_{tail}} \frac{S_{tail}}{S_w} + C_{Do_{fus}} \frac{S_{fusefrontal}}{S_w} \quad (4.8)$$

In order to arrive at the complete aircraft drag coefficient, the induced drag was found by assuming a minimum power required flight condition, namely,

$$C_{Do} = C_{Di} \quad (4.9)$$

Thereby, the total aircraft drag coefficient was found to be twice the parasitic drag coefficient. Since the induced drag coefficient was known, the optimum lift coefficient was then found using the definition of the induced drag coefficient,

$$C_{Lopt} = \sqrt{C_{Di} \pi e A R_{wing}} \quad (4.10)$$

The maximum lift to drag ratio was then found using the optimum lift coefficient divided by the aircraft drag coefficient,

$$\left(\frac{L}{D}\right)_{MAX} = \frac{C_{Lopt}}{C_{Dplane}} \quad (4.11)$$

The weight of the ball payload was found by simply multiplying the number of balls by the weight per ball. This weight was then added to the empty weight of the aircraft with the electronics installed to arrive at a total aircraft weight for the ball sorties. This weight was then used to determine the ball sortie lift coefficient. This lift coefficient was then used to determine the ball sortie lift to drag ratio. The power required for the ball sorties was then estimated using the following equation:

$$PR_{balls} = V_{flight} T_{R_{balls}} \quad (4.12)$$

Where the thrust required for flight during the ball sorties is,

$$T_{R_{balls}} = \frac{W_{balls}}{\left(\frac{L}{D}\right)_{balls}} \quad (4.13)$$

The power required for flight for the steel sorties was found by the available power, and average throttle setting,

$$PR_{steel} = \frac{(\#motors)(MaxPower / motor)(\%Power_{steel})}{100} \eta_o \quad (4.14)$$

where η_o is the overall propulsive efficiency. In order to evaluate the takeoff performance, it was necessary to find the available takeoff thrust. This was found by simply dividing the available power by the takeoff velocity, as given by the following equation:

$$T_{Takeoff,avail} = \frac{(\#motors)(MaxPower / motor) \left(\frac{\%P_{Takeoff}}{100} \right)}{V_{Takeoff}} \eta_o \quad (4.15)$$

The next parameter needed to evaluate the takeoff performance was the drag at takeoff,

$$D_{Takeoff} = C_{D,plane} \frac{1}{2} \rho V_{Takeoff}^2 S_{wing} \quad (4.16)$$

Once the takeoff velocity, thrust and drag were known, the maximum weight of the aircraft was found for the specified takeoff distance of 200 ft,

$$W_{\max} = \frac{(64.4)(X_{\text{Takeoff}})(T_{\text{Takeoff}} - D_{\text{Takeoff}})}{V_{\text{Takeoff}}^2} \quad (4.17)$$

The estimated empty weight was then subtracted from this to arrive at the steel payload weight, since the steel sortie was assumed to be the heaviest. Once the steel payload weight was found as a function of tennis balls via the drag coefficient's dependency on the speed loader size, the energy used was found by the product of the thrust and the effective distance traveled. This was compared to the total battery energy available at the start, and the percent battery used was checked such that it remained within the safety limit of 10% energy in reserve, set forth by the team's electrical specialist. The steel payload weight was simultaneously checked against the ball payload weight to ensure that there was not more ball weight than steel weight, since the takeoff performance was evaluated for the steel weight. Once the total number of balls and total steel weight were known, the total flight score was found as described in the rules. The Rated Aircraft Cost was also found for each particular configuration. This then allowed an overall score to be found for each payload configuration. This overall score was the total flight score divided by the Rated Aircraft Cost with an assumed report score equal to 1. The configuration resulting in the highest overall score was selected as the "Almost Heaven" design.

4.4 Optimization Scheme Results

In the optimization scheme, the wing area was varied from 8 sq.ft. to 13 sq.ft. in 1 sq.ft. increments. For each wing area, the number of tennis balls was varied from 10 to 100 in increments of 10 balls. For each number of tennis balls (at each wing area) the overall score was recorded as shown in Figure 4.1. The highest overall score occurred at the maximum wing area of 13 sq.ft. and 100 tennis balls; however, upon inspection of Figure 4.2, as the wing area was increased above 12 sq.ft., the percent usage of the battery increased above about 90% which put the energy used above the safety limit of 10% in reserve. Therefore, for safety, the wing area was selected as 12 sq.ft. Since the maximum score for any wing area (Figure 4.1) occurred at the maximum number of balls, 100 tennis balls was selected as the payload. The weight of the tennis balls was lower than that weight required by the restricted takeoff distance; as a result, the steel payload was selected as 13.44 pounds (see Figure 4.3). Table 4.2 shows the configuration parameter values for the final aircraft.

4.5 Structural design

The minimum and maximum load factors, n_{neg} and n_{pos} , express the maneuvering ability of an aircraft as a multiple of the acceleration due to gravity. Based on the typical limit load factors of a general aviation aircraft, the limit load factors were determined to be $n_{\text{pos}} = 3.0$ and $n_{\text{neg}} = -1.0$. The V-n diagram (Figure 4.3) depicts the limit load factors as a function of airspeed. The positive and negative lift limit curves were calculated using the following equation:

$$n = \frac{0.5 \rho_{\text{alt}} V^2 S_W C_{L_{\text{max}}}}{W_{\text{TO}}} \quad (4.18)$$

4.6 Wing Structure Analysis

Once the weights of each component were determined (Table 4.3), the load, shear, and moment forces acting on the wing were calculated. To determine the forces acting upon the wing in the y-z and the x-z planes, the lift distribution, weight distribution, drag distribution and thrust of the motors on the wing were needed.

The lift along the span of the wing was calculated using an elliptical lift approximation. This was possible since the wing was tapered and twisted to achieve a nearly elliptical lift distribution. The span was divided into 3" sections. Next, the distributed load of the wing was calculated along the span. Then concentrated loads of the power plant and landing gear were then added and the load distribution was calculated (see Figure 4.4). The span-wise drag distribution on the wing was calculated, along with the concentrated force of the thrust. These were then plotted in Figure 4.7. Using a trapezoidal approximation to calculate the area under the curve, the shear diagrams and moment diagrams were calculated for each loading direction (see Figures 4.5, 4.6, 4.8, and 4.9).

4.7 Fuselage Structure Analysis

Using the component weights from Table 4.3 the load diagram of the fuselage was determined. The weight of each component was treated as a distributed load and the power plant, avionics, and wing weights were lumped together. Since the wing is attached to the fuselage at the leading and trailing edges, the reaction forces at these locations were calculated as shown in Figure 4.10. Using the Figures of Merit established in Section 3, an aluminum tube or a carbon fiber tube would meet the criteria to construct the fuselage. Once other components of the aircraft were designed, it was determined that an aluminum pipe would be easier to work with. Even though the carbon fiber tube is significantly lighter than the aluminum one, the carbon fiber tube could only be purchased in 6' lengths whereas the aluminum could be purchased in 12' lengths. It was determined that the use of additional materials to join the carbon fiber tubes would add weight comparable to the weight of the aluminum tube and require more work to fabricate the connections. Another downside to the carbon fiber tube was that it could not be threaded (through the wall) like the aluminum. This ability to thread the aluminum tube allows connections to the tail, nose gear, and the wing to be made simpler.

4.8 Preliminary Design Results

The preliminary design resulted in a fixed wing area, number of tennis balls, and steel payload weight. The values of these parameters were based upon some initial assumptions, which are listed in Table 4.2, along with the final designed values for the final configuration. The optimization output is listed in Table 4.1.

Table 4.1 Optimization output

# balls	Fuse L	Fuse radius	Sfuse	Swet fuse	Empty W	ss eff	sb eff	ball time
10	5.10	0.058	0.010	1.85	19.3	4450	6900	197
20	7.20	0.087	0.024	3.92	19.8	4450	6900	197
30	6.12	0.077	0.019	2.96	19.6	4450	6900	197
40	7.16	0.116	0.042	5.20	20.0	4450	6900	197
50	8.20	0.173	0.094	8.93	20.8	4450	6900	197
60	7.16	0.260	0.212	11.70	21.3	4450	6900	197
70	8.00	0.260	0.212	13.07	21.6	4450	6900	197
80	8.62	0.260	0.212	14.08	21.8	4450	6900	197
90	9.24	0.260	0.212	15.09	22.0	4450	6900	197
100	10.07	0.260	0.212	16.45	22.3	4450	6900	197

steel time	swap time	Re,Lfuse	Cf fuse	CDo, fuse	CDo, plane	CDI	CD,plane	CL, opt
191	53.04	2.27E+06	0.004	1.170	0.012	0.012	0.025	0.507
191	53.04	3.20E+06	0.004	1.085	0.013	0.013	0.027	0.530
191	53.04	2.72E+06	0.004	1.077	0.013	0.013	0.026	0.521
191	53.04	3.19E+06	0.004	0.929	0.015	0.015	0.029	0.551
191	53.04	3.65E+06	0.004	0.811	0.018	0.018	0.035	0.608
191	53.04	3.19E+06	0.004	0.674	0.023	0.023	0.046	0.697
191	53.04	3.56E+06	0.004	0.693	0.024	0.024	0.047	0.702
191	53.04	3.83E+06	0.004	0.707	0.024	0.024	0.048	0.706
191	53.04	4.11E+06	0.004	0.720	0.024	0.024	0.048	0.709
191	53.04	4.48E+06	0.003	0.738	0.024	0.024	0.049	0.714

L/D max	Wballs	Wplane TB	CL balls	L/D balls	TVballs	Tballs req'd	TVsteel	Tsteel
20.6	1.25	20.6	0.295	12.0	120.3	1.72	281.9	4.03
19.8	2.50	22.3	0.319	11.9	131.1	1.87	281.9	4.03
20.1	3.75	23.3	0.334	12.9	126.6	1.81	281.9	4.03
19.0	5.00	25.0	0.358	12.3	142.0	2.03	281.9	4.03
17.2	6.25	27.0	0.387	11.0	172.7	2.47	281.9	4.03
15.0	7.50	28.8	0.412	8.9	227.0	3.24	281.9	4.03
14.9	8.75	30.3	0.434	9.2	230.2	3.29	281.9	4.03
14.8	10.00	31.8	0.455	9.6	232.6	3.32	281.9	4.03
14.8	11.25	33.2	0.476	9.9	235.0	3.36	281.9	4.03
14.7	12.50	34.8	0.497	10.2	238.0	3.40	281.9	4.03

Table 4.1 Optimization output cont'd

Ttakeoff, avail.	Dtakeoff	W w/ steel allowed	Steel W	TFS	Fuse Cost	Empty Wcost	Rated A/C Cost	OVERALL SCORE
8.32	0.860	39.13	19.8	63.4	25.4	1435	7.88	8.041
8.32	0.938	38.72	19.0	64.9	33.8	1476	8.09	8.023
8.32	0.906	38.89	19.3	70.0	29.5	1457	7.98	8.766
8.32	1.016	38.32	18.3	70.9	33.6	1502	8.11	8.741
8.32	1.235	37.16	16.4	69.2	37.8	1576	8.27	8.370
8.32	1.624	35.13	13.8	65.4	33.6	1632	8.24	7.940
8.32	1.647	35.00	13.4	68.2	37.0	1659	8.34	8.187
8.32	1.664	34.91	13.1	71.4	39.5	1679	8.40	8.490
8.32	1.681	34.83	12.8	74.5	42.0	1700	8.47	8.790
8.32	1.703	34.71	12.4	77.3	45.3	1727	8.57	9.025

Energy used	% Batt used	Ws-Wb
116717	56.5	19
123825	60.0	16
120906	58.6	16
130795	63.3	13
149634	72.5	10
180847	87.6	6
182658	88.5	5
183965	89.1	3
185250	89.7	2
186938	90.5	0

Table 4.2 Aircraft parameters – Final Values

Parameter	Value	Units
Landing Gear Frontal Area	0.18	ft ²
Horizontal Tail Area	3.00	ft ²
Vertical Tail Area	1.68	ft ²
Wing Aspect Ratio	8.33	
Wing Span	10.00	ft
Wing Taper Ratio	0.50	
Wing Root Chord	1.60	ft
Wing Tip Chord	0.80	ft
Wing Area	12.00	ft ²
Horizontal Tail Volume Coefficient	0.80	
Vertical Tail Volume Coefficient	0.07	
Tail Boom Length	5.00	ft
Fuselage Length	8.34	ft
Fuselage Diameter	0.115	ft
Speed Loader Length	6.00	ft
Speed Loader Diameter	0.46	ft
Overall Propulsive Efficiency – Geared Motor/Propeller System	0.42	
Battery rating	2,400.00	mA-hr
# cells	36	
Battery Energy	217,940.70	ft-lb
%Power – Cruise	65.00	
%Power – Takeoff	95.00	
# motors	2	
CDo, gear – streamlined	0.01	
CDo, wing	0.01	
CDo, horizontal tail	0.01	
CDo, vertical tail	0.01	
Assumed Oswald Efficiency	0.80	
Max Current Draw	35.00	Amps
Max power per motor	0.939	Hp
Steel Sortie Distance (no wind)	4,000.00	ft
Ball Sortie Distance (no wind)	6,000.00	ft
# steel sorties	3	
# ball sorties	2	
Wing Maximum Lift Coefficient with Flaps Deployed	1.20	
Maximum Takeoff Distance – no headwind	200	ft
Average Flight Velocity	70.00	ft/s
Wing Reynold's Number	534,257.35	
Typical Wind Speed	30.00	ft/s
Actual Stall Velocity	49.54	ft/s

Table 4.3 Weight component fractions for the steel and tennis ball sorties

Part	Steel sortie		Tennis ball sortie	
	Weight per part (lb)	Fraction of total weight (%)	Weight per part (lb)	Fraction of total weight (%)
<i>Flap Pushrod L</i>	0.011	0.034	0.011	0.033
<i>Flap Pushrod R</i>	0.011	0.034	0.011	0.033
<i>Flap Servo L</i>	0.097	0.30	0.097	0.29
<i>Flap Servo R</i>	0.097	0.30	0.097	0.29
<i>Fuselage</i>	1.72	5.38	1.72	5.22
<i>H pushrod</i>	0.011	0.034	0.011	0.033
<i>H Servo</i>	0.097	0.30	0.097	0.29
<i>Main Batt L</i>	2.49	7.79	2.49	7.56
<i>Main Batt R</i>	2.49	7.79	2.49	7.56
<i>Main Gear L</i>	1.01	3.15	1.01	3.06
<i>Main Gear R</i>	1.01	3.15	1.01	3.06
<i>Main Wheel L</i>	0.16	0.51	0.16	0.49
<i>Main Wheel R</i>	0.16	0.51	0.16	0.49
<i>Motor L</i>	0.93	2.92	0.93	2.83
<i>Motor R</i>	0.93	2.92	0.93	2.83
<i>NG pushrod</i>	0.01	0.03	0.01	0.03
<i>Nose Brake</i>	0.03	0.10	0.03	0.10
<i>Nose Gear</i>	0.50	1.56	0.50	1.52
<i>Nose Pant</i>	0.07	0.21	0.07	0.20
<i>Nose Wheel</i>	0.16	0.51	0.16	0.49
<i>Prop L</i>	0.053	0.16	0.053	0.16
<i>Prop R</i>	0.053	0.16	0.053	0.16
<i>Rx</i>	0.070	0.22	0.070	0.21
<i>Rx Batt</i>	0.21	0.65	0.21	0.63
<i>Speed Control L</i>	0.12	0.38	0.12	0.37
<i>Speed Control R</i>	0.12	0.38	0.12	0.37
<i>Steel Payload</i>	13.44	40.76	12.5	39.01
<i>Tail</i>	0.65	2.03	0.65	1.97
<i>Tennis Ball Payload</i>	12.50	39.01	0.00	0.00
<i>V pushrod</i>	0.011	0.034	0.011	0.033
<i>V Servo</i>	0.10	0.30	0.10	0.29
<i>Wheel Pant L</i>	0.067	0.21	0.067	0.20
<i>Wheel Pant R</i>	0.067	0.21	0.067	0.20
<i>Wing</i>	6.00	18.73	6.00	18.19

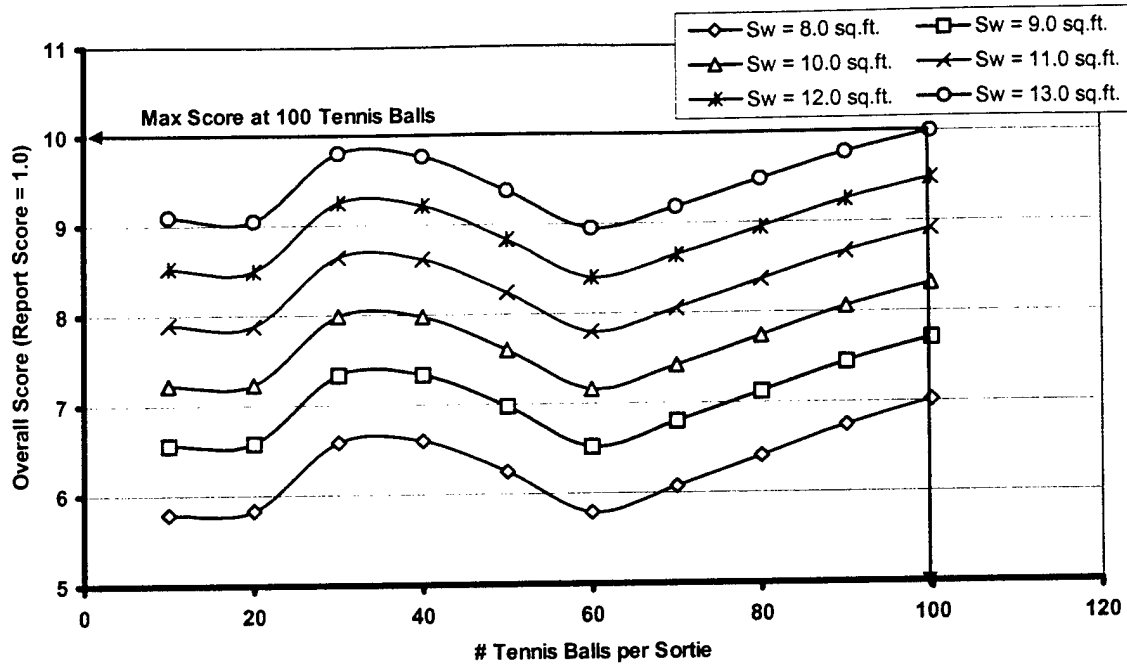


Figure 4.1 Overall Score Dependency on Number of Tennis Balls – Note variations that occur when the speed loader dimensions change to accommodate more balls.

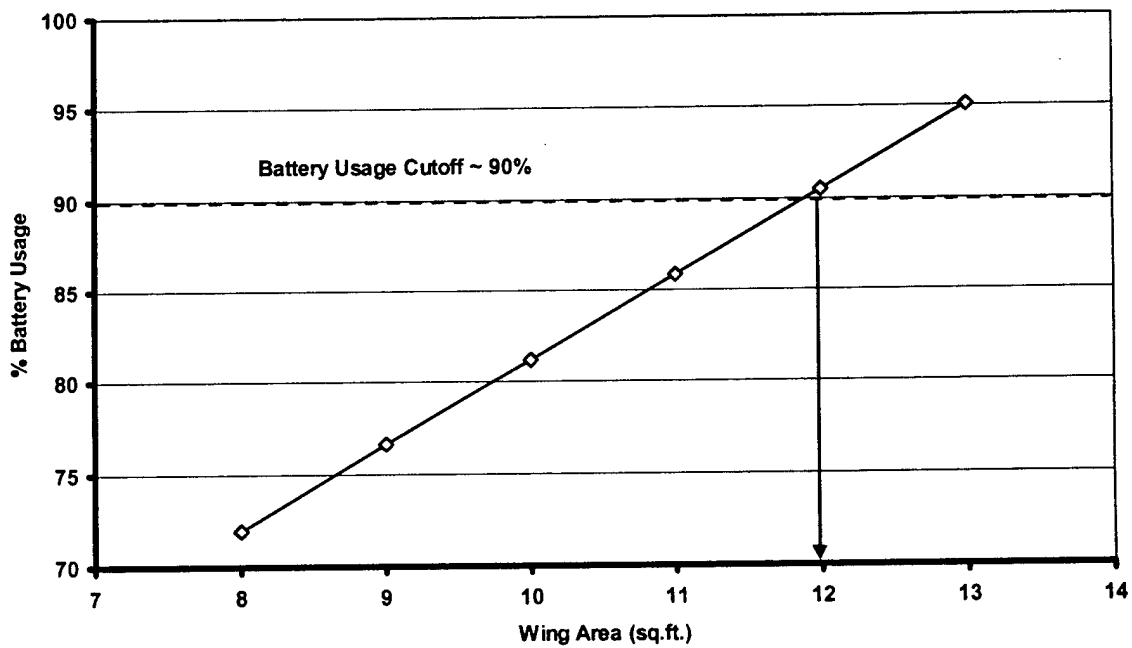


Figure 4.2 Battery Usage Dependence on Wing Area for 100 Tennis Balls – Battery Cutoff determined from typical 2,400 mA-hr cell fast discharge curves.

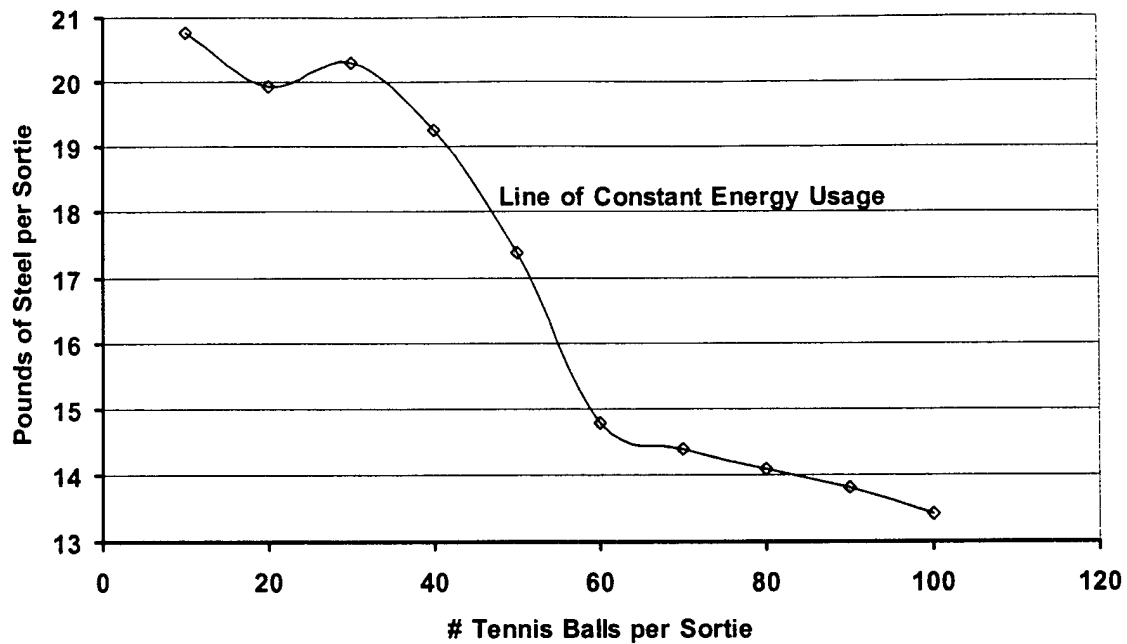


Figure 4.3 Comparison of possible payload options for equivalent energy use – Irregularities in curve are due to the changes in the speed loader dimensions to accommodate different numbers of balls.

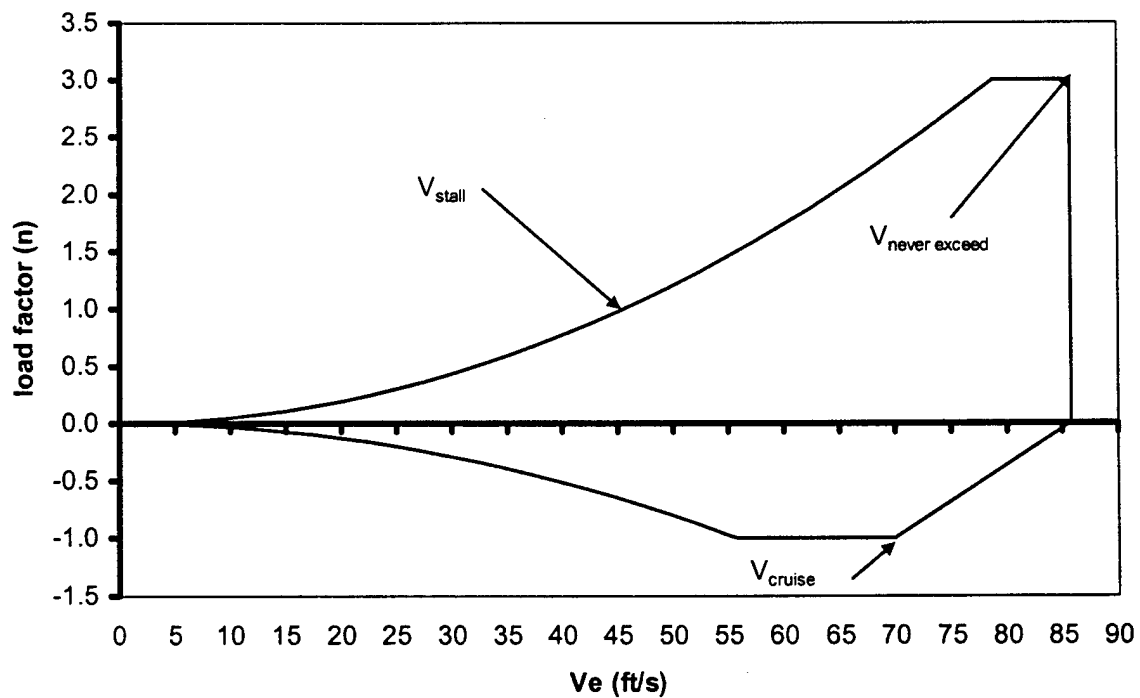


Figure 4.3 V-n diagram – Defines the flight speed envelope which must be adhered to for ensured structural integrity

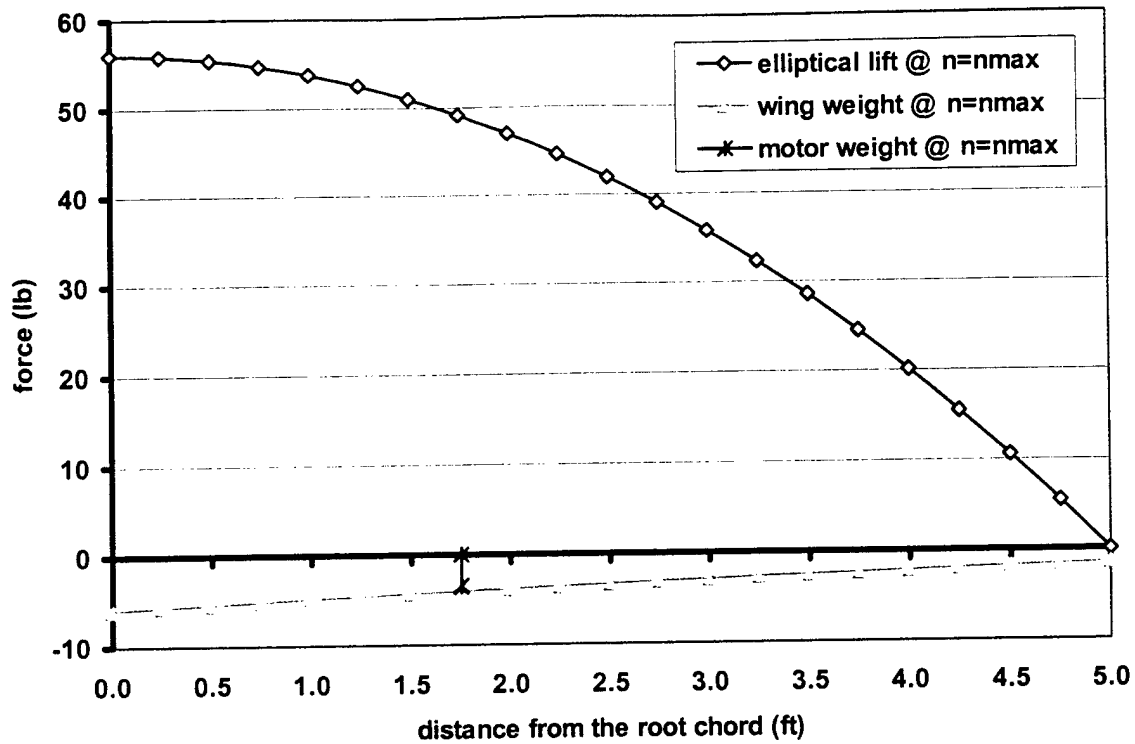


Figure 4.4 Flight load diagram due to lift and weight at load factor $n=n_{max}$

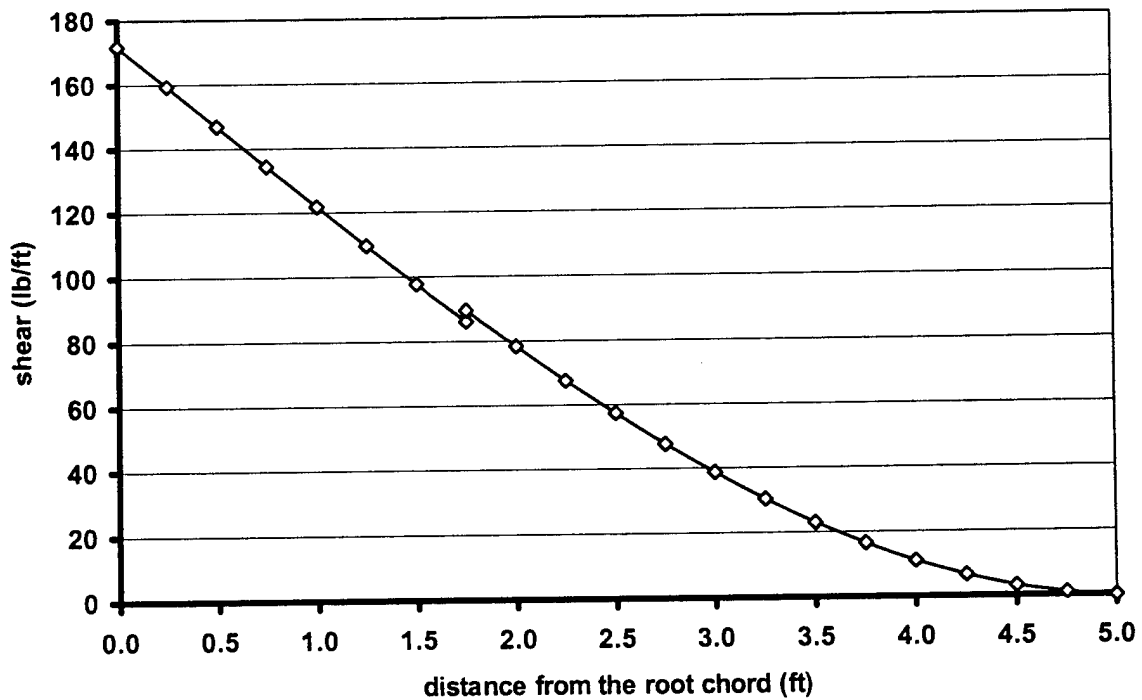


Figure 4.5 Flight shear diagram due to lift and weight at load factor $n=n_{max}$

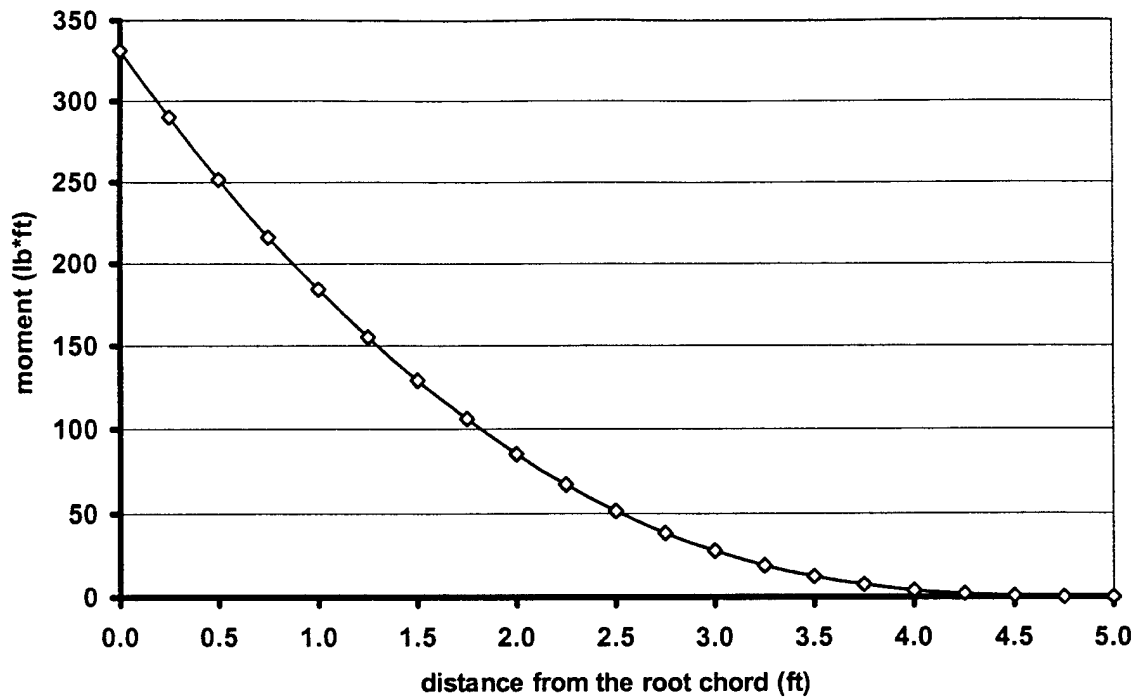


Figure 4.6 Flight bending moment diagram due to lift and weight at load factor $n=n_{max}$

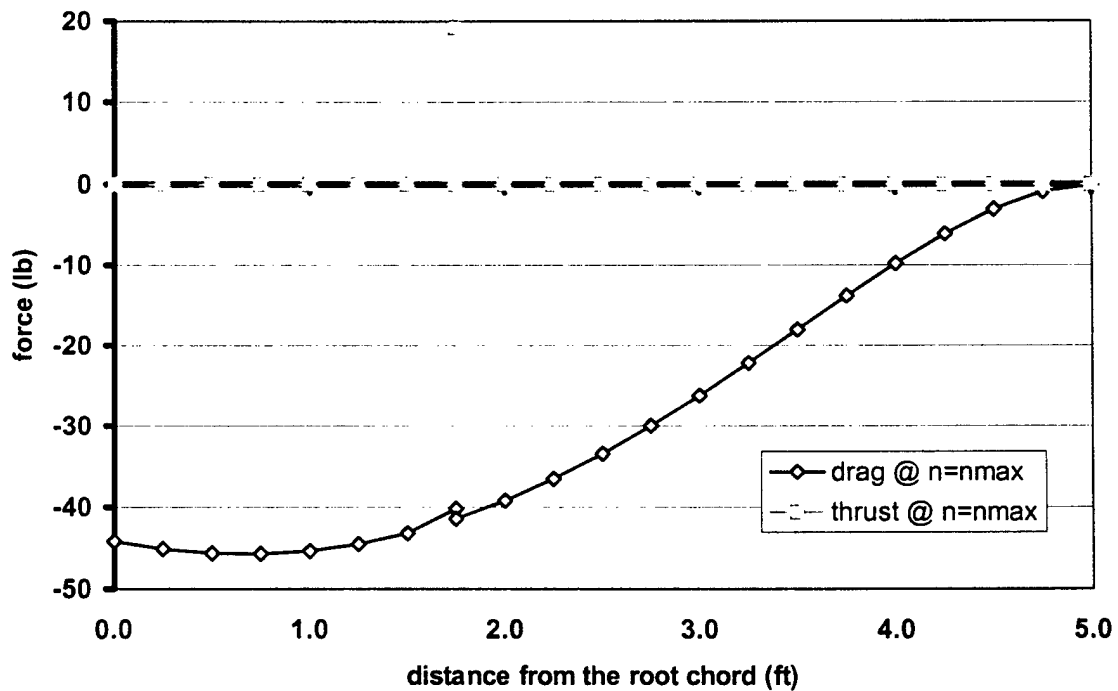


Figure 4.7 Flight load diagram due to drag and thrust at load factor $n=n_{max}$

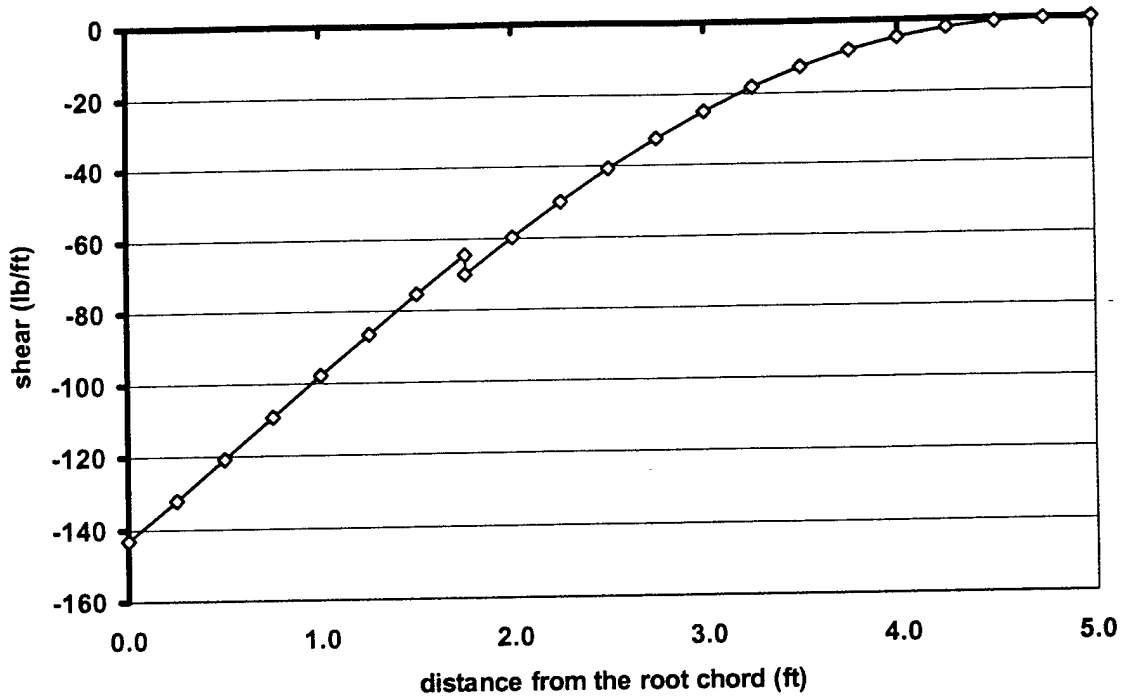


Figure 4.8 Flight shear diagram due to drag and thrust at load factor $n=n_{\max}$

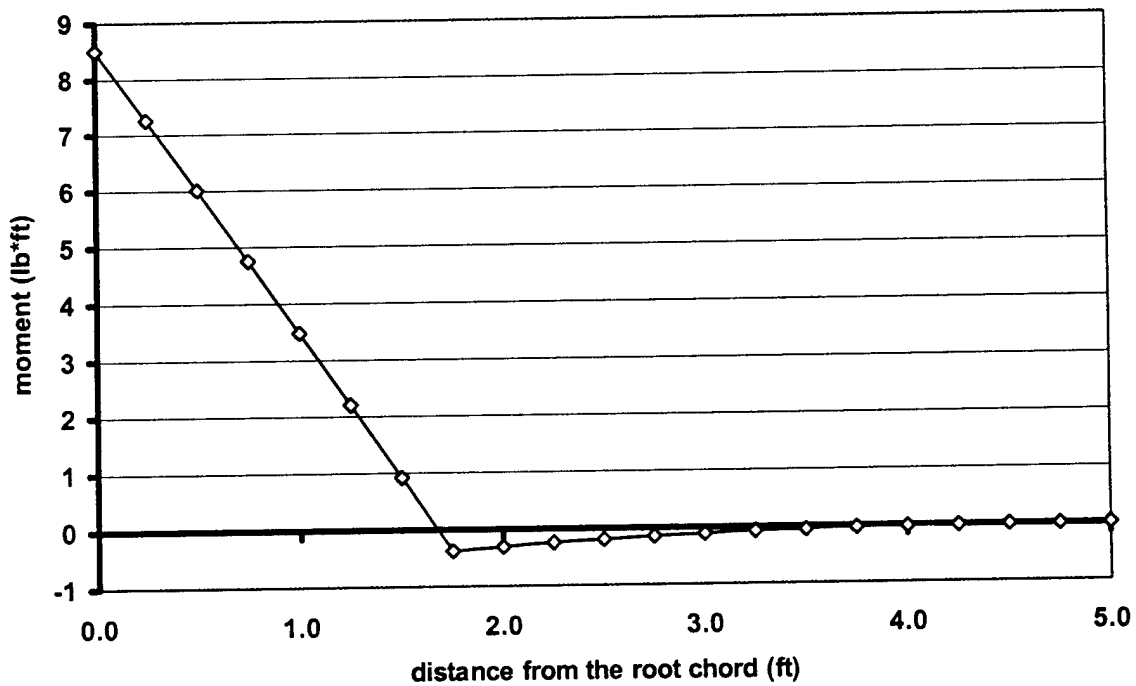


Figure 4.9 Flight moment diagram due to drag and thrust at load factor $n=n_{\max}$

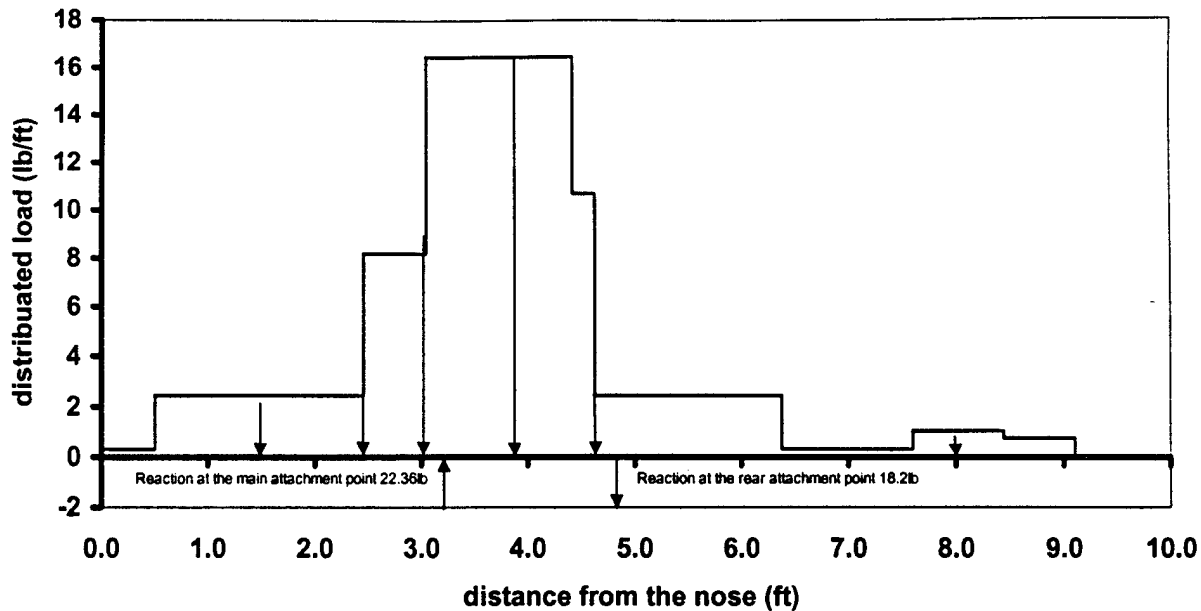


Figure 4.10 Load diagram of the fuselage

5. Detail Design

After the wing area, number of balls and steel weight per sortie were found in the preliminary design phase, the detailed design was undertaken to determine the airfoil, propeller, motor locations, aileron size, tail size and tail control surface sizes, as well as the tail location, wing twist and incidence. Consideration was also given to turning, climb, and landing performance.

5.1 Detailed Design – Aircraft Parameters Group

5.1.1 Airfoil Selection

The airfoil selection was a very critical part of the detailed design, since the airfoil affects the the cruise speed, takeoff performance, stall speed and handling qualities near stall conditions as well as the overall aerodynamic efficiency.

The two most important qualities that were investigated when searching for an airfoil to use was the stall performance and the handling qualities near stall. These were considered most important because the WVU team has lost two entries in previous years due to poor stall performance. This year's team was determined to not allow this to happen again.

In order to have good roll control near stall conditions, it is imperative that the flow over the wing not separate at moderate to high angles of attack. The air flow over the wing will be closer to separating and stalling when it encounters a disturbance in the flow. This disturbance may be a sharp leading edge. One way to help prevent this is to select an airfoil that has a relatively large leading edge radius. This translates into an airfoil with a larger thickness not less than 15%, typically. The flow can maintain its

momentum when it has a larger radius of curvature rather than a smaller one, as is encountered in a thinner airfoil.

The other quality considered by the APG when selecting an airfoil was the stall performance. The lift curve should be smooth and continuous near the region of stall. Lift curves displaying a sharp drop in lift coefficient at high angles of attack were avoided.

These required properties led the APG to select the NACA 4415 airfoil for use on the WVU entry. The lift performance curve can be seen in Figure 5.1.

5.1.2 Propeller Selection

In order to select a pair of propellers, the APG used the commercially available software package, "ElectriCalc," (Version 2.03, copyright, 1999 by SLK Electronics, L.L.C., all rights reserved). The major requirements for the propeller were that it had to have a low drop-off of thrust with increasing flight velocity, and it had to have mass properties such that the load it placed on the motor did not cause the motor to draw more than the limited 40 amps. Several propellers were evaluated in "ElectriCalc" and the results prompted the APG to select the TopFlight 15x8 prop for use on the WVU entry.

5.1.3 Aileron Sizing

The dual-use ailerons (flaperons) were sized according to historical trends, based on previous entries as well as reference [1]. An aileron chord to wing chord ratio of 0.28 and an aileron span to wing span ratio of 0.35 were selected in order to provide enough roll control and maximum lift coefficient for takeoff as well as a large enough drag coefficient for increased landing performance. There was some flexibility in the actual aileron size, since the deflection angle could be adjusted.

5.1.4 Horizontal Tail Sizing and Location

The horizontal tail was sized using the tail volume coefficient method, according to the equation,

$$S_H = \frac{c_H (MAC_w) S_w}{L_H} \quad (5.1)$$

where c_H is the horizontal tail volume coefficient selected from reference [1]. The distance from the wing to the tail was defined such that there was sufficient rotation for takeoff and such as to place the cg in a proper location. The elevator chord was selected from historical data from previous entries to be 30% of the horizontal tail mean aerodynamic chord.

5.1.5 Vertical Tail Sizing

The vertical tail was also sized using the tail volume coefficient method. The equation for the vertical tail area is,

$$S_V = \frac{c_V b_w S_w}{L_V} \quad (5.2)$$

where c_V is the vertical tail volume coefficient selected from reference [1]. The rudder chord was also selected from historical data from previous entries to be 30% of the vertical mean aerodynamic chord. The location of the vertical tail was selected so that the root chord of the vertical tail would match that of the horizontal tail. This provided an easier construction method. The size of the vertical tail also

depended on the location of the motors on the wing. The closer the motors are placed to the wing tips, the larger the vertical tail had to be to maintain control with one motor off. In order to minimize the size of the vertical tail, the motors were placed as close to the fuselage as possible, allowing one inch of clearance between the prop and the fuselage.

5.1.6 Wing Incidence, Twist, Taper, and Dihedral

In order to provide the proper amount of lift, the wing incidence was determined to be 7.8 degrees at the root using the following equation:

$$i_{root} = \frac{C_{L_{ROOT}}}{C_{L_{u, wing}}} + \alpha_o \quad (5.3)$$

and the tip incidence angle was found to be 4.8 degrees using the following equation:

$$i_{tip} = \frac{C_{L_{TIP}}}{C_{L_{u, wing}}} + \alpha_o \quad (5.4)$$

where these incidence angles were designed to provide the same average lift as an untwisted elliptic wing planform [9]. The terms, $C_{L_{Root}}$ and $C_{L_{TIP}}$ were defined such that the area under the actual lift distribution curve matched the area under the elliptical lift distribution curve.

Since no simple technique for selecting a dihedral angle exists, the dihedral was set to 2 degrees based on historical data from previous designs as well as reference [1]. The wing taper was selected to be 0.5 based on the stall patterns of highly tapered wings. For model aircraft wings that are tapered more than about 0.45, the stall progresses from the tip to the root from the trailing edge to the leading edge, thus causing the loss of aileron control before the aircraft is totally stalled. As a result, the taper ratio of 0.5 was selected as a safe estimate.

5.1.7 Landing Gear Selection

During the detail design phase, two types of landing gears were considered; fixed and retractable. A retractable landing gear would provide a more aerodynamically efficient aircraft, requiring less power for flight, and less battery energy usage through a decreased drag coefficient; however, the retractable option increased the complexity of the design and provided another source of failure within the aircraft. The advantages were weighed against the disadvantages and the decision was made to use a fixed landing gear, since it was easier to build, was much more reliable, and was less expensive than a retractable system.

5.1.8 Longitudinal Static Stability Analysis

In order to ensure a stable aircraft, a longitudinal static stability analysis was performed in which the total aircraft aerodynamic center location was found and the center of gravity was adjusted such that the static margin was greater than or equal to a preset value. The aircraft aerodynamic center, or neutral point was found according to the following equation:

$$\bar{X}_{ac} = \frac{C_{L_{\alpha}} \bar{X}_{ac_H} - C_{m_{\alpha, FUSE}} + \eta_H \frac{S_H}{S_W} C_{L_{\alpha, H}} \frac{\partial \alpha_H}{\partial \alpha} \bar{X}_{ac_H} + \frac{F_{P_a}}{q S_W} \frac{\partial \alpha_P}{\partial \alpha} \bar{X}_P}{C_{L_{\alpha}} + \eta_H \frac{S_H}{S_W} C_{L_{\alpha, H}} \frac{\partial \alpha_H}{\partial \alpha} + \frac{F_{P_a}}{q S_W}} \quad (5.5)$$

where the propeller force terms,

$$\frac{F_{P_a}}{q S_W} \quad (5.6)$$

have been neglected and accounted for by simply adding 5% to the required static margin. The downwash terms, $\frac{\partial \alpha_H}{\partial \alpha} = 1 - \frac{\partial \epsilon}{\partial \alpha}$ have been found using empirical methods as discussed in reference [raymer]. The fuselage pitching moment contribution was determined using the following equations:

$$C_{m_{\alpha, FUSE}} = \frac{K_f W_f^2 L_f}{c S_W} \quad (5.7)$$

$$K_f = 0.0000001x^3 + 0.000006x^2 - 0.0002x + 0.0066 \quad (5.8)$$

where x is the percent fuselage length position of the root quarter chord. The wing and tail lift curve slopes were found by using 2D airfoil data for each and adjusting the slope to account for 3D effects.

Once the aerodynamic center location was known, the components of the aircraft were arranged such that the center of gravity provided the proper static margin, i.e., the aerodynamic center was far enough behind the center of gravity location. The payload center of gravity was placed at the aircraft center of gravity to ensure that the empty flying qualities were unchanged. Tables 5.1 and 5.2 show the values of the component locations and the parameters discussed above, respectively.

5.1.9 Turning, Landing, and Climb Analysis

The ability to maintain altitude during a turn was taken into account in the design of the flaperons as well as the vertical tail. During the turning maneuver, the flaps will be deployed and appropriate rudder given in order to maintain lift. During landing the flaps are deployed to avoid stalling the aircraft at the slower speed. Once touchdown has occurred the brake will be used to stop the roll of the aircraft. Since the brake is activated along with the down elevator a pitching moment is applied to the aircraft acting downward on the nose, helping to keep the aircraft on the ground. The maximum rate of climb was found to be 1.61 ft/sec.

5.2 Assessment of available materials

The preliminary structural design began with an assessment of the materials available to the team. These materials included those left over from previous years, those that were donated this year, and a realistic list of materials to be bought. Using previous aircraft as a starting point, and the Figures of Merit described in Table 3.2 it was determined that composite materials, balsa wood, foam, adhesives, and other basic construction materials would be needed. Due to cost restraints, high strength composite

materials such as carbon fiber and Kevlar were unable to be purchased. However, 3k carbon fiber, 1.7oz Kevlar 49 and various epoxies were donated to the team. One and two pound density foam was donated and was used to construct plugs. Balsa wood, adhesives, servos, push rods, etc. could be purchased from model vendors.

5.3 Comparison of different laminates

Ideally, 1k plain weave carbon fiber or carbon fiber prepreg would have been used to construct the necessary components of the aircraft. Carbon fiber provides a high strength to weight ratio. In the prepreg form, the fiber volume fraction is higher than what can be achieved using hand lay-up. The composite matrix provides less strength than the fiber therefore a higher fiber volume fraction would provide a lighter and stronger component. 1k plain weave carbon fiber would allow more freedom in varying the laminate to achieve the required strength. Due to the high cost of 1k carbon and the lack of proper facilities (large-scale oven) to use prepreg neither of these materials were used.

The available materials of 1.7oz plain weave Kevlar 49 and a loose weave 3k carbon fiber were made into different laminates for evaluation. Using last year's design as a starting point, three laminate combinations were analyzed. Table 5.3 is a comparison of the following laminates three layers of [0,90] 1.7oz Kevlar 49, one layer of [0,90] 1.7oz Kevlar 49 and one layer of [0,90] 3k carbon fiber, and one layer of [0,90] 3k carbon fiber sandwiched between one layer of [0,90] 1.7oz Kevlar 49 on either side. As can be seen in Table 5.3 the laminate of one layer of 3k carbon sandwiched between the layers of Kevlar 49 provides a higher first ply failure and fiber failure values than the other laminates. Another advantage of this laminate is that the Kevlar is a plain weave, whereas the carbon fiber is a loose weave. The plain weave is easier to work with, since the epoxy can be spread without moving the fibers out of alignment. During construction of the wing, each layer will be laid out in the mold dry, then the epoxy will be worked into it.

5.4 Truss-Core Sandwich Composite Stringers

The stringers were designed to avoid the need for a spar. There are two advantages to not having a spar. These are weight reduction and ease of construction. The construction is simplified because the strengthening members are added during the lay-up of the skin. A spar would have to be built separately and fitted into the wing. This would consist of building a plug, a mold, and then the spar. Adding the strengthening members during the initial construction assures that the upper and lower wing skins are adhered to their respective supports. When attaching a spar to the skins, one cannot be certain that the connection with the skin is bonded well. This is because the second skin is blindly attached to the spar. This can cause delamination during flight, resulting in a structural failure as well as altered wing aerodynamics. The strengthening members were constructed from 1" thick, $1 \frac{lb}{ft^3}$, foam sheets that were cut into 1.25" wide strips with 45° beveled edges. These foam strips were then oriented so that they interlocked with each other; i.e., each piece was alternated so that the beveled sides match as seen in the drawing package. Composite material was layered between the foam strips in a zigzag pattern. This pattern formed a corrugated structure similar to cardboard stiffening. This method reduced the shear

flow in the wing. The 45° bevel allowed the composite material to be laid around the stringer, so that the vacuum bag could conform to the shape. The stringers were placed along the quarter chord of the wing.

5.5 Truss-Core Sandwich Composite Stringer Analysis

Composite materials are orthotropic materials; their properties differ in the 1, 2, 3 directions. The material properties of the carbon fiber/epoxy located in the webs of the truss core are at +45° and -45° in their respective locations. To calculate the material properties in these directions, a coordinate transformation matrix was used:

$$[C] = [T]^T [C'] [T] \quad (5.9)$$

where $[C]$ is the stiffness matrix, $[C] = [S]^{-1}$, in the global axis and $[T]$ is the transformation matrix:

$$[T] = \begin{bmatrix} \pm \cos\theta & \pm \sin\theta & 0 \\ \pm \sin\theta & \cos\theta & 0 \\ 0 & 0 & 1 \end{bmatrix} \quad (5.10)$$

where the \pm varies depending on which web the properties are calculated for. $[S]$ is the compliance matrix:

$$[S] = \begin{bmatrix} 1/E_1 & -\nu_{12}/E_1 & -\nu_{13}/E_1 & 0 & 0 & 0 \\ -\nu_{12}/E_1 & 1/E_2 & -\nu_{23}/E_2 & 0 & 0 & 0 \\ -\nu_{13}/E_1 & -\nu_{23}/E_2 & 1/E_3 & 0 & 0 & 0 \\ 0 & 0 & 0 & 1/G_{23} & 0 & 0 \\ 0 & 0 & 0 & 0 & 1/G_{13} & 0 \\ 0 & 0 & 0 & 0 & 0 & 1/G_{12} \end{bmatrix} \quad (5.11)$$

Laminates consisting of [0,90] Kevlar 49-carbon fiber-Kevlar 49, [0,90] Kevlar 49-carbon fiber, and [0,90] carbon fiber were modeled in "CADEC-Macromechanics" based on the material properties in Table 5.3. For a more accurate analysis of the wing, five stations were designated at equal increments of the wing semi-span. These sections were then modeled in "CADEC-Thin-Walled-Beams." "CADEC-Thin-Walled-Beams" was also used to analyze the stringer and airfoil geometry. First, each type of cell (see Drawing Package) was analyzed separately, so that they could be added to the airfoil as a concentrated stiffness. The EA (axial stiffness) and GJ (torsional stiffness) values were found for each concentrated stiffness and were then added to the airfoil model. Each of the concentrated stiffnesses were then placed at the appropriate locations, according to drawing of the airfoil as shown in the Drawing Package. The test section was then evaluated and values for EA and GJ were calculated for the airfoil at each station. The results from CADEC showed that the Kevlar 49 - carbon fiber - Kevlar 49 laminate would provide adequate strength to support the aircraft at load factor of $n_{pos} = 3.0$.

5.6 Fuselage Structural Analysis

The fuselage consist of a 1-3/8" OD and 0.058" wall thickness aluminum pipe with a Young's Modulus $E = 10.1E6$ psi, modulus of rigidity $G = 3.7E6$ psi, and Poisson's ratio $\nu = 0.36$. Once the load diagram of the fuselage was calculated (Figure 4.10), IDEAS Master Series 8 was used to model the loads on the fuselage. The fuselage attaches to the wing at three locations: 1" back from the LE, 7" back from the LE, and 13" back from the LE. These locations were modeled with zero degrees of freedom. The loads were then placed as distributed loads in their respective locations. Shell elements were used to mesh the pipe. Figure 5.3 displays the results of the von Mises stress. The maximum stress is $1.47E3$ psi and occurs where the pipe attaches to the wing. Since this year's aircraft weighs approximately 15 lbs more than last year's plane, the deflection of the pipe when the plane was fully loaded was a major concern. Figure 5.4 shows the displacement. As can be seen, the maximum displacement of $8.72E-2$ in occurs at the tail.

5.7 Landing Gear Structural Analysis

The landing gear structure is crucial to an aircraft. This is evident in the aircraft for the competition, since multiple sorties require several takeoffs and landings. If the landing gear were to fail, several key aircraft components could be damaged. Therefore, the landing gear must be able to withstand not only the weight of the aircraft, but the force generated due to landing. The maximum static load of the main landing gear was calculated using the following equation:

$$(Max \ Static \ Load) = W \frac{N_a}{B} \quad (5.12)$$

where W is the weight of the aircraft, N_a is the distance from the nose gear to the aft cg, and B is the distance from the nose gear to the main gear. The maximum static load was calculated to be 36.7lbs.

Using last year's landing gear as starting point, 1/4" steel was used to construct the landing gear. To determine if the landing gear would withstand the maximum static load the following equation was used to calculate the buckling load of a single piece of 1/4" steel.

$$P_c = \frac{\pi^2 EI}{2L^2} \quad (5.13)$$

The above equation is for a fixed free member and the buckling load was calculated to be 30.48 lbs per gear. Since the dynamic landing load was found to be 105 lbs total, (assuming a 3g landing), extra struts were added to strengthen the gear.

5.8 Payload Configuration

The results of the APG's optimization dictated that the frontal area of three tennis balls be used. Next, came the task of minimizing the length of the speed loader. Three different stacking arrangements were compared to determine which had the minimum length. AutoCAD was used to draw and measure the length of each arrangement. First, the tennis balls were arranged in a triangle and then stacked directly on top of each other. This arrangement (#1) produced a length of 84.5". Next, the tennis balls were stacked with three tennis balls in a triangle then a fourth tennis ball placed in the middle, to obtain a

pyramid shape. This arrangement (#2) produced a length of 95.25". Finally, the tennis balls were arranged in a triangle with another set of tennis balls on top, also in a triangle arrangement, rotated 180°. This arrangement (#3) produced a length of 72", therefore, #3 was selected. Figure depicts each arrangement.

Table 5.1 Center of Gravity Calculation Table.

Component	Weight (lb)	Distance From mac/4 (in)	Moment (lb-in)
<i>Nose Gear</i>	0.44	58.9	25.9
<i>Nose Wheel</i>	0.1628	58.9	9.59
<i>Nose Brake</i>	0.033	58.9	1.94
<i>Nose Pant</i>	0.0671	58.9	3.95
<i>Pole</i>	1.715428	-7.48	-12.8
<i>Motor</i>	0.93412	5.75	5.37
<i>Motor</i>	0.93412	5.75	5.37
<i>Prop</i>	0.0528	7.625	0.403
<i>Prop</i>	0.0528	7.625	0.403
<i>Speed Control</i>	0.12166	2.69	0.327
<i>Speed Control</i>	0.12166	2.69	0.327
<i>Rx</i>	0.0704	-7.32	-0.515
<i>Rx Batt</i>	0.20812	-7.3	-1.52
<i>Main Batt</i>	2.4948	2.62	6.54
<i>Main Batt</i>	2.4948	2.62	6.54
<i>H Servo</i>	0.0968	-61.06	-5.91
<i>V Servo</i>	0.0968	-61.06	-5.91
<i>Flap Servo</i>	0.0968	-7.14	-0.691
<i>Flap Servo</i>	0.0968	-7.14	-0.691
<i>Wing</i>	4.9896	-4.99	-24.9
<i>Tail</i>	0.649	-58.1	-37.7
<i>Main Gear L</i>	0.001408	-8	-0.0113
<i>Main Gear R</i>	0.001408	-8	-0.0113
<i>Main Wheel L</i>	0.1628	-8	-1.30
<i>Main Wheel R</i>	0.1628	-8	-1.30
<i>Wheel Pant L</i>	0.0671	-8	-0.537
<i>Wheel Pant R</i>	0.0671	-8	-0.537
<i>H pushrod</i>	0.011	-61.06	-0.672
<i>V pushrod</i>	0.011	-61.06	-0.672
<i>NG pushrod</i>	0.011	58.9	0.648
<i>Flap Pushrod L</i>	0.011	-7.14	-0.0785
<i>Flap Pushrod R</i>	0.011	-7.14	-0.0785
Xcg (in) =	-1.74	from wing quarter chord	

Table 5.2 Stability variable values

Parameter	Value	Description of Parameter
$C_{L\alpha}$	0.079/deg	3-D Wing Lift Curve Slope
X_{acw}/MAC	0.294	Non-Dimensional Wing Aerodynamic Center Location
$C_{M\alpha fus}$	0.0017	Fuselage Pitching Moment Coefficient
η_H	0.96	Dynamic Pressure Ratio for Horizontal Tail
$C_{L\alpha H}$	0.06/deg	Horizontal Tail Lift Curve Slope
$\Delta\epsilon_H/\Delta\alpha$	0.495	Downwash Parameter
$\Delta\alpha_H/\Delta\alpha$	0.505	Horizontal Tail Effectiveness Parameter
X_{ach}/MAC	3.97	Non-Dimensional Horizontal Tail Aerodynamic Center Location
K_f	0.024	Empirical Fuselage Pitching Moment Factor

Table 5.3 Material properties of Kevlar 49/Epoxy and Carbon/Epoxy and comparison of laminates using available materials

Property	Kevlar 49/Epoxy	Carbon/Epoxy	Property	Kevlar 49 (3 ply)	Kevlar 49/Carbon	Kevlar 49/Carbon/Kevlar 49
E_1 (psi)	1.10E+07	2.06E+07	E_x (psi)	5.56E+06	7.62E+06	7.40E+06
E_2 (psi)	7.98E+05	1.49E+06	E_y (psi)	5.56E+06	6.18E+06	7.40E+06
G_{12} (psi)	3.00E+05	1.04E+06	G_{xy} (psi)	3.00E+05	8.00E+05	7.63E+05
ν_{12}	0.34	0.27	ν_{xy}	0.046	0.041	0.038
F_{1t} (psi)	2.00E+05	2.65E+05	*FPF	3.66E+03	4.82E+03	4.99E+03
F_{2t} (psi)	5.00E+03	8.27E+03	*FF	1.17E+04	1.87E+04	1.57E+04
F_6 (psi)	6.40E+03	1.03E+04	*Tsai-Wu Failure Criterion			
F_{1c} (psi)	8.50E+04	1.59E+05				
F_{2c} (psi)	2.00E+04	3.31E+04				
F_4 or F_5 (psi)	7.06E+03	-				

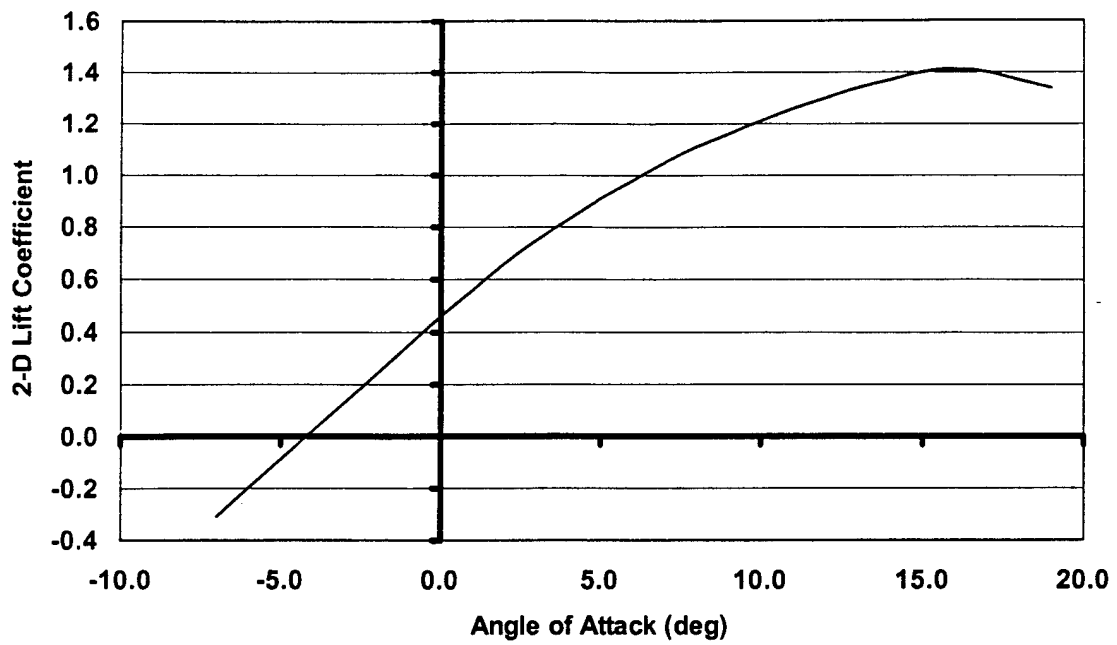


Figure 5.1 NACA 4415 2D Lift Curve – Reynolds number $6.5E5$

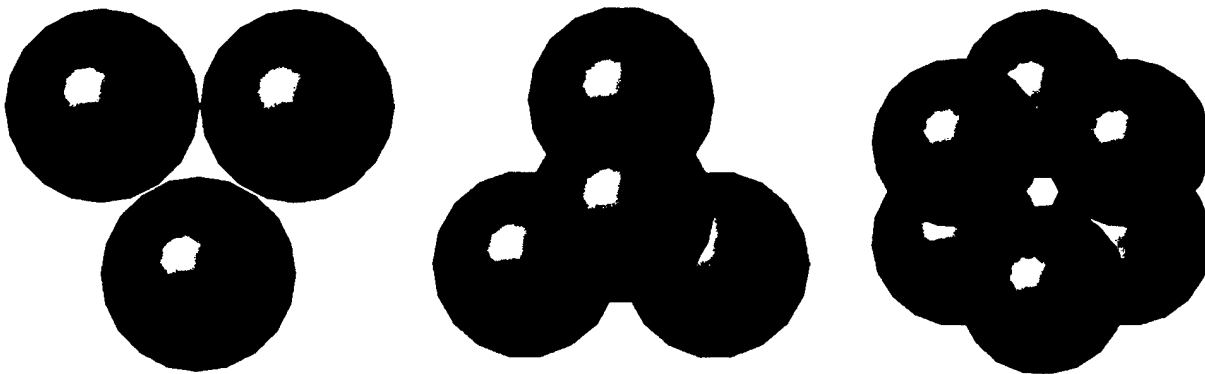


Figure 5.2 Comparison of tennis ball configurations #1, #2, and #3 respectively

C:\Fuselage\fuselage6.mf1
 RESULTS: 3- B.C. 1, STRESS 3, LOAD SET 1
 STRESS - VON MISES MIN: 0.00E+00 MAX: 1.47E+03
 DEFORMATION: 1- B.C. 1, DISPLACEMENT 1, LOAD SET 1
 DISPLACEMENT - MAG MIN: 0.00E+00 MAX: 8.72E-02
 FRAME OF REF: PART

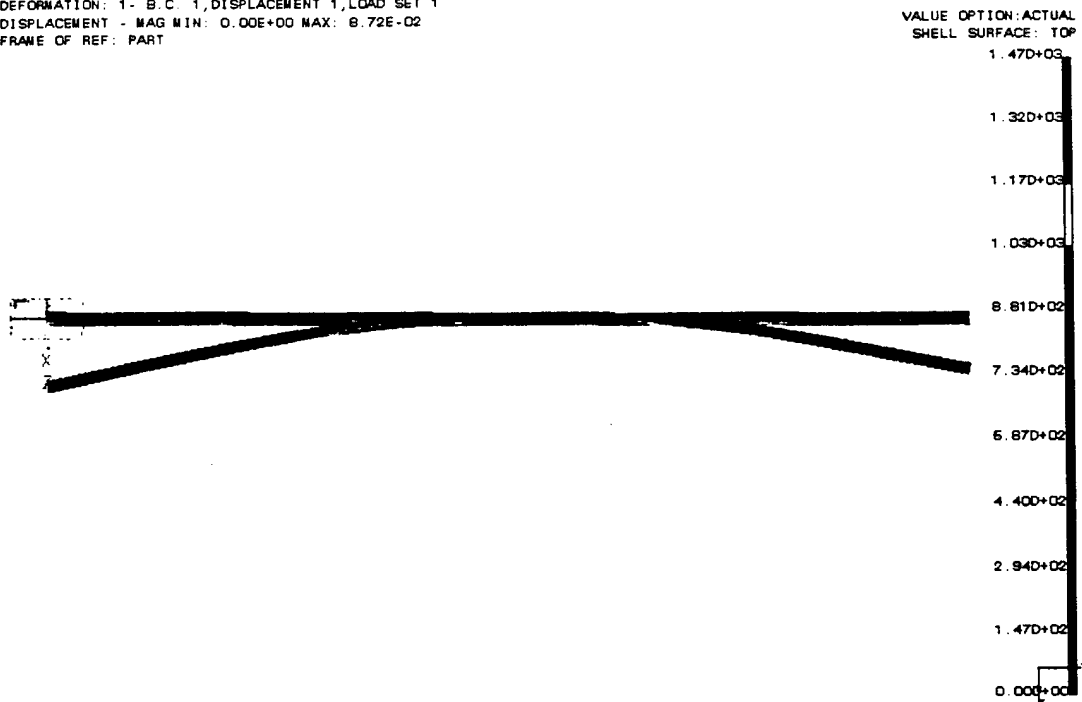


Figure 5.3 von Mises stress of the fuselage using IDEAS Master Series 8

C:\Fuselage\fuselage5.mf1
 RESULTS: 1- B.C. 1, DISPLACEMENT 1, LOAD SET 1
 DISPLACEMENT - MAG MIN: 0.00E+00 MAX: 8.72E-02
 DEFORMATION: 1- B.C. 1, DISPLACEMENT 1, LOAD SET 1
 DISPLACEMENT - MAG MIN: 0.00E+00 MAX: 8.72E-02
 FRAME OF REF: PART

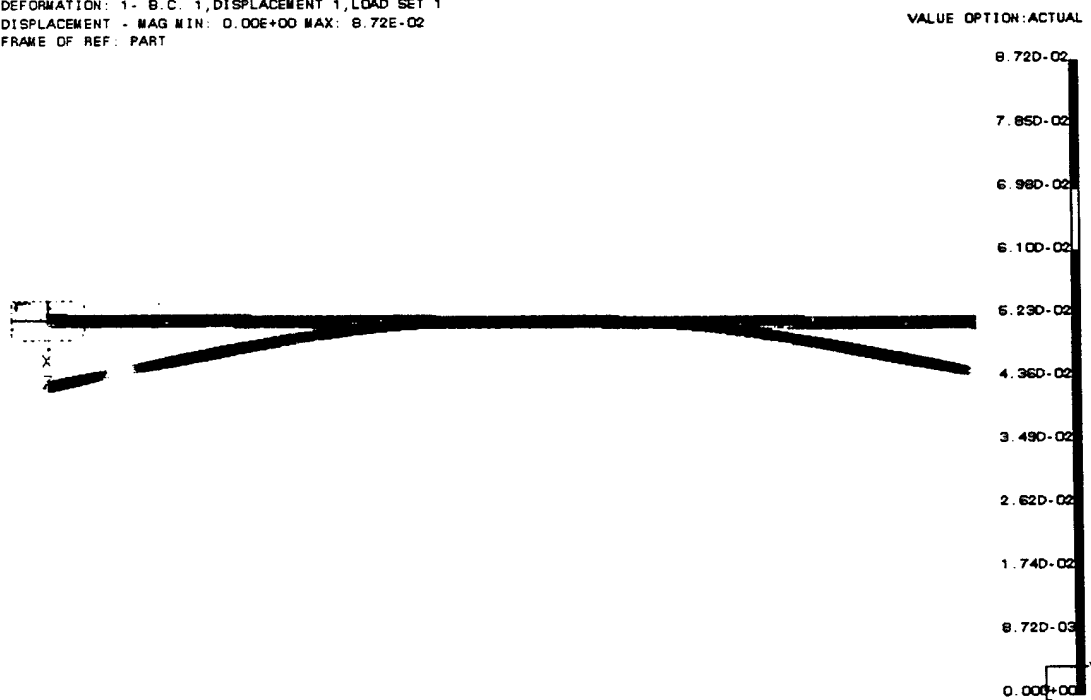
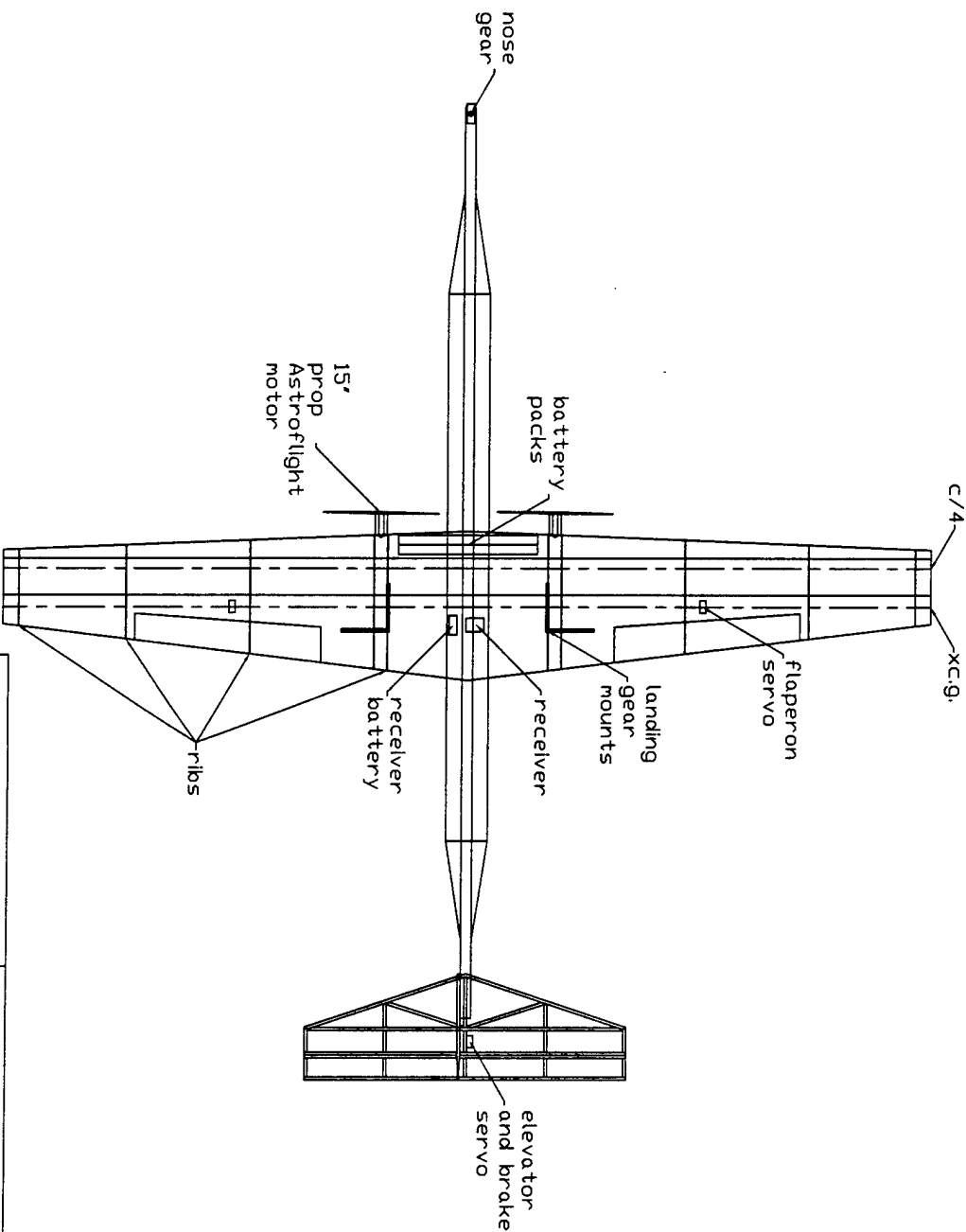
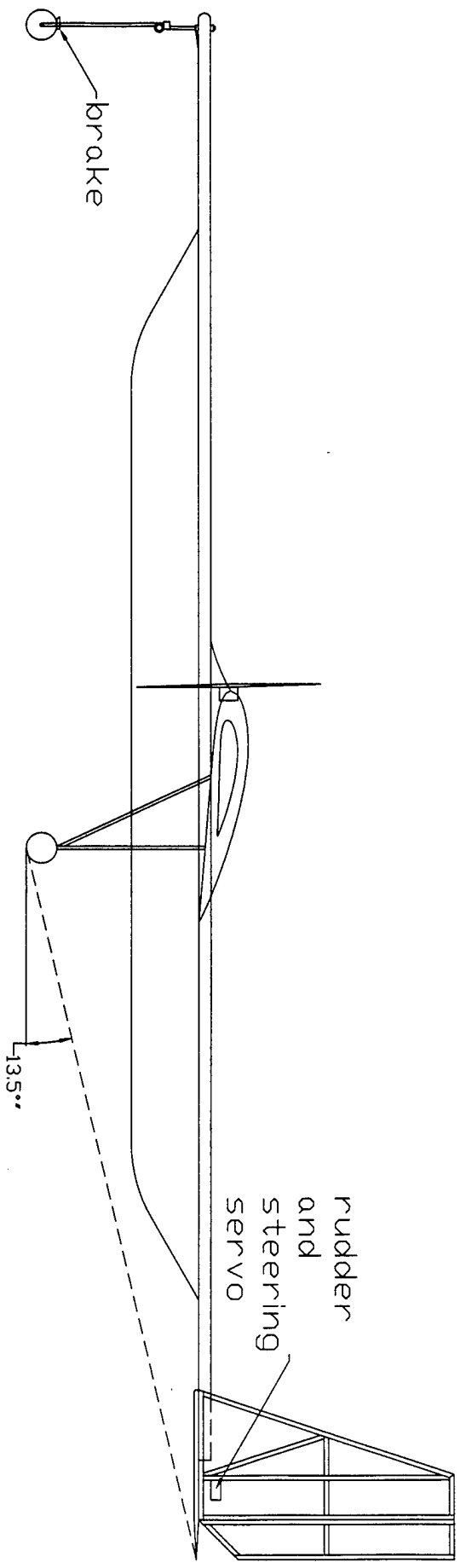


Figure 5.4 Displacement of the fuselage using IDEAS Master Series 8



Wing Parameters	
Span	10'
Root Chord	19.2"
Tip Chord	9.6"
Angle of Twist	2.98°
Dihedral	2°
Angle of Attack	7.81°
Area	12ft ²
Aspect Ratio	8.33
Taper Ratio	0.5
Tail Parameters	
Span	41.5"
Root Chord	13.75"
Tip Chord	7"

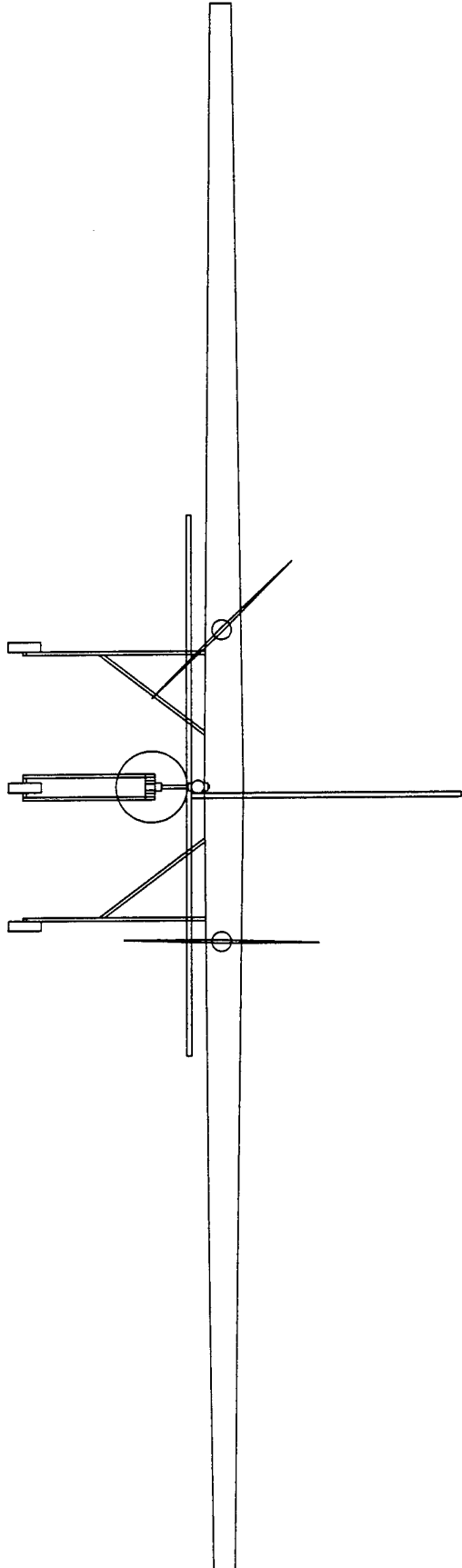
West Virginia University Morgantown, WV 26506	Almost Heaven Top View Scale 0.8"=1'	Drawn by: K. Ford and T. Scarborough
--	---	---



West Virginia University
Morgantown, WV 26506

Almost Heaven Side View
Scale 1/4"=1'

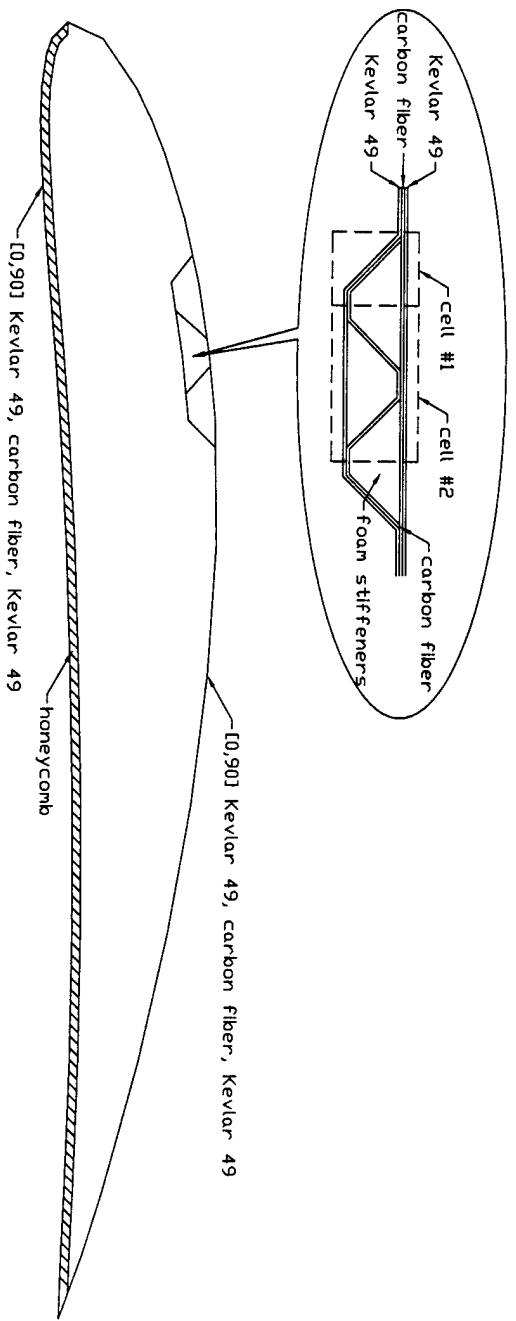
Drawn by: K. Ford
and T. Scarberry



West Virginia University
Morgantown, WV 26506

Almost Heaven Front View
Scale 1/4"=1'

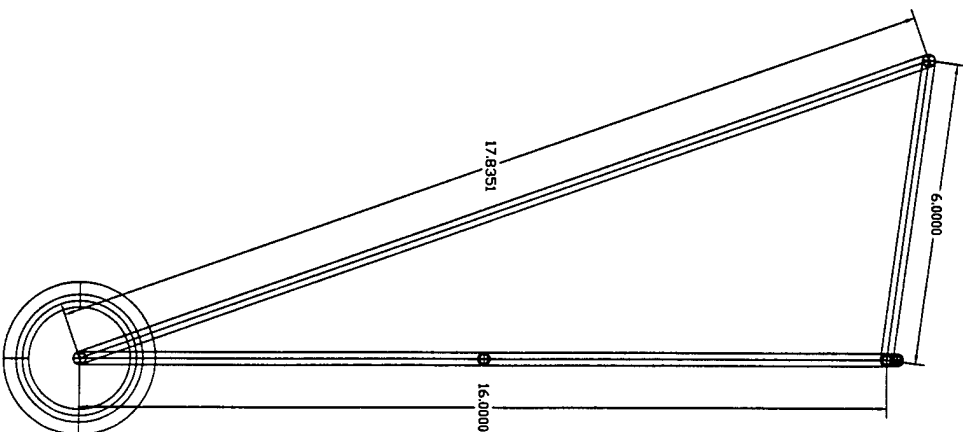
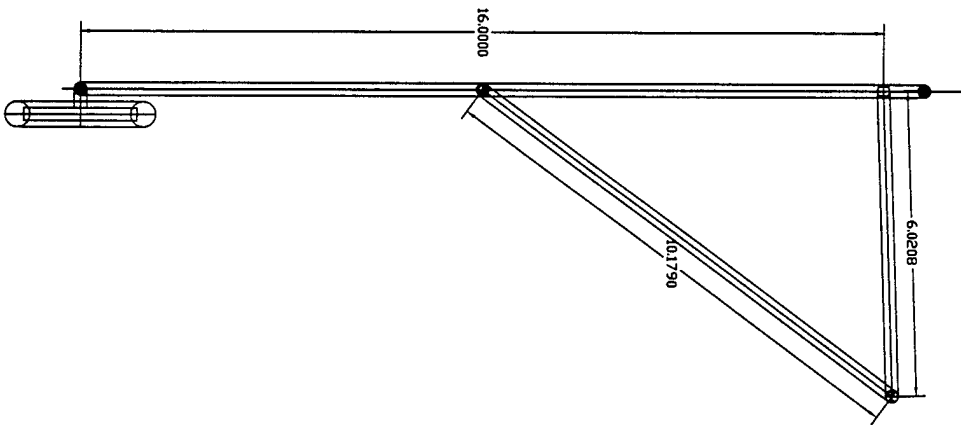
Drawn by: K. Ford
and T. Scarberry



West Virginia University
Morgantown, WV 26506

Almost Heaven
Wing Structure

Drawn by: K. Ford



West Virginia University
Morgantown, WV 26506

Almost Heaven
Landing Gear

Drawn by: K. Ford

6. Manufacturing Plan

The fabrication and assembly of the aircraft components needed to be done quickly and within the limitations of the team's skill and available equipment at the University. During the construction of the aircraft time was a nemesis. Having an aircraft in the air is the ultimate goal, but class work, delivery delays, and learning appropriate construction techniques require time. To overcome this, the team division described in the Management Summary was vital. It maximized the amount of time spent constructing the aircraft and allowed every team member to be involved in several aspects.

6.1 Wing

Due to the success of last year's innovative wing design incorporating the Ford-Guiler super beam, the same concept was used to fabricate this year's wing. Hand lay-up and vacuum bagging were used to construct the wing. This method for producing composite components was selected due to the availability of the necessary tools. Vacuum bagging material had been previously used and the necessary materials had been donated. Prepreg and filament winding were considered due to their higher fiber volume fraction, but were quickly abandoned since there was no access to the respective machinery.

Once hand lay-up and vacuum bagging were selected as the construction method, a plug was needed. The plug was produced from low-density foam using an electric hot wire. The hot wire was guided along the contours of balsa wood templates that were tacked to the ends of the foam. This produced a roughly shaped plug. The plug was then lightly sanded to remove any large imperfections. Next, 1/16" balsa wood was used to sheet the wing, using spray adhesive, which was then covered with monocoat, creating a smooth surface. Plywood was then used to create a flange along the chord line of the wing, creating a division between an upper half and lower half of the mold. Then the upper half was covered with the following release agents: 3 layers of mold release wax and 3 layers of polyvinyl acetate (PVA). The plug was then covered with a layer of surface coat, followed by several layers of e-glass/epoxy. These layers of materials were allowed to cure for 24 hours and then 1/4" plywood stiffeners were secondarily bonded to the shell to give it rigidity when the plug was removed. Once this cured for the manufacturer's recommend mold release time, the flange was removed and the process was repeated to create the lower mold. Once the plug was removed, the mold surfaces were filled with Bondo™ filler putty and glazing compound to fill in any imperfections. This process was repeated with sanding in-between to create a smooth glass-like surface. To prepare the mold prior to use, 3 layers of mold release wax, and 3 layers of PVA were applied in the same manner as they were applied to the plug.

Hand lay-up along with vacuum bagging was used to construct the wing. These techniques were used because of their low cost, ease of use, and weight reduction gained by the removal of the excess epoxy through the bleeder/breather layers. First the different layers of carbon fiber and Kevlar were cut to fit the mold and the foam stiffeners were cut on a band saw. The layers were then placed inside each mold and resin was then applied to it. Brushes, rollers, and straight edged plastic were then used to

evenly spread the resin and work it into the material. A Layer of 3 mil perforated polyethylene called "perf-ply" was then placed over the epoxy-impregnated fabric. A layer of plastic filament batting to form a breather layer followed. The breather layer allows a vacuum pump to remove vapors and draw excess resin into the batting. All of this was covered by a 6 mil layer of polyethylene to form a bag when sealed around the edges with tape. A pump capable of creating a vacuum of 26 inches of mercury was then connected to the bag. The vacuum pump was then turned on and adjusted to 13 inches of mercury. The vacuum of 13 in/hg could not be exceeded because the foam in the stiffeners would begin to collapse. The vacuum allowed pressure to compress the layers of the composite and also removed any excess epoxy.

6.2 Fuselage

The fuselage's structural requirements were that it must be able to support the speed loader, nose gear and tail loads and be capable of containing the push rods for the brakes and steering. These requirements were met by using a pipe. From the design analysis of the fuselage, an aluminum pip was used to fabricate the fuselage.

This allowed the fuselage to be dismantled for transportation purposes and each section to be replaced if needed. Pieces of aluminum were machined to the outer diameter of the aluminum pipe and were epoxied and bolted to the wing, at the leading, midchord, and trailing edges of the root. This gave three positions for the fuselage to be attached to the rest of the aircraft structure.

In an effort to lower the rated aircraft cost the same servos for the rudder and elevator were used to control the steering and braking respectively. Control of the rudder and elevator were deemed more critical than control of the steering and braking. The servos were then located on the tail to minimize the number of critical connections that needed to be made on the field.

6.3 Speed Loader

The rules of the competition state that the speed loader must be able to contain both the steel and tennis ball payload. To reduce drag a cylinder was used as the shape of the speed loader. The speed loader was constructed from one layer of 3k carbon fiber. A 6" piece of PVC pipe was used as the mold. The carbon fiber was laid up on the outside of the pipe and vacuum bagged. Once the epoxy cured, the carbon fiber was cut along its length. Next, the edges were overlapped and adhered together so that the diameter of 5.5" could be obtained. This shape made it easy to store the tennis balls by simply dropping them in the cylinder. However, the steel proved to be more difficult to store. The steel payload needed to be rectangular pieces and could not be tapped or have any other type of mechanical faster attached to it. To store the steel, foam blocks were cut in a cylinder shape that fit inside the speed loader. The foam block that stores the steel payload was cut in half and a rectangular shape was cut out so that the steel could fit inside.

Another aspect of the speed loader was the fact that it had to be exchanged with a new one between flights. Several different methods such as: ski boot buckles, hose clamps, etc were all considered to attach the speed loader to the fuselage. However, the simplest idea prevailed. Zip ties

were used. They provided the needed strength and could be quickly attached and taken off with a pair of wire cutters.

6.4 Tail

The tail was constructed using the balsa wood build-up method described in 3.2 Balsa Wood Build-up. AutoCAD was used to generate 1:1 scale drawing of the tail structure. The drawing was printed and taped to a flat surface. Wax paper was then used to cover the drawing so that adhesives would not adhere to the drawing. 3/8" square balsa wood stock was then cut to the appropriate lengths, laid over the drawing, and bonded with glue. This structure was then covered with monocoat.

6.5 Landing Gear

As discussed in section 5.7 Landing Gear Structural Analysis 1/4" steel was strong enough to withstand the maximum static load of the aircraft. The landing gear is depicted in the Drawing Package. One can see that the landing gear is braced on each side. The supports were used to strengthen the main struts and to reduce the effect of any side forces exerted on the landing gear. The supports were welded at each joint.

6.6 Power Plant

The power plant consisted of two Astroflight motors mounted in the leading edge of the wing. Previous year's aircraft experienced difficulties with motors mounted forward of the fuselage. Even though the weight added by the motors and the distance forward of aircraft's c.g. helped to balance the airplane, the added structure provided unnecessary weight. The previous aircraft had used a plywood "plank" to attach each motor. The "plank" acted like a canard which caused handling problems with the aircraft. Another reason for mounting the motors in the wing was to shorten the length of the wires running from the speed controllers and batteries to each motor. Last year's aircraft had trouble with interference due to the length of the wires. This interference caused the motors to cut out periodically.

The motor mounts were made of 1.75" O.D. and 0.058" wall thickness aluminum pipe. This pipe was machined into an "L" shape so that the motors could lie in the half pipe section (refer to the Drawing Package). The cylindrical remaining section of the pipe was then attached to two ribs inside the wing. Fiberglass-epoxy was wrapped around the pipe and the ribs to provide a strong connection. Hose clamps were then used to secure the motors to the pipe. Hose clamps provided adequate strength to secure the motors in place, while providing quick and easy access to the motors.

6.7 Final Assembly

Perhaps the biggest improvement of this year's aircraft over previous years is the way the components were assembled. A great deal of time was wasted assembling and disassembling the aircraft for transportation. Problems also arose when servos needed to be reconnected at the flying field. If the servos are not properly connected, flight performance problems could occur and the aircraft could even crash. The aircraft can be disassembled into two components: the wing – landing gear – motor section and the fuselage – tail – nose gear section. The sections are connected with three bolts that run through extensions under the wing that bolt through the aluminum pipe (fuselage). Power to the

elevator/brake and rudder/steering servos have also been made. This configuration eliminated the error associated with disconnecting and reconnecting the elevator/brake or rudder/steering servos or disassembling other crucial aircraft components.

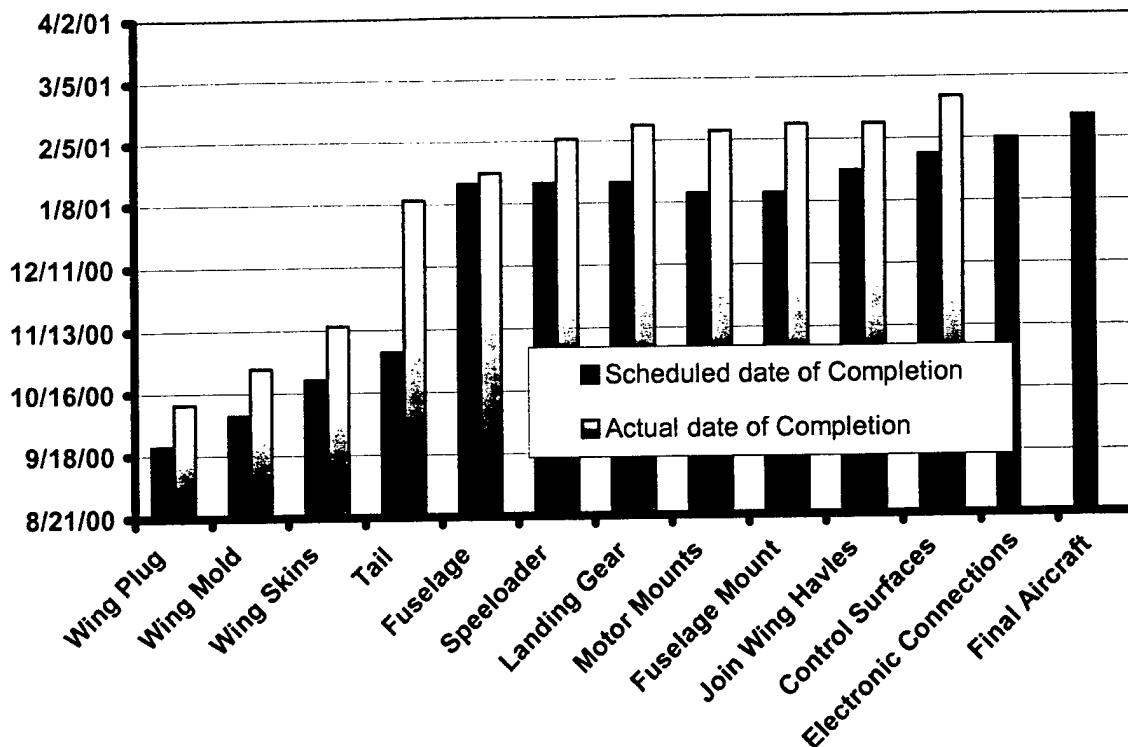


Figure 6.1 Manufacturing Milestone Chart

7. References

- [1] Raymer, Daniel P., "Aircraft Design: A Conceptual Approach Third Edition," American Institute of Aeronautics and Astronautics, Inc., Reston, VA 20191
- [2] Barbero, Ever J., "Introduction to Composite Materials Design," Taylor and Francis, Inc., Philadelphia, PA 19106
- [3] Tomblin, John; Chaffin, Michael; Rexrode, Timothy; Ringler, Todd, "Detailed Structural Design of the F-120 Fuselage MAE 162," Presented to Dr. Nithiam Sivaneri August 11, 1989, Morgantown, WV 26505
- [4] Sivaneri, N. "MAE 160 Design Project," West Virginia University, Morgantown, WV, 1999
- [5] Anderson, John D. Jr., "Fundamentals of Aerodynamics," McGraw-Hill, Inc.
- [6] Sun, C. T., "Mechanics of Aircraft Structures," John Wiley and Sons, Inc.
- [7] Ford, Kevin J., "UAV Truss-Core Sandwich Composite Wing," Mechanical and Aerospace Engineering Department, West Virginia University, Morgantown, WV 26505
- [8] Scarberry, Thomas T., "Electric Model Aircraft Propeller Analysis," Mechanical and Aerospace Engineering Department, West Virginia University, Morgantown, WV 26505

[9] <http://cms.access.wvu.edu:8900/>, accessed online February 2001, Loth, John L.

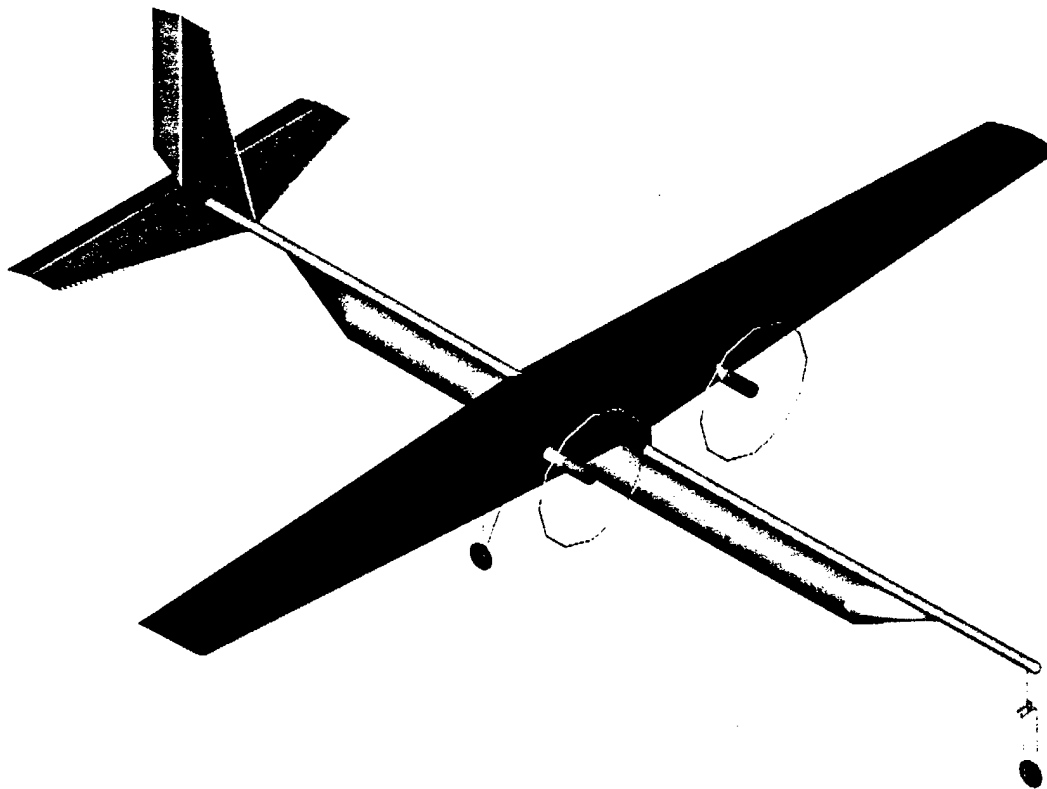
[10] Anderson, John D., "Introduction to Flight, 3rd Edition," McGraw Hill, 1989.

ALMOST HEAVEN
WEST VIRGINIA UNIVERSITY

Addendum Phase

April 19th – 21st, 2001

Cessna ONR – Student Design/Build/Fly Competition



DEPARTMENT OF MECHANICAL AND AEROSPACE ENGINEERING

WEST VIRGINIA UNIVERSITY

MORGANTOWN, WV 26506

i. Table of Contents

i. Table of Contents	1
1. Executive Summary.....	3
2. Management Summary	4
3. Conceptual Design	5
3.1 Aircraft Parameters	6
3.1.1 <i>Alternative Concepts Investigated</i>	6
3.1.2 <i>Number of Motors</i>	6
3.1.3 <i>Number of Wings</i>	6
3.1.4 <i>Number of Speed Loaders</i>	6
3.2 Material Selection and Construction Techniques.....	7
3.2.1 <i>Balsa Wood</i>	7
3.2.2 <i>Foam Build-up</i>	7
3.2.3 <i>Composite Materials</i>	7
3.2.4 <i>Other Materials</i>	8
3.3 Conceptual Design Results	8
4. Preliminary Design	10
4.1 Design Parameters Investigated	10
4.1.1 <i>Wing Area</i>	10
4.1.2 <i>Number of Tennis Balls</i>	10
4.1.3 <i>Steel Payload Weight</i>	11
4.2 Preliminary Design Rating System.....	11
4.3 Analytical Methods Used	11
4.4 Optimization Scheme Results	14
4.5 Structural design	14
4.6 Wing Structure Analysis	15
4.7 Fuselage Structure Analysis	15
4.8 Preliminary Design Results	15
5. Detail Design	25
5.1 Detailed Design – Aircraft Parameters Group.....	25
5.1.1 <i>Airfoil Selection</i>	25
5.1.2 <i>Propeller Selection</i>	26
5.1.3 <i>Aileron Sizing</i>	26
5.1.4 <i>Horizontal Tail Sizing and Location</i>	26
5.1.5 <i>Vertical Tail Sizing</i>	26
5.1.6 <i>Wing Incidence, Twist, Taper, and Dihedral</i>	27
5.1.7 <i>Landing Gear Selection</i>	27

5.1.8 Longitudinal Static Stability Analysis	27
5.1.9 Turning, Landing, and Climb Analysis	28
5.2 Assessment of available materials	28
5.3 Comparison of different laminates	29
5.4 Truss-Core Sandwich Composite Stringers	29
5.5 Truss-Core Sandwich Composite Stringer Analysis	30
5.6 Fuselage Structural Analysis.....	31
5.7 Landing Gear Structural Analysis.....	31
5.8 Payload Configuration	31
6. Manufacturing Plan	41
6.1 Wing	41
6.2 Fuselage.....	42
6.3 Speed Loader	42
6.4 Tail.....	43
6.5 Landing Gear.....	43
6.6 Power Plant	43
6.7 Final Assembly	43
7. References	44
8. Lessons Learned	46
8.1 Wing	46
8.2 Avionics	46
8.3 Weight comparison.....	46
8.4 Test Flight Analysis	47
8.5 Improvements for Next Year	47
9. Rated Aircraft Cost.....	47
9.1 Breakdown of the Rated Aircraft Cost.....	47
9.2 Manufacturer's Empty Weight Multiplier.....	48
9.3 Rated Engine Power	48
9.4 Manufacturing Man Hours	48
9.4.1 WBS 1.0 Wing.....	48
9.4.2 WBS 2.0 Fuselage/Pods.....	48
9.4.3 WBS 3.0 Empenage	49
9.4.4 WBS 4.0 Flight System.....	49
9.4.5 WBS 5.0 Propulsion System.....	49
9.5 Overall Score.....	49

8. Lessons Learned

During the construction of the aircraft, several modifications were made. These modifications stemmed from construction flaws and from factors that were overlooked in the design phase of the aircraft. Flaws in the plug used to make the wing proved to cause most of the difficulties during construction. The tail servo locations and the landing gear were modified as well.

8.1 Wing

Overall, the construction techniques used to fabricate the aircraft worked well. Nonetheless, flaws in construction were present. This was due to a wide range of experience and skill in construction of the team members.

Of all the components of the aircraft, the wing had the most flaws. As stated earlier the wing was constructed of composite materials using hand lay-up and vacuum bagging techniques. First, a male plug was produced, then a mold, and finally the wing itself. This meant that any flaws in the plug would be visible in the mold and thus visible in the wing. As a result of the flaws in the plug and mold, the wing endured several mistakes. Some of these were cosmetic while some were aerodynamic. Using balsa wood and monocoat to sheet the plug was the first mistake. The balsa wood did not adhere well to the foam core and the monocoat wrinkled causing imperfections in the mold. These imperfections in the mold were fixed by filling them with surface filler. The balsa wood not adhering properly caused other problems. The dimensions of the wing and the shape of the airfoil were slightly altered. It was felt that these alterations would not cause enough problems to justify rebuilding another plug and mold. The team felt that if they had to do over again they would construct the plug from foam core and cover it with light weight fiberglass and bondo. The other aircraft components were not as complicated to construct as the wing was. Therefore, these components did not have the same flaws the wing did.

8.2 Avionics

The servos located on the tail, rudder-steering and elevator-brake, were moved to make connections easier. Each servo was mounted directly behind the fuselage. The first advantage of this configuration was that it made it easier to run the pull-pull steering system and brake line to the nose gear. The steel cables run above the fuselage and through the wing-fuselage assembly. The second advantage was that this made it easier to run the servo wire to the receiver. The wire runs through the fuselage and into the wing, which houses the receiver.

8.3 Weight comparison

The empty weight of the aircraft is 24.5lbs. This is 4.5 pounds overweight. Most of the extra weight is in the wing. The weight of the wing is 8 pounds compared to the estimated 6 pounds. Several factors were overlooked on the estimate of the empty weight of the wing. First, the added weight of the control surfaces was not taken into account. The control surfaces were cut out of the wing and then trimmed with balsa wood and covered in fiberglass. The locations where the hinges mounted to the wing and control surfaces were strengthened with additional balsa wood. Another area where additional weight was added was the motor mounts. Fiberglass was wrapped around the aluminum pipe and bolts

were ran through the pipe to attach it to the adjacent ribs. The tail and wing-fuselage assembly also weighed more than what was estimated. Due to the additional weight of these components the cg of the aircraft was off. To compensate for this 1lb of lead was melted and fit inside the fuselage in front of the nose gear.

8.4 Test Flight Analysis

The first flight of the aircraft took place on April 4th, 2001 at Jackson Mill, West Virginia. Several empty flights were made so that the aircraft could be controls could be trimmed. Upon flying empty the it was noticed the aircraft was underpowered. Once the test flights were the team determined that they had overestimated the power of the motors in the design program. During the weeks leading up the competition the team plans on working on reducing the weight of the aircraft and recalculating the payload that can be flown at the competition. One thought is to possibly replace the 1lb lead weight with a third motor to gain extra power. Hopefully, in the few weeks a lighter, more powerful aircraft can emerge.

8.5 Improvements for Next Year

Organization, communication, and work ethic are perhaps the biggest improvements that need to be made for next year's team. The team leaders found it difficult to bring the team members together to work on the aircraft. Several team members were counted on to perform certain tasks and ended up doing nothing. Because of this most of the work fell on the shoulders of the team leaders.

For next year, several flights of this year's aircraft need to be video taped and analyzed. The takeoff distances and battery life need to be measured. Using these values the design program can be corrected.

9. Rated Aircraft Cost

The overall score of each team is a function of three parameters: the report score, flight score, and the rated aircraft cost (RAC). Each of these components is then further broken up into subsections. The report score is a summation of the proposal and addendum phases. The flight score is a summation of one-fifth the number of tennis balls transported and the weight of steel transported of each flight. The RAC is a more complicated score to tabulate. It is based on the "simplicity" of the aircraft and is calculated from a formula set forth by the competition officials. The following equation is used to calculate the overall score of the aircraft.

$$Total \ Score = \frac{Written \ Report \ Score \cdot Total \ Flight \ Score}{Rated \ Aircraft \ Cost} \quad (9.1)$$

As one can observe to obtain the highest total score and win the competition, one must maximize the written report score and the total flight score while minimizing the RAC. Upon further examination of the RAC one will notice that minimizing the RAC and maximizing the total flight score are a closely related process.

9.1 Breakdown of the Rated Aircraft Cost

The overall rated aircraft cost (RAC) is calculated by the equation:

$$RAC, (\$thousands) = \frac{A \cdot MEW + B \cdot REP + C \cdot MFHR}{1000} \quad (9.2)$$

In the above equation, A, B, and C represent values of multipliers used to convert aircraft characteristics into manufacturing hours. The Manufacturer's Empty Weight Multiplier (MEW), Rated Engine Power (REP), and the Manufacturing Man Hours (MFHR) are a breakdown of the different aircraft components to be converted to man-hours. A more detailed explanation of these parameters is described below.

9.2 Manufacturer's Empty Weight Multiplier

The manufacturer's empty weight multiplier, MEW, is comprised of the weight of the aircraft without the batteries or the payload. Of all the parameters that constitute the RAC the MEW affects the total flight score more than any other. Every additional pound the aircraft weighs increases the RAC by 0.1 point. Each pound saved on the construction of the aircraft can be replaced with an increased payload weight. This is crucial to the total score. Each additional pound of steel is multiplied by a factor five. Using these observations one sees that not only does the MEW affect the RAC it also affects the amount of payload carried which can make a significant change in the total score. In equation 9.2 A represents the manufacturer's empty weight multiplier and was given a value of \$100/lb. The MEW of 'Almost Heaven' is 2.45.

9.3 Rated Engine Power

The rated engine power, REP, was calculated using the following equation:

$$REP = \#engines \cdot Amp_{fuse} \cdot 1.2V / cell \cdot \#cells \quad (9.3)$$

In equation 9.2 B represents the rated engine power multiplier and was given a value of \$1/Watt. The aircraft uses two engines, 36 battery cells, and a 40Amp fuse. The REP of 'Almost Heaven' is 3.46.

9.4 Manufacturing Man Hours

The manufacturing man hours, MFHR, further breaks down the components of the aircraft into the work breakdown structure, (WBS), and takes into account the number of wings and their size, the number of fuselages/pods, and their size, the number of horizontal and vertical surfaces, the number of servos used, and the number of motors and propellers used. In equation 9.2 C represents the manufacturing cost multiplier and was assigned a value of \$20/hr. Table 9.1 is summary of the total number of manufacturing hours assigned to each component of the WBS. A value of 174.36 was used for the MFHR.

9.4.1 WBS 1.0 Wing

To achieve the highest total score possible the optimization program gave the results that the aircraft should have one wing with an area of 12ft² and two control surfaces. The rules state that 15hrs per wing, 4hrs per square foot of projected area, 2hrs per strut or brace, and 3hrs per control surface were to be used in the calculation of WBS 1.0. The total number of hours for WBS 1.0 is 69hrs (refer to Table 9.1).

9.4.2 WBS 2.0 Fuselage/Pods

WBS 2.0 consists of the number of fuselages and or pods and their respective lengths. 5hrs per body and 4hrs per foot of length were assigned to the components of the aircraft. Three components of the aircraft fall under this category, the fuselage and motor mounts. The length of the fuselage is 8.34' and the length of each motor mount that extends past the leading edge of the wing is 0.5'. The total number of hours for WBS 2.0 is 52.36hrs (refer to Table 9.1).

9.4.3 WBS 3.0 Empenage

WBS 3.0 is the number of vertical and horizontal surfaces on the aircraft. 5hrs were assigned for the construction of these components with an additional 5hrs per vertical surface and 10hrs per horizontal surface. The aircraft is comprised of 1 vertical surface and 1 horizontal surface. The total number of hours for WBS 3.0 is 20hrs (refer to Table 9.1).

9.4.4 WBS 4.0 Flight System

WBS 4.0 is the number of servos and controllers used on the aircraft. 5hrs were assigned for the basic flight control system. An additional 2hrs were assigned for each servo and controller used. The aircraft has 4 servos adding 8hrs to the MFHR (refer to Table 9.1)

9.4.5 WBS 5.0 Propulsion System

WBS 5.0 is the number of motors and propellers or fans used on the aircraft. 5hrs per motor, propeller, and fan were assigned. The aircraft has 2 motors and 2 propellers adding 20hrs to the MFHR (refer to Table 9.1)

9.5 Overall Score

Even though the overall score cannot be determined until the actual competition, the RAC component was calculated using the following equation:

$$RAC, (\$thousands) = \frac{100 \cdot 24.5 + 1 \cdot 3456 + 20 \cdot 174.36}{1000} = 9.39 (\$thousands) \quad (9.4)$$

Table 9.2 is a comparison of the values for each airframe dependent parameter in the cost model. Figure 9.1 is a comparison of the different components of the RAC and the percentage that each adds to the overall RAC. As can be seen the REP is the largest contribution to the RAC. This occurs because the design uses the maximum allotted weight for the batteries and 2 motors. The MEW is the second largest contributor to the RAC. Better construction skills and time construct another aircraft would lower the empty weight. The value of the RAC may change by the time of the competition. Some additional weight may be added to the aircraft due to repairs or other unforeseen occurrences.

Table 9.1 Work Breakdown Structure for the aircraft

	component	characteristic	hours per characteristic	total number of hours per component
WBS 1.0 Wings	<i>number of wings</i>	1	15	15
	<i>wing area (ft²)</i>	12	4	48
	<i>struts and braces</i>	0	2	0
	<i>control surfaces</i>	2	3	6
WBS 2.0 Fuselage/Pods	<i>number of bodies</i>	3	5	15
	<i>total length of bodies (ft)</i>	9.34	4	37.36
WBS 3.0 Empenage	<i>basic cost</i>	-	5	5
	<i>number of vertical surfaces</i>	1	5	5
	<i>number of horizontal surfaces</i>	1	10	10
WBS 4.0 Flight System	<i>basic cost</i>	-	5	5
	<i>number of servos or controllers</i>	4	2	8
WBS 5.0 Propulsion System	<i>number of engines</i>	2	5	10
	<i>number of propellers or fans</i>	2	5	10
total number of hours				174.36

Table 9.2 Comparison of the airframe dependent parameters in the cost model

Airframe Parameter	RAC (\$ thousands)
Manufacturer's Empty Weight, MEW	2.45
Rated Engine Power, REP	3.46
WBS 1.0 Wing	1.38
WBS 2.0 Fuselage and Motor Mounts	1.05
WBS 3.0 Empenage	0.40
WBS 4.0 Flight System	0.26
WBS 5.0 Propulsion System	0.40
Total RAC	9.39

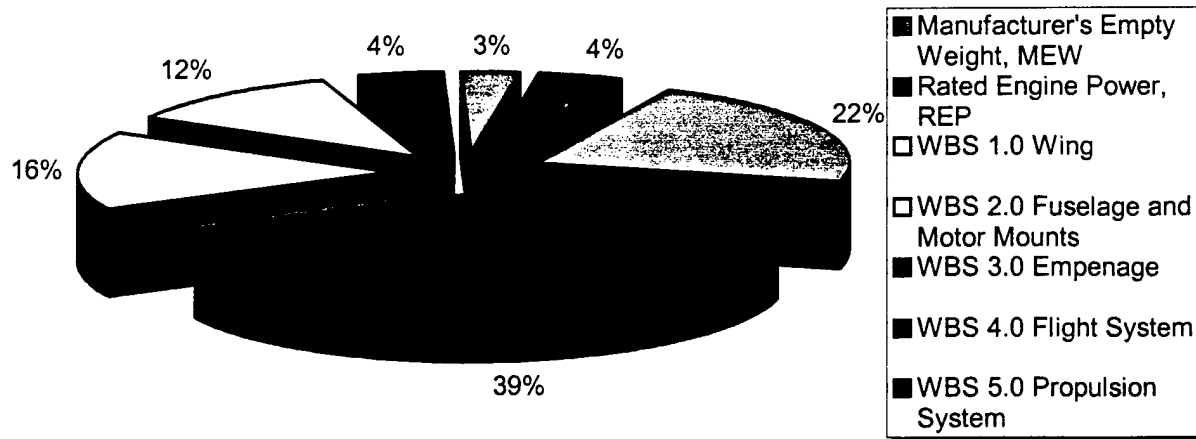


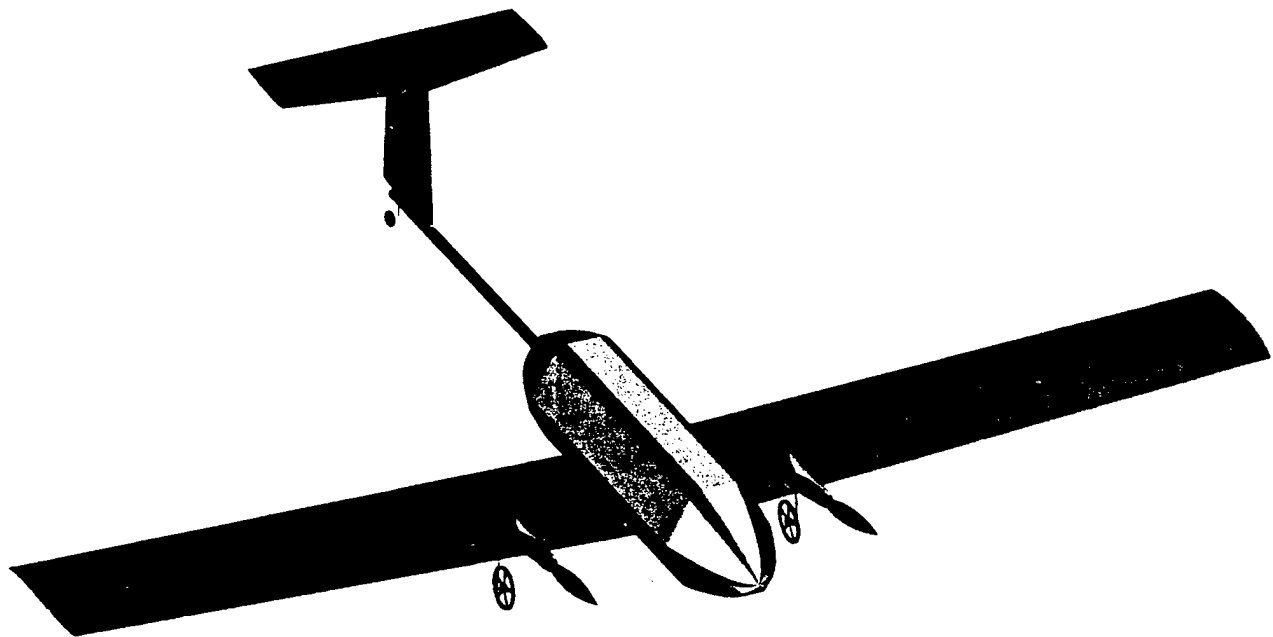
Figure 9.1 Comparison of the component's contribution to the rated aircraft cost



UNIVERSITY OF CALIFORNIA, SAN DIEGO

Proposal Phase Design Report

Submitted March 13, 2001



TLAR II

Table of Contents

1	<i>Executive Summary</i>	4
1.1.1	Objectives	4
1.1.2	Analytical Tools	4
1.1.3	Conceptual Design Phase Outline	5
1.1.4	Preliminary Design Phase Outline	5
1.1.5	Detail Design Phase Outline	5
2	<i>Management Summary</i>	7
2.1.1	Team Architecture	7
2.1.2	Task Scheduling	8
2.1.3	Milestone Chart	8
3	<i>Conceptual Phase</i>	9
3.1	Stage I – Feasibility Analysis	9
3.1.1	Airfoil	10
3.1.2	Wings	10
3.1.3	Empennage	11
3.1.4	Fuselage	12
3.1.5	Landing Gear	13
3.1.6	Propulsion and Power System	13
3.1.7	Structural System	14
3.1.8	Conceptual Design Phase – Stage I Summary	14
3.2	Stage II – Generalized Analysis	16
3.2.1	Wings	17
3.2.2	Empennage	17
3.2.3	Fuselage	18
3.2.4	Landing Gear	19
3.2.5	Propulsion and Power System	19
3.2.6	Structural System	20
3.2.7	Conceptual Design Phase – Stage II Summary	21
4	<i>Preliminary Design Phase</i>	22
4.1.1	Wings	22
4.1.2	Empennage	23
4.1.3	Fuselage	24
4.1.4	Landing Gear	26
4.1.5	Propulsion and Power System	26
4.1.6	Structural System	27
4.1.7	Preliminary Design Phase Summary	29
5	<i>Detail Design</i>	30
5.1	General Sizing	30
5.1.1	Weight Estimate	30
5.1.2	Wing Performance	30
5.1.3	Motor Thrust Available	30
5.2	Flight Performance Calculations	31
5.2.1	Takeoff Performance	31
5.2.2	Rate of Climb	31
5.2.3	Turning Radius	31
5.2.4	Range and Endurance	32
5.2.5	Static Stability	32

5.2.6	Systems Architecture	33
5.2.7	Detail Design Summary	34
5.3	Drawing Package	35
5.3.1	Three View	35
5.3.2	Structural Component Dimensions	36
5.3.3	Flight Component Dimensions	37
5.3.4	Conceptual Configurations	38
5.3.5	Detailed Configuration, Tennis Ball Packing, and Flight Equipment Location	39
6	Manufacturing Plan	40
6.1	FOM Reasoning/Discussion	40
6.2	Component Manufacturing Description	40
6.2.1	Spar Structure	40
6.2.2	Wing Joiner	41
6.2.3	Wing Joiner Carrier Box	41
6.2.4	Torsion Rod	42
6.2.5	Wing Airfoil	42
6.2.6	Wing Cores	42
6.2.7	Spar Assembly	43
6.2.8	Wing Skins	43
6.2.9	Final Wing Assembly	43
6.2.10	Stabilizers	43
6.2.11	Main Landing Gear Strut	44
6.2.12	Gear Blocks	44
6.2.13	Wheels	44
6.2.14	Tail Landing Gear	45
6.2.15	Speed Loaders	45
6.2.16	Fuselage	45
6.2.17	Boom	46
6.3	Assemblies	46
6.3.1	Wing Core Assembly	46
6.3.2	Wing panel Assembly	46
6.3.3	Boom Assembly	46
6.4	Manufacturing Timeline	47
7	Proposal Phase References	48

List of Figures

FIGURE 2-1	MILESTONE CHART	8
FIGURE 6-1	MANUFACTURING TIMELINE	47

List of Tables

TABLE 1-1	FINAL DESIGN SPECIFICATIONS	6
TABLE 2-1	TEAM MEMBER PROFILES AND ASSIGNMENT AREAS	7
TABLE 3-1	DESIGN PARAMETER FOM ANALYSIS – STAGE I	9
TABLE 3-2	DESIGN PARAMETER FOM ANALYSIS – STAGE II	16
TABLE 5-1	GENERAL SIZING	34
TABLE 5-2	SYSTEMS ARCHITECTURE	34

TABLE 5-3 FLIGHT PERFORMANCE DATA.....	34
--	----

1 Executive Summary

Student members of the American Institute of Aeronautics and Astronautics (AIAA) at the University of California, San Diego designed and built a remote-controlled aircraft for the 2001 AIAA Design/Build/Fly Competition to apply and broaden their knowledge of aircraft design and manufacture.

Certain design aspects of the aircraft were dictated by restrictions imposed by the rules of competition, but within those restrictions, there was freedom for individualized design of a remote controlled electrically powered aircraft. The aircraft must fly sorties consisting of a light, high volume payload alternating with a heavy, low volume payload. The high volume payload is limited to no fewer than 10 and no more than 100 tennis balls, while the high weight payload is comprised of at least 5 lbs. of steel. It must also have a take-off distance of less than 200 ft., a wingspan of no more than 10 ft., and a total dry weight of less than 50 lbs. The power limitations dictate that the aircraft use less than 5 lbs. of batteries.

1.1.1 Objectives

In order to meet these requirements, the team first established a set of design goals that the final aircraft configuration should meet. To maximize the score, it was decided to design the aircraft to carry a maximum of 20 lbs. of steel, 100 tennis balls, and cruise at 60 MPH. Ideally, the aircraft would complete three light and two heavy sorties within the time allotted, while meeting the functional requirements of the design as specified by the rules stated above.

Experience gained from the previous year's entry, "TLAR I", was beneficial in designing the new aircraft. This year, the team began the project with a better overall understanding of the design process, materials, design trade-offs and time constraints. This experience and knowledge, coupled with the Figures of Merit (FOMs) and design parameters, enabled the team to work more efficiently and effectively.

1.1.2 Analytical Tools

Several analytical tools were used throughout the entire design process. The most important was Microsoft Excel, which was used for everything from calculations of weight-and-balance, number of sorties expected, climb rate, take-off distance, and turn radius, to financial analysis and Rated Aircraft Cost (RAC). General aviation design principles and equations were used in determining exact dimensions and specifications. The mathematical toolbox, Matlab 5.1, was used to perform numerical analysis of flight performance of the chosen wing configuration. Finally, the programs AutoCAD 2000 and PRO/E 2000i were crucial tools used to visualize and present aircraft design ideas.

FOMs and Design Parameters were chosen to provide requirements to ensure that the design would meet the functional requirements dictated by the contest administrators, as well as the design goals as defined by the UCSD AIAA team. They were applied to each stage within the entire design process to analyze the strengths and weaknesses of each component as well as those of the overall

aircraft configurations. The design process used to determine the final configuration began with the Conceptual Design Phase (CDP). Next was the Preliminary Design Phase (PDP) followed by the Detail Design Phase (DDP), from which emerged the final configuration of the aircraft.

1.1.3 Conceptual Design Phase Outline

The CDP consists of two stages, Stage I and Stage II. Stage I incorporates a range of ideas for each component that was considered. The FOMs of Stage I were geared towards eliminating ideas that were intuitively and/or obviously impractical. These FOMs centered on material availability, handling characteristics, RAC, ease of transportation and complexity of manufacture in relation to time and skill level required. Stage I analysis resulted in component concepts that were determined to be viable. These components were assembled into three different configurations that initially met the design parameters and FOMs. The three configurations were then progressed into Stage II.

The goals of applying Stage II FOMs were to maximize the overall flight score, minimize the RAC, and develop a preliminary aircraft design. Stage II FOMs focus on an in depth analysis of the components, with specific attention to payload access, construction feasibility, propulsion and maximizing strength to weight ratios, operator and component safety, difficulty of repairs, component and interfacing strength, and payload capacity. The analysis of Stage II resulted in a single overall design configuration, at which point, the question was raised of whether it met the functional and design goal requirements. If it was determined that the configuration met these requirements, it continued into the PDP. Otherwise, it was reiterated through Stage II of the CDP in an attempt to optimize the configuration with alternate component designs.

1.1.4 Preliminary Design Phase Outline

Once an overall design configuration was decided upon, the next step was to conduct a more thorough and detailed analysis of the configuration using the PDP FOMs. The main purpose of the PDP was to optimize sortie performance, RAC, and structural integrity of each component individually, and as part of the entire configuration. Specific design parameters, such as sizing, materials, connection interfaces, and exact location of each part within the assembly were also determined. These, combined with optimization of power requirements, led to a complete detailed aircraft configuration.

1.1.5 Detail Design Phase Outline

The DDP was less focused on actual aircraft configuration design as compared to the previous two phases. The focus in this section was on determining the flight performance of the detail configuration to discern whether or not the design met the functional requirements. To complete these calculations the team made use of performance analysis techniques suited to propeller driven general aviation and radio controlled aircraft. These techniques were validated by the previous year's design, "TLAR I" and used to determine characteristics such as takeoff distance, turn radius, stall speed and sortie times.

Though manufacturing related FOMs had been applied to eliminate ideas throughout the both the Conceptual and Preliminary Design Phases, in the Manufacturing Phase, each component underwent a rigorous investigation as to the best method of construction possible. Specific FOMs were developed to take into consideration the restrictions of skill level, availability of materials and machinery as well as time constraints and cost.

The final product of the design process was a configuration in which each component satisfied the contest functional requirements, design goals as well as the FOMs of each category. The resulting design was a simple, two-engine, single fuselage, low mono-wing aircraft with a 10 ft. wingspan and a 74 in. nose-to-tail length. The specific details of the aircraft are given in Table 1.1.

Table 1-1 Final Design Specifications

Design Parameter	Specification
Aircraft Dry Weight	19.6 lbs.
Light Payload Capacity/Weight	100 Tennis Balls/12.85 lbs.
Heavy Payload Capacity/Weight	Steel/15 lbs.
Main Wing Configuration	Low Mono-Wing
Main Wing Airfoil	Eppler-214
Wing Span	10 ft.
Length	74 in.
Motor	Graupner Ultra 3300/7 (x2)
Rated Aircraft Cost	6.54
Final Flight Score	98.1

2 Management Summary

2.1.1 Team Architecture

The 2001 UCSD Design/Build/Fly project team consisted of sixteen undergraduates with diverse backgrounds. At the first general project meeting, an open discussion took place on how to best approach the task. The project manager, Andrew Mye, discussed the importance of utilizing the strengths of each member while emphasizing the importance of equal contributions to the project in order for success to be achieved. The team was broken down into the various subgroups of wings, tail, airfoil, fuselage, structural system, landing gear, propulsion & power plant and fundraising. The team member profiles and assignment areas are shown in Table 2.1.

Table 2-1 Team Member Profiles and Assignment Areas

Name	Year	Major	CAD Programs			Matlab	Technical Writing	Machining	Assignment Area
			Pro/Engineer	AutoCAD	SolidWorks				
Andrew Mye	Sr	ME	x	X	x	x	x	x	Structural system, Fuselage
Justin Smith	Sr	AE	x	X	x	x	x	x	Empennage, Propulsion & Power Plant
Kari Goulard	Sr	ME	x	X		x	x	x	Landing Gear
Guy Watanabe	Sr	AE		X	x	x	x	x	Wings
Maziar Sefidan	Sr	ME		X		x	x	x	Landing Gear
Joshua Adams	Sr	ME		X		x	x	x	Empennage
Joshua Hu	Sr	AE		X		x	x	x	Airfoils
Chad Valenzuela	Jr	AE	x	X			x		Airfoils
Annie Powers	So	AE		X		x	x	x	Wings, Fundraising
Mark Shtayerman	So	AE		X					Wings
Tyson Wooten	So	AE		X		x			Fundraising
Gregory Burton	So	ME		X		x			System Architecture
David Tamjidi	So	BE		X		x			System Architecture
John Moretti	Fr	AE		X		x			Fundraising
Andrew Tchieu	Fr	AE		X					Fundraising

Weekly meetings were set in which the team could discuss design ideas, obstacles and possible alternatives for further optimization. Each meeting was documented in order to keep everyone up-to-date and ensure that progress stayed on schedule. This management structure provided an efficient means of accomplishing necessary goals, overcoming design challenges and subgroup collaboration. In addition, this structure was conducive to timely completion of each subgroup's particular responsibility.

2.1.2 Task Scheduling

In early September, the group decided upon a schedule of completion dates. Each subgroup was expected to complete tasks by a certain deadline. The chart below (Figure 2.2) depicts the planned and actual dates of completion (D.O.C.) of each major event. Problems that were encountered completing these tasks were quickly resolved through teamwork and subgroup collaboration. The subgroup dependencies were as follows

Flight Characteristics & Performance:

Airfoil ⇔ Wings ⇔ Empennage ⇔ Propulsion & Power Plant

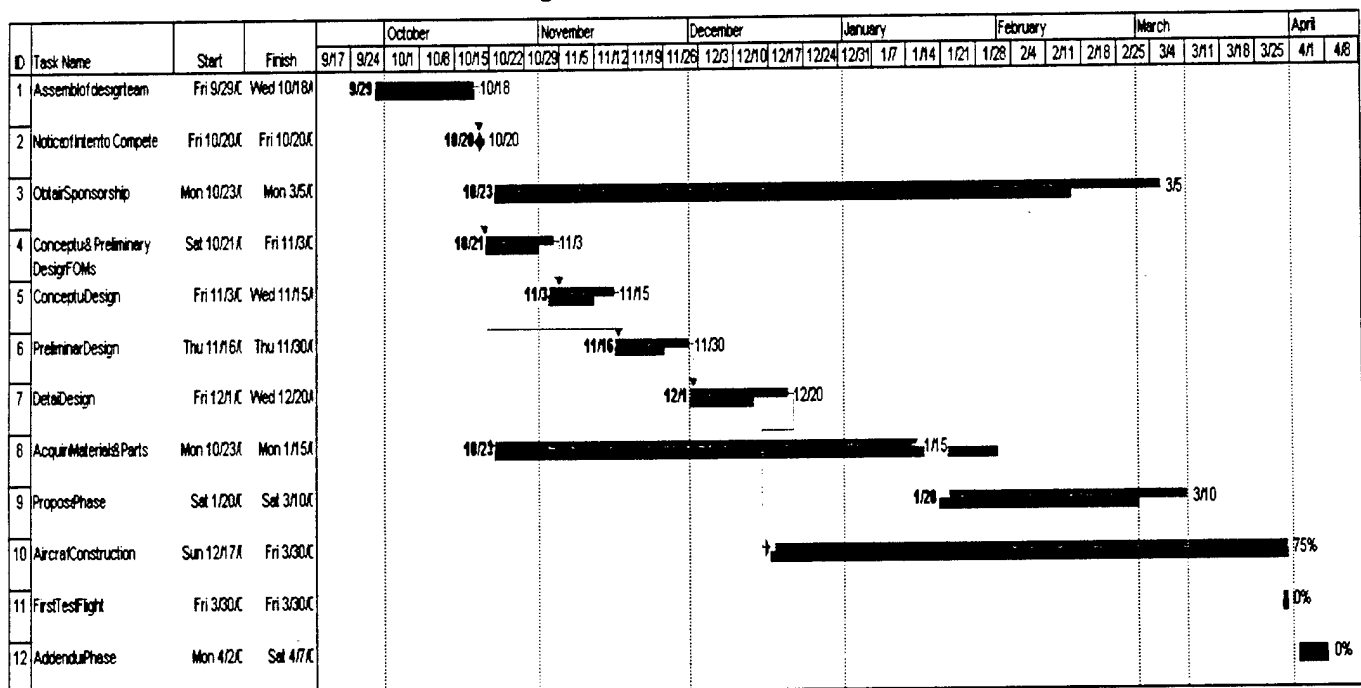
Component Interfaces:

Wings ⇔ Structural System ⇔ Fuselage ⇔ Empennage

Structural System ⇔ Landing Gear

2.1.3 Milestone Chart

Figure 2-1 Milestone Chart



Legend: Grey dotted lines = Proposed duration of task. Proposed start and finish dates are indicated in the cells on the left.

Blue solid lines = Actual duration of task. Actual start and finish dates are indicated on both ends of line.

Percentage = Percentage of task completed.

The purpose of Stage I was to apply FOMs to eliminate and analyze concepts for aircraft components that were proposed during brainstorming sessions at the beginning of the design process. The goal was to produce a set of desirable components to incorporate into three conceptual aircraft designs. The Stage I FOMs consisted of five primary areas. First, material availability required that any material not commercially available or unreasonably expensive be ruled out. Second, handling characteristics were used to eliminate concepts that were initially thought to have poor ground or flight performance. Third, designs that did not promote ease of transportation were dismissed from consideration. The fourth consideration for Stage I was simplicity and tooling. Simple structures are easier to analyze and build without necessarily losing functionality or performance characteristics. These guidelines established a solid set of conceptual components to consider for the aircraft.

3.1.1 Airfoil

When choosing an airfoil, the lift to drag ratio was the most important feature to be considered. For the final design, an aircraft constrained by take-off distance, an airfoil that maximized lift while minimizing drag was necessary. Three airfoils were analyzed in order to obtain their respective coefficients of lift and drag. The three airfoils considered were SD7003, SD7037 and E214. When calculating the C_L and C_D coefficients, a Reynolds number of between 200,000 and 300,000 was considered, which was determined by an average cruise velocity of 60 MPH.

The maximum lift and drag coefficients calculated for airfoil SD7003 were 0.79 and 0.0142, respectively. The maximum lift and drag coefficients calculated were 0.78 and 0.012, respectively, for airfoil SD7037. For the E214, the maximum lift and drag coefficients were found to be 1.43 and 0.017, respectively. While the SD airfoils have excellent drag values, they fall short of the Eppler airfoil with regards to maximum lift. The lift created by this airfoil was determined to be sufficient for the application of flight given the 200 ft. takeoff distance limit.

An added benefit in choosing this airfoil was that it was used in the design of last year's aircraft and preformed well. Also, the templates for this airfoil were kept from last year and reduced tooling time and cost.

3.1.2 Wings

The wings are a primary defining characteristic of an aircraft. In this year's design, they were optimized to the role of the aircraft's flight objectives. Other primary, secondary and tertiary structures were designed around the general wing structure. In this design process, there were limitations imposed by contest rules, flight conditions, and structural feasibility. The initial design parameters being investigated were wing configuration and wing planform. The available wing configurations included a bi-wing and a high, mid, and low placement mono-wing. The considered wing types were delta, elliptical, and rectangular. The intent of the Stage I wing analysis was to eliminate design parameters based on FOMs to determine their applicability to the design goals. FOMs that were used consisted of handling characteristics, RAC, ease of transportation, and complexity of manufacture.

3.1.2.1 Transportability

Transportation was a major concern that needed to be addressed early in the design phase. All parts had to be sufficiently compact to be transported via air. The wings of the aircraft, with a maximum wingspan of 10 ft., would require a box inconveniently large and costly to ship. Thus, it was determined during Stage I that the wings would have to be constructed in at least 2 (half-span) parts.

3.1.2.2 Wing Configuration

The wing configurations presented as options represented the traditional configurations that were well documented. One of the basic limitations was that the payload was to be carried within the fuselage. Thus the mid-wing was immediately eliminated as it would restrict the useable fuselage volume and complicate the construction of a speed loader. The other configurations would not pose this problem and were therefore left for further analysis.

3.1.2.3 Wing Planform

Delta: A delta wing was eliminated immediately as a design possibility due to the fact that it is optimized for transonic and supersonic flight.

Elliptical: Elliptical wings, which feature a constantly varying chord length, were eliminated due to their difficulty of manufacture.

Rectangular: Only a rectangular wing satisfied the initial set of FOMs and was selected for further analysis in Stage II.

3.1.3 Empennage

The tail surfaces of TLAR II will be referred to as empennage, and are an essential part of an aircraft's control and stability. The primary function of empennage is crucial to the operation of the aircraft and must be subjected to the most critical and fundamental FOMs.

Existing empennage configurations were selected from documented styles. They were analyzed based on the experience of the team members gained in last year's competition and through application of basic FOMs. The goal of the first stage of the CDP was to complete the analysis of proven empennage configurations so as to select three designs to investigate further in the second stage.

The purpose of empennage is to provide stability, and pitch/yaw control. The three main FOMs were handling characteristics, RAC, and ease of manufacture. Other FOMs, such as material availability, ease of transportation, and reparability were not considered explicitly in this section, as the materials of all designs were understood to be the same, and the types of tails were assumed to be equally transportable and repairable.

3.1.3.1 Tail Configuration

Canard: A canard configuration would reduce the required control surfaces at the rear of the aircraft to a single vertical stabilizer. The benefit of a reduction in control surfaces at the rear, however, would be negated by the complexity of both pitch and roll capabilities integrated into the aileron control.

While this configuration had benefits that included main wing stall prevention and less control surface actuators, the design, analysis and fabrication was complex and was eliminated for these reasons.

Conventional: Major benefits of a conventional design were ease of construction and lightweight design. However, the low placement of the horizontal stabilizer usually puts it in the wake of the main wing, "washing out" the airflow over the horizontal stabilizer and rendering elevator control ineffective. This configuration was eliminated due to its poor efficiency, susceptibility to damage and loss of control.

"T": The most important benefit of the "T"-Tail design is that the horizontal stabilizer is above the turbulence from the body and main wing, thus allowing the horizontal control area to be reduced. It also acts as an endplate for any control deflections caused by the vertical fin, which increases the vertical fin's efficiency and allows a reduction in the fin's area. This allowed a large reduction in weight and the "T" style tail was deemed the first design to be considered in Stage II.

Cruciform: The fourth concept examined was the cruciform design, a hybrid of the Conventional and the "T"-Tail. It was determined that this style shared several benefits of both, but was difficult to construct and the end plate effect from the "T" was lost. For those reasons, this design was eliminated.

"V": The next configuration investigated was the "V"-Tail design, which was efficient because it eliminates one wing tip vortex, decreasing induced drag. The design was discarded due to its many disadvantages, including high control surface complexity, and an induced opposite roll when given rudder input.

Inverted "V": The inverted "V", by contrast, produces favorable yaw-roll coupling. Elevator control was less affected by turbulent wake from the fuselage and main wing, and the use of only two control surfaces reduced the number of servos needed for both rudder and elevator control. This design had bad ground clearance and complex control surface design. However, it was kept for further analysis because of the good turning characteristics and the reduced drag of one less wing tip vortex.

"H": This was deemed a good design, as turbulence from the fuselage does not flow around the vertical fins. The vertical fins also prevent spillover of the elevator with an end plate effect, therefore eliminating drag from tip vortices induced by elevator input. Although this design is complex, it was kept for further analysis as it worked well with a twin-body design.

3.1.4 Fuselage

The fuselage serves as a primary structure of the aircraft and acts as a critical load path for the aircraft to transmit forces between the tail and wings, in addition to housing flight equipment and payload. Design of the fuselage is somewhat dependent on the design of the wing and tail because it links the components. The FOMs that were used to optimize the design parameter of structural reinforcement were ease of manufacture, strength to weight ratio, handling characteristics, and cost. The three types of fuselage structural reinforcement investigated were trusses, monocoque, and semi-monocoque.

3.1.4.1 Structural Reinforcement

Truss: A truss structure in the fuselage has a relatively good strength to weight ratio, but may interfere with the payload volume. Trusses are very difficult to manufacture, so it was immediately dismissed as means of reinforcement in the fuselage.

Monocoque: A monocoque design has good torsional strength, but it is weak in bending, which is the type of load transferred by the tail to the fuselage. The required skin thickness needed to support these bending loads would increase the weight significantly and therefore it was eliminated as a design parameter.

Semi-Monocoque: A semi-monocoque structure combines the torsional strength of the skin with bending strength that can be customized for the aircraft by means of stringers and ribs. This type of configuration allows the strength to be customized for specific loads. A semi-monocoque fuselage has the best attributes and was the choice for structural reinforcement of the fuselage.

3.1.5 Landing Gear

The functional requirement of the main landing gear is to absorb and dissipate landing loads effectively. The design parameters considered included tail dragger, quadracycle, bicycle and tricycle. During Stage I of the CDP various landing gear configurations were screened according to the established FOMs, such as ease of manufacture and ground handling characteristics.

3.1.5.1 Landing Gear Configurations

Bicycle: The bicycle landing gear configuration consisted of two in-line wheels straddling the CG of the fuselage and another wheel on each wing for balance. Due to complexity of manufacture and poor ground handling characteristics, the bicycle design was immediately eliminated.

Others: At this stage of the design, the remaining three landing configurations were all kept for further evaluation in Stage II.

3.1.6 Propulsion and Power System

The propulsion design began with little knowledge about the overall configuration of the aircraft, so the initial decisions related to propulsion choices were based on experience gained from last year's project.

The amount of power available to propel the aircraft is dependent upon the total power of the system and the efficiency of the entire propulsion system. To maximize this number, given that the battery power was limited by weight restrictions, a maximally efficient engine/propeller combination was chosen. Optimizing the efficiency of the motor as well as motor configurations while lowering the REP was the goal of the propulsion design portion of the conceptual phase.

The battery weight restriction of 5 lbs. limited the number of battery cells to 38, which amounted to approximately 40 volts. For standard radio controlled propulsion systems, 40 volts exceeded the rated power of many motor possibilities. While a motor's power is related to the input voltage, they can normally withstand higher voltages. Problems experienced in last year's competition showed that this

was not a desirable arrangement, yet it was determined that a single motor design was still a valid concept. Concerns for power as well as those regarding additional weight of this year's design did necessitate that a dual-motor configuration also be proposed.

Dual-Motor: The dual-motor configuration featured the simple option of powering both motors with a single 38-cell battery pack or two separate propulsion systems, each with 19 cells. The concern with over powering the motors determined that the two separate packs was the most reliable configuration.

Single-Motor: Initially, due to concerns with overpowering the single motor, the single motor configuration was developed with a maximum of 19 cells connected to the motor. However, due to the lower thrust of this configuration, the single motor connected to 38 cells was considered instead. This design was included along with the dual-motor configuration for analysis in Stage II.

3.1.7 Structural System

The structural system was required to provide efficient "load paths" which resolve forces experienced during landing and flight sequences. The spar structure, which reinforces the wings, and the wing carry-through, which transmits the bending loads through the fuselage, are the two major components of the structural system. When considering viable structural configurations it was noted that several options placed constraints on other component design solutions. These affected components included the wing planform (swept and tapered), wing configuration (biplane, delta and monoplane) and fuselage parameters. Several of these concepts were analyzed during Stage I of the CDP to effectively meet the various requirements of the structural system. Various spar cross-sectional geometric shapes were also considered for each of the competing component designs. These included the box beam, hollow cylindrical, solid rectangular and I-beam cross-sections.

The primary objective of the Stage I screening process was to eliminate design concepts that were complex, difficult to transport, raised the RAC, or difficult to repair or replace. The structural system design ideas that remained following the application of the Stage I FOMs are as follows:

Spar Structure: Initial concepts that were considered were the one, two, and three piece spars. The only design that failed to satisfy the transportation and ease of manufacture FOMs was the one piece model and was therefore discounted. The remaining concepts are described in detail during the CDP Stage II.

Wing Carry-through: The strut braced concepts that were initially proposed were disposed of due to poor manufacturing and strength to weight ratio ratings. The remaining design concepts were the bending beam and ring frame carry-through models.

3.1.8 Conceptual Design Phase – Stage I Summary

The CDP Stage I was focused on the development of initial aircraft designs that feature various component concepts that were determined to have merits applicable to the mission goal. By the end of the first stage, concepts that were immediately discernable as inadequate had been eliminated. Any

remaining concepts were combined into several configurations. These configurations would be evaluated further in the second stage of the CDP as to their individual component interactions and total system performance.

The decisions made when combining the components into complete configurations were somewhat arbitrary. However, each component that survived the first stage was examined to determine its ability to interact with other components. For example, it was immediately clear that an inverted V tail configuration could not be combined with a tail-dragger landing gear configuration. Equally obvious was the fact that an "H" tail configuration was well suited to a twin fuselage design. For each component, this process was done to piece compatible components together and develop three aircraft configurations.

The first configuration, designated "C-01", featured twin fuselages mounted over a low mono-wing. The twin motor powerplant concept fit this configuration as well as the "H" tail concept. The tail dragger concept was modified to include two tail wheels and the payload was accessed through twin hinged hatches.

"C-02", the second configuration employed a single fuselage with a high mono-wing concept. The high wing necessitated the use of the tricycle landing gear concept and allowed, due to the height of the fuselage, an inverted "V" tail mounted to a tail boom. The single motor mounted to the front of the fuselage also required that the payload access be from the rear of the fuselage.

"C-03", the third configuration was built around the implementation of a bi-plane wing concept. For this concept, wing spacing was known to be a concern with regards to fuselage height and susceptibility to crosswinds. To reduce this weakness, the fuselage was split into to canted pieces, which fit very well with the application of the quadracycle landing gear concept. To allow the payload access on the front of the fuselage, the single motor powerplant was implemented in a separate nacelle mounted under the upper wing. The remaining tail concept was a "T" tail and was well suited to this configuration due to the raised position of the horizontal stabilizer away from the wake of the two main wings.

These designs were taken as the concepts examined in the second stage of the CDP. There, they are analyzed with regards to component interaction and initial flight characteristics while further determination of RAC and ease of manufacture was performed.

3.2 Stage II – Generalized Analysis

Table 3-2 Design Parameter FOM Analysis – Stage II

Design Parameters – Stage II		Figures of Merit – Stage II (x weighting)												
		Ease of Construction (x2)	Ease of Transport (x1)	Personnel Safety (x1)	Component Safety (x1)	Component Interactions (x2)	Sortie Performance (x2)	Difficulty of Repairs (x1)	Rated Aircraft Cost (x1)	Cost (x1)	Motor Aerodynamic Flow (x2)	Motor Access/Mounting Ease (x1)	Motor Cooling (x1)	Sum of Ratings
Wing Types	Low Mono-wing	1	-	-	-	1	0	0	0	0	-	-	-	4
	Bi-plane	-1	-	-	-	-1	0	0	0	0	-	-	-	-4
	High Mono-wing	1	-	-	-	0	0	0	0	0	-	-	-	2
Wing Structure and Materials	Rib Structure	-1	0	0	-1	-1	0	-	-	1	-	-	-	-3
	Foam Core	1	0	0	0	0	0	-	-	0	-	-	-	2
Structural System	Two Piece	0	-	-	-	0	-	0	0	-	-	-	-	0
	Three Piece	0	-	-	-	1	-	0	0	-	-	-	-	2
	Bending Beam	1	-	-	-	1	-	0	0	-	-	-	-	4
	Ring Frame	-1	-	-	-	-1	-	0	0	-	-	-	-	-4
Tail Structure	Twin Body H	0	0	0	0	-1	0	0	0	0	-	-	-	-2
	Inverted V-tail	0	0	0	-1	0	0	0	0	-1	-	-	-	-2
	T-tail	1	0	0	0	1	1	0	0	0	-	-	-	6
Fuselage Configuration	Single	1	0	-	-	0	1	0	0	0	-	-	-	4
	Dual	-1	0	-	-	-1	0	-1	-1	0	-	-	-	-6
Fuselage Materials	Fiberglass	0	0	-	-1	0	1	1	0	0	-	-	-	2
	Aircraft Grade Plywood	-1	0	-	-1	0	1	0	0	1	-	-	-	0
	Kevlar	0	0	-	1	0	-1	1	0	-1	-	-	-	-1
	Carbon Fiber Reinforced Kevlar	-1	0	-	1	1	1	1	0	-1	-	-	-	3
Landing Gear	Tail-Dragger	1	-	-	-	0	1	-	0	0	-	-	-	4
	Tricycle	-1	-	-	-	-1	0	-	-1	-1	-	-	-	-6
	Quadracycle	-1	-	-	-	-1	1	-	-1	-1	-	-	-	-5
Power Plant	1 motor 38 cells	-	-	-	-	-	-	-	-	-	-1	0	0	-2
	2 motors 19 cells each	-	-	-	-	-	-	-	-	-	0	1	1	2

Stage II of the CDP was necessary to obtain our final aircraft characteristics. This stage rendered the designs that promoted a finished product which satisfied all of the design parameters. FOMs for Stage II included ease of construction, payload access and capacity, strength to weight ratio, difficulty of repair, component and interfacing strength, and component/personnel safety. The application of these

FOMs to specific design parameters resulted in a final set of components that, when assembled, produced an aircraft design with all of the desired characteristics.

3.2.1 Wings

Wing FOMs in Stage II focused mainly on structural complexity and construction. The FOMs were applied to the determination of the best wing type.

3.2.1.1 Wing Type

Bi-wing: The bi-wing implemented in "C-03" failed to satisfy the ease of manufacture FOM as it required the fuselage to be reinforced in multiple places and had the possible necessity of external bracers. The increased difficulty of manufacturing and additional induced drag thus eliminated it as a design concept.

High Mono-wing: "C-02" featured a high mono-wing design. This carried the benefit of large ground clearances for propellers (for wing mounted motors). It was however, a major challenge in terms of designing fuselage mounted landing gear which would not interfere with the payload. This was therefore eliminated due to the structural stipulations.

Low Mono-Wing: "C-01" configuration featured the low mono-wing which was demonstrated effective in TLAR I. Landing gear length was minimized, allowing for lighter and/or stronger struts. Torsion load transfer can be accomplished with limited interference with fuselage layout. The drawback of low propeller clearance was shown to be inconsequential compared to the benefits, thus this configuration was selected for further development.

3.2.2 Empennage

The goal for the second stage of the CDP of empennage was to analyze the interaction of the surviving Stage I conceptual designs as combined with the rest of the aircraft. The primary focus areas were the structural and aerodynamic dependencies and interactions with other components in the design under the application of further FOMs.

The sorties that TLAR II will fly consist of steep climbs, tight turns and short landings. And, as the wetted surface area of a particular design is very much constrained by the stability desired for the aircraft, the focus of the empennage design moved to the reduction of drag from wingtip vortices rather than viscous drag.

"Twin Body H": In the conceptual design "C-01", the "Twin Body H" configuration was implemented. While the construction was viewed as reasonably simple and sturdy, a couple of disadvantages were immediately apparent. This design required having two fuselages and an additional servo, both of which effect the RAC and add to the aircraft weight. While the structural and aerodynamic properties of this design were favorable, the added cost to the overall weight and RAC of the aircraft was too much to consider it further for the final design.

Inverted "V": The second design, "C-02," which featured a tricycle landing gear and high tail boom, provided the opportunity to apply the "Inverted V" configuration due to the fact that it would have

enough ground clearance. Aerodynamically, the concept was free of major concerns related to interaction with the fuselage and main wing. Some structural concerns, stemming from experience with tail booms not being rigid enough in last year's competition, were brought up with this design; however, the experience gained last year enabled more accurate analysis of design requirements for stability.

While the aerodynamic and structural constraints were satisfied by this configuration, there were distinct drawbacks related to the complexity of the control design and the ease of manufacture. This increased complexity eliminated the possibility of an Inverted "V" configuration.

"T" Tail: The third Stage I conceptual design "P-03" featured the "T-tail" configuration. To prevent tail surface washout and related loss of stability, the high placement of the horizontal stabilizer was essential. The fact that this configuration was proven in the flight competition last year added to the simplicity and efficiency of this design and led to the decision that it would be the final choice as a tail configuration for TLAR II.

3.2.3 Fuselage

Stage II fuselage design involved the evaluation of the fuselage design possibilities within the various configurations. The FOMs used to ensure that the design goals were met included ease of construction, payload access, RAC and component and interfacing strength. The three aircraft configurations considered were titled "C-01", "C-02", and "C-03" and each inspired unique fuselage design styles. The three design styles were: Dual fuselage for "C-01", single fuselage for "C-02", and a custom designed twin canted fuselage for "C-03". An analysis of the characteristics of these three styles was necessary to decide which will best satisfy the FOMs.

"C-01" Dual Fuselage: Two fuselages allow for each fuselage to have less projected area which, with a streamlined design, reduces drag. The problems with this design included a dramatic increase in the RAC, complexity, interfacing strength concerns and possible construction difficulty. This design was dismissed due to failure to satisfy the FOMs.

"C-02" Single Fuselage: The second design style featured a single fuselage that would house the payload and flight equipment. This configuration was considered because it provides good airflow around the fuselage, maintains interfacing strength and would not affect the RAC drastically. In addition, efficient access to the payload is granted via a hatch located at the end of the fuselage. This design meets all the FOMs and was thus considered a viable design option.

"C-03" Dual Fuselage: The third style considered was the dual diagonal fuselage design of configuration P-03. This design provides good airflow around the fuselage and, due to canting, is less susceptible to crosswinds. It was a variation on the dual fuselage, and would also be difficult to manufacture, increase RAC and raise concerns about payload capacity and access. This design failed to satisfy many of the FOMs and was duly eliminated.

3.2.4 Landing Gear

In Stage II of the CDP, advantages and disadvantages of each remaining landing gear configuration were explored as they related to specific design choices made for other components of the aircraft. The two major considerations focused on were ground handling, and minimization of weight and drag.

3.2.4.1 Landing Gear Configuration

Tricycle: "C-02" featured the tricycle arrangement. Because the center of gravity is ahead of the main wheels, the aircraft would be inherently more stable on the ground and can be landed at a fairly large "crab" angle. In addition, this configuration required one extra gear block and steering servo for the nose landing gear, which added more weight to the design and increased the RAC. This concept therefore did not satisfy the Stage II FOMs and thus was not a feasible landing gear configuration.

Quadracycle: This configuration has good ground handling stability and an improved strength to weight ratio due to the lack of struts. However, two wheels require servos for steering ability, thereby increasing the RAC greatly. Because of these reasons, the Quadracycle was eliminated as a viable configuration.

Tail dragger: The tail dragger landing configuration provided ample propeller clearance by angling the nose off the ground. In addition, it was more simple to configure, as connecting the tail wheel to the same servo that controls the rudder, the aircraft is more easily controlled on the ground and construction was simplified. This dual use for a servo provided an excellent reduction in RAC, and therefore the tail dragger design was chosen as the final landing configuration.

3.2.5 Propulsion and Power System

The three configurations developed in Stage I of the CDP provide a basis for the propulsion requirements that needed to be met. At this stage however, thrust or specific efficiency requirements were not determined. Instead, FOMs such as power limitations of the motor and a low REP were applied to the design parameters such as number of motors and number of batteries per motor. This was similar to the FOM/design parameter process applied during Stage I of the conceptual phase, however here it was applied in parallel with analysis of the interaction with the other components in the design. This was accomplished by applying FOMs relating to aerodynamic flow of the thrusting air, ease of construction and motor/controller cooling to determining the final rating of each design.

Twin Motor: The conceptual aircraft configuration "C-01" featured a twin engine design mounted to twin separate fuselages. This lent itself excellently to the two-motor/two battery pack configuration. There were no power limitation concerns with this configuration as 20 volt motors were readily available for radio controlled aircraft applications. It had excellent access to clean air into the prop but the thrusting flow was disturbed by the fuselage that was located immediately behind the propeller. It was clear that the fuselage design was a drawback to many of the benefits of having two motors. Attaching the motors

directly to the wings on each side of a single fuselage would give all of the benefits of having twin motors without any of the disadvantages of the twin fuselage design.

Single Motor: The two concepts "C-02" and "C-03" featured very similar implementations of the single motor design which resulted in very similar FOM/Design Parameter analyses. The major concern, as noted before, with the single engine configuration was running radio-controlled motors at higher voltages than designed for. The thrust, mounting/access ease, cooling and REP were all comparable to the two-motor configuration discussed previously and there was only a slightly lesser rating given to the aerodynamic flow properties due to larger fuselage interference.

Summary: The most important factor in analyzing these configurations was the REP. With two motors connected to smaller individual packs, the basic REP was identical to a single motor connected to a single larger battery pack. Combined with the realization that wing mounted twin engines would have better cooling, aerodynamic flow and mounting/access ease, it was determined that the best power plant configuration was a wing-mounted twin-motor design with each motor connected to its own 19-cell power supply.

3.2.6 Structural System

The purpose of Stage II for the structural system was to evaluate the individual strength as well as the interface strength within the various configurations. The Stage II FOMs that were pertinent to the structural system were RAC, component interaction and ease of construction. Through the application of these FOMs the individual structural components remaining from Stage I are evaluated. The structural system components were evaluated as follows:

3.2.6.1 Spar Structure

The shear and bending stress increases approaching the fuselage interface, therefore in the interest of weight conservation, the size of the spar structure could be made to vary. In all CDP aircraft configurations, it was also determined that torsional loads were a major concern, needing to be addressed by the design of the spar structure.

Two piece: The two piece spar model consisted of two separate spar lengths, one from the wing tip to half of the wing span, and the other continuing to the wing's root. The exact size would be determined by the existing stresses due to the shear and moment. However, the required torsional strength was not sufficient enough to consider this design further.

Three-piece: The three piece model is a variation of the two piece model, the only difference being the addition of a small torsion pin near the leading or trailing edge. The size, and therefore weight, of the main spar could be further reduced, since the pin would absorb the torsional stresses. An additional benefit of the pin was its ability to accurately maintain the wing angle of attack. This model satisfied the Stage II FOMs and thus was considered a feasible spar design.

3.2.6.2 Wing Carry Through

The wing carry through component is required to absorb the maximum stresses due to lift without having to rely upon the fuselage for additional strength.

Ring frame: The ring frame design is composed of several bulkheads, which absorb and transmit the stresses produced by the wings. The weight and volume of these bulkheads did not satisfy the Stage II FOMs and was eliminated.

Bending beam: The bending beam's sole purpose is to absorb the bending stresses produced by the wings. The ability to vary the shape and required volume required make it an optimal choice for this structural component. Consequently, this concept remained as a viable design option within the various aircraft designs.

3.2.7 Conceptual Design Phase – Stage II Summary

The combined Conceptual Stage I and Stage II had the goal of determining a final configuration for the aircraft design. For each possible component of the configuration: airfoil; wing; tail; fuselage; landing gear and power supply, design parameters were defined and then eliminated through the application of FOM to determine the best final choices for the preliminary aircraft design.

The result of this process was the aircraft designated as "TLAR 1.9", a design very close to the final design, "TLAR II", though lacking final sizing and optimization of the components. "TLAR 1.9" features a single aerodynamically faired cylindrical fuselage riding over a low mono-wing. The payload access, through the nose of the fuselage, was facilitated by the symmetric mounting of two motors to the leading edges of the wings. Similar to last year's design was the implementation of a "T" tail configuration on a tail boom extending from the center of rear of the fuselage. This lengthened design allowed the use of the tail dragger landing gear to increase the lateral stability of the aircraft on the ground. Overall the preliminary design was simple and efficient and reflects the great effort put forth in the conceptual design to determine the best choice for each concept.

4 Preliminary Design Phase

As the design of the aircraft progresses, estimates for actual design specifications need to be made. The PDP of the design focuses on completing the initial calculation and estimation of general sizing, performance, and configuration with regards to the final aircraft design created in the second stage CDP.

During this process, techniques developed for the design of propeller driven general aviation aircraft were used to a large extent. Standard aerodynamic theories, such as Prandtl's lifting line method, were also implemented in computer algorithms to analyze the aerodynamic properties of the wing. While these techniques are not expected to be exact, they were implemented with confidence as their accuracy was validated by TLAR I in last year's competition. Overall, these proven methods provided excellent analysis results while directly exposing the design team to the fundamental principles of aircraft design.

As the CDP was highly focused on determining design parameters and FOMs to apply to the design process, so was the PDP. Here, however, the considerations that need to be made are more related to the optimization of flight performance and aircraft component interaction, than with the broader concerns examined in the previous sections. For each area of the preliminary phase, design parameters and FOMs will be applied as suit that particular area, and will be described locally. Overall, we are still concerned with component and personnel safety, structurally and aerodynamically favorable component interaction, ease of manufacture and construction, and a low RAC.

4.1.1 Wings

The wings PDP deals with the general sizing of the wing and associated components as well as materials selection. Wing geometry was chiefly governed by necessary flight characteristics and optimized by RAC concerns.

Materials: Strength to weight ratio was a primary FOM in this stage, as was cost. The goal was to maximize the strength to weight ratio, while also considering the implications to construction. Aircraft grade plywood is relatively cheap and lightweight. Manufacturing a wing with this material, however, is a complicated task. The wing would have to be made out of a series of ribs, each of which had to be individually assembled and shaped. The difficulty of this fails to satisfy the ease of construction FOM. A composite wing holds several advantages over the plywood wing. It was easier to construct and was considerably stronger while being comparable in weight. The structure and procedure were established by TLAR I in the 2000 competition. Composite wings are somewhat more expensive than plywood, but the increased ease of construction caused their use for the final wing structure.

Wing Geometry: The rectangular wing planform selected out of the CDP required optimization to reduce unnecessary drag and maximize lift and stability. Many geometric characteristics either had an adverse impact on performance or simply were not applicable to a model aircraft. Adaptations such as sweep and wing twist were not considered due to complexity of design and manufacture.

The wing sizing was begun with a desired aspect ratio of at least 8. Given the span limitation of 10 ft., this gave an initial root chord value of 15 in. However, minimizing drag due to vortices at the wingtips was a major concern. Therefore, taper ratio was introduced to approximate the lift distribution of an elliptical planform. Reduced lift at the wing tips reduces the pressure gradient and the tendency of air to move from high to low pressure areas. Due to the complexity of tooling a template in the suitable airfoil shape, only relatively high ratios were deemed practical. A taper ratio of 0.9 was settled on as a compromise between performance and practicality, which gave a tip chord of 13.5 in.

Stability: Documented performance characteristics of the chosen planform and low wing configuration led to some concern over roll axis stability. The low wing configuration creates a pressure buildup during a banked turn due to side-slipping (the fuselage interferes with airflow over the upwind wing). This causes a tendency for the aircraft to roll into a turn as the leading wing loses lift. To compensate for this, a dihedral angle was introduced to roll the aircraft back to its stable flight position. Due to the lack of a simple method to calculate the appropriate dihedral angle, empirical data was used to determine that, for radio controlled aircraft design, a 3° dihedral is most effective.

Control Surfaces: The type and location of control surfaces were dependent, in part, upon the rest of the primary aircraft structures. The available options included flaps, ailerons, or a hybrid control surface. Achieving the necessary level of control was the principal concern, followed by the impact to the RAC and building complexity.

Flaps were considered to increase lift during takeoff in order to minimize the takeoff distance. However, initial calculations on the lifting capacity of the wing suggested that the aircraft would have no trouble lifting off in 200 ft. Additionally, the inclusion of flaps would add significantly to the RAC (+6 hrs for 2 flaps +4 hrs for 2 servos). Spoilerons were chosen in place of ailerons to ensure control of the rolling/turning of the aircraft at low airspeeds. They are hybrid structures combining spoiler effects with aileron control surfaces. They help the flow stay attached to the wing during slow, high AOA flight, ensuring that the ailerons do not stall before the main part of the wing. They can also be used after touch down to reduce the lift of the main wing and ensure that the aircraft stays on the ground. Typical sizing of an aileron structure is approximately 25% of the span, extending to the outer edge of the wing. Thus our initial control surfaces were each 30 inches long.

4.1.2 Empennage

The preliminary phase of the Tail design focused on the initial determination of the sizes of the vertical and horizontal members, the size of the control surfaces, and the placement of the tail surfaces away from the aircraft's CG. Other design parameters considered at that point in the design were material choices, and manufacturing techniques. The main FOMs that were applied to these design parameters were ease of construction and stability.

General Sizing: The Tail sizing calculations used were a combination of general aviation and R/C aviation empirical data relations. Specifically to design the volume coefficient of both the horizontal and vertical members as well as the size of the elevator and rudder control surfaces.

The sizes of the tail components are functions of their distance from the CG of the aircraft and main wing size. Empirical data gives a function for tail volume coefficient, which is the standard method of approximating initial tail size, dependant on these parameters (equations shown below). Modifications to this empirical relationship for a T-tail allowed the vertical coefficient to be reduced by approximately 5% due to end plate effect of the horizontal member. Also, with the engines mounted on the leading edge of the wings, the tail arm was given to be 50% of the fuselage length as measured from the mean aerodynamic chord of the main wing.

Typical values used for the volume coefficients depend on the type of aircraft and, from experience for homebuilt aircraft, are approximated as 0.5 and 0.03 for the horizontal and vertical respectively. With these available parameters, and the size of the aircraft configuration at this stage giving an arm of 36 in, the initial sizes of the tail sections were determined to be 310 in² for the horizontal and 125 in² for the vertical.

$$Area_{HorizontalStabilizer} = (Coefficient_{HorizontalVolume}) (MAC_{MainWing}) (Area_{MainWing}) / (Arm_{HorizontalStabilizer})$$

$$Area_{VerticalStabilizer} = (Coefficient_{VerticalVolume}) (Span_{MainWing}) (Area_{MainWing}) / (Arm_{VerticalStabilizer})$$

An empirical approach was utilized in the preliminary sizing of the tail control surfaces. Guidelines derived from empirical data suggest that the rudders and elevators be approximately 25% of the tail chord, while extending from the tail boom to about 80-90% of the tail span. Given these areas and control surface relationships, as well as an Aspect Ratio and Taper Ratio of 4.2 and 0.77 proven successful for TLAR I, the horizontal stabilizer was determined to need a span, root chord, tip chord and elevator chord and span of 36.0, 9.6, 7.4, 2.5, and 36.0 inches respectively. With the Aspect Ratio and Taper Ratio of 1.5 and 0.8, again from TLAR I, the vertical stabilizer was determined to need a span, root chord, tip chord and elevator chord and span of 13.5 in, 10.25 in, 8.25 in, 3.0 in, 11.25 in respectively.

Manufacturability: A major design parameter for the tail preliminary design was material choice. Similar to the main wings, FOMs such as availability, workability and strength to weight ratio must be applied to all material choices.

Materials such as Steel were eliminated directly due to the high weight and poor workability. Aluminum has better workability, is lighter in weight, but its complexity of manufacturing was the reason it was eliminated. Another considered technique was a rib/spar structure of aircraft ply, which is lightweight and strong, but again very complex and time consuming to manufacture. The materials that were finally chosen fitted well with the most simple of available manufacturing techniques which was a foam core, fiberglass skin structure. These materials provide excellent strength to weight ratios and the ability to manufacture the components quickly with tools already available from the construction of TLAR I.

4.1.3 Fuselage

Optimization of the fuselage included determining a viable support structure and the necessary dimensions for maximum payload capacity. In order to determine the necessary dimensions for the fuselage a packing structure for the tennis ball speed loader was needed. The FOMs that were

considered pertinent during this design phase were interfacing and component strength, weight and payload access.

A satisfactory packing arrangement was found following several attempts to find an arrangement that was not too long or too wide. This arrangement consisted of three balls side by side on the bottom row, four in the middle row and three on the top row. This arrangement of ten formed a single cross section (See Drawing Package), therefore ten of these sections met the design goal of one hundred T-balls. The dimensions of this packing arrangement and, thus the speed loader, were 26" in length, 10.4 in width and ~7.5" in height. At this point the fuselage dimensions can be determined and a support structure can be designed.

In order to avoid payload access problems, the fuselage dimensions would have to be slightly larger to accommodate the batteries and flight equipment. The room created would also have to accommodate a support structure for the wing carry-through and boom interfaces. Working closely with the structural system group allowed for mutually beneficial solutions. This provided room for a support structure. The support structures considered were a keelson, longeron and box & stringer arrangement. The FOMs were individually applied to determine the feasibility of the support structure design concepts.

Keelson: The first design concept considered was the keelson, which is essentially a panel that runs along the length of the bottom of the fuselage. This panel would have to be quite strong and large in order to transfer and absorb loads effectively, which raised concerns of weight and payload accessibility. Thus the keelson design concept was dismissed.

Longerons: The next design concept that was considered was the longeron support structure. Longerons are planks that run longitudinally along the fuselage wall. Similar to the keelson design concept, weight and payload access were questionable and thus this design concept was dismissed.

Box & Stringer Arrangement: The box and stringer arrangement consists of a box type structure at the wing interface and stringers that run laterally and axially. Working closely with the structural system team, the wing interface was designed such that the fuselage actually "rode" on the wing joiner, thus reducing the needed strength of the fuselage. The stringers would provide the strength necessary to absorb bending stress from the boom as well as provide stiffness for the fuselage skin. Two plates at the rear of the fuselage would provide a means of attaching the boom and transferring loads to the stringers. This design concept met all of the FOMs and was thus chosen as the support structure for the fuselage.

Final Sizing: The final size of the fuselage was determined to be 45" in length, 10.75" in width and 9.75" in height. The box structure consisted of two plates on each wall of the fuselage running the length of the wing root (15"), two running across the fuselage, where the spar structure enters, forming a box. The boom interface plates are located 2" and 4" inches from the rear of the fuselage across the entire structure.

4.1.4 Landing Gear

At this stage, more emphasis was placed on general sizing to limit minimize weight and drag. It was necessary to optimize the landing gear configuration as well as specific components associated with the landing gear including gear struts, wheels, and gear blocks.

Landing Configuration: At this point, the preliminary calculations and design of the tail dragger could be completed. The tail-down angle of the tail dragger should be about 8-10 degrees with the gear in static position. To prevent the aircraft from overturning, the main wheels should be laterally separated beyond 25 degrees angle off the center of gravity as measured from the rear in a tail-down attitude. This was evaluated to be a distance of approximately 20 in. from the aircraft centerline at the spar location.

Gear Struts: A number of materials were considered for the gear strut, which was designed to interface with the wing spar, including steel, aluminum, and carbon. Carbon and steel would provide the most strength, while aluminum and carbon would be the lightest. Due to the difficulty of manufacturing and lack of impact strength, carbon struts were eliminated as a feasible option. Aluminum, despite its reduced weight, would not guarantee the performance requirements needed and was also eliminated. Due to the proven performance of the previous year's struts, a steel piano wire torsional configuration was chosen for the design of the struts. With this design, the majority of the force of the impact of landing would be absorbed by the torsional loading of the piano wire, and would not be directly transferred to the gear block and ultimately the wing.

Wheels: For the construction of the wheels, rubber and aluminum were considered. Due to the weight of the rubber and the fact that traction was not a major concern, the front wheels were constructed from aluminum. Due to the fact that the expansion joints in the runway could cause takeoff problems if the front wheels were too small, the wheels were designed to be 4 in. in diameter and ¼ in. in thickness. The rear wheel, however, would only absorb 10% of the impact of the landing, so its size could be considerably smaller. For this reason, and to simplify construction, a standard rubber model aircraft wheel of 1.5 in. diameter was chosen.

4.1.5 Propulsion and Power System

The propulsion choices that were made in the conceptual phase of the paper were based on general power management, motor life, and RAC concerns. In the PDP, there was a lot more known about the aircraft configuration and more precise propulsion system design could be conducted.

In limiting the motor type and manufacturer, the contest organizers made the determination of motor type a fairly narrow search. From efficiency data of Astro and Graupner motors, the Astro motors were eliminated immediately. Upon analysis of the available Graupner motors, the only class that were seen as applicable due to thrust requirements and power available were the Ultra 3300 series. These motors are designed to run off of 20 volts and turn a direct drive propeller.

With the class of motor selected, manufacturer supplied data relating motor current draw to the efficiency, output wattage and RPM was used to determine exactly which 3300 series model would be used. Assuming a maximum current draw of 35 Amps, safely below the 40 Amp limit, the 7 wind series

was compared to the 8 wind. At this current level, the efficiency, output wattage and RMP were found to be 81.4%, 565 Watts, and 7000 RPM, respectively, for the 8 wind motor. By contrast, at the same current level, the 7 wind motor gave an efficiency, output wattage and RPM of 83.5%, 650 Watts, and 8300 RPM, respectively. Given the added efficiency and RPM output of the 7 wind model, it was chosen as the motor for the final design.

The propeller choice was made from a decision for a cruise speed of 60 mph, at a current setting below maximum. The Graupner Ultra 3300/7 motor operates most efficiently at a current draw between 23 and 29 Amps. At this setting and RPM, a 14" diameter x 12" pitch propeller gives a speed of approximately 70 mph. This factor of safety will be verified during flight testing to determine if an alternate propeller will be needed. For efficiency during glides and descents, experience gained during last year's competition dictated the use of a thin carbon fiber folding propeller, which is durable, light and has less drag in flight when not powered.

The final step in determining the power system was the choice of batteries. The weight, voltage and current limit was dictated in the rules, so the batteries were chosen based on durability, availability and cost. The Sanyo 2400 batteries that were used in last year's competition performed very well under raised current levels and fast discharging, so their reliability had been proven. This fact, combined with their increased availability and reduced cost this year, led to them being selected.

The final configuration for the power plant of TLAR II featured two Graupner 3300/7 motors, each separately powered and controlled, by 19 Sanyo 2400 batteries and turning carbon fiber thin folding props of 14" diameter and 12" pitch.

4.1.6 Structural System

The principal objectives of the PDP for the structural system were to maximize the strength to weight ratio without adversely affecting the payload capacity and access. Focus was placed on structural integrity, to avoid failure under flight and landing loads and component interfacing, as most systems fail at joints and interfaces.

Application of theory from solid mechanics and statics provided the basis upon which necessary design adjustments were made. These adjustments were the variation of the cross-section of the spar structure and the fuselage/wing interface method. In order to determine the best cross-section for the spar structure, stress and static analyses were conducted via the use of Microsoft Excel. Optimization of the fuselage/wing interface involved the determining the maximum stresses, for which it was necessary to determine the maximum load experienced (during banked turns). The following equations were utilized to determine the necessary values of maximum moment and bending loads:

$$\text{Newton's Law: } \sum F = ma$$

$$\text{Moment Equation: } M = Fd$$

$$\text{Maximum Bending Stress: } \sigma = \frac{Mc}{I}$$

$$\text{Moments of Inertia: } I_x = \int_A y^2 dA \text{ \& } I_y = \int_A x^2 dA$$

4.1.6.1 Spar Structure Optimization:

The wing's thickest point was chosen as the location for the spar structure so as to allow the furthest distance, 'c', from the neutral axis for bending. At the wing root and tip the thicknesses were 1.6875" and 1.4", respectively. At specific points along the span, the values of 'c' and 'M' were fixed thus allowing for variation of the moment of inertia by varying the cross-sectional area. The above equations were used, along with values for a 35 lb. aircraft travelling at 60 mph, to calculate the following load values:

Maximum G Force (with safety factor): 9.35

Maximum Load (per wing panel): 1410.9018 oz.

Maximum Moment: 38873.284 in.-oz.

Moments of Inertia: I-Beam: 0.0348635 in⁴ Rectangle: 0.059582 in⁴

Maximum Bending Stress: I-Beam: 57173.497 psi Rectangle: 33454.2 psi

Although the maximum bending stress can be taken by both the rectangular and I-beam sections, the I-Beam cross-section was chosen due to the weight savings that it would provide.

4.1.6.2 Wing Carry Through Optimization:

Optimization of the bending beam involved evaluating possible methods of interfacing with the spar structure. Inserting a wing joiner with a wing carrier box internal to the wing and extending the spar structure into the fuselage were the only method that were deemed feasible.

Weight savings could be attained by several methods, including replacing the shear web in the spar structure with a box carrier. The joiner could also be made from lightweight composite materials. Fuselage weight could also be reduced as its required strength is minimized due to the isolation from bending loads.

Through the application of the FOMs, specifically strength to weight ratios and overall component weight, the wing joiner with wing carrier box proved to be the best method to optimize the wing carry through component of the structural system. Integration of the carrier box with the I-beam cross-section was accomplished by allowing the carrier box to replace the shear web of the I-beam cross-section. The flange of the I-beam (spar cap), would run from wing tip to root, thus providing a method of connecting the two separate entities. The required spar cap thickness was calculated at various stations along the span, which determined the height of the shear web as well as the carrier box.

The moment and shear calculations determined the carrier box wing dimensions to be 10" length, .5" width, 1.24" height and wall thickness of .0625". I-beam shear web would taper from 1.24" at the carrier box interface to 1.35" at the wing tip and have a constant thickness of .375". The difference in height between the wing and web, being the spar cap thickness, provided a lay-up schedule for the

material chosen during the manufacturing phase. The wing joiner dimensions were calculated as 1.24" in height, .375" in width, with a 26.75" horizontal length.

4.1.7 Preliminary Design Phase Summary

The PDP analyzed the preliminary configuration as developed in the CDP with regard to the determination of exact sizing and component interaction. Design parameters that were related to the purpose of sizing the components were defined locally. FOMs such as component and personnel safety, structurally and aerodynamically favorable component interaction, ease of construction, and a low RAC were the primary factors determining much of the component design. Most general sizing calculations that were done were based upon those used in designing propeller driven general aviation and radio controlled aircraft. Precise calculations on flight performance will be completed during the DDP now that the detail configuration of TLAR II has been established.

5 Detail Design

The goal of the DDP was to optimize the sizing and design parameters that were developed in the PDP with regard to flight and takeoff performance. Similar to the PDP, the primary performance analysis techniques used were those applied to propeller driven general aviation aircraft. The calculation of basic characteristics, such as lift and thrust, allowed for the computation of more specific flight characteristics such as takeoff distance, rate of climb and endurance. In each section of the PDP, individual component weights were estimated.

5.1 General Sizing

5.1.1 Weight Estimate

Estimates based on experience gained from last year's design were assembled into a preliminary weight estimate of 30 lbs. Upon completion of the DDP and construction of the aircraft, the final value for aircraft weight was **32.3 lbs**. While heavier than first estimated, it was still well within the competition rules and design limitations of the aircraft.

5.1.2 Wing Performance

The detailed performance calculations of the main wing were based upon Prandtl's classic lifting line theory. Prandtl's theory was implemented numerically in Matlab code and run with the sizing parameters developed in the PDP. When given inputs for wing dimensions of span, root chord length, aspect ratio, $\alpha_{CL=0}$, the program gave an output of $C_{L\alpha=0}$ of 0.324, and a C_{Lmax} of 1.05. These values were reduced from the theoretical infinite wing data by approximately 26%, which was relatively efficient despite the low aspect ratio and a high taper ratio. However, by altering the values of the taper ratio, it was possible to achieve an 20% reduction. Any further reduction in tip chord could result in a weak wing structure and ineffective control surface area. The final values for $C_{L\alpha=0}$ and C_{Lmax} of **0.325** and **1.136** respectively, were realized with a root chord of 15 in. and tip chord of 13 in. This gave the final wing an aspect ratio of 8.6, taper ratio of 0.867, planform area of 1680 in². An important quantity resulting from these refined sizing and performance characteristics was a wing loading, W/S, of **2.77 lbf/ft²**.

5.1.3 Motor Thrust Available

While the static thrust of an engine was a necessary calculation related to the determination of performance characteristics such as takeoff distance and rate of climb. Analysis of power supplied being reduced by the inefficiency of the motor and propeller was used to indicate the amount of power available to actually propel the aircraft. Having determined the number of cells to power each motor in the preliminary phase, the total power available to the motor was calculated using the equation $P = VI$, giving an available power of 712 Watts. With a combined efficiency of 0.75, the thrust developed per engine was **4.75 lbs**. This gave a final thrust-to-weight ratio of **0.29**.

5.2 Flight Performance Calculations

In optimizing sortie performance, it was necessary to evaluate takeoff, rate of climb and range/endurance characteristics as well as static stability. While dynamic stability was also a concern, for a fairly conventional design as TLAR II, dynamic instability has proved to be highly transient in modes that are easily controlled by a skilled pilot.

5.2.1 Takeoff Performance

The takeoff profile for TLAR II was essential, as it was a competition constraint. It was determined for takeoff that the rotate/stall speed needed was **45.3 ft/s**, while the actual takeoff speed was **49.8 ft/s**.

For the Reynold's number (~200,000 to 300,000 based on M.A.C.) at which the takeoff was performed, the induced drag of the aircraft was small enough to be approximated to zero. This enables the approximation of integrating Newton's second law over the ground run of the aircraft. This integration of the acceleration can be reduced to the following equations from reference 1:

$$\left(\frac{1}{2gK_A} \right) \ln \left(\frac{K_T + K_A V_f^2}{K_T + K_A V_i^2} \right) \quad \text{with} \quad K_T = \left(\frac{T}{W} \right) - \mu, \quad \text{and} \quad \frac{\rho}{2(W/S)} (\mu C_L - C_{D_0} - KC_L^2)$$

A ground roll of **165 ft** was calculated for a rolling resistance factor (μ) of 0.05 and a total takeoff distance of **185 ft** with a 1.0 rotate factor. While this seems close to the distance limit, the likelihood of winds being present during the competition will shorten the actual takeoff distance. If this is not the case, and taking off within the limit proves difficult, reducing the payload may be considered.

5.2.2 Rate of Climb

The rate of climb (R/C) is the vertical component of the aircraft velocity. It can be expressed in terms of weight (W), perpendicular component of drag (W_D) and velocity (V). W_D is a function of thrust (T) and drag (D), therefore yielding:

$$\frac{R}{C} = \frac{(T - D) \times V}{W}$$

The best climb rate will occur at the velocity for maximum lift to drag ratio, L/D_{\max} . Although the thrust produced by the propeller and corresponding power available changes with the airspeed, an approximation was made to show that the maximum lift to drag depends only on the values for the parasite drag coefficient, C_D and the wing's aspect ratio, AR.

$$\frac{L}{D_{\max}} = 0.886 \sqrt{\frac{AR}{C_D}}$$

Using these formulas, the rate of climb for the aircraft was calculated to be **710 ft/min**.

5.2.3 Turning Radius

The turning radius gives an indication of how much distance, time and power are needed to perform a turn and is necessary because it affects sortie flight time and power management.

The turn radius calculations began with the assumption that the turn will be made at the cruise speed of 60-MPH. The equation

$$n = \frac{(V_{cruise})^2 (C_{L_{max}})}{2(W_{aircraft})} (Area_{wing})$$

gave a load factor of 3.78 for the turn. From this, and geometry, a bank angle of 74 degrees and turn radius value of **66 ft** was calculated.

5.2.4 Range and Endurance

Range and endurance characteristics are essential performance indicators for an aircraft designed to participate in timed, limited fuel flight profiles. The range figure of TLAR II was based on the power available and the power that the flight profile will require, so that a determination of the number of sorties possible can be made.

Initially, this was done by examining TLAR II in steady flight. The power available is the number of cells multiplied by the power rating for each cell. This equated to 1 battery pack multiplied by 2400 milliAmp-hours for a total of 2.4 Amp-hours. This allows **6.4 minutes** of flight time at the current setting of 22.6 Amps, which subsequently gave a cruise range of **7.0 miles**.

While this flight time was less than the flight period, an Excel spreadsheet was used to determine the detailed flight plan and current setting breakdown for the entire mission profile, with gliding and powered back cruises to be ample for the completion of a ten minute flight period. The final estimate for the number of flight sorties possible was five.

5.2.5 Static Stability

The ability of the aircraft to return to trimmed flight, if it was somehow deflected, was an important consideration. Due to the symmetry of the aircraft about the centerline of the fuselage, it was possible to achieve some roll stability of the design, with the selection of 3° dihedral in the preliminary phase. The focus was placed on the pitch stability (the directional stability was already addressed in the sizing of the vertical tail stabilizer). A well designed aircraft that has good static stability, historically will also behave well dynamically.

The pitch stability is related to how the main wing and horizontal stabilizer work together to correct pitch deflection. For TLAR II, this was especially critical due to the choice of a symmetrical airfoil for the tail. To prevent excessive corrective elevator deflection during steady flight, the pitching moment of the airfoil needs to be balanced by the placement of the center of gravity relative to the center of pressure of the wing. Assuming that any pitch deflections would be small, the pitch static stability is directly dependent on the horizontal stabilizer. The calculations focused on determining the exact placement of aircraft CG for a desired Stability Margin of 0.3. This margin is the geometrical distance between the location of the CG and the location of the neutral point. The neutral point was determined with the following equation along with design parameters defined earlier in the paper.

$$x_{np} = x_{AerodynamicCenter} + V_i \left[1 - \left(\frac{4}{AR_{MainWing}} \right) \right]$$

With a few iterations, this allowed the placement of the wing at the optimum position for stability. The main wing leading edge was located at 18 in from the nose of the aircraft, which places the CG directly on the spar location. Additional pitch stability was achieved through decalage (angle between the horizontal stabilizer and the main wing), which was initially set at 1° and will be finalized during flight testing.

5.2.6 Systems Architecture

The Systems Architecture describes the electrical components used to fly the aircraft including the batteries, servos, receivers, and handset. The number, location, and type of motors and batteries were determined in the propulsion section of the PDP. Determining the types of servos remained.

Given the values obtained for the torque required by each servo, two different servos (HS-225MG and HS-545BB) manufactured by Hitec RCD Inc. were chosen for the rudder, elevator, and aileron controls. The HS-225MG, capable of 55-67 ^{oz}/_{in} of torque was used to control the elevator. The HS-225MG was also used for the rudder, despite the rudder having less control surface area than the elevator, because the same servo controls both the rudder and the rear wheel. The spoilerons however require more torque to control due to higher surface area, therefore a more powerful servo, HS-545BB, capable of 62-73 ^{oz}/_{in} of torque was used.

(Tables on Next Page)

5.2.7 Detail Design Summary

Table 5-1 General Sizing

Design Parameter	Size
Aircraft Dry Weight	20.9 lbs.
Light Payload Capacity/Weight	100 Tennis Balls/12.85 lbs.
Heavy Payload Capacity/Weight	Steel/15 lbs.
Battery Pack Weight	5 lbs.
Main Wing Configuration	Low Mono-Wing
Main Wing Airfoil	E214
Main Wing Area	1680 in ²
Taper Ratio	0.867
Aspect Ratio	8.57
Number of Motors	2
Propeller Size	14" x 12" (x2)
Total Thrust	9 lbs.
Horizontal Stabilizer Area	310 in ²
Vertical Stabilizer Area	125 in ²
Tail Airfoil	NACA 0009
Fuselage Height	9.75 in
Fuselage Length	45 in
Fuselage Width	10.75 in

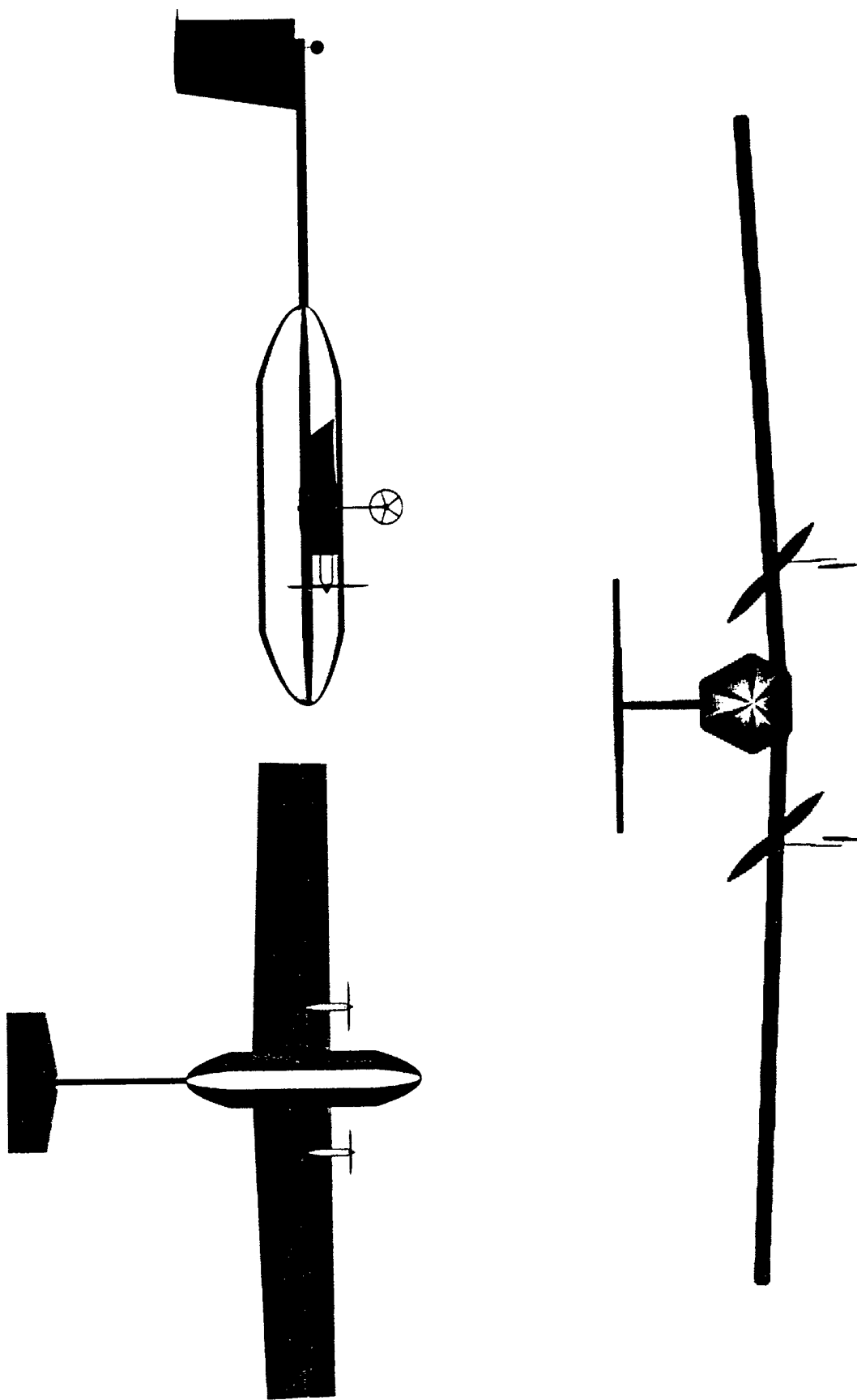
Table 5-2 Systems Architecture

Component	Description (Amount)
Motors	Graupner Ultra 3300/7 (2)
Servos	HS-225MG (2), HS-545BB (2)
Batteries	Sanyo 2400 (2 sets * 19 cells = 38 total)
Receiver	HPD-07RB (PCM)
Handset (Radio)	Prism 7X (PCM)

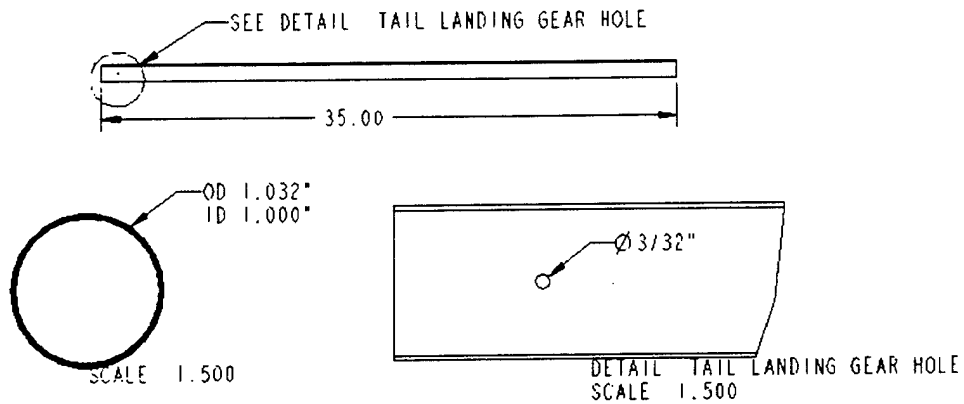
Table 5-3 Flight Performance Data

Design Parameter	Performance
Cruise Speed	60 mph (88 ft/s)
Takeoff Distance	185 ft
Climb Rate	710 ft/min
Turning Radius	66 ft
Payload/Gross Weight Ratio	0.39
Cruise Endurance	6.4 min
Sortie Endurance (# of Sorties Flown)	5
Rated Aircraft Cost	6.54
Final Flight Score	98.1

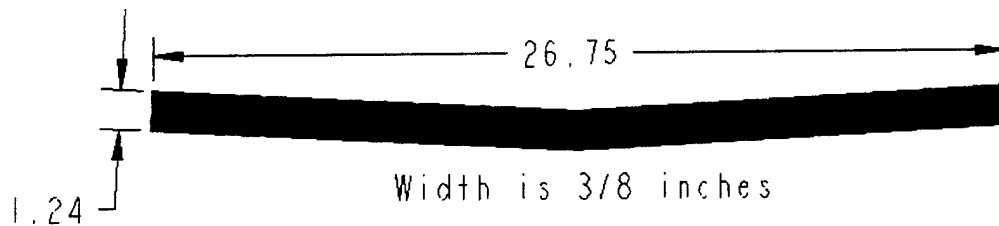
TLAR II: Three View



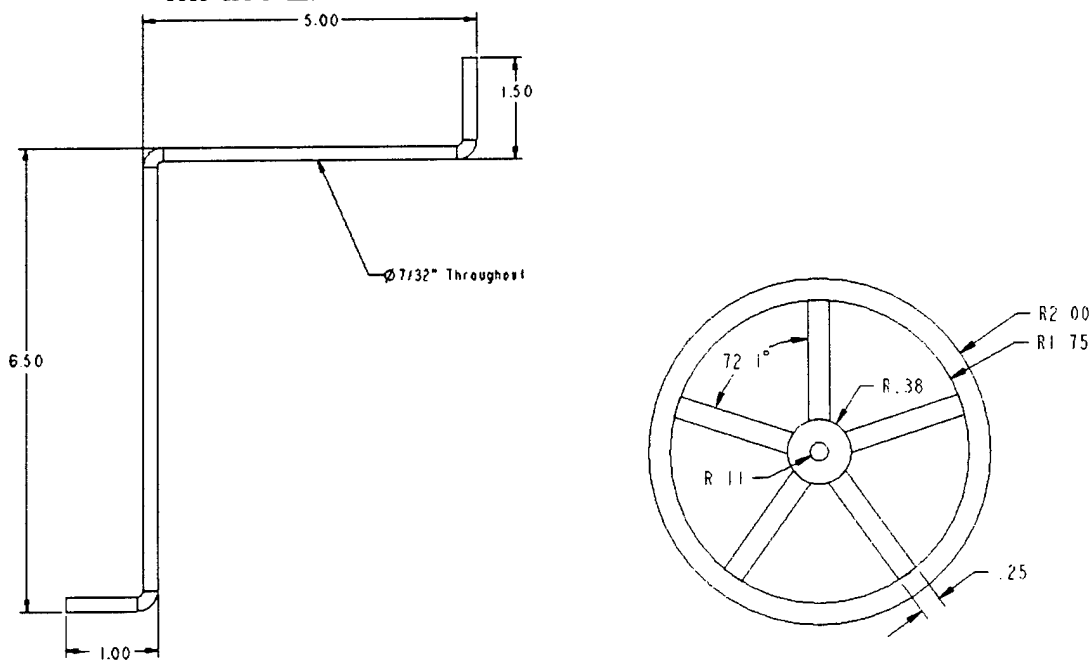
BOOM



WING JOINER

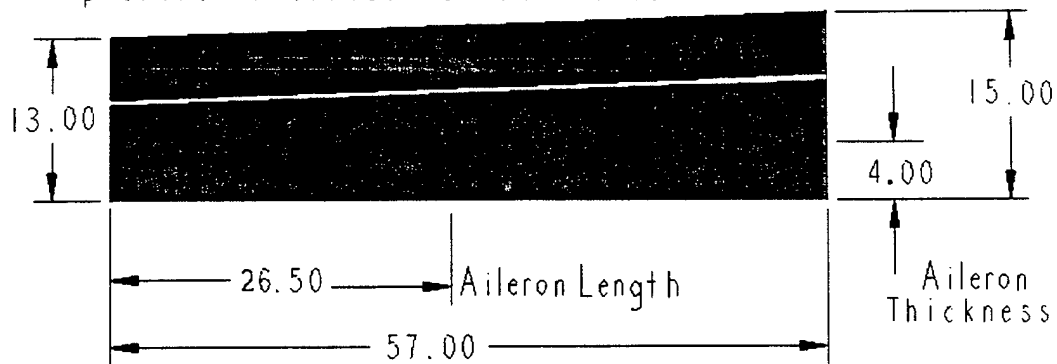


MAIN LANDING GEAR STRUT & WHEEL

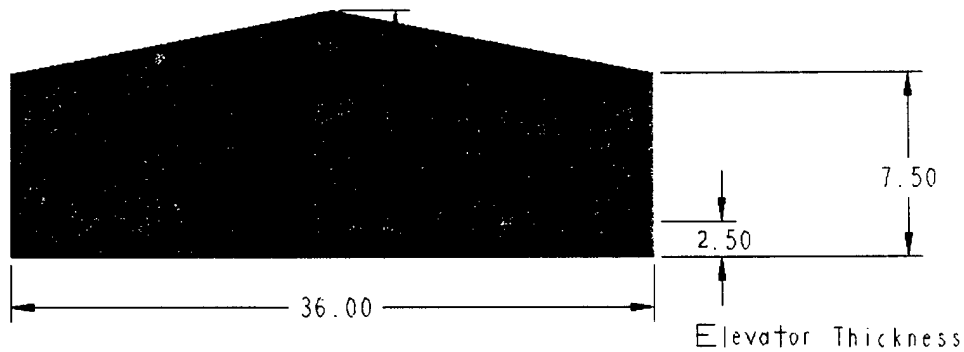


WING PANEL

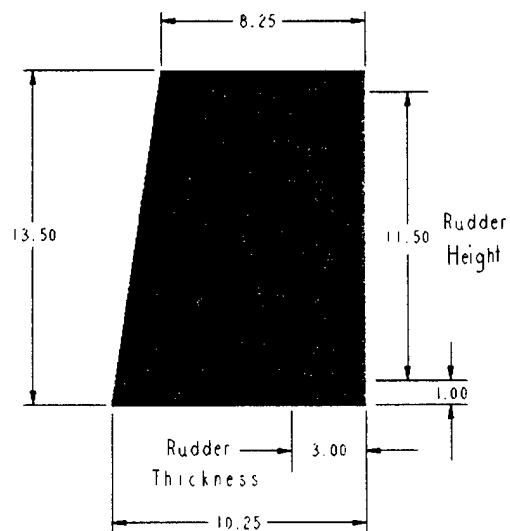
Root Chord Thickness is 1.6875 inches
Tip Chord Thickness is 1.4 inches



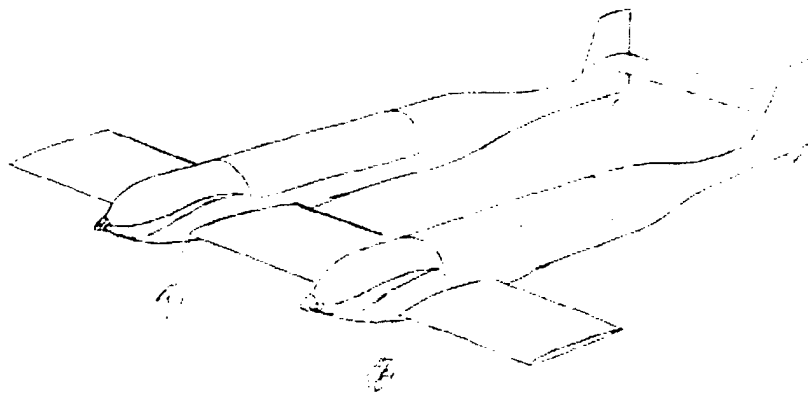
HORIZONTAL STABILIZER



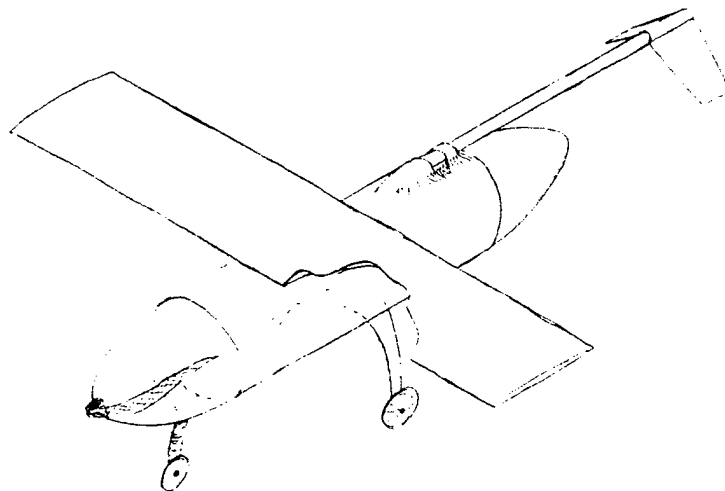
VERTICAL STABILIZER



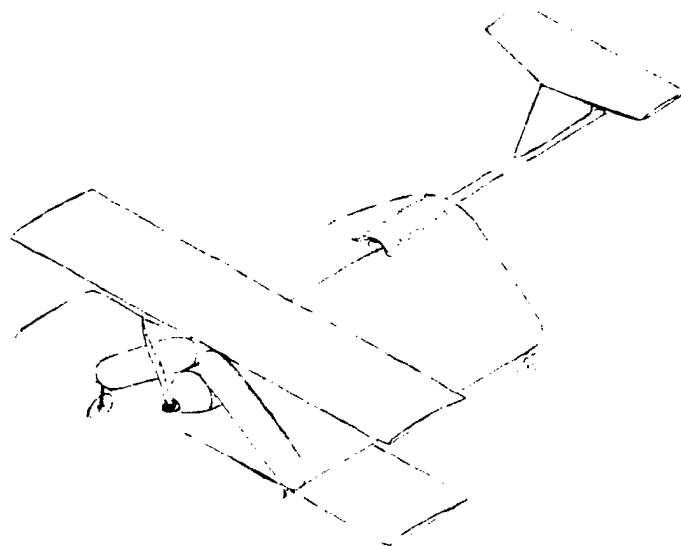
"C-01"



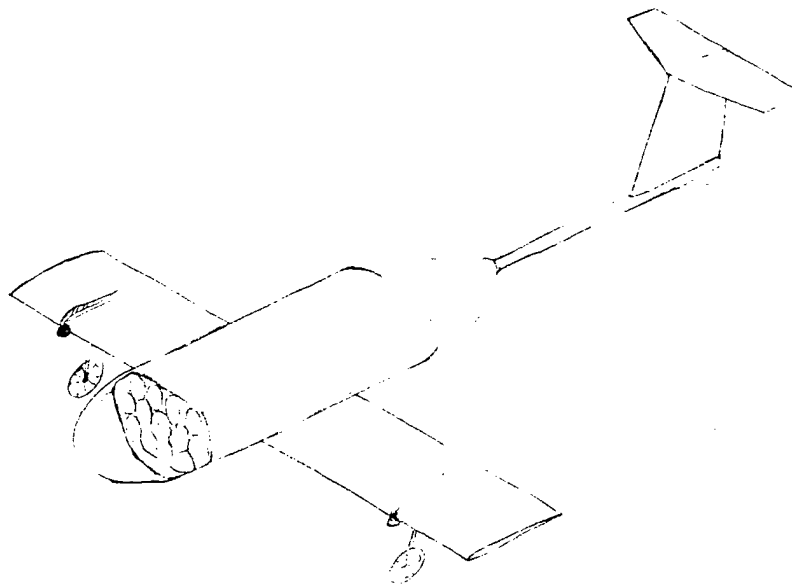
"C-02"



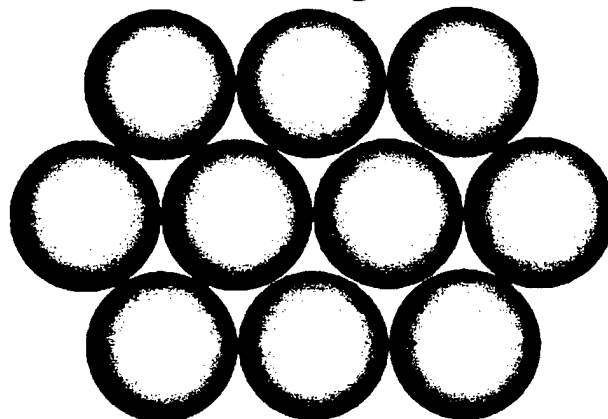
"C-03"



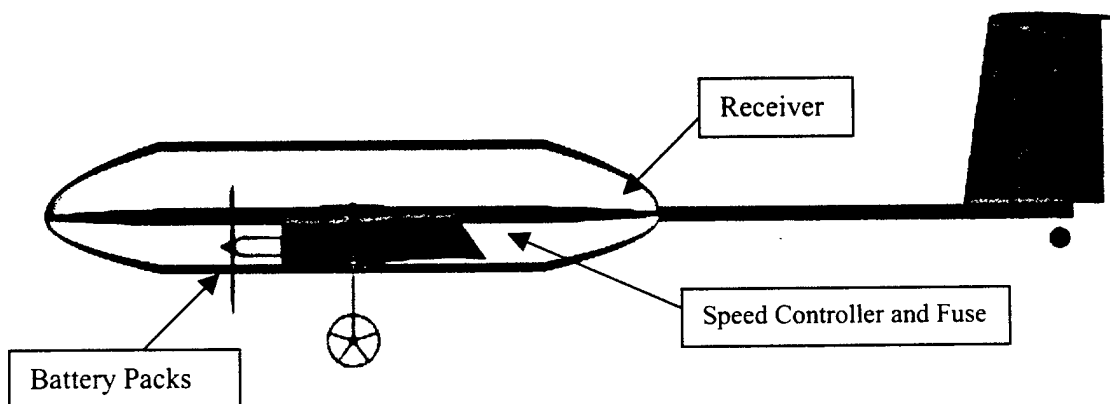
TLAR II



Tennis Ball Packing Arrangement



Flight Equipment Locations



6 Manufacturing Plan

Logistics and required skill level to manufacturing component design ideas imposed constraints on design options. The manufacturing constraints were continually considered in order to avoid conflicts between a chosen design idea and the ability to construct it. The manufacturing FOMs were used to screen construction techniques and materials based on skill level, physical properties, component and interfacing strength, and logistics. The material FOMs were sometimes used to eliminate construction methods, while construction FOMs were sometimes used to eliminate materials. The order in which the various components and assemblies were completed are shown in the manufacturing timeline presented in section 6.4.

6.1 FOM Reasoning/Discussion

Materials: Materials were screened due to their strength-to-weight ratios, availability, cost and required skill level.

Construction Techniques: "Home-built" construction with limited techniques were the only methods available to the team due to limited experience with an autoclave, time restrictions, and the unavailability of a large CNC machine. Construction FOMs are composed of required skill level, machinery, tools, tooling time, robustness and ease of repair.

6.2 Component Manufacturing Description

6.2.1 Spar Structure

The spar structure assembly consists of the torsion rod, shear web, spar cap, wing joiner, and the wing joiner carrier box.

Spar Cap Materials: The spar cap absorbs the majority of the bending stress and is of variable thickness. A carbon material was best suited for this component because of its high axial load capacity.

Spar Cap Construction Techniques: 12 K carbon tows were cut into the required lengths to match the required thickness at the various stations along the wing. The lengths that were required were determined by the lay-up schedule in the structural system PDP. The strands of 12 K carbon tow were wet-out with epoxy and then laid into the groove between the shear web and wing surfaces.

Shear Web Materials: The shear web is only required to give spacing between the spar caps and to absorb a nominal amount of shear stress. Material FOMs were applied to various lightweight materials in order to extract the best material. The materials investigated for the shear web were carbon plate, balsa, and Aircraft plywood. Despite the high tensile strength of carbon, the thinness a plate raised concerns about buckling and was eliminated. Aircraft plywood was eliminated due to its high relative weight, leaving the balsa wood board as the ideal choice since it was light, required low skill level, and was the cheapest of the three choices. The specific type of board used was vertical end-grain balsa wood.

Shear Web Construction Techniques: The only construction technique explored was to cut it to the required dimensions and epoxy the end-grain balsa pieces together. The wood was cut into 2-inch tall sections, which were then glued together with Cyano-Acrylate (CA) to make two 60-inch lengths. The shear webs were then cut to the height specified by the spar cap thickness at the particular station along the span.

6.2.2 Wing Joiner

This component joins the wing halves and must be strong enough to withstand the concentrated bending loads from landing and turning.

Materials: The materials investigated for the wing joiner were 12K-carbon tow and 6061 aluminum. The aluminum was quickly eliminated in favor of the carbon tow due to the skill level required to machine the necessary geometry as well as tooling time. The light-weight and high strength characteristics of the carbon tow made it the ideal choice for the wing joiner.

Construction Techniques: The methods that were considered for fabrication of a wing joiner were to use an autoclave or to do a manual "wet-lay up". The autoclave required that a complex mold be made. The "wet-lay up" process was chosen since it satisfied the required skill level and tooling time FOMs. Construction of the "wet-lay up" mold began by using the LaserCAMM in the Undergraduate Machine Shop to cut an acrylic sheet into the proper shapes. After the acrylic pieces were bolted to a melamine board, approximately 350 yarns of 12K-carbon tow were whetted with epoxy and placed in the gap. Once the carbon was laid properly, another melamine board was clamped over the newly laid spar. Once the epoxy had hardened, the wing joiner was removed and the surfaces finished to ensure exact dimensions.

6.2.3 Wing Joiner Carrier Box

The purpose of the wing joiner carrier box is to act as a stiff sheath for the wing joiner while transferring loads from the wings.

Materials: The materials considered for the wing joiner carrier box were carbon tow, Kevlar, and fiberglass cloth. Since all three had desirable properties, a combination of the three was used. Unidirectional 12K carbon and 1.2-oz/yd² fiberglass cloths provided strength and structural stiffness, while two layers of 1.8-oz/yd² Kevlar increased impact strength of the carrier box.

Construction Techniques: The only method investigated for the wing joiner carrier box was to mold it around the wing joiner itself. This ensured a tight fit and reduced the chance of failure due to fatigue at the joint. A single layer of fiberglass was wrapped around the wing joiner. Once cured, the fiberglass sheath was cut off of the wing joiner and bonded back together using CA. Coating the wing joiner with a mold release, the fiberglass sheath was slid onto the joiner. Unidirectional 12K carbon tow was cut and bonded to the fiberglass, with the carbon laid along the length of the wing joiner. After the carbon had cured, two layers of Kevlar were wrapped around the existing lay up. After the lay up

hardened, the edges were cut to ensure the proper dimensions and the sides were “roughened” to create a good bonding surface.

6.2.4 Torsion Rod

The torsion rod serves to absorb wing torsion loads.

Materials: The materials considered for the torsion rod were a 1095 cold rolled steel piano wire with a $\frac{7}{32}$ -inch diameter and a 1/4-inch diameter 6061 aluminum rod. The aluminum was chosen because of the larger diameter (to increase moment of inertia) and lower weight.

Construction Techniques: Cutting the aluminum rod into two 6-inch lengths was the only necessary tooling required.

6.2.5 Wing Airfoil

Airfoil Templates: The first step in the process of fabricating the wings was to make Eppler 214 airfoil templates.

Materials: The materials considered for the airfoil templates were 6061 aluminum, aircraft plywood and Formica. Since the hot wire method was the desired cutting process for the wing cores, it was necessary for the chosen material to be smooth for the wire path, and not melt under hot wire temperatures. Formica was the clear choice due to smooth surface finish and low thermal conductivity.

Construction Techniques: The two techniques for construction of airfoil templates considered were the “cut-and-paste” and a CNC machine cutting method. The “cut-and-paste” process was used because it was easier. Using data points obtained from the UIUC Database, printouts of the airfoil for chord lengths of 15, 14, and 13 inches were created. This included the root, tip, and midpoint of the spans of the airfoils. Printouts were bonded to the Formica, which were then cut into the shape of the airfoil.

6.2.6 Wing Cores

The purposes of the wing core are to maintain the airfoil cross-sectional shape and to contribute to the composite strength.

Materials: The materials considered were aircraft ply, and blue and EPS foam. Using aircraft ply, would result in a design using a rib structure overlaid with MonoKote, while the foam design could form a solid core for composite lay up. The foam was chosen because a solid core was more structurally sound and required less construction. The stiffness and compressive strength of the blue foam and low weight of the EPS foam made both of them viable choices for the core. A combination of blue and white EPS foam was used. The dense blue foam provides stiffness and the less dense white EPS foam conserves weight.

Construction Techniques: The two construction techniques investigated for cutting the foam core were utilization of a large CNC machine and a hot-wire cutting process. The CNC machine was immediately eliminated due to the unavailability. The hot-wire technique satisfied the logistical issues and the skill level requirements.

In order to accommodate the length of the hot-wire bow, the foam blocks were cut into quarter span sections. Blue foam was used from the leading edge to the thickest point of the wing, while EPS foam was used from the thickest point to the trailing edge. The blue and white foam sections were set against each other and the wing templates were set in the foam. After the reference pins were inserted into the foam blocks, the hot wire was drawn through the foam, following the template, creating the desired E214 airfoil cross-section.

6.2.7 Spar Assembly

The spar assembly, which consists of the shear web, carrier box, and two landing gearblocks, was coated with epoxy and pressed between the blue and EPS foam wing halves. Epoxy was used to bond the 12K-carbon tow spar caps to the balsa shear web and carbon/Kevlar carrier box. The aircraft ply hard points for the motor nacelles, torsion rod, and fuselage interface were placed in the wings. The entire wing structure was vacuum bagged to extract the excess resin and to ensure optimum bonding strength.

6.2.8 Wing Skins

The functional requirement of the wing skin is to provide a smooth surface for airflow over the wings, which reduces parasitic drag. The skin is also required to provide torsional strength to dissipate stresses generated during flight.

Materials: Carbon and fiberglass cloths were the materials considered for the wing skins. Carbon cloth was eliminated due to high cost and difficulty of working with the dimensions that were required. Fiberglass cloth was chosen because it was cheap and easy to work with.

Construction Techniques: The use of foam as the core excluded the possibility of using an autoclave, therefore a wet lay up process was needed. Fiberglass was laid at a 45° bias over Mylar. Each wing core was then sandwiched between the sheets of fiberglass/Mylar. The whole assembly was then placed in a vacuum bag to compress the fiberglass/Mylar. After the epoxy had finished curing, the wings were removed from the vacuum bag, the Mylar was peeled off and the excess fiberglass was trimmed or sanded off.

6.2.9 Final Wing Assembly

The fiberglass covering the hard points was trimmed off, allowing access to the plywood below. The spoilerons were cut out and trimmed to allow enough clearance for full range of motion. The recesses to hold the servos were cut into the wings and the wing tips were cut at a 45-degree angle. Fiberglass was then adhered to the exposed core surfaces to provide strength.

6.2.10 Stabilizers

The airfoil decided on for the horizontal and vertical stabilizers was the NACA 0009. The same materials and construction techniques were chosen for the two stabilizers.

Materials: The horizontal and vertical stabilizers were made from foam and fiberglass for the cores and skins, respectively. The only difference from the wings was that only blue foam was used. To provide stiffness and strength unidirectional carbon cloth was laid along the span at half the chord length. The final material used in the tail was aircraft ply that acted as hard points at the interface with the boom.

Construction Techniques: The final lay-up of the stabilizers was exactly the same as the wings.

6.2.11 Main Landing Gear Strut

The gear struts need to withstand fatigue and to absorb the majority of the loads applied at landing.

Materials: The materials considered were carbon, 6061 aluminum and 1095 cold rolled steel piano wire. The carbon was eliminated due to lack of impact strength and tooling time. Aluminum was eliminated due to strength and stiffness concerns. Cost, prior experience, high strength and durability made piano wire the ideal choice.

Construction Techniques: Prior experience with 1095 cold rolled steel piano wire eliminated the need to investigate other construction techniques. In order to obtain the necessary strength and shape the piano wire was (cold) bent then stress relieved at 600°F. This was repeated until the desired shape had been obtained. The strength of the steel was thus preserved and the residual stress at the joints was relieved.

6.2.12 Gear Blocks

Materials: The two possible materials investigated were aluminum and aircraft ply. Tooling time required caused the aluminum to be eliminated. Aircraft ply was chosen since tooling time, cost and skill level were nominal.

Construction Techniques: Prior experience with the materials and component design eliminated the need to investigate construction techniques. The aircraft ply was cut into the required dimensions and then stacked together and bonded with epoxy. A second layer of plywood consisted of two pieces, thinner than the first layer, for the landing gear strut. Epoxy was applied to T-nuts that were pressed into the wood to hold the bolts that would keep the piano wire in place.

6.2.13 Wheels

Materials: Two possible materials for the wheels were aluminum and high-density rubber. The rubber was easily eliminated as a viable material due to weight and strength issues. The aluminum had a lower weight while meeting the strength and durability requirements. Thinner aluminum wheels, compared to thick rubber, decreased aerodynamic drag.

Construction Techniques: Two possible methods for constructing the wheels were by hand or with a small CNC that was available. The tooling time and skill level required to machining the aluminum by hand was excessive thus the CNC method was chosen. In addition, use of the CNC made it possible to decrease the wheel weight since a more complex geometry could be cut. After the wheels had been drafted with Pro-Engineer, the drawings were converted to a file that was read by the CAM program,

MasterCAM, which directed the machine's movements. The 6061 aluminum pieces were cut into five-spoked wheels. The spokes converged at a hub at the center of the wheel into which two bearings could be inserted. A rubber O-ring was placed in the grooves cut into the outer edge of the wheels to act as a "tire" in order to provide traction and increase ground handling.

6.2.14 Tail Landing Gear

Materials: The tail landing gear strut was made from 1095 cold-rolled steel piano wire because of cost and strength FOMs. It was decided that a standard 1.5-inch RC model aircraft wheel would suffice as the tail wheel, because it saved construction cost and time.

Construction Techniques: The cold bend and stress relief technique was employed for fabricating the tail gear strut. After the final shape had been achieved, the wheel was attached to one end of the strut, which was then connected to the servo by an additional control arm. Milled fiber mixed with epoxy was used to attach the tail gear assembly to the rudder.

6.2.15 Speed Loaders

Materials: Carbon tow and cloth, Kevlar, and fiberglass cloth were viewed as the only viable materials. The carbon cloth and fiberglass were both eliminated due to issues concerning durability, cost and required skill level. Kevlar met durability and cost requirements and was therefore the ideal choice of materials for the speed loaders.

Construction Techniques: A mold was needed to fabricate the speed loader. The two construction methods considered were the use of a CNC machine and taping the tennis balls together to attain the required geometry. The taping method required the least tooling time and skill level and consequently was chosen.

Tennis balls were taped together over which Mylar sheets were laid to provide a smooth surface to which the epoxy and the Kevlar cloth would not adhere. Two plies of Kevlar were used to construct the loader, which was then stiffened with carbon tow.

6.2.16 Fuselage

Materials: The three materials investigated for the fuselage were Kevlar, carbon cloth, and fiberglass cloth. The need for a stringer arrangement within the fuselage made carbon cloth a viable choice. Kevlar was also kept as a possible material since it met durability requirements. The fiberglass was eliminated since strength and impact strength requirements were not met.

Construction Techniques: The two possible methods for construction of a mold were a CNC machine or by forming one using the tennis ball speed loader and a pieces of foam to obtain the necessary cross-sectional shape. The CNC machine was eliminated due to the unavailability of a large enough machine and the time required to program. Therefore the loader/foam method for constructing the fuselage was used. The foam blocks were cut and sanded to form the desired shape of the nose cones. Three-ply of 1.8-oz/yd² Kevlar and one-ply of 2-oz/yd² fiberglass were to be used to form the fuselage skin. A speed loader, wrapped in plastic, and a female mold made from mylar, were used to form the

Kevlar and glass plies in the required shape. The nose and tail cone structures were formed from sections of blue foam, which were then attached to the loader/mold assembly. Aircraft plywood bearing walls and 12 K carbon tow stringers were incorporated to increase structural stability.

6.2.17 Boom

The functional requirements for the boom were stiffness and bending strength to support loads from the tail and landing gear.

Materials: Two materials that were considered for the boom were carbon and aluminum. The carbon was chosen over the aluminum due to issues with weight and stiffness.

Construction Techniques: Due to prior experience with carbon tubes, no additional construction techniques were investigated. A 60" long (1" ID x .032" WT) carbon tube was cut to the necessary 35" length. Aircraft ply was bonded to the inner diameter to provide strength for the connection to the vertical stabilizer and tail gear.

6.3 Assemblies

6.3.1 Wing Core Assembly

The spar cap thickness, landing gearblocks, and the wing halves were needed to assemble the main spar. Niches in the balsa shear web were cut where the landing gear blocks would be attached. Shims were used to bond the shear web to the wing cross-section at the correct height, which, at the half-span length, is equal to the spar cap thickness. Epoxy was applied to the landing gear blocks, which were then connected to the carrier box.

6.3.2 Wing panel Assembly

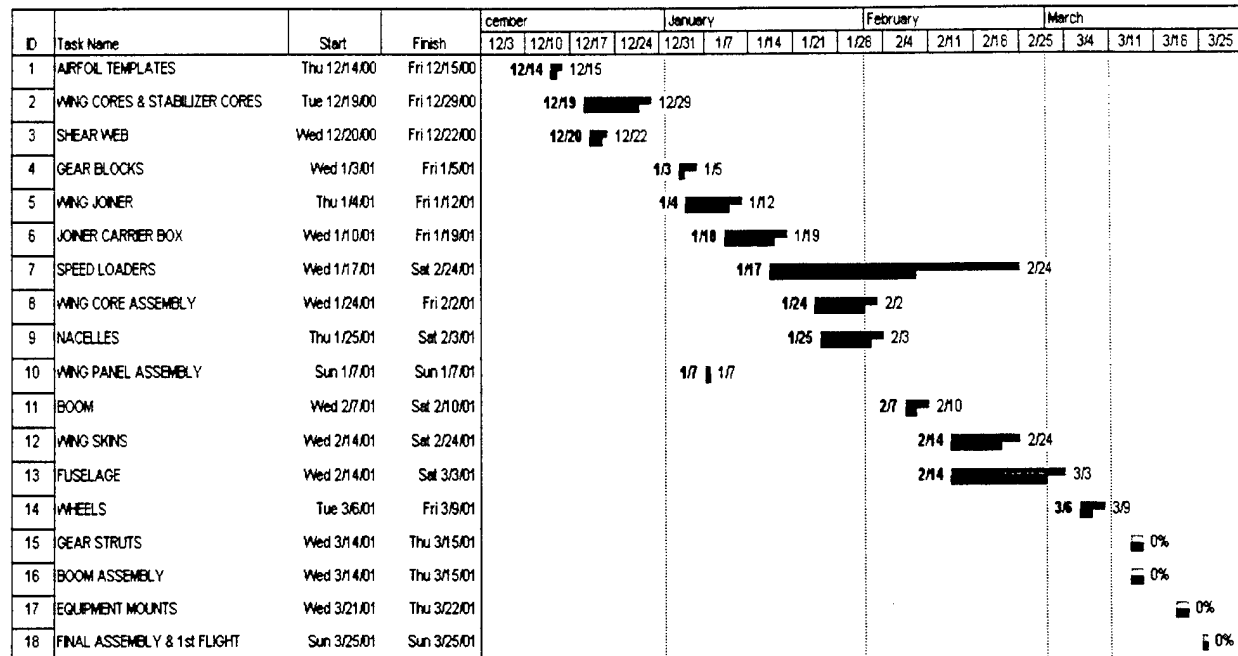
12 K carbon tow was cut in the lengths required by the lay-up schedule that was determined during the spar structure preliminary design phase. The lengths were then wet out and layered on top of the shear web within the wing core assembly. Motor nacelle hard points were installed and Mylar was layered over the wet carbon tow and the whole assembly was placed in a vacuum bag.

6.3.3 Boom Assembly

Using an epoxy and cavitex mixture, aircraft plywood was installed in the tail of the fuselage. The boom was then bonded to this structure to provide a load transfer path.

6.4 Manufacturing Timeline

Figure 6-1 Manufacturing Timeline



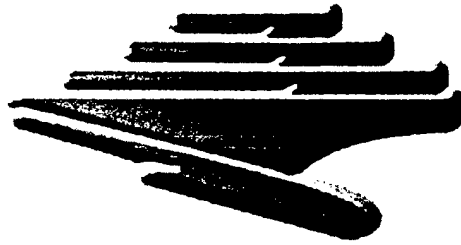
Legend: Grey dotted lines = Proposed duration of task. Proposed start and finish dates are indicated in the cells on the left.

Blue solid lines = Actual duration of task. Actual start and finish dates are indicated on both ends of line.

Percentage = Percentage of task completed.

7 Proposal Phase References

1. Raymer, D.P., Aircraft Design: A Conceptual Approach, AIAA Education Series, 1989.
2. Simons, M., Model Aircraft Aerodynamics, Argus Books, 3rd edition, 1994.
3. Lennon, A., The Basics of R/C Model Aircraft Design, Air Age Inc., 1996.
4. McCormick, B.W., Aerodynamics Aeronautics and Flight Mechanics, John Wiley and Sons, 2nd edition, 1995.
5. Nelson, R., Flight Stability and Automatic Control, McGraw Hill, 1989.
6. Stinton, D., The Design of the Airplane, Van Nostrand Reinhold, 1983.

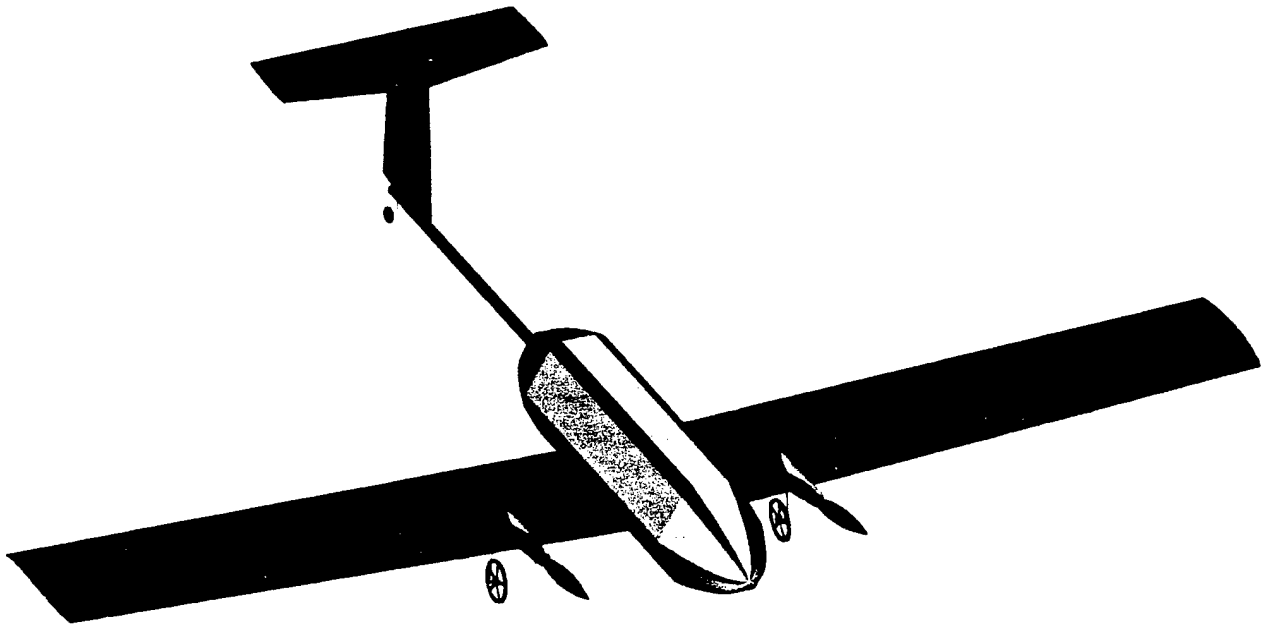


UCSD

UNIVERSITY OF CALIFORNIA, SAN DIEGO

Addendum Phase Design Report

Submitted April 10th, 2001



TLAR II

Table of Contents

1	<i>Executive Summary</i>	4
1.1.1	Objectives	4
1.1.2	Analytical Tools	4
1.1.3	Conceptual Design Phase Outline	5
1.1.4	Preliminary Design Phase Outline	5
1.1.5	Detail Design Phase Outline	5
2	<i>Management Summary</i>	7
2.1.1	Team Architecture	7
2.1.2	Task Scheduling	8
2.1.3	Milestone Chart	8
3	<i>Conceptual Phase</i>	9
3.1	Stage I – Feasibility Analysis	9
3.1.1	Airfoil	10
3.1.2	Wings	10
3.1.3	Empennage	11
3.1.4	Fuselage	12
3.1.5	Landing Gear	13
3.1.6	Propulsion and Power System	13
3.1.7	Structural System	14
3.1.8	Conceptual Design Phase – Stage I Summary	14
3.2	Stage II – Generalized Analysis	16
3.2.1	Wings	17
3.2.2	Empennage	17
3.2.3	Fuselage	18
3.2.4	Landing Gear	19
3.2.5	Propulsion and Power System	19
3.2.6	Structural System	20
3.2.7	Conceptual Design Phase – Stage II Summary	21
4	<i>Preliminary Design Phase</i>	22
4.1.1	Wings	22
4.1.2	Empennage	23
4.1.3	Fuselage	24
4.1.4	Landing Gear	26
4.1.5	Propulsion and Power System	26
4.1.6	Structural System	27
4.1.7	Preliminary Design Phase Summary	29
5	<i>Detail Design</i>	30
5.1	General Sizing	30
5.1.1	Weight Estimate	30
5.1.2	Wing Performance	30
5.1.3	Motor Thrust Available	30
5.2	Flight Performance Calculations	31
5.2.1	Takeoff Performance	31
5.2.2	Rate of Climb	31
5.2.3	Turning Radius	31
5.2.4	Range and Endurance	32
5.2.5	Static Stability	32
5.2.6	Systems Architecture	33

5.2.6	Systems Architecture	33
5.2.7	Detail Design Summary	34
5.3	Drawing Package	35
5.3.1	Three View	35
5.3.2	Structural Component Dimensions	36
5.3.3	Flight Component Dimensions	37
5.3.4	Conceptual Configurations	38
5.3.5	Detailed Configuration, Tennis Ball Packing, and Flight Equipment Location	38
6	Manufacturing Plan	39
6.1	FOM Reasoning/Discussion	39
6.2	Component Manufacturing Description	39
6.2.1	Spar Structure	39
6.2.2	Wing Joiner	40
6.2.3	Wing Joiner Carrier Box	40
6.2.4	Torsion Rod	41
6.2.5	Wing Airfoil	41
6.2.6	Wing Cores	41
6.2.7	Spar Assembly	42
6.2.8	Wing Skins	42
6.2.9	Final Wing Assembly	42
6.2.10	Stabilizers	42
6.2.11	Main Landing Gear Strut	43
6.2.12	Gear Blocks	43
6.2.13	Wheels	43
6.2.14	Tail Landing Gear	44
6.2.15	Speed Loaders	44
6.2.16	Fuselage	44
6.2.17	Boom	45
6.3	Assemblies	45
6.3.1	Wing Core Assembly	45
6.3.2	Wing panel Assembly	45
6.3.3	Boom Assembly	45
6.4	Manufacturing Timeline	45
7	Proposal Phase References	47
8	Lessons Learned	48
8.1	Introduction	48
8.2	Time Management	48
8.3	Teamwork	48
8.4	Design Process	48
8.5	Theoretical vs. Actual	48
8.6	Finance	49
8.7	Final Configuration vs. Proposal Design	49
8.7.1	Fuselage	49
8.7.2	Nosecone	49
8.7.3	Motor Nacelles	50
8.7.4	Power System Fuse Choice	50

8.7.5	Servo Installation	50
8.7.6	Speed Loader	50
8.8	Areas of Improvement	51
8.8.1	Time Management	51
8.8.2	Wing Area	51
8.8.3	Flaps	51
8.8.4	Materials and Experience	51
9	Aircraft Cost Model	52
9.1	Rated Aircraft Cost	52
9.2	Expense Summary (*Donated or last year's equipment)	52
9.2.1	Airframe Expenses	52
9.2.2	Control System Expenses	53
9.2.3	Propulsion System Expenses	53
9.2.4	Travel Expenses	53
9.2.5	Payload and Ground Support Expenses	53
9.2.6	General Expenses (Photocopies, Report Printing, Binding and Shipping)	53
9.2.7	Total Project Expense	53

List of Figures

FIGURE 2-1	MILESTONE CHART	8
FIGURE 6-1	MANUFACTURING TIMELINE	45

List of Tables

TABLE 1-1	FINAL DESIGN SPECIFICATIONS	6
TABLE 2-1	TEAM MEMBER PROFILES AND ASSIGNMENT AREAS	7
TABLE 3-1	DESIGN PARAMETER FOM ANALYSIS – STAGE I	9
TABLE 3-2	DESIGN PARAMETER FOM ANALYSIS – STAGE II	16
TABLE 5-1	GENERAL SIZING	34
TABLE 5-2	SYSTEMS ARCHITECTURE	34
TABLE 5-3	FLIGHT PERFORMANCE DATA	34

8 Lessons Learned

8.1 Introduction

Throughout the design process, many important lessons were learned and valuable experience was gained. The success of this project relied on the diverse backgrounds and skills contributed by each team member. This included experience with composite materials, structural and aerodynamic analysis, machining techniques, electronics, power systems, computer programs, team/time management, and fundraising.

8.2 Time Management

Establishing a management structure and starting the design process as early as possible allowed room to deal with unforeseen obstacles. An early start enabled the conceptual phase of the design to be completed so that the basic aircraft layout was defined. With this layout, estimations for manufacturing timelines and expenses set a baseline for planning the rest of the project. As the manufacturing process continued, preliminary and detail design could be completed with more information of the actual aircraft characteristics, resulting in the optimum design.

It was important to set a timeline with realistic goals at the start of the project and then adhere to it throughout the design process. One example was planning the Proposal Phase paper well in advance. An outline was created and sections were divided among team members to distribute the workload.

8.3 Teamwork

Creating an organized team was essential in order to allocate responsibilities among the team members. One of the major lessons learned working as a team, was that productivity can decrease with too many people assigned to one element of the project. Delegating separate individual responsibilities allowed specialization. Incorporating each team member's concepts and ideas about their specialized areas into the final design was a process that a great deal was learned from. Dealing with trade off issues between the various component configurations was important to realize the optimum design.

8.4 Design Process

While many of the senior team members had taken advanced design courses, a lesson that was learned early was that the classroom is an ideal. With a short term project, it was found that less complex designs which enabled more simple analysis and took less time to manufacture were desirable. Experience gained from the design classes, combined with practical experience gained by last year's team members provided knowledge that was shared by the newer team members to learn from and apply to their efforts for this year. By providing this knowledge openly, the full talent of every team member could be used most effectively.

8.5 Theoretical vs. Actual

A lesson that was learned last year and re-affirmed with this year's design was that the actual characteristics of TLAR II differed from the designed theoretical characteristics. With even the most careful manufacturing techniques, the components will inevitably change. For example, as the propeller diameter changes, so will the required landing gear length, as the weight increases or decreases so will

the required engine thrust. These types of trade-offs were needed throughout the construction even with the extensive factors of safety used during the proposal phase of the design. This is a very important point to realize for any design process.

8.6 Finance

Working within a set budget emulated a real-world design setting. Due to the limited budget, the team was required to rely heavily on analysis to ensure that fabrication went smoothly and to avoid errors that could potentially increase the amount of materials needed. One of the main fundraising techniques learned last year was how to create a well-written proposal package. In addition, establishing and maintaining good relationships with sponsors and keeping them up-to-date on the project was important.

8.7 Final Configuration vs. Proposal Design

The final configuration of the aircraft design essentially remained the same as the proposal design although changes to several components were required. These changes were made in order to ensure effective component interfacing, increased strength and eased payload access. Also, decreasing the RAC (via weight reduction, etc) and having a more robust structure was a goal for many of the changes to the design. The following are component-wise breakdowns of deviations from the proposal design:

8.7.1 Fuselage

The initial fuselage design was altered due to changes in the cross-sectional shape when the tail cone was attached. In order to maintain the required shape, the box structure proposed for stiffening the fuselage was extended to run the length of the fuselage. Adhering the aircraft plywood box structure to the carbon/Kevlar skin with epoxy caused the skin to bond to the box structure thus providing a means of maintaining the correct cross-sectional shape. In addition, this also formed a platform to place the payload on in order to prevent it from shifting during flight.

The total length of the fuselage needed to be increased from the proposed design due to lessons learned from manufacturing imprecision. The C.G. of the aircraft was designed to be located at the wing joiner, however this was not necessarily assured. To allow for a margin of error with the construction, it was desired to have room in the forward section of the fuselage to move the battery pack forward and aft, to adjust the C.G. the increased factor of safety and flexibility was determined to be valuable enough to offset the increased RAC.

The incorporation of a faring was necessary in order to maintain interfacing strength and aerodynamic efficiency between the wing carry through structure and fuselage. The faring was constructed from a combination of blue foam and aircraft plywood. The wood was cut to match the root airfoil and adhered to the foam, which was sanded to match the fuselage shape. This structure was then permanently bonded to the fuselage with epoxy.

8.7.2 Nosecone

The method of attaching the nosecone to the fuselage required careful consideration due to the necessity for quick payload exchanges. The initial design made use of tabs to ensure proper placement

and Velcro straps for attaching it to the fuselage. This was deemed unacceptable as the tabs would interfere with the payload exchange and would weigh too much. The final design utilized plastic hinges attached to the upper surface of both the fuselage and nosecone. This design ensured that the was always aligned with the fuselage and allowed for quick access to the cargo bay thus decreasing the time required during each pit stop.

8.7.3 Motor Nacelles

Motor nacelle design and construction was necessary due to the desire for the placement of the motors outboard of the fuselage to be aerodynamically faired and structurally sound. Initially it was believed that the motors could be inserted into a recess cut into the leading edge of the wing, but this was determined to be infeasible due to strength and structural stability issues.

The motor nacelle construction method made use of Kevlar molded over an existing RC model aircraft fuselage mold. Following the curing process, the nacelle was removed from the mold and cut to match the airfoil profile of the leading edge. Three hard points made from composite panel were bonded to the Kevlar and holes were made to attach them to the wings. A firewall, also made from composite panel, was fabricated and adhered to the opening of the nacelle providing a means to mount the motor.

8.7.4 Power System Fuse Choice

In the Detail Design Phase, it was calculated that the aircraft would cruise at a current draw of 22.6 Amps. With an additional allowance for takeoff and climb out power, a conservative draw of 30 Amps was estimated. Also, selecting a lower rated fuse was found to reduce the RAC considerably, on the order of 10% per 10 Amps. This reduction in RAC, combined with the expected current draw of the propulsion system enabled the choice for a fuse rated at 30 Amps to be made.

8.7.5 Servo Installation

Originally the servos were going to be installed by imbedding them in the foam and gluing them in place. The compressive strength of the foam was seen as a potential point of failure resulting in ineffective servo control.

Cutouts were made to accommodate the size of the servos then aircraft grade plywood surfaces were secured with epoxy to the bottom of the niche. The servos were then attached with silicon-based glue to the hard surface. Silicon glue was used because it provides sufficient strength as well allowing for easy servo replacement in case of servo failure.

The servo for the rudder also controlled the tail wheel and thus a higher torque servo was required. Since the servo was wider than the vertical stabilizer, it was necessary to place tape over the exposed part of the servos to ensure secure placement.

8.7.6 Speed Loader

The design of the speed loaders was changed slightly in order to decrease the payload exchange time as well as to decrease the weight. The initial speed loader design utilized Kevlar as both the body and the ends ("caps") of the speed loaders. The ability to access the payloads and to attach a handle

raised serious design concerns, thus design alterations were required in order to meet these issues. The final design replaced one of the "caps" with a mesh bag that could be opened with a drawstring. This provided a means to access the payload as well as to form a handle that would be necessary to extract it from the cargo bay.

The construction method chosen to fabricate the "cap" was to bond the mesh to the Kevlar body-skin via the use of epoxy and one layer of fiberglass. The fiberglass was wetted out with epoxy and "sandwiched" the mesh to the Kevlar.

8.8 Areas of Improvement

Experience from last year's project was extremely useful as it helped to improve the project in all aspects from time management to construction techniques. However, there were still several areas that could use improvement. These areas are described below.

8.8.1 Time Management

The initial designs for this year's aircraft were completed in November and manufacturing began in December – much earlier than last year. However, this design was more complex and it was still difficult to finish the manufacturing of the airplane in time to perform comprehensive testing of the components through test flights. In short, time management is a priority, and the timeline of completion dates, especially with regards to the paper, needs much improvement.

8.8.2 Wing Area

This year's design incorporated the same airfoils as last year's model, despite the difference in performance requirements. Improvements may have been possible through investigation of a larger spectrum of airfoils.

8.8.3 Flaps

The addition of flaps to the TLAR II wings could possibly benefit both take-off and landing performance by increasing the effective angle of attack and low-speed lift. However, the design of dedicated flaps is complex and increases the number of required servos thus increasing the RAC.

8.8.4 Materials and Experience

It is always better to overestimate than underestimate when it comes to materials and time. For example, the Kevlar was delivered late and even then, there was not enough. Also, it would be useful if more people had machine shop experience, especially of the more complex machinery such as a CNC machine, and had more comprehensive knowledge of analysis tools such as FEA and CAD programs like CosmosWorks, Pro-Mechanica, Pro/Engineer and SolidWorks.

9 Aircraft Cost Model

9.1 Rated Aircraft Cost

RAC (Rated Aircraft Cost, in thousands of dollars) = **A*MEW+B*REP+C*MFHR**

A = \$100/lb.

MEW = Manufacturer's Empty Weight (lbs.)

B = \$1/Watt

REP = Rated Engine Power (Watts)

C = \$20/hour

MFHR = Manufacturing Man Hours (hours)

MEW = 13.1 lbs.

REP = Number of motors * 30 Amps * 1.2 Volts/cell * Number of cells

= 2 * 30 Amps * 1.2 Volts/cell * 19 cells

= 1368 Watts

WBS Number and Name	Scoring Values	Design Description
#1-Wings	15 hr/wing + 4 hr/sq. ft Projected Area (PA) + 2 hr/strut + 3 hr/control surface	1 Wing PA = 11.67 ft ² 0 struts 2 ailerons
#2-Fuselage and/or Pods	5 hr/body + 4 hr/ft of length extending from LE of wing	1 Fuselage (44") 2 Nacelles (4" x 2) 4.33 ft = \sum of Lengths
#3-Empennage	5 hr (basic) + 5 hr/Vertical Surface + 10 hr/Horizontal Surface	1 Vertical Surface 1 Horizontal Surface
#4-Flight Systems	5 hr (basic) + 2 hr/Servo or Controllers	4 Servos 2 Speed Controllers
#5-Propulsion Systems	5 hr/Motor + 5 hr/propeller	2 motors 2 propellers

MFHR = \sum **WBS** = Wing + Fuselage + Empennage + Flight Systems + Propulsion Systems

= (15*1 + 4*11.67 + 2*0 + 3*2) + (5*3+4*4.33) + (5+5*1+10*1) + (5+2*6) + (5*2+5*2)

= 67.68 + 32.32 + 20 + 17 + 20 = 154.00 hours

A * MEW = (\$100/lb.) * (13.1 lb.) = \$ 1310.00

B * REP = (\$1/Watt) * (1368 Watts) = \$ 1368.00

C * MFHR = (\$20/hour) * (157.00 hours) = \$ 3140.00

RAC = (A*MEW+B*REP+C*MFHR) / 1000 = (\$1310.00 + \$1368.00 + \$3140.00) / 1000

FINAL RAC = \$5.818

9.2 Expense Summary (*Donated or last year's equipment)

9.2.1 Airframe Expenses

Item	Cost
Plywood	\$ 98.34
Hardware (adhesives, tools, paint, etc)	\$ 121.53
Component Materials (Piano wire, foam, tubing, etc)	\$ 111.00
Composite Materials (Kevlar, Carbon and Glass)	\$ 517.34
TOTAL COST	\$ 848.21

9.2.2 Control System Expenses

Item	Cost
Transmitter (Hitec RCD Prism 7X PCM)	\$ 334.01
*Receivers (3 Hitec RCD HPD-07RB PCM)	\$ 355.54
*Aileron Servos (4 Hitec RCD HS-225 MG)	\$ 150.81
*Rudder Servos (2 Hitec RCD HS-545 BB)	\$ 64.63
*Elevator Servos (2 Hitec RCD HS-545 BB)	\$ 64.63
TOTAL COST	\$ 945.60

9.2.3 Propulsion System Expenses

Item	Cost
Motors (4 Graupner Ultra 3300/7)	\$ 975.14
*Speed Controls (3 120-A DMA controllers)	\$151.00
Propellers (4 DMA folding carbon 15"x7")	\$ 86.20
*Fuses (6 30-A Car audio Fuses)	\$ 29.09
Spinners (3 DMA carbon fiber)	\$ 32.33
Battery Packs (4 19-cell Sanyo 2400 mAh)	\$ 430.00
TOTAL COST	\$ 1703.76

9.2.4 Travel Expenses

Item	Cost
Airfare (12 People)	\$ 2907.00
Hotel (4 rooms for 4 nights)	\$ 1206.80
Car Rental (2 Mini-Vans for 5 days)	\$ 518.62
Gasoline (estimated value)	\$ 150.00
TOTAL COST	\$ 4782.42

9.2.5 Payload and Ground Support Expenses

Item	Cost
*Deep Cycle Battery	\$ 62.54
*Battery Charger	\$ 800.00
*Tennis Balls (100)	\$ 90.61
Steel Bars (3)	\$ 15.42
TOTAL COST	\$ 971.57

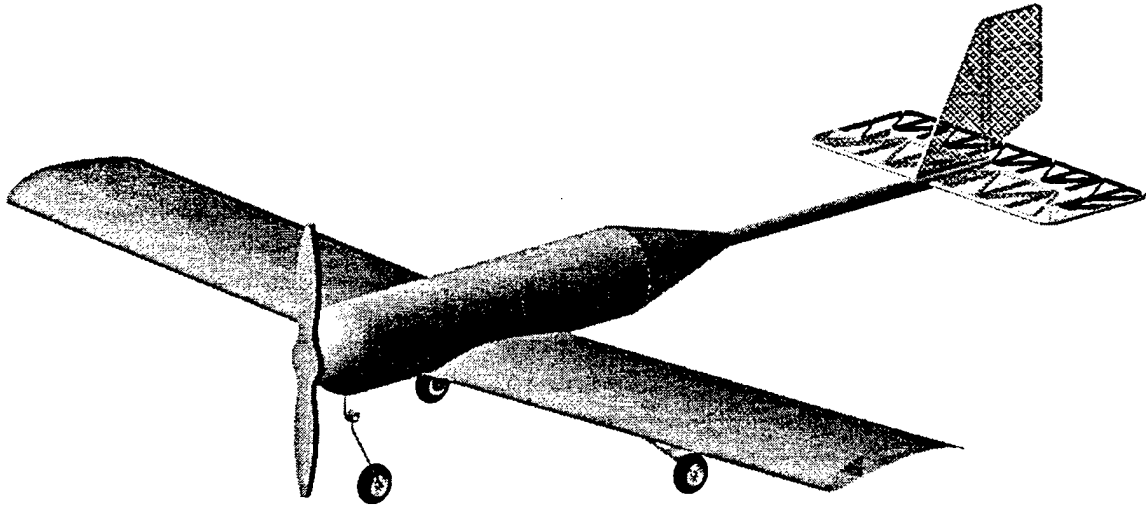
9.2.6 General Expenses (Photocopies, Report Printing, Binding and Shipping)

Item	Cost
Proposal Phase Report	\$ 219.15
Addendum Phase Report (estimated value)	\$ 150.00
PhotoCopies	\$ 12.62
TOTAL COST	\$ 381.77

9.2.7 Total Project Expense

Item	Cost
Airframe	\$ 848.21
Control System	\$ 945.60
Propulsion	\$ 1703.76
Travel	\$ 4782.42
Payload and Ground Support Expenses	\$ 971.57
General Expenses	\$ 381.77
GRAND TOTAL	\$ 9633.33

No Excuse



2000 – 2001

*AIAA Cessna/ONR Student Design/Build/Fly
Competition
Design Report*

Wichita State University

March 2001

Table Of Contents

1.	Executive Summary.....	3
2.	Management Summary	6
3.	Conceptual design.....	9
3.1.	Design Parameters.....	9
3.2.	Figures of Merit – Conceptual design phase.....	12
3.3.	Design Parameter results – Conceptual stage.....	14
3.4.	Discussion of rated aircraft cost	14
3.5.	Initial Sizing – Conceptual Stage.....	14
4.	Preliminary Design	17
4.1.	Propulsion.....	17
4.2.	Aerodynamics.....	18
4.3.	Structures	27
5.	Detail Design	29
5.1.	Performance Measures	29
5.2.	Handling Qualities:	31
5.3.	Component Selection and System Architecture.....	32
5.4.	Cost and Manufacturing Consideration	32
5.5.	Innovative Design Approaches.....	34
6.	Manufacturing Plan.....	35
6.1.	Wing Construction	35
6.2.	Fuselage.....	36
6.3.	Speed Loaders	36
6.4.	Tail.....	36
6.5.	Landing Gear.....	37
6.6.	Figures of Merit for Manufacturing Processes.....	37
	Detailed Drawing Package	41

1. Executive Summary

A design team was put together to produce an entry for the AIAA/Cessna/ONR Student Design/Build/Fly competition. The requirements of the competition were to build a radio-controlled airplane that could perform two different prescribed missions at the contest site, Webster Field, St Inigos, Maryland on the weekend of April 20th to 22nd 2001. The first mission profile was to fly with at least 5 lb of steel plate for one lap of the course. The second profile was to fly two laps with between 10 and 100 tennis balls.

The design team was divided into different functional groups that worked closely together to produce the aircraft design. The functional groups were Aerodynamics, Propulsion Systems, Stability and Control, and Structures.

The aerodynamics group developed a Matlab program to analyze the lift and drag of the aircraft. This program was used to find the optimum wing size. The aerodynamics group also investigated possible airfoils for the wing. This investigation resulted in a number of candidates that were put into the program. The aerodynamics group also completed much of the performance analysis within the same computer program.

The propulsion systems group analyzed the motor, propeller, and controllers for use on the airplane. This was accomplished using separate programs for the analysis of the motor and propeller, and comparing the results of the combinations.

The stability and control group found the size of the horizontal tail, vertical tail, and control surfaces required to produce a flyable airplane. This group also helped to define the longitudinal position of the components in order to give desired stability characteristics. The stability group developed Matlab programs to assist in the iterations required to place the components and size the tail.

The structures group considered materials for construction and structural component sizing to satisfy the loading on the airplane. The structure was designed to have the lowest possible weight within the manufacturing capabilities of the group. The material choice was made dependent on the application and loading of the individual components. Programs were developed to analyze the major components of the aircraft separately and to meet the individual requirements for that component.

Initial design concepts were rated according to criteria referred to as figures of merit. These figures of merit drew from prior knowledge of the team members and some simple analysis to narrow the initial choices from 48 configurations to that of 25. The initial concepts included four fuselage designs, from a box to a lifting airfoil, four landing gear designs, and three tail designs. Many materials were considered for each design with the best material varying with the chosen design.

The conceptual design stage led to the rough initial configuration. Analyzing the figures of merit, as well as flight scoring possibilities, it was determined that a maximum allowable wingspan would prove to be the best choice. The propulsion system was also formed into shape with the determination that a single motor and propeller combination would provide the required thrust and lend to the minimum cost of the aircraft. Size and weight estimations were performed on the various fuselage configurations, thus helping to eliminate oversized and heavy configurations.

During the preliminary design stage, the airplane emerged in a more definite shape. The major components were sized to accommodate a maximum score while staying within propulsion, weight, and other restrictions. With the major components sized, static stability could then be determined to give way to the horizontal and vertical tail size. The various configurations were iterated and cross-referenced with each other to determine a final design configuration that would perform with desired characteristics.

The final design stages looked more deeply into the characteristics of the aircraft. After close consideration of all details, a final configuration resulted. The aircraft would have a single, low, two-piece wing, utilizing the Selig 1223 airfoil. The wing would span 10 feet, and have an area of 13.5 square feet. The fuselage would have a round, torpedo shape, with two separate speed loaders. The tail would be a conventional configuration, mounted on a straight, round tube behind the fuselage. The aircraft would be able to accommodate one hundred tennis balls, and provide enough lift to carry twenty five pounds of steel.

Detail Design Configuration

Configuration:	Low Wing
Fuselage type:	Torpedo Shaped
Airfoil:	Selig 1223
Wing Span:	10 ft.
Wing Area:	13.5 ft ²
Wing Loading (max):	3.33 lb/ft ²
Empty Weight:	20 lbs.
Total Length:	8 ft.
Max. GTOW:	45 lbs.
Motor:	Astroflight Cobalt 90
Propeller:	19x11
Payload:	100 Tennis Balls/25 lbs. Steel

2. Management Summary

The design team for the AIAA/Cessna/ONR Student Design/Build/Fly competition consisted of eleven members. Six seniors made up the primary design group, with involvement of one other senior, and four underclassmen. All team members are aerospace engineering majors.

The team was divided into four functional groups to complete the design process. The four groups were Aerodynamics, Propulsion Systems, Stability and Control, and Structures. The team members worked within these groups to develop the design with two weekly discussions about the overall design. Due to the small size of the design team there was a large amount of cross-functional work undertaken by the team members. The work share is shown in the following figure, 2.1.

The team worked to a schedule set early in the design process. Due to complications, construction of the model began over a month later than scheduled. The timeline can be seen in the following figure, 2.2.

The team had one team member that took on the responsibility of drawing the entire detail design in a CAD drafting package. The information from the rest of the group was put into the detailed drawing to check for interferences and other possible design problems. This proved to be very useful in determining optimal cargo layout and placement.

	Brian Brown	Ian Goodman	Hung Lam	Jason Nickel	Wei-min Ooi	Soon Cheong Tan	Additional Team Members
Conceptual design							
Design Parameters	5	5	5	5	5	5	5
Initial Aerodynamics Analysis	0	0	0	0	4	5	2
Initial Structural Analysis	2	5	0	2	0	0	2
Initial Stability and Control Analysis	0	3	4	0	4	3	2
Initial Propulsion Analysis	5	0	2	5	0	0	3
Initial Performance Analysis	0	2	0	0	2	5	2
Figures of Merit	5	5	5	5	5	5	5
Preliminary design							
Preliminary Aerodynamics Analysis	0	0	0	0	3	5	1
Preliminary Structural Analysis	4	5	0	4	0	0	0
Preliminary Stability and Control Analysis	0	3	5	0	5	3	2
Preliminary Propulsion Analysis	5	0	0	5	0	0	2
Preliminary Performance Analysis	0	0	2	0	3	5	0
Detailed design							
Detailed Aerodynamics Analysis	0	0	0	0	2	5	1
Detailed Structural Analysis	4	5	0	4	0	0	1
Detailed Stability and Control Analysis	0	4	5	0	5	2	0
Detailed Propulsion Analysis	5	0	0	5	0	0	0
Detailed Performance Analysis	0	0	3	0	4	5	1
Drafting Package	5	1	1	1	1	1	0
Manufacturing Plan							
Wing Manufacturing Plan	5	3	0	5	0	2	2
Tail Manufacturing Plan	5	3	2	5	2	0	2
Fuselage Manufacturing Plan	5	3	0	5	0	0	1
Landing Gear Manufacturing Plan	5	3	0	0	0	0	1
Propulsion System Manufacturing Plan	5	0	0	5	0	0	1

Figure 2.1. Share of the group's on the "No Excuse" design project. A value of 5 indicates maximum involvement with a value of 0 indicating little.

Event	Planned Start	Planned Finish	Actual Start	Actual Finish
Overall Planning				
Conceptual Design Phase	10/9/00	11/1/00	10/9/00	12/1/00
Preliminary Design Phase	11/2/00	1/10/01	12/2/00	2/12/01
Final Design Phase	1/11/01	1/25/01	2/13/01	3/1/01
Construction	1/26/01	3/5/01	3/2/01	
Report Preparation	1/26/01	3/1/01	2/27/01	3/11/01
Aerodynamics Group				
Wing Design	10/9/00	12/1/00	10/9/00	1/10/01
Tail Design	11/9/00	1/11/01	11/9/00	2/12/01
Fuselage Design	10/9/00	12/1/00	10/9/00	2/12/01
Structures Group				
Fuselage Design	11/9/00	1/10/01	11/9/00	2/20/01
Wing Design	11/9/00	1/10/01	11/9/00	1/10/01
Tail Structure Design	12/9/00	1/20/01	12/9/00	2/20/01
Landing Gear Design	1/10/01	2/10/01	1/10/01	2/20/01
Propulsion Systems Group				
Motor Selection	10/9/00	12/9/00	10/9/00	1/10/01
Propellor Selection	10/9/00	12/9/00	10/9/00	1/10/01
Design Drawings	12/10/00	2/10/01	11/20/00	3/2/01

Figure 2.2. Milestone Chart of the project showing the major events in the design of the airplane

3. Conceptual design

During the conceptual design phase over forty variables and configurations were considered. Figures of merit were used to help narrow the number of items to be further investigated. The parameters and figures of merit investigated are outlined in the following section.

3.1. Design Parameters

3.1.1. Wing Planform

The decision for the planform of the wing was made between three options. The first choice was an elliptical planform. This design offered superior aerodynamic characteristics but inferior manufacturing characteristics. The second design was a tapered wing. The tapered wing offers good aerodynamic characteristics but also has manufacturing qualities that were undesirable. The third choice was a rectangular wing planform. The rectangular wing offered manufacturing characteristics that were vastly superior because of the constant cross section. The disadvantage of the rectangular wing planform is that it is less efficient aerodynamically.

3.1.2. Wing configuration

The placement and number of wings were both considered at an early stage. Configurations with bi-wings and mono-wings were contemplated. Each wing was also considered with winglets. The placement of the mono-wing was considered in a low, mid, or high position on the fuselage. For construction and scoring purposes, the bi-wing was dropped from consideration, as was the addition of winglets. The best placement of the mono-wing was considered to be a low wing design. The low wing allowed the structural weight of the fuselage to be decreased by not requiring the load of the landing to be transferred to a high wing. The low wing design also facilitated the use of speed loaders that would fit in the top of the fuselage and act as the upper fuselage surface.

3.1.3. Wing Structure

The structural arrangement, weight and material usage were important parameters in the wing design. The structural arrangements considered utilized two spars. The reason for the two-spar arrangement was so the main spar could carry most of the aerodynamic loads of the wing while the rear spar could be used to carry the loads developed by the aileron. The use of ribs between the spars also allowed for an increase in the moment of inertia about the vertical axis. The skin of

the wing was contemplated to be either a solid component, to help carry the bending and shear loading of the wing, or to be a thin fabric-like covering, to reduce weight. The spars were considered in varying cross-sectional arrangement. The cross-sections considered were an I-beam, a C-section beam, a hollow circular tube, and a solid rectangular beam. For strength and weight considerations the solid rectangular beam was ruled out at this stage. The material usage in the wing would depend greatly on the configuration decided upon. For a solid skin the whole wing would be constructed from composite fibers, but for a thin fabric skin design the wing could be fully constructed of wood. For the purposes of increased strength to weight the fully wooden designs were ruled out in favor of using a composite or metal spar arrangement.

3.1.4. Tail configuration

The purpose of the tail is to provide stability and control in pitch and yaw. Three concepts were considered during the initial design, a conventional, T, and V tail. The V configuration would reduce the overall tail surface area but due to the surfaces providing both pitch and yaw control, the operation of the configuration is more complex than with more conventional designs. The T-tail and conventional designs separate the pitch and yaw control. This separation makes the design easier to both analyze and operate. The T-tail configuration has a disadvantage over the conventional tail in that the vertical surface has to transfer the loading of the horizontal surface to the tail boom increasing the weight of the structure. Therefore the best configuration for the tail was concluded to be the conventional tail attached directly to the tail boom.

3.1.5. Tail boom

By using a tail boom, the moment arm for the empennage could be increased without lengthening the fuselage. This adaptability allows for a larger flight envelope. Two configurations were considered for the tail boom. One configuration used a box beam comprising a composite skin around a honeycomb core. The other configuration was based around a hollow circular beam. The circular beam offers superior aerodynamic and torsion characteristics and for these reasons was considered for further investigation. Three variations in the longitudinal shape of the tail boom were also considered. Two shapes, a z-shape and a straight beam at an angle, were considered to increase the ground clearance and hence the rotation angle. The third solution was to use a boom coming straight from the rear of the airplane.

3.1.6. Fuselage

The fuselage had to be designed with the dual loading of tennis balls and steel weights in mind. The requirement for carrying a large number of tennis balls required a large internal volume. Four fuselage configurations were considered. The first configuration was a rectangular box shape. This configuration gave good usable internal volume but had poor drag characteristics. The second design used a vertically oriented airfoil. This had very good drag qualities, but the internal volume and loading were considered to be bad design qualities. The third configuration used an airfoil shape to help in lifting the weight of the airplane. This design paid a drag penalty but this was considered to be less than the lift generated. The fourth design used a cylindrical fuselage with aerodynamic fairings both at the nose and at the tail. At this stage both the lifting fuselage and cylindrical fuselage were considered for further investigation.

3.1.7. Material selection for the fuselage

The material used in construction of the fuselage was slightly dependent of the fuselage design but all had the requirement of transferring all loads with the minimum possible weight. The materials investigated were wood, aluminum, carbon fiber, glass fiber and plastic. The woods considered were balsa and spruce. Both woods are easy to machine and provide good qualities in tension, although lacking the high strength to weight ratio of the composites but is considered for lower stress uses. The aluminum provides good strength but also has a high density. The weight of any aluminum part plus the difficulty in forming complex shapes ruled out aluminum from further consideration. Carbon and glass fiber provide very good strength to weight properties. Both composite materials were considered for high strength parts. Thermoplastic was considered for use as a fairing where the material would not undergo heating and where high strength was not a requirement but maintaining the rigid shape was desired.

3.1.8. Landing gear

The landing gear had to be designed in such a way as the aircraft could withstand several strong landings while being light in weight and generating low drag. The aircraft would also have to exhibit good ground handling characteristics. Two materials were considered for use in the landing gear. Aluminum exhibits favorable strength characteristics that are desired in the landing gear. Composite materials also provide good strength characteristics for lighter weight. The manufacturing of either material into the landing gear would prove equally difficult. Several designs were considered for the landing gear configuration. A tail dragger configuration was

considered due to its light weight and low drag. This was rejected due to unfavorable ground handling characteristics though. A bicycle landing gear was investigated for the good drag characteristics but again, like the tail dragger, was rejected due to problematic ground handling characteristics as well as manufacturing complications. Finally, a tricycle gear was contemplated due to the good strength to weight attributes. The tricycle gear does have unfavorable drag characteristics but has good ground handling qualities. The tricycle gear was considered the best solution and was the only design investigated further in depth.

3.1.9. Propulsion system

The requirements of the propulsion system were to provide the maximum thrust while using the minimum battery power in order to give the longest flight duration. The propulsion system also had to be capable of providing a peak thrust that would allow the aircraft to take off within 200 ft. The flight duration must at a minimum be one flight sortie and at maximum should be ten minutes. The three components of the propulsion system that were considered at this stage were the propeller, motor and the batteries. The exact number of cells was determined during the preliminary design stage. The restrictions on the motor type imposed by the competition rules limited the choices, however the exact size and composition of the motor and gear ratios would be decided during the next design phase. The propeller size and pitch angle would depend heavily on the overall weight of the airplane and the power available from the motor, thus would also be left for a later design stage.

3.2. Figures of Merit – Conceptual design phase.

Figures of merit were chosen in a manner that would help the team eliminate some of the design variables from further investigation. Particularly high on the list of difficulty was the manufacturability of the airplane, therefore this parameter received a weighting factor of 1.5. Other important factors were cost and strength to weight ratio each given a weighting factor of 1.5. The remaining factors considered were power consumption, handling characteristics and cargo holding ability.

3.2.1. FOM - Manufacturability

This figure of merit took into account the manufacturability of the aircraft. The ability to form the material into the desired shape, the difficulty machining of the material, the complexity of the shape and most importantly, the time required were all rated with varied scores depending on team member's experience and expertise.

3.2.2. FOM - Strength to weight ratio

In order to carry the maximum payload the weight of the airplane structure needs to be reduced. The material to do this must exhibit a high strength to weight ratio. The major structural consideration is the tip-loading test to be performed at the competition. Therefore more than any other component, the wing must exhibit the high strength qualities.

3.2.3. FOM - Power Consumption

The weight of the airplane and the drag induced by the components of the airplane are the major factors in this figure of merit. Without adequate consideration to drag reduction, a plane that generates more drag than thrust can quickly be designed. Additional points were given to any parts that would create more drag than another.

3.2.4. FOM - Handling Characteristics

The ground controllability and air handling characteristics were considered under this figure of merit. Points were put on characteristics that took away from the plane's stability and ease of maneuverability.

3.2.5. FOM - Cost

The cost of the design included both the physical cost of the materials and the cost in man hours to construct parts. This was an important figure of merit due to the finite amount of finances available. Construction time was also considered a cost, and thus was also scored heavily.

3.2.6. FOM - Cargo Holding Ability

The cargo holding ability figure of merit was used to factor the fuselage and wing changes that would impact the cargo volume and ease of using a speed loader. Whenever a design was considered that would reduce the amount of cargo that could be carried, without increasing the fuselage size, then points were placed against the concept.

3.3. Design Parameter results – Conceptual stage

The results of the figure of merit analysis can be seen in Figure 3.1. Each parameter was rated with a score depending on whether there was a relative advantage to using that parameter. A score of -1 denoted a disadvantage, 0 denoted a neutral outcome and 1 denoted an advantage. The sums of the factors are added up in the score column. The decision column is used to denote the parameters that will have further analysis (FA) or eliminated (E) from consideration.

3.4. Discussion of rated aircraft cost

The overall size of the airplane for a given weight range will be fairly similar due to the aerodynamic qualities of the wing and the manufacturers empty weight which is a direct relation to the size. Materials such as carbon fiber can be used to reduce the weight of certain components. Our team has attempted to use materials that are best suited to the task while reducing weight. The one factor that can be varied to have the most effect on the rated airplane cost is the motor and batteries. By running with one larger motor instead of two the motor cost is approximately halved. If the amp rating of the motor can also be reduced while still providing the required thrust, the cost is reduced greatly.

3.5. Initial Sizing – Conceptual Stage

Once the results from the figures of merits were known, the initial sizing was undertaken. Each functional group developed computer programs to help in the analysis of the design.

The aerodynamics group calculated the wing size based on the take off distance requirement and a maximum take off weight of 45lb. The wing size was found to be 14 ft². The wing used the maximum span allowed by the competition rules producing a chord of about 1.5 ft. The drag produced by the wing was found to be 4 lbs.

The aerodynamics group also investigated the shape of the fuselage and considered the drag produced. Two fuselage designs were investigated. The first was the lifting airfoil design. This fuselage design produced some lift to aid the wing in lifting the airplane. During analysis it was found that the drag induced by the fuselage was more than the thrust produced by the motor and propeller. This design was quickly abandoned. The second design was a cylindrical fuselage with a hemispherical nose and conical tail. This design had a much lower total drag than the airfoil design. The cylindrical fuselage also had the bonus of having no change in characteristics during rolling maneuvers.

Design Parameters - Conceptual Phase			Figures of Merit - Conceptual Stage							
			Manufacturability	Power consumption	Strength to weight	Handling characteristics	Cost	Cargo Holding	score	decision
			1.5	1	1.5	1	1.5	1		
Wing Planform	elliptical		-1	1			-1		-2	E
	tapered		0	1			0		1	E
	rectangular		1	0			1		3	FA
Wing configuration	w/ winglets	bi-wing	-1	1		0	-1	-1	-3	E
		high mono-wing	0	1		0	0	0	1	E
		mid mono-wing	0	1		0	0	-1	0	E
		low mono-wing	0	1		0	0	1	2	E
	w/o winglets	bi-wing	-1	0		0	-1	-1	-4	E
		high mono-wing	1	1		0	1	0	4	FA
		mid mono-wing	1	1		0	1	-1	3	E
		low mono-wing	1	1		0	1	1	5	FA
Wing structure	Skin	solid	0	0	0		-1		-1.5	FA
		fabric	0	0	-1		0		-1.5	FA
	Spar	I-beam	-1		1		1		1.5	FA
		C-section	-1		1		1		1.5	FA
		Circular	0		1		0		1.5	FA
		Solid	1		-1		-1		-1.5	E
	Material	Composite	1		1		-1		1.5	FA
		Wood	1		0		0		1.5	FA
		Foam and composite	1		1		-1		1.5	FA
		Wood and composite	1		1		-1		1.5	FA
Tail Configuration	T-Tail		0		-1	1			-0.5	E
	V-tail		-1		0	0			-1.5	E
	Conventional		1		0	1			2.5	FA
Tail Boom	Box beam		1		0				1.5	E
	Hollow circular beam		1		1				3	FA
	Z-shape		-1	-1	0		-1		-4	E
	Angled		0	-1	1		0		0.5	E
	Straight		0	0	1		0		1.5	FA
Fuselage	Rectangular Box		1	-1	0	-1		1	0.5	E
	Vertical Airfoil		-1	1	0	0		0	-0.5	E
	Airfoil lifting body		-1	-1	0	0		0	-2.5	E
	Cylindrical		-1	1	1	0		1	2	FA
Fuslage Material	Wood		1		0		1		3	FA
	Composite		1		1		0		3	FA
	Aluminum		1		0		0		1.5	E
	Plastic		1		0		1		3	FA
Landing Gear	Configuration	Tail-dragger	1	0	0	-1	0	0	0.5	E
		Tricycle	0	-1	1	1	0	1	2.5	FA
		Bicycle	0	0	0	0	0	1	1	E
		Retractable	-1	1	-1	0	-1	-1	-4.5	E
	Material	Aluminum	0		0		1		1.5	FA
		Composite	0		1		0		1.5	FA
Propusion System	Motor	1	0	0		0	0		0	FA
		2	0	-1		0	-1		-2.5	E
	Propeller	1	0			0	0		0	FA
		2	0			0	-1		-1.5	E
	Cells		N/A	N/A	N/A	N/A	N/A	N/A	N/A	FA

Figure 3.1 Figures of Merit – Conceptual stage. Each parameter was given a score for the relevant figure of merit ranging from -1 to 1.

As part of the aerodynamics group's analysis, the performance of the airplane was calculated. The design was found to fly at approximately 50 ft s^{-1} and would complete up to 4 sorties within the given flight period.

The propulsion group worked to find a motor and propeller combination that would, at the minimum, produce thrust equal to the drag at the desired flight speed and complete one sortie. A number of propeller and motor combinations were found that could provide the required output. The major impact on other groups was the size of the propeller. Landing gear, fuselage structure, and other various aspects were affected by the different choices. At this stage of the design the propeller was found to have a diameter of 24 inches and a pitch of 16 degrees.

The structures group developed the wing structure with the tip loading requirement being the major constraint. The forces developed in the tip loading test were in excess of the lifting loads possible by the wing. Two wing designs were developed with different structural materials while different manufacturing techniques were investigated. One design used two wooden spars with composite spar caps. The remainder of the wing shape was constructed of foam covered with monocote. The second design used a fully composite construction with both the skin and spars being constructed as one part. With the use of weight saving techniques, the two designs weighed nearly the same.

The fuselage was analyzed as being constructed of composite material. The design would use stiffeners in the keel and on either side of the fuselage to provide longitudinal stiffness. It would also utilize bulkheads for torsional and lateral stiffness.

The main landing gear would be constructed of a flat plate of aluminum bent into the desired shape. The nose landing gear would be built with a swept nose wheel in an attempt to use passive nose wheel steering.

4. Preliminary Design

4.1. Propulsion

The propulsion system, consisting of the motor, propeller, and batteries, make up an integral part of the aircraft. It is up to the propulsion system to provide adequate power to allow the aircraft to liftoff within given constraints, while maintaining battery life for the duration of the various flights. Several different choices were considered as described.

4.1.1. Battery Selection

The first thing that was looked at was the battery selection. The battery selection process looked at two main concerns. First, the weight of the batteries was considered. A maximum of five pounds of batteries were allowed given in the rules for the competition. Taking the voltage and amperage draw requirements of the motor, the amount and size of the batteries could be determined to fit within the five-pound limit. Using standard Ni-Cad batteries, a chart was constructed to display the maximum amount of batteries versus energy that was attainable given the constraints set aside. This allowed the number of batteries to be determined early on so that the motor and propeller could be chosen around them.

4.1.2. Motor Selection

The motor, either Graupner or Astroflight, was an important part of the propulsion system. Various sizes of motors were considered, as well as the number of motors. It was determined early in the design phase that a single motor could provide adequate thrust to perform accordingly. Motor information was collected from suppliers, as well as numerous hand calculations performed to determine the optimum motor for success. Motor and propeller sizing and thrust availability was related back and forth to the aerodynamics group to help optimize the combination.

4.1.3. Propeller Selection

Due to the size of the propeller not being a factor in the cost equation, a range of propeller sizes were researched. The range of propellers studied varied from two to four blades with diameters of 10 to 28 inches and blade angles of 6 to 16 degrees. A computer analysis program was written to find the propeller performance and efficiency at a given rotation speed. The propeller was then mated to a motor that could provide the desired rotation speed with maximum

efficiency. The best propeller and motor combination was then selected. The optimum propeller was found to have a diameter of 19 inches and a blade angle of 10 degrees. Below is a power available Vs. power required curve generated by the propeller analysis program. This graph shows where the aircraft can fly as a function of aircraft weight.

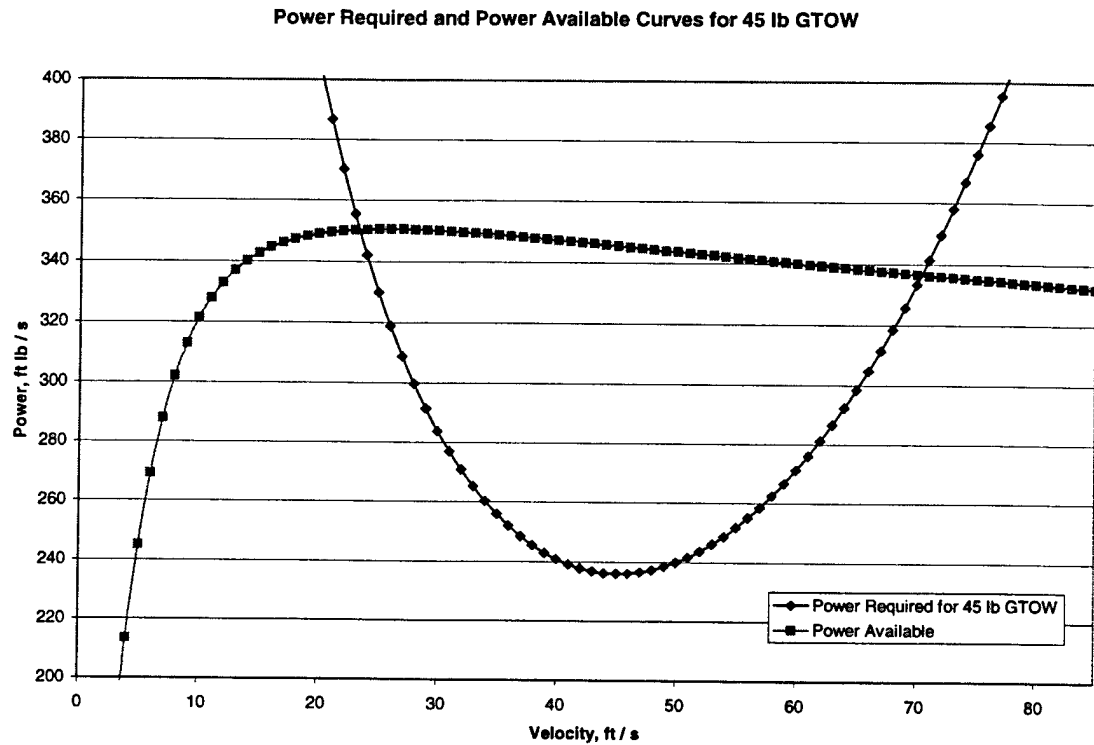


Figure 4.1. Graph of the power required and power available for a GTOW of 45 lb with the desired motor and propeller combination

4.2. Aerodynamics

4.2.1. Airfoil Selection and Wing Sizing

A design tool was developed in Matlab for the wing sizing of the DBF aircraft. The tool development process included formulation of the necessary equations by hand followed by the development of the program using those equations. The program calculated the wing area required to meet the 200-ft takeoff distance constraint for a selected airfoil, and the power required to fly the aircraft.

The wing size should not be too large, otherwise there would be unnecessary costs in the manufacturing process. However, if the wing were too small, there would not be enough lift generated to fly the aircraft. In addition, the wing area is a very important factor in meeting the 200-ft takeoff requirement. The airfoil selection is also sensitive. If an airfoil selected does not have a high C_L , the aircraft would be unable to takeoff within the 200-ft constraint unless it had a large wing area.

The airfoils selected have a max coefficient of lift of about 1.7 to 2.0. Selection of a high lift airfoil was to aid in reducing the required wing area, which in turn would reduce costs. The equations used to determine the takeoff distance required for a given wing area were as follows:

$$q = \frac{1}{2} \rho V^2$$

$$a = \frac{T - D - \mu(W_{total} - L)}{m}$$

$$L = q(S_{wing} C_{l_{max_{wing}}} + S_{fuse} C_{l_{max_{fuse}}})$$

$$D = q(S_{wing} C_{d_{max_{wing}}} + S_{fuse} C_{d_{max_{fuse}}})$$

$$TOD = TOD + V * t + \frac{1}{2} a * t^2$$

$$V = V + a * t$$

The program was then written to iterate for wing areas ranging from 1 to 50 ft², aircraft weight from 1 to 55 lbs (maximum gross takeoff weight (GTOW) per regulations), and a time period ranging from 1 to 20 seconds in steps of 0.1 seconds.

Some of the constants in the above equations may be varied to view the effects or trends. Aspects such as different wing coefficients, total takeoff weight, and thrust available were iterated to display trends. From this, more accurate information about the effects of varying particular aspects of the plane could be derived. All these possibilities were analyzed and shall be discussed later.

Safety factors were taken into account for the various aspects of the airfoil selection. Safety factors were necessary to accommodate for manufacturing tolerances and additional buffer for error correction. The takeoff distance was constrained to 180 ft (10% reduction), the maximum C_L 's of the airfoils were reduced by 15-20%, and rotation was set at 70% takeoff speed.

Figure 4.2 shows the wing area and maximum takeoff weight possible to meet the takeoff constraint of 200 ft with the Selig 1223 airfoil and a thrust of 10 lbs. The unshaded area is the “no-fly” zone.

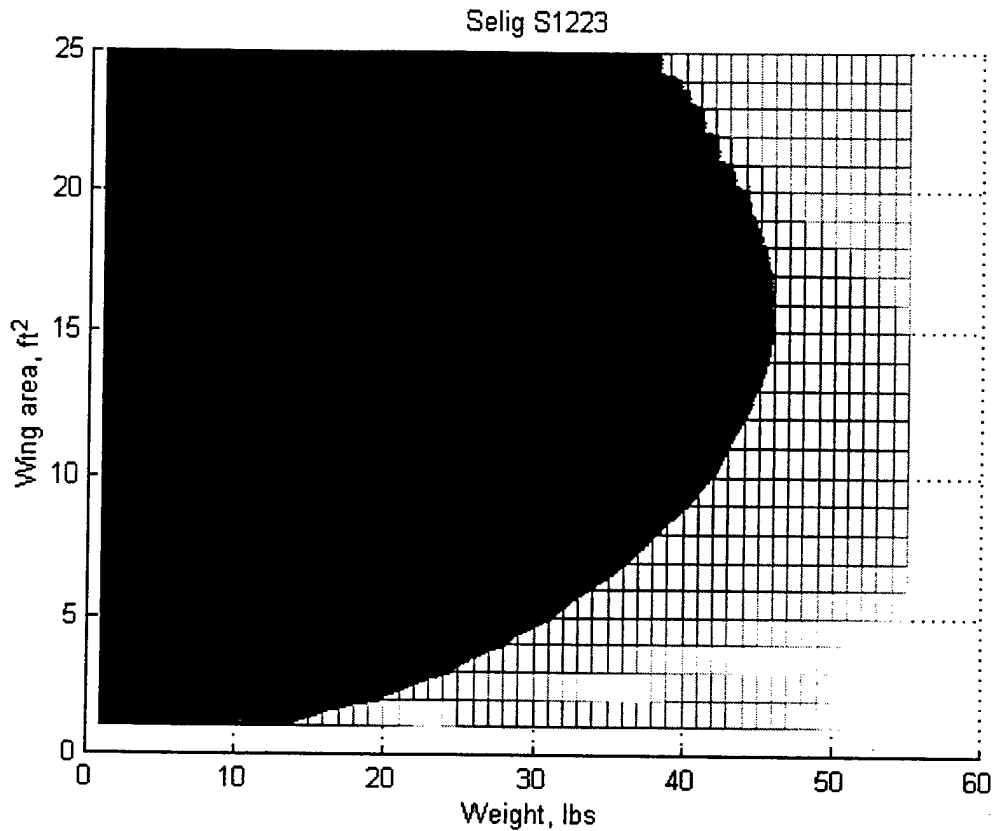


Figure 4.2. Takeoff distance required with 10 lbs. of thrust, airfoil Selig 1223 ($C_{Lmax} = 1.8$). Shaded area meets takeoff constraint.

4.2.1.1. Change in C_L (Airfoil type)

As the C_L decreases, the wing area required increases. From the above-mentioned figure, the trend can be seen visibly by an upward shift of the shaded area, this implies that the wing area required to meet the takeoff constraint is larger with a lower C_L . Compare with figure 4.3 which shows the Wortmann FX63137B airfoil ($C_{Lmax} = 1.45$). Investigating the two graphs, it is quickly noted the maximum (rightmost point) weight possible to take off is different between the two graphs.

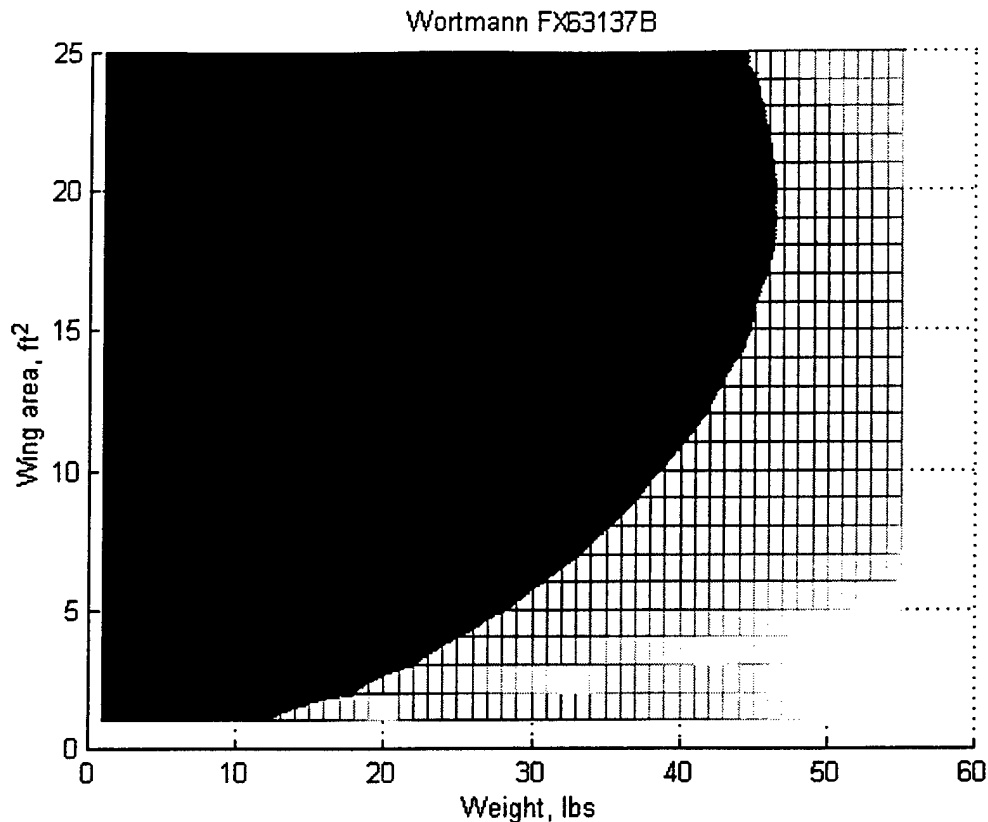


Figure 4.3. Takeoff distance required with 10 lbs. of thrust, airfoil producing $C_{Lmax} = 1.45$. Note upward shift of shaded region indicating larger wing area required to meet takeoff constraint.

4.2.1.2. Change in Thrust

As thrust is decreased, the same shaded region shifts toward the left. Figure 4.4 shows this effect with the Selig1223 airfoil and 6 lbs of thrust. Similar plots were constructed using various expected thrust availabilities producible by the motor and propeller combination. The results pointed toward the Selig 1223 airfoil and depending on the desired maximum GTOW, a wing size could then be determined. The desired GTOW was determined from the flight configuration program, and then using the combination of the two, an optimal solution for the aircraft was determined.

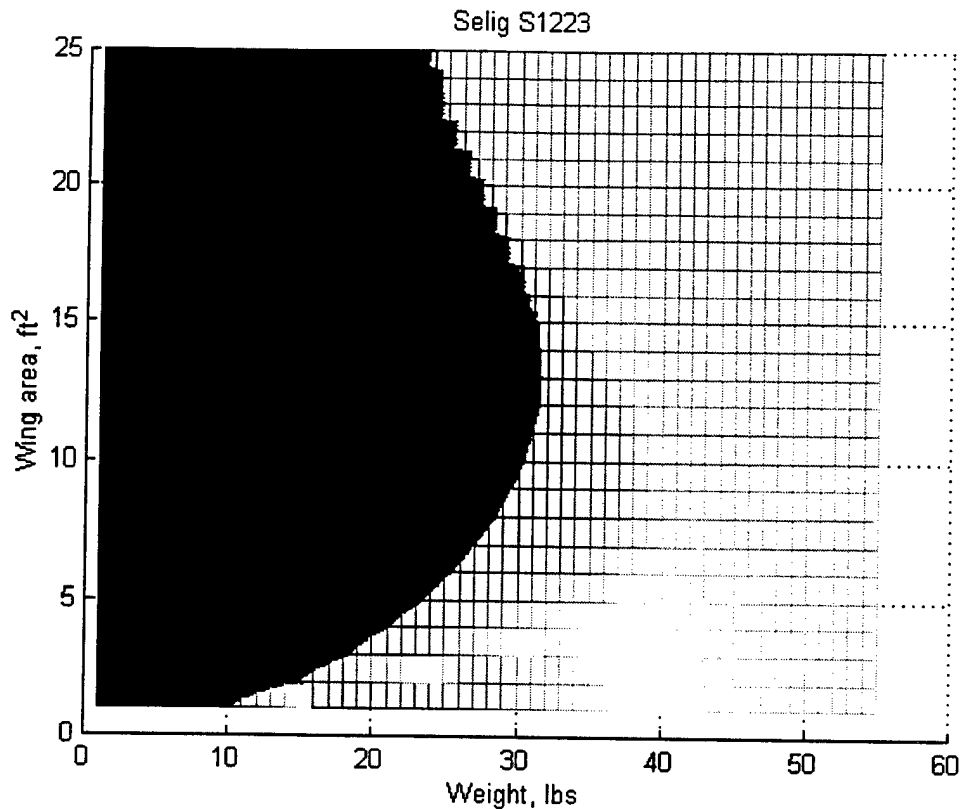


Figure 4.4. Takeoff distance required with 6 lbs. of thrust, airfoil Selig 1223 ($C_{Lmax} = 1.8$).

4.2.2. Flight configuration

In order to determine whether a big plane that could carry a lot of payload, or a small plane that could fly many laps was required, a program was written in Matlab to determine the optimum configuration of flights. Preliminary calculations indicated that energy was not a concern, but the time restriction of 10 minutes was the limiting factor. With that in mind, it seemed that all possible configurations provided a maximum of four flights (2 tennis balls and 2 steel flights), thus the maximum possible weight is desired for a higher flight score. The change in wing area affects the total score by a marginal amount, and since the maximum number of tennis balls and the maximum amount of steel would provide the highest score. The minimum wing area to achieve this was desired to reduce the rated aircraft cost. Going back to figure 4.2, the wing area required is 13.5 ft² and the maximum GTOW is 45 lbs. This is based on 10 lbs of thrust available from the motor and propeller.

4.2.3. Fuselage

The two shapes considered were a lifting body fuselage (airfoil shaped) and the torpedo shaped (round tube and front end, tapered tail) fuselage. The lifting body fuselage was thought up to aid in adding more lift and thus reduce the wing area. However, due to its low aspect ratio and large thickness, the total drag resulting from this fuselage was massive. Thus, the torpedo shaped fuselage was chosen to reduce drag to a minimum.

The internal layout of the fuselage had to be carefully planned in order to maximize the use of space within the body. This would keep the fuselage size to a minimum thus reducing weight, drag, and cost. By drawing the fuselage shape in CATIA®, we were able to fit tennis balls into the fuselage virtually. The final configuration was a 5-foot long 9-inch diameter fuselage. Drawing number 1845-905-2 shows the speed loader and 1845-901 shows the speed loader in the fuselage. For manufacturing and reloading purposes, the speed loader will be split into two sections.

4.2.4. Tail Boom

After considerations and calculations, a tube tail boom was chosen. The tube shape was chosen for the ease of manufacturing and it provides excellent stiffness qualities. It was projected that the tail was going to have enough ground clearance thus moving the tail to a higher location was unnecessary. A tail safety wire was added to prevent damage to the tail if the pilot over pitches the nose during takeoff.

4.2.5. Horizontal Tail Sizing and Position

Candidate airfoils were selected based on low Reynolds number (around 500,000) data. Symmetric, half symmetric and cambered airfoils were selected with various lift coefficients, drag coefficients, and moment coefficients. A program was written to find the horizontal tail area using given inputs of wing coefficients, tail and wing location, as well as center of gravity location. The program iterated horizontal stabilizer area and aspect ratio to solve moment equations, static margin, and handling qualities. Graphical representations of these values were produced. Trends were found by varying tail inclination, wing, center of gravity, and tail location. With the trends, handling qualities were considered and the combination that produced the best result was chosen. Other candidate airfoils were then input to the program. Candidate airfoils that produced better result (required less tail area) were then studied in detail by varying tail inclination and

airplane configuration again. Through iterations, the optimal tail size, location, and airfoil were selected as shown below.

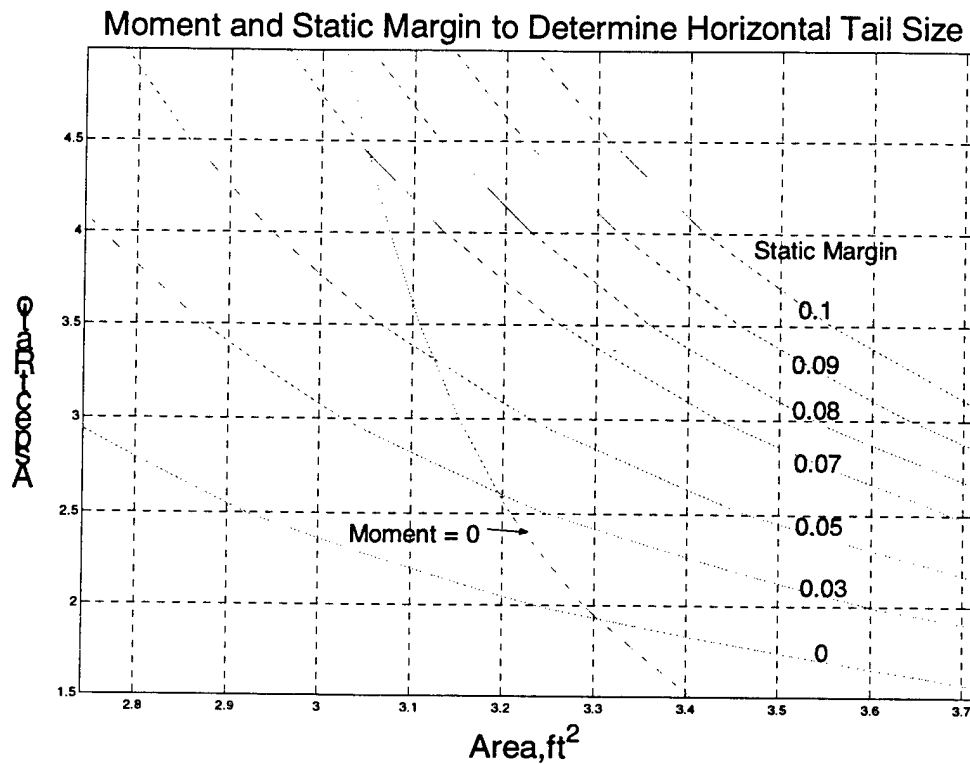


Figure 4.5 Graph of the Moment and Static Margin used to Determine Horizontal Tail Size

4.2.5.1. Elevator Sizing

A Matlab code was written to optimize elevator size. The program iterates elevator deflection to solve for moment, hinge moment, total aircraft lift, and elevator deflection required to maintain maneuvering conditions. All the values were then plotted on a graph to generate an envelope with given constraints such as available lift, control power conditions and thrust. The elevator for No Excuse has a chord of 0.287 ft (35% of tail chord) and the full span of the horizontal tail.

Table 4.1 Configuration of the horizontal tail and longitudinal stability values

Airfoil		USNPNS-4
Aspect ratio		4.5
Area		3.05 ft ²
Span		3.74 ft
Chord		0.82 ft
Locations:		
X- location (from front of fuselage):		
	Neutral point	1.8456 ft
	Wing location	1.5 ft
	Center of gravity location	1.75 ft
	Tail length	8 ft
Height (from center line of fuselage)		
	Neutral point height	0 ft
	Wing height	-0.167 ft
	Center of gravity height	0 ft
	Tail height	0 ft
	Landing Gear Drag	-0.8 ft

4.2.6. Vertical Tail Sizing

The vertical stabilizer was sized based on determining the yawing stability derivative. The derivative was estimated by varying the area and the aspect ratio that would give the approximate information to size the tail. It was calculated for a plate flat, that the vertical stabilizer has a span of 1.22 ft and an aspect ratio of 1.04.

The rudder is sized by determining the yawing derivative. It is determined that the chord is 50 percent of the vertical stabilizer. The rudder is also sized to handle a sideslip direction from $\pm 41.3^\circ$. The rudder is founded to have an area of 0.71 ft², a span of 1.22 ft, and a chord of 0.58 ft.

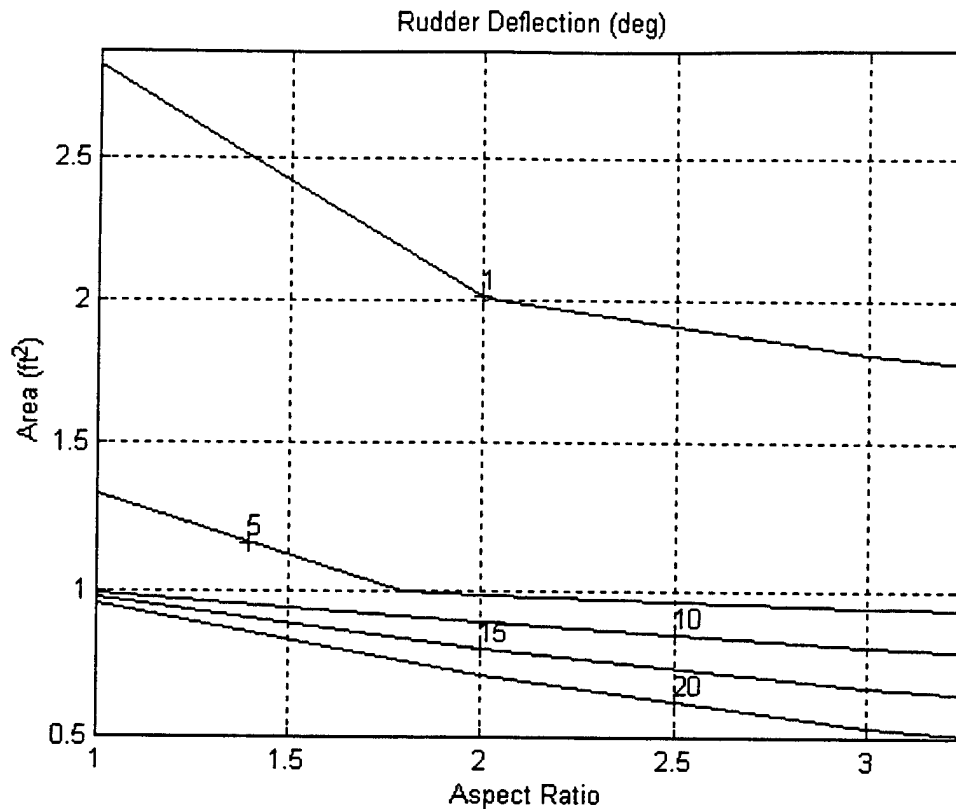


Figure 4.6: Vertical Stabilizer Sizing accounting for the Rudder Deflection

4.2.7. Wing and Aileron Configuration

Dihedral on the wing provides rolling stability. The dihedral determined from empirical data was 2.5° for the low wing configuration. Ailerons were sized in order to provide rolling control. The aileron chord was determined to be 20 percent of the main wing chord due to structural consideration in the design process. Each aileron has a length of 3 ft and a chord of 0.3 ft.

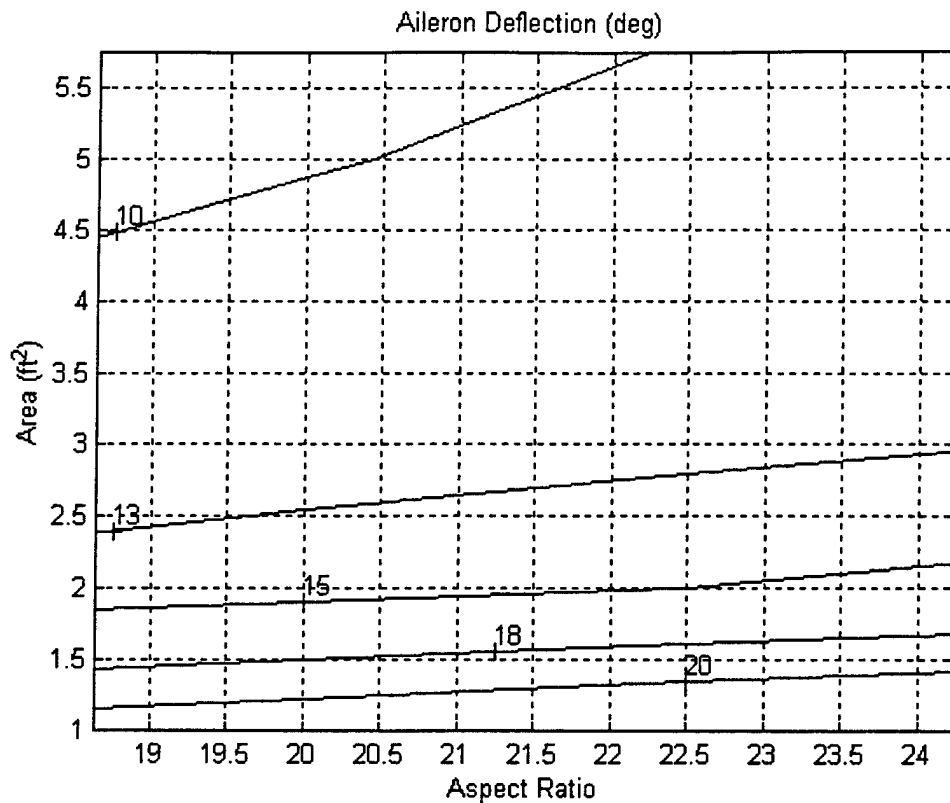


Figure 4.7: Aileron Sizing due to the Deflection

4.3. Structures

4.3.1. Wing

Given the flight configuration and aerodynamic loads, the wing was found to need to be fully composite. It comprised of two spars, one at 25% chord and one at 80% chord. The composite material was chosen due to an excellent strength to weight ratio, and by reducing the weight of structures, we could increase the payload, thus obtaining a higher score. The wing was analyzed using shear flow methods. The maximum bending stress in the wing was found to be approximately 7,000 lb/in². The maximum shear stress was 47 lb/in². Both of these values are below the maximum allowable stresses and thus permitted the wing to be lightened by removing some of the structure.

4.3.2. Fuselage Structure

The fuselage is comprised of a composite skin as well as a composite strengthening keel. There are two stringers running the length of the fuselage to provide longitudinal stiffness. There are two bulkheads, one at the front for the engine mounting, and one at the tail for the tail boom mounting. There will be brackets attached to the keel and fuselage. The wings will slide in through the side of the fuselage, allowing the spars to be bolted onto the brackets. The batteries will be secured along the floor of the fuselage between the two strengthen keels.

5. Detail Design

5.1. Performance Measures

5.1.1. Takeoff

The takeoff distance constraint was used to determine the wing size and GTOW and thus corresponds to 180ft (10% safety factor). The approximate takeoff time was calculated to be 8.5 seconds.

5.1.2. Endurance

The best endurance for the aircraft can be determined by cruising at the minimum power required to fly. Figure 5.1 shows the power required for wing areas of 10, 13.5 and 18. The uppermost line corresponds to area of 18 followed by 13.5 and 10. The bottom curve is the lift produced at that flight speed and the horizontal line is the lift required to fly. From this figure, the minimum flight speed required to fly is about 51 ft/s. The power required at that flight speed is approximately 281 ft-lbs/s. The energy available from the batteries (assuming 70% efficiency) was approximately 136,500 ft-lbs. This would result in an endurance time of 8 minutes. Note that this number was acquired if the aircraft instantaneously acquires flight speed.

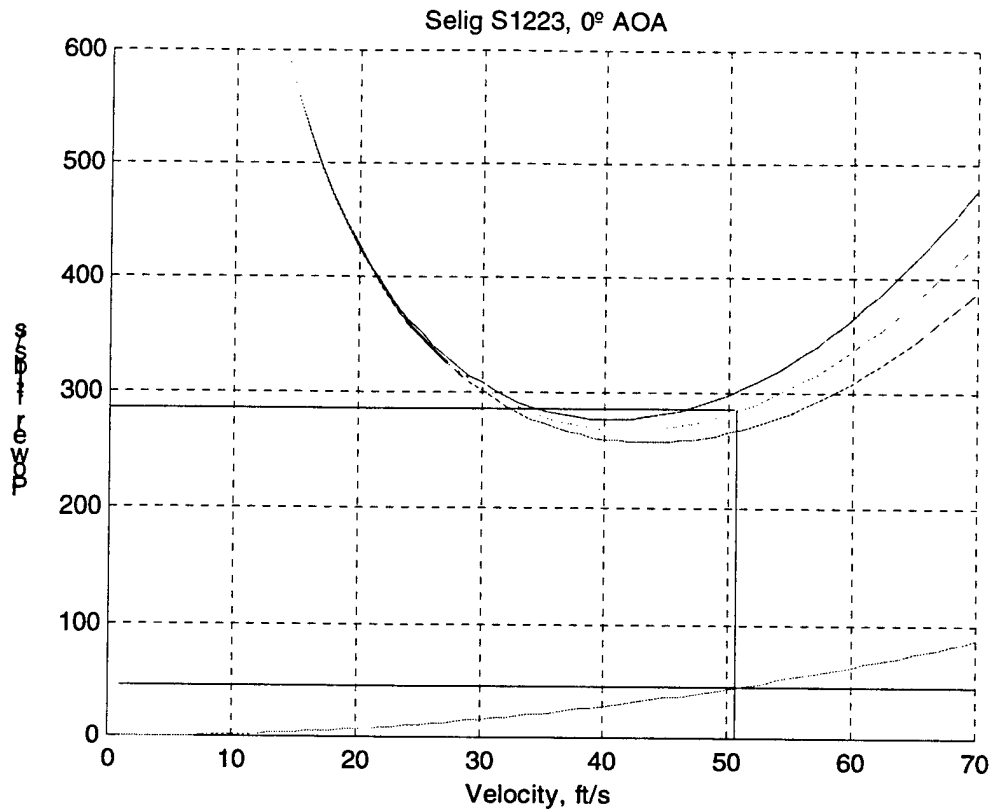


Figure 5.1. Power required (top) curves and Lift produced (bottom).

5.1.3. Range

The best range for the aircraft can be achieved by flying at the best L/D velocity. This can be determined graphically from figure 5.2, and for a wing area of 13.5 ft^2 , this flight speed was approximately 55 ft/s. Based on this flight speed, we can approximate the endurance of the aircraft based on the battery energy available and the power required to fly at this flight speed and from there obtain the maximum range. The approximate drain on the batteries at that flight speed was approximately 305 ft-lbs/s. This corresponds to an endurance time of approximately 7.46 minutes which results in a maximum range of 24,618 ft. Note that this number was acquired assuming that the aircraft instantaneously acquires flight speed.

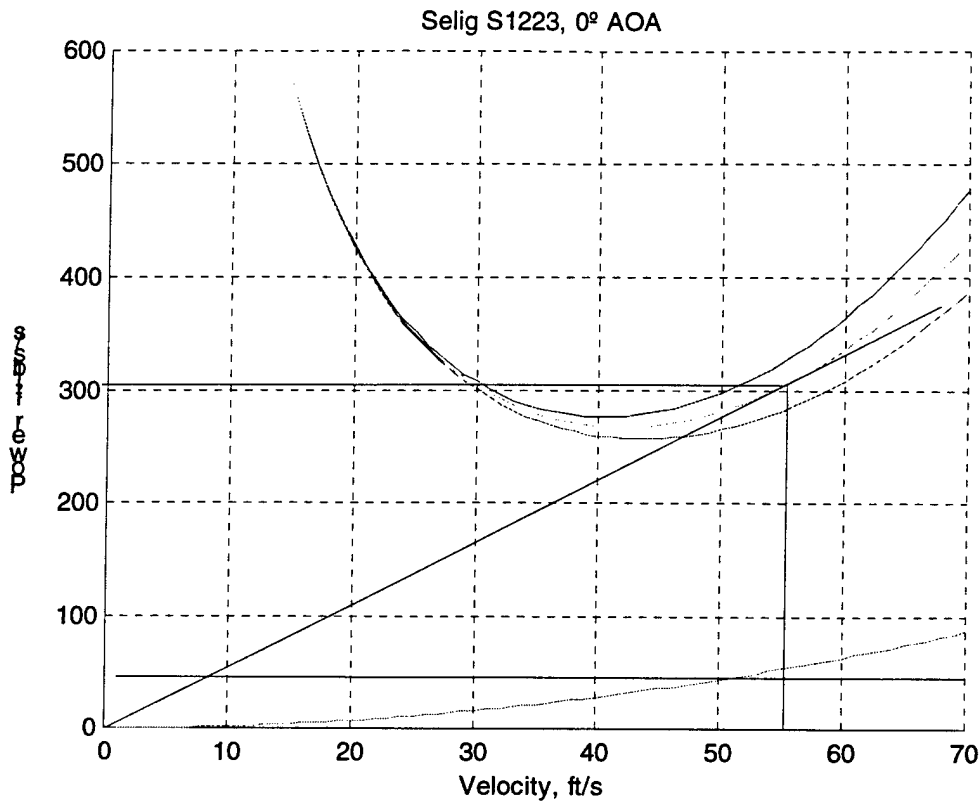


Figure 5.2. Power required (top) curves and Lift produced (bottom).

5.2. Handling Qualities:

The aerodynamic derivatives for use in finding the handling qualities are the roll mode, spiral mode, dutch roll, yaw rate, and roll rate. The derivatives for the aerodynamic force and the moment were found using a Matlab program. The results can be seen in Table 5.1.

Table 5.1: Aerodynamic Derivatives

Lateral Derivatives	Value
C_{yp}	0
C_{np}	-0.0187
C_{lp}	-0.1361
C_{yr}	-2.8880
C_{nr}	-0.2022
C_{lr}	-0.0228

To overcome the effects of turbulence, dynamic analysis was carried out. A Matlab program was set up to calculate short period, natural frequency, and damping ratio for selected horizontal tail size at various maneuvering conditions. If the short period mode was not satisfied, a new tail size was chosen, and the script was ran again.

The short period of natural frequency and damping ratio were satisfactory for No Excuse. The static margin for the selected tail is 0.073. The dynamic handling qualities found using the aerodynamic coefficients can be seen in Table 5.2

Table 5.2: Dynamic Modes

Short Period	Natural Frequency (1/sec)	Damping Ratio (1/sec)	Period (sec)
Longitudinal	0.2485	0.4248	25.3
Roll	1.4410	0.1478	4.36
Spiral	1.1304	0.1361	5.56
Dutch Roll	4.5121	0.2022	0.96

5.3. Component Selection and System Architecture

Motor and propeller were selected as a pair, but were analyzed separately. Analysis was performed to determine the best propeller and motor combination that would generate the most amount of thrust while using the least amount of power. It was decided that a 19-inch prop with a 10-degree pitch angle, and an Astroflight Cobalt 90 electric motor, were the best combination for the aircraft. Since there is only one motor, it was placed in the center of the fuselage in a tractor configuration.

Batteries and servos were available from the previous year's competition. It was felt that buying new components would not be of significant advantage, therefore these older batteries and servos were used. All batteries are located on the bottom of the fuselage while the servos for the ailerons, and vertical and horizontal tail are all located near their respective control surfaces.

5.4. Cost and Manufacturing Consideration

Aircraft cost was a major concern during the design phase. Using the aircraft cost model as a guide, an effort was made to minimize rated aircraft cost as much as possible without sacrificing aircraft performance. It was decided early that a single wing would be best, both in terms of aircraft cost and performance. The ten-foot wing span limit was enough to provide a large

enough wing area to fly, therefore a second wing would not have been beneficial. Similarly, a single engine was desirable for several reasons. It cost less, allowed for a single reinforced structure in the center of the fuselage rather than several on either the wings or in a cumbersome pusher/puller configuration on the fuselage, and because a single motor draws less current from the batteries than multiple motors. Once it was found that a single motor swinging one propeller would generate enough thrust to fly, a second motor was deemed unnecessary.

Great care was also taken to ensure that the plane that was designed was a plane that could be built. The materials used to construct the plane were chosen based on the structural needs as well as the amount of difficulty involved in construction. Composites offered high strength with low weight, however, the amount of work involved in building composite structure was high. Consequently, composites were used only for the wings and in part of the fuselage where high strength was a necessity. The tail boom is a solid aluminum tube requiring minimal manufacturing changes. The tail itself is constructed of balsa wood, which is very easy to construct with and maintains a good aerodynamic shape.

One area that was of great concern was the speed-loaders. The nature of the competition required that the plane have multiple speed-loaders, all of which needed to be exactly the same, and that they have a large volume as well as high strength. Building individual loaders out of balsa would have taken up too much time, and since each loader would have been custom made, no two speed-loaders would have been exactly the same. In order to alleviate these problems, it was decided that a thermo-former machine would be used to lay plastic over a mold of the loader. This would ensure that each speed-loader was the same exact size. It was also decided that since the fuselage was a long tube shape, the speed-loader could act as the top of the fuselage. This would make changing loaders quicker and easier on the ground crew. Because the thermo-former machine was limited on the size of part it could make, it became necessary to have two loaders in the fuselage at one time. This worked out well since it allowed for a separating ring to be installed in the fuselage which could separate the two speed-loaders as well as aid in fuselage rigidity. This design also allowed for easy access to the batteries and servos stored under the speed-loaders on the bottom of the fuselage.

5.5. Innovative Design Approaches

By designing the speed-loaders to act as part of the outer surface of the fuselage, the team reduced the time taken for loading and unloading the aircraft. The shape of the loader was designed around the shape of the tennis ball payload to minimize the volume required.

The wing attachment to the fuselage afforded the team a chance for innovation. In the early design phase the necessity of transportation dictated that the airplane would need to be taken into several parts. The decision was made to construct the wing from two sections that would join at the fuselage. The attachments would take the load from the wing and transfer them to the fuselage. The attach points would also provide a support for the speed-loaders.

6. Manufacturing Plan

The final design of No Excuse called for several intricate manufactured products. Those pieces of the design will be detailed below, as well as the process went about to manufacture them. The schedule for the construction phase of the project can be seen in figure 6.1. The team conducted a study into the feasibility of different construction methods using figures of merit. The results of the figures of merit study can be seen in figure 6.2.

6.1. Wing Construction

The wing of No Excuse needed to be strong, yet as light as possible. For that reason, several designs were considered. Firstly, a fully balsa and monocote construction was considered. This design was set aside due to several problems. The major problem of a balsa constructed wing was the need for exact ribs to be cut out. This would require either a form and press to be utilized, which was not disposal, or the ribs were to be cut out by hand. Cutting the ribs out by hand would be the only choice we had. This would lead to a very inaccurate wing, due to all hand cut ribs having a slight variation, and that variation carrying its way into the wing. The next alternative considered was a fully foam wing construction, with two composite spars running the length of the wing. Although carefully considered, this option was also turned down. The Selig 1223 airfoil used on No Excuse had a very thin rear airfoil section. This section of the wing would be under high stresses, and fear existed that the foam would flex, thus taking away performance characteristics desired. The final design of No Excuse called for a complete carbon fiber construction, still using the two composite spars. Carbon fiber was selected over kevlar and fiberglass for various reasons. Kevlar was turned down due to the expense. Carbon fiber was in abundance, and at our disposal, so the purchase of kevlar was an expense that we were not willing to take on. Fiberglass was also closely considered, again due to the abundance of material available. We eventually finalized on carbon fiber due to the increased strength and decreased weight over fiberglass. In all cases, a two piece wing construction was considered a must. The ten foot wing would have to be transported in one manner or another, and would prove to be very cumbersome if left as one large section. With two five foot sections, it was thought that transportation would be much easier.

Foam wings were cut and constructed, then they were cut into three main sections. The front leading edge section stopped at the first spar. This section was covered in carbon fiber, cured, and then the foam was removed. A section of the foam was also cut between the spars, again covered, cured, and then the foam removed. Ailerons were cut from the remaining trailing edge, and then the various parts of the trailing edge were covered, cured, and then the foam was again

removed for weight savings. The front and rear spar was fashioned from pre-impregnated carbon fiber, cured, and then cut to proper size. The entire assembly of leading edge, front spar, mid section, rear spar, and trailing edge was then assembled and bonded. To insure the overall strength of the assembly, one layer of carbon fiber was laid up around the assembly, and was again cured. The ailerons were mounted on the wing, and the servos were also retrofitted into the assembly.

6.2. Fuselage

First cut construction method of the fuselage consisted of forming aluminum sheeting to the proper shape. This was quickly dismissed due to the imperfections the forming process would create. A nine inch diameter PVC pipe was located to form the fuselage. The PVC was cut to dimensions, and then three layers of carbon fiber were laid up around the tube to provide an adequate baseplate for the plane. Two bulkheads were cut, fitted, and laminated into the front and back of the fuselage. These two bulkheads would support the tail and the motor. A third, frame was constructed and placed near the center of the fuselage for torsional rigidity. Two balsa stringers were laminated along the sides of the fuselage to help disperse loads along the length of the fuselage. Additional stringers were placed along the bottom of the fuselage for added bending and torsional strength. Two custom fitted walls were placed at the front and rear spar location of the wing for attachment points.

6.3. Speed Loaders

Two separate speed loaders were to be utilized. This would require the manufacture of several speed loaders that were exactly the same. The loaders was considered to be made from a balsa frame, and then covered in a cloth or plastic. It was feared that this method of construction would not handle steel loads. A plastic thermo-form method was considered that would allow for enough strength to handle the steel loads, as well as remain as light as possible. For this, a plastic thermo-form machine was utilized. Molds were made of the bottom and top halves of the speed loader. Several plastic loaders were built with the two halves of the loaders bonded together. This was the only manufacturing process considered for the construction of several exactly the same speed loaders.

6.4. Tail

The horizontal tail was constructed using a full foam construction with two composite spars. The elevator was cut from the foam, and two carbon fiber spars were fit into the foam. Balsa was used

to provide additional stiffness in the elevator. The vertical tail was constructed as a flat plate. The frame and inside struts were all made of balsa wood. The assembly was then covered in monocoque. The rudder is of the same construction method. The tail boom was purchased as is, and then was cut to length. Slots and holes were cut into end of the tail boom to allow for vertical and horizontal stabilizer attachments.

6.5. Landing Gear

The nose landing gear was purchased with the spring helical manufactured. The landing gear just needed to be bent into the swept configuration to accommodate passive steering. The main landing gear was cut from a flat pattern into a sheet of aluminum. The aluminum was then formed around the fuselage. With the primary bend in place, the two sides were folded back up, and the final bends were preformed. This proved to be the most efficient method of constructing the main landing gear.

6.6. Figures of Merit for Manufacturing Processes

The figures of merit for the construction phase were analyzed in order to find the best construction methods for the airplane. The team wanted to reduce the construction time, difficulty and cost. The following sections describe each figure of merit and the results can be seen in figure 6.1.

6.6.1. FOM - Availability of Supplies

Time was of essence, so the supplies chosen had to be readily or available within a short period of time. The use of supplies that were going to be hard to locate and purchase were eliminated from the choices of manufacturing processes. Such processes were given a negative one value. If the material was readily available, and could be located and purchased within a reasonable time, then a score of one was assigned.

6.6.2. FOM - Skill Level

This category investigated the amount of skills required to manufacture components through the different processes. A negative value was assigned if there was a high skill level required, and there was no team member with the necessary skills. A null value (0) was assigned if a high skill level was required, but there were team members that possessed such skills. A positive value

was assigned if the manufacturing process required little skill, or team members were highly enough skilled to overcome any complications in the manufacturing process.

6.6.3. FOM - Tolerances

A high tolerance was needed to maintain the performance characteristics of the aircraft. If a manufacturing process was thought to increase the deviation from what the actual shape should be, then a negative value was assigned. When the manufacturing process was such that tight tolerances could be held, then a positive value was assigned.

6.6.4. FOM - Costs

The cost of the aircraft was an important aspect to keep in mind. Costs not only included direct costs, but indirect and sunk costs, such as excess time required, as well. When a manufacturing process was introduced that would be costly, either to us directly, or to any other party involved, then it was assigned a negative value.

6.6.5. FOM - Strength

Since strength to weight ratios were a major concern, a figure of merit was assigned for all manufacturing configurations. If a particular manufacturing process would yield a product that was weak in comparison to the other methods, it was assigned a negative value. If the process yielded a stronger component, it was assigned a positive value.

6.6.6. FOM - Equipment Necessary

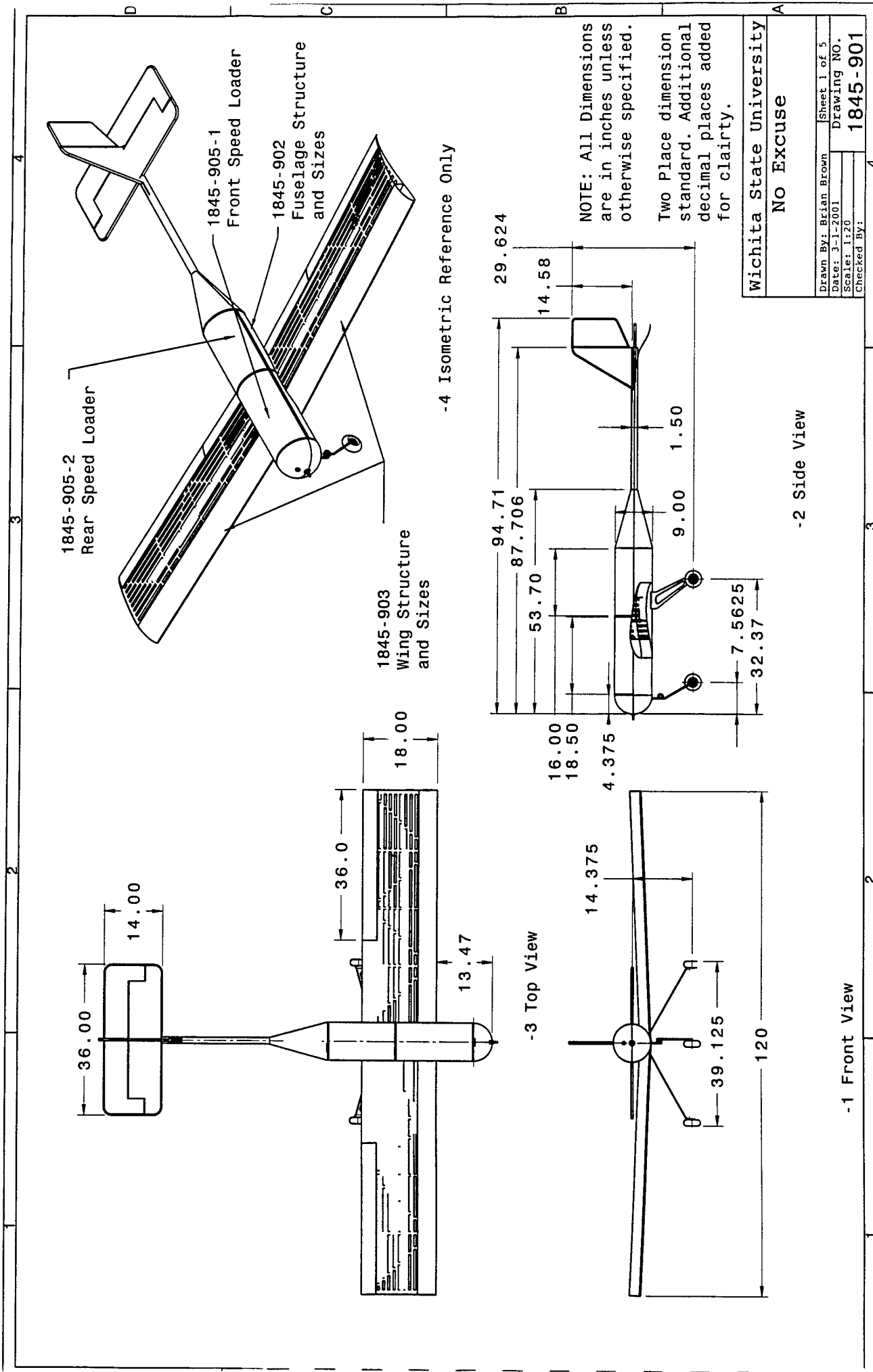
The various manufacturing methods required different machinery to construct the components. If the machinery was available, with team members knowledgeable in the operation of such machinery, then a positive value was assigned to the figure of merit. Otherwise, a negative value was assigned to indicate either no knowledge of the machine operation, or no machine was at our disposal.

Event	Planned Start	Planned Finish	Actual Start	Actual Finish
Wing Construction				
Cut Wing Shapes from Foam	1/26/01	2/2/01	3/2/01	3/8/01
Form Spars	2/3/01	2/10/01	3/9/01	
Lay-up Wing Sections	2/3/01	2/10/01	3/11/01	
Assemble Whole Wing	2/11/01	2/15/01		
Lay-up Around Assembly	2/16/01	2/20/01		
Fuselage Construction				
Form Shell	1/26/01	2/10/01	3/2/01	
Attach Stringers	2/11/01	2/14/01		
Attach Bulkheads	2/15/01	2/20/01		
Speed Loader				
Create molds	1/26/01	2/10/01	3/2/01	
Form loaders	2/11/01	2/20/01		
Tail Construction				
Cut Balsa for Vertical Tail	1/26/01	2/1/01	3/2/01	3/6/01
Construct Vertical Tail	2/2/01	2/10/01	3/7/01	3/10/01
Cut Foam For Horizontal Tail	2/10/01	2/14/01	3/2/01	
Form Spars for Horizontal Tail	2/15/01	2/20/01		
Assemble Horizontal Tail	2/20/01	2/25/01		
Cut Final Size of Tail Boom	2/20/01	2/25/01	3/10/01	
Landing Gear Construction				
Form shape	2/10/01	2/28/01	3/2/01	
Attach to fuselage	3/1/01	3/3/01		
Install Systems	2/21/01	3/5/01		

Figure 6.1 Milestones in the construction phase

Component	Investigated Methods	Availability of Required Supplies	Skill Level (Required and available)	Tolerances	Costs	Strength	Equipment Necessary	Results
Wing	Balsa	0	0	-1	1	-1	-1	-2
	Solid Foam	0	-1	0	0	0	0	-1
	Carbon Fiber	1	0	0	-1	1	0	1
	Balsa/Carbon Fiber Mix	0	0	0	-1	0	-1	-2
Wing Spars	Carbon Fiber	1	0	1	-1	1	1	3
	Fiberglass	1	0	1	-1	0	1	2
	Hardwood	0	0	0	-1	0	0	-1
Fuselage	Carbon Fiber	1	0	1	-1	1	1	3
	Wood	0	0	-1	1	-1	-1	-2
	Wood/Aluminum Skin	-1	-1	-1	0	0	-1	-4
Landing Gear	Aluminum	-1	1	1	0	1	0	2
	Carbon Fiber	1	0	0	-1	1	-1	0
Tail Boom	Filament Wound	-1	-1	1	-1	1	1	0
	Aluminum Tube	0	0	1	1	1	1	4
Vertical Tail	Carbon Fiber	1	0	0	-1	1	1	2
	Balsa	0	1	1	1	0	1	4
Horizontal Tail	Solid Foam	0	-1	0	0	0	0	-1
	Balsa	0	1	-1	1	-1	-1	-1
	Foam/Carbon Fiber Mix	1	0	-1	-1	1	0	0

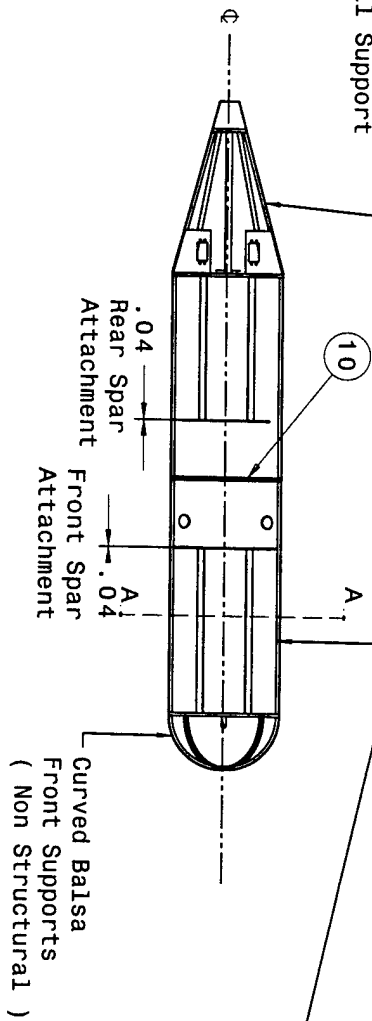
Figure 6.2 Figures of Merit for the construction phase of the project.



Wichita State University	
No Excuse	
Drawn By: Brian Brown	Sheet 1 of 5
Date: 3-1-2001	Drawing NO.
Scale: 1:20	1845-901
Checked By:	

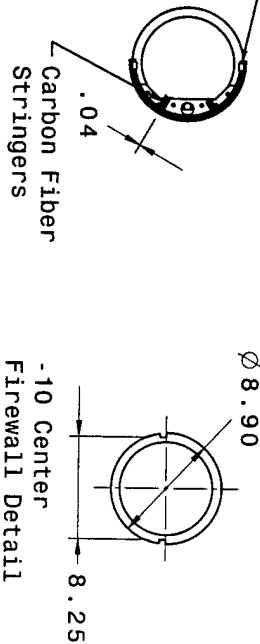
.25x.25 Balsa Struts
for Tail Support

.25x.5 Balsa Stringers



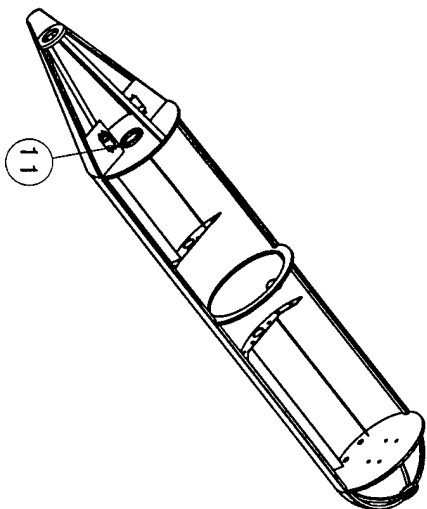
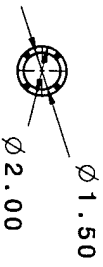
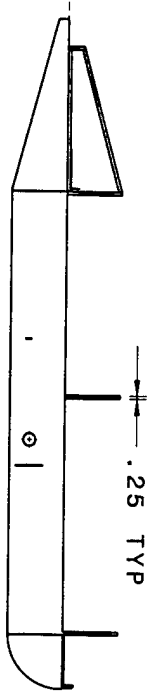
-1 Top View

-3 A-A Section View



-10 Center
Firewall Detail

-2 Side View



Isometric view
Scale: 1:10

-11 Tail Mount
Detail
Scale: 1:5

Wichita State University	
No Excuse	
Fuselage Structure	
Drawn By: Brian Brown	Sheet 2 of 5
Date: 3-1-2001	Drawing NO.
Scale: 1:20	1845-902
Checked By:	

Cut to match
Fuselage

Full Assembly
Front Wing

Full Assembly
Side View

Trailing Edge

Aileron

Rear Spar

Mid Section

Slots cut into
Mid Section
to allow for
weight savings.

Front Spar

Leading Edge Section

Three Piece
Two Spar
Construction
Reference

2.00

.350

59.00

60.00

Front Spar
Front View

Rear Spar
Front View

Wichita State University

No Excuse

Wing Structure

Drawn By: Brian Brown

Date: 3-1-2001

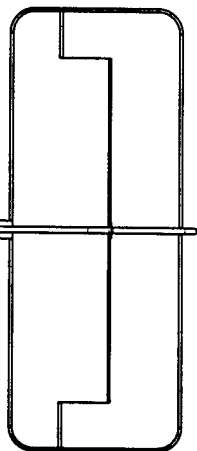
Scale: 1:10

Checked By:

Sheet 3 of 5

Drawing NO.

845-903



Receiver
Battery Pack

Tail Servos
(Linkage runs
length of tail
boom)

Receiver

JR Servo
(One Per Aileron)

Note: Outer skin and mid
section removed for clarity.

Passive Steering system
will be spring loaded. No servo
will be used.

Astroflight Motor
and Gearbox

Sanyo 1700 SCR Batteries

Astroflight 204D
Speed Controller

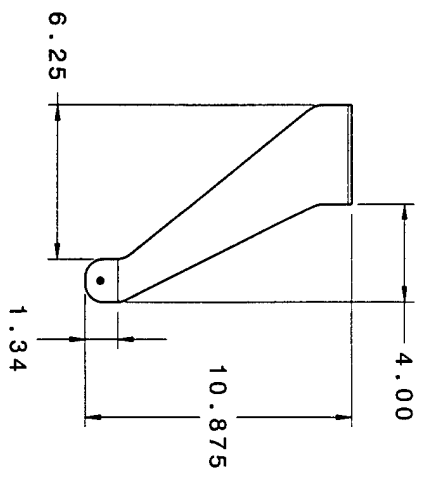
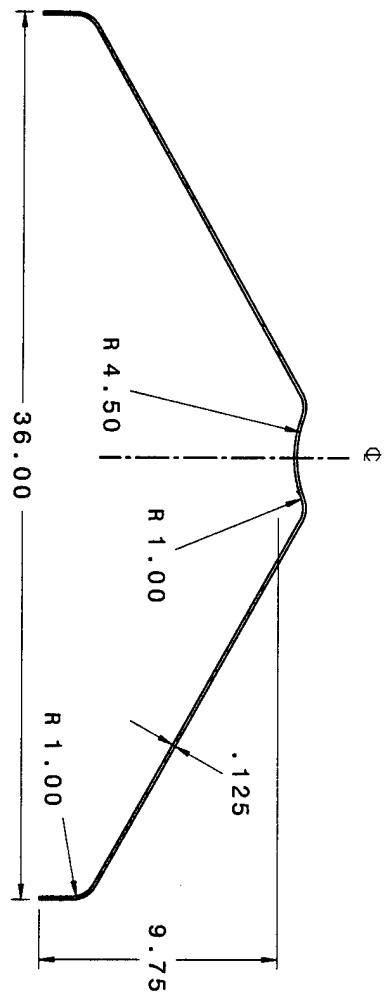
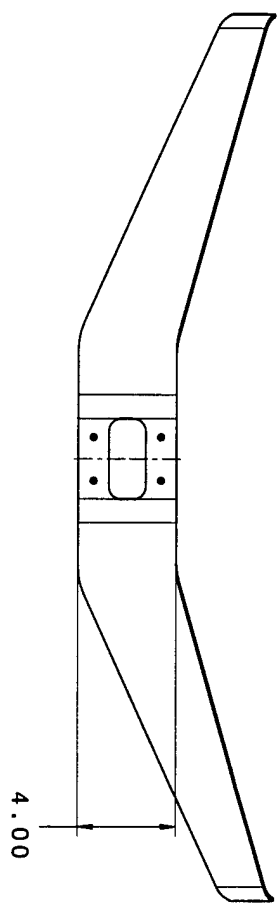
Wichita State University

No Excuse

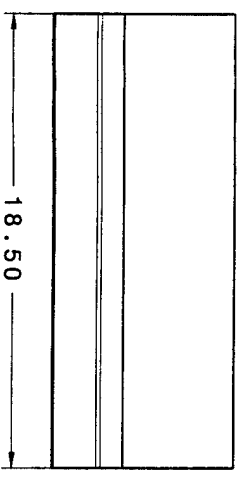
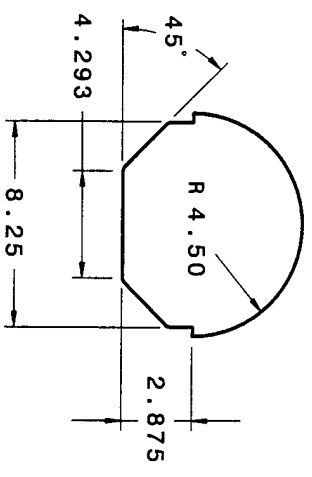
Flight Systems

Drawn By: Brian Brown
Date: 3-1-2001
Scale: 1:20
Checked By:

Sheet 4 of 5
Drawing NO.
1845-904



Landing Gear Front View



Other Speed Loader is 2.5" Shorter.

Wichita State University

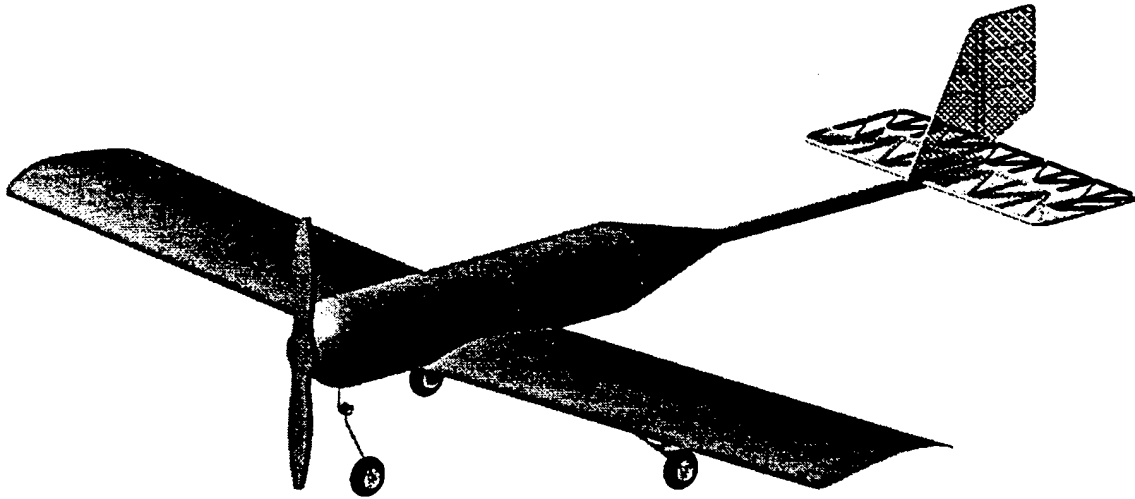
No Excuse

Misc Parts

Drawn By: Brian Brown
Date: 3-1-2001
Scale: 1:5
Checked By:

Sheet 5 of 5
Drawing NO.
845-905

No Excuse



*2000 – 2001
AIAA Cessna/ONR Student Design, Build, Fly
Competition
Addendum Phase Report*

Wichita State University

April 2001

Addendum Report Table of Contents

1.	Lessons Learned	3
1.1.	Aircraft Differences	3
1.1.1.	Wing.....	3
1.1.2.	Horizontal Tail	3
1.1.3.	Propeller.....	3
1.1.4.	Fuselage	3
1.2.	Areas of Improvement in Manufacturing for Next Design.....	4
2.	Aircraft Cost	5
2.1.	Rated Aircraft Cost.....	5
2.2.	Manufacturing Man Hours (MFHR).....	6

1. Lessons Learned

1.1. Aircraft Differences

During the construction and finalization of the design several changes were made to the airplane. Each change is documented in the following section.

1.1.1. Wing

The wing design was changed during the construction phase. The trailing edge was found to be too thin to be made from a foam core. The decision was made to construct the trailing edge and aileron from balsa wood covered with monocote. The trailing edge still retained the flight qualities required but was far easier to construct while also decreasing the weight of the component. The thickness of the wing skin was reduced after testing and calculation. The skins were reduced from 0.04 inches to 0.02 inches in thickness. This change increased the maximum bending stress in the wing from 7,000 lb/in² to 14,000 lb/in². The shear stress also doubled from 47 lb/in² to 94 lb/in². The change in stress levels is still far below the yield for the material. The weight of the entire wing was reduced by almost half from the original design.

1.1.2. Horizontal Tail

The original plan called for a horizontal tail that was constructed using a foam core, composite spars and monocote covering, due to the difficulties encountered during construction of the wing the tail was made from balsa wood covered with monocote. The design used 12 ribs spaced evenly along the span. The ribs were sandwiched between solid spar caps with a spar web running the span of the tail between the caps.

1.1.3. Propeller

The propeller size was increased from the original 19-inch diameter to 20-inch diameter when the manufacturer we desired to purchase the propeller from fell through. We changed to a Zinger propeller of 20-inches to allow us to produce similar thrust levels without changing the other propulsion components.

1.1.4. Fuselage

The changes in the fuselage since the original design are mainly cosmetic. The tail cone was shorted due to the amount of wasted space within the cone. The nose fairing was lengthened slightly due to the

difficulty in finding or constructing a suitable mold in the time available. Both changes had minimal aerodynamic effect on the airplane.

1.2. Areas of Improvement in Manufacturing for Next Design

Given the opportunity to build the aircraft again, several changes in manufacturing would be implemented. Most of the manufacturing difficulties arose from constructing the wing. Failing to account for our limited skills in composite molding increased the time of construction. The lay-up of the composite material was the only section taken into account. We failed to add in the time it takes to gather the extra materials needed. Although not a significant part of the lay-up process, it added significant overall time. The mold generation also required a significant amount of time. The proper molds were not readily available, therefore molds had to be created from other sources. Now that the required skills have been attained, construction of a new aircraft would prove to be much faster.

If a new design opportunity arose, a less cambered wing airfoil would have been chosen. The trailing edge of the current airfoil becomes very thin, and created many complications in construction. The initial plan was to create the trailing edge from composite material, although after further investigation, balsa was found to be necessary. The balsa construction allowed for the trailing edge to become thin, while holding the required shape. The less cambered wing would also allow for a simpler, more uniform construction from composite material. Given the opportunity, we would still use composite rather than balsa for its superior strength to weight ratio.

The manufacturing process changes described would not only decrease the production time, it would also decrease the cost of the aircraft. By utilizing a simpler wing airfoil section, it would have taken less time to create the molds and then lay-up the wing. It is also felt that the accuracy of the wing would also be increased with a simpler design, since the current high cambered wing required extensive sanding to obtain the required shape.

2. Aircraft Cost

2.1. Rated Aircraft Cost

Coef.	Description	Value
A	Manufacturers empty weight multiplier	\$100 /lb.
B	Rated Engine Power multiplier	\$1 /watts
C	Manufacturing Cost multiplier	\$20 /hr.
MEW	Manufacturers Empty Weight	17 lbs.
REP	Rated Engine Power: # engines * Amp * 1.2V/cell * # cells	1728 Watts
Amp	Value of inline fuse	40 Amps
# Engines	Astroflight Cobalt 90	1 engine
# cells	Sanyo 1700	36 cells
MFHR	Manufacturing Man Hours: MFHR = Σ WBS hrs.	149 hrs.
Rated Aircraft Cost (\$, thousands)	$\frac{(A*MEW + B*REP + C*MFHR)}{1000}$	5.048

The **Rated Aircraft Cost** for "No Excuse" totals to **\$5,048**. The configuration of the propulsion system composes of thirty-six cells of 1.2 volt Sanyo 1700 batteries, rated at 1700 mA/hr, that powers an Astroflight Cobalt 90 motor. A 40 Amp fuse is placed between the battery pack and the controller. The motor will swing a 20" propeller with 10° pitch. This combination, when run at full open throttle, provides 16 lbs of static thrust.

2.2. Manufacturing Man Hours (MFHR)

WBS1.0 Wing:	
15 hr./wing	1 wing
4 hr./sq. ft. Projected Area	13.5 sq. ft.
2 hr./strut or brace	0
3 hr./control surface	2 ailerons + 1 elevator + 1 rudder
WBS 2.0 Fuselage and/or Pods:	
5 hr./body	1 fuselage + 2 speed loaders
4 hr./ft of length	3.75 ft
WBS 3.0 Empenage:	
5 hr. basic	1 unit
5 hr./vertical surface	1 surface
5 hr./horizontal surface	1 surface
WBS 4.0 Flight Systems:	
5 hr. basic	1 unit
2 hr./servo or controller	4 servos
WBS 5.0 Propulsion Systems:	
5 hr./engine	1 engine
5 hr./ propeller	1 propeller
Total WBS hrs. (MFHR)	149 hrs.

State University of New York at Buffalo



2000/20001 Design/Build/Fly Competition

“Undecided”
A.K.A. “Black Magic”

Proposal Phase
March 2001

Table of Contents

1. Executive Summary	3
2. Management Summary	4
3. Conceptual Design	5
3.0 Introduction	5
3.1 Aircraft Requirement	5
3.2 Conceptual Design Process	5
3.3 Conceptual Design Configuration	8
4. Preliminary Design	9
4.0 Introduction	9
4.1 Weight Sizing	9
4.2 Propulsion System	9
4.3 Airframe Configuration & Sizing	10
4.4 Preliminary Design Configuration	11
5. Detail Design	12
5.0 Introduction	12
5.1 Final Performance Data	12
5.2 Component Selection and System Architecture	13
5.3 Final Design	15
5.4 Drawing Package	16
6. Manufacturing Plan	21
6.0 Introduction	21
6.1 Main Wings	21
6.2 Fuselage	22
6.3 Tail	23
6.4 Engine Mounts	24
6.5 Landing Gear	24
6.6 Figures of Merit	24
7. Appendix	26
7.0 References	26

1. Executive Summary

We, the students of the University at Buffalo (UB) chapter of the American Institute of Aeronautics and Astronautics (AIAA), have undertaken the task of designing and building an aircraft for the 2000/2001 Cessna/Office of Naval Research (ONR) Student Design/Build/Fly Competition. The AIAA sponsored competition will be held in St. Inigos, Maryland at Webster Field, which is part of the Patuxent River Naval Base, on April 20-22, 2001.

The competition gives undergraduate engineering students an opportunity to design, build, and fly an unmanned, electric powered, propeller driven aircraft that must conform to the rules as set out by the judges. The aircraft must successfully navigate around an upwind and downwind pylon set 500 feet from the starting line, carrying a small volume "heavy payload" of steel, or a large volume "light payload" of tennis balls, alternating payloads for each sortie. The team must do this as many times as possible in a ten-minute time period.

The teams will be judged on their design report, the number of sorties flown, and the rated aircraft cost that is outlined in the rules. These elements will be put into a formula by the judges and a score will be given to each team. The team with the highest score will win the competition.

It is the goal of the UBAIAA to win the 2001 Cessna/ONR DBF Competition. With an understanding of this year's rule changes we are confident that we have a strong grasp and understanding of where we as competitors need to be. The new wingspan limit, longer takeoff distance and the reduction of motor selection have all played a major role in directing us to a successful design.

This year's requirement for payload is very different from last year's. With careful planning an accurate design was constructed to maximize our chance for success. Flexibility was a large part of the brainstorming design, taking into consideration that the categories of payload were so different. The ability of our plane to hold both the minimum amount of steel (5 lbs) and the maximum amount of tennis balls (100) was an important characteristic to our design team, understanding that the payload is certainly a point producer.

The tools used for each design phase were based mostly on Dr. Jan Roskam's series, *Airplane Design*. Team members used the books in the series to produce viable configurations in the conceptual and preliminary design phases and to do the sizing of the aircraft in the detail design phase. Custom spreadsheets in Microsoft Excel were used prolifically to test measurements and to get a visual account of exactly where our design and design methods were heading. For instance, a spreadsheet was used to examine the tradeoffs between thrust-to-weight ratios, power-to-weight ratios, aspect ratios and desired payload. This approach formed the basis of the sizing of the aircraft during the preliminary design phase. Another spreadsheet was compiled during the detailed design phase to examine the performance of the design. The spreadsheet was based on techniques outlined in *Fundamentals of Aerodynamics*, by John D. Anderson.

2. Management Summary

Due to the high level of student interest in the design of the DBF aircraft, two separate and unbiased teams were formed in order to create a strong thought process with the initial design. One team based their designs primarily on fuselage and engine usage while the other found itself trying to use different materials and wing designs to optimize the aircraft.

Eventually each team had a strong handle on its own specialized areas of attack. Combining the two "brains" proved very efficient and the cooperating design glued together like two pieces of a puzzle. Our team then consisted of 5 senior aerospace engineering students, 5 junior aerospace engineering students, 3 sophomore aerospace engineering students, and 3 freshman aerospace engineering students.

The team was then broken up into sub-teams, which were aerodynamics, propulsion, materials, and structures. Each sub-team researched independently during the week and presented its work during our weekly design team meeting. There we discussed all possible options to come up with our final design. It was very important that each aspect of this design team was attended to in order to understand fully all the characteristics of aerospace design. Careful, decisive planning and proper attention to details has been the method of thinking since day one.

When the team was initially organized, a preliminary timeline was developed. This acted as a guide to show the team where they were and where they should be in the design process. Table 2.1 shows a summary of the preliminary timeline.

Table 2.1 Preliminary Timeline

	SEPTEMBER
	Begin Research
Week 1	Select and Organize Team
Week 2	
Week 3	Selection of Overall Config.
Week 4	Material Research
	OCTOBER
	Continue Research
Week 1	Aerodynamics Research
Week 2	Propulsion Research
Week 3	Conceptual Design
Week 4	Letter of Intent due before Oct. 31
	NOVEMBER
	Finalize Design
Week 1	Preliminary Design
Week 2	
Week 3	Detail Design
Week 4	
	DECEMBER
	Begin Construction
Week 1	Manufacturing Plan
Week 2	Exec. & Mgmt. Summaries
Week 3	
Week 4	
	JANUARY
	Continue Construction
Week 1	Edit and Refine Design Report
Week 2	
Week 3	
Week 4	
	FEBRUARY
	Finish Construction
Week 1	Edit and Refine Design Report
Week 2	
Week 3	
Week 4	
	MARCH
	Ground and Flight Test
Week 1	Finalize Design Report
Week 2	Proposal Phase due March 13
Week 3	Lessons Learned
Week 4	Aircraft Cost Model
	APRIL
	Complete Flight Test
Week 1	
Week 2	Addendum Phase Due April 10
Week 3	Competition: April 20-22
Week 4	

3. Conceptual Design

3.0 Introduction

The conceptual design evolved in two ways. We formed two teams and began to design very different airplanes. Unintentionally, each team ended up working on different aspects of the design. While one team focused on fuselage design and engine usage, the other team focused on materials and wing design. The many ideas that were thought up under these topics were discussed and evaluated by the individual teams. These teams were then brought together and final decisions were made. The following sections will describe what team decisions were made and why.

3.1 Aircraft Requirements

The primary aircraft requirements set forth in the competition rules are as follows:

- Wingspan is limited to 10 feet.
- Battery pack weight is limited to 5 lbs.
- Gross takeoff weight must be less than 55 lbs.
- Motors must be brushed, from Astroflight or Graupner.
- Take off distance is 200 ft.

3.2 Conceptual Design Process

A number of design parameters and configurations were discussed. We began with the C-Sketch design method to start our brainstorming process. With the C-Sketch design method, each person starts with a blank sheet of paper and has three minutes to sketch anything that they desire. Then the sheet of paper is passed to the next person to add or remove whatever they see fit. This process was continued until each person received his or her original sketch. We found this design method to provide us with an excellent basis to begin our further design.

The options discussed in this initial phase were then evaluated using a Figures of Merit chart. The design parameters were given scores on a 0-10 scale. The resulting design is then evaluated and . Table 3.1 shows the Figures of Merit chart used. The parameters are then discussed to explain each selection.

3.2.1 Wing Design

Two basic wing configurations were discussed, mono-wing, and bi-wing. Having seen success with bi-wing aircrafts in the past, we leaned toward this type of configuration. It was decided that the benefit of added lift of the bi-wing configuration made up for the drawbacks of added weight and drag. The options for the wing planform shape were elliptical, tapered, and rectangular. With each type of planform having specific advantages, the rectangular wing configuration is the easiest for use to build and work with.

Table 3.1 Figures of Merit												
Score Weight	Manufacturing		Aerodynamics		Structure			Performance			Cost	Total
	Ease	Time	Lift	Drag	Strength	Weight	Volume	Speed	Stability	Maneuv.		
	9	8	9	3	7	7	9	3	5	4	5	
General Config.												
Bi-Plane	6	6	7	5	6	5	7	5	7	5	6	420
Mono-Plane	6	7	5	6	6	5	5	6	7	5	6	398
Flying Wing	5	7	8	8	7	6	4	8	3	5	5	408
Aft-fuselage												
Single	8	8	N/A	6	7	5	7	6	5	5	7	399
Twin Boom	3	3	N/A	4	6	5	4	4	5	5	4	253
Stabilizer												
V-Tail	5	5	N/A	5	3	6	N/A	5	4	4	4	234
T-Tail	6	6	N/A	6	5	4	N/A	6	8	7	6	299
Low Horizontal	7	7	N/A	5	4	5	N/A	5	5	5	6	287
Wing Config.												
Straight	7	7	7	4	7	6	N/A	4	5	5	7	377
Swept	3	3	7	5	4	4	N/A	6	5	5	4	268
Dihedral	4	4	N/A	N/A	5	4	N/A	N/A	6	4	5	202
Taper	3	3	5	5	6	4	N/A	6	5	6	4	268
Landing Gear												
Tail-Dragger	7	7	N/A	5	5	7	N/A	6	6	4	6	312
Tricycle	7	6	N/A	5	7	6	N/A	5	6	7	5	315
Motor Selection			(Thrust)									
Single	6	6	3	5	N/A	6	N/A	5	5	5	6	276
Double	4	4	9	5	N/A	5	N/A	5	5	5	5	284

3.2.2 Material Selection

The next major decision was what material should be used to build the wings. Balsa wood is light and durable if used correctly. Carbon fiber has a higher strength to weight ratio, but can be harder to employ. Our team has had some experience with carbon fiber, but more with balsa wood. After considering each possibility, carbon fiber composite with a foam core was chosen to be the design for our wings. The foam core weighs a fraction of what a wood core would weigh, and the carbon fiber will hold the shape of the airfoil. A goal with using the carbon fiber was to construct each wing and the center struts as one component. With proper reinforcements this would provide a strong mid-section to attach our motors to. The carbon fiber will provide enough strength to support the aircraft and payload during flight, landings, and take-offs, and to pass the wing tip test performed at the competition. Therefore it was decided that adding a spar in each wing would increase the strength without adding too much weight.

3.2.3 Fuselage Design

The design parameters that govern the fuselage are:

- Payload volume and disposition
- Frontal and side area
- Wing, tail, and landing gear mounting
- Payload accessibility

We first had to decide how we wanted to carry the payload in the aircraft. From previous experience we found that having the payload inside the fuselage (being inserted and removed from the nose) looks nice and is practical but drastically increases the time it takes to change the payload between runs. In the DBF competition the faster the payload can be removed and replaced the better. Consequently a quick release method was considered.

During our research phase we came across Vincent J. Burnelli and his Flying Fuselage. Vincent J. Burnelli "wanted to incorporate maximum efficiency in the realm of air transport. The unorthodox result pioneered the wide-body cabin and the lifting-fuselage design." Burnelli's design was basically a large airfoil shaped fuselage. For our application, however, this type of design is impractical. A large fuselage like Burnelli's would cause too much drag.

Analyzing all the design parameters, we came up with a thin aerodynamic fuselage where the payload can be inserted into the top of the fuselage and 'snapped' in. See the Detail Design Section for further details.

3.2.4 Empennage Design

A T- tail design was chosen for our plane where the horizontal stabilizer is located at the top of the vertical stabilizer. This design was chosen over a conventional tail design and a V-tail design. For an aircraft of this scale, the T- tail design will provide more stability and easier construction. Both the horizontal and vertical stabilizers will be carbon fiber with a foam core. Each stabilizer will be a symmetric airfoil to reduce drag. It was decided that the horizontal stabilizer would be cut into two halves. A carbon rod was inserted about 8" into each half with a 1 ½" gap of carbon rod separation. The vertical stabilizer will be connected to the horizontal stabilizer via this carbon rod. A tail boom will be used to connect the T- tail to the fuselage.

Two types of tail boom designs were discussed, a single and twin tail boom. Using a single boom results in less weight, and less drag. Using a twin tail boom provides better torsion stability, and higher strength, but it adds weight. We chose a single carbon fiber rod as our tail boom. The carbon fiber rod is extremely lightweight and is very strong; therefore we felt this was our best option.

3.2.5 Landing Gear Design

Since landing gear is an essential component in any aircraft, much effort must be put forth when designing and constructing it. Our first thought was to have hinged landing gear with spring shocks. Due to the difficulty in design, added weight, and drag this concept was not chosen for our final design. Retractable landing gear was also taken into consideration. Retractable landing gear significantly

reduces drag on the aircraft during flight, but adds too much weight. Single wire strut landing gear was chosen for our final design. The wire strut landing gear is lightweight, low cost, low drag, and can be designed to provide enough strength for a 5-G landing. Landing gear disposition was chosen to be tricycle configuration with a steerable nose gear.

3.2.6 Propulsion System

The DBF Aircraft requirements state that our aircraft must be propeller driven and electric powered with an unmodified, over the counter model electric motor. All motors must be from the Graupner or Astro Flight families of brushed electric motors. In order to obtain an adequate power loading above 80 Watts per pound, which is a general guideline for model aircraft, total power must be no less than 2500 Watts for the target weight of 30 lbs. This specification narrowed our choice of motors. It was decided to use two Astro 60 geared brushed electric motors that produce 1300 Watts each.

Placement of these motors required additional research. Three options of motor placement were reviewed. One motor could be placed on the nose and one on the midsection of the top bi-wing configuration, which would require a larger landing gear to prop clearance. Both motors could be placed on either side of the top wing, which would require the addition of structure for strength, or both motors could be placed on the midsection of the wing configuration in a push-pull design. The nose-mounted configuration would present a ground clearance problem because the landing gear would have to be too large to accommodate the large-diameter propellers. The push-pull design was decided against because of the close proximity of the two motors. The pusher motor would be receiving "dirty" air from the tractor motor. The disposition that was selected for further design is the side-by-side motor configuration.

3.3 Conceptual Design Configuration

After the conceptual design was completed the aircraft was ready to go to the preliminary design phase. Table 3.2 is a summary of the conceptual design.

Table 3.2 Conceptual Design Configuration

Configuration	Biplane
Light Payload	100 Tennis Balls
Heavy Payload	5 Lb. Steel
Wing Span	10 feet
Wing Area	20 ft ²
Chord Length	12 in.
Airfoil	SD7062
Aspect Ratio	10
Wing Separation	12 in.
Wing Stagger	6 in.
Weight	30 Lb.
Overall Length	10 ft
Overall Height	34 in.

4. Preliminary Design

4.0 Introduction

Design parameters were a major consideration in designing this plane because these are what the design team was limited by. Many of these parameters could be handled without much manipulation. The major design parameters that are discussed here are weight, propulsion system, airframe configuration, and sizing.

4.1 Weight Sizing

This design parameter was probably the most restrictive of all because according to the competition rules the TOGW (take-off gross weight with payload) must be less than 55 lb. This is a more than generous number for the task that was to be undertaken. By decreasing the weight of the aircraft an increase in power efficiency and battery life can be expected while wing loading and cost can be decreased. Based on mission requirements and past experience, a target weight of no more than 30 lb TOGW was set.

4.2 Propulsion System

The propulsion system consists of the two (2) motors, propellers and battery pack. Selection of each was based on competition rules and design requirements.

4.2.1 Motor Selection

This design parameter was partly taken care of by the judges at the competition. In this years rules the motors were to be from the Graupner or Astro Flight families of brushed electric motors. These motors will be limited to a maximum of 40 Amp current draw by means of a single 40 Amp fuse in the line from the battery pack positive terminal to the motor controller. This rule basically brought our options down to two companies and a single type of motor. After much research and careful consideration the motor that was decided on was the AstroFlight Cobalt 60 Geared, providing approximately 1300 Watts each. Because of our planes target TOGW we needed motors that would have a power loading of at least eighty (80) watts per pound or a total power of 2400 watts. The reason that two motors with power ratings of 1300 watts each were chosen is because they would satisfy the thrust requirements presented from our design.

4.2.2 Battery Selection

Contest rules state that battery packs could not weigh more then 5 lb total with all connections made. We needed to try and figure out the right combination of batteries, cells, and formations in order to satisfy our parameters. While trying to limit the weight of the batteries themselves it was necessary to have enough power to produce sufficient thrust to the two motors. It was decided that the five pounds of

batteries would be sufficient by linking the batteries into a mix of parallel and series setups. Calculations for the amount of milliamp-hours (mAh) and for total run time were done using the five-pound weight limit on test stands built by the AIAA team and evaluated for a couple of different configurations. The task of choosing the batteries was daunting and challenging. The batteries that we were looking to find had to be lightweight and high capacity. Our first set of batteries that we found were very light weight with a medium to high power output, but unfortunately they were out of production for a while. The final selected was the Sanyo 1700AUL Nicad.

4.3 Airframe Configuration & Sizing

This part of the design was particularly critical because our goal as a team was to design and build the lightest aircraft possible. In order to optimize most of the other parameters for the aircraft this step must be very well done. While there are many different designs for fuselages only one would be able to make the final cut for our design. It was decided that the fuselage would be nothing more than a structural element that could carry cargo. We minimized the area and made the shape aerodynamic to increase lift and decrease drag. The components that are discussed more in detail are the wings, empennage, and fuselage.

4.3.1 Wing Configuration & Sizing

The competition rules state that the wingspan could be no more than 10 feet. This was one of the primary constraints that were used in designing the wings. In order to design a wing, the aspect ratio, chord length, position of fuselage and tail, and the position of the motors have to be taken into account. To maximize the wing area while keeping the aspect ratio relatively high, a biplane configuration having a ten-foot wingspan with a one-foot chord length was used, thus the area of the wings would be doubled while staying within the span and aspect ratio limits. The main drawback of the biplane design is greater drag, however due to the relatively low speed this is outweighed by the higher lift capabilities. One of the biggest problems in designing the wings was how to configure the struts and reinforcements that connect the wings. It was decided that two center struts and two end struts was the best configuration because of their high strength and their high resistance to torsional flexing. The spacing and stagger of the wings is also a major concern in a biplane configuration. A review of prior aircraft showed that a spacing of one chord length and a stagger of $\frac{1}{2}$ chord length are optimal. A discussion of airfoil selection will be presented in the detail design.

4.3.2 Empennage Sizing

The Empennage was designed using the tail volume method presented in Roskam's *Aircraft Design*. The tail volume coefficients are a critical part in the design of a plane and extensive analysis was done in order to optimize the design. Based on previous model aircraft, tail volume coefficients in the range of 0.5 to 0.7 for the horizontal, and 0.03 to 0.06 for the vertical were targeted.

4.3.3 Fuselage Sizing

By analyzing the function that the fuselage would have in this aircraft it was decided that it should be just a shell in order to minimize weight. The fuselage would have basically a bottom and two side panels, and it would resemble a box beam cut in half and hollowed out with the resulting area that was left filled in with the cargo-carrying device. This design would create a complete fuselage that was low drag while at the same time eliminating any added weight for the cargo-carrying container. This basic design helps to reduce weight, drag, and cost.

4.4 Preliminary Design Configuration

The final configuration for this aircraft took into account the conceptual design and made several modifications. The areas that had the most modifications from the conceptual phase were: tail volume, wings, airfoils, and fuselage. These areas were of great concern and were felt that optimization should be used extensively in these areas. The basic style of the aircraft remained unchanged after all these modifications with only minor adjustments in most areas. Our conceptual design resulted in a biplane that was low-weight, low-drag, high-lift, had two motors, and a cargo-carrying container that would 'blend' into the aircraft. These basic parameters stayed the same throughout the preliminary design stage. The modifications that were done used the conceptual design ideas while tweaking the smaller and more minor details. Table 4.1 summarizes the preliminary design configuration.

Table 4.1 Preliminary Design Configuration

Configuration	Biplane
Light Payload	100 Tennis Balls
Heavy Payload	5 Lb. Steel
Wing Span	10 feet
Wing Area	20 ft ²
Chord Length	12 in.
Airfoil	SD7062
Aspect Ratio	10
Wing Separation	12 in.
Wing Stagger	6 in.
Weight	30 Lb.
Wing Loading	16.7 oz/ft ²
Motor(s)	AstroFlight 60 Geared
Horizontal Tail Area	288 in ²
Vertical Tail Area	180 in ²

5. Detail Design

5.0 Introduction

For the detail design, the team performed a complete analysis of the airplane selected from the preliminary design phase. Final performance data, including take off performance, handling qualities and g load capability, range and endurance, and payload fraction were evaluated and qualified. Detailed component selection and system architecture will be included in this section. The design team primarily used Microsoft Excel to evaluate and optimize the necessary design parameters.

5.1 Final Performance Data

Following the preliminary design phase, the aircraft was placed through a more detailed evaluation. Specifically, design parameters such as required lift, thrust, and endurance were estimated. The design was then verified as meeting these requirements and adjusted accordingly.

5.1.1 Take Off Performance

As stated in the rules, the aircraft must take off within 200 feet. To meet this requirement, the design team looked at the available thrust from the motors and the lift of the wings. The aircraft must accelerate to take off speed within the 200-foot limit. The estimated take off speed is 44 feet/sec. This requires an acceleration of 4.84 feet/sec^2 to take off within the 200 feet. For a gross weight of 30 lb a total thrust of 72 oz is needed to achieve this acceleration. This is well within the range of the motors; as each provide about 100 oz thrust. It was decided that the take off acceleration requirement is not a problem needing further analysis.

5.1.2 Handling Qualities

During the contest flight, the aircraft must perform 5 basic maneuvers: take off, left 180° turn, right 360° turn, left 180° turn, and landing. Since these maneuvers are fairly simple, the design team used basic aircraft modeling experience to design the control surfaces. Past experience has demonstrated that the aircraft is rarely in straight and level flight. Therefore, the design team decided that a detailed control surface analysis would be unnecessary and time-consuming; only a basic approach was taken during the control surface sizing.

The following guidelines were used to determine proper control surface areas: Ailerons should be 10% of the wing area. The rudder area should be 20% of the vertical tail area. The horizontal tail is configured as a full-flying tail or stabilator, so an analysis of the proper deflection angle was attempted. The resulting control surface sizing is summarized in Table 5.1.

Although this design approach may seem crude, previous modeling experience has demonstrated that any discrepancies or handling problems can usually be fixed by properly adjusting radio settings and servo control throws.

Because the aircraft is not designed to perform complex aerobatics, the required G-load capacity is relatively low. The design team decided that the aircraft should be designed to sustain a 3-G turn. The landing gear, however, was designed to sustain a 5-G load to accommodate the inevitable rough landing. A ¼-inch wire strut will be shaped to provide the correct ground clearance and main gear separation.

5.1.3 Range and Endurance

The nature of the competition requirements and flight pattern dictate that range is not as important as endurance. Because of the time limit and battery pack weight limit, the aircraft was designed to provide maximum efficiency so as to decrease power consumption and increase endurance.

5.1.4 Payload Fraction

The payload fraction is included in Table 5.1.

5.2 Component Selection and System Architecture

After the preliminary design was complete, the team proceeded to work on the details of each component while keeping in mind the main goal of reducing weight and cost. The aircraft was then analyzed as both individual components and as a whole to verify that each component and system worked together properly.

5.2.1 Wings

The wing planform remained unchanged from the preliminary design. The dimensions are summarized in Table 5.1. The airfoil chosen in the preliminary design was the SD7062. Its lift, drag, and moment characteristics were analyzed to obtain the proper incidence angle. An angle of 2° was found to give the optimum lift to drag ratio during cruise flight.

Finding a way to mount the struts and fuselage to the wings proved to be a difficult task. The wing was designed to be a carbon fiber shell wrapped around a foam core with a spar. The team did not want to cut any large mounting holes in the shell because it would drastically decrease the strength of the carbon laminate. An innovative solution was designed where small carbon fiber tubes would be glued to the front and back of the spar at certain points before the carbon fiber shell is placed on the wing. This would provide the necessary hard points to which the fuselage and struts would be attached.

5.2.2 Tail

As stated previously, the tail surfaces were sized using the tail volume method. This method involves choosing an appropriate volume coefficient for each tail surface, then calculating the tail surface area and distance behind the center of gravity. The equations used are:

$$\bar{V}_h = \frac{S_h \cdot x_{AC}}{S_w \cdot \bar{c}_w} \quad 5.1$$

$$\bar{V}_v = \frac{S_v \cdot x_{AC}}{S_w \cdot b_w} \quad 5.2$$

where S_w , S_h , and S_v are the areas of the wing, horizontal stabilizer, and vertical stabilizer, respectively; x_{AC} is the distance from the center of gravity to the aerodynamic center of each surface; c_w is the chord length of the wing; and b_w is the span of the wing. For the horizontal tail, the volume coefficient should be in the range of 0.5 to 0.7. That for the vertical tail should be between 0.03 and 0.06. The stability of the plane increases with the volume coefficient, but only up to a certain value after which the tail would be too large and heavy. The results of these calculations are summarized in Table 5.1.

One of the strongest benefits to incorporating a stabilator rather than a standard tail with elevator is the fact that the tail incidence is controlled by the radio; it is not built into the plane. Although it adds some complexity to the manufacturing process, it reduces the amount of calculations necessary to obtain the proper incidence angle. Additionally, the ability to trim the stabilator in flight gives the pilot extra control over the aircraft.

5.2.3 Fuselage

The main function of the fuselage is to hold the payload. The shape is therefore primarily governed by the size and disposition of the large volume payload, the tennis balls. Since the optimum stacking configuration was found to be 4 by 1 by 25 balls in width, height, and length, the fuselage was designed to be a flat rectangular box with slightly larger dimensions than the payload box.

Additional aerodynamic considerations for the fuselage were the nosecone and wing fairing. Since the nose holds no structural value, a simple lightweight aerodynamic nosecone was added to the front of the main fuselage to decrease drag. An aerodynamic fairing was designed into the fuselage to provide smooth airflow under the bottom wing.

5.2.4 Wing Struts

The main struts connect the wings and provide a mounting location for the motors. Simple flat plates were designed to have enough strength to support the aerodynamic forces generated by the wings, as well as the thrust of the motors. The leading edge is rounded and the trailing edge is sanded to a point for less drag. The electrical wires to the motor are routed through the strut to the motor mounts, providing a fully faired route from the controller to the motor. This feature further decreases drag.

5.2.6 Landing Gear

The disposition of the landing gear is an important factor when considering static ground stability. As a general guideline, the main gear should be placed so as to make a 15° angle with the center of gravity. As stated in the preliminary design, the landing gear must be strong enough to sustain a 5-G landing. Structural analysis revealed that a $\frac{1}{4}$ -inch wire strut provides enough strength to meet this requirement.

5.2.8 Control Systems

A standard radio control system is used to pilot the aircraft. The onboard system consists of the radio receiver, radio battery pack, four servos, and electric wheel brakes. There is one servo for each tail surface and one for each aileron. The aileron servos are mixed with flap control to form flaperons.

The tail servos are mounted in the aft fuselage. Flexible pushrods running through the tail boom connect the servos to the control surfaces. Special linkages running through the vertical tail are required to actuate the stabilator. The aileron servos are located in the fuselage above the trailing edge on the bottom wing. Torque rods embedded in the inboard section of the trailing edge link the servos to the ailerons. The main advantage of this system is that all the controls are completely hidden, drastically reducing the drag.

5.3 Final Design

After completing the conceptual, preliminary, and final design phases, the final aircraft is ready for the competition. Table 5.1 shows a summary of the geometry, propulsion, and payload for the final design.

Table 5.1 Final Design Configuration

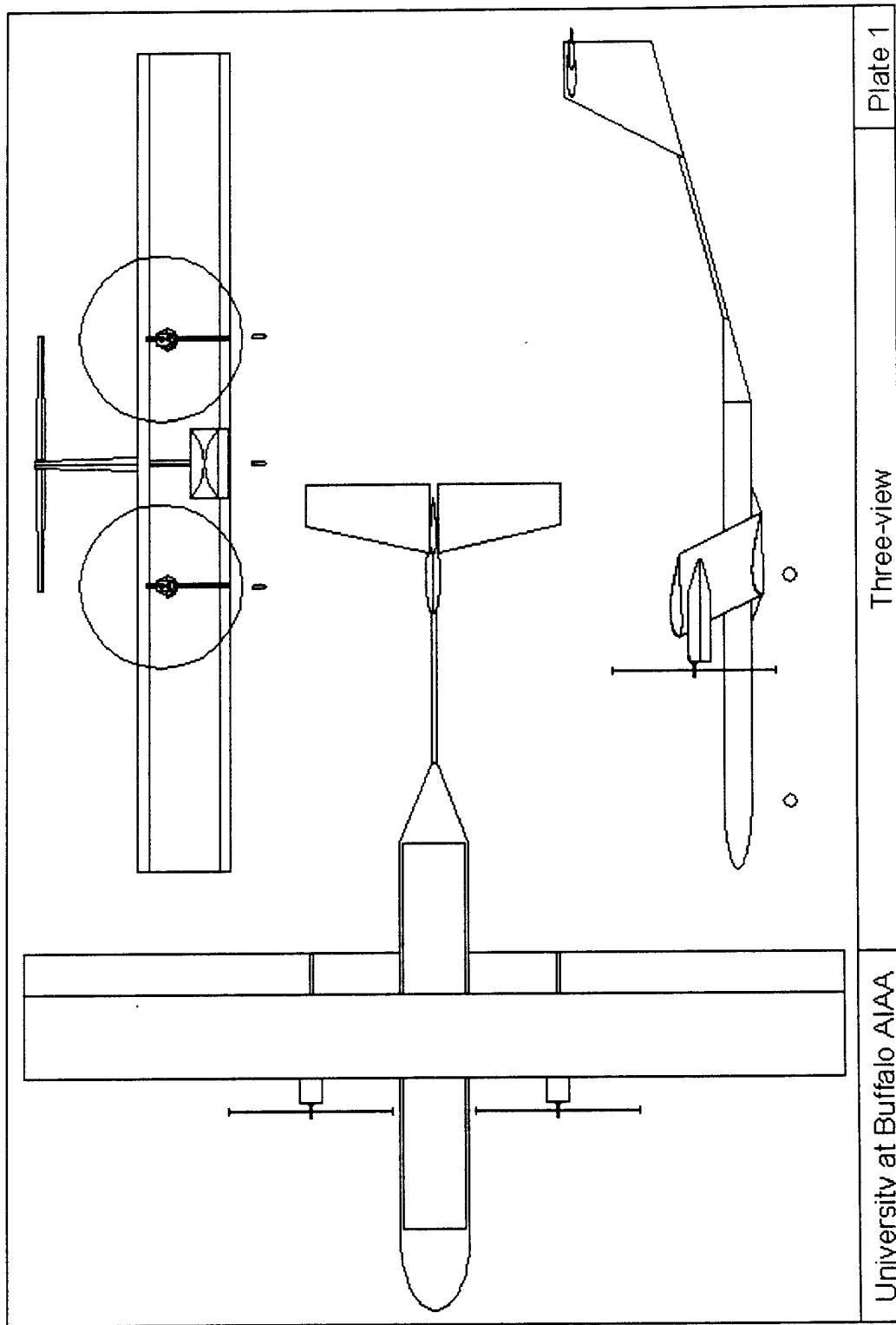
Configuration	Biplane
Light Payload	100 Tennis Balls
Light Payload Fraction	0.42
Heavy Payload	5 Lb. Steel
Heavy Payload Fraction	0.17
Wing Span	10 feet
Wing Area	20 ft ²
Chord Length	12 in.
Airfoil	SD7062
Aspect Ratio	10
Wing Separation	12 in.
Wing Stagger	6 in.
Weight	30 Lb.
Wing Loading	16.7 oz/ft ²
Overall Length	10 ft
Overall Height	34 in.
Motor(s)	AstroFlight 60 Geared
Propeller	18 x 10
Horizontal Tail Area	288 in ²
Distance Behind CG	76 in
Vertical Tail Area	180 in ²
Distance Behind CG	170 in

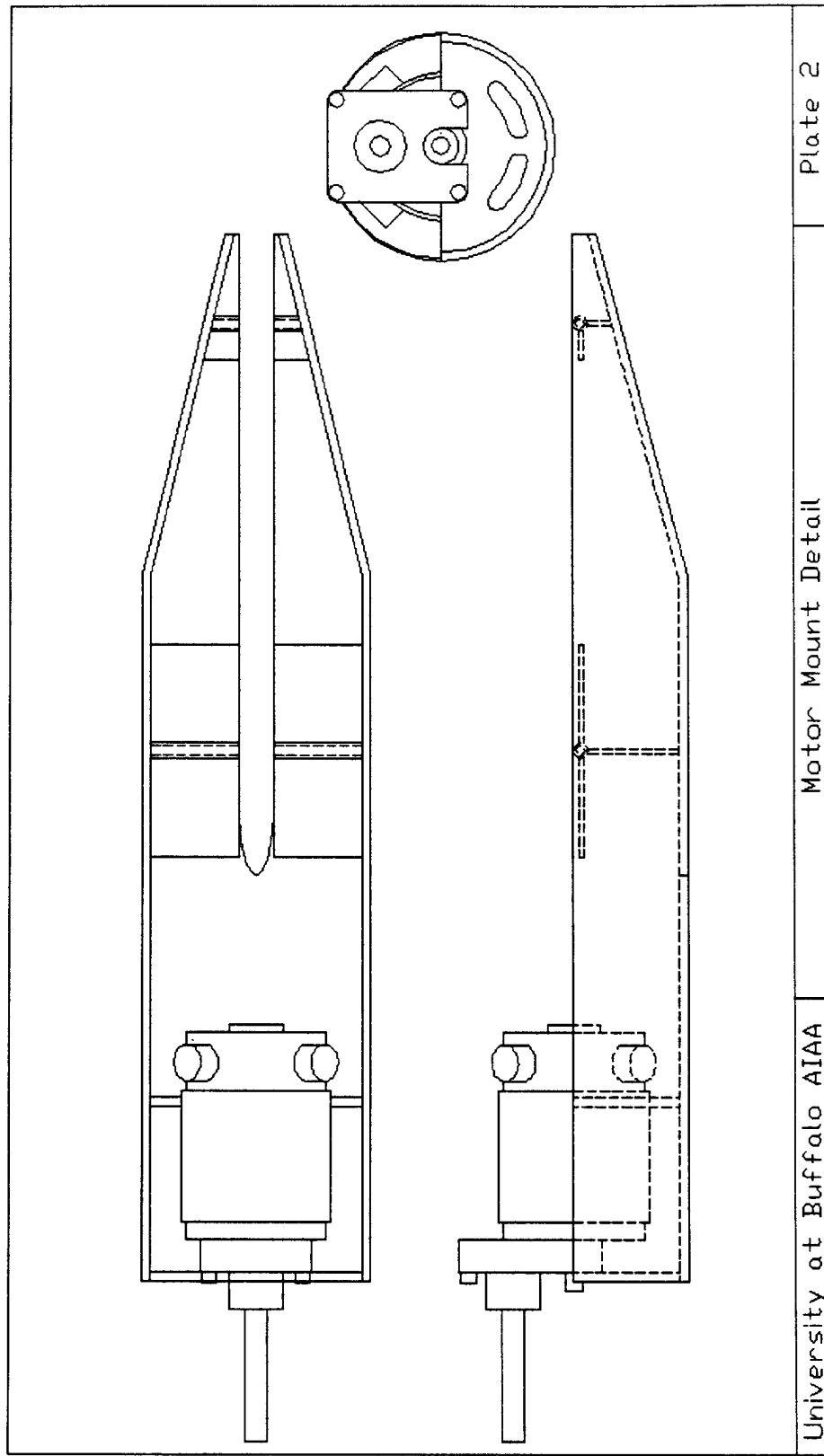
5.4 Drawing Package

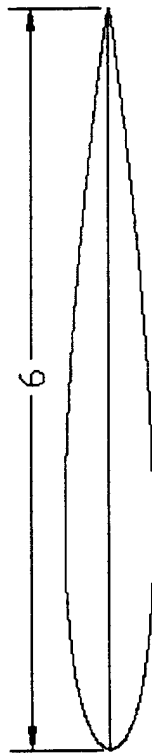
The drawing package was prepared to supplement the design report with graphical depictions of various aspects of the design.

5.4.1 Drawing Package Index

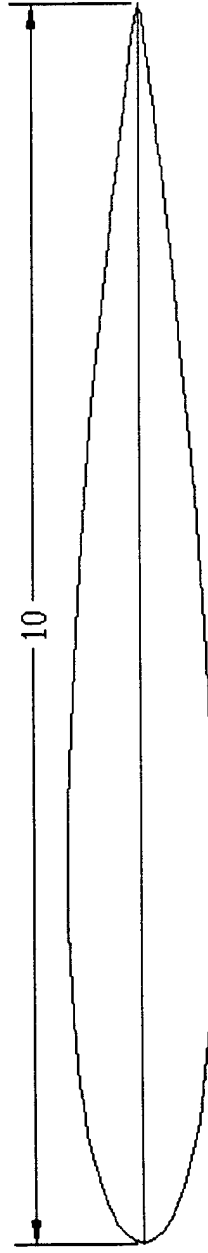
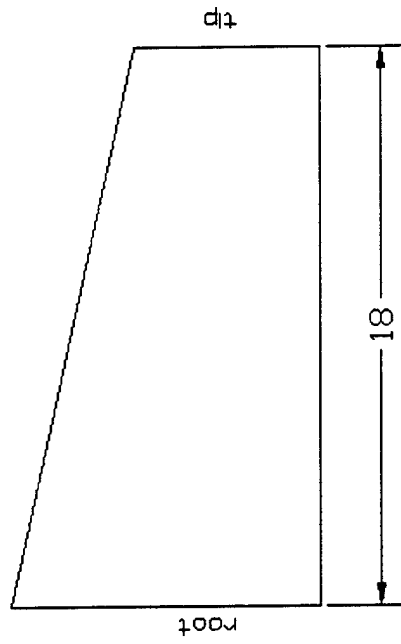
Plate	Description	Page
1	Three-view	17
2	Motor Mount Detail	18
3	Horizontal Tail Layout	19
4	Vertical Tail Layout	20







TIP - 6" chord - NACA 0012 AIRFOIL



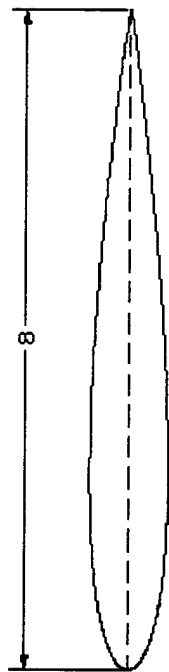
ROOT - 10" chord - NACA 0012 AIRFOIL

All dimensions in inches

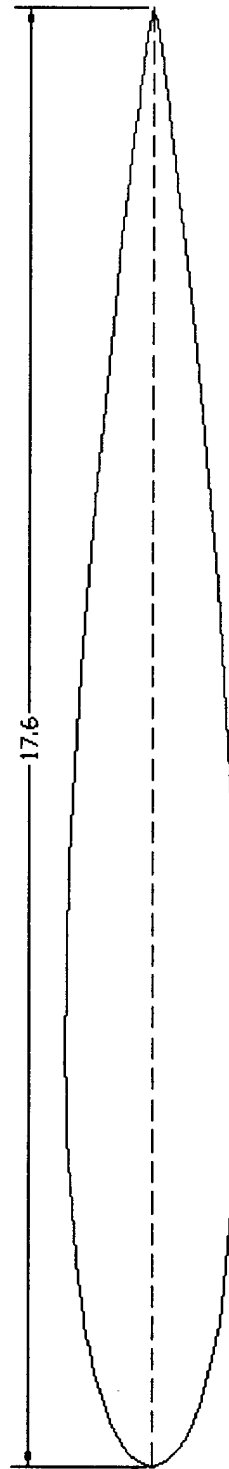
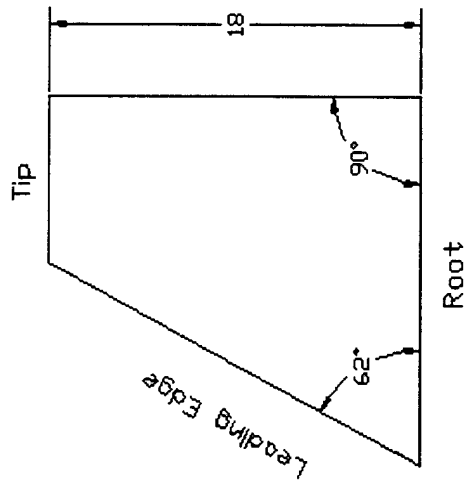
University at Buffalo AIAA

Horizontal Tail Layout

Plate 3



TIP - 8" chord - NACA 0012 AIRFOIL



ROOT - 17.6" chord - NACA 0012 AIRFOIL

All dimensions in inches

University at Buffalo AIAA	Vertical Tail Layout	Plate 4
----------------------------	----------------------	---------

6. Manufacturing Plan

6.0 Introduction

The design and analysis of an airplane is only half of the task in this project. There is still the actual production of a working airplane. Many different methods of manufacture exist for the different components of this airplane; however, there is a certain degree of expense and skill required for some of these processes. Each part of the airplane is compiled along with the figures of merit in Figure 6.1. These were used to determine the best methods for constructing a lightweight, structurally sound, high performance aircraft.

6.1 Main Wings

The process of deciding a construction method for the wings was the most time consuming in the project. This was due in part to the critical importance of a lightweight wing that could support the entire airframe in flight. There were three methods discussed in the conceptual design section for the wing: a traditional spar and balsa wood rib wing, a hollow carbon fiber shell, and a foam core with a spar. Through numerical analysis of the particular figures of merit, it was decided to construct a wing with a foam core and spar.

The first step in the manufacture of the wings was cutting the foam to the shape of the chosen airfoil. The foam that was used in construction had to be low density, for weight savings, but had to be strong enough to resist being crushed when it was placed in a vacuum bag for laminating, a procedure that will be discussed later. A polystyrene foam block measuring 12' x 1' x 1' is used to cut the shape of the airfoil. This block provides enough volume to create a one-piece foam core for each wing.

Next, airfoil coordinates are entered into AutoCAD to produce a three-dimensional model of the wing. A computer-guided machine with a hot wire attachment is used for the cutting of the foam block. This machine provides more accuracy and a smoother surface for applying a laminate. Though this method costs more, the time savings are significant due to the lack of sanding and surface preparation needed.

The foam wing is then cut into four (4) span wise sections. The first section is the leading edge, the next is the area where the spar is placed, the third section is the middle part of the wing, and the last section cut is the trailing edge. The main stresses will be placed on the second section of the foam wing. This is where the spar is placed.

For spar construction the second section of foam cut is used as the core. A carbon braided sleeve and uni-directional carbon fabric is placed over this piece of foam and a thick layer of epoxy is applied. This whole spar is put inside a vacuum bag for curing. The vacuum bagging process allows the outside air pressure to be evenly distributed across the entire length of the spar. This method is fairly inexpensive and produces a lightweight spar by squeezing out excess epoxy and securely bonding the carbon fiber to the core.

The foam was used as a core for the spar because it was already shaped to the airfoil correctly. If balsa wood is used for the spar, it must be sanded to the correct shape before the carbon fiber is applied. However, the foam is weaker than balsa wood, but the carbon fiber laminate over the entire wing will provide much needed strength in the wing.

The next step is to combine the first three sections of the foam core to produce a one-piece wing section. A thin bead of five-minute epoxy is applied between each section and they are pressed together to form a foam core with a carbon fiber spar. However, before the wing is laminated, all hard points and other internal structures must be built into the wing. This will provide secure mounting for the fuselage, main struts, and wingtip struts.

For mounting the ailerons, a ten foot long piece of ½-inch balsa is glued to the end of the third section of the foam core. This provides a secure place to attach the hinges for the ailerons. After that, pairs of 1/8-inch ID carbon tubes are mounted on the front and back of the spar at each strut and fuselage mounting location. These provide sockets into which the mounting pins are inserted. The same will be done to both wings, creating a solid wing-strut structure.

After all of the internal structure are in place, the wing is laminated in carbon fiber and vacuum bagged. The carbon fiber fabric is placed on the wing and a sufficient layer of epoxy is applied. Next, a sheet of peel ply is placed over the wing before it is placed in the vacuum bag. The peel ply is fiberglass cloth coated with Teflon, which allows excess epoxy to be lifted away from the carbon fiber leaving a lightweight, smooth surface wing. The whole wing is left in the bag for twelve hours before it is opened. The wing is at maximum strength in approximately three days. The long curing time is due to the use of extra slow hardener in the epoxy, which provides higher strength than the quick cure hardener. This was chosen over Monokote and balsa laminate because it is lighter weight and provides increased structural rigidity for the wing. Also, the addition of team members with experience in laminating carbon fiber made this a useful method of construction.

6.2 Fuselage

In the Conceptual Design section, the shape of the fuselage was presented as a simple rectangular block with a rounded foam nose cone. This shape has good structural characteristics and is also simple to manufacture. This is critical in this part of the airplane because all of the structural components meet at the fuselage. Also, the fuselage has to carry the cargo for the competition.

The two competing ideas for constructing the fuselage were a balsa frame with a Monokote covering or using a foam core and carbon fiber laminate. Although the balsa frame is cheaper, the carbon fiber shell that can be made is lighter, stronger, and requires less time to build. Also, if needed, balsa strips can be added to the carbon fiber shell for extra reinforcements.

The first step, as with the wings was to cut a piece of foam to the shape of the fuselage. This was done through the computer-guided cutting method described in section 6.1 for the main wings. A

large groove is cut down the middle of the fuselage as a place for the cargo container, battery pack, receiver, and servos to be mounted.

The tail is mounted by placing the boom into a sleeve molded into the rear of the fuselage and inserting steel pins through the boom to secure it. Lateral and longitudinal forces are transmitted to the sleeve and torsional forces are transmitted through the pins.

After all of the internal structures are attached to the foam, there are three layers of carbon fiber placed on the foam section oriented at 90°, 45°, and 90° with respect to the walls of the fuselage. By putting the carbon fiber fabric in different directions, the torsional rigidity of the fuselage can be greatly increased. This whole lay-up is then placed in a vacuum bag. The vacuum bagging procedure for the fuselage is identical to the procedure done for the main wings. The only difference here is that the foam core is melted out with acetone in the end to leave a hollow carbon shell.

The last section of the fuselage that is constructed is the nosecone. This is a simple procedure because it is not a structural component. A block of foam measuring 10" x 10" x 4" is hot wire cut to a rough aerodynamic shape and then sanded to a nice smooth surface. A single layer of carbon fiber is used to cover the nose cone. The finished nosecone is then glued to the front of the fuselage.

6.3 Tail

For the manufacture of the tail, two main designs were considered. The first design involved using foam cores and carbon fiber laminates. The second method considered was a balsa wood frame covered in Monokote. However, weight is a major disadvantage with the balsa wood construction. This could be seen through the use of sample sections of the same size that were built for testing. Also, the balsa wood section took more man-hours to build.

The horizontal stabilizer is constructed as stabilator, which means the whole horizontal rotates to control the pitch of the airplane. This saves the team from having to attach an additional control surface to the horizontal stabilizer. The stabilator is constructed with a carbon rod inserted at aerodynamic center of the cross section. The rod runs from the tip of the left side of the stabilizer to the tip of the right side. This whole structure is then laminated with carbon fiber and vacuum bagged.

The vertical stabilizer is constructed through the same lay up process as the horizontal stabilizer. However, this surface requires a rudder to be attached. This is done by gluing a piece of balsa to the trailing edge and inserting the hinges that will attach the rudder. The next step is to cut a circular groove into the bottom of the stabilizer. This will act as a cradle for the tail boom, which will be glued in with an epoxy and chopped carbon mix. There is a second groove cut in the top of the vertical stabilizer for the horizontal stabilizer. This groove is lined with Teflon tape so the horizontal stabilizer can rotate smoothly. This whole structure is vacuum bagged in identical manner to the wings and fuselage.

After all of the laminating is done, the horizontal stabilizer is placed on the top of the vertical stabilizer. A cap is placed on the top of this to prevent separation of the horizontal and vertical stabilizer.

The carbon rod used for the tail boom is epoxied into place in the bottom groove of the vertical stabilizer. The whole tail structure can then be mounted to the fuselage in the manner discussed in section 6.2.

6.4 Engine Mounts

It was decided by the team to place the engines on the main struts in front of the top wing. This is done by mounting a flat plate on each of the main struts, the details of which can be seen in the drawing package. The firewall, which prevents the engine from detaching the main strut, is constructed out of a flat carbon plate. This was seen as a lighter weight alternative to steel or aluminum and could be attached just as easily. The wires from the engines are then routed through grooves cut into the main struts, and then to the battery pack in the fuselage.

6.5 Landing Gear

The final landing gear design for this airplane is based on the tricycle style. However, the rear landing gear is mounted to the bottom wing and not the fuselage. This is done by routing piano wire through each of the main struts and then through the bottom wing. This design is more stable and fairly lightweight compared to using a hinge design that attached to the sides of the fuselage.

The nose wheel assembly used is commercially available and is rated for model aircraft of this size. It is controlled by a separate servo connected to the same channel as the rudder. This provides good ground handling and allows for easier hookup than routing a control rod from the rudder servo.

6.6 Figures of Merit

The following figures of merit provide the design team with the manufacturing characteristics of each component of the airplane. This was important in deciding how to go about construction the airplane outlined in the Detail Design section. The merit parameters are as follows: availability, cost, required skill level, time required, strength.

6.6.1 Availability

This was extremely important to the design team when deciding what materials to use. There had to be material vendors available that could supply the team with the proper dimensioned and cost effective materials. A score of 0 was given if the product was not available and a score of 4 was given if the product was easily attainable.

6.6.2 Cost

The airplane built had to be cost effective. The team raised enough money to purchase some fairly exotic materials, but these had to be used in only the most essential components. A score of 0 is for and extremely expensive material and a score of 4 is for a relatively inexpensive material.

Table 6.1 Manufacturing Figures Of Merit

		Availability	Cost	Skill Level	Time Required	Strength	Total
Weight Factor		3	1	2	3	2	
Wing Struture	Foam Wing w/ Spar	4	3	4	3	4	40
	Balsa Wood Ribs	4	4	3	2	3	34
	Carbon Fiber Shell	4	2	1	4	3	34
Spar	Balsa Wood w/ Carbon Sleeve	4	3	3	3	4	38
	Foam Spar w/ Carbon Sleeve	4	4	3	3	4	39
Fuselage	Balsa Frame w/ Monokote	4	4	4	2	3	36
	Carbon Fiber Shell	3	3	3	4	4	38
Landing Gear	Carbon Fiber Struts	2	1	4	4	4	35
	Piano Wire Gear	4	4	4	3	4	41
Horizontal Stabilizer	Balsa w/ Monokote	4	3	3	2	3	33
	Foam w/ Carbon Laminate	4	4	3	4	4	42
Vertical Stabilizer	Balsa w/ Monokote	4	3	3	2	3	33
	Foam w/ Carbon Laminate	4	4	3	4	4	42
Tail Boom	Carbon Rod	4	3	4	4	4	43
	Aluminum	4	4	3	4	3	40
Motor Mount	Carbon Plate	4	4	4	4	4	44
	Steel Plate	4	3	4	3	4	40
	Aluminum Plate	4	4	4	3	3	38

6.6.3 Required Skill Level

This year's team was fortunate to have the advice of many experienced builders. This allowed looking into processes that are somewhat more advanced. However, it was still important to stay within the scope of reality because reading a book on carbon lay-ups is different from actually doing it. A score of 0 is for expert skill level and a score of 4 is for beginner skill level.

6.6.4 Time Required

Time is always against a team in a design competition of this magnitude. The plan is to have the airplane built at least two weeks before competition. This allows enough time for testing the plane as a whole. All of the manufacturing has to be done relatively quickly in time for the competition. A score of 0 is for a very time consuming method and a score of 4 is for a fast manufacturing method

6.6.5 Strength

A strong plane is critical to surviving the sorties in the competition. This is where choice of material can make or break an airplane. A score of 0 is for a weak structure and a score of 4 is for structurally sound component.

7. Appendix

7.1 References

1. Anderson, John D., Jr., *Fundamentals of Aerodynamics*, McGraw-Hill, New York, NY 1991
2. Donaldson, Bruce K., *Analysis of Aircraft Structures*, McGraw-Hill, New York, NY 1993
3. Roskam, Jan, *Airplane Design Part I: Preliminary Sizing of Airplanes*, DARcorporation, Lawrence, KS 1997
4. Roskam, Jan, *Airplane Design Part II: Preliminary Configuration Design and Integration of the Propulsion System*, DARcorporation, Lawrence, KS 1997

State University of New York at Buffalo



2000/20001 Design/Build/Fly Competition

“Undecided”
A.K.A. “Black Magic”

Addendum Phase
April 2001

8.0 Lessons Learned

8.1 Aircraft Differences

As we began our construction of the aircraft we learned that the final design does not always end up as it was originally intended. Our most significant changes were those made to lessen the weight of the aircraft. These changes were realized after finding easy ways to reduce weight and add strength to the overall aircraft design during manufacturing. Changes were made from the original design so that construction of the aircraft would fit into our timetable and budget. Changes were also made due to purchasing and delivery problems that occurred during the construction phase.

The changes that were made are as follows

- Fuselage was constructed out of carbon fiber covered balsa wood as opposed to a foam core
- The cargo container was also made out of carbon fiber covered balsa as opposed to a foam core
- The main spar in the wings was constructed out of balsa wood as opposed to foam core
- The size of the container and the fuselage were increased due to incorrect data on the size of the tennis balls
- Two battery cells were removed from the final design so as to meet the weight requirements for the battery pack

The fuselage and cargo container changes were made due to incorrect sizing of the USTA official tennis ball size. So both the length and width of the aircraft needed to be increased to satisfy this discrepancy. This error was discovered during the construction phase and it was decided since we did not have enough foam on hand and it would be too expensive and take too much time to re-cut the foam we would just build the fuselage and the cargo container out of balsa wood and cover it with carbon fiber.

The balsa spar was used as opposed to a foam spar due to the foams inability to avoid warping during the carbon fiber curing process. It was decided to laminate two layers of balsa wood together and offset the joints of the balsa where the pieces were glued together. This added strength to the spar so that it would not warp during the curing process. It was then covered with a carbon fiber braided sleeve to once again increase the strength of the spar.

Two battery cells needed to be removed from our battery pack due to incorrect weight data on the cells before delivery. Once the cells were weighed we needed to reduce the weight, so it was decided to remove two cells: one from each motor pack. This would put us under the competition battery weight restriction with out significant power loss to motors.

8.2 Aircraft Improvements

To achieve a maximum score, the design team limited the payload to the maximum of 100 tennis balls. The team realized that this limited the number of payload configurations possible. By using a fewer balls, the power requirements would not be as high and more flights may be possible.

Materials should be ordered early in the design process so as to obtain accurate weight and dimension specifications. Additionally, a lighter weight carbon fiber weave could have been used. The weight of the carbon fiber used was 5.8 oz per square yard. The lighter weight 2.9 oz. weave would have provided adequate strength, and would also reduce the weight of the aircraft.

The type of foam used in this design was not very sandable, and presented problems where an exact shape was necessary. In future designs, a smaller cell type of foam with better surface workability should be used.

Finally, a more specific timetable should be developed and strictly adhered to. Extra time factors should be included in the scheduling to accommodate vendor and shipping mistakes and errors in manufacturing.

9.0 Rated Aircraft Cost Model

The Rated Aircraft Cost provides a guideline for estimating the cost of an actual aircraft with this design. The cost in thousands of dollars is calculated as follows:

$$Cost(\$thousands) = \frac{A \cdot MEW + B \cdot REP + C \cdot MFHR}{1000}$$

where MEW is the Manufacturers Empty Weight, REP is the Rated Engine Power, and MFHR is the Manufacturing Man Hours. The coefficients A, B, and C are the cost multipliers for each parameter. The Rated Aircraft Cost for this design is provided in table 9.1.

9.1 Manufacturers empty weight.

The Manufacturers Empty Weight is the final weight of the aircraft without payload and batteries. This is multiplied by the MEW coefficient 'A' in the cost equation.

9.2 Rated Engine Power.

The Rated Engine Power is calculated by multiplying the number of engines, the current rating of the fuse, the number of volts per cell, and the number of cells. This is then multiplied by the REP coefficient 'B' in the cost equation.

9.3 Manufacturing Man Hours.

The Manufacturing Man Hours is calculated by adding the prescribed assembly work hours for each component. This is then multiplied by the MFHR coefficient 'C' in the cost equation.

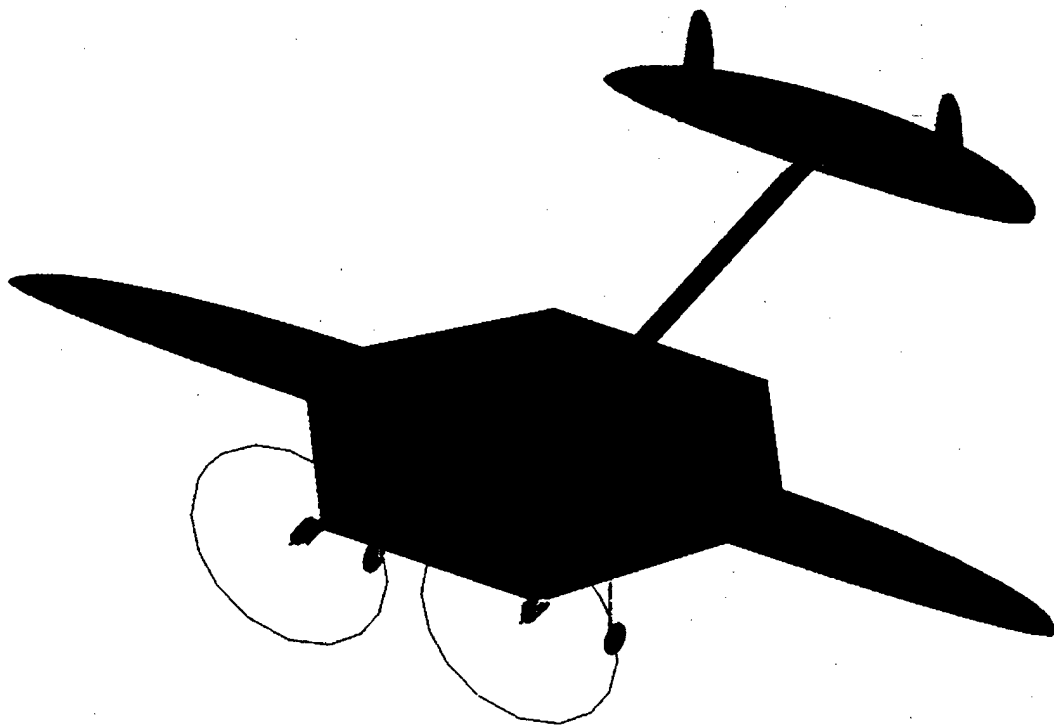
Table 9.1

Rated Aircraft Cost, \$(Thousands) = (A*MEW + B*REP + C*MFHR)/1000

Cost (\$Thousands)	8.2940			
Coefficient				
A (/lb)	B (/watt)	C (/hour)		
100	1	20		
MEW (lb)				
Airframe weight (lb)	12.5			
REP	2604			
# engines	Fuse Amp	1.2 V/cell	# cells	
2	35	1.2	31	
MFHR	222			
Wing(s)	item	value	hrs/item	hrs
	wing(s)	2	15	30
	Area (ft ²)	22	4	88
	Strut or brace	4	2	8
	Control Surface	2	3	6
	TOTAL			132
Fuselage	item	value	hrs/item	hrs
	body(s)	1	5	5
	length (ft)	7	4	28
	TOTAL			33
Empennage	item	value	hrs/item	hrs
	basic	1	5	5
	Vert surface	1	5	5
	Horiz surface	1	10	10
	TOTAL			20
Flight System	item	value	hrs/item	hrs
	basic	1	5	5
	servo/controller	6	2	12
	TOTAL			17
Propulsion Systems	item	value	hrs/item	hrs
	engine(s)	2	5	10
	propeller(s)	2	5	10
	TOTAL			20

*2000/2001 AIAA Foundation
Cessna/ONR Student Design Build Fly Competition*

Design Report
Proposal Phase



"A"
Utah State University
March 2001

Table of Contents

	<u>Page #</u>
1. Executive Summary	2
1.1 Conceptual Design.....	2
1.2 Preliminary Design.....	3
1.3 Detail Design.....	4
2. Management Summary	5
2.1 Architecture of the Design Team	5
2.2 Configuration and Schedule Control.....	5
3. Conceptual Design	8
3.1 Design Parameters and Aircraft Configurations	8
3.2 Figures of Merit	11
3.3 Quantitative Analysis of Selected Parameters	12
3.4 Analytical Tools	14
3.5 Configuration Selection.....	17
4. Preliminary Design	18
4.1 Prototype Testing	18
4.2 Figures of Merit	20
4.3 Design Parameters Investigated.....	20
4.4 Analytic Methods Used	22
4.5 Configuration Selection.....	24
4.6 Engineering Requirements	26
5. Detail Design.....	27
5.1 Component Selection and Systems Architecture	27
5.2 Performance Analysis	44
6. Manufacturing Plan	47
6.1 Figures of Merit	47
6.2 Results	49
6.3 Overview of the Manufacturing Plan	50
7. References	50

1. EXECUTIVE SUMMARY

A team of students at Utah State University has chosen to compete in this year's Cessna/ONR Student Design Build Fly Competition. The competition involves designing and building a propeller driven, electric powered, unmanned R/C airplane capable of flying different payloads around a designated course as many times as possible within a ten-minute period. The airplane must be able to complete at least three ten-minute scoring periods.

The goal of the design team was to design and build an airplane that would achieve the highest possible score. The total competition score is based on the weight of steel and number of tennis balls carried during the three best ten-minute scoring runs, a written report documenting the design of the airplane, and a rated aircraft cost. The written report will be judged and scored by AIAA officials.

The engineering process that led to the final aircraft design was divided into three phases. These were the conceptual design phase, the preliminary design phase, and the detail design phase.

1.1. Conceptual Design

To aid the team in selecting the best possible airplane, the design team was divided into five major aircraft-component groups: Wing, Empennage, Fuselage, Landing Gear, and Power Plant groups. A sixth group called the Flight group was created to coordinate the mission profile and the component design groups. Team members from each group were assigned tasks to study different concepts to be combined into various airplane design configurations. The team rated each airplane configuration based on criteria referred to as the figures of merit. Concepts were screened based on the contest design constraints, payload capacity (heavy and light loads) and rated aircraft cost. The goal of the conceptual design phase was to choose a few of the most promising concepts for further analysis.

1.1.1. Design Alternatives. The considered alternatives encompassed the following areas: wing planform, wing configuration, empennage structure, fuselage shape and size, landing gear type, and power plant. The team compared the advantages and disadvantages of elliptical and rectangular wing planforms. Possible wing configurations investigated were mono-wing and bi-wing. For the tail structure, T-tail, V-tail, canard and conventional configurations were investigated along with the possibility of using a flying wing design (no tail). The fuselage shapes and sizes that were considered consisted of vertical and horizontal airfoil shapes specially modified to accommodate payloads between one and ten tennis balls wide (or high) and six and twelve tennis balls long. The advantages of retractable landing gear and fixed landing gear were investigated. All brushed motors from Astroflight, with available motor specification data, were considered against a wide range of commercially available propellers of varying diameter, pitch and number of blades. Every motor-propeller combination was applied to each possible airplane configuration to help optimize power plant performance. Multiple motor combinations were also studied, as the 40-amp fuse severely limited the amount of thrust that one motor was allowed to produce.

Aircraft properties analyzed for all of these cases were gross airplane weights from 10 to 55 pounds, wing planform areas from 5 to 30 square feet, and wing spacing (bi-wing only) from 6 inches to 3 feet. Since the number of possible design alternatives was on the order of millions, generalized aircraft models were used to estimate the characteristics of each configuration.

1.1.2. Design Tools. The team wrote a FORTRAN computer program called DBF2001 to perform a detailed score analysis for each configuration. The program was comprised of six main subroutines: WING, EMPENNAGE, FUSELAGE, LANDING GEAR, POWER, and FLIGHT. Each subroutine quantitatively evaluated each design alternative mentioned above using results from previous design teams and aerodynamic theory. After modeling an airplane using each of the aforementioned

subroutines, the FLIGHT subroutine estimated the performance of each airplane configuration, and then used the POWER routine to determine battery power used as well as time elapsed for each sortie.

To determine aircraft characteristics, the program WINGS2001 (see Phillips and Snyder 2000) was utilized. WINGS2001 was chosen over classical panel and CFD codes because of its accuracy and fast computation time, allowing for the analysis of a large number of different aircraft configurations.

1.1.3. Conceptual Design Results. The program DBF2001 analyzed 24 different concept combinations for varying wing area, wing loading, and payload capacity. For each wing area, wing loading and payload capacity, different power plant configurations were analyzed. For each concept, an optimal airplane configuration was found. The design team defined the optimal airplane configuration as the aircraft capable of achieving the highest score. The best configuration found during conceptual design was a mono-wing with an elliptical planform, a wing area of 7.8 square feet, and a fuselage composed of airfoil sections sized to facilitate a payload capacity of 80 tennis balls. With a wingspan of ten feet and retractable landing gear, this aircraft was powered by two Astroflight 625 3.1:1 motors each turning a 17.5x12 propeller. DBF2001 predicted that the optimal airplane would be able to carry a 10-pound steel payload, would have a rated aircraft cost of 5.86, and would yield a total score of 13.31. Three other configurations received very nearly the same score and were also selected for further analysis in preliminary design.

1.2. Preliminary Design

During the preliminary design phase the four concepts selected from the conceptual design phase were studied in greater detail using improved analytical methods. Potential flow models of each aircraft concept were created to yield more accurate predictions of aerodynamic performance. The goal of the preliminary design phase was to select the optimum aircraft from the competing concepts and establish a specific set of engineering requirements to be used in the detail design phase.

1.2.1. Design Alternatives. Several of the airplane characteristics were refined based on the results of conceptual design. These included fuselage size, wing area, and gross weight. Fuselage size was limited to allow only single-layer ball configurations of 7x9, 7x10, 8x9, 8x10, 8x11, 8x12, 9x9 and 9x10. The tennis ball configurations are expressed as $m \times n$, where m is the number of balls in the span direction, and n is the number in the chord direction. Wing areas were limited to a range of 3 to 8 square feet and gross weight was restricted to the range of 17 to 40 pounds.

Because the design team now had a better idea of how the final design would be configured, the team set out to select materials and material properties that would allow the final selected airplane to be built in a lightweight fashion. Materials were evaluated for construction of the main wing, fuselage, landing gear, tail boom, and empennage. Cross sections that would provide the highest strength to weight ratios were evaluated for the landing gear, wing spar, and tail boom.

1.2.2. Design Tools. In order to obtain more accurate estimates of the aerodynamic characteristics of the aircraft configurations being considered, 90 different airplanes of varying configuration and wing area were modeled using the USU potential flow program WINGS2001. Results were obtained from these models for a range of gross weight and airspeed. The team also modified several assumptions in the DBF2001 program subroutines. These modifications provided a more accurate estimate of the actual weight and dimensions. In order to test the viability of the aircraft concepts, a prototype aircraft was designed, built, and flight-tested. Concerns about deep stall and the handling qualities of elliptical wings were addressed. The prototype testing identified design challenges and helped establish engineering requirements and areas for possible improvement in the final design.

1.2.3. Preliminary Results. The modified version of DBF2001 returned an aircraft performance model that better reflected the physical behavior of the actual aircraft. This optimal aircraft consisted of a fuselage sized to carry an 8x10 tennis ball configuration, with a wingspan of ten feet, retractable landing gear in a tail dragger configuration, an elliptical wing area of 4.89 square feet, and the same power plant as that selected during conceptual design. Predicted performance showed that the optimal airplane could carry 14.75 pounds of steel with a rated aircraft cost of 5.49 and attained a total score of 16.82. From the results of the preliminary design analysis, specific engineering requirements to be used in the detail design phase were specified.

1.3. Detail Design.

For the detail design phase, the final aircraft was refined using the optimal aircraft configuration and the engineering requirements determined in the preliminary design phase. The goal of this phase was to optimize the aerodynamics of the airframe, the power plant configuration, and the structural components of the aircraft. After completing the aircraft aerodynamic and structural design, the team predicted the performance of the airplane for the contest flight criteria, performed a detailed static and dynamic stability analysis, and prepared the design for fabrication.

1.3.1. Design Alternatives. Alternatives in the airframe design were investigated for best possible performance. These included wing area, longitudinal position of the wing, spanwise length of the fuselage-to-wing transition, fuselage airfoil design, empennage location and size, and mounting angles for the wing and horizontal tail. Design decisions were made based on aerodynamic efficiency, controllability, weight, and manufactureability. Component placement was also examined in detail. A detailed power plant analysis was performed to select an optimum motor-propeller-battery combination that would meet the engineering requirements while maintaining the highest possible propulsive efficiency.

1.3.2. Design Tools. The detailed design optimization analysis was performed using several computer analysis codes. Aerodynamic analysis was performed using the USU potential flow program WINGS2001, a USU airfoil design panel code named AIRFOIL2000, and an internet airfoil analysis program named CALCFOIL. The motor-propeller efficiency analysis was performed using a USU program named GPROPS. The structural analysis and drafting was accomplished using SDRC's I-DEAS solid modeler and finite element analysis software. Flight test data from the prototype aircraft was also used in the detail design process.

1.3.3. Detail Results. The detail design phase finalized the complete aircraft design. The final airframe optimization further decreased the minimum thrust required for steady level flight by 12.7 percent. The power plant optimization resulted in an efficiency increase of 3.6 percent. The final airframe structure was designed and analyzed to meet the wingtip test as well as landing and flight loads. Dynamic flight analysis showed that the aircraft displayed divergent phugoid and spiral modes. These divergent modes were evaluated and considered to be non-critical to the handling qualities necessary to meet mission requirements. With an adequate safety margin, the final aircraft was calculated to complete three sorties loaded with 15.13 pounds of steel and three sorties loaded with 80 tennis balls. For the final airplane a rated aircraft cost of 5.476 and an overall score of 17.057 was predicted.

2. MANAGEMENT SUMMARY

In the fall of 2000, a team of Utah State University engineering students was assembled with the intent of designing and building an aircraft that would successfully compete in this year's Cessna/ONR Student Design/Build/Fly Competition. The team consisted of fourteen seniors (ten aerospace engineering students and four mechanical engineering students), eight underclassmen majoring in aerospace and mechanical engineering, and two mechanical engineering graduate advisors.

2.1. Architecture of the Design Team

It was obvious that the organization of the team needed to be very dynamic. A project manager was selected to help the team become more agile and effective in executing its responsibilities. The project manager was responsible for coordinating the administrative and technical efforts of the group. For the design phases, the team was divided into task-oriented groups based on expertise and training, and a leader was assigned to each group as shown in Table 2.1.

<i>Project manager: Nick Alley</i> <i>Treasurer: Robert Judd; Procurement: Jason Slack; Logistics: Erick Johnson</i>			
Aerodynamics <i>Leader: Brian Anderson</i>	Propulsion <i>Leader: Quinn Kelly</i>	Structures <i>Leader: Chad Earl</i>	Dynamics & Control <i>Leader: George Tripp</i>
Nick Alley B. Allen Gardner Jerome Jenkins Robert Judd Quinn Kelly Vit Sun George Tripp	Bryce Harris Jason Slack	Nick Alley Jeff Hibsmann Jared Jeffries Erick Johnson Robert Judd Underclassmen	Brian Anderson B. Allen Gardner Bryce Harris Jerome Jenkins Jason Slack Vit Sun

Table 2.1. Organizational structure of the design team.

Under the direction of the project manager, the group leaders were responsible for dividing up the group's workload among its members. Figure 2.1 shows how each team member was involved in the design, analysis, and construction of the airplane. A rating of 5 indicates maximum involvement by the student and a rating of 0 indicates no involvement.

2.2. Configuration and Schedule Control

The team set forth a schedule to visualize the major and minor project milestones and the time periods in which they were to be realized (see Figure 2.2). The project manager was responsible for maintaining the schedule and ensuring that milestones were being met.

Each week the entire team met with faculty advisor Dr. W. F. Phillips. During these meetings each individual group reported their progress and future goals to the team. This provided a forum for interdisciplinary discussion of problems and overall status of the project. At other times during the week, groups met individually either to work on tasks as a group or to discuss the manner in which their designs could be improved. Additionally, group leaders communicated the status of assigned tasks to the project manager daily.

Each and every member was vital to the success of the project as every goal set forth by the team was completed as a team.

	Nick Alley	Brian Anderson	Chad Earl	Bryce Harris	Jeff Hibsmann	B. Allen Gardner	Jared Jeffrey	Jerome Jenkins	Erick Johnson	Robert Judd	Quinn Kelly	Jason Slack	Vit Sun	George Tripp	Underclassmen	Graduate Students
3. Conceptual Design	5	5	5	5	5	5	5	5	5	5	5	5	5	5	3	5
3.1 Design Parameters - Initial Phase	5	5	5	5	5	5	5	5	5	5	5	5	5	5	3	5
3.2 Figures of Merit - Initial Phase	5	5	5	5	5	5	5	5	5	5	5	5	5	5	3	5
3.3 Quantitative Analysis	5	5	5	5	5	5	5	5	5	5	5	5	5	5	3	5
3.3.1 Wing Analysis	1	0	0	0	0	5	0	0	0	5	0	0	5	0	1	3
3.3.2 Empennage Analysis	1	0	0	0	0	0	0	0	0	0	0	5	0	5	1	4
3.3.3 Fuselage Analysis	1	0	5	0	5	0	5	5	5	0	0	0	0	0	1	3
3.3.4 Power Plant Analysis	1	0	0	5	0	0	0	0	0	0	5	0	0	0	1	0
3.4 Numerical Analysis	5	5	2	2	2	2	2	2	2	2	3	2	2	0	0	4
3.5 Configuration Selection	5	5	5	5	5	5	5	5	5	5	5	5	5	5	0	5
4. Preliminary Design	4	5	3	4	4	4	4	5	4	4	4	4	5	5	1	3
4.1 Prototype Construction and Testing	5	2	3	4	5	0	4	5	4	5	0	3	5	2	2	1
4.2 Figures of Merit	1	3	0	0	0	3	3	5	3	3	0	0	5	0	0	0
4.3 Refinement of Design Parameters	5	0	0	0	5	0	3	4	3	2	3	0	0	2	0	0
4.4 Refined Numerical Analyses	1	5	0	3	0	4	0	0	0	0	5	4	5	4	0	5
4.5 Configuration Selection	1	5	3	3	0	4	0	2	0	0	4	0	0	4	0	0
4.6 Engineering Requirement Selection	5	1	0	0	0	3	0	3	0	0	0	3	3	3	0	0
5. Final Design	5	5	5	5	5	5	5	5	5	5	5	5	5	5	2	5
5.1 Configuration Optimization	2	5	0	5	0	5	0	5	0	5	5	5	5	5	0	5
5.1.1 Airframe	1	5	0	2	0	4	0	5	0	2	3	3	4	5	0	3
5.1.2 Propulsion Systems	2	1	0	5	0	0	0	0	0	0	5	0	0	0	0	0
5.1.3 Structural Systems	5	0	5	0	5	2	5	3	5	5	0	3	0	0	0	3
5.1.4 Control System	5	0	0	0	0	0	0	0	3	5	0	5	0	0	0	0
5.1.5 Final Configuration	5	3	3	2	2	2	3	4	4	0	4	3	1	5	0	4
5.1.6 Assembly Drawings	1	0	5	0	5	0	5	0	5	0	0	0	0	0	5	0
5.2 Performance Analysis/Optimization	2	0	5	0	5	0	5	0	5	0	0	0	0	0	2	0
5.2.1 Take-off and Clime	1	0	5	3	5	0	5	0	5	3	0	0	0	0	0	2
5.2.2 Range, Endurance and Payload	1	1	3	1	3	1	3	2	3	3	0	0	0	3	0	5
5.2.3 Handling Qualities	4	5	0	3	0	4	0	2	0	0	4	0	0	4	0	0
6. Manufacturing Plan	5	2	1	5	4	1	3	2	5	5	2	5	3	2	2	2
6.1 Figures of Merit	1	0	0	5	0	0	0	0	0	5	0	0	0	0	0	0
6.1 Manufacturing Process Selection	5	0	0	0	3	0	3	0	5	5	0	3	0	0	0	0
6.3 Detail Manufacturing Plan	5	0	0	3	0	0	0	0	0	5	0	5	0	0	0	0
Final Airplane Construction	5	3	1	3	5	1	3	5	5	5	2	4	5	2	3	2
A. Documentation of Design	4	5	4	4	5	4	4	5	4	4	4	5	5	4	3	5
A.1 Journal	2	5	2	2	2	2	2	5	2	2	2	5	5	2	2	2
A.2 Letter of Intent	0	0	0	0	0	0	0	3	0	0	0	0	0	0	0	5
A.3 Final Report	5	5	1	5	3	5	1	5	1	5	5	5	5	5	0	4
A.4 Addendum Report	0	0	5	0	5	0	5	0	5	0	0	0	0	0	0	1
B. Drafting Package	0	0	5	0	5	0	5	0	5	0	0	0	0	0	5	0

Figure 2.1. Personnel Assignments. A summary of how each member of the design team contributed to the completion of the project goals. A 5 indicates maximum involvement by the student.

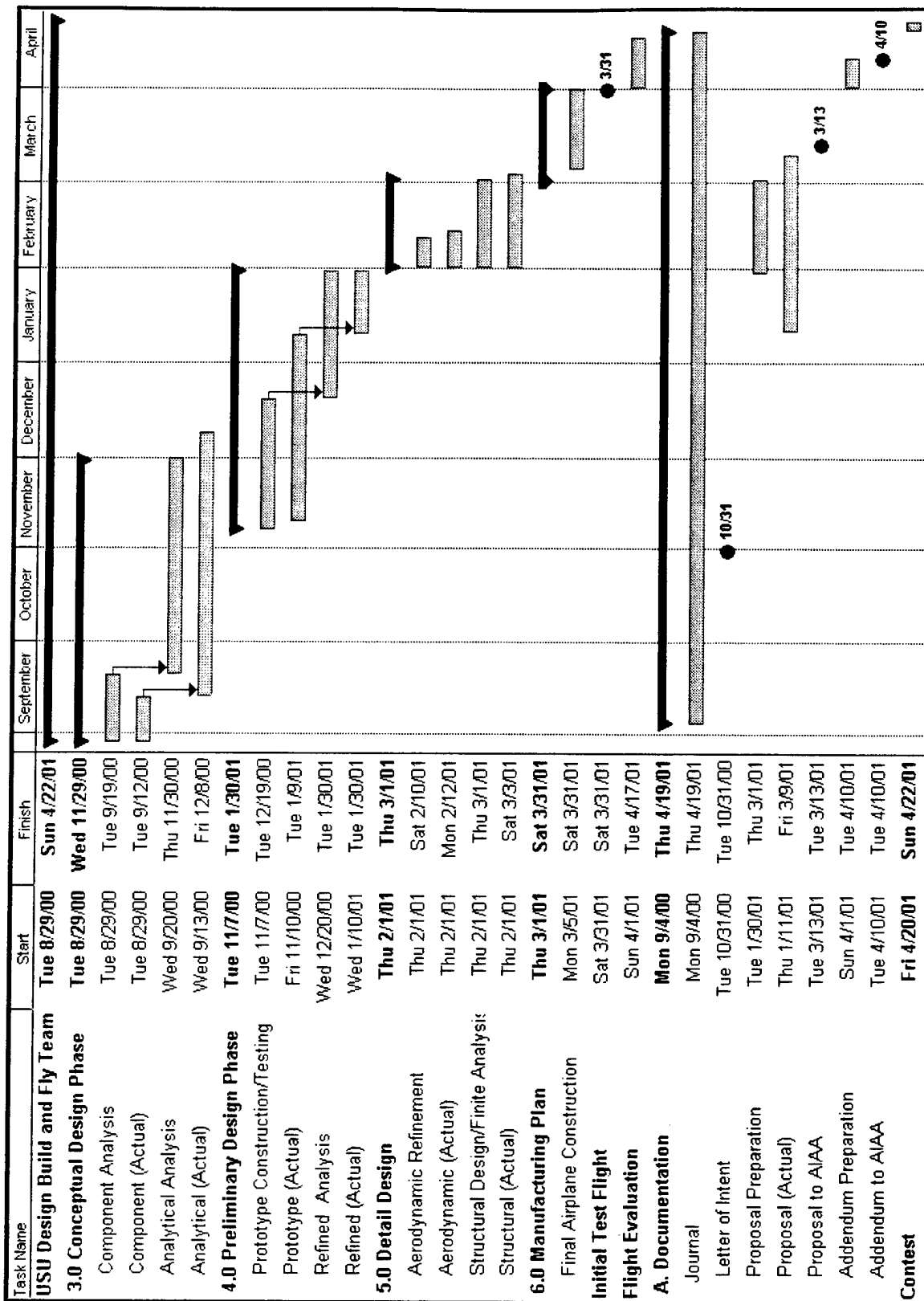


Figure 2.2. Project Schedule. This schedule illustrates the project milestones and time periods designated for each design phase. The blue bars represent the planned schedule while the pink bars show the time periods over which the events actually occurred.

3. CONCEPTUAL DESIGN

During the conceptual design phase, the team members investigated different airplane design parameters that could be used to construct the final airplane. After identifying the parameters, each was studied further by modeling complete airplane designs with different combinations of these parameters. Each airplane design was numerically evaluated using a FORTRAN program written by the design team. Each design received a rating based on weighted figures of merit. The results of the ratings determined the designs that were either eliminated or further analyzed in the preliminary design phase.

3.1. Design Parameters and Aircraft Configurations

Key design parameters and aircraft configurations were identified during the conceptual design phase. These were investigated and rated based on figures of merit to determine the design features that would be advantageous to analyze in greater detail. At this point, any aircraft configuration that was deemed too difficult to build or incurred too high a rated aircraft cost was eliminated.

3.1.1. Wing Planform. The team desired to design the most efficient airplane possible while still maintaining good handling characteristics. Though it is not a factor in rated aircraft cost, the choice of wing planform can have a significant effect on the performance of an airplane. Planform shapes evaluated included: tapered, rectangular, and elliptical.

Previous experience by team members and other USU design teams has shown that low Reynolds numbers encountered at the wing tips of small aircraft having tapered wings result in poor handling qualities. Therefore, the tapered planform shape was not considered further in conceptual design.

The rectangular planform was evaluated because of its aerodynamic stability and ease of construction. Using the rectangular wing would eliminate a large amount of uncertainty, as there is a considerable amount of planform data and construction experience gained from previous USU teams.

According to aerodynamic theory, the elliptical wing out-performs the rectangular wing. The lift slope and the span efficiency factor for the elliptic wing are greater for any aspect ratio. Previous teams eliminated the concept of elliptical planforms due to construction complexity. Manufacturability was of less concern to the team this year because of access to machinery that is able to precisely cut elliptical wings shapes. However, the team was concerned about the handling characteristics of an elliptical planform, as an elliptical wing tends to have very low Reynolds numbers at its tip, which may cause the tip to stall before the rest of the wing.

Elliptical and rectangular planforms were chosen for analysis in the conceptual design phase.

3.1.2. Wing Configuration. Wing configuration also greatly affects the performance of an airplane. Depending on the given wing configuration, greater lift slopes may be obtained, efficiencies increased, drag reduced, and structural requirements simplified. For the conceptual design phase, mono-wings without winglets, and bi-wings without winglets were considered. Winglets were not considered for either case because of the small performance advantage compared to the large rated aircraft cost penalty.

The greatest advantage of using a bi-wing is the increase in lift that is created by two wings as opposed to one. Because of this extra lift a heavier payload could be carried, resulting in a higher total score. However, due to the interaction between the two wings, the lift per unit wing area is not as high for a bi-wing as it is for a mono-wing having the same aspect ratio. With an allowable wingspan of ten feet, a mono-wing could efficiently create the required lift. Furthermore, rated aircraft costs increase due to the penalty placed on a bi-wing configuration.

An efficient mono-wing with a large wingspan avoids higher rated aircraft costs and is more easily manufactured. However, the bi-wing configuration may enable more payload to be carried.

3.1.3. Fuselage Configuration. The fuselage is the backbone of the airplane. It must possess the structural strength to withstand the forces induced on the assembly by the wings, tail, landing gear, payload, and motor. It must contain the payload, batteries, servos and other electrical equipment. The fuselage must also be aerodynamically efficient, lightweight, and easily manufactured. It may need to be large enough to carry one hundred tennis balls, and must allow for fast and easy loading and unloading of payload. Four basic fuselage shapes were considered: a vertical fuselage with two different airfoil shapes, and a horizontal fuselage with two different airfoil shapes.

The first shape considered was a vertical airfoil shape. An airfoil is the most aerodynamically efficient shape available. It would be relatively easy to fabricate and facilitate simple wing and landing gear mounts. By cutting the fuselage airfoil at its point of maximum thickness, and placing a constant-thickness extension between the two-airfoil halves, the fuselage becomes very space efficient. Tennis balls are easily stacked in the resulting shape. The vertical fuselage is most advantageous for a biplane. The engine could also be mounted sufficiently high to allow for a large propeller and small landing gear, resulting in increased efficiency and ground handling qualities. The only real disadvantage of this shape is its susceptibility to cross winds.

The horizontal airfoil shape was also considered. Not only does it have very low drag, but unlike the vertical airfoil, the horizontal airfoil could provide some lift. It is not as susceptible to cross winds as the vertical airfoil. Attachment of the wings and landing gear would be relatively simple, and it could be designed to provide the required strength. Like the vertical fuselage shape, the horizontal fuselage is space efficient. The horizontal airfoil shape is best suited to a monoplane. Its only disadvantage is increased difficulty in placing the engine high enough to utilize a large propeller.

Modified NACA 0012 and NACA 0015 airfoil sections were both considered as fuselage sections during conceptual design. Both airfoils are symmetric and easy to manufacture. The NACA 0012 has less parasitic drag than a NACA 0015 airfoil for a given planform area and the flow is mostly laminar at the design Reynolds number. A NACA 0015 airfoil, however, allows for higher angles of attack before the onset of stall because of its thickness. The total length of the fuselage using a NACA 0015 airfoil can be up to twenty percent shorter for a given maximum thickness. Fuselage length is an important factor in the rated aircraft cost, as shorter fuselages equate to lower rated aircraft costs.

3.1.4. Empennage Configuration. The empennage is used to control and stabilize the airplane in pitch and yaw. In conceptual design a tail structure was selected, sized, located, and evaluated based on performance and stability. Five different tail structures were initially considered: T-tail, V-tail, canard configuration, flying wing (no tail), and conventional tail.

A conventional tail consists of a horizontal and vertical stabilizer located aft of the center of gravity, with the vertical stabilizer located above the horizontal stabilizer. This mounting configuration is relatively strong, as each surface supports only its own weight. The conventional tail is easily manufactured and analyzed. It has been well researched and proven in past aircraft designs.

A T-Tail resembles a conventional tail, except the horizontal stabilizer is located at the top of the vertical stabilizer. The T-Tail is more aerodynamically efficient than the conventional tail because the horizontal stabilizer is in a region of reduced downwash, but stiffness requirements of the tail assembly require more structure to support the raised horizontal stabilizer. Manufacture of the T-Tail is also more complex, as the elevator control linkages must be transferred through the vertical stabilizer.

A V-Tail uses two surfaces aligned in a V-shape to provide stability in pitch and yaw. A V-Tail can be lighter than a conventional tail but requires a more complex structure to analyze, build, and operate.

A canard configuration places the control surface forward of the center of gravity. Because a canard will generally carry positive lift, this configuration can be aerodynamically more efficient at cruise and make the plane difficult to stall. However, takeoff performance is compromised.

A flying wing (no tail) accomplishes stability by altering the shape of the main wing using sweep, twist, and different airfoil sections. Rated aircraft cost would be reduced because no vertical or horizontal surfaces would be present. This configuration could also reduce drag and increase efficiency but is much more difficult to design to insure proper stability, control, and handling qualities.

The conventional tail was selected for analysis because of its simplicity and proven performance.

3.1.5. Landing Gear Configuration. Landing gear affects the performance of an airplane in the air and on the ground. Quality landing gear has low drag characteristics and is lightweight, without compromising strength and handling. The two types of main gear considered were fixed and retractable gear.

Traditional solid spring landing gear common to RC-Modelers has been time tested to be the most reliable landing gear available. It can be manufactured to be strong, durable and lightweight. However, the drag produced while in flight is considerable.

Properly constructed retractable landing gear has no drag while in flight. The problems with retractable landing gear are increased weight, mounting complexity, and reliability. Use of retractable gear also warrants the addition of a servo, increasing the rated aircraft cost.

Both traditional and retractable landing gear were selected for detailed analysis. Due to its relative unimportance to the outcome of the conceptual and preliminary design phases, the decision to use taildragger or tricycle landing gear was deferred to the detail design phase.

3.1.6. Power Plant. The power plant consists of three major components: motor, batteries, and propeller. The power plant must be able to do two things for the airplane to complete its mission. First, it must provide enough thrust to accomplish liftoff within 200 feet. Second, it must provide enough power to fly for at least the time required for one scoring sortie, and at most there must be enough power to fly for a ten-minute time period. The closer the battery can come to allowing the full ten-minute time interval, the higher the achievable score.

Power consumption was a major concern. The competition rules specify a maximum of five pounds of propulsive batteries. Based on the findings of previous teams, optimal performance is gained through the use of all five pounds of NiCad batteries. A number of battery cell layouts were considered in order to find the configuration that minimized the power drawn from the batteries.

For conceptual design, all brushed Astroflight motors were considered using the available motor specification data. Multiple motor combinations were also considered. The 40-Ampere fuse requirement could make multiple motors a necessity as one motor, drawing under 40 amperes, may not be able to take off in the allotted distance. Use of multiple motors, however, imposes a higher rated aircraft cost.

Commercially available propellers coupled with various motor and battery configurations were considered in conceptual design.

3.1.7. Aircraft Configurations. From different combinations of the above design parameters 24 aircraft configurations were selected for detailed analysis during the conceptual design phase. These are shown in Fig. 3.1. Many other aircraft configurations could have been considered. However, because of the very limited time allocated for conceptual design, the team had to consider the tradeoff between the number of configurations investigated and the level of detail used to optimize each of the chosen configurations. It was decided that a better final design would probably result, if fewer configurations were analyzed in greater detail.

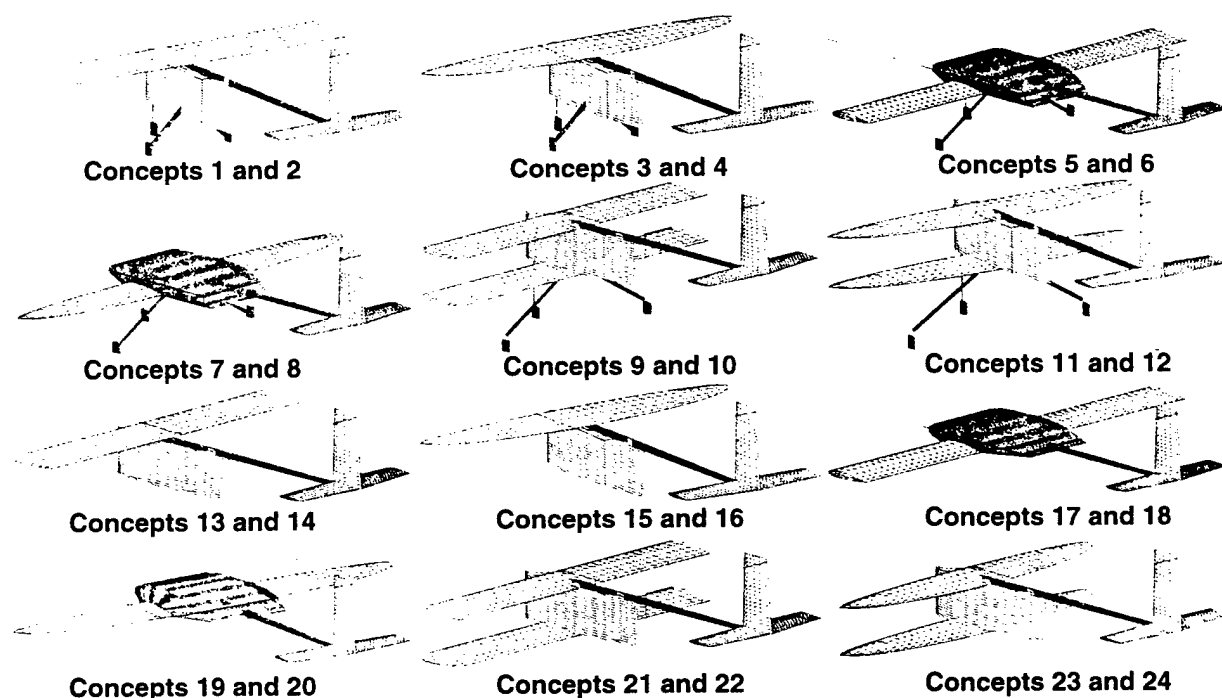


Figure 3.1. Aircraft configurations considered during the Conceptual Design Phase. Because the subtle difference between a NACA 0012 and NACA 0015 fuselage cannot be readily seen, only the NACA 0015 fuselage is shown. Refer to Table 3.1 for more detail.

3.2. Figures of Merit

A figure of merit is a way to quantify and compare the benefits and drawbacks of a given design concept. The figures of merit were selected for conceptual design in an attempt to produce the highest possible flight score at the competition. Only three parameters directly affect the flight score. These are, the weight of steel carried, the number of tennis balls carried, and the rated aircraft cost. Handling qualities were judged to be very important and to have a significant effect on the flight score. However, handling qualities were not considered during the conceptual design phase because the analytical tools used were not sufficient to acquire a true representation of the handling qualities. This factor was instead deferred to the detail design phase. Therefore, the following three figures of merit were chosen based on the scoring criteria for the competition: heavy payload, light payload, and rated aircraft cost.

3.2.1. Heavy Payload. The total score depends on the weight of steel that a given design can carry. Competition rules state that the minimum weight of steel that can be carried is five pounds. The maximum weight of steel is limited by a maximum gross airplane weight of 55 pounds. For each pound of steel carried on a heavy payload sortie, the raw flight score increases by one point.

3.2.2. Light Payload. The second contributor to the total score is the number of tennis balls carried by the selected design. The competition rules state that a minimum of 10 tennis balls and maximum of 100 may be carried during a light payload sortie. A raw score of one point is accumulated for every five tennis balls carried on a light payload sortie.

3.2.3. Rated Aircraft Cost. Rated aircraft cost was included in the figures of merit both as a contest requirement and as a method of quantifying the cost of the concepts being studied. Because the total score is inversely proportional to the rated aircraft cost, the higher the cost, the lower the overall score.

Concept ID	Design Parameters					Figures of Merit			Results	
	Landing Gear N=non-retractable R=retractable	Wing Planform E=elliptical R=rectangular	Wing Type M=mono-wing B=bi-wing	Fuselage Type V=vertical H=horizontal	Fuselage Airfoil	Best Number of Tennis Balls	Best Weight of Steel (pounds)	Best Rated Aircraft Cost (k\$)	Best Total Score	Decision
1	N	R	M	V	0012	80	16.5087	6.595	12.362	E
2	N	R	M	V	0015	90	14.5435	6.228	12.786	E
3	N	E	M	V	0012	80	16.5283	6.638	12.290	E
4	N	E	M	V	0015	90	14.5619	6.268	12.712	E
5	N	R	M	H	0012	80	13.5464	5.822	12.477	E
6	N	R	M	H	0015	80	14.2699	5.749	13.012	FA
7	N	E	M	H	0012	80	13.7433	5.778	12.675	E
8	N	E	M	H	0015	80	14.4664	5.690	13.251	FA
9	N	R	B	V	0012	90	16.4938	6.996	11.646	E
10	N	R	B	V	0015	80	17.2039	6.925	12.073	E
11	N	E	B	V	0012	80	16.5007	7.034	11.587	E
12	N	E	B	V	0015	80	17.2104	6.948	12.037	E
13	R	R	M	V	0012	70	12.8325	6.456	12.468	E
14	R	R	M	V	0015	70	13.4548	6.394	12.882	E
15	R	E	M	V	0012	70	12.8514	6.512	12.371	E
16	R	E	M	V	0015	70	13.4734	6.434	12.810	E
17	R	R	M	H	0012	70	9.7504	5.951	11.973	E
18	R	R	M	H	0015	80	9.8049	5.913	13.092	FA
19	R	E	M	H	0012	70	9.9066	5.903	12.149	E
20	R	E	M	H	0015	80	9.9831	5.859	13.305	FA
21	R	R	B	V	0012	80	12.2652	6.934	12.229	E
22	R	R	B	V	0015	80	12.9832	6.848	12.695	E
23	R	E	B	V	0015	80	14.9922	7.209	12.896	E
24	R	E	B	V	0012	80	14.2825	7.296	12.452	E

Table 3.1. The design parameters and figures of merit that were used to screen competing design concepts. Those concepts with the greatest total score were selected for further analysis. The "FA" in the decision column stands for further analysis and the "E" stands for eliminate.

3.3. Quantitative Analysis of Selected Parameters

3.3.1. Wing Analysis. For mono-wings, chord length was varied from 6-inches to 3-feet and each wing was modeled in a simulation program, WINGS2001. For each wing the lift slope and the span efficiency factor were computed. This was done for both the rectangular and elliptical wing shapes. Bi-wing chord length was varied from 6-inches to 3-feet, wing spacing was varied from 6-inches to 3-feet, and each wing was modeled in WINGS2001. Again span efficiency factor and the lift slope were computed for both the elliptical and rectangular planforms. The results of the analyses performed for the mono-wing and bi-wing planforms were interpolated using a least-squares fit to obtain expressions used in the WING subroutine discussed in Section 3.4.2.

The wing area and gross weight of previous years' airplanes were measured to obtain an empirical expression for computing wing weight as a function of wing area and total airplane weight. This expression also was used in the WING subroutine discussed in Section 3.4.2.

3.3.2. Empennage Analysis. The main focus for the initial design of the empennage was to develop first order estimates for dimensions and weight. The analysis consisted of four parts: determining the surface areas for the empennage, determining the required properties of the tail boom, optimizing the design of the empennage for weight, and calculating the empennage parasitic drag coefficient.

The required surface area of the empennage was determined in order to provide pitch and yaw stability for the airplane. The pitch stability analysis was based on the moment distribution of the airplane along a fuselage reference line. The aerodynamic centers of the wing and horizontal stabilizer and the center of gravity of the airplane were all assumed to lie on the fuselage reference line. The lift slopes for the wing and horizontal stabilizers were calculated using finite wing theory for an elliptical wing. The horizontal stabilizer lift slope included the theoretical downwash of an elliptical wing.

Stability was determined by examining the derivative of the pitching moment about the center of gravity of the airplane. The amount of stability was quantified by referencing the neutral point to the center of gravity using the standard definition of the static margin. Using the static margin, the required horizontal stabilizer area was determined as a function of wing area, lift slope, and distance from the center of gravity. The vertical stabilizer was assumed to have 55 percent the area of the horizontal stabilizer in the conceptual design phase.

The weights of the horizontal and vertical surfaces were calculated from the volume computed for the surfaces multiplied by the density of foam and balsa. For the conceptual design the tail was optimized to minimize weight. The required stiffness was computed from an aeroelastic control loss constraint.

Figure 3.2 shows a plot of tail weights as a function of tail boom length for a sample airplane configuration. The figure shows that for this configuration, the minimum weight occurs at a tail boom

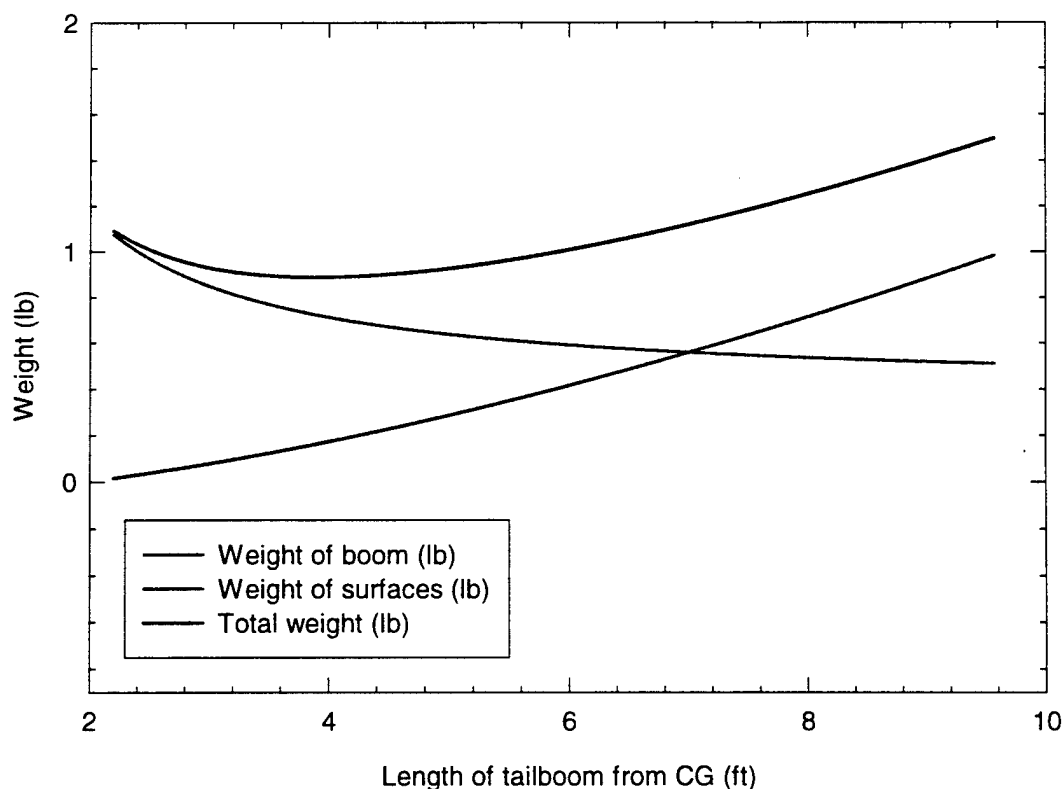


Figure 3.2. Tail weight as a function of tail length for a sample airplane configuration.

length of 3.5 feet. The length corresponding to minimum tail weight could later be used as a guideline in iterating with respect to the rated aircraft cost. Since the tail boom length was included in the fuselage portion of the rated aircraft cost, the optimum tail may not exactly correspond to the minimum tail weight.

The parasitic drag for the horizontal and vertical surfaces was determined using NACA 0009 airfoil data. The drag for the wing was determined using the best-fit equations developed from WINGS2001. The tail boom drag coefficient was assumed to be 1.0, based on the frontal profile area of the tail boom.

3.3.3. Fuselage Analysis. Efficient use of a fuselage with a NACA 0015 or NACA 0012 airfoil requires cutting the airfoil at the location of maximum thickness and inserting a constant thickness section large enough to enclose an entire payload. Given a thickness for a NACA 4-digit series airfoil, the chord length is fixed. If the thickness is increased by stacking multiple layers of tennis balls, the overall length of the fuselage is increased even though the payload bay length shrinks. Stacking tennis balls two or three balls high thus increases the overall length and total parasitic drag due to increased surface and frontal area. A single layer of tennis balls yields the shortest, as well as the thinnest fuselage resulting in less drag and fuselage weight. A single layer of tennis balls was determined to be the optimum configuration for the fuselage because it gave the best combination of drag and rated aircraft cost.

3.3.4. Power Plant Analysis. An analysis of battery configuration, in an effort to optimize battery capacity, was performed. Additional optimization was performed in the DBF2001 program (see Section 3.4) by finding the best motor/propeller/battery combinations.

Analysis was performed for 10 different NiCad cells, ranging from 500 milliamp-hours to 5000 milliamp-hours per cell. The cells were assumed to have a voltage per cell of 1.1 V and a resistance per cell of about 0.004 Ohms. A program was written to determine the optimal configuration for the maximum number of cells in the five-pound limit. Some of this weight (0.72 lbs) was allotted for cables, battery connectors and wrapping, leaving 4.28 pounds for cells. This decision was based on the weight and number of cells in last year's flight battery pack. The code analyzed every possible cell combination for a given required voltage, and the battery configuration giving the highest capacity was chosen for that voltage. For configurations requiring two or three motors, two and three packs were used, respectively. These configurations were also optimized. After the program found the best combinations for all the given voltage levels, three of the voltages were selected along with their corresponding battery capacities and resistances. These results were tabulated. For two and three motor configurations, the output was 19.8 volts at 0.072 Ohms, and 13.2 volts at 0.048 Ohms, respectively. At these three levels, capacity increases for a decrease in voltage. This shows that if the aircraft could run a lower voltage motor, significant increases in battery capacity would result, along with a lower overall battery resistance. These levels were defined and utilized in the POWER subroutine discussed in Section 3.4.6.

3.4. Analytical Tools

The design team wrote a FORTRAN computer program called "DBF2001" to find which aircraft configuration would obtain the highest total score. This program and its subroutines are described below.

3.4.1. Program Architecture. DBF2001 served as a main routine calling several subroutines to perform specific tasks in the conceptual evaluation. For each case, the WING, FUSELAGE, TAIL and LANDING GEAR subroutines calculated aerodynamic and structural characteristics; the POWER subroutine determined power plant characteristics; the FLIGHT subroutine predicted mission profile performance; and the RAC subroutine computed rated aircraft cost. The inputs required by the program were the different aircraft parameters considered: landing gear type, wing planform shape, wing type, fuselage orientation, fuselage airfoil, and number of tennis balls and their configuration. The program also iterated

on gross aircraft weight and wing loading. After the complete aircraft configuration was defined by calling the WING, FUSELAGE, TAIL, LANDING GEAR, and POWER subroutines, DBF2001 calculated the total possible laps using the FLIGHT subroutine, then computed a flight score. The total score was found by dividing the flight score by the rated aircraft cost. The aforementioned subroutines are described below. See Figure 3.3 for a flowchart of the program.

3.4.2. WING subroutine. The WING subroutine was used to obtain the aerodynamic and weight characteristics for each configuration considered. The WING subroutine consisted of a model of the main wing and fuselage. This model was chosen so a comparison of the design configurations could be accomplished with reduced complexity, while maintaining as accurate and broad a solution as necessary in the conceptual phase. To reduce complexity further, each concept incorporated a Selig-Donovan 7062 airfoil shape based on desirable flight characteristics at the design Reynolds number of 400,000.

The input to the WING subroutine was the same aircraft characteristics that were iterated in the main program. These variables were: planform area, wing spacing (bi-wing configuration only), number of wings (bi-wing or mono-wing), planform (rectangular or elliptical), and gross airplane weight.

To model wing performance and wing weight, the WING subroutine utilized interpolated data acquired by WINGS2001 and measurement of past years' airplanes, as discussed in Section 3.3.1.

The outputs of the WING subroutine for each iteration were: lift slope, parasitic drag coefficient, zero-lift angle of attack, wing weight, and number of control surfaces and servos included in the wing structure.

3.4.3. TAIL subroutine. The TAIL subroutine was used to calculate the size and location of tail surfaces for required longitudinal and lateral stability of each aircraft. The subroutine was based on a force and moment analysis that estimated the horizontal and vertical surface areas needed to provide static

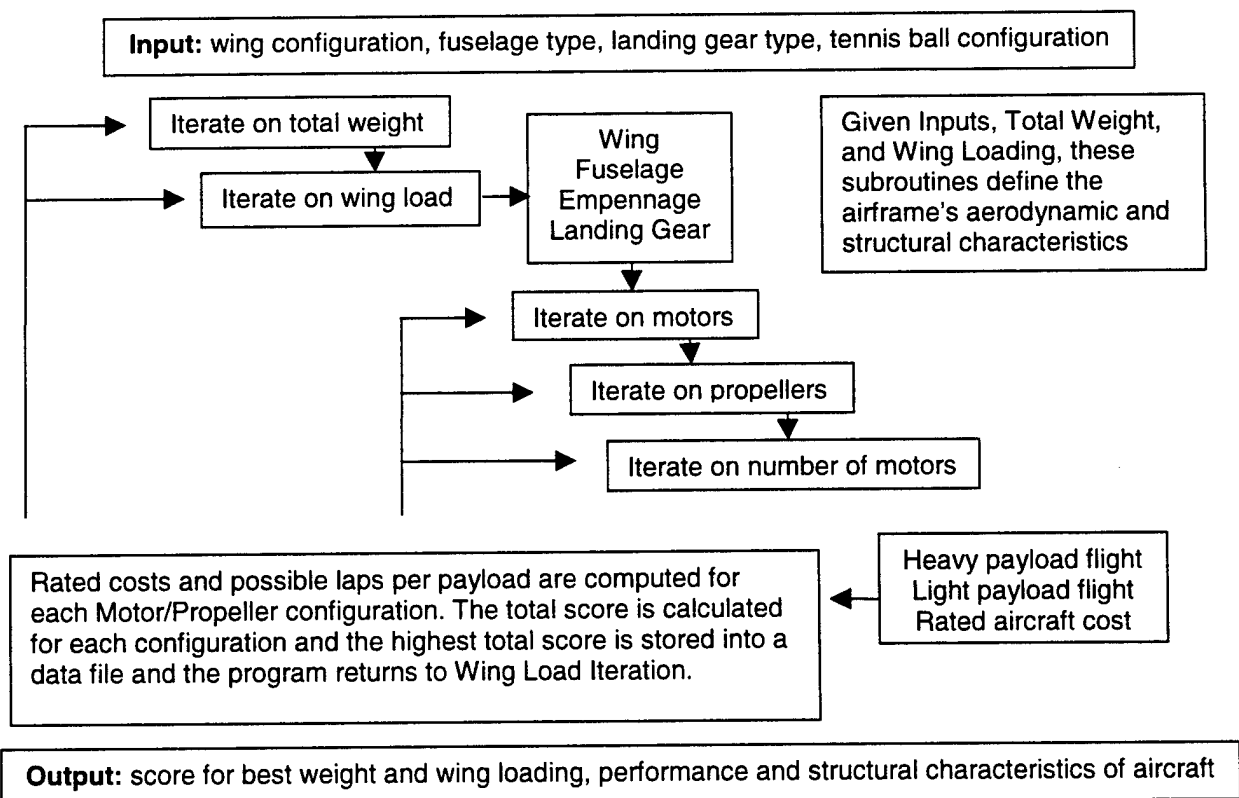


Figure 3.3. Program "DBF2001" Flowchart

stability. Using an iterative process that accounts for aeroelastic effects, drag, and stability requirements, the TAIL subroutine generated an optimal tail design for a given wing configuration. This optimal tail design was based on minimizing weight. The primary outputs of the TAIL routine were the required tail boom stiffness, empennage weight, empennage surface area, and location. The TAIL subroutine also calculated the empennage parasitic drag coefficient.

3.4.4. FUSELAGE subroutine. The FUSELAGE subroutine estimated the size, weight, and parasitic drag coefficient of the fuselage for a specific orientation, payload configuration, and NACA four-digit airfoil number. The light payload (tennis balls) was assumed to be carried in a constant thickness section inserted at the point of maximum thickness of the airfoil. The number of tennis balls, accounting for payload configuration, was then used to determine the specific payload area.

The subroutine used the parameters described above to compute the fuselage dimensions. To compute the fuselage length, the subroutine divided the maximum thickness by the last two digits of the NACA number. The airfoil length was added to the payload bay length to acquire the total fuselage length. Area and perimeter calculations determined the planform area and the perimeter using equations for the NACA four digit airfoils. The weight of the fuselage was estimated using provisions for a main spar, balsa skin, monokote covering, payload support plate, motor mounts and internal structure. The volume and surface area of this structure was estimated and multiplied by the material weights to yield the estimated weight of the fuselage section. The configuration was different depending on the orientation of the fuselage. Finally, a polynomial fit from known drag coefficients was used to estimate the parasitic drag coefficient for the fuselage.

3.4.5. LANDING GEAR Subroutine. This subroutine computed the weight and parasitic drag coefficient for the landing gear. The inputs to this subroutine were gross weight of the airplane and gear type (retractable, non-retractable). The subroutine used the weights of previously built landing gear and a Lagrangian interpolation scheme to estimate the weights for the non-retractable gear. For retractable gear, the program fixed the weight of the gear as specified by the manufacturer. A parasitic drag coefficient of 1.0 was assigned for both non-retractable and retractable configurations based on the frontal area of the landing gear.

3.4.6. POWER subroutine. To help optimize the design of the airplane components, the POWER subroutine was written. This portion of the program computed the power in Amps being used by a given motor/propeller/battery combination for a specified flight condition (takeoff, cruise, turning, etc).

A database containing 11 different electric motors in 110 different gearing and voltage combinations was used. A propeller database with 69 propellers ranging from 12 to 32 inches in diameter was also utilized. Some 3- and 4-blade propellers were included. The POWER subroutine then used a propeller code called EPROPS to determine available thrust and required power at a given airspeed.

A variation of the POWER subroutine computed the thrust produced by each motor/propeller combination from zero airspeed to the liftoff velocity. This thrust/airspeed data was used with a second-order polynomial fit to obtain an expression relating thrust and airspeed. This expression was then used to integrate the thrust over the takeoff and to determine the energy used from the batteries.

3.4.7. FLIGHT subroutine. The objective of the FLIGHT subroutine was to quantitatively evaluate each airplane configuration using flight performance as the criteria. Each airplane configuration was comprised of wing, empennage, landing gear, fuselage, and motor/propeller combination. Aided by the POWER subroutine the FLIGHT routine determined if the motor/propeller combination would satisfy the 200-foot takeoff distance, and also calculated the milliamp-hours used by the aircraft configuration per lap around

the course. The time and milliamp-hours needed for each mission task was computed. In performing the analysis, each sortie was divided into five sections: ground roll, transition (climb to obstacle clearance height), steady coordinated turn, steady level flight, and descent. Time to re-configure each payload (steel or tennis balls) was also included in the analysis.

3.4.8. RATED AIRCRAFT COST subroutine. This subroutine was used to calculate the rated aircraft cost from the guidelines provided by the competition officials. All inputs to this subroutine were obtained from the WING, TAIL, FUSELAGE, LANDING GEAR and POWER subroutines.

3.5. Configuration Selection.

The airplane configuration with the highest score for the conceptual design phase was determined to be an elliptical mono-wing, with retractable landing gear and a horizontal NACA 0015 fuselage sized to carry an eight by ten (8x10) tennis ball configuration. The wing area was 7.8 square feet. The airplane was able to fly three heavy payload sorties, with 10 pounds of steel, and three light payload sorties, with eighty tennis balls. For propulsion, two Astroflight 625 motors were selected, each turning a 17.5-inch diameter by 12-inch pitch propeller. This airplane configuration had a rated aircraft cost of 5.86. The total score was 13.31 points. A graphical representation of the results obtained for this design is shown in Figure 3.4. The final ranking chart for each figure of merit was included as Table 3.1. The accuracy of the approximations used during the conceptual design process was not sufficient to eliminate designs using rectangular wing planforms and non-retractable landing gear. As can be seen from Table 3.1, the difference between the highlighted scores was not sufficient to make a clear-cut decision as to which designs should be eliminated. Furthermore, the reliability of the retractable landing gear and the handling characteristics of elliptical planform wings presented a concern. Thus, concepts 6, 8, 18, and 20 were all considered in the preliminary design phase.

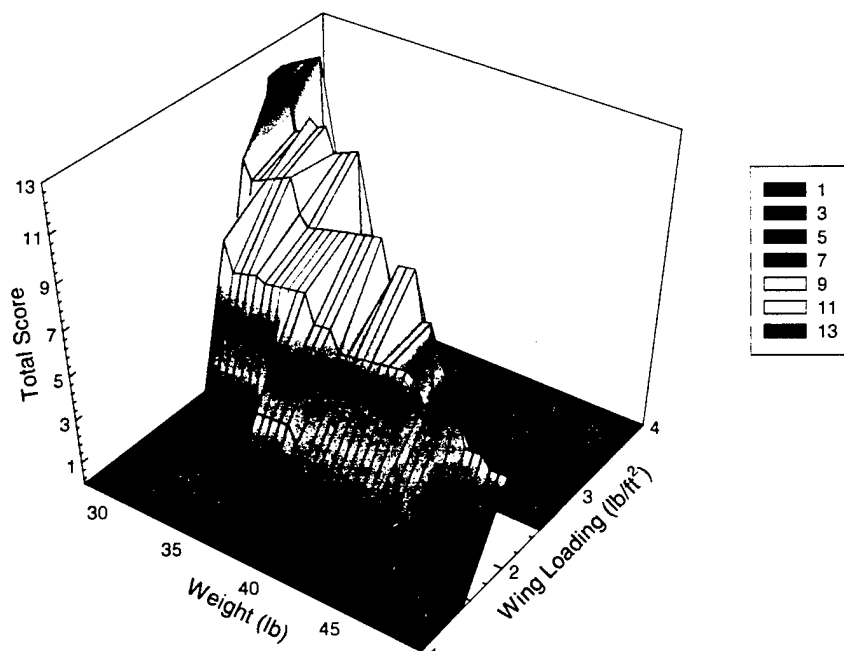


Figure 3.4. A three-dimensional plot of results obtained from the conceptual design for the highest-scoring configuration. A score of zero in the figure corresponds to the inability of the airplane design to meet the 200-foot takeoff distance. A top score of 13.31 was achieved.

4. PRELIMINARY DESIGN

During conceptual design, the program "DBF2001" was used to perform an exhaustive search over a wide range of airplane configurations. This was done to find the aircraft configurations that would best satisfy the mission requirements. These mission requirements were to carry the maximum number of tennis balls and the largest amount of steel through as many sorties possible in a ten-minute period with an airplane of cost effective design. Each design selected from the conceptual design phase included a mono-wing configuration with a modified NACA 0015 horizontal fuselage. Designs with retractable and non-retractable landing gear, as well as elliptical and rectangular wing planforms were included. These configurations were designated as concepts 6, 8, 18 and 20 in Fig. 3.1 and table 3.1.

The first objective of the preliminary design phase was to determine which of these four aircraft configurations would best meet the mission requirements. The second objective was to specify engineering requirements to be imposed on the final design. These objectives were accomplished using improved analytical tools combined with prototype testing.

Because the configurations selected from the conceptual design phase predicted unconventional airplanes in terms of relative fuselage to wing size, it was deemed necessary to use more accurate analytical models in the preliminary design phase. This task was performed using WINGS2001. The team also modified several assumptions in the DBF2001 program subroutines to provide a more accurate estimate of each configuration's performance. Also, because of the unconventional nature of the configurations chosen in conceptual design, a prototype was built to test various ideas and concepts to ensure that the results predicted by aerodynamic theory could be applied to real flight performance.

4.1. Prototype Testing.

A prototype airplane was built to test some of the unique and relatively untried concepts that defined the designs selected from the conceptual design phase. Specific concerns were raised about deep stall induced by a large horizontal fuselage and the handling characteristics of elliptic wings. The prototype was designed and built with elliptic wings and the capacity to hold 100 tennis balls. Traditional solid spring tricycle landing gear was included because of its proven reliability. The motor from last year's DBF project was used on the prototype to save cost. As a result of building and testing the prototype, the concerns about deep stall and handling characteristics were resolved and the team gained valuable construction experience.

4.1.1. Prototype Deep Stall Test. A large horizontal fuselage, when stalled, could cause a wake that would disrupt the flow over the tail surfaces. This could result in loss of pitch control and induce an unrecoverable deep stall. Figure 4.1 illustrates how the wake might intersect the tail surface during stall.

To test for this effect, a steel A-frame structure with a pivoting joint was mounted to a truck. The prototype was bolted to the pivoting joint, allowing free rotation in pitch (see Figure 4.1). This "poor man's wind tunnel" made it possible to simulate the airplane flying close to stall speed at high angles of attack. The truck was driven as close to the calculated stall speed of 22.5 miles per hour as possible. A pilot riding in the truck used remote elevator control to vary angle of attack from 0 to 30 degrees.

Several runs were made and the plane showed no signs of pitch control loss. The plane returned to its neutral horizontal position from every offset, showing deep stall not to be a significant problem.

4.1.2. Prototype Handling Characteristics. An elliptic wing produces the minimum induced drag for a given lift coefficient and aspect ratio. However, this wing planform shape introduces some control concerns. Since the Reynolds number approaches zero at the wingtips, circulation, lift properties, and stall characteristics are difficult to predict. This factor could possibly cause the aircraft to enter a spin,

threatening total control loss of the airplane. From previous experience it was known that tapered wing planforms on R/C aircraft have poor lateral control characteristics due to small Reynolds numbers near the wingtips. These wings also display undesirable stall behavior since the flow separation propagates from the wingtips toward the fuselage, resulting in aileron control loss before full stall occurs. Therefore, it was important to test the handling qualities before further design refinements were carried out.

During flight, the aircraft was controllable and displayed adequate maneuverability and handling qualities. When stalled, the aircraft experienced full aileron control loss causing the airplane to rotate about its longitudinal axis, dropping a wing. However, since the center of gravity was positioned properly, the airplane pitched down at full stall and aileron control was recovered quickly. This experiment proved that elliptical wings have the necessary flight characteristics to meet the mission requirements.

One of the concepts tested using the prototype was the application of large faired surfaces to the landing gear. This would cut drag and potentially increase lift at no added cost. Because of the anhedral associated with such surfaces, they would be destabilizing to the airplane in roll. To determine the effect of this instability, faired surfaces were applied to the landing gear of the prototype after it had successfully flown with non-faired landing gear. The prototype handled well with the faired gear and the pilot experienced no difficulty controlling the plane.

The prototype was initially designed with a center of gravity (CG) at the wing spar coincident with the quarter chord of the wings. The horizontal stabilizer was sized to have a static margin of 0.20 accordingly. On the first test flight, the pilot felt that the airplane was tail-heavy and did not have sufficient stability for safe flight, although he was able to land safely. The CG was moved forward 1-inch corresponding to a static margin of 0.235. The pilot felt he had sufficient control but recommended that the CG be moved forward even further. The CG was moved again to a location of 2.5-inches forward of

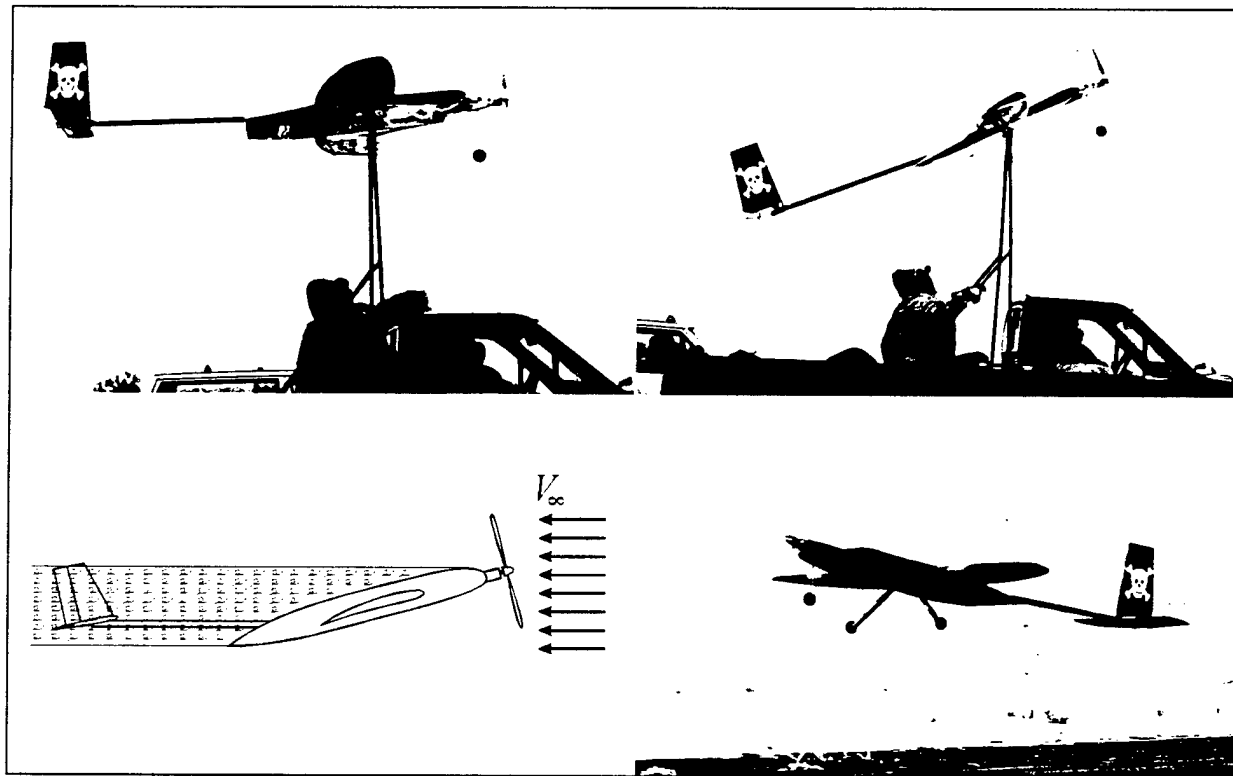


Figure 4.1. Prototype testing: stall recovery tests and first free flight.

the spar. This position of the CG gave the airplane a static margin of 0.29. The pilot felt that the airplane handled very well with the CG at that location. It was decided that a static margin of 0.25 would provide sufficient stability without sacrificing performance. This static margin was set as an engineering requirement for the remainder of the design process.

4.1.3. Structural and Manufacturing Lessons Learned. By building the prototype, the team discovered that balsa-sheeted-foam wing construction was very heavy and proved to be much stronger than required. In addition, the sheeting process was difficult and used an excessive amount of glue. This added to the weight of the already heavy foam structure.

4.1.4. Prototype Conclusions. As the prototype test flights proved, the elliptical planform wings had the necessary handling characteristics to meet the mission requirements. The team also proved that the complex geometry of elliptical wings could be constructed. Since elliptical wings provide a more efficient lifting surface than rectangular wings, elliptical planform wings were chosen for further design. Considering the results of test flights with faired landing gear, it was also determined that a fixed landing gear configuration could be fitted with a fairing to reduce drag and increase lift at no added cost. All fixed landing gear from this point was analyzed as faired landing gear.

4.2. Figures of Merit

A figure of merit is a way to quantify and compare the benefits and drawbacks of a given design concept. Figures of merit were selected for the preliminary design to narrow all possible design parameters to a number of combinations where the best possible airplane design would emerge.

4.2.1. Manufacturability. An important constraint on the team was the requirement to actually construct the airplane. Not all members of the team had experience building model aircraft. Simple designs would lend themselves to a more simple construction process, decreasing the time and skill required to manufacture the airplane. The design team had access to all of the facilities and equipment at Utah State University, as well as CNC machinery. It would be difficult to build proposed designs that called for equipment and experience not readily available within the team and the University.

4.2.2. Power Consumption. Power consumption was a major design consideration for the team. The contest rules stated that a maximum of five pounds of propulsive batteries could be carried in the airplane. Mission requirements demanded the design of an airplane that efficiently maximized the number of scoring sorties flown while carrying the maximum number of tennis balls and maximum amount of steel. As the weight of the airplane increased, the power required to take-off in 200 feet also increased. Therefore, weight was a considerable factor in the power consumption. Also, designs that were more aerodynamically efficient resulted in lower drag on the airplane, decreasing the power required for take-off and flight. It was important to select design parameters that were light and aerodynamically efficient.

4.2.3. Strength-to-Weight Ratio. Many factors defined the structural strength requirements for the airplane. Competition rules require that the airplane be capable of passing the "Wingtip Test". This test simulates a 2.5-g wing loading by supporting the maximum gross weight of the airplane at the wingtips. The airplane must withstand severe landing loads. The materials and structures chosen to constitute the airplane must be as light as possible and still be able to withstand these loadings.

4.3. Design Parameters Investigated

In the preliminary design phase, the parameters from conceptual design were refined. These were wing area, fuselage size and landing gear. Competing concepts for landing gear, wing, wing spar, fuselage, tail boom, and empennage designs, as well as for construction materials were filtered.

4.3.1. Landing Gear Configuration. The landing gear must be strong enough to support the airplane while remaining sufficiently flexible to absorb energy upon landing. It must also be lightweight and provide good handling characteristics while on the ground. The two landing gear types considered in the preliminary design phase were tricycle and taildragger configurations, in both retractable and faired form. Fixed landing gear was considered because of its strength and reliability; retractable gear because of its low drag in flight.

Tricycle gear provides good handling characteristics during takeoff and landing while a tail dragger configuration is lighter and produces less drag. After considering the skill and experience of the pilot, the tail dragger configuration was selected for further consideration in final design.

4.3.2. Landing Gear Shapes. The fixed main landing gear was of typical solid spring construction. The structures group optimized weight and form by designing a hollow rectangular aluminum shape of sufficient strength to support a 1.5-g maximum gross weight load. Aluminum was an ideal material because of its flexibility. Deflection was limited to prevent a prop strike in the taildragger configuration and a fairing was added to reduce drag. The tailwheel would be a manufactured item, as would retractable gear, should it prove to be the choice in final design.

4.3.3. Wing/EmPennage Structure and Materials. Five wing/emPennage construction methods were considered: foam core with carbon composite sheeting, carbon composite sheeting (no core), foam core with balsa sheeting, foam core with spar and balsa sheeting, and balsa ribs with spar and balsa sheeting.

Although carbon composites have superior strength to weight ratios, they were eliminated due to lack of experience laying up carbon fiber composites on complex geometry. The foam core wing with balsa sheeting could be easily manufactured but might lack the stiffness necessary to pass the wingtip test without an internal spar. A wing made from balsa ribs, balsa skin and constructed with an internal spar would be sufficiently strong and lighter than a foam core wing.

4.3.4. Spar Cross Section and Materials. The wing spar is a primary wing support member. Spar cross sections considered were a hollow circular spar, a tapered hollow circular spar, a box beam, and a tapered box beam. A circular composite spar would be easy to manufacture as well as both stiff and strong. The rectangular box spar, however, could be designed to more efficiently carry bending stresses and is suitable for either composite or wood construction. Tapering both spar shapes would increase the strength to weight ratio by placing material at the high stress areas near the wing root.

Spar materials investigated were aluminum, spruce, balsa wood, fiberglass and carbon composites. Aluminum had sufficient strength but was not as light or stiff as composite materials. Spruce would be effective, but only if used in the construction of a box beam spar. Balsa wood did not have the necessary strength to survive the wingtip test. Fiberglass or carbon fiber composite were good choices due to their high strength, but fiberglass lay-ups could be heavy without experience using the material. Carbon fiber has a high strength to weight ratio and has been used in past years, making it a desirable alternative.

4.3.5. Tail Boom Cross Section and Material. The tail boom must be sufficiently stiff to ensure that the airplane does not experience elevator control reversal at high speeds. Calculations predicting change in horizontal stabilizer attitude as a function of elevator deflection, airspeed, and tail boom stiffness were made. From these calculations an engineering requirement was implemented that required the boom to be stiff enough to experience no more than 10% control loss at flight speeds of 100 fps.

Two different cross sections were considered for the construction of the tail boom: a box beam and hollow circular cross section. A box beam cross section could be designed to provide the necessary stiffness, but would not be as aerodynamically efficient. A hollow, circular, composite cross section is

easier to construct than a box beam and has excellent torsional stiffness. Because of the high stiffness requirement necessary to prevent control loss, carbon fiber composite was chosen for the tail boom material. The availability of a local carbon fiber winding facility removed many manufacturing concerns.

4.3.6. Materials to Construct Fuselage. The fuselage must support the weight of the payload while providing a secure mount for the wings, tail boom, motors, and landing gear under various loads. A combination of materials was considered for the fuselage. Lighter materials would be used in low stress areas, while stronger, heavier materials would be used in high stress areas.

Materials considered were balsa wood, plywood, foam, fiberglass, carbon composites, and aluminum. Balsa wood is light, easily obtained, and used extensively in model aircraft construction. It has a very low density and a reasonable modulus of elasticity giving it an excellent stiffness to weight ratio. Two types of plywood were examined: Microlite (3-ply) and Aircraft (5-ply). Both types of plywood have low densities, reasonable moduli of elasticity and are readily available. Plywood would be well suited for high stress areas. Styrofoam has a low density, but also a low modulus of elasticity. Styrofoam must be used as a composite core with a balsa skin to provide adequate stiffness and form. This requires large amounts of epoxy, increasing the weight of the structure. Similar wood structures can be built to provide the required stiffness while using less material, and at a fraction of the weight of Styrofoam composite construction.

Fiberglass structures are widely used by R/C modelers in the construction of lightweight glider fuselages and engine cowlings. However, the "glassing" expertise of the design team was extremely limited. Carbon fiber composites are very stiff and like fiberglass, are very strong. Unfortunately, they are difficult to manufacture in complex shapes like the fuselage. Aluminum has a relatively high density and modulus of elasticity. Aluminum used in large quantities in an aircraft of this scale is not efficient. Therefore, these three materials were eliminated for use in the fuselage.

4.3.7. Fuselage Size. The size of the fuselage determines the number of tennis balls that can be carried by a given airplane configuration. Thus, this parameter has a direct effect on the total possible flight score. Fuselage size was studied further in preliminary design to obtain more refined approximations for the aerodynamics that affected the airplane with such a large fuselage. Although an 8x10 ball configuration was selected during the conceptual design phase, it was still possible a maximum score had not been obtained due to the accuracy limits of the model used in that phase. During accuracy refinement the ball configurations considered were 7x9, 7x10, 8x9, 8x10, 8x11, 8x12, 9x9 and 9x10.

4.3.8. Wing Area. Increasing wing area can improve aircraft performance. However, a stiff penalty is assessed in the rated aircraft cost for large wing areas. In the preliminary design, wing areas ranging from approximately 3.0 to 8.0 square feet in 1 square foot increments were considered.

4.3.9. Figure of Merit Results. The figures of merit for preliminary design are displayed in Table 4.1. Each design parameter was analyzed based on each figure of merit and rated from -2 to 2 relative to a reference highlighted in yellow in the table. Those design concepts with the highest scores were kept for detail design and the remaining design concepts were eliminated. FA denotes all concepts kept for detail design, and E denotes concepts eliminated. A weighting factor of 2 was applied to power consumption as it directly affects the total score, while a factor of 1 was applied to manufacturability and strength to weight ratio. Fuselage size and wing area was not included with the other design parameters considered in the preliminary design phase in Table 4.1. They were instead optimized as described in the following section.

4.4. Analytical Methods Used

Analytical methods were used to determine which of the remaining aircraft configurations would best meet the mission requirements. These methods were also used to better specify the engineering

requirements imposed on the final design. Tools used to implement this analysis were more detailed models used in WINGS2001 and a refined version of DBF2001.

4.4.1. Modeling in WINGS2001. A model of each configuration was created in WINGS2001. Tail size and position was held constant to be optimized during detail design. Data was collected to determine lift and drag curves for all the designs so more accurate approximations could be made in DBF2001.

The selected wing area from the conceptual design phase was 7.8 square feet. While creating the data collection matrix, wing area was centered on this value. The main wing area was varied in increments of one square foot starting at a minimum area defined by a minimum allowed root chord of 9.6-inches and increasing up to a maximum wing area of 9.8 square feet. Multiple wing areas were applied to each of the eight fuselages depending on the root chord allowed by the fuselage size. Faired and retractable landing gear were also included in the WINGS2001 models.

During the design of the prototype, it was determined that an optimum lift to drag ratio could be achieved by adjusting the mounting angles of the wing relative to the fuselage. This created an evenly distributed lift profile across the different airfoil shapes. To avoid favoring configurations that arbitrarily

Design Parameters		Manufacturability 4.2.1	Power Consumption 4.2.2	Strength/Weight Ratio 4.2.3	Result	Decision
Weight Factor		1	2	1		
Landing Gear 4.3.1	Tail Dragger	0	0	0	0	FA
	Standard Tricycle	0	-1	0	-2	FA
	Retractable	-1	1	0	1	FA
Cross Sections 4.3.2	Hollow Circular Beam	0	0	0	0	E
	Box Beam	1	1	1	4	FA
Wing/Emppennage Structure and Materials 4.3.3	Foam Core & Balsa Sheeting	0	0	0	0	E
	Foam Core & Composite Covering	-2	0	1	-1	E
	Foam Core w/ Spar and Balsa Sheeting	0	0	1	1	E
	Balsa Ribs w/ Spar and Balsa Sheeting	1	1	2	5	FA
	Carbon Composite (no core)	-2	0	2	0	E
Spar Structure 4.3.4	Hollow Circular Shaft	0	NA	-1	0	E
	Tapered Hollow Circular Shaft	0	NA	0	0	E
	Box Beam	1	NA	0	0	E
	Tapered Box Beam	1	NA	2	1	FA
Materials to Construct Spar 4.3.4	Aluminum	0	NA	0	0	E
	Spruce	1	NA	1	2	FA
	Balsa Wood	1	NA	-1	0	E
	Fiberglass Composite	1	NA	-1	0	E
	Carbon Fiber Composite	1	NA	2	3	FA
Tail Boom 4.3.5	Box Beam Cross Section	0	0	0	0	E
	Hollow Circular Cross Section	1	1	0	3	FA
Materials to Construct Fuselage 4.3.6	Balsa Wood	2	NA	2	4	FA
	Poplar Plywood	2	NA	1	3	FA
	RC Plywood	2	NA	1	3	FA
	Styrofoam	2	NA	-1	0	E
	Fiberglass composite	-2	NA	0	-2	E
	Carbon Fiber Composite	-2	NA	1	-1	E
	Aluminum	0	NA	0	0	E

Table 4.1. Figures of Merit for the Preliminary Design Phase.

had a better wing-fuselage balance, the fuselage of each design was modeled with a lift slope and zero lift angle of attack equal to the lift slope and zero lift angle of attack values for the wings. The tail in each of the models was modeled as an all-flying tail to simulate a tail mounted for no elevator balance at the model test condition. These measures helped to ensure evenhanded comparison between all configurations. Relations for lift coefficient as a function of angle of attack and drag coefficient as a function of lift coefficient were found. Plots were generated for each airplane design to show these relations. An example of these plots is shown in Figure 4.2. The relations for lift coefficient and drag coefficient were used in a modified version of DBF2001 to more accurately predict aircraft performance.

4.4.2. Modified Computer Program. DBF2001 was modified in order to obtain quantitative comparisons between the different airplane designs and make use of the data taken from WINGS2001. These modifications provided a more accurate estimate of the actual weight and dimensions of each design and improved aircraft performance predictions. The aircraft performance section of DBF2001 was modified to incorporate the data taken from WINGS2001. All aerodynamic parameters were computed, where possible, using the lift and drag relations obtained from WINGS2001. In conceptual design, DBF2001 iterated on gross weights from 10 to 55 pounds. Based on the gross weights of the highest scoring conceptual configurations, this range was refined to 20 to 40 pounds. Retractable and fixed-faired gear (non-retractable) were analyzed for comparison. The same motors and propellers from conceptual design, along with multiple motor and propeller combinations, were analyzed.

4.5. Configuration Selection

The results of the preliminary design program are shown in Table 4.2. An example of the results from the program is shown as Figure 4.3 for the design selected.

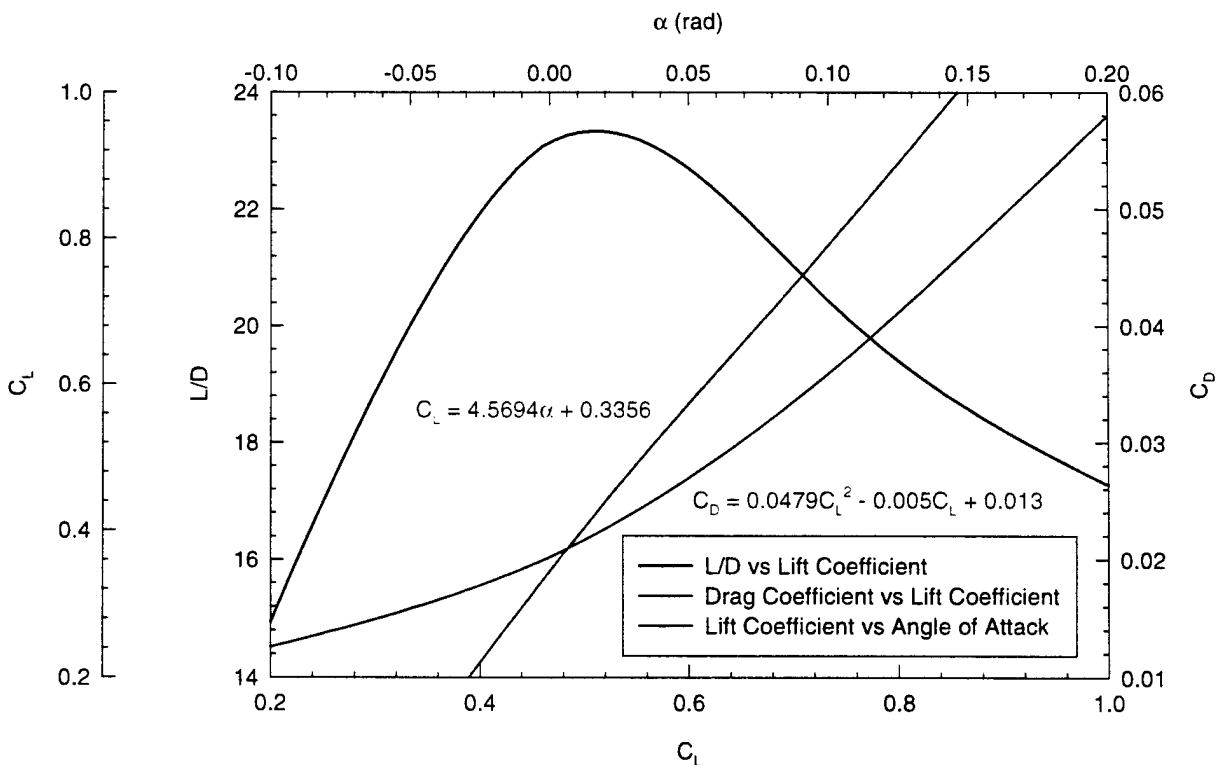


Figure 4.2. Lift/drag characteristics obtained from WINGS2001 for the preliminary design configuration.

	Config.	Wing Area	Weight	Score	RAC	Results
NONRETRACTABLE	7 x 9	4.052	33	14.219	5.19	E
		5.052	34	14.011	5.35	E
		6.052	36	14.315	5.51	E
		7.052	37	14.097	5.67	E
	8 x 9	4.320	34	14.638	5.31	E
		5.320	36	14.885	5.48	E
		6.320	37	14.664	5.64	E
		7.320	36	13.526	5.79	E
	8 x 10	3.893	34	15.243	5.30	E
		4.893	36	15.474	5.47	E
		5.893	36	14.763	5.62	E
		6.893	34	13.202	5.75	E
	9 x 9	7.893	33	12.120	5.90	E
		4.593	36	15.457	5.45	E
		5.593	37	15.203	5.61	E
		6.593	36	14.059	5.76	E
	9 x 10	4.117	36	16.137	5.44	E
		5.117	36	15.399	5.59	E
		6.117	35	14.250	5.73	E
		7.117	33	12.710	5.87	E
RETRACTABLE	7 x 9	4.052	32	15.939	5.22	E
		5.052	33	15.751	5.38	E
		6.052	35	16.108	5.53	E
		7.052	32	13.834	5.68	E
	7 x 10	4.669	33	16.539	5.37	E
		5.669	34	16.333	5.52	E
		6.669	33	15.093	5.67	E
		7.669	32	13.950	5.80	E
	8 x 9	4.320	33	16.683	5.35	E
		5.320	34	16.469	5.50	E
		6.320	33	15.218	5.65	E
		7.320	37	14.081	5.81	E
	8 x 10	8.320	38	13.309	5.96	E
		3.893	33	17.590	5.33	E
		4.893	33	16.815	5.49	FA
		5.893	32	15.595	5.62	E
	9 x 9	6.893	37	14.405	5.78	E
		7.893	36	13.523	5.93	E
		4.593	34	17.374	5.47	E
		5.593	33	16.089	5.62	E
	9 x 10	6.593	32	14.869	5.77	E
		7.593	37	13.836	5.94	E
		4.117	32	17.349	5.44	E
		5.117	31	16.060	5.59	E
	8 x 11	6.117	36	14.785	5.75	E
		7.117	35	13.617	5.90	E
		3.463	31	17.435	5.30	E
		4.463	32	17.211	5.46	E
	8 x 12	5.463	31	15.933	5.61	E
		6.463	35	14.224	5.76	E
		7.463	34	13.078	5.92	E
		3.034	30	17.790	5.29	E
		4.034	35	16.213	5.45	E
		5.034	35	15.481	5.60	E
		6.034	35	14.785	5.75	E
		7.034	33	13.157	5.89	E

Table 4.2. Results from the preliminary design program DBF2001. The design chosen for further analysis in detail design is highlighted. (FA: Further Analysis; E: Eliminated)

The design selected in Table 4.2 did not achieve the highest score predicted by DBF2001. The highest scoring configurations had elliptic wings with very small root quarter chords. The program output showed that the larger the fuselage and smaller the wings, the larger the score. This can be partially explained by the penalty for larger main wing areas in the rated aircraft cost. The designs shown in Table 4.2 are not consistent with reality. Airplanes having main wings with root chords under eight inches are not modeled accurately in WINGS2001 because low Reynolds numbers are not accounted for. Therefore, the team decided to select the configuration that corresponded to a more conservative lifting line estimate. This airplane consisted of a wing area of 4.89 square feet, an 8x10 tennis ball configuration and retractable landing gear with tail dragger configuration. This airplane had a rated aircraft cost of 5.49 and achieved a total score of 16.82.

4.6. Engineering Requirements

The engineering requirements were established during preliminary design. These requirements were used to constrain the optimization process used for detail design. They are as follows:

Gross Weight: 33 lbs	Tail Boom Stiffness: Allow less than 10% control loss at 100 fps
Tennis Ball Capacity: 80 balls	Wing Planform: Elliptical
Light Payload Laps: 3	Wing Span: 10 ft
Heavy Payload Laps: 3	Landing Gear: Retractable
Static Margin: 0.25	Batteries Specifications: 5 lbs, 2400 mah

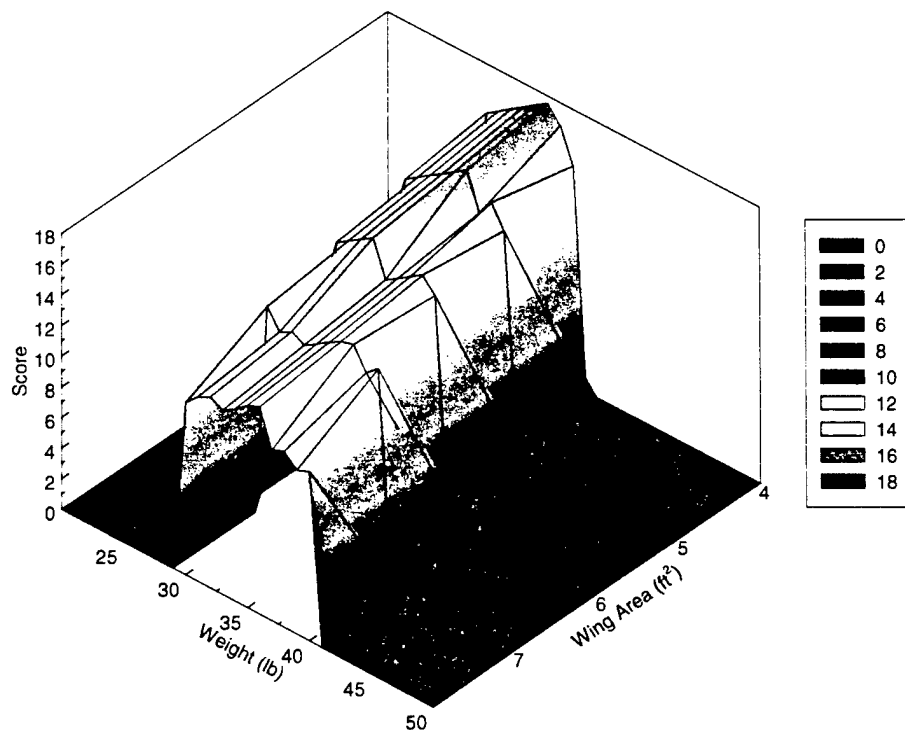


Figure 4.3. Three-dimensional plot showing the results of the selected airplane configuration from preliminary design—a fuselage 8x10 ball configuration with elliptical planform wings and retractable landing gear. A maximum score of 16.815 was predicted for this design.

5. DETAIL DESIGN

During the detail design phase, the design team took the aircraft configuration selected during the preliminary design phase and refined it into a final aircraft design. This refinement consisted of three major tasks: optimizing the aerodynamics of the airframe, optimizing the power plant configuration, and designing and analyzing the structural components of the aircraft. Each of these tasks presented design problems; the solutions are addressed in this section. Upon completion of the aircraft design, a final flight performance analysis was carried out. This analysis examined the static and dynamic stability of the aircraft and made predictions for the performance of the aircraft under the competition conditions.

5.1. Component Selection and Systems Architecture

In order to optimize the design of the final aircraft, several aspects of the aircraft design were studied in detail. The main categories of study were aerodynamic efficiency, power plant efficiency, and structural design. The overall goal was to increase the flight performance of the aircraft. This was accomplished by lowering the thrust required for flight by increasing aerodynamic efficiency, increasing the efficiency of the power plant by optimizing the motor/propeller combination, and designing a minimum weight structure to meet the loading requirements. The aircraft configuration was modeled in WINGS2001, and various properties of the model were varied and iterated upon. Parameters modified were wing-mounting angle, fuselage cross-section, size and shape of the transition section of the fuselage, and tail planform, mounting angle, and height. After this refinement was complete, the power plant was matched to the aircraft for the design flight conditions using a program called GPROPS which calculated available thrust, input power required, and the efficiency of motor/propeller combinations. A full solid model of the airplane was generated using SDRC's I-DEAS, and a finite element model of the entire aircraft was created and solved.

5.1.1. The Aerodynamic System. The aircraft chosen from the preliminary design was an optimal aircraft with respect to ball configuration and wing area. Preliminary design parameters such as fuselage airfoil shape, fuselage transition shape, axial wing position, and center of gravity location were based on the design of the prototype aircraft and were not optimized for each preliminary design configuration. The main focus of the airframe design was to vary these aircraft parameters to determine aerodynamic trends and find the optimum airframe for the final aircraft.

The USU DBF 2000 team examined many airfoils for last year's DBF 2000 competition airplane. Of these airfoils, the Selig-Donovan 7062 and Eppler 387 displayed the best aerodynamic performance. The major differences separating the two airfoils were maximum lift coefficient and cross-sectional area. The SD7062 airfoil has a maximum lift coefficient of 1.663 compared to the E387 maximum lift coefficient of 1.27. As far as aerodynamic efficiency for cruise, both airfoils are excellent with the E387 providing a slight improvement over the SD7062. The SD7062 was chosen for its higher maximum lift coefficient. The increased thickness of the SD7062 also better facilitated the main wing spar design for smaller wings of small chord.

For conceptual design, the horizontal fuselage was assumed to be a NACA 0015 airfoil with a straight box section inserted in the region of maximum thickness (see Figure 5.1). This fuselage shape was used to simplify the payload section of the prototype but was not optimized aerodynamically. As employed on the prototype, the symmetric compound airfoil had to be rotated 4.3° relative to the wings to generate the necessary lift to balance the plane. This angle of attack also allowed the fuselage to generate enough lift to create a more uniform lift distribution across the span of the aircraft. In order to carry this lift more

efficiently, the fuselage was modified to have characteristics similar to the more efficient SD7062 airfoil. To match the camber line of the SD7062 airfoil, the fuselage airfoil needed to have a design section lift coefficient of 0.5 while having a constant thickness section to house the tennis ball payload.

To solve this problem an airfoil was designed using AIRFOIL2000 (an airfoil mapping and pressure-calculating program written by Dr. Warren Phillips). This airfoil is shown in Fig. 5.1. Figure 5.2 shows a plot of the coefficient of pressure on the upper and lower surfaces of two airfoils, the final design fuselage airfoil (Compound USU 483419-1214.20), and the prototype symmetric fuselage airfoil (Compound NACA 0015). Note the undesirable large adverse pressure gradient on the upper surface of the compound NACA 0015 shown in Figure 5.2 by the bottom red line. This large gradient near the nose of the airfoil could cause early flow separation and was one of the characteristics that was changed. Both pressure curves were generated for a lift coefficient of 0.5, which corresponded to an angle of attack of 0.0° for the final design fuselage airfoil and an angle of attack of 4.3° for the symmetric prototype fuselage airfoil.

Figure 5.2 further illustrates the advantage of the final design fuselage airfoil over the prototype symmetric airfoil. The figure displays the upper and lower pressure distributions for both airfoils corresponding to lift coefficients of 1.4 as might be reached during takeoff. It is highly probable that the compound NACA 0015 airfoil will stall before the compound USU airfoil due to the large adverse pressure gradient near the nose of the compound NACA 0015.

To validate the decision for the final fuselage airfoil, this airfoil and the symmetric compound NACA 0015 airfoil were analyzed using a panel code to predict lift and drag from the website <http://beadecl.ea.bs.dir.de./airfoils/calcofoil.htm>. The software uses a simple bubble method to predict the flow separation point on the upper and lower surfaces of the airfoil. The compound USU airfoil reached a lift coefficient of 1.34 before any flow separation occurred. The symmetric compound NACA 0015 airfoil had drastic separation after reaching a lift coefficient of 0.63.

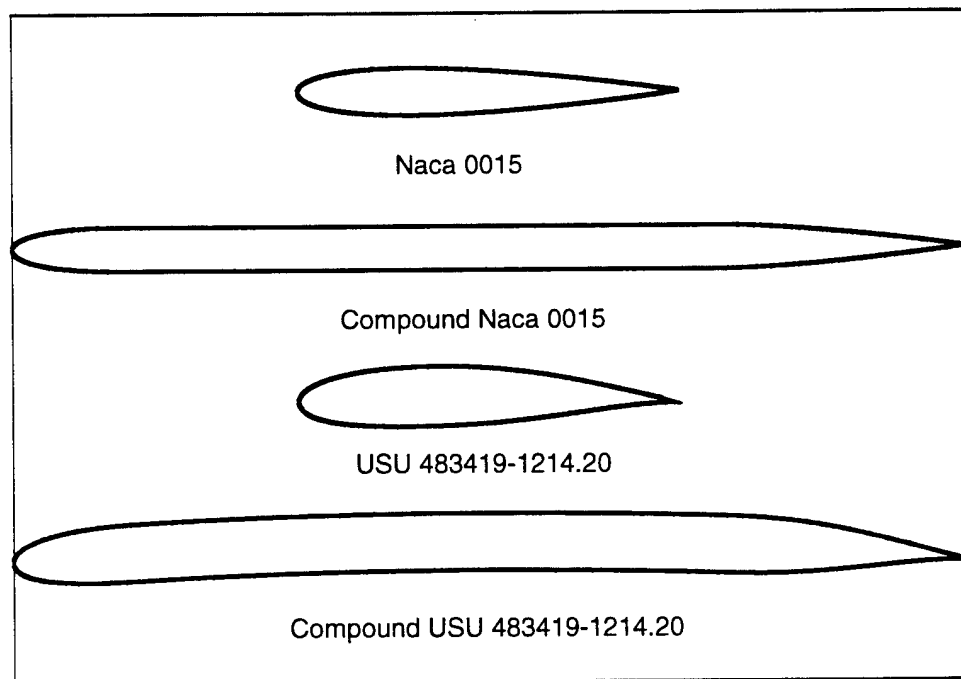


Figure 5.1. Cross-Sections of Airfoils Examined in Detail Design.

To compare the performance of the cambered fuselage airfoil with the symmetric airfoil, potential flow models of both aircraft were created. The cambered fuselage yielded two distinct counteracting aerodynamic trends: an increase in lift on the fuselage, and an increase in the nose-down pitching moment caused by the fuselage. Increasing lift on the fuselage increased the efficiency of the aircraft. Increasing the pitching moment required more negative lift on the tail for stability and decreased the aircraft efficiency. Overall, the increase in efficiency due to lift slightly outweighed the effects of negative lift on the tail. Based on the improved stall characteristics of the cambered fuselage as well as the slight gain in overall aerodynamic efficiency, the cambered fuselage airfoil (USU 483419-1214.20) was chosen.

In preliminary design, the transition from the fuselage to wing was made using a transition fairing with a span-wise length of 6 inches on each side of the fuselage. Since the optimum preliminary design aircraft contained a high aspect ratio wing, an analysis was performed to determine whether it was more aerodynamically efficient to use a fairing that made a more gradual transition to the wing. Holding the wing area constant, fairing transitions were examined with span-wise lengths of 6-16 inches.

For a span of 10 feet, increasing the fairing while holding wing area constant required an increase in the wing root chord. This allowed the circulation to be distributed more evenly over the fuselage and wing. This reduced the vorticity shed from the fuselage and increased the efficiency of the aircraft. As seen in Figure 5.3, increasing the transition length from 6 to 14 inches decreases the minimum thrust required. As the transition length is increased beyond 14 inches, the loss of efficiency due increasing the wing chord outweighs any gain from decreasing vorticity shed from the fuselage.

The next phase of the airframe design focused on making slight variations to wing planform area. Wing areas of 3.89 ft² through 4.89 ft² were examined for aircraft with fuselage transition span-wise

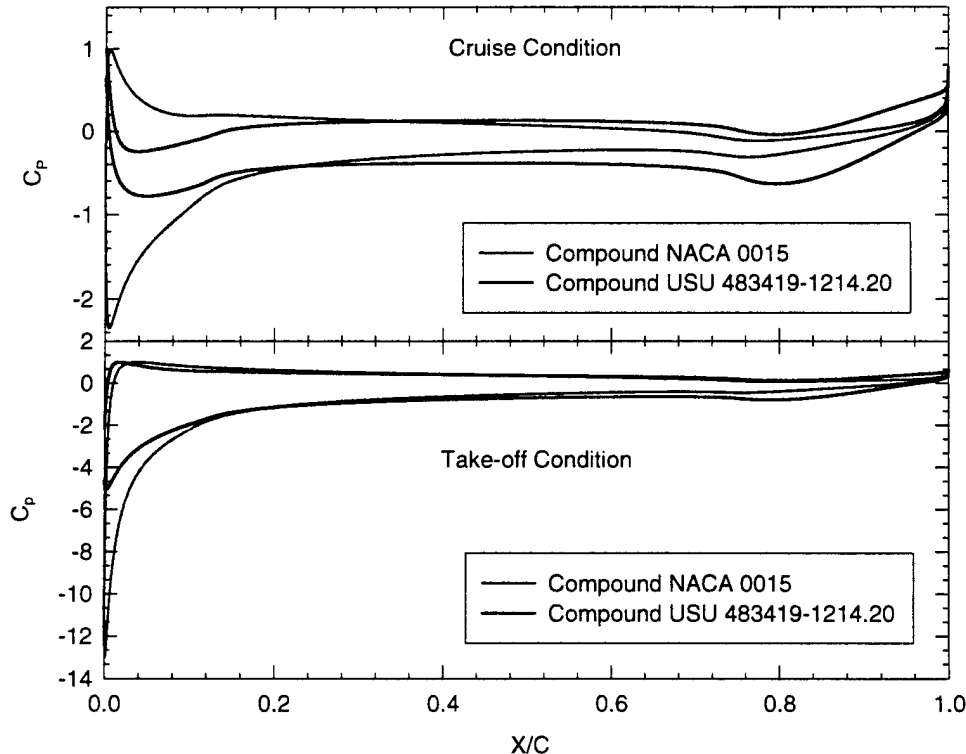


Figure 5.2. Pressure Distribution of Selected Airfoils for Cruise and Takeoff Conditions.

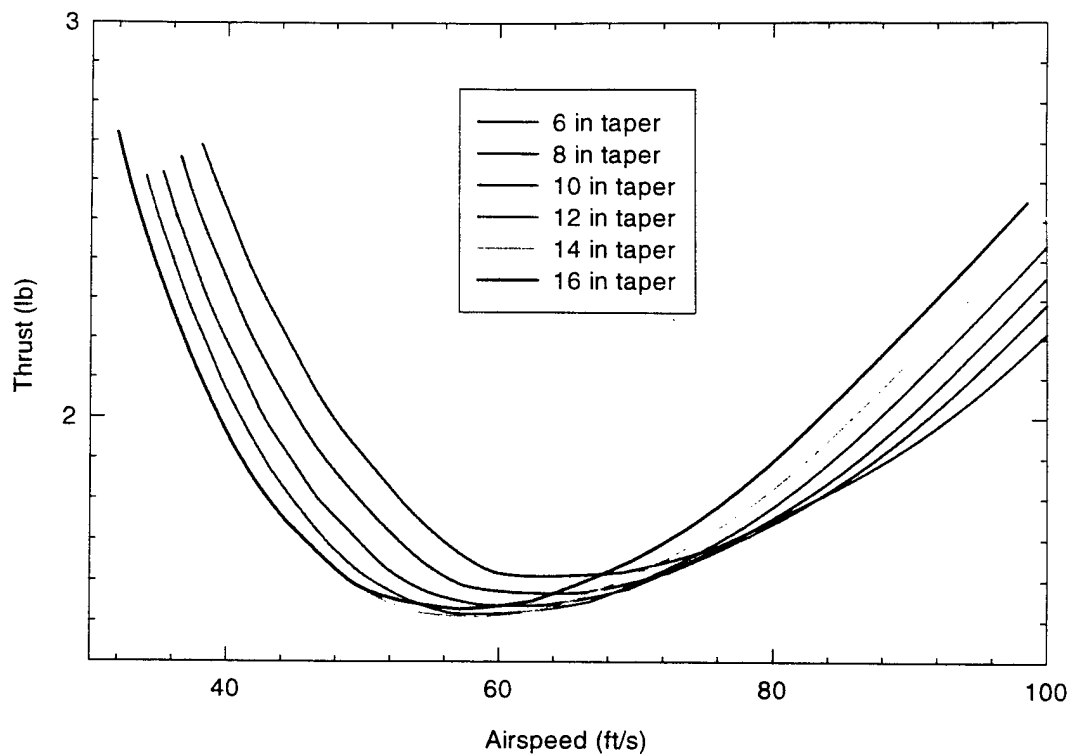


Figure 5.3. Thrust vs. airspeed for aircraft with various fairing lengths.

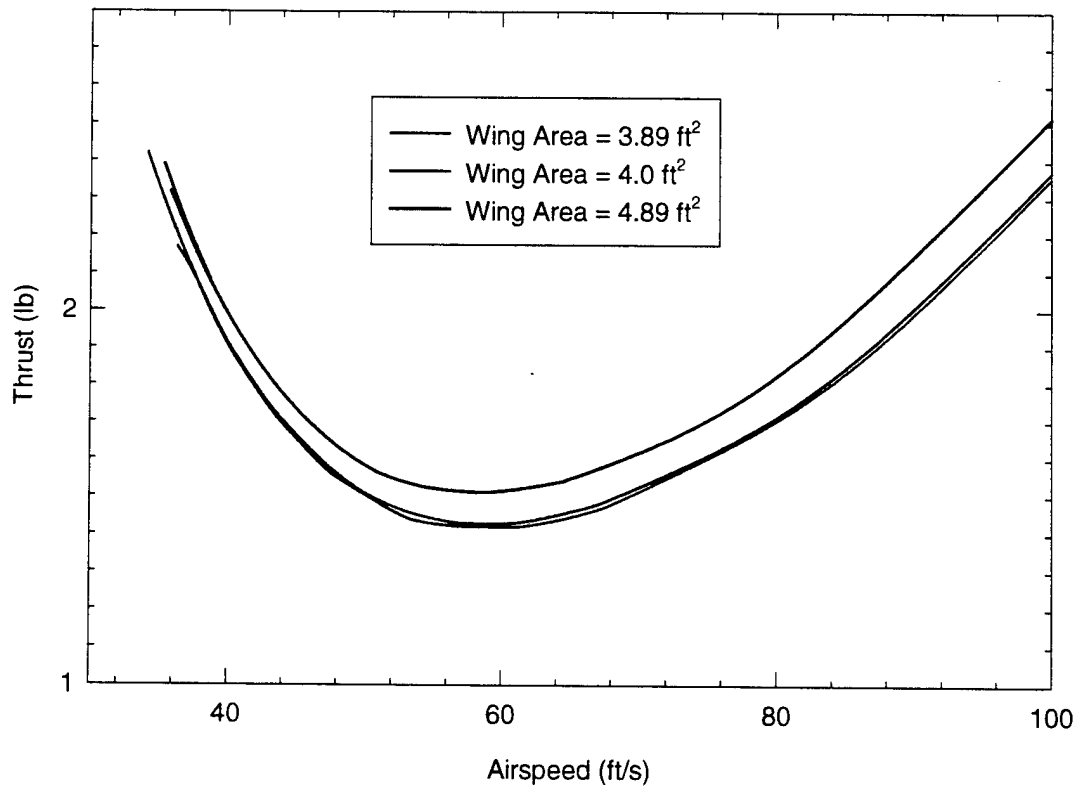


Figure 5.4. Thrust vs. airspeed for different values of wing planform area.

lengths of 11-14 inches. The limits of this wing area range represented the two optimum designs predicted by the preliminary design. In all cases examined, decreasing the wing area increased the total score (see Figure 5.4). Decreasing the wing area also affected the optimization of the fuselage transition fairing. For smaller wing areas, the fuselage transition length reached an optimum at lower values. For wing areas lower than 4.0 ft², the root chord of the main wing fell below 10 inches. After reviewing the analysis, a wing planform area of 4.0 ft² was chosen.

The preliminary design placed the axial location of the wing ¼ chord at the center of the fuselage payload section. This design was chosen to place the aerodynamic center of the wing near the center of gravity for payload configurations. Since the competition rules never require the aircraft to be flown without payload, an analysis was performed to determine if an alternate axial wing location would increase aerodynamic efficiency. The aerodynamic optimum occurred when the wing ¼ chord was located 14 inches aft of the fuselage nose (see Table 5.1). Although this wing location was aerodynamically optimal, it generated several stability problems. Table 5.1 displays the minimum thrust and horizontal stabilizer area required for each axial position of the wing ¼ chord. Although the thrust required is minimized for a wing located 14 inches aft of the fuselage nose, the required stiffness of the tailboom and the increased horizontal stabilizer area increase the aircraft empty weight. After considering all factors, it was determined that the overall small gain in aerodynamic efficiency was not worth the design challenges of dramatically increasing the size of the horizontal stabilizer.

Through the initial aerodynamic optimization, aerodynamic trends of the fuselage and wing structure were studied while holding the tail location and area constant. Initially, the tail design used to locate the general optimums shown in Figures 5.3 and 5.4 was taken from the prototype aircraft and was the same tail design used in all preliminary design calculations. The final stage of the aerodynamic optimization included individually sizing and positioning the horizontal stabilizer for each aircraft configuration.

To simplify the iteration process during the airframe optimization, each aircraft was statically balanced by rotating the entire aircraft to a given angle of attack and using an all-flying tail to balance the pitching moment. After the final geometry of the fuselage, wing, and horizontal stabilizer were defined, the mounting angles of the wing, and horizontal stabilizer were adjusted to achieve the minimum drag lift coefficient during steady level flight for a thrust angle of zero with no elevator deflection. The final mounting angles of the wing and horizontal stabilizer were respectively 3.75° and 1.85°. This adjustment improved the optimum lift to drag ratio of the aircraft from 21.4 to 22.5.

Aircraft Configuration		Airframe Efficiency		Horizontal Stabilizer	
Axial Wing Location*	Transition Length (in)	Minimum Thrust (lbf)	Airspeed (ft/s)	Area (ft ²)	Lift (lbf)
11	10	1.83	58	5.37	-0.38
12	10	1.51	57	5.78	0.22
14	10	1.36	55	5.42	-0.63
16	10	1.41	56	4.96	-1.41
20	10	1.55	61	3.14	-3.0
20	11	1.55	60	3.80	-2.9
20	12	1.54	59	4.32	-3.0

* distance measured aft of the fuselage nose in inches

Table 5.1. Airframe optimization.

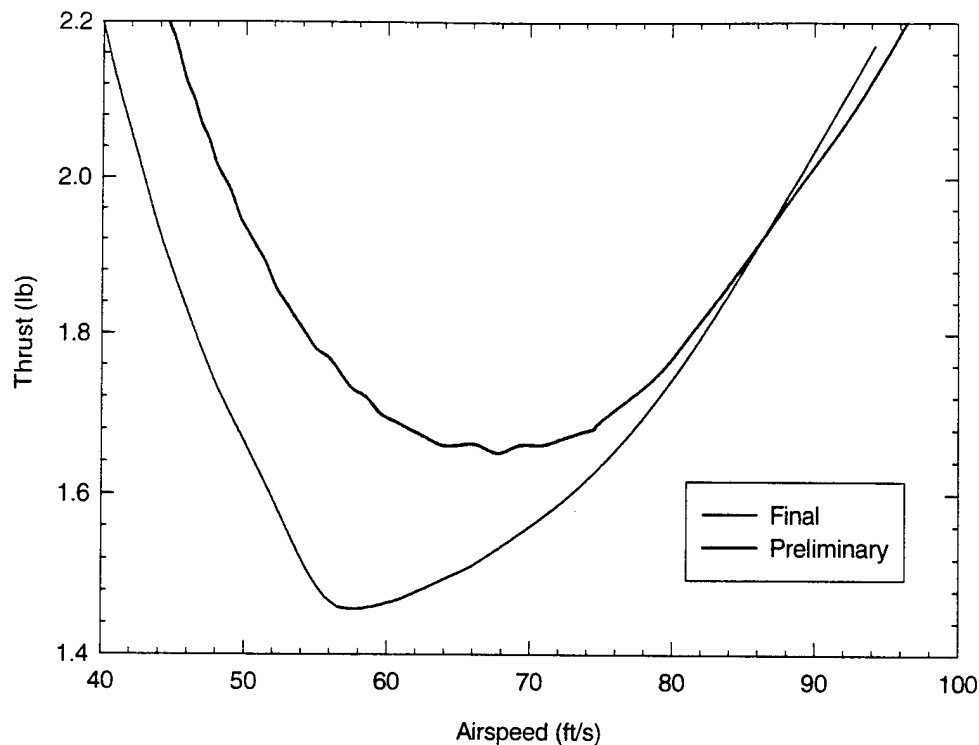


Figure 5.5. Thrust vs. airspeed for the preliminary and final aircraft designs.

The final results of the airframe optimization are presented in Figure 5.5. This figure compares the thrust versus velocity curves for the final and preliminary airframe designs. By aerodynamically optimizing the preliminary design airframe, the thrust required for steady level flight decreased for airspeeds below 90 ft/s. This represents an improvement over the entire airspeed region expected for the final aircraft design. The minimum thrust required for steady level flight decreased by 12.7%. This decrease in thrust corresponds to a 10 ft/s decrease in minimum drag velocity. To maintain the minimum drag velocity of the preliminary airframe, a reduction in thrust of 7.3% was predicted.

5.1.2. The Propulsion System. To optimize the power plant and match it to the finalized aircraft airframe, a detailed analysis was performed. It was known that a larger diameter propeller turning at a slower angular velocity would result in the highest propeller efficiency. However, an electric motor develops maximum efficiency at a certain rotational speed corresponding to a particular torque, which is unique to every motor. This speed may not be the optimal speed for a given propeller. It was therefore desirable to compare many propellers and motors in order to find the optimal match for the airframe.

In past years, the only tool available to examine the power plant was a program called EPROPS. The only available way to verify the predictions was from static thrust measurements. It was found that the output from EPROPS with a safety factor of two conservatively reflected the actual static performance. However, there was no way to assure that the calculations were correct for flight conditions.

This year a different approach was taken. Goldstein's (1929) vortex theory was used. In this theory, Goldstein assumed a helical vortex trailing behind the rotating propeller. In order to verify the accuracy of Goldstein's theory, USU graduate students collected data for rotating propellers in a wind tunnel. The data was compared to calculations from Goldstein's vortex theory and EPROPS. The results presented in Figs. 5.6 and 5.7 show that Goldstein's model is a better method of predicting propeller performance.

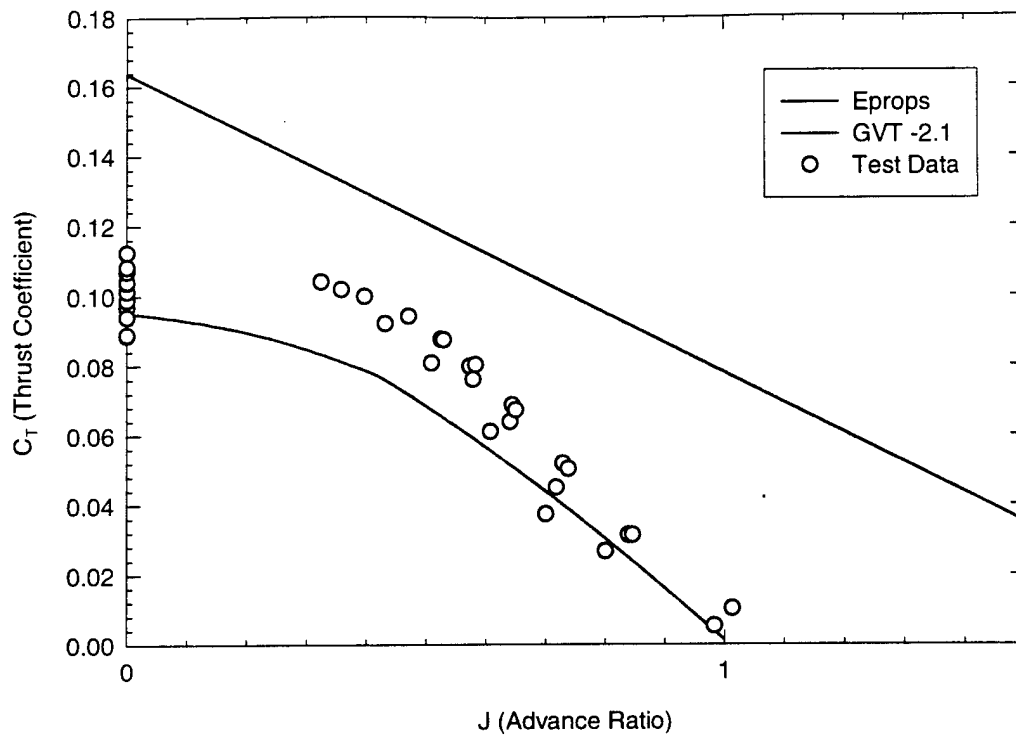


Figure 5.6. Thrust Coefficient vs. Advance Ratio for the 12 x 10 propeller.

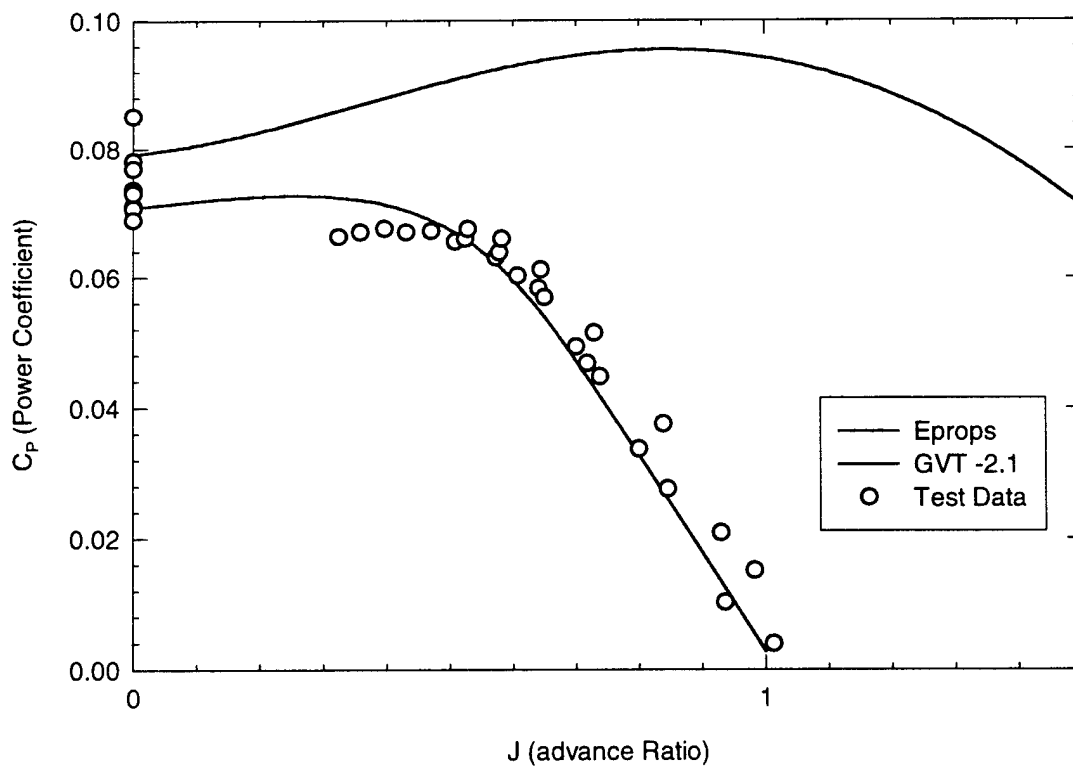


Figure 5.7. Power Coefficient vs. Advance Ratio for the 12x10 propeller.

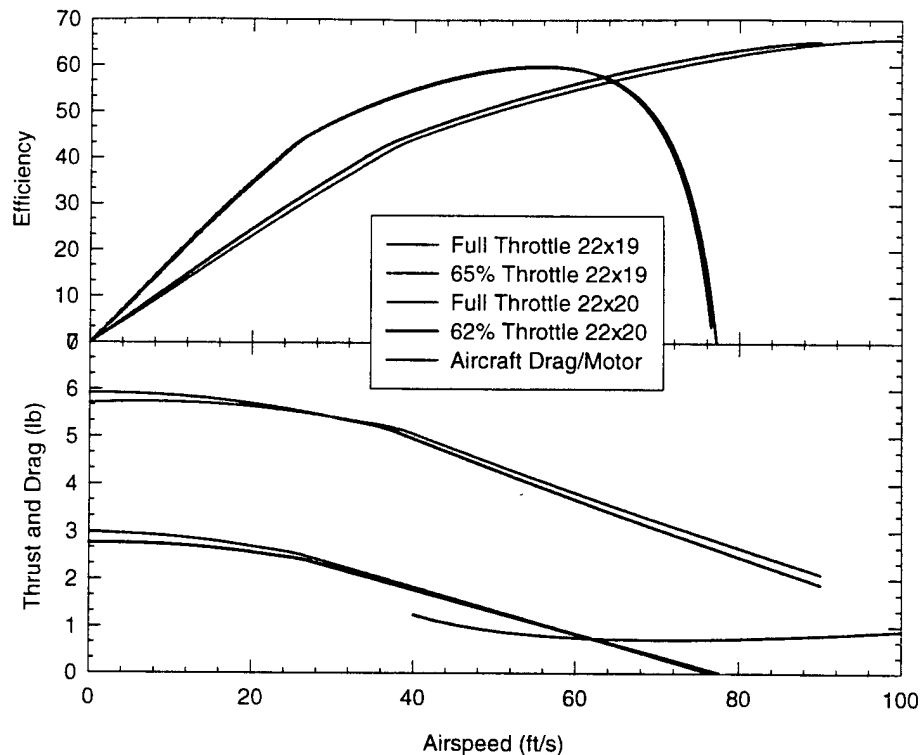


Figure 5.8. Efficiency and Thrust for the 22 x 19 and 22 x 20 propellers mounted on the Astroflight 640 motor with a 3.1:1 Gear Ratio.

The program EPROPS was modified by the design team to use Goldstein's vortex theory to compute propeller performance. All of the propellers from the conceptual and preliminary design databases were run through the program, now known as GPROPS. Five Astroflight motors were considered: the 625, 627, 640, 642, and 643, with 1.6:1 and 3.1:1 gear ratios. The optimal motor/propeller combination for the cruise conditions of 61 feet per second and 1.6 pounds total thrust required was the 640 motor, 3.1:1 gear ratio, and a 22 x 19 two-blade propeller. Figure 5.8 contrasts the properties of the 22 x 19 and the 22 x 20 propellers—the two best combinations from this analysis.

5.1.3 The Structural System. To predict displacements and stresses in the final design, the structures group performed a more rigorous stress analysis than had been done in previous competitions. The objective of this analysis was to ensure structural integrity for the wingtip test and flight loads, while reducing overall airframe weight.

Static, linear elastic, small displacement analysis of the airframe structure was undertaken using finite element techniques. This method allowed analysis to be performed on complex geometry and unusual boundary conditions in a reasonable length of time. The finite element capability of I-DEAS, a powerful software package with Drafting, Modeling and Simulation modules, was used. The software provided considerable flexibility in mathematically modeling a structure as complex as an airplane and also provided the graphics tools necessary to evaluate and display the interaction of components.

Load cases included the wingtip test, a landing load, and in-flight loading. Contest specifications required that the airplane be subjected to a wingtip test when loaded to maximum gross weight. During design, the wingtip test was considered to be the maximum load. The landing case was intended to simulate a hard landing and was the second highest load on the airplane. In-flight loads simulated steady

flight of the loaded airplane in a 1.65-g, 60° steep turn at maximum gross weight. It showed the structural response of members under uniformly loaded flight conditions.

The geometry of the airplane was defined using solid modeling. The structures group was prepared to model and analyze two structural concepts for the wing: a solid composite wing made of foam with a balsa skin and integral spar; and a stick built wing of rib and skin construction built around a main spar. The stick framing technique was found to be the lightest construction method for the aircraft. This method was well adapted to the use of thin shell elements for the finite element analysis. Thin shell elements were a good compromise for internal rib, spar and tail boom members that could have been modeled as beam elements. They allowed for easy attachment of ribs to the skin elements while producing a reasonably sized model for analysis. Quadratic, triangular Mindlin plate elements available in I-DEAS were used to provide the shape needed to define complex geometry while providing adequate representation of deformations due to bending. Three different materials were used in the model: balsa wood, plywood and carbon fiber composite. Identifying the elements by material groups simplified the construction of the meshed model and provided advantages when reviewing stresses.

Geometric symmetry about the longitudinal axis of the airplane was used to reduce model size. In this way, half the airplane could be modeled with the same accuracy as a full model solution. Boundary conditions were applied to the model through the use of restraints and loads. This proved to be challenging for the symmetrical model under the various loading conditions.

Three separate boundary and load sets were created to simulate the different loading cases. For each model (except the landing configuration) the steel payload was used to balance moments about the pitch axis. After the airplane was balanced, applicable boundary conditions were applied and a solution set obtained. The steel payload was determined by subtracting the manufacturer's empty weight and fuel (batteries) from the maximum gross weight.

For the wingtip test, translation was prevented in the vertical and longitudinal directions at the wingtips. Symmetrical restraints were configured along centerline nodes and a fictitious rotational restraint about the pitch axis was added near the spar centerline. The CG was placed at the spar centerline to facilitate the test at the contest. Material densities were assigned a one-G load down; component loads (i.e. motors, batteries, landing gear, servos) were placed at their appropriate fixed locations on the airplane; the steel payload was positioned over the spar at the center of gravity. From the solution of this load and boundary set, the fictitious moment that developed at the pitch axis restraint was balanced to zero with a force couple comprised of the payload. The model was solved again to confirm that the pitch axis moment was sufficiently close to zero.

Figure 5.9 shows the results for the wingtip test. The stress distribution was used to determine likely locations from which to remove or add material to improve the strength to weight ratio of the airplane. This model had a plywood spar with a yield strength of approximately 5,000 psi. The maximum stress was determined to be 3,000 psi, providing for a factor of safety of 1.67. Balsa skin stresses were low. The maximum displacement at the wingtip was 2.6 inches.

For the in-flight load case, translation was prevented in the vertical and longitudinal directions at the end of the tail boom. Rotation about the pitch axis was also prevented at this point. Symmetrical restraints were configured along the centerline and fixed loads were the same as in the wingtip test. Uniform pressures were applied to the lower surfaces of the airplane as determined in the aerodynamic analysis for a maximum gross weight configuration. The steel payload was distributed symmetrically about the CG, 2.5-inches in front of the spar as predicted by the aerodynamics group. The lift pressures

were scaled up or down in subsequent analyses until the pitching moment at the tail restraint became zero. The resulting vertical reaction was the aerodynamic horizontal stabilizer balancing force (due to a judicious choice of restraint). The reaction computed by I-DEAS was 1.47 lbf.; WINGS2001 had predicted 1.5 lbf. This provided the team with confirmation of the overall modeling consistency.

Figure 5.10 shows stresses from in-flight loads for a 1.65-g steep turn. The maximum stress occurs on the composite tailboom and has a magnitude of 2,000 psi. The stress at this location is due to the downward lift generated by the empennage during flight. Wingtip deflection is 1.7 inches.

For the landing load case, the load configuration for the in-flight model was used. Loads were modified to represent a 1.5-g static load down. Ten percent of the payload force was also applied in the longitudinal direction through the CG. For this restraint set, translation was prevented in the vertical and longitudinal directions and rotation restrained about the pitch axis at the end of the main gear leg. This member was approximated as a beam element with the shape and material configuration much the same as the manufactured gear assembly. The strut was rigid-linked to fuselage connection points to simulate attachment of the manufacturer's steel assembly. The objective was to determine stress concentrations in the fuselage at these locations to determine reinforcement options. Maximum stress was 2,000 psi in the attachment areas of the gear box. Results of the landing case are shown in Figure 5.11.

The wing spar had to be strong enough to withstand a wingtip test at maximum gross weight. The prototype aircraft was designed with the wing spar pinned into the fuselage section. This allowed for excessive movement at the wing root to fuselage interface. For the final aircraft, the wing spar was designed to be continuous from wingtip to wingtip. The analysis performed during detail design showed that a carbon fiber spar would not be required, and a spruce-plywood box spar would be adequate.

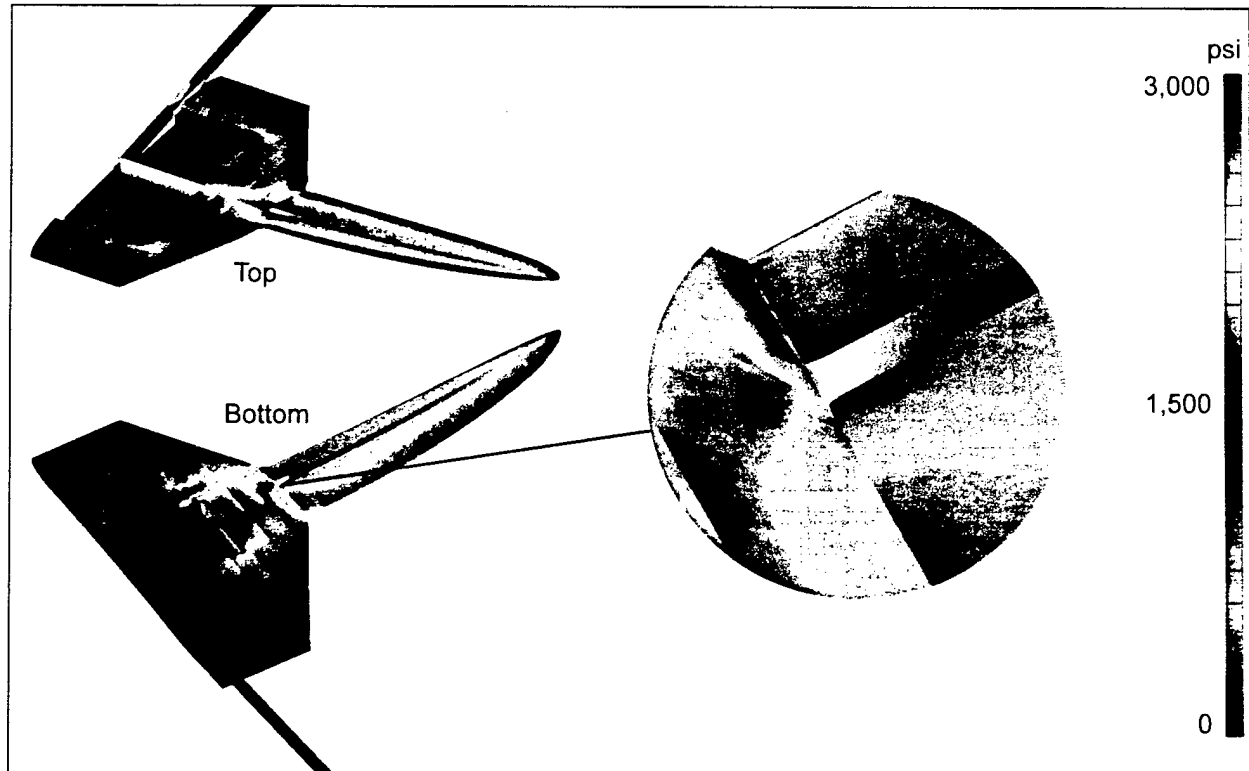


Figure 5.9. Stress Distribution from Wingtip Test Load Conditions.

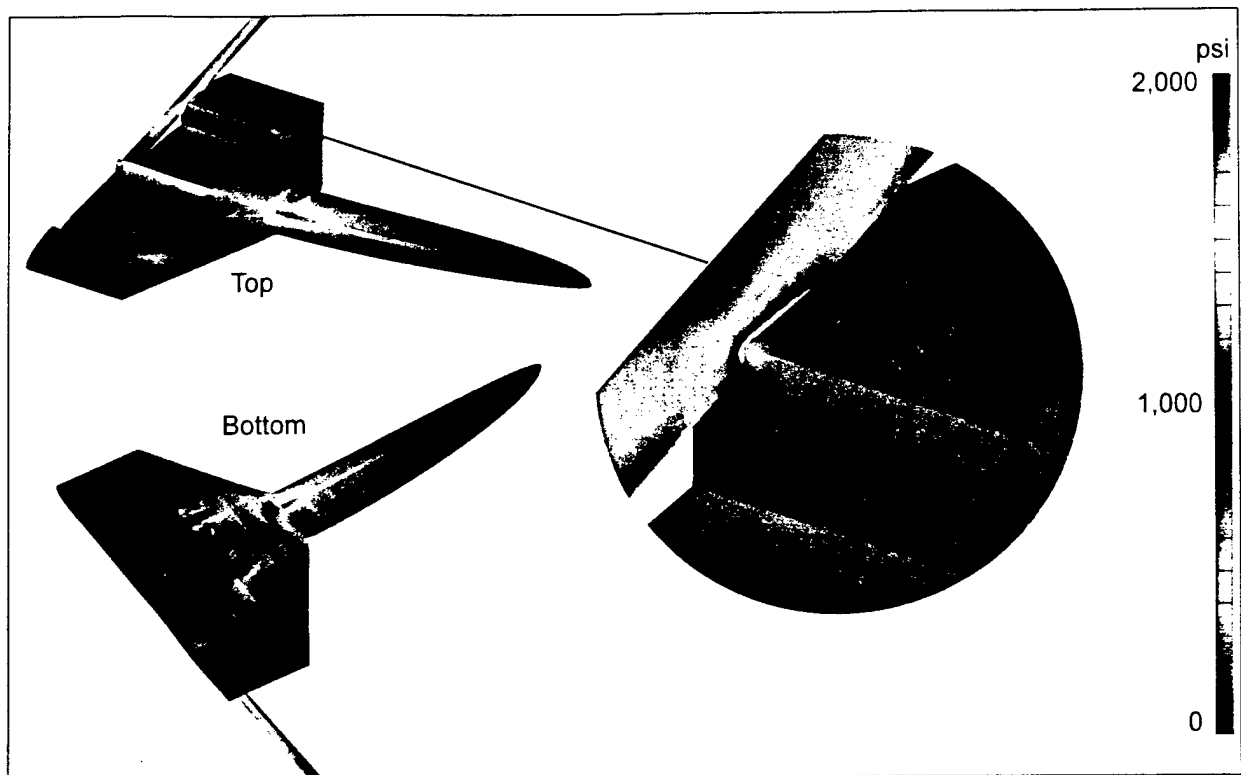


Figure 5.10. Stress Distribution from the 1.65-g Flight Load Conditions.

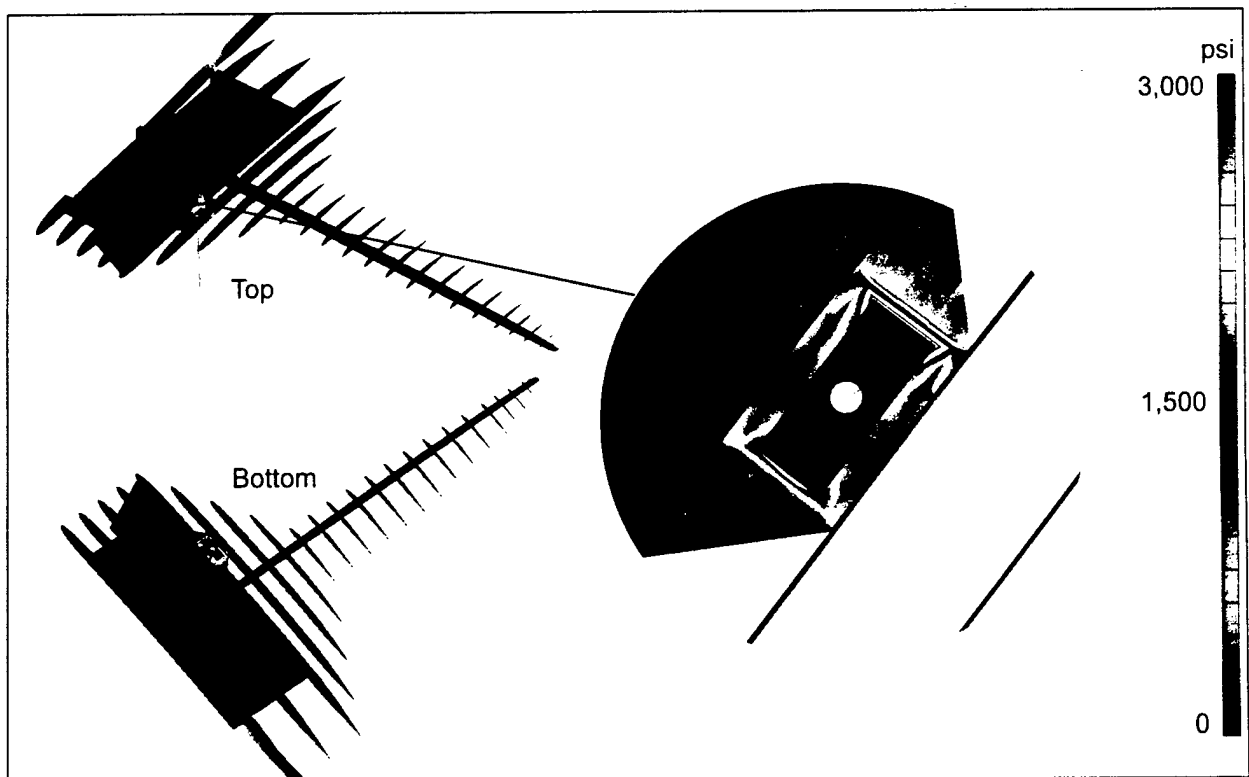


Figure 5.11. Stress Distribution from the Landing Load Conditions.

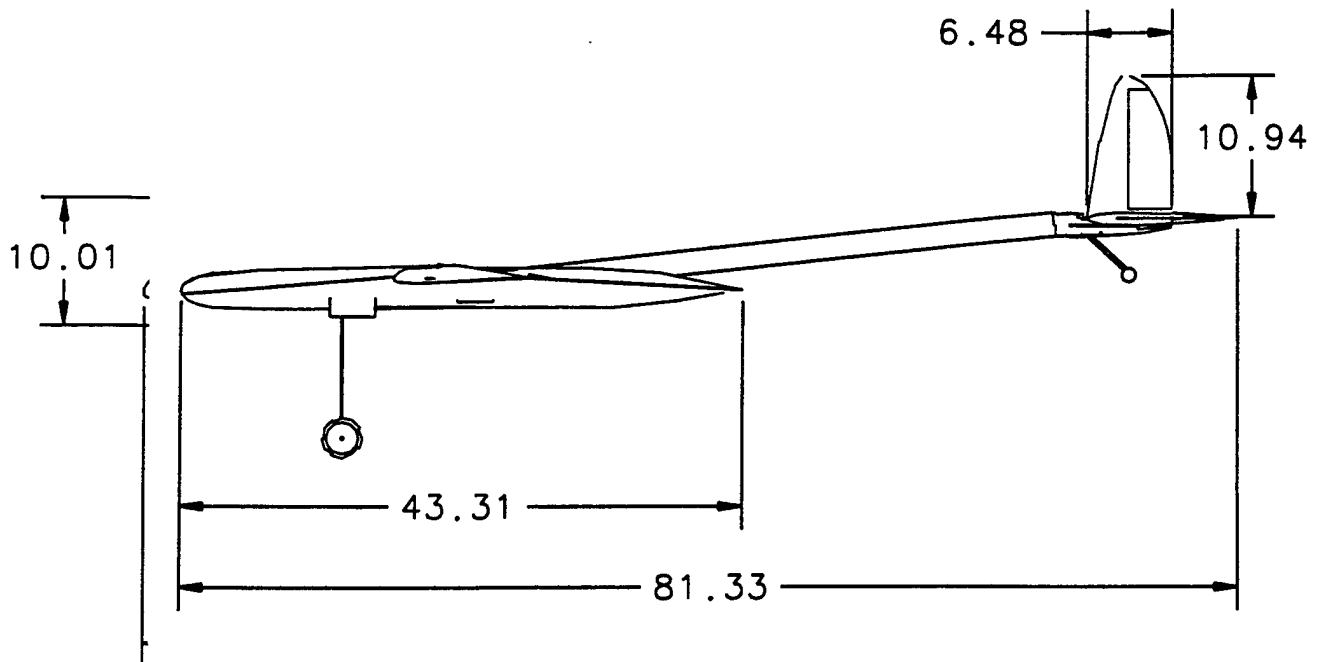
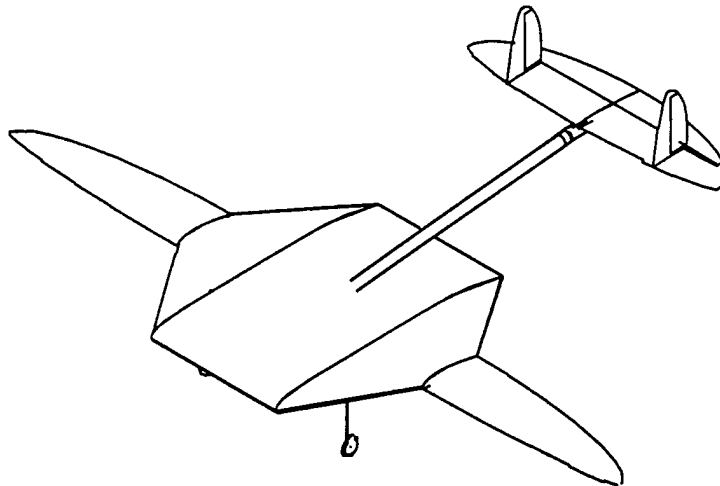
5.1.4. The Control System. Using WINGS2001, the ailerons were sized to provide a dimensionless rolling rate of 0.10 at a deflection of 10° . The elevator was sized at 35% of chord. This allowed for the airplane to be balanced near stall using about -12° of elevator. The rudder was sized conservatively to provide good ground handling characteristics for the taildragger configuration. A 40% flap was chosen. This size was also checked to ensure that the rudder could balance the thrust-induced moment if one of the motors failed and the other motor was run at full throttle. This required 6° of rudder deflection.

For a taildragger configuration handling characteristics are important during takeoff. Sufficient airflow can be supplied early in the takeoff by positioning tail control surfaces in the slipstream of the propeller. This could be done in two ways. The empennage could consist of two vertical surfaces placed directly behind the two propellers or a belt drive system could be used to drive a center propeller with two motors. The belt drive system was rejected due to reliability concerns. Despite the increase of 5 hours in the Rated Aircraft Cost, the empennage was redesigned to have two vertical surfaces. This solution had the least effect on the total score for the aircraft.

5.1.5. Final Configuration. The final aircraft configuration is shown in Table 5.2 and in the following assembly drawings.

Wing Airfoil:	Selig-Donovan SD 7062
Fuselage Airfoil:	USU 483419-1214.20
Horizontal & Vertical Stabilizer Airfoil:	NACA 0009
Wing Span:	10 ft
Elliptic Wing Area:	4 ft ²
Horizontal Stabilizer Area:	3.142 ft ²
Total Vertical Stabilizer Area:	0.647 ft ²
Aileron Area (per Wing):	0.50 ft ²
Elevator Area:	0.96 ft ²
Total Rudder Area:	0.26 ft ²
Wing Mounting Angle:	0.0°
Horizontal Stabilizer Mounting Angle:	-1.9°
Center of Gravity Location (from nose):	1.37 ft
Maximum Gross Weight:	33.0 lbf.
Steel Capacity:	15.13 lbf.
Tennis Ball Capacity:	80
Landing Gear Type:	Retractable, Tail Dragger
Motors:	2 x Astroflight 640
Propellers:	22 x 19
Predicted Rated Aircraft Cost:	5.476
Total Predicted Score:	17.057

Table 5.2. Final Airplane Configuration.



29.72 -

1	000-001	AILERON LEFT		5
1	000-001	AILERON RIGHT		4
1	004-000	EMPENNAGE ASSEMBLY		3
1	003-000	WING ASSEMBLY		2
1	002-000	FUSELAGE ASSEMBLY		1
QTY REQD	DRAWING IDENTIFYING NO	NOMENCLATURE OR DESCRIPTION	MATERIAL SPECIFICATION	ITEM NO
PARTS LIST				

PARTS LIST

UNLESS OTHERWISE SPECIFIED
DIMENSIONS ARE IN INCHES
TOLERANCES ARE:
FRACTIONS DECIMALS ANGLES
±.005 ±.002 ±.005
DO NOT SCALE DRAWING

MATERIAL
FINISH
MATERIAL SUPPLIER ACT. WT. CALC. WT.

CONTRACT NO.

UTAH STATE UNIVERSITY DESIGN, BUILD, FLY, 2001

APPROVALS

DATE

TITLE

DRAWN

JJ

3-10-01

CHECKED

ISSUED

SIZE

DWG NO.

B

000-000

DESIGN

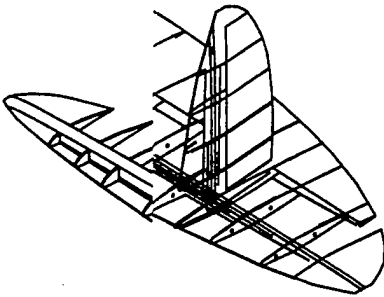
DBF 2001 TEAM

SCALE NTS

SHEET 1 OF 5

3-VIEW DRAWING

NOTE:
BALSA SHEETING REMOVED
TO SEE INNER COMPONENTS



1	001-011	ELEVATOR SERVO	11
1	001-010	RUDDER SERVO	10
1	001-009	SPEED CONTROLLER	9
1	001-008	RECEIVER BATTERY PACK	8
1	001-007	LANDING GEAR SERVO	7
2	001-006	AILERON SERVO	6
2	001-005	BATTERY PACK	5
2	001-004	MOTOR	4
2	001-003	AIR TANKS	3
1	001-002	LEFT LANDING GEAR ASSEMBLY	2
1	001-001	RIGHT LANDING GEAR ASSEMBLY	1
QTY REQD	DRAWING IDENTIFYING NO	NOMENCLATURE OR DESCRIPTION	MATERIAL SPECIFICATION
			ITEM NO

PARTS LIST

UNLESS OTHERWISE SPECIFIED
DIMENSIONS ARE IN INCHES
TOLERANCES ARE:
FRACTIONS DECIMALS ANGLES
± .XX ± .XXX ±
DO NOT SCALE DRAWING

CONTRACT NO.

UTAH STATE UNIVERSITY DESIGN, BUILD, FLY, 2001

MATERIAL

FINISH

MATERIAL SUPPLIER

ACT. WT

CALC WT

APPROVALS

DATE

TITLE

DRAWN

JJ

3-6-2001

CHECKED

ISSUED

DESIGN

DBF2001 TEAM

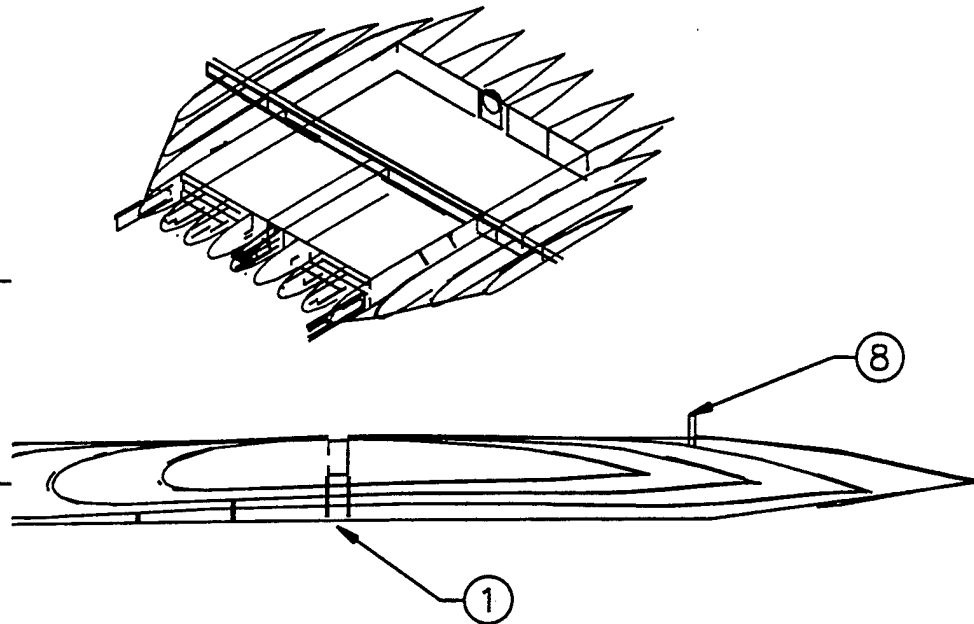
SIZE DWG NO.

B

001-000

SCALE NTS

SHEET 2 OF 5



NOTE:

1. TAPERED RIBS 3" APART
2. FUSELAGE FRONT RIBS 3" APART
3. FUSELAGE REAR RIBS 5" APART

1	002-018	FRONT LEADING EDGE		18
2	002-017	TAPER LEADING EDGE		17
2	002-016	TAPER RIB 4		16
2	002-015	TAPER RIB 3		15
2	002-014	TAPER RIB 2		14
2	002-013	TAPER RIB 1		13
1	002-012	REAR RIB ASSY		12
1	002-011	FRONT RIB ASSY		11
1	002-010	LEFT BATTERY SUPPORT PLATE		10
1	002-009	RIGHT BATTERY SUPPORT PLATE		9
1	002-008	REAR TAIL BOOM SUPPORT		8
1	002-007	FRONT TAIL BOOM SUPPORT		7
1	002-006	LEFT MOTOR MOUNT		6
1	002-005	RIGHT MOTOR MOUNT		5
1	002-004	TAIL SERVO MOUNT ASSY		4
1	002-003	L LANDING GEAR MOUNT ASSY		3
1	002-002	R LANDING GEAR MOUNT ASSY		2
1	002-001	PRIMARY SUPPORT ASSEMBLY	X	1
QTY REQD	DRAWING IDENTIFYING NO	NOMENCLATURE OR DESCRIPTION	MATERIAL SPECIFICATION	ITEM NO

PARTS LIST

UNLESS OTHERWISE SPECIFIED
DIMENSIONS ARE IN INCHES
TOLERANCES ARE:
FRACTIONS DECIMALS ANGLES
2 .XX+ .XX- 2
DO NOT SCALE DRAWING

CONTRACT NO.

UTAH STATE UNIVERSITY DESIGN, BUILD, FLY, 2001

APPROVALS

DATE

TITLE

DRAWN

JJ

3-6-2001

FUSELAGE ASSEMBLY

CHECKED

ISSUED

SIZE DWG NO.

B

002-000

MATERIAL SUPPLIER

ACT. WT

CALC WT

DESIGN

DBF2001 TEAM

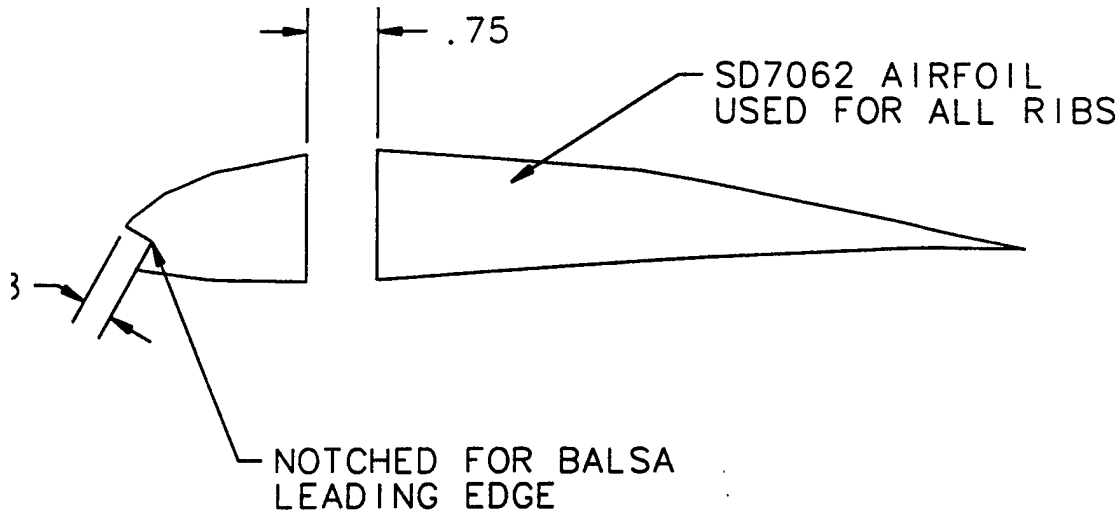
SCALE NTS

SHEET

3 OF 5

NOTES:

1. SHEET OVER THE WING RIBS WITH 1/16 INCH MEDIUM BALSA WOOD
2. ALL RIBS ARE 1/16 INCH THICK
3. SPACING BETWEEN ALL RIBS IS 2.98 INCHES



2	003-019	LEADING EDGE		19
2	003-018	WING RIB 12		18
2	003-017	WING RIB 11		17
2	003-016	WING RIB 10		16
2	003-015	WING RIB 9		15
2	003-014	WING RIB 8		14
2	003-013	WING RIB 7		13
2	003-012	WING RIB 6		12
2	003-011	WING RIB 5		11
2	003-010	WING RIB 4		10
2	003-009	WING RIB 3		9
2	003-008	WING RIB 2		8
2	003-007	WING RIB 1		7
2	003-006	TAPER SECTION RIB 3		6
2	003-005	TAPER SECTION RIB 2		5
2	003-004	TAPER SECTION RIB 1		4
1	003-003	LEFT WING TIP		3
1	003-002	RIGHT WING TIP		2
1	003-001	SPAR		1
QTY REQD	DRAWING IDENTIFYING NO	NOMENCLATURE OR DESCRIPTION	MATERIAL SPECIFICATION	ITEM NO

PARTS LIST

UNLESS OTHERWISE SPECIFIED
DIMENSIONS ARE IN INCHES
TOLERANCES ARE:

FRACTIONS DECIMALS ANGLES
± .XX ± .XXX ±
DO NOT SCALE DRAWING

MATERIAL

FINISH

MATERIAL SUPPLIER

ACT. BY

CALC BY

CONTRACT NO.

UTAH STATE UNIVERSITY DESIGN, BUILD, FLY, 2001

APPROVALS

DATE

TITLE

DRAWN

JJ

3-10-01

WINGS ASSEMBLY

CHECKED

ISSUED

SIZE DWG NO.

B

003-000

DESIGN

DBF2001 TEAM

SCALE NTS

SHEET

4 OF 5

5.2. Performance Analysis

The final aircraft configuration was examined using a modified version of the preliminary design program. Changes were made to the power plant predictions to incorporate the propeller efficiency predictions from Goldstein's vortex theory. In addition, hand calculations were made for climb rate of the aircraft. Static and dynamic stability predictions were made, verifying the controllability and handling characteristics of the final airplane. The results are presented in the following sections.

5.2.1. Takeoff and Climb. The modified preliminary program was run for the conditions of 33 lbf. gross weight using the optimal power plant described above. The estimated takeoff distance for the competition aircraft was 141 feet, and the available static thrust was 11.9 lbf.

At an airspeed of 52 ft/s, WINGS2001 gave a lift to drag ratio of 20.05 at steady level cruise. With the gross weight of 33 lbf, this equates to a drag of 1.646 lbf. At steady level flight, this is also the thrust required. From GPROPS, the total available thrust for both motors was 8.61 lbf. The following relation is an approximation for the climb rate of an aircraft, for small angles of attack and small climb angles:

$$V_c = \frac{VT_A - V_D}{W}$$

In this expression, V_c is the climb rate, V is airspeed, D is drag (or thrust required), T_A is thrust available, and W is gross aircraft weight. The climb rate at these conditions was calculated to be 505 ft/minute.

5.2.2. Range, Endurance and Payload. The range and endurance were calculated using a modified version of the preliminary design program DBF2001. The final aircraft was modeled in WINGS2001 and the aerodynamic characteristics were coded into the program in place of the previous estimates. The GPROPS subroutines were also included to give a more accurate prediction of the power consumption around the flight course. Predicted range as it applies to the competition was three sorties carrying 15.13 lbf. of steel and three sorties carrying eighty tennis balls. This distance was traveled in 9:56, assuming 30-second payload changeover times between sorties. The expected endurance of the aircraft (flying these sorties until battery exhaustion) was 21 minutes. The battery energy consumed was small—only an estimated 8227 Amp-seconds out of the 17280 Amp-seconds (4800 mAh) available in the five lbf. of propulsive batteries. This prediction seemed optimistic, but allowed for a large factor of safety in the power consumption calculations.

5.2.3. Handling Qualities. The horizontal stabilizer was sized and placed to give a static margin of 0.25, which was determined to be adequate during the prototype testing. The vertical stabilizers were sized to give a yaw stability derivative of 0.003 per degree, close to that recommended by Nelson (1998). To be conservative for the taildragger configuration, an additional safety margin of 10% vertical surface area was then added to the vertical stabilizers. This resulted in a final yaw stability derivative of 0.003306. This configuration gave a roll stability derivative of 0.001615 per degree, which considered effects not only from the main wing, but also the destabilizing vertical offset of the empennage. This was judged to be close enough to the standard of 0.0015 per degree recommended by Nelson (1998).

Dynamic analysis of the final aircraft was investigated for steady flight conditions including level flight at 61 ft/s, climb out at 52 ft/s, and descent 52 ft/sec. For each condition, the necessary angle of attack, elevator deflection, and thrust were calculated and applied for balanced flight. A linear dynamic analysis of these balanced flight conditions was then performed. The rigid body 6-DOF equations were used to obtain the longitudinal and lateral modes from the generalized eigenproblem. The results of this dynamic analysis are given in Tables 5.3 through 5.8.

Longitudinal Derivatives			
Derivative	Value	Derivative	Value
$C_{L,\alpha}$	5.330	$C_{x_b,\alpha}$	0.3761
$C_{L,\dot{\alpha}}$	0.6928	$C_{z_b,\alpha}$	-4.914
$C_{L,0}$	0.3110	$C_{m,\alpha}$	-2.008
$C_{D,\alpha}$	0.002431	$C_{z_b,\dot{\alpha}}$	-0.8587
$C_{D,\dot{\alpha}}$	0.0004480	$C_{x_b,\dot{\alpha}}$	-0.002045
$C_{D,0}$	0.01525	$C_{x_b,q}$	-0.1431
$C_{m,0}$	0.000002007	$C_{z_b,q}$	-4.441
$C_{m,\dot{\alpha}}$	-3.623	$C_{m,q}$	-33.07

Table 5.3. Longitudinal aerodynamic force and moment derivatives with respect to non-dimensional velocities and angular rates.

Lateral Derivatives			
Derivative	Value	Derivative	Value
$C_{y_b,\beta}$	-0.4354	$C_{y_b,r}$	0.4081
$C_{l,\beta}$.001248	$C_{l,r}$	0.4720
$C_{n,\beta}$	0.4775	$C_{n,r}$	-0.4478
$C_{y_b,p}$	-0.001616	$C_{y_b,\dot{r}}$	0.2166
$C_{l,p}$	-1.651	$C_{l,\dot{r}}$	0.02349
$C_{n,p}$	-0.1024	$C_{n,\dot{r}}$	-.1583

Table 5.4. Lateral aerodynamic force and moment derivatives with respect to non-dimensional velocities and angular rates.

Dimensionless Eigenvalues			
Mode	Steady-Level Flight $\gamma = 0^\circ$ $V = 61$ ft/sec	Climb-out $\gamma = 8^\circ$ $V = 52$ ft/sec	Descent $\gamma = -4^\circ$ $V = 52$ ft/sec
Short Period	$-0.02536 \pm 0.02347i$	$-0.02546 \pm 0.02328i$	$-0.02546 \pm 0.02328i$
Phugoid	$0.0000607 \pm 0.004957i$	$0.0001641 \pm 0.006938i$	$0.0001613 \pm 0.006967i$
Roll	-0.8106	-0.80571	-0.8056
Spiral	0.01491	0.0231187	0.02319
Dutch Roll	$-0.1150 \pm 0.4113i$	$-0.1199 \pm 0.4216i$	$-0.1200 \pm 0.4215i$

Table 5.5. Dimensionless Eigenvalues corresponding to rigid body motion at different flight conditions.

	Damped Natural Frequency (1/sec)	Undamped Natural Frequency (1/sec)	Damping Rate (1/sec)	Damping Ratio (1/sec)	Period (sec)	99% Damping Time (sec)
Short Period	3.484	4.746	3.484	0.7340	1.949	1.322
Phugoid	0.6810	0.6810	-0.008345	0.01225	9.227	Divergent
Roll	0.000	0.0000175	9.889	0.0000491	-	0.4657
Spiral	0.000	0.0000175	-0.1819	0.0000491	-	Divergent
Dutch Roll	5.152	5.340	1.403	0.2627	1.219	3.283

Table 5.6. Dynamic modes corresponding for steady level flight airspeed of 61 ft/sec.

	Damped Natural Frequency (1/sec)	Undamped Natural Frequency (1/sec)	Damping Rate (1/sec)	Damping Ratio (1/sec)	Period (sec)	99% Damping Time (sec)
Short Period	2.726	4.040	2.982	0.7380	2.305	1.544
Phugoid	0.8125	0.8128	-0.0922	-0.02365	7.733	Divergent
Roll	0.000	0.0000189	8.379	0.0000404	-	0.5496
Spiral	0.000	0.0000189	-0.2404	0.0000404	-	Divergent
Dutch Roll	4.385	4.559	1.247	0.2736	1.433	3.693

Table 5.7. Dynamic Modes for a steady climb angle of 8.0° and airspeed of 52 ft/sec.

	Damped Natural Frequency (1/sec)	Undamped Natural Frequency (1/sec)	Damping Rate (1/sec)	Damping Ratio (1/sec)	Period (sec)	99% Damping Time (sec)
Short Period	2.726	4.040	2.982	0.7381	2.305	1.545
Phugoid	0.8159	0.8161	-0.01889	-0.02315	7.701	Divergent
Roll	0.000	0.0000611	8.378	0.0001304	-	0.5497
Spiral	0.000	0.0000611	-0.2412	0.0001304	-	Divergent
Dutch Roll	4.384	4.558	1.248	0.2738	1.433	3.691

Table 5.8. Dynamic Modes for a steady decent angle of -4.0° and airspeed of 52 ft/sec.

The phugoid mode was found to be divergent with a period of 9.277 seconds. The doubling time for this mode was 83.061 seconds. This divergence was not initially expected. The divergence is primarily due to low drag (Phillips 2000). Because the aircraft will be under visual control at all times and the period is large compared with the reaction time of the pilot, phugoid divergence should not be a problem.

The spiral mode was also found to be divergent, with a doubling time of 3.811 seconds. A divergent spiral mode is fairly common in general aviation and represented no threat to the controllability of the aircraft since the airplane would always be under visual control.

The lateral complex eigenvalue pair is the Dutch roll mode. It displayed a period of 1.219 seconds with a 99% damping time of 3.283 seconds at steady level flight. A serious problem can arise with the dutch roll mode when the damping time is very near the reaction time of the pilot, as the correction the pilot applies will actually excite the motion further. The pilot was made aware of the possible overcorrecting dangers for the dutch roll mode.

6. MANUFACTURING PLAN

The culmination of months of research and analysis depend, to a large degree, on the feasibility, accuracy, and detail of the manufacturing plan. The team took great care in preparing the construction processes and considering the manufacturing options available. To help facilitate the manufacturing plan, a manufacturing schedule was made. Figure 6.1 shows this schedule, which lists the major components of the airplane and the time periods over which they are to be built and tested. A number of manufacturing processes were then investigated; Table 6.2 lists these processes and the figures of merit used to compare them.

6.1. Figures of Merit

A list of figures of merit was prepared specifically for the manufacturing plan. The list helped the team be more objective when choosing the manufacturing processes for the various components of the airplane. It was designed to aid the team in the elimination of construction techniques that would be too costly, too time consuming, or too difficult to realize. The figures of merit were availability, required skill level, time required, reliability, and cost.

6.1.1. Availability. An obvious limiting factor to the choice of any manufacturing process is the availability of the material or equipment required to carry out that process. If the team could not gain access to necessary materials or machinery, the process received a -1. If lead times were long or access was difficult the process received a 0. If everything necessary was readily attainable the process received a 1.

6.1.2. Required Skill Level. Many manufacturing processes require extensive training and skill to execute effectively. Table 6.1 lists the skills that are required to carry out the manufacturing processes considered and the number of team members possessing those skills. If a process was beyond the expertise available to the team, it received a -1. If a process had to be outsourced or was only within the capabilities of a few team members, it received a 0. If the majority of the team members could readily carry out the process, it received a 1.

6.1.3. Time Required. The team must adhere to a tight schedule. A little more than a month was scheduled to build and test the airplane. If a process required a time period of two weeks or more, it was given a -1. If a process could be completed within a two week to four-day period, it was given a 0. Any process that could be realized in four days or less was given a 1.

6.1.4. Reliability. It was essential that each process be able to reliably produce components that met the airplane's design and strength requirements. If a process was undependable and thus unable to produce

Available or Required Skills	Available or Required Skills											
	CNC Milling	Lathe Operation	Wood Working Skills	Carbon Filament Winding	Carbon Composite Lay-ups	Foam Hot-Wiring	Balsa/Plywood Framing	Balsa Sheeting	Fiberglass Shelling	Fiberglass Stripping	Monokote Application	R/C Airplane Modeling
Number of Personnel	1	3	14	4	0	3	6	8	1	7	4	3

Table 6.1. Skill Matrix

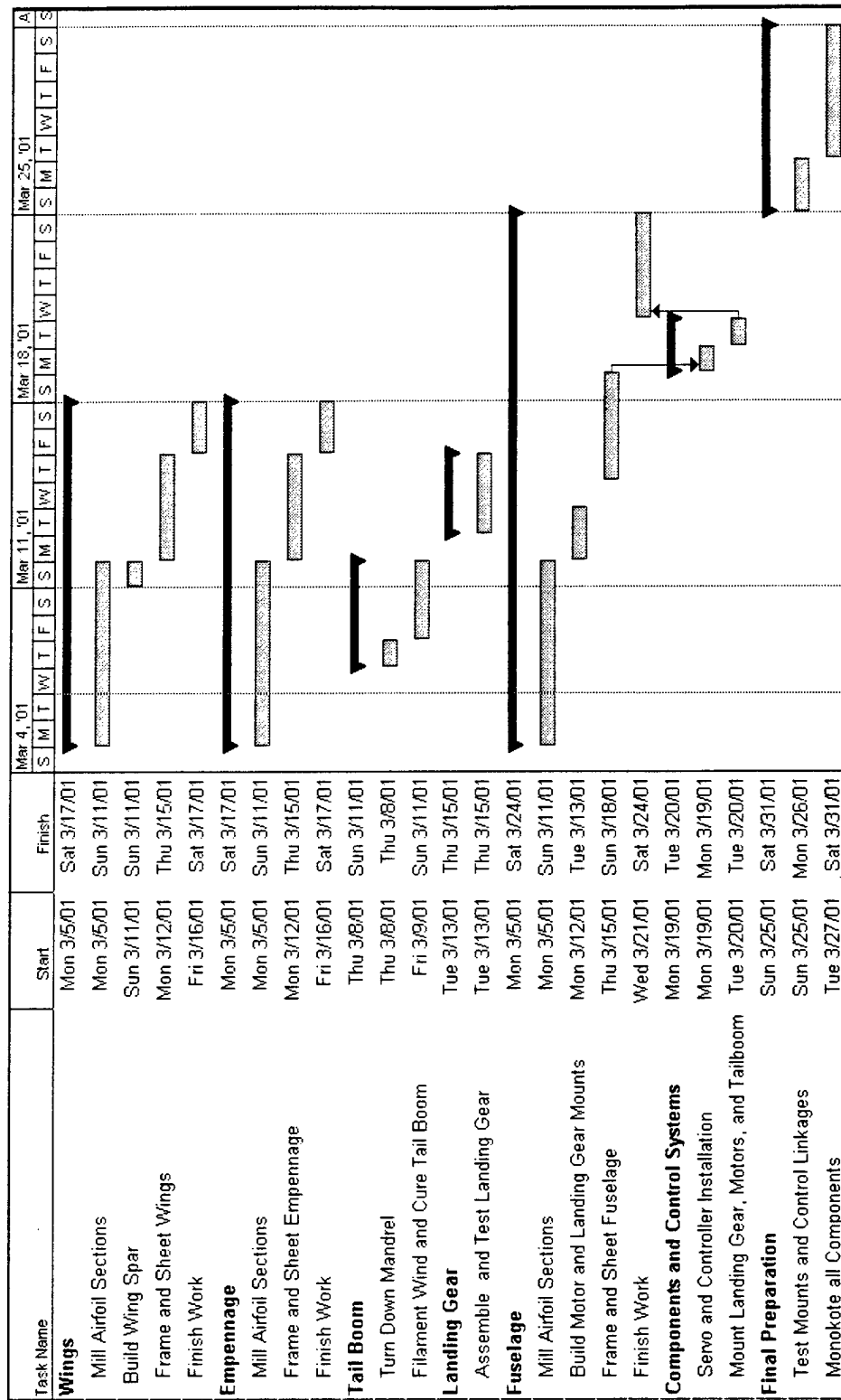


Figure 6.1. Manufacturing Schedule. This figure illustrates the milestones and time allotted for the building and testing of the airplane. The manufacturing schedule was vital in the organization of the manufacturing plan as it allowed the team to visualize the time periods required for each process and the order in which they will occur.

		Figures of Merit 6.1					
		Availability 6.1.1	Required Skill Level 6.1.2	Time Required 6.1.3	Reliability 6.1.4	Cost 6.1.5	Results 6.2
Weighting Factor		2	1	2	2	1	
Wings and Empennage	Foam Core & Composite Covering	0	-1	-1	0	0	-3
	Foam Wing w/ Spar and Balsa Sheet	1	0	0	0	1	3
	Ribbed Spar Structure	1	0	1	1	1	7
	Carbon Composite (no core)	0	-1	-1	-1	0	-5
Wing Spar	Carbon Composite Lay Up	0	-1	0	0	0	-1
	Plywood Framing	1	1	1	1	1	8
Tail Boom	Manual Lay Up	0	-1	0	0	0	-1
	Filament Wound	1	0	1	1	1	7
Motor Mount	Carbon Fiber Mounting Posts	1	0	1	0	1	5
	Plywood Plate	1	1	1	1	1	8
Landing Gear	Outsource	1	1	1	1	1	8
	In-House	0	-1	-1	0	-1	-3
Fuselage	Balsa/Plywood Framing	1	1	1	1	1	8
	Foam Sheeted w/ Balsa	1	0	0	1	1	5
	Carbon Fiber Composite	0	-1	-1	1	1	0
	Fiberglass "Shell" Method	0	-1	-1	1	-1	-2
	Fiberglass "Strip" Method*	1	1	1	1	1	8

*Must be used in conjunction with another process

Table 6.2. Figures of merit for the manufacturing plan.

desirable components it was given a score of -1. If a process' reliability was questionable it was issued a 0. If a process could reliably produce quality components it was given a 1.

6.1.5. Cost. A relatively tight budget limited the cost of the final airplane and individual team members were required to raise the funds necessary for its construction. While the actual cost of manufacturing will not affect the final score, it will affect the team's ability to complete the project. Manufacturing processes that were beyond the financial means of the team received a -1. Any process inexpensive enough for the team to pay for received a 0. If a process was very inexpensive or donated free of charge it received a 1.

6.2. Results.

The manufacturing processes were chosen using the results of the figures of merit in Table 6.2. The wing and empennage will be constructed using balsa ribs. The wing spar will be constructed using wood framing techniques. The tail boom will be a filament-wound carbon fiber tube. The motor mount will be made from a plywood plate. Robart Inc. will manufacture the main landing gear. The fuselage will be a balsa and plywood framed structure reinforced with epoxy and small fiberglass strips.

6.3. Overview of the Manufacturing Plan.

The following sections briefly describe the manufacturing processes to be used in the fabrication and assembly of major components of the aircraft. Detailed engineering specifications and manufacturing instructions were prepared as part of a separate document associated with the detail drawing package.

6.3.1. Wings and Empennage. The wing and empennage are important components of any airplane. It was imperative that the wing and tail provide the calculated aerodynamic characteristics while maintaining their structural integrity. Balsa wood rib construction was determined to be the best possible manufacturing process for the wing and empennage.

Ribs and wingtips will be fabricated from balsa wood using a NC machining process. A tapered box beam will be constructed from spruce (flanges) and Microlite plywood (webs). Each web will be milled in three sections to match the taper of the wing and fuselage. Once the ribs, tips, and wing spar have been manufactured, the wing and tail surfaces will be assembled and sheeted in a custom jig machined from 6-pound Styrofoam. Before sheeting, the servo mounts will be installed at the spar and servo extension wires will be routed along the spar to the wing root. Control surface framing will be installed at this time. Sheeting will be done over the servo mounts and control surface framing. Construction of the empennage follows the same process as the wings with the exception of the spar.

6.3.2. Tail Boom. A thin-walled circular tube made of carbon fiber composite will serve as the tail boom. This tube will be constructed using a filament-winding machine, which winds pre-preg carbon fiber filaments around a steel mandrel. After the boom is wound, it will be cured at 310°F for four hours. After cooling the mandrel will be removed.

6.3.3. Fuselage. All major fuselage parts will be CNC machined. Highly stressed areas will be constructed of plywood or a balsa/plywood composite, while low stress areas will be constructed of balsa. The parts will be assembled as shown in the drawing package using epoxy and wood glue. The landing gear mounts will be reinforced to support the commercially obtained retractable landing gear. The motor mounts will be attached to the side plates using ¼-inch bolts and epoxy. The framed sections of the fuselage will be sheeted with balsa. The sheeted fuselage will then be fitted with the tail boom mounts and the tail boom. The fuselage top will be fabricated and attached to the fuselage. The servos and control linkages will be installed last. The fuselage will be sanded and covered with monokote.

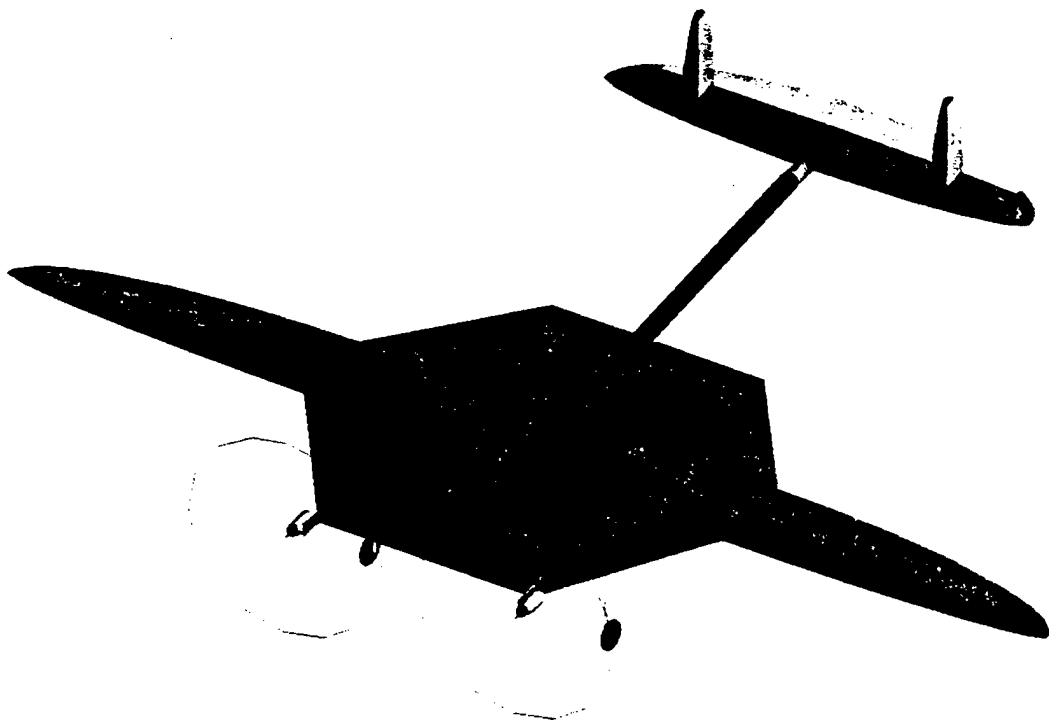
6.3.4. Controls. The control surfaces framed into the wings and empennage will be cut out, finished and hinged to the main structure. Holes will be cut into the bottom surfaces of the wings to gain access to the servo mounts. Control horns and cables will be attached and servos installed. Empennage servos will be located in the fuselage and linked to the elevator and rudders by pull-pull cables routed through the tail boom to the control horns of the empennage.

REFERENCES

- Goldstein, S., (1929), "On the Vortex Theory of Screw Propellers," *Proc. Roy. Soc.* **A123**, 440.
- Nelson, R. C., (1998), *Flight Stability and Automatic Control*. 2nd edition, McGraw-Hill, New York.
- Phillips, W. F., (2000), "Phugoid Approximation for Conventional Airplanes," *AIAA Journal of Aircraft*, Vol. 37, No. 1.
- Phillips, W. F., (2000), "Improved Closed-Form Approximation for Dutch Roll," *AIAA Journal of Aircraft*, Vol. 37, No. 3.
- Phillips, W. F., and Snyder, D. O., (2000), "Modern Adaptation of Prandtl's Classic Lifting-Line Theory," *AIAA Journal of Aircraft*, Vol. 37, No. 4.

*2000/2001 AIAA Foundation
Cessna/ONR Student Design Build Fly Competition*

Design Report
Addendum Phase



“A”
Utah State University
April 2001

Table of Contents

	Page #
1. Executive Summary	2
1.1. Conceptual Design	2
1.2. Preliminary Design	3
1.3. Detail Design	4
2. Management Summary	5
2.1. Architecture of the Design Team	5
2.2. Configuration and Schedule Control	5
3. Conceptual Design	8
3.1. Design Parameters and Aircraft Configurations	8
3.2. Figures of Merit	11
3.3. Quantitative Analysis of Selected Parameters	12
3.4. Analytical Tools	14
3.5. Configuration Selection	17
4. Preliminary Design	18
4.1. Prototype Testing	18
4.2. Figures of Merit	20
4.3. Design Parameters Investigated	20
4.4. Analytic Methods Used	22
4.5. Configuration Selection	24
4.6. Engineering Requirements	26
5. Detail Design	27
5.1. Component Selection and Systems Architecture	27
5.2. Performance Analysis	44
6. Manufacturing Plan	47
6.1. Figures of Merit	47
6.2. Results	49
6.3. Overview of the Manufacturing Plan	50
7. References	50
8. Lessons Learned	51
8.1. Modifications to Improve Takeoff Performance	51
8.2. Modifications to Improve Aircraft Structure	53
8.3. Cost-Benefit Analysis for Aircraft Modifications	56
8.4. Suggested Improvements for a Next-Generation Design	57
9. Aircraft Cost	58
9.1. Manufacturer's Empty Weight (MEW)	59
9.2. Rated Engine Power (REP)	59
9.3. Manufacturing Hours (MFHR)	59
9.4. Results	60

8. LESSONS LEARNED

Several modifications to the aircraft design were made. These modifications were made because of improved analytical tools, longer than expected procurement times, manufacturing difficulties and improved manufacturing procedures. These modifications included increased wing area for better takeoff performance, a lighter tailboom, and the use of a Kevlar strip to provide added strength to the wing spar. In order to minimize the number of mistakes during the manufacturing process, a quality assurance plan including an inspection and certification procedure was established. Alternatives for a next-generation design were also considered during the manufacturing process.

8.1. Modifications to Improve Takeoff Performance

Two of the greatest uncertainties affiliated with the analytical tools used to design the proposed aircraft and predict its performance were those associated with the propeller and stall analysis. Since both available thrust and stall speed have a dramatic effect on takeoff distance, confidence in the predicted takeoff performance was low. From the outset, it was known that this would be the case. Original plans called for testing the competition aircraft and making any required adjustments by changing the propellers, motors and/or batteries. Shortly after construction began, it was realized that fabrication delays combined with longer than expected procurement times would make extensive testing impossible. Final propeller and motor selection would need to be accomplished solely through the use of analytical tools and the experimental data that was already available. When this was realized, a second analytical effort was launched in parallel with the aircraft construction. The objective of this effort was to improve both the propeller analysis and the stall analysis so that propellers and motors could be ordered with greater confidence.

8.1.1. Improved Propeller Analysis. The computer program (GPROPS) used for propeller analysis in the preliminary and detail design phases was based on Goldstein's vortex theory. Predictions from this program were compared with wind tunnel data taken at USU and it was observed that GPROPS would often under-predict the torque required to turn a propeller at a given airspeed.

Goldstein's vortex theory requires a section drag coefficient for the propeller blades. The drag is integrated over the length of the propeller in order to determine the power required for a given operating condition. For GPROPS, the computation of section drag coefficient is broken up into three ranges in angle of attack. The first provides an expression for drag coefficient in the range of linear lift below stall. The third is an expression for drag on a flat plate nearly perpendicular to the airflow at angles of attack above 85 degrees. The middle expression is a second order polynomial fit between the other two. To better match the GPROPS predictions with the test data, the method of calculating the section drag coefficient was changed. The drag coefficient of the first expression was increased and a cubic polynomial was used in the interpolation region (15 to 85 degrees).

A motor test was also performed to validate the performance predictions for the propellers chosen for the final aircraft. This test was also carried out to verify the prediction that the 22x19 propeller would outperform the 22x20. The motors were mounted to a test stand, with instrumentation to give thrust, current and voltage readings. Temperature measurements were also collected to see how the electrical resistance of the motor varied with temperature. The results for the test are shown in Figure 8.1. These results show that the performance of the purchased motors and propellers was consistent, and that GPROPS is conservative in its predictions of static thrust for a given current. The electrical resistance of the motors was nearly constant over an operating temperature range of 75° to 175° F. The test results also show that the 22x19 propeller produced more static thrust for any given current draw.

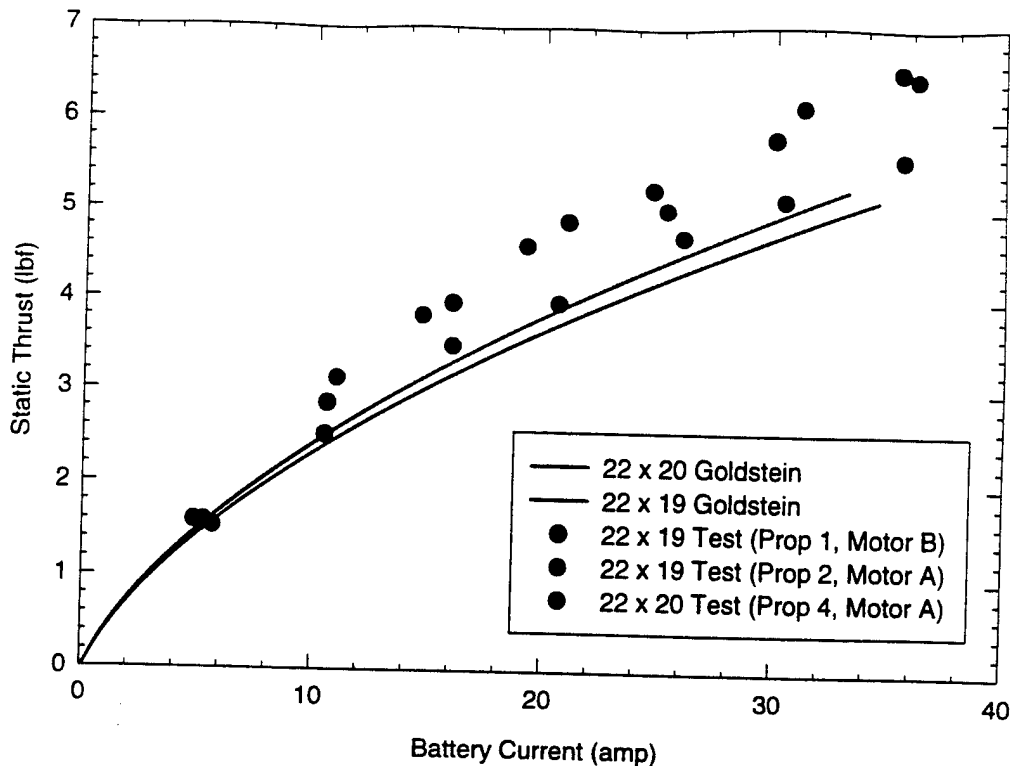


Figure 8.1. Test results for the Astroflight 640 motor with various propellers with Goldstein's vortex theory predictions from zero to full throttle.

8.1.2. Improved Stall Analysis. The stall analysis carried out in the preliminary and detail design phases used a two-dimensional approximation to predict the maximum section lift coefficient for the airfoil sections used to construct the wing and fuselage. From this analysis, it was estimated that the airplane would stall at approximately 41 feet per second with the heavy payload and 37 feet per second with the light payload. Takeoff performance predictions were made using these stall speeds. However, since no attempt was made to account for the three-dimensional effects of downwash on the wing, confidence in the estimated stall speeds and the resulting takeoff distances was low.

Using WINGS2001, which accounts for lifting surface interactions, the lift coefficients for each of the major lifting surfaces (wing, fuselage and horizontal tail) were computed for steady level flight at various airspeeds. Lift versus airspeed relations for the wing and fuselage were plotted and compared with the maximum lift coefficient for the airfoil used to construct the lifting surface. The intersection of these lines determined the stall speed for each section. Data was collected for two different root chord lengths and is shown in Figure 8.2. For the values of the wing root chord shown, the main wing will stall before the fuselage. Because the heavy payload configuration will stall before the light payload configuration, analysis of stall speed was limited to airplanes with a heavy payload configuration.

The data shown in Figure 8.2 was used to improve the stall speed predictions for the proposed aircraft. Using the lift-airspeed curves shown in Figure 8.2, a lift coefficient of 1.6 for the proposed main wing (SD7062 airfoil) with a chord of 10 inches corresponds to a stall speed of 47 feet per second. This result is significantly different from the stall speed predicted during the preliminary and detail design phases of 41 feet per second. To realize a more optimal takeoff performance, wing area was increased to reduce the stall speed.

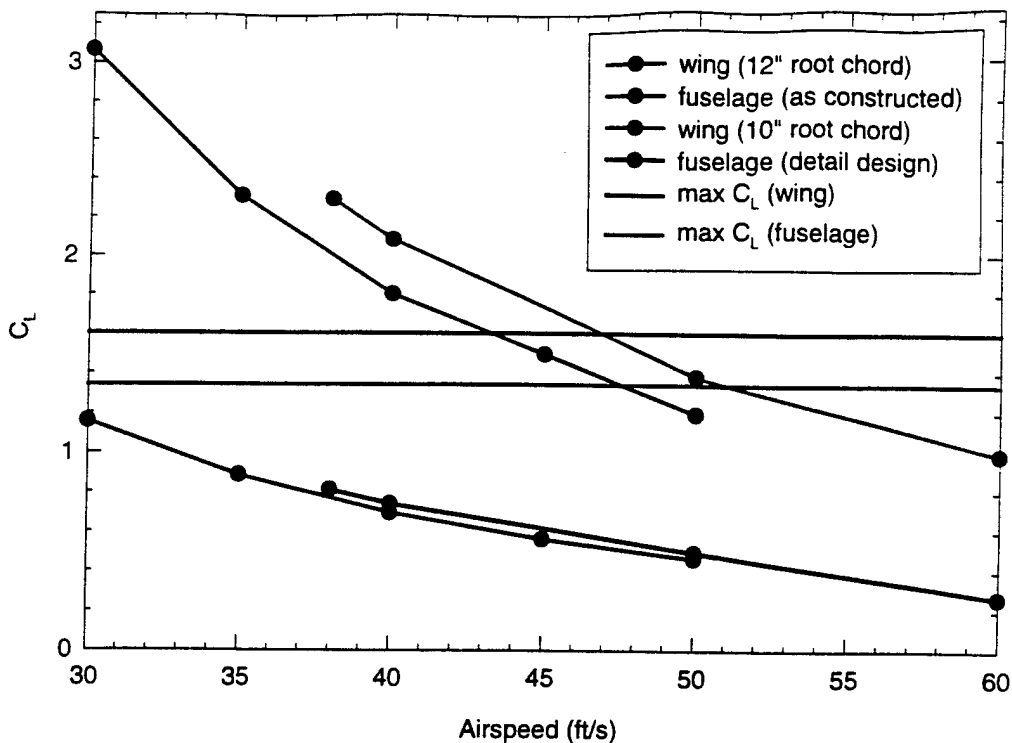


Figure 8.2. Improved stall speed calculation results.

8.1.3. Wing Modification. Using the improved stall speed predictions in the takeoff analysis, the predicted takeoff distance increased from the detail design phase value of 155 feet to 196 feet. To provide a larger safety factor in the takeoff, the wing area was increased. Although increasing the wing area adversely affects the total score possible at the competition due to an increase in rated aircraft cost, it was decided that the safety factor for takeoff was worth the penalty.

The design team was comfortable with the safety factor afforded by a predicted takeoff distance of 185 feet; therefore, a wing area corresponding to this takeoff distance was sought. The root chord of the main wing corresponding to a 185-foot takeoff distance was found to be 12 inches using the improved stall speed analysis and results from previous design phases. In modifying the main wing from a 10-inch root chord to a 12-inch root chord, the wing area increased by 0.83 ft². This increase in wing area corresponds to an increase in rated aircraft cost of 0.07 thousand dollars.

8.2. Modifications to Improve Aircraft Structure

For the team to achieve the highest possible score at the competition, it was necessary that the airplane be structurally sound. Considerable effort was exerted to manufacture a wing spar capable of withstanding the load introduced by the wing tip test. Test results from the fabricated wing spar, along with finite element analysis, were used to determine the maximum certifiable gross weight, which has a large effect on the achievable score at the competition. A lighter tailboom was also manufactured. Other procedures were used to ensure a high standard of quality in the completed aircraft structure.

8.2.1. Fabrication and Testing of the Wing Spar. A practice spar was fabricated to better understand the wing spar construction process. This practice spar provided information about the adequacy of a box-beam design, feasibility of tapering the spar in all directions, and the possibility of using a continuous spar across the span of the airplane.

Due to the scarcity of aircraft grade spruce, the practice spar flanges were built using Douglas Fir. The flanges and web of the box-beam were milled on the edges to maximize the adhesive surface area. Dovetail tension and compression joints were used in the flanges to join the two halves at the center, while a shear plate reinforced the web sections. Slow-set epoxy was used for assembly.

The practice spar was loaded at the center while simply supporting the tips. A load of 16 pounds was applied before it was decided that the box-beam design and construction process would be adequate. Fabrication and testing of the practice spar showed that the advantages of tapering the width of the spar were small compared with the associated manufacturing difficulties. The joints used to connect the two halves in the practice spar were cumbersome and significantly weaker than alternative methods. It was also difficult to maintain the webs and flanges true and plumb.

Using the lessons learned from the practice spar, the final spar was fabricated around an aluminum mandrel using aircraft grade spruce for the flanges and Microlite plywood for the web. The mandrel was included to connect the two spar halves during test flights. At the competition, the spar will be epoxied into place. By simply supporting the spar near its ends and loading the middle of the spar, force-deflection data was obtained for comparison with a finite element model. The finite element model was used in determining the maximum certifiable gross weight of the airplane.

8.2.2. Determination of the Final Certified Maximum Gross Weight. Since the wing tip test is the most severe load the airplane will experience, a more detailed structural analysis of the wing spar was performed to determine the maximum load the spar could carry before yielding and ultimate failure. With knowledge of this load, the plane can be tested to its full payload potential, allowing maximum flexibility in selecting payload at the competition.

The first step in the detailed analysis was to determine as accurately as possible the elastic modulus of the spar. This was accomplished by simulating the spar test with a finite element model. The model was constructed using the same materials, cross-section and boundary conditions as the spar test using the I-DEAS software. The finite element model was solved with static, linear elastic, small displacement theory. The elements used to generate the model were quadratic triangular Mindlin shell elements. The solution process to obtain the material properties used in the model for Microlite plywood was iterative. Values for Young's Modulus (E) were guessed until the deflections of the finite element model matched those of the spar test. The spar test data compared with results from the finite element model are shown in Figure 8.3. This gave $E=0.7 \times 10^6$ psi for the plywood and $E=1.8 \times 10^6$ psi for spruce.

The wing spar was originally designed using a published tensile yield strength of 6,700 psi as the failure criterion for the Sitka Spruce flanges. No published data was available for the ultimate tensile strength of aircraft grade Sitka Spruce. However, published data for other similar woods, such as West Coast Douglas Fir and Eastern White Pine, indicated that the ultimate tensile strength was probably much greater than the published yield strength. To verify this fact and to establish a better failure criterion, tensile tests were performed. Seven tensile test samples were cut from pieces of spruce left over from the fabrication of the spar. These were all pulled to failure. All samples failed between 13,900 and 14,990 psi. From this data an ultimate tensile failure criterion of 14,000 psi in the spruce flange was established for use in determining of the maximum gross weight for the aircraft.

Finally, the loads that would result in yielding and failure of the spar assembly components were predicted. Another finite element model was constructed of the spar and spar box to simulate the spar glued into the fuselage. Symmetry along the centerline of the airplane was used. This analysis predicted

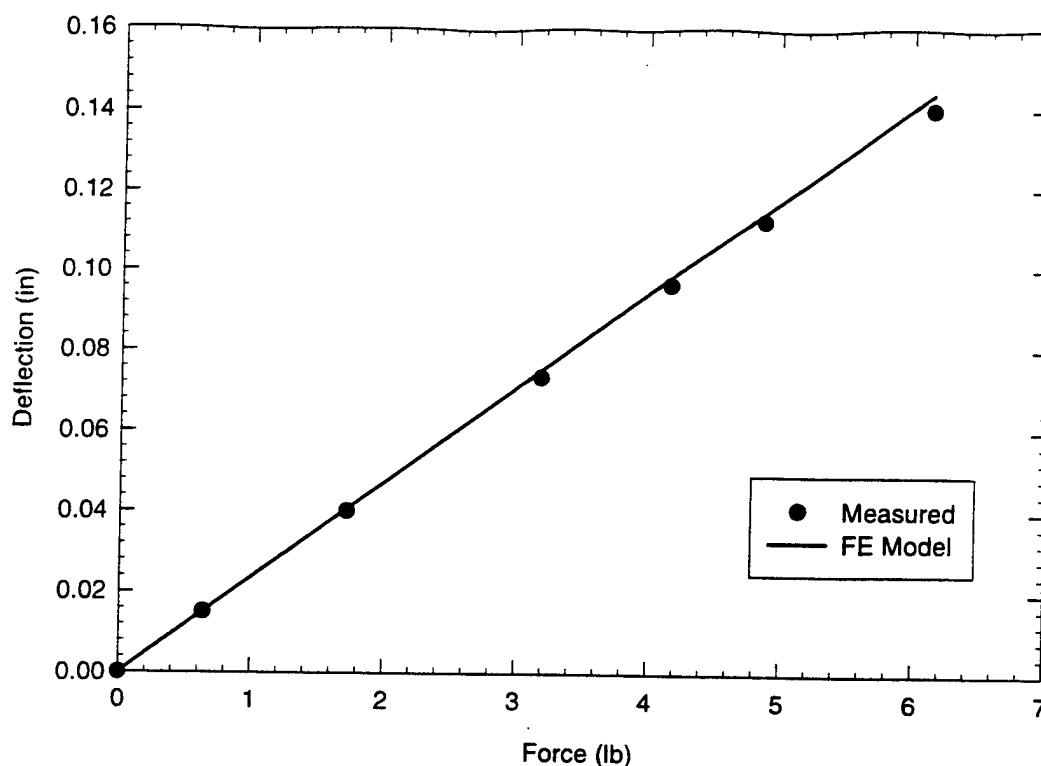


Figure 8.3. Force-deflection curve for the final wing spar, including results of the FE model used to determine the maximum certifiable gross weight.

that the wingtip test load at compressive yield would correspond to a gross weight of 40 pounds, tensile yield would occur at a gross weight of 54 pounds, and the gross weight at ultimate tensile failure was predicted to be 114 pounds. These values were calculated using a factor of safety of 1.0. While unity is a low safety factor for this type of analysis, there is an implicit safety factor when the airplane is assembled. This is due to the wing skin supporting some of the load. This was neglected in the finite element model of the spar. The finite element model that was used in the detail design phase included the wing skin and showed its effect to be significant. Based on the results of this analysis, it was decided that the competition aircraft could be safely wingtip tested to a maximum gross weight of 55 pounds. Stress distributions in the spar flanges and the shear webs are shown in Figure 8.4 for the design gross weight of 33 pounds.

8.2.3. Modifications to the Final Aircraft Structure. The stiffness requirement imposed on the tailboom during the final design phase was that the boom must allow a maximum of 10% control loss at two times the minimum drag velocity. The team felt that this requirement was unnecessarily strict and that the tail boom could be made lighter while maintaining sufficient control. The design was modified to 80% of the stiffness imposed by the final design requirements. In the final tailboom, 30 degree fibers were used instead of 45 degree fibers. This allowed one layer to be removed from the boom. A spare tail boom was also fabricated to be used as a replacement should the installed boom fail. Due to problems at the winding facility, the team opted to lay-up the composite tailboom by hand.

A Kevlar strip was added to the bottom of the tension side of the wing spar to provide added strength. In addition to the strength provided by the Microlite plywood and spruce used to construct the wing spar, the Kevlar strip reduced concern about the possibility of failure during the wing tip test.

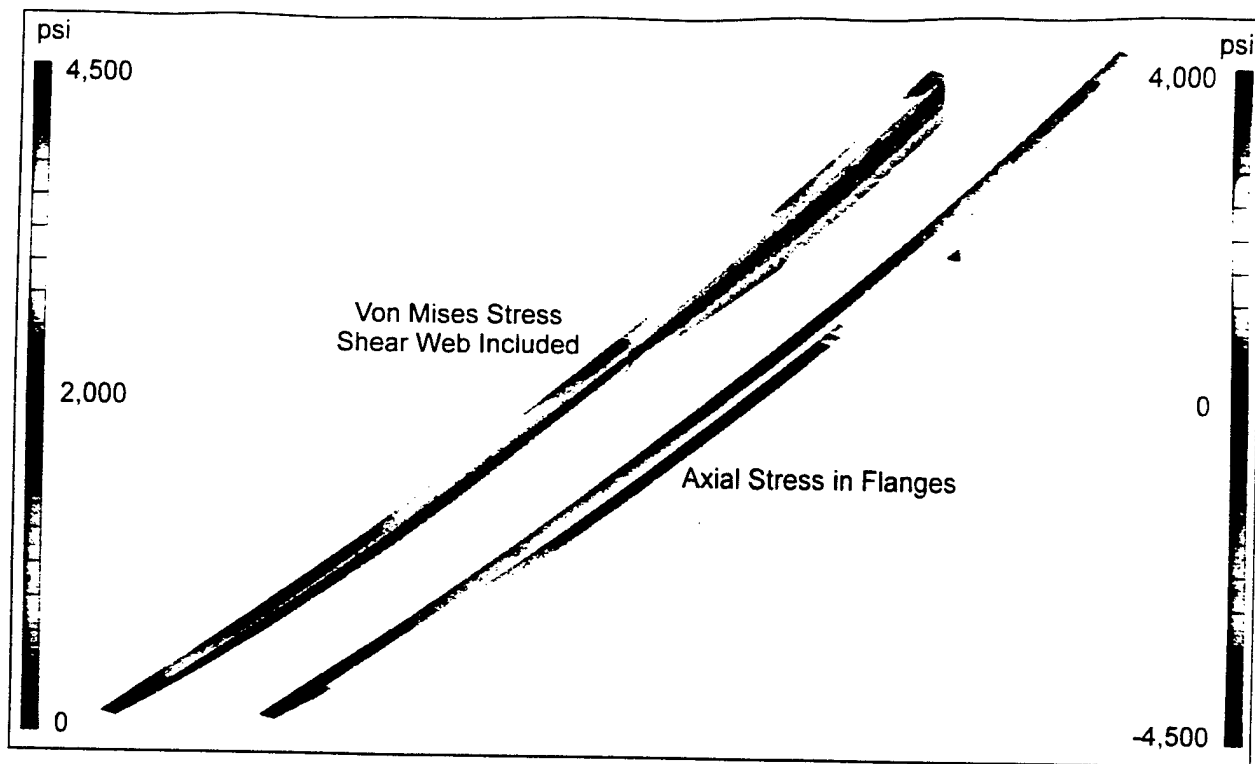


Figure 8.4. Stress distributions in the spar flanges and shear webs.

8.2.4. Quality Assurance and Certification. Mistakes can occur during the fabrication of any product. This can lead to differences between the proposed design and the actual product. During fabrication, a number of processes required skills where the design team as a whole did not have much experience. In order to minimize the effect of any errors and in order to ensure that the airplane be built in a timely fashion, a quality assurance and certification procedure was established. Inspection and certification forms for each major airplane component were created. For the manufacturing process to proceed, four people inspected each component: a structural engineer, an engineer responsible for that particular component, a structural advisor and an aerodynamic advisor. These four people ensured that the component was structurally and aerodynamically sound, and was fabricated according to the design specifications. After inspection was completed and the quality of the component was determined to be sufficient, each of the inspectors signed the form. An example of an inspection and certification form is shown as Figure 8.5. A schedule of inspection times was also constructed to help ensure that deadlines were met. The scheduled date and time for each inspection were included at the top of each Inspection and Certification form.

8.3. Cost-Benefit Analysis for Aircraft Modifications

Each of the design modifications discussed in the sections above was made to increase the likelihood of achieving the highest possible score at the competition. A summary of how these modifications accomplished this task is included in the following sections.

8.3.1. Time and Cost Required to Implement Modifications. As a result of increasing the wing area (Section 8.1.3), one day was lost to cut the new ribs required for the modified wing. An increase in the rated aircraft cost (RAC) of 0.07 thousand dollars along with a small increase in weight due to the added material was also incurred. By eliminating the width-tapering originally planned for in construction of the

QUALITY ASSURANCE
Inspection and Certification Form

5. Internal Wing Inspection

Scheduled Date and Time: 28-March, 3:30 PM

- Purpose:** a) Certify the integrity of the internal structural members of the wing.
b) Certify that the wing surfaces have the correct aerodynamic shape and size.
c) Certify that the control surfaces on the wing are the correct size and shape.

Requirements: All internal structural elements of the wing must be completed and still exposed. Some of the sheeting may be applied but none of the structural elements may be covered in such a manner as to make inspection impossible or extremely difficult. The external shape of the wing must be completely defined and all sheeting supports must be in place. The location and extent of all control surfaces must be clearly marked but not cut.

Signatures:


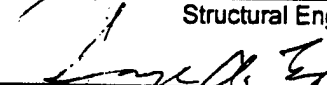
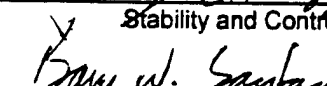
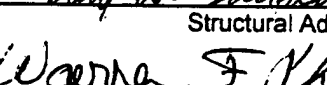
 _____ Structural Engineer	<u>3/28/01</u> Date	<u>11:42 p.m.</u> Time
 _____ Stability and Control Engineer	<u>3/28/01</u> Date	<u>10:40 p.m.</u> Time
 _____ Structural Advisor	<u>3/28/01</u> Date	<u>10:42 p.</u> Time
 _____ Aerodynamic Advisor	<u>3/28/01</u> Date	<u>10:42</u> Time

Figure 8.5. Example Inspection and Certification form.

wing spar (Section 8.2.1), a very small penalty in the *RAC* was induced because of added material. The time and cost to add a Kevlar strip to the bottom of the wing spar (Section 8.2.3) were negligible. New tailboom construction techniques (Section 8.2.3) required approximately five hours of added construction because team members performed the fabrication manually.

8.3.2. Improvements Realized. By increasing the wing area, improved stall characteristics for the airplane and a decrease in takeoff distance of 10 feet were realized. Eliminating width-tapering in the wings spar greatly simplified construction. Addition of Kevlar tape to the wing spar increased the strength of the spar with virtually no added cost. Improved tailboom construction provided a lighter tailboom, decreasing the *RAC*.

8.4. Suggested Improvements for a Next-Generation Design

During the proposal design phase, the design of the empennage was changed from a single vertical stabilizer to two vertical stabilizers, in order to increase yaw control during takeoff. This design change resulted in an increased rated aircraft cost. With sufficient time, airplanes with empennage configurations having only one vertical stabilizer could be tested, and if found to provide sufficient ground control, it may be possible to eliminate one of the vertical stabilizers.

Analysis of the final airplane in WINGS2001 showed that 2.9 pounds of negative lift was required on the tail during steady level flight. A canard design could provide the necessary pitch stability with positive lift. However, it was not feasible to implement such a major design change due to time constraints.

An increased score could be realized by moving the servos, controllers and tailboom mount into unused portions of the fuselage. By creating extra space in the payload area, up to eight additional tennis

balls could be accommodated. This translates to an increased flight score of 1.6 points for every tennis ball sortie flown.

A more aesthetically pleasing tailboom could be constructed. During the fabrication of the tailboom, the shrink-wrap was applied in a direction opposite the carbon fibers. This caused some wrinkling along the surface of the tailboom. Although this mistake did not penalize the tailboom significantly in terms of stiffness, another tailboom could be fabricated using the correct shrink wrap application in order to eliminate any wrinkling.

Because battery and motor efficiency decreases with increasing temperature, the current design could be improved to provide better heat transfer between the batteries, the motors and the air. The batteries could be more exposed to the airflow, providing improved ventilation. Airfoil-shaped fins or cowlings could be used to help cool and improve motor efficiency.

The area where the greatest improvement could be made was not associated with the design of the airplane but rather with the fabrication process and the production of engineering detail drawings. Because contest rules did not allow the inclusion of a complete detail drawing package in the design report, the team was lulled into thinking that the production of such a drawing package was of low priority. As a result, the detail drawing package was not completed until after fabrication of the airplane had begun. This turned out to be a very big mistake. The team learned that it is nearly impossible to accurately fabricate an engineered structure without a complete set of detail drawings. Costly mistakes were made in the fabrication process that had to be corrected by refabricating several parts of the airplane. In every case these mistakes could have easily been caught on paper, if the detail drawing package had been completed before fabrication of the airplane was begun. For the production of any next-generation aircraft this team would strongly recommend that a complete set of detail drawings be produced, checked, and approved before any construction is started.

9. AIRCRAFT COST

The total score that can be obtained at the Design, Build, Fly Competition is a function of three parameters: the written report score, the total flight score, and the rated aircraft cost (*RAC*). The total contest score is computed as

$$\text{Total Score} = \frac{\text{Written Report Score} \times \text{Total Flight Score}}{\text{Rated Aircraft Cost (RAC)}}$$

In order to achieve the highest possible score, it was required that the design team maximize scores for the written report and flight sorties, while minimizing the *RAC*.

The aircraft cost model used to compute the *RAC* approximates the cost of the final aircraft in thousands of dollars. While this aircraft cost model is only approximate, it provides valuable insight into the design process and was an important factor in each of the design phases. The *RAC* is comprised of three factors: manufacturer's empty weight (*MEW*), rated engine power (*REP*), and manufacturing hours (*MFHR*). It is computed using the formula

$$RAC = \frac{MEW \times A + REP \times B + MFHR \times C}{1000},$$

where the constants *A*, *B*, and *C* are used to convert the units of each factor into dollars. The *MEW* multiplier, *A*, was assigned the value of \$100 per pound. The *REP* multiplier, *B*, has a value of \$1 per

watt, and the *MFHR* multiplier, *C*, has a value of \$20 per hour. A detailed description of the *RAC* variables is provided below.

9.1. Manufacturer's Empty Weight (*MEW*)

The manufacturer's empty weight (*MEW*) is the weight of the aircraft measured in pounds, without the payload and batteries. For every pound of aircraft weight, not only is the total payload capacity of the airplane decreased by one pound, but the *RAC* increases by 0.1 as well. The *MEW* for the aircraft as designed and built is 14.40 pounds.

9.2. Rated Engine Power (*REP*)

The rated engine power (*REP*) is a measure of the power available to the aircraft. The *REP* is computed using the formula

$$\text{Rated Engine Power (REP)} = \text{Number of Engines} \times \text{Number of Cells} \times 1.2 \frac{\text{volts}}{\text{cell}} \times 40 \text{ amps},$$

where the number of cells is the number of batteries connected to each motor. For the proposed aircraft, there are two engines, each connected to an individual battery pack containing 18 cells. Therefore, the *REP* is computed as

$$\text{Rated Engine Power (REP)} = 2 \text{ Engines} \times 18 \frac{\text{Cells}}{\text{Engine}} \times 1.2 \frac{\text{Volts}}{\text{Cell}} \times 40 \text{ Amps} = 1728 \text{ watts}.$$

9.3. Manufacturing Hours (*MFHR*)

The manufacturing hours (*MFHR*) were used to approximate the amount of time required for the construction of the final aircraft. The *MFHR* is broken down into several different groups described by the Work Breakdown Structure (*WBS*). The total *MFHR* is computed by calculating and summing each of the *WBS* hours. Table 9.1 shows the *MFHR* for the final aircraft. The individual *WBS* values are also shown. The total *MFHR* for the final aircraft is 141.40 hours.

9.3.1. WBS: Wing(s). According to the Work Breakdown Structure as given in the contest guidelines, each wing was assessed a 15-hour charge. For each square foot of projected planform area, including the area of any winglets, braces, and struts, a 4-hour charge was included. An additional 2 manufacturing hours were assessed for each winglet, strut, and brace; while 3 manufacturing hours were charged for each control surface. Table 9.1 shows that the constructed aircraft was assessed a Wing *WBS* charge of 40.88 hours.

9.3.2. WBS: Fuselage. Each fuselage and pod on the aircraft was assigned a 5-hour manufacturing time. For each foot of fuselage and pod length, an additional 4-hours of manufacturing time were added. Table 9.1 shows a total Fuselage *WBS* charge of 36.52 hours.

9.3.3. WBS: Empennage. By charging 5 hours for each vertical control surface and 10 hours for each horizontal control surface, the *WBS* value for the empennage was calculated. A basic empennage manufacturing time of 5 hours was included with the manufacturing times for the control surfaces. The Empennage *WBS*, as shown in Table 9.1, is 25 hours.

9.3.4. WBS: Flight Systems. A basic manufacturing time of 5 hours was assessed for the construction of the aircraft's flight systems. Additionally, each servo and speed controller used in the aircraft was charged another 2 hours of manufacturing time. For the final aircraft, Table 9.1 shows a Flight Systems *WBS* of 19 hours.

Work Breakdown Structure (WBS)	WBS Components	Airplane Characteristics	Number of Assigned Hours	Total Number of Hours
Wings	# of Wings	1	15	15
	Projected Area (ft ²)	4.97	4	19.88
	# of Braces & Struts	0	2	0
	# of Control Surfaces	2	3	6
	Wing WBS:			40.88
Fuselage	# of Bodies	1	5	5
	Total Length (ft)	7.88	4	31.52
	Fuselage WBS:			36.52
Empennage	Basic	-	5	5
	# Vertical Surfaces	2	5	10
	# Horizontal Surfaces	1	10	10
	Empennage WBS:			25
Flight Systems	Basic	-	5	5
	# of servos/controllers	7	2	14
	Flight WBS:			19
Propulsion System	# of engines	2	5	10
	# of propellers/fans	2	5	10
	Propulsion WBS:			20
	Total MFHR Hours:			141.4

Table 9.1. The manufacturing hours assigned to each aircraft component according to the Work Breakdown Structure (WBS).

9.3.5. WBS: Propulsion Systems. For each motor, propeller, or fan used to power the aircraft, 5 manufacturing hours were charged. Table 9.1 shows that the final aircraft used 2 engines and 2 propellers, resulting in a Propulsion Systems WBS of 20 hours.

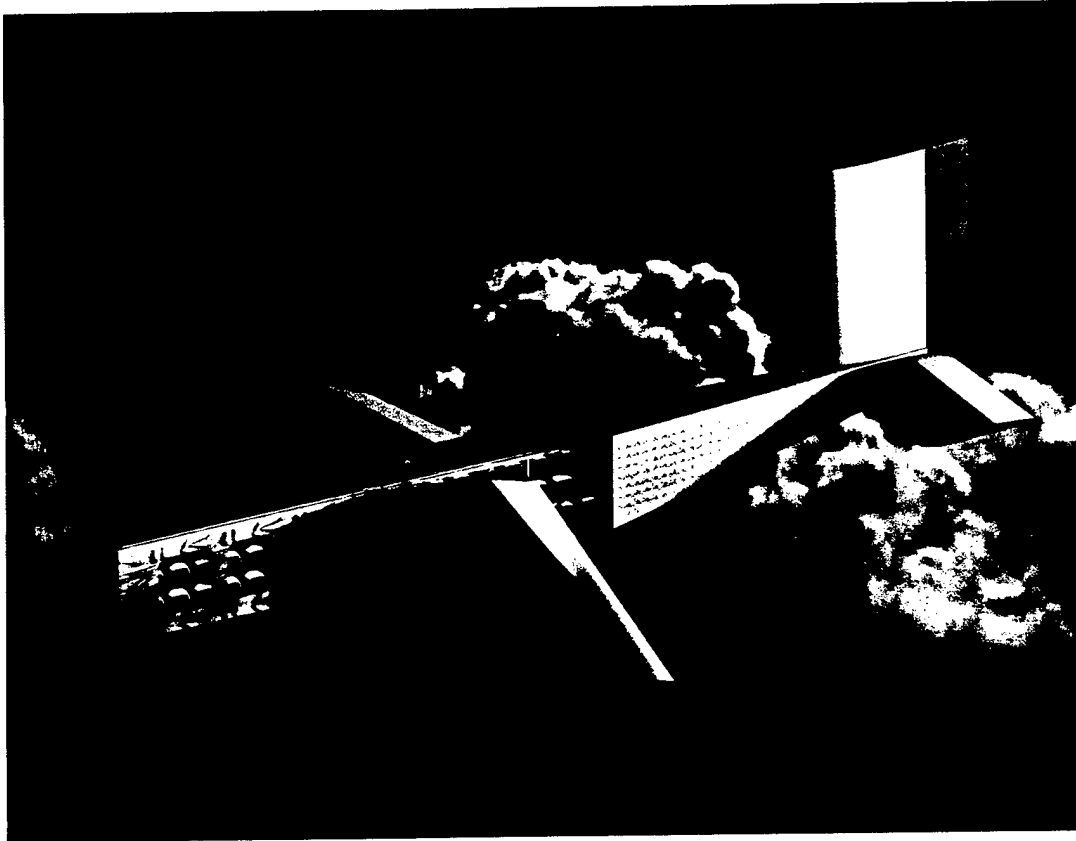
9.4. Results

As can be seen from the detail above, every component of the aircraft has a significant role in the determination of the RAC. For the constructed aircraft, the final RAC is:

$$\begin{aligned} \text{Rated Aircraft Cost (Thousands of \$)} &= \frac{MEW \times A + REP \times B + MFHR \times C}{1000} \\ &= \frac{14.40 \text{ lbs} \times \frac{\$100}{\text{lbs}} + 1728 \text{ watts} \times \frac{\$1}{\text{watt}} + 141.40 \text{ hours} \times \frac{\$20}{\text{hour}}}{1000} \end{aligned}$$

$$\text{Rated Aircraft Cost (Thousands of \$)} = 5.996$$

Final Design Report RPP-4



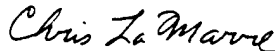
AIAA Student Design/Build/Fly Competition

Webster Field, Maryland

**Department of Aeronautical and Astronautical Engineering
University of Illinois at Urbana-Champaign**

13 April 2001

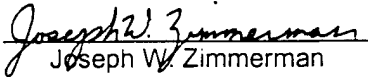
2001 Project Team
Report Contributors



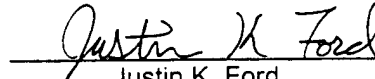
Christopher M. LaMarre



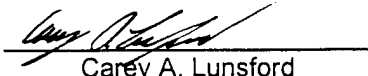
Michael S. Sexauer



Joseph W. Zimmerman



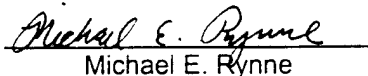
Justin K. Ford



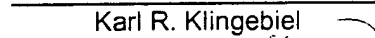
Carey A. Lunsford



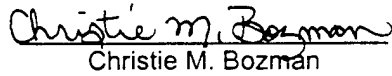
Ann Peedikayil



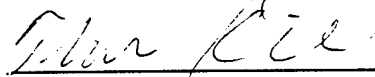
Michael E. Rynne



Karl R. Klingebiel



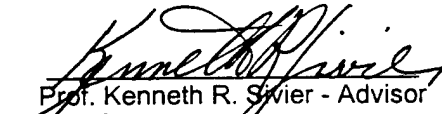
Christie M. Bozman



Theresa Kidd



Jason M. Merret



Prof. Kenneth R. Svier - Advisor



Andy P. Broeren - Advisor

Other Members

Mike Cross - Pilot
AnnMarie Cross - Pilot
Suzanne M. Vig - Finance
Aaron T. Dufrene - Manufacturing

Jeffery M. Lazzaro - Manufacturing
Tom Krenzke - Manufacturing
Leah Stefanos - Finance

Acknowledgements

This year's project owes its success to many sources. We would like to take this opportunity to acknowledge their help and support. We thank Jim Schmidt and Hobbico for their continued support and sponsorship of the team through donations of building materials and tools. We also thank Mike and AnnMarie Cross, the team pilots, for their time, patience, and advice. We thank the Department of Aeronautical and Astronautical Engineering for the use of shop space, monetary support, and the use of its wind tunnel. We also thank the College of Engineering and AIAA Region III for their monetary support. Finally, we would like to thank Prof. Kenneth Sivier and Dr. Andy Broeren for their continued guidance and support through all phases of this design process.

Table of Contents

1.0 Executive Summary	1
2.0 Management Summary	2
3.0 Conceptual Design	5
3.1 System Requirements	5
3.2 Figures of Merit and Configuration Selection	5
3.3 Configuration Selection	6
3.4 Initial Motor Selection	6
3.5 Estimated Score Analysis	6
3.6 Conclusion	7
4.0 Preliminary Design	11
4.1 Design Parameters Investigated	11
4.2 Aerodynamics	11
4.3 Propulsion	12
4.4 Performance	13
4.5 Tail Sizing and Stability Analysis	14
4.6 Preliminary Design Summary	15
4.7 Results of the Test Flights	15
4.8 Lessons Learned from Prototype	15
5.0 Detail Design	25
5.1 Introduction	25
5.2 Aerodynamics	25
5.3 Propulsion	25
5.4 Weights and Balances	26
5.5 Performance	26
5.7 Tail Sizing and Stability Analysis	27
5.8 Final Design Summary	27
6.0 Manufacturing Plan	38
6.1 General Requirements	38
6.2 Manufacturing Process	38
6.3 Manufacturing Process for the Prototype Aircraft	39
6.4 Modifications Needed for Competition Aircraft	40
6.5 Manufacturing Process for Competition Aircraft	40
6.6 Cost Reduction Methods	41

1.0 Executive Summary

This report represents the design processes and results for the University of Illinois' entry into the Fifth Annual AIAA Student Design/Build/Fly Competition. The final design, RPP-5 *Accipiter*, is the product of detailed aerodynamic and performance analyses. The design processes discussed in this report rely on both experimental data, acquired through the construction and testing of a prototype aircraft, and analytical modeling. The aircraft is designed to satisfy all of the competition requirements and maximize its contest score.

The design process began with the analysis of four different configurations using Figures of Merit. Configurations analyzed were the flying wing, canard, monoplane, and biplane. The flying wing and the canard were eliminated because of handling and stability concerns. The biplane configuration was also eliminated because of a higher rated cost estimation and awkward ground operations. Different variants of the remaining monoplane configuration were then evaluated. The characteristics varied included the number of motors, and payload size. Propulsion systems that met the minimum thrust and duration requirements were coupled with the monoplane variants and the resulting combinations were put into the rated cost model. The results of the conceptual design process indicated that a conventional, single-engine monoplane would have the lowest rated cost for a given payload.

The preliminary design consisted of experimental and analytic studies of aircraft configuration and performance. Studies employed at this stage were additional figures of merit and takeoff, climb, and cruise energy analyses. Experimental design tools used were propulsion testing and flight testing. The flight testing of the prototype aircraft provided analytic information for the improvement of the takeoff, climb and cruise models as well as practical information for the improvement of flight handling qualities and construction methods.

The prototype aircraft met all the design requirements, but was hampered by high drag and poor flight handling qualities. This resulted in high energy usage for the payload carried. The competition aircraft's design corrects these issues and results in a more efficient airplane. The final design, RPP-5 *Accipiter*, satisfies all of the requirements described in the 2000-2001 Rules and Vehicle Design Specifications and is designed to carry a payload of 14 lbs. of steel or 100 tennis balls with a gross weight of 32 lbs. Four to five sorties are expected with full payload at a cruise velocity of 60 ft/s.

The University of Illinois at Urbana-Champaign is proud to submit this design to the sponsors of the AIAA Design/Build/Fly Competition.

2.0 Management Summary

The conceptual design stage began during the summer of 2000, shortly after the rules were released. The core group that met during this time consisted of members from the previous year's team, the advisors, and the pilots. The team had informal weekly meetings and was able to progress through the conceptual design and most of the preliminary design stages during the summer. This progression allowed construction of the prototype to begin before the fall semester began.

When classes began in August 2000, the team switched to a more organized structure. New members were recruited and assigned to departments. Each department was headed by an experienced team member, with other members working within that department. Many individuals participated in more than one department. Each department was responsible for investigating a particular design area and reporting to the rest of the team so that important decisions could be made as a team. Departments and their respective participants are listed in Figure 2.1.

The entire team was led by the project heads. The project heads were responsible for organizing meetings, procuring materials, and tending to administrative concerns. During the entire design process, the project heads worked closely with the advisors and pilots to ensure the design process ran smoothly. The project leaders and the advisors met to discuss the details and overall progress of the design. The pilots served as advisors for aircraft handling, construction details, and procurement.

The team met weekly to keep all members informed of the project's progress. Departments with multiple members had additional meetings to work on that department's specific responsibilities. Construction was accomplished primarily on the weekends. After the prototype aircraft was constructed members from all departments participated in flight testing the aircraft on the weekends.

An overall project milestone chart was established in order to keep the team on schedule. Limited participation caused some delays in the flight testing of the prototype, but otherwise has not significantly altered the timeline. The milestone chart is shown in Fig. 2.2.

UIUC DBF Participants

Chris LaMarre -project head
 Joseph Zimmerman -assistant project head
 Professor Kenneth Sivier -faculty advisor
 Dr. Andy Broeren -advisor
 Mike Cross -pilot / advisor
 AnnMarie Cross -pilot / advisor

Aerodynamics

Christie Bozman*
 Joseph Zimmerman*
 Michael Rynne
 Alfred Pang
 Vincent Lee

Building Crew

Carey Lunsford*
 Michael Rynne*
 Aaron Dufrene
 Jeffery Lazzaro
 Tom Krenzke

Fundraising and Finances

Leah Stefanos*
 Suzanne Vig*

Graphics and Design

Michael Sexauer*

Performance

Jason Merret*

Propulsion

Karl Klingebiel*

Stability and Control

Tracy Kidd*

Weights and Balances

Justin Ford*

Writing and Editing

Ann Peedikayal*
 Chris LaMarre
 Joseph Zimmerman

* denotes department head

Figure 2.1: Team Architecture

	Jun	Jul	Aug	Sep	Oct	Nov	Dec	Jan	Feb	Mar	Apr
Preliminary Design Studies	■										
Continued Configuration/design Studies	■	■									
Design of Prototype		■	■								
Construction of Prototype			■	■	■						
Propulsion Testing				■	■						
Flight Testing of Prototype					■	■	■				
Evaluation of Flight Test Results						■	■				
Evaluation of Prototype Design						■					
Write "Proposal Phase" report						■	■	■	■		
Final Design of Competition Aircraft						■			■	■	
Construction of Competition Aircraft							■	■	■		
Flight Testing of Competition Aircraft										■	■
Engineering Open House Display										■	■
Final Modifications										■	■
Write "Addendum Phase" report										■	■
Attend Competition											■

Figure 2.2: Project Timeline

3.0 Conceptual Design

3.1 System Requirements

The aircraft system requirements are specified in the 2000-2001 Rules and Vehicle Design. The system design objective is to achieve the highest score possible by optimizing the payload-to-sortie ratio while adhering to the contest constraints. After reviewing the rules, the following major design drivers were determined:

- Minimum payload of 5 lbs. of steel or 10 tennis balls
- Maximum of 5 lbs. of batteries
- 200 ft. takeoff limit
- Good flying qualities
- Quick payload changes
- Durability to withstand repeated landings
- Low cost and ease of manufacture

The rated cost and the energy available for flight were determined to be the principal constraints of the conceptual design. In general, larger aircraft that carry more payload will have a higher rated cost and a higher gross weight as compared to smaller aircraft. As a result of the battery limitation, larger aircraft may not complete as many sorties as smaller aircraft carrying less payload. Therefore, a smaller aircraft could achieve a higher final score than a large one could achieve. The optimum configuration and payload size had to be determined. Using the aircraft cost model, approximate costs were calculated for the prototype configurations as discussed in the next few sections of the report. In addition, each of the configurations was analyzed using a simple takeoff model to ensure that it could meet the 200 ft. takeoff limit. Once the costs of the conceptual designs were determined, the single flight and total flight scores were estimated.

3.2 Figures of Merit and Configuration Selection

The complexity of this year's competition required Figures of Merit (FOMs) to evaluate the configurations. The FOMs used are defined below:

- **Rated Cost:** this represents the estimated rated cost of the configuration. A lower cost design will result in a higher final score than a higher cost design.
- **Complexity:** how difficult the configuration will be to construct. A complex design is susceptible to errors and will take longer to construct than a simple design.
- **Durability:** ability to withstand repeated landings. A robust aircraft will be easier to maintain than a fragile one.
- **Ground operations:** the time required to change the payload between sorties and the batteries between flights. A design with a quicker turn around time will have more flight time than one with a slower turn around time.

- **Stability and Handling:** the aircraft must be stable, maneuverable, and possess good stall recovery characteristics. An aircraft with better handling characteristics is more desirable than one with poor handling characteristics.
- **Monetary Costs:** the capital needed for materials and equipment in order to construct the aircraft. An inexpensive aircraft is more likely to be funded than an expensive one.

The Figures of Merit ratings are presented in Table 3.1. Each Figure of Merit was assigned a numerical scale from 1 to 5 so that quantitative analysis of a configuration could be made. Each Figure of Merit also has a multiplier that represents its importance. FOMs with a higher multiplier were deemed more crucial to the design than those with a lower multiplier.

3.3 Configuration Selection

Four general configurations were studied during the conceptual design phase. These were the flying wing, canard, monoplane, and biplane. Within each of these general configurations, there existed variations in numbers of motors and payload sizes.

The four configurations were initially analyzed using FOMs. The canard and flying wing configurations were eliminated due to higher complexity and stability and control issues. The biplane configuration was eliminated due to a higher estimated rated cost and awkward ground operation characteristics. As can be seen in Table 3.2, the monoplane configuration received the highest rating, and was therefore the only configuration to be analyzed further.

3.4 Initial Motor Selection

One of the major changes in this year's contest rules was the specification that only brushed, electric motors from the Astroflight or Graupner product lines be used. Because the team had no prior experience with brushed motors, choosing the new propulsion system became a priority. It was important for the motors to be selected and acquired early in the design process so that propulsion testing could begin as soon as possible. Selecting the motors at this point in the design allowed the team to remain on task and gain a working knowledge of the brushed motor performance for preliminary design work.

Both the Astroflight and Graupner product lines were researched on the internet. The motors that were in current production were then simulated using Motocalc™¹. This program evaluates combinations of motors, propellers, gearboxes and batteries and was used to narrow considerations to three motors that met the approximate thrust and runtime requirements. The Cobalt 60 was seen as the best choice based on the facts that it could meet the estimated thrust requirement, unlike the Cobalt 40, and was less expensive, more widely available, physically smaller and significantly lighter than the Cobalt 90. Two Astro Flight Cobalt 60 motors were purchased for propulsion testing and use in the prototype aircraft.

3.5 Estimated Score Analysis

After the motor and monoplane configuration were selected, different variants of the monoplane configuration were investigated using an estimated score analysis. The different variations considered were number of motors, number of control surfaces, wing area, and propulsion systems. The rated cost

of a baseline monoplane was computed and served as a reference for other variants. This baseline was chosen to have a single motor with no pods and traditional tail surfaces. A payload fraction of 0.53 was selected based on historical data from past competition aircraft. Its wing area and thrust requirements were based on a simple, team-written takeoff analysis code. A baseline propulsion system to meet this thrust requirement was generated by Motocalc™.

The variants and baseline aircraft were compared using the rated cost model. A sample of this comparison is provided in Table 3.3. It can be seen that certain features such as the number of control surfaces did not have a significant impact on the rated cost. Other features such as wing area had a significant impact, but the rated cost model was insufficient to set this parameter at this stage in the design. The largest impact on the rated cost of the variants was the propulsion system.

The variants were compared using not only the rated cost model, but also an estimated scoring model encompassing rated cost and flight score estimations. Using flight test data from last year's designs, a single motor variant was estimated to have the ability to complete one or two more scoring sorties than a dual motor variant. Based on a flight score analysis, sorties with an equal weight of tennis balls and steel, corresponding to 100 tennis balls and 13 lbs. of steel, would achieve the highest flight score for the energy consumed. A sample of the estimated score analysis is provided in Table 3.4, and it can be seen that the single motor variants achieve higher scores than the dual motor variants.

3.6 Conclusion

Based on the FOMs, all configurations except the monoplane were eliminated. From the estimated score analysis, it was determined that a single motor variant of this would offer optimal performance. Therefore, the result of the conceptual design was that a single motor monoplane configuration would be analyzed further.

Table 3.1. Figures of Merit Ranking

Figure of Merit	Ranking		
	5	3	1
Rated Cost	Low Cost	Average Cost	High Cost
Complexity	Simple	Average	Complex
Durability	Durable	Average	Fragile
Ground operation	Fast/Easy	Moderate	Slow/Difficult
Stability and Handling	Stable	Average	Unstable
Monetary Cost	Inexpensive	Moderate	Expensive

Table 3.2. Final Concept Rating

Figure of Merit	Multiplier	Concept			
		Monoplane	Biplane	Canard	Flying wing
Rated Cost	5	3	2	4	5
Complexity	5	5	4	3	2
Durability	3	5	4	4	4
Ground Operation	3	4	3	4	5
Stability and Handling	4	5	5	4	3
Monetary Cost	5	5	4	4	4
Totals		112	91	95	94

Table 3.3. Rated Costs for Sample Variants

Parameter(s) Changed from baseline	Baseline	No Flaps	Wing Area	Propulsion	Propulsion	Twin Motor	Twin Motor wing area
payload	13.00	13.00	13.00	13.00	13.00	25.00	25.00
payload fraction	0.53	0.53	0.53	0.45	0.53	0.60	0.60
total weight	24.53	24.53	24.53	28.89	24.53	41.67	41.67
empty weight	11.53	11.53	11.53	15.89	11.53	16.67	16.67
Weight Cost	1152.83	1152.83	1152.83	1588.89	1152.83	1666.67	1666.67
engines	1.00	1.00	1.00	1.00	1.00	2.00	2.00
cells/engine	26.00	38.00	20.00	36.00	30.00	19.00	19.00
amps	25.00	25.00	25.00	20.00	20.00	25.00	25.00
Engine Cost	780.00	1140.00	600.00	864.00	720.00	1140.00	1140.00
span	10.00	10.00	10.00	10.00	10.00	10.00	10.00
chord	1.00	1.00	1.50	1.00	1.00	1.50	1.75
wing area	10.00	10.00	15.00	10.00	10.00	15.00	17.50
control surfaces	4.00	2.00	4.00	4.00	4.00	4.00	4.00
fuse length	5.00	5.00	5.00	5.00	5.00	6.00	6.00
Pods	0.00	0.00	0.00	0.00	0.00	2.00	2.00
pod length	0.00	0.00	0.00	0.00	0.00	0.75	0.75
servos	6.00	4.00	6.00	6.00	6.00	6.00	6.00
engines	1.00	1.00	1.00	1.00	1.00	2.00	2.00
propellers	1.00	1.00	1.00	1.00	1.00	2.00	2.00
Construction Cost	2680.00	2480.00	3080.00	2680.00	2680.00	3680.00	3880.00
Total Rated Cost	4.61	4.77	4.83	5.13	4.55	6.49	6.69

Table 3.4. Final Scores for Sample Variants

Parameter(s) Changed from Baseline	Baseline	No Flaps	Wing Area	Propulsion	Propulsion	Twin Motor	Twin Motor Wing Area
payload	13.00	13.00	13.00	13.00	13.00	25.00	25.00
Total Cost	4.61	4.77	4.83	5.13	4.55	6.49	6.69
5 sorties							
tennis balls	100.00	100.00	100.00	100.00	100.00	Not deemed possible from energy analysis	
lbs. steel	13.00	13.00	13.00	13.00	13.00		
tennis balls	100.00	100.00	100.00	100.00	100.00		
lbs. steel	13.00	13.00	13.00	13.00	13.00		
tennis balls	100.00	100.00	100.00	100.00	100.00		
<i>flight score</i>	<i>86.00</i>	<i>86.00</i>	<i>86.00</i>	<i>86.00</i>	<i>86.00</i>		
Total Score	18.64	18.02	17.79	16.75	18.89		
4 sorties							
tennis balls	100.00	100.00	100.00	100.00	100.00	100.00	100.00
lbs. steel	13.00	13.00	13.00	13.00	13.00	25.00	25.00
tennis balls	100.00	100.00	100.00	100.00	100.00	100.00	100.00
lbs. steel	13.00	13.00	13.00	13.00	13.00	25.00	25.00
<i>flight score</i>	<i>66.00</i>	<i>66.00</i>	<i>66.00</i>	<i>66.00</i>	<i>66.00</i>	<i>90.00</i>	<i>90.00</i>
Total Score	14.31	13.83	13.66	12.86	14.50	13.87	13.46
3 sorties							
tennis balls						100.00	100.00
lbs. steel	Deemed unrealistically low from energy analysis					25.00	25.00
tennis balls						100.00	100.00
<i>flight score</i>						<i>65.00</i>	<i>65.00</i>
Total Score						10.02	9.72

4.0 Preliminary Design

4.1 Design Parameters Investigated

The preliminary design phase was used to set the final configuration of the prototype aircraft. After the test flights of the prototype aircraft, the results from this section were evaluated and either used as stated in this section or reanalyzed and then used as the preliminary design for the competition aircraft.

The conceptual design work revealed a number of important vehicle sizing and performance design areas that were addressed in the preliminary design. These areas were:

- Aircraft Gross Weight and Payload Size
- Flight Reynolds Number
- Wing Planform Shape
- Tail Sizing for Stability
- Takeoff Performance
- Propulsion Data

4.2 Aerodynamics

The first aerodynamic concern addressed in the prototype design was wing airfoil selection. Initially, a broad range of airfoils designed for low-speed, high-lift applications was studied. These included the S1210, S1223, SD7062, SG6042, and SG6043. These airfoils were evaluated using the wind tunnel data, provided in Lyon et al.², for an estimated takeoff Reynolds number of 300,000. In terms of C_{lmax} , the S1223 offered the best performance. However, this airfoil is highly under-cambered. A wing using it would be difficult to build without the use of special construction techniques. As a result, airfoils having a large degree of under-camber were eliminated from the list of candidate airfoils. The SG6043 was chosen because it provides a relatively high C_{lmax} of 1.65 without complicating construction.

While the wing airfoil was selected based on maximum lift coefficient and ease of construction, the tail airfoil selections were governed by maintaining low drag. The NACA 0009 was chosen for both the horizontal and vertical tails. This airfoil provides low drag with a reasonable thickness, maintaining ease of construction. See Figure 4.1 and 4.2 for profiles and lift curves for the SG6043 and NACA 0009 respectively.

After airfoil selection was complete, the wing planform was established. Using the takeoff analysis code previously mentioned, the exposed planform area was set at 12.67 ft.². From Raymer³, a taper ratio of 0.45 is suggested for attaining a nearly elliptical lift distribution corresponding to low induced drag. This factor, along with the requirement for a thick inboard wing panel to accommodate the removable-wing tube, led to the possibility of a tapered wing being used. The inboard wing section could also be made thicker than the aluminum tube that it would accept, allowing dihedral to be built into the wing. If the spar location was chosen to be at 34% chord, the thickest point of the airfoil, this would result in a sweep of nearly 6 degrees and natural directional stability (Raymer³).

After the aerodynamic benefits of using a taped wing had been established, it was necessary to decide if these outweighed the extra complexity and build time of this design. Figures of Merits were used to decide between the tapered wing described above and a more conventional constant chord wing design. The following FOMs were used in this analysis:

- Drag Reduction: the relative amount of induced drag that a wing generates.
- Complexity/Build Time: the time needed to build the proposed wing.
- Stability: the relative benefit of having increased flight stability.

The Figures of Merit ratings are presented in Table 4.1. Each Figure of Merit was assigned a numerical scale from 1 to 5 so that quantitative analysis of a configuration could be made. The final rankings of each design are shown in Table 4.2. It was decided that the benefits of the tapered wing offset the increased construction time, and the wing was set to have a root chord of 27 inches and a tip chord of 11 inches to meet previously mentioned requirements.

With the airfoil selected and the planform determined, the performance characteristics of the prototype's wing was evaluated. This was done using a team-written, nonlinear, lifting line program that uses the airfoil sectional lift curve and the wing geometry as inputs and calculates the lift curve for the wing. The program calculated a wing $C_{L \max}$ of 1.5. The effect of flaps on the wing lift curve was estimated, using the method given in Raymer³, to yield a $C_{L \max}$ of 1.8 for the optimal flap deflection of 45°. This flap deflection recommendation is based on larger aircraft, but served as a first approximation.

Finally, the parasite drag coefficient of the prototype airframe was determined. This was done by calculating the parasite drag contributions of the wing, fuselage, and tail surfaces and summing them according to the method given in Roskam⁴. The resulting drag buildup for the prototype aircraft is provided in Table 4.1. C_{D0} for the prototype was 0.0417. This value is relatively high and is primarily the result of the low fineness ratio of the nose as can be seen in Fig. 4.3.

4.3 Propulsion

After the initial motor selection was made, a Model Air Tech™ belt drive with interchangeable pulleys to obtain ratios of 4:1 and 5:1 was ordered. New mounts to accommodate the Cobalt 60 were designed, machined and added to the existing thrust testing apparatus along with a new Interface™ load cell to measure the thrust. This setup was designed for use both inside a wind tunnel, for thrust testing over a range of airspeeds, and for static thrust testing outside the tunnel. Thrust testing was first used to obtain realistic values of the maximum attainable thrust and then used to evaluate the accuracy of thrust and runtime predictions from Motocalc™. All tests were conducted using 36 battery cells, the most allowed under the 5 lbs. battery limit. Propulsion system data, corrected for tunnel effects, were gathered for different gearbox combinations and the largest diameter propellers that could reasonable be tested in the wind tunnel. Figs. 4.4 and 4.5 show a sample of the data collected in the wind tunnel. Data were also obtained from static thrust tests. Motocalc™ predictions were obtained for each of the test points and

compared to the experimental data. For this case Motocalc™ does not accurately predict thrusts for propulsion systems in the size range tested and actually overestimates static thrust and underestimates thrust at airspeed. However, the wind tunnel thrust tests yielded an important result: there is no significant drop in amperage with increasing airspeed, as was previously assumed in the performance codes.

Using the test data for calibration of Motocalc™, it could now be used as a more accurate analysis tool. It was used to predicted that a readily available wooden 27 x 27 propeller on the 5:1 belt reduction drive and using 36 Sanyo 2000 mAh cells to power motor, would provide the necessary thrust for the prototype aircraft.

4.4 Performance

4.4.1 Takeoff & Climb

A takeoff-and-climb analysis was performed to determine the takeoff distances, takeoff and climb times, and takeoff energies for various combinations of weight, C_{Lmax} , final altitude, and zero-lift drag coefficient. It was deemed best that the aircraft have the capability to perform the required mission without a headwind. To analyze the takeoff performance, a computer program was written using a fourth-order Runge-Kutta solver for the aircraft's equations of motion. Initial models for the thrust were estimated using Motocalc™ software and experimental thrust data obtained in the wind tunnel. Motor system models were then developed, using Motocalc™, and incorporated into the takeoff code to provide an estimation of the energy usage.

The baseline performance inputs are presented in Table 4.4. Despite the fact that the wind tunnel data did not support Motocalc's predictions, the propeller and motor data from Motocalc™ were used as the performance inputs for lack of a more accurate model.

All of the results for the takeoff and climb analysis are a function of takeoff weight. The effects of maximum lift coefficient on takeoff and climb performance were studied. As expected, increasing the maximum lift coefficient decreases the takeoff distance, and as a result, the electrical energy required decreases, as shown in Figs 4.6 and 4.7. It is interesting that the efficiency (shown in Fig. 4.7 and based on the ratio of the required mechanical energy to the electrical energy used) also decreases with increased C_{Lmax} . The difference between the electrical and mechanical energy is significant, and the analysis results support previous flight test data and help explain the difference. The main reason for the large difference in the energies is the motor system efficiency. The calculation of mechanical energy assumes an ideal situation and is the minimum required energy to complete the maneuver.

Fig. 4.8 shows that as the maximum lift coefficient increases, the climb energy increases. The total of the takeoff and climb energies is approximately constant for varying maximum lift coefficients. Therefore, as the takeoff energy decreases, due to an increase in maximum lift coefficient, the climb energy increases. A very interesting result is that as the weight increases for a given C_{Lmax} , the energy usage increases initially then decreases. This is due to the fact that the takeoff has a parabolic dependence on airspeed while thrust has a linear dependence on airspeed.

The results of the zero-lift drag coefficient variation were as expected. The analyses showed that the variation of zero-lift drag coefficient, from 0.035 to 0.045, had little effect on the takeoff distance and required energy. The rolling friction and acceleration were the driving factors during the takeoff roll. In the climb, the drag coefficient variation had a more pronounced effect. As expected, the energy required in climb increased as the drag coefficient increased, as is shown in Fig 4.9. An increase in zero lift drag coefficient of 50% resulted in a maximum of 6% increase in energy usage.

Changing the altitude at the end of climb has no effect on the takeoff roll, but the climb energy varies considerably. Figure 4.10 shows that as the end-of-climb altitude increases so does the energy usage. In addition, Figure 4.10 shows that as the end-of-climb altitude increases, the climb final velocity decreases. The end-of-climb airspeed also decreases as the takeoff weight increases. The end-of-climb airspeed is a very important factor since it must be above the stall speed for a given turn load factor (determined by the turn airspeed and the turn radius). If the end-of-climb airspeed is below the stall speed for a given set of turn parameters, the aircraft will stall. The analysis showed that this requirement was just as difficult to meet as the takeoff distance requirement.

4.4.2 Flight Energy Usage Analysis

In order to accurately determine the performance of the aircraft, a detailed energy analysis was performed. As in the takeoff and climb analysis, the energy used was computed for all segments of the flight. The results from the takeoff and climb analysis were used as inputs for the flight energy calculations. The remaining segment energies were computed using airspeeds to determine the forces on the aircraft and using the course layout to determine the distances flown. The analysis assumed constant speed throughout the flight regime except during takeoff and climb. For the initial analysis, it was assumed that the aircraft would be able to complete 5 sorties in one flight. This was based on experience and initial results of the program development.

The weight, drag, and cruise speed of the aircraft were studied to determine the effects on the sortie and flight energies. Both the time and energy usage increases as weight increases as shown in Figure 4.11. Increasing cruise speed, however, decreases flight time as seen in Figure 4.12. Figure 4.12 also shows that the flight energy initially decreases and then increases as the cruise speed increases. This variation in flight energy usage corresponds directly to the drag polar of the aircraft. The minimum energy usage occurs near a flight velocity of 60 ft/s.

The steady level turn performance is an important factor in the performance of the aircraft and was analyzed. As Figure 4.13 demonstrates, a slow, small diameter turn requires the lowest energy. Increasing the turn diameter by 15 ft slightly increases the energy usage.

4.5 Tail Sizing and Stability Analysis

Volume coefficients and historical data from Raymer³, were used to size the horizontal and vertical tail surfaces. Results from this analysis, have been included in Table 4.5. The sizing of the control surfaces was also based on historical data from Raymer³.

4.6 Preliminary Design Summary

After an exhaustive and detailed preliminary design analysis had been performed, the following parameters were chosen for the prototype aircraft. A takeoff Reynolds number of 300,000 resulted in the choice of the SG6043 airfoil for the wing and the NACA 0009 for the tail surfaces. This gives a $C_{L \text{ max plane}}$ of 1.5. An Astro Flight Cobalt 60, 11turn, brushed motor, turning a 27 x 27 on a 5:1 gear ratio and powered by 36 2000mah Sanyo cells was to be used as the propulsion system for the aircraft.

With a gross takeoff weight of 35 lbs., a payload of 12 lbs., and 15 lbs. of thrust, the prototype aircraft was able to takeoff before the 200 ft. limit. Four or five sorties were expected from the available energy. With the center of gravity at 33% mean chord the static margin was 14.81%. Figure 4.3 shows the external configuration of the prototype.

4.7 Results of the Test Flights

Although limited, the flight-test program provided some good insight to the performance calculations. It showed that the electrical energy prediction was close to the actual energy consumed. The difference observed between the wind tunnel thrust data and the Motocalc™ data used in the performance calculations explains the difference between the flight energy predictions and the actual energy consumed during the flight tests.

The flights tests also brought to attention reliability and handling problems that would have to be addressed in the competition design. The short tail moment arm of the tail dragger configuration resulted in the loss of yaw control after the tail wheel lifted off at low speeds during the takeoff roll. The flight test program was cut short when the belt drive failed in flight resulting in a forced landing and moderate damage to the aircraft.

4.8 Lessons Learned from Prototype

The design, building and flight testing of the prototype provided valuable lessons that were incorporated into the design of the competition aircraft. These lessons included:

- Drag on the competition aircraft must be decreased by reducing the fuselage frontal area.
- Tricycle landing gear must be used to maintain controllability before rotation.
- Weight should be reduced to improve energy performance.
- A more reliable reduction unit for the motor should be used.

Table 4.1: Figures of Merit Ranking

Figure of Merit	Ranking		
	5	3	1
Drag Reduction	Low Drag	Moderate Drag	High Drag
Complexity/Build Time	Simple/Fast	Average	Complex/Slow
Stability	Strong	Moderate	Neutral

Table 4.2: Wing Design Rating

Figure of Merit	Wing Design	
	Tapered	Constant Chord
Drag Reduction	4	2
Complexity/Build Time	3	5
Stability	3	1
Total	10	8

Table 4.3: Prototype Drag Buildup

Component	C_{D_0}
Wing	0.0126
Fuselage	0.0234
Horizontal Tail	0.0034
Vertical Tail	0.0023
Total C_{D_0}	0.0417

Table 4.4: Baseline Prototype Performance Inputs

Weight (lbs)	36
Span (ft)	9
MGC (ft)	1.68
S (ft ²)	15.125
AR	5.355
C_{D_0}	0.0417
E_o	0.8
CLMax without Flaps	1.4
CLMax with Flaps	1.5
Altitude (ft)	35
Turn Speed (ft/s)	50
Turn Diameter (ft)	125
Cruise Speed (ft/s)	65
Crew Time (s)	10

Table 4.5 Prototype Specifications

Tail Attributes	Horizontal Tail	Vertical Tail
Area	480 in ²	352 in ²
Span	40 in	16 in
Mean Aerodynamic Chord	12 in	22 in
Aspect Ratio	3.333	1.375
Taper Ratio	1	1
Airfoil	NACA 00009	
Elevator	33% of horizontal tail chord	N/A
Rudder	N/A	33% of vertical tail chord
Wing Attributes		
Mean Aerodynamic Chord	20 in	
Wing Area	2053 in ²	
Taper Ratio	0.38	
Wing Aerodynamic Center	5 in*	
Ailerons	25% chord, 40%span	
Aircraft Attributes		
Center of Gravity	6.27 in.*	
Neutral Point	6.92 in. *	
Static Margin; power off	14.81%	

* measured from root chord leading edge

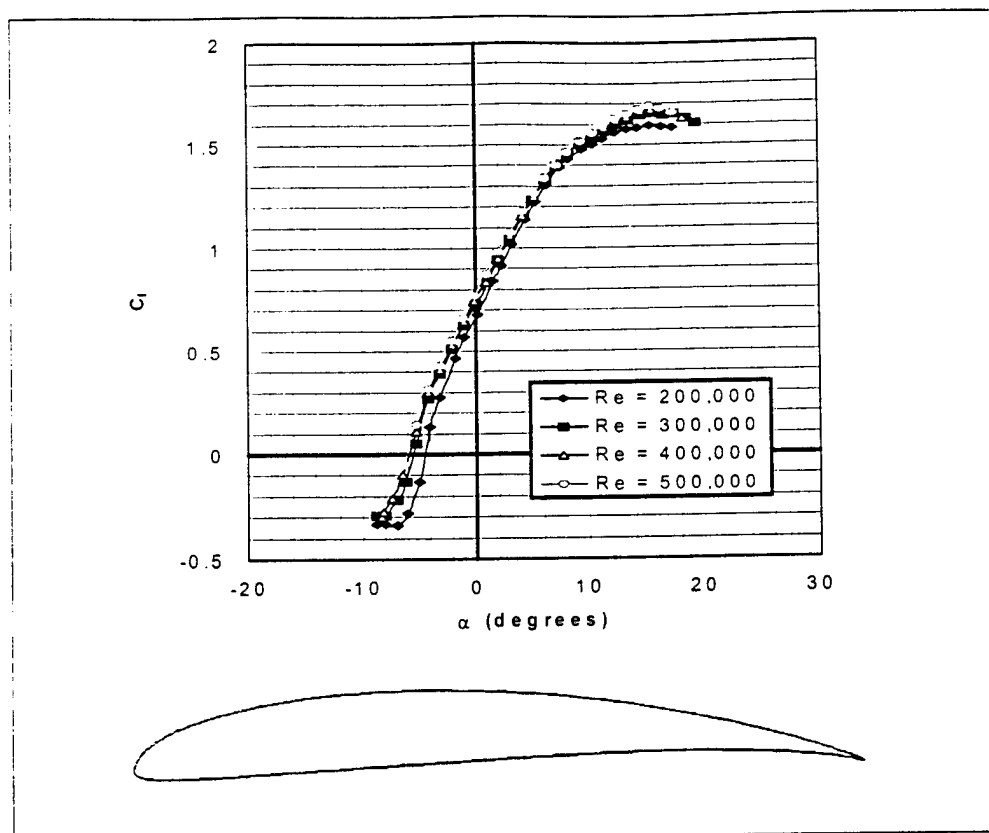


Figure 4.1: SG6043 Data

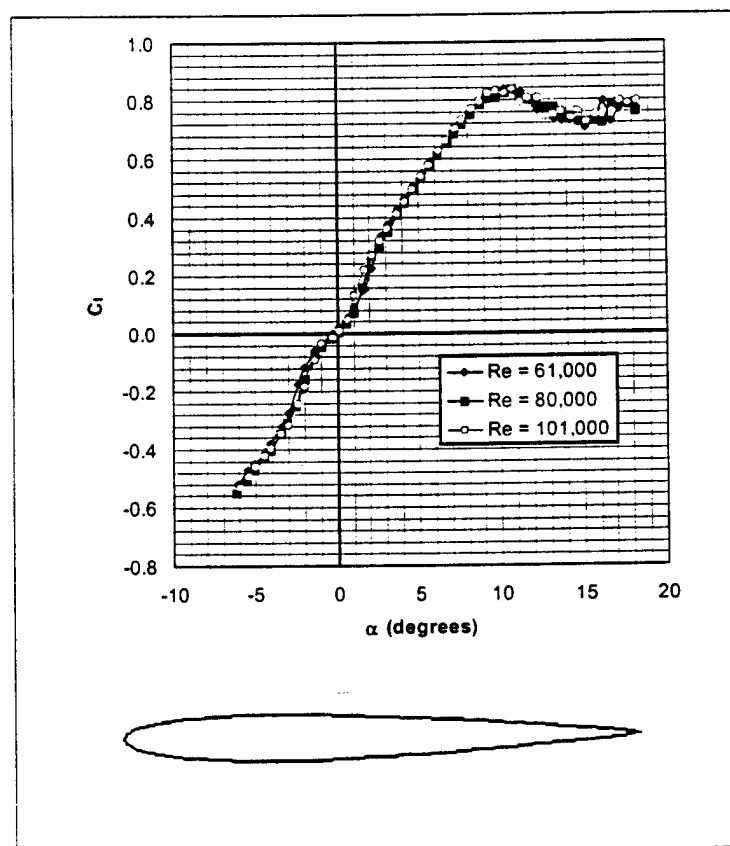
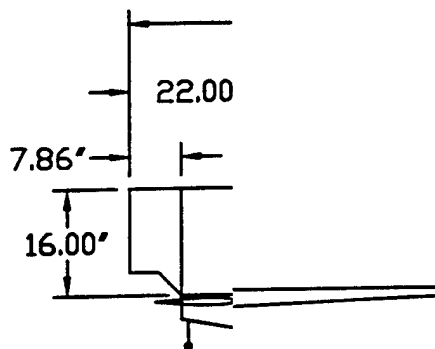
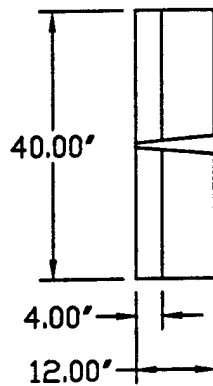


Figure 4.2: NACA 0009 Data



University of Illinois at Urbana

Aeronautical and Astronautical Engineering (Dimensions in inches)

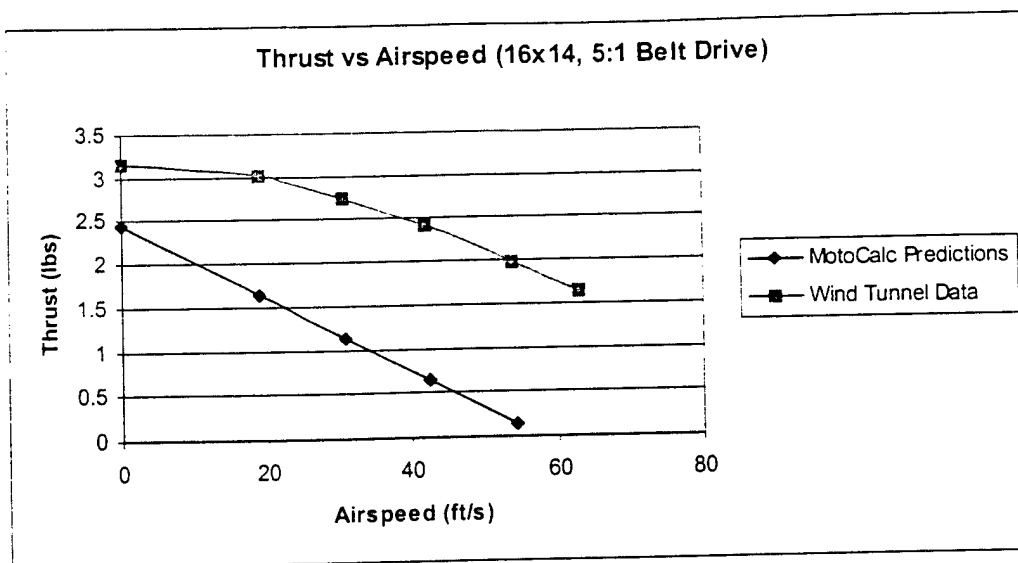


Figure 4.4. Thrust versus Airspeed

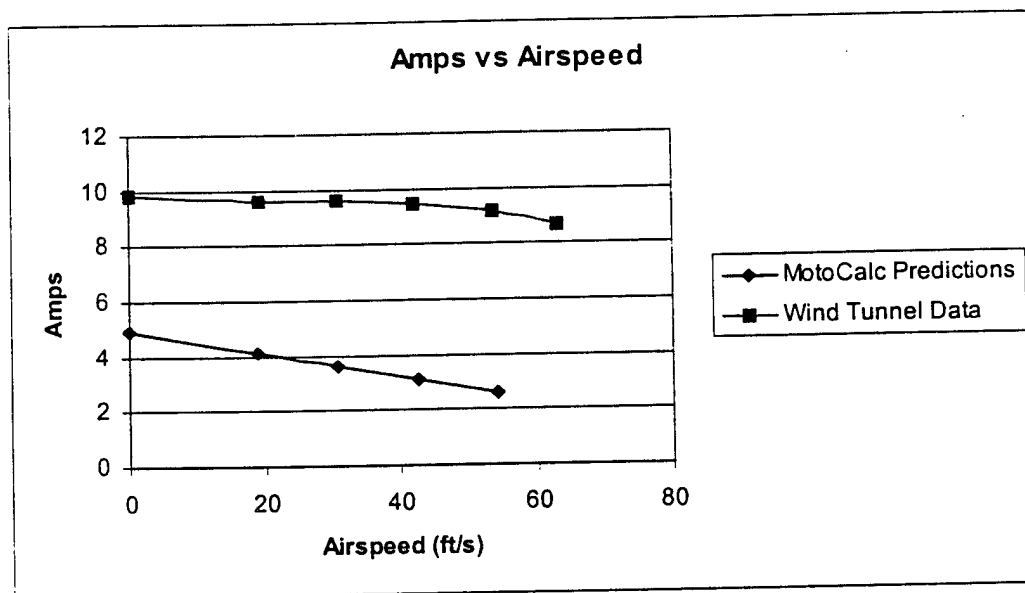


Figure 4.5 Amperage versus Airspeed

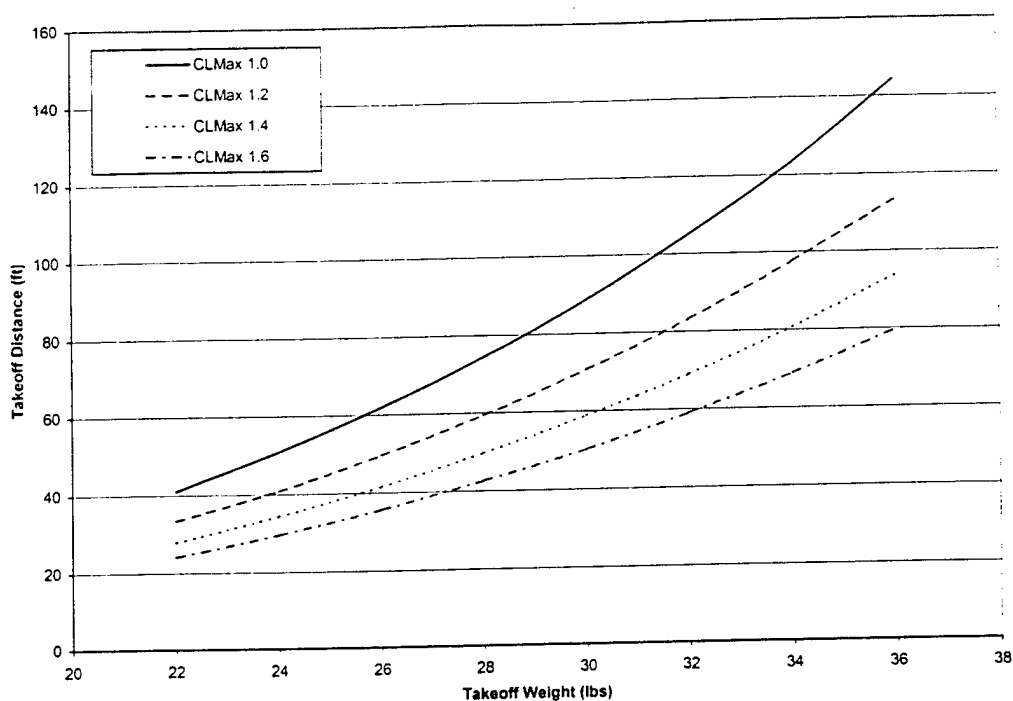


Figure 4.6: Effect of Lift Coefficient on Takeoff Distance

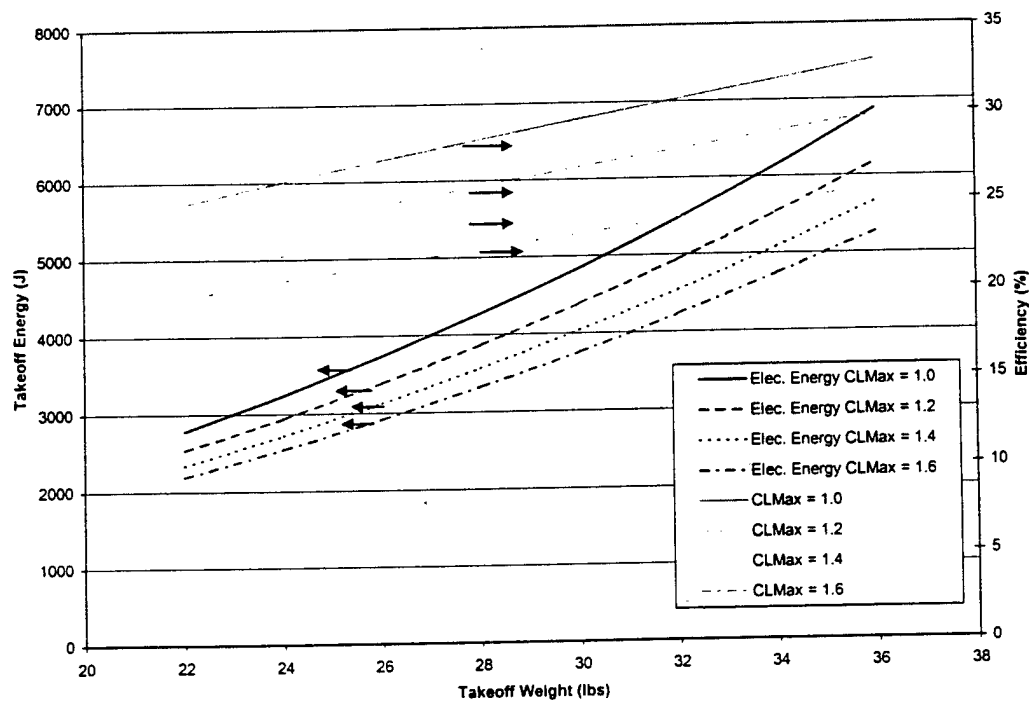


Figure 4.7: Effect of Lift Coefficient on Takeoff Energy

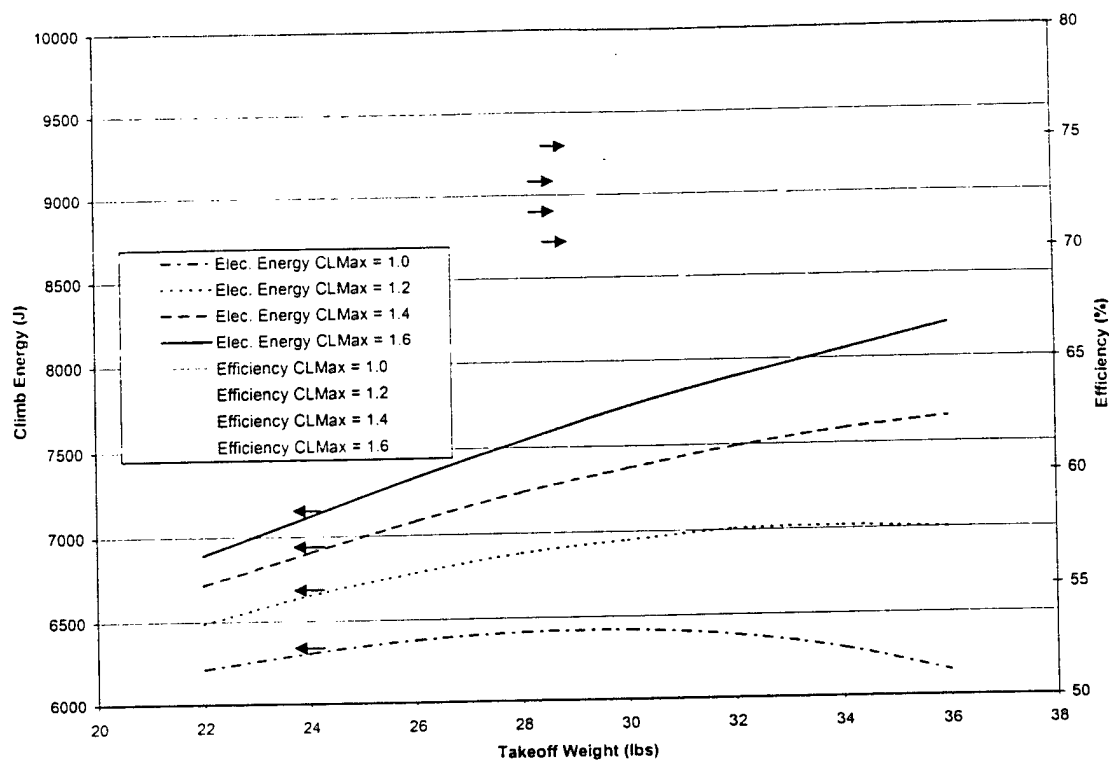


Figure 4.8: Effect of Lift Coefficient on Climb

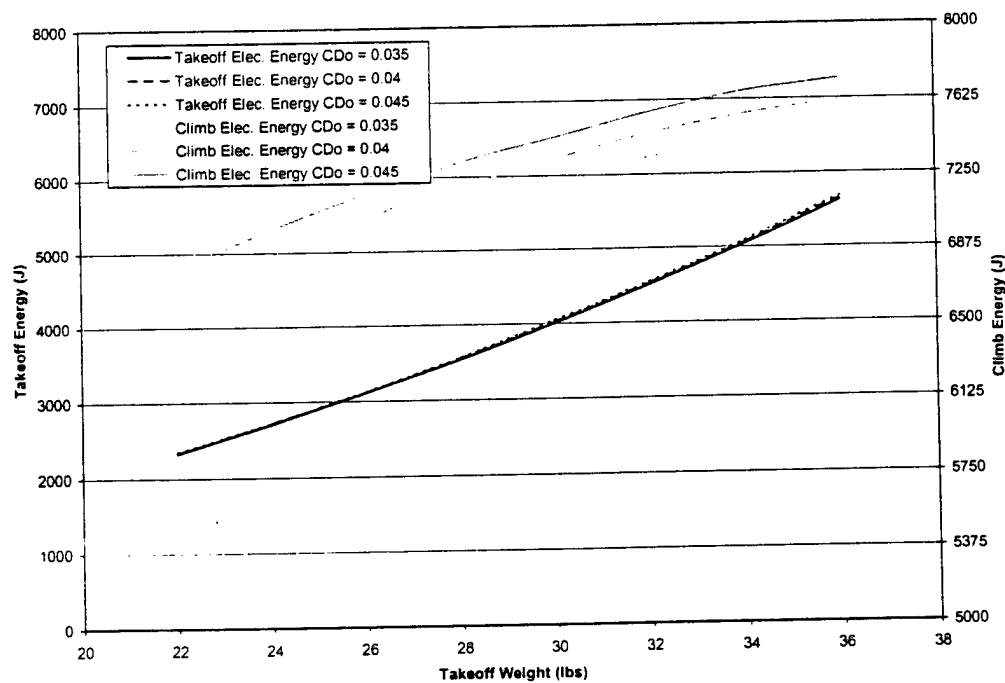


Figure 4.9: Effect of Drag Coefficient on Takeoff and Climb Energy

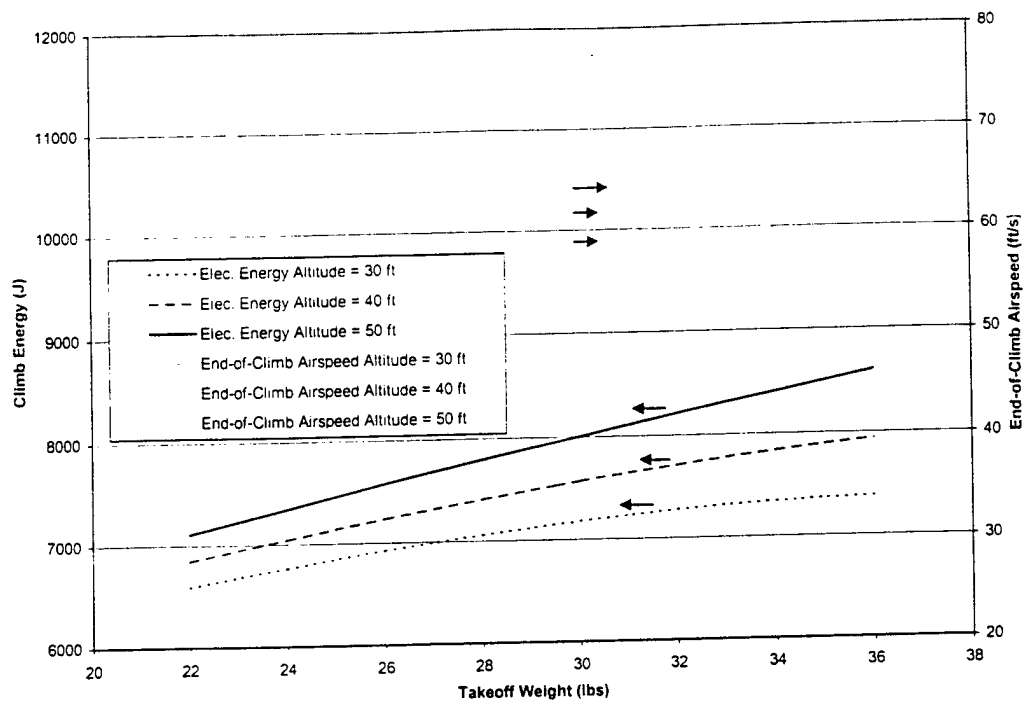


Figure 4.10: Effect of the End-of-Climb Altitude on Climb Performance

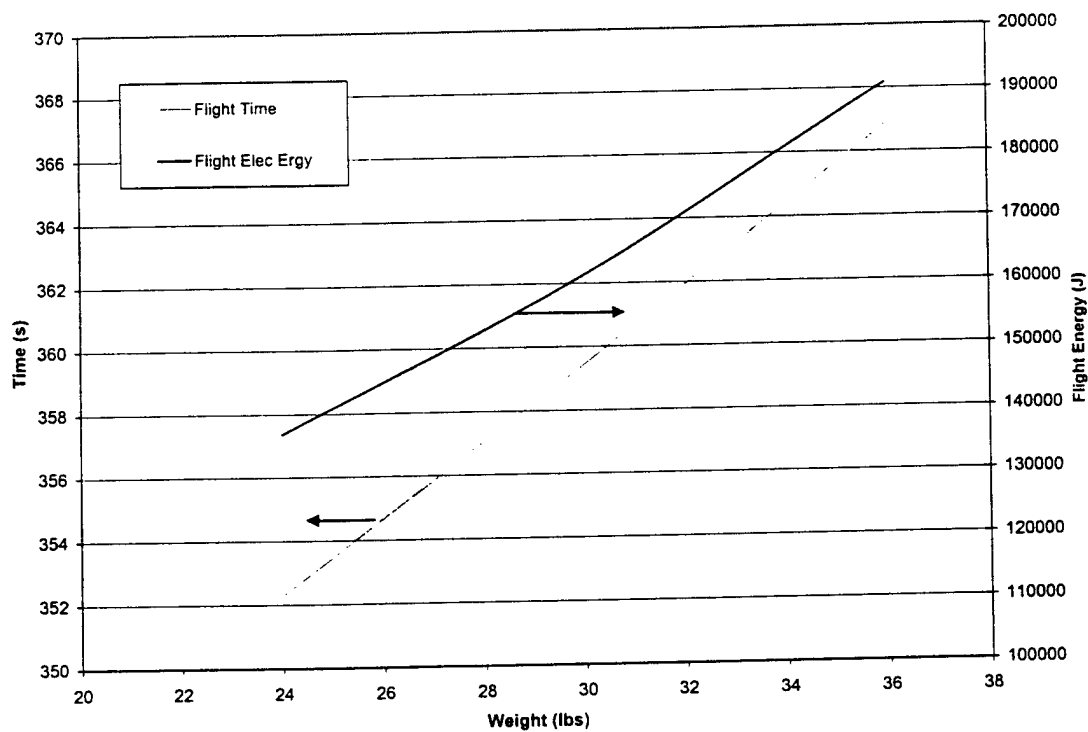


Figure 4.11: Effect of Weight on Flight Time and Energy

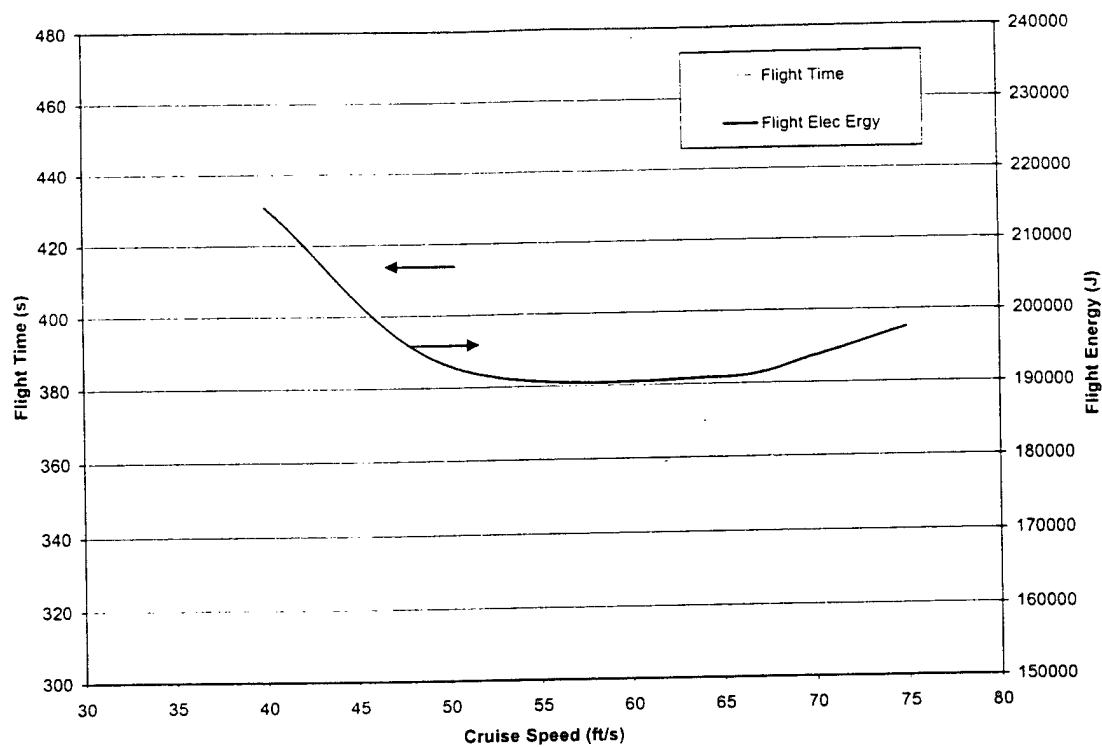


Figure 4.12: Cruise Airspeed Effect on Flight Time and Energy

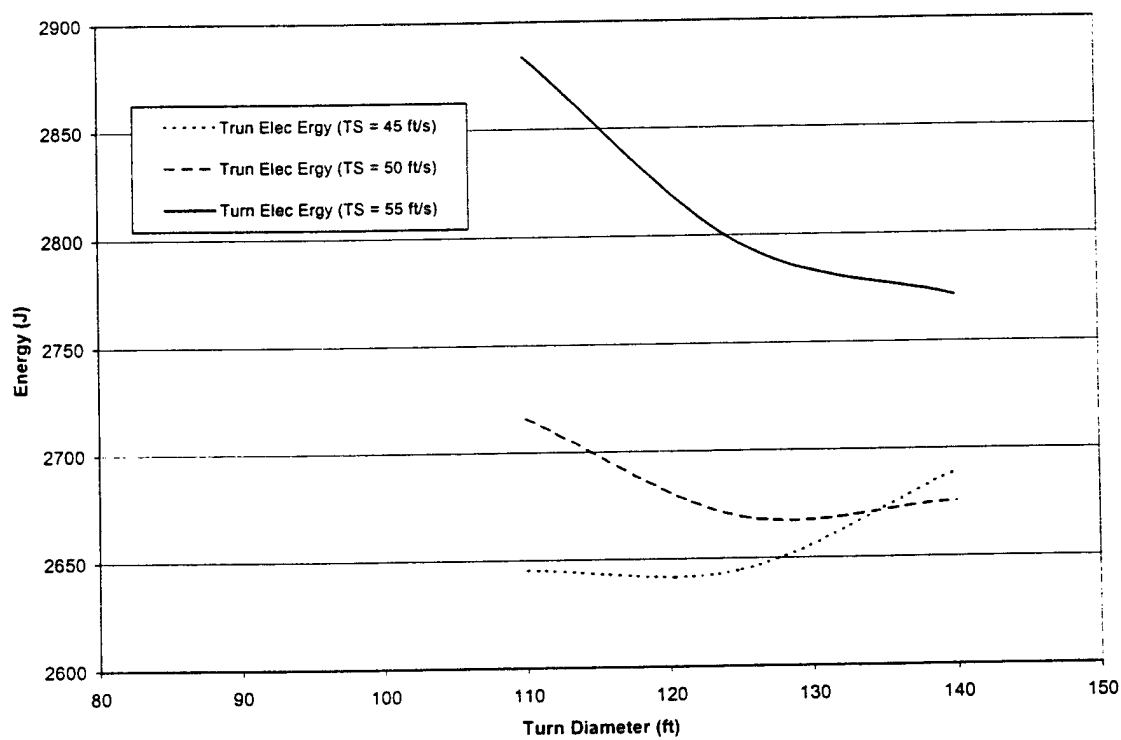


Figure 4.13: Turn Speed and Diameter Effect on Turn Energy

5.0 Detail Design

5.1 Introduction

This section contains the detail design analysis for the competition design RPP-5 *Accipiter*.

5.2 Aerodynamics

Because the prototype wing panels were reused for the competition aircraft, the aerodynamic analysis of the competition wing was simplified. The reduction in the fuselage width resulted in a slight change in wing reference planform, decreasing the area and span while increasing the taper ratio. When the new planform was analyzed, using the lifting-line program described in Section 4.2, little change was noted in the wing's performance. Fig. 5.1 shows lift curves, at a takeoff Reynolds number of 400,000, for the competition aircraft, along with sectional lift data for the SG6043 airfoil.

The increase in fuselage fineness ratio reduced aircraft drag. Using the analysis method discussed in Section 4, the competition aircraft showed a 50% decrease in the parasite drag due to the fuselage when compared to the prototype. A comparison of the drag buildups, determined for each aircraft using the method in Roskam⁴, is provided in Table 5.1. The drag estimation method used in preliminary design is based heavily on theoretical values, and a more realistic method was desired. Therefore, a method utilizing experimental data was developed. Drag data given in Lyon et al.² for the SG6043 and in Selig et al.⁵ for the NACA 0009 were used for the wing and tail surfaces. Data given in Hoerner⁶ provided realistic estimates for the drag of the fuselage and landing gear. The wing/fuselage interference drag was estimated as 20% of the total wing drag. A drag buildup for the competition aircraft components using this method, including the wing and interference, is provided in Table 5.2.

Using these parasite drag data and the lift curve computed with the lifting line program, an aircraft drag polar was constructed. For this calculation, the wing was assumed to have zero incidence angle with respect to the fuselage. The fuselage drag was modeled as a function of angle of attack, estimated to increase by the percent increase in frontal area. These methods represent a conservative approach. The estimated drag polar for the competition aircraft is provided in Fig. 5.2, while L/D is plotted as a function of angle of attack in Fig. 5.3. The maximum L/D given on this graph corresponds to the optimal cruise angle of attack.

The results of this detailed aerodynamic analysis are an aircraft $C_{L \max}$ of 1.5, and an aircraft $C_{D \min}$ of 0.042. The induced drag coefficient at zero angle of attack is roughly 0.008. The maximum lift-to-drag ratio of 10.92 occurs at an angle of attack near 1 degree.

5.3 Propulsion

Due to reliability problems that occurred with the belt drive reduction unit during the prototype flight test, it was decided that a geared reduction unit should be used on the competition aircraft. Propulsion data also suggested that a smaller diameter propeller could be used with a different gear ratio producing the same thrust for only a small energy consumption penalty. Therefore, a 24 x 24 propeller will be used on the competition aircraft. Further propulsion testing and analysis will be performed prior to test flights of the competition aircraft.

5.4 Weights and Balances

The total weight of the aircraft and its center of gravity are both key parameters that will dictate the aircraft's necessary lift, its performance, and its stability. Obviously both can be measured once the aircraft is built, but it is convenient to estimate the weight and the c.g. in order to use these values for other parts of the design process. The best method for predicting the total aircraft weight and c.g. is to estimate the weight of each component that will be added to the aircraft and find the approximate location of these components relative to vertical and horizontal reference axes. AutoCad 2000 was used to create drawings of the aircraft. These drawings were analyzed to find the volume of the wood and metal components used in the wings, tail, and fuselage of the aircraft. The weight of each component was then predicted using its volume and material density. Electronic and mechanical components were weighed and their location was referenced off the building plans.

The component weights and centers of gravity of all items were then compiled in a spreadsheet using Microsoft Excel. Table 5.3 shows a sample of the spreadsheet used with the approximated weight of each object, its position relative to the nose of the aircraft and the bottom of the fuselage. These individual components were summed to obtain weight and c.g. approximations for the whole aircraft. The calculated total weight of the competition aircraft is 18.6 lbs., and its center of gravity is 31 inches from the nose and 4.5 inches above the bottom of the fuselage.

5.5 Performance

5.5.1 Takeoff and Climb

Using the new inputs for the motor, aerodynamics, and the competition aircraft geometry an analysis similar to the prototype takeoff and climb analysis was performed. This analysis starts with a takeoff roll followed by a rotation when the aircraft reaches takeoff speed. The climb portion begins as soon as the aircraft leaves the ground and continues until the aircraft reaches the first turn. In order to simplify the analysis the altitude at the beginning of the first turn was specified so that the takeoff roll and the final altitude would determine the climb angle while the ground distance remained constant at 500 ft. Since the payload may vary between sorties, all of the takeoff and climb results are functions of the aircraft weight. The inputs for the competition aircraft analyses have been included in Table 5.4.

The takeoff performance for the competition aircraft is presented in Figs. 5.4 through 5.6. With no headwind, a 36 lbs. aircraft will takeoff in 95 ft while using 6220 J of energy. As the headwind increases to 20 ft/s, the takeoff distance decreases to 23 ft. and the energy usage decreases to 3051 J. Figure 5.6 shows that the energy required to climb increases as the headwind increases. With no headwind the competition aircraft requires 9038 J to climb out and with a 20 ft/s headwind the aircraft requires 13138 J. The increase in required energy is due to the increased time of the climb. The airspeed is constant, but the ground speed is slower so the aircraft takes longer to reach the initial turn.

5.5.2 Energy Usage

The energy analysis for the competition aircraft should give a good estimation of the number of sorties that the aircraft can perform. A single 36 cell 2400 mAh battery pack ideally contains 373248 J of

energy. As in the prototype energy analysis sorties with one 360° turn (steel payload sortie) and sorties with 2 laps and no 360° turn (tennis ball sortie) were analyzed. Unlike the prototype analysis six sorties were assumed to make up a flight due to the increased battery capacity. The results of the energy analysis have been included in Tables 5.5 and 5.6. Table 5.5 presents a breakdown of each of the sortie types. The majority of the energy time is spent in the turn segments for the steel payload sortie. In the tennis ball sortie approximately the same amount of energy is consumed in the turn segments as in the straight segments, whereas more time is spent in the turn segments.

Table 5.6 shows the flight energy consumption for a variety of cases. Four cases were considered: a baseline case of 36 lbs. at 65ft/s airspeed, a 36 lbs. and 80 ft/s airspeed case, a 40 lbs. weight and 65ft/s airspeed case and, a 40 lbs. and 80 ft/s case. Increasing the airspeed increases the flight energy by 189 mAh. Therefore, it will be important to maintain lower cruise airspeeds to conserve energy. Increasing the weight also increases the energy consumption. A 4 lb. increase in weight will increase the energy consumption by 270 mAh. Increasing the weight by 4 lb. and increasing the cruise speed has a drastic effect increasing the energy usage by 402 mAh.

Even though the electrical energy calculations have improved the energy consumption prediction, they are still very optimistic. Based on prototype flight test results and the previously mentioned inaccuracies in Motocalc™, it is unlikely that the aircraft will be able to complete six laps. Using a 50% error of margin on the energy predictions, the reference case will consume 2310 mAh of energy. Experience with the batteries has demonstrated that the batteries will not be able to produce the entire capacity with enough voltage to fly. Therefore the aircraft will complete five scoring sortie for each flight.

5.7 Tail Sizing and Stability Analysis

The stability analysis of the RPP-5 was completed using methods found in Raymer³ and Roskam⁷. Unlike the prototype tail sizing, which was based on historical data, the competition aircraft was sized based on stability-and-control analyses. Table 5.7 lists final design values for the RPP-5 tail surfaces along with stabilizer and control surface sizing. Control surface percentages were kept unchanged from the prototype values. Final stability values of C_{m_α} , C_{n_β} , and C_{l_β} are -0.6468 rad^{-1} ,

0.145 rad^{-1} , and -0.137 rad^{-1} respectively, with a stable static margin of 14.18 %.

Analyses of longitudinal and lateral trim conditions are summarized in Figs. 5.7 and 5.8. Airfoil data from Selig et al.⁵ were used for the elevator trim plot analysis. The trim curves have a peculiar shape, caused by the use of these airfoil data.

5.8 Final Design Summary

The design features incorporated into the final design were the result of lessons learned from the prototype aircraft and further analysis. Since the competition aircraft uses the same wing panels as the prototype the parameters are similar. The planform area and taper ratio have changed due to a

decreased fuselage width, while the $C_{L \text{ max plane}}$ remains at 1.5. The parasite drag coefficient for the competition aircraft is 0.042.

The competition aircraft also features a removable wing and horizontal tail. The payload is easily accessible from a hatch in the top of the aircraft, and is split in to two equal containers housed on either side of the wing spar bulkhead. Figure 5.9 shows the external configuration of the competition airplane.

Performance analysis for the aircraft estimates that five sorties with full payload can be achieved using the 2400 mAh battery packs. Stability and control analyses showed the aircraft to be stable with a static margin of 14.18% with the center of gravity located at 33% mean chord. The final design, RPP-5 *Accipiter*, satisfies all of the requirements described in the 2000-2001 Rules and Vehicle Design Specifications and is designed to carry a payload of 14 lbs. of steel or 100 tennis balls with a gross weight of 32 lbs. Four to five sorties are expected with full payload at a cruise velocity of 60 ft/s.

Table 5.1: Parasite Drag* Breakdown Comparison

	Prototype Aircraft	Competition Aircraft
Component	C_{D0}	C_{D0}
Wing	0.0126	0.0124
Fuselage	0.0234	0.0116
Wing/Fuselage Interference	Not Included	Not Included
Horizontal Tail	0.0034	0.0025
Vertical Tail	0.0023	0.0019
Landing Gear	Not Included	Not Included
Total C_{D0}	0.0417	0.0285

*From Roskam

Table 5.2: Competition Aircraft Drag

Component	$C_D @ \alpha = 0$	$C_D @ \text{Minimum Drag}$
Wing	0.0282	0.0183
Fuselage	0.0096	0.0127
Wing/Fuselage Interference	0.0056	0.0037
Horizontal Tail	0.0018	0.0018
Vertical Tail	0.0011	0.0011
Landing Gear	0.0041	0.0041
Total C_D	0.0504	0.0417

Table 5.3: Sample Competition Aircraft Weight Buildup

Weights and Balances					
All distances measured from nose and bottom of aircraft					
Item	Qty	Unit Weight (lbs)	Total Weight(lbs)	Horizontal CG	Vertical CG
Fuselage:					
Batteries	38.00	0.13	5.00	24.22	0.51
Firewall	1.00	0.25	0.25	6.17	4.74
Bulkhead #1	1.00	0.09	0.09	30.90	5.34
Bulkhead #2	1.00	0.08	0.08	32.65	5.35
Bulkhead #3	1.00	0.06	0.06	48.57	4.78
Side panels	2.00	0.43	0.86	23.59	5.20
Bottom truss	1.00	0.03	0.03	32.53	0.19
Wing Tube	1.00	0.52	0.52	31.84	8.31
Top Rails	2.00	0.08	0.15	49.39	9.25
Bottom Rails	2.00	0.08	0.15	49.59	1.50
Propeller	1.00	0.68	0.68	0.63	7.61
Main Gear	1.00	1.41	1.41	35.16	-1.25
Nose Gear	1.00	0.54	0.54	5.67	-1.00
Rudder Servo	1.00	0.16	0.16	85.94	7.11
Elevator Servos	2.00	0.16	0.32	87.98	8.71
Steering Servo	1.00	0.16	0.16	6.92	3.00
Motor and Gearbox	1.00	1.90	1.90	3.25	7.75
Motor mount	1.00	0.30	0.30	6.17	7.86
Speed Controller	1.00	0.13	0.13	6.50	0.46
Receiver	1.00	0.08	0.08	6.50	0.38
AI support for side panels	2.00	0.11	0.21	36.12	0.44
Cardboard tube	2.00	0.10	0.20	31.84	8.31
Carbon-fiber spar	4.00	0.16	0.63	31.84	8.31
Basla shear web	2.00	0.04	0.08	27.69	8.31
Servos	2.00	0.16	0.32	41.06	6.49
Rudder Ribs	7.00	0.01	0.07	94.99	17.44
Vertical Tail Sheeting	1.00	0.05	0.05	87.74	19.41
Rudder Sheeting	1.00	0.06	0.06	94.99	17.44
Leading Edge Support	1.00	0.02	0.02	82.85	18.69
Trailing Edge Support	1.00	0.61	0.61	92.23	18.69
Elevator Ribs	12.00	0.00	0.00	92.24	8.75
Horizontal Tail Sheeting	1.00	0.08	0.08	86.84	8.75
Leading Edge	2.00	0.01	0.03	82.98	8.75
Trailing Edge	2.00	0.03	0.07	90.33	8.75
Mounting Tube	2.00	0.05	0.10	89.35	8.75
CA Glue	6.00	0.13	0.75	24.32	2.58
Payload:					
Tennis Balls	102.00	0.13	12.95	31.84	5.64
Steel (14 lb)		7.00	14.00	31.84	0.63
Empty Aircraft Total:			18.65	31.12	4.51
Aircraft w/ tennis balls Total:			31.60	31.41	4.97
Aircraft w/ 14 lb steel Total:			32.65	31.43	2.84

Table 5.4: Competition Aircraft Performance Inputs

Weight (lbs)	36
Span (ft)	8.5542
MGC (ft)	1.63
S (ft ²)	13.9391
AR	5.25
CLMax without Flaps	1.5
CLMax with Flaps	1.5
Altitude (ft)	35
CD	$CD = -0.101788C_L^3 + 0.42357C_L^2 - 0.31537C_L + 0.10844954$
Turn Speed (ft/s)	50
Turn Diameter (ft)	125
Cruise Speed (ft/s)	65
Crew Time (s)	10

Table 5.5: Baseline Competition Aircraft Sortie Breakdown

Sortie Type 1 (Steel Payload)						
Segment	Time (s)	% Time	Mech. Energy (J)	% Mech. Energy	Elec. Energy (J)	% Elec. Energy
Takeoff	4.7	7.4	1556.4	7.1	6220.8	17.2
Climb	8.7	13.7	5310.2	24.4	9037.6	25.0
Turns	15.7	24.8	9442.2	43.3	14691.3	40.6
Straight	15.4	24.3	4218.2	19.4	4780.8	13.2
Descent Straight	4.6	7.3	1265.5	5.8	1434.2	4.0
Descent	4.3	6.8	0.0	0.0	0.0	0.0
Payload Change	10.0	15.8	0.0	0.0	0.0	0.0
Totals	63.4	100.0	21792.4	100.0	36164.8	100.0
Sortie Type 2 (Tennis Ball Payload)						
Segment	Time (s)	% Time	Mech. Energy (J)	% Mech. Energy	Elec. Energy (J)	% Elec. Energy
Takeoff	4.7	5.0	1556.4	5.2	6220.8	13.6
Climb	8.7	9.2	5310.2	17.6	9037.6	19.8
Turns	15.7	16.7	9442.2	31.2	14691.3	32.1
Straight	46.2	49.0	12654.5	41.9	14342.3	31.4
Descent Straight	4.6	4.9	1265.5	4.2	1434.2	3.1
Descent	4.3	4.6	0.0	0.0	0.0	0.0
Payload Change	10.0	10.6	0.0	0.0	0.0	0.0
Totals	94.2	100.0	30228.7	100.0	45726.3	100.0

Table 5.6: Sortie and Flight Summaries

Flight Summary for the Baseline Case					
	Time (s)	Mech. Energy (J)	Elec. Energy (J)	Elec. Energy (mAh)	Efficiency (%)
	462.7	156063.2	245673.2	1540.6	63.5
Flight Summary for the Cruise Airspeed = 80 ft/s Case					
	Time (s)	Mech. Energy (J)	Elec. Energy (J)	Elec. Energy (mAh)	Efficiency (%)
	422.9	189537.4	274980.9	1729.1	68.9
Flight Summary for the Weight = 40lbs Case					
	Time (s)	Mech. Energy (J)	Elec. Energy (J)	Elec. Energy (mAh)	Efficiency (%)
	501.8	174787.0	281569.0	1810.7	62.1
Flight Summary for the Cruise Airspeed = 80 ft/s and Weight = 40 lbs Case					
	Time (s)	Mech. Energy (J)	Elec. Energy (J)	Elec. Energy (mAh)	Efficiency (%)
	462.0	200366.8	302058.6	1942.5	66.3

Table 5.7: Competition Aircraft Specifications

Tail Attributes	Horizontal	Vertical
Area	360 in ²	300 in ²
Span	36 in	20 in
Mean Aerodynamic Chord	12 in	15 in
Aspect Ratio	2.5	1.333
Taper Ratio	1	1
Airfoil	NACA 00009	NACA 00009
Elevator	33% of horizontal chord	N/A
Rudder	N/A	33% of vertical chord
Wing Attributes		
Mean Aerodynamic Chord	20 in	
Wing Area	2053 in ²	
Taper Ratio	0.38%	
Wing Aerodynamic Center	5 in*	
Ailerons	25% chord, 40%span	
Aircraft Attributes		
Center of Gravity	6.6 in.*	
Neutral Point	7.0773 in. *	
Static Margin: power off	14.18%	

* measured from root chord leading edge

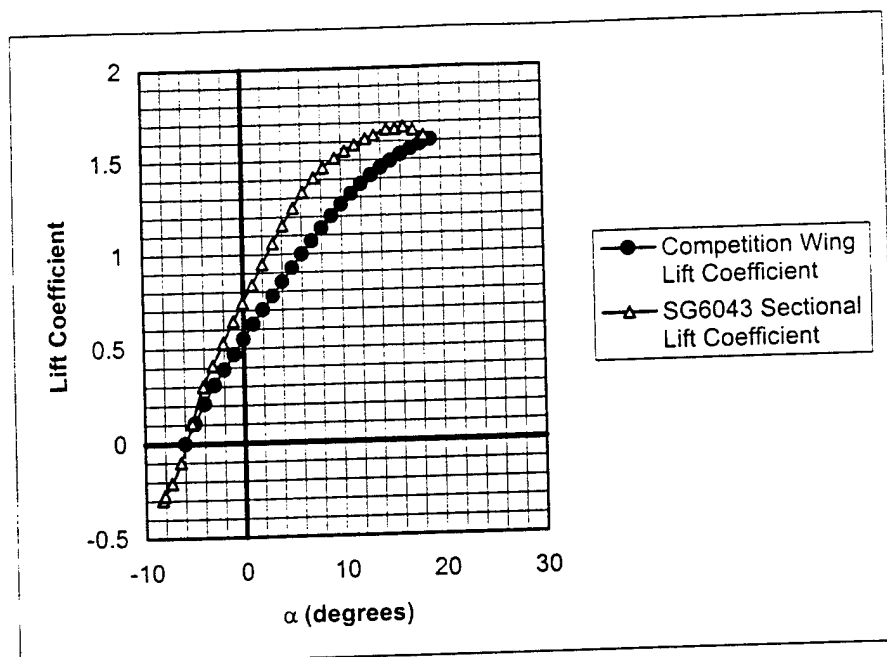


Figure 5.1: Competition Aircraft Lift Curve

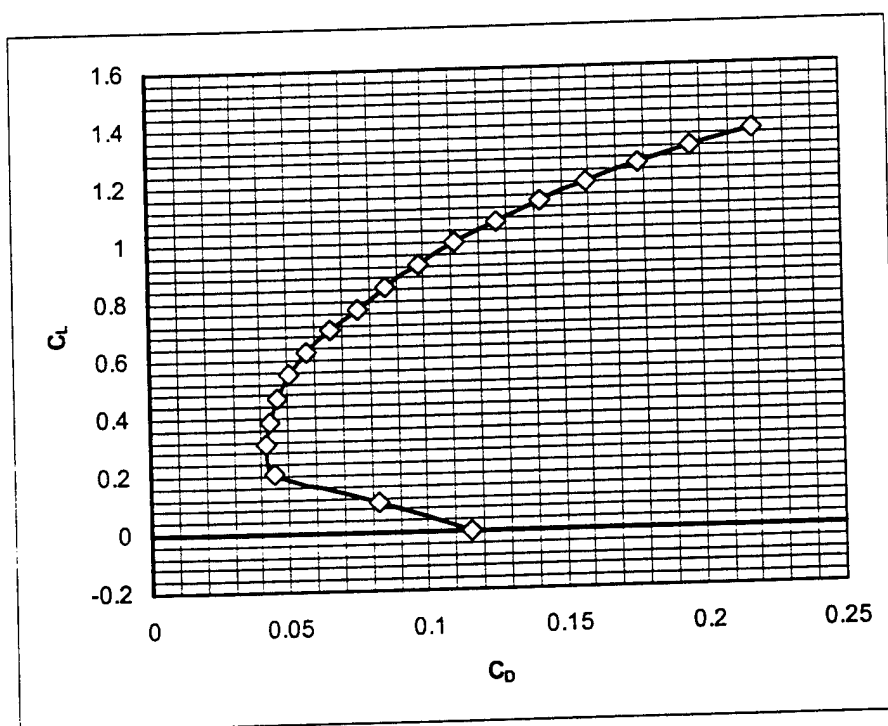


Figure 5.2: Competition Aircraft Drag Polar

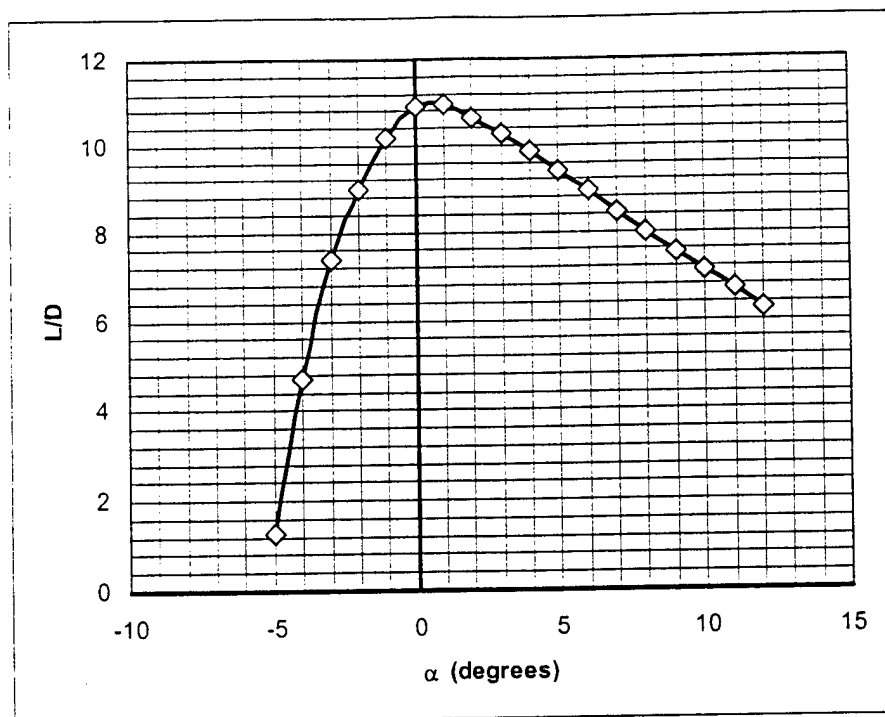


Figure 5.3: Competition Aircraft L/D versus Angle of Attack

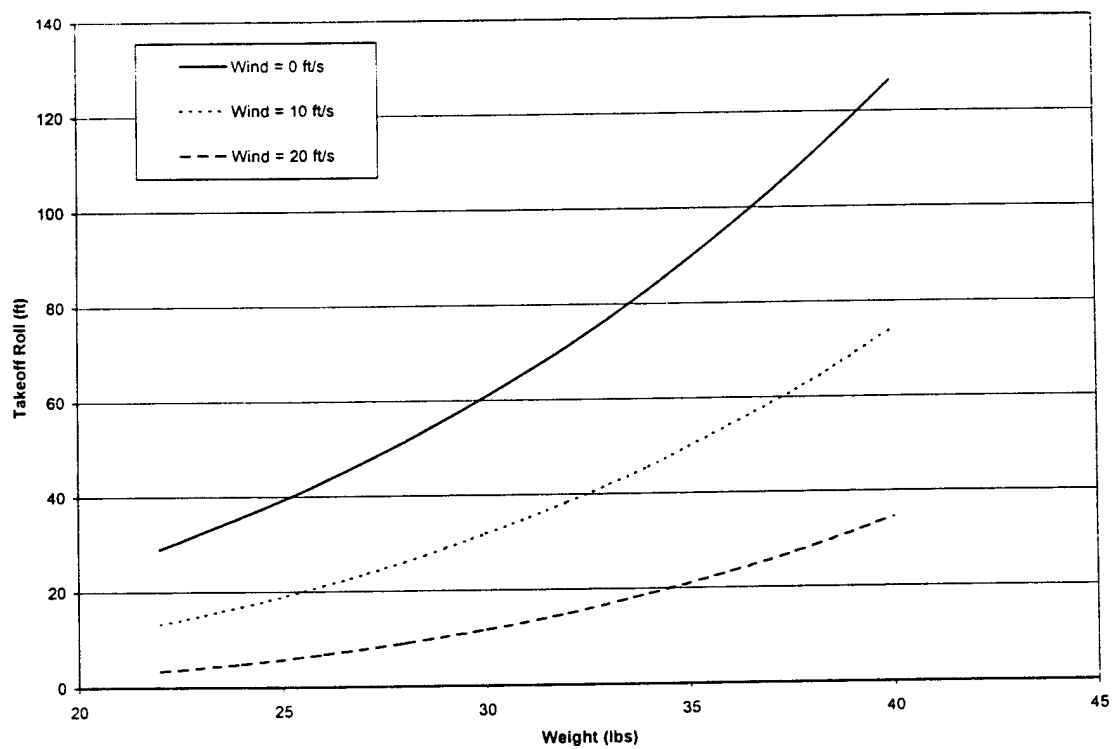


Figure 5.4: Takeoff Roll with Wind Effect

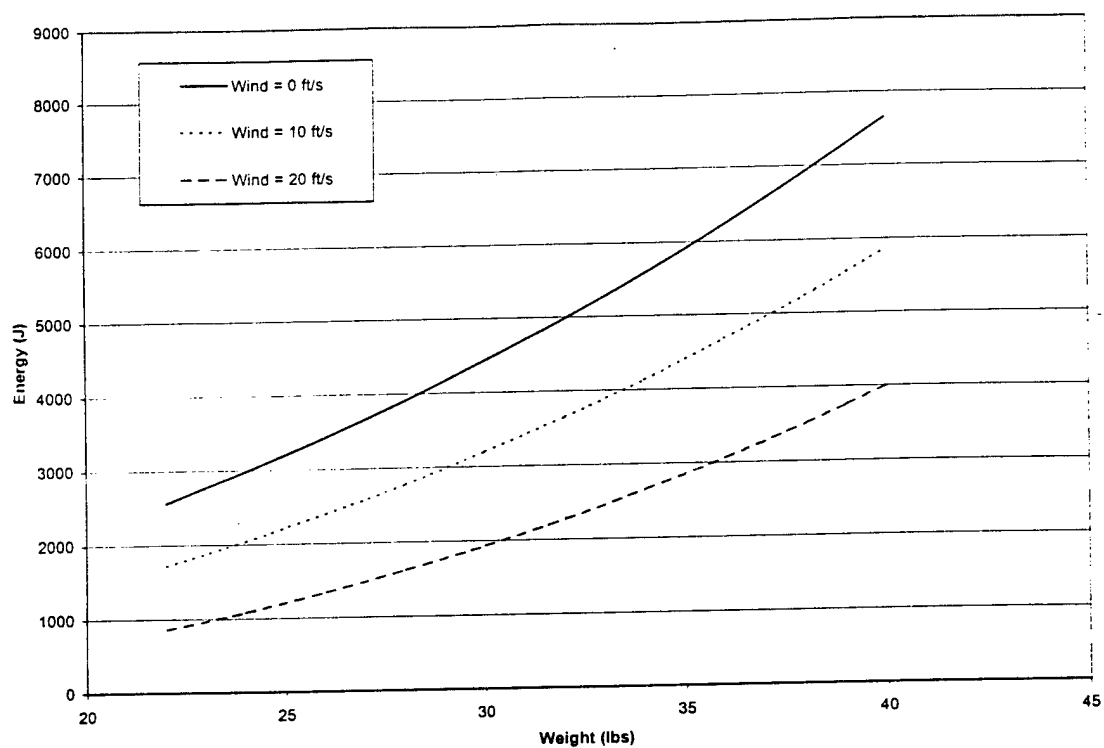


Figure 5.5: Takeoff Energy with Wind Effect

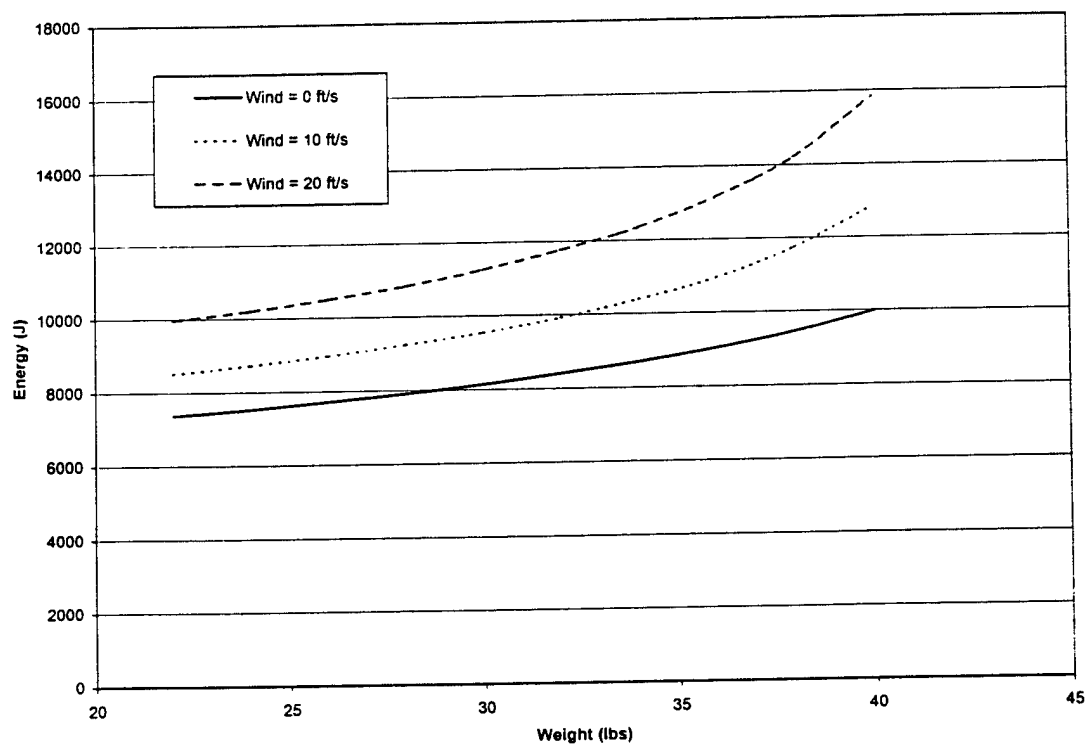


Figure 5.6: Climb Energy with Wind Effect

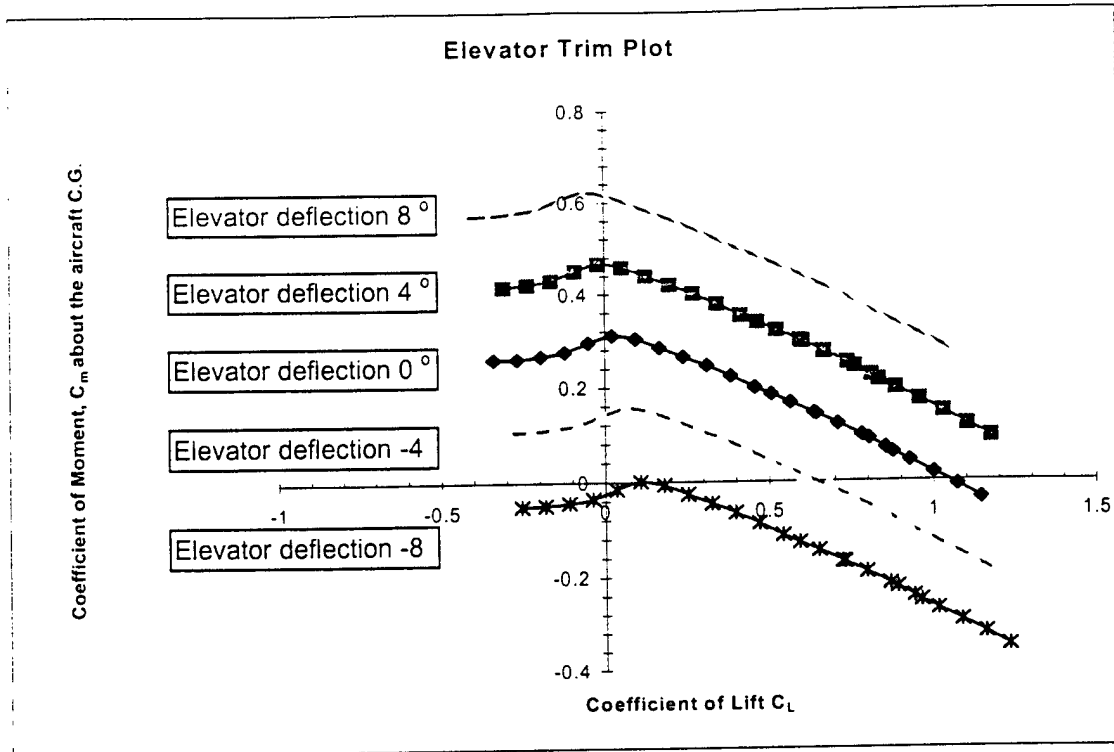


Figure 5.7: Elevator Trim Plot

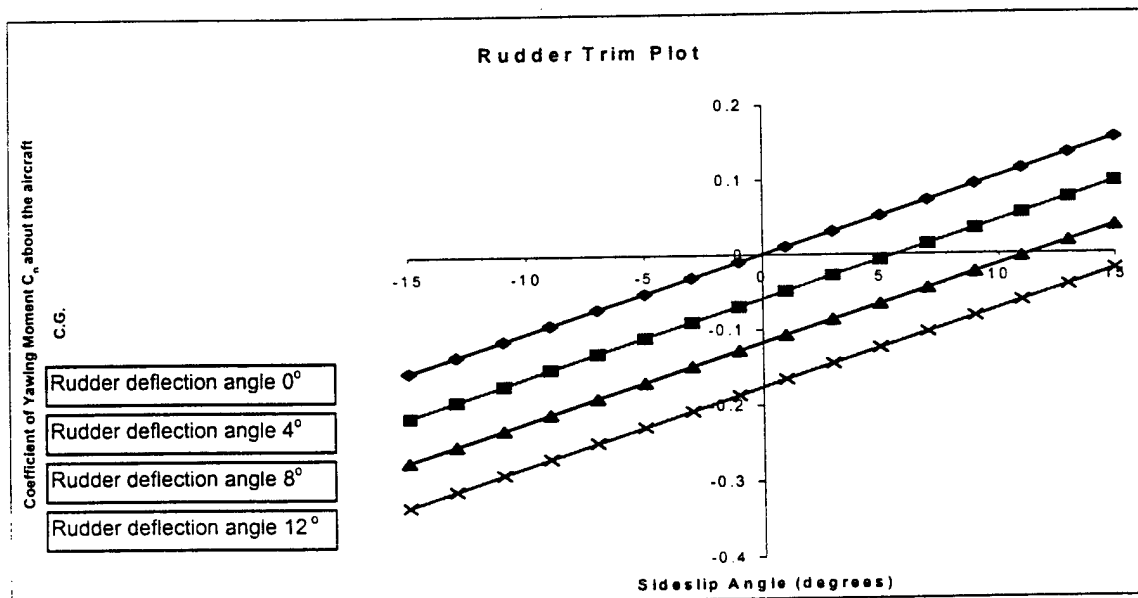
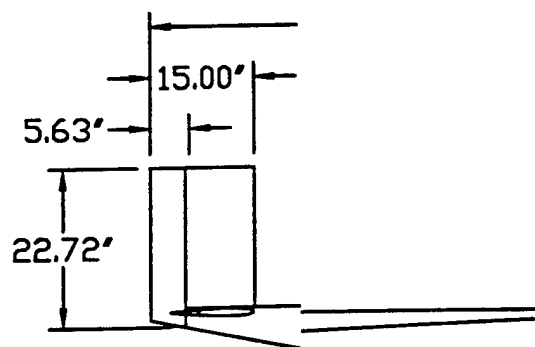
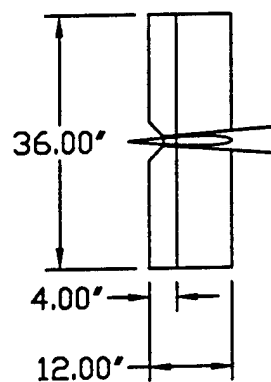


Figure 5.8: Rudder Trim Plot



University of Illinois at Urban

Aeronautical and Astronautic dimensions in inches)

6.0 Manufacturing Plan

6.1 General Requirements

The overall component requirements and design drivers used to select the manufacturing processes were:

- The aircraft must be large enough to carry 100 tennis balls and durable enough to carry 13 pounds of steel.
- The aircraft must withstand handling, transportation, payload weight, and repeated takeoffs and landings.
- The wings and tail must be removable for transportation purposes.
- The aircraft must be built in a way that allows easy access to the payload and battery packs.
- Materials used must be cost effective and have modest strength to weight ratios.

6.2 Manufacturing Process

Possible construction techniques were investigated for the fuselage, wing, and empennage. The methods considered are common to model aircraft construction.

6.2.1 Fuselage

The construction methods considered for building the fuselage were traditional built up and fiberglass skin over wooden longerons and formers. Fuselage shape could either be cylindrical or rectangular with square or rounded corners.

6.2.2 Wings

The wing assembly needed to be strong while remaining light to achieve low Rated Aircraft Cost. Two construction techniques, fiberglass composite and traditional built up wing, were considered. Less traditional construction methods, such as a D-tube leading edge, were considered to improve upon the built-up method.

6.2.3 Empennage

Like the wing, the tail could be traditionally built up or constructed of fiberglass with a foam core. Due to transportation restrictions, the horizontal stabilizer needed to be removable. For strength, with the traditional method, the tail construction could utilize either a spar or cross-bracing between the ribs.

6.2.4 Figures of Merit

In order to determine which manufacturing process would be used, the following Figures of Merit were employed.

- Accuracy: how true to the plans the completed aircraft and the wing (due to the required airfoil accuracy) could be constructed.
- Durability: the ability of the aircraft to withstand flight conditions.

- Ease of Construction: the skill necessary to build the design.
- Material Availability: the ease of acquiring building materials.
- Material Cost: the monetary expense of the chosen materials.
- Speed of Construction: the amount of time in which the components can be completed.
- Structural Strength: the ability of the components to support loadings.
- Weight: the total weight of the aircraft.

The Figures of Merit rankings are presented in Table 6.1. Each Figure of Merit was assigned a numerical rating from 1 to 5 so that quantitative analysis of the manufacturing processes could be made. Unlike the FOMs in Section 3, each manufacturing FOM carries equal weight. Table 6.2 shows the final ranking for the construction methods considered for the wing. Fuselage construction methods are ranked in Table 6.3.

It was decided that a traditional built-up method of construction would be used for the wings, which would feature a D-tube leading edge and carbon fiber spar. The decision to use the built-up construction for the wings was primarily due to the ease and speed of construction. As seen in Table 6.2, the built-up balsa leading edge and the D-tube ranked the same. However, the D-tube was chosen due to its lower weight despite its longer build time. On the basis of Table 6.3 it was decided that the fuselage would have plywood sides. These building methods were used for both the prototype and competition aircraft.

6.3 Manufacturing Process for the Prototype Aircraft

The traditional built up method was chosen for the prototype aircraft, based on the FOMs analysis. Once these construction methods were selected, it was necessary to move on to more detailed construction concerns for primary aircraft structures. The timeline for the construction of the prototype aircraft XRPP-4 *Drag Queen* is provided in Figure 6.1. See Fig. 4.3 for the external configuration of the prototype.

The fuselage design featured a constant taper from the firewall to the tail to eliminate areas of stress in the longerons. The fuselage had four longerons; the top two were made of $\frac{1}{2}$ inch by $\frac{1}{4}$ inch basswood, and the bottom two of $\frac{1}{4}$ inch by $\frac{1}{4}$ inch basswood. The payload compartment had $\frac{1}{8}$ inch plywood sides. Both the wings and horizontal stabilizer were removable, requiring the fuselage to contain two cardboard tubes to accept the aluminum tubes used to attach these components. To minimize weight, $\frac{1}{8}$ inch plywood with lightening holes was used for the bulkheads. The front bulkhead was made of $\frac{1}{4}$ inch plywood to provide the necessary support for the motor mount and batteries. The payload compartment consisted of two bays, one ahead of the spar bulkhead and one behind. Compartment sizing was chosen to keep the center of mass located at 33% of the wing chord whether loaded or unloaded. The aft fuselage structure was a cross-braced truss structure that provided torsional stiffness.

A built up wing was used for the prototype. Because the wings were to be made detachable, a cardboard tube was built into the inboard wing structure to accept the aluminum tube used to join the

wings to the fuselage. The cardboard tube interlocks with carbon fiber spars and a balsa shear web forming the base structure of the wing. The ribs were made of $\frac{3}{32}$ inch balsa with most of the central material removed for weight reduction. A D-tube leading edge, formed from $\frac{1}{64}$ inch plywood, was used to provide torsional stiffness.

The tail was also a traditional built-up design. Like the wing, the horizontal tail includes an aluminum tube for easy removal. Because the horizontal tail does not experience the same loads as the wing, no central spar was used, saving weight. To add torsional stiffness, the top and bottom surfaces of the horizontal tail were sheeted with $\frac{1}{16}$ inch balsa. The vertical tail was built in a similar manner, but was permanently mounted to the fuselage structure.

6.4 Modifications Needed for Competition Aircraft

Construction and flight testing of the prototype revealed changes that would have to be made for the competition aircraft. The fuselage needed to be completely redesigned with less complexity to reduce construction time and improve ground operations. A stronger main landing gear was needed because the prototype gear was bent during landings. Further weight reduction methods would also have to be investigated.

6.5 Manufacturing Process for Competition Aircraft

The competition aircraft was constructed using methods similar to those employed in manufacturing the prototype. The timeline for the construction of the competition aircraft RPP-5 is presented in Fig. 6.2.

A basswood and balsa truss fuselage with $\frac{1}{8}$ inch plywood sides was used for the competition aircraft. The fuselage was also lengthened, while reducing the frontal area, so it carried the same number of tennis balls. To reduce fuselage weight, truss work was employed as much as possible and plywood reinforcement was used sparingly. A lightweight but strong material was needed for the firewall to withstand forces exerted by the motor. Balsa laminated with fiberglass was used for the firewall.

Due to time restrictions, the wing used on the prototype was modified and reused on the competition aircraft with plans to build another wing if time permits. Modifications made to the prototype wing included removing the balsa root rib and replacing it with a $\frac{1}{8}$ inch plywood root rib. The areas between the first two ribs and the last two ribs were sheeted with balsa to improve durability.

The tail surfaces were constructed using balsa leading and trailing edges. Sheeting was used near the roots of both stabilizers to reduce twisting caused by aerodynamic loads. Like the wing, the horizontal stabilizer uses an aluminum tube for easy assembly and removal. The horizontal stabilizer does not have a spar because it does not experience the same loads as the wings. Weight was reduced significantly by eliminating the horizontal tail spar. The elevators and rudder were sheeted on both sides to increase the accuracy in building and to increase control authority. Micro-servos were housed inside the stabilizers for easier connection to the control surfaces.

Both types of payload have identical sets of boxes that fit snugly into the cargo area of the fuselage. The boxes have been designed to place the steel payload as close to the center of gravity as possible. The tops of the boxes can be unscrewed and removed to meet the requirement that payloads be interchangeable. A removable cowl allows access to the motor for necessary maintenance and repairs. Nose gear and the steering servo were attached to the firewall and a custom manufactured main gear was used.

6.6 Cost Reduction Methods

The fuselage, wings, and empennage were constructed out of balsa, basswood, and plywood. All of these materials are easily attainable and relatively inexpensive. Wings for the competition aircraft are the same wings used on the prototype, eliminating the need for new material to build another set. Much of the epoxy and glue was still available from the previous year's project.

Table 6.1: Construction Figures of Merit

Figure of Merit	Ranking		
	5	3	1
Strength	Strong	Adequate	Weak
Ease of Construction	Easy	Moderate	Difficult
Speed of Construction	Fast	Moderate	Slow
Weight	Light	Moderate	Heavy
Durability	Durable	Moderate	Fragile
Accuracy	Accurate	Moderate	Inaccurate
Material Availability	Readily Available	Moderately Available	Obscure
Material Cost	Cheap	Affordable	Expensive

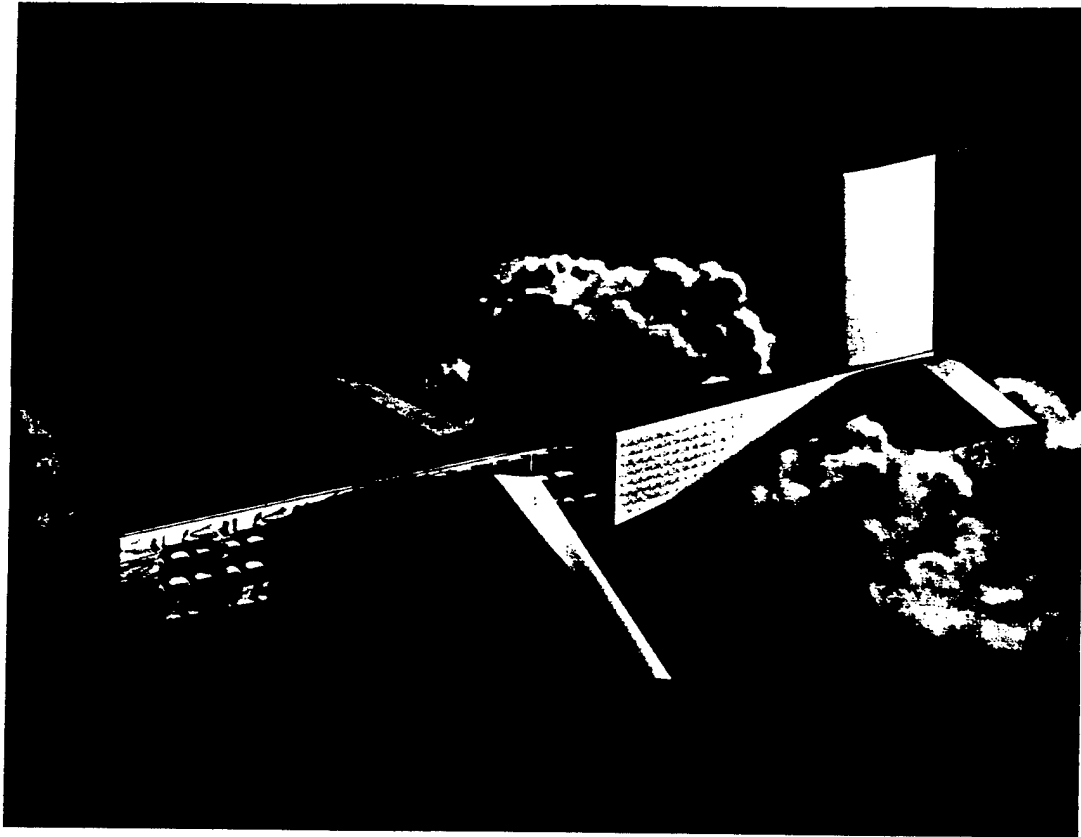
Table 6.2: Wing Figure-of-Merit Results

	Built Up With Balsa Leading Edge	Built Up With D-tube Leading Edge	Built Up With Carbon Fiber Spar	Foam Core With Fiberglass
Strength	3	4	5	5
Ease of Construction	5	3	4	1
Speed of Construction	5	4	4	2
Weight	3	5	5	1
Durability	3	2	5	5
Accuracy	3	5	4	5
Material Availability	5	5	3	3
Material Cost	5	4	3	2
Total	32	32	33	24

References

1. Motocalc. Vers. 5.01 Computer Software. Capable Computing, Inc. 1998.
2. Lyon, C.A., Broeren, A.P., Gopalarathnam, A., Girguere, P., and Selig, M.S., *Summary of Low-Speed Airfoil Data - Vol. 3*, SoarTech Publications, Virginia Beach, VA. Dec. 1997
3. Raymer, D.P., *Aircraft Design: A Conceptual Approach*, 3rd ed., AIAA Education Series, Washington, D.C., 1999
4. Roskam, J., *Airplane Design: Part VI: Preliminary Calculation of Aerodynamic, Thrust and Power Characteristics*, Roskam Aviation and Engineering Corporation, Ottowas, KS. 66067, 1987.
5. Selig, M.S., Guglielmo, J., Broeren, A.P., and Giguere, P., *Summary of Low-Speed Airfoil Data - Vol. 1*, SoarTech Publications, Virginia Beach, VA. June 1995.
6. Hoerner, Sighard F., *Fluid Dynamic Drag; Practical Information on Aerodynamic Drag and Hydrodynamic Resistance*, Midland Park, NJ, 1965
7. Roskam, J., *Airplane Flight Dynamics and Flight Controls*, Roskam Aviation and Engineering Corporation, Ottowas, KS. 66067, 1990

Final Design Report RPP-5



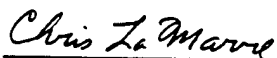
AIAA Student Design/Build/Fly Competition

Webster Field, Maryland

**Department of Aeronautical and Astronautical Engineering
University of Illinois at Urbana-Champaign**

10 April 2001

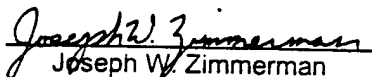
2001 Project Team
Report Contributors



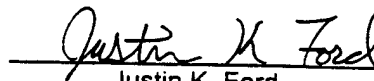
Christopher M. LaMarre



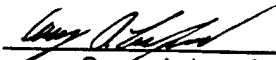
Michael S. Sexauer



Joseph W. Zimmerman



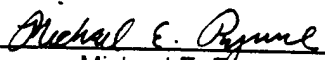
Justin K. Ford



Carey A. Lunsford



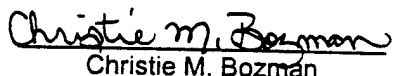
Ann Peedikayil



Michael E. Rynne



Karl R. Klingebiel



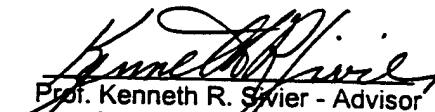
Christie M. Bozman

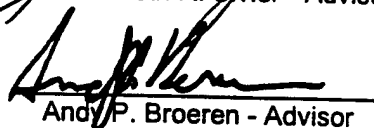


Theresa Kidd



Jason M. Merret


Prof. Kenneth R. Swier - Advisor


Andy P. Broeren - Advisor

Other Members

Mike Cross - Pilot
AnnMarie Cross - Pilot
Suzanne M. Vig - Finance
Aaron T. Dufrene - Manufacturing

Jeffery M. Lazzaro - Manufacturing
Tom Krenzke - Manufacturing
Leah Stefanos - Finance

Table of Contents

1.0 Executive Summary	1
2.0 Management Summary	2
3.0 Conceptual Design	5
3.1 System Requirements	5
3.2 Figures of Merit and Configuration Selection	5
3.3 Configuration Selection	6
3.4 Initial Motor Selection	6
3.5 Estimated Score Analysis	6
3.6 Conclusion	7
4.0 Preliminary Design	11
4.1 Design Parameters Investigated	11
4.2 Aerodynamics	11
4.3 Propulsion	12
4.4 Performance	13
4.5 Tail Sizing and Stability Analysis	14
4.6 Preliminary Design Summary	15
4.7 Results of the Test Flights	15
4.8 Lessons Learned from Prototype	15
5.0 Detail Design	25
5.1 Introduction	25
5.2 Aerodynamics	25
5.3 Propulsion	25
5.4 Weights and Balances	26
5.5 Performance	26
5.7 Tail Sizing and Stability Analysis	27
5.8 Final Design Summary	27
6.0 Manufacturing Plan	38
6.1 General Requirements	38
6.2 Manufacturing Process	38
6.3 Manufacturing Process for the Prototype Aircraft	39
6.4 Modifications Needed for Competition Aircraft	40
6.5 Manufacturing Process for Competition Aircraft	40
6.6 Cost Reduction Methods	41
7.0 Lesson's Learned	45
7.1 Propulsion Testing	45
7.2 Flight Tests and Energy Analysis	45

7.3 Comparison of Final Design to Proposed Design	46
7.4 Areas for Improvement	47
8.0 Aircraft Rated Cost	50

7.0 Lesson's Learned

7.1 Propulsion Testing

Before the competition aircraft was completed, a new gearbox was built and two Bolly 24x24 Carbon fiber propellers were obtained. Static testing showed that only 8 lbs. of thrust could be obtained from the 24x24 propellers with a 4:1 gear ratio. This was approximately 4 lbs. below the Motocalc™ prediction. This was insufficient thrust for takeoff within the 200 ft. limit with a 36 lb. gross takeoff weight. The decision was made to return to the Zinger 27x27 wooden propeller, with a 5:1 gear ratio, that had been used on the prototype aircraft. This combination produces 13 lbs. of static thrust and was known to be sufficient from its use on the prototype aircraft.

Other problems were also encountered in propulsion testing. Motor vibration is believed to have caused the loosening of two screws that secured the motor to the gearbox. The loss of these screws led to the motor twisting it's way off the gearbox and damaging the gearbox. A second gearbox was prepared. The failure points were reinforced with epoxy and all screws were secured using Locktite™. In addition, the shaft was lengthened to increase propeller-cowling clearance.

A preliminary energy use study was also performed. The bench-mounted propulsion system was run for 1.0 minute, allowed to rest for 30 seconds, run for 1.5 minutes, allowed to rest for 30 seconds, and then the sequence was repeated. The 1.0 minute run represents the estimated time for sorties carrying steel weights, the 1.5 minutes for the time for sorties carrying tennis balls, and the 30 seconds for ground change time. Runs were conducted at 20, 25 and 30 amperes using both battery packs. During the periods when the motor was being run, energy consumption, voltage, current, rpm, and thrust were monitored. These tests suggested that 5 sorties could be completed at a 20 amp. current draw, 4 sorties at 25 amps., and only 3 sorties at 30 amps. This was a crude approximation since the drop in amperage, although shown in wind-tunnel tests to be small, and thrust with increasing airspeed were not taken into consideration. Also, the current draw for the duration of a sortie would not be constant.

7.2 Flight Tests and Energy Analysis

7.2.1 Flying Qualities

After construction of the competition aircraft was completed, a flight test program was begun. An initial familiarization flight showed the aircraft to be stable and adequately powered. Ground handling had been improved by the change to a tricycle landing gear with a steerable nose wheel. During initial flights a severe pitch up moment induced by downwash on the horizontal tail resulting from flap deployment was discovered. Because more roll control authority was desired and flaps were not needed to make the takeoff requirement, both control surfaces were replaced with full-span ailerons. This improvement in roll control also reduced the rated cost of the aircraft.

The initial familiarization flight revealed the need to reduce the aerodynamic load on the horizontal tail, eliminating the negative elevator deflection needed to trim the aircraft in level flight. The c.g. was moved forward from 33% to 30% MAC. This increased the static margin of the aircraft to 17.85% and improved the handling of the aircraft.

7.2.2 Flight Tests

The goal of the flight test program was to collect energy data in order to establish an optimum program to fly at the competition and to later use for energy analysis. Test flights accurately simulated the contest course layout. The runway was marked off in 10 ft. increments and turn judges were positioned 500 ft. from the starting line. Spotters, data recorders, and timers were positioned along the course. This made it possible to time the aircraft in each segment of the flight. Watts, amperage, and voltage readings were relayed to a ground monitor via an onboard camera. These data, combined with the flight times recorded, allowed an accurate determination of the energy consumption for each flight segment. A sample flight data sheet is shown in Table 7.1. The camera system also allowed for consistency in flights, as amperage drawn at any point could be adjusted by the pilot in real time to match a predetermined level. The onboard meter also monitored the amount of energy used from the battery pack. With this information, it could be determined how much energy was needed to fly each type of sortie with a given payload as well as the how much energy was still available for future sorties.

In order to reduce energy consumption, it was necessary to determine the optimal cruise power consumption. To find this optimal power setting, the aircraft was flown upwind and downwind for a thousand feet at several levels of motor current. Data on the time and energy consumed at each current level are shown in Table 7.2. These data show that maintaining a 20 ampere current achieved the best efficiency for a 12 lb. payload. This current represents the best lift-to-drag ratio for reducing power consumption. This corresponds to a cruise velocity of 67 ft/s, which was close to the predicted 65 ft/s cruise velocity.

Once the cruise power setting was established, concentration shifted toward determining the total sortie energy used for the various payloads. Based upon the earlier energy analyses, the original intention was to complete four scoring sorties per flight period. The initial strategy was to fly two flights of each sortie type, using 14 lbs. of payload on each sortie; 100 tennis balls weigh about 14 lbs. This would achieve a flight score of 68; 40 points for the two tennis ball sorties, and 28 points for the two steel sorties. After attempting to fly these sorties, it was discovered that the battery pack voltage dropped below that required to sustain safe flight during the fourth sortie. Further tests revealed that the energy used on the steel sorties varied from about .420 Ah with 12 lbs. of steel to about .550 Ah with 22 lbs. of steel. Energies for different sorties and payloads are shown in Table 7.3. It could be seen that one steel sortie with 20 lbs. of steel would achieve the same score as two sorties flown with half that weight, and consume less energy. In addition, it was observed that a steel sortie carrying 20lbs. achieved the same score as a 100 tennis ball sortie while consuming less energy. Taking these results into consideration, it was realized that a higher score could be achieved by flying three sorties per flight with increased weight during the steel sorties. Therefore, it was decided that the contest flight schedule should consist of a 20 lb. steel sortie, a tennis ball sortie, and another 20 lb. steel sortie. This order of sorties offers a margin of safety in energy consumption or allows the possibility of flying a higher steel payload depending on flight conditions.

7.3 Comparison of Final Design to Proposed Design

The competition aircraft incorporates a few minor design changes that should be addressed. These changes were based on test data, observed handling qualities, and efforts to improve aerodynamics. A few of these changes resulted directly from the testing phases previously discussed. The first change was the decision to use the Zinger 27x27 wooden propeller in place of the Bolly 24x24. The second change was replacing the flaps with full span ailerons. The third change was the relocation of the c.g. to 30% MAC. In addition to these changes, a new engine cowling was made in an effort to increase aerodynamic efficiency and provide increased engine and battery cooling. Also, the landing gear was reinforced with an aluminum plate to reduce flexing of the gear on landing.

7.4 Areas for Improvement

During the course of this year's design work, the project could have been improved by directing more attention to certain design procedures such as analysis, testing and administration. These improvements should be employed during design work for next year's competition.

The most important area requiring improvement is propulsion testing. Because currently available software propulsion simulations proved inaccurate, a wider range of propeller, gearbox, and motor combinations should be run in both static and wind tunnel tests. This would allow for the most efficient combination to be found, and allow direct prediction of propulsion performance. This requires that more time and resources be allocated to propulsion testing.

The next improvement is in the area of structural analysis. A more thorough structural analysis, including the use of finite element analysis of the aircraft, would have given a better indication of the behavior of the aircraft structure under flight loads. This could lead to reduction of the airframe weight and a lower rated cost. In order to accomplish this task, a department should be dedicated to structural analysis in next year's project.

In addition to performing more analyses, better documentation of the analyses that are performed would be beneficial. This not only allows for a more thorough design report, but also gives future teams an understanding of the design processes done in past years. Weekly status reports and more stringent deadlines would improve efficiency and keep all departments updated and on task.

Additional improvements can also be made through utilizing available engineering software. Current software programs could be used to not only provide building plans and drawings, but to perform structural analysis and weights estimates. Instructing future team members in the use of this software would streamline design analyses.

Finally, more consideration to the construction details should be incorporated into the design phase. Sacrificing a small increase in the weight of the aircraft would be a worthwhile design compromise if it allows the airframe to be built more accurately and in less time.

Table 7.1: Sample Flight Data Sheet

Sortie # and type: 21-23 contest simulation					
	Date		31-Mar	31-Mar	31-Mar
		units			
	Flight #	Date-#	3-31-21	3-31-22	3-31-23
	Sortie #		21	22	23
	# of tennis balls		0	102	
	weight	lbs	22	13	20
	Lap weight		-	-	-
	Battery name		yellow	yellow	yellow
	Battery voltage	V	50.2	46.9	46.2
	Energy	Amp/hrs	0	0.61	1.243
	with 360=Y w/o 360=N		Y	N	Y
0	start	sec	0	0	0
1	Take Off	sec	8.62	8.22	9.2
	TO dist	ft	165	167	175
	Lap 1		17.65		
3	Beginning of 1st Turn	sec	17.65	17.55	17.15
4	End of 1st Turn	sec	25.26	-	24.39
5	Beginning of 360 Turn	sec	34.85	-	31.23
6	End of 360 Turn	sec	50.07	-	34.79
7	Beginning of 2nd Turn	sec	54.4	35.24	40.53
8	power off	sec	-	-	
9	End of 2nd Turn	sec	1.03.09	42.08	57.4
	Lap 2				
	Beginning of 1st Turn	sec		1.00.64	
	End of 1st Turn	sec		1.04.55	
	Beginning of 360 Turn	sec		-	
	End of 360 Turn	sec		-	
	Beginning of 2nd Turn	sec		1.17.99	
	power off	sec		-	
	End of 2nd Turn	sec		-	
10	touchdown	sec	1.13.00	1.32.00	1.06.00
11	End of roll out	sec			
12	End of sortie	sec			
13	Payload change	sec			
	overall sortie flight time	sec			
	Battery voltage	V	46.9	46.2	44.5
	Energy	Amp/hrs	0.61	1.243	1.768
	Max rate of climb	ft/min			
	Max altitude	ft			
	crew change time	sec			
	total energy used	Ah	0.61	0.633	0.525

Table 7.2: Cruise Power Setting for 12 lbs. Payload

Amperes	Time (s)	Velocity (ft/s)	Energy Used (J)
30	12.00	83.33	360.00
30	12.31	81.23	369.30
25	12.57	79.55	314.25
25	13.60	73.53	340.00
20	14.73	67.89	294.60
20	15.00	66.67	300.00
17	34.68	28.84	589.56
17	35.49	28.18	603.33

Table 7.3: Average Energy Consumption

Type	Payload (lbs.)	Energy (Ah)
Steel	12	0.431
Steel	12	0.408
Steel	16	0.428
Steel	16	0.483
Steel	16	0.413
Steel	20	0.494
Steel	20	0.489
Steel	20	0.609
Steel	20	0.525
Steel	22	0.610
Tennis Balls	12	0.634
Tennis Balls	12	0.544
Tennis Balls	13	0.609
Tennis Balls	13	0.802
Tennis Balls	13	0.633
Tennis Balls	14	0.610
Tennis Balls	14	0.606
Tennis Balls	14	0.636
Tennis Balls	14	0.665
Tennis Balls	16	0.613
Tennis Balls	16	0.575
Tennis Balls	16	0.627

8.0 Aircraft Rated Cost

The rated cost of the aircraft was computed using the cost model provided in the 2000/01 Rules and Vehicle Design. A breakdown of the rated cost is provided in Tables 8.1 and 8.2.

Table 8.1 Aircraft Rated Cost Parameters

A	Manufacturers Empty Weight Multiplier	\$100/hour		
B	Rated Engine Power Multiplier	\$1/watt		
C	Manufacturing Cost Multiplier	\$20/hour		
MEW	Manufacturers Empty Weight			
		Weight	15	
		Total	15	
REP	Rated Engine Power			
		Amps	40	
		Cells	36	
		Motors	1	
		Volts/cell	1.2	
		Total	1728	
MFHR	Manufacturing Man Hours			
	Wing	15 hours/wing	1	15
		4 hours/sq. ft.	14.04	56.16
		2 hours/strut	0	0
		3 hours/control surface	2	6
	Fuselage	5 hours/body	1	5
		4 hours/ft.	8.75	35
	Empennage	5 hours basic	1	5
		5 hours/vertical	1	5
		10 hours/horizontal	1	10
	Flight Systems	5 hours basic	1	5
		2 hours/servos, controller	9	18
	Propulsion Systems	5 hours/engine	1	5
		5 hours/propeller	1	5
			Total	170.16

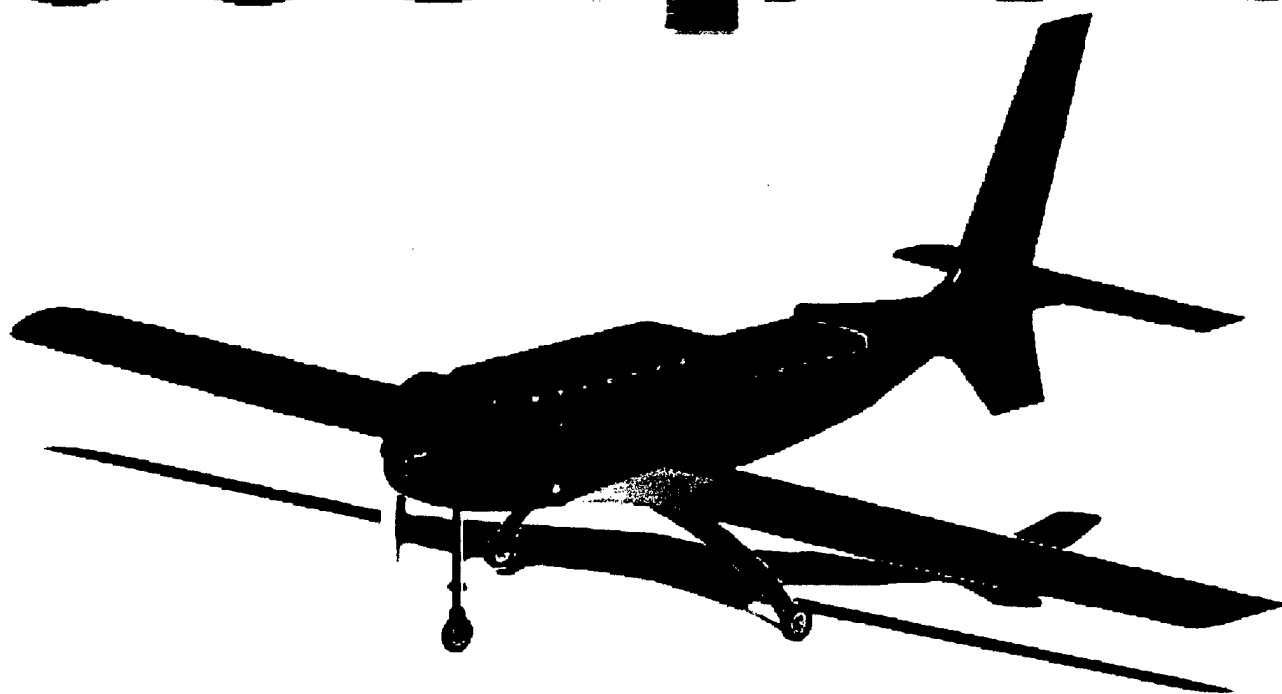
Table 8.2: Aircraft Rated Cost

A*MEW	1500
B*REP	1728
C*MFHR	3403.2
Total Aircraft Rated Cost	6.6312

USC Aero Design

Presents:

Scorpion



USC UNIVERSITY OF
SOUTHERN CALIFORNIA



AeroVironment

GWS 2010



**The
Skunk
Works**

LOCKHEED MARTIN

BOEING

Raytheon



NORTHROP GRUMMAN

Table of Contents

ii. Awesome Features Diagram	ii
1. Executive Summary	1
2. Management Summary	5
2.1. Aero Surfaces & Fuselage.....	6
2.2. Landing Gear & Lab Manager.....	6
2.3. Controls & Propulsion.....	7
2.4. Flight Tests.....	7
2.5. Construction.....	7
2.6. Conceptual and Preliminary Design.....	7
2.7. Report Editor.....	7
2.8. Information Technology & Design Spreadsheet Development.....	7
2.9. Propulsion Testing & Weights and Balance.....	8
2.10. Configuration and Structural Design & Structural Sizing.....	8
3. Conceptual Design	8
3.1. Alternative Concepts Investigated.....	8
3.2. Detail Design Parameters.....	8
3.3. Design Descriptions.....	9
3.4. Subjective Figures of Merit.....	9
3.5. Analytic Figures of Merit.....	11
4.0. Preliminary Design	13
4.1. Design Tools.....	13
4.2. Optimization Parameters.....	20
4.3. Configuration.....	22
4.4. Wing.....	23
4.5. Tail.....	23
4.6. Brakes.....	24
4.7. Landing gear.....	24
5. Detailed Design	25
5.1. Performance Data.....	25
5.2. Modeling Process.....	26
5.3. Payload Design.....	26
5.4. Fuselage Aerodynamic Design.....	27
5.5. Structural Design.....	27
5.6. Wing Structure.....	28
5.7. Landing Gear.....	32
5.8. Component Mounts.....	33
5.9. Cooling Design.....	35
5.10. Nose Design.....	36
6. Drawing package	37
7. Manufacturing Plan	41
7.1. Manufacturing Method Down Select.....	41
7.2. Construction Methods.....	41
7.3. Construction.....	44
7.4. Scheduling.....	47

Cargo Box: Designed to fit 100 Tennis balls with minimal volume.

100 Tennis Balls: Packed for lowest volume.

Self-Aligning wing mount: Designed to set the wing at the correct incidence.

Exhaust fins: Designed to maximize airflow around motor and other sub-components.

Integral bulkheads: Designed to simplify construction process, and keep high tolerances.

Low pitch, large diameter prop to meet current requirements.

AstroFlight Gearbox to let the high revving motor drive the large prop.

Frangible motor mount: Designed to fail in a crash, protecting the front bulkhead

Heat Sink: Designed to let the motor run at very low temperatures.

Steerable Nose Gear: for improved ground handling

1 Piece carbon fiber landing gear: Designed to sustain a single wheel landing at 6 G's.

Carbon-Balsa spar designed for a 4.5G load.

1 piece dorsal and ventral fin to avoid over-rotation

Offset Horizontal: To avoid flat spins if it should stall.

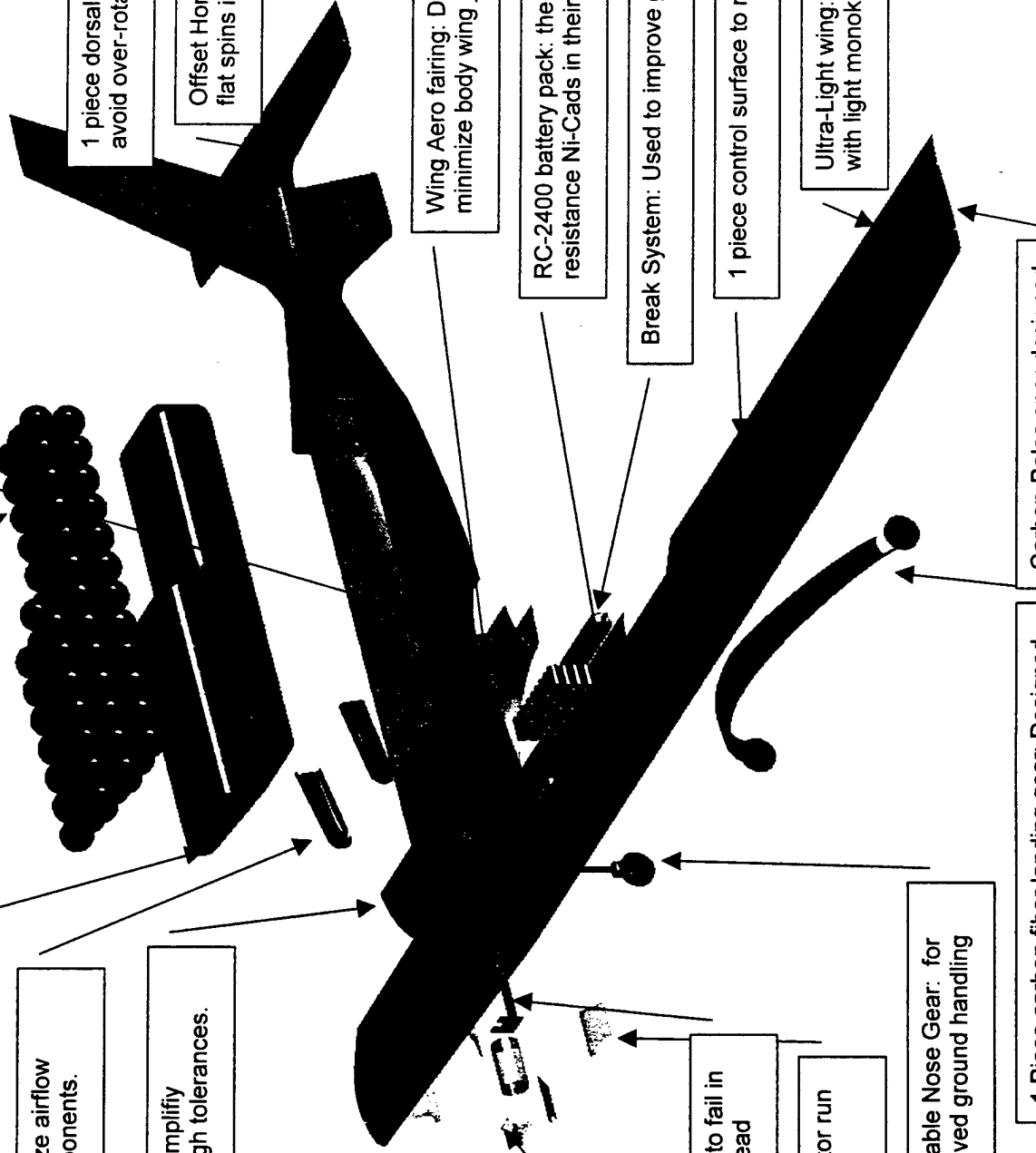
Wing Aero fairing: Designed to minimize body wing junction drag.

RC-2400 battery pack: the lowest internal resistance Ni-Cads in their class

Break System: Used to improve ground handling.

1 piece control surface to minimize cost

Ultra-Light wing: Foam core with light monokote cover.



1. Executive Summary

The University of Southern California's Student Aero Design Team will participate in the 2000-2001 AIAA/Cessna/ONR Student Design/Build/Fly Competition. This contest draws teams of college students from across the country to compete in a remote controlled electric aircraft contest. Each year's contest brings a new set of rules and requires a new design, keeping teams from refining one design year after year. This year's contest requires teams to create a plane capable of carrying the greatest weight of steel and/or number of tennis balls over a 1000-foot pylon course in 10 minutes. When carrying steel, the plane must take off within 200 feet, cruise to the first pylon, turn 180°, complete a 360° turn in the opposite direction, cruise to the second pylon, turn 180°, land and taxi back to the starting line. When carrying tennis balls, the plane must take off within 200 feet, complete two consecutive empty laps, land, and taxi back to the starting line. Figure 1.1 describes the flight profile for a sortie with steel, and a sortie with tennis balls flies two laps around the pylons without the 360° turn.

The contest also imposes severe constraints on the plane's design. It set a span limit of 10 feet and a maximum aircraft weight of 55 pounds. No lighter-than-air or rotary-wing planes are allowed. The plane can only be driven by commercially available, unmodified brushed electric motors from Graupner or AstroFlight turning propellers. Gear or belt reduction is allowed and current is limited to 40 amps or less by a fuse between the power supply and the speed controller. The motor power supply must use only commercially available nickel cadmium batteries and can weigh no more than five pounds. The propellers must be commercially made but may be clipped. The propulsion system must incorporate a disarmed lockout for safety, all connectors must be fully insulated, and the batteries must be shrink-wrapped. No payload can be carried within the wing, and payload must be fully faired and enclosed. Each pound of steel or five tennis balls carried earns the team one point. The plane must carry at least five pounds of steel and between 10 and 100 tennis balls. The judges determine the final aircraft score by multiplying the sum of the points earned in the best three scoring flights by the report score and dividing by the rated aircraft cost. This rated aircraft cost incorporates such measures of cost and complexity as battery and motor count, fuse rating, gross weight, wing area and servo count. Creating a successful plane required the respect of many different constraints, severely impacting our design.

USC's entry in the 2000-2001 contest, the *SCorpion*, resulted from a thorough design process. During last year's contest USC's team evaluated a comprehensive list of alternative configurations including a baseline high-winged monoplane, flying wings, canards, and a risky but attractive joined wing design. Using this same evaluation, many of the same configurations have been eliminated leaving the two best configurations, a monoplane design and a biplane design, for further study. Modifying the primary analysis spreadsheet to accommodate biplane configurations revealed that they offered negligible benefits while requiring much more effort in design and construction. The decision was made to pursue a monoplane design.

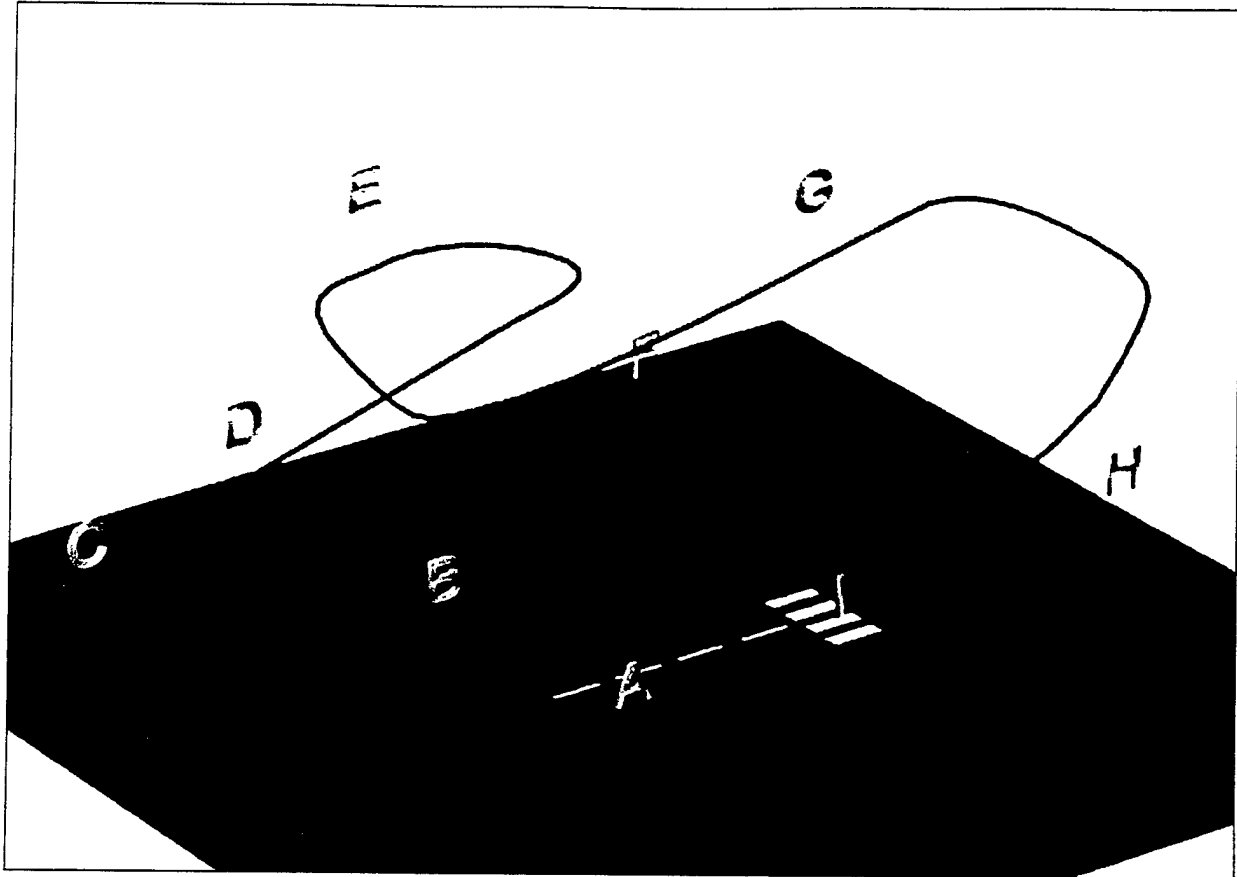


Figure 1.1. Flight profile of steel sortie (A- Takeoff, B- Climb, C-180° Turn, D-Cruise, E- 360° Turn, F- Cruise, G- 180° Turn, H- Descent, I- Landing)

The focus then shifted into plane optimization. An interactive, multidisciplinary spreadsheet was the key analytical tool for optimization. Simultaneous development of the aircraft's three-view by the configurator validated the viability of the analysis. It was evident early in the design process that the cost model would heavily penalize multiple motor configurations. Multiple motors also added to aircraft weight, construction time, actual cost and flight risk. The team's entry in last year's contest validated the feasibility of propelling a large aircraft with a single motor, and the decision was made early on to pursue only single-motor designs.

This year a new emphasis was placed on testing. At the start of the year the decision was made to build a prototype aircraft that would fulfill all the contest requirements. Intended to serve as a flying test bed for the propulsion system and as a construction tutorial for the new team members, *SCarface* used a fuselage derived from last year's plane and had few weight optimizations. To enhance its usefulness for testing, it incorporated airspeed, battery voltage and altitude downlinks and was built very robust to withstand the anticipated crashes. The tests gave many of the new crew experience in construction and flight testing and revealed that the battery life was only 65% of the predicted value. The team also conducted motor and propeller tests on a thrust stand. The thrust, current draw and RPM data collected

USC Aero Design Team "SCorpion"

revealed that the propellers were somewhat more efficient than had been assumed. These data were integrated into the spreadsheet analysis and were used in the design of the prototype plane, *SCarface*, and also served as the flying test bed for *SCorpion's* power plant.

Observations from previous year's contests revealed the importance of payload access and ground handling. An effective braking system significantly reduced ground time and the risk of running off the runway and enabled more scoring flights. A strong braking system placed on the wheels favored a tricycle landing gear, which also improved ground controllability. A tricycle landing gear arrangement with pneumatic brakes was chosen. The cartridge-based, top loading payload system proven in last year's contest was modified for the new payload requirements. This led to a low wing design, which also allowed for a lighter attachment structure with shorter load paths.

The great impact of maneuverability on flight performance made stability and control the focus of much attention. To aid in this analysis, the stability and control tool from the previous contest was refined and integrated into the main analysis spreadsheet. This revealed that reducing the tail length decreased rated cost more than the larger tail hurt performance. The stability and control spreadsheet helped choose aerodynamic parameters that gave an acceptably stable plane with good stall characteristics and low gust response. To meet takeoff field requirements while minimizing drag, the use of wing flaps increased lift at takeoff and reduced wing area at cruise. The stability and control goal was to allow the pilot to fly the plane to its aerodynamic limits without struggling to keep it aloft.

The primary analytical spreadsheet had as its main outputs the total points scored per flight and the vehicle cost. The ratio of payload to cost provided a single measure to evaluate each intermediate design. The team converged on two related configurations using different motors, providing a backup plan if the best motor proved unsuitable or problematic. The addition of a temperature analysis spreadsheet to the mission model allowed us to evaluate the propulsion system cooling requirements. This analysis largely determined the placement of propulsion components. The analysis favored 13-18lb payload planes over very large planes, and small configurations suffered heavily from fixed costs like wing count. The data gained from the thrust bench and from testing *SCarface* resulted in a lower theoretical score for every configuration but did not significantly alter the optimum design.

Weight and construction considerations now drove the increasingly detailed design of the evolving plane. Data and experience gathered from the prototype plane aided these decisions. The analysis spreadsheet emphasized the absolute criticality of weight to takeoff field length and overall performance. Whenever presented with a choice between durability and reduced weight, the lighter plane was chosen with the accepted risk. Crashworthiness was minimized unless it had a very small impact on weight. A set of spare parts taken to the contest and faith in the team's skills in composite repair will compensate for this decreased durability.

Most components were designed for minimum weight using structural analysis spreadsheets. A wing loading analysis spreadsheet helped design a lightweight structure. The wing is made of foam with a single spar consisting of a pair of carbon fiber caps with a balsa shear web placed at the wing 30% chord. Carbon sheeting at the leading edge, and the monokote covering provide span wise and torsional

USC Aero Design Team "SCorpio"

rigidity respectively. A composite landing gear analysis provided accurate prediction of the landing gear deflection and optimized its design for the required height width, aircraft weight and design landing acceleration. The landing gear featured all-composite construction, allowing a significantly improved strength-to-weight ratio over aluminum. Joining the landing gear and wing mounts at a single hard point improved structural efficiency. A set of carbon fiber-nomex honeycomb bulkheads served to stiffen the composite aerodynamic shell, and both served as primary structure. The composite motor mount was designed to fail gracefully in a crash, protecting the motor and motor shaft. The motor had an additional heat sink as well. The nose gear and braking system were purchased from manufactures we had used in the past, but were of lighter construction. To minimize servo and control surface count and weight, the plane used a single servo in each wing driving flaperons.

Aircraft construction began in January. The use of a lost-foam method eliminated the need for a fuselage mold and saved two weeks. The aircraft met its weight target and was mostly finished by mid-February. *SCorpio's* first flight took place on March 3 (shown in Figure 1.2) and revealed a strong flyer.



Figure 1.2. Landing approach on *SCorpio's* first flight.

2. Management Summary

USC's Aero Design Team consisted of four faculty and industry advisors, a core group of experienced upperclassmen, and a number of new arrivals and peripheral members. Dr. Ron Blackwelder and Mark Page served as the faculty advisors. Wyatt Sadler and Stuart Sechrist, both from Aerovironment, Inc., were the team's industry advisors. The student leaders included Nathaniel "Rusty" Palmer, Jacob Evert, Cheng-Yuan (Jerry) Chen, David Lazzara, Phillippe Kassouf, Charles Heintz, George Sechrist, Tim Bentley, George Cano, Michael Mace, and Scott Oishi. The team was roughly divided into Design/Report and Construction sections and had a semiformal command structure. Positions were assigned according to experience and interest; the responsibilities were somewhat fluid, with team members helping out when and where needed.

Dr. Ron Blackwelder, who served as secretary and treasurer, was also our liaison with the school. Mark Page, an adjunct Professor at USC who is also chief aerodynamicist at Swift Racing, advised the team on aerodynamics and helped develop the analysis spreadsheet. Stuart Sechrist and Wyatt Sadler, both alumni of the DBF competition, helped construct the plane. Wyatt also served as the primary pilot. The team structure is depicted in Figure 2.1.

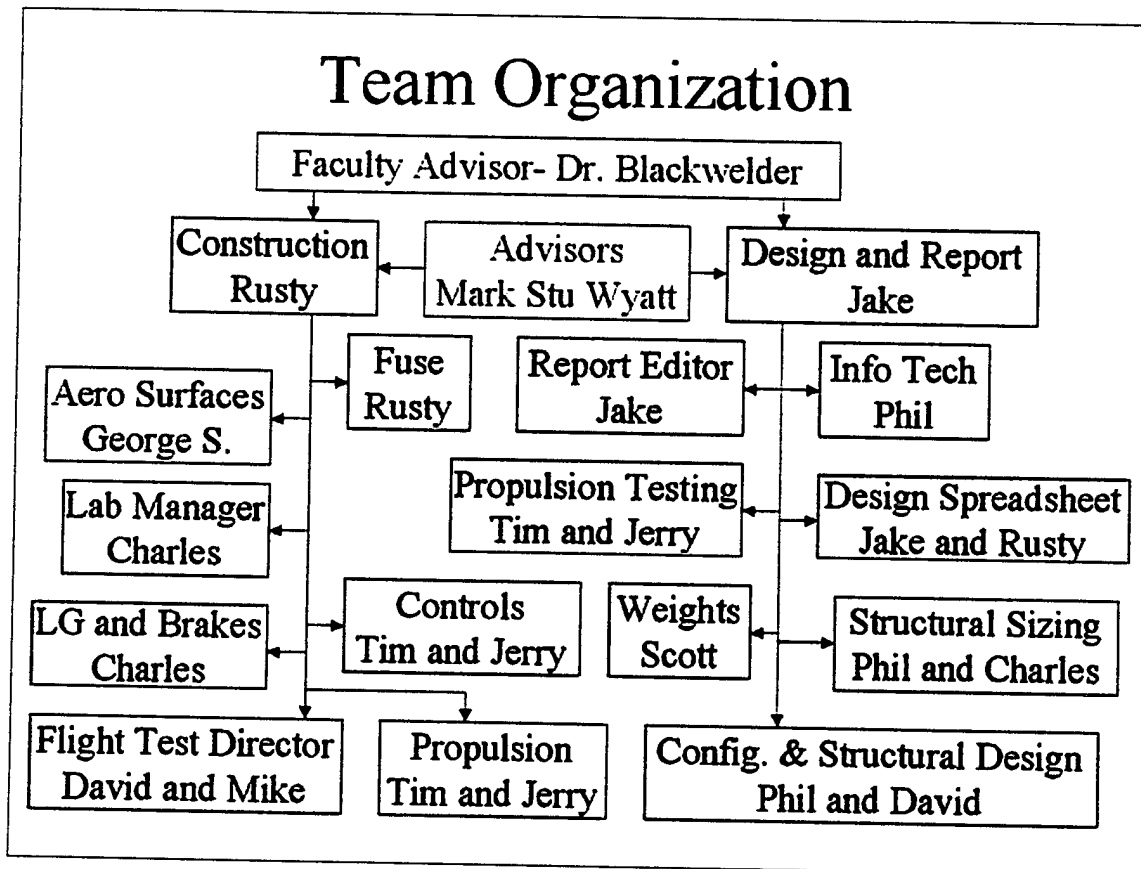


Figure 2.1. Team organizational Structure

USC Aero Design Team "SCorpion"

The responsibilities for the construction section were to construct the prototype and final planes, plus all necessary test pieces and replacement parts. The construction section captain was Nathaniel "Rusty" Palmer, a senior in Aerospace Engineering who also acted as a co-group leader. Our pilot, Wyatt Sadler, also lent considerable input and assistance to the fabrication of both aircrafts. The construction section was divided into several areas of responsibility, including Aero Surfaces, Fuselage, Landing Gear and Brakes, Lab Manager, Controls, Propulsion, and Flight Testing.

Design Process Schedule		Sept	Oct	Nov	Dec	Jan	Feb	Mar
Task	Team Member	1 2 3 4	1 2 3 4	1 2 3 4	1 2 3 4	1 2 3 4	1 2 3 4	1 2 3 4
Conceptual Design								
Mission simulator functional	Rusty	X						
Biplane analysis added to mission simulator	Jake		X					
Biplane study	Jake		X					
Preliminary Design								
SCarface Flight Test	Rusty							
SCarface design	David	X						
SCarface construction	Rusty		X					
SCarface flight testing	Rusty			X				
Motor Test								
Thrust stand operational	Jerry		X					
Battery life study	Jerry		X					
Propulsion system testing	Jerry		X					
SCorpion Design								
Mission simulations	Jake	X						
SCorpion configuration frozen	Jake				X			
Payload configuration completed	Phil			X				
Wing design	George			X				
Fuselage design	Phil			X				
Propulsion system design	Jerry			X				
Landing gear design	Charles			X				
Report								
Subsections in	Team captains			X				
Report editing	Jake						X	
Due date								X

Projected time is this color
 Actual time is this color
 X is when the task actually started

Figure 2.2. Scorpion design schedule outline

2.1. Aero Surfaces & Fuselage

The responsibilities of the Aero Surfaces group included designing and building the wing, the horizontal and vertical stabilizers, and the control surfaces. George Sechrist was in charge of this group. The Fuselage group, led by Nathan Palmer, had the responsibility of constructing the plane's fuselage and the integrating the various components that are installed into it.

2.2. Landing Gear & Lab Manager

The Landing Gear and Brakes group was responsible for constructing and installing the nose and main landing gears, the brakes, the wheels and the steering system. Our lab manager, Charles Heintz, took on this responsibility. As the Lab Manager, he was also in charge of keeping the lab clean and organized.

USC Aero Design Team "SCorpion"

2.3. Controls & Propulsion

The Controls group took responsibility for the radio and servo systems and the servo linkages. The Propulsion group was tasked with constructing and testing the entire power plant and power supply, as well as designing and constructing the motor mount. Jerry Chen led both of these groups with aid from Tim Bentley.

2.4. Flight Tests

The Flight Test group was in charge of organizing the test flights and collecting and processing data. David Lazzara and Mike Mace led this team.

2.5. Construction

The construction section was assisted by a number of underclassmen that lent their time when needed. These people include Tyler Golightly, Amanda Lim, George Cano, Tim Schoen, Jonathan Hartley, Stephanie Gallet, Oakley Trinh, Tai Merzal, Syed Alsagoff and Doris Pease.

2.6. Conceptual and Preliminary Design

The Conceptual and Preliminary Design section was lead by Jacob Evert, a senior in Aerospace Engineering, a co-group leader. The areas of responsibility under this were coordination of Information Technology, Propulsion Testing, Design Spreadsheet Development, Weights and Balance, Structural Sizing, and Configuration & Structural Design.

2.7. Report Editor

The Report Editor was responsible for collecting the various report pieces from other group members, organizing them, and editing them into a final report. Jake Evert also took on this task.

2.8. Information Technology & Design Spreadsheet Development

The Information Technology group, led by Phil Kassouf, created the computer graphics in this report and helped prepare materials for presentations and our sponsors. The Design Spreadsheet Development group updated, refined and integrated the various analysis spreadsheets used to design the plane. Jake Evert and Nathan Palmer were responsible for this, with considerable aid from Mark Page.

2.9. Propulsion Testing & Weights and Balance

Jerry Chen and Tim Bentley headed the Propulsion Testing group, which conducted extensive propulsion system testing to refine our models and test the flight hardware. The Weights and Balance group was tasked to update the design spreadsheet's weight models and monitor the plane's weight and c.g. as construction progressed. Scott Oishi took primary responsibility.

2.10. Configuration and Structural Design & Structural Sizing

The Configuration and Structural Design group was responsible for the overall design of the plane. David Lazzara configured the prototype plane, while Phil Kassouf configured the final plane. Charles Heintz directed the Structural Sizing group, which was in charge of sizing the plane's structure.

3. Conceptual Design

3.1. Alternative Concepts Investigated

3.1.1. List of initial concepts

This year's team discussed several aircraft configurations, including flying wing, tandem motor monoplane, joined wing, and a canard monoplane. A preliminary study of these concepts quickly eliminated them because there were no significant rule changes from the previous year's contest, where these concepts were also less valuable. Efforts then focused on a much more competitive design study between a biplane and monoplane.

3.2. Detail Design Parameters

3.2.1. Design philosophy

The design approach for this team was best described by the term K.I.S.S. (Keep It Simple Stupid). The simplest design resulted in the fastest, lightest, and cleanest aircraft. The speed of manufacturing was key because mistakes made in either the design or manufacturing phase could be discovered long before the contest date. Flight tests also identified mistakes as the actual aircraft performance and characteristics were displayed. Improving these errors would result in a better contest score.

To implement this design philosophy the team was divided into two sub groups. The first group built a prototype aircraft named *SCarface* and used it to gather data in test flights. The prototype was also a backup contest plane. If *SCorpion* were not completed on time, the *SCarface* aircraft would be used at the contest instead.

USC Aero Design Team "SCorpion"

The second group worked with the Excel spreadsheet model optimizing and comparing the final two configuration options. This proved to be a successful venture since early flight test results changed the modeling program in such a way that it favored one configuration: the monoplane.

3.3. Design Descriptions

3.3.1. Monoplane

A conventional low wing monoplane was the team's baseline configuration for four years. Its success in industry made it an obvious choice considering its good handling characteristics, flight performance, and decent efficiency. Most of all, the team had experience with the configuration.

3.3.2. Biplane

A biplane configuration was a strong contender in the competition during the last few years. As a result, the team wished to look much more closely at this configuration against a more general design study of multiple configurations. Since there was a ten-foot wingspan limit this year, the need for more effective wing area was reduced. The complicated wing support structure of the biplane was also complicated to build and had more difficult cargo access than a low-wing monoplane.

3.4. Subjective Figures of Merit

The following eight criteria were used to compare the monoplane to the biplane: ease of manufacturing, ease of assembly and repair, robustness of construction, elegance of structural design, flight handling qualities, ground handling, payload accessibility, and experience with design. Using these figures of merits (FOMs), the team discussed and ranked each configuration out of five points. The results from this discussion were summarized in Table 3.1.

3.4.1. Ease of manufacturing

Ease of manufacturing was an important consideration. A simple plane required less time to build and generally performed better. Repair time also reduced when fewer components could be damaged. The monoplane received a five because it contained fewer parts and the biplane received a three.

3.4.2. Ease of assembly and repair

A configuration with common and easily repairable materials was needed. Repairing an aircraft within 30 minutes of its crash ensured the points scored for the sorties completed. Due to the complex structure involved supporting a biplane, repairing a biplane would take longer than a monoplane. As a result, the biplane received a three in this category. The monoplane received a five for its fast repair in past experience.

USC Aero Design Team "SCorpion"

3.4.3. Crash worthiness

For Scorpion, the team used a new design philosophy. Instead of designing for large impact loads (8g's or greater), some robustness was sacrificed to reduce weight. The use of a flying prototype and longer flight-test sequence to gain experience and test components resulted in a more mature final aircraft and reduced the level of crashworthiness deemed desirable. It was still an important figure of merit, but the stability of a design was now a consideration.

The biplane's stability decreased the likelihood of crashes. The monoplane's short load paths and concentrated structure made it inherently more robust. Neither design had an overall advantage, so a tie was awarded.

3.4.4. Elegance of structural design

The elegance of *SCorpion's* structural design was in its simplistic nature and minimal weight contribution. The payload compartment needed extra space for payload shift to ballast the aircraft c.g. after its construction. A biplane's complex upper-wing structure reduced flexibility to payload access and had long load paths. Much of the monoplane's structure, though, had short load paths that concentrated at the landing gear attachment points. As a result, the biplane received a three, and the monoplane scored a five.

3.4.5. Flight handling qualities

Stability and control was implemented into *SCorpion's* design for flying in various weather conditions. A large static margin (SM) reduced sensitivity to small disturbances, yet an upper limit in SM allowed aircraft rotation for takeoff. Easy landings were necessary because each scoring flight included multiple landings. A biplane, with its increased wing area and aspect ratio, had the most stable approach on landing and received a five. The monoplane's lower aspect ratio required a faster rate of sink and was less gust sensitive. However this increased the landing loads and allowed less time for pilot correction against strong wind gusts. The monoplane received a score of three.

3.4.6. Ground handling qualities

Since each scoring flight had a time limit, minimizing ground time improved the flight scores. Maneuvering with power to the start line was beneficial because payload exchange could not occur until the plane stopped at this point. Steady maneuvering lowered the chances of tipping. The lower c.g. of a monoplane made it less likely to tip during ground maneuvers, thus receiving a five. The biplane received a four.

USC Aero Design Team "SCorpion"

3.4.7. Payload accessibility

Easily accessed payload is easily exchanged. During a complicated payload exchange, nervous bumbling fingers may slow the payload exchange process. Thus the payload needed simple accessibility and removal. A speed loader was the best choice for quick and easy payload removal. Taking the payload from the top of the fuselage reduced the number of obstacles surrounding the payload as well. The high wing of a biplane prevented a large hatch to accommodate the payload and received a three. The low wing of the monoplane easily accommodated a top hatch and received a five.

3.4.8. Experience with design

There was a definite learning curve involved with design. To under take an exotic untested design did make good use of the team's experience and skills. A simple configuration similar to previously built aircraft reduced the time needed to build the final plane. The team's construction experience was taken into account for the design of this year's plane. Given the desire to finish the construction with enough time to test fly, the monoplane received a five. The biplane received a one because no team member had experience in fabricating a biplane.

From the subjective FOM discussion, the monoplane scored the best against a biplane configuration. In order to justify this basic down select, time was spent upgrading the mission model spreadsheet to simulate a biplane. A more analytic method was used to make the final configuration selection.

Figures of Merit	Monoplane	Biplane
1. Ease of manufacturing	5	3
2. Ease of assembly and repair	5	3
3. Crash worthiness	4	4
4. Elegance of structural design	5	3
5. Flight handling qualities	3	5
6. Ground handling qualities	5	4
7. Payload accessibility	5	3
8. Experience with design	5	1
Sum Totals	37	26

Table 3.1 Ranking summary for the monoplane and biplane configurations (5=Best, 1=Unfavorable)

3.5. Analytic Figures of Merit

3.5.1. Cost determination model

The cost determination function was written into the mission spreadsheet model. Geometry parameters from the mission model were sent to the cost equation. Each configuration was optimized in the mission model and then assigned a cost.

3.5.2. Configuration analysis model

A detailed analytic performance analysis was obtained using simulation macros in the mission spreadsheet. The final decisions between the two configurations were based on the outputs from this spreadsheet. A variety of payload weights were surveyed in the mission model. Mission parameters were optimized in the mission model after inputting this year's contest rules and both the monoplane and biplane configurations. The results of the design study, including predicted cost and final score, were shown in Figure 3.1.

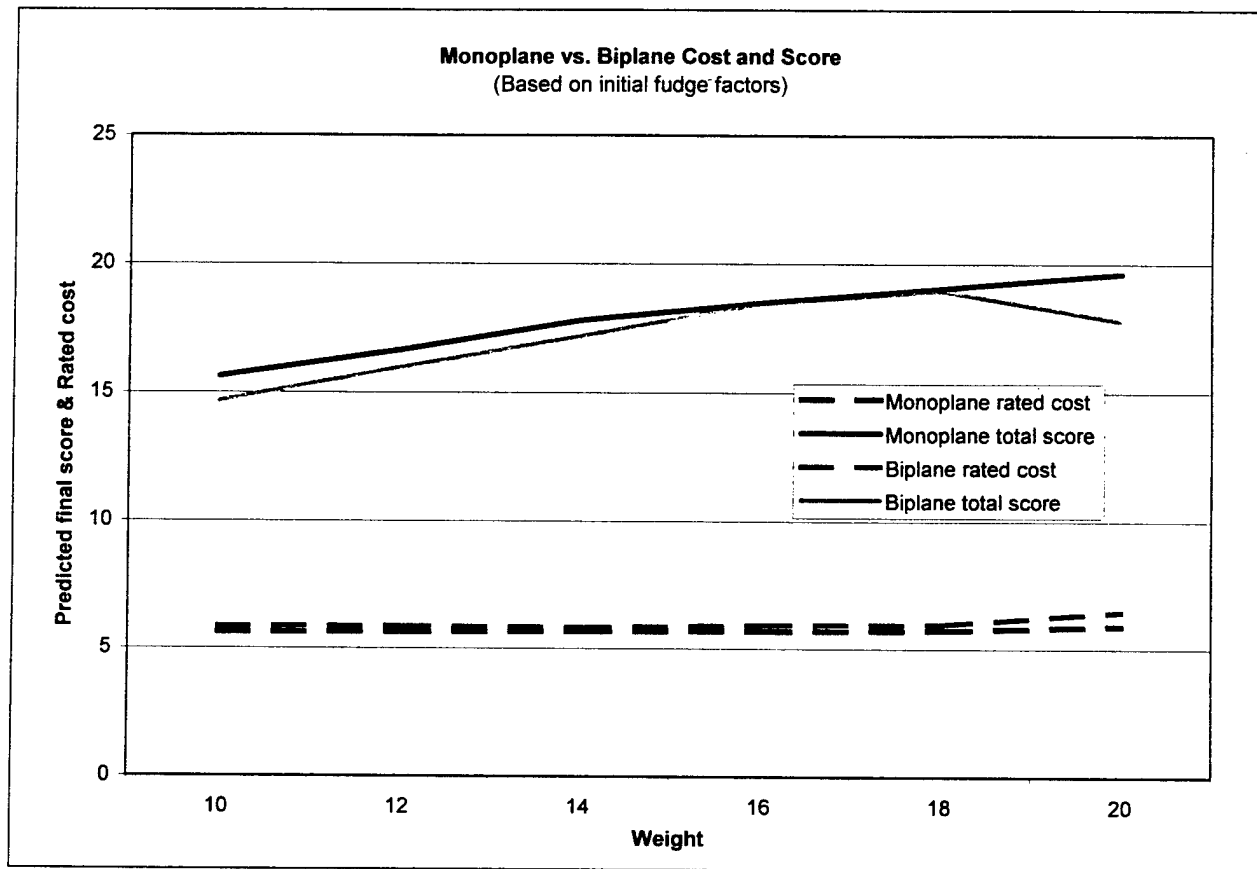


Figure 3.1. Rated cost and final score curves for various weights in monoplane and biplane configuration.

4. Preliminary Design

4.1. Design Tools

4.1.1. Mission model

The mission simulator, called "Mission" was an Excel spreadsheet originally written to support the 1997/1998 AIAA efforts. It consists of an Excel workbook with several spreadsheets that model various components of the aircraft during a scoring flight. It models all legs of the flight including: takeoff, cruise, turning flight, descent, landing, and ground handling. Some of the different modeling spreadsheets include: electrical, propulsion, weights, cost and aerodynamics. All these pages take geometry inputs from the user and rapidly evaluate different aircraft configurations and score the design based on payload carried and the cost of the craft. Some of these inputs are: airfoil type, wing area, propeller diameter and advance ratio, motor and gearbox type and count, battery type and count, and amount of payload carried. "Mission" derives its primary parameters from these inputs plus throttle setting, airspeed, initial altitude, aircraft weight, and load factor of each leg. This data from each sheet is used to calculate the energy consumption, time required, and altitude change for each leg. The output consists of the sum of the total energy and time consumed and predicts how many sorties will be completed given the initial parameters and constraints. The overall score is determined by multiplying the total number of sorties completed by the amount of payload carried then dividing by the calculated cost of the airplane. Figure 4.1 shows the organizational structure of "M".

Over the years, "Mission" has been modified to more accurately predict performance based on previous years data. This year, the flight test data from SCarface was incorporated. For example, last year the team added a thermal analysis model for the motor, battery pack, and controller based on Newtonian cooling and convective heat transfer. This feature also included a complete thermal time history. This year's flight profile and cost function were added to "Mission" at the start of school year, and the team initiated a careful design analysis. In addition, a "save configuration" feature that copied all inputs to an archive was added. This allowed rapid comparisons with earlier baselines and last year's plane.

USC Aero Design Team "SCorpion"

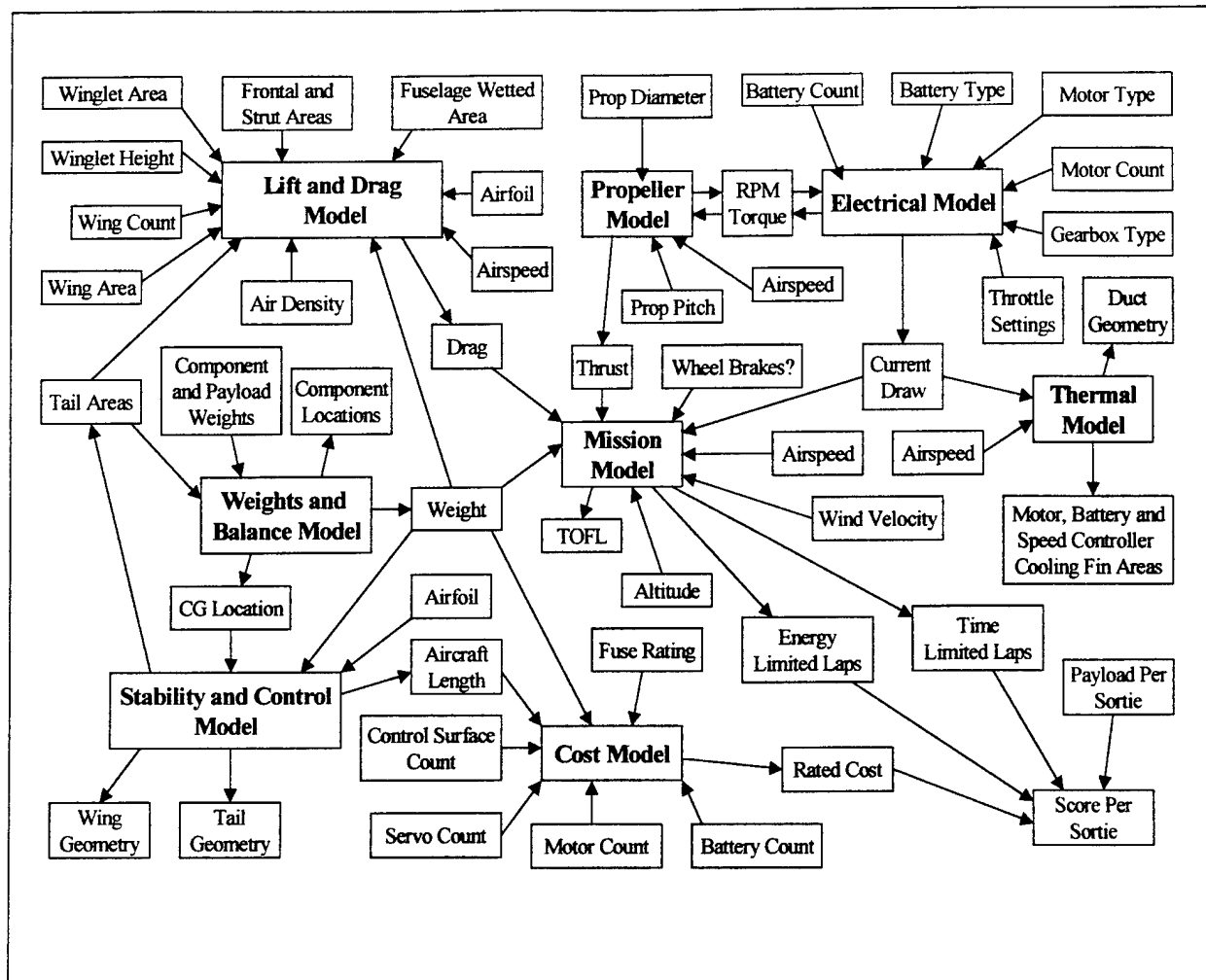


Figure 4.1. "Mission" organizational chart

Since wind is a non-trivial contributor to energy consumption, a wind effects model was added to this year's analysis. Wind was accounted for in all flight phases except for takeoff where it would be non-conservative. Upwind penalties were found to be larger than downwind credits on both energy and time. A wind of 15fps (10mph) was selected as a reasonable value for moderately adverse winds. All future design work assumed this level of wind. As a result of this modification, the airplane optimized at slightly higher flight speeds to counteract wind effects.

Concern over poor climb performance last year prompted the addition of rate-of-climb (ROC) versus airspeed plots for the 2 payload cases. A minimum ROC of 300fpm seemed necessary for acceptable altitude loss in the first turn. Figure 4.2 showed whether the airplane lost climb rate with reducing airspeed (backside handling), which can make landing difficult. This year's plane was found to have a much better ROC than last year's plane. Also, ROC became a tie-breaker between the final two configurations with similar total scores. Finally, macros were added to accelerate convergence for the user. These include; wing area convergence to a target TOFL, top-of-climb altitude convergence to

maintain a 30ft minimum en-route altitude, and throttle convergence to balance energy and time-limited lap scores (this was found to always improve overall score).

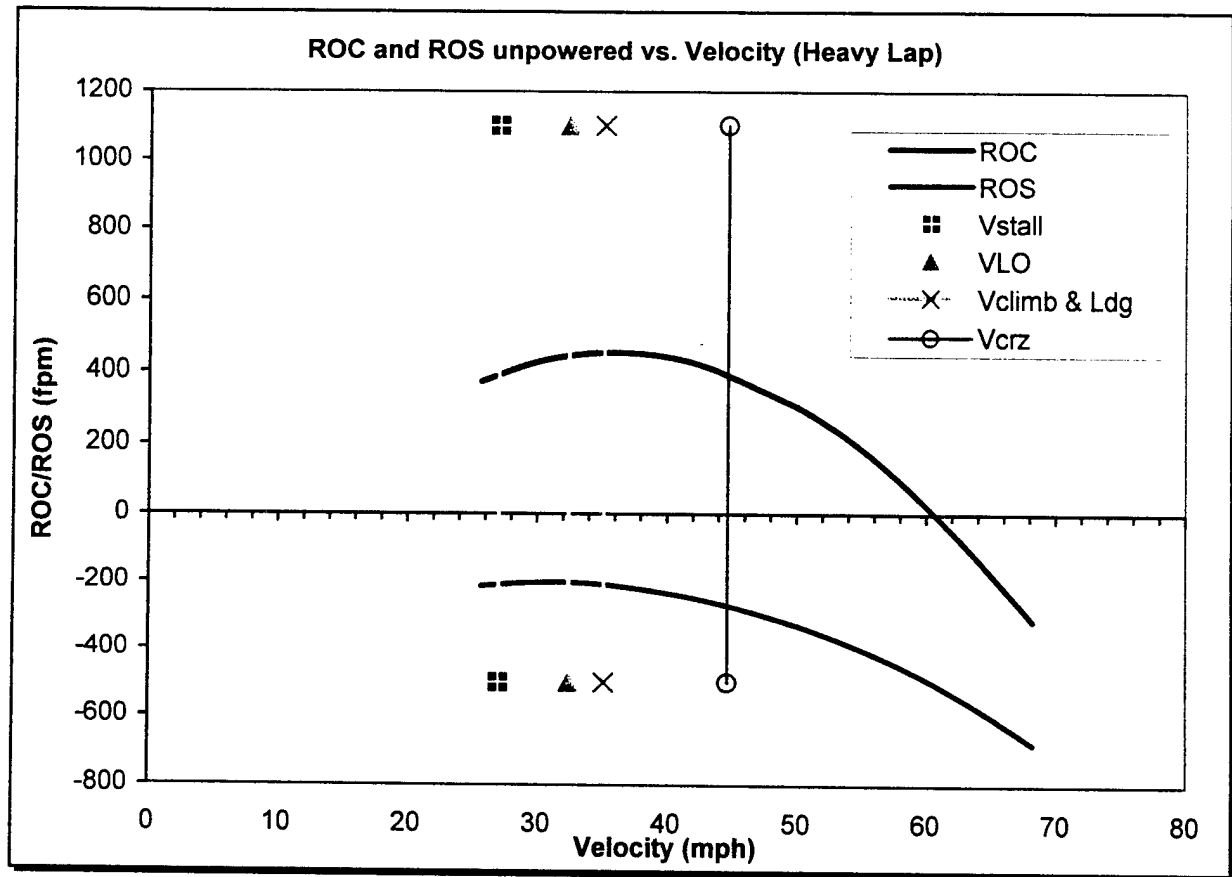


Figure 4.2. Rate of Climb and Rate of Sink chart generated by "Mission"

This page was later expanded to summarize all the parameters that could be useful in the field during flight-testing. In this way discrepancies with the spreadsheet were immediately detected. The summary sheet lists target flight speeds, takeoff field length, recommended control deflections, target c.g., static thrust, static rpm, flap-to-elevator gearing ratio, and aileron-to-rudder gearing ratio. As a result of having a prototype aircraft, the accuracy of the predictions could be determined. Now the team could rely with confidence on the performance predicted from "Mission". With these new additions, many configurations were evaluated to arrive at the best design solution.

4.1.2. Electrical model

The electrical model is designed to analyze electrical motors used for small aircraft. The equations programmed into "Mission" follow the analysis presented by R.J. Boucher (1995). Inputs into this page include: throttle setting for each leg, propeller diameter and pitch, number of battery cells, volts per cell etc. taken from the input page of "Mission". Using the selected motor, battery, and gearbox type, it calculated the values of torque, voltage, current loaded and unloaded, and resistance. The electrical

USC Aero Design Team "SCorpion"

model sets an initial value of current, and the propeller page provides efficiencies and coefficients of thrust and power. It then feeds this data into a set of formulae to calculate thrust, motor RPM, and power. A feature in Excel called "goal seek" then adjusts current draw until it matches the current needed to spin the propeller at the desired RPM. This current is then used to find the energy consumption, thrust produced, and total system efficiency to export to the front page of "Mission".

4.1.3. Propeller model

This model takes the propeller diameter and pitch and generates a map of thrust and power coefficients, C_T and C_p respectively. A plot of these coefficients and efficiencies (Figure 4.4) was then generated from this data and brought to test flights for comparisons with actual measured thrust. During test flights, differences between the predicted and measured thrust resulted in another efficiency multiplier added to the propeller model.

4.1.4. Weight model and stability & control

The weight of the plane is calculated by summing the weights of the individual components. For the constructed materials, a weight estimate was made from the calculated volume of material used in the design multiplied by the density of the specific material. For pre-manufactured parts, i.e. motor, propeller, batteries etc., their weights were stored in their respective models. The weight page looks up the component weights from each of the component pages and adds them to find the total weight of the aircraft.

Since "Mission" calculates weights for all of the significant sub-components it was decided to install last year's balance spreadsheet directly into "Mission". At the same time, the stability & control spreadsheet provided by Mark Page (team advisor) was installed in "Mission" as well. A 2-view drawing of the airplane appears on the S&C page. The estimated actual c.g. location was added to the 2-view drawing so it could be readily compared to the desired c.g. for S&C. Shifting the wing position on the fuselage allowed the designer to balance the airplane by aligning the two c.g.s. Target stability criteria were modified based on test flying with the prototype, and an S&C pass/fail alert was added to the global pass/fail test. Figure 4.5 shows the weights model, and Figure 4.6 shows the S&C model.



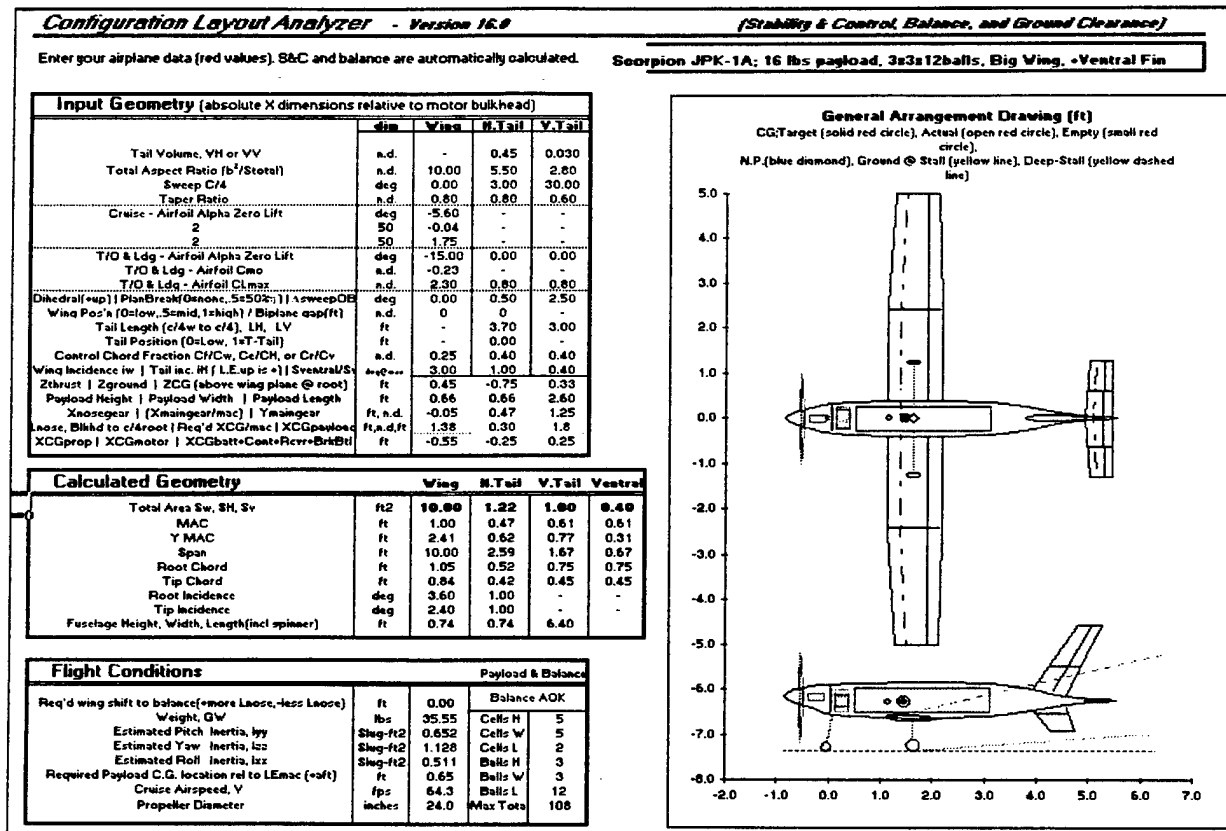


Figure 4.5. S&C summary page

4.1.5. Cost model

The model for calculating the cost function of *SCorpio* was obtained from the rules of the contest. Cost parameters such as fuselage length, wing area, motor count, battery count etc. were drawn from the input page by the cost model in "Mission". Calculating the cost of *SCorpio* was a relatively simple programming task in Excel.

4.1.5. Aerodynamic (lift and drag) model

Several airfoils taken from an already existing airfoil database were analyzed to find the optimal one for the final airplane. The Lift to Drag ratio, angle of attack, and stall speed were some of the data taken into consideration in the choice of the wing's airfoil shape. A comparison of the drag polars generated by several different airfoils, shown in Figure 4.7, proved the LA-203 to be the best choice for this particular plane. The plotted drag polar using the C_l and C_d data from our analysis provides an indication of how to fly the plane and possible aerodynamic problems that might occur in flight.

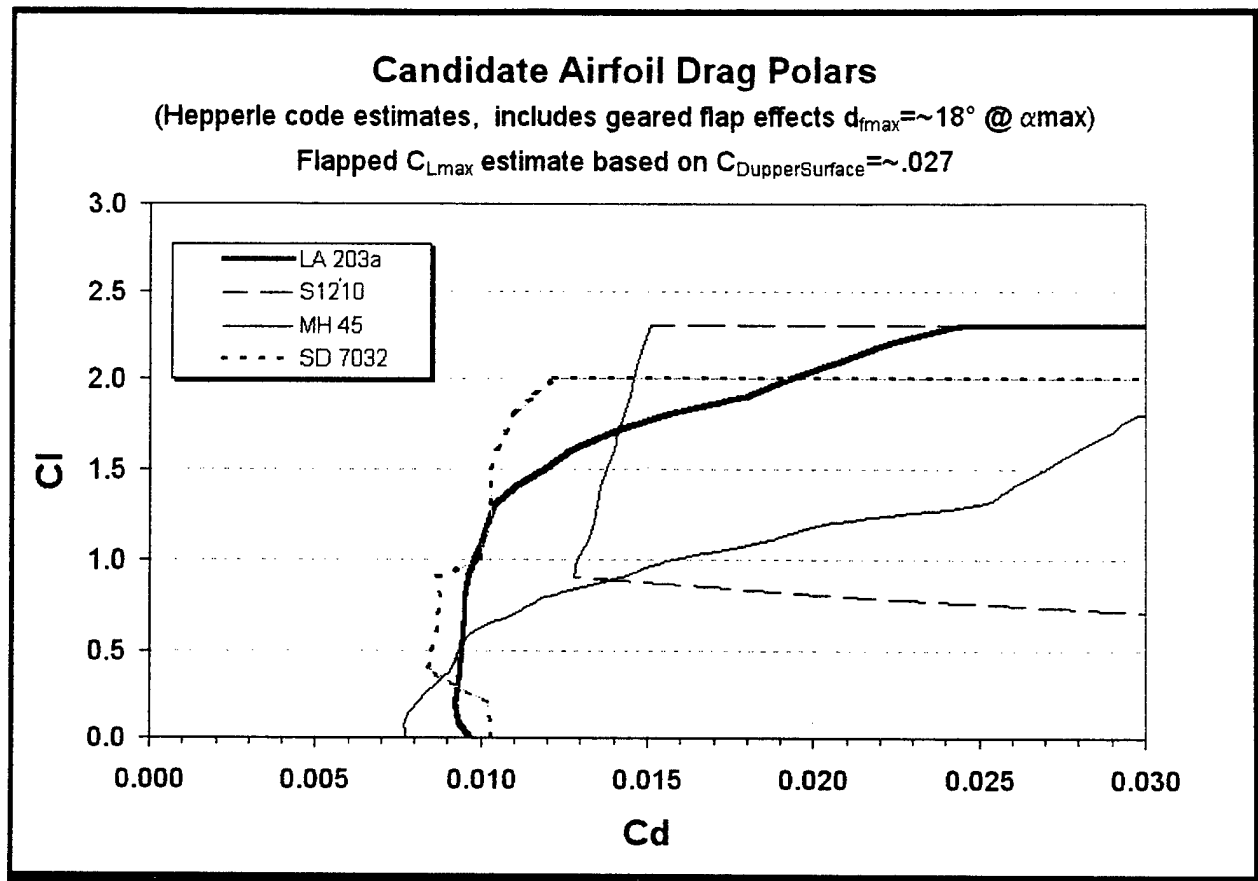


Figure 4.6. Drag Polar of four competing airfoils: LA 203a, SD 7032, S1210, MH 45

4.1.6. C.G. optimization model

The fuselage was the main structure to which the other airplane components were attached. The proper c.g. location was needed for the aircraft to have nominal longitudinal control qualities. A balance spreadsheet located in "Mission", shown in figure 4.5, was used to balance the aircraft for a design c.g. location at 30% of the wing root chord (measured from its leading edge). The location of each component, such as the receiver, battery pack, payload, brake system, and motor, was measured with respect to the motor bulkhead. Knowing the weight of each component, the expected location of the c.g. was then determined. If the design c.g. location was not reached, then the wing position was changed to correct the problem. The payload c.g. was located near the empty aircraft c.g. so that the presence (or lack thereof) of the payload did not normally cause a large C.G. shift but it could be used to trim the aircraft.

4.1.7. Thermal analysis model

Overheating caused much trouble in previous electric aircraft. To model and design for these conditions, "Mission" included a thermal model that covered the motor, battery, and speed controller. This is discussed in detail in the detailed design section.

4.2. Optimization Parameters

Once the biplane configuration had been ruled out, the task remained to optimize the monoplane. The following parameters carried the most weight in terms of affecting aircraft performance.

4.2.1. Payload

The amount of payload carried has a large effect on final score of any craft. Since a considerable amount of time and energy is expended in landing, ground handling, take-offs, etc. the analysis showed that a plane carrying 100 tennis balls will do better than a plane carrying any smaller number. Since 100 tennis balls weigh approximately 13.2 pounds, a similar amount of weight in steel should be carried. The key to the optimization process is to find the point of diminishing returns between the added score of payload and the additional cost of wing area.

4.2.2. Wing area

Wing area contributes greatly to aircraft performance. Wing area affects TOFL requirements and ROC. To put more payload on a given plane, the wing area must increase to provide lift for the added weight. Since the cost increases with wing area, there is an optimal wing area in the design.

4.2.3. Airfoils

Energy consumption and TOFL dominated the airfoil selection. The aircraft's low Reynolds makes exotic airfoils attractive. The lift and drag of the wing has a direct relationship to the airfoil shape. An airfoil must have a very blunt face, so that a C_D is a minimum at operating C_L 's.

4.2.4. Winglets

Winglets have a desired effect of increasing the effective span of the wing, therefore reducing its induced drag. But winglets come with a price in the cost model. The 10' wingspan limit allowed for a sufficient span to a point where the increased benefits of winglets did not outweigh their cost. Additional weight would have to be added to meet the design requirements of lifting the craft by the tips. These factors influenced the decision to fly without winglets.

4.2.5. Propeller diameter/pitch

Propeller size determines such things as thrust, and current draw. Available thrust affects TOFL, cruise speed and ROC. Current draw has proven to be a key parameter in this design. The amount of current the motor draws is modeled in the cost function. As a result, the motor wants to spin faster and use a smaller prop to draw less current. But, in order to take off with all necessary payload, a large prop is desired to produce sufficient static thrust to take off and the larger prop will draw more current. A reduction in current by 10 amps (i.e. 30A max current vs. 40A) will produce a 5% decrease in cost. So a tradeoff between static thrust and aircraft cost must be made.

USC Aero Design Team "SCorpion"

Along with diameter, an increase in pitch will produce increases in static thrust and current draw. Gearboxes allow for a larger prop and may even reduce the current draw depending on their gear ratio. Again, an optimization must be employed to find the optimal pitch and current draw.

4.2.6. Motor type/count

The rules of this year's contest limit the type of motor to be used. The predicted performance of these motors were taken from their manufacturers and placed in "Mission". These few motors were then paired with gearbox and propeller combinations for analysis. The design analysis found two motors, the FAI 60, and the Pattern 90 that out performed the others as shown in Figure 4.8. Both motors produce similar scoring configurations, but flight tests may determine the more reliable of the two.

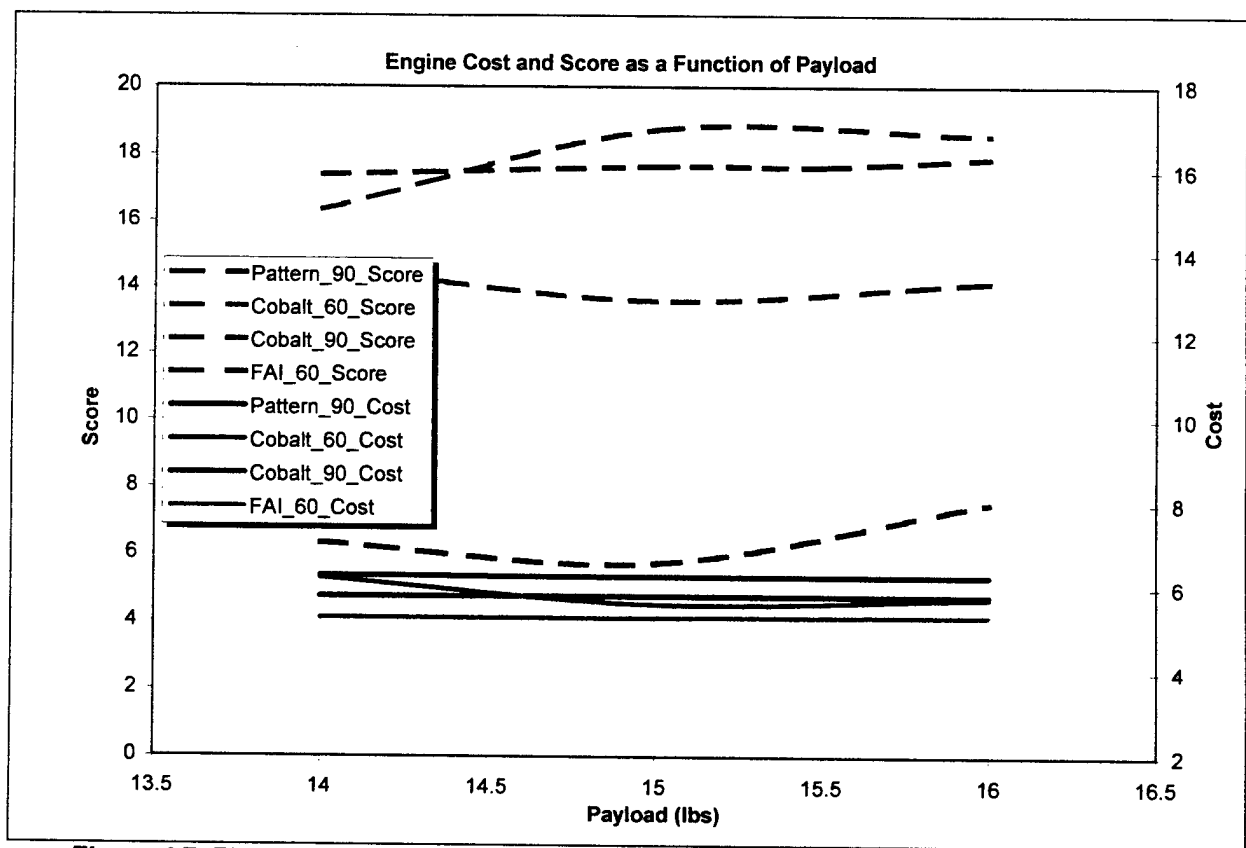


Figure 4.7. Plot showing rated cost and final score of competing motors for a range of weights

4.2.7. Battery type/count

The rules allow a maximum of five pounds of Ni/Cad batteries to fly the plane for ten minutes. Energy consumption was modeled very carefully in "Mission". After last year's flying showed actual battery lives having 50% of their predicted values, an independent study was undertaken to understand this problem. It was determined that draining a battery pack at such high currents adds additional losses due to heat and nonlinear internal resistance. As a result, the competition plane was designed with a much lower battery life expectancy than the prototype, as discussed in the next section.

4.2.8. Battery life expectancy

After extensive bench and flight-testing with the battery packs, the team discovered that at discharge rates near 35 amps the batteries yielded 65% of their predicted capacity. The SCarface flight test confirmed this 65% battery life factor. Aircraft optimized with an 80% battery life that then had a 65% battery life inserted into the design-spreadsheet produced an average decrease in final score of almost three points (~17%). By optimizing the cruising velocities and the payload weights the team produced an aircraft that performed well under these conditions. Ultimately, the optimization of the aircraft using the 65% battery life factor resulted in a decrease of the final score by one and a half points (~8%) compared to the earlier results.

4.3. Configuration

4.3.1. Fuselage structure

The 100-tennis ball payload set the shape of the aircraft. Tennis balls had a low density and were difficult to package efficiently. In addition, a single removable cartridge containing the cargo (i.e. a speed loader) was desirable to speed ground handling. These constraints placed stringent conditions on the location of the bulkheads and load paths. Also, for stability purposes the payload C.G. must be near the aircraft C.G. since two very different payloads were being used. Most of the fuselage design process occurred in the detailed design section.

4.3.2. Motor location

The cost function and mission simulators highly favored single motor configurations. These configurations reduced weight and cost without adversely affecting performance. The prop clearance and C.G. issues associated with pusher propeller designs made them highly unfavorable, so a nose mounted tractor configuration was adopted.

4.3.3. Payload access

Front, rear, side, and top loading configurations were analyzed. The nose-mounted motor made access through the nose undesirable. Loading through the tail would disrupt the load paths from the tails to the main structure, making it an undesirable solution. Hatches in the side, aft, or bottom interfered with the wing, landing gear, or tail surfaces. These other hatch options also needed greater fuselage structural integrity to support the wing, which increased their overall weight. A top hatch would restrain the payload on all four sides. Gravity would also assist in keeping the payload inside the fuselage during flight. The lack of benefits of the alternative configurations and their problems led to the selection of a top-loading configuration.

4.4. Wing

4.4.1. Dihedral

The use of dihedral in the wing was closely examined. Wing dihedral would offer distinct benefits to the aircraft's stability. However, wing dihedral would complicate the wing design. Continuous wing spars are highly favorable since they are lighter, simpler, and stronger. A continuous, properly supported spar with dihedral would weight significantly more than a part without dihedral. Dihedral also impacts handling in crosswinds. Even though dihedral added a restoring moment to a crosswind disturbance, the period of that action was not small enough for easy landing. Flat wings are less sensitive to gusts, reducing problems on landing. Despite the stability benefits of dihedral in the wing, the team decided to use a flat wing.

4.4.2. Low or high wing

The wing location severely impacted the aircraft configuration. High wing configurations have better tip clearance than low mounted wings, allowing for shorter landing gears. However, high wing configurations complicate top loading payload arrangements since the wing spar interferes with the hatch. Low wing designs also experience more ground effect for improved lift at takeoff and a shorter TOFL. Having a low wing also shortens the load path between the landing gear, spar, and fuselage structure. This eases design and manufacturing and reduces weight. Low wing configurations have several benefits over high wing configurations.

4.5. Tail

4.5.1. V-tail

A V-tail configuration was initially favored because of its simplicity of mounting and the fact that it has fewer surfaces to make. They do not give an advantage in wetted area, however. To account for the shortened fuselage, the tail would have to be large. This would make it impossible to fit a V-tail in a small shipping box unless it incorporated removable joiners. These joiners would increase tail weight, and would be fairly difficult to make for a V-tail. Ultimately the greater difficulty and minimal benefits associated with the V-tail led to a conventional tail choice.

4.5.2. T-tail

Prior experience with T-tails, found that they tended to be heavy. Although the extra tail arm is helpful, this year's focus on weight made a T-tail undesirable.

4.5.3. Ventral fin

As the design progressed it became apparent that the plane would need something to limit its maximum ground angle. This would prevent it from taxiing in deep stall rather than taking off. The need to fair a long skeg made it desirable to have this serve some aerodynamic purpose. The vertical tail was

thus shifted downwards, with the reinforced lower portion serving as the ground angle limiter. The need to have the tails be one piece for cost equation reasons led us to offset the horizontal from the vertical tails, with the sweep of the vertical compensating somewhat from its more forward location.

4.5.4. Offset vertical tail

The location of the vertical fin with respect to the horizontal stabilizer was important in characterizing the airplane spin tendencies. A flat-spin, or any loss of rudder authority, was possible if the stabilizer stalled in front of the fin. This would result in the rudder seeing turbulent air and becoming useless for lateral control. Avoiding this scenario meant placing the stabilizer far enough behind the fin to ensure that a stalled stabilizer did not affect the majority of the flow over the rudder. A ventral fin also provided redundancy in case the vertical fin was stalled and also prevented inverted spins.

4.6. Brakes

Ground handling qualities are a very important design parameter. The time limit of the flights makes good ground maneuverability important since it reduces taxi time. Brakes allow the aircraft to approach the starting line at high speed and then decelerate at a high rate, significantly reducing taxi time. They also help prevent the aircraft from rolling off the runway and sustaining damage. The rather minimal weight and cost of the braking system and the good results from it in the last contest led to its inclusion in SCorpion's final design.

4.7. Landing gear

When brakes are applied to the main gear, a strong pitch down moment must be reacted. Having a nose gear is the best way to react this load. A tail dragger configuration would have to have enough weight on the main gear to prevent the plane from tipping over and breaking the propeller. The c.g. location to accomplish this would make rotating for takeoff difficult. Also, nose gear configurations protect the propeller since they limit the ground angle in tip-forward situations. Since brakes are being used, a tricycle gear is the most desirable configuration.

5. Detailed Design

5.1. Performance Data

The detailed design process used data from the mission simulator as its foundation. Table 5.1 shows the most important data:

Plane Data			Steel Payload Stability Calculations			
Motor	AstroFlight Cobalt-60 or Pattern-90		Conditions @ Min Airspeed			
Gearbox	AstroFlight 2.7:1		CLmax Trimmed	n.d.	1.92	
Batteries	36 RC-2400		Elevator req'd to Stall Wing	deg	-7.2	
Controller	AstroFlight 204D		Sideslip Angle for Fin Stall	deg	11.1	
Props	Zinger 24x16 or Mens 24x14		Max Recommended Rudder Throw	deg	25.00	
Fuse	35 Amps		Max Sideslip Angle using max Rudder	deg	9.82	
10 ft^2 wing area			Max allowable crosswind for T/O & Ldg mph	5.5		
10 ft wingspan						
LA 203a airfoil			Ground Handling			
			Rollover Angle	deg	49.18	
			Pitchover Angle	deg	54.34	
Predicted Performance Data			Tipback Angle	deg	8.99	
Payload	100 tennis balls	16 lbs steel	Wingtip Strike Clearance	deg	10.92	
Weight w/ Payload	32.8 lb	35.6 lb	Minimum Cornering Radius	ft	8.06	
TOFL	123 ft	150 ft	Max Yaw Acceleration,dy/dt2	deg/s2249		
ROC	500 ft/min	450 ft/min	Stability Characteristics			
n turn (g's)	2.3	1.9	Pitch Stability, Static Margin	%mac	0.16	
V Lift-Off (ft/s)	46	48	Pitch Frequency (@ Cruise)	Hz	1.54	
V Climb (ft/s)	49	52	Pitch Damping Ratio (@ Cruise)	n.d.	0.77	
V Touchdown (ft/s)	49	52	Directional Stability, CnBeta	1/deg	0.00	
V Cruise (ft/s)	67	63	Yaw Frequency (@ Cruise)	Hz	1.13	
V stall (ft/s)	38	40	Instantaneous Roll/Yaw in a side gust	n.d.	0.11	
Energy limited laps	2.96 laps		Lateral Stability	1/deg	1E-04	
Time limited laps	2.96 laps					

5.2. Modeling Process

5.2.1. Solid modeling

The solid model represented the plane at a 1:1 scale ratio. Purchased components such as the batteries, motor, landing gear wheels, servos and speed controller were measured and drawn to scale. The specifications laid down in the Performance Analysis process determined the rough placement of these components and the dimensions and locations of many of the manufactured parts. However, if the configuration warranted a design feature that the Performance Analysis did not previously consider, such as a ventral fin, the simulator was updated to analyze the effects of the new feature.

5.2.2. C.G. determination

The Weights and Balance model helped refine the locations of each major component as new designs were checked against the balance model. When placing a component in its intended position proved impractical, the balance model was adjusted and another component was moved. This process was aided by the realization that the plane did not need to fly without payload, allowing the payload to act as ballast. This ongoing c.g. optimization ensured that the c.g. was at 30% wing root chord, preventing stability and control problems.

5.3. Payload Design

5.3.1. Preliminary analysis

The configuration analysis process began with the configuration of the payload. The objective was to design the most compact payload cartridge able to carry 16 pounds of steel or 100 tennis balls. This meant maximizing the packing efficiency of the balls and efficiently integrating the payload with the aircraft. Some preliminary designs featured tennis balls in hexagonal close-packed arrangements but these did not integrate well with the wing, complicated the cartridge design and tended to be rather long. Cubical cartridges have the highest volume to surface area ratio of any rectangular ball arrangement since they most closely approximate a sphere. The optimal ball configuration was five balls wide by four balls high by 5 balls long (refer to drawing package). Equation 5.1 shows how the ratio of volume to surface area depends on the size of the package:

$$\frac{V}{SA} = \frac{x^3}{6x^2} = \left(\frac{1}{6}\right)x, \quad (5.1)$$

where $\frac{V}{SA}$ is the ratio of volume to surface area and x is the length of the side of the cartridge. This also reveals that the frontal cross sectional area of the cartridge increases with length by a factor of x^2 .

5.3.2. Payload detailed design

Practical considerations entered in to the next stage of the payload design process. The frontal area of the cartridge was limited to half the area of one side of the cartridge, or

$$\frac{SA_{Side}}{SA_{frontal}} \geq 2, \quad (5.2)$$

and the length was constrained so that the overall length of the cargo box did not exceed 36 inches. These constraints were satisfied by a cargo box 3 balls wide by 12 balls long for the first two layers with the remainder of the balls on a third layer. Also, the front of the payload cartridge was angled to facilitate payload ejection.

5.4. Fuselage Aerodynamic Design

To minimize flow separation and drag, the fuselage profile was designed to be second derivative smooth. Unigraphics' solid modeling abilities enabled this by allowing the configurator to analyze the slope of the surface geometry. The output of Unigraphics' surface analysis tool is a graphic that displays the derivatives of the slopes of many points on the fuselage. The surface geometry was then adjusted to eliminate discontinuities. Using the second derivative smooth constraint allowed the aft section of the fuselage to taper tighter than otherwise possible, reducing the length of the fuselage.

5.5. Structural Design

The plane's structural design consisted of a load-bearing shell stiffened with bulkheads. This design has been refined over many years and yields a reasonably light aircraft with an excellent aerodynamic shape. It is also quite durable and very easy to repair.

5.5.1. Shell

The shell was constructed from carbon fiber. Most of the shell used two layers, although the region between the nose and main landing gears incorporated six layers. The fuselage bottom was molded to the wing's root chord airfoil to permanently set the wing incidence angle. The shell had aerodynamic tail mounts molded into it, permanently setting the tail incidence angle and eliminating the need for fillets. A balsa strip set into the side of the fuselage helped stiffen the hatch region.

5.5.2. Bulkheads

Carbon fiber-Nomex honeycomb sandwich bulkheads stiffened the shell and supported concentrated loads like those from the motor mount. These bulkheads were attached to the shell with carbon fiber strips, and the spaces around cutouts in the bulkheads were filled with potting compound to

prevent delamination under load. The bulkheads were placed to accommodate the plane's major components. There were three of them: the forward, traverse and rear bulkheads.

5.5.3. Forward bulkhead

The motor mount and nose landing gear mount required two primary hardpoints in the forward bulkhead. To mount these, the fuselage design included a vertical bulkhead near the nose of the plane. This had large air passages cut into it to allow for airflow to the batteries and speed controller. The area in front of this bulkhead housed the motor and nose landing gear.

5.5.4. Traverse bulkhead

The combined wing and main landing gear mount required another major hardpoint. The traverse bulkhead connects the top of the forward bulkhead with this hardpoint. It forms a triangle with the forward bulkhead and the stiffened skin. The area under this bulkhead housed the battery packs, speed controller, fuse and nose gear servo. A large hole was cut into this bulkhead to allow access into this compartment and reduce weight.

5.5.5. Rear bulkhead

A third bulkhead was required to stabilize the aft fuselage and restrain the cargo from sliding aft. Most of this bulkhead was removed to reduce its weight. The payload compartment was directly in front of this bulkhead. The area behind the bulkhead housed the brake air system, the receiver and receiver battery pack and the tail servos.

5.6. Wing Structure

The structural integrity of the wing was directly dependant on its spar. A linear statics model was used to determine the loads, moments, and stresses along the wing with for a given loading. The wing spar needed to resist a minimum 4g load factor with 50% safety factor.

The maximum predicted load was determined as follows:

$$F_L = C_{g's} \frac{(W_{total} - W_{wing})}{2} SF, \text{ Lift due to weight and max loading (lb.)} \quad (5.3)$$

$C_{g's}$ = max loading coefficient (g's)

$SF = 1.5$, safety factor (n.d.)

W_{total} = aircraft weight (lb.)

W_{wing} = assumed wing weight (lb.)

The tapered wing planform created an elliptical lift distribution with the highest load concentrated at the fuselage side of body. Equation 5.4 showed the analytical description for this loading with x measured from the centerline:

$$w(x) = \frac{4}{\pi} \frac{F_L}{L^2} \sqrt{L^2 - x^2}, \quad (5.4)$$

where L designates the direction along the semi span. Integrating Equation 5.4 over the wing semi span provided the formula for the maximum loading [Equation 5.3]. Therefore, the concentrated load at any distance x from the centerline was found by integrating the area under the curve, as shown in Equation 5.5:

$$F_{L,d} = \int_{-L}^{L-d} w(x)dx = -\frac{F_0 L}{2} \left[\frac{\pi}{2} - \sin^{-1} \left(1 - \frac{d}{L} \right) - \frac{L-d}{L^2} \sqrt{2Ld - d^2} \right]. \quad (5.5)$$

$$\begin{aligned} F_0 &= \text{Lift @ } x = 0 \text{ (i.e., centerline)} \\ &= w(0) \\ &= \frac{4F_L}{\pi L} \end{aligned}$$

Though the term F_0 defined the maximum load in the elliptical distribution, it was neglected because lift from the wing section passing through the fuselage was as a second-order affect due to the wing-fuselage and landing gear interference with the flow and propeller wash.

The center of lift for the area under the lift curve was calculated using the formula,

$$\bar{x}_d = \frac{\int x dA}{\int dA} = \frac{\int x w(x) dx}{F_{L,d}} = \frac{F_0}{3LF_{L,d}} (L^2 - d^2)^{3/2}, (\text{in.}) \text{ with } dA = w(x)dx \quad (5.6)$$

Results from these equations were substituted into the following formulae to calculate shear, moment, bending stress, bending radius, moment of inertia, and core crushing. Not shown are formulae used to calculate shear stress, spar cap strain, spar cap-to-web face wrinkling, and spar cap-to-foam face wrinkling.

- Shear $V_x = F_{L,d}, (\text{lb.})$
- Bending Stress $M_x = F_{L,d}(\bar{x}_d - x), (\text{in} \cdot \text{lb.})$
- Bending Radius $r = \frac{EI}{bM_x} (SF), (\text{n.d.})$
- Moment of Inertia $I = \frac{1}{12}bh^3, (\text{in}^4)$
- Core Crushing $\sigma_{core} = \frac{\sigma_t}{r}, \text{core crushing (psi)}$

Table 5.2. Equations used in spar design

The spar was located at 30% root chord because it coincided with the thickest cross-section of the LA203a airfoil and the center of lift. Maximizing the spar thickness increased the spar moment of inertia and bending radius and reduced the local bending stress, among other effects.

The spar profile came under careful consideration. Tubular spars had excellent resistance to torsion but are not optimal under bending and are difficult for the team to construct. I-beam spars were excellent in bending but were not optimal under torsion, were difficult to construct, and had concentrated loads at the web-spar junction that acted as weak points. A rectangular spar profile was selected for its continuous cross-section, ease of construction, and rigidity under bending and torsion.

The spar sizing process analyzed fiberglass, carbon fiber, aluminum, balsa and spruce spar materials. Carbon fiber was the clear favorite for the spar caps because of its high strength- and stiffness-to-weight ratios, minimizing spar weight. The shear web was moderately loaded in shear and compression, favoring balsa for its low density. Figures 5.1 and 5.2 show the shear and moment diagrams for the wing semi span. The spar cap and shear web stresses were plotted against the ultimate loading stress of the material in Figures 5.3 and 5.4. The compression loads experienced by the shear web sized the spar width to 3/8 inches.

The spar was designed for ease of construction and minimum weight. Structural joiners are complicated, heavy, and failure prone, so they were avoided by making the spar one piece. The spar height tapered to match the local thickness-to-chord ratio of the airfoil, a property modeled in the analysis.

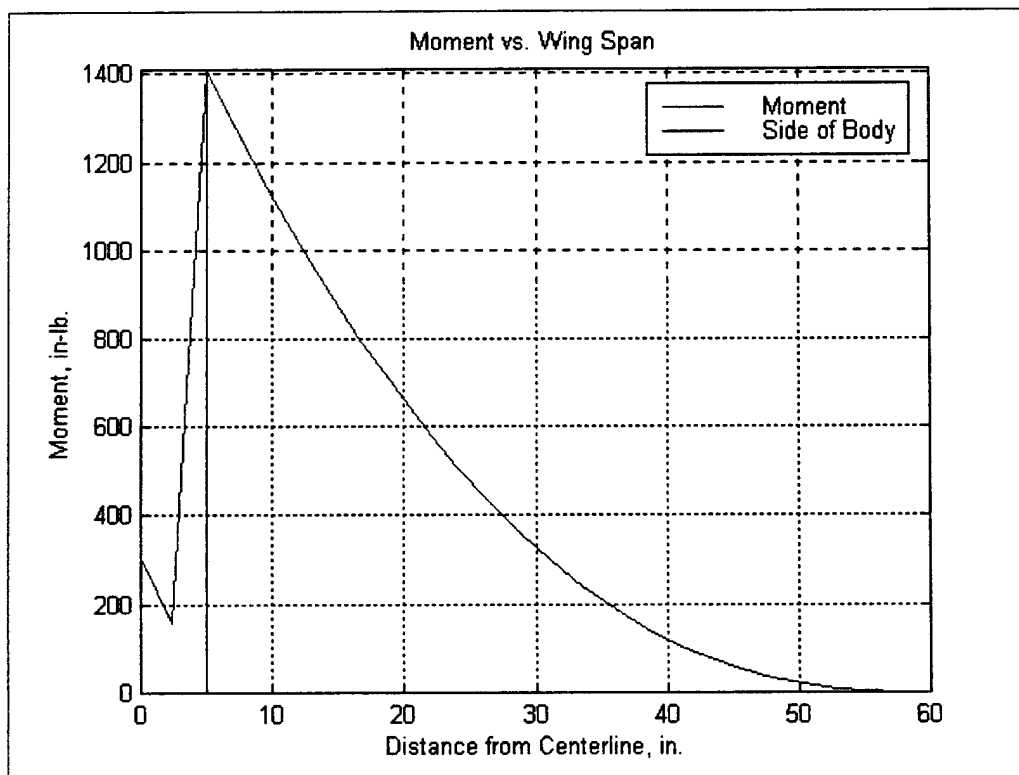


Figure 5.1. Moment distribution across the wing semi span

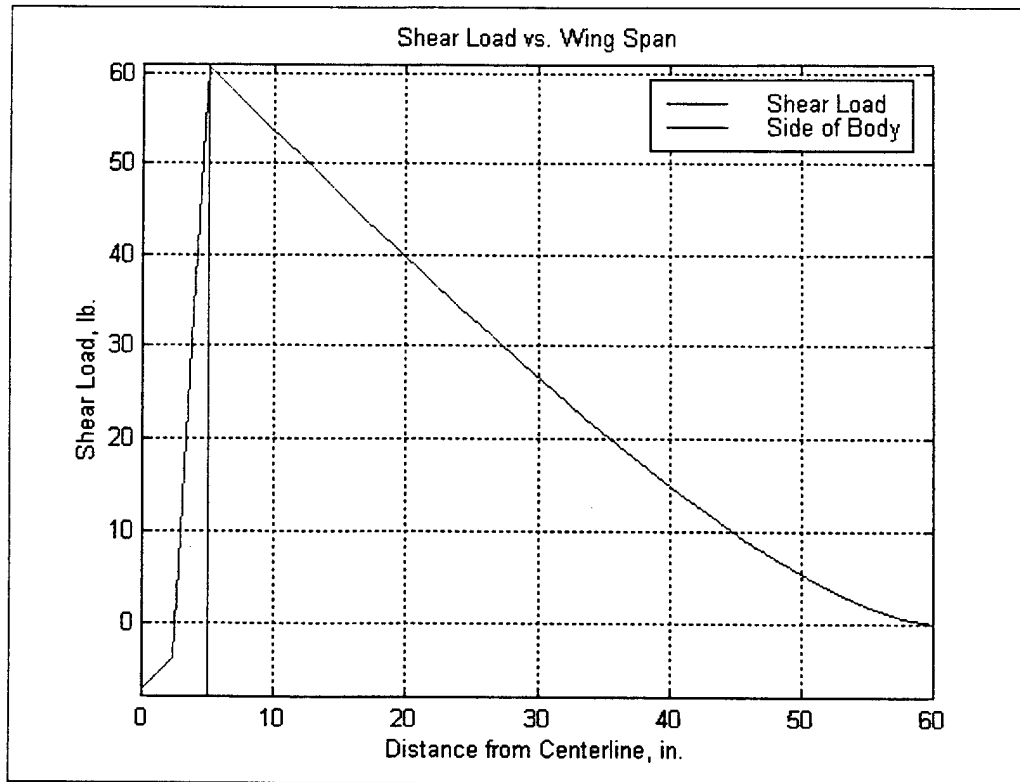


Figure 5.2. Shear distribution across the wing semi span

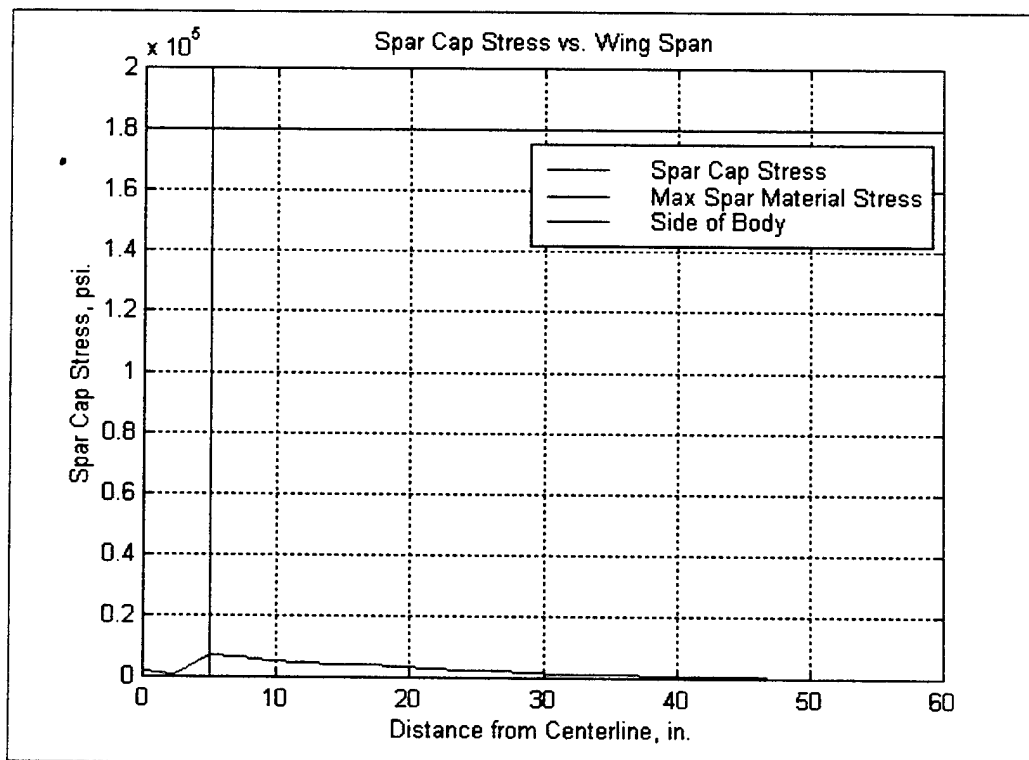


Figure 5.3. Spar cap stress distribution across the wing semi span

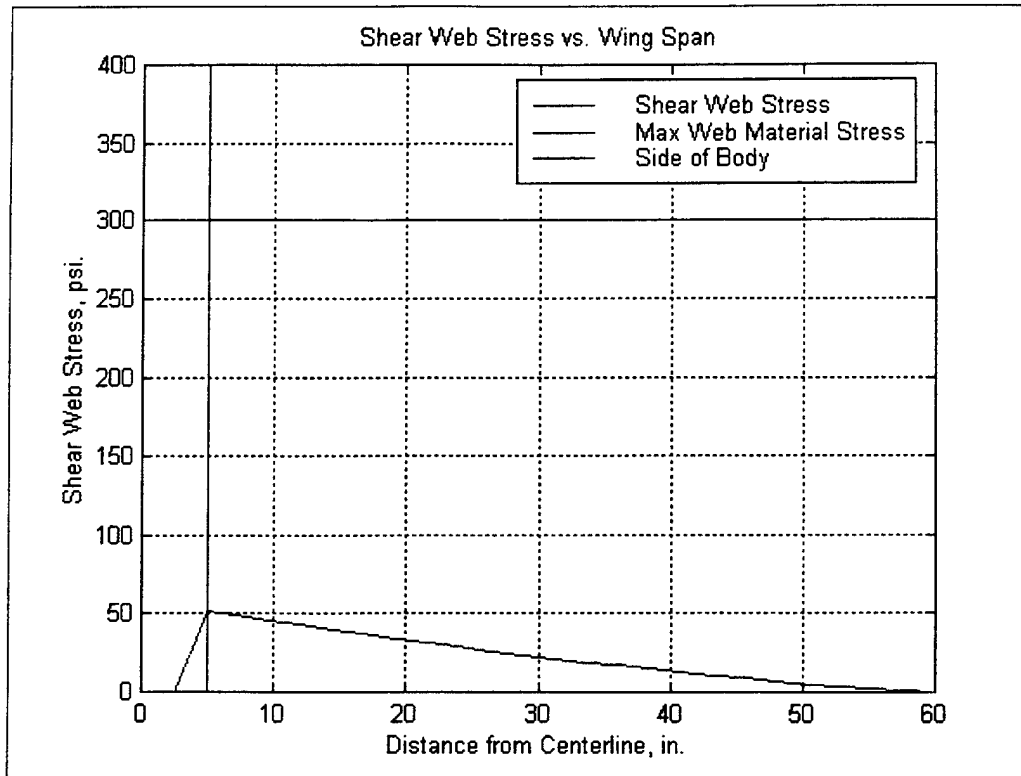


Figure 5.4. Shear web stress distribution across the wing semi span

5.7. Landing Gear

5.7.1. Nose gear

We purchased our nose gear from Robart, Inc. because they had performed well in the past. The nose gear was attached to the forward bulkhead using a steel mount included with the strut. The strut was lengthened by four inches by adding a section of threaded rod and aluminum.

5.7.2. Main gear

The main landing gear was designed on Solid Landing Gear Design, a piece of custom software written by Blaine Rawdon, one of our industry advisors. The main inputs into the Excel spreadsheet were the aircraft weight, the vertical and horizontal distances from the axles to the fuselage mounting bolts, the angle between the c.g. and the main wheels and the height of the c.g. Other inputs were the sink rate, the maximum load factor during landing and the limit shear and axial stresses of the materials.

After determining the geometry and layup schedule of the gear, the design tool produced a graphic showing the shape of the gear when unloaded and at maximum deflection. The program also graphed the stress and strain along the landing gear. The optimum number of layers was found by adjusting the design until the levels of stress and strain were mostly uniform and beneath the material's limit. The landing gear was designed to survive a one-leg touchdown at the maximum sink rate. The final

landing gear design had forty-two layers of unidirectional carbon fiber running along the curve of the gear and eight running across the curve.

A major landing gear design goal was to combine the wing and landing gear mounts into a single hardpoint that straddled the spar. This simplified the load paths and lightened the attachment structure. To achieve this goal it was necessary to sweep the landing gear 5° aft. Since the landing gear design tool did not support this, the landing gear data were imported into Unigraphics and the sweep was added. The landing gear was then analyzed on COSMOS, a finite-element analysis program linked to Unigraphics. A check on the stress levels during landing resulted in the addition of four plies running along the curve of the gear.

Parameter	Value
Design sink rate	9.12 ft/s
Design aircraft weight	40 lbs
Design load factor	4.5 gs plus 1.5 safety factor
Maximum distance between struts	28.7 in
Height	8.25 in
Sweep	5 degrees

Table 5.3. Summary of the landing gear design parameters.

5.8. Component Mounts

5.8.1. Motor mount

The motor mount had a balsa core wrapped in carbon fiber. This part was designed to fail where the motor boom joined the rest of the mount. The motor mount was secured to the forward bulkhead with three nylon bolts, and plywood doublers were bonded to the mount at these places to reinforce the boltholes. The motor was secured to the pylon with screws in front and a pipe clamp in back, as seen in Figure 5.5.

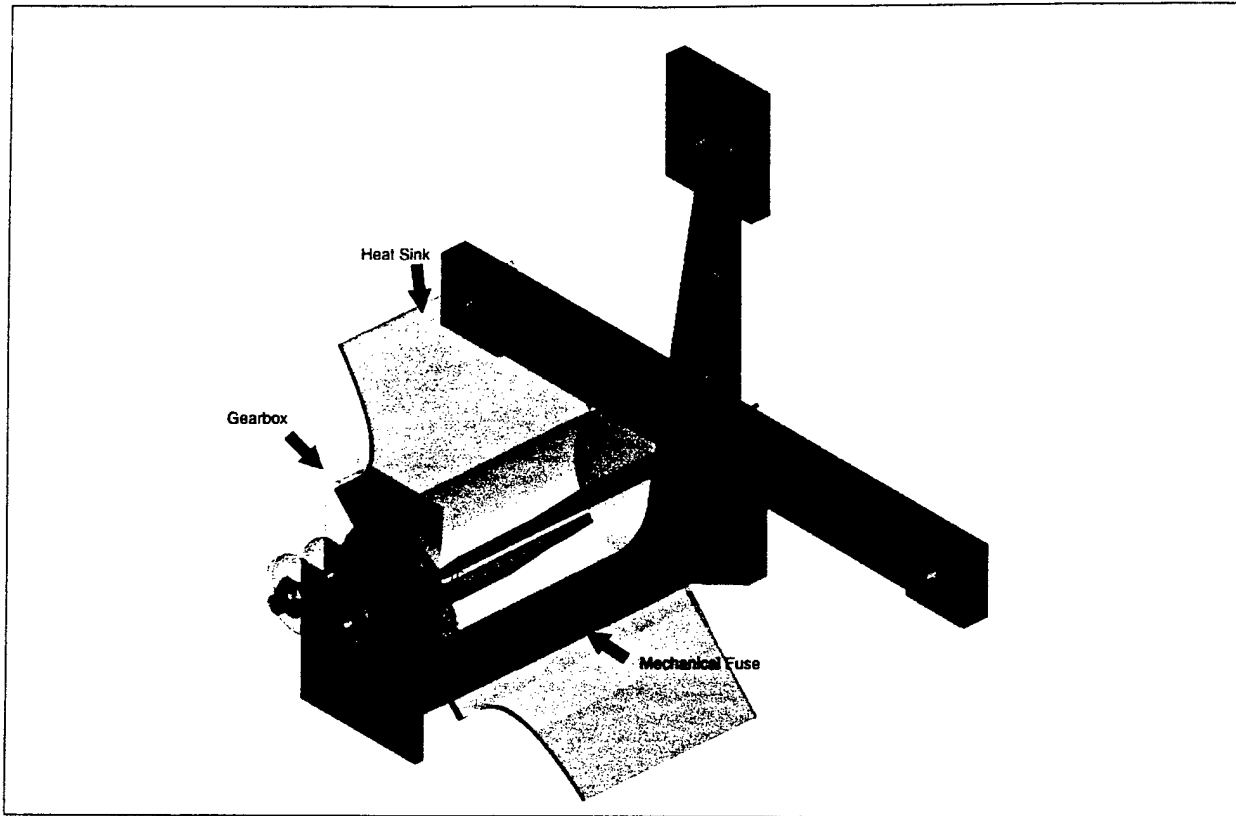


Figure 5.5. Detailed motor mount illustration.

5.8.2. Tail mounts

The tails mounted to the fuselage with structural fairings molded into the fuselage. The horizontal and vertical tails were secured to their mounts with tape.

5.8.3. Wing and main landing gear mount

The wing fit into a saddle molded into the fuselage. The wing and main landing gear mounted to the shell with a single set of four nylon bolts secured with nuts and washers.

5.8.4. Payload mount and access

The payload was accessed through a hatch on top of the fuselage. The hatch opened to the side and was secured with a Kevlar fiber hinge on one side and a latch on the other. The payload was secured with Velcro tape.

5.8.5. Electronics mounts

Most electrical components were mounted to the fuselage with Velcro. Additionally, the batteries fit into raised channels in the fuselage.

5.9. Cooling Design

Cooling the propulsion system was not a trivial consideration. Without careful design, motor overheating can cause in-flight failures and battery overheating reduces energy capacity, can shorten battery life and can cause catastrophic failure. The thermal model predicts the temperature of the motor, battery pack and speed controller over the course of the mission using a Newtonian cooling method with forced convective heat transfer to model heat flow. The outputs from the thermal model are depicted in Figure 5.6. The cooling design process involved adjusting the component cooling fin area to keep component temperatures within their manufacturer's tolerances. The required duct areas (shown in the drawing package) were determined by the serial nature of the cooling flow and the battery's temperature requirements. Table 5.4 lists the important data for the design of the cooling system.

	Motor	Battery	Controller	
Length of cooling surface	3.75	3.5	2.4	in
Behind motor's airflow?	-	Yes	Yes	
Behind batteries' airflow?	No	-	Yes	
Behind controller's airflow?	No	No	-	
Area of Inlet	16.00	10.67	1.33	sq-in
Area of duct at object	12.00	8.00	1.00	sq-in
Area of exit	8.00	5.33	0.67	sq-in
Surface area of bare object	0.17	1.25	0.05	sq-ft
Heatsink fin surface area	30.00	0.00	0.00	sq-in
Number of Fins	8	-	-	
Width of Fins	0.02	-	-	in
Length of Fins	3.00	-	-	in
Height of Fins	1.25	-	-	in

Table 5.4. Cooling system data

The aircraft was designed to ensure sufficient airflow over the propulsion system elements. The thermal analysis section of "Mission" calculated the necessary duct geometry and cooling fin area. The nosecone was shaped to provide the inlet and duct area for the entire propulsion system. Room was left around the battery packs to give them sufficient airflow. Exhaust holes were cut into the rear of the battery compartment, and faired vents were placed over these holes to enhance their suction.

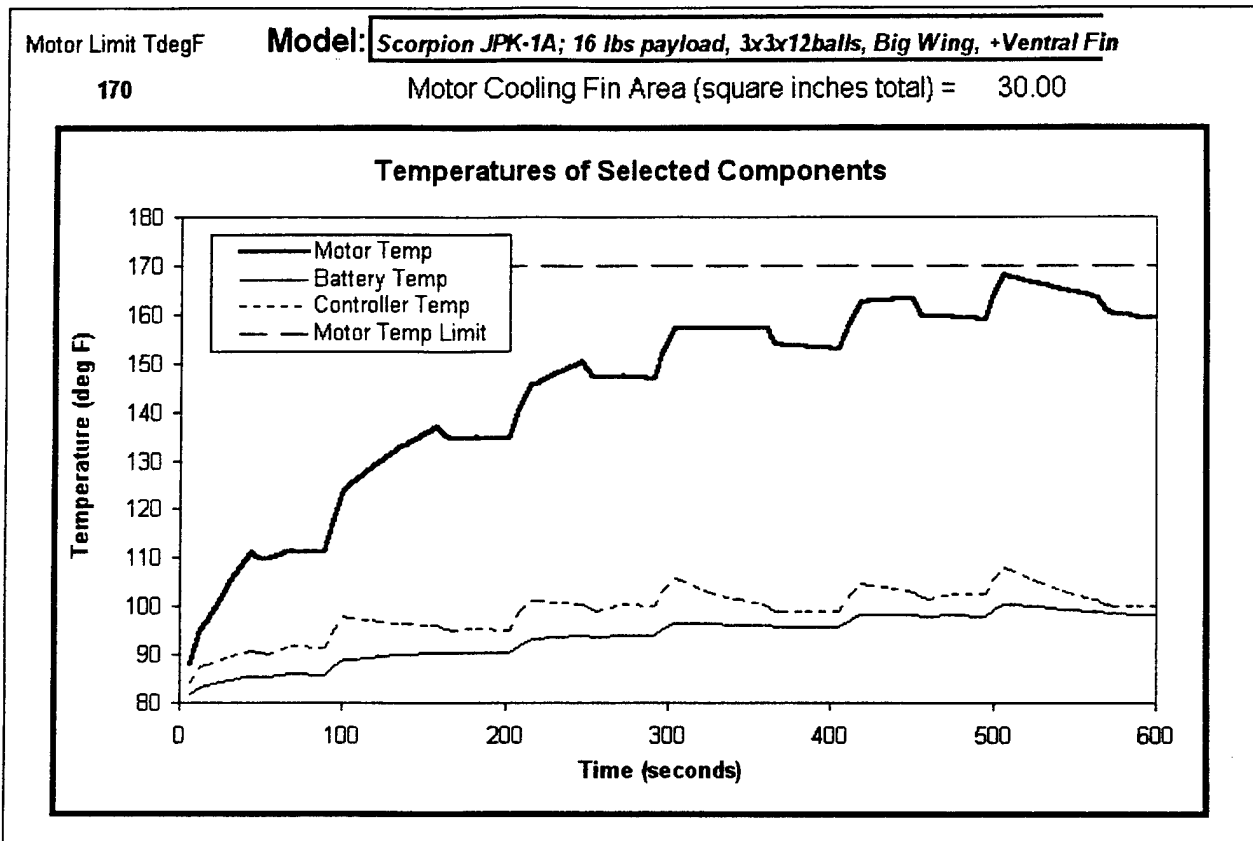


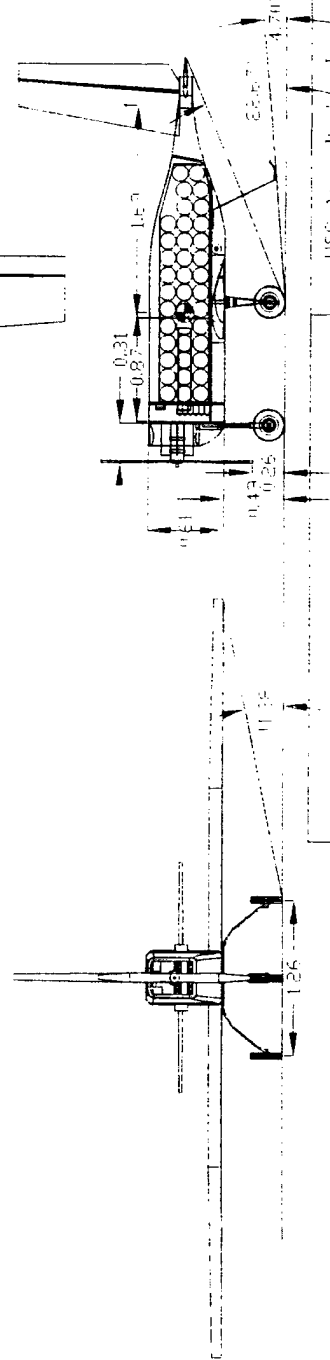
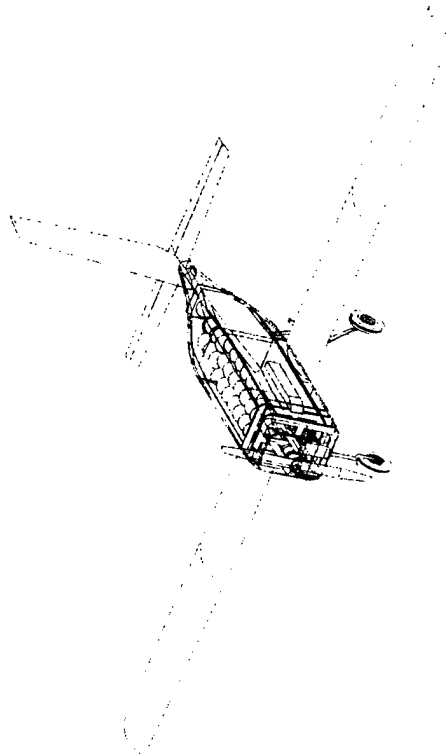
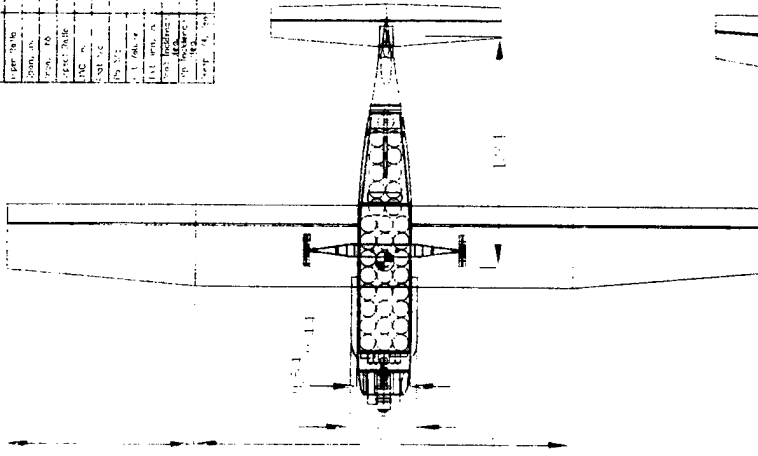
Figure 5.6. Motor, controller, and battery temp vs. time for a scoring flight modeled by "Mission"

5.10. Nose Design

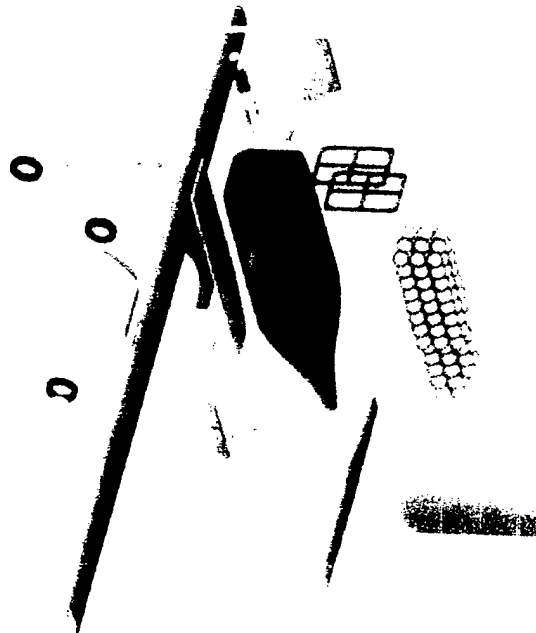
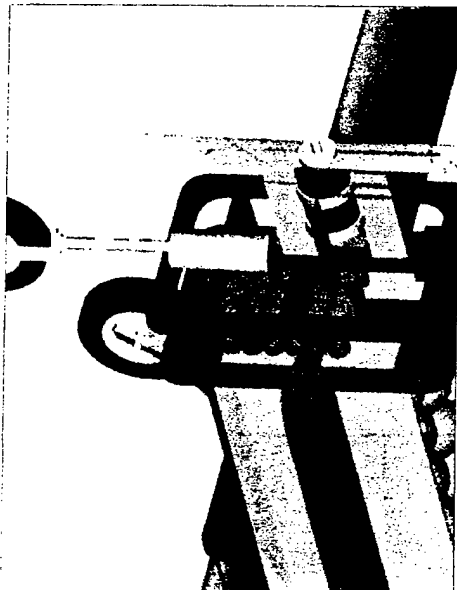
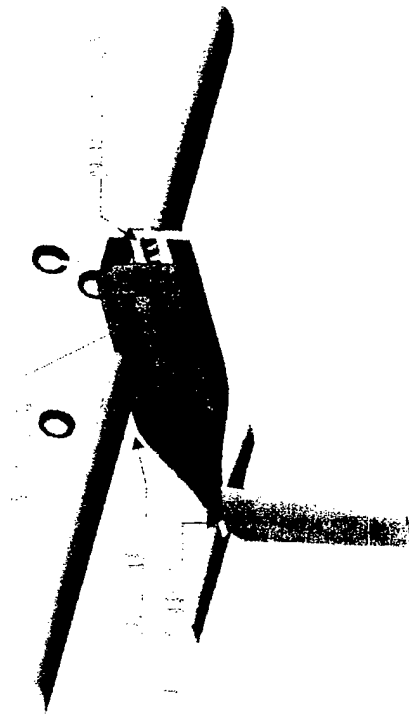
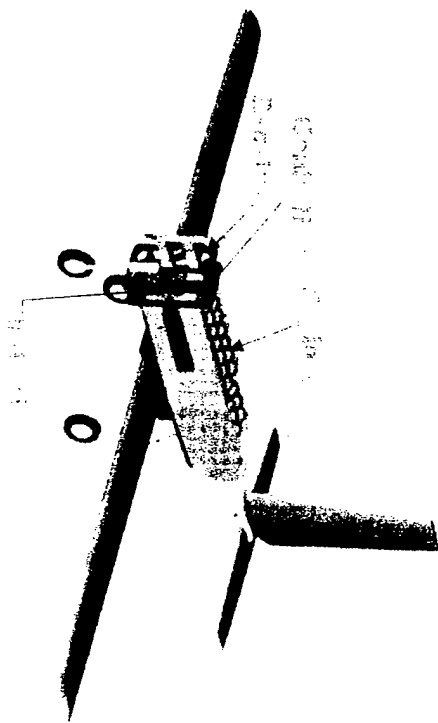
The nose section of the plane was expected to take only air loads, so its weight could be minimized. A hollowed, removable foam cowling formed the nose of the plane, minimizing weight and allowing for good motor access. The cowling was contoured on the inside, ensuring good airflow inside the cooling duct.

6. Drawing Package

NO.	DESCRIPTION	QTY	UNIT	REMARKS
1	WING	2	PC	
2	WING RIB	12	PC	
3	WING RIB	12	PC	
4	WING RIB	12	PC	
5	WING RIB	12	PC	
6	WING RIB	12	PC	
7	WING RIB	12	PC	
8	WING RIB	12	PC	
9	WING RIB	12	PC	
10	WING RIB	12	PC	
11	WING RIB	12	PC	
12	WING RIB	12	PC	
13	WING RIB	12	PC	
14	WING RIB	12	PC	
15	WING RIB	12	PC	
16	WING RIB	12	PC	
17	WING RIB	12	PC	
18	WING RIB	12	PC	
19	WING RIB	12	PC	
20	WING RIB	12	PC	
21	WING RIB	12	PC	
22	WING RIB	12	PC	
23	WING RIB	12	PC	
24	WING RIB	12	PC	
25	WING RIB	12	PC	
26	WING RIB	12	PC	
27	WING RIB	12	PC	
28	WING RIB	12	PC	
29	WING RIB	12	PC	
30	WING RIB	12	PC	
31	WING RIB	12	PC	
32	WING RIB	12	PC	
33	WING RIB	12	PC	
34	WING RIB	12	PC	
35	WING RIB	12	PC	
36	WING RIB	12	PC	
37	WING RIB	12	PC	
38	WING RIB	12	PC	
39	WING RIB	12	PC	
40	WING RIB	12	PC	
41	WING RIB	12	PC	
42	WING RIB	12	PC	
43	WING RIB	12	PC	
44	WING RIB	12	PC	
45	WING RIB	12	PC	
46	WING RIB	12	PC	
47	WING RIB	12	PC	
48	WING RIB	12	PC	
49	WING RIB	12	PC	
50	WING RIB	12	PC	
51	WING RIB	12	PC	
52	WING RIB	12	PC	
53	WING RIB	12	PC	
54	WING RIB	12	PC	
55	WING RIB	12	PC	
56	WING RIB	12	PC	
57	WING RIB	12	PC	
58	WING RIB	12	PC	
59	WING RIB	12	PC	
60	WING RIB	12	PC	
61	WING RIB	12	PC	
62	WING RIB	12	PC	
63	WING RIB	12	PC	
64	WING RIB	12	PC	
65	WING RIB	12	PC	
66	WING RIB	12	PC	
67	WING RIB	12	PC	
68	WING RIB	12	PC	
69	WING RIB	12	PC	
70	WING RIB	12	PC	
71	WING RIB	12	PC	
72	WING RIB	12	PC	
73	WING RIB	12	PC	
74	WING RIB	12	PC	
75	WING RIB	12	PC	
76	WING RIB	12	PC	
77	WING RIB	12	PC	
78	WING RIB	12	PC	
79	WING RIB	12	PC	
80	WING RIB	12	PC	
81	WING RIB	12	PC	
82	WING RIB	12	PC	
83	WING RIB	12	PC	
84	WING RIB	12	PC	
85	WING RIB	12	PC	
86	WING RIB	12	PC	
87	WING RIB	12	PC	
88	WING RIB	12	PC	
89	WING RIB	12	PC	
90	WING RIB	12	PC	
91	WING RIB	12	PC	
92	WING RIB	12	PC	
93	WING RIB	12	PC	
94	WING RIB	12	PC	
95	WING RIB	12	PC	
96	WING RIB	12	PC	
97	WING RIB	12	PC	
98	WING RIB	12	PC	
99	WING RIB	12	PC	
100	WING RIB	12	PC	

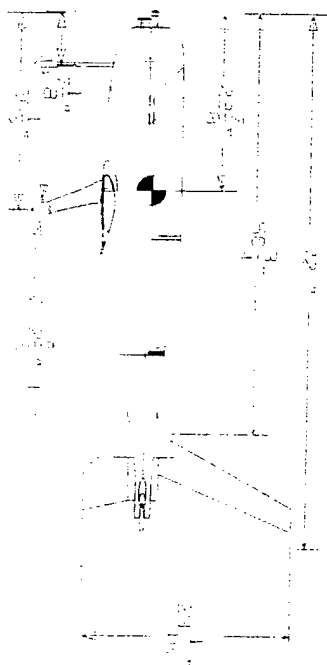
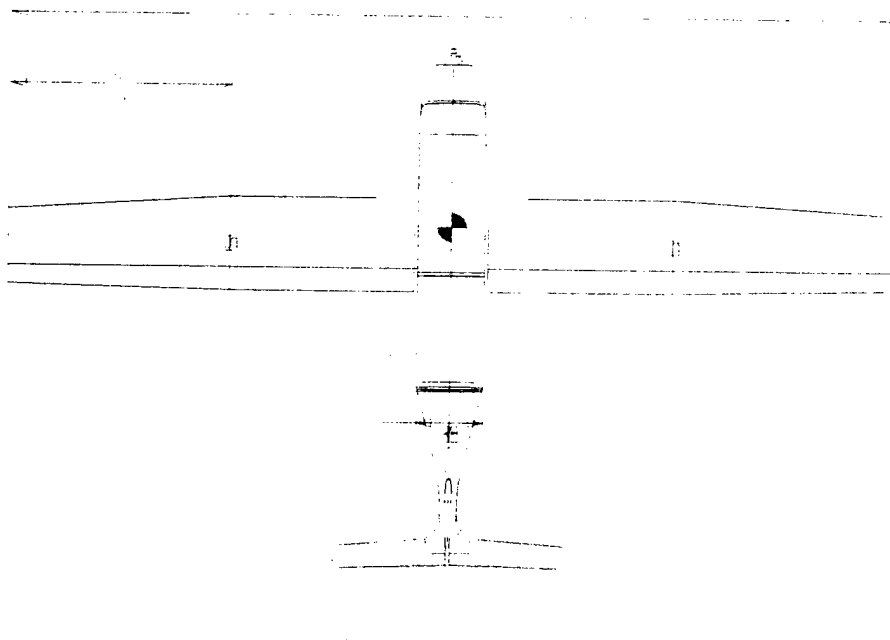
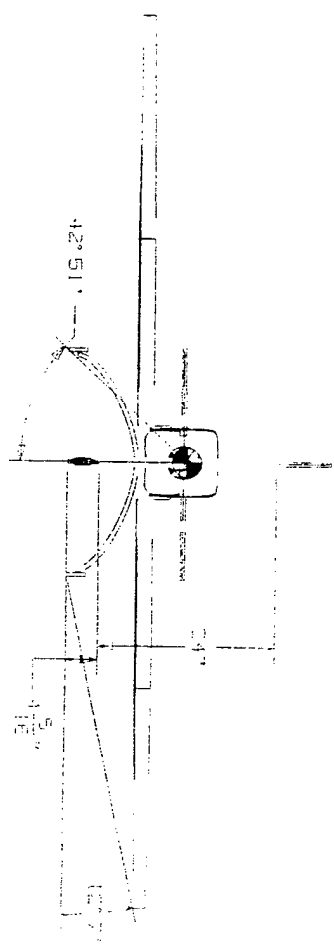


1500 Aer. Design Team 2000 2001
 BUCKUP DRAWING FILE CONCEPT 02
 07-JOHN-11 DRAWN BY: DAVID LAZZARA



$\frac{1}{\sqrt{\pi}}$

Figure 1 illustrates the experimental setup. A subject is seated at a table, viewing a video screen. A camera is positioned above the screen. A horizontal bar is placed on the table, with a vertical rod attached to it. The rod is connected to a motor unit. The motor unit is connected to a power source. The power source is connected to a control unit. The control unit is connected to a computer. The computer is connected to a data acquisition system. The data acquisition system is connected to a plotter. The plotter is connected to a printer. The printer is connected to a storage unit. The storage unit is connected to a network. The network is connected to a server. The server is connected to a database. The database is connected to a user interface. The user interface is connected to a user.



7. Manufacturing Plan

From the previous years in the USC Aero Design team, a combination of composite fuselage with a covered foam wing provided the best construction results. The carbon composite fuselage provided the strength needed to transfer loads through the skin and bulkheads. Constructing the wing and tail sections out of foam allows for easy and very precise duplication of the desired airfoil shape using a hotwire cutting technique. An additional advantage of both materials is that they can be repaired rather easily in case of a crash.

7.1. Manufacturing Method Down-Select

7.1.1. Cost

The "virtual" cost of student labor was deemed the most expensive resource. As a rule, any manufacturing process that reduced time or skill demand was selected. In the first semester, most of the team was trained in wet lay-up and hot-wire processes. Table 7.1, a skill matrix for the team, shows the team possessed a large group of skills.

	CAD Drawings	Hot-Wire Foam Cutting	Wet Lay-Up & Vac-Bag	Hand Shaping	Electronics & Systems	Monokote Application
Nathan P.	2	1	1	1	-	-
Phil K.	1	2	2	1	1	2
Dave L.	1	-	-	-	-	-
George S.	-	1	1	1	-	1
Tim B.	-	-	-	-	2	-
Charles H.	-	-	-	1	-	-
Jerry C.	-	-	2	1	1	2

Table 7.1. Skills Matrix- 1=Highly skilled, 2=capable, Bold-type denotes the lead fabricator.

7.2. Construction Methods

Due to time constraints and labor shortages, it was determined that the best way to build the aircraft would be to keep all the required construction techniques as simple as possible. All experienced team members and the industry advisors gave input before any major construction task was undertaken. This input determined what possible construction techniques would lead to the best balance between ease of construction and part quality.

The fuselage construction for the prototype, SCarface, was fairly simple. It was determined that the fuselage for this year's competition aircraft would be very similar to the fuselage used last year, and therefore it was decided that the prototype airplane would use last year's fuselage molds. This allowed the team to make a rough estimate of a competition aircraft quickly in order to gain valuable knowledge from flight tests. Minimal design and construction time took precedence over part quality and minimal weight. In constructing the competition plane, SCorpion, quality took precedence over speed. Experience gained by members while working on SCarface allowed for increased part quality with reduced construction time.

Previous construction experience showed that the best results in manufacturing the fuselage came from using composites to provide a stiff, load-bearing skin. This structure is reinforced in key areas with bulkheads, which take the brunt of the loads. For the final aircraft, SCorpion, a decision had to be made about the construction method that was going to be used. The possible construction methods included: Lost foam method, balsa build-up, and the foam buck and mold.

7.2.1. Construction method FOMs

The previously discussed construction methods were then ranked according to the following construction FOMs: Crash worthiness, construction complexity, experience with design, required construction time, and construction accuracy. The results of the following discussion are summed in Table 7.2.

7.2.2. Lost foam method

The "lost foam" method of construction was well suited for reducing weight. This involved using a hot wire to cut the fuselage foam buck and embedding each bulkhead into the foam. Carbon fiber with epoxy was wrapped around the buck and cured. Once the buck was completely cured, the top hatch was cut out and acetone was poured into structure to melt out the enclosed foam.

The benefit to this method lay in preserving the shape of the fuselage while all fillets, hatches, and junctions were molded as one piece. This process limited the amount of composite material used, which kept the fuselage weight low. At the same time, the fuselage was sufficiently stiff and load paths were sufficiently strong to survive moderate crash loads without serious damage.

The team had not used this method before. To evaluate it and gain experience with it the team constructed several test articles. Those parts were successful and demonstrated that the "lost foam" method gave good results and had a moderate learning curve.

7.2.3. Balsa build-up

A balsa structure was the most lightweight construction option. Balsa structures are not very crashworthy and are difficult to repair. Past experience showed that crashes were extremely likely and that a balsa structure would have a poor chance of surviving the flight tests.

The complexity of balsa construction was also discouraging. A detailed plan for every truss member in the fuselage was necessary for this structure to match the aircraft specifications. Despite the fact that balsa wood was an easy material to work with, the structural shortcomings outweighed the ability to construct a fuselage quickly.

The team's experience in balsa construction was limited. Balsa had been used in creating bulkheads, wing spar shear webs, and sheeting for the wing and empennage but had not recently been used to construct a fuselage. This limited construction experience would have complicated fuselage construction. Building accurately to tight specifications required careful work over a long period of time. The tight construction and test flight schedule made the learning curve inherent in this different fuselage technique a problem.

7.2.4. Foam buck and mold

This construction method was used extensively in the past and made consistently robust aircraft able to survive crashes. The amount of composite material used in this process was often excessive because the fuselage contained flaws requiring filler material and composite patches. This haphazard approach to fuselage construction and repair added unnecessary weight to the aircraft.

The complexity of this construction method was minimal due to the high level of experience the team had in using it. This experience also showed that the molding process was very time-consuming. Tremendous effort was exerted in perfecting the mold before the fuselage was built. This was an inefficient building method because the mold was generally used only once. This method would be most efficient if more than one aircraft were created with it. Also, accurate fuselage contours were sometimes difficult to create without filler material and much sanding of rough edges. Bulkheads created independent of the skins often did not fit the fuselage cross-section as expected, requiring extra patchwork with more composite material. This addition of extra material increased the aircraft weight noticeably.

USC Aero Design Team "SCorpion"

Figures of Merit	"Lost-Foam Method"	Balsa Structure	Foam Buck & Mold
Crash Worthiness	2	1	3
Construction Complexity	3	1	2
Experience with Design	2	1	3
Required Construction Time	2	3	1
Construction Accuracy	3	1	2
<hr/>			
Total Score			
(Highest score = most favorable)	12	7	11

Table 7.2. Summary of manufacturing method rankings and FOM used (Best = 3 while Unfavorable = 1).

7.2.5. Conclusions

After extensive discussions, the team decided to proceed with the lost foam method. Despite the close rankings and the strong desire to stick with current methods, the team decided to expand their techniques in the interest of quickly building a better plane.

7.3. Construction

7.3.1. Fuselage

The new "lost foam" construction process for SCorpion was not complicated. Figure 7.1 shows SCorpion's fuselage during this construction phase. The team was adequately skilled in creating foam bucks and carbon-fiber layups. Extreme detail was not needed because the composite structure was easily formed to the buck's contours. The lack of small, precisely machined pieces in the structure simplified construction.

This method efficiently used time and labor. One buck was created to make only one fuselage. Extra work in creating a mold was eliminated and the time consuming woodwork of a balsa structure was also avoided. This concept reduced the fuselage construction time to one week, compared to two or three weeks construction time needed when a foam buck and mold were used.

Construction followed the aircraft drawings with high accuracy because the foam buck and bulkhead attachments assured that the bulkheads were aligned and correctly sized to fit the fuselage profile. The front bulkhead became the common datum plane for referencing aircraft features such as the wing, tail, landing gear and c.g. locations.



Figure 7.1. Photograph of SCorpio's fuselage during construction

7.3.2. Wing

The wing was built using 1 lb. foam because it had a low density yet resisted damage from point loads fairly well. The root chord on the wing was 1.05 ft, and the tip chord was 0.84 ft. Full-scale drawings of the wing airfoil were made in Unigraphics at the wing root, taper break point, and tip. The full-scale airfoil sections were pasted onto 1/8" particleboard. Two sets of templates were made for the upper and lower half of the wing airfoil. A hotwire was used to cut the wing from 4 blocks of foam (two blocks for each semi span) using these templates.

Since they were more highly loaded than the main wing, the wing flaperons were made of 2 lb. foam using the airfoil templates described above. They were strengthened with fiberglass sheeting and one ply of carbon fiber to act as a spar in resisting torsion. The flaperon servos were glued into the foam core beneath the wing at its quarter span and the servo horns were glued to load spreaders in the flaperon skins.

The wing spar was designed with a 50% safety factor to counteract the moment and shear generated by the lift from the wing and a maximum 4g landing load. A blade spar 3/8" x 2" was the optimal design. Pre-preg carbon fiber spar caps sandwiched the end grain balsa shear web. Carbon fiber layers tapered from the centerline to the wing tip and the whole spar was wrapped in Kevlar to avoid peeling under adverse loads. A slot through the entire airfoil was hot wired across the wing at 30% of its

root chord. The carbon fiber-balsa spar was secured in the slot with epoxy. After the epoxy cured, a 1/64" plywood blade was embedded into the wing's leading edge along the whole span to protect the leading edge from mishandling. The wing tips were covered with 1/16" balsa to protect the foam core against mishandling and a cartwheel crash.

Another decision involved the material of which the leading edge of the wing was made. Balsa is fairly strong, but it was difficult and time consuming to carve it to the correct shape. Carbon fiber and fiberglass are both strong and easy to work with, but they are also fairly heavy. The test flights revealed that Mylar is very good at holding an airfoil shape, and even light Mylar would make for an effective leading edge. Thus, a foam leading edge sheeted in Mylar was selected for *SCorpion*.

Hard points were inserted into the wing for landing gear and fuselage attachment. Using the root chord airfoil templates, two balsa attachment structures were created. Two 1/8" x 6" balsa strips with grain perpendicular to the airfoil chord line were sandwiched between two 1/2" x 6" balsa strips with grain parallel to the airfoil chord line. This structure was held together with epoxy and inserted into slots 3 1/2" from the centerline. The same was done on the opposite side of the centerline. Two layers of 3" wide fiberglass strips were wrapped around the wing section enclosing each hard point. This fiberglass distributed load from the wing/landing gear/fuselage attachment over the attachment structures. Once the fiberglass strips cured, two holes with 1/4" diameter were drilled 3" apart in each hard point with a drill-press. Another hard point was inserted at the flaperon-wing junction near the centerline. Past experience showed that this region of the wing suffered extensive damage from crashes. A plywood hard point resisted the crushing loads acting on this portion of the wing and saved time in repairs after a crash. The plywood block measured 1" x 1" x 16" and was centered about the centerline. The sections of the foam core unsupported by the plywood were strengthened with 1/16" balsa.

The wing was covered with monokote without an underlying balsa skin. Low temperature monokote was used to avoid melting the foam core. The surface tension of the monokote skin coupled with the spar structure provided torsional rigidity for the wing. The flaperons were taped at their hinge line to the balsa and plywood structure in the wing.

7.3.3. *Empennage construction*

The elevator and rudder were both hot wired from 1 lb. foam using airfoil templates and covered with two layers of 3/4 ounce fiberglass. These parts were vacuum bagged under 15" HG and cured at room temperature.

Carbon fiber strips were cured on both sides of the airfoil in the horizontal stabilizer and vertical fin to provide rigidity against bending. A carbon fiber rod was embedded into the leading edge of the ventral fin and coated with Kevlar. This rod provided a skeg that set the ground angle limit to avoid stalling the wing during rotation on takeoff. The horizontal and vertical stabilizers were independent of the fuselage and inserted into gloves molded into the fuselage. The elevator and rudder servos were placed in the aft section of the fuselage instead of the tails, improving airflow over the tail, easing construction,

and making the servos easily replaceable. Servo horns were glued to the upper airfoil surface to prevent damaging the servo horns during rotation.

7.3.4. Landing gear

Past experience provided confidence in constructing composite landing gears similar to those employed in *SCarface's* configuration. Using the landing gear design spreadsheet and Unigraphics the landing gear's shape and layup schedule were calculated. Pre-impregnated carbon was used instead of standard wet layup carbon because of its greater stiffness and uniformity in thick layups. The lay-up schedule called for forty-four layers of unidirectional carbon running along the curve of the gear with a layer running across the curve every eight plies.

The fabrication process involved curing the part at high temperature and under pressure. Bending two sheets of aluminum to match the frontal view of the landing gear created the mold. The layup schedule was symmetric from the bottom mold to the top to prevent warping. The top plate of the mold was clamped to the bottom mold with the carbon in the middle, and the whole assembly was placed in an oven to cure the resin. After the gear had cured, a plot of the gear's profile was attached to the top surface of the part and a Dremel cutoff tool was used to remove excess material. Holes were then drilled in the top of the part for attachment to the wing and the fuselage.

7.4. Scheduling

Scheduling was critical to the design process because of the limited time available. Schedules were constructed for each major discipline, including the fuselage, landing gear, aero surfaces, controls and propulsion groups. Construction began after the first meeting of the year on January 11th and the first flight was scheduled for February 17th. This was a very aggressive schedule, but delays were acceptable. Figure 7.2 shows the milestones in *SCorpion's* construction.

Construction proceeded on several parts in parallel with the labor pool of unassigned underclassmen helping out where needed. No major problems occurred during construction but the plane was not ready by the 17th, requiring that the first flight be pushed back a week. The weekend of February 25th was rainy but a flight was attempted. The plane did not take off because water beading up on the wing disrupted its lift and the takeoff speed was not sufficient to blow the beads off. The next flight attempt on March 3rd was successful although *SCorpion* sustained minor damage from a crash.

USC Aero Design Team "SCorpion"

SCorpion Manufacturing Milestones		Responsible	Jan 14-20	Jan 21-27	Jan 28-Feb 3	Feb 4-10	Feb 11-17	Feb 18-24	Feb 25-Mar 3
Task	Team Member		SMTWTFS	SMTWTFS	SMTWTFS	SMTWTFS	SMTWTFS	SMTWTFS	SMTWTFS
Fuselage Group		Mark							
Fuselage buck finished				X					
Fuselage laid up				X	X				
Foam and peel ply removed					X				
Bulkheads and raw edges reinforced					X				
Tail gloves finished						X			
Hatch completed and installed								X	
Wing mounts drilled								X	
Landing Gear Group		Charles							
Main Gear / Brakes									
Main gear designed					X				
Main gear laid up						X			
Main gear trimmed							X		
Wheels and axles attached								X	
Pneumatics in								X	
Nose Gear									
Received nose gear						X			
Nose gear mounted to fuse							X		
Nose gear extension in								X	
Servo linkage in								X	
Wing									
Sparcups laid up				X					
Shear web built					X				
Spar assembled					X				
Cores out					X				
Spar installed						X			
Servos installed						X			
Wing mount installed							X		
Leading edge reinforced and sheeted							X		
Wing filled/sanded to profile								X	
Trailing edge reinforced and sheeted								X	
Wing monokoted								X	
New control surfaces out						X			
Control surfaces sheeted						X			
Control surface hardpoints installed							X		
Hinges taped								X	
Tail									
Cores out				X					
Cores sheeted					X				
Control surfaces sheeted					X				
Ventral skag installed						X			
Hardpoints installed							X		
Hinges taped								X	
Controls Group		Tim + Jerry							
Electronics									
Wing wiring harnesses installed						X			
Fuselage-mounted servos wired							X		
Receiver installed								X	
New Piz battery pack constructed									X
Mechanical									
Elevator and rudder servos installed						X			
Wing control horns and linkages installed							X		
Tail control horns and linkages installed								X	
Heavy Electronics / Propulsion Group		Tim + Jerry							
Fabricate motor mount					X				
Wire propulsion system						X			
Install temporary circuit breakers							X		
Install battery pack mounts								X	
Assemble and test SCorpion propulsion system								X	
Flight Schedule		David							
Plane complete								X	
Attempted first flight									X
First flight!									X

Figure 7.2. Manufacturing Schedule for SCorpion

USC Aero Design

Presents:

Scorpion

Design Report-Addendum
April 10, 2001
2000-2001 AIAA/Cessna/ONR
DBF Competition



LSC UNIVERSITY OF
SOUTHERN CALIFORNIA

 **AeroVironment**

GWServo



**The
Skunk
Works**

LOCKHEED MARTIN


BOEING

Raytheon



NORTHROP GRUMMAN

Table of Contents

ii. Awesome Features Diagram	ii
1. Executive Summary	1
2. Management Summary	5
2.1. Aero Surfaces & Fuselage.....	6
2.2. Landing Gear & Lab Manager.....	6
2.3. Controls & Propulsion.....	7
2.4. Flight Tests.....	7
2.5. Construction.....	7
2.6. Conceptual and Preliminary Design.....	7
2.7. Report Editor.....	7
2.8. Information Technology & Design Spreadsheet Development.....	7
2.9. Propulsion Testing & Weights and Balance.....	8
2.10. Configuration and Structural Design & Structural Sizing.....	8
3. Conceptual Design	8
3.1. Alternative Concepts Investigated.....	8
3.2. Detail Design Parameters.....	8
3.3. Design Descriptions.....	9
3.4. Subjective Figures of Merit.....	9
3.5. Analytic Figures of Merit.....	11
4.0. Preliminary Design	13
4.1. Design Tools.....	13
4.2. Optimization Parameters.....	20
4.3. Configuration.....	22
4.4. Wing.....	23
4.5. Tail.....	23
4.6. Brakes.....	24
4.7. Landing gear.....	24
5. Detailed Design	25
5.1. Performance Data.....	25
5.2. Modeling Process.....	26
5.3. Payload Design.....	26
5.4. Fuselage Aerodynamic Design.....	27
5.5. Structural Design.....	27
5.6. Wing Structure.....	28
5.7. Landing Gear.....	32
5.8. Component Mounts.....	33
5.9. Cooling Design.....	35
5.10. Nose Design.....	36
6. Drawing package	37
7. Manufacturing Plan	41
7.1. Manufacturing Method Down Select.....	41
7.2. Construction Methods.....	41
7.3. Construction.....	44
7.4. Scheduling.....	47
8. Lessons Learned	51
8.1. Flight Tests.....	51
8.2. Propulsion System Tests.....	52
8.3. Design Changes.....	55
8.4. Changes for next year.....	57
9. Costs	58
9.1. Rated Engine Power.....	58
9.2. Manufacturing Hours.....	58
9.3. Manufacturers Empty Weight.....	58
9.4. Rated Aircraft Cost.....	59

8. Lessons Learned

The biggest lesson from last year's contest entry was the need to test fly early. It was a goal set and achieved this year: the team was able to flight test a prototype, *SCarface*, and use it to learn and implement new discoveries into the final design. The contest plane, *SCorpio*n, was also built on an accelerated schedule to allow for extensive flight-testing. The team was also able to do some extensive testing on the propulsion system. Energy problems limited last year's performance, so the primary focus of this testing was to refine the battery life model. Extensive data resulted in better modeling of available energy, and an optimized combination of motor, gearbox, and propeller was chosen. The following sections depict these lessons learned.

8.1. Flight Tests

This year a new emphasis was placed on testing. Flight-testing a prototype would provide valuable performance data and give new team members experience with building a composite aircraft when the time came to build *SCorpio*n. Documented are some findings from the flight test experiences.

8.1.1. Use of flight cards

A significant amount of time was spent test flying *SCarface* and *SCorpio*n. Many different performance parameters and aircraft characteristics were measured to compare with predicted values. This required a well-organized flight test regime; thus one team member was charged with creating a flight test plan. Flight cards were created prior to each test flight and used to dictate the schedule of test flights. Each card represented a unique test flight with different objectives and aircraft configuration, including varying payload weight, propeller type, motor type, flight path definition, and performance checks regarding stability and control, ground handling, takeoff performance, and battery life. In addition, all flight cards required various velocity measurements, battery voltage measurements, TOFL measurement, and flight times. Static thrust and tachometer tests were also conducted to verify the propulsion system. Rolling resistance tests and temperature measurements for the motor, batteries, and speed controller were recorded as well.

The flight cards were also used to brief the pilot before each test flight and organize team members to perform certain tasks. All measured quantities were recorded on their corresponding flight card for each test flight. Pilot comments and debriefing notes were listed on the flight cards. This data were compared with predicted values on the flight cards to change the test schedule when a specific issue required more attention. After all test flights were conducted for a given day, the collected data were plotted in comparison to predicted values using an estimated uncertainty.

8.1.2. Pre-flight checklists

A formal pre-flight checklist was not used during initial test flights. In one incident, though, a hatch was not secured and it opened during flight, which caused the loss of control of the aircraft. Thus a formal pre-flight check list was integrated into the flight cards and each team member was given a list of responsibilities to complete before the aircraft was allowed to takeoff. Responsibilities included aircraft handler, propulsion captain, controls captain, radio captain, landing gear and brakes captain, electronics captain, and various data collecting jobs. If a problem occurred again, a specific individual would be responsible instead of the group as a whole. More efficient work also resulted from the pre-flight checklist because each person in attendance assisted in a specified manner and decreased the time needed to prepare the aircraft.

8.1.3. Removable Motor Mount

The plane's original design called for removable motor mounts designed to break in a severe crash. This saved the gearbox and propeller on several occasions during flight-testing. Having several spare motor mounts, and making them easily replaceable, eased motor maintenance and greatly reduced the turnaround time between flights.

8.1.4. Addition of Skegs

The ventral fin was designed partly as a ground angle limiter to prevent wing stall during takeoff. The limiting angle was approximately 10 deg., which included the limiting angle plus 3 deg. of margin to assure liftoff after rotation. In *SCorpio*n's first flight test, the pilot indicated that the ventral fin did not provide ample rotation for liftoff. Thus the ventral fin was shortened to provide approximately 20 deg. of rotation. Succeeding test flights proved this new rotation limit permitted liftoff. However, during takeoff the wing stalled consistently. A return to the 10 deg. ground angle limit was necessitated to avoid wing stall on takeoff. In retrospect, this angle was always sufficient. The failure to liftoff in the first flight test was attributed to wing stall caused by raindrops on the wing. *In situ* video footage by an onboard camera observed the wing during acceleration and depicted a laminar bubble formation near the wing leading edge (as seen by a row of water drops neatly arranged on the leading edge) and separation towards the trailing edge. Thus the ground angle limit was not the cause of a failed liftoff.

Rather than rebuild the ventral fin, a skeg was added to the fin to reset the ground angle limit. If future troubles are associated to the reduced ground angle limit, the skeg can be easily shortened.

8.2 Propulsion System Tests

*SCorpio*n's propulsion system includes the propeller, gearbox, motor, speed controller, fuse, switch and batteries. In previous contests, battery life and the reliability of the propulsion system had been issues, so a primary goal of this year's effort was to thoroughly test the propulsion system. Another

goal was to validate and refine the mission simulator by testing each motor with several different propellers.

8.2.1. Constraints and Methodology

Meeting the contest's take-off field length (TOFL) requirements required approximately 10 lb of static thrust. The maximum current draw on the motor was set at 40 amps by the contest rules. Maximizing efficiency was the overall goal for the propulsion system, and this involved maximizing static thrust and minimizing current draw for a given input voltage.

Shaft rotation speed is a linear function of voltage for electric motors, so an easy way to measure power consumption is to multiply the current draw by the rotation speed. A good method for comparing the performance of different propulsion system configurations is to normalize their power consumption with their static thrust. This power consumption factor is calculated using Equation 8.1:

$$C_P = \frac{A * \omega}{T}, \quad (8.1)$$

where C_P is the thrust normalized power consumption factor, A is the current draw in amperes, ω is the rotation speed in RPMs, and T is the static thrust in pounds. The motor and propeller combination with the lowest C_P in the operating thrust range is the most desirable.

The flight motors and batteries were selected using the mission spreadsheet and their performance was validated through motor testing. Several tests using different voltages were run for each motor and propeller combination. A simple battery discharge test at constant throttle and a full mission simulation measured battery life. The data obtained during propulsion system testing was used to establish reliability and validate and refine the mission simulator.

8.2.2. Equipment

The test stand included a 3000-watt DC power supply, voltmeter, ammeter, thermometer, tachometer, and a load cell for measuring thrust. A notebook computer running a LabVIEW program collected current, voltage and temperature data while the thrust and propeller rotation speed data were collected by a load cell and tachometer and entered by hand.

8.2.3. Procedure and Results

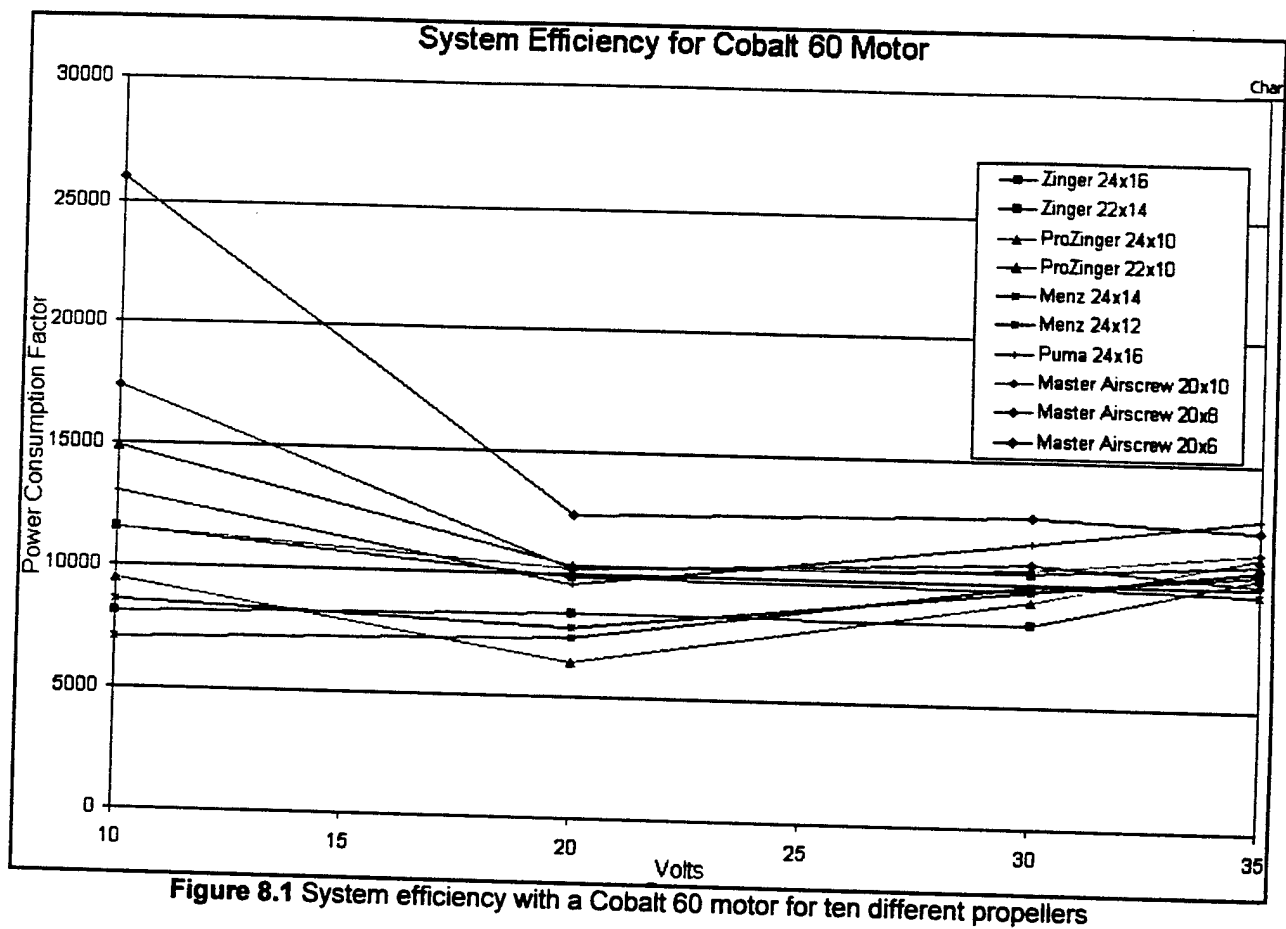
The first test involved determining the propulsion system efficiency for the Cobalt 60 and Pattern 90 using several different propellers. Each combination was run at voltages between 10 and 35 volts. At each voltage increment data was collected on the rotation speed, voltage, current, and static thrust. The data for the Cobalt 60 are listed in Figure 8.1. The motor was run with a heat sink sized by the mission simulator.

The full propulsion system tests used the same configuration, but with the motor connected to the battery pack instead of the power supply. The first test had the speed controller set to a constant 80% throttle setting. The motor was run until the batteries ran completely out of power.

The second test used varying throttle settings chosen to give thrust levels calculated from the mission simulator. Figure 8.2 shows the results for the mission simulation test.

8.2.4. Conclusions

The Cobalt 60 and Menz 24x14 produced the highest static thrust and rotation speed, while the Pattern 90 and Zinger 24x16 had a lower current draw and maximum temperature. The higher static thrust and lower weight of the Cobalt 60 power plant made it the favored choice, while the Pattern 90 was retained as a backup. The constant throttle test drained the batteries in less than 600 seconds. However, the four full sorties achieved in the mission simulation test exceeded the mission simulator's pessimistic predictions. With careful flying, three full sorties were attainable.



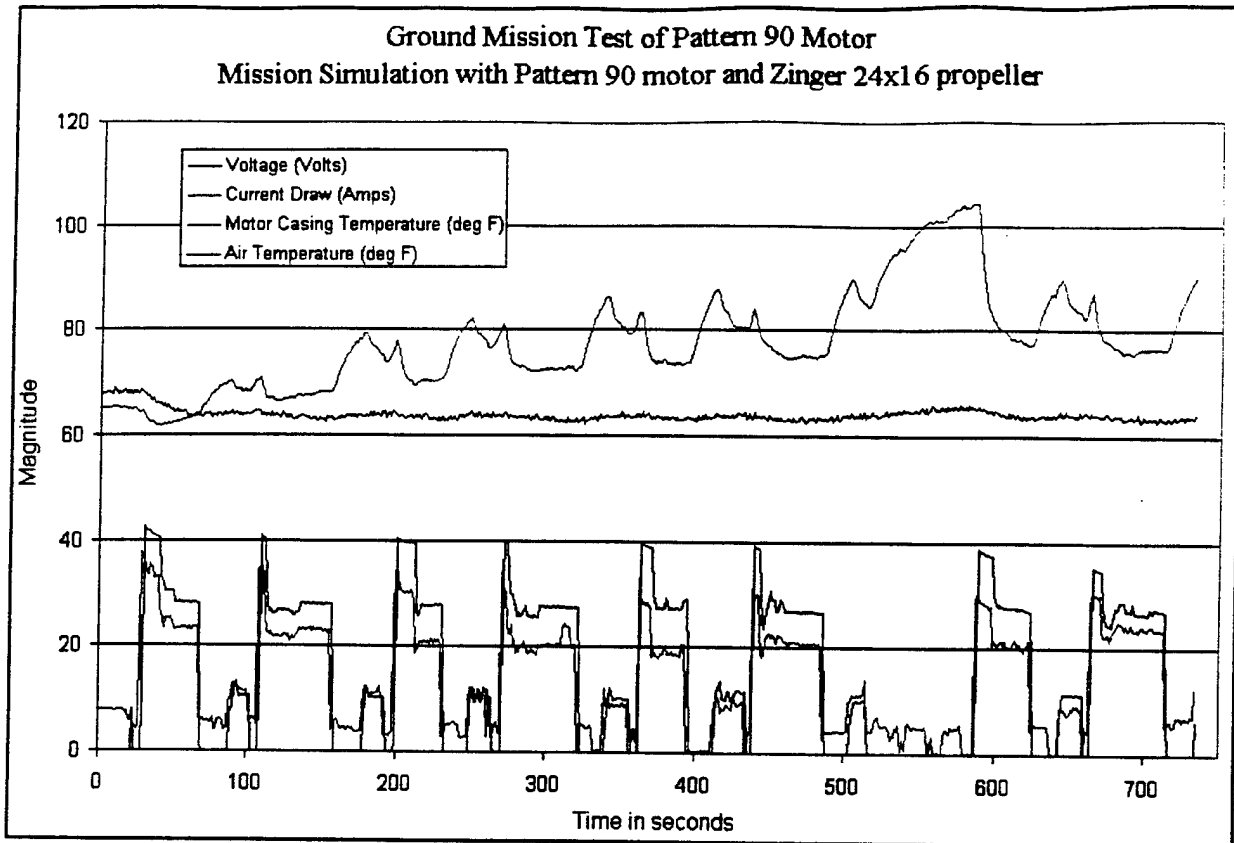


Figure 8.2 Voltage, current draw, and motor casing temperature during a mission simulation

8.3. Design Changes

8.3.1. Wing washout

The plane was originally designed with two degrees of washout in the outboard panels of the wing to avoid tip stalls. During flight-testing, the wingtips consistently stalled on takeoff at high angles of attack. Extra washout would allow the pilot greater stability at high angles of attack. One more degree of washout was incorporated in the root section of the wing (totaling 3 degrees at the tips). The reason the washout was increased from the root was to avoid over-loading the tips, and to minimize drag.

8.3.2. Stiffer spars

Static load tests on the wing spar indicated a lack of stiffness in its construction. This permitted excessive wing bending such that the wing was slightly but permanently bowed after numerous c.g. tests, when *SCorpio* was lifted by the wing tips. The new wing incorporated carbon fiber spar caps with 3 extra layers of carbon fiber and the same spar width. No other issues with the spar were found because it performed well during flight and survived hard landings. Wing bending due to static loads should be reduced substantially.

8.3.3. Reduced Front Bulkhead

The original design had the motor and nose landing gear attached to a bulkhead at the front of the fuselage. A series of crashes shattered this structure and damaged the fuselage skin in that area. The rebuilding process created the opportunity for an improved design. Consideration of the load paths in the nose revealed that most of the loads encountered in a hard landing flowed directly from the motor mount to the fuselage skin. The purpose of the forward bulkhead was primarily to react loads from the nose gear during a hard landing, for which its design was not ideal.

In the new design, most of the upper bulkhead was eliminated to save weight. The motor mount was attached to small hard points at the sides and top of the fuselage. The motor mount would stiffen the forward fuselage. The nose gear attached to a L-shaped aluminum bracket designed to bend in a hard landing but otherwise be unbent on the flight line. This was in turn mounted to the lower fuselage, eliminating the need for the forward bulkhead.

8.3.4. Nose gear re-design

The nose gear was originally mounted to the forward bulkhead. This transmitted crash loads to the forward bulkhead and damaged it substantially. A piece of L shaped sheet aluminum was used to mount the nose gear strut to the lower fuselage. This was stiffened longitudinally by using Zip ties to pretension it against a carbon fiber rod spanning the width of the fuselage. This would absorb crash loads as the Zip tie broke and the aluminum underwent plastic deformation, and the system could be easily repaired by bending the bracket back into a L-shape and replacing the Zip tie. Mounting the steering servo to the nose strut minimized its exposure to danger. Flight tests revealed that this design performed well but that it permitted excessive side-to-side shimmy during sharp turns, so it was modified with a rod attached to the bend in the L and mounted to hardpoints in the sides of the fuselage. A composite nose strut was also designed and built, and this performed well and saved significant weight.

8.3.5. Hatch re-design

Initially, the hatch was secured with a tape hinge on one side of the plane and a latch on the opposite side. Yet this design had inherent flaws. If the latch opened in flight, it would introduce a severe drag increase and yawing moment causing the pilot to lose control. Therefore, a front hinge was designed to secure the hatch. If this hatch became loose in flight, the hatch would only lift slightly and have a low effect on the overall plane drag. This hinge design also reduced weight by a few ounces because the latch mechanism contained only low-weight structure (e.g., a locking pin).

8.3.6. Vertical tail sizing

In SCorpio's initial test flights, the rudder did not provide enough control authority in yaw. A 16% increase in rudder area was incorporated. This improved the aileron-rudder interconnection gain reducing the adverse yaw at maximum aileron deflection.

8.3.7. Tail surface stiffening

Test flights also demonstrated that the tail surfaces were not strong enough in bending. It was noted that when the plane banked and pulled a high "g" turn, the horizontal tail would bend and the vertical tail would flutter. The initial tail design was lightweight and consisted of 2 layers of 0.5 oz. fiberglass laid at 45 degrees from each other. Rough calculations had indicated that this would be sufficient to minimize the twist and bending of the tail, but flight tests proved otherwise. So laying a 1" wide uni-directional carbon spar on either side of the surface for added stiffness during flight stiffened the tail surfaces.

8.4. Changes for next year

The team discusses improvements for future contests at the end of each contest year. This step helps avoid repeating mistakes from previous years. Improvements in communication and in manufacturing issues would help the team function more efficiently in the next competition.

8.4.1. Communication

A new team structure was devised for this year. The team broke into two groups; one building a proto type aircraft, and the other designing the competition aircraft. During the process of building the prototype aircraft, several changes were made to the design. Due to a lack of communication between the design team and the manufacturing team, the prototype's tail sizes were too small. Fortunately, trailing edge extension strips (TEX's), proved to be a quick fix to the design problem. But, if the team is to continue the dual nature of design, an established structure of communication must be formed to ensure that every member of the team is updated with the most current design.

8.4.2. The use of tape in SCorpio

Tape was used to secure payload, electronics, telemetry systems, and other components to the fuselage. This was an inefficient way of securing components and was often inadequate for holding certain components, such as the steel payload. A secure payload box was thus designed to avoid payload shift, provide a frozen payload c.g., and minimize pre-flight preparation. Similar designs were done for the electronics and telemetry systems.

8.4.3 Manufacturing Plans

There were instances when manufacturing plans or templates were not provided at designated times. This hindered manufacturing because builders often did not have sufficient information for completing a part and needed to postpone construction. Slow progress also resulted when templates were not provided on time. A complete task list of required templates and their needed dates must be implemented in future competitions. Template files should also be readily accessible by any team

member in order for builders to access them at any time. A team web page containing these files is one possible solution for this issue.

9. Costs

The Rated Engine Power (REP), Manufacturing Man Hours (MFHR) as based on the supplied WBS structure, and the Manufacturers Empty Weight (MEW), and final Rated Aircraft Cost (RAC) for the competition plane *SCorpion*, is listed in Table 9.1. Equation 9.1 calculates the final competition score:

$$TotalScore = \frac{N_s * (P_p) * RS}{RAC} \quad (9.1)$$

where N_s is the number of completed sorties, P_p is points from the payload (tennis balls and pounds of steel), and RS is the Report Score.

9.1. Rated Engine Power

The REP for *SCorpion* was calculated with Equation 9.2:

$$REP = Ne * FA * 1.2 * Nc \quad (9.2)$$

where Ne is the number of engines, FA is the size of the electrical fuse in Amps, and Nc is the number of cells in the battery pack. The rated engine power has units of Watts. The cost equation charges one dollar for each Watt of power in the rated propulsion system. *SCorpion's* REP is 1512 W and has an associated cost of 1.512 (\$thousands).

9.2. Manufacturing Hours

Each element in the WBS structure was listed and assigned a value. The associated amount of work hours for each element was summed in the MFHR cel in the table. The cost of labor in the rated cost equation is 20 dollars/hr. The total amount of man-hours for *SCorpion* is 138.24 hours with an associated cost of 2.765 (\$thousands).

9.3. Manufacturers Empty Weight

Removing the entire payload and the batteries from the fuselage, and balancing the plane on the scale about the c.g determined the weight of *SCorpion*. The final MEW of the aircraft was 14.7 pounds. According to the cost model, the cost of empty weight is 100 dollars/pound. The final associated cost of the MEW was 1.470 (\$thousands).

9.4. Rated Aircraft Cost

The rated aircraft cost for SCorpio is described in Equation 9.3:

$$RAC = \frac{\$100 * MEW + \$1 * REP + \$20 * MFHR}{\$1000} \quad (9.3)$$

The final value of RAC is in units of thousands of dollars and has a value of 5.747 (\$thousands).

Aircraft Rated Cost Summary				
Aircraft dependant parameters	Value	Dimension	Component Cost	
Rated Engine Power				
Nengines =	1	n.d.	1	n.d.
Amps =	35	A	35	A
Ncells =	36	n.d.	43.2	V
REP =			1512	Watts
Cost Subtotal =			1.512	\$(Thousands)
Manufacturing Man Hours				
Nwings =	1	n.d.	15	hrs
Sw =	10	ft^2	40	hrs
Nstruts =	0	n.d.	0	hrs
Ncontrolsurfaces =	2	n.d.	6	hrs
Nbody =	1	n.d.	5	hrs
Lf =	6.31	ft	25.24	hrs
Nvertical tail =	1	n.d.	5	hrs
Nhorizontal tail =	1	n.d.	10	hrs
Nservos =	6	n.d.	12	hrs
Nengines =	1	n.d.	5	hrs
Nprops =	1	n.d.	5	hrs
Empennage Basic Cost =			5	hrs
Flight Systems Basic Cost =			5	hrs
MFHR =			138.24	hrs
Cost Subtotal =			2.765	\$(Thousands)
Manufacturers Empty Weight				
Empty Gross Weight =	14.7	lbs		
MEW =			14.7	lbs
Cost Subtotal =			1.470	\$(Thousands)
Total Rated Aircraft Cost =			5.747	\$(Thousands)

Table 9.1. Breakdown of manufacturing hours and rated aircraft cost

Cessna/ONR Student Design, Build, and Fly Competition
Naval Air Station
Patuxent River, MD

2000/2001 Contest Year
5th Annual Event

San Diego State University
“Full Monty”

Design Report
(Proposal Phase)

	Page #
1. Executive Summary.....	(1 – 4)
Figure 1.1: Conceptual Design Configuration.....	2
Figure 1.2: Preliminary Design Configuration.....	3
Figure 1.3: Design And Mission Requirements.....	4
2. Management Summary.....	(5 – 6)
Figure 2.1: Milestone Chart.....	6
3. Conceptual Design Phase.....	(7 – 12)
3.0 Conceptual Design.....	7
3.1 Design Considerations.....	7 – 11
3.2 Figures Of Merit (FOMs)	11 – 12
4. Preliminary Design Phase.....	(13 – 23)
4.0 Introduction.....	13
4.1 Wing Design.....	13 - 19
4.2 Fuselage Design.....	20
4.3 Drag Analysis.....	21 - 22
4.4 Summary.....	23
5. Final Design Phase.....	(24 – 25)
5.0 Introduction.....	24
5.1 Takeoff Distance.....	24 – 25
5.2 Stability.....	25
Detailed Drawing Package.....	(26 – 27)
Three-View Drawing.....	26
Internal Structure.....	27
Control System.....	27
6. Manufacturing Phase.....	(28 – 29)
6.0 Introduction.....	28
6.1 Manufacture & Assembly of Major Parts.....	28
6.2 Figures Of Merit (FOM) Included.....	29
6.3 Results.....	29

1.0 Executive Summary

San Diego State University (SDSU) students involved in the Design, Build, and Fly competition have completed their contest entry to compete in April 2001 at the Cessna/ONR sponsored event. Their design comprises an unmanned, remote controlled, propeller powered airplane capable of flying a course set up by contest officials. SDSU will compete against a number of colleges around the nation.

The primary goal of this contest is to obtain as many points as possible through several methods, the team receiving the most points will be declared the winner. These methods include the report phase, where a report detailing the different aspects of the aircraft fabrication process, from initial design considerations to detailed design to a final manufacturing description is submitted. Another phase involves the actual competition, where different numbers points are awarded for aircraft performance in achieving different mission parameters. The total of these scores is tallied, and the highest score wins.

One of the initial concerns of the SDSU team was the fact that the number of people available and willing to work on the project was low. Also, practically no one on the team had actual experience in any of the areas, such as initial design and manufacturing, required to construct an airworthy aircraft for this event. Previous entries by former SDSU students could not be used because of changes in the design mission and design failures. The competition this year, therefore, required the few students to learn how to properly design an aircraft, how to analyze its performance, how to build what was created on paper, and how to effectively conduct flight tests that would yield meaningful results.

The SDSU team did not have the analysis resources to complete detailed research on the aircraft. Since previous SDSU entries did not do well in competition, and no reports were available to understand what an effective design process would require, the team had to develop from the ground up ways to efficiently and accurately design an aircraft. Student experience was minimal in the design process so in consequence, the only four seniors involved in the project had to constantly refer to the aircraft design class they concurrently were taking. Overall, it was difficult to see where the design was going without someone who could offer advice on the progress of the project.

Initial design considerations floated around several designs. These designs included single and bi wing, and single and double boom fuselage. Although there were many ideas, it was known that substantial design analysis could not be taken because of time constraints. It was difficult for any extensive analysis to be done because of manpower issues. Instead of performing several different analyses for all of the proposed configurations and finding which one had the best performance for the lowest cost, other decision guidelines were used. Low manpower was the principal limiting factor, so considerations in manufacturing time and difficulty was taken into account. Also, since time was limiting both construction efforts and analysis efforts, a simple yet effective design was decided to be the best way for the SDSU team to go. The conceptual design included deciding how the plane was to perform, including considerations for amount of payload the aircraft could carry. Since score depended on the

type and amount of payload carried, maximizing this amount was desired. Results for the conceptual design are presented in the following figure.

Figure 1.1 Conceptual Design Configuration

Airplane Type:	High Speed Swept Wing (F18 Design)
Tails:	Horizontal & Two Vertical
Payload:	100 Tennis Balls / Equal Weight In Steel
Payload Carrying System:	Speed Loader
Total Airplane Weight:	35.0 lbs
Wing Span:	7.0 ft
Wing Area:	7.0 ft ²
Wing Loading:	5.0 lbs/ ft ²
Total Length Of Airplane:	74.5 inches
Motor:	Astro Cobalt 40
Battery:	Sanyo 2000
Propeller:	18.0inch diameter

As information was made available and our conceptual design critiqued by model aircraft hobbyists, it became a concern that the team's initial efforts had been overzealous. After making some new estimations to cruise velocities, weight, and airfoil selection, a new configuration was achieved. Since the new cruise velocity was reduced, a change to the weight of the plane or the wing was required. Again, since the team was pressed for time, very conservative estimations were made at this point. It was agreed that a design exceeding performance estimations would be the best route to go. It was decided that the maximum TOGW would be reduced and the wing area increased to provide a much lift as possible. Maximum thrust available in the motor was also decided to be at a conservative value. These decisions were necessary, because of the limited resources available, in an effort to speed up the design process and to get the aircraft into production. Results for the preliminary design are presented in the following figure.

Figure 1.2 Preliminary Design Configuration.

Airplane Type:	Standard Un-swept Wing
Tails:	Horizontal & One vertical
Payload:	56 Tennis Balls / Equal Weight In Steel
Payload Carrying System:	Speed Loader (Fuselage Latch-On)
Fuselage:	8.0inch diameter
Total Airplane Weight:	26.0 lbs
Wing Span:	8.0 ft
Wing Area:	8.0 ft ²
Wing Loading:	3.25 lbs/ ft ²
Total Length Of Airplane:	74.5 inches
Motor:	Astro Cobalt 40
Battery:	Sanyo 2000
Propeller:	16.0inch diameter

At the completion of the preliminary design configuration, the design and mission requirements for the aircraft were met. A summary of the design and mission requirements is presented at the end of this section. However, due to limited resources, construction was not completed in time for flight tests. Therefore, since the detail design phase included refinements to the aircraft design to improve performance, this phase of the design is not available at this time. After construction has been completed and a few flight tests done, improvements will include reducing wing area to reduce weight. This is predicted because the cruise velocity used to size the wing seems to be low, but there is no data available to give a better estimation. Other improvements include changing the payload loading system and manufacturing process to reduce TOGW.

Figure 1.3 Design and Mission Requirements

Airplane Type:	Standard Un-swept Wing
Tails:	Horizontal & One vertical
Payload:	56 Tennis Balls / Equal Weight In Steel
Payload Carrying System:	Speed Loader (Tail Cone Out)
Fuselage:	6.0inch diameter
Airfoil:	NACA 4418
Total Airplane Weight:	26.0 lbs
Wing Span:	8.0 ft
Wing Area:	8.0 ft ²
Wing Loading:	3.25 lbs/ ft ²
Total Length Of Airplane:	74.5 inches
Motor:	Astro Cobalt 40
Battery:	Sanyo 2000
Propeller:	16.0inch diameter

Figure 1.3 Design and Mission Requirements

Airplane Type:	Standard Un-swept Wing
Tails:	Horizontal & One vertical
Payload:	56 Tennis Balls / Equal Weight In Steel
Payload Carrying System:	Speed Loader (Tail Cone Out)
Fuselage:	6.0inch diameter
Airfoil:	NACA 4418
Total Airplane Weight:	26.0 lbs
Wing Span:	8.0 ft
Wing Area:	8.0 ft ²
Wing Loading:	3.25 lbs/ ft ²
Total Length Of Airplane:	74.5 inches
Motor:	Astro Cobalt 40
Battery:	Sanyo 2000
Propeller:	16.0inch diameter

communication was happening across the team. The following figure show how the team laid out the game plan and in actuality when each milestone came into effect.

Figure 2.1 Milestone Chart

<div> <div>Oct-00</div> <div>Nov-00</div> <div>Dec-00</div> <div>Jan-01</div> <div>Feb-01</div> <div>Mar-01</div> <div>Apr-01</div> </div>			
	Target	Planned	Actual
Conceptual Stage	Fund Raising Ideas	Apr-00	Apr-00
	Fund Raising Process	May-00	May-00
	Finish AE460A (FA/18) Military Jet Trainer Design	Oct-00	Oct-00
	Finalize: a-configuration details	Nov-00	Nov-00
	b-drawings	Nov-00	Nov-00
	c-sketches/corrections	Nov-00	Nov-00
	d-design on "AAA" software	Nov-00	Nov-00
	**** Exams/No Work Scheduled/Collect Donations ****	Dec-00	Dec-00
Preliminary Design	Refine Ideas To A Bare Minimum	Beg Jan, 01	Beg Jan, 01
	Finalize: a-wings	Mid Jan, 01	End Jan, 01
	b-fuselage	Mid Jan, 01	End Jan, 01
	c-tails	Mid Jan, 01	End Jan, 01
	d-speed loader	Mid Jan, 01	End Jan, 01
	Preliminary Iterations	End Jan, 01	Beg Feb, 01
	Preliminary Drawings	End Jan, 01	Beg Feb, 01
	Final Iterations	End Jan, 01	Beg Feb, 01
Detailed Design	Final Drawings	Beg Feb, 01	Mid Feb, 01
	Obtain Parts List	Beg Feb, 01	Mid Feb, 01
	Obtain Best Possible (Cheap) Sources/Vendors	Beg Feb, 01	Mid Feb, 01
	Divide Into Three Assembly Groups:		
	1-Finish Fuselage & Internal Structure	Mid Feb, 01	Beg Mar, 01
	2-Finish Wing & Tails	Mid Feb, 01	Beg Mar, 01
	3-Finish Landing Gear & Speed Loader	Mid Feb, 01	Beg Mar, 01
	Build & Test Fly	End Feb, 01	Mid Mar, 01
	Modifications (If Necessary)	End Feb, 01	Mid Mar, 01
	Test Fly w/Full Load	End Feb, 01	Mid Mar, 01
Report Preparation	Appoint People To Prepare Report	Oct-00	Oct-00
	Collect Minutes From Each Group/Group Meeting	End Jan, 01	Mid Feb, 01
	Review DBF Rules For Report Writing	End Jan, 01	Mid Feb, 01
	Prepare Rough Draft	End Jan, 01	End Feb, 01
	Finish Report	End Jan, 01	Beg Mar, 01
	Proof Read	Beg Feb, 01	Beg Mar, 01

communication was happening across the team. The following figure show how the team laid out the game plan and in actuality when each milestone came into effect.

Figure 2.1 Milestone Chart

<div> <div>Oct-00</div> <div>Nov-00</div> <div>Dec-00</div> <div>Jan-01</div> <div>Feb-01</div> <div>Mar-01</div> <div>Apr-01</div> </div>			
	Target	Planned	Actual
Conceptual Stage	Fund Raising Ideas	Apr-00	Apr-00
	Fund Raising Process	May-00	May-00
	Finish AE460A (FA/18) Military Jet Trainer Design	Oct-00	Oct-00
	Finalize: a-configuration details	Nov-00	Nov-00
	b-drawings	Nov-00	Nov-00
	c-sketches/corrections	Nov-00	Nov-00
	d-design on "AAA" software	Nov-00	Nov-00
	**** Exams/No Work Scheduled/Collect Donations ****	Dec-00	Dec-00
Preliminary Design	Refine Ideas To A Bare Minimum	Beg Jan, 01	Beg Jan, 01
	Finalize: a-wings	Mid Jan, 01	End Jan, 01
	b-fuselage	Mid Jan, 01	End Jan, 01
	c-tails	Mid Jan, 01	End Jan, 01
	d-speed loader	Mid Jan, 01	End Jan, 01
	Preliminary Iterations	End Jan, 01	Beg Feb, 01
	Preliminary Drawings	End Jan, 01	Beg Feb, 01
	Final Iterations	End Jan, 01	Beg Feb, 01
Detailed Design	Final Drawings	Beg Feb, 01	Mid Feb, 01
	Obtain Parts List	Beg Feb, 01	Mid Feb, 01
	Obtain Best Possible (Cheap) Sources/Vendors	Beg Feb, 01	Mid Feb, 01
	Divide Into Three Assembly Groups:		
	1-Finish Fuselage & Internal Structure	Mid Feb, 01	Beg Mar, 01
	2-Finish Wing & Tails	Mid Feb, 01	Beg Mar, 01
	3-Finish Landing Gear & Speed Loader	Mid Feb, 01	Beg Mar, 01
	Build & Test Fly	End Feb, 01	Mid Mar, 01
	Modifications (If Necessary)	End Feb, 01	Mid Mar, 01
	Test Fly w/Full Load	End Feb, 01	Mid Mar, 01
Report Preparation	Appoint People To Prepare Report	Oct-00	Oct-00
	Collect Minutes From Each Group/Group Meeting	End Jan, 01	Mid Feb, 01
	Review DBF Rules For Report Writing	End Jan, 01	Mid Feb, 01
	Prepare Rough Draft	End Jan, 01	End Feb, 01
	Finish Report	End Jan, 01	Beg Mar, 01
	Proof Read	Beg Feb, 01	Beg Mar, 01

constructed with a solid foam core and lined with plastic sheeting was feasible. Because of the rectangular wing, the airfoil section was constant along the span; this made construction easy in that the foam could be cut shaped. It was not necessary to set up structural webs internal the wing for support. The foam would serve as the load carrier, and the plastic lining would ensure the smooth shape of the airfoil all along the span. Other materials such as fiberglass were considered, but even though the added strength of the fiberglass would help as another load carrying structure, the added weight might be high. Even if the foam and plastic lining approach were not strong enough, an I-beam spar running inside the foam would not be difficult to fabricate and assemble.

3.1.2 Fuselage

The primary consideration in designing the fuselage was to maximize the internal payload capacity. Since flight sorties had to be completed with both tennis balls and steel blocks, it was necessary to determine the number of tennis balls allowable in any configuration. Initial efforts were made to research maximizing volume, and it was found that volume efficiency, defined as the number of tennis balls in a given volume, increased as the balls were organized in a certain pattern. This pattern required a single tennis ball at the center of the formation, and additional tennis balls were added surrounding the center. In a planar configuration, the pattern would look like one tennis ball surrounded by six other tennis balls. However, it was obvious that even though volume efficiency increased quickly as more balls were placed in the formation, the fuselage also quickly increased in size, thus affecting aerodynamic performance.

Other considerations made to fuselage design were overall strength, time and ease of manufacture, and ease of integrating the other components-wing, vertical and horizontal stabilizer, and landing gear. A lifting body design was suggested, however the required investment in research and design would greatly overshoot what the team had available. Again, limitations in time and manpower limited the team greatly in the choices for design routes.

It was quickly realized that manufacturing skill level would play a role in what configuration the team chose. It was agreed that the simplest and most feasible design would be a hollow cylinder fuselage. Although not very imaginative, this design had the manufacturing and aerodynamic characteristics we could work with in the short time we had. Strength in the fuselage would be sufficient for conceptual design, and it would not be difficult for later improvements in strength and rigidity if the design called for it. Also, because the material chosen to build the fuselage with was fiberglass, it was agreed that a fuselage could be manufactured quickly using a foam mold.

Component attachment was also considered in the design, but because manufacturing time and performance analysis was seen to be as relatively easy to do for the cylindrical fuselage, attachment was view only as a secondary consideration. The team decided that attachment would be done with separate structures to transfer loads between all of the components.

constructed with a solid foam core and lined with plastic sheeting was feasible. Because of the rectangular wing, the airfoil section was constant along the span; this made construction easy in that the foam could be cut shaped. It was not necessary to set up structural webs internal the wing for support. The foam would serve as the load carrier, and the plastic lining would ensure the smooth shape of the airfoil all along the span. Other materials such as fiberglass were considered, but even though the added strength of the fiberglass would help as another load carrying structure, the added weight might be high. Even if the foam and plastic lining approach were not strong enough, an I-beam spar running inside the foam would not be difficult to fabricate and assemble.

3.1.2 Fuselage

The primary consideration in designing the fuselage was to maximize the internal payload capacity. Since flight sorties had to be completed with both tennis balls and steel blocks, it was necessary to determine the number of tennis balls allowable in any configuration. Initial efforts were made to research maximizing volume, and it was found that volume efficiency, defined as the number of tennis balls in a given volume, increased as the balls were organized in a certain pattern. This pattern required a single tennis ball at the center of the formation, and additional tennis balls were added surrounding the center. In a planar configuration, the pattern would look like one tennis ball surrounded by six other tennis balls. However, it was obvious that even though volume efficiency increased quickly as more balls were placed in the formation, the fuselage also quickly increased in size, thus affecting aerodynamic performance.

Other considerations made to fuselage design were overall strength, time and ease of manufacture, and ease of integrating the other components-wing, vertical and horizontal stabilizer, and landing gear. A lifting body design was suggested, however the required investment in research and design would greatly overshoot what the team had available. Again, limitations in time and manpower limited the team greatly in the choices for design routes.

It was quickly realized that manufacturing skill level would play a role in what configuration the team chose. It was agreed that the simplest and most feasible design would be a hollow cylinder fuselage. Although not very imaginative, this design had the manufacturing and aerodynamic characteristics we could work with in the short time we had. Strength in the fuselage would be sufficient for conceptual design, and it would not be difficult for later improvements in strength and rigidity if the design called for it. Also, because the material chosen to build the fuselage with was fiberglass, it was agreed that a fuselage could be manufactured quickly using a foam mold.

Component attachment was also considered in the design, but because manufacturing time and performance analysis was seen to be as relatively easy to do for the cylindrical fuselage, attachment was view only as a secondary consideration. The team decided that attachment would be done with separate structures to transfer loads between all of the components.

could be used to power the aircraft, but a question arose as to how long the motors could be run. Total battery weight to run the motors was limited as set by contest rules, so there was only a certain amount of electrical power available to produce thrust. The team could only come up with a limited amount of information regarding the motors that would possibly be used in the aircraft. However, understanding that range and endurance played a significant part in obtaining a high flight score led to the conclusion that a single engine set up was the best course of action at this point without further investigation.

The type of engine to be used was fixed at the inception of the project. No funds were available and conservative estimates of the funds able to be raised seemed to show that the team could not purchase another engine. Previous teams had used an engine for the designs, and it was understood that the available motor could sufficiently power the current team's design. Because the team had decided to stay with a single motor design, it was fortunate that there was already a motor that could be used without having to purchase another one.

Moreover, the propeller chosen to attach to the motor was selected on the basis of the amount of thrust it could produce. Weight was not an issue for the selection since all propellers weighed almost the same, and if there were any difference, it would have not significantly affected the overall weight of the plane by much. Limited data was again available for the different propellers that could be used with the motor the team had, but a propeller was chosen without regard for diameter and pitch. Thrust production was the primary concern.

The team had limited resources to spend on analysis, and it was decided that the maximum amount of batteries allowed for the engine would be used to power the aircraft. Without analyzing the potential range, endurance, and time the aircraft could fly, it would be impossible to say the number of batteries required for the mission. Although the extra weight of the batteries certainly reduces the amount of payload the aircraft can carry, the team was sure that going with the decision to include as much power available was the safest route.

3.1.5 Control Surfaces

Control surface design was not considered to be as important as the previous sections. Because of the nature of the mission capability-carrying cargo as far as is possible- the handling qualities did not require special attention. In contrast to another type of aircraft where maneuvering might be a concern, the transport type aircraft in this project only needs to takeoff, land, and make some turns. Adequate control surface sizing needed to be done, but extensive analysis was not needed. Fortunately, this decision favored the team because of the limited manpower resources.

Horizontal and vertical stabilizers were to be sized using models from current transport aircraft. Balance was all that was needed for the stabilizers, and a symmetric airfoil was chosen for both parts on the aft tail.

The use of flaps was decided to be necessary to takeoff in the required distance set by contest rules. In addition, to make the design simpler, these flaps would serve as both lift increasing devices and

could be used to power the aircraft, but a question arose as to how long the motors could be run. Total battery weight to run the motors was limited as set by contest rules, so there was only a certain amount of electrical power available to produce thrust. The team could only come up with a limited amount of information regarding the motors that would possibly be used in the aircraft. However, understanding that range and endurance played a significant part in obtaining a high flight score led to the conclusion that a single engine set up was the best course of action at this point without further investigation.

The type of engine to be used was fixed at the inception of the project. No funds were available and conservative estimates of the funds able to be raised seemed to show that the team could not purchase another engine. Previous teams had used an engine for the designs, and it was understood that the available motor could sufficiently power the current team's design. Because the team had decided to stay with a single motor design, it was fortunate that there was already a motor that could be used without having to purchase another one.

Moreover, the propeller chosen to attach to the motor was selected on the basis of the amount of thrust it could produce. Weight was not an issue for the selection since all propellers weighed almost the same, and if there were any difference, it would have not significantly affected the overall weight of the plane by much. Limited data was again available for the different propellers that could be used with the motor the team had, but a propeller was chosen without regard for diameter and pitch. Thrust production was the primary concern.

The team had limited resources to spend on analysis, and it was decided that the maximum amount of batteries allowed for the engine would be used to power the aircraft. Without analyzing the potential range, endurance, and time the aircraft could fly, it would be impossible to say the number of batteries required for the mission. Although the extra weight of the batteries certainly reduces the amount of payload the aircraft can carry, the team was sure that going with the decision to include as much power available was the safest route.

3.1.5 Control Surfaces

Control surface design was not considered to be as important as the previous sections. Because of the nature of the mission capability-carrying cargo as far as is possible- the handling qualities did not require special attention. In contrast to another type of aircraft where maneuvering might be a concern, the transport type aircraft in this project only needs to takeoff, land, and make some turns. Adequate control surface sizing needed to be done, but extensive analysis was not needed. Fortunately, this decision favored the team because of the limited manpower resources.

Horizontal and vertical stabilizers were to be sized using models from current transport aircraft. Balance was all that was needed for the stabilizers, and a symmetric airfoil was chosen for both parts on the aft tail.

The use of flaps was decided to be necessary to takeoff in the required distance set by contest rules. In addition, to make the design simpler, these flaps would serve as both lift increasing devices and

plane could fly faster and therefore more laps to score higher in the flight phase of the contest. However, whatever design was chosen, strength could not be sacrificed for weight. Where ever possible, composite materials were used to keep low weight but to also keep strength.

3.2.4 Cost

The ultimate goal of the sponsors of this competition is to give an insight into the real world engineering work. As in any real world applications final product must be attractive enough to encourage the end user to purchase the product that was built with lot of time and effort. However, one of the main factors that the end user considers is how costly that particular item is. Therefore, cost of one of the main FOMs.

Also, careful consideration needed to be given to the overall cost of the unit since only a limited amount of funds were available to achieve a difficult task.

Figure 3.1 Figures of Merit, Conceptual Phase

Airplane Type:	High Speed Swept Wing (F18 Design)
Tails:	Horizontal & Two Vertical
Payload:	100 Tennis Balls / Equal Weight In Steel
Payload Carrying System:	Speed Loader
Total Airplane Weight:	35.0 lbs
Wing Span:	7.0 ft
Wing Area:	7.0 ft ²
Wing Loading:	5.0 lbs/ ft ²
Total Length Of Airplane:	74.5 inches
Motor:	Astro Cobalt 40
Battery:	Sanyo 2000
Propeller:	18.0inch diameter

plane could fly faster and therefore more laps to score higher in the flight phase of the contest. However, whatever design was chosen, strength could not be sacrificed for weight. Where ever possible, composite materials were used to keep low weight but to also keep strength.

3.2.4 Cost

The ultimate goal of the sponsors of this competition is to give an insight into the real world engineering work. As in any real world applications final product must be attractive enough to encourage the end user to purchase the product that was built with lot of time and effort. However, one of the main factors that the end user considers is how costly that particular item is. Therefore, cost of one of the main FOMs.

Also, careful consideration needed to be given to the overall cost of the unit since only a limited amount of funds were available to achieve a difficult task.

Figure 3.1 Figures of Merit, Conceptual Phase

Airplane Type:	High Speed Swept Wing (F18 Design)
Tails:	Horizontal & Two Vertical
Payload:	100 Tennis Balls / Equal Weight In Steel
Payload Carrying System:	Speed Loader
Total Airplane Weight:	35.0 lbs
Wing Span:	7.0 ft
Wing Area:	7.0 ft ²
Wing Loading:	5.0 lbs/ ft ²
Total Length Of Airplane:	74.5 inches
Motor:	Astro Cobalt 40
Battery:	Sanyo 2000
Propeller:	18.0inch diameter

This airfoil was chosen by referring to Abbott and VonDoenhoff's Theory of Wing Sections (1949). Wing drag is discussed in a later section.

Wing shape and configuration had already been chosen in the conceptual phase of design. Thus, wing planform area was easy to calculate because of the rectangular shape. Once the estimate of the required wing area was completed, further analysis on wing takeoff and landing performance was necessary.

4.1.2 High Lift Devices

Although the estimated cruise velocity was assumed to be a constant speed, that is takeoff, cruise, and landing speed would be the same, takeoff distance was an important consideration. This distance was set by contest rules, and the aircraft had to be off of the ground within that distance. Because takeoff distance is the sum of the distance covered in accelerating the aircraft to takeoff speed and then lifting the plane, it was necessary to reduce takeoff speed. In order to generate more lift to lift the plane during takeoff, a decision was made to install flaps at the trailing edges of the wings. In addition, to maximize lift generation, the flaps were to extend the wing tips. In effect, they would be full span flaps. Again, Nicolai was referenced to size the flaps.

In the model, it was first necessary to construct a basic C_l vs. angle of attack (α) graph for the airfoil. This was done by referencing the NACA 4418 data in Abbott and VonDoenhoff. Once this had been done, analysis could be done on the addition of flaps to the airfoil. Since the airfoil is a two-dimensional section, adding flaps to the airfoil would be comparable to adding full span flaps. According to Nicolai, adding plain trailing edge flaps results in a change of the α corresponding to zero lift (α_{0L}).

$$\Delta\alpha_{0L} = -(dC_l/d\delta_f)(1/C_{l\alpha})\delta_f K'$$

Where $C_{l\alpha}$ is the section lift curve slope (per radian), K' is the correction for non-linear effects, $dC_l/d\delta_f$ is the change in C_l for a change in δ_f (flap deflection in degrees, positive downward). K' and $dC_l/d\delta_f$ are values found in Nicolai (9-10,11). Once the change in zero lift angle of attack had been calculated, it was possible to construct the C_l vs. α plot for the airfoil. The results for the NACA 4418 are as follows.

Curve labeled as "line 1" is the basic airfoil plot of lift coefficient vs. angle of attack. The second line and the third line show the change of the plot with flap deflections of 10 and 30 degrees respectively.

This airfoil was chosen by referring to Abbott and VonDoenhoff's Theory of Wing Sections (1949). Wing drag is discussed in a later section.

Wing shape and configuration had already been chosen in the conceptual phase of design. Thus, wing planform area was easy to calculate because of the rectangular shape. Once the estimate of the required wing area was completed, further analysis on wing takeoff and landing performance was necessary.

4.1.2 High Lift Devices

Although the estimated cruise velocity was assumed to be a constant speed, that is takeoff, cruise, and landing speed would be the same, takeoff distance was an important consideration. This distance was set by contest rules, and the aircraft had to be off of the ground within that distance. Because takeoff distance is the sum of the distance covered in accelerating the aircraft to takeoff speed and then lifting the plane, it was necessary to reduce takeoff speed. In order to generate more lift to lift the plane during takeoff, a decision was made to install flaps at the trailing edges of the wings. In addition, to maximize lift generation, the flaps were to extend the wing tips. In effect, they would be full span flaps. Again, Nicolai was referenced to size the flaps.

In the model, it was first necessary to construct a basic C_l vs. angle of attack (α) graph for the airfoil. This was done by referencing the NACA 4418 data in Abbott and VonDoenhoff. Once this had been done, analysis could be done on the addition of flaps to the airfoil. Since the airfoil is a two-dimensional section, adding flaps to the airfoil would be comparable to adding full span flaps. According to Nicolai, adding plain trailing edge flaps results in a change of the α corresponding to zero lift (α_{0L}).

$$\Delta\alpha_{0L} = -(dC_l/d\delta_f)(1/C_{l\alpha})\delta_f K'$$

Where $C_{l\alpha}$ is the section lift curve slope (per radian), K' is the correction for non-linear effects, $dC_l/d\delta_f$ is the change in C_l for a change in δ_f (flap deflection in degrees, positive downward). K' and $dC_l/d\delta_f$ are values found in Nicolai (9-10,11). Once the change in zero lift angle of attack had been calculated, it was possible to construct the C_l vs. α plot for the airfoil. The results for the NACA 4418 are as follows.

Curve labeled as "line 1" is the basic airfoil plot of lift coefficient vs. angle of attack. The second line and the third line show the change of the plot with flap deflections of 10 and 30 degrees respectively.

coefficient from the previous construction of lift coefficient vs. alpha plot. With these changes, the basic wing C_L vs. alpha can be made.

To account for flap deflection, the change in maximum lift coefficient must be known. According to Nicolai 9-21, this change is equal to

$$\Delta C_{Lmax} = \Delta C_{lmax}(S_{WF}/S_W)K_A$$

Where K_A is a correction for wing sweep. This factor can be found in Nicolai 9-22. ΔC_{lmax} can be found from the previous construction of the airfoil lift coefficient vs. angle of attack plot. S_{WF} is the area of the part of the wing influenced by the flap. In this case, the flap extends all the way to the wingtips, so the flap covers the whole span of the wing. Since the whole span is covered, the whole wing is influenced by the presence of the flaps. S_W is the wing planform area. Since ΔC_{Lmax} is known for a given flap deflection, another lift coefficient vs. alpha curve can be constructed. Figure 4.2 shows the results for the wing design.

coefficient from the previous construction of lift coefficient vs. alpha plot. With these changes, the basic wing C_L vs. alpha can be made.

To account for flap deflection, the change in maximum lift coefficient must be known. According to Nicolai 9-21, this change is equal to

$$\Delta C_{Lmax} = \Delta C_{lmax}(S_{WF}/S_W)K_\Lambda$$

Where K_Λ is a correction for wing sweep. This factor can be found in Nicolai 9-22. ΔC_{lmax} can be found from the previous construction of the airfoil lift coefficient vs. angle of attack plot. S_{WF} is the area of the part of the wing influenced by the flap. In this case, the flap extends all the way to the wingtips, so the flap covers the whole span of the wing. Since the whole span is covered, the whole wing is influenced by the presence of the flaps. S_W is the wing planform area. Since ΔC_{Lmax} is known for a given flap deflection, another lift coefficient vs. alpha curve can be constructed. Figure 4.2 shows the results for the wing design.

All Deflections are Flap Deflections
Airfoil: NACA 4418

Inputs

α_{0L} , deg	-3.8
$C_{l\alpha}$, per deg	0.105
α_{climax}	14
α_{break}	7.2
α_{max}	1.53

cl_{α} , per rad	6.016
-------------------------	-------

Addition of Flaps: Plain Flaps

C_l/c	0.20
dC/ddf	3.8

Table 1. C_l vs. Alpha Points	
Alpha, deg	C_l
-3.8	0
7.2	1.155
14	1.53
18	1.38

zero lift
break
stall
end

Table 2. Deflection Info, from reference		
deflection, deg	K'	delta α_0L
0	1.000	0.000
10	1.000	-6.316
20	0.870	-10.991
30	0.680	-12.886
40	0.600	-15.159
50	0.550	-17.370
60	0.510	-19.328

Table 3. Delta α stall, from refer	
deflection, deg	delta α stall
0	0
10	-0.40
20	-1.00
30	-1.80
40	-3.00
50	-4.30
60	-5.80

A parameter

4

Table 4. Alpha Changes due to Flap				
Deflection, deg	zero lift	break	stall	end
0	-3.80	7.20	14.00	18.00
10	-10.12	6.80	13.60	17.60
20	-14.79	6.20	13.00	17.00
30	-16.69	5.40	12.20	16.20
40	-18.96	4.20	11.00	15.00
50	-21.17	2.90	9.70	13.70
60	-23.13	1.40	8.20	12.20

Table 5. Estimation of delta C_{lmax} at Various Flap Deflections	
Deflection, deg	delta C_{lmax}
0	0.000
10	0.520
20	-1.530
30	1.020
40	-1.530
50	-1.530
60	-1.530

Table 6. C_l at Various Flap Deflections				
deflection, deg	zero lift	break	stall	end
0	0.00	1.16	1.53	1.38
10	0.00	1.68	2.05	1.90
20	0.00	-0.38		-0.15
30	0.00	2.18	2.55	2.40
40	0.00	-0.38		-0.15
50	0.00	-0.38		-0.15
60	0.00	-0.38		-0.15

Figure 4.3 Calculation Results for NACA 4418 Airfoil for Various Flap Deflections

All Deflections are Flap Deflections
Airfoil: NACA 4418

Inputs

α_{0L} , deg	-3.8
$C_{l\alpha}$, per deg	0.105
α_{clmax}	14
α_{break}	7.2
C_{lmax}	1.53

$C_{l\alpha}$, per rad	6.016
-------------------------	-------

Addition of Flaps: Plain Flaps

C_l/c	0.20
dC_l/ddf	3.8

Table 1. C_l vs. Alpha Points	
Alpha, deg	C_l
-3.8	0
7.2	1.155
14	1.53
18	1.38
	zero lift
	break
	stall
	end

Table 2. Dedeflection Info, from reference		
deflection, deg	K'	delta a_{0L}
0	1.000	0.000
10	1.000	-6.316
20	0.870	-10.991
30	0.680	-12.886
40	0.600	-15.159
50	0.550	-17.370
60	0.510	-19.328

Table 3. Delta a stall, from reference	
deflection, deg	delta a stall
0	0
10	-0.40
20	-1.00
30	-1.80
40	-3.00
50	-4.30
60	-5.80

A parameter 4

Table 4. Alpha Changes due to Flap				
Deflection, deg	zero lift	break	stall	end
0	-3.80	7.20	14.00	18.00
10	-10.12	6.80	13.60	17.60
20	-14.79	6.20	13.00	17.00
30	-16.69	5.40	12.20	16.20
40	-18.96	4.20	11.00	15.00
50	-21.17	2.90	9.70	13.70
60	-23.13	1.40	8.20	12.20

Table 5. Estimation of delta C_{lmax} at Various Flap Deflections	
Deflection, deg	delta C_{lmax}
0	0.000
10	0.520
20	-1.530
30	1.020
40	-1.530
50	-1.530
60	-1.530

Table 6. C_l at Various Flap Deflections				
deflection, deg	zero lift	break	stall	end
0	0.00	1.16	1.53	1.38
10	0.00	1.68	2.05	1.90
20	0.00	-0.38		-0.15
30	0.00	2.18	2.55	2.40
40	0.00	-0.38		-0.15
50	0.00	-0.38		-0.15
60	0.00	-0.38		-0.15

Figure 4.3 Calculation Results for NACA 4418 Airfoil for Various Flap Deflections

4.2 Fuselage Design

Since the basic shape for the fuselage was determined in the conceptual phase of design, further analysis on geometry was not necessary. Internal components such as the batteries, remote controller receiver, and structure to mount the engine were all initially placed as near together as possible so that additional payload would not change the center of gravity much. No lift was going to be generated for the fuselage; its only use was to house all of the aircraft's necessary parts and payload. However, aerodynamic drag was going to be a major consideration. This will be discussed in a later section.

4.2 Fuselage Design

Since the basic shape for the fuselage was determined in the conceptual phase of design, further analysis on geometry was not necessary. Internal components such as the batteries, remote controller receiver, and structure to mount the engine were all initially placed as near together as possible so that additional payload would not change the center of gravity much. No lift was going to be generated for the fuselage; its only use was to house all of the aircraft's necessary parts and payload. However, aerodynamic drag was going to be a major consideration. This will be discussed in a later section.

$$\Delta C_{D_{\text{gear}}} = \Delta f_{LG} A_{LG} / S_W$$

Where A_{LG} is the landing gear head on area. For the first iteration, the landing gear structure was neglected in the calculation of the head on area, thus the only area considered was the head on wheel area. Structure area was neglected because it was deemed that it would not affect the landing gear drag by any significant amount.

4.3.4 Total Drag Calculation

The total drag for the aircraft as described by Nicolai is

$$C_D = C_{D0} + K' C_L^2 + K'' (C_L - C_{L_{\min}})^2$$

Where C_{D0} is the total zero lift drag coefficient calculated by totaling the C_{D0} 's of the wing, fuselage, and landing gear in the case of the SDSU design. $C_{L_{\min}}$ is the lift coefficient for the wing when the angle of attack is zero. K' and K'' are factors determined from Nicolai. These K 's are called the drag due to lift factors. Once the K 's are determined, the total drag on the aircraft for a given C_L can be calculated, and a figure of the results for the SDSU preliminary design follows.

CL vs. CD

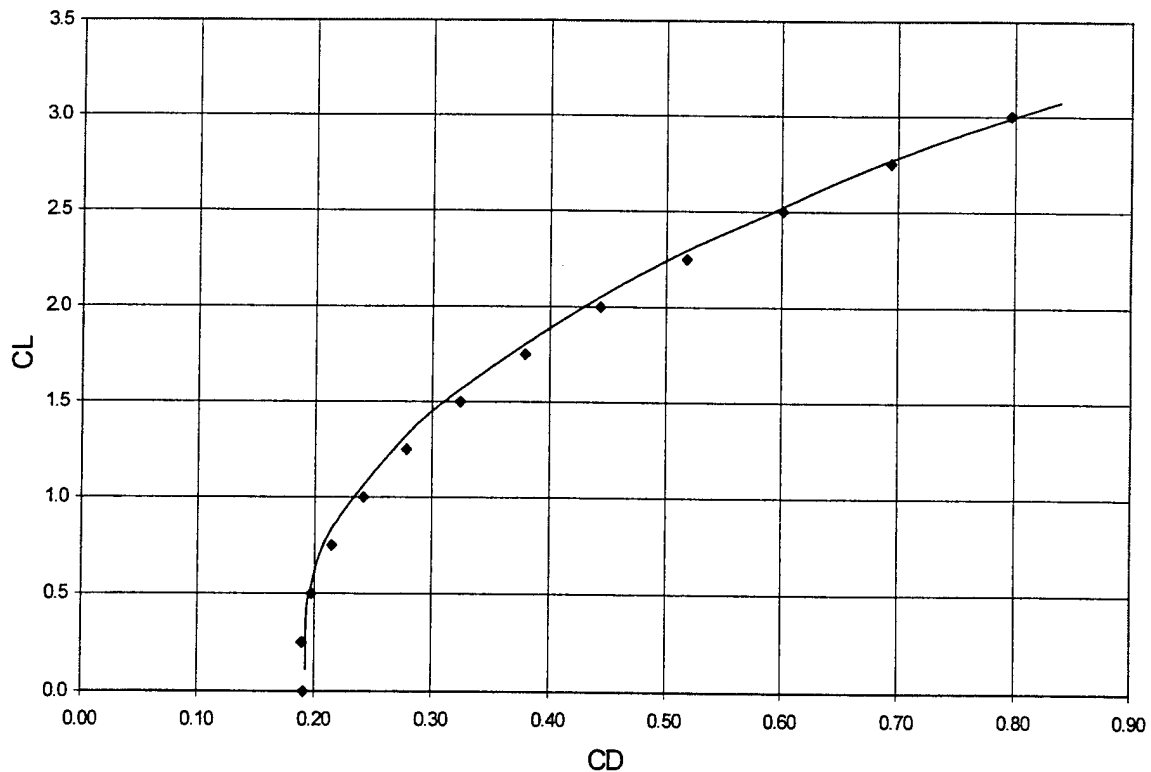


Figure 4.3 Lift Coefficient versus Drag Coefficient Results

$$\Delta C_{D_{\text{gear}}} = \Delta f_{LG} A_{LG} / S_w$$

Where A_{LG} is the landing gear head on area. For the first iteration, the landing gear structure was neglected in the calculation of the head on area, thus the only area considered was the head on wheel area. Structure area was neglected because it was deemed that it would not affect the landing gear drag by any significant amount.

4.3.4 Total Drag Calculation

The total drag for the aircraft as described by Nicolai is

$$C_D = C_{D0} + K' C_L^2 + K'' (C_L - C_{Lmin})^2$$

Where C_{D0} is the total zero lift drag coefficient calculated by totaling the C_{D0} 's of the wing, fuselage, and landing gear in the case of the SDSU design. C_{Lmin} is the lift coefficient for the wing when the angle of attack is zero. K' and K'' are factors determined from Nicolai. These K 's are called the drag due to lift factors. Once the K 's are determined, the total drag on the aircraft for a given C_L can be calculated, and a figure of the results for the SDSU preliminary design follows.

CL vs. CD

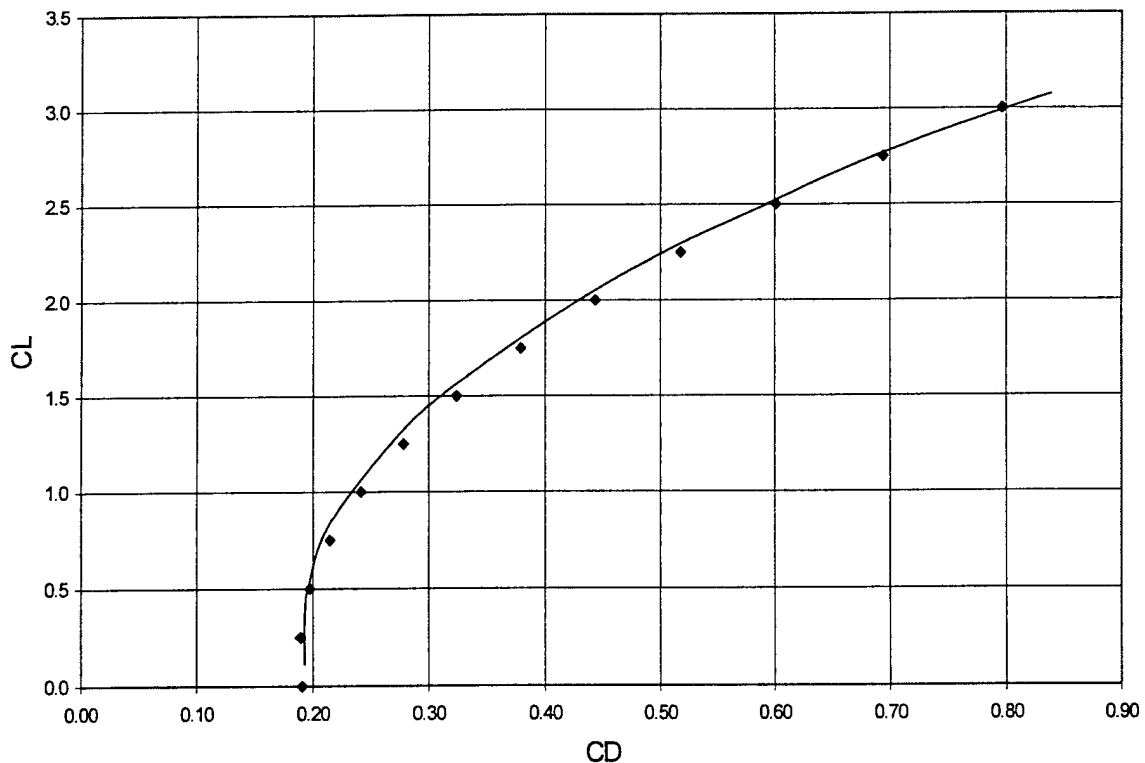


Figure 4.3 Lift Coefficient versus Drag Coefficient Results

5.0 Introduction

The conceptual and preliminary design phases gave the basic characteristics of the aircraft. The conceptual phase brought out the basic geometry and layout of the plane. It also included initial estimates on the total aircraft empty weight, payload weight, and the internal volume available for storage. The preliminary phase took the design further, going into aerodynamic analysis by determining the lift generated by the wing and the total drag acting on the plane. The detail design phase put all of the previously analyzed aspects of the plane to determine how well it will perform.

The only performance related requirements of the contest were that the aircraft had to takeoff within the designated 100 foot limit, it had to run a number of sorties and survive, and had to be able to takeoff and land many times. Taking off and landing are mostly dependent on the strength of the landing gear, and are not considered to be a part of the aerodynamics performance. The detail design is primarily concerned with the amount of ground roll the aircraft needs to take off, and the stability aspects of the aircraft.

5.1 Takeoff Distance

As in the previous sections of the preliminary design phase, Nicolai's Fundamental of Aircraft Design was used to estimate takeoff distance. According to Nicolai, the takeoff distance is "the distance required to accelerate from zero initial velocity to takeoff speed and climb over a 50 foot obstacle." There were no specifications on a 50 foot obstacle in the contest rules, so take off distance was defined to be the distance to get the aircraft from zero initial velocity to off the ground.

5.1.1 Estimation of Takeoff Velocity

In the conceptual design phase, the takeoff velocity was assumed to be the same as the cruise velocity. However, Nicolai provides a better estimation.

$$V_{TO} = 1.2[(W_{TO}/S)2/(\rho C_{Lmax})]$$

Where W_{TO} is the takeoff weight of the aircraft, which in this case was the same as the cruise weight and landing weight, and C_{Lmax} is the maximum lift coefficient for a particular flap setting. This value can be determined from the wing lift coefficient vs. angle of attack graph constructed in section 4.1.2. It was noted that the higher lift coefficient led to a decrease in takeoff velocity. Because W_{TO} was known and a maximum lift coefficient could be determined from the flap analysis done in the previous phase of design, a good estimate of the takeoff velocity could be made.

5.1.2 Estimation of Takeoff Distance

According to Nicolai, assuming the acceleration of the aircraft to be constant in the takeoff segment, then the takeoff distance could be estimated by

5.0 Introduction

The conceptual and preliminary design phases gave the basic characteristics of the aircraft. The conceptual phase brought out the basic geometry and layout of the plane. It also included initial estimates on the total aircraft empty weight, payload weight, and the internal volume available for storage. The preliminary phase took the design further, going into aerodynamic analysis by determining the lift generated by the wing and the total drag acting on the plane. The detail design phase put all of the previously analyzed aspects of the plane to determine how well it will perform.

The only performance related requirements of the contest were that the aircraft had to takeoff within the designated 100 foot limit, it had to run a number of sorties and survive, and had to be able to takeoff and land many times. Taking off and landing are mostly dependent on the strength of the landing gear, and are not considered to be a part of the aerodynamics performance. The detail design is primarily concerned with the amount of ground roll the aircraft needs to take off, and the stability aspects of the aircraft.

5.1 Takeoff Distance

As in the previous sections of the preliminary design phase, Nicolai's Fundamental of Aircraft Design was used to estimate takeoff distance. According to Nicolai, the takeoff distance is "the distance required to accelerate from zero initial velocity to takeoff speed and climb over a 50 foot obstacle." There were no specifications on a 50 foot obstacle in the contest rules, so take off distance was defined to be the distance to get the aircraft from zero initial velocity to off the ground.

5.1.1 Estimation of Takeoff Velocity

In the conceptual design phase, the takeoff velocity was assumed to be the same as the cruise velocity. However, Nicolai provides a better estimation.

$$V_{TO} = 1.2[(W_{TO}/S)^2/(\rho C_{Lmax})]$$

Where W_{TO} is the takeoff weight of the aircraft, which in this case was the same as the cruise weight and landing weight, and C_{Lmax} is the maximum lift coefficient for a particular flap setting. This value can be determined from the wing lift coefficient vs. angle of attack graph constructed in section 4.1.2. It was noted that the higher lift coefficient led to a decrease in takeoff velocity. Because W_{TO} was known and a maximum lift coefficient could be determined from the flap analysis done in the previous phase of design, a good estimate of the takeoff velocity could be made.

5.1.2 Estimation of Takeoff Distance

According to Nicolai, assuming the acceleration of the aircraft to be constant in the takeoff segment, then the takeoff distance could be estimated by

6.0 Introduction

The group investigated several processes to manufacture each one of the necessary parts for the airplane through the method of trial and error, our primary analytical method. The FOM's factored into the manufacturing plan included availability, required skill levels and cost.

6.1 Manufacture and Assembly of Major Parts

6.1.1 Wings and Tail

As foretold, the SDSU group used trial and error to decide how to manufacture and assemble the major parts of the vehicle. Lack of experience forced the group into the utilization of this costly method. The wings portray one example of this.

The first method of wing building attempted is as follows. First, a template of metal was constructed to conform to the shape of the desired airfoil. Then, a hot wire was used to cut a large piece of foam into the shape of the template. The wing-shaped foam was coated with resin, wrapped around with a layer of fiber, and then coated with more resin. After the resin dried, bubbles were still found in the fiberglass. The students had the option of sanding down the bubbles, but this would have taken away from the strength of the material. Hence, a second wing was constructed.

The second attempt succeeded. After shaping the foam with the hot wire, a spar made of carbon fiber was inserted through the length of the wing to give added strength. Mylar was then layered around the wing.

The tail was constructed exactly like the second method, but without a spar.

6.1.2 Fuselage

The SDSU group succeeded at making the fuselage during the first attempt. A hot wire was used to shape a piece of foam into a tube. After the foam was coated with resin, great care was taken to ensure that no bubbles formed while fiber was wrapped around. More resin was added, and any bubbles found were pierced with a needle and smoothed out. After the resin dried, the foam was slid out.

The back cone front cones for the fuselage were constructed in the same way, with similar success.

6.1.3 Landing Gears

Two attempts were made at building the landing gear. In the first attempt, a strip of aluminum was bent into a "μ" shape, with the center curve able to mate with the curvature of the bottom half of the fuselage. At both ends of the curve, the strip would take a sharp, pointed turn downwards. The strip would then straighten out on each side, forming the legs that would carry the wheels. Unfortunately, when the

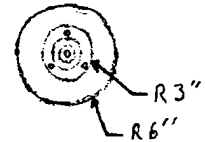
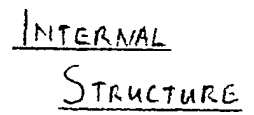


FRO

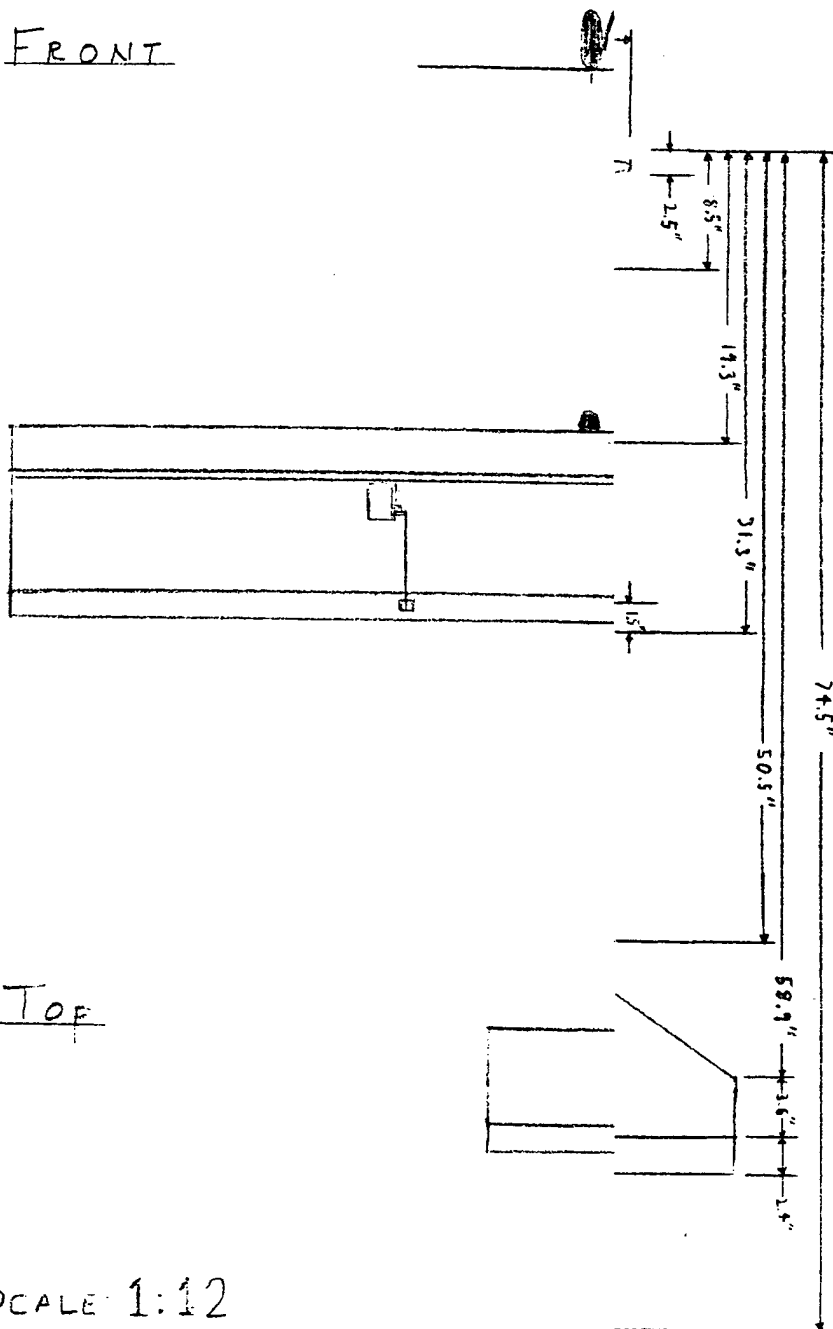


Top

SCALE

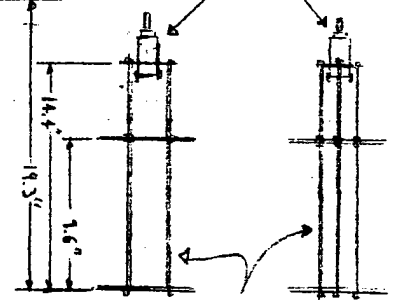


FRONT



TOF

MOTOA
COBALT 40



BATTERY
RELIEVER
AND SPEED
CONTROL BAY
(SEE EXPLODED
INTERNAL
STRUCTURE
CUTAWAY)

SCALE 1:12

aluminum was bent, the two pointed spots became extremely brittle, rendering the entire strip useless for a sixty pound cargo which would cause breakage at the two sharp points upon impact during landing.

For the second attempt, a strip of aluminum was used again. The students decided to cut the aluminum strip into two pieces and bend one of them to fit the curvature of the fuselage. The other piece of the strip was bent into the shape of a parabola. The two strips were bolted together as if they were a type of hyperbola. Holes were drilled through the bottom of both legs so that the wheels could be attached.

6.2 Figures of Merit

The figures of merit factored into the manufacturing plan included availability, required skill levels and cost.

6.2.1 Availability

The availability of materials for the students to use for the project depended on the recommendations of experienced remote control airplane builders. The advice of experienced builders was invaluable as to finding out where to go to obtain materials. The availability of equipment to shape the materials was not a difficult challenge. The students simply used equipment at San Diego State University.

6.2.2 Required Skill Level

Members of the group did possess some of the required skills that were necessary for the building of the airplane, including electrical assembly skills and fiberglass manufacturing. The students working on the landing gear acquired the skill on how to bend and shape aluminum from the on-campus aerospace laboratory technician.

6.2.3 Cost

The funds for the manufacturing process needed to be raised. The only cost of the process was the materials used, since the students were allowed to use the necessary shaping and drilling equipment for free.

6.3 Results

The trial and error method showed that, in order for an airplane to be built in the most efficient way, careful planning must be involved. As beginners, the students really had no other recourse than to investigate and try different methods of manufacturing techniques.

Cessna/ONR Student Design, Build, and Fly Competition
Naval Air Station
Patuxent River, MD

2000/2001 Contest Year
5th Annual Event

San Diego State University
"Full Monty"

Design Report
(Addendum Phase)

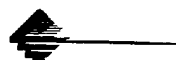


Table of Contents

	Page #
1. Executive Summary.....	(1 – 4)
Figure 1.1: Conceptual Design Configuration.....	2
Figure 1.2: Preliminary Design Configuration.....	3
Figure 1.3: Design And Mission Requirements.....	4
2. Management Summary.....	(5 – 6)
Figure 2.1: Milestone Chart.....	6
3. Conceptual Design Phase.....	(7 – 12)
3.0 Conceptual Design.....	7
3.1 Design Considerations.....	7 – 11
3.2 Figures Of Merit (FOMs)	11 – 12
4. Preliminary Design Phase.....	(13 – 23)
4.0 Introduction.....	13
4.1 Wing Design.....	13 - 19
4.2 Fuselage Design.....	20
4.3 Drag Analysis.....	21 - 22
4.4 Summary.....	23
5. Final Design Phase.....	(24 – 25)
5.0 Introduction.....	24
5.1 Takeoff Distance.....	24 – 25
5.2 Stability.....	25
Detailed Drawing Package.....	(26 – 27)
Three-View Drawing.....	26
Internal Structure.....	27
Control System.....	27
6. Manufacturing Phase.....	(28 – 29)
6.0 Introduction.....	28
6.1 Manufacture & Assembly of Major Parts.....	28
6.2 Figures Of Merit (FOM) Included.....	29
6.3 Results.....	29
7. Lessons Learned	
7.0 Introduction.....	30
7.1 Design Modifications.....	30

7.2	Next Generation Improvements.....	32
8.	Rated Aircraft Cost	
8.0	Introduction.....	34
8.1	Manufacturers Empty Weight.....	34
8.2	Rated Engine Power.....	34
8.3	Manufacturing Man Hours.....	34
8.4	Results.....	36

7.0 Lessons Learned

Minimal modifications were made to the aircraft after the proposal phase of the design. Major changes or improvements were not made due to insufficient resources such as time, money, and manpower. Aircraft manufacture continued well beyond the proposal phase, and a limited time remained for flight worthy tests before the conclusion of the addendum phase. Therefore, the overall configuration of the aircraft has not changed, and any changes made to the aircraft were small.

7.1 Design Modifications

7.1.1 Wing and Wing Sub Systems

The primary goal in the wing design was to provide enough lift for the design payload. Results from the flight tests would determine if the preliminary design met specifications.

However, since an important factor was not researched in the preliminary phase, namely engine data, the wing could have not been sufficiently designed. Estimates were made as to the thrusts the motor could produce, based on the previous experience of some of the team members. The results from the flight tests showed the inaccuracy of the estimates. Maximum design payload was tested to be half of the original value, significantly different to the preliminary design value.

Manufacturing difficulties also arose in the process. Due to the large wingspan, it was difficult to construct a wing with a constant section. It was determined that the wing would have to be cut into pieces such that ease of manufacture was at the point where a wing could be sufficiently produced. Initial estimates on wing construction were also underestimated, which led to large lag times in the overall manufacture of the aircraft.

Sufficient design was not completed for the wing subsystems- flaperon servos that would mount internal the wing. Manufacturing difficulty arose with servo implementation; exact locations for the servos were not determined and construction slowed.

Wing mount was not sufficiently designed also. The manufacturing team had many concerns regarding the original wing mounting procedure using rubber bands to secure the wing to the mount and fuselage. Although this configuration did not fail in initial flight tests, adequate data was not given to the manufacturing team as to the feasibility of the mount.

In initial flight tests, damage was caused to the aircraft in the difficulty to properly control it. It is unknown whether this was caused by poorly sized control surfaces, however it can be said that the stability and control of the aircraft was not sufficiently examined. This area in design needs to be adequately researched.

Future endeavors in this design shall require accurate manufacture's data and lab-tested data by the students of the motor. This will inevitably lead to an accurate design of the wing. Other requirements include a better understanding of all of the considerations of wing design, including allowances for extra weight accumulated during manufacturing, mounting considerations, and most importantly, considerations as to how the wing will be manufactured. Plans for manufacture should be included in the total design phase to optimize the time utilized in construction.

7.1.2 Fuselage

No significant changes were made to the fuselage at this time. However, considerations are being made in the reduction in the length of the fuselage accounting for the reduction of the maximum payload carrying capacity.

A tail gear was mounted to the rear of the fuselage. The only encountered problem seemed to be the strength integrity of the gear, which was easily solved by increasing the load carrying structure on the tail gear.

Flight tests did not reveal any necessary modifications that had to be made.

Future design considerations must include the primary type of payload carried by the aircraft. Manufacturing difficulties were not as significant in this component, however plans should also be included in the total design phase to increase efficiency in construction.

7.1.3 Landing Gear

Again, flight tests did not reveal any necessary changes required for a more efficient design. The landing gear structure held up under the load, and was designed sufficiently, if not well beyond operating limits.

Future considerations require an in-depth analysis of the structure to increase the main gear weight efficiency. Payload could be increase with a decrease in the landing gear weight while remaining at adequate strength levels.

Due to the simplicity in the design, manufacturing difficulties were not significant. There were minor struggles in construction, and a simple analysis of the tools available for manufacturing should account and reduce the minor construction difficulties.

7.1.4 Propulsion Systems

During the initial flight test, damage was suffered by the motor system. At this point, it is unknown whether the motor is salvageable. A new motor will be purchased and tests will resume to determine the final aircraft's performance.

No significant changes will be made to any of the motor systems. Although the mount for the motor separated from the fuselage, it was seen that this was only caused by the flight test mishap.

7.1.5 Control Systems

Initial flight tests yielded several results for improving the design of the flight control surfaces. During the manufacturing process, the control surfaces were reduced to account for ease in construction. Although the significance of this decision was not exactly known, it was also decided that more control power could be integrated after initial flight tests were concluded.

During the flight tests, it was seen that control was difficult in turning the aircraft. More rudder and aileron power was needed to perform the required maneuvers designated in the contest rules. Although new surfaces need to be constructed, the original size of the surfaces from the preliminary design will be implemented to correct problems in aircraft control.

Since the primary material chosen for the control surfaces was balsa, manufacturing was dependent on the size of wood to work with. Because of its weight, a minimal amount of wood was desired and therefore the control surfaces were reduced.

Future considerations should include an adequate sizing of the control surfaces. All of the surfaces should be overestimated to ensure aircraft control.

7.2 Next Generation Improvements

Initial flight tests were satisfactory for the SDSU design. This ground up design was plagued with problems ranging from significant limited resources in experience and knowledge to a huge time constraint placed on all of the team members. Next generation aircraft should have a steady base and foundation to design an aircraft. Methods used in this project can be used to modify the design. As the results from the flight tests show, the aircraft was flightworthy. However, tests needed to be done to correct airflow problems, interference problems, and other problems that might deviate the real life aircraft from the one designed on paper.

Improvements should include maximizing wing loading through better choices in airfoils and changing manufacturing processes. Aircraft drag did not seem a factor that can be reduced all that much, therefore, ways should be explored in increasing total thrust. Considerations

should include going to multiple engines (many transport type aircraft utilize this), increasing engine performance, and reducing the total empty weight. Analysis should be done in the propulsion area to get a better estimate of the aircraft's performance.

8.0 Rated Aircraft Cost

This part of the design gives a value to the aircraft designed. Since it is a part of the overall total score for the design including flight performance scores, it is a vital benchmark on the efficiency of the design. The total score for the contest for each aircraft is given by the following:

$$\text{Total Score} = \frac{\text{Written Report Score} * \text{Total Flight Score}}{\text{Rated Aircraft Cost}}$$

Therefore, to increase the total score, the rated aircraft score (RAC) should be minimized. The RAC considers the aircraft design in its components and assigning a standard value to each part and system. The following is a calculation of the RAC for the SDSU designed aircraft.

$$\text{Rated Aircraft Cost, \$ (Thousands)} = (A * \text{MEW} + B * \text{REP} + C * \text{MFHR}) / 1000$$

Where the values for the coefficients and variables are given in the Table 8.1 which was supplied in the contest rules.

8.1 Manufacturers Empty Weight

Calculation of the Manufacturers Empty Weight (MEW) was determines to be the total aircraft empty weight without payload and batteries. It was important to reduce the MEW to reduce the total score for the aircraft. Since this fact was being multiplied by \$100/lb, this factor significantly contributes to the RAC. MEW for the SDSU design was determined to be 13.26lbs.

8.2 Rated Engine Power

Another factor in the determination of the RAC is the Rated Engine Power (REP). According to the contest rules, REP is dependent on the number of engines, the value of the inline fuse from the battery to the speed controller, and the number of cells in the battery system. Again this value should be reduced to minimize RAC to increase total score. As given in the contest rules, the REP is determined from the following formula

$$\text{REP} = \# \text{ engines} * \text{Amp} * 1.2 \text{ V/cell} * \# \text{ cells}$$

REP for the SDSU design was determined to be 1728 watts.

8.3 Manufacturing Man Hours

The third element in calculating the total score of the aircraft was the number of hours required to build the components of the airplane. This values was calculated using the

breakdown structure prescribed in the contest rules. The following table gives values for the different man hours put into each component.

WBS		Airplane Characteristics	Number of Assigned Hours	Total Number of Hours
Wings	Basic	1	15	15
	Projected Area (ft ²)	8	4	32
	# Strut/Brace	1	2	2
	# Control Surface	5	3	15
Fuselage	# bodies	1	5	5
	Total Length (ft)	6	4	24
Empenage	Basic	-	5	5
	Vertical Surface	1	5	5
	Horizontal Surface	1	10	10
Flight Systems	Basic	-	5	5
	# Servos	5	2	10
Propulsion System	# Engines	1	5	5
	# Propellers/Fans	1	5	5
Total Hours				123

Table 8.1 Summary of WBS

8.3.1 Work Breakdown Structure

8.3.1.1 Wings

The Work Breakdown Structure (WBS) for the wing was dependent on a basic assumed manufacturing time, in addition to allowances for the projected area, the number of struts and braces, and the number of control surfaces on the wing. Values are presented in the previous table.

8.3.1.2 Fuselage

Similar to the wings, the WBS for the fuselage accounted for the number of bodies and the total length of the fuselage.

8.3.1.3 Empenage

WBS for the empennage included a basic time for manufacture, plus allowances for the vertical and horizontal surfaces.

8.3.1.4 Flight Systems

WBS for the Flight Systems included allowances for a basic manufacturing time and the number of servos used in the aircraft

8.3.1.5 Propulsion System

WBS for the propulsion systems included allowances for the number of engines in the design and the number of propellers used.

8.4 Results

From the previous calculations, the total Rated Aircraft Cost can be calculated. As it can be seen:

$$\text{RAC} = \text{Rated Aircraft Cost, \$ (Thousands)} = (A \cdot \text{MEW} + B \cdot \text{REP} + C \cdot \text{MFHR}) / 1000$$

$$\text{RAC} = [(\$100/\text{lb}) \cdot (13.26\text{lb}) + (\$1/\text{watt}) \cdot (1728\text{watt}) + (\$20/\text{hr}) \cdot (123\text{hr})] / 1000$$

$$\text{RAC} = 5.51 \text{ (Thousands of \$)}$$

Coef.	Description	Value
A	Manufacturers Empty Weight Multiplier	\$100 / lb.
B	Rated Engine Power Multiplier	\$1 / watt
C	Manufacturing Cost Multiplier	\$20 / hour
MEW	Manufacturers Empty Weight	Actual airframe weight, lb., without payload or batteries
REP	Rated Engine Power	# engines * Amp * 1.2 V/cell * # cells " Amp " will be the value of the inline fuse from the battery to the controller.
MFHR	Manufacturing Man Hours	Prescribed assembly hours by WBS. MFHR = \sum WBS hours WBS 1.0 Wing(s): 15 hr/wing. + 4 hr/sq. ft. Projected Area + 2 hr/strut or brace + 3 hr/control surface WBS 2.0 Fuselage and/or pods 5 hr/body. 4 hr/ft of length WBS 3.0 Empenage 5 hr.(basic) + 5 hr./Vertical Surface + 10 hr./Horizontal Surface WBS 4.0 Flight Systems 5 hr.(basic) + 2 hr./servo or controller WBS 5.0 Propulsion Systems 5 hr./engine + 5 hr./propeller or fan

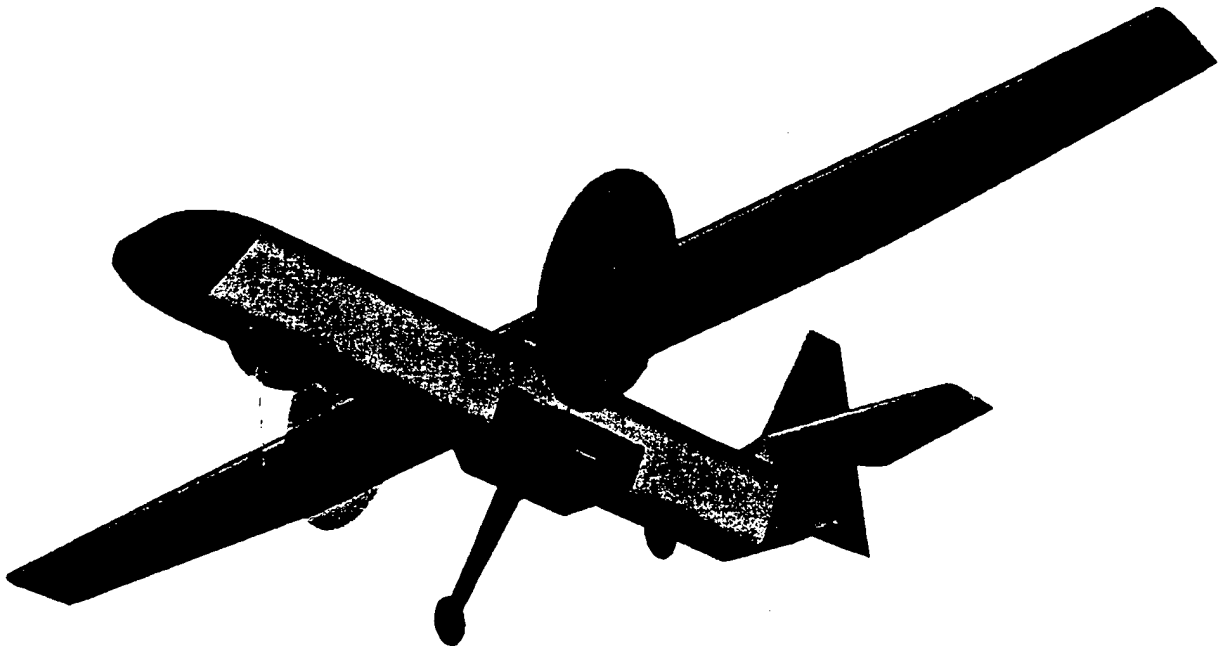
Table 8.2 Contest Rules for determination of RAC

**2000/2001 AIAA Foundation
Cessna/ONR Student Design/Build/Fly Competition**

DESIGN REPORT – PROPOSAL PHASE
MARCH 6, 2001



Department of Aerospace Engineering
Mississippi State University



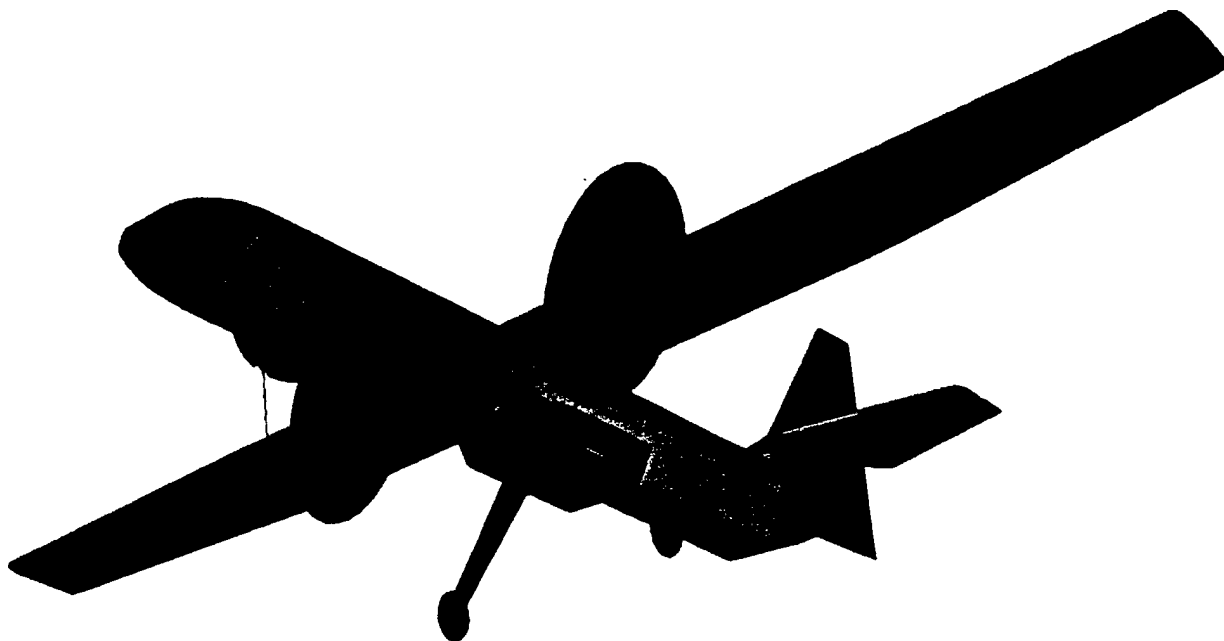
"Carbon Goose"

**2000/2001 AIAA Foundation
Cessna/ONR Student Design/Build/Fly Competition**

DESIGN REPORT – PROPOSAL PHASE
MARCH 6, 2001



Department of Aerospace Engineering
Mississippi State University



"Carbon Goose"

Table of Contents

1. Executive Summary.....	1
2. Management Summary	4
2.0 Introduction	4
2.1 Team Member Summary and Assignment Areas	5
2.2 Project Milestones.....	8
3. Conceptual Design Phase	9
3.0 Introduction	9
3.1 Figures of Merit	9
3.2 Design Concepts.....	10
3.3 Scoring of Design Concepts	14
3.3.1 Scoring of Concept 1	14
3.3.2 Scoring of Concept 2	14
3.3.3 Scoring of Concept 3	14
3.3.4 Scoring of Concept 4	15
3.3.5 Scoring of Concept 5	15
3.4 Conclusion	15
4 Preliminary Design Phase	16
4.0 Introduction	16
4.1 Figures of Merit	17
4.2 Numerical Optimization	17
4.2.0 Introduction.....	17
4.2.1 Design Variables	17
4.2.2 Design Constraints	18
4.2.3 Objective Function.....	19
4.3 Simplified 3-Dimensional Discretized Optimization	19
4.4 Final Selection of Parameters.....	20
4.5 Tail Sizing.....	21
4.6 Fuselage Design Concepts.....	22
4.7 Final Results	24
4.8 MathCad Code Listing	25
5. Detail Design	32
5.0 Introduction	32
5.1 Performance Data and Flight Handling.....	32
5.2 Component Selection.....	33
5.3 Systems Architecture	33

5.3.1 Radio System	33
5.3.2 Propulsion Architecture	34
5.4 Drawing Package	35
6. Manufacturing Plan	39
6.0 Introduction	39
6.1 Figures of Merit	39
6.2 Project Milestones	40
6.3 Fuselage Plug Construction	40
6.3.1 Main Fuselage Construction Steps	41
6.4 Mold Construction	41
6.4.1 Mold construction steps	41
6.5 Spar Construction	41
6.5.1 Spar Construction Steps	42
6.6 Wing Construction	42
6.6.1 Wing Construction Steps	42
6.7 Tail design	43
6.8 Systems Pod Design	44
Bibliography	45

1. Executive Summary

Because of the growing interest in remotely controlled aircraft shown by the students, the Department of Aerospace Engineering at Mississippi State University formed a Design/Build/Fly team for this competition. This was treated as an extracurricular activity with the students receiving no special credit in any of their courses. By joining the team, students sought an opportunity to further their education in aircraft design and development. The team consisted of twelve student members and one faculty advisor.

The goal of the competition is for each team to design, fabricate, and demonstrate the flight capabilities of an unmanned, electric powered, radio controlled airplane, which can meet the mission requirements. The airplane must perform two types of missions: large volume/light weight and small volume/heavy weight. The first mission consists of carrying as many tennis-balls (a maximum limit of 100-balls and minimum limit of 10-balls) around a closed pattern for two laps. The second mission consists of carrying steel blocks with a minimum of 5 lb. around a closed pattern for one lap with a 360-degree turn on the downwind leg. There is an allotted time of 10 minutes to fly as many missions (sorties) as possible. The restrictions on the plane are:

- The gross weight must be less than 55 lb.
- The wing span must be less than 10 ft.
- The take-off roll must be less than 200 ft.
- The battery pack to power the engines must be less than 5 lb.
- The pilot must be a member of the Academy of Model Aircraft (AMA).

The team was divided into six groups: Structures, Propulsion, Stability/Control, Performance, Flight Testing, and CAD. Each group held its own meetings but reported back to the team on their progress once a week during the regular meetings.

Five design concepts were considered in the conceptual design phase. When the Figures of Merit were applied to them, two concepts emerged as acceptable candidates: the conventional aircraft design and the conventional aircraft design with a "V"-tail. Because of the lack of adequate performance data and the complexity associated with the flight control system, the "V"-tail design concept was eliminated in favor of the conventional design configuration.

The preliminary design was conducted using two different approaches. One using a formal mathematical optimization technique based on four design variables, and the other using a one-dimensional optimization analysis based on MathCAD. Although the approaches were different, both converged on nearly the same design. In order to estimate the Manufacturers Empty Weight, the design analysis was based on historical values for the horizontal and vertical tails. A more detailed analysis was performed based on stability requirements once all other parameters were optimized. All top-level design specifications are listed in Table 1.1.

Table 1.1. Top-level design specifications.

Parameter	Value
Gross Weight	28.9 lb
Wing Area	7.3 ft ²
Wing Span	120 in
Fuselage Length	70 in
Horizontal Tail Area	286 in ²
Vertical Tail Area	150 in ²
Engine Type	Astro Flight Cobalt 15
Gearbox Type	Astro Flight 3.69:1
Prop Size	14X8
Number of Engines	2
Payload Capacity (steel)	12.9 lb
Payload Capacity (balls)	100
Endurance (at 70% average throttle)	8.8 min

The fuselage shape was determined by selecting a design that would have a small cargo length and frontal area accommodating a 100 tennis ball arrangement. The preliminary studies conducted by the Performance group indicated that the steel block weight would impose a more stringent requirement on the aircraft performance than the tennis-ball volume. Hence, the design of the fuselage focused primarily on the cross-sectional geometry that would accommodate carrying the maximum number of balls allowed in the competition with a reasonable constraint on the fuselage length. The cross-sectional geometry selected used a 5 ball trapezoidal arrangement per cross-sectional cell. Twenty of these cells arranged along the fuselage length comprise the cargo bay. The trapezoidal arrangement not only satisfied the design objectives, but also used cargo volume more efficiently.

Two different construction methods were considered: classic built-up and film-covered construction, and manual composite lay-up manufacturing. After application of the Figures of Merit, the composite construction was selected, mostly due to the decreased part construction time (resulting in easy reproducibility of the airplane) and superior structural characteristics.

A detailed design analysis provided the performance and handling characteristics as listed in Table 1.2.

Table 1.2. Predicted performance characteristics.

Parameter	Value
Takeoff distance	180 ft.
Maximum climb rate (loaded)	220 ft/min
Maximum climb rate (unloaded)	420 ft/min
Stall speed dirty	27.8 mph
Stall speed clean	31.1 mph
Cruise speed ($C_L=1.0$)	39.3 mph
Minimum turning radius (level turn at cruise speed)	75 ft
Maximum roll rate	75 deg/sec
G-load capacity	$\pm 15g$
Cruise endurance (including takeoff)	10 min
Cruise range	6.55 mi
Static Margin	27%

The performance characteristics reflect a reasonable, if narrow, performance envelope for an airplane designed to perform the specified mission involving the two alternate sorties.

The aircraft design chosen for this configuration is shown in Figure 1.1.

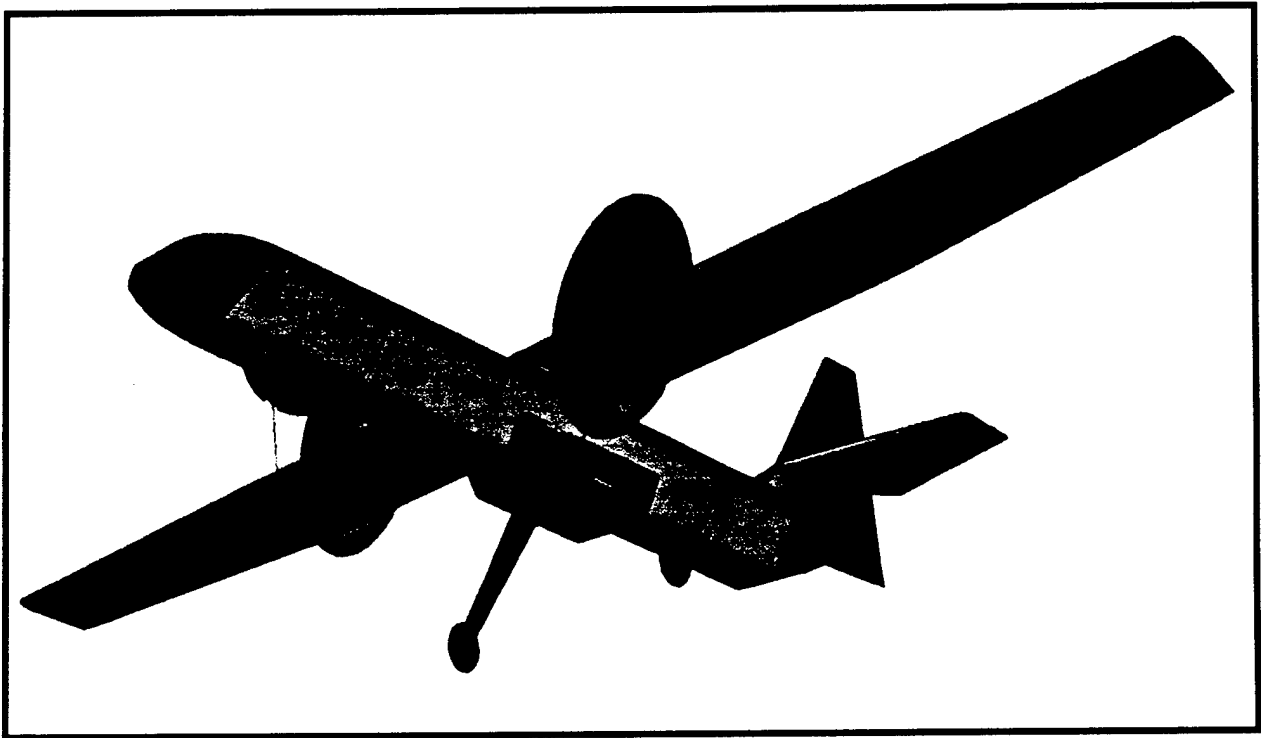


Figure 1.1 Design Chosen Named the "Carbon Goose"

Finally, a detailed manufacturing plan was developed and is presented herein.

2. Management Summary

2.0 Introduction

The Design/Build/Fly team consisted of twelve members: three freshmen, two sophomores, four seniors, and three graduate students all belonging to the Department of Aerospace Engineering at Mississippi State University. In their first official function, the team selected a faculty advisor and elected a team leader. It was intended that the advisor would suggest on the design and manufacturing of the aircraft, and the team leader would perform the administrative duties for the team. The team held regular weekly meetings with each lasting approximately two hours.

The team was divided into six groups: Structures, Propulsion, Stability/Control, Performance, Flight-testing, and CAD. The team leader selected the group leaders who organized meetings and reported to the team on their progress. The selection of group members was based on the members' qualifications and group requests. Because of the large number of groups, team members served in more than one group.

An administrative committee was also formed, which consisted of the team and group leaders. The duties of this committee were to acquire funding for support of this project, request the purchasing of materials, and manage the budget. Funding was requested and was provided by the Department of Aerospace Engineering and the College of Engineering. A member of the committee was designated as the sole authority for all purchasing. This arrangement helped to organize and manage the purchasing of required items and related bookkeeping activities.

2.1 Team Member Summary and Assignment Areas

- Masoud Rais-Rohani Associate professor of Aerospace Engineering and faculty advisor to the team. He has advised teams in similar competitions, and he brings these experiences to the team.
- Bryan L. Gassaway Graduate student. He was elected the team leader. His duties included scheduling, communicating with group leaders, arranging transportation to and lodging at the contest site, and working within different groups when needed.
- John L. Freudenthal Graduate student. He was appointed the leader of the Performance group and co-leader of the Flight-testing group. He is AMA certified and has built and flown remotely controlled aircraft for 12 years. He brought his experience and knowledge to the Performance group and collaborated with the Propulsion and Stability/Control groups.
- Michael L. McNabb Graduate student. He was appointed the group leader of the Structures and CAD groups. He has taken courses in the analysis of composite structures and worked in the field of composites for more than five years. He also collaborated with the Performance group.
- Jeremy M. Sebens Senior. He was appointed the leader of the Propulsion group. He is a laboratory technician for the department and is experienced in conducting tests involving the subsonic wind tunnel. He performed wind tunnel tests of different engine and propeller combinations with his group. He has flown remotely controlled aircraft for eight years. He also collaborated with the Performance and Flight-testing groups.
- Robbi A. Jouben Senior. He was appointed the leader of the Stability/Control group. His duties included the sizing of the horizontal and vertical tails, control surface sizing, control power analysis, and aerodynamic control load analysis. He also collaborated with the Structures group.

Anthony J. Fabiszak	Senior. He was appointed as the co-leader of the Flight-testing group. He is knowledgeable in the field of composite structures and played a major role in the manufacturing of the airplane. He is also AMA certified and has designed, built, and flown remotely controlled aircraft for more than ten years. He also collaborated with the Structures group.
Michael S. Cancienne	Senior. He replaced a team member who left because of a co-op position. Even though he did not participate in the design of the airplane, his skills in composite materials and manufacturing proved quite handy.
K. Erin Wahlers	Sophomore. She played a supportive role in the performance calculations and helped with the mathematical software development. She also collaborated with the CAD group.
Matthew J. Monti	Sophomore. He played a supportive role in the manufacturing of the airplane. His duties included the making of the wing and tail templates for the airfoils. He also collaborated with the Structures and CAD groups.
M. Jordan Haines	Freshman. He was involved with propulsion calculations and wind tunnel measurements. He helped with acquiring funding from the College of Engineering.
David J. Bodkin	Freshman. He helped with the manufacturing of the airplane and provided support to the Stability/Control group.
H. Fred Bufford	Freshman. He helped with the manufacturing of the airplane and provided support to the Propulsion group.

Table 2.1 was created to quantify the involvement of each member. A value of zero means no participation by that member in the specified area, and a value of five means maximum participation.

Table 2.1 Member's Involvement in Assigned Areas

	Bryan Gassaway	John Freudenthal	Michael McNabb	Jeremy Sebens	Robbi Jouben	Anthony Fabiszak	Michael Cancienne	K. Erin Wahlers	Matthew Monti	M. Jordan Haines	David Bodkin	H. Fred Bufford
Structures:												
Wing	0	0	5	0	0	4	3	0	2	0	0	0
Fuselage	0	0	5	0	0	4	3	0	2	0	0	0
Tail	0	0	4	5	0	3	3	0	2	0	0	0
Manufacturing:												
Wing	3	3	4	3	3	5	4	3	3	3	3	0
Fuselage Plug	4	2	4	4	1	4	4	1	2	3	3	1
Fuselage	/	/	/	/	/	/	/	/	/	/	/	/
Ball Carrier	/	/	/	/	/	/	/	/	/	/	/	/
Horizontal and Vertical Tail	/	/	/	/	/	/	/	/	/	/	/	/
Component tray	/	/	/	/	/	/	/	/	/	/	/	/
Proposal Report	5	3	5	5	2	1	0	0	0	0	0	0
Flight Testing:												
Pilot	/	/	/	/	/	/	/	/	/	/	/	/
Ground Crew	/	/	/	/	/	/	/	/	/	/	/	/
Other	/	/	/	/	/	/	/	/	/	/	/	/
Propulsion	0	3	0	5	0	0	0	0	0	3	0	3
Performance:												
Design Optimization Tool	5	2	3	3	0	0	0	2	0	0	0	0
MathCad	3	3	5	5	0	0	0	2	0	0	0	0
CAD:												
Components	0	0	4	0	0	0	0	0	4	0	0	0
Engine Mounts	0	0	3	3	0	2	0	0	0	0	0	0
Wing	0	0	5	0	0	3	0	0	0	0	0	0
Fuselage	0	0	5	0	0	3	0	0	0	0	0	0
Horizontal and Vertical Tail	0	0	4	2	0	4	0	0	0	0	0	0
Stability & Control:												
Horizontal and Vertical Tail Sizing	0	5	0	0	4	0	0	0	0	0	2	0
Servo Selection	4	0	0	4	0	0	0	0	0	0	2	0
Control Surface Sizing	0	4	0	4	0	4	4	0	0	0	2	0
Administration:												
Budget	5	2	2	2	2	2	0	0	0	0	0	0
Funding	5	0	0	4	0	0	0	2	0	2	0	0
Purchasing	0	0	0	5	0	0	0	0	0	0	0	0

0 – No Involvement 5 – Maximum Involvement

 Incomplete activity

2.2 Project Milestones

As shown in Table 2.2, the project was broken into four phases: Design and Sizing, Manufacturing, Proposal Report, and Flight Testing.

Phase I focused on the design analysis involving the Structures, Propulsion, Stability/Control, and Performance groups. The planned completion for this phase was November 30, 2000, and the actual completion was January 31, 2001. The delay was due to exam conflicts, winter vacation, and difficulty with the performance optimization task.

Table 2.2. Project Milestones

Phase	Planned Date of Completion	Actual Date of Completion
Phase I: Design and Sizing	November 31, 2000	February 1, 2001
Phase II: Manufacturing	January 31, 2001	N/A
Phase III: Proposal Report	February 28, 2001	March 7, 2001
Phase IV: Flight Testing	April 16, 2001	N/A

Phase II focused on the manufacturing of the airplane. It was originally scheduled under the assumption that the Arboga CNC milling machine at Raspet Flight Research Laboratory would be operational. However, in January 2001, the milling machine went offline for repairs and would not be online until the end of May 2001. Since the consensus of the group was still to use composite construction to manufacture the airplane, the molds were made by hand. The completion date of this phase is anticipated to be March 16, 2001.

Phase III involved writing the proposal report. Due to the manufacturing deadlines, the report was delayed by one week. Several group leaders helped the team leader in writing with this report.

Phase IV, involving flight testing, was originally scheduled to last two months. Delays in phases I and II will reduce the time that will be devoted to this task. However, the team is confident that the airplane will be built and flight-tested well in advance of the completion date. The week of spring break will be used to make up for the lost time.

3. Conceptual Design Phase

3.0 Introduction

The conceptual design phase was carried out in a series of group discussions, in which team members developed and presented ideas on the configuration of the airplane. These ideas were limited to aircraft configuration only; specific design parameters such as sizing, engine selection, and airfoil selection – to name a few – were reserved for the preliminary design phase. Concepts were evaluated based on Figures of Merit (FOM's); and based on the final evaluation, a basic configuration was selected.

3.1 Figures of Merit

The FOM's were chosen based on performance, Rated Aircraft Cost, manufacturability, weight lifting capacity, and innovation. Each FOM was given a value ranging from zero to four (four indicating a very important FOM). The FOM's and their assigned weight factors are listed in Table 3.1.

Table 3.1 Conceptual Design Figures of Merit and Associated Weight Factors

FOM	Description	Weight
1. Takeoff Performance	Capability of the airplane to take off in less than 180 ft	4
2. RAC	Rated Aircraft Cost of the airplane	4
3. Cruise Performance	Performance of the airplane during mission sorties	3
4. Manufacturability	Ease of construction	2
5. Weight Lifting Capacity	Capability to be built to 55 lb GW	2
6. Innovation	Design Innovation	0.5

FOM's 1 and 2 are considered to be most important. These two parameters directly relate the total FOM score and airplane requirements. FOM 3 was important because about 75% of the flight time will be spent in cruise. Manufacturability, FOM 4, was necessary to give some information on the fabrication of a design. The FOM on Weight Lifting Capacity was chosen as to allow for the possibility that the sizing of the Preliminary Design Phase might call for an aircraft of the maximum gross weight, 55lb. While the FOM on Innovation was given a very small weight factor, it reflected the desire of the team to experiment with some new ideas without compromising the integrity of the selected design concept.

3.2 Design Concepts

Concept 1: Twin-engine, Twin-boom, A-tail Airplane with Cargo Pod

This concept, as shown in Figure 3.1, called for a quasi-elliptical wing with two booms extending rearward from the engine pods, terminating in an A-tail. The wing was based on current advanced glider designs which have been shown to yield very high Oswald efficiency numbers. This design was also very modular in nature, with all payload carried in a central pod. This trait would have allowed easy re-use of the airframe for other research projects, as well as eliminating the need for an internal speed loader.

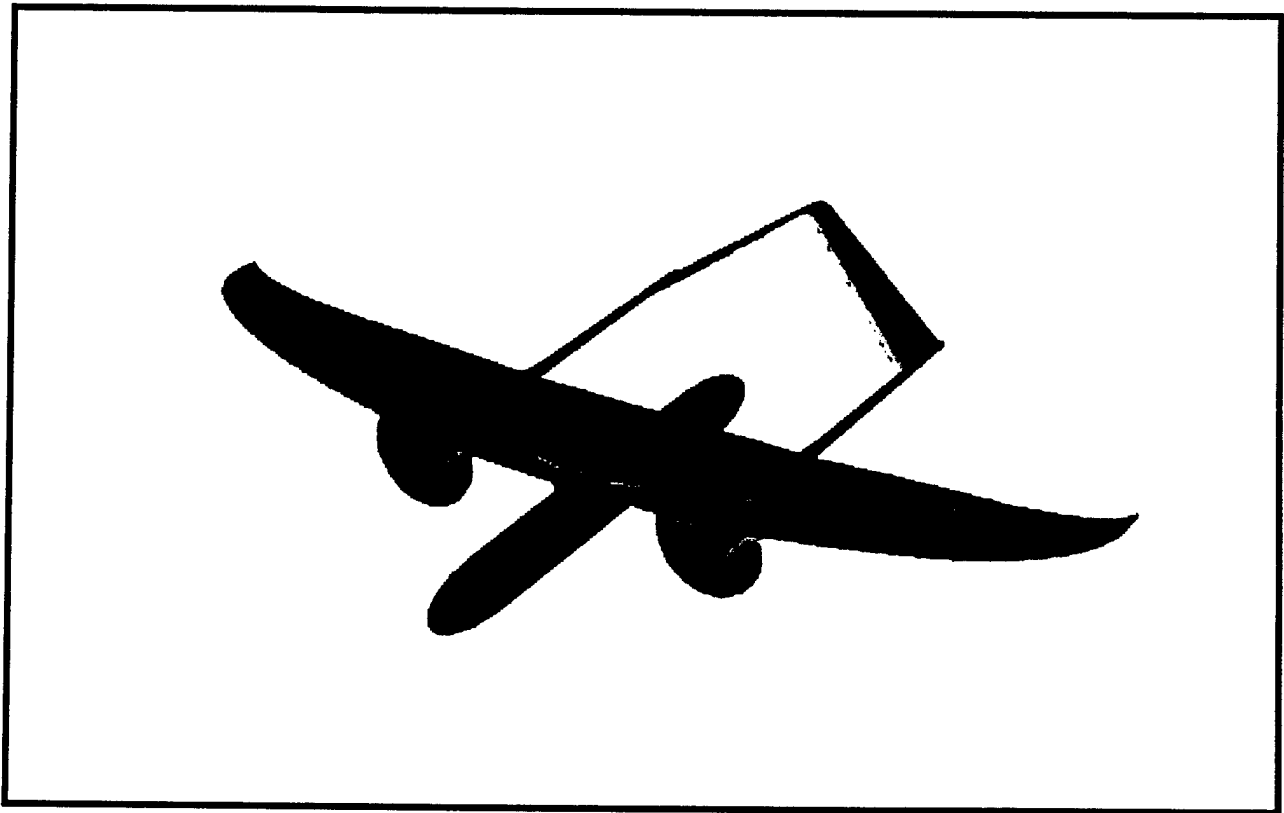


Figure 3.1. CAD rendering Concept 1

Concept 2: Conventional Single-, Twin-, or Tri-engine Airplane

This configuration consisted of a "standard" airplane with one, two, or three engines. While this design was a great deal less interesting and attractive to the team than concept 1, it was easily recognizable that it offered simple manufacture. The conceptual drawing presented in Figure 3.2 shows the twin-engine concept.

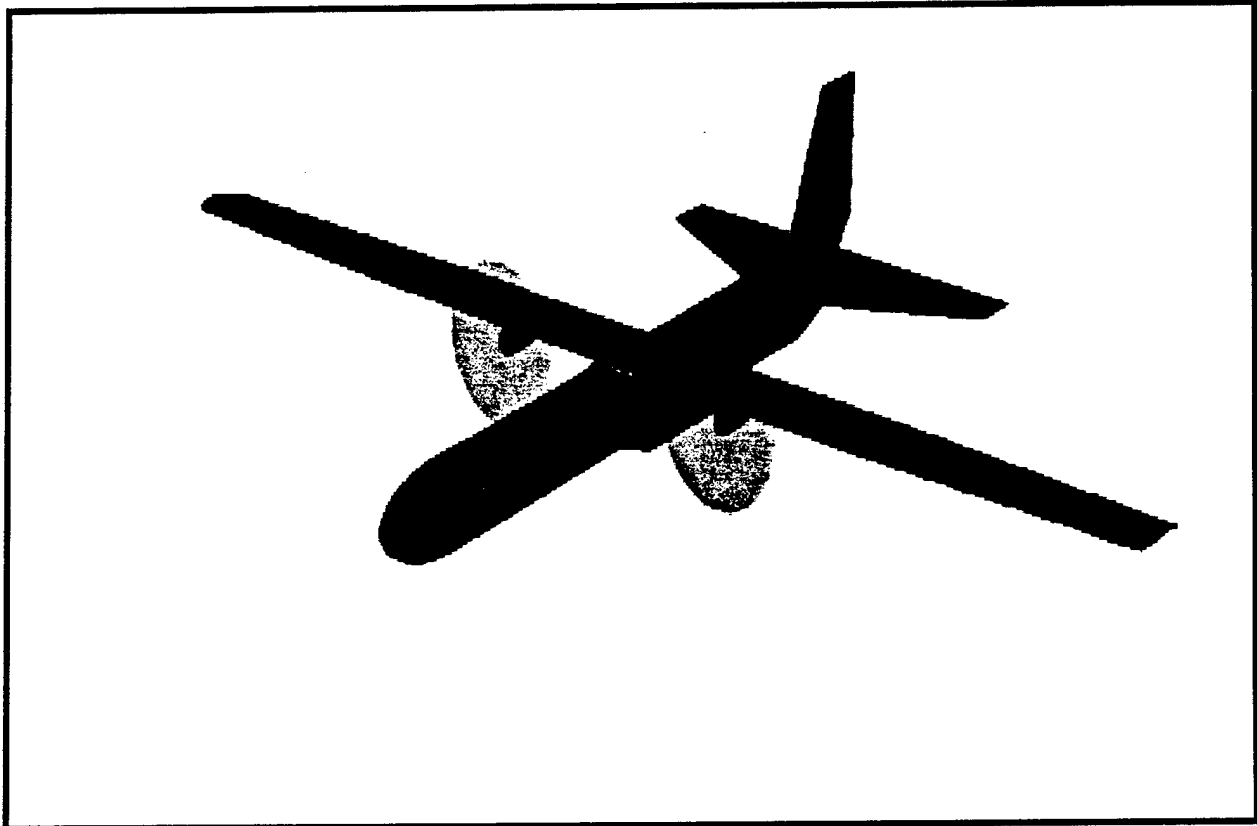


Figure 3.2. CAD rendering of Concept 2

Concept 3: Conventional Single-, Twin-, or Tri-engine Airplane with "V"-tail

This configuration was identical to 3.2.2, but used a V-tail, rather than a standard empennage. A conceptual drawing is presented in Figure 3.3.

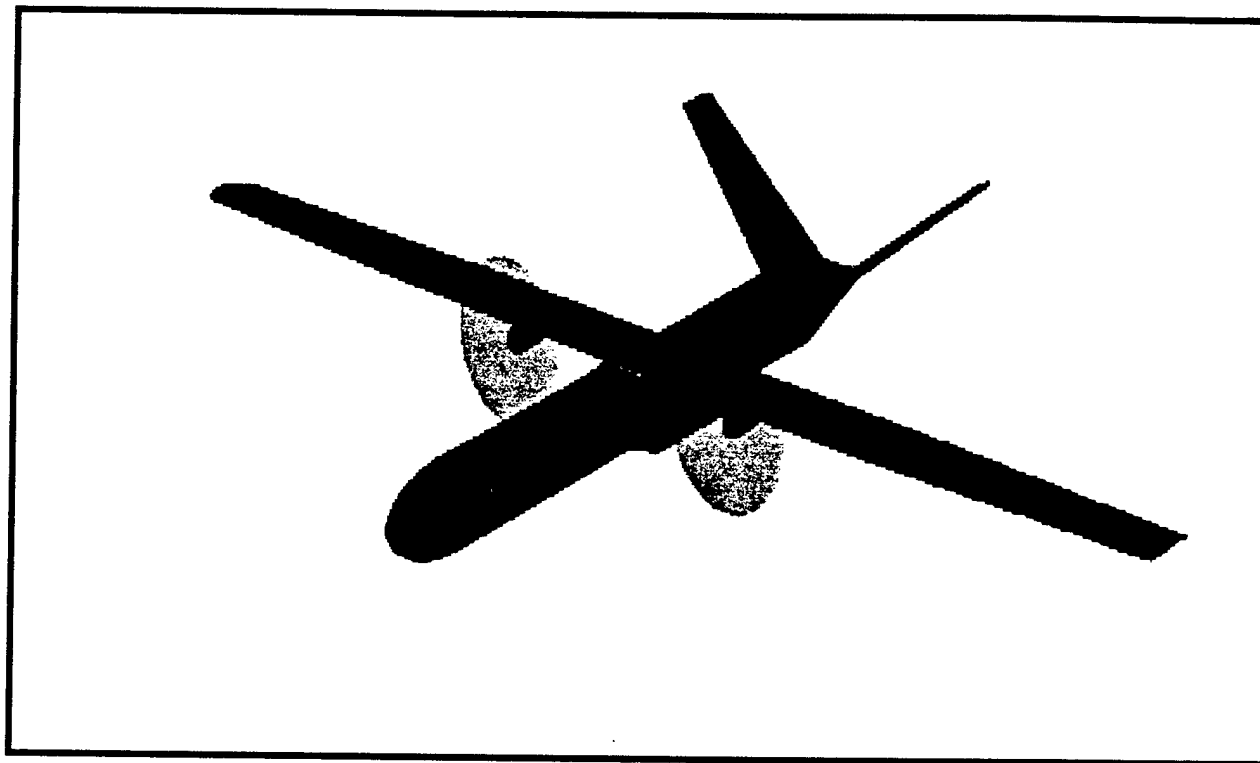


Figure 3.3. CAD rendering of Concept 3

Concept 4: Single-engine Flying Wing with Cargo Pod

This configuration consisted of a large flying wing with a cargo pod. Without a tail and with a reduce number of control surfaces, a significant cost advantage is achieved. No conceptual drawing was prepared for this concept.

Concept 5: Single-engine Canard

This configuration described a single-engine (pusher) canard type airplane. The canard was considered because of its efficiency. With the horizontal stabilizer providing lift, rather than downforce, the airplane functions more efficiently through all phases of its flight envelope. Again, no conceptual drawing was prepared for this concept.

3.3 Scoring of Design Concepts

Each design was scored based on all Figures of Merit. Each configuration was assigned a score ranging from -2 to 2, with 2 indicating greatest fitness. The scores were tabulated according to the formula for FOM score expressed as

$$\text{FOM Score} = \sum_{i=1}^6 S_i W_i \quad (3.1)$$

where S_i and W_i are the score and weight factor for the i^{th} FOM, respectively. The scores are shown in Table 3.2.

Table 3.2. Figure of Merit Scoring

FOM (Weight Factor)	Design Concept				
	1	2	3	4	5
Take-off Performance (4)	2	2	2	-1	2
Rated Aircraft Cost (4)	-2	1	1	2	1
Cruise Performance (3)	2	1	1	1	1
Manufacturability (2)	0	1	1	2	1
Lifting Capacity (2)	1	1	1	0	2
Innovation (0.5)	2	0	0	1	1
Total	9	19	19	11.5	17.5

3.3.1 Scoring of Concept 1

This design was favored by nearly all team members before actual quantification of the FOM. However, the design fell from favor under objective scrutiny. While performing well in all other FOM's, the design suffered badly in the RAC category, largely because of the three long bodies, each of which had to be scored as a "fuselage".

3.3.2 Scoring of Concept 2

The "conventional airplane" was not initially favored by the team, but given its fair performance in all FOM's and its lack of an "Achilles Heel" (a trait possessed by all other concepts, save number 3), this concept rapidly rose to favor.

3.3.3 Scoring of Concept 3

While this concept was presented to the team separately from number 2, the team soon realized that the two possessed identical fitness traits according to the chosen FOM's.

3.3.4 Scoring of Concept 4

The flying wing concept seemed promising in early evaluation because of its extremely low cost factor and ease of manufacturing. However, this concept suffered in takeoff performance and lifting capability due to the unavailability of high lift devices.

3.3.5 Scoring of Concept 5

The canard offers very high efficiency because of the fact that the horizontal stabilizer actually produces lift, but the concept suffered in the manufacturability area, as the team was wary of the more exacting design required by this type of airplane.

3.4 Conclusion

After considering the results of the FOM scoring, the team decided to carry forward Concepts 2 and 3, deferring the decisions on tail and propulsion to the next design phase. Many lessons were learned by the team during this phase, resulting in the abandonment of an attractive but technically flawed designs (Concepts 1, 4, and 5) for those that were not as glamorous or initially appealing (Concepts 2 and 3). In order to achieve the highest possible score, aesthetics and efficiency were sacrificed for greater utility.

4 Preliminary Design Phase

4.0 Introduction

In this design phase, the Performance group set out to determine the major sizing parameters for the airplane. These parameters included the takeoff gross weight, wing area, wing span, engine type, number of engines, fuselage length, and the corresponding payload capacities. The group was divided into two subgroups to investigate the design space in an attempt to maximize the total score as defined in the competition rules.

Each subgroup devised a different strategy for achieving an optimal design. One subgroup formulated the problem as a constrained optimization problem involving four continuous design variables: wing span, aspect ratio, payload weight for steel, and payload volume for tennis balls, and two discrete variables: engine type and quantity. The fuselage length was determined by the volume capacity of 100 tennis balls (explained later in Section 4.6), and the gross weight was determined by a highly detailed weight model involving all of the design variables. The engine parameters were treated as constants in the optimization process. The engine type and quantity, being discrete variables, were adjusted outside of the optimization loop.

The other subgroup, through careful selection and examination of simplifying assumptions, defined a design space involving only three design variables: takeoff gross weight, engine type, and number of engines. All other variables were either set as constants or were found to be dependent upon these three through the use of a detailed weight and performance model. Since both engine type and quantity are discrete variables, the design space was discretized with the optimum design found through one-dimensional optimization analysis.

The hopes of convergence between the two teams did not immediately materialize. Since both groups were building their codes from scratch, a great deal of troubleshooting was necessary in order to converge to an optimal set of design variables. However, once all assumptions were unified, and all discrepancies were eliminated from the codes, the results did indeed converge as initially hoped.

4.1 Figures of Merit

Only one Figure of Merit was used: Total Score. The team felt that any design capable of flying satisfactorily in all phases of the mission had only one real measure of fitness, that being the score the design would achieve. Based on this reasoning, the problem became a relatively simple optimization problem that was independently approached by the two subdivisions of the Performance group.

4.2 Numerical Optimization

4.2.0 Introduction

An analysis code was developed and coupled with the general purpose optimization tool, DOT [1] to perform the optimization analysis. The optimization problem sought to determine the optimal vector of design variables, X that

$$\begin{aligned} \text{Min. } & f(X) \\ \text{s.t. } & g_i(X) \leq 0 \quad i = 1, 2 \\ & x_j^L \leq x_j \leq x_j^U \quad j = 1, 2, 3, 4 \end{aligned} \quad (4.1)$$

Where $f(X)$ is the objective function chosen to be the total score, and $g(X)$ is the vector of inequality design constraints on thrust and gross weight. The design variables are limited by lower and upper side constraints defined by X^L and X^U vectors, respectively. Figure 4.1 shows the flow chart of the algorithm used for this optimization.

4.2.1 Design Variables

The selected design variables and corresponding lower and upper limits are listed in Table 4.1. The limits on the design variables were based on the contest rules [2] and preliminary a performance analysis.

Table 4.1. Side Constraints on Design Variables.

Design Variable	Minimum	Maximum
Wing Span	80 in	120 in
Aspect Ratio	5	15
Number of Balls	10	100
Weight of Steel	5 lb	30 lb

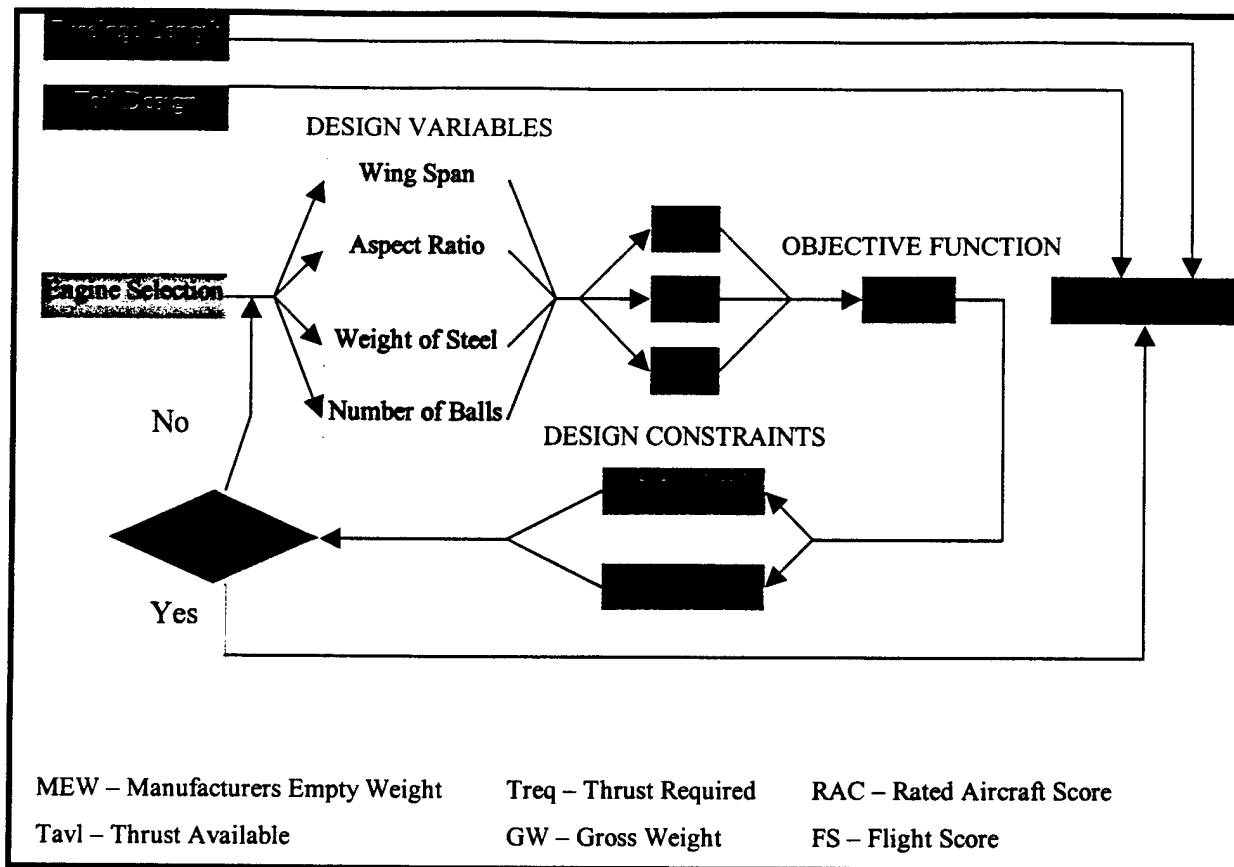


Figure 4.1. Flow Chart for DOT Algorithm

4.2.2 Design Constraints

The design constraints were selected based on contest rules and engine performance, and formulated as

$$\frac{T_{req}}{T_{avl}} - 1 \leq 0 \quad (4.2a)$$

$$\frac{GW}{55} - 1 \leq 0 \quad (4.2b)$$

Equation (4.2a) limits the required thrust to that available while Eq. (4.2b) imposes an upper limit on the airplane gross weight.

4.2.3 Objective Function

The objective function is the overall score, which is a combination of the Flight Score, Report Score, and the Rated Aircraft Cost.

$$\text{SCORE} = \frac{\text{Report Score} \cdot \text{Flight Score}}{\text{Rated Aircraft Cost}} \quad (4.3)$$

Since the Report Score is an unknown variable and simply a multiplier of the overall score, the Report Score is dropped from the objective function.

$$\text{MODIFIED SCORE} = \frac{\text{Flight Score}}{\text{Rated Aircraft Cost}} \quad (4.4)$$

The Flight Score [2] was calculated based on the design variables concerning cargo and on the assumption of four sorties. The Rated Aircraft Cost (RAC) is a highly detailed model based on all design parameters.

The results of this numerical optimization are given in Table 4.2.

Table 4.2. Numerical Optimization Results for Various Engine Configurations

Design Variable	Engine Type*		
	Cobalt 15 Geared	Cobalt 25 Geared	Cobalt 40 Geared
Wing span, ft	10	10	10
Aspect Ratio	13.7	12.6	12.1
Wing area, ft ²	7.3	7.9	8.1
Gross Weight, lb	25.8	28.2	30.6

* In twin configuration

4.3 Simplified 3-Dimensional Discretized Optimization

Two members of the Performance group approached the problem differently, with the hope of using MathCad to perform the optimization. The extremely visual nature of this software package would allow very simple examination and modification of the program. After careful examination, the decision was made to use the takeoff gross weight, engine type, and number of engines as design variables. Wing span and fuselage length were set as constants, while wing area and payload capacity were determined based on the three design variables. Again, optimization was performed with takeoff performance in

mind, using the same modified score equation (Eq. 4.4) as was used in the numerical optimization approach. Once an optimum design emerged, it was tested for fitness in cruise. A design was considered fit for cruise if its cruise speed (at C_L of 1.0) was more than 5 mph slower than the V_{max} of the engine/prop combination used.

Since both engine type and number of engines were discrete variables, the design space was discretized into a series of one-dimensional optimizations. These optimizations were performed, and an optimum design was determined. This optimum design was then tested for cruise capability, which it passed with a comfortable margin of safety.

4.4 Final Selection of Parameters

After many hours of unification sessions, in which the two performance groups troubleshot each other's code, a unified solution emerged. Therefore, the simplifying assumptions of the MathCad optimization were correct, and the MathCad optimization was used for further development of the design. (This optimization is included in Section 4.7.) Figure 4.2 shows the Score vs. Weight curves for single and twin engine configurations using Astro Flight 90, 60, 40, 25, and 15 size engines. Trimotor configurations were eliminated from the optimization because they could not carry enough battery capacity to complete a flying period and still stay below the 5lb battery constraint. From the plot, the airplane equipped with two 15's generates the highest score. This airplane was, therefore, tested for fitness in cruise and passed easily. With these parameters selected, only tail sizing and fuselage configuration remained.

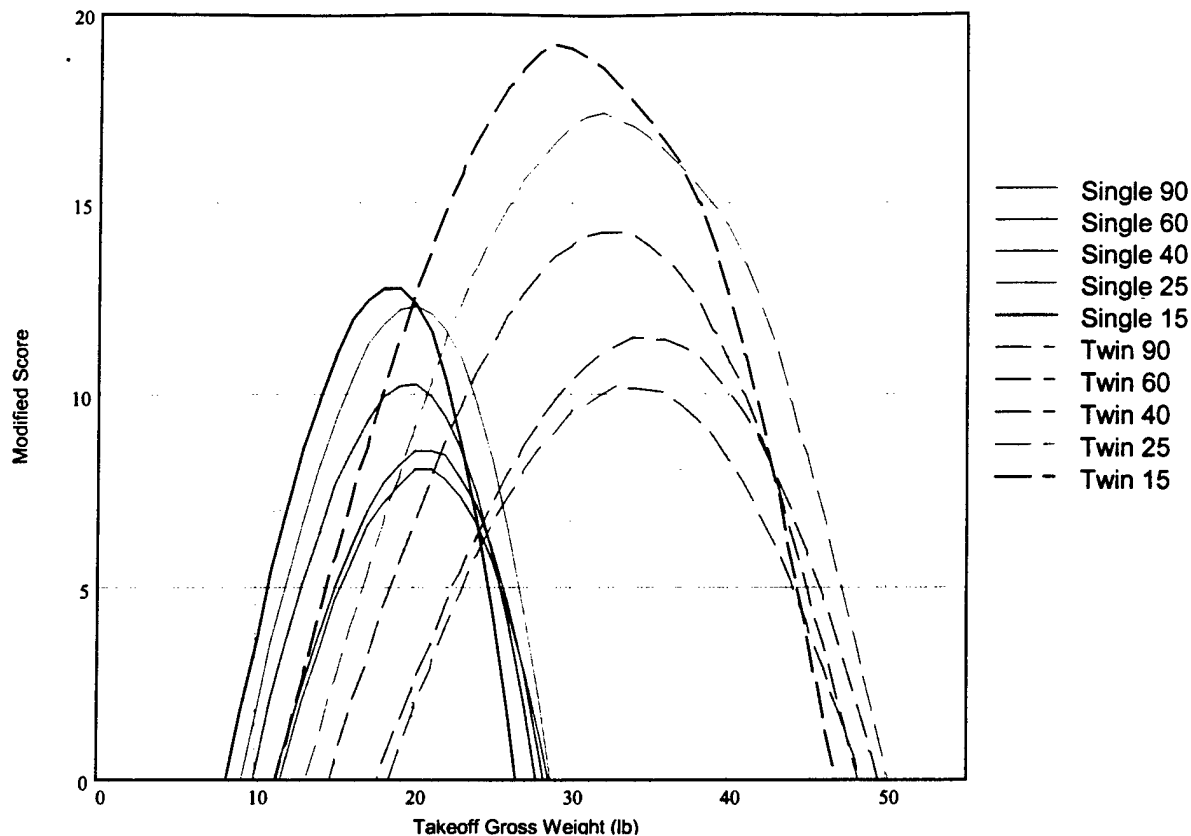


Figure 4.2. Modified Score vs. Weight Plots

4.5 Tail Sizing

While simple historical data on full-scale transports were used to determine tail sizing for the optimization weight model, a proper sizing based on stability requirements was necessary. Based on the lack of available resources on V-tail design, the team decided to construct the airplane with a conventional tail.

The horizontal tail surface was sized and positioned according to data published in NACA-TR-648 [6]. The tail moment arm was considered set by the minimum fuselage length necessary to hold 100 tennis balls and very basic streamlining components, such as the nose and tail sections. An analysis was performed for a stabilizer that was mounted flat on the fuselage and for a stabilizer that was mounted in various cruciform positions on the vertical fin. The team decided to mount the horizontal stabilizer in a cruciform position low on the fin. The chosen position corresponded to a Horizontal Tail Effectiveness (HTE) of 65% for design cruise conditions and was not mounted very high on the fin. This position was a good compromise that resulted in a moderately sized stabilizer with a mounting only slightly more

complex than the simplest fuselage mounting. A "T"-tail was not considered because of increased structural complexity.

The driving factor in determining the design of the vertical tail of the aircraft was the ability of the tail to gradually damp out any oscillations from a rudder impulse. The vertical tail sizing was determined through solving for the derivative of the yawing moment with respect to sideslip angle ($C_{n\beta}$). For this analysis, the value of $C_{n\beta}$ was set to be 0.11, and the necessary vertical tail area was calculated to be 140 in². As a method of verifying the results, the derivative of the rolling moment with respect to the sideslip angle ($C_{L\beta}$) was then compared to and found to be similar to existing aircraft of this type.

4.6 Fuselage Design Concepts

The fuselage design was determined by selecting a design that would have a small cargo length and frontal area given 100 tennis balls. These criteria were based on the request for proposals (RFP) [2] and drag measurements. Figure 4.3 shows possible design configurations for the fuselage. Design concept A obviously has the shortest required length, but the frontal areas required careful examination.

Design concept A is a trapezoidal configuration that has 5 balls in each cross-sectional cell. This configuration was quickly dubbed the "Olympic" configuration due to its resemblance to the Olympic symbol. For 100 tennis balls, concept A would have 20 stations. For this number of stations, the cargo length was 52.75 in. For this configuration, the frontal area was 33.4 in².

Design Concept B is a rectangular configuration that has 4 balls per cross-section, and Design Concept C is a helical configuration with 4 balls per cross-section. For 100 tennis balls, Concepts B and C would have 25 stations, resulting in a cargo length of 65.94 in. The frontal areas for Concepts B and C are 25.6 in² and 33.4 in², respectively. While concept B had less frontal area than A, this parameter was less important than the fuselage length, which actually makes up part of the total score.

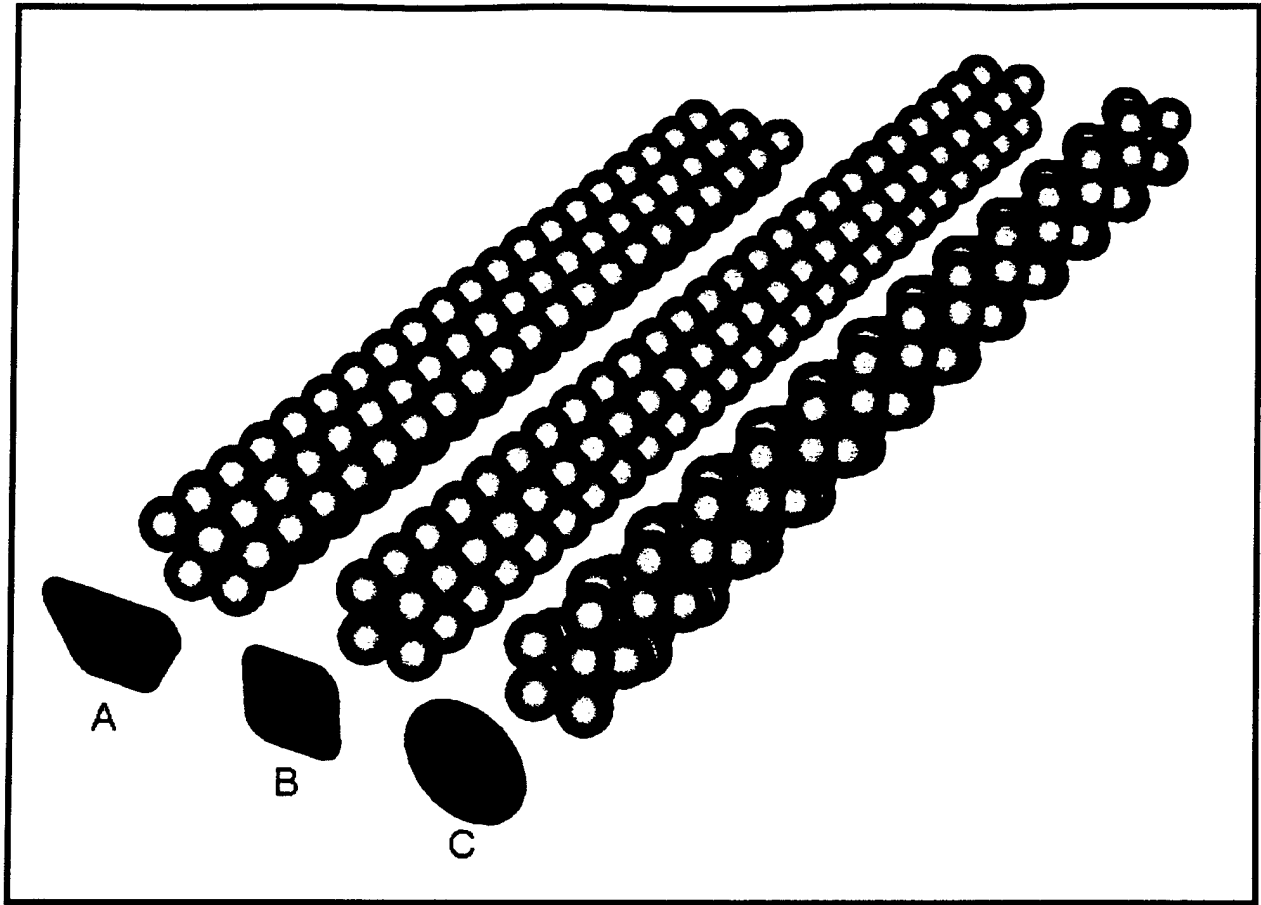


Figure 4.3. Fuselage Design Concepts for 100 Tennis Ball Capacity

4.7 Final Results

With the optimization analysis complete, a list of the actual parameters computed was prepared. These results are tabulated below. Surprisingly, the maximum score for the aircraft does not occur at gross weight values approaching the 55 lb. limit but rather at the gross weight that allows the aircraft to carry 100 tennis balls (the maximum allowed). These results surprised the team at first, but it was soon realized that tennis balls offer a greater score-to-weight ratio. Therefore are worth more to the actual score. Adding further lifting capacity (beyond the weight of 100 tennis balls) does not provide an advantageous score-to-cost ratio, so this is the point at which the maximum occurs.

Table 4.1. Calculated Sizing Parameters

Parameter	Value
Target Takeoff Gross Weight	28.9 lb
Wing Area	73 ft ²
Wing Span	120 in
Fuselage Length	70 in
Horizontal Tail Area	286 in ²
Vertical Tail Area	140 in ²
Engine Type	Astro Flight Cobalt 15
Gearbox Type	Astro Flight 3.89
Prop Size	14X8
Number of Engines	2
Payload Capacity (steel)	12.9 lb
Payload Capacity (balls)	100
Endurance (at 70% average throttle)	8.8 min
Modified Score	19.28

4.8 MathCad Code Listing

Constant Definitions

Define constants relevant to performance:

$s_{LO} := 180\text{ft}$ Maximum Takeoff Distance (with 20 ft buffer)
 $b := 10\text{ft}$ Wingspan
 $C_{Lmax} := 2.0$ For takeoff run with flaps deployed
 $C_{Lmaxclean} := 1.6$ Without flaps
 $C_{Lcruise} := 1.0$ Lift Coefficient for cruise
 $\mu_r := 0.11$ Coefficient of rolling resistance (estimated)
 $\rho := 0.0023769 \frac{\text{slug}}{\text{ft}^3}$ Density of air at sea-level standard conditions

Define Motor Performances:

$Amp_{40} := 29A$ $Amp_{25} := 30A$ $Amp_{15} := 29A$ $Amp_{60} := 34A$ $Amp_{90} := 22A$
 $Cells_{40} := 22$ $Cells_{25} := 19$ $Cells_{15} := 15$ $Cells_{60} := 30$ $Cells_{90} := 30$
 $T_{st_{40}} := \frac{116}{16}\text{lbf}$ $T_{st_{25}} := \frac{115}{16}\text{lbf}$ $T_{st_{15}} := \frac{100}{16}\text{lbf}$ $T_{st_{60}} := \frac{110}{16}\text{lbf}$ $T_{st_{90}} := \frac{133}{16}\text{lbf}$
 $v_{max_{40}} := 43\text{mph}$ $v_{max_{25}} := 46\text{mph}$ $v_{max_{15}} := 50\text{mph}$ $v_{max_{60}} := 53\text{mph}$ $v_{max_{90}} := 38\text{mph}$
 $EW_{40} := \frac{12.5}{15} \cdot \text{lbf}$ $EW_{25} := \frac{11}{15} \cdot \text{lbf}$ $EW_{15} := \frac{8.5}{15} \cdot \text{lbf}$ $EW_{60} := 1 \cdot \text{lbf}$ $EW_{90} := 1 \cdot \text{lbf}$

Define densities for weight calculations:

Density of foam core Density of fiberglass Density of carbon rod Density of Balsa
 $\rho_{FoamCore} := 6.0 \cdot \frac{\text{lbf}}{\text{ft}^3}$ $\rho_{Fiberglass} := \frac{2}{16} \cdot \frac{\text{lbf}}{\text{yd}^2}$ $\rho_{Carb_Rod} := 95 \cdot \frac{\text{lbf}}{\text{ft}^3}$ $\rho_{Balsa} := 10 \cdot \frac{\text{lbf}}{\text{ft}^3}$

Define Component Weights:

Single Cell
(SR Max 3000)

$$W_{\text{cell}} := \frac{2.55}{16} \text{ lbf}$$

Landing Gear

$$W_{\text{LG}} := 1.5 \cdot \text{lbf}$$

Speed Control
(Astro 204D)

$$W_{\text{Speed}} := \frac{3}{16} \cdot \text{lbf}$$

Receiver
(JR R629S)

$$W_{\text{Rx}} := \frac{1}{16} \cdot \text{lbf}$$

Engine Mount

$$W_{\text{engmt}} := \frac{3}{16} \cdot \text{lbf}$$

Servo
(FMA S355AM)

$$W_{\text{servo}} := \frac{2.58}{16} \cdot \text{lbf}$$

Receiver Flight Battery

$$W_{\text{flightbatt}} := \frac{5.6}{16} \cdot \text{lbf}$$

Performance Equation Definitions

Define expression for wing area required as function of weight and propulsion:

$$T(V, \text{Engines}, \text{Engtype}) := \text{Engines} \cdot \left(T_{\text{st}_{\text{Engtype}}} - \frac{T_{\text{st}_{\text{Engtype}}}}{V_{\text{max}_{\text{Engtype}}}} \cdot V \right)$$

Linear approximation of thrust to velocity relationship. Verified as conservative by experimentation.

$$a(V, W, \text{Engines}, \text{Engtype}) := \frac{T(V, \text{Engines}, \text{Engtype}) - \mu_r \cdot W}{\frac{W}{g}}$$

Acceleration based on thrust and an assumed constant resistance force equal to rolling resistance force at zero velocity

Based on these functions, the takeoff run can be simulated with the following pseudoprogram, obtaining the velocity at the end of the run (point of rotation):

```

VLO(W, Engines, Engtype) :=
    x ← 0ft
    V ← 0mph
    timestep ← 0.01s
    while x < sLO
        V ← V + a(V, W, Engines, Engtype) · timestep
        x ← x + V · timestep
    V
    
```

Based on this function, the wing area required for a given TOGW and propulsion configuration can be determined:

$$S_{\text{req}}(W, \text{Engines}, \text{Engtype}) := \frac{W}{\frac{1}{2} \cdot \rho \cdot V_{\text{LO}}(W, \text{Engines}, \text{Engtype})^2 \cdot C_{L\text{max}}}$$

MEW - Manufactured Empty Weight

Wing Data - Foam core glass overlay construction

$$c_{avg}(S) := \frac{S}{b} \quad \text{Average chord of wing}$$

$$t_{max_airfoil}(S) := .14 \cdot c_{avg}(S) \quad \begin{array}{l} \text{Max thickness} \\ \text{of airfoil} \end{array}$$

$$HeightSpar := 0.03 \cdot \text{in}$$

$$WidthSpar := 0.5 \cdot \text{in}$$

$$CoreWing_Vol(S) := 0.0883 \cdot c_{avg}(S) \cdot S$$

$$WWing_Core(S) := \rho_{FoamCore} \cdot CoreWing_Vol(S)$$

$$NumWingLay := 4$$

$$WWing_Skin(S) := 1.5 \cdot NumWingLay \cdot S \cdot \rho_{Fiberglass}$$

$$WSpar(S) := (2 \cdot b \cdot HeightSpar \cdot WidthSpar \cdot \rho_{Carb_Rod}) + (t_{max_airfoil}(S) - 2 \cdot HeightSpar) \cdot WidthSpar \cdot b \cdot \rho_{Balsa}$$

$$WWing(S) := 1.1 \cdot (WWing_Core(S) + WWing_Skin(S) + WSpar(S))$$

Fuselage Data

$$FuseLength := 70 \cdot \text{in}$$

$$FusePerimeter := 22.58 \cdot \text{in}$$

$$NumFuseLay := 2$$

$$WFuse_Skin := 1.5 \cdot FuseLength \cdot FusePerimeter \cdot NumFuseLay \cdot \rho_{Fiberglass}$$

$$WFuse := 1.2 \cdot WFuse_Skin$$

Tail Data

$$HtailArea(S) := 0.2 \cdot S \quad CoreHtail(S) := .1417 \cdot \text{in} \cdot HtailArea(S)$$

$$VtailArea(S) := 0.1 \cdot S \quad CoreVtail(S) := 0.1417 \cdot \text{in} \cdot VtailArea(S)$$

$$WTail_Core(S) := (CoreHtail(S) + CoreVtail(S)) \cdot \rho_{FoamCore}$$

$$NumTailLay := 4$$

$$WTail_Skin(S) := 1.5 \cdot NumTailLay \cdot (HtailArea(S) + VtailArea(S)) \cdot \rho_{Fiberglass}$$

$$WTail(S) := 1.1 \cdot (WTail_Skin(S) + WTail_Core(S))$$

Payload Carriage

Propulsion/Radio/Other Data

$$W_{Carriage} := \frac{WFuse}{2}$$

$$W_{Radio} := 6W_{servo} + W_{Rx} + W_{flightbatt}$$

$$W_{Prop}(Engines, Type) := (EW_{Type} + W_{engmt}) \cdot Engines + W_{Radio} + W_{Speed} + W_{LG}$$

TOTAL MEW:

$$MEW(S, Engines, Engtype) := 1.1 \cdot (WWing(S) + WFuse + WTail(S) + W_{Carriage} + W_{Prop}(Engines, Engtype))$$

REP - Rated Engine Power

$$\text{REP}(\text{Engines}, \text{Type}) := \text{Engines} \cdot \frac{\text{AmpType}}{\text{amp}} \cdot 1.2 \cdot \text{CellsType}$$

MFG HR - Manufacturing Man Hours

A. Wing

$$\text{wings} := 1 \quad \text{wingtime} := 15 \cdot \text{hr} \cdot \text{wings}$$

$$\text{Propulsion Data/Other} \quad \text{wingareatime}(S) := 4 \frac{\text{hr}}{\text{ft}^2} \cdot S$$

$$\text{brace} := 0 \quad \text{bracetime} := 2 \text{hr} \cdot \text{brace}$$

$$\text{ctrlsurf} := 4 \quad \text{ctrlsurftime} := 3 \cdot \text{hr} \cdot \text{ctrlsurf}$$

$$\text{Wingcost}(S) := \text{wingtime} + \text{wingareatime}(S) + \text{bracetime} + \text{ctrlsurftime}$$

B. Fuselage & Pods

$$\text{body} := 1 \quad \text{bodytime} := 5 \cdot \text{hr} \cdot \text{body}$$

$$\text{Length} := \text{FuseLength} \quad \text{lengthtime} := 4 \cdot \frac{\text{hr}}{\text{ft}} \cdot (\text{Length} + 6 \text{in})$$

$$\text{Bodycost} := \text{bodytime} + \text{lengthtime}$$

C. Empenage

$$\text{vertical} := 1 \quad \text{verttime} := 5 \cdot \text{hr} \cdot \text{vertical} \quad \text{Basecost} := 5 \cdot \text{hr}$$

$$\text{horiz} := 1 \quad \text{horiztime} := 10 \cdot \text{hr} \cdot \text{horiz}$$

$$\text{Empcost} := \text{Basecost} + \text{verttime} + \text{horiztime}$$

D. Flight Sys

$$\text{servos} := 8 \quad \text{servotime} := 2 \cdot \text{hr} \cdot \text{servos} \quad \text{basetime} := 5 \cdot \text{hr}$$

$$\text{Fgtsyscost} := \text{basetime} + \text{servotime}$$

E. Propulsion

$$\text{enginetime}(\text{Engines}) := 5 \cdot \text{hr} \cdot \text{Engines}$$

$$\text{proptime}(\text{Engines}) := 5 \cdot \text{hr} \cdot \text{Engines}$$

$$\text{Propcost}(\text{Engines}) := \text{enginetime}(\text{Engines}) + \text{proptime}(\text{Engines})$$

Total MFG HR:

$$\text{MFHR}(S, \text{Engines}) := \frac{\text{Wingcost}(S) + \text{Bodycost} + \text{Empcost} + \text{Fgtsyscost} + \text{Propcost}(\text{Engines})}{\text{hr}}$$

RAC - Rated Aircraft Cost

$$\text{RAC}(W, \text{Engines}, \text{Engtype}) := \left(\frac{\begin{aligned} &\frac{100}{\text{lbf}} \cdot \text{MEW}(S_{\text{req}}(W, \text{Engines}, \text{Engtype}), \text{Engines}, \text{Engtype}) \dots \\ &+ \text{REP}(\text{Engines}, \text{Engtype}) \dots \\ &+ 20 \cdot \text{MFHR}(S_{\text{req}}(W, \text{Engines}, \text{Engtype}), \text{Engines}) \end{aligned}}{1000} \right)$$

Flight score

$$\text{Payload}(W, \text{Engines}, \text{Engtype}) := (W - \text{MEW}(S_{\text{req}}(W, \text{Engines}, \text{Engtype}), \text{Engines}, \text{Engtype})) \dots \\ + (-\text{Cells})_{\text{Engtype}} \cdot \text{Engines} \cdot W_{\text{cell}}$$

$$\text{Numballs}(W, \text{Engines}, \text{Engtype}) := \begin{cases} 100 & \text{if } \text{Payload}(W, \text{Engines}, \text{Engtype}) > 100 \cdot \left(\frac{2.063}{16} \text{lbf}\right) \\ \frac{\text{Payload}(W, \text{Engines}, \text{Engtype})}{\frac{2.063}{16} \text{lbf}} & \text{otherwise} \end{cases}$$

$$\text{FlightScore}(W, \text{Engines}, \text{Engtype}) := 3 \cdot \frac{\text{Payload}(W, \text{Engines}, \text{Engtype})}{\text{lbf}} \dots \\ + 3 \cdot \frac{\text{floor}(\text{Numballs}(W, \text{Engines}, \text{Engtype}))}{5}$$

Total Score (without effect of report score)

$$\text{Score}(W, \text{Engines}, \text{Engtype}) := \frac{\text{FlightScore}(W, \text{Engines}, \text{Engtype})}{\text{RAC}(W, \text{Engines}, \text{Engtype})}$$

Other performance parameters of interest:

$$V_{\text{stall}}(W, \text{Engines}, \text{Engtype}) := \sqrt{\frac{2 \cdot W}{\rho \cdot C_{L_{\text{max}}} \cdot S_{\text{req}}(W, \text{Engines}, \text{Engtype})}}$$

$$V_{\text{stallclean}}(W, \text{Engines}, \text{Engtype}) := \sqrt{\frac{2 \cdot W}{\rho \cdot C_{L_{\text{maxclean}}} \cdot S_{\text{req}}(W, \text{Engines}, \text{Engtype})}}$$

$$V_{\text{cruise}}(W, \text{Engines}, \text{Engtype}) := \sqrt{\frac{2 \cdot W}{\rho \cdot C_{L_{\text{cruise}}} \cdot S_{\text{req}}(W, \text{Engines}, \text{Engtype})}}$$

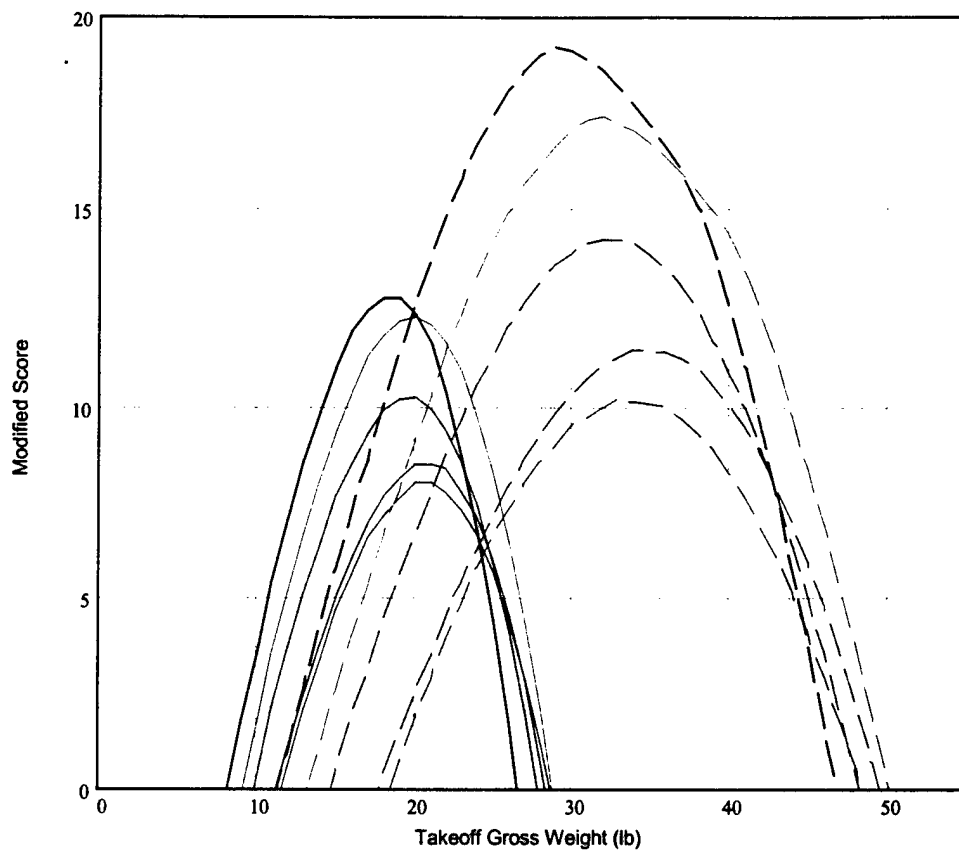
$$\text{Wingloading}(W, \text{Engines}, \text{Engtype}) := \frac{W}{S_{\text{req}}(W, \text{Engines}, \text{Engtype})}$$

$$\text{Ratio}(W, \text{Engines}, \text{Engtype}) := \frac{\text{MEW}(S_{\text{req}}(W, \text{Engines}, \text{Engtype}), \text{Engines}, \text{Engtype})}{W}$$

Score Plot

W1 := 5lbf, 6lbf.. 55lbf

(working series for plots)



—— Single 90
—— Single 60
—— Single 40
—— Single 25
—— Single 15
- - - Twin 90
- - - Twin 60
- - - Twin 40
- - - Twin 25
- - - Twin 15

Final Optimization

Since the highest score results from the twin 15 configuration, the exact optimum TOGW and corresponding wing area can be determined:

$$\text{Score}_{2_15}(W) := \text{Score}(W, 2, 15) \quad W := 30\text{lb} \quad (\text{guess value for optimization})$$

$$W_{\text{star}_{2_15}} := \text{Maximize}(\text{Score}_{2_15}, W) \quad W_{\text{star}_{2_15}} = 28.931\text{lb}$$

$$S_{\text{req}}(W_{\text{star}_{2_15}}, 2, 15) = 7.313\text{ft}^2$$

The current optimum is an airplane weighing 28.9 lbf, with a wing area of 7.3 sq. ft. and powered by two Astro Flight 15s. Its fitness for cruise must now be tested:

$$V_{\text{cruise}}(W_{\text{star}_{2_15}}, 2, 15) = 39.339\text{mph}$$

This value is a good deal lower than the V_{max} of the Astro 15 with 14X8 prop, so the airplane is fit for flight in both takeoff and cruise.

$$\text{Payload}(W_{\text{star}_{2_15}}, 2, 15) = 12.906\text{lb}$$

$$\text{Numballs}(W_{\text{star}_{2_15}}, 2, 15) = 100$$

5. Detail Design

5.0 Introduction

With the preliminary analysis completed, a more detailed analysis was performed. With general sizing parameters in hand, the task of developing a detail design for the airplane unassigned to the CAD and Structures groups.. This included establishing the remainder of the performance and handling characteristics, the component selections, and systems architecture. Detail drawings of the aircraft are included: a 3-view drawing, systems components, payload configuration, and locations of propulsion and flight control systems.

5.1 Performance Data and Flight Handling

With the final parameters of the design complete, the team performed a detailed analysis of the airplane's performance and handling qualities. These results are presented below in Table 5.1.

Table 5.1 Performance Characteristics

Parameter	Value
Takeoff distance	180 ft
Maximum climb rate (loaded)	220 ft/min
Maximum climb rate (unloaded)	420 ft/min
Stall speed dirty	27.8 mph
Stall speed clean	31.1 mph
Cruise speed (CL=1.0)	39.3 mph
Minimum turning radius (level turn at cruise speed)	75 ft
Maximum roll rate	75 deg/sec
g-load capacity	±15g
Cruise endurance (including takeoff)	10 min
Cruise range	6.55 mi
Static margin	27%
Payload fraction (Payload/GW)	44.6%

These performance figures represent the complete analysis of the selected design. Dynamic stability analysis was not performed, as the aircraft will be under visual control at all times. The only possible occasion, for a radio-controlled airplane to encounter a displacement followed by a stick-fixed flight condition, would be a loss of radio signal. However, for the purpose of this competition, this situation does not exist. Signal loss will result instead in activation of the airplane's fail-safe mode, which is essentially a self-destruct.

The flight handling characteristics of the airplane are those of an airplane designed to get a heavy payload off a short runway and carry it around a course. While the climb rate is somewhat anemic, this reflects the fact that a great deal of power is being devoted to lifting weight. The roll rate and turning radius result in an airplane that is reasonably maneuverable, but by no means aerobatic. Also, the airplane is quite strong, with the wing (the most fragile component of the airplane) being rated for ± 15 g's.

5.2 Component Selection

With the basic design complete, it was necessary to select the off-the-shelf components that would be used in the aircraft. Based on the number of channels needed, the team decided to use an eight-channel system, and eventually selected the JR XP8103DT. The receiver chosen was a JR R649 PCM. For servo selection, it was decided to use one type of servo to drive all control surfaces. This decision was made for the purpose of easy design and component interchangeability in the event that quick repairs or component replacement might become necessary. Initial examination revealed that the flaps were the surfaces that would experience the highest hinge moments, and therefore these hinge moments were the constraining factor for servo selection. The hinge moment coefficient for our flaps was determined to be approximately 0.5, resulting in a hinge moment of 74 oz-in at 60 degrees deflection [5]. To support this load, the 355AM dual ball-bearing, all metal-gear servo from FMA Direct, was chosen. This servo is capable of outputting 104 oz-in of torque, giving a reasonable factor of safety. The metal-gear servo was chosen over a similar nylon-gear servo in order to maximize reliability and durability.

The main landing gear selected were 30 lb. capacity fiberglass gear from TnT Landing Gear with polyethylene scooter wheels selected for their low rolling resistance. For the nose gear, an adjustable dual-strut nose gear from Fults was selected, using the same wheel. Nose gear steering is to be provided by a JR NES-537 servo. All linkages were designed from 4/40 all threaded rod with Du-Bro Kwik-Link clevises.

The engines selected were the AstroFlight Cobalt 15 with a 3.69:1 gearbox. For propellers, the team selected Freudenthaler Aeronaut 14X8 Carbon Fiber folding propellers, which will be locked in the unfolded position.

5.3 Systems Architecture

5.3.1 Radio System

The radio receiver is placed in the systems bay, along with its battery pack. Servo wires for wing control surfaces are run externally up the fuselage sides and into wiring access tubes in the wings. Tail servo wires are run along the bottom of the fuselage exterior and into the tailcone area, through which they enter the tail itself. Nose gear servo wiring is run forward along the

bottom of the fuselage. All servos drive their control surfaces through direct external linkages. The control model is set up with the following channel assignments.

Table 5.2 Radio channel assignments

Channel	Assignment
1	Throttle
2	Aileron (Right)
3	Elevator
4	Rudder
5	Aileron (Left)
6	Flap (Right)
7	Flap (Left)
8	Unused

With each control surface controlled by its own servo, it becomes possible to improve flight handling by enabling mixing between channels. The following mixes will be used for control purposes:

Table 5.3 Radio Mixes

Mix	Description
Aileron to Flap	Enables entire trailing edge of wing to enhance lift by using ailerons as flaps
Flap to aileron	Enhances roll control by using flaps as ailerons
Flap to Elevator	Enables tighter turning and more efficient rotation on takeoff

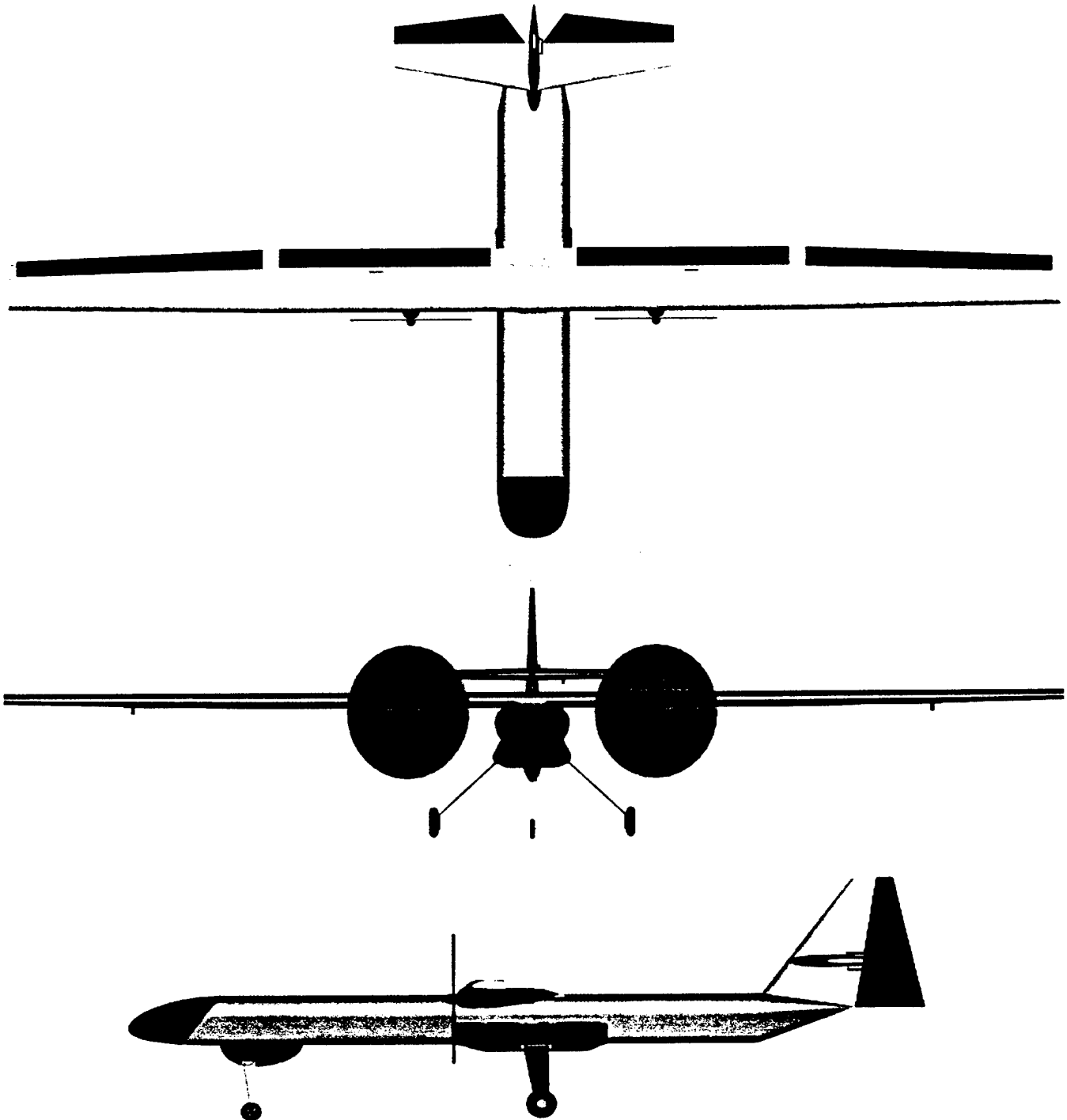
Additionally, mixes will be used to "dial out" any unwanted control coupling (i.e. to allow flat skidding turns for approach path adjustment).

5.3.2 Propulsion Architecture

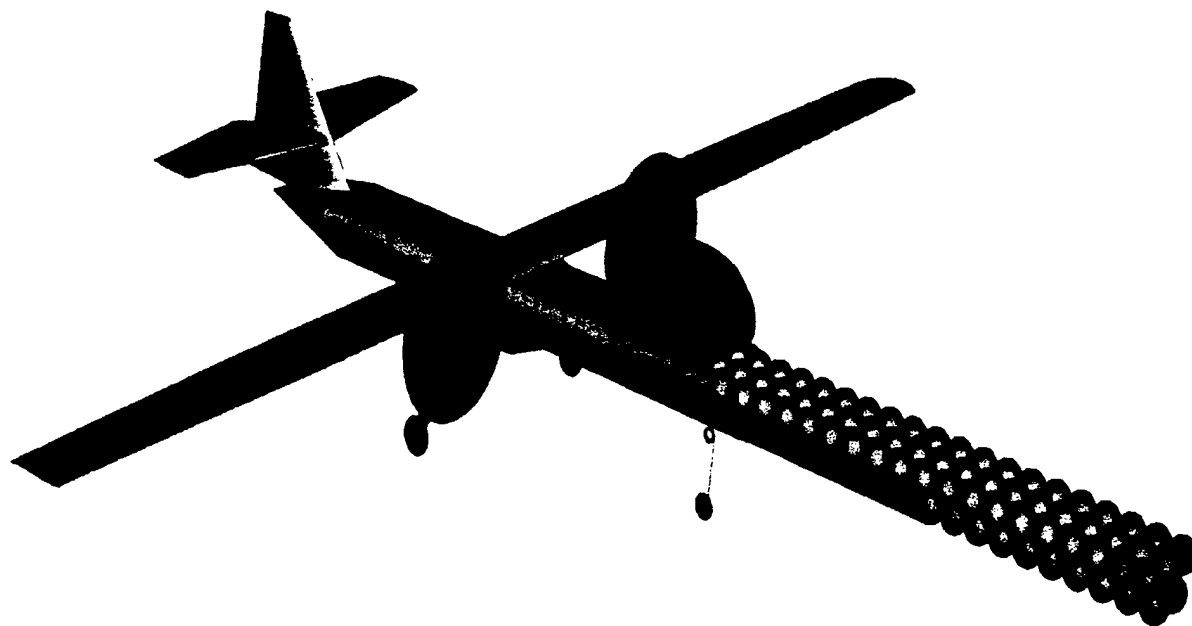
Each motor has its own independent electrical drivetrain consisting of battery, speed control, and motor, all connected by 14 gauge wiring. Both speed controls are controlled by the same radio channel.

5.4 Drawing Package

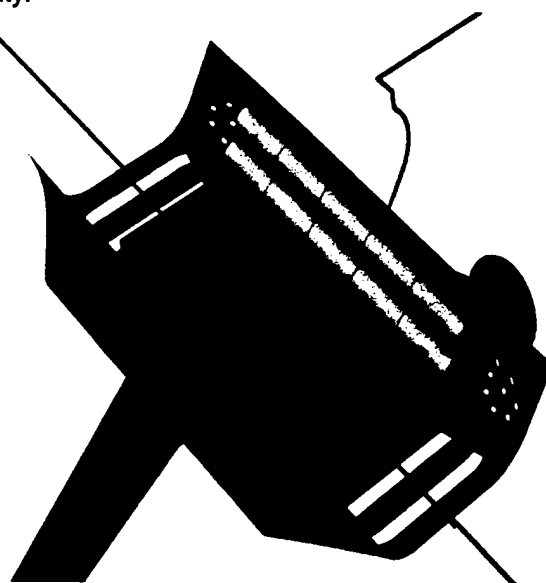
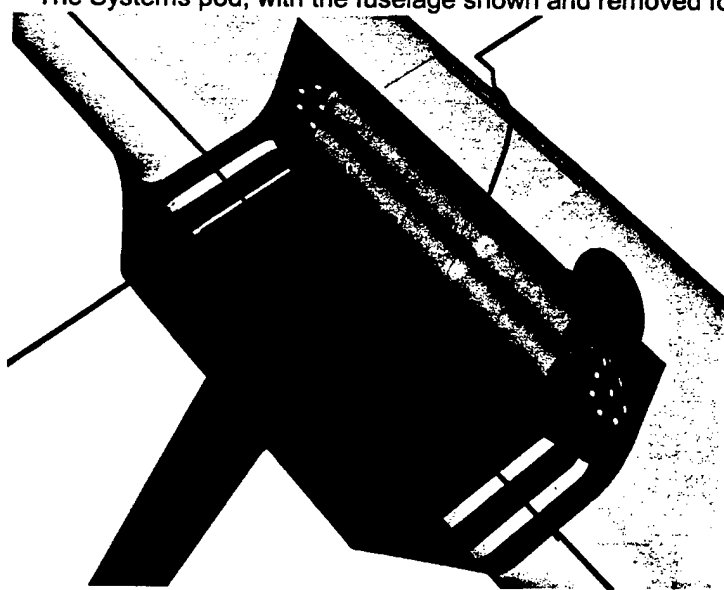
Three-view drawing of the airplane:



A view demonstrating the loading mechanism and ball arrangement:



The Systems pod, with the fuselage shown and removed for clarity.

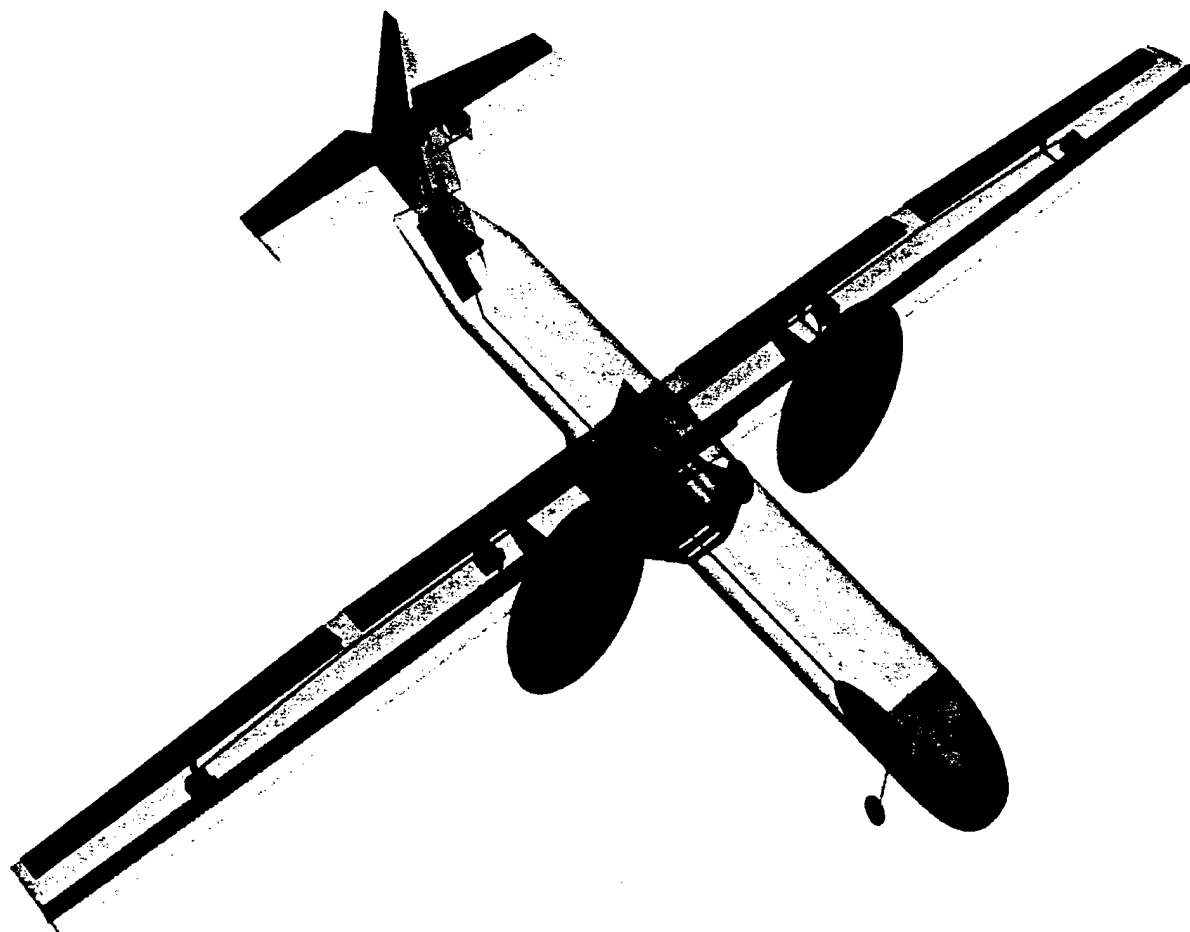


Receiver

Receiver Battery

Engine Battery

A "ghost view" of the airplane, showing all major components:

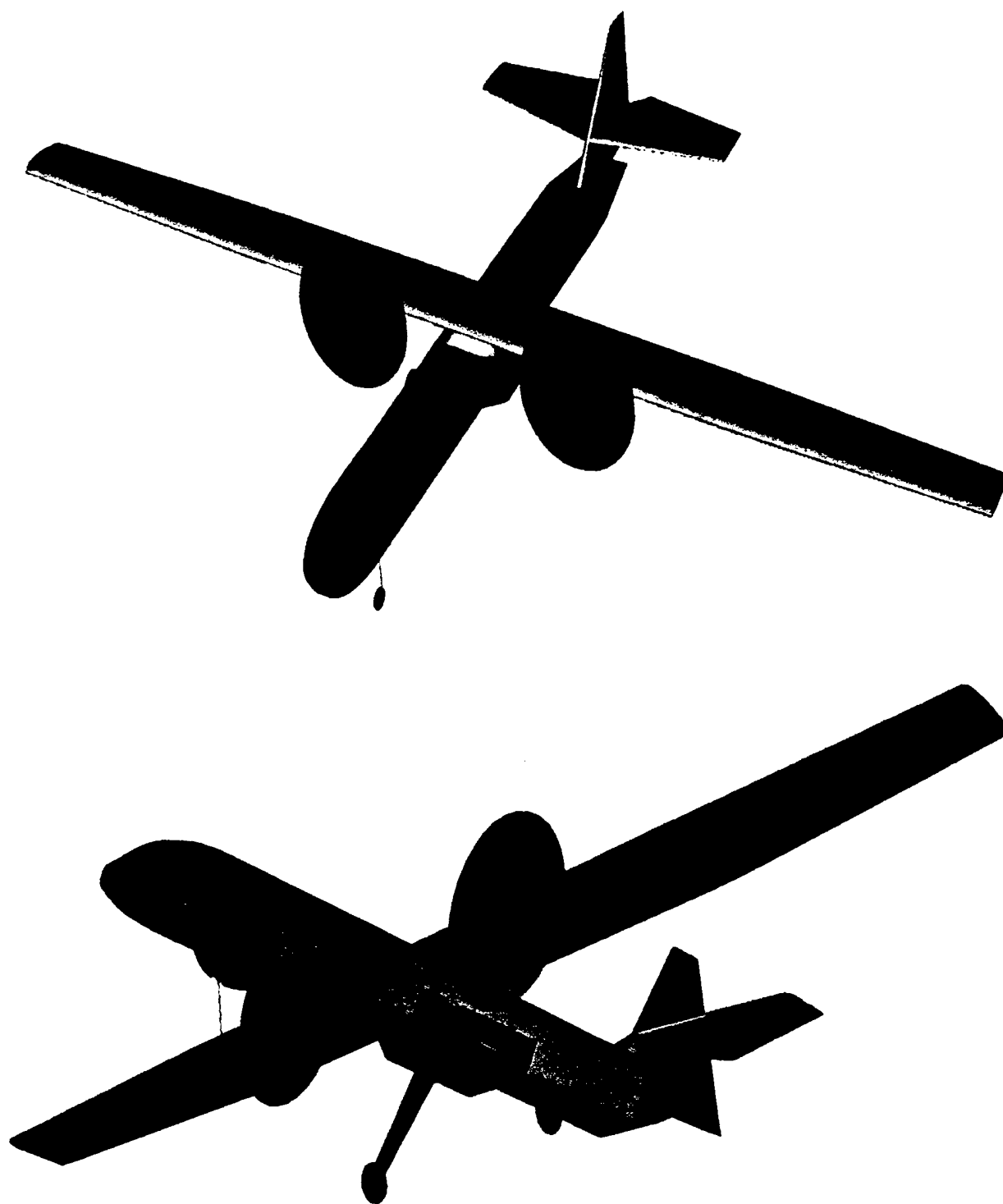


Receiver

Receiver Battery

Engine Battery

Isometric views of the airplane:



6. Manufacturing Plan

6.0 Introduction

Before the aircraft could be fully designed, however, it was necessary to determine the construction plan. The team essentially had three choices for construction techniques: classic built-up balsa and hardwood structure covered in shrink-wrap film; composite construction with manual mold construction; and composite construction with CNC-milled molds. Soon after the team officially came into existence, the 5-axis CNC milling machine at Raspet Flight Research Laboratory at MSU was taken offline for repairs. This reduced the number of options to two. Since three members of the team were trained as composite technicians, and the team decided to construct the airplane nearly entirely from composite materials.

6.1 Figures of Merit

In order to quantify and verify the decision on manufacturing process, the following Figures of Merit were selected.

Table 6.1 Manufacturing Figures of Merit and Associated Weight Factors

FOM	Description	Weight
1. Strength-to-Weight Ratio	Drives Manufacturers Empty Weight and Score	3
2. Availability	Describes how easily the materials can be purchased	2
3. Part Construction Time	Time it takes to make multiple parts	2
4. Tooling Time	Time it takes to prepare for part construction	2
5. Skill Level Required	Skill required for construction	1
6. Cost	Monetary cost of construction	1

FOM 1 was considered to be the most important of these FOM's because this Figure drives the Manufacturers Empty Weight, which in drives the Rated Aircraft Cost. FOM 6 was considered to be the least important because the budget was set before the type construction was decided and allowed for either of the two construction methods. FOM's 3 and 4 were chosen because these two quantities are important in the event that another part needs be made due to unforeseen circumstances.

The analytical method used to select the design process was based on the score of all Figures of Merit. Each method was assigned a score from -2 to 2, with greater numbers indicating greater fitness. The scores were tabulated according to the formula described by Eq. (3.1). The scores and results are presented in Table 6.2.

Table 6.2. Figure of Merit Scoring

Figures of Merit (Weight Factor)	Design Concept	
	Built-up Design	Composite Design
Strength to Weight Ratio (3)	0	2
Availability (2)	2	1
Part Time Construction (2)	-1	1
Tooling Time (2)	2	0
Skill Required (1)	0	-1
Cost (1)	1	0
Total	7	9

As shown in Table 6.2, the composite construction method would be the preferred option in this case.

6.2 Project Milestones

For scheduling purposes, the Project Milestones are listed in Table 6.3 were set.

Table 6.3. Project Milestone chart for manufacturing phase

Steps	Scheduled Completion
Section 6.3 Plug Construction	March 8, 2001
Section 6.4 Mold Construction	March 12, 2001
Section 6.5 Spar Construction	March 15, 2001
Section 6.6 Wing Construction	March 17, 2001
Section 6.7 Tail Construction	March 14, 2001
Section 6.8 System's Pod	March 14, 2001

6.3 Fuselage Plug Construction

The fuselage was designed to be constructed as a monocoque structure, with 3/8 in. plywood mounting blocks for landing gear and a wing saddle all molded into the lay-up. To allow for easy insertion and removal of a speed-loader, no structure or components were placed in the interior of the fuselage cargo section. The fuselage mold will be constructed by first making a male plug using a glass-over-foam construction method. Foam will be cut and sanded to shape, then covered with fiberglass and painted. The nose cone is to be molded separately by a similar process.

6.3.1 Main Fuselage Construction Steps

1. Start by plotting the fuselage cross-section.
2. Glue the shape onto a sheet of metal and cut out the shape to create a template.
3. Cut the foam plug using a hot wire and using the templates as guides.
4. Lay two layers of light weaved fiberglass for protection against bumps.
5. Paint and sand for a smooth surface.
6. Glaze surface with mold release.

6.4 Mold Construction

From the plug, a female mold can be cast. This female mold will allow easy construction of multiple fuselages. In order to allow the fuselage to be molded in one piece, the mold was broken at the maximum-width height (high water mark) of the fuselage. With the female mold constructed, four layers of 2.0 oz/yd² fiberglass were laid with all mounting blocks installed between the second and third layers. To join the two halves, an in-mold overlapping scheme will be used. Any seams from the joining process will be sanded for a smooth transition. Graphite powder is included in the resin lay-up for color; so after curing overnight, the fuselage will be all but complete. The only step remaining will be to bond two 0.25 in. plywood blocks into the tail cone for tail mounting purposes.

6.4.1 Mold construction steps

1. Create parting tray at high water mark.
2. Put a layer of resin and graphite dust on the plug and parting tray to highlight any bubbles that may be present.
3. Lay three layers of light weave fiberglass to make a smooth surface that matches the contours of the male plug.
4. After three layers of fiberglass has cured, lay ten layers of heavy weave fiberglass to give the female mold strength.
5. After the fiberglass has cured, pull off the female mold, and reset the parting tray for the side of the plug.

6.5 Spar Construction

Design of the wing began with its major structural members (i.e., the spars). The design was undertaken with the goal of making a main spar capable of fulfilling the "lifted at the tips" constraint entirely on its own. While this will obviously result in an overbuilt wing, the team had found earlier that if the spar was made to a reasonable size to fit the wing, it resulted in a spar of more than adequate strength. The final main

spar cross section design consisted of two unidirectional carbon laminate caps, each 0.5 in. X 0.030 in. bonded to a Rohacell foam spar core. The design then called for a braided carbon fiber sleeve to be laid up around this assembly. Analysis showed this spar to be capable of supporting a 90 lb. concentrated load at the center when supported at the tips. The team considered narrowing the spar but decided to hold it at 0.5 in. for ease of assembly and increased strength in the drag direction, as the weight savings from narrowing the spar proved negligible.

The rear spar was designed in a similar fashion, except the spar caps were omitted, so the spar consisted only of braided carbon-fiber tube laid up around a Rohacell core.

6.5.1 Spar Construction Steps

1. Cut the spar caps to length.
2. Cut the Rohacell spar core to shape including the taper.
3. Test fit the spar caps and Rohacell cores and bond together
4. After curing, feed the braided sleeve over the spar and pull tight.
5. Bond the sleeve and vacuum bag to get good adhesion.

6.6 Wing Construction

The wing was designed as a "glass-over-foam" wing with a 60 in. constant-chord center section and 30 in. tip panels tapered around the quarter-chord. The root chord was set at 9.3 in., and the tip chord set at 6.975 in. for a total wing area of 1043 in². The design called for a one-piece wing with a full-length main spar and an auxiliary rear spar extending through the constant-chord section. Plywood mounting blocks were incorporated for engine mounting purposes, and the wing was designed to be attached to the fuselage by four nylon bolts. Flaps were extended through the center section and ailerons through the tip panels.

The wing cores were designed to be cut from "pink foam" – Dow Foamula 250, a common material for foam wing cores. Two degrees of washout were built into the tip panels. Bays and slots were removed for all components to be installed internally in the wing.

6.6.1 Wing Construction Steps

1. Start by plotting the airfoil shape at both ends of the section that are going to be cut out.
2. Glue the shape onto a sheet of metal and cut out the shape to create a template.

3. Stick the templates on either end of the foam that has been cut out to the correct length.
4. Make sure cutting wire has sufficient tension and heat applied to it.
5. Take the wire and carefully run it along the template to cut out the shape. Make sure you enter and exit the foam at the same time.
6. Keep the extra foam that is not part of the wing core. This will be used as cradles during the wrapping process.
7. After airfoil shape is cut out of foam cut away places for spars, ribs, engine mounts, wiring tubes, wing-fuse mounts, etc.
8. Bond in the spars and set the cores aside.
9. Cut Mylar to shape of the wing with a 1.5 in overlap.
10. Wax the Mylar and paint the wing color wanted on the Mylar.
11. Make ribs by placing two layers of glass on ends of the foam where ribs will go, cutting the glass so that there is a 0.5 in to 1 in lip that lays on the top and bottom of the airfoil.
12. Lay up fiberglass skins on Mylar and sandwich core between them.
13. Place the wing in a vacuum bag and place it back in the cradles from step 5
14. Apply vacuum and allow the wing to cure overnight.
15. Cut ailerons and flaps out of cured wing.
16. Bond hinges for flaps and ailerons to the skin near ribs.
17. Cut slots or pockets for the servo mounts out of the wing.

6.7 Tail design

The tail was designed to be manufactured as a single removable unit. The vertical tail was designed with a taper from 17 in. chord at the root to 4 in. at the tip. The horizontal tail was designed with a root chord of 12 in. and a tip chord of 6 in. These surfaces used an SD8020 tail surface airfoil and were designed with two layers of 2 oz. fiberglass over foam cores only. The horizontal tail surfaces are joined through the fuselage by two hardwood dowels. Elevator and rudder were both set at 40% chord, and the elevator was split to allow rudder travel to 30 degrees. The two elevator halves are joined by a u-shaped steel torque rod, and elevator travel was set at 20 degrees in both directions.

6.8 Systems Pod Design

Since no componentry was allowed in the fuselage itself, it became necessary to design a pod to carry such items as the receiver, batteries, and speed controllers. In order to minimize the inertial loads and moments induced upon the airframe by the large concentrated mass of the batteries, the components were placed in a systems pod attached to the base of the fuselage and landing gear. The battery packs were designed as a triangular prism constructed from 3 sticks of 5 cells each. Each pack (one for each engine) was placed outboard of the landing gear, with holes drilled in the fairing to allow cooling air to flow over them. The speed controls (one per engine) were placed ahead of the landing gear on the floor of the component tray, and the receiver and its battery pack were placed aft of the gear.

Bibliography

1. Design Optimization Tools User's Manual, Vanderplaats Research and Development, Inc., 1999.
2. AIAA Student Design/Build/Fly Competition, March 7, 2001,
<<http://amber.aae.uiuc.edu/~aiaadb/>>.
3. Anderson, J. D., Introduction to Flight, 4th Edition, McGraw-Hill, Boston, MA, 1999.
4. Anderson, J. D., Fundamental of Aerodynamics, McGraw-Hill, Boston, MA, 1981.
5. Etkin, B.E, Reid, L. D., Dynamics of Flight: Stability and Control, 3rd Edition, Wiley, New York, NY, 1996.
6. Lennon, A., Basics of R/C Model Aircraft Design, Air Age Inc., Wilton, CT, 1996.
7. Nelson, R. C., Flight Stability and Automatic Control, 2nd Edition, McGraw-Hill, Boston, MA, 1998.
8. Abbott, I. H., Von Doenhoff, A. E., Theory of Wing Sections: Including a Summary of Airfoil Data, Corrected Version, Dover, New York, NY, 1959.

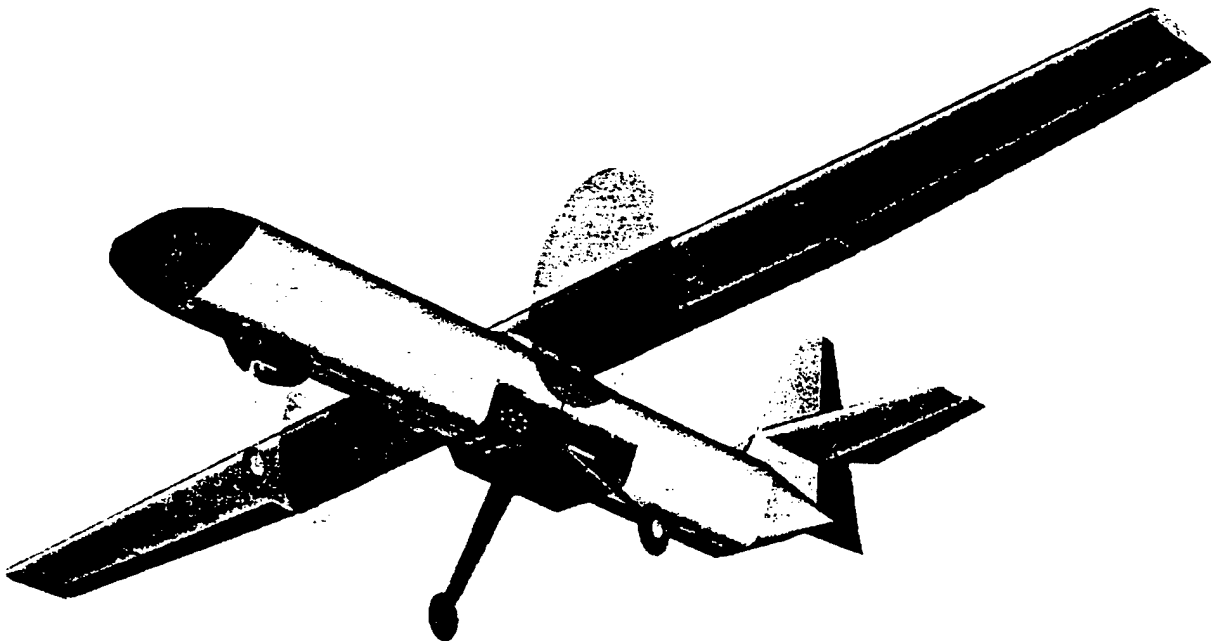
**2000/2001 AIAA Foundation
Cessna/ONR Student Design/Build/Fly Competition**

DESIGN REPORT – ADDENDUM PHASE

APRIL 9, 2001



Department of Aerospace Engineering
Mississippi State University



"Carbon Goose"

Table of Contents

1. Executive Summary.....	1
2. Management Summary	4
2.0 Introduction	4
2.1 Team Member Summary and Assignment Areas.....	5
2.2 Project Milestones.....	8
3. Conceptual Design Phase.....	9
3.0 Introduction	9
3.1 Figures of Merit	9
3.2 Design Concepts.....	10
3.3 Scoring of Design Concepts	14
3.3.1 Scoring of Concept 1.....	14
3.3.2 Scoring of Concept 2.....	14
3.3.3 Scoring of Concept 3.....	14
3.3.4 Scoring of Concept 4.....	15
3.3.5 Scoring of Concept 5.....	15
3.4 Conclusion	15
4 Preliminary Design Phase	16
4.0 Introduction	16
4.1 Figures of Merit	17
4.2 Numerical Optimization	17
4.2.0 Introduction.....	17
4.2.1 Design Variables	17
4.2.2 Design Constraints	18
4.2.3 Objective Function.....	19
4.3 Simplified 3-Dimensional Discretized Optimization	19
4.4 Final Selection of Parameters.....	20
4.5 Tail Sizing.....	21
4.6 Fuselage Design Concepts.....	22
4.7 Final Results	24
4.8 MathCad Code Listing	25
5. Detail Design	32
5.0 Introduction	32
5.1 Performance Data and Flight Handling.....	32
5.2 Component Selection.....	33
5.3 Systems Architecture	33

5.3.1 Radio System	33
5.3.2 Propulsion Architecture	34
5.4 Drawing Package	35
6. Manufacturing Plan	39
6.0 Introduction	39
6.1 Figures of Merit	39
6.2 Project Milestones	40
6.3 Fuselage Plug Construction	40
6.3.1 Main Fuselage Construction Steps	41
6.4 Mold Construction	41
6.4.1 Mold construction steps	41
6.5 Spar Construction	41
6.5.1 Spar Construction Steps	42
6.6 Wing Construction	42
6.6.1 Wing Construction Steps	42
6.7 Tail design	43
6.8 Systems Pod Design	44
Bibliography	45
7. Lessons Learned	46
7.0. Introduction	46
7.1 Challenges Encountered	46
7.1.1 Mold Construction and Composite Fabrication	46
7.1.2 Inaccuracy of Initial Weight Estimate	47
7.1.3 Center of Gravity	47
7.2 Design Modifications	47
7.2.1 Battery Placement	47
7.2.2 Rear Spar	48
7.2.3 Propeller Selection	48
7.2.3 Nosewheel Selection	50
7.2.4 Brakes	50
7.2.5 Control Characteristics	50
7.3 Improvements Possible for Future Designs	50
7.3.1 Weight model refinement	50
7.3.2 Center of Gravity Model Refinement	50
8. Rated Aircraft Cost	52

7. Lessons Learned

7.0. Introduction

This project proved to be highly educational for all members of our team. The experience of manufacturing and flying what we had actually designed from scratch was very rewarding. However, the project was not without its challenges. The lessons we learned in the process of manufacturing and testing our airplane are summarized in this addendum report.

7.1 Challenges Encountered

7.1.1 Mold Construction and Composite Fabrication

Of all project tasks, the prototype construction was found to be the most challenging. Most of the difficulties we encountered in trying to meet the schedule were rooted in our underestimation of the time and effort involved in manual construction of a composite mold to a fairly tight tolerance. The two-step process of making a male plug and using it to construct a female mold that was subsequently used for fuselage layup was very tedious, and required many hours of repeated sanding and sealing of the male plug. The manufacturing schedule was not kept as rigidly as it should have been. This meant that the final 20% improvement in the tool consumed approximately 50% of the total tool making effort. With all that said, the final product was of considerably good quality considering the limited experience of the team as a whole.

The student members with experience in composite construction had mentioned that the composite fabrication is mainly in making the tool, and that making the actual part would take a minimal amount of time. That was truly the case. It was clear from the start that unlike the traditional balsa construction in which the aircraft is build gradually piece by piece, the composite construction required 95% of the effort in making the mold and the rest in making the part. The low part count composite construction in many ways is superior to the built-up method, and the finished product is lighter and much stronger in comparison. The overall experience was perhaps a bit overwhelming to the uninitiated members of the team, but they all hung in there and finished the job.

Upon completion of the fuselage mold and the cutting of the wing and tail foam cores, we completed the construction of the prototype in about 25 days.

7.1.2 Inaccuracy of Initial Weight Estimate

Upon completion of the aircraft, it was weighed, and was discovered to be approximately 4 lb. overweight. This was caused by a combination of factors, ranging from heavier-than-expected landing gear to excess resin in the layup of composite parts. A correction factor was applied to the weight model used for optimization, and optimization was performed again, resulting in a negligible change in the configuration of the aircraft, but registering a substantially decreased payload capacity. This problem could have been quite serious, but luckily did not affect the critical wing area measurement.

7.1.3 Center of Gravity

With the airframe complete, the team checked the C.G. location, only to find that it was substantially aft of its predicted (and necessary) position. Initial attempts at ballasting the nose required nearly 2 lb. of lead in the nose of the aircraft, which was deemed unacceptable by the team. This problem probably arose from the fact that nearly all of the components and structure of the airplane are near or behind the C.G. location, and most of the weight model inaccuracy affected the rear portion of the aircraft. The solution adopted is detailed below.

7.2 Design Modifications

7.2.1 Battery Placement

In order to correct the C.G. problem, the team decided to move the most portable and heaviest components of the aircraft – the batteries. By fastening a plywood support plate to the underside of the fuselage, it became possible to move the battery packs forward by about 10 inches. This balanced the airplane properly without the added weight of ballast. It did become necessary to create an extended systems pod by molding two parts and cutting them in such a way as they could be mated together. This done, the C.G. problem was corrected without an appreciable weight increase.

7.2.2 Rear Spar

During construction of the wing, it was decided that while the composite main spar design was excellent, constructing a similar rear spar offered very little advantage over a simple plywood spar. The decision was made to bond in a full-height spar made from 1/8" aircraft plywood. This spar proved to be more than adequate, and simplified wing construction dramatically, reducing manufacturing time.

7.2.3 Propeller Selection

While the team initially selected lightweight folding propellers from Freudenthaler, wind tunnel testing showed these propellers to be inferior to APC fixed-blade propellers, generating less static thrust and having a lower V_{max} . Based on these tests, the team decided to use the less expensive APC propellers for the final airplane.

Table 7.1. Propeller Performance

Propeller	Static Thrust	V_{max}
Freudenthaler 14X8	75 oz	85 ft/s
APC 14X8	84 oz	90 ft/s

(all tests performed at 18 Volts input)

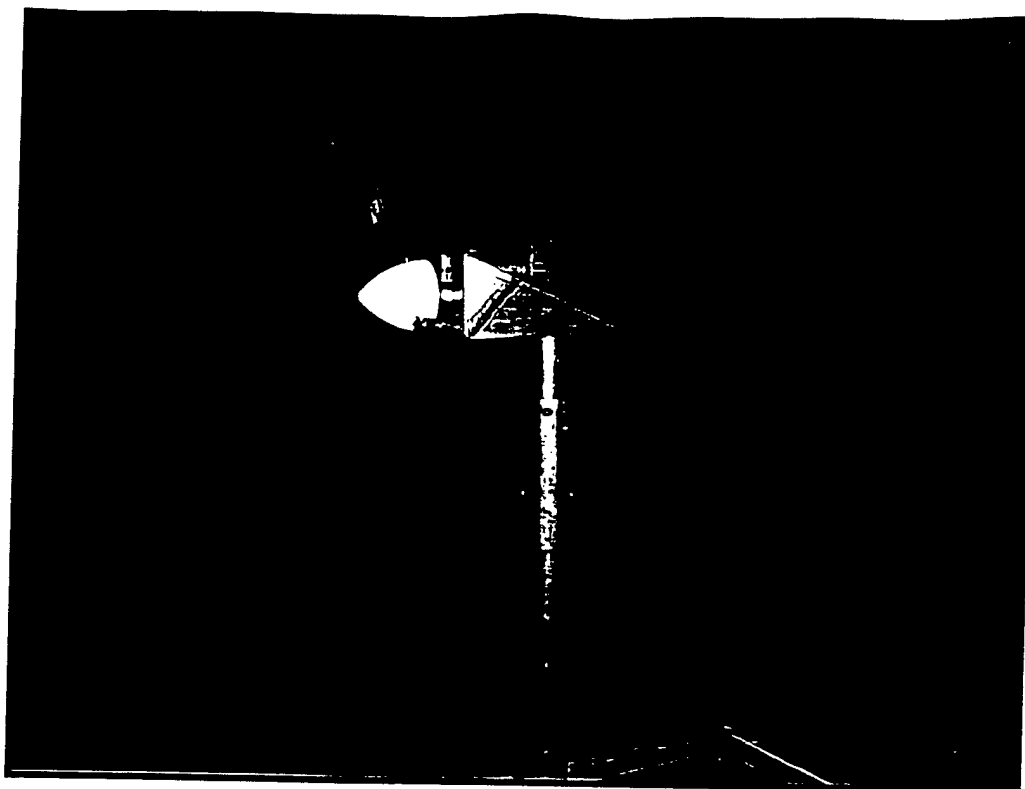


Figure 7.1. Propeller Testing Apparatus

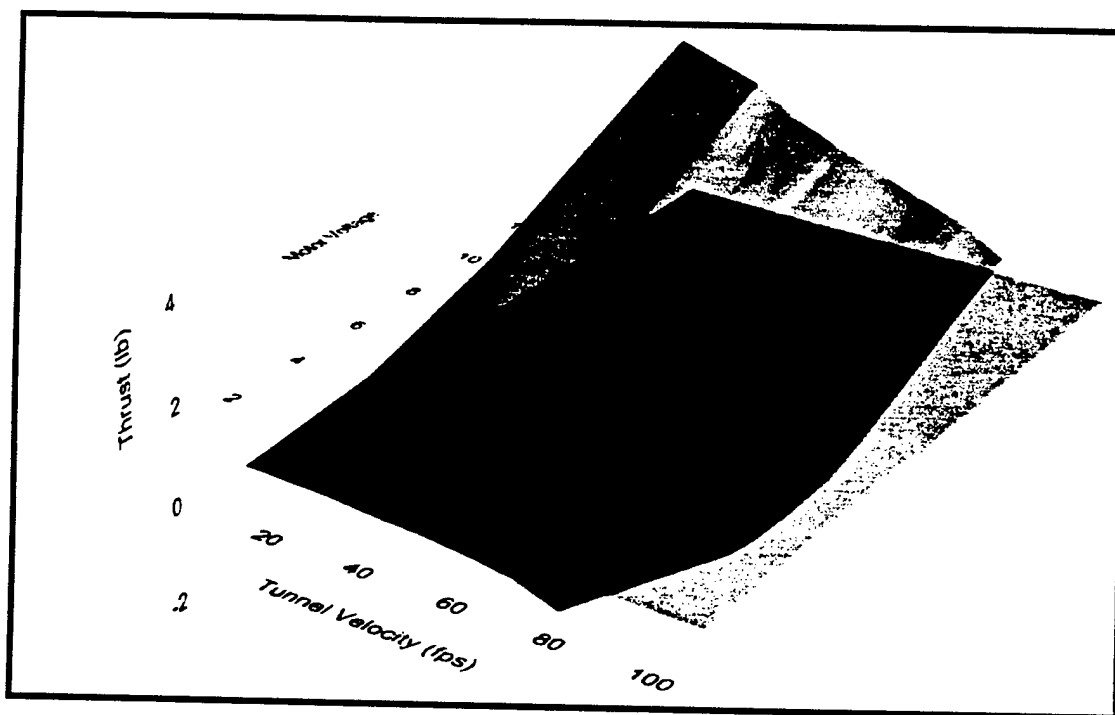


Figure 7.2. Propeller Performance Surface

The wind-tunnel tests actually supported the use of a linear approximation of engine thrust through the takeoff roll, but the team was disappointed to be unable to obtain the advertised value of 100 oz. of static thrust.

7.2.3 Nosewheel Selection

Initially, the team planned to use the same type of scooter wheels on the main gear and the nosewheel. However, to improve ground handling, the decision was made to use a soft rubber wheel instead. This did not result in a large increase in rolling resistance, and ground handling proved to be excellent.

7.2.4 Brakes

Because the wheels selected had a very low rolling resistance, the aircraft demonstrated a tendency to roll a rather long distance after landing. In order to combat this, brakes were added to the wheels. While this did result in a slight increase in Rated Aircraft Cost, the team felt that the addition was justified in order to reduce the time required to retrieve the airplane for payload changes.

7.2.5 Control Characteristics

At the time of this writing, the aircraft has had four successful flights. The handling qualities in all parts of the flight envelope were satisfactory. The flight tests indicated some areas where improvements could be made. This included increasing the yaw control for cross wind conditions expected at the competition site. The trim conditions were typical for this class of airplanes and will not require any changes to the aircraft.

7.3 Improvements Possible for Future Designs

7.3.1 Weight model refinement

In order to increase the accuracy of the design optimization, it would be very helpful to have in hand a refined weight model based on this year's experience. To develop such a model would require component-by-component weight analysis, which could then be correlated with the expected results to help troubleshoot the model. With this in hand, the optimal design could be more easily determined.

7.3.2 Center of Gravity Model Refinement

While this goes hand in hand with the previous item, it would make the manufacturing of the aircraft easier if components did not have to be moved in order to balance the airplane.

Refinement of the C.G. model would allow the elimination of the need for drastic on-the-fly engineering.

8. Rated Aircraft Cost

The Rated Aircraft Cost (RAC) is described as follows:

$$RAC = \left(\frac{\$100}{\text{lbs}} \cdot \text{MEW} + \frac{\$1}{\text{Watt}} \cdot \text{REP} + \frac{\$20}{\text{hr}} \cdot \text{MFHR} \right) / 1000$$

The parameters of this equation are described and listed in Table 8.1. Using these listed values, the RAC is 5.8706 (\$ Thousands) or \$5,870.60.

Table 8.1 Rated Aircraft Cost Parameters and Values

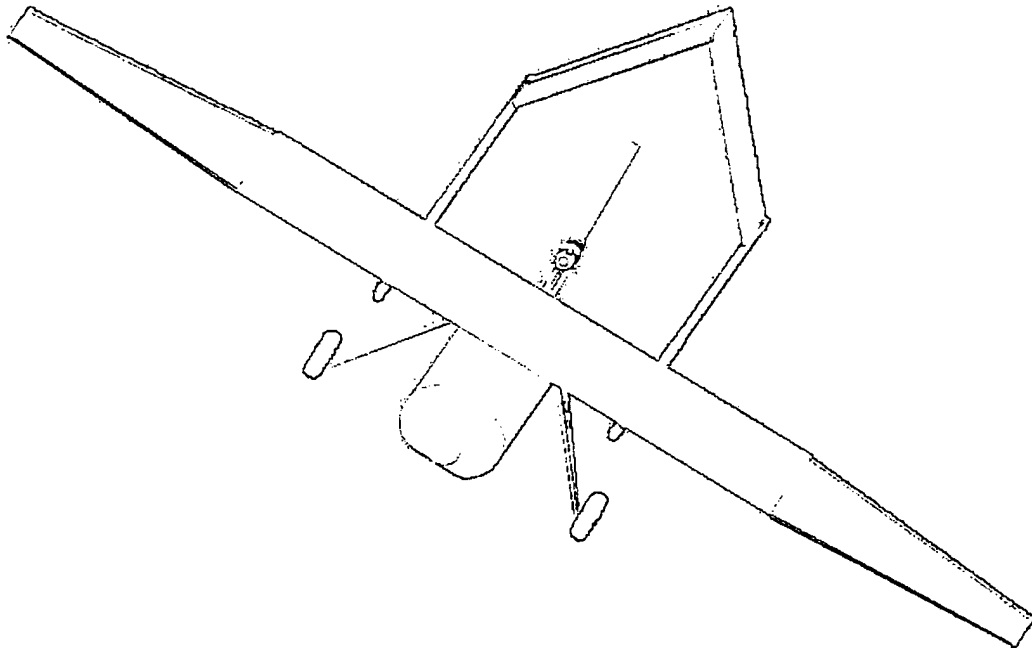
Parameter	Description	Value
Manufacturers Empty Weight (MEW)	16 lbs	16 lbs
Rated Engine Power (REP)	2 engines (15 cells*1.2 V/cell * 30A)	1080 Watts
Manufacturing Hours (MFHR)		
Wing	15 hrs * 1 wing	15hrs
	4 hrs * 7.3 ft^2	29.2 hrs
	3 hrs * 4 control surfaces	12 hrs
	Wing Total	56.2 hrs
Fuselage	15 hrs * 1 fuselage	15 hrs
	4 hrs*5.83 ft	23.33 hrs
	Fuselage Total	38.33 hrs
Empennage	5 hrs (basic)	5 hrs
	5 hrs *1 vertical surface	5 hrs
	10 hrs *1 horizontal surface	10 hrs
	Empennage Total	20 hrs
Flight Systems	5 hrs (basic)	5 hrs
	2 hrs * (8 servos + 2 controllers)	20 hrs
	Flight Systems Total	25 hrs
Propulsion Systems	5 hrs * 2 engines	10 hrs
	5 hrs * 2 propellers	10 hrs
	Propulsion Total	20 hrs
Manufacturing Hours Total		159.53 hrs

MASTER COPY

2000-2001

**AIAA FOUNDATION CESSNA/ONR
STUDENT DESIGN BUILD FLY COMPETITION**

ISTANBUL TECHNICAL UNIVERSITY



"THE BOSPHORUS BLUE"

Design Report – Proposal Phase

March 13, 2001

ISTANBUL

INDEX

1. Executive Summary	3
1.1 Introduction	3
1.2 Range of Design Alternatives	4
1.3 Design Tools	4
2. Management Summary	6
2.1 Architecture of the Design Team	6
2.2 List of Design Personnel and Assignment Areas	8
2.3 Milestone Chart	9
3. Conceptual Design	10
3.1 Introduction	10
3.2 Design Parameters	11
3.2.1 Fuselage Cross Section Geometry	11
3.2.2 Wing Planform	12
3.2.3 Wing Vertical Location	12
3.2.4 Propeller Location	13
3.2.5 Motor Location	13
3.2.6 Tail Arrangement	13
3.2.7 Landing Gear Configuration	14
3.3 Figures of Merits	15
3.3.1 Power Consumption	15
3.3.2 Payload Access	15
3.3.3 Manufacturing	16
3.3.4 Rated Aircraft Cost	16
3.3.5 Conceptual Design Result	20
4. Preliminary Design	21
4.1 Design Parameters	21
4.1.1 Propulsion System Analysis	21
4.1.1.1 Battery Type	22
4.1.1.2 Motor Type	22
4.1.2 Wing Analysis	22
4.1.2.1 Aspect Ratio	22
4.1.2.2 Taper Ratio	22
4.1.2.3 Oswald Efficiency	22
4.1.3 Airfoil Analysis	23
4.1.3.1 Airfoil Thickness	23
4.1.3.2 Airfoil Efficiency	23
4.1.3.3 Airfoil Maximum Lift Coefficient	23
4.1.4 Fuselage Length	23
4.1.5 Tail Longitudinal Location	24
4.1.6 Landing Gear Length and Location	24
4.1.7 Fuselage Nose and Empennage Geometry	24
4.2 Figures of Merits	24
4.2.1 Battery Internal Resistance	24
4.2.2 Current Capacity to Battery Weight Ratio	24
4.2.3 Motor Efficiency	25
4.2.4 Motor Output Torque	25
4.2.5 Motor Constant	25
4.2.6 Aerodynamic Efficiency	25
4.3. Analytic Methods Used	25
4.4 Sizing Calculations and Configurations Data	26
4.4.1 Battery Selection	26
4.4.2 Motor Selection	26

4.4.3 Wing Analysis Results	28
4.4.4 Airfoil Analysis Results	29
4.4.5 Payload Optimization	32
4.4.6 Determination of Tail Longitudinal Location	33
4.4.7 Determination of Landing Location	33
4.4.8 Nose and Empennage Geometry Selection	34
<u>5. Detail Design</u>	35
5.1 Performance Data	35
5.2 Component Selection and Systems Architecture	37
5.3 Drawing Package	38
<u>6. Manufacturing Plan</u>	42
6.1 Introduction	42
6.2 Schedule	42
6.3 Manufacturing Process Selection	42
6.3.1 Material Selection	42
6.3.2 Process Selection	44
6.3.3 Wing	45
6.3.4 Battery	46
6.3.5 Tail, Flaps and Ailerons	47
6.3.6 Fuselage	47
6.3.7 Motor Mount Assembly	47
6.3.8 Landing Gear	48

1.1 INTRODUCTION

The annual Cessna/ONR Student Design/Build/Fly Competition organized by AIAA gives students an opportunity to students to present and evaluate their own skills. It is a good chance for those who aim at planning out their future on aeronautics and have the background and knowledge capacity to come up with solutions to the problems that may arise while designing an aircraft.

A group of seven students from the Department of Aeronautics and Aerospace at Istanbul Technical University will be attending this year's competition with the aircraft they designed and manufactured, **The Bosphorus Blue**. The fly-off will be at Webster Field, part of the Patuxent River Naval Base, in St. Ignis, Maryland, between April 20 and April 22 2001.

What was asked of the entering teams was to build an electric motored, remote controlled, unmanned aircraft and has it fly two types of mission profiles within a given period of flight with different types of payloads. As is stated by the rules and regulations set, it was not allowed for the airplane to carry any payload inside the wing, the wing span was limited to 10 feet and the take-off distance to 200 feet; the different types of payloads the airplane would carry in each of the sorties of the flight period were determined as steel, for the Heavy Payload Task, and tennis balls, for the Light Payload Task; and finally only the brushed electric motors of certain companies were allowed to be used. In addition, the battery pack that would provide power for the electric motor was supposed to weigh maximum of 5 pounds. A fuse placed between the motor and the battery would prevent the motor to receive a current over 40 amperes.

The total flight score and rated aircraft cost, judges' major criterion for the evaluation process at the competition, were effective in determining the outline of the design. Final score was directly proportional with the total flight score and inversely proportional with the rated aircraft cost. In order for the team to get the highest score possible, it was necessary to design an aircraft that would have the best flight performance, namely one that would carry as many tennis balls, one hundred being the maximum, and as much steel weight as possible, and in the mean time have the minimum cost rate.

During the initial design phases of **The Bosphorus Blue**, light, simple configurations with easy loading and unloading systems were considered. For this reason, bi-plane and flying wing configurations were ignored at the very beginning. The effects of the length of the fuselage on rated cost made the team think of light weighted and vertical body configurations. Limitations on the propulsion system had an enormous effect on the number of motors, and thus the general configuration of the entire aircraft.

All of the effects listed above were taken into consideration during the design phase, the pros and cons of alternatives were discussed, so that at each step, the team could select what would reach the desired position in the competition to finally come up with the eventual configuration. There was a share of duties among the team members at this point to make it less demanding to judge the proposed motor, body and wing groups and alternative designs.

1.2 RANGE OF DESIGN ALTERNATIVES

At first, the aircraft was thought to have two motors and two bodies, each having enough volume to carry 50 tennis balls. It was planned to attach the booms behind each body to the H tail. (Fig 1.a) Evaluating this configuration made it clear that there could be difficulties in loading and unloading, and that the cost rate would come out to be very high due to the fact that this design would have a long total fuselage length. The configuration was discarded because of the difficulty in loading and unloading due to the existence of two wings, even though a single body could have been used.

Secondly, it was thought the plane would have a wing beneath it, a removable speed loader with the capacity of holding 100 tennis balls on top of it, and the booms sticking out from behind the wings to be attached to the T tail. (Fig 1.b) This configuration was discarded because of the structural complexity of the fuselage because of the landing gear, the motor and the wing attached to it, and that this would increase the empty weight of the plane.

Then, the aircraft was planned to have its wing on top, two motors, boom behind the wing, a reversed V-tail and a pod beneath the body. (Fig 1.c) The removable pod under the wing made loading and unloading simpler. On top of that, attaching the landing gear and the motors to the wing make the body heavier. It made the team consider the wing merely for reasons of structural concerns.

Lastly, it was attempted to minimize the rated cost by building a vertical body with a symmetrical airfoil cross-section. A configuration with two wings seemed to be the only possible solution to increase the stability of such a vertical body during flight, landing and take-off. It was decided that unloading would be difficult in such a configuration if the team had to use only one motor.

1.3 DESIGN TOOLS

Four computer programs, Microsoft Excel, AutoCAD 2000, MotoCalc and Drag Estimator were used while designing the aircraft. AutoCAD 2000 was used in the conceptual and detail design phase. Pre-sizing was done with that program. The three dimensional sketches drawn in AutoCAD made it easier to evaluate whether or not each of the new concepts brought up by the design group were appropriate for the geometry of the airplane.

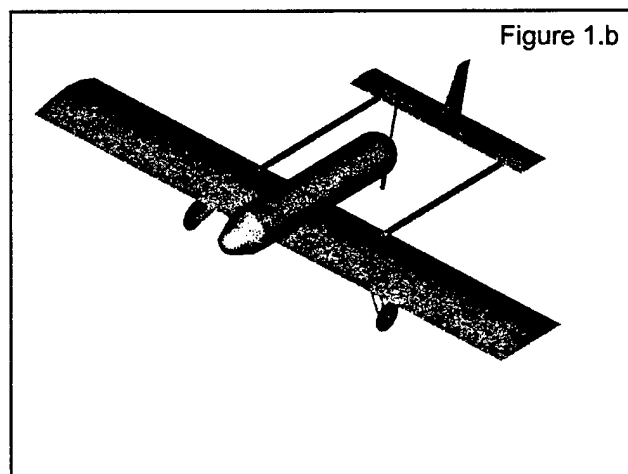
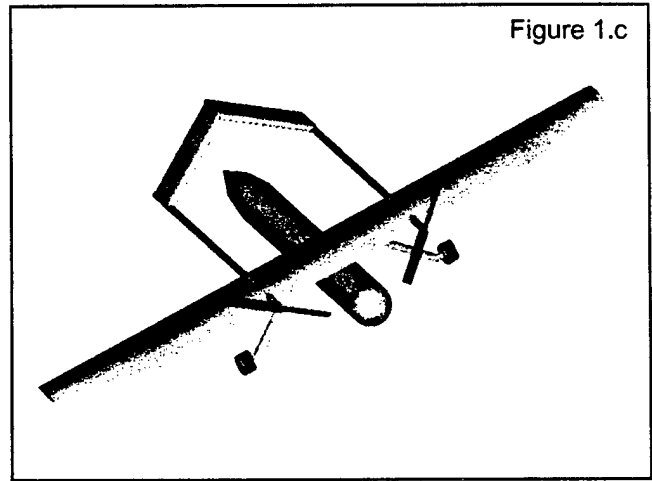
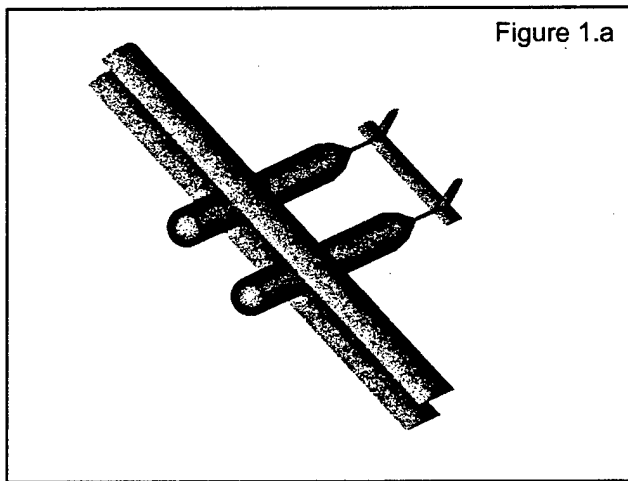
Microsoft Excel, MotoCalc and Drag Estimator were used in the preliminary design phase. A table of coefficients by which various rated aircraft costs could be compared was formed using the calculation sheets that were formed in Microsoft Excel, and thus the rated aircraft costs of each configuration were compared. In this manner, it was thought to select the configuration with the optimum rated aircraft cost.

After that, the selected propulsion system was put in MotoCalc to examine the plane's performance during flight and in different throttle settings. MotoCalc is a program analyzing the performance of a certain propulsion system. The motor, battery, propeller and gearbox databases, entering the properties of the plane during analysis into the control menu and the possibility of limiting the amount of current dragged, just like it is in the competition, made it more straight forward to choose the propulsion system.

Drag Estimator is a program guessing a plane's drag force once its approximate configuration has been submitted. It is with the aid of this program that it was determined whether or not the power system would provide the performance expected of the aircraft.

During the detailed design phase, performance of the aircraft was evaluated with the calculation tables in Excel, based on methods taken from various consulted sources on flight mechanics. Moreover, two and three-dimensional sketches of the final configuration were drawn in AutoCAD.

Figure 1.1 Some sketches of investigated design alternatives



2.1 ARCHITECTURE OF THE DESIGN TEAM

The Bosphorus Blue, the design team formed within the Istanbul Technical University to join the 2001 Student Design-Build-Fly competition organized by American Institute of Aeronautics and Astronautics, abbreviated as AIAA, consisted of eight people, project coordinator Oguzhan Aydin, a senior student, Ergin Esirgemez, another senior student, Arda Mevlutoglu, Altug Tufekcioglu, Ozgur Omeroglu, Serkan Kale and Elmas Anli, sophomores, and Oguz Dogansoy, the pilot. Even though the fact that the team neither had enough number of people nor enough experience was an impediment, surpassing this obstacle through a disciplined work plan and a rational management structure was possible. Members were categorized into two main work groups, namely the design group and the management group, depending on their skills and areas of interest, each of which had a different strategy of fulfilling its mission. What each group was responsible of completing can be seen in Chart 2.1, a short summary of which is that the design team was in charge of the design, and the management team was in charge of planning and carrying out the entire project. Each member of **The Bosphorus Blue** had separate duties for both of these work groups that he was responsible from.

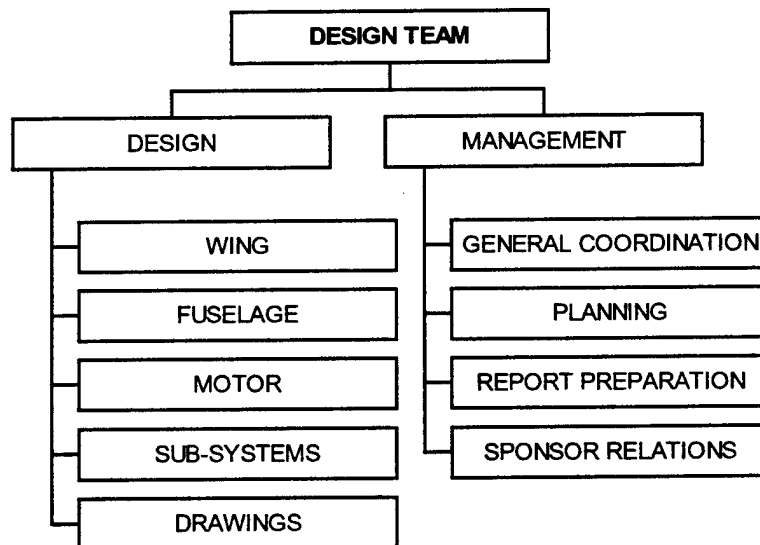


Chart 2.1: Architecture of the design team

The fuselage group, a sub-group of the design group, worked on designing an aerodynamically and structurally optimized fuselage to get the highest score on the competition. The second job of this group was to determine the best design among numerous others and judging them on grounds of ground handling, loading and unloading, which would be vital during the competition. The motor group was responsible of determining the appropriate propulsion system, in accordance with the competition rules, and testing how it would perform during the two flight assignments. The wing group was responsible of

coming up with the wing design that is most appropriate to the motor configuration, fuselage concept and the strategy taken. Designing a wing of the desired strength came only after calculating the aerodynamic forces that would act upon the aircraft. The group called sub-systems was responsible from designing the sub-systems, such as the landing gear and the control system, that would work in perfect harmony with the other systems of the aircraft and designing the aircraft in accordance with the targeted design. The drawing person helped the design team come to better conclusions about the configuration alternatives that were examined during different stages of the design by drawing their three dimensional sketches to scale. He also prepared the drawing package that is supposed to appear on the proposal phase report.

The general coordination group, a sub-group of the management group, assembled meetings, took attendance and generated the group's communication between the faculty advisor and the AIAA representative. The planning person checked to see whether the design was being carried out as was planned. One person was responsible from writing the reports since both would be submitted in English and had to be comprehensible and in a certain format. One person was responsible from arranging the trips to the provided work site and back, because the technical sponsor was located in a distant city and the trips had to be pre-planned. This person also coordinated the group's communication with the financial sponsor and dealt with purchasing equipment.

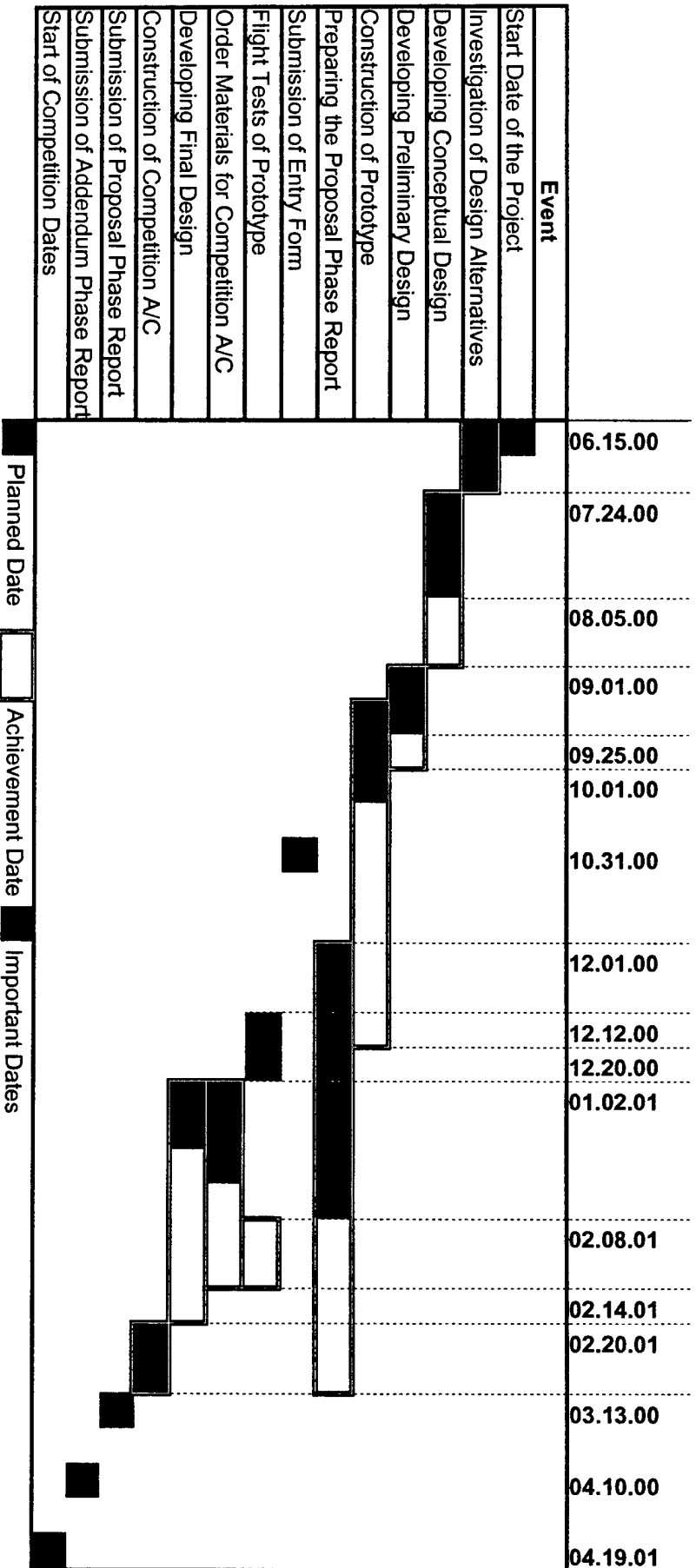
Such work groups could work efficiently by constantly communicating with each other. Each group preferred to pay attention to the remarks of other groups rather than taking an introvert strategy. There were meetings held every Saturday at school's Aviation Branch Room so that each group could keep up with the others. What was done during these meeting was to evaluate the previous week, determine what phase of the project was reached and assign new jobs for the upcoming week. In presence of delay in a plan, the reasons of this problem and new short-term strategies were figured out in order to eliminate the problem. These meetings, run by Professor Suleyman Tolun, the advisor, helped the project move on more openly and flow smoothly. In addition, the mailing list made it possible for the team members to announce progresses, share the problems faced and discuss solutions with each other on weekdays.

2.2 LIST OF DESIGN PERSONNEL AND ASSIGNMENT AREAS

<u>Personnel Assignment Areas</u>		Oguzhan Aydin	Ergin Esirgemez	Altug Tufekcioglu	Serkan Kale	Arda Mevlutoglu	Ozgur Omeroglu	Elmas Anli
DESIGN	Wing		✓					
	Fuselage	✓	⑩					
	Motor	✓						
	Sub-Systems	✓	⑩	✓	⑩		⑩	
	Drawing				✓			
MANAGEMENT	General Coordination	✓						
	Planning	⑩	✓					
	Report Preparation	✓	⑩				⑩	✓
	Sponsor Relations		✓	✓				
Manufacturing of Prototype		⑩	⑩	✓	⑩	✓	⑩	⑩
Manufacturing of Competition Aircraft		⑩	✓	✓	✓	⑩		

✓ Fully ⑩ Partially

2.3 MILESTONE CHART



3.1 INTRODUCTION

In this very first stage of the design phase, team members were in total agreement that construction of a lightweight aircraft and a propulsion system, which made efficient use of the motor, battery and propeller within the boundaries of the competition rules were the major concerns of designing a highly competitive aircraft. Besides, a design with high aerodynamic efficiency, increasing the time span of endurance by letting the aircraft consume less energy, was another matter to be discussed on the way towards reaching the desired performance. So the design team focused on how to make the major components, meaning the fuselage and the wing, lightweight and aerodynamically efficient while keeping their capabilities at the highest level to accomplish the missions. Several design concepts were investigated in order to reach the most competitive features, as described below.

At first, the main load carrier fuselage concept was investigated. This concept brought up the idea of a fuselage, which is a joint structure for the wing, landing gear and the propulsion system, with a mission of carrying certain payloads. It was seen after sketching this design that the fuselage weight increased excessively due to the supporting structures needed when the fuselage was to have a required rigidity to resist the masses of the landing gear, wing and the propulsion system. The compulsory interruption of the wing and the landing gear on the fuselage made load access even more difficult.

Secondly, concepts of a lifting body and an aerodynamically ideal fuselage were investigated. The primary aim of this concept was to build a fuselage within the restrictions of the competition which generates additional lift on top of its conventional mission, or a fuselage, which may not generate lift but require the least thrust to accelerate into take-off at the required distance because of its high aerodynamic efficiency. After some discussions on the alternative configurations, team members noticed that creating a lifting body rather than a body having an airfoil cross-section as required by the competition rules needed highly developed optimization techniques and numerous wind tunnel tests. Moreover, the wing would interrupt the fuselage and the landing gear, meaning a payload access problem would arise.

Then, another design proposing to build a fuselage that carries nothing but the payload and a wing that the landing gear and propulsion system are located on came about. This way, the fuselage could be a lightweight construction, as it would only carry the payload. The wing would be structurally strengthened to pass the wing tip test, and thus could easily resist the impact of masses of the landing gear and the static masses of the propulsion system. By the aid of the configuration sketches drawn, it was seen that the length and the weight of the landing gear increased, but this proposal was still advantageous because of its lightweight fuselage and easy constructible nature.

3.2 DESIGN PARAMETERS

After discussing some major configuration possibilities, team members tried to determine the parameters, which would guide them into reaching an optimum configuration through this design process. The competition rules and the performance targeted were the major concerns when selecting the design parameters, and it is defined in detail below why the team selected each design parameter at the conceptual design level.

- Fuselage Cross-Section Geometry
- Wing Planform
- Wing Vertical Location
- Propeller Location
- Motor Location
- Tail Arrangement
- Landing Gear Configuration

3.2.1 Fuselage Cross Section Geometry

The fuselage would to be used to carry the designated type of payloads for each mission. The fuselage could also carry battery packs, motor and other electrical components in a section separate from that of the payload. However, the design team considered the possibility of carrying the electrical equipments in the wing or in a separate structure attached to wing. So the fuselage was primarily designed to carry rectangular steel blocks and tennis balls. Tennis balls required much more space with respect to steel blocks, so the cross section alternatives were compared as if the fuselage would only be carrying tennis balls. The team assumed that the aircraft would carry one hundred tennis balls, which let them determine the fuselage fines ratio of each alternative. Several fuselage designs were investigated, paying attention to the method of judgment mentioned above.

A fuselage with a rectangular cross section was easy to construct, but had a low packing density because of the sharp corners and could easily be affected by cross winds.

A fuselage with a square cross section was commonly easy to construct. The aspect of packing density made this advantageous with respect to the rectangular cross-sectioned design because there is no loss of space due to the symmetry with respect to two axes.

A circular fuselage cut from the lower side to create a plain base to allow the wing and the landing gear to be installed easily had the best packing density, but a smaller number of balls fit into the cross-section. This gave way to a long fuselage with high fines ratio.

A cross section of filleted-corner rectangular had an aerodynamically advantageous fines ratio and a high packing density, but this kind of a fuselage had relatively more blunt nose and empennage sections, which promoted undesired flow separations behind the fuselage.

A vertical airfoil shaped fuselage was aerodynamically the most advantageous alternative with its high aerodynamic efficiency; but its small packing density made it less favorable and the difficulty of

connecting the wing and the fuselage without disturbing the payload space restricted the designer to evaluate other configuration alternatives.

3.2.2 Wing Planform

As was in every discussion of the design, efficiency was the major concern of the wing design. Because of the constraints competition rules set on the power availability, it was necessary to design a less power-consuming wing. In this phase, the team had a point of view that was concerned only about the matter of efficiency.

The team considered three planforms for the main wing. The considered planforms were elliptical, rectangular, and tapered wings. Prandtl wing theory proves that the elliptical wing planform has the best aerodynamic efficiency, in comparison to the other two wing planforms. However, an elliptical planform was difficult to manufacture.

The untapered rectangular wing was the easiest to build. Rectangular wing had a constant chord along the span, a small stall velocity, but approximately 7% more drag than an elliptical wing with the same aspect ratio due to lift. Therefore, the aerodynamic efficiency of the rectangular wing was less than that of the elliptical wing.

The tapered wing produced a lift distribution close to the ideal, namely the elliptical. Hence, its aerodynamic efficiency was more than that of the rectangular wing. The tapered wing was also simple to manufacture, compared to an elliptical wing.

3.2.3 Wing Vertical Location

Wing vertical location was selected as a design parameter because of its great influence on structural weight and ground handling characteristics. Three different alternatives were considered as part of this discussion.

A high wing design had structural benefits. When the wing passes through the fuselage, the fuselage had to be stiff around the cutout area, which would add to the weight of the fuselage. However, passing the wing attachment structure over the fuselage or attaching the fuselage below the wing would increase drag due to the increase in frontal area. In a high wing design, propeller(s) would have sufficient ground clearance without excessive landing gear length.

A mid-wing arrangement had structural disadvantages due to a wing attachment structure passing through the fuselage the way explained above. It also weakened the ground handling capabilities by interrupting the payload space.

A lower wing arrangement required a long landing gear to provide sufficient propeller clearance. Payload access seemed to be easier with a clear upper side of the fuselage. Still, once again, to prevent interruption of the payload-carrying volume, the fuselage needed to have a wide cross-section.

3.2.4 Propeller Location

Propeller is such an important component of the propulsion system that its satisfactory performance must be assured for a competitive performance. Its interaction with the other components must be considered as well. At this phase, the interaction problem was discussed by only considering its location.

A pusher location has the propeller behind the attachment point. The pusher location is more often used because of its advantages. Most importantly, it reduces aircraft skin friction drag, because the pusher location allows the aircraft to fly in undisturbed air. Moreover, the airflow induced by a pusher propeller will prevent airflow separation despite a blunt empennage. The pusher may require longer landing gear, because the aft location causes the propeller to dip closer to the runway as the nose is lifted for take-off.

A tractor installation has the propeller in front of its attachment point. The tractor location places the propeller in undisturbed air. However, the aircraft flies in turbulence caused by the propeller wake, which increases the aircraft skin friction drag.

3.2.5 Motor Location

Wing mounting of the motor is generally used for multiengine designs. Wing mounting motors reduces wing structural weight through a span loading effect and fuselage drag by removing the fuselage from the propeller wake. For the low-wing design, wing mounted motors may require longer landing gears. The propeller would be halfway in the wake from under the wing and halfway that from over the wing. The pressure differences between these two wakes could cause the propeller to lose efficiency and produce vibrations.

Upper fuselage pods tend to be used in need of a huge propeller clearance; but the nose pitching caused by high thrust line had to be considered for good control characteristics. In this arrangement, it was not mandatory to construct a massive structure to constraint the motor to wing because the wing would be stiffened.

Fuselage mounted design would have difficulty in payload access. This arrangement would also lengthen the fuselage while increasing its structural weight for the motor is attached to the fuselage.

3.2.6 Tail Arrangement

The tail had to be aerodynamically efficient with the least amount of wet area possible and lightweight while it had the required control and stability features. In this phase, without the exact knowledge of the desired control and stability characteristics, the tail arrangement and geometry could only depend on the provided wetted area of the tail and a general account on the benefits of the geometry and arrangement on control and stability.

The team only considered boom-mounted type of tail arrangements because of their simplicity in contrast to the sophisticated conventional tails. The easily compatible nature of twin-boom arrangement

with a vast amount of probable motor number and location variations let the team feel free about the motor related discussions.

A boom mounted conventional tail having a mid-mounted horizontal tail provides adequate stability and control; but as the distance between the booms gets longer, the need for a longer propeller and the length and the weight of the horizontal tail increase. This widely used type of tail arrangement loses its control advantages because it ends up at an unreasonable structural weight when there are excessive distances between booms.

A conventional tail design with a high horizontal tail is inherently heavier than a conventional mid-horizontal tail, because the vertical tail must be strengthened to support the horizontal tail. However, this type of tail has some compensating advantages due to the end plate effect. The T-tail allows a smaller vertical tail and lifts the horizontal tail clear of the wing wake and prop wash, which makes it more efficient, and hence allows reduction of its size. On the other hand, due to the required propeller clearance, these benefits no longer exist when there is a long distance between the booms.

As for the boom mounted inverted-V tail arrangement, the V shape is intended to reduce the wetted area. Vertical and horizontal tail forces are the result of the horizontal and vertical projections of the force exerted upon the inverted-V surfaces. Using both surfaces for each control reduces the wetted area and the tail structural weight.

3.2.7 Landing Gear Configuration

Landing gear is one of the major components of the aircraft and must be placed correctly for excellent landing and take-off performance. The common options for the landing gear arrangement were discussed as shown below.

The tail dragger landing gear has two main wheels in front of the c.g. and auxiliary wheel(s) at the tails shorter than the forward wheels. The tail dragger gear provides more propeller clearance for the tractor type propellers, but not quite the same for the pusher type propellers. It has less drag and weight compared to the other configuration alternatives, but it is inherently unstable because the c.g. is located behind the main landing gear. This causes the turn to be tighter until a ground loop is encountered and the aircraft drags a wing tip, makes the landing gear collapse or runs off the side of the runway. The pilot must therefore align the aircraft almost perfectly with the runway at touchdown while trying to keep the aircraft almost stable with quick rudder controls in order to prevent this.

The tricycle type landing gear, which has two main wheels aft of the c.g. and an auxiliary in front of c.g., has the c.g. ahead of the main wheels, so the aircraft is stable on the ground.

The quadricycle landing gear has wheels on four sides of the fuselage. All the gears are of the same length, so this configuration requires a flat take-off and landing attitude.

3.3 FIGURES OF MERITS

3.3.1 Power Consumption

One of the major constraints the competition rules had on the design was the amount of power the propulsion system would provide. It was permissible for the motor to draw a maximum current of forty amperes from the five-pound battery pack. To increase the number of sorties to be flown and the payload weight to be carried, it was necessary to build a light weight and aerodynamically efficient aircraft. The aircraft would require less power for take-off and lifting more payloads as it had less weight and more aerodynamic efficiency.

The overall arrangement and smoothness of the fuselage could have a major effect on aerodynamic efficiency. Well-arranged and longitudinally smooth contoured aircraft components create less flow separation, which increases aerodynamic efficiency. Minimizing wetted area is one of the most powerful considerations for virtually all aircraft because wetted area directly affects the friction drag.

Fuselage wetted area is minimized by tight internal packaging and a low fines ratio. In order to reduce drag caused by the airflow separation, the aft-fuselage deviation from the free stream direction should be smooth. Nevertheless, as the fuselage gets smoother and smoother, its length and weight, and eventually the rated aircraft cost, increase as well.

However, the airflow induced by the pusher type propeller will prevent separation despite contour angles of up to 30 degrees or more.

Locating opposing forces near each other can minimize the size and weight of the structural constituents. The primary forces are lift of the wing and opposing weight of the major parts of the aircraft, such as the landing gear, propulsion system and payload. As the wing provides the lift force, locating the heavy weight items as close to the wing as possible can reduce load path distances. This leads to a concept of locating major components on the wing.

3.3.2 Payload Access

Payload access directly affects the number of sorties flown. Load and unloading tens of tennis balls and rectangular steel blocks would be less time consuming if there was a well-prepared arrangement. The team must complete the mission flights and exchange the payloads in ten minutes. Basically, the less time the aircraft spends on the ground, the more time it has to fly.

The fuselage where the payload must be carried should be cleared of other components' interference. For instance, a tractor type propeller may avoid front access while the tail hinders the aft side access to the fuselage. In addition, the fuselage must be free of wing interruptions, which restrict easy payload access.

3.3.3 Manufacturing

The designed aircraft needed to have an easily constructible nature, meaning it needed to be produced using unsophisticated tools and materials. The required tools and materials had to be readily

available at the school facilities or provided by the sponsor. The manufacturing process should not have required highly qualified manufacturing skills which would be difficult to be met by the inexperienced team members when such a big scale model aircraft building is at stake.

It is a fact that an easily constructible aircraft is also easily repairable. In case of a possible crash during test or competition flights, it should be easy to repair the aircraft and continue flying in a limited amount of time, as mentioned in the competition rules.

3.3.4 Rated Aircraft Cost

The rated aircraft cost was discussed according to Table 3.3.4.1 for each design parameter. The effect of the fuselage on the rated cost was only related to its length, which was related to nothing but the number of tennis balls that fit into a cross section of the fuselage. In other words, the option with the greatest number of balls in its cross section would be the shortest, and thus would result in the least rated aircraft cost.

As far as the wing vertical location was concerned, different alternatives would have different results on the empty weight of the aircraft, each of which would affect the rated aircraft cost in a different respect. Complexity of the structural system would increase the weight. For this reason, simplicity of high wing configuration would give way to lightness, and thus have the least contribution to the rated aircraft cost.

As for the tail configuration, when the tail is an inverted-V and the same surfaces are used for both states of control, economizing from both the horizontal and the vertical empennage surfaces would minimize the tail's effect on the rated aircraft cost.

A tricycle landing gear demanded a nose wheel in front of the fuselage. Since the spot where the nose wheel would be placed needed to be stiffened, the empty weight of the fuselage, and thus the rated aircraft cost would increase. When it came to a tail dragger, there would be no extra addition to the empty weight because the main landing gear would be attached to the already-stiffened wing, which means it would no longer be necessary to stiffen any other part. On the other hand, the fact that the landing gear goes around the fuselage implied a longer and heavier landing gear. The same result was true also of the quadricycle configuration. Under these circumstances, there was no gigantic difference between the landing gear alternatives as far as their effects on the rated aircraft cost went.

Motor location was quite effective on the empty weight of the aircraft and the fuselage length when a rated-aircraft-cost-concerned approach was taken. If the motor was placed within the fuselage, the joints would have to be structurally supported. If a propeller with a big radius was used, the landing gear would need to be enormously elongated in order to provide the necessary propeller clearance.

Placing the motor in the wing would not make the wing heavier because the wing, which already was structurally supported, would require no extra stiffening. In the configuration with the wing on top, landing gears would not be too long since the propeller provided clearance for the motors in the wings. Taking these into consideration, one might lead to think the wing mounted motor consideration was the

most desirable, but that is possible only when two motors are used. According to the rated aircraft cost model though, rated aircraft cost increase as the number of motors and propellers increase. When a single motor and a single propeller are used in the upper fuselage pod mounted configuration, the landing gear length would be reasonable since the propeller clearance would be enough for the motor placed on a pod on the wing. In spite of these advantages, the weight of the pod mounted on the wing would increase the empty weight of the aircraft. Eventually, in a single motor configuration the upper fuselage pod mounted configuration was the most suitable, as far as the rated aircraft cost was concerned.

Aircraft Cost Model

$$\text{Rated Aircraft Cost, \$ (Thousands)} = (A * \text{MEW} + B * \text{REP} + C * \text{MFHR}) / 1000$$

Coef.	Description	Value
A	Manufacturers Empty Weight Multiplier	\$100 / lb.
B	Rated Engine Power Multiplier	\$1 / watt
C	Manufacturing Cost Multiplier	\$20 / hour
MEW	Manufacturers Empty Weight	Actual airframe weight, lb., without payload or batteries
REP	Rated Engine Power	# engines * Amp * 1.2 V/cell * # cells "Amp" will be the value of the inline fuse from the battery to the controller. Maximum value is 40A, but a lower current fuse may be used, and REP adjusted accordingly.
MFHR	Manufacturing Man Hours	Prescribed assembly hours by WBS (Work Breakdown Structure). MFHR = \sum WBS hours WBS 1.0 Wing(s): 15 hr/wing. + 4 hr/sq. ft. Projected Area + 2 hr/strut or brace + 3 hr/control surface Note: Winglets, end-plates, and biplane struts ARE included in the Projected Area calculation. WBS 2.0 Fuselage and/or pods 5 hr/body. 4 hr/ft of length WBS 3.0 Empenage 5 hr.(basic) + 5 hr./Vertical Surface + 10 hr./Horizontal Surface WBS 4.0 Flight Systems 5 hr.(basic) + 2 hr./servo or controller WBS 5.0 Propulsion Systems 5 hr./engine + 5 hr./propeller or fan

Table 3.3.4.1: Aircraft Cost Model

Ranking Chart of Design Alternatives

Design Parameters		Figures of Merits						
		Power Consumption		Payload Access 1-3	Manufacturability 1-2	Cost* 1-10	Final**	Decision
		Aerodynamic 1-3	Weight 1-4					
Fuselage Cross-Section Geometry	Rectangular	1	1	1	2	7	1.4	E
	Square	1	2	2	2	7	1	E
	Filletted-Corner Rectangular	3	4	3	1	5	0.4	FA
	Circular	2	3	3	1	10	1.1	E
Wing Planform Shape	Elliptical	3	1	N/A	1	N/A	5	E
	Tapered	2	2	N/A	2	N/A	6	FA
	Rectangular	1	2	N/A	2	N/A	5	E
Wing Vertical Location	High-Wing	2	3	3	2	6	0.6	FA
	Mid-Wing	2	1	1	1	10	2	E
	Lower-Wing	2	3	3	2	7	0.7	E
Propeller Location	Pusher Type	3	2	3	2	N/A	10	FA
	Tractor Type	1	2	1	2	N/A	6	E
Motor Location	Wing Mounted	2	4	3	2	6	0.5	FA
	Upper Fuselage Pod Mounted	3	3	3	2	7	0.6	FA
	Fuselage Mounted	3	2	2	1	10	1.4	E
Tail Arrangement	W Mid-Mounted Horizontal Tail	1	2	2	2	10	1.4	E
	W High-Mounted Horizontal Tail	2	2	2	2	10	1.2	E
	Inverted V tail	3	4	2	2	7	0.5	FA
Landing Gear Configuration	Tail Dragger	3	4	3	2	8	0.6	FA
	Tricycle	2	2	2	1	8	1.1	E
	Quadricycle	2	2	3	1	10	1.2	E

E = Eliminated FA = Further Analysis N/A = Not Applicable

** Final = Cost/(Power Consumption+Weight+Payload Access)

When the cost is not applicable to the design parameter the sum of FOM points decided the final.

Chart 3.1: Ranking Chart of Design Alternatives

3.3.4 Conceptual Design Result

The team chose the fuselage with a filleted-cornered rectangular cross-section because this configuration could possess a reasonable fuselage length and fines ratio even when it held the maximum number of balls. This was advantageous both for purposes of rated aircraft cost and aerodynamic efficiency.

The design team took into account the aerodynamic efficiency and the manufacturing ease of three wing planform alternatives. The team decided to build a tapered wing since its aerodynamic efficiency was close to that of an elliptical wing even though it was simpler to build than an elliptical wing.

Choosing the motor location as upper fuselage pod mounted helped the motor rotate a high-radius propeller without adding too much to the length of the landing gear. On top of these, its effect on the empty weight was less, compared to the other single motor location configurations, as described above. Since a multi-engine configuration would be further analyzed, the team decided to investigate the wing mounted motor alternative too.

Pusher type propellers prevented the propeller wakes from disturbing the wing. Additionally, this configuration increased the general aerodynamic efficiency of the aircraft by decreasing the effect of fuselage induced flow separation.

Determining the wing vertical location as high wing caused structural simplicity. The empty weight was kept at the minimum by mounting all the main components on to the already-supported wing.

The tail arrangement was chosen to be an inverted-V because of its aerodynamic efficiency, the fact that it can allow a single servo to be used, and that the necessary tail areas remain at the minimum.

CONCEPTUAL DESIGN RESULTS

Fuselage Cross-Section Geometry	<i>Filleted Cornered Rectangular</i>
Wing	<i>Tapered Mono Wing</i>
Wing Vertical Location	<i>High Wing</i>
Propeller Location	<i>Pusher</i>
Motor Location	<i>Upper Fuselage Pod Mounted for Single Motor Wing Mounted for Multi Motor Configurations</i>
Tail Arrangement	<i>Inverted "V" Tail</i>
Landing Gear Configuration	<i>Tail Dragger</i>

4.1 DESIGN PARAMETERS

The design parameters investigated during the preliminary design stage are as follows.

- Propulsion System Analysis
 - Battery Type
 - Motor Type
- Wing Analysis
 - Aspect Ratio
 - Taper Ratio
 - Oswald Efficiency
- Airfoil Analysis
 - Airfoil Thickness
 - Efficiency
 - Airfoil Maximum Lift Coefficient
- Fuselage Length
- Tail Longitudinal Location
- Landing Gear Location
- Fuselage Nose and Empennage Geometry

4.1.1 Propulsion System Analysis

As mentioned in the first stages of conceptual design, optimization of efficiency and maximum thrust available from the motor was one of the major concerns of the design team. Since the team had a limited power source to use, the motor had to convert the input power to output torque efficiently. A motor could perform for longest time span of duration at its maximum efficiency-operating regime. So in this stage, the team tried to find the most efficient motor. In order to know the operating regime, however, the team had to decide how many volts and amperes the battery pack would provide the motor with. Because these in direct relations with the battery cell type, the team had to make a decision on the battery type first.

The manufacturer advised not to think much of the other parts of the propulsion system, like the motor controller and the propeller, once a certain motor and battery combination has been selected. Thus, the team found it unnecessary to carry out a propeller and a motor controller analysis.

The team was required to use only Astro Flight and Graupner brushed electrical motors on the aircraft. After a quick research, it was noticed that Graupner motors generally had less output power compared to Astro Flight motors. Insufficiency of the amount of information available on Graupner motors urged the team to investigate Astro Flight motors only.

4.1.1.1 Battery Type

The competition rules limited the maximum current to be drawn from the battery pack to 40 amperes and the maximum battery pack weight to 5 pounds. The main purpose of the battery was to provide the maximum power to the motor in watts. Taking into account that the product of volts and amperes drawn by the motor gives the input power, it became apparent that maximum numbers of cells had to be used and maximum amperes of current had to be provided by the battery pack in order to provide the maximum input power. Thus, the team tried to select the battery type, which was capable of providing approximately 40 amperes and had the highest number of cells when the total pack weight was 5 pounds.

4.1.1.2 Motor Type

For this section, the goal of the team was to find the motor, which had a current of 35-40 amperes when it functions most efficiently and uses the number of cells figured out in the solutions to the previous section.

4.1.2 Wing Analysis

4.1.2.1 Aspect Ratio

Aspect ratio is defined as the square of the span divided by the area. It affects flying performance and energy consumption. A wing with a large aspect ratio, compared to others with the same area, provides more lift coefficient. Moreover, the induced drag coefficient for a finite wing with a general lift distribution is inversely proportional to the aspect ratio. When the aspect ratio is increased, $C_{l_{max}}$ also increases and tip vortex decreases. Another effect of aspect ratio arises when the stall angle is changed. A lower aspect ratio wing will stall at a higher angle of attack than a higher aspect ratio wing.

4.1.2.2 Taper Ratio

Taper ratio is the ratio between the tip chord and the centerline root chord. Taper affects the distribution of lift along the span of the wing. Actually, minimum drag due to lift, or "induced" drag, occurs when the wing is elliptical, which was difficult to build. By using the tapered wing the distribution of lift could be close to elliptical lift distribution. Taper also reduces undesired effects of the constant-chord rectangular wing.

4.1.2.3 Oswald Efficiency

Oswald efficiency factor is also related to the induced drag. The wing's taper ratio and wash-out angle were determined based on a comprehensive study of the wing shape's effect on the Oswald efficiency factor. Oswald efficiency factor is related to the aspect ratio as shown in the equation below.

The Oswald efficiency factor would equal 1 only for an elliptical wing. Therefore, for a tapered wing, e is always less than 1. The Oswald efficiency factor is between 0.7 and 0.85 for a typical tapered wing.

4.1.3 Airfoil Analysis

Airfoil selection is the one of the important parts in preliminary design phase. The design team considered three design parameters to select the available airfoil for the desired performance. These parameters were thickness, efficiency, and maximum lift coefficient.

4.1.3.1 Airfoil Thickness

The aircraft had to verify the structural requirements of the competition. Therefore, thickness was one of the important parameters in the selection of airfoil. According to the design requirements, all aircraft needed to be lifted at one lift point at each wing tip to justify adequate wing strength. Therefore, airfoil thickness had to be enough for this wing strength. Thickness also affects drag, maximum lift and stall characteristics. If thickness increases, the form drag of airfoil and weight of wing would also increase. However, an increase in thickness would provide an increase in the maximum lift coefficient and a decrease in the stall angle.

4.1.3.2 Airfoil Efficiency

Aerodynamic efficiency was also taken into account as a design parameter to obtain good flight performance. According to the competition rules, the aircraft would lift steel blocks and tennis balls. Two different missions meant two different take-off gross weights. Since the wing had to be adequate for take-off for two different mission tasks, the airfoil had to have best aerodynamic efficiency. Aerodynamic efficiency is defined as the ratio of the lift coefficient to the drag coefficient (C_l/C_d). Augmentation in aerodynamic efficiency means lifting heavier payload with minimum amount of power.

4.1.3.3 Airfoil Maximum Lift Coefficient

The other design parameter was the maximum lift coefficient. This parameter depends upon the airfoil shape, Reynolds number and wing or flap geometry. Maximum lift coefficient of airfoil had to be selected by taking the maximum take-off gross weight into consideration. Estimating the maximum lift coefficient was difficult. Values of maximum lift coefficient vary between 1.2 and 2.0 for a wing that has no flaps.

4.1.4 Fuselage Length

Because of the relation between the rated aircraft cost and fuselage length and weight, the team decided to investigate the fuselage length as a design parameter. Since the fuselage cross-section was selected in the conceptual design phase, the length of the fuselage depended only on the number of

tennis balls to be carried. Thus, the team had to make an optimize the relation between the payload to be carried and the fuselage length.

4.1.5 Tail Longitudinal Location

Tail longitudinal location was seen to be important because of its effect on the control of the aircraft. The effectiveness of the tail in generating a moment about the center of gravity is proportional to the force produced by tail and the tail moment arm. The primary purpose of a tail is to encounter the moments produced by the wing. Eventually, the tail size was be in some way related to the wing size.

4.1.6 Landing Gear Length and Location

In the conceptual design phase, the landing gear arrangement was selected as a taildragger. Its location had to be decided very carefully to eliminate the disadvantages in ground control. Additionally, its location affects the propeller clearance during landing or take-off.

4.1.7 Fuselage Nose and Empennage Geometry

According to the competition rules, the payloads have to be carried in a closed geometry. The length and the cross-section of the fuselage had already been decided up until this stage. The last elements of the fuselage were the nose and empennage geometries of the fuselage. The team noticed that two different effects acted inversely on the way to decide on one of these geometries, which were aerodynamic efficiency and the rated aircraft cost. In order to make the fuselage aerodynamically efficient, slender nose and empennage geometries were needed. What was derived considering the effect of the fuselage length on the rated aircraft cost calculation was that it would be an absolute design failure to use slender geometries since it would not be useful to carry payloads. Thus, the team referred to the wind tunnel test data of several nose geometries.

4.2 FIGURES OF MERITS

4.2.1 Battery Internal Resistance

To provide the motor with the maximum amount of power, the battery pack had to provide the highest current within the limits of the competition rules. A battery's capacity to provide higher amperes of current depends on its internal resistance. For a battery to provide current above 35 amperes, its internal resistance must be below 4 mOhm.

4.2.2 Current Capacity to Battery Weight Ratio

While evaluating the optimum battery cell weight, the team had noticed a linearity between the battery cell weight and current capacity. The team decided to select the battery type according to the ratio of current capacity to the battery cell weight. With this ratio, the team was able to evaluate the current

capacity provided by each pound weight of the battery cell. The cell became more suitable for the project as this ratio got higher.

4.2.3 Motor Efficiency

The motor had to be arranged so as to operate at its most efficient regime with the provided voltage and current, as mentioned before. The motor efficiency shows how much of the input power is converted to torque. There are two types of losses. Copper losses are the product of the square of the motor's operating current and the motor resistance; and iron losses are the product of the motor's no load current and the input voltage. The motor operates most efficiently when these losses are equal. The team calculated the efficiency of each motor at provided volts and amperes.

4.2.4 Motor Output Torque

The torque production ability of the motor determines how big the propeller that can be driven by the motor is. It also determines the available thrust coming in from the propulsion system. Output torque can be expressed as a function of the product of the motor torque constant and the motor operating current. The torque value was calculated for each motor type.

4.2.5 Motor Constant

Motor constant is a very effective figure of merit that tells how good a motor is. The larger the number, the better the motor. It can be expressed as motor torque constant (K_t) divided by the square root of motor resistance. This is a comparison of the torque produced by motor and the power consumed by the internal losses of the motor.

4.2.6 Aerodynamic Efficiency

Aerodynamic efficiency can be determined as L/D . If the aerodynamic efficiency increases, the consumption of energy will decrease and the payload can be increased for the same thrust. In the case of airfoil selection can be made following the figures that show the aerodynamic characteristics of the airfoil. For the wing, it is known that elliptical lift distribution is the best efficient distribution, therefore the lift distribution of the tapered wing was tried to be close to that of an elliptical wing.

4.3 ANALYTIC METHODS USED

Calculation methods regarding the motor and the batteries were either learned from manufacturers or taken from amateur modelers. Internal losses were calculated using methods used in electrical subjects. Information that manufacturers gave did not seem to be reliable, thus the team members were not glad about their own results. The only way to verify calculations was trial-and-error, which apparently was not logical for reasons of time and cost. In calculations regarding the battery, the

output voltage of the NiCad battery, which normally is 1.2 V, was taken to be 1.1 V, so as to leave some margin for possible errors. Motor calculations depended on the manufacturer's test results.

Statistical information taken from Aircraft Design: A conceptual Approach by Daniel P. Raymer was consulted with while carrying out calculations regarding the location of the landing gear. Placement of the landing gear was done taking into account the limitations that arise from the geometry and structure of the aircraft.

The distance between the tail and the wing mean aerodynamic chord was determined using statistics on big scale radio controlled model aircrafts. This methods was used making the assumption that a statistical approach gives sufficient solutions when the sample has characteristics close to those of the design.

The only source of error in the payload optimization made to determine the fuselage length was assumed weight to be added to the fuselage weight when placing another row of balls. This weight was found building a sample piece. Error percentage was lowered with this practical data.

Determination of fuselage nose and empennage geometries came after some wind tunnel test results. Since the experiments were conducted at values close to the Reynolds number aircraft being designed, it was possible to compensate for error percentage.

Some airfoil information was taken from volumes I-III of the University of Illinois at Urbana Champaign's Low Speed Airfoils. For NACA airfoil, the test data was taken from Abbott and Doenhoff's book. Aerodynamic characteristics of the airfoils were calculated using the 2-D Panel Method and compared to wind tunnel test data.

To determine the lift distributions of the wing, Prandtl's Classical Lifting Line Theory was used. The philosophy of this theory was taken from Fundamentals of Aerodynamics written by Anderson J.D.

4.4 SIZING CALCULATIONS & CONFIGURATION DATA

4.4.1 Battery Selection

All the available Sanyo and SR batteries with internal resistances below 4 mOhm were listed in Table 4.4.1.1 and eliminated depending on their ratios of current capacity to battery cell weight. SR 2400 Max was selected, as seen from the table. When the pack weight is considered, SR2400 MAX has 36 cells.

4.4.2 Motor Selection

In table 4.4.2.1, some motor possibilities were compared according to selected figures of merits for the motor at the figured number of battery cells in the previous section and the maximum available current. The team found out that Cobalt90 10T #22 is the most suitable motor type providing the required performance at the highest efficiency rate.

Battery Type	Current Capacity (mAh)	Cell Weight (gr)	Internal Resistance mOhm	Available Cell #	Current Capacity/Cell Weight mAh/gr	Decision
SR 1300 MAX	1300	40	< 4	57	32,7	E
SR 1600 MAX	1600	51	< 4	44	31,3	E
SR 2000 MAX	2000	53	< 4	43	37,9	E
SR 2400 MAX	2400	54	< 4	42	44,5	FA
SR 3000 MAX	3000	70	< 4	32	42,8	E
SANYO N-1400SCR	1400	53	4	42	26,4	E
SANYO N-1800SCR	1800	56	4	40	32,1	E
SANYO N-1700SCR	1700	54	4	42	31,5	E
SANYO N-1700SCK	1700	56	4,1	40	30,4	E
SANYO N-1900SCR	1900	54	4	42	35,2	E
SANYO N-2000 CK	2000	80	4,1	28	25,0	E

Table 4.4.1.1: Battery Selection Table

<u>Motor Types</u>	SINGLE MOTOR			
	Efficiency @ 36 cells & 40 Amp	Torque (inc. oz)	Motor Constant (Kt/R_o^2)	Decision
Cobalt 90 10T#22 Kt:5,35 Ro:0.111 Io:3	%81.4	214	434	FA
Cobalt 90 11T#23 Kt:5,89 Ro:0.550 Io:2.5	%40	235	19.5	E
Cobalt 60 10T#23 Kt:4,62 Ro:0.150 Io:2,5	%78.5	185	205	E
<u>Motor Types</u>	TWIN MOTOR			
	Efficiency @ 18 cells for ea. & 40 Amp	Torque (Total)	Motor Constant	Decision
Cobalt 40	%70.5	159.2	136	E

8T#20

Kt:1,99 Ro:0.121 lo:2.0

E= Eliminated FA = Further Analysis

Kt (inc.oz./amp), Ro (ohm), lo (A)

Table 4.4.2.1 Motor Selection Table**4.4.3 Wing Analysis Results**

The team decided on the value of aspect ratio by scrutinizing the statistics of well-designed UAV and cargo aircraft. Afterwards, the value of aspect ratio varied between 6 and 7. The planform of the wing was to have 80 cm of the wing rectangular, starting from the root and the remaining 70 cm tapered to the tip, to increase aerodynamic efficiency. The comparison of the three planform is shown in Figure 4.4.3.1. It is shown that the tapered lift distribution is close to elliptical lift distribution. The team also tried to have the Oswald efficiency factor close to 0.85 to have good aerodynamic efficiency. Thus, the aspect ratio is close to 6.83 according to the equation.

$$e = 1.78 * (1 - 0.045A^{0.68})^{0.64}$$

After determining the aspect ratio, the area of wing could be found easily from the definition of aspect ratio. The area of wing could be obtained as 14.64 ft² using the equation below. To estimate the required wing loading, the team decided to investigate the changing wing loading with all values of the lift coefficient in the take-off as a first approximation.

$$A = \frac{b^2}{S_{ref}}$$

C_{lmax}	1.2	1.4	1.6	1.8
W/S	3.012	3.514	4.016	4.518

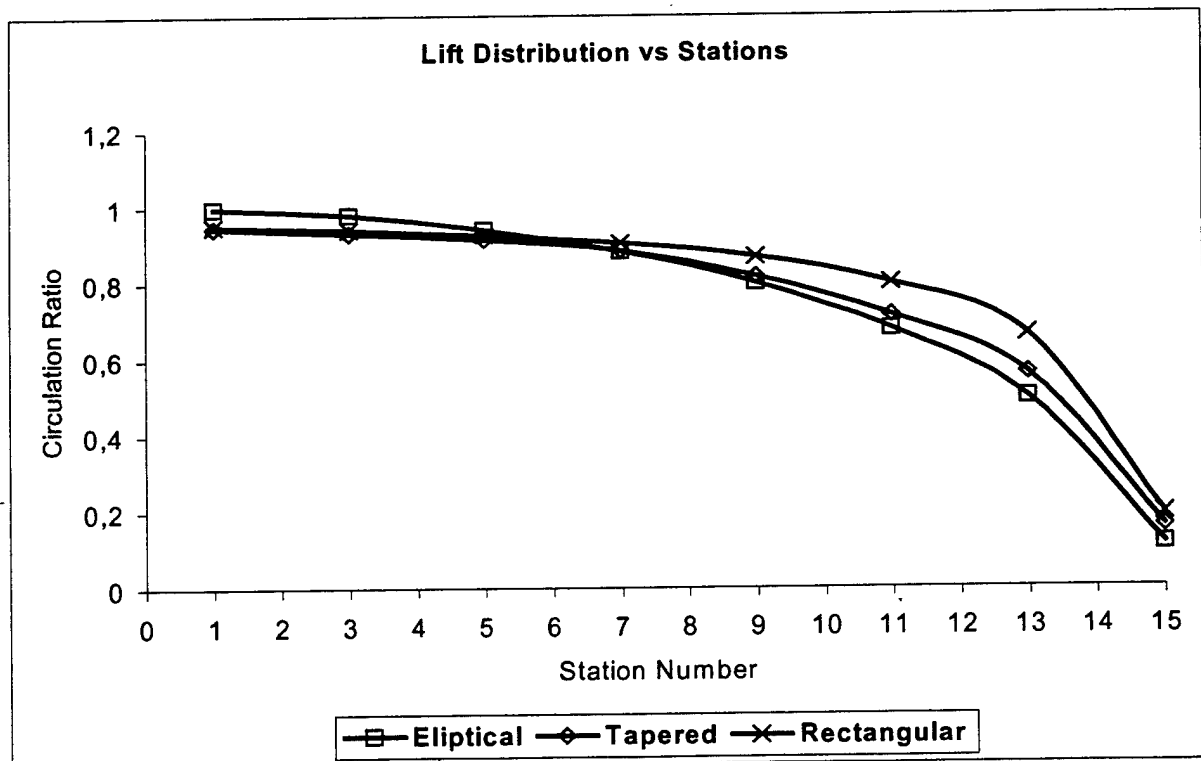


Figure 4.4.3.1: Lift distribution for the three planforms along the semi span stations.

(The data are calculated from Prandtl's Lifting Line Theory. Circulation ratio is the ratio of Γ/Γ_0 .)

4.4.4 Airfoil Analysis Results

The team compared the four airfoils according to design parameters mentioned above. These airfoils are S822, E231, AVISTAR, and NACA 4415. When analyzing the airfoil, the 2-D Panel method was used and the wind tunnel test data were compared. Since the aircraft operates in low Reynolds number, the airfoil characteristics were investigated at Reynolds number of 400000. The Figure from 4.4.4.1 to 4.4.4.4 shows the changing of lift and drag coefficient vs. angle of attack for each investigated airfoil type. Afterwards, the efficiency variation of each airfoil was compared with the angle of attack. At the end of this stage, it was seen that NACA 4415 had the best aerodynamic efficiency; therefore, the team decided to select NACA 4415 profiles for further analysis.

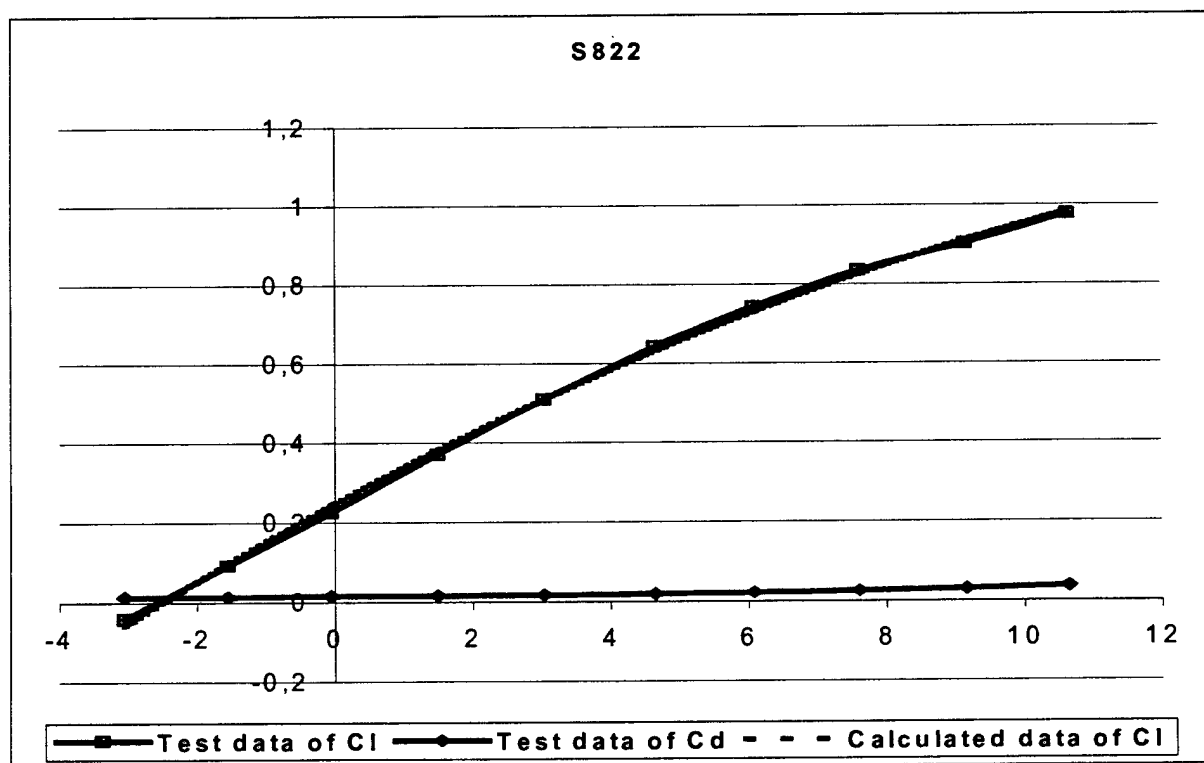


Figure 4.4.4.1: Coefficient drag and lift characteristics of S822 at Average Reynolds number of 401400. Test data was compared to the calculated data using 2-D Panel Method.

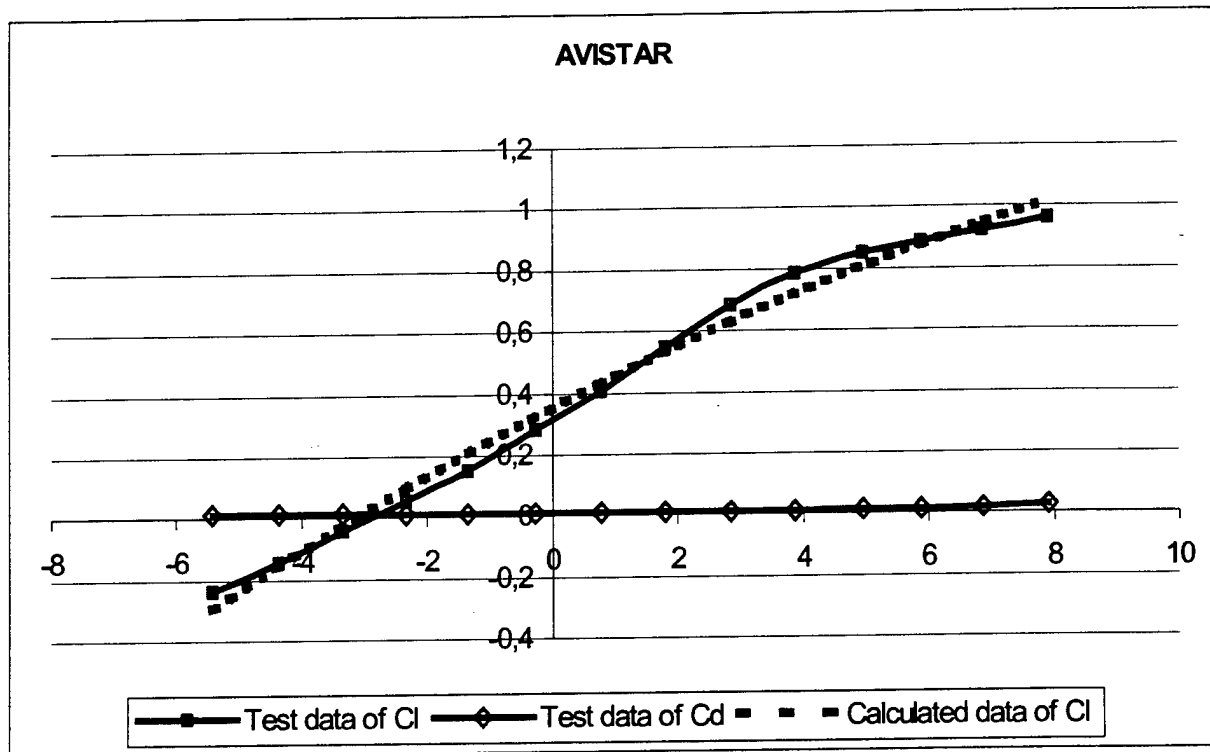


Figure 4.4.4.2: Coefficient drag and lift characteristics of AVISTAR at Average Reynolds number of 402100. Test data was compared to the calculated data using 2-D Panel Method.

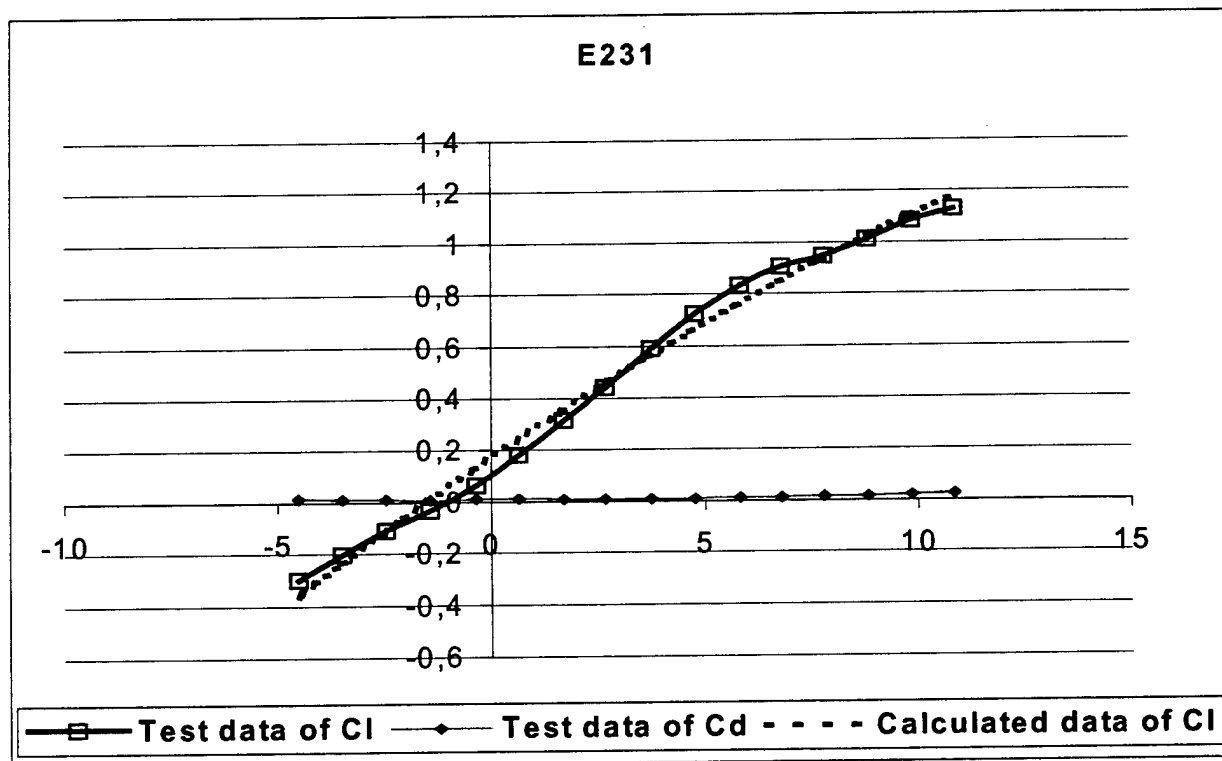


Figure 4.4.4.3: Coefficient drag and lift characteristics of AVISTAR at Average Reynolds number of 400400 Test data was compared to the calculated data using 2-D Panel Method.

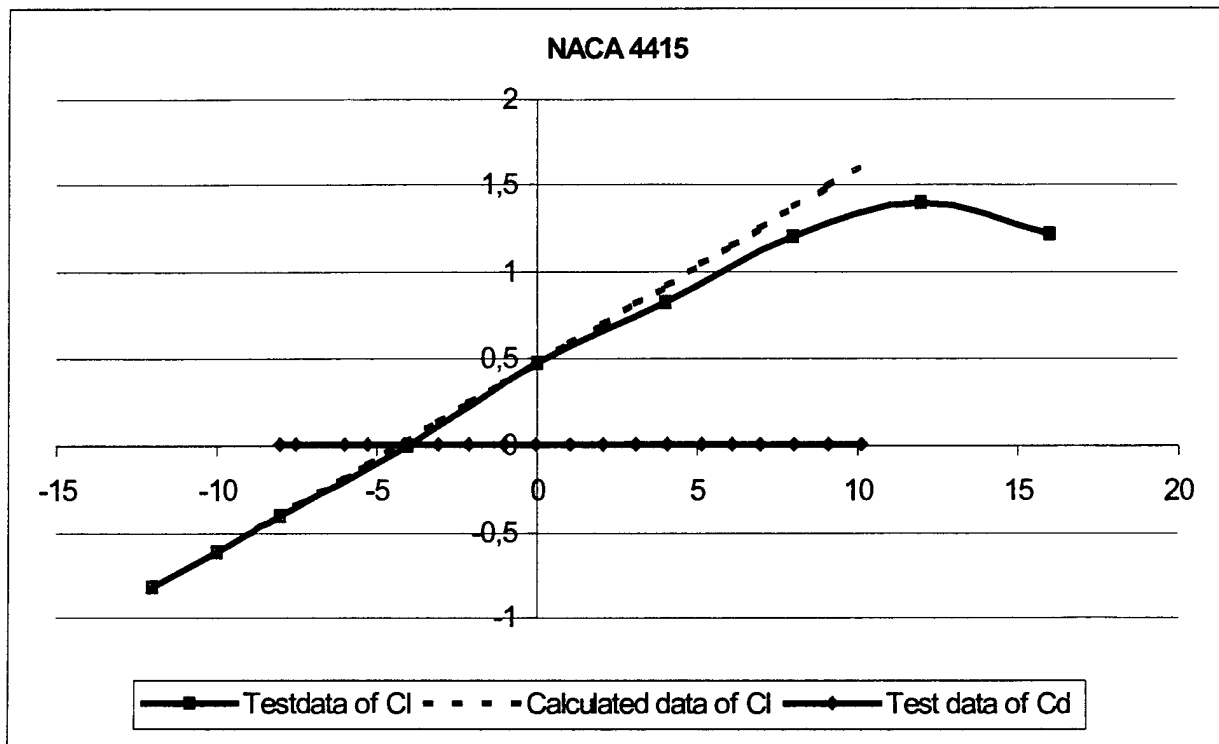
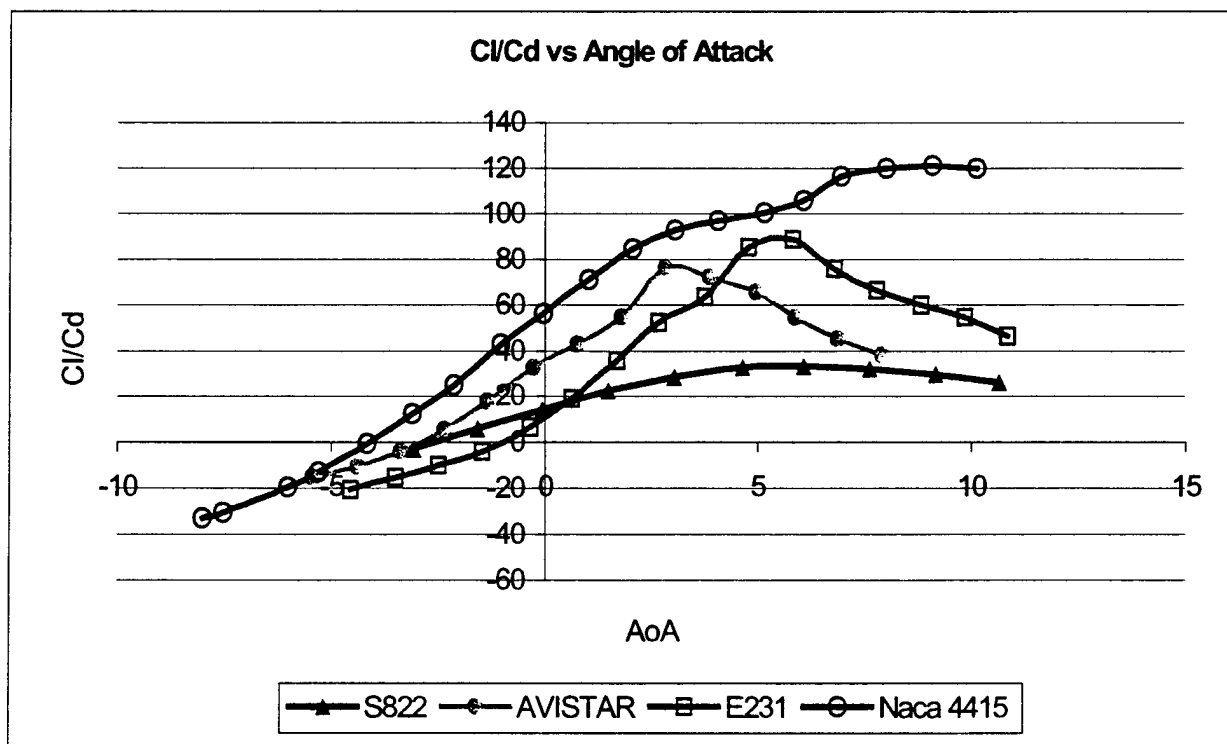


Figure 4.4.4.4: Coefficient drag and lift characteristics of NACA 4415 at Average Reynolds number of 400000 Test data was compared to the calculated data using 2-D Panel Method.



4.4.5 Payload Optimization

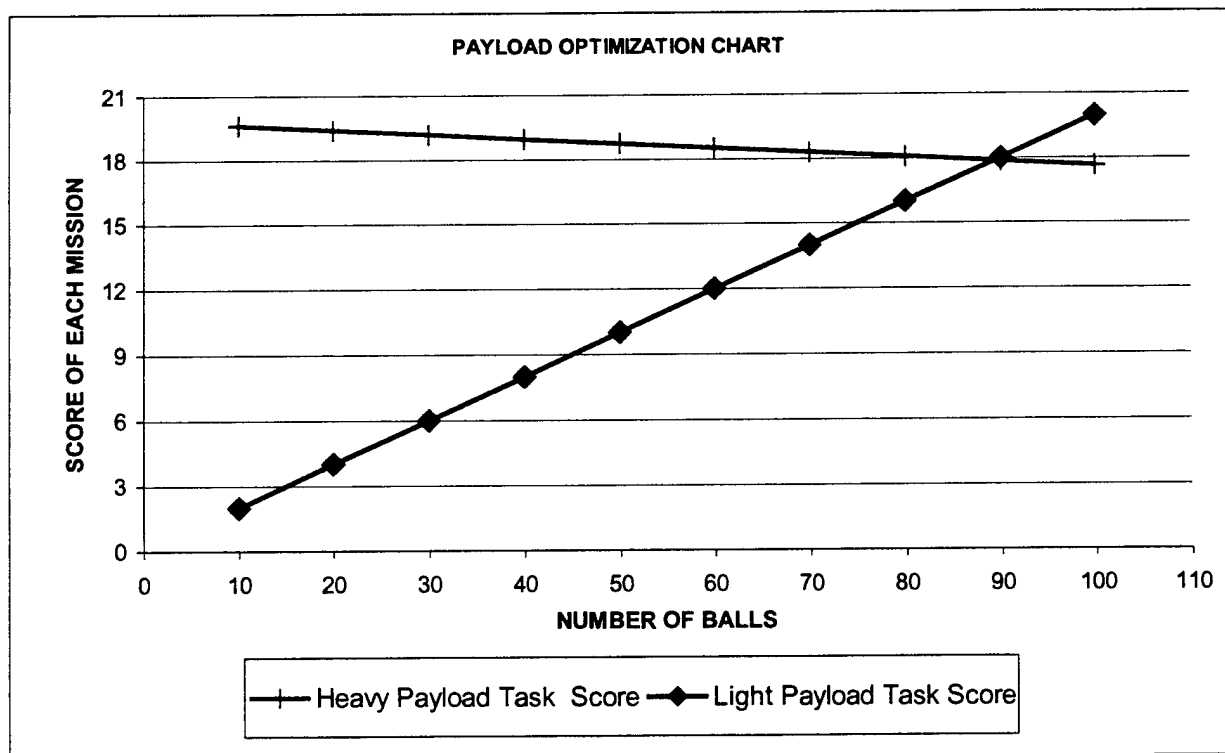
Payload Optimization Table						
Number of Balls	Heavy Payload Weight (lb)	Heavy Payload Task Score	Light Payload Task Score	Cost	Final Score	Decision
10	19,62	19,62	2	5,87	368	E
20	19,4	19,4	4	5,89	397	E
30	19,18	19,18	6	5,9	427	E
40	18,96	18,96	8	5,92	455	E
50	18,74	18,74	10	5,94	484	E
60	18,52	18,52	12	5,96	512	E
70	18,3	18,3	14	5,97	541	E
80	18,08	18,08	16	5,99	569	E
90	17,86	17,86	18	6,01	597	E
100	17,64	17,64	20	6,02	625	FA

E= Eliminated FA= Further Analysis

Table 4.4.5.1 Payload Optimization Table

The team estimated a try total payload weight was about 19,84 lb (9 kg). The calculated weight contribution of each row of ten balls due to fuselage elongation was 0,22 lb, so the team came up with an equation relating each amount of payload and the final score by decreasing 0,22 pounds of heavy payload for each group of ten balls added. Additionally, the aircraft rated cost calculated for each payload alternative was added to this equation.

It was noticed that carrying 100 tennis balls and 17.64 lb of heavy payload tops. This also determines the fuselage length for the highest score. According to this optimization, the fuselage length was found to be 2,15 ft. (65,8 cm)



4.4.6 Determination of Tail Longitudinal Location

Using the relation between the tail location and wing area, the team refined a statistical ratio between the wing area and the distance of wing mean aerodynamic chord to the quarter length of horizontal tail surface. According to this ratio, the tail had to be located 4.19ft (128 cm) away from the wing mean aerodynamic chord.

4.4.7 Determination of Landing Location

The landing gear length and location were determined according to the statistical data to provide a proper propeller clearance. The center of gravity should fall between 15-25 degrees behind the vertical line measured from the main landing gear. The tail down angle needed to be about 10-15 degrees with the gear static position. If the center of gravity was way too forward, the aircraft would tend to nose over; and loop on ground if it was far too back. To prevent the aircraft from turning over, the main wheels needed be laterally separated beyond a 25-degree angle off the center of gravity as measured from the rear in a tail down attitude.

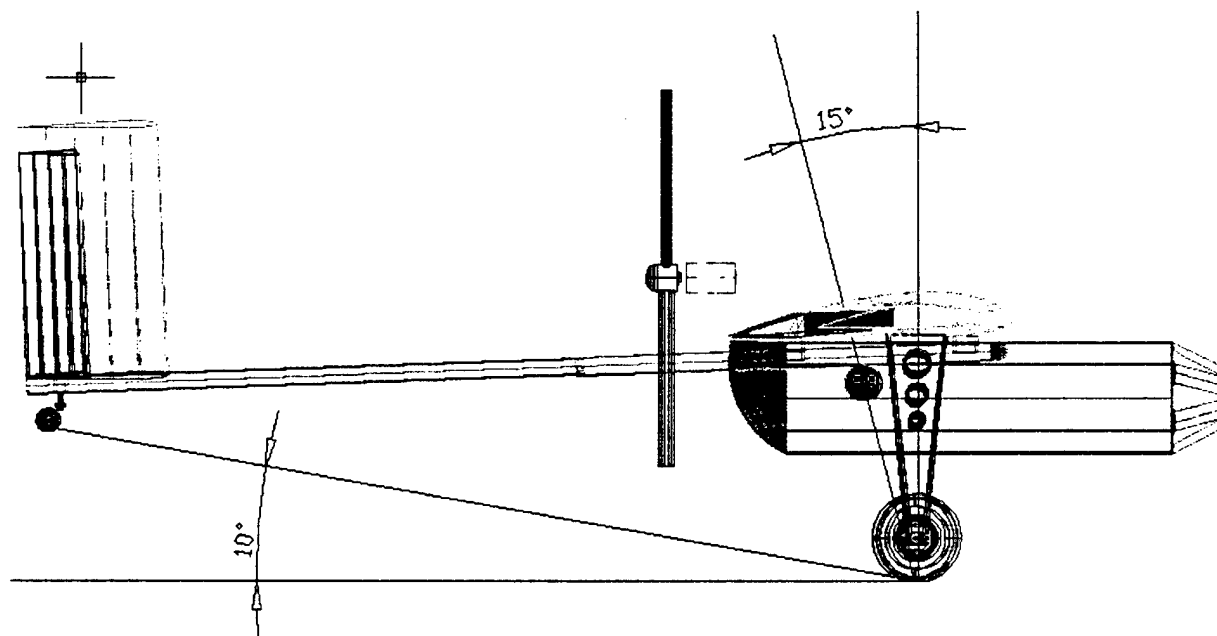


Figure 4.4.7.1 Figure Showing the Installation of Landing Gear

4.4.8 Nose and Empennage Geometry Selection

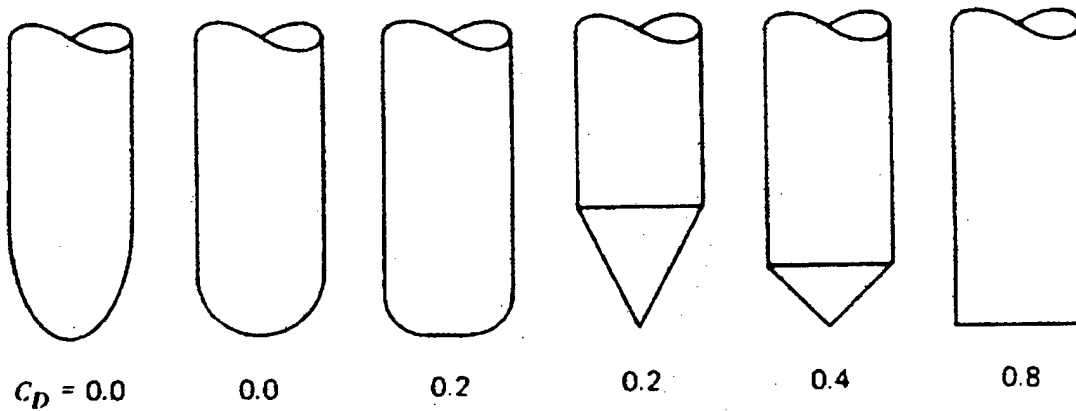


Figure 4.4.8.1 Investigated Nose Geometries

Some wind tunnel tests belonging to several fuselage nose geometries were investigated. The third figure, corner-rounded blunt nose geometry was selected for offering reasonable drag coefficient with the least length. Empennage geometry designed to have the least length when rounded to caused less airflow separation

PRELIMINARY DESIGN RESULTS

Wing Area:	14.64 ft ²
Wing Span:	10 ft
Airfoil:	NACA 4415
Tail Location:	4,19 ft. back from the mean aerodynamic chord.
Fuselage Length:	2.15 ft
Type of Motor:	Cobalt 90 10T #22
Number of Motors	1
Type of Cells:	SR 2400 MAX
Number of Cells:	36
Propeller:	26x14
Available Max. Thrust:	150 oz.

5.1 PERFORMANCE DATA

The competition rules were calling the competitor aircraft to land and take off within a 200 ft. of runway distance. Assuming that the thrust is constant and neglecting the drag and friction forces, an equation giving the shortest ground roll distance possible was obtained. This simple equation was extracted from equation 5.1 and was very useful as a rough estimate of the take-off ground run required because it needed only the lift-off velocity and the thrust-to-weight ratio of the aircraft.

$$T = \frac{W}{g} V \frac{dV}{dX} \quad (5.1)$$

Indeed, drag and friction forces were not totally ignored. It was assumed that dissipative forces were usually less than 10-20% of the aircraft maximum take-off thrust. Knowing that the maximum thrust available from the propulsion system is 150 oz., the team set the available thrust to a value of 120 oz. for the calculations as the %20 of maximum available thrust were consumed by dissipative forces.

	Takeoff Performance Data	
	Heavy Payload Flight	Light Payload Flight
Ground Roll Distance (X_{GR})	164 ft (50 m)	115.3 ft (35.15 m)
Payload	27 lb (12.2 kg)	100 ea. Tennis Ball = 13.2 lb (6 kg)
Lift-off Velocity (V_{LO})	41 ft/s (12.5 m/s)	40.78 ft/s (12.43 m/s)
Tire Required for Lift-off (t_{LO})	8 seconds	6 seconds
Takeoff Gross Weight	46.73 lb. (21.2 kg)	33.07 lb. (15 kg)
Rolling Friction Coefficient	0.03	0.03
Takeoff Lift Coefficient $C_{L_{TO}}$	1.6	1.4
Takeoff Drag Coefficient $C_{d_{TO}}$	0.18	0.15
Thrust to Weight Ratio (T/W) _{TO}	0.20	0.28
Wing Loading (W/S) _{TO}	3.19 lb/ft ² (152 N/m ²)	2.21 lb/ft ² (108 N/m ²)

Table 5.1.1: Takeoff Performance Data

The load factor or g-loading during a turn is the acceleration due to lift expressed as a multiple of the standard acceleration due to gravity. Load factor (n) can be determined as the lift to weight ratio. In level flight, without any turns, the load factor is equal to 1. In the case of a turning flight, the load factor is related to the bank angle ϕ . For a sustained turn, in constant altitude, the load factor is calculated using the equation below.

Flight Type	Load Factor
Structure Limit	2,5
Level Flight	1
Sustained Turn	1.53

$$n = \frac{1}{\cos(\phi)} = \frac{qC_L}{W/S}$$

Since the designed aircraft is symmetrical about the centerline, changes in angle of attack will have little or no influence upon yaw and roll. Therefore, the stability and control analysis can be investigated in two parts, longitudinal and lateral directional analysis. To analyze the terms in these two parts, semi empirical method was used since the evaluation of the terms was difficult without wind tunnel data. For dynamic stability, it is tried to calculate first order of pitching and yaw damping derivatives in level flight using design aircraft velocity. The results are shown in Table 5.1.2 and 5.1.3

Table 5.1.2 Longitudinal Stability Derivatives and Values

Pitching moment derivative	C_{m_α}	-0.035
Wing pitching moment derivative	C_{m_w}	0.077
Fuselage pitching moment derivative	$C_{m_{\alpha, fus}}$	0.00367
Coefficient of Moment about Center of Gravity	$C_{m, cg}$	0.319

Table 5.1.3 Lateral Stability Derivatives and Values

Yawing moment due to aileron deflection	$C_{n_{\delta_a}}$	-0.0035
Wing yawing moment due to sideslip	$C_{n_{\beta_w}}$	-0.0213
Wing yawing moment	$C_{l_{\beta_w}}$	-0.043
Yaw-moment derivatives with respect to sideslip	C_{n_β}	0.0343
Pitching-moment derivatives with respect to sideslip	C_{l_β}	0.0335
Roll moment coefficient	C_l	-0.0013
Yaw moment coefficient	C_n	-0.0024

Table 5.1.4 Damping Derivatives

Pitching damping derivatives	C_{m_q}	-0.0058
Yaw damping derivatives	C_{n_r}	-0.0037

5.2 COMPONENT SELECTION & SYSTEMS ARCHITECTURE

As required by the contest rules, the **Bosphorus Blue** used commercially available Astro Cobalt 90 10T #22 brushed motor. This motor was powered by two packs of SR2400 MAX with 18 cells in each.

An Astro Model 204D speed control was used. It was specially designed for six to thirty six cells type airplane models. The 204D uses the latest digital technology and is very efficient at all throttle settings.

An Astro Superbox Model 714 gearbox was used. It had 1:2.7 gear ratio. Model 714 uses 60-tooth stainless steel spur gear and 22-tooth pinion gear.

The batteries were delivered with screened and matched cells. The nickel straps used between the cells were very special. Besides, having strain relief formed into them, six welds were used per strap end. In addition, stacks of straps were used between cells for a total of many welds resulting in the lowest pack impedance, which would deliver the highest possible current.

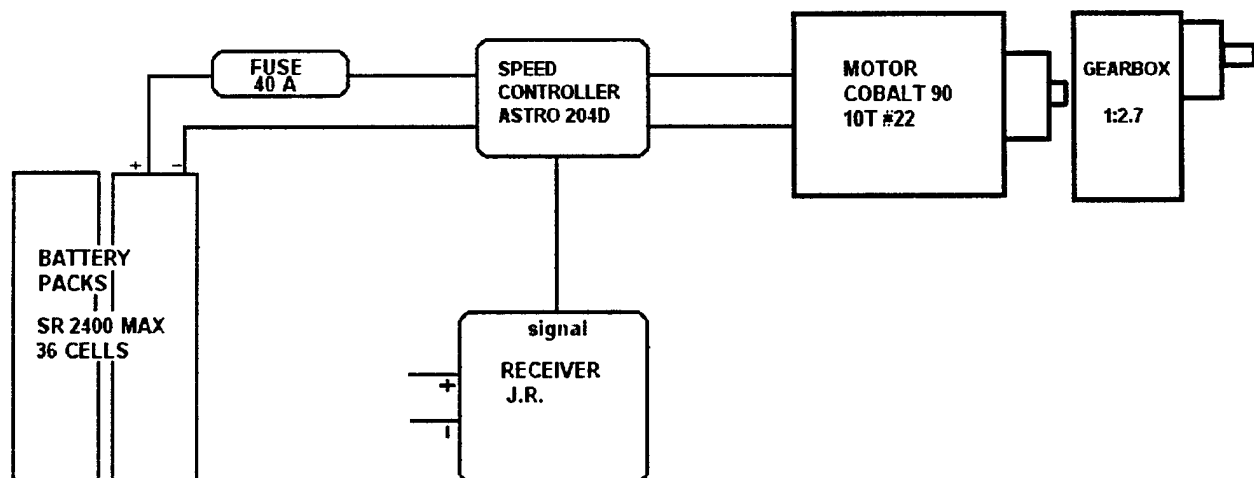
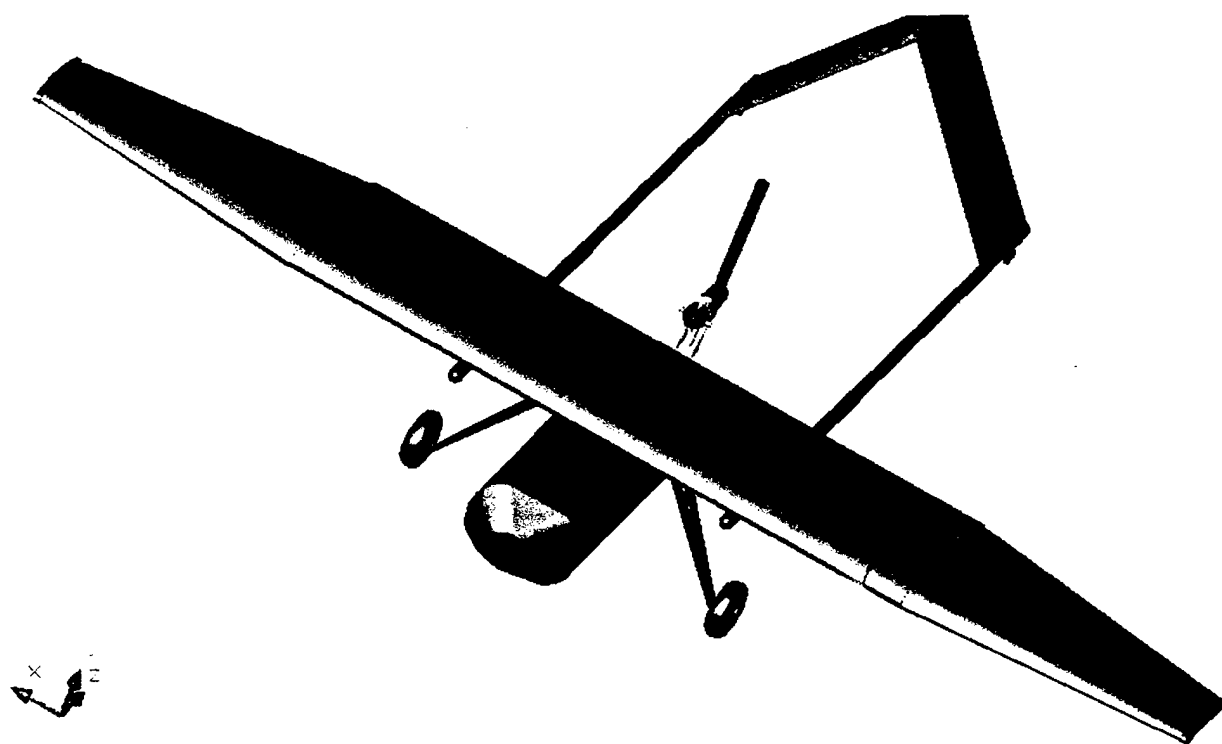
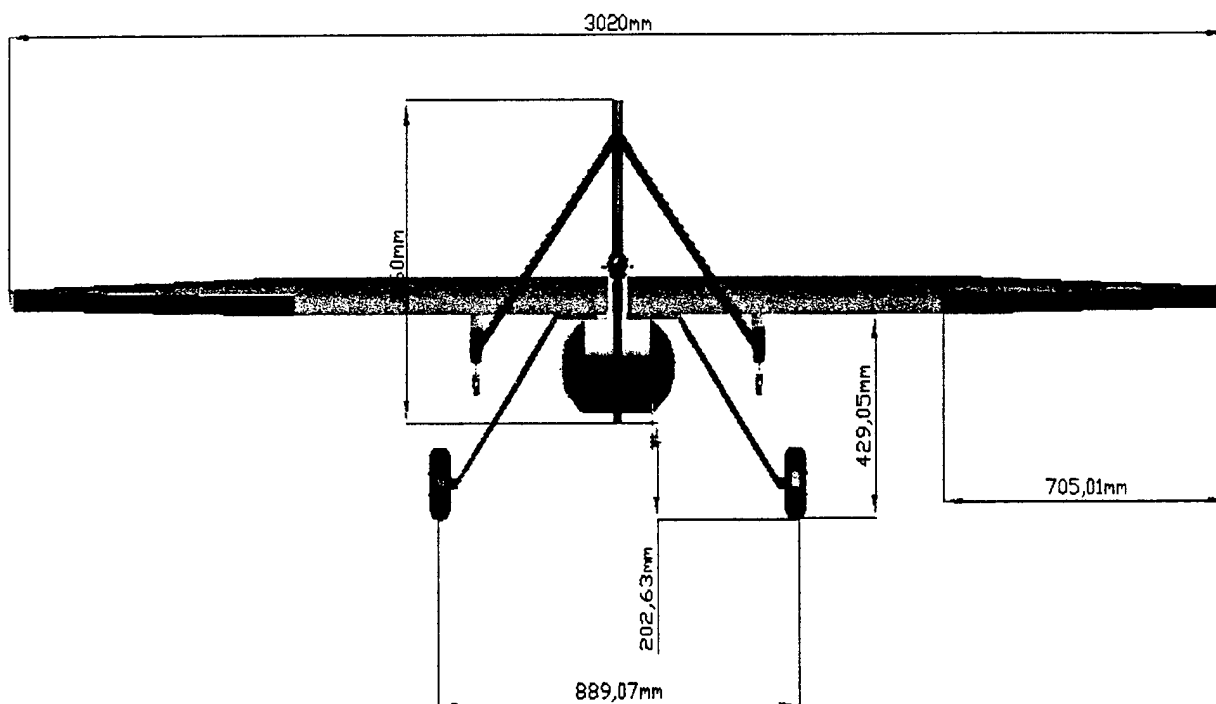
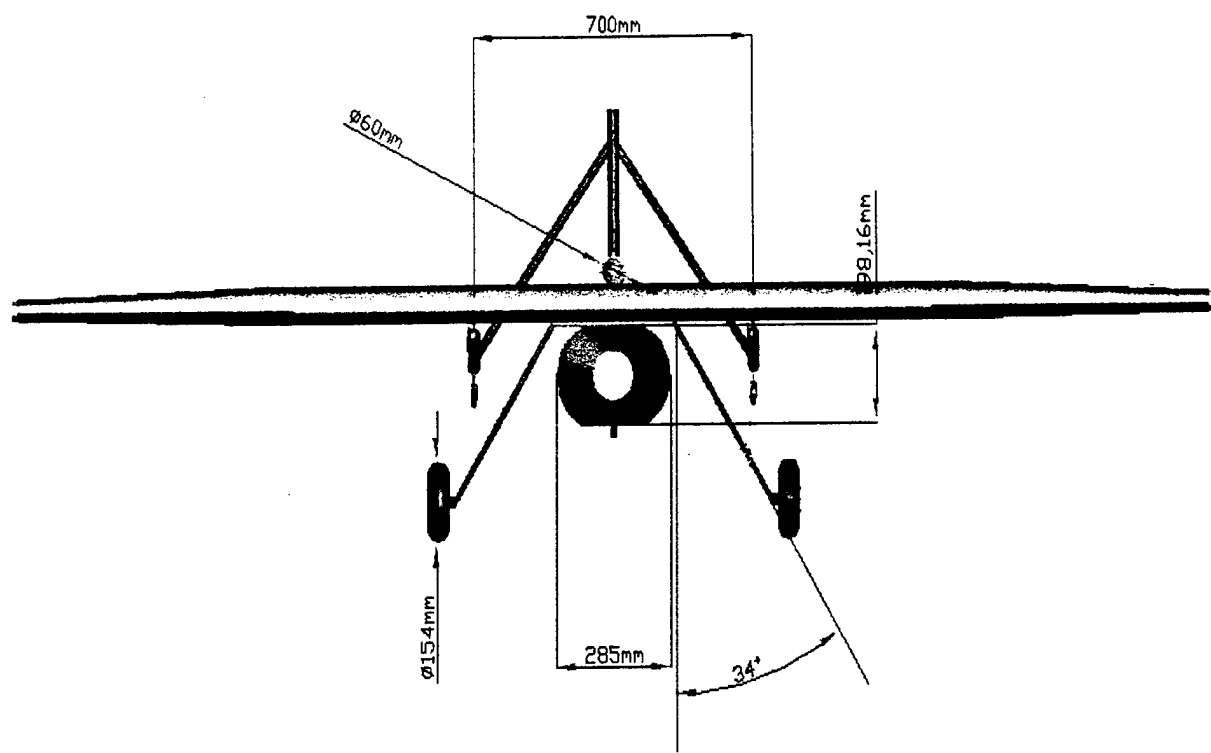


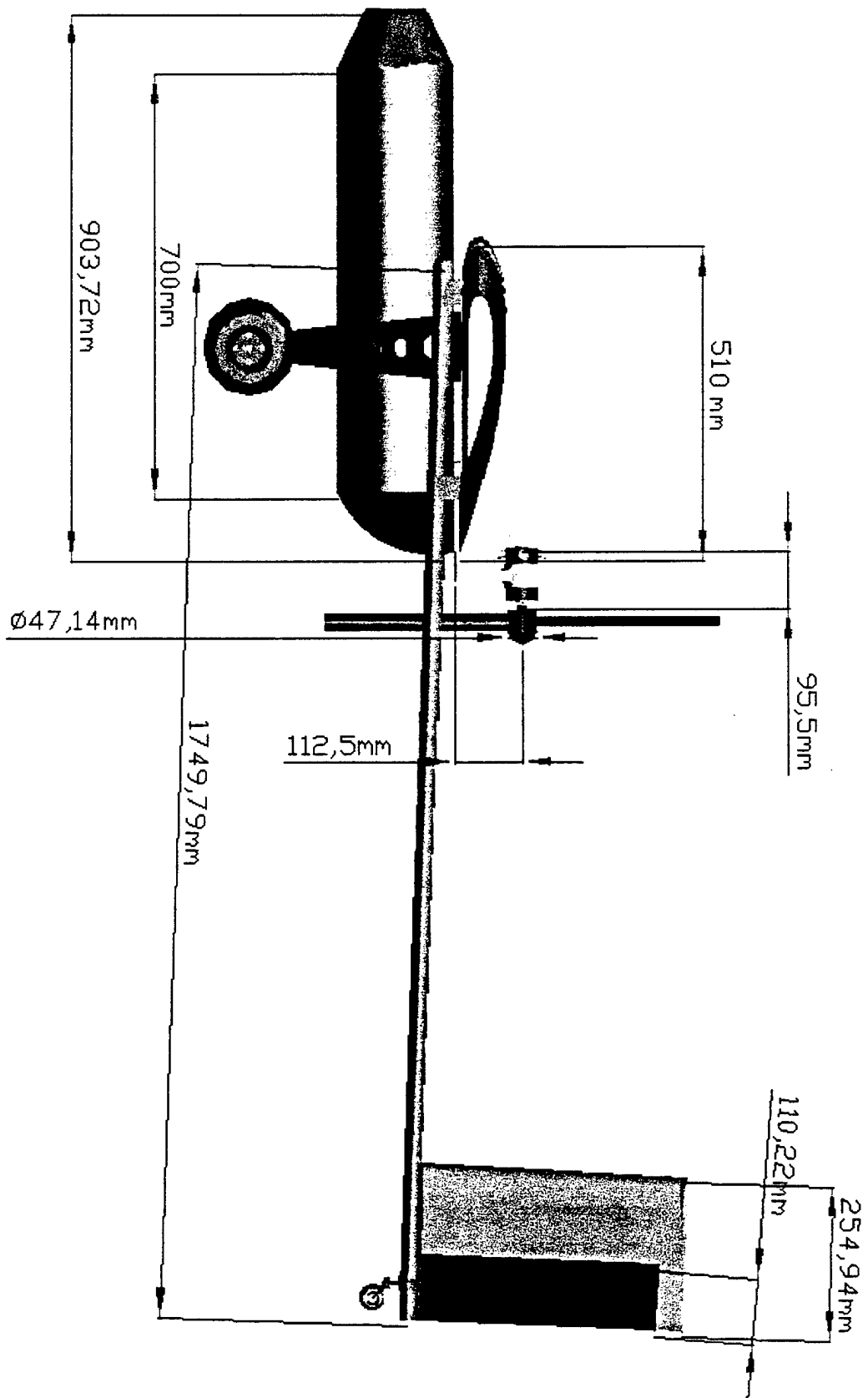
Figure 5.2.1: Propulsion System Architecture

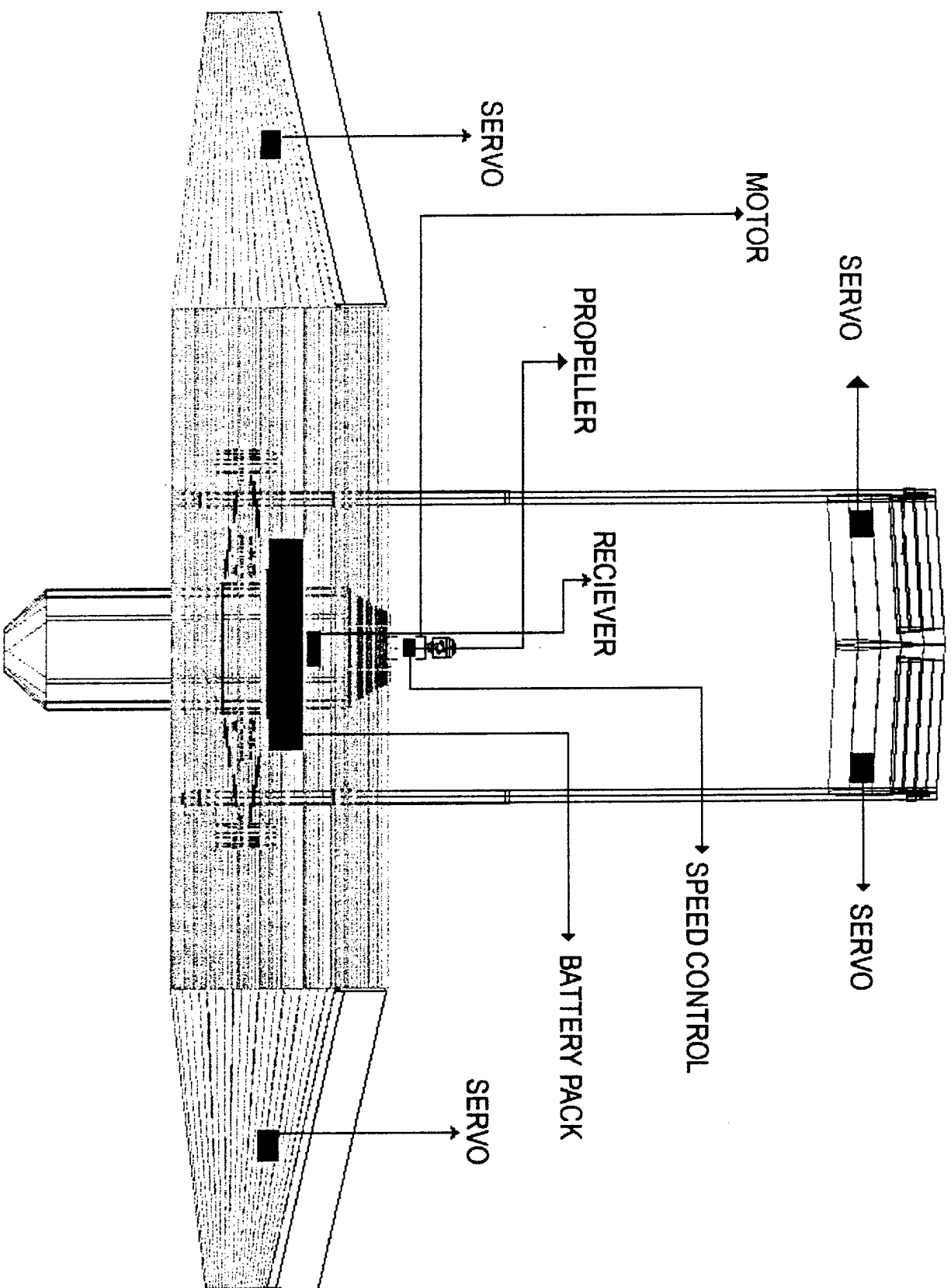
5.3 Drawing Package











6.1 INTRODUCTION

The designed aircraft consists of seven main parts, namely the wing, the fuselage, the landing gear, the motor block, the battery pack, the tail booms and the tail. Since the battery pack would be placed within the wing, it was not needed to produce a separate part for it. Booms with the desired properties could be bought off the market anyway, so it was not necessary to produce booms. That is why only five parts were manufactured.

6.2 SCHEDULE

Scheduling had to be done prior to the manufacturing process. A prototype had to be manufactured and tested first. Manufacturing the final aircraft would only come afterwards. The sponsor had its workshops in a distant city, and all the members of the team were enrolled as full-time students. Under these circumstances, manufacturing needed to take place during the intervals when the school was on holiday. There periods were the month before school started in fall, the two weekly national holidays and the semester break. The initial plan was to start building the prototype in fall and finish up in the first of the two national holidays and the semester break. The team kept up with the timetable, and conducted the flight test in the semester break. The final aircraft would have been manufactured in the second national holiday, but it had to be delayed because the proposal report was due shortly after that time. Manufacturing had to take place at the end of March. Considering that members became experienced with the procedure, manufacturing and flight tests were to be done the last week of March when the students would take a week off and not go to school.

6.3 MANUFACTURING PROCESS SELECTION

6.3.1 Material Selection

In order to manufacture the components mentioned above, materials of the desired characteristics were to be chosen. For this reason, all the materials that could possibly be used in this process were listed and judged according to the criterion that were thought to be crucial. Results were collected in a table.

Materials that could have been used can be categorized into two, namely wood and composite materials. Wood had the possibilities of balsa and beech; and composites had the possibilities of fiberglass, graphite and Kevlar. In the mean time, manufacturing those pieces with profiles, such as the wing or the tail, could demand the usage of foam.

Figures of merits used to evaluate materials could be categorized depending on the degree to which they were a priority. First degree priority had to be given to those that simply could not have been omitted, while second degree priority were given to those that were still important but could be ignored

when there was a matter of choice. The main purpose was to manufacture the lightest aircraft that would be strong enough. Price and availability of materials were also effective in this procedure.

The most essential FOMs used in choosing materials were strength, weight, manufacturability and cost. Strength was needed because the main goal was to build the lightest and strongest aircraft possible. The flight missions and judges' method of evaluation implied these. Weight, as explained above, had to be as small as possible, in order to build a highly competitive aircraft, since it was desired to build a light aircraft that would complete the payload tasks. Manufacturability was essential, as well, because working on materials that are not easy to produce could halt the entire project if the team ran out of that particular material. Last, but not the least, cost had to be taken into consideration not to force the sponsor provide the team with materials it could not afford. Trial-and-error could work with economical materials, but not with overpriced ones.

Second-degree FOMs were not the main reasons to choose or reject a material, but they still needed to be considered if a high score was aimed at. The material chosen had to be repairable because even if the aircraft built was perfectly designed and manufactured by all means, it would have to be repaired within a single day in case of an accident in the first sortie. Reliability was a measure of how deformed the material would be over time. Availability was a criteria because it would have been time consuming and unaffordable to be in pursuit of materials with low availability. The experience factor was an indication of how used the team members were to that particular material. Working on materials people were unfamiliar with would be problematic and time consuming. The material chosen had to be capable of being used with others because it was clear more than one single material would be used in the entire manufacturing process. Flexibility was important as well, since high rigidity could end up in a crack or a break.

	WOOD		COMPOSITE (+foam)		
1st degree Priority	Balsa	Beech	Fiberglass	Graphite	Kevlar
Strength	-2	1	1	2	0
Weight	2	-2	1	2	1
Manufacturability	1	1	2	2	-1
Cost	-1	2	1	-2	-1
Result	L	L	G	L	L
2nd degree Priority					
Reparability	-1	-1	2	0	0
Reliability	-2	-1	2	2	2
Availability	2	2	2	-2	-1
Experience	2	1	2	0	1
Use with Other Materials	1	1	2	1	-2
Flexibility	1	-1	1	0	2
Result	L	L	G	L	L

G: General Usage L: Limited Usage

Table 6.3.1.1: Material Selection Table

Grading was straightforward and simple. A material was given a 2 if it was superb on grounds of that property, a 1 if it was satisfactory, a -1 if it was below average and a -2 if it was totally unsatisfactory.

Taking all of these into consideration, it was decided to use fiberglass and epoxy. The sponsoring firm had a partial influence on this decision because they were familiar with those materials and had plenty of them. In some parts, though, it was needed to use other materials. For instance, carbon fiber was used in the landing gear, because it would carry the entire weight, and in the strap to be used as a spar, even though carbon fiber is precious and rare, since it is not heavy.

The next step was deciding on the foam. There were three types of foam available. P-15 was light but had low strength. P-30 was twice as dense and stronger. Blue foam was very strong but it was too heavy. Foam type would be selected after deciding on the type of wing.

6.3.2 Process Selection

The next phase was deciding on the manufacturing technique. A different method would be used for each part since all five pieces had totally different properties.

The team took one piece at a time and examined all the possible ways it could be produced. Combining this examination procedure with the information from the table above, the most advantageous methods were selected and put into practice. The figures of merit used are as follows.

Experience Methods nothing was known about could be problematic, so the most well known methods were tried to be used, while the most advantageous were tried out as well.

Time: Since the workshop was in another city, manufacturing processes were carried out in huge blocks of time. There was one-month period in the summer, after the students were done with their internship, a two-week period in the semester break and two one-week periods during national holidays. What was scheduled to be finished at the end of each of these sessions, thus time-consuming methods were not preferred.

Manufacturing devices: Methods that required equipment that was not ready to be used would have been time consuming, so they were not preferred as well.

Materials: Methods that required the usage of the materials that seemed to be advantageous according to the table above were preferred.

Size of the work piece: The fact that methods that may seem to be advantageous when working on larger pieces might lose their advantages when it comes to smaller scale work pieces was taken into consideration.

Portability: It needed to be easy to carry the aircraft or repair it if it were broken. Moreover, if there was a change in the design, it needed to be easy to just disconnect the pieces and do the necessary rearrangements. There was such a change in the design of the fuselage, which was not hard to deal with due to this property.

6.3.3 Wing

The plan was to mount all the other parts directly onto the wing, meaning the entire weight would act upon it. Additionally, it had to withstand 2 G, due to its length. For these reasons, the wing had to be strong. On the other hand, a light wing meant a light aircraft since this part took the most part among all the others. A wing with both of these properties would either be of foam or of a coated, contoured and sparred skeleton. The contoured system would have been fragile and time-consuming to build. In addition, it would be difficult to mount pieces like the landing gear onto such a system. Thus, it was decided to build the wing using foam.

First two things to decide on were whether or not foam would be coated and whether or not there would be any spars. An un-sparred wing had to be totally strong. The flaps would open up and the landing gear would exert some force on a part of the sparred wing. Additionally, strength of the wing would decrease when the wing was punctured to make holes for the screws, or when the batteries were placed. Instead of a standard sparred wing, the top and the bottom of the wing, where the spar would be, could be covered with strips of unidirectional carbon, or a torsion-box could be built. It was preferred to build a torsion-box out of fiberglass since carbon was not available. This way, the spar ended up being lighter, and also easier to construct. All the attachments on the wing were done straight on this torsion-box, and thus strengthened.

Except for the torsion-box, which would carry the entire weight, and the joints between the wing and the other parts, the wing had to be of maximum strength and minimum weight. For this reason, P-15 type foam was chosen since it was the least dense type. Shaping up the foam as desired could only be hand-made, using the electric-heated metal wire. The wing consisted of two 70 cm tapered pieces and a 160 cm flat piece. Since the largest block of foam available was a meter cube, the 160 mid-section was manufactured as two 80 cm pieces, while the 70 cm pieces could be manufactured as two separate 70 cm pieces. A rectangular prism of dimensions larger than the sizes mentioned above was cut for each of the four pieces. Two wooden plates with the shape of the parts of the wing profile were screwed on opposite sides of the foam prisms and then the foam was cut by going along the side of those wooden plates with the hot wire. Tapered parts were cut likewise, screwing a larger plate on one side and a smaller one on the other, and moving the wire relatively slower along the smaller one. In short, the wing was cut in four slices.

As for the torsion-box, there were two possible methods to use. Either the place where the torsion-box would be placed would be carved out and a torsion-box manufactured separately would be placed there, or the rectangular part of the wing would be worked on. The first option was eliminated because of the trouble of mounting that external piece onto the rest of the wing. At this point, it was necessary to cut off a piece along the wing where the torsion-box would be made. That was done before attaching the four parts that formed the wing because there was no wire long enough to cut a piece off a 3 meter wing. Other than that, it was difficult to cut through the epoxy used on surfaces of attachment. By

taking out the part where the torsion-box would be, each of the four pieces was now further divided into three pieces. Bands of fiberglass, cut a few centimeters in excess so that the vertices did not remain uncovered, were placed on the foam block that would form the torsion box. The other two slices of wing that would be stuck on the torsion-box were also covered with epoxy. The top of the wing was covered with the 135 gr/m² fiberglass which was light.

The remainders of the foam block from which the wing was extracted were used as a female mold. They were first covered with nylon sheets so that no epoxy stuck to it. All of the pieces that form the wing, except for the ailerons, cut out of the wing, were laid into this mold. Secondly, each group of four neighboring parts of the wing were glued to each other using 5 minute epoxy. Some mass was placed on the female mold and the whole thing was left to dry overnight. The next day, the bottom side and the leading edge was covered with 135 gr/m² epoxy and left to dry for another night.

Then the rectangular foam made of four parts, which would stay in the torsion-box, was dealt with by covering its top, sides, and finally its bottom with epoxy and then the fiberglass bands. Fiberglass options were 200 gr/m² and 300 gr/m² unidirectional and 135 gr/m². Using unidirectional would give the strongest result since the force exerted on the torsion-box would be longitudinal, however unidirectional was expensive and hard to find. On the other hand, 135 gr/m² or 200 gr/m² could be unsatisfactory. It was not for sure whether or not 200 gr/m² fiberglass would be satisfactory on its own. Since the prototype had to be extremely strong, vertical spots were to be covered using a single layer of 300 gr/m² fiberglass while the horizontal spots were to have one layer of 200 gr/m² fiberglass and one layer of unidirectional.

Some parts of the wing needed additional strengthening. For instance, all the pieces mounted on the wing would be done so by the means of screws, and since they could not have been screwed directly onto foam, blocks of beech were stuck on there with 5 minute epoxy and coated with fiberglass. Similarly, wingtip and the spot where the ailerons would be placed were covered with 1 cm thick balsa which were stuck into place using 5 minute epoxy. This process gave the wingtip the desired shape and more strength. Ailerons had the chance of being dipped into the wing. One more spot, the place where the servos would be placed, needed such a process. Like it was done for the screws, blocks of balsa with holes big enough for servos to be placed were fixed on the wing. The landing gear, some screws of the fuselage and the forward screws of the booms would be screwed right next to the torsion-box, so that no extra strengthening was necessary. Cables connecting the servos and the receiver were dipped into the wing.

The result was that manufacturing of the wing was completed. Ailerons and flaps would be manufactured along with the tail since they were of similar shape and size.

6.3.4 Battery

The battery was placed within the wing so that it would be close to the motor and create no drag. The only difficulty regarding this was to find the place where the wing would be cut up. Cutting the top

would spoil the airflow. For this reason, it was thought to have a lid below the wing. The wing was cut from below, a piece of foam in the shape of the battery pack was carved out, and the pack was placed there. That spot was covered like the motor block. Placing it under the motor block could save some weight, but that would mean dismounting the entire motor. Thus, the batteries were at the edge of the plate on which the motor laid. The strength of the wing remained unchanged, so long as the torsion-box remained untouched.

6.3.5 Tail, flaps and ailerons

There were three options to manufacture the designed V-tail and the ailerons: coating foam with fiberglass, coating foam with balsa, and a contoured wing. The third option would take long to put into practice and hinder the placement of servos inside. As for fiberglass, even the 135 gr/m² type would have been too heavy. Coating P-15 foam with thin sheets of balsa would give the lightest tail, thus it was decided to manufacture the tail and the ailerons as such. Balsa was coated with film so that external factors such exhaust or rain could not damage it. The film was heated along the sides and stretched by blowing warm air onto it, and then fixed in place. Parts of the ailerons close to the wing had enough inclination to allow the opening of the aileron and coated with balsa. Afterwards, ailerons and the wing were hinged to one another on their balsa parts. Booms were made by cutting fishing lines in the desired length. The tail was hooked on to the booms and fixed with epoxy. The top of the V-tail was attached by ankernors, which let the tail be portable.

The tail servos were placed close to the booms. Parts of the tails close to the booms were carved and servos were placed there. The cables connecting these servos and the receiver were taped onto the booms.

6.3.6 Fuselage

The fuselage did not have to be very strong since it would only carry payload. It was formed by cutting a foam block with the aid of two profiles in the shape of a fuselage and covering it with fiberglass. Then it was covered from the interior as well, leaving a thickness of 0.5 cm and left to dry. Thus, the fuselage made of scarce foam and epoxy was light and strong, because of the sandwich system applied. The nose and the empennage were also made of grounded foam covered with fiberglass. To make both the nose and the empennage portable, a 1 cm notch was carved into the interior of the fuselage.

The fuselage was mounted to the wing from the back and the front with thin strips of metal that were easy to find. These strips allowed the fuselage to be dismounted effortlessly, which allowed loading and unloading to be done effortlessly. A rail system could have been used instead, but it would not only be hard to manufacture, but manufacturing a strong rail would also mean a lot of weight.

6.3.7 Motor Mount Assembly

The motor block was supposed to be mounted to the wing and stick up from there, so that the propeller could rise from the ground. For this reason, either the wing would be strengthened, or a strut would stick upwards from across the booms. Building two separate struts would mean adding a lot of extra weight, so it was decided to connect the motor block directly to the wing.

The wing could have been re-coated with fiberglass for purposes of strengthening, but it was not preferred because it would damage the airflow above the wing and be too heavy. Strengthening the bottom side of the wing and mounting the motor block there was done instead. The bottom surface would be worked on for the battery pack anyway. Additionally, there was a distance between this surface and the fuselage as much as the thickness. This way, the attachment point where most of the load acts upon did not have to be portable since motor block was attached to a wide plate screwed in six places on to the beech blocks dipped into the wing. Since the carrier strut went through a part of the trailing edge of the wing, that part was also strengthened using a fine layer of balsa.

6.3.8 Landing Gear

Designing the landing gear could only come after deciding whether it would be a tricycle or a taildragger. The nose landing gear was eliminated from the very beginning because the fuselage, the only place forward enough for the wheels to be mounted, was too fragile for this purpose. Booms could be elongated forwards, but that would mean adding a lot of extra weight. In addition, the center of gravity was far too behind, meaning a nose wheel would make it mandatory to place the main landing gear much more to the back.

On the other hand, if there was a tail wheel, the main landing gear could be attached to some holes near the torsion-box, meaning no extra strengthening would be necessary, meaning there would be no more extra weight. Putting the tail wheel to the far back of the booms was a simple task. It had a disadvantage though. It would be harder to control the aircraft as it ran on the ground. Setting a connection between the tail servos and the wheels solved this problem.

After deciding to build a tail dragger, the tail wheel had to be configured. Building a typical tail wheel meant connecting the booms with a third one and fastening the wheel to the mid-point of it, which does not only increase weight, but also the drag. On top of that, a third servo would have to be placed to control that single wheel. If one wheel was attached to the ends of each boom though, neither an extra boom to connect the other two, nor an additional servo would be necessary. Thus, it was decided to use two wheels in the tail.

After that was done, properties of the main landing gear had to be decided upon. The main landing gear had to be strong because it would carry the entire load, while it had to be flexible so that not a huge amount of force would act upon the wing. The fuselage or the propeller could hit the ground though, if it was too flexible. The team had initially thought of using carbon when manufacturing the landing gear but, once again, there was a problem of availability. Following all of these, two alternatives seemed to be the most appropriate. A V-shape landing gear out of fiberglass was the first of these. If it was too flexible, the desired degree of flexibility could be reached by coating it with a couple more layers

of fiberglass, through trial-and-error, and without wasting anything. Additionally, extra weight could be thrown off by making holes on certain parts of the landing gear, without decreasing the strength.

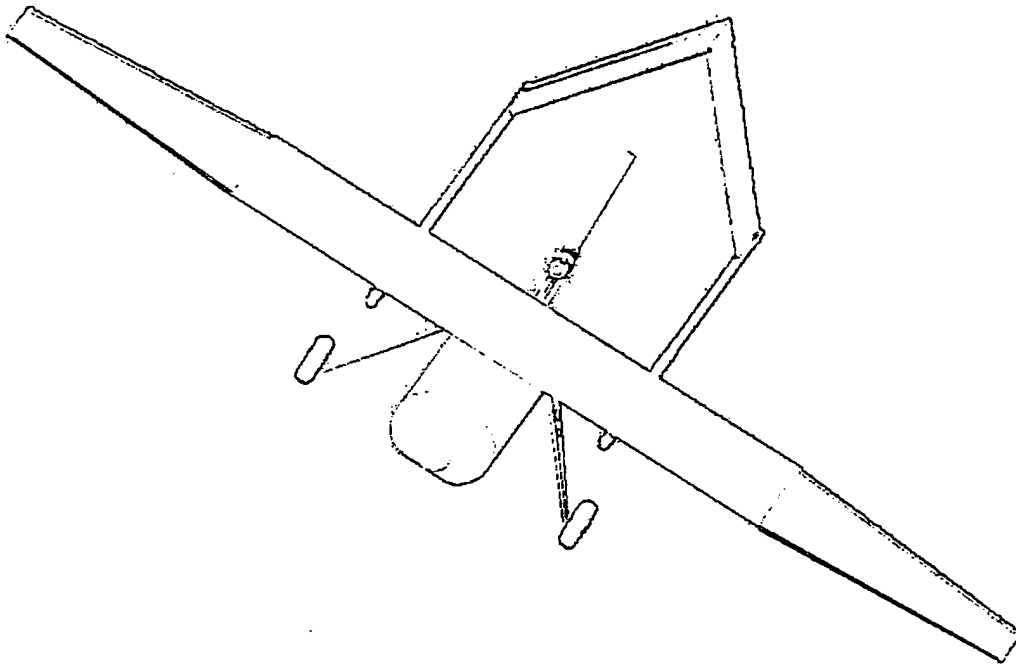
The other alternative was a spring-wheel system placed under a boom or a rigid strut made of fiberglass, following the example of commercial airplanes. Flexibility of the system could be adjusted by changing the spring on the wheel; however, manufacturing such a system was difficult, and the already-made ones were too heavy. Thus, this system was not used.

The final decision was to use a V-shape landing gear made of fiberglass. The joining part of the V-shape was made a bit long so that the wheels could be far apart enough to not to crush into the fuselage. The landing gear was manufactured by cutting a block of foam and coating it.

2000-2001

**AIAA FOUNDATION CESSNA/ONR
STUDENT DESIGN BUILD FLY COMPETITION**

ISTANBUL TECHNICAL UNIVERSITY



"THE BOSPHORUS BLUE"

Design Report – Addendum Phase

April 10, 2001

ISTANBUL

1. LESSONS LEARNED

After having some flights with the aircraft configured as described in the proposal phase, the team decided to revise some components of the aircraft to enhance its performance. These revisions were requiring some changes on the wing and landing gear.

The team noticed that the prototype aircraft wing was heavier than the estimated value due to the excessive use of fiberglass and epoxy. When manufacturing the competition aircraft in spite of using fiberglass of 300 gr/m^2 we used the lighter 135-gr/m^2 type, which provided the necessary strength as well.

Locating the tapered tips of the wing with a dihedral angle made another important change. By the prototype it was seen necessary for the stability. The angle of dihedral configured by the help of statistics as 3° .

A new landing gear manufactured for the final aircraft. It is seen from the prototype that the current landing gear structure was flexible to carry impact loads during hard landings. So a new landing gear manufactured which was a structurally reinforced type of the first one.

2. AIRCRAFT COST

Rated Aircraft Cost	6,07
---------------------	------

Coef.	Description	Value	
A	Manufacturing Emty Weight Multiplier	100	\$ / lb.
B	Rated Engine Power Multiplier	1	\$ / watt
C	Manufacturing Cost Multiplier	20	\$ / hour
MEW	Manufacturers Empty Weight	15,5	(Actual Airframe Weight, lb. , without payload or batteries)
	# Engines	1	
	Amp.	35	
	# cells	36	
	1,2 V / cell	1,2	
REP	Rated Engine Power	1512	Watt
	WBS 1.0 Wing(s)		
	15hour/wing	1	
	4hr./sq.ft . Projected Area	14,96	
	2hr./strut or brace	0	
	3hr./ control surface	4	
WBS 1.0	Total Hour	86,84	
	WBS 2.0 Fusulage / or Pods		
	5hr./ body	1	
	4hr./ft.of lenght	2,95	
WBS 2.0	Total Hour	16,8	
	WBS 3.0 Empenage		
	5hr. basic	5	
	5hr./ Vertical Surface	1	
	10hr. / Horizontal Surface	1	
WBS 3.0	Total Hour	20	
	WBS 4.0 Flight Systems		
	5hr. basic	5	
	2hr./servo or controller	6	
WBS 4.0	Total Hour	17	
	WBS 5.0 Propulsion System		
	5hr./ Engine	1	

	5hr./propeller or fan	1
WBS 5.0	Total Hour	10
MFHR		150,64



Università degli Studi di Roma "La Sapienza"

Facoltà di Ingegneria

Corso di laurea in Ingegneria Aerospaziale



AIAA/CESSNA/ONR Student Design/Build/Fly Competition 2000/2001

DESIGN REPORT

Proposal phase

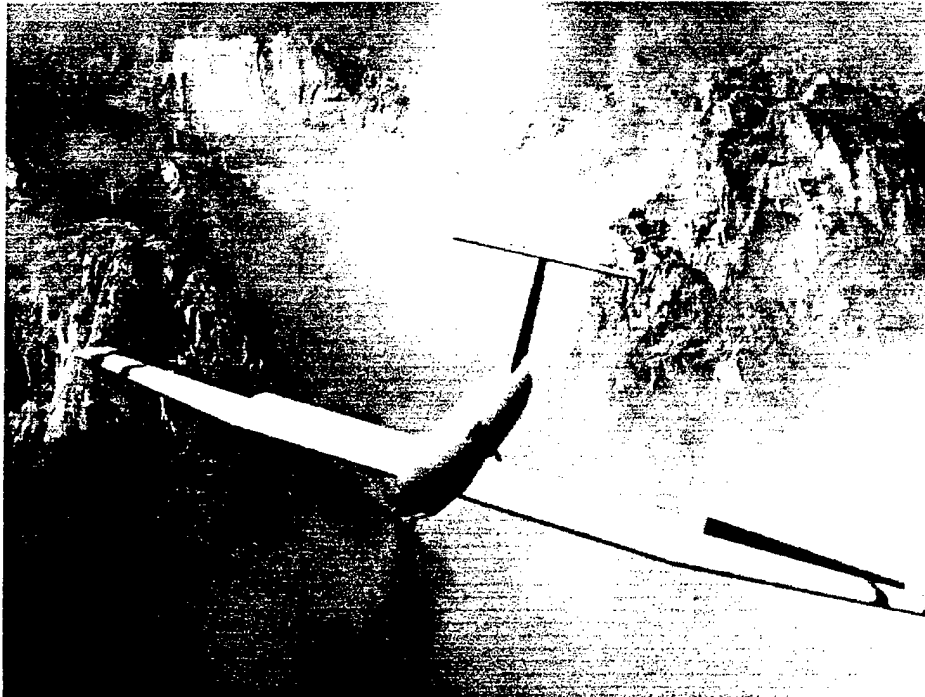


Table of Contents

1. Executive Summary	1
2. Management Summary	3
2.1. Team Architecture	3
3. Conceptual design	5
3.1. Introduction.....	5
3.2. Airplane Concepts and FOMs	5
3.3. Take-off Analysis.....	9
3.4. Preliminary Airfoil Analysis	10
3.5. Power Plant Analysis.....	10
3.6. Final Results.....	11
4. Preliminary Design	13
4.1. Introduction.....	13
4.2. Analytical Aerodynamic and Power Plant Models	13
4.3. Mission Assignment	17
4.4. Optimization Algorithm and SIM1 Description	19
4.5. Wing Analysis, Airfoil Selection and Surfaces Sizing	21
4.6. Structural Design.....	24
5. Detail Design.....	34
5.1. Introduction.....	34
5.2. Flight Mechanics	34
5.3. Structures.....	37
5.4. Propulsion	39
6. Manufacturing Plan	47

1. EXECUTIVE SUMMARY

An increased number of students from "La Sapienza" University joined the 2000/2001 AIAA/Cessna/ONR 'Design Build Fly' (DBF) Competition, spurred by the fair results achieved on the previous edition. The new team has took advantage of the facilities and the organizatory frames build by the old team, and keep on improving them, in the attempt to exploit at a maximum degree the great opportunities offered by such a competition. The cooperation between "La Sapienza" University and "G. Galilei" Technical High School, which had been started on the occasion of the DBF 99/00, has been continued and improved. A joint-venture, called 'Lapis', is currently at the study: it should allow students from "La Sapienza" to make practical and research experiences beyond the DBF as well. Students from "La Sapienza" have had the availability of "G. Galilei" labs and facilities; on the other hand, they have been involved in a series of lessons to "G. Galilei" students with the aim of integrating the contents of the standard Technical High-School programs.

The goal of the present DBF competition is to design and build a propeller driven, electric powered, unmanned RC airplane capable of meeting two different mission requirements, which are determined by the kind of payload carried and the pattern to be flown. The two payloads are 'heavy' and 'light', and they consist respectively of steel and tennis balls. The former must weight 5 lbs as a minimum; the latter must be in the range from 10 up to 100 balls, and could be considered as a 'bulky' payload, which contrasts with the 'heavy' payload.

A number of constraints has been placed by the contest officiators. They range from dimensional limits to required performance, i.e. the take-off distance must be 200 ft maximum. The required kind of electric motor has been changed from last edition's *brushless* to the *brushed* one. A cost formula has been given once again, which takes account of motor power, airframe dimensions, layout and weight.

The first meetings were held on June 2000. A preliminary time schedule and team subdivision were established by September, after having focused the main areas of development. It was decided to stress the wind-tunnel aerodynamic analysis of low Reynolds airfoils and of the whole final aircraft, to be reproduced in a scaled model; it was also decided to build the aircraft both exploiting the acquired experience in the making of wooden structures and improving the knowledge about composite materials. Wind-tunnel tests were decided also to acquire data about the power-plant performance, with a particular concern about the problem of having the propeller performance charts available.

The alternative concepts considered ranged initially from a conventional monoplane to a tandem wing airplane, including a canard layout and a biplane configuration. The team felt immediately the contrast between the 'bulky' payload and the 'small-and-heavy' one, and orientated itself to the development of a software tool, which included this and other items in an optimization routine.

Executive Summary

A great effort has been made on the organizatory side, with the efforts of the six students who took part to the previous DBF directed to manage about 25 new entries. In the light of the 99/00 experience, a strong stress was posed on the area of fund raising, with people in the team who was charged with specific responsibilities.

The team has used a number of software tools, which have been useful during the whole design process. Many of them were self-written routines. MOFIPO is a potential flow program to solve the aerodynamics flow field generated by several lifting surfaces. SIM1 is a simulator which allowed to compare the performances of different airplane configurations and to chose the optimum size of the best configuration by maximizing the final score on a complete flying period; it is based on a number of simplifying assumptions which allow to reduce the number of variables to be considered. DYN is a routine, which calculates the performances data required in the 'Final Design' section of this report. All of these programs have been written with the aim to be used and improved in the circumstance of further editions of DBF. Other commercial and shareware tools have been used to solve both structural and propulsive problems; among them, the program *Elica* provided by Mr. E. Padovano.

The team wish to thank all the people who offered their help: Prof. Guido De Matteis, team advisor; Prof. Giuseppe D'Ascenzo, rector of "La Sapienza" University; Prof. Gianni Orlandi, rector's assistant; Prof. Filippo Sabetta; Prof. G. Santucci; Prof. Franca De Zardo, "G. Galilei" head-mistress; Prof. Giorgio Sforza, "G. Galilei" teacher; Prof. Ascenzi; the technicians at "G. Galilei" labs. The team does not neglect the help it received from AIDAA, thanks to the concern of Ernesto Vallerani, AIDAA Chairman, Prof. M. Marchetti and Prof. Castellani. We also wish to thank Prof. G.P. Romano, Mr. Angelo Silvagni, for his suggestions about the power-plant management, and all the people whose name is not quoted above. The team is grateful to student Renato Chiesa, who momentarily transferred his interest from the ships to the airplanes and helped us to build the glass-fiber composite components of the airframe.

2. MANAGEMENT SUMMARY

2.1. Team architecture

The number of students who decided to participate in the DBF 2000/2001 was initially over thirty people. Six among them had taken part in the previous edition, and as a consequence of that they were chosen to be the responsible for the organization of the work. One of them was elected 'chairman' of the team, with the task to harmonize the work of the sub-teams. In fact, four technical groups were formed corresponding to the four technical areas defined during the initial meetings: *aerodynamics*, *flight mechanics*, *structures* and *propulsion*. Another group, called *marketing*, was created to raise funds; its members come from the quoted technical groups. Each group has been leaded from a *group tutor*.

Each team member was given the opportunity to decide the group to join and to change to another group if desired. After a few weeks, everyone had decided where to stay all the time of the competition.

A treasurer was elected to monitor the funds availability. One of the students was given the task to create an Internet site (<http://theflyingcenturions.jump.to>). Another student has been responsible to keep the contacts with the contest administrator. The team advisor have had mostly a role of support in the definition of the joint-venture between "La Sapienza" University and the "Galilei" High School, and helped the team to obtain the important support given by the administrative departments of the University. Some people were involved in the additional effort to strengthen the joint-venture quoted above and to organize it. One of the team members was assigned to the written reports, with the responsibility of gathering together the contributions coming from the five groups.

An additional task assignment process became necessary when the team started to build the airframe and the wind tunnel models. Each team member among those who wished to participate in the manufacturing activity was initially required to give his/her availability one day of the week as a minimum. There were no assignments referred to the specific components of the airframe, and this system showed its limits when people got disoriented about the work to be done. It was realized that it would have worked better to form small groups linked to each specific component. The team turned to the new system, and each team member had the opportunity to choose one or more among the components of the airframe or among those of the wind-tunnel models. A daily logbook was available at the "Galilei" labs, where the member had to sign in and to describe briefly his/her daily work.

Three levels of meetings have been utilized so far. Major items have been discussed during 'plenary meetings' involving all the team members from all the groups, on a twenty days time schedule. During these meetings each group could have been informed about the others' work; general tasks were assigned; deadlines were given and checked and the configuration control was made. At a lower level, each group decided its own meeting time schedule, under the responsibility of its *group leader*. At an

Management Summary

intermediate level, the five *group leaders* have had a short number of meetings where general issues have been settled without having to face the obvious difficulties raised up by the large number of people to gather up in a 'plenary meeting'.

The team had to face the difficulties raised up by the sudden or scheduled commitments occurred to some of its members. Lessons at "La Sapienza" Faculty of Engineering are scheduled from September to December and from March to May, with intermediate periods devoted to the exams. Besides, some people come from other towns apart from Rome and have had to leave the team for short periods.

The high number of people who have taken part in this edition has allowed a better distribution of the workload. Besides, it has given the chance to split two of the four groups into sub-groups. This chance has been used by the *structures* group to explore two different solutions for the fuselage structure, which have been studied and built separately; the *flight mechanics* group split itself into two sections when it had to manage the analysis of the performances and of the flying qualities of the final aircraft.

The official way to exchange information between the team members is via e-mail. A form containing the members' addresses has been updated all the time.

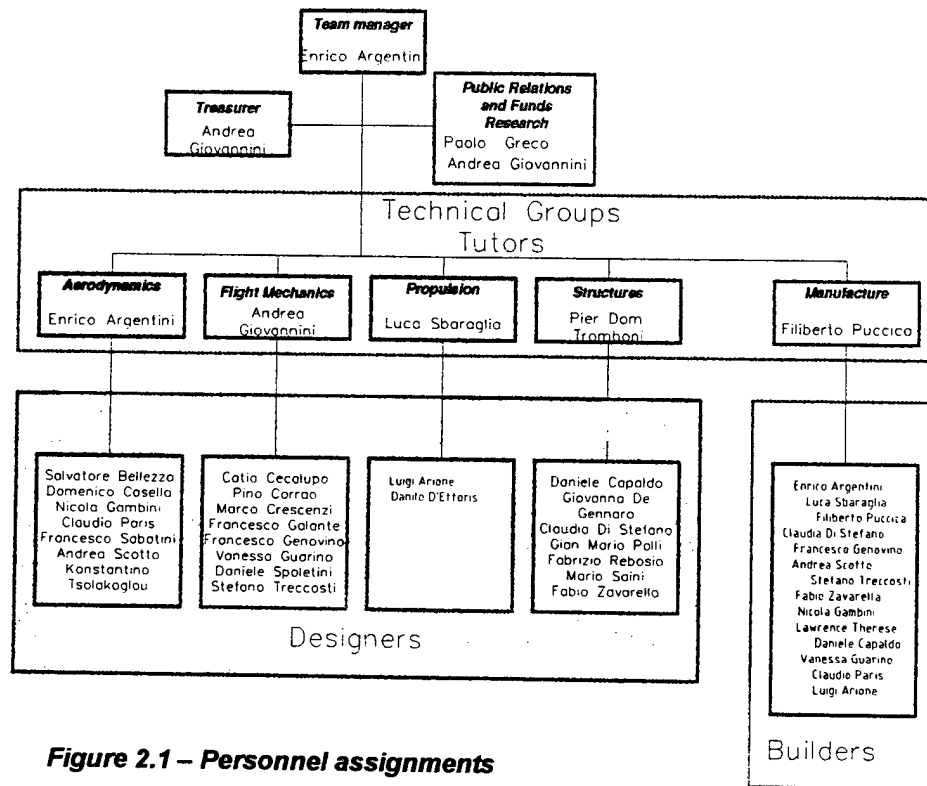


Figure 2.1 – Personnel assignments

3. CONCEPTUAL DESIGN

3.1. Introduction

The goal of the *conceptual design* phase is to select the airplane concept which best suit the mission required. Only one among the competing concepts will generally survive to this stage, the one which offers the greatest potential to be developed during the following stages.

Some items are required to be settled up during the early stages of the design: 1) to invent a number of different airplane concepts; 2) to describe their physical behaviour by some analytical models; 3) to screen those features which cannot be translated into formulas by the use of some *figure of merits* (FOMs). These items have been managed by all the technical groups. In particular, all the team members were involved in the proposal of different airplane concepts.

The analytical models' development was started during the conceptual stage, but the results were considered useful during the following stage, *preliminary design*, since the sizing process would have had to be focused on only one among the competing concepts. On the other hand, the configuration selection process showed to be acceptably executable on the basis of previous years data, observations and experiences. Some basic analytical studies have been done at this stage, involving a take-off run analysis, a first selection of suitable airfoils and a preliminary study about the optimum number of motors to install onboard.

3.2. Airplane Concepts and FOMs

Four concepts emerged from the early 'plenary meetings' which took place on Summer 2000: 1) conventional monoplane; 2) canard monoplane; 3) tandem wing with horizontal tail; 4) biplane. (see Figure 3.1)

The team chose to screen initially the competing concepts by a short number of FOMs: each FOM was given a 'weight coefficient' to take into account its relative importance. The following FOMs were chosen ('weight coefficient' are given within brackets which range from 0.5 to 1.5): *ease of building* (1); *battery consumption* (1.5); *maneuverability* (1); *stability* (1); *Rated Aircraft Cost* (1.5); *degree of confidence* (1); *mass distribution* (0.5); *ease of payload loading* (1.5). (see the table on next page).

Degree of confidence, maneuverability and stability

The first solution, *conventional monoplane*, is well known and easy to model: this can result important during the design as the designers can trust more in the figures obtained from their calculations. Besides, a high degree of confidence will translate into less wind-tunnel tests to be done, and the time saved will be addressed to other areas. Another advantage is the availability of data such as the DATCOM deriving

Conceptual Design

formulas for the stability and control analysis, which can be found on many texts and manuals and have been developed for the use with conventional airplane. This aspect has been considered along with the *maneuverability* and *stability FOMs* to guarantee good flying qualities for the final airplane.

A low degree of confidence could have been obtained on the third solution, since it is difficult to foresee the interaction effects among the lifting surface wakes and the lifting surface themselves; but this concept had been explored by the Italian team on DBF 98/99, and so its degree of confidence has been increased.

Configuration selection by FOM screening process	Ease of building	Battery Consumption	Handling Characteristics	Stability	RAC	Confidence	Mass Distribution	Ease of Payload Handling	Total FOMs result
<i>Weighting Factor</i>	1	1,5	1	1	1,5	1	0,5	1,5	
Configuration 1	5	3	4	4	3	5	5	5	37
Configuration 2	3	4	5	3	4	2	1	4	32
Configuration 3	2	3	3	5	4	3	3	4	31,5
Configuration 4	3	3	3	4	2	2	4	3	27

Weighting Factors range from 0 to 1.5 - FOMs values range from 0 to 5

Mass distribution and Rated Aircraft Cost

A positive feature of the conventional monoplane is its good mass distribution. Although the airplane is not required to fly without payload, it will certainly fly with different payload weights (the minimum *heavy payload* weight is 5 lbs, compared with a minimum *light payload* weight of 1.3 lbs or so); an excursion range of the center of gravity (CG) has to be allowed, and this can be easily managed if the empty-weight CG is located near the center of the payload bay. But mass distribution cannot be discussed without considering some aerodynamic features of the airplane. Each reasoning about CG locations depends on where the neutral point (NP) is located, under the condition that the latter falls behind the CG to ensure the airplane to be longitudinally stable (this condition is not strictly necessary on a piloted aircraft, but it is better to respect it). The NP position is strongly determined by the size and the relative position of the lifting surfaces, and in a conventional monoplane or in a *canard* it is located near the main wing. Another factor to be taken into account is the lift sharing on the lifting surfaces, which is obviously influenced by the relative distance of the CG from each lifting surface (main wing, horizontal tail, canard and so on...).

As the airplane has to lift a 'bulky' payload of tennis balls (depending on how many balls are carried, of course: 100 balls fill roughly 0.04 cubic meter or 2400 cubic inches), the payload bay could take a lot of the internal volume available. When trying to size a canard airplane with these concepts in mind, one immediately realize that the internal volume, potentially available to be used as a payload bay, which is placed between the main wing and the canard cannot be utilized, because the more the CG travels toward the canard, the bigger is the lift to be generated by the canard itself; this drives to an aerodynamically inefficient design. Three solutions could be found. The first solution is to place the power plant at the rearward end of the fuselage, or on the main wing (as seen on the Beechcraft *Starship*). By the way, to place a propeller ahead of a canard wing is prone to cause a pitch-up at stall, since the energized propeller stream delays the stall of the canard. The second solution is to carry back the payload, bringing it near the main wing. This could work but it has two disadvantages: first, the fuselage length is increased, resulting in a worse RAC; second, there is a lot of room not used for any purpose except than spacing the canard from the wing. This condition is not symmetrical with spacing the horizontal tail from the main wing of a conventional airplane, since in the former case a streamlined shape has to be given to the fuselage, which brings to an heavy and internally empty fuselage forward section. In the latter case, a shrunk fuselage rear section can be used, which can collapse even into a tail boom (so it has been done by the Italian team on the previous DBF). The third solution is to stress the role of the canard wing, enlarging its surface to a value comparable with that of the former 'main wing'. The drawback to face with is that the NP will be placed near the front wing (since the rear wing suffers from the strong downwash caused by the front wing) and this doesn't allow to properly exploit the fuselage section between the two wings. To correct that, one could place a horizontal tail, which draws back the NP and permit to center the payload inside the quoted fuselage section. This previously studied three-lifting-surfaces concept has been revisited this year by an attempt to reduce front wing dimensions to those of a canard, in such a way as to avoid it were considered as a 'wing' in the RAC formula. Besides, a canard with a flapped trailing edge is considered as a 'wing', and this would lower the RAC: hence, canard surfaces have been always thought of as all-moving surfaces.

Another drawback of the canard solution is that it's hard to get the necessary moments to trim a flapped main wing, which could become a serious problem because the short-take-off performance imposed by the contest officiators. This issue is partially alleviated by the always positive lift generated by a canard wing.

As far as the biplane concept is concerned, it has as a good mass distribution as the conventional monoplane has, but with a RAC likely worse (which could be compensated by the likely increased payload carried).

Ease of building

This FOM evaluates the complexity of the competing concepts from a structural point of view. Complexity will become time spent during the manufacturing work, and this brings to the better FOMs obtained by the concepts with less lifting surfaces. It should be noted that each lifting surface requires a structural joint to the rest of the airframe, and consequently an increase in weight, time-to-design and time-to-build.

Ease of payload loading

During the flight period, the ground crew has to reach the payload bay to switch between the payloads. This task must be performed quickly and safely (both for the people and the airplane), and an upper bay-door is generally the better solution, since the fuselage back is likely less than 0.5 m above the ground. An upper door can be easily obtained on a low wing monoplane, while it becomes hard to place it on the back of an high wing airplane, since the load-carrying components of the wing structure will limit the opening available. This is also the case of a biplane airplane. To solve such a problem, one could open the fuselage on a transverse plane, either in a forward or in a backward fuselage section; some drawbacks will rise if, for example, a power plant is placed in the nose, since the structure have to withstand the thrust-driven loads and to be discontinuous at the same time. Indeed, wherever the opening may be placed, it will determine a discontinuity in the structures of the airframe. Separate pods have been rejected since they make RAC worse and penalize the aerodynamic performance due to the increased wetted area and the added interference drag.

Battery consumption

By this FOM, the team tried to take into account the overall aerodynamic efficiency of the design, which influences the required thrust to fly at a given speed and weight and hence the energy absorption from the NiCd batteries onboard. The canard solution was thought to be the most efficient, since it should diminish the overall trim drag of the lifting system. The three lifting surfaces concept could be even more efficient (as the fair performances of the Piaggio/Gates P180 design seems to show), but it would be necessary a binding work to get the best sizing and positioning of the lifting surfaces, and low Re numbers definitely don't make the work easier (*see the following Analytical Models section*). However, if a conventional monoplane had to be chosen, its cruise trim drag could be minimized by a proper positioning and mounting angles of main wing and tail.

Several other issues were considered during this stage. A few team members started to think about the payload containers to be built, looking at different solutions, which ranged from wooden structures to hydraulic plastic pipes (to be lightened by skin openings). The 'DBF classic' trade study between 'light

Conceptual Design

and fast' and 'heavy and slow' aircraft was delayed to the next design stage, since it doesn't depend on which concept has been chosen to be further developed.

One important decision was to avoid a retractable landing gear if an heavy airplane had to be built: this saves both weight and room inside the fuselage for the nose wheel at least, and it is definitely hard to design a retractable leg capable of sustaining the relatively high landing loads which can be expected to be developed at a high-wing-loading-RC-airplane touchdown. A study on a carbon fiber composite landing gear was assigned to some members of the structures group.

A FOM-based study was made to establish which wing planform had to be chosen for the preliminary design analysis. Results are shown in the table below.

Wing planform selection by FOM screening process	Ease of building	Battery Consumption	Confidence	Mass Distribution	Ease of Payload Handling	Total FOMs result
<i>Weighting Factor</i>	1	1,5	1	0,5	1,5	
Rectangular wing	5	3	5	4	4	22,5
Elliptical wing	1	5	3	5	5	21,5
Trapezoidal wing	3	4	5	5	5	24
<i>Weighting Factors range from 0 to 1.5 - FOMs values range from 0 to 5</i>						

3.3. Take-off Analysis

The take-off runway available this year has been set by the contest officiators at 200 ft (60 m). This value is bigger than last year (100 ft / 30 m), but it can still influence the final design. There are two reasons which determine its importance: first, the final score is still proportional to the payload weight, so that an heavy airplane could result from the optimization process; second, the type of electric motor has changed to the *brushed* type, which is likely to show lower performances. On the other hand, allowable wingspan has been increased from 7 to 10 ft (2.1 to 3 m), which could help to carry more weight; indeed, we preferred to think of increased wing span as a mean to increase the aspect ratio, which, on turn, increase the aerodynamic efficiency (last year Italian airplane had a low wing aspect ratio, say 4.5).

Since many design variables are unknown on the conceptual design stage, mainly the take-off weight, it is convenient to analyze the take-off performances as a function of the thrust-to-weight and weight-to-wing surface ratios. A third parameter should be taken into account, which is the airplane maximum lift coefficient, $C_{L\text{ MAX}}$. A safety coefficient equal to 1.15 divides the maximum allowed W/S, in order to permit

the take-off with partially charged batteries. The results from this analysis are shown in Figure 3.2. $C_{L \text{ MAX}}$ values have been considered to range up to 1.5, because the low Reynolds numbers, which can be expected at typical take-off speeds (say below 15 m/s, 50 ft/s), are prone to not allow higher maximum lift coefficients.

3.4. Preliminary airfoil analysis

The aerodynamic group analyzed a great number of airfoils, which could have been suitable to the mission requirements. Flight speeds from 15 to 25 m/s were assumed, together with typical wing loading from 12 to 16 kg/squared meters. A cruise lift coefficient of about 0.6 was assumed, from last year experience. With those values in mind, the following airfoils were selected to be further analyzed on next design stages.

Preliminary Airfoil Selection	$C_{L \text{ MAX}}$	$C_D @ C_{L \text{ MAX}}$	$C_D @ C_L = 0.6$
SD 7032	1.400	0.0341	0.0080
S 7012	1.174	0.0326	0.0100
S 4083	1.327	0.0246	0.0083
E 387	1.277	0.0287	0.0079

3.5. Power Plant Analysis

Upon the likely hypothesis of an airplane weight of roughly 15 kg (33 lbs), the propulsion group began to study how is the total efficiency of a power plant influenced by the number of cells-motor-controller-propeller groups (*power groups*) installed onboard.

The value of η_{τ} , the efficiency of a single group, is given by the total product among the propeller, motor and controller efficiencies η_e , η_m , η_c , where:

$$\eta_e = \frac{PF}{PA} \quad \eta_m = \frac{PA}{PDc} \quad \eta_c = \frac{PDc}{PD}$$

and

PF = power transferred to the air stream

PA = shaft power

PDc = controller output power

PD = available battery power (given)

This gives:

$$\eta_{\tau} = \frac{PF}{PA} * \frac{PA}{PDc} * \frac{PDc}{PD} = \frac{PF}{PD}$$

Let us consider a power plant composed by a number $n \geq 2$ of power groups and let them be identical (i.e. formed by the same components). We have:

$$\eta_{\tau} = \frac{\sum_{i=1}^n \eta_e^i * \eta_m^i * \eta_c^i * PD^i}{PD} = \frac{n * \eta_e^i * \eta_m^i * \eta_c^i * \frac{PD}{n}}{PD} = \eta_e^i * \eta_m^i * \eta_c^i$$

In other terms, the total efficiency of the power plant can be expressed in the same way as in the single power group case. On the other hand, the motor and the controller efficiencies are proportional to their size, or the maximum electric power they can manage. The net result will be that, if the influence of the propeller and battery efficiencies is neglected, a better total efficiency can be expected from a power plant composed by only one group. The following table seems to confirm this result:

Comparison between single and double motor installation	Efficiency		
	η_m	η_c	η_{τ}
One motor and controller (Graupner 3450/7 / Astroflight 204D)	0.86	0.998	0.85
Two motors and controllers (Graupner 3300/4 / Astroflight 217D)	0.83	0.937	0.778

3.6. Final Results

At the end of the conceptual design stage, the team had chosen to carry on the development a conventional, single-motor-and-propeller monoplane design, which had to be sized on next stage.

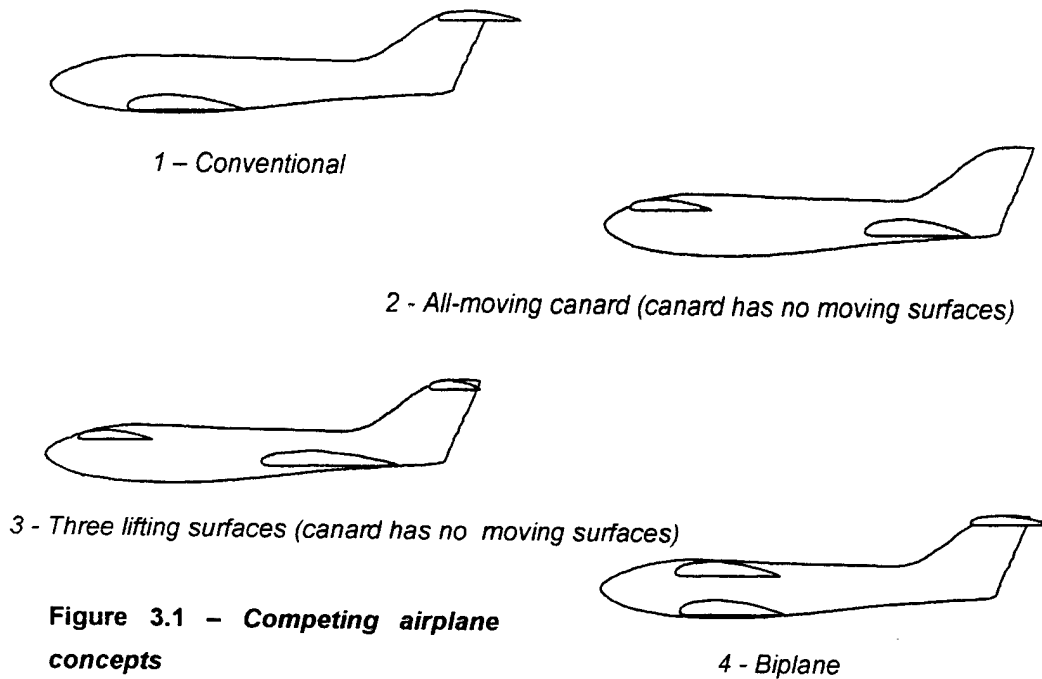


Figure 3.1 - Competing airplane concepts

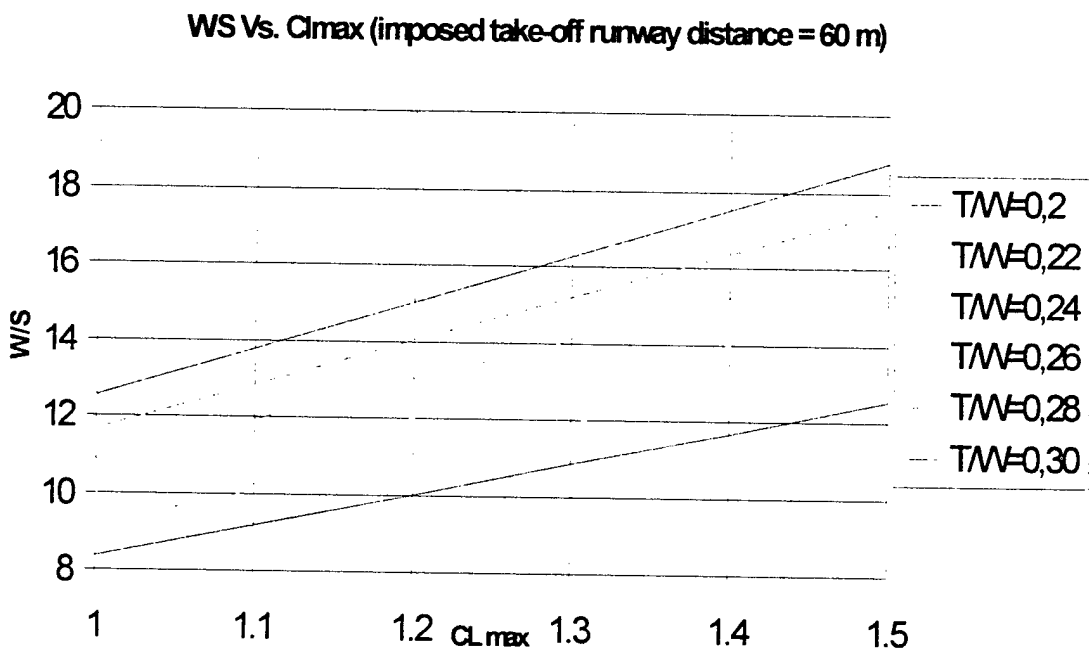


Figure 3.2 - Take-off analysis

4. PRELIMINARY DESIGN

4.1. Introduction

The main task accomplished on this design stage has been to size the concept selected on the 'conceptual design' stage – low wing monoplane, conventional tail arrangement – to meet the mission and design requirements and to give as much points as possible. As more and more issues were settled up and the geometry of the airplane became clearer, each technical group has been drove to solve specific matters. The items to be developed have been: 1) to model the aerodynamic characteristics of the airframe; 2) to model and to study the power plant; 3) to model the mission assignments; 4) to insert the developed models into a computer program which makes use of an optimization criterion to find the best design; 5) to analyze and to size aerodynamically the main wing and to analyze different structural solutions for the wing and the fuselage. Assignments 1 and 5 were given to the aerodynamic group, the latter involving also the structures group; assignment 2 was given to the propulsion group; the flight mechanics group faced items 3 and 4, with the contribution of the aerodynamic group.

We will explain this matter starting by the models' description; then, the optimization computer routine will be presented. Indeed, the goal of the models is to allow the program to be written: each model will translate into a subroutine which will correlate some variables each other, so to have a balanced ratio between unknown variables and 'equations' available. To explain this further, one could think about things such as the 'horizontal tail volume coefficient', which ties together four fundamental variables – wing and horizontal tail surfaces, mean aerodynamic wing chord and relative distance between wing and tail – to respect a value given by the designers according to general design criteria.

4.2. Analytical Aerodynamic and Power Plant Models

One of the major concerns to deal with in such a competition as the DBF, is the low Reynolds (Re) number at which the airframe components have to operate. Re is usually in the range from 200.000 to 400.000, due both to the low speeds (which can reach values under 15 m/s) and the small size of the components (i.e. airfoil chords range typically from 0.2 to 0.5 m). Small components (like landing gear wheels) reach $Re < 80.000$. Within these ranges, it is difficult to find affordable data in classic aerodynamics textbooks and manuals, mostly devoted to the manned aircrafts. Fortunately, there are a few databases collecting low- Re airfoils' data, and this allows to settle up the modeling of the lifting surfaces. Another way is to test components in a wind-tunnel, which has been made by the team but at a reduced level, since the wind tunnel available at the Faculty had to be shared with many others.

4.2.1. Initial Fuselage, Wing and Tail Drag Estimation

To have a first guess value of the fuselage and wing drag we have used two self-written *MATLAB*® functions: *DragFus* and *DragWing*.

DragFus calculates, from the angle of attack and the front and wetted area of the fuselage, the effective front area and find the form drag using a typical value of the coefficient of drag for slender bodies ($C_d = 0.08$). The skin friction drag is calculated by a simplified flat plane model, which takes into account the wetted area and the Re number referred to the fuselage's length and uses the well-known flat-plane relationships to give the value of the skin friction coefficient; a fully developed turbulent flow is assumed on the whole fuselage skin. Summing the two terms calculated by the procedure discussed above, we guessed to have found a value for the total fuselage drag greater than the actual one.

DragWing starts from the following data: wing area, wing span, taper ratio and the angle of attack, to find the mean aerodynamic chord (MAC), the aspect ratio, the wetted area and the front area of the wing (a typical value for the relative thickness of 10% is assumed). An approximated lift coefficient is calculated from the angle of attack. Like *DragFus*, *DragWing* find the zero-lift drag of the wing (i.e. the form and the skin friction drag); then it calculates the induced drag given a classical elliptical load distribution. Under this hypothesis, the induced drag depends on the aspect ratio and the coefficient of lift; besides, the elliptical load hypothesis has been assumed since the aerodynamic group set it as a target, to minimize the induced drag of the final airplane. In spite of this, *DragWing* tends probably to underestimate the induced drag; on the contrary, it overestimates the zero-lift drag, since the competing airfoils evaluated by the aerodynamic group are characterized by low drag coefficients at intermediate values of lift coefficient (i.e. on cruise condition).

The horizontal and vertical tail contribution to the overall drag was calculated by the quoted flat-plane model. A constant value of $C_d = 0.012$ was obtained by this way; the influence of lift coefficient both on the profile drag and on the induced drag was neglected.

The final estimate of the drag buildup by all the components of the airframe was likely a bit greater than the actual one, but the model utilized didn't take into account the interactions among the various boundary layers (i.e. interference drag), which increases the total drag.

4.2.2. Weight Estimation

Two are the contributions to the take-off weight of the airplane. The first component is the empty weight, calculated by summing up the airframe and the power plant weight; this weight must be guessed from some source. The second component is the payload weight, which is not really assigned, since the payload has been treated as a variable to be determined in the optimization process.

As far as the influence of this process on the empty weight is concerned, it treats the component sizes as independent variables, so the components weights have to be calculated from their sizes. We had two

Preliminary Design

ways available to execute such calculations. The first was to freeze the structural arrangement of the main components (i.e. wing, fuselage...), calculate the size of the internal structural elements (i.e. spar, ribs...) of those components according to the given main component size and then sum up each element's weight according to materials' properties data (i.e. density). The second way was based on statistical data collected during the last two years (i.e. wing weight as a function of wing area and method of construction): the latter way is simpler than the former, and it was chosen and inserted into the program.

Example of approximate data for initial weight estimation of some components		DENSITY		WEIGHT
		[kg/m ²]	[kg/m]	[kg]
COMPONENT	WING (WITH SERVOS)	2.000		
	HORIZONTAL TAIL (W.S.)	1.800		
	VERTICAL TAIL	1.500		
	CARBON FIBER TAIL BOOM		0.370	
	WOODEN PROPELLER		0.330	
	MAIN LANDING GEAR WHEEL			0.10
	WING SECTION LINKAGE SPAR			0.03
	ALUMINIUM LANDING GEAR			0.4

4.2.3. Power Plant Performance Estimation & Components Selection

Performance Estimation

The development of a good power plant performances prediction has showed itself to be as important as hard to obtain. The power plant is composed by three groups: the battery pack(s), the electric motor(s) with their accessories, and the propeller(s) (possibly geared to the motor by a reduction box). The restrictions imposed by the DBF rules on the type and brand of the electric motor that must be used have made the work a little bit easier. The motor is relatively easy to model. A few data are sufficient to characterize the motor: the no load current, the internal resistance and the 'motor constant' K_T . These data are available from motor manufacturers. Refined data estimation was made with the help of Mr. A. Silvagni, who allowed the team to obtain precise results by his fixed-point test stand (see *Final Design section for more details*). A derived datum necessary to the performance prediction is the battery current with respect to the flight speed, given the throttle setting. A main concern remained about the description

of the propeller performances, which are unavailable on such a kind of product as the small scale model aircraft propellers are. The most desired data are the *thrust coefficient*, C_T and the *torque coefficient*, C_Q curves. The propulsive group early began to work on this difficult matter, and definitive results began to be available at the time of the end of the preliminary design phase. Two ways were followed, one based on a numerical simulation and the other based on wind-tunnel tests. The former was performed by using *Elica*. This program considers the propeller blade as composed by a number of finite elements and requires both geometrical (i.e. local chord to blade radius ratio) and aerodynamic (i.e. zero lift line angle) data referred to each blade element.

The curves obtained from *Elica* were used by *Motor1*, a program developed by Mr. Luca Cistriani, who took part at DBF 98/99. Batteries are modeled by an empirical relation by Mr. E. Padovano which relates voltage, V and current, A by two constants a and b according to: $V = aA^b$.

An example of the final results is given in Figure 4. 1 The somewhat oscillating behavior of the thrust and current curves at low speed values is due to the uncertainties in the numerical simulation if a high blade angle of attack take place, as it is the case at low speeds and high propeller's RPM values. The wind tunnel test had to be postponed due to unavailability of the wind tunnel; they will be started in a few days since now, but the results will be hardly available before this report's sending deadline. However, it makes sense to carry them on since those data could be useful during the in-flight tests that will take place before the contest fly-off.

The same test stand used to determine the motor constants was useful to obtain true fixed-point thrust values, which have a predominant role in the take-off run prediction. Besides, one can use these results to correct the uncertain low-speed portion of the numerically derived propeller curves.

The format to be given to the final results coming from the power plant simulation was a couple of matrices describing numerically the relationships:

$$\begin{aligned}\text{THRUST} &= F(\text{AIRSPEED, THROTTLE SETTING}) \\ \text{BATTERY CURRENT} &= F(\text{AIRSPEED, THROTTLE SETTING})\end{aligned}$$

The two functions are calculated on a coarse mesh and written on the mass memory to be available to the program *SIM1*. A *SIM1*'s subroutine reads the data and executes a data interpolation on a mesh whose size is controlled by the user, according to the accuracy required on each particular design phase.

Components' selection by FOMs

A set of candidate power plant components has been selected by a FOM-based process before further analyses would have been done, in order to restrict the number of candidates components and to reduce

Preliminary Design

the time required for such analyses. These FOMs are both of a technical and of a commercial nature, and are shown in the following tables.

Motor Selection by FOMs	Maximum power efficiency	Weight	Cost	Ease to find	Compatibility with over-the-counter controllers/propellers/cells	TOTAL
Weighting Factor	5	3	1	4	5	
Graupner 3450/7	3	3	3	3	3	54
Graupner 3500/8	3	2	2	3	3	50

Propeller Selection by FOMs	Maximum power efficiency	Weight	Cost	Ease to find	Compatibility with over-the-counter controllers/propellers/cells	TOTAL
Weighting Factor	5	4	1	4	4	
Menz	3	3	1	3	3	52
APC	3	1	2	3	3	45

Controller Selection by FOMs	Internal Resistance	Maximum current	Cost	Ease to find	Compatibility with over-the-counter controllers/propellers/cells	TOTAL
Weighting Factor	5	4	1	4	5	
Astroflight	3	3	3	3	3	57

Note: no other useful controller have been found on commerce

NiCd Cells Selection by FOMs	Capacity to Weight Ratio	Cost	Ease to find	Compatibility with over-the-counter controllers/propellers/cells	TOTAL
Weighting Factor	5	1	4	5	
Sanyo RC2400	3	2	3	3	44
GM 2400	3	1	2	3	39

4.3. Mission Assignments

Preliminary Design

Flight Pattern Model

A flight pattern model had to be inserted into the optimization program to calculate the flight performances (i.e. speed, bank angle etc.) required to get the optimum final score. The main concern was about the presence of two different payloads, each of them with its own flight pattern: the resulting high number of variables had to be lowered in some way, both to shorten the computing time and make the program writing easier. The flight mechanics group chose to model a single 'equivalent flight pattern' (EFP) which would have given the same single-flight period final score result as in the two 'real' patterns case. The EFP model is based on the concept of 'score to time ratio'; in other words, 'points obtained per given time period'. First, a single scoring criterion has to be found, since the heavy payload is scored on weight and the light payload is scored on number of balls carried. By assuming an average tennis ball weight of 0.058 kilos and assumed that the weight of payload is the same, independently from its nature, we obtain a score ratio of:

$$S_T/S_S = 1.5$$

(S_T = score with a tennis balls payload; S_S = score with a steel payload). To compare the scores obtained according a time criterion, we consider a second ratio whose terms are the respective flight pattern lengths flown in both cases, L_T/L_S . This ratio depends on how the turns are flown, or the load factor used.

Patterns' lengths ratio	Distance flown on straight legs [m]		L _T /L _S
	Payload		
	Distance flown on turns [m]		
	Tennis balls, L _T	Steel, L _S	
40	1360	760	1.8
100	1600	1000	1.6
140	1760	1160	1.5

Since the 'tennis balls' pattern contains a greater number of straight legs than the other pattern (3 vs. 1) and the number of turns is the same, we may assume that the average flight speed on a single flight pattern will be greater in the former case. Hence, passing from a distance ratio, L_T/L_S , to a new time-based ratio, T_T/T_S (T_X = total time to complete a single flight pattern, carrying the 'X' type of payload), we may expect it to be a bit lower than the other, which conducts to:

$$T_T/T_S \cong S_T/S_S = 1.5$$

To define an equivalent flight pattern we sum up straight and turn legs from the 'heavy' pattern (1S+4T) and the 'light' one (3S+4T), which gives 4S+4T. Accordingly, the EFP will be defined as 2S+2T (see Figure 4.2). The last step is to define the single EFP score per unit weight of payload carried. Let Q be the weight which gives 1 point at the end of a single 'steel' lap; on the following 'tennis balls' lap Q will give 1.5, and the total score will be 2.5. Hence, we have to assign 1.25 points every time an EFP lap is concluded (and a payload weight Q has been carried) to get the same result as the real case is (see figure 4.3).

4.4. Optimization Algorithm and SIM1 description

The rules of the competition assign a score according to the relationship:

$$\text{Score} = \text{Written Report} * (\text{Total Flight Score} / \text{Rated Aircraft Cost})$$

With a given 'written report score', the result depends on the ratio 'Total Flight Score / Rated Aircraft Cost' (from now on, 'Real Flight Score', or 'RFS'). The 'Total Flight Score' depends directly on how high the payload carried is on a single flight period. The 'Rated Aircraft Cost' is influenced by the size and mass of the airframe and by the size of the power plant. An obvious relationship exists between these two terms since the more payload is carried, the bigger and heavier is the aircraft. Hence, the score will be a number which couples payload and airframe, and a way to treat this nonlinear problem should be found. According to this, the team started the development of a *MATLAB*® program, *SIM1*, which simulates a whole flight period under some simplifying assumptions.

4.4.1. *SIM1* Description

The *MATLAB*® program *SIM1* was created to simulate the required mission. The flight pattern used has been the EFP (see 0, Flight Pattern Model).

The program manages a short number of parametric variables describing the *airframe* structural and aerodynamic characteristics, the quantity of *payload* carried and the *flight performances* on the flight pattern. These variables are incremented in the main loop of the program by a series of nested *for...next* sub-loops: their optimum combination with respect to the maximum RFS obtained is given as the output, together with the final RFS obtained. A group of 'assigned' variables is defined in the initial program lines, before the main loop is executed. These variables belong to the same three groups quoted above, but they can be accessed and modified by the user only before executing the program. This expedient was used to diminish the number of variables cycled in the nested loops, so that the overall computational

Preliminary Design

time is reduced (it would increase exponentially with the number of variables). The user will modify these variables according to his/her own judgment and intuition. Typical values are: V_h , volumetric horizontal tail volume coefficient = 0.6; V_v , volumetric vertical tail volume coefficient = 0.04; $S_{wing}/S_{tail} = 5$. A W/S , wing loading < 20 Kg/m² check is executed during the internal loops not to excess the performances to be required from the structures.

Before entering the main loop, the program loads from the mass memory the power plant performances data. A take-off run performance check is executed just after having assigned a new *payload* quantity. The runway available is set to 50 m (170 ft) to take a margin over the effects of degraded batteries' performances to be expected as time goes by during the flight period. The simulation is stopped when either the flight time (10 minutes) is ended or the residual energy available in the batteries becomes lower than 40% of the initial value.

The payload is assigned as a weight quantity equal for both steel and tennis balls; the number of tennis balls is then calculated. On the early simulations, a fuselage 'rubber sizing' was used, allowing it to vary with tennis balls payload volume. Since the program gave about 100 balls as optimum result, from then on the fuselage size has been fixed according to that result.

A typical SIM1 output is showed below. The results are quite similar to the parameter of the final configuration.

Airplane Parameters		Mission Parameters	
Wing surface [m ²]	1.136	'Light' payload [no. of balls]	100
Wing span [m]	3.04	'Heavy' payload [lbs]	16
Wing chord [m]	0.38	Take-off distance [m]	48.4
Take-off weight [kg]	15.7	Take-off speed [m/s]	15.4
Wing loading [kg/m ²]	13.83	Speed- C_L on straight legs [m/s – nadn*]	17 – 0.77
Total length [m]	2.12	Speed- C_L on turn legs [m/s - nadn]	18 – 0.89
RAC	6.174	Load factor – bank angle on turns [naden – deg]	1.3 - 40
SIM1 Output *naden = not a dimensional number		Total laps	4
		Time [sec]	472
		Final RFS	10.37

It should be noted that the airplane will stop flying because batteries have ran out, but more than two minutes are still available before the flight period ends. The airplane must be able to carry the maximum

allowed tennis balls number or an equivalent steel weight, at least during the first pattern flown. This datum was transferred to the structures group, who took care of the consequent structural design.

4.5. Wing Analysis, Airfoil Selection and Surfaces Sizing

4.5.1. MOFIPO

The aerodynamic characteristics of the lifting surfaces have been analyzed by a self-written *MATLAB*® program, *MOFIPO*, which is based on the classic potential flow lifting line model. Each lifting surface is modeled by a 'modified horse-shoe' vortices distribution. The vortices are symmetrical with respect to the vertical plane (X-Z plane), and both a sweep and a dihedral angle may be assigned. More interacting lifting surfaces are allowed. The capabilities of *MOFIPO* were increased by adding a small subroutine whose inputs are the local (along the lifting surface) angle of attack and C_d vs. C_l curve(s) of the airfoil(s) which are used for the lifting surfaces. A profile drag of the lifting surface may be calculated which likely approximates the real case if the aspect ratio is not too low (say > 5). Induced drag calculation is performed by a separate subroutine and final 'true' C_D vs. C_L curves for the finite aspect ratio lifting surface may be obtained. Four more results have been obtained from *MOFIPO*: 1) it has been the basic tool to optimize the wingspan load distribution; 2) it allowed to check for first wing section along the wingspan to stall; 3) it permitted to calculate the predominant wing and tail contribution to the neutral point location; 4) upwash and downwash angles ahead of and behind of the wing were obtained to be used on longitudinal stability calculations (i.e. for the determination of the fuselage, tail and propeller contributions to the total pitching moment).

Using *MOFIPO*, the aerodynamic group has found the optimal design of the wing. Two iterations have been necessary, since the first result was a high aspect ratio wing ($AR = 9.96$; $S = 0.9 \text{ m}^2$) which was optimized for cruise condition but unable to satisfy the take-off requirement with a minimum safe margin. After having assumed a safe margin on the take-off run, the required wing surface increased to 1.136 m^2 , with $AR = 7.92$.

4.5.2. Airfoil selection

The final airfoil chosen by the aerodynamic group was the SD-7032, whose characteristics are given in figure 4.4. This airfoil showed to be the airfoil which best matches the required cruise condition. It has an adequate $C_{l_{max}} = 1.4$ and a smooth behavior on stall.

4.5.3. Aerodynamic Design of the Wing

Preliminary Design

To size up the wing we have begun from the take-off limit. The preliminary design of the whole model and an estimation of the total weight and drag give for the fuselage:

Diameter	Length	Wetted area	Front area
0.25 m	2 m	1.5 m ²	0.05 m

Wing span is $\sim 3\text{m}$ and wing surface is $\sim 1\text{ m}^2$ (to have an aspect ratio of about 8-10). Maximum take-off weight is $\sim 150\text{ N}$ and total drag coefficient is guessed as $C_D \sim 0.07$.

The preliminary sizing has been made to carry the maximum load (100 tennis balls) while the estimation of the drag has been made with a *MATLAB®* program that, given the geometry, calculates separately the fuselage and wing drag, as explained above. The result is to overestimate the total drag, but this tends to foretell worst take-off performances.

From the foreseen propulsive performance we have a thrust of $\sim 50\text{ N}$ and $V_{TO} > 15\text{ m/s}$ (from the given field length).

Considering a take-off speed of 13 m/s , is requested for the wing $C_{Lmax} = 1.3$; hence, for the airfoil $C_{Lmax} = 1.4$. For the cruise we will have $C_L = 0.6$. At the beginning we designed a rectangular wing $3 \times 0.3\text{m}$, then an area $S = 0.9\text{m}^2$ and an aspect ratio $AR = 10$. For this wing, with an angle of attack of 15° , Mofipo gave us $C_D \sim 0.0524$, $C_L \sim 1.2325$ and a coefficient for the parabolic polar ($C_D = k C_D^2$) $k \sim 0.0345$. To reduce the induced drag we have then considered a wing with taper ratio $\lambda = 0.5$ that, again for 15° , gives $C_D \sim 0.0523$, $C_L \sim 1.2674$ and $k \sim 0.0326$ and permits a greater C_L of the wing given the maximum C_L for the airfoil.

The following idea was to consider a double tapered wing, i.e. a wing composed of two parts with different taper ratios. This permit to have a load distribution near to the elliptical one, so to reduce the induced drag and to have a nearly constant spanwise C_L .

The optimization of the cruise later executed by the flight mechanics group gave us a wing surface $1,13\text{ m}^2$ which, considering the wing span limit, leads to $AR \sim 8$. The new wing geometry and the lift distribution are shown in figure 4.6. Again at $\alpha = 15^\circ$ we have $C_D \sim 0.0604$, $C_L \sim 1.2225$ e $k \sim 0.0404$ (the higher value of k is caused by the lower aspect ratio).

4.5.4. Drag polar of complete wing

Figure 4.5 shows the total (parasite + induced) drag polar of complete wing calculated by MOFIPO. Output data were fitted by a second order polynomial curve, which has been used in following calculations. This curve features a linear term, which is due to the original airfoil polar curve. Another complete wing drag polar had been calculated for the first wing designed by the aerodynamic group, the

one with $AR = 9.96$, which was even more sensitive to the airfoil polar curve, since the 'parabolic' induced drag component was obviously lower.

4.5.5. Tail surfaces size and positioning

Both the horizontal and the vertical tails have been initially sized up by using typical volumetric tail volume coefficient ($V_h = 0.5$; $V_t = 0.04$), whose values were used by the SIM1 software to get a good first guess value of tail areas. Chord values have been chosen in order to avoid too low Re numbers.

	S [m²]	Span [m]	Chord [m]
Horizontal tail	0.18	0.90	0.20
Vertical tail	0.11	0.44	0.25

Airfoil selected was NACA 0009 in both cases. The horizontal tail had been initially placed in a conventional low position. This would have been corrected later (see *Detail Design section*).

4.5.6. Aileron size

Ailerons have been sized using the classic flap theory which takes into account the aileron span, deflection, δ_A , and zero lift line rotation due to δ_A . Ailerons are placed on the tapered (outer) wing portion. A stationary roll rate of 100 deg/ s has been imposed at $V = 20$ m/s and $\delta_A = 20$ deg. Equating the roll moment due to the damping roll effect, and the one due to the aileron, we have:

$$\frac{1}{4} \rho U S C_{l_p} b^2 \Delta p_{st} = \frac{1}{2} \rho U^2 S C_{l_{\delta A}} b \delta_A \quad (4.1)$$

where C_{l_p} and $C_{l_{\delta A}}$ are, respectively, the roll damping coefficient and the aileron control power coefficient. The latter depends on τ , flap efficiency, which is a well-known function of the aileron chord to wing chord ratio. Hence, aileron chord may be sized by solving eq. 4.1 with respect to τ and using the quoted function. Final result is $c_a/c_w = 0.20$.

4.5.7. Elevator size

To size the elevator, a landing maneuver was considered, which should be the most critical condition encountered during the flight. Following the same reasoning as in the aileron case, a function of τ was used, that is:

$$x_{cg} = x_{ac} - \frac{C_{m_\delta}}{C_{L_{Max}}} \left[\delta_{Max} + \frac{\alpha_w - \varepsilon - i_w + i_l}{\tau \eta} + \frac{C_{m_{ac}} + C_{m_f} + C_{m_p}}{C_{m_\delta}} \right] \quad (4.2)$$

Eq. 4.2 represents the moment equilibrium around CG. Since $C_{m_\delta} = -a_l \bar{V} \eta \tau$, Eq. 4.2 may be solved with respect to τ , and elevator chord may be found. Final result is $c_\theta/c_w = 0.25$. Deflection angle is 20 deg. The same result has been obtained by considering the take-off rotation maneuver. A lower c_θ/c_w might have been chosen with an higher deflection angle (i.e. 0.20 percent vs 25 deg), but this has been avoided since the flap loose its effectiveness at high deflection angles.

4.6. Structural Design

4.6.1. Fuselage and containers

Following the suggestions received by the flight mechanics group and the aerodynamic group, which showed the advantages of a fuselage fineness ratio, *length/diameter*, equal of greater than 5, the structures group began to design the fuselage. At the same time the team faced the design of the payload containers which had to be placed inside the fuselage. The best solution was found to be characterized by the following features:

- a approximately cylindrical (circular section) payload bay with the tennis balls disposed on 15 layers, each composed by 7 balls
- a streamlined fuselage nose section which carries the power plant (*see Detail Design section*)
- a tapered aft section, 'tail cone', which transfers the tail loads to the central section of the fuselage. The tail cone is 0.66 m long, and it is reinforced by an internal carbon fiber boom (length = 0.4 m), which carries the tail planes.
- tennis balls and steel blocks are both secured internally to the containers. Number of containers inside the fuselage is three to reduce each container's length, in such a way as to avoid any trouble caused by flexibility.
- containers are put inside the fuselage throughout an opening on its back. The opened section is 0.4 m long

Containers have been realized with a simple wooden structure and have an internal mechanism that allows locking the steel blocks. A graphical description of the arrangement quoted above is given in Figure 4.11.

Preliminary Design

The fuselage central section was required by the flight mechanics group to have a flat bottom, in such a way as to allow the wing to be shifted along the longitudinal direction. Besides, the flat bottom makes easier to put and slip the payload containers inside. The central section is 1.15 m long; diameter is 0.255 m. The flat bottom is 0.137 m wide. The greatest loads on the fuselage are the ones due to wing and tail lift forces; the vertical tail gives a further transversal load of about 30 N and a torque moment related to that load. Spars are made of lime wood, and they are sized up to a load factor, $n = 2$ and a safety coefficient of 1.5. Cover's spars are sized up to compression loads only. The front frame is sized up to carry the loads generated by the power plant.

The balsa wooden skin carries the whole torsional resistance. The fuselage section is basically a single closed section beam. The shear flow distribution, q , produced by the torque T due to the propeller and the differential use of the control surfaces is:

$$q = \frac{T}{2A}$$

Figure 4.7 shows the shear flow distribution calculated between each pair of frames. Balsa cover is assumed to be 3 mm thick.

The structure group obtained the structural design of the fuselage by a *FORTTRAN* program. This software is composed of two parts: the first one (*Momenfus*) studies the stresses distribution due to the aerodynamic and mechanical loads acting on the structures; the second one (*Dimension*) sizes up the structural members: fuselage frames, spars and the stressed skin.

Momenfus

It calculates the shear distribution along with the bending and torque acting on the fuselage central section, which is supposed to be loaded by tail and engine actions at its endpoints, and by the wing loads. The full payload case is considered as a distributed load per unit length. From the translational and rotational equilibrium the diagrams shown in figure 4.8a are obtained, using the semi-coque theory.

Dimension

Outputs from *Momenfus* are used by *Dimension* to calculate the size of spars and of the skin. A beam model has been used. Spars are spaced by 30 degrees, and an open section is present, which allows enough room to load/unload the payload. The second step is the determination of the minimum number of frames, which is calculated using the Euler's formula for critical load. A safety coefficient $c_s=3$ has been used. The program calculates the stresses acting on the frame placed at the wing root. The frame's shape is circular: the inner radius is the container radius plus 0.5 cm, and the outer radius is the fuselage

one. Results are shown in fig. 4.8b. To determine the minimum dimension of each structural member, the maximum stress value is compared with the physical limit of the material used, multiplied by c_s .

4.6.2. *Wing structural design*

In our previous experiences, we were used to build only wooden wings with traditional beams and ribs structure. But this year we decided to renounce (to the) easy construction of the wing just to be more competitive in terms of performances. We designed a composite wing, made of a polystyrene matrix, covered with thin panels of obece/lime wood. The wing root has been strengthened with the insertion of a 50 cm long glass fiber reinforced plastic beam (see Figure 4.9).

The wing analysis started from the analytic model of beam. The taper of wing was simulated considering two different sections of the beam: the first section is referred to the beam portion extending from the root to 0.7m span; the second is referred to the beam portion extending from 0.7m to tip (the total half wing span is 1.5m). The cover thickness was determined according to the hypothesis it brings the whole bending resistance. The condition of maximum bending load consists in the structural verification the aircraft will undergo before joining the contest: to be lifted by the wing tips. We examined how the stress distribution due to bending changes according the cover thickness. Logically, the largest stresses are localized on the wing root. Set the maximum weight of the aircraft at 150 Newton, a load factor $n = 2$, a fail-safe factor $k = 1.5$ and a half wing weight $W = 5$ Newton, we determined the bending moment working along the half wing; we focused our attention to the wing root section and to the 0.7m span section. The load carrying sections don't match with the geometrical ones, and are described in figure 4.10. Such a configuration describes an initial approximation of the tapered wing; it has minor resistance than the real model as it carries the wing tip section for 0.7m wing span. Final results are shown in figure 4.10.

Preliminary Design

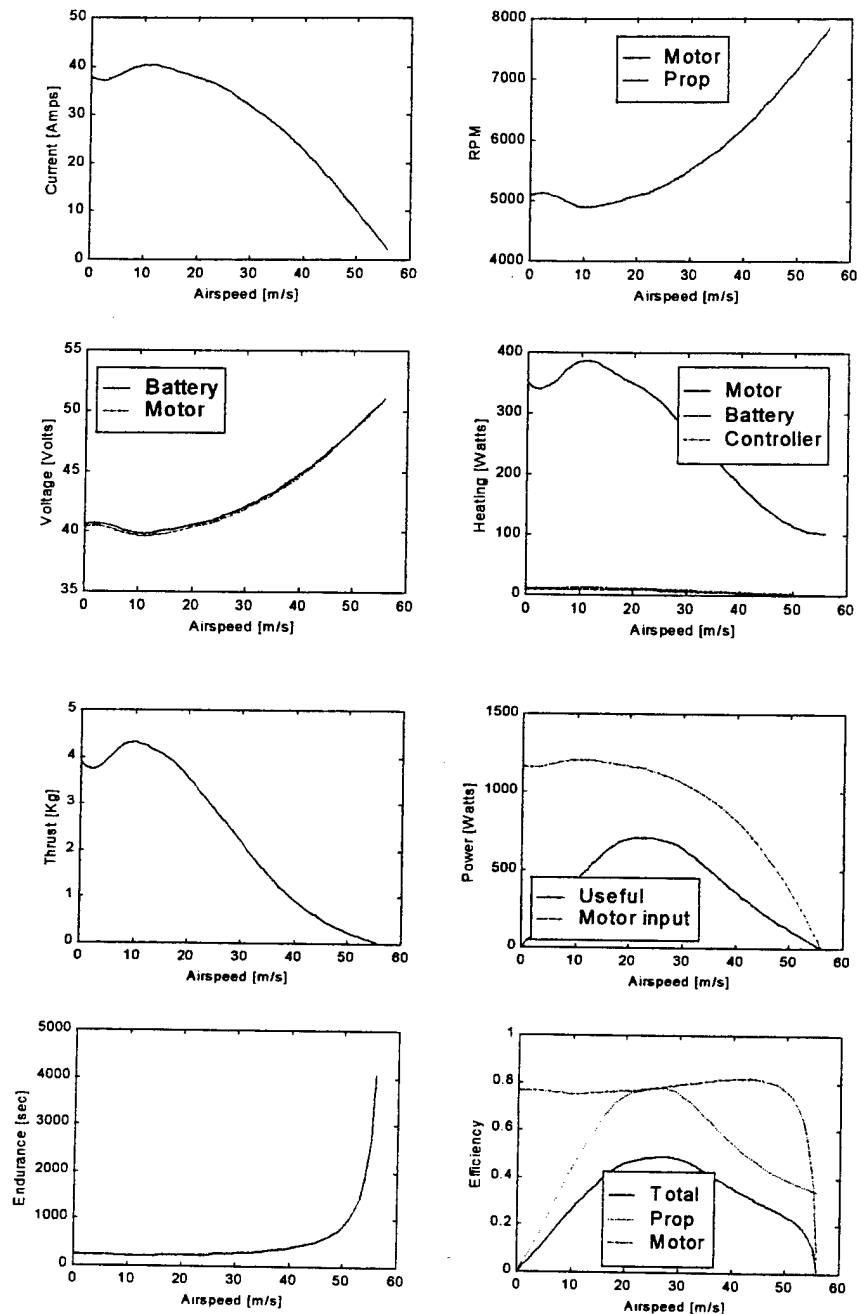


Figure 4. 1 – A ‘MOTOR1’ output – Input data: Graupner3450/7 – Menz 21”x11” – Gear ratio 2.15:1 – 36 x Sanyo2400 NiCd cells – Controller: Astroflight 204D - Throttle setting: 100%

Preliminary Design

'Tennis ball' flight pattern: $3 S + 4 T$ ($S = 300 \text{ m}$)
'Steel' flight pattern: $1 S + 4 T$ ($T = f(\text{speed, load factor})$)

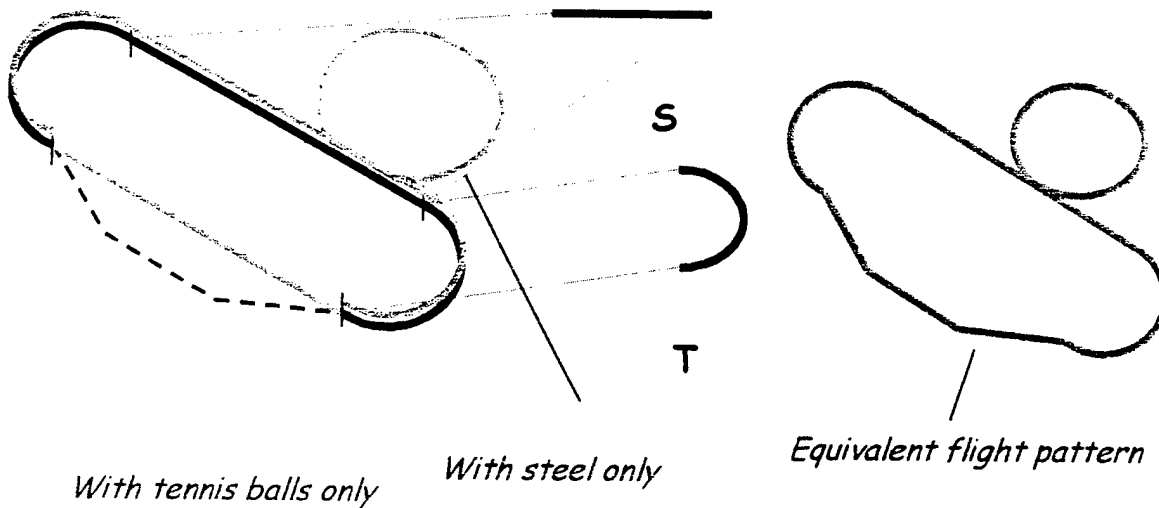


Figure 4. 2 – Assigned and equivalent flight patterns

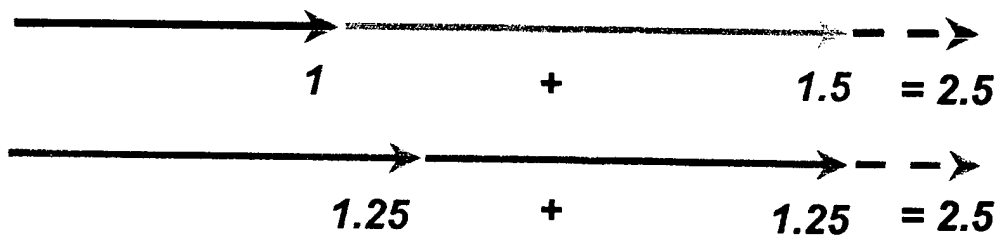


Figure 4.3 – Equivalent flight pattern score

Preliminary Design

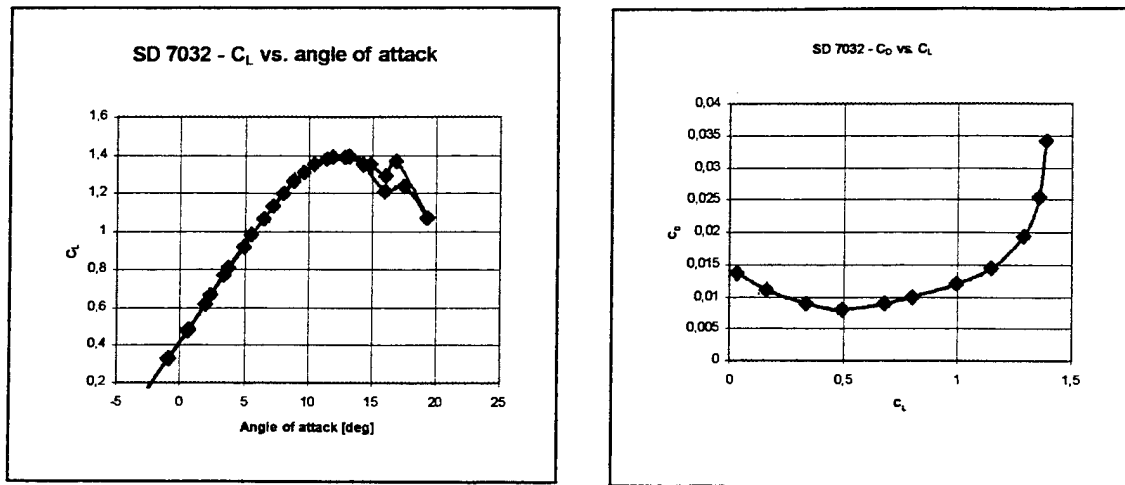


Figure 4. 4 – SD 7032 airfoil characteristics

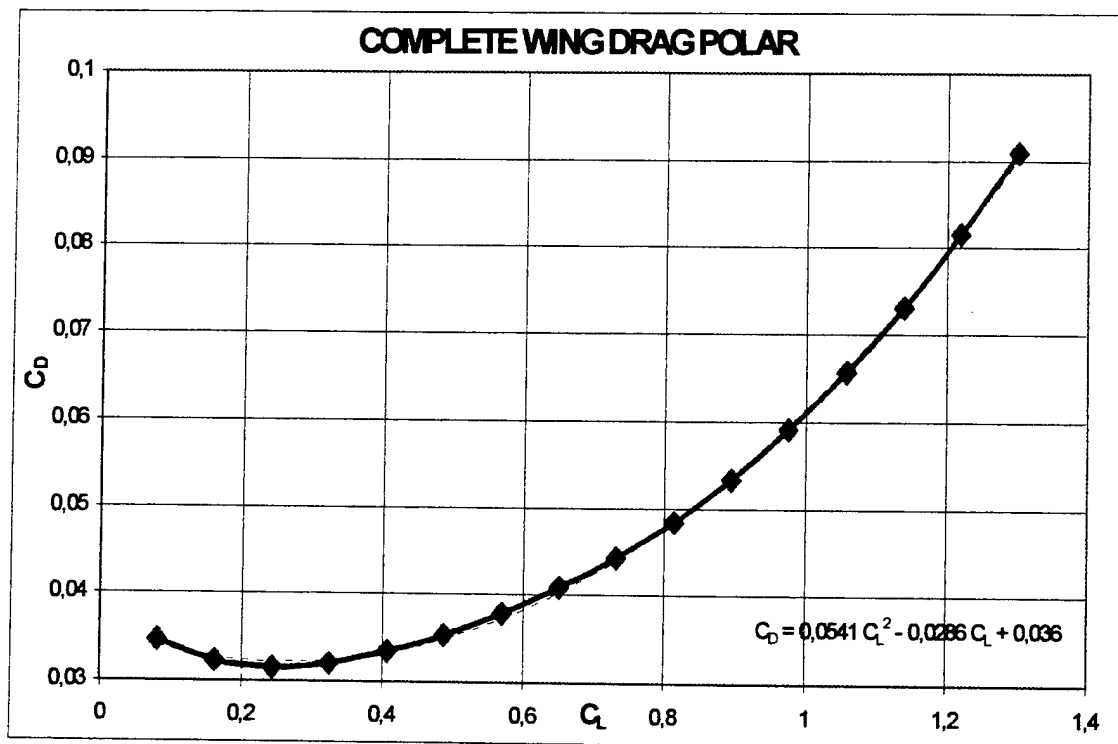


Figure 4. 5 – Complete wing drag polar

Preliminary Design

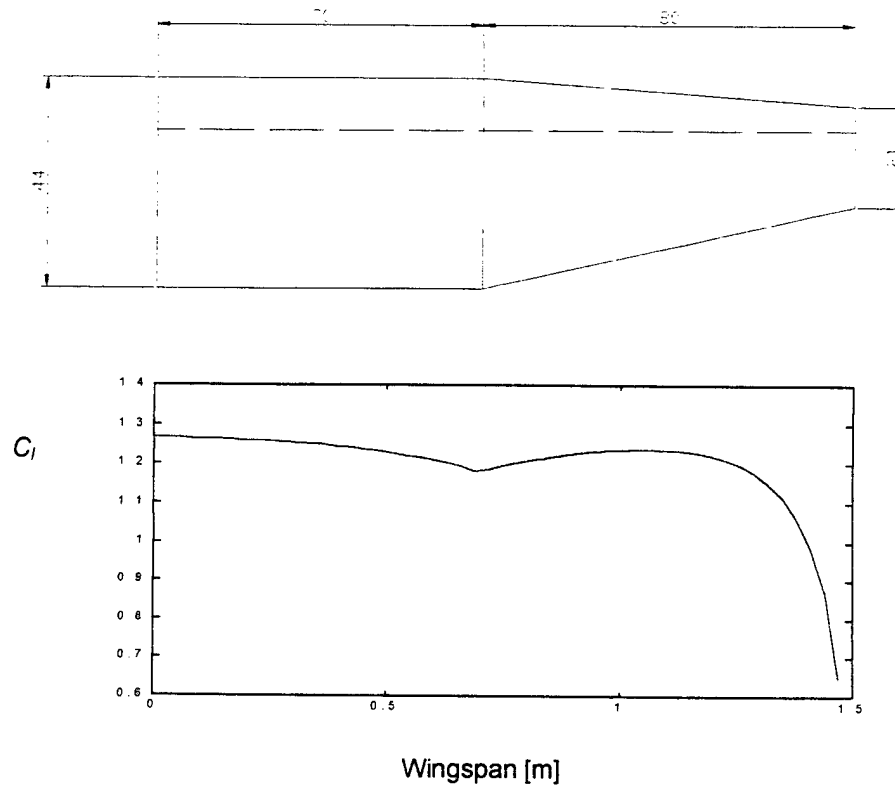


Figure 4.6 – Lift coefficient distribution along the wingspan – AOA = 15°

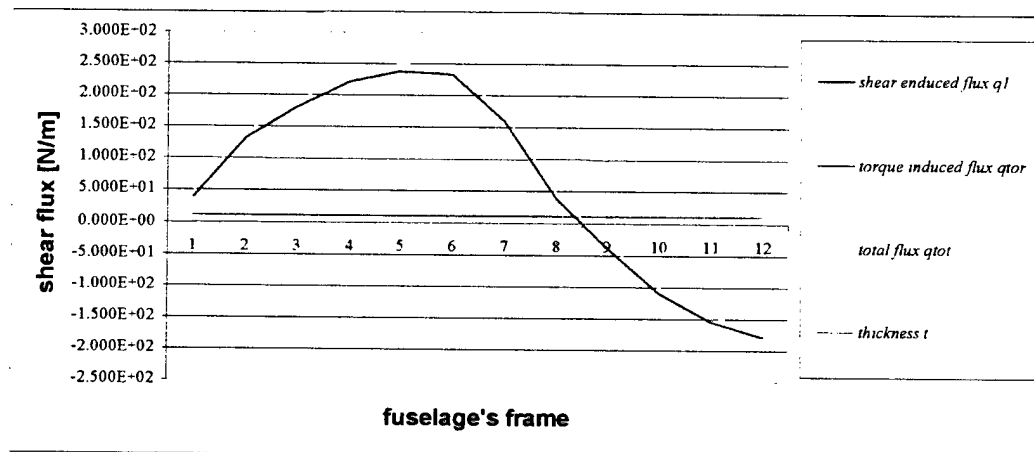
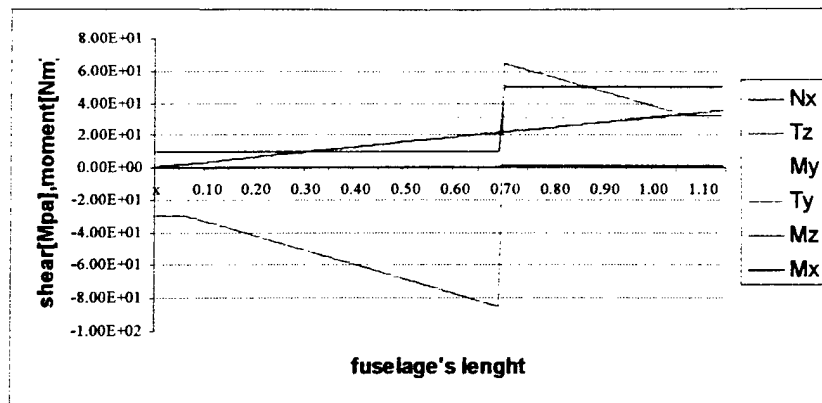
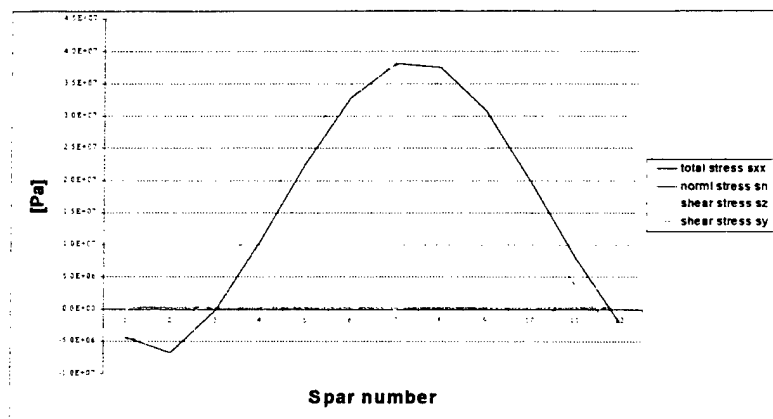


Figure 4.7 – Frames' shear flux

Preliminary Design



a



b

Figure 4. 8 – a) Shears and moments – b) normal and shear stresses

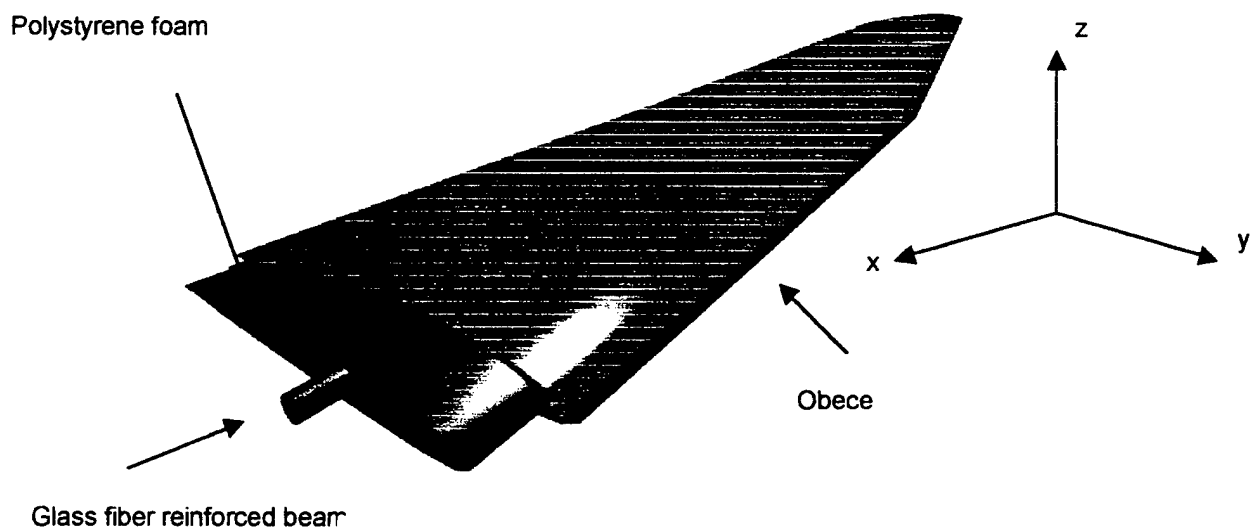
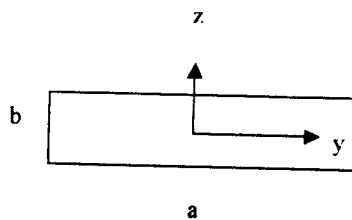
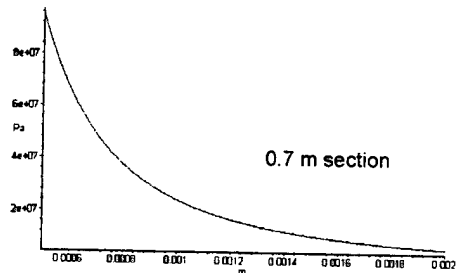
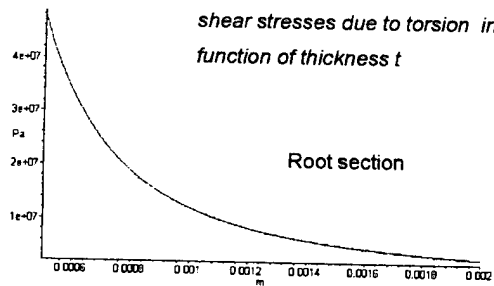
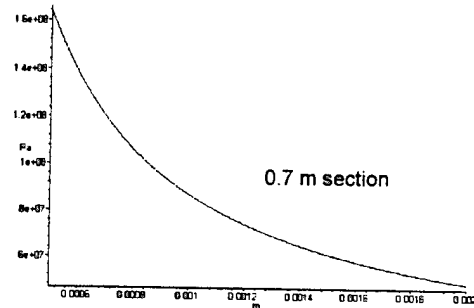
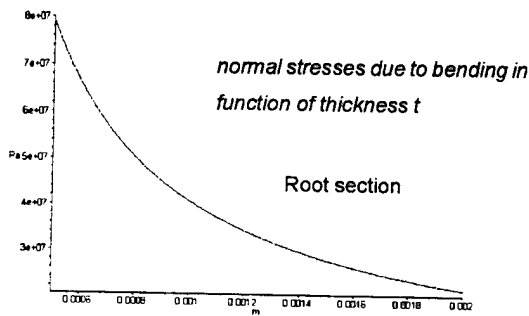
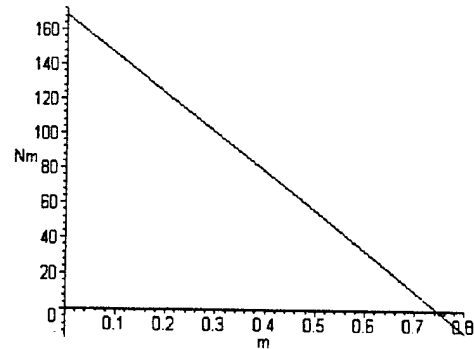
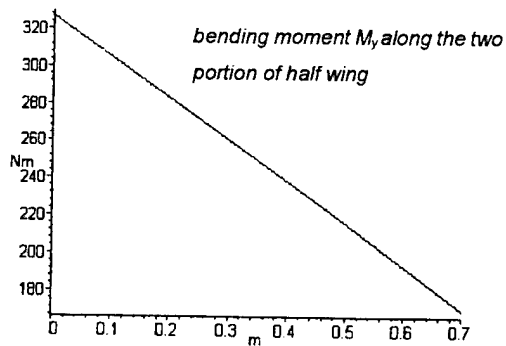


Figure 4.9 – Wing structure

Preliminary Design



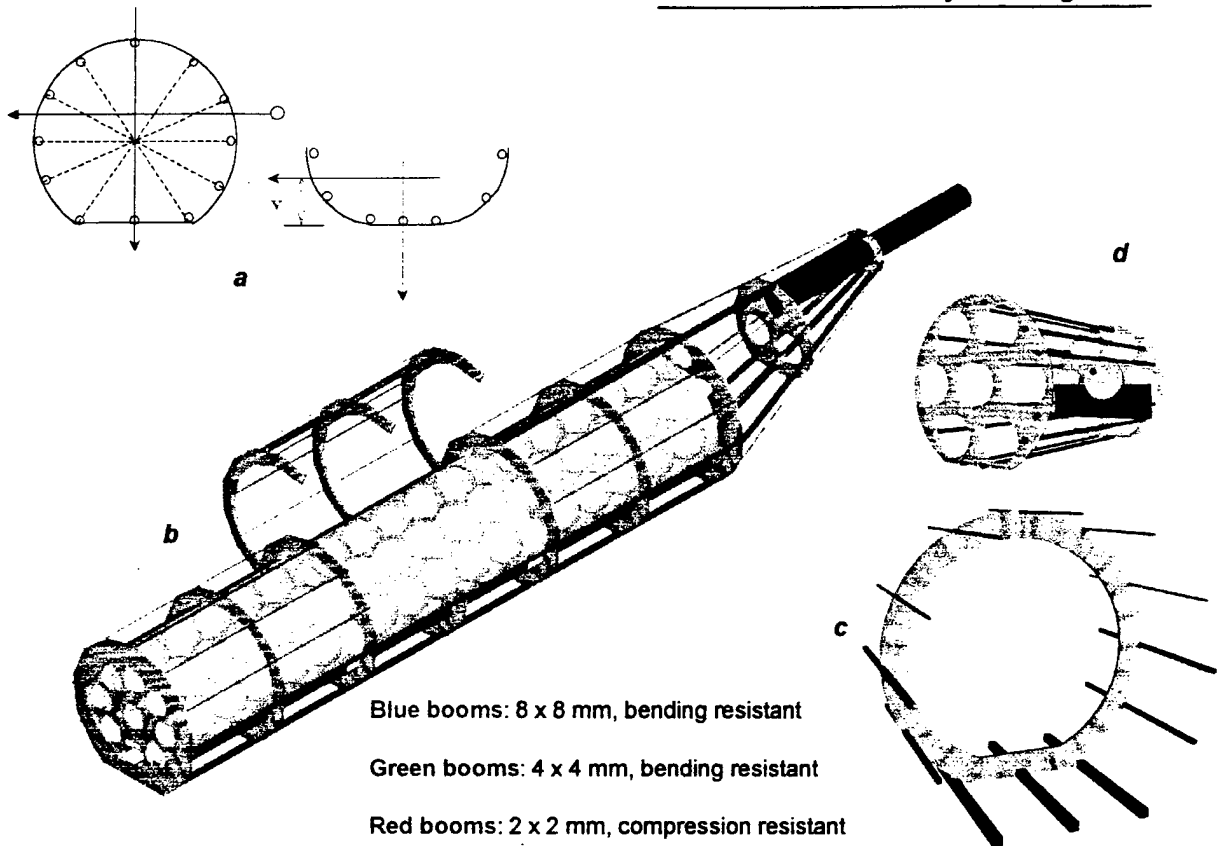
Root section [0.7 m section]

$a = 0.2$ [0.1] m

$b = 0.04$ [0.02] m

bending moment $M_y = 326.45$ [170] Nm

Figure 4.10 – Structural analysis of the wing



**Figure 4. 11 – a) Fuselage section schemes with principal inertia axes - b) fuselage view
– c) frame and spars assembly – d) a container with a steel block locked inside**

5. DETAIL DESIGN

5.1. Introduction

This section shows the results from a number of optimization studies that have driven to the final design; some analyses of the final airplane performances are included as well. Arguments are ordered by the design area they belong to.

5.2. Flight Mechanics

5.2.1. *Wing distance from center of gravity*

The wing may be positioned (on ground) in the longitudinal sense. This allows to correct possible unsatisfying flying qualities and/or performances, since the analytical models used could fail at low Re numbers. Besides, we studied the effects of wing position vs. CG in order to minimize the trim drag. Results are shown in figure 5.1. Trim drag reduction was considered as the main goal to be obtained, but wing excursion toward the nose is limited by a dangerous static margin reduction.

5.2.2. *Refined horizontal tail sizing and positioning*

The horizontal tail was initially positioned at the rearward end of the fuselage, starting just below the vertical tail plane root chord. When the group members studied the effect of wing positioning on trim drag (see above), they decided to increase the static margin, which had been decreased to values about 10%, by both taking the horizontal tail away from the wing downwash and increasing the tail surface and aspect ratio. A series of trade studies have been made, whose final result is a T-tail configuration with horizontal tail surface, $S_h = 0.253 \text{ m}^2$; chord $c_h = 0.23 \text{ m}$ and span, $b_h = 1.10 \text{ m}$. Aspect ratio is 4.78. During the trade studies, an aspect ratio of about 6 had been taken into account, but it was considered to be too high with a dangerous hazard of reduced tail stall angle of attack. A positive effect of T-tail arrangement is the increased effective vertical tail aspect ratio, which allows lesser vertical tail area and weight. Horizontal tail position has been checked by methods found in literature to be properly positioned with respect to the pitch up and deep stall risks. Further analysis will be done by half-model wind-tunnel testing. *Note: on every analysis concerning the static margin, a contribution due to propeller and fuselage has to be added. This contribution has been calculated to be: $\Delta sm_{\text{due to fus}} = -3\%$; $\Delta sm_{\text{due to prop}} = -4\%$.*

5.2.3. *Performances and flying qualities analysis*

The characteristics to be analyzed on the final design stage may be divided into two groups: *performances and flying qualities*. The former group deals with speeds, rate of climb etc. The latter mainly

concerns the airplane dynamic around its center of gravity. The two terms were linked in a self-written flight simulation program, *SIM2*, which integrates the equations of motion. *SIM2* contains an 'autopilot' subroutine in order to track a given flight path. At the actual stage of development, *SIM2* takes into account only the longitudinal dynamics terms (i.e. no turns allowed); in spite of that, it has been useful to refine such things as wing and tail mounting angles and to check the predicted performances. Both the longitudinal and the lateral-directional motions have been studied separately by a classic eigenvalues approach. In this case, the equations of motion have been linearized around the cruise condition at level flight.

The non-dimensional stability derivatives were calculated mainly by using the classic DATCOM methods.

Performances

Required Thrust

The flight mechanics group has studied the airplane performances using the power plant and aerodynamics models given by the propulsion and aerodynamic groups and described into the previous section. Results are shown in figures 5.2 and 5.3.

Curves of figure 5.3 are given with weight (expressed in Newton) as a parameter. One shouldn't be surprised by the lesser drag that the airplane shows at high speed when it is heavily loaded, with respect to a lower weight case. This is due to the combined effect of the wing drag curve and of the trim drag. The mounting angles of wing and horizontal tail are studied in order to have an unloaded horizontal tail in a full payload cruise condition, i.e. $C_{L_{HTAIL}} \cong 0$ at $V = 17$ m/s. At higher flight speeds, say 30 m/s, things change. Look at the following table:

Weight [N]	M_w [Nm]	L_w [N]	L_T [N]	C_{Lw}	C_{Dw}	C_{Lht}
80	-24.65	60.16	19.84	0.128	0.0330	0.142
170	-24.65	158.0	12.00	0.272	0.0316	0.086

Due to the wing drag curve, at low C_{Lw} values (i.e. from 0 to 0.35) the C_{Dw} has a parabolic behavior with a minimum at $C_{Lw} = 0.27$; at lower C_{Lw} values, the smaller the C_{Lw} , the greater the C_{Dw} . Because the C_{Lht} required to trim the airplane results greater at low weights, the horizontal tail induced drag will be higher as well, which makes things worse.

The study of g-load capability has shown that the airplane is able to reach a g-factor equal to 2 (which is the structural limit) between 18,7 and 28,5 m/s. At higher speed the g-factor maximum reachable becomes to decrease. The behavior of the g-factor vs. speed is described in figure 5.2 .

Range/Endurance

Range and endurance performances have been obtained at $V = 17$ m/s, which implies a total drag of about 15.5 N. With these inputs inserted into *Motor1*, the results showed by the figure 5.2 have been obtained. They will be verified during the flight test before the contest, and are expected to vary with the propeller installed.

Take-off run

Results from a numerical simulation of the take-off run are given in figure 5.4. The airplane is assumed to execute the whole take-off run at $C_L = 1.3$, which is on the conservative side since the high induced drag developed in such a condition. Thrust available has been scaled to the 85% over the maximum available, which should allow battery saving at the first take-off at least.

Flying qualities**Longitudinal dynamics**

The following table shows the non-dimensional and the dimensional longitudinal derivatives of our airplane, and the moment of inertia around Y body axes:

$C_{L,\alpha}$	$C_{D,\alpha}$	$C_{M,\alpha}$	$C_{M,\dot{\alpha}}$	$C_{M,q}$
5.2513	0.3571	-1.1851	-4.551	-7.210
Z_α	X_α	M_α	$M_{\dot{\alpha}}$	M_q
-68.23	5.21	-15.66	-0.698	-1.1041
J_y [kg m ²]	6			

The longitudinal dynamic shows the following modes:

Mode	Eigenvalues	Period [sec]
Short period	$-2.9597 \pm 3.4351i$	1.38
Phugoid	$0.0520 \pm 0.7104i$	8.82

The phugoid mode is slightly divergent, but since the about nine seconds period, this is not a problem for a good pilot, and the team has a great pilot ☺!

Lateral-directional dynamics

Detail Design

The following table shows the non-dimensional and the dimensional lateral-directional derivatives of our airplane, and the moment of inertia around X and Z body axes:

$C_{y,\beta}$	$C_{l,\beta}$	$C_{n,\beta}$	$C_{l,p}$	$C_{n,p}$	$C_{l,r}$	$C_{n,r}$
-0.438	-0.1	0.1343	-0.4412	-0.087	0.171	0.1389
Y_β	L_β	N_β	L_p	N_p	L_r	N_r
-15.446	-29.211	15.542	-11.524	0.9	4.4662	-1.4372
J_x [kg m ²]	2.091	J_z [kg m ²]	5.278	J_{xz} [kg m ²]	-0.396	

where: Y = lateral force; L = moment around x-axis; N = moment around z-axis; β = sideslip angle; p = rolling rate; r = yawing rate. *Note: font has been increased to 12 points to improve readability.*

The resulting lateral-directional modes are listed below:

Mode	Eigenvalues	Period [sec]
Dutch roll	$-1.2930 \pm 4.4060i$	1.37
Spiral	0.0643	0
Roll	-11.5128	0

These are satisfying, since roll is highly damped and Dutch roll is damped as well. The slightly divergent spiral mode could become a problem only if the team wouldn't have a great pilot (see above) ☺!

5.3. Structures

5.3.1. Alternative Fuselage

An alternative solution for the fuselage has been considered, which features a truss structure rather than a frames-and-spars one. Total weight should be lower in the first case. To prove this, a structures sub group is building the truss fuselage. Its section is octagonal, which implies a total of ten faces (two front and rear faces plus eight side faces). The number of elements (rods or struts) on each face is $N_e = 2N_n - 3$, where N_n is the number of nodes (see Figure 5.5).

Truss geometry	Rods	Nodes
Front (or rear) face	17	10
Side face	13	8

The resulting structure is then statically determined. Ritter's method has been used in this study in order to find the stresses acting on each rod.

5.3.2. *Wing Finite Element Analysis*

Settled the thickness of the cover we have verified our results by finite elements analysis. We described the structure with laminate elements using *Femap+MscNastran*® programs. We considered materials to be isotropic and homogeneous. The cover is always 1mm thick. The laminate elements are different in thickness to approximate the airfoil: this means that inner matrix thickness changes along the wing span. The load bearing airfoil has a 0,26m long chord at the root and a 0,13m long chord at the tip. The wing root is fixed and the wing tip is loaded with a vertical force of 225N (actually the vertical force consists in the half full aircraft weight: max 80N). The total wing tip translation measure about 8cm. This value, as the whole structure tensional status will be reduced by the presence of the glass reinforced plastic beam. The highest stress value of the cover reaches 13 MPa at the root area, very far from the limit stress of lime wood. The inner polystyrene matrix is almost unloaded as the maximum stress doesn't reach 1 MPa. Results are shown in figure 5.7, along with the first two modes and related pulsations.

5.3.3. *Horizontal tail*

Wooden horizontal tail structure is sized up to carry both flexional and torsional loads. It is based on a single-spar (flexional loads) and D-box (torsional loads) scheme. The tapered, lime-wood-made spar is located at maximum thickness point of the airfoil. The central section is reinforced to allow the vertical tail assemblage (see Figure 5.6).

5.3.4. *Vertical tail*

Vertical tail structure is similar to the horizontal tail one just quoted above. Vertical tail was required to be strengthen since it has to transfer the horizontal tail loads to the fuselage. This matter has been studied by the structural group, which took into account those loads, including the vertical tail tip torque moment induced by asymmetrical additional span loading on the horizontal tail during a roll maneuver. Two small additional carbon fiber spars were inserted into the vertical tail wooden structure mainly to ease the assembly between vertical tail and horizontal tail and between vertical tail and fuselage. The assembly is required to be detachable for transport reasons.

5.3.5. *Forward fuselage section*

The glass fiber and epoxy resin composite nose fuselage section has been statically analyzed and sized up by mean of a finite element model. This model consists of a quadrangular shell element mesh (thickness = 0.001 m) shown in figure 5.8. The nose section transfers to the fuselage the loads given by the power plant actions (thrust, torque) and weight. Maximum torque has been guessed to be 1.5 Nm. The total power plant weight is 30 N. Maximum Von Mises stress and maximum strain are respectively $\sigma_{\max} = 418 \text{ MPa}$ and $\epsilon_{\max} = 9\text{E-}2 \text{ mm}$. Both of them are below the limits of the glass fiber composite used to build this component.

5.3.6. Tail cone

The tapered aft section of the fuselage has been modeled as a beam fixed at one end. The sizing has been made on the smaller tail cone frame, which adds safety to the results. Loads acting on this section are direct aerodynamic loads and the loads transferred to the section from horizontal and vertical tail surfaces. Frames are spaced by 0.19 m and are 4 mm thick.

Tail cone sizing	Spar number								
	1	2	3	4	5	6	7	8	9
Maximum stress [MPa]	7.220	0.306	0.306	5.230	5.970	5.970	5.230	0.306	0.306
Area [m²]	6.4e-5	4.0e-6	4.0e-6	1.6e-5	6.4e-5	6.4e-5	1.6e-5	4.0e-5	4.0e-5

Note: spars are numbered clockwise from upper spar (see Fig 5.9)

5.4. Propulsion

The selected final motor is the *Graupner 3450/7*, geared 2.15:1. Results from bench test obtained with the help from Mr A. Silvagni are given in figure 5.10.

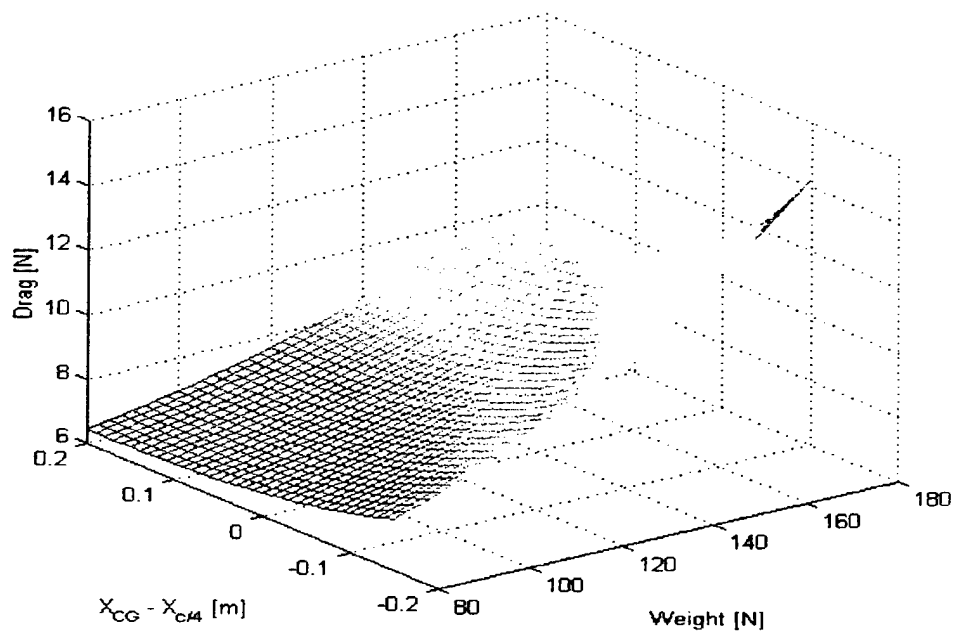


Figure 5.1 – Drag effects due to wing distance from CG

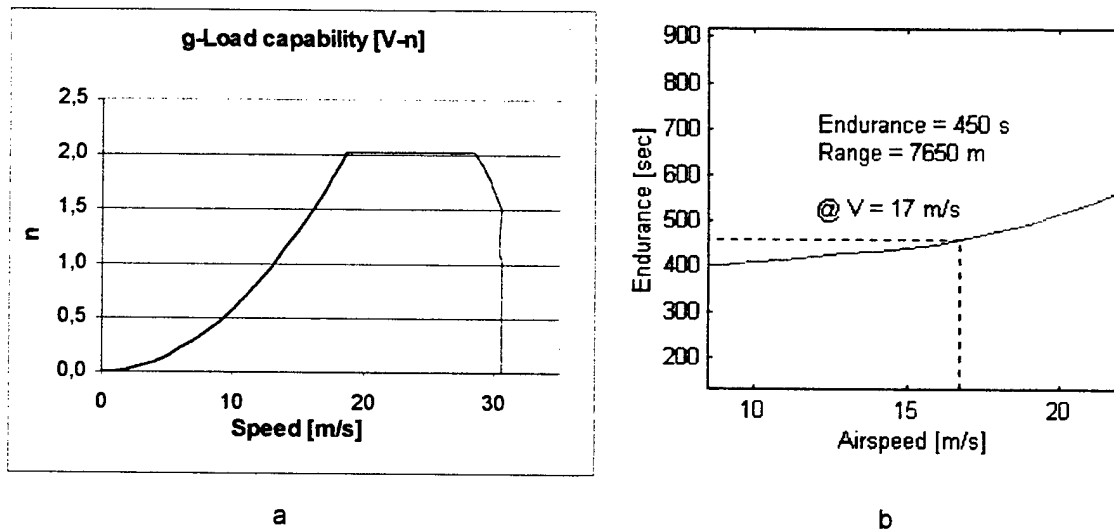


Figure 5.2 – a) G-Load Capability – b) Range & Endurance

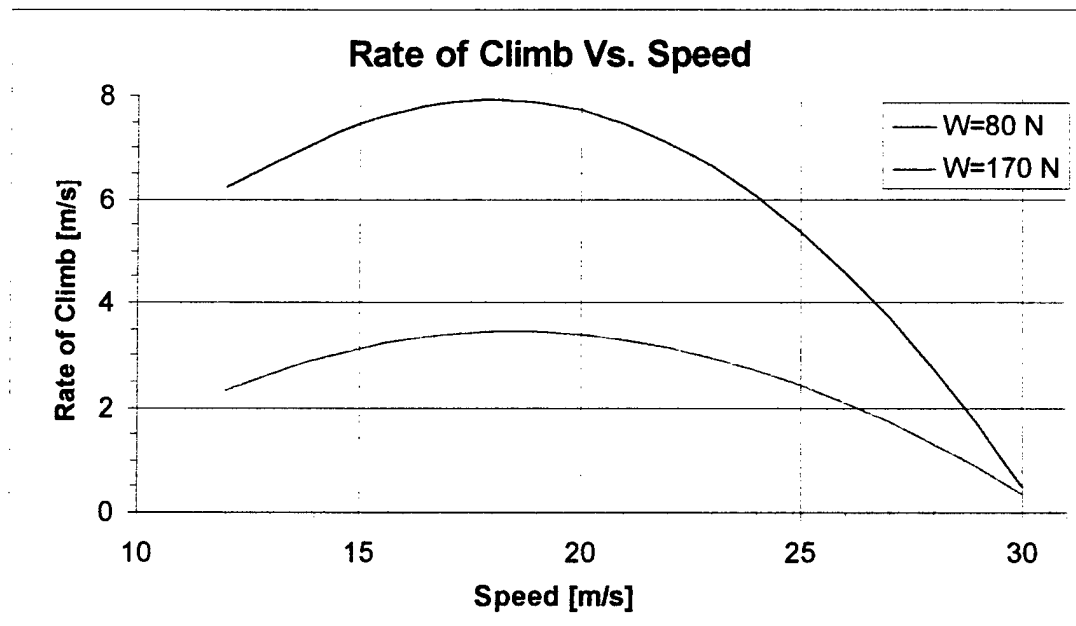
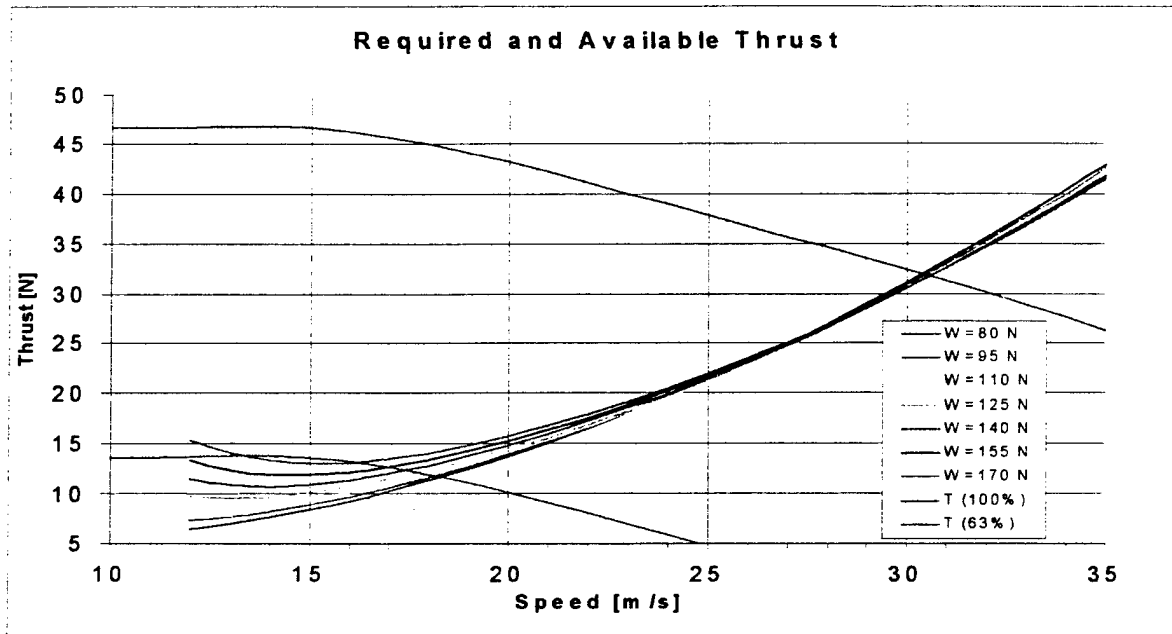


Figure 5. 3 – Airplane Performances

TAKE-OFF ANALYSIS @ Thrust/Maximum Thrust_{|_{V=0}} = 0.85, $C_L = 1.3$

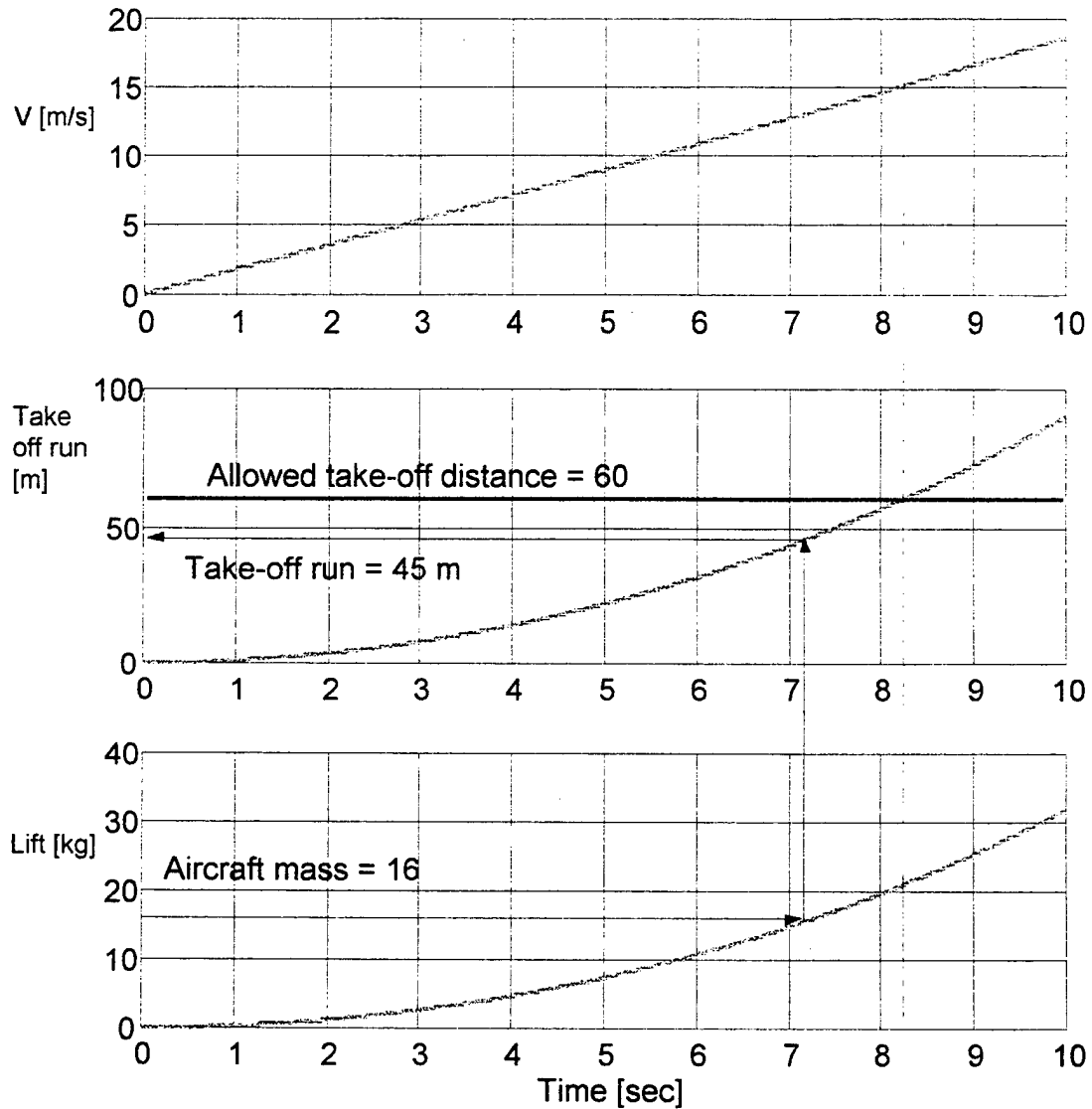


Figure 5.4 – Take-off performances

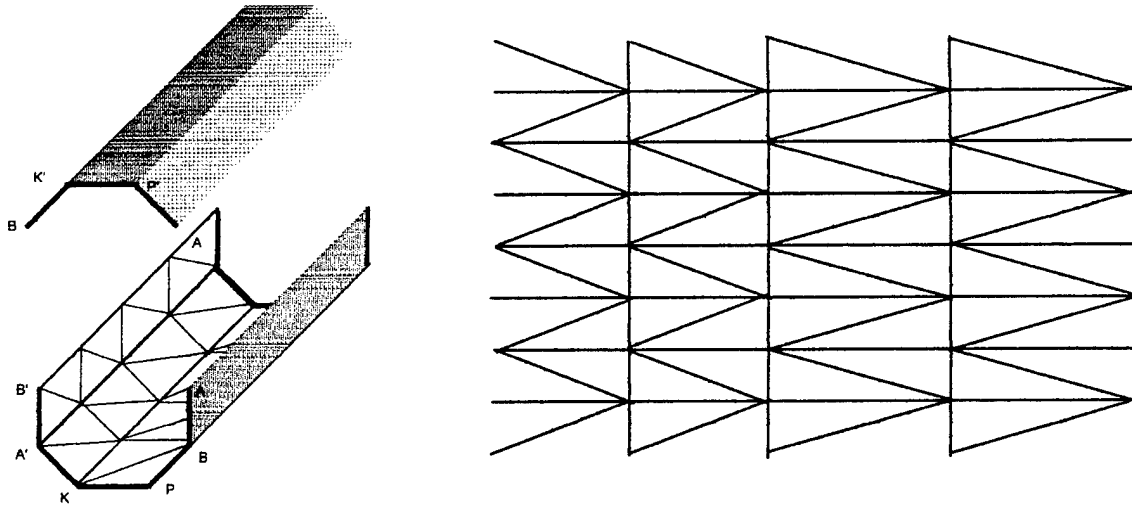


Figure 5.5 – Truss fuselage

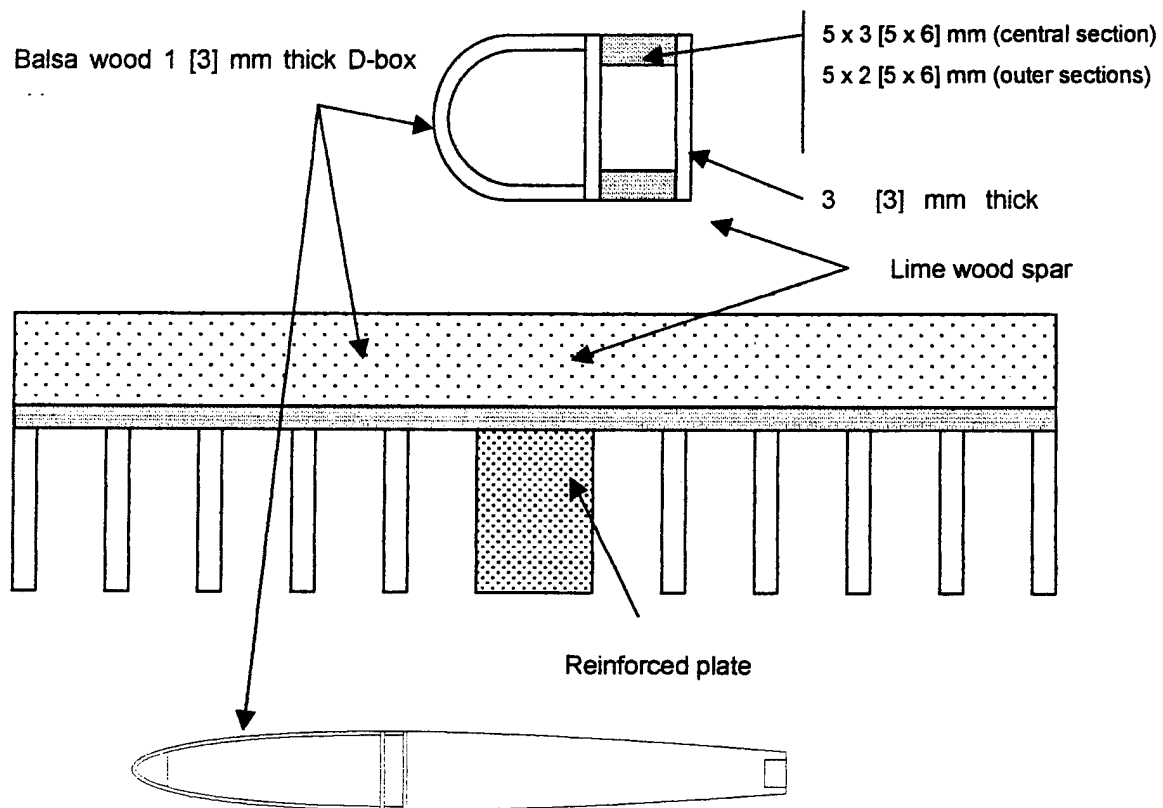


Figure 5.6 – Horizontal and vertical tail structure

(Note: data between [...] are referred to the vertical tail; vertical tail plan form is tapered (see Drawing Package))

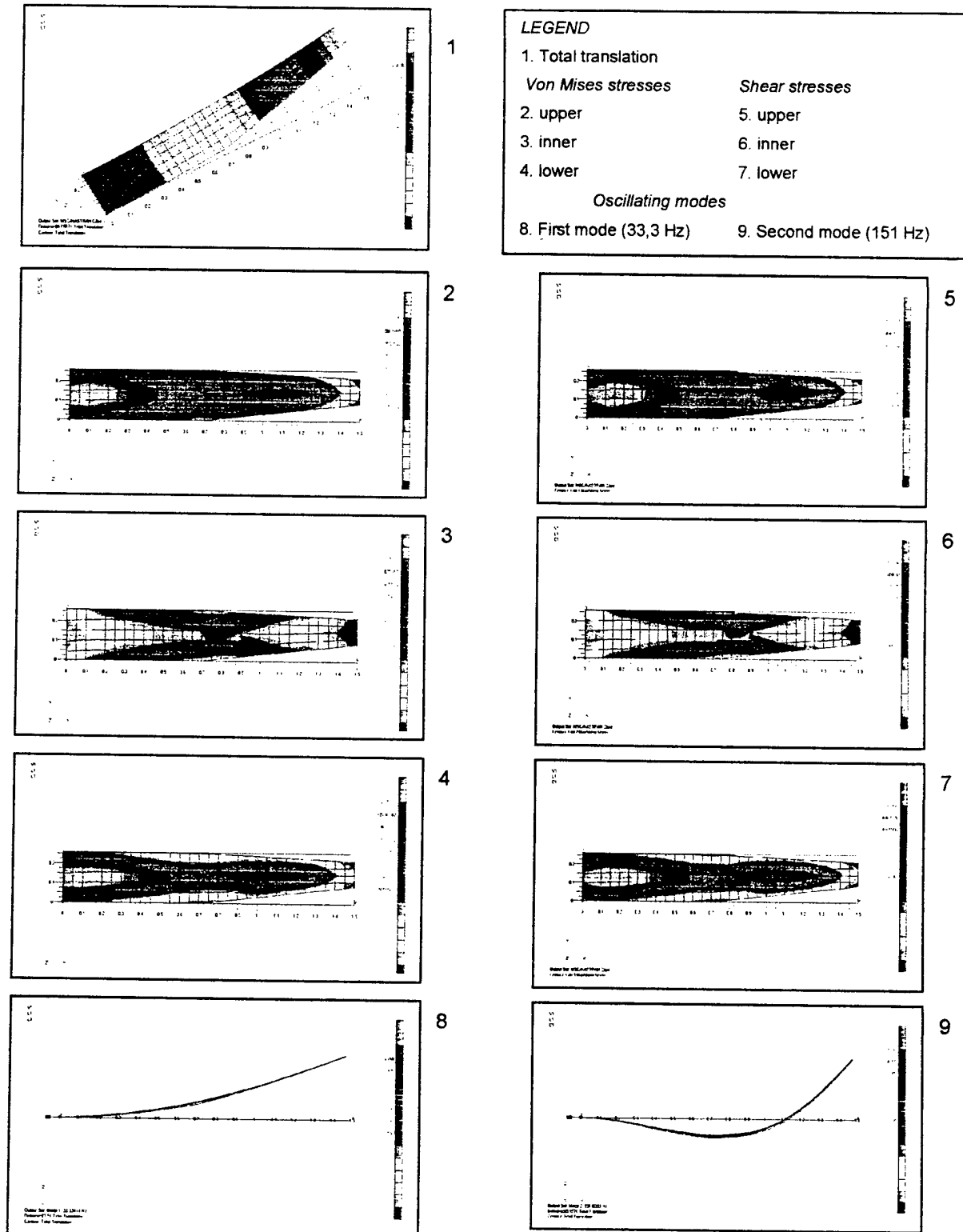


Figure 5.7 – Finite elements analysis of the wing

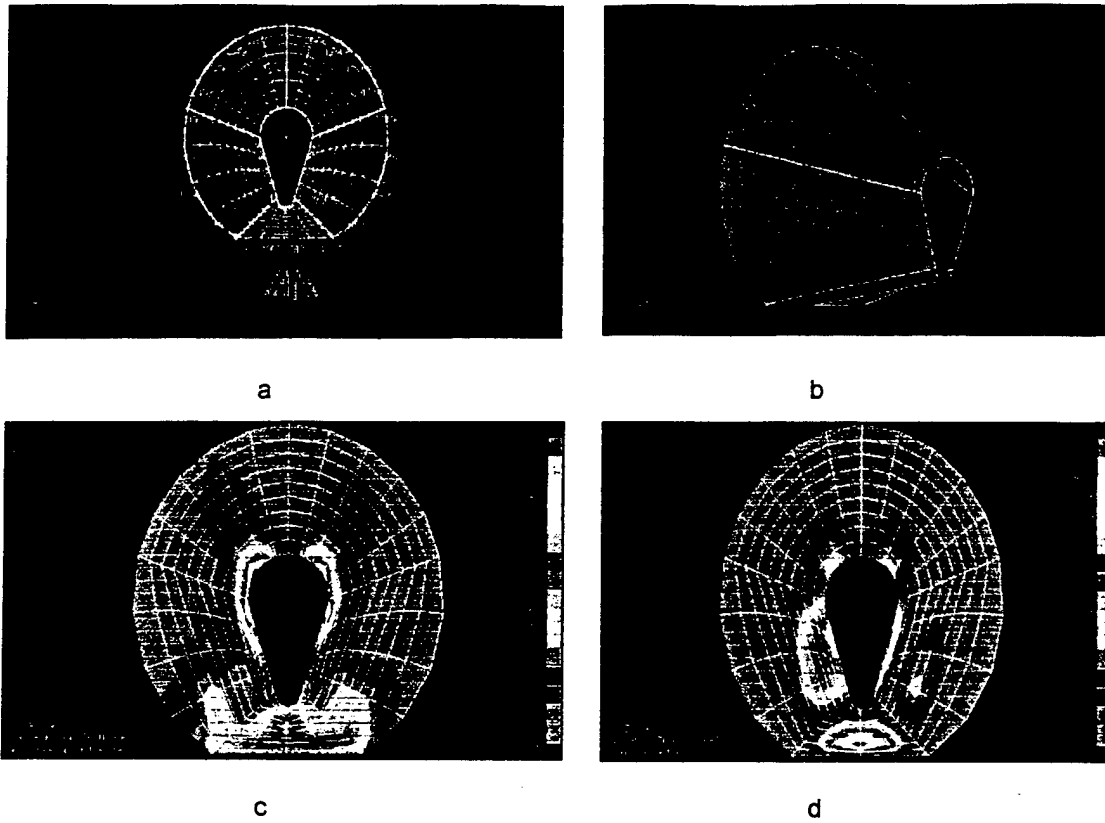


Figure 5.8 – a) nose fuselage section mesh model – b) solid rendering – c) Plate top Von Mises stress – d) Total translation

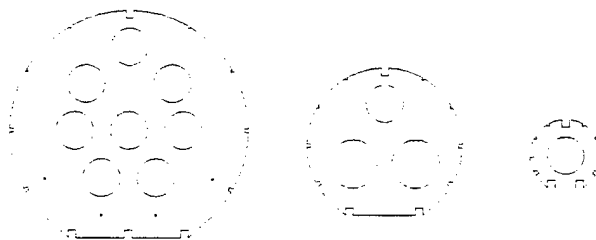


Figure 5.9 – Tail cone frames

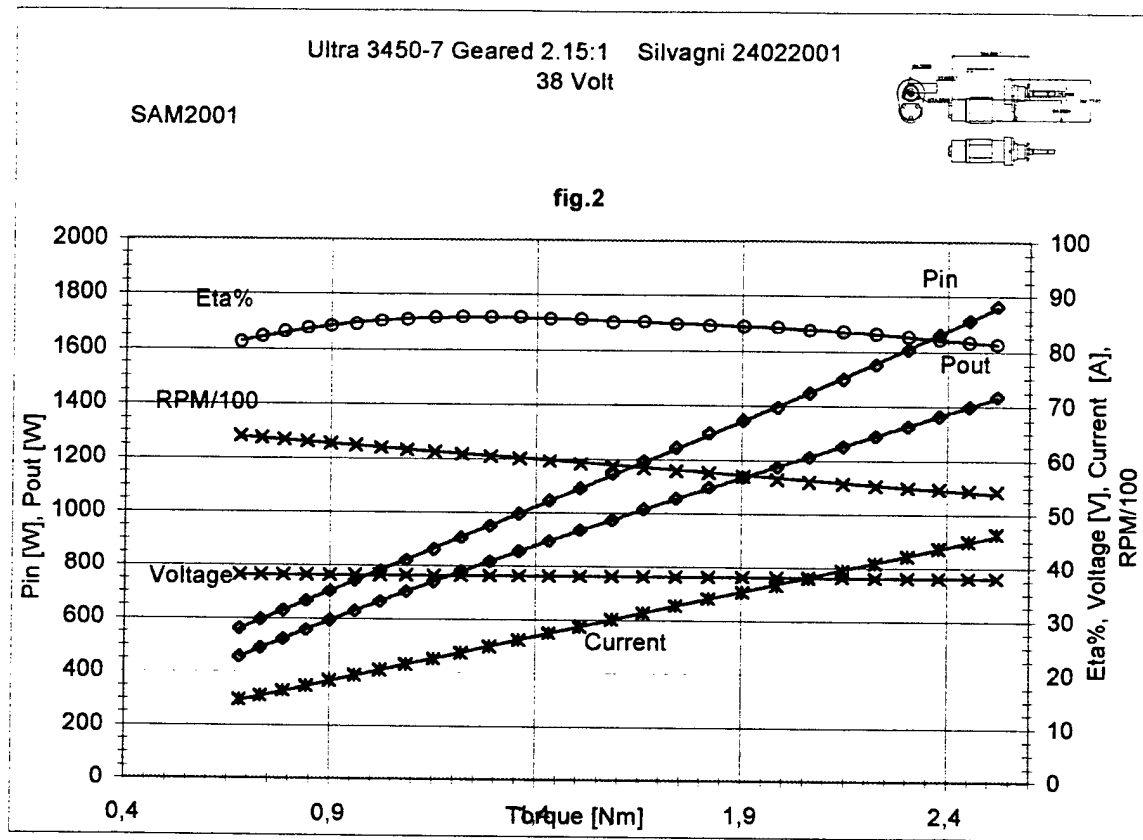


Figure 5.10 – GRAUPNER 3450/7 motor performances (static bench test)

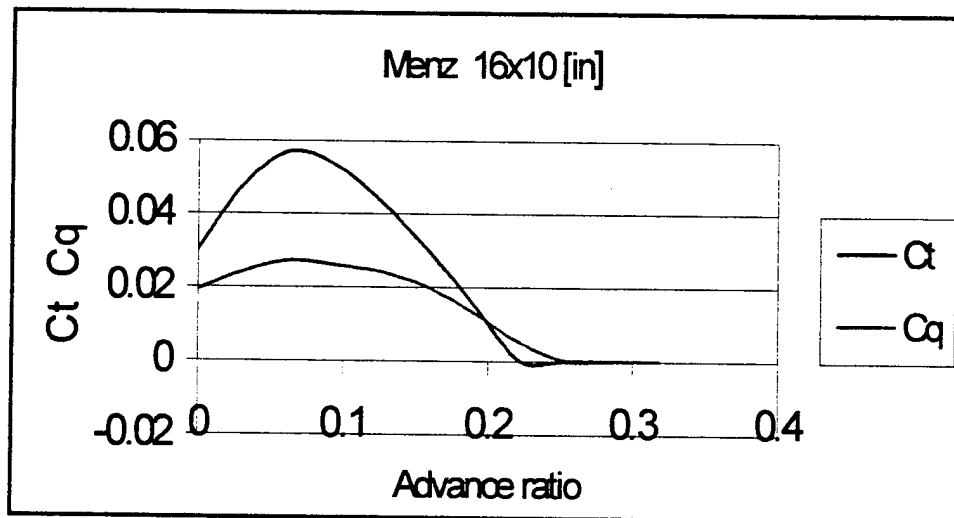


Figure 5.11 – Propeller thrust & torque coefficient curves

6. MANUFACTURING PLAN

The base materials used to construct the airplane are: balsa, ply-wood and lime-tree. These kind of woods are typically used in model aircraft applications; we have appreciated their lightness and fair mechanical characteristics. Besides, they are easy to work and cheap to buy.

The manufacturing process of these materials was made in the laboratory of the "I.T.I.S. Galileo Galilei", using the experience of the last year, where we could test different technology of building.

In this point of view we have used alternative techniques of manufacturing, not conventional structure, tested advanced materials and organized all the person of the DBF Group in a much more rational system to reach a better efficiency.

Advanced materials, as glass and carbon fiber are, were used particularly to build stronger structural critical point, as the connection between wings and body, the connection of the landing gear, and the spars nodes.

The nose section of the engine was made by cold-rolling over a stamp of a 0°-90° glass fiber material.

We have realized a second body with the truss technique, making stronger the nodes with wire of fiber glass, to compare with the classical structure with regular rib and spars.

The most particular technology have been used to build the wing. It consists in a sandwich where the bread is balsa and the meat is polystyrene!

To realize all these different parts with different technology we divided the group in sub-groups, every sub-group realized a part of the model aircraft under the control of a tutor of the manufacturing. Each sub-group has assimilated different know-how, and has studied different technology of manufacturing.

In this way we have written out a calendar to realize the plan, each sub-group have given the time to finish of their own works, so we could make some flight test to confirm the goodness of our choice.

The milestone table, with the division into sub-groups and the scheduled timing is reported in the following page. To this one should add eight more days for the structural and system assembly.



Università degli Studi di Roma "La Sapienza"

Facoltà di Ingegneria

Corso di laurea in Ingegneria Aerospaziale



AIAA/CESNA/ONR Student Design/Build/Fly Competition 2000/2001

DESIGN REPORT

Addendum phase

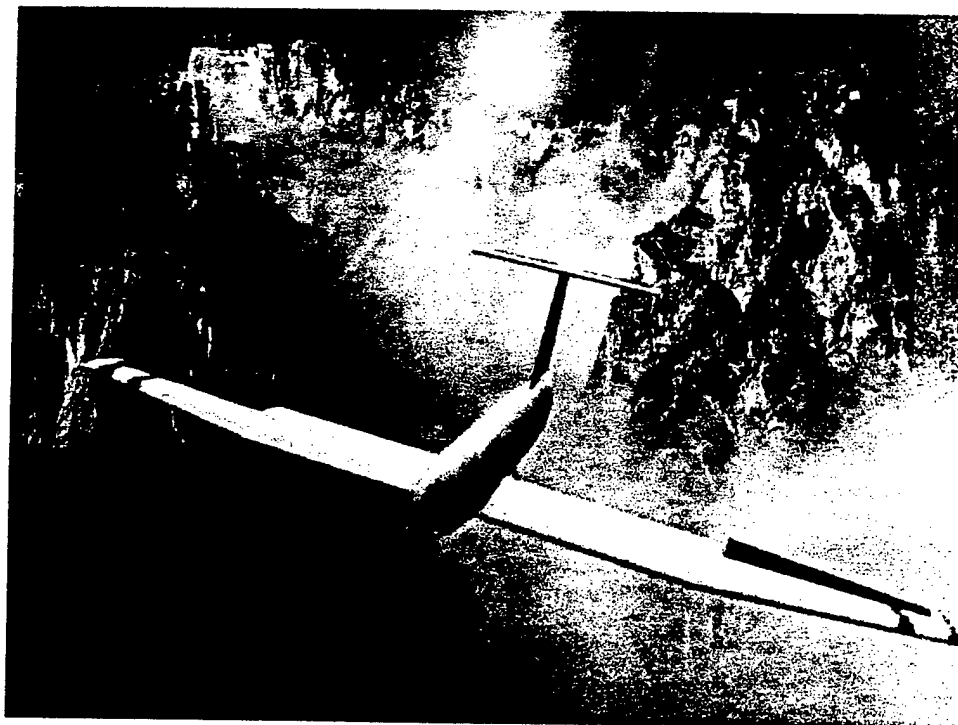


Table of Contents

1. Executive Summary	1
2. Management Summary	3
2.1. Team Architecture	3
3. Conceptual Design	5
3.1. Introduction.....	5
3.2. Airplane Concepts and FOMs.....	5
3.3. Take-off Analysis	9
3.4. Preliminary Airfoil Analysis	10
3.5. Power Plant Analysis	10
3.6. Final Results	11
4. Preliminary Design	13
4.1. Introduction.....	13
4.2. Analytical Aerodynamic and Power Plant Models	13
4.3. Mission Assignment.....	17
4.4. Optimization Algorithm and SIM1 Description.....	19
4.5. Wing Analysis, Airfoil Selection and Surfaces Sizing	21
4.6. Structural Design	24
5. Detail Design.....	34
5.1. Introduction.....	34
5.2. Fight Mechanics	34
5.3. Structures	37
5.4. Propulsion	39
6. Manufacturing Plan	47
7. Lessons Learned.....	50
7.1. Introduction.....	50
7.2. Wing	50
7.3. Fuselage.....	50
7.4. Empenage	51
7.5. Speed loaders	51
7.6. Wind tunnel tests	51
8. Aircraft Cost	57
8.1. Calculation of the coefficients	57

7. LESSONS LEARNED

7.1. Introduction

Since the Proposal Phase the project have had several changes which interested many parts of the airplane. All the changes were thought during the manufacturing process when new problems, unknown in the design phase, rose up. We noticed that the weight evaluation of final aircraft has been sufficiently correct, contrary to the time scheduling. The major lesson we have learned is to improve information sharing between groups. In fact, each group has worked without considering as primary objective to let their results be immediately accessible by other groups. It has caused an unhappy growing of manufacturing time.

7.2. Wing

At the beginning the wing has been designed with an obece cover 1 mm thick, but the following structural analysis brought us to halve the thickness of the cover in the attempt to save weight (guaranteeing the structural resistance). It was needed to save weight because, for evident delivery necessities, the wing has been split into three sections. Then several reinforcements were needed, to guarantee the structural continuity of the assembled wing, with the following final weight increasing (*see figure 7.1*).

The three wing portions are: the central segment, which represents the rectangular part of the wing and is fixed to the flat bottom of the fuselage with four nylon screws, with a span of 1.4 m and a chord of 0.44 m; the two tip sections 0.8 m long, with a 5° dihedral and tapered till 0.21 m.

The reinforcements are two beams which cross the central section and on it are linked the other two sections of the wing. The main beam is made of lime, has a rectangular cross section (0.5 x 4 cm) and it is located in the maximum thickness of the airfoil. The dihedral angle for the tip section is guaranteed by the shape of the extremities of the beam. The secondary beam is placed 8 cm behind the main one. It is a carbon tube with a diameter of 1 cm and is drown in the polystyrene.

A delicate problem rose up for the presence of the main beam: high bending moment on the wing would break the cover of the wing near the junction of wing portions. So we have decided to reinforce these parts of the cover with a single layer of glass fiber.

We have modified also the aerodynamics of the wing; to gain lift during the take off run, and to save cells' power, two flaps have been added in the rectangular part of the wing. (*see figure 7.2*). All this changes have raised the Rated Aircraft Cost (we add 2 servos for the flaps and so 2 new control surfaces) and extended the manufacturing time.

7.3. Fuselage.

Little changes have involved the fuselage. On the bottom of the cargo bay we have placed a 0.3 mm thick sheet of layered wood to let the speed loaders slip more easily into the fuselage.

To improve the cooling of the brushes of the engine, a glass fiber duct from the air inlet in the nose has been shaped.

7.4. Empenage.

The link between the vertical surface and the large (1.1 m span) horizontal one has been reinforced using on each part a coat of glass fiber.

7.5. Speed loaders.

Wood made speed loaders have revealed to be laborious to build; in fact it takes up to 30 pieces to assembly a single one. Furthermore they request great attention and time to fulfill a load/unload cycle. So we have considered to design a new configuration of speed loaders using glass fiber. They consist in a single cylindrical piece with an opening to permit cargo loading/unloading (see figure 7.3). The new speed loaders have the same weight of the wooden ones (about 130 g.) but they have increased the easiness of loading operations. Problems have raised for fixing the steel bars, so because of we are not sure of the correctness of the system arranged to fix the heavy payload we are going to bring both speed loaders configuration, and we will choose the right one after judges clearance. The price of this alternative solution has been two days of working.

7.6. Wind tunnel tests

After several efforts, we have gained access to the wind tunnel of our faculty.

Since we had short time, also to leave the tunnel for the didactic activity, we limit our tests to two models:

1. A section of wing with a chord of 44 cm (like the root of the actual wing) and a span of 50 cm, with a mobile surface. Thanks to it, we can verify the profile polar we had and the flap theory we used to size the ailerons and the equilibrator.
2. A complete half-model, i.e. a model of the whole airplane, split up by its plane of symmetry. With this model we should valuate the interaction among the parts of the airframe (wing, fuselage, tail planes) and have the confirm of our choice for the position of the tail horizontal plane (high or low). The model is 1:3 scale, so to work near the dynamic similitude at a wind speed of about 40 m/s (the maximum operative speed of the tunnel) and remain in the part of the section where the flow is nearly uniform, (section of about 70 cm in diameter). The model is 50 cm wide a 70 cm long.

For the tests on the section of wing (whose span is 50 cm) two "screen" at the tips are needed, to have a flow as bidimensional as possible. One screen will be used also for the tests on the half-model, to achieve the symmetry condition.

The models are mainly made of wood, with reinforces in aluminum, plastic and glass fiber. There are also weights to make the models more stable in the airflow at the higher speeds. Anyway the total weight should be about 3.5 kg, not to exceed the maximum carrying capacity of the balance (5 kg).

In the first day we have spent at the tunnel we have calibrated the balance, i.e. we have weighted note masses to find the constants of the linear law that link the output voltage with the load. Then we mounted the section of wing without the screens and made some measurements at various AOA and various flap deflections. With the data collected we have made the two graphics in fig. 7.4. It's evident the low value of the slope of the lift curve (about 1.7) due to the low aspect ratio (about 1!).

The next day we have mounted the screens and made other tests on the airfoil, the results are shown in figure 7.5. As we expected the lift slope was increased arriving to the value 2.3. The increase is so low perhaps due to a non-perfect effectiveness of the tip screens. The high stall angle (near 20°) and the low value of the lift coefficient were probably caused by the roughness of the surface that forces the flow to be turbulent also at low Reynolds number. In fact we have had problem applying the plastic cover, which wasn't perfectly smooth. It is to be noticed that the polar curve from our data is very similar to the one supplied by Selig.

From the data we collect we can also find the value of the flap efficiency $\tau = \frac{d\alpha_{aero}}{d\delta}$, i.e. the rotation of the zero lift line per flap deflection. The actual value (about 0.5) is very near the theoretical one we used to size the mobile surfaces of the airplane.

We have tested models with two different tail surfaces arrangements: conventional, with low horizontal surface, and "T" configuration, with the horizontal surface on the tip of the vertical one.

The results are shown in figure 7.6, and display that the T arrangement, which we selected, brings to a little resistance decrease, which don't justify the increase of the structural manufacturing complexity, but is also to notice that the T configuration lead the horizontal surface out from the wing's wake, increasing the overall efficiency of the aircraft.

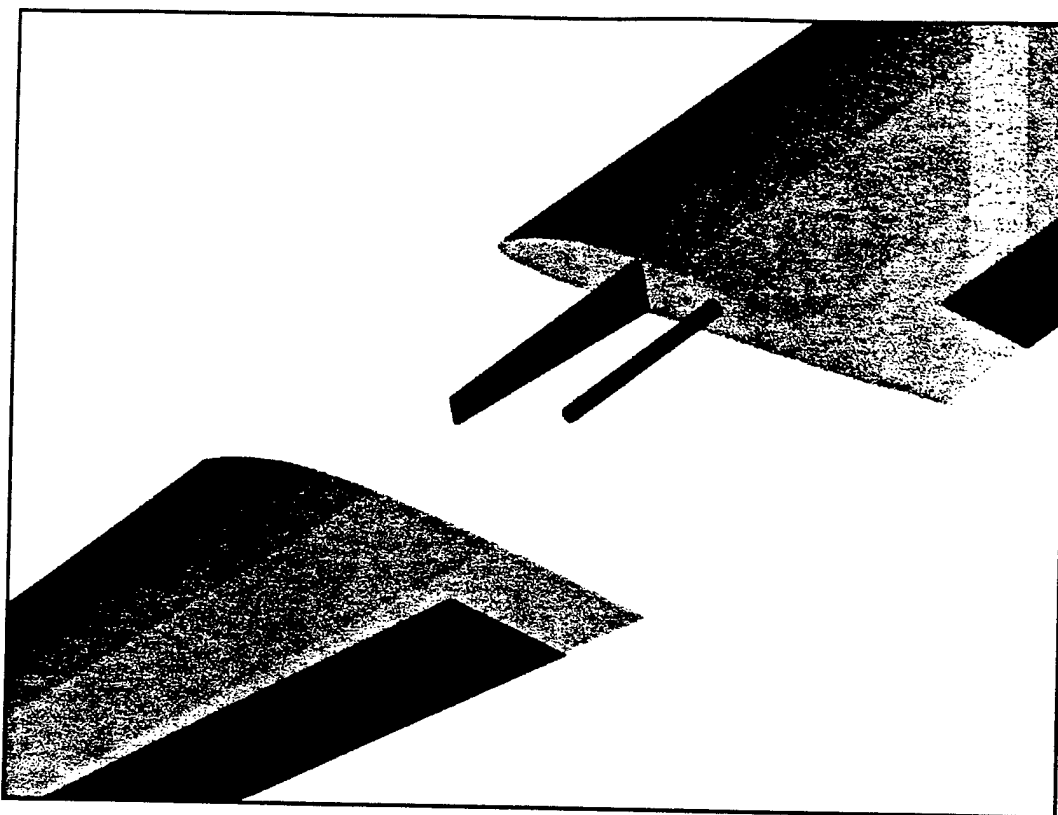


Figure 7.1 – Wing junction particular

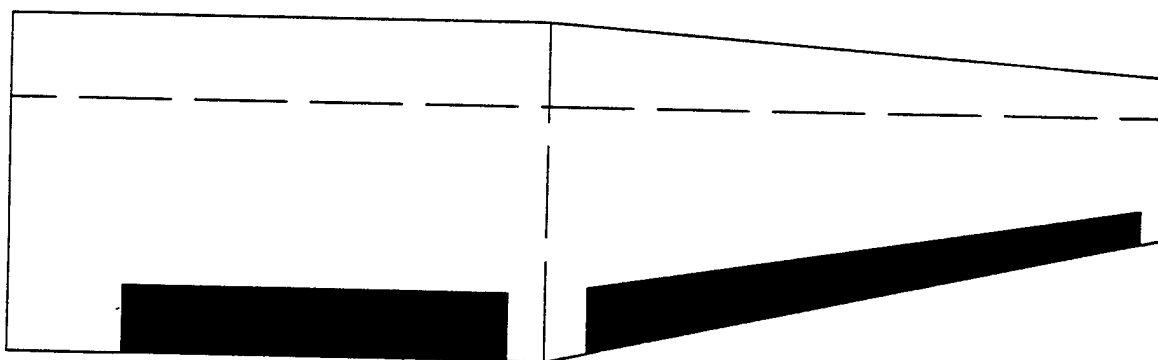


Figure 7.2 – Half wing control surfaces

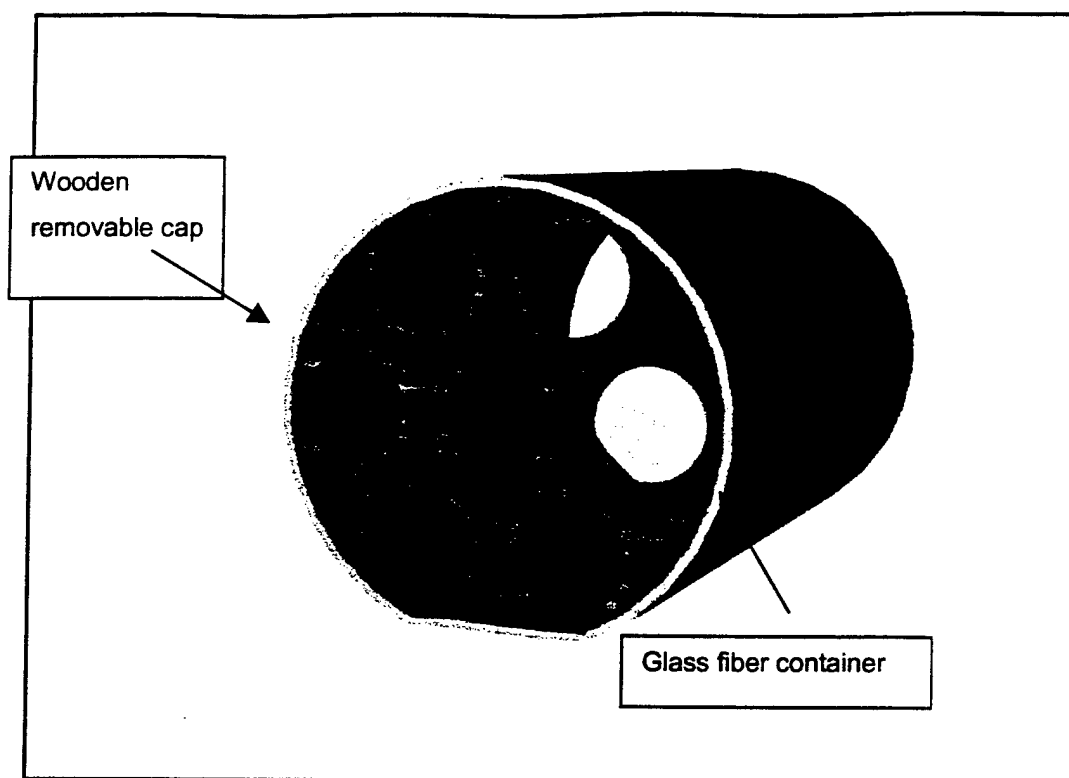


Figure 7.3-Glass fiber speed loader

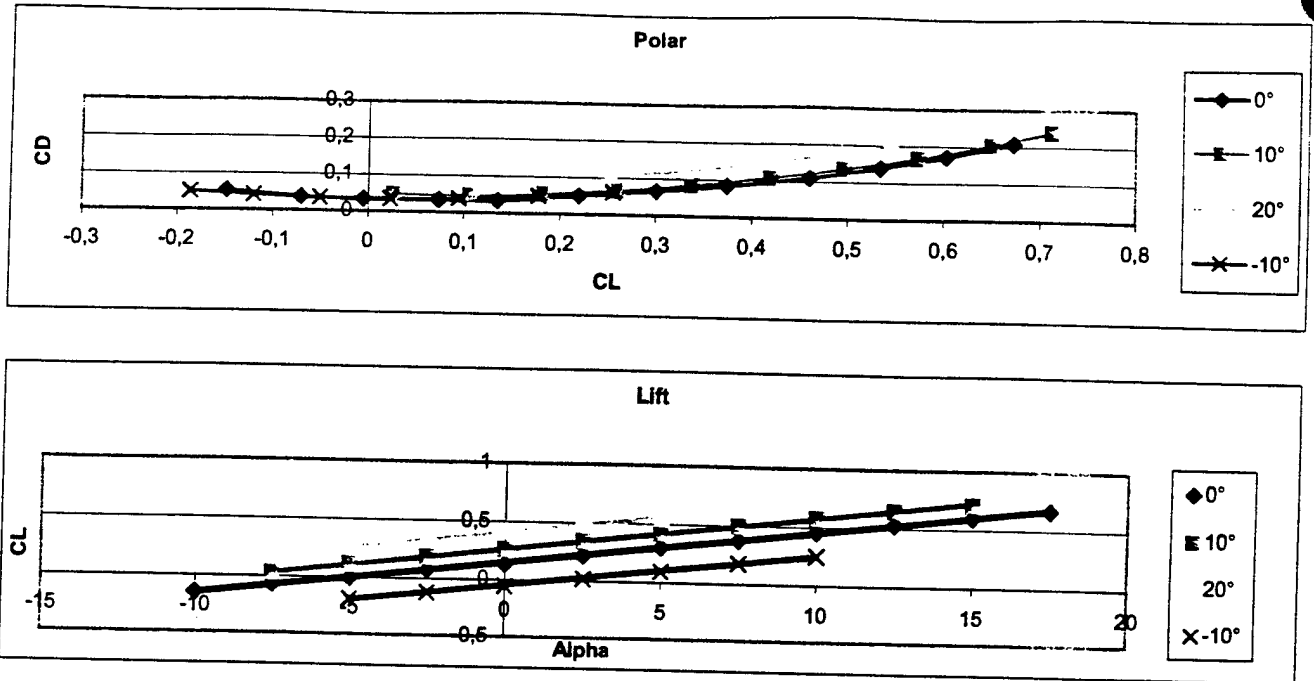


Figure 7.4-Results of wind tunnel test of the portion of wing without screens

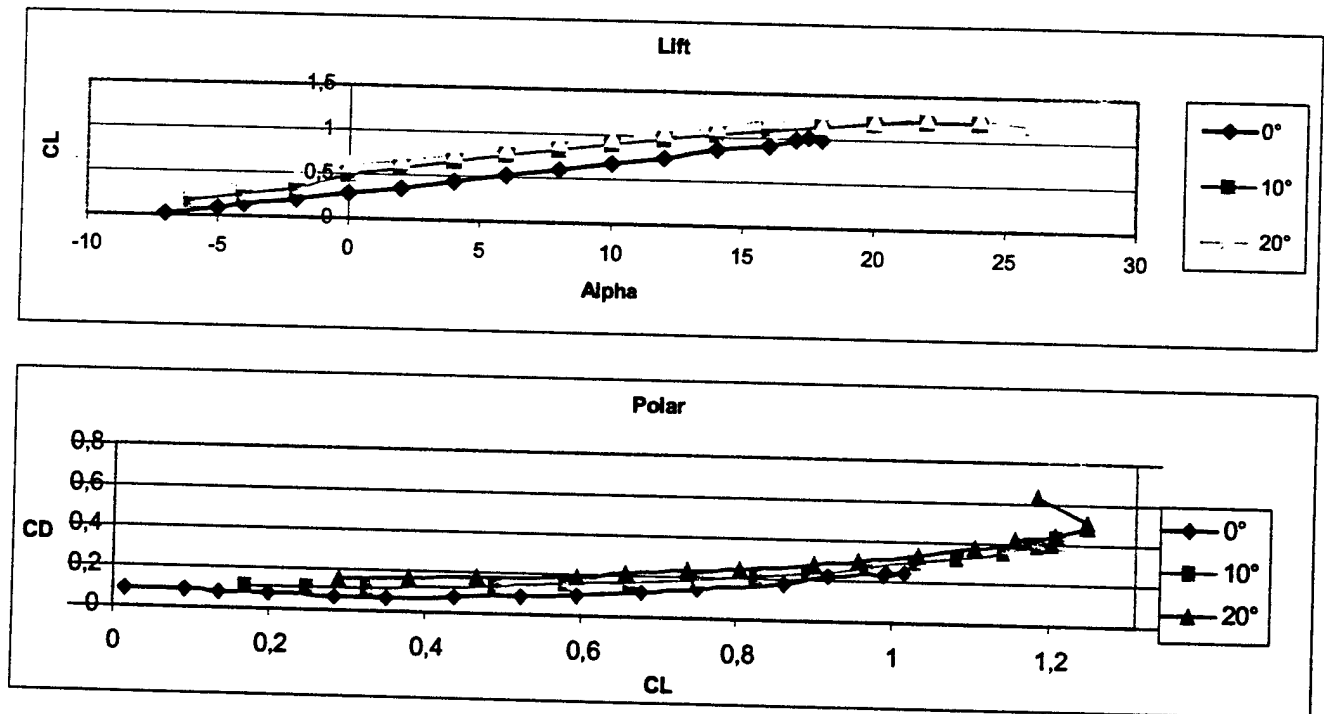


Figure 7.5- Results of wind tunnel test of the portion of wing with screens

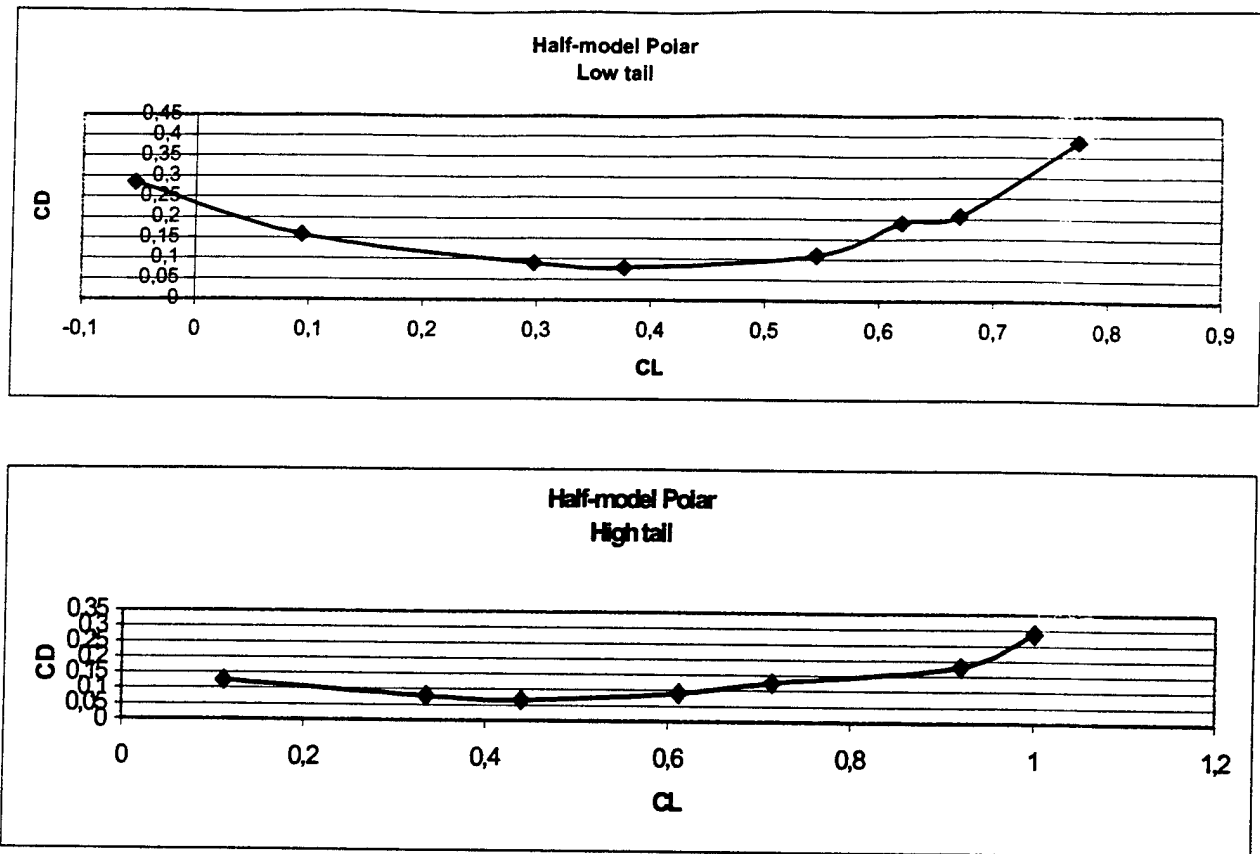


Figure 7.6-Low and high tail polar comparison

8. AIRCRAFT COST

Is to be considered that a big airplane brings more payload than a small one, and then it should earn a higher Total Flight Score. To penalize the big airplanes and so put into evidence the global efficiency of the project (under the points of view of the structural and the aerodynamic design, of the flight mechanics and the payload dealing) has been introduced the Rated Aircraft Cost (R.A.C.) that, being proportional to the weight and the length of the airplane, to the power of the propulsion system and to the complexity of the architecture, tends to lower the final score of the bigger or more complex airplanes.

The Rated Aircraft Cost provides an estimation of money (thousands \$) needed to build the model. It's very important to minimize this value considering that it affects the score according to the formula:

$$\text{SCORE} = \frac{\text{Written Report Score} * \text{Total Flight Score}}{\text{Rated Aircraft Cost}}$$

The R.A.C. consists in this simple expression

$$\text{R.A.C.} (\$ \text{ Thousands}) = \frac{A \times \text{MEW} + B \times \text{REP} + C \times \text{MFHR}}{1000}$$

8.1. Calculation of the coefficients

A (Manufacturers Empty Weight multiplier)

\$100/lb.

B (Rated Engine Power multiplier)

\$1/watt

C (Manufacturing Cost multiplier)

\$20/hour

MEW (Manufacturers Empty Weight)

16.97 lb.

REP (Rated Engine Power)	# of engines	1	1776 watts
	Amp	40	
	# of cells	37	

Aircraft cost

(Work Break Structure)

WBS	Wing	# of wings	1	75.64 hours
		Projected area	12,16 sq. ft.	
		# of struts or braces	0	
		# of control surfaces	4	
	Fuselage	# of body	1	31.9 hours
		Length	6,72 ft.	
	Empenage	# of vertical surfaces	1	20 hours
		# of horizontal surfaces	1	
	Flight Systems	# of servos or controllers	8	21 hours
	Propulsion Systems	# of engines	1	10 hours
		# of propellers or fans	1	

MFHR (Manufacturing Man Hours)

158.54 hours

The resultant R.A.C. of the aircraft is:

R.A.C. (Rated Aircraft Cost)

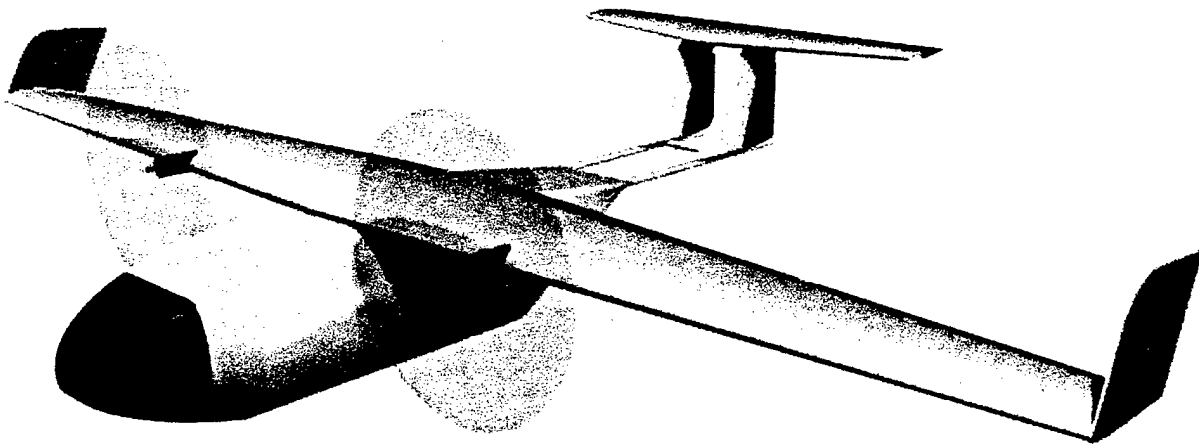
6.64 \$ (Thousand)

*MASTER
COPY*

AIAA / CESSNA / ONR

Student Design / Build / Fly Competition

Proposal Report



Middle East Technical University

Team Anatolian-Craft

March 2001

1. EXECUTIVE SUMMARY	1
2. MANAGEMENT SUMMARY	4
3. CONCEPTUAL DESIGN	8
3.1. INTRODUCTION	8
3.2. FIGURES OF MERIT (FOM)	8
3.3. INITIAL PHASE	9
3.4. INITIAL GUESS SIZING	15
3.5. SELECTION PHASE	17
4. PRELIMINARY DESIGN	19
4.1. INTRODUCTION	19
4.2. WING GEOMETRY OPTIMIZATION	19
4.3. AIRFOIL SELECTION	20
4.4. TAIL GEOMETRY OPTIMIZATION	23
4.5. CONTROL SURFACE OPTIMIZATION	23
4.6. FUSELAGE OPTIMIZATION	23
LANDING GEAR OPTIMIZATION	25
4.8. ENGINE SIZE AND BATTERY OPTIMIZATION	25
5. FINAL DESIGN	30
5.1. STABILITY AND CONTROL ANALYSES DATA	30
5.2. COMPONENT SELECTION AND SYSTEM ARCHITECTURE	31
5.3. CONCLUSION	32
5.4. STRUCTURAL ANALYSIS OF FUSELAGE MAINFRAME	35
5.5. DRAWING PACKAGE	36
6. MANUFACTURING PLAN	41
6.1. INTRODUCTION	41
6.2. FIGURES OF MERIT –MANUFACTURING PLAN	41
6.3. WING CONSTRUCTION	43
6.4. TAIL CONSTRUCTION	44
6.5. POWER SYSTEM INTEGRATION	45
6.6. FUSELAGE	45
6.7. LANDING GEAR	47
6.8. RESULTS	47
7. REFERENCES	49

1. EXECUTIVE SUMMARY

The team Anatolian-Craft is a design group, working under the AIAA Student Branch at Middle East Technical University (METU) Aeronautical Engineering Department. The team attended to the AIAA DBF 1999/2000, last year. After the announcement of the rules for the DBF 2000/2001 on 11th of June 2000, the team arranged for its first meeting. The organizational structure of the team is considered and the goal of the team is defined to be "Designing, Building and Flying the simplest possible UAV, which can carry the maximum payload according to the rules of the competition".

The aim of this year's competition is to design, manufacture, and fly an electrically powered UAV which can fly maximum number of sorties within a time period of ten-minutes carrying a payload of tennis balls up to 100, which is referred to as "light payload" and carrying steel blocks with a minimum weight of 5 pounds and is referred to as "heavy payload" during consecutive sorties. The goal of the team is chosen as to carry the maximum amount of light payload, because of its advantages in scoring with respect to the heavy payload.

A group of senior students, referred to as "the design sub-group", were assigned the task of investigating the initial parameters for the design of the UAV, while working together with the experienced members of the Team Anatolian-Craft on modeling. The design procedure was initiated by forming a database, including those successful UAV's which flew at the previous AIAA competitions. This database helped to formulate the basic concepts for the present design.

The design sub-group then formed the work break down structure for the design by forming special components such as the fuselage, power systems, wing and empennage, and the landing gear.

Many factors were considered in selecting the final design configuration. These were; the safety, structural strength, cost, speed of loading the cargo, power consumption, ease of manufacturing, stability and performance and the ease of transportation over seas. A trade-off analysis is carried out and the most efficient configuration is selected while keeping in mind during all phases of design, the motto; "The simplest design is the best design".

The parameters that are considered for the design of the fuselage are the ease of loading, structural strength without excessive weight and the ease of manufacturing. The concept of speed loader system is also considered in the design of the fuselage. The fuselage of the existing military cargo aircraft, such as

C-160 and CN-235 are examined and the fuselage of the present design is decided upon which would allow the easiest loading/unloading capability.

The configuration that can lift and carry the desired payload is designed according to the consideration of the aerodynamic efficiency, stability and performance, ease of transportation and manufacturing. The simplest of all the configurations analysed is the mono-wing. The design based on the conventional wing and tail configuration has a higher chance of success. The selection of the airfoil is also very important. The airfoil selected must be easy to manufacture and stable enough to improve the handling characteristics of the aircraft while increasing its performance during the flight. Changing the configuration of the wing can solve some of the problems which may be faced during the calculations and tail design other than conventional. The design sub-group investigated various alternative designs other than the conventional configuration. However, the configuration that is reached at the end of the preliminary design phase was the conventional monoplane wing with pi-tail configuration.

Preliminary Design Revised Parameters	
Payload Capacity	14.44 lb. (39 liters)
Wing Area	12.78 ft ²
Aspect Ratio	8.25
Taper Ratio	0.45
Leading Edge Sweep Angle	2.95°
Airfoil	Modified Clark Y
Tail Configuration	π -tail
Flap Chord to Wing Chord Ratio	18%
Aileron Chord to Wing Chord Ratio	16%
Fuselage Length	6.3 ft
Fuselage Material	Aluminum 2024
Landing Gear Material	Aluminum 2024
Type of Motors	Astro Flight Cobalt 60
Number of Motors	2
Type of Cells	SR 2400
Number of Cells	36
Propeller	22" x 14"

Table 1.1 – Preliminary Design Revised Parameters

In addition, the power system is designed considering the cost, safety, and performance as the main factors. The motors that were already available to the team had the highest priority, since their cost was a major factor. The calculations also showed that the available motors were suitable since they met the power requirement of the design.

Last design consideration was the landing gear where a tri-cycle configuration with solid spring main gear and steerable nose gear was chosen because of the improved capability of the system during taxing.

The final configuration attained with the forgoing considerations is presented in Table 1.1

During the final design phase, the structural strength, the performance and the stability analysis of the final configuration are analyzed. The stability analysis program, coded in MATHCAD programming language, is employed to find out the stability characteristics of the aircraft. The stability characteristics of the aircraft are found to be satisfactory. The performance parameters for the aircraft are calculated and are found to be satisfactory as well. For the structural strength of the aircraft, ANSYS, finite element analysis software, is used and the results showed that the structure was safe enough. Detail drawings were done with the help of AutoCad R14; and also as another analytical tool, Motocalc was used in order to calculate the engine performances.

Detailed design of the fuselage is performed while considering the following factors such as; payload and battery access doors, electronic controller and servo motor locations, electrical and controller wire locations, connectors, switches and ease of assembly and disassembly during loading and unloading of the cargo. Also the materials selected are re-considered according to the figures of merit. This analysis ended up with an electrically powered UAV, completely satisfying the maximum light payload requirement set forward by the RFP. This procedure gave the configuration presented in Table 1.2

Cruise Speed	37 Knot
Stall Speed	19.4 Knot
Maximum Speed	40.82 Knot
Range	28.8 mi
Endurance	9'45' at 18.5 m/s
Take-off Ground Roll	49.5 ft.
Landing Ground Roll	196.85 ft

Table 1.2 –Final Design Performance Parameters of the UAV

2. MANAGEMENT SUMMARY

The team Anatolian-Craft started to the AIAA 2000/2001 DBF Competition UAV Project with 25 members, 23 of which are undergraduate students, and 2 of which are graduate students during the Summer of 2000. 13 of these 23 students were seniors, 4 of them were juniors, and 6 of them were sophomores. At the final stages of the project, 2 freshman students integrated to the team whereas 1 senior, 2 juniors, 4 sophomores and 1 graduate student left the team, leaving the team with a total of 19 students.

At the initial stages of the project, the team was divided into 3 sub-groups. These teams were the design sub-group, logistics sub-group and sponsorship sub-group where all 3 sub-groups were responsible to the team-leader and gave report to the team-leader on regular basis during meetings held weekly. A leader to each sub-group was assigned whose responsibility was to organize the sub-group and get the jobs done assigned to the group. Figure 2.1 shows the organizational structure of the team and the inter group coordination realized:

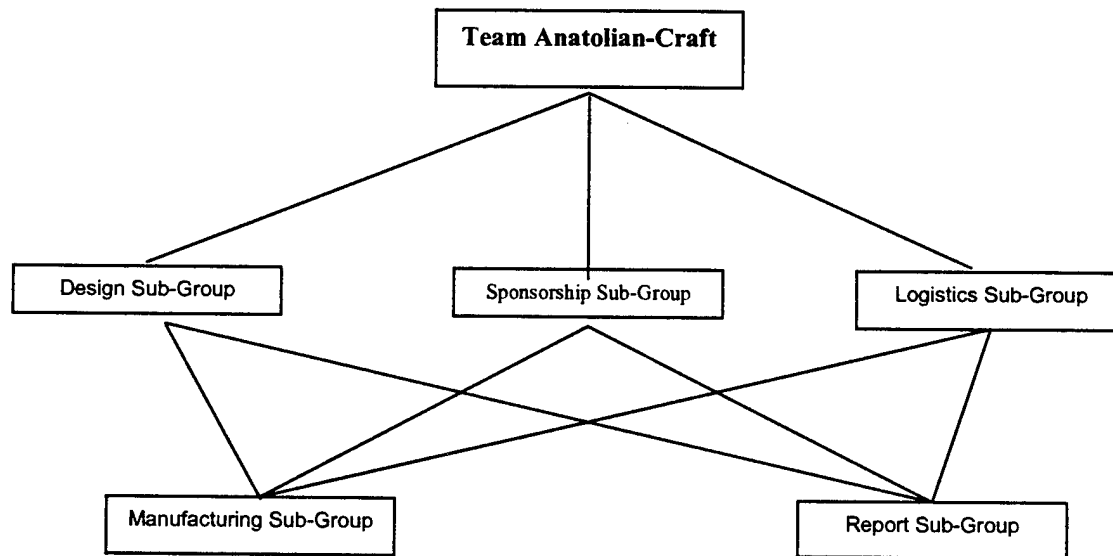


Figure 2.1 – Structural Chart of the Team

The design sub-group was responsible from the conceptual, preliminary and detail design of the UAV, analysis of the design and detail drawings of the parts of the UAV. The Logistics sub-group was

responsible from supplying all any kind of support to the design team such as written documents, computer software, web searches and material. This team was generally formed with underclassman with the idea that they gain experience about the design and the organization of the team and that they become ready for the design missions that will be given to them following years. The sponsorship sub-group was responsible to support the team by finding financial support to the team to cover the costs of manufacturing the UAV, the travel costs for the team members and the shipping cost of the UAV to the competition site.

Also a treasurer and a person in charge of archiving were assigned at the beginning of the project.

After the design process was over two new sub-groups were created to organize the manufacturing and the report writing processes. Each member of the team, who was previously a member of the sub-groups, has taken a new responsibility on these two newly formed sub-groups. Manufacturing sub-group searched for alternative production methods and the ease of production of the parts that were designed by the design sub-group. Alternative materials were searched for production that will reduce the cost of the project, reduce the weight and decrease the workload. Also a detailed timetable, which is presented in Table 2.2, is prepared and the materials are ordered after the production method and the ease of production of the parts are confirmed by the manufacturing sub-group. However this did not mean that the work of the initial sub-groups was over. The changes suggested by the manufacturing team put the design team into work again for suggested modifications in the design. In the meantime the logistic sub-group carried on with their search and supplementing the requested materials.

The design sub-group was formed by senior students, who were taking the Aeronautical Engineering Design Course. This gave the team the advantage to further analyze and modify their design according to the knowledge acquired in this design course. The design sub-group modified the design during their weekly study hours of the course under the supervision of the advisor.

During the regularly held weekly meetings of the team, the team leader directly assigned tasks to the logistic subgroup leader following the requests coming from the design sub-group and the sponsorship sub-group. So the logistics sub-group leader was the person who was responsible for any incomplete job. The logistics sub-group leader assigned the given job to one of his group members but he personally followed the task until the job was completed. In case the job was not completed the leader did the job himself or assigned it to another member who was more capable of doing the job on time. So that there was an auto-control mechanism within the system. In addition, the Anatolian-Craft Team leader was personally responsible to the project advisors for any incomplete job. The weekly team meetings, in which

each sub-group leader gave a report to the team leader and the weekly study hours, in which the team leader gave a report to the project advisor, became a successful method of controlling the progress of the project. The reason for the delayed jobs was mostly due to the lack of material.

Besides the successful organizational structure of the team, the team spirit and the desire of each member of the team to reach the final goal to which each member of the team believed strongly, was the reasons for success of the team.

The assignment areas of the group members is tabulated in Table 2.1

Name of the Member	Function at the Team
Fikri Akcali/AE/SR	Teamleader and Design sub-group leader. Organized the communication between the sub-teams. Arranged communication with AIAA. Arranged the meetings.
Candas Ozdogu/AE/SR	Design sub-team member and Sponsorship sub-team leader. Contributed to ordering materials from abroad and the written report.
Onur Baylan/AE/SR	Design sub-team member. Contributed into manufacturing process and the written report.
Ozan Sakarya/AE/SR	Design Sub-team member and contributed to manufacture. He also worked on the final format of the written report.
Ayca Yetere/AE/SR	Design-Sub team member and Contributed to the manufacturing and the written report.
Yasser El-Kahlout/AE/SR	Design sub-team member. Contributed to the manufacturing process and was responsible from R/C settings.
Jaffar Hajibrahim/AE/SR	Design sub-team member. Contributed to the manufacturing process.
Azra Timur/AE/GRAD	Contributed to the design as an advisor.
Ilter Duran/AE/SR	Logistics sub-team leader. Contributed in the manufacturing process.
Mine Alemdaroglu/AE/JR	Logistics sub-team member and contributed to the manufacturing and the written report.
Halil Kutay/AE/JR	Logistics sub-team member and contributed to the manufacturing process.
Sema Simsek/AE/SR	Logistics sub-group member. Contributed to the manufacturing process and kept the archive of documents and the members information and continuity.
Serdar Cora/AE/SR	Logistics sub-team member. Contributed to the material assurance, report writing.
Nebi Calli/AE/SO	Logistics and sponsorship sub-group member. Contributed to the manufacturing process.
Evm Dizemen/AE/SO	Logistics sub-group member. Contributed to the manufacturing process.
John Montgomery/AE/SR	Contributed to the manufacturing process.
Baris Atakan/AE/SR	Sponsorship sub-team member. Contributed in the manufacturing process and the report.
Oguzhan Ayisi/AE/FR	Sponsorship sub-team member.
Sercan Soysal/AE/FR	Sponsorship Sub-team member and contributed to the manufacturing process.

Table 2.1 – Assignment areas of the group members

Management Summary

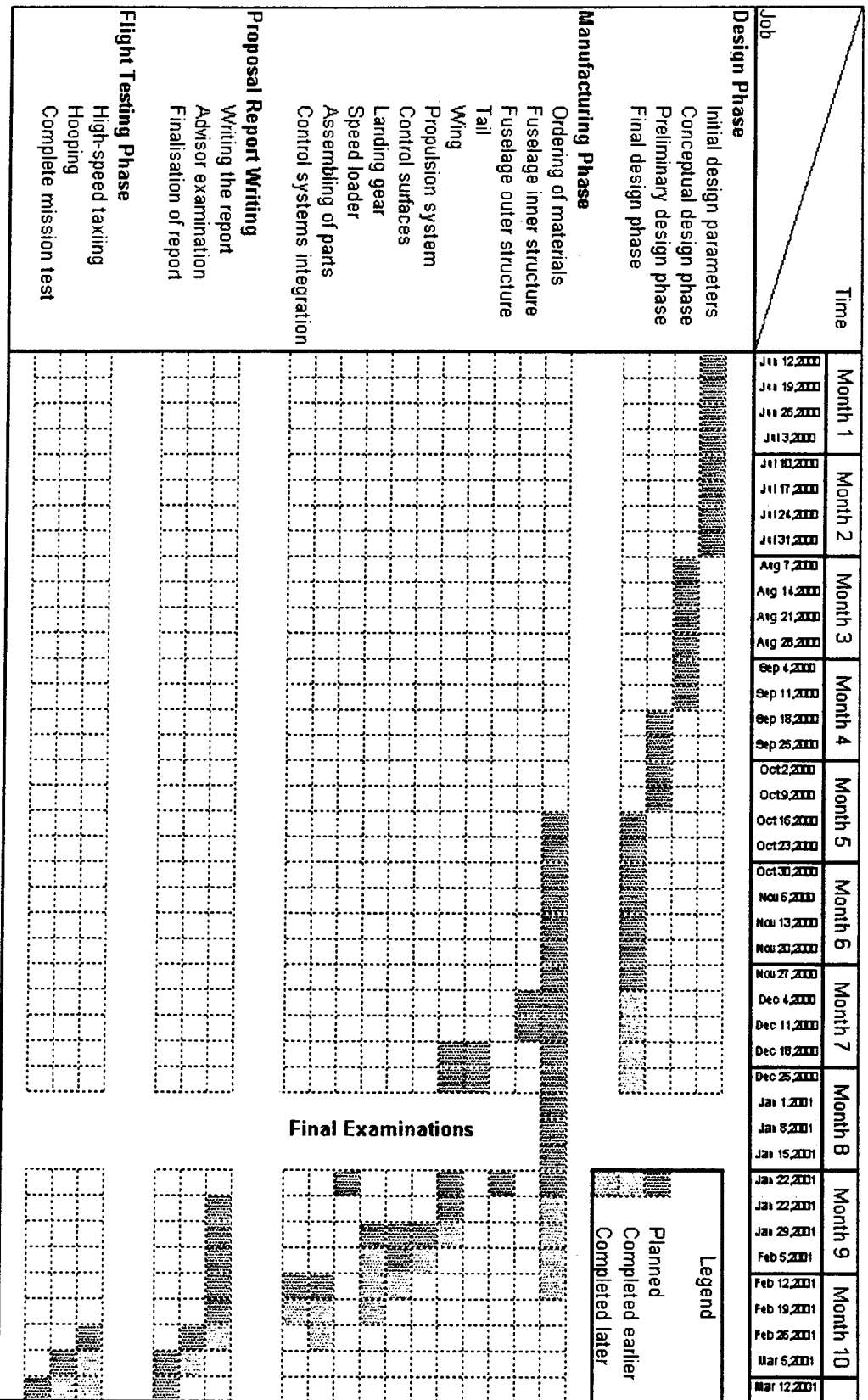


Table 2.2 – Timetable

3. CONCEPTUAL DESIGN

3.1. Introduction

The conceptual design phase was divided into two parts, initial phase and selection phase. During the initial phase, members of the team exchanged their ideas about what can be done and how it can be done. During the selection phase further analysis was done to choose the best configuration for each component of the aircraft. For this purpose, initially the figures of merit were introduced and more detailed analysis will be supplied in the following sections.

3.2. Figures Of Merit (FOM)

Manufacturability: One of the most constraining criterion of the design phase was the skill required to build the UAV. Since not all the team members were experienced in building model aircraft, the aim of the team was designing a simple UAV while optimizing its performance. This would also lead to a shorter manufacturing time. The team had a chance to use the facilities and the equipment of the Aeronautical Engineering Department of Middle East Technical University. It would be also a very difficult task for all the team members to build a complex and a complicated UAV since non-of the team members were professional model makes.

Power Consumption: Power consumption was another important criterion, since the weight of the batteries used were limited, thus the team tried to design an optimum UAV that will fly maximum number of flying sorties while carrying the maximum payload, as stated in the rules.

As the weight of the aircraft increased, the power required to take off in the limited take-off distance is increased. So the weight was an important factor in determining the power consumption of the UAV. In addition, an aerodynamically efficient design decreased the power required, since it decreased the drag on the aircraft.

Specific Strength: Many factors affect the structural strength of the aircraft. The wings should be able to carry the entire weight of the UAV, the fuselage must be strong enough to carry the payload, the landing gears must withstand high impact landings, etc. All these major factors were taken into consideration in determining the materials and the manufacturing techniques used.

Speed Loading: According to the rules of the competition, the time of flight of the UAV is limited, thus the loading/unloading time for the cargo must be minimized. The cargo door and the fuselage were designed according to these parameters, which will minimize the loading time between each sortie.

Handling: Handling characteristics are important parameters in designing the UAV. The UAV must be well controllable in the ground, must have short take-off and landing distances. In addition, the UAV should be easily controlled during its flight with different payloads, and must withstand adverse atmospheric conditions.

Cost: Since each team was required to fund the total cost of their UAV, cost was a very important figure of merit and therefore the cost of the UAV should be minimized. Hence, utmost attention had to be given to the selection of the material used and the cheapest but the correct material should be chosen for the task.

Stability: The stability of the aircraft directly affects its handling qualities, thus designing a stable UAV was the goal of the team. The UAV should be easily controlled on the ground and in flight, since it will fly with different payloads having different weights around a predetermined course and should be capable of withstanding windy conditions.

Performance: Since the take-off distance and the battery weight are limited, a high performance aircraft is necessary that could meet these design limitations. The aircraft should have short take-off and landing distances and its aerodynamic performances must be optimized in order to carry the maximum load with minimum power requirement.

Transportation: As the UAV will be manufactured in Turkey and will be transported to the USA for the AIAA DBF competition, the UAV needed to be easily assembled/disassembled and fit to a minimum amount of volume within the volume and size limitations set by the airlines.

3.3.Initial Phase

In this section rough estimations were made for the initial size of the aircraft, the wing and the tail shape, the amount of payload to be carried, the structure of the fuselage to carry the desired payload, the engines to be used and the landing gear to carry the aircraft. After examining the rules for this year's competition, it was observed that every 5-tennis balls carried was equivalent to carry a pound of solid bar and since 5-tennis balls weighs less than a pound the team decided to design an aircraft with a

substantial cargo volume to carry 100 tennis-balls. The following design parameters were investigated during the initial phase of the conceptual design stage:

Wing Planform: The options considered for the wing geometry were rectangular, elliptical and tapered. Each of these shapes had distinct advantages and disadvantages. The rectangular wing was superior to others for its ease of production but it had shortages when considered aerodynamically. On the other hand the elliptical wing had the best lift distribution but as it is well known to manufacture an elliptical wing is a time consuming process. Therefore a tapered wing was considered next. It is known that for a certain taper ratio and a quarter chord sweep angle, a tapered wing could produce a lift distribution similar to that of an elliptical wing. This will shorten the manufacturing time and give a satisfactory lift distribution.

Next, the aspect ratio (AR) was chosen to be larger than 8 in order have a greater change in C_L for a smaller change in α . After this the taper ratio was chosen to be 0.45, which produced a lift distribution close to the elliptical (ideal) wings'. This resulted in a drag due to lift (induced drag) less than 1% more than the ideal elliptical wing.

Wing Configuration: The team investigated two different wing configurations for this mission with and without winglets. Namely these were monoplane and bi-plane wing configurations. Each one had its own advantages and disadvantages. Bi-plane wing configuration is considered when low structural weight is more important to the design than the aerodynamic efficiency or when low speed is required without complicated high lift devices or excessive wingspan. There is a reduction of 30 % in induced drag for a bi-plane when compared to a monoplane of equal span. On the other hand monoplane wing configuration is much more efficient than the bi-plane, therefore a carefully manufactured monoplane configuration will lead the same lift force with less structural weight.

Wing Structure and Materials: Two types of construction were considered for the wing. One is to construct it from ribs and the other is to use a foam core. The rib construction is supposed to be lighter and stiffer but on the other hand it is much more difficult to construct because it requires precise manufacturing which is difficult for a tapered wing. Even though there are some disadvantages for the foam core structure, by using appropriate stiffeners like spars and sheeting these disadvantages can be minimized. In order to cover the foam one can use either balsa wood sheet or composite material (such as glass fiber + epoxy, carbon fiber + epoxy, etc.). The composite materials yield a stiffer but also heavier structure than the balsa wood. Since composite materials are expensive and hard to manufacture, the balsa wood sheeting will be further analyzed.

Spar Structure: The spar provides the primary structural strength of the main wing. It was designed to withstand variety of loads, which the wing will experience during flight. The two parameters that affected the initial design of the spar were its weight and its strength. The main variables that governed these parameters were the cross-sectional geometry of the spar and the material characteristics.

The geometry considered for the beams cross section included an I-beam, a circular cross section, a solid rectangular beam, a box beam and a multi-box beam. An I-beam has the greatest moment of inertia and therefore the greatest strength about the horizontal axis; however, the strength about the vertical axis is small. An I-beam would also be very difficult to manufacture using lightweight materials.

A circular cross section has equal moments of inertia about both the horizontal and vertical axes providing equal strength in all directions. However, this design makes the spar unnecessarily heavy. A solid rectangular beam is the strongest, but like the circular shaft, much of the material towards the center of the beam is relatively unstressed. The solid rectangular beam is simple to manufacture, yet it has a low strength to weight ratio.

The box beam has the greatest strength about the horizontal axis, similar to an I-beam, but also has good strength characteristics about the vertical axis. The box beam is hollow, decreasing the amount of wasted material, which helps reducing the weight of the spar. But on the other hand it would still be hard to produce this type of spar for the wing considered. On the other hand a continuous multibox material can be used as a spar by giving it the desired thickness. A market search for such a material was made and a suitable spar material was found which will be given in more detail at the Spar material section.

Spar Material: Different types of spar materials were taken into consideration. From comparatively light materials; such as balsa, hardwood, fiberglass and polycarbonate to heavier materials such as aluminum and carbon fiber composites were investigated. The purpose was to determine the spar material with the greatest specific strength, which would be sufficient for the expected loading on the wing.

Aluminum has a high strength; however, it is a very dense material compared to the other materials considered. Aluminum may not be the best material for the construction of the spar because the strength to weight ratio is lower than the composite materials considered. The machining processes also make it difficult to manufacture the desired shapes using aluminum.

Hardwood and balsa wood are widely used and easy to find but the low strength to weight ratio and the difficulties in manufacturing complex geometries are disadvantages of these materials. Also the strength characteristics are not uniform within these materials.

Although fiberglass has better strength characteristics than wood, it has a lower specific strength than carbon based composite materials such as carbon fiber or polycarbonate. Even though polycarbonate materials have a less specific strength than carbon fiber composites, according to the strength tests performed, these materials met the necessary criteria. Another important criterion for deciding the spar material is its availability in the market.

Tail Structure: A conventional tail consists of horizontal and vertical stabilizers located aft of the center of gravity by means of a tail boom. The horizontal and vertical stabilizers are mounted to the tail boom structure with the horizontal stabilizer located at the bottom of vertical stabilizer. This configuration is easy to manufacture, analyze, and has been well researched and proven in most of the successful aircraft designs.

Although T-tail has many drawbacks, spin recovery characteristics are good. Because of the fact that, the flow coming out of the horizontal tail surface does not intersect with the vertical tail surfaces. There is always uniform, fresh airflow coming to the vertical tail surfaces since they are situated at the tips of the horizontal tail. These advantages are accompanied with an increase in the structural weight and a stall recovery problem.

H-tail is used primarily to position the vertical tails in an undisturbed air during high angle of attack conditions or to position the rudder in the prop-wash on multi engine aircraft to enhance one-engine-out control. The H-tail is heavier than the conventional tail, but its endplate effect allows a smaller horizontal tail.

Even though H-tail seems better for this design, its weight may cause a stability problem since it makes the CG move aft. Therefore a conventional tail will be considered in further analysis.

Control Surfaces: Primary control surfaces are ailerons, flaps, elevator and rudder. The sizing of those surfaces was very important as maneuverability and stability is affected by their sizing.

Before considering the areas of the control surfaces, a decision between flap-aileron and aileron and flap combination had to be made. Based on the experience gained last year a flap and an aileron combination is decided to be used, as the aircraft is more controllable.

In order to have enough maneuvering capability, depending on very rough calculations, the ailerons should be 15% of the wing chord and 40% of the wingspan. Nearly the remaining part of the wing span

(50%) was decided to be used for the flaps, as high amount of lift might be necessary for take off due to the fact that the take off distance is limited to 200-ft.

For the remaining control surfaces, the most common values were chosen, which were 40% of the chord and 100% of the span of the horizontal stabilizer for elevator and 50% of the chord and 80% of the span of the vertical stabilizer for rudder.

Fuselage Structure: As it was explained before, carrying five tennis balls instead of one pound of steel bar was more advantageous according to the DBF competition rules. Therefore, the team decided to design the fuselage to carry as many tennis balls as possible. The first task was to find out the smallest possible container, which would be sufficient to hold 100 tennis balls. After this was accomplished, a compartment in the fuselage structure was designed to carry and support the container. Also the payload should be accessed easily and quickly as an important parameter of the design.

Since the wing and tail will be mounted onto the fuselage, which will also be carrying the payload as well as the batteries, it had to be made of a stiff material. Therefore, it was thought that aluminum beams could be used. Figure 3.1 shows the structure of the fuselage of the design.

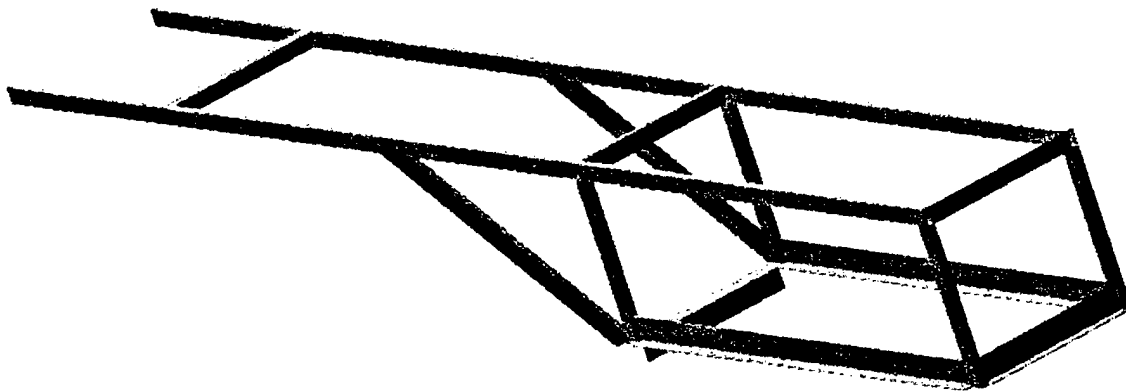


Figure 3.1 – Fuselage inner structure

The booms of the fuselage structure were designed such that their upper surfaces would be flat in order to provide a suitable place for the wing and the tail. The bottom of the structure is designed such that it would support the payload easily without using excessive means of securing. By preparing a sliding mechanism the payload will be loaded fast and easily.

Fuselage Shape and Material: After deciding upon the inner structure of the fuselage, the team thought of several methods to make the fuselage aerodynamically efficient as well. The task was simple. To prepare the lightest and most efficient shape and cover the aluminum structure inside. Since all the load is expected to be carried by the inner structure the covering did not have to be strong. Therefore the team decided to use foam material for the covers, and if extra stiffness would be needed thin fiberglass clothing would be introduced over them. By using foam the desired shape could be easily given to the fuselage and most efficient one among these would be an airfoil shape, since it would produce the minimum drag.

Landing Gear: The landing gear configuration had a direct effect on the ground handling characteristics of the aircraft. Landing gear configuration became an important parameter as the team realized that multiple take-off and landings would be a demanding part of the competition. In order to satisfy the design mission, an efficient landing gear configuration is needed to be designed. Three types of landing gear arrangements were considered. They are discussed in detail below:

A retractable gear eliminates drag on the landing gear while the airplane is in flight. However, multiple takeoffs and landings require greater power consumption to raise and lower the landing gear for takeoff and landing. Also, it is more difficult to manufacture a retractable landing gear that would be strong enough to support the weight of the aircraft.

A tail dragger design was considered because of the decreased drag on the landing gear during flight. A tail dragger design provides the necessary strength to support the airplane on landing and takeoff. However, tail dragger designs are more difficult to control on the ground.

The third design developed was a standard tricycle landing gear. The tricycle landing gear can easily be manufactured to support a heavy airplane. This landing gear provides satisfactory ground control but increases the drag. Also, tricycle gear arrangement is suitable to the desired payload loading system. The tricycle landing gear was selected for further analysis because it provided the desired ground control and structural strength.

Power Plant: Since the team was required to fund the aircraft construction, engine cost was one of the important criterion in deciding the engine to be used. Not knowing the actual size of the UAV made it

even more difficult to choose the engines to be considered at the very initial stages of the design, thus a wide range of engines and propellers were inspected. Multiple motor combinations were also possible, depending on the size of the UAV

Using NiCad batteries was also a requirement of the competition, so batteries with high capacity were subject to use. Another consideration about the cells is their weight. The total weight of the cells to power the motor should be less than 5 lb, which constraints the variety of cells that can be used.

Propellers may be of wood or reinforced nylon, but in the conceptual design, the size of the propeller can be selected as the optimum propeller that the selected motor can run. But although the wooden propellers make noise more than the nylon propellers, their efficiencies are higher than nylons. As there is not such a limitation for noise, to use the more efficient wooden propellers is reasonable. The size of the propeller is a function of the electric motor selection.

3.4. Initial Guess Sizing

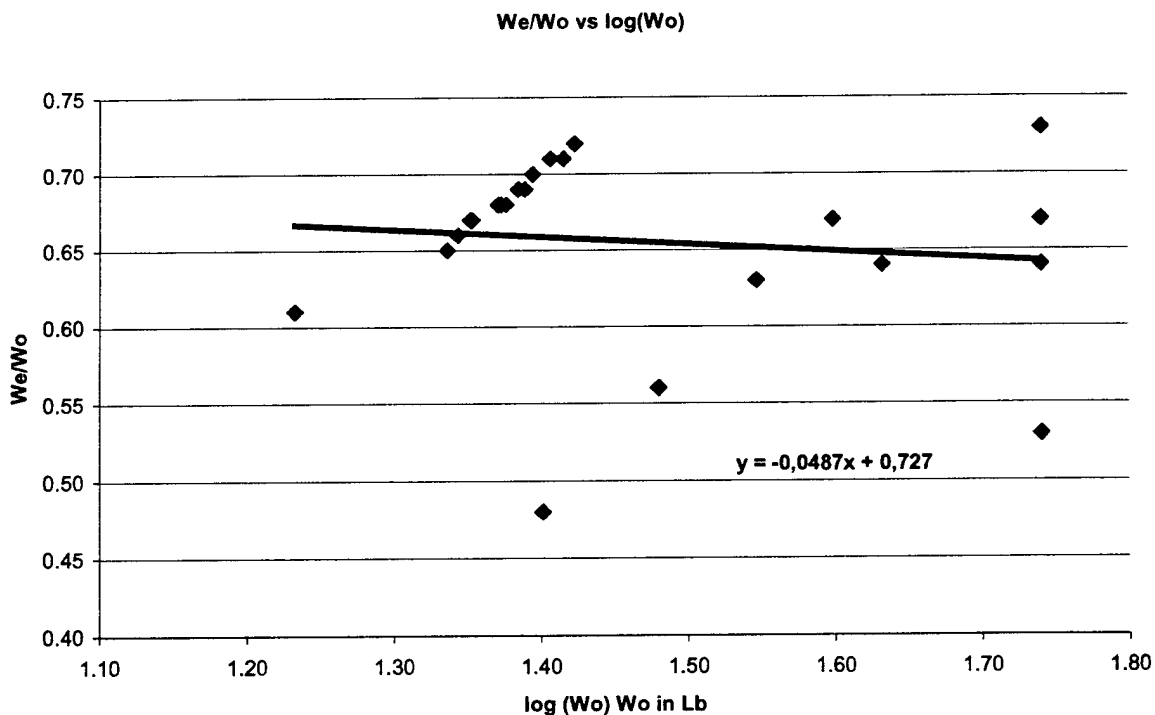


Figure 3.2 – W_e/W_o vs $\log(W_o)$ for similar UAV's

In order to make a first guess sizing for this aircraft the formulas in Reference 1 were introduced. Using data of past years' successful competitors of AIAA/DBF Competition, Figure 3.2 was plotted.

From the graph:

$$A=0.727 \quad c=-0.0487$$

K_{ws} = variable sweep constant = 1 (for fixed sweep)

After manipulating the formulas in Reference 1 for W_0 (Takeoff Gross Weight) one obtains:

$$W_0 = \frac{14.44}{1 - 0.727 * W_0^{-0.0487}}, \text{ where } W_0 \text{ is in lbs}$$

Equation 3.1

In order to solve the above equation a trial and error method was used and it is found that **$W_0=37$ lb.** satisfied the equation, and the entire payload, **$W_p= 14.44$ lb.**, could be carried. Therefore for this to be accomplished the empty weight of the aircraft should not exceed **$W_e= 22.56$ lb.**

Therefore the total weight of the aircraft is roughly estimated to be as 37 lb. Again referring to the competitor study, and the searches that are done about the engine performance lead us to a statistical data such that; to take-off with 10 ft span if W_0 vs. Power Required for take-off statistics are plotted, an equation between Power and Total weight is found (Power Required = $25,371W_0 - 31,25$) from which it is found out that the power required for take-off is 908 Watts. From previous experience, the team is more familiar with Astro flight motors. So the alternatives are Astro Cobalt 90 (1200 watts), Cobalt 60 (1000 watts) and Astro Cobalt 40 (800 watts). For an electric motor, 70% efficiency is quite a good approximation. Then the possible configurations are Two Cobalt 60, two Cobalt 40 or a puller-pusher combination of any of these two motors. But this configuration may cause problem in loading. Then wing mounted Cobalt 40s or Cobalt 60s are preferred. This can be finalized after further analyzing the engines with a software (Reference 3) after some other basics of the UAV such as, its wing area and aerodynamic constants are estimated.

Also from past experience, it was obviously seen that the cells need to be able to provide sufficient current to the motor in unit time with high discharge rates. Otherwise the motor will not be fed by enough

current resulting with lower rpm's than desired during the take off. Therefore, it was concluded that high capacity NiCad cells of SANYO and SR BATTERIES for electric flight must be searched initially.

3.5.Selection Phase

The design parameters were investigated based on the figures of merit (FOM) and presented in Table 3.1. The design parameters were rated from -1 to 1. A -1 indicates that this parameter causes a disadvantage, while 1 indicating the parameter was advantageous. If the parameter does have neither specific advantages nor disadvantages, namely neutral, it is assigned a 0. A N/A was assigned if the figure of merit did not apply. Those design parameters with the greatest total score were selected for further analysis. The "FA" in the decision column stands for further analysis and the "E" stands for eliminate. The configurations marked **bold** are the ones that are selected.

Rated Aircraft Cost: An important parameter in selecting the aircraft configuration was the rated aircraft cost. It was clear that the total score was very much depended on this parameter and therefore intensive attention was paid to it. Design team worked on different aircraft combinations and prepared a simple Excel program, which gives the rated aircraft cost for the desired configuration. Considering a conventional aircraft, while keeping everything else constant:

- Every extra engine introduces an increase of approximately 25 % to the rated aircraft cost.
- Increasing the number of wings from one to two will introduce approximately an increase of 20 %.
- Adding an extra servo or a controller will increase rated aircraft cost approximately 1 %.

Other parameters were also investigated but it was seen that the effect of these were not significant. Number of cells were kept constant during all calculations because it was determined before that the total limit for cell weight would be used.

According to these calculations, a conventional aircraft to carry the desired payload would have a rated aircraft cost of about 9000.

Design Parameters		Figures Of Merit								
		Manufacturability	Power Consumption	Specific Strength	Speed Loading	Handling	Cost	Stability	Total	Decision
Weighting Factor		1.5	1.5	1.5	1.5	1	1	1		
Wing Planform	Rectangular	1	-1	N/A	N/A	0	1	-1	0	E
	Elliptical	-1	1	N/A	N/A	0	-1	0	-1	E
	Tapered	0	0	N/A	N/A	-1	1	1	1	FA
Wing Configuration	Monoplane w/ winglets	0	0	1	N/A	1	0	1	3.5	FA
	Monoplane w/o winglets	1	1	1	N/A	1	1	0	6.5	FA
	Biplane w/ winglets	-1	1	0	N/A	0	-1	-1	-2	E
	Biplane w/o winglets	0	0	0	N/A	0	-1	0	-1	E
Wing Structure	Wooden Rib	-1	1	0	N/A	N/A	-1	N/A	-1	E
	Foam & Wood Sheet	1	1	-1	N/A	N/A	1	N/A	2.5	FA
	Foam & Composite Sheet	0	0	1	N/A	N/A	-1		0.5	E
	Foam & Wood Sheet with Spar	1	0	1	N/A	N/A	0	N/A	3	FA
Spar Structure	I-Beam	-1	-1	1	N/A	N/A	-1	N/A	-2.5	E
	Solid Rectangular	1	-1	0	N/A	N/A	1	N/A	1	E
	Circular Cross Section	1	0	0	N/A	N/A	1	N/A	2.5	E
	Box Beam	1	1	1	N/A	N/A	0	N/A	4.5	FA
	Multi-box Beam	1	1	1	N/A	N/A	1	N/A	5.5	FA
Spar Material	Wood	1	0	-1	N/A	N/A	1	N/A	1	E
	Fiberglass	-1	1	1	N/A	N/A	-1	N/A	0.5	E
	Polycarbonate	1	1	1	N/A	N/A	0	N/A	4.5	FA
	Aluminum	0	-1	1	N/A	N/A	0	N/A	0	E
	Carbon Fiber	-1	1	1	N/A	N/A	-1	N/A	0.5	E
Tail Structure	Conventional	1	1	0	N/A	0	1	-1	3	FA
	T-Tail	0	-1	0	N/A	0	0	1	-0.5	E
	H-Tail	-1	0	0	N/A	1	-1	0	-1.5	E
Tail Boom	Box Beam	0	0	0	N/A	1	1	N/A	2	FA
	Circular Beam	1	0	1	N/A	-1	0	N/A	2	FA
Fuselage	Rectangular	1	-1	N/A	N/A	0	1	-1	0	E
	Axisymmetric	0	0	N/A	N/A	0	1	0	1	E
	Airfoil Shape	-1	1	N/A	N/A	1	0	1	2	FA
Fuselage & Tail Material	Hard-Wood	1	-1	-1	N/A	N/A	1	N/A	-0.5	E
	Composite	-1	1	1	N/A	N/A	-1	N/A	0.5	E
	Aluminum	0	0	1	N/A	N/A	0	N/A	1.5	FA
Landing Gear	Retractable	-1	0	N/A	1	1	-1	N/A	0	E
	Tricycle	1	-1	N/A	1	1	0	N/A	2.5	FA
	Tail Dragger	1	-1	N/A	-1	0	0	N/A	-1.5	E

Table 3.1 – Rating of Configurations

4. PRELIMINARY DESIGN

4.1. Introduction

The main purpose of the preliminary design phase is to refine the design parameters that were decided in the conceptual phase. Those parameters need to be investigated deeply from many points of view, which are known to be figures of merit. These figures of merit, as explained before, are structural strength, cost, speed loading, power consumption, and ease of manufacture, stability, performance and ease of transportation. The already narrowed down configurations in conceptual design phase were considered in detail during the preliminary design phase, to find out the most proper design parameters within the specified limits.

4.2. Wing Geometry Optimization

The basic design parameters that are relevant to wing geometry are aspect ratio, wing sweep and taper ratio. In the conceptual design phase the importance of each was explained and the limiting values for each parameter were discussed. However now in the preliminary design phase it is possible to choose the most appropriate value for each one and to improve the pre-assigned values.

To have an optimum aspect ratio drag, structural weight and lift reduction were considered. It was decided to have an aspect ratio greater than 8 in the conceptual design. As a result, to have an aspect ratio of 8.25 was found to be optimal due to the fact that it is high enough to provide less drag, and low enough not to form much stress at the wing and fuselage joints. Also the structural weight is not high, so the wing doesn't need to be strengthened too much, which reduces the weight of the wing as well.

Although a high aspect ratio was chosen, the wing tip vortices were still a problem; so having end plates as an addition was found out to be a good solution. Yet the team thought that this end plates might cause some problems in the case of sidewind and also in transportation. So it was decided to have end plates that can easily be mounted to the wing tips when the sidewind was not a concern. Further investigations and flight tests performed in windy conditions will show their effectiveness and a decision will be taken whether it is necessary or not to use the endplates.

It is quite known that the best lift distribution is obtained by an elliptical planform so the team tried to obtain the closest distribution to the elliptical lift distribution. But as building of such a planform requires skilled labor and time, it was decided to have a wing with proper leading and trailing edge sweeps and a taper ratio that would do good enough as an elliptical planform. For the taper ratio, the well-known value

of 0.45 was used and the sweeps were chosen accordingly to obtain the best fitting geometry into the desired ellipse (Figure 4.1), also considerations must be given the propeller clearance for engines that might be mounted onto the wing. Even though, when rib structures were considered, building of a tapered wing is much more difficult than building a rectangular wing, the team kept on with that idea, searching for another manufacturing technique. Finally it was decided to have an inner structure formed totally of foam, covered with balsa sheets on top, with embedded spar material. This construction technique will be explained in more detail at Section 6.3

Another important concept that was kept in mind during the preliminary design period was the fact that the wing had to be transported overseas, so that it had to be disassembled into smaller components and volume quite easily. Due to this fact, the wing is designed as two pieces.

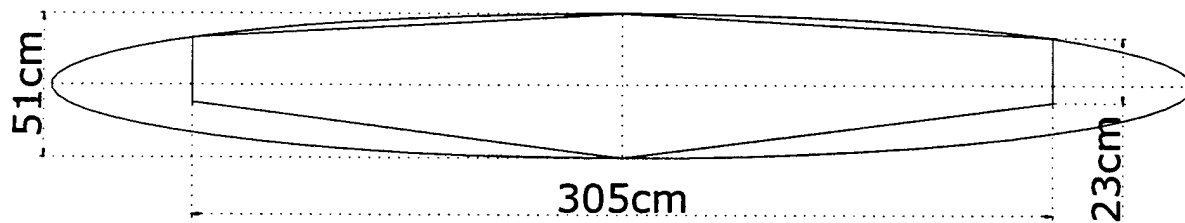


Figure 4.1 – Wing in an Ellipse

4.3. Airfoil Selection

After setting the wing geometry parameters, the airfoil selection has to be completed as another important parameter. In order to select the airfoil, the group searched for an airfoil with:

- High design lift coefficient to reduce the wing area and weight.

- High maximum lift coefficient to reduce the take off distance (due to the 200-ft limitation).
- Low drag for using the limited thrust in the most efficient way.
- High stall angle of attack as the recovery in any case of stall at low altitude is difficult.
- Ease of manufacturing due to the simple techniques that has to be used for manufacturing.

In addition to the above characteristics the thickness of an airfoil, which directly affects the performance of an airfoil, has to be considered. Stall characteristics of an airfoil are directly related with its thickness. Fat airfoils ($t/c > 14\%$) stall from trailing edge. The turbulent boundary layer increases with angle of attack. At around 10 degrees the boundary layer begins to separate, starting at the trailing edge and moving forward as the angle of attack is further increased. The loss of lift is gradual. The pitching moment changes only a small amount. Also the airfoils with moderate thickness (t/c 6-14%) have gradual loss of lift because of the reattachment of the flow after separation near the nose. By using the above reminders two airfoils was chosen for final selection: Modified Clark-Y and SD 8040

To obtain the characteristics of both airfoils, a code (Reference 7) was used to analyze the two-dimensional airfoil lift characteristics by using a 2nd order panel method with linear varying vortex distributions. The program requires inputs like Reynolds number, angle of attack limits, flap deflection angle and the coordinates of the airfoil, and delivers outputs like velocity distribution on the airfoil surface, C_l vs. angle of attack and C_l vs. C_d graphs. To be on the safe side the program was double-checked by using airfoils with available wind tunnel data and found out that this program is accurate enough and gave reliable results for our calculations.

By looking at the outputs of this program (Figure 4.2 and Figure 4.3) Modified Clark-Y becomes a more reasonable choice. It was seen that the velocity distribution of Modified Clark-Y is more suitable than SD 8040. However their drag coefficient is not a distinguishing characteristic, it can be said that Modified Clark-Y airfoil has a better C_l characteristic than the SD 8040. Even though SD 8040 can offer a reduction in total wing weight, Modified Clark-Y was selected due its better aerodynamic characteristics.

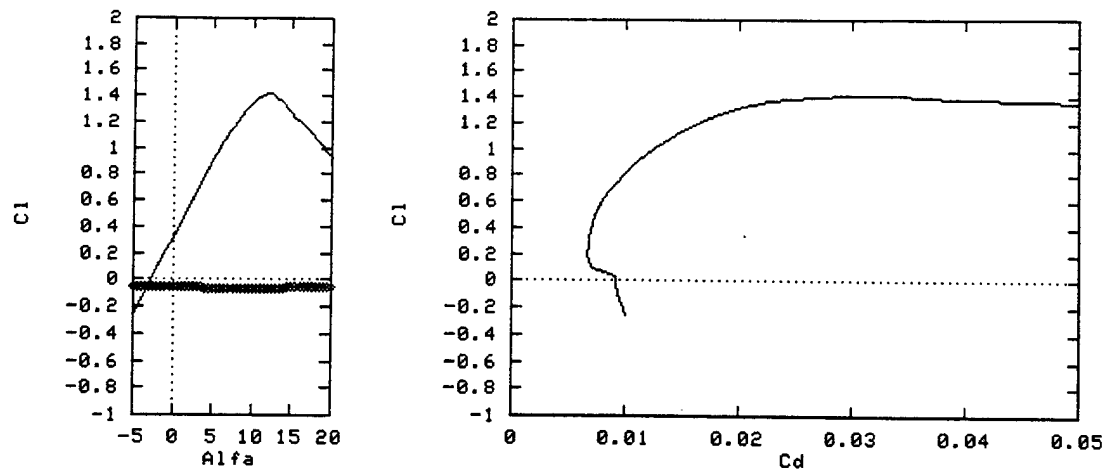


Figure 4.2 – Aerodynamic Characteristics of SD8040

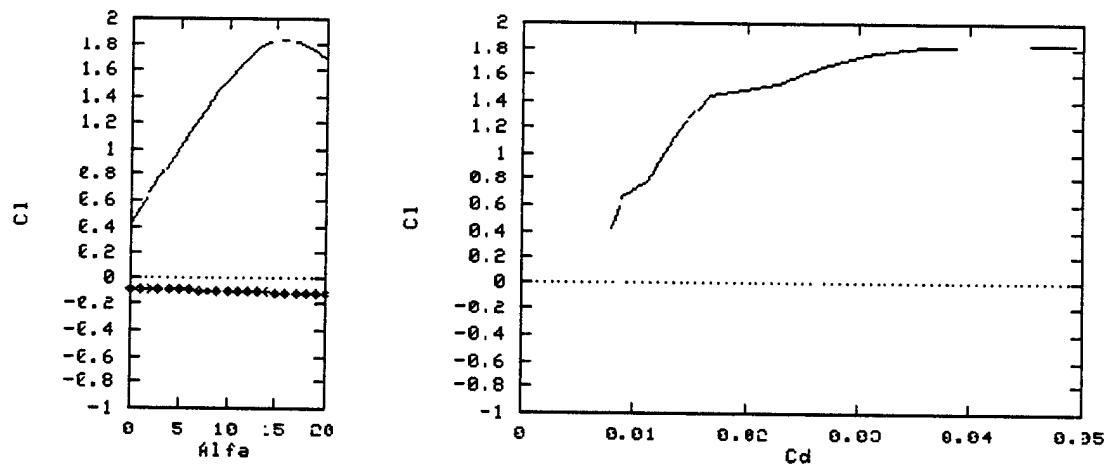


Figure 4.3 – Aerodynamic Characteristics of Modified Clark Y

4.4. Tail Geometry Optimization

The tail arrangement was a conventional tail at the conceptual design phase. As a design study, the spin recovery and stability contribution of this tail arrangement is studied out in detail. To avoid wing wake for a stall condition, the limits of the tail height was determined and then spin recovery characteristics were studied. To have adequate rudder control, in other words enough unblanketed rudder area, team decided to move the horizontal stabilizer above the vertical stabilizer, having a T shaped tail arrangement. Then the height of the total empennage rose as a problem. In order to find a solution for this problem, a new arrangement was considered. The new arrangement which was formed of a horizontal stabilizer on top of two vertical stabilizers, which can be called as a π -tail, actually comes out to be a very proper configuration due to its manufacturing ease, as there were two booms coming out of the fuselage to the tail. As a final decision two vertical stabilizers were selected although the team was aware of the fact that manufacturing two identical vertical stabilizers would be a hard task.

Finally the stability contribution of the tail was considered by using very rough calculations and it was decided to increase the area of the horizontal tail. Of course all those changes affected the structure of the empennage and to strengthen the horizontal and the vertical tail, and the joints between them came out as a necessity.

4.5. Control Surface Optimization

In the very beginning of the design period, the decision between a flapaeron and a flap and an aileron combination was made and an area ratio was determined. The values for the aileron location and area were found sufficient enough to do the desired maneuvers; however the predetermined flap areas didn't provide the necessary lift for the take-off condition. In order to obtain the desired lift, the flap areas were increased. Also by refining this parameter a necessity for redetermining the hinge line occurred. So the hinge line that was previously parallel to the trailing edge came out to be parallel to the horizontal axis of the wing. It was done so that the hinge line of the flap is always at the same percent of the airfoil, so the lift is distributed evenly when the flap is deflected. Finally the areas of the rudder and elevator were changed respectively by the ratio with which all the vertical and horizontal tail areas were changed.

4.6. Fuselage Optimization

Fuselage optimization is one of the most important parts of the design because even though the main structure was already decided the material selection is quite critical. The mainframe had to support both the forces applied by the lifting surfaces and by the landing gear. This led the team to face a problem of

choosing between, an over safe and heavy structure, or, light and low-strength structure. At this point, since using composite materials wasn't considered, the optimum metal with highest strength and the lowest density was searched and aluminum was chosen as the building material of the mainframe not just from the stiffness and weight point of view but also from manufacturing point of view. Even though this selection was a little expensive, it was the most proper material to use. However, after this selection the job even became harder as the best aluminum alloy had to be found. The materials available on the market for selection were Al 2014-T6, Al 2024-T3 and Al 7075-T6. Between those materials, Al2014 was not preferred as it has the same density with the Al 2024 but a lower strength. Al7075 has the highest strength among all of them and the same density with the others but this doesn't satisfy all the means, as it is not available in the market with the desired dimensions. After deciding the material a market search was done to find L-beams, T-beams and box beams necessary to build up the mainframe. As a result the cross-sectional geometry of the booms coming out of the fuselage to the tail was changed because of the unavailability of the desired beams in the market. Those booms, previously designed as box beams, became tubes with new calculated dimensions (Figure 4.4). This change also affected the fuselage supports, used to fix the wing, in a favorable way, by providing more ease of manufacture.

Another change done in the preliminary design period was reducing the boom lengths. This was done because of the refinement done in the tail areas. The boom lengths were shortened slightly in order not to affect the maneuvering capability of the aircraft.

When the mainframe design was finished the team considered possible locations for placing the battery pack keeping in mind that it is the next heaviest part to the payload. Not to cause any unbalancing moments, the sides of the fuselage are eliminated. The bottom of the fuselage was a candidate place however as the landing gear is directly fixed to the mainframe there was no room for the battery pack and in the event of an unexpected crash during landing, the whole battery pack could be damaged. Therefore the top of the fuselage was chosen for the battery pack location due to ease of access to the battery pack at this location. Also the place of the batteries need to be as forward as possible to keep the center of gravity location forward.

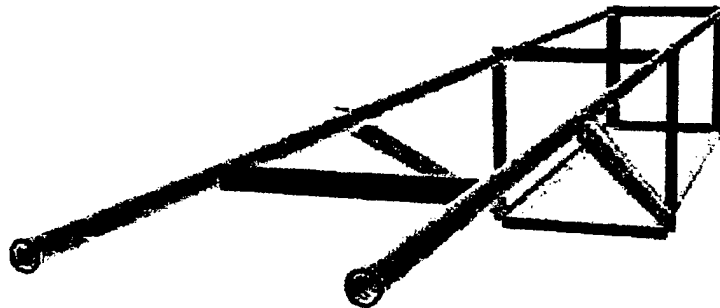


Figure 4.4 – Mainframe Drawing

4.7.Landing Gear Optimization

Landing gear configuration was already decided at the conceptual design phase. Solid spring type main landing gear as the one used on Cessna 172 aircraft is the easiest to manufacture for the main landing gear. To have the spring effect, steel is generally used. While searching for the landing gear material, the team realized that landing gear made of steel would be over safe and the aircraft would be carrying unnecessary dead weight. Again, aluminum was chosen as the material for the landing gear structure not only because of its weight and stiffness advantages but also because of its flexibility.

4.8.Engine Size and Battery Optimization

For the optimization of the engine at the very beginning there was a roughly determined trust to weight ratio calculated by using the available statistical data. However, those data were insufficient for an electric powered aircraft so a search was done to learn more about the electric powered flight. By examining all the resources that were available, an approximate value for the power required was found. The electric

motor suppliers catalogues were investigated while keeping the competition rules in mind. To have minimum number of engines possible, Graupner motors were eliminated, since they were not powerful enough. The 5-lb battery weight limit further complicated the motor selection procedure. However after a little search the team found out that this limit would amount to 36-40 batteries and this would supply power to too many possible motor selections. So from the Astro Flight motor family three motors were selected; FAI 40, Cobalt 40, and Cobalt 60. None of these engines is powerful enough by itself so it was decided to have a solution with two-engine combination located on the wings.

From the motor selections above, FAI 40 turns out to be the most proper one because of its power and number of batteries requirement (which will affect the duration). However the team had to give up on that motor because of the 40-ampere limitation of the competition.

In order to analyze the selected motors (Astro Flight -Cobalt 40, Cobalt 60) a program (Reference 3) was used. MotoCalc is a program for predicting the performance of an electric model aircraft power system, based on the characteristics of the motor, battery, gearbox, propeller, speed control and the aerodynamic data of the aircraft. MotoCalc will predict the current, voltage at the motor terminals, input power, output power, power loss, motor efficiency, motor rpm, power-loading, system efficiency, propeller rpm, static thrust, pitch speed, and run time. It can also do an in-flight analysis for a particular combination of components, predicting lift, drag, current, voltage, power, efficiency, rpm, thrust, pitch speed, and run time at various flight speeds. It can also predict the stall speed, hands-off level flight speed, maximum level flight speed, rate of climb, and power-off rate of sink.

Before using the MotoCalc in order to narrow down the possibilities for the battery pack, it was decided to use either the Sanyo 2000 or the SR 2400 batteries since they are not heavy, so they can be packed together to provide enough power within the 5-lb limitation.

To find out the most proper condition that can provide 10 minutes of flight time with 200 ft take off distance and an adequate speed; analysis were made with MotoCalc, for too many combinations of motors, batteries and propellers. Performance calculations for each motor are presented in Figure 4.5 and Figure 4.6 Finally it was decided to use two Cobalt 60 motors with 22"x14" propellers, with 36 SR 2400 batteries.

In-Flight Analysis

Sea Level

Motor: Astro Cobalt 40 8T#20 #640; 682 RPM/V; 0.121 Ohms; 2A idle.

Battery: Sr max 2400; 22 cells; 2400mAh; 0.003 Ohms/cell.

Speed Control: Astro 204; 0.005 Ohms; High rate.

Drive System: Astro superbox; 2 motors (parallel); 16x8 (const=1.31) geared 3.1:1.

Airframe: Anatolian craft; 1748sq.in; 546.5oz; 45oz/sq.ft; Cd=0.055; Cl=0.65; Clmax=1.51.

Stats: 24 W/lb in; 19 W/lb out; 27 MPH stall; 41 MPH level @ 101% (25:49); -49ft/min @ -1.1°; -246ft/min @ -5.3°.

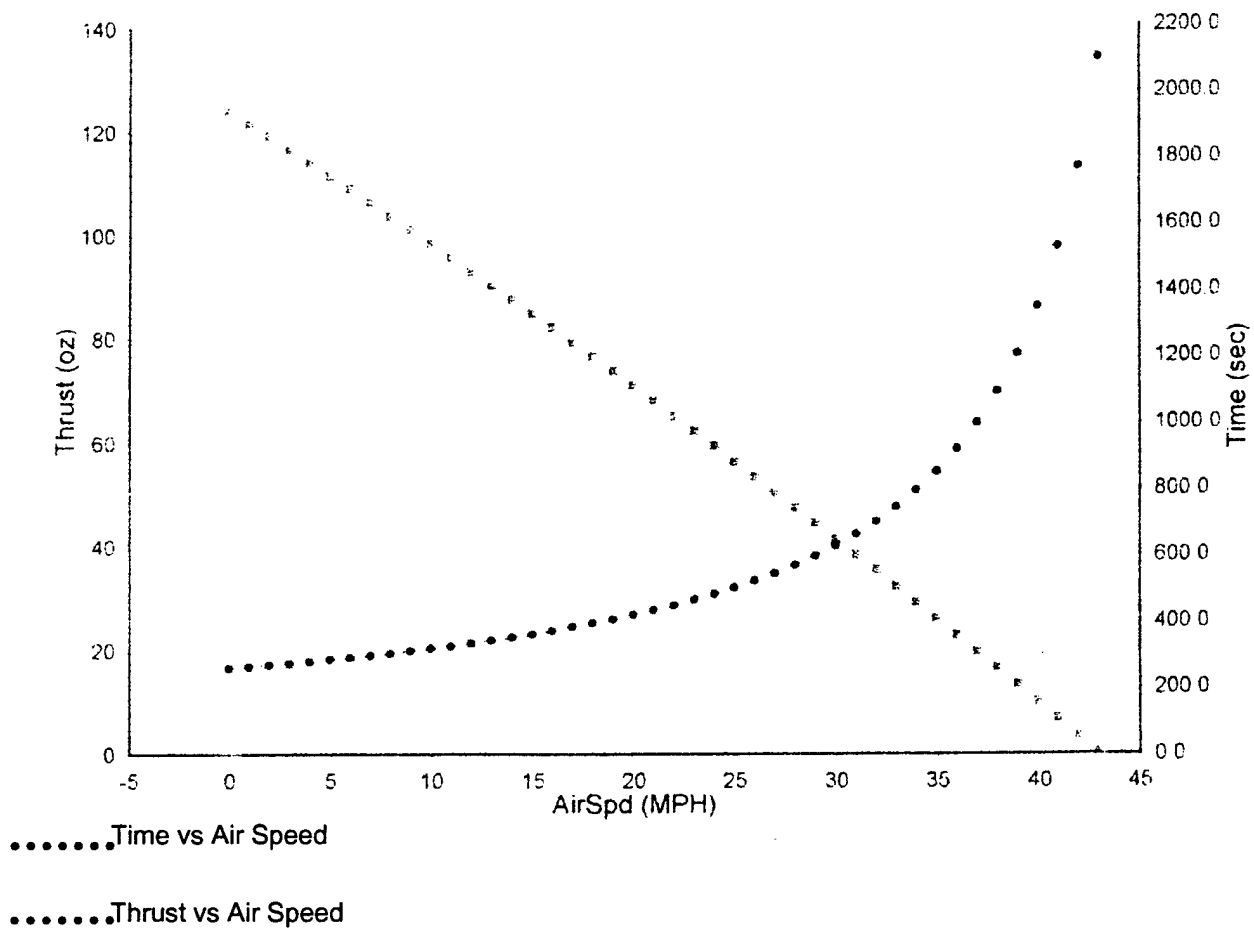


Figure 4.5 – Performance Analysis of Cobalt 40

In-Flight Analysis

Sea Level

Motor: Astro Cobalt 60 11T#23 #661; 347 RPM/V; 0.103 Ohms; 2.5A idle.

Battery: sr max 2400; 36 cells; 2400mAh; 0.003 Ohms/cell.

Speed Control: Astro 204; 0.005 Ohms; High rate.

Drive System: Astro superbox; 2 motors (parallel); 22x14 (const=1.31) geared 3.1:1.

Airframe: Anatolian craft; 1748sq.in; 591.1oz; 48.7oz/sq.ft; $C_d=0.055$; $C_l=0.65$; $C_{lmax}=1.51$.

Stats: 60 W/lb in; 50 W/lb out; 28 MPH stall; 43 MPH level @ 84% (12:29); 608ft/min @ 12.6°; -255ft/min @ -5.3°.

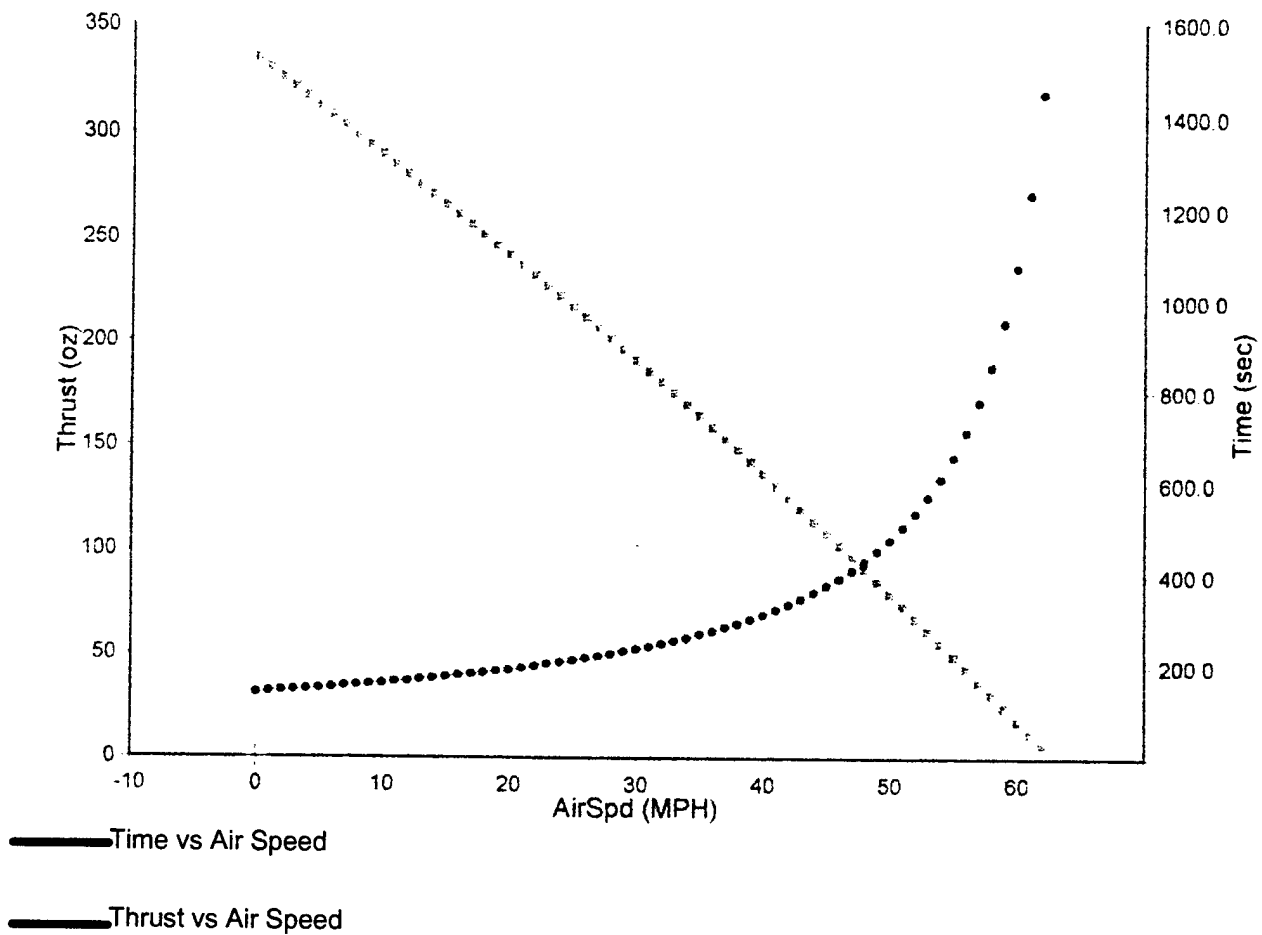


Figure 4.6 – Performance Analysis of Cobalt 60

Summary of Refined Design Parameters

Preliminary Design Revised Parameters

Payload Capacity	14.44 lb. (39 liters)
Wing Area	12.78 ft ²
Aspect Ratio	8.25
Taper Ratio	0.45
Leading Edge Sweep Angle	2.95°
Airfoil	Modified Clark Y
Tail Configuration	π -tail
Flap Chord to Wing Chord Ratio	18%
Aileron Chord to Wing Chord Ratio	16%
Fuselage Length	6.3 ft
Fuselage Material	Aluminum 2024
Landing Gear Material	Aluminum 2024
Type of Motors	Astro Flight Cobalt 60
Number of Motors	2
Power of Motor	1000 W
Type of Cells	SR 2400
Number of Cells	36
Propeller	22" x 14"

Table 4.1 – Preliminary Design Revised Parameters

5.FINAL DESIGN

5.1.Stability and Control Analyses Data

According to the approach given in Reference 1, longitudinal, lateral, and directional stability analyses of Anatolian UAV were performed. The neutral point location and the static margin of the aircraft were found to be 0.748 m and 0.062 m respectively.

Applying the trim analysis, the rudder and the elevator deflections for several cases were calculated. The spin recovery criteria (SRC) were found to be 2.85×10^{-3} .

Hence, all the stability criteria were satisfied showing that the aircraft would be able to cruise and maneuver within the skills of the pilot.

Simple code written in Mathcad and developed in METU allowed the team to calculate the modal characteristics of Anatolian.

The longitudinal stability and control analysis is very important in determining the requirement of stability augmentation system (SAS). Phugoid (long period) and short period eigenvalues of the aircraft can be given as follows:

$$\lambda_{1,2} = -6.205 \pm 0.418i \quad (\text{Phugoid Mode})$$

$$\lambda_{3,4} = -0.013 \pm 0.407i \quad (\text{Short period Mode})$$

Where,

$$\lambda = -\eta \pm \omega i \quad \eta = -\zeta \omega_n \quad \omega = \omega_n \sqrt{1 - \zeta^2}$$

ω_n is the undamped natural frequency [rad/s], ζ is the damping ratio

The period, time and number of cycles to half amplitude, undamped natural frequency and damping ratio are readily obtained once the eigenvalues are known. They are tabulated in Table 5.7. It can be seen from the above eigen values, that the linearized longitudinal Anatolian behaves in a classical manner with short period and phugoid modes in the longitudinal direction.

The aircraft would be able to complete the course by the help of the flight experience of the pilot. Lateral/directional stability was investigated by using the approach given Reference 1. The output is given in Table 5.8.

5.2. Component Selection and System Architecture

Propelling system: Twin Astro Flight Cobalt 60 Electric Motors Model 714 Super Box ratio 3:1 are used to propel the UA V. For the engine selected, a pack of 36 cells should be used because of the total cell weight limit of 5 lb. A pack of 36 cells weighs 4.275 lb. So both of the engines will be powered by a single pack of SR Max 2400 batteries. Two wooden Ultra 22x14 2-blade propellers are used. The motor and the propeller assembly will be mounted on the wing. The motor gives 4000 static rpm, 37 Volts, 34 Amps, 1000 Watts, 110-oz. thrust and 53 mph speed ideally with this propeller. This motor is one of the high output power motors available in the market, which will function with the stated number of batteries (since battery weight is limited by the contest rules). 204D Speed Control (ESC) Airplane Futaba is used. The ESC must be a high quality device that our UAV will have a high temperature increase because of high power motor, so our ESC is heat-protected. But this high quality ESC unfortunately increases the cost.

This ESC works in a range of 6-36 NiCad Cells, with max 50 Amps, 2800 switching rate, weighs 30 gram (54 gram with wires) and connectors supplied with zero loss. All of the components of the designed UA V readily available and can be found in any hobby store.

Control system: Our control system is a Futaba Digital proportional radio control unit, with nine-channel PCM 1024Z transmitters. It is a good choice with respect to the contest rules since it has the fail-safe feature for any fail condition. It also satisfies all of our needs in controlling our UA V. It has a dual mode gyro function, which allows selecting two different settings within one flight condition. These capabilities ease the landing and take-off because it increases the usage of ailerons and flaps. It has a frequency synthesizer that allows flying on any unused channel, which we must fly at. This radio control is also programmable and has the ability of servo reversing. It has the capability to reverse the rotation of a servo with a flip of a switch. It is easy to use and has flexibility during installation.

We have used 3 Futaba S-3102 micro-servos, which are micro-sized, metal gear, and 5-pole motor, has 54.1 oz.-in of torque and 3 Futaba S-9204 servos, which are gold plated and deliver 131.9 oz.-in of torque and 1 Futaba S-9202 servo, which are ball bearing, gold plated and deliver 69.5 oz.-in of torque. We have used two servos for ailerons, two for flaps, one for the nose landing gear, one for the rudder and one for the elevator. Micro-servos are used to control the ailerons and the elevator only. They all have ball

bearing supported output shafts except for Futaba S-9204. It is known (from our previous experiences) that these torque are large enough for actuating the control surfaces.

Our receiver is Futaba RI29DP, which is compatible with our radio control unit. Its dual-conversion style filters the signals twice for maximum clarity. This radio control and receiver system includes all NiCads and is available on the 50 & 72 MHz.

According to the competition rules, all aircraft radios must have a fail-safe operation mode, the details of which are given in the RFP. Research was done to collect information about how to manufacture such a system.

5.3.Conclusion

Performance data is investigated in this chapter, including the take-off and the landing performances, handling qualities, range and endurance, and payload fraction, including the component selection and systems architecture. Also structural analysis of the fuselage main structure was performed using the ANSYS finite element structural analysis software. Also the stability analyses were performed using a code written in MATHCAD by the team. Details of the computations performed are tabulated below.

Payload Weight	14.44 lb
Empty Weight	22.56 lb
Electrical components Weight	8.81 lb
Take off Weight	37 lb
Payload fraction	0.5

Table 5.1 Weight Estimates

Take Off Ground Roll	49.5 ft (Friction Coeff.= 0.05)
Velocity at Lift off	29.27 ft/s
Drag at Lift off	3.565 lb
Thrust at Lift off	3.48 lb
Takeoff Lift coefficient	1.94
Takeoff Drag coefficient	0.274

Table 5.2 Take off Performance Data

Climb Angle	31.6 deg
Climb Rate	6.96 m/s
Total distance traveled to clear 10 m obstacle	198.23 ft
Climb Lift coefficient	2.049
Climb Drag Coefficient	0.0264

Table 5.3 Climb Performance Data

Load Factor (g load capability)	3.45
Sustained Turn Rate at Sea Level	1.645 rad/s
Instantaneous Turn Rate at Sea Level	1.45 rad/s

Table 5.4 Turning Performance Data

Cruise Speed	37 Knot
Stall Speed	19.4 Knot
Maximum Speed	40.82 Knot
Range	28.8 mi
Endurance	9"45' at 18.5 m/s
Cruise Lift Coefficient	1.674
Cruise Drag Coefficient	0.0261

Table 5.5 Cruise Performance Data

Touchdown Speed	46.5 ft/s
Landing ground Roll	196.85 ft (Friction Coeff. =0.4)
Landing Lift Coefficient	1.936
Landing Drag Coefficient	0.0263

Table 5.6 Landing Performance Data

Parameters	Phugoid (Long Period)	Short Period
$T_{1/2}$	55.003	0.111
Period	15.436	15.046
$N_{1,2}$	3.563	7.391×10^{-3}
ω_n	0.407	6.219
ζ	0.031	0.998

Table 5.7 Longitudinal Modal Characteristics

Parameters	Dutch Roll
$T_{1/2}$	1.164
ω_n	6.4646
ζ	0.12758
Period	1.363
$N_{1,2}$	0.854

Table 5.8 Lateral/Directional Modal Characteristics

5.4. Structural Analysis of Fuselage Mainframe

In order to find out if the mainframe will collapse under the expected loads a series of tests were performed both physically and theoretically. For the analysis of the mainframe, ANSYS program (Reference 9) was used. The mainframe was represented as beams and by using multiple elements more accurate results were obtained. The moments of inertia and material properties were given to the program. Next thing was to determine and simulate the maximum expected loads and moments (Including the factor of safety and competition regulations). To do this maximum take-off gross weight (37 lb) was multiplied with 3g (Competition regulation), which turned out to be 111 lb. Then this load was distributed over the entire mainframe with the accompanying moments. While doing this, majority of the load was applied to the wing section and the rest of the loading was applied to the tail. The displacement graphics were obtained for this loading. It was observed that the greatest deformations occurred in the loading directions. All the other directions showed minor deformations; therefore the displacements for the loading direction are given in Figure 5.1. All the dimensions are in millimeters.

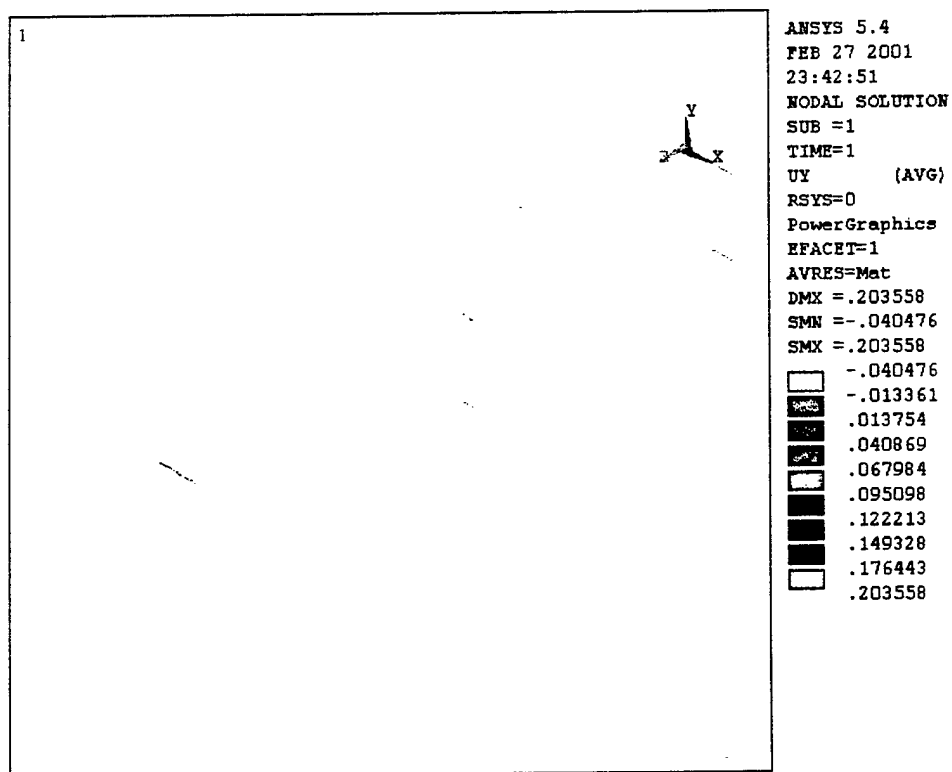


Figure 5.1 – Structural Analysis of the Mainframe

5.5.5. Drawing Package

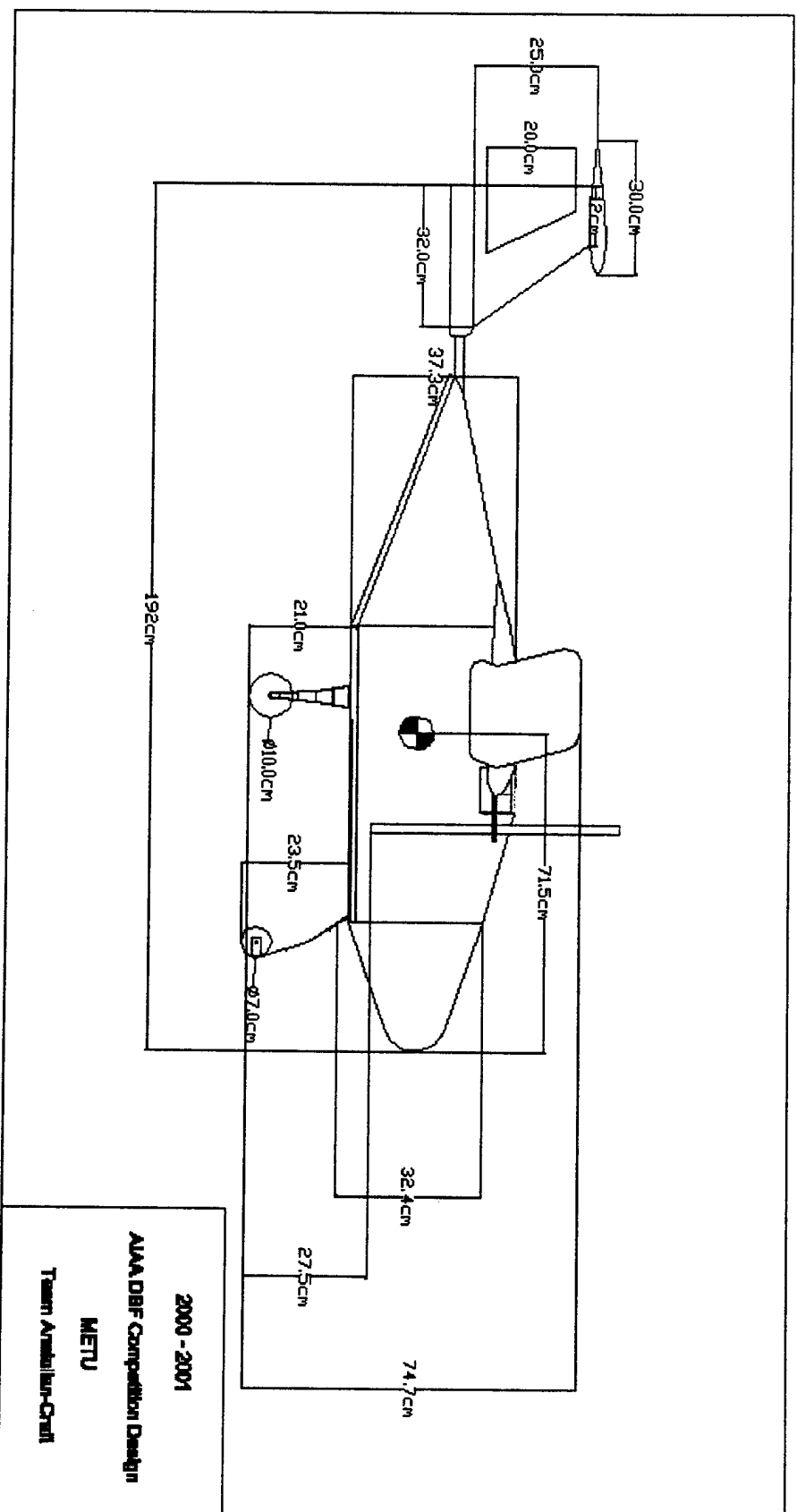


Figure 5.2 – Side View of the Aircraft

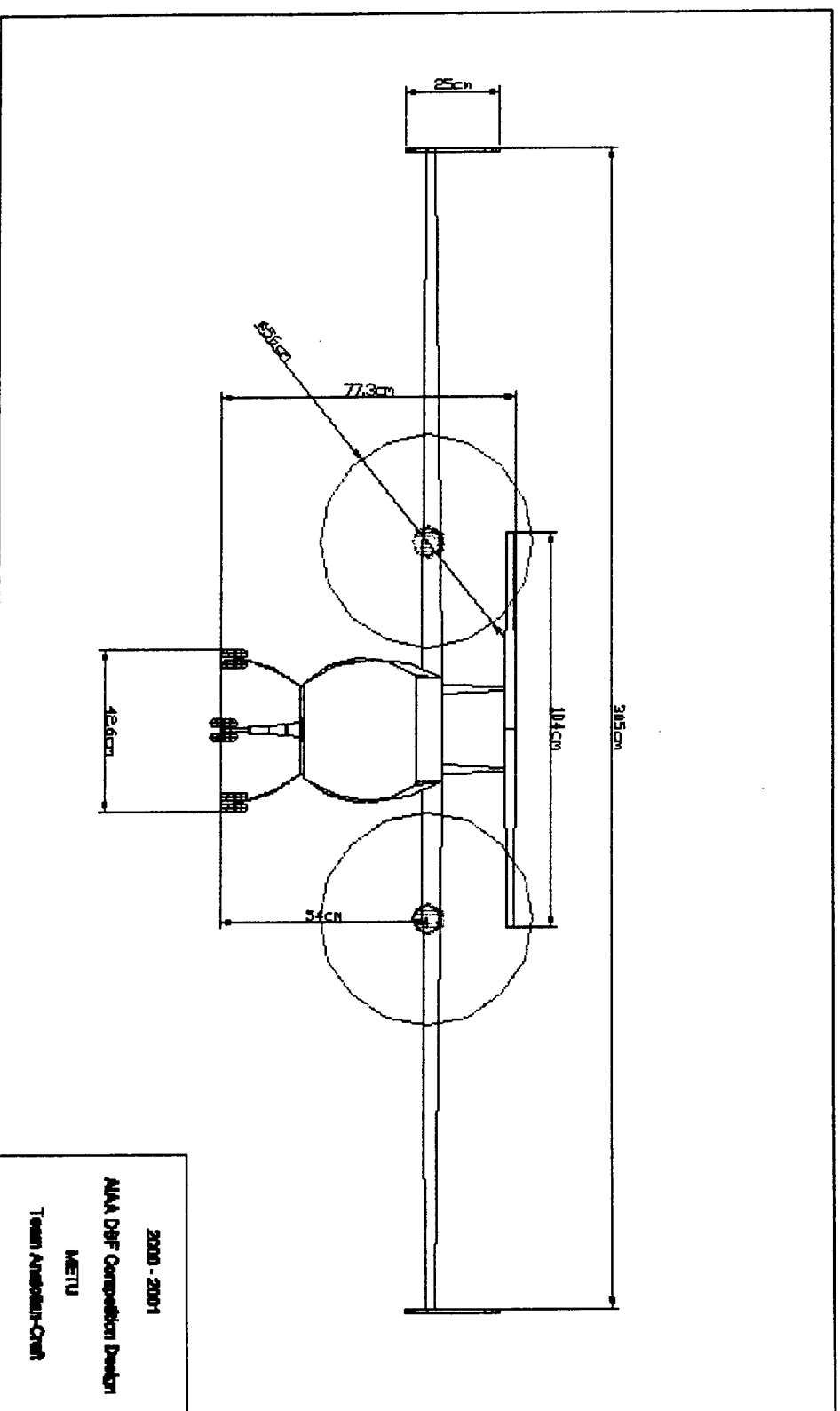


Figure 5.3 – Front View of the Aircraft

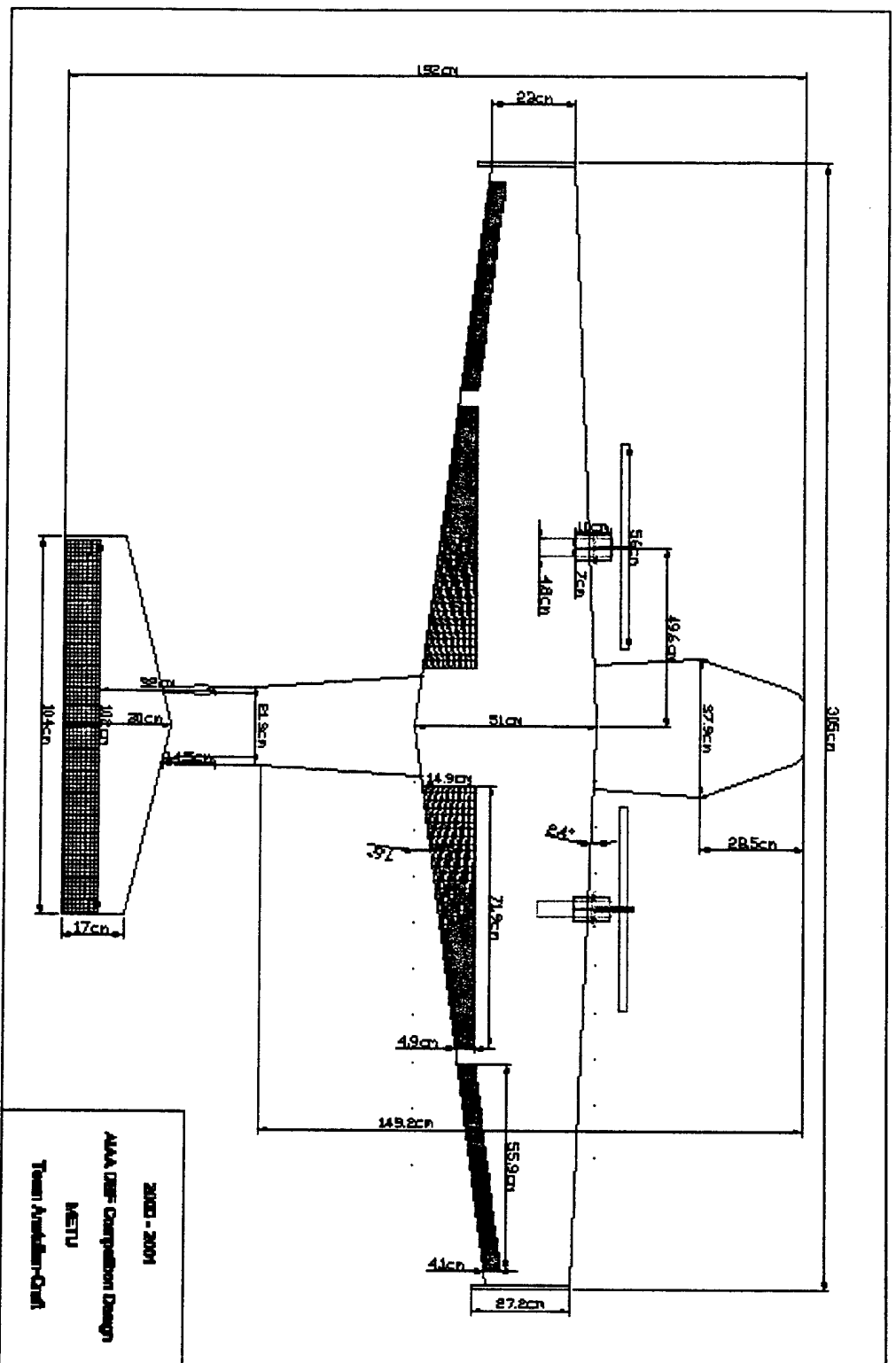


Figure 5.4 – Top View of the Aircraft

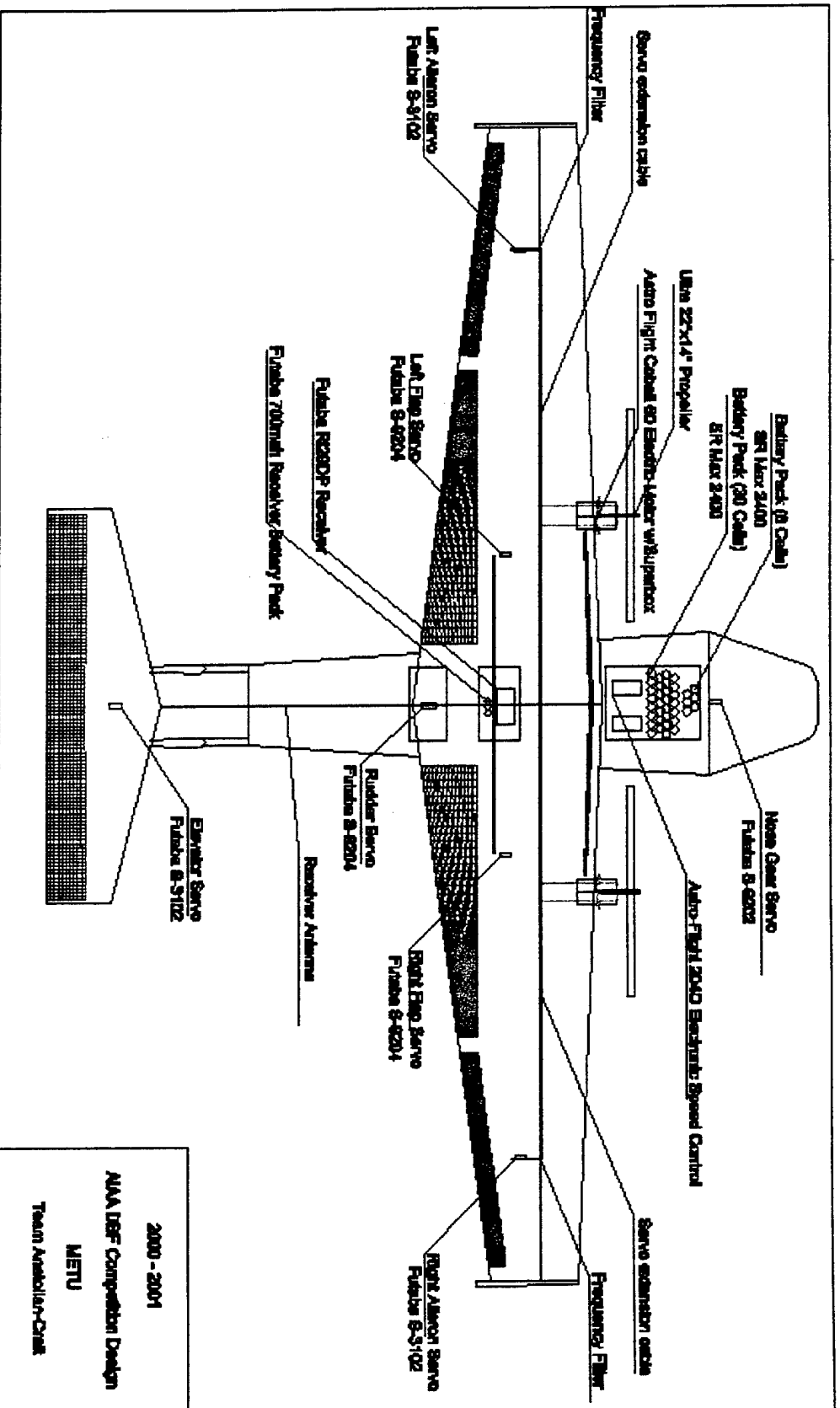


Figure 5.5 – Component Layout of the Aircraft

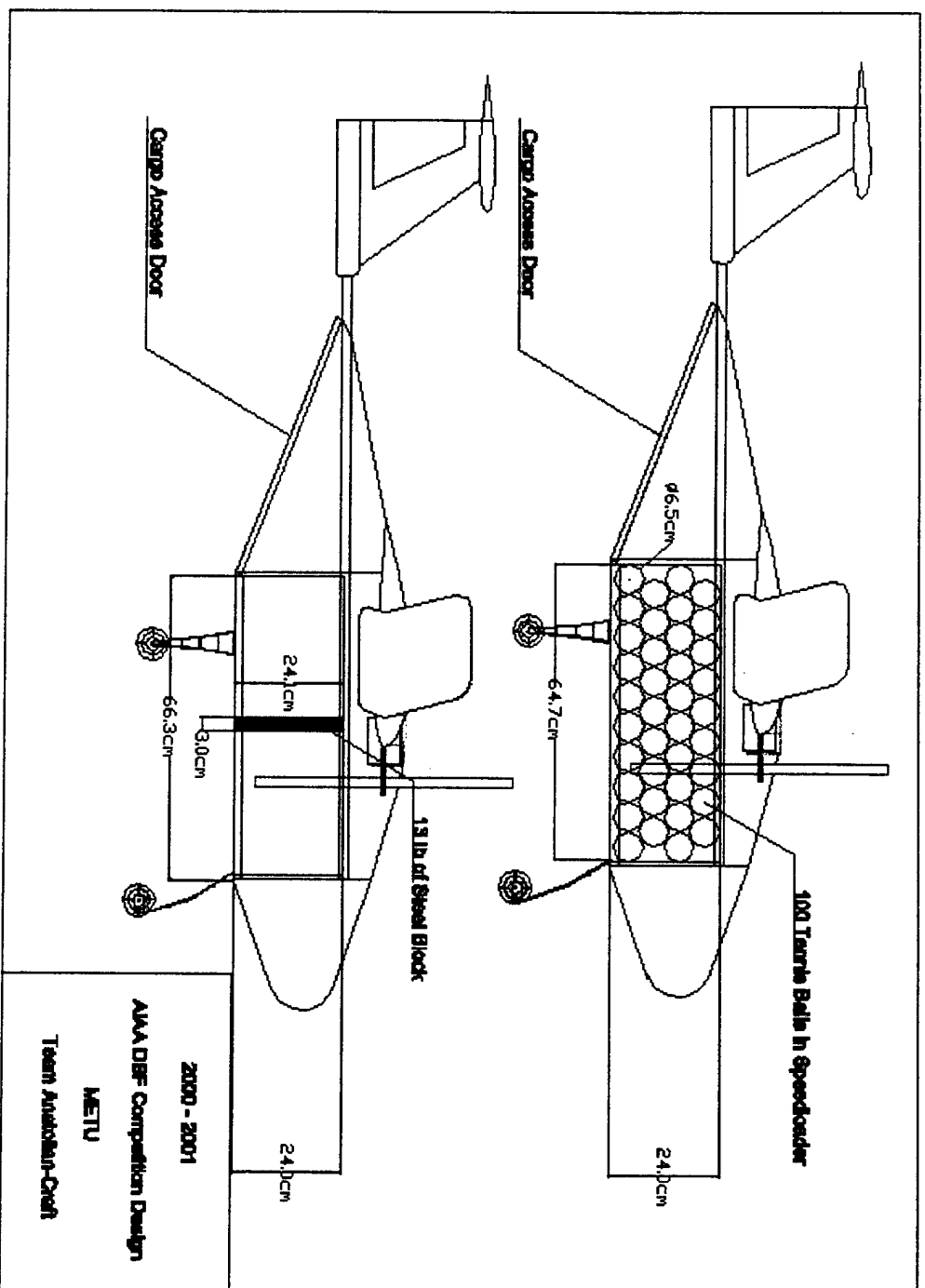


Figure 5.6 – Cargo Layout of the Aircraft

6. MANUFACTURING PLAN

6.1. Introduction

After completing the numerical analysis, next step was manufacturing the aircraft. As a first step, manufacturing processes for different parts of the aircraft were determined. It was the most important part of the manufacturing process, because the aircraft must be manufactured with minimum weight and with greatest strength while maintaining the desired structural integrity of the airplane. Table 6.1 shows all the manufacturing processes employed for different parts of the aircraft.

6.2. Figures of Merit –Manufacturing Plan

The figures of merit considered during the manufacturing process were availability, ease of manufacturing, workload, precision, structural strength and cost. According to the figures of merit, the processes that are going to be used in the manufacturing were selected. All the possible methods rated and are shown in a figure, which shows the reason why the process is selected. The following points were considered during this selection.

Availability: The material and the equipment that is required to produce a part of the aircraft were considered under availability. During the consideration of the manufacturing process, a material or equipment that is unavailable was eliminated. If material availability was low, it was assigned with a score of -1, and if material is readily available it was assigned a score of 1 at the figure.

Work Loads: Required man-hours that would be needed to complete a process were also rated. A process which requires large amount of time and man power to complete, was scored with -1, and a score of 1 was given to processes that required less time for construction.

Ease of Manufacture: Required skill level, which was needed to manufacture the part, was rated under ease of manufacture. Processes that will increase the workload were tried to be eliminated. This figure of merit scored -1 for the processes that required specialized skill. A score of 1 is assigned to manufacturing processes that required little or no experience.

Precision: In manufacturing process of some parts of the aircraft, it would be impossible to have large amounts of tolerances. This part should be manufactured very precisely. A score of -1 was given to manufacturing processes which required high precision and a score 1 was given to processes which required relatively high tolerances.

Structural Strength: Structural strength was a very important part of the manufacturing process. Processes that were used in the construction should provide desired strength. If the structural strength desired could not be met, a -1 was assigned. A 1 was assigned if the process provided the structural strength.

Cost: Manufacturing processes should not require high cost. A manufacturing process that requires high cost was scored with a -1, a component that could be built with less cost, a score of 1 was assigned.

		Availability	Manufacturability	Work Loads	Precision	Structural Strength	Weight	Cost	Result
	Weighting Factor	2	1	1	2	2	2	2	
Main Wings	Balsa Wood Rib Construction	1	1	-1	-1	1	1	1	6
	Foam Wing With Spar	1	1	1	1	1	0	0	8
Spar	Aluminum	0	-1	1	1	1	-1	0	2
	Chopped Carbon Fibers & Resin	-1	-1	-1	0	1	0	-1	-4
	Polycarbonate Multi-box	1	1	1	0	0	1	1	8
Horizontal Stabilizer	Balsa-Wood Rib	1	-1	-1	-1	1	1	1	4
	Complete Foam	1	0	1	1	1	0	0	7
Vertical Stabilizer	Balsa-Wood Rib	1	-1	-1	-1	1	1	0	2
	Complete Foam	1	0	1	1	1	0	0	7
Fuselage Floor	Chopped Carbon Fibers & Resin	-1	-1	-1	0	-1	0	-1	-6
	Carbon Fiber Laminates	0	-1	-1	0	1	0	-1	-2
	Solid Spruce Wood	1	1	1	0	0	-1	1	4
	Polycarbonate Layer	1	1	1	1	0	1	1	10
Fuselage Main Frame	Carbon Fiber Shell	0	-1	-1	0	1	0	-1	-2
	Spruce Wood	1	1	1	0	0	-1	1	4
	Aluminum Beam Structure	1	0	1	1	1	1	1	11
Landing Gear	Steel Plate	1	1	1	1	1	-1	1	8
	Aluminum Plate	1	1	1	1	1	1	1	12
Motor	Embedded Structure	1	0	-1	0	0	1	0	3
	Mounting Plate	0	1	1	1	1	-1	0	4
Cargo Container	Balsa Ply Sheets	1	1	-1	-1	-1	1	1	2
	Aluminum	0	-1	0	1	1	-1	-1	-1
	Polycarbonate Sheets	1	1	1	0	0	1	1	8
Fuselage Cover	Balsa Wood	1	1	-1	-1	-1	0	1	0
	Foam	1	1	1	1	-1	1	1	8
Nose	Balsa Wood	1	1	-1	-1	-1	0	1	0
	Foam	1	1	1	1	-1	1	1	8
	Carbon Fiber Laminates	0	-1	-1	0	1	-1	-1	-4

Table 6.1 – Manufacturing Processes Considered

6.3.Wing Construction

Construction of the wing was the major part of the manufacturing phase. The wing should be as light as possible with the greatest possible strength. During the conceptual design phase, two different manufacturing processes were investigated for the construction of the main wing. These were balsa wood rib construction and solid foam core wing with load carrying spar construction. Due to the inexperience in the balsa wood rib construction and considering the figures of merit, foam core with load carrying spar was chosen as the best manufacturing process for the wing.

Three main elements were used in the wing construction. These were balsa wood, polycarbonate and polystyrene foam. Polystyrene foam was the major element of the wing. It was used to maintain the desired shape of the airfoil across the span of the wing. According to low weight with high modulus of elasticity consideration, 10 kg/m^3 density foam was used in the wing manufacturing. At the beginning, lower density foam was used however because of single spar configuration wing did not seem to have the required strength. So the wing is manufactured again from 10 kg/m^3 foam. The airfoil models were constructed from hard wood for mid, tip and root sections of the wing. With the help of airfoil models, foam cores were cut by using an electric hot wire-cutting device. Each wing was constructed from two parts of foam core since it was difficult to cut the wing as a single piece. The remaining part of the foam core was used as a mold for the wing while covering the foam with balsa sheets. Then these two components of each wing were bonded together with an epoxy coated balsa plate between them to strengthen the structure of the wing.

Three different materials were considered for the construction of the spar. These were polycarbonate spar, aluminum spar and e-glass fiber or carbon fiber composite spar. In the consideration of cost and strength analysis polycarbonate was the most suitable choice for spar material. With the help of the sawing and milling machines, polycarbonate was given a taper, in order to make it fit into the wing. The multi-box structure of the polycarbonate allowed us to pass all the wires of the control surfaces from the spaces between the multi-box structures.

After the construction of the spar, foam core wing and the spar were connected. As a first step, the volume that the spar will occupy was cut off from the foam and the foam and spar were bonded together with epoxy.

Next step was the wood sheeting of the wing. Balsa wood sheets of $1,5\text{mm} \times 100\text{mm} \times 1000\text{mm}$ were bonded to obtain a balsa sheet, which is equal to the wing in area. This process was repeated for both the lower and upper the surface of the wing. Then using the mold pieces that are previously obtained, the

foam is sandwiched between the balsa placards at the upper and lower surfaces. Epoxy, which was thinned by methyl alcohol, was applied to both foam and the balsa placard surfaces. Keeping the placards under a high pressure over 12 hours resulted in a balsa sheet covered foam core, which formed the main structure of the wing.

After covering the wing, the leading edge of the wing was constructed from balsa blocks. The reason to use balsa on the leading edge was the ease of shaping the balsa wood to obtain accurately the desired leading edge geometry of the airfoil profile.

The control surfaces were cut off from the main wing and balsa wood was placed into the hinge locations of the control surfaces where the hinges will be mounted.

Last step of the wing construction was to place the linkages which will connect the right and the left wing parts together and the manufacturing of the end plates. End plates were made from the balsa wood. For end plate construction, two pieces of balsa wood were connected to each other with the help of balsa glue. An important factor in the end plate construction is that, direction of fibers in each lamina of the balsa wood was perpendicular to each other so that the endplate was strong in both directions. In the connection of two wings, aluminum tubes with carbon fiber wound around them were used. For each wing, two aluminum tubes were used for the connection. The aluminum tubes in the right wing fit tightly to the tubes that are embedded into the right wing so that the wing can be separated into two parts anytime. This feature is designed solely for transportation purpose. At the end of the wing construction, e-glass composite was used to strengthen the connection parts of the wing and engine mount part of the wing, since these parts will carry more stress when the aircraft is in flight.

6.4.Tail Construction

For tail construction, again two types of manufacturing processes were considered; balsa wood rib construction and foam core tail construction without load carrying spar. Due to the lack of experience of team members in rib construction technique and the strength problems and manufacturing difficulties faced with the rib construction for the tapered shapes, foam core construction was also preferred for the manufacturing of the tail.

Same procedure as used in the wing construction was applied for the construction of the tail. The only difference was the spar construction and foam type. In tail construction, there was no need for a load carrying spar, so higher density foam should be used to have the required strength. Therefore, 15 kg/m³ density foam core was used.

The most important consideration in the tail construction was the connection between the horizontal and the vertical tails. According to the preliminary design, horizontal tail should be placed on top of the vertical tails, however this caused some strength problems at the connection point. To overcome this problem e-glass fiber composite was used to strengthen the connection of the horizontal and vertical tails.

6.5.Power System Integration

During the conceptual and the preliminary design phases, it was decided to use two wing-mounted electric motors. It was also found out that the required propeller was 22"x14" and the power would be supplied by 36 batteries. The batteries were consisted of two packs, a pack of 30 batteries and a pack of 6 batteries because of the battery charger capacity. So two different packs were prepared and placed on the nose of the aircraft, where they balanced the moments that are caused by the weight of the tail.

Two different methods were studied to determine the method that could be used to attach the engines to the leading edge of the wing. First method was to insert the engine inside the wing and support it by hard wood to increase the structural strength. Second method was to use aluminum engine mounts to attach the motors to the wing. First method was eliminated because it was structurally insufficient to prevent the vibration that could be caused by the engine. Aluminum mounting plates were fixed to the wing with four screws at the upper surface of the wing and fiber reinforced nuts and lock-tight was employed to prevent the vibration on these screws. Two of these screws were also connected to the aluminum connection tube of the wing to increase the structural strength of the engine mounting. Teflon was used in the contact points between the mounting plates and the motors to decrease the vibration effect. This manufacturing technique did not require complicated final adjustments and it did not require high level of skilled labor.

6.6.Fuselage

The possible manufacturing procedures for the fuselage was manufacturing the fuselage from hardwood supported balsa wood structure, manufacturing the fuselage from composite material and manufacturing the fuselage from aluminum beams.

From experience, it is decided that hardwood supported balsa wood structure had advantages in the availability of the materials but the weight of the structure is high because of the strong mainframe, needed to support the landing gear, wing and the payload.

Also composite structures were difficult to manufacture due to the unavailability of the tools, and the high cost of manufacture.

The final option was building an aluminum boom structure, which will carry the cargo and also distribute the loads of the wing, landing gear and tail to the mainframe. Also the structural analyses that are performed by ANSYS software gave satisfactory results. This structure would be covered with any material such as balsa plywood or foam to achieve a reasonable aerodynamic efficiency.

The boom structure had to be stiff enough to prevent fluttering of the tail. Aluminum 2024 T3 was chosen as the material for the boom structure. Aluminum 2024 T3 is widely used in aviation industry because of its high specific strength and stiffness. Aluminum 4043 was used as the welding material for the structure.

A specially designed structure was necessary to mount the wing tightly on the upper booms, which were hollow cylinders. Also some space was necessary to place the electronic equipment between the upper booms of the fuselage and the wing. It was a design goal to be able to move the wing along the longitudinal axis, for the further modifications and fine-tuning for stability; so a fixed support was not used. Two aluminum supports, which were able to slide freely on the upper two booms, were used. These booms were made from aluminum 6061 T6; which was more efficient than 2024 T3 for accurate welding process. The supports were fixed with screws on the booms, so it was possible to remove or replace them to any location along the fuselage.

The fuselage cover was free of stress, so a simple and light structure was necessary. The three options for fuselage cover were polycarbonate sheets, balsa plywood and foam. The foam structure was lightest and easiest to shape; so it was chosen. 4mm thick polycarbonate sheets were used for the access doors made on the fuselage to reach the cargo, electronic equipment and the batteries.

The batteries, servos and other electronic structure were mounted on more dense foam, which was placed between the upper booms and wing. The foam that is fixed to the booms carries the batteries and the other electronic devices over the fuselage. The foam is fixed to the booms with Velcro so that it allows moving the batteries and the devices along the booms to move freely the cg location to the desired position.

The cargo container was made of 3mm thick polycarbonate sheets. This was the lightest and the easiest material for manufacturing the container with the desired dimensions. The loading is performed by inserting the container from the aft cargo access door of the aircraft as used by the military cargo aircraft.

The tail attachments were made with screws on the tail booms, which enabled further modifications on tail placement along the longitudinal axis, for stability considerations.

The outer structure of the fuselage is covered with foam to increase the aerodynamic efficiency of the structure and to decrease the drag.

The nose of the fuselage was also prepared from foam, since this was the easiest material to shape. It was also covered with epoxy-fiber composite for more stiffness in case of any high impact landing.

6.7.Landing Gear

The tri-cycle landing gear is selected at the design phase. For the main landing gear, the simplest and the lightest possible option was a sheet metal landing gear. The possible materials considered were steel and aluminum. The spring effect of an arc shaped steel was considered to be effective, but it was observed after manufacturing the component that this structure was too heavy for the design. So the same structure was remanufactured from aluminum. The main landing gear was fixed to the lower beams of the aluminum frame structure with screws. This would again permit further modifications in the longitudinal stability of the aircraft.

The nose gear was manufactured from two parallel steel springs which were welded together to increase their strength without losing the spring effect. A servo is connected to the nose gear that is working parallel with the rudder to improve the steering during ground taxiing.

6.8.Results

In Table 6.1, the techniques of manufacturing used during the project are presented. The manufacturing technique for the wing and tail is selected to be foam core structure with balsa covering. A polycarbonate multi-box spar is inserted inside the foam core of the wing to increase its structural strength. The fuselage was manufactured from, Al 2024 T3 frame structure composed of cylindrical and L-beams with Al 4043 weldings. An Al 6061 T6 wing mount is screwed to the fuselage to support the wing. A polycarbonate rectangular box is selected as a cargo container that can be inserted into the fuselage from the cargo access door. Aluminum solid spring main landing gear is selected because of its light weight and strength. Two parallel steel springs are employed as the nose gear, which provide good steering and enough impact resistance. Finally a smooth aerodynamic shape is given to the fuselage by covering it with profiled foam patches. The nose of the fuselage is also manufactured from profiled foam and covered with fiberglass and epoxy for imparting additional impact resistance to the nose. Finally wings are attached to the aluminum wing mounts on the fuselage frame by Teflon bolts for reduced weight and vibration transfer. The timetable for manufacturing is presented in Table 2.2.

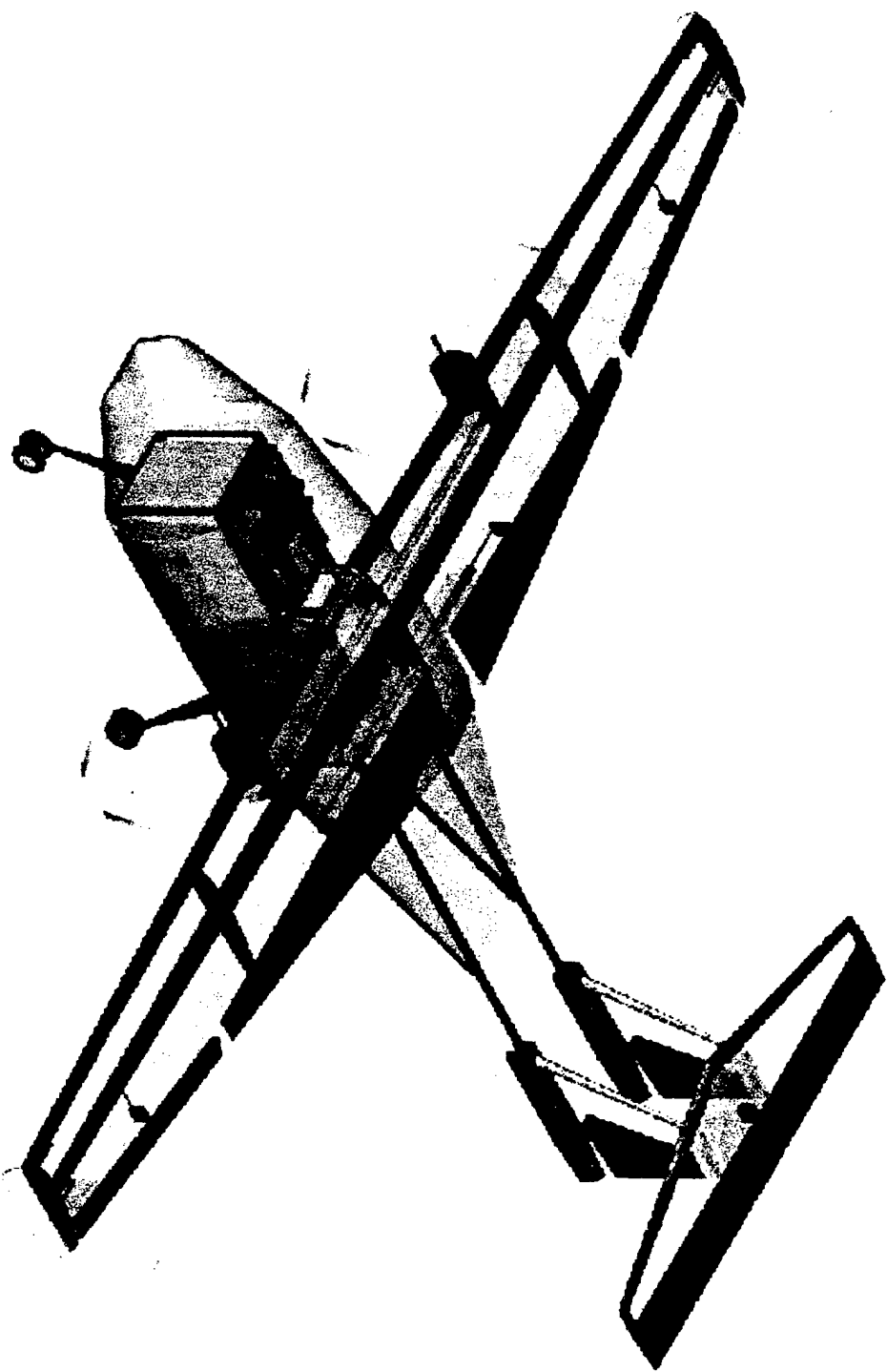


Figure 6.1 – Detailed 3D Drawing of the Aircraft

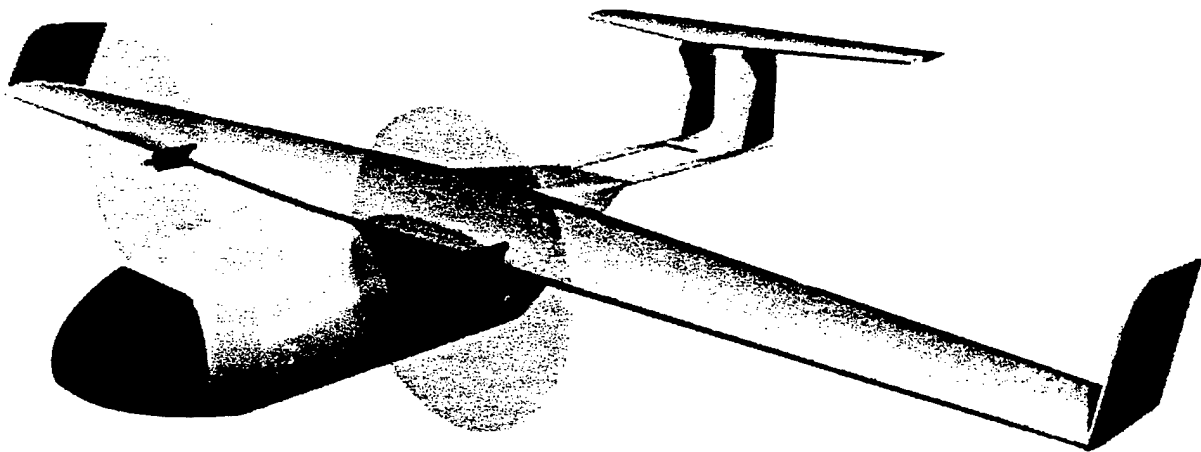
7. REFERENCES

1. Raymer D.P., *"Aircraft Design: A Conceptual Approach"*, AIAA Education Series, Second Edition, 1992.
2. Roskam J., *"Airplane Design"*, Parts 1-8, Roskam Aviation and Engineering Corporation, Second Printing, 1989.
3. Motocalc Version 5.01, Copyright 1997 – 1998, Capable Computing.
4. Microsoft © Excel 97, Copyright 1985 – 1996, Microsoft Corporation.
5. Microsoft © Word 97, Copyright 1983 – 1996, Microsoft Corporation.
6. MathCad , Copyright 1986 – 1997, MathSoft Corporation.
7. Analyze an Airfoil, <http://beadec1.ea.bs.dlr.de/Airfoils/calcfoil.html>
8. AutoCAD Release 14.0, Copyright 1982 –, AutoDesk Inc.
9. Utah University, Wing and a Prayer Team, *"AIAA 99/00 DBF Competition Best Written Report"*, 2000.
10. Munson K., *"Unmanned Aerial Vehicles and Targets"*, Jane's Information Group, 1996.
11. UIUC Airfoil Coordinates Database, http://amber.aae.uiuc.edu/~mselig/ads/coord_database.html
12. Ansys © Version 5.7, Copyright 1995 – 2000, Ansys Inc.

AIAA / CESSNA / ONR

Student Design / Build / Fly Competition

Addendum Report



Middle East Technical University

Team Anatolian-Craft

April 2001

7. LESSONS LEARNED **2**

7.1 INTRODUCTION **2**

7.2 FLIGHT AND GROUND TESTS **2**

7.3 IMPROVEMENT AREAS **3**

8. AIRCRAFT COST **8**

8.1 INTRODUCTION **8**

8.2 RATED AIRCRAFT COST MODEL **8**

8.3 RESULTS **10**

7. LESSONS LEARNED

7.1 Introduction

The team learned some lessons from the mistakes made during the manufacturing phase and the ground and flight tests. However, the manufactured aircraft has only slight differences from the one, depicted at the proposal phase. Many of the mistakes were easily corrected by simply redesigning and replacing or by simply improving some parts of the aircraft. Within the problems, the team encountered the main landing gear and the nose landing gear problems were the most time consuming parts of the whole aircraft.

7.2 Flight and Ground Tests

- Test # 1: (10.03.2001) 30 minutes, Clear weather N-NE 10 knots.
Purpose: To test the engines, landing gear functionality and to evaluate the performance of the aircraft during taxiing.
Procedure: The aircraft was tested with 2-kg payload. The power supply was composed of two packs containing 30 and 2 batteries. Firstly, the engines were run while the aircraft was fixed and then the aircraft was tested on ground (taxiing). During taxiing the aircraft was let to run 30 meters and afterwards completed a 180° turn and returned to point where it had started.
Observations: The engines worked properly without causing any problems both when the aircraft was fixed and when it was taxiing. During taxiing it was observed that the nose landing gear was not designed appropriately since it was bending inwards during the forward motion of the aircraft. Also the position chosen for the servo control of the nose landing gear was not good this it was causing difficulties in controlling the landing gear orientation.
- Test # 2: (25.03.2001) 45 minutes, Clear weather N-NW 15 knots.
Purpose: To test the revised nose landing gear and flight performance of the aircraft.
Procedure: The aircraft was tested first with 30 tennis balls of payload. Power supply consisted of two packs of 30 and 2 batteries respectively. The first step was the taxiing of the aircraft 30 meters along the runway and turning back to the starting point. Afterwards another payload of 70 tennis balls was inserted and again the taxiing performance along the same route was tested. After finishing the ground tests 70 tennis balls were removed during the flight tests. First step of the flight test was taking off and landing immediately. The aim was to determine the stability of the aircraft.
Observations: The ground tests were completed successfully both with 30 and 100 tennis balls of payload. The new nose landing gear was strong enough to withstand the static loading and the loads during taxiing. The aircraft performed very well during the takeoff. However while approaching for landing, when the pilot decreased the thrust it was observed that the engines failed, consequently the aircraft landed with high velocity, damaging the main landing gear. One side of the main landing gear

deflected nearly 40° outboard, No other damage was observed. (Figure 7.1).

Test # 3: (30.03.2001) 35 minutes, Clear weather N 9 knots.
 Purpose: To test the engines and the new main landing gear.
 Procedure: The aircraft was loaded with 2 kg of payload. The Power supply was composed of two packs each containing 30 and 6 batteries respectively. The aircraft was tested on the run way just performing the usual taxiing route, the trim adjustments were also examined by running the motors when the aircraft stayed fixed.
 Observations: The ground test showed that the new main landing gear design and the trim adjustment of the engines were successful. However while testing the engines it was observed that as the RPM of the engines decreased the wing started vibrating as a consequence of the unbalance problem of one of the propellers.

Test # 4: (31.03.2001) 20 minutes, clear weather N-NE 3 knots.
 Purpose: Evaluating the flight performance of the aircraft.
 Procedure: The flight tests were performed with 2 kg of payload. The power supply was composed of two packs each containing 30 and 6 batteries respectively. The aircraft was tested by performing the following mission task:
 Takeoff / Climb / 3000 ft of cruise / Landing
 Observations: Aircraft completed the whole mission task without any problem. (figure 7.2)

7.3 Improvement Areas

Wing: There were only slight changes on the wing, as the manufactured parts resulted to be quite close to the ones designed at the proposal phase. There were some misleading characteristics of the wing observed after the manufacturing. Yet, all those defects were corrected before any ground and flight tests.

The team decided to remove the end plates that were included in the design at the proposal phase. It was decided that the endplates would cause problems at crosswind and gust conditions during flight and taxiing. Since the cruising altitude is not very high, any instability caused by the crosswind conditions could lead to a crash. The team decided to replace the end plates simply by rounded wingtips.

It was observed that the gap between the control surfaces and the wing was too much, which would cause unnecessary amount of air to leak from lower surface to the upper surface through these gaps. The remedy to this problem was to use a thin sheet of acetate to cover over these openings.

Fuselage: The characteristics of the fuselage were found satisfactory enough during manufacturing and ground and flight tests. However, to save some weight and to improve the aerodynamic characteristics of the aircraft it was decided to have thinner foam coverings thereby

reducing the total cross sectional area of the fuselage. Other than reducing the thickness of the foam coverings of the fuselage, nothing was changed.

Landing gear: Before any ground and flight tests, the landing gears seemed to be sufficiently strong. However, the first ground test showed that the nose landing gear was bending inwards during taxiing due to the heavy loading on it during the forward acceleration of the aircraft. The team designed a new nose landing gear, which was more stronger than the first one and capable to withstand high loads during forward acceleration (Figure 7.3). This new nose landing gear proved to be successful during the second ground test. The fixture of the front landing gear to main structure of the fuselage was also changed. The landing gear was attached to the metallic frame of the fuselage from two points: the lower and the upper transverse bars of the frame. This new attachment of the front landing gear to the main frame was more beneficial and correct since the bending stresses created was distributed more evenly over the landing gear. In addition, the spring was made stiffer by increasing the diameter of the spring wire and by heat treating it after bending it in coil form.

After solving the problem with the "nose landing gear" the team performed a second test in which the aircraft took off and cruised for some distance successfully. However, the landing was not properly done due to the problems caused by the trim settings of the throttle. This misfortune clearly proved that the main landing gear was not also designed appropriately when taking into considerations that high impact landings that can always take place. A new main landing gear was designed. The team added strut wires that prevent the bending of the main landing gear outward during high impact landing conditions (Figure 7.4). For this new design of the landing gear heat-treated aluminum was used to decrease its weight and improve its strength. The fourth flight test proved the reliability of the new landing gear.

Engine and Batteries: All the ground and flight tests showed that there was no problem due to the engines. In the proposal phase, it was decided that a pack of 36 batteries would be used. However, the team considered that it was not necessary to use 36 batteries as it might overload the electronic speed controllers. For first tests, 32 batteries were used, composed of a 30 battery pack and another 2 battery pack (due to the fact that the battery charger permits 30 batteries at one time). With this power supply flight, time became a problem. The pack of 2 batteries was consumed earlier than the larger pack because of the unbalance of the packs caused by different charging currents applied by the charger, to the respective packs. This resulted in a reduction of the RPM of the engines and therefore of the thrust before the battery pack was completely emptied. Hence, in order to increase the flight time, the team decided to take a chance by using a

pack of 36 batteries. During the ground and flight tests the high voltage did not cause any problems for the speed controllers, provided longer flight period for the engines.

Propellers: During the second ground test the team realized that there was a large amount of vibration on the wing. At firstly it appeared as an "engine mounting" problem. However, it was soon discovered that an unbalance in one of the propellers was causing this problem. So the propellers were checked for an unbalance and an unbalance was found on one of the propellers. The propeller was re-balanced by simply painting the lighter side of the propeller with a heavy acrylic paint.

Radio Control and Servos: During the first flight test, while the aircraft was cruising, both of the engines stopped, as a result of the pilots attempt to decrease the throttle. The team first thought this was an "engine problem". However, it was understood that the trim settings of the radio controller were not done properly. Upon checking, it was found that the elevator trim and the throttle trim were reversed. This caused any trim given to the elevator during the flight, to decrease the throttle setting. This gave us a big lesson: it showed that even though the aircraft may be all right, it can crash easily because of improper radio settings. Therefore, this showed us that the pre-flight checks must always be done properly. So the team double-checked all the R/C settings.

The nose landing gear steering servo controller appeared to be a problem at the start of the ground tests. The location of the servo (right under the nose towards the left side) was not chosen appropriately and was causing problems while maneuvering. It was also creating additional drag. The team decided that placing it inside the nose would be the most appropriate place for the servo controller since this would reduce the drag and would facilitate the control of the landing gear.

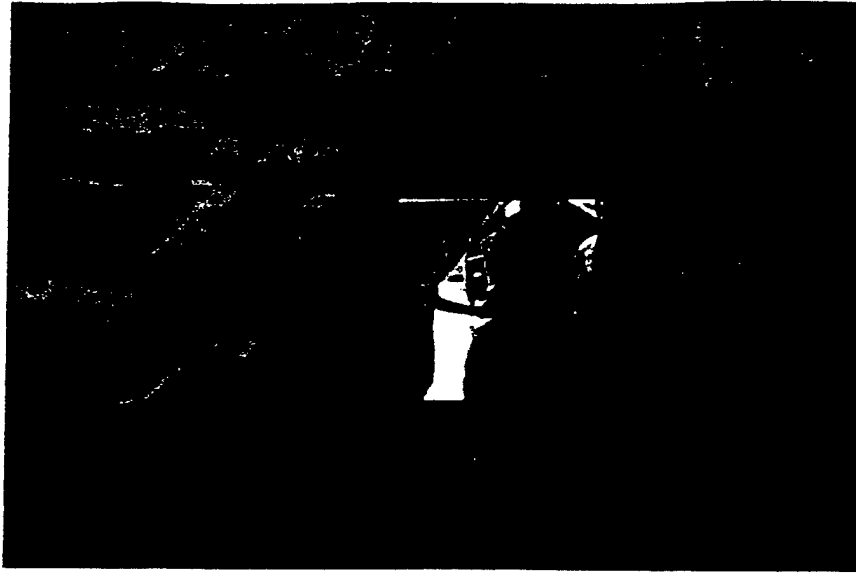


Figure 7.1 Damaged landing gear during landing (Test # 2)



Figure 7.2 Anatolian craft at flight (Test # 4)

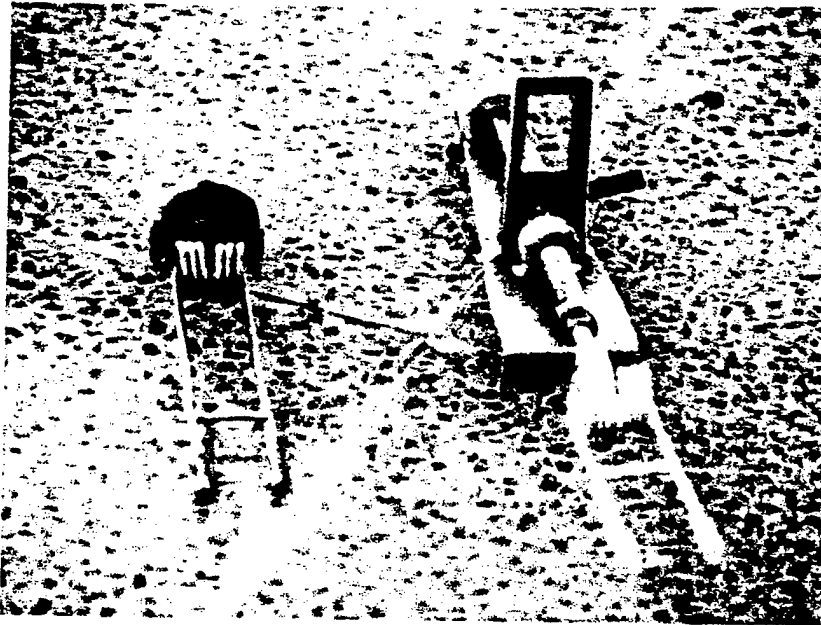


Figure 7.3 Old design (left) new design (right)

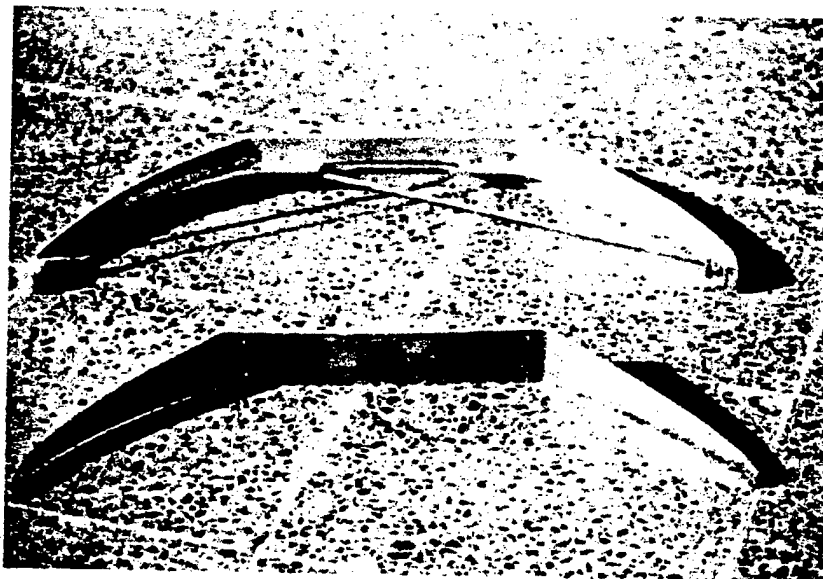


Figure 7.4 Old design (below) new design (above)

8. AIRCRAFT COST

8.1 Introduction

Each team's overall score will be computed from their *Written Report Score*, *Total Flight Score* and the *Rated Aircraft Cost* using the formula:

$$\text{Score} = \frac{\text{WrittenReportScore} * \text{TotalFlightScore}}{\text{RatedAircraftCost}} \quad (8.1)$$

Since, apart from the performance of the model, the total score is dependent on the Rated Aircraft Cost, the team worked for obtaining the highest flight score possible for the lowest rated aircraft cost. So an optimization was done for the ratio of the total flight score and the rated aircraft cost.

The Rated Aircraft Cost formula (equation 8.2) contains 3 variables which are *Manufacturers Empty Weight*, *Rated Engine Power* and *Manufacturing Man Hours*. These variables are reduced as much as possible without sacrificing from the performance of the aircraft in order to obtain high flight scores.

$$\text{Rated Aircraft Cost, \$ (Thousands)} = (A * \text{MEW} + B * \text{REP} + C * \text{MFHR})/1000 \quad (8.2)$$

8.2 Rated Aircraft Cost Model

Coefficient	Description	Value
A	Manufacturers Empty Weight Multiplier	\$100/lb
B	Rated Engine Power Multiplier	\$1/watt
C	Manufacturing Cost Multiplier	\$20/hour
MEW	Manufacturers Empty Weight	Actual airframe weight, lb., without payload or batteries
REP	Rated Engine Power	# engines*50A*1.2V/cell * # cells
MFRH	Manufacturing Man Hours	Prescribed assembly hours by WBS (Work Breakdown Structure). MFHR = WBS hours WBS 1.0 Wing(s):

		15hr/wing + 4hr/sq.ft Projected Area + 2hr/strut or brace + 3hr/control surface WBS 2.0 Fuselage and/or Pods 5hr/body 4hr/ft of length WBS 3.0 Empennage 5hr (basic) +5hr/Vertical Surface +10hr/Horizontal Surface WBS 4.0 Flight Systems 5hr (basic) +2hr/servo or controller WBS 5.0 Propulsion System 5hr/engine +5hr/propeller or fan
--	--	--

Table 8.1 Aircraft Cost Model

Manufacturers Empty Weight: The actual airframe weight without payload or batteries is manufacturers empty weight as indicated before and is 22.491 lb.

$$\text{MEW} = 22.491 \text{ lb.}$$

Rated Engine Power: The aircraft is using two Astro Cobalt 60 engines, each consuming a maximum of 35 Amperes. Since 35-Ampere fuses were not available, the team had to use 40 Ampere fuses instead. The motors run on 36 batteries of 1.2 Volts each.

$$\text{REM} = 2 * 40 \text{ Amp} * 1.2 \text{ V/cell} * 36 \text{ cells}$$

This calculated value for REM is 3456 watts.

Manufacturing Man-Hours: This variable is used to approximate the working hours for building up the aircraft. Working hours for five parts were added up in order to compute the MFHR. The work brake down structure is as follows:

		Aircraft parameters	Multiplier	Total Working Hour
Wing	# of wings	1	15 hr	15 hr
	Projected Area	12.78 ft ²	4 hr	51.12 hr
	Strut or Brace	-	2 hr	-
	Control Surface	4	3 hr	12 hr
Fuselage	# of bodies	3	5 hr	15 hr
	Length of the fuselage	6.3 ft	4 hr	25.2 hr
	Length of the pods	0.51	4 hr	4.08 hr
Empennage	Basic	-	5 hr	5 hr
	Vertical Surface	2	5 hr	10 hr
	Horizontal Surface	1	10 hr	10 hr
Flight Systems	Basic	-	5 hr	5 hr
	# of servo	7	2 hr	14 hr
Propulsion Systems	# of engines	2	5 hr	10 hr
	# of propeller	2	5 hr	10 hr
Total Working Hours :				186.4 hr

Table 8.2 Brake down of manufacturing hours

8.3 Results

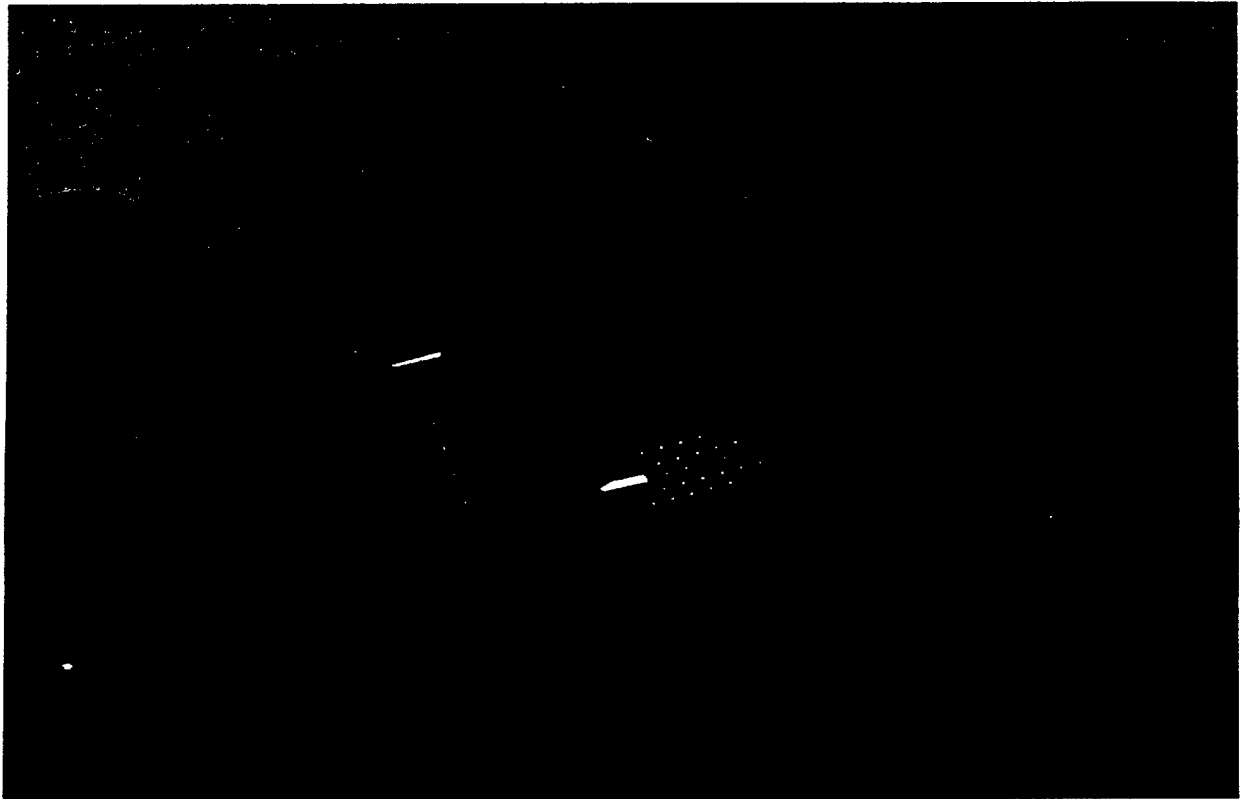
The total rated aircraft cost is:

$$\text{Rated Aircraft Cost} = \frac{(\$100/\text{lb} * 22.491\text{lb} + \$1/\text{watt} * 3456\text{ watt} + \$20/\text{hr} * 186.4)}{1000}$$

Rated Aircraft Cost, \$ (Thousands)=9.433

**AIAA Student Design/Build/Fly
Competition**

THE GPA Killer



By:

The University of Texas at Austin
2000/2001 Design/Build/Fly Team

Table of Contents

1.0 Executive Summary.....	1
2.0 Management Summary.....	2
3.0 Conceptual Design.....	4
3.1 Alternative Concepts Investigated.....	4
3.2 Design Parameters Investigated.....	5
3.3 Figure of Merits.....	7
3.4 FOM – Ranking Importance Factors.....	9
3.5 FOM Matrix.....	10
4.0 Preliminary Design.....	11
4.1 Preliminary Aerodynamics Design.....	11
4.2 Preliminary Structural Design.....	16
4.3 Preliminary Propulsion Design.....	30
5.0 Detail Design.....	31
5.1 Performance Data.....	31
5.2 Component Selection and Systems Architecture.....	32
5.3 3-View Drawing Package.....	41
5.4 Innovative Solutions, Manufacturing Processes, and Cost Reduction.....	43
6.0 Manufacturing Plan.....	45
6.1 Wing Spar.....	45
6.2 Wing.....	46
6.3 Fuselage.....	46
6.4 Vertical Stabilizers.....	47
6.5 Landing Gear.....	47
6.6 Motor Mounts.....	47
6.7 Longerons.....	48
6.8 Joints.....	48
6.9 Combining the components.....	48
6.10 Timeline/Manufacturing Milestones.....	49
7.0 References.....	50

1.0 Executive Summary

Students at the University of Texas at Austin's Department of Aerospace Engineering and Engineering Mechanics have designed and built an RC electric airplane. The purpose of this project was to compete in this year's Cessna/ONR Student Design, Build, Fly Competition held at Webster Field in St. Inigos, Maryland on April 20 – 22, 2001. The mission profile is to take off, perform a heavy payload task, land, perform 2 light payload tasks and land. The mission profile may be repeated for a higher score within a 10 minute period.

The criterion used to evaluate each of the design concepts during the conceptual design phase focused on maximizing the overall score. The UT DBF team's highest priority, then, was the estimated flight score. The other four criterion were also considered in evaluation of each design concept: total score normalized by the Rated Aircraft Cost (RAC), crash resistance, and feasibility. The team then devised four possible design concepts, including a flying wing design, a biplane design, a monoplane design, and a canard tandem wing design. Each concept was evaluated based on the selected criteria in as analytical fashion as possible, and, using a Figure of Merit matrix, it was determined that the canard tandem wing design was the most suitable for the competition.

After deciding the tandem wing was optimum, the next step was to size the plane and perform other preliminary design tasks. LinAir was used at this stage to size proper airfoils and front tail dimensions. In regards to the propulsion system, both Electricalc and Matlab computer programs were used to match aerodynamic requirements of the tandem configuration with the propulsion components. Meanwhile, part of the UT DBF team performed materials testing in effort to determine the lightest and strongest materials for each structural component. These tests confirmed that the tandem wing design was a viable and successful design, the team moved on to the detailed design stage.

Like the preliminary design stage, the detail design stage can be divided into three sections: aerodynamics, structures, and propulsion. Matlab code was developed to determine the stability of the airplane under various design parameters. Using this code, an optimal configuration of the engines was determined. In addition, the code aided in determining other vital characteristics such as center of gravity and aerodynamic center locations and the total moment acting on the plane. The location of the landing gear, fuselage, and wing with respect to the tail came soon after determining these quantities. Next, the propulsion components were placed on a test stand and numerous thrust tests were performed in order to determine the airplane's running time, total available thrust, and top speed. All testing and design tools ultimately led to a detailed design package for the University of Texas at Austin's DBF airplane, The G.P.A. Killer.

The G.P.A. Killer is a canard-style tandem wing airplane. Its wingspan is 10 feet with a chord of 1.5 feet. It requires three pusher engines—two on the front tail and one centered on the wing. The fuselage is totally removed from the lifting bodies, and final dry weight is 25 pounds.

2.0 Management Summary

The UT DBF team's motto for this year was "Everybody Does Something." In designing the team architecture, then, it was necessary to consider each person's knowledge and skill level.

The overall team leader is Mr. Aproorva Bhopale. He is the most experienced DBF member and has unusually proficient leadership skills. Mr. Bhopale divided the DBF team into three groups: the Propulsion team, the Aerodynamics team, and the Structures team. As the leader, Mr. Bhopale served as overall coordinator between the three groups.

The leader of the Propulsion team was Mr. Bhopale. His group consisted of four members: Mr. Steve Miranda, Mr. Chris Moore, Ms. Miranda Murdock, and Mr. Nathan Stauffer. The propulsion team selected batteries, engines, propellers, and all electrical equipment. The primary goal of the Propulsion team was to maximize thrust provided to the airplane, and the secondary goal was to minimize the weight of these components.

The leader of the Aerodynamics team was Mr. Ravi Prakash. Members of Mr. Prakash's group include Mr. Philippe Hemple, Mr. David Hughling, Mr. Paul Mears, Mr. Nikhil Rao, Ms. Sue Schmidt, and Mr. Ahbi Shah. The Aerodynamics team's primary goal was to size the aircraft and optimize the lift generated.

The leader of the Structures team was Ms. Theophania Dick Tingley. Members of Ms. Tingley's group include Ms. Amanda Babcock, Mr. Paul Bauman, Mr. Millan Diaz-Aguado, Mr. Clint Kam, Mr. Rodolfo Madrid, Mr. Chris Rivera, and Mr. Brandon Rodgers. The Structures team's primary goal was to select manufacturing processes which minimized the weight of the airplane.

The entire UT DBF team met on Sundays throughout the year to discuss the progress of each group. At this time, topics affecting all teams, such as engine placement, were decided on.

In light of the motto "Everybody Does Something", the group leader's task was to keep every member busy. Every group consisted of students from every level of the aerospace engineering program. The upper division students performed most design work. However, in effort to assure that the DBF team endures for years to come, lower division students were encouraged to assist in the design process and likewise, upper division students were encouraged to teach. During the construction phase, all groups combined to build the UT DBF airplane, called the GPA Killer. When a team member had "nothing" to do, it was the group leader's responsibility to provide a task. In turn, when a group had "nothing" to do, it was Mr. Bhopale's responsibility to motivate the group.

In scheduling the DBF timeline, the most time-intensive work was to occur during school breaks. As Figure 2.1 shows, the dates that each event was actually completed were consistently late. Most work still occurred during break; however, unexpected problems always seem to happen regardless of how much planning is given to do a task. During peak times, every team member worked approximately 30 hours per week. During less demanding times, team members worked only about 2 hours per week.

UT DBF found the aforementioned team structure and philosophy to be highly successful. The design process proceeded with little problems associated with team architecture.

UT DBF Timeline

Activity	Date Due	Date Accomplished	Assigned to
Assemble Design team	7/4/00	6/18/00	Apu
Purchase basic Supplies for plane (epoxy, dremmel bits, etc...)	7/18/00	7/29/00	Structures team
Complete and document conceptual design phase	8/1/00	8/14/00	Aerodynamics Team/Entire group
Form teams and set structure of group	9/12/00	10/5/00	Entire group
Purchase propulsion components	10/2/00	11/19/00	Propulsion team
Complete and document preliminary design phase	10/2/00	1/16/01	Aerodynamics team
Letter of intent due	10/31/00	10/31/00	Apu
Complete and document detail design phase	11/21/00	2/14/01	Aerodynamics team
WINTER BREAK: Those who stay in Austin area will construct design. Those who go home to be with family will write rough drafts of parts 1, 2, and 6 of proposal report	Last day of finals: 12/19/00 First day of Spring semester: 1/17/01	3/01/01 —	Entire group
Construction complete—first test run	2/6/00	2/28/01	
Start arranging travel, drivers licenses go to Timothy	2/6/00	3/05/01	Miranda
Rough draft of proposal report due	2/20/00	3/01/01	Entire group
Written proposal due	COB 3/13/01	3/12/01	Taffy
Rough draft of Addendum Due	4/2/00	4/2/00	
Addendum due COB 4/10/01			Taffy
DBF CONTEST	4/20 -04/22	4/20 - 4/22	

Figure 2.1: DBF milestone timeline.

3.0 Conceptual Design

3.1 Alternative Concepts Investigated

The team investigated several types of airplanes to determine the design best suited for this competition. First, the design parameters were recognized. Next, the conceptual designs were created. The Aerodynamics, Propulsion and Structure groups optimized these designs for the competition. A Figure of Merits (FOM) was created to determine the best design to proceed with.

3.1.1 Flying Wing Concept

The first design concept was a flying wing powered by a single pusher engine as demonstrated in fig 3.1.1a. The flying wing was a modified and scaled up reproduction of the 1998 airplane that was used by the UT DBF team. Since most of this airplane's design flaws were already remedied in 1998, it would have taken very little time to design the airplane and modify it to our needs. A rough analysis of this concept has shown that it possesses a low Rated Aircraft Cost (RAC) and could do more laps than an "average" airplane, which could possibly compensate for its smaller payload. The airplane does have some problems mainly pertaining to engine placement, payload access, and clearance for rotation during takeoff. Further analysis showed that the flying wing requires an S shaped airfoil, which has a positive coefficient of moment. These airfoils traditionally have a low coefficient of lift, which means the airplane will have to either carry fewer payloads or have a significantly larger wingspan to lift sufficient payload. In other words, this airplane design is meant to travel light and fast.

3.1.2 Tandem wing Concept

The second design concept was a two-winged airplane as demonstrated in fig 3.1.1b. Over 30% of the lift of this airplane comes from the canard. According to the DBF FAQ question number 11 in the Cost Formula Questions, [1]:

"11. Question: Just how big can a canard or horizontal be before it is considered a wing?

Answer: If there are multiple flying surfaces, and there is no overlap between the surface, the largest area one is considered a wing. If the "other" surfaces have a high-lift system, they will be considered to be a second (or third) wing. "

Since the surface area of the canard is not counted in the RAC of the airplane, the airplane's performance for it's Rated Aircraft Cost is significantly higher than other airplanes. Due to the extremely large wing area, the takeoff thrust and coefficient of lift of the airplane can be reduced.

A rough analysis of this airplane showed that it would have high performance scores, a moderate aircraft cost, and due to the extra weight of the canard wing, the tandem wing can have a very low stall speed meaning a high probability of surviving an engine failure. On the other hand, the airplane will be difficult to stabilize since the aerodynamic center of lift will be harder to find.

3.1.4 Traditional Design Concept

The fourth concept design was a traditional design airplane with a single engine configuration as shown in fig 3.1.1c. The simplicity of the design and its wide use were why this design was an appealing concept. Most general aviation aircraft have been built using this general design. The team considered this design because it was both easy to evaluate and was most likely to work. Furthermore, the airplane constructed previous year was a traditional monoplane.

3.1.5 Biplane Concept

The fifth concept design was a biplane with a single engine as shown in fig 3.1.1d. Biplanes had several advantages over the other designs. Biplanes had the best turning radius. In addition, due to the large amount of wing area, a biplane had the ability to safely return back to ground in case of an engine failure. Further more, biplanes have done exceptionally well in competition in previous years.

3.2 Design Parameters Investigated

All of the concept designs were analyzed using the parameters listed below:

1. Cost
2. Time
3. Contest requirements
4. Payload configuration

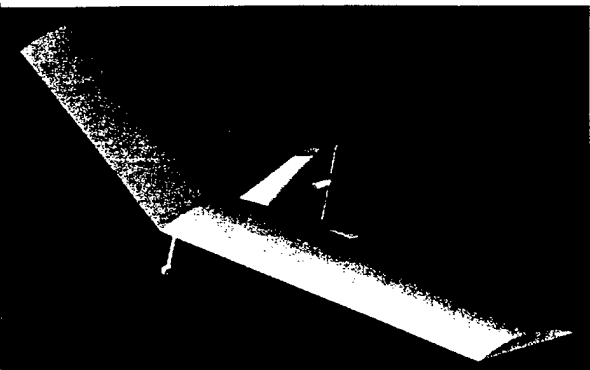
3.2.1 Cost

The cost of the product is always an important consideration for the product's design. Due to the need for a lightweight aircraft, expensive high-performance items were essential. The team concluded from previous experiences that the project's quality should not be compromised in place of price. If the team could afford a more reliable high-performance component, it would be a wiser investment for the entire plane. As shown in Figure 3.6 at the end of this, items that had the propensity to be expensive with quality, such as engines and batteries, were some of the team's more costly investments.

3.2.2 Time

Since all the members of this year's team are full time college students and most of them also have part time jobs, time was a very important parameter deciding design for the airplane. All airplane designs had to be constructed with average construction time being 3 hrs per member per week. Estimates of time construction were made using advice of experienced modelers and veterans of previous dbf projects.

FLYING WING SPECS	
Empty Weight (lbs)	17.7
Wing Span (ft)	15
Wing Area (sq ft)	15
Payload capacity	
Steel (lbs)	15.3
Tennis Balls	50
Sorties of Steel	3
Sorties of Tennis balls	2
Estimated RAC	\$6,018
Estimated Flight Score	1285
Flight Score/RAC	640.4018

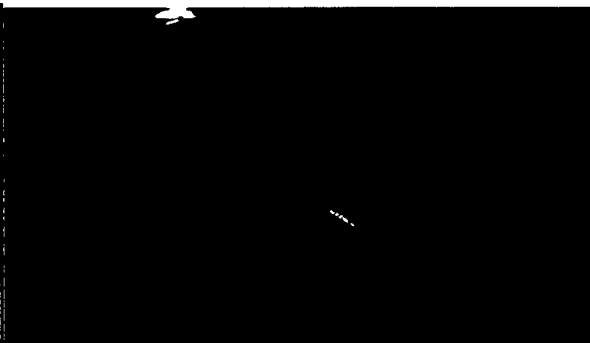


TANDEM WING SPECS	
Empty Weight (lbs)	23
Wing Span (ft)	15
Wing Area (sq ft)	25*
Payload capacity	
Steel (lbs)	32
Tennis Balls	100
Sorties of Steel	2
Sorties of Tennis balls	2
Estimated RAC	\$7,392
Estimated Flight Score	1753
Flight Score/RAC	711.5449



* Canard wing area = 10 ft², Main Wing area = 15 ft²

BIPLANE SPECS	
Empty Weight (lbs)	23.6
Wing Span (ft)	10
Wing Area (sq ft)	20
Payload capacity	
Steel (lbs)	20.4
Tennis Balls	100
Sorties of Steel	2
Sorties of Tennis balls	2
Estimated RAC	7788
Estimated Flight Score	1395.994
Flight Score/RAC	537.748



MONOPLANE SPECS	
Empty Weight (lbs)	0
Wing Span (ft)	10
Wing Area (sq ft)	15
Payload capacity	
Steel (lbs)	0
Tennis Balls	0
Sorties of Steel	0
Sorties of Tennis balls	0
Estimated RAC	\$0
Estimated Flight Score	7788
Flight Score/RAC	0

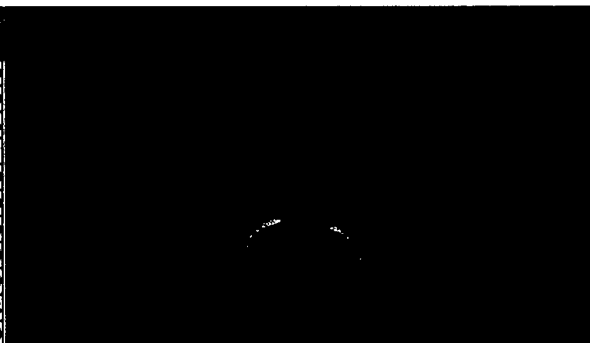


Figure 3.1: Conceptual Designs.

3.2.3 Contest requirements

According to contest guidelines: the wingspan of the airplane was not to exceed ten feet the battery pack weight cannot exceed 5 lbs. The airplane must take off in less than 200 feet. The airplane weight including the payload must not exceed 55lbs. The airplane in the fully loaded configuration must be able support its weight when held by its wingtips. The payload of the conceptual design was to hold at least 5 lbs of steel, and between 10 and 100 tennis balls.

3.2.4 Payload access

In order to maximize the amount of sorties completed in the given amount of time, the airplane's payload must be removed in the least amount of time possible.

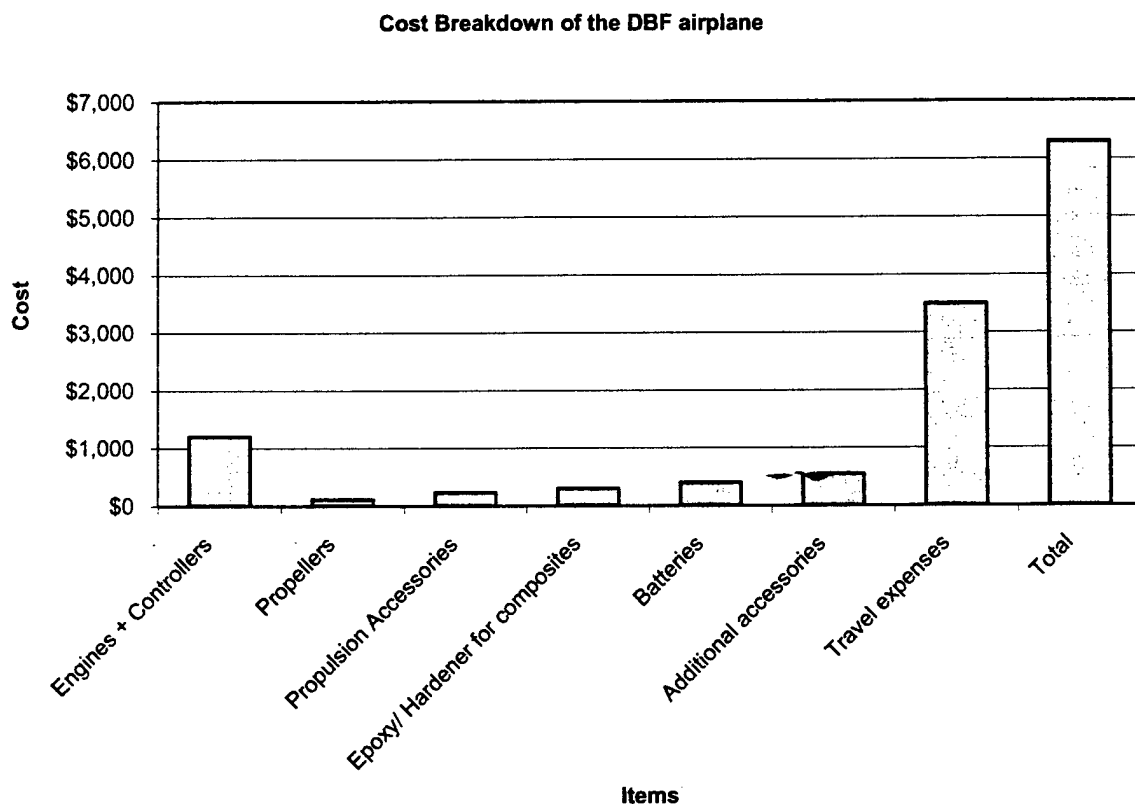


Figure 3.2: Projected Budget for Concept Design

3.3 Figure of Merits

All of the concept designs were compared using the figures of merit listed below. The concept that has the best total score based on the figure of merits would proceed through the design process and be constructed. The figure of Merits are listed below:

3.3.1 Final Score

The main objective of this competition is to get the highest final score. The final score is determined by the report grade multiplied by total flight score divided by RAC. The conceptual design most likely to win will be the one that has the highest flight score compared to its RAC.

The first step to obtain a flight score was to determine the RAC of the airplane. The Structures team obtained a rough estimate of the weight of the airplane. This information was used to determine the Manufacturers Empty Weight section of the RAC. The Propulsion team obtained a rough estimation of the propulsion RAC and the Aerodynamics team obtained a rough estimate of the flight performance and sizing of the airplane. All of the information was combined to obtain a rough estimate of manufacturing RAC. Once all the sections of the RAC were determined, the group proceeded to determine the flight score of the airplane.

The Aerodynamics group estimated the aircraft's performance using some simple assumptions such as the thrust was 10 lbs on all airplanes, the CI of the wings all airplanes except the flying wing was 1.9, since the flying wing has a S shaped airfoil, it's CI was assumed to be 1.2. The airplanes were sized to reasonable dimensions and an estimated flight score was calculated.

The estimated flight score was divided by the estimated RAC of each conceptual design to get an estimated Final Score. Table 3.3.1 shows the estimated Final Score of the Airplane.

AIRPLANE	Normalized Score	Actual Score	RAC	Flight Score
BIPLANE	0.76	537.75	7788.00	1395.99
MONOPLANE	0.91	845.67	8854.00	1432.10
TANDEM	1.00	1711.54	7392.00	1753.25
FLYING WING	0.90	840.40	8018.00	1284.85

Table 3.3.1

3.3.2 Crash Resistance

For the past 2 years, the UT DBF team has experienced major damage caused by crashes less than a week before competition. These crashes have played a crucial role in the quality of the team's airplane at the competition. In 1999 the team was unable to compete due to a severe crash. In 2000, the team had to rebuild the entire fuselage in 3 days. This led to a catastrophic failure in the landing gear during the competition. In order to have an airplane that can be extensively flight-tested and be extremely resistant to crashes, the airplane has to have a large wing area. Generally, the larger the wing area, the slower the stall speed for the airplane. A slower airspeed means a softer crash. The estimated Crash Resistance Score is shown in the table below.

AIRPLANE	Normalized Score	Wing Area (ft ²)
BIPLANE	1	20
MONOPLANE	0.8	15
TANDEM	0.825	
FLYING WING	0.8	15

*10 ft² canard and 15 ft² main wing

Table 3.3.2

3.3.3 Feasibility

According to previous experience and advice from expert modelers, the feasibility of the airplane is directly dependent on the weight of the airplane. Usually, the heavier the airplane is, the more structure is required to reinforce it. The Structures team estimated weight of the airplane using construction techniques they were familiar with. The table below shows the weights of the conceptual designs.

Airplane	Normalized Score	Weight (lbs)
BIPLANE	0.75	23.6
MONOPLANE	0.88	20.06
TANDEM	0.77	23
FLYING WING	1.00	17.7

Table 3.3.3: Feasibility Score.

3.4 FOM—Ranking and Importance Factors

Narrowing down which design concept is best started by ranking which factor of merit is the most valuable for the team. In order of decreasing importance, the team's priorities were:

1. Final Score
2. Crash Resistance
3. Feasibility

The top priority for building the model is its performance. The higher the Final Score, the better the airplane is. The second priority is the Crash Resistance. The airplane has to be able to survive reasonable crashes. The last priority is Feasibility. The lower the weight of the airplane, the less complex the airplane, and the better chance of it working.

3.5 FOM Matrix

All of the figures of merit scores were entered in the matrix below to determine the best design concept for the contest. According to the matrix the best airplane is the Tandem Wing Concept.

AIRPLANE	X3 Score	X2 Crash Resistance	X1 Feasibility	TOTAL
TANDEM	3.00	2.00	0.77	5.00
FLYING WING	2.70	1.20	1.00	3.90
BIPLANE	2.27	1.60	0.75	3.87
MONOPLANE	2.72	1.20	0.88	3.92

Table 3.5

4.0 Preliminary Design

In assessing the preliminary design parameters, the team found it most effective to divide tasks into three groups: aerodynamic preliminary design, propulsion preliminary design, and structures preliminary design. Throughout the preliminary design stage, integration of these separate design groups played a vital role in the overall airplane design.

4.1 Aerodynamic Preliminary Design

All preliminary design centered on the Aerodynamics team's work in the sizing of the airplane. Important to note is that the plane was assumed to be a completely rigid body, and thus elements of aeroelasticity were neglected.

4.1.1 Design Parameters

The mission profile for the DBF competition was, in general, to take off, climb to an unspecified altitude, fly in a circle, descend, and land. The minimum height ambiguity in the DBF rules allowed a liberal amount of variation with the take off performance calculations. Since the DBF rules set a maximum weight value for the entire plan, all preliminary design calculations were performed using 55 lbf. as the gross weight. Under the above assumptions, the following parameters were used in the preliminary aerodynamic analysis of the plane:

1. Lift. Adequate lift is an essential design element in airplane design. For level flight, the lift must be 55 lbf. Since a minimum altitude was not specified in the rules, the lift required for the take-off phase simply has to be greater than 55 lbf.
2. Static and Dynamic Stability. As a simple guideline for dynamic stability, aircraft must have a dynamic damping ratio, ζ , as high as possible while remaining below zero. In addition, the airplane must be statically stable.
3. Drag. A proper airplane sizing will have minimal drag—particularly in the fuselage.

4.1.2 Figure of Merits

There are three figures of merit considered in optimizing the airplane's performance given the stated parameters. Considered first was the lift. As with most airplane designs, a high amount of lift is desirable. As a design condition, the airplane design must provide adequate lift for an angle of attack range of $-15^\circ < \alpha < 15^\circ$. Measured next was static and dynamic stability. The UT DBF team has found, from previous experience, that a high amount of stability not only makes the plane more crash resistant but also decreases the complexity of the design. Evaluated last is the drag. Because of the relatively small size of the airplane, it is assumed that the drag generated will be small with respect to the other aerodynamic forces generated. However, drag should still be considered a FOM in effort to fully optimize the GPA Killer.

4.1.3 Analytic Methods Used and Sizing of the airplane

In evaluating the required lift, it was assumed that in order to maximize lift, the wing would have a span of 10 ft. Similarly, the tail, which also produces lift, would have a span of 9.5 ft. The first step in maximizing the lift was to select a proper airfoil.

The Aerodynamics team used an iterative method to optimize the lift generated by the ideal airfoil. As a general design condition, the selection process started with assigning initial conditions for the airfoil. These were a coefficient of lift, C_L , of 1.5 and a Reynolds number, Re , of 300,000. Next, the group members visited the UIUC Airfoil Data website [2] and gathered data for all airfoils which met these criteria. At this point, the team had C_L and C_D data for a range of α between 0° and 15° . In order to narrow the airfoil selection further, the team used a program called LinAir. Given the values for C_L and C_D , LinAir calculated a variety of design ratios, such as the zero-lift angle of attack drag coefficient and the moment coefficient (C_{D0} and C_M) for each airfoil. The desired airfoil would produce a minimal, yet slightly positive (nose down) moment about the airfoil's center of pressure and also produce sufficient lift throughout the entire range of angle of attack. The airfoil which best matched these conditions was the Selig S1210. This airfoil would work for both the canard (tail) and the main wing, with the chord of the main wing and the chord of the canard being 1.5 ft. and 1.0 ft., respectively.

When evaluating static and dynamic stability, it was convenient to divide each type into two categories: longitudinal and lateral stability. Since the canard airplane is symmetric about the center of gravity/aerodynamic center axis and, during thrust tests, the gyroscopic effects of the propellers were small, the airplane is statically stable in the lateral direction. However, now that symmetry about the cg-ac axis is crucial to stability, all further sizing will bear this as a design parameter.

A more detailed analysis of the static lateral stability will aid in sizing the vertical tail, rudders and rudder deflection. Two factors, the total side area (TSA) and the tail moment arm were essential to sizing the vertical tail. To begin sizing, the side areas and location of the side area of each component was determined using the dimensions and approximated component shapes. The TSA was determined by:

$$TSA = \frac{((\sum A_{comp}) * coa)}{\sum A_{side}}$$

where A_{comp} is the area of each component, coa is the center of area, and A_{side} is side area of each component. The location of the TSA was calculated to be 3.2147 ft from the tail spar. Standard design convention shows that the TSA should be located at the cg plus 25% of the tail moment arm. The length of the tail moment arm is defined as the distance from the cg to the center of area of the tail. With the cg and TSA known, the tail size, and thus the side area and center of area of the tail,

could be set such that the proper TSA may be achieved. This method, however, proved to be rather difficult due to the numerous geometric complications of the aircraft.

For example, the tail needed to be placed under the rear wing to provide not only a fairing for the tail spar but also a wing buffer in the event of over rotation of the aircraft during a rough landing. If over rotation were to occur, the tail would strike the ground first, thus reducing the possibility of damage to the rest of the aircraft. However, the length of the tail must allow for adequate ground clearance during take off. This limiting factor for tail dimensions did not allow for the proper TSA to be achieved. The difference between the optimal TSA and the actual TSA was found to be 6.31in^2 . Although this discrepancy exists, the optimal tail volume coefficient was used to determine the effectiveness of the tail. Tail volume coefficient, V_{vt} is defined by the equation:

$$V_{vt} = \frac{(VTA * TMA)}{(.5 * WA * Wingspan)}$$

where VTA is the Vertical Tail Area, TMA is the Tail Moment Arm, and WA is the Wing Area. As the value of V_{vt} increases, the more effective the response of the aircraft will be due to the tail. A comparison of the V_{vt} of our aircraft ($V_{vt} = 0.0793$) and that of the Lockheed Martin C-5 Galaxy ($V_{vt} = .1$) was used since both aircraft are not intended to have large yaw responses due to the tail. The value for V_{vt} and TSA for our aircraft is acceptable provided that the predicted yaw will not be so great that the aircraft may become unstable in the vertical axis when the rudder is deflected.

A detailed analysis of static stability in the longitudinal direction is essential in the sizing of the aircraft. Analysis of static longitudinal stability will determine several aircraft sizing characteristics, including wing and tail placement, angles of incidence for both the tail and the wing, engine configuration, and location of the center of gravity (cg) and the aerodynamic center (ac). To begin the process of assessing static longitudinal stability, a computer model of the aircraft was needed. The use of MatLab allowed for a computational model of the aircraft to be built and optimized.

The first step in the modeling process was to determine a reference datum from which the location of every element of the aircraft would be measured. General aircraft design convention suggests that the reference datum be located near the front of the aircraft. To simplify moment and position calculations, the quarter cord of the front wing was chosen as the reference datum.

Next, the Aerodynamics team used LinAir to configure the locations of the tail with respect to the wing. LinAir used airfoil data given on the UIUC Internet website [2], the wing and tail span, and the basic design concept configuration as input. LinAir then output the optimal lifting wing and tail configuration for a canard design concept and the necessary angles of incidence for the tail and wing. The main wing spar is oriented 3 ft. behind and 6 in. above the canard spar. The angles of incidence for the canard and the wing are 4° and 0° , respectively.

Aircraft design and performance depends heavily on the location of the center of gravity. Actual calculations of the cg are very difficult when beginning the aircraft design process due to the number of variables such as weight and component cg. To counter this problem, a trial cg was 'fixed' at some initial location on the aircraft. This allowed the aircraft to be designed around the fixed cg constraint. When choosing a fixed cg location, standard design convention shows it is necessary to choose a location that will place the cg in front of the ac. Placement of the cg in front of the ac will cause a tendency for the aircraft to pitch nose down. To complicate decisions concerning the trial cg position, the ac was not known when the design process began since an airfoil design had not yet been determined. However, it was known, from the wing area, that the rear wing would produce approximately 60% more lift than the front wing. Thus, a good approximation of the ac position can be calculated by:

$$X_{ac} = \left(\frac{L_{front} * X_{front} + L_{rear} * X_{rear}}{L_{front} + L_{rear}} \right)$$

where L is the lift and X is the position from the reference datum of each wing. This calculation placed the ac position at 2.3 ft from the reference datum. Preliminary dimensions of the aircraft components did not allow for the cg to be placed in front of the ac. The initial fixed cg was placed at 2.5 ft from the reference datum. Although this cg location did not conform to design convention, the team decided to accept this configuration as an experimental test of the aircraft design.

To calculate the actual cg dimension, the location and size of each component of the aircraft had to be modeled. To simplify calculations, approximate shapes of each component were assumed. The longerons, tail spars, battery packs, and tails were all modeled as rectangles. Both fuselage bodies and the two wings were each modeled as ellipses, while the three tires for the landing gear were modeled as circles. The center of gravity of each component, except for the wings and tails, was assumed to be the geometric center of each piece. By reviewing construction design methods proposed by the Structures team, the quarter cord of each wing and tail was used as their cg. The cg data for each component and their locations were then entered into the MatLab code.

Motor placement was also a very important issue with which to contend, since the thrust produced by the rear motor(s) would impart a nose down, or positive, moment about the aircraft cg. Initial moments calculated without the addition of motor weights and trusts showed a nose up (negative) -5 ft-lbf moment about the cg. When motors were included, several problems arose while trying to balance the thrust moments produced by the rear motor(s) and the moments produced by the weights of each motor. By placing two motors at the rear of the aircraft, a +4 ft-lbf moment was induced due to thrust while at full throttle 0 ft-lbs were provided by motor weight. Summing all moments showed a -1ft-lbf moment about the cg. Thus the aircraft would experience a constant nose up pitching moment. If one motor was placed in the rear and two in front, the sum of moments

yields a +4.5 ft-lbf moment. This proved much better than the previous configuration, but these were still only approximate values.

Selection of an airfoil allowed for the computation of lift values for both the front and rear wings, thus permitting the calculation of actual moments about the cg due to lift. Lift values also allowed angles of attack for each wing to be selected such that the aircraft would produce enough lift for the aircraft to become not only airborne, but also stable. Table 4.1.1 was used to determine the lift values at various airspeeds and angles of attack.

Air Density		Velocity(ft/s)	Weight(lbf)					
2.37E-03		31	45					
Front Wing			Front Wing	Rear Out	Rear Prop	Rear Total		
9.5 Cl	alpha(deg)	Lift(lbf)	Lift(lbf)	Lift(lbf)	Lift(lbf)	Lift(lbf)	ac	Total Lift
Rear(In Prop Wash)	1.25	0	11.08891894	7.708151	8.519535	16.2276863	2.227723	27.3166052
7.125	1.36	1	12.0647438	8.386468	9.269254	17.6557226	2.227723	29.7204664
Rear(Out Prop Wash)	1.47	2	13.04056867	9.064786	10.01897	19.083759	2.227723	32.1243277
7.875	1.58	3	14.01639354	9.743103	10.76869	20.5117954	2.227723	34.528189
	1.69	4	14.9922184	10.42142	11.51841	21.9398318	2.227723	36.9320502
	1.8	5	15.96804327	11.09974	12.26813	23.3678682	2.227723	39.3359115
	1.9	6	16.85515679	11.71639	12.94969	24.6660831	2.227723	41.5212399
	2	7	17.7422703	12.33304	13.63126	25.964298	2.227723	43.7065683
	2.09	8	18.54067246	12.88803	14.24466	27.1326914	2.227723	45.6733639
	2.16	9	19.16165192	13.31968	14.72176	28.0414418	2.227723	47.2030938
	2.19	10	19.42778598	13.50468	14.92623	28.4309063	2.227723	47.8586923
		front	rear	total lift	Xac(ft)	Xcg		
for takeoff(31ft/s)	alpha(deg)	12	8			2.25		
	lift(lbf)	19	27	46	2.201087			
for cruise(37ft/s)	alpha(deg)	5	0					
	lift(lbf)	22	23	45	1.916667			
for cruise(35ft/s)	alpha(deg)	4	3					
	lift(lbf)	19	26	45	2.166667			

Table 4.1.1: Lift values at variable velocities and angle of attack

As the dimensions and weights of the aircraft components were decided, a formal weight and balance of the aircraft was calculated and the cg was found to be 2.25 ft aft of the reference datum. This cg, although behind the ac, was accepted as a test value.

In regards to dynamic longitudinal stability, it is assumed that, for this mission, phugoid mode oscillation is negligible due to the short flight time. For the short-period mode oscillation, however, the dynamic effects on the airplane are significant. As stated in the design parameters section, the damping ratio is to be as high as possible, yet below 1.0. A typical design parameter for a minimum damping ratio is .33 for the short period mode [3]. This value is for a highly tapered and swept subsonic jet, which in principle is less dynamically stable in the longitudinal direction than the our plane's straight wing design. Based on this comparison, it may be determined that the airplane is dynamically stable in the longitudinal direction.

A useful guide to maximizing the dynamic lateral stability is minimizing the mass moment of inertia, I , about the symmetric axis. A plane design with a high I about this axis carries a high amount

of roll when disturbed by a wind gust or simple turn. When the weight is not as distributed, or the mass moment of inertia is minimal, the plane will have a higher dynamic resistance to sudden changes in sideslip angle. Since the wing and tail configuration has been set in the lift analysis and the static stability in the longitudinal direction, the fuselage configuration must be adjusted to control the dynamic lateral stability. The three-engine configuration determined in the previous paragraphs means that a single fuselage centered on the cg, although desired, is impossible. The closest fuselage configuration to the cg possible is to have two pods just outside of the longerons. The longerons will be located one on each side of the main wing propeller.

Since the sizing and configuration of the wing, tail, and vertical stabilizers has already been finalized, the analysis of drag will be used in sizing the fuselage. Already determined is that the fuselage is to have 2 pods; however, in effort to conserve the rated aircraft cost, the team decided that a thin connecting piece that bears a steel payload will attach the two pods together, thus qualifying the aircraft as having a single fuselage configuration under DBF rules. In addition, the volume capacity of the fuselage will be big enough to hold the maximum allowable 100 tennis balls (50 tennis balls per pod). The final design condition, in order to maximize lift, was that the fuselage must not interfere with the laminar airflow over the entire wing and tail configurations.

Drag is defined as a function of density, velocity, drag coefficient, and planform area. Ambient air density and velocity were not considered in this analysis. A minimal fuselage cross-section area would be a circle with either a 4 ball layer configuration, a 7 ball "honeycomb" configuration, or a similar 19 tennis ball "honeycomb" configuration. A simple model for wetted planform area, S , can be expressed as:

$$S_{wet} = \pi r^2 h$$

where r is the radius of fuselage and h is the length of the cylindrical body. The wetted area for the 4 ball configuration, the 7 ball configuration, and the 19 ball configuration is 1540 in², 1145 in², and 1696 in², respectively. Therefore, the optimal configuration for the fuselage is two cylinders holding 8 rows of 7 "honeycomb" configured tennis balls. The caps placed on the end of each cylinder will hold 4 balls. In addition, in order to reduce pressure drag, the caps of each cylinder were tapered as much as the overall aircraft configuration would permit.

4.2 Structures Preliminary Design

4.2.1 Wing Spar Design

Once the plane design was established, investigations of the wing spar design began. Four options for spar design were presented: an all carbon fiber spar wrapped around a Styrofoam core, a shower curtain aluminum spar, a carbon fiber weave wrapped around the shower curtain aluminum spar, and an aluminum alloy spar.

The figure of merits used were strength (x4.0), the inverse of the weight of a five foot section (x3.0), the modulus of elasticity of the spar design (x3.0), a uniform cross section (as ranked zero to one, x2.0), and the estimated ability and skill required to make the spar, also as ranked (x1.0). These figure of merits were chosen and weighted according to their importance in a spar's ability to perform. To accurately determine the strength of the possible candidates load tests were performed on the spars.

Before performing the tests, the maximum bending moment that the airframe would experience during flight was analyzed. This was considered the minimum moment that any spar used would have to withstand if it were to be used in the wing. After examining the flight profile, the structures team determined that the maximum loading that the wing would incur was going to be during the structural verification on the ground, in which the plane will be lifted by the wing tips, experiencing roughly the loading in a 2.5 g turn. Since the center of gravity (cg) does not lie along the quarter chord of the main wing, the judges have allowed us to lift the plane by the wing tips and the front canard.

As shown in Figure 4.2.1-a, the structural verification test will induce three loads on the airframe due to the weight of the fully loaded plane: R1, R2, and P. In Figure 4.2.1-b, the side view of the airframe is shown in which by summing the forces and moments about the cg we find:

$$\begin{aligned} R1 + R2 + P &= W \\ \text{and} \\ X * (R1 + R2) &= Y * P \end{aligned}$$

where W is the total weight of the airplane, and X and Y are the respective distances of the loads from the cg. We can then solve these equations for R1 + R2 and P to get:

$$P = \frac{W * X}{Y + X} \quad (1)$$

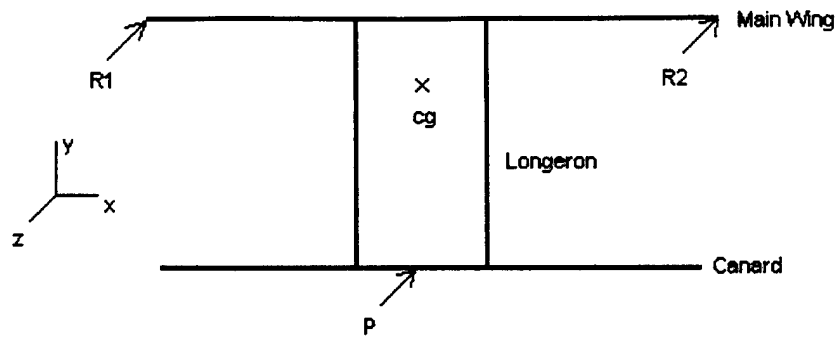
$$R1 + R2 = \frac{W * Y}{Y + X} \quad (2)$$

If the cg is assumed to act along the middle of the main spar shown in Figure 4.2.1-c, then W1 equals W2. Summing the moment about the cg yields:

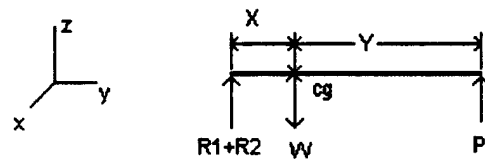
$$L1 * R1 + \frac{L2}{2} * W2 = L3 * R2 + \frac{L2}{2} * W1.$$

By assuming that L1 and L3 are equal (as planned):

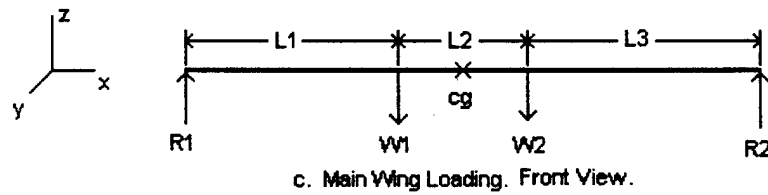
$$R1 = R2 \quad (3)$$



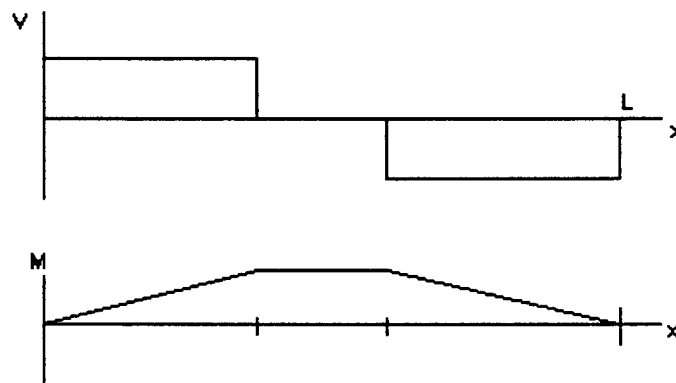
a. Airframe loading during structural verification: Top View.



b. Side view of loading.



c. Main Wing Loading. Front View.



d. Shear and Moment diagrams for Main Wing.

Figure 4.2.1: Airframe analysis for the spar design.

By substituting (3) into (2):

$$R1 = R2 = \frac{W * Y}{2 * (Y + X)} \quad (4)$$

where W equals 45 pounds, the expected weight of the plane and payload, and Y and X have been determined by the aerodynamic analysis placement of the cg to be 2.5 ft and 1.25 ft respectively. Plugging these values into (4), $R1=R2= 15 \text{ lbf}$ is found.

Looking at the bending moment diagram shown in Figure 4.2.1-d, the maximum bending moment reaches peaks at $x = L1$. Because the design is not finalized, the assumption of L1 equals 5 ft is made so that our wingspan is within the maximum 10 ft. This means that the spar would experience a maximum moment of 75 ft-lbf at the spar connection.

The first spar design examined was the single layer of carbon fiber wrapped around a Styrofoam rod. This was done by applying a three-point bending load as shown in Figure 4.2.2-a. Under this configuration, the spar withstood a force, P, of 45 pounds applied at the center of the spar before yielding. As expected, the spar broke 45 degrees relative to the weave of the carbon fiber; however, the spar supported a much lower load than theory would predict.

As shown in Figure 4.2.2-b, the maximum moment of such a setup occurs at the midpoint of the spar, and from the diagram the maximum moment experienced when the spar snapped was equal to $R1 * L/2$ or, 28.125 foot-pounds (ft-lbf). To determine the ultimate strength (the same as the yield stress for carbon) of the spar, σ_u , the following flexure relation was used:

$$\sigma_u = \frac{M * y}{I}, [4] \quad (5)$$

The spar geometry, shown in Figure 4.2.2-c, gives a moment of inertia, I, equal to .021525 in^4 . Since the maximum stress experienced by the spar is the point of interest, y is equal to .5 in. Using these values along with the experimentally determined moment, M, that the spar held, the ultimate strength of the spar is found to be 108.1 MPa. The published value for the ultimate strength of carbon fiber is 500 MPa, meaning our spar should have been able to withstand a moment approximately 5 times what it did in experiment, or 130 ft-lbf. If the spar had performed as expected, it would have easily met the required 92 ft-lbf load and only weighed half a pound.

Unfortunately, carbon fiber's strength depends dramatically on how well the weave is set up in the epoxy and the relative smoothness in the lay up (i.e. no kinks in the cross-section). With our construction methods, a spar without some deviation from a circular cross-section and a crease down the centerline (where the weave met back up with itself) was never produced.

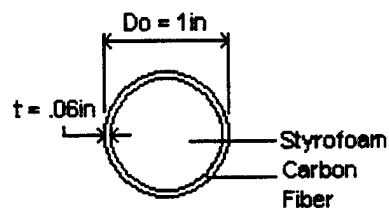
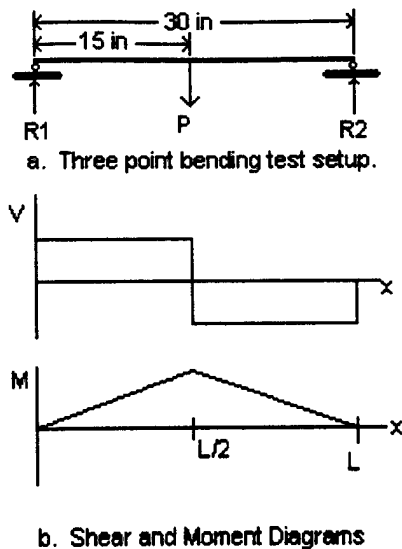


Figure 4.2.2: Three point bending test.

Next, a strip cut from the aluminum spar candidate was tested to yield. A screw driven loading device, shown in Figure 4.2.3 was used to create strain in the test piece. Two rotating screws in the device were attached to a movable plate such that as the screws rotated, the plate that the screws were connected to moved up or down. A load cell and a strain gage were attached to the sample piece to gather the stress and strain data. The data was fed into Labview, which then plotted the data in stress versus strain format. The point at which the linear relation between the stress and strain ended determined the yield stress, this was recorded as 20 ksi for the aluminum test piece. Rearranging (5), using $\sigma_y = 20$ ksi, $I = 1.077 \times 10^{-6} \text{ ft}^4$, and $y = .5$ as the maximum moment location, it was found that this spar design could withstand 6.205 ft-lbf.

Finally, a carbon wrapped aluminum rod was tested with an applied tip load. In the test configuration the spar was attached to a worktable by two C-clamps and a tip load was applied at 4 feet along the spar by pressing upward with a scale contacting a worm clamp attached to the spar, as shown in figure 4.2.4. A ruler was taped to a piece of Styrofoam with zero set at the position of the unloaded tip so as to measure the deflection of the tip.

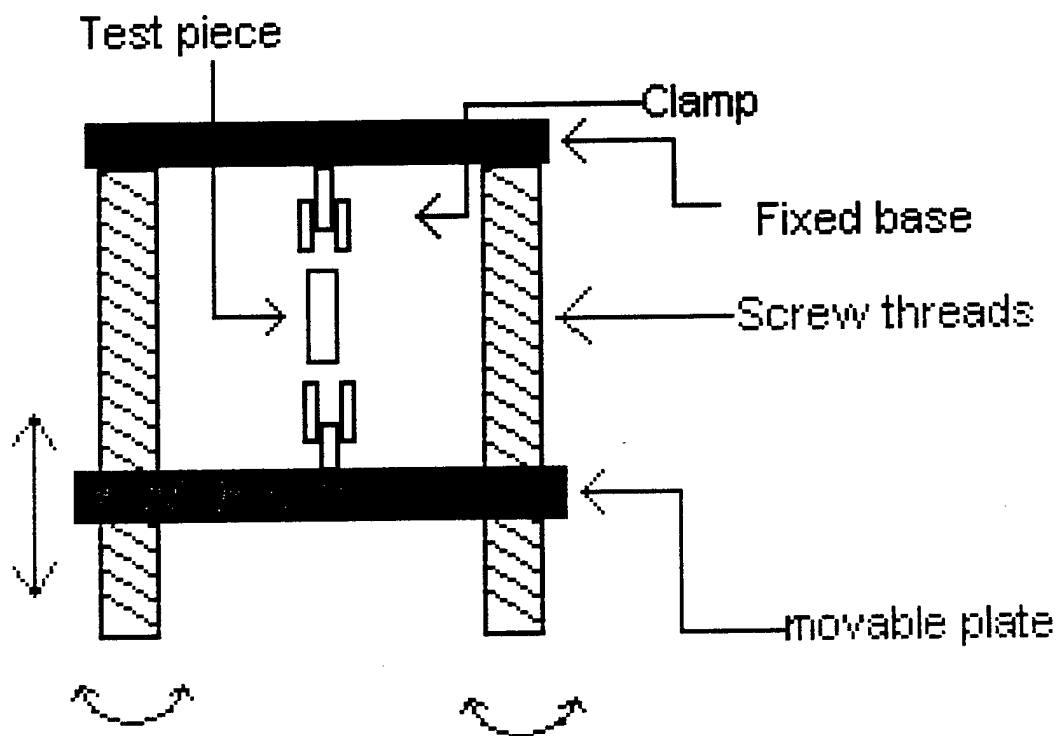


Figure 4.2.3: Test Apparatus for Aluminum yield strength.

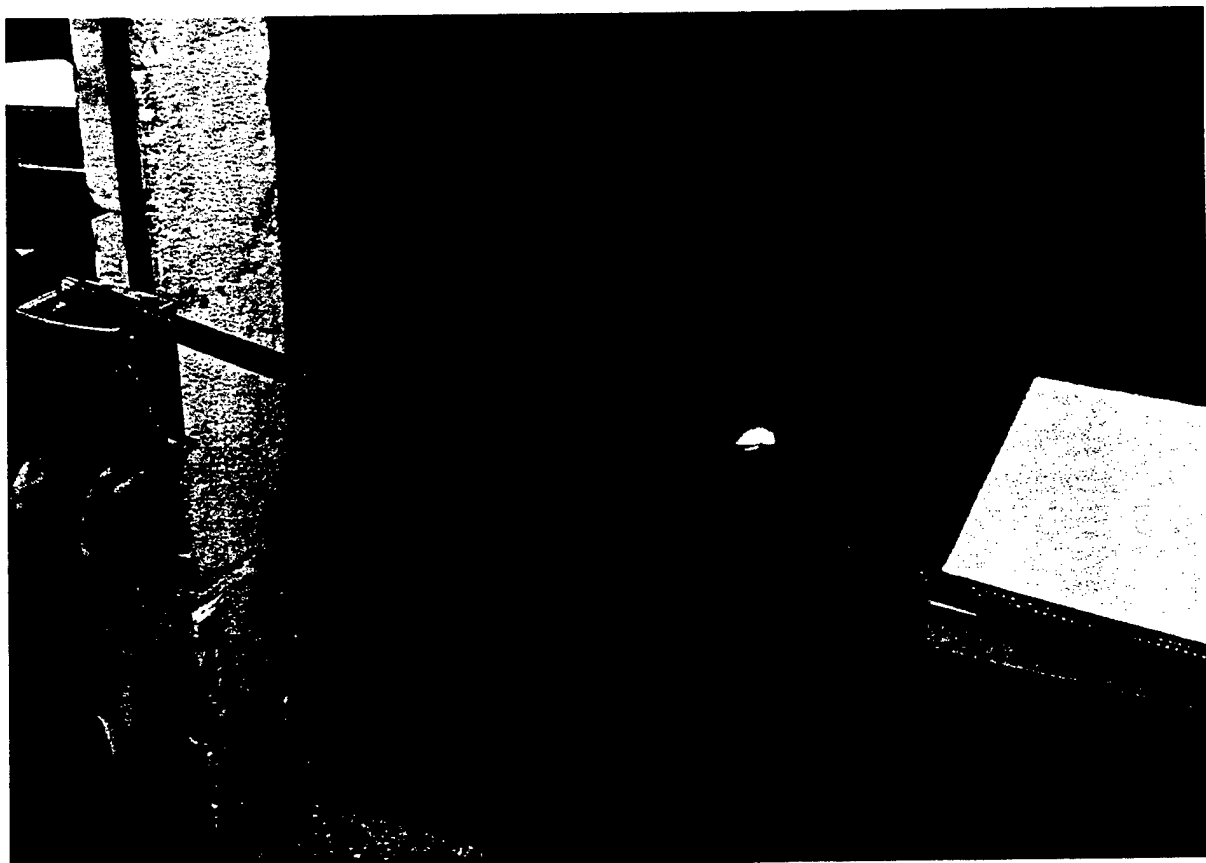


Figure 4.2.4: Spar Deflection test setup.

The force applied was gradually increased in increments of 1 pound and the displacement was read off of the ruler for each loading. The load was increased up to 23 lbf, at which point the bar was experiencing a maximum moment of 92 ft-lbf at the clamps. This corresponds to a factor of safety of 1.3 for the loading with five-foot wing spars.

The spar was not tested to yield because it successfully handled the desired load with a factor of safety, thus we cannot calculate the spar's yield stress. From the resulting graph of displacement versus applied load, as shown in Figure 4.2.5, we can see that the displacement was linearly proportional to the loading and from the curve fit (shown in red) the modulus of elasticity of the beam can be found to compare our hybrid spar design with other pure metal spars.

From Figure 4.2.5, the curve fit has a slope of .031098 ft/lbf. From Bernoulli-Euler beam theory we can derive that the deflection due to a tip loading would be [3]:

$$\delta = \left(\frac{L^3}{3 * E * I} \right) * P, [4] \quad (6)$$

where δ , the deflection at the wing tip, is linearly related to the tip loading by a slope of $L^3/(3 * E * I)$.

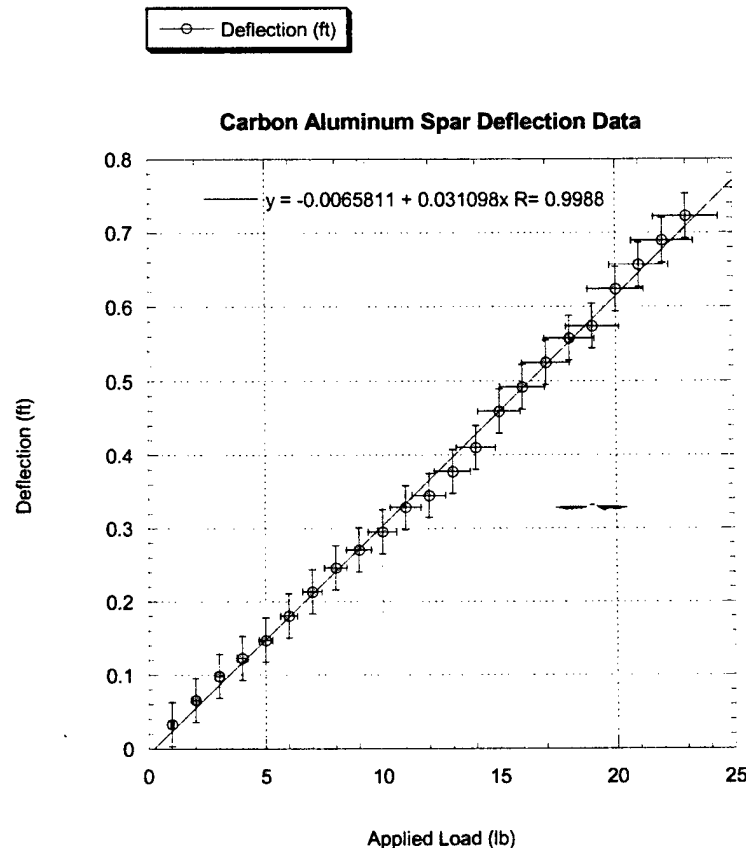


Figure 4.2.5: Deflection data from spar test.

The length of our test spar was 4 ft and the moment of inertia, I , of the carbon aluminum spar was $4.987 \times 10^{-6} \text{ ft}^4$. Using the curve fit's slope and rearranging (6), a value for E , the modulus of elasticity of the spar, is found to be 137550 ksi. This is much higher than the modulus of elasticity of other pure metal designs; for example, aluminum's modulus of elasticity is around 10000 ksi. This means that, for our hybrid spar configuration, the wing tip deflection will be much less than for other spar designs.

Another attractive quality to the aerodynamics group was that the hybrid spar could withstand a very high bank angle during flight giving the aircraft the ability for a tight turn radius. As defined in [3], the bank angle, μ , is:

$$\mu = \cos^{-1}\left(\frac{W}{L}\right), [3]. \quad (7)$$

where W is the total weight of the plane, at most 55 lbf, and L is the maximum distributed load that the wing can withstand. Based on the strength of the Aluminum/carbon design, the L that the wings should be able to withstand is 147.2 lbf. Using (7) we find that $\mu = 68.1$ degrees.

The team also examined, using the theoretical values from a materials properties table, how well an aluminum alloy (6061-T6) spar would perform. For a spar with a constant cross section and a thickness of .06 in, the aluminum design could withstand a maximum moment of 98.6 ft-lbf (using eq. 5) and would weigh approximately .3635 lbf for a 5-ft section. Unfortunately, this spar would be relatively difficult to manufacture because the aluminum would have to be turned down in a lathe to get the desired .06 in thickness.

The final method that was considered to add strength was to wrap a second layer of carbon to the carbon/Styrofoam spar. After testing the single wrapped hybrid spar, however, it was decided to use the carbon wrapped aluminum instead because adding another layer of carbon weave would have doubled the weight of the carbon fiber weave, making it heavier than the carbon/aluminum spar. All the while, the carbon/Styrofoam spar would still be very difficult to manufacture. Using the results from the above tests, the spar design was chosen based on the figure of merit matrix, as shown in Figure 4.2.6, to be the carbon fiber on the shower curtain rod.

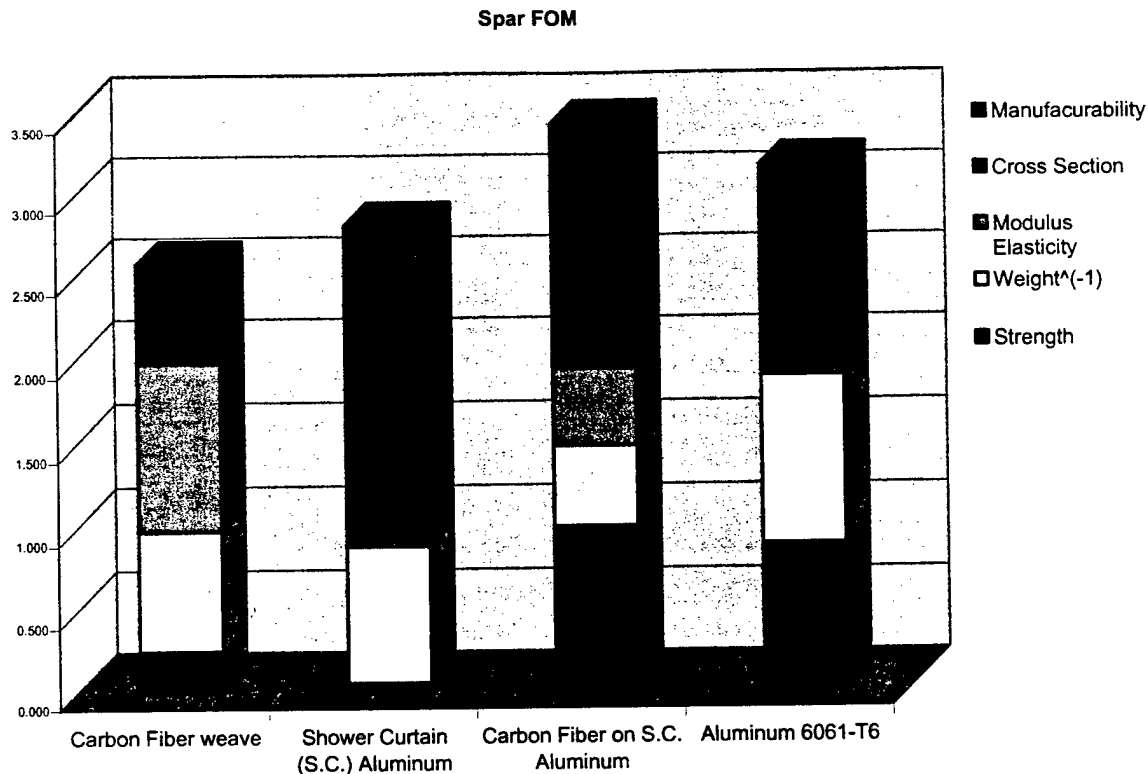


Figure 4.2.6: Results of FOM analysis on the wing spar

4.2.2 Wing Design

There were three considerations for the design of the wing sections: a solid Styrofoam wing, second a ribbed Styrofoam design, and third, a ribbed balsa wing; all were to be coated with Econokote. Because the spar, which would run through the quarter chord of all the above designs, is designed to support the load of the plane, the wing structure need not support any load. Instead the wing design must be light and hold the shape of the airfoil during flight. Because of this, the figure of merits used for the wing design were inverse weight ($\times 3.0$), the smoothness of the airfoil ($\times 2.0$), and the estimated skill involved in building the design ($\times 1.0$).

The first design examined was the solid Styrofoam configuration. The advantage of this design was the constant shape of the airfoil as well as the speed and ease with which a wing section could be made. However, a five-foot section of a wing constructed with this method weighs .74 lbs.

The next design considered was to use Styrofoam ribs to reduce the weight. This method yielded a wing that weighed only .38 lbs and had only a slight loss of airfoil shape. The only disadvantage to the method was the skill and time required to cut the Styrofoam ribs accurately.

The last design evaluated was using balsa ribs as an alternative to the Styrofoam ribs. Not only was this design very laborious and difficult to reproduce consistently, but it weighed more

than the Styrofoam ribbed wing and had a worse dimple effect; that is, where the Econokote bowed inward in-between the ribs. Therefore, the Styrofoam rib wing configuration based on the Figure of merit graph shown in Figure 4.2.7 was chosen.

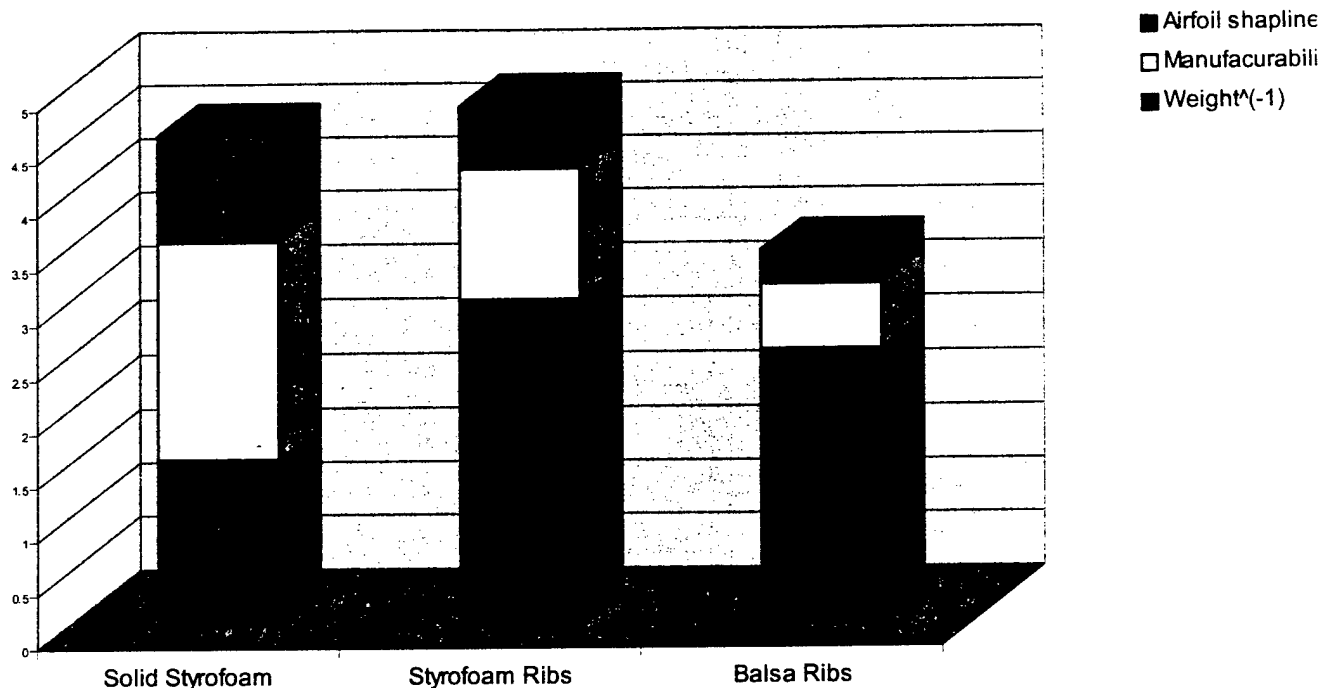


Figure 4.2.7: Figure of merit chart for Wing designs.

4.2.3 Fuselage Design

Because of the difficulty in carrying both the steel and the tennis balls in the same fuselage, only two designs were proposed. The first was a single structure in which all 100 tennis balls and all 25 pounds of steel would be carried; the second was two cylindrical canisters which would split the payload. The figures of merit used were the estimated airflow disruption by the fuselage (x4.0), the strength of the fuselage attachment design to the airframe (x3.0), the inverse of the weight (x2.0), and the manufacturability of the design (x1.0).

The single payload box design, because of the volume of 100 tennis balls, would interrupt the airflow over the rear airfoil. Also, this design was found to be more difficult to attach to the longerons. The dual cylinder design on the other hand was found to be readily attachable and air disruption was not as much of a danger compared to the single box design. The cylinders did weigh slightly more, however, and were not as easy to manufacture. Figure of merit analysis, shown in Figure 4.2.8, showed that the two cylindrical fuselages was the best choice.

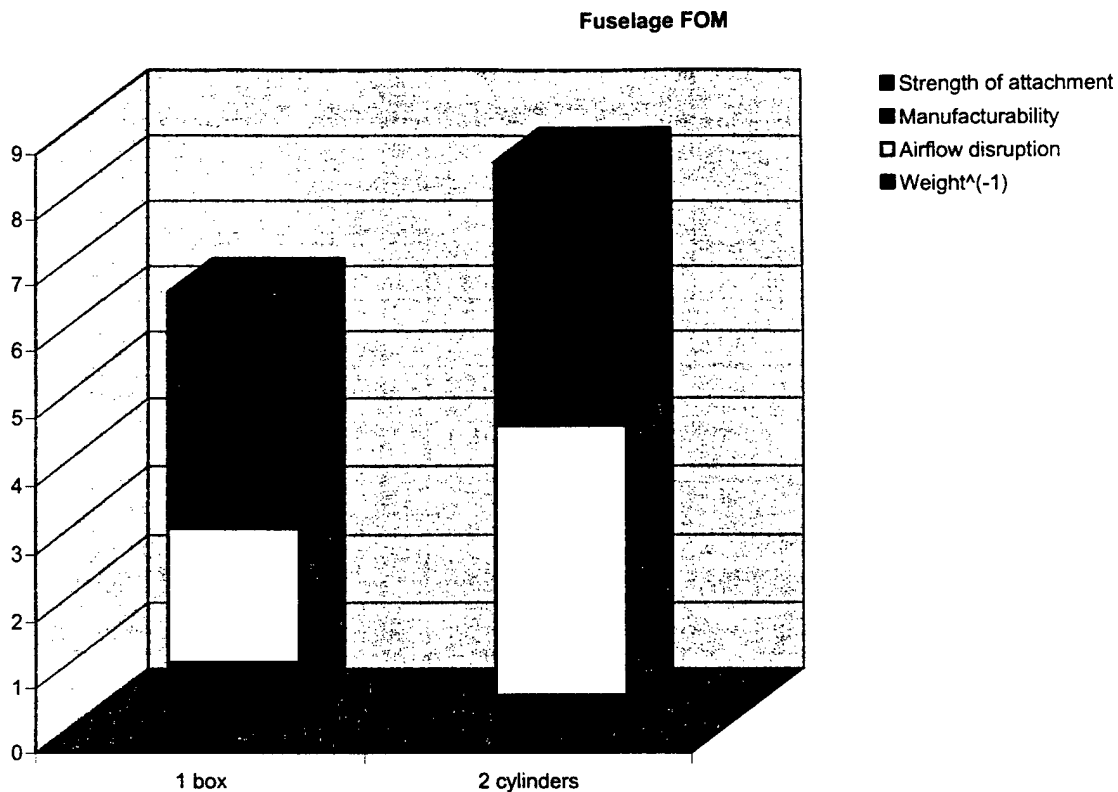


Figure 4.2.8: FOM analysis of fuselage designs.

4.2.4 Vertical Stabilizer Design

The three stabilizer design considerations were a stabilizer constructed out of Styrofoam with Econokote, one made of fiberglass and foam, and one with foam ribs. The figure of merits for the stabilizer design were the inverse weight ($\times 2.0$), the manufacturability ($\times 1.0$), and the airfoil shape uniformity ($\times 1.0$).

The foam/Econokote stabilizer was easily made and held had a constant airfoil shape over the entire surface. It was, however, slightly heavier than the ribbed foam stabilizer, which was difficult to manufacture and was not entirely uniform over the surface. The fiberglass/foam stabilizer was heavy and hard to make, but had a uniform cross section. As shown in Figure 4.2.9, the optimum stabilizer was the solid foam and Econokote design.

Vertical Stabilizer FOM

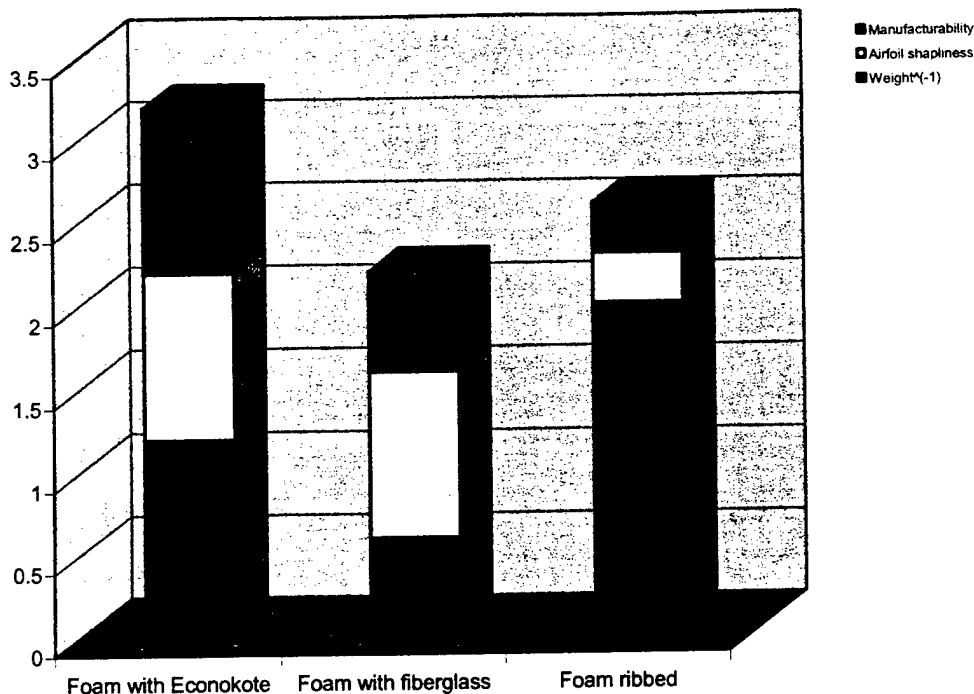


Figure 4.2.9: FOM analysis for the vertical stabilizers.

4.2.5 Longerons Design

The Structures team decided to use the existing carbon/aluminum spars that were being made for the wings since they were found to be very strong, inexpensive, and were already being made in excess.

4.2.6 Joint Design

Three designs for the connection joints between the wings and longerons were examined: a carbon wrap with microfiber in epoxy, a wooden dowel T-joint, and a PVC pipe. The figure of merits for the joints were the inverse weight of the joints (x4.0), the joint's strength (x3.0), the modularity, or ease of replacement if the plane were to crash, (x2.0), and the manufacturability of the joint (x1.0).

The carbon wrap was found to be incredibly strong, but too heavy to justify its use. It was also nearly irreplaceable if the plane were to crash or if one of the joints were to break. The T-joint, on the other hand, was relatively strong and light, and was easily replaceable by another wooden dowel if it were to break. The last design examined was the PVC pipe which was easy to make, but too weak. Based on the results shown in Figure 4.2.10, the wooden T-joint was chosen.

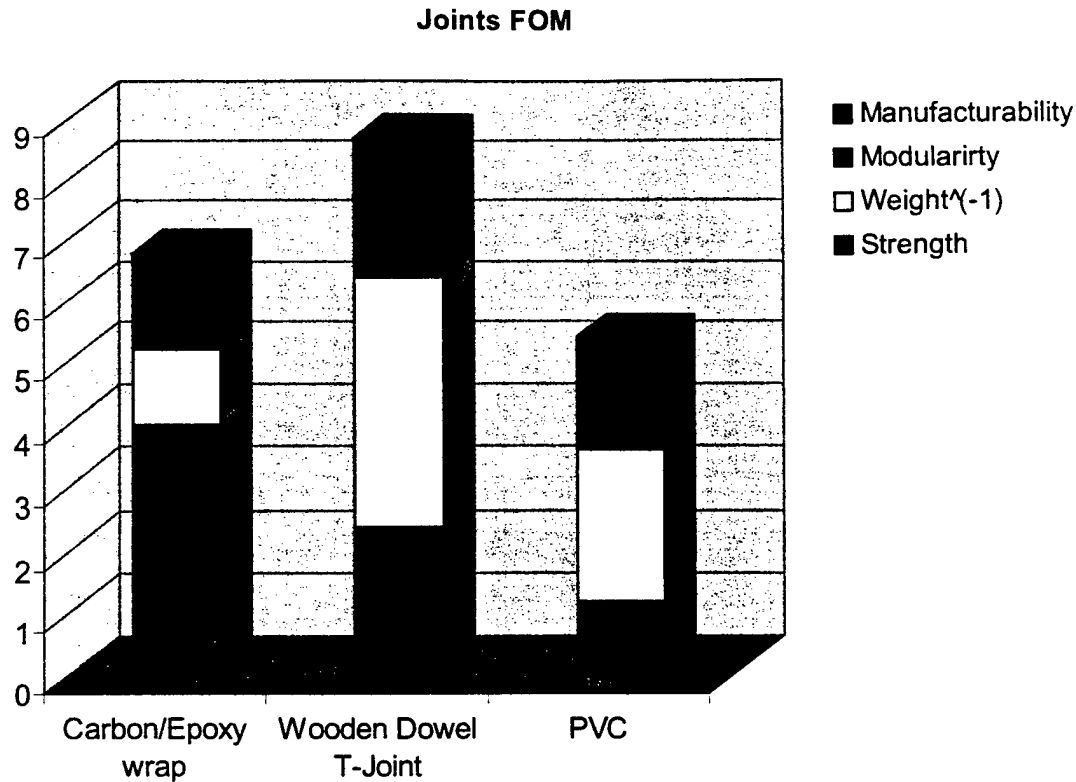


Figure 4.2.10: FOM analysis for joint configurations.

4.2.7 Landing Gear Design

The previous year's front landing gear was found to perform well and was easy to configure, so no changes were made to its design. The main landing gear, however, had to be built to withstand a much heavier loading and three designs were put forward to accomplish this task. The figure of merits for the landing gear were strength (x3.0), inverse weight (x2.0), and manufacturability (x1.0).

In the first design, shown in Figure 4.2.11-a, a standard aluminum plate was to be attached to the longeron. This design was weak and costly, but light. The second design, shown in Figure 4.2.11-b, was to epoxy a carbon fiber weave to a liteply plate. The wood was used to stiffen the landing gear in compression, and the carbon fiber was to increase the strength in tension. This design was of medium strength and easy to make, but it was heavy. The last gear design considered, shown in Figure 4.2.11-c, was to use the carbon/aluminum spar used for the wing design because of its strength, and availability. As shown in Figure 4.2.12, the carbon/Aluminum spar configuration was chosen.

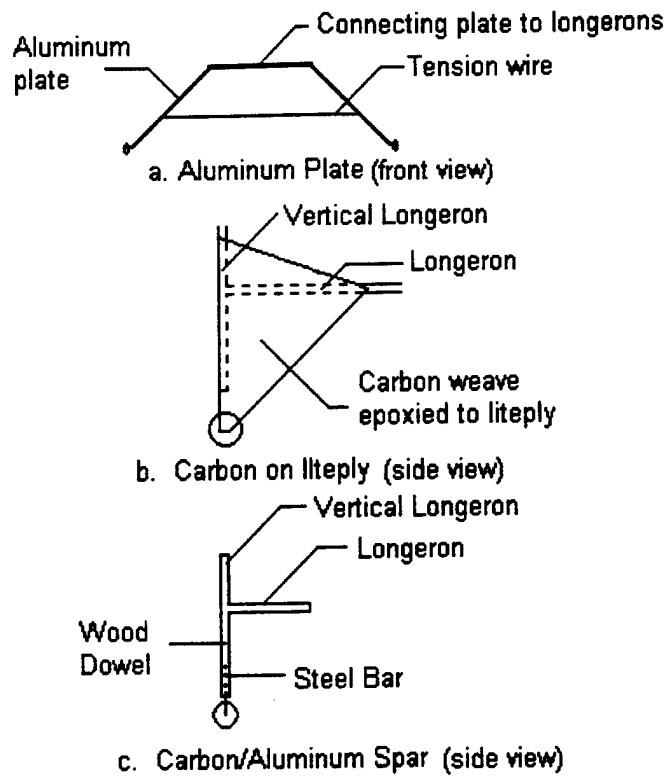


Figure 4.2.11: Various landing gear concepts considered.

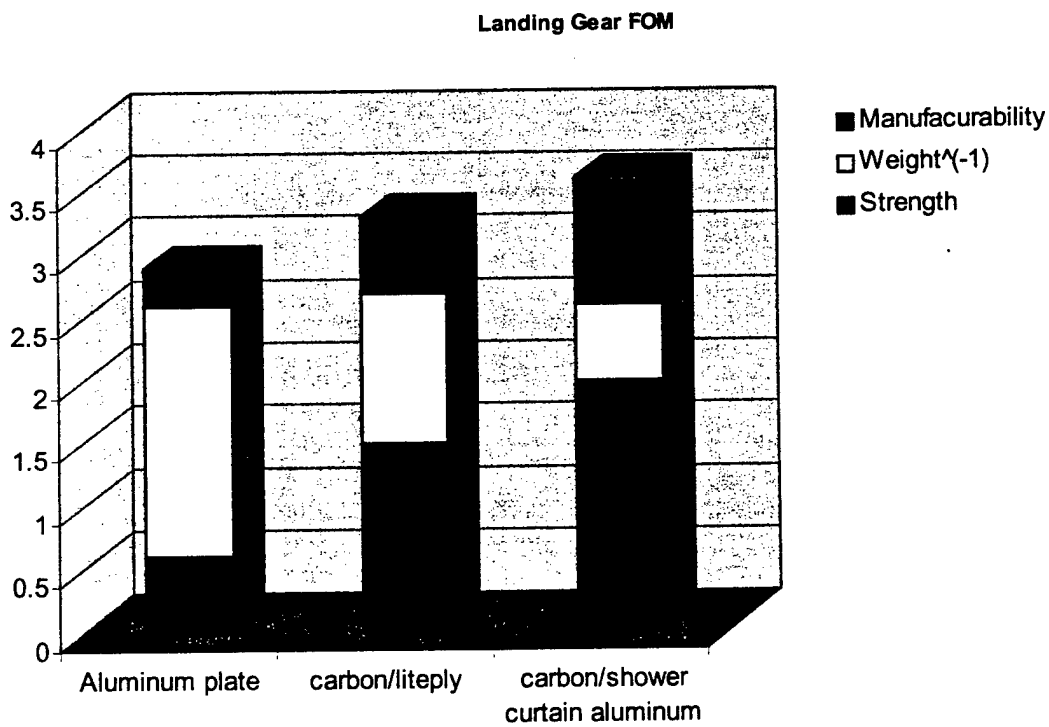


Figure 4.2.12: FOM analysis for the landing gear.

4.3 Propulsion Preliminary Design

4.3.1 Preliminary Design Parameters:

The first parameter of the propulsion design consisted of the contest rule parameters, which state that all propulsion of the airplane is to be powered by a Nickel Cadmium battery pack whose weight does not exceed 5 lbs and brushed Astroflight or Graupner electric motors. Aerodynamics group set the second parameter of the design to be 10 lbf of thrust. Figure 4.3.1 shows 10 lbf is the amount of thrust needed for a 45 lb airplane to takeoff in 200 feet. The third parameter is a minimum 4 minutes of flight time at full throttle. This is the minimum full throttle time needed for a ten minute run, (the rest of the 10 minutes will be spent on ground or gliding). The fourth parameter is "off the shelf propellers". This limits the diameter, pitch and airfoil shape of the propeller. The fifth parameter is gearing. Due to our manufacturing capability the team cannot build custom gearboxes for the motors. Therefore, the gearing will be limited to "off the shelf" gear boxes. The sixth parameter is cost of propulsion. The budget of the DBF airplane prohibits the battery cost not to exceed \$500 for the batteries, \$500 for the controllers, and \$1000 for the motors.

4.3.2 Minimum energy needed for takeoff

According to the DBF rules, there is a 5 lb maximum limit on the Ni-Cad battery pack to power the airplane. The amount of energy in a battery pack determines the amount of thrust and the duration of the thrust provided by the electric engines. The minimum requirement of energy needed for takeoff was calculated to be 2712 joules, which was calculated using 10 lbf of thrust and 200 ft of runway. The takeoff time was calculated to be 5 seconds, this means 543 joules/second or 700 watts (after accounting for inefficiencies) for takeoff.

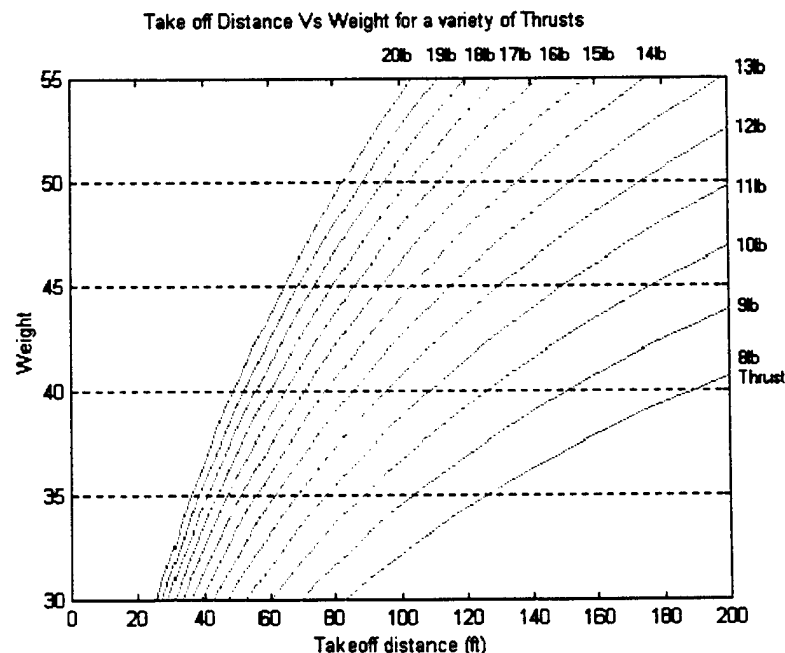


Figure 4.3.1: Take off distance vs. Thrust.

5.0 Detail Design

5.1 Performance Data

The following list provides an easy-to-reference list of final performance data for the GPA Killer. All of the calculations used to compute the aerodynamic data were calculated by hand using *Introduction to Airplane Flight Mechanics* by Dr. D.G. Hull [3,5].

Geometry—

Fuselage —

Diameter	9 in
Length	35 in
Wetted area	2882.2 in ²

Wing—S1210

Thickness ratio (t/c)	.125
Maximum thickness	.25
Peak suction	.25
Root/tip chord (c)	18 in
Span (b)	120 in
Sweep (qc, ac, etc..)	0 degrees
Planform area (s)	2160 in ²
Aspect ratio (AR)	6.66
Taper ratio (λ)	1
X-coordinate of ac (ξ)	4.5 in
Y-coordinate of ac (η)	30 in
Wetted area	4320 in ²
i_w	0 degrees

Horizontal tail—S1220

Thickness ratio (t/c)	.125
Root/tip chord	12 in
Span (b)	114 in
Sweep (qc, hc, etc..)	0 degrees
Planform area (s)	1368 in ²
Aspect ratio (AR)	9.5
Taper ratio (λ)	1
X-coordinate of ac (ξ)	3 in
Y-coordinate of ac (η)	28.5 in
Wetted area	4320 in ²
i_H	4 degrees

Vertical Tail Geometry

Thickness ratio	.156
Chord (c)	8 in
Span (s)	12 in
Sweep (qc, hc, etc..)	0 degrees
Planform area (s)	96 in ²
Aspect ratio (AR)	1.5
Taper ratio (λ)	1
X-coordinate of ac (ξ)	2 in
Y-coordinate of ac (η)	3 in

Wetted area 4320 in²
Aerodynamics at Re = 300000, $v = 16.1$ ft/s $\alpha = 0$ degrees

Wing

α_0	-5.87 degrees
$C_{l\alpha}$.08389 1/degree
ac/c	.25
C_{m0}	-.001
$C_{L\alpha}$.366
C_{mac}	-.001

Horizontal Tail

α_0	-5.87 degrees
$C_{l\alpha}$.08389
ac/c	.25
C_{m0}	-.001
$C_{L\alpha}$.368
C_{mac}	-.001

Wing-Body

α_{0L}	5.87 degrees
$C_{L\alpha}$.783
C_{mac}	≈ 0.00

Airplane aerodynamics

e_a	.5637
e_o	4.43
h_h	.9
C_{Do}	.01
C_{Lo}	.895
C_{La}	.4575
C_{LdE}	0 (no flaps)
x_{acwb}	3.0 ft.
x_{ach}	.25
V_H	.0793
C_{mo}^A	1.80
C_{ma}^A	.00915
C_{mdE}^A	0 (no flaps)
X_{AC}	2.23
X_{cg}	2.25

The weight of the plane before its maiden flight was 27 lbf with the fuselage. This means that the maximum payload capacity of the airplane is 28 lbf, making a payload fraction of 51%. Two flight tests were conducted prior to the submission of this report. Both were conducted without payload and if these tests were successful, the plane would be loaded. Also, at the test site, the back wing motor was not operating, but the team decided to go ahead with the flight test since it could be a simulation if the third motor were to go out in competition.

The first test was simply to observe the stability of the aircraft and, therefore, was only lifted off the ground a few inches to avoid significant damage. Take-off distance was unobservable since the vertical height obtained by the airplane was very small. The pilot noticed no uncontrollable tendencies of in-flight performance, so the team decided to increase the altitude in the next flight to further test the aircraft.

In the second flight test, take-off distance was approximately 50 feet, which was in good agreement with aerodynamic predictions. The plane reached about 5 feet in the air when the pilot noticed a nose up tendency in the aircraft. With full elevator up and throttle cut, the nose continued up until the plane reached approximately 20 ft. altitude and fell straight to the ground.

The exact causes of the crash have yet to be determined, but the team is examining possibilities of the cg being too far back in flight, the lack of operation of the back wing motor causing instability, initial aerodynamic predictions of lift forces on the wings being incorrect, and/or the manufacturing of the airfoil was not close enough to the specified one. Causes of the crash will be included with the report addendum.

5.2 Component selection and systems architecture

5.2.1 Ni-Cad Battery optimization

The amp-hour rating of the battery determines the time duration of the battery's output at a certain load. For example, if a 5 amp-hour battery is being drained at 5 amps, the battery will last 1 hour. In order to maximize the energy density of the battery pack, the batteries have to last just long enough for the 10 minute run. To determine the amp-hour rating needed for the batteries, the estimated time of flight and power consumption was determined. Table 5.2.1 shows the estimated time of power use.

According to Table 5.2.1, the airplane will be able to do 4 sorties, 2 tennis ball and 2 steel weight, in 10 minutes. The total time for full throttle required for the batteries is 4 minutes. Due to safety considerations, the UT-DBF Team does not want to exceed 35 amps, this will ensure that the airplane is not disqualified or fails in flight with a 40 amp fuse. The 35 amp max means that a airplane is not disqualified or fails in flight with a 40 amp fuse. The 35 amp max means that a

Action	Throttle%	Time for action (s)	Full Throttle Time (s)	Time (min)
Takeoff with steel payload	100	7	7	0:07
Climb + Turn	100	29	29	0:36
Loop	100	6	6	0:42
Descend+Turn	0	29	0	1:11
Total time full throttle for steel run			42	
Reload time	0	1:00	0:00	2:11
Takeoff with tennis ball payload	100	6	6	2:17
Climb + Turn	100	29	29	2:46
Turn (.75 throttle)	75	29	22	3:15
Turn (.75 throttle)	75	29	22	3:44
Descend+Turn	0	29	0	4:13
Reload time	0	1:00	0:00	5:13
Total time full throttle for tennis ball run		77	79	
Total time of full throttle for both sets of runs			1:21	

Table 5.2.1: Estimate of time required.

battery pack of at least 2.3 amp-hours is required. To satisfy this requirement, the battery packs must consist of batteries connected in series with capacities of 2.3 amp-hours or greater, or a pack consisting of several parallel battery packs whose sum of amp-hrs exceeds 2.3 amp-hrs.

Battery efficiency is represented by the battery's internal resistance, which determines the amount of watts the battery losses while outputting the power. To maximize the airplane's performance, the battery pack should contain the greatest amount of energy within the 5 lb limit and have the lowest possible internal resistance. In order to find the best Ni-Cad battery suited for the competition, the propulsion team investigated 177 different Ni-Cad batteries to find the most energy dense Ni-Cad batteries available on the market.

According to our research, the Panasonic High Capacity series, the Sanyo E series, and SR batteries were exceptionally good because they had a significantly larger joule per gram ratio than their counterparts. Additionally, it was determined that these batteries can provide the minimum power required for takeoff. These batteries were configured in packs which had amp-hr ratings greater than 2.3. The batteries with an amp-hr rating less than 2.3 were connected in parallel till they had an amp-hr rating greater than 2.3 and then "stacked up" in series till the battery pack weight is 5 lbf and the batteries which had an amp-hr rating greater than 2.3 were

simply “stacked up” in series till their weight was 5 lbf. Taking the internal resistance of the battery into account, the batteries were then analyzed for their power output. Figure 5.2.1 shows the results and the winning batteries’ specifications are shown in Table 5.2.2.

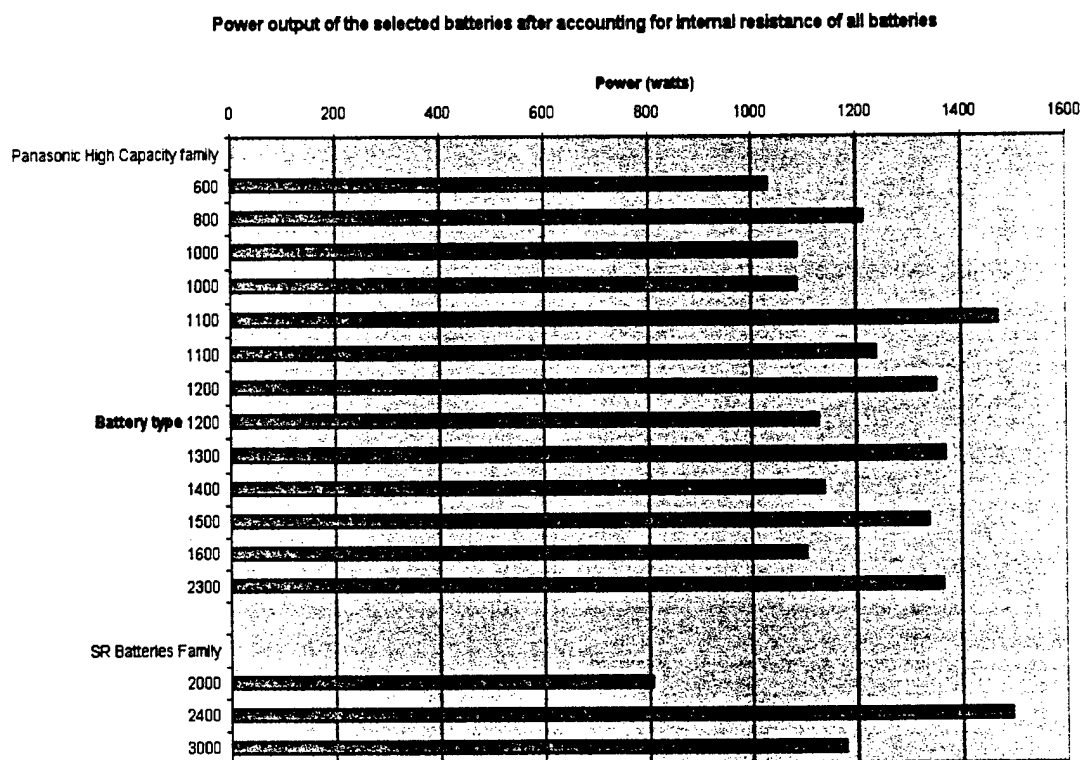


Figure 5.2.1: Battery power output.

SR Batteries 2400 Max		Info
Mah		2400
Weight(g)		53.86
Watt-hrs/g		0.05
Internal Resistance (mOhm)		3.8
Battery Packs Needed		1.00
Batteries in a 5lb pack		40.00
Voltage		48.00
Amps		35.00
Total Internal Resistance (Ohms)		0.15
Power out		1493.80

Table 5.2.2: 2400 mAh SR Batteries Specifications.

5.2.2 Figures of Merits for Propulsion Component Selection

The Propulsion team proceeded to create the figure of merits to judge the propulsion system. The team decided that the most important figure of merit (FOM) was thrust (x5.0). According to the Aerodynamics group, the largest problem in flying a heavy payload will be accelerating the aircraft to takeoff speed in the 200 ft runway distance. Therefore the more thrust the engine creates, the more steel the airplane will be able to carry.

The second most important FOM was determined to be the propeller diameter (x4.0). According to the Structures group, the taller the landing gear, the larger the forces it will experience on a landing, causing a tall landing gear to be stronger and heavier to overcome the forces caused by the large moment arm. Propellers with diameters smaller than 18" were given a score of 4, while propellers with diameters larger than 18" were penalized by multiplying the inverse normalized diameter with the multiplier. For example, a 26" propeller will have a value of $(18/26) \times 4$, so its score is, 2.8.

The third most important FOM was determined to be the adaptability of the motor (x3.0). This FOM accounted for engine changes that might happen in the future due to design changes, defective engines, or damaged motors in an airplane crash. This FOM accounts for the number of possible motor/gearbox configurations that allow this motor with or without the gearbox to be used on the airplane. The number of configurations is divided by the maximum number of configurations of any motor to obtain a normalized value then this is multiplied by the adaptability multiplication factor. For example, the most versatile motor appears in 10 different configurations and the least versatile motor appears twice. Therefore, the score for the least versatile motor will be $(2/10) \times 3$ or 0.6 while that of the most versatile motor is 3.

The fourth most important FOM was rated aircraft cost (RAC) of the propulsion system (x2.0). The estimated RAC was determined by the following formula:

$$\begin{aligned} & \$5010 \text{ (the estimated base cost for the tandem wing)} \\ & + (\text{the number of total watts the motors will consume}) \\ & \quad + \$100 \times \text{the number of engines used} \\ & \quad + 100 \times \text{the weight of the engines} \end{aligned}$$

The power consumption of the motor was determined from the output of electricalc. The weight of engines was obtained from the website of the manufacturers.

The last FOM was reliability of the motors (x1.0). The reliability of the propulsion system was based on the number of motors on the airplane (the more motors on an airplane, the less the chance of crash if a motor fails) and the gear ratio of the motors. The formula for the reliability, R, was:

$$R = 0.2 \times \text{number of motors}$$

Adding 0.2 to R if the motors are direct drive (direct drive motor is more reliable than a geared motor), this gives a max score of 1 for a propulsion system with 4 direct drive motors and a minimum score of 0.2 for a single geared motor.

Three different methods were used to evaluate the motors. The first method was obtaining specifications from the manufacturer. The second involved modeling motor/propeller configuration in Matlab. The third, and most accurate, was modeling the motor and propeller configuration in Electricalc software.

The Propulsion team found that the first method of obtaining manufacturer's specifications was not applicable to our airplane due to the size and weight of the airplane. Both companies have a wide list of recommended propeller/motor/gearing/battery configurations, however they all produce a fraction of thrust the airplane needs. The Propulsion team then proceeded to develop a Matlab code to optimize the propulsion system, but the output failed to correlate with real results. Finally, the team bought a software package called Electricalc. The input of the program is the motor, propeller, gearing and battery data. Electricalc outputs the thrust of the system at a given throttle.

5.2.3 Verification of Thrust Predictions Using a Static Test Stand

Since Electricalc was extensively utilized to predict the optimal propeller blade geometry, blade sizing and shaft power, it was necessary to verify the accuracy of Electricalc with static engine trials. The propulsion team selected four propeller blades for the initial blade sizing trials. Each of the propellers was independently tested on an engine mounted to a static test stand as shown in Figure 5.2.2. The propeller thrust was measured with a scale mounted on the engine moment arm the RPM was measured with a tachometer mounted to the test stand.

The tests were done using several different propellers and a Maxcim max-15 motor. A constant power source of 13.7 volts and 10 amps was used to power the motor. According to Figure 5.3.3, Electricalc calculations were reasonably consistent with the results of the static test stand test. In addition to confirming the reliability of Electricalc, the static test stand trials revealed several other important conclusions. Since the 14x6 propeller generated only 1.75 lbs of thrust, then at least six engines would be needed to generate the 10 lbf of thrust. Since six engines have problems with reliability and cost per engine, the test revealed a need for a larger diameter propeller with an optimized pitch and corresponding engine to reduce the number of needed engines.

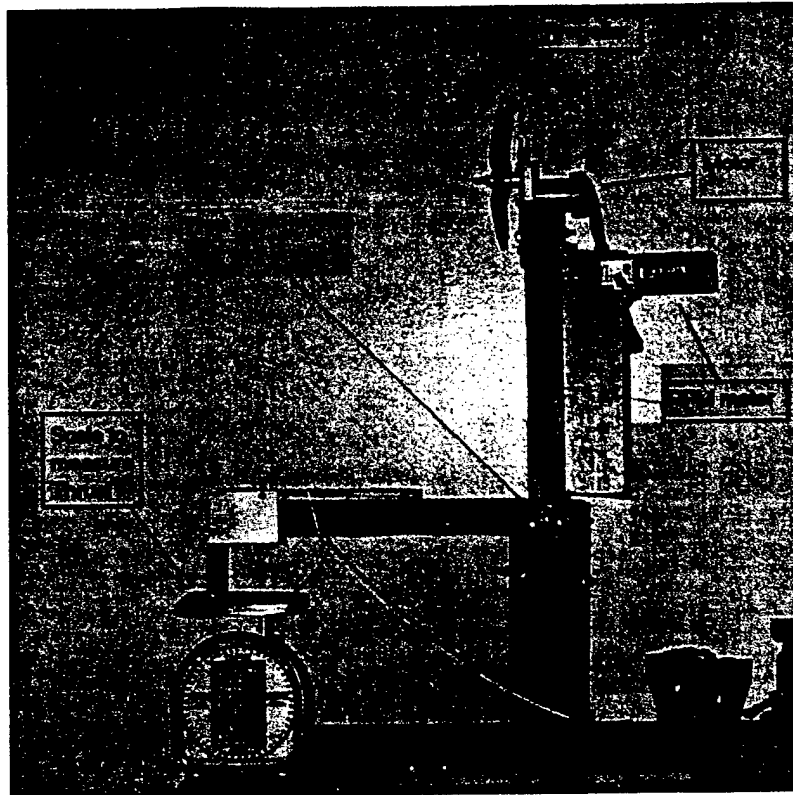


Figure 5.2.2: Motor Test Stand.

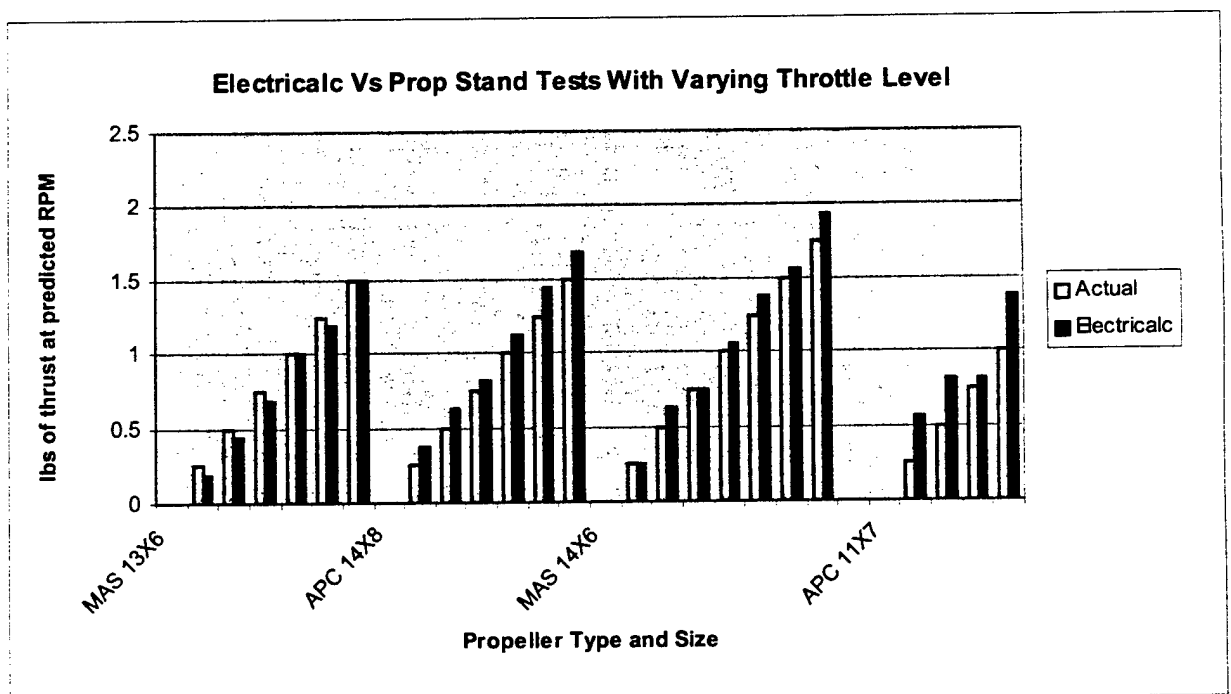


Figure 5.2.3: Comparison of Electricalc with actual Static thrust tests.

5.2.4 Motor/Propeller/Gearing optimization using Electricalc

The Electricalc user interface requires 4 different input parameters to give an output of thrust. Figure 5.2.4 shows the interface console of Electricalc. The first parameter is power in which the number of cells, their voltage, internal resistance, and amp-hours of the battery pack was entered. Since the battery pack has already been optimized, this was kept constant with cell count =36, cell internal resistance = 3.8 mOhm, ESC mOhm = 15 (power lost to wiring), and mA-hr=2400. The next parameter is motor, where the Astroflight and Graupner motors with their accessorized gearboxes were entered. The third parameter is the drive parameter in which the most efficient diameter/pitch ratio is usually 2:1. In order to optimize the propulsion system, the pitch and diameter are set so that the amp level in the motor parameter is approximately 35amps. Usually this value is about 1-4 amps above or below 35 amps, therefore the pitch is slightly varied to bring the amp level closer to 35 amps. This pitch and diameter selection is checked with what dimensions are available on the market, and the closest to this value that creates an amp loading not exceeding 35 amps is selected. This is the optimal engine/motor/gearbox configuration.

All the motors with their respective gearboxes were optimized with the propellers and rated on the figure of merits. It was noticed that all the Graupner motors were too small for the airplane so only Astroflight motors were used for this analysis.

Figure 5.2.5 shows the result of this analysis. According to the results the winning configuration was an Astroflight 625 motor with a model 713 gearbox which has a 3.1:1 gearing ratio. The 3-engine configuration was found to be optimal and should produce 17.9 lbf of thrust. The optimal propellers were found to be of 21 in diameter and 10 in pitch. The motors were calculated to have a run time of 4.36 minutes. The power consumption rate of all motors combined was 1400 watts. In case of motor failures, the motors could be rewired for a 2 motor or a 1 motor flight having smaller propellers with dimensions of 17x8 and 12x7 respectively. Both of these configurations were calculated to provide over 10 lbf of thrust so the team can still compete with 2 damaged motors. These configurations also stayed within the design parameters.

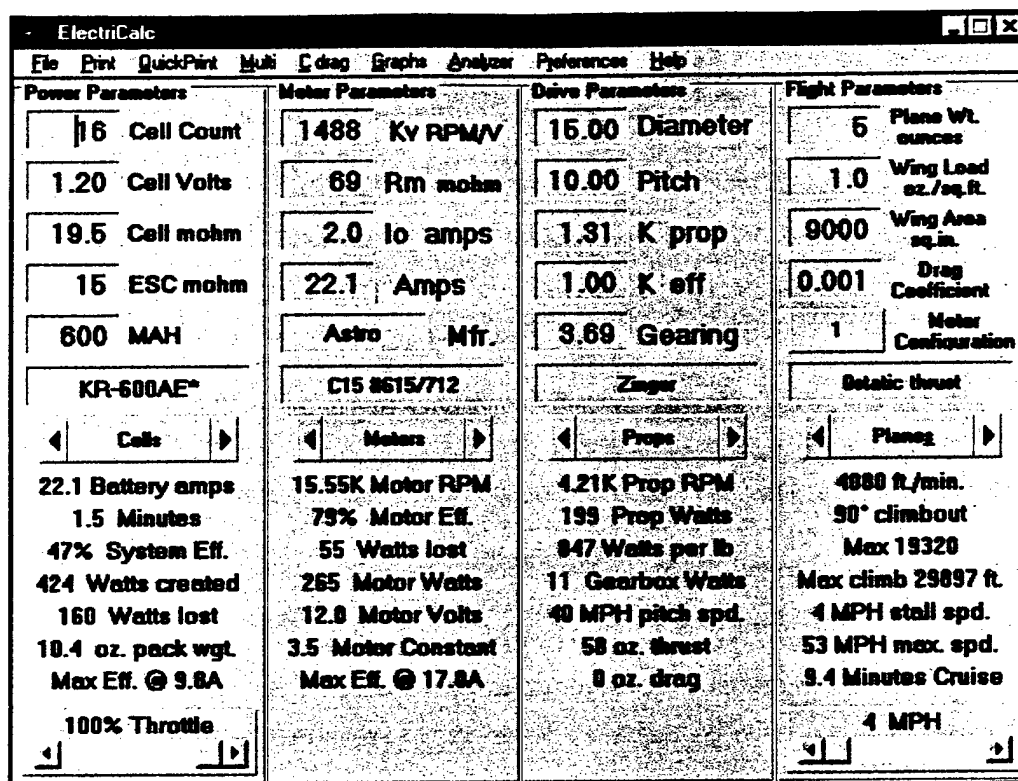


Figure 5.2.4: Electricalc console.

FOM Results of Engine/Propeller/Gearbox Configuration

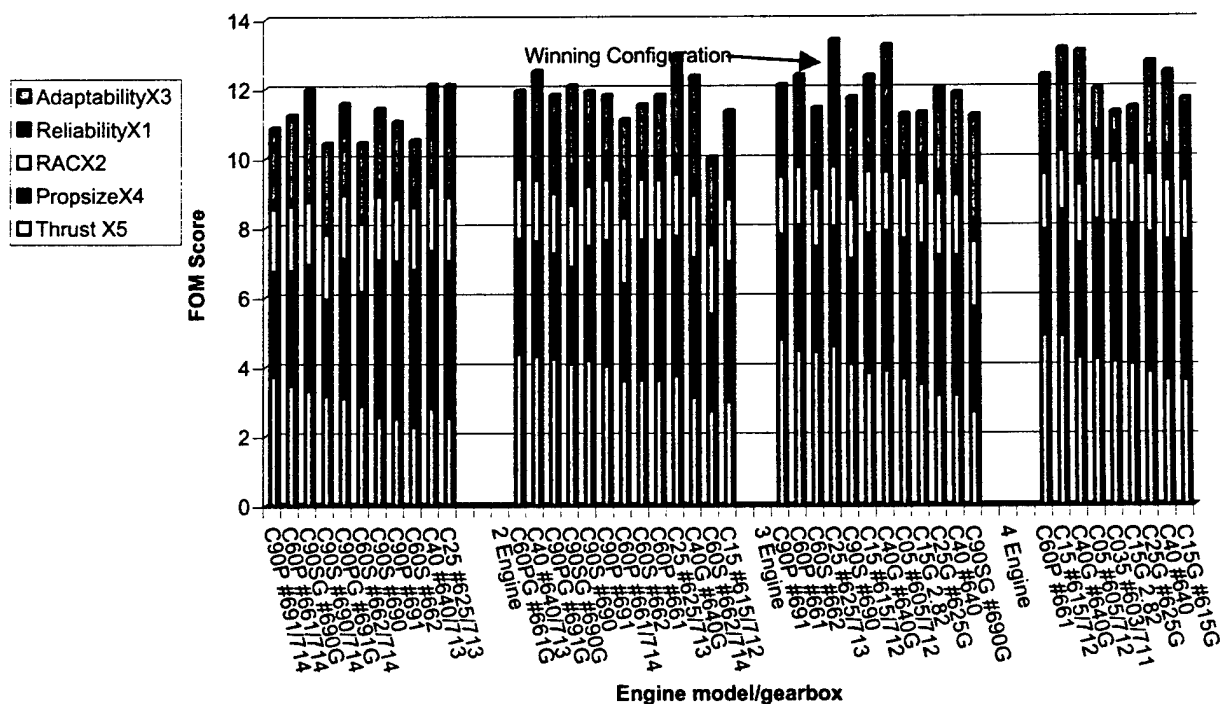


Figure 5.2.5: Figure of Merit breakdown for motor configuration.

The winning configuration, an Astroflight 625/713 motor with Master Airscrew 21x10 propeller, was tested for its static thrust and duration. The test was performed on the same test stand shown in Figure 5.2.2. Propeller thrust and power consumed data was taken approximately every half-pound of thrust that the propeller produced and is shown in Figure 5.2.6. The actual thrust at full throttle was measured to be 5.25 lbf per engine meaning that the total thrust for the three motors would be 15.75 lbf. The actual amperage was measured at 29 amps. Both of these values were slightly lower than our expectations. According to Electricalc, the thrust should have been 6 lbf per engine and the measured amps to be 33 amps. In conclusion, the motors have 12.5% less thrust than expected but can fly 14% longer than expected. The Propulsion team is in the process of investigating the inconsistencies between Electricalc and actual data. The Propulsion team believes that vorticies at the ends of propellers might be the cause of the error. The motors can propel the airplane for approximately 5 minutes at full throttle, which exceeds the minimum requirements for the airplane of 10 lbf thrust for 4 minutes as needed for the competition.

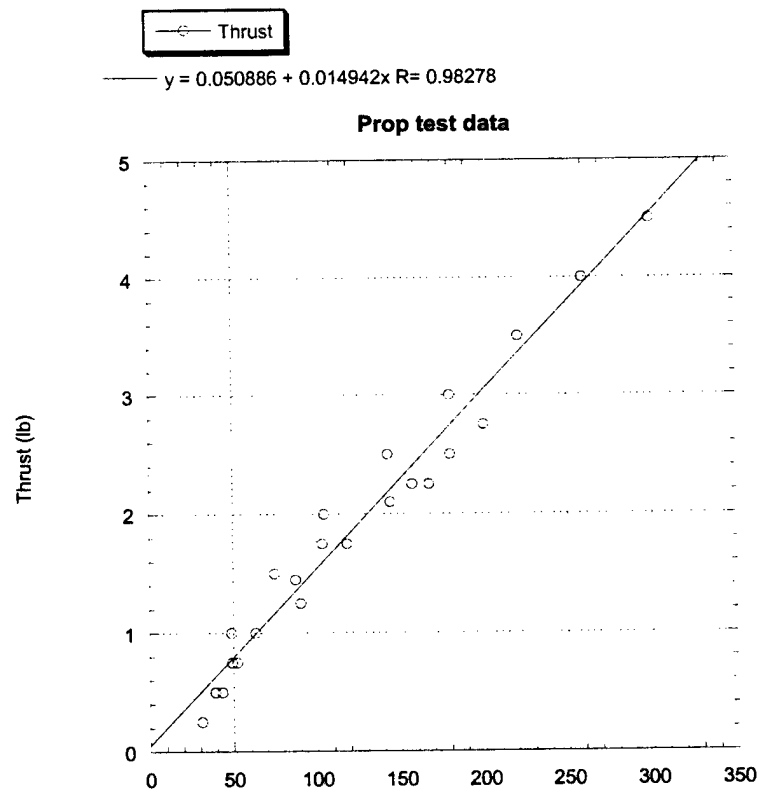
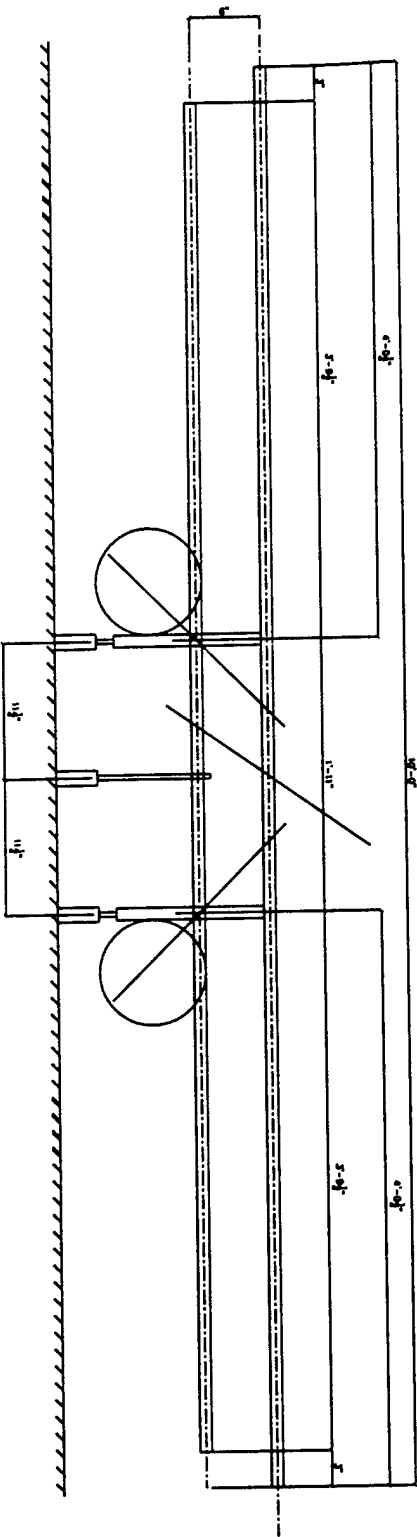
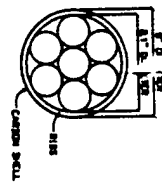
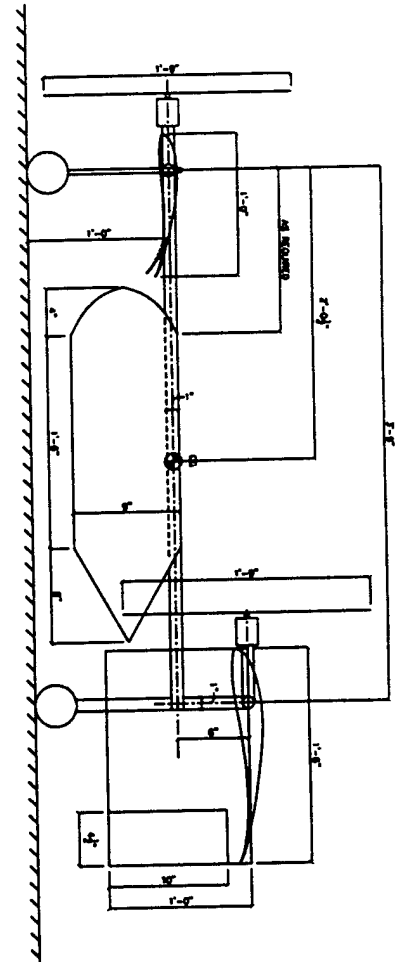
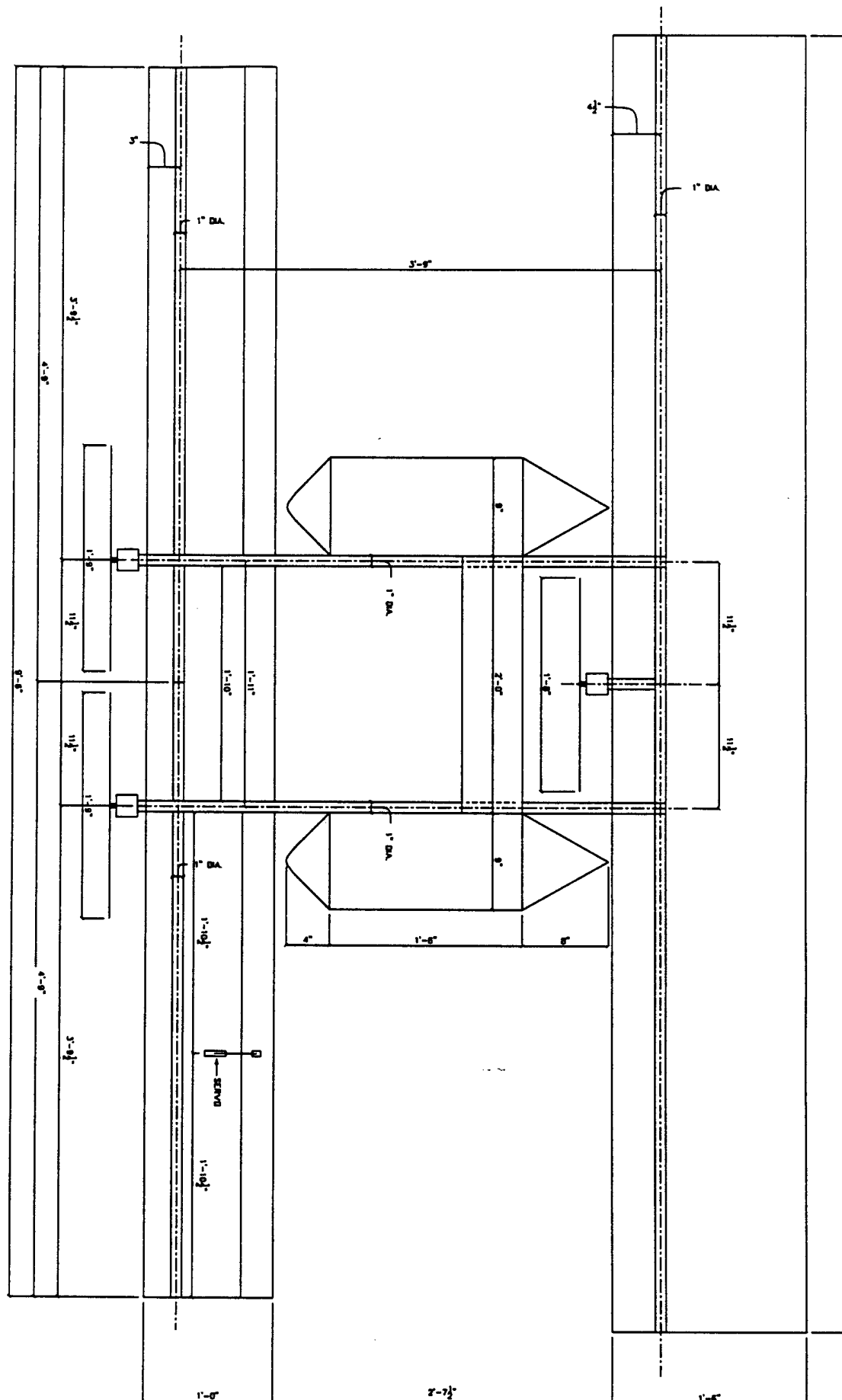


Figure 5.2.6: Propellor test data from selected motor configuration.



Front View

Aerial View



5.4. Innovative solutions, manufacturing processes, and cost reduction

5.4.1 Wooden dowel T-Joints

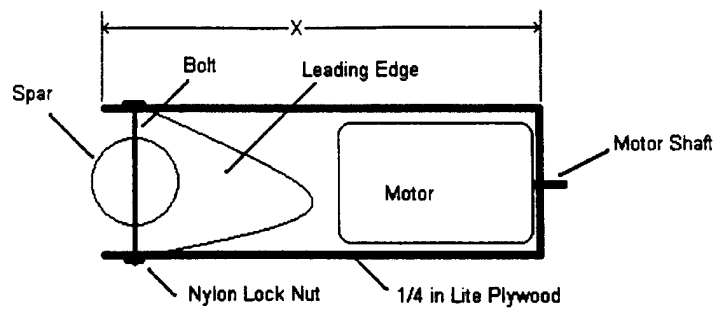
With the airframe design finalized, the team was faced with the difficult task of joining the sections together in a way that allowed modularity so that the plane could be shipped in several pieces, and yet still have enough structural strength in the joints to withstand the loading subjected to the wing spars. Several designs were proposed, but all failed to be both portable and strong. The wooden dowel T-Joints, however, were the solution. They allowed the wing sections to be connected by drilling holes through both spars that are to be joined and then through a wooden dowel. The dowel was then inserted into the spar and a bolt placed through the holes on each side to secure the sections. This proved to be a light and strong method of joining the wing sections while allowing quick assembly and transport.

5.4.2 Motor mounts

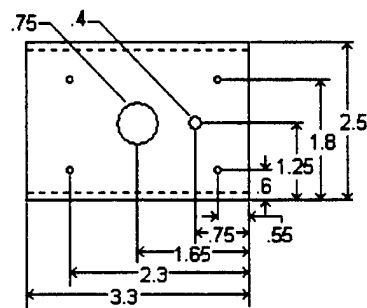
Once the design of the airframe was finalized, and the placement of the motors determined, the team found that, to maintain the portability of the plane required by the long shipping distance, the only motor mount design that would not require extensive modification of the airframe was one in which two main plates attached to the spar as shown in Figure 5.4.1. The design difficulty arose from problems attaching a circular motor (with set screws on its rectangular face) to a circular spar. As seen in the figure, the design was to attach the motor to a flat plate with holes drilled for the shaft and the set screws. This front plate was then attached to two plates that had holes drilled through which bolt slide through to attach the mount to the wing spar. For the front canard, which has a smaller leading edge, the length of these plates (dimension X in Figure 5.4.1) was 7.125 in and for the rear wing the plate length was 9 in. This design also had the advantage of serving as the connection element for the front canard sections.

5.4.3 Vertical Tail positioning

The vertical stabilizer was sized by the Aerodynamic group in the preliminary design and could have been either one large symmetric airfoil in the center of the rear wing, or it could have been two separate tails placed symmetrically on the back wing. Once it was realized that the selected landing gear were symmetrically and vertically mounted from the quarter chord of the main wing the decision was made to mount the tails on the landing gear spars. By using two tails attached to the landing gear, it was noted that we could fare the landing gear to reduce drag and solve the problem of placing the tails onto the small circular spar, the only structural element in the wing that they could attach to otherwise.



a. Motor Mount - Side View



b. Motor Mount - Front View

Figure 5.4.1: Engine Mount diagrams (dimensions in inches).

5.4.4 Canard surface

The most innovative feature about the plane is the large forward canard. The aircraft needed a lot of lift due to the excessive weight of the plane and the payload. By adding the canard the aircraft gained a significant amount of lift with no added rated aircraft cost (minus the additional weight cost of the plane). By essentially doubling the airfoil surface area, the aircraft was able to handle a much larger lift distributed across the wings surface. This in turn allowed the plane to pull a 68 degree bank angle versus a 42 degree angle.

6.0 Manufacturing Plan

When considering the process of manufacturing, the methods of previous UT-DBF teams played a key role in deciding what methods to implement. This included, but was not limited to, methods that gave way to a plane crash and techniques that yielded better performance of the aircraft. Library research was also conducted to assess construction methods.

To simplify the manufacturing plan, the plane was divided into components to be considered independently. These include the wing spar, the wing, the fuselage, the vertical stabilizers, the landing gear, the motor mounts, the longerons, and the joints. Each component was evaluated according to a figure of merit matrix to assess its manufacturability. Of highest priority was the availability and cost of the component. This was chosen since the piece cannot be manufactured if materials cannot be obtained. The next figure of merit was the skill level required of the team members in manufacturing the part. This was considered since it would be easier to construct a component if team members had already had experience with the manufacturing methods involved. Then, the ability to mass-produce the component was measured. The team had chosen crash resistance as a figure of merit in conceptual design by having several spare parts for each component so the plane could be easily repaired. The final merit considered was the time required to manufacture the component. The team's time was valuable since work on the plane must be negotiated with time in school, and therefore the less time building the airplane, the better. All figures of merit are weighted equally. Figure 6.1 illustrates the figure of merit matrix and the results of analysis.

The manufacturing analysis was not the deciding factor for each component of the airplane. Rather, it served as a figure of merit in preliminary design for deciding the materials of which the plane will consist and how to construct them.

6.1 Wing Spar

Four processes for manufacturing the wing spar were investigated: a carbon fiber wrapped aluminum shower curtain rod, carbon fiber wrapped Styrofoam, an aluminum shower curtain rod, and a 6160 T6 aluminum bar. Numerical analysis yielded the carbon fiber wrapped aluminum as the spar of choice.

To manufacture the spar, the carbon fiber was first cut to match the dimension of the aluminum tube. Next, 3M Super 77 was applied to the carbon to aid in keeping the carbon correctly aligned with aluminum rod. The carbon was then wrapped around the aluminum in such a fashion that air bubbles were minimized and was completely wrapped around the pipe. West System 105 resin and the corresponding 205 hardener were applied to the carbon. Once sufficiently covered, the rod was then cured in a vacuum bag at room temperature for approximately 12 hours. Once dried, the spar was sanded to remove any inconsistencies incurred from the curing process.

6.2 Wing

Since the team must fly to the competition, it was necessary to construct a wing that was easily disassembled and transported. To achieve this, the team decided in preliminary design that the wing and canard will consist of three pieces: two outer sections each spanning 4 ft. and a middle section that would be 22 in. in length. Three concepts were evaluated for the structure of each wing component. First evaluated was a solid Styrofoam wing with the spar running through it. The second was a solid foam leading edge, a foam ribbed mid-section, and a solid foam trailing edge. Also, a balsa ribbed mid-section with foam leading and trailing edges was considered. All wing styles would be covered with Econokote to provide greater structural strength and to give the wing its shape. The figure of merit analysis yielded the second concept as optimal.

To produce an accurate airfoil shape in the leading edge, rib structure, and trailing edge; airfoil templates were constructed. The appropriate airfoil design was stored in AutoCad and then printed to paper. Next, these paper outlines were glued to Formica plates and cut. The templates were placed on the ends of a well sized piece of Styrofoam and a hotwire was used to cut the Styrofoam. Once the leading edge and correct number of ribs were cut, they were glued to the spar using 3M Super 77 adhesive. Econokote was then applied to this section. The trailing edge could not be constructed with the main parts of the wing since it is much thinner and a much more delicate piece of Styrofoam; therefore, a different method must be used to ensure its stiffness in flight.

To achieve this stiffness, the Styrofoam trailing edge was covered with Elmer's glue and HP translucent bond paper was applied to the surface. Once the glue dried, the trailing edge was covered with Econokote and attached to the main portion of the wing. After the wing was fully constructed, airfoil shaped balsa ribs coated with carbon fiber were attached (using Super 77) at the ends of each portion of the wing to provide structural rigidity.

6.3 Fuselage

Two concepts for the fuselage were considered in the design of the airplane. The first consisted of a single unit which would carry 100 tennis balls and 25 pounds of steel. The second consisted of two cylindrical containers which would each carry 50 tennis balls and 10 pounds of steel. Both would consist primarily of carbon fiber and liteply. Preliminary design narrowed the choice to the cylindrical containers.

To manufacture the fuselage, a styrofoam mold was first made of one half of the conceptualized cylinder. Next, a carbon fiber piece was laid into the mold and epoxy applied. Curing took place at room temperature for approximately 12 hours. Once cured, excess carbon was removed and the fuselage sanded. This process was repeated and the two halves were joined with carbon fiber strips. In a similar fashion, carbon fiber caps were manufactured to lessen aerodynamic drag.

6.4 Vertical Stabilizers

Three designs were considered for manufacture of the vertical stabilizers. First was a solid foam rudder coated in Econokote. Next was a solid foam rudder coated with fiber glass. Then, a "wing style" rudder that was ribbed with foam and covered with Econokote was evaluated. Numerical calculations showed the first design to be optimal.

To manufacture the foam, a process similar to that of wing construction was used. First, templates are made using AutoCad printouts glued to Formica. Next, a hotwire cuts out the Styrofoam to the shape of the airfoil. The cut Styrofoam pieces were then attached to the T-joint that joined the wing, landing gear, and longerons by gluing the pieces in place and applying Econokote. Last, the translucent bond paper with Elmer's glue was applied to the foam to provide stiffness in the rudder and Econokote was ironed onto the surface.

6.5 Landing Gear

Three concepts were evaluated for the design of the main landing gear, all involving direct connections to the longerons. First considered was a design similar to that of the previous teams: an aluminum plate attached to each longeron with a wire connecting each gear for structural stability. Next was a carbon coated liteply plate converging to the wheel at the base. Considered last was attaching the gear to an extension of the rods that extended vertically to the wing. Figure 4.2.11 (in section 4.2) illustrates all of these landing gear concepts. Matrix analysis concluded that the third concept for construction of the main landing gear was the most efficient to manufacture. With regards to the front gear, the structures team decided to use the design implemented by the previous year's team. That is, a steel rod connecting the wheel mechanism to the body of the plane.

Central to the construction of the main landing gear concept was the T-joint used in connecting the wings and longerons. The same materials used in manufacturing the spar were used to extend the rear portion of the plane down to three in. from the ground. A wooden dowel was epoxied into place at the lower end of the extension, which served as brace for the steel rod that housed the wheel mechanism.

The front landing gear was of similar construction; the wheel mechanism was connected to a steel rod. This rod was attached to the wing spar and penetrated the surface of the wing. This allowed the pilot the ability to steer the airplane on the ground (via a servo) without diverting power from the motors.

6.6 Motor Mounts

To manufacture the motor mounts, appropriate dimensions were measured for the Liteply plates and then cut. Next, holes were drilled in the front plate to accommodate the shaft and securing screws for the motor. Then, two holes were drilled in the longer plates to fit through the previously

drilled holes in the wing spar. The three plates were then epoxied together at the edges and filleted with microfiber. Once the motors are installed, the mounts are bolted into place on the wing and canard.

6.7 Longerons

Two designs were considered for the longerons. First was a carbon fiber tube with a Styrofoam core. Second was an aluminum tube wrapped with carbon fiber; the same as used in spar construction. The second design was chosen in preliminary design. Since the longerons are exactly the same as the spars, the procedure for manufacturing the longerons is also the same.

6.8 Joints

Three concepts were evaluated for use in connecting the wings to the longerons: a carbon fiber weave with microfiber epoxy, a T-joint made of wooden dowel, and PVC pipe. Numerical results indicated that the T-joint would be optimal.

The wooden dowels were bought at a local hardware store. After each was cut to the proper length, holes were drilled through the center of each piece for bolt placement. On each side of these holes, washers were epoxied into place to aid in securing the bolt. This is the male part of the T-joint. The female part of the T-joint consisted of a much shorter piece of dowel with a hole drilled down the center of the vertical axis. On one end, a securing nut was epoxied into place to receive the bolt from the male part of the joint; this end was fed into the longeron. The pieces fit together and the bolt was tightened into place, securing the wing to the longeron.

6.9 Combining the components

In integrating all of the components of the entire aircraft, the main body of the plane was first assembled. The center sections of the wing and canard were connected to the two longerons via the T-joints. For attaching the longerons to the center wing sections, holes needed to be predrilled at the end of each spar section to give the correct angle of attack for the wing and canard. A single $\frac{1}{4}$ in. bolt could then be attached to each side of the wing section and the longerons.

After the main section of the plane was built, then the two outer parts of the wing and canard were connected. To do this, holes were drilled on one appropriate side of each wing to allow a bolt to connect the wing/canard to the T-joint. The T-joint could then be slid into the hollow spar and the bolt attached, completing the wing and canard.

Finally, the landing gear was attached. To connect the front gear mechanism, a hole was drilled down the center of the spar in the middle section of the canard. A bronze bushing was then epoxied into the hole to serve as a bearing in which the steel rod would rotate. The steel rod was aligned in the hole and secured using an axle collar. On the surface of the wing, the servo used to rotate the front wheel was attached with four #2 screws to a small plywood plate.

6.9 Timeline/Manufacturing Milestones

Table 6.1 illustrates the manufacturing timeline used by the DBF team. As seen, the team fell behind schedule numerous times. This is mainly due to problems encountered during the design process (as should be expected). There were several major developments during this process that caused the design of the aircraft to evolve.

The initial design of the aircraft called for a carbon fiber wrapped Styrofoam spar. Following numerous difficulties with manufacturing, this design was ruled out in favor of the carbon fiber wrapped shower curtain rod. This design proved to be strong enough for both spars and longerons. The design was also extremely economical. The carbon fiber was readily available as a donation from the Hexcel corporation and the shower curtain rods were inexpensive and easily accessible at a nearby hardware store. The next problem was how to connect these pieces together.

After some research, wooden dowels proved to be a very capable joint. Not only was manufacturing this part straightforward, but it was also very economical. Wooden dowels sufficed for both dimension and strength. The strength requirement is needed since it joins components that loaded very heavily and the joint transfers this loading. When transferring the load, the joint distributes the loading more throughout the structure thereby minimizing point loads experienced by the structure of the aircraft.

Task	Date Due	Actual Completion
Calculate Payload Configuration and Construct necessary parts	October 31, 2000	November 5, 2001
Construct Spar in Wing, Begin Landing Gear	November 30, 2000	January 7, 2001
Construct wing	December 22, 2000	January 9, 2001
Construct Fuselage	Winter Break (1/12/2001)	February 12, 2001
Insert Propulsion Components	Winter Break (1/16/2001)	February 26, 2001
Construct and insert landing gear	Winter Break (1/16/2001)	February 25, 2001
CONSTRUCT PLANE – bring all components together	February 6, 2001	February 26, 2001

Table 6.1: The timeline.

- Cost
- Time Required
- Mass-producibility
- Skill Level
- Availability

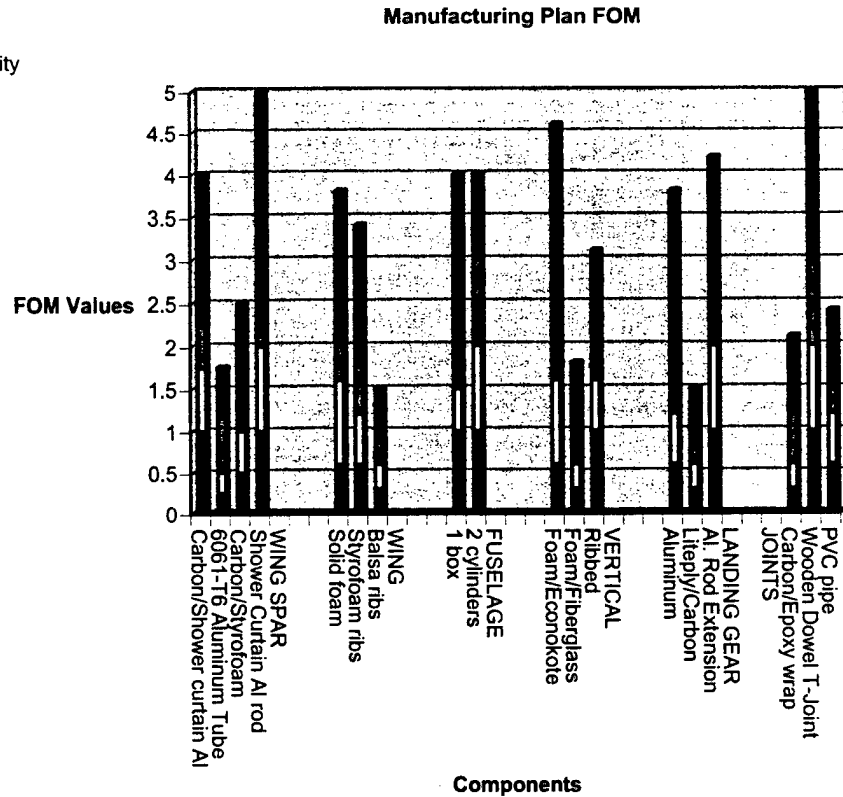


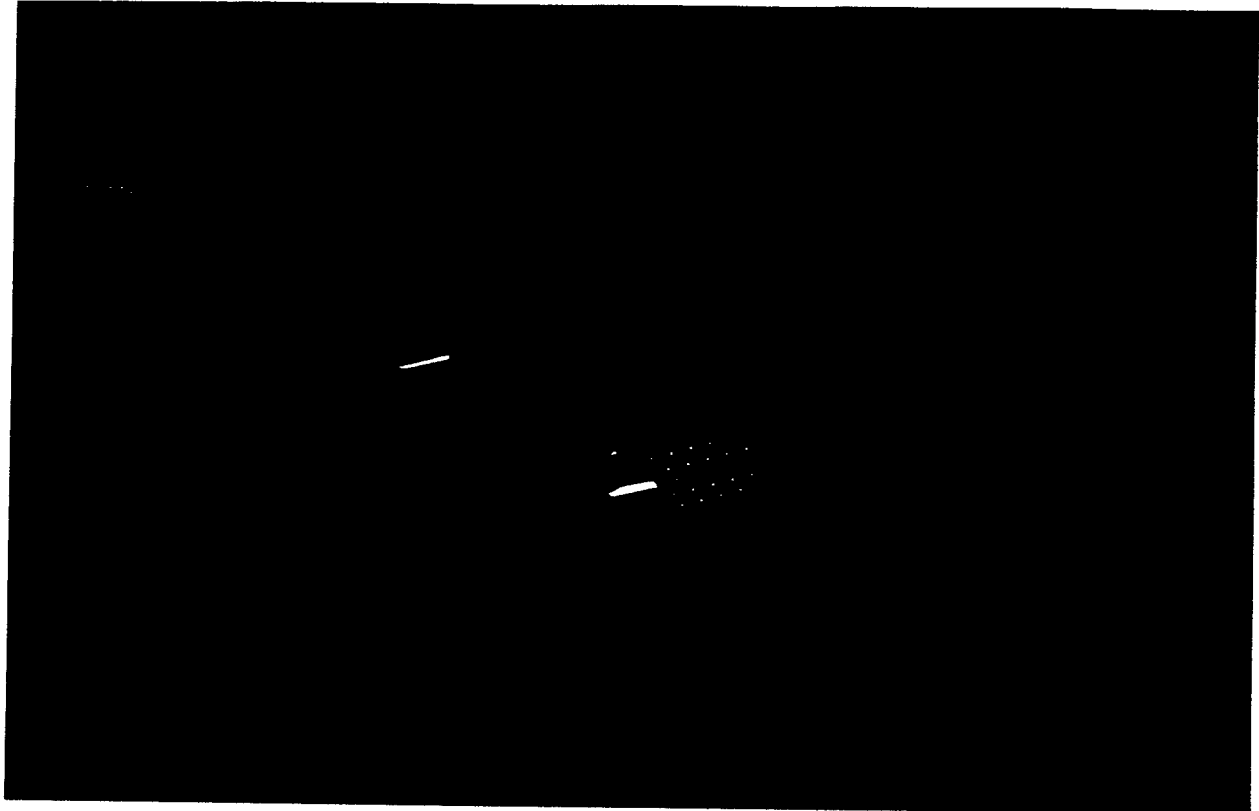
Figure 6.1: Plot of the figures of merit for each component.

7.0 References

- [1] <http://amber.aae.uiuc.edu/~ajadbf/00faq.html>, date accessed: November 23, 2000.
- [2] <http://opus.aae.uiuc.edu/~selig/ads.html>, date accessed: September 11, 2000.
- [3] D. G. Hull, Introduction to Airplane Flight Mechanics. Austin: UT Press, 2000.
- [4] R. R. Craig, Mechanics of Materials, 1st ed. New York: John Wiley & Sons, 1996.
- [5] A. Lennon, R/C Model Aircraft Design. Connecticut: Air Age Inc., 1986.
- [6] R. R. Craig, Structural Dynamics. New York: John Wiley & Sons, 1981Wiley & Sons, 1996.

**AIAA Student Design/Build/Fly
Competition**

THE GPA Killer



By:

The University of Texas at Austin
2000/2001 Design/Build/Fly Team

Table of Contents

1.0 Executive Summary.....	1
2.0 Management Summary.....	2
3.0 Conceptual Design.....	4
3.1 Alternative Concepts Investigated.....	4
3.2 Design Parameters Investigated.....	5
3.3 Figure of Merits.....	7
3.4 FOM – Ranking Importance Factors.....	9
3.5 FOM Matrix.....	10
4.0 Preliminary Design.....	11
4.1 Preliminary Aerodynamics Design.....	11
4.2 Preliminary Structural Design.....	16
4.3 Preliminary Propulsion Design.....	30
5.0 Detail Design.....	31
5.1 Performance Data.....	31
5.2 Component Selection and Systems Architecture.....	32
5.3 3-View Drawing Package.....	41
5.4 Innovative Solutions, Manufacturing Processes, and Cost Reduction.....	43
6.0 Manufacturing Plan.....	45
6.1 Wing Spar.....	45
6.2 Wing.....	46
6.3 Fuselage.....	46
6.4 Vertical Stabilizers.....	47
6.5 Landing Gear.....	47
6.6 Motor Mounts.....	47
6.7 Longerons.....	48
6.8 Joints.....	48
6.9 Combining the components.....	48
6.10 Timeline/Manufacturing Milestones.....	49
7.0 References.....	50
8.0 Lessons Learned.....	51
8.1 Aircraft differences from the PROPOSAL design and justification.....	51
8.2 Areas for improvement in the next design and manufacturing process.....	57
8.3 Time and cost required to implement change/improvement realized.....	58

8.0 Lessons Learned

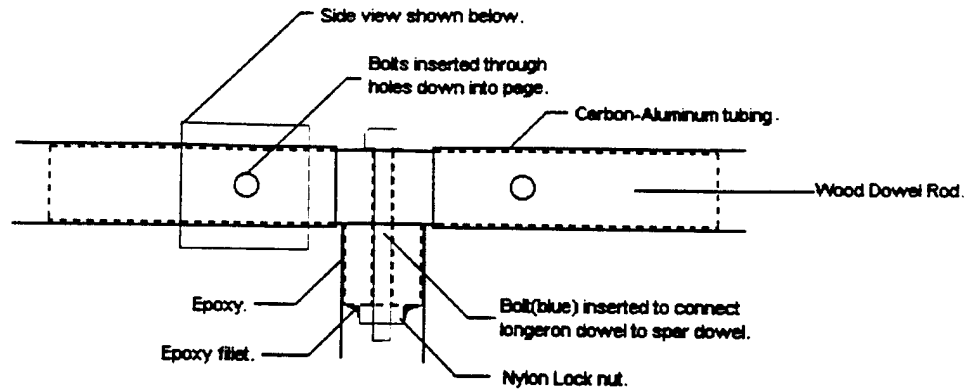
8.1 Aircraft differences from the PROPOSAL design and justification

At the time of writing the proposal, the initial design described had not yet been successfully flown. After further flight testing, it was discovered that there were problems with the rotational stiffness of the airframe and with the wing spar connections to the wooden dowel T-Joints. During one such flight, the plane was unable to come out of a turn because of the wing's ability to rotate by a small amount around the T-Joints, causing a variable angle of attack on the wings.

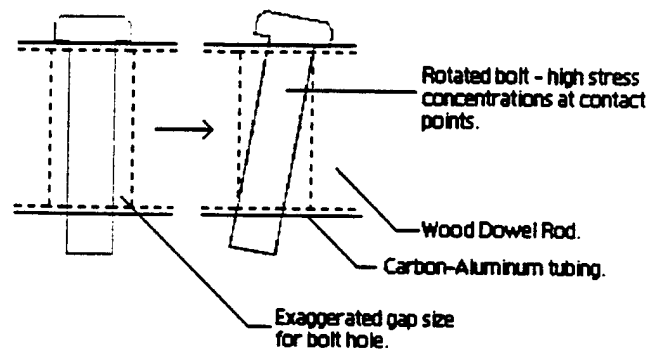
8.1.1 Improved spar connection to T-Joints

The main problem with the original connection design, shown in Figure 8.1.1-a was the inaccuracy in drilling holes in the wing spar and the wooden dowel. Once the bolts were put through the holes, the connection was found to allow slight rotation about the bolt, as shown in Figure 8.1.1-b. This allowed the left and right side of wings to have separate angle of attacks, and for the wings to flutter during flight. Another disadvantage with the bolt design was the weight of the bolts themselves. While not weighing much individually, each bolt weighs approximately 1/10 of a pound, there were a total of 10 bolts, meaning a pound of bolts were on the plane. One of the strong points of the bolt ~~method~~ design was the modularity of the design, allowing us to detach and attach the wing to the main frame for transport. After one of the test flights, however, it was found that when the bolts were over-tightened, the spar deformed and pinched the wooden dowel, preventing removal of the wing. Finally, drilling holes in the wooden dowels created stress concentrations that weakened the strength of the wooden dowel, increasing the probability of failure.

The solution, shown in Figure 8.1.2-a and 8.1.2-b respectively, was to abandon the bolt connection method altogether for the spar - T-joint interface. Instead, epoxy was used to permanently attach one side of the T-joint to the main frame of the plane and to attach the other side, which leads out to the wing, by slitting the wing spar on the top and bottom with a triangular cut about 1 in. deep and 1/10 in. wide. The spar was then fastened to the wooden dowel by tightening a worm-clamp around the spar and squeezing it tightly to the T-joint. This turned out to be a very rigid connection that allowed virtually no rotation and required no holes in the T-joints. This method was also 3/4 lbf lighter than the previous method for the entire plane and it allowed us to more carefully monitor any permanent pinching of the spar while providing more precise control over the wing's angle of attack. Also, by attaching one end permanently with epoxy the wooden dowel was able to be shortened considerably because the load created during bending was distributed along the entire surface instead of two point loads where the tips of the wood dowels came into contact with the spar.



a. Original T-joint design.



b. Side view of bolt rotation.

Figure 8.1.1: Original T-Joint Design.

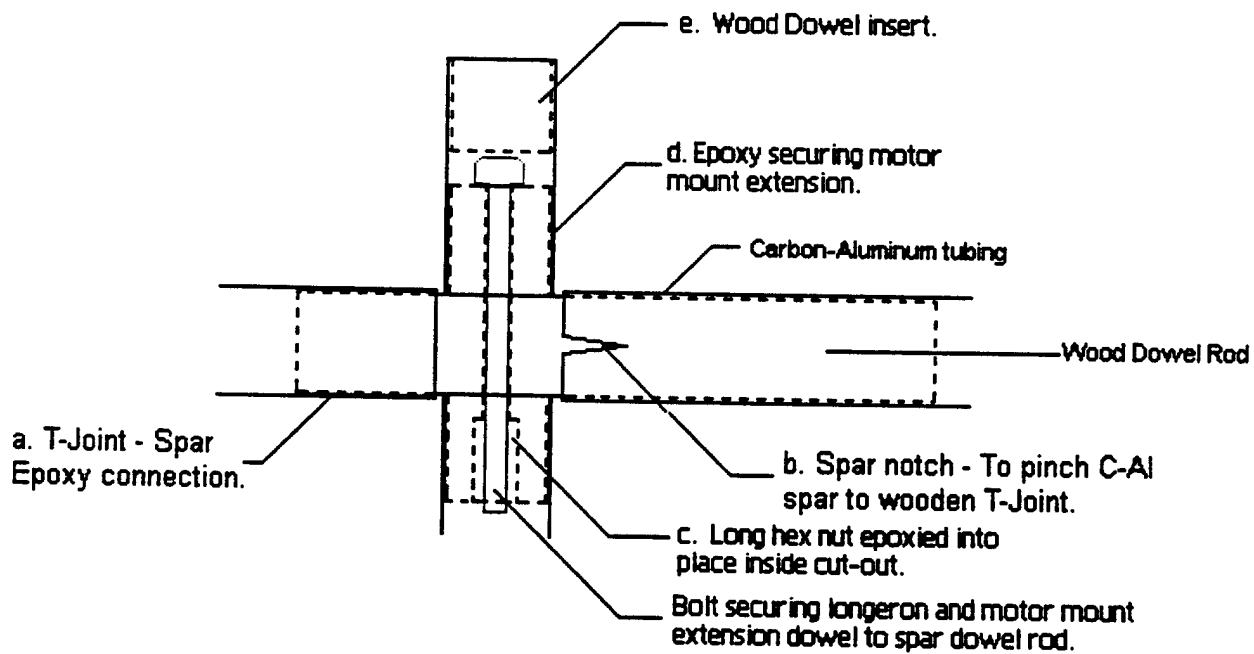


Figure 8.1.2: New T-Joint Design.

After repeated assembly and disassembly on the trips to and from the flight test location, another problem with the T-joints manifested. An epoxied nut at the end of the longeron dowel, shown in Figure 8.1.1-b, tightened the bolts that connect the longeron wood dowel to the spar wood dowel. However, after repeated use, the nuts started to shear off of the wooden dowel, keeping us from attaching the longeron to the wing spar via the T-joint. To solve this problem, instead of using a standard nut immersed in epoxy, the hole was drilled larger 3/4 in. into the longeron dowel and a long hex nut epoxied into the hole (Figure 8.1.2-c). The epoxy should hold better because of the larger surface area and the nut's downward (in the Figure) motion will be restricted by the ledge resulting from the varying drill sizes.

8.1.2 Motor mount connection stability

Another deficiency of the original design was the motor mount's stiffness. Not only were the mounts relatively heavy at 3/8 lbf apiece, but they were found to vibrate at low throttles. Worried about the fatigue that could be caused by the propeller's vibrational excitation of the motor mounts, the structures team examined different other mount designs and came up with a stiffer, lighter, and easier to manufacture mounting system.

The new engine mount is shown in Figure 8.1.2-d and is merely an extension of the longeron past the wing spar. Essentially a wooden dowel was drilled down the center so that the bolt previously attaching the longeron dowel and the spar dowel now also runs through another dowel section around which the Carbon-Aluminum tubing is epoxied. The engine is then tightly clamped onto the circular spar by using two worm clamps. Using two clamps eliminates rotational motion in the vertical direction (with respect to the ground) and when tightened sufficiently, they easily restrict any rotation about the spar itself. It was also found that the clamps kept the motor from oscillating and sliding along the spar. To keep the Carbon-Aluminum tubing from collapsing from the clamps, a wooden dowel spacer was added, shown in Figure 8.1.2-e.

8.1.3 Stabilization of front canard connection

The canard was initially connected to longerons by bolts as shown in 8.1.4a. This connection allowed the canard to rotate on the 2 longerons as shown in 8.1.4 b. This problem was solved by attaching 2 carbon reinforced aluminum tubes as shown in 8.1.4c. The carbon reinforced aluminum tubes were fused to the longerons using carbon fiber string and cyanoacrylate (super glue).

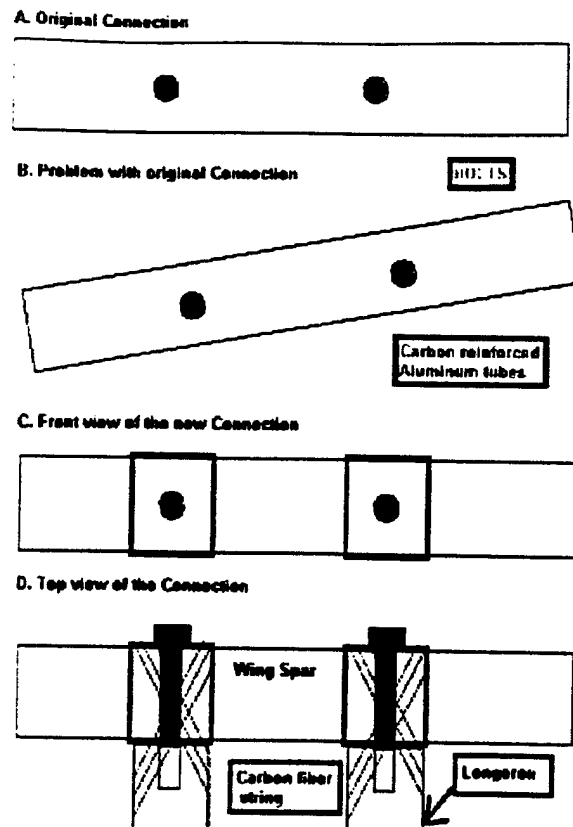


Figure 8.1.3 Stabilization of the canard with respect to the longerons

8.1.4 Fuselage

After final assembly of the aircraft, it was noted that the weight of the airplane was excessive. The team immediately examined the fuselage as a culprit for weight burden. Examining each component of the airplane, the fuselage pods were found to make up 17% of the total airplane weight (excluding payload). This was attributed to the excessive use of epoxy in the carbon fiber pods.

Another problem associated with the carbon pods was connecting them to the longerons. The pods are of a circular cross-section, as well as the longerons. Hence, the mount would have to connect two cylinders. This turned out to be a very difficult task, structurally. The connection would consist of a crossbar between the two longerons and connecting the pods to each end of the bar. The crossbar would be of the same material as the spar; that is, an aluminum shower curtain rod wrapped in carbon fiber. The bar would then be attached to the longerons. Not only was this connection very heavy, needing several bolts and a heavy crossbar, but the way the pods attached, significant pre-stresses were present from the moment each pod exerts at the end of the crossbar. The team lacked the confidence that the connection would hold during landing.

Further problems with the connection were encountered when attempting to load and unload the pods. The connection had several places that needed attending when switching out the cargo. The pods themselves also proved very difficult to load and unload. The interior was not structured to hold tennis balls in such a way as to restrict their movement inside the pod. Hence, the tennis balls could not be moved in an efficient way to limit the ground time of the airplane.

The caps on the cylindrical pod were also difficult to secure. The front covering was secured using a strip of carbon fiber epoxied around the connecting edge. It was very secure, but increased the weight of the already heavy pods. The rear cap was secured using several small bolts. The greatest disadvantage associated with the bolts was the length of time needed to unscrew all of them to be able to switch out the payload.

Finally, the time required to manufacture each pod was very high. One of the main goals of the design was modularity. This implied several spare parts would be made. In order to make spare pods, a great deal of time would have to be invested in manufacturing them, taking away time from other aspects of the aircraft.

To remedy the problems with the fuselage design, the two-pod concept was abandoned completely. Instead, a single, symmetrical airfoil shaped pod was created. First, templates were made resembling the cross-section shown in Figure (8.1.3). Then, a hotwire was used to cut Styrofoam into a top and bottom section. Next, a shear web made out of four, square balsa rods and two balsa plates was installed to provide structural stiffness in the Styrofoam so it could sustain the weight imparted by 100 tennis balls and 20-25 pounds of steel.

There are several advantages to this new design. First, the weight was decreased by half compared to the carbon pods. Next, loading and unloading of both the pod itself and the cargo are greatly simplified. The pod will not need to be disconnected to remove the payload; a side plate was installed on the pod that is easily removed. The foam was cut such that the pod forms around the shape of the tennis balls. Hence, plastic capsules can be constructed to hold "strings" of tennis balls that can be efficiently removed and loaded. Also, steel blocks can be slid into the slots very easily. The pod connection to the longerons is similar to that of the two carbon pods. Wooden dowels were attached to the shear web section with epoxy and a bolt attaches the pod to the longerons. Since the pod attaches directly beneath the longerons, the pre-stresses in the bolts are minimal and the connection should be able to endure landing. Another consequence of the pod being attached underneath is that the distance between it and the ground is smaller than the distance between the propeller and the ground. Hence, if the front landing gear were to break away upon landing, the fuselage would serve as a cushion to keep the propeller from striking the ground.

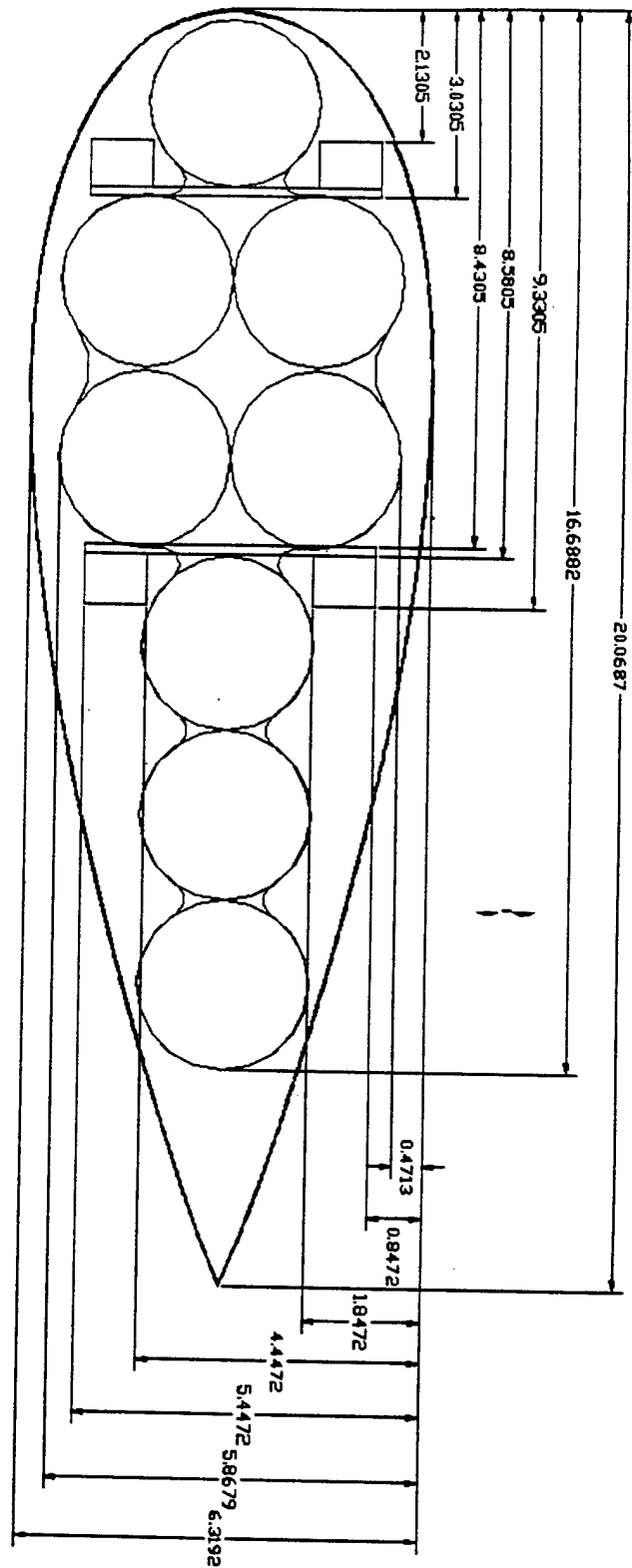


Figure 8.1.4 Fuselage

8.1.5 Adhesion of foam ribs to wing spar

The wings and the canards were initially glued to the spars by Super 77 contact adhesive. After moderate use, it was noticed that the glue's adhesion to the foam ribs and leading edges was not very strong since direct contact was required for a good adhesion. After extensive testing it was determined that Great Stuff, an aerosol foam sealant was determined to be the best available adhesive to bond the spar to the foam ribs. It's biggest advantage was that it filled in all gaps between the spar/leading edge/ribs while minimizing weight. Figure 8.1.5 shows a diagram of the wing section with the Great Stuff colored as white and blue checkers.

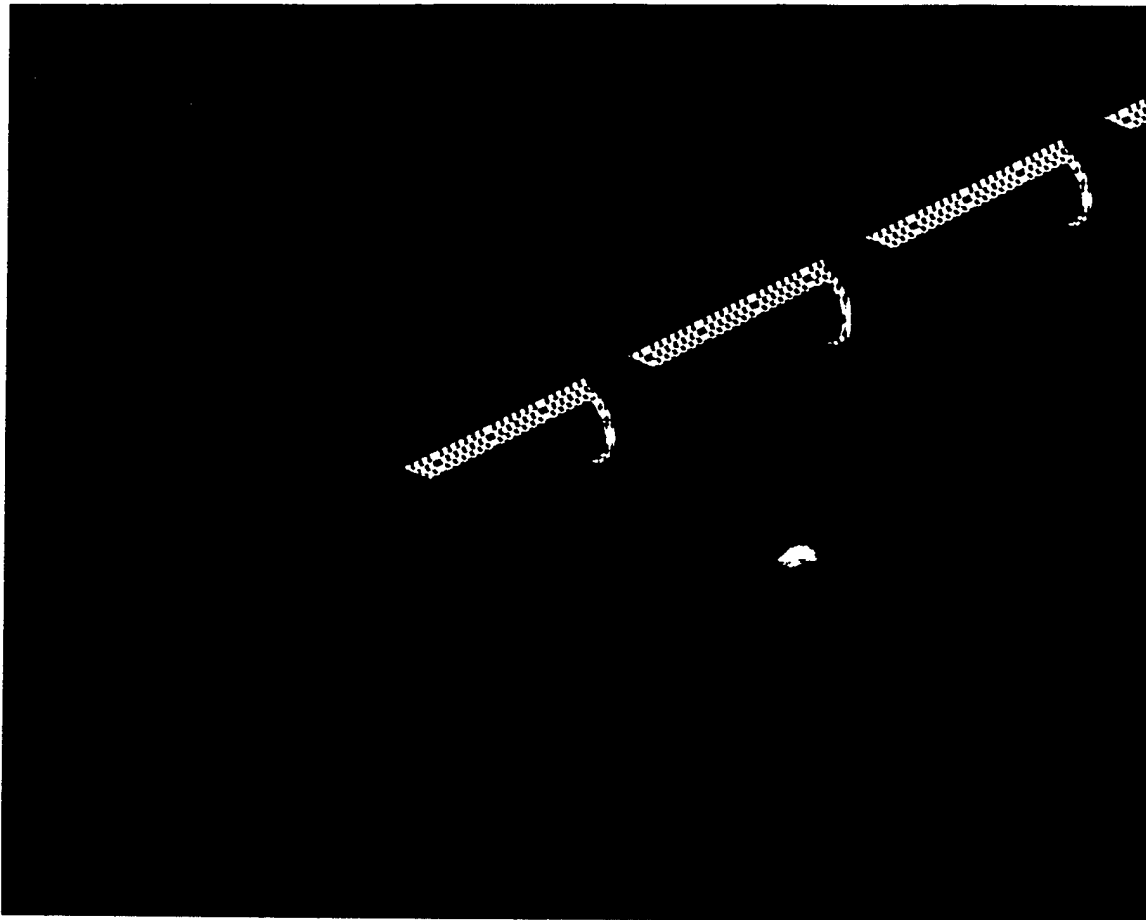


Figure 8.1.5 Great stuff used for adhesion of spar to wing structure

8.2 Areas for improvement in the next design and manufacturing process

One improvement foreseen by the structure's team is replacing the hollow tube with a wing box and shear web design for the wing spar. It's weight is much less and provides more stiffness in the wing. To achieve this, flat carbon plates would be epoxied together, forming

in the wing box and the other parts of the wing could be attached similarly to the current design. This would not present a great deal of difficulty with all of the experience the team has gained this year using the carbon fiber, but some re-design would be necessary which is always cumbersome.

Another slight improvement would be to add steel wire connecting the wing tips to the rear landing gear. The gear is quite stiff and would provide ample resistance to the tensile force in the wire. The purpose of the wire would be to lessen the wing tip deflection. This would not be very difficult to add to the airplane since all that would be needed is the correct length of wire and a worm-clamp to attach the wire to the wing tip. Hence, the time involved would be minimal.

During testing, the team noticed that the plane had a tendency to rotate about the front wheel on the ground. This was especially noticeable in high winds; the plane tended to tip over very easily. One remedy was to place a second wheel on the front, making the landing gear total 4. This would be a last resort since it would increase the weight quite a bit and, hence, increase the rated aircraft cost. Also, the work and time required to enact the changes would be excessive.

Another design change that could be investigated would be optimizing the weight and strength of the longerons. Larger diameter rods could be used to increase the stiffness of each boom, but of course this would add weight to the aircraft. An investigation could be carried out to determine the optimal configuration of the longerons. As with any design change, the amount of time required would be a great deal as well as the time to implement the changes on the current aircraft.

8.3 Time and cost required to implement change/improvement realized

The estimated time for the wing box is approximately 6 days. Due to the generous donation of carbon fiber from Hexcell, and leftover epoxy from the project, the cost will be negligible.

The estimated time for the steel wire is one day. The cost of the steel wire is virtually negligible, however, a more detailed analysis needs to be done on if this modification is absolutely need and the impact of this on the RAC since this will be counted as a strut.

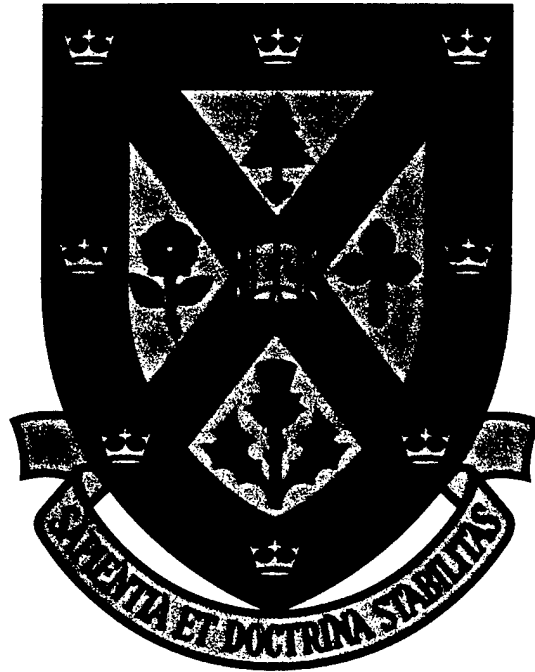
The estimated time for an installation of a second nose gear is approximately 4 days. There will be cost of about \$20 for the spring and wheel.

The estimated time for further optimization of longeron is 8 days. The cost of the change is unknown since the price will vary greatly depending on the type of rod the team chooses.

Input		
Description	Input	Cost \$ (Thousands)
Empty weight (lbs)	21	2100
Engine Power Cost		
# of Engines	3	
Amp Fuse (40 amp max)	30	
# of Cells	12	
Total Power Cost		1296
Building Cost		
Wings		
# of Wings	1	
Sq. ft of Projected Area	15	
# of struts or braces	0	
# of control surfaces	0	
Total Wing Cost		1500
Fuselage/ Pods		
Number of fuselages	1	
Fuselage length (ft)	1.67	
Total fuselageCost		233.33
Empenage		
# of Vertical Surfaces	2	
# of Horizontal Surfaces	1	
Total Empenage cost		500
Flight Systems		
# of Servos/Controllers	5	300
Propulsion system		
# of engines	3	
# of propellers	3	
Total Propulsion System Cost		600
Rated Aircraft Cost		6529.33

2001 AIAA DBF Competition Design Report

Proposal Phase



Queen's University at Kingston

"Absolute Toque"

Department of Mechanical Engineering

Department of Engineering Physics

March 13, 2001

List of Nomenclature	2
1.0 Executive Summary	3
1.1 Major Development Areas	3
1.2 Design Tool Overview	4
2.0 Management Summary	5
2.1 Personnel and Configuration	5
2.2 Scheduling	6
3.0 Conceptual Design	8
3.1 Initial Figure of Merit	8
3.2 Examined Designs	10
3.3 Screening the Three Designs	11
3.4 Analysis of the "Prototype"	11
3.5 "Absolute Toque"	12
3.6 Shrouds	12
3.7 Design Summary	13
4.0 Preliminary Design	15
4.1 Take-off Gross Weight (TOGW) Estimation	15
4.2 Propulsion Systems Selection	15
4.3 Wing Area and Airfoil Selection	17
4.4 Aspect Ratio	19
4.5 Wing Platform	19
4.6 Horizontal Stabilizer Sizing	19
4.7 Vertical Stabilizer Sizing	20
4.8 Fuselage Design and Sizing	21
5.0 Detail Design	24
5.1 Weights	24
5.2 Payload Fraction	25
5.3 Drag	25
5.4 Wing Sizing and Performance	26
5.5 Tail Sizing and Performance	27
5.6 Propulsion	28
5.7 G-Loading	29
5.8 Take-off Performance	30
5.9 Endurance and Range	31
5.10 Shrouds	32
5.11 Stability	33
5.12 Control Systems	35
6.0 Manufacturing Plan	41
6.1 Wing Construction	41
6.2 Fuselage Construction	42
6.3 Tail Construction	42
6.4 Figure of Merit	43
6.5 Evaluation and Selection	44
6.6 Description of Construction Techniques Employed	45
References	50

A	Parasite drag coefficient	T	Maximum airfoil thickness
A_{wetted}	Wetted area	V	Velocity
AOA	Angle of attack	V_{max}	Maximum cruise speed
AR	Aspect ratio	V_{min}	Minimum cruise speed (stall speed)
a_m	Average acceleration on ground roll	V_{mean}	Mean velocity on takeoff roll
Ac	Aerodynamic centre	V_{stall}	Stall speed
B	Induced drag coefficient	V_{TO}	Takeoff speed
C	Chord	W	Fuselage Width
C_D	Coefficient of drag	W	Weight
C_{Dpara}	Coefficient of parasite drag	X_{CG}	Position of CG
$C_{Dinduced}$	Coefficient of induced drag	X_{ACW}	Position of wing aerodynamic center
C_f	Skin friction drag coefficient	X_{ACH}	Position of stabilator aerodynamic center
CG	Center of gravity	X_{NP}	Position of stability neutral point
C_L	Coefficient of lift of wing	α	Angle of attack
C_{Lh}	Coefficient of lift of stabilator	β	Angle of bank
$C_{L\alpha}$	Derivative of C_L with respect to AOA	ρ	Air mass density
C_{Lmax}	Maximum coefficient of lift	σ	Maximum stress
C_M	Coefficient of pitching moment	ϵ	Downwash angle
C_p	Power coefficient	η	Efficiency
C_t	Thrust coefficient	θ	Pitch Angle
D	Propeller diameter	μ	Dynamic viscosity
D	Drag	γ	Kinematic viscosity
d_c	Climb-out distance		
d_r	Ground roll distance		
d_{TO}	Take-off distance		
E	Wing efficiency factor		
G	Acceleration due to gravity		
FOM	Figure of merit		
H	Altitude		
I	Mass moment of inertia		
K	Form factor		
L	Lift		
M	Mass		
M	Pitching moment		
R	Turning radius		
Re	Reynold's number		
S_h	Stabilator planform area		
S_w	Wing planform area		
T	Thrust		
TOGW	Takeoff gross weight		

List of Nomenclature

1.0 Executive Summary

This year's entry to the Design/Build/Fly (DBF) marks the most ambitious aircraft Queen's has ever fielded in our 12 year history of entering either the SAE's heavy lift competition or in more recent years, the AIAA's DBF competition. With a wingspan of 3m (10'), a length of 2.4m (8') and an all-up weight of 7.7kg (17lbs.) without cargo, "Absolute Toque" is one big electric airplane. Learning from our experiences with last year's entry "Obsidian", we've changed our construction techniques, streamlined our design, and improved our power system to the point where we're confident that this will be our most successful year ever.

1.1 Major Development Areas

"Absolute Toque", so named to give reference to the team's northern heritage, exhibits several new and innovative design features and construction techniques in an attempt to produce the lightest and most efficient aircraft possible. Variables such as laminar flow airfoils and bicycle undercarriages were tested on a full-sized prototype aircraft, and a senior research project led to the incorporation of shrouded propellers to this year's entry – a valuable increase in available thrust in this current-limited event.

In the early days of conceptual design, our team studied the payload criteria, and with the help of a simple spreadsheet, came to the conclusion that a large, light airplane with a 100 tennis ball capacity would be the most competitive in this challenge.

With the decision to build a large plane made, the team studied the propulsion systems available and quickly established that the updated motor limitations would have a drastic effect on the aircraft's design. For the first time, Queen's could truly tailor a power system to the specific mission goals without having to base our design choices around an existing propulsion system. With this knowledge, the team decided to design around a pair of Astroflight FAI-40 cobalt motors and a pair of 18 cell Sanyo 2400 mAh NiCd battery packs, as they provided the best energy density and efficiency.

A pusher configuration was chosen due to its increased efficiency, and design work began to incorporate the power system and 100-tennis ball bay into a high-winged, T-tailed aircraft with a very long cylindrical fuselage. Although a flying wing was also investigated, The "Flying Pencil" proved to be an interesting concept and was subsequently refined into a prototype aircraft with a shorter fuselage of a larger diameter. The testing with this aircraft brought about our decision to return to a traditional airfoil and tricycle undercarriage, and the resulting design was "Absolute Toque", a low winged, streamlined aircraft with twin shrouded propellers.

1.2 Design Tool Overview

1.2.1 Conceptual Design

Throughout the conceptual design phase of Absolute Toque's development, a variety of tools were used to develop and evaluate different aspects of the aircraft's design. These ranged from researching old documents and studies on various components, making use of a spreadsheet detailing the *rated aircraft cost* penalty of the various designs, to actually building a working prototype to test the ideas under examination.

This research allowed the team to compare a variety of different designs with proven theory from several respected sources, and then actually perform our own research to see if the technology could be applied by our design with limited resources. This allowed us to narrow down the permutations in design in preparation for the preliminary design stage.

1.2.2 Preliminary Design

Once the team entered this portion of the design process, the techniques used became more analytical than the quantitative methods used in the conceptual design. The *rated aircraft cost* spreadsheet was still used, but to screen slight variations of Absolute Toque's design rather than the large structural variations examined in the previous section. Component weight was measured, estimated, or obtained from manufacturing specification sheets to allow for some first iteration values to be generated. Simple aerodynamic formulae were used to determine such things as the coefficient of lift and tail sizing, and to determine areas that needed further development.

Computer software in the form of ElectriCalc and MotoCalc were used to obtain an estimation of how much thrust the chosen electric motors would produce across their given flight envelope. These figures were used in the development of the shrouds, providing information on the sizing of the shroud unit as well as providing suitable propeller choices.

1.2.3 Detail Design

The final stage of the design process meant a transition to purely analytical methods. Classical aeronautical theory was used to determine such things as drag, stall speeds, takeoff rolls, and turning radii. The use of a master spreadsheet reduced the hours of number crunching, and helped the team quickly see the effect of slight design changes.

The final values were used to produce the drawing package. "Absolute Toque" was drafted into AutoCAD 14 to obtain the required construction drawings and to ensure that the components mated correctly.

2.0 Management Summary

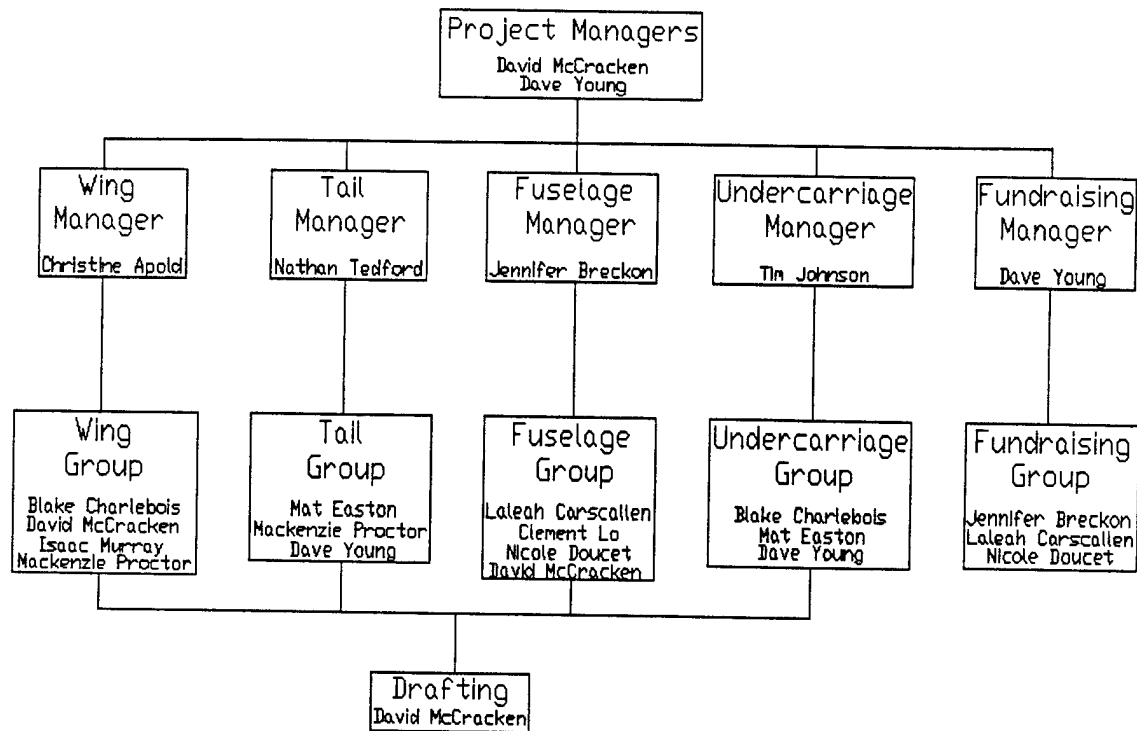


Figure 2.1 Organizational Structure

2.1 Personnel and Configuration

The management structure chosen for this year's aero design team was based loosely on the functional matrix style organizational plan. The design tasks during the initial portion of the year were broken down into four subgroups, with fundraising and finances being added as a fifth group. All team members were expected to be on at least two teams, to increase the knowledge each student would obtain about the various components of the aircraft.

Four of the subgroups were each tasked with the research, development, and design of one major component of the aircraft, with the fifth group being responsible for approaching outside companies to try and secure donations in the form of cash, product discounts, or access to tooling. Rough sketches and CAD drawings were submitted by each subgroup to David McCracken, who drew up the finalized working drawings of the aircraft.

In the initial part of the year, the entire team met once a week with either of the project managers, David McCracken or Dave Young. The project managers would send an email to all members to announce the time and location. The purpose of these group meetings was to bring all of the five

subgroups together to allow each team to report on their progress and to allow the entire group to offer suggestions to any problems that arose. These meetings also helped ensure that there was adequate communication between the subgroups, and that each component would mate properly with the aircraft.

Also during this time period, separate meetings were held with the various subgroups. These meetings were called by the respective subgroup managers and were set at different times based on the schedules of the members in question. These meetings were also announced to the project managers, so that either David or Dave could attend the meeting and help with the component design. It should be noted that during these meetings, the project managers were not the group leaders. It was felt that the aircraft configuration would benefit by leaving the younger students in charge of the various components, as this would ensure that everyone on the team had a chance to be an active participant in the design process. By making sure everyone was involved with the design, the actual construction of "Absolute Toque" would progress much more rapidly.

After the design had been finalized, the subgroups were disbanded for the construction portion of the year. Shop hours set by the project managers, which were then emailed to everyone on the team every few days. This allowed team members to work around their own schedules and to decide when they would be able to come in and build for a few hours. The shop hours were set to ensure that there would be a senior member of the team present to help the newer members learn the construction techniques required. This system ensured that every team member, regardless of prior building experience, was able to contribute to the assembly of "Absolute Toque"

2.2 Scheduling

To ensure that the project would be able to meet its goals within the time allotted for the task, a Gantt chart timeline (see Figure 2.2) was set in the week after the team's first introductory meeting. Based on previous D/B/F experience, the project managers were able to make what was felt as reasonable assumptions of the amount of time each task would take throughout the year. As can be seen on the Gantt chart, most of the estimations were very close to the actual time required. Fundraising was a little optimistic, but we were able to secure several large companies in the extra time. The remainder of process had enough slack in the form of the winter break to bring the schedule back on target.

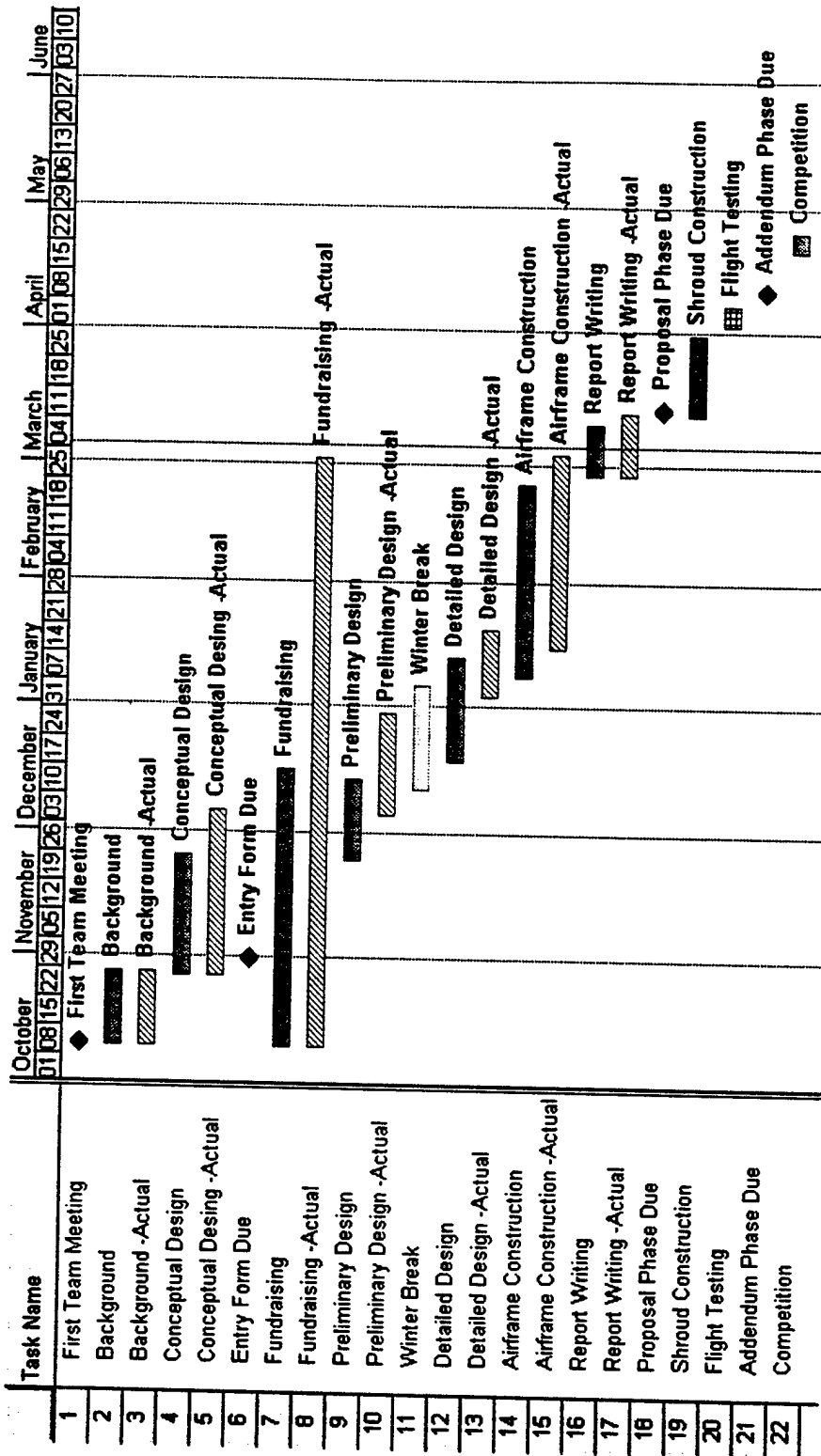


Figure 2.2 Schedule Control

3.0 Conceptual Design

This year's DBF aircraft is a progression of design, building on experience from our '99-'00 entry 'Obsidian'. Although changes to the cost penalty system have increased the feasibility of operating a multi-motored aircraft, the essence of the competition – to build the most efficient aircraft – has not changed.

Before any airframe design was started, the team examined the cargo to be transported this year. Quick calculations (see figure 3.4) revealed that a maximum score would be obtained if the full 100 tennis balls were carried on as many sorties as possible, with the amount of steel being a lesser goal. The tennis balls weigh approximately 6 kg (13 lbs) and result in a score equal to that earned by carrying 9 kg (20 lbs) of steel. It was felt that the reduction of weight to be carried more than made up for the increase in airframe size required to house this volume of tennis balls. As such, the team settled on building a "large" plane.

The next thing considered by the team before any airframe design was started was the power system. With the new requirement of having to use brushed motor(s), the team was able to start with a fresh sheet of paper, allowing the motor to be tailored to the task at hand. An examination of the AstroFlight and Graupner product line revealed that there was a large selection of motors of various power outputs, meaning that the design would not be limited to a single motor option.

Once these decisions had been made, the team set up a FOM to help narrow down the number of aircraft criteria. By examining fuselage cross-section, airfoil choice, tail configuration, and undercarriage design, the team was able to narrow the field down to three competing designs.

3.1 Initial Figure of Merit

3.1.0 Figures of Merit

Fuselage Cross-section

The cross-sectional shape of the fuselage was the first criterion examined. The plane could have a round cross-section, a square cross-section, or it could be a blended design. The blended design results in the lowest parasitic drag, but they tend to be harder to build and heavier than the more traditional designs.

Airfoil Selection

Two families of airfoils were examined this year. The first was the traditional "flat-bottom" airfoils developed by NACA and Eppler. These wings are "tried and true" and generally produce an aircraft with good lifting abilities and without unpleasant flight characteristics. The second family is known as "laminar flow" airfoils. They are specially shaped to delay the formation of a separation bubble on the top of the

wing. The desirable reduction in drag is tempered by the increased weight of the structure required to achieve an accurate profile and with the notoriously poor stalling characteristics of these airfoils.

Tail Configuration

The tail configuration of the aircraft was also considered. The conventional tail is light, yet less efficient, resulting in a requirement for more area, which increases drag. A V-tail is light, yet has been known to create control problems in violent flight maneuvers. A T-tail is heavier, yet more efficient, producing less drag.

Undercarriage

The three types of undercarriage examined are tricycle, bicycle, and tail-dragger. The tricycle gear produces the most drag, yet offers the best ground handling. The bicycle gear is more complex as it requires out-riggers in the wings to give ground stability. This advantage of this design is that it produces a very clean airframe for flight. A tail-dragger possess better drag characteristics than a tricycle gear, but has poor ground handling in windy conditions.

3.1.2 Figure of Merit Criteria

The following criteria were selected by the team to help identify the most promising aircraft configuration:

Drag: The drag of the component in question is important as it adds to the drag of the total airframe. In high wind situations, valuable battery power is lost fighting for headway, when a sleeker plane would have no trouble. This FOM was given a weight of 4.

Weight: Similar to drag, the weight of each component is added to produce the total aircraft weight. A wise man once said, "it's easier to take one gram from 100 parts than to take 100 grams from one part." The same principle applies here. This FOM was given a weight of 5.

Performance: The design of the part is crucial to producing the best aircraft. If one option performs the same task slightly better than the competition, then it receives a higher score. This FOM was given a weight of 4.

Ease of Manufacture: The best design in the world is useless if cannot be built, or requires skills or equipment beyond what the team possesses. A higher rating indicates its relative ease of production. This FOM was given a weight of 4.

		Drag (4)	Weight (5)	Performance (4)	Ease of Manufacture (4)	Total
Fuselage	Round	4	5	4	5	77
	Square	3	5	4	5	73
	Blended	5	3	5	2	63
Airfoil	Flat-Bottom	3	5	4	5	73
	Laminar	5	4	5	4	76
Tail	Conventional	3	5	4	5	73
	V-Tail	4	5	2	3	61
	T-Tail	5	4	5	4	76
Undercarriage	Tricycle	2	4	5	5	68
	Bicycle	5	4	4	4	72
	Tail-Dragger	3	4	4	4	64

Table 3.1 –Initial Figure of Merit

3.2 Examined Designs

3.2.1 "Flying Pencil"

The initial design examined by the team was dubbed the "Flying Pencil" due to its distinctive elongated fuselage. It featured a cylindrical fuselage large enough to carry 100 tennis balls in four tubes of 25. Steel would also be carried in these tubes. The battery pack was mounted in the tail-cone to balance the plane around the aft-mounted, high wing. Twin pusher motors were mounted on pylons from the rear of the wing. A twin motor set up reduced the ground clearance requirements and the cost associated with a large single propeller, as well as provided a convenient cargo nose hatch. The design featured a T-tail for increased elevator effectiveness and to keep the control surfaces out of the propeller slipstream. The aircraft also sported a bicycle undercarriage with retractable outriggers to reduce drag. See Fig 3.3.

3.2.2 "Flying Wing"

The second design was a radical departure from anything Queen's has ever built. A flying wing with a single front-mounted motor would house the cargo in an elongated center section lifting body. The wings would be cranked in an inverted gull-wing configuration to permit a very short undercarriage to be used. The use of a cranked center section would also allow the plane to maintain some yaw control without the need for a separate vertical fin, and provide adequate propeller clearance. See Fig 3.3.

3.2.3 "Prototype"

The third design was dubbed the "Prototype", because it was in line for production. The aircraft was very similar to the "Flying Pencil", but the fuselage was of a larger diameter to permit the cargo (both tennis balls and steel) to be carried in 7 tubes instead of four. This allowed the fuselage to be shortened to a more reasonable length than the "Flying Pencil". The wing was changed to a mid-wing configuration to reduce interference drag and to reduce the length of undercarriage needed. See Fig 3.3.

3.3 Screening the Three Designs

Once the team had selected three designs to study further, another FOM was set up that studied how the various airframes compared with respect to drag, weight, performance, ease of manufacture, and their respective *Rated Aircraft Cost (RAC –see figure 3.5)*. The weighting of the respective criteria remained the same as it was for the component selection process in 3.1. The FOM Rated Aircraft Cost was calculated by dividing 5 by the RAC, then multiplying by 10. This is a heavy rating as it was felt that this criterion had a huge effect on the team's final score and standing at the competition. See Figure 3.2

Once the screening FOM was completed, the "Prototype" aircraft was constructed. This was done to gain experience with the construction techniques required for the design, in particular the foam/fiberglass composite required for the fuselage. The aircraft also served as a test-bed for the innovative ideas suggested in the initial Figure of Merit, such as the laminar flow airfoil and the bicycle landing gear.

Upon completion of the airframe and flight trials, the team unfortunately had to re-examine several of the initial design ideas, as some of the designs incorporated into the "Prototype" were not found to be as beneficial as the theory would predict.

Aircraft Concept	Drag (4)	Weight (5)	Performance (4)	Ease of Manufacture (4)	Rated Aircraft Cost (5)	Total
Flying Pencil	4	4	4	4	7.2	75.2
Flying Wing	5	5	3	2	10.0	75
Prototype	4	4	5	5	7.3	83.3

Table 3.2 –Screening the Three Designs

3.4 Analysis of the "Prototype"

Our experiences with the "Prototype" can be summarized as:

- The aircraft was too heavy. The airframe weighed 6.8kg (15lbs) instead of the predicted 5.5kg (12lbs) –a 25% overshoot.
- The laminar flow wing did not adapt well to balsa construction. There were difficulties in keeping the correct airfoil profile across the span of the wing. Research indicated that these airfoils must be as accurate as possible or they do not retard the formation of a turbulent layer.
- The mid-wing design proved to be very difficult to transport. A 3.05m (10') wing permanently affixed to a 1.22m (4') portion of the fuselage was very awkward to transport. The team did not want to go with a two piece wing as it would make proper fairing with the fuselage difficult, would introduce weaknesses and would be heavier than a one-piece wing.
- The bicycle undercarriage with retractable outriggers was too delicate for this type of UAV. The outrigger units were too flimsy; yet making them stronger would add a weight penalty. The system

was already heavier than a conventional undercarriage and far less reliable. The bicycle gear did hold promise however for a future design, as its low drag design was very impressive.

- The cargo location required the full 6kg (13lb) payload to be in place at all times to balance the weight of the battery pack in the tail. This configuration was undesirable, as it did not permit cargo weight to be varied to account for local flight conditions.

In conclusion, the team decided to return to a conventional flat-bottom airfoil for reduced weight and ease to manufacture. The mid-wing design was dropped in favor of a low-wing design, allowing the wing to be removed for transport and reducing landing gear length. The bicycle undercarriage was replaced by a more conventional tricycle arrangement. Finally, the cargo bay was moved so that it would center over the aircraft's center of gravity. The batteries were moved from the tail to a position just in front of the wing, their weight counteracting the weight of the motors behind the wing.

3.5 "Absolute Toque"

The team's decision to radically change the design of the aircraft from that of the "Prototype" led to the development of what subsequently became "Absolute Toque". The cargo bay was angled so that it would allow enough room for the wing to be installed below it. This had a three-fold advantage: the bay could now be longer, permitting a return to four tubes of 25 tennis balls and reducing the fuselage diameter; the wing would not interfere with the cargo, permitting the tennis balls to be centered over the wing while still retaining the ease of single hatch loading; and the angle elevated the tail enough to rotate the aircraft for takeoff while still using a short landing gear. The round fuselage profile of the initial FOM was retained, as was the T-tail. The low wing permitted the installation of a tricycle undercarriage with a wide wheelbase for improved ground handling. Analysis of the Rated Aircraft Cost (figure 3.5) indicated that this airframe would be slightly more competitive than the "Prototype" due to the decreased number of servos required by not having a retractable undercarriage.

3.6 Shrouds

Research undertaken for a senior design thesis led to shrouded propellers being included on "Absolute Toque". These units are ideal for increasing thrust at low speeds due to the low pressure created over the lip of the shroud from air accelerating into the propeller. The shrouds also increase efficiency by eliminating the formation of vortices from the tips of the propellers. The shroud unit also serves to straighten the airflow behind the propeller and prevents the contraction of the slipstream that occurs behind a propeller in a free-propeller system. As long as the aircraft remains below the point where the drag of the shroud unit equals the increase of thrust from it (the "critical point"), then there is a net increase in thrust from the unit. The critical point is usually around 36m/s (80mph) and as these

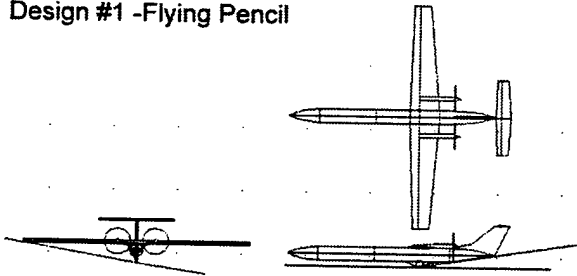
UAVs operate below that speed for much, if not all, of their flight profile, it was felt that they'd be a worthy addition to our entry this year.

3.7 Design Summary

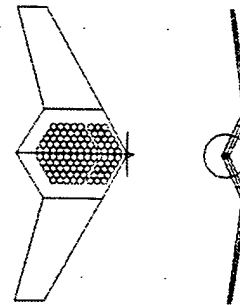
The final aircraft "Absolute Toque" (see figure 3.3 and figure 3.5) has the following specifications:

- 100 tennis ball capacity held in four tubes of 25 inside the fuselage, centered over the plane's center of gravity
- The steel cargo would be carried as long strips (rectangles) that would be placed in the bottom ball tubes, distributing their weight along the fuselage floor.
- Low-wing configuration utilizing a flat-bottom type airfoil.
- Tricycle undercarriage with a wide stance for excellent ground handling.
- A T-tail to raise the stabilizer above the shroud units and slipstream.
- Round fuselage cross-section, with fairings where appropriate.
- Twin motors fitted with shrouds, located at the behind the wing.
- Two battery packs, one for each motor, located in front of the wing to balance the motors.
- A Rated Aircraft Cost of 6.8672 based on preliminary weight estimates.

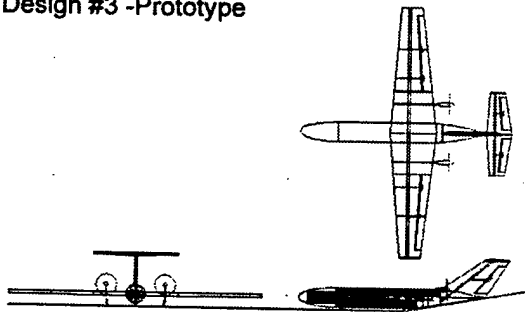
Design #1 -Flying Pencil



Design #2 -Flying Wing



Design #3 -Prototype



Design #4 -Absolute Toque

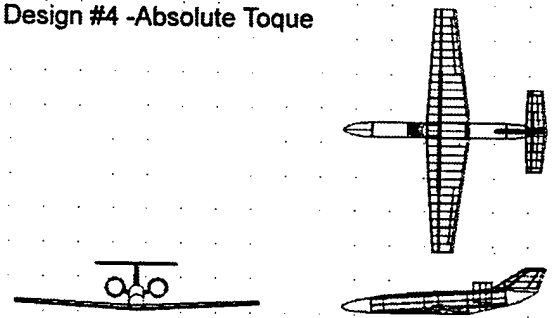


Figure 3.1: Various designs examined

	Small Plane	Medium Plane	Large Plane -less steel	Large Plane -more steel	Large Plane - max steel
# of Tennis Balls	20	50	100	100	100
# of Tennis Ball Flights	3	3	2	2	2
Amount of Steel (lbs.)	5	6.25	6.25	12.5	18
# of Steel Flights	2	2	2	1	1
Total Flight Score	22	42.5	52.5	52.5	58

Table 3.3 -Payload/Scoring Figure of Merit

AIAA Design/Build/Fly 2000/2001					
Rated Aircraft Cost Spreadsheet		Flying Pencil	Flying Wing	Prototype	Absolute Toque
Coef.	Description				
A	Manuf. Empty Weight Multiplier (\$/lb)	100	100	100	100
MEW	Manufacturers Empty Weight (lb)	13	8	12	12
	Sum A*MEW (\$)	1300	800	1200	1200
B	Rated Engine Power Multiplier (\$/Watt)	1	1	1	1
	# Motors	2	1	2	2
	Amperage	40	40	40	40
	# Cells per motor	18	36	18	18
REP	Rated Engine Power (Watt)	1728	1728	1728	1728
	Sum B*REP (\$)	1728	1728	1728	1728
C	Manufacturing Cost Multiplier (\$/hour)	20	20	20	20
	# Wings	1	1	1	1
	Projected Area (sq/ft)	12.16	18.55	13.34	13.36
	# Struts or Braces	0	0	0	0
	# Control Surfaces	2	2	2	2
	# Fuselages	1	0	1	1
	Length of Fuselages	9.22	0	7.41	7.96
	# Pods	2	1	2	2
	Length of Pods	0.71	0.25	0.83	0.67
	# Vertical fins	1	0	1	1
	# Horizontal fins	1	0	1	1
	# Servos or Controllers	8	4	10	9
	# Propellers or Fans	2	1	2	2
MFHR	Manufacturing Man Hours	195.36	124.2	197.32	196.96
	Sum C*MFHR (\$)	3907.2	2484	3946.4	3939.2
Total (\$1,000s)		6.9352	5.012	6.8744	6.8672

Table 3.4 -Rated Aircraft Cost Analysis

4.0 Preliminary Design

4.1 Take-off Gross Weight (TOGW) Estimation

The first step in the preliminary design phase was estimating the gross weight of the aircraft, as this parameter is crucial in determining its size and performance. To determine the TOGW, it was necessary to compile the individual weights of known components and to estimate the weights of various airframe structures.

A cargo capacity of 100 tennis balls yields a cargo weight of 5.7 kg (12.5 lbs.). Because the steel payload will not exceed the weight of the tennis balls, the performance design of the aircraft was based on the tennis ball mission TOGW. A large airframe would be needed to carry this voluminous payload and research was done to investigate previous competition aircraft weights. With careful weight management and engineering, an empty airframe weight of 5.5 kg (12.1 lbs.) was expected. Along with a 2.3kg battery pack (5 lbs.) and the payload, a **TOGW of 13.5 kg (29.7lbs.)** seemed reasonable.

4.2 Propulsion Systems Selection

4.2.1 Motor Selection

The new changes to the 2000/2001-contest year dictated that all motors must be from the AstroFlight or Graupner lines of brushed motors. Graupner motors were quickly ruled out due to the efficiency advantage obtained by using AstroFlight's cobalt magnet motors. Astroflight also has a solid reputation of providing reliable, long lasting motors that are able to handle the abuse of high voltage and high currents associated with a competition of this type.

A major rule of thumb within the electric flight community is that a minimum of 120 watts/kg be used for rise of ground (ROG) flight. This is considered marginal for smaller sport radio-controlled airplanes but for larger aircraft that operate at higher Reynolds numbers, performance would be adequate for a heavy lift aircraft. Previous competition experience has also verified this rule, providing an excellent starting place for motor section. This meant that Absolute Toque would require a total of approximately 1600 watts, split between two motors.

MotoCalc and ElectriCalc, commercial software packages, were used to compare the various possible configurations of motor, gearbox, propeller, and batteries for their efficiency, thrust, pitch speed and estimated run-time. With a twin configuration already selected in the conceptual design phase, it was determined from these software packages that twin Astroflight FAI 40's would provide the necessary power. Each of these motors are rated to 900 watts maximum output, providing the necessary **1600 watts** total power required. Larger motors, such as the more powerful AstroFlight FAI 60 weigh and cost almost twice as much as the AstroFlight FAI 40. With a limited battery pack capacity, more power output

would result in a shorter run time, requiring the motors to run at a partial throttle setting where brushed motor speed controllers are less efficient.

4.2.2 Battery Selection

The voltage and the current define the power of the motors. With the maximum current set by the contest rules at 40 amps, the only way to increase motor output power is to increase the number of cells. The AstroFlight FAI 40's, though rated to 18 cells, can easily handle up to 20. Thus it was desirable to find approximately 36 to 40 cells that would weigh 2.3kg (5lbs.) or less. The batteries were selected by comparing the weight, capacity, internal resistance and power density. Sanyo **2400 mAh** cells were found to have the highest power density while still allowing **36 cells** to be used, providing 18 cells per motor.

4.2.3 Propeller and Gearing Selection

In order to maximize the efficiency of the power system, a careful balance between the propeller pitch speed and thrust must be maintained. This can be done by gearing the motor to swing a larger propeller, at a slower pitch speed. An initial pitch speed of **33.5 m/s (75 mph)** was chosen as a starting point (based on experience and rough calculations) in order to obtain an approximate propeller diameter. An AstroFlight helical gearbox with a 1.63:1 gear ratio would turn a **10.5"** by **7"** propeller with an approximate pitch speed of 34 m/s (76 mph) and provide an approximate **22.5 N (5 lbs.)** of static thrust (**45 N, 10 lbs**, total aircraft thrust). This gives a thrust to weight ratio of approximately 1:3 and an approximate maximum aircraft velocity of **25 m/s (55 mph)** with an assumed drag coefficient of 0.03 (a worst-case cruise drag scenario based on the calculated value of last years aircraft, "Obsidian").

4.2.4 Shroud Sizing

In an attempt to increase the propulsion performance with the limited battery pack capacity, it was decided to attempt to use propeller shrouds. The design of the shrouds was based entirely on an undergraduate thesis completed by 4 students, 3 of them members of the Queen's Aero Design Team. The thesis involved the design and development of a variable geometry shroud for small scale UAV's. From this thesis, it was determined that fixed shrouds would provide a significant efficiency increase by reducing tip losses and straightening the efflux flow. Properly sized shrouds would also create their own thrust due to the low pressure created over the leading edge radius of the inlet lip, provided that the inlet area is greater than the exit area. This is achieved by using a cambered airfoil cross section. The inner diameter of the shrouds is of course dictated by the diameter of the propeller, and the outer diameter by the camber and thickness of the ring airfoil. The chord of the shroud is based on maintaining a smooth airfoil shape, about 0.3 m (12 in). Final dimensions will be examined in the detailed design. Because the use of shrouds is considered experimental, provisions were made to use regular open propellers. Hence, as a worst-case scenario, the initial design of the aircraft and its performance is based on un-shrouded propellers.

4.3 Wing Area and Airfoil Selection

The wing area and airfoil were chosen based on the lift requirements over the mission profile, stall characteristics, and induced drag estimates. The FOM used in the selection is as follows, with each of the above criteria being given a rating on a scale of 5, with 5 being desirable.

4.3.1 Airfoil Selection Figure of Merit

C_l at the Best Lift to Drag (L/D) Angle of Attack

The C_l at best L/D was used to gain insight into the amount of lift the wing would produce while operating at peak efficiency. This was considered important since the more lift the airfoil generates, the smaller the wing area can be, thus reducing drag and weight.

Maximum C_l

The maximum C_l was considered to be important as this determines the stall speed, take-off speed, and maximum g-loading for a fixed wing area. Due to the requirement for take-off within a limited distance and the energy advantage obtained by minimizing the amount of time in climb, a moderately high C_l was considered advantageous. Extremely high C_l airfoil can create excessive induced drag.

Stall Characteristics

Like many other parameters, this FOM arises from past experience. An airfoil with a more docile stall increases the time available to react and increase the likelihood of recovery. The stalling characteristics were compared based on published lift, drag, and pitching moment data

Induced C_d at Expected Cruise AOA

Due to the restrictions on available battery power, drag reduction is of primary importance. The airfoils were compared at the expected cruise C_l , where the drag will have the most influence on performance.

Manufacturing Ease

The difficulty in constructing the airfoil must also be taken into consideration. Complex high lift airfoils usually possess thin trailing edges and concave undersides which, in order to maintain structural rigidity, require heavier structures that are more time consuming and complicated to build.

	C_l at best L/D AoA	Maximum C_l	Stall Characteristics	Induced C_d at Cruise	Manufacturing Ease	Total
Clark Y	4	4	5	4	5	22
Eppler 193	5	4	5	5	5	24
Naca 64-612	5	5	4	4	4	22

Table 4.1 Airfoil Figure of Merit

4.3.2 Airfoil Section and Wing Area

A compromise between wing area, surface drag and induced drag must be made, as well as the above FOM's taken into consideration. A larger area wing has a higher parasitic drag, but a lower induced drag, as it does not require an airfoil with as high coefficient of lift. The larger wing area however requires more structure and has a slightly increased weight. The opposite is true for a small platform wing. It was decided that a wing area of approximately **1.16 m² (1800 in²)** would produce a comfortable wing loading of **121 g/dec² (40 oz/ft²)** and allow a flat bottom airfoil to provide the necessary C_l . The flat bottom airfoil, being lighter to construct, would offset the weight of having the larger wing area and provide a lower induced drag. From this, the C_L at cruise was determined from the standard lift equation. Three-dimensional effects reducing the overall lift of the wing will be more thoroughly examined in the detailed design when the final wing configuration has been selected.

$$C_{Lmin} = \frac{2L}{\eta \rho S_w V_{max}^2}$$

Where η is the efficiency of the wing, assumed to be 0.9, and L is the total lift required, equal to the TOGW of 13.5 kg (29.7 lbs.).

This gives a required C_L of 0.35 ± 0.1 at max a velocity 25 m/s (55mph) and a C_L of **0.42 ± 0.1** at a cruise speed of **22.5 m/s (50 mph)**. The stall speed would be determined by the maximum coefficient of lift obtainable from the airfoil. Most flat-bottomed airfoils have a maximum C_l at approximately 1.3 ± 0.1 with a well designed wing being able to achieve 90% of this maximum C_l . Thus a stall speed of approximately **12.8 m/s (27 mph)** can be achieved with a wing C_L of 1.2 ± 0.1 . It was also desired to have an aircraft capable of maneuvering with a G loading of at least 2.5 at cruise speed, which gives a required maximum C_L of 1.05 ± 0.1 , well within that of a normal flat bottomed airfoil.

The maximum takeoff distance is one of the primary design considerations is determining the airfoils maximum C_l . If the C_l of the airfoil were not high enough to allow takeoff within the set distance, high lift devices would need to be incorporated. With the preliminary weight, thrust, and wing area known, and by setting the takeoff distance to 61 m (200 ft), a minimum C_l for take off was determined to be 0.52 ± 0.1 , achievable by many airfoils.

As such, the wing was required to have a C_{Lmin} of **0.35** and a C_{Lmax} of **1.2**. Airfoil lift and drag data were obtained from the UIUC Low-Speed Airfoil Test program and several airfoil texts and their performance examined with regard to the FOM's and the desired values calculated above. The final selection made was the **Eppler 193**, with a C_L of 0.33 and a C_D of 0.0071 at its minimum drag angle of 0° , and a maximum C_l of 1.31 as the angle of attack approaches the critical angle of approximately 12° . An angle of incidence of approximately 2 degrees would be needed to provide the lift at cruise velocity. The Eppler 193 airfoil has slightly less drag than the Clark Y airfoil used in previous years aircraft, yet still has advantages of similar high lift and mild stall characteristics that are familiar to the team.

4.4 Aspect Ratio

A higher aspect ratio will reduce the induced drag of the aircraft, thus allowing for a faster cruise speed for the same power. Thus all of the 3.05 m (10ft) maximum wing span will be utilized in order to increase efficiency. With the wing area having been previously selected as 1.16 m² (1800 in²) and a 3.05 m (10ft) span, an average chord of 0.38 m (15 in) was required for a constant chord wing. However, as discussed in the conceptual design, a taper platform would be used in order to approximate the lift distribution of an ellipse. This resulted in an aspect ratio of **8**, which is quite respectable for a high lift aircraft with a restricted wingspan.

4.5 Wing Platform

A taper ratio of **0.45** was used to approximate lift distribution that an ideal ellipse wing platform would provide, allowing a substantial reduction in induced drag. This required a **root chord of 0.56 m (22 in)** and a **tip chord of 0.25 m (10 in)** to provide approximately 1800 in² of wing area plus the section of wing interrupted by the fuselage carry-over. The Eppler 193 is a thin airfoil used mainly on gliders with a thickness of only **10.5%**, meaning the root airfoil will be an acceptable **0.058 m (2.3 in)** root thickness. However, at the wing tip this would result in a wing thickness of only 0.026 m (1.05 in), which was thought to be too thin to survive the wingtip lift test. Increasing the wing tip airfoil thickness to **15%** would not only strengthen the wing structure, but also increase the airfoils lift potential, in turn preventing wing tip stalls. The resistance to wing tip stalling has been deemed necessary after watching last year's aircraft "Obsidian" spiral into the ground. Thus a wing tip thickness of **0.038 m (1.5 in)** was selected.

4.6 Horizontal Stabilizer Sizing

The design considerations used to determine the required tail surface dimensions are stability and control authority. The wing is capable of approximately 2.5g before stalling (see section 4.3.5), and the Eppler 193 has a moment coefficient of approximately -0.095 for a cruise angle approximated at of 2°. The stabilizer must be capable of overcoming both the pitching moment of the wing and the moment caused by a finite separation between the center of gravity and the center of pressure on the wing (assumed for now to be within 0.0254 m or 1 in. of each other). The tail must then still provide enough torque for control. This leads to the inequality:

$$X_{ach} \frac{1}{2} C_{Lh} \rho S_h V^2 \geq \frac{1}{2} C_M \rho S_w V^2 c + 2.4 X_{ack} W + I \ddot{\theta}$$

From this, the product of stabilizer maximum coefficient of lift, surface area, and distance from the center of gravity ($X_{ach} C_{Lh} S_h$) can be found. In order to minimize its size and reduce drag, the tail is placed as far aft as feasible to give it a large moment arm on which to act. In the design of Absolute Toque, this is achieved through the length of the fuselage cargo compartment alone, without the need for a tail boom.

It is common practice to use a stabilizer that is approximately 20 to 22% percent of the wing area and an elevator that is 40% of the stabilizer area. With the slow speeds and multiple takeoffs and landing in this competition, pitch authority was deemed very important. With no penalty for stabilizer area, an area that is 22% of the wing was preferred. It has been found that a **0.24 m² (370 in²)** stabilizer located **1.27 m (45 in.)** from the CG would require a C_l of approximately 0.2 ± 0.1 . This would be easily provided by a **NACA0009 airfoil** (C_{Lmax} of 1.3) (ref. 7), which has the desired horizontal stabilizer qualities of low drag and zero pitching moment. These will be further quantified in detailed design.

The horizontal stabilizer platform is also designed with a taper ratio to reduce its induced drag. However, in order to prevent the Reynolds numbers at the tip of the stabilizer from becoming too small, a taper ratio of only 0.7 was used. An aspect ratio close to 5 was also desired in order to reduce induced drag. This resulted in a root chord of 0.27 m (10.5 in) and a tip chord of 0.2 m (7.5 in), a 1.02 m (40 in) span and a 4.8 aspect ratio.

As decided upon in conceptual design, a T-tail design would be used. Construction of this design is only marginally heavier than a conventional tail, yet is upwards of 30% more efficient. Raising the horizontal stabilizer into clean air greatly increases its effectiveness while still reducing interference drag by reducing the number of joints between rudder, tail and fuselage.

4.7 Vertical Stabilizer Sizing

The vertical stabilizer supports the horizontal stabilizer and must be quite stiff to withstand this loading. The tip chord of the vertical fin was set to the same as the horizontal stabilizer root chord in order to minimize interference drag at the junction. In order to increase its rigidity, and to allow room for servo mounting, a slightly thicker tip airfoil, a **NACA 0015** was used. Because of the effective slant of the fuselage, the aft end of the fuse is raised up, minimizing the height of the vertical fin needed to clear the shrouds. The vertical fin height was set to 0.25 m (10 in), which raises the horizontal tail out of both the downwash from the wing and the possible turbulent flow created by the shrouds at high angles of attack. In order to provide enough yaw stability, the root chord of the fin was adjusted to provide enough area. For an airplane to be stable in yaw, the Center of Lateral Area should be about 25% back from the center of gravity. In the preliminary AutoCAD design, quick area moment calculations were done to show that the area selected was adequate for yaw control. Also, common model design practice states that the vertical tail area should be approximately 50% of the horizontal tail area used. Thus a vertical fin area of **0.12 m² (180 in²)** would be employed, resulting in a root chord of 0.61 m (24 in) and a **NACA 0009** root airfoil. This heavy taper provides a very rigid vertical fin. The vertical fin was also swept so as to increase the horizontal tail moment arm and to improve appearance. Further analysis of vertical fin height is done in the detail design section.

4.8 Fuselage Design and Sizing

4.8.1 Fuselage Design Considerations

During the preliminary design stage, several design parameter and sizing trades were considered. While innovative design and construction methods were investigated, they were weighed against ease of manufacture and functionality. The decision of airframe design depended upon trades between simplicity of construction, strength, weight and reduction of drag. The following aspects of performance were considered in lofting the fuselage geometry.

Efficiency

The layout chosen for the fuselage should optimize the space required for the airframe structure while also limiting the fuselage's overall size. The placement of the balls was the main factor contributing to the preliminary design of the most efficient airframe possible.

Manufacturing Ease

The preliminary design of the airframe should limit the cost and time required for its construction. Also, shop tooling and facilities must be considered.

Functionality

The fuselage must function properly as a cargo-carrying aircraft that requires repeated removal and loading of the cargo. The design feature used for access to the cargo must be both quick and rugged due to the rushed nature of cargo insertion/removal. Provisions must be made to support both ball and steel cargos.

Structural Rigidity

The airframe structure must be sufficiently strong and stiff to account for the substantial payload and the repeated landings that the aircraft will encounter. The structure must also be rigid enough to prevent flexing that could reduce horizontal or vertical stabilizer effectiveness. The type of materials used and the thickness chosen for the primary structural components of the aircraft depended on their ability to withstand the expected loading.

Drag Penalty

The design of the airframe should minimize the amount of parasitic and interference drag created by the fuselage. This will reduce the power required for cruise and increase overall top speed, increasing motor run time. All junctions between airframe components should be smoothly faired in order to reduce interference drag. Any fuselage upsweep should be less than 15° to prevent separation drag.

4.8.2 Fuselage Size

The design of the fuselage is based on the considerations above, with its length dictated by both the cargo hold and the length required for the tail moment arm. The cargo is configured in four tubes, sized to be one tennis ball in diameter and 25 in length. This meant that the cargo hold would be 1.67 m (66 in) in length, and when centered over the wing 1/3 chord (predicted center of gravity) and the addition of a 0.38 m (15 in) tail cone, would prove a long enough tail moment arm. The steel payload would also be carried in these four tubes. Long strips of steel (rectangular) the length of the cargo hold would distribute the load over the foam inner structure and prevent the cargo from shifting while over the centre of gravity. The fuselage contours are based a cylindrical shape 0.19 m (7.5 in) in diameter with a nose and tail cone, wing fairing and a slight curvature added to the fuselage top to reduce drag. This tube is placed on a slant, centered over the wing 1/3 chord (predicted CG location on wing) in order to have the aircraft balance with and without cargo and to shorten the nose gear and vertical tail height. The wing is then faired into the bottom of the fuselage. The shrouded propellers are mounted to the sides of the fuselage on airfoil shaped pylons located behind the wing. The length of these pylons is a compromise between having a short moment arm for structural rigidity and a long arm to prevent interference drag and the shroud "swallowing" the fuselage boundary layer. A preliminary pylon length of 0.064 m (2.5 in) was chosen. The battery compartment is located in the front wing fairing, while the radio control equipment resides in the trailing edge fairing.

4.8.3 Cargo Access

Access to the cargo hold is facilitated through the removable nose cone. This nose cone is held on by 3, quarter-turn fasteners, which allow quick removal between flights. The cargo is easily removed from all 4 tubes through this hatch.

4.8.4 Speed Loader

In order to speed up the time to load and unload the cargo, a speed loader will be utilized. The loader consists simply of a long fabric bag the length of the cargo tube. Both the tennis balls and steel strips will fit in these bags and can be easily removed. This method of speed loading was though to be the lightest and easiest solution.

4.9 Undercarriage Design

The tricycle landing gear design used for Absolute Toque must be designed to absorb the landing shock and to provide excellent ground handling qualities. A main wheel stance of $\frac{1}{4}$ of the wingspan was chosen to prevent an upset in high crosswinds. The nose gear is located as far forward on the main fuselage as possible. Because the propellers are mounted high on the fuselage, the length of the nose and main gear need only to be based on the provision of providing adequate clearance for rotation and

the wing tips. A gear length of 0.11 m (4.5 in) allowed slightly over 15 degrees of rotation and 0.2 m (8 in) of wing tip to ground clearance. The main landing gear was positioned 0.05 m (2 in) behind the center of gravity so that when the aircraft rotates on takeoff, the wheels remain behind the center of gravity.

Dual ball bearing supported aluminum wheels, 0.089 m (3.5 in) in diameter, are used for the main gear. Because the aluminum does not deform, the rolling resistance is very low. However, these wheels are prone to sliding sideways in crosswinds, necessitating that duct tape be placed around the rim for friction. (Many rubber compounds have been tried, but duct tape has consistently worked the best).

The nose gear supports less weight, so a standard 0.063 m (2.5 in) model aircraft wheel was used. The higher friction of this wheel provides better directional control on takeoff.

Gear struts are formed from bend $\frac{1}{4}$ in diameter music wire. The main gear uses a torsion bar design for shock absorption, where as the nose gear uses a dual coil.

Item	Imperial	Metric	Item	Imperial	Metric
Propulsion			Horizontal Stabilizer		
Motor	AstroFlight		Airfoil	NACA 0009	
	FAI 40 G		Area	363 in ²	0.233 m ²
Speed Controller	Astro 204D		Span	40.0 in	1.06 m
Cells	36, 2400mAh		Root Chord	10.5 in	0.267 m
Gearing	1.63:1		Tip Chord	7.5 in	0.191 m
Propeller	10.5 by 7		MAC	9.08 in	0.231 m
Static Prop Thrust	10 lbf	44.5 N	Thickness	0.75 in	0.019 m
Run Time (100%)	3.4 min	3.4min	Aspect Ration	4.8	4.8
Motor Efficiency	80%	80%	Taper	Double Taper	
Wing			Taper Ratio	0.714	0.714
Airfoil	Eppler 193		Elevator Area	144 in ²	0.093 m ²
Wing Area	1764 in ²	1.138m ²	Elevator Span	36 in	0.914 m
Span	120 in	3.05 m	Elevator MAC	4.01 in	0.102 m
Root Chord	22.0 in	0.559 m	Tail Moment Arm	45.0 in	1.14 m
Tip Chord	10.0 in	0.254 m	Vertical Stabilizer		
MAC	16.75 in	0.425 m	Airfoil	NACA 0015	
Wing Thickness	2.25 in	0.057 m	Area	183 in ²	0.118 m ²
Aspect Ratio	8.16	8.16	Root Chord	24.0 in	0.610 m
Taper	Double Taper		Tip Chord	11.0 in	0.279 m
Taper Ratio	0.455	0.455	MAC	18.3 in	0.465 m
Aileron Area	165 in ²	0.106 m ²	Height	10.0 in	0.254 m
Aileron Length	39.4 in	1.0 m	Rudder Height	9.0 in	0.229 m
Aileron MAC	4.18 in	0.106 m	Rudder MAC	5.07 in	0.129 m
Fuselage			Rudder Area	45.6 in ²	0.029 m ²
Length	89.0 in	2.26 m	Velocities		
Max Height	12.0 in	0.30 m	V _{max}	55.4 mph	26.1 m/s
Width	7.5 in	0.19 m	V _{cruise}	49.9 mph	23.5 m/s
Fuselage Diameter	7.5 in	0.19 m	V _{stall}	27.2 mph	12.1 m/s

Table 4.2. Summary of aircraft geometry based on both preliminary design and detailed design calculations.

5.0 Detail Design

Drawings of the final aircraft design are presented at the end of this section. These drawings include detailed two-dimensional drawings and the templates used for construction.

The design of any airplane is a highly iterative process, involving many changes to the initial preliminary design before arriving at the final configuration. To accommodate this, a spreadsheet was developed that performed the necessary calculations while only requiring airfoil properties and some aircraft geometry input. The detailed calculations for the shroud design and performance also make use of a spread sheet that gives detailed analysis for a given power output, testing prop sizes from 0.15 m (6 in) to 0.41m (16 in) props and their associated shroud geometry.

5.1 Weights

An estimate of the components, structure and payload to be carried was tabulated. Airframe structure was calculated based on volume approximations of the materials used in the construction of each part, and by using data obtained from last years aircraft. Care was taken not to underestimate the weight of the aircraft, as all primary design features require an accurate approximation of this weight in their calculations. A summary of weight is presented below.

DESCRIPTION	WEIGHT (lbs)	WEIGHT (N)	NUMBER	SUBTOTAL (lbs)	WEIGHT (N)
Tennis Ball	0.125	0.556	100	12.5	55.6
Steel Block	2.00	8.90	3	6.00	26.7
Battery Pack	5.00	22.2	1	5.00	22.2
Receiver	0.125	0.566	1	0.125	0.556
Servos	0.125	0.556	6	0.750	3.34
Landing Gear	0.5	2.225	1	0.5	2.225
Wheels	0.125	0.556	3	0.375	1.67
Wing	3.25	14.5	1	3.25	14.5
Tail	1.25	5.57	1	1.25	5.57
Fuselage	3.50	15.6	1	3.5	15.6
Motor	0.688	3.06	2	1.375	6.12
Speed Controller	0.075	0.334	2	0.150	0.667
Gear Box	0.094	0.417	2	0.188	0.834
Shroud	0.442	1.99	2	0.884	3.98
Receiver Battery	0.183	0.812	1	0.183	0.812
Hardware	0.250	1.11	1	0.250	1.11
Prop	0.125	0.556	2	0.250	1.11
Take Off Gross Weight with Tennis Balls				30.4	135
Take Off Gross Weight with Steel Blocks				23.9	106
Empty Flying Weight				17.9	79.6
Airframe Weight				12.9	57.4

Table 5.1. Aircraft Weights

5.2 Payload Fraction

Payload fraction is a measure of the payload's contribution to the take-off gross weight of the aircraft. The payload fraction of Absolute Toque with the tennis ball payload is **0.411**. Much of the airframe weight is being put towards creating a large cargo hold for a relatively light cargo, giving a below average payload fraction.

5.3 Drag

In order to make accurate predictions of the flight speed and acceleration, the drag on the aircraft must be calculated. In this basic estimation, the total drag is taken to be the sum of parasitic drag and the induced drag from the wing. This approximation does not take into account interference drag caused by the junction of various parts. This form of drag can be reduced considerably if proper drag reduction techniques are incorporated as in the case with Absolute Toque.

5.3.1 Parasitic Drag Coefficient

Parasite drag was estimated using the "component build-up" method. A flat-plate skin friction drag coefficient (C_f) for fully developed turbulent flow is calculated for each major component of the aircraft and then multiplied by a "form factor" (k) that estimates losses due to form drag:

$$C_{dPara} = \sum \left[\frac{k \times C_f \times A_{wetted}}{S_w} \right]_{component} \quad C_f = \frac{0.455}{(\log_{10} Re)^{2.56}} \quad Re = \frac{V \times L}{\gamma}$$

Component	$A_{wetted} (m^2)$	Re	C_f	t/c	k	$C_{dparasitic}$
Wing	2.28	757270	0.00486	0.0572	1.07	0.0104
Fuselage	1.72	4023701	0.00361	11.9	1.1	0.0575
Wheels	0.036	180841	0.00646	0.0625	1.13	0.000224
Gear Struts	0.002	11303	0.0125	1.00	1.8	0.000036
Horizontal Stab.	0.469	410659	0.00547	0.0188	1.02	0.00220
Vertical Stab.	0.295	827561	0.00478	0.0254	1.03	0.00122
Shrouds	0.393	444982	0.00538	0.1	1.21	0.00215
Total						0.0220

Table 5.2. Parasitic Drag Estimate

The total parasitic drag estimate is **0.022**, which seems reasonable for an aircraft of this shape and size. In order to help reduce parasitic drag, the skin of Absolute Toque will have very smooth Mylar skin on flight surfaces and a polished epoxy fuselage.

5.3.2 Induced Drag Coefficient

The induced drag coefficient is dependent on a proportionality factor "K" and the square of the C_L (for moderate angles of attack). K is dependent on an Oswald efficiency factor "e" and the aspect ratio of the wing. In order to reduce the induced drag, Absolute Toque utilized the maximum wing span limit in order to increase the aspect ratio. Winglets and endplates were considered as ways to minimize the induced drag. However, the rules state that the length of the winglets be added to the wing span in determining the overall span. With a set limit of 3.05 m (10ft), a smaller wingspan would have been needed to accommodate the winglets, making this an undesirable trade off. Wing tip endplates have been known to add more interference drag than any reduction in induced drag they may provide.

$$e = 1.78(1 - 0.045 \times AR^{0.68}) - 0.64 = 0.816 \quad K = \frac{1}{\pi A e} = 0.0488 \quad C_{D_{\text{induced}}} = K C_L^2 = 0.0488 C_L^2$$

5.3.3 Total Drag

The total drag is based on its velocity at which the aircraft travels. While the Reynolds number term in the parasitic drag equation does change with velocity, its effects are negligible for a calculation of this accuracy. The induced drag coefficient does depend heavily on velocity however due to the C_L term. Thus the coefficient of drag at a known airspeed and C_L is given by $C_D = 0.022 + 0.0488 C_L^2$. The actual drag force experienced by the aircraft is given by $D = 0.5 C_D \rho V^2 S_w$.

5.4 Wing Sizing and Performance

5.4.1 Wing Planform

The dimensions proposed in the preliminary design were further refined in an attempt to increase the accuracy of the wing performance calculations. The wing area was recalculated using the detailed AutoCAD drawings, accounting for the fuselage carry-over and taper. The wing area was finalized at **1.14 m² (1764 in²)** with a tip chord of **0.254 m (10 in)** and a root chord of **0.559m (22 in)** (unchanged from the preliminary design). The maximum wing loading with full cargo is **1165 g/dec² (39.7 oz/in²)**.

5.4.2 Aileron Sizing

The ailerons were sized based on historical data for effective control. A 50% semi-span, 25% wing chord aileron was used. These ailerons do not extend all the way to the wing tip in order to prevent flutter, which can be caused by wing-tip vortices. The ailerons used are Frise ailerons, which create drag when deflected upward, helping to yaw the airplane into the turn. A sealed hinge line increases effectiveness an extra 15%. The aileron area is **0.106 m² (165 in²)** each.

5.4.3 Stall Velocity

An airfoil efficiency factor, η , of 90% was used to relate 2-dimensional airfoil data to a 3-dimensional wing. This value accounts for lift losses at the tip and slight inaccuracies in the airfoil construction (laser cut parts minimize construction inaccuracies). This reduces the maximum coefficient of lift of the Eppler 193 from 1.31 to 1.19. Thus the stalling speed can be calculated by the equation.

$$V_{STALL} = \sqrt{\frac{2Mg}{\eta C_{l_{max}} \rho S_w}} = 12.8 \text{ m/s}$$

This results in a stall speed of **12.8 m/s (27.2 mph)** (fast, but not unreasonable).

5.4.4 C_L at Cruise and Maximum Velocity

In order to determine maximum velocity and the resulting C_L at these velocity, several iterations must be done. By iterating between velocity and C_L values, a final cruise and maximum velocity were found. The cruise velocity was taken to be 90% of the maximum velocity.

	Velocity	Velocity	C_L
V_{CRUISE}	23.5 m/s	49.9 mph	0.43
V_{MAX}	26.1 m/s	55.4 mph	0.36

Table 5.3. Maximum and Cruise Velocities

5.4.4 Wing Incidence

With the known cruising velocity, the angle of incidence for the wing was determined. This angle provides the model with the correct lift for level flight at the cruise velocity, taking the aspect ratio (AR) and platform taper in effect.

$$\alpha = \frac{a_0 + 18.24 \times C_{L_{cruise}} \times (1.0 + T)}{AR} = 2.1^\circ$$

Where, a_0 = the angle of attack of the wing at $C_{L_{cruise}}$

T = planform adjustment factor for aspect ratio (Fig 4., pg 6, Lennon, Andy, "Basics of Model Aircraft Design")

The pitching moment of the wing at the cruise velocity and angle of incidence was calculated to be **-31.0 N/m (-2193 oz/in)**.

5.5 Tail Sizing and Performance

5.5.1 Horizontal Stabilizer Platform

The horizontal tail has an area of **0.234 m² (363 in²)**, which is 22% of the wing area. A tip chord of 0.191 m (7.5 in), a root chord of 0.267 m (10.5 in) and a span of 1.02 m (40 in) gives an aspect ratio of 4.8. Historic guidelines suggest an elevator area of between 30 and 40 percent for effective pitch control. An elevator area of **0.093 m² (144 in²)** was used, representing 40% of the stabilizer area.

5.5.2 Horizontal Stabilizer Lift

Basic model airplane guide lines suggest that the horizontal tail be placed approximately 2.5 times the mean aerodynamic wing chord from the neutral point of the wing to the neutral point of the stabilizer. The neutral point of both airfoils is assumed to be at the $\frac{1}{4}$ chord. This guideline would suggest a 1.06 m (42 in) tail moment arm. However, due to fuselage sizing which is constrained by the cargo hold size, the moment arm was slightly extended to **1.14 m (45 in)**.

With a pitching moment of -31.0 N/m (-2193 oz/in) and a tail moment arm of 1.14m (45 in) the horizontal tail must provide a down force of **39.3 N (54.1 oz)** assuming 90% stabilizer efficiency. This down force is provided by the negative lift from the stabilizer airfoil, requiring a $C_{l_{stab}} = -0.21$.

5.5.3 Horizontal Stabilizer Incidence

The angle of incidence to provide this C_L was taken from published airfoil data and was shown to be -2.21° for two-dimensional flow. Using the same equation as the wing to account for the effects of an aspect ratio of 4.8, the tail incidence becomes -3.11° .

The down wash from the wing and its effect on the stabilizer must be taken into account. The horizontal moment arm and the height of the stabilizer from the wing were calculated and their values were used with charts (Figure 2, pg 40, Lennon, Andy; "Basics of RC Model Aircraft Design" ref 10.) to provide the correct tail incidence required. A final incidence of -1.6° is used.

5.5.4 Vertical Stabilizer Platform

The vertical stabilizer platform remained unchanged from the preliminary design. The rudder area was set at 25% of the vertical stabilizer as recommended by historical guidelines. As the chance of having a motor out condition are very slight with electric propulsion, this value was deemed adequate. The resultant rudder area is **0.029 m² (46 in²)**.

5.6 Propulsion

Motor and propeller selection remained unchanged from the preliminary design. Twin AstroFlight FAI 40's will provide the aircraft with sufficient power. An AstroFlight helical gearbox with a 1.63:1 gear ratio would turn an APC 10.5" by 7" propeller with an approximate pitch speed of **34 m/s (76mph)** and provide an approximate 22.5 N (5 lbs) of static thrust (**45 N, 10lbs, total aircraft thrust**). At a predicted amp draw of **40.8 amps**, full throttle duration of the 36 cell, 2400 mAh battery pack is **3.4 minutes**. The computer radio will limit the current to stay below 40 amps at full throttle static draw so as not to blow a fuse. As the prop unloads in the air, amp draw will be reduced. Because much of the mission sortie is flown at a partial throttle setting, flight times will be higher than the predicted 3.4 minutes.

5.7 G-Loading

In predicting the maximum g-load the aircraft is capable of handling, two major parameters were investigated. Firstly, the aircraft's structural capabilities were estimated with a calculation of the spar's maximum allowable bending stress. Predictions were then made on the accelerated stall properties of the wing, using published lift data for the selected airfoil.

5.7.1 Structural Loading

A **G-load rating of 4** was assigned as a prediction of the maximum loading the airplane would experience under normal flying condition and while at the maximum TOGW. From here the size and strength of the wing could be determined.

For calculations, the assumption was made that the wing spar carried all wing loads and that the spar would experience heavier loads than any other aircraft part. Thus, the maximum bending stresses the spar can handle will determine the G-load capability of the plane.

The wing manufacturing plan calls for an "I" beam spar to be used, with a carbon laminate for each flange and a vertical grain balsa shear web. Thus, the maximum bending stresses these elements can handle will determine the G-load capability of the plane. As nearly all G-loadings placed on the airframe would be positive, this puts the upper spar into compression and the lower into tension. Thus the number of carbon fibre laminates would be different for each spar flange. From these assumptions, the cross sectional area of these respective materials could be calculated.

The maximum bending moment experience by the wing was calculated using basic force and moment analysis and found to be **55.6 kN/m (3419 lbf/in)** at the root, dropping to zero at the wing tip. The second moment of inertia (I_y) was calculated for the area of the carbon fiber cross section. With the known distance to the neutral plane (z), the bending stress could be calculated using the equation:

$$\sigma_x = \frac{M \cdot z}{I_y}$$

The dimensions of the upper spars (stock sizes) were then iterated to achieve a safety factor of approximately 1.5 (to account for lamination defects) with positive 4 G loading. It was found that 4 layers of carbon fiber on a 0.0381 (1.5) in by 0.0064 m (0.25 in) piece of balsa was required for the bottom spar. Because the compressive properties of carbon fiber are much lower than its tensile strength, 7 layer of fiber were necessary for the top spar. In order to be sure that the spar did not fail in shear, vertical grain shear webs were used to join the two spar halves together.

Because the stress in the spar goes to zero at the tip, a tapered spar was used to reduce the overall weight. The spar tapers from 0.0381 m (1.5 in) to 0.019 m (0.75 in) at the tip.

5.7.2 Accelerated Stall Characteristics

The minimum controlled level turning radius for an airplane is determined by the maximum radial acceleration the wing can sustain before an accelerated stall. The maximum G-load that can be produced by the aircraft is given by the ratio of the maximum lift available from the airfoil to the lift generated in steady level flight. The angle of bank at which the wing can still provide the necessary lift for the airplane is given by:

$$\cos\beta = \frac{C_{L_{cruise}}}{C_{L_{max}}}$$

Thus the **maximum angle of bank is 69°**. The maximum radial acceleration before the onset of an accelerated stall is calculated using the equation:

$$\tan\beta = \frac{a_{stall}}{1 \cdot g}$$

This gives a loading of **2.56g's**. Thus, if the aircraft more than 2.56g lateral acceleration, the maximum lift available from the wing will be exceeded and a accelerated stall will occur.

From this data the minimum radius of turn with no altitude loss is **20m (65 ft)** as given by the equation:

$$R = \frac{V_{cruise}^2}{a_{stall}}$$

5.8 Take-off Performance

Take-off distance is broken into three components: ground roll, rotation distance, and climb-out distance. Rotation distance is assumed to be negligible for this calculation.

5.8.1 Ground Roll

$$d_g = \frac{V_{TO}^2}{2 \cdot a_{mean}}$$

The ground roll distance (d_g) of the aircraft is given by:

$$\text{where, } M \cdot a_{mean} = \left[T_{mean} - (A + B \cdot C_{L_{cruise}}^2) \frac{1}{4} \rho V_{Mean}^2 S_w - \mu (W - C_{L_{cruise}} \frac{1}{4} \rho V_{Mean}^2 S_w) \right]$$

Take-off speed (V_{TO}) is taken as 15% above stall speed:

$$V_{TO} = 1.15 \cdot V_{stall}$$

The C_L and C_D used in this equation are the values at cruise speed, as the plane can be considered in level flight while on the ground with its wing angle of incidence relative to the runway. Static thrust is estimated from the available motor data from ElectriCalc. This yielded a ground roll acceleration of **3.00 m/s² (9.85 ft/s²)**. The ground roll is **36.0 m (118 ft)**, well under the 200ft limit. These distances are given under a no wind condition.

5.8.2 Climb out Distance

The climb out angle for the aircraft is given by the equation: $\tan\vartheta = \frac{T}{W} - \frac{D}{L}$

A **climb angle of 13.4°** is achieved. If this rate of climb were held constant so that there is no gain in velocity after lift off, a distance of **42 m (137 ft)** would be needed to reach an altitude of 10 m (32.8 ft). The performance under these assumptions is as expected for a heavily loaded aircraft. To increase the climb rate, the aircraft should be allowed to accelerate to its minimum drag velocity in level flight, at which point the excess power at this velocity can be used for climb.

5.9 Endurance and Range

5.9.1 Minimum Drag Velocity

Because parasitic drag increases with increasing velocity and induced drag decreases, there exists a point of minimum drag. The velocity at which this minimum drag occurs is also where minimum thrust is required, as thrust is equal to drag. The minimum drag velocity is given by:

$$V_{\min \text{ drag}} = \left(\frac{B}{A} \right)^{1/4} \left(\frac{2Mg}{\rho S_w} \right)^{1/2}$$

Where A and B correspond to the parasitic and induced drag respectively. The minimum drag velocity for Absolute Toque is **16.9 m/s (37.7 mph)** at which only **8.9 N (2.0 lbf)** of thrust are required.

5.9.2 Endurance

The aircraft achieves maximum endurance when flying at its minimum throttle setting. This is achieved at $V_{\min \text{ drag}}$ where the lowest thrust is required. The ElectriCalc commercial software package is used to estimate the endurance of the aircraft with the selected motor and battery arrangement. It was found that $V_{\min \text{ drag}}$ could be achieved with a minimum throttle setting of 41%. At this setting, ElectriCalc estimated a run-time of 26.7 minutes. Due to electrical losses in the wire leads, losses in the speed controller, and difficulty in maintaining $V_{\min \text{ drag}}$, a conservative estimate of 90% of this value was taken. Thus the endurance of Absolute Toque is **24 minutes**. However this estimate neglects power needed for take-off, climb-out, and landing.

5.9.3 Range

The maximum range characteristics of an electrically powered aircraft differ from those of a gas-powered plane, as motor efficiency drops at increased throttle settings. The maximum range of the aircraft is achieved not at the best lift-to-drag velocity, but at the lowest possible throttle setting—at the endurance throttle setting. To calculate the range, the endurance prediction of 24 minutes is multiplied by the endurance velocity of 16.9 m/s (37 mph). This method produces a maximum range value of **24.3 km (15.1 miles)**. This range is assuming zero wind conditions and neglects the power needed for takeoff, climb, landing and energy loss maneuvers.

5.10 Shrouds

5.10.1 Shroud Sizing

The inside diameter of the shroud is of course set by the diameter of the propellers, which will now be referred to as the rotor. A modified Clark Y airfoil is used as the basis for the shroud ring airfoil design, with its leading edge radius modified to 6% of the rotor diameter in order to prevent separation. The leading edge of the airfoil is angled outward, leaving the trailing edge perpendicular to the tip of the rotor. This allows the shroud to create its own thrust from the acceleration of incoming air over the leading edge of the shroud. The shroud airfoil is 0.3 m (12 in) in chord and 0.043 m (1.675 in) in thickness.

5.10.2 Stator Design

Stators are small curved airfoils that support the motor inside the shroud while also straightening the airflow efflux behind the prop. Proper design of the stators increases efficiency by regaining the kinetic energy of the rotation in the rotor efflux. By considering the rotor as a cascade of blades, and taking the resultant of the axial, radial and $\frac{1}{2}$ the tangential flow, the angle of the flow over the stators can be calculated using vortex theory. The stator must impart an equal flow but in the opposite direction. By evaluating this flow in segments along the length of the stator, the required C_L could be obtained along the length of the stator. Four stators were used, each with a C_L of 2.82.

5.10.3 Shroud Thrust

In order to evaluate thrust, Weissinger's approximation is employed. This provides a good approximation of thrust provided the camber is not too extreme. For this approximation, the shroud is replaced with a ring vortex at its $\frac{1}{4}$ chord, and then satisfying boundary conditions at its $\frac{3}{4}$ chord. Vortex theory predicts the static shroud thrust to be **9.31 N (2.09 lbs)**, and the cruise shroud thrust to be **2.11 N (0.473 lbs)** (per shroud). This corresponds to a **42%** increase in static thrust and a **9.4%** increase in cruise thrust. Only testing of the completed shroud will verify these figures, but the results are promising.

5.10.4 Rotor Efficiency.

The reduction of tip losses greatly increases the efficiency of the rotor. A standard propeller uses the last 3% of its blade to reduce tip losses, yet this contributes very little to the thrust of the system. By trimming a 0.279 m (11 in) propeller to 0.2667m (10.5 in), the motor can now turn the 0.2667m (10.5 in) propeller while producing the same power output as a 0.279 m (11 in) propeller. This results in an efficiency increase of **7%**, and creates an additional **3.9 N (0.875 lbs)** of static thrust.

5.10.5 Shroud Drag Estimate.

As shown above, the thrust increase associated with shrouded propellers diminishes with increasing flight speed. To be practical, the shroud must provide more thrust in cruise than the drag it produces. The drag of the shroud, because it is a ring airfoil, has been limited to a parasitic drag analysis, similar to that done for the rest of the airframe. The resultant drag force at cruise is **1.66 N (0.373 lbs)**, which is about 21% less force than the shroud generates in thrust.

5.10.6 Shroud Weight Estimate.

The weight of the shrouds is very important to the overall performance of the aircraft. A detailed weight approximation was performed within the thesis based on volume calculations of the materials used. The weight of a shroud for a 0.267 m (10.5 in) rotor was estimated to be **1.99 N (0.442 lbs)**. This corresponds to a **2.96 %** increase in GTOW, which is considered negligible for the potential thrust increase. The weight of the shrouds was previously incorporated into the sizing and performance of the aircraft.

5.10.7 Performance Increase From Shrouds.

The primary performance increase associated with shrouds is the low speed thrust. This in turn greatly effects takeoff and climb performance. With an all up increase in static thrust of **50.3 %**, **67.6 N (15.2 lbs)** of force are created. This significantly shortens the takeoff run from **36.0 m (118 ft) to 23.1 m (75.8 ft)**. The resultant climb angle is increased from **13° to 22°**. The thrust from the shrouds does quickly drop off however as velocity increase, but the increase in rotor efficiency continues to produce and additional **8%** more thrust than an open propeller. However, with a quick takeoff and climb, less battery capacity will be needed per flight, possible allowing another scoring lap.

5.11 Stability

Static stability is achieved when the forces on the aircraft created by a disturbance to the flight path push the aircraft back in the **direction** of its original state. Dynamic stability is achieved when the dynamic motions of the aircraft will eventually return the aircraft to its original state (motions are damped). Without the software to perform a dynamic stability analysis to any degree of accuracy, the stability analysis presented here has been limited to static stability. However, for most modes of flight, static stability analysis will be sufficient for an aircraft with a conventional layout such as "Absolute Toque".

5.11.1 Longitudinal Stability

The maximum allowable distance between the center of gravity of the aircraft and the location of the $\frac{1}{4}$ chord neutral point of the wing was determined using the following stability criterion:

$$\frac{dC_{M(CoG)}}{dL} = \frac{x}{c} - \eta_H \left(\frac{S_H}{S_w} \right) \left(\frac{l_H}{c} \right) \left(\frac{a_H}{a} \right) \left(1 - \frac{d\epsilon}{d\alpha} \right) + \frac{dC_{Mf}}{dC_L} \leq 0$$

The marginally stable case value of x , the distance from the $\frac{1}{4}$ chord, was found by setting the above inequality to zero and evaluating. This yielded a value of 44.4%, which means that for the aircraft to be longitudinally stable, the center of gravity can be located at no more than 44.4% of the wing chord from the leading edge. The difference between the actual center of gravity and the maximum allowable center of gravity is termed the static margin. With the predicted center of gravity at 30% of the mean aerodynamic chord, a **static margin of 0.144** is achieved. This is a sufficient value for good longitudinal stability.

5.11.2 Lateral-Directional Stability

In order to provide directional stability, the moments about the center of gravity must be such that the derivative of the yawing moment is less than zero. In order to determine the yawing moment derivative about the center of gravity, the pitching moment derivative of the fuselage and vertical fin must be evaluated. The derivative of the pitching moment of the fuselage in the case of "Absolute Toque" will be negligible because the fuselage areas ahead of and behind the center of gravity are equal. The derivative of the vertical fin pitching moment can be expressed by:

$$\frac{dC_{mfin}}{d\theta} = \left(\frac{dC_{Lfin}}{d\alpha} \right) \left(\frac{S_{fin}}{S_w} \right) \left(\frac{l_H}{c} \right)$$

Where $dC_{Lfin}/d\alpha$ is the slope of the lift curve of the vertical fin, S_{fin} is the vertical fin area, S_w is the wing area, l_H is the tail moment arm and c is the mean aerodynamic chord of the wing. The value of the vertical fin pitching moment derivative was evaluated to be 1.6. This value is subtracted from the fuselage pitching moment derivative to determine stability.

$$\frac{dC_{mCG}}{d\theta} = \frac{dC_{mFuselage}}{d\theta} - \frac{dC_{mfin}}{d\theta}$$

The evaluated derivative was found to be 1.6, which is greater than zero indicating that the aircraft was directionally stable.

This results in a **lateral-directional pitching moment derivative of -1.6**, meaning the aircraft exerts a restoring force in the direction opposite the disturbance and is hence statically stable.

5.11.3 Roll Stability

Based on historical data, **6° of wing dihedral** would provide sufficient roll stability for an unswept low wing. As an aircraft with dihedral banks, it begins to slide slip towards the lowered wing, effectively increasing the wings angle of attack and increasing its lift. This provides a restoring force to level the wings.

5.12 Control Systems

5.12.1 Receiver and Programming

Control of the aircraft is provided by a **Futaba 8 channel PCM** transmitter and receiver with its failsafe programmed as per competition rules. Each control surface has its own servo and receiver channel, allowing programmable mixing to be incorporated. Ailerons are programmed to provide differential control for more up throw than down. Slight rudder application is also programmed to operate in conjunction with the ailerons to provide coordinated turns. Each motor system is on its own channel as well, allowing motor rpm of each motor to be synced at all throttle settings.

5.12.2 Flight Pack Battery

A five cell, **600mAh, NiMh** battery pack is used to power the receiver and servos. This pack size is large enough to complete several missions, but will be peak charged again after each ten-minute flight. The **6.0V** system increases power to all servos for a minimal weight gain.

5.12.3 Servo Selection

All servos must provide quick, accurate and strong control authority to the flight surfaces. Any slop in the control set-up could lead to flutter, and possible departure of that control surface. To reduce this risk, all servos are dual ball bearing supported. While many mini servos have static load torques capable of moving the flight surfaces, their fragile gear sets are unable to handle sudden dynamic loads. For this reason, standard sized servos with metal gears are used. In order to select the proper servo, the load on each control surface must be calculated. The torque on the servo can be calculated with the equation below.

$$T = 8.5 \times 10^6 (C^2 V_{\max}^2 L \sin(S_1) \tan(S_1) / \tan(S_2)) = \text{oz} / \text{in}$$

Where T is the torque in oz/in, C is the control surface chord, L is the control surface length, S_1 is the max control surface deflection (assumed to be 20°), S_2 is the maximum servo deflection from center (30° each way for most servos). The maximum torque on each flight surface was calculated. The aileron servos experienced the highest flight load of all the surfaces with a load of **49.5 N/cm (69 oz/in)** each. After viewing many servos and comparing their torque, weight, speed and price, the **Hitec 645 MG Super Torque Metal Servo** was selected. At 6.0V, this servo provides 94.2 N/cm (133 oz/in) at a speed of $20^\circ/\text{sec}$ in 57.5 g (2.1 oz) package. While the power output of this servo may seem like overkill in a static loading, the extra torque provides a factor of safety against dynamic loads. It was decided to use this servo exclusively for the entire aircraft, as the weight differences between other servos were minimal. It also meant that only one type of spare would be needed for the entire aircraft.

5.13 Aircraft Safety

5.13.1 Fuses

In order to comply with the contest rules, a fuse on the motor power line must be used in order to keep currents below 40 amps. This also protects the motor and speed controller from drawing too much current if for some reason the propeller should become jammed. These fuses will be pulled from the aircraft while loading and unloading cargo to disarm the motors (See Fig 5.1)

5.13.2 Data Acquisition System

One of the difficulties of flying an electric powered RPV is monitoring the capacity left in the batteries. Low batteries can result in an airplane losing power suddenly in the air. In order to prevent this, an AstroFlight Whatt meter has been incorporated into the aircraft structure. This device will measure the voltage of the battery pack, the amperage draw and the amount of charge that is left the batteries. By recording the number of mAh that were put into the motor when charging, the capacity left in the batteries can be quickly determined. The ground crew will check this value while changing cargos to determine if there is enough capacity left to perform another sortie. (See Fig 5.1)

5.13.3 Airborne Warning System

In the heat of competition, there may come a time when another flight is attempted without sufficient battery power. To guard against a complete power outage, a strobe light will be fitted to Absolute Toque that will flash when the main battery pack drops below a certain voltage. A comparator circuit will compare the main battery pack voltage to a reference battery. When the pack voltage drops below a preset value of about 0.95 V per cell (experimentation will determine the exact voltage), a xenon strobe light will begin to flash, alerting the pilot that the battery pack is about to drop off, and to land immediately. (See Fig 5.1)

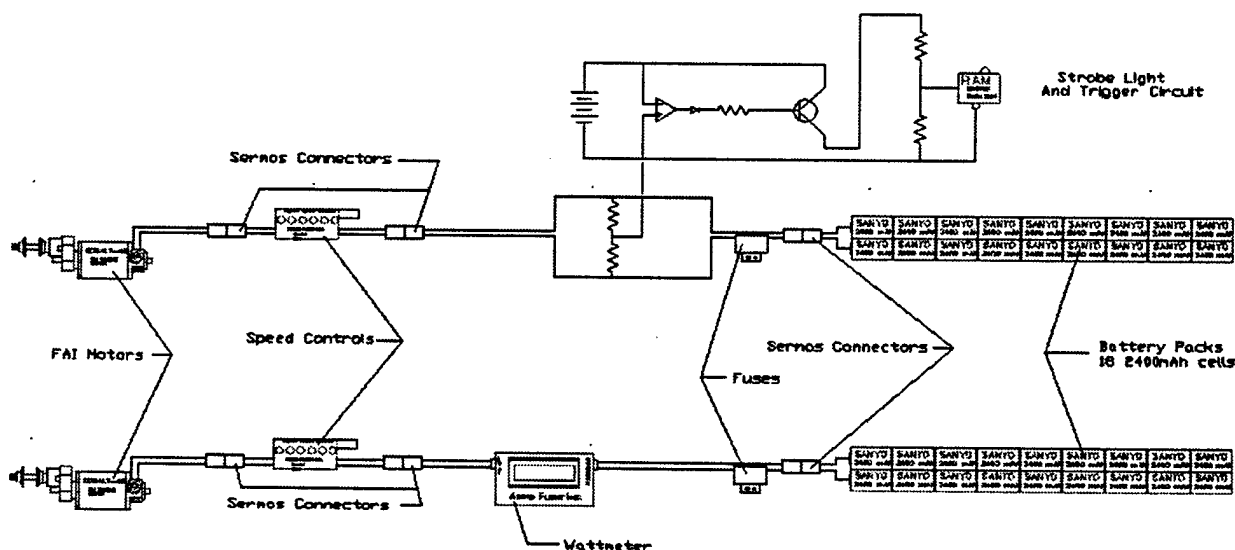
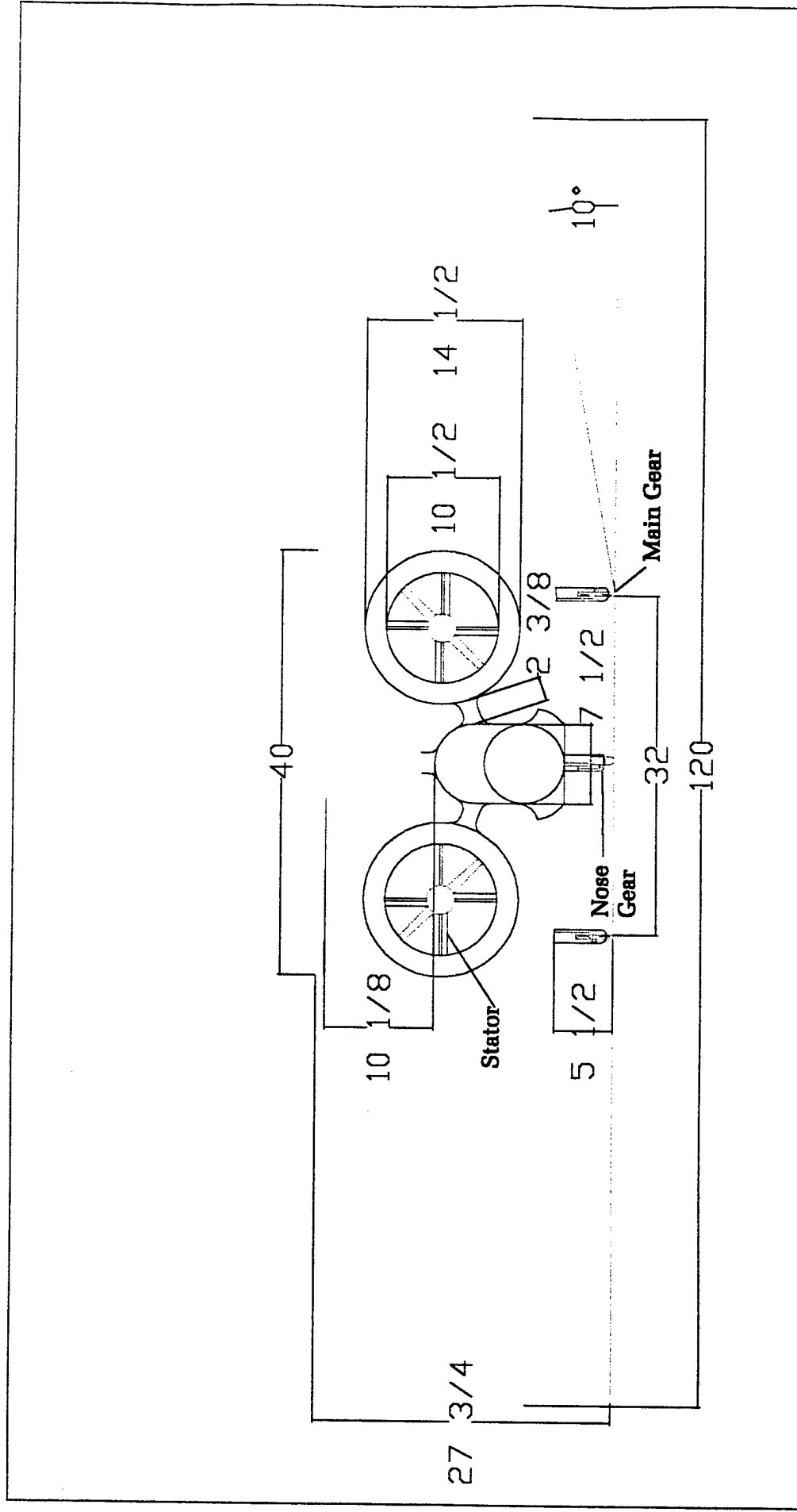
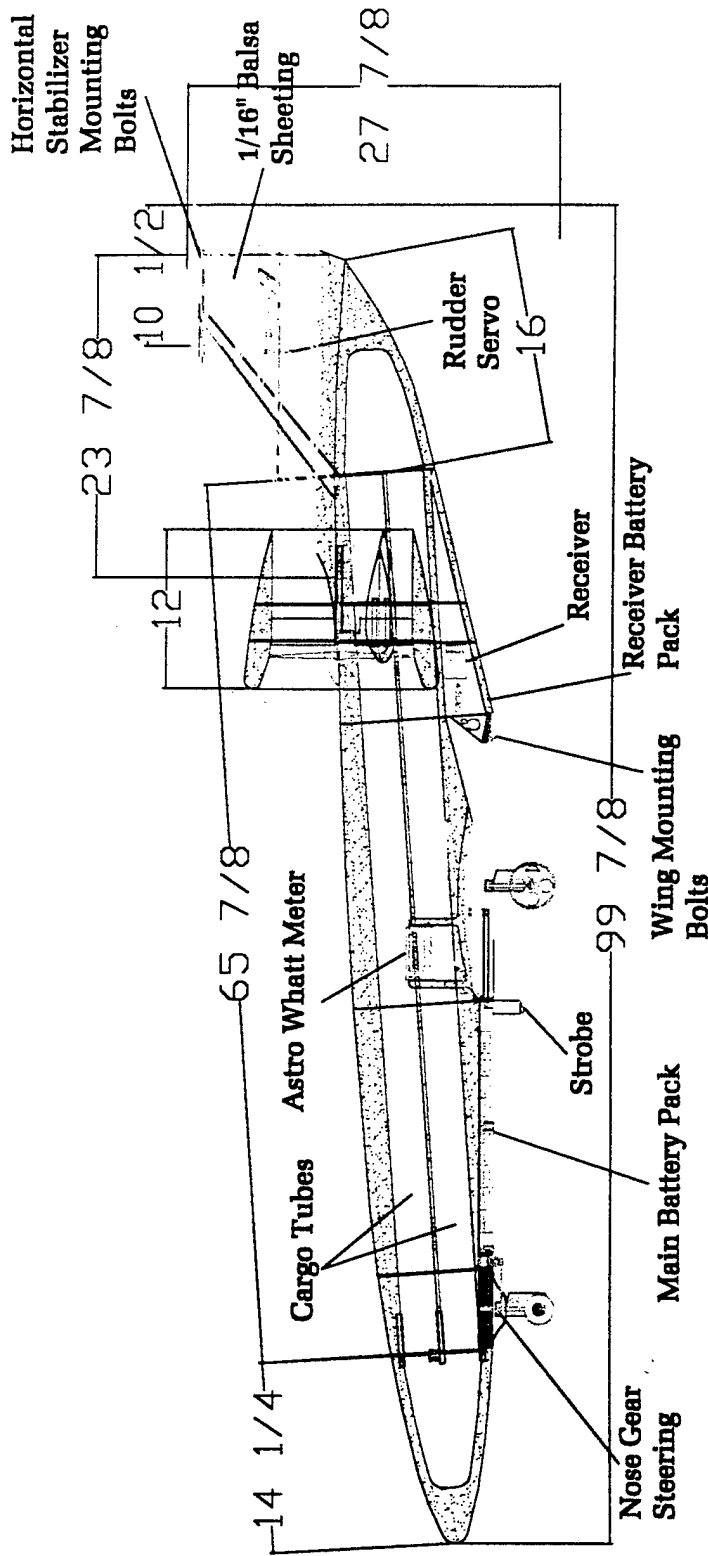


Figure 5.1 Absolute Toque's Wiring Diagram



<i>Absolute Toque</i>	
Queen's Aero Design Team 2000/2001 AIAA D/B/F Competition	
Dimensioned Front View Dimensions are in Inches	

Spruce	Aircraft Plywood
Hardware	White Foam
Carbon Fiber	



Absolute Toque

Queen's Aero Design Team
2000/2001 AIAA D/B/F Competition

Dimensioned Side View

Dimensions are in Inches

Left Side of Fuselage Removed For Clarity

Spruce

Aircraft Plywood
Hardware
White Foam
Carbon Fiber

Absolute Toque

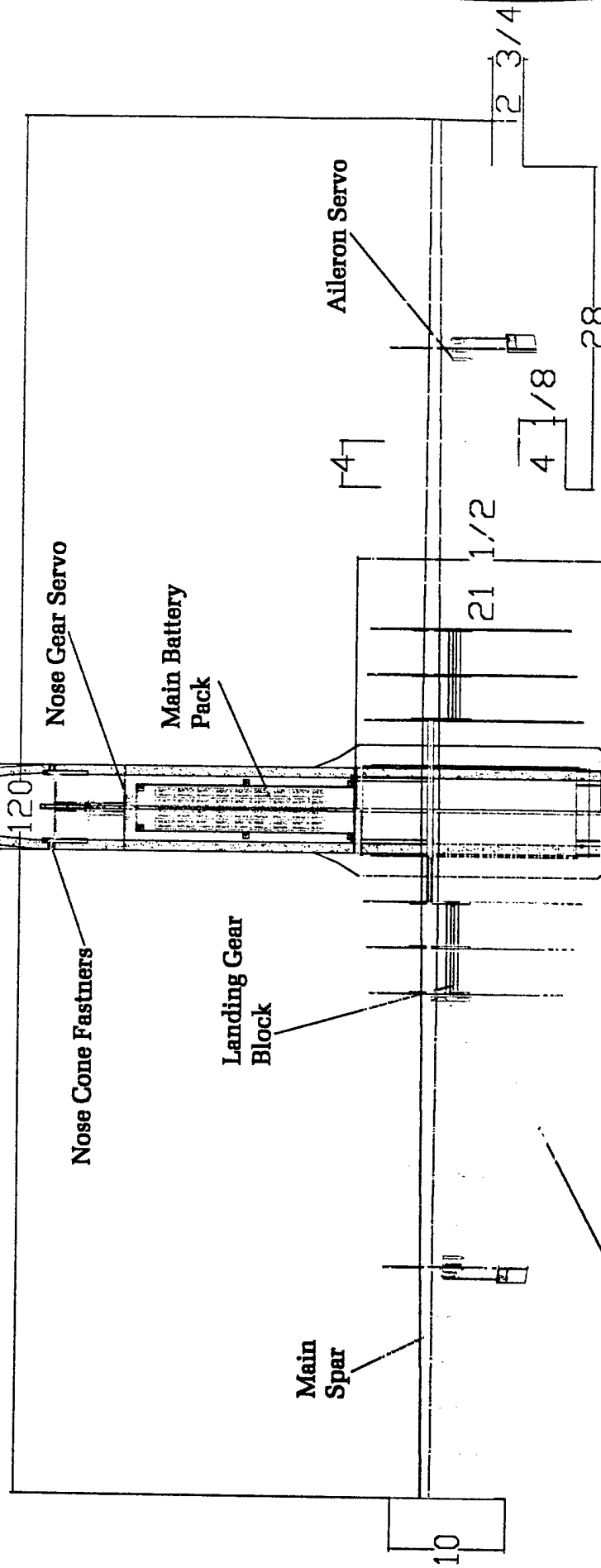
Queen's Aero Design Team
2000/2001 AIAA D/B/F Competition

Dimension Top View

Dimensions are in Inches

Right Hand 1/16" Balsa Sheeting
Removed for Clarity

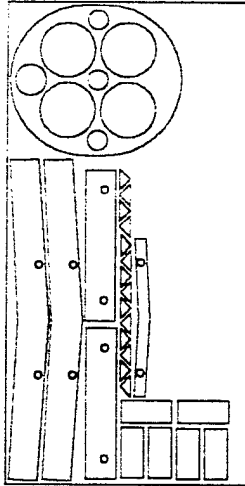
7 1/2



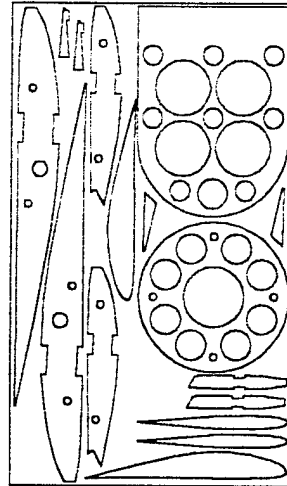
Spruce

Aircraft Plywood
Hardware
White Foam
Carbon Fiber

**1/8"
Aircraft
Ply**

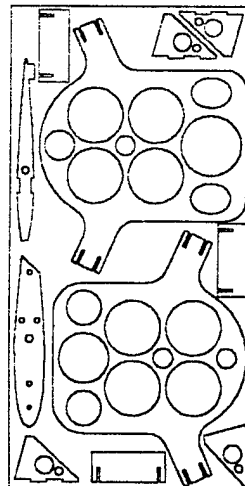


**1/16"
Aircraft
Ply**

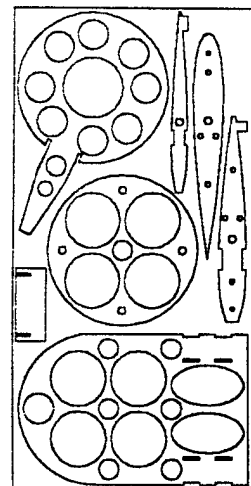


**1/16
Balsa**

**1/8"
Aircraft
Ply**



**1/8"
Aircraft
Ply**



Absolute Toque

Queen's Aero Design Team
2000/2001 AIAA D/B/F Competition

Laser Cut Parts

Aircraft Plywood Formers and Ribs
Balsa Ribs

6.0 Manufacturing Plan

Absolute Toque's design can be broken down into three separate components, each of which employs a different construction technique. Different methods of building the wing, fuselage, and tail appendage were analyzed and the best choices were determined with a figure of merit matrix.

6.1 Wing Construction

6.1.1 Foam and Fiberglass

This technique involves cutting a wing from low density foam using a hot-wire cutting apparatus. The wing cores are then strengthened by the addition of a balsa, spruce or carbon fiber spar. Provision is then made for flap and aileron actuation installation, and then the entire surface is coated with one or two layers of fiberglass or carbon cloth. This results in a structurally strong wing without too much effort. The chief disadvantage of this technique is that the weight can become prohibitive.

6.1.2 Built-up Construction

Built-up construction is the oldest and most traditional form of building a wing; unfortunately, it is also the most time consuming. Ribs are cut in an airfoil shape from thin balsa or aircraft plywood and are then positioned on a jig so that there are 4 to 6 inches between each one. The spars, made of balsa, spruce, carbon fiber, or of some combination, are glued in and a shear web of cross-grained balsa is positioned to form the web of the I-beam structure. Leading and trailing edges are formed by gluing balsa to the front and back of the ribs, and the whole structure is then sanded to ensure a streamlined shape. Thin balsa sheeting is applied from the leading edge back to the spar on both the top and bottom of the wing, forming a strong D-tube structure, which is good in torsion. The whole structure is then covered with a thin plastic film to form a smooth airfoil surface. This technique forms a light, rigid structure.

6.1.3 Carbon Fiber Monocoque

This technique is the most technically demanding of the three choices presented here. An airfoil is drawn up in a 3-D modeling computer program and is transmitted to a computer controlled milling machine. The machine must mill two female molds, one for the top of the wing, the other for the bottom of the wing, from a temperature stable material. The molds are then prepared and pre-impregnated carbon fiber is laid up into the cavity. The mold is then placed under vacuum in an autoclave and baked at approximately 120 degrees Celsius for three hours. Once cooled, the wing halves are released from their molds and are carefully sanded and glued together. This technique requires very complex and expensive facilities, materials, and expertise; however, it results in a very light, strong wing.

6.2 Fuselage Construction

6.2.1 Foam and Fiberglass

This construction technique is something Queen's discovered last year while preparing the tail booms of our '99/00 entries "Obsidian" and "Minnow". A foam block is shaped and hollowed with a hot-wire foam cutter, then a thin layer of fiberglass is applied to the exterior. This structure is tough, light, and produces an excellent surface finish.

6.2.1 Built-up Construction

This form of construction stretches back to the first days of both full-sized and model aircraft flight. Many thin strips of wood (balsa on model planes) connect several wooden formers to produce the fuselage frame. This frame is then covered by doped paper or silk, or in more recent times, by a shrinkable plastic film. This method is labor intensive, yet produces a very light structure. However, this type of structure requires extensive repair after a crash.

6.2.2 Carbon Fiber Monocoque

This technique makes use of expensive composite materials to produce a very strong and lightweight fuselage. A mold of the required fuselage shape is made up of a heat resistant material. Several layers of pre-impregnated carbon fiber are laid up onto the mold, a sheet of thin structural honeycomb (which acts as a shear web for the carbon) is placed into the lay-up, and then more carbon fiber is laid up on top. The assembly is vacuum bagged and then heated until the epoxy cures. This technique requires access to expensive materials, equipment, and expertise, but can produce excellent results. The chief disadvantage is that it is nearly impossible to repair after a mishap, and joining parts can be difficult. The other difficulty in working with this material is that it requires approximately 7 hours to lay up and cure a part, regardless of its size.

6.3 Tail Construction

6.3.1 Foam and Fiberglass

A strong and smooth airfoil can quickly be made by cutting the required shape from medium density foam and then adding a single layer of fiberglass. The fibreglassed surface is then covered by a sheet of thin plastic and the whole assembly is placed in a vacuum until the epoxy has hardened. The plastic sheets can then be peeled away, leaving a perfectly finished tail surface. While this method of construction can result in a perfectly sculpted complex airfoil, it tends to be heavier than the other options available.

6.3.2 Sheet Balsa

By far the easiest way to construct a tail, thick, light sheet balsa can be cut in the required planform shape and then the edges can be rounded with a sanding block. Although the tail does not take a proper streamlined shape, the extra drag is usually accepted for the ease of construction. This method of construction is durable, but is heavy and prone to warping with changes in temperature and humidity.

6.3.3 Built-up Construction

A built-up tail is the lightest, but most fragile option under consideration. Construction is very similar to a built-up wing, with a set of evenly spaced ribs joined by a double spar and shear web, and the leading and trailing edges. Sheeting is sometimes extended right to the trailing edge to give a slight increase in torsional stiffness. The chief disadvantage of this design is that it is very time consuming to construct. Also worth considering is that the tiny balsa structure that makes up a built-up surface is vulnerable to damage, especially on a portion of the plane that is often accidentally banged and knocked during storage and transportation.

6.4 Figure of Merit

To choose the best combination of manufacturing processes for Absolute Toque, a qualitative figure of merit was conceived to evaluate each technique's merits and weaknesses in an easily interpreted chart. Five criteria were selected, weight, structure, time, skill, and expense, and each construction method was given a qualitative score that illustrates its performance in each category. The separate categories are described in detail below.

Weight

In a high performance competition aircraft, flight performance dictates who will win, and who will be defeated, or worse, who will crash. If the aircraft design is effective and well planned out, then building weight is the one element that can seriously affect every aspect of the flight envelope. Where it is reasonable, a builder should always strive to make the components as light and efficient as possible. Thus, this was selected as the first criterion in the FOM.

Strength

Structural failure is expensive and can be dangerous under the wrong conditions. To ensure that the aircraft will be able to withstand the loads experienced in flight and on the ground, structural integrity was chosen as the second criterion in the FOM.

Skill

To produce the required components of the aircraft, the selected construction technique must either be known to the team or it must be easy to learn. Also worth considering is that more experience with the specified building technique produces a more accurate final product and less waste, thus it is desirable to choose methods that are familiar to a larger number of team members. Skill was selected as the third criterion in the FOM.

Expense

Among the various construction techniques discussed, there is a huge difference in cost. This is because some techniques use exotic materials or machining, while the more mundane and traditional techniques make use of the builder's individual skill rather than a complex mould or machine. As Absolute Toque was built with our meager budget in mind, the cheaper option is often worth pursuing due to fiscal necessity. As such, the expense of the construction technique was chosen as the fourth entry into the FOM.

Time

The final item worth considering when evaluating the construction choices is the length of time that the method requires. Absolute Toque was designed and built on a 100% volunteer basis because Queen's does not offer course credit towards participation in a design competition. As all design and construction must be made around the demands of a full engineering course load, time is a precious commodity and was given a place in the FOM.

6.5 Evaluation and Selection

6.5.1 Analytical Method

Each construction technique was evaluated in terms of each of the five criteria listed above. The weight of the method was estimated in ounces. The strength of the method was given a rating on a scale from 0 to 10, with 10 being the most robust choice. The FOM's "skill" category indicates the percentage of team members familiar with the particular construction method. The cost of the method was estimated using a Canadian dollar value with American funds also indicated (\$1.53CDN=\$1.00US). The final entry, time, was given a value of the estimated construction hours required for each method.

Total scores were tabulated with the following equation, which weights the relative importance of each of the criteria.

$$\text{Total} = 80/\text{weight} + \text{strength}/2 + \text{skill}/20 + 200/\text{expense} + 80/\text{time}$$

	Weight (oz)	Strength	Skill	Expense		Time	Total
				Can\$	US\$		
Wing							
Foam and Fiberglass	72	8	90	120	78.43	30	13.94
Built-up Construction	72	5	90	150	98.04	20	14.00
Carbon Fiber Monocoque	64	5	0	3000	1960.78	100	5.37
Fuselage							
Foam and Fiberglass	64	8	90	150	98.04	30	13.75
Built-up Construction	96	5	50	200	130.72	42	8.74
Carbon Fiber Monocoque	72	5	40	2000	1307.19	60	7.04
Tail							
Foam and Fiberglass	20	8	40	6	3.92	5	59.33
Sheet Balsa	24	9	100	6	3.92	3	72.83
Built-up Construction	16	5	90	4	2.61	5	78.00

Table 6.1 Manufacturing Process Evaluation

6.5.2 Selection

The Figure of Merit indicated that built-up construction techniques would be suitable for the flight surfaces (wing and tail), and that a foam and fiberglass composite would be the best choice for the fuselage. The methods we employed during the construction of these components are described below.

6.6 Description of Construction Techniques Employed

6.6.1 Flying Surfaces

Once the Figures of Merit indicated that both the wing and the tail surfaces would utilize built-up construction techniques, work began with drafting software to produce the set of working drawings necessary for this type of construction. In a built-up surface, be it a wing or a vertical fin, the airfoil shape is created by cutting out pieces of balsa wood with the proper profile, which are subsequently known as 'ribs'. The exact shape of the ribs depends on their spacing along the flight surface. This spacing can range from 10cm (4inches) between ribs as on "Absolute Toque's" wing, or can be less for the smaller flight surfaces.

The CAD program must produce a set of outlines, which can then be cut from balsa. While the traditional method involves printing these outlines out, gluing the template to the balsa, and then cutting the piece with a knife, our team was fortunate enough to receive sponsorship in the form of the use of the equipment of a professional laser cutting service. The laser eliminated the inaccuracies created through the printing/gluing/cutting technique, as the balsa can be laser cut directly from the original CAD

drawings. The use of laser cutting also saved the team valuable time, as we were able to spend an hour removing the parts from their stock sheets rather than a week laboring with a razor knife and scroll saw.

Once the ribs are cut, it's time to prepare the spars. The spars are made from a laminate of balsa wood and linear carbon fiber. The carbon fiber is applied in a wet lay-up process over the balsa spar and then vacuum bagged until the epoxy sets. The spars are then trimmed to the correct dimensions and then set aside until required.

The next stage of the wing construction is setting up the ribs. The ribs must be aligned on a pair of threaded rods to ensure that their position and spacing is correct. Each rib is held in place by a washer and nut on each side, with a total of four washers and nuts per rib. This arrangement allows minute adjustments to be made before any glue is applied, but can still be removed once the wing has enough structure in place to support its own weight.

With the ribs in place, the bottom spar is glued into its prepared position. The shear webs (their task is to act like the web of an I-beam) are then prepared and glued in their position between the ribs. It's this step where having a rib spacing of 10cm (4inches) becomes important. Balsa is sold in either 7.62cm (3inch) or 10cm (4inch) widths. By spacing the ribs accordingly, time can be saved by not having to trim each shear web. Weight can be saved at this stage by tapering the shear webs' width to account for the reduced loading conditions at the wing tips.

Once the shear webs have been installed, the top spar can be glued in place. This forms the final section of the wing's I beam, and the increase in wing rigidity is apparent as soon as it is in place. The leading and trailing edges are then glued in place, increasing the torsional rigidity of the unfinished wing until the wing sheeting can be installed. The threaded rods of the wing jig are removed, and the resulting wing panel can be handled to install servo mounts, hinge points, landing gear mounts and wing dowels.

One innovation developed by Queen's this year involves the trailing edge of the flight surfaces. Having these surfaces taper back to a razor sharp trailing edge reduces the drag of the structure, but they are very hard to build in this fashion with conventional techniques. To remedy this, a layer of thick fiberglass was laid up between two sheets of balsa wood. When the assembly was cured, a piece suitable for the trailing edge was cut out and then glued in place on the wing or tail structure. The balsa allowed a good glue bond to be made with the structure at the front of the trailing edge yet could be progressively sanded away until there was only the thin layer of cured fiberglass at the rear edge of the wing. This results in a very straight, strong, and streamlined trailing edge.

"Absolute Toque" features a wing built with 6 degrees of dihedral to improve the aircraft's stability. Once the required wing hardware is installed, the left and right wing panels are joined with the aid of a specifically designed wing brace at the spars made from aircraft plywood. The assembly is then wrapped in carbon fiber for strength and left to cure.

The newly joined wing is now ready to be sheeted. 1/16" balsa sheet is glued from the leading edge to the top and bottom spar, producing a "D-tube" wing structure. This structure gives the wing its required torsional rigidity and helps to maintain the wing's proper airfoil profile in flight. The center section of the

wing is fiber-glassed at this point to help ensure that the wing joint retains the strength for the required mission profile.

Once the fiberglass has cured, the wing is filled and sanded to prepare for covering. Servomotors are installed in their bays, wired, and tested. The wing is then covered with a self-adhesive heat-shrinkable Mylar, which protects the balsa structure as well as bridging the open bays between ribs. Other than the installation of the control surfaces, covering is the final stage in constructing a built-up flight surface.

6.6.2 Fuselage Construction

The construction of the foam/fiberglass composite used for Absolute Toque's fuselage begins by splitting up the solid model created in a 3D-modelling program into manageable sections. The cross-sections at these points are printed out, glued onto Formica material, and then cut out with a scroll saw to form templates to be used with a hot-wire foam cutter. The team then cuts out and glues up several sheets of "white" foam into blocks from which the various segments of the fuselage can be cut.

Once the glue is dry, the templates are affixed to their correct location on the foam blocks, and then the fuselage sections are cut out with the hot-wire foam cutter. This device is nothing more than a piece of thin wire stretched on a frame, with 6 volts running through it to heat the wire. The wire reaches temperatures hot enough to melt its way through a foam block, and the use of templates permits virtually any shape to be cut in this fashion.

The fuselage segments are then glued together to permit some rough sanding of the various profiles to be done. When the rough profile has been settled on, the segments are separated (the use of a mild adhesive allows this), and plywood bulkheads are glued in between the blocks where necessary. The plywood bulkheads allow hard points such as the wing and shroud pylon to be secured to the fuselage.

When the fuselage has been assembled again, the motor mounts, wing hold-downs, battery tray, nose gear, and fuse block are installed and faired into the structure where appropriate (smaller pieces of white foam are used for this). The whole structure is filled with lightweight filler and sanded to prepare for the fiberglass.

The fiberglass is applied in pieces as large as possible to reduce the number of seams that must be dealt with later. A high grade finishing epoxy is used, and various pigments can be added at this point to provide color to the final fuselage. Black carbon is used for "Absolute Toque". The fiberglass must be left for two days to dry before sanding.

Once dry, the fuselage is sanded with a medium grit sandpaper. Care must be taken to not penetrate the fiberglass layer as this would create a weak spot in the fuselage's stressed skin. A second layer of thinned epoxy can be added after this sanding to ensure that the weave of the fiberglass cloth is filled, resulting in a smooth surface. The assembly is left for another two days to cure.

Once cured, the whole fuselage is wet sanded with 400 and 600-grit sandpaper. The resulting surface is then waxed with a high-grade paste wax and then buffed to a shine.

6.6.3 Shroud Construction

The construction of the shrouds on "Absolute Toque" required some thought to ensure that the finished product would be able to withstand the forces on them during flight. The initial step is to build a motor mount that can also house the speed control. Although milled aluminum was considered for this portion of the shroud, manufacturing the aluminum to fit the elliptical casing of the motor proved to be beyond the capabilities of our team. As a second choice, several layers of fiberglass was formed around the motor itself, with waxed paper ensuring that the motor could be removed from the cured fiberglass.

The next step is to construct the outer part of the shroud unit. Using templates and the hot-wire foam cutter as was done for the fuselage, a ring is cut from a suitably prepared foam block. The resulting ring is hand-sanded with specially shaped sanding blocks until it is formed to the required airfoil profile. The ring airfoil is then cut for the addition of plywood rings, which serve as a hard point for the attachment of the shrouds to the fuselage pylons.

The next step is to make up the shroud's stator vanes. These are cut from foam and then fiber-glassed with a heavy cloth to ensure that they do not flex under load. It would be disastrous to have the motor move relative to the outer shroud as this would permit the rotor to touch the inside of its race, ruining the shroud unit.

Once the stators have dried and have been sanded, they are securely fastened to the motor mount with epoxy and strips of fiberglass cloth. Care must be taken to ensure that the alignment of the stator vanes relative to the propeller position and subsequent airflow is maintained throughout the gluing process.

This assembly is then affixed to the inside of the foam ring, and the entire shroud is fiber-glassed to maintain structural integrity. After a wet sanding, the motor and speed control can be installed and the shroud unit can be attached to the motor pylons on the fuselage.

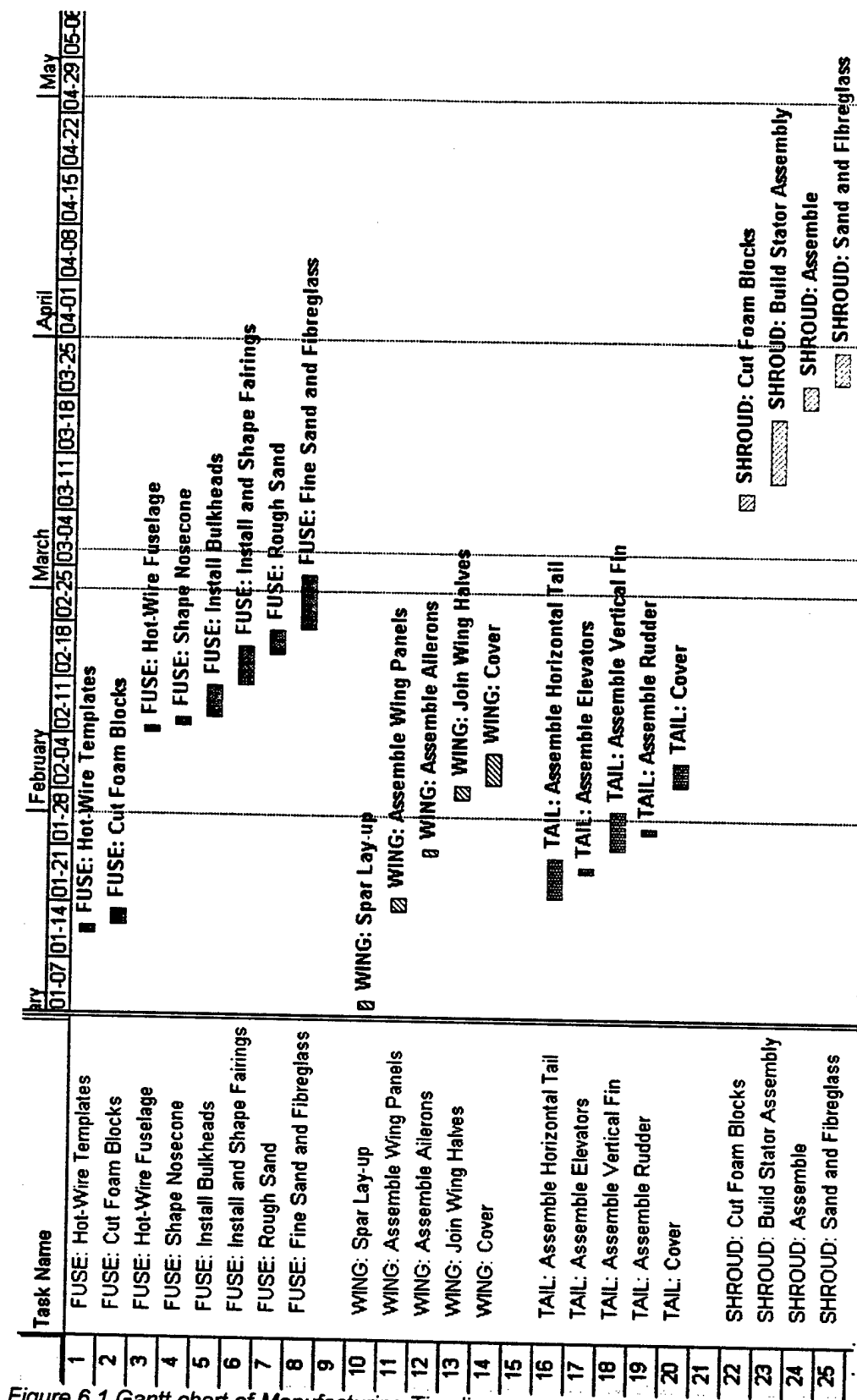


Figure 6.1 Gantt chart of Manufacturing Timeline

References

1. Eppler, Richard. Airfoil Design and Data. Springer-Verlag: Germany. 1990.
2. Easton, Matt; McCracken, David; Splinter, Joe; Young, Dave. "*Design of a Variable Geometry Propeller Shroud*" Undergraduate Design Project, Department of Mechanical Engineering. December, 2000.
3. Foster, Steve. "*Undercarriage Design for Queen's Cargo Aircraft*." Undergraduate Thesis Project, Department of Mechanical Engineering. March, 1994.
4. Horton, Johanna Lisa. "*Cargo Aircraft Stability Analysis*." Undergraduate Thesis Project, Department of Mathematics and Engineering. April, 1993.
5. McCormick, Barnes. Aerodynamics, Aeronautics, and Flight Mechanics, second edition. John Wiley & Sons, Inc.: New York. 1995.
6. Munson, Young, and Okiishi. Fundamentals of Fluid Mechanics, second edition. John Wiley & Sons, Inc.: New York. 1994.
7. Raymer, Daniel. Aircraft Design: A Conceptual Approach. AIAA Education Series. American Institute of Aeronautics and Astronautics, Inc.: Washington, D.C. 1989.
8. Abbott, Ira. Theory of Wing Sections. McGraw-Hill Book Company Inc.: Toronto. 1949.
9. White, Frank M. Fluid Mechanics, 4th Edition. McGraw-Hill Book Company Inc.: Toronto. 1999.
10. Lennon, Andy. Basics of R/C Model Aircraft Design. Y. DeFrancesco: Ridgefield, CT. 1999.

2001 AIAA DBF Competition Design Report

— *Addendum Phase* —



Queen's University at Kingston

"Absolute Toque"

Department of Mechanical Engineering

Department of Engineering Physics

April 10, 2001

List of Nomenclature.....	2
1.0 Executive Summary.....	3
1.1 Major Development Areas	3
1.2 Design Tool Overview	4
2.0 Management Summary	5
2.1 Personnel and Configuration	5
2.2 Scheduling.....	6
3.0 Conceptual Design	8
3.1 Initial Figure of Merit	8
3.2 Examined Designs	10
3.3 Screening the Three Designs.....	11
3.4 Analysis of the "Prototype"	11
3.5 "Absolute Toque"	12
3.6 Shrouds	12
3.7 Design Summary	13
4.0 Preliminary Design	15
4.1 Take-off Gross Weight (TOGW) Estimation	15
4.2 Propulsion Systems Selection.....	15
4.3 Wing Area and Airfoil Selection	17
4.4 Aspect Ratio.....	19
4.5 Wing Platform	19
4.6 Horizontal Stabilizer Sizing	19
4.7 Vertical Stabilizer Sizing	20
4.8 Fuselage Design and Sizing	21
5.0 Detail Design	24
5.1 Weights.....	24
5.2 Payload Fraction.....	25
5.3 Drag.....	25
5.4 Wing Sizing and Performance.....	26
5.5 Tail Sizing and Performance	27
5.6 Propulsion	28
5.7 G-Loading.....	29
5.8 Take-off Performance	30
5.9 Endurance and Range	31
5.10 Shrouds	32
5.11 Stability.....	33
5.12 Control Systems.....	35
6.0 Manufacturing Plan	41
6.1 Wing Construction.....	41
6.2 Fuselage Construction.....	42
6.3 Tail Construction.....	42
6.4 Figure of Merit	43
6.5 Evaluation and Selection.....	44
6.6 Description of Construction Techniques Employed	45
References	50
7.0 Lessons Learned.....	52
7.1 Changes From the Proposal.....	52
7.2 Next Generation Improvements.....	55
8.0 Aircraft Cost.....	58
8.1 Final Score Equation.....	58
8.2 Rated Aircraft Cost.....	59

7.0 Lessons Learned

7.1 Changes From the Proposal

Throughout the construction stage of "Absolute Toque" several design changes were required in order to improve the final performance of the aircraft. Most of these design changes were quite minor, as the detailed CAD drawings minimized part interference and improved fit of components.

7.1.1 Wing

The precision of the laser cut parts meant that wing construction proceeded very smoothly. Nylon wing-tip skids were added to prevent the wing's covering from being scuffed or torn.

7.1.2 Horizontal Stabilizer

The horizontal stabilizer was built very early in the construction phase, before servos had been bought. It had been originally designed to have the servos completely internal to the structure, but this proved very difficult to do while building, as the stabilizer is quite thin. As such, the servo body sticks out slightly into the air stream. The servo is flush with the surface at the spar, but sticks out 2 mm (0.08 in) at the sub trailing edge where the elevator is hinged. This protrusion, while minimal, was not called for in the plans and slightly increases drag.

7.1.3 Vertical Stabilizer

Because the hinge line of the rudder is swept, deflection caused the rudder to interfere with the fuselage and horizontal tail, due to the rudder thickness. To remedy this, the top and bottom of the rudder were sanded at an angle (thickness wise) to allow increased deflection without increasing the gap.

7.1.4 Fuselage

No structural airframe changes were made during the construction phase to the fuselage. However, the receiver battery was moved to behind the forward wing hold down former in order to help achieve the correct aircraft balance. Also, a nylon skid was placed at the rear of the fuselage to protect the fiberglass in the case of over-rotation.

7.1.5 Undercarriage

The nose gear was changed from 2.25 inches in diameter to 2.5 inches due to availability.

7.1.6 Shrouds

The most significant design change occurred with the shrouds. Originally the shrouds were design to accommodate a 0.267 m (10.5 in) rotor. This diameter was chosen based on the ElectriCalc (commercial

software) prediction that a 0.267 m (10.5 in) propeller on a geared 5-turn AstroFlight FAI 40's would draw 42 Amps at full throttle. The 0.267 m (10.5 in) inner diameter shrouds were built before motor testing, as the motors had not been retimed for gearbox operation yet. Upon retiming the motors, a problem emerged. The motors drew 46 Amps on only a 9x6 propeller (un-shrouded) at full throttle, much higher than ElectriCalc predictions. After checking ElectriCalc again, it was noted that the predicted performance of the 4-turn AstroFlight FAI 40 motors closely matched the actual performance of our motors. The motors were checked for the number of windings and confirmed to be the 5-turn motors that we had expected. At this stage in development, and after having already purchased 3 motors, it was decided nothing else could be done other than to reduce the shroud diameter.

The shroud inside diameter was reduced to 0.203 m (8.0 in) to accommodate a cut down 0.228 m (9.0 in) propeller. The smaller diameter rotor allowed a thinner ring airfoil to be used while still maintaining a lip radius of 6% the rotor diameter. The maximum ring airfoil thickness was reduced from 0.051 m (2.0 in) to 0.038 m (1.5 in). A new shroud airfoil cross section was also employed in order to further prevent separation. In the old shrouds, a straight taper from the leading edge to the trailing edge was used. The new shrouds have a gradually increasing taper from leading edge to trailing edge. The new shrouds are also 0.051 m (2.0 in) longer in order to reduce the taper angle.

White foam was used exclusively in the construction of the original shrouds due to its low density. Unfortunately, the foam's mechanical properties became a problem at the trailing edge of the shroud where the thickness became very thin, and resulted in a jagged trailing edge. To prevent this on the new shrouds, a layer of pink foam was used at the trailing edge. This foam is much stronger than white foam and allowed for a smooth trailing edge with minimal weight gain.

The new shrouds will undergo further testing to determine their effectiveness, but initial results seem to show an increase in static thrust. The low-pressure area around the leading edge lip can be easily felt with a finger.

It is interesting to note that the spread sheet developed in the undergraduate thesis project for shroud propulsion predicted that a 0.21 m (8.25 in) inner diameter shroud be used, based on momentum and vortex theory and a power input of 700 watts (as achieved from the AstroFlight FAI 40s).

7.1.7 Weight

During construction, every attempt was made to reduce weight as much as possible. Even so, the actual aircraft weight is more than that predicted in the design phase. Table 7.1 provides a break down of the airframe weight, comparing predicted weight to actual weight.

Component	Predicted Weight (N)	Predicted Weight (lbs)	Actual Weight (N)	Actual Weight (lbs)
Tennis Ball	55.6	12.5	55.6	12.5
Steel Block	26.7	6.00	26.7	6.00
Battery Pack	22.2	5.00	21.8	4.90
Receiver	0.556	0.125	0.556	0.125
Servos	3.34	0.750	3.34	0.750
Landing Gear	2.225	0.50	3.34	0.750
Wheels	1.67	0.375	1.67	0.375
Wing	14.5	3.25	18.1	4.06
Tail	5.57	1.25	6.68	1.50
Fuselage	15.6	3.50	22.2	5.00
Motors	6.12	1.375	6.12	1.375
Speed Controllers	0.667	0.150	0.667	0.150
Gear Boxes	0.834	0.188	0.834	0.188
Shrouds	3.98	0.884	6.68	1.50
Receiver Battery	0.812	0.183	1.11	0.250
Hardware	1.11	0.250	1.11	0.250
Props	1.11	0.250	1.11	0.250
Take Off Gross Weight With Tennis Balls (Actual)			151	33.9
Take Off Gross Weight With Steel (Actual)			122	27.4
Empty Flying Weight (Actual)			95.3	21.4
Airframe Weight (Actual)			73.5	16.5

Table 7.1 Predicted Weight compared to actual airframe weight. Differences in Blue.

It is evident that the increase in weight is due mainly to the wing and fuselage structures. During the preliminary design phase, the weight of the covering on the wing was neglected. This alone accounts for nearly 2.23 N (0.5 lbs) of the increased wing weight. The fuselage predicted weight, being a new method of construction, was a considerable underestimate. The fuselage weight was initially estimated based on crude volume and surface area measurements and appropriate material densities. The shrouds were also estimated in the same way and were again severely under estimated. Unfortunately, this technique did not account for the additional glue and filler added in construction and can be considered inaccurate in dealing with hand applied, wet lay-up fiberglass. During construction it was felt that there was very little material that could be removed from the structure to reduce weight while still maintaining structural rigidity. The data gained in terms of weight measurements will prove useful in future designs utilizing this construction method.

7.1.9 Performance

The increased takeoff weight has the detrimental effect of reducing performance. In order to determine if "Absolute Toque" would still accomplish the mission sortie, performance predictions were re-calculated with the increased takeoff weight. Table 7.2 provides a summary of predicted performance changes between the proposal aircraft and the actual aircraft.

Performance Feature	Proposal		Actual	
TOGW	135 N	30.4 lbs	151 N	33.9 lbs
Velocity for Minimum Drag	16.9 m/s	37.7 mph	17.8 m/s	39.9 mph
Thrust for Minimum Drag	8.93 N	2.01 lbf	9.46 N	2.24 lbf
Stabilizer Incidence	0.200 °		0.010 °	
Wing Incidence	2.10 °		2.73 °	
Spar Safety Factor (4G load)	1.63		1.46	
Stall Velocity	12.8 m/s	27.2 mph	13.5 m/s	28.7 mph
Range	20.5 km	12.8 mi	17.9 km	11.1 mi
Endurance	23.3 min		19.2 min	
Turning Radius	19.9 m	65.1 ft	22.6 m	74.4 ft
Accelerate Stall G Loading	2.56		2.25	
Take Off Distance	34.5 m	113 ft	43.2 m	142 ft
Climb Out Angle	13.4 °		11.5 °	
Wing Loading	1300 g/dec ²	44.2 oz/ft ²	1165 g/dec	39.7 oz/ft ²

Table 7.2 Predicted Performance Changes due to Increased TOGW.

The decrease in performance, while unfortunate, does not reduce the performance to a level where the mission sortie is compromised. Flight tests will prove if less cargo weight needs to be carried to offset the increased airframe weight.

7.2 Next Generation Improvements

7.2.1 Design Improvements

There are several areas of "Absolute Toque's" design that can be improved upon in a next generation design in order to further increase its competitiveness. It should be noted that "Absolute Toque" is a second-generation design based on the "Prototype" that was designed and built earlier this year. Many major design changes were made between these two designs, including different wing placement, fuselage cargo layout and undercarriage design. Even with this previous refinement, the team has still found several areas that would improve upon "Absolute Toque's" design.

- The weight estimation was too optimistic. While still substantially less than the "Prototype", the actual weight of "Absolute Toque" was off by 11.5% from what was thought to be a conservative preliminary estimate. Had this weight been accounted for in the preliminary design, modifications could have been done to improve the aircraft's performance. In a third generation design, a higher TOGW than that predicted by volume and density measurements should be accounted for. This would lead to a slightly larger wing and tail area.
- The undercarriage can be improved through replacing the wire torsion bar gear with working Oleo struts. Unfortunately, preliminary budget estimates ruled out the purchase of commercial units. It was too late in the construction phase to change to Oleo struts after additional funding had been secured. Due to the large number of what can be considered less than graceful landings, it is

thought that a trailing link design would provide the most robust gear. Several commercial gear sets, such as those used on large radio controlled jets, are available for this application.

- The motors used generate considerable heat when being pushed to their limits. This can reduce their performance and seriously damage the motors if they are subjected to these conditions for any length of time. In order to remove heat from the motors, an aluminum motor mount should be used. An full aluminum motor mount was to be used on "Absolute Toque", but the elliptical housing on the AstroFlight FAI 40 made the mount too difficult to machine. Very close tolerances must be maintained for effective heat transfer through the contact area, even when heat transfer grease is used. A fiberglass mount was used during actual construction which provided the tight fitting, rigid mount needed for a shrouded propeller. While effective at holding the motor, it covers the outer casing, reducing forced convection over the motor.
- The speed control mounts behind the motor and is supported out in the open on two beams. This is a less than ideal situation as it creates turbulence, reducing the effectiveness of the shroud. For "Absolute Toque", proper cooling was considered more important than reducing this turbulence. However, with careful design, a pod casing for the speed control could have been made which both increases heat transfer by directly channeling flow over the speed controller and reducing turbulence in the wake.
- The horizontal stabilizer should be slightly increased in thickness in order to allow the elevator servos to remain completely enclosed within the structure, reducing drag.
- More room needs to be created within the fuselage to allow components to be moved. This would allow the center of gravity to be easily moved by shifting components and not by adding nose or tail weight.

The time and cost to implement these improvements was estimated and the results are shown in the summary table below.

Improvement	Time (hrs)	Cost (\$ US)	Comments
Weight Savings	10	100	Time need to thoroughly evaluate all areas of the design to reduce airframe weight.
Undercarriage	2	300	Oleo struts are expensive, but require little time over a regular gear to install.
Motor Mounts	12	50	Takes considerable time for the actual design, drawings and creation of tool paths. Actually machining time would be about an hour per mount. Using shop facilities within the University, the only cost is for materials.
Speed Controller Pod	6	20	Testing of several fiberglass pods would require some time, but costs would be negligible.
Thicker Stabilizer	0	0	This requires no additional time or money over the previous stabilizer.
Room to Balance Aircraft	3	0	During the design stage, extra time should be taken to find more room within the airframe where components can be move in order to shift the center of gravity.
TOTAL	33 hrs	\$ 470	The total cost to implement these changes is quite high but possible with increased fundraising. The additional man hours to implement the changes is small if it can be spread throughout the entire school year.

Table 7.3. Time and Cost to Implement Design Improvements.

7.2.2 Manufacturing Improvements.

Improvements in manufacturing practices can greatly improve the accuracy and performance of the aircraft being built. Several areas of improvements within in the manufacturing process were noted throughout the construction of "Absolute Toque" which should be implemented in the next generation design.

- A 10-foot long, perfectly flat building surface is of prime importance for improving the accuracy of all aspects of construction. It would allow the wing, fuselage and tail to be built warp free.
- The wing jig currently used requires washers and nuts to be threaded onto a long steel rod to position the ribs in place. By replacing the nuts with large wheel collars and the threaded rod with a smooth one, the time to construct the wing would be greatly reduced.
- Reduce airframe weight wherever possible. It is often easy to say that "an ounce will not affect a 30 lb airplane", but these ounces quickly add up. An attitude must be developed where every component is looked at for possible ways to reduce its weight. This attitude was adopted during the construction of "Absolute Toque", but there is definitely room for improvement.
- The use of an epoxy thinner may have been able to reduce the weight of the fiberglassed fuselage. It was noted that while the finishing epoxy had an hour-long pot life, it would slowly begin to thicken after approximately 20 minutes.

- The use of a proper incidence meter to align the wing and horizontal stabilizer at the right incidence would reduce trim drag.
- Laser cutting greatly increased the accuracy of construction. Approximately 90% of the wood pieces within the aircraft were cut by laser. The goal should be to have accurate enough drawings so that 99% of the wood can be laser cut. Not only does this increase accuracy, it also reduces weight (allows increased use of lightening holes) and reduces the number of hours to construct the airframe.
- Only two-dimensional detailed drawings were drawn this year. While they were more than adequate for the construction of the aircraft, a three-dimensional rendering of the model would prove very useful in certain area of the design. Unfortunately due to the complex compound curves present on "Absolute Toque", a model of any accuracy could not be developed with our available software. A detailed solid model would allow accurate weight estimates and check for part fit. Moments of inertia could also be found for use in stability analysis.

These manufacturing improvements require very little money to implement and would greatly improve the precision of the final aircraft.

8.0 Aircraft Cost

8.1 Final Score Equation

The final score for each team is a combination of the Report Score, Total Flight Score and the Rated Aircraft Cost. The Report score is a mark between 1 and 100 representing the quality of report submitted. The Total Flight Score is the sum of the number of pounds of payload carried during three sorties. The Rated Aircraft Cost is a model used to determine the cost of the aircraft based on its size, power and complexity. Its purpose is to drive teams to create efficient and innovative aircraft designs. The relationship between these three scores is given by the equation below:

$$SCORE = \frac{\text{Written Report Score} * \text{Total Flight Score}}{\text{Rated Aircraft Cost}}$$

From the above equation it is evident that to obtain highest overall score, the Written Report and Total Flight Score must be maximized while the Rated Aircraft Cost is minimized. The Report Score has little to do with the actual design of the aircraft (provided that there is some innovation with the design). Thus it is important to look at Total Flight Score and the Rated Aircraft Cost, which are closely related. As determined during the conceptual design phase, the larger the payload capacity, the higher the Total Flight Score and the higher the Rated Aircraft Cost (due to increased airframe size). "Absolute Toque" attempts to carry the maximum payload with the lowest rated aircraft cost.

8.2 Rated Aircraft Cost

The Rated Aircraft Cost is a model to approximate the cost of the aircraft in dollars. It provides a way to compare the different design costs within the competition, as each team will undoubtedly have different procurement costs. The Rated Aircraft Cost is given by the formula below, with the variables being described in subsequent sections.

$$\text{Rated Aircraft Cost, \$ (Thousands)} = (A * \text{MEW} + B * \text{REP} + C * \text{MFHR}) / 1000$$

8.2.1 Manufactures Empty Weight (MEW)

The Manufactures Empty Weight is the weight of the aircraft in pounds without the batteries or payload. In order to convert this weight to a dollar value, the coefficient "A", which has a value of \$100, is multiplied with the MEW. Thus for every pound of airframe weight, the Rated Aircraft Cost increases by 0.1. The Manufactures Empty Weight of "Absolute Toque" is 16.5 lbs.

8.2.2 Rated Engine Power (REP)

The Rated Engine Power is the number of watts produced by the aircraft's propulsion system. Because the power output is dependent on the motor size, motor load, cell make, cell count, and the throttle setting, an equation is used to provide a simple measure of the power available. This is given by the equation:

$$\text{REP} = \# \text{ engines} * \text{Amp} * 1.2 \text{ V/cell} * \# \text{ cells.}$$

"Absolute Toque" has two independent power systems with each motor running on 18 cells and using a 40 Amp inline fuse. Thus the REP is calculated for each motor and then added together. The REP was calculated to be:

$$\text{REP} = 1 * 40 \text{ Amps} * 1.2 \text{ V/cell} * 18 \text{ cells} + 1 * 40 \text{ Amps} * 1.2 \text{ V/cell} * 18 \text{ cells} = 1728 \text{ watts}$$

The REP is then multiplied by the coefficient "B", which has the value of 1\$ per watt.

8.2.3. Manufacturing Man Hours (MFHR)

The Manufacturing Man Hours value is used to approximate the number of hours it takes to construct the airframe based on its size and complexity. The MFHR is broken down into several sections as dictated by the Work Break Down Structure (WBS). The sum from all the hours from the WBS is the total MFHR. The coefficient "C" is used to assign the value of \$20 per manufacturing hour.

WBS	Assigned Hours	Aircraft Dependant Parameter	Hours Subtotal
1. Wings	15 hr / wing	1 wing	15
	4 hr / ft ² wing area	12.2 ft ² wing area	48.8
	2 hr / strut or brace	0 struts or braces	0
	3 hr / control surface	2 control surfaces	6
WBS Wing Total			69.8
2. Fuselage / Pods	5 hr / body	1 fuselage, 2 shrouds	15
	4 hr / ft of length	9.67 ft total length	38.7
WBS Fuselage/ Pod Total			53.7
3. Empennage	5 hr basic	1 empennage	5
	5 hr / vertical surface	1 vertical surface	5
	10 hr / horizontal surface	1 horizontal surface	10
WBS Empennage Total			20
4. Flight Systems	5 hr basic	1 control system	5
	2 hr / servo or controller	6 servos, 2 motor controllers	16
WBS Flight Systems Total			21
5. Propulsions System	5 hr / motor	2 motors	10
	5 hr / propeller	2 propellers	10
WBS Propulsions Systems Total			20
TOTAL MHFR			184.5

8.2.4. Final Value

The Total Rated Aircraft Cost for "Absolute Toque" was calculated to be:

$$\text{Rated Aircraft Cost, \$ (Thousands)} = (\$100/\text{lbs} \times 16.5 \text{ lbs} + \$1/\text{watt} \times 1728 \text{ watts} + \$20/\text{hr} \times 184.5 \text{ hrs}) / 1000$$

$$\text{Rated Aircraft Cost, \$ (Thousands)} = 7.07$$

This value, which is high compared to aircraft in last year's competition, is due to the increase in size needed to be competitive this year.

THE CITY COLLEGE OF NEW YORK



CITY HAWK

PROPOSAL PHASE REPORT

DESIGN, BUILD & FLY COMPETITION
AMERICAN INSTITUTE OF AERONAUTICS AND ASTRONAUTICS

TABLE OF CONTENTS

EXECUTIVE SUMMARY	3
MANAGEMENT SUMMARY	4
CONCEPTUAL DESIGN REPORT	
1. Introduction	5
2. General Anatomy of the fuselage	5
3. Airfoil Selection	8
4. Rated Aircraft Cost	9
5. Conceptual Design Configuration	10
 PRELIMINARY DESIGN REPORT	 11
1. Wing	11
2. Enpanage	12
3. Fuselage	14
4. Center of gravity	14
5. General Aerodynamic Characteristics	15
 DETAIL DESIGN	 28
1. Fuselage Design	29
2. Power Plant	30
 MANUFACTURING PLAN	 33
1. Preliminary wing	33
2. Wing Stand	34
3. Prototype Wing	34
4. Fuselage	35
5. Landing Gear	35
6. Finite Element analysis	36
 FINAL AIRPLANE CONFIGURATION AND DRAWING PACKAGE	 40
 REFERENCES	 44

Executive Summary

Our chosen airplane configuration for carrying out the specific tasks is a monoplane, propelled by a single electrically driven engine. Aerodynamic design is a balancing act between lift and drag and other vector forces involved (i.e. thrust). Therefore, the aerodynamic characteristics of the aero structure are based on the design of the wing, the fuselage, the ailerons, elevators, rudders as well as landing gear. The most important aerodynamic characteristics are the coefficient of lift and the coefficient of drag. We know that most of the drag. We know that most of the lift is determined by the wing configuration. Moreover, one must be extremely careful as to choose the proper airfoil profile. The correct airfoil profile should optimize the lift without inducing a considerable amount of drag. In addition, the designer must choose the proper profile and cross section for the fuselage. The fuselage will tend to produce an increase in drag. We optimize lift, and maneuverability while inducing minimum drag. The same methodology applies to the ailerons, rudders and elevators.

Since the correct selection of the wing depends on its profile. A careful analysis and comparison was performed among a *family* of airfoil profiles. Our selected profiles come from the NACA (4 digit) family of airfoils. The analysis was performed in Sub-3D. This aerodynamic software helps to approximate the aerodynamic properties of the airfoils. The quantities that we are mainly concerned with are the coefficient of lift and the coefficient of drag. The airfoil chosen based on its numerical figure of merit was NACA 6412. Both, lift and drag are a function of geometry and Mach number. In actual atmospheric conditions the latter one may change. Therefore, we have to concentrate on studying the effects of varying the airfoils' geometry. A thorough analysis was performed on each of the above-mentioned airfoils. Logically, the best approach is to corroborate computational results with experimental evidence. However, this may be extremely difficult to do without the proper aerodynamic testing facilities. We were forced to build a wing set-up, specifically designed for our wing's dimensions. However, based on computer simulations, we chose the airfoil that optimized lift while induced minimum drag. The latter criterion was applied for choosing the cross section of the fuselage.

Management Summary

The following is the list of students taking part of the design competition and the assignment areas

Design	Manufacturing	Power Plant	Fundraising
Christian Rojas	Julian Canizales	Andres F. Quintana	Christian Rojas
John Okogun	Cesar A. Gomez	Dondit Sutoyo	Andres F. Quintana
	Jorge A. Franco	Kashif Husain	
		Kirk Phillips	

Table 1: Division of labor

The following is a list of the faculty members involved in the supervision of the contest

Prof. Damian Rouson

Prof. Ali Sadegh

We would like to mention the following professors that offered their help and their expertise

Prof. Yanis Andreopoulos

Prof. Peter Ganatos

CONCEPTUAL DESIGN REPORT

1. Introduction

From the start, the awareness of our lack of both experience and expertise forced the group to start from a simple design and modify it as we improved our knowledge base. The initial design chosen was to a C-130 Hercules. That is, a cylindrical fuselage that is tapered at the end below the tail. A wing that would have a rectangular platform mounted on top of the fuselage, that is, a high wing. With a carriage right underneath the wings which will be the location of the center of gravity. The thrust will be provided by a single propeller mounted in front of the fuselage. With our limited knowledge, our concern throughout has been ease of manufacturing.

1.1 Fuselage The fuselage could be a cylinder or a rectangular box. A cylinder will be difficult to fabricate as opposed to a rectangular box, due its characteristic roundness. Evidently, a cylindrical fuselage will have less drag than a rectangular fuselage. At this stage of the design, ease of manufacture was considered more important than drag. Theoretically, with enough thrust we can always overcome the drag, termed as brute force. Thus, a rectangular box fuselage was chosen.

1.2 Wings Usually professional engineers design the fuselage first then design a wing that will carry the fuselage effectively. For our group our main focus was to design a good wing, then design a fuselage that the wing could carry. The obvious difference is that professional aeronautical engineers design airplanes that carry payload or specific cargo. On the other hand our main purpose was to fly a contraption.

2. General Anatomy of the Airplane

2.1 Vertical Wing Location There are four major kinds, high wing, low wing, mid-wing and parasol. The high wing is the most desirable, for its aerodynamic characteristics, stability and ease of manufacture. Aerodynamically, the high wing unlike the low wing and the mid-wing has its upper surface uninterrupted, giving it a better lift to drag ratio. The inherent stability of a high wing makes it require little or no dihedral. This also plays a role in ease of manufacture. The parasol wing is not very visually appealing and may add weight because of the extra strength required to hold it and its support in place.

<u>Wing Location</u>	<i>FOM: Aerodynamics</i>	<i>FOM: Stability</i>	<i>FOM: Visual Appeal</i>	<i>FOM: Ease of Manufacture</i>	<u>Total</u>
High Wing	1	1	1	1	4
Low Wing	0	0	1	0	1
Mid-Wing	0	0	1	0	1
Parasol	0	0	0	0	0

Table 1

2.2 Dihedral Angle A wing with dihedral has better stability than the same wing Without dihedral. Dihedral is harder to manufacture than a flat wing, because it is essential for both wings to have the same angle. The same goes for cathedral and is worse for gull. Also, making it a high wing can compensate for the lack of dihedral on a flat wing.

<i>Dihedral</i>	<i>FOM: Ease of Manufacture</i>	<i>Total</i>
Dihedral	0	0
Flat	1	1
Cathedral	0	0
Gull	0	0

Table 2

2.3 Wing Platform The major wing platforms have distinct stall progressions. For a tapered wing the stall progression begins to occur at the outboard regions. This can be very undesirable for two reasons. The first reason is that a stall in this region will result in loss of lift in this area and will induce a roll on the aircraft. The second reason is that the loss of lift in this region causes a loss of control to an aileron. This is most undesirable when the aircraft is close to the ground. This can be corrected by twisting the wing towards the wing tip. Thus the outboard regions will have less angle of attack than the wing root; this is called wash out. Aerodynamic twist can also resolve this problem. This is using a better airfoil at the tip than at the root. These corrections would be very difficult to manufacture.

The stall progression for a rectangular wing begins at the root. This is where we want it to stall. The aileron continues to be effective right up to the break of the stall. Also, the elliptical wing platform stalls evenly over the span. Both platforms are acceptable for aileron control during stall progression.

Ease of manufacture breaks the tie between the elliptical platform and the rectangular platform. The elliptical platform is even harder to fabricate than the tapered platform, due to its elliptical nature. The rectangular platform has a constant chord from tip to root. The Swept platforms and the delta platform are also very difficult to fabricate and sweep decreases the efficiency of a wing at slow speeds.

Wing Platform	FOM: Ease Manufacture	of	FOM: Stall Progression	Total
Elliptical	0		1	1
Rectangular	1		1	2
Tapered	0		0	0
Swept Back	0		Not Determined	0
Delta	0		Not Determined	0
Swept Forward	0		Not Determined	0

Table 3

2.4 Wing Structure The cantilever is beneficial because it will reduce the total drag of the aircraft. While the strut-braced is beneficial because of the strength of the wings. Due to this tie in merit, this design parameter will be further investigated during the preliminary design stage. The ease of manufacture of both is comparable.

Wing Structure	FOM: Ease of Manufacture	FOM: Drag	FOM: Wing Strength	Total
Cantilever	1	1	0	2
Strut-braced	1	0	1	2

Table 4

2.5 Number of Wings Monoplanes generate less total drag than biplanes and other multi-planes. Most of all, fabricating one wing that can carry a specific payload within the standard design constraints is more efficient and will be easier to manufacture.

Number of Wings	FOM: Ease Manufacture	of	FOM: Drag	Total
Monoplane	1		1	2
Biplane	0		0	0
Tri-plane	0		0	0

Table 5

2.6 Thrust Method One propeller as a tractor or a pusher or two propellers mounted on the wings. Mounting the propellers on the wing would be very difficult and require added strength to the wings. Since the payload might have to be accessed through the rear of the aircraft, the tractor was decided upon.

<i>Thrust Method</i>	<i>FOM: Ease of Manufacture</i>	<i>FOM: Access of Payload</i>	<i>Total</i>
Single engine Tractor	1	1	2
Single engine Pusher	1	0	1
Multi-engine (wing mounted)	0	1	1

Table 6

2.7 Landing Gear The options are tricycle, bicycle and tail wheel (tail dragger). Noticeable, student pilots generally learn how to fly in tricycle landing gear aircrafts. This is mainly because of the lack of complication in taxiing, landing and take off operations which is characteristic of a tail dragger. Thus, tricycle landing gear was opted for.

<i>Landing Gear</i>	<i>FOM Lack of Complication Handling</i>	<i>Total</i>
Tricycle	1	1
Tail Wheel	0	0

Table 7

2.8 Tail Arrangement The conventional is the best tail arrangement for this design. This arrangement can be described as follows. A single vertical tail mounted above the horizontal stabilizer. A double vertical stabilizer or triple tail would be used to avoid rolling moments that occur with large fins. Since we do not expect to need large fins, a single vertical tail will be sufficient. The vertical tail will not be swept because this achieves nothing is achieved for light aircrafts. This tail arrangement is the easiest to fabricate.

In terms of spin recovery, the horizontal tail tends to blank out the vertical tail. This can be avoided with a T-tail or a V-tail. Using a V-tail creates mounting complications and additional weight due to necessity of heavier supporting structure is necessary for a T-tail. It is noticeable that most light aircrafts that suffer tail structural damage from flutter have T-tails. Also, the nature of the expected performance does not warrant a consideration of spin recovery. Spin usually occurs with large sudden deflections of the elevators to effect in a steep climb followed by a large deflection of the rudder. For simplicity, this situation will not be taken into account. Another advantage of the T-tail as well as the V-tail is that the surfaces are placed out of the downwash of the wing. This can be avoided in the conventional tail configuration by placing the horizontal stabilizer in a different horizontal plane than that of the wing. Although the V-tail reduces drag due to reduction of interference drag, it is an inherently complicated control system. Moreover, V-tails are susceptible to dutch rolls.

<u>Tail Configuration</u>	<u>FOM Ease of Manufacture</u>	<u>FOM Weight</u>	<u>Total</u>
<u>Conventional</u>	<u>1</u>	<u>1</u>	<u>2</u>
<u>T-tail</u>	<u>0</u>	<u>0</u>	<u>0</u>
<u>Triple tail</u>	<u>0</u>	<u>0</u>	<u>0</u>
<u>V-tail</u>	<u>0</u>	<u>1</u>	<u>1</u>

Table 8

3. Airfoil Selection

Airfoil	Thickness	Camber	Leading Edge Radius	Trailing Edge Angle	Figures of Merit
Clark YH	0.1190	0.0247	0.0753	16.8797	
Göttingen 188	0.0894	0.0432	0.1149	12.5079	
Göttingen 398	0.1173	0.0367	0.0440	17.4813	
Göttingen 285	0.1385	0.0485	0.0425	22.3401	
Clark Y	0.1171	0.0343	0.0128	15.4473	

Design Parameters

3.1 Flat Bottom The Aircraft will be in a high wing configuration whereby the wing is mounted on the top of the fuselage, which is flat. Thus a flat-bottomed airfoil will be desirable mainly because of the ease of construction. Also, limiting the profile to have a flat bottom greatly diminishes the amount of airfoils that may be considered at this stage.

3.2 Leading Edge Radius If the leading edge radius of the profile is too small it could lead to early separation even right at the leading edge. Thus a sharper leading edge might have a higher stalling speed. A lower stalling speed is desirable.

3.3 Camber A cambered airfoil produce more lift than a non-cambered airfoil. Thus an airfoil of high camber produces more lift than an airfoil of less camber. Unfortunately the more camber an airfoil has the more drag it will produce. A trade off is required here. A good flap for a moderately cambered airfoil could compensate for lift during take off and landing, and thereby achieve moderate drag, flap unextended, during cruise conditions. Though, the drag and lift of an airfoil of high camber is beneficial during landing. An average airfoil has a 2% camber, though a 4% camber is used more often in light aircraft and in-between is a good compromise. Higher camber also increases the pitching moment of the wing. This will cause a need for larger stabilizing surfaces resulting in higher drag.

3.4 Thickness: Light aircrafts generally have 12% to 15% thickness. Since our aircraft might be considered an ultralight aircraft, a little less than 12% thickness may then be desirable. Much less than 12% could result in a heavy wing and one that cannot be supported internally, since the spar occupies the point of maximum thickness. In general higher thickness and camber leads to slower stall progression.

3.5 Wing Incidence Angle: This is the angle between the wing root chord line and the fuselage reference line. The *fuselage reference line* of our conceptual design will be parallel to the ground, that it horizontal. A non-zero wing incidence angle is advantageous for a *design point* at cruising speeds, because of the high lift to drag ratio of the wing. In terms of field lengths, this may lead to shorter takeoff distances, but also may lead to longer landing distances. Another disadvantage of a non-zero wing

incidence angle is that a sudden increase in the angle of attack may increase the probability of stalls due to the proximity to the critical angle. A zero wing incidence angle may give the pilot better chances of regaining control of the aircraft under such a sudden change.

3.6 Trailing Edge: The sharper the trailing edge the better. A sharp trailing edge establishes the Kutta-Joukowski condition.

4. Rated Aircraft Cost, \$ (Thousands) = (A*MEW + B*REP + C*MFHR)/1000

Coeff.	Description	Value
A	Manufacturers Empty Weight Multiplier	\$100/lb.
B	Rated Engine Power Multiplier	\$1/Watt
C	Manufacturing Cost Multiplier	\$20/hour
REP	Rated Engine Power	# of Engines * Amp * 1.2V/cell * # of cells "Amp" will be the value of the inline fuse from the battery to the controller. Maximum value is 40A, but a lower current fuse may be used, and REP adjusted accordingly.
MFHR	Manufacturing Man Hours	Prescribed assembly hours by WBS (Work Breakdown Structure). WBS 1.0 Wing(s): 15 hr./wing + 4 hr./sq. ft. Projected Area + 2 hr./strut or brace + 3 hr./control surface Note: Winglets, end plates, and biplane struts ARE included in the Projected Area calculation WBS 2.0 Fuselage and/or pods 5 hr./body + 4 hr./ft of length WBS 3.0 Empennage 5 hr. (basic) + 5 hr./Vertical Surface + 10 hr./Horizontal Surface WBS 4.0 Flight Systems 5 hr. (basic) + 2 hr./servo or controller WBS 5.0 Propulsion Systems 5 hr./engine + 5 hr./propeller or fan

Rated Aircraft Cost, \$ (Thousands) = [(100(20)+1(1425.6)+20(141))/1000=6.2456

5. Conceptual Design Configuration

- 1- Wing: The wing configuration is a rectangular planform, high wing with zero dihedral, because of ease of manufacture and inherent stability. The airfoils that have been chosen for further analysis are Gottingen 285 for it's thickness, camber and relatively flat bottom, and Gottingen 188 for it's flat bottom.
- 2- Fuselage: The fuselage will have a rectangular cross-section and be shaped like a box with a tapered rear.
- 3- Empenage: The tail will be conventional.
- 4- Thrust: The aircraft will be a single engine tractor.
- 5- Landing Gear: The landing gear will be tricycle.
- 7- Cargo Bay: The cargo will be housed below the wing at the center of gravity.
- 8- Wing Span: 10 feet
- 9- Total Weight: 55 lbs

Preliminary Design Report

1. Wing

1.1 Airfoil Selection(1) The Gottingen 285 (GOE 285) and the Gottingen 188 (GOE 188) were the airfoils from the conceptual design stage selected for further analysis. The airfoil analysis was done using an internet-based software at the web address, <http://beadec1.ea.bs.dlr.de/Airfoils/calcofoil.htm>. The analysis proved that GOE 285 is a superior airfoil than GOE 188. The coefficient of lift (Cl) of GOE 285 at zero angle of attack is 0.40, and that of GOE 188 is 0.33. Thus GOE will create greater lift at an angle of attack of zero and at subsequent angle of attacks. The Lift to drag (L/D) of GOE 285 is 29.4239 and that of GOE 188 is 9.5796. Though GOE 188 has a smaller nose down pitching moment than GOE 285, its lift to drag is too low for it to be considered any further.

Airfoil	FOM Cl	FOM L/D	FOM Pitching Moment	Total
GOE 285	1	1	0	2
GOE 188	0	0	1	1

Table 1

1.2 Airfoil Selection(2) After the above analysis had been completed another airfoil was discovered and introduced, NACA 6412. This airfoil was argued to be better and since it was comparable to GOE 285 in thickness and camber, the group decided to analyze it. It was analyzed using the same software used to analyze GOE 285 and GOE 188. The coefficient of lift of NACA 6412 at zero angle of attack is 0.63 and its lift to drag 42.8488. Though its moment coefficient at zero angle of attack is more negative than that of GOE 285, the decision at this discovery was unanimous, NACA 6412 would be used.

Airfoil	FOM Cl	FOM L/D	FOM Pitching Moment	Total
NACA 6412	1	1	0	2
GOE 285	0	0	1	1

Table 2

Airfoil	Cl (@ 0 AOA)	L/D (@ 0 AOA)	Cm (@ 0 AOA)
NACA 6412	0.63	42.8488	-0.1263
GOE 285	0.40	26.4239	-0.0651
GOE 188	0.33	9.5796	-0.0234

Table 3: Summary of airfoil force characteristics. Re = 200000

1.3 Flaps and Ailerons Flaps are used to increase the camber of a wing thus increasing its coefficient of lift at a specific angle of attack. Ailerons are used for roll control and to ensure lateral stability. Each flap and each aileron will require its separate servo for deflection. To save weight, time, money and manufacturing difficulty, the use of flaperons was decided upon (the March issue of Custom Planes passively encouraged this selection).

1.4 Flaperon Deflection The flaperon deflection was analyzed with the same software that analyzed the airfoils. The percent of flap, and angle of the flap deflection were analyzed. The percentage of chord to be used for the flaperon considered were 25% and 35 % the deflection angles were 10 degree and 20 degrees.

% of Chord and Angle of Deflection		Cl
---------------------------------------	--	----

	<u>L/D</u>	
25% and 10 deg.	81.4818	1.02
25% and 20 deg.	83.2425	1.40
35% and 10 deg.	69.9879	1.00
35% and 20 deg.	74.4322	1.36

Table 4: Summary of flaperon deflection analysis. $Re = 300000$

The lift and the drag characteristics are preferable for a 25% chord flaperon. The high force characteristics will improve the take off performance thus decreasing take off field length and the flaperon could serve as spoilers during landing thus decreasing the landing field length.

% of Chord	<u>FOM</u> <u>L/D</u>	<u>FOM</u> <u>Cl</u>
25%	1	1
35%	0	0

Table 5: Figures of Merit for % of chord.

1.5 Dimensions(1) The aspect ratio of a light aircraft ranges from 5 to 7. Since our aircraft is smaller than a light aircraft, the following calculations are based on an aspect ratio of 5.

$$AR = 5$$

$$\text{Span, } b = 10 \text{ ft}$$

$$\text{Chord, } C:$$

$$AR = b / C$$

$$C = 10 / 5 = 2 \text{ ft}$$

$$\text{Wing Area} = 10 \text{ ft} * 2 \text{ ft} = 20 \text{ ft}^2$$

$$\text{Wing Loading, } n = 55 \text{ lbs} / (20) \text{ ft}^2 = 2.75 \text{ lbs/ft}^2$$

1.6 Dimensions(2) A seven foot wing was fabricated to test its structural integrity and wing loading. Part of the results of the test showed that a nine foot wing span would be preferable than a ten foot wing span, because the wing is fabricated in three foot sections; and adding a one foot section in the middle, for the width of the fuselage, reduced the wing's structural integrity and put it's zero dihedral at risk. The test wing had an aspect ratio of 7. Inspection of the wing showed that an aspect ratio of 5 may prove difficult to manufacture in such a manner as to reduce separation due to uneven surfaces, and would increase weight by its internal supports. So the Aspect ratio was increased to six. In this manner, the overall weight of the aircraft including the payload could be reduced for better performance. However, for now the gross weight would be kept at 55 lbs.

$$AR = 6$$

$$\text{Span, } b = 9 \text{ ft}$$

$$\text{Chord, } C:$$

$$AR = b / C$$

$$C = 9 / 6 = 1.5 \text{ ft}$$

$$\text{Wing Area} = 9 \text{ ft} * 1.5 \text{ ft} = 13.5 \text{ ft}^2$$

$$\text{Wing Loading, } n = 55 \text{ lbs} / (13.5) \text{ ft}^2 = 4.07 \text{ lbs/ft}^2$$

2. Empenage

2.1 Horizontal Stabilizer (Longitudinal Stability) Since the wing produces a pitching moment about its aerodynamic center and the lift it generates also produces a pitching moment, to trim the aircraft a horizontal stabilizer fitted with an elevator is employed. These provide longitudinal stability that is stability in pitch. A graph of pitching moment vs. angle of attack results in a line with a negative slope, this is evident from the table of the values below. Negative pitching moment is a nose-down moment.

<u>Angle of Attack</u>	<u>Cm</u>
------------------------	-----------

0	-0.1263
1	-0.1278
2	-0.1286
3	-0.1301
4	-0.1317
5	-0.1334
6	-0.1349
7	-0.1365
8	-0.1381
9	-0.1395
10	-0.1397

Table 6: Values of alpha vs. Cm

Trim will be achieved partially by the nose-up moment of the wing lift (L_w) forward of the CG and partially by the nose-up moment of the downward lift of the tail at a moment arm of ' l_t '. The natural nose down pitching moment, which is about the aerodynamic center, is equal to the wing lift moment and the tail moment.

$$M_{ac} = L_w * l_w + L_t * l_t$$

Evidently a larger ' l_t ' will result in a smaller ' L_t '. As a result to result to reduce weight and have a sufficient ' l_t ' a tail boom will be used and the fuselage will be shortened.

2.2 Horizontal Stabilizer Airfoil This airfoil is usually a symmetric airfoil. NACA 0012 was chosen over NACA 009 for its better lift characteristics with a 25% chord elevator at 25 degrees deflection, and its thickness.

Airfoil	FOM Lift Characteristics	Total
NACA 0012	1	1
NACA 009	0	0

Table 7: Figures of merit for Horizontal stabilizer airfoil

Horizontal stabilizers are usually placed at a negative angle of incidence.

2.3 Horizontal Stabilizer Dimensions The horizontal tail volume coefficient for light aircrafts ranges from 0.5 to 0.7. The large degrees of flap will require greater horizontal tail surface, thus a larger horizontal tail coefficient to provide maximum longitudinal stability.

Tail Volume coeff, $C_{tv} = 0.7$

Tail Volume, $V_t = C_{tv} * S_w * C = 0.7 * 13.5 * 1.5 = 14.175 \text{ ft}^3$

Tail arm(determined from fuselage), $l_t = 2.25 + 0.5 + 1.25 = 4.0 \text{ ft}$

Tail Area, $S_h = 14.175 / 4 = 3.5 \text{ ft}^2$, Approximated to 4 ft^2 for added stability.

Tail Span, $b_h = 4 \text{ ft}$

Tail Chord, $C_h = 1 \text{ ft}$

Elevator = 25% of chord

The horizontal stabilizer is usually considered to be a third of the size of the wing.

Wing Area, $S_w = 13.5 \text{ ft}^2$

Tail Area, $S_h = 4 \text{ ft}^2$

$S_h / S_w = 4 / 13.5 = 0.296$ (approximately $1/3$)

2.4 Vertical Stabilizer (Directional Stability)

Directional Stability is provided by the fin and the rudder. The degree of directional stability like the degree of longitudinal stability is proportional to the size the control surface, in this case the fin and rudder. And, also the distance from the CG. A larger area results in

a larger side force and a greater distance from the CG results in a greater moment arm. An increase in either of the parameters will result in a larger restoring moment. The sizes of these parameters are also proportional to the amount of yaw control and weathercocking done by the rudder and fin respectively.

2.5 Horizontal Stabilizer Airfoil This airfoil is a symmetric airfoil. NACA 0012 will also be used for the vertical stabilizer, for the reason outlined above.

2.6 Vertical Stabilizer Dimensions A simple rule used in RC flight was learned from the DBF 2000 report of the California Polytechnic State University. The rule states that the vertical tail be half of the horizontal tail. Thus,

Tail Span, $b_v = 2$ ft

Tail Chord, $C_v = 1$ ft

Rudder = 25 % of chord

3. Fuselage The fuselage will house the payload, the engine, the batteries and support the weight of the wing as well as the tail boom. The fuselage will comprise of three sections. The first and third sections are similar to a pyramid sawn off at the middle and with its rectangular base lying in the vertical plane. These rectangular bases are to be attached to the second section of the fuselage at both ends. This section will be a rectangular box.

The first section will house the engine. The second section will house the payload as well as support the weight of the wing. The third section will house the battery pack and will provide access for the tail boom into the fuselage for structural support.

A fuselage with a rectangular cross section is susceptible to crosswinds and sideslips during a turn. As a result to ensure lateral stability fuselage effect was taken into consideration. To provide for upwash over the second section that is rectangular, the wing which is 1.5 ft in chord length will be mounted at the rear of this section leaving 1 ft of the top of the section in front of the leading edge of the wing. Thus total length of the second section will be $1 \text{ ft} + 1.5 \text{ ft} = 2.50 \text{ ft}$.

The first section will be 0.75 ft long and the third section will be 0.50 ft long. The total length of the fuselage without the tail boom is, $0.75 + 2.50 + 0.50 = 3.75 \text{ ft}$.

A fineness ratio of a fuselage is three. If it is high than this the fuselage will create more drag, and if it is less than three the drag created by the fuselage will be even worse.

Fineness ratio = length of fuselage / height of fuselage = 3

Therefore,

Height of fuselage = $3.75 / 3 = 1.25 \text{ ft}$

To minimize the lateral cross section the width = 1 ft

4. Center of Gravity The center of gravity of the aircraft will be calculated by measuring the difference in weight between the nose gear and the main gear.

General Aerodynamic Characteristics

The general aerodynamic characteristics of the aero-structure are based on the design of the wing, the fuselage, the ailerons, elevators, rudders as well as landing gear. Aerodynamic design is a balancing act between lift and drag. The most important aerodynamic characteristics are the coefficient of lift and the coefficient of drag. We know that most of the lift will be produced by the selected wing configuration. Moreover, one must be extremely careful as to choose the proper airfoil profile. The correct airfoil profile should optimize the lift without inducing a considerable amount of drag. In addition, the designer must choose the proper profile for the fuselage. The fuselage will tend to produce an increase in drag. We optimize lift, and maneuverability while inducing minimum drag. The same methodology applies to the ailerons, rudders and elevators.

Additional Airfoil Preliminary Design Report

As mentioned before the correct selection of the wing depends on its profile. A careful analysis and comparison was performed. Our selected profiles come from the NACA (4 digit) family of airfoils. Our analysis was performed in Sub-3D. This aerodynamic software helps to approximate the aerodynamic properties of the airfoils. The quantities that we are mainly concerned with are the lift coefficient and the drag coefficient. A thorough analysis was performed on each of the above-mentioned airfoils. Once again, aerodynamic design is a balancing act between lift and drag. Logically, the best approach is to corroborate computational results with experimental evidence. However, this may be extremely difficult to do without the proper aerodynamic testing facilities.

Our analysis started with computing the approximate coefficient of lift and the coefficient of drag. The selected conditions for testing included the proper wind speed, angles of attack for the airfoil and ailerons. We expected the coefficient of lift and the coefficient of drag to be functions of the speed of the flow and of the angle of attack. Obviously, it is expected that an increase in the speed of the flow will induce a proportional change in lift and drag. However, our simulations are clear in showing that the increase in drag is only fractional when compared to the corresponding change in lift. Most importantly, we wanted to know the effects of curvature, thickness and the location of its maximum curvature on the aerodynamic characteristics of the airfoil profile. In addition, we preferred to use a total wingspan of 7 feet, and a cord value of 1 foot. Given our wing configuration, the taper ratio is equal to unity. This arrangement provides simplicity and elegance while facilitating manufacturing.

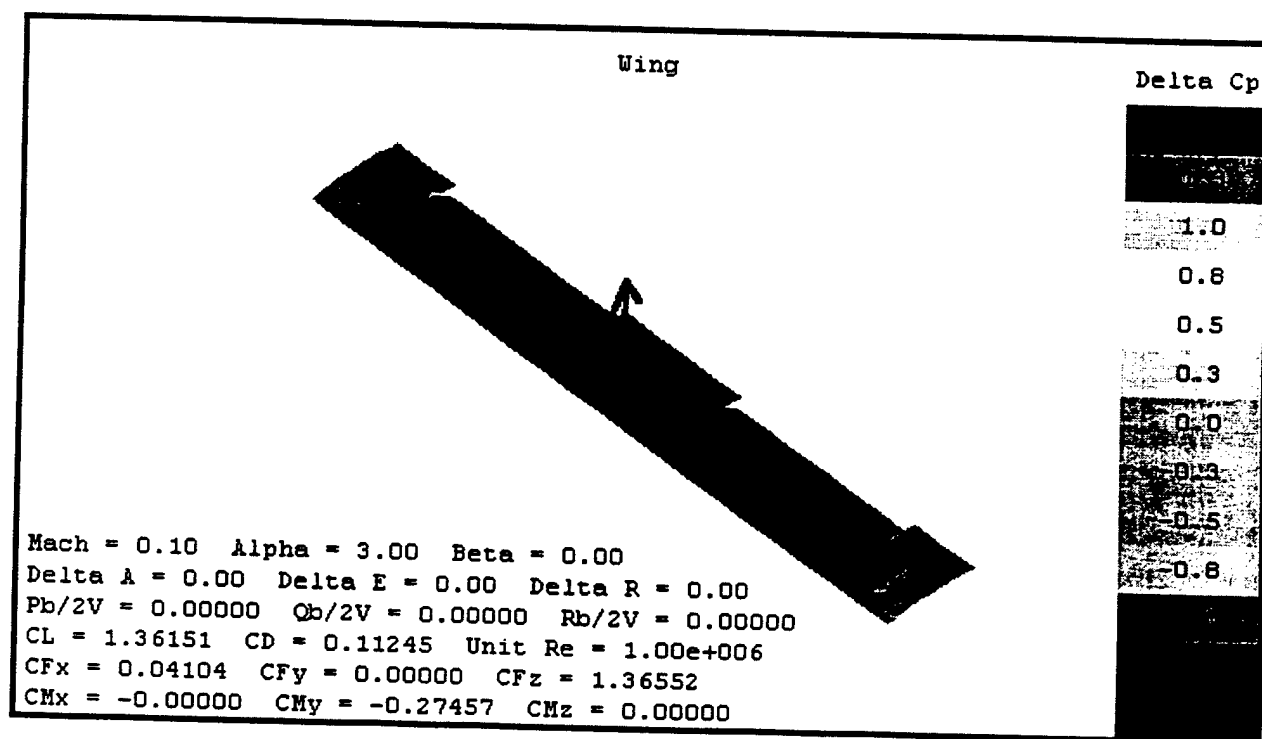
NACA 5412

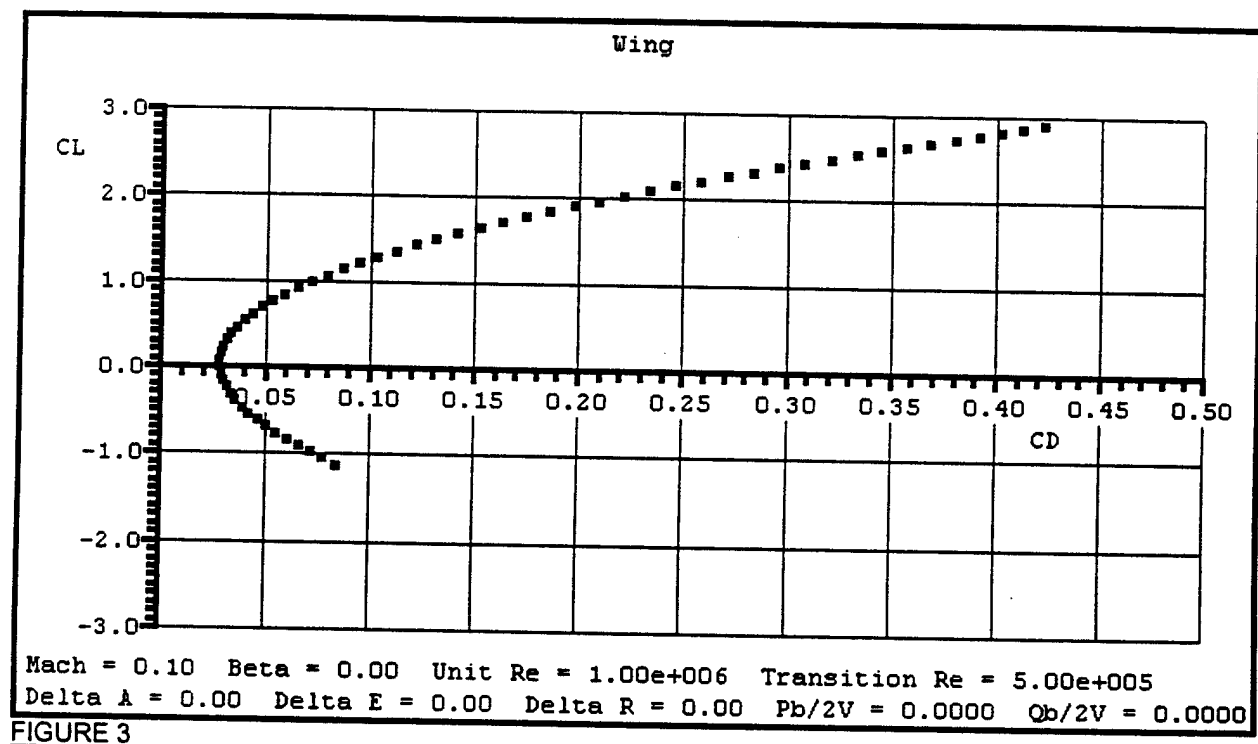
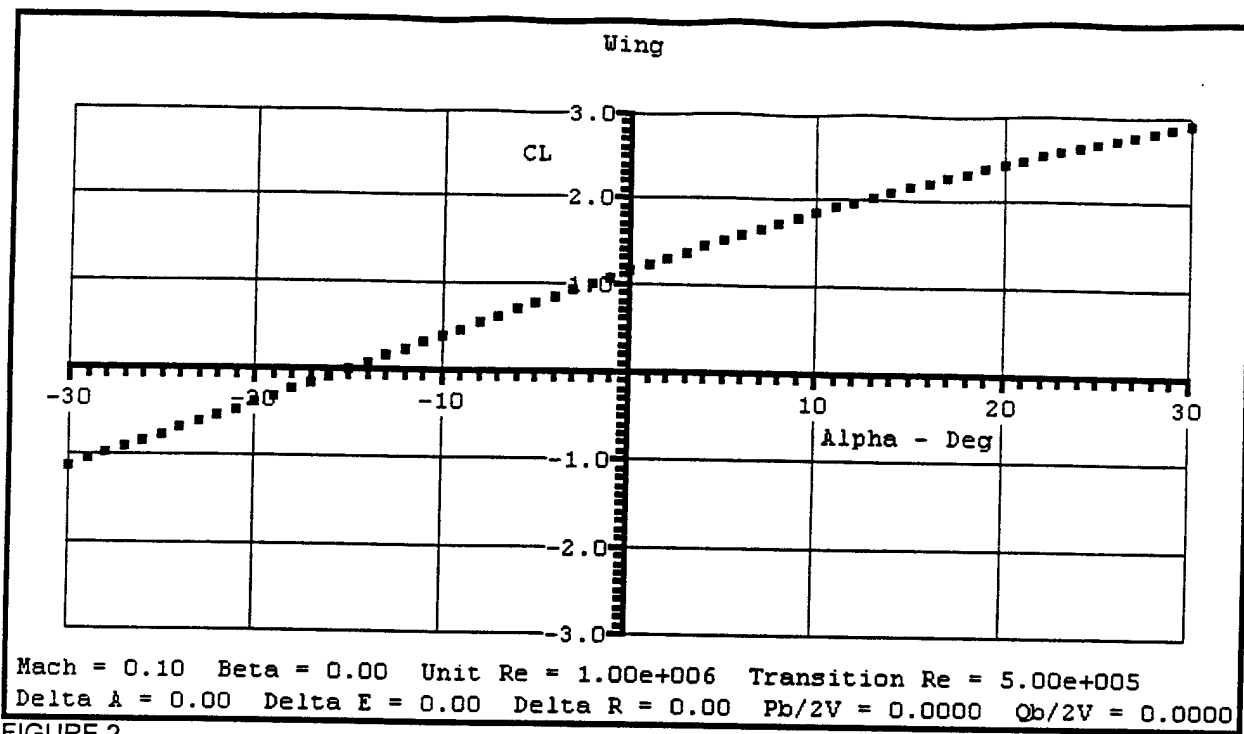
Once again, we started by computing the approximate coefficient of lift and the coefficient of drag. The selected conditions for testing included the proper wind speed, angles of attack for the airfoil and ailerons. We expected the coefficient of lift and the coefficient of drag to be functions of the speed of the flow and of the angle of attack. Given the conditions shown in FIGURE 1, the value for the coefficient of lift was found to be 1.36151. In contrast, the coefficient of drag was found to be 0.11245. Deductively, we may say that the magnitude of the coefficient of drag is about a tenth of the value of the lift coefficient. However, we must go beyond that. We must explore the relation between a change in airfoil geometry and its corresponding change in aerodynamic properties. In fact, we expect an increase in camber (NACA 1st Digit) to be followed by a proportional increase in lift and drag. Changes in drag will be relatively small compared to changes in lift. Therefore, we must explore the impact of varying the camber as well as the location of its maximum value (NACA 2nd Digit).

Furthermore, we may expect an increase in lift as we increase our angle of attack. Our main limitation will be stalling or separation in the boundary layers at a maximum angle of attack. A simplified relation between angle of attack and coefficient of lift is plotted in Figure 2. Notice that at an angle of attack of 3 degrees, the approximate value of the lift coefficient is 1.36.

As we expected, the coefficient of drag is approximately one tenth of the lift coefficient. In reality the coefficient of drag is about 12% of the lift coefficient value. Figure 3 illustrates this relation. Our next step will be to simulate the changes in lift coefficient with respect to the location of maximum camber (NACA 2nd Digit). We will repeat the same procedure for different values of curvature (camber) and its point of maximum value (NACA 2nd Digit).

FIGURE 1 NACA 5412





NACA 5512

Following our procedure, we start by computing the approximate coefficient of lift and the coefficient of drag. Again, the selected conditions for testing included the proper wind speed, angles of attack for the airfoil and ailerons. Given the conditions shown in FIGURE 4, the value for the coefficient of lift was found to be 1.39988. In fact, we have succeeded in increasing the value for the coefficient of lift. However, the new coefficient of drag was found to be 0.11723. Once again, we may say that the magnitude of the coefficient of drag is about a tenth of the value of the lift coefficient. We have observed that changes in airfoil geometry affect our lift and drag values.

In addition, we may expect an increase in lift as we increase our angle of attack. Our main limitation will be stalling or separation in the boundary layers at a maximum angle of attack. A simplified relation between angle of attack and coefficient of lift is plotted in Figure 5. Notice that at an angle of attack of 3 degrees, the approximate value of the lift coefficient is 1.39.

As we expected, the coefficient of drag is approximately one tenth of the lift coefficient. In reality, the coefficient of drag is about 12% of the lift coefficient value. Figure 6 illustrates this relation.

NACA 5512

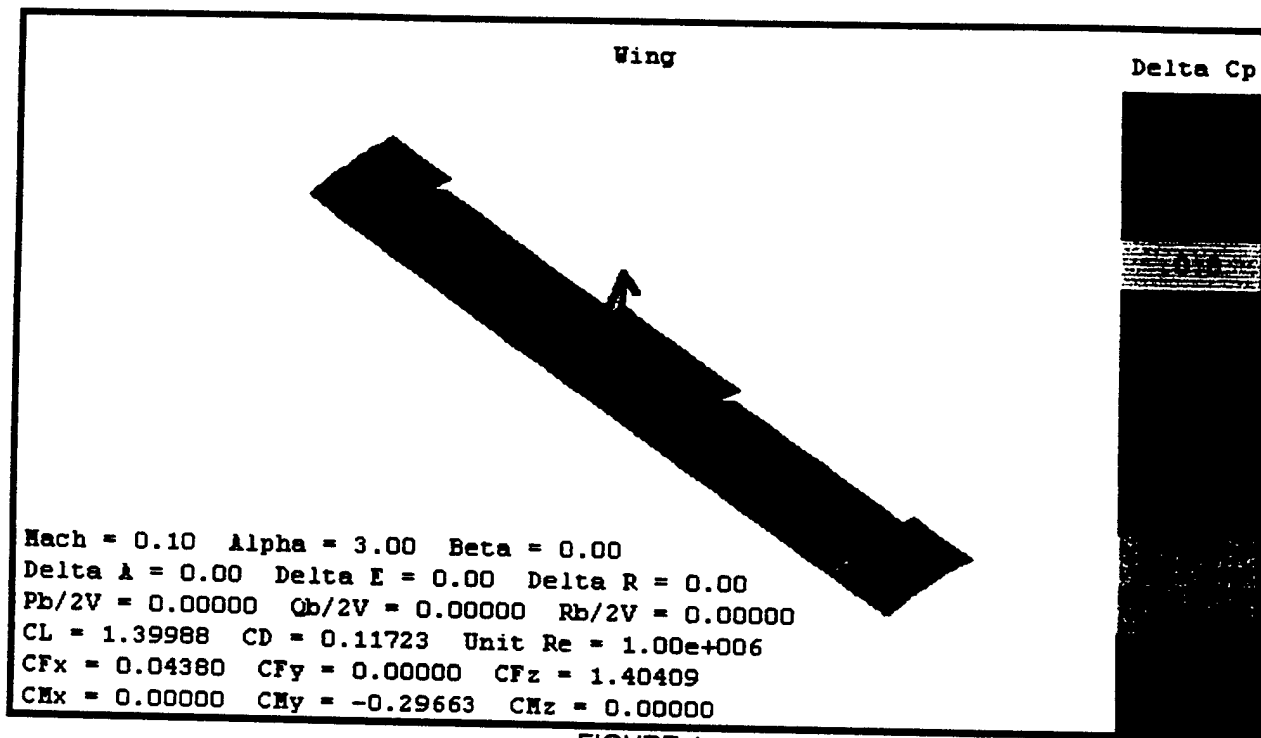


FIGURE 4

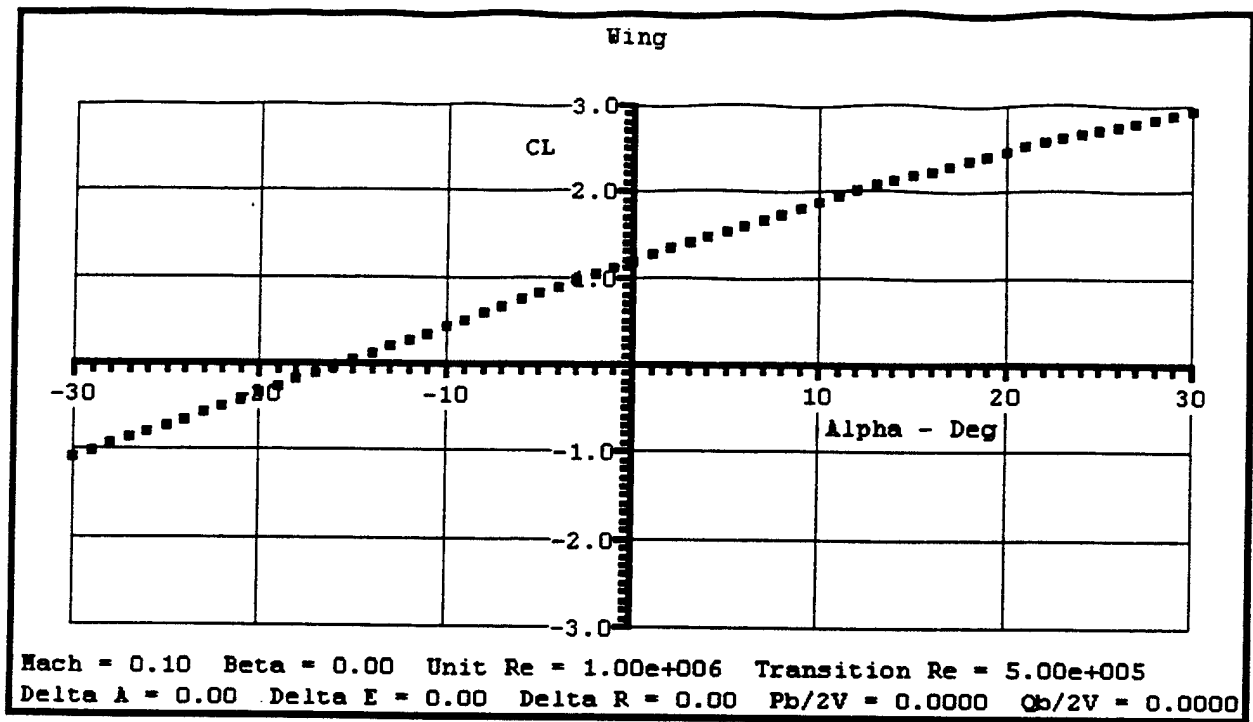


FIGURE 5

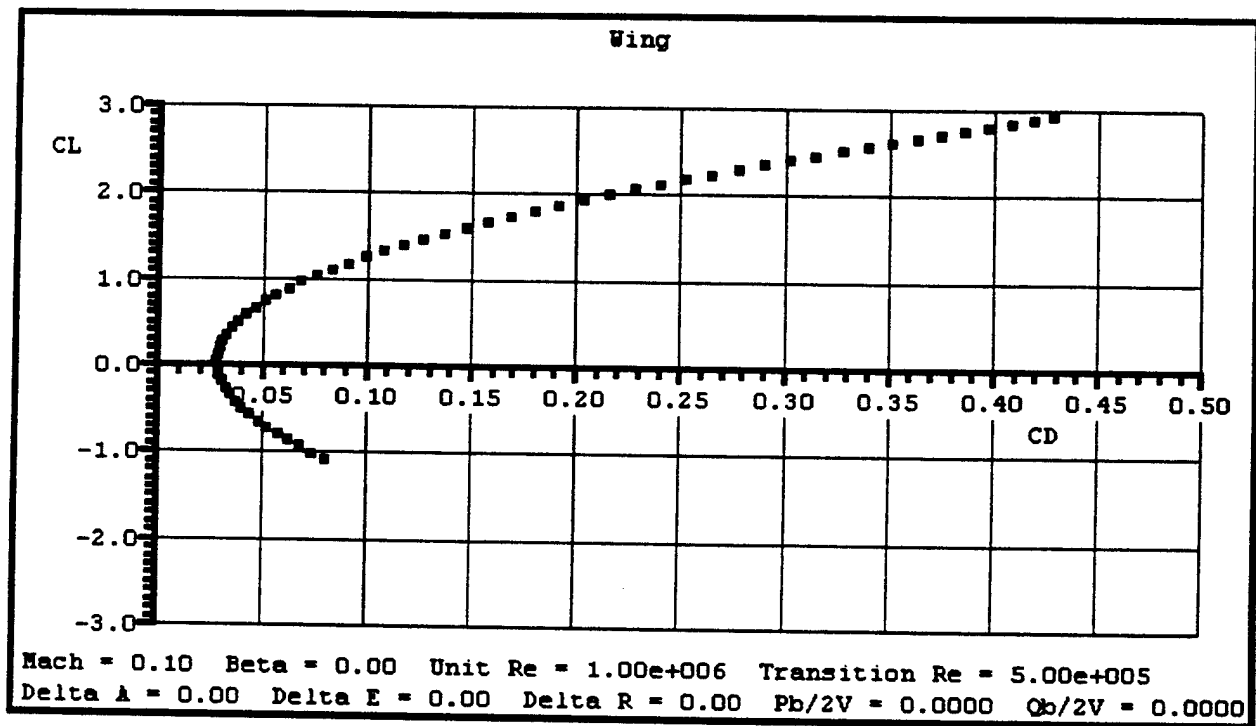


FIGURE 6

Following our procedure, we start by computing the approximate coefficient of lift and the coefficient of drag. Again, the selected conditions for testing included the proper wind speed, angles of attack for the airfoil and ailerons. Given the conditions shown in FIGURE 7, the value for the coefficient of lift was found to be 1.45282. In fact, we have succeeded in increasing the value for the coefficient of lift. However, the new coefficient of drag was found to be 0.12409. Once again, we may say that the magnitude of the coefficient of drag is about a tenth of the value of the lift coefficient. We have observed that changes in airfoil geometry affect our lift and drag values. Therefore, we must explore the impact of varying the camber as well as the location of its maximum value (NACA 2nd Digit). In fact, we have *discovered* that increasing the distance of its maximum value as measured from the airfoil's leading edge (NACA 2ND Digit) may increase the lift coefficient.

Our main limitation will be stalling or separation in the boundary layers at a maximum angle of attack. A simplified relation between angle of attack and coefficient of lift is plotted in Figure 8. Notice that at an angle of attack of 3 degrees, the approximate value of the lift coefficient is 1.5. As we expected, the coefficient of drag is approximately one tenth of the lift coefficient. In reality, the coefficient of drag is about 12% of the lift coefficient value. Figure 9 illustrates this relation.

NACA 5612

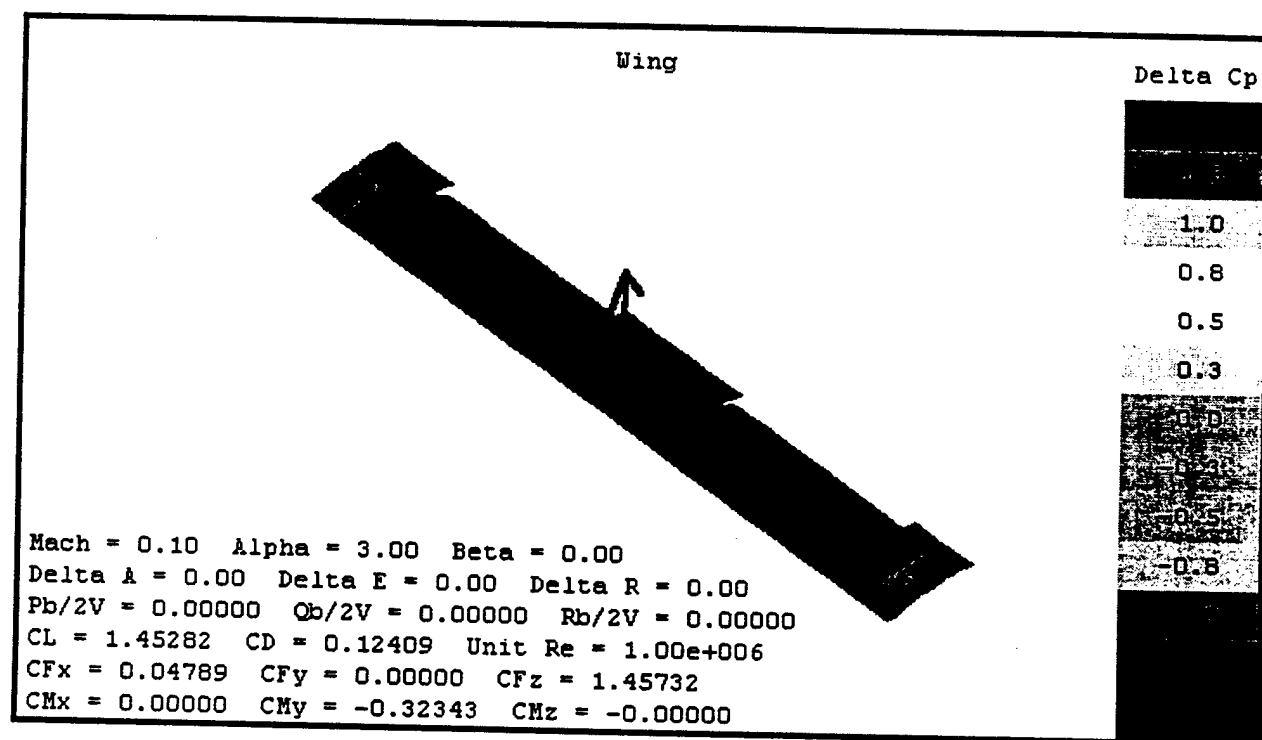


FIGURE 7

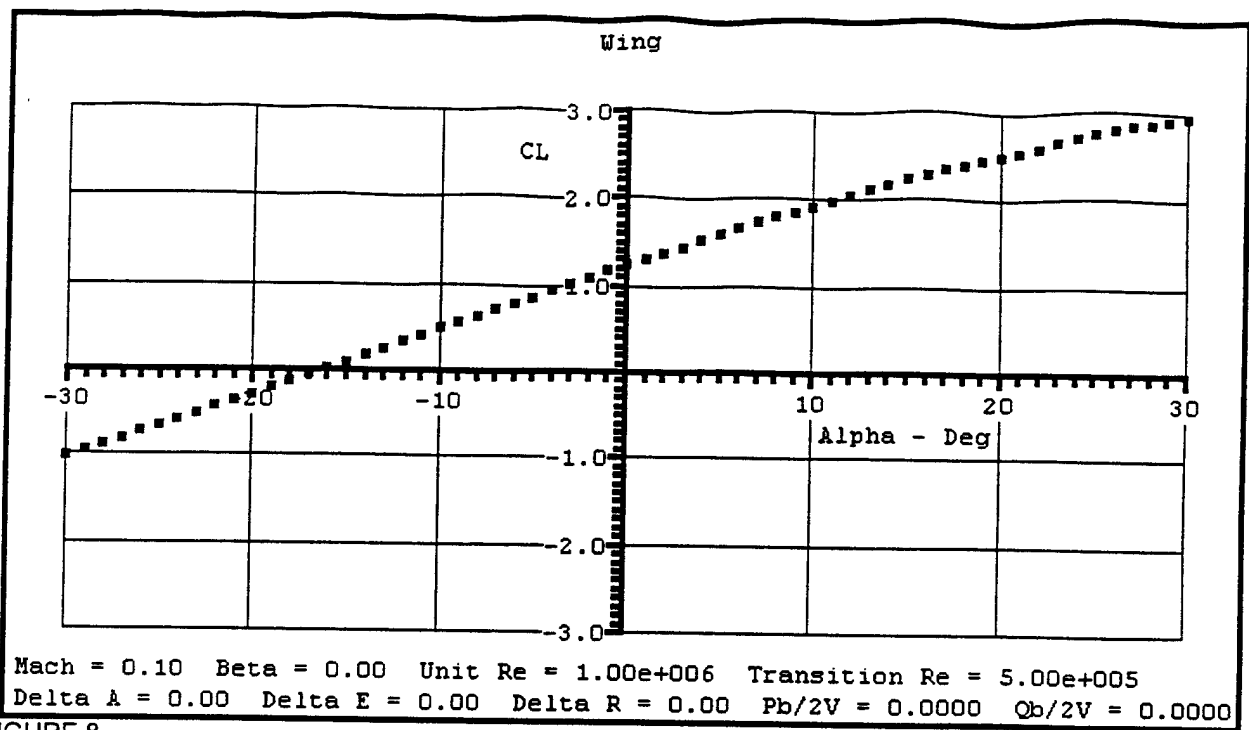


FIGURE 8

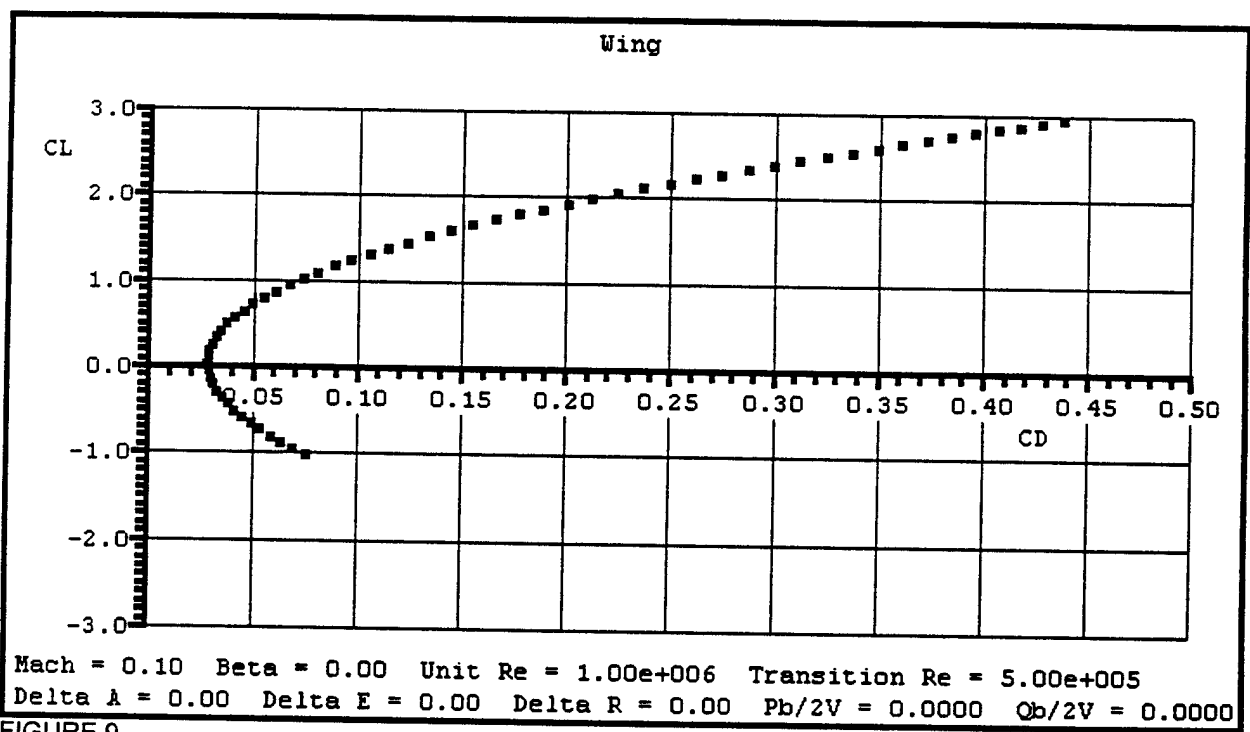


FIGURE 9

NACA 6412

We have explored the idea of increasing the location of maximum camber (NACA 2nd Digit). Now, we are ready to simulate the effects of both, an increase in camber as well as in increase in its point of maximum value. Again, the selected conditions for testing included the proper wind speed, angles of attack for the airfoil and ailerons. Testing conditions are provided in FIGURE 10, the value for the coefficient of lift was found to be 1.46365. In fact, we have succeeded in increasing the value for the coefficient of lift. However, the new coefficient of drag was found to be 0.13087. Again, we have *verified* that increasing the distance of its maximum value as measured from the airfoil's leading edge (NACA 2nd Digit) increases the lift coefficient.

A simplified relation between angle of attack and coefficient of lift is provided in Figure 11. Notice that at an angle of attack of 3 degrees, the approximate value of the lift coefficient is 1.46. As we expected, the coefficient of drag is approximately one tenth of the lift coefficient. In reality, the coefficient of drag is about 12% of the lift coefficient value. Figure 12 illustrates this relation.

NACA 6412

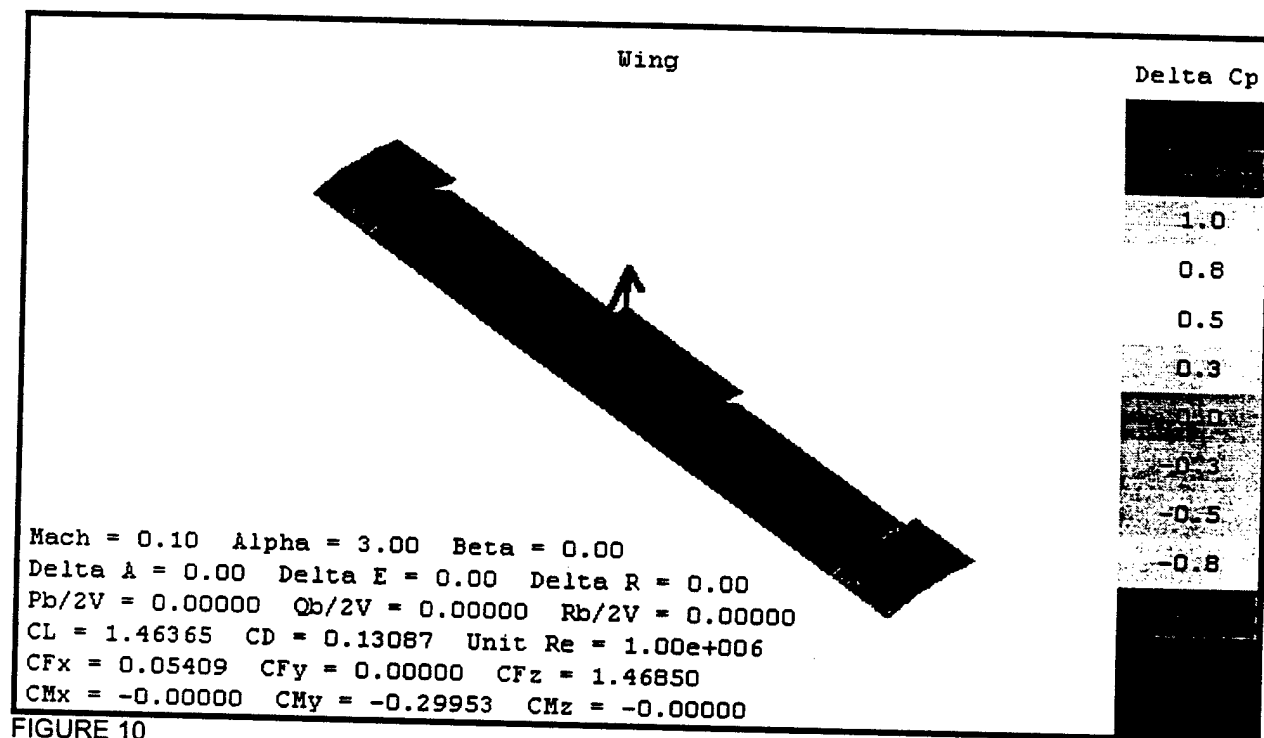


FIGURE 10

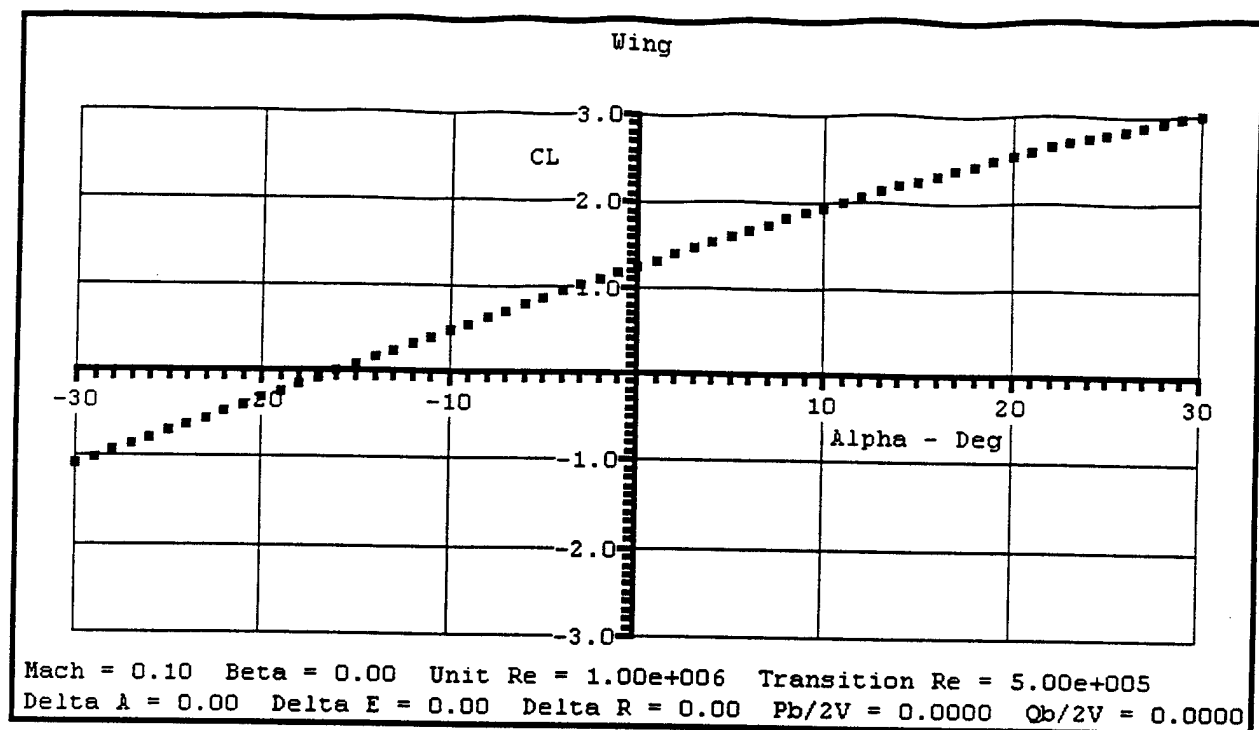


FIGURE 11

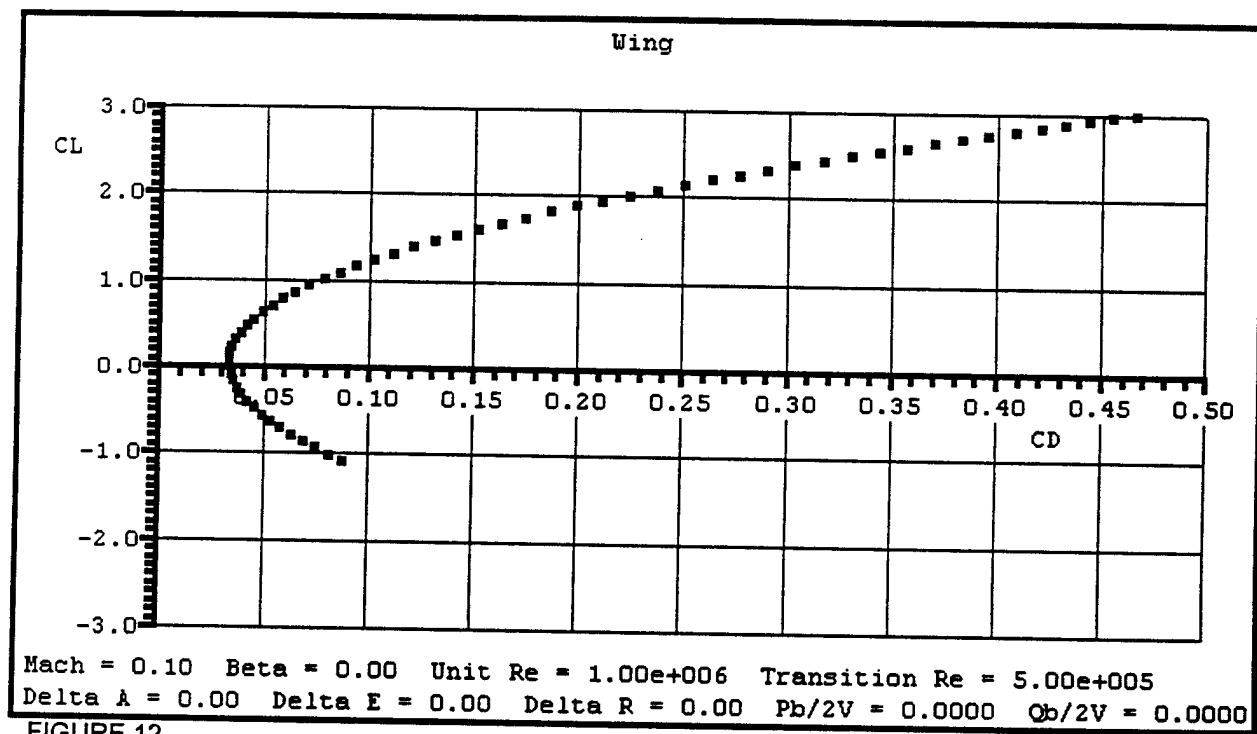


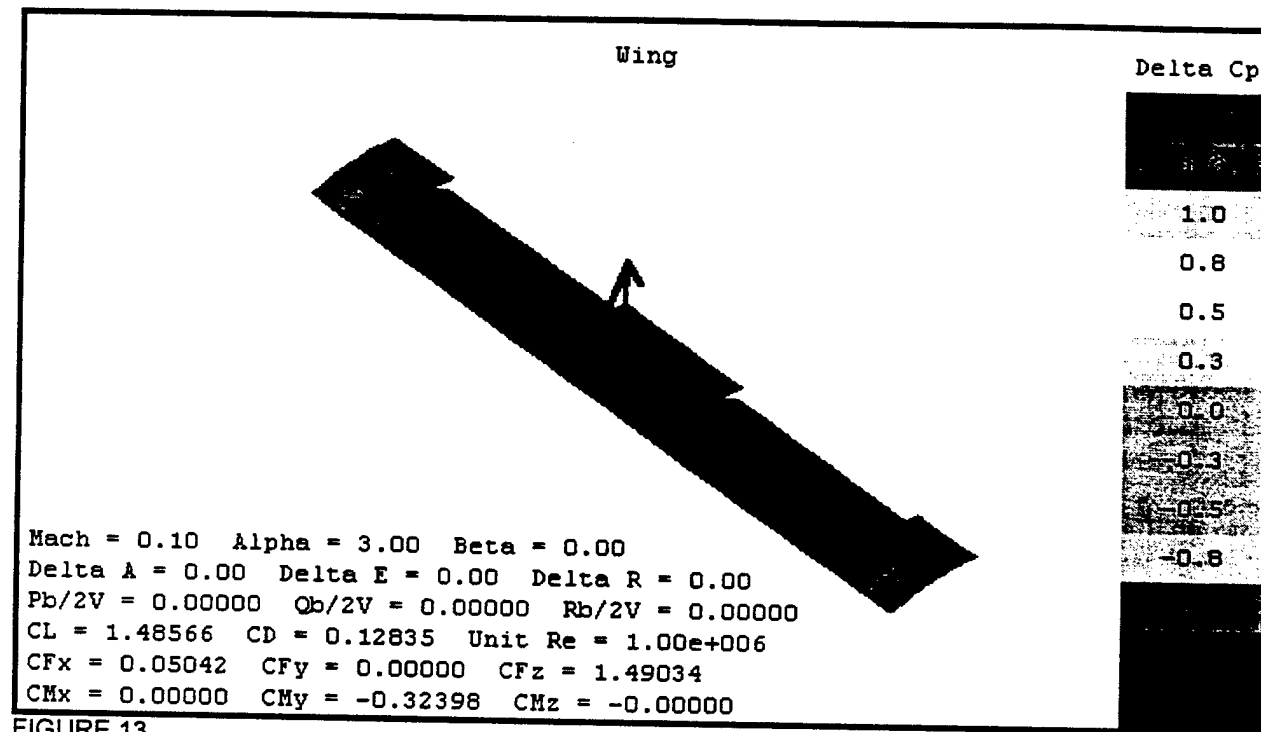
FIGURE 12

NACA 6512

As usual, the selected conditions for testing are shown in FIGURE 13. The value for the coefficient of lift was found to be 1.48566. In fact, we have succeeded in increasing the value for the coefficient of lift. However, the new coefficient of drag was found to be 0.12835. We have *verified* that increasing the curvature (camber) as well as the distance of its maximum value as measured from the airfoil's leading edge (NACA 2nd Digit) may increase the lift coefficient.

However, it is extremely important to notice that this particular airfoil has provided a higher lift but a slightly less drag, thus providing a great advantage. The angle of attack versus coefficient of lift is plotted in Figure 14. Notice that at an angle of attack of 3 degrees, the approximate value of the lift coefficient is 1.48. As we expected, the coefficient of drag is approximately one tenth of the lift coefficient. In reality, the coefficient of drag is about 12% of the lift coefficient value. Figure 15 illustrates this relation.

NACA 6512



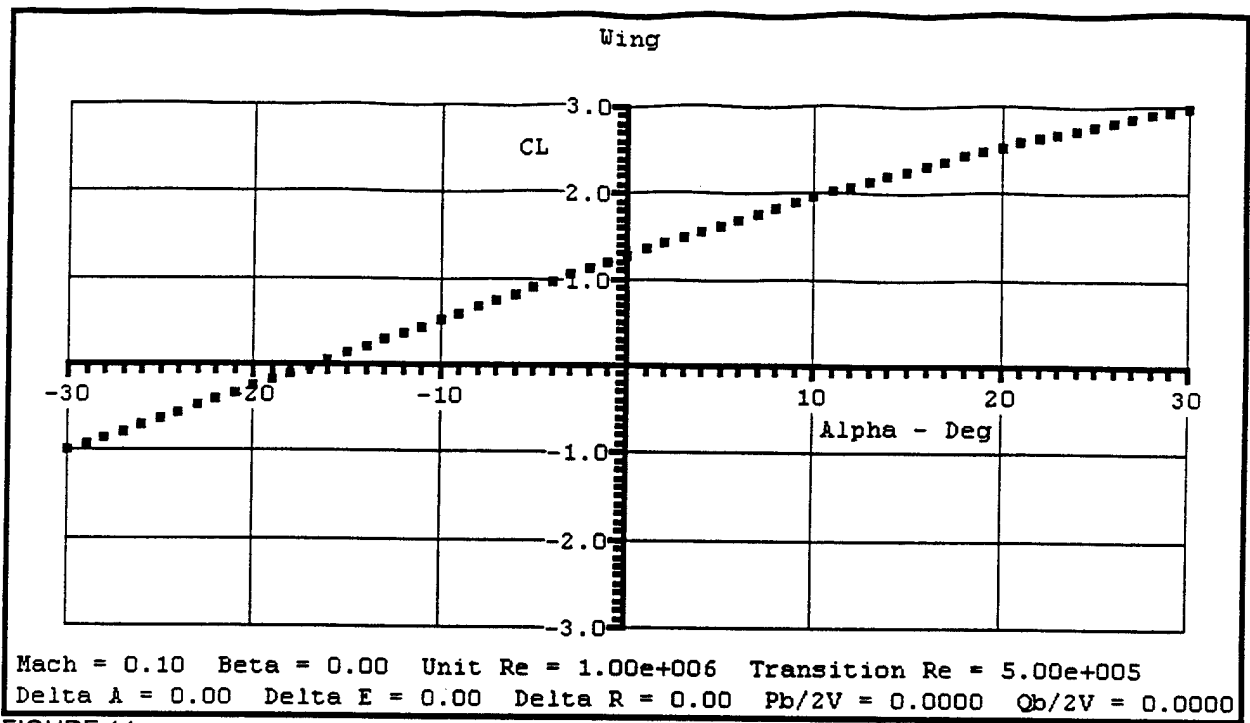


FIGURE 14

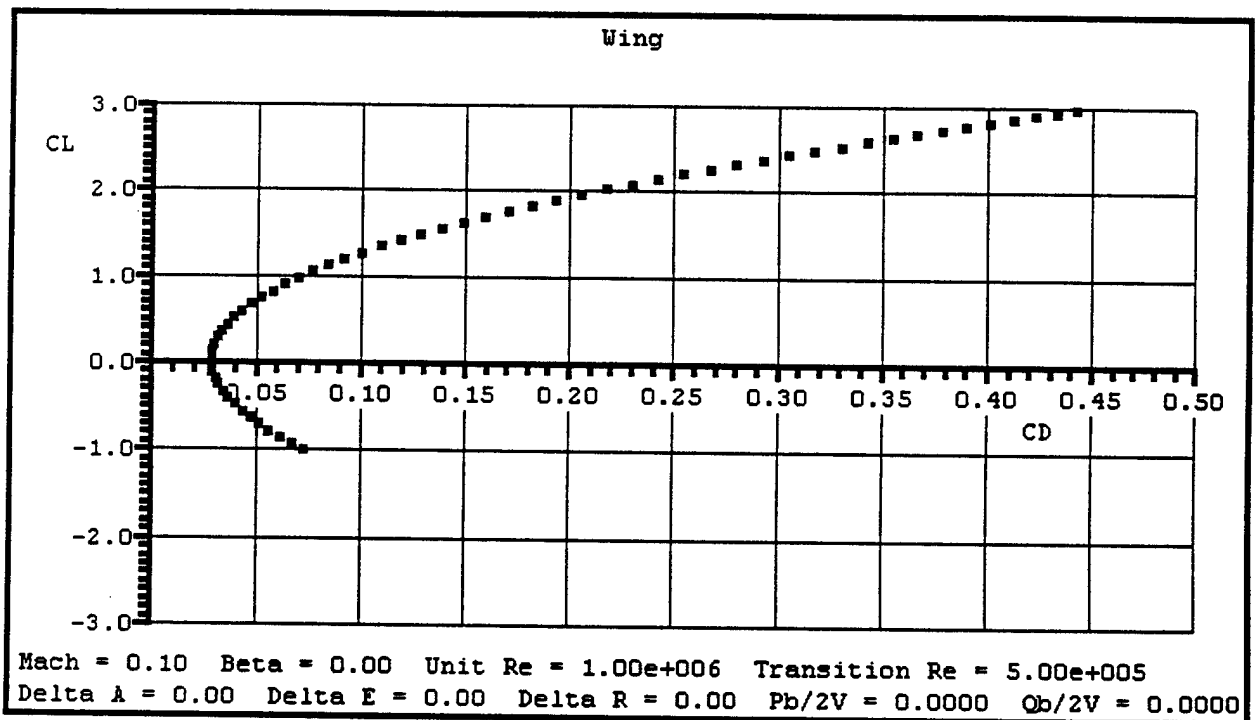


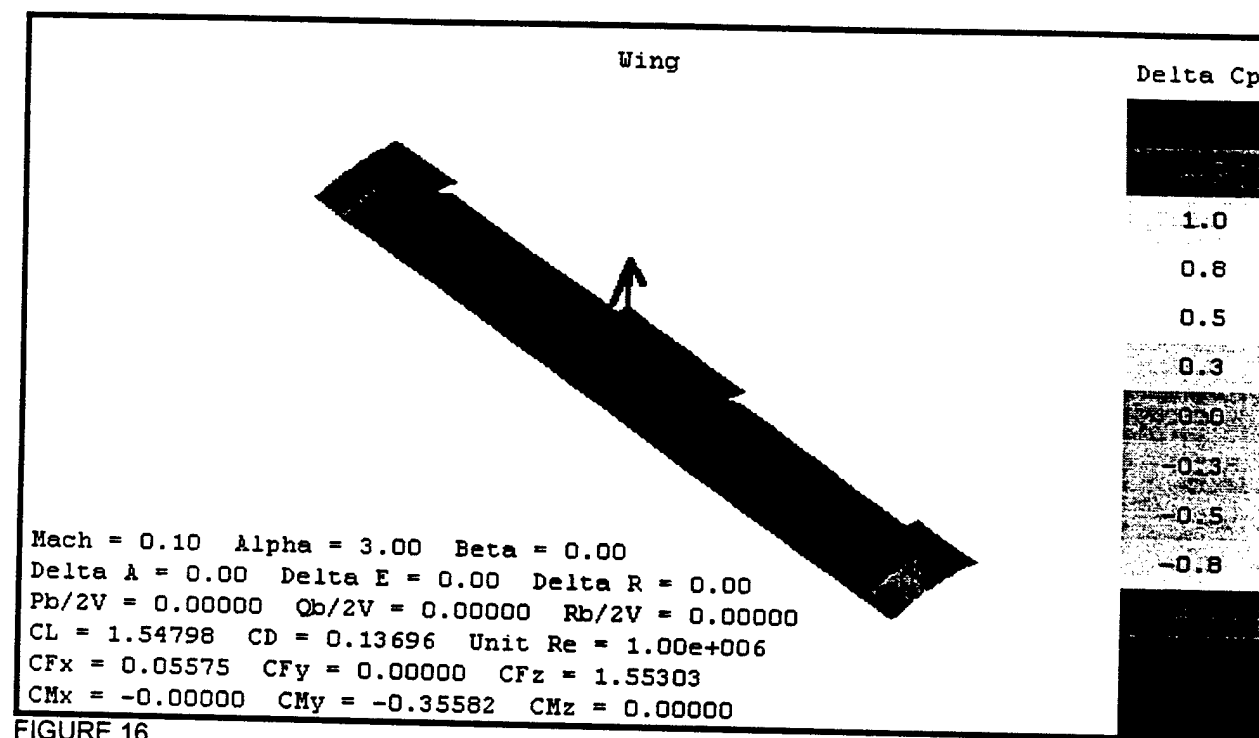
FIGURE 15

NACA 6612

We have succeeded in obtaining a higher lift wing at the minimum possible drag. As usual, the selected conditions for testing are shown in FIGURE 16. The value for the coefficient of lift was found to be 1.54798. In fact, we have succeeded in increasing the value for the coefficient of lift. However, the new coefficient of drag was found to be 0.13696. This value is greater than the drag value for NACA 6512 (previous analysis). This particular airfoil may provide more lift, but that comes at the expense of more drag.

Once again, the angle of attack versus coefficient of lift is plotted in Figure 17. Notice that at an angle of attack of 3 degrees, the approximate value of the lift coefficient is 1.54. As we expected, the coefficient of drag is approximately one tenth of the lift coefficient. In reality, the coefficient of drag is about 12% of the lift coefficient value. Figure 18 illustrates this relation.

NACA 6612



DETAIL DESIGN

We have explored the idea of increasing the lift while minimizing induced drag. We have simulated the effects of both, an increase in camber as well as an increase in its point of maximum value. We have succeeded in obtaining a higher lift wing at the minimum possible drag. Based on our simulations, our choice of airfoil is NACA 6512. This airfoil profile will be used for the elevators as well.

1. Fuselage design

The general aerodynamic characteristics of the aero-structure are based on its geometry, including the landing gear. Once again, aerodynamic design is a balancing act between lift and drag. The most important aerodynamic characteristic of the fuselage is the coefficient of drag. We will minimize its value. We recall that gliders have a great advantage over regular configurations, they minimize drag. With that in mind, we proceed to design a glider-like fuselage. Figure 19 provides a glimpse of our original design. Notice the sharp edges at the front and back of the fuselage. Our optimized model is shown in Figure 20.

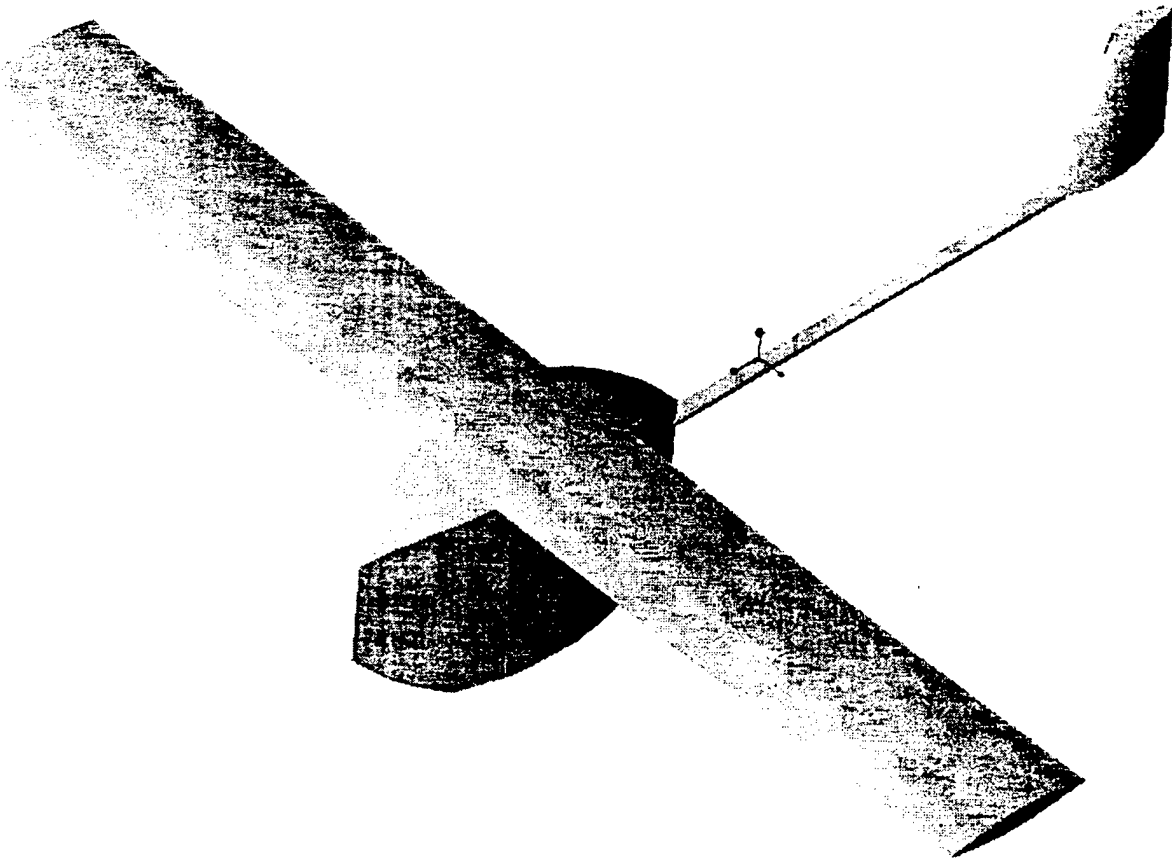


Figure 19 Original Design

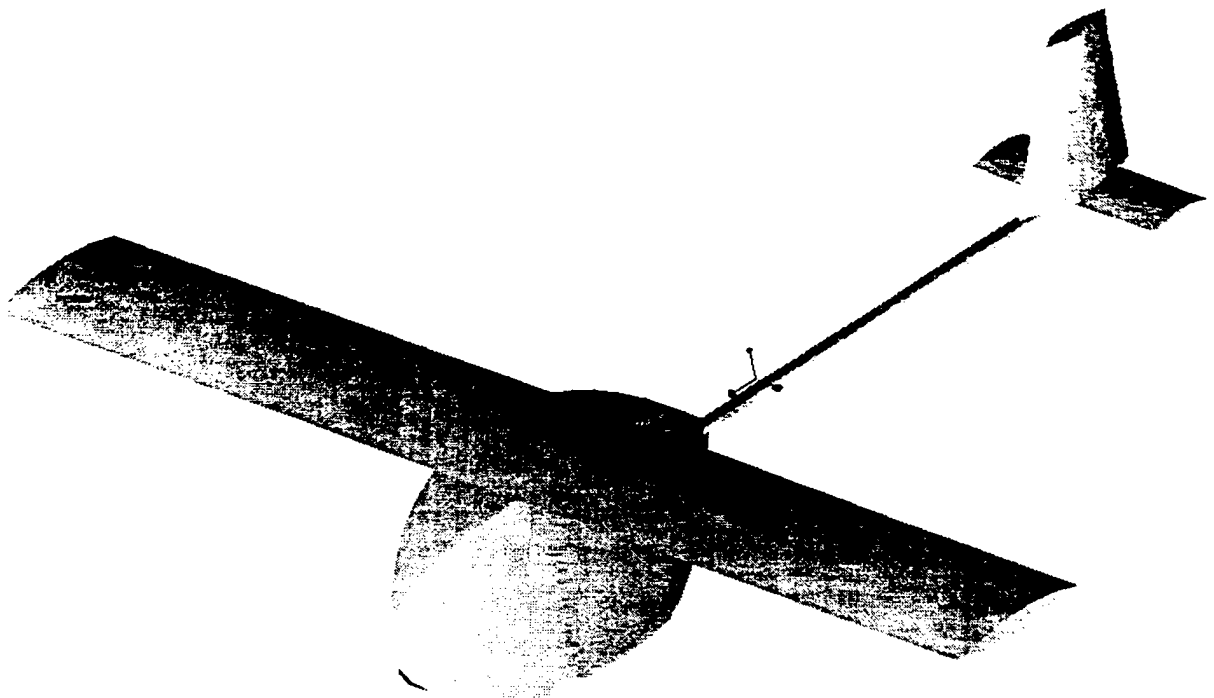


Figure 20. Optimized Design

Since the most important aerodynamic characteristic of the fuselage is the coefficient of drag, we will minimize its value. We recall that gliders have a great advantage over regular fuselage configurations, they minimize drag. With that in mind, we chose a glider-like fuselage. Our optimized model is shown in figure 20.

2. Power Plant

One of the most important and difficult aspects about building an airplane is the selection of the appropriate power plant. The power plant must provide enough thrust to accomplished the tasks set for this competition. These tasks include liftoff within 200 feet, flying around a field carrying a heavy payload and a volume payload in a specific time period. The power plant must provide with the necessary thrust and power to fly for at least ten minutes. The power plant consist mainly of the engine the battery pack and the propeller. These parts have to be selected and manipulated carefully in order to accomplish the best performance needed.

Another important part in the power plant is the speed controller, which is the accelerator for the motor. The selection of an adequate controller was very important for energy conservation.

We analyzed all the family of motor from the astro-flight company and tried to narrow down our selection base on the size and weight of the airplane.

For this design we used over the counter NiCad batteries as determined by the rules of the competition. Another power constraint and weight constraint was the maximum number of cells to be used dictated by the five pound limit.

The propeller selection was made based on the weight of the airplane and the wing design. Propellers are made of wood or reinforced nylon and should be commercially produced.

2.1 Motor analysis

The biggest obstacle for the design of the airplane was the weight of the airplane with the max payload and specially the five-pound battery limit. The main concern was to complete the highest number of laps with the heavy payload and volume payload and maximize the potential power supplied by the cells.

Our approach was as follows:

- We investigated what kind of airplane we were going to design based on the wing and fuselage set up. Based on these designs we were able to calculate the wing area, length fuselage cross-section.
- We proceeded to determine the handling characteristics. Our design concept has the characteristics of a very large airplane with over 1000 sq. in. of wing area.
- We studied many profiles for the wing and after many trials and optimizations we decided to use
- We determine the total weight: $\text{Total weight} = \text{wing loading} \times \text{wing area}$
- We chose an appropriate power loading. For this airplane the power levels go from 50 to 100 watts / pound
- We determine the peak power needed: $\text{Peak power} = \text{power loading} \times \text{weight}$
- We estimated a static current needed. A good starting point is to choose a current that gives 6-7 minutes. With the use of throttle, the static draws yield 8 to 10 minutes of good flight.
- We determine the number of cells. Since good Ni-Cad deliver approximately 1 volt per cell: $\text{Number of cell} = \text{peak power} / \text{current}$
- Determine the motors. For this step we decided to use a series layout for the cells. For this competition only brushed motors are accepted.
- We decided to use a gear. Most motors have to be gear to turn the large propellers necessary for efficient thrust.

With the previous information we were able to tabulate different input to get the values necessary to perform the tasks assigned. Having reached some conclusions we narrowed down or selection of motors.

We then determined the weight of the power system and the radio. We looked up the weight of the motor and gear box and multiply it by 2. The weight of the battery was five pounds.

With this information we were able to calculate how much can the airframe weigh.

To choose the right propeller we had to find certain speeds for our model

- First we calculated the stall speed
- The desired flight speed is recommended to be twice the stall speed. This is more than adequate for any bomber or transport. At three to four times the stall speed, good maneuvering and fighter type performance is achieved
- For our design the stall speed is $22.83\text{mph} \times 2 = 45.66$
- The transport/bomber is only going to be 85 to 90 percent efficient so the prop speed will have to be 45.66×1.15 (15% addition to be safe) = 52.52 mph
- To find the prop speed: Prop speed = pitch x rpm.
- The desired flight speed was figured to be 52.52mph. A good average rpm for geared cobalt 25/40 is 6500rpm. With this basic estimation we can calculate the pitch. For transport/bombers types a pitch ratio of 2:1 is good

In the real world electric motors are not 100% efficient and our propellers are not 100% efficient. Both motors and propellers when used properly and in their design ranges should provide efficiencies of 70% to 85%. The motor that we used which is available from Astro Flight, delivers high power at efficiencies of 78% to 82%. The thin carbon fiber scimitar propeller blades available from Hobby Lobby can deliver thrust at efficiencies between 75% and 85% depending on aerodynamic loading.

We will present the expected range with a real motor and a real propeller installed in the model. We can expect our model to have a range between

Flying Weight

17 lbs.	16 lbs.	15 lbs.	14 lbs.	13 lbs.
<u>Glide Ratio</u>				
10: 1	15:1	20:1	25:1	30:1
80% Efficiency				
38 laps	61 laps	87 laps	116 laps	150 laps
75% Efficiency				
36 laps	57 laps	81 laps	109 laps	141 laps

The power needed for level flight as we mention before is a function of wingspan, weight, and shape factor. If we assume a streamline model not unlike a Sailplane, the shape factor will be close to 4.0. Using this value of shape factor and a combined propulsive efficiency for motor and propeller of 50% we can construct the following table.

Weight	6 Ft Span	8 ft span	10 ft span	12 ft span	14 ft span
18 pounds	138 watts	104 watts	83 watts	69 watts	59 watts
19 pounds	147 watts	113 watts	90 watts		
20 pounds	156 watts	122 watts	97 watts		

For take off and climb out our model will need an excess power over that needed for level flight of 50 watts per pound. This power level will produce a climb rate of about 400 feet per minute and should be adequate for the 200-foot runway. The take off power required for the same configurations used before are show here.

Weight	6 ft span	8 ft span	10 ft spa
17 pounds	450 watts	418 watts	399 watts
18 pounds	480 watts	446 watts	425 watts
19 pounds	510 watts	474 watts	451 watts
20 pounds	540 watts	502 watts	477 watts

The propulsion system should be able to handle up to 400 watts at take off. Maximum efficiency in the cruise mode should be as high as possible at power levels between 50 watts and 100 watts. Candidate Systems include the FAI-25 and FAI-40 motor frames with the new astro super high ratio gearbox.

Model						
Number	627	627G	642	642G	643	643G
Motor						
Name	FAI-25	FAI-25	FAI-40	FAI-40	FAI-40	FAI-40
	Direct	Geared	Direct	Geared	Geared	Direct

MANUFACTURING PLAN

Introduction

From the beginning, we knew that this was a manufacturing challenge. Our main problem was that none of the members of our team had any experience in building a remote control airplane. Therefore, our first task was to find information, and collect information on the different techniques used for building remote control airplanes. After this preliminary research was concluded, we learned that the fuselage had to be to build with wood. Three types of wood were recommended for the construction of the fuselage, balsa for the airplane surface, and spruce for the skeleton interior. Plywood was recommended for places where extra strength was needed. We also found two techniques for constructing an airplane wing, namely, using balsa wood ribs, and using a solid foam core.

Several books explained the difference between this two building techniques, however the explanations were unsatisfactory. We needed to know which technique best suited our needs. We decided to try simple but effective techniques. We bought the necessary materials and tools and embarked in the exploration of these building techniques. We constructed two small models, one made out of foam and the other made out of balsa wood. All of our members agreed that balsa wood was easier to cut and manipulate, for this reason, we decided to use balsa as the main material for the construction of the wing.

1. Preliminary wing.

Our first model was GOT 185. Our design team gave us this airfoil because of its physical characteristics, its flat bottom, the curvature of the camber, and the length of the chord. Because of the flat bottom characteristics this airfoil was fairly easy to build. The purpose of the building of the airfoil was to test its lift capacity as well as its strength. The first step in building our wing was to get a print out of the airfoil with its actual measurements. Once we had the outline of the airfoil the next step was getting it drawn into the balsa wood sheet. Once this was done we drew as many ribs as necessary. The second step was to cut out the individual ribs from the balsa sheets this was done with a modeling knife. We cut from the highest point on the rib to the trailing edge to take advantage of the wood grain, for it takes the blade away from the drawn line and eliminates the chance of undercutting.

Once all the ribs were cut, we held them together with a clam in order to cut the notches (all at once using a small handsaw). The notches were located at a distance of one third of the chord from the leading edge and at two thirds of the chord from the leading edge. These specifications were given by the design team. Once the notches were cut we proceeded to sand all the ribs until they were all even. This is a very important step because it has a lot of influence on the aerodynamic performance of the wing. Now that the ribs were done, struts were introduced and glued into the notches, each rib was separated by a

distance of three inches. For this first design only four struts were used, two on the top and two on the bottom. We let the glue cure for 24 hours and then we proceeded to the sheeting of the wing.

Applying the sheet of balsa to the wing was one of the most difficult and frustrating tasks, because all the pieces were to be placed precisely in order to have a smooth surface. First we applied carpenters' glue in all the edges of the wing skeleton. Then, we placed the sheets carefully, just avoiding any gaps between them. Once the wing was fully covered by balsa wood we continued by covering the surface with shrink paper in order to protect it from humidity, since balsa wood is so sensitive to humidity.

2. Wing stand.

For the testing of the wing in the wind tunnel we needed to build a stand that would fit in a tunnel with a 4 by 4 feet cross sectional area. The purpose of this stand was to measure the lift capacity of our wing. We knew that manufacturing of this stand was not our primary objective so we did not want to spend a lot of time and effort on its construction. The manufacturing team proposed a very simple design that included two vertical parallel circular rods separated by a distance of three and a half feet. The rods were held in place two wooden blocks with circular holes drilled into them where the rods were inserted, these blocks were then themselves screwed to a flat wooden surface.

Linear bearings were to move up and down along the rods, these bearing were connected to a metal platform, which would hold the wing, as the wing would lift. In summation, the mechanism would work as follows. Once the wind tunnel is turned on, the wind would create a lift on the wing. It will also create a drag. However, since the wing is constrained by the platform, which would only move up and down, this drag force would be canceled and only the lifting force would act on the wing. This lift force can be measure by putting weights on the wing.

3. Prototype Wing

After the preliminary results, we decided that The GOT 185 did not have the lift needed in order to achieve our goals, so we needed to test a new airfoil. The design team gave us the NACA 6512. The same procedure followed for the construction of the preliminary wing was followed in the construction of this wing. Once test wing for the NACA 6512 was build we put it in the win tunnel the tested its lift. When the tests were done, we concluded that the results for NACA 6512 were satisfactory and we proceeded to build a full-scale prototype. The wing was to have a seven feet wing span and the chord was to be one foot long.

Since we did not have seven feet long struts we have to find a way to build a seven feet long wing with three feet long struts. We decided to build three parts of the wing separately and then connected then in a way that the final wing would have the require length. The three parts were called the right wing the second

part was the center wing and the third part was called the left wing. The center wing was constructed with three feet long struts, but only one foot of its length, from the middle out, would have ribs going across them. The extra two feet, one foot at each side, overlap with the right wing and the left wing and serve as the connecting parts. The left wing and the right wing were also constructed with three feet long struts, but now two feet of their length were cross with ribs. These two feet were measure from the left tip of the struts for the left wing and from the right tip of the struts for the right wing. The extra foot left without ribs overlap with the center wing and serves as the connection part.

4. Fuselage

For the construction of the fuselage we would use a very simple and straight procedure. The interior structure is a simple box with the measurement previously specified by the design team. This box will be divided into small compartments where the different peaces will be placed, always taking in consideration the desired position of the center of gravity. Since the surface of the fuselage is a curved surface in order to have better aerodynamic characteristics, we will use thin sheets of balsa wood to build this curved surface. It is important to mention that the surface will not have any structural value it is there only to improve the aerodynamic of the plane. One of the primary elements of the fuselage is its fast loading capabilities this is done by having a railing system at the bottom of the fuselage. These rails will serve as a guide to the retractable container that will carry the paid load. At the back of the fuselage extra structural strength will be needed to ensure that the fuselage will be able to resist the bending moments that will be created by the tail of the plane. A truss system that connects the fuselage and the tail was designed to account for these moments.

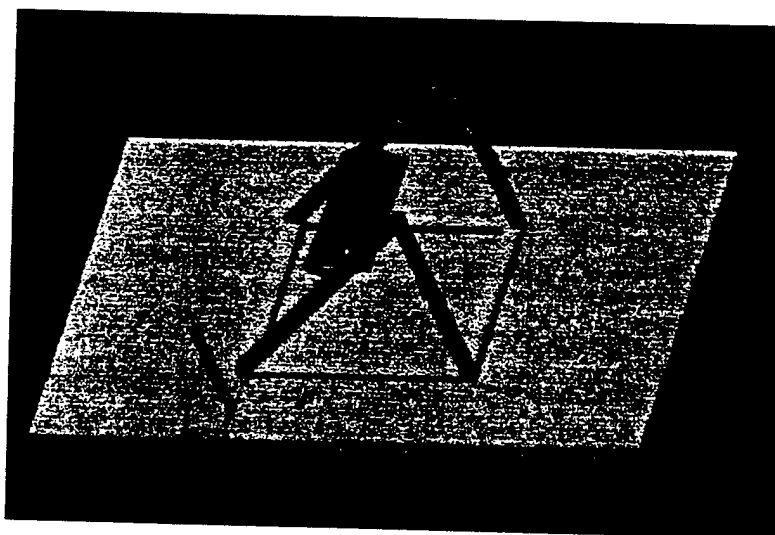
5. Landing gear

After taken into consideration as to whether to buy the lading gear from a commercial remote control airplane dealer or to design a landing gear ourselves, we decided that purchasing a landing gear was a better choice. We purchased a tricycle landing gear; the front wheel will be placed at the tip of the airplane and the main landing gear will be placed just behind the center of gravity. Each wheel will have wheel pants in order to decrease the drag. Additional padding for the wheels will be added in order to have a smooth landing.

6. Finite Element Analysis on Wing

One of the most crucial aspects of the design is the prediction of the bending moments across the wing. Finite Elements Analysis was employed in solving the task. Moreover, a good engineer is always compelled to exercise good judgement when using Finite Element Methods.

We applied Finite Element Analysis to the wing. Bending moments will be produced as the aerostructure takes off. Under general conditions, the wing will undergo bending as well as stresses due to torsion. As a good exercise, we designed a special apparatus for testing the wing under static pressure (please see figure below). The process is intended to simulate the some of the bending load conditions that the wing will be subjected to. We loaded the wing with 10 pounds of load. At this particular value we appreciated considerable deflections. When we reached approximately 22 pounds, the wing underwent failure. Finite Element Analysis was employed in determining the stress distribution along the wing. The results obtained help us to visualize the stress field along the wing. Thus facilitating a better response to solve the problem. Finite Element Analysis helps us to determine that the bending moment along the wing will be much higher closer to the fuselage. Therefore, solving the problem requires reinforcing that specific part as supposed to the entire structure. This helped us to save not only time but also some additional use of materials. However, one must be very careful when approaching Finite Element Methods results. The figures below describe the failure conditions that occurred in our static test. Most importantly, they also show the same response for a reinforced wing.



Wing Stand

Displacement Mag
Max +4.3898E-04
Min +0.0000E+00
Original Model
Max Disp +4.3898E-04
Load: load1



+3.902E-04

+3.414E-04

+2.927E-04

+2.439E-04

+1.951E-04

+1.463E-04

+9.755E-05

+4.878E-05

Z

"window1" - anlysj - anlysj

Displacement Mag
 Max +4.3404E-04
 Min +0.0000E+00
 Deformed Original Model
 Max Disp +4.3404E-04
 Scale 2.0736E+03
 Load: load1



+3.858E-04

+3.376E-04

+2.894E-04

+2.411E-04

+1.929E-04

+1.447E-04

+9.645E-05

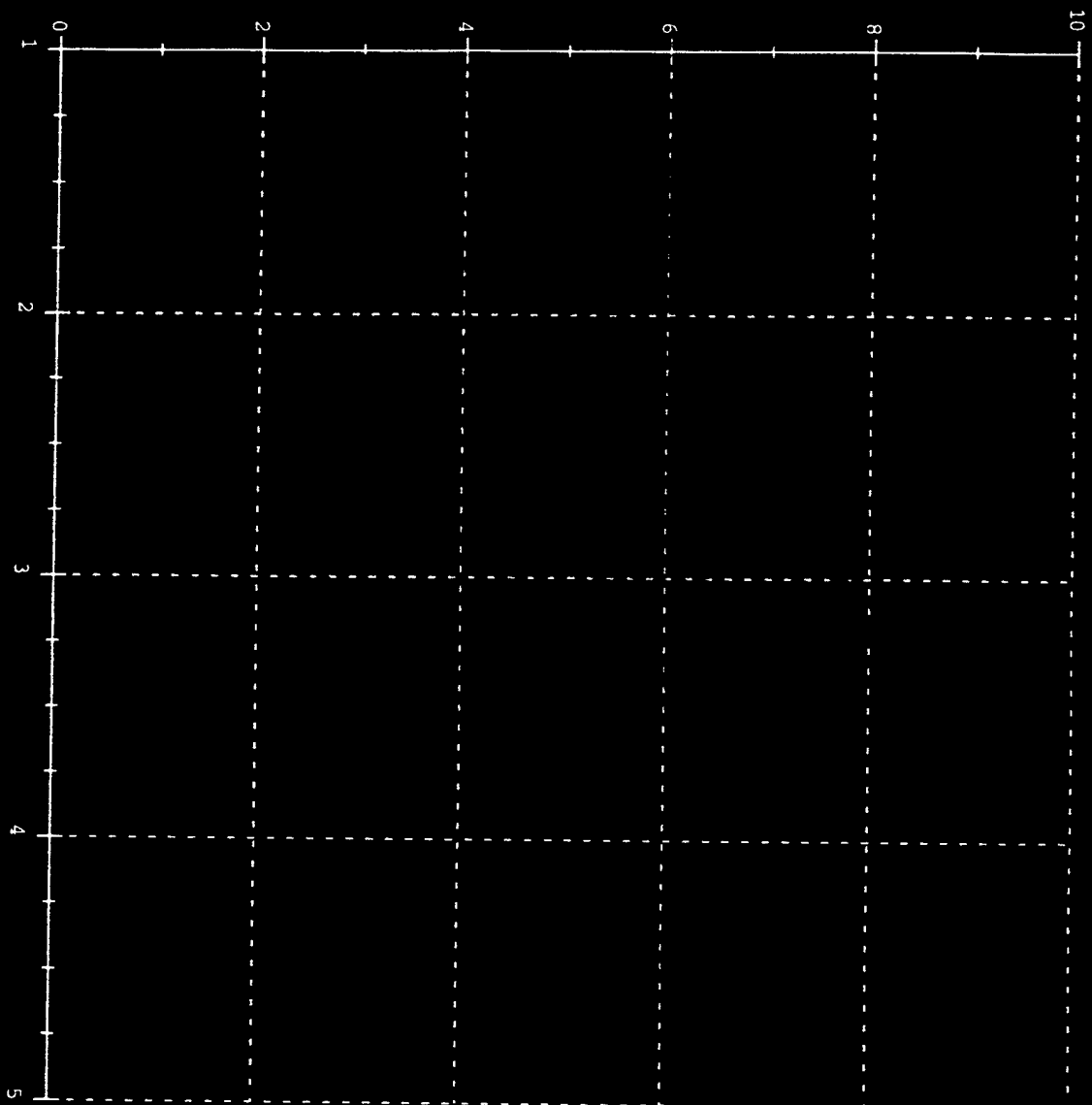
+4.823E-05

z

"window1" - anlysl - anlysl

strain_energy
P-Pass
Load: load1

strain_energy



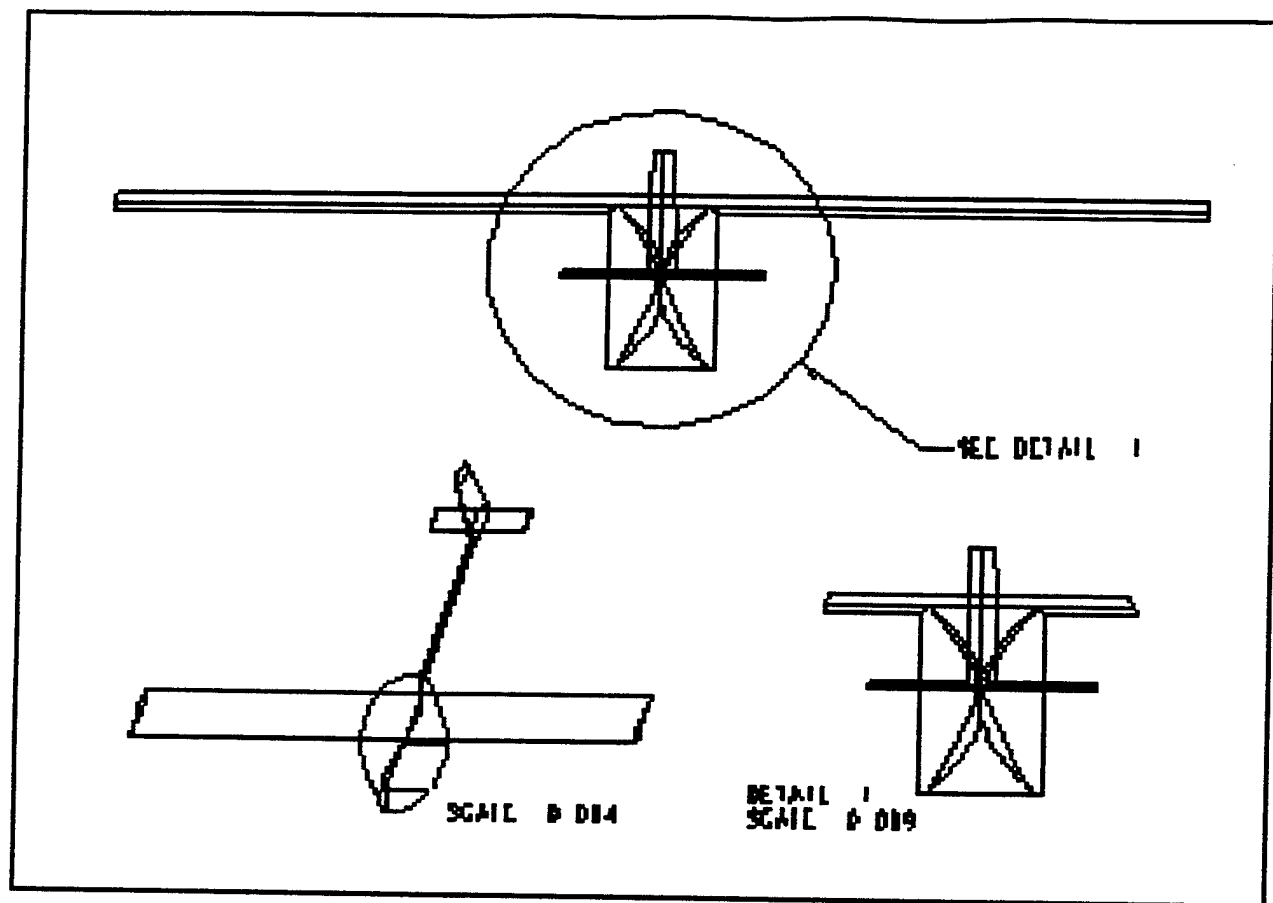
"window2" - analys3 - analys3

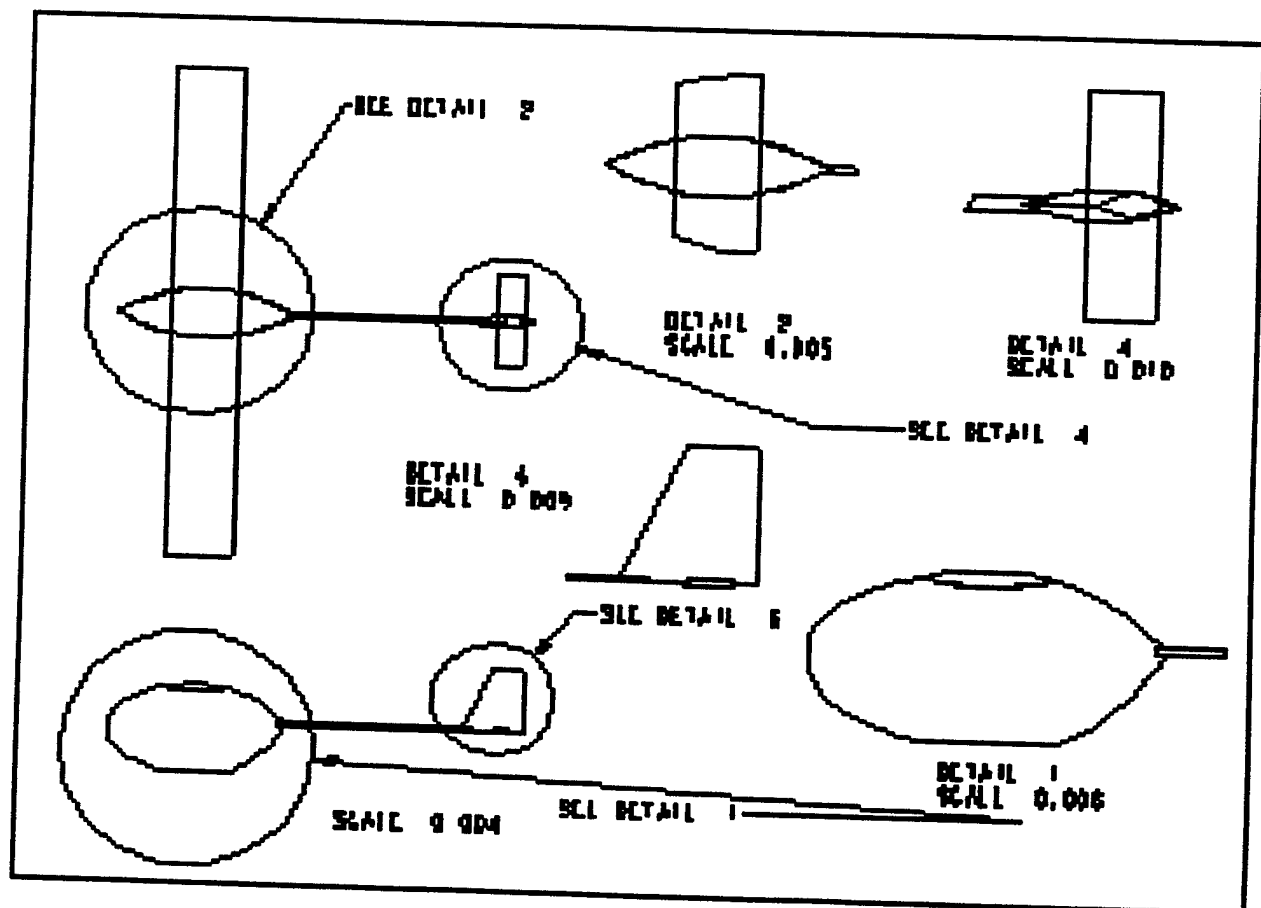
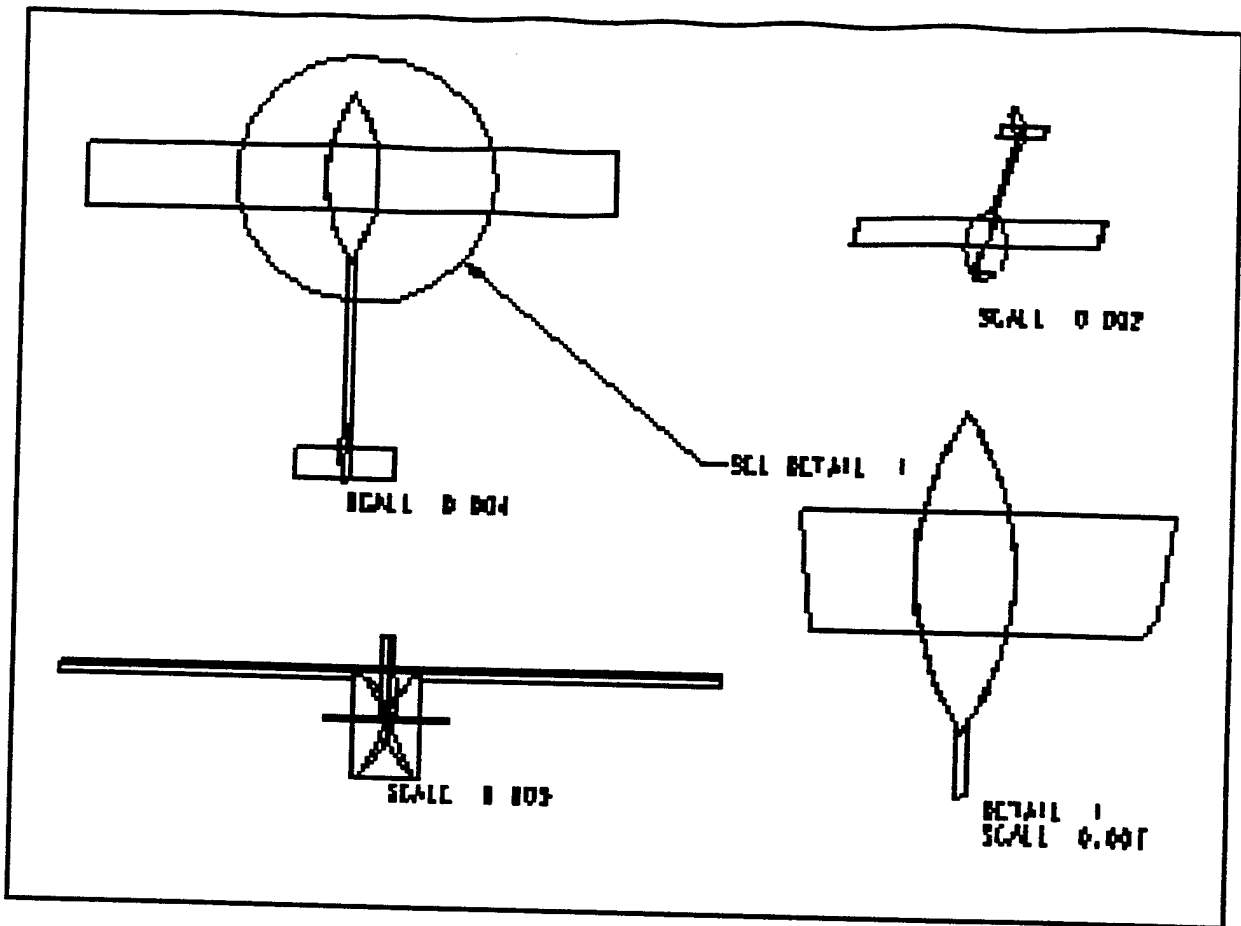
FINAL AIRPLANE CONFIGURATION AND DRAWING PACKAGE

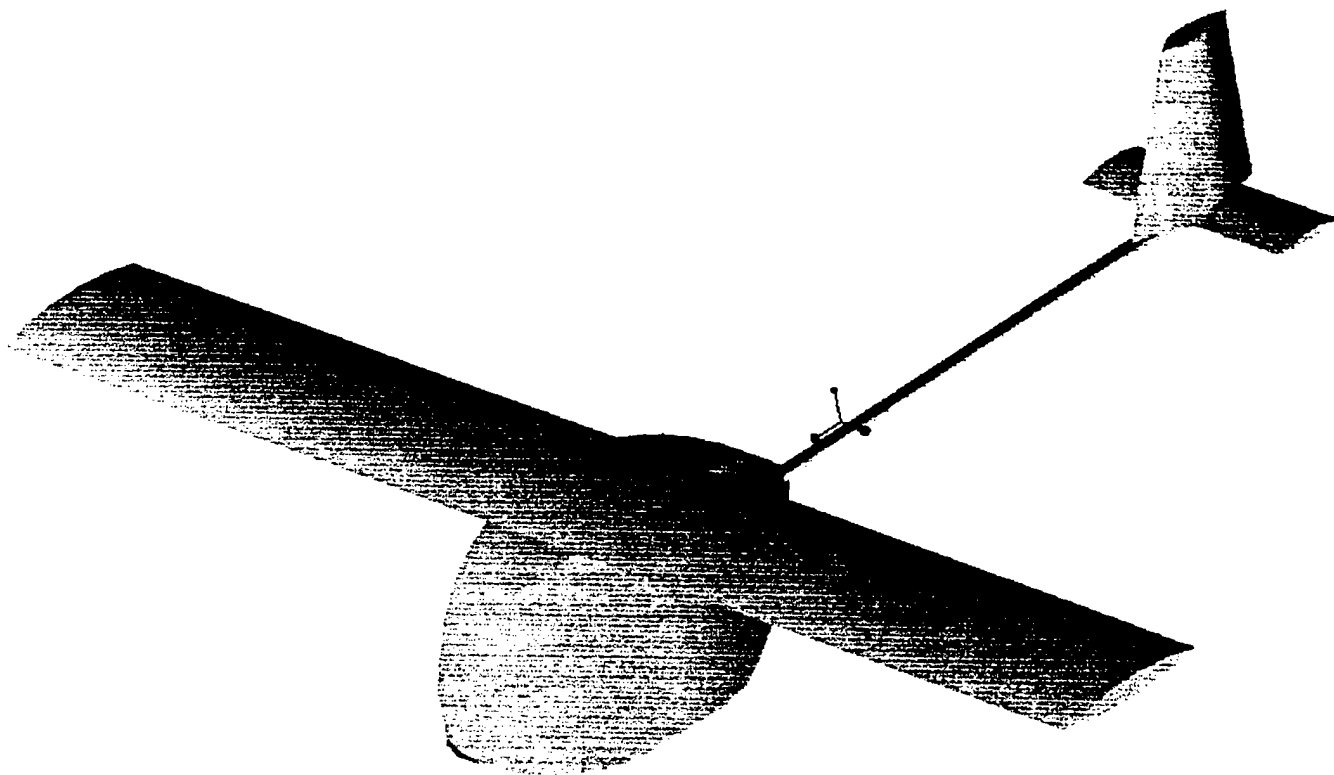
Payload Capacity	Heavy payload	8 lb of steel
	Volume payload	40 tennis balls
Wing configuration		Monoplane
Wing airfoil		NACA 6512
Wing area		10.5 square feet
Wing angle		2
Mounting angle of Horizontal Stabilizer		2
Horizontal stabilizer area		4 square feet
Vertical stabilizer area		2 square feet
Tail airfoil	horizontal	NACA 0012
	Vertical	NACA0012
Fuselage length		3.75 feet
Motor		1- Astro flight 643G FAI-40 Geared
Propeller		22x12
Total loaded weight		33
G load capacity		2.5
Rated aircraft cost		6.2456

Drawings

TECHNICAL DRAWINGS







References

Astroflight website

Electrics. Shawn Keith. Model Airplane News

Fundamental of Aerodynamics, by John David Anderson. 1984. McGraw-Hill. United States of America

Fundamentals of Flight. Second edition. Shevell Richard S. Prentice Hall

Getting Started in Radio Control Airplanes. By Yarrish, Gerry. Model Airplane News

The illustrated guide to Aerodynamics. Second edition. Smith. H.C

Theory of Flight. Von Mises

THE CITY COLLEGE OF NEW YORK



CITY HAWK

ADDENDUM PHASE REPORT

DESIGN, BUILD & FLY COMPETITION
AMERICAN INSTITUTE OF AERONAUTICS AND ASTRONAUTICS

TABLE OF CONTENTS

LESSONS LEARNED	3
------------------------	----------

IMPROVEMENTS TO CONCEPTUAL DESIGN

1. Introduction	3
2. General Improvements	3
3. New Airfoil Selection	4
4. Flaps and Ailerons	5
5. Flaperon Deflection	5
6. Dimensions	6
7. Stabilizers Values	7
8. Fuselage	8
9. Center of Gravity	9

AIRCRAFT COST ANALYSIS

1. Cost Analysis for Aircraft	10
2. Optimized Design Configuration	10
3. Final Design	11

LESSONS LEARNED

INTRODUCTION

Aerodynamic design is a balancing act between lift, drag and other vectorial forces involved (i.e. thrust). Therefore, the aerodynamic characteristics of the structure are based on the design of the wing, the fuselage, the ailerons, elevators, rudders as well as landing gear. The correct airfoil profile should optimize the lift without inducing a considerable amount of drag. We optimize lift, and maneuverability while inducing minimum drag. The same methodology applies to the ailerons, rudders and elevators.

Since the correct selection of the wing depends on its profile. A careful analysis and comparison was performed among a *family* of airfoil profiles. Our selected profiles come from the NACA (4 digit) family of airfoils. The analysis was performed in Sub-3D. The quantities that we are mainly concerned with are the coefficient of lift and the coefficient of drag. Originally, the airfoil chosen based on its numerical figure of merit was NACA 6412. However, a second thorough analysis was performed on each of the above-mentioned airfoils. Logically, the best approach is to corroborate computational results with experimental evidence. However, this may be extremely difficult to do without the proper aerodynamic testing facilities. Based on our second general analysis we chose NACA 6512 as the airfoil to be used in our design. Its general aerodynamic characteristics were discovered to be better than the ones for NACA 6412.

GENERAL IMPROVEMENTS

1. Wing

1.1 New Airfoil Selection(1) As mentioned before, we started with The Gottingen 285 (GOE 285) and the Gottingen 188 (GOE 188) were the airfoils from the conceptual design stage selected for further analysis. The airfoil analysis was done using an internet-based software at the web address, <http://beadec1.ea.bs.dlr.de/Airfoils/calcofoil.htm>. The analysis proved that GOE 285 is a superior airfoil than GOE 188. The coefficient of lift (Cl) of GOE 285 at zero angle of attack is 0.40, and that of GOE 188 is 0.33. Thus GOE will create greater lift at an angle of attack of zero and at subsequent angle of attacks. The Lift to drag (L/D) of GOE 285 is 29.4239 and that of GOE 188 is 9.5796. Though GOE 188 has a smaller nose down pitching moment than GOE 285, its lift to drag is too low for it to be considered any further. After a second analysis, we decided to choose NACA 6512 for its aerodynamic properties, including its lift to drag ratio value.

Airfoil	FOM	FOM	FOM	Total
	Cl	L/D	Pitching Moment	
GOE 285	1	1	0	2
GOE 188	0	0	1	1

Table 1

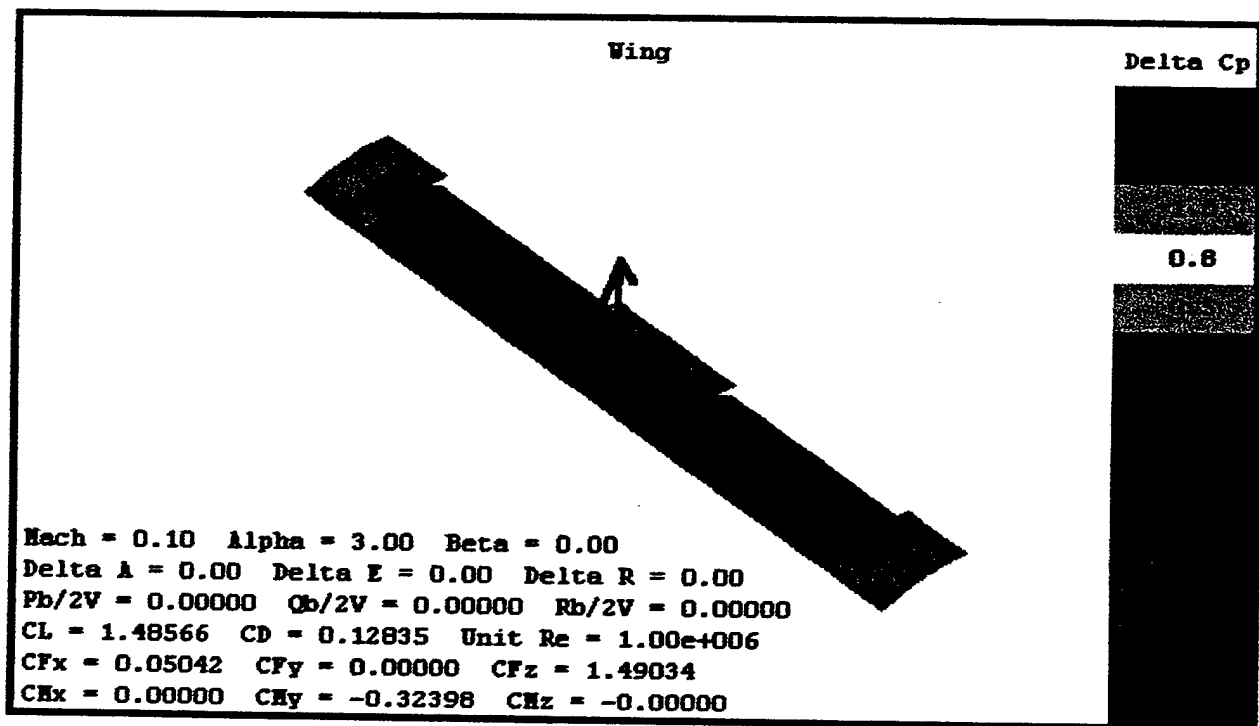
1.2 Airfoil Selection(2) After the above analysis had been completed another airfoil was discovered and introduced, NACA 6412. This airfoil was argued to be better and since it was comparable to GOE 285 in thickness and camber, the group decided to analysis it. It was analyzed using the same software used to analyze GOE 285 and GOE 188. The coefficient of lift of NACA 6412 at zero angle of attack is 0.63 and its lift to drag 42.8488. Though its moment coefficient at zero angle of attack is more negative than that of GOE 285, originally, the decision at this discovery was unanimous, NACA 6412 would be used. However, after a secondary analysis we decided to use NACA 6512.

<u>Airfoil</u>	<u>FOM</u> <u>Cl</u>	<u>FOM</u> <u>L/D</u>	<u>FOM</u> <u>Pitching Moment</u>	<u>Total</u>
NACA 6512	1	1	0	2
GOE 285	0	0	1	1

Table 2

<u>Airfoil</u>	<u>Cl (@ 0 AOA)</u>	<u>L/D (@ 0 AOA)</u>	<u>Cm (@ 0 AOA)</u>
NACA 6512	0.63	42.8488	-0.1263
GOE 285	0.40	26.4239	-0.0651
GOE 188	0.33	9.5796	-0.0234

Table 3: Summary of airfoil force characteristics. Re = 200000



NACA 6512 (NEW CHOSEN AIRFOIL).

1.3 Flaps and Ailerons Flaps are used to increase the camber of a wing thus increasing its coefficient of lift at a specific angle of attack. Ailerons are used for roll control and to ensure lateral stability. Each flap and each aileron will require its separate servo for deflection. To save weight, time, money and manufacturing difficulty, the use of flaperons was decided upon (the March issue of Custom Planes passively encouraged this selection). Given our corrected airfoil profile, the control surface for the ailerons will be affected as well.

1.4 Flaperon Deflection The flaperon deflection was analyzed with the same software that analyzed the airfoils. The percent of flap, and angle of the flap deflection were analyzed. The percentage of chord to be used for the flaperon considered were 25% and 35 % the deflection angles were 10 degree and 20 degrees. However, after further analysis we decided to increase the deflection angles for the ailerons, thus increasing the lift produced.

% of Chord and Angle of Deflection	<u>L/D</u>	<u>Cl</u>
25% and 10 deg.	81.4818	1.02
25% and 20 deg.	83.2425	1.40
35% and 10 deg.	89.9879	1.00
35% and 20 deg.	74.4322	1.36

Table 4: Summary of flaperon deflection analysis. $Re = 300000$

The lift and the drag characteristics are preferable for a 25% chord flaperon. The high force characteristics will improve the take off performance thus decreasing take off field length and the flaperon could serve as spoilers during landing thus decreasing the landing field length.

% of Chord	<u>FOM</u> <u>L/D</u>	<u>FOM</u> <u>Cl</u>
25%	1	1
35%	0	0

Table 5: Figures of Merit for % of chord.

1.5 Dimensions(1) The aspect ratio of a light aircraft ranges from 5 to 7. Since our aircraft is smaller than a light aircraft, the following calculations are based on an aspect ratio of 5.

$$AR = 5$$

$$\text{Span, } b = 10 \text{ ft}$$

$$\text{Chord, } C:$$

$$AR = b / C$$

$$C = 10 / 5 = 2 \text{ ft}$$

$$\text{Wing Area} = 10 \text{ ft} * 2 \text{ ft} = 20 \text{ ft}^2$$

$$\text{Wing Loading, } n = 55 \text{ lbs} / (20) \text{ ft}^2 = 2.75 \text{ lbs/ft}^2$$

1.6 Dimensions(2) A seven foot wing was fabricated to test its structural integrity and wing loading. Part of the results of the test showed that a nine foot wing span would be preferable than a ten foot wing span, because the wing is fabricated in three foot sections; and adding a one foot section in the middle, for the width of the fuselage, reduced the wing's structural integrity and put it's zero dihedral at risk. The test wing had an aspect ratio of 7. Inspection of the wing showed that an aspect ratio of 5 may prove difficult to manufacture in such a manner as to reduce separation due to uneven surfaces, and would increase weight by its internal supports. So the Aspect ratio was increased to six. In this manner, the overall weight of the aircraft including the payload could be reduced for better performance. However, for now the gross weight would be kept at 55 lbs.

$$AR = 6$$

$$\text{Span, } b = 9 \text{ ft}$$

$$\text{Chord, } C:$$

$$AR = b / C$$

$$C = 9 / 6 = 1.5 \text{ ft}$$

$$\text{Wing Area} = 9 \text{ ft} * 1.5 \text{ ft} = 13.5 \text{ ft}^2$$

$$\text{Wing Loading, } n = 55 \text{ lbs} / (13.5) \text{ ft}^2 = 4.07 \text{ lbs/ft}^2$$

2. Empenage

2.1 Horizontal Stabilizer (Longitudinal Stability) Since the wing produces a pitching moment about its aerodynamic center and the lift it generates also produces a pitching moment, to trim the aircraft a horizontal stabilizer fitted with an elevator is employed. These provide longitudinal stability that is stability in pitch. A graph of pitching moment vs. angle of attack results in a line with a negative slope, this is evident from the table of the values below. Negative pitching moment is a nose-down moment.

Angle of Attack	Cm
0	-0.1263
1	-0.1278
2	-0.1286
3	-0.1301
4	-0.1317
5	-0.1334
6	-0.1349
7	-0.1365
8	-0.1381
9	-0.1395
10	-0.1397

Table 6: Values of alpha vs. Cm

Trim will be achieved partially by the nose-up moment of the wing lift (L_w) forward of the CG and partially by the nose-up moment of the downward lift of the tail at a moment arm of ' l_t '. The natural nose down pitching moment, which is about the aerodynamic center, is equal to the wing lift moment and the tail moment.

$$M_{ac} = L_w * l_w + L_t * l_t$$

Evidently a larger ' l_t ' will result in a smaller ' L_t '. As a result to result to reduce weight and have a sufficient ' l_t ' a tail boom will be used and the fuselage will be shortened.

2.2 Horizontal Stabilizer Airfoil This airfoil is usually a symmetric airfoil. NACA 0012 was chosen over NACA 009 for its better lift characteristics with a 25% chord elevator at 25 degrees deflection, and its thickness.

Airfoil	FOM Lift Characteristics	Total
NACA 0012	1	1
NACA 009	0	0

Table 7: Figures of merit for Horizontal stabilizer airfoil

Horizontal stabilizers are usually placed at a negative angle of incidence.

2.3 Horizontal Stabilizer Dimensions The horizontal tail volume coefficient for light aircrafts ranges from 0.5 to 0.7. The large degrees of flap will require greater horizontal tail surface, thus a larger horizontal tail coefficient to provide maximum longitudinal stability.

Tail Volume coeff, $C_{tv} = 0.7$

Tail Volume, $V_t = C_{tv} * S_w * C = 0.7 * 13.5 * 1.5 = 14.175 \text{ ft}^3$

Tail arm(determined from fuselage), $l_t = 2.25 + 0.5 + 1.25 = 4.0 \text{ ft}$

Tail Area, $S_h = 14.175 / 4 = 3.5 \text{ ft}^2$, Approximated to 4 ft^2 for added stability.

Tail Span, $b_h = 4 \text{ ft}$

Tail Chord, $C_h = 1 \text{ ft}$

Elevator = 25% of chord

The horizontal stabilizer is usually considered to be a third of the size of the wing.

Wing Area, $S_w = 13.5 \text{ ft}^2$

Tail Area, $S_h = 4 \text{ ft}^2$

$S_h / S_w = 4 / 13.5 = 0.296$ (approximately $1/3$)

2.4 Vertical Stabilizer (Directional Stability) Directional Stability is provided by the fin and the rudder. The degree of directional stability like the degree of longitudinal stability is proportional to the size the control surface, in this case the fin and rudder. And, also the distance from the CG. A larger area results in a larger side force and a greater distance from the CG results in a greater moment arm. An increase in either of the parameters will result in a larger restoring moment. The sizes of these parameters are also proportional to the amount of yaw control and weathercocking done by the rudder and fin respectively.

2.5 Horizontal Stabilizer Airfoil This airfoil is a symmetric airfoil. NACA 0012 will also be used for the vertical stabilizer, for the reason outlined above.

2.6 Vertical Stabilizer Dimensions A simple rule used in RC flight was learned from the DBF 2000 report of the California Polytechnic State University. The rule states that the vertical tail be half of the horizontal tail. Thus,

Tail Span, $b_v = 2 \text{ ft}$

Tail Chord, $C_v = 1 \text{ ft}$

Rudder = 25 % of chord

3. Fuselage The fuselage will house the payload, the engine, the batteries and support the weight of the wing as well as the tail boom. The fuselage will comprise of three sections. The first and third sections are similar to a pyramid sawn off at the middle and with its rectangular base lying in the vertical plane. These rectangular bases are to be attached to the second section of the fuselage at both ends. This section will be a rectangular box.

The first section will house the engine. The second section will house the payload as well as support the weight of the wing. The third section will house the battery pack and will provide access for the tail boom into the fuselage for structural support.

A fuselage with a rectangular cross section is susceptible to crosswinds and sideslips during a turn. As a result to ensure lateral stability fuselage effect was taken into consideration. To provide for upwash over the second section that is rectangular, the wing which is 1.5 ft in chord length will be mounted at the rear of this section leaving 1 ft of the top of the section in front of the leading edge of the wing. Thus total length of the second section will be

$1 \text{ ft} + 1.5 \text{ ft} = 2.50 \text{ ft}$.

The first section will be 0.75 ft long and the third section will be 0.50 ft long. The total length of the fuselage without the tail boom is, $0.75 + 2.50 + 0.50 = 3.75 \text{ ft}$.

A fineness ratio of a fuselage is three. If it is high than this the fuselage will create more drag, and if it is less than three the drag created by the fuselage will be even worse.

Fineness ratio = length of fuselage / height of fuselage = 3

Therefore,

Height of fuselage = $3.75 / 3 = 1.25$ ft

To minimize the lateral cross section the width = 1 ft

4. Center of Gravity The center of gravity of the aircraft will be calculated by measuring the difference in weight between the nose gear and the main gear.

4. Rated Aircraft Cost, \$ (Thousands) = (A*MEW + B*REP + C*MFHR)/1000

Coeff.	Description	Value
A	Manufacturers Empty Weight Multiplier	\$100/lb
B	Rated Engine Power Multiplier	\$1A/Watt
C	Manufacturing Cost Multiplier	\$20/hour
REP	Rated Engine Power	# of Engines * Amp * 1.2V/cell * # of cells "Amp" will be the value of the inline fuse from the battery to the controller. Maximum value is 40A, but a lower current fuse may be used, and REP adjusted accordingly.
MFHR	Manufacturing Man Hours	Prescribed assembly hours by WBS (Work Breakdown Structure). WBS 1.0 Wing(s): 15 hr./wing + 4 hr./sq. ft. Projected Area + 2 hr./strut or brace + 3 hr./control surface Note: Winglets, end plates, and biplane struts ARE included in the Projected Area calculation WBS 2.0 Fuselage and/or pods 5 hr./body + 4 hr./ft of length WBS 3.0 Empennage 5 hr. (basic) + 5 hr./Vertical Surface + 10 hr./Horizontal Surface WBS 4.0 Flight Systems 5 hr. (basic) + 2 hr./servo or controller WBS 5.0 Propulsion Systems 5 hr./engine

	+ 5 hr./propeller or fan
--	--------------------------

Rated Aircraft Cost, \$ (Thousands) = $[(100(20)+1(1425.6)+20(120))/1000]=5.8256$

5. Optimized Design Configuration

- 1- Wing: The wing configuration is a rectangular planform, high wing with zero dihedral, because of ease of manufacture and inherent stability. The airfoils that have been chosen for further analysis are Gottingen 285 for it's thickness, camber and relatively flat bottom, and Gottingen 188 for it's flat bottom.
- 2- Fuselage: The fuselage will have a rectangular cross-section and be shaped like a box with a tapered rear.
- 3- Empenage: The tail will be conventional.
- 4- Thrust: The aircraft will be a single engine tractor.
- 5- Landing Gear: The landing gear will be tricycle.
- 7- Cargo Bay: The cargo will be housed below the wing at the center of gravity.
- 8- Wing Span: 10 feet
- 9- Total Weight: 55 lbs

OPTIMIZED FINAL DESIGN

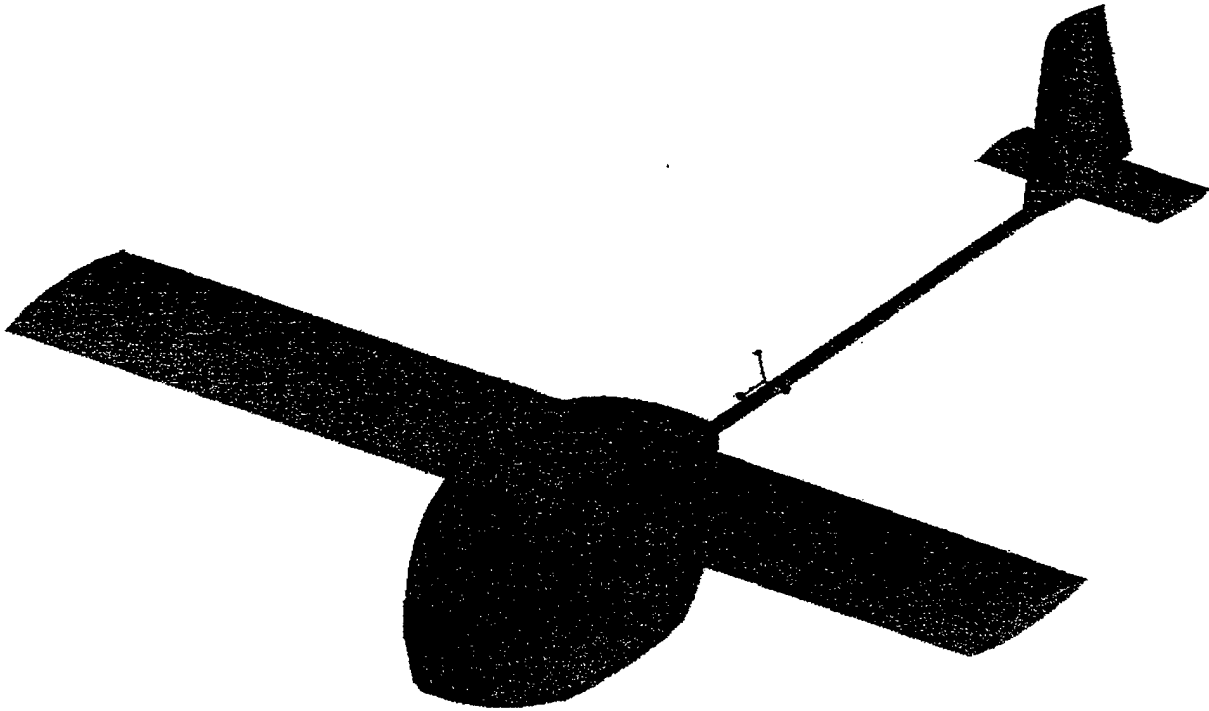
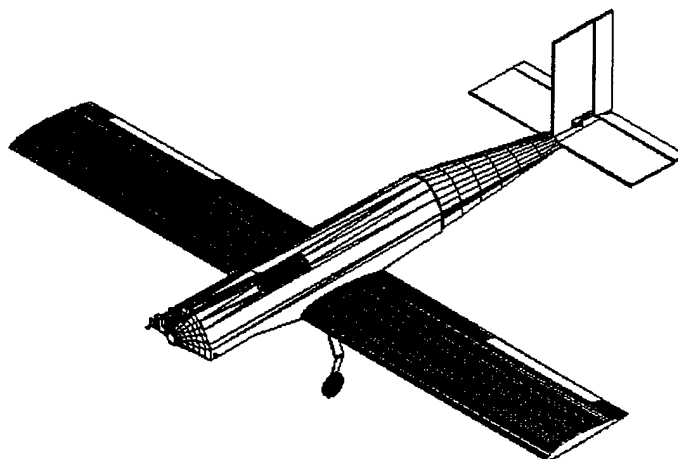


Figure A. Optimized Design

Since the most important aerodynamic characteristic of the fuselage is the coefficient of drag, we will minimize its value. We recall that gliders have a great advantage over regular fuselage configurations, they minimize drag. With that in mind, we chose a glider-like fuselage. Our optimized model is shown in figure A. Notice that despite of its apparent similarity, this model has a new chosen airfoil -NACA 6512. Same applies to the ailerons and flaps and entire aerostructure.

**2000/2001 AIAA
*Cessna/ONR Student Design, Build, Fly Competition***

Design Report



“MU-2”

**Miami University
Oxford, Ohio**

March 2001

Table of Contents

Executive Summary

Problem Statement.....	1
Summary of Design of Development.....	1
Overview of Design Tools Used.....	1

Management Summary

Architecture of Design Team.....	3
Management Structure.....	3
Project Milestone Chart.....	4

Conceptual Design

Alternate Concepts Investigated	7
Design Parameters Investigated and Figures of Merit Used.....	8
Rated Aircraft Cost Summary.....	10
Features That Produced the Final Configuration Selection.....	13

Preliminary Design

Design Parameters / FOM Explanation.....	14
Configuration / Sizing data.....	15
Tail Position.....	17
Aileron Span.....	17
Special Features.....	18

Detailed Design

Performance Data.....	19
Aerodynamic Factors.....	19
Handling Qualities.....	19
Takeoff Analysis and Climb Performance.....	20
Flight Performance Analysis.....	22
Component Selection.....	27
AutoCAD Drawing Package.....	33
Configuration Solutions Tail-to-Fuselage Attachment.....	37
Wing-To-Fuselage Attachment.....	37
Landing gear-To-Wing Attachment.....	38
Motor Mount Configuration.....	38
Estimated Weight.....	40

Manufacturing Plan

FOM for Manufacturing Processes	41
Purchased Products.....	41
Tail.....	42
Fuselage.....	42
Nose cone.....	43
Rear Fuselage Attachment.....	43
Wing.....	44
Wheels.....	44
Motor Mount.....	45
Wiring.....	45
Manufacturing Milestone Chart.....	46

EXECUTIVE SUMMARY

problem statement

The contest rules ask student design teams to "design, fabricate, and demonstrate the flight capabilities of an unmanned, electric powered, radio controlled aircraft that can best meet the specified mission profile." After reviewing the mission profile and subsequent rules and regulations, our team set out to design and build the best airplane, according to the rated aircraft cost model (explained later in the report). The main purpose of this competition is to apply engineering and aeronautic knowledge to a real life scenario, incorporating analysis, design, and manufacturing. The culmination of these efforts will be the judging of this report documenting our design, as well as the flight score our aircraft accumulates in the air.

summary of design development

Our approach to accomplishing this task started with brainstorming ideas based on our involvement in past design, build, and fly competitions, and this year's contest rules. Preliminary designs were considered, that included such variations as the number of wings, where to carry the payload, and shape of the fuselage. For instance, we considered making the plane a low, single-wing plane or a bi-wing plane with structured supports. We also considered different shapes and sizes for the fuselage, such as circular, boxed, or a mixture. After careful consideration and brainstorming, we decided to carry the payload internal to the fuselage (especially because the internal wing area is not an option). Design decisions were attacked in an iterative manner. For example, the number of internal "tunnels" was disputed, ranging from two to five. This decision depended on the overall length of the plane and the type of weight distribution that comes about from subsequent design and building. This design approach has proven to be very effective and efficient in completing our task.

Our team consists of ten students, three of which are in manufacturing engineering, and the rest are involved with aeronautics. Once a preliminary design was selected, we formed sub teams to consider some of the different components including, the wing, fuselage, propulsion, tail, and landing gear. We decided to include one engineering student in each group to provide an engineering perspective to each component. These teams met independently to work on each component and the whole group met weekly to ensure compatibility in the design of the components. Our plan is to have the aircraft built and ready for testing as early as possible to give us ample time for testing and trial runs.

overview of design tools used

We used many different, but very helpful design tools in all phases of design development. For example, in our conceptual design stage, we used basic tools such as rated aircraft cost analysis, FOM analysis, and research from previous designs.

In considering more advanced design necessity, we looked to AutoCAD 14, ElectriCalc, and Microsoft Excel to develop a model of the preliminary designs as well as to determine the rated aircraft cost of each

one. We also figured in basic aeronautic principles of thrust and drag graphs and average speed readouts to select certain motor and propeller systems for analysis.

When it came to the detailed design portion of the project, we relied heavily on AutoCAD 14, ElectriCalc, Stability and Control Program, and Take Off and Climb Performance Program.

✦ *AutoCAD 14* is a computer-aided design package that allowed us to visualize the detailed aspects of our aircraft in both a two-dimensional and three-dimensional workspace. It is the basis behind all of our modeling design and component analysis.

✦ *ElectriCalc* is a computer program that enabled our team to determine the aircraft's propulsion systems, which in our case was a D/C brush motor. It was used to find the optimal motor, battery, and propeller combination. We investigated various parameters of the aircraft design, such as the weight of the airplane, surface area of the wing, type of motors used, as well as many other different inputs. ElectriCalc's output included the aircraft's thrust and drag, the life of our batteries, as well as graphs of the different inputs and output parameters we chose to compare.

✦ *Stability and Control Program (SCAP)* is a program mainly used in the Aeronautics Department at Miami. It is used to estimate the stability of aircraft including inputs for the location of the center of gravity, length from the nose to leading edge of tail, and other overall dimensions of the aircraft. We studied Alpha angles, which deal with how far the aircraft veers from its longitudinal axis in the vertical direction and Beta angles, the yaw, or how far it veers in the horizontal direction.

✦ *Takeoff and Climb Performance Program (TACP)* is another program used in Miami's Aeronautics Department. This program is based on the equations of motions that were obtained by relating aircraft acceleration to the thrust, drag, and rolling friction forces. Engine and propeller data that was obtained from Electricalc were entered as inputs to TACP as well. This program was chosen because it was written for previous aircraft design projects and was easy to use and offers accurate results.

MANAGEMENT SUMMARY

architecture of design team

Our particular design team is a collaboration of people with one common interest—that of designing, building, and flying a plane in this contest. We all have our own individual reasons for this interest, but it is a shared interest just the same. Three students represent the Manufacturing Engineering Department at Miami, while the others are active in Aeronautics study. Majors and programs of study range from Engineering to Management to Finance to Chemistry to Physics. Table 1 shows the team members and their particular areas of expertise.

Table 1: personnel and assignment areas

Name	Class	Major	Design Group	Skills/Tasks
Ben Kessing	Sr. (5th yr.)	EGM	Propulsion	Motor Analysis Builder Manufacturing knowledge
Ryan Walton	Sr.	EGM	Propulsion	Propulsion Analysis Grant proposal Builder/tester
Chris Ruifrok	Jr.	Finance	Propulsion	Propulsion Analysis Builder/tester
Steve Wittman	Sr.	Marketing	Wing	Wing Design Builder/tester
Tyler Martin	Sr.	Economics	Wing	Wing Design Builder/tester
Tommy Joyner	Sr.	EGR	Wing	Wing Design Builder/tester
Steve Parlato	Sr.	EGR / EGM	Fuselage / Landing gear	Fuselage design Builder/tester Landing gear design
Sarah Wyse	Jr.	Zoology	Fuselage	Fuselage design Builder/tester
Lenny Marsh	So.	Marketing	Fuselage	Fuselage design Builder/tester
Scott Foster	Sr.	Chemistry	Tail	Tail design Tail builder Team leader
Rauolle Rausch	Jr.	Physics	Propulsion	Performance analysis
Dr. James Stenger				EGR Advisor
Dr. Richard Walker				Aeronautics Advisor
Tom Schroeder				Aeronautics Advisor

*EGR – Manufacturing Engineering, EGM – Engineering Management, Manufacturing specialty

management structure

The team is also blessed with three advisors, one from the Manufacturing Engineering Department and two from Aeronautics. Their main tasks from a management standpoint are to give us guidance and suggestions for all aspects of the project. The team is also divided into smaller subsections—ones for the

wing, fuselage, propulsion system, and tail. This resulted in a more complete understanding of the workings of the entire plane by separating members with diverse backgrounds. Each smaller group worked on its individual area throughout the week, then we met as an entire group each week to discuss consequent areas of success, those which need improvement, and possible concurrent changes to the current design with regard to the ease of manufacturing. Design decisions were made by consensus within the subgroups and relayed to the entire team at the weekly meetings for review and discussion. This management structure has minimized conflict and produced a team working towards a common goal.

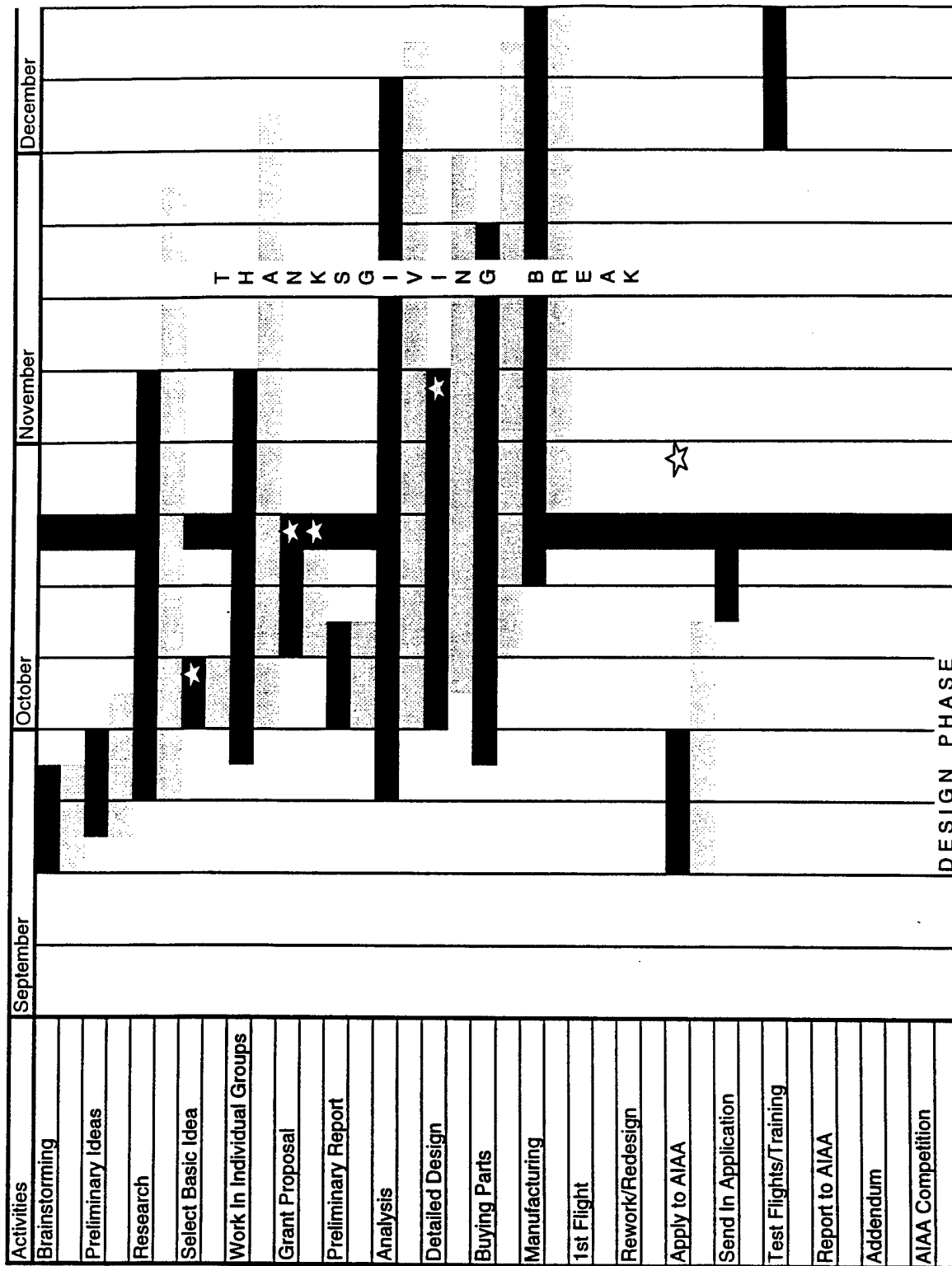
Various members of the group were assigned specific assignments throughout the duration of the project. The member with the most experience in the field of building model airplanes was the emergent leader, but each member at times asked for specific actions of the other members. Team members worked together to help bridge the gaps in our educational backgrounds.

A detailed schedule was also developed at the onset of the project, with identifiable key goals and milestones. As the project progressed, another chart was kept to mirror as closely as possible the actual progression of the project. The detailed milestone chart is included below, where the identifiable stages of the project are shown along with team planned and actual progress.

milestone chart

Figure 1 shows our milestone chart. Planned and actual activities are shown with a key explaining the differences. Milestones are marked with stars for the major turning points in the project and specific goals the group has determined to be very important.

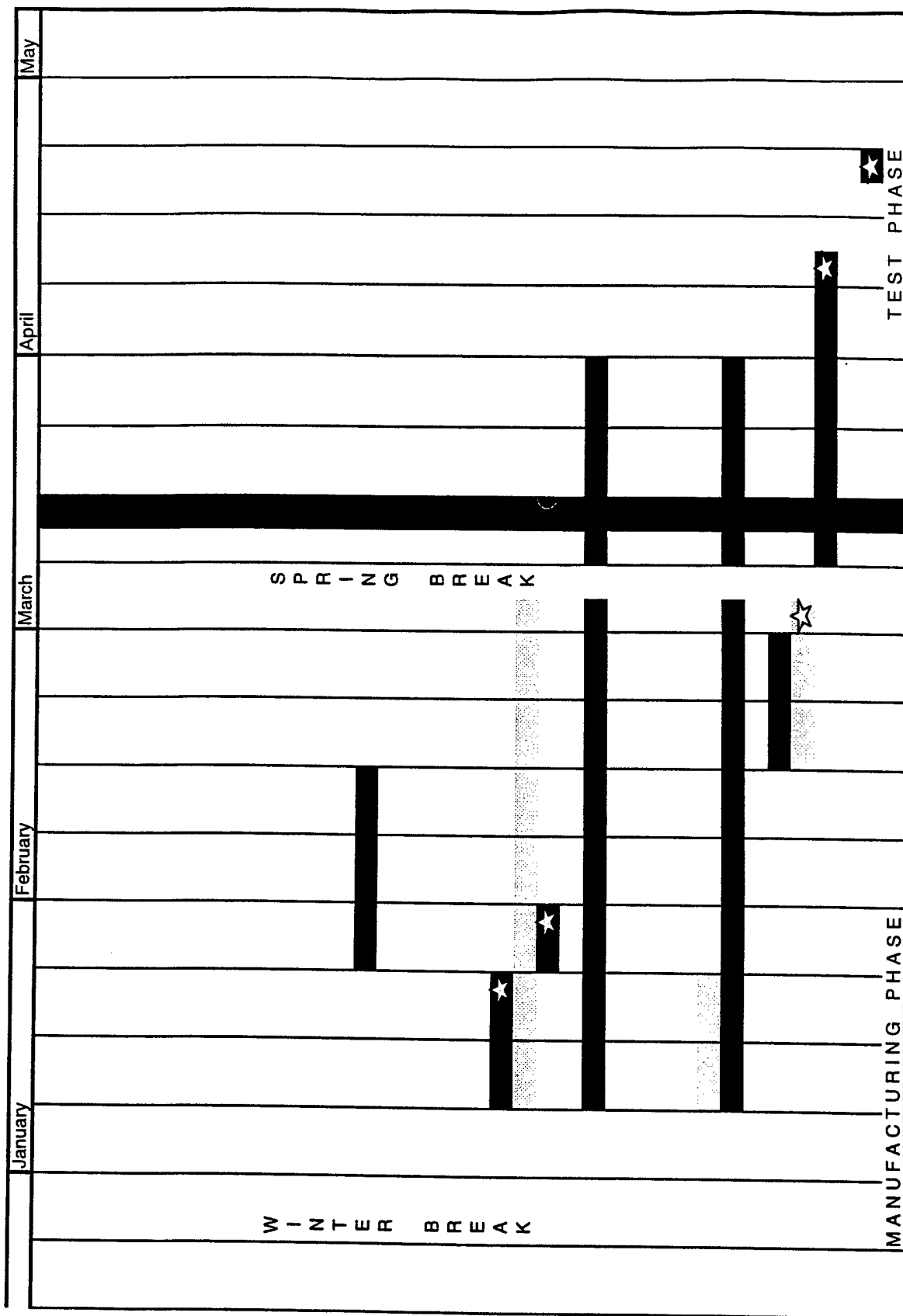
Figure 1: Milestone of MU-2 Project



■ planned
 ■ actual

*events that have yet to occur are not documented as actual, only as planned
 ☆ planned milestones are marked with stars

Figure 1 cont



CONCEPTUAL DESIGN

alternate concepts investigated

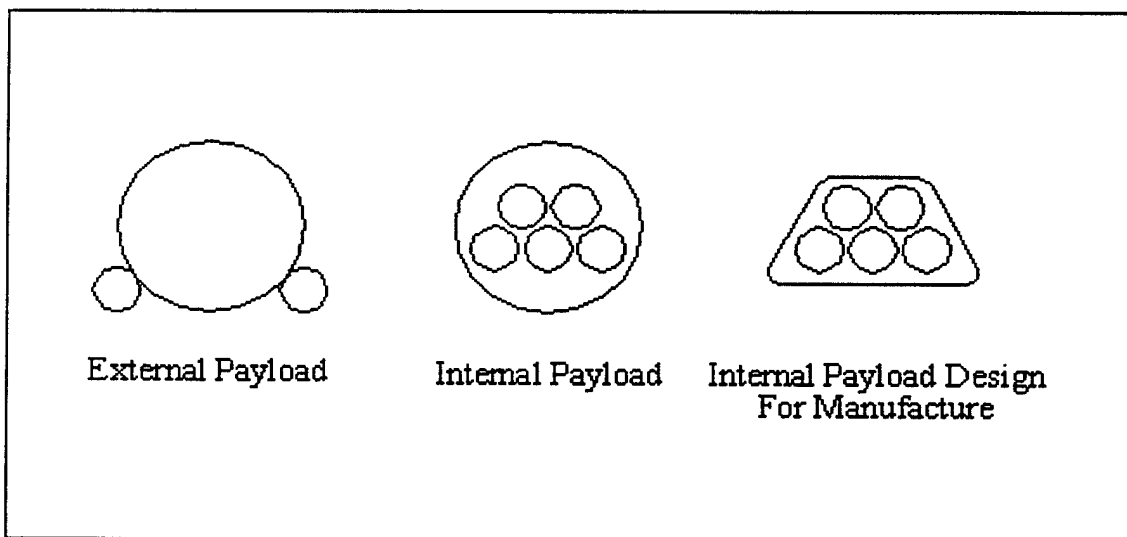
Before we approached the basic tasks of design and analysis, we first congregated to compile some preliminary ideas. Afterward, we decided on the criteria we would use to evaluate each idea, leading to our preliminary sketches of the plane and its components.

We first had to develop and analyze the type of plane we would design and build. We came up with two main designs-- the bi-plane or the single wing plane. Both have their advantages and disadvantages. For example, the bi-plane will allow for more lift, having twice the wing surface area. On the other hand, this design adds weight to the plane and adds complexity to the easy loading of competition payload, which contradicts with our goal of keeping the plane as light as possible and doing well on the flight scores. It also adds to the rated aircraft equation with the excess number of supports needed for wing stability. The single wing plane obviously does not have the lift advantages that the bi-plane possesses, but it is lighter and will be much easier to fly. The single wing plane also allows for the quick-loading procedure we need for faster turnaround time and better flight scores.

Once we considered the alternatives, we chose the single wing plane, mainly because of its ease to manufacture and its lightweight properties. Both of these factors will contribute to a better overall score.

The main point-scoring objective lies in the decision of where to carry the different payloads, internally or externally. We brainstormed three possible ideas, which are represented by the drawings below:

Figure2: Possible Payload Configurations



The first idea consisted of a solid fuselage and tubes on the outside used for carrying the different payloads. This design would increase both weight and drag, but the tubes are positioned for quick loading and unloading. The second design is a modification of the first, taking the load and making it internal to the fuselage. This change reduced some of the weight that would have come from the external tubes and the area of Styrofoam occupying along the length of the fuselage. With a better design than the one with which we started, we continued to try to make the fuselage design even better. A third design was proposed as an upside down u-shaped fuselage with the payload compartments cut out of the Styrofoam. Again, this design has its pros and cons. The right angles formed near the bottom will eliminate the air pockets formed by the second design's circular shape. The square bottom is not the most technically aerodynamic design, but our wing placement and attachment makes this design the most desirable.

There are three main areas for possible wing placement-- under the fuselage, above the fuselage, or attached to the side. As a group, we decided that the best way we had to attach the wings was with model-specific glue. Bearing this in mind, we considered the overall implications of putting the wing in each place. Attaching the wing to the sides of the fuselage seemed like the worst idea. If for some chance the glue's hold loosened a bit, surely the wings would fly off and the plane would crash. The same holds true for putting the wings over the fuselage. Any tearing or quick gust of wind might rip the wings up and away from the heavy load. The likely solution was to attach the wings under the fuselage. A quick gust of wind simply pushes the plane higher in the air, and if the glue starts to loosen, the flight itself pushes the wing up into the fuselage where it belongs. The only possible downfall is the force generated on the tips of the wings in addition to the weight of the plane, but we will offset this with carbon-fiber sheets in an I-beam formation for increased support.

In other areas, we took less time deciding on component decisions. One example was the overall wingspan. We decided that if the design analysis allowed for the maximum 10' wingspan, we would use all ten. This greatly increases the surface area exposed to the forces of flight. We also had to consider things like the length of the fuselage and where to affix the motor. The fuselage design and placement was chosen to be long enough to carry five tunnels of twenty tennis balls each. The tail length will depend on the necessary balancing of the aircraft on the quarter-chord point ($1/4$ of the way across the cross-section of the wing). Balancing the aircraft here is good practice and will make the plane much easier to control during flight missions. Motor placement will also follow this principle for balance.

design parameters investigated and figures of merit used

After our team brainstormed a number of different ideas, we decided on which designs to consider for further analysis toward a final design. The three main ideas our team chose were the biplane, the low-wing monoplane with outside containers, and the low-wing monoplane with internal compartments, as was stated earlier. It was then from these three ideas that our design team had to choose as the one that

would be the basis of our final design, which would be the plane that our group would use for the detailed design. In choosing our final design, the different members thought up of various design parameters that were pertinent to developing an effective aircraft.

The deciding parameters and their mission features were as follows:

speed of loading: This parameter is critical to the plane's scoring potential in the contest. Each time the plane competes; it has only 10 minutes to fly as many laps as possible, including changeover time. The less time it takes to change over between different payloads, the more time is spent in the air. The more laps completed, the higher the subsequent score.

carrying capability: This parameter is also critical to the plane's scoring potential. The more tennis balls (and more steel) the plane is able to fly with, the higher scoring potential the plane carries.

manufacturability: Another critical parameter, the easier a plane is to manufacture, the less time will be spent in building it. This often leads to lower cost, as well as more time for test flights and alterations before the contest.

stability: This has to do with the plane's ability of preventing itself from veering horizontally and vertically from its line of flight. A plane that is unstable in flight is very hard to control.

maneuverability: This has to do with the ease of banking, climbing or diving the aircraft. Our concern here would only be with its turning ability. The sharper its banking angle, the less time will be spent traveling around the 360-degree loop. Since these designs are so large, and will be around the same weight, their banking maneuverability will not differ by that much from one another.

aerodynamics: This has to do with the flow of air across the surfaces of the plane. The more aerodynamic the plane is, the less drag is induced upon it. This parameter was not weighted much, due to the fact that the planes will not be going more than 40 mph. By concentrating on the curvature of the plane, the time and cost spent in manufacturing the surface topography will not be offset much by what is gained in speed.

safety: This parameter was ranked last, because any plane entered into the contest has to have the same safety requirements, in that if the transmission signal fails, the plane will automatically dive and bank away from where any spectators will be. Each different idea would have the same type of motor, and it would always be disengaged during the changeover period. There could possibly be a slight chance that one of the outboard containers on the mono-wing design could come loose during flight, and

put some ground personnel at risk, but this was the only safety risk that differed from the other ideas we considered.

rated aircraft cost summary

The rated aircraft cost was only one aspect of our selection process although it had a significant bearing on our performance. For each of our three preliminary designs we calculated a predicted rated aircraft cost using the equation provided by the contest. Once the aircraft cost was calculated, it was then divided by the predicted payload capacity for three flight scores to obtain a cost per point estimate.

Our first design was a biplane design. This design would provide more lift due to the dual wing system, but had a very high cost. Our intentions were to carry the payload in the struts between the wings, but this design didn't allow us to carry many tennis balls. Table 2 shows a breakdown of the estimated rated aircraft cost for the biplane design.

Table 2: Figure-of-Merit Analysis of Biplane Preliminary Design

		Cost (\$)
Weight (lb)	24	2400
Total Power (W)	1221	1221
# of Wings	2	600
Square footage of wing	21	1680
# of struts or braces	6	240
# of control surfaces	5	300
# of fuselages	1	100
Length of fuselage (ft)	5	400
# of tails	1	100
# of verticle surfaces	1	100
# of horizontal surfaces	1	200
# of flight systems	1	100
# of servos or controllers	6	240
# of engines	1	100
# of props or fans	1	100
Rated Aircraft Cost (\$)		\$7,881.00
In Thousands (\$1000)		7.88

Expected load (tennis balls)	30
Expected load (steel)	20
Expected total points (3 scoring runs)	78
Rated Aircraft Cost	\$7,881.00
Cost per point	\$101.04

Our second design was a single wing design, with the load carried outside the fuselage in tubes. This design would provide easier loading, but added unnecessary cost due to the additional weight and fuselages. This design also didn't allow us to carry many tennis balls. The drag was also a negative aspect of this design. Table 3 is a breakdown of the estimated rated aircraft cost.

Table 3: Figure-of-Merit Analysis of External Load Preliminary Design

		Cost (\$)
Weight (lb)	23	2300
Total Power (W)	1221	1221
# of Wings	1	300
Square footage of wing	15	1200
# of struts r braces	0	0
# of control surfaces	3	180
# of fuselages	3	300
Length of fuselage (ft)	7.03	562.4
# of tails	1	100
# of verticle surfaces	1	100
# of horizontal surfaces	1	200
# of flight systems	1	100
# of servos or controllers	4	160
# of engines	1	100
# of props or fans	1	100
Rated Aircraft Cost (\$)		\$6,923.40
In Thousands (\$1000)		6.92

Expected load (tennis balls)	40
Expected load (steel)	15
Expected total points (3 scoring runs)	69
Rated Aircraft Cost	\$6,923.40
Cost per point	\$100.34

Our third design was also a single wing design, with the load carried inside the fuselage in holes. This design would provide easy loading, as well as reducing the weight of the fuselage by hollowing it out.

This design allows us to carry the maximum amount of tennis balls. The drag was also reduced in this design. Table 4 is a breakdown of the estimated rated aircraft cost for this design.

Table 4: Figure-of-Merit Analysis of Internal Load Preliminary Design

		Cost (\$)
Weight (lb)	22	2200
Total Power (W)	1221	1221
# of Wings	1	300
Square footage of wing	15	1200
# of struts r braces	0	0
# of control surfaces	3	180
# of fuselages	1	100
Length of fuselage (ft)	7.03	562.4
# of tails	1	100
# of verticle surfaces	1	100
# of horizontal surfaces	1	200
# of flight systems	1	100
# of servos or controllers	4	160
# of engines	1	100
# of props or fans	1	100
Rated Aircraft Cost (\$)		\$6,623.40
In Thousands (\$1000)		6.62

Expected load (tennis balls)	100
Expected load (steel)	15
Expected total points (3 scoring runs)	105
Rated Aircraft Cost	\$6,623.40
Cost per point	\$63.08

From the three designs, our third is obviously the best choice. It has the lowest rated aircraft cost and provides the lowest cost per point. The first two designs were pretty similar in cost per point estimates, but the biplane had a much higher rated aircraft cost. Table 5 summarizes the Figures-of-Merit (FOM) and Cost for each design. The rated aircraft comparison shows that design three with the single wing and hollow fuselage will maximize our performance and our scoring potential.

Table 5: Final ranking chart for each design for each FOM

Rank Multiplier	FOM	D1	D2	D3
1.5	Aerodynamics	3	5	8.5
3	Speed of loading	8	10	9
3	Carrying capacity	6	9	9
3	Manufacturability	6.5	8.5	10
2.5	Stability	8	5	8
2	Maneuverability	5	4	8
1	Safety	7	8	8.5
TOTAL		103	118.5	141.25

Design 1 - biplane

Design 2 - low wing w/ outside tube containers

Design 3 - low wing w/ internal longitudinal compartments

features that produced the final configuration selection

Some of the features that had a major influence on our selection in this stage were the rated aircraft cost and the ranking chart. The rated aircraft cost is important because it is a major factor in our total score. The lower the rated aircraft cost the better. The ranking chart gave us a way to see all of the features we were looking for in perspective. We were able to compare the features of the various designs analytically and choose base on a quantitative value for each design.

PRELIMINARY DESIGN

After considering in detail our preliminary ideas and conceptual design parameters, we decided on a basic preliminary design. Following basic contest rules and guidelines as well as our own personal goals for the competition, we investigated many issues and finally discussed how our ideas related to the FOM's chosen. We also will explain the configuration of the most detailed component part of this design, the fuselage. We will also talk about some of the design considerations and special features used in the preliminary design of the fuselage.

design parameters and FOM explanation

First, we looked at aerodynamics, being that the first issue would be whether or not the plane would fly. We looked at potential thrust vs. drag issues, lift, and take-off length with each design. The take-off analysis is very important to the success of the missions, being that the requirement set forth is that the plane be able to take-off in less than 200 feet. The other design parameters considered are basic to the design of any plane. The lift and drag comparisons were computed using ElectriCalc, and the assumptions put into the program were accurate as far as weight, propeller size and motor used. From all the data received, we rated the different designs according to this hypothetical performance in the table below. With thorough investigation and significant belief that the analysis done here is correct, we gave this category a rank multiplier of 1.5, also assuming a lower importance, being that this factor will be used all other designs.

Two other areas we chose to focus on were speed of loading and carrying capability, both of which relate to the number of points scored during competition. Since we are planning on carrying the maximum number of tennis balls (100) and the same weight in steel payload (12.5 lbs.), we believed this area to be of the utmost importance, giving both of them rank multipliers of 3.0. The easier and faster we can load and unload the different payloads, the better our chances are of completing more sorties and gaining the maximum number of points per ten-minute trial. Most of this analysis is hypothetical, based on our beliefs looking at the different designs. We ranked the different designs on these characteristics, and as supposed, all were very similar.

The next area we considered was manufacturability, considering how easy or difficult the entire manufacturing process would be, depending on the overall geometry and assembly of the designs (the FOM's used to decide the manufacturing plan will be discussed in a later section). The biplane received the lowest score in this category due to the difficulty introduced in assembling the wing portions. The other two designs were very similar, differing only where the wings would be placed and the difficulty surrounding the respective manufacturing.

Next, we performed a preliminary stability analysis on all three designs. The biplane and the low wing plane were shown to react very similar to each other, based on the handling data from SACP (stability and control program). Analysis results deal with the banking angles, climbing and diving capabilities of the aircraft. The analysis also includes turning ability, considering the 360° loop in the contest rules as a major factor in ultimate contest scoring.

We next looked at maneuverability, a topic in which we were limited due to the nature of this type of analysis. From our readings and personal accounts of people who have flown planes like this, we assumed certain design rankings. We hope that these personal experiences with flying are correct, and not simply personal preference. In this particular area, we have done the best we can with what we had.

Safety, a consideration built into all three designs, was the last criteria we considered. We looked at safety as a necessity, not a choice. Because of this, we ranked safety with a multiplier of 1, being that the other design parameters would help to make decisions.

configuration/sizing data

One of the design parameters set forth in the beginning was to maximize our plane's scoring potential. We can accomplish this by maximizing the amount payload, as well as keeping our plane's weight down (thus, minimizing the power required to fly). With this in mind, we determined how long to make the fuselage compartment. We knew the maximum diameter of each tennis ball is 2.625 inches. If we had one compartment to hold the balls, we would need a fuselage that was $(2.625 \times 100) = 262.5$ inches, or almost 22 feet long. That would be quite ungainly.

For ease of loading/unloading and balance, we wanted to have an equal amount of tennis balls to fit into each compartment. We also did not want a fuselage that was wider than its length, because that would increase the drag acting on the plane, and stability and handling would decline. If we went with 4 compartments of 25 tennis balls each, the fuselage length would be 65.625 inches, or almost 5.5 feet long. If we went with 5 compartments of 20 balls each, the total length would be 52.5 inches, or 4.375 feet long.

For aerodynamic qualities, we wanted the top surface to have a smooth, rounded contour. Since we were going to attach the wings to the bottom of the fuselage, we thought we could improve the ease of manufacturability by having a flat surface on the bottom. In this way, there would be more surface contact between the top portion of the wing and the bottom of the fuselage, thus making the wing more secure to the fuselage. With a flat bottom surface, we decided it would be better to have five compartments of 20 balls each. Two compartments would be bored out of the top portion and three would be bored out of the bottom portion. In this arrangement, the 5 tennis ball compartments can be

located closer to one another, thus reducing the wasted excess material in between them, which would have occurred by having two compartments on top and two on the bottom.

The second aspect on our minds was the weight. We wanted to make the fuselage out of Styrofoam. Styrofoam is a very light material, and the fuselage is one of the largest components of the plane. We had between 0.65 and 0.7 inches between the tennis ball compartments and the outside surface of the fuselage. This was done because the Styrofoam material becomes weaker as sections of it get thinner, and it is easier to chip off thinner sections. This would be possible during quick changeover. We do not want the chance of a crack propagating from inside one of the compartments to the outside surface while in flight. By having 0.7 inches between the bottom three sections and the bottom surface, there is much more untouched Styrofoam area to insert the two tail booms, and less worry about them ripping out of the fuselage while the plane is in flight. The rear side of the fuselage consists of a 1-½ inch thick wall. This prevents the balls from falling out the back. During the quick changeover part of the sortie, the balls are to be inserted into the front of the fuselage all at once. This thick wall section in the wall provides increases durability by preventing the tennis balls from tearing through the back wall as they are rolling down their respective compartments.

We then decided on where to cut out the slot for the metal block (or blocks). We were going to have slots cut out on the top section, perpendicular to the ball compartments, and have the blocks slide down into them. Then it occurred to us. Why cut away more of the fuselage, and risk cutting down on its supportability, when we could find a way to insert the blocks into the compartments themselves? We then decided that instead of two or three blocks, one could have one long steel rod that could be inserted into the middle compartment on the bottom row. In doing this, the steel rod will be lined up with the center of gravity of the plane, and there will be no moments that could result as the plane banks while carrying the steel cargo. Slotted inserts at the front and back of the fuselage can secure the ends of the steel rod. The flat portions of the upper sides of the fuselage are ideal for securing the battery pack. No grooves or holes will have to be dug out of the fuselage itself when trying to fasten a flat battery to a round surface.

One of the key areas of attaining proper stability and control in the aircraft's flight is a properly designed tail. The purpose of the tail is to act as the stabilizing component of the aircraft, which counters any unwanted movements by the wing. The tail is divided into two sections, the vertical and horizontal tail. The horizontal tail consists of a fixed horizontal stabilizer. Attached behind this is a moveable control surface, the elevator, which changes the lift on the horizontal tail, and thereby controls the angle of attack and lift of the wings. The vertical tail consists of a fixed vertical stabilizer, with a moveable rudder that is connected behind it.

We thought that since our plane had such a large wing, the tail would have to be large as well. When calculating initial tail sizing requirements, we found that the tail volume not only depended largely of the size of the wing, but also on the length of the tail arm. Our tail arm is going to consist of two carbon fiber tubes, which extend from inside the bottom rear of the fuselage to the rear bottom edge of the Balsa wood tail assembly. The reason we used two rods as opposed to a single rod was to minimize the effect of twisting caused by the aerodynamic torque about the tail. This torque could cause the tail to slightly shift away from its vertical position about the tail arm, which could drastically reduce the stability of the plane. Instead, this torque will be applied to two rods side-by-side, sharing the torque between them, and decreasing the torque applied to each member.

For the initial tail sizing, we used two separate equations. One is for estimating the vertical tail volume required for maintaining stability, while the other estimates the horizontal volume required for stability.

$$\text{Vertical tail volume: } S_{vt} = (c_{vt} * b_w * S_w) / L$$

C_{vt} is equal to a coefficient which is based on the aircraft type (ranges from .02 to .09), b_w is wing span, S_w is equal to the wing area, and L is equal to the length of the tail arm. We can see that as the wing area increases, the volume needed for the vertical tail increases as well. As the length of the tail arm increases, the volume needed for the vertical tail decreases.

$$\text{Horizontal tail volume: } S_{ht} = (h_{vt} * C_w * S_w) / L$$

h_{vt} is equal to the horizontal tail volume coefficient (ranging from .05 to 1.0), C_w is the length of the mean wing chord, S_w is equal to the wing area, and L is equal to the length of the tail arm. We can see again that as the wing area increases, the volume needed for the vertical tail increases as well. As the length of the tail arm increases, the volume needed for the vertical tail decreases. The horizontal component has been determined to be 3 square feet. The vertical component has been determined to be 1.72 square feet.

tail position

Positioning the tail was directly connected to both its size as well as the stability coefficients of the airplane. Therefore an initial position has been calculated and used for both calculation of the tail volume as well as the required area of the tail parts. After the tail sizing was accepted by the design team, the SACP was used in order to determine an optimum value for both pitch and yaw stability coefficients $c_{m\alpha}$ and $c_{m\beta}$ and to ensure a high static margin. (Numerical results are presented in the detail design section)

aileron span

The sizing of the ailerons, as well as their positioning has mainly been determined based on the experience of the pilot. After last years experience with the combined flaps and ailerons, the team decided this year to use the same combination again, in order to minimize the weight. After consulting

aircraft design literature, the team decided to design the ailerons/flaps based on the pilot's experience with model airplanes. This led to an aileron span of 24 inches.

special features

The bottom corners of the fuselage profile were going to be radii at first. Since the wings would be sitting under the fuselage, these radii would create air pockets along the two bottom lengths of the fuselage, producing unfavorable stability and handling. The squared corners will not only prevent this, but will also reduce the surface area of the fuselage, which reduces our overall cost. Our nose cone will have the same profile as the fuselage, but will come to a rounded point.

The rear end of the fuselage will not be left flat. If it is, there will not be a smooth flow of air along the surface of the fuselage. Instead, there will occur an area of high pressure at the front of the plane, and a subsequent area of almost no pressure behind the fuselage. This vast difference in air pressure will adversely affect the stability and handling of the aircraft. This smooth transition from the back of the fuselage to the tail can be accomplished simply by gluing carbon strips from the rear circumference of the fuselage to the tail assembly. As a result, a smooth airflow will occur, and the pressure differential will be negligible.

DETAILED DESIGN

performance data

During the detail design phase, the aerodynamics of the airplane selected from the Preliminary Design Phase has been analyzed. The Stability and Control program has been used to obtain optimal values for the stability of the airplane and the Takeoff and Climb performance program has been used to optimize takeoff distance and climbing performance. The design team considered static stability as well as the static margin but did not analyzed the aircraft's dynamic stability.

aerodynamic factors

In order to obtain any quantitative and comparable results out of the different analytical methods used, it was necessary to agree upon some common factors. Those factors have all been measured either on the actual aircraft parts, taken out of reference material or have been calculated (or approximated) based on those measurements. All measurements and all results obtained from any calculations have been rounded pessimistically, so that the final aircraft performance exceeds all expectations. These factors are summarized in Table 6.

Factor	Value
Empty Weight	20
Takeoff Weight	33
Reference Area, S	15
CD0	0.0228
Rolling Friction Coefficient	0.6
Aspect Ratio	6.6666
Propeller Dimensions	27 x 20

Table 6 – Summary of the common factors used in analytical calculations

handling qualities

The basic concept of stability is simply that an aircraft returns to its initial state after it has been disturbed. The performed stability analysis was mainly concerned with static stability, dynamic stability has been neglected. This decision has been made since the past experience has shown that a statically stable aircraft has, at most times, expectable dynamic stability properties. In order to obtain some information about the aircraft's stability, the pitching and yaw moment derivatives have been approximated using numerical methods and analyzed. The wing, the fuselage, the tail and the engines cause the main contributions to those pitching moments and therefore the total value has been calculated for those components. The design team used the SACP program to analyze the pitching and yaw moment derivatives change with angle of attack and at different (low) velocities. The results of this analysis are illustrated in Figure 3 and Figure 4.

The design team wanted to obtain a high static stability, comparable to that of modern general aviation and transport aircrafts. This should ensure that keeping the aircraft in the desired flight position would not divert the pilot flying the aircraft. The high negative value for the pitching moment derivative $c_{m\alpha}$ shows clearly that the aircraft is largely above the given limit for modern transport aircrafts, based on the $c_{m\alpha}$ plot in Figure 3. The design team also tried to obtain a large moment derivative $c_{m\beta}$. The static margin, which determines the longitudinal stability of the airplane, has been calculated to be 0.1198. This clearly identifies this stability and makes it similar to that of transport aircrafts, based on the plot of Figure 4.

Upon finishing the stability analysis part, it has been decided that if during the flight test, the pilot would conclude that the aircraft is too inert, a simple change in the location of the battery pack would change the stability of the aircraft through changing center of gravity. Even though this scenario is not expected, the pitching stability of the aircraft could be easily changed.

takeoff analysis and climb performance

The detailed takeoff analysis was performed with the TACP program. The stall velocity was calculated and the lift off velocity has been taken to be 1.1 times the stall velocity. Based on those calculations the takeoff distance has been calculated to be 131 ft. The aircraft has been calculated to have a rate of climb of 458 feet per minute in the loaded configuration. This ensures that the aircraft is able to achieve a safe altitude of 50 feet after only 6.6 seconds of flight time. These results are plotted in Figure 5.

Figure 3

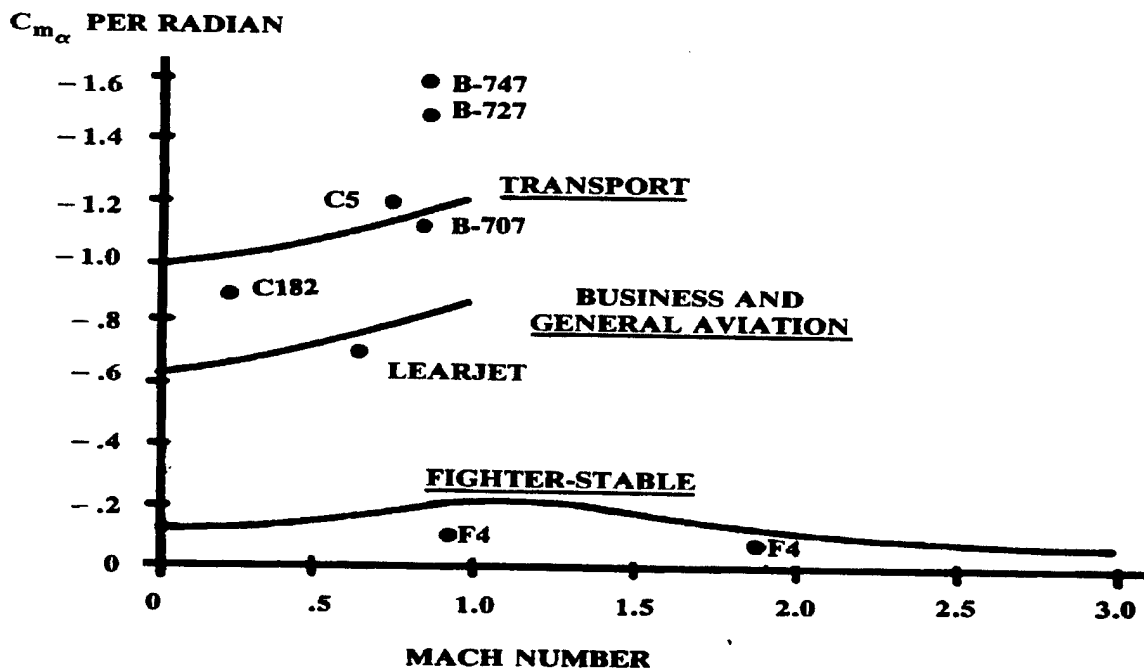


Figure 4

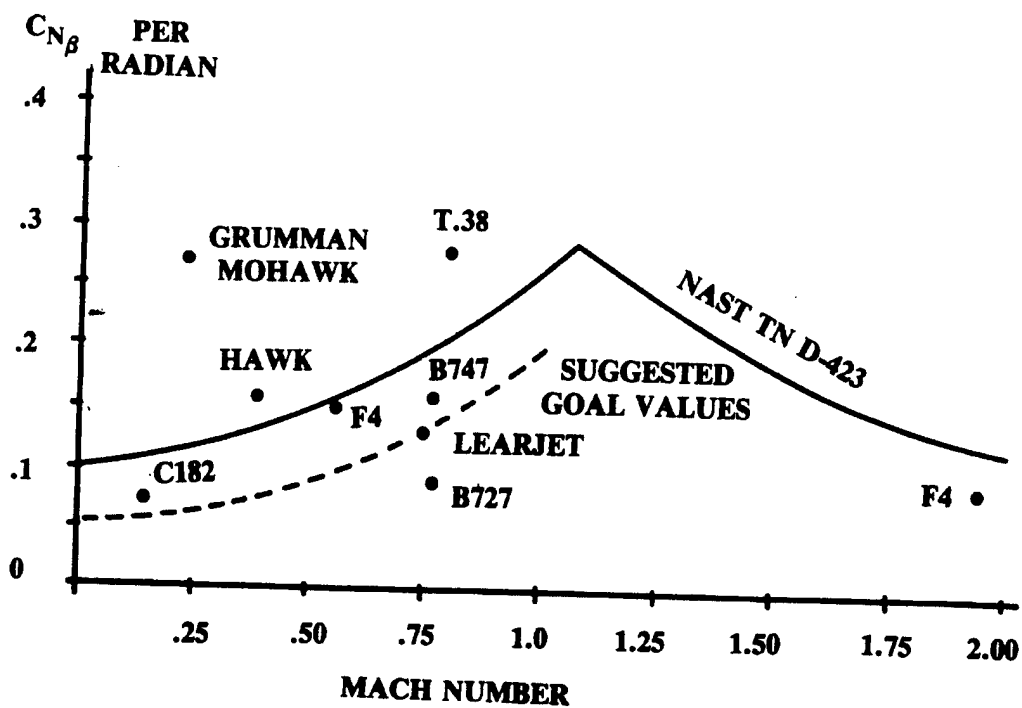
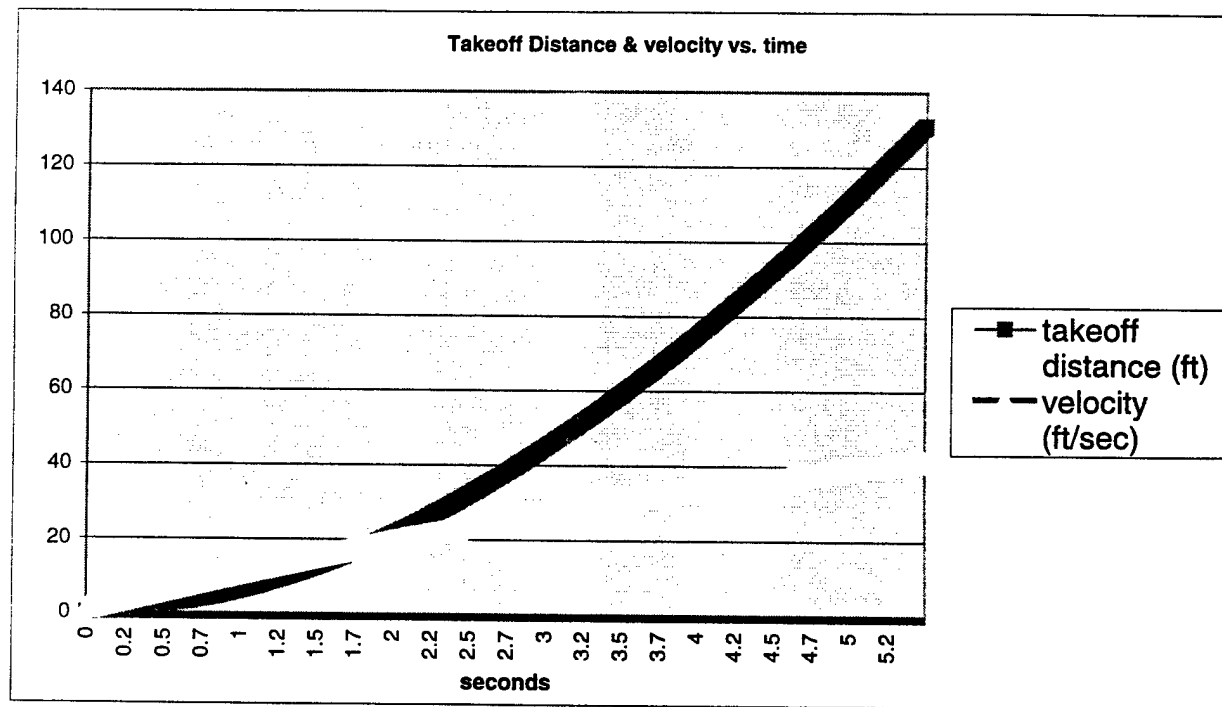


Figure 5



flight performance analysis

A TK Solver program was produced to verify analytically the aircraft's performance using methods discussed in Fundamentals of Flight, by John D. Anderson. The drag of the different components of the aircraft has been approximated using methods described by Hoerner. Carrying a hundred tennis balls or a 13 pounds of steel, the aircraft would fly then with wing loading of .42. The empty weight of the airplane was approximated to be 22 pounds and the maximum payload was taken to be 13 pounds. The stall speed was calculated to be about 29 ft/s.

The flight plan for the aircraft has been portioned up into the different tasks and based on the calculated performance of the aircraft the required times and power for completing those tasks have been calculated. For both Take-off and climb portion the design team used a full power setting, whereas the optimal airspeed for the cruise portion has been determined, to be achieved with an 85% thrust setting. For both Final approach and taxiing on the ground the thrust setting has been determined to be 75%. With the help of Electricalc, the needed currents have been calculated and the required power was obtained.

100 Tennis Ball Mission Segments							
Take-off	Climb	Cruise	Turns	Final	Taxi	Total	
6	7	45	23	10	10	101	Time, sec
48	54	287	186	24	24	623	Battery. mAh
100	100	85	100	50	50		Throttle, %
29	29	23	29	10	10		Battery Amps

Table 7 shows the predicted time and the approximated power the aircraft will need in order to complete each portion of the flight plan for the 100 Tennis Ball Mission.

Thirteen Pounds of Steel Mission Segments							
Take-off	Climb	Cruise	Turns	Final	Taxi	Total	
6	7	15	23	10	10	73	Time, sec
48	54	96	186	24	24	432	Battery. mAh
100	100	85	100	50	50		Throttle, %
29	29	23	29	10	10		Battery Amps

Table 8 shows the predicted time and the approximated power the aircraft will need in order to complete each portion of the flight plan for the heavy payload mission.

Out of Tables 7 and 8, it can be seen that the total required power for 1 set = 623 mAh + 432 mAh = 1055 mAh. Since our battery pack is 2400 mAh, we should be able to fly two sorties with tennis balls and 2 sorties with steel. This would ensure a safety factor of 12.1 %.

The design team concluded that in order to ensure an optimal endurance of the plane over the given time period, a power setting of 85% of thrust would be optimal in order to complete the steady flight portion of the flight plan. A thrust setting of 85% allows the airplane to fly at velocity of 66.15 feet per second. The required angle of attack for the aircraft in order to maintain steady level flight is 4.26 degrees.

By approximating the ground time between sorties to be thirty seconds, the aircraft should be able to complete seven scoring laps in the given ten minute period. This number has been obtained by flying four laps with the light payload task and three laps with the heavy payload task.

After the aircraft performance had been evaluated, the design team was concerned with the endurance of the battery pack. Therefore a careful analysis of the required power for the different portions of the flight plan has been made, in order to ensure that this limiting factor would not influence the scoring potential of the aircraft.

Section of the Flight Pattern	Full Load (mAh)	Unloaded
Takeoff	15.54305556	0
Climb	17.41666667	8.5
Turns	34.83333333	31.16667
Cruise	55.97222222	45.36111
Landing	70.55555556	56.5
Taxi	0	0
Total	194.3208333	141.5278

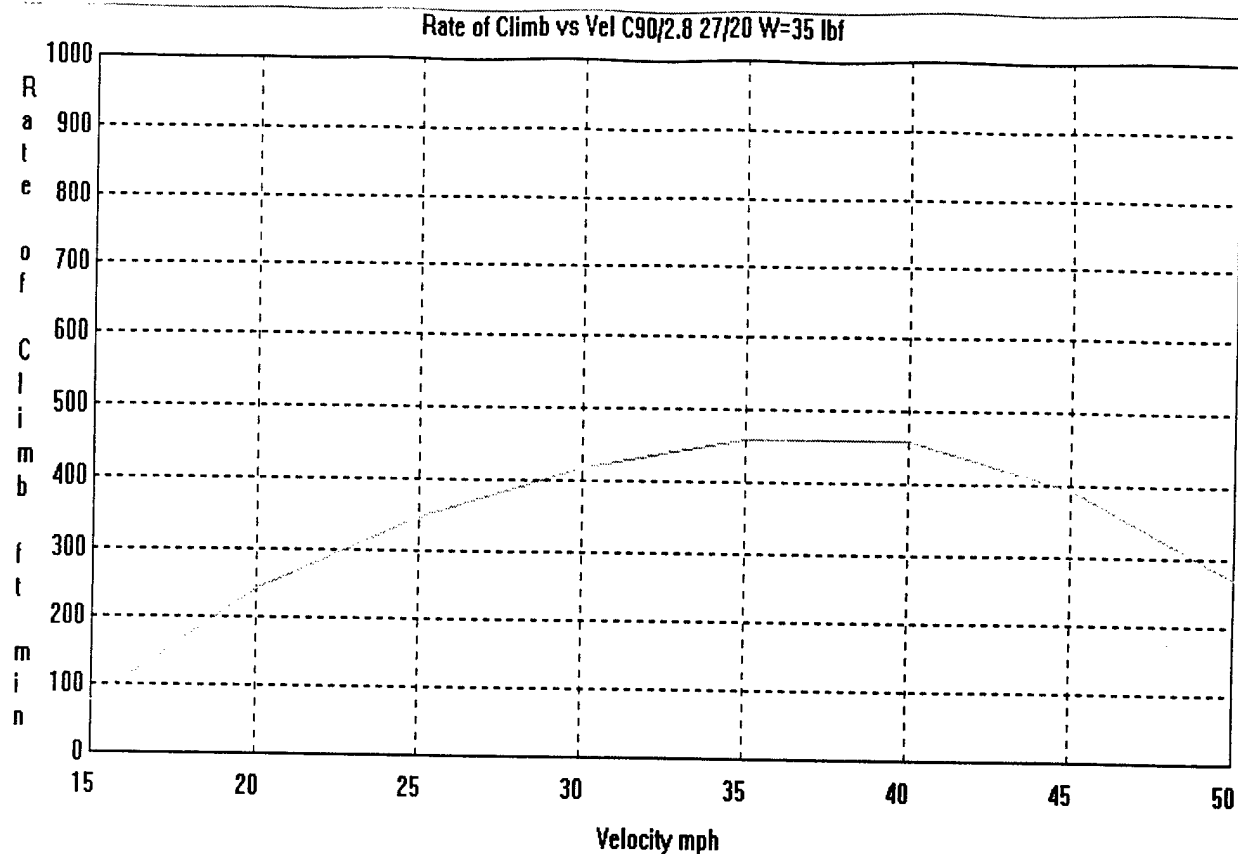
Table 9 shows the power needed by the AstroFlight C90 with a 27/20 Zinger Wood Propeller

According to obtained results for the required power, the design team concluded that the aircraft should be able to complete the expected task of seven scoring laps.

rate of climb vs. velocity graph

The rate of climb is a function of excess power and weight. More specifically, rate of climb is calculated by dividing excess power by the weight of the aircraft. The weight of the aircraft used to derive this graph is thirty-five pounds, our estimate for the combined total weight of the airplane at completion. Excess power is found by subtracting the values from the power required curve from the values on the power available curve at each velocity point. Upon analyzing the data we calculated that the maximum rate of climb occurs between the velocities of thirty-five and forty miles per hour. During this range of velocity the rate of climb for our aircraft reaches four hundred and eighty miles feet per minute. Beyond forty miles per hour the rate of climb of the aircraft declines as the amount of excess power also declines. Power required and available values were calculated using TK Solver, and the graph, Figure 6, was created.

Figure 6: Rate of Climb vs. Velocity



lift coefficient required for 1.5 & 2 G turns vs. velocity graph

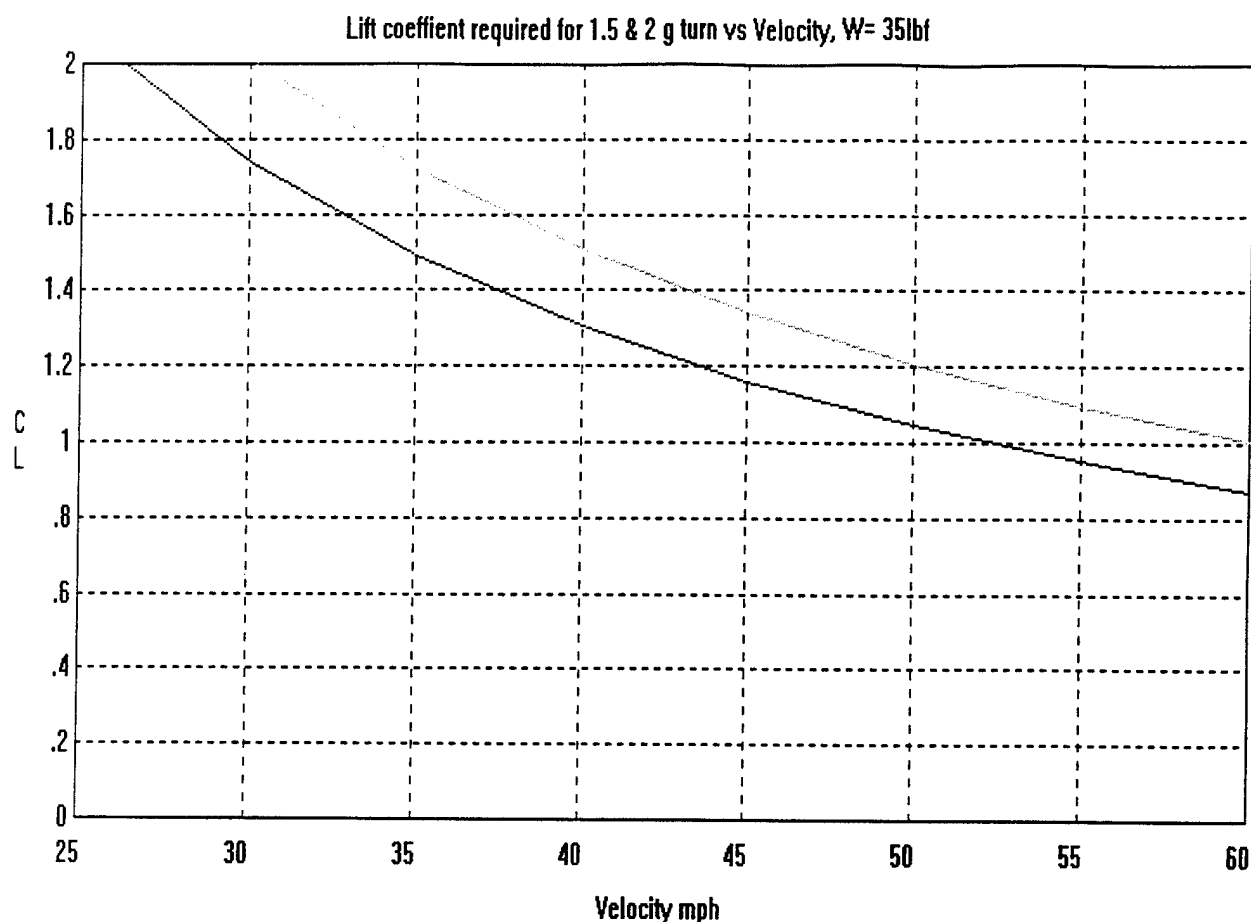
The lift coefficient is defined using the variables of lift, dynamic pressure, and the wing reference area.

The equation for the lift coefficient is:

$$C_L = L / q S$$

Furthermore, dynamic pressure is a function of density and velocity, such that dynamic pressure equals $.5\rho v^2$. The wing reference area for our airplane is fifteen square feet. Of all the variables involved in the calculation of the lift coefficient, lift is the only factor affected by G-loading. Due to the fact that as the G-load upon the wing is increased, as a result of a steep turn, the area of the wing actually producing lift is decreased. As a result the lift coefficient required slowly decreased as velocity increases because by increasing your velocity you are producing more lift and negating the lift lost during G-loading. A graph, (Figure 7), was created using outputs from equations entered into TK Solver.

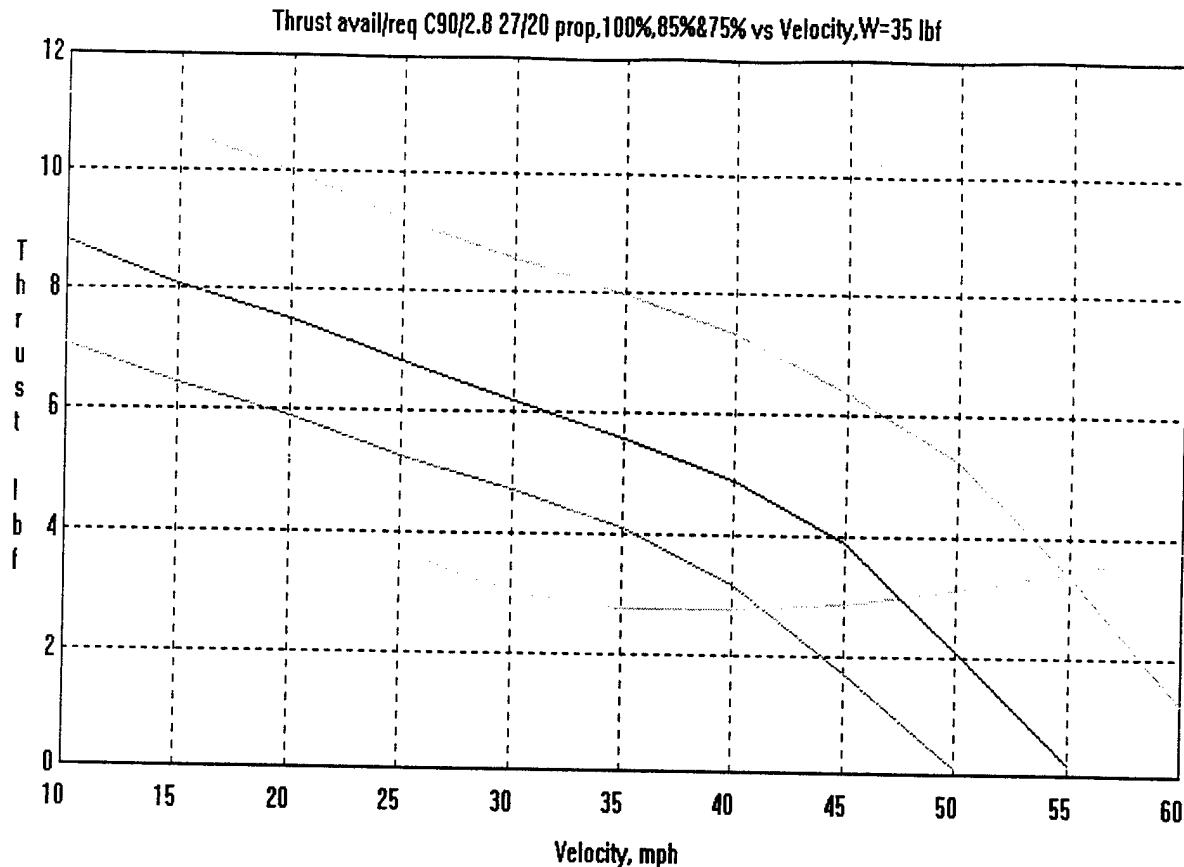
Figure 7



thrust available/power required vs. velocity graph

Using TK Solver we calculated the thrust available and required. Thrust available was calculated using data from ElectriCalc using throttle settings of 100%, 85%, and 75%. The thrust required curve, shown in light blue on the graph, is calculated by dividing the weight of the aircraft by the ratio of lift to drag. These values were then graphed along a rational range of velocity values. The three remaining curves show the thrust available, the green curve representing the throttle at 100%, the dark blue curve at 85%, and the red curve the throttle at 75%. The intersection of the thrust required curve and the thrust available curve represent the maximum velocity the aircraft can fly at. At a throttle setting of 100% the aircraft can fly at 55 mph, at 85% throttle it can fly up to 47.5 mph, and at 75% throttle the aircraft can attain slightly over 40 mph. The thrust output at all of these values falls around three pounds of force. Figure 8 shows a graph of these results.

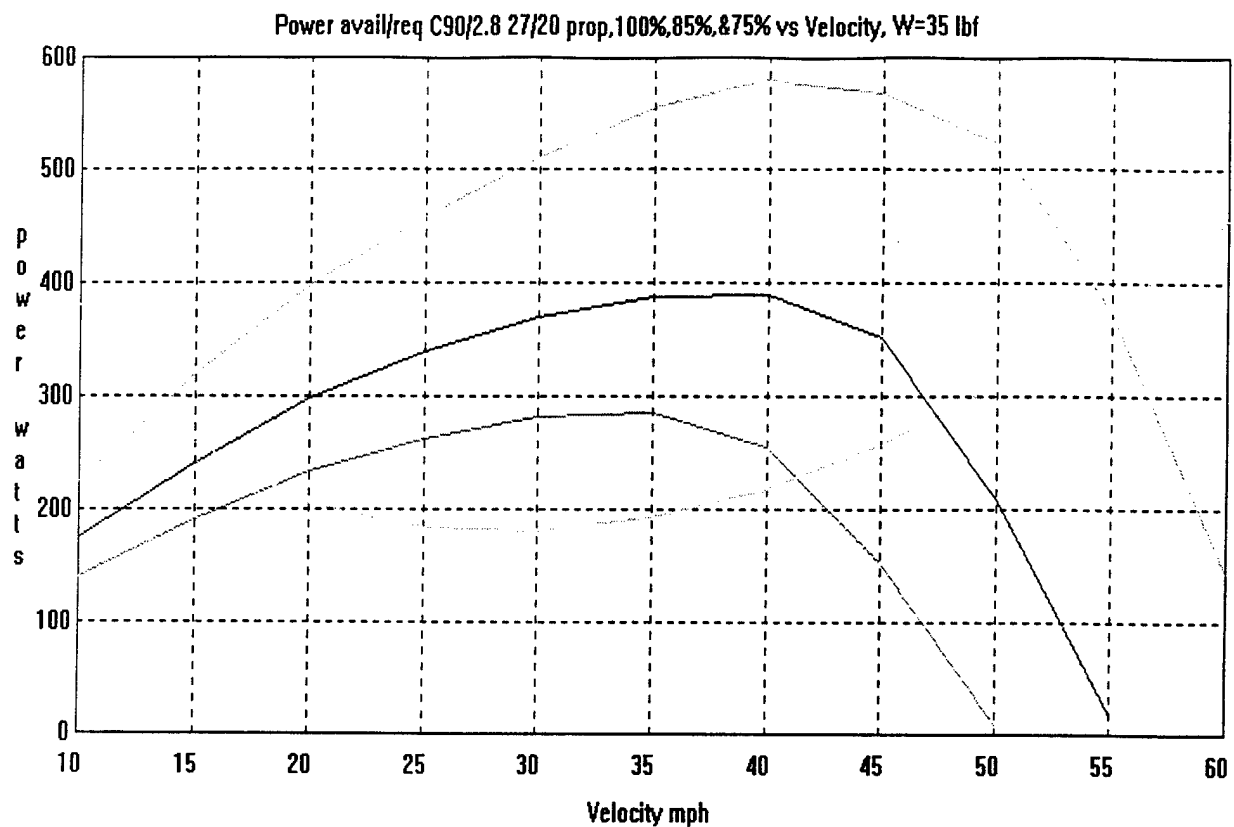
Figure 8:



power available/power required vs. velocity graph

Using equations entered into the program TK Solver we calculated outputs of power available and required and then entered them into an Excel spreadsheet. Power is simply a function of force multiplied by velocity, the force obviously being thrust. The resultant power figure is then stated in watts. As displayed on the graph in green the maximum power output at 100% throttle is 585 watts occurring at a velocity of 40 mph. At 85% throttle, shown in dark blue, the maximum power output is 390 watts occurring at a velocity of 40 mph. Finally, at a 75% throttle setting maximum power output is 285 watts occurring at 35 mph. The power required curve is shown in light blue. It begins to decline as velocity increases as a result of the airplane overcoming lift-induced drag while it eventually leads to a minimum power required value and then increases as a result of zero-lift drag. The most efficient velocity for straight-and-level flight is denoted where there is the largest spread between the power available and power required curves. For a throttle setting of 100%, the optimal cruising velocity is 40 mph. At 85% throttle the optimal cruising velocity is 35 mph. Finally, at 75% throttle the optimal cruising velocity is 30 mph. Figure 9 shows a graph depicts this description.

Figure 9:



component selection

motor

We were constrained to having to buy our brush motor from one of two companies, AstroFlight and Groupner. Since AstroFlight had more information on their website, and are pioneers in the model aircraft propulsion business, our team decided to stick with AstroFlight for investigating motors.

Since our plan was to carry the maximum payload of 100 tennis balls, we looked at the larger motors available. Through our research, we found that it was recommended to have a propulsion system that produced around 40 watts / pound. In the beginning of the year, our team set a rough estimate of the leaded plane's weight to be about 30 pounds. This would equate to a propulsion system that would produce at least 1200 watts. The two configurations from AstroFlight that would have 1200 watts would be two Astro C-60's or one Astro C-90. Our two ideas were to use the two Astro C-60's, connected by a belt, to drive one propeller shaft, or to have one motor. The two C-60's idea was dropped, due to the fact that two motors were not as efficient in driving one propeller as a single motor. Another reason was that two motors would cost twice as much in our Rated Aircraft Cost than just one motor. The final reason was that a single motor would drive the thrust back along the plane's c.g., which results in better handling

qualities. If one of the C-60's died during flight for some reason, the thrust from the other motor would produce a moment, causing the plane to spin and become unstable.

Based upon our ElectriCalc analysis, it soon became apparent that a gearbox was needed. Connecting the propeller to a direct drive system would spin the propeller too fast, and the 2.8-to-1 gearbox was the only gearbox available for the Astro C-90.

battery pack

Our battery pack had a limitation of 5 pounds and could not produce more than 40 amps. Our three choices were 2000, 2400, or 5000 milliamp-hours. The 5000 mAh pack was ruled out first, due to the fact that the cells in the battery pack were quite large. It would only take a few of these cells to have a 5-pound pack. Fewer cells mean fewer volts, which means less R.P.M's. More amps would be required to get the necessary volts, and the maximum of 40 amps was not enough to acquire amount of volts needed, based on our ElectriCalc predictions. The 2400 pack was better than the 2000 pack because it turned out that we could have a greater capacity with the 2400 mAh at the expense of one less cell. Less weight is always a plus in our design.

propeller

In picking our propeller, we used ElectriCalc by inputting the various properties of our aircraft. We wanted a propeller that would have the motor draw as close to 40 amps as well as provide for the longest battery life. More amps mean more volts, which equates to higher rpms, and longer battery life equates to less time needed to recharge the batteries. With this in mind, we chose to buy a 27 – 20 propeller. The 27-inch diameter provided the proper thrust and the largest amount of watts under 40, and the 20-inch pitch gave our plane a theoretical pitch speed that was twice as much as it's stall speed, which is a rule of thumb among aircraft designers.

control system

A Futaba 8UAP, eight channel, 1024 PCM transmitter was used with stock components. This system was purchased for the AIAA DBF competition three years previous because of its mixing capabilities, programmability, and fail-safe capability. Mixing was of particular interest because we can mix a flap function into the ailerons while maintaining aileron function. This allows us to gain the advantages of flaps without the cost of adding additional servos, and complexity of adding the flaps themselves. Due to the fact that each aileron was controlled with its own servo, we needed a transmitter and receiver that could accommodate the extra servo and program its function. The fail-safe program function is necessary to ensure safety should the receiver lose contact with the signal.

The servos used for each surface were Futaba S3001. These particular servos weigh 1.59 oz each, produce 41.7 oz-in of torque, and have a speed of .22sec/60°. This torque and speed combination is more than adequate for our application.

The large dimensions of this year's contest required servo leads in excess of fifty-four inches!

Due to the voltage drop over this length we upgraded our receiver battery pack from a 4.8V, 600-mah NiCad pack to a 6.0V, 600-mah NiCad pack. The extra voltage is necessary because the long servo lead length causes a tremendous voltage drop. At lower voltages servos will have difficulty centering correctly and jitter unnecessarily, especially once the pack has been partially drained.

brake system

Once the design team had decided to build a conventional tail wheel airplane, the decision was made that a brake system would not be required. Even though an effective braking system would reduce the time between landings and reloading, it has been concluded that the conventional tail wheel design chosen would already produce enough drag. The drag produced by the tail wheel gear has been calculated to be 0.0037 lbf. Furthermore the design team concluded that the additional weight added to the aircraft would not be justified by the short time gain during the landing/reloading process.

landing gear

Among the things we looked at in the design of our landing gear were the positioning of the landing gear, the stroke, the bending and torsional stresses in the cross section of the landing gear's shape, and buckling in the vertical portion of the gear.

In doing research on landing gear configurations, we found some standard dimensions for our tail wheel type of undercarriage. The two front landing gears should be a certain distance below the center of gravity and apart from one another, such that the angle between a line running from the bottom of a wheel to the plane's center of gravity and the runway's surface is no more than 60 degrees. Also, in this tail wheel undercarriage set up, the two front wheels lie slightly ahead of the center of gravity, such that the angle between a line running from the bottom of the wheels to the plane's center of gravity forms an angle between 13 and 17 degrees with respect to the runway. In drawing out our overall dimensions of our landing gear design, we took these to values into consideration.

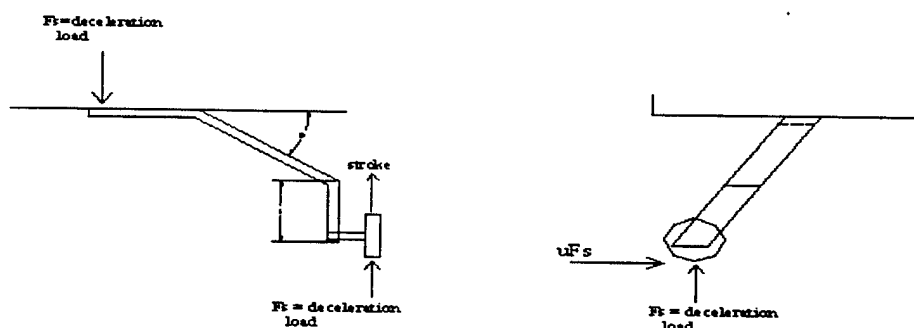
The stroke is the vertical distance the landing gear deflects upon the force of landing. The goal is to keep this deflection low enough that the vertical portion of the landing gear does not get pressed up into the bottom of the wing. The length of the landing gear was determined from where the motor sits on the fuselage, and how much vertical distance there is between the tip of the propeller blades and the runway. We want the stroke to be low enough so that the momentary decrease in the height of the landing gear does not cause the propeller to hit the runway, and snap off. Figure 10 describes the forces generated upon the landing gear during landing.

Stroke is a function of the deceleration force, the angle between the bottom of the wing and the vertical portion of the landing gear, the length of the gear, the cross section's moment of inertia, and the modulus

of elasticity of the material being considered. The deceleration load is based on the weight of the aircraft. For our purposes, we used 40 pounds, which is the upper limit of the range we wanted our plane to weigh. $F_s = (\text{plane's weight} * \# \text{ of gears}) / 2$. Our plane is going to have three landing gears, two under the wings and one at the tail. This gives an F_s value of 60 pounds. The two front landing gears will absorb this force, since they will hit the ground before the back gear. We utilized a spreadsheet that was developed by last year's design team in calculating the stroke for our set up. Last year's plane had a tricycle landing gear set up, and they used this spreadsheet for their plane's two rear landing gears. This same analysis can be used on our design's two front landing gears. Its inputs are the plane's weight, the angle between the landing gear and the

Figure 10

Front Landing Gear Diagram



$$\text{Stroke} = F_s * (\sin 20) * (l^3) / (3EI)$$

l = gear leg length
 E = Material Modulus of elasticity
 $I = (1/12) * b * h^3$
 u = coefficient of friction between wheels and ground

wing, and the moment of inertia of the cross section. The output is stroke, in inches. The strokes for all of our landing gear shapes turned out to fall between .1 and .5 inches, which ensures that no harm would be done to the plane upon landing.

The material we plan on using to manufacture the landing gear is aluminum. Aluminum weighs less than steel, and it is easier to bend into angles than steel, too. Many airplane models have carbon fiber landing gears. Carbon fiber is very lightweight, yet very strong. We could not think of an easy way that one could bend a carbon fiber tube in our processes lab, without damaging the tube itself, let alone bending it to our desired curvature.

We then looked in the McMaster Carr hardware-supply catalog to see what the standard thickness was of 6061 aluminum sheets. These turned out to be .125, .19, .25, .375, and .5 inches. We analyzed an aluminum plate that would utilize each of these thicknesses, with widths between 2 inches and 4

inches. By referring back to Figure 10, the two critical cross sections in the landing gear are at A and B. At section A, F_s , which is 60 pounds, times w , will produce a bending stress σ . Different values were calculated for σ , based on the varying cross sections of the different cross section possibilities. A torsional stress, τ , will also be produced around the cross section at point A. Torsional stress is equal to $T \cdot (3a + 1.8b) / (a^2 \cdot b^2)$, where a and b are the thickness and width for each size of cross section. Figure 6 shows that this torsional stress is caused by the deceleration force, F_s , multiplied by the distance h . The frictional force between the wheel and the ground, times the distance v , causes another torsional stress. This acts in the opposite direction.

The third area of analysis was considering buckling in the vertical portion of the landing gear, to which the front wheels are attached. This section of the landing gear was treated as a column. For each cross section considered, we found the critical load that the "column" could support, and compared this value to F_s that acts on the column at landing. As long as the F_s is less than this critical load, the vertical portion of the landing gear will not buckle.

The last area of the landing gear that was analyzed was the axle for each wheel. If these axles yield in any way, the alignment of the front wheels will be off, thus making it very hard to control the plane during the next take-off. There will be a bending moment being applied to the axle upon landing, due to the deceleration force, F_s , multiplied by the length of the axle. The bending moment causes a maximum bending stress at the surface of the steel pin and screw serving as the axle. The length of our axle will extend no more than 0.5 inches from the landing gear, and will probably be 0.25 inches in diameter. This will equal the bending stress, $\sigma = Mc/I = 19.6$ ksi. The yield strength of 1020 Alloy steel, from which our screw is manufactured, is 42 ksi, so the axle will not yield.

A new spreadsheet was used to analyze our landing gear dimensions. Using the moment of inertia and the cross sectional area of the landing gear, we were able to calculate the radius of gyration (ρ , which is a $(I/A)^{.5}$). L_e/ρ is the slenderness ratio of the vertical portion of the landing gear. The L_e , or equivalent length was taken as 3.8576 inches, or 0.8 times 4.822 inches. This was done because we assumed the vertical legs of the landing gears to be pin supported at one end and the top end fixed, as can be seen in our design. The slenderness ratio is a number that is used to determine how which equation to use in determining what the critical load, P_{cr} , is for that column. This tangency point is calculated as $(2\pi^2 E / S_y)^{.5}$.

Next the torsional and bending stresses that are developed at the cross section where the landing gear is attached to the plane were calculated. These stresses were compared to the yield stress of the Aluminum, to determine if the landing gear will plastically deform upon landing. This torsional stress was first calculated for a landing gear that was perpendicular with the surface,

upon landing. This was done before we determined that the front wheels should be ahead of the plane's center of gravity. Torsional stress developed in an angular landing gear, like our design, was found. The 60-pound forces down the next column represents the deceleration force, which was compared to the critical load that the vertical portion of the landing gear can withstand. Since all these values are greater than the 60-pound deceleration force, we know that the bottom portion of the landing gear will not collapse.

Figure 11

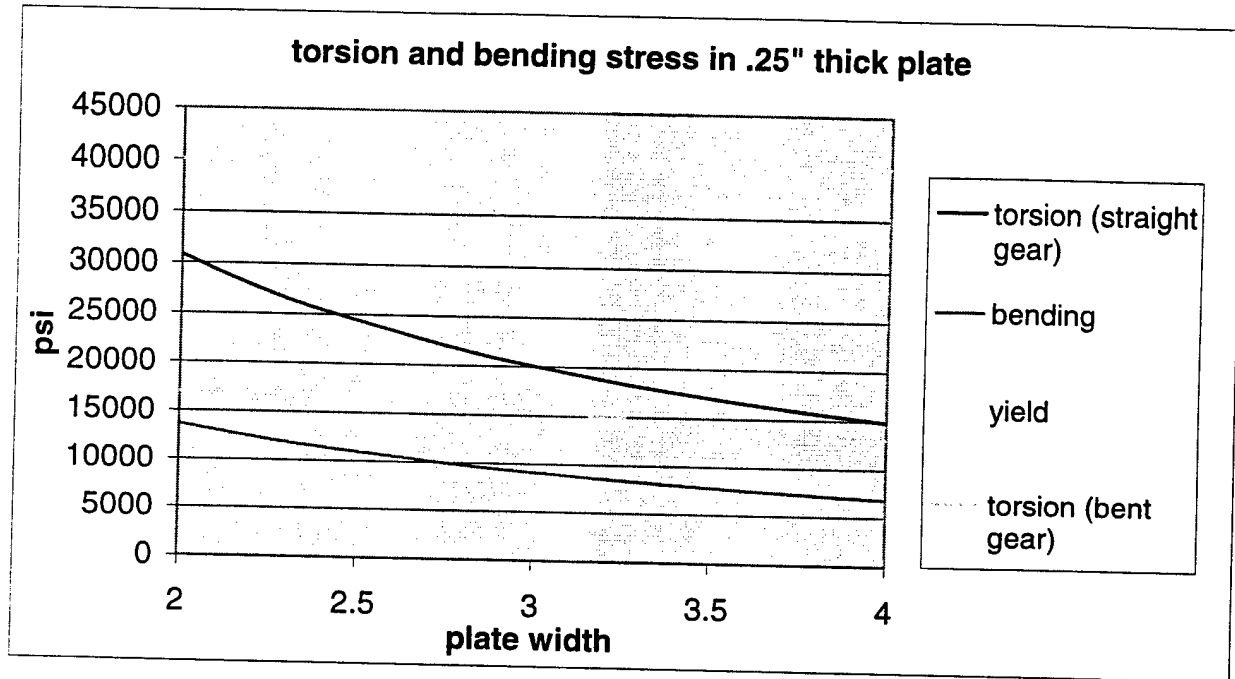
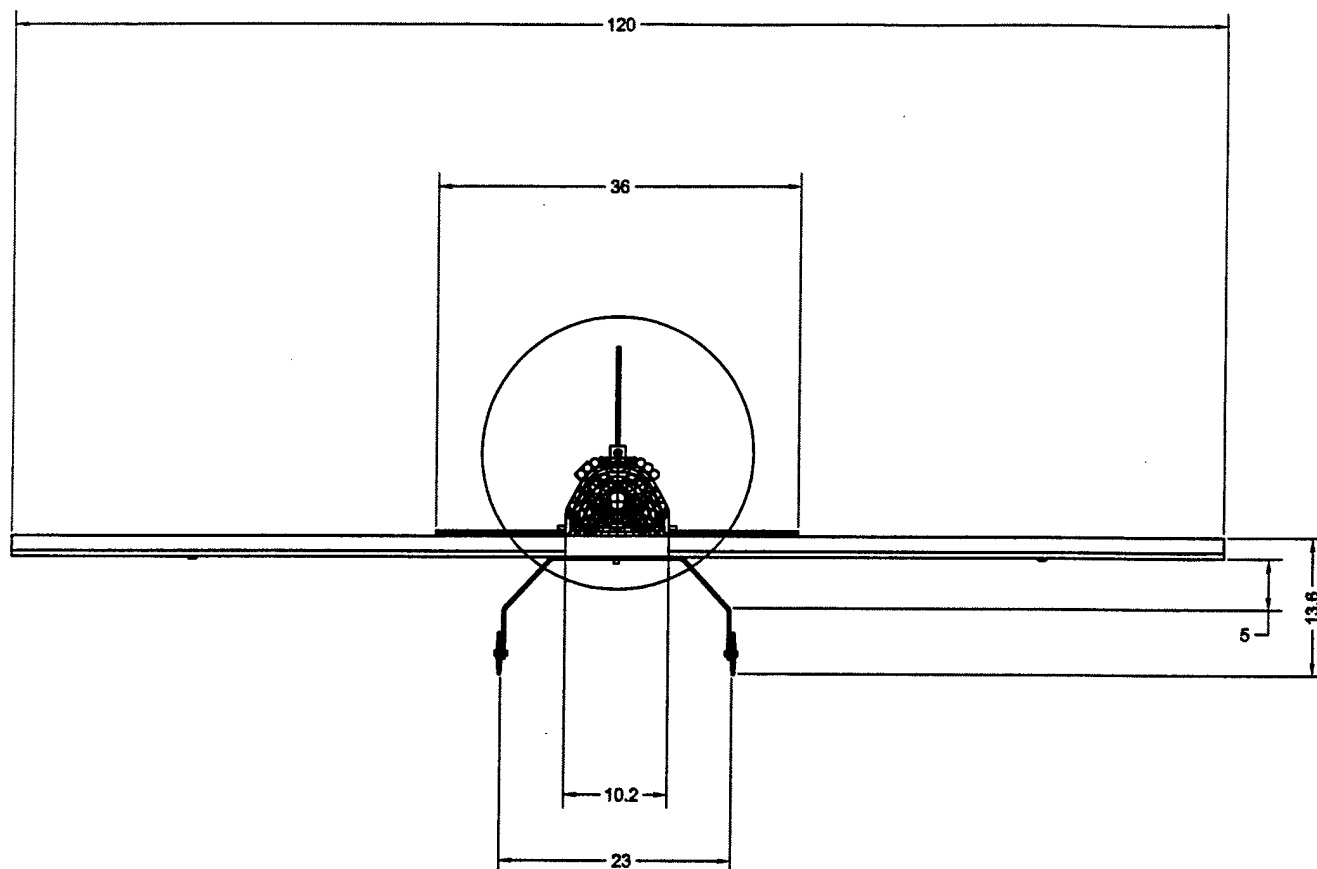


Figure 11 shows the plot that was generated from this data. It depicts a graph of the torsion and bending stresses that are developed in a 0.25-inch-thick landing gear, with respect to the various widths. The top horizontal line at the top is the material's yield strength. One can see that a safe configuration would be to utilize a cross sectional area of 0.25 inches, since the bending stress and the torsional stress for both a straight and an angular front landing gear configuration will not yield.

About a week after we designed our landing gear, we found an outside contractor that constructs landing gears solely for model aircraft. We decided that it would be safer with attaching a professionally built landing gear that we knew would work, as opposed to trying out one we built. The company used the same material, 6061 Aluminum, as we were intending to use. The company then replied to our design inquiry we had sent them a week later, informing us that our design was stable, but it would be more stable with a 0.25" X 2" cross section, utilizing no lightening holes like the ones on our design. Our plot, Figure 11, confirms this. A 0.25" X 2" cross section will provide for a much higher yield strength, making this landing gear very sturdy. The following pages are the detailed drawings of the MU-2.



MIAMI UNIVERSITY

OXFORD, OHIO 45056

FILE

Figure 12
MU-2
Front View

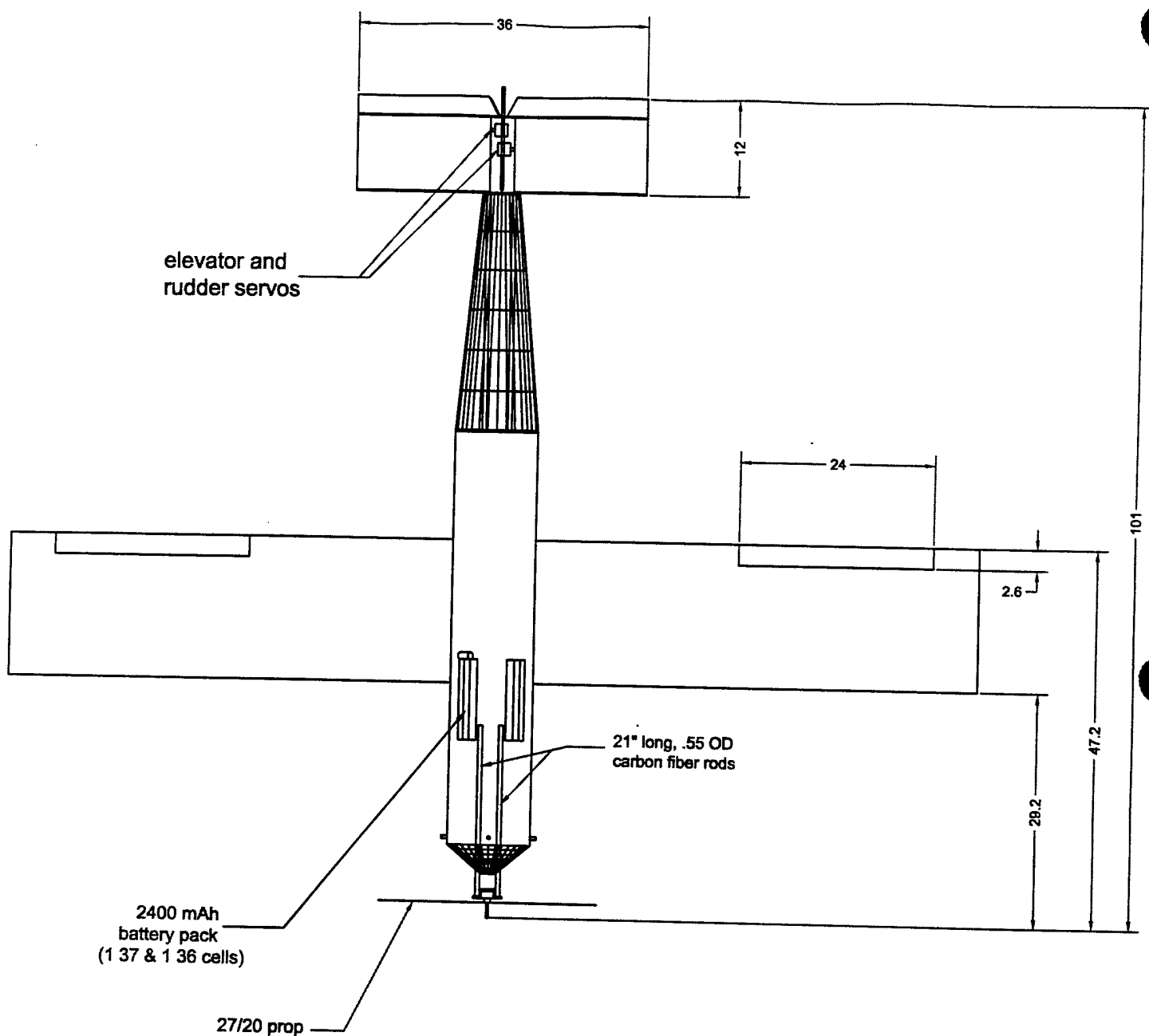
NAME: MU AIAA Design Team

DATE: 3/5/01

SCALE: 1" = 20"

DRAWING NO.
1

33



MIAMI UNIVERSITY

OXFORD, OHIO 45056

TITLE

Figure 13
MU-2
Top View

NAME: MU AIAA Design Team

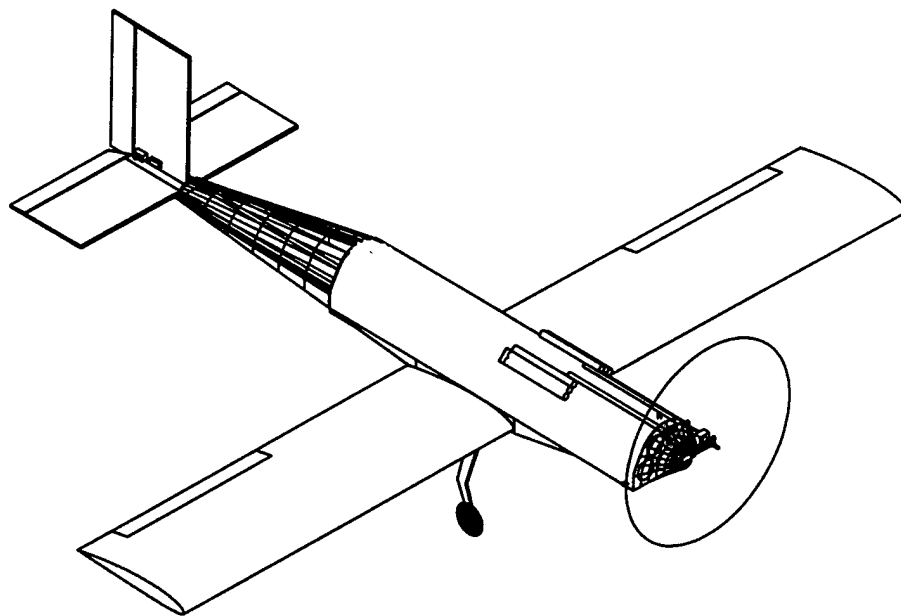
DATE: 3/5/01

SCALE: 1" = 20"

DRAWING NO.

2

34



MIAMI UNIVERSITY

OXFORD, OHIO 45056

TITLE

Figure 15
MU-2
Isometric View

NAME: MU AIAA Design Team

DATE: 3/5/01

SCALE: NTS

DRAWING NO.

4

36

configuration solutions

tail-to-fuselage attachment configuration

The initial idea of attaching the tail section to the rear fuselage was to bore out two holes into the bottom of the fuselage face. The holes would be situated such that one hole would be in between the two bottom compartments, where most of the excess Styrofoam lies. These holes would align with the distance between the centers of the carbon fiber rods extending from the tail section. After the tail rods are inserted and glued into the fuselage, carbon fiber cloth would be fastened from the end of the fuselage compartment to the front of the tail section. This would cover up the exposed rods, and provide for a smooth flow of air across the back of the fuselage. When we tested the soundness of this method by clamping the ends of the tail rod inserts in a similar manner to how they would be fastened into the bottom of the cargo compartment, we decided that a better configuration was needed. The large tail structure was too unstable to be supported by two thin carbon rods, and it kept oscillating back and forth with the slightest torque applied to either one of the rods.

The solution was to have more of the length of the rods to be secured by the Styrofoam. The closer to the tail that the securing force was clamped, the less the tail structure moved. This is why we added a rear section to the compartment of the fuselage. This would be an attachment, made of Styrofoam, that would be glued to the back face of the cargo compartment and around both the rods at the point where they meet the tail structure, as can be seen in our drawing of the plane (Figures 12-15). The bottom of this ferring would be flat and flush with the bottom of the rest of the fuselage. Two grooves would be cut out along the length of the bottom face, into which the tail rods would be fastened. There would be no holes bored out of the rear face of the cargo compartment. Instead, additional grooves were cut out of the bottom surface of the fuselage, which would line up with the grooves in the rear ferring. The top side of the rear wing ferring would also have grooves cut out that align with the grooves of the fuselage, which would form to holes into which the two tail rods could be glued and secured.

wing-to-fuselage attachment configuration

We felt that it would be easier to attach the wing to the flat bottom of the fuselage, as opposed to gluing some special feature on the fuselage to hold the wing over the fuselage. One possible attachment method was to cut out a groove into the top of the finished wing, which would be as wide as the flat bottom of the fuselage. The wing would be situated such that the chord would be flush and parallel to the bottom surface of the fuselage. After some thought, we decided to scrap this idea. The thickness of the wing gets thinner going from the front to the back edge. If a groove were cut out of the wing, there would hardly be any material on the back edge of the wing where the groove is cut out. This would result in a significant loss of structural stability in the wing. The thinned out section of the wing would also be the location where the fuselage is attached, which could increase the chances of a crack or tear to propagate throughout the wing.

The configuration we chose to go with is much more stable than the previous idea. Instead of cutting out a groove in the top surface of the wing, a Styrofoam "platform" was made. This platform was simply the excess material used in cutting out the wing sections, and was glued around the center portion of the wing on which the fuselage will set. This will provide for a flat upper wing surface to mate with the flat underside of the fuselage. This wing addition would also sit around the rounded leading edge of the wing and the pointed trailing edge of the wing. By looking at the wing's profile, the section that in under the fuselage had a flat top surface and a flat, vertical surface over the front and back ends of the wing. Two thin slots would then be cut out into the top surface of the wing and through the bottom surface. These slots would be situated at such a distance apart that they just clear either side of the fuselage. Through these two slots would fit a thin strip of aluminum and a metal O-clamp. The aluminum strip would wrap around the fuselage, and the O-clamp would be tightened over the strip. This would tightly secure the wing to the fuselage, without ripping into the fuselage with support screws.

Finally, for better aerodynamic qualities, two triangular Styrofoam ferrings were cut out. One would be glued to the front vertical surface of the wing and one to the back vertical surface, underneath the fuselage. These ferrings will prevent the airflow from hitting a flat surface underneath the fuselage, as well as preventing the wings from swiveling back and forth during flight.

landing gear-to-wing attachment configuration

The last step in analyzing the landing gear is how to connect it to the bottom of the wing. We know that the center of the top, horizontal component of the landing gear will align up with the quarter-chord point on the wings, which is the location of the aerodynamic center of gravity. Our first idea was to drill two rows of holes along the top section of the landing gear and along the bottom of the wing. Plastic inserts would be glued into the drilled holes in the bottom of the wing. The torque applied to this top section of the plate will want to rip out the screws in the front row and press in the screws in the back row.

Instead of screwing into the bottom of the wing, long, slender bolts would be screwed into the top surface of the wing and into the mounting holes on the landing gear, and nuts underneath the horizontal Aluminum plate would secure the landing gear. The fact that these bolts would be screwed into carbon fiber strips glued to the top and bottom surfaces of the wing, makes it nearly impossible for the bolts to be ripped out of the wing upon landing.

motor mount configuration

Our first idea for mounting the motor to the fuselage was to place it directly on top of the fuselage, above the front face. A groove that had the contour of the cylindrical motor would be cut out, into which the motor would be placed. This would prevent the motor from swiveling right and left due to the thrust caused by the propeller. A clamp that would fit around the round contour of the motor and the sides of the fuselage could be manufactured by bending a long strip of metal. Some type of clamp would then attach below the front end of the fuselage, and pull the ends of the clamp together, thus holding the motor in place. The problem with this motor mounting configuration was that there was little room for a nose cone

to be placed on the front end of the fuselage. The length of the nose cone is based on the space between the front face of the fuselage and the propeller blades. With this set up, our nose cone would almost be as flat as the front side of the fuselage.

The configuration we thought would be more ideal would have the motor located out in front of the front fuselage face, which would provide more room for a nose cone. Two carbon fiber rods would be fastened to either side of the motor. Two shallow grooves would be routed out along the top of the fuselage. The ends of the carbon fiber rods would lay in these grooves, where they would be glued in place. Then, a piece of Styrofoam that matched the contour of the top of the fuselage would be glued over the two rods. For added strength, a strip of carbon fiber cloth would be wrapped around the top and bottom of the front end of the fuselage, so as to prevent the thrust from pulling the motor assembly off the fuselage. This is the configuration that is shown in our drawing.

estimated weight

The weight of the aircraft is vital to analyzing the performance of our design. From the aircraft's weight we can determine how much power is required to fly the plane, how long the take-off length we will need, and how fast the plane will travel, among others. In estimating the weight of the aircraft, we gathered a list of all the materials that we are expecting to use in the construction of this aircraft. The weight of each material component was calculated by taking its volume times the material's density. Some of the material densities were found by going to the online materials catalog, www.matweb.com. Here, many of the material properties for almost every single type of material could be found, including density. For other materials that we either could not find on this site, or that there were such a large variety of a particular type of material, we simply took a section of known volume of the material, and weighed it on a digital scale. For some of the volumes for our more complicated components, like the fuselage, the wing, the tail, and our proposed landing gear design, we simply drew three-dimensional drawings of these on AutoCAD, and used the mass properties to find their volumes. Once we had the densities and volumes of all our materials, we were able to get an estimate of our plane's weight. The AIAA set the maximum weight for the loaded plane at 55 lb. We wanted to analyze our plane by assuming it weighs between 40 and 55 pounds, to ensure that our wings could support the load from the wingtips, and that it will be able to take off well below the maximum take-off distance of 200 feet. Table 10, on the following page, is a list of our estimated weights of each component for our plane.

Table 10: Estimated Weight

Plane Component	Estimated Weight
<i>Fuselage.....</i>	0.9 lb
<i>Rear Fuselage attachment.....</i>	0.1 lb
<i>Wing.....</i>	2.8 lb
<i>Tail section.....</i>	2.1 lb
<i>Two carbon fiber spar rods.....</i>	0.1876 lb
<i>Motor.....</i>	2.0 lb
<i>Propeller.....</i>	0.5 lb
<i>Battery pack.....</i>	5.0 lb
<i>Landing gear.....</i>	0.95 lb
<i>Two front wheels.....</i>	0.4375 lb
<i>Tail wheel.....</i>	0.25 lb
<i>Carbon fiber wing spar.....</i>	0.15 lb
<i>Cargo (tennis balls or steel).....</i>	12.5 lb
<i>Estimated weight of glue used.....</i>	1.0 lb
<i>Servos and wiring.....</i>	2.0 lb
Total Weight	31.775 lb

MANUFACTURING PLAN

The beginning of the manufacturing phase of this project leads us to evaluate and determine different methods to make each part of the plane. Most of the components are made out of Styrofoam, and therefore have the same manufacturing considerations. As is commonplace with any manufactured product, some components must also be purchased. We have included a list of those parts that we bought from outside vendors and an explanation of our reasoning in those cases. Table 11 is the FOM charts for the manufacturing processes considered for the major components of our aircraft, as well as a narrative about the ultimate decisions made in each case.

fuselage, wing, nose cone, rear fuselage attachment, ferrings

Table 11

rank	consideration	wire cutter	hand saw	CNC
2	Experience	9	7	7
2	Ease of use	9	6	7
2	Final finish	7	5	9
1	Sanding/filler required	8	5	10
3	Time necessary	10	6	5
TOTAL		88	59	71

After considering the above three methods, we chose to use the wire cutter system. This consists of a metal wire that is connected to a power source. This current running through the wire heats the wire up, which melts the Styrofoam along the cutting path. This system has been used before in similar projects, so we had members with experience in this area, a vital part of the decision criteria. Once this method was chosen, we developed identical templates in the shape of the component we were making, then ran the electrically charged wire around the outside edge of the templates, simply melting away the Styrofoam and forming a smooth base for our eventual component. For the tubes within the fuselage, we started by running a hot rod through the fuselage to make room for the wire. Then, we simply followed the same method as described above.

purchased products

We chose to purchase those components that were either demanded by contest rules or too difficult in our⁷ estimation to manufacture ourselves with a certain degree of professionalism. The brush motor and the battery packs are specified in the project rules. These we purchased and installed using makeshift assembly fixtures that we made. We also purchased the controller, in line with the other parts of the propulsion system already decided. Other than those components dictated by the contest rules, we bought the landing gear. We had plans to originally make this ourselves, but we stumbled across a local business that specializes in making landing gear for small model airplanes, among other things. With this company's expertise, we decided to use their landing gear instead of making our own.

tail

The main goals in designing the tail assembly were strength, cost, and most importantly, weight. Balancing an airplane is the most crucial last step before flight, as we have discovered from previous years' experiences in the contest. We knew we would be combating tail heaviness. We could achieve our strength and weight goals by using carbon fiber sheeted foam; however, it is very expensive. Due to this, we designed the tail assembly out of balsa and spruce. The leading edges, tips, and trailing edges of each stabilizer were made of 0.25 inch square spruce. The stringers between the tips were 0.25 inch square balsa. This structure was extremely light, but still very flimsy. From here, we covered the top and bottom of each stabilizer with .0625 inch balsa. The resulting structure was extremely rigid, very light, and inexpensive.

After the dimensions of the tail were found, full size plans were drawn. Both the vertical and horizontal stabilizers were constructed using quarter inch square spruce and balsa sticks. Spruce was used at the leading edge, tips, and trailing edge to provide rigidity. All of the stringers were quarter inch square balsa. Both stabilizers were sheeted with .0625 inch balsa, enclosing the stick structures. The rudder and elevator halves were constructed in similar fashions but were not sheeted. The elevator torque rod, situated between the two elevators, was then made out of .0625" music wire and is partially enclosed with brass. Next, we cut holes on the vertical stabilizer near the base for the elevator and rudder servos. Appropriate mounting tabs were installed for both the servos and control horns. The tail mounting blocks were shaped from half-inch balsa to fit between the two half-inch carbon fiber tail booms. The two mounting blocks sandwich the vertical stabilizer mounting tabs between them while providing an adhesive surface for the horizontal stabilizer. The rudder and elevator halves were then hinged and the tailpieces were covered with Econokote and Monokote. The entire tail assembly (two tail booms, vertical and horizontal stabilizers, tail mounting blocks) was glued together at once using thirty-minute epoxy. Then, the tail wheel bracket was mounted and tail wheel installed, followed by the rudder and elevator halves being glued on. Finally, the servos and control horns were installed and connected.

fuselage

We decided to use an NC mill to manufacture the fuselage templates, since we set tight tolerances on the locations of the payload compartments. The program for the Anilam CNC mill required us finding the points we needed for the profile, loading them into the Anilam in the proper format, and setting the tool, cutting speed, and other crucial parameters. Once the program was written, it could be checked using a "draw mode," which allowed us to see if the program was correct by drawing the finished part first. Once it was determined that the program was correct, we had to secure and zero the workpiece. When the workpiece was ready, we began cutting.

We used two 0.125-inch sheets of aluminum on top of each other to make two identical templates. Once we had the templates cut out, we cut the fuselage and the wing out of the Styrofoam using the foam wire cutter. The fuselage was too large for one sheet of Styrofoam, so we glued two sheets together before cutting it. To cut these holes we had to drive a hot rod through the entire length of the Styrofoam so that the wire from the foam cutter could be guided through. To guarantee that our hot rod went straight through the Styrofoam, we machined a guide out of aluminum that fits in the hole of the template. This guide forces the hot rod to be straight as it is sent through. Once all the initial holes were made, we then ran the wire cutter around the templates and made the basic outer (and inner) designs.

nose cone

The nose cone of the plane was manufacturing in the same method as the wings and the fuselage with the wire cutter. A smaller, hand-held hot wire cutter was used, due to the small length of the nose. Three blocks of blue Styrofoam were glued together, up to the desired length of our nose. After the glue dried, one of the steel fuselage templates was fastened to one side of the Styrofoam block with screws. On the other face, a two-inch outer diameter washer with holes drilled into it was fasten with two screws as well. The wire cutter was heated up with the power source, and the nose was cut out with the hot wire being guided along the perimeter of the fuselage template and the outside circumference of the washer. The flat front of the nose was then rounded down with a sander. EconoKote was then glued onto the nose. Then we heated up a small steel rod and pressed it into the top and bottom sides of the nose cone, about 0.25 inch from the fuselage face to make holes for the wood dowels. Finally, wood dowels were glued into the holes. The dowels provide fastening tabs so that the nose cone can be quickly removed to gain access to the load compartments.

rear fuselage attachment

In order to add rigidity to the tail and reduce drag off the back of the fuselage, we had to extend the fuselage over the carbon fiber tail booms from the rear portion of our cargo section of the fuselage leading edge of the tail. In construction of the aft portion of the fuselage, we began by gluing together a series of foam blocks 2" x 34" x 12". We tack glued the sheets together and attached the templates from the fuselage to the block and cut it down to the desired shape using similar methods and machinery from the wing. In addition to cutting the block to the shape of the fuselage, we cut it down to the 29.5" length of the carbon fiber tail booms running between the forward part of the fuselage and the tail. To taper the fuselage we cut out an elliptical template approximately 4" x 2" with rounded edges. After cutting the template, we attached the fuselage template and the elliptical rear template to the block of foam and cut it to shape. In order to reduce weight we decided to hollow this piece out. In doing this, we separated the original sheets of foam that form the aft section of the fuselage. When apart, we removed the center section of the two middle pieces of foam in the structure by using the hotwire cutter. Next, we reassembled the structure using 30-minute epoxy. Once the epoxy had cured, we used a router to form channels on the bottom side of the aft fuselage to accommodate the carbon fiber tail booms. Finally, we

attached the rear fuselage section to the carbon fiber tail booms running between the forward fuselage and the tail.

wing

Our design for the basic wing design used the entire allotted ten-foot wingspan. Constructing a lightweight, strong wing while keeping cost in mind, proved to be a monumental task. We decided to use Styrofoam as the main material for our wing because it is light, strong, and cheap, costing \$22 for a four-foot by eight-foot sheet. However, the foam alone would not support the weight of our fuselage and cargo, so we added carbon fiber spars to provide the necessary rigidity. Traditionally, foam model airplane wings are sheeted with 3/16" balsa. However, due to weight restrictions we left out this part and covered the foam directly with EconoKote.

Once we chose an airfoil, we made two templates out of aluminum. Due to the large set up time involved with the Anilam, we decided to cut the airfoil templates out using a band saw and then grind it to exact shape. To do this, we first blued the workpiece, and then traced a cardboard template of the airfoil (generated using AutoCAD) on it, scratching away the blue die, leaving the profile. Then we cut out the airfoil using the band saw, giving ourselves about .0625 inch all the way around, recognizing it is too difficult to be much more accurate with the band saw. We then smoothed the edges using the grinder.

We placed numbers on the templates in identical locations for reference while cutting the wing. Next, we cut blue foam to the length and width and the templates were installed on each end. After cutting the wings using the wire cutter, the two wing cores were joined with thirty-minute epoxy. The leading edge of the wing was cut off at the quarter-cord point using a table saw. Soft carbon-fiber cloth was cut to length and laid between the two halves of the wing and epoxy applied. Once cured, the second spar was completed approximately three inches behind the first spar. Next, the bottom spar was installed using hard carbon-fiber along the length of the wing between the two main vertical spars using thirty-minute epoxy. The final spar was installed on the top of the wing between the two main vertical spars and is four feet long. Next, we installed a rectangular piece of plywood 0.125 inches long and the landing gear mounting plate on the bottom of the wing. Due to the flimsy nature of the foam at the trailing edge, we replaced the last inch of the trailing edge with trailing edge stock balsa. Next the ailerons were cut, servo wells were dug, and servo mounted tabs were installed. A channel was cut for each servo leading from the servo to the center of the wing. The ailerons were made out of balsa block stock, and hinged appropriately using Robart hinges. Next, we filled the depressions in the wing with filler and sanded them smooth. After installing the servo extensions, we finished by covering the wing with Econokote.

wheels

The wheels were manufactured out of two 4-inch diameter, 0.5 inch thick, PVC disks. The 1-inch and 0.5 inch lightning holes, as well as the 0.5 inch center hole, were drilled out on a drill press. Each disk was

inserted into a lathe, and the both faces were turned down from 0.5 inch in the center to 0.25 inch at the perimeter. We used a ball-nose mill to cut out the 0.25-inch groove around the circumference of each wheel. Then, 0.25-inch diameter rubber o-ring material was cut to the proper length and fastened into the outer grooves with rubber cement. We next inserted bearings into each side of the center hole, to provide for smoother spinning. A nut and bolt serve as the axle, which is inserted into the two bottom holes on the landing gear.

motor mount

The components of the motor mount assembly consist of the Astro 90 electric motor that was ordered, two strips of 0.25 inch Aluminum, two 0.55-inch outer diameter carbon fiber tubes, two dowel rods, and four setscrews. The two strips were milled down with an end mill that ensured both pieces were the same size and had square ends. A hole was then drilled into the center of one strip. This hole was then sanded out until the metal strip could be press fit onto the hub in the center of the motor's back face. Two smaller holes were drilled on either side of the center hole so the cooling openings on the motor were not covered up. The two metal strips were then clamped together, and put into a mill. A drill bit that was slightly larger than the outer diameter of the carbon fiber rods was used to drill into each end of both strips. These holes were measured at such a distance apart that both carbon fiber rods would run parallel along either side of the motor, as can be seen in Figures 13-16.

The front plate was inserted into the fixture on the mill and a groove was milled out down the center of the plate. This groove ensures that there is clearance for the gear shaft on the front of the motor. The front Aluminum strip was fastened to the front side of the motor with the bottom two mounting screws on the front extension of the motor. Then, 0.125-inch holes were drilled into both ends of each metal strip, into the sides of the rod holes. Then these tiny holes were tapped. The two metal strips were fastened to the ends of the motor. Two pieces of 0.5 inch wood dowel rods were turned down on a lathe until they could be press fit inside the carbon fiber rods, and both were cut to a length such that they would extend from the front metal strip to the back one. When the carbon fiber tubes were inserted into the outer holes of both the metal pieces, the wooden dowels were inserted into the carbon fiber rods, and the setscrews were inserted into the tapped holes and were tightened against the rods. These setscrews serve to prevent the rods from slipping out of the holes in the metal mounting pieces. The wooden dowels that were inserted into the carbon rods prevent the setscrews from cracking the walls of the carbon fiber rods.

wiring

Before the Econokote was placed on the fuselage and wing surfaces, grooves were cut out using a heating gun. The grooves were cut out along the bottom wing surface, from each aileron servo to the point where the side of the fuselage meets the top of the wing. A groove was cut along the top of the rear fuselage attachment, for the wiring to attach to the tail servos. All the distances from the servos to the area on top of the fuselage where the receiver is planned to be located were measured. Each set of wiring consisted of a red, white, and black wire, braided together. All necessary connections were

soldered together, with shrink fit heated over them, to prevent any connections from being pulled apart. The wiring was then taped to the fuselage. Grooves were not cut into the fuselage, for fear of adversely affecting its structural stability.

gantt chart

On the following pages is a pictorial account of the work we have done on the project, both planned and actual. For the most part, we stayed on track, with the occasional delay due to late component delivery or unavoidable school holiday schedules and subsequent time away from active work. Our schedule is broken down into phases and milestones are marked according to group performance and overall project goals, Figure 16 on the next page. Major project milestones are marked with stars.

Figure 16: Manufacturing Schedule

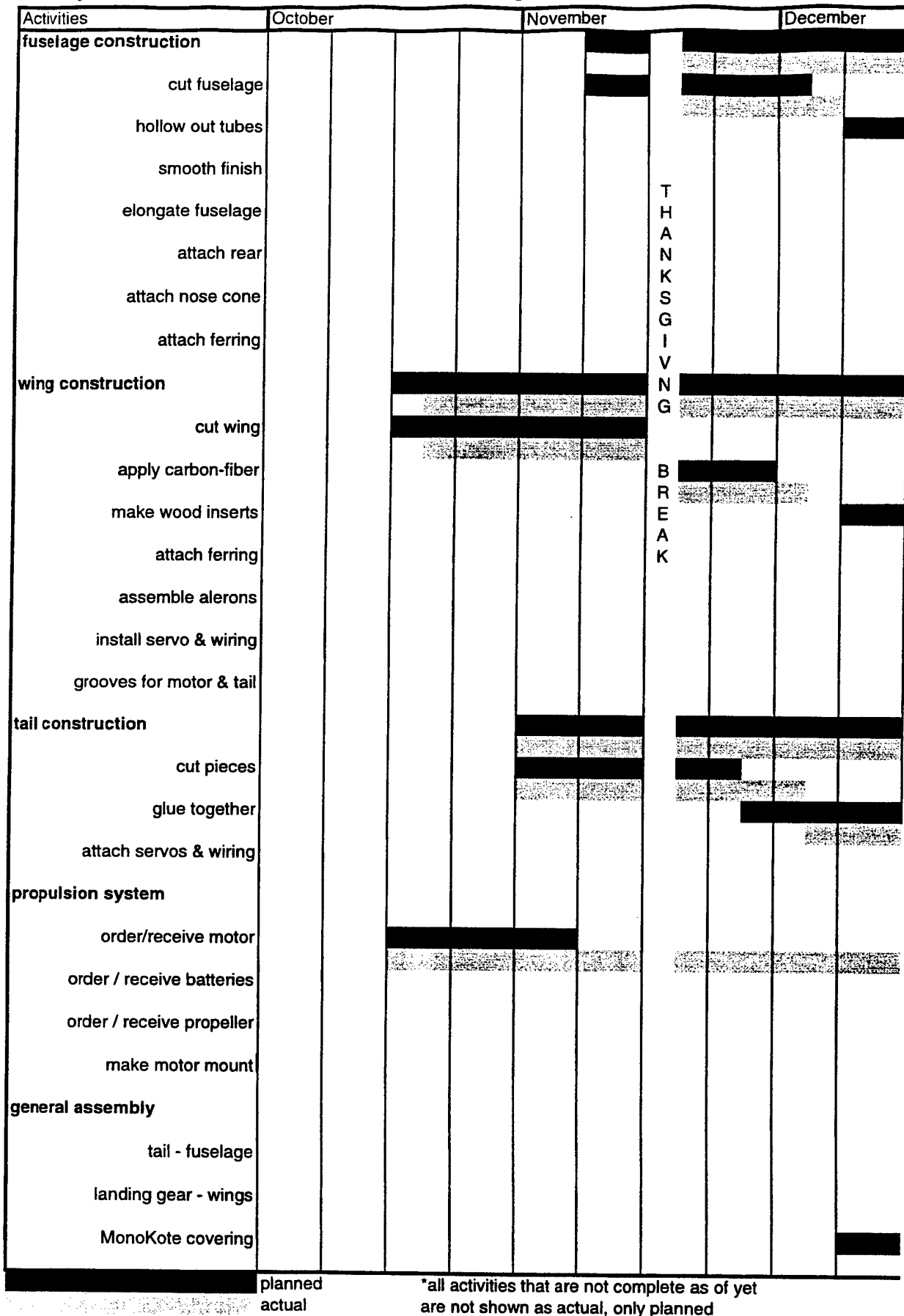
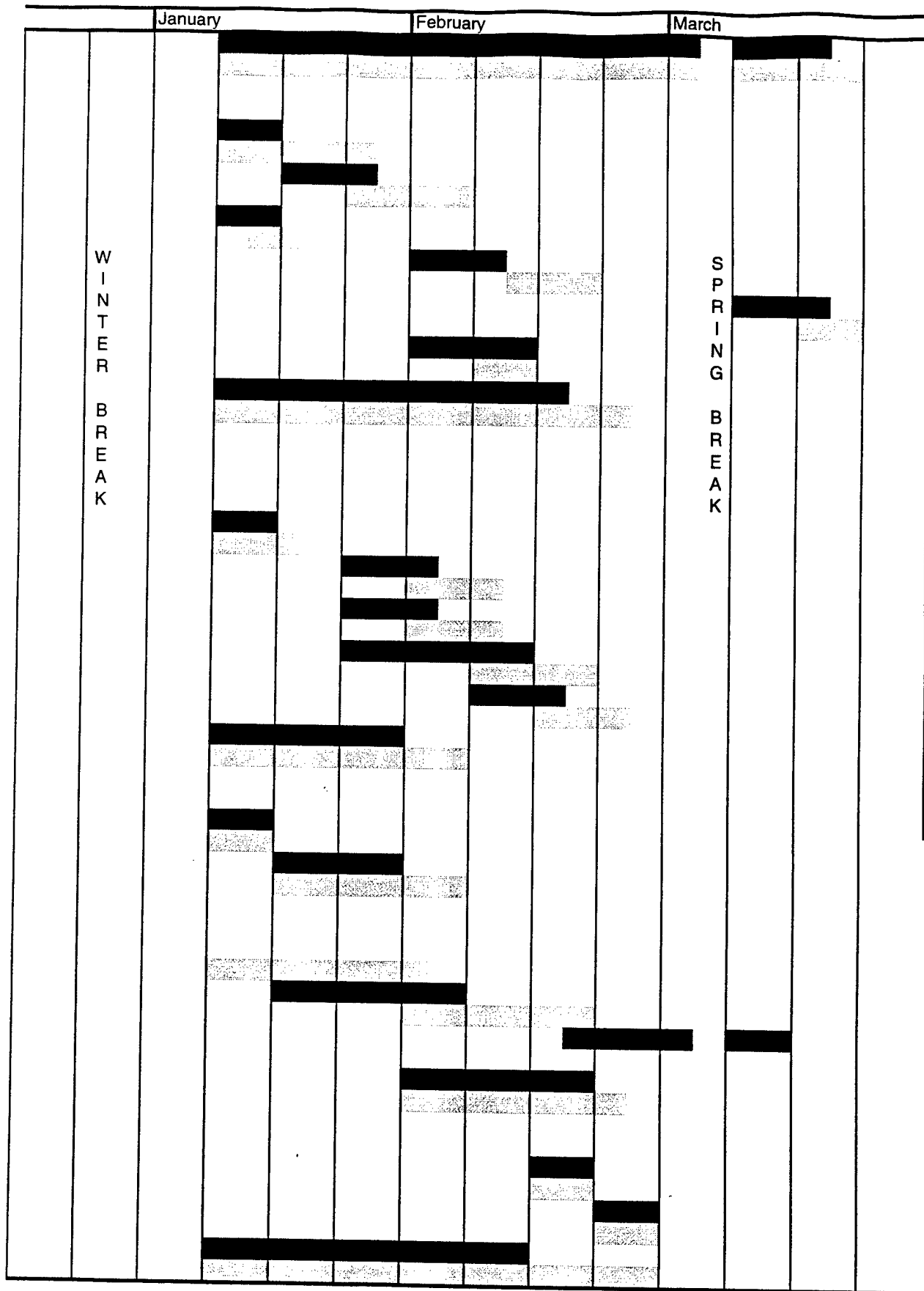
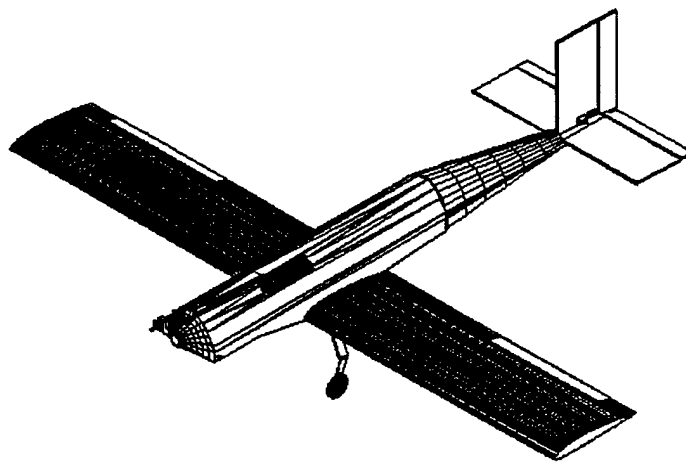


Figure 16 cont



**2000/2001 AIAA
Cessna/ONR Student Design, Build, Fly Competition
Design Report – Addendum**



“MU-2”

**Miami University
Oxford, Ohio**

April 2001

Table of Contents

Executive Summary

Problem Statement.....	1
Summary of Design of Development.....	1
Overview of Design Tools Used.....	1

Management Summary

Architecture of Design Team.....	3
Management Structure.....	3
Project Milestone Chart.....	4

Conceptual Design

Alternate Concepts Investigated	7
Design Parameters Investigated and Figures of Merit Used.....	8
Rated Aircraft Cost Summary.....	10
Features That Produced the Final Configuration Selection.....	13

Preliminary Design

Design Parameters / FOM Explanation.....	14
Configuration / Sizing data.....	15
Tail Position.....	17
Aileron Span.....	17
Special Features.....	18

Detailed Design

Performance Data.....	19
Aerodynamic Factors.....	19
Handling Qualities.....	19
Takeoff Analysis and Climb Performance.....	20
Flight Performance Analysis.....	22
Component Selection.....	27
AutoCAD Drawing Package.....	33
Configuration Solutions Tail-to-Fuselage Attachment.....	37
Wing-To-Fuselage Attachment.....	37
Landing gear-To-Wing Attachment.....	38
Motor Mount Configuration.....	38
Estimated Weight.....	40

Manufacturing Plan

FOM for Manufacturing Processes	41
Purchased Products.....	41
Tail.....	42
Fuselage.....	42
Nose cone.....	43
Rear Fuselage Attachment.....	43
Wing.....	44
Wheels.....	44
Motor Mount.....	45
Wiring.....	45
Manufacturing Milestone Chart.....	46

Lessons Learned

Introduction.....	49
Fuselage.....	49
Rear Fuselage Fairing and Tail.....	50
Wing.....	50
Nose Cone.....	50
Landing Gear and Wheels.....	51
Propulsion System.....	51
Wing-to-Fuselage Connection.....	51
Manufacturing Improvements.....	52
Testing Improvements.....	52
Weight.....	52

Aircraft Cost Model

Manufacturer's Empty Weight.....	54
Rated Engine Power.....	54
Manufacturing Man Hours	
Wings.....	55
Fuselage.....	55
Empenage.....	55
Fight Systems.....	55
Propulsion Systems.....	55
Aircraft Cost Summary.....	56
Results.....	56

LESSONS LEARNED

introduction

The manufacturing of our plane was moving along at a steady pace. On our first flight test, we flew the plane at an empty weight. The plane performed well, considering the effects of the high winds on the empty plane, and the fact that it appeared to be tail-heavy. On the second flight test, the plane was loaded with 80 tennis balls. Again, its takeoff and flight performance characteristics seemed to be quite good. However, after a few minutes of flying time, the signal between the controller and the receiver experienced some interference, and apparently was lost. The result was that the plane went into the radio fail-safe mode, resulting in an immediate dive from approximately 100 feet, and crashed. The wing was broken in numerous places, the fuselage was a complete wreck, a propeller blade was torn, and the landing gear was slightly bent from the impact. However, the entire section of the rear fuselage attachment and the tail were essentially intact. The wing ailerons were unscathed, too. The motor still worked, although the gearbox was bent. With this drastic turn of events, we went into a rebuilding phase. All necessary material was ordered as quickly as possible. The controller, the servos and wiring, and the receiver were sent out to be tested and serviced. The fact that the motor was still in working condition was the only reason the team was able to continue this design project, due to the fact that we had no time to wait another two months for a new motor. The Astro C-90 motor was sent out to be tested, and a new gearbox was made for it as well. The new, rebuilt plane differs slightly with our initial design. To meet the time constraints imposed by participation in the contest, we had to use as much of the surviving parts of the plane as possible, and were limited in the amount of redesign we could do and implement. However, we used the rebuilding as an opportunity to incorporate as many improvements into our design as possible.

fuselage

The fuselage compartment was completely wrecked. There were a few design changes in the new plane's fuselage. We made new templates for cutting out the fuselage. The outside perimeters of the templates were extended .25 inches. This allowed for more thickness between the fuselage surface and the interior compartment walls, in order to give more structural stability to the fuselage. The spacing of the hole locations was extended, slightly, and the diameters of the holes were enlarged from 2.625 inches to 2.75 inches. This was done to 1) decrease the amount of time spent sanding out the five compartments, and 2) to allow the tennis balls to roll down the compartments more quickly. A new, longer hot-wire cutter was made. This was of the same design as the one we used for the first plane, but the wire in the new one was longer than the length of the fuselage. This allowed us to cut out the fuselage in one piece, instead of cutting out two sections, and then gluing on additions to achieve the desired length, which adds weight. The same white Styrofoam was used, to keep the weight to a minimum. The top and bottom

grooves for holding the motor mount and the tail attachment were cut out with the router as previously. A carbon fiber strip was glued along the top and bottom length of the fuselage. These strips added increased stability and resistance to bending caused by the thrust from the motor.

rear fuselage fairing and tail

This section of the plane was almost completely intact, except for where one of the carbon fiber rods was ripped out of the side of the lower tail structure. This rod was easily glued back in place, and Monokoted over. On our first plane, the end of the fairing on the rear section dipped down at the point where it was connected to the tail, which resulted in a hidden surface. On the rebuild, this section was smoothed, so the air will hit the entire surface of the fairing. On the face of this rear attachment was glued a .25-inch thick section of the larger fuselage, with the bottom surfaces aligned with each other. After the fuselage compartment was glued to this inserted section, the exposed portions were sanded down to allow for a smooth transition from the larger fuselage cross section to the smaller rear fairing's cross section.

wing

The wings were cut out in the same manner as before. The main difference with the new wing design is in the carbon spar insert. The previous wing support utilized two vertical carbon fiber strips (one at the quarter-chord point and one three inches behind it), as well as a carbon fiber strip along the top surface and one along the bottom surface, situated in between the two vertical spars. We tested the strength with one vertical spar, and then with the second vertical spar, and we found no real improvement in tip-to-tip strength. It was the top and bottom strips that significantly strengthened the wing. With this in mind, we decided that an I-beam spar configuration would be just as effective as the "box" configuration. The vertical spar was located at the quarter-chord point, as before. Instead of using the stiff, carbon fiber strips, we chose to use carbon fiber netting. We found that this netting, when soaked through with epoxy, was just as strong as the solid carbon fiber strips, but were not as brittle. This proved to be effective. The aileron cut outs were done in the same way as before, with the same ailerons from the first plane. All holes for servos, wiring, hole-clamps, and screws for landing gear are in the same locations.

nose cone

The nose cone was manufactured in the same manner as our first nose cone. It is larger, though, since the new fuselage cross section is larger. In order to accommodate the two extra balls for holding the steel rods, two cut outs were made into the inside face of the nose, which aligned with the two upper compartments.

landing gear and wheels

The landing gear was easily realigned back into its original form. Two new wheels were made. On the original wheels, the stretching of the rubber was used to hold the rubber o-ring onto the wheels. The force of landing would tear the rubber from the outer outer grooves of the wheels. On the rebuild, we used epoxy to glue the rubber o-ring around the PVC wheels or a secure fit. The method in securing the wheels to the legs of the landing gear was also improved. The original set-up used a floating-axle configuration, in which one nut is used on the inside faces of the landing gear legs. This was changed to a solid-axle configuration, in which two nuts are used to secure each wheel to the landing gear legs. One nut would be between the wheel and the outside face of the leg, and the second nut would be screwed to the inside face. This was done to prevent any wobbling of the wheels.

propulsion system

The motor and all electrical components were sent out to be tested and repaired. For our new design, the motor is attached out in front of the fuselage as described in the Proposal, except that it is inverted. Due to the configuration of the motor, this allows for the line of thrust to be closer to the longitudinal center of gravity of the plane, which will provide for better handling capabilities. The two rods of the motor mount were glued into the two top grooves, and secured with carbon fiber netting wrapped around the front section of the fuselage. The battery pack is situated on top of the fuselage instead of along the sides as depicted in the Proposal Report. Two side rails, made from Styrofoam, are glued along the upper section of the fuselage, in order to keep the two battery packs together. The battery packs were moved up closer to the front spars of the motor mount, to overcome the plane's tail-heavy flight characteristics. The locations and paths of all wiring are still the same as before. The receiver is located more towards the rear of the plane, as far away from the batteries as possible. This should eliminate or minimize any possible interference caused by the proximity to the batteries. The first plane's propeller was a 27/20. Being pressed for time to build a new plane, we looked at whatever sizes of propellers were available, and the closest size we found, and that was also in stock, was the 27/18. We purchase this for our rebuild plane.

wing-to-fuselage connection

The same clamping configuration was used on both planes. When we lifted the front of our original plane up, the fuselage tended to shift up and down about the spot where the clamp was. To eliminate this shifting tendency, a second pair of slots was cut out in the wing, and an additional clamp was used to secure the fuselage to the wings. This addition keeps the fuselage more secure.

manufacturing improvements

We were quite pleased with how well the hot wire cut through the Styrofoam. We could not think of any better manufacturing system than the hot wire. However, by taking more time in building a hot-wire cutter, the tension in the wire could be better maintained, and more accurate cuts that would cut down on sanding time, could have been achieved.

testing improvements

While testing the new plane, the fail-safe setting will not be used. This is done to improve the survivability of the plane in the chance that the signal gets interrupted again. We are assuming that less damage would be done to the plane if it can glide and crash land horizontally, instead of going immediately into a banking dive, and hitting the ground nose first.

weight

The weight of the airplane components is listed in Table 12. Despite the larger actual weight, our team believes that this was the lightest weight that could be achieved in our design, using the materials at hand. The discrepancy between actual and estimated weight can be explained from differences in the volumes between the design found on AutoCAD for each of the separate components and the actual components, and the determination of materials' densities. Another problem we had was in trying to estimate the weight of the epoxy used. Since we used stronger blue Styrofoam, we forewent gluing on a thin layer of Balsa wood over the entire wing surface. We simply applied the Econokote onto the Styrofoam. This wing design would definitely be lighter than the same one with Balsa covering. We used the lighter, white Styrofoam for the fuselage compartment, since this was one of the largest sections of the plane. To reduce weight further, the rear fuselage fairing could have been hollowed out more, but we took out a good deal of Styrofoam to begin with, and felt that the small weight advantage would not equal the decrease in strength. Drilling lightening holes in the Aluminum landing gear could have taken out between a quarter to a half a pound, but we were set on having a sturdy landing gear (we had a bad experience with our landing gear in last year's contest). A carbon fiber propeller would have slightly cut down on weight compared to our wooden propeller, but we could not find any carbon fiber props in the size for which we were looking. The use of carbon fiber rods in the motor mounts and the tail section were ideal, since they are very light with very high material strengths. We could not have gone much lighter in this area. Weight was a critical design issue throughout the design and manufacturing process. The lower the weight, the less power required and the lower rated aircraft cost.

Weight (lb) of plane components	Estimated	Actual
Wings (incl. Carbon Fiber Spars and Epoxy)	3.45	5.38
Fuselage, Nosecone, Rear Fairing, Tail Section, Rear Wheel	3.35	4.19
Main Landing Gear and Wheels	0.95	1.5
Propulsion: (Motor, Propeller, Battery Pack, Receiver, Servos, and Wiring)	9.5	9.74
Motor Mount, Carbon Fiber Netting, 2 Metal Hose Clamps	0.9	0.9125
Total Airplane Weight	17.34 lb	21.72 lb

Table 12: Estimated Airplane Weight vs. Actual Airplane Weight

Aircraft Cost Model

The rated aircraft cost is one of the three main components in our total score for the competition. The other two components are the total flight score, which is based on our performance at the competition, and the written report score.

The function that relates these three elements is shown below:

$$\text{Total Score} = \frac{\text{Written Report} * \text{Total Flight Score}}{\text{Rated Aircraft Cost}}$$

For us to be as competitive as possible, it was crucial for us to maximize our written report score and our total flight score, while minimizing our rated aircraft cost. To minimize the rated aircraft cost, we calculated the cost for each preliminary design we had, and chose the design that would provide the best cost per point ratio. This ratio was determined by estimating the total flight score based on the design, or what we predicted each design could carry, and divided that value by the rated aircraft cost. This allowed us to maximize our scoring potential by using good design selection methods, choosing the lowest cost per point ratio.

To determine the rated aircraft cost, we were provided with an equation that accounts for most of the possible elements in a plane of this type. The equation provided a standardized way of costing each element in the design to make the scoring system consistent for all entrants. The rated aircraft cost equation is shown below:

$$\text{\$ (Thousands)} = \frac{A * \text{MEW} + B * \text{REP} + C * \text{MFHR}}{1000}$$

A detailed description of the variable is provided below

manufacturers empty weight (MEW)

The MEW is the weight of the plane excluding the payload and batteries. The multiplier "A" is assigned the value of \$100 per pound. Our plane weighs 21.72 pounds. It was important to keep this weight down, as this is a large portion of the total rated aircraft cost. Another consideration in keeping the weight down was that since the total loaded weight could not exceed 55 lbs., there needed to be plenty of weight available for the payload in order to maximize our total flight score.

rated engine power (REP)

The REP was calculated using the following formula:

$$\text{REP} = \# \text{ of engines} * 40A * 1.2 \text{ V/cell} * \# \text{ of cells}$$

The REP is the number of Watts used. The multiplier "B" is assigned the value of \$1 per Watt. Our team decided to use 37 cells in our design, giving us a REP of 1221 Watts. Keeping this value low is also important because it is a significant part of the rated aircraft cost as well.

manufacturing man hours (MFHR)

The MFHR provides a way to estimate the hours spent manufacturing the plane based on the plane's characteristics. This is also to keep the costing as objective as possible. The multiplier "C" is assigned the value of \$20 per hour. The MFHR is broken down into different parts of the plane including the wings, fuselage, empenage, flight systems, and propulsion systems.

wings

The wings are assessed a standard 15 hours per wing, as well as, four hours per square foot of projected area, two hours per strut or brace, and three hours per control surface. We have one wing that has 15 square feet of projected area. We also have three control surfaces. Since it is a single wing craft we had no need for struts or braces. The total number of hours for the wing is 84 hours.

fuselage

The fuselage is assessed a standard five hours per body and an additional four hours per foot of length. We have one single fuselage that is 7.03 feet long, which gives us 33.12 hours for our fuselage.

empenage

The empenage has a basic five hours as well as five and ten hours respectively per each vertical and horizontal surface. Our tail is standard with only one horizontal and one vertical surface, giving us 20 hours for our empenage.

flight systems

The flight systems have a basic five hours and an additional two hours per servo or controller. Our design has three servos and/or controllers giving us a total of 11 hours for our flight systems.

propulsion systems

The propulsion systems were assessed five hours for each engine and each propeller or fan. Our plane had one engine and one fan, giving us 10 hours for our propulsion system.

The total number of hours for our plane is 155.2, which is our MFHR.

Table13 shows the entire breakdown of the cost model, explained above, giving us the rated aircraft cost for our plane.

Table 13 - Aircraft Cost Summary

Description	Characteristics	Hours	Cost
1. Manufacturers Empty Weight (lbs)	21.72	N/A	\$2,172.00
2. Rated Engine Power (Watts)	1221	N/A	\$1,221.00
3. Manufacturing Cost (\$)			
3.1 Wings			
Number of wings	1	15	\$300.00
Area of wings (sq. ft.)	15	60	\$1,200.00
Number of struts	0	0	\$0.00
Number of control surfaces	3	9	\$180.00
3.2 Fuselage			
Number of fuselages	1	5	\$100.00
Length of fuselage (ft.)	7.03	28.12	\$562.40
3.3 Empenage			
Number of vertical surfaces	1	5	\$100.00
Number of horizontal surfaces	1	10	\$200.00
3.4 Flight Systems			
Basic	N/A	5	\$100.00
Number of servos or controllers	4	8	\$160.00
3.5 Propulsion Systems			
Number of engines	1	5	\$100.00
Number of propellers	1	5	\$100.00
		Total Cost:	\$6,495.40
		Rated Aircraft Cost:	6.4954

results

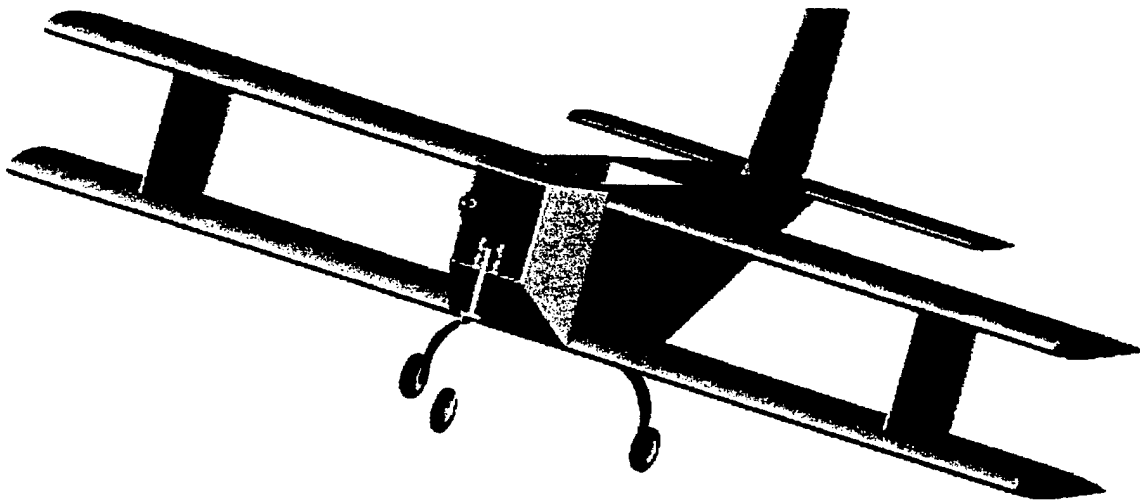
It is evident that there are many factors that can affect the rated aircraft cost. Our final cost calculation is shown below:

Rated Aircraft Cost (Thousands of \$) =

$$\frac{\$100/\text{lb} * 21.72 \text{ lbs} + \$1/\text{Watt} * 1221 \text{ Watts} + \$20/\text{hour} * 155.2 \text{ hours}}{1000}$$

Rated Aircraft Cost (Thousands of \$) = 6.4954

AIAA Design Build Fly Competition: Written Report



Submitted by:

The student chapter of the AIAA at the University of Arizona
Department of Aerospace and Mechanical Engineering
Tucson Arizona
March 13th 2001

TABLE OF CONTENTS

Executive Summary	1
Management Summary	2
Conceptual Design	6
Preliminary Design	10
Detailed Design	18
Manufacturing Plan	21

Executive Summary

The Aircat 2001 is an airplane that is completely designed and built from the ground up. The entire production of this aircraft took place in Tucson, Arizona, at the University of Arizona. This project is currently overseen by two faculty advisors: Dr. Larry B. Scott, and Dr. Sergey V. Shkarayev. Both faculty members have extensive knowledge and expertise in aircraft design and performance. The actual design and construction of the airplane was completed by the student chapter of the American Institute of Aeronautics and Astronautics.

The design process began in July of 2000, and construction was completed December 1st, 2001. Five days later, the airplane had already made history with its first award, the "Best Overall Design Project" for the Aerospace department at the university. That was only the beginning of its fabled history.

The first flight occurred on the morning of the 10th of February, and it was an unprecedented success. No adjustments were necessary, and the plane performed flawlessly.

The Aircat 2001 is a paramount success. It has single handedly redefined the careers and ambitions of its designers and builders, while providing new challenges and achievements with each passing day.

Many different designs were investigated, ranging from low wing to high wing aircraft in accordance with a myriad of sizes & shapes. Some designs resembled the Aircat 2000, (a traditional high wing craft), and still others resembled small scale C-130 cargo transports. Based largely on experience from the previous year, the optimal configuration of the positives of each design were compiled to form the new design of the Aircat 2001.

Many design tools were used in each phase of the design. The preliminary designs were largely composed of CAD drawings and engineering sketches. Once the final design structure was selected, a more formal PRO-E drawing was produced, and then numerous pages of Excel spreadsheets optimized the anticipated sizing criterion and performance data. From that point on, construction began.

All in all, this project has been a huge success from the beginning, one that has had few setbacks. The Aircat 2001 was bred to be a winner, and it has been a winner from it's first formal appearance to its peers. It's success will surely be continued in April.

Management Summary

The University of Arizona's AIAA 2001 design/build/fly team is comprised of a wide range of students. These members vary in age, experience, and cultural background. The team has been in place since August of 2000, with most of its upper division management already in position from the 1999-2000 competition.

Management Structure

The management structure of the team consists of a club/team President, a Project Coordinator, and a Chief Builder/Director of Funding. These three persons oversee the entire project from beginning to end. This includes preliminary design, detailed design, construction, testing, & fundraising.

Matthew Angiulo: Matt Angiulo is currently a senior majoring in Aerospace Engineering. He is the club/team president and is responsible for everything included in the student AIAA chapter, along with overseeing the DBF project as a whole. Some of Matt's major responsibilities include managing the organization of the team members, conducting weekly meetings, delegating tasks & responsibilities, and also to act as the liaison to the Tucson Professional Chapter of the AIAA. Moreover, Matt is in charge of our community & business outreach, which includes public presentations of the project, academic recruitment, and the management of spending & procurement.

Patrick Haley: Patrick Haley is a sophomore majoring in Mechanical Engineering. He serves as the project coordinator for our contest entry. He is responsible for keeping the team on schedule with the project. This includes assigning weekly tasks & goals for the team. He is also responsible for providing the president with detailed itemizations of parts & supplies needed for the project. Patrick is also in charge of presenting weekly progress reports to the general club meetings. More importantly, he serves as the manager of the team members who work on the project. This includes solving all of the day to day problems that occur with the project and team members. He serves as a single point of contact for interfacing between project issues, concerns, and their solutions.

Keith Brock: Keith Brock, a sophomore in Aerospace Engineering, is the Chief Builder/Director of Funding for our project. He was selected to this position due to his long time relationship with the aircraft industry, and extensive experience with R/C aircraft and their components. This knowledge enables Keith to not only supervise and lead the design and construction of the airplane, but to also spearhead the fundraising effort by targeting specific companies in the Southwest who can further our success. Keith is responsible for corresponding with the project coordinator on progress and future development of the airplane. He acts as the foreman for our contest entry, and is present at every weekly building session. Most importantly, Keith serves as the aircraft pilot, and is fully AMA and IMAA certified. He is responsible for scheduling test flights of the airplane, and specific tasks will be accomplished during those flights.

Project Team Members/Personnel

The general club members are responsible for the implementation of goals and objectives set forth by contest regulations and tasks assigned by the management structure. The team members have a wide range of abilities which provides a fun, challenging, and rewarding project environment. This in turn provides the club with a range of design ideas and construction techniques.

Adam Tate, Valerie Thurston, Patricia Chapman and Eduardo Placencio: Aerospace Engineering seniors. Adam, Valerie, Patricia, and Eduardo act as agents linking the project to the classroom via utilization of the airplane as a senior design project. These four people are responsible for the specific design calculations and overall numerical performance and sizing analysis of the airplane. They also act as mentors to the younger members of the club through academic experience and personal maturity. The seniors and their overall design calculations are overseen weekly by a senior faculty member. This acts as a system of checks and balances which allows for the highest success with the least amount of error. The seniors also are responsible for the computer drawings of the aircraft.

Team Members:

- Patrick Craine - Aerospace Engineering, senior, is responsible for stability and control.
- Court Wainwright - Aerospace Engineering, junior, is the payload specialist.

- Tom Cote - Aerospace Engineering, junior, is the Engineering Student Council representative.
- Brent Hampton - Aerospace Engineering, sophomore, web site maintenance.
- Troy Stevenson - Aerospace Engineering, freshman, is a builder.
- Motoyuki Aki - Aerospace Engineering, junior, is a builder.
- Vincent Kuok Lan Do - Aerospace Engineering, junior, is a builder.
- Victoria Stubbs - Biology, freshman, is the club photographer and shop assistant.

Project Schedule

<u>DATE</u>	<u>DESCRIPTION</u>
9/7/00	AIAA Chapter Meeting (Introduction)
9/7/00-9/14/00	Delegation of Project Assignments/Teams
9/14/00	AIAA Chapter Meeting (Progress Report)
9/14/00-9/21/00	Complete Final Design Criteria
9/21/00	AIAA Chapter Meeting (Progress Report)
9/21/00-9/28/00	Begin Preliminary Analysis of Design Criteria
9/28/00	AIAA Chapter Meeting (Progress Report)
9/28/00-10/5/00	Finalize Preliminary Analysis of Design Criteria
10/5/00	AIAA Chapter Meeting (Progress Report)
10/5/00-10/12/00	Finalize Engine & Propeller Purchase based on Design Criteria
10/12/00	AIAA Chapter Meeting (Progress & Budget Report)
10/12/00-10/19/00	Begin Construction of Prototype
10/19/00	AIAA Chapter Meeting (Progress & Construction Report)
10/19/00-10/26/00	Continue Construction of Prototype
10/26/00	AIAA Chapter Meeting (Progress & Construction Report)
10/26/00-11/03/00	Continue Construction of Prototype
11/03/00	AIAA Chapter Meeting (Progress & Construction Report)
11/03/00-11/10/00	Finalize Construction of Prototype

11/10/00	AIAA Chapter Meeting (Progress & Final Construction Report)
11/10/00 – 11/17/00	Testing of Prototype
11/17/00	AIAA Chapter Meeting (Progress, Testing & Budget Report)
11/17/00-11/24/00	Testing & Modification of Prototype based on Test Results
11/24/00	NO MEETING /THANKSGIVING HOLIDAY
12/1/00	AIAA Chapter Meeting (Progress Report)
12/1/00-12/15/00	Final Completion of Airplane Prototype & Project

Conceptual Design

Mission Design

The mission requirements for this year's competition make the design of the aircraft a complicated process. Because of the volume and weight differences of the payload specifications, designing a small fuselage to handle the steel requirements would limit the number of tennis balls that can be carried by the fuselage. Whereas, if the fuselage is designed in order to maximize the number of tennis balls carried, the steel carrying capacity would not be affected, but the added structural weight would be a drawback. This payload dilemma was the major challenge set forth by the mission requirements. As a consequence, the conceptual designs that were investigated included an airfoil-shaped fuselage, round fuselages, variable height and width profile fuselages, and blended wing/body fuselages.

Greater lift generation is needed because of the size of the fuselage needed to carry a maximum number of tennis balls. Due to this fact, monoplanes and biplanes were also investigated. Based on past experiences with radio-controlled planes and the experiences of last year's competition, the team decided that the most lift generation and greatest success would be achieved with a biplane configuration.

Propulsion

As shown in the above mission requirements, the conceptual design of our aircraft had to be structured around the propulsion system. This was necessary due to the large amount of weight that needed to be flown. Our team made it a point to do the conceptual design of the airplane *around* the motor. By doing this, we were able to eliminate early the downstream problems that can occur with an under-powered prototype.

It was stated in the mission requirements that our competition entry was limited to only two vendors of motors, Graupner and Astro Flight. Extensive research was done to idealize motor performance for our conceptual design. This was necessary in that as stated above, our future conceptual designs were to center around this decision. Therefore, up front motor selection was of paramount importance.

As a result of these findings, and for specific reasons that will be illustrated later in the report, the Astro Flight Cobalt 90 motor was selected as the optimal choice for our project.

Lift Generation

The mission requirements of this year's competition require us to simply lift a lot of weight. When it all comes down to it, the competition is a straight lifting competition. The winning team is the one who can lift the most weight in the most efficient manner. Therefore, airfoil selection was important in analyzing the different conceptual designs.

The blended wing/body design was eliminated due to the sheer complexity of the structure. It was decided that although the structure was very efficient and high tech, this design would simply be too difficult to build with the resources that were available to us. Basically, the "keep it simple" philosophy was adopted here.

The low wing conceptual designs that existed were very traditional in nature. Both designs included tail driven landing gear with conventional style wing structures. Of all of the conceptual designs, these proved to be the most practical. They were fairly easy to visualize through to their final stages. Low wing aircraft tend to be very low drag, but traditionally do not perform as well structurally for high lifting applications. We found that to be the major drawback with those designs.

The only other conceptual designs for the wings were biplane and standard high wing configurations. Based on the experience from last year's plane, the standard high wing aircraft typically had a high amount of wing loading based on the given propulsion arrangement. Based largely upon the underachievement of last year's entry, the high wing configuration was kept at bay.

As a result of these discussions and analyses of the conceptual designs, the biplane configuration was chosen. High camber airfoils were adapted for reasons that will be shown later in the report.

Fuselage

The mission requirements for the competition illustrate a need for a strong, sturdy fuselage. As stated before, this was one of the major conceptual design challenges that was presented in this year's competition. Two roads were provided, a team could either carry lots of

tennis balls and score a few times with high volume, or score more frequently with smaller volume.

The conceptual designs for our fuselages centered around the payload capacity. The traditional low wing concepts had smaller fuses with smaller payload bays. These planes were designed to fly quickly around the track by doing many laps with a small amount of payload. The larger biplane and high wing configurations had much larger fuselages, which in turn acted in an opposite manner with the smaller ones. The larger fused conceptual designs would carry larger payloads only a few times around the track.

Last year's experience was huge here. It was decided that for reasons that will be shown later, a smaller fuselage design would only limit our abilities down the road. This was important in that the conceptual designs were intended to focus around the motor and power output, and we wanted to give the motor every opportunity to perform at its best. In that respect, a larger, havier fuselage design was implemented.

Rated Cost Table

The following table outlines the values for each component of the cost index.

Table # 1: Rated Cost

<i>Manuf. Empty Weight Multiplier "A"</i>	\$100 / pound
<i>Rated Engine Power Multiplier "B"</i>	\$1 / watt
<i>Manuf. Cost Multiplier "C"</i>	\$20 / hour
<i>Rated Engine Power</i>	1728
<i>Manufacturing Man Hours (total)</i>	236
<i>Manuf. Empty Weight</i>	12 pounds
<i>Overall Rated Cost</i>	\$7,648.00

Summary

The conceptual design phase of this year's project was a very important one. It allowed the team to thoroughly investigate all of the possible configurations for the design. These designs ranged from complex fuselage structures to simple low wing designs. The most important fact in this stage of the design process is twofold. Firstly, all of the designs centered on the mission requirements set forth by the competition. All designs aimed at completing the given competition requirements in the most efficient manner possible. Secondly, all of the designs centered around the propulsion system. This allowed the team to work with a free mind that in the end, the plane would have a great chance of flying in that enough power would be available to complete the mission.

Preliminary Design

Design Parameters

Many various design parameters were investigated in designing the aircraft. The main parameters range from payload capacity to lift generation to propulsion. The main goal of these parameters is to provide the lightest, most powerful airplane possible. For example, last year's competition entry, the Aircat 2000, was the lightest plane at the competition. We wanted this year's plane to mirror that accomplishment. This allows for a higher payload capacity, which thereby generates more points for our team in the competition.

Lift Generation

As stated earlier, the mission requirements for this year make it necessary to have over achieving wings. These combined with ample power output would in theory produce a winning aircraft. One of the major problems with our entry for last year's event was that it simply did not produce enough lift to carry the liters of water. Furthermore, the wing loading was too high. This year's design focused around better airfoil selection, along with maintaining the same building techniques that provide a functional, ultra lightweight airfoil.

The main characteristics that were investigated were high lift, low Reynolds number behavior, and aspect ratio.

FOM = Percent camber / chord length.

FOM = Lift coefficient / thickness.

We wanted an airfoil that had a fairly high camber airfoil to produce high lift, but that was also structurally sound. The trade-off for the high cambered airfoil is that it produces a large amount of drag. We also needed an airfoil with a significantly high lift coefficient (for example: $1.3 < C_L < 1.7$ un-flapped). This will allow for a modest amount of lift production.

The next figure of merit investigated was that of a monoplane versus a biplane configuration. Going along with the same philosophy from before, it was determined that a biplane configuration would produce more overall lift given our fixed wing span requirement and

manufacturing process. This fit in with the mission requirements in that the biplane configuration provides a more structurally stable lifting device. The biplane configuration also reduced the wing loading of the airplane, which was another advantage over last year's entry. We believe it is necessary to have a structurally strong lifting device in order to carry the steel blocks necessary for the mission.

Another figure of merit that was investigated was the use of a flap system in order to increase the effective wing area for take-off and landing. This would enable for a much more stable and productive airfoil. Plane flaps and slotted flaps were analyzed and were given figures of merit, which maximized extended lift coefficient while reducing construction complexity. It was decided that after building a prototype slotted Fowler Flap, that this flap system would give us the most lift increase to our airfoil.

From these figures of merit along with the use of computer software (such as Excel and MATLAB), the following optimal specifications were decided upon.

Table # 2: Airfoil Characteristics/Lift Characteristics

<i>Airfoil Type</i>	Eppler E396 LRN airfoil
<i>Camber</i>	6%
<i>Chord Length</i>	18 inches
<i>Span</i>	96 inches
<i>Thickness at maximum chord</i>	2.34 inches
<i>Flap System</i>	Fowler .015c slotted system
<i>Flap gap length</i>	.25 inches
<i>Lift coefficient (flapped)</i>	2.5
<i>Lift coefficient (un-flapped)</i>	1.55
<i>Wing loading</i>	2.4 pounds/feet squared

Horizontal Tail

The preliminary design of the horizontal stabilizer was to produce a tail that would be able to counteract the nose up moment generated by the wings of the plane. For that reason, an inverted Clark Y airfoil was selected as the horizontal tail. This produces a nose down moment, which in turn yields a very stable aircraft.

Landing Gear

The mission of our plane and for the competition this year is to successfully carry a lot of payload. The responsibility for getting this payload safely on and off the ground lies squarely on the landing gear. In conjunction with the mission requirements, a strong gear is needed, but it must also be lightweight. The lighter the gear, the more weight that can be supported in the payload bay, and this of course yields the team a better score.

The main figure of merit that was considered for the landing gear was the following:

$$\text{FOM} = \text{strength} / \text{weight}.$$

Our landing gear from last year's entry proved to be the only redeemable quality from last year's aircraft and was thereby replicated for this year's plane. The main gear is made of 30 alternating layers of bi-directional carbon graphite with three-ounce fiberglass. It was then vacuum molded into form with epoxy. This provides us with an incredibly flexible, yet strong, landing gear. The main gear has been weight tested to 75 pounds yet it only weighs 2.2 pounds. The nose gear was selected based on its ability to provide spring resistance and good steering capabilities. This gear setup was selected over a "taildragger" system because it has a much lower tendency to "weather vain" on takeoff.

Furthermore, in an emergency situation, the plane could be converted to a "taildragger" setup. This conversion could take place if a hard landing occurred and fatally damaged the nose gear. This conversion would allow the plane to continue to compete, even after heavy damage to the gear. This is just another safety factor included in the preliminary design of the landing gear.

This combination of nose and main gear systems provide the airplane with a tricycle take-off/landing platform that is more that strong enough to support the weight of the plane plus any hard landings that the plane might make.

Propulsion

Because of the limited selection of motors specified in the mission for this year, we have decided to use the best possible motor that was available to us. One of the major problems for last year's entry was a lack of power, and this was the major decision for choosing this motor. We used the power coefficient as the driving figure of merit.

$$\text{FOM} = \text{Power out} / \text{Power in}$$

Based on this FOM, we selected the Astro Flight Cobalt 90 motor. It provides the most output power per input power allowed for completing the mission. Supporting the gearbox and engine with a suitable engine mount proved to be a difficult task. In order to solve this problem, our team constructed a sturdy aluminum engine mount.

The Astro Flight Cobalt 90 allows us to use the optimal propeller, which maximizes acceleration during take-off. This is an important parameter because take-off distance is regulated by the contest rules.

Batteries were an important variable due to the fact that they comprise the largest single empty weight factor in the airplane. Therefore the following FOM was optimized in battery selection:

$$\text{FOM} = \text{power output} / \text{weight}$$

From an extensive analysis of available over-the-counter batteries, it was decided that the Sanyo 2400 NiCad cells were the best option for our power system. For example: using the Sanyo batteries, it is possible to use 36 cells plus their wiring and still come within the five pound contest battery weight maximum. However, if we used the Sanyo 3000 series NiCad batteries, the cell limit would be approximately 30. This scenario would produce less voltage, which in turn would lower the engine RPM, thereby reducing thrust. Overall, this combination of motor, propeller, gearbox, and battery configuration yield an overwhelming static thrust figure of 14.5 pounds. This thrust value illustrates our optimized configuration.

Table # 3: Engine/Power Specifications

<i>Engine Type</i>	Astro Flight Cobalt 90
<i>Gearbox Type</i>	Astro Flight Super-box 2.75:1
<i>Battery/Cell Type</i>	Sanyo 2400 mAh Nickel Cadmium
<i>Number of Batteries/Cells</i>	36
<i>Propeller Type</i>	Mejlik carbon fiber
<i>Propeller Dimensions</i>	28 x 12
<i>Maximum Power Output</i>	1600 Watts at 80% efficiency
<i>Power Input</i>	20 Amps
<i>Propeller RPM</i>	2700 rpm
<i>Brake Horse Power</i>	1.4
<i>Speed Controller</i>	Astro Flight 60 Amp speed controller

Payload Capacity

The driving goal for this year's project was to accomplish the set forth mission of carrying the most payload possible, while doing so quickly and efficiently. More specifically, one of our main goals was to design and construct an aircraft that could carry near its own weight. This was the major FOM that we aimed for as a team. Based upon last year's results, we theorized that it would take at least that amount of ability to have a chance at winning the competition.

Furthermore, it was discovered that last year's project was too small in nature. For example, a vast amount of time was wasted trying to squeeze parts and wires into cramped places. As a consequence of that, this year's plane was designed with the builder in mind. Ample room exists to manipulate cargo, adjust batteries and servos, and to vary the CG location as the need should arise.

The payload capacity was one of the most scrutinizing factors in selecting a design for our project. We discovered that in many of our members' conceptual designs, the payload bay was secondary in nature, and not nearly adequate to make the sorties worthwhile.

As a result of this, the Aircat 2001 was designed AROUND its payload bay, tailored to the mission of this year. It was designed from the ground up and from the beginning as a transport aircraft.

The following table expresses the specifications and abilities of our project with respect to the payload capacity & payload delivery.

Table # 4: Payload Bay Specifications

<i>Bay Location</i>	Above lower wing at 25% MAC
<i>Max # of Tennis Balls carried</i>	68
<i>Max pounds of steel carried</i>	15
<i>Delivery Mechanism</i>	EasyLoader System
<i>Aircraft Empty Weight</i>	17 pounds

Internal Spar

The mission for our plane calls for the need to have an adequately strong wing structure in order to accomplish the lifting requirements in the mission. For this reason, it was necessary to devise a spar for our lower wing that would be incredibly lightweight, yet could be strong enough to support the aircraft takeoff weight plus an adequate margin of safety.

Our payload bay is supported mainly by the lower wing and it's internal spar. This spar consists of a sleeve joint of balsa stock wrapped and adhered with three ounce fiberglass. This matrix is in turn held together with thin CA glue. This technique allows for a very lightweight, very strong lifting surface. Our spar has been weight tested to over 35 pounds, more than enough to cover the max takeoff weight of the aircraft, plus a reasonable margin of safety for the plane.

Material selection played an important role in this part of the preliminary design phase. Materials were needed that could provide the necessary yield strength, but were not too heavy in nature. This provided our team with an interesting engineering dilemma. We liked the idea of using balsa as the main wood structure, due to the fact that it is very lightweight in nature. However, we have found from past experience that balsa stock has a tendency to shear in the lateral direction.

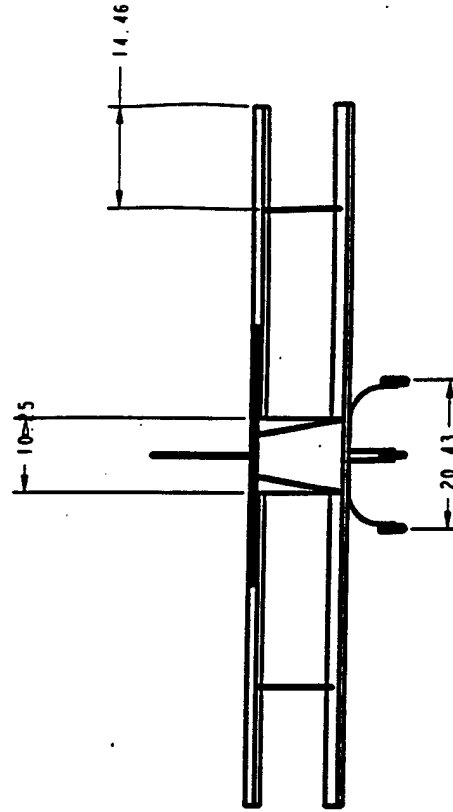
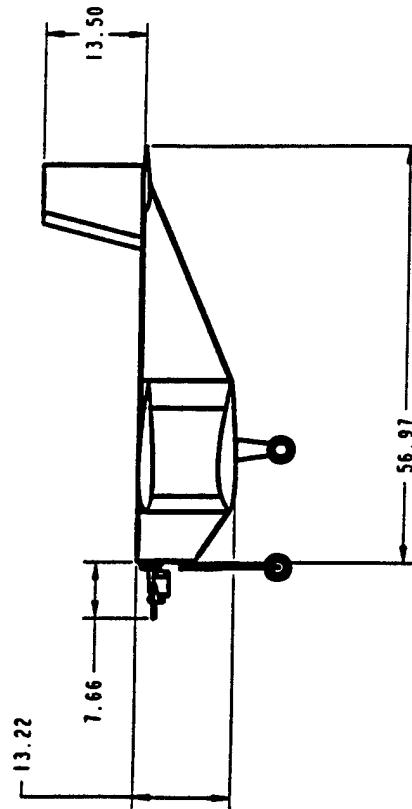
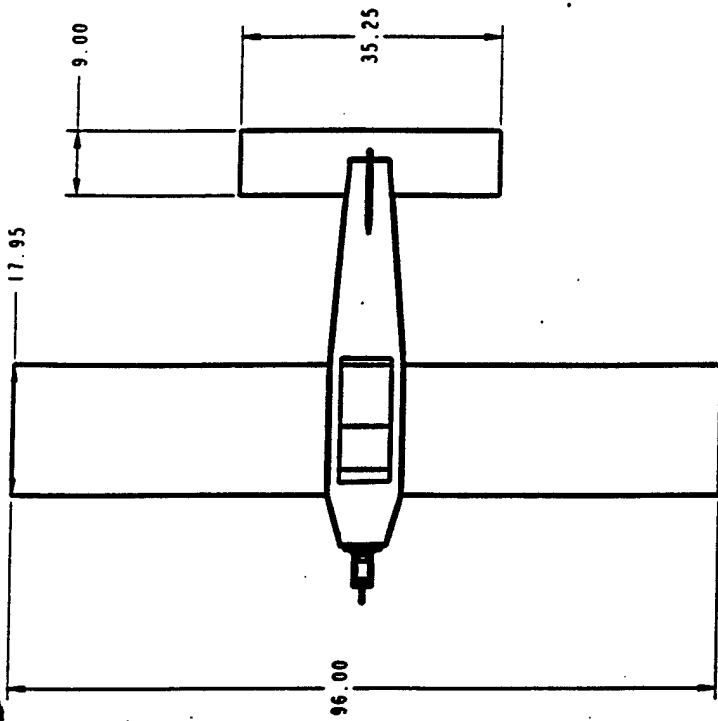
In order to compensate for this, the joint in the spar was cut to a scarf joint, thereby increasing the effective bond area of the joint. This in turn made the joint stronger, which made our spar and plane stronger. In order to compensate for the weak lateral yield strength, the stock pieces were adhered together longitudinally. This increased the strength of the spar dramatically.

Finally, in order to improve the strength of the spar, the spar was covered with fiberglass and then covered in CA glue. This really strengthened the spar in all directions, and produced little center point deflection at 35 pounds. Finally, the spar was installed into the lower wing.

Summary

The final configuration of the Aircat 2001 is one of complete success. The airplane has been successful from the beginning; it won the "Best Overall Design" for the department five days after construction was completed. The airplane can carry over 60 tennis balls, and over 12 pounds of steel. This, combined with an overachieving engine, has provided us with a winning design. Our landing gear has a substantial safety factor built in, which allows for a nice margin of error in inclement weather. Our airfoils and control surfaces are literally "parachutes" when it comes to providing adequate lift to drag performance.

All in all, the design for the Aircat 2001 is one of championed success. It was handcrafted and designed with simple computer spreadsheets and a lot of personal calculations. Very rarely do a small group of people accomplish so much, especially perfectly from the beginning. Teamwork and a passion for long hours of dedication have made the Aircat 2001 the pillar of flight that it has become.



UNIVERSITY OF ARIZONA		University of Arizona	
AIRCAL 2001 CR2 Edition		Airca 2001 CR2 Edition	
Foam and Fiberglass		Foam and Fiberglass	
English		English	
Model 101		Model 101	
Date: 10/1/01		Date: 10/1/01	
By: [Signature]		By: [Signature]	
For: [Signature]		For: [Signature]	
Total: 1.000		Total: 1.000	

Detailed Design

This section of the technical report illustrates the overall performance characteristics of the aircraft. The data is generally given in tabular format for ease of presentation.

Performance

The following table defines the takeoff performance for our aircraft.

Table # 5: Takeoff/Landing Data

<i>Takeoff Field Length</i>	200 feet
<i>Takeoff Ground Roll Distance</i>	20 – 200 feet
<i>Takeoff Velocity</i>	25 feet/sec (18 mph)
<i>Takeoff Power</i>	80% (1024 W)
<i>Landing Field Length</i>	200 feet
<i>Landing Run Distance (Empty Weight)</i>	50 feet
<i>Landing Run Distance (Max Payload Weight)</i>	96 feet
<i>Landing Power Range</i>	0% to 100% dependent on flight conditions
<i>Landing Velocity Range</i>	10 ft/sec to 35 ft/sec (6.8 mph to 24 mph)
<i>Overall Aircraft Handling</i>	Excellent
<i>G Load</i>	1.6

Payload

The following table gives the payload types, specs, and configurations for our aircraft.

Table # 6: Payload Specifications

<i>Mission 1 Payload</i>	15 pounds of steel
<i>Mission 2 Payload</i>	68 tennis balls
<i>Mission 1 Payload Weight</i>	15 pounds
<i>Mission 2 Payload Weight</i>	9.82 pounds
<i>Aircraft Empty Weight</i>	17 pounds
<i>Payload Transfer Mechanism</i>	EasyLoader System
<i>Payload Fraction</i>	.882 or 88.2%

General Component Selection & System Architecture

As expected with such a large project, hundreds of components make up the success story of the Aircat 2001. These components range from the 2024 aluminum engine mount to the tiny bell cranks added to the flap servos for equal deployment. They all work in harmony to produce a uniform mechanism of flight.

Due to the large number of components and parts associated with this project, only the major, more general pieces will be presented, with the general assumption that the reader assumes a basic R/C aircraft background.

The following two tables illustrate the components of the aircraft, along with the general system architecture and aircraft type.

Table # 7: General Aircraft Components

<i>Airfoils</i>	Eppler E396 Low Reynolds Number airfoils
<i>Flaps</i>	Fowler single slotted system
<i>Ailerons</i>	Standard Bi-directional
<i>Vertical Tail</i>	Carbon graphite & epoxy matrix
<i>Main Landing Gear</i>	Carbon graphite, foam, & epoxy matrix
<i>Nose Gear</i>	15 inch single wheel system
<i>Horizontal Tail</i>	35 inch foam with Econokote covering
<i>Servos</i>	Futaba High Torque standard servos
<i>Rods & Connectors</i>	Great Planes assortment
<i>Control Surface Hinges</i>	Great Planes standard size CA hinges
<i>Engine</i>	Astro Flight Cobalt 90
<i>Batteries</i>	Sanyo 2400mAh Ni-Cad
<i>Receiver</i>	Hitec standard 6 channel receiver
<i>Radio</i>	Prism Programmable 6 Channel Radio
<i>Camera</i>	X10 Security Camera with transmitter
<i>Propeller</i>	Mejlik 28 x 12 forged carbon graphite
<i>Coloring</i>	Airbrushed latex model paint
<i>Covering (Fuselage)</i>	3 ounce fiberglass
<i>Covering (Airfoils & Control Surfaces)</i>	Econokote model covering
<i>Struts</i>	Bi-directional polyethylene matrix
<i>Spar</i>	Balsa wrapped in fiberglass

Table # 8: General System Architecture

<i>Aircraft Configuration</i>	Traditional biplane
<i>Payload Configuration</i>	Transport
<i># Of Engines</i>	1
<i>Retractable Landing Gear</i>	No
<i>Aircraft Empty Weight</i>	17 pounds
<i>Aircraft Takeoff Weight</i>	32 pounds
<i>Span</i>	8 feet
<i>Chord</i>	18 inches
<i>Propulsion</i>	Electric
<i>CG location</i>	25 % from front of aircraft

Manufacturing Plan

In choosing the best way to build the aircraft and the materials to use, we mostly looked at building the plane from foam core and reinforcing it with a fiberglass covering for the fuselage and Econokote for the wings. This method was decided upon because it produced the lightest plane from last year's competition. The foam is also easier to work with and modify within a short amount of time.

Airfoils

Because of the size of the wings, 8' x 1.5', along with the airfoil shape that was chosen, we used three inch thick foam and cut the wings in four foot sections using a hot wire foam cutter. We had to cut in four foot sections because of the length limitation of the hot wire. A template of our chosen airfoil was made and then transferred to plywood to make two solid forms to be traced by the hot wire. These templates were then attached to the ends of the foam sections. Four wing sections were cut in this manner. The edges were then cut off to allow room for the control surfaces. Two wing sections were then joined together by a spar to form the bottom wing. The top wings were shortened to account for the space that the fuselage takes and wood reinforcements were added to the inside edge of the sections so that they could be attached to the fuselage using bolts.

The spar of the bottom wing is made of four balsa leading edge pieces glued together and reinforced with a covering of three-ounce fiberglass and thin CA glue. The spar was inserted into the pre-cut groove that was made from the template and the hotwire. The two wing sections were then glued together to create a continuous bottom wing.

The control surfaces were cut from the same foam and covered with 1/32" balsa wood and Econokote. Tracks were designed and made from plywood for the Fowler flap system. These four tracks were then attached to the flaps and attached to the wing. Channels and pockets were cut with a soldering gun so that the servo controls would sit flush within the wing. The wing was then covered with Econokote.

Fuselage

The fuselage foam was cut in a similar manner as the wings. With the help of an overhead projector, an outline of the fuselage was traced onto a sheet of 4' by 8' by 2" foam. This tracing was cut out and used to cut six more pieces of foam, with one piece being only half the thickness of the rest, giving a total of seven fuselage pieces. A cargo bay, battery bay and servo tray were then cut from the inside 5 pieces. The pieces were then tacked together. The angles of the fuselage were cut with the hot wire to give it its streamlined shape. The corners were then rounded using sandpaper. Once the sanding was finished, all of the sides were covered with three ounce fiber glass and secured with thin CA glue. To create a smoother finish over the fiberglass, filler was used to fill in the small gaps and crevices.

Landing gear

The landing gear design and choice of materials is based on the mission requirements for last year's competition entry. It is made of 30 alternating layers of carbon graphite and three ounce fiber glass with a 2:1 ratio of fiberglass to graphite. Strips of the material were cut. A mold made of 2 x 4 wood, was shaped and then covered with resin to prevent the layers from becoming adhered to the mold. The layers were then placed over the mold with a layer of epoxy separating each layer of material. Once the 30 layers were laid, the mold was vacuum-bagged overnight to ensure that the layers were completely formed to the mold. After the epoxy finished drying, the gear was cut and sanded to get rid of the rough edges and reduce the weight of the landing gear. Holes were then drilled for mounting to the fuselage and for wheel mounting.

Vertical Tail

The vertical tail was made in the same manner as the landing gear. It is made of four layers of carbon graphite surrounding a foam core. A shape for the vertical tail was cut from 1/4" thick foam. Two layers of the carbon graphite were laid down with layers of epoxy in between, the foam was placed, and then the next two layers of carbon graphite were laid with more epoxy. The

"sandwich" of foam and carbon graphite was vacuum-bagged overnight and cut down to size when dry. The leading edge was smoothed out using micro-balloons and epoxy.

Cowling

In order to create a place for the motor to be mounted, the nose of the fuselage was cut off before it was fibreglassed. This was then covered and painted to be used as the mold for the plastic. Clear plastic was heated and formed to fit over the nose mold and vacuumed until it cooled. The plastic was removed from the mold and cut to fit the nose of the aircraft. A firewall was cut out of plywood and glued to the nose of the aircraft to provide stability for the motor mount. Cooling ducts were also added around the lower 20 % of the cowling. These enabled the motor and gearbox to self cool themselves as the plane flies.

Control Surfaces

The control surfaces of our project were constructed in a similar manner to that of the vertical and horizontal tail, They were cut to the optimized size from the foam material, and were then covered to form a lightweight, yet strong control surface. Control rods and clevises were then added to attach the control surfaces to the servo systems.

Horizontal Tail

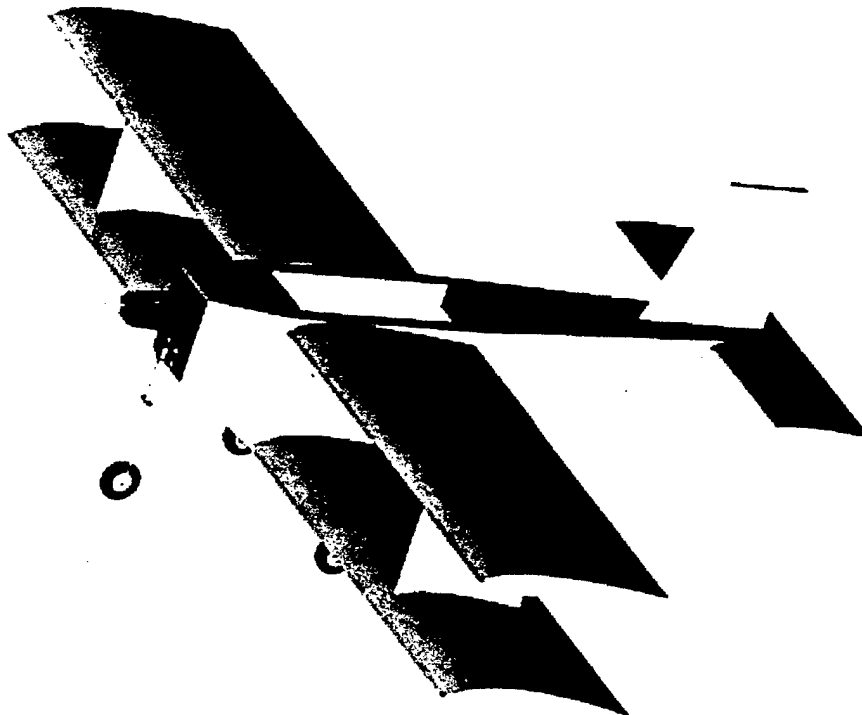
The horizontal stabilizer was constructed of an inverted Clark Y airfoil made of foam, and then covered with Econokote. The airfoil was inverted in order to provide a counteracting pitching moment to the lifting moment produced by the wings. This allowed for a more stable aircraft. The elevator was made of balsa stock that was cut to size and then Econokoted.

Summary

The manufacturing process for this project was one centered around cost effectiveness and material optimization. The best materials for the job were chosen, and if the cost was too high, money was raised to purchase the material, or a cheaper solution was utilized.

One of the best things about our manufacturing process was that it was a total team effort. Everyone chipped in, and everyone contributed to the overall team chemistry in the laboratory. As a consequence of that, our project was rarely behind schedule and was always moving ahead with forward progress.

AIAA
Design Build Fly Competition
Addendum



Submitted by:

University of Arizona
AIAA Student Chapter
Department of Aerospace and Mechanical Engineering
Tucson Arizona

Lessons Learned

The Aircat 2001 has changed in a few areas since the "Proposal Phase" of the written report. For example, the lower wing was replaced with a newer, stronger version; the nose gear was modified for increased structural support; an air induction scoop was added to the lower portion of the plane in order to properly cool the batteries. Also, the struts were modified to fit the new wing, and were also reduced in area.

All of these modifications have increased the chance of success of the Aircat 2001. The plane is now stronger, and thereby able to carry more payload, which in turn produces a higher score for our team. The nose gear is stronger, which will prevent buckling failure on hard landings. An increased cooling system for the batteries has increased engine performance and overall engine efficiency. Finally, the newly formed struts have provided the airframe with increased stiffness and overall increased compressive strength. All in all, these modifications have greatly helped our aircraft, and our chances of winning the competition.

New Lower Wing

Our previous lower wing included a complex Fowler flap system, which was originally designed to increase the overall lift coefficient of the lower wing. This in turn would produce more lift, and thereby carry more payload. However, the tradeoffs for this system outweighed the benefits. The flap system caused a large increase in drag, and also added considerable weight to the trailing edge of the aircraft.

The goal of this newly constructed wing was to remove the flap system, since it was unnecessary to the performance of the airplane. This would in turn reduce the weight of the airplane, and also reduce the drag. The result is a new lower wing that produced less drag, and weighed less.

In order to maximize the newly saved weight, we installed a stronger, larger spar. This new spar is constructed in a traditional wing box configuration, with balsa filling in the middle, and plywood flanges for the outside. This spar was then wrapped at the middle joint with 3 ounce fiberglass. This new spar can hold a total weight of 45 pounds, whereas the previous wing and spar could only support 32 pounds. Ultimately, this allows us to carry 20 pounds of payload, instead of 15.

This new lower wing is a huge success. We can carry more payload, and the plane flies faster with the reduced profile drag implied from the flap removal. This new wing doesn't limit us, whereas the previous wing did.

Nose Gear Bracing

In early March, we test flew the airplane. The winds at the flight field were sustained at 15 m/s. Our goal was to try and see how the plane would fly in windy conditions, much like the ones we expect for the competition in Maryland.

The airplane flew very well in the wind, however it stalled on the landing due to the incredibly strong head wind. Upon crashing, the nose gear buckled inward and caused it to shear off from the firewall. This was an obvious problem. Our team knew immediately that this could not happen at the competition, so a support solution was investigated.

Many designs were looked at; they ranged from complex fork braces to simple firewall reinforcement methods. After much discussion, a simple support brace was added to the nose gear. This aluminum tube brace was installed in a fork design to the engine mount, and was then tied to the screw mount of the nose gear using "zip ties."

This new brace resists the motion of the gear to shear inward, and thereby increases the rigidity of the nose gear mount to the firewall. This has proved to be a lightweight, structurally adequate solution to our problem.

Air Induction

During the flight testing of the airplane, our team noticed that the batteries were getting very hot during flight. The reason for this is twofold. Firstly, they were simply doing a lot of work. 36 cells drawing 40 amps of current is simply a big task, no matter what the electrical system is. Secondly, the fuselage and battery compartment are made of foam, which acts as a huge insulator to the inside. The heat dissipated by the batteries was staying inside the battery compartment, as was not leaving the aircraft.

As a solution to this, an air induction scoop was added to the bottom of the airplane, just ahead and below the battery compartment. The fuselage under the scoop was sanded to a 40° angle, which helps to shoot the air up into the battery compartment during flight. Furthermore, a circular section was cut from the top of the battery compartment to allow the incoming air to leave the inside of the plane.

The result of this was an air cooled induction system which drastically cooled the batteries during flight. This will, in turn, increase battery life and has already shown a more consistent performance from the battery pack.

Wing Struts

If our team had to name one area of improvement on the plane, they would undoubtedly say the struts. Our previous struts were incredibly strong and did an outstanding job at supporting the wings. However, they just didn't fit right. They were large and bulky, and one even overhung from the leading edge of the wing. This, of course, produced an incredible increase in drag, which reduced the performance of the wing.

Our new struts are smaller, and have been molded to fit our newly constructed wing. They fit perfectly into their mounts and really do an excellent job of supporting the wings. This was a nice change because all along, this was an area of concern for the team. Now that they are fixed and tested, a overachieving wing has been produced.

Lessons Learned

This competition has been a true learning experience. From the beginning, the engineering process of designing, testing, and modifying parts has been utilized. The result has been an incredibly successful project and a team that is much closer and smarter than they were before.

One of our biggest lessons that we learned was to not over-engineer the plane. Our entry for last year's competition produced the desire to make a superior aircraft for this year. As a result of this, some parts of the aircraft were overdone, such as the flap system. On paper, the design and performance of the flap system was great, but the time and effort that was spent implementing them was unnecessary. The airplane's engine exceeded expectations, and the airfoil produced more lift than expected, so the flaps were simply not needed.

Another one of our lessons was to incorporate the knowledge of all our team members. Our seniors have an outstanding ability to apply their knowledge of fundamentals to calculations and design specifics. In turn, our underclassmen have an outstanding knowledge of real life R/C aircraft, and their construction. This marriage of talents provided our project with the best possible resources necessary to complete the success of our airplane.

RATED AIRCRAFT COST

The following tables contain the rated cost index for the Aircat 2001, CR2 edition.

Table 1: Given Cost Parameters:

DESCRIPTION	VALUE
Manufacturers Empty Weight Multiplier	\$100/pound
Rated Engine Power Multiplier	\$1/Watt
Manufacturing Cost Multiplier	\$20/hour

Table 2: Manufacturers Empty Weight:

DESCRIPTION	VALUE
Airframe Weight (minus payload and batteries)	12 pounds

Table 3: Rated Engine Power:

DESCRIPTION	VALUE
# of Engines	1
Amperage	40
# of Cells	36
Multiplier (1.2V/Cell)	1.2
TOTAL REP	1728 Watts

Table 4: Manufacturing Man Hours:

DESCRIPTION	QUANTITY	TOTAL
1.0 WING		
15 hr/wing	2 wings	30 hrs
4 hrs/sq ft projected area	25.8 square feet	103.2 hrs
2 hrs/strut	2 struts	4 hrs
3 hrs/control surface	6 control surfaces	18 hrs
TOTAL		155.2 hrs
2.0 Fuselage		
5 hrs/body	1 body	5 hrs
4 hrs/ft of body length	5.5 feet long	22 hrs
TOTAL		27 hrs
3.0 Empenage		
5 hrs basic		5 hrs
5 hrs/vertical surface	1 vertical tail	5 hrs
10 hrs/horizontal surface	1 horizontal stabilizer	10 hrs
TOTAL		20 hrs
4.0 Flight Systems		
5 hrs basic		5 hrs

2 hrs/servo or controller	4 servos, 1 speed controller	10 hrs
TOTAL		15 hrs
5.0 Propulsion Systems		
5 hrs/engine	1 engine	5 hrs
5 hrs/propeller	1 propeller	5 hrs
TOTAL		10 hrs
TOTAL HOURS	155.2 + 27 + 20 + 15 + 10	227.2

Using values from tables 1-3, the following total aircraft cost was determined.

Total Rated Aircraft Cost =

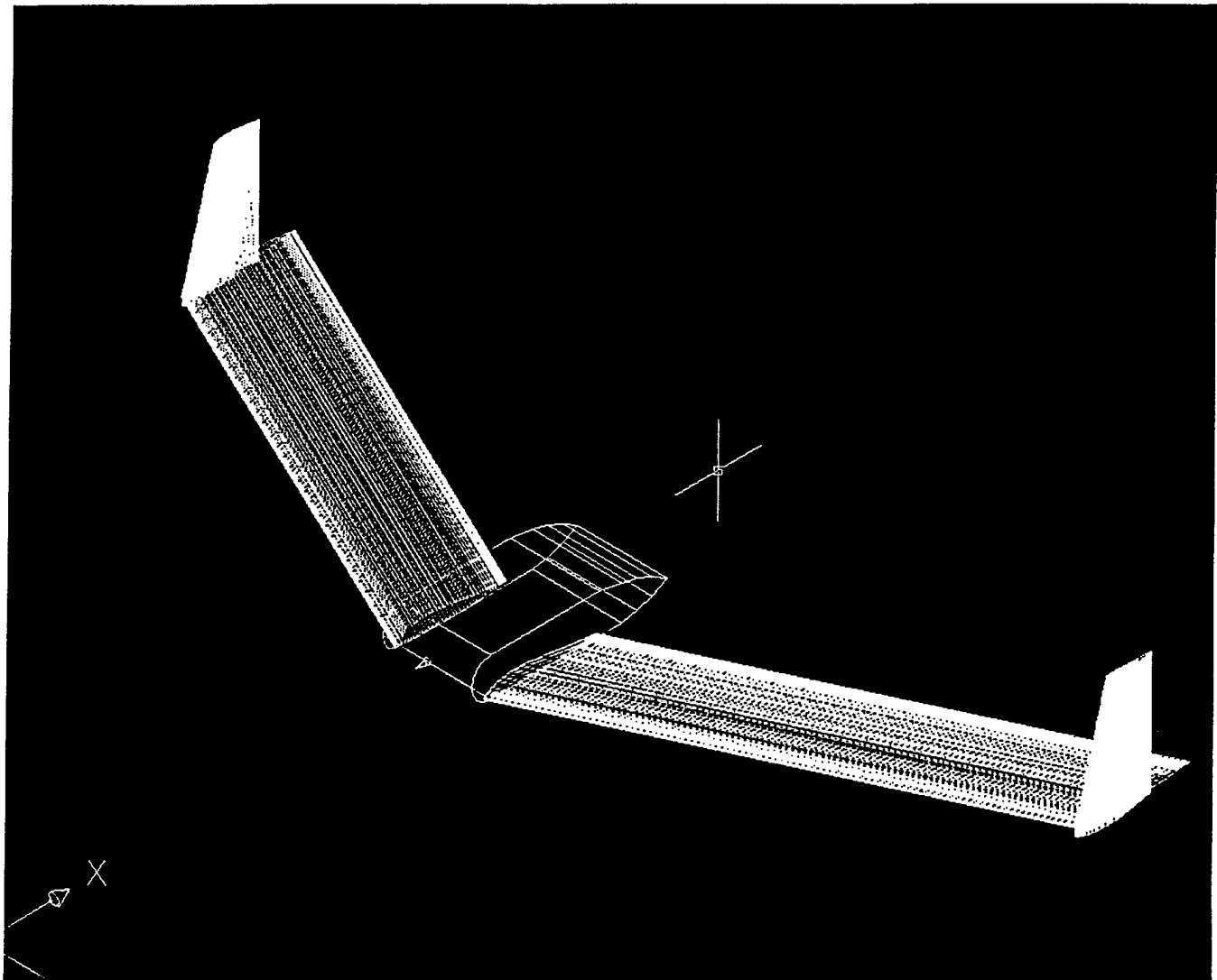
$$[(\$100/\text{pound}) \times (12 \text{ pounds}) + (\$1/\text{Watt})(1728 \text{ Watts}) + (\$20/\text{hr}) \times (227.2 \text{ hrs})]$$

1000

= 7.472

2000/2001 AIAA Foundation
Cessna/ONR Student Design Build Fly
Competition

Design Report



Virginia Polytechnic Institute and State University

March 2001

Table of Contents

	Page #
Executive Summary.....	3
Management Summary.....	6
Conceptual Design Phase.....	9
Introduction.....	9
Possible Concepts.....	9
Design Parameters.....	9
Excel Spreadsheet.....	10
Preliminary Design Phase.....	15
Introduction.....	15
Wing.....	15
Fuselage.....	16
Speed Loader.....	16
Systems.....	16
Detail Design Phase.....	22
Introduction.....	22
Wing.....	22
Fuselage.....	22
Systems.....	22
Manufacturing Plan.....	24
Introduction.....	24
Wing.....	24
Fuselage.....	24
Speed Loader.....	25
Systems.....	25
Appendix 1 -References.....	27
Detailed Drawing Package.....	28

Executive Summary

During the 2000-2001 school year, a group of aerospace undergraduate students at Virginia Polytechnic Institute and State University decided to compete in the Cessna/ONR Student Design/Build/Fly Competition. To enter this contest, the team had to create, optimize and fly a remote controlled aircraft. The AIAA sponsored contest will be held on April 20th through April 22nd, 2001 at the Office of Naval Research in St. Inigos, Maryland.

The Design/Build/Fly Competition consisted of designing an unmanned, electric powered, radio controlled aircraft that best met the specifications laid out in the mission profile. This profile included flying the aircraft around a set course with two payloads. Payloads were tennis balls for the light payload, and steel bars for the heavy payload. The team could attempt to fly as many missions as possible within a ten-minute time limit.

The long-range goal of the team was to build an aircraft capable of winning the competition. To do this, the aircraft had to achieve the best overall score. Scoring included the written report score, multiplied by the total flight score, all divided by the rated aircraft cost. The total flight score was a combination of the three best single flight scores attained during the flight part of the competition. The team decided to attempt to maximize the report score and minimize the rated aircraft score so that the team had an edge entering the flying portion of the contest.

The team initially divided into several subgroups so that several aircraft configurations could be looked at all at once. Each subgroup consisted of an upperclassman and an underclassman. The pairs were given a single concept to investigate so that the best aircraft configuration could be used in the competition. The upperclassmen looked at the performance-oriented analysis of each concept, while the underclassmen aided the upperclassmen and looked into the cost analysis for each concept. The aircraft configurations considered were: a flying wing concept, a Vari-eze concept, a twin fuselage concept, a conventional concept, and a biplane concept.

The performance-oriented members in each pair were encouraged to use an Excel spreadsheet created to evaluate each concept. The Excel spreadsheet combined the methods of Raymer, Tornbeek and methods in a forthcoming book by British professor Lloyd Jenkins. The Excel spreadsheet required several inputs: mission variables, wing variables, fuselage variables, tail variables, power variables and flight system variables. Some of these variables were held constant between concepts, while others were modified with each concept. During the conceptual phase, the Excel spreadsheet was used to find the efficiency of the aircraft as well as the overall rated aircraft cost in numbers that could be easily compared. The flying wing was found to be the most efficient and cost effective at the end of the conceptual phase.

Conceptual Design Data	
Wing Weight (pounds)	1.972169
Fuselage Weight (pounds)	0.761795
Energy Required to Fly a lap with light payload	1470.978
Energy required to fly a lap with heavy payload	6233.447
Number of cycles flyable	3
Flight Score	143.7745
Rated Aircraft Cost Score	62.05644

Figure 1.1: Data for Conceptual Design Phase

This chart shows the data calculated for the flying wing during the conceptual design phase and it was used to compare this stage with the other two design phases.

Preliminary Design Phase

After choosing an aircraft configuration, the team that looked into performance and cost of the flying wing shifted to looking into optimizing the flying wing for the preliminary design phase. The other groups, which had their designs set aside then switched to looking at weight saving building materials and cost reducing construction practices.

The preliminary design phase also consisted of adjusting from depending on the Excel spreadsheet to doing the calculations by hand. It was found that the spreadsheet was producing a maximum heavy payload flight speed of 90 feet per second, as well as a few other marginal errors. Components were added to the Excel spreadsheet to begin to calculate take off and landing distances, which we checked with hand calculations.

In the preliminary design phase, it was decided to change the wings from being small in size with tapering to larger wings with constant chord. The change was necessitated by the need to withstand a set amount of wing loading and improve Reynolds numbers at the wing tips. The fuselage was also altered to handle the change in loading at the root of the wing.

Members of the team also began to investigate the best possible ways to load the most amount of payload in the aircraft in the quickest time. It was decided to use lightweight balsa wood speed loaders to facilitate in the loading and unloading of payload.

During the preliminary stage two models were built. The first was an eighth scale model made out of balsa wood. It was used to check overall static stability of the design. The second model was a half scale model, which was used to test dynamic stability, aerodynamics, flight controls, and to test the skills of the team members to see who would be most proficient in building the full sized aircraft.

Preliminary Design Data	
Wing Weight (pounds)	3.163329
Fuselage Weight (pounds)	0.778842
Energy Required to Fly a lap with light payload	1201.293
Energy required to fly a lap with heavy payload	9350.171
Number of cycles flyable	2
Flight Score	118.3509
Rated Aircraft Cost Score	45.53714

Figure 1.2: Data for Preliminary Design Phase

This chart shows the data calculated for the flying wing during the preliminary design phase and it was used to compare this stage with the other two design phases.

After the preliminary design phase was complete, the team moved on the final design phase. In this phase, the last adjustments of the configuration of the aircraft were made. Information gathered from building and flying the half scale model was integrated into the team's plane for construction of the full-scale model and placement of the servos.

A final building crew was chosen from those that had helped in building the half scale model and had shown proficiency in technique and speed. The speed loaders were completed and the payloads were placed in each loader. These were then tested in the aircraft to adjust for fit, movement during flight, and to also allow the ground crew to test ease of exchanging payloads. The final aircraft will be test flown and any last minute glitches will be ironed out in the last few days before the contest.

Final Design Data	
Wing Weight (pounds)	3.25
Fuselage Weight (pounds)	1.0
Energy Required to Fly a lap with light payload	1250.01
Energy required to fly a lap with heavy payload	5500
Number of cycles flyable	4
Flight Score	108.45
Rated Aircraft Cost Score	44.52

Figure 1.3: Data for Detail Design Phase

This chart shows the data calculated for the flying wing during the detail design phase and it was used to compare this stage with the other two design phases.

Management Summary

A design team was created at Virginia Polytechnic Institute and State University so that an aircraft could be designed and built for the 2000-2001 Cessna/ONR Student Design/Build/Fly Competition. This year's team consisted of one graduate student, four seniors and eight underclassmen, all of which were majoring in aerospace engineering. While there are several organizational methods to this year's team, it allowed for everyone to gain experience in different areas, as well as allowing for the strengths of team members to be used.

The design team was split into several pairs of students to begin the design process. These pairs were given an aircraft concept to research and present to the entire team with the opinion of whether the design would be feasible as a contest entry. The design pairs were vital to the initial design phase of the whole design process. Without design pairs looking at many concepts at once, valuable time would have been wasted and a more feasible configuration may have been missed because of time constraints.

The team met as a whole once a week to discuss the findings of the design pairs during the first semester of school. The team leader was then responsible for relaying what had happened at the weekly meetings to the faculty advisor, Dr. Fred Lutze, so that the team could receive feedback from him. Once a concept was chosen, the team moved to meeting bi-weekly, and the design pairs were dissolved. The team was then split into separate groups to optimize the chosen design. These groups are listed in Figure 2.1. It was decided to also have a meeting on Saturday's for any member that could attend to build the models and to test fly them.

During the building process, the team organization was altered for the last time. There were three subgroups in the final months. The first subgroup included those building the aircraft as well as those procuring building materials. The second group involved those rechecking all the calculations and correcting any problems found during the test flight of the half-scale model, as well as creating the drawing package needed for the final report. The third group began writing the report and obtaining all the data needed for the report from the second group.

In the beginning of the design process, the members decided to create a Ghannt chart so that deadlines were not missed, and all members were kept up to date on the next goal. The chart is reproduced in Figure 2.2. A website was also created so that members could easily exchange files, exchange research information, and could email the entire group. Several members of the team put in more hours than other team member did to make sure that all deadlines were met. With careful organization, a willingness of all team members to give of their time, and a plan of action that was adhered too, all the goals set out for the design team at the beginning of the whole process were met.

	RODNEY BAJNATH	STEPHEN BANAS	GEOFFREY BUESCHER	VICTOR COLLAZO- PEREZ	ERNIE KEEN	ANDY KROHN	TIM MILLER	DZELAL MUJEZINOVIC	HENRICK PETERSEN	ROBERT SIDELL	RACHAEL TESTERMAN	MICHAEL ZAUBERMAN
Concept Research	2	0	5	4	5	0	5	2	3	0	3	2
Concept Evaluation	2	0	5	4	5	0	5	2	3	0	3	2
Optimization Stage:												
Structures	0	0	5	0	3	0	2	0	0	5	0	0
Stability and Control	0	2	5	3	5	2	3	0	3	3	0	0
Payload	5	4	5	3	4	2	4	3	0	4	0	5
Manufacturability	3	4	5	3	4	4	5	2	2	4	0	4
Aerodynamics	0	0	3	2	5	3	3	0	5	3	0	0
Configuration	3	3	5	4	4	4	5	2	3	3	1	3
Engine	0	4	0	0	0	0	3	0	0	5	1	0
Cost	3	3	4	3	4	4	5	2	0	4	2	2
Building Stage:												
Wings	3	5	4	4	5	5	5	0	0	5	2	0
Fuselage	0	4	5	3	2	5	5	2	0	4	0	0
Speed Loaders	5	2	4	3	2	3	3	4	0	3	0	5
Landing Gear	0	5	2	0	0	3	5	0	0	5	0	0
Systems	2	5	3	4	4	5	4	2	0	5	0	1
Material Procurement	0	0	0	0	0	3	5	0	0	5	5	0
Fundraising	5	0	5	5	5	0	5	5	0	0	5	5

Figure 2.1: Management Summary

This figure shows how each member of the design team contributed to the completion of the aircraft. A ranking of 5 indicates maximum involvement and a ranking of 0 indicates no involvement.

Ghannt Chart of Important Goals			
Investigate configurations	26 days	Tuesday 9/19/00	Tuesday 10/24/00
Pick a Configuration	1 day	Tuesday 10/24/00	Tuesday 10/24/00
Optimization	82 days	Wednesday 10/25/00	Monday 01/15/01
Alter Excel Code	59 days	Wednesday 10/25/00	Monday 1/15/01
Research chosen configuration	27 days	Wednesday 10/25/00	Thursday 11/30/00
Build 1/8 Scale Model	32 days	Friday 12/1/00	Monday 1/15/01
Build 1/2 scale model	29 days	Tuesday 1/16/01	Friday 2/23/01
Finalization	40 days	Monday 2/26/01	Sunday 4/22/01
Set configuration in stone	1 day	Tuesday 2/27/01	Tuesday 2/27/01
Fly 1/2 scale mode	1 day	Wednesday 2/28/01	Wednesday 3/10/01
Begin to build the final aircraft	25 days	Monday 2/26/01	Sunday 4/1/01
Test fly final aircraft	10 days	Monday 4/2/01	Friday 4/13/01
Repair any test flight damage	5 days	Friday 4/13/01	Thursday 4/19/01
Contest	3 days	Friday 4/20/01	Sunday 4/22/01

Figure 2.2 Organizational Chart

This chart was used to keep the team on track and to make sure that deadlines were not missed. All dates are actual start and completion dates.

Introduction

The conceptual design phase was divided into two parts. The first part of the conceptual phase involved all of the team members investigating various designs to see which would give the best results. The second part of the conceptual phase had the team choosing a design based on criteria shown below.

Possible Concepts

Conceptual design of the aircraft began by the team's brainstorming different concepts that might fulfill the mission requirements. The concepts included such unconventional options as lifting bodies and twin-fuselage designs, but these more radical possibilities, though given serious consideration, were judged to provide little advantage per rated aircraft cost. The wing bending moment reduction that would be obtained from a twin-fuselage design's distribution of payload away from the centerline held potential to reduce wing weight, but this potential was unlikely to be fulfilled considering the already low weight of the wing and the limited capability for structural analysis of a wing likely to be made of composite materials; the cost function for a twin-fuselage aircraft, however, would increase significantly, especially since either two motors or an additional engine pod would likely be required. In contrast, the lifting body would save on the cost function by eliminating a wing, but was judged extremely unlikely to give acceptable performance.

The remaining concepts from the initial brainstorming were a conventional monoplane with aft-mounted tail, a biplane, a canard or tandem wing aircraft, and a flying wing. The monoplane was considered a baseline design that could be built and controlled easily. The biplane would add wing area, likely helping performance, but with cost function penalties for both the extra wing and the extra wing area. The tandem wing was thought to avoid the biplane's cost function penalty for adding wing area by counting the smaller of the two lifting surfaces as a horizontal tail, carrying a flat cost rather than one proportional to planform area. The flying wing would have the lowest possible cost function by minimizing the fuselage length and eliminating the empennage; further, its lift to drag ratio would benefit from the low wetted area, and its weight should also be reduced by eliminating nonlifting components. The stability and trim difficulties inherent in selecting the flying wing or canard/tandem wing option were noted and accepted as design issues that could be managed later in the design process.

Design Parameters

Four senior- and junior-level students were each assigned one of the four concepts to analyze for scoring potential. To provide a common base for analysis, a method of weight estimation was developed using data taken directly from the previous year's contest winner's final report, which gave detailed geometric data along with an explicit weight breakdown of the aircraft.

Conceptual Design

The weight model used is given in Figure 3.1; weights for system components used in Figure 3.1 such as servos are representative values obtained from surveying available hardware. A common method was also needed to estimate drag, so a buildup method was employed with component drag coefficients taken from a handout provided in a senior design course. Figure 3.2 contains selected entries from this handout.

Figure 3.1: Conceptual design weight model		
COMPONENT	WEIGHT	SOURCE
Wing	0.3939 lb/ft ² of planform area	From 2000 Utah State report
Tail (horizontal and vertical)	0.2325 lb/ft ² of planform area	From 2000 Utah State report
Fuselage (includes receiver)	0.4090 lb/ft ² of wetted surface	From 2000 Utah State report
Battery	5 lb	Assumed will use max allowable
Propeller	2.4 oz per propeller	Assumed based on values in Jim Ryan's R/C weight estimation spreadsheet (Ref. 1)
Motor	0.02 oz per watt of available power	Very rough fit to AstroFlight brushed motors (weights found on AstroFlight website, Ref. 2)
Servos	2 oz per servo	Assumed based on values in Jim Ryan's R/C weight estimation spreadsheet (Ref. 1)

Figure 3.1: Conceptual Design Weight Model

The figure above shows how weights were estimated during the conceptual design phase.

Figure 3.2: Conceptual design drag buildup model		
COMPONENT	C _D	REFERENCE AREA ON WHICH C _D IS BASED
Wing	0.007	Planform area
Tail surface	0.0091	Planform area
Streamlined body	0.05	Frontal area
Landing gear	FACTOR of 1.2	Multiply by total C _D buildup

Figure 3.2: Conceptual Design Drag Buildup Model

The figure above was used to estimate the drag that would occur on each component listed above.

Excel Spreadsheet

One approach to the assigned analysis resulted in the development of an Excel spreadsheet that could easily be adapted for use in analyzing all the concepts under examination. The spreadsheet accepts as inputs geometric parameters to define the aircraft configuration for use in weight and drag calculations with the models described above. An Oswald efficiency factor E must be assumed and input and the total drag can then be calculated by assuming a parabolic drag polar. At a certain weight—for a certain loading of payload—thrust required for steady level flight can be computed, and the power required as well by multiplication by an input cruise velocity. To determine the battery energy required in a single lap, the drag in cruise is multiplied

by the distance flown for a single lap and divided by the efficiencies in the propulsion system. Defining a "cycle" as one lap with heavy payload and two laps with light payload, as the Required for Proposal (RFP) flight profile specifies payload carriage, the energy per cycle is found by summing the energies over the three laps. Given total battery energy, the product of battery voltage and energy rating, the range in "cycles" is calculated by dividing the battery energy by the energy required for each cycle.

Since the flight period is limited to ten minutes, the maximum range may not actually be achievable, and the cruise velocity becomes more important. Time on the ground swapping payloads and getting back into the air must be assumed and added to the flight time for each cycle, and then the total time-limited number of cycles that can be flown may be found. The minimum of either this number of cycles or the energy-limited number of cycles discussed above then can be used with the scoring formula in the RFP to calculate the score for a flight at that loading and geometry.

Cost must be considered, too, though, so the spreadsheet again uses the geometric parameters and other inputs to the cost function to evaluate the components of the cost model contained in the RFP. Dividing the flight score by the cost for a given configuration and loading provides the most valuable figure of merit for the concept, the cost-specific flight score (CSFS), a quantity to be maximized in selecting a concept with which to proceed to preliminary design.

The spreadsheet is highly idealized but provides a quick means of evaluating each concept, and to simplify the spreadsheet's development and use, several relationships and constraints were omitted. Although a cell was provided for the amperage of the fuse limiting the motor's current, this value was used only in the cost function and was assumed at 40 Amps, as team members were not familiar enough with radio-controlled airplane battery packs to determine the voltage across a combination of cells. The takeoff distance constraint was also ignored at this stage of design.

A huge array of variables enter into the spreadsheet calculation of CSFS, and to limit the design space, those about which least was known, or which could be least manipulated were given assumed values. Figure 3.3 lists the variable parameters held invariant between the different configurations:

Figure 3.3: Variables held constant between concepts in conceptual design stage	
Estimated time to land, change payload, take off (s):	60
Wing Oswald efficiency factor:	0.8
C_{Lmax} :	1.6
Number of battery cells:	9
Voltage per cell (V):	1.2
Battery voltage-specific energy (mA-h):	7000
Motor electrical efficiency:	0.8
Propeller efficiency:	0.8

Figure 3.3: Variables Held Constant Between Concepts in Conceptual Design Stage
This figure shows which variables were not changed in the analysis for each concept.

Conceptual Design

With a means of evaluating the CSFS for a configuration, the maximum possible CSFS for each of the four concepts under examination was needed. The goal-seeking capabilities of Microsoft Excel, which can maximize, minimize, or set a value for a single cell by manipulating other cell values subject to user-input constraints, were put to use here. CSFS was selected for maximization, and Figure 3.4 lists the parameters that were varied in the optimization. Many other parameters were made functions of these variables in the spreadsheet to simplify the optimization; for instance, the number of propellers was set equal to the number of motors, and the fuselage geometry was made a function of the number of tennis balls to be carried, by different formulas depending on the fuselage cross section and payload layout envisioned. Figure 3.5 lists constraints used explicitly in the optimization.

Figure 3.4: Independent variables used in MS Excel CSFS optimization	
Heavy (steel) payload weight	
Cruise velocity, heavy payload	
Number of tennis balls in light payload	
Cruise velocity, light payload	
Wing span	
Wing aspect ratio	
Number of motors	

Figure 3.4: Independent Variables Used in Microsoft Excel CSFC Optimization

The figure above lists the variables that were altered between each concept during the conceptual phase.

Figure 3.5: Constraints used in MS Excel CSFS optimization, with origin of constraint	
Heavy (steel) payload weight ≥ 5 pounds	RFP requirement
Number of tennis balls in light payload ≥ 10	RFP requirement
Wing span ≤ 10 feet	RFP requirement
Wing aspect ratio ≤ 12	Assumed structural limit
Motor rated power ≤ 500 Watts	RFP requirement
Number of motors an integer	Physical possibility
Aircraft heavy payload gross weight < 55 pounds	AMA requirement (RFP)
Heavy payload C_L at cruise $< C_{Lmax}$	Aircraft cannot fly stalled
Heavy payload power required at cruise \leq propulsive power available	Aircraft must have sufficient power to cruise
Aircraft light payload gross weight (lb) ≤ 55 pounds	AMA requirement (RFP)
Light payload C_L at cruise $< C_{Lmax}$	Aircraft cannot fly stalled
Light payload power required at cruise \leq propulsive power available	Aircraft must have sufficient power to cruise

Figure 3.5: Constraints Used in Microsoft Excel CSFS Optimization, With Origin of Constraint

The figure shows the constraints given in the contest rules.

Conceptual Design

After the spreadsheet converged on a solution maximizing the CSFS, all values were checked visually to be sure no completely unreasonable numbers had been developed by the spreadsheet. Sometimes additional constraints had to be added to resolve solutions that were physically impossible, such as negative wingspans and aspect ratios. Once the solver had produced a reasonable solution, however, several input variables would be changed from their determined optimum values and the solver re-started to verify that the maximum CSFS found was not a local maximum only. Three or four verifications producing approximately the same CSFS were considered to confirm that this value was the maximum obtainable from a concept.

It was found in the original solutions obtained for each concept that extraordinarily high cruise velocities, from 120 to 150 feet per second, were being used to maximize CSFS. These values were thought unreasonable and likely a result of inaccurately modeling the capabilities of the propulsion system since constant efficiencies were used regardless of power demand. Rather than attempt a more detailed analysis of the batteries, motor, and propeller, an additional constraint was imposed limiting cruise speeds to a more reasonable (though still felt to be high) 90 feet per second.

Figure 3.6 gives the flight score, cost function, and maximum CSFS obtained for each concept and shows that the flying wing was determined to hold the highest scoring potential. Figure 3.7 compiles the geometric and mission parameters that produced this score. It was this baseline configuration that was then selected to move forward to the preliminary design stage.

Figure 3.6: Optimized concept scores				
CONCEPT	Monoplane	Biplane	Canard/Tandem Wing	Flying Wing
Flight score	133	133	145	143
Cost function	\$3126	\$3663	\$3078	\$2315
Cost-specific flight score	0.0426/\$	0.0364/\$	0.0472/\$	0.0618/\$

Figure 3.6: Optimized Concept Scores

The figure listed above shows the comparison of several calculations for the various configurations that were investigated.

Conceptual Design

Figure 3.7: Maximum-CSFS flying wing concept definition	
Heavy payload weight (lbs.):	45.5
Cruise velocity, heavy payload (ft/s):	90
Number of tennis balls:	10
Cruise velocity, light payload (ft/s):	90
Wing span (ft):	7.74
Wing aspect ratio:	12
Wing area (ft ²):	5.0
Winglet area (ft ²):	0.1
Number of control surfaces:	4
Main fuselage radius (in):	3.3
Main fuselage length (in):	7.7
Nose length (in):	4
Fuselage tailcone length (in):	4
Total fuselage length (in):	15.7
Motor rated power (W):	500
Number of motors:	1
Number of servos:	5
Aircraft empty weight (lb):	4.25

Figure 3.7: Maximum CSFS Flying Wing Concept Definition

The figure above shows the best cost-specific flight score that could be achieved with the conceptual flying wing.

Introduction

During the preliminary design phase, the flying wing configuration was optimized. This included the planform and airfoil selection of the wing. The fuselage and component placement within the fuselage was also considered.

Wing

After the conceptual phase of the design was complete, the team no longer used the Excel spreadsheet as its primary source for data. The Excel spreadsheet was utilized for rechecking calculations and for estimating take off and landing figures. Calculations were done by hand using formulas from aerodynamic, stability and control and propulsion classes. Doing calculations by hand was found to be more accurate and less stressful than manipulating the computer code.

The primary configuration of the aircraft was a flying wing. The team decided to look at two different wings for the aircraft. The first was a tapered wing with the second being a constant chord wing which was a little larger than the first. The shape of the wings was vastly different, but they used the same airfoil as their basic structure. This airfoil was the EH 3.0/12. This airfoil was chosen for its low pitching moment, and high thickness. The airfoil was found during an internet search for flying wing information from the B²Streamlines website, and performance data for this airfoil was found on an UIUC website. A low pitching moment airfoil was desired so that control surfaces could be more effective. The thicker airfoil was chosen for its increased camber, which helped create the lift necessary for the wing.

When the hand calculations for the two wings were compared, a decision for the final wing configuration was reached. The tapered wing's calculations showed that this design possibly could not takeoff within the required distance, when carrying the heavy payload. On further inspection, the tapered wing resulted in a wing loading that was higher than practical. Another concern was that the stability of the design would be effected because the tapered wing would have Reynolds numbers that were too low. Calculations for the constant chord wing were more favorable. With the constant chord wing, the design could take off within the required takeoff distance. It also brought the wing loading into a more comfortable range, and improved the Reynolds number at the tips. The problems with the constant chord wing were that it would weigh more, it had a higher cost function, and drag increased. The improved takeoff performance and increased ease of manufacturing offset these negatives. Thus, the team chose to use the constant chord wing for the final design.

Fuselage

During the preliminary design, several fuselage concepts were considered. The main configurations of these were circular and rectangular cross-sections. A rectangular cross-sectioned fuselage was chosen for its ease of manufacture and integration of the wing to the fuselage. The rectangular fuselage also allowed for a wider fuselage, with a smaller cross-section. A wider fuselage accomplished our goal of creating a design with a minimum cost function. Wider fuselages can hold more payload with a shorter fuselage, reducing the cost. One drawback to the rectangular fuselage shape was that it had more aerodynamic drag than the circular shape. This was overcome with a streamlined fuselage that resembled a wing airfoil, which had the added benefit of creating more lift.

Speed Loader

The cross-section of the fuselage determined to cross-section of the speed loader. The team realized it would be easiest to mate a flat-bottomed rectangular speed loader into a rectangular fuselage. The team's priority was to carry as much weight as possible, and carry the minimum number of tennis balls. This provided a smaller aircraft that allowed a smaller drag penalty. The team also found that designing for one pound of steel weight was easier to accommodate than five tennis balls. These numbers were taken from the scoring part of the contest rules, and represented a score increase that was an integer.

Systems

Placement of the engine, payload, and batteries were considered after the outline of the fuselage was determined. Some of the configurations tried were rear-facing aft mounted, and forward-facing front mounted engines. Payload configurations included placement under and above the wing. The team decided that top mounting the payload would be more efficient since mounting the payload under the wing provided poor access to it during changes. The two payloads have very different weights, and could potentially have a significant effect on the design's center of gravity. Therefore, the payload was placed at the design's aerodynamic center so that the two payloads didn't have a degrading effect on its stability.

The engine and batteries were the only items remaining that had to be placed such that the aircraft remained balanced and efficient. Propeller strikes were a major concern in placing the engine in an aft and rearward facing position. Forward placement of the engine was the only way to reduce the risk of a propeller strike. Placing the engine in the front of the aircraft, and the desire for orderly ground matters concluded in a tricycle landing gear for the plane. In order to keep the aircraft balanced, the batteries had to be placed as far aft as possible. The final choice in engine and propeller were left to the detailed design.

Constant Wing Loading Curves

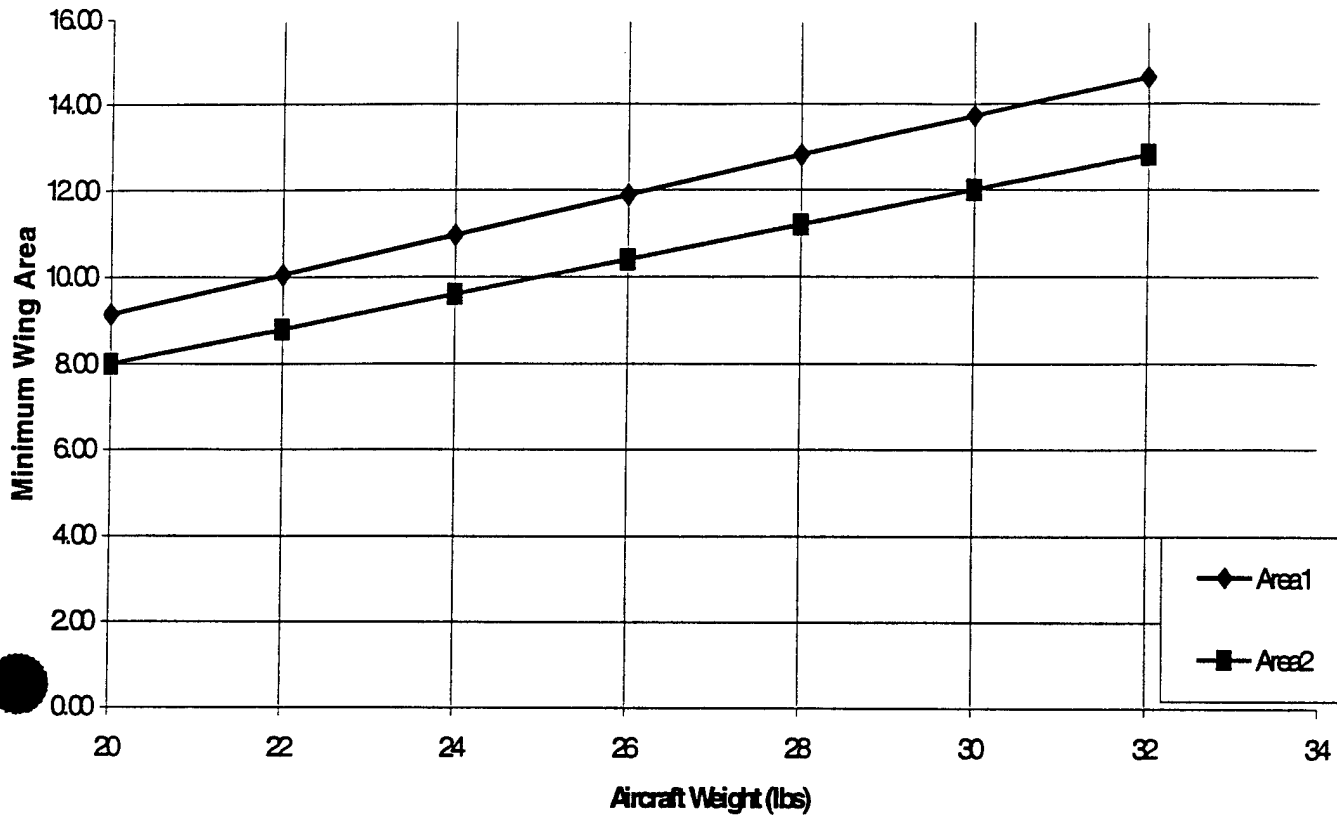


Figure 4.1: Graph of wing loading.

The Chart above details the minimum wing area needed for the given aircraft weight, with area 1 being the constant chord wing and area 2 being the tapered wing.

Preliminary Design

Figure 4.2: Calculations for Take-off time and distance					
Fric. Coeff.	K	Vstall, no flaps	Vto, no flaps	Vstall, flaps	Vto, flaps
0.020	0.0393	37.448	44.937	34.455	41.346
Static Thrust (lb.)	Weight (including 12 lb. airframe)			Grav. Accel.	
5.000	32.000			32.200	
Cl,ground (Clg)	Cd,ground (Cdg)	a (for thrust equation)		a,flaps	
0.254	0.015	-0.00105		-0.00160	
Calculations for A and B					
A		B, no flaps		B, flaps	
4.387		-0.00093		-0.00149	
Take off distance (ft):					
No flaps		Flaps			
191.577		153.717			

Figure 4.2: Take off calculations

The chart above is the list of the calculations made in the Excel spreadsheet for take off distance.

4.3 Complete analysis of flying wing in preliminary design phase	
CONSTANTS	
Tennis ball weight (lb.):	0.128906
Course distance (ft):	2376.991
Number of landings per cycle:	2
Time available to fly (min):	10
Manufacturer's Empty Weight Multiplier (\$/lb.):	100
Rated Engine Multiplier (\$/W):	1
Manufacturing Cost Multiplier (\$/h):	20
INPUTS	
MISSION	
Heavy payload weight (lb.):	44.90783
Cruise velocity, heavy payload (ft/s):	60
Number of tennis balls:	11.02811
Cruise velocity, light payload (ft/s):	60
Estimated time to land, change payload, take off (s):	60
WING	
Wing span (ft):	8.855935
Wing span (for cost purposes)	9.641935
Wing aspect ratio:	9.765861
Wing area (ft ²):	8.030792
Wing area (for cost purposes)	8.816792
Wing Oswald efficiency factor:	0.8
Wing planform area-specific weight (lb/ft ²):	0.3939

Wing planform area C_{D0} :	0.007
Number of wings:	1
Number of struts or braces:	0
Number of control surfaces:	4
C_{Lmax}	1.6
FUSELAGE	
Main fuselage side radius (in):	3.259
Main fuselage flat section width (in):	0
Main fuselage length (in):	7.443977
Nose length (in):	8
Fuselage tailcone length (in):	0
Total fuselage length (in):	15.44398
Main fuselage wetted area-specific weight (lb/in ²):	0.00284
Number of bodies:	1
Fuselage cross-sectional area C_{D0} :	0.05
TAILS	
Number of vertical tail surfaces:	0
Number of horizontal tail surfaces:	0
Horizontal tail area (ft ²):	0
Vertical tail area (ft ²):	0
Tail planform area-specific weight (lb/ft ²):	0.2325
Tail planform area C_{D0} :	0.0091
Landing gear C_{D0} factor:	1.2
POWER	
Battery weight (lb.):	5
Number of battery cells:	6
Voltage per cell (V):	1.2
Battery voltage-specific energy (mA-h):	3000
Motor rated power (W):	500
Motor fuse value (A):	40
Motor power-specific weight (lb./W):	0.00125
Number of motors:	1
Motor electrical efficiency:	0.8
Number of propellers:	1
Propeller weight (lb.):	0.15
Propeller efficiency:	0.8
FLIGHT SYSTEMS	
Number of speed controllers:	1
Speed controller weight (lb.):	0.125
Number of servos:	2
Weight per servo (lb.):	0.125
CALCULATION	
Wing induced drag coefficient K:	0.040743

Wing weight (lb.):	3.163329
Main fuselage cross-sectional area (in ²):	33.36711
Main fuselage circumference-equivalent radius (in):	3.259
Main fuselage cross-sectional area-equivalent radius (in):	3.259
Fuselage wetted area (in ²):	274.24
Fuselage weight (lb.):	0.778842
Tail weight (lb.):	0
Motor weight (lb.):	0.625
Total servo weight (lb.):	0.25
Battery energy per cell (mA-V-min):	216000
Total battery energy (mA-V-min):	1296000
Total battery energy (ft-lb.):	57352.12
Available thrust power (W):	320
Available thrust power (ft-lb./s):	236.017
Available propulsive energy (ft-lb.):	36705.36
Light payload weight (lb.):	1.421593
Aircraft C _{D0} :	0.010131
Aircraft empty weight (lb.):	10.09217
Minimum velocity, unloaded (ft/s):	25.70172
Drag coefficient C _D at V _{min} , unloaded:	0.114432
Aircraft L/D at V _{min} , unloaded:	13.98205
Thrust required at V _{min} , unloaded (lb.):	0.721795
Power required at V _{min} , unloaded (ft-lb./s):	18.55137
Aircraft heavy payload gross weight (lb.):	55
Lift coefficient C _L at cruise, heavy payload:	1.6
Drag coefficient C _D at cruise, heavy payload:	0.114432
Aircraft L/D at cruise, unloaded:	13.98205
Thrust required at cruise, unloaded (lb.):	3.933616
Power required at cruise, unloaded (ft-lb./s):	236.017
Aircraft light payload gross weight (lb.):	11.51376
Lift coefficient C _L at cruise, light payload:	0.334946
Drag coefficient C _D at cruise, light payload:	0.014702
Aircraft L/D at cruise, light payload:	22.78221
Thrust required at cruise, light payload (lb.):	0.505384
Power required at cruise, light payload (ft-lb./s):	30.32303
Energy required to fly single lap with heavy payload (ft-lb.):	9350.171
Energy required to fly single lap with light payload (ft-lb.):	1201.293
Energy required to fly cycle of one heavy lap, two light laps (ft-lb.):	11752.76

Number of cycles flyable:	3.123128
Time required per cycle (s):	238.8496
Number of cycles flyable in time available:	2.512042
Number of cycles flown:	2.512042
Flight score:	118.3509
COST FUNCTION	
Manufacturer's Empty Weight (lb.):	5.09217
Rated Engine Power:	288
MFHR	
Wing assembly time (h):	58.94107
Fuselage/pod assembly time (h):	10.14799
Empennage assembly time (h):	0
Flight system assembly time (h):	11
Propulsion system assembly time (h):	10
Total assembly time (h):	90.08907
Total rated aircraft cost (\$1000):	2.598998
Cost-specific flight score:	45.53714

Figure 4.3: Complete analysis of flying wing in preliminary design phase

The figure above shows all constraints placed upon the flying wing, as well as all the inputs for the Excel spreadsheet. This spreadsheet was used to recalculate all numbers that were calculated by hand.

Introduction

The detailed design of the aircraft was determined once the preliminary design phase was completed. This included material selection for the wing and fuselage. Other aspects decided in the detailed design were the selection of the engine, batteries, and propeller.

Wing

Based on information from last year's Virginia Tech Design/Build/Fly entry, the team chose to build a blue foam core wing skinned in bi-directional carbon fiber. The wing would include an I-beam of two layers of bi-directional carbon fiber inserted at the quarter chord of the wing. The wing tips will be built from the same blue foam, and covered in four-ounce fiberglass. The glassing of all aspects of the aircraft will be done with 24-hour curing model epoxy. Part of the reasoning behind selecting this method of construction was carbon fiber leftover from last year. This diminished our cost to produce the wing, an important factor in our design because of our limited budget.

Fuselage

The fuselage was based off of a $\frac{1}{4}$ inch sheet of plywood that the engine, payload, wing were attached to. This sheet was 12 inches wide, the same width of the fuselage. The streamlined portions of the fuselage were constructed from blue foam and basswood. The blue foam was covered with four-ounce fiberglass. The streamlined portions of the fuselage are the portions in front and behind of the payload and wing. The speed loader that contains the payload will be constructed of a balsa frame with balsa and plywood skins. The wing and speed loader will be attached through 4 common steel bolts attached with locknuts. Again, the impetus behind these selections was the abundance of plywood from previous years, and the inexpensive cost of blue foam.

Systems

The aircraft's power is an important part of the design. This was hampered by the team's inexperience with electric motors and electrical theory. After significant use of the shareware version of MotoCalc these aspects were determined. The team decided to go with an AstroFlight Cobalt 60 motor with an AstroFlight Superbox, and AstroFlight 204D speed controller. These components were chosen because of ease of access to AstroFlight's website and information. The AstroFlight Cobalt 60 also satisfied the engine's power requirements, and fit within the contest's requirement of brushed motors. The Superbox gearbox was included with the engine, simplifying its choice, and the use of the engine. Power to the engine will be provided through 40-amp fuse. It will come from 13 cells in 3 banks of Sanyo 2400 NiCad batteries. The decision to use these batteries was because they were leftover from previous years, and they provided the

Detailed Design

energy required to fly the mission. A 20-inch composite propeller was determined to pull the aircraft along.

A specific landing gear wasn't chosen because none investigated fit the team's requirements. The team did not want to repeat the errors of the Virginia Tech's entry last year. The team was looking for a gear that provided a significant amount of flex without breaking. This was a design parameter because this would let the gear suck the plane into the ground, rather than bouncing it off the ground. This is an important part of the design, and hasn't been finalized at this time.

Figure 5.1: Calculations for Detail Design	
Area of Wing	11.25 feet ²
Aspect Ratio	7.2
Taper Ratio	1
Sweep of the leading edge	25°
M	1.05 feet
Mean Aerodynamic Chord	1.25 feet
Y bar	2.25 feet
Neutral Point of the Wing	0.22
Neutral Point of the Aircraft	0.244
h_n	0.144
a_{wb}	4.44 per radian

Figure: 5.1 Calculations For Detailed Design

This figure shows the final calculations of the stability and control data for the detail design of the aircraft.

Figure 5.2: Key Features that Distinguish the Detail Design
Streamlined Fuselage
Constant Chord Wing
Large Wing Tips
EH 3.0/12 Airfoils
Twenty Five Degrees of Sweep

Figure 5.2: Key Features that Distinguish the Detail Design

The figure above shows the features of the detailed design, which distinguishes it from the conceptual and preliminary designs.

Introduction

The manufacturing of this aircraft was completed in three main parts, the wing, the fuselage, and the speed loader. These aspects were done simultaneously to reduce production time depending on the number of team members available, and the progress completed on each aspect.

Wing

The wing was built in three sections: the left panel, the right panel, and the center section. The planform of the wing panels were marked out on the blue foam with a black Sharpie pen, with extra triangles added at the either side of the panels. The triangles were added so that the wing will be the correct wing span after the wing sweep angle has been cut out of the panels. The airfoils were hot-wired from the all three foam planforms using a Featherlite system, and then the wing cores were hot-wired along the quarter chord. A channel was carved from the leading edge of the aft section of the wing exposed by the quarter chord cut to accommodate servo wire. Each wing section will be glassed separately. The glassing process started with the adhesion of the two strips of bi-directional carbon fiber to the trailing edge side of the forward part of the wing exposed by the quarter chord cut of the wing. The two wing parts were attached together, while the epoxy was still wet. While this was taking place another group wetted down the carbon fiber skin, which was placed over the wing after the two wing parts have been attached. A final strip of four-ounce fiberglass was wetted and placed at the leading edge of the wing. Mylar wing covers were placed around the wing. This was all placed in a vacuum bag cradled by the excess wing core foam and allowed to cure for 24 hours. Once the wing had setup the wings were removed, and the wing sweep was cut from wings. This cost unused carbon fiber, but this was outweighed by the increased ease of setting up the wing in the vacuum bag. The wingtips were constructed in a similar manner, only skinned in four-ounce fiberglass instead of carbon fiber.

The wing panels were attached by cutting small balsa wing holder that was epoxied in the exposed foam core of the wing. This allowed the team to make sure the wings were set at the same angle of attack at predetermined positions along the wingspan. After the placeholders had dried, the wings were glassed together with four-ounce strips at the two joints, covered with Mylar and vacuum bagged. The wing tips were joined the same way.

Fuselage

The fuselage was built up from the plywood plate. Two vertical stations were built onto this plate. One acting as the firewall the engine would be bolted to. Another bulkhead divided the payload and wing from the electronics section of the fuselage. From the second vertical bulkhead a lower surface extended, made of basswood. The rest of this section was built from foam shaped to fit the streamlined outline of the aft portion of the fuselage and glued to the basswood

Manufacturing Plan

sheet. Space for the batteries, receiver, and other electronics were carved from this blue foam. The front portion of the fuselage was built up in the same manner, with a portion cut out for the engine and gearbox. Once the shape of both the fore and aft section of the fuselage was determined it was covered with four-ounce fiberglass and then vacuum bagged. The wing was attached to the undersurface of this plywood plate, with foam epoxied to the bottom of the plywood sheet so the wing was attached at the correct angle of attack. This foam was not glassed to reduce weight, and to ease the placement of the wing to the fuselage.

Speed Loader

The speed loader was built up from a balsa frame. The frame was constructed of one-quarter inch square cross-sectioned stringers, and 5-Minute epoxied at the corners of the box. The bottom of the box was cut from one-quarter inch plywood, while the other five sides were skinned in one-quarter inch balsa to save weight. For the tennis ball cargo, strips of the "hook" side of velcro were epoxied to the inside of the top and bottom of the speed loader to secure the tennis balls in-flight. A foam block was cut to fit inside the speed loader, with holes cut in it to accept the steel. The foam would act to stabilize the steel in-flight. Different foam inserts were cut to accommodate different steel payloads. Two Metal "L" brackets were epoxied to forward side of the speed loaders, with one on the left and right side of the speed loader, two inches from the rear of the speed loader. The brackets already had holes drilled in the bottom of the "L" to accept a bolt through. Holes were drilled through the fuselage and wing in corresponding places. Locking nuts were epoxied to the plywood plate of the fuselage, above the drilled holes. The bottom of the wing was counter sunk so the bolt's heads wouldn't be seen by the flow. Next wings were bolted to the fuselage through the epoxied bolts. Then one of the speed loaders was placed over the exposed bolts, and bolted in place with four more locknuts. The excess bolt showing from these final bolts were marked. Then the bolts were removed, and cut to size to save weight.

Systems

Once all the aspects of the aircraft had been built, and checked for fitting the systems of the aircraft were installed. Holes were dug in the underside of the wing where the servos were to be placed. Servo wires were run down the channel along the quarter chord of the wing. A hole was cut out of the center section of the wing where all the servo wires exited the wing, and ran through the back bulkhead to the electronics section. The servos were attached to a one-eighth inch piece of basswood; the basswood was then epoxied into the cut out holes. The control surfaces were cut out of 3/16-inch balsa, and control horns were epoxied to their lower surface. The bottom of the wing where the flaps would be placed was carved out so that the flaps would fit flush with the bottom of the wing. All the surfaces were fiberglass taped in position. Metal control-arms were cut to length and connected to the servos and control surfaces. The engine was screwed in place, and control wires were run to the electronics part of the fuselage. They ran

along the underside of the plywood plate, and were taped to it so that they would not get fouled with other wires.

Figure 6.1: Tasks to be Performed During the Building Phase		
Task	Skill Level Needed	Number of team members available for task
Template Making	3	2
Hot Wiring Foam	1	2
Sanding Foam	1	1
Applying Epoxy	5	4
Vacuum Bagging	5	4
Sanding Down Cured Parts	2	1
Adding Control Surfaces	2	3
Adding Servos	2	3
Building Speed Loader	1	2
Assembling Final Product	4	4

Figure 6.1: Tasks to be Performed During the Building Phase

This figure shows the tasks that had to be completed during the building process, the difficulty of the task with a 5 indicating a difficult task and a 0 indicating an easy task. The number of team members is the minimum number of people that is needed to complete each task.

References

1. Jim Ryan's weight estimation spreadsheet. Linked from
<http://members.aol.com/kmyersefo/page31.htm>
2. "AstroFlight Inc. Sport & FAI Motors." <http://www.astroflight.com/motors.html>
3. Utah State 1999-2000 Design Build Fly Report
<http://amber.aae.uiuc.edu/~aiaadbf/99reports/>
4. <http://www.halcyon.com/bsquared/EH.html>
5. <http://amber.aae.uiuc.edu/~m-selig/flyingWingAfs/>
6. <http://www.motocalc.com>

HOKIE BIRD 5

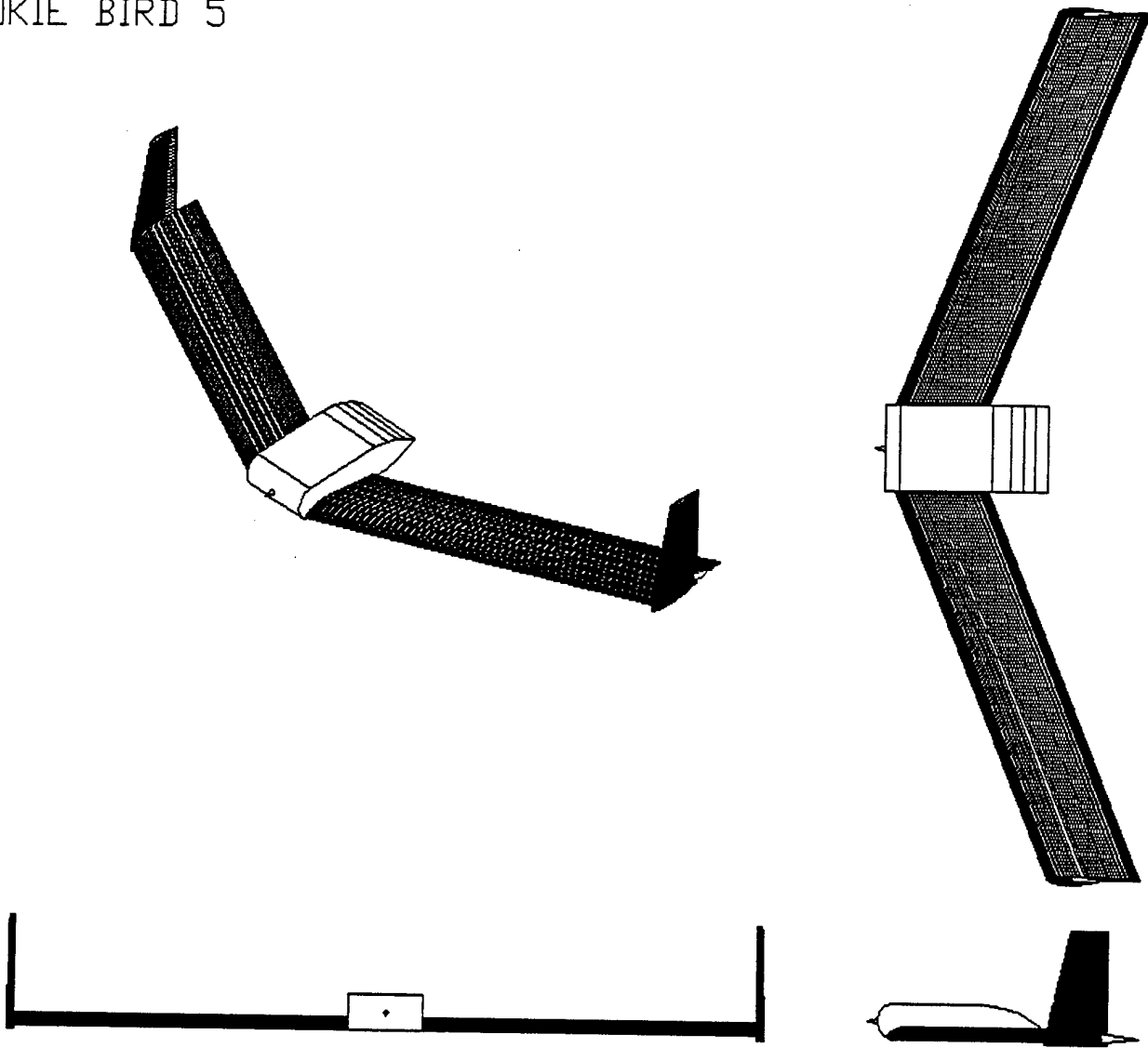


Figure 7.1: Three-View Drawing of the Aircraft

The figure above shows the three view drawing of the aircraft. Dimensions are on subsequent drawings.

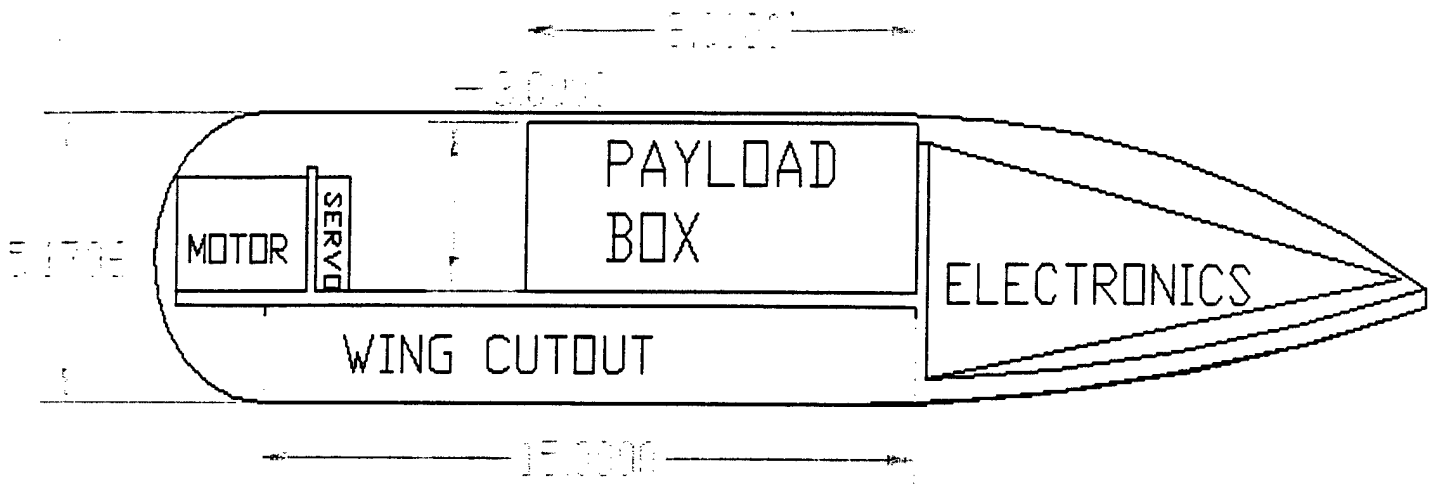


Figure 7.2: Fuselage Layout

The figure above is the layout of the fuselage. All measurements are in inches.

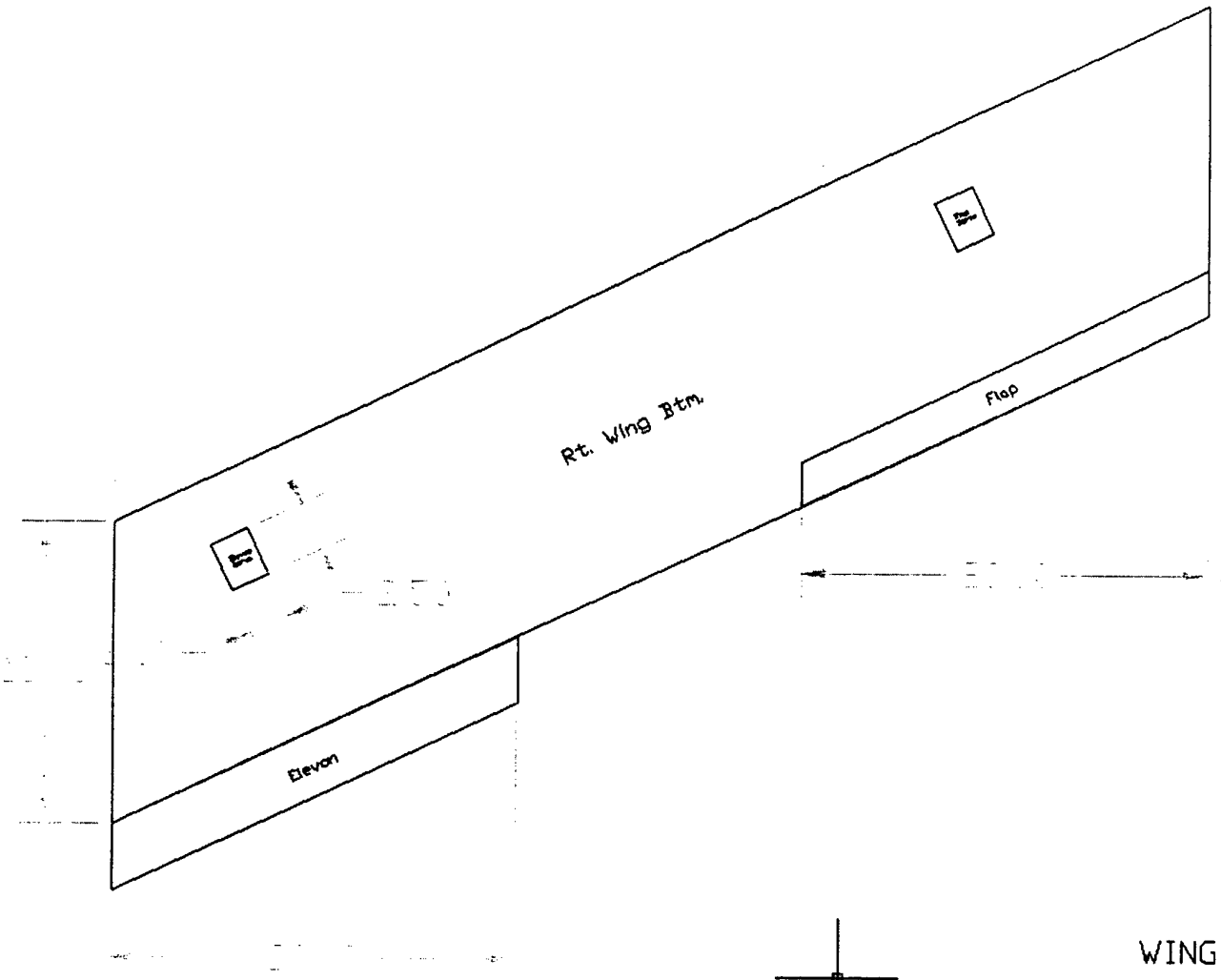
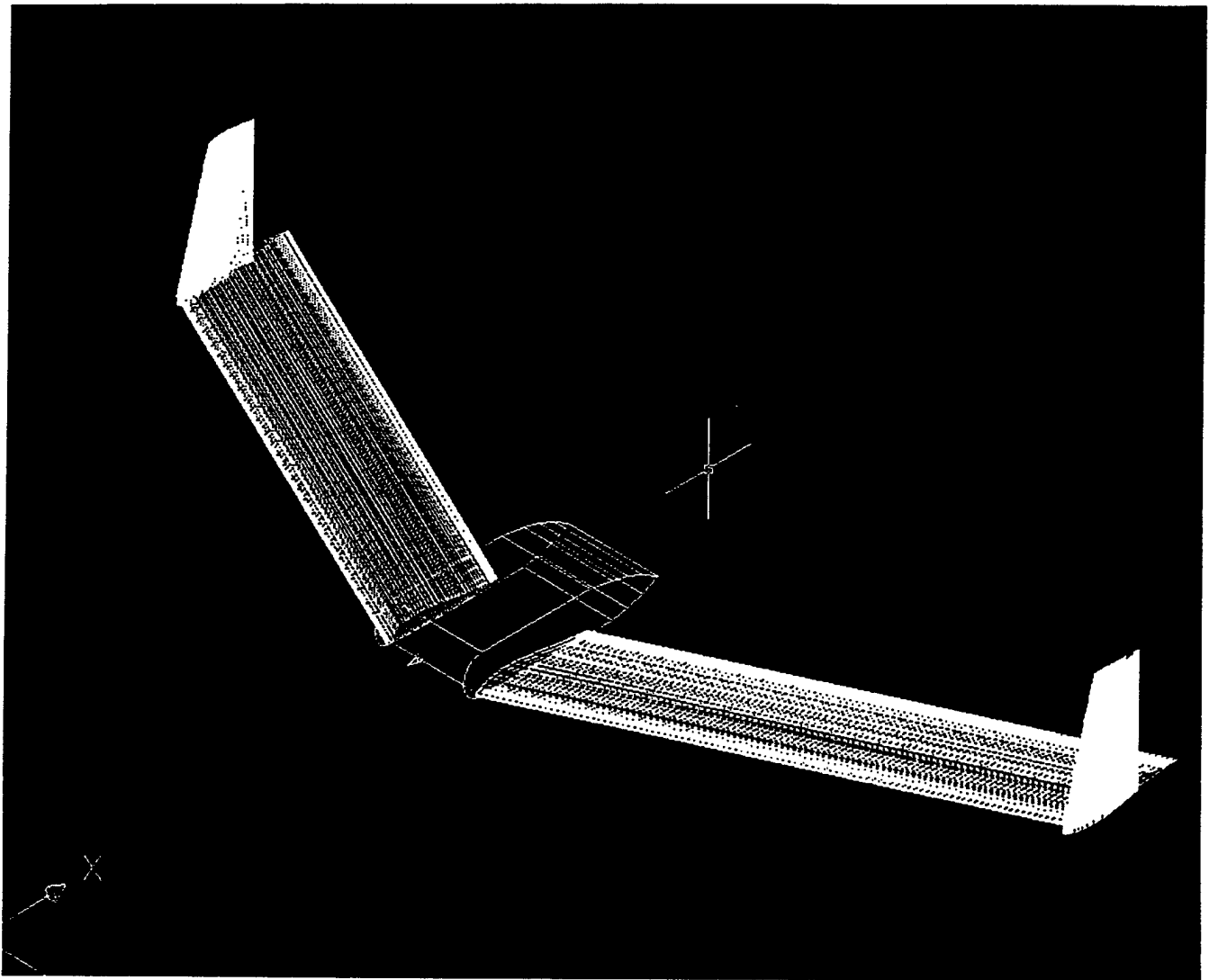


Figure 7.3: Wing Layout

The figure above shows the layout of the wing with the servos, flaps and elevons. All measurements are in inches.

2000/2001 AIAA Foundation Cessna/ONR Student Design Build Fly Competition

Addendum Report



Virginia Polytechnic Institute and State University

April 2001

The Design/Build/Fly team from Virginia Polytechnic Institute and State University has successfully attained the goals set for the manufacturing and development of the aircraft that will be its entry in the AIAA/Cessna/ONR Design/Build/Fly competition which started at the beginning of the 2000 school year and culminated April 20th through April 22nd, 2001 at the Office of Naval Research in St. Inigos, Maryland.

Several changes occurred in the overall design between the entry of the design report and the final manufacturing of the aircraft. Most of the changes were done to the wings. Drag rudders were added to the wing because yaw control was needed during take off. The wing tips were made smaller and the thickness was also lessened. This was done because it was found that larger wing tips were too stable. During testing with the half-scale model, the larger tips caused a greater amount of weathercocking to occur. The reducing of the tips also helped to reduce the wing area, which reduced the rated aircraft cost score slightly. In addition to reducing the size of the tips, their placement was also altered. The wingtips were placed with their trailing edges lining up with the trailing edge of the wing. This change is not shown on the cover of the addendum due to the requirements of the contest that the cover of the report and the addendum be the same. For the quarter chord I-beam, only one strip of bi-directional carbon fiber was used, instead of the two strips that were originally going to be used. This reduced not only the weight but also the cost to the team, since less carbon fiber had to be purchased.

Changes were also made to the payload box, the fuselage, and the landing gear was designed. Carbon fiber was added to the top of the payload box to increase strength during the inverted testing. Also, a body panel was added around the payload box to improve the aerodynamic flow over the fuselage. Holes were drilled in the fuselage plate such that no structural integrity was lost but weight was removed from the aircraft. The aircraft landing gear was designed so that structural integrity improved over designs that were researched from previous years. The main landing gear was made with leftover bits of Carbon Fiber from previous year's attempts, using a white foam core that was less dense than the blue foam we used for the wings. The less dense foam was chosen because it was also left over from previous years, and lightened the overall weight of the design. A steel rod was used for the nose wheel instead of the strut that was used in previous years' designs. The landing gear was designed to be able to absorb the shock from possible imperfect landings, while remaining cost effective to the team.

Several things could be improved in terms of design and manufacturing for next year's aircraft. The fuselage would also be designed with weight reduction, and ease of construction in mind. The fiber glassing and hot-wiring techniques were rudimentary at best this year. The four and a half foot semi-span wings proved difficult to hotwire, because bowing in the hotwire caused imperfections in the wing; an alternative method was devised which refined in following years. In addition, the wings were too thick to fit inside a single layer of blue foam. Methods of attaching two panels of blue foam were investigated, however none provided a solution that was cost effective, easy to manufacture, or to the level of perfection desired. Fiber glassing will improve in years to come because the number of team members with experience will rise from none to six. In addition this experience will be taught to rising members earlier in the manufacturing of test models. The fiber glassing of leading edge would be improved in future years because the leading edge pinched together during vacuum bagging. Because of this, time was wasted sanding and refiber-glassing the leading edge to the appropriate shape. Too much time was consumed while refining the placement and function of aircraft systems. Experience gained during the design of the aircraft this year will alleviate the need for in-depth study of system placement. More time would be allocated in the final design construction to improve the application of these systems.

The analysis of the conceptual designs would be improved with a greater number of team members experienced in evaluation of conceptual designs. Thus, the flying wing concept would be reconsidered with its stability problems included in the analysis of the design. During the course of the design and construction of the aircraft several mathematical and aerodynamic theories were challenged. These included Pythagoras' theorem for right triangles, that wing center sections should be included in aspect ratio calculations. Realizing these theorems have already been sufficiently verified could save significant time during the final design and construction. Time could also be saved in future years by producing only one scale model of the design, and having this completed before winter break. Time management in general will be improved. Quintessential in this time management is beginning the written and construction aspects of the design earlier in the spring semester. Gathering materials necessary for the construction of the final aircraft would also be done at the same time.

All the above-mentioned changes would be cost effective as well as time saving, which would be beneficial to the team.

The design is to have black carbon fiber wings with "Hokie Bird 5" stenciled on the upper left wing, in accordance with the contest specifications. On the upper right wing, a Penske Trucking decal may be placed, pending their support. A white VT may be stenciled on the bottom

of one of the wings if test flights determine insufficient visibility of the aircrafts attitude. The fuselage and wingtips will be covered in maroon wrapping paper dotted with orange Virginia Tech "VTs."

Transportation of the aircraft is being negotiated with Penske Trucking. The details of this donation are still being solidified. If it does not work out, we are planning to use a team member's personal vehicle.

On the following pages the Rated Aircraft Cost is determined. The Rated Aircraft Cost score was calculated using a formula provided in the contest rules and regulations.

Rated Aircraft Cost

Rated Aircraft Cost, \$ (Thousands) = $(A \cdot \text{MEW} + B \cdot \text{REP} + C \cdot \text{MFHR}) / 1000$

A: Empty Weight Multiplier -- \$100 / pound

B: Rated Engine Power -- \$1 / watt

C: Manufacturing Cost -- \$20 / hour

MEW: Manufacturers Empty Weight – Actual weight without batteries or payload

REP: Rated Engine Power – number of engines * Amps * 1.2Volt/cell * number of cells

MFHR: Manufacturing Man Hours – the sum of work breakdown hours, which are listed below.

MEW:

The manufactures empty weight of the aircraft was calculated by weighing the empty aircraft in the aerospace shop. The total wing weight was 6 pounds. The fuselage and speed loaders weighed 6 pounds. This means that the total empty weight of the aircraft was 12 pounds. This was heavier than first estimated, but still manageable with the engine chosen.

REP:

Only one engine was used for this aircraft. It was decided to use the full 40 amps and to have 39 cells. Multiplying all the pieces of the equation together, the total REP equaled 1872.

MFHR:

The manufacturing man-hours include all areas of the aircraft. The table on the next page shows the work break down as well as the calculated work hours.

Table 1.1 Manufacturing Plan for the Aircraft and Total Cost		
Structure	Work Break Down	Total Cost
Wing	15 hours per wing	15
	4 hours per square foot of area	61
	2 hours per strut or brace	0
	3 hours per control surface	24
Fuselage	5 hours per body	5
	4 hours per foot of length	10.5
Empennage	5 hours basic	0
	5 hours per vertical surface	0
	10 hours per horizontal surface	0
Flight Systems	5 hours basic	5
	2 hours per servo / controller	14
Propulsion system	5 hours per engine	5
	5 hours per propeller or fan	5
TOTAL MFHR		144.5

Table 1.1: Manufacturing Plan for the Aircraft and Total Cost.

The above table shows the work hours calculated for each part of the aircraft. These work hours were used in the final determination of the rated aircraft cost.

Total Rated Aircraft Cost:

$$RAC = ((100 * 12) + (1 * 1872) + (20 * 144.5)) / 1000$$

$$RAC = 5.962$$